34TH ANNUAL CONFERENCE ON MASS SPECTROMETRY AND ALLIED TOPICS

TABLE OF CONTENTS

INTRODUCTION v

CORPORATE MEMBERS vi

ASMS BOARD OF DIRECTORS viii

MASS SPECTROMETRY LOCAL DISCUSSION GROUPS ix

34TH ANNUAL CONFERENCE ON MASS SPECTROMETRY & ALLIED TOPICS

LISTING OF EXTENDED ABSTRACTS xi

MONDAY MORNING ORAL SESSIONS
Liquid Chromatography/Mass Spectrometry 1
Symposium: Hybrid Mass Spectrometry 17

MONDAY MORNING POSTER SESSIONS
Fragmentation Mechanisms 28
Symposium: Expert Systems 52
Toxicology 66

MONDAY AFTERNOON ORAL SESSIONS
Applications of Ion Activation 85
Lipids 107
Symposium: Ion Image Processing & Analysis in SIMS . 124

MONDAY AFTERNOON POSTER SESSIONS
Elemental Analysis and Isotope Ratios 134
Instrumentation 154
Environmental 183

TUESDAY MORNING ORAL SESSIONS
Instrumentation FT/MS 212
Environmental Mass Spectrometry 234
Symposium: Isotopic Tracers in Mineral Nutrition . . 260

TUESDAY AFTERNOON POSTER SESSIONS
Computer Applications 276
Biochemistry 308
Biochemistry II 341

TUESDAY AFTERNOON ORAL SESSIONS
Symposium: Environmental Applications of MS 369
Instrument Development and Biological Applications . 377
Isotope Ratios and Elemental Analysis 401

TUESDAY EVENING POSTER SESSIONS
Ion Activation 416
Medicinal Chemistry and Biomedical Applications . . 445
Chlorinated Environmental Contaminants 476

WEDNESDAY AFTERNOON ORAL SESSIONS
Symposium: Bioactive Molecules 502
Ionization: New Developments 507
Cluster Ions 529

WEDNESDAY AFTERNOON POSTER SESSIONS
Ion Chemistry 549
Liquid Chromatography/Mass Spectrometry 566
Ion Chemistry II 600

THURSDAY MORNING ORAL SESSIONS
Symposium: MS in Molecular Biology 620
Desorption Ionization - Mechanisms and Methods . . . 632
Ion Activation Methods 661

THURSDAY MORNING POSTER SESSIONS
Organic Analysis 687
Instrumentation 707
Organic Analysis II 736

THURSDAY AFTERNOON ORAL SESSIONS
Symposium: Time-of-Flight Mass Spectrometry 762
Soft Ionization: Peptide Analysis 774
Ion-Molecule Reactions 794

THURSDAY AFTERNOON POSTER SESSIONS
Fuels and Polymers 817
Peptides 842
New Developments in Ionization Methods 870

FRIDAY ORAL SESSIONS
Mass Spectrometry in Biochemistry 896
High Mass Analysis and Instrument Development . . . 931
Ion-Neutral Complexes 969

FRIDAY POSTER SESSIONS
Drug Metabolism: Environmental 999
Drug Metabolites 1031
Surfaces; General Analytical 1058

FEATURE LECTURES
Plenary Lecture: The Growing Role of Mass Spectrometry in Molecular Biology, by Klaus Biemann, Massachusetts Institute of Technology 1077

Introductory Lecture: Tandem Mass Spectrometry: Coming of Age, by Richard A. Yost, University of Florida 1090

Introductory Lecture: Twenty Years of Chemical Ionization, by Alex G. Harrison, University of Toronto 1103

INDEX OF AUTHORS 1117

REPORTS OF INTEREST GROUPS AND WORKSHOPS
Academic Mass Spectrometry Laboratories 1131
Solids and Surface Analysis 1132
How to Manage an Environmental Laboratory 1134
Availability of Metal Stable Isotopes 1135
Multicollectors in the Real World 1136
Quantitative Organic Analysis 1137
Young Mass Spectrometrists 1138
Biomedical Applications 1140
Education 1141
Environmental 1143
Good Laboratory Practices 1144
History 1145
Ion Physics and Instrumentation 1146
Isotope Ratios 1148
Qualitative Organic Studeis 1149

MINUTES OF THE ASMS BUSINES MEETING 1150

MEMORIAL PAGE 1152

MINUTES OF ASTM COMMITTEE E-14 1153

MINUTES OF ASTM COMMITTEE D-2 1155

MIDDLE AGE TURKS (MAT) vs. YOUNGER MASS SPECTROMETRISTS (YMS) 1157

REPORT OF THE PRESIDENT 1162

DIRECTORY OF MEMBERS AND 34TH ANNUAL CONFERENCE PARTICIPANTS
U.S.A. 1164
CANADA 1231
FOREIGN 1235

CITATION NOTICE

This volume contains the abstracts of papers presented at the 34th Annual Conference on Mass Spectrometry and Allied Topics. It is intended that this volume be distributed only to members of ASMS and conference registrants; therefore, it is not considered to be a publication.

References to individual abstracts contained in this volume should be cited as follows:

Author(s); title; presented at the 34th Annual Conference on Mass Spectrometry and Allied Topics, Cincinnati, OH, June 8-13, 1986.

INTRODUCTION

This bound volume is the official record of the 34th Annual Conference on Mass Spectrometry and Allied Topics held in Cincinnati, Ohio, June 8-13, 1986. The extended abstracts provide a timely view of research and innovations in mass spectrometry and a historical record. In the back of this volume are workshop and interest group reports and a directory of names, addresses and telephone numbers of members and conference attendees. The value of this record is a reflection of the care taken by each contributor in preparing the manuscripts and reports, and in meeting the publication deadline.

The efforts of Mrs. Judith Watson of Professional Association Management in compiling the bound volume and arranging for timely printing and distribution in a cost effective manner are gratefully acknowledged. This volume also reflects the dedication of Gerry Meisels, the Vice President for Programs, in arranging the technical program.

It is the desire of the Board of Directors of ASMS that the Bound Volume be a valuable asset to the members of this Society. Comments or suggestions directed toward making this a more useful resource are appreciated.

Charles N. McEwen
Editor and Member-at-Large
ASMS Board of Directors

NOMENCLATURE

A list of defined terms appears on pages 920-940 of the Bound Volume for the 32nd Annual Conference on Mass Spectrometry and Allied Topics held May 27 - June 1, 1984, in San Antonio, Texas.

1986 CORPORATE MEMBERS

ATOMIKA INC
PO BOX 77070
PITTSBURGH PA 15215
PHONE: 412/963 8202

BALZERS HIGH VACUUM
8 SAGAMORE PK RD
HUDSON NH 03051
PHONE: 603/889-6888

BIO-ION
PO BOX 15045
UPPSALA S-75215
PHONE: 018-104440

CAMBRIDGE ISOTOPE LABS
20 COMMERCE WAY
WOBURN MA 01801
PHONE: 617/938-0067

COLORADO GROUP
WAL INC
GOLDEN CO 80403
PHONE: 303/278-9521

COMPUCHEM
PO BOX 12652
RES TRI PK NC 27709
PHONE: 919/549-8263

DETECTOR TECHNOLOGY INC
PO BOX K-300
BROOKFIELD MA 01506
PHONE: 617/867-7156

EXTREL
250 ALPHA DRIVE
PITTSBURGH PA 15238
PHONE: 412/782-3884

FINNIGAN CORP
355 RIVER OAKS PKWY
SAN JOSE CA 95134
PHONE: 408/946-4848

GALILEO ELECTRO-OPTICS
GALILEO PARK
STURBRIDGE MA 01518
PHONE: 617/347-9191

HEWLETT PACKARD
1601 CALIFORNIA AVE
PALO ALTO CA 94304
PHONE: 415/857-6090

INFICON LEYBOLD-HERAEUS
6500 FLY ROAD
E SYRACUSE NY 13057
PHONE: 315/437-0377

IONSPEC
ONE LONGSTREET
IRVINE CA 92714
PHONE: 714/857-0793

JEOL LTD USA
11 DEARBORN ROAD
PEABODY MA 01960
PHONE: 617/535-5900

JOHN WILEY & SONS
605 THIRD AVE
NEW YORK NY 10158
PHONE: 212/850-7063

KRATOS ANAL INSTRUMENTS
170 WILLIAMS DR
RAMSEY NJ 07446
PHONE: 201/934-9000

LINDEN-CHROMASSPEC
PO BOX 3451
PRINCETON NJ 08542
PHONE: 609/452-1451

M-SCAN INC (US)
PO BOX 5368
WILMINGTON DE 19808
PHONE: 302/453-8151

MASSPEC INC
275 TURKEY CREEK RD
BARTLESVILLE OK 74003
PHONE: 918/335-2707

MSD ISOTOPES
PO BOX 899
QUEBEC H9R 4P7
PHONE: 514/697-2823

NERMAG
10 KINGSBRIDGE ROAD
FAIRFIELD NJ 07006
PHONE: 713/442-0970

NICOLET INSTRUMENT
5225 VERONA RD
MADISON WI 53711
PHONE: 606/271-3333

NUCLIDE CORPORATION
642 E COLLEGE AVE
STATE COLLEGE PA 16801
PHONE: 814/238-0541

ONEIDA RESEARCH
ONE HALSEY ROAD
WHITESBORO NY 13492
PHONE: 315/736-3050

PERNICKA CORPORATION
112 RACQUETTE DR
FORT COLLINS CO 80524
PHONE: 303/224 0220

PHRASOR SCIENTIFIC
1536 HIGHLAND AVE
DUARTE CA 91010
PHONE: 213/357-3201

R J BRUNFELDT CO

BARTLESVILLE OK 74005
PHONE: 918/336-4467

SCIENTIFIC GLASS ENGIN
2007 KRAMER LANE
AUSTIN TX 78758
PHONE: 512/837-7190

SCIEX INC
55 GLENCAMERON RD
THORNHILL ONT L3T 1P2
PHONE: 416/881-4646

SHIMADZU SCIENTIFIC INSTR
7102 RIVERWOOD DR
COLUMBIA MD 21046
PHONE: 301/997-1227

SHRADER ANALYTICAL LAB
3814 VINEWOOD
DETROIT MI 48208
PHONE: 313/894-4440

SPECTROSCOPY
195 MAIN STREET
METUCHEN NJ 08840
PHONE: 201/549-3000

SPECTROSPIN AG
INDUSTRIESTRASSE 26
CH-8117 FAELLAN
PHONE: 01/825 48 55

TEKNIVENT CORPORATION
10774 TRENTON AVE
ST LOUIS MO 63132
PHONE: 314/429-7272

TMS ANAL SERVICES
6264 LAPAS TRAIL
INDIANAPOLIS IN 46260
PHONE:

TOFTEC
PO BOX 12877
GAINESVILLE FL 32604
PHONE: 904/472-2668

VACUMETRICS
2261 PALMA DRIVE
VENTURA CA 93003
PHONE: 805/644-7461

VESTEC CORP
9299 KIRBY DRIVE
HOUSTON TX 77054
PHONE: 713/521-2599

VG INSTRUMENTS INC
300 BROAD ST
STAMFORD CT 06901
PHONE: 203/322-4546

AMERICAN SOCIETY FOR MASS SPECTROMETRY
BOARD OF DIRECTORS
1985-1986

PRESIDENT	R. Graham Cooks Department of Chemistry Purdue University West Lafayette, IN 47907
VICE-PRESIDENT for PROGRAMS	Gerry G. Meisels College of Arts & Sciences 1223 Old Father Hall University of Nebraska Lincoln, NE 68588
VICE-PRESIDENT for ARRANGEMENTS	Catherine E. Costello Massachusetts Institute of Technology Department of Chemistry Cambridge, MA 02139
SECRETARY	Robert T. McIver, Jr. Department of Chemistry University of California Irvine, CA 92717
TREASURER	James J. DeCorpo Naval Sea Systems Command Code 05R32 Washington, DC 20362
MEMBER at LARGE	Charles N. McEwen E. I. du Pont de Nemours Experimental Station 228 Wilmington, DE 19898
MEMBER at LARGE	Gordon Wood Vice President, Academic University of Windsor Windsor, Ontario N9B 3P4
ASTM REPRESENTATIVE	Terrence R. Ashe ESSO Petroleum Post Office Box 3022 Sarnia, Ontario N7T 7M1
PAST PRESIDENT	Catherine C. Fenselau Johns Hopkins University Department of Pharmacology Baltimore, MD 21205
SOCIETY OFFICE	ASMS Post Office Box 1508 East Lansing, MI 48823
Telephone:	517/337-2548

CONTACTS FOR LOCAL MASS SPECTROMETRY DISCUSSION GROUPS

ATLANTIC CANADA
W D JAMIESON
NRC
1411 OXFORD STREET
HALIFAX, NOVA SCOTIA B3H 3Z1
902/426-8279

AUSTIN
JOHN W CHINN
DEPT OF CHEMISTRY
UNIV OF TEXAS
AUSTIN, TX 78712
512/471-7344

BOSTON
LAUREN YELLE
ARTHUR D LITTLE INC
15 ACORN PARK
CAMBRIDGE, MA 02140
617/864-5770

BRITISH COLUMBIA
GUENTER EIGENDORF
DEPT OF CHEMISTRY
UNIV OF BRITISH COLUMBIA
VANCOUVER, B C V6T 1Y6
604/228-3235

CENTRAL NEW MEXICO
T R HENDERSON
5609 DON FELIPE CT S
ALBUQUERQUE, NM 87105
505/844-4267

CONNECTICUT
H Y GUH
PFIZER
EASTERN POINT ROAD
GROTON, CT 06340
203/441-4260

DELAWARE VALLEY
LEW KILMER
SK & F LABS
15 W SPRING GARDEN STREET
PHILADELPHIA, PA 19101

INTERMOUNTAIN
THOMAS R SHARP
CHEMISTRY DEPT
UNIV OF UTAH
SALT LAKE CITY, UT 84112
801/581-4177

MADISON-CHIC-MILWAUKEE
STEVEN P CEPA
ABBOTT LABORATORIES
ANALYTICAL RESEARCH DEPT
ABBOTT PARK, IL 60064
312/937-7539

MICHIGAN
BRIAN MUSSELMAN
DEPT OF BIOCHEMISTRY
MICHIGAN STATE UNIV
EAST LANSING, MI 48824

MID-OHIO
ALAN G MARSHALL
CHEMICAL INSTRUMENT CTR
176 WEST 19TH AVENUE
COLUMBUS, OH 43210
614/422-3446

NORTH JERSEY
DON SEDGWICK
ALLIED CORPORATION
PO BOX 1021 R
MORRISTOWN, NJ 07960
201/455-2977

NORTHEAST OHIO
FRANK BOCKHOFF
SOHIO RESEARCH CENTER
4440 WARRENSVILLE ROAD
CLEVELAND, OH 44128
216/581-5600

OKLAHOMA
DAVID BATTISTE
PHILLIPS RESEARCH CTR
150 PETROLEUM LAB
BARTLESVILLE, OK 74004
918/661-3444

OTTAWA
JOHN HOLMES
UNIV OF OTTAWA
DEPT OF CHEMISTRY
OTTAWA, ONTARIO K1N 9B4
613/231-2239

PITTSBURGH
LAN K WONG
UNIV OF PITTSBURGH
804 SALK HALL
PITTSBURGH, PA 15261
412/624-3268

RESEARCH TRIANGLE PARK
J RONALD HASS
TRIANGLE LABORATORIES
PO BOX 13485
RES TRI PK, NC 27709
919/541-3872

ROCKY MOUNTAIN
TOM MCCLURE
MANVILLE CORP
PO BOX 5108
DENVER, CO 80217
303/978-5484

SAN FRANCISCO BAY AREA
BILL HADDON
35 WILLOW AVENUE

LARKSPUR, CA 94939
415/486-3693

SOUTHEAST TEXAS
BESSIE FAN
SHELL DEVELOPMENT BRC
PO BOX 481
HOUSTON, TX 77001
713/663-2147

SOUTHERN CALIFORNIA
TERRY LEE
CITY OF HOPE RESEARCH CTR
1450 E DUARTE ROAD
DUARTE, CA 92621
818/359-8111

SYRACUSE
DON BRACKEN
GE COMPANY, BLDG EP3, ROOM 23
PO BOX 4840
SYRACUSE, NY 13221
315/456-2441

TORONTO
GLENYS FOSTER
MIN OF ENVIRONMENT, OTC
PO BOX 213
REXDALE, ONTARIO M9W 5L1
416/248-3755

WASHINGTON DC
MARK ROSS
NAVAL RESEARCH LABORATORY
CODE 6110
WASHINGTON, DC 20375
202/767-3551

MONDAY MORNING ORAL SESSIONS

LIQUID CHROMATOGRAPHY/MASS SPECTROMETRY

THERMOSPRAY LC/MS ANALYSIS OF THREE AMINE SALTS COMPARING AMMONIUM ACETATE AND AMMONIUM TRIFLUOROACETATE BUFFERS IN A PULSED AND CONTINUOUS BUFFER MODE 1
*JAKUBOWSKI,E M,CHOU,F E AND SMITH,J R

MODIFICATION OF A FINNIGAN THERMOSPRAY INTERFACE TO ALLOW DISCHARGE CHEMICAL IONIZATION OF THE THERMOSPRAY VAPOR 3
*ZAKETT,D,KALLOS,G J AND SAVICKAS,P J

COLLISION INDUCED DECOMPOSITIONS IN THE THERMOSPRAY ION SOURCE 5
*BENCSATH,F A AND FIELD,F H

DETERMINATION OF ACRYLAMIDE IN SUGAR BY THERMOSPRAY MULTIDIMENSIONAL LIQUID CHROMATOGRAPHY-MASS SPECTROMETRY 7
*KALLOS,G J AND CUTIE,S S

SENSITIVITY AND SELECTIVITY IN THERMOSPRAY IONIZATION 9
*RUDEWICZ,P AND STRAUB,K

SUPERCRITICAL FLUID CHROMATOGRAPHY/MASS SPECTROMETRY USING A MOVING BELT INTERFACE 11
BERRY,A J,*GAMES,D E AND PERKINS,J R

CAPILLARY SUPERCRITICAL FLUID CHROMATOGRAPHY-MASS SPECTROMETRY FOR THE ANALYSIS OF LABILE AND NONVOLATILE COMPOUNDS 13
*KALINOSKY,H T,UDSETH,H R,WRIGHT,B W AND SMITH,R D

THERMOSPRAY MASS SPECTROMETRY APPLYING A DUAL BEAM VAPORIZER 15
BUTFERING,L,SCHMELZEISEN-REDEKER,G AND *ROLLGEN,F W

SYMPOSIUM: HYBRID MASS SPECTROMETRY

HYBRID MASS SPECTROMETERS 17
*COOKS,R G,WRIGHT,L G AND O'LEAR,J D

GUIDED ION BEAM MASS SPECTROMETRY: KINETIC ENERGY DEPENDENCE OF ION-MOLECULE REACTIONS 19
*ARMENTROUT,P B

SOLVING PROBLEMS WITH A HYBRID MS/MS INSTRUMENT OF EBQ GEOMETRY 21
*BUSCH,K L AND DIDONATO,G C

ION/MOLECULE REACTIONS IN THE COLLISION REGION OF A HYDRID MASS SPECTROMETER 23
CAMPANA,J E,TONDEUR,Y,FREAS,R B,TABET,J C AND *MISSLER,S R

STUDIES WITH A HYBRID TANDEM MASS SPECTROMETER OF QEB GEOMETRY 25
GLISH,G L AND *MCLUCKEY,S A

A HYDRID BEQQ MASS SPECTROMETER FOR STUDIES IN GAS-PHASE ION CHEMISTRY 27
*HARRISON,A G AND YOUNG,A B

MONDAY MORNING POSTER SESSIONS

FRAGMENTATION MECHANISMS

WAGNER-MEERWEIN REARRANGEMENT IN THE GAS PHASE 28
*CAO,Z-M,SUN,Z-L,DONG,Z-W AND ZHANG,X-M

ION STRUCTURES AND KETO-TO-ENOL ISOMERIZATION IN DIALKYLMETHYLPHOSPHONATES 30
*HOLTZCLAW,J R AND WYATT,J R

DECHLORINATION REACTIONS INDUCED BY FAST ATOM BOMBARDMENT OF GLYCOPEPTIDE ANTIBIOTICS 32
*SIEGEL,M M,MCGAHREN,W J AND ELLESTAD,G A

FRAGMENTATION OF ALIPHATIC HYDROCARBONS: n-DECANE DIMERS 34
*HOFFMANN,E

FABMS AS A MONITOR FOR ORGANIC REACTIONS: CYANOGEN DRIVEN AMIDE BOND FORMATION AND CYANOGEN CONDENSATION REACTIONS 36
*DAY,R A AND MOTHERSOLE,S

THE DETERMINATION OF A REACTION PATHWAY BY GC/MS ANALYSIS FOR CROTONALDEHYDE AND SECONDARY AMINES 38
*NERO,V P AND KAPUSCINSKI,M M

MASS SPECTRAL DEALKYLATIONS OF METHOXYQUINOLINIUM AND MYTHOXYISOQUINOLINIUM IODIDES 40
*BARBUCH,R J,PEET,N P AND KARRICK,G L

MASS SPECTRAL ANALYSIS OF PYRAZOLO [4,3-c]QUINOLINE-3-ONES: ARYL MIGRATIONS ON ELECTRON IONIZATION 41
METZ,S,PADMANABHAN,G AND *STOGNIEW,M

FRAGMENTATION PROCESSES STUDIED BY GC/MS/MS AND ISOTOPE LABELLING 43
*HSU,C S AND FARCASIU,D

MASS SPECTROMETRY OF N,N-DIMETHYLAMINO-CYCLOHEXANOLS: MECHANISM OF FRAGMENTATION DETERMINED BY DEUTERIUM LABELLING 45
*CHENG,M T

FORMATION OF NEW C-C BONDS IN SULFON ENAMIDES UPON EI INDUCED SO2 ELIMINATION 47
SUTER,M,WINKLER,I,STEINAUER,R AND *SCHLUNEGGER,U P

FAB MASS SPECTRAL OBSERVATIONS ON NEW CATIONIC PLATINUM ORGANOMETALLIC COMPLEXES 49
KOWALSKI,M,*SHARP,T R AND STANG,P J

FRAGMENTATION PATTERNS OF METAL CHELATES IN SIMS DUE TO THE USE OF SILVER FOILS 51
*WENCLAWIAK,B

SYMPOSIUM: EXPERT SYSTEMS

EXPERT SYSTEMS: A POSTER SYMPOSIUM 52
WONG,C

TOOLS AND RULES FOR STRUCTURAL INTERPRETATION OF MS/MS SPECTRA 54
WADE,A P,PALMER,P T,HART,K J AND ENKE,C G

A KNOWLEDGE BASED SYSTEM FOR TUNING MS/MS INSTRUMENTS IN VARIOUS OPERATIONAL MODES 56
*GREGG,H,BRAND,H R AND WONG,C M

DEVELOPMENT OF AN EXPERT SYSTEM FOR HIGH RESOLUTION DIODE LASER SPECTROSCOPY 58
VARGHESE,P AND GARRELL,J

AN EXPERT SYSTEM FOR COMBINED INTERPRETATION OF MASS AND INFRARED SPECTRA 60
CURRY,B

INTELLIGENT TUTORING SYSTEMS AS EXPERT SYSTEMS 62
CUNNINGHAM,R,SCHULTZ,J AND BONAR,J

A SYSTEM FOR INTERACTIVE GRAPHICS-ORIENTED MULTIVARIATE ANALYSIS 64
*WINDIG,W AND MEUZELAAR,L C

TOXICOLOGY

ACCURATE MASS DETERMINATIONS OF MACROCYCLIC TRICHOTHECENE MYCOTOXINS USING A LC-MS INTERFACE AS AN AUTOMATED INLET 66
*MISSLER,S R,GIBBS,P H,JARVIS,B B,COMEZOGLU,F T AND WELLS,K

CHARACTERIZATION OF 6 TRICOTHECENE METABOLITES BY ELECTRON IMPACT, METHANE POSITIVE CHEMICAL IONIZATION AND NEGATIVE CHEMICAL IONIZATION AS THE TMS AND TFA DERIVATIVES 68
*HANEY,C A,HAGLER,W M AND SWANSON,S P

ANALYSIS OF MYCOTOXINS IN BLOOD BY CAPILLARY COLUMN-AMMONIA CHEMICAL IONIZATION MASS SPECTROMETRY 70
*D'AGOSTINO,P A,PROVOST,L R AND DROVER,D R

THERMOSPRAY LC/MS ANALYSIS OF MYCOTOXINS AS A FUNCTION OF ELECTROLYTE CONCENTRATION AND MODE OF IONIZATION 72
RAJAKYLA,E,LAASASENAHO,K,SAKKERS,P AND *FOERST,D

METABOLISM OF PROPYL HOMOLOGUES OF THE TETRAHYDROCANNABINOLS STUDIED BY GC/MS 74
*HARVEY,D J AND BROWN,N K

GC/MS ANALYSIS OF DERIVATIZED METABOLITES OF POLYNUCLEAR AROMATIC HYDROCARBONS 76
*CHESS,E K,BEAN,R M AND THOMAS,B

STRUCTURAL CHARACTERIZATION OF DNA ADDUCTS BY MASS SPECTROMETRY 78
*DIETRICH,A M,HARVEY,T M AND HASS,J R

TANDEM MASS SPECTRAL STUDIES OF CARCINOGEN-MODIFIED OLIGONUCLEOTIDES 80
*DINO,J J,GUENAT,C R,GASKELL,S J AND KAUFMAN,D G

MASS SPECTROMETRIC CHARACTERIZATION OF AMINO- AND NITRO-SUBSTITUTED MPTP ANALOGUES AS STUDIED BY GC/MS AND FTMS 81
*WEISZ,A,MARKEY,S P AND SHIH,M -C

GC/MS STUDIES ON URINARY METABOLITES OF TETRALIN IN FISCHER RATS EXPOSED BY GAVAGE 83
*YU,K O,LLEWELLYN,B M,OLSON,C T AND SERVE,M P

MONDAY AFTERNOON ORAL SESSIONS

APPLICATIONS OF ION ACTIVATION

SOFT IONIZATION/TANDEM MASS SPECTROMETRY 85
*HANSEN,G AND HATCH,F

DIFFERENTIATION OF ISOMERIC OXYGEN-18 LABELED NUCLEOTIDES USING FAST ATOM BOMBARDMENT-TANDEM MASS SPECTROMETRY 87
*MALLIS,L M,RAUSHEL,F M AND RUSSELL,D H

REMOTE SITE FRAGMENTATION: A STRUCTURALLY SENSITIVE FRAGMENTATION 89
*TOMER,K B,JENSEN,N J AND GROSS,M L

MECHANISMS OF REMOTE-CHARGE-SITE FRAGMENTATION OF FAB-DESORBED FATTY ACID CARBOXYLATES 91
*JENSEN,N J,TOMER,K B AND GROSS,M C

AMINO ACID SEQUENCING OF FRESH WATER BLUE-GREEN ALGAL TOXIC PEPTIDES BY FAST ATOM BOMBARDMENT TANDEM MASS SPECTROMETRIC TECHINIQUES 93
*KRISHNAMURTHY,T,SZAFRANIEC,L,SARVER,E W,HUNT,D F, SHABANAWITZ,J,CARMICHAEL,W C AND MISSLER,S

ROLE OF HYDROGEN TRANSFERS IN THE FORMATION OF [M-X]+ IONS FROM ETHYL HALOSUCCINATES UNDER ELCTRON IMPACT 95
BORNSTEIN,D,DOMON,B,*MANDELBAUM,A,MUELLER,D AND RICHTER,W J

APPLICATIONS OF A HIGH MASS TANDEM MASS SPECTROMETER TO THE CHARACTERIZATION OF PROTEINS 97
*SCOBLE,H A,COSTELLO,C E AND BIEMANN,K

INVESTIGATION OF PARAMETERS AFFECTING THE COLLISIONAL ACTIVATION OF HIGHER MASS MOLECULES 99
*CERNY,R L,TOMER,K B AND GIBLIN,D E

COLLISIONAL ACTIVATION OF CATIONIZED FATTY ALCOHOLS AND ACIDS: ENERGETICS OF REMOTE SITE DECOMPOSITIONS AND STRUCTURAL INFORMATION 101
*ADAMS,J AND GROSS,M L

A STUDY ON THE EFFECT OF ALKALI METAL CATIONIZATION ON THE DISSOCIATION REACTIONS OF POLAR ORGANIC MOLECULES 103
*MALLIS,L M AND RUSSELL,D H

SIMULTANEOUS AND ACCURATE ANALYSIS OF TRACE LEVELS OF SIMPLE AND MACROCYCLIC TRICHOTHECENES BY LC/THERMOSPRAY-MS AND TANDEM MASS SPECTROMETRIC TECHNIQUES 105
*KRISHNAMURTHY,T,SARVER,E W AND BECK,D J

LIPIDS

FAST LC/MS/MS FOR THE DTERMINATION OF PHYTOESTROGENS 107
*COVEY,T AND HENION,J

STEROID PRODUCTION IN THE PREMATURE AND NEWBORN. GC/MS OFFERS INSIGHT INTO PHYSIOLOGY OF ADRENAL GLAND 109
*FENNESSEY,P,GOTLIN,R,HAMBIDGE,S,FENNESSEY,K AND PIKE,A

MEASUREMENT OF URINARY ARACHIDONIC ACID (AA) METABOLITES BY HIGH RESOLUTION GAS CHROMATOGRAPHY-NEGATIVE ION CHEMICAL IONIZATION-MASS SPECTROMETRY FOLLOWING PURIFICATION BY IMMUNOAFFINITY CHROMATOGRAPHY 110
*VRBANAC,J J,ELLER,T D,HUBBARD,H L,BAKER,R H,HALUSHKA,P V AND KNAPP,D R

THE METABOLISM OF PROSTAGLANDIN D2 IN MAN: APPLICATIONS OF MASS SPECTROMETRY 112
*SWEETMAN,B J,PRAKASH,C,ROBERTS,L J AND BLAIR,I A

ANALYSIS OF LEUKOTRIENES, PROSTAGLANDINS AND OTHER METABOLITES OF ARACHIDONIC ACID BY THERMOSPRAY HPLC/MS 114
*VOYKSNER,R D AND BUSH,E D

NEGATIVE ION MASS SPECTROMETRY IN STUDIES OF HUMAN PLATELET ACTIVATION 116
*BLAIR,I A,SWEATT,J D,REDDY,K AND LIMBIRD,L E

SELECTIVE CHEMICAL MODIFICATION OF LIPOXYGENASE METABOLITES FOR ELECTRON CAPTURE NEGATIVE CHEMICAL IONIZATION 118
*MCCARRAHER,L C AND WATSON,J T

QUANTITATIVE ASPECTS OF LC/MS ANALYSIS OF PHOSPHOLIPIDS 120
ABDEL-MAKSOUD,H M,*EVANS,J E,JUNGALWALA,F B AND MCCLUER,R H

BACTERIAL PHOSPHOLIPID ANALYSIS BY FABMS 122
*PRAMANIK,B N,ZECHMAN,J,DAS,P R,BARTNER,P L,HORAN,A C AND MORTON,J B

SYMPOSIUM: ION IMAGE PROCESSING & ANALYSIS IN SIMS

PROCESSING AND ANALYSIS OF IMAGES FROM A CAMECA ION MICROSCOPE 124
*BRIGHT,D S

ION IMAGING: METHODOLOGY AND APPLICATION TO BIOLOGICAL SYSTEMS 126
*MORAN,M G AND MORRISON,G H

IMAGE DEPTH PROFILING FOR THREE DIMENSIONAL ELEMENTAL MAPPING 128
*BRYAN,S R,LINTON,R W AND GRIFFIS,D P

APPLICATIONS OF SECONDARY ION MASS SPECTROMETRY IMAGE ANALYSIS IN MATERIALS SCIENCE 130
*NEWBURY,D E

HIGH RESOLUTION SCANNING ION MICROSCOPY USING LIQUID METAL ION SOURCES 132
*LEVI-SETTI,R

MONDAY AFTERNOON POSTER SESSIONS

ELEMENTAL ANALYSIS & ISOTOPE RATIOS

PRECISION MASS SPECTROMETRIC ANALYSIS OF PURITY AND SPECIALTY GAS AT PPB LEVELS 134
*WAGNER,G,LASER,B,SCHMIDT,W AND GEISE,U

ANALYSIS OF SOLIDS BY LASER ABLATION PLASMA SOURCE MASS SPECTROMETRY 136
*ARROWSMITH,P

STUDY OF ION OPTICS AND IONIZATION POTENTIALS IN RELATION WITH MATRIX EFFECTS OF INDUCTIVELY COUPLED PLASMA/MASS SPECTROMETER 138
*BEAUDET,S,CHTAIB,M AND SCHMIT,J P

LASER MICROPROBE MASS ANALYSIS OF MICROCIRCUIT CONTAMINANTS 140
*SCHMIT,J P,BEAUDET,S AND MADORE,G

THE INFLUENCE OF SOURCE PARAMETERS ON INDUCTIVELY COUPLED PLASMA-MASS SPECTROMETRY 142
*VICKERS,G H,WILSON,D A,HIEFTJE,G M AND ZANDER,A T

NONRESONANT MULTIPHOTON IONIZATION OF LASER-SPUTTERED NEUTRALS 144
*SCHUELER,B AND ODOM,R W

ANGAL: AN AUTOMATED LABORATORY FOR NOBLE GAS ISOTOPE DILUTION MASS SPECTROMETRY 146
*LEICH,D A,HUNT,G F,MCCRORY,G,STUCKEMEYER,S R AND VELSKO,C

NOVEL GASEOUS POLYATOMIC LANTHANIDE OXIDE SPECIES DETECTED BY FAB MS 148
*KAHWA,I A,HSIEH,T C,LAINE,R A AND SELBIN,J

ACCURACY AND PRECISION OF HYDROGEN-2/HYDROGEN-1 ISOTOPE RATIO MEASUREMENTS BY ZINC REDUCTION OF WATER SAMPLES OF NATURAL ABUNDANCE & BIOLOGICAL FLUIDS 150
*WONG,W W,LEE,L S AND KLEIN,P D

RESONANCE IONIZATION MASS SPECTROMETRY OF LA AND BA 152
*GREEN,L W,MACDONALD,R G AND SOPCHYSHYN,F

INSTRUMENTATION

REMOVING METASTABLES FROM ANGLE-RESOLVED MASS SPECTROMETRY 154
*MOORE,C,JENNINGS,K R AND EVANS,S

METHODOLOGY FOR THE DETERMINATION OF ABSOLUTE TOTAL CROSS-SECTIONS IN A QQQ INSTRUMENT 156
*MARTINEZ,R T AND DHEANDHANOO,S

AN INTEGRATING TRANSIENT RECORDER FOR TIME ARRAY DETECTION 158
*NEWCOME,B,ERICKSON,E,YEFCHAK,G,DAVENPORT,M AND HOLLAND,J

CALIFORNIUM-252 PLASMA DESORPTION FOURIER TRANSFORM ION CYCLOTRON RESONANCE MASS SPECTROMETRY 160
VISWANADHAM,S K,*WELLER,R R,HERCULES,D M,GIAM,C S AND VISWANADHAN,S K

DESIGN AND ANALYTICAL APPLICATIONS OF A NEW HIGH MASS TANDEM MASS SPECTROMETER 162
*LYON,P A,HUNT,S L,EVANS,S AND TUDGE,H

PARTICULATE ANALYSIS VIA SPUTTER ATOMIZATION/RESONANCE IONIZATION MASS SPECTROMETRY 164
*GOERINGER,D E,CHRISTIE,W H AND MCKOWN,H S

FOURIER TRANSFORM ION CYCLOTRON RESONANCE MASS SPECTROMETRY AT LOW MAGNETIC FIELDS 166
*HEARN,B A,BAYKUT,G AND EYLER,J R

SOME RESULTS USING RF BURST EXCITATION AS A TOOL FOR INVESTIGATION OF PHENOMENA IN THE FTMS CUBIC ION TRAP 167
HUANG,S K AND *REMPEL,D L

EFFECTIVENESS OF VELOCITY COMPACTION FOCUSING IN COMPENSATING FOR INITIAL TEMPERATURE DISTRIBUTION OF ION SOURCE PLASMA 169
*MUGA,M L

MANITOBA II: A TIME-OF-FLIGHT MASS SPECTROMETER WITH IMPROVED RESOLUTION 171
*TANG,X,BEAVIS,R,ENS,W,SCHUELER,B AND STANDING,K G

AM IMPROVED TIME OF FLIGHT MASS SPECTROMETER 173
*ROCKWOOD,A L

ABSORPTION-MODE FT/ICR MASS SPECTRA: SOLVING THE PHASE PROBLEM 175
CRAIG,E C,*SANTOS,I AND MARSHALL,A G

A TRAP AND PULSE TECHNIQUE FOR ENHANCING SIGNALS FROM ION/MOLECULE REACTIONS IN THE CENTRAL QUADRUPOLE OF A TRIPLE QUADRUPOLE MASS SPECTROMETER 177
*DOLNIKOWSKI,G G AND KRISTO,M

MICROCOMPUTER-ASSISTED LINKED SCANNING WITH A KRATOS DS-55 DATA SYSTEM 179
*JONES,G G AND NUTTER,G L

MULTI-PARALLEL MICRO-BORE COLUMNS FOR FAST GC AND GC/MS ANALYSIS 181
EPSTEIN,P,MCKELLOP,K AND *HATCH,F

ENVIRONMENTAL

APPLICATION OF LIQUID IONIZATION MASS SPECTROMETRY TO ANALYSIS OF COAL TAR AND PITCH 183
FUJIOKA,Y AND *TSUCHIYA,M

THERMOSPRAY LC/MS/MS ANALYSIS FOR AZO DYES SPIKED IN WASTEWATER 185
*BETOWSKI,L D,PYLE,S M,BALLARD,J M AND SHAUL,G M

GC/MS ANALYSIS OF ORGANIC POLLUTANTS IN PONCE AIR PARTICULATE: ASSESSMENT OF REGIONAL AND LOCAL INFLUENCES 186
*INFANTE,R,CARRASQUILLO,A,IRIZARRY,J,LEBRON,J,NEGRON,N AND PENA,L

ENVIRONMENTAL APPLICATIONS OF THE THERMOSPRAY LC/MS INTERFACE: PART I. DYES AND SELECTED POLLUTANTS 188
*FLORY,D A AND MCLEAN,M A

NEW DEVELOPMENTS IN HERBICIDES ANALYSIS BY THERMOSPRAY LIQUID CHROMATOGRAPHY-MASS SPECTROMETRY 189
*SHALABY,L M

A COMPARISON OF THERMOSPRAY CONDITIONS FOR ORGANOPHOSPHATE PESTICIDES 191
*FRANCL,T J,KRASKE,P J AND THOMSON,M L

THE DETERMINATION OF ORGANOHALIDES IN WHIRLPOOL SPAS BY GC/MC 193
*BENOIT,F M AND JACKSON,R

RAPID DETERMINATION OF VOLATILE POLLUTANTS IN AQUAEOUS SAMPLES VIA FLOW INJECTION MASS SPECTROMETRY 195
*LANGVARDT,P W,BRZAK,K A AND KASTL,P E

A GC/MS DESIGN FOR THE ANALYSIS OF VOLATILE AND EXTRACTABLE ORGANICS WITHOUT COLUMN CONVERSION 197
*TERNES,T N,GRINDSTAFF,Q G AND JONES,M P

FAST, COST EFFECTIVE IDENTIFICATION OF GROUND POLLUTION SOURCES 199
*SMITH,J S,WEISS,M,SHEPPERD,D A AND WESTON,R F

A DETAILED MASS SPECTROMETRIC STUDY OF DFTPP 201
*TONDEUR,Y,NIEDERHUT,W,BONAPARTE,K AND CAMPANA,J E

DEVELOPMENT OF ION ABUNDANCE CRITERIA FOR QUADRUPOLE GC/MS ANALYSIS 203
DONNELLY,J R,TONDEUR,Y,*SOVOCOOL,G W AND MITCHUM,R K

REVISED QUALITY INDEX FOR THE EPA/NIH MASS SPECTRAL DATA BASE 205
*TERWILLIGER,D T,IRELAND,J C AND BUDDE,W L

EXPANDED DATA BASE OF 120,000 MASS SPECTRA OF 100,000 COMPOUNDS 207
TWISS-BROOKS,A B,STAUFFER,D B,LOH,S,ZHANG,M -Y AND *MCLAFFERTY,F W

THE UTILIZATION OF A SECTOR MASS SPECTROMETER FOR PERFORMING ENVIRONMENTAL GC/MS ANALYSES 208
*GRINDSTAFF,Q G,TERNES,T N AND ALMOND,M F

AN EVALUATION OF SP-2331 AND ULTRA 2 CAPILLARY COLUMNS FOR THE GC-MS ANALYSIS OF PCDDs AND PCDFs IN DIELECTRIC FLUIDS 210
*HARDIN,E D,STEWART,P B,KABAY,M C,CAMPBELL,T W,HAYES,D A AND SHORE,F L

TUESDAY MORNING ORAL SESSIONS

INSTRUMENTATION: FT/MS

INCREMENTAL/DECREMENTAL HIGH RESOLUTION SELECTED ION MONITORING FOR EVALUATING INSTRUMENT PERFORMANCE 212
*ROBOZ,J,ALLAN,A AND CHU,M

ION-MOLECULE REACTIONS IN A QUADRUPOLE COLLISION CELL USING A MASS SPECTROMETER OF BEQQ GEOMETRY 214
*YOUNG,A B

QUANTITATIVE ELEMENTAL ANALYSIS BY LASER IONIZATION MASS SPECTROMETRY (LIMS) 216
*ODOM,R W AND NIEMEYER,I C

EVIDENCE CONCERNING THE IDENTITY OF SECONDARY PARTICLES IN POST-ACCELERATION DETECTORS 218
WANG,G H,ABERTH,W AND *FALICK,A M

A MULTIQUAD TRIPLE ANALYZER MS/MS/MS 220
*BEAUGRAD,C,DEVANT,G,ROLAND,C AND JAOUEN,D

THE DESIGN AND DEVELOPMENT OF A QUINQUEQUADRUPOLE MASS SPECTROMETER 222
*MORRISON,J D,STANNEY,K A AND TEDDER,J

SUPERCRITICAL FLUID CHROMATOGRAPHY-FOURIER TRANSFORM MASS SPECTROSCOPY 224
*HENION,J,LEE,E,CODY,R AND KINSINGER,J

THE EFFECTS OF MAGNETIC FIELD INHOMOGENEITIES ON FTICR SPECTRA 226
*LAUKIEN,F H

TAILORED EXCITATION FOR FT/ICR MASS SPECTROMETRY 228
*MARSHALL,A G,WANG,T-C L AND RICCA,T L

MAXIMUM ENTROPY METHOD IN FOURIER TRANSFORM MASS SPECTROMETRY 230
*RAHBEE,A

ACCURATE MASS MEASUREMENTS MADE WITH SOFT IONISATION TECHNIQUES - A NEW APPROACH ALLOWED BY A UNIQUE ELECTROMAGNET DESIGN 232
BATEMAN,R H,OWEN,R,PARR,V C AND *WOOD,D

ENVIRONMENTAL MASS SPECTROMETRY

INTERLABORATORY COMPARISON OF ELECTRON ENERGY DISTRIBUTIONS IN NCI MASS SPECTRA 234
*DOUGHERTY,R C,WOLFF,B,BUDDE,W L,EICHELBERGER,J,HITES,R A, STIMLER,E,GRIMSRUD,E P AND SEARS,J

THE ROLE OF NEGATIVE ION MASS SPECTROMETRY IN THE DETECTION OF POLYCHLORINATED DIBENZOFURANS, BIPHENYLOLS AND DIPHENYL ETHERS IN MICHIGAN SPORT FISH 236
PRICE,H A,*SCHEEL,R H,WARREN,L AND WELCH,R L

THE QUANTITATION OF TOXAPHENE IN ENVIRONMENTAL SAMPLES USING NEGATIVE ION MASS SPECTROMETRY 238
*SWACKHAMER,D L,CHARLES,M J AND HITES,R A

THE METHANE ENHANCED NEGATIVE ION MASS SPECTRA OF DIPENYL ETHANE DERIVATIVES SUCH AS DDT 240
*STEMMLER,E A AND HITES,R A

NEGATIVE ION CHEMICAL IONIZATION MS AS AN ENVIRONMENTAL METHOD - RESIDUE DETERMINATION OF ALACHLOR METABOLITES IN EDIBLE ANIMAL PRODUCTS 242
*SMITH,R G,ALLAN,J M,HORNER,L M,LAUER,R,NORD,P J AND KLEIN,A J

INVESTIGATIONS OF THE MECHANISMS RESPONSIBLE FOR ISOMERIC DISCRIMINATION OF POLYCYCLIC AROMATIC USING NEGATIVE ION CHEMICAL IONIZATION 244
*BUCHANAN,M V,WISE,M B AND RUBIN,I B

ELECTRON CAPTURE PROCESSES AT REDUCED PRESSURES FOR SELECTIVE CHROMATOGRAPHIC DETECTION 246
*WISE,M B AND BUCHANAN,M V

DETERMINATION OF PAH AND ALKYLATED-PAH IN PARTICULATE EXTRACTS USING NEGATIVE ION CHEMICAL IONIZATION MASS SPECTROMETRY 248
*HILBERT,L R

GAS CHROMATOGRAPHIC/MASS SPECTROMETRIC ANALYSIS OF BIOLOGICALLY IMPORTANT AROMATIC AMINES 250
STILLWELL,W G,BRYANT,M S AND *WISHNOK,J S

DETERMINATION OF TRACE LEVELS OF ALIPHATIC AMINES IN AIR BY GC/SURFACE IONIZATION MASS SPECTROMETRY 252
*FUJII,T AND KITAI,T

DETECTION OF SUBSTITUTED POLYNUCLEAR AROMATIC HYDROCARBONS BY SECONDARY ION MASS SPECTROMETRY 254
*LEIBMAN,C P,MAMANTOV,G AND TODD,P J

MASS SPECTROMETRIC CHARACTERIZATION OF PRODUCTS OF PYROLYSIS AND COMBUSTION OF UTILITY MATERIALS 256
*MAZER,S,RUBEY,W AND DELLINGER,B

DIFFERENTIATION OF POSITIONAL ISOMERS OF POLYCHLORINATED BIPHENYLS USING TRIPLE QUADRUPOLE MS AND AMMONIA AS THE COLLISION GAS: APPLICATION OF AN ION-MOLECULE REACTION STUDY 258
*WHITE,E L,BURSEY,M M AND KENAN,W R

GAS CHROMATOGRAPHY-MASS SPECTROMETRY STUDIES ON BUTYLTINS AND THEIR ANALYSES IN ENVIRONMENTAL SAMPLES 259
*GREAVES,J

SYMPOSIUM: ISOTOPIS TRACERS IN MINERAL NUTRITION

THERMAL IONIZATION MASS SPECTRAL ANALYSIS FOR STABLE ISOTOPE STUDIES OF MINERAL METABOLISM IN HUMANS 260
*TURNLAND,J R

STUDIES OF CALCIUM METABOLISM USING ISOTOPE DILUTION-THERMAL IONIZATION MASS SPECTROMETRY 262
*YERGEY,A L,COVELL,D G,VIEIRA,N E AND MUENZER,J

ISOTOPE RATIOS BY INDUCTIVELY COUPLED PLASMA-MASS SPECTROMETRY FOR MINERAL BIOAVAILABILITY STUDIES 264
*SERFASS,R E,THOMPSON,J J AND HOUK,R S

QUANTITATION AND USE OF STABLE ISOTOPES OF CALCIUM IN CALCIUM NUTRITION STUDIES 266
JIANG,X,LU,Y-M,SMITH,D L,SHU,I AND WEAVER,C M

MASS DISCRIMINATION PHENOMENA IN FAST ATOM BOMBARDMENT MASS SPECTROMETRY OF METAL STABLE ISOTOPES 268
*MILLER,L V,PEIRCE,P,GOSS,C,HAMBIDGE,K M AND FENNESSEY,P V

AN 18O/16O WATER-CARBON DIOXIDE EXCHANGE SYSTEM FOR ISOTOPE RATIO MEASUREMENTS OF MICROLITER QUANTITIES OF WATER SAMPLES OF NATURAL ABUNDANCE AND BIOLOGICAL FLUIDS 270
*WONG,W W,LEE,L S AND KLEIN,P D

IONIZATION MECHANISMS AND OPTIMIZATION OF THE GLOW DISCHARGE IONIZATION SOURCE 272
*HESS,K R AND HARRISON,W W

PARAMETRIC EBALUATION OF THE HOLLOW CATHODE ATOMIZATION/IONIZATION SOURCE FOR SOLIDS ANALYSIS 274
*KING,F L AND HARRISON,W W

TUESDAY MORNING POSTER SESSIONS

COMPUTER APPLICATIONS

THE EFFECT OF SMOOTHING ON THE PRECISION AND ACCURACY OF QUANTITATIVE GC-MS DATA 276
THORNE,G C AND *GASKELL,S J

AN AUTOMATED PROCESS FOR THE IDENTIFICATION OF VOLATILE AND SEMIVOLATILE COMPOUNDS IN HUMAN ADIPOSE TISSUE - RESULTS OF AN NHATS STUDY 278
*ONSTOT,J,STANLEY,J,REMMERS,J AND BREEN,J

IDENTIFICATION OF ORGANIC COMPOUNDS USING AUTOMATED MS/MS SPECTRAL/ SUBSTRUCTURE CORRELATION 280
*HART,K J,WADE,A P,PALMER,P T AND ENKE,C G

USE OF AN ADVANCED GC/MS DATA PROCESSING ENVIRONMENT FOR THE COMPARISON OF CHROMATOGRAPHIC PATTERNS 282
*HUGHES,B M

IMPROVEMENTS TO PBM/STIRS FOR THE IDENTIFICATION OF UNKNOWN MASS SPECTRA 284
*STAUFFER,D B,LOH,S AND MCLAFFERTY,F W

PROCEDURE FOR REAL-TIME QUALITY CONTROL OF GAS CHROMATOGRAPHY/MASS SPECTROMETRY DATA 286
*CODY,J T

EMPIRICAL FORMULA DETERMINATION BY TRIPLE QUADRUPOLE MASS SPECTROMETRY 288
*PALMER,P T AND ENKE,C G

INTERACTIVE DATA ACQUISITION AND INSTRUMENT CONTROL FOR A SECONDARY ION MASS SPECTROMETER 290
*FLURER,R A AND BUSCH,K L

USE OF CROSS-CORRELATION METHOD FOR RATIO MEASUREMENTS 292
CELIKKAYA,A AND *SUZER,S

COMPUTER-BASED SYSTEMS FOR CORRELATING MOLECULAR STRUCTURES WITH MASS SPECTRAL DATA: METHODS FOR GENERATING MOLECULAR SUBSTRUCTURES AND FOR INCORPORATING FRAGMENTATION RULES 294
*SIEGEL,M M,BAUMAN,N AND CARTER,G T

AUTOMATIC PROCESSING OF QUANTITATIVE MULTIPLE-ION-DETECTION DATA 296
*ROHWEDDER,W K AND WOLF,D J

A SPECTRAL DATA MANAGEMENT SYSTEM 298
*MCCLUSKY,G A,WERNESS,S C,DEJOHN,D E AND SHIH,M H

AN INEXPENSIVE WAY TO ANALYZE THE OPTICS OF ELECTROSTATIC, SURFACE-IONIZAT ION SOURCE CONFIGURATIONS 300
*BALESTRINI,S J

AUTOMATED INTERPRETATION OF COMPLEX CAPILLARY GC/MS DATA 302
*LEGENDRE,M G,LIU,R H AND BERNI,R J

AN ENHANCED PC VERSION OF THE SIMION ELECTROSTATIC LENS DESIGN PROGRAM 304
*DAHL,D A AND DELMORE,J E

THE LKB-2091 CAPILLARY GAS CHROMATOGRAPH/MASS SPECTROMETER/DATA ANALYSIS SYSTEM USING THE IBM-AT 306
*MCGOWN,S R AND WALLER,G R

BIOCHEMISTRY I

THE DETRMINATION OF THE LOCATION AND NATURE OF AMINO ACID SUBSTITUTIONS IN BIOSYNTHETIC BACTERIO-OPSIN 308
*ALLMAIER,G,CHAO,B,KHORANA,H G AND BIEMANN,K

HPLC/MS IN THE CLINICAL ANALYSIS OF POLAR CORTICOSTEROIDS AND GLUCURONIDES 310
LIBERATO,D,ESTEBAN,N AND SHACKLETON,C H L

ANALYSIS OF FOLATES BY FAST ATOM BOMBARDMENT AND TANDEM MASS SPECTROMETRY 312
*CLIFFORD,A J,JONES,A D AND MISSLER,S R

PICOLINYLDIMETHYLSILYL ETHERS: NEW DERIVATIVES FOR THE STRUCTURAL DETERMINATION OF FATTY ALCOHOLS BY GC/MS 314
*HARVEY,D J

RAPID INJECTION PORT DERIVATIZATION AND NEGATIVE ION GCMS DETECTION OF DEUTERIUM-LABELLED 4-PYRIDOXIC ACID 316
GREGORY,J F AND *TOTH,J P

DETECTION OF DEUTERIUM-LABELLED FOLACIN BY TRIFLUOROACETIC ANHYDRIDE/ TRIFLUOROETHANOL DERIVATIZATION AND NEGATIVE ION ELECTRON CAPTURE GCMS 317
GREGORY,J F AND *TOTH,J P

APPLICATION OF LASER DESORPTION-FOURIER TRANSFORM MASS SPECTROMETRY TO ANALYSIS OF POLYSACCHARIDES 319
*COATES,M L,NUWAY-SIR,L AND WILKINS,C L

STUDIES OF DEOXYNUCLEOSIDES BY FABMS 321
CHATTOPADHYAYA,R,WELLS,J L AND SENSHARMA,D K

QUANTITATIVE ANALYSIS OF ADENOSINE BY GAS CHROMATOGRAPHY-MASS SPECTROMETRY SELECTED ION MONITORING AND STATISTICAL COMPARISON OF THE RESULTS WITH +A RADIOIMMUNOASSAY 323
*BALLARD,K D,KNAPP,R G,ELLER,T D,WEBB,J G,NEWMAN,W H AND KNAPP,D R

ELEMENTAL ANALYSIS OF BIOLOGICAL MEMBRANES BY INDUCTIVELY COUPLED PLASMA/ MASS SPECTROMETRY 325
*SCHMIT,J P,HEIDHART, S,CHTAIB,M AND BELIVEAU,R

ASSESSMENT OF VITAMIN A STATUS BY ISOTOPE DILUTION GC/MS 327
CLIFFORD,A J,*JONES,A D,TONDEUR,Y,FURR,H C AND OLSON,J A

CHARACTERIZATION OF OLIGORIBONUCLEOTIDES UP TO 24 MER (M/Z 13726) BY SECTOR TYPE MASS SPECTROMETER 329
*MATSUO,T,SAKURAI,T,MATSUDA,H,MATSUGI,M AND IKEHARA,M

CURIE-POINT PYROLYSIS OF SOME DIPEPTIDES CONTAINING AROMATIC AND HETERCYCLIC AMINO ACID RESIDUES BY GC/MS 331
SMITH,G G,BOON,J J AND *REDDY,S G

MASS SPECTROMETRY OF DINITROPYRENE-NUCLEOSIDE ADDUCTS 333
*QUILLIAM,M A,ANDREWS,P J,GERGELY,R J,MCCARRY,B E,BRYANT,D W AND MCCALLA,D R

COMBINED LC/MS AS AN AID IN THE PREPARATIVE FRACTIONATION OF COMPLEX MIXTURES 335
*QUILLIAM,M A,HOO,K,BERRY,T AND GAMES,D E

MASS SPECTROMETRY OF T-BUTYLDIMETHYLSILYL DERIVATIVES OF CYTOKININS 337
*WONG,D C,HOCART,C H AND LETHAM,D S

MASS SPECTROMETRIC STUDIES OF CYTOKININ METABOLITES IN RELATION TO RETARDATION OF LEAF SENESCENCE 339
*WONG,O C,ZHANG,R AND LETHAM,D S

BIOCHEMISTRY II

QUANTITATIVE ANALYSIS OF PGE2 AND THE MAIN URINARY METABOLITES OF PGI2 AND TXA2 BY PACKED AND CAPILLARY COLUMN GC/NCI-MS IN HUMAN AND IN RAT 341
*MARTINEAU,A AND FALARDEAU,P

ANALYSIS OF PROSTAGLANDINS FROM CEREBROSPINAL FLUID BY CAPILLARY COLUMN GAS CHROMATOGRAPHY/NEGATIVE ION CHEMICAL IONIZATION MASS SPECTROMETRY 343
*YERGEY,J AND SALEM,N

DEUTERATED 4-AMINOBUTANAL DIETHYL ACETAL AS AN IN VIVO PRECURSOR TO THE NEUTROTRANSMITTER, GABA 345
*VICCHIO,D AND CALLERY,P S

THE USE OF SPECIFICALLY LABELLED ACYL [18 O]- DIHYDROXYACETONE PHOSPHATE TO STUDY GLYCERYL ETHER BIOSYNTHESIS - QUANTITATION BY FAB AND GC-MS 347
*WEINTRAUB,S T,PETERSON,D M,FRIEDBERG,S J,MARTINEZ,R A AND STOOTER,P L

IDENTIFICATION OF LONG CHAIN BASES IN INOSITOL SPHINGOPHOSPHOLIPIDS FROM LEISHMANIA DONOVANI 349
*JAYASIMHULU,K AND KANESHIRO,E S

METABOLISM OF PAF BY THE ISOLATED PERFUSED RAT LUNG 351
*HAROLDSEN,P E,VOELKEL,N F AND MURPHY,R C

ANALYSIS OF COMPLEX CARBOHYDRATE MIXTURES BY HPLC-FABMS 353
*HER,G,SANTIKARN,S AND REINHOLD,V N

CARBOHYDRATE MAPPING BY MASS SPECTROMETRY: A NOVEL METHOD FOR IDENTIFYING ATTACHMENT SITES OF ASN-LINKED SUGARS IN GLYCOPROTEINS 355
CARR,S A,*ROBERTS,G D AND JOHNSON,W

THE STRUCTURE OF THE REPEATING OLIGOSACCHARIDE UNIT OF THE CAPSULAR POLYSACCHARIDE OF STREPTOCOCCUS PNEUMONIA TYPE 19B 357
*PHILLIPS,L R,EGAN,W AND LEE,C -J

STRUCTURAL ELUCIDATION OF CONSTITUENT FATTY ACIDS AND ALCOHOLS FROM RAT MEIBOMIAN SECRETION USING GC/MS OF THEIR NICOTINATE & PICOLINYL DERIVATIVES 359
*HARVEY,D J,DUERDEN,J M AND TIFFANY,J M

QUANTITATIVE ANALYSIS OF PHOSPHOLIPID MOLECULAR SPECIES BY THERMOSPRAY LC/MS 361
*KIM,H-Y AND SALEM,N

PHOSPHOLIPID/ALKALI ION BINDING CONSTANTS STUDIED BY FAST ATOM BOMBARDMENT MASS SPECTROMETRY 363
*DEMIREV,P

NCl-GC-MS OF FLUORINATED IMINE AND IMIDE DERIVATIVES OF BIOGENIC PHENYLALKYL AND INDOLEALKYL AMINES 365
*DURDEN,D A

SELECTIVE ADSORPTION OF PEPTIDES IN PLASMA DESORPTION MASS SPECTROMETRY 367
NIELSON,P F,ROEPSTORFF,P,CRAIG,A G AND CRAIG,A G

TUESDAY AFTERNOON ORAL SESSIONS

SYMPOSIUM: ENVIRONMENTAL APPLICATIONS OF MASS SPECTROMETRY

THE ROLE OF THE MS IN INDOOR AIR QUALITY ANALYSIS 369
*BAYER,C W AND BLACK,M S

APPLICATIONS OF LC/MS/MS TO THE DETERMINATION OF AZO DYES IN ENVIRONMENTAL SAMPLES 371
*HENION,J AND BRUINS,A

EVALUATION OF THE BIOAVAILABILITY OF CHEMICALS TO FISH USING GC/MS AND LC/MS 373
*KUEHL,D W,BUTTERWORTH,B C AND BURKHARD,L

TRACING GROUNDWATER CONTAMINATION WITH A STATIC COLLECTION DEVICE AND MS 375
*VOORHEES,K J,MALLEY,M J,HICKEY,J C,KLUSMAN,R W AND BATH,W W

INSTRUMENT DEVELOPMENT & BIOLOGICAL APPLICATIONS

ENHANCED LSIMS PERFORMANCE USING A SUBAMBIENT SAMPLE PROBE 377
*FALICK,A M,WALLS,F C AND LAINE,R A

COMPARISON BETWEEN GAS PHASE AND LIQUID PHASE IONIZATION FOR LC/MS/MS USING AN ATMOSPHERIC PRESSURE ION SOURCE 379
*BRUINS,A AND HENION,J

A CONTINUOUS FLOW FAB PROBE FOR THE INTRODUCTION OF AQUEOUS SOLUTIONS 381
*CAPRIOLI,R M,FAN,T AND COTTRELL,J

SUPERCRITICAL FLUID INJECTION OF NONVOLATILES WITH RESONANT TWO-PHOTON IONIZATION DETECTION IN SUPERSONIC BEAM MASS SPECTROMETRY 383
*LUBMAN,D M

PULSED LASER DESORPTION WITH RESONANT TWO-PHOTON IONIZATION DETECTION IN SUPERSONIC BEAM MASS SPECTROMETRY 385
*TEMBREULL,R AND LUBMAN,D M

THERMOSPRAY LIQUID CHROMATOGRAPHY/MASS SPECTROMETRY FOR THE IDENTIFICATION OF METABOLITES: COMPARISONS WITH OTHER DESORPTION IONIZATION METHODS 387
*UNGER,S E,MCCORMICK,T J,WARRACK,B M,LAN,S J,SWANSON,B, EVERETT,D AND MITROKA,J

DEUTERIUM-LABELED CHLOLESTEROL AS AN INTERNAL STANDARD IN THE ANALYSIS OF OXIDATED STEROLS 389
*WASILCHUK,B A,LE QUESNE,P W AND VOUROS,P

HIGH SENSITIVITY AND HIGH RESOLUTION PROBE ANALYSIS OF INDOLEAMINES USING A DUAL CELL FTMS 391
*MARKEY,S P AND SHIH,M -C

FAB MS/MS VS DCI MS/MS: APPLICATION TOWARDS POLAR MOLECULES 393
*MAACK,F,BEAUGRAND,C AND DEVANT,G

PRACTICAL APPLICATIONS OF ON-LINE LIQUID CHROMATOGRAPHY/FAST ATOM BOMBARDMENT MASS SPECTROMETRY 395
*STROH,J G,COOK,J C,RINEHART,K L AND SNYDER,W C

A NEW INSTRUMENT FOR CHROMATOGRAPHY/SIMS 397
*DIDONATO,G C AND BUSCH,K L

BIOMOLECULES INVESTIGATED BY MULTIPHOTON IONIZATION MASS SPECTROMETRY 399
*GROTEMEYER,J,BOESL,U,WALTER,K AND SCHLAG,E W

ISOTOPE RATIOS & ELEMENTAL ANALYSIS

ABSOLUTE ISOTOPIC REFERENCE MATERIALS FOR SAFEGUARDS MEASUREMENTS 401
*CRAWFORD,D W

ISOTOPIC DILUTION MASS SPECTROMETRY MEASUREMENTS OF PLUTONIUM IN INPUT SOLUTIONS TO THE HANFORD PLUTONIUM-URANIUM EXTRACTION FACILITY 403
LAGERGREN,C R AND *BAKER,E S

MASS SPECTROMETRIC MEASUREMENT OF ULTRA SMALL QUANTITIES OF ACTINIDES 0
*PERRIN,R E,CAPPIS,J H,KNOBELOCH,G W,EFURD,D W AND ROENSCH,F R

ISOTOPIC ANALYSIS OF LITHIUM 405
*GREEN,L W,LEPPINEN,J J AND ELLIOTT,N L

APPLICATION OF ELECTRON ENERGY STUDIES TO RESONANCE IONIZATION MASS SPECTROMETRY 407
*SMITH,D H,YOUNG,J P AND DONOHUE,D L

INTERFACE PROPERTIES OF A QUADRUPOLE ICP/MS SYSTEM 409
*BROWNER,R F AND ZHU,G

ION KINETIC ENERGIES IN INDUCTIVELY COUPLED PLASMA MASS SPECTROMETRY 410
*FULFORD,J E AND DOUGLAS,D J

INTERFERENCES IN INDUCTIVELY COUPLED PLASMA-MASS SPECTROMETRY 412
*WILSON,D A,VICKERS,G H,HIEFTJE,G M AND ZANDER,A T

GLOW DISCHARGE MASS SPECTROMETRY APPLIED TO THE DIRECT ANALYSIS OF SOLIDS 414
CANTLE,J E,*SANDERSON,N E,NAYLER,R,JACKSON,P AND CHARALAMBOUS,P

TUESDAY EVENING POSTER SESSIONS

ION ACTIVATION

EFFECT OF EXPERIMENTAL CONDITIONS ON THE COLLISIONALLY-ACTIVATED DECOMPOSITION SPECTRA OF STEROID GLUCURONIDES 416
*GUENAT,C,COLE,R B AND GASKELL,S J

OPTIMISATION OF ANALYTICAL PARAMETERS FOR THE TANDEM MASS SPECTROMETRY OF COMPOUNDS OF BIOCHEMICAL INTEREST USING A HYBRID SECTOR/QUADRUPOLE INSTRUMENT 418
*GASKELL,S J,THORNE,G C AND PORTER,C J

COLLISIONALLY ACTIVATED DECOMPOSITION OF POLY (ETHYLENE GLYCOL) S: AN INVESTIGATION OF THE GENERAL UTILITY OF THE COLLISIONAL ACTIVATION TECHNIQUE WITH LARGE MOLECULES 420
*KIPLINGER,J P AND BURSEY,M M

ANOTHER STRATEGY FOR PRODUCING REMOTE-CHARGE SITE FRAGMENTATIONS OF FATTY ACID POSTIVE IONS 422
*DETERDING,L

STRUCTURAL STUDIES OF SUBSTITUTED CYCLIC PERFLUOROALKANESULFONATES USING FAST ATOM BOMBARDMENT COMBINED WITH TANDEM MASS SPECTROMETRY 424
*HUNT,S L,LYON,P A,BEHR,F E,WINTER,L D AND CERNY,R L

A NOVEL APPROACH FOR AUTOMATIC ELUCIDATION OF SPECTRAL SUBSTRUCTURE RELATIONSHIPS IN MSn SPECTRA 426
*WADE,A P,PALMER,P T,HART,K J AND ENKE,C G

A METHOD TO DETERMINE THE ELEMENTAL COMPOSITIONS OF DAUGHTER IONS IN MIKES SPECTRA 428
*BOZORGZADEH,M H AND LAPP,R L

FOURIER TRANSFORM ION CYCLOTRON RESONANCE MASS SPECTROMETRY OF ORGANOMETALLICS 429
*MULLEN,S L AND MARSHALL,A G

THE STRUCTURE OF THE IONS FORMED BY NO. LOSS FROM DINITROBENZENE AND DINITROTOLUENE ANIONS 431
*GLISH,G L,MCLUCKEY,S A AND FRIAR,D L

NEUTRALIZATION-REIONIZATION MS: CHARACTERIZATION OF NEUTRAL SPECIES BY SEPARATE COLLISIONAL DISSOCIATION 433
*FENG,R,WESDEMIOTIS,C AND MCLAFFERTY,F W

PHOTODISSOCIATION OF NEGATIVE IONS GENERATED BY LSIMS 435
*WELCH,M J AND WHITE,E

INTERNAL ENERGY DISTRIBUTIONS OF ANIONS AND CATIONS ACTIVATED IN ION/ATOM AND ION/SURFACE COLLISIONS 437
*WYSOCKI,V H,KENTTAMAA,H I,COOKS,R G,SYKA,J AND STAFFORD,G

SOME APPLICATIONS OF MS/MS TO STRUCTURE DETERMINATION 439
BECKER,G W,BRIGGS,B S,DEBONO,M,GILLIAM,J M,MOLLOY,R M AND *OCCOLOWITZ,J L

CHARACTERIZATION OF A PHYSALAEMIN-LIKE IMMUNOREACTIVE PEPTIDE BY TANDEM DOUBLE-FOCUSSING MASS SPECTROMETRY 441
*HARVAN,D S,WILSON,W E AND BOYD,R K

CALIFORNIUM-252 PLASMA DESORPTION MASS SPECTROMETRY OF SKIN LIPIDS 443
*PANNELL,L K,YANG,Y-M,SOKOLOSKI,E A AND FALES,H M

MEDICINAL CHEMISTRY & BIOMEDICAL APPLICATIONS

ANALYSIS OF SOME SUBSTITUTED PYRIDINE C-NUCLEOSIDES BY MICROBORE DLI/LC-MS 445
*ESMANS,E L,BELMANS,M,VRIJENS,Y,LUYTEN,Y,ALDERWEIRELDT,F C, WOTRING,L L AND TOWNSEND,L B

MECHANISM OF CATIONIZATION OF OLIGOSACCHARIDES AND NUCLEOSIDES IN LASER DESORPTION-FOURIER TRANSFORM MASS SPECTROMETRY 447
*CHIARELLI,M P

MASS SPECTROMETRY OF ELECTROPHORE LABELLED DNA BASES AND NUCLEOSIDES. PENTAFLUOROBENZYL AND CINNAMOYL DERIVATIVES 449
TRAINOR,T M,FISHER,D H,ADAMS,J,GIESE,R W AND *VOUROS,P

IDENTIFICATION OF BACTERIA BY ANALYSIS OF THE GROWTH MEDIUM VIA MS WITH CI 451
*CONWAY,D C,LOPEZ,H AND QUARLES,J M

QUANTITATION OF POLYOLS IN SERUM AND TISSUES FOR DIAGNOSIS OF FUNGAL INFECTIONS 453
*JAYASIMHULU,K AND WONG,B

IDENTIFICATION OF THERMAL DEGRADATION PRODUCTS OF COMPOUNDS COSYNTHESIZED IN THE PRODUCTION OF PHENCYCLIDINE (PCP) 455
*JONES,L A AND HANEY,C A

A COMPARISON OF IONIZATION METHODS FOR THE ANALYSIS OF TECHNETIUM RADIOPHARMACEUTICALS 457
*MCCORMICK,T J,UNGER,S E,TREHER,E AND NUNN,A

FAB MASS SPECTRA OF 4-HYDROPEROXY-CYCLOPHOSPHAMIDE DERIVATIVES DERIVATIVES 459
*BOYD,V L,BONE,W M,PHILLIPS,L R AND ZON,G

CHARACTERIZATION OF ANTHRACYLINES BY USING FAST ATOM BOMBARDMENT MASS SPECTROMETRY 461
*DAS,C,SESHADIRI,R,ISRAEL,M AND DESIDERIO,D M

MATRIX-ASSISTED MOLECULAR SIMS OF QUINOME ANTIBIOTIC, SAFRAMYCIN Y SERIES 463
*SUZUKI,M,HARADA,K -I,MASUDA,K,TATEMATSU,A AND ARAI,T

ANALYSIS OF AMPICILLIN BY THERMOSPRAY HIGH-PERFORMANCE LIQUID CHROMATOGRAPHY MASS SPECTROMETRY IN BIOLOGICAL FLUIDS 465
*SUWANRUMPHA,S AND VESTAL,M L

THE APPLICATION OF THERMOSPRAY TO THE STUDY OF THE MECHANISM OF THE CONVERSION OF MODIFIED AVC - TRIPEPTIDES TO PENCILLINS AND CEPHAMS BY CELL FREE ENZYMES 467
*APLIN,R T,MCDOWELL,M AND ROLLINS,K

ANALYSIS OF THE CURIE-POINT PYROLYSIS PRODUCTS OF SOME DIPEPTIDES AND THEIR DIKETOPIPERAZINES BY GC/MS 468
SMITH,G G,BOON,J J AND *REDDY,S G

A CANDIDATE DEFINITIVE METHOD FOR URIC ACID 470
ELLERBE,P,MEISELMAN,S,WELCH,M J AND WHITE,E

ISOTOPE DILUTION MASS SPECTROMETRY UTILIZING ELECTRIC DEFLECTION PLATE SWITCHING 472
*MEISELMAN,S,ELLERBE,P,WELCH,M J AND WHITE,E

DISTINCTION OF ISOMERIC - & -ASPARTAME BY THERMOSPRAY LC/MS 474
*STAMP,J A,GARTEIZ,D A AND LABUZA,T P

CHLORINATED ENVIRONMENTAL CONTAMINANTS

SURVEY OF THE "ORTHO EFFECT" IN PCB MASS SPECTRA 476
*SOVOCOOL,G W AND DONNELLY,J R

DETERMINATION OF PCB CONTENT IN HAZARDOUS WASTE FROM SPECIFIC ISOMERS 478
*CHOW,C S AND KRECISZ,J M

ANALYSIS OF MULTIPLE COMBUSTION SOURCE FEED MATERIALS FOR DIOXIN PRECURSORS 480
*BURSEY,J T,WAGONER,D E,MCGAUGHEY,J F,MESSER,E E,MILES,A J, PALAZZOLO,M A,OBERACKER,D F AND SOUTHERLAND,J H

NEGATIVE CHEMICAL IONIZATION MS/MS FOR IDENTIFICATION OF CHLORINATED COMPOUNDS IN NORTHERN SHARK LIVER 482
*GUEVREMONT,R,YOST,R A,JAMIESON,W D AND SIM,P G

THE IDENTIFICATION OF A POTENTIAL INTERFERENCE IN THE ANALYSIS OF CHLORINATED DIBENZO-P-DIOXINS AND DIBENZOFURANS 484
*ORTH,R,FUHRMANN,J,WUEBBELS,J,NOBLE,R AND HILEMAN,F

IDENTIFICATION OF CHLORINATED BIPHENYLENES AND OTHER POLYCYCLIC AROMATIC COMPOUNDS FORMED FROM THE INCINERATION OF PCB-DIELECTRIC FLUIDS AT A CAPACITOR PLANT'S DISPOSAL SITE 486
*PETERMAN,P H,SMITH,L M,STALLING,D L AND PETTY,J D

MINIMIZING INTERFERENCES IN GC/MS ANALYSIS FOR TETRACHLORODIBENZO-P-DIOXINS 488
DONNELLY,J R,TONDEUR,Y,NIEDERHUT,W J AND *SOVOCOOL,G W

LABORATORY STUDIES AT CDC INVOLVING DIOXINS 490
*PATTERSON,D G,NEEDHAM,L L AND SAMPSON,E J

PERSISTENCE OF 2,3,7,8-TCDD IN RHESUS MONKEYS: ANALYTICAL METHODOLOGY AND PRELIMINARY RESULTS 492
*PAN,J C,WEERASINGHE,N C A,MEEHAN,J L AND BOWMAN,R E

THE QUANTITATION OF CHLORINATED BIPHENYLS, DIBENZODIOXINS AND DIBENZOFURANS USING RESPONSE FACTOR ESTIMATION 494
*SAUTER,A D AND DOWNS,J J

MASS SPECTRAL CHARACTERIZATION OF THE THIRTY-EIGHT ISOMERS OF TETRACHLORODIBENZOFURAN 496
CHITTIM,B G,SAFE,S,MCKINNON,H S,WADDELL,D S AND *BOYD,R K

ANALYSIS FOR POLYCHLORINATED BIPHENYLENES IN HUMAN ADIPOSE TISSUE NY NEGATIVE CHEMICAL IONIZATION 498
*PATTERSON,D G,ALLEY,C C AND BARNHART,E R

GC/MS STUDIES IN SUPPORT OF SYNTHESIS OF STANDARD REFERENCE MATERIAL FOR DETERMINING THE CHLORINATED PYRENE CONTENT OF BIOLOGICAL SPECIMENS 500
*ALLEY,C C,BARNHART,E R,PATTERSON,D G,MAGGIO,V L AND ASHLEY,D L

WEDNESDAY AFTERNOON ORAL SESSIONS

SYMPOSIUM: BIOACTIVE MOLECULES

LEUKOTRIENES AND PLATELET-ACTIVATING FACTOR: LIPID MEDIATORS OF THE ACUTE HYPERSENSITIVITY REACTION 502
*MURPHY,R C,CLAY,K L AND CHILTON,F H

PHARMACOLOGY OF THE PARKINSONIAN SYNDROME PRODUCING NEUROTOXIN MPTP - THE ROLE OF MASS SPECTROMETRY 504
*MARKEY,S P,JOHANNESSEN,J N,MARKEY,C J,BACON,J P,SAVITT,J M AND HANSELMAN,D S

ROLE OF FAB-MS IN STRUCTURAL ANALYSIS OF PEPTIDES 506
*FRASER,B A

IONIZATION: NEW DEVELOPMENTS

FURTHER ADVENTURES WITH AN ELECTROSPRAY ION SOURCE 507
*WHITEHOUSE,C M,LEVIN,F,MENG,C K AND FENN,J B

LASER MASS SPECTRA OF SOLUTIONS AT AMBIENT PRESSURE 509
*MORELLI,J J,ROSNACK,K J AND HERCULES,D M

UV LASER INDUCED DESORPTION IONIZATION STUDIED WITH PRISM INTERNAL REFLECTION AND TIME-OF-FLIGHT MASS SPECTROMETRY 511
YANG,M,*MILLARD,J R AND REILLY,J P

ALKALI SPECIFIC CATION ATTACHMENT AND FRAGMENTATION IN LDMS 513
*LINDNER,B AND SEYDEL,U

HIGH RESOLUTION TIME-OF-FLIGHT MASS SPECTROMETER USES LASER DESORPTION AND RESONANCE IONIZATION 515
*FREY,R,WEISS,M,KAMINSKI,H AND WEISS,G

ELECTRON CAPTURE AGENTS AS MODIFIERS FOR INCREASED CIMS SENSITIVITY 517
*HATCH,F,HANSEN,G,MCKELLOP,K AND EPSTEIN,P

UNUSUAL HIGH PRESSURE ELECTRON CAPTURE MASS SPECTRA OF FLUORANIL AND CHLORANIL 519
SEARS,L J AND *GRIMSRUD,E P

ELECTROPHILIC MODIFIER GASES IN CI: ENHANCEMENT OF THE POSITIVE CI RESPONSES OF ANALYTES IN TRACE ANALYSIS 521
*JOHNSON,J V AND YOST,R A

DETECTION OF CHLORINE ADDUCTS UNDER CONDITIONS FOR ELECTRON CAPTURE NEGATIVE CHEMICAL IONIZATION MASS SPECTROMETRY 523
*KASSEL,D,KAYGANICH,K AND WATSON,J T

MATRIX-LESS FAST ATOM BOMBARDMENT MASS SPECTRAL CHARACTERIZATION OF DIAZENIUM AND HYDRAZONIUM CATIONIC COMPOUNDS 525
SANDERS,C G,*SHARP,T R AND ALLRED,E L

IRON(I) CHEMICAL IONIZATION AND GC/FTMS FOR LOCATING DOUBLE BONDS 527
*PEAKE,D A AND HUANG,S K

CLUSTER IONS

COLLISION-INDUCED AND UNIMOLECULAR DISSOCIATION OF CARBON DIOXIDE CLUSTERS, STUDIED WITH A TANDEM MOLECULAR BEAM-QUISTOR-QUADRUPOLE INSTRUMENT 529
ROMANOWSKI,G,GABLING,R -H AND *WANCZEK,K P

CARBON CLUSTERS OF HIGH MASS DURING INFRARED LASER DESORPTION OF AROMATIC POLYMERS 531
*BROWN,C E,KOVACIC,P AND WILKIE,C A

REACTIONS OF SILICON CATION CLUSTERS 533
*CREASY,W R,MCELVANEY,S W AND O'KEEFE,A

POSITIVE AND NEGATIVE CLUSTER IONS OF PHOSPHORIC AND SULFURIC ACIDS 535
*SHARP,T R AND JONES,H K

EFFECT OF GAS PHASE ION MOLECULE REACTIONS ON THERMOSPRAY SEPCTRA 537
ALEXANDER,A J AND *KEBARLE,P

PHOTOELECTRON SPECTROSCOPY OF NEGATIVE CLUSTER IONS 539
*SNODGRASS,J T,COE,J V,FREIDHOFF,C B,MCHUGH,K M AND BOWEN,K H

SPECTROSCOPIC AND THERMODYNAMIC INFORMATION FOR TRANSITION METAL CLUSTER IONS MFe+ 541
*HETTICH,R L AND FREISER,B S

RELATIONSHIP BETWEEN STRUCTURE AND REACTIVITY FOR METAL CLUSTERS FORMED IN ION-MOLECULE REACTIONS IN GROUP 6 METAL CARBONYLS 543
REENTS,W D,*MECKSTROTH,W K AND RIDGE,D P

DISSOCIATIONS OF METAL CARBONYL CLUSTER IONS 545
*FREAS,R B,ROSS,M M,CAMPANA,J E AND RIDGE,D P

METAL ACETYLACETONATES REVISITED: NEW MASS SPECTRAL EVIDENCE FOR POLYMERIC CHEMISTRY 547
*BUSCH,K L AND DIDONATO,G C

WEDNESDAY AFTERNOON POSTER SESSIONS

ION CHEMISTRY II

THE ION-STABILIZING EFFECT OF THE TRIMETHYLSILYL GROUP 549
BARTMESS,J E AND *THOMAS,D

NEW SOURCES OF ELECTRON IMPACT PRODUCED ANIONS 550
BARTMESS,J E AND *CROWDER,C

SUBSTITUENT EFFECTS ON GAS PHASE ELIMINATION PROCESSES 551
BARTMESS,J E AND SUMPTER,T

OBSERVATION OF CARBON-HELIUM IONS 552
*YOUNG,S E AND COGGIOLA,M J

UNIMOLECULAR DECOMPOSITION OF HEPTYL IONS IN THE MICROSECOND TIME SCALE 554
*GUENAT,C,STAHL,D AND GAUMANN,T

SOLVENT AND CONCENTRATION EFFECTS ON THE FORMATION AND STABILITY OF POSITIVE AND NEGATIVE CLUSTER IONS OF TETRA-ALKYLAMMONIUM HALIDE SALTS 556
*TOLUN,E AND TODD,J F J

RADIATIVE RELAXATION OF PHOTOEXCITED C6H6+ AND C6D6 IONS 558
*SO,H Y AND DUNBAR,R C

THERMOCHEMICAL PROPERTIES OF POTASSIUM CATIONS 560
*EVANS,D H,KEESEE,R G AND CASTLEMAN,A W

TUNING THE EFFECTIVE AUTONEUTRALIZATION LIFETIME OF SF6- 562
DELMORE,J E AND *APPELHANS,A D

A TPEPICO-MS STUDY OF THE FRAGMENTATION OF DIMETHYL SULFOXIDE 564
ZHA,Q,NISHIMURA,T AND *MEISELS,G G

LIQUID CHROMATOGRAPHY/MASS SPECTROMETRY

THE USE OF A THERMOSPRAY INTERFACE TO A MASS SPECTROMETER AS A FLOW REACTOR FOR IN-SITU THERMAL DEGRADATION STUDIES: APPLICATIONS TO BETA- LACTUM ANTIBIOTICS 566
*SIEGEL,M M,ISENSEE,R K AND BECK,D J

ANALYSIS OF NAPHTHENES AND ORGANOMETALLIC FERROCENE-TYPE DERIVATIVES BY NORMAL PHASE LIQUID CHROMATOGRAPHY/THERMOSPRAY MASS SPECTROMETRY 568
*WANG,T H,MCLEAN,M AND VESTAL,C H

CRITICAL PARAMETERS EFFECTING THERMOSPRAY PERFORMANCE 570
*ROBINS,R H AND CROW,F W

ELUENT pH AND THERMOSPRAY SPECTRA: DOES THE CHARGE ON THE ION IN SOLUTION INFLUENCE THE SPECTRUM? 572
*SMITH,R W,PARKER,C E,JOHNSON,D M AND BURSEY,M M

MIXED-MODE COLUMN THERMOSPRAY LC/MS 574
*LLOYD,J R,COTTER,M L,OHORI,D AND OYLER,A

THE DEVELOPMENT OF NOVEL SAMPLE INTRODUCTION TECHNIQUE FOR FAB MEASUREMENT 576
*MIZUNO,T,ITAGAKI,Y,ITO,Y,TAKEUCHI,T,ISHII,D AND GOTO,M

DEVELOPMENT AND PERFORMANCE OF A DISPOSABLE MOVING BELT LC-MS INTERFACE 578
*DEMAIO,W AND VESTAL,M L

COMPARISON OF RESULTS FROM PACKED AND OPEN TUBULAR CAPILLARY COLUMN SFC/MS 580
*UDSETH,H R AND SMITH,R D

GRADIENT ELUTION LIQUID CHROMATOGRAPHY/MASS SPECTROMETRY USING A MONODISPERSED AEROSOL GENERATION (MAGIC) INTERFACE 582
*ABBEY,L E,BOSTWICK,D E,WINKLER,P C,PERKINS,D D
AND BROWNER,R F

AN INVESTIGATION OF OPERATIONAL PARAMETERS AND REPRODUCIBILITY OF THE MONODISPERSED AEROSOL GENERATION LC/MS INTERFACE 584
*PERKINS,D D,WINKLER,P C,ABBEY,L E AND BROWNER,R F

ELECTROSPRAY LC/MS WITH AN API TANDEM QUADRUPOLE MS 585
*BRUINS,A AND COVEY,T

THERMOSPRAY LIQUID CHROMATOGRAPHY-MASS SPECTROMETRY USING A DOUBLE FOCUSSING MAGNETIC SECTOR INSTRUMENT 587
*GREATHEAD,R J,PARILLO,R J,CHAPMAN,J R,PRATT,J A E,CLENCH,M R
AND MELLON,F A

ANTIBIOTICS: LOW LEVEL DETECTION USING THERMOSPRAY LIQUID CHROMATOGRAPHY/ MASS SPECTROMETRY 589
*GOODLEY,P C

THERMOSPRAY LC/MS ANALYSIS USING AMMONIA GAS CHEMICAL IONIZATION 591
GARTEIZ,D A,BLAKLEY,C R AND *OSTERMAN,R M

ENVIRONMENTAL APPLICATIONS OF A NEW THERMOSPRAY LC/MS INTERFACE FOR BENCHTOP MASS SPECTROMETERS 593
VESTAL,C H AND *GARTEIZ,D A

STUDIES ON SIZE AND CHARGE DISTRIBUTION OF DROPLETS FORMED IN THERMOSPRAY 595
*KATTA,V AND VESTAL,M L

STUDIES WITH THERMOSPRAY LIQUID CHROMATOGRAPHY-MASS SPECTROMETRY 596
*BUCHNER,J D AND WILLOUGHBY,R C

A NEW SOURCE AND PROBE FOR THERMOSPRAY APPLICATIONS 598
*JONES,D S,KROLIK,S T AND PARR,V C

ION CHEMISTRY II

PHOTOELECTRON SPECTROSCOPY OF SeO-, TeO-, SeO2-, Se2-, Te2-, Te3- AND P2 600
*SNODGRASS,J T,COE,J V,FREIDHOFF,C B,MCHUGH,K M AND BOWEN,K H

MEASUREMENT OF THE RADIATIVE RELAXATION RATE OF PHOTOEXCITED IODOBENZENE USING TWO-LIGHT-PULSE PHOTODISSOCIATION: EVIDENCE FOR AN INFRARED MULTIPHOTON MODEL FOR RELAXATION 602
*ASAMOTO,B AND DUNBAR,R C

COLLISIONAL QUENCHING OF PHOTOEXCITED BROMOBENZENE IONS 604
*AHMED,M S AND DUNBAR,R C

DIAGNOSTIC STUDIES OF THE FLOW DYNAMIC EFFECT ON RATE COEFFICIENTS OBTAINED WITH A SELECTED ION FLOW TUBE (SIFT) 606
*SHUL,R J,UPSCHULTE,B L,PASSARELLA,R,KEESEE,R G AND CASTLEMAN,A W

INTRODUCTION AND DETECTION OF CLUSTER IONS IN A FOURIER TRANSFORM MASS SPECTROMETER 608
*REENTS,W D,BONDYBEY,V E AND MANDICH,M L

CHAINLENGTH EFFECTS IN THE GAS PHASE CHEMISTRY OF TRANSITION METAL- AND METAL CONTAINING-IONS WITH UNSATURATED ORGANIC MOLECULES 610
*STEPNOWSKI,R M AND ALLISON,J

HETERONUCLEAR TRANSITION METAL CLUSTER IONS IN THE GAS PHASE. REACTIONS OF MFe+ (M=Cu, Nb, La) WITH SMALL HYDROCARBONS 612
HUANG,Y,FREISER,B S,*TEWS,E C,BUCKNER,S W AND MACMAHON,T

HIGH ENERGY COLLISION EFFECT ON ACTIVATION OF UNIVALENT METAL ION-ALCOLHOL COMPLEXES 614
*HUANG,S K AND HOLMAN,R W

A STUDY OF THE DISTONIC RADICAL CATION ADDUCTS OF BENZENE WITH OLEFINS AND PROPYLENE 616
*HOLMAN,R W,GROSS,M L AND WARNER,C D

FORMATION AND REACTIONS OF SiH5- IN THE GAS PHASE 618
*HAJDASZ,D AND SQUIRES,R R

THURSDAY MORNING ORAL SESSIONS

SYMPOSIUM: MS IN MOLECULAR BIOLOGY

A MULTIDISCIPLINARY APPROACH TO MOLECULAR NEUROBIOLOGY 620
*MARSHAK,D R

MOLECULARBIOLOGICAL APPLICATIONS OF FAB-MS 622
*GROTJAHN,L AND STEINERT,H

STRUCTURAL STUDIES OF INTACT COMPLEX CARBOHYDRATES OBTAINED FROM GLYCOPROTEINS AND GLYCOCONJUGATES OF BIOLOGICAL INTEREST USING CESIUM ION LIQUID SECONDARY ION MASS SPECTROMETRY 624
*BURLINGAME,A L

MASS SPECTROMETRIC MEASUREMENT OF OPIOID BRAIN PEPTIDES 626
*DESIDERIO,D M

ENZYMES AND MASS SPECTROMETRY: A NATURAL COMBINATION 628
*CAPRIOLI,R M

RECENT STUDIES IN THE ANALYSIS OF BIOPHARMACEUTICALS BY MASS SPECTROMETRY 630
*CARR,S A,ROBERTS,G D,HEMLING,M E,KILLMER,L B,JOHNSON,W AND MENTZER,M

DESORPTION IONIZATION: MECHANISMS & METHODS

A NEW TECHNIQUE FOR THE MASS SPECTROMETRIC ANALYSIS OF NONVOLATILE COMPOUNDS 632
*BOMBICK,D D,KASSEL,D B AND ALLISON,J

NEW DEVELOPMENTS IN ELECTROCHEMICAL/FAST ATOM BOMBARDMENT MASS SPECTROMETRY 634
*BARTMESS,J E AND PHILLIPS,L R

ANALYTE, MATRIX AND SOLVENT EFFECTS ON ION CURRENT PROFILES OBSERVED IN THERMALLY-ASSISTED FAB (TA-FAB) 635
*ACKERMANN,B L,HOLLAND,J F,HEINE,C E AND WATSON,J T

ORGANIC SECONDARY ION EMISSION FROM SULFURIC ACID SOLUTIONS 637
*LEIBMAN,C P,MAMANTOV,G AND TODD,P J

ROLE OF GAS-PHASE BASICITIES IN FABMS 639
*SUNNER,J,KULATUNGA,R AND KEBARLE,P

THE STUDY OF PEPTIDE-COLLOIDAL GOLD CONJUGATES BY TIME-OF-FLIGHT SIMS 641
*MAIN,D E,BEAVIS,R,ENS,W,SCHUELER,B AND STANDING,K G

COMPARISON OF MOLECULAR ION YIELDS FOR KeV ION AND 252Cf FISSION FRAGMENT BOMBARDMENT 643
*ENS,W,BEAVIS,R,MAIN,D,TANG,X AND CHAIT,B T

THE ROLE OF SURFACE CHEMISTRY IN THE SECONDARY ION MASS SPECTROMETRY OF LIQUID SURFACES 645
*LIGON,W V AND DORN,S B

SURFACE SUPPLY OF SAMPLE MOLECULES BY ION MIGRATION IN FAB MS 647
WIRTH,K P,WONG,S S AND *ROLLGEN,F W

ON THE VALIDITY OF THE PREFORMED ION MODEL IN FAB MS 649
SUNNER,J,KULATUNGA,R AND *KEBARLE,P

MATRIX PHYSICAL PROPERTIES AND THEIR EFFECTS ON ANALYTE SURFACE CONCENTRATION 651
*TODD,P J

LOW TEMPERATURE PARTICLE BOMBARDMENT (FAB/SIMS) MS OF METHANOL 653
*KATZ,R N,CHAUDHARY,T AND FIELD,F H

LASER DESORPTION FOURIER TRANSFORM MASS SPECTROMETRY OF PORPHYRINS 655
BROWN,R S AND *WILKINS,C L

FAST ATOM BOMBARDMENT INDUCED ADDUCT ION FORMATION IN THE MASS SPECTRA OF ALKYLPYRIDINIUM CHLORIDES 657
*KEOUGH,T

ON THE NATURE OF (M+nH)+ IONS (N=1,2,3,) IN FAST ATOM BOMBARMENT MASS SPECTROMETRY 659
*MUSSELMAN,B D

ION ACTIVATION METHODS

COLLOSIONAL MASS SPECTROMETRY OF GASEOUS PROTONATED AMINES 661
*REINER,E J AND HARRISON,A G

STRUCTURE OF IONS IN THE ION CHEMISTRY OF (CF3)2NO AND (CF3)2NONO STUDIED BY COLLISION-INDUCED DISSOCIATION IN A BROAD ENERGY RANGE WITH A HIGH MAGNETIC FIELD FT ICR SPECTROMETER 663
PARK,J -W AND *WANCZEK,K P

CHARGE INVERSION AND NEUTRALIZATION-REIONIZATION MASS SPECTRA OF ALKOXIDE ANIONS 665
*MERCER,R S AND HARRISON,A G

MS/MS BY ION-ELECTRON COLLISIONS IN FTMS 667
*CODY,R B AND FREISER,B S

DISSOCIATIVE AND REACTIVE COLLISIONS BETWEEN MOLECULAR IONS AND SURFACES 669
*MABUD,M A AND COOKS,R G

ISOTOPIC LABELLING STUDIES IN THE NONRESONANT MULTIPHOTON IONIZATION/ FRAGMENTATION OF ANILINE 671
*ZIMMERMAN,J A AND O'MALLEY,R

STRUCTURE ELUCIDATION OF ISOMERS BY MULTIPHOTON IONIZATION/FRAGMENTATION 673
CHANG,T C AND *JOHNSTON,M V

SIMPLIFICATION OF ION PHOTODISSOCIATION SPECTRA 675
GOSS,S P AND *MORRISON,J D

LASER-ION BEAM PHOTODISSOCIATION STUDIES: THE DISSOCIATION REACTIONS OF Fe3(CO)x+ AND C)4(CO)x+ 677
*TECKLENBURG,R E AND RUSSELL,D H

INFRARED MULTIPHOTON DISSOCIATION OF SOME PROTONATED OXYGEN-CONTAINING HYDROCARBONS. COMPETITIVE PHOTODISSOCIATION CHANNELS AND THEIR RELATIONSHIP TO MULTIPLE PROTONATION SITES 679
*BAYKUT,G,WATSON,C H AND EYLER,J R

INFRARED MULTIPHOTON DISSOCIATION OF LASER DESORBED IONS 681
*WATSON,C H,BAYKUT,G AND EYLER,J R

THE PHOTOFRAGMENTATION OF METHYL-HEXENES IN A FT-ICR MASS SPECTROMETER 683
*RAPIN,J,BENSIMON,M AND GAUMANN,T

INTERNAL ENERGY DEPOSITION IN ION TRAP MASS SPECTROMETRY 685
*LOURIS,J,BRODBELT,J,COOKS,R G AND STAFFORD,G

THURSDAY MORNING POSTER SESSIONS

ORGANIC ANALYSIS I

FAST ATOM BOMBARDMENT MASS SPECTROMETRY OF POLAR COMPOUNDS IN VEGETABLE OILS 687
*SANDERS,R A,CHARPENTIER,B A AND KEOUGH,T

ANALYSIS OF METAL ION CHEMICAL IONIZATION MASS SPECTRA FOR TEN TRANSITION METAL IONS WITH KETONES, ALDEHYDES AND THERS USING PATTERN RECOGNITION 689
*FORBES,R A,TEWS,E C,HUANG,Y,FREISER,B S AND PERONE,S P

THE CHARACTERIZATION OF BENZYL ESTERS OF CARBOXYLIC ACIDS USING SELF CHEMICAL IONIZATION FOURIER TRANSFORM ION CYCLOTRON RESONANCE MASS SPECTROMETRY 691
*WELLER,R R,FANG,Y AND GIAM,C S

LIMITS OF DETECTION IN MASS SPECTROMETRY: AN ATTEMPT TO BRING ORDER OUT OF CHAOS 693
KROLIK,S T AND *MILLARD,B J

FIELD IONIZATION MASS SPECTRA OF SYNTHETIC PYRETHROIDS 695
*HU,H C AND ROSEN,R T

CHARGE EXCHANGE FAB-MS OF LOW MOLECULAR WEIGHT ALCOHOLS. APPLICATION TO THE ANALYSIS OF GINGEROLS AND SHOGAOLS 696
*ROSEN,R T,HO,C-T,CHEN,C-C AND HARTMAN,T G

THE APPLICATION OF CI/MS ANALYSIS FOR NONIONIC SURFACTANTS AND THE LOTUS 1-2-3 698
*WANG,J-S,QUA,A AND ROSENBERG,I

4-PHENYL-1,2,4,-TRIAZOLE-3,5,-DIONE IN THE ANALYSIS OF CONJUGATED DIENES 699
*YOUNG,D,DECOSTA,B,HOLICK,M F AND VOUROS,P

A MASS SPECTROMETRIC STUDY OF THE VAPORIZATION OF BIS(4-DIMETHYLAMINOPHENYL) SQUARAINE AND ITS DERIVATIVES 701
LAY,K Y,*BLUETT,L J AND BAILEY,F C

NEGATIVE CHEMICAL IONIZATION MASS SPECTROMETRY OF SOME NITRO COMPOUNDS 703
*DAS,P R AND PRAMANIK,B N

ANALYSIS OF RESIN ACIDS IN PULP AND PAPER INDUSTRY EFFLUENTS BY FUSED SILICA CAPILLARY COLUMN GC/MS 705
*MESSIER,F,FOUQUET,A,GRAVEL,G AND COLGAN,D

INSTRUMENTATION

HIGH SENSITIVITY FAB/EI USING A DIP GUN ON A MAGNETIC SECTOR 707
*PEREL,J,MAHONEY,J F AND GREATHEAD,R

HARDWARE PEAK-FINDING FOR RELIABILITY AND INCREASED SCAN RATES 709
*KRISTO,M J AND NEWCOME,B H

CONSTANT-NEUTRAL-LOSS AND PARENT-ION SCANS ON A KRATOS MS-50TA 711
*GIBLIN,D E AND LAPP,R L

POSITIVE/NEGATIVE ION SOURCE ELECTRONICS CONVERSION FOR THE FINNIGAN 4000/4500 712
*STAUFFER,J L

MODIFICATIONS TO THE FIELD CONTROL AND SCAN CIRCUITRY OF A CEC 21-110B MASS SPECTROMETER FOR IMPROVED LINEAR MASS SCANS AND HIGH RESOLUTION DATA ACQUISITION 714
*RAMALEY,L,MASON,F G,DALTON,T E AND JAMIESON,W D

MOBILE MASS SPECTROMETRY - THE INSTRUMENT COMES TO THE PROBLEM 716
*GALLAHER,K L,GIBSON,J H,KOSMAN,J,ROSENHAMMER,D G AND TELLER,R

NOVEL QUADRUPOLE GEOMETRY FOR REDUCTION OF IONIZATION RELATED NOISE 718
*SYKA,J E P,SCHOEN,A E,CEJA,P C AND SMITH,R M

NEW METHODS AND CONCEPTS IN DIGITAL CONTROL OF A QUADRUPOLE MS/MS INSTRUMENT 720
*STEINER,U AND SOKOLOW,S

ION TRANSMISSION CONSIDERATIONS FOR TANDEM QUADRUPOLE MASS SPECTROMETRY 722
*SCHOEN,A E AND SYKA,J E P

THE DESIGN OF A NEW DOUBLE FOCUSSING MASS SPECTROMETER 724
BRUNNEE,C,MARKWARDT,U,BRACHMANN,K,JUNG,G AND *PESCH,R

EFFECTS OF WINDOWING UPON FTMS SIGNALS 726
*HANNA,D A AND GOODMAN,S

NEW SOFTWARE FOR THE CONTROL AND ANALYSIS OF SELECTED ION MONITORING EXPERIMENTS 728
*WARBURTON,G A,MOORE,C,KENNERLEY,S AND RYAN,P A

LOW MASS DETECTION IN FTMS BY AUTOMATIC UNFOLDING OF ALIASED PEAKS 730
*CODY,R B,KINSINGER,J A AND GOODMAN,S

AN EI SOURCE OPTIMISED FOR LOW LEVEL POLLUTANT ANALYSIS BY GC-HRSIR 732
*GREEN,B N,GRAY,B W,GUYAN,S A AND KROLIK,S T

A CALIBRANT FOR ACCURATE MASS MEASUREMENT IN HIGH RESOLUTION CIMS 734
*EVANS,M J,MALTAIS,L AND BERTRAND,M J

ORGANIC ANALYSIS II

ADVANTAGES AND LIMITATIONS OF "BATCH" MASS SPECTROMETRIC METHODS FOR MIXTURE ANALYSIS 736
*KASSEL,D B,BOMBICK,D D AND ALLISON, J

COMPARISON OF CI AND EI DIRECT INJECTION CAPILLARY GC/MS METHODS FOR THE ANALYSIS OF SELECTED MEAT FLAVOR PRINCIPLES USING A PURGE-AND-GAP TECHNIQUE 738
*LIU,R H,LEGENDRE,M G,BERNI,R J,KUAN,J W,VERCELLOTTI,J R AND DUPUY,H P

GC/MS OF FLUORINATED REFERENCE MATERIALS 740
*KING,R W

ANOMALOUS MASS SPECTRA IN THE GC/MS CHARACTERIZATION OF SOLVENTS AND VOLATILE COMPOUNDS 742
*SACK,T M AND TIMMONS,L

ANALYTICAL APPLICATIONS OF HEAD SPACE - GC/MS/IR 744
*CITERIN,R,GALLAHER,K L,KOLLAR,R G,MARKELOV,M AND BOCKHOFF,F M

MASS SPECTRAL IDENTIFICATION OF ARTIFACTS FORMED IN SILYLATION REACTIONS 746
*LITTLE,J L AND CRAWFORD,J L

TANDEM MASS SPECTROMETRY FOR THE DETERMINATION OF TRACE LEVELS OF LSD IN HUMAN URINE 748
*JOHNSON,J V,LEE,M R,LEE,M S AND YOST,R A

DETERMINATION OF 2,4,6-TRINITROTOLUENE AND ITS METABOLITES IN URINE OF MUNITION WORKERS BY MICRO-LC/MS 750
*YINON,J AND HWANG,D -G

DEVELOPMENT OF A CONFIRMATORY TEST FOR EXPOSURE TO 3-QUINUCLIDINYL BENZILATE (BZ) 752
*BYRD,G D,SNIEGOSKI,L T AND WHITE,E

VOLATILE ORGANIC COMPOUND ANALYSIS BY GAS CHROMATOGRAPHY WITH THE ION TRAP DETECTOR 754
*JOHNSON,E,PETIT,E AND MELANSON,E

THE DEVELOPMENT OF THERMOSPRAY MASS SPECTROMETRY COMBINED WITH ELECTROCHEMICAL REDOX PROCESSES 756
*GETEK,T A

DIRECT ION EVAPORIZATION OF IONIC ORGANIC AND INORGANIC COMPOUNDS IN THERMOSPRAY HPLC/MS 758
*VOYKSNER,R D

FORMATION OF (M-1)- OR (M+OAc)- IONS IN NEGATIVE ION THERMOSPRAY MASS SPECTROMETRY 760
*PARKER,C E,SMITH,R W AND BURSEY,M M

THURSDAY AFTERNOON ORAL SESSIONS

SYMPOSIUM: TIME-OF-FLIGHT MASS SPECTROMETRY

DEVELOPMENT OF TIME-OF-FLIGHT MASS SPECTROMETER SYSTEMS 762
*WOLLNIK,H

SECONDARY ION TOF MASS SPECTROMETERS AND DATA SYSTEMS 764
*STANDING,K G,BEAVIS,R,BOLBACH,G,ENS,W,LAFORTUNE,F,MAIN,D, SCHUELER,B,TANG,X AND WESTMORE,J B

VELOCITY COMPACTION - THEORY AND PERFORMANCE 766
*MUGA,L

IMPROVED PERFORMANCE OF A TANDEM QUADRUPOLE TIME-OF-FLIGHT MASS SPECTROMETER 768
*GLISH,G L,MCLUCKEY,S A AND MCKOWN,H S

A NEW HIGH RESOLUTION MASS SPECTROMETER 770
*YANG,M AND REILLY,J P

HIGH RESOLUTION TIME-OF-FLIGHT MASS SPECTROMETRY WITH LASER DESORPTION AND LASER IONIZATION SOURCE 772
BOESL,U,*GROTEMEYER,J,WALTER,K AND SCHLAG,E W

SOFT IONIZATION: PEPTIDE ANALYSIS

APPLICATIONS OF FAB/MS TO THE CHARACTERIZATION OF MAMMALIAN PEPTIDE HORMONES 774
*FAULL,K F,BECK,O,TYLER,A N,ROTH,K A,LORENZ,R G AND BARCHAS,J D

MULTIPLE REACTION MONITORING OF LEUCINE ENKEPHALIN FOR QUANTIFICATION AT THE FEMTOMOLE LEVEL 776
*DAS,C AND DESIDERIO,D M

STUDIES OF PEPTIDES BY FAB MASS SPECTROMETRY 778
*GIBSON,B W,WILLIAMS,D H,POULTER,W L,NAYLOR,S AND FINDEIS,A F

FABMS ANALYSIS OF DISULFIDE BONDS IN HEN EGG WHITE LYSOZYME AND BOVINE RIBONUCLEASE A 780
*YAZDANPARAST,R,DIXON,J E AND SMITH,D L

ANALYSIS OF LYSOZYME DERIVED TRYPTIC PEPTIDES BY FAST ATOM BOMBARDMENT AND TANDEM MASS SPECTROMETRY 782
*HARTMAN,T G,ROSEN,R T,GOVINDARAJIN,S,HO,C -T AND ROSEN,J D

FAB-MS OF PROTEINS - ENZYM-AIDED SEQUENCE DETERMINATION OF PEPTIDES AND IDENTIFICATION OF PEPTIDES & IDENTIFICATION OF PARTICULAR AMINO ACIDS 784
*HAFOK,CH,MAURER-FOGY,I AND SCHMID,E R

ENZYMATIC HYDROLYSIS AND ELECTROHYDRODYNAMIC IONIZATION: AN APPROACH TO KINETICS AND STRUCTURE 786
*COOK,K D AND MURAWSKI,S L

PROTEIN SEQUENCING BY TANDEM MASS SPECTROMETRY 788
*YATES,J,HUNT,D F AND SHABANOWITZ,J

THE ROLE OF A MATRIX IN PEPTIDE MAPPING BY PLASMA DESORPTION MASS SPECTROMETRY 790
*CRAIG,A G,ENGSTROM,A,BENNICH,H,KAMENSKY,I,LINDBERG,M S L, ROEPSTORFF,P,SELF,R,SALEHPOUR,M,JONSSON,G AND SUNDQVIST,B U R

AMINO ACID SEQUENCE OF CALMODULINS USING FAB/MASS SPECTROMETRY WITH CONVENTIONAL SEQUENCING TECHNIQUES 792
*SCHAEFER,W H,LUKAS,T J AND BLAIR,I A

ION MOLECULE REACTIONS

THE ELECTRONIC AND GEOMETRIC STRUCTURE OF THE TRANSITION METAL CARBYNE CATIONS ScCH+, TiCH+, VCH+ AND CrCH+ 794
MAVRIDIS,A,ALVARADO-SWAISGOOD,A AND *HARRISON,J F

THEORETICAL STUDY OF THE EFFECT OF A PERMANENT DIPOLE MOMENT ON THE KINETIC ENERGY RELEASE IN THE DISSOCIATION OF NASCENT ION-MOLECULE CLUSTERS 795
*BASS,L

KINETICS OF GAS PHASE METAL IONS 797
*SIGSWORTH,S,DIFAZIO,L,LEUCHTNER,R,KEESEE,R G AND CASTLEMAN,A W

IDENTIFICATION AND ELCTROPHILIC REACTIVITY OF PRODUCTS FROM 2-METHYLPROPANE AND FIRST ROW TRANSITION METAL CATIONS USING A MS/MS/MS QUADRUPOLE TRIPLE SECTOR 799
MESTAGH,H,MORIN,N,*ROLANDO,C,BEAUGRAND,C AND MAACK,F

THE INTERACTION OF GAS PHASE TRANSITION METAL IONS WITH ALKANES: IS BUTANE MORE STRONGLY BOUND TO Cr+ THAN CO? 801
*ALLISON,J,HANKINSON,D J,HARRISON,J F AND HUNT,P M

FTMS STUDIES OF Sc+ -LIGAND COMPLEXES: ISOMER DIFFERENTIATION USING COLLISION-INDUCED DISSOCIATION, ION/MOLECULE REACTIONS AND H/D EXCHANGE REACTIONS 803
*LECH,L M AND FREISER,B S

GAS PHASE ION-MOLECULE REACTIONS OF Fe- AND Co- WITH THIOLS, SULFIDES AND DISULFIDES USING FOURIER TRANSFORM MASS SPECTROMETRY 805
*SALLANS,L,LANE,K R AND FREISER,B S

THE EFFECT OF ION KINETIC ENERGY IN ION/MOLECULE REACTIONS USING FTMS 807
*MCELVANY,S W,O'KEEFE,A AND MCDONALD,J R

SLOW DISCHARGE REACTIONS IN THE GAS PHASE - EXPERIMENTS AND INTERPRETATION 809
RICHARDSON,D E,CHRIST,C S,SHARPE,P AND *EYLER,J R

GAS PHASE CHEMISTRY OF THE BENZENE RADICAL CATION: REACTION WITH 1,3-BUTADIENE 811
*WARNER,C D AND HOLMAN,R W

HYDROXIDE INITIATED GAS PHASE CHEMISTRY OF QUINONES 813
*JOHNSON,C L AND WILKINS,C L

ION/MOLECULE REACTIONS OF PROTONATED ALCOHOLS WITH ACETIC ACID IN THE TRIPLE QUADRUPOLE MASS SPECTROMETER 815
*DOLNIKOWSKI,G G AND WATSON,J T

THURSDAY AFTERNOON POSTER SESSIONS

FUELS & POLYMERS

DIRECT QUALITATIVE AND QUANTITATIVE CHARACTERIZATION OF SOLID RUBBER SAMPLES BY LASER PROLYSIS MASS SPECTROMETRY (PY-MS) 817
*MCCLENNEN,W H,RICHARDS,J M,MEUZELAAR,H L C,PAUSCH,J B AND LATTIMER,R P

CHEMICAL AGING AND THERMAL STABILITY OF POLY(ARYL-ETHER-ETHER-KETONE) [PEEK] 819
*GRAYSON,M A AND WOLF,C J

ANALYSIS OF CHLORINE-CONTAINING POLYMERS BY DIRECT PYROLYSIS MASS SPECTROMETRY 821
*MCGUIRE,J M AND BRYDEN,C C

IDENTIFICATION OF ORGANIC ADDITIVES IN RUBBER VULCANIZATES USING MASS SPECTROMETRY 823
*LATTIMER,R P,HARRIS,R E,RHEE,C K AND SCHULTEN,H -R

FIELD DESORPTION MASS SPECTRAL ANALYSIS OF HIGH MOLECULAR WEIGHT POLYMERS 825
MALEKNIA,S D AND *COSTELLO,C E

POLYMETHYLENE LINKAGES IN TANDEM MASS SPECTROMETRY ANALYSIS OF COAL REDUCTION PRODUCTS 827
*WOOD,K V,PACHUTA,R R AND NARAYAN,R

STRUCTURAL ANALYSIS OF POLYCYCLIC TERPANES AND AROMATIC STEROIDS BY MS/MS AND HRMS 829
*BOCKHOFF,F M,BARWISE,A J,DROZD,R J AND KRUGE,M A

NEGATIVE ION CHEMICAL IONIZATION MASS SPECTROMETRY FOR ISOMER DIFFERENTIATION OF NITROGEN HETEROCYCLIC, SULFER HETEROCYCLIC AND MIXED NITROGEN-SULFER HETEROCYCLIC COMPOUNDS 831
*CAMPBELL,J A,KALLOS,G,HERMANN,E,PATRICK,D,LEE,M AND CASTLE,R

MASS SPECTROMETRIC STUDIES OF THE PUMPING OF METHAN BY THERMAL CRACKING AND GETTERING 833
*PANG,E K

ANALYSIS OF A DIESEL FUEL SEDIMENT BY HIGH RESOLUTION MASS SPECTROMETRY 835
*GRIGSBY,R D,TANG,S -Y AND STURM,G P

MASS SPECTROMETRIC ANALYSIS OF COAL PRODUCTS BEFORE AND AFTER TREATMENT WITH MOLTEN CAUSTIC 837
*SCHMIDT,C E,DOUGLAS,L J AND UTZ,B R

MOLECULAR BEAM MASS SPECTROMETRIC STUDIES OF COAL DUST-AIR FLAMES 839
*GREENE,F T AND O'DONNELL,J E

THE APPLICATION OF THERMOSPRAY LC/MS AND THERMOSPRAY LC/MS/MS TO THE ANALYSIS OF EPOXY GRAPHITE COMPOSITE MATERIALS 840
*LITTON,J F,SELOVER,S J,WAKEFIELD,M R AND TUELL,T M

PEPTIDES

COMPUTER ASSISTED INTERPRETATION OF FAST ATOM BOMBARDMENT MASS SPECTRA OF PEPTIDES 842
*LEE,T D AND SPAYTH,V

STUDIES ON THE KINETICS OF HYDROLYSIS OF LARGE POLYPEPTIDES BY ENDOPEPTIDASES USING FABMS 844
*SEIFERT,W E AND CAPRIOLI,R M

ASSIGNMENT OF DISULFIDE BOND LINKAGES IN SYNTHETIC N-POMC (1-28) BY FAB MASS SPECTROMETRY 846
*CHAKEL,J A,RAMACHANDRAN,J,NIXON,M,FEISTNER,G,BARCHAS,J B AND FAULL,K F

ANALYSIS OF PEPTIDE MIXTURES AND TRYPTIC DIGESTS BY GRADIENT LIQUID CHROMATOGRAPHY/THERMOSPRAY MASS SPECTROMETRY 848
ROBINS,R H AND *CROW,F W

STRUCTURAL ANALYSIS OF TISSUE PLASMINOGEN ACTIVATOR GLYCOPROTEIN BY MASS SPECTROMETRY 850
*CARR,S A,ROBERTS,G D AND JOHNSON,W

MS AND MS/MS IN THE STRUCTURAL ANALYSIS OF THIOREDOXINS AND INVERTASE 852
*JOHNSON,R S,MATHEWS,W R AND BIEMANN,K

TANDEM MASS SPECTROMETRY OF OLIGOPEPTIDES 854
*MARTIN,S A AND BIEMANN,K

ACCURATE MASS MEASUREMENTS IN FAB-MS OF AN UNKNOWN, SECRETIN-LIKE PEPTIDE (MW 3111) 856
*FEISTNER,G J,GREEN,B N,FAULL,K F,TATEMOTO,K AND BARCHAS,J D

STUDIES OF PROTEIN SEQUENCING BY ON-LINE ENXYMATIC HYDROLYSIS, AND LC-THERMOSPRAY MS 858
*YANG,L,STACHOWIAK,K AND DYCKES,D F

MOLECULAR WEIGHT DETERMINATION OF ENDOGENOUS AND CLONED EPIDERMAL GROWTH FACTORS AT THE PICOMOLE LEVEL BY WEIN LSIMS 860
ABERTH,W,GIBSON,B W,*BURLINGAME,A L,DIAUGUSTINE,R P AND WALKER,M P

MASS SPECTROMETRIC ANALYSIS OF MIXED DISULFIDES OF PEPTIDE DERIVATIVES 862
*ALAI,M AND FENSELAU,C

THE USE OF FAB-LCMS FOR THE ANALYSIS OF HIGH MOLECULAR WEIGHT PEPTIDES 864
BORDOLI,R S,FAIRBROTHER,A E,*KROLIK,S T AND WRIGHT,H J

FAB MASS SPECTROMETRY AS A TOOL IN PEPTIDE SYNTHESIS 866
SCHAFER,W,PESCH,R,RAPP,U AND DIELMANN,G

BIOMEDICAL MASS SPECTROMETRY TO m/z 3000 WITH A QUADRUPOLE SYSTEM 868
*JARDINE,I,LISEK,C A,TSARBOPOULOS,A,SCANLAN,G S AND SMITH,D C

NEW DEVELOPMENTS IN IONIZATION METHODS

DI-ISOPROPYL ETHER AS A SELECTIVE CI REAGENT GAS 870
*BARRY,R AND MUNSON,B

MEMBRANES AND CELL WALLS AS PROBES FOR DESORPTION TECHNIQUES 872
*HELLER,D N,FENSELAU,C,COTTER,R J,UY,M,TANAKA,T,KISHIMOTO,Y, DEMIREV,P,OLTHOFF,J AND HONOVICH,J

LASER DESORPTION/FOURIER TRANSFORM MASS SPECTRAL ANALYSIS OF HETEROCYCLIC AROMATIC POLYMERS 874
*BROWN,C E AND KOVACIC,P

FAB SPECTRUM CHANGES OF CsI/NaI MIXTURES IN A VOLATILE MATRIX AN EXACT MASS MATRIX FOR FAB 876
*METRAL,C J

POST SPUTTERING EI FAB MS 878
*LEHMAN,J P AND GILLEN,G

A COMPARISON OF 8 KEV FAB AND 30 KEV CAESIUM ION BOMBARDMENT FOR THE DESORPTION OF LARGE BIOMOLECULES 880
ELLIOTT,G,*COTTRELL,J S AND EVANS,S

SURFACE IONIZATION MASS SPECTROMETRY OF ORGANICS; I.N-CONTAINING ALIPHATIC ORGANICS 882
*FUJII,T AND KITAI,T

SELECTIVE REACTANT IONS IN CHEMICAL IONIZATION MASS SPECTROMETRY: TRIMETHYLSILYL ION 884
*ORLANDO,R AND MUNSON,B

LASER DESORPTION FT-ICR WITH AN EXTERNAL ION SOURCE 886
KOFEL,P,*ALLEMANN,M AND GROSSMANN,P

DESIGN OF A PULSED NOZZLE FOR SUPERCRITICAL FLUID/MASS SPECTROMETRY 888
*PANG,H M,*SIN,C H,LUBMAN,D M AND ZORN,J

ATMOSPHERIC PRESSURE MASS SPECTROMETRY WITH LASER-PRODUCED IONS 890
*KOLAITIS,L AND LUBMAN,D M

CLUSTERS OF WATER UNDER ATMOSPHERIC PRESSURE STUDIED BY FIELD IONIZATION AND LIQUID IONIZATION MASS SPECTROMETRY 892
*TSUCHIYA,M,AOKI,E AND OTSUKA,K

DEVELOPMENTS IN HIGH FIELD IONIZATION MASS SPECTROMETRY 894
*LAGNA,W M,CALLERY,P S,MUSSER,S M AND ROBBINS,R C

FRIDAY ORAL SESSIONS

MASS SPECTROMETRY IN BIOCHEMISTRY

THE ROLE OF LC/MS IN THE CHARACTERIZATION OF NEW NUCLEOSIDES FROM TRANSFER RNA 896
*EDMONDS,C G,HASHIZUME,T,MCCLOSKEY,J A,GUPTA,R AND STETTER,K O

FAST ATOM BOMBARDMENT COMBINED WITH TANDEM MASS SPECTROMETRY FOR MODIFIED NUCLEOSIDES AND NUCLEOTIDES 898
*TOMER,K B,CERNY,R L,DEINZER,M,CAVALIERI,E AND EASTMAN,A

ISOLATION AND STRUCTURE ELUCIDATION OF A UNIQUE HYPERMODIFIED NUCLEOSIDE FROM E. COLI TRANSFER RNA 900
*PHILLIPSON,D W,EDMONDS,C G,CRAIN,P F,SMITH,D L AND MCCLOSKEY,J A

DETERMINATION OF THE 2-HYDROXY- AND 2-KETOACID METABOLITES OF VAL, LEU AND iLEU IN SERUM: A STABLE ISOTOPE DILUTION ASSAY 902
*MAMER,O A,LASCHIC,N S AND SCRIVER,C R

STRUCTURE DETERMINATION OF SCH 13384 COMPONENTS I & V BY FAST ATOM BOMBARDMENT (FAB) MASS SPECTROMETRY 903
*PRAMANIK,B N,GANGULY,A K,MORTON,J B,CHAN,T M,BARTNER,P L, SARRE,O AND GIRIJAVALLABHAN,V M

NEGATIVE ION CHEMICAL IONIZATION MASS SPECTROMETRY OF 2,4-DINITROPHENYL PEPTIDES 905
*WILLIAMS,T D AND ANDEREGG,R J

THERMOSPRAY MASS SPECTROMETRY OF AMINOGLYCOSIDE ANTIBIOTICS 907
*GETEK,T A AND ALEXANDER,T G

STRUCTURAL DETERMINATION OF LIPID A FROM GRAM NEGATIVE BACTERIA USING LASER DESORPTION MASS SPECTROMETRY 909
*HONOVICH,J,QURESHI,N,TAKAYAMA,K AND COTTER,R J

STRUCTURE ELUCIDATION OF THE ANTIGENTIC OLIGOSACCHARIDE ISOLATED FROM CELL WALL OF STREPTOCOCCUS SANGUIS (MITIS) 34 (Ss34) 911
BUSH,A,FENNESSEY,P,MCINTIRE,F AND *TJOA,S

ANALYSIS OF SOME FURSARIUM MYCOTOXIN METABOLITES BY THERMOSPRAY HPLC/MS 913
*VOYKSNER,R D,HANEY,C A,HAGLER,W M AND SWANSON,S P

THE IMPACT OF TAMOXIFEN, AN ANTI-TUMOR AGENT, ON STEROID METABOLISM IN THE TUMOR-BEARING RAT AS ASSESSED BY METABOLIC PROFILING 915
*LEARY,J J AND WELSCH,C W

12-HYDROXYEICOSATETRAENOIC ACID METABOLISM IN PSORIATIC HUMAN SKIN: GC-MS ANALYSIS 917
*MALLET,A I

THERMOSPRAY LIQUID CHROMATOGRAPHY-MASS SPECTROMETRY OF CARBOHYDRATES 919
*HSU,F F,EDMONDS,C G AND MCCLOSKEY,J A

MASS SPECTRAL MEASUREMENT OF INDIVIDUAL BACTERIA PARTICLES IN AIR 921
*SINHA,M P

THERMOSPRAY LC/MS IN STUDIES IF BIOMEDICAL AND CLINICAL INTEREST 923
*LIBERATO,D J,ESTEBAN,N V AND YERGEY,A L

DIFFERENTIATION OF VALPROIC ACID METABOLISM IN FIVE PATIENTS WITH HEPATOPATHY 925
*MATSUMOTO,I,KUHARA,T,INOUE,I,MATSUMOTO,M AND OHKURA,T

MASS SPECTRAL DETERMINATION OF THE EMPIRICAL FORMULAS AND COMPOSITIONS OF PEPTIDES BY FABMS 927
BERTRAND,M J,*THIBAULT,P,EVANS,M J AND ZIDAROV,D

CAPABILITIES AND LIMITATIONS OF TANDEM MASS SPECTROMETRY FOR THE IDENTIFICATION OF DRUG METABOLITES 929
*LEE,M S,YOST,R A AND PERCHALSKI,R J

HIGH MASS ANALYSIS & INSTRUMENT DEVELOPMENT

FRAGMENTATION BEHAVIOR OF HIGH MASS MOLECULES 931
*DEMIREV,P,FENSELAU,C,OLTHOFF,J AND COTTER,R J

A COMPARISON OF BIOPOLYMER FRAGMENTS GENERATED BY DIFFERENT METHODS OF SAMPLE DESORPTION AND THOSE INDUCED BY COLLISION: WHAT IS RELEVANT? 933
*REINHOLD,V N,SANTIKARN,S AND HER,G R

CHARACTERIZATION OF CARBOHYDRATE-INSULIN CONJUGATES USING FAST ATOM BOMBARDMENT MASS SPECTROMETRY 935
MYHRE,D V,*KEOUGH,T AND MCCRACKEN,M S

HIGH FLUX PARTICLE BOMBARDMENT TOF MASS SPECTROMETRY II 937
*OLTHOFF,J,HONOVICH,J AND COTTER,R J

ANALYSIS OF BIO-ORGANIC MOLECULES BY PLASMA DESORPTION MASS SPECTROMETRY 939
*KAMENSKY,I,LINDBERG,M S L,CRAIG,A G,ENGSTROM,A,BENNICH,H, NIELSON,P F,ROEPSTORFF,P,SELF,R,JONSSON,G,HAKANSSON,P AND SUNDQVIST,B U R

A RAPID, SENSITIVE MASS SPECTROMETRIC METHOD FOR INVESTIGATING MICROSCALE CHEMICAL REACTIONS OF SURFACE ADSORBED PEPTIDES AND PROTEINS 941
*CHAIT,B T AND FIELD,F H

A NEW MASS SPECTROMETRIC TECHNIQUE FOR INVESTIGATING MICROSCALE ENZYME CATALYZED CHEMICAL REACTIONS OF SURFACE BOUND PEPTIDES AND PROTEINS 943
*CHAIT,B T,CHAUDHARY,T AND FIELD,F H

TANDEM QUADRUPOLE FOURIER TRANSFORM MASS SPECTROMETRY: NEW DEVELOPMENTS 945
*SHABANOWITZ,J,HUNT,D F AND RUSSELL,D H

SOLID-STATE SIMS FOURIER-TRANSFORM MASS SPECTROMETRY OF HIGHER MOLECULAR WEIGHT COMPOUNDS 947
*AMSTER,I J,LOO,J A,FURLONG,J,WANG,B H,WILLIAMS,E R AND MCLAFFERTY,F W

MOLECULAR WEIGHT DETERMINATION AT HIGH MASS BY QUADRUPOLE MASS SPECTROMETRY 949
LYNAUGH,N,*MCDOWALL,M A AND SMITH,D C

TIME-OF-FLIGHT SECONDARY ION MASS SPECTROMETRY OF POLYURETHANES 951
*BLETSOS,I V,HERCULES,D M,VANLEYEN,D AND BENNINGHOVEN,A

OPTIMIZATION OF NITROCELLULOSE AS AN OVERLAYER MATRIX FOR 252-cf-PLASMA DESORPTION MASS SPECTROMETRY OF BOVINE INSULIN 953
*HILL,J C,PHELPS,R G AND MACFARLANE,R D

THE PERFORMANCE OF A NEW TANDEM HIGH MASS INSTRUMENT FOR BIO-ORGANIC MS-MS APPLICATIONS 955
BATEMAN,R H,BORDOLI,R S,GREEN,B N,LEE,G W AND *MILLARD,B J

A MODIFIED DOUBLE-FOCUSING MASS SPECTROMETER WITH SIMULTANEOUS ION DETECTION FOR HIGH MOLECULAR WEIGHT COMPOUNDS 957
*BOERBOOM,A J H AND MEUZELAAR,H L C

OPERATIONAL CHARACTERISTICS OF TWO CHANNEL ELECTRON MULTIPLIERS USED IN MASS SPECTROMETRY 959
*SOMSSICH,P F

DUAL-MODE DETECTION FOR EXTENDED DYNAMIC RANGE IN MS/MS 961
*KRISTO,M J AND ENKE,C G

CONTINUING DEVELOPMENTS OF ADVANCED ION TRAP INSTRUMENTATION 963
*KELLEY,P E,SYKA,J E P,CEJA,P C,STAFFORD,G C,LOURIS,J N, GRUTZMACHER,H F,KUCK,D AND TODD,J F J

EXTENSIONS TO COMBINED CHROMATOGRAPHY-MASS SPECTROMETRY ON A DOUBLE FOCUSSING MAGNETIC SECTOR INSTRUMENT 965
*CHAPMAN,J R,RAMSEY,E D AND PRATT,J A E

THE USE OF HIGH RESOLUTION AND ACCURATE MASS MEASUREMENTS IN GC/MS USING FOURIER TRANSFORM MASS SPECTROMETRY 967
*KINSINGER,J A

ION-NEUTRAL COMPLEXES

ISSUES REGARDING THE ROLES OF ION-NEUTRAL COMPLEXES AS INTERMEDIATES IN UNIMOLECULAR DISSOCIATIONS 969
*MCADOO,D J

ION-MOLECULE COMPLEXES IN 2ND ORDER REACTIONS. ISOTOPE EFFECTS ON ALKYL CATION DEPROTONATION 971
*REDMAN,E W AND MORTON,T H

ION-MOLECULE COMPLEXES IN 1ST AND 2ND ORDER REACTIONS: CONNECTING TWO KINETIC REGIMES 973
*MORTON,T H,REDMAN,E W AND STAMS,D A

SITE SPECIFICITY OF A H REARRANGEMENT CANCELLED BY SUBSEQUENT H EXCHANGES IN ION-NEUTRAL COMPLEXES 975
*LONGEVIALLE,P A

PHOTOELECTRON SPECTROSCOPY OF THE NEGATIVE IONS: TeH- AND TeO- 977
*FREIDHOFF,C B,COE,J V,SNODGRASS,J T,MCHUGH,K M AND BOWEN,K H

EXPERIMENTAL AND THEORETICAL CHARACTERIZATION OF AN ION-NEUTRAL COMPLEX MEDICATED REACTION, CH4 ELIMINATION FROM CH3OCH(CH3)2 979
*GRIFFIN,L,TRAEGER,J,HUDSON,C AND MCADOO,D

ENERGY RANGES OF ION-NEUTRAL COMPLEX FORMATION: ALKANE ELIMINATIONS FROM IONIZED KETONES 981
*TRAEGER,J C AND MCADOO,D J

ION-NEUTRAL COMPLEXES AS INTERMEDIATES IN FORMATION OF "MCLAFFERTY + 1" (CH3CO2H2+) IONS FROM C5H1002+ ISOMERS 983
*HUDSON,C E,GRIFFIN,L L,BROIDA,E AND MCADOO,D J

ION/MOLECULE COMPLEXES AS INTERMEDIATES OF THE FRAGMENTATION OF PROTONATED ARYL KETONES 985
*GROTZMACHER,H-F AND FILGES,U

HEAT OF FORMATION FOR THE 1-METHYLALLYL CATION BY PHOTOIONIZATION MASS SPECTROMETRY 987
*TRAEGER,J C

ELECTRON AFFINITIES OF COMPOUNDS M AND PRESENCE OF M- AND CLUSTERS OF M- IN NEGATIVE ION CHEMICAL IONIZATION 989
CHOWDHURY,S AND *KEBARLE,P

TIME-OF-FLIGHT STUDIES OF METASTABLE SECONDARY ION DECAYS 991
*SCHUELER,B,ENS,W,MAIN,D E AND TANG,X

THERMAL ENERGY CHARGE TRASFER REACTIONS OF AR+ AND AR2+ 993
*PASSARELLA,R,UPSCHULTE,B L,SHUL,R J,KEESEE,R G
AND CASTLEMAN,A W

THEORETICAL AND EXPERIMENTAL STUDIES OF THE DICATION OF NITRIC OXIDE 995
WETMORE,R W AND *BOYD,R K

KINETIC ISOTOPE EFFECT IN THE FRAGMENTATION OF ENERGY-SELECTED IONS 997
*NISHIMURA,T AND MEISELS,G G

FRIDAY POSTER SESSION

DRUG METABOLISM; ENVIRONMENTAL

CHARACTERIZATION OF ENCAINIDE METABOLITES BY FAB/MS 999
*SWEETMAN,B J,MAYOL,R F,LABUDDE,J A AND BLAIR,I A

A CAPILLARY COLUMN GC/NEGATIVE ION CHEMICAL IONIZATION METHOD FOR DETERMINATION OF CHLORAMPHENICAL IN SWINE MUSCLE 1001
*HOFFMAN,M K AND CHAMBERLAIN,T N

QUANTITATIVE DETERMINATION OF RIMANTADINE BY GC-MS 1003
*FUKUDA,E K,RODRIGUEZ,L C,CHOMA,N AND GARLAND,W A

APPLICATION OF 252CF PLASMA DESORPTION MASS SPECTROMETRY TO THE ANALYSIS OF SULFATE, GLUCURONIDE AND GLUTATHIONE CONJUGATES 1005
*ALAI,M,DULIK,D AND PALLANTE-MORELL,S

CHARACTERIZATION OF D AND L MANDELIC ACID AND PHENYLGLYCINE sec-BUTYL ESTER DIASTEREOISOMERS FROM DIAZOTIZED AMPICILLIN AND -LACTAMASE I 1007
*BOUZIANE,C AND DAY,R A

QUANTITATIVE ANALYSIS OF TERBUTALINE BY THERMOSPRAY LC/MC 1009
*HAYES,M,BAX,M AND ALKALAY,D

BILIARY METABOLITES OF CYCLOSPORINE IN LIVER TRANSPLANT PATIENTS 1011
*WONG,L K,HASHEM,H,VENKATARAMANAN,R,BUCHNER,J AND WILLOUGHBY,R

ACCURATE MASS HPLC-MS OF A PHOTOAFFINITY DERIVATIVE OF COLCHICINE 1013
*WEINTRAUB,S T,FLOYD,L J,BARNES,L D AND WILLIAMS,R F

MASS SPECTRAL ANALYSIS OF PHENOTHIAZINE N-OXIDES 1015
*MCKAY,G,EDOM,R,HAWES,E M,HUBBARD,J W AND MIDHA,K K

METABOLISM OF NAFIDIMIDE IN CANCER PATIENTS BY THERMOSPRAY LC/MS 1017
NEWMAN,R A,MCLEAN,M A AND GARTEIZ,D A

QUANTITATION OF NOVEL AMINO ACIDS AND SUGARS BY THERMOSPRAY LC/MS/MS AND LC/MS IN BIOLOGICAL SAMPLES 1019
*COUTANT,J E AND CHAN,K Y

THE USE OF ION/MOLECULE REACTIONS FOR SELECTED REACTION MONITORING IN GC/MS/MS ANALYSES 1021
*KINTER,M T AND BURSEY,M M

BENCHTOP SUPERCRITICAL FLUID CHROMATOGRAPHY/MASS SPECTROMETRY DETERMINATION OF CORTICOSTEROIDS 1023
*LEE,E D AND HENION,J D

QUANTITATION OF THE ARYLEICOSANOID -PENTYL-3-(2 QUINOLINYLMETHOXY)- BENZENEMETHANOL IN HUMAN PLASMA BY SIM GC/MS 1025
*BROWN.S Y AND CHOI,R L

THE USE OF MS AND MS/MS FOR DRUG RELATED STUDIES 1027
*ASHCROFT,A E,GREATHEAD,R J AND KIMBER,M L

LASER MICROPROBE MASS ANALYSIS OF INDUCTRIAL ATMOSPHERIC DUST PARTICLES 1029
*BEAUDET,S,SCHMIT,J P AND LESAGE,J

DRUG METABOLISM

SEPARATION AND IDENTIFICATION OF THE OPTICAL ISOMERS OF 3-METHOXY-17- METHYLMORPHINAN AND 17-METHYLMORPHINAN-3-OL IN URINE SAMPLES AS (-) MENTHYL CARBAMATE DERIVATIVES BY CAPILLARY COLUMN GC/MS 1031
*WILSON,R L AND SAMS,R A

STUDIES OF BETA-ADRENERGIC BLOCKER DRUGS WITH LIQUID CHROMATOGRAPHY MASS SPECTROMETRY 1032
*WILLOUGHBY,R C,BUCHNER,J D,PIRONE,A J AND ASSENZA,S P

A COMPARISON OF FAB-MS/MS AND HPLC-MS/MS FOR THE ANALYSIS OF CATECHOLAMINE METABOLITES 1033
*RUDEWICZ,P AND STRAUB,K

A PHARMACOKINETIC COMPARISON OF TRICLOPYR AND ITS BUTOXYETHYL ESTER IN FISCHER 344 RATS 1035
*KASTL,P E,VEENSTRA,G E AND HERMANN,E A

DETECTION AND IDENTIFICATION OF SUFENTANIL AS ITS HEPTAFLUOROBUTYRL DERIVATIVE BY CAPILLARY GC/MS WITH NEGATIVE CHEMICAL IONIZATION 1036
*NOONAN,J S AND SAMS,R A

FAST ATOM BOMBARDMENT MASS SPECTROMETRY AND FAST ATOM BOMBARDMENT MASS SPECTROMETRY/MASS SPECTROMETRY OF THREE GLUTATHIONE CONJUGATES OF ACETAMINOPHEN 1038
*LAY,J O,POTTER,D W AND HINSON,J A

DESORPTION CHEMICAL IONIZATION AND FABMS STUDIES OF THREE GLUCURONIDE METABOLITES OF DOXYLAMINE 1040
*LAY,J O,KORFMACHER,W A,MILLER,D W,SIITONEN,P,HOLDER,C L AND GOSNELL,A B

IDENTIFICATION OF METABOLITES OF 3,4-DICHLOROBENXYLOXYACETIC ACID (3,4-DCBAA) BY HPLC, EI-MS AND LC-MS 1042
*PEFFER,R C,ZEMAITIS,M A,WONG,L K AND ALVIN,J A

THERMOSPRAY LC-MS/MS FOR RAPID PROFILING OF DRUG METABOLITES 1044
*STRAUB,K,RUDEWICZ,P,GUTZAIT,L AND MICO,B

APPLICATION OF SIR AND DEFOCUSSING METASTABLE SIR TO THE IDENTIFICATION OF FLUPHENAZINE 5-SULFOXIDE IN MAN AFTER INTRAMUSCULAR FLUPHENAZINE DECANOATE 1046
*EDOM,R W,MCKAY,G,BROOKS,P W,HUBBARD,J W AND MIDHA,K K

GAS CHROMATOGRAPHY-FAST ATOM BOMBARDMENT-MASS SPECTROMETRY OF CARBOXYLIC ACIDS 1048
*GALLEGOS,E J

CORRELATION OF DEGRADATION PRODUCT PROFILES FROM AQUATIC HUMIC SUBSTANCES AS DETERMINED BY GC/MS WITH 13C-NMR SPECTRAL CHARACTERISTICS 1050
*NORWOOD,D L,CHRISTMAN,R F AND HATCHER,P G

CHEMICAL IONIZATION STUDIES OF T-BUTYLDIMETHYLSILYL DERIVATIVES OF ENVIRONMENTAL ORGANIC CONTAMINANTS 1052
*HEADLEY,J V

THE USE OF COMBINED SUPERCRITICAL FLUID CHROMATOGRAPHY-MASS SPECTROMETRY TO CHARACTERIZE CAROTENOID PIGMENTS 1054
*FREW,N M,JOHNSON,C G AND BROMUND,R H

THE IMPACT OF SAMPLE COLLECTION TECHNIQUES AND SOURCES OF BACKGROUND CONTAMINATION ON GC/MS DATA FOR ENVIRONMENTAL SAMPLES 1056
*ROSECRANCE,A E,SCHREIBER,J M AND RATHBUN,C A

SURFACES; GENERAL ANALYTICAL

ON THE EXAMINATION OF SURFACE FILMS BY Cf-252 PDMS 1058
SHOWELL,J S,*FALES,H M,SOKOLOSKI,E A,YANG,Y-M AND PANNELL,L K

ANALYSIS OF BIOMOLECULES ATTACHED TO SURFACES BY SIMS AND ESCA 1059
*KIDWELL,D A AND COLTON,R J

EFFECT OF PRIMARY ION BEAM PARAMETERS ON THE SECONDARY ION MASS SPECTROMETRY OF AN EXEMPLARY BIOMOLECULE 1061
*COLE,R B,GUENAT,C,HASS,J R AND LINTON,R W

NEUTRAL SIMS OF GALLIUM ARSENIDE 1063
*HINDENLANG,D M AND SEDGWICK,R D

ENHANCED DETECTION OF POSITIVE OR NEGATIVE IONS UNDER SELECTIVE ILLUMINATION ON O2 OR Cs AND COINCIDENT MEASUREMENT OF PHOTOEMISSION ACCOMPANIED BY SPUTTERING DUE TO ION BOMBARDMENT 1065
OHSHIMA,M,SHINOMIYA,T,TAMURA,H,SUGIYAMA,Y,NAMIKI,A,NISHIGAKI,S AND *NODA,T

FLUORINE ANALYSIS BY TIME-RESOLVED MASS SPECTROMETRY 1067
*HEMBERGER,P H,BECKMAN,R J AND HEATON,R C

PYROLYSIS MASS SPECTROMETRY OF ANTIMONY OXIDE-ORGANOHALOGEN FLAME RETARDANTS IN PLASTICS 1069
*GALE,P J,BENTZ,B L AND LEE,W M

DEVELOPMENT OF A CURIE POINT PYROLYSIS INLET FOR THE FINNIGAN ION TRAP DETECTOR 1071
*RICHARDS,J M,STOLK,H T,MCCLENNEN,W H AND MEUZELAAR,H L C

LASER DESORPTION FT/ICR MASS SPECTROMETRY: ANALYSIS OF INVOLATILES AND ELECTRODE SURFACES 1073
*SHOMO,R E,HSU,A T AND MARSHALL,A G

MODIFICATION OF A FINNIGAN-MAT TRIPLE STAGE QUADRUPOLE FOR ORGANIC SIMS OF SOLID SURFACES 1075
*BENTZ,B L,GALE,P J AND HONIG,R E

Thermospray LC/MS Analysis of Amine Salts Comparing Continuous and "Pulsed" Modes of Buffer Introduction: E.M. Jakubowski, F.E. Chou, and J.R. Smith; U.S. Army Medical Research Institute of Chemical Defense, Aberdeen Proving Grounds-Edgewood Area, MD, 21010-5425.

Direct ionization thermospray LC/MS analysis requires the addition of an ammonium salt to the LC solvent system. Normally, a solution of 0.1N ammonium acetate buffer is added continuously to the solvent system somewhere prior to the thermospray interface. An alternate method is to add the salt only to the sample liquid matrix. On injection, the sample is contained in a pulse of buffer. The "pulsed" method achieves excellent sensitivity while minimizing the amount of material flowing into the mass spectrometer. Some of the benefits gained by this method include a lower background noise, better peak shape, lower incidence of capillary blockage, and simplified data handling. At present, the pulsed method can only be used in direct injection, a column in many cases would separate the solute from the ammonium salt.

Table 1 indicates the typical operating environment used for direct injection, direct ionization thermospray LC/MS. Figures 1 and 2 show ion chromatograms for the pulsed and continuous methods of analyzing the indicated amines. All of the peaks shown in figures 1 and 2 represent injections of 10 nanograms amine/20 microliter solvent. Continuous and pulsed methods are used to develop concentration versus peak area ratio curves for four pyridostigmine concentrations from 1 to 16 nanograms in various matrices. Selective ion monitoring of the pyridostigmine 110 M/e ion and the edrophonium(internal standard) 152 M/e ion are utilized in the determination of the standard curves and the results are shown in table 2.

Table 1
LC/MS Operating Environment

Mass spec.:	Finnigan 4500
LC interface:	Vestec TSP
Injector:	Rheodyne 7125
Buffers:	0.1N AA or TAAS
LC solvent:	100% water or 55%ACN:45%water
Flow rate:	1.2 ml/min
Trap coolant:	liq.nitrogen
Inject. vol:	20 microliter

Table 2
Linear Regression Analysis
(solvent matrix)

Buffer/Mode	Statistics		
(55%ACN:45%water)	slope	y-int	corr
0.1N AA/cont	0.337	-0.005	0.993
0.1N AA/pulse	0.390	-0.013	0.981
0.1N TAAS/cont	2.074	0.009	0.979
0.1N TAAS/pulse	2.886	0.029	0.992
(100% water)			
0.1N AA/cont	2.712	0.197	0.999
0.1N AA/pulse	2.822	0.098	0.992
(100% water)			
(serum matrix)			
0.1N AA/cont	0.240	0.000	0.970
0.1N AA/pulse	0.206	0.000	0.950

The contrast between figures 1 and 2 indicates the advantages of the pulse method. Compounds such as acetylcholine would not be observed using the continuous mode but in the pulse mode they are clearly evident. The results of table 2 indicate that the continuous and pulse modes yield comparable standard curves. Trifluoroacetate ammonium salt (TAAS) produces usable thermospray ions and is a promising substitute for ammonium acetate (AA). The serum matrix method utilized the cartridge cleanup procedure of Ellen et al.(J Chrom,vol 228,pp 235,1982) this phase of the assay needs more work to increase the precision and accuracy.

FIGURE 1

RECONSTRUCTED ION CHROMATOGRAM OF SELECTED COMPOUNDS ACTIVE IN CHOLINERGIC SYSTEMS:

Continuous Buffer Mode (0.1N amm.ace.,3inj/compd.)

compound	
1	atropine
2	2-PAM
3	physostigmine
4	benactyzine
5	aprophen
6	TMB-4
7	neostigmine
8	acetylcholine

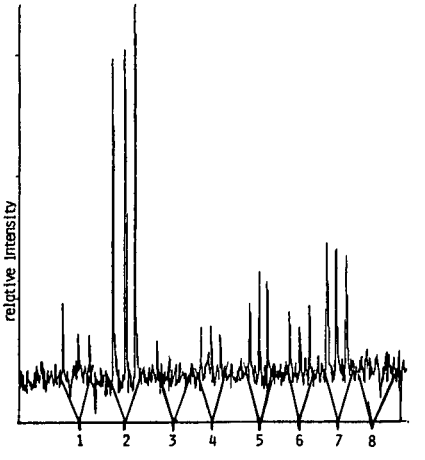

FIGURE 2

RECONSTRUCTED ION CHROMATOGRAM OF SELECTED COMPOUNDS ACTIVE IN CHOLINERGIC SYSTEMS:

Pulsed Buffer Mode (water carrier,3inj/compd.dis.in 0.1N amm.ace.)

compound	
1	atropine
2	2-PAM
3	physostigmine
4	benactyzine
5	aprophen
6	TMB-4
7	neostigmine
8	acetylcholine

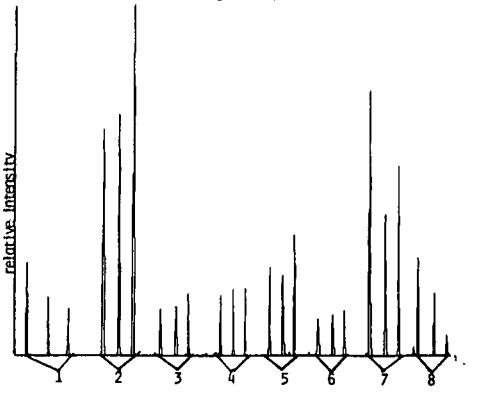

MODIFICATION OF A FINNIGAN THERMOSPRAY INTERFACE TO ALLOW DISCHARGE CHEMICAL IONIZATION OF THE THERMOSPRAY VAPOR. Don Zakett, G. J. Kallos, and P. J. Savickas; The Dow Chemical Company; Analytical Laboratories, 574 Building, Midland, Michigan 48667

A standard Finnigan Thermospray (TSP) LC/MS interface has been modified by the addition of discharge ionization. This feature allows operation of the TSP interface in the chemical ionization mode, which substantially increases its versatility since the requirement for buffered LC eluents or post column addition of reagents to promote ionization of the sample has now been eliminated. The modified interface accommodates conventional LC flow rates (1.0-1.4 mL/minute) and permits use of unbuffered normal and reverse phase eluent systems. The modifications to the standard interface are inexpensive and easily implemented. The voltage required to operate the discharge was obtained from the adjustable power supply normally used for the Townsend Discharge. Use of discharge chemical ionization allows successful analysis of many compounds with low and moderate polarity which could not be analyzed using buffered eluent systems.

The modifications to the standard TSP source block are shown in Figures 1 and 2. A hole was drilled approximately midway between the LC vaporizer tip and the mass spectrometer sampling cone to allow placement of the insulated discharge electrode (needle). The discharge was typically operated at -1.2 kV.

Figure 3 shows the DCI/TSP mass spectrum obtained for adenosine in a non-buffered mobile phase of 70/30 H_2O/MeOH. The relative abundance of 136+ versus 268+ (<10%) indicates the interface does not produce extensive thermal decomposition. The full scan mass spectrum (sum of 10 scans; no background subtraction) for an injection of 2 ng of adenosine is given in Figure 4 and demonstrates excellent full scan sensitivity. The response for injection of 1 ng Acridine, MW 179, is shown in Figure 6. Here, the mobile phase was 100% CH_3-CN with full scan mass spectra taken over the range of 135-400 amu. The single ion chromatogram for m/z 180+ (MH+) is shown in this figure and indicates subnanogram (scanning) sensitivities can be obtained by DCI/TSP/MS.

Mixed (CI and/or Charge Exchange) ionization is often observed for compounds with low or moderate polarities as shown in Figure 5 for Biphenyl.

The voltage applied to the repeller electrode can cause additional fragmentation by collisional activation as ions are extracted into the mass spectrometer. This effect is most apparent in non buffered mobile phases as shown in Figure 7 for adenosine where the protonated molecular ion is almost totally eliminated from the mass spectrum by CAD in changing the repeller from 60 V to 90 V. It was not possible to cause CAD in a buffered mobile phase without DCI (conventional thermospray ionization) over the repeller voltage range studied as shown in Figure 8.

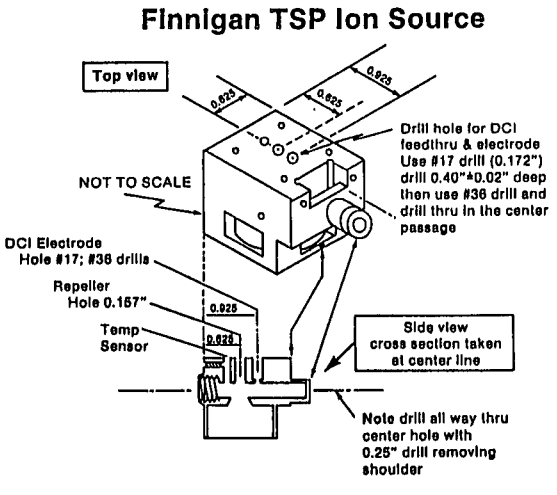

FIGURE 1

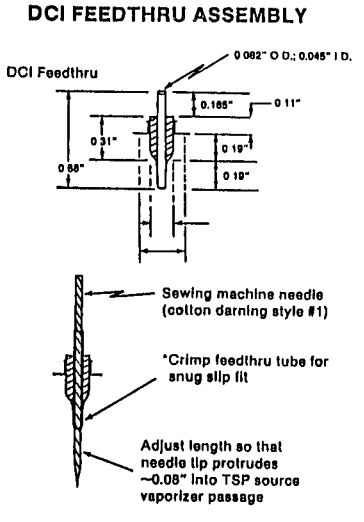

FIGURE 2

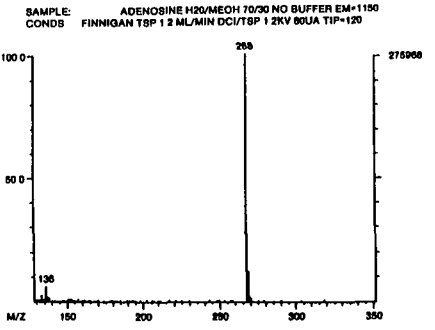

FIGURE 3

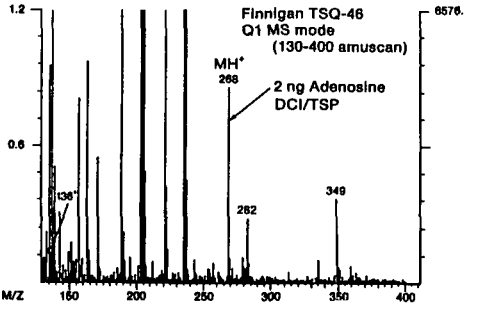

FIGURE 4

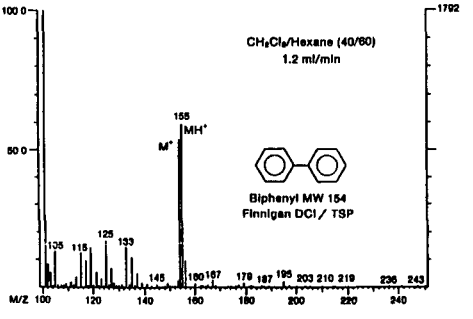

FIGURE 5

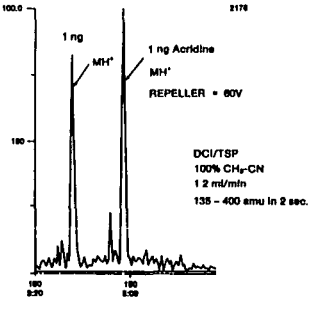

FIGURE 6

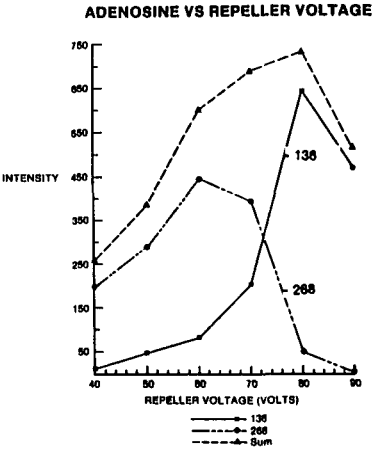

FIGURE 7

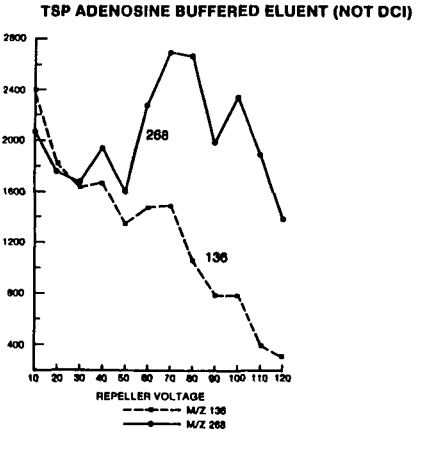

FIGURE 8

COLLISION INDUCED DECOMPOSITION IN THE THERMOSPRAY ION SOURCE

F.A. Bencsath and F.H. Field
The Rockefeller University
New York, N.Y. 10021

Though several workers reported sub-nanogram even picogram sensitivity [1,2] in certain thermospray MS [3] works, the basic sensitivity of this hyphenated method is at least two orders of magnitudes less than that of the GC-MS. One obvious reason of it is the wasteful processing of the ions generated in the source: most of them land in the cryopump which maintains the low pressure in the source and about 1% of them leaks into the analyzer region. In order to lessen the waste, we equipped our home-built thermospray LC-MS interface and ion source in a Biospect quadrupole mass spectrometer with a retarding electrode as described by Lewis and Smith [4], placing it about 2 mm downstream from the ion sampling cone in the source. In order to control the source pressure we inserted a flow restriction valve in the cryopump line and attached a differential manometer downstream, very close to the source. The application of a 0-500 V potential to the retarding electrode caused appreciable changes in the spectra in agreement with the finding of Lewis and Smith, and we studied this phenomenon as a function of source pressure and the retarding potential.

We found:

1. The total ion current (TIC) increased continously and strongly with the retarding potential up to about 500 V, at which point electric breakdown (discharge) occurred. This phenomenon was indicated by the sudden rise of the electrode current from about 1 μA to 1 mA within 20-25 V potential increment.

2. The characteristics of the spectra began to change when the retarding potential exceeded 150-200 V in that the lower mass fragment ions were formed with greater relative intensity. Thus, with the commonly used 1:3 methanol/water/0.05M NH_4Ac system increasing the retarding potential decreased the relative intensity of the dominant $CH_3OH.NH_4^+$ cation with a concomitant rise in the intensities of fragment ions NH_4^+ between 150-300 V, $CH_3OH_2^+$ from 300 V, and CH_3^+ above 350 V (Fig. 1). This fragmentation is probably the result of energetic collisions caused by acceleration of the ions in the retarding field.

3. The changes in the spectrum characteristics caused by high retarding potential could be reversed by increasing the pressure in the source. The higher the retarding potential was set, the higher source pressure was necessary to suppress the secondary processes (Fig. 2). This behavior supports our assumption about collision induced decomposition, since the extra energy the ions obtain between collisions is equally dependent both on field strength and the length of the free path which are linear functions of the retarding potential and the reciprocal pressure, accordingly.

The intensity enhancement and the collision induced decomposition also occurs with ions of solutes in the thermospray system. Thus in the spectrum of adenosine (Fig. 3) the MH^+ molecular ion at m/z 268 was the dominant ion below 400 V retarding potential and at 2.5 torr source pressure, and the BH_2^+ fragment at m/z 136 was a minor one. This relationship was reversed at 500 V. The intensity increase of the molecular ion m/z 268 was 13 fold at 400 V. A more extensive fragmentation of the molecular ion was observed with the tripeptide $(L\text{-}ALA)_3$. At 150 V retarding potential, the only ions in the spectra were the MH^+ and $M+NH_4^+$ quasi-molecular cations. At 480 V, five intense fragment ions enriched the spectrum with meaningful structural information. (Fig. 4).

Both the sensitivity and fragmentation enhancement caused by the retarding electrode is useful, the latter being a potential tool for structure elucidation.

Acknowledgement:

This work was supported in part by the Division of Research Resources, National Institutes of Health

References.

1. R.D. Voyksner, J.T. Bursey, E.D. Pellizari, Anal. Chem. 56, 1507 (1984).
2. T.R. Covey, J.B. Crowther, E.A. Dewey, J.D. Henion, Anal. Chem. 57, 474 (1985).
3. C.R. Blakley, J.J. Carmody, M.L. Vestal, Anal. Chem. 52, 1636 (1980).
4. I.A.S. Lewis and D.C. Smith, ASMS 1984, San Antonio, p. 803.

TSP SOLVENT SPECTRA AT DIFFERENT RETARDING ELECTRODE POTENTIALS

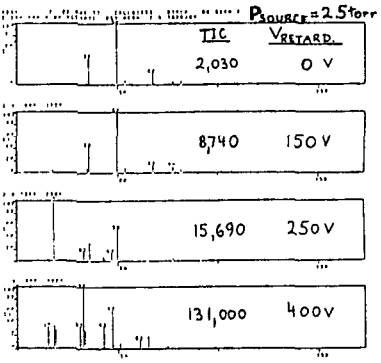

SOLVENT: (25% MEOH + 75% WATER), 0.05M NH_4Ac

Fig. 1.

PRESSURE DEPENDENCE OF THE INTENSITIES OF $MeOH \cdot NH_4^+$ AND $MeOH_2^+$ AT DIFFERENT V_R-s.

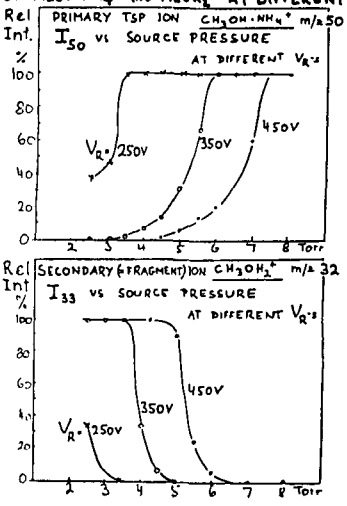

Fig. 2.

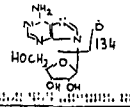

Adenosine (MW 267)
TSP spectra at different V_R-s.

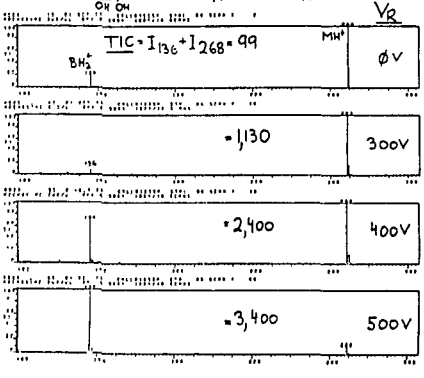

Fig. 3.

TRI-L-ALANINE TSP SPECTRA AT DIFFERENT RETARDING POTENTIALS

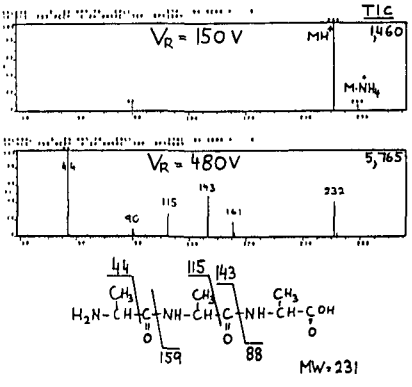

Fig. 4.

DETERMINATION OF ACRYLAMIDE IN SUGAR BY THERMOSPRAY MULTIDIMENSIONAL LIQUID CHROMATOGRAPHY-MASS SPECTROMETRY, G. J. Kallos and S. S. Cutie', The Dow Chemical Co., Analytical Laboratories, 574 Building, Midland, Michigan 48667

Results presented in this paper illustrate the versatility of the thermospray liquid chromatographic-mass spectrometric technique (TSP LC/MS) for the determination of trace levels of acrylamide in sugar. The interest has been generated because this compound was reported[1,2] to show some biological activity. Since acrylamide monomer is the raw material for making polyacrylamide, residual monomer may be present in polyacrylamide which is used in the sugar industry as a flocculant. An analytical technique for determining ppt levels of this monomer in refined sugar has, therefore, been developed.

The acrylamide is derivatized with bromine[3], separated by multidimentional reversed phase liquid chromatography and detected with mass spectrometry through a thermospray interface. This technique is shown to be superior to the moving-belt interface in its ability to provide molecular mass information from a thermally labile low volatility compound. Since sugar is known to contain numerous nitrogenous compounds, the multidimensional liquid chromatographic separation has been developed in order to avoid interferences present in the sugar matrix. Limits of about 200 ppt can be achieved through the TSP LC/MS without any significant evidence of thermal decomposition.

The LC set up consisted of a Varian Ternary Gradient Liquid Chromatograph Model 5560 (Varian, 220 Humboldt, Sunnyvale, CA 94086) with UV-200 programmable UV-VIS detector, and a Waters M-600 pump (Waters Associates, Milford, MA) that was used for the post column addition of buffers. The samples were injected with a Rheodyne 7125 injector and separated with a Rheodyne 7125 injector and separated on a 25 cm x 4.6 mm, Partisil 10 ODS-2 column (Whatman Chemical Separation Inc., Clifton, NJ). A similar column was used in the multi-dimensional separation with a Rheodyne 7001 pneumatic actuated second valve to switch the chromatographic flow. The TSP interface (Vestec, Houston, TX) was installed on a Finnigan 4500 quadrupole mass spectrometer. The moving-belt interface (Finnigan MAT Company, San Jose, CA) was installed on the same Finnigan MS. The optimal temperatures for 40% methanol in water of 1 ml/min in multidimentional separation and postcolumn addition of 0.3 ml/min 0.25 M trifluoroacetic acid were vaporizer T_1 = 130°C, vaporizer Tip T_2 = 197°C, source block T_3 = 243°C and aerosol T_4 = 229°C. The mass spectrometer was operated in the selected ion recording mode covering ions at m/z 230, 232, and 234 for the dibromopropionamide derivative and m /z 72 and 90 for acrylamide.

The MS detector response for the calibration of acrylamide in water was found to be linear with a dynamic range of at least three orders of magnitude. However, the direct procedure was found to be unacceptable in the complex sugar matrix. The alternate route was to derivatize the acrylamide to dibromopropionamide for easy extraction out of the sugar matrix and to analyze by TSP LC/MS[4]. A linear calibration curve of this derivative was obtained with similar dynamic range as that of acrylamide. The calibration study was carried out in the entire ppb and low ppm range. The precision of the TSP LC/MS procedure for the dibromopropionamide derivative was found to be ±3.2% for 1σ.

The methane chemical ionization mass spectra obtained by the solids probe and LC/Ms moving belt introduction shown in Figure 1 exhibit a protonated-molecular ion at m/z 230 (2 Br) and intense protonated acrylamide ion at m/z 72 particularly more pronounced in the moving belt interface. The thermospray ionization mass spectrum shown in Figure 2 did not show any significant thermal decomposition, but a very intense protonated molecular ion at m/z 230 (2 Br), when trifluoroacetic acid was used. A single Partisil 10 ODS-2 column coupled to the thermospray LC/MS system, as shown in Figure 3a contained many interferences. Therefore, a multidimensional chromatographic LC approach was applied with the use of two Partisil 10 ODS-2 columns and most of the interferences in the sugar blank were removed as it can be seen in Figure 3b. A typical total ion chromatogram of a spiked sample and a standard of 98 ppb dibromopropionamide derivative is shown in Figure 4. The results of the recovery experiments are shown in Table 1. The variability of the values reported for the recoveries may be a function of the derivatization procedure and stability of the dibromo derivative in water.

REFERENCES

1. Dow Report "Recent Acrylamide Monomer Toxicity Data and Its Importance To You The Monomer Customer", November 1984.
2. Johnson, K. A.; Gorzinski, S. J.; Bodner, K. M.; Campbell, R. A.; Wolf, C. H; Froedman, M. A.; Mast, R. W.; "Chronic Toxicity and Uncogenicity Study on Acrylamide", Submitted for publication in Toxicology and Applied Pharmacology, 1985.
3. Brown, L.; Rhead, M.; Analyst (London) 1979, 104, 391-399.
4. Blakley, C. R.; Vestal, M. L., Anal. Chem. 1983, 55, 750-754.

FIGURE 1 METHANE CHEMICAL IONIZATION MASS SPECTRA OF DIBROMOPROPIONAMIDE

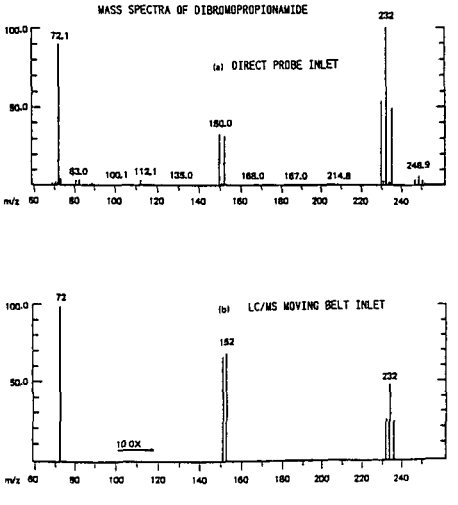

FIGURE 3 LC/MS TOTAL ION CHROMATOGRAM OF SUGAR SAMPLE

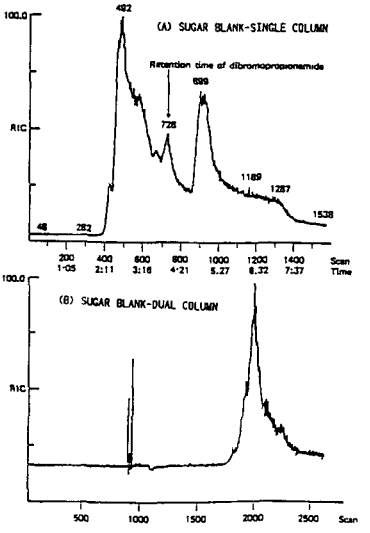

FIGURE 2 THERMOSPRAY IONIZATION MASS SPECTRUM OF DIBROMOPROPIONAMIDE

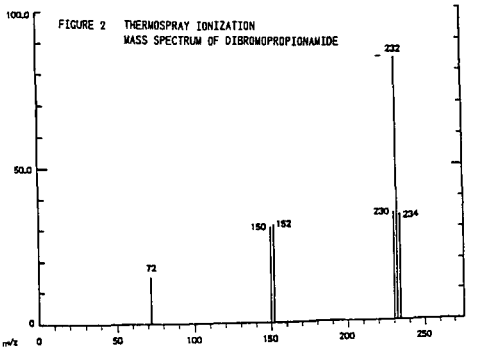

TABLE I

RECOVERY DATA OF ACRYLAMIDE IN SUGAR SAMPLES

Sample ID	Amount Added (ppt)	Amount Found (ppt)	% Recovered Corrected for Blank
Water Blank		320	
1	200	30	15
2	800	240	30
3	800	320	40
4	800	270	34
5	2000	890	45
6	2000	610	31

FIGURE 4. THERMOSPRAY LC/MS TOTAL ION CHROMATOGRAMS OF DIBROMOPROPIONAMIDE

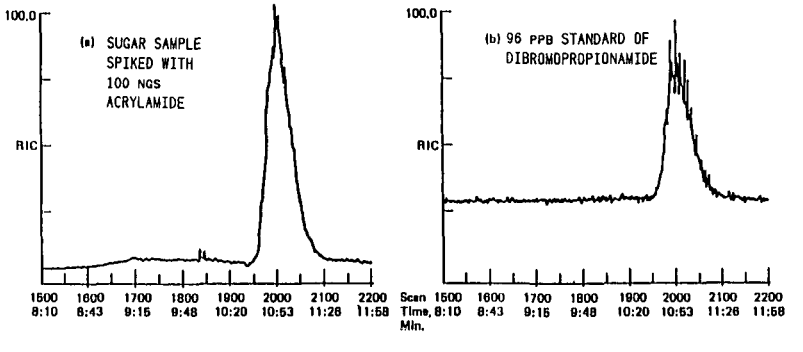

Sensitivity and Selectivity in Thermospray Ionization. Patrick Rudewicz and Kenneth Straub; Smith Kline and French Laboratories, Dept. of Drug Metabolism, 709 Swedeland Road, Swedeland, PA, 19479.

Introduction

Recently, gas-phase ion/molecule reactions have been shown to be an important process in thermospray (TSP) ionization. Using single ion monitoring experiments, Bursey and co-workers observed that when aniline elutes under TSP conditions using an ammonium acetate buffer, the gas-phase order of basicity is followed; i.e., NH_4^+ protonates aniline (1). In another study, TSP ionization has been shown to have two distinct stages (2). In the first stage, primary TSP ions are formed by field-induced ion evaporation from superheated droplets. In the second stage, ionization may take place by gas-phase ion/molecule reactions, depleting the primary TSP ions and forming product ions. Since gas-phase ion/molecule reactions are an important ionization mechanism for moderately volatile analytes, we have investigated the question of whether the marked sensitivity differences for compounds reported in NH_3 CI (3) are present in TSP using an ammonium acetate buffer. In addition, we have explored the possibility of selective ionization using buffers containing basic compounds such as pyridine or tripropylamine. This approach is directly analogous to achieving selective ionization in chemical ionization (CI) by employing weak Brønsted acids as the reagent ions.

Experimental

Thermospray LC-MS experiments were carried out using a Finnigan thermospray ion source and controller interfaced to a tandem quadrupole mass spectrometer, ("TSQ 15", Finnigan-MAT, San Jose, CA). The thermospray operating temperatures were: vaporizer 140 °C; jet 190-195 °C; aerosol 220-230 °C. An electron filament was not employed. The HPLC system consisted of a Beckman model 320 gradient controller and two model 114 pumps (Beckman, Berkeley, CA), connected to a model 7520 loop injection valve (Rheodyne, Cotati, CA).

Discussion

In NH_3 chemical ionization (CI) the molar sensitivities (total sample ionization/mole) for compounds with proton affinities (PA) 3-4 kcal/mole less than the PA of NH_3 (204 kcal/mole) are significantly lower than those of more basic compounds having PA's greater than NH_3 (3). A similar decrease in sensitivity with decreasing PA has been observed in our laboratory in TSP experiments using an aqueous 0.05 M ammonium acetate buffer. As shown in Figure 1, TSP sensitivities decrease significantly as the PA of the sample falls below that of NH_3: the TSP sensitivity for acetophenone (PA=205.4 kcal/mole) is 50 times greater than that for cyclohexanol (PA=193 kcal/mole). Cyclohexanol, benzoic acid, and ethyl acetate give only $(M+NH_4)^+$ ions in their TSP spectra. Methyl benzoate and acetophenone give both $(M+NH_4)^+$ and MH^+ in a ratio which is strongly dependent upon source conditions. These sensitivity differences are in agreement with a gas-phase mechanism since the dissociation energies of gas-phase ionic hydrogen bonds, $AH^+ \cdots B$, have been shown to decrease as the difference between the proton affinities of A and B increase (4). No detectable TSP ion current was observed for either toluene (PA=189.8 kcal/mole) or phenol (PA=196.3 kcal/mole) in agreement with previously reported NH_3 CI studies on these compounds (5).

To investigate the possibility of selective ionization of analytes through manipulation of buffer composition, the thermospray ionization efficiencies of four bases of known proton affinities (PA) were studied using both an ammonium acetate and a pyridinium acetate buffer system. The bases used for this study were adenine (PA=224 kcal/mole), cytosine (PA=224 kcal/mole), uracil (PA=208 kcal/mole), and thymine (PA=209 kcal/mole). Under these TSP conditions using a 0.05 M NH_4OAc buffer, the major primary ion in the TSP spectrum is NH_4^+, 65 % of the total ionization. When 50 ng samples of the four bases are run with an NH_4OAc buffer roughly similar responses are observed, 7142 ± 800, Table 1. The two bases with PA's close to that of NH_3 (PA=204 kcal/mole), cytosine and uracil, give abundant MH^+ and $(M+NH_4)^+$ ions.

The bases of higher PA's, adenine and cytosine, give mostly MH^+ ions in their TSP spectra. With a 0.025 M pyridinium acetate solution, the major TSP primary ion is the pyridinium ion, 80% of the total ionization. When 50 ng samples of the four bases are run using a pyridinium acetate buffer, the two compounds of higher PA, adenine and cytosine have roughly similar sensitivities, 7381 ± 600; whereas thymine and uracil give much smaller responses, ≅ 200.

The difference in responses of the four bases with the two different buffers can be explained in terms of gas-phase ion/molecule kinetics. Since the PA's of the all four bases are greater than the PA of NH_3, proton transfer from the ammonium ion to each of the bases is an exothermic process and should be highly efficient, proceeding at close to the collision rate. The proton affinity of pyridine, however, is 220.8 kcal/mole and proton transfer from the pyridinium ion to thymine and uracil is an endothermic process and should have a very low reaction efficiency. Alternatively, if protonated thymine and uracil are desorbing directly from solution, neutral pyridine would deprotonate these species.

These results demonstrate that gas-phase ion/molecule reactions are important in the production of sample ions in TSP ionization and that TSP sensitivities for moderately volatile neutral analytes may be predicted using a gas-phase model. In addition, as shown by the above experiment, selective ionization of analytes may be achieved by modifying the TSP primary (reagent) ion spectrum. This is easily accomplished by changing the composition of buffers, either post-column or pre-column.

---

1. Bursey, M.M.; Smith, R.W.; Gaskell, S.J. Anal. Chem. 1985, 57, 2597-2599.
2. Alexander, A.J.; Kebarle, P. Anal. Chem. 1986, 58, 471-478.
3. Weinkam, R.J.; Toren, P.C. Paper presented at the 31st Annual Conference on Mass Spectrometry and Allied Topics, Boston, MA, 1983.
4. Davidson, W.R.; Sunner, J.; Kebarle, P.J. J. Amer. Chem. Soc. 1979, 101, 1675-1679.
5. Keough, T.; DeStefano, A,J. Org. Mass Spectrom. 1981, 16, 527-533.

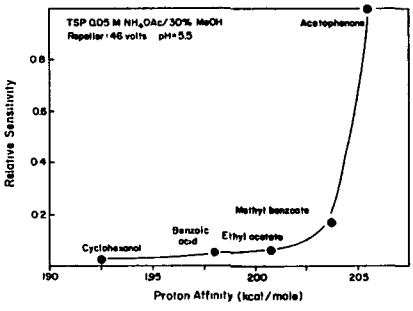

TABLE I

0.05 Ammonium Acetate Buffer pH=5 5

Compound	PA (kcal/mole)	$(M+H)^+$	$(M+NH_4)^+$	Total
Adenine	224	8028	35	8064 ± 986
Cytosine	224	7062	355	7417 ± 567
Thymine	209	4304	1846	6150 ± 431
Uracil	208	3734	3204	6938 ± 1300

0.025 Pyridinium Acetate Buffer pH=5 5

Compound	PA (kcal/mole)	$(M+H)^+$
Adenine	224	7803 ± 447
Cytosine	224	5959 ± 567
Thymine	209	228 ± 84
Uracil	208	< 200

SUPERCRITICAL FLUID CHROMATOGRAPHY/MASS SPECTROMETRY USING A MOVING BELT INTERFACE

A.J. Berry, D.E. Games and J.R. Perkins
Department of Chemistry, University College, P.O. Box 78, Cardiff CF1 1XL, U.K.

INTRODUCTION

A supercritical fluid has a combination of gas-like and liquid-like properties, which, when such a fluid is used as a chromatographic mobile phase, result in favourable transport of solutes through a chromatographic column. Supercritical fluid chromatography (SFC) is complementary to both gas chromatography (GC) and high-performance liquid chromatography (LC). In contrast to GC, solute does not have to be vaporized for analysis and better chromatographic efficiencies, differing selectivities and more rapid analyses are obtainable than with LC. In addition, a wide range of detectors can be used with SFC. Both conventional LC columns[1] and fused silica bonded capillary[2] columns have been used for SFC. The former approach offers speed of analysis and method development, ease of obtaining good quality preparative samples and use of a wide range of modifiers. The latter approach enables chromatographic efficiencies approaching those of capillary GC to be obtained.

Our major interest in SFC has been in interfacing the technique with a mass spectrometer, since the gas volumes generated from the mobile phase are much lower than with LC and hence interfacing should be easier. SFC/MS has been effected with packed columns, using molecular beam techniques[3], a capillary inlet[4] and a modified direct liquid introduction LC/MS probe[5]. In the latter approaches only a relatively small portion of the eluent from the chromatograph could be handled by the mass spectrometer. Use of capillary SFC enables the mass spectrometer to handle all the column eluent and both EI and CI mass spectral data can be obtained[6]. However, it should be noted that in the former case there will be limitations in which modifiers can be used.

We have interfaced both packed and capillary SFC to our mass spectrometers and in this paper we will discuss our experiences with the former approach.

EXPERIMENTAL

SFC was performed on a Hewlett-Packard 108B liquid chromatograph modified for SFC operation. 100 x 4.6mm columns packed with 5μ silica or aminobonded silica were used with carbon dioxide modified with varying amounts of methanol or methoxy ethanol. SFC/MS interfacing was effected to both Finnigan 4500 and VG 70/70E mass spectrometers using moving belt LC/MS interfaces and a modified Finnigan thermospray deposition device. The spray deposition was connected in-line to the chromatograph via a 'T' piece between the UV detector exit and the outlet back-pressure regulator. In order to use the full density range for SFC, the end of the stainless steel tubing used in the spray deposition device was slightly crimped. The spray deposition device was connected to a 6 volt power supply which was adjusted through a rheostat to prevent freezing of the mobile phase at the tip. In all other respects the moving belt interfaces were used as for LC/MS.

RESULTS AND DISCUSSION

Use of a moving belt interface for SFC/MS enables a large proportion of the eluent from the SFC to be handled and also has the advantage of provision of conventional EI and CI mass spectral data. Initial studies were conducted with mixtures of polynuclear aromatic hydrocarbons and xanthines. In both cases, excellent TIC traces were obtained showing little loss of chromatographic performance. EI spectra obtained gave excellent matches with library spectra and could be scanned from 40u. For a mixture of sulphonamides methane CI was necessary to obtain molecular weight information. The technique has been used to study a crude Ergot fermentation extract and EI data obtained was in excellent agreement with that previously reported for the mixture by LC/MS[7], but SFC/MS had the advantage of performing the analysis in ten minutes as opposed to one hour. This approach to SFC/MS has also been shown to be

amenable to studies of coumarin rotenticides and carbamate pesticides and studies of other classes of compound are in progress.

CONCLUSIONS

SFC/MS using a moving belt interface has been effected. The approach enables a large proportion of the eluent from the SFC to be handled and conventional EI and CI mass spectra to be obtained. Because of the better efficiency obtainable by SFC, SFC/MS analysis is more rapid and detection limits are better than with LC/MS. The limitations of this approach to SFC/MS are those that are apparent in moving belt LC/MS, i.e. thermal decomposition at low levels with labile compounds and the limitations to compounds which are amenable to EI and CI mass spectrometry unless surface ionization techniques are used.

REFERENCES

1. D.R. Gere, Science, 1983, 222, 253.
2. J.C. Fjeldsted and M.L. Lee, Anal. Chem., 1984, 56, 619A.
3. L.G. Randall and A.L. Wahrhaftig, Rev. Sci. Instrum., 1981, 52, 1283.
4. T.H. Gouw, R.E. Jentoft and E.J. Gallegos, in K.D. Timmerhause and M.S. Barber (Edts) "High Pressure Science & Technology", Vol. 1., Plenum Press, New York, 1977, p. 583.
5. J.B. Crowther and J.D. Henion, Anal. Chem., 1985, 57, 2711.
6. B.W. Wright, H.T. Kalinoski, H.R. Udseth and R.D. Smith, J. High Resolut. Chromatogr. Chromatogr. Commun., 1986, 9, 145.
7. C. Eckers, D.E. Games, D.N.B. Mallen and B.P. Swann, Biomed Mass Spectrom., 1982, 9, 162.

CAPILLARY SUPERCRITICAL FLUID CHROMATOGRAPHY-MASS SPECTROMETRY FOR THE ANALYSIS OF LABILE AND NONVOLATILE COMPOUNDS*, H. T. Kalinoski, H. R. Udseth, B. W. Wright, and R. D. Smith, Chemical Methods and Separations Group, Chemical Technology Department, Pacific Northwest Laboratories, (Operated by Battelle Memorial Institute), Richland, Washington 99352.

Supercritical fluid analytical techniques are attracting increasing attention for high resolution separation and analysis of labile, less volatile and higher molecular weight compounds (1-4). Capillary column supercritical fluid chromatography (SFC) allows both high resolution separations and high-speed analysis based upon rapid pressure programming methods (5). The interface of capillary SFC with mass spectrometry has provided the selectivity and sensitivity required for identification and confirmation, as well as the basis for extension to more polar fluid systems with greater solvating power. Mass spectrometry overcomes the limitations of other chromatographic detectors, such as low sensitivity, inapplicability to many analytes, solvent incompatability, and lack of specificity, while the use of supercritical fluids avoids the constraints of liquid chromatographic introduction, such as lower chromatographic resolution, and the solvent limitations, effluent splitting, thermal lability and volatility requirements of gas phase detectors. The continuing evolution of capillary SFC-MS has produced interface designs which can be near routinely applied with fluids such as carbon dioxide while providing for the transport of truly nonvolatile compounds to the mass spectrometer ionization region. The molecular weight range of compounds capable of being analyzed by SFC-MS appears limited only by the range of the mass spectrometer; mass spectra of compounds of 2000 dalton have been obtained with quadrupole SFC-MS. The same interface design is also used for supercritical fluid extraction-mass spectrometry (SFE-MS) (1,6) where the superior solvating ability and gas-like transport properties of supercritical fluid solvents are exploited for extraction and characterization of complex, often otherwise intractable, materials.

Recent advances in the understanding of supercritical fluid phase behavior has led to the increased use of polar modified fluids for SFC-MS of more polar analytes. Fluid mixtures have been prepared that retain mild thermal conditions and allow full exploitation of the selectivity offered by supercritical fluids through control of fluid pressure (and, therefore, density). These mixtures have been utilized for analysis of thermally labile polar analytes, higher molecular weight mixtures, such as polyglycols, as well as extraction of polar materials from natural matrices. Other aspects of mass spectrometric analysis previously demonstrated as being compatible with direct supercritical fluid introduction, such as choice of ionization or tandem MS/MS analysis (1-6), are also possible when modified fluids are used.

*This work was supported by the U. S. Department of Energy, Office of Health and Environmental Research under Contract DE-AC06-76RLO-1830.

1. R. D. Smith, B. W. Wright and H. R. Udseth, "Supercritical Fluid Technology"' Penninger, J.M.L.; Radosz, M.; McHugh, M. A.; Krukonis, V. J., Eds.; Elsevier, Amsterdam, 1985; 191-223.

2. R. D. Smith, H. R. Udseth and B. W. Wright, J. Chromatogr. Sci. 1985, 23, 192-199.

3. B. W. Wright, H. T. Kalinoski, H. R. Udseth and R. D. Smith, J. H. R. C. and C. C. 1986, 9, 145-153.

4. H. T. Kalinoski, B. W. Wright, and R. D. Smith, Biomed. Environ. Mass Spectrom. 1986, 13, 33-34.

5. R. D. Smith, H. T. Kalinoski, H. R. Udseth and B. W. Wright Anal. Chem. 1984, 2476-2480.

6. R. D. Smith, H. R. Udseth and B. N. Hazlett, Fuel, 1985, 64, 810-815.

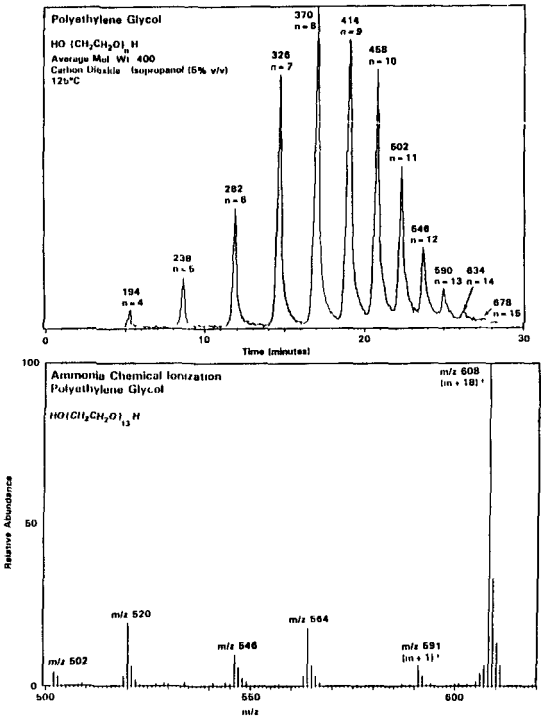

SFC-MS separation of a 400 average molecular polyethylene glycol sample using an isopropanol modified-carbon dioxide fluid (upper) and the ammonia CI mass spectrum of the n=13 oligomer from the sample (lower).

THERMOSPRAY MASS SPECTROMETRY APPLYING A DUAL BEAM VAPORIZER

L. Bütfering, G. Schmelzeisen-Redeker and F.W. Röllgen

Institute of Physical Chemistry, University of Bonn, Wegelerstr. 12
D-5300 Bonn, FRG

The use of a single beam thermospray vaporizer as a HPLC/MS interface and for ionization of solute molecules has several limitations: Solvents of high dielectric constant such as water and an electrolyte are necessary to provide the reagent ions for ionization of the solute. Samples insoluble in such solvents are not amenable to this mode of ionization. Therefore, for electrolyte free LC-eluates ionization of the vaporized molecules in the so-called jet chamber by EI or an electrical discharge and ionization by post-column addition of the electrolyte is frequently applied. A further limitation of TSP regarding the use of microbore columns is the minimum flow rate required for ion formation by vaporization of the liquid.

A TSP system employing two independently heatable capillary vaporizers has been constructed for HPLC/MS on-line coupling to overcome these limitations /1/. (Fig. 1). Parallel directly heated capillaries (0.1 i.d., 0.4 o.d.) terminate 1 mm apart in the jet chamber. One capillary vaporizer is used for introduction of the eluate (i.e. the sample solution), while the other generates the reagent ions, i.e. ammonium ions from an aqueous ammonium acetate solution for ionization of sample molecules. The dual beam TSP interface of Fig. 1 is an improved version of the one reported last year in San Diego employing two indirectly heated capillary vaporizers.

We have studied the properties of a dual beam in comparison to a single beam TSP system. For the single beam experiments only one of the two capillaries in Fig. 1 was utilized. Test compounds were mainly arginine, sucrose and chloramphenicol which are all soluble in water and therefore amenable to both the dual and the single beam techniques. The following results were obtained:

1. For a number of compounds (mol. weights $m/z < 400$, limited by the quadrupole) the level of fragmentation was similar in both modes of TSP ionization. However, for sucrose a more abundant molecular ion signal could be obtained by the dual beam technique.
2. For water soluble compounds the ionization efficiency in the dual beam mode of operation is about the same as in the single beam mode (Fig. 2). Of course, polar and non-polar (aromatic) compounds not soluble in water could be ionized by the dual beam technique only. Non-polar solvents were successfully applied.
3. For the sample solutions flow rates down to 30 µl/min, only limited by the HPLC-pump utilized, could be applied (Fig. 3). Therefore the dual beam technique appears promising for use with microbore columns.
4. The ionization phenomena observed in both modes of TSP ionization suggest that there is no principal difference in the ion formation mechanism. In the dual beam technique ion formation can be attributed to the coalescence of charged and uncharged droplets or particles in the mixing region of both jets followed by a decay of these droplets or particles, and to ion-molecule reactions between desolvated ions and neutrals.

/1/ L. Bütfering, G. Schmelzeisen-Redeker and F.W. Röllgen, J.C.S. Chem. Comm. 1986, 579.

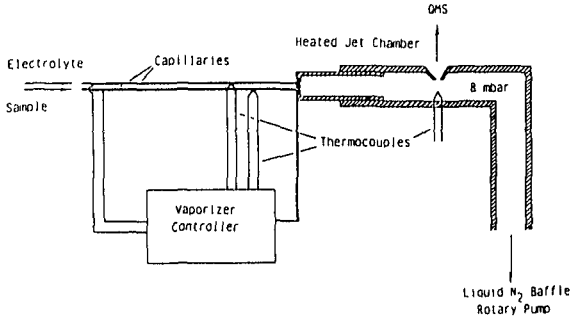

Fig.1: Dual Beam Thermospray System

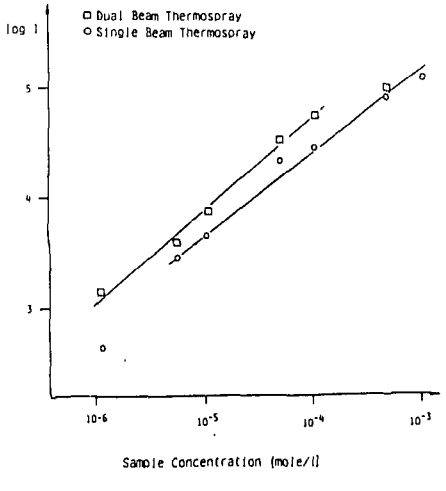

Fig.2: $(M+NH_4)^+$ Intensity of Chloramphenicol as Function of Sample Concentration

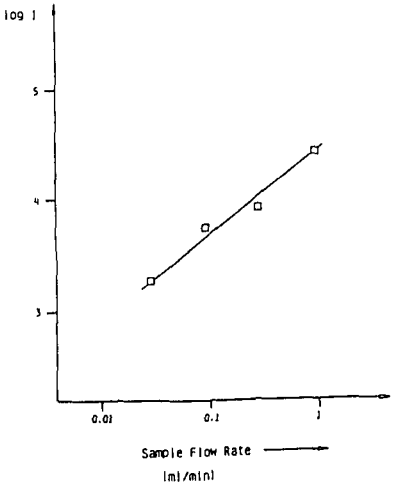

Fig.3: $(M+NH_4)^+$ Intensity of Sucrose as Function of Flow Rate

HYBRID MASS SPECTROMETERS

R. Graham Cooks, L.G. Wright and J.R. O'Lear, Purdue University, Chemistry Department, West Lafayette, IN 47907.

Hybrid instruments, those with more than one type of mass analyzer, were first built (1) as MS/MS instruments for the purpose of combining the best capabilities of sector and triple quadrupole machines. Following the development of the BQQ instrument (1) other hybrids have been described (2), including combinations of high resolution instruments with quadrupoles, eg. BEQQ (2), EBQQ (3) and QQEB (4), as well as time-of-flight/sector combinations (5).

Hybrids are versatile instruments as a consequence of their use of several types of analyzers. In the BEQQ design, which is emphasized here, both low and high energy ion beams are available for collisional activation and photodissociation experiments, exact mass measurements can be performed, and access is possible to ion/molecule reactions in the super-thermal range. Hybrid instruments have performance characteristics over a wide range of measurements which probably make them the preeminent analytical mass spectrometers, not excluding four-sector and FTMS instruments.

This presentation attempts to illustrate the power and promise of these instruments by concentrating on two recent discoveries which have been facilitated by the capabilities of hybrids (i) new types of MS/MS scans and (ii) polyatomic ion/surface interactions, especially surface-induced dissociation (SID).

New Types of Spectra

Hybrids can be used to obtain improved performance in established types of spectra and to produce new types of spectra.

Figure 1 illustrates three different experiments in which hybrids can be used to obtain improved performance in a MIKES spectrum. A MIKE spectrum can be viewed either as a kinetic energy spectrum or as a daughter ion spectrum, depending upon whether the focus is on the masses or the kinetic energy distributions of the fragment ions. Using a BEQQ, a scan of the quadrupole mass analyzer at fixed electric sector setting mass-resolves a particular peak in the energy spectrum (a); a scan of the electric sector at a fixed analyzer quadrupole setting energy-resolves a particular daughter ion (b), while both E and Q can be synchronously scanned (6) in order to mass resolve all components of the MIKES spectrum, so producing a well-resolved daughter ion spectrum (c). Examples of performance in mode (a) is shown in Figure 2.

A consideration (7) of the MS/MS experiment has revealed a hierarcy of spectra proceding from a zero "order" case, reaction monitoring, through first order spectra such as the well-known parent, daughter and neutral change spectra, to higher order spectra. In the useful first order class the results of a scan are a single mass/abundance listing. There are six (7) (and only six (8)) such spectra based on two reactions occuring in sequence in the mass spectrometer. Two additional MS/MS/MS scans are possible but these are of different order. One of the new scans of particular interest in studies on ion structure and reactivity is the reaction intermediate scan. This is a scan which recognizes all intermediates falling between a selected parent and a selected daughter ion.

The well-known rule that even-electron (closed shell) ions tend, for reasons of energetics, not to fragment to give odd-electron fragment ions is nicely exemplified in a reaction intermediate scan for benzyl methyl ether ($M^{+\cdot} \diamond 52^{+\cdot}$). All the intermediates in the spectrum, viz. 78, 92, 106 are odd-electron species since both parent and daughter are such.

Reaction intermediate spectra are often expected to be isomer specific as shown for 2-, 3- and 4-octanone ($M^{+\cdot} \diamond 43^{+\cdot}$) (Figure 3). Most interestingly, it is possible to efficiently seek new fragmentation routes by examining these spectra. Hence, in the case of 3-octanone the expectation that the daughter ion at 85^+ is the product of γ-cleavage with reciprocal hydrogen transfer, $+ \overset{\overset{\displaystyle OH}{\|}}{C_2H_5\text{-}C}\text{-}CH{=}CH_2$ is inconsistent with the observation that this ion is an intermediate to m/z 43. The mechanism of $C_3H_7^{\cdot}$ loss from ionized 3-octanone is therefore highlighted as being worthy of further examination.

Ion/Surface Interactions

The development of ion/surface interactions as a means of characterizing organic ions was facilitated by the availability of a BQ hybrid instrument, the mechanical and operational flexibility of which was designed to encourage a search for new experiments (1). A variety of ion/surface processes have been observed, chief among them (i) reflection (ii) charge transfer (iii) chemical reactions and (iv) collisional excitation. Only surface-induced

dissociated (SID) is discussed here. The characteristics of this technique, besides the fact that MS/MS data are taken without addition of collision gas to the mass spectrometer, are (i) the energy deposited in the ion ($\Delta\varepsilon$) is controlled by the collision energy (ii) high values of $\Delta\varepsilon$ are possible and (iii) the distribution of $\Delta\varepsilon$ can be narrow compared to that for gas phase excitation. The large energy deposited by SID is illustrated by the breakdown curve of $SiEt_4^{+\cdot}$, where internal energies ranging from 3 eV to ca. 30 eV can be supplied (Figure 4). This capability surely is a powerful new feature of mass spectrometry, especially in view of the difficulty of fragmenting larger biological molecules in gas phase collisions and the consequent difficulty in obtaining structural information in this way.

References:

1) G.L. Glish, et al. Int. J. Mass Spectrom. Ion Phys. 41 157 (1982)
2) A.E. Schoen, et al. Int. J. Mass Spectrom. Ion Proc. 65 125 (1985)
3) B.N. Green, et al. Fresenius Z. Anal. Chem. 316 217 (1983)
4) G.L. Glish, et al. Anal. Chem. 56 2291 (1984)
5) J.F. Holland, et al. Anal. Chem. 55 997A (1983)
6) F.M. Harris, et al. Int. J. Mass Spectrom. Ion Proc. 58 273 (1984)
7) J.N. Louris, et al. Anal. Chem. 57 2918 (1985)
8) A.P. Wade, et al. to be published

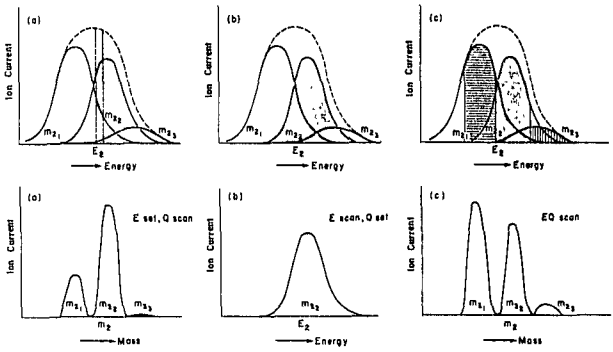

Figure 1. MIKES spectra and improved scans obtainable using a hybrid.

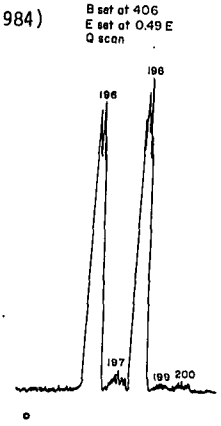

Figure 2. Scan mode (a), Figure 1.

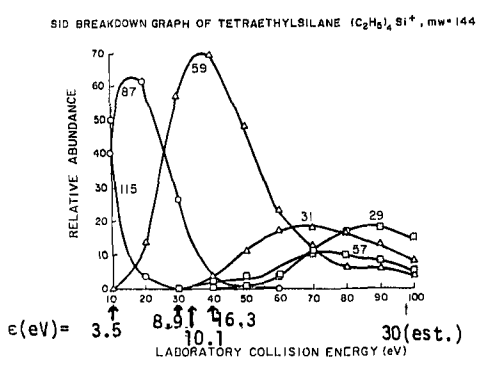

Figure 4. Breakdown curves for surface-induced dissociation showing large energy deposition.

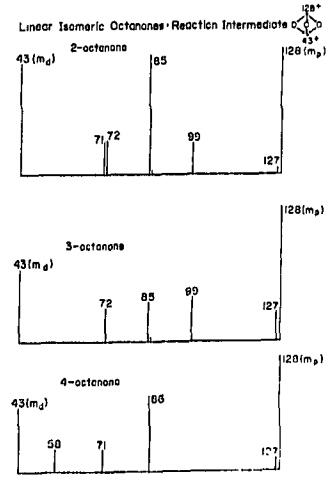

Figure 3. Reaction intermediate spectra distinguish isomers.

GUIDED ION BEAM MASS SPECTROMETRY:
KINETIC ENERGY DEPENDENCE OF ION-MOLECULE REACTIONS

P. B. Armentrout, Chemistry Department
University of California, Berkeley, CA 94720

Hybrid mass spectrometers have the potential for being powerful tools in the field of chemical physics. We have developed a guided ion beam tandem mass spectrometer, a.k.a. BOQ (O = octopole) hybrid, for the measurement of absolute cross sections of ion-molecule reactions over a very wide kinetic energy range, 0.1 to 1000 eV in the laboratory frame. Requirements for such an apparatus include complete collection and transmission of ions through the reaction and analysis regions, good control of the ion energy, and efficient detection. High resolution is not a required feature. In this regard, the analysis mass spectrometer was chosen to be a quadrupole mass filter which when used judiciously at low resolution can provide nearly complete transmission while accepting ions with a wide range of kinetic energies and a large angular distribution. The detector is a scintillation ion counter comprised of a high voltage (25-30 kV) conversion dynode and scintillator and phototube. The key feature of the BOQ when compared with conventional tandem mass spectrometers is the rf-only octopole which surrounds the reaction region. Similar in concept to the central rf-only quadrupole in QQQ instruments, the octopole provides a radial trap for the reactant and product ions. This ensures that all ions are collected and transmitted to the analysis quadrupole without losses. In addition, the octopole allows low ion energies to be easily obtained. This is accomplished again by trapping the ions which prevents loss of the beam due to space charge effects. An octopole field is superior for these purposes compared with a quadrupole field because it is more homogeneous and thus has better trapping properties. In addition, the radial well in the octopole is quite flat such that ion energies are perturbed very little, Figure 1.

Applications of this apparatus include a variety of measurements on the dynamics of ion-molecule reactions (1-3), analysis of the effects of electronic excitation on reactions (4-6), mechanistic studies of transition metal chemistry (7), measurements of thermochemical data for both ions and neutrals, particularly of transition metal chemistry (8-11).

[1] J. L. Elkind and P. B. Armentrout, J. Phys. Chem. 88, 5454-6 (1984).

[2] Kent M. Ervin and P. B. Armentrout, J. Chem. Phys. 83, 166-89 (1985).

[3] M. E. Weber, J. L. Elkind and P. B. Armentrout, J. Chem. Phys. 84, 1521-9 (1986).

[4] J. L. Elkind and P. B. Armentrout, J. Phys. Chem. 89, 5626-36 (1985).

[5] J. L. Elkind and P. B. Armentrout, J. Chem. Phys. 84, 4862-71 (1986).

[6] J. L. Elkind and P. B. Armentrout, J. Am. Chem. Soc. 108, 2765-7 (1986).

[7] N. Aristov and P. B. Armentrout, J. Am. Chem. Soc. 108, 1806-19 (1986).

[8] K. Ervin, S. K. Loh, N. Aristov, and P. B. Armentrout, J. Phys. Chem. 87, 3593-6 (1983).

[9] N. Aristov and P. B. Armentrout, J. Am. Chem. Soc. 106, 4065-6 (1984).

[10] J. L. Elkind and P. B. Armentrout, Inorg. Chem. 25, 1078-80 (1986).

[11] R. Georgiadis and P. B. Armentrout, J. Am. Chem. Soc. 108, 2119-26 (1986).

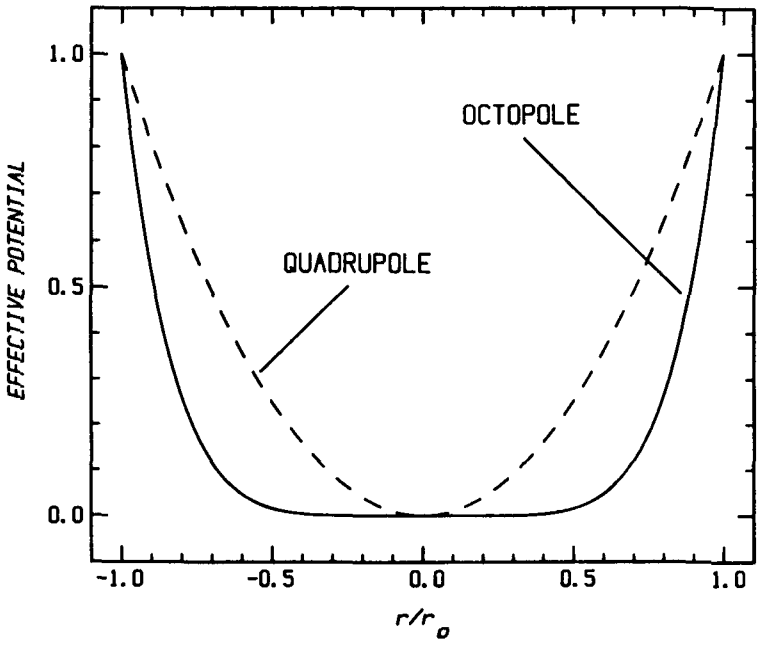
1.0
0.5
0.0
EFFECTIVE POTENTIAL
OCTOPOLE
QUADRUPOLE
-1.0
-0.5
0.0
0.5
1.0
r/r_o

Figure 1

SOLVING PROBLEMS WITH A HYBRID MS/MS INSTRUMENT OF EBQ GEOMETRY

Kenneth L. Busch and Gerald C. DiDonato
Department of Chemistry, Indiana University, Bloomington, IN 47405

MS/MS experiments explore changes in ion mass, ion charge, or ion reactivity (Δm, Δz, and ΔH, respectively). Hybrid instruments offer higher resolution for products and reactants, but can also be used for experiments which involve sequences of reactions. We have used a hybrid instrument of EBQ geometry (Kratos MS80RFAQQ) in studies of organometallic ion structures, intercomparisons of ionization methods for the production of ions from onium salts, derivatization chemistry in the study of simple biological mixtures, and the effects of liquid matrices on FAB mass spectra .

Mass spectra of organometallic compounds contain high mass polymeric ions for which the isotopic envelope expands over tens of daltons, and relatively abundant doubly-charged ions. High resolution parent ion selection is required for unambiguous MS/MS data. Figure 1 contains the daughter ion MS/MS spectrum of $[V(acac)_3-CH_3]^{2+}$ formed in the EI mass spectrum of vanadium acetylacetonate. The parent ion (measured m/z 166.5291) is selected at an instrument resolution of 7500 to separate it from an adjacent ion at $VO(acac)^+$ (measured m/z 165.9860) that is more than 140 times as abundant, and its ^{13}C isotope. Since the doubly-charged ion produces singly-charged fragments upon collision, daughter ions are observed with m/z ratios greater than that of the parent ion selected.

The FAB spectra of guanosine and uridine contain $(M+2H)^{+\cdot}$ and $(M+3H)^+$ ions in addition to $(M+H)^+$. Exact mass measurements confirm the addition of hydrogen, but very high resolution is required to separate the hydrogen-containing ions from ^{13}C and ^{15}N isotopic contributions. The presence of hydrogenated products can be confirmed in a parent ion MS/MS spectrum of $(M+H)^+$ (or a constant neutral loss spectrum for 1 or 2 daltons). The parent ion MS/MS spectrum of $(M+H)^+$ for guanosine contains ions $(M+2H)^{+\cdot}$, $(M+3H)^+$, and $(M+H+glycerol)^+$. Gross has suggested that the mechanism for formation of $(M+2H)^{+\cdot}$ and $(M+3H)^+$ ions involves multiple protonation of the nucleoside followed by one and two electron reduction during desorption. No evidence for multiply-charged ions were found in the parent ion MS/MS spectrum of $(M+2H)^{+\cdot}$ of guanosine, which did however, contain a signal for $(M+2H+glycerol)^+$. In other MS/MS experiments, the protonated molecular ion was established as a precursor to $(M-H)^{+\cdot}$. Both unit mass resolution of the daughter ions and accurate mass measurement of the indicated parent ions are needed in these experiments.

Since FAB mass spectra contain abundant signals for ions preformed in solution, derivatization reactions for the analysis of specific functional groups have been developed. The ionic derivatives exhibit characteristic fragment ions and losses in MS/MS which can be used to pinpoint reactive components in a complex mixture. The daughter ion MS/MS spectra of the derivatives of steroids formed by Girard's T contain a large trimethylammonium ion. A parent ion MS/MS spectrum for this selected daughter ion highlights the Girard's T derivatives in a mixture. Similarly, a constant neutral loss spectrum for loss of trimethylamine provides the same information (Figure 2). Exact mass measurements provide the empirical formulas for the reactive species.

The intact cation at m/z 309^+ of triphenylpyrylium tetrafluoroborate is found in its electron ionization, direct exposure probe electron ionization, and fast atom bombardment mass spectra. We have compared the daughter ion MS/MS spectra of 309^+ generated by these ionization methods with the daughter ion MS/MS spectrum of 309^{2+} formed in the electron ionization mass spectrum, and the daughter ion MS/MS spectrum of 309^+ formed by electron ionization, but acquired by a linked scan (B/E) of daughter ions formed in into the first field free region (FFR1). Since there are two separate collision regions in the hybrid mass spectrometer, a new experiment (ΔH, Δm) is used to examine the daughter ion MS/MS spectra of ions which have survived a collision in FFR1 without undergoing a change in mass or in charge. Figure 3 compares the daughter ion MS/MS spectra of 309^+ formed by direct exposure probe electron ionization obtained without (top) and with (bottom) helium collision gas introduced into FFR1. The relative abundances of most of the ions in the spectrum are not affected. However, the ratio of the peaks at m/z 202 and 203 shows a reproducible change. The increase in the $202^+/203^+$ ratio with the introduction of gas into FFR1 is also observed in daughter ion MS/MS spectra obtained with electron ionization.

A similar experiment was used in a study of the FAB spectrum of thiamine hydrochloride, which contains the intact cation at m/z 265, but also a fairly abundant ion at m/z 357, the adduct between the thiamine cation and a glycerol molecule. The daughter ion MS/MS spectrum of m/z 357 (Figure 4, top) contains an ion at m/z 238 (not present in the daughter ion MS/MS spectrum of 265^+) which indicates substantial interaction between

the thiamine and the glycerol, perhaps with structural rearrangement. When helium is added to FFR1, the relative abundance of m/z 238 in the daughter ion MS/MS spectrum of the survivor ion (Figure 4, bottom) increases.

The direct exposure probe, with both electron and chemical ionization, has been used to provide mass spectra for several compounds which otherwise must be analyzed by FAB. The DEI mass spectrum of thiamine hydrochloride (Figure 5) indicated thermal degradation and polymerization of the molecule. An ion at m/z 265 in the DEI spectrum was confirmed by exact mass measurement to have the same empirical formula as expected for the intact cation. Its presence as part of a series of polymeric ions suggested, however, that its structure may not be the same. The daughter ion MS/MS spectra of 265^+ ions of identical masses, but formed by fast atom bombardment (top) and direct exposure probe electron ionization (bottom) are compared in Figure 6. Under identical MS/MS conditions, the spectra are significantly different, with the ion at m/z 235 signalling the change in reactivity of the ion.

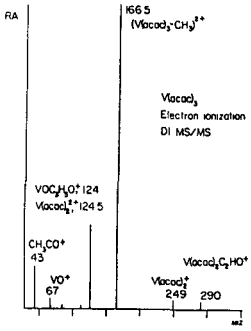

Figure 1

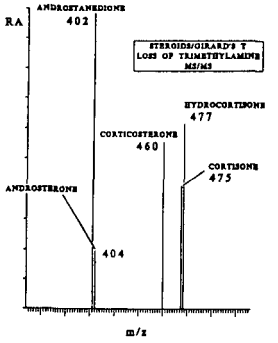

Figure 2

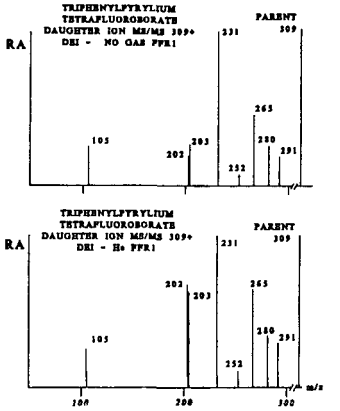

Figure 3

Figure 4

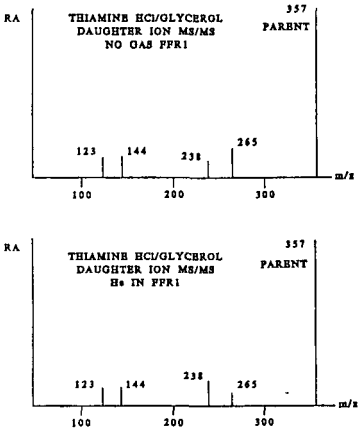

Figure 5

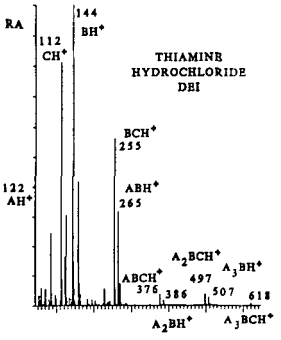

Figure 6

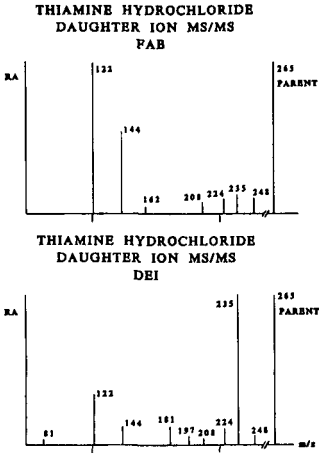

ION/MOLECULE REACTIONS IN THE COLLISION REGION OF A HYBRID MASS SPECTROMETER

Joseph E. Campana and Yves Tondeur, Environmental Research Center, University of Nevada, Las Vegas, NV 89154
Royal B. Freas, Naval Research Laboratory, Chemistry Division, Washington, DC 20375
Jean Claude Tabet, Laboratory for Organic Synthesis, Ecole Polytechnique, Palaiseau 91120, France
Steven R. Missler, P.O. Box 425
Texaco Houston Research Center, Bellaire, TX 77401

Low-energy (E_{lab} = 0 - 30 eV) ion/molecule reactions have been observed and studied in the RF-only quadrupole (collision region) of a hybrid MS/MS having an EBQ_1Q_2 geometry. Reactions of organic reactants with both sputtered metal species and organic ions were contrasted with results obtained in complementary experiments using other state-of-the-art mass spectrometric methods.

The origin of metal/organic cluster ions observed within a novel CI/FAB ion source [1] were confirmed using the hybrid mass spectrometric collisionally-activated reaction spectrometry (CARS) technique. In the CI/FAB ion source, metal/organic cluster ions can originate by ion/molecule reactions of sputtered ionic metal species with organic reactants or by the particle-induced desorption of metal/organic species (from the chemisorption of the organic reactant on the metal substrate). In the hybrid MS/MS experiments atomic and cluster ions of copper and cobalt, sputtered from metal foils in a conventional FAB ion source, were mass-selected with the first double-focusing (EB) mass spectrometer. The mass-selected ions were reacted with isobutane at low-translational energies in the collision quadrupole (Q_1) and the metal/isobutane reaction products formed were mass-analyzed with the second quadrupole (Q_2). The results indicated that reactions of sputtered ionic metal species with isobutane are facile. A variety of copper/organic species were observed: $[CuC_4H_{10}]^+$, $[Cu(C_4H_{10})_2]^+$, $[Cu_3C_4H_{10}]^+$, $[Cu_3(C_4H_{10})_2]^+$ and $[Cu_3(C_4H_{10})_3]^+$, which are the same as those observed using the CI/FAB technique [1].

Bimodal distributions of product ions were observed with increasing energy of the reactant ions for all the metal species studied (Co^+, Cu^+, Cu_3^+). Figure 1 shows typical distributions, it is thought that these bimodal distributions result from sequential and different reactions occurring in the reaction quadrupole under the multiple collision conditions. For example, they may result from collisionally-activated reactions followed by collisionally-activated dissociations of the product ions. With cobalt, product ions are observed that result from the oxidative insertion of the metal in carbon-carbon bonds ($[CoC_3H_6]^+$, $[CoC_3H_6(C_4H_{10})]^+$) and carbon-hydrogen bonds ($[CoC_4H_8]^+$, $[CoC_4H_8(C_4H_{10})]^+$).

Reactions of organic species formed in an EI or CI source were studied also. Reactants with large differences in proton affinities reacted by proton transfer, for example,

$$[CH_2OH]^+ + NH_3 \longrightarrow NH_4^+ + \text{products}.$$

Reactants with similar proton affinities, for example, protonated acetone or protonated isopropanol with acetone, gave complex products. Protonated acetone reacts with acetone to give the protonated dimer, the acetone radical cation, and the reaction products ($C_3H_8O_2^{+\cdot}$ (m/z 76), $C_6H_{11}O^+$(m/z 99), $C_6H_{12}O_2^{+\cdot}$(m/z 116)) solvated by one and two acetone molecules. The first two reaction products (m/z 76 and 99) may originate from the dissociation of higher order products. While the species corresponding to the protonated dimer of acetone would be thought to be a proton-bound dimer, a hemiaketal product $(CH_3)_2C{=}O^+C(CH_3)_2OH$ formed by nucleophilic attack of acetone on protonated acetone can best explain the origin of the products observed at m/z 76 and m/z 99.

Protonated acetone and the stoichiometrically equivalent [protonated isopropanol-H_2] species formed in the ion source were reacted with acetone in the collision quadrupole. Significant differences in the product ion abundances were noted (Figure 2).

In contrast the MIKES/CID spectra (High-energy 8 KeV collisions) of these two species yielded superimposable collision spectra. This result indicates that CARS is a more sensitive probe of structure and/or internal energy than high-energy collisional dissociation.

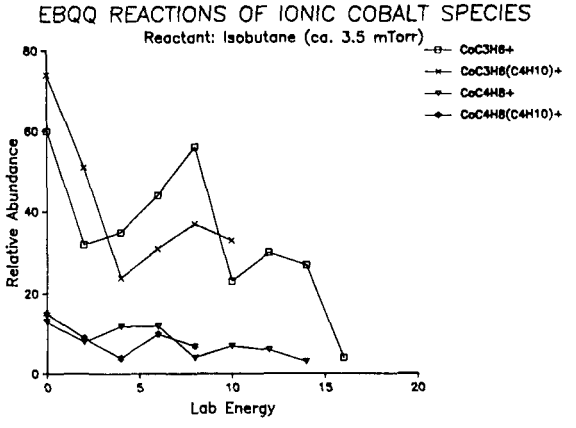

Figure 1. Ion abundances of product ions formed from the reaction of Co^+ (formed by sputtering in the FAB Source) and isobutane in the collision quadrupole.

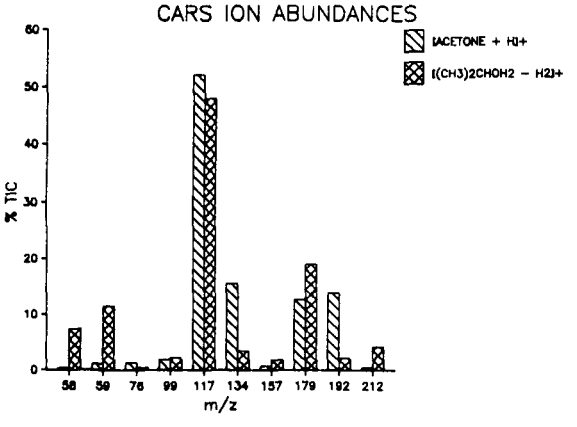

Figure 2. Comparison of ions observed in the collisionally-activated reaction spectrum of protonated acetone and the stoichiometrically-equivalent [protonated isopropanol-H_2] species reacted with acetone (collision energy = 0 eV; pressure: 3 x 10^{-5} torr). Collision spectra obtained by MIKE/CID gave superimposable spectra.

REFERENCE

1. R.B. Freas and J.E. Campana, J. Amer. Chem. Soc. 1985, 107, 6202.

STUDIES WITH A HYBRID TANDEM MASS SPECTROMETER OF QEB GEOMETRY

G.L. Glish and S.A. McLuckey
Analytical Chemistry Division
Oak Ridge National Laboratory, Oak Ridge, TN 37830

A year ago at this meeting we described the interfacing of a quadrupole mass filter (Q) to the front of a high resolution sector mass spectrometer (an MS50) in which the electric sector (E) precedes the magnetic sector (B). The new instrument, referred to as a QEB spectrometer, falls into the category of the so-called "hybrid" mass spectrometers which combine quadrupoles with sectors. This particular hybrid mass spectrometer is unusual in that the quadrupole precedes the sectors as opposed to the reverse, more common sequence.

The addition of the quadrupole mass filter to the front of the MS50 provides a number of new capabilities which significantly enhance the instrument as a research tool(1). Some of these capabilities are listed below:

1. unit mass resolution parent ion selection with high mass resolution daughter ion analysis(2)
2. elimination of spurious peaks common to constant B/E linked scans
3. ion/molecule reactions subsequent to the first stage of mass analysis
4. variable collision energy collision activated dissociation (CAD) and collisional activation (CA) in the eV range
5. eV collision energy CAD followed by keV collision energy CAD
6. eV collision energy CA followed by keV collision energy CAD
7. CAD of ion/molecule reaction products from the first reaction region.

Figure 1 shows a schematic of the QEB instrument. Figure 2 shows a representation which emphasizes the regions of the instrument in which reactions can occur the charged products of which can be mass analyzed. These regions are referred to as reaction regions and are abbreviated as R.R. The capabilities listed above can be realized by analyzing by one or more scanning modes the products from one or more reaction regions.

These capabilities are illustrated with particular emphasis on ion/molecule reactions in R.R.1. For example, Figure 3 shows a partial spectrum of charged products from the reaction of mass analyzed $C_2H_4^{+\cdot}$ with neutral ethylene in R.R.1 obtained by scanning the magnet with the electric field fixed. This spectrum shows the major ions observed in the mass region above that of the mass-selected ion and therefore result from reactive collisions. The reaction presumably proceeds through the formation of an excited $C_4H_8^{+\cdot}$ ion

This work was supported by the U.S. Department of Energy, Office of Basic Energy Sciences, through Contract DE-AC05-840R21400 with Martin Marietta Energy Systems, Inc.

By acceptance of this article, the publisher or recipient acknowledges the U S Government's right to retain a nonexclusive, royalty-free license in and to any copyright covering the article

which fragments predominantly through two major competitive reaction channels. These are the loss of H· and its consecutive reactions and the loss of CH_3· and its consecutive reactions. Cis-2-butene, another source of $C_4H_8^{+\cdot}$, has been used to illustrate some of the ways a compound can be characterized in R.R.1. via reactive collisions. For example, charge exchange experiments of the longitudinal type have been performed with $Ne^{+\cdot}$ and $Kr^{+\cdot}$ as reagent ions. Experiments are also described in which H_3^+ and D_3^+ are used as the reagent ions.

A unique feature of the quadrupole/sector sequence hybrid is the capability to form an ion in R.R.1 under controlled conditions and subsequently obtain a high collison energy CAD spectrum of that ion (capability number 7 listed above). An example is given in Figure 4 which shows the 8 keV collision energy CAD spectrum of the $C_4H_8^{+\cdot}$ ion formed in R.R.1 by reaction of 25 eV translational energy $H_2^{+\cdot}$ with cis-2-butene. The CAD was induced in R.R.2 and the charged products analyzed by scanning the MS50 portion of the instrument at constant B/E.

1. G.L. Glish, S.A. McLuckey, E.H. McBay and L.K. Bertram, Int.J. Mass Spectrom. Ion Proc., In Press.

2. G.L. Glish and S.A. McLuckey, Anal. Chem., In Press.

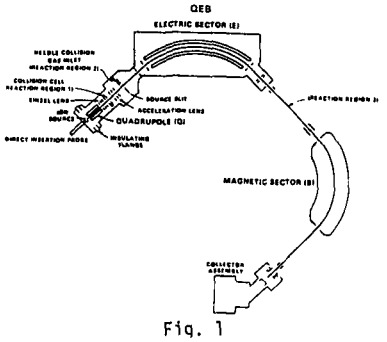

Fig. 1

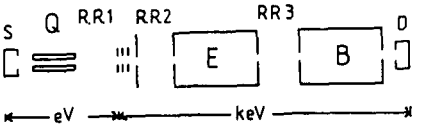

Fig. 2

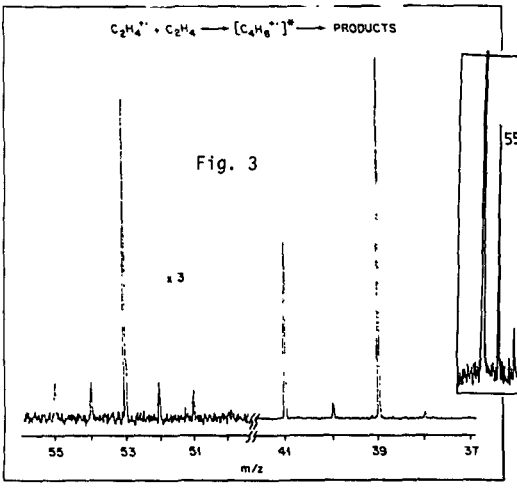

Fig. 3

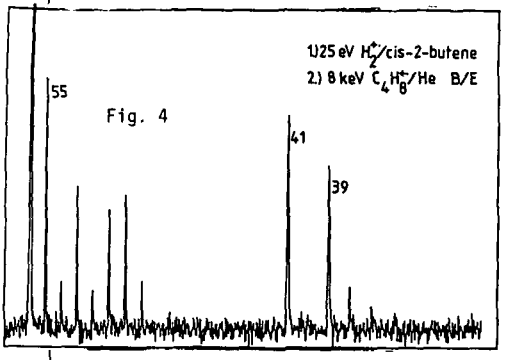

Fig. 4

A HYBRID BEQQ MASS SPECTROMETER FOR STUDIES ON GAS-PHASE ION CHEMISTRY

A. G. Harrison and A. B. Young
Department of Chemistry
University of Toronto
Toronto, Canada M5S 1A1

The Ontario Regional Ion Chemistry Laboratory (ORICL) was established to provide a regional centre for fundamental and applied research in gas-phase ion chemistry. The instrument chosen for the laboratory is a hybrid mass spectrometer of BEQQ geometry shown schematically in the figure. The BE section consists of a VG Analytical ZAB-2F instrument(1) which has a mass range of 1750 at the full accelerating voltage of 8 kV and a masimum resolution (10% valley) of 100,000 in the double-focussing mode. The instrument is equipped with two collision cells and an intermediate deflector electrode in the field-free region between the magnetic and electric sectors. Gas cell 2, the bias voltage on which is continuously variable up to ±5 kV, is the standard cell used for high energy collisional (MIKES) studies. Gas cell 1, which is not electrically isolated from ground, and the ion beam deflector electrode, which can be floated at up to ±3 kV, are used in neutralization-reionization experiments (2).

The high resolution BE stage is followed by a series of electrostatic lenses which reshape the ion beam from a rectangular to a circular cross-section and retard the beam prior to admission into an r.f.-only quadrupole (Q_1) which acts as a collision gas cell. The final quadrupole (Q_2) has a mass range of 1500 amu·at an operating frequency of 1.36 MH_z. At full mass the peak-to peak r.f. amplitude on Q_2 is 6 kV and the resolving d.c. voltage is approximately 980 V. Q_1 has a d.c. bias voltage applied to it which is continuously variable from ± 8 kV (ion source voltage) to ± 7.5 kV giving collision energies from 0 to 500 V. Similarly the analyzing quadrupole Q_2 is floated at a d.c. bias voltage continuously variable from ± 8 kV to ± 7.4 kV allowing the ion translational energy through this quadrupole to be adjusted. For low energy CID experiments this bias voltage is scanned with the mass of the daughter ions to maintain constant translational enrgy in the analyzing quadrupole. In addition, linked scans of the electric sector and quadrupole voltages are possible.

A port is provided to admit a laser beam coaxially with the ion beam in the field-free region between B and E. In addition, ports are provided to admit laser beams to gas cells 1 and 2 and to cross the ion beam with a laser beam just prior to entry into Q_1.

A full description of the instrument and examples of its use in gas-phase ion chemistry studies has been submitted to Int. J. Mass Spectrom. Ion Processes.

1. R.P. Morgan, J.H. Beynon, R.H. Bateman and B.N. Green, Int. J. Mass Spectrom. Ion Phys., 28 (1978) 171.

2. J.K. Terlouw, W.M. Kiesdamp, J.L. Holmes, A.A. Mommers and P.C. Burgers, Int. J. Mass Spectrom. Ion Processes 64 (1985) 245.

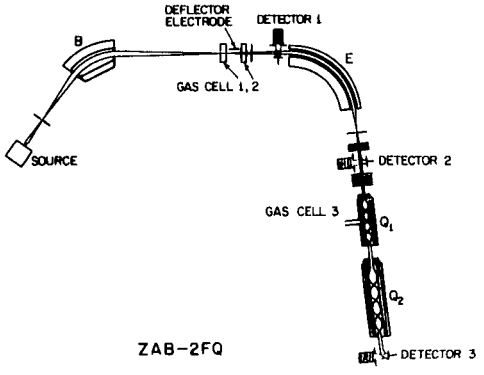

WAGNER-MEERWEIN REARRANGEMENT IN THE GAS PHASE

Cao, Z-M., Sun, Z-L., Dong, Z-W., and Zhang, X-M.
Dalian Institute of Technology, Dalian, China.

INTRODUCTION

Parallels have been found between well-known ionic reactions in solution, such as aldol condensation[1], Michael addition[2], pinacol rearrangement[3] and Beckmann rearrangement[4], and their gaseous counterparts. Wagner-Meerwein rearrangement is an intramolecular migration of an alkyl or aryl group with its pair of electrons from a β-carbon to the adjacent carbocationic center. This kind of rearrangement is often met in solution during S_N1 hydrolysis where two or three alkyl or aryl groups are on the β-carbon. The objective of this paper is to study the parallelism between Wagner-Meerwein rearrangement in solution and that in the gas phase. Alcohols of the neopentyl-type were used as the precursors of the carbenium ions which were formed through water loss of the protonated molecular ions of the alcohols. These even-electron ions tend to undergo ion-electron recombination producing free radicals. But before neutralization the ions had time to rearrange. In order to examine the rearrangement of carbenium ions in gas phase, the novel but well-established method of "Tandem Mass Spectrometry of Radical Species"[5] was used. From the neutral loss in the CID spectrum, the structure of the trapped radical, hence that of the rearranged ion, can be deduced (see Eq. 1).

EXPERIMENTAL

This work was done on a reverse geometry double focusing ZAB-2F mass spectrometer. Methane was used as the reacting gas. Tetracyanoethylene (TCNE) was used as the radical trapping agent and was obtained from Aldrich Chemical Co. Methyl- and phenyl-t-butylcarbinols were synthesized according to the classical method from t-butyl-magnesium chloride and acetaldehyde and benzaldehyde respectively. Their purity was checked by GC and their structures confirmed by ^1H NMR.

RESULTS AND DISCUSSION

Fig. 1 gives the NI CID spectrum of $[TCNE\cdot radical\text{-}CN]^-$ ion derived from methyl-t-butylcarbinol. As the structure of the trapped radical is identical to that of the carbenium ion at the moment of trappkng, it is evident that loss of t-butyl radical and H in the CID spectrum typifies the structure of the carbenium ions which have not undergone Wagner-Meerwein rearrangement, while the occurrence of the rearrangement is characterized by the loss of isopropyl radical. From the comparison of the peak intensities of C_4H_9 and C_3H_7 losses, it can easily be seen that most of the original carbenium ions have undergone Wagner-Meerwein rearrangement. This indicates that Wagner-Meerwein rearrangement takes place in the gas phase as well as

in solution. It is interesting to note that in the CID spectrum there is a peak of considerable intensity of losing ethyl radical. It seems that part of the original carbenium ions has been transformed into ions of the structure -C-C-C-C-C-. No explanation can be given to such an isomerization which awaits further investigation.

Phenyl-t-butylcarbinol gave a negative ion spectrum in which the intensity of the mother ion to selected for MS/MS analysis was so low that it was impossible to get a CID spectrum. Probably, this might be due to the fact that carbenium ions of benzylic-type structure are so stable on account of the presence of resonance that it is difficult for them to be attacked by electrons to form radicals. It seems that the method of "Tandem Mass Spectrometry of Radical Species" is unsuitable to be used for deducing the structures of benzylic-type carbenium ions.

ACKNOWLEDGEMENT

The authors wish to thank Professor Jian-Guo Huang of Nankai University for his generous and invaluable assistance in performing the negative ion MS/MS of the samples.

REFERENCES

1. C. Wesdemiotic and F. W. McLafferty, Org. Mass Spectrom. 16, 381 (1981)
2. J. H. J. Dawson and N. M. M. Nibbering, Int. J. Mass Spectrom. Ion Phys. 33, 3 (1980)
3. H. E. Audier, et al., Nouv. J. Chim. 4, 531 (1980)
4. Hans-Fr. Grutzmacher and Christian Romer, Org. Mass Spectrom. 17, 318 (1982)
5. C. N. McEwen and M. A. Rudat in "Tandem Mass Spectrometry" (F. W. McLafferty Ed.), Chapt. 20.

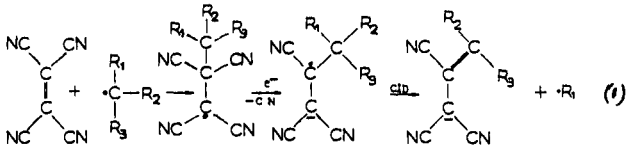

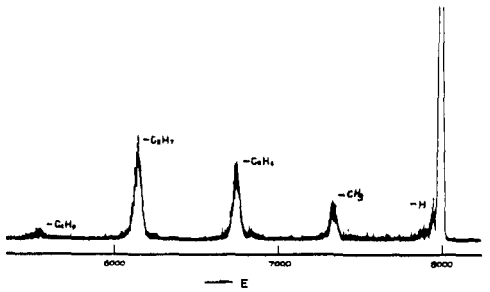

ION STRUCTURES AND KETO-TO-ENOL ISOMERIZATION IN DIALKYLMETHYLPHOSPHONATES

James R. Holtzclaw
Honeywell, Inc.
13350 U.S. Hwy. 19 So.
Clearwater, Fla. 33546

Jeffrey R. Wyatt
Code 6110
Naval Research Laboratory
Washington, D.C. 20375

Previously[1] we have shown that the DMMP molecular ion undergoes an essentially complete keto-to-enol isomerization , resulting in a structure that cannot readily loose the phosphorus- bound methyl group to produce the m/z 109 ion by CID.

Keto-to-enol isomerization for the DMMP molecular ion can occur by several different mechanisms, Figure 1 . The results from deuterium labelling experiments (P-CH_3 replaced by P-CD_3) show that limited H/D scrambling accompanies loss of formaldehyde in the electron ionization spectrum, This data suggests that a rapid keto-to-enol isomerization occurs followed by a slower loss of formaldehyde and is consistant with the isomerization mechanism involving sequential 1,4-hydrogen migrations.

Additional support for an isomerization mechanism involving sequential 1,4-hydrogen migrations is provided by a MIKES/CID study of methylphosphonic acid (MPA). One might expect keto-to-enol isomerization for the MPA molecular ion to be a favored process because the resulting enolic isomer, Figure 2, has three resonance structures that should contribute significantly to the overall stability of the enolic structure. However, the MIKES/CID spectrum of the MPA molecular ion exhibits a very abundant daughter ion corresponding to loss of $\cdot CH_3$ and thus suggests that a keto-to-enol isomerization has not occurred. If this is the case, then sequential 1,4-hydrogen migrations rather than 1,3- or sequential 1,2-hydrogen migrations must be the preferred process for keto-to-enol isomerization.

Keto-to-enol isomerization also occurs for the molecular ion of diethymethylphosphonate (DEMP). A comparison of the EI spectrum of DEMP and the MIKES/CID spectrum of the DEMP molecular ion (Figure 3) reveals several differences that are similar in nature to the differences observed for DMMP. In particular the daughter ion corresponding to loss of $\cdot CH_3$ (m/z 137) is completely absent in the MIKES/CID spectrum. The validity of assigning an enolic structure to the DEMP molecular ion was confirmed by comparing the MIKES/CID spectrum of the DEMP molecular ion with an isobaric ion known to have the enolic structure. Fragment ions from DEMP that possess a pentavalent phosphorus exhibit MIKES/CID spectral features that are similar to those observed for the molecular ions of DMMP and DEMP.

The dialkylmethylphosphonates provide a striking example of the fact that ions sampled in the MIKES/CID experiment do not necessarily have the same structure as ions initially formed in the ion source. In fact, the DMMP and DEMP molecular ions sampled by the MIKES/CID experiment have undergone an essentially complete keto-to-enol isomerization.

All available data suggests that the keto-to-enol isomerization for the DMMP molecular ion occurs by sequential 1,4-hydrogen migrations. This isomerization has been demonstrated for both the DMMP and DEMP molecular ions and is postulated to be a common process for molecular and fragment radical cations of the dialkylmethylphosphonates that possess a pentavalent phosphorus atom.

[1] James R. Holtzclaw, Jeffrey R. Wyatt, and Joseph E. Campana, Org. Mass Spectrom. 20, 90 (1985).

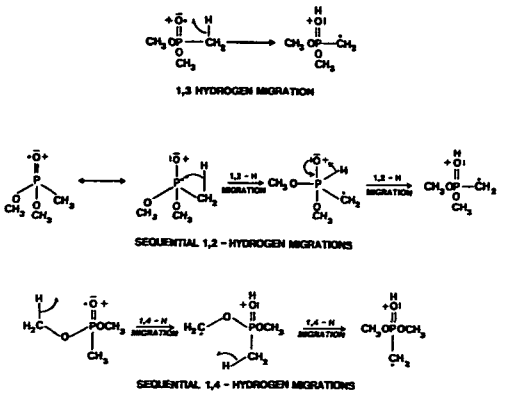

Figure 1. Possible reaction mechanisms for keto-to-enol isomerization of the DMMP molecular ion.

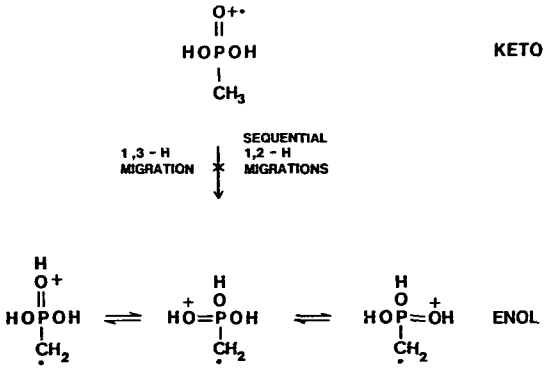

Figure 2. Keto-to-Enol Isomerization for the Methylphosphonic Acid Molecular Ion and the Resonance Structures for the Enotic Isomer.

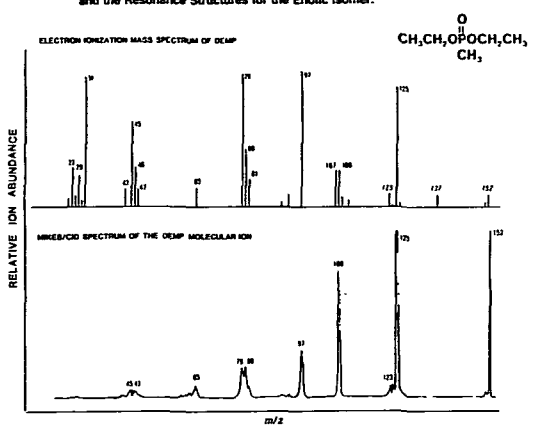

Figure 3. A comparison of the electron ionization mass spectrum of DEMP and the MIKES/CID spectrum of the DEMP molecular ion.

Dechlorination Reactions Induced by Fast Atom Bombardment of the Glycopeptide Antibiotics Vancomycin and Avoparcin

Marshall M. Siegel*, William J. McGahren, George A. Ellestad

American Cyanamid Company, Medical Research Division
Lederle Laboratories, Pearl River, NY 10965

Vancomycin I ($C_{66}H_{75}N_9O_{24}Cl_2$, M.W. 1447), a member of the glycopeptide class of antibiotics, is used to suppress intestinal microfloura and Gram positive bacteria. During studies aimed at identifying impurities present in vancomycin, an analytical standard of the sulfuric acid salt of vancomycin was prepared using preparative high performance liquid chromatography. To verify the purity of this standard, fast atom bombardment (FAB) mass spectra in both the positive and negative ionization modes were obtained. Important fragment ions correspond to the losses of the vancosamine and the disaccharide moieties. The most unusual features of the FAB spectra are the appearances of ions corresponding to a monochlorinated form of vancomycin, $(M+H-Cl+H)^+$, $(M+HSO_4-Cl+H)^-$ and $(M+HSO_4-Vancosamine+H-Cl+H)^-$, with significant intensities relative to the corresponding molecular ion adducts (Figure 1). These results were unexpected since the high purity of the sample was confirmed by ^1H and ^{13}C NMR studies where no resonances corresponding to the monochlorinated forms of vancomycin were detected.

To further understand the origin of the ions corresponding to the monochlorinated form of vancomycin, the highly purified sample was studied by *Californium-252 plasma desorption (CfPD)* MS and by FAB/MS/MS. No ions corresponding to a monochlorinated form of vancomycin were observed in the positive or negative ionization CfPD mass spectra (Figure 2) or in the positive ionization FAB/MS/MS daughter ion spectrum of the $(M+H)^+$ parent ion of vancomycin. One perhaps would have expected to observe the monochlorinated vancomycin in the CfPD spectrum since CfPD is a much more highly energetic ionizaton process than FAB. The absence of the monochlorinated vancomycin in the FAB/MS/MS data is not so surprising since in a low pressure gaseous system it is highly unlikely for a chorine atom to be replaced by a proton. These results confirm our suspicion that the ions corresponding to a monochlorinated form of vancomycin originated as an artifact of the FAB ionization process.

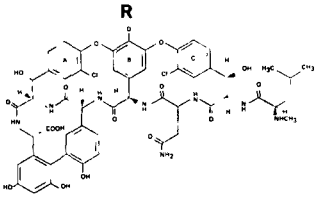

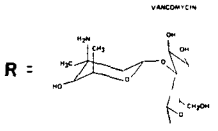

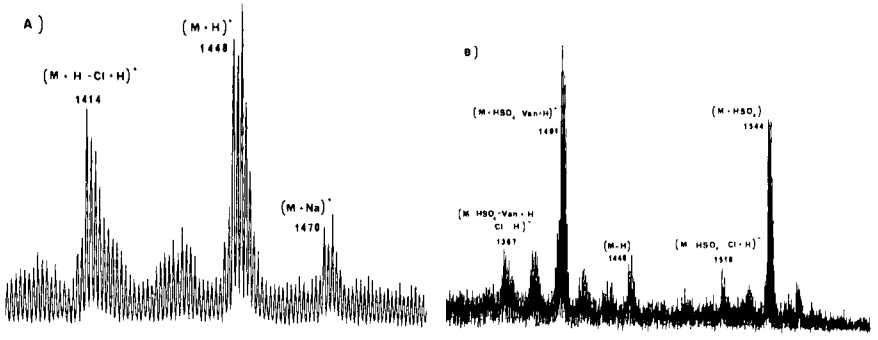

Fig. 1. Molecular ion region of FAB/MS of vancomycin a) Positive ionization mode, b) Negative ionization mode.

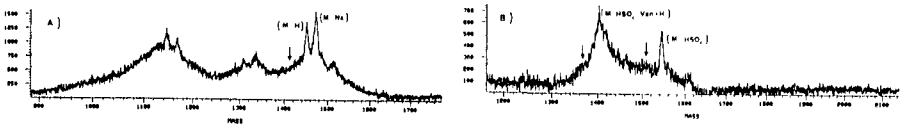

Fig. 2. Molecular ion region of CfPD/MS of vancomycin a) Positive ionization mode, b) Negative ionization mode. Arrows indicate where corresponding monodechlorinated vancomycin ions were observed in the FAB mass spectra.

The FAB data suggest that the formation of monochlorovancomycin is generated during the FAB ionization process in the condensed phase via a free radical mechanism which precedes the ionization process, viz.,

$$M \xrightarrow{FAB} (M\text{-}Cl)^{\cdot} \xrightarrow{+H^{\cdot}} (M\text{-}Cl)^{\cdot}\text{+}H^{\cdot} \xrightarrow{+H^{+}} [(M\text{-}Cl\text{+}H)\text{+}H]^{+}$$

$$(M\text{-}Cl\text{+}H)^{\cdot}\text{+}H^{\cdot} \xrightarrow{+HSO_4^{-}} [(M\text{-}Cl\text{+}H)\text{+}HSO_4]^{-}$$

In the condensed phase mechanism described above, the first step is the formation of a monochlorovancomycin free radical which is followed by the abstraction of a proton from the FAB matrix. The final step is the ionization of the monochlorovancomycin via adduct formation.

The dichloro containing glycopeptide epi-β-avoparcin ($C_{89}H_{101}N_9O_{36}Cl_2$, M.W. 1941), a stereoisomer of β-avoparcin, was studied by CfPD. Abundant molecular ion adducts [$(M+Na)^+$ and $(M+HSO_4)^-$] as well as fragment ions were observed but no ions corresponding to a chlorine-hydrogen exchange reaction were present. β-Avoparcin ($C_{89}H_{101}N_9O_{36}Cl_2$, M.W. 1941) and D-galactosyl-β-avoparcin ($C_{95}H_{111}N_9O_{41}Cl_2$, M.W. 2103) were also studied by FAB/MS. In both cases, abundant $(M+H)^+$ ions as well as less abundant $(M+H\text{-}Cl+H)^+$ ions were observed. The latter ions were apparently generated by a chlorine-hydrogen exchange reaction induced by the bombardment of the fast atoms.

FRAGMENTATION OF ALIPHATIC HYDROCARBONS: n-DECANE DIMERS.

E. de HOFFMANN
University of Louvain - Departement of Chemistry
Pl. Pasteur,1 1348 Louvain-la-Neuve Belgium

Solid state gamma ray irradiation of n-decane leads to a mixture of hydrocarbons, with a dehydro-dimers fraction[1]. Fig. 1 shows the FID GC of these eicosan hydrocarbons obtained from a mixture of perhydro- and perdeutero-n-decane, and the mass chomatograms under CI/CH_4 conditions for the perhydro (mass 281), mixed (masses 301 and 302) and perdeutero (mass 322) pseudo-molecular $(M-H)^+$ or $(M-D)^+$ ions. Fragmentation of n-eicosan has been studied[2]. n-Hexane and n-heptane fragmentation have been reported in detail[3,4] but little has been done on ramified aliphatics[5]

The structures of these eicosan isomers were determined by examination of the EI fragmentation. Fig. 2 shows a typical spectrum. Low mass ions did not give information on the structure. All spectra showed intense peaks at masses 141 and 140 for perhydro compounds, and small peaks at higher masses. These were detected by EI/SIM as shown in fig. 3. Examination of these fragments show that more intense ions appear in one or two pairs corresponding to the loss of a total of nine carbon atoms for each pair. This is in agreement with a dehydro-bridging between two unrearranged n-decane molecules as shown by the exemple in fig. 4.

This interpretation is confirmed by the fact that all the 15 possible isomers shown in fig. 5 are detected and uncompletely resolved peaks are consistent with expected diastereoisomers pairs. Numbering of the formulas appear on the chromatographic trace.

As may be seen from fig. 3, fragments of mass 141 and 140 are in about the same intensity ratio for all peaks. Fig. 6 shows this as a function of the retention indice, with the corresponding 162 and 160 traces for the deuterated compounds. The intensity ratio for the latter vary markedly from one compound to the other, and the 160/162 ratio is much higher than the 140/141 one. Those isomers that have a "branched" shape, numbered 9,10,12 and 13 in fig. 5, have markedly distinct intensity ratios, and do not vary from perhydro to perdeutero. The perdeutero compounds are less polar than their hydrogenated counterparts, as shown by their lower retention times in fig. 1. Furthermore, there is practically no H/D scrambling in the lower masses fragments of the mixed dimers. Thus, the molecular ion does not appreciably rearrange before fragmentation. The carbon-deuterium bond is stronger than the carbon-hydrogen one, so that these result are not in agreement with the, unlikely, loss of $H^{\bullet}$ or $D^{\bullet}$ from the 141 or 162 ions. The sensitivity to the structure suggest that the lost atom is transfered to the neutral, probably through a temporary complex between the cation and the neutral radical. The chromatographic retention time is indeed a function of the compactness of the molecules, which could also favor the complex. Perhydro and branched compounds might react by another pathway.

References

1. B. Tilquin, Th. Baudson, P. Claes, O. Claesson and A. Lund, Journal of Phys. Chem., 86, 3324 (1982).
4. A. G. Brenton, C. J. Porter, I. Howe and J. H. Beynon, Advances in Mass Spectrometry, vol. 8A, 573-576, Heyden and son, 1980.
3. A. Lavanchy, R. Houriet and T. Gäuman, Org. Mass Spectrom., **13**, 410 (1978).
4. A. Lavanchy, R. Houriet and T. Gäuman, Org. Mass Spectrom., **14**, 79 (1979).
5. D. R. Nelson, C. L. Fatland, R. W. Howard, C. A. McDaniel, G. J. Blomquist, Insect Biochem., vol. 10, 409-418 (1980).

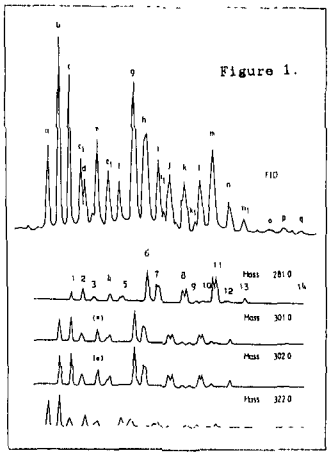

GC FID and CI/SIM traces

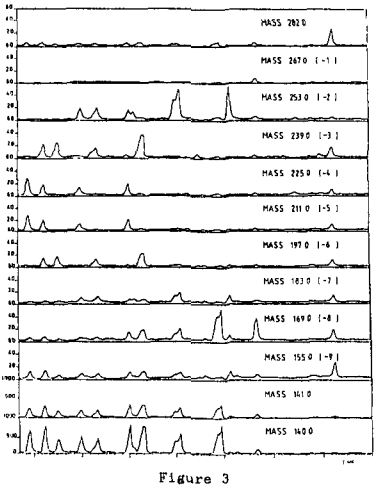

Figure 3
Selected fragment monitoring under EI

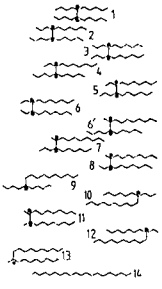

Figure 5.
The 15 isomers Asymetric carbons are stared

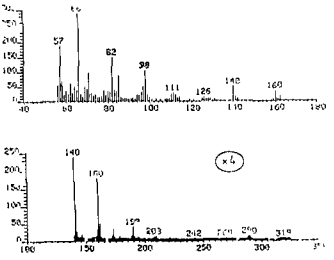

Figure 2
Typical spectrum of a mixed H/D isomer

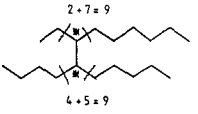

Figure 4.
Typical high-masses fragments. the sum of lossed carbon atoms is always 9

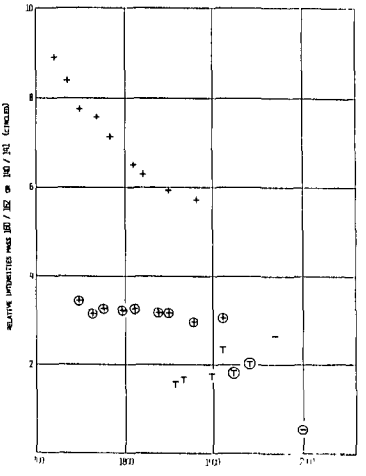

Figure 6
160/162 and 140/141 abundances ratio versus retention indices

FABMS AS A MONITOR FOR ORGANIC REACTIONS: CYANOGEN (C_2N_2) DRIVEN AMIDE BOND FORMATION AND CYANOGEN CONDENSATION REACTIONS

R. A. Day, S. Mothersole and M. E. Madis

Department of Chemistry
University of Cincinnati
Cincinnati, Ohio 45221

Many reactions proceed through intermediates to the desired product(s) and generally one finds side-products and by-products. In many cases these compounds are labile, highly polar and/or ionic. FABMS provides a means to detect, identify and characterize a large number of the components of a reaction mixture. We report here two types of reactions involving C_2N_2: (1) The novel condensation of carboxylates and amines to form amide bonds in peptides and proteins driven by C_2N_2. (2) The reaction of C_2N_2 with certain organic bases to produce highly fluorescent products of analytical interest. C_2N_2 is notorious for the succession of condensation products formed with amines and with itself under various conditions. Many of these products are unstable, and to date, essentially none of them have been identified. We use a Kratos MS80/DS55 equipped with a Phrasor DIP probe. In general, sorbitol was used as the matrix allowing higher T when needed and gave fewer background peaks. In peptide condensations FAB allows monitoring the reactants and products where confirmation is the main objective and no C_2N_2 is incorporated: no further derivatization is required. Detection of frequently seen, but as yet uncharacterized, ionic, labile, C_2N_2 adducts can be effected. FAB is providing, for the first time, structural data on products incorporating the elements of C_2N_2. For example, C_2N_2 condensation with guanidine is known; but the labile fluorescent precursor(s) have not been described.

C_2N_2 Driven Amide Bond Formation

It was first noted that C_2N_2 provided the driving force for amide bond formation in proteins (see Ref. 1-5) and subsequently in model compounds (Ref. 5 and this report). To date, no one has reported significant yields of amides from inter-molecular condensation. Here, we note that peptide cyclization and lactam formation occur readily. FABMS was crucial in the confirmation of this due to the fact that the cyclization may also occur adventitiously under certain conditions of derivatization and mass spectral analysis. The results for some dipeptides are shown in Table I.

Table 1. Model System to Study Amide Bond Formation:

$$\text{Dipeptides} \xrightarrow{C_2N_2} \text{Diketopiperazines}$$

Peptide	Solvent	Approximate Time to completion
L,L-PRO-PRO	DMSO	<<5 min
	DMF	<<5 min
	Pyridine	<30 m
	H_2O	∿1 week
	MeOH	< 5 m
L,L-LEU-LEU	DMF	< 1 hour
	DMSO	< 5 min
	H_2O	∿2 weeks
	MeOH	∞
L,D-LEU-LEU	DMF	∿ 10 min
	DMSO	< 5 min
GLY-GLY	80% DMF/20% H_2O	∿ 1 day

Reactions were carried out at room temperature (∿21°). C_2N_2 was at 1 atm. Reactions were monitored by TLC, ion-exchange chromatography, NMR. Products were confirmed by FAB-MS. (Direct inlet and/or some derivatization methods can give the DKP artifactually.)

The lactams from 5 to 7 membered rings form readily as well (Table II).

Table II. Simple Lactam Formation:

$$\omega\text{-Amino Acids} \xrightarrow{C_2N_2} \omega\text{-Lactams}$$

ω-Amino Acid	Solvent	Approximate Reaction time
γ-Aminobutyric	DMSO	15 m
	DMF	15 m
δ-Amino Valeric	H_2O	> 1 week
	MMF*	3H (~ 90%)
ε-Amino Caproic	H_2O	3d
	MMF	10 m

*MMF = monomethylformamide

FABMS of the parent peptide (Table I) or ω-amino acid (Table II) showed MH^+ and a loss of OH. Negligible amounts of MH-18 were seen. The cyclic peptide or lactam showed a strong MH^+ which was 18 amu less than the parent compound. While the FAB-MS of these compounds is trivial, its use to confirm the reaction is not. Likewise FAB-MS affords the confirming data that has consistently ruled out the occurrence of any inter-molecular condensations.

Cyanogen Condensation Products

Cyanogen rapidly forms fluorescent condensation products and under certain circumstances affords the brownish-black "final" product, paracyanogen. The structures of these intermediates have not been reported to date. Various amines cause the reaction to proceed more rapidly. Hexamethylene tetramine and guanidine salts are the most effective; use of the former provides the basis of a C_2N_2 assay that is free of CN^- and OCN^- interferences (6). The latter affords a series of intermediates which were partially characterized by FAB-MS. The postulated reaction sequence is depicted in Figure 1 (below).

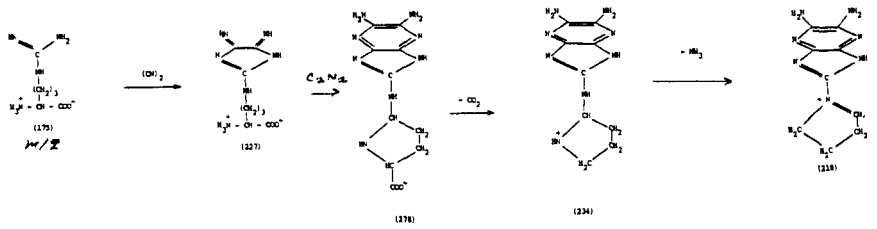

References

1. J. Willet and R. A. Day, Biophysics J. 45, 250 (1984).
2. J. W. Kirley and R. A. Day, Biochem. Biophys. Res. Commun. 126, 457 (1985); ibid., 130, 1324 (1985).
3. J. W. Kirley and R. A. Day, Fed. Proc. 44, 1811 (1985).
4. J. W. Kirley, R. A. Day and G. P. Kreishman, FEBS Lett. 193, 145 (1985).
5. R. Tharp and R. A. Day, Fed. Proc. 45, 1614 (1986).
6. S. Mothersole, M. S. Thesis, University of Cincinnati (1986).

THE DETERMINATION OF A REACTION PATHWAY BY GC/MS
ANALYSIS FOR CROTONALDEHYDE AND SECONDARY AMINES

V. P. NERO and M. M. KAPUSCINSKI
TEXACO RESEARCH CENTER, BEACON, NEW YORK 12508

The reaction of crotonaldehyde with various secondary amines does not only produce the expected amine carbonyl addition product, but also leads to the formation of methylbenzaldehyde and a variety of other products. The analysis of the intermediate reaction products by electron impact and chemical ionization gas chromatography / mass spectrometry lead to a probable reconstruction of the reaction pathway for these types of reactions.

The reaction of aldehydes and secondary amines will initially form a hemiaminal. If there is an adjacent hydrogen to the hemiaminal, water will be eliminated to give a carbon-carbon double bond and form an enamine. (1)

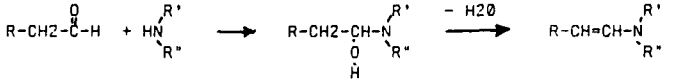

A similar product is obtained when there is an available hydrogen alpha to a carbon-carbon double bond which is conjugated to the carbonyl group of the aldehyde, but now a dienamine can be produced. When, as in this case, crotonaldehyde 1 and N-methylpiperazine 2 are reacted, the expected product, N-methyl,N'-(1-butadienyl)piperazine 3 is produced.

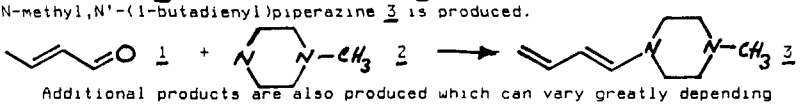

Additional products are also produced which can vary greatly depending upon the concentration of reactants. The dienamine 3 is the major product when the reaction is performed using an excess of the N-methylpiperazine 1. All products were identified by interpretation chromatographic / mass spectra. The spectra were obtained using electron impact, chemical ionization, and accurate mass conditions. Relative yields were estimated from the GC/MS total ion chromatograms for each reaction.

When an excess crotonaldehyde is present the dienamine 3 procedes to react further via a Diels-Alder reaction to form the cyclohexenyl aldehyde product 4. The reaction of dienamines as dienes has been documented. (2) The aminocyclohexenyl aldehyde product 4 subsequently eliminates the secondary amine to form 2-methylcyclohexadienylcarboxaldehyde 5.

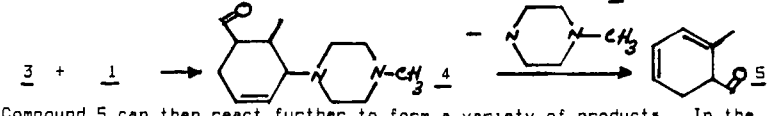

Compound 5 can then react further to form a variety of products. In the presence of air it will be oxidized to form 2-methylbenzaldehyde 6 as the major product. (The identification of the methylbenzaldehyde was confirmed by comparison with the GC retention time and mass spectrum of an authentic sample.) When the reaction is run under a nitrogen atmosphere considerably less methylbenzaldehyde is formed.

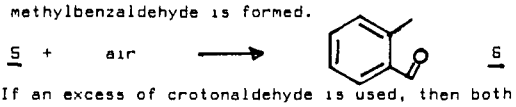

If an excess of crotonaldehyde is used, then both the methylbenzaldehyde and the cyclohexadienyl carboxaldehyde will react further to form aldol condensation products. The initial aldol product of the benzaldehyde 6 leads to the formation of 3-methyl-4-oxo-4-(o-tolyl)-butanal 7.

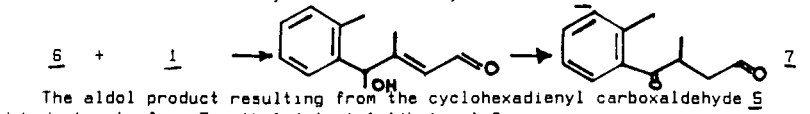

The aldol product resulting from the cyclohexadienyl carboxaldehyde 5 dehydrates to form 3-methyl-4-(o-tolyl)butenal 8.

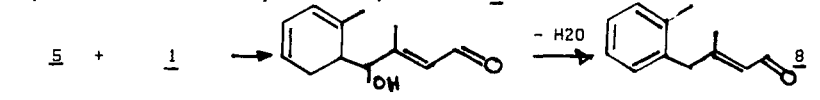

When the reaction is performed using an excess of N-methylpiperazine, then the benzyl amine compound 9 is formed.

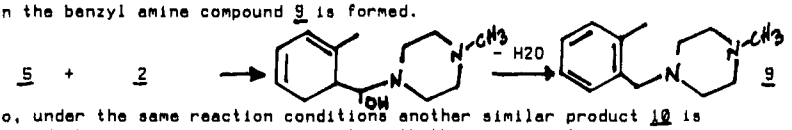

Also, under the same reaction conditions another similar product 10 is produced when excess piperazine reacts with the amino cyclohexenyl carboxaldehyde 4 formed in the Diels-Alder reaction.

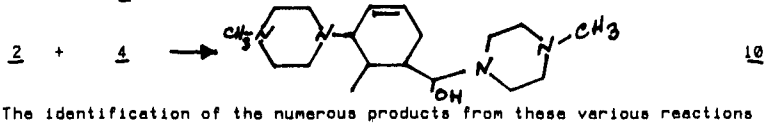

The identification of the numerous products from these various reactions was greatly simplified by the use of gas chromatography / mass spectrometry. The chromatograms for the principal reactions and their corresponding mass spectra with accurate mass elemental compositions for the parent ion follow:

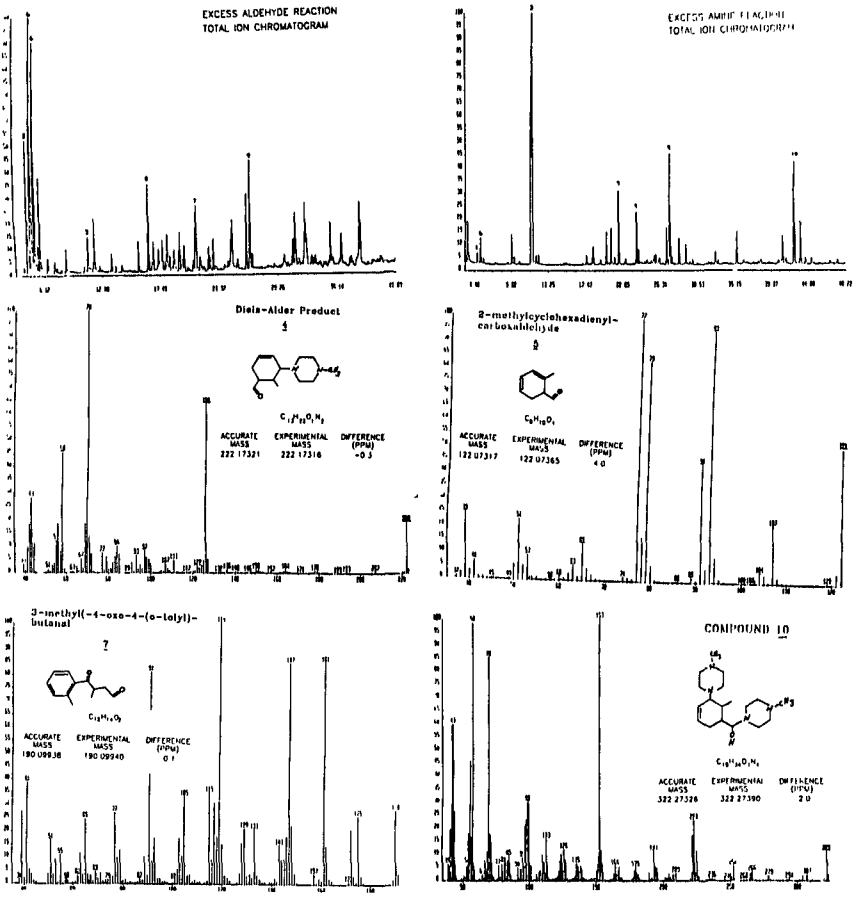

REFERENCES

1. Szmuszkovicz, Advan. Org. Chem 4, 1-113 (1963), pp. 9-12
2. M. Petrzika & J.I. Grayson, Synthesis, 753 (1981)

MASS SPECTRAL DEALKYLATION OF METHOXYQUINOLINIUM AND METHOXYISOQUINOLINIUM IODIDES,

Robert J. Barbuch, Norton P. Peet and Gregory L. Karrick, Merrell Dow Research Institute, Indianapolis Center, Indianapolis, IN 46268.

This paper describes mass spectral dealkylations of methoxyisoquinolinium iodides 1 a-d and methoxyquinolinium iodides 2 a-d.

We had earlier observed demethylation of the 6,7-dimethoxyisoquinolinium iodide 3. Compound 3 is an intermediate in the synthesis of glaucine, a potent antitussive agent. We found that 6-methoxyisoquinolinium iodide 1 a undergoes O-demethylation, and to a greater extent than does 7-methoxyisoquinolinium iodide 1b.

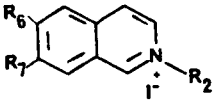

1 a R_2=Et, R_6=OMe, R_7=H
b R_2=Et, R_6=H, R_7=OMe
c R_2=nPr, R_6=OMe, R_7=H
d R_2=nPr, R_6=H, R_7=OMe

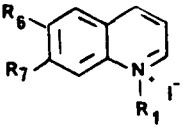

2 a R_1=Et, R_6=H, R_7=OMe
b R_1=Et, R_6=OMe, R_7=H
c R_1=nPr, R_6=H, R_7=OMe
d R_1=nPr, R_6=OMe, R_7=H

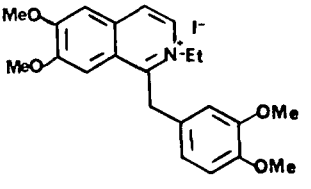

3

The radical cation from 1 a is resonance stabilized while that derived from 1 b is not. The analogous methoxyquinolinium iodides were also prepared. The 7-methoxyquinolinium iodide 2 a undergoes O-demethylation, since the radical cation is resonance stabilized, while O-demethylation of 6-methoxyquinolinium iodide 2 b does not result in a resonance stabilized cation. Propyl salts 1 c, 1 d, 2 c, and 2 d were prepared to rule out the unlikely possibility that cleavage beta to the quaternary nitrogen was a dealkylation pathway.

MASS SPECTRAL ANALYSIS OF PYRAZOLO [4,3-c]QUINOLINE-3-ONES:ARYL MIGRATIONS ON ELECTRON IONIZATION

Stephanie Metz, G. Padmanabhan and Martin Stogniew, Drug Development Department, Pharmaceuticals Division, CIBA-GEIGY Corporation, Suffern, NY 10901

INTRODUCTION

The Electron Ionization (EI) mass spectra of novel derivatives of pyrazolo [4,3-c]quinoline-3-one are described. These compounds (Figure I), which are potential anxiolytic agents, are substituted in either the 1- or 2-pyrazolo position by aryl or alkyl groups. The mass spectra of all the aromatic substituted compounds showed a loss of m/z 56 and/or 57, suggesting a collapse of the pyrazole moiety (loss of N_2CO and/or N_2COH) with aryl rearrangement to the quinoline ring. Figure II is the EI partial mass spectrum of CGS 9896, representative of the aromatic substituted compounds examined. To our knowledge, aryl migrations involving a pyrazole ring system of this type are unreported; however, aryl rearrangements have been reported for azobenzenes[1] and dioxopyrazolidines[2] In this abstract, we report the results of our studies and propose a mechanism which includes the collapse of the pyrazole ring and the aryl rearrangement.

EXPERIMENTAL

1. Electron Ionization experiments were performed for all compounds in Figure I by solid heat probe (300 - 400°C) on a Kratos MS-25 by the authors. All compounds were run at 70 eV; selected compounds were run over a range of 20 - 70 eV.
2. Exact Mass Measurements were performed on selected ions for CGS 8216, CGS 9896, CGS 11092, CGS 13713 and CGS 18803. These experiments were performed on a Finnigan MAT 8200 Mass Spectrometer by Charles Shimanskas, CIBA-GEIGY, Ardsley, NY.
3. MS/MS experiments were performed for the parent and selected daughter ions of CGS 9896. These experiments were performed by James Buchner, Extrel Corporation, Pittsburgh, PA on an Extrel ELQ-400-3 triple quadrupole mass spectrometer.
4. Deuterium Exchange was performed by dissolving the compound in deuterated media. The compound was precipitated and filtered, and the mass spectrum recorded.

Figure I. Compounds Studied

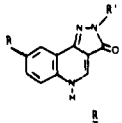

Compound No	R	R'
CGS 8216	H	
CGS 9896	H	
CGS 9895	H	
CGS 11040	CH_3O	
CGS 10678	F	
CGS 11068	H	
CGS 15975A	F	

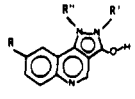

Compound No	R	R'	R''
CGS 10649	CH_3O		----
CGS 10632	Cl		----
CGS 10650	F		----
CGS 11092	H	--	

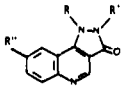

Compound No.	R	R'	R''
CGS 18959	C_3H_7	H	H
CGS 18603	C_4H_9	H	H
CGS 13713	C_2H_5		H
CGS 15458		H	Cl

Figure II. Mass Spectrum of CGS 9896

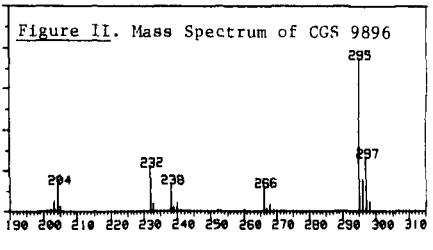

RESULTS AND DISCUSSION

The EI spectra of the aromatic substituted derivatives of [4,3-c]-quinoline-3-one show losses of m/z 56 and 57, which have been identified by exact mass measurements as CON_2 and $COHN_2$. Similarly, losses of m/z 28 and 29 have been shown to consist of CON_2 and $COHN_2$. Shown in Figure III are the results from the MS/MS data obtained from CGS 9896. The parent ion (m/z 295) loses COH followed by loss of N_2 and Cl. This pathway results in the collapse of the pyrazole ring with aryl migration. Another pathway involving loss of COCl followed by N_2 results in a similar ion. This evidence supports a stepwise process; however, until further MS/MS experiments are performed, we cannot rule out a concerted reaction mechanism.

EI spectra have been recorded for selected aliphatic substituted compounds. Although these derivatives also lose m/z 29 and 56, exact mass measurements have established that these losses are structurally different; consisting of hydrocarbons rather than CO or CON_2 eliminations.

The aryl rearrangement of azobenzene with loss of N_2 has been studied[1]. Our results are similar to those of the azobenzene study in that aryl substituents do not affect the degree of migration. Moreover, these migrations occur over a wide range of energy (20 - 70 eV) in both studies. Aryl substituted compounds tend to show loss of the substituents before migration, which may explain why there is little correlation between the substituent and the rearrangement products.

This set of compounds has one readily exchangeable hydrogen. Exchange with deuterium produced labelled material at 60 - 80% of theoretical yield. CGS 8216, CGS 9896 and CGS 11092 all showed incorporation of the label which was retained during the rearrangement process, suggesting that the hydrogen lost during the collapse of the pyrazole moiety originates either on the aryl ring or alpha to the quinoline nitrogen. CGS 18803, the one aliphatic compound which is consistent with the exact mass measurement identifying the ions as ethyl and butyl losses.

In conclusion, evidence is presented for the collapse of a pyrazole ring and aromatic rearrangement from aryl substituted pyrazolo[4,3-c]-quinoline-3-ones. This process does not occur for aliphatic derivatives. Shown in Figure IV is a generalized proposed stepwise rearrangement mechanism.

Figure III. MS/MS Tree for CGS 9896

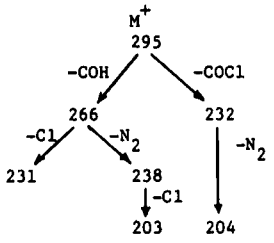

Figure IV. Proposed Aryl Migration

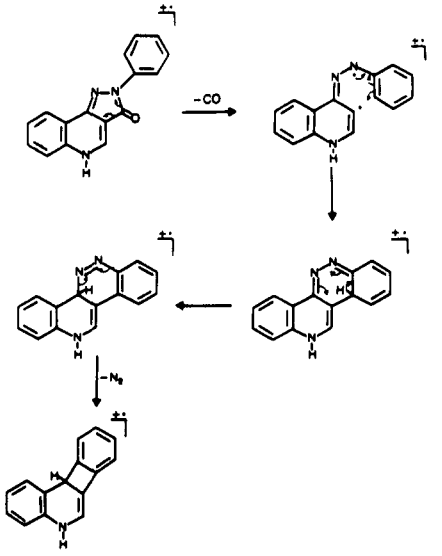

---

1 J. H. Bowie, G. E. Lewis and R. G. Cooks, J. Chem. Soc., B, 1967, 621

2 R. A. Locock, R. E. Moskalyk, L. G. Chatten and L. M. Lundy, J. Pharm. Sci., 1974, 1896.

FRAGMENTATION PROCESSES STUDIED BY GC/MS/MS AND ISOTOPE LABELLING: C. S. Hsu and D. Farcasiu; Exxon Research and Engineering Company, Route 22 East, Annandale, NJ 08801.

Isotope labelling has been commonly used for studying the fragmentation scheme of vapor-phase ions in a mass spectrometer. Using single-stage mass spectrometry, however, can lead to incorrect schemes due to insufficient information. Mass spectrometry/mass spectrometry (MS/MS), coupling two mass spectrometers in tandem, provides additional dimensions in mass spectrometric analysis. The additional stage can provide information about fragment ions, precursor ions, and the functionality of ionic species of interest. It, therefore, improves the specificity obtained by single-stage mass spectrometry, yielding unequivocal, or less ambiguous, information about ionic structure and fragmentation.

We used a Finnigan triple-stage quadrupole (TSQ-46B) mass spectrometer to investigate the fragmentation processes of vapor-phase carbocations generated from 3-methyl-2-butyl trifluoroacetate and its deuterated analogs. ^{18}O labelled esters were also used to confirm several processes involving oxygen-containing ionic species. During the analysis, GC was used to eliminate the interference of isobaric fragments from other components. To improve the sensitivity of MS/MS, ions from Q1 in the TSQ-46B were collided with argon with a collision energy of 20 eV.

Figure 1 shows the single-stage mass spectra of 3-methyl-2-butyl trifluoroacetate and its deuterated analogs. As shown in Figure 2, the first route postulates the formation of the m/z 113 ion without information from deuteration because alkyl loss is possible with a charge residing on the fragment that contains heteroatoms. However, the second route is suggested from observed mass shifts of deuterated analogs of the m/z 113 ion. The mass shifts indicate that the m/z 113 ion contains a portion of the C_5H_{11} skeleton. Is this a correct route for the formation of the m/z 113 ion from the molecular ion? Single-stage quadrupole (low resolution) mass spectrometry could not answer this question, while MS/MS was able to answer the question.

Results indicated that the second proposed route was incorrect. Figure 3 shows the daughter spectra of the m/z 113 ion and its deuterated analogs. The presence of the m/z 69 ion in all of the spectra suggests a CF_3 moiety in the m/z 113 ion structure. Further information on the origin of the m/z 113 ion and its deuterated analogs can be obtained from their parent spectra, shown in Figure 4.

The same approach can positively identify the fragmentation processes of other ionic species from 3-methyl-2-butyl trifluoroacetate. Figure 5 summarizes the fragmentation scheme of 3-methyl-2-butyl trifluoroacetate via a loss of an isopropyl group. Although complex rearrangement does occur, no hydrogen scrambling occurs in the ionic species that contain heteroatoms.

For the hydrocarbon ions that contain no heteroatoms, such as $C_5H_{10}^+$ and $C_5H_{11}^+$ ions, hydrogen scrambling was found. Figure 6 shows the daughter spectra of the $C_5H_{11}^+$ ion and its deuterated analogs. The scrambling process in the deuterated $C_5H_{11}^+$ ion was nearly complete before loss of alkanes and alkenes; for the $C_5H_{10}^+$ ion, on the other hand, the scrambling process is not complete before loss of alkyls and ethylene.

Ionic species that contain heteroatoms should be selected for locating deuterium in the products of acid-catalyzed reactions using deuterated acids. The use of hydrocarbon ions which would undergo hydrogen/deuterium scrambling should be avoided.

Figure 1

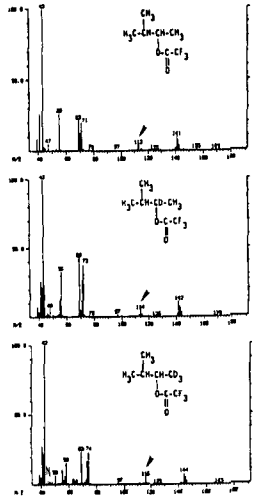

Figure 2

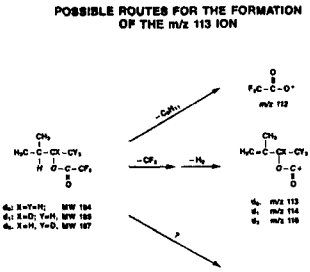

Figure 3

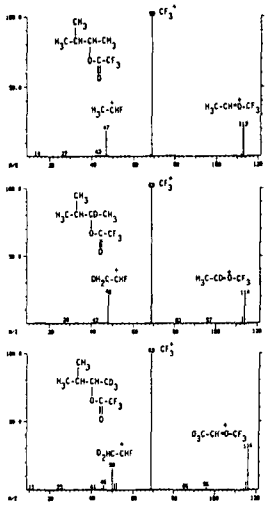

Figure 4

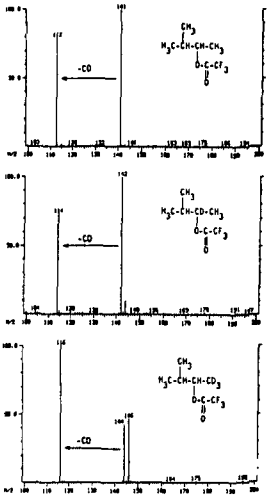

Figure 5

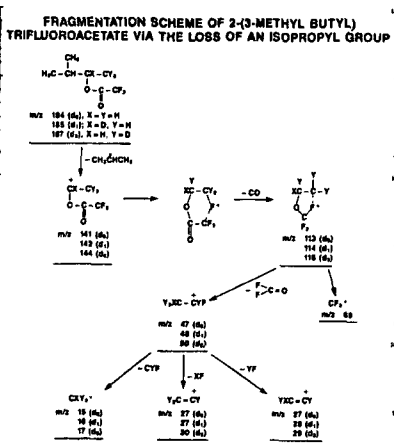

Figure 6

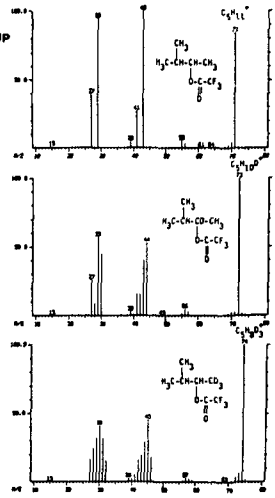

MASS SPECTROMETRY OF N,N-DIMETHYLAMINOCYCLOHEXANOLS: MECHANISM OF FRAGMENTATION DETERMINED BY DEUTERIUM LABELING

Michael T. Cheng, Stauffer Chem. Co., Richmond, California 94804

The mass spectrometric study of aminocyclohexanols can be treated in two perspectives. One is the radical induced alpha-cleavage (and subsequent cleavages) with initial ionization taking place on the nitrogen lone pair of electrons, the other is the elimination of small neutral molecules, water or an amine. Unlike cyclohexanediols, the intensity of the ions due to the loss of small neutrals in the mass spectrum of aminocyclohexanols are low. The subject of this study is to determinate the mechanism of carbon skeletal fragmentation of aminocyclohexanols.

It is known that 90% of the molecular ion current of 2-aminoethanol is carried by a species resulted from the removal of one non-bonding electron on nitrogen, only 10% is carried by a species resulted from the removal of one non-bonding electron on oxygen. It appears that for N,N-dimethylaminocyclohexanols the percentage of charge carried by the oxygen atom is even less. Therefore, the initial ionization involves the removal on one non-bonding electron from the nitrogen atom forming the molecular ion. Subsequent radical initiated alpha-cleavage causes the ring scission and forming a ring opened radical cation, the radical then abstracts a proton in a five and a six-member ring fashion followed by cleavage and forming the stable immonium ion. The fragmentation of the 1,2-, 1,3-, and 1,4-N,N-dimethylaminocyclohexanols are described in Schemes 1, 2, and 3, respectively.

The molecular ion (i) of the 1,2-isomer (Scheme 1) has two potential sites for radical induced alpha-cleavage, bond A and bond B. Bond A is more highly substituted than bond B, therefore cleaving bond A and forming the cation radical ii is the energetically favored route. The radical in ii then abstracts a proton in a six member (path a) and five-member (path b) ring transition state followed by another alpha-cleavage to produce the ions at m/z 84 and m/z 98, respectively. Since the six-member ring transition state is the favored process, therefore, the m/z 84 ion is the most intense ion in the spectrum. This mechanism is confirmed by the mass spectrum of the deuterium labeled analog. As shown in Scheme 4, the m/z 84 and m/z 98 ions are shifted to m/z 85 and m/z 99, respectively, the others are also shifted by the corresponding amount. The mass spectrum of the labeled and non-labeled 1,2-N,N-dimethylaminocyclohexanol is shown in Figure 1.

The molecular ion (iv) of the 1,3-isomer also has two bonds for alpha-cleavage (Scheme 2). However, unlike the 1,2-isomer, the two bonds (A and B) in the 1,3-isomer have similar substitution, therefore they are cleaved with approximately the same frequency. The resultant radical cation (v and vi) can abstract a proton in a six-member and a five-member ring transition state followed by another alpha-cleavage to produce the corresponding ions. The ions at m/z 84 and m/z 100 are the two most intense ions because six-member ring proton abstraction is the favored pathway. This mechanism is confirmed by the mass spectrum of the deuterium labeled analog as shown in Scheme 5.

The 1,4-isomer has an axis of symmetry, therefore the two bonds for alpha-cleavage in the molecular ion are degenerate. The radical cation (ix) abstracts proton in the analogous manner (Scheme 3), the m/z 84 and the m/z 114 ions are from proton abstraction in the six-member and five-member ring transition state, respectively. And the deuterium labeled analog shows the corresponding mass shifts (Scheme 6).

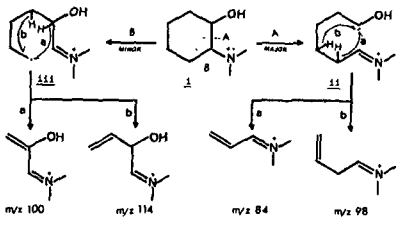

Scheme 1

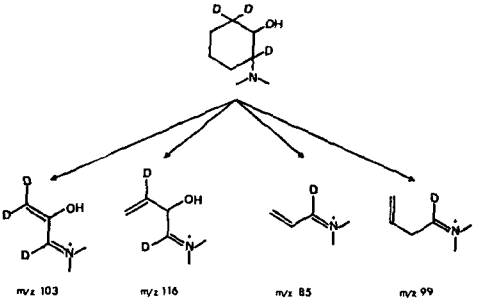

Scheme 2

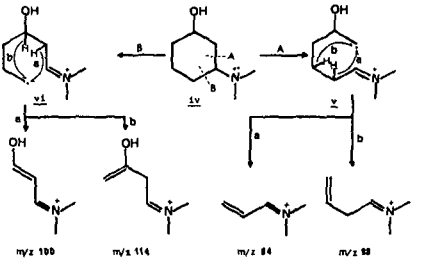

Scheme 3

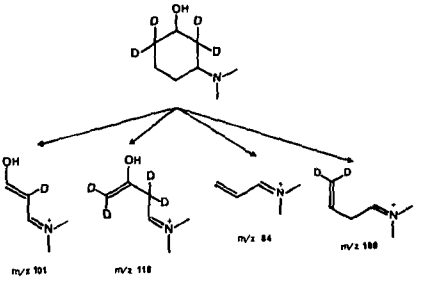

Scheme 4

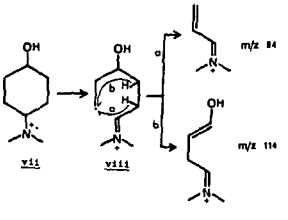

Scheme 5

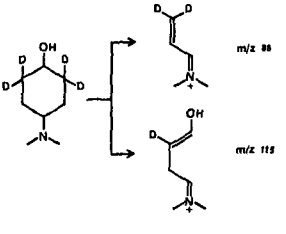

Scheme 6

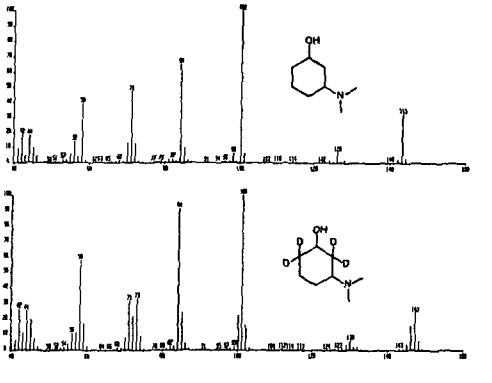

Figure 1

FORMATION OF NEW C-C BONDS IN SULFON ENAMIDES UPON EI INDUCED SO_2 ELIMINATION

M. Suter, I. Winkler, R. Steinauer, R. Lauber, U.P. Schlunegger
Department of organic chemistry, University of Berne,
Freiestrasse 3, CH-3012 Berne, Switzerland

Brown and Djerassi [1] postulated a general mechanism for the rearrangement of sulfon amides I requiring a strong basicity of Z (Z ≠ carbon).

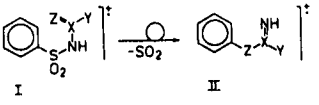

In the case [2] of the sulfon enamide IV generated by loss of acetic acid upon electron impact ionisation (70 eV) from acetic acid (N-tosyl prolinyl)ester III (Mc Lafferty rearrangement) the exocyclic methylene carbon becomes similar to "Z". During the following SO_2 elimination a new C-C bond between this "Z" carbon and the aromatic ring system is formed. This has been demonstrated by deuterium labelling experiments and MIKE spectrometry [3].

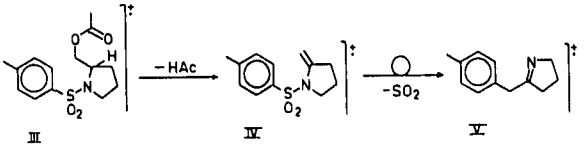

At this point the question arose, where "Z" is linked to the benzene ring - in ortho, meta, or para position to the methyl group of the former toluene sulfonic acid rest. It has been shown that it must be in the para position (the former SO_2 group position) by comparing the CID-MIKES spectra of V with those of synthesized ortho, meta and para analogues [4,6].

Additionally to the enamide IV generated in the mass spectrometer, 12 different sulfon enamides VI have been synthesized in vitro and analysed by MIKES, CID-MIKES, and constant neutral loss scans (2FFR).

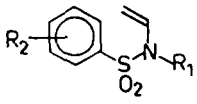

VI

R1 = $-CH_3$

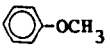

R2 = $-o,m,p-CH_3$

$-o,m,p-NO_2$

They behave analoguously to IV. The SO_2 elimination reaction is enhanced by electron donating substituents like R1 = $O-CH_3$ and R2 = $-CH_3$. A strong ortho effect (R_2 in ortho position) inducing additional rearrangements has been observed [5].

[1] P. Brown & C. Djerassi
Angew. Chem. 79, 481 (1967)

[2] W. Wiegrebe, U.P. Schlunegger, E.G. Herrmann
Pharm. Acta Helv. 49, 253 (1974)

[3] R. Steinauer, Diplomarbeit, University of Berne 1977

[4] M. Suter, Diplomarbeit, University of Berne 1982

[5] I. Winkler, Ph.D. Thesis, University of Berne 1984

[6] M. Suter, R. Lauber, in preparation 1986

FAB MASS SPECTRAL OBSERVATIONS ON NEW CATIONIC VINYL ORGANOPLATINUM COMPLEXES[1]

Mark H. Kowalski, Thomas R. Sharp and Peter J. Stang
Department of Chemistry, The University of Utah, Salt Lake City, Utah 84112, U.S.A.

Oxidative addition reactions of a series of vinyl trifluoromethanesulfonates (triflates) to $Pt(PPh_3)_4$ yield stable, crystalline 16-electron Pt(II) complexes of the general structure given below, containing a sigma-bonded vinyl ligand and a non-coordinating triflate anion. We have utilized fast atom bombardment (FAB) mass spectrometry as one of an arsenal of chemical and spectroscopic techniques for characterizing these structures.

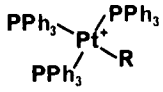

1, R = methyl
2, R = 2-propenyl
3, R = isobutenyl
4, R = 1-cyclohexenyl
5, R = 2-methyl-1-cyclohexenyl
6, R = 2-cyclohexyl-1-ethenyl
7, R = p-NO_2-phenyl

Reaction of $Pt(PPh_3)_4$ with a 3-fold excess of the appropriate vinyl triflate in toluene at room temperature produced the indicated compounds in high yield within a few hours[2]. These compounds were examined by +Ve FAB-MS in either a m-nitrobenzyl alcohol (NBZ) matrix (Aldrich, 98%) or a mixed 18-crown-6 crown ether/tetraglyme (18Cr6) matrix[5] without any unusual handling precautions and without further purification of the matrix. Observations were made with a VG Analytical 7070-E mass spectrometer operating at +5 KV, resolving power 1000-2000, scanning over m/z 90-1300 at 20 sec/decade. Samples were bombarded with 6.0-7.0 KeV Ar^o from an Ion Tech saddle field source operated at 1.0-1.5 mAmp. Repetitive scan spectra were recorded by a VG DS2050 datasystem, mass calibrated with the cluster ion spectrum of H_2SO_4[3,4].

Partial spectra of compounds 2 and 6 are shown. Data on the fragmentation of the other compounds examined are given in Table I. All of the data given in Table I are of observations made from the NBZ matrix. Spectra of compounds 5 and 6 were also recorded from the 18Cr6 matrix. From this limited examination, the NBZ matrix is superior in that it produces substantially less background and a higher analyte signal intensity. The fragmentation intensities appear to be approximately the same in both matrices.

Molecular weights are confirmed, and isotope patterns resulting from polyisotopic platinum are consistent with predictions. Intensities of the molecular cation signals are small when present. Some of the compounds show small intensities at $[M-R]^+$. The structurally significant fragment, $Pt(PPh_3)_2R^+$, resulting from loss of one PPh_3 ligand from M^+, is the base peak in all spectra. A prominent additional feature of these spectra, illustrated in the figures, is the presence of low intensity signals showing the characteristic Pt isotope pattern which appears 17 mass units above each of the major fragment ions. We suggest that these signals arise by replacement of the very labile PPh_3 ligand by a hydroxyl ligand. As noted above, no extraordinary precautions were taken to exclude trace amounts of H_2O from the matrices used. This behavior is consistent with known solution chemistry of these compounds. One PPh_3 ligand is readily displaced in solution by any of a number of alternate ligands possessing a lone pair of electrons, such as the halides, cyanide, water, etc.

The $Pt(PPh_3)_4$ synthetic precursor was also examined. The spectrum consists principally of $Pt(PPh_3)_3^+$ base peak and losses of PPh_3. No molecular ion was observed. The isotope clusters 17 mass units above the primary ions are also prominent. Indeed, the spectrum of all the compounds in Table I below $Pt(PPh_3)_2^+$ are identical with the spectrum of $Pt(PPh_3)_4$.

The most interesting point to note is that significant spectral intensities correspond to loss of $C_6H_5^{\bullet}$ from PPh_3, producing ions, for example, of structures $Pt(PPh_3)_2(PPh_2)^+$ and $Pt(PPH_3)(PPh_2)^+$. This behavior, consistent within this entire series of cationic compounds, is in distinct contrast to that of other systems which we have studied, in which fragmentation occurs principally at the metal-ligand bonds, and very seldom at bonds within any of the organic ligands. One exception is of a neutral $Pt(PPh_3)_2C_2H_2$ pi complex[5], in which the ethylene ligand appeared to cleave. We have reexamined this compound and found similar behavior to that of the Pt(II) complexes reported here, suggesting that this originally neutral Pt(0) complex may be undergoing oxidation to a Pt(II) compound under our observation conditions. This property of showing relatively facile intra-ligand fragmentation appears to be a property of the Pt(II) oxidation state. In all of the other stable Pt(0) neutral complexes previously reported[5], intra-ligand fragmentation did not occur. Cottee et al.[6] report that their Pt(II) complexes containing triethyl phosphine ligands also fragment internally to the ligand, showing first loss of $C_2H_5^{\bullet}$, then successive losses of C_2H_4 from $[Pt(PEt_3)_2]^+$ as prominent features of their spectra.

Table I:

Relative intensities of structurally significant fragments in the +Ve FAB mass spectra of several cationic Pt(II) vinyl complexes from a m-nitrobenzyl alcohol matrix.

#	Compound Ligand name (ligand mass)	m.w.[1]	Ion Intensities[2] M^+	$[M-PPh_3]^+$	$[Pt(PPh_3)_2]^+$	$Pt(PPh_3)_2-Ph]^+$
1	R = methyl (15)	996	9.0	100	89	15
2	R = 2-propenyl (41)	1022	3.0	100	68	10
3	R = isobutenyl (55)	1036	1.5	100	60	10
4	R = 1-cyclohexenyl (81)	1062	0.0	100	41	13
5	R = 2-methyl-1-cyclohexenyl (95)	1076	0.5	100	32	5
6	R = 2-cyclohexyl-1-ethenyl (95)	1076	5.0	100	44	14
7	R = p-NO_2-phenyl (122)	1103	5.0	100	66	12

1. Calculated using most abundant ^{195}Pt isotope.
2. Intensities are normalized to the ^{195}Pt-containing peak in the $[M-PPh_3]^+$ ion cluster. All intensities are of the ^{195}Pt-containing peak.

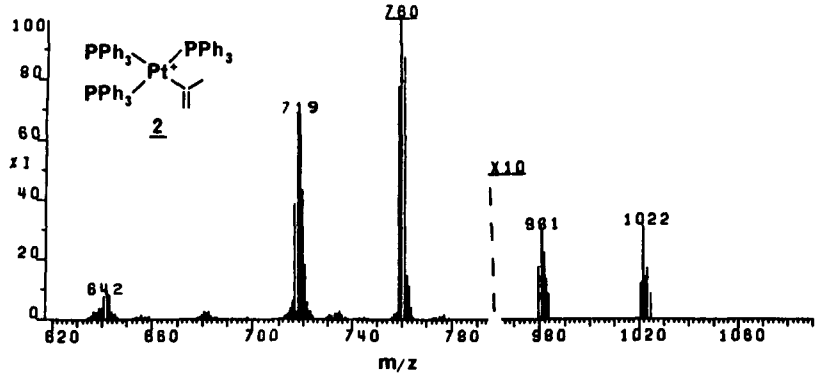

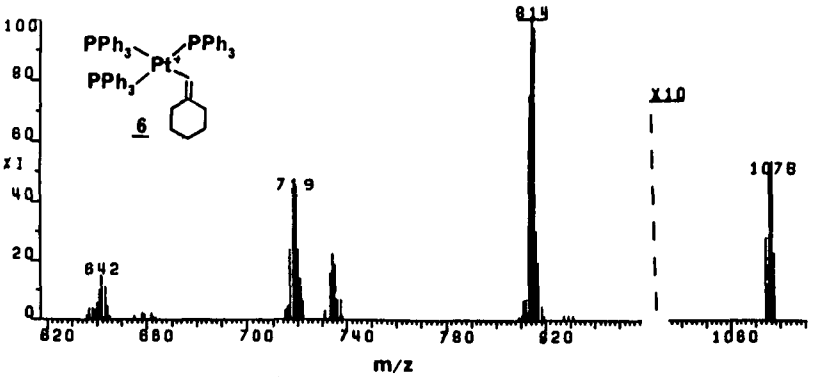

---

1. Supported by National Science Foundation grant CHE-8419099. Instrumentation obtained with funds from National Science Foundation grants CHE-8100424 and CHE-8310031.
2. M.H. Kowalski, P.J. Stang (1986). **Organometallics** (in press).
3. T.R. Sharp, H.K. Jones (1986). **These Proceedings.**
4. T.R. Sharp (1986). **Org. Mass. Spectrom.** 21, (in press).
5. T.R. Sharp, M.R. White, J.F. Davis, P.J. Stang (1984). **Org. Mass Spectrom.** 19,107.
6. F.H. Cottee, J.A. Page, D.J. Cole-Hamilton, D.W. Bruce (1985). **J. Chem. Soc., Chem. Comm.**, 1525.

FRAGMENTATION PATTERNS OF METAL CHELATES IN SIMS DUE TO THE USE OF SILVER FOILS

B.Wenclawiak, Dept. of Chemistry, University of Toledo, Toledo, Ohio 43606

Three different classes of metal chelates have been investigated by secondary ion mass spectrometry (SIMS):

1) beta-diketonates (O-M-O six membered chelate ring)

2) 8-hydroxyquinolinates (O-M-N five membered chelate ring)

3) diethyldithiocarbamates (S-M-S four membered chelate ring)

In addition to fragments observed in EI-MS and FAB-MS, SIMS revealed ions, which were due to the loss of the heteroatom or heteroatom group. This had been observed earlier [1], but was not discussed in detail.

The loss of whole ligands during ionization is common in metal chelate mass spectrometry. The molecular ion minus one ligand ion is usually the largest metal containing fragment. Additional fragments, especially of simple ligands like acetylacetone are rare. Introducing larger residual groups in the beta-diketone ligand gives rise to additional fragments, e.g. 2,2,6,6-tetramethylheptane-3,5-dionates lose butyl from the ML_3 or ML_2 during CAD-MS-MS experiments.

For a number of metal chelates with different ligands and central ions additional fragments have been observed during SIMS experiments. Cationization due to the target material (Ag) or impurities (Na) are common and expected. Cooks and Walton [1,2] described self cationization and cationization by another first row transition metal.

The SIMS spectra of $Cr(tod)_3$, $Rh(Ox)_3$, $Ir(Ox)_3$, and $Ni(DDTC)_2$ show fragments, which are due to the loss of O, CO, and S. The loss of S was also reported for an ion of $Fe(DDTC)_3$ [1,2]. Neither of these ions have been observed with any other ionization technique. $VO(acac)_2$ does not show the loss of O in EI-MS but in SIMS.

Not all chelates investigated show these losses. This may be due to the treatment of the support material, the matrix chosen, and the chelate itself. Especially the stability of the central ion to the heteroatom (Pearson) may contribute.

The loss of O, CO, and S could be explained by the following reaction scheme: Cleavage of the chelate ring, reaction of the heteroatom with the supporting silver foil, finally the cleavage of the heteroatom (group) from the ligand.

[1] Pierce J.; Busch K.L.; Walton R.A.; Cooks R.G.; J.Am.Chem.Soc. 1981, 103, 2583
[2] Pierce J.; Busch K.L.; Cooks R.G.; Walton R.A.; Inorg.Chem. 1982, 21, 2597

Acknowledgements: The author wishes to thank Prof. Dr. A. Benninghoven and Dr. W. Sichtermann for the use of the SIMS, and Dr. R.E. Sievers and Dr. R.M. Barkley for the use of the FAB-MS.

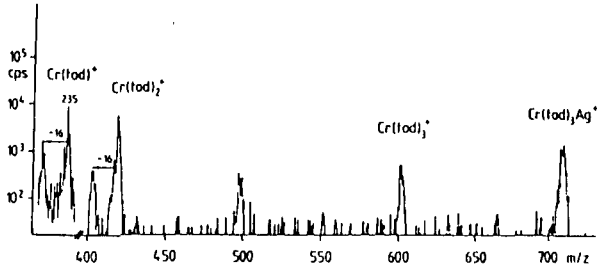

SIMS of Cr-2,2,7-trimethyloctane-3,5-dionate

EXPERT SYSTEMS: A POSTER SYMPOSIUM

Organized by: Carla M. Wong, Lawrence Livermore National Laboratory, P.O. Box 808, L-365, Livermore, CA 94550

Machines, even some of the most sophisticated computers, are essentially stupid. Although they may be able to perform fantastic feats of memory and calculation, basically they only follow their programmed orders, and thus they lack the ability to deal with the slightest unforeseen contingency. But engineers and programmers keep building "smarter" machines all the time, and we may well ask ourselves how far this trend can go. Will we really, some day, be able to build a machine that "thinks"? There are many potential applications for a machine able to work unattended and adjust to unexpected changes, because machines never sleep or become bored.

One of the most promising approaches to artificial intelligence (AI) is the development of "expert systems." The idea is to give the computer a vast store of knowledge (provided by human experts) together with a set of rules for manipulating what it "knows" to arrive at correct conclusions. Although the computer seldom models the exact decision-making process of the human expert, it can make valid inferences and supply an understandable explanation of its reasoning. Present applications of expert systems include such complex tasks as process control, medical diagnosis, genetic engineering design, military threat assessment, and geologic survey interpretation.

The process for developing an expert system is called knowledge engineering. This involves acquiring and organizing a human expert's knowledge and using the heuristic, representational, and rule-based techniques of AI to encode this information for the computer. In turn, the computer uses some of these same techniques to manipulate this store of knowledge.[1-4]

At present, most computerizing of equipment and interpreting of data are accomplished by traditional algorithms. In these applications, the computer's programs are totally defined, stepwise procedures. In contrast, the symbol-manipulation program of an expert system solves problems by logical or plausible rules of inference rather than by calculation. An expert system is capable of making educated guesses and of analyzing the results of trial calculations to correct its initial assumptions.

One of the most important features of an expert system is its "transparency." A typical computer using algorithmic problem-solving techniques accepts input and prints out the answer without explanation. The system is essentially opaque, only the programmer knows how the computer arrived at the result. The expert system, in contrast, displays the reasoning behind its decisions (i.e., is transparent). This enables the user either to accept the result with confidence or, if a flaw is detected in the reasoning, to change the decision. One way to do this is to add new information to the knowledge base. Another is to change the reasoning rules or heuristics of the expert system.

These characteristics make expert systems well suited for solving problems that require high levels of expertise. Typical applications involve interpretation of data that are voluminous or very repetitive or that come at unpredictable intervals. Other applications involve problems requiring more years of experience and more related background information than any one person can acquire. The very nature of these problems ensures that the human experts who can deal with them are themselves scarce.

The participants in this session will present an oral 6-7 minute overview of their expert system, a 4' x 8' poster, and computer demonstrations of their application, which

Work performed under the auspices of the U.S. Department of Energy by the Lawrence Livermore National Laboratory under contract number W-7405-ENG-48.

will run continuously throughout the Symposium time period. The computers will be strategically located to coordinate demonstrations with their respective poster description. (The computers represent AI-LISP processing environments, PC-environments, and traditional mini-type computers which have been generously loaned to us for this occasion.) Extended abstracts will be available as will summary handouts on hardware, software and services available in the AI-Expert System community.

Some of the participants are developing their first expert system and some have developed many systems. They are using many different programming environments of varying complexity (LISP code, PSL, expensive knowledge engineering environments, expert system shells, and traditional algorithmic programming languages).

The problem types to be demonstrated are all familiar to mass spectrometrists, even if the actual problem domain is not. We have problems in structure elucidation, compound identification, tuning and controlling complex instruments or processes and training new people. We will see how expert systems address these areas. Also, most of us are concerned with chemical reactions and development of new materials (drugs, polymers, metals, etc.) and one of our speakers has an expert system to develop new metals (alloys).

Finally, all of us like to compare more familiar, traditional methods with new ones, so we have addressed SIMPLEX optimization vs. AI-Tuning in one poster, and, the concepts illustrated by multivariant statistical analysis and pattern recognition are shown in another.

REFERENCES

[1] C. Wong, R. W. Crawford, J. C. Kunz, and T. P. Kehler, "Application of Artificial Intelligence to Triple-Quadrupole Mass Spectrometry," in *Proc. IEEE Nuclear Science Symposium* (1984, in press).

[2] A. Barr and E. A. Feigenbaum, *The Handbook of Artificial Intelligence* (William Kaufmann, Inc., Los Altos, CA, 1982), Vol. I and II.

[3] P. R. Cohen and E. A. Feigenbaum, *The Handbook of Artificial Intelligence* (William Kaufmann, Inc., Los Altos, CA, 1982), Vol. III.

[4] C. M. Wong, *et al.*, "Development of a Totally Computer-Controlled Triple Quadrupole Mass Spectrometer Systems," *Rev. Sci. Inst.* **54**, 996-1004 (1983).

TOOLS AND RULES FOR STRUCTURAL INTERPRETATION OF MS/MS SPECTRA,

A.P. Wade[1], P.T. Palmer, K.J. Hart and C.G. Enke*,

The Chemistry Department, Michigan State University, East Lansing, MI 48824

[1] also of: The Information Technology Research Unit, British Petroleum Research Centre, Chertsey Road, Sunbury-on-Thames, Middlesex, TW16 7LN, UK

Artificial intelligence and machine learning methodologies are being developed for automatic structure elucidation from MS/MS (and MS^n) data. The goal of this is to produce an intelligent system for structural elucidation which has in its feedback loop a triple quadrupole mass spectrometer, controlled by an expert system. This MS/MS instrument will carry out diagnostic and confirmatory experiments, each time feeding its results back through interpretive tools to its intelligent controller. An MS/MS instrument yields more data about a given compound than does a conventional MS system. Daughters, parent-to-daughter transitions and neutral losses may be directly observed. Thus an extra dimension of information is made available in which sets of features due to particular substructures are less overlapped than in MS.

Software tools are being developed to facilitate automated substructure identification and structure elucidation. These tools identify rules which help diagnose the presence of particular substructures in unknowns. These substructures then constrain the number of structures consistent with known empirical formula data, and so are a major aid in structure elucidation. As "expert system" interpretation of the rules, match factors and other known chemical data is developed, improvements in performance are expected. The existing tools will now be described:-

MAPS: The "Method for Analysing Patterns in Spectra" software is written in InterLISP-D and runs on a Xerox 1108 AI Workstation. It deduces, without prior knowledge, the relationships that exist between the presence of substructures in molecules and the characteristic features they produce in MS/MS spectra. Once enough of these relationship rules are known, and at a high enough level of certainty, MAPS can use them to predict the presence (and sometimes the absence) of substructures in an unknown, irrespective of whether the MS/MS spectra of that compound have ever been taken before. The MAPS functions:

* Add known compounds into a current training set MS/MS database and then apply a number of tests to the MS/MS data.

* Deduce substructure / spectral feature correlations: Features that appear to be characteristic of particular substructures are empirically identified and stored as "rules" (see below). These express the correlation of MS/MS spectral features with particular fragments of molecules.

```
RULE 11
IF   [10/15] Line in neutral loss spectrum at m/z 16      CH4
AND  [9/15]   ..  ..  ..  ..  ..  .. m/z 27      C2H3
AND  [15/15]  ..  ..  ..  ..  ..  .. m/z 28      C2H4
AND  [7/15]   ..  ..  ..  ..  ..  .. m/z 29      C2H5
AND  [6/15]   ..  ..  ..  ..  ..  .. m/z 30      C2H6
AND  [8/15]  Line in daughter spectrum at m/z 27         C2H3
AND  [11/15] Line in daughter spectrum at m/z 29         C2H5
THEN Functionality indicated is ETHYL
```

The "[x/y]" in each clause indicates that that feature was found in x of the y training set compounds having the ETHYL substructure. Only clauses that correlate highly or almost exclusively with that substructure are allowed. So far, MAPS has identified sets of features which correlate with 29 substructures. Most give good discrimination. Heuristics are being added to filter out "false" correlations which can occur in the rules. These are artifacts of the database and decrease as the database grows.

* Evaluate unknowns: Not all of the spectral features associated with the presence of a particular substructure are seen in the spectra of *every* compound which contains that substructure. However, in many cases a sufficient proportion will be observed for the association to be made. Decreasing the confidence level which indicates the presence of a particular substructure increases both the number of successful inferences and the likelihood of errors. The set of indicated substructures is "filtered". Those identified are then passed as input to GENOA.

* Analysis of deductive reliability: By comparing the rules against "unknowns" (or the spectra of the training compounds), the substructures which are correctly (or incorrectly) identified as present (or absent) can be noted.

EFG: The Empirical Formulae Generator produces a list of all empirical formulae consistent with a given set of elemental composition constraints. These constraints may be obtained from MS/MS data.

GENOA: The GENOA program (from the Stanford DENDRAL project) generates all molecular structures consistent with a given empirical formula. An unconstrained run may take hours and generate thousands of possible structures. The list of possibilities consistent with the known empirical formula is greatly constrained if the presence (or absence) of single (or multiple) occurrences of discrete (or overlapped) substructures is known. This substructure information is provided by MAPS. If MAPS identifies the substructures correctly, the structure of the unknown will lie within the set of structures generated by GENOA.

Acknowledgements: We thank Finnigan MAT for use of the Xerox 1108 and acknowledge support from NIH grant GM-28254.

A Knowledge Based System for Tuning MS/MS Instruments in Various Operational Modes

Hugh Gregg, Hal Brand and Carla Wong
Lawrence Livermore National Laboratory
P.O. Box 808 L-310, Livermore, CA 94550

Mass spectrometers have traditionally been tuned by an operator "tweaking" the instrument control knobs until an oscilloscope display of the spectrum looks right. This is a time consuming process that yields a set of parameters that produce a compromise or average tune over the mass range of interest. This compromise tune necessarily trades off signal intensity at each end of the mass range for sensitivity at the other mass extreme. To obtain maximum sensitivity over a large mass range, the instrument needs to be tuned over many small mass ranges, and the control computer must sequence through the sets of tuning parameters while scanning the full mass range. However, manually tuning an instrument over many small mass ranges consumes time that would be better used for sample preparation.

At LLNL, we have developed a tuning system for our triple quadrupole mass spectrometer based on the knowledge engineering environment (KEE, trademark of IntelliCorp) running on a Xerox 1109 lisp processor. This system is able to tune the TQMS in both normal MS operations and MS/MS operations, and results in increased sensitivity throughout the mass range (see Figures 1 and 2).

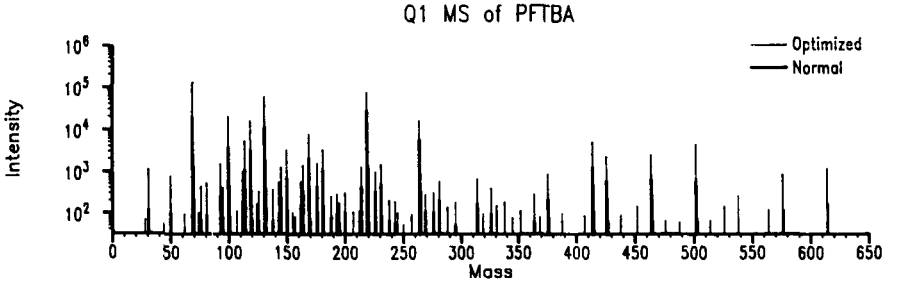

Figure 1

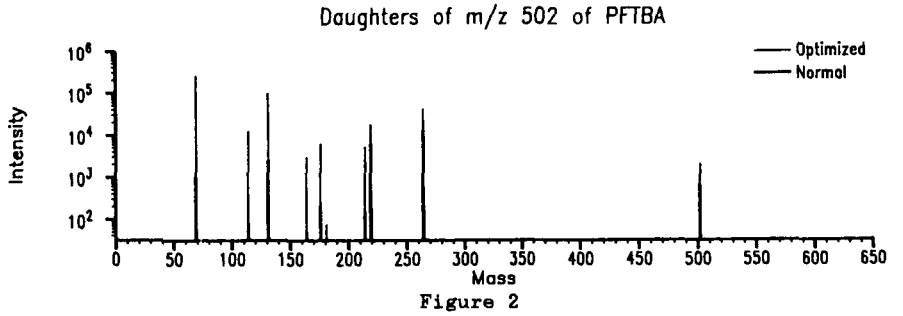

Figure 2

Work performed under the auspices of the U.S. Department of Energy by the Lawrence Livermore National Laboratory under contract number W-7405-ENG-48.

The knowledge based tuning system that we have implemented simulates a person tuning the instrument; a knob is selected and "tweaked" (adjusted) for the maximum desired result. The desired result is either the signal intensity, or a measure of the peak "goodness" (a combination of peak shape parameters and intensity). After one knob has been tweaked, another is selected and tweaked until no more knobs can be selected, at which point the tuning on the selected ion is complete.

Three major classes of knowledge are relevant to tuning the TQMS:

1) Knowledge to tune the instrument and evaluate the output.
2) Knowledge about the instrument itself.
3) Knowledge to interface to the instrument control computer.

KEE provides four basic mechanisms for representing and using knowledge: frames, methods, rules and active values. Frames permit static knowledge to be represented in a class/sub-class/member inheritance hierarchy (e.g. the instrument knowledge shown in Figure 3, the control hierarchy). Methods provide a mechanism for representing procedural knowledge in LISP code with an object-oriented interface and control structure (most of the code used in system is implemented as methods). Rules provide an alternative mechanism for representing procedural knowledge with KEE providing both forward and backward chaining control structures (the knob selection and tweak function selection are implemented as rules). Finally, active values provide a mechanism for attaching procedural knowledge in the form of methods or rules to frames (used for display purposes, and to link the tuning system to the instrument control computer). The use of a tool, such as KEE, that integrates several knowledge representation schemes significantly decreases system development time over procedural languages, and results in a system where the knowledge encoding is easily seen, understood and modified.

A unique feature of our tuning system is the ability to create and tweak "linked" knobs. A linked knob consists of one primary knob, and one or more secondary knobs which track the primary knob at some offset. As an example, if we vary the quad 2 collision energy (field axis offset) without linked knobs, we obtain the lower curve in Figure 4. However, if we link quad 3 field axis and lenses as secondary knobs to the primary quad 2 field axis, we obtain a factor of 25 increase in signal intensity.

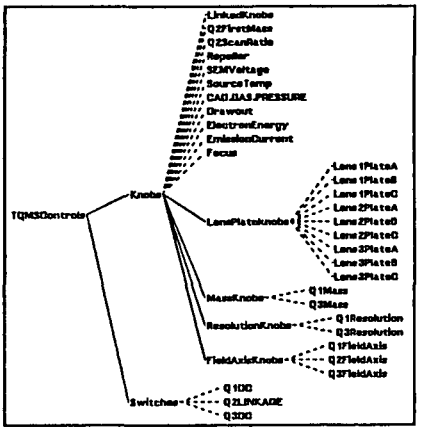

Figure 3

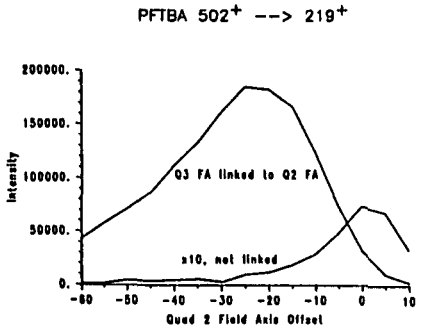

Figure 4

DEVELOPMENT OF AN EXPERT SYSTEM FOR HIGH RESOLUTION DIODE LASER SPECTROSCOPY

Philip L. Varghese and Joel T. Garrell
The University of Texas at Austin
Department of Mechanical Engineering
Austin, Texas 78712

OPTEX is an expert system, designed to integrate the data acquisition, numeric processing, and graphic capabilities of a laboratory microcomputer to assist the spectroscopist in diagnosing and correcting system problems associated with high resolution measurements made with diode lasers. The data transferred to the computer are analyzed and interpreted using empirically developed rules to diagnose sub-optimal settings of experimental parameters. The system has initially been configured to provide suggestions to the experimenter on how to change experimental conditions to correct problems detected. The ultimate objective of this work is to transfer control of the laser and key experimental apparatus to the computer which will act as an "intelligent" data acquisition and analysis system.

Tunable infra-red diode lasers provide the means to perform extremely high resolution absorption spectroscopy in the wavelength range from 3 to 30 microns, on a wide variety of molecules of practical importance. Potential applications include pollutant detection, monitoring of reactive intermediates for process control, and studies of chemical kinetics. The use of diode lasers has been restricted primarily to research laboratories because of the high degree of expertise required to obtain suitable laser operation at the precise wavelength of interest. A typical diode laser experiment is quite complex requiring several experimental parameters to be optimized simultaneously. Slight shifts in optical alignment, feedback into the laser, interference fringes from multiple reflections and a variety of other factors must be considered when tuning the laser to a new frequency and optimizing an experiment. The laser must be made to operate in a stable mode and any mode-hopping detected. The identification of mode-hopping by visual inspection of the laser output power, as monitored by a detector and displayed on an oscilloscope, takes considerable training and continuous attention. Since microcomputers are often used for data acquisition in the laboratory we wished to investigate the possibility of adding some "intelligence" to the data acquisition and analysis process to assist in a complex experiment.

OPTEX is a rule-based classification system which determines if the data are valid or invalid, and suggests possible remedies for system malfunctions appropriate to the diagnosis. In its current configuration the system contains over 50 rules which describe the effects of 6 key system components on the signals from the infra-red detectors which are digitized and stored on the computer. These rules represent the "knowledge base" that OPTEX has. In addition to the knowledge base, expert systems have an "inference engine" which uses the knowledge base to operate on data supplied at run time and arrive at conclusions when solving specific problems. The expert system development package we used (described below) provided the inference engine. When provided with input data the inference engine uses backward chaining to determine if additional data are needed to arrive at a conclusion.

The rules comprising the knowledge base are a series of IF - (Condition) - THEN (Conclusion 1) - ELSE - (Conclusion 2) statements. Examples of rules from OPTEX are:

(1) IF: An abrupt change in the spacing of the fringes on the etalon trace is very pronounced
THEN: Mode hop is present - Probability=90/100

(2) IF: [BOTH DET OUT LN2] > 0.5
THEN: System is operating improperly; data will be invalid - Probability=100/100
and System is operating properly - Probability=0/100
and Both detectors are probably out of liquid nitrogen
and Check both detectors for liquid nitrogen, and add if necessary.

Data on experimental conditions are input via a menu of screens with multiple choice questions. To assist the user in making choices there are several split screen displays, with the experimental data and reference data provided on the right half of the screen, and the question and answers on the left half. Since the expert shell has no graphics

capabilities, these questions are asked in an external graphics program and the responses passed to the expert program.

OPTEX functions as an assistant, i.e. the system is interactive and depends on operator input in arriving at its conclusions. The task of diagnosing system malfunction has been divided into two parts. The infra-red detector data acquired are displayed on the computer screen and the operator is asked a series of questions regarding its quality, with reference spectra being displayed for reference and ease of comparison. This allows the pattern recognition task, which is "easy" for humans but "difficult" for the computer to be performed by the human operator, while the interpretation of the pattern which requires expertise is left to the computer. Although this is not as useful as automatic detection, the system helps identify sometimes subtle flaws by focusing the operator's attention to specific details, and by providing reference patterns for comparison.

The development of an expert system is greatly facilitated by the use of an expert system development shell, particularly if the features of the shell are well matched to the application. Most shells provide for relatively easy construction of the knowledge base and provide the inference engine which operates on input data in conjunction with the knowledge base to arrive at conclusions when solving specific problems. Recently several development shells have become available that do not require programming in LISP or PROLOG and which can be run on relatively small (and inexpensive) microcomputers. We constructed OPTEX using an expert system development shell supplied by EXSYS, Inc. We discuss this shell below to illustrate the features and limitations of such systems.

EXSYS has a number of features which made it suitable for our application. It provides a rule editor which allows for easy building and modification of rules in the knowledge base. It can be interfaced with external programs, so that results of complex calculations on spectra can be passed to the expert module if necessary. It permits confidence measures to be assigned to intermediate and final conclusions via a "probability" scheme. This is important since several different problems can be manifested by similar symptoms in the detector signals and several different symptoms are generally combined when arriving at a conclusion. It has a limited explanation facility. If the user asks WHY at any stage the program displays the rule(s) used. Explanations can be built into the notes and references associated with each rule. The program is compact and hence can be installed on a microcomputer. It executes quickly which is important because we ultimately wish to automate the decision process completely and obtain a real time control system.

A limitation of the development shell (for our application) is that it does not handle graphics internally. We resolve this problem by running the graphics intensive portion of the program external to the expert program itself, and pass the information obtained to the expert. Another limitation of the development package is that it does not automatically generate rules from examples, and hence the knowledge base is static until the rules are specifically modified or extended. Thus (unlike most humans) OPTEX does not automatically accumulate knowledge with time. This advanced feature is available on systems which run on special purpose machines or mainframe computers. Additionally, the current version of EXSYS (3.0) has an inference engine which uses backward chaining only to determine what data are required to arrive at a conclusion and requests information appropriately. Problem solving efficiency, and hence execution speed, would increase with a combination of forward and backward chaining.

OPTEX is a system under active development. It demonstrates what can be achieved by adding some pseudo-intelligence to the microcomputers frequently dedicated to data acquisition. Future work will be aimed at automating the pattern recognition portion of the program, so that the system can identify mode-hops, interference effects, noisy data, etc. Upon completion of this phase the task of monitoring and controlling the laser and other key experimental equipment will be transferred to the computer so that the machine itself implements the changes initially programmed as suggestions to the operator. Successful completion of this phase the system will make high resolution diode laser spectroscopy a much more routine research tool and a far more attractive diagnostic for industrial applications.

Acknowledgements: This work was supported in part by the National Science Foundation under Grant No. CBT-8404277, and the University Research Institute, and Bureau of Engineering Research at UT Austin. We gratefully acknowledge the donation of the computer hardware by and software by the Academic Information Systems Division of IBM through Project QUEST at UT Austin, and the expert system development shell by EXSYS, Inc.

An Expert System for Combined Interpretation of Mass and Infrared Spectra

Bo Curry, Hewlett-Packard Company
Chemical Systems Dept., Palo Alto, CA 94304-1209

The Plato project is an ongoing effort to apply the techniques of Artificial Intelligence to the interpretation of analytical data and the determination of molecular structures. In its present form, the program interprets mass spectra, gas phase infrared spectra, and elemental analysis information. It concludes with a list of molecular substructures believed to be present in the unknown compound. The current system also provides tools to assist the user in assembly of substructures to form complete candidate structures, and in testing candidate structures for consistency with the original data.

An expert system such as Plato is designed to function as an assistant to, rather than a replacement for, a human expert. It is not yet possible to endow a computer program with a depth of physical insight comparable to that of a human. On the other hand, the program can remember and consistently apply thousands of empirical rules. Also, few spectroscopists are simultaneously expert at interpreting mass spectra, infrared spectra, and other kinds of spectral data. In keeping with its role as an assistant, Plato explains its reasoning process and presents its results in a form which a chemist can understand. The user can suggest possibilities to the program and resolve ambiguities which are too difficult for it.

We have developed Plato on an HP-9000/320 workstation running the HP-UX operating system and the Common Lisp Development Environment. This provides a powerful dedicated processor and a rich programming environment. Most of the code for Plato was written in Lisp. It communicates with programs written in other languages through operating system calls and direct linking of foreign subroutines into the Lisp environment.

Plato was designed to be able to use data from multiple sources in a single analysis. The use of different kinds of spectra greatly increases the number of functional groups which can be reliably identified. Different classes of compounds are more readily detected with one technique or another. Ketones, for example, are difficult to detect from mass spectra but conspicuous in the infrared. Interferences which cause difficulties in the interpretation of one kind of spectrum may have little effect on another. Use of multiple spectra also improves specificity. By working back and forth between spectra, substructures which are suggested by one spectrum may be confirmed, and their chemical environment elaborated, by another.

To facilitate the use of different data sources, Plato is composed of modules which interact with each other in specialized ways. The primary modules are the Controller, the Reasoner, and a committee of data Experts. The chemical knowledge of the system is stored in a hierarchy of about 900 chemical substructures. The chemical knowledge base also serves as a "blackboard", on which information needed by all modules is stored.

Each of the data Experts is responsible for the interpretation of a single kind of input data. It maintains its own private rules and data, and can read the blackboard, but not write on it. The Experts communicate only with the Controller.

The currently implemented data Experts are the STIRS Expert, the IR Expert, the element Expert, and the human Expert. STIRS (1) is a well-known Fortran program for the interpretation of low-resolution mass spectra. The STIRS Expert calls up STIRS to run in the background, then translates its results into a form usable by Plato. The IR Expert is a rule-based interpreter which uses about 1000 correlations between IR bands and substructures. It also searches for distinctive patterns of bands. The element Expert uses partial elemental analysis information to constrain the suggested substructures. The human Expert provides an interface for the user to assert or deny the presence of particular substructures.

The Controller controls the flow of information by exchanging messages with other modules. It begins the analysis by assembling a committee of data Experts competent to deal with the input data. It then solicits suggestions from each Expert on the committee. These initial suggestions are made by the Experts without consultation. The Controller sends the initial suggestions to the Reasoner, which combines them to form an initial guess at the substructures present in the unknown. The Controller then systematically investigates each substructure believed to be present. During the search, it asks each committee member to evaluate the likelihood of the substructures, and to suggest the most specific chemical environment for the substructure which is consistent with its data. For example, the STIRS Expert may initially suggest the presence of an ester group. During the search, the Controller will ask each Expert if this is consistent with its data, and what kind of an ester it might be. The IR Expert might respond that its data support the presence of a saturated acid ester, or of a methyl ester, or whatever. Once no further specialization is possible, the analysis is over.

When one of the data Experts determines the presence or absence of a substructure, it

communicates this finding by reporting a piece of "evidence" back to the Controller. A piece of evidence has a value which indicates the degree to which the data supports the presence or absence of the substructure.

The evidence supplied by the data Experts must be combined to form a consistent set of conclusions about the compound under investigation. This is the task of the Reasoner module, which combines items of evidence to form "beliefs". A belief is generated for each of the 900 defined substructures. The belief records the total support for the presence or absence of that substructure, derived from all the evidence collected so far. It also records the supporting evidence. The value of the belief is posted to the blackboard so the other modules can use it while interpreting their data. The Reasoner also notices contradictions, and refers the offending evidence back to the originating Experts for reconsideration.

Plato also incorporates an Explanation module, which is able to read the reasons recorded by the Reasoner for each belief. In this way it determines which original pieces of evidence were responsible for the belief. The data Expert which generated the evidence is responsible for explaining how the evidence is justified by the input data.

The program has been tested in several modes. Individual infrared rules were tested on 1800 compounds from the EPA gas-phase IR library. All compounds in the library were analyzed using IR data only. The combination of mass and infrared spectra has been tested for about 200 selected compounds. Since most of the spectra in the libraries have negligible noise levels, a systematic series of tests on noisy spectra is currently underway.

The results of these tests have been encouraging. The IR only tests on the EPA library showed an average recall rate (percentage of substructures correctly reported) of over 60% for 134 selected substructures. The reliability (percentage of reported substructures which were correct) was over 80%. Our more limited tests combining mass and infrared spectra show large increases in recall (to over 80%) and smaller improvements in reliability.

The current system is by no means complete. We are continuing to expand the IR rule base to improve performance for classes of compounds not well represented in the EPA library. We are also investigating rule-based mass spectrum interpretation methods to supplement STIRS.

The Plato system represents a promising method of automatically combining quite different interpretation methods to obtain a consistent determination of the structure of an unknown compound. The anticipated advantages of combining data from multiple sources have been confirmed.

(1) Haraki, K. S.; Venkataraghavan, R.; McLafferty, F. W. Anal. Chem. 1981, 53, 386-392.

Intelligent Tutoring Systems as Expert Systems

Robert Cunningham, Jamie Schultz, and Jeffrey Bonar

Intelligent Tutoring Systems
Learning Research and Development Center
University of Pittsburgh

At the Learning Research and Development Center (LRDC) we are developing intelligent tutoring systems as practical expressions of the principles of learning and teaching that are emerging from research on novice cognition. Our approach is to build on past AI experience with intelligent tutoring systems [Sleeman and Brown 82], but using our research to provide explicit objectives, diagnostic strategies, and guidance on instructional approaches. In this presentation we discuss our tutors as expert systems and present two example systems: *BRIDGE*, an intelligent tutor for computer programming and *SMITHTOWN*, an intelligent tutor for basic microeconomics.

Three Kinds of Expertise

In our intelligent tutors we draw on three kinds of expertise. *Domain expertise* characterizes the knowledge and strategies needed for expert performance in a domain. In the formal science and math domains we are using for our tutors, this knowledge consists of straightforward principles, definitions, and procedures.

Novice conceptions are the second kind of "expertise" in an intelligent tutor. These are the conceptions (often *mis*conceptions) used by novices when understanding and problem solving in a domain. There is considerable evidence that novices have detailed, systematic, and errorful conceptions of how a domain works [Resnick 83]. In order to effectively understand novice errors, the intelligent tutor must know about typical alternative novice conceptions.

Intelligent tutors must also use *teaching expertise*. This expertise captures how effective teachers actually instruct students in a domain. This knowledge may be a set of skill components, ordered in difficulty. In this case, the tutor selects more difficult problems by requiring the use of more difficult skill components. A different strategy involves representing the knowledge as concepts to be taught, ordered by conceptual dependence (see [Bonar, Cunningham, Schultz 86]). With such a conceptual approach, the tutor constructs problems by combining knowledge stored in several different domain concepts. More difficult problems are constructed from concepts with more dependencies. In either case, the teaching expertise must be used to assess a student's knowledge and construct the next problem on which a student is to be tutored.

SMITHTOWN: An Intelligent Tutor for Microeconomics

Smithtown is a simulation of an imaginary town where the student has control of certain economic variables. S-he observes the effect variable changes have on the overall picture of the town. By discovering variable relations the student is able to to discover underlying economic principles. To learn from Smithtown, the student must possess good scientific inquiry skills. To facilitate this we are constructing an unobtrusive intelligent coach that is concerned primarily with a student's preformance as a scientist. The coach examines the student's interrogation skills and provides feedback when detecting floundering behavior.

When the student sits down at the computer, s-he is introduced to the to the simulated town of Smithtown (see figure). The first menu contains the markets currently available in *Smithtown*. The student uses this menu to select a good or service to investigate Next, a menu of economic indicators relevant to the economics of *Smithtown* appears. These indicators include average income, population, weather, consumer preference index, and number of suppliers. After the student has or has not made changes to the indicators, s-he is presented with a 'Things to Do' menu. The student can see the effect of market manipulations on price, quantity demanded, quantity supplied, surplus, or shortage. Using this information the student may:

1. Adjust the market price or have the computer make a price adjustment,

2. Use the inquiry tools to assist in the investigation (e.g., make a notebook entry of the market data), or

3. Select an experimental framework.

The experimental frameworks let the student manipulate the market in various systematic ways and observe the effects.

BRIDGE: An Intelligent Tutor for Programming

Our research has uncovered two sorts of representations that are critical to modeling users learning about programming:

- informal schemas used by non-programmers to describe simple procedures and specifically repeated actions [Bonar86], and

- informal schemas used by expert programmers to capture the strategies and tactics implicit in a detailed procedural description

Using these two kinds of schemas, we have developed *Bridge*, an intelligent tutorial environment for elementary computer programming. Students use informal language to express possibly incomplete and incorrect ideas about how an algorithm should run. Our coach guides them in shaping their informal account into a formal plan using the expert schemas and then into an actual runnable program. Our trials with students show several benefits of this approach: the student need not understand all details of the problem and programming language before beginning, the coaching provided by the program is situated in the context of specific difficulties encountered by the student, and, by interacting with informal and formal planning languages, students learn important aspects of programming expertise.

References

[Bonar 86] Bonar, Jeffrey G.
Mental Models of Looping.
Technical Report, Learning Research and Development Center, University of Pittsburgh, 1986.

[Bonar, Cunningham, Schultz 86]
Bonar, Jeffrey G., Cunningham, Robert, and Schultz, Jamie.
An Object Oriented Architecture for Intelligent Tutoring.
In *Proceedings of the ACM Conference on Object Oriented Programming Systems, Languages, and Applications.* Association for Computing Machinery, September, 1986.

[Resnick 83] Resnick, Lauren B.
A New Conception of Mathematics and Science Learning.
Science 220:477-478, April, 1983.

[Sleeman and Brown 82]
Sleeman, Derek, and Brown, John Seely.
Intelligent Tutoring Systems.
Academic Press, London, 1982.

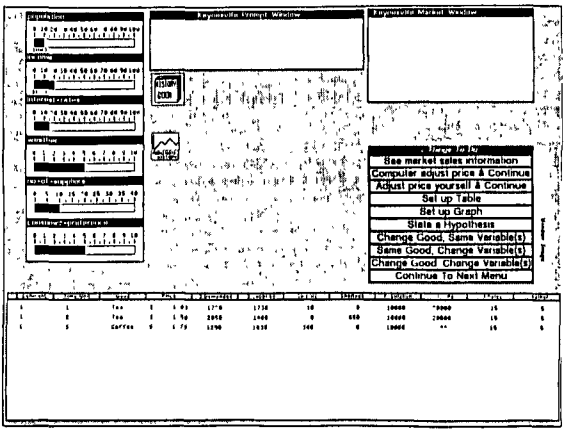
Hypothesis Market Window
Hypothesis Prompt Window
Do Next Step
Do Step
Do Step
Do

SIGMA,
A SYSTEM FOR INTERACTIVE GRAPHICS-ORIENTED MULTIVARIATE ANALYSIS

Willem Windig and Henk L.C. Meuzelaar
Biomaterials Profiling Center, University of Utah
Salt Lake City, Utah 84108

Application of modern chromatographic and spectrometric techniques often results in large amounts of data. In order to get a reliable insight into the structure of the data set, the use of multivariate data analysis methods is a prerequisite. Multivariate analysis techniques can be used for: (a) data reduction, (b) noise reduction, (c) integration of different data sets, and (d) chemical interpretation. The SIGMA program developed at the University of Utah Biomaterials Profiling Center, performs all these multivariate analysis tasks in an interactive, graphics-oriented manner (see Table I).

TABLE I
DESCRIPTION OF MAIN SIGMA OPTIONS

MAIN OPTIONS	DESCRIPTION
INPUT-OUTPUT	Reading, writing or adding files.
SET UP MATRIX	All changes in the data matrix, e.g., scaling, weighting, normalization, deletion of variables/objects.
UNIVAR STAT	Univariate statistics of variables, e.g., mean, variances, skewness, kurtosis, reproducibility and characteristicity.
OBJECT	Statistics on the objects (spectra) e.g., scatter and normalization fit values.
MULTIVARIA	Multivariate analysis techniques, e.g., factor analysis, discriminant analysis and multi-set canonical correlation analysis.
ROTATE	Graphical rotation, variance diagram (interactive, visually assisted oblique rotation method) and target rotation.
DISPLAY	Printing and plotting of results on screen or printer, in the form of bar ("spectra"), point, contour or polar plots.

(a) Data Reduction

If the number of variables is large, displaying differences by simple means such as 2- or 3-dimensional plots becomes impractical. Due to correlations between variables, it is generally possible to calculate independent linear combinations of the correlated variables, resulting in a considerable data reduction. This type of data reduction is accomplished by factor analysis. The limited number of independent variables ("factors"), makes it possible to display the data with a few plots of the intensities ("scores") of the factors.

(b) Noise Reduction

Discriminant analysis is a variation of factor analysis. Factor analysis describes the total variance in a data set as efficiently as possible, whereas discriminant analysis describes the ratio of the "between-group variance" and the "within-group variance" as efficiently as possible. The between-group variance is a measure for the differences between predefined groups of samples ("signal") and within-group variance measures the differences within the groups ("noise"). This generally results in an additional data reduction and an enhanced signal-to-noise ratio. Analogous with factor analysis, the intensities of the discriminant functions are called "discriminant scores".

(c) Integration of Different Data Sets

Determination of the common parts of different data sets, e.g. MS and IR data, by canonical correlation analysis often gives insights that cannot be obtained from the separate data sets. Furthermore, the unique parts of the data sets will show the relative merits of the techniques. The results of canonical correlation analysis have the same form as the results of the abovementioned techniques, namely linear combinations of the original variables and their scores for each of the data sets.

(d) Chemical Interpretation

The linear combinations of the variables, as defined by factor analysis (or the other techniques described above) show the cause of the differences displayed by the scores. A plot in the form of a bar graph is called a factor/discriminant spectrum. Since factors and discriminant functions are defined on mathematical grounds, a rotation generally is necessary in order to obtain meaningful factors, e.g. spectra of pure components from a data set of mixtures. SIGMA has unique interactive capabilities to locate and extract natural factors [1] (see Figure 1).

The SIGMA program has the following unique combination of capabilities when compared to other multivariate statistical packages such as ARTHUR, SPSS and BMDP: SIGMA (a) runs on a microcomputer; (b) is user-friendly; (c) is interactive; (d) is dedicated to spectral pattern recognition; and (e) can extract natural factors (e.g., chemical components from a mixture data set.

References:

1. W. Windig and H.L.C. Meuzelaar, Anal. Chem. 56 (1984) 2297-2303.

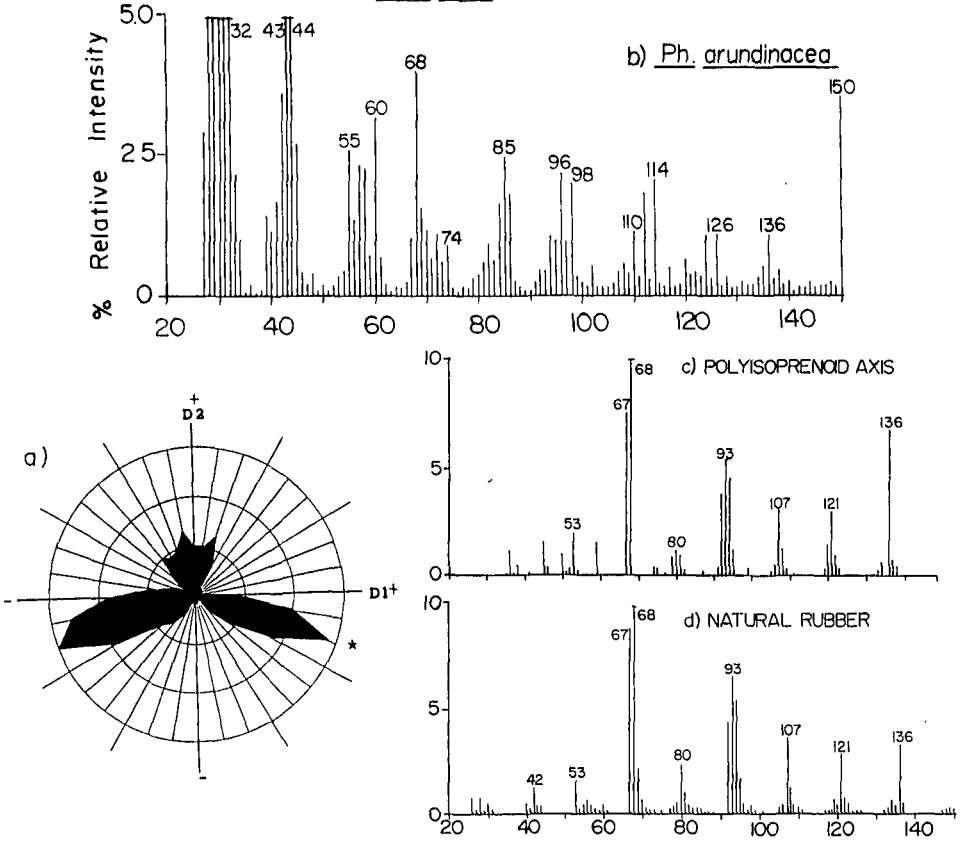

Figure 1. The Variance Diagram (VARDIA) plot (a) of the first two discriminant functions obtained on a "data set" of 8 different grass species (see (b) for one of the grass spectra). The maxima in the VARDIA indicate a correlated behavior of the mass variables. The mathematically extracted spectrum (c) of the maximum indicated by a * shows a clear polyisoprenoid pattern (as can be concluded after comparison with a model spectrum of natural rubber in (d).

ACCURATE MASS DETERMINATION OF MACROCYCLIC TRICHOTHECENE MYCOTOXINS USING A LC-MS INTERFACE AS AN AUTOMATED INLET: S. R. Missler[1] and P. H. Gibbs, U. S. Army Medical Research Institute of Infectious Diseases, Frederick, MD 21701; B. B. Jarvis, F. T. Cömezoğlu, and K. Wells, University of Maryland, College Park, MD 20742

A liquid chromatography-mass spectrometry interface of the moving belt design was used as an inlet for a high resolution mass spectrometer to facilitate acquisition of accurate mass information on a number of novel macrocyclic trichothecene mycotoxins. Accuracy and precision of the technique were verified using a model consisting of three experiments run at one week intervals, and comprised of 10 - 11 injections per experiment with 4 - 8 scans for each injection. Precision was determined by measuring the variances between:

1. experiments, EXP, which was a measure of reproducibility;

2. peaks within an experiment, PEAK (EXP), which was a measure of repeatability;

3. scans within a peak in an experiment, SCAN (PEAK, EXP), which was a measure of the determination error.

Figure 1 is a typical mass chromatogram of m/z 630 for Baccharanoid B12 diacetate, a macrocyclic trichothecene of known structure used to obtain accurate mass data for each of the three experiments. Note that peak widths were less than 30 seconds, enabling total acquisition within five minutes for ten injections.

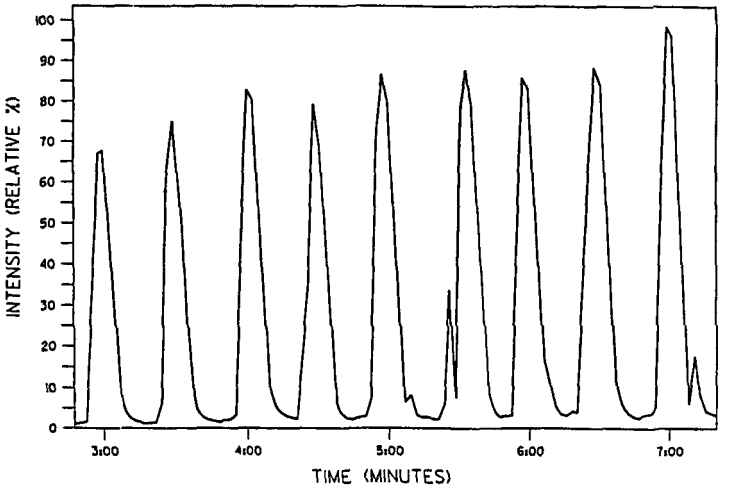

FIGURE 1

[1]Current address: Texaco Houston Research Center, 5901 S. Rice Avenue, Bellaire, Texas 77401.

Tables 1 and 2 summarize the statistical evaluation of mass determinations from this model. In the evaluation of accuracy from Table 1, data were shown to be normally distributed about 0 ppm error, with 95% (2 SD) of all variance for a single measurement falling within a ± 10 ppm window. From Table 2, 97% of this variance was shown to arise from determination error (scan to scan variance). Therefore, the repeatability and reproducibility of mass measurement inherent in the instrument was essentially unaffected by the presence of the interface.

TABLE 1

STATISTICAL EVALUATION OF MASS ANALYSIS

Experiment	n	Mean ppm	Standard Deviation ppm[2]	Accuracy[1] $p < 0.05$	Dispersion[2] $p < 0.05$
1	60	1.8	5.1	0.009	>0.15
2	54	0.2	6.0	0.79	<0.01
3	46	-0.1	2.6	0.84	0.40
Overall	160	0.7	5.0	0.068	>0.15

[1]Test of the accuracy of the mean using null hypothesis, mean ppm = 0, $p < 0.05$.

[2]Test of the dispersion about the mean using goodness of fit to normal distribution, $p < 0.05$.

TABLE 2

ESTIMATES OF COMPONENTS OF VARIANCE[1]

Factor	MM (Type 1)[2]	MIVQUE[3]	ML[4]	% of Total Variance[5]
EXP	0.74	0.76	0.25	2.78
PEAK (EXP)	-1.78	-1.52	0.00	-
SCAN (PEAK, EXP)	25.82	25.55	24.18	97.22

[1]Larger value for a factor is proportional to its contribution to variance.
[2]Method of moment (Type 1).
[3]Minimum Variance Quadratic Unbiased Estimators.
[4]Maximum Likelihood.
[5]Derived from MM (Type 1).

This technique was then applied to the analysis of 28 novel macrocyclic trichothecenes isolated in the laboratory of BBJ. While four compounds did not produce observable molecular ions, all other measurements were within ± 10 ppm of expected values and had standard deviations of less than 7 ppm[2]. Total acquisition time for this analysis was less than 16 minutes.

CHARACTERIZATION OF 6 TRICOTHECENE METABOLITES BY ELECTRON IMPACT, METHANE POSITIVE CHEMICAL IONIZATION AND NEGATIVE CHEMICAL IONIZATION AS THE TMS AND TFA DERIVATIVES

C. A. Haney,[1] W. M. Hagler, Jr.,[1] and S. P. Swanson[2]

1. North Carolina State University, Raleigh, NC 27695
2. University of Illinois, Urbana, IL 61801

Natural occurrence of tricothecene mycotoxins in feedstuffs and their effects on poultry and livestock consuming contaminated feedstuffs is well documented (1,2). Because the metabolism of tricothecenes is rapid, occurring in several organs and sites within cells via several enzyme reactions, the parent toxin halflife is short (3). Therefore, a thorough investigation of the analytical performance for the resulting metabolites is essential. The tricothecene metabolites investigated include de-epoxy HT-2, de-epoxy T-2, de-epoxy scirpentriol, de-epoxy deoxynivalenol, de-epoxy monoacetoxyscierpenol and 3'-hydroxy-T-2. Analysis of derivatized tricothecenes by GC/MS is rapid, sensitive and specific. However, both the derivative and the mode of ionization selected affect the sensitivity of the analysis.

Electron impact analysis of the TMS and TFA derivatives show similar sensitivities in standards. However, the predominant fragment ions are low mass making this technique unsuitable for MID screening of urine extracts.

All of the metabolites can be analyzed by positive chemical ionization as the TMS derivatives. The sensitivity in urine extracts is excellent (detection limits less than 1 ng MID). The spectra consist of small $[M+H]^+$ ions (1-10%) with many fragment ions. In general, the predominant fragment ions are characteristic of the toxin metabilites. De-epoxy scirpenetriol, de-epoxy DON and de-epoxy MAS are exceptions. The base peaks are under 250 amu with the more characteristic fragment ions of low abundance. MID screening for the metabolites in urine extracts show considerable background interferences in the mass channels (Figure 1).

The TFA derivatives are especially sensitive by negative chemical ionization. The spectra are simple, consisting of a large molecular ion and a few characteristic fragment ions making this a useful approach to MID screening. Additionally, the background noise in the higher mass channels is considerably reduced (Figure 2).

1. Vesonder, R. F. "Tricothecenes: Chemical, Biological and Toxicological Aspects." Y. Urno, editor, Vol. 4. Elsevier, NY, 1983.

2. Hsu, I. C., Smalley, E. B., Strong, F. M., Ribelin, W. E. Appl. Microbiol. 24 (1972 684.

3. Corley, R. A., Swanson, S. P. and Buck, W. B. J. Agric. Food Chem. 33 (1985 1085-1089.

TMS - Urine Extract 6ng/μl spike MID/PCI

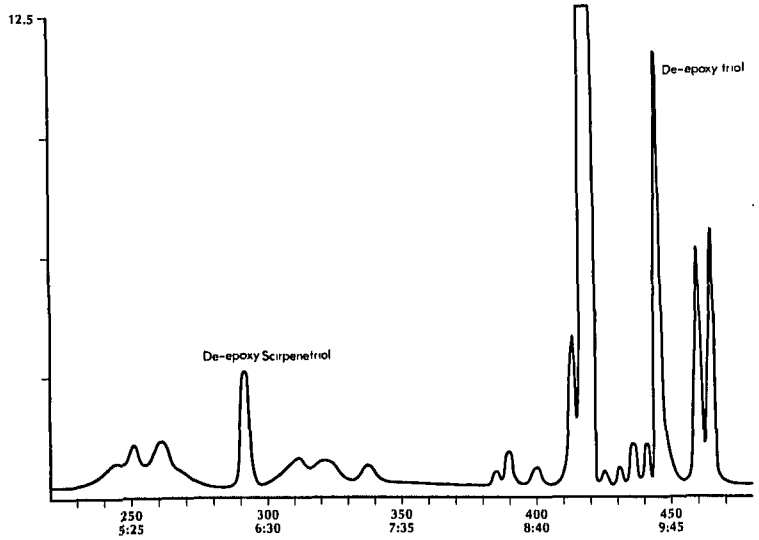

FIGURE 1: POSITIVE ION MID MASSES 467 AND 567

TFA - Urine Extract 6ng/μl spike MID/NCI

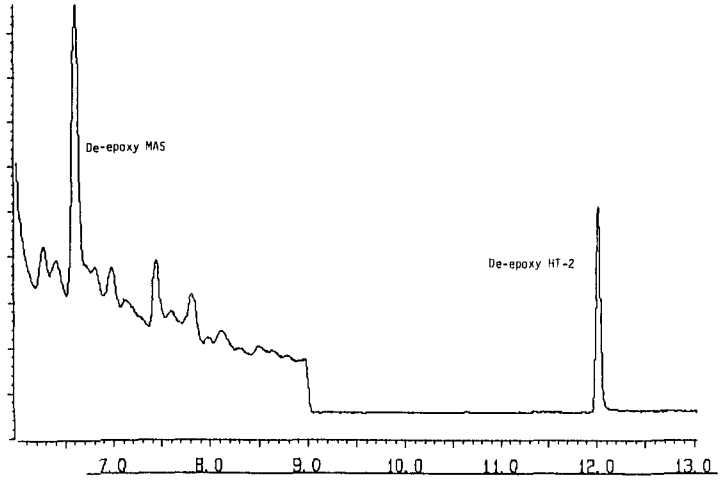

2: NEGATIVE ION MID MASSES 227 AND 600

ANALYSIS OF MYCOTOXINS IN BLOOD BY CAPILLARY COLUMN-AMMONIA CHEMICAL IONIZATION MASS SPECTROMETRY, Paul A. D'Agostino, Lionel R. Provost and David R. Drover, Defence Research Establishment Suffield, Ralston, Alberta, Canada, TOJ 2NO

Trichothecene mycotoxins, a group of naturally occurring sesquiterpenoid compounds, are of analytical interest due to their potential presence in agricultural products and their alleged use as chemical warfare agents in Southeast Asia. Monitoring requirements have resulted in the development of a number of analytical techniques for their detection. These methods include thin layer chromatography, high performance liquid chromatography (HPLC), supercritical fluid chromatography (SFC), gas chromatography (GC) and tandem mass spectrometry. Gas chromatography-mass spectrometry methods are often favoured due to the availability of instrumentation and the sensitivity and specificity of these methods. Most of the GC-MS methods utilize derivatization prior to analysis.

We report the development and evaluation of a capillary column GC-MS method for mycotoxins in human blood that does not require derivatization. Mass spectral determinations were performed under ammonia chemical ionization (CI) conditions, a technique recently reported for HPLC-MS (1, 2) and SFC-MS (3) analysis of mycotoxins. Abundant $(M+H)^+$ and/or $(M+NH_4)^+$ pseudo-molecular ions were observed under the conditions selected with considerably less fragmentation than was observed during electron-impact analysis. Sample detection limits of 0.7, 3.6 and 3.3 ng/g blood ($S/N \geq 3:1$) were estimated based on the selected-ion-monitoring (SIM) detection of two characteristic ions for T-2 toxin (T2), diacetoxyscirpenol (DAS) and HT-2 toxin (HT2) respectively.

Capillary column GC-MS analyses were performed on a VG Micromass 70/70E mass spectrometer equipped with a Varian 3700 gas chromatograph under the following conditions: (GC Column: 15 m x 0.32 mm ID J+W DB-5, Temperature Program: 50°(2 min) 10°/min 300°C (8 min), Injection Mode: Cold on-column at 50°C, Source Pressure: 5 x 10^{-6} Torr NH_3; Source Temperature: 160°C, Emission Current: 500 µA; Electron Energy: 50 eV). $(M+NH_4)^+$ and $(M+1+NH_4)^+$ ions were monitored for T2, HT2 and DAS during accelerating voltage stepping SIM analysis of blood extracts. $(M+H)^+$ and $(M+1+H)^+$ ions were monitored for T-2 triol (T2T), $(M+H)^+$ and $(M+H-H_2O)^+$ for verrucarol (VER) and, $(M+H)^+$ and $(M+NH_4)^+$ for deoxynivalenol (DON).

Blank blood and a set of blood samples spiked with a number of mycotoxins in the 0-500 ng/g range were received from the Centre for Disease Control (Atlanta, GA) as part of an interlaboratory exercise. All blood was stabilized with heparin and 0.5% sodium fluoride prior to delivery and stored at 4°C prior to analysis. Black and Read's clean-up scheme (4), illustrated in Figure 1, was used for all blood samples.

Figures 2 and 3 illustrate typical ammonia CI mass spectra for the six mycotoxins under study. Abundant $(M+H)^+$ and/or $(M+NH_4)^+$ pseudo-molecular ions were observed for all mycotoxins during capillary column GC-MS analysis. Selected-ion-monitoring traces for the determination of T2, HT2 and DAS in human blood are illustrated in Figures 4 to 6 respectively.

This method was recently compared to two methods which utilize heptafluorobutryl and pentalfluoropropionyl derivatives. The results of this laboratory were good and all laboratories were in agreement as to the relative amounts of T2 and DAS in the set of spiked blood samples. No false positive were reported.

References

1. R.D. Voyksner, W.M. Hagler Jr., K. Tyczkowska and C.A. Haney, JHRC + CC, 8 (1985) 119.
2. S.R. Missler, 33rd ASMS, San Diego, CA, May 26-31 1985, pp. 659-660.
3. R.D. Smith, H.R. Udseth and B.W. Wright, J. Chromatogr. Sci., 23 (1985) 192.
4. R.M. Black, R.W. Read, P. Begley, B.E. Foulger and P.D. Jeffery, "The Detection of Trace Levels of Trichothecene Mycotoxins in Blood (U)", CDE, Porton Down, UK, Technical Paper No. 397, March 1985, UNCLASSIFIED.

5 mL Blood + 10 mL Acetone (vigorously shaken)

↓

Centrifuge and Decant Aqueous/Acetone Layer

↓

Concentrate and Load onto C_{18} Sep-Pak

↓

Rinse with 2 mL H_2O (discard)

↓

Elute with 2 mL 40:60 $MeOH/H_2O$

↓

Further Elute with 3 mL 90:10 $MeOH/H_2O$

↓

Add 2.4 mL H_2O and Extract with 2 × 5 mL CH_2Cl_2

↓

Dry Through 2 g Na_2SO_4

↓

Concentrate to Dryness

↓

Dissolve in 100 μL Acetone Prior to GC-MS Analysis

Fig 1

BLOOD CLEAN-UP SCHEME

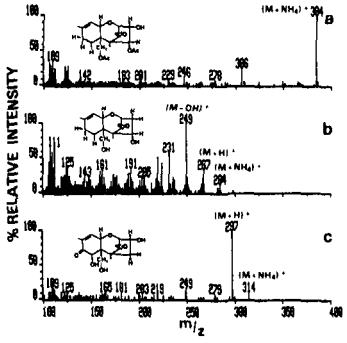

Fig 2

AMMONIA CI MASS SPECTRA OF a) DAS, b) VER AND c) DON OBTAINED DURING GC-MS ANALYSIS

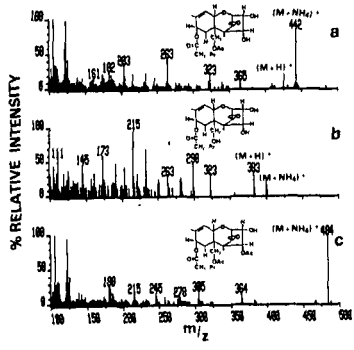

Fig 3

AMMONIA CI MASS SPECTRA OF a) HT2, b) T2T AND c) T2 OBTAINED DURING GC-MS ANALYSIS

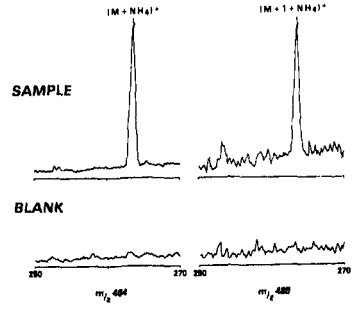

Fig 4

T2 IN BLOOD EXTRACT AT 2.2 ng/g AND CORRESPONDING BLANK

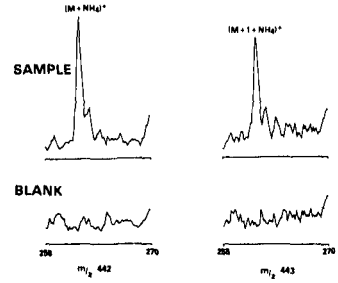

Fig 5

HT2 IN BLOOD EXTRACT AT 4.5 ng/g AND CORRESPONDING BLANK

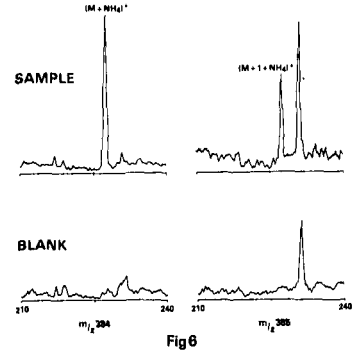

Fig 6

DAS IN BLOOD EXTRACT AT 9.9 ng/g AND CORRESPONDING BLANK

THERMOSPRAY LC/MS ANALYSIS OF MYCOTOXINS AS A FUNCTION OF ELECTROLYTE CONCENTRATION AND MODE OF IONIZATION

Eero Rajakyla, Finnish Sugar CO., Kantvik ,Findland;
Katri Laasasenaho, University of Helsinki, Helsinki, Findland;
Peter Sakkers, Hewlett-Packard Nederland BV, Amstelveen, Netherlands;
and Denis Foerst, Hewlett Packard SID, Palo Alto, California, 94303

The mycotoxins Deoxynivalenol (DON), Patulin, Diacetoxyscirpenol (DAS), HT-2 Toxin, T-2 Toxin, Zearalenone, and Ochratoxin A were subjected to a series of LC/MS Thermospray experiments in order to find a set of optimum conditions for analysis of these mycotoxins in food.

When ammonium acetate buffers (0.005 Molar) are used during the Thermospray introduction of HPLC effluents into a mass spectrometer, ions are formed by processes that are not fully understood. This filament off mode of ionization has termed rapid ion formation. This ionization process is extremely soft; most of the time, ions are formed only in the region of the molecular ion. Adduct ions with ammonia and organic solvent are frequently observed. When the buffer concentration was changed to 0.001 Molar there was a significant change in the mass spectra of three of these mycotoxins. Deoxynivalenol (DON) contains the parent molecular structure of the homologous series DON, DAS, HT-2 Toxin, and T-2 Toxin. The last three members of the group differ from DON in that free hydroxyl groups of the parent compound are esterified with acetic acid, or that a keto group has been reduced and esterified with 2-methylbutanoic acid. Figures 1 and 2 give the mass spectra of these four mycotoxins. In all cases, when ester groups are present, the mass spectra obtained at 0.001 Molar ammonium acetate exhibit a large degree of fragmentation when compared to 0.005 Molar buffer. The mass spectra in Figures 1 and 2 were obtained using the filament on mode of ionization. Clearly, at 0.001 Molar ammonium acetate, the ionization process is harder than at a 0.005 Molar concentration. Quantitative analysis is favored at the lower buffer concentration because structure interpretation is possible due to the wealth of fragmentation ions.

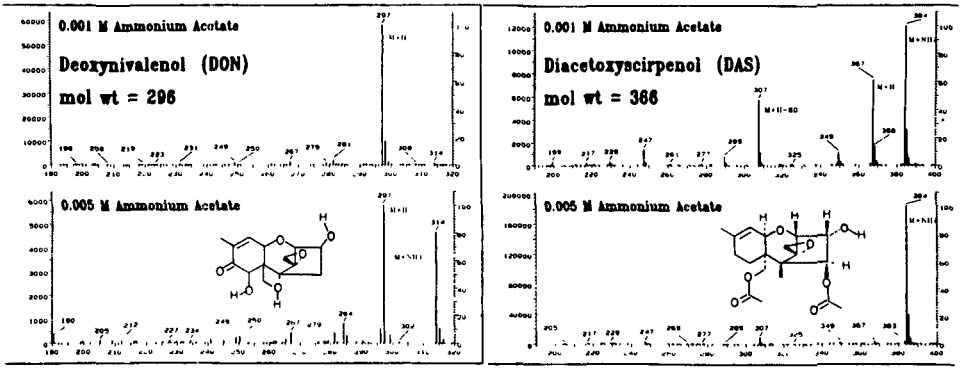

FIGURE 1. Thermospray Mass Spectra of DON and DAS

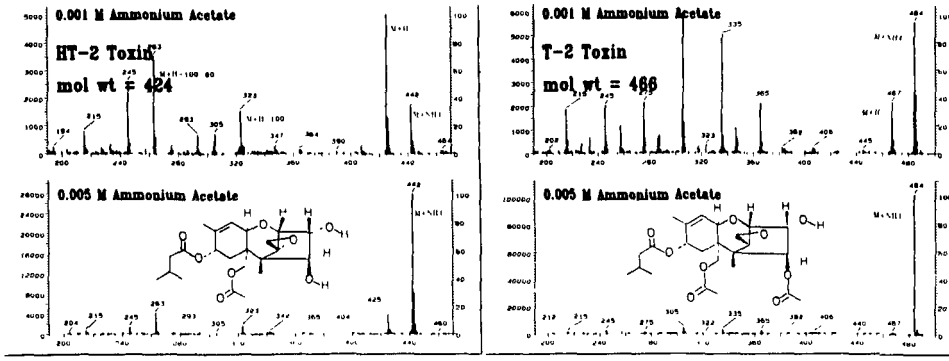

FIGURE 2. Thermospray Mass Spectra of HT-2 and T-2 Toxin

Sensitivity improves for these same three mycotoxins when the buffer is present at 0.005 M. The sensitivity for DON drops when the buffer concentration is raised.

The remaining three mycotoxins (Patulin, Ochratoxin A, and Zearalenone show little fragentation at either buffer concentrations which were studied. The raw abundance for the base peak of Patulin decreased when the buffer concentration was raised, but increased for Ochratoxin A and Zearalenone. Changing the buffer concentration showed an effect on the chromatography of Ochratoxin A and Zearalenone. Their elution order reversed when the buffer concentration was changed. Quantitative analysis is favored at a higher electrolyte concentration with electron assisted ionization conditions.

When the electron assisted mode of ionization (filament on) was compared to the filament off mode, the filament on mode was more sensitive by a factor of five.

Patulin exhibited the poorest sensitivity of these seven mycotoxins. The compound's molecular weight is such that the solvent ions masked the presence of the analyte when 3 ng were injected into the LC/MS system. T-2 Toxin exhibited the best sensitivity for Thermospray LC/MS analysis. The signal-to-noise ratio in excess of 400 for the ion at m/z 484 when 3 ng was injected and the mass spectrometer was operated in the selected ion monitoring mode.

EXPERIMENTAL The LC was an HP 1090A and the MS was an HP 5988A equipped with an HP Thermospray interface. The mass spectrometer was tuned and optimized using a 25 ug/mL solution of polypropylene glycol. A Resolution ODS (150 x 4.6 mm ID) column packed with VYDAC 201 HSB (5 microns) was used for all chromatography. Gradient elution was used; 8 minute linear gradient from 40% to 70% acetonitrile. The aqueous phase was adjusted to a pH of 3 using acetic acid and buffered with 0.001 or 0.005 M ammonium acetate.

METABOLISM OF PROPYL HOMOLOGUES OF THE TETRAHYDROCANNABINOLS STUDIED BY GC/MS

D.J. Harvey and N.K. Brown

University Department of Pharmacology, South Parks Road, Oxford, OX1 3QT, UK.

The psychoactivity of marihuana and related drugs obtained from Cannabis sativa is associated with compounds known as cannabinoids and, in particular with delta-9-tetrahydrocannabinol (delta-9-THC, Ia). Major cannabinoids contain a pentyl side-chain but also present are lower homologues, particularly those with propyl chains, whose relative abundance in some samples can approach that of the pentyl compounds. No study appears to have been reported on their metabolism even though they contribute to the drug's pharmacological profile. This paper reports a study of the metabolism of propyl-delta-9-THC (Ib) and the related propyl-delta-8-THC (IIb)

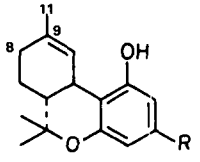

I

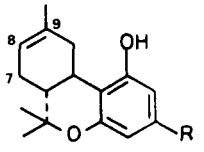

II

a, R = C_5H_{11}

b, R = C_3H_7

The propyl homologue of delta-8-THC and its 3-deuterio-analogue was synthesized by condensation of 1,3-dihydroxy-5-propyl benzene with (1S)-(-)-verbinol and (1S)-(-)-[^{2}H]-verbenol respectively (1). The corresponding delta-9-isomers were synthesised from these compounds by chlorination and dehydrochlorination (2). For the metabolite study, these compounds were administered IP to male Charles River CD-1 mice and metabolism was allowed to proceed for 1 hour before the animals were killed. Hepatic metabolites were extracted with ethyl acetate, isolated by chromatography on Sephadex LH-20 (3) and converted into TMS, perdeuterio-TMS, methyl ester/TMS and methyl oxime/TMS derivatives for examination by GC/MS. Metabolic samples were also reduced with lithium aluminium deuteride to correlate structures of oxidized metabolites with those of the hydroxylated analogues. GC/MS data were recorded with a VG Micromass 12B mass spectrometer interfaced to a VG 2050 data system and via a glass jet separator to a Varian 2440 gas chromatograph which was fitted with a 2 m x 2 mm glass column packed with 3% SE-30 on 100 - 120 mesh Gas Chrom Q.

Delta-9-THC

Six metabolites were identified from this compound, all were products of hydroxylation and four were oxidized further to carboxylic acids. These are listed in Table 1 together with the major ions in the mass spectra of their TMS derivatives.

TABLE 1

Metabolites of propyl-delta-9-THC identified in mouse liver

Metabolite	Major ions in the mass spectrum of the TMS derivative.					Metabolite abundance[a]
	M^+	$[M - 15]^+$	Base	Other ions		
11-OH	446[b]	431	343			5
	(7)	(5)				
11-COOH	460	445	343	275		100
	(40)	(37)		(1)		
8-alpha,11-di-OH	534	-	444			5
	(12)					
2'-OH,11-COOH	548	433	117	504	431	30
	(41)	(48)		(25)	(34)	
8-alpha-OH,11-COOH	548	533	458	443		20
	(2)	(5)		(12)		
2',8-alpha-di-OH,11-COOH	636	621	117	546	502	15
	-	(4)		(14)	(3)	

a = Abundance relative to the major metabolite.
b = m/z and (relative abundance)

Identification of the metabolites was based on the mass spectra of the various group-specific derivatives and by comparison with the mass spectra of TMS derivatives of the corresponding metabolites of delta-9-THC (4). Administration of the deuterated analogues to mice and comparison of the mass spectra of the extracted products with those of the non-deuterated compounds enabled those GLC peaks produced by metabolites to be identified. Thus, the 11-hydroxy and acid metabolites were characterized by base peaks formed by elimination of the 11-substituent, metabolites containing an 8-alpha-hydroxy group were characterized by abundant losses of trimethylsilanol and the presence of hydroxylation in the 2'-position (side-chain) gave rise to the base peak at m/z 117. In addition, the presence of 2'-hydroxylation produced a weaker ion representing loss of butanone (m/z 504 and 502 respectively in the spectra of the 2'-mono- and 2',8-alpha-di-hydroxy derivatives of propyl-delta-9-THC-11-oic acid).

Delta-8-THC

Five metabolites were identified from this cannabinoid as listed in Table 2.

TABLE 2

Metabolites of propyl-delta-8-THC identified in mouse liver

Metabolite	Major ions in the mass spectrum of the TMS derivative.					Metabolite abundance
	M^+	$[M - 15]^+$	Base	Other ions		
11-COOH	460	445	460	275	290	100
	(100)	(19)		(57)	(15)	
2'-OH,11-COOH	548	533	117	502		20
	(44)	(20)		(25)		
7-alpha-OH,11-COOH	548	533	443	275	458	60
	(30)	(22)		(43)	(86)	
7-beta-OH,11-COOH	548	533	548	275	458	35
	(100)	(21)		(96)	(13)	
7-alpha,11-di-OH	534	519	341	429	444	30
	(7)	(3)		(49)	(15)	

Identification of propyl-delta-8-THC-11-oic acid and 7-alpha,11-dihydroxy-propyl-delta-8-THC was based on the similarity of their mass spectra with those of the corresponding pentyl homologues where synthetic standards were available. The 7-alpha- and 7-beta-hydroxy-derivatives of propyl-delta-8-THC-11-oic acid were again identified by spectral similarities with the pentyl homologues, this time from material obtained by metabolism of 7-alpha- and 7-beta-delta-8-THC by the mouse. The spectra of the hydroxy acids showed marked similarities with those of the corresponding C_5 compounds, particularly in the abundance of the molecular ion which was much higher in the spectrum of the beta (equatorial) isomer. In contrast, the relative abundance of the $[M - TMSOH]^+$ ion (m/z 458) was much lower (13%) in the spectrum of this isomer.

Routes of metabolism shown by these two cannabinoids were thus similar to those observed for the pentyl homologues but with differences in the relative abundances of certain metabolites. Hydroxylation at C-11 and oxidation to the corresponding carboxylic acid was the major metabolic transformation. Further hydroxylation led to hydroxylated analogues of both the 11-hydroxy- and 11-acid metabolites. A greater proportion of the metabolites of these propyl homologues appeared as acids than was seen with the pentyl homologues. This was particularly marked by the relatively low concentration of the 11-monohydroxy THC's and the absence of any other monohydroxy metabolite; delta-9-THC itself is metabolised to 8-alpha-hydroxy-delta-9-THC in equivalent concentration to the 11-hydroxy metabolite. This is thought to reflect the lower lipophilicity of the propyl homologues which reduces the availability of the drugs to the membrane-bound cytochrome P-450 oxidases and increases the amount of oxidation by cytosolic enzymes such as alcohol dehydrogenase.

This work was supported by the Wellcome Trust and NIDA.

1. R. Mechoulam, P. Braun and Y. Gaoni, J. Am. Chem. Soc., 1972, 94, 6159.
2. T. Petrzilka, W. Haefliger and C. Sikemeier, Helv. Chim. Acta, 1969, 52, 1102.
3. D.J. Harvey, B.R. Martin and W.D.M. Paton, J. Pharm. Pharmacol., 1977, 29, 482.
4. D.J. Harvey, Biomed. Mass Spectrom., 1981, 8, 579.

ANALYSIS OF DERIVATIZED METABOLITES OF POLYNUCLEAR AROMATIC HYDROCARBONS BY GC AND GC/MS

E. K. Chess, B. L. Thomas, D. L. Springer, D. B. Mann, D. J. Hendren and R. M. Bean

Biology and Chemistry Department, Pacific Northwest Laboratory, Richland, WA 99352

A number of recent scientific studies have correlated the carcinogenic potential of certain organic compounds with the ability of their metabolites to form chemical bonds with deoxyribonucleic acids (DNA)[1,2,3]. The correlations are strong enough to suggest that analysis of DNA for bound metabolites can provide an estimate of individual exposure to carcinogens[4,5]. Although some methods have very recently evolved for determining total DNA binding[6,7], methods are not readily available for the identification of the bound organic compounds because of the very low concentrations involved. Concentrations of adducted compounds in environmentally-exposed tissues are typically on the order of one adduct per 10^6 to 10^7 DNA bases (about 0.1 to 1 nanograms per milligram of DNA). We are currently developing methodologies that will allow analysis of the metabolites after hydrolysis from the DNA by gas chromatography (GC) and GC/mass spectrometry (GC/MS). The objective of the research is to develop methods for the dosimetric analysis of DNA-adducts that will permit identification and quantification of the adducted species, permitting estimates of exposure to individual carcinogenic compounds.

The analytical methodolgy will consist of several steps: isolation of DNA from target cells (initially mouse skin), acid hydrolysis of the DNA to cleave the bound metabolites[8], and isolation, derivatization, and quantification by GC/MS of the released metabolites. Initial development work has focused on methods for analyzing the well-characterized metabolites of benzo(a)pyrene, B[a]P, a potent mammalian carcinogen. These metabolites, 3-hydroxy-, 7,8-dihydro-7,8-dihydroxy-, 7,8,9, 10-tetrahydro-7,8,9-trihydroxy-, and 7,8,9,10-tetrahydro-7,8,9,10-tetrahydroxy-B[a]P, are relatively light and heat sensitive, and require derivatization of the polar hydroxyl groups prior to analysis by GC. Several types of derivatives (permethyl, peracetyl, and trifluoroacetyl) for each metabolite have been prepared and are being tested to determine which type of derivative will offer the best performance in terms of stability and sensitivity for the analysis of trace levels of metabolites isolated from biological systems. Electron impact (EI), methane chemical ionization (CI), and electron capture negative ion chemical ionization (NICI) are being evaluated to determine which mode of ionization offers the best overall sensitivity and selectivity.

Permethylated derivatives were prepared using the method of Hakamori[9] and were analyzed by GC and GC/MS using relatively short (<10 m) fused silica capillary columns (SE-54 and DB-5, J&W Scientific) at temperatures <280 °C. All derivatives were found to chromatograph very well, with no tailing or evidence of thermal decomposition using splitless injection. Molecular ions were found for all modes of ionization, but the CI spectra generally contained more extensive fragmentation than did the EI spectra. The EI mass spectra provided the most diagnostic fragmentation information related to the structure of the ion. For example, the prominent molecular ion (m/z 376) of the permethylated tetrahydrotetrol (Figure 1) undergoes a retro-Diels Alder reaction, expelling a molecule of 1,2-dimethoxyethene containing C-8 and C-9 from the B[a]P ring structure, resulting in the fragment ion at m/z 288. This ion then loses a methyl radical, primarily originating from the methoxy group attached to C-10 (B[a]P numbering system), to produce the base peak fragment ion at m/z 273. This fragmentation pathway has been confirmed by deuterium labeling experiments.

The peracetate and trifluoroacetate derivatives were successfully prepared using standard derivatization procedures with acetic anhydride[10] or MSTFA[11], respectively, for all metabolites except the 7,8-dihydrodiol, which appeared to either dehydrate under the reaction conditions or decompose during analysis, resulting in chromatograms which contained peaks for both a derivatized and underivatized mono-hydroxy-B[a]P. Some peracetate and trifluoroacetate derivatives appeared to undergo thermal decomposition during GC and GC/MS analysis using conventional splitless injection. On-column injection has been shown to improve the analysis both qualitatively and quantitavely by reducing both injector discrimination and thermal decomposition. As anticipated, the peracetate derivatives all display retention times which are several minutes longer than their permethyl analogs, indicating a comparative decrease in volatility. The EI mass spectra of the acetates display the diagnostic loss of acetic acid for acetates attached to a partially hydrogenated aromatic ring, and the loss of ketene for acetates attached to a fully aromatic ring. CI and NICI mass spectra of the tetrahydrotetrol acetate and perfluoroacetate display very weak molecular ions and strong peaks for fully aromatic fragment species.

Initial experiments to determine the detection limits of the derivatized metabolites indicated that <0.6 pg of permethylated and ~0.05 pg of the peracetylated tetrahydrotetrol could be detected during single ion monitoring (SIM) GC/MS analyses using a mass selective detector (Hewlett-Packard). These levels of sensitivity are sufficient to detect the amounts of DNA-bound metabolites isolated from laboratory animals exposed to relatively high levels of carcinogens, and may be sufficient to detect the hydrolyzed metabolites at levels that can be isolated from environmentally-exposed systems. Approximately 1 mg of DNA isolated from 2 mg of mouse skin which had been treated with ^{3}H-labelled B[a]P was subjected to acid hydrolysis, and the released B[a]P-tetrols derivatized by permethylation. GC/MS analysis (multiple ion monitoring @ m/z 273, 288, 376) accounted for 620 pg of B[a]P-tetrol, or approximatedly 13% of the radiolabel in the DNA before acid hydrolysis. This number has not been corrected for estimates of losses from extractions, derivatization, or transfers.

Results from the initial methodology development stages of this assay indicate to us that GC/MS analysis can provide the specificity required for the quantitative determination of derivatized B[a]P-tetrahydrotetrol isolated from DNA adducts, and that SIM privides the sensitivity expected to be sufficient for the quantification of DNA-adducted PAH metabolites that have been formed as a result of environmental exposure to PAH.

This work has been supported by the Department of Energy Office of Health and Environmental Research under contract # DE-AC06-76RLO 1830.

Literature Cited.

1. Brookes, P., and P. D. Lawley. **1964.** *Nature* **202**:781-4.
2. De Serres, F. J., B. L. Gledhill, and W. Sheridan, Eds. **1985.** *Environ. Health Perspec.* **62**:3-231.
3. Sims, P., P. L. Grover, S. Swaisland, and A. Hewer. **1974.** *Nature* **252**: 326-27.
4. Wogan, G. N., and N. J. Gorelick. **1985.** *Environ. Health Perspec.* **62**:5-18.
5. Shugart, L. **1985.** *J. Toxicol. Environ. Health* **15**: 255-63.
6. Gupta, R. C., M. Vijayara, J. Reddy, and K. Randerath. **1982.** *Carcinogenesis* :1081-92.
7. Santella, R. M., L.-L. Hsieh, C.-D. Lin, S. Viet, and I. B. Weinstein. **1985.** *Environ. Health Perspec.* **62**:95-99.
8. Rahn, R. O., S. S. Chang, J. M. Holland, and L. R. Schugart. **1982.** *Biochem. Biophys. Res. Commun.* **109**: 262-68.
9. Hakamori, S. **1964.** *J. Biochem. (Tokyo)* **55**:205-8.
10. Knapp, D. R. **1979.** Handbook of Analytical Derivatization Reactions, John Wiley and Sons, New York, NY. pp. 30-33.
11. Sullivan, J., and L. Schewe. **1977.** *J. Chromatogr. Science* **15**: 196-7.

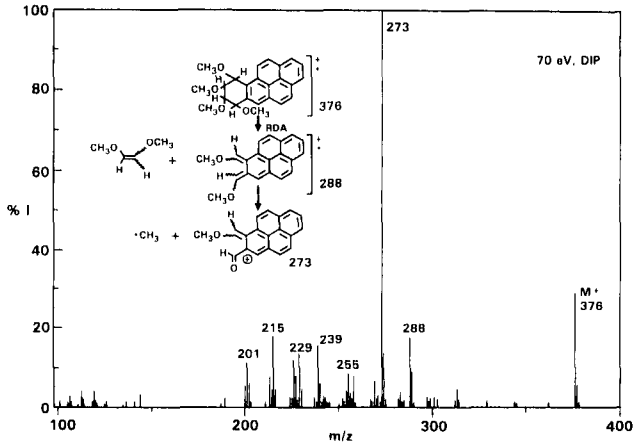

FIGURE 1. 70eV Mass Spectrum of the Permethyl Derivative of B[a]P-Tetrahydrotetrol.

STRUCTURAL CHARACTERIZATION OF DNA ADDUCTS BY MASS SPECTROMETRY

Andrea M. Dietrich, J. Ronald Hass, Christian R. Guenat*

University of North Carolina, Chapel Hill, NC 27514
* NIEHS, P.O. Box 12233, Research Triangle Park, NC 27709

Formation of DNA adducts, or the covalent bonding of foreign chemicals to the DNA bases, is thought to be a critical early step in chemical carcinogenesis. Standard methods for in vitro production and detection of DNA adducts include reacting DNA with a specific chemical, followed by degradation of the DNA to free nucleotides or nucleosides. Presence or absence of modified bases is determined from chromatographic elution data with detection by UV, fluorescence, scintillation counting or autoradiography. These methods yield little information on the actual structure of the adduct, if present. Mass spectrometry is a desirable analytical method for providing structural information concerning the modified bases.

In this research mass spectrometry was utilized to characterize the nucleoside adducts 1,N^6-ethenodeoxyadenosine (formed from the reaction of DNA with vinyl chloride) and 7-methyldeoxyguanosine (formed from reaction of DNA with methylmethanesulfonate or dimethyl sulfate) (Singer and Grunberger, 1983). Standard chemicals were purchased from Sigma. EI analyses were performed with a VG-7070F, and FAB analyses with a VG-ZAB-4F equipped with an Ion Tech FAB source using xenon gas at 8kV.

Direct probe positive ion EI at 70 and 15 eV analyses of the modified and unmodified nucleosides produced ions principally characteristic of the free base and sugar moieties with transient or absent molecular ions. This required rapid heating to 350-400°C, and as expected, thermal degradation resulted, particularly with guanosines. To increase sample volatility for direct probe EI and GC/MS analyses, the traditional approach of forming trimethylsilyl (TMS) ethers with BSTFA in pyridine was applied (McCloskey, 1974). This technique produced characteristic cations at $[M]^{+\cdot}$, $[M-15]^+$, $[B+H]^{+\cdot}$, $[B+2H]^+$, $[B+H+TMS]^+$, (B is defined as the fragment ion for the base). This method has the advantage of indicating the number of derivatizable groups on the nucleoside or base; this information can be utilized to determine if reactive amino, hydroxyl or enolizable carbonyl functional groups have been blocked. In the case of 1,N^6-ethenodeoxyadenosine, the 6-amino group can no longer derivatize after modification by vinyl chloride (Figure 1), so that the $[B+H+TMS]^+$ ion present in deoxyadenosine is only $[B+H]^{+\cdot}$ in 1,N^6-ethenodeoxyadenosine.

Positive ion FAB, with thioglycerol and glycerol plus oxalic acid as matrices, produced characteristic ions at $[B+H]^+$, $[M+H]^+$, $[2M+H]^+$, and either $[M+Glycerol+H]^+$ or $[M+Thioglycerol+H]^+$, depending upon the matrix, for both modified and unmodified deoxyadenosine and deoxyguanosine (Figure 2). $[M+H]^+$ was the base peak, and $[B+2H]^+$ was 50% intensity. Thioglycerol proved to provide better ion intensities than glycerol plus oxalic acid. The detection limit for deoxyguanosine alone was about 600 ng on the probe tip.

Deoxyguanosine was reacted with the 1,2 oxide of benz(j)aceanthrylene, and the reaction mixture analyzed by HPLC/UV/Fluorescence to determine the presence of modified adducts. HPLC fractions indicative of PAH modified deoxyguanosine were analyzed by FAB-MS. Unfortunately, the amount of sample present was likely below the detection limit, and no ions indicative of the parent or modified nucleoside, parent or modified base were detected. Additionally, the HPLC fraction contained various anions, cations and other species which dominated the FAB spectrum.

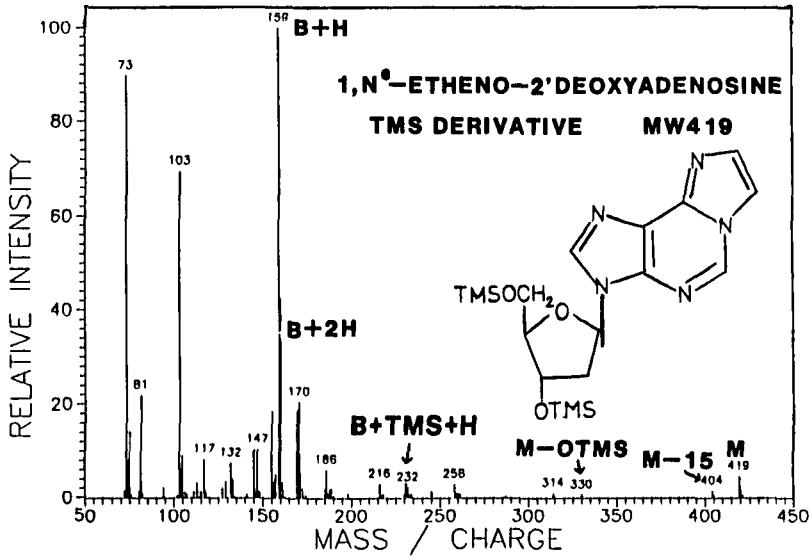

Figure 1: Electron ionization spectrum (70 eV) of 1,N^6-etheno-2'deoxyadenosine.

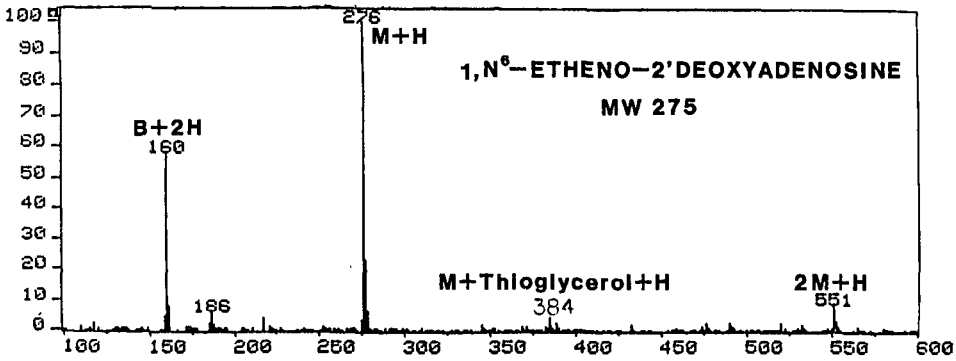

Figure 2: FAB spectrum in thioglycerol matrix for 1,N^6-etheno-2'deoxyadenosine

1) **Singer, B.**, D. Grunberger; Molecular Biology of Mutagens and Carcinogens; Plenum Press, NY; 1984.

2) McCloskey, J.A.; "Mass Spectrometry" in Basic Principles in Nucleic Acid Chemistry; P.O.P. Ts'o (ed.); Academic Press, NY; pp.209-309, 1974.

TANDEM MASS SPECTRAL STUDIES OF OLIGONUCLEOTIDES

John J. Dino, Jr.[1,2], Christian R. Guenat[1], Simon J. Gaskell[1], and David G. Kaufman[2]

1. National Institute of Environmental Health Sciences, RTP, NC 27709
2. Department of Pathology, University of North Carolina, Chapel Hill, NC 27514

Mass spectral studies were performed on oligonucleotides possessing a variety of chain lenghts and base compositions. This work is part of a study to isolate and identify previously uncharacterized polar products of interactions between benzo[a]pyrene (BP) metabolites and DNA. Previous investigations have indicated that these products may consist of oligonucleo tides of indeterminate lengths modified with metabolites of BP. As a prelude to the above-mentioned study, the current work examines mass spectral behavior of unmodified oligonucleotides. This is believed to be a logical first step in the examination of modified material.

Initial studies examined oligonucleotides in double-focusing or MS/MS modes with positive ion FAB analysis on a VG ZAB 4F mass spectrometer with BEEB configuration. Using glycerol/oxalic acid as matrix, oligonucleotides gave protonated molecular ions: 5' TTC 3' (m/z 836), 5' AGCT 3' (m/z 1174), 5' TCTAGA 3' (m/z 1791). [M+H+Na]+ ions were low or non-existent. Little usable fragmentation occurred from [M+H]+ or [M+H+Na]+ ions.

Collisionally activated dissociation (CAD) experiments were performed on protonated molecular ions using the collision cell between MS1 and MS2 (in the third field-free region). Glycerol/oxalic acid was used as matrix. The collision gas was helium at a pressure which gave approximately 50% attenuation of the parent ion beam. Fragment ions of 5' AGCT 3' included m/z 950 (loss of dT), m/z 940 (loss of dA), m/z 661 (loss of CpT) and m/z 611 (loss of ApG). Fragment ions of 5' TTC 3' included m/z 612 (loss of dT) and m/z 529 (loss of dCMP).

With dithiothreitol/dithioerythritol (5:1) as matrix, oligonucleotides gave clusters with sodium, whose sizes corresponded to the number of phosphate groups. This is a diagnostic tool since it gives the oligonucleotide chain length. When combined with the molecular weight, this allows predictions of base compositions.

A major concern of this work is the small amounts of carcinogen modified material produced by in vitro and in vivo systems. To that end, experiments were done to optimize the glycerol/oxalic acid matrix using 5' TTC 3' as test compound. Judgement criteria were the signal-to-noise ratio of [M+H]+ and the ratio of [M+H]+ to [M+H+Na]+ (where present). It was found that these ratios could be optimized by adding .04 g aliquots of oxalic acid to .25 ml glycerol. The optimum mixture was .12 g oxalic acid in .25 ml glycerol.

The optimized matrix was then used to determine a practical lower detec tion limit, using 5' AGCT 3' as test compound. 25, 12.5 and 6.25 μg were applied to the probe. Positive ion FAB analysis was used. The lower limit was between 6.25 and 12 μg of 5' AGCT 3'. When 6.25 μg 5' AGCT 3' were applied in dithiothreitol/dithioerythritol (5:1), an intense sodium ion cluster (maximum S/N=10:1) was observed, indicating that even less material might be needed with this matrix.

Mass Spectrometric Characterization of Amino- and Nitro-Substituted MPTP Analogues as Studied by GC/MS and FTMS

A. Weisz, M.-C. Shih, and S.P. Markey
Laboratory of Clinical Science, National Institute of Mental Health,
Bethesda, Maryland 20892

The neurotoxin MPTP (1-methyl-4-phenyl-1,2,3,6-tetrahydropyridine) has the unique property of lesioning the substantia nigral brain cells in man and certain laboratory animals. We have synthesized several MPTP analogues in order to determine the molecular requirements of the neurotoxin as well as to provide ligands for the preparation of MPTP antibodies.

SYNTHESIS, MASS SPECTRA, AND DISCUSSION

Nitration of 4-phenylpyridine results in a mixture of 2'-, 3'-, and 4'-nitro-4-phenyl pyridines which were separated by fractional crystalization and flash chromatography. These isomers show very marked differences in their fragmentation patterns (Fig. 1). The 3'- and 4'-isomers exhibit loss of 30 daltons (NO) from the molecular ion, producing the m/z 170 ion, whereas the 2'-isomer loses CO (28 daltons) as shown by high resolution mass spectrometry, producing the m/z 172 ion as the base peak in the spectrum. The loss of CO by ortho-nitrobiphenyl has been previously reported(1) and the 2'-nitro-4-phenylpyridine represents another example of this unusual fragmentation. An attempt to explain the formation of the m/z 172 ion was based on the fact that the pyridine-ring hydrogen atom is sterically accessible to the nitro group in the ortho-isomer (Fig. 2). This explanation is analogous to the mechanisms suggested for the CO loss in ortho-nitrobiphenyl(1) and 1-nitronaphthalene(2). In the meta- and para-isomers, the nitro group is spatially remote from this hydrogen atom and this fragmentation does not occur. Rather, the loss of the NO (ion m/z 170), common for the nitro compounds, is observed. The higher intensity of the m/z 170 ion in the spectrum of the para-isomer is due to the greater resonance stabilization available to the pyridine phenoxy ion derived from that isomer relative to that derived from the meta-isomer. This behavior is similar to that of the meta- and para-nitrobiphenyls.(1)

N-methylation of the nitrophenylpyridines and reduction of the pyridine to the tetrahydropyridine ring produced nitro-MPTP analogues. Reducing the nitro groups yielded the amino-MPTP analogues. Differences in fragmentation patterns between the meta- and para- vs ortho-position isomers was also observed in these two sets of compounds (Fig. 3 and 4). Based on the high resolution mass spectra an attempt was made to account for this behaviour. To elucidate the mechanisms of these fragmentations measurements of metastable transitions and specific deuterium labeling are planned.

FTMS has been used to determine accurate masses and assign elemental compositions in this study. MS/MS measurements of the MPTP and pyridine derivatives by FTMS has proven to be impossible because of their high proton affinity. During the time required to excite unwanted fragment ions from the source cell prior to CID, the molecular ion or specific

fragment under investigation was protonated, and simple electron impact processes were no longer observed. It may be possible at lower source pressures (< 10^{-8}) to study EI ions by a second electron impact process (EIEIO) as proposed by Cody & Freiser.(3)

References

1. S. Meyerson, I. Puskas, and E.K. Fields, J. Am. Chem. Soc. 88, 4974 (1966).
2. J. Harley-Mason, T.P. Toube, and D.H. Williams, J. Chem. Soc. (B), 396 (1966).
3. R.B. Cody and B.S. Freiser, Anal. Chem., in press (1986).

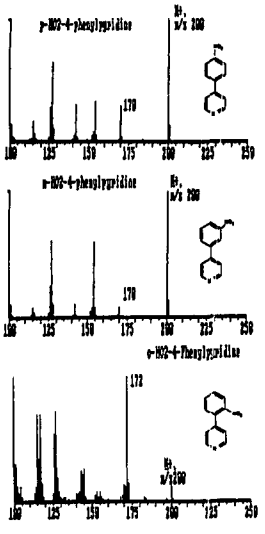

Figure 1

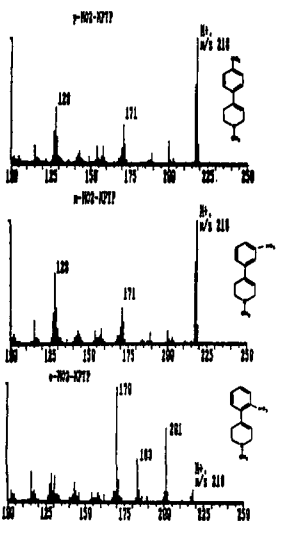

Figure 3

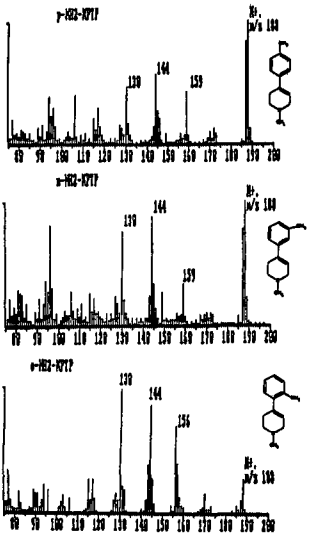

Figure 4

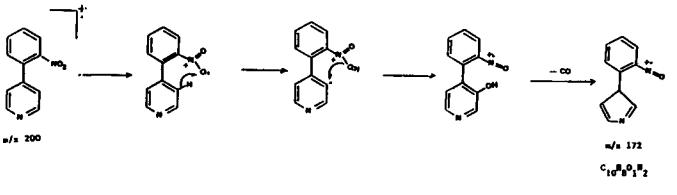

Figure 2

GC/MS STUDIES ON URINARY METABOLITES OF TETRALIN IN FISCHER RATS EXPOSED BY GAVAGE

K.O. Yu, B.M. Llewellyn, C.T. Olson and M.P. Serve

Harry G. Armstrong Aerospace Medical Research Laboratory
Toxic Hazards Division
Hazard Assessment Branch
Wright-Patterson AFB OH 45433-6573

Long term inhalation of cyclic hydrocarbons such as JP-10 and decalin cause kidney damage in male rats, but not in controls or in females. These lesions do not occur in either sex of other species while male rats appear sensitive to the kidney damage caused by hydrocarbons. The objective of this study was to identify the urinary metabolites of rats exposed to tetralin by gavage and to determine if there was a difference in metabolism between male and female rats. Tetralin is a C_{10} isomer of JP-10 and decalin, and is used as a degreasing agent and as a solvent for naphthalene, fats, resins, oils and waxes.

Male and female rats (N=6) were exposed to 0.5 mL tetralin/Kg body weight every other day for 14 days and urine collected. Urine was hydrolyzed at 37°C with β-glucuronidase sulfatase (pH 4) for 16 hrs. Urinary metabolites were extracted using a CLIN ELUT column with methylene chloride. Concentrated extracts were analyzed by GC/MS. The identification of metabolites were accomplished by matching GC retention times and MS fragmentation patterns of pure compounds previously prepared or purchased.

GC/MS analyses of rat urine confirmed the presence of 1- and 2-tetralol, 2-hydroxy- and 4-hydroxy-1-tetralone, and 1,2- and 1,4-tetralindiol. No differences in metabolites were observed between males and females. Control rats were employed in all experiments. This study showed that hydroxylation and oxidation to keto alcohols were the major metabolic pathways for tetralin in rats exposed by gavage.

1-TETRALOL

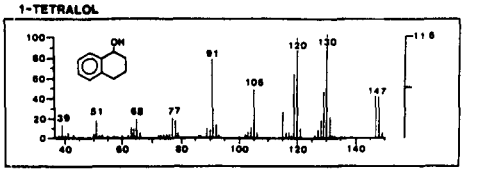

2-TETRALOL

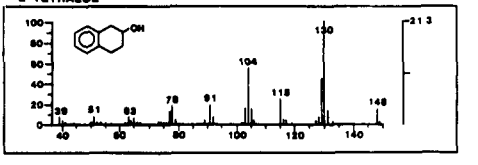

2-HYDROXY-1-TETRALONE

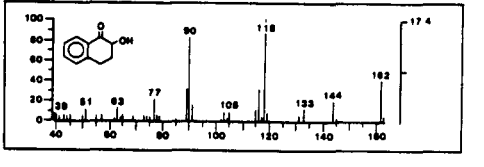

4-HYDROXY-1-TETRALONE

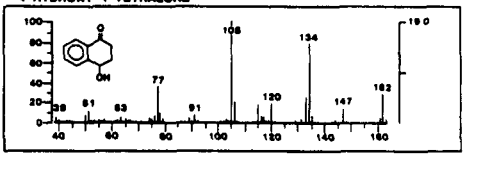

1,2-TETRALINDIOL

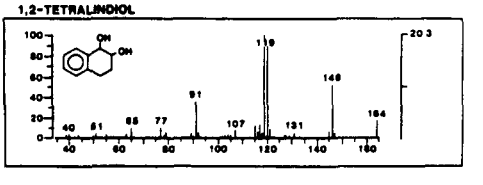

1,4-TETRALINDIOL

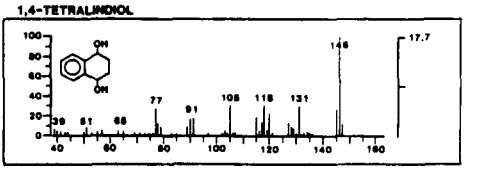

SOFT IONIZATION/TANDEM MASS SPECTROMETRY":

Gordon Hansen and Frank Hatch;
Boehringer Ingelheim Pharmaceuticals, Inc.,
90 East Ridge Road, Ridgefield CT 06877

Soft ionization techniques such as Fast Atom Bombardment and Chemical Ionization are often the method of choice for MS/MS studies because of their ability to produce intense molecular ions with little fragmentation.

A hybrid MS80 EBQQ tandem mass spectrometer has been employed to study the daughter ion spectra of ions formed by a variety of soft ionization methods. Daughter ion scans of protonated molecular ions obtained at low collision energy (5-30 ev) have been shown to be sensitive to changes in the method of ionization. Differences in the spectra have been observed which may be attributable to differences in the site of protonation as well as in the internal energy of the parent ion.

The 10 ev daughter ion scans for the MH^+ of Phenacetin obtained from the CH_4 and NH_3 chemical ionization are shown in FIG. 1. Ions at m/z 138 and 152 in the daughter ion spectrum from the methane CI protonated molecule ion result from protonation and cleavage of the amide and ether bonds respectively. The daughter ion scan of the ammonia CI protonated molecule ion contains only the 138 ion-cleavage of the amide, the most basic site on the molecule and most likely site for proton transfer from the NH_4^+ reagent ion.

FIG. 2. is a plot of daughter ion intensity vs. collision energy for the MH^+ ion of caffeine produced by CH_4 and NH_3 CI. In each case, the ion profiles for the daughter ions produced from the NH_4^+ protonated molecule ions are offset towards higher collision energy. This energy shift may be due to differences in the internal energy of the parent ion. Kenttämma[1] and Glish[2] have reported differences in low energy daughter ion spectra which have been attributed to different parent ion internal energy.

In order to investigate these effects further we have conducted a series of experiments designed to measure this energy shift in daughter ion spectra as CIMS conditions are changed. The energy shifts observed with changes in source pressure, repeller voltage, reagent gas and MH^+ vs. $M + C_2H_5^+$ product ion are listed in Table 1. In each case the daughter ion profiles are shifted to higher energy for parent ions formed with lower internal energy. The observed collision energy shifts agree with theoretical energy differences based on thermochemical calculations. These energy affects should be considered when low energy daughter ion spectra are obtained and may become an important factor in the development of soft ionization MS/MS quantitative methods.

1. Kenttämma, OMS 20, p. 703 1985

2. Glish et al. 33rd Annual Conference ASMS, 1985
San Diego Ca.

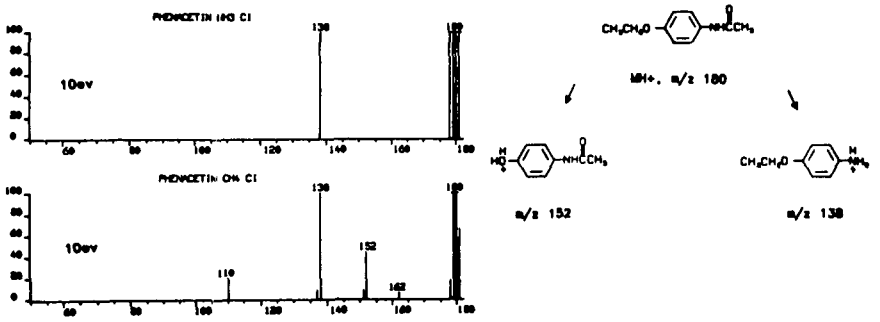

FIG. 1 PHENACETIN, DAUGHTERS OF MH+

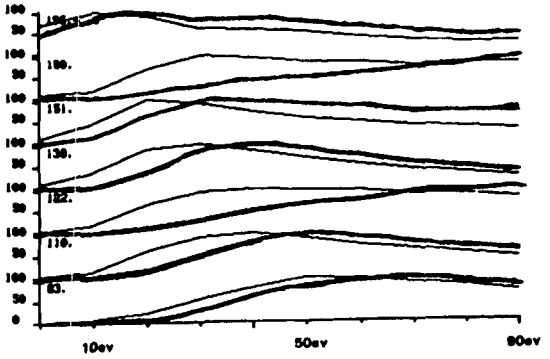

FIG. 2 CAFFEINE, DAUGHTERS OF MH+ VS. COLL. ENERGY
— NH3 CI, — CH4 CI

TABLE 1 AVERAGE ENERGY SHIFTS

-INCREASE IN SOURCE PRESSURE (CH4 CI)
60 MICRONS > 225 MICRONS
SHIFT = 8.6 KCAL/MOL
225 MICRONS > 375 MICRONS
SHIFT = 13 KCAL/MOL

-INCREASE IN REPELLER VOLTAGE (0-5V)
SHIFT = 18 KCAL/MOL
5EV = 19.6 KCAL/MOL (CENTER OF MASS EN)

-CH4 VS. NH3 CI (MH+, CAFFEINE)
SHIFT = 31.3 KCAL/MOL
PA(NH3)-PA(CH4) = 36.5 KCAL/MOL

-MH+ VS. (M+C2H5)+ (CH4, CAFFEINE)
SHIFT = 23 KCAL/MOL
PA(C2H4)-PA(CH4) = 33 KCAL/MOL

DIFFERENTIATION OF ISOMERIC OXYGEN-18 LABELED NUCLEOTIDES USING FAST ATOM BOMBARDMENT-TANDEM MASS SPECTROMETRY

L. M. Mallis, F. M. Raushel and D. H. Russell
Department of Chemistry
Texas A & M University
College Station, Texas 77843.

The positional isotope exchange technique (PIX)[1] has proven to be a valuable tool in elucidating the mechanistic pathways of many enzyme-catalyzed reactions. This technique has been used with reactions involving phosphoryl transfer, followed by ^{31}P-NMR or derivatization followed by mass spectrometry. Several studies concerning the analysis and structure elucidation of phosphorylated nucleotides using fast-atom bombardment (FAB) ionization have been reported,[2] however in many cases the number and abundance of structurally significant fragment ions is low making it difficult to determine the structure of isotopically labeled (oxygen-18 [^{18}O]) positional isomers.

[A] [B]

Recently, we reported that the dissociation reactions of organo-alkali metal ion complexes are influenced by the alkali metal binding site, enhancing the structurally significant fragment ions formed.[3] In these studies the $[M+Na]^+$ ions of uridine-6-^{18}O-triphosphate (6-^{18}O-UTP, positional isomers [A] and [B]) are formed by using FAB ionization and analyzed by using tandem mass spectrometry (TMS). The collision-induced dissociation (CID) reactions of the nucleotides are studied in the mass-analyzed ion kinetic energy (MIKE) scan mode.

To evaluate the use of tandem mass spectrometry (TMS) to determine the extent to which the PIX reaction has occurred, unlabeled UTP was analyzed. In the FAB-TMS spectrum of unlabeled UTP plus sodium (m/z 506, see Figure 1) ions at m/z 345 and m/z 329 are observed corresponding to loss of $H_3P_2O_6$ and $H_3P_2O_7$, respectively. These two ions are necessary to elucidate the integrity of the beta-gamma bridging oxygen, i.e., whether an oxygen-18 is present at this position. It is interesting to note that the Na^+ ion seems to interact more strongly with the triphosphate chain of the nucleotide. For example, ions at m/z 121, 201, and 281 which correspond to H_3PO_4Na, $H_4P_2O_7Na$ and $H_4P_3O_{10}Na$, respectively, are observed in the FAB-TMS spectrum of unlabeled UTP plus sodium. In the FAB-TMS spectrum of the oxygen-18 labeled UTP plus sodium (m/z 518) fragment ions at m/z 345 and 329 are observed which correspond to loss of $H_3P_2O_6$ and $H_3P_2O_6O$, respectively, viz., oxygen-16 located at the beta-gamma bridging position (see Figure 2). After the PIX reaction has been performed the fragment ion at m/z 345 would be shifted to higher mass due to the presence of oxygen-18 at the beta-gamma bridging position. The FAB-TMS spectrum of labeled UTP plus sodium (after the PIX reactions was performed; see Figure 3) shows fragment ions at m/z 347 and m/z 329 corresponding to loss of $H_3P_2O_5O$ and $H_3P_2O_6O$, respectively. This indicates that the beta-gamma bridging oxygen has been exchanged with an oxygen-18 atom.

The PIX reaction occurs (see Scheme 1A) by cleavage of the terminal alpha-beta biphosphate group, free rotation about the alpha-beta bridging oxygen followed by reformation of the triphosphate nucleotide (see Scheme 1A). In the narrow scan FAB-TMS spectrum of labeled UTP (after the PIX reaction) fragment ions at m/z 433 and m/z 414 corresponding to loss of H_2PO_2O and H_3PO_3O are observed (see Figure 4). This suggests that after cleavage of the terminal biphosphate, free rotation perpendicular to the alpha-beta bridging oxygen causes an alpha phosphate labeled oxygen to become the beta gamma bridging oxygen (see Scheme 1B). This additional pathway would account for the high percent incorporation of oxygen-18 at the beta-gamma bridging position after the PIX reaction.

---

[1]Midelfort, D. F.; Rose, I. A. *J. Biol. Chem.* 1976, *251*, 5881.
[2](a)Slowikowski, D. L.; Schram, K. H. *Nucleos. Nucleot.* 1985, *4*, 309. (b)Slowikowski, D. L.; Schram, K. H. *Nucleos. Nucleot.* 1985, *4*, 347. (c)Hilscher, L. W.; Hanson, C. D.; Russell, D. H.; Raushel, F. M. *Biochem.* 1985, *24*, 5888.
[3]Mallis, L. M.; Russell, D. H. *Anal. Chem.* 1986, *58*, 1076.

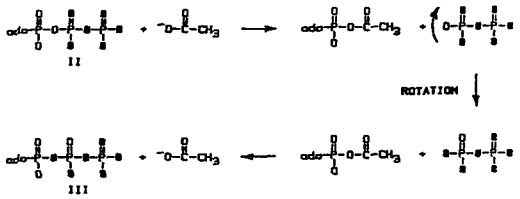

Scheme 1A

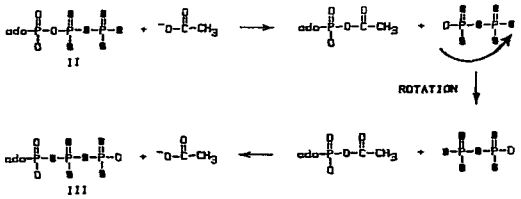

Scheme 1B

Figure 1

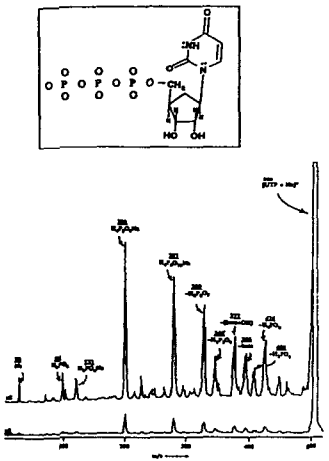

Figure 2

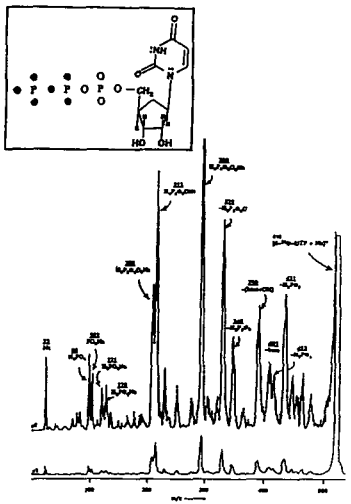

Figure 3

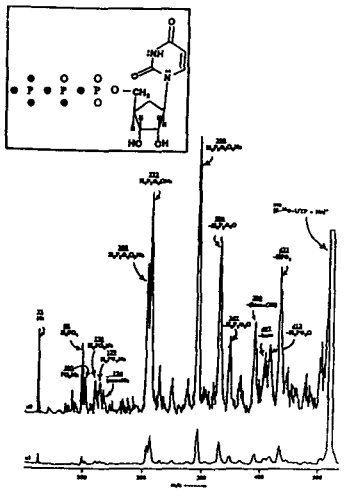

Figure 4

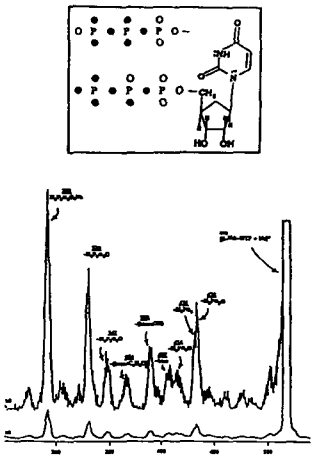

REMOTE SITE FRAGMENTATION: A STRUCTURALLY SENSITIVE FRAGMENTATION

K.B. Tomer, N.J. Jensen, and M.L. Gross; Midwest Center for Mass Spectrometry, Department of Chemistry, University of Nebraska, Lincoln, NE 68588

During the past several years we have been investigating the utility of high energy (8 keV translational energy) collisionally activated decompositions for structure elucidation. The high translational energy collision process can result in the conversion of 10-30 eV of translational energy into internal energy. This makes high energy reaction channels accessible to ions which are not readily observed in ions with the usual range of internal energies. As a result of the high energies we have been able to observe a class of reactions in which the fragmentations occur remote from the charge site (1). These reactions are most readily observed in closed-shell ions.

The first experimental evidence for these reactions was observed in CAD spectra of the $(M-H)^-$ anions of long-chained fatty acids (2). Since these reactions occur remote from the charge site, charge-induced rearrangements are not observed. Thus, these reactions are useful for structure determination. An early example was the determinations of double bond location in fatty acids. More recently, structural determination of modified fatty acids and complex lipids and mixture analysis by remote site fragmentation have been reported.

A recent application is the determination of fatty alcohols by reverse derivatization to their sulfates followed by MS/MS.

The CAD spectrum of the sulfate derivative of an acetylenic alcohol, 7-tetradecyn-1-ol is shown in Fig. 1. Relatively abundant allylic cleavages separated by a four carbon gap in the fragmentation pattern locates the position of the triple bond. Ions a and c are formed by losses of the elements of C_nH_{2n+2} and C_nH_{2n-2} respectively. Ion b arises by homolytic cleavage of the allylic bond to yield a radical and a distonic radical anion.

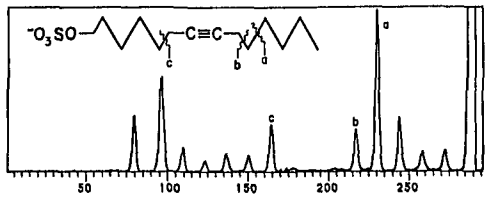

Fig. 1. MS/MS spectrum of the $(M-H)^-$ anion of 7-tetradecyn-1-ol sulfate.

The CAD spectrum of a urofuran acid, a urinary metabolite isolated by Professor G. Spiteller, Univ. Bayreuth, FRG, is an example of the application of remote-site fragmentation to structure elucidation of substituted fatty acids. Loss of the elements of C_nH_{2n+2} is initiated at the carbon-terminus of the alkyl chain and is interrupted by the presence of the furan ring.

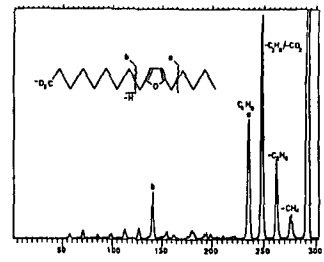

Fig. 2. MS/MS spectrum of the $(M-H)^-$ anion of a urofuran acid. Peaks a and b represent cleavages alpha to the heterocycle ring.

Although these reactions were initially observed in fatty acids or derivatives this chemistry is observed for a variety of compounds.

Remote site fragmentation of alkaloid modified nucleotides yields ions characteristic of the various portions of the molecule. In the example in Fig. 3, the charge is localized on the phosphate group while fragmentations occur by non-charge mediated hydrogen transfers.

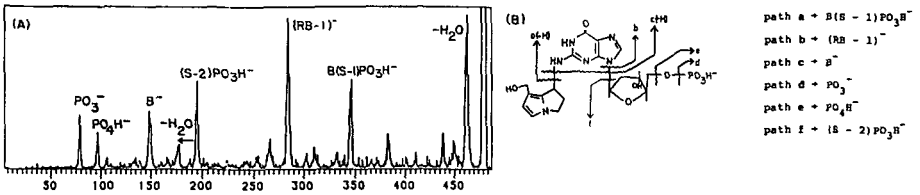

Fig. 3. A) MS/MS spectrum of the $(M-H)^-$ anion of dehydroretronecine adduct with guanosine-5-monophosphate.

Fig. 3. B) Fragmentation scheme of the MS/MS spectrum of the $(M-H)^-$ anion of dehydroretronecine adduct with guanosine-5-monophosphate.

Steroid sulfates undergo reaction primarily at the opposite end of the molecule from the charge site. These fragmentations are sensitive to stereochemistry. As an example the loss of CO can be used to distinguish the stereochemistry at the C-5 position in 17-sterol sulfates shown in Fig. 4. The more sterically hindered 5β-isomer expels CO to a significantly greater extent than does the 5α-isomer.

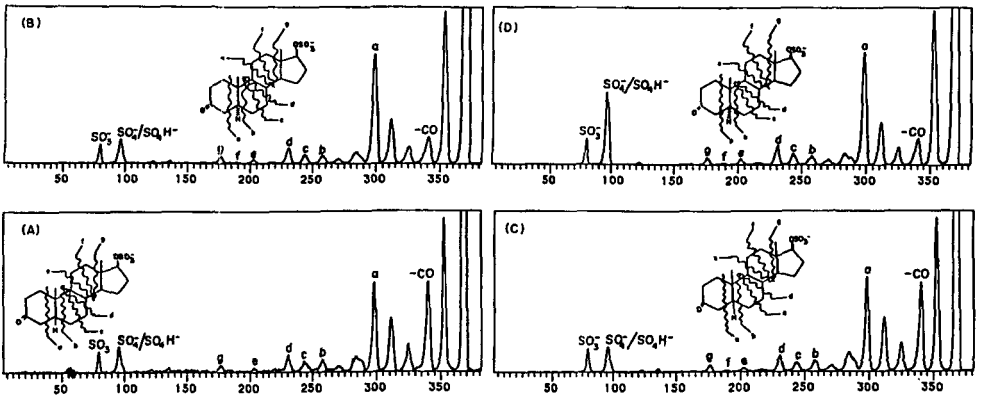

Fig. 4. A) MS/MS spectrum of $(M-H)^-$ ion of 17β-Hydroxy-5β-Androstan-3-one sulfate.
B) MS/MS spectrum of $(M-H)^-$ ion of 17β-Hydroxy-5α-Androstan-3-one sulfate.
C) MS/MS spectrum of $(M-H)^-$ ion of 17α-Hydroxy-5β-Androstan-3-one sulfate.
D) MS/MS spectrum of $(M-H)^-$ ion of 17α-Hydroxy-5α-Androstan-3-one sulfate.

In conclusion remote-site fragmentations of closed-shell ions are sensitive probes for structure determination.

References

1) Jensen, Tomer, Gross JACS 107, 1863 (1985).

2) Tomer, Crow, Gross JACS 105, 5487 (1983).
7 (1983).

MECHANISMS OF REMOTE-CHARGE-SITE FRAGMENTATION OF FAB-DESORBED FATTY ACID CARBOXYLATES

N.J. Jensen, K.B. Tomer, and M.L. Gross, Midwest Center for Mass Spectrometry, Department of Chemistry, University of Nebraska, Lincoln, NE 68588.

Several classes of closed-shell ions decompose upon collisional activation in a manner that does not rely upon charge initiation (1). For saturated acids, these fragmentations, which we have termed remote-charge-site, presumably involved parallel 1,4 hydrogen eliminations with subsequent losses of the elements of C_nH_{2n+2} initiated from the alkyl terminus. Water loss is the only other significant fragmentation. Water losses are observed for both unimolecular and collisionally activated decompositions of long-chained saturated acids. In fact, a low abundance H_2O loss is the only fragmentation seen for the unimolecular decompositions.

We have explored the mechanism of this H_2O loss by collisionally activating the $(M - H)^-$ anions of 2,3-d_2-octanoic acid; 2,2-d_2-octanoic acid, and 4,4-d_2-dodec-7-enoic acid. As the spectra of Fig. 1 show, 2,3-d_2-octanoic loses HDO, 2,2-d_2-octanoic loses D_2O. Thus, both hydrogens involved in the water loss are originally attached to the C-2 of the acid chain. The mechanism of the H_2O loss process is not readily apparent. Several workers including DePuy (2,3) and Nibbering (4) have suggested ion-molecule complexes as intermediates for gas-phase reactions of anions. Hence, we propose that the H_2O loss may occur via an ion-molecule complex as shown below:

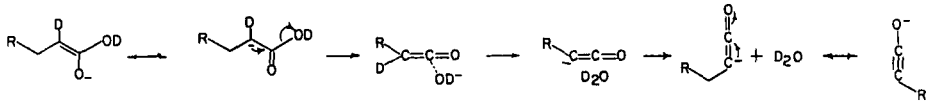

The effect of the presence of an unsaturated site in the carbon chain on the remote-charge-site fragmentation process is another interesting consideration. A double bond causes an interruption of the fragmentation series, as vinylic and olefinic bonds are not cleaved. However, the fragmentation at the allylic position distal to the charge and one C-C bond more remote and the C_nH_{2n} loss involving the allylic bond more proximate to the charge are considerably enhanced. Careful examination of the CAD spectrum of 7-dodecenoic acid (Fig. 2) shows that the fragmentation at the distal allylic position involves the loss of C_3H_6 and yields the ion $C_9H_{14}O_2^{-\cdot}$. The formation of a radical anion as a result of collisional activation of the even electron $(M - H)^-$ anion is unusual. Furthermore, considering the remote-site-fragmentation process by which the ions of the fragmentation series arise, this ion is proposed to be a distonic ion (Structure A).

$$\cdot CH_2\text{-}C{\equiv}C\text{-}(CH_2)_n\text{-}COO^-$$

A

Nibbering (4) has proposed the occurrence of such species for propyne and acetone radical anions formed via a dissociative resonance processes and for the radical anion produced by the collisionally induced loss of a methyl radical from the even electron $(M - H)^-$ ion of methoxyacetonitrile. Further examination of the collisionally activated decompositions of the $(M - H)^-$ ions of other monounsaturated acids shows that formation of a radical anion is not unique to 7-docecenoic acid, but is a typical fragmentation at the distal allylic position.

The collisionally activated decomposition of double bond-containing fatty acids were compared with those of a set of analogous compounds containing triple bonds. The fragmentations of the $(M - H)^-$ anions of 7-dodecynoic acid, 7-tetradecynoic acid and 9-tetradecynoic acid are representative examples (Fig. 3). These fragmentations are quite similar to those of the dienoic acids. The formation of a daughter ion with the formula C_nH_{2n+1} at the site of the triple bond is a significant feature of the fragmentation and, as in the case of the similar fragmentation the dienoic acids, appears to be a distonic anion. The relative abundance of the radical anion as compared to the ion formed from cleavage of the C-C bond adjacent to it on the alkyl side of the chain is less for the acelylenic acids than for the dienoic acids. Daughter ions formed as the result of the loss of 72μ are an unusual feature of the fragmentation of acids with triple bonds in the 7-position. These ions are the result of a rearrangement reaction which is a process distinct from remote-charge-site decomposition.

References

(1) Jensen, N.J.; Tomer, K.B.; Gross, M.L., JACS, 107, 1863 (1985).
(2) Grabowski, J.J.; DePuy, C.H.; Bierbaum, V.M., JACS, 105, 2565 (1983).
(3) Squires, R.R.; Bierbaum, V.M.; Grabowski, J.J.; DePuy, C.H., JACS, 105, 5185 (1983).
(4) Nibbering, N.M.M., Rec. Trac. Chim., 100, 297 (1981).

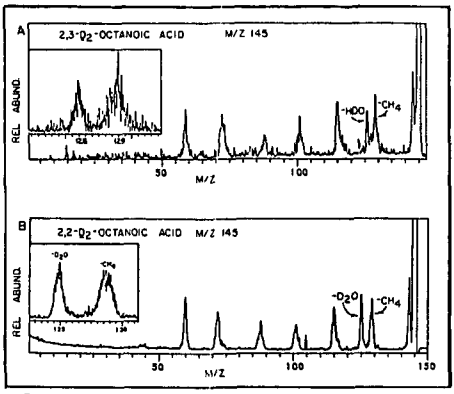

FIG 1

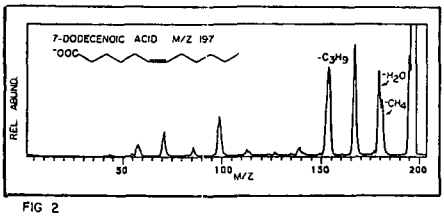

FIG 2

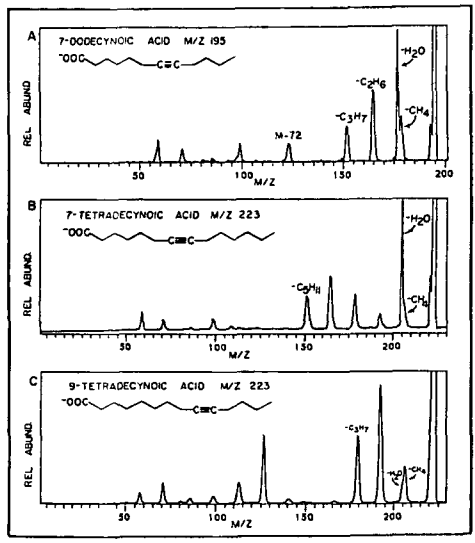

FIG 3

AMINO ACID SEQUENCES OF FRESH WATER BLUE-GREEN ALGAL TOXIC PEPTIDES BY FAST ATOM BOMBARDMENT TANDEM MASS SPECTROMETR IC TECHNIQUE

Thaiya Krishnamurthy, Linda Szafraniec, and Emory W. Sarver
U.S. Army Chemical Research, Development and Engineering Center
Aberdeen Proving Ground, Maryland 21010-5425

Donald F. Hunt and Jeffrey Shabanowitz
University of Virginia
Charlottesville, Virginia 22901

Wayne W. Carmichael
Wright State University
Dayton, Ohio 45435

Stephan Missler
USAMRIID, Ft. Detrick
Frederick, Maryland 21701-5011

Olav Skulberg
Norwegian Institute for Water Research
N Oslo 3, Norway

Geoff Codd
The University
Dundee DD1-4HN United Kingdom

Some blue-green algal blooms found in fresh water lakes and ponds have been found to be toxic, and linked to cattle loss and human health hazards in several countries. The compounds isolated from these toxic blooms have been found to be either hepatotoxic or neurotoxic. The algal growth, and thus the toxin production, is facilitated by increased environmental pollution and eutrophication of natural waters. The available information on chemical structures and properties of these toxins, required for the detection and clean-up of the contaminated water sources, is very limited. Hence, we have recently conducted investigations in order to elucidate the structures of several blue-green algal toxins.

A hepatotoxin isolated from blue-green algal (Microcystis Aeruginosa) blooms found in natural fresh water lakes in Norway, was found to be a peptide with the molecular weight of 994 Daltons, based on the amino acid analysis and fast atom bombardment (FAB) mass spectrum of the peptide. Absence of sequence ions in the FAB mass spectrum of the toxin and the formation of a linear peptide on hydrolysis of the intact peptide indicated it to be a cyclic peptide. The identity of all the amino acid moities and their sequences in the peptide were deduced as,

—Ala—Leu—Masp—Arg—Adda—Glu—Mdha—,

based on the FAB-collisionally activated dissociation (CAD) mass spectrum of the intact peptide and its hydrolysate. The proposed sequence (Figure) was confirmed by the FAB-CAD mass spectral data of the chemical reaction products of the toxin. The diacids

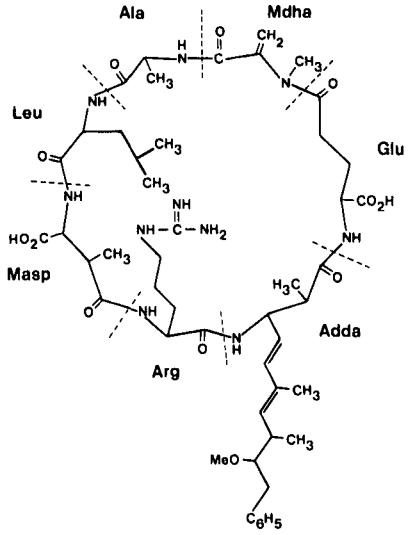

Figure. AKERSTOX

in the molecule were found to be iso linked based on the FAB-CAD mass spectrum of the deuterated linear peptide (hydrolysate). The nmr spectra of the intact peptide corroborated the identities and linkages of the amino acids present in the molecule. The configurations of the amino acids are unknown at this point. The same toxin was also detected in the algal blooms found in fresh water lakes in Canada (Anabena flos-aquae), Scotland and the USA (Microcystic Aeruginosa).

Similarly, other toxic peptides isolated from the various species of blue-green algal blooms also were investigated. The identities of amino acids, and their sequences were established using only a few nanomoles of the intact peptides and FAB tandem mass spectrometric data. The results are listed in the Table.

Table.
SEQUENCE OF AMINO ACIDS IN BLUE-GREEN ALGAL PEPTIDES

M.W.	AMINO ACID SEQUENCE	ORIGIN	
		SPECIES*	COUNTRY
980‡	—Ala—Leu—Asp—Arg—Adda—Glu—Mdha—	MA, FA	USA, CANADA (S23G1)
		GO	NORWAY
998	Ala—Leu—Asp—Arg—Adda—Glu—Mdha	GO	NORWAY
1012	Ala—Leu—Masp—Arg—Adda—Glu—Mdha	MA	SCOTLAND (7820)
			NORWAY
1009‡	—Ala—Leu—Asp—Arg—Adda—Glu—Dha—	GO	NORWAY
1023‡	—Ala—Leu—Asp—Arg—Adda—Glu—Dha—	RO	NORWAY

* MA, MICROCYSTIS AERUGINOSA; AF, ANABENA FLOS—AQUAE, GO, GREEN OSCILLATORIA, RO, RED OSCILLATORIA

‡ CYCLIC PEPTIDES

ROLE OF HYDROGEN TRANSFERS IN THE FORMATION OF $[M-X]^+$ IONS FROM ETHYL HALOSUCCINATES UNDER ELECTRON IMPACT.

D. Bornstein[a], B. Domon[b], A. Mandelbaum[a], D. Mueller[b], and W.J. Richter[b]
[a]Department of Chemistry, Technion-Israel Institute of Technology, Haifa, Israel
[b]Ciba-Geigy, Ltd., Basel, Switzerland

Gas phase protonated diethyl maleate and its geometrical isomer diethyl fumarate can be readily differentiated by a low energy CID experiment: the former eliminates ethanol while the latter exhibits loss of one and two molecules of ethylene.[1]

Diethyl chloro- and bromosuccinates 1 eliminate the halogen atom from their molecular ions under electron impact. Low energy CID spectra indicate that the resulting $[M-X]^+$ ions are mixtures of O-protonated diethyl maleate (>90%) and fumarate (<10%).[2] No analogous loss of halogen has been observed in the electron

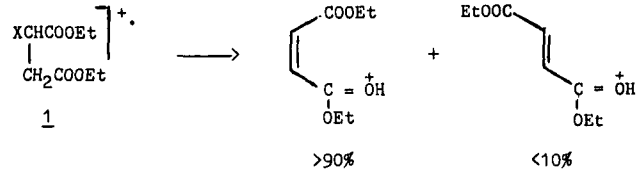

impact mass spectra of the corresponding dimethyl halosuccinates.

A surprising difference has been observed between the electron impact mass spectra of the isomeric mixed methyl ethyl halosuccinates 2 and 3. The loss of the halogen occurs only in 2 (with the ethyl group remote from the halogen) while 3 gives rise to abundant $[M-C_2H_4-CO_2]^{+\cdot}$ ions.

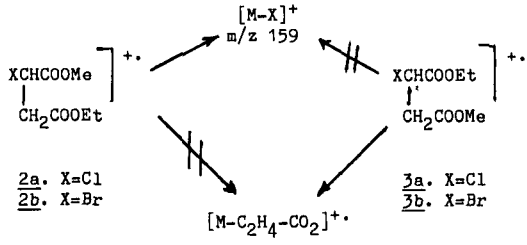

Low energy CID measurements indicate that more than 90% of the m/z 159 $[M-X]^+$ ions formed from 2a and 2b have the structure of protonated methyl ethyl maleate which is characterized by elimination of methanol and ethanol. Deuterium labelling was applied to elucidate the mechanism of the formation of the $[M-X]^+$ ion from 2.

$[M-Br]^+$ ion formed from methyl, d_5-ethyl bromosuccinate 2c eliminates CH_3OD under low energy CID conditions indicating that a deuterium atom migrates from the ethyl group to a carbonylic oxygen in the course of the loss of the halogen atom from 2 under electron impact.

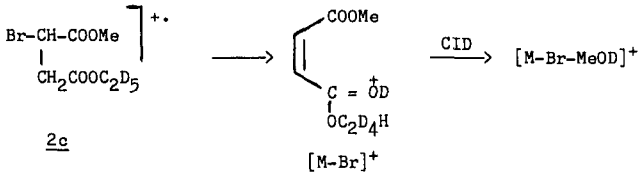

$[M-X]^+$ ion formed from methyl, 1-d_2-ethyl bromosuccinate 2d eliminates only CH_3OH under CID conditions indicating that a hydrogen atom originally from position 2 of the ethyl group is attached to the carbonylic oxygen in this case:

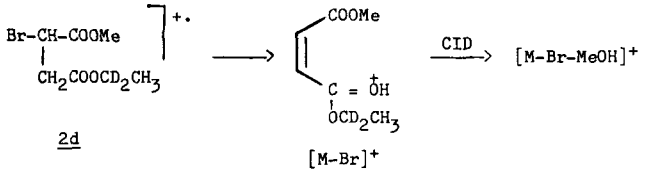

The results of the labelling experiments lead to the conclusion that the elimination of the halogen atom from halosuccinates 2 under electron impact is a multistep process including at least two specific hydrogen migrations. One hydrogen atom from C-2 of the ethyl group is transferred to the carbonylic oxygen. Another hydrogen atom from the succinic part of 2 must also migrate to allow formation of the double bond after loss of the halogen atom. The following mechanism is suggested to explain all the above facts:

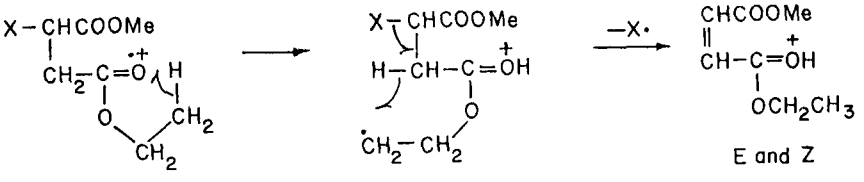

A

The formation of the intermediate distonic ion A is of interest in the context of understanding the mechanism of McLafferty rearrangement and analogous processes.

REFERENCES

1. A. Weisz, A. Mandelbaum, J. Shabanowitz, D.F. Hunt, Org. Mass Spectrom., 19, 238 (1984).
2. A. Weisz, A. Mandelbaum, W. Blum, B. Domon, D. Muller, W.J. Richter, J. Shabanowitz, D.F. Hunt, Org. Mass Spectrom., submitted for publication.

APPLICATIONS OF A HIGH MASS TANDEM MASS SPECTROMETER TO THE CHARACTERIZATION OF PROTEINS

H. A. Scoble, C. E. Costello and K. Biemann, Department of Chemistry, Massachusetts Institute of Technology, Cambridge, Massachusetts 02139

The primary structure of several proteins has been investigated to evaluate the utility of high mass and tandem mass spectrometry for problems involving structural characterization. Past research from our laboratory has indicated the need for high field instruments since the molecular weights of peptides formed in proteolytic and chemical digests inevitably go beyond the practical mass range of most instruments. The use of the 4-sector mass spectrometer (JEOL HX110/HX110) has allowed us to answer specific questions concerning certain structural features of the proteins under study.

Alanyl-tRNA synthetase (ARS) binds to a specific DNA sequence as part of a transcriptional control mechanism and information is available on the general location of the catalytic sites. An amino terminal subunit of ARS, approximately 48000 daltons, has full ATP-inorganic pyrophosphate activity in that it forms the aminoacyl adenylate just as effectively per mole as the native enzyme. A smaller N-terminal fragment (T1) generated by limited tryptic digestion is only 20% as active as the larger fragment. Since adenylate formation is a reaction common to all tRNA synthetases, establishing the C-terminal sequence of the T1 fragment would delineate the region of the catalytic site. Although the exact location of the C-terminus of the T1 fragment was not known, it was thought to contain between 2 and 42 amino acids since the primary structure of the intact ARS is known. Fifteen nanomoles of the carboxymethylated T1 subunit from E. coli ARS was treated with cyanogen bromide and the resulting peptides separated by reversed-phase high performance liquid chromatography. Fast atom bombardment mass spectromtric analysis of the fractions from the digest revealed a peptide with an MH^+ of 3074.3 which could not be attributed to any cyanogen bromide peptide from the enzyme. Assuming complete random cleavage of intact ARS, six peptides are found which are within a 0.5 amu window of the 3074.3 peptide. Of these six peptides, only one would be generated by a combination of trypsin followed by cyanogen bromide, and additionally is the only peptide from the C-terminal region of the T1 fragment . Thus, the T1 fragment of ARS extends from amino acid positions 1 to 368. It should be noted that these mass assignments were made at unit mass resolution. However, since the information content at unit mass resolution is no greater than that at lower resolution, we see no need in routinely operating at greater than 1000 resolution for two-sector experiments. In the course of this investigation, we have also noted that under the conditions of CNBr digestion (70% formic acid), extensive formylation of the peptides can occur. This fact must be kept in mind if only very small quantities of protein under study are available.

In another study, a calcium binding protein (CBP) of unknown function was isolated from salmon. The majority of the primary structure had been determined using gas phase sequencing techniques, however, the N-terminus was blocked and thus not amenable to classical sequencing methodologies. Ten nanomoles of an N-blocked amino terminal peptide was available for sequence determination using a four-sector tandem mass spectrometer. In preliminary two-sector experiments, many protonated molecular ions were detected indicating the original ten nanomole sample was the a mixture of many componenents. The sample was then separated chromatographically into seven fractions labeled CBP1 through CBP7. The two must abundant peptides, CBP1 and CBP2, differed in mass by 18 amu while the other five differed in mass by 28 amu or 56 amu from CBP1 and CBP2. The only information we had about the peptide was that it was N-blocked; however, from our previous experience with cyanogen bromide digests, it appeared that these peptides represented homoserine and homoserine lactone derivatives and also their formylated derivatives. Comparison of the MS/MS spectra of CBP1 (MH^+ 1018.5) and CBP2 (MH^+ 1000.5) revealed that these two peptides were structurally similar. The 18 amu difference allowed us to easily recognize which fragments were originating from the N-terminus and which were originating from the C-terminus. The MS/MS spectra of CBP1 is shown in Figure 1. Using the Roepstorff and Fohlman nomenclature [1], fragment ions corresponding to B_1 through B_5 can be identified indicating the sequence is AcSer-Asp-xLeu-Trp-Val- . Fragment ions from the Y series allow assignment of the sequence AcSer-Asp-xLeu-Trp-Val-(Gln or Lys)- . Since we know the peptide contains a C-terminal homoserine or homoserine lactone, the sequence of the peptide must be AcSer-Asp-xLeu-Trp-Val-(Gln or Lys)-(Gln or Lys)-Hse/Hsl. Derivatization of the peptide with phenylisothiocyanate, which will react with free N-terminal amino groups or the ϵ-amino

group of lysine, followed by MS/MS analysis indicated that the sequence at postions 6 and 7 is -Gln-Lys- . The final question to be resolved concerned the assignment of position 3 as Leu or Ile. Since there is an A_3 ion and a small corresponding A_3-42 ion (loss of C_3H_6) and no A_3-28 (loss of C_2H_4), position 3 must be leucine.

The information provided by comparing the homoserine and homoserine lactone containing peptide greatly facilitated the MS/MS interpretation since N-terminal and C-terminal fragment ions could easily be distinguished. The complete interpretatation of the homoserine lactone containing peptide would have been considerably more difficult without the added information provided by the homoserine peptide, since two set of ions (Y_3,B_3 and Y_5,B_5) have nearly identical masses. Also, in the spectrum of the lactone containing peptide, there was a small ion in the region bounded by B_3 and B_4 which could have indicated Ser-Ala or Ala-Ser rather than Trp. Since this ion was not present in the free acid spectrum and both spectra contain a strong Trp immonium ion (m/z 159), the assignment was made as Trp. In addition to placing the Lys at postion 7, the phenylisothiocyanate derivatized peptides contained B_6 and B_7 ions which were not present in the underivatized spectra.

REFERENCES

1. P. Roepstorff and J. Fohlman, Biomed. Mass Spectrom. 11, 601 (1984).

This work was supported by grants from the National Institutes of Health (Grants RR00317 and GM05472). We thank Dr. John H. Collins for providing us with the salmon calcium binding protein.

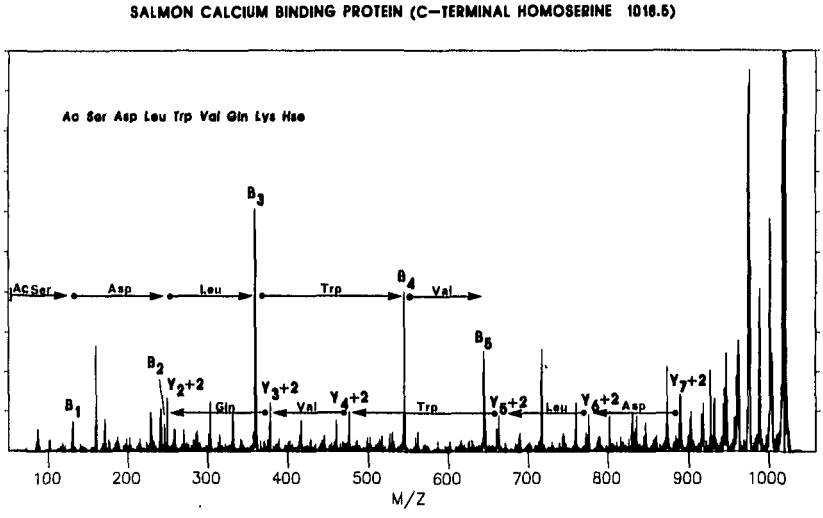

FIGURE 1. MS/MS spectrum of N-blocked N-terminal peptide from a calcium binding protein isolated from salmon. The mass spectrum was recorded at 30 Hz filtering and 50% parent ion reduction using helium as the collision gas. The resolution of both MS-1 and MS-2 was 1:1000. Scan time from 50 to 1018.5 was approximately 2 minutes. The sample matrix was glycerol/HOAc. Fragment ion nomenclature is that of Roepstorff and Fohlman [1].

INVESTIGATION OF PARAMETERS AFFECTING THE COLLISIONAL ACTIVATION OF HIGHER MASS MOLECULES

R.L. Cerny, K.B. Tomer, D.E. Giblin, Midwest Center for Mass Spectrometry, Dept. of Chemistry, University of Nebraska, Lincoln, NE 68588.

Early studies of the collisional activation process considered many of the parameters affecting the activation of the sample ion. In these studies, helium was determined to be the collision gas of choice as its use minimized scattering of the main beam. The high ionization potential of helium also limits the competitive process of collision gas ionization. However, these conclusions were based on the activation of small molecules such as methane. There have been few studies which consider high mass ions. We report here on the use of Ar and Xe for the CA of higher mass ions desorbed by FAB.

The amount of energy available to an ion upon CA becomes more important for the higher mass species. Equation 1 shows that this energy is dependent on the mass of the sample ion and the mass of the collision

$$E_A = M_T E / (M_T + M_I) \qquad \text{Equation 1}$$

E_A = available energy in center of mass system
E = kinetic energy of the ion
M_T = mass of the target (collision gas)
M_I = mass of the ion

gas. As the mass of the sample ion increases, the energy available to that ion decreases. This infers a decrease in the effectiveness of collisional activation in the study of higher mass ions.

More energy can be made available to higher mass ions by increasing the mass of the collision gas (to Ar or Xe) or by increasing the average number of collisions an ion undergoes. Shown in Fig. 1 are the CAD spectra of the methyl ester of Substance P (1-7) with He collision gas pressures sufficient to supress the ion beam by 50,75,90, and 99%.

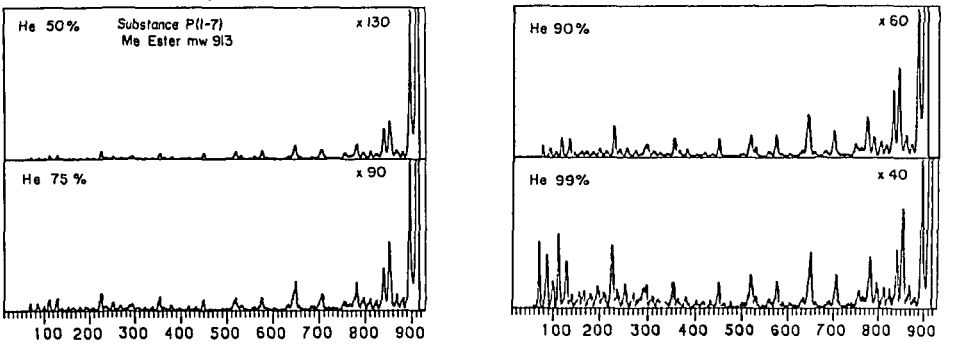

Figure 1

There is a pronounced increase in the abundance of lower mass fragment ions as the percentage of beam suppression is increased. At 50% beam suppression, of those ions undergoing a collision, ≈80% will be involved in only one collision. In contrast, at a 90% beam suppression level, >70% of the ions will undergo multiple collisions. These multiple collisions result in an increase in energy available to the ion. It is important to note that increasing the suppression does not significantly distort the high-mass fragmentations observed at lower pressures.

Shown in Fig. 2 are the CAD spectra of the same Substance P(1-7) ion with either Ar or Xe as the collision gas with 50% beam reduction. The increase in available energy due to the increased mass of the collision gas also results in more abundant low-mass fragment ions as compared to using He at 50% beam reduction.

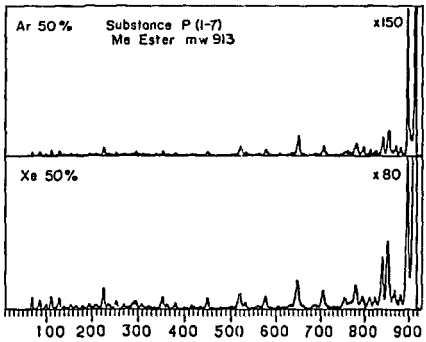

Figure 2

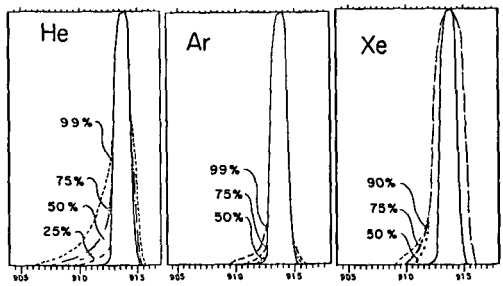

Figure 3

Another feature observed in CAD spectra is the "foot" or "tail" on the main beam likely due to sample ions which have undergone at least one collision but have not fragmented (see Fig. 3). The abundance of these non-fragmented ions is much more significant when He is used as the collision gas indicating a lower efficiency in the transfer of energy. However, instrumental design may also play a role, since sample ions scattered by collision with He may still fall within the acceptance angle of MS-II. Scattered sample ions resulting from collision with the heavier Ar or Xe atoms, will be deflected more and may be outside the acceptance angle.

The mass shift of fragment ions to lower masses due to translational energy loss can be problematic in the assignment of fragment ions. The observed mass shift is substantially smaller when higher mass target gases are used. For example, the A_5 fragment ion of the peptide Substance P has a mass of 579.4 u. The observed masses in the CAD spectra are 576.3 u with He, 578.5 u using Ar, and 577.7 u for Xe. Again, there may be some instrumental discrimination involved, since He-scattered ions may still be measured and would appear at lower energy (mass).

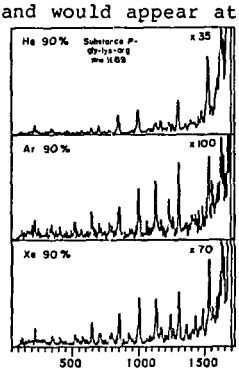

Figure 4

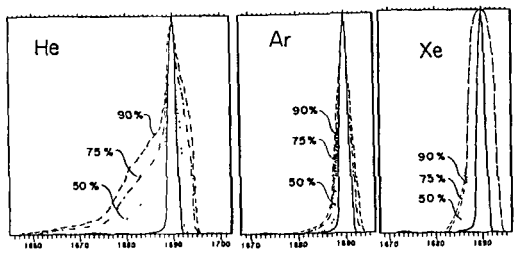

Figure 5

The advantages of using a heavier collision gas are much more pronounced for higher mass samples. (See Figs. 4 and 5 for Substance P-gly-lys-arg mw=1689). The CAD spectra are improved by making more energy available to the system through heavier target gases and increased collision probabilities. From these preliminary studies, it appears that it is important to choose CA parameters which provide sufficient energy to promote useful fragmentations of the sample ion. For low mass ions (<500), He works quite well; CA of higher mass ions benefits from the use of heavier collision gases.

COLLISIONAL ACTIVATION OF CATIONIZED FATTY ALCOHOLS AND ACIDS: ENERGETICS OF REMOTE SITE DECOMPOSITIONS AND STRUCTURAL INFORMATION

Jeanette Adams and Michael L. Gross, Midwest Center for Mass Spectrometry, Department of Chemistry, University of Nebraska, Lincoln, NE 68588-0362

Fast atom bombardment (FAB) and collisional activation tandem mass spectrometry (CA MS-MS) provide a simple and direct method for determining structural features of nonderivatized fatty alcohols and acids. The fatty alcohols and acids are cationized with alkali metal ions on the FAB probe tip and are collisionally activated. Activated ions decompose giving remote charge site fragmentations (1) clearly indicating hydrocarbon chain length and other structural features. CA decompositions of cationized oleyl alcohol also provide an estimate of internal energy required for the remote decompositions.

CAD spectra of monounsaturated alcohol $(M + Li)^+$ ions (Figure 1A), acid $(M + Li)^+$ ions (Figure 1B), and acid $(M + 2Li - H)^+$ ions (Figure 1C) clearly show hydrocarbon chain

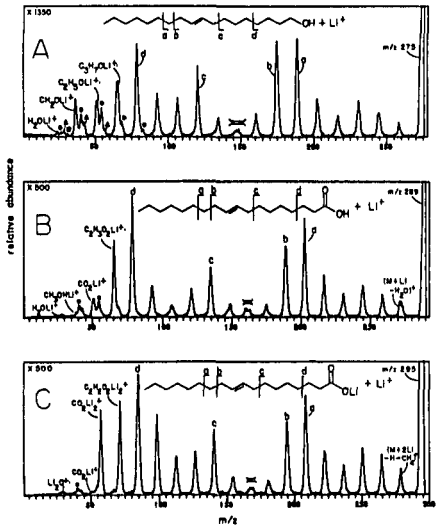

Figure 1. Cad spectra of oleyl alcohol $(M + Li)^+$ ions (A), oleic acid $(M + Li)^+$ ions (B), and oleic acid $(M + 2Li - H)^+$ ions (C).

length and double bond location. The major ion series is from losses of the elements of C_nH_{2n+2}. CA of cationized deuterium-labelled alcohols and acids show the probable mechanism to be 1,4-hydrogen eliminations giving alkenes and either terminally-unsaturated cationized alcohols (eq. 1) or cationized fatty acids (eq. 2).

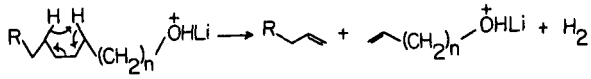

(1)

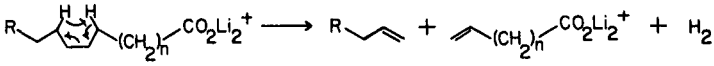

(2)

CAD spectra of cationized polyunsaturated alcohols and acids also show location of double bonds. Spectra of polyunsaturated acid $(M + 2Li - H)^+$ ions, in contrast with $(M - H)^-$ anions (2), distinctly show perterbation of the remote fragmentation pattern with

obvious correlation to double bond location (Figure 2A, B). Where locating double bonds is impossible in $(M - H)^-$ anions (2), CAD spectra of $(M + 2Li - H)^+$ ions clearly show double bond location (Figure 2C, D).

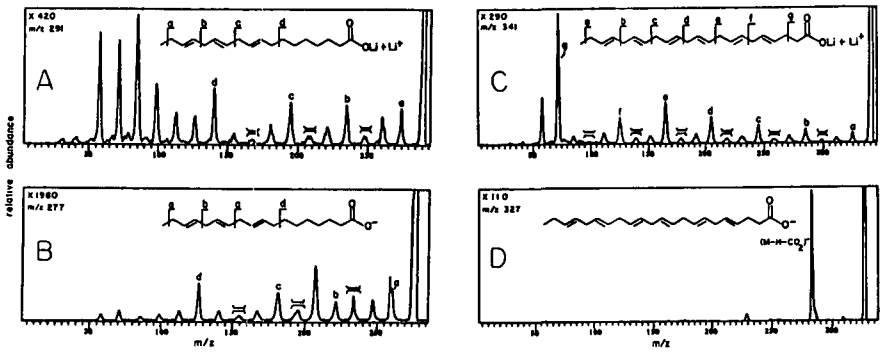

Figure 2. CAD spectra of linolenic acid $(M + 2Li - H)^+$ ions (A) and $(M - H)^-$ anions (B); and of 4, 7, 10, 13, 16, 19-docosahexaenoic acid $(M + 2Li - H)^+$ ions (C) and $(M - H)^-$ anions (D).

CA decompositions of other acid $(M + 2Li - H)^+$ ions provide an obvious advantage over CA of the corresponding $(M - H)^-$ anions. In such cases shown in Figure 3, CAD spectra of $(M + 2Li - H)^+$ ions allow complete structure determination while $(M - H)^-$ anions decompose giving no structural information.

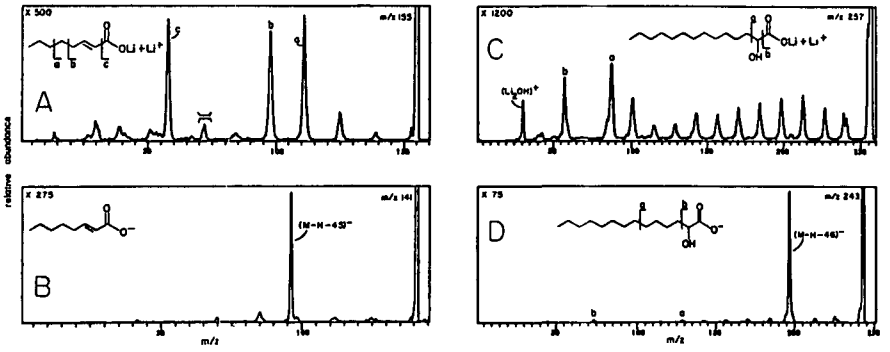

Figure 3. CAD spectra of 2-octenoic acid $(M + 2Li - H)^+$ ions (A) and $(M - H)^-$ anions (B); and of 2-hydroxytetradecanoic acid $(M + 2Li - H)^+$ ions (C) and $(M - H)^-$ anions (D).

Internal energy required for the remote decompositions is estimated by comparing CA decompositions of oleyl alcohol $(M + Li)^+$ and $(M + Na)^+$ ions to enthalpies of solvation of the alkali cations (3). After correcting for chain length effects (4,5), the energy required for the remote decompositions is estimated to be 1.5-2.0 eV.

References

(1) Jensen, N.J.; Tomer, K.B.; Gross, M.L. J. Am. Chem. Soc. 1985, 107, 1863-1868.
(2) Jensen, N.J.; Tomer, K.B.; Gross, M.L. Anal. Chem. 1985, 57, 2018-2021.
(3) Dzidic, I.; Kebarle, P. J. Phys. Chem. 1970, 74, 1466-1474.
(4) Woodin, R.L.; Beauchamp, J.L. J. Am. Chem. Soc. 1978. 100, 501-508.
(5) Lias, S.G.; Liebman, J.F.; Levin, R.D. J. Phys. Chem. Ref. Data 1984, 13, 695-808.

A STUDY ON THE EFFECT OF ALKALI METAL CATIONIZATION ON THE DISSOCIATION REACTIONS OF POLAR ORGANIC MOLECULES

L. M. Mallis and D. H. Russell

Department of Chemistry
Texas A & M University
College Station, TX 77843

Ions formed by the attachment of alkali metal ions (A^+) are frequently the most abundant ions in fast atom bombardment (FAB) ionization mass spectra of polar organic molecules. Since polar organic molecules (i.e., peptides, sugars, nucleotides, etc.) contain highly polar functional groups, and these functional groups have different H^+ and A^+ ion affinities, it follows that the binding sites of H^+ and A^+ ions may differ. Therefore, the site of attachment for H^+ and A^+ ions, and the structure of the ionic complexes may result in significant differences in the collision-induced-dissociation (CID) spectra. Recently, we reported that the highly branched structure and the basic nature of the histidyl R-group (i.e., the imidazole ring nitrogen) lead to marked changes in the CID spectrum of hippuryl-L-histidyl-L-leucine (HHL).[1] Due to the nature of the sodium ion interaction, structurally significant fragment ions are observed in the CID spectrum of $[M+Na]^+$ ions which were not previously observed in the corresponding CID spectrum for the $[M+H]^+$ ions.

To investigate the site of interaction of the alkali metal ion (Na^+) with basic amino acid residues, organo-alkali metal ions of gly-his and gly-trp were formed by using FAB ionization and analyzed using tandem mass spectrometry. Several fragment ions provide information on the site of interaction of the sodium ion with the molecule. For example, in the CID spectrum of gly-his plus sodium (m/z 235), fragment ions are observed at m/z 132, 98 and 81 which correspond to the histidyl residue (plus sodium) without the carboxy terminus, cleavage of the carboxy terminus and loss of the histidyl R-group (plus sodium) and the glycyl residue (plus sodium), respectively (see Figure 1B). These three ions provide evidence for the site of interaction of the sodium ion as shown in Figure 1A. It is interesting to note that in all cases the sodium ion remains with the observed fragment ions. In the CID spectrum of gly-trp plus sodium (m/z 284) fragment ions are observed at m/z 181, 154 and 98 which correspond to the tryptophan residue (plus sodium) without the carboxy terminus, the tryptophan R-group (plus sodium) and the glycyl residue plus NH (plus sodium), respectively (see Figure 2B). These three ions provide evidence for the site of interaction of the sodium ion with this molecule as shown in Figure 2A.

Looking at the CID spectrum of gly-his-arg-pro plus sodium (m/z 488) a competitive interaction of sodium with the arginine and histidine R-groups would be expected. For example, the most abundant fragment ion in the CID spectrum is observed at m/z 374 corresponding to cleavage of the proline residue (see Figure 3B). This ion could be formed due to the interaction of the sodium ion with the R-groups of histidine and arginine as shown in Figure 3A. Ions at m/z 277 and m/z 261 are assigned to arg-pro (plus sodium) and arg-pro with a simultaneous loss of OH (plus sodium), respectively (Figure 3B) and correspond to a stronger interaction of the sodium ion with the arginine R-group. The ions at m/z 234 and m/z 189 are assigned to gly-his (plus sodium) and gly-his plus CO-NH (plus sodium) and correspond to a stronger interaction of the sodium ion with the histidine R-group (see Figure 3A).

We have recently initiated studies aimed toward understanding the effect amino acids with titratable R-groups have on the binding site and relative binding energy of alkali metal ions to peptides. It is thought that as the R-group pK_a increases for a specific amino acid, the relative alkali metal binding energy should increase thus dictating the site of interaction of the alkali metal with the peptide (see Figure 4). It is interesting to note that when amino acids with titratable R-groups are present in the same molecule, the trend is still observed. For example in the CID spectrum of angiotensin II plus sodium (m/z 1069, see Figure 5) the five most abundant fragment ions in the spectrum are assigned as fragments arising from interaction of the sodium ion with a particular R-group (i.e., Arginine, pK_a 12.5; Tyrosine, pK_a 10.1; Histidine, pK_a 6.0). For example the fragment ions at m/z 953 and m/z 746 are assigned as loss of the aspartic acid residue and loss of the aspartic acid and phenylalanyl residues, respectively, corresponding to interaction of the sodium ion with the arginine R-group. The fragment ions at m/z 530 and m/z 485 are assigned as asp-arg-val-his and asp-arg-val-his with a simultaneous loss of the valyl R-group, respectively, corresponding to interaction of the sodium ion with the tyrosine R-group. The fragment ion at m/z 780 is assigned to cleavage of the prolyl-phenylalanyl residues corresponding to interaction of the sodium ion with the histidine R-group. If a plot of percent relative intensity of total fragment ion current (peak areas calculated by FWHM) versus the pK_a of the particular amino acid residues one gets a graph as shown in Figure 6. Therefore it is proposed that the interaction of alkali metal ions is dictated by the most basic site of a molecule and that for peptides is dependant upon the pK_a of the R-groups present.

[1]Mallis, L. M.; Russell, D. H. *Anal. Chem.* 1985, *58*, 1076.

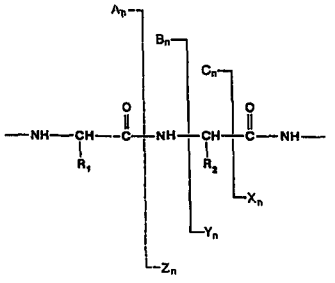

General case dissociation reactions for Peptides

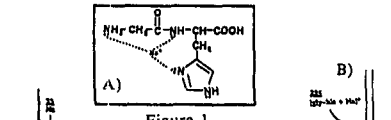

Figure 1

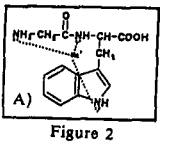

Figure 2

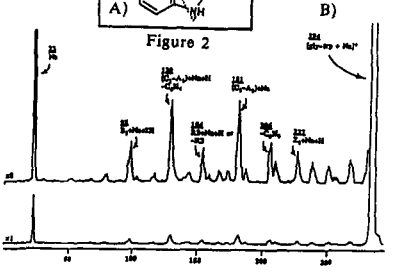

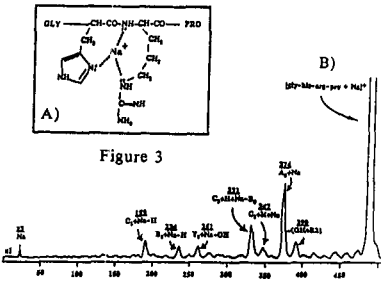

Figure 3

Figure 4

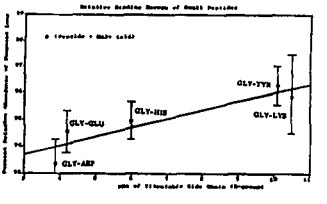

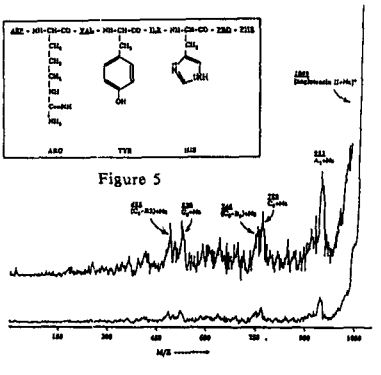

Figure 5

Figure 6

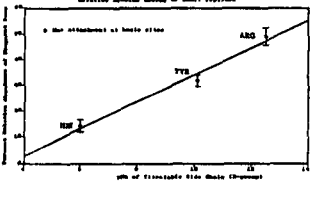

SIMULTANEOUS AND ACCURATE ANALYSIS OF TRACE LEVELS OF SIMPLE AND MACROCYCLIC TRICHOTHECENES BY LC/THERMOSPRAY - MASS SPECTROMETERIC AND TANDEM MASS SPECTROMETRIC TECHNIQUES.

Thaiya Krishnamurthy, and Emory W. Sarver
Research Directorate
US Army Chemical Research & Development Center
Aberdeen Proving Ground, MD 21010-5423 U.S.A.

Debra J. Beck, and Robert Isensee
Oneida Research Services
One Halsey Road, Whitesboro, NY U.S.A.

Trichothecenes (Figure 1) are toxic metabolites from various species of imperfect fungi. Economic losses and human health hazards due to these toxins have been observed and reported in several instances. The toxic nature of these trichothecenes combined with their frequently reported occurrence in various types of samples makes it imperative that any suspected samples be analyzed decisively and accurately with excellent sensitivity. However, until recently such methodologies were unavailable.

The complex polar structures of trichothecenes pose challenges in the development of simple GC/MS methods of analysis for these compounds. Extensive chemical modifications and/or derivatization procedures are required prior to their separation by GC. Earlier we reported several GC/NICIMS, DCI (positive and negative ions)-MS/MS, LC/MS, LC/MS/MS, and direct Thermospray-MS/MS methods of analysis for both simple and macrocyclic trichothecenes. The major disadvantage of all of these procedures is that, despite their efficiency or adequacy, only few compounds of similar structure could be analyzed by a single method.

However, we have recently developed LC/MS and LC/MS/MS (Figure 2) methods for the detection and quantification of most of the known trichothecenes representing all types, during a single analysis. The compounds are ionized under Thermospray conditions, and selectively monitored at pre-designated intervals during the analysis for increased sensitivity and selectivity. The total analysis time for the detection of 33 trichothecenes, by these procedures, is less than 30 minutes. The developed methods were applicable for the quantitative analysis of several true samples. Picogram and nanogram levels of these trichothecenes were detected under the mass spectrometric and tandem mass spectrometric conditions, respectively.

Figure 1.

TRICHOTHECENE MYCOTOXINS

SIMPLE TRICHOTHECENES

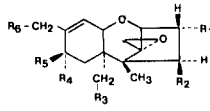

T-2 toxin, etc

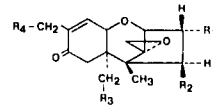

Deoxynivalenol, etc

MACROCYCLIC TRICHOTHECENES

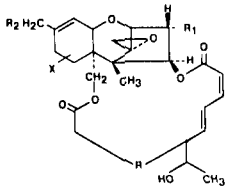

Roridins, Baccharinoids

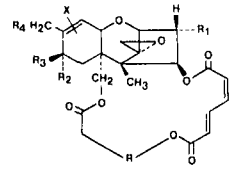

Verrucarins

Figure 2.

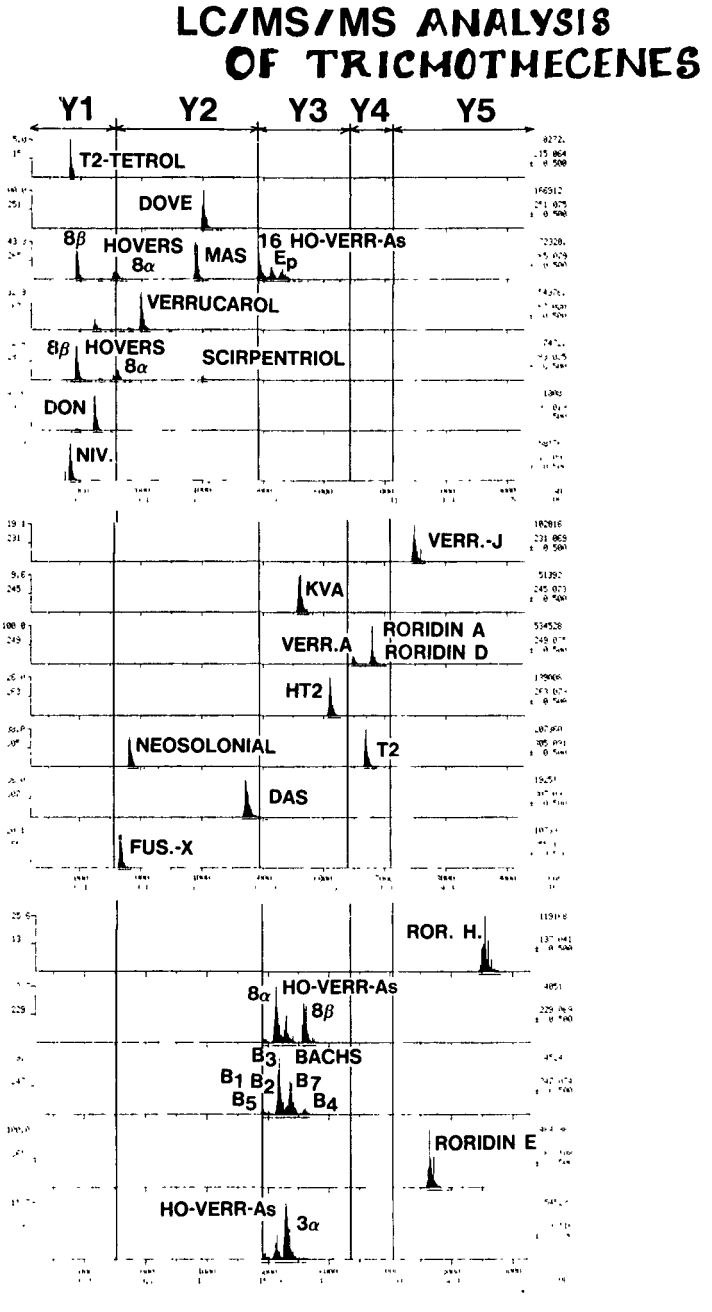
LC/MS/MS ANALYSIS
OF TRICHOTHECENES
Y1
Y2
Y3
Y4
Y5
T2-TETROL
DOVE
8β
HOVERS
8α
MAS
16 HO-VERR-As
Ep
VERRUCAROL
8β
HOVERS
8α
SCIRPENTRIOL
DON
NIV.
VERR.-J
KVA
VERR.A
RORIDIN A
RORIDIN D
HT2
NEOSOLONIAL
T2
DAS
FUS.-X
ROR. H.
8α
HO-VERR-As
8β
B3
BACHS
B1
B2
B7
B5
B4
RORIDIN E
HO-VERR-As
3α

FAST LC/MS AND LC/MS/MS FOR THE DETERMINATION OF PHYTOESTROGENS AND DRUGS IN FOOD MATERIAL, Thomas Covey and Jack Henion, Drug Testing and Toxicology, NYS College of Veterinary Medicine, Cornell University, 925 Warren Drive, Ithaca, New York 14850

INTRODUCTION

LC/MS techniques have matured so as to now be capable of high sample throughput analyses. We have been reporting the use of an API ion source as an important means achieving routine LC/MS by a variety of ionization modes (1-5). The essential important aspect of this system is the ion source at atmospheric pressure which circumvents many of the problems associated with introducing liquids into an ion source with low pressure requirements. The API source is also easy to access, clean, and permits simple LC/MS interface designs. Some of the advantages of using HPLC as a means of sample introduction into a mass spectrometer include minimum sample pretreatment and large volume sample injections, lack of thermal degradation of the analyte, and mild ionization. Mild ionization is achieved using chemical ionization (at atmospheric pressure in this case) or by mechanisms involving the desorption of preformed ions from solution droplets (2-5). Using the collision capabilities of MS/MS, structural information and analytical specificity can be derived from the abundant molecular ion species produced. With the APCI source, collisionally activated dissociation (CAD) can also be achieved before the first mass analyzer yielding fragment ions under single MS conditions and providing the capability for grandaughter ion analysis (6).

In this presentation we report the use of fast LC/MS and LC/MS/MS with an API source, heated pneumatic nebulizer interface (1) and atmospheric pressure chemical ionization for the determination of compounds of regulatory and health in the food supply Specific examples include the phytoestrogen coumentrol found present in alfalfa sprouts and the growth promoting drugs dexamethasone, trenbolone, and melengestrol determined in fortified bovine liver samples. An example is shown of the analytical utility of the pre-mass filter CAD capability of the API source when doing LC/MS on the alfalfa extracts.

EXPERIMENTAL

A Sciex TAGA 6000E quadrupole MS/MS equipped with an API ion source and heated pneumatic nebulizer (Sciex, Inc.) was used for this work. CAD in the central quadrupole collision cell was performed at collision energies of 70 eV and collision a gas thickness of 2×10^{14} atoms/cm^2 (2.0×10^{-5} torr). Selected reaction monitoring on 4 daughter ions of the targeted analyte was done for the low level determinations. CAD before the first quadrupole is accomplished in the free jet expansion of nitrogen from the API source into the analyzer vacuum region and collision energy was adjusted to 70 eV through control of the lenses in this region. LC/MS selected ion monitoring on 4 daughter ions of coumestrol in the alfalfa extracts was done during these experiments.

The HPLC equipment consisted of two Waters model 6000 pumps and a Perkin Elmer ISS 100 autosampler. The LC column was a Perkin Elmer 4.6 mm x 3 cm packed with 3 micron particles bonded with C18 for the fast LC/MS/MS and a 8 cm column for the LC/MS operated with 70/30 methanol/.1 M NH_4OAc mobile phase at a flow rate of 1 mL/min, while the entire effluent was introduced into the ion source.

RESULTS

Using an HPLC autosampler and the LC/MS/MS system described, rapid repetitive analyses of complex biological samples can be performed. The short, 3 cm cartridge columns provide short retention times and fast analyses, provided the added specificity of the MS/MS is employed to detect the analyte within a large amount of co-eluting matrix. For the coumestrol in the alfalfa extracts, repetitive injections every minute are shown in the figure below with a lower detection limit of approximately 0.5 ppb. Similar detection limits can be obtained using LC/MS SIM on 5 CAD fragment ions but this requires longer columns and analysis times on the order of 10 - 15 minutes per sample to separate the analyte from the matrix components. For the growth promoting drugs dexamethasone, trebolone, and melengestrol, repetitive injections every 2 minutes were made and analyses in the 1 - 5 ppb range were obtained.

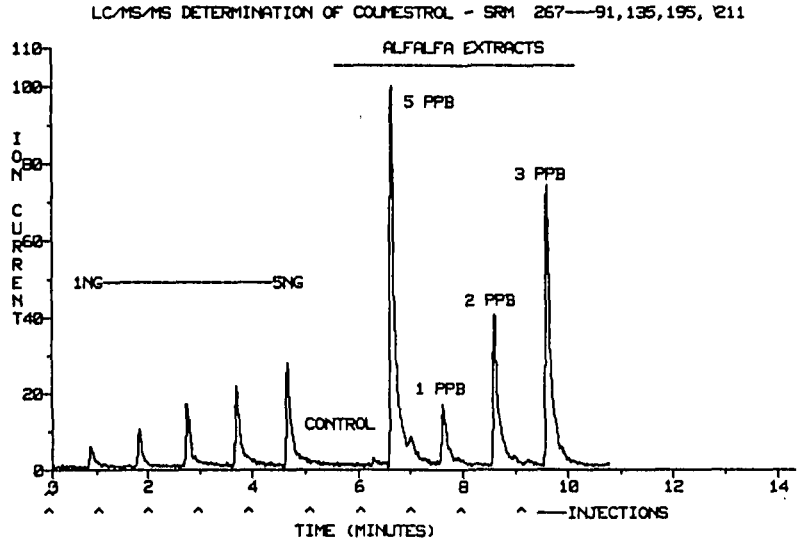

ACKNOWLEDGEMENTS

We thank the United States Department of Agriculture Agricultural Research Service, Food Safety and Inspection Service and the New York State Racing and Wagering Board Drug Testing and Research Program for financial support of this work.

REFERENCES

1. Covey, T., Henion, J.; presented at the Pittsburg Conference on Analytical Chemistry; Atlantic City, 1986, #856.
2. Bruins, A., Covey, T., Henion, J.; presented at the 34th Annual Conference on Mass Spectrometry and Allied Topics; Cincinnati, 1986, #TOE 2
3. Bruins, A.; Ibid. #WPB 11
4. Henion, J. and Bruins, A., Ibid. #TOD 3
5. Thompson, B.A.; Ibid; San Antonia, 1984, 190.
6. Dawson, P.H., French, J.B., Buckley, J.A., Douglas, D.J., Simmons, D. 1982. Org. Mass Spectrom. 17(5), 212-219.

STEROID PRODUCTION IN THE PREMATURE AND NEWBORN. GC/MS OFFERS INSIGHT INTO PHYSIOLOGY OF ADRENAL GLAND. Fennessey, P.V., Gotlin, R.W., Hambidge, S.J., Fennessey, K.D., and Pike, A.W. University of Colorado Health Sciences Center, Denver, Colorado

The urinary steroid profile from the newborn has been difficult to use as a tool to evaluate the adrenal function of this age group. The principle reason for this is the existence of two distinct types of adrenal tissue and the resulting excretion of large amounts of steroids that are unsaturated in the 5 position. Furthermore, in the immediate postpartum period the residual maternal hormonal levels have been considered as being an important factor in disturbing the observed urinary steroid profile. By one year of age the profile shows only normal steroids and except for the absolute levels of C-19 compounds the are essentially those of "little" adults. We decided to follow the excretion patterns of all the steroids produced using samples obtained from both premature and term infants. In this manner, we hoped to gain some insight into questions about the amounts, types and source(s) of the 5-ene steroids and the underlying physiological changes that caused the observed transition(s).

After obtaining informed consent from the parents, twenty four hour urine samples were collected from infants who were drug free and healthy. Follow-up samples were obtained on as many of the infants as was possible in an attempt to obtain longitudinal profiles. This sample collection continued on a (2-4) samples a month basis until the observed profile was essentially normal.

The unusual steroids seen in the premature are dominated by compounds that are derived from pregnenolone (5-Pregnen-3ßol-20 one). These were easily identified by a peak at m/z 129 in the spectra obtained from the MOX, TMS derivatives. This ion is produced from the derivatized steroids with a 3 hydroxy -5ene structure in the A/B rings. Profiles of this ion were used to locate and identify pregnenolone metabolites.

By following the quantitation production of these compounds we were able to accurately plot the development and subsequent involution of the fetal zone of the human adrenal. A task that was heretofore only measured by following the histology from autopsy sample. Surprisingly this zone develops and involutes and on a time basis that is independent of parturition. The maximum output (and presumably the termination of the growth cycle) of the fetal zone appear at a time equivalent to 38 ±2 weeks gestational age. Further, the adult zones appear to have grown to a size equal to the fetal zone at a time equivalent to 50 ±2 weeks gestational age.

This data was obtained on healthy infants and provides us with a new tool that can be used to follow basic physiological parameters of human adrenal development. Additional studies on sick premature and term infants may reveal the possible interrelationship of stages of adrenal development and the child's ability to cope with the stress and/or illness.

MEASUREMENT OF URINARY ARACHIDONIC ACID METABOLITES BY HIGH RESOLUTION GAS CHROMATOGRAPHY-NEGATIVE ION CHEMICAL IONIZATION MASS SPECTROMETRY FOLLOWING PURIFICATION BY IMMUNOAFFINITY CHROMATOGRAPHY.

J.J. Vrbanac[1], T.D. Eller[1], L.H. Hubbard[1], R.L. Baker[1], P V. Halushka[1,2], I.A. Blair[3] and D.R. Knapp[1]. Departments of Cell and Molecular Pharmacology and Experimental Therapeutics[1] and Medicine[2], Medical University of South Carolina, Charleston, SC 29425, and Division of Clinical Pharmacology[3], Vanderbilt University, Nashville, TN 37232.

Purification procedures necessary for quantitative GC/MS measurement of arachidonic acid metabolites in various biological matrices can be extensive. These procedures are particularly lengthy for urine samples. We have previously reported the development of immunoaffinity colums which sufficiently purified urinary TXB_2 and 6-keto-$PGF_{1\alpha}$ such that in subsequent analysis by high resolution GC-negative ion chemical ionization-MS (HRGC-NICI-MS) an interference free chromatogram was observed. The columns were constructed using agarose as the supporting matrix. We have subsequently noted interferences when using these columns. These interferences could be chromatographically resolved from the compound of interest by using *t*-butyldimethylsilyl derivatives (tBDMS) in place of trimethylsilyl (TMS) derivatives. However, a more satisfactory solution was to remove the source of interferences by using a silica supporting matrix in the construction of these columns.

The immunoaffinity columns were prepared by covalently bonding isolated IgG fractions to functionalized silica. To isolate the IgG fractions, rabbit prostaglandin E_2 (PGE_2), thromboxane B_2 (TXB_2) and 6-keto-prostaglandin $F_{1\alpha}$ ($6KPGF_{1\alpha}$) antisera were treated separately in the following manner A 5ml sample of antiserum was combined with 5ml of phosphate buffer and passed over a column containing staphylococcus aureus protein A immobilized on agarose The column was washed with 50 ml PBS and bound proteins eluted with 10 ml 1% acetic acid in 0.15 M NaCl. The eluates were adjusted to pH 8.0 with solid $NaHCO_3$. A 5g portion of hydroxysuccinimidyl SP500 silica gel (Serva, Westbury, NY) was combined with this purified IgG fraction and rotated for 2 hours at ambient temperature The silica was capped by addition of 100 µl of neat ethanolamine and rotating 45 minutes more. The gel was placed in polypropylene syringes containing a porous polypropylene frit and stored in PBS with 1% sodium azide at 4°C. Acidified urine samples were extracted with ethyl acetate, dried and the extract reconstituted in 1.3 ml PBS. The samples were loaded on the immunoaffinity column and allowed to equilibrate for 15 minutes. Columns were washed with 3 X 5 ml PBS, 2 x 5 ml distilled water and bound material was eluted with 10 ml 95% acetonitrile. Samples were dried under N_2 and methoxime (MO), ester (methyl, ME, or pentafluorobenzyl, PFB) and ether (TMS of tBDMS) derivatives were formed. The performance of these columns was evaluated using HRGC and both NICI-MS and electron impact MS (EI-MS). The NICI evaluation required PFB esters (monitoring M^--181, M^--PFB) and the EI evaluation employed tBDMS ethers (monitoring M^+-57; M^+-*t*-butyl). NICI analyses were performed either on a NERMAG R10-10C GC/MS or a modified GC/MS system consisting of Extrel C-50/C-150 electronics and 3/8 inch quadrupole rods, Finnigan 3200 vacuum system and ion source, and a Teknivent Vector 1 data system. EI analyses were performed using a HP 5970B Mass Selective Detector system. Results of NICI analysis are shown in figures 1-3. The results of EI analysis are seen in Figures 4-5 (dual peaks seer in Figs. 3-5 are due to syn- and anti-isomers). Traces in Figures 2-5 were obtained using the same urine sample. Surprisingly, the EI traces were as free from interferences as the NICI traces and the data obtained for 6-keto-$PGF_{1\alpha}$ using EI was cleaner than the NICI data (comparison shown in Figure 6).

In summary, we have developed silica based immunoaffinity columns for TXB_2, 6-keto-$PGF_{1\alpha}$ and PGE_2 which can be used repeatedly. Our data indicate that silica is superior to agarose in these applications Interference free chromatograms obtained in subsequent GC/MS analysis were noted for both NICI and EI modes of operation.

Supported in part by NIH grants RR01239 and HL29566.

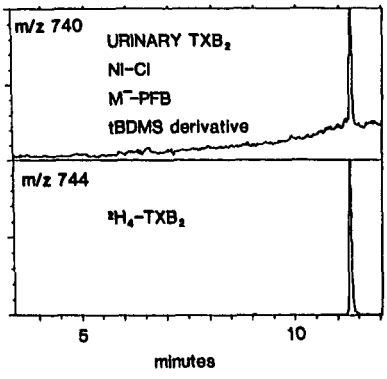

Figure 1

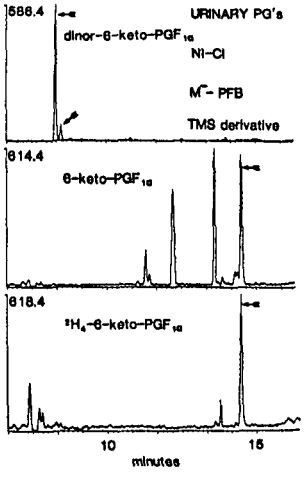

Figure 2

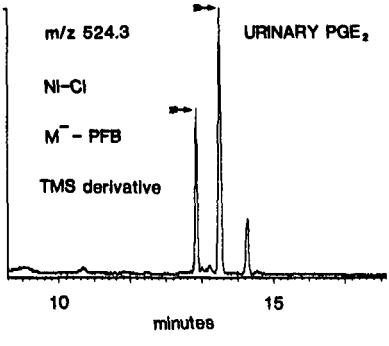

Figure 3

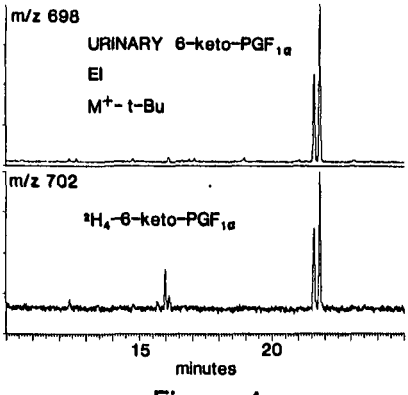

Figure 4

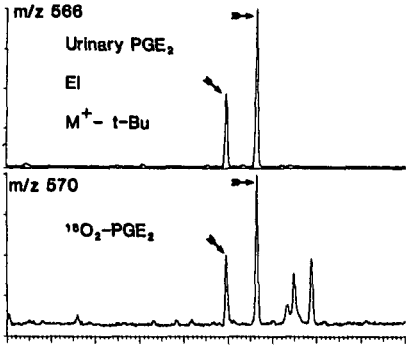

Figure 5

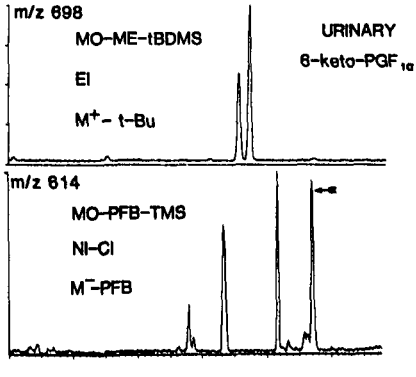

Figure 6

THE METABOLISM OF PROTAGLANDIN D_2 IN MAN: APPLICATIONS OF MASS SPECTROMETRY

B.J. Sweetman, C. Prakash, L.J. Roberts, and I.A. Blair, Department of Pharmacology, Vanderbilt University, Nashville, Tennessee 37232

We have previously investigated the metabolism of prostaglandin D_2 (PGD_2) is the monkey and characterized by GC/MS some 20 urinary metabolites, containing either a PGD or a PGF ring. This study now has increased clinical relevance because of the recent finding that patients having systemic mastocytosis can produce up to 150 times more PGD_2 than normal, and this can be an important mediator of vasodilatory episodes associated with the disease. It is now known that PGD_2 is the major prostaglandin produced by the mast cell. Some 16 metabolites of PGD_2 were isolated from the urine of a female patient having systemic mastocytosis. These were structurally-similar to the previously identified monkey metabolites but did include several isomeric forms which had not previously been seen. Several of the major urinary metabolites which had tetranor-PGF structures appeared to have the unusual 11-β configuration. This configuration of the 11-hydroxyl group appears to arise as a product of a specific 11-keto reductase enzyme. The occurrence of metabolites of PGD_2 containing the PGF_2 ring puts doubt on previous studies which have relied on the quantitation of PGF_2 metabolites as an index of $PGF_{2\alpha}$ production. The occurrence of PGF_2 metabolites containing the 11-hydroxyl group in the presumed β-configuration potentially provides a means for specific quantitation of PGD_2 production.

With these facts in mind we devised a synthetic scheme directed towards the unambiguous total synthesis of the proposed metabolites of PGD_2, both as a means of confirmation of the proposed structures of metabolites of PGD_2 isolated from urine as well as to provide a basis for the future development of a GC/MS assay specific for PGD_2.

The synthesis of 9,11 dihydroxy-15-oxo-2,3,18,19-tetranorprost-5-ene-1,20-dioic acid was successfully accomplished. The major metabolite of PGD_2 proposed in man is the hemiketal, δ-lactone of this structure. The synthetic scheme involved oxidation of the Corey lactone with dicyclohexylcarbodiimide in DMSO followed by a Wittig-Horner condensation of the ylid derived from levulinic acid gave the expected eneone. Hydrogenation and conversion of the ketone to thioketal was followed by formation of t-BDMS derivative and reduction with diisobutyl aluminum hydride giving the lactol which was condensed with the appropriate ylid under Wittig conditions to give the protected ortho ester, thioketal t-BDMS derivative. Removal of t-BDMS followed by hydrolysis of the ortho ester and esterification with diazomethane gave the thioketal dimethyl ester. The thioketal group was removed using ceric ammonium mitrate to give the expected product.

During the course of this synthetic scheme, all the synthetic intermediates and by-products were characterized using both positive ion and negative ion fast atom bombardment mass spectrometry and this technique has proved to be a highly useful adjunct to nuclear magnetic resonance in the structural elucidation of these molecules. Some unexpected reactions occurred during the course of the synthesis, one of which was a trans-esterification during the butyl lithium reaction to a mixture of butyl and methyl esters which tended to persist through the synthetic scheme. In addition, we were able to document the formation of a sulfoxide formed from the thioketal under some conditions.

As an example, the positive ion FAB spectrum of the ortho ester, t-BDMS, thioketal derivative (Figure 1) indicate of the spectra obtained that trans-esterification had occurred during reaction with butyl lithium. This spectrum showed pairs of peaks 42 M.U. apart attributed to matrix adduct, MH^+ and a fragment ion originating by fission of the ortho-ester for the mixture of methyl and butylesters.

Negative ion fast atom bombardment also proved to a useful technique in characterization of this series of compounds and associated products. Figure 2 shows the spectrum of a di-pentafluorobenzyl t-BDMS deriative which was also amenable to GC/MS analysis. However, GC/MS analysis with negative ion chemical ionization detection indicated the presence of one PFB ester group whereas the negative ion FAB spectrum provided clear evidence for two PFB groups, together with other structural information.

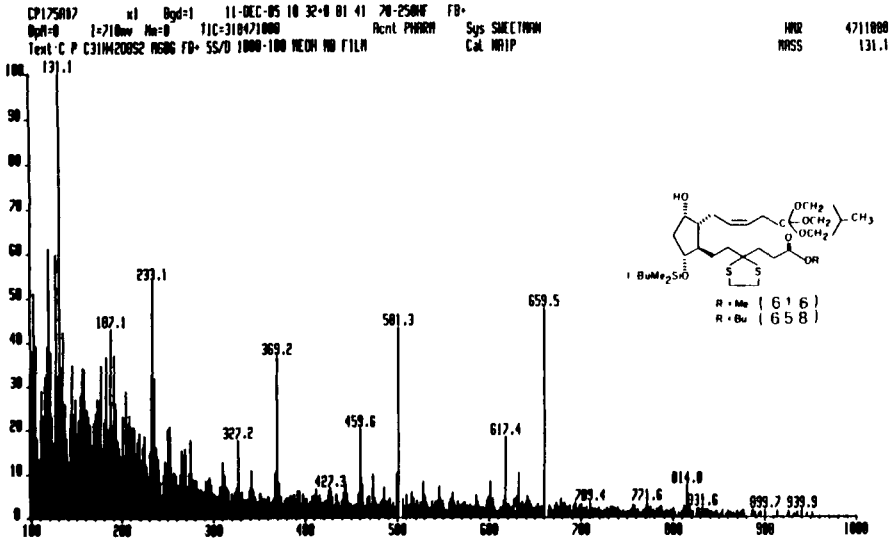

Figure 1. Positive Ion FAB mass spectrum of o-ester, t-BDMS, thioketal derivative.

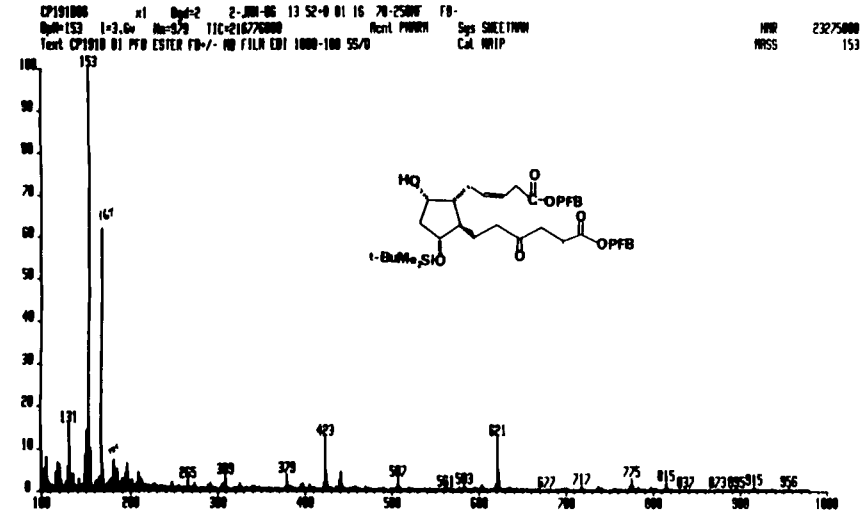

Figure 2. Negative Ion FAB spectrum of di-PFB ester + BDMS derivative.

Now having successfully completed the synthesis of the 11-α-hydroxyl series of compound, we are applying similar methods to the synthesis of the 11-β-hydroxyl series of compounds. In general, both positive and negative ion fast atom bombardment mass spectrometry have proved to be quite useful techniques in characterizing these small molecules of synthetic origin. FAB-MS is best used in conjunction with both NMR and GC/MS analysis.

Supported by NIH grants RR-01688, GM-15431 and RR-05424.

ANALYSIS OF LEUKOTRIENES, PROSTAGLANDINS, AND OTHER METABOLITES OF ARACHIDONIC ACID BY THERMOSPRAY HPLC/MS

Robert D. Voyksner[1] and Ernie D. Bush[2]; (1) Analytical and Chemical Sciences, Research Triangle Institute, P. O. Box 12194, Research Triangle Park, NC 27709; (2) Wellcome Research Laboratories, Research Triangle Park, NC 27709.

Metabolites of arachidonic acid are of great interest due to their implication in inflammatory reactions and neurotransmission. Anti-inflammatory drugs such as aspirin have been shown to inhibit production of certain metabolites or enhance other metabolities. To accurately map pathways inhibited or enhanced by drugs under investigation, sensitive and specific analytical methods are needed. The metabolites of interest include: leukotrienes (LTs), hydroxy-fatty acids (HETEs), and prostaglandins (PGs). Typically, GC/MS techniques have been used to monitor the metabolic pathways but, due to specific derivatization requirements for some of the metabolites, the pathways cannot be monitored simultaneously. Thermospray HPLC/MS has offered a very specific and sensitive means to monitor all arachidonic acid metabolites.

Individual analysis of the arachidonic acid metabolites using positive and negative ion detection with thermospray or filament chemical ionization indicated that thermospray ionization with positive ion detection was the most sensitive and information-rich mode of operation. Thermospray ionization produced ion currents from 1.2 to 2.0 times more intense than filament chemical ionization in the positive ion mode. The spectra for all the metabolities show $[M+NH_4]^+$ ions with fragments from sequential losses of water. The LTs, however, did not produce a molecular ion. The cleavage of the thio-carbon bond for the LTs was the highest m/z ion detected. Due to this cleavage, the thermospray spectra for LTC_4, LTD_4, and LTE_4 were virtually identical, and identification had to be based on HPLC retention time. The thermospray spectra for the HETEs were not sufficiently unique to differentiate the three individual metabolities. 15-HETE could be identified in the presence of the 5- and 12-isomers due to the difference in the relative ion intensities. The 5- and 12-isomers had to be identified by HPLC retention times. Other isomers including PGD_2 and PGE_2 (MW 352) and thromboxane B_2 (TXB_2) and 6-keto $PGF_{1\alpha}$ (MW 370) could be identified by the difference in relative intensities of the fragment ions as well as the HPLC retention time.

Negative ion detection using either thermospray or filament chemical ionization showed a factor of 5 to 10 less ion current than positive ion detection. Also, the information obtained from the negative ion spectra was nearly identical to the information obtained from the positive ion spectra. The $[M-H]^-$ ion and losses of water from the $[M-H]^-$ ion were the main peaks detected. The LTs were not detected in the negative ion mode at 200 ng levels.

The 14 arachidonic acid metabolites were separated by HPLC as shown in Figure 1. The separation was performed on a Zorbax ODS (DuPont, Wilmington, DE) 25 cm x 4.6 mm column using a mobile phase of 55% methanol for 20 min, 66% methanol for 20 min, 77% methanol for 20 min, and 100% methanol for 20 min (1). The remainder of the solvent was water buffered with acetic acid (0.08%) and brought to a pH of 6.2 with sodium hydroxide. The flow rate was 1.4 mL/min. The ammonium acetate (0.3 M) necessary for thermospray ionization was added postcolumn at a flowrate of 0.4 mL/min. Chromatographic separation of the HETEs, LTs and some of the PGs (TXB_2, 6-keto-$PGF_{1\alpha}$, PGD_2, and PGE_2) was required for identification due to the similarity of the thermospray spectra of the isomers of each class of metabolities. In order to achieve the desired sensitivity for the metabolites in plasma, multiple ion detection was employed. The two major peaks of each metabolite were monitored during the HPLC/MS analysis. Figure 2 shows representative selected ion profiles of the base peak of some PGs, LTs and HETEs for a 1 ng injection (LTs correspond to 40 ng). As shown in these chromatograms, many of the metabolities could be detected in the ng range and lower. The LTs as a class were not sensitive to thermospray HPLC/MS. Estimated detection limits for these metabolites appeared about a factor of 20-30 higher than the other metabolites.

Derivatization of the arachidonic acid metabolites was evaluated to increase sensitivity and gain spectral specificity. The thermally-induced methylation reaction of the carboxylic acid metabolite with trimethylanilinium hydroxide (TMAH) is possible with the heat supplied by the vaporizer and source. The esterification occurs as depicted below:

$$R\text{-}COO^- + (CH_3)_3NC_6H_5^+ \xrightarrow{\Delta} R\text{-}COOCH_3 + (CH_3)_2NC_6H_5$$

The arachidonic acid metabolites were chromatographed in the free acid form with the TMAH solution being added coaxially postcolumn such that derivatization occurred in

the heated thermospray interface. The HPLC/MS spectra of the esterified metabolites exhibited a similar fragmentation pattern to that observed with the free acid except the ions detected were 14 daltons higher due to methylation (Figure 3). Also, the TMAH derivative showed a factor of 3-6 increase in the ion current over the ion current for the free acid.

Pre-column derivtization was also evaluated for PGs. Chloro or bromo ethyl diethyamine reacts with carboxylic acids to form a triethyamine (TEA) derivative as shown below:

$$R\text{-}COOH + Cl\text{-}CH_2\text{-}CH_2\text{-}N(CH_2\text{-}CH_3)_2 \xrightarrow{\Delta} R\text{-}COOCH_2\text{-}CH_3\text{-}N(CH_2\text{-}CH_3)_2 + HCl$$

This derivative is very sensitive in both thermospray and filament CI modes of operation since the amine increases the molecules' proton affinity, favoring formation of $[M+H]^+$ ions. The spectra for the derivative shows an $[M+H+TEA]^+$ ion (m/z 454 for $PGF_{2\alpha}$) with few fragments. The derivative exhibits about 10-15 better sensitivity for $PGF_{2\alpha}$ than the free acid.

Reference

(1) D.C. Henke, S. Kouzan, and T.E. Eling, Anal. Biochem., 140, 87 (1984).

Acknowledgement

The authors would like to thank Burroughs Wellcome Co., Research Triangle Park, North Carolina, for the support of this research.

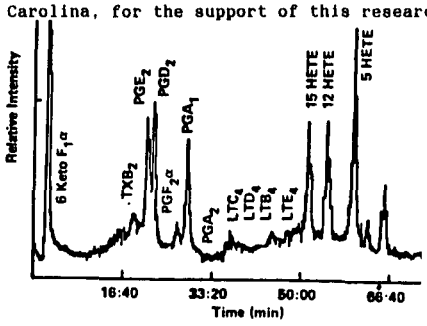

Figure 1

HPLC/MS total ion current chromatogram for the analysis of 14 arachidonic acid metabolites.

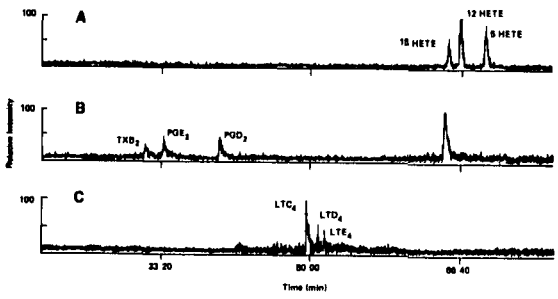

Figure 2

Selected ion monitoring chromatograms for: (A) m/z 317 for 1 ng of PGD_2, PGE_2, and 6-keto $PGF_{1\alpha}$; (B) m/z 303 for 1 ng of 5-, 12-, and 15-HETE; and (C) m/z 301 for 40 ng of LTC_4, 20 ng of LTD_4 and LTE_4.

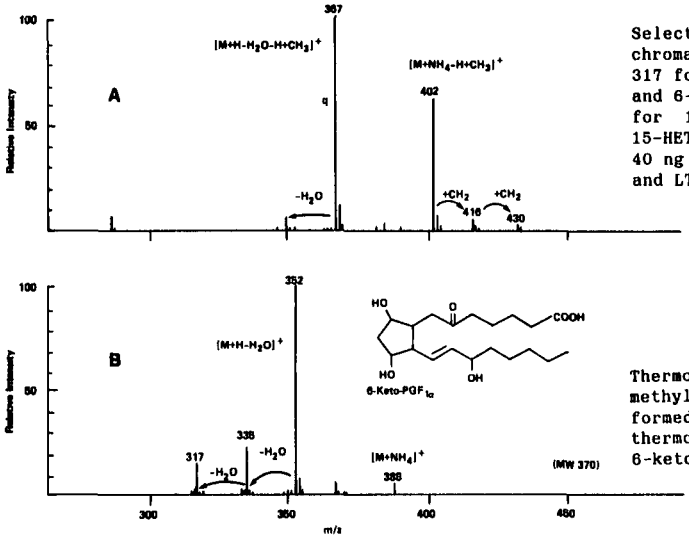

Figure 3

Thermospray spectra of (A) the methyl ester of 6-keto-$PGF_{1\alpha}$ formed with TMAH in the thermospray source and (B) of 6-keto-$PGF_{1\alpha}$ as a free acid.

NEGATIVE ION MASS SPECTROMETRY IN STUDIES OF HUMAN PLATELET ACTIVATION

L.A. Blair, J.D. Sweatt, K. Reddy, and L.E. Limbird, Department of Pharmacology, Vanderbilt University, Nashville, Tennessee 37232

The mobilization of arachidonic acid subsequent to activation of human platelets by various stimuli occurs through a number of pathways. For example, thrombin causes accelerated phosphatidyl inositol turnover and generates inositol phosphates and diacyl glycerol via the phospholipase C enzyme. Free arachidonic acid is then liberated from the diacylglycerol or from a mono-acyl glycerol after further hydrolysis. In contrast, it has been proposed that epinephrine-stimulated human platelet aggregation involves activation of phospholipase C indirectly as a result of arachidonic acid metabolism. The present study was initiated in order to determine which enzymic pathways of arachidonic acid release are involved in epinephrine-induced arachidonic acid mobilization in human platelets.

Human platelets were obtained from aspirin-free healthy male donors and prepared by centrifugation through a step-wise bovine serum albumin gradient followed by filtration through a Sepharase-2B column. A thromboxane (TX) receptor antagonist (SQ 29548) was added to the platelet preparation to prevent TXA_2-mediated aggregation and secretion from occurring. Epinephrine (10μM) was used as the stimulus. Initial experiments using platelets pre-labelled with ^3H-arachidonic acid or the use of analytical techniques based on radioimmunoassay were unable to detect released archidonic acid or prostanoids. It was then decided to employ the highly sensitive technique based on negative ion chemical ionization mass spectrometry (NICIMS) for the analysis of prostanoids. Prostanoid synthesis was determined 2 min after stimulation of human platelets with epinephrine. The incubations were terminated by the addition of 1M formic acid (final pH 3.5). To the incubation mixture was added 2ng each of $^2H_4$-$PGF_{2\alpha}$, $^2H_4$-PGE_2 and $^2H_4$-6-oxo-$PGF_{1\alpha}$ and extraction was carried out on Sep-Pak cartridges. The prostanoids were then converted to methoxime, pentafluorobenzyl (PFB) ester, trimethylsilyl (TMS) ether derivatives and analyzed by capillary column GC/NICIMS. Selected ions monitored corresponded to $(M\text{-}PFB)^-$ as shown in Figure 1. Quantification was carried out by use of extracted standard curves, unknown concentrations were determined by interpolation from these standards.

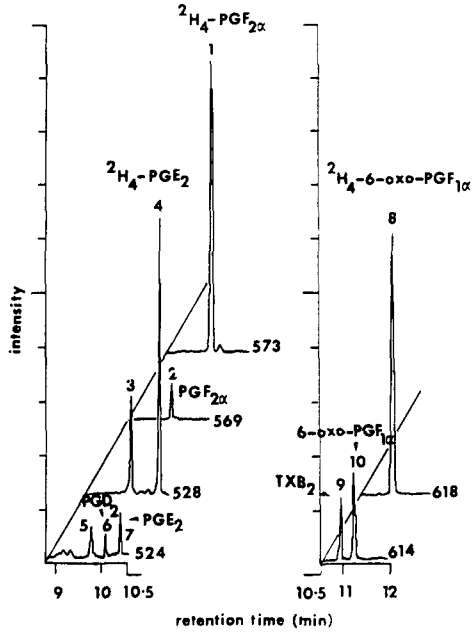

Figure 1. Selected ion current profile of a mixture of prostanoids using capillary column GC/NICIMS. Ions monitored correspond to $(M\text{-}PFB)^-$ for the relevant prostanoids.

In initial experiments a high background of TXB_2 was observed in the platelet preparation making it difficult to monitor small changes what may have occurred in response to epinephrine. In order to overcome the high basal TXB_2 concentrations, experiments were carried out in the presence of a TX synthase inhibitor (L63557) so that any formed PG endoperoxides (PGG_2, PGH_2 would be converted to PGs $F_{2\alpha}$, E_2 and D_2 rather that TXB_2 (Figure 2). We had previously shown that there was relatively low concentration of these PGs in the platelet preparation.

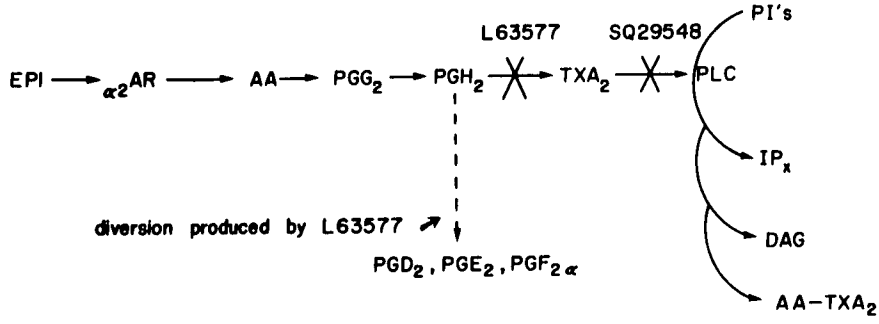

Figure 2. Experimental design for platelet activation experiments.

Stimulation of the platelets in the presence of the TX receptor antagonist (SQ29548) and the TX synthase inhibitor (L63557) caused an approximate two-fold increase in the production of $PGF_{2\alpha}$, PGD_2 and PGE_2 compared with control un-stimulated platelets (Table 1).

Table PG synthesis after stimulation of human platelets with 10μM epinephrine in the presence of a TX receptor antagonist (1μM, SQ29548) and a TX synthase inhibitor (100μM, L63557).

PG	Stimulation	Subject1*	Subject 2	Subject 3
$PGF_{2\alpha}$	Vehicle	48 ± 3	116 ± 16	90 ± 15
	Epinephrine	112 ± 7	290 ± 29	270 ± 31
PGE_2	Vehicle	126 ± 12	117 ± 13	31 ± 5
	Epinephrine	257 ± 36	274 ± 42	75 ± 15
PGD_2	Vehicle	162 ± 39	100 ± 20	28 ± 13
	Epinephrine	358 ± 37	205 ± 14	75 ± 14

* PG synthesis is expressed as pg/3x10^8 platelets/2 min (mean ± SEM; n=3).

These data show that epinephrine stimulation caused activation of a phospholipase enzyme which released a small pool of arachidonic acid that was converted to the PG endoperoxides. In the presence of the TX synthase inhibitor the endoperoxides were converted to PGs. In the absence of a TX synthase inhibitor the endoperoxides would be converted to TXA_2. Under normal circulstances (absence of a TX receptor antagonist), the TXA_2 would then activate a phospholipase C enzyme resulting in the release of more arachidonic acid and the production of more pro-aggregatory cyclooxygenase metabolites. In conclusion, negative ion mass spectrometry has provided evidence that a small pool of arachidonic acid is mobilized after epinephrine stimulation of human platelets.

Supported by NIH grants HL25182, GM15431, AM26657-061A and a grant-in-aid from the American Heart Asociation.

SELECTIVE CHEMICAL MODIFICATION OF LIPOXYGENASE METABOLITES FOR ELECTRON CAPTURE NEGATIVE CHEMICAL IONIZATION

Linda C. McCarraher and J. T. Watson
Department of Chemistry
Michigan State University
East Lansing, MI, 48824

The objective of our work is to investigate whether certain lipoxygenase metabolites of arachidonic acid can be selectively modified by chemical means to a structure having improved volatility over the parent compound. Ideally, the chemical modification scheme also would bring out any latent electrophilic character which could be used to advantage in electron capture negative chemical ionization mass spectrometry. In addition, the ideal scheme would selectively modify only the analyte by virtue of its structural features, thereby discriminating against chemical background which would either not be volatilized or not be converted to an electrophilic species or both.

The allylic hydroxyl moiety in many of the lipoxygenase metabolites seemed to be a good candidate for a distinguishing structural feature that might be exploited for analytical advantage. If the allylic hydroxyl could be oxidized with a mild oxidizing agent to the α,β-unsaturated ketone, such a reaction might be the basis of selectively converting allyl hydroxylated compounds to more volatile analogs while leaving other hydroxylated compounds unchanged in a more polar, less volatile form. In this way, a selective chemical reaction might discriminate against such chemical background, whereas the usual approach of using a derivatizing reagent such as BSTFA would convert all hydroxylated compounds to volatile species.

To test this hypothesis, the model compound 13-hydroxy-$\Delta^{9,11}$-octadecadienoic acid (lipoxygenase metabolite of linoleic acid) and 12-hydroxystearic acid were treated with MnO_2 in pet ether. As shown by the scheme in Figure 1, a mild oxidizing agent can be used to selectively modify the allylic hydroxy moiety. However, treatment of the oxidized product with diazomethane is required prior to vapor phase analysis, thus, only partial discrimination against chemical background is achieved with the mild oxidation reaction.

Figure 2 is an array of selected segments of GC-MS data to show the relative responses of the indicated model compounds to EC-NCI detection and to show their gas chromatographic behavior. The top row shows that, as expected, the compounds give approximate equimolar responses by FID. The second row indicates that the compound with the α,β-unsaturated system is selectively ionized over those without it, although the response of the pentafluorobenzyl (PFB) derivative is approximately 9 x greater.

The vapor phase properties of the 13-keto-18:2-ME are demonstrated and the retention times are shown to represent the relative elution pattern. The model compound 12-OTMS-18:0-PFB was included to represent the derivative used in the currently available method (1). Comparisons of the α,β-unsaturated ketone electrophore and the PFB derivative with regard to sensitivity, retention time, and vapor phase properties suggest that this approach to chemical modification of allyl-hydroxy compounds may offer advantages of overall selectivity in the analysis of complex mixtures for certain lipoxygenase products of arachidonic acid.

The oxidation of 15-hydroxyeicosatetraenoic acid to 15-keto-eicosatetraenoic acid was possible using MnO_2, however yields of the ketone were quite small even after extended oxidation. Another oxidizing reagent, dichlorodicyanobenzoquinone (DDQ), which is suitable for oxidizing allylic hydroxyls is being evaluated. While DDQ has proven to be much more efficient in the chemical conversion of 15-HETE to 15-keto-ETE, we must optimize the kinetics, yield, and isolation procedures for the 15-keto-ETE. Once those are established, we will determine the EC-NCI response and study this chemical modification procedure with realistic biological samples to evaluate its utility in discriminating against chemical background.

Acknowledgement: This work was supported in part by a grant (RR-00480) from the Biotechnology Research Program, Division of Research Resources, National Institutes of Health.

1. Balazy, M., Murphy, R. C. Anal. Chem., 58: 1098, (1986).

Figure 1. The selectivity of the MnO_2 reaction conditions for the model compound, 13-OH 18:2-ME (allylic hydroxyl) over 12-OH 18:0 18:0-ME (isolated hydroxyl).

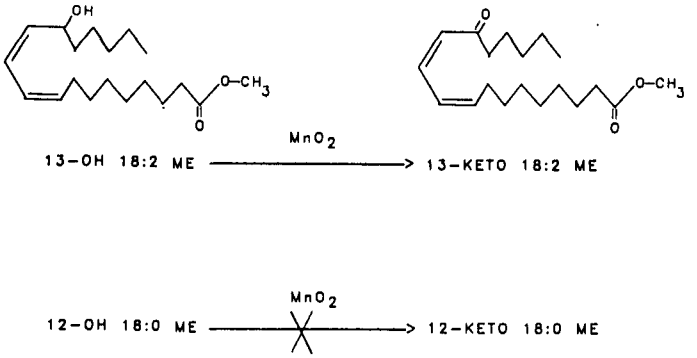

Figure 2. Responses of structurally different C-18 compounds to a universal detector (FID) and a selective detector (EC-NCI). All chromatographic peaks result from approximately the same amount of analyte injected on a DB-1 15m megabore column. Methane EC-NCI was accomplished using a modified HP5985A GC-MS.
EC-NCI conditions were: CH_4 pressure = 1.8 x 10^{-4} torr
source temperature = 155°C
Emission = 300μA
Electron Energy = 105eV

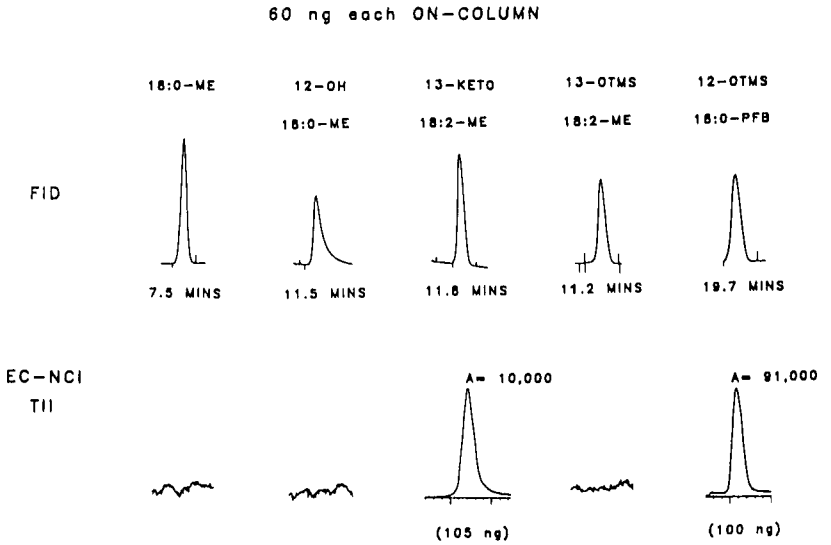

QUANTITATIVE ASPECTS OF LC/MS ANALYSIS OF PHOSPHOLIPIDS

Hamdy M. Abdel-Maksoud, James E. Evans, Firoze B. Jungalwala
and Robert H. McCluer, E. K. Shriver Center, Waltham, MA.

Phospholipids (PLs) are abundant structural components of all biological membranes. They also play important functional roles in many cellular processes. The molecular composition of PLs is heterogeneous with respect to the type of polar base present (e.g. serine, ethanolamine, choline or inositol), and the position, chain length and degree of unsaturation of the fatty acyl or alkyl moieties. Convenient methods for the separation and sensitive quantitative analysis of individual molecular species of PLs are needed to advance research into their biological roles. Conventional HPLC with UV detectors have variable and limited sensitivity dependent on the degree of unsaturation of the phospholipids. Thus, direct quantitation of phospholipids with an unknown degree of unsaturation is not possible with the ultraviolet detection mode. Alternately, HPLC-MS (1) was found to be the most direct and efficient technique of analysis and quantitation of phospholipids. This report describes a LC-MS method for the rapid quantitative analysis of PLs in biological mixtures.

Experimental

HPLC was performed with a Spectra Physics (model 8700) gradient pump and Brownlee cartridge, 10 cm x 2.0 mm spherical silica (5 um) column. The column was eluted with a linear gradient of solvent A, dichloromethane-methanol-water 93:6.5:0.5 (by volume) and solvent B, dichloromethane-methanol-water 65:31:4 (by volume), prgramming from 12% B to 45% B in 10 min and then to 100% B in 2 min at a flow rate of 0.6 ml/min. The phospholipids were dissolved in dichloromethane-methanol 1:1 (by volume) at a concentration of about 1 ug/ul and 5 ul injected. The HPLC solvent was applied as a fine stream to the moving polyimid belt of a Finnigan HPLC-MS interface to achieve an even coating.

The stream was formed by inserting a 10-cm section of polyimid-coated fused silica capillary GLC column (0.25 mm i.d.), pulled to a fine orifice. The sample evaporator heater was at 300° C and the cleanup heater was at 210° C. A Finnigan model 4500 mass spectrometer was used with ammonia (0.5 torr) as the CI reagent gas. The ion source was at 150° C. Positive ion spectra were obtained by the system under the control of a Teknivent model 56K MS data system. MS data were collected from m/z 100-850 with 14 second scans.

Results and Discussions

A reconstructed plot of the total ion current after HPLC-MS analysis of standard mixture (5 ug each) is shown in Figure A. Fairly good reproducibility was achieved under the experimental conditions. All the phospholipids were well resolved. The specific ion plots for m/z 141, 198, 105, and 142 are also shown in Figure A. These ions are fairly specific for the individual phospholipid bases. Thus m/z 105, specific for PS, is not found to be associated with other phospholipids. Similarly, m/z 141 is relatively specific for ethanolamine-containing phospholipids, whereas m/z 142 is specific for choline-containing phospholipids, and m/z 198 is found to be associated only with inositol-containing phospholipids. The mass spectral analysis of the earlier peak (PE) showed that it contained alk-1-enylacylglycerophosphoryl-ethanolamine, m/z 587 corresponding to plasmalogen with 18:1-18:2.

Female mouse kidney extract analyzed under the same conditions was found to contain mainly PE, PC, and SP (Figure B). Individual phospholipids were chromatographically resolved to some extent based on molecular species. Sphingomyelin was resolved into two peaks. Mass spectral analysis showed that the front peak contained mostly long-chain fatty acid-containing sphingomyelin such as 24:1 (m/z 630) whereas the later peak contained mostly short-chain fatty acid-containing sphingomyelin such as 16:0 (m/z 520).

Standard curves for PE, PS, PC, PI, and SP were obtained by chromatography of a mixture containig from 1 to 16 ug of each of these lipids (Figure C). All standard curves except that for PE showed good linearity when the area response for the TIC or

reconstructed ion chromatograms for base ions and diglyceride ions were used. The curves for the ethanolamine and diglyceride ions from PE showed an exponential increase in response with the amount injected.

The effect of the fatty acid chain length and unsaturation on the detector response was studied for synthetic PC's. Increasing number of carbons decreases the response linearly when the ratio of the area for the TIC to that for m/z 142 was plotted against the total number of fatty acid carbons. However, the degree of unsaturation did not seem to have measurable effect (Figure D). When the area ratio for the diglyceride ions (e.g. M^{+}-182) to that for m/z 142 was used the decrease in response was more drammatic and appeared to be exponential (Figure E).

This work was supported by N.I.H grants HD 05515, NS 16447 and NS 15037.

Reference:

(1) Jungalwala, F.B., Evans, J.E. and McCluer, R.H. (1984), J. Lipid Res., 25: 738-749.

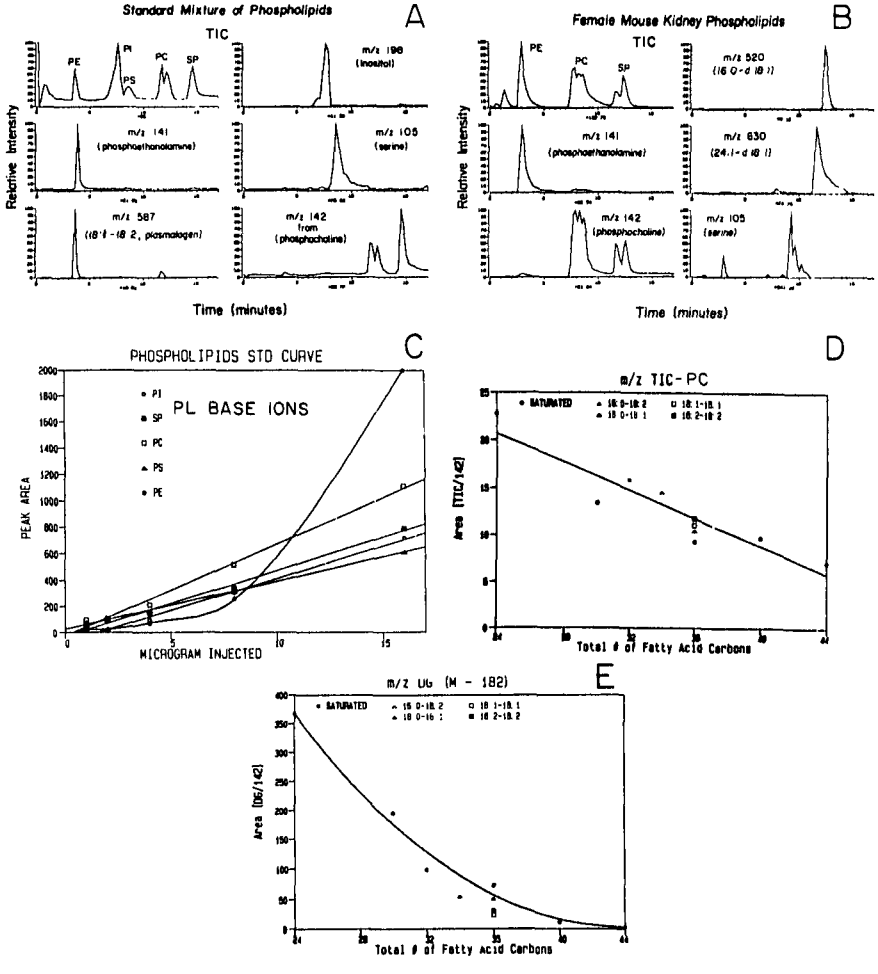

BACTERIAL PHOSPHOLIPID ANALYSIS BY FABMS

B.N. Pramanik, J.M. Zechman, P.R. Das, P.L. Bartner, A.C. Horan, and J.B. Morton. Schering Corporation, Bloomfield, NJ 07003, USA.

The analysis of bacterial phospholipids by fast atom bombardment mass spectrometry (FABMS) is reported. FABMS was found to be a useful method for analyzing phospholipid mixtures and information of value in bacterial taxonomy and identification was obtained. Stable molecular ions and characteristic fragment ions were displayed which permitted the identification of phosphatidyl (P)-choline, P-ethanolamine and its methylated forms, P-glycerol and P-inositol. Information regarding the length of the acylated fatty acids, their degree of unsaturation, and the presence of hydroxyl groups was also obtained.

Phospholipids were extracted from lyophilized cells by a modification of the method of Bligh and Dryer. In this procedure, the phospholipids were extracted by heating 5 minutes at 100°C in chloroform:methanol (1:2) and mixing 3 h at room temperature in chloroform:methanol:0.3% NaCl (1:2:0.8). Phospholipids present in the resulting lipid fraction were analyzed without further purification. Mass spectra were obtained on a Finnigan MAT 312 operating at an accelerating voltage of 3 KeV and employing a SS-200 data system.

A total of 19 organisms representing several genera of actinomycetes, 2 strains of Escherichia coli and 1 strain each of Proteus mirabilis and Pseudomonas aeruginosa have been examined. A representative spectrum of the phospholipids from the actinomycete Microbispora parva is shown in Fig. 1. A fragment ion present at M/Z 142 ($HO-CH_2-CH_2-NH_3^+$) indicated that P-ethanolamine (PE) was present (spectrum not shown). Diacyl and monoacyl fragment ions representing the fatty acid components are present in the regions of M/Z 551-609 and 311-355, respectively. These results taken together allow the identification of the PE species which are present as molecular ions in the region M/Z 706-750. For example, the molecular ion at M/Z 736 represents PE acylated with a hydroxylated C_{16} and a saturated C_{18} fatty acid and gives rise to acylated fragment ions at M/Z 595, 329, and 341. As additional evidence for this interpretation, the hydroxylated and non-hydroxylated PE classes were partially separated and isolated by TLC using chloroform:methanol:H_2O (65:25:4). The polar component corresponding to PE with a hydroxylated fatty acid produced a FABMS spectrum enriched in molecular ions at M/Z 708, 722, 736, and 750 (Fig. 2A). In contrast, the non-polar component corresponding to PE with non-hydroxylated fatty acids produced molecular ions at M/Z 706, 720, and 734 (Fig. 2B). These results were supported by high resolution MS and MS/MS studies.

Each organism examined varied with respect to the types of phospholipid classes present and/or the nature of the acylated fatty acids. The FABMS spectra were therefore highly characteristic of individual bacterial species. Compare Fig. 1 with the FABMS profiles of phospholipids from Proteus mirabilis (Fig. 3) and the actinomycete SCC 1789 (Fig. 4). These results suggest the use of FABMS as a method for rapid bacterial phospholipid analysis and identification.

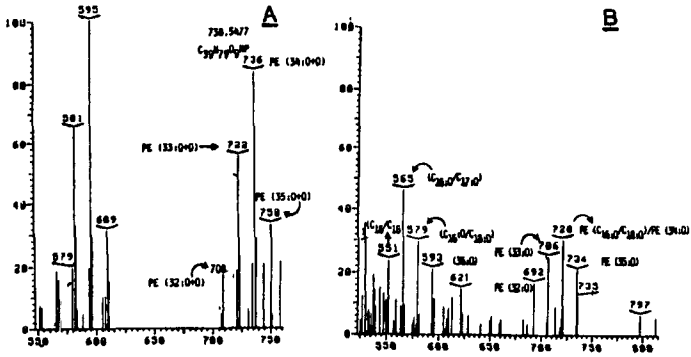

FIG. 2. FABMS OF POLAR (A) AND NON-POLAR (B) COMPONENTS OF MICROBISPORA PARVA SEPARATED BY TLC

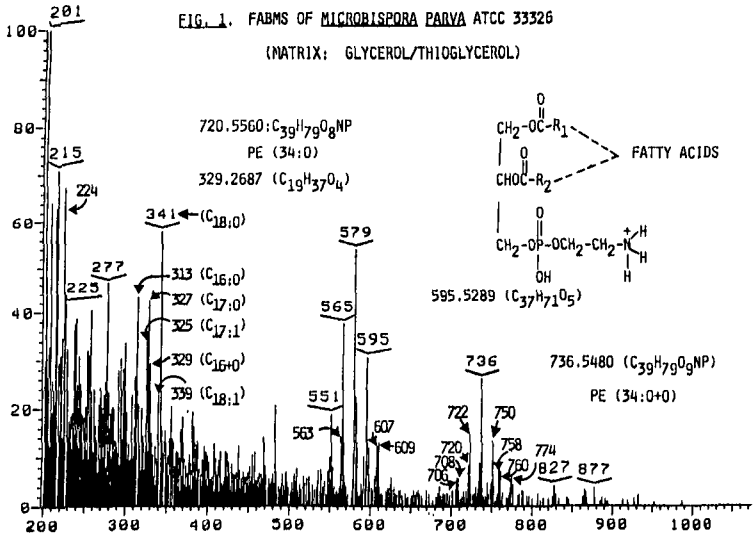

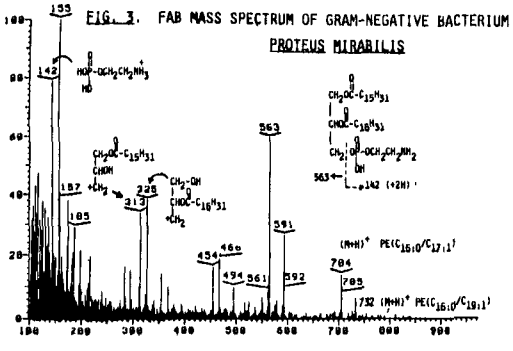

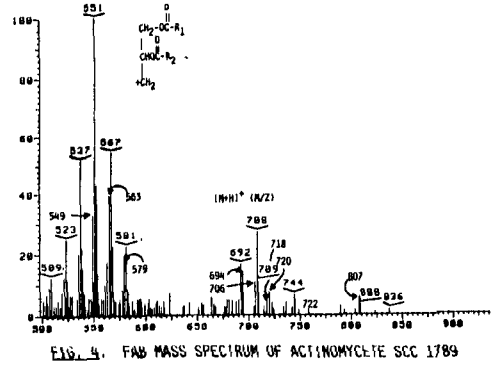

FIG. 4. FAB MASS SPECTRUM OF ACTINOMYCETE SCC 1789

PROCESSING AND ANALYSIS OF IMAGES FROM A CAMECA ION MICROSCOPE

David S. Bright
National Bureau of Standards
Gaithersburg, MD. 20899

A few image processing and analysis techniques are here illustrated that have been useful in extracting information from ion microscope images of discrete particles. In particular, an algorithm is presented to select particles from an image, an essential step in measuring the isotope ratios of the particles. Preliminary results are shown for a field of particles and the five major isotopes of Barium.

Images of particles taken on the ion microscope (Figure 1) have characteristics that make it difficult to select the particles. Selecting a particle means determining a 'blob' or a contiguous set of pixels that correspond to the particle. One characteristic is shown by the mesh plot in Figure 2, where the saddle between the two largest peaks is higher than the shorter peak nearby. Using one threshold, either the two brightest particles will not be resolved or the dimmer particle nearby will not be detected. Another characteristic is that the particles do not have uniform size ,shape or intensity (cf. Figure 1 with log of intensities, Figure 3) and some are very close together. It is not obvious how to use the more conventional mask filtering or cross correlation techniques. The third characteristic is that the edges of the particles are not sharp. If they were, the gradient of the image would give edges of the bright and dim particles alike, which in turn could be used to locate the particles themselves.

The algorithm presented here involves setting a number of intensity thresholds, and keeping track of what the blobs do as the threshold is gradually increased. During this process, the blobs shrink and split (imagine horizontal sections of Figure 2, taken at higher and higher levels). If a blob splits then each piece is treated as a distinct blob if it has an area above a set minimum area A_{min} (small noise areas are rejected in this way). The piece is retained if it gradually erodes away without splitting again. The concept is shown in Figure 4, where each arrow represents an increase in the threshold in going from one shape to the next. In this case, the object to the upper left is composed of several particles. At the lowest threshold setting, the entire object is selected, as shape 'A'. This shape splits into two pieces, one of which again splits. The letter 'X' denotes that the blob has eroded below A_{min} at that threshold. The pieces kept in this example are then C, D and E.

The results can be seen in Figures 3 and 5, where in each, a rectangle is drawn to just enclose the particle or blob of interest. The log of the intensities of the images are displayed to make the dimmer particles more visible. The the rectangles in figure 3 were obtained by setting a uniform threshold at a level to select as many particles as possible. Note that many bright particles are fused and that many dim ones are missed. Figure 5 shows the results of applying the algorithm, where practically all of the particles are selected.

Particle locations were determined for the brightest image, ie. Barium 138. For each particle, isotope ratios were measured from this image and the four other images of the four other major isotopes by using the average intensities in the corresponding rectangles.

The results for 84 particles (horizontal lines) and the 5 isotopes (134 ... 138 , vertical bands, left to right) are shown in Figure 6, as deviations from the naturally occuring value. The bar at the top represents a deviation in percent abundance, of 2% negative (darker shade to the left) or 2% positive (lighter shade, to the right). The top particles are the brightest, and have better values because correction for background is less of a problem. The dimmer particles at the bottom are barely above background intensity.

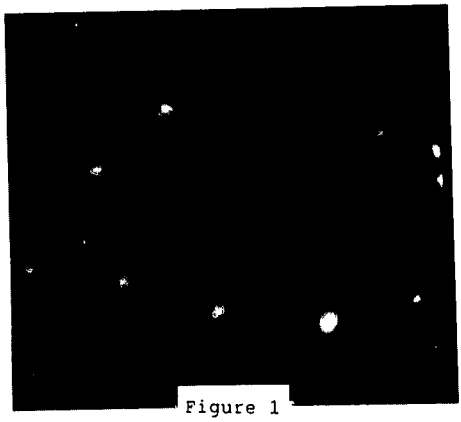

Figure 1

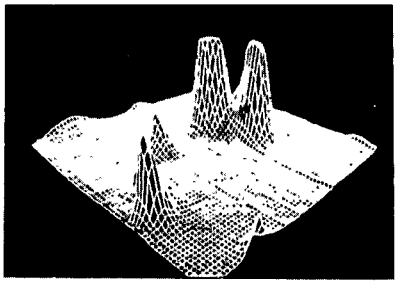

Figure 2

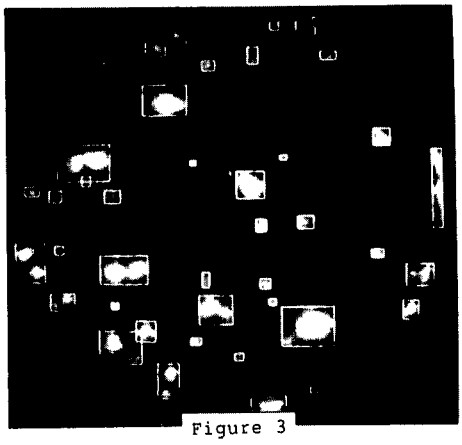

Figure 3

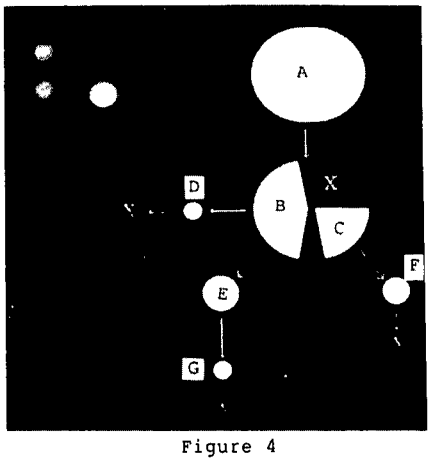

Figure 4

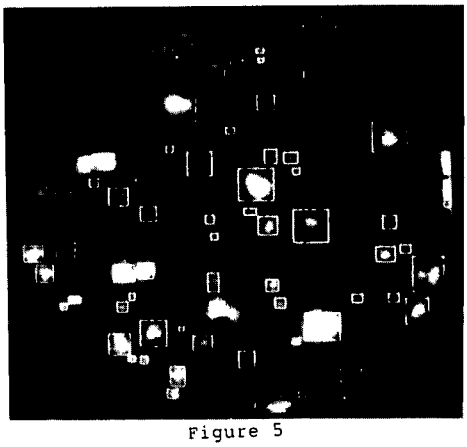

Figure 5

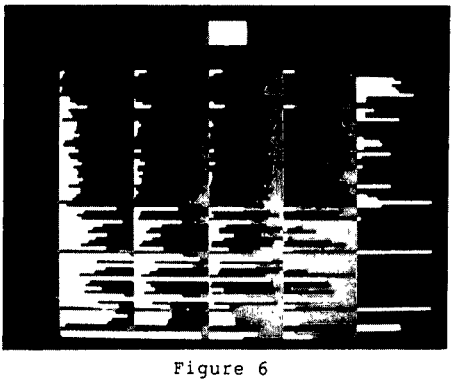

Figure 6

ION IMAGING: METHODOLOGY AND APPLICATION TO BIOLOGICAL SYSTEMS

M.G. Moran and G.H. Morrison
Department of Chemistry, Cornell University, Ithaca, New York, 14853

Introduction

Imaging has traditionally played an important role in the investigation of biological systems. This is primarily due to the fact that visual inspection of biological specimens is one of the most efficient methods of correlating the structure of the system under study and its function. Light microscopy is the oldest method of imaging biological samples and has contributed greatly over the years to understanding of life processes. Development of newer methods of imaging in this century such as electron and ion microscopy have pushed the investigation of the structure/function relationship to new depths. These advances, coupled with the application of digital computer manipulation of image data are on the verge of ushering in a new era in the study of biologicals at the cellular and subcellular level.

This report will deal primarily with issues related to ion microscopy and how this technique can enhance our knowledge of the role chemical elements play at the cellular level. Various applications of imaging and image processing to the elucidation of elemental distributions in biological soft tissue samples will be discussed.

Ion microscopy is based on secondary ion mass spectrometry (SIMS). Positive secondary ions are sputtered from the sample surface when bombarded with a beam of monoenergetic primary ions. A stigmatic instrument such as the Cameca IMS-3f focuses the sputtered ions into a modified Nier-Johnson mass spectrometer. The mass filtered ion image impinges on a microchannelplate and can be imaged by a 35 mm camera or a low light level video camera. In this way, the spatial distribution of elements of physiological interest such as Na, K, Ca, Mg can be recorded. The principles of stigmatic ion imaging and scanning ion microscopy have been extensively discussed in the literature [1,2].

Image Processing - Methodology

Ordinary 35 mm photography is a quick simple way of recording ion images for qualitative work. For more demanding applications such as quantitative work and multielement image depth profiling a computer controlled data acquisition system is a must [3,4]. Since SIMS involves destructive sampling and generation of large amounts of data, a computer controlled video recording system has been proposed by the authors [5]. This system can record a virtually unlimited amount of data on video tape in real time for subsequent digitization and off line processing. Additionally, acquisition methodology can be made flexible enough to accommodate temporal changes in experimental conditions.

Amendment of raw image data usually means conversion of each image pixel value into a number proportional to concentration of the element of interest. This has been attempted for Ca distribution in plant root tip cells using a modified implanted internal standards quantification scheme [6]. However, this method is not considered to be entirely satisfactory.

Image Processing - Applications

As methodology matures, image processing will be an increasingly important tool in aiding analysis of biological SIMS data. An important area is sample preparation. Ca, Mg, Na, K are all readily soluble in water and highly diffusible in biological samples. Thus, any sample preparation technique for imaging work must satisfy two important criteria. The native element distribution must be preserved while rendering the sample amenable to high vacuum conditions. Imaging of samples is also an excellent way to evaluate various sample preparation schemes [7]. Additionally, imaging is well suited to evaluating any sample pretreatment. An example is the modification of Na/K ratios in normal rat kidney cells as a function of exposure time to the inhibitor ouabain [8].

Any quantification scheme in biological SIMS must deal with matrix effects and differential sputtering. A method recently proposed to evaluate the severity of matrix effects is to integrate through the profile of an implanted element. Ideally the implanted element should be one that is potentially influenced by sample heterogeneity. Beryllium has been used for this purpose in our laboratory [9]. If matrix effects are absent, the integral of the image depth profile of the implant should be a featureless image. This was found to be approximately the case in ashed biological thin sections.

Conclusion

Ion imaging is a relatively new field which has a considerable way to go before reaching its full potential. However, its promise for quantitative work, kinetic studies of ion transport and 3 dimensional analysis of biological systems more than justifies further research in this area.

References

1. G.H. Morrison, G. Slodzian, Anal. Chem., 47, p. 932A, (1975).
2. R. Levi-Setti, G. Crow, Y.L. Yang, Scanning Electron Microscopy II, p. 535 (1985).
3. B.K. Furman, G.H. Morrison, Anal. Chem., 52, p. 2305, (1980).
4. S.R. Bryan, W.S. Woodward, D.P. Griffis, R.W. Linton, J. Micros., 138, p. 15, (1985)
5. J.T. Brenna, M.G. Moran, G.H. Morrison, Anal. Chem., 58, p. 428, (1986).
6. W.C. Harris, S.C. Chandra, G.H. Morrison, Anal. Chem., 55, p. 1959, (1983).
7. S. Chandra, G.H. Morrison, C.C. Wolcott, J. Cell Biol. (In press).
8. S. Chandra, G.H. Morrison, Science, 228, p. 1543, (1985).
9. J.T. Brenna, G.H. Morrison, Anal. Chem., (In press).

Image Depth Profiling for 3-Dimensional Elemental Mapping

S.R. Bryan, R.W. Linton, and D.P. Griffis*

Department of Chemistry, University of North Carolina, Chapel Hill, NC 27514
*Engineering Research Services Division, North Carolina State University, Raleigh, NC 27650

The high detection sensitivity, spatial resolution, and depth profiling capabilities of secondary ion mass spectrometry (SIMS) can be combined with digital imaging technologies to produce 3-dimensional elemental maps of the near-surface region of solids [1-3]. These maps are generated by acquiring a series of mass-selected digital ion images at specific time intervals while continuously sputtering the sample surface. Each successive image shows the lateral (x-y) distribution of the element of interest at successively greater depths (z) from the surface. This mode of SIMS analysis, called image depth profiling (IDP), is performed with either an ion microprobe or an ion microscope [4].

In order to fully automate IDP acqusition, a microcomputer-based digital imaging system [5] has been developed for a Cameca IMS-3f ion microscope (Figure 1). The imaging system has been interfaced to the HP 9845B microcomputer, which controls the ion microscope, to synchronize peak switching of the mass spectrometer with digital image acquisition and storage during a multielement IDP. Each image is digitized into a 244 x 248 array of 8-bit pixels (picture elements). In an IDP containing 50 data sets, the 3-dimensional distribution of each element profiled is characterized within the imaged volume by a 244 x 248 x 50 array of intensities.

Once an IDP has been acquired and stored on disk, the data may be processed and displayed in a variety of ways [4]. One of the most powerful post-acquisition processing techniques is the reconstruction of local area depth profiles (LADP). An LADP is reconstructed by summing the pixel intensities from any area within the image field, ranging from a single pixel to the entire image field, and plotting the intensity sum from each image in the IDP vs. sputter time or depth.

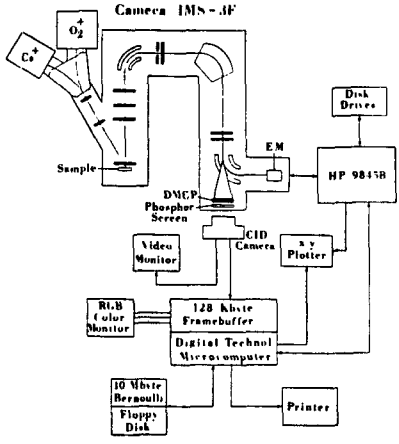

Figure 1. Block diagram of the experimental set-up used for acquiring digital image depth profiles.

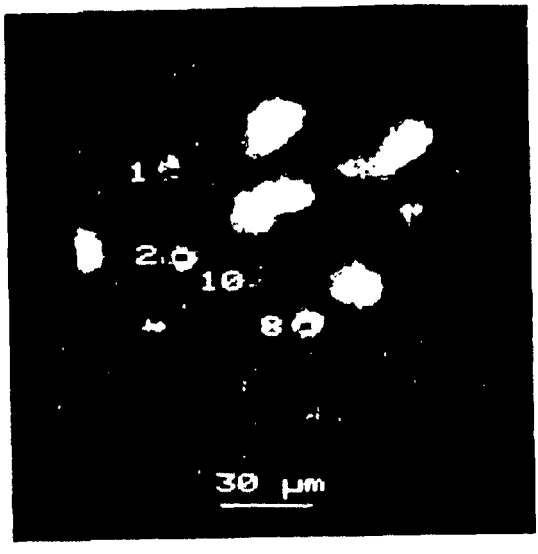

Figure 2. A digital Ti image from a 150 um diameter area containing several fly ash particles. Local area depth profiles were generated from the square black areas within each particle.

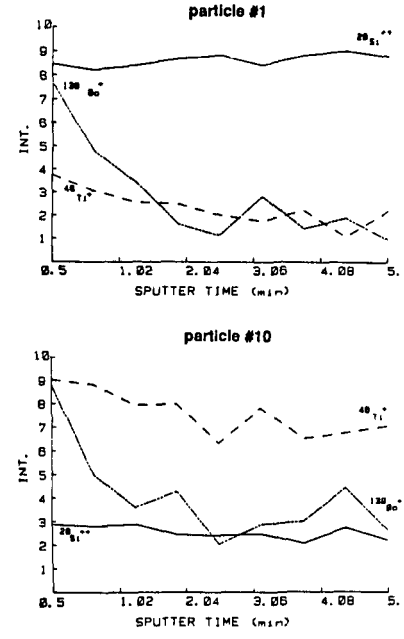

Figure 3. Local area depth profiles from particles 1 and 10 (see Figure 2). Total sputtered depth is approximately 1 um. Intensity range for both plots is from 30 to 148 intensity units/pixel.

IDP of Trace Elements in Fly Ash Particles

A study was undertaken to determine the feasability of using IDP to characterize the depth distribution of trace elements within individual micrometer size fly ash particles and to determine the variation in concentration of these elements from particle to particle. An example of the type of results obtained using IDP is given in Figures 2 and 3. An IDP of Si, Ti, and Ba was acquired from a 150 um diameter area containing several individual particles. Figure 2 is a Ti image from the IDP with the individual particles of interest numbered. The square black area within each numbered particle indicates the 3 x 3 pixel region chosen for generating a LADP.

Figure 3 shows a LADP from particles 1 and 10. These plots illustrate the ability to distinguish between elements which are surface enriched (Ba) and those which are more uniform in concentration with depth (Si and Ti). Also, by comparing the relative elemental intensities from LADP's of different particles, it is possible to determine the variation in elemental composition from particle to particle.

References

1. F.G. Rudenauer and W. Steiger, Mikrochim. Acta Suppl. **2**, 375 (1981).
2. A.J. Patkin and G.H. Morrison, Anal. Chem. **54**, 2 (1982).
3. S.R. Bryan, W.S. Woodward, R.W. Linton and D.P. Griffis, J. Vac. Sci. Technol. **A3**, 2102 (1985).
4. F.G. Rudenauer, Surf. Interface Anal. **3**, 132 (1984).
5. S.R. Bryan, W.S. Woodward, D.P. Griffis, and R.W. Linton, J. Microsc. **138**, 15 (1985).

Applications of Secondary Ion Mass Spectrometry Image Analysis in Materials Science

Dale E. Newbury
National Bureau of Standards
Gaithersburg, MD 20899

Compositional mapping by microanalysis techniques is developing as an important tool in materials science for the characterization of specimens on the micrometer and sub-micrometer spatial scales. In order to solve many problems, an analytical approach which makes use of several imaging/analysis methods is especially powerful. Secondary ion mass spectrometry (SIMS) in the form of the ion microscope or ion microprobe provides capabilities for light element and trace element imaging which can augment information derived from other forms of microscopy and microanalysis, e.g., optical microscopy (OM), scanning electron microscopy (SEM), electron probe microanalysis (EPMA), etc. The utilization of information from multiple techniques has now become practical with the development of digital imaging and compositional mapping techniques. Two examples of applications to materials science problems will illustrate the synergistic nature of the results which can be obtained [1].

(1) Reaction-bonded silicon carbide displays strong anomalous contrast in secondary electron emission when imaged in the SEM [2]. The differences observed in secondary electron emission could not be correlated with any compositional variation which could be detected with EPMA at concentration levels of the order of 0.1%. SIMS images of a trace aluminum constituent reveal a pattern of segregation which closely matches the pattern of secondary electron emission observed in the SEM, as shown in Figures 1(a) and 1(b). In order to confirm this apparent correlation, it was necessary to use image processing to apply compensation for relative distortion of the SEM and SIMS images. The SIMS image was modified by a warping function which was applied by manually selecting 25 tie points which were recognized to correspond in the two images. The warping function produced the image in Figure 1(c). The degree of matching between the SEM image and the warped SIMS image was then further studied by means of image processing functions. For example, edge highlighting of the warped SIMS image was accomplished by applying a either threshold function, as shown in Figure 1 (d), or a gradient function (a two-dimensional spatial derivative). By means of color overlay techniques, the edge-highlighted SIMS image could be overlaid on the original SEM image, producing a composite image from which the correlation between the behavior of the secondary electron emission and the distribution of aluminum in the microstructure could be recognized. The aluminum constituent is believed to segregate during partial melting during the reaction-bonding process. The aluminum modifies the band structure of the semiconductor silicon carbide, thus modifying the secondary electron coefficient.
(2) Aluminum-lithium alloys form an important class of high strength-to-weight structural materials [3]. The lithium constituent at concentration levels below 10 wt% cannot be directly analyzed by any other microanalytical techniques except SIMS. SIMS images of lithium distributions reveal a variety of metallurgical phenomena, including precipitation of intermetallic compounds, denuding of grain boundaries in over-aged alloys, and anomalous surface structures produced by conventional optical metallography preparations. This latter artifact is illustrated by the images shown in Figures 2(a) and 2(b). Figure 2(a) shows the lithium distribution at the surface of the as-polished specimen, while Figure 2(b) shows the distribution after sputtering to remove the surface layer. The distribution of lithium is profoundly different between the two locations, suggesting that the surface has been affected by the metallographic preparation, rendering it non-representative of the interior of the specimen.

References

1. Newbury, D., Bright, D., Williams, D., Sung, C.M., Page, T., and Ness, J., Secondary Ion Mass Spectrometry SIMS V, ed. A. Benninghoven, R.J. Colton, D.S. Simons, and H.W. Werner (Springer-Verlag, Berlin 1986) 261.
2. Sawyer, G.R. and Page, T.F., J. Mats. Sci., 13 (1978) 885.
3. Williams, D.B., in Aluminum-Lithium Alloys, ed. T.H. Sanders and E.A. Starke (Metallurgical Society of AIME, 1980) 89.

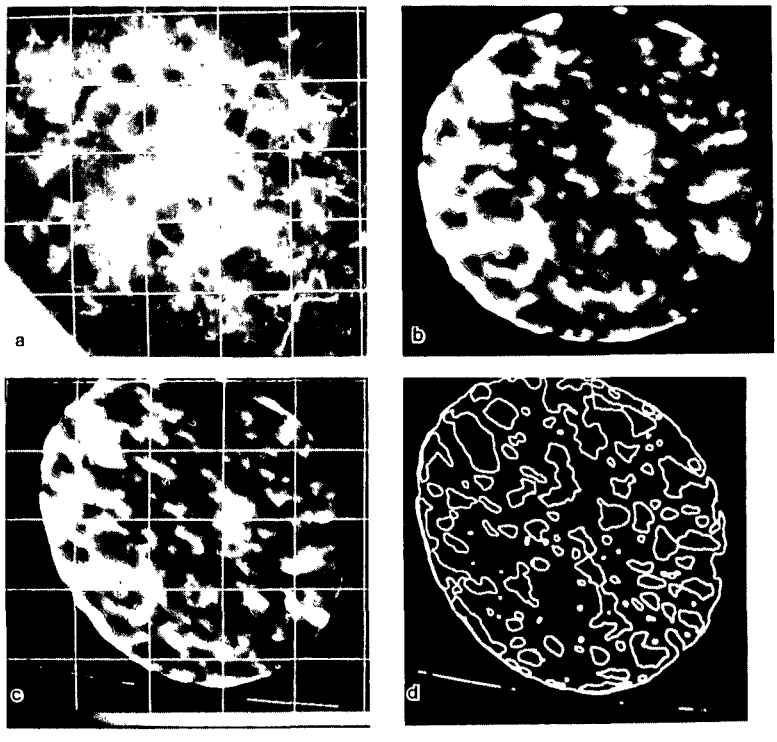

Figure 1 Reaction-bonded silicon carbide: (a) SEM image with contrast in the secondary electron signal; (b) SIMS image of a trace aluminum constituent; (c) SIMS image after application of image warping function; (d) SIMS image after application of thresholding function to outline grains.

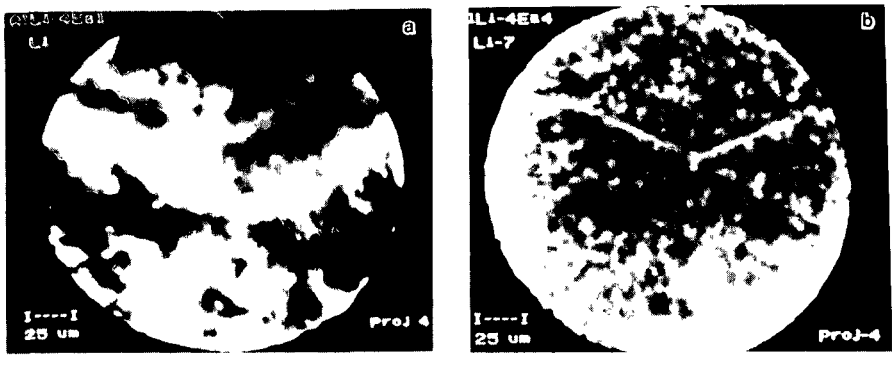

Figure 2 Aluminum-3.6 weight% lithium alloy: (a) lithium image of as-polished surface at onset of sputtering; (b) lithium image after sputtering to reveal the bulk structure of the alloy.

HIGH RESOLUTION SCANNING ION MICROSCOPY USING LIQUID METAL ION SOURCES

R. Levi-Setti

The Enrico Fermi Institute(*) and Department of Physics
The University of Chicago, Chicago, IL 60637

Liquid Metal Ion Sources (LMIS), in view of the quasi-point-like geometry of their emitting region and confined emission cone, possess brightness ($\sim 10^6$ A $cm^{-2}sr^{-1}$) which is adequate for the realization of high current density ($\sim$1 A cm^{-2}), finely focused ($\lesssim$ 20 nm) probes. Commonly used versions of LMIS consist of a W needle wetted with a metal of choice (Ga,In,Au etc.) protruding from a heated reservoir.(1) The phenomena initiated by the interaction of fast ions with solids determine the contrast mechanisms relevant to SIM imaging of surfaces. A wider spectrum of contrast signals is available in SIM than in electron probe instruments, reflecting the complexity of the atom-atom interaction. In addition to Ion-induced Secondary Electrons (ISE), copious emission (sputtering) of either positive or negative Ion-induced Secondary Ions (ISI) or neutral Atoms (ISA) stem from the ion bombardment of solids. All these secondaries carry information about the solid. The ISE or positive ISI signal can be collected for imaging of the surface topography and material contrast (Z- and crystallographic).(2) By Secondary Ion Mass Spectrometry (SIMS), both positive and negative ISI's can be analyzed to yield mass-resolved images (isotopic maps), mass spectra and depth profiles.(3)

Both the virtual source size ($\lesssim$40 nm) and the energy spread of the emitted ions (5-10 eV) determine the lower limit to the useful probe size in LMIS conventional electrostatic focusing columns. Both contributions are about an order of magnitude larger than the corresponding case for a field emission electron probe. Aside from the Gaussian image of the source, of size $d_g = Md_s$, with M the magnification, d_s the virtual source size, the final spot size in a LMIS column is dominated by the chromatic size $d_c = C\,\alpha\,\Delta E/E$, where C is the chromatic aberration coefficient of the lens system, α the probe semiangle, E the probe energy and ΔE the FWHM of the ion energy spectrum. Since the probe current is given by $I = \pi\alpha^2 dI/d\Omega$, where $dI/d\Omega$ is the angular intensity, for such a chromatically limited system we have that $I = \pi(d_c^2/\Delta E^2)(dI/d\Omega)\cdot(E/C)^2$. It follows that the probe current density $J = 4(dI/d\Omega)/\Delta E^2\cdot(E/C)^2$ is independent of α and of the probe size. This also means that the probe current decreases with the square of the probe size, a behaviour which severely constrains the use of very small probes. As can be seen, a reduction in C and ΔE would reduce the chromatic spot size linearly, and increase the current density quadratically, at a given α and E. Similar improvements ensue from an increase in the primary energy.

In the UC-HRL SIM(3), the current of a 40 keV Ga^+ probe, at 20 nm spot size, is 1-2 pA. A particularly efficient SIMS system in this instrument has made it feasible to take unique advantage of probe currents at this level in selected applications demanding that the sputtered depth be limited to a few surface atomic monolayers. Favorable problems involve the mapping of segregated components of elements of low ionization potential or high electron affinity which, at concentration unity, yield counting rates as high as 10^5 cps/pA. A reduction of spot size below 20 nm appears problematic on account of the possible limit set by the Gaussian image of the source, and not very useful for SIMS from the above intensity considerations in addition to the fact that the lateral size of the collisional cascade initiated by the primary ions is estimated $\sim$10 nm. In practice, since the image resolution depends on the signal to noise ratio, and this increases linearly with d_c, a significant trade-off in image quality is achieved by operating at beam diameters larger than the above limits.

From the standpoint of relative efficiency in the yields of positive vs negative ISI's, 40 keV Ga^+ and In^+ probes have been found comparable to a 15 keV O^- probe (3).

The images shown in Fig.1 were obtained with a 20 pA 40 keV Ga^+ probe of 70 nm diameter. This value corresponds to the 90% fall-off width of the Al^+ SIMS signal in scans across a sharp Al edge. Fig. 1 a) is an ISE image of a fossil diatom skeleton, showing good topographic contrast. Fig. 1 b) is an Al^+ SIMS map of an Al bar pattern deposited on a Si wafer, fabricated at the National Research and Resource Facility for Submicron Structures at Cornell University (courtesy M.T. Bernius). The image 90% fall-off width of the edge of the bars is 35 nm from microdensitometry. Fig. 1 c) and d) are

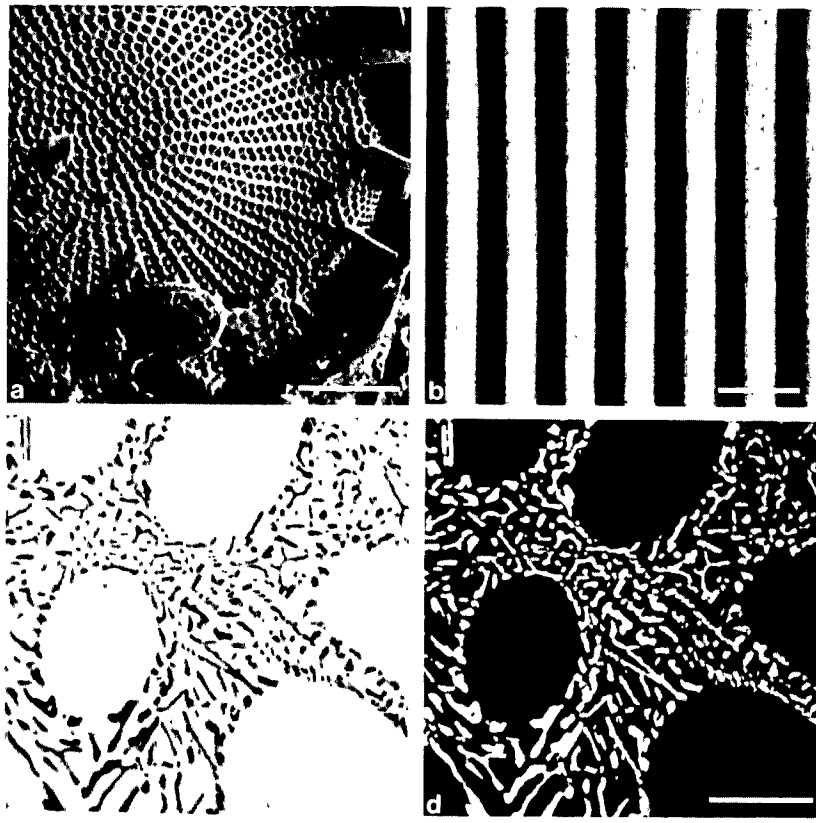

Fig. 1. Images obtained with the UC-HRL SIM/SIMS using a 20 pA Ga^+ probe of 70 nm diameter.
a) ISE image of a fossil diatom skeleton (SiO_2). Scale bar = 5 μm.
b) Al^+ SIMS map of Al bar pattern on Si. The images's 90% fall-off width at the bar edges is 35 nm. The bar width is 0.4 m. Scale bar = 1 μm.
c,d) Al^+ and Si^+ SIMS maps of polished section of Al-based alloy, containing 7% (wt) Si. The area shown corresponds to a dendritic eutectic Al-rich phase. Scale bar = 10 μm.

* * *

respectively SIMS mass-resolved images of the distribution of aluminum and silicon in an Al-based alloy (courtesy A. Lodding). All images contain 1024 x 1024 pixels.

Our instrument is routinely applied to a vast range of interdisciplinary applications involving imaging microanalysis of metals and alloys, semiconductors, ceramics, and of mineralized and soft biological material[4]. The Ga LMIS, operated at residual pressure in the 10^{-10} Torr range, have lifetimes in excess of 1000 hours of stable operation, prior to requiring replenishment.

* Work supported by the NSF Materials Research Laboratory at the University of Chicago.
(1) P.D. Prewitt and E.M. Kellogg, Nucl. Instr. Methods in Phys. Res. B6 (1985) 135.
(2) R. Levi-Setti, Scanning Electron Microsc. 1983; I:1.
(3) R. Levi-Setti, G. Crow, and Y.L. Wang, Scanning Electron Microsc. 1985; II:535.
(4) R. Levi-Setti, G. Crow, and Y.L. Wang, SIMS V, (Springer-Verlag, 1985), 132.

Precision Mass Spectrometric Analysis of Purity and Specialty Gases at PPB Levels

G. Wagner, B. Laser, W. Schmidt and U. Geise
Finnigan MAT, Bremen, West Germany

OBJECTIVE

Purity Gases (like Helium 5.5, Argon 6.0, Oxygen 5.5) and Specialty Gases (such as Phosphine, Arsine, Silane) are used in many high technology processes at high purity demand. Any impurity exceeding the safety margin of such processes may ruin its productivity, the quality of its products and its economy.

The fast, direct, unambiguous and quantitative determination of all kinds of gasesous trace impurities in Purity and Specialty Gases is a complex analytical task. It can be resolved with high reliability by mass spectrometry, if mass spectrometry is utilized to its fullest capabilities.

MASS SPECTROMETRIC SOLUTION

Linearity, stability and a large dynamic range for peak detection and acquisition are standard with the Finnigan MAT Model 271/45 magnetic sector type mass spectrometer. For Purity and Speciality Gas analysis, these specific capabilities of the Model 271/45 mass spectrometer are utilized:

1. MULTIPLET RESOLUTION FOR TRACE DETECTION

   Automated adjustment between 250, 1400, 3000 and 8000 resolution (10% valley definition) provides separation of most mass multiplets in complex gas mixtures. The data systems's interaction with the mass spectrometer, for its control, for data acquisition as well as data evaluation fulfills the enhanced requirements of multiplet resolution:

   - Mass calibration automated, reliable and precise to ± half a peak width at 3000 resolution.
   - Mass and chemical assignments accurate for multiplet.
   - Matrix evaluation automated and flexible according to mass resolution.
   - Multiple regression evaluation for automated analysis of an unknown number of unknown components.
   - Automatic selection of calibration spectra.

   Classical rules of quantitative mass spectrometry are considered: background subtraction, correction of fractionation, closure of total sample pressure with component's partial pressures.

2. SAMPLE TRANSFER WITHOUT FURTHER CONTAMINATION

   For Purity and Specialty Gas analysis, all the elements for the transfer of sample gas from the pressurized gas container to the ion source of the mass spectrometer need to perform with lowest possible sample contamination. Such "clean" sample transfer is provided by combining two new modules:

   A. Inlet system with continuous flow and with pressure reduction in a stainless steel capillary;
   B. Pressure reduction valve with two additional gas lines, either for flushing (with helium or argon) or for flow split.

   Using these inlet modules, the sample contamination by air components is less than 3 ppm within five minutes after connecting a new sample cylinder.

3. DIRECT COMPARISON OF SAMPLE AND REFERENCE GAS

The use of two similar capillary lines for Sample and Reference gas inlet, employing a change-over valve combination, well known in gas isotope analysis, to maintain a steady sample/matrix gas flow, provides the following improvements:

A. The background becomes stable at ppb level with constant flow of matrix gas.

B. With stable background, the direct comparison of sample gas with a well-known standard gas provides very reliable analytical results.

According to our analytical experience, purity gas standards with a level of total impurities below 2 ppm are now available.

4. LOW ION-MOLECULE ARTIFACT ION GENERATION

The interaction of sample gas with components or cracking products from former samples deposited on the ion source, as well as the interaction of ion already produced in the ion source with fresh sample gas molecules, may lead to significant artifact ion intensities, in ppm level trace gas analyses. Generally, a low ion source temperature (150 °C), a large sample flow (ion source pressure at 3×10^{-6} mbar) and a low electron emission (10 µA) optimize the Model 271/45 mass spectrometer system for low artifact ion intensities caused by sample/residue reaction. Remarkably, this instrument provides such a high sensitivity that even at the low electron emission of 10 µA and at multiplet resolving power of M/ΔM 250, the trace detection limits are well below 100 ppb.

"ARGON 7.0"

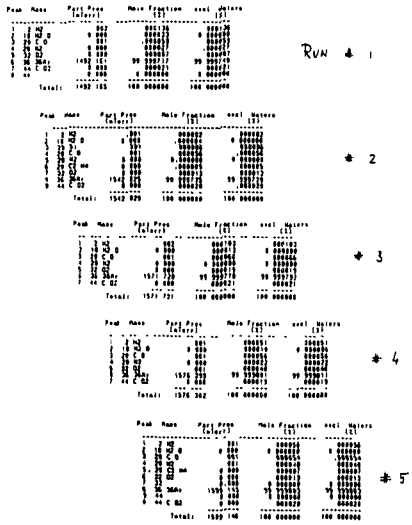

Repetitive Analysis of an Ultrahigh Purity Argon to Approach the Real Trace Impurity Concentrations

An ultrahigh purity argon specified by its vendor to be "ARGON 7.0" with a total concentration of trace impurities below 0.1 ppm (99.99999% argon) was analyzed on the Finnigan MAT 271/45 mass spectrometer system.

Five subsequent analytical runs provide the following general results:

1. The total trace impurities with run #4 and #5 are leveling off at 2 ppm.
2. The first three analytical runs show a continuous change from higher to lower concentrations, caused by continuous decontamination of pressure reduction valve and transfer lines by sample gas.
3. Hydrogen, carbon monoxide and nitrogen amount to 0.5 ppm each. Oxygen and carbon dioxide are at the 0.2 ppm level in the final result.

   The maximum 0.1 ppm level of total impurities claimed by the gas vendor cannot be approved.

For these analyses, the Finnigan MAT 271/45 mass spectrometer system was used at very good vacuum conditions. The total residual gas pressure at the ion source was 2×10^{-7} Torr, providing very stable background at low intensity.

ANALYSIS OF SOLIDS BY LASER ABLATION PLASMA SOURCE MASS SPECTROMETRY

P. Arrowsmith, SCIEX®, 55 Glen Cameron Road, Thornhill, Ontario, L3T 1P2, Canada

Inductively coupled plasma source mass spectrometry (ICP/MS) has rapidly become an important technique for elemental analysis, due to its high sensitivity. Conventional sample introduction systems which convert a solution into an aerosol and allow a small proportion to pass into the plasma are restricted to soluble materials and discard up to 98% of the sample. Sample introduction by direct laser ablation of solids with subsequent gas flow transport of the ablated particulate material into the ICP offers a number of advantages.

1) Order of magnitude improvement in transport efficiency.
2) Reduced cooling of the plasma due to the absence of solvent and consequent reduction in levels of molecular ions such as oxides.
3) Rapid analysis with minimal sample preparation of most solids including semiconductors, ceramics and polymers. Powdered materials such as minerals and biological samples can be fused or pressed with a suitable binder.
4) The ~10μm diameter of a focussed laser beam allows inhomogeneous samples to be analyzed with high spatial resolution.

Until the present work, sample introduction by laser ablation has been confined to low repetition rate pulsed lasers for both ICP/optical emission (1) and ICP/MS (2). The resulting signal is in the form of a transient, typically 0.5 s in duration due to spreading of the ablated particles in the sample cell and transport line. There are two problems associated with such a signal. Determination of up to 40 masses with a single channel quadrupole-based ICP/MS gives poor duty cycle or low sample rate per mass and optimization of the signal with respect to, for example, laser beam focus, is extremely tedious. For these reasons a relatively high (10-20 Hz) repetition rate Nd:YAG laser was used in the present work to obtain a continuous signal (typical measurement time 0.1 s).

The laser was operated in Q-switched mode and pulse energies of ~150 mJ at λ=1.06μm were sufficient for ablation of a wide range of materials. The transport line from the ablation cell (see Figure 1) was connected to the sample inlet of the ICP torch in a standard SCIEX® ELAN® 250 ICP/MS. There are three modes of operating the system.

1) A single laser pulse in conjunction with peak hopping the ICP/MS allows up to 10 elements in a 10-100μm area of the sample to be determined with good precision (5% RSD). The signal at each sample point can be displayed or accumulated in separate mass bins to give a quantity proportional to the total amount of that element in the sample. Accumulation of background is minimised by gating the laser pulse to the start of the data acquisition period.
2) The 10 Hz repetition rate laser together with a peak hopping MS give a continuous signal for each selected mass. With a static sample, depth profiling in 1-5μm steps is possible although there is a fall-off in signal due to defocussing of the laser beam. By translating the sample in the X,Y plane under microcomputer control a steady signal can be maintained for homogeneous materials. For inhomogeneous samples the spatial distribution of elements is obtained. Because the duty cycle is greatly improved (compared to transient signals) and there are no systematic variations in signal this mode is also preferred for analytical work.
3) Alternatively, a sequential scan of the MS in conjunction with the 10 Hz laser gives a complete mass spectrum of the sample, as shown in Figure 2.

Techniques for quantitative analysis have also been investigated. The chief problem is that the amount of material ablated is unknown and varies from sample to sample. For these reasons some form of internal standardization is preferred. The internal standard must be of known concentration in both the sample and standard (if available) and should give an unsaturated signal, e.g. a minor isotope of a matrix element. Figure 3 shows analytical curves for seven elements in a series of NBS microprobe standard steels with ^{60}Ni as an internal standard. Accuracies are approximately 20% and detection limits are 0.1-1 ppm for all elements. If standards are not available then relative response factors R(element)/R(internal standard) derived from multielement solution analysis can be used. Finally, if all isotopes of the internal standard element are saturated, the signal may be brought on scale by detuning one of the electrostatic lenses in the ICP/MS.

REFERENCES

(1) T. Ishizuka and Y. Uwamino, Spectrochim. Acta 38B, 519 (1983).
(2) A.L. Gray, Analyst 110, 551 (1985).

Fig. 1 SCHEMATIC OF LASER ABLATION CELL

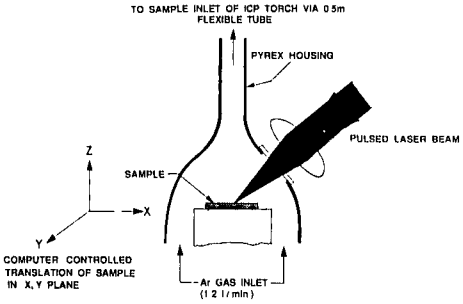

Fig 2 NBS STEEL SRM #664 (CONCENTRATIONS IN PPM)

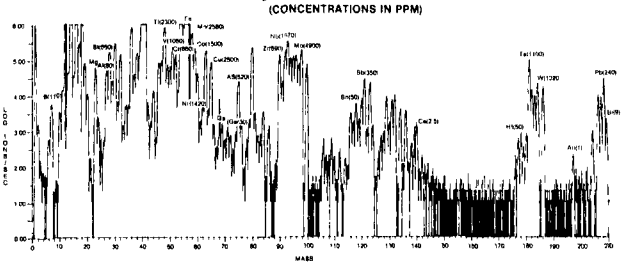

Fig. 3
ANALYTICAL CURVES FOR NBS MICROPROBE STANDARD STEELS (SRM Nos. 661-664) AND IRON (SRM No. 665).
INTERNAL STANDARDIZATION ON ^{60}Ni

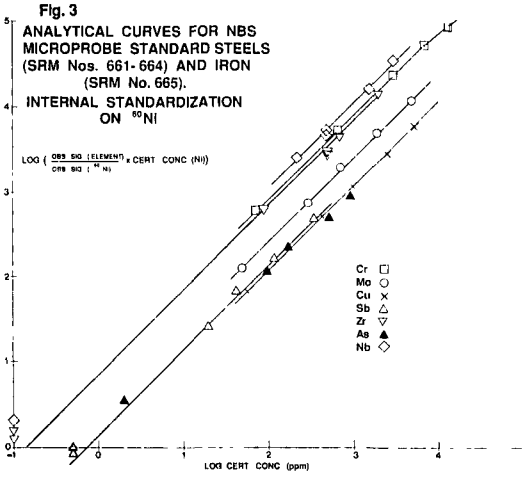

STUDY OF ION OPTICS AND IONIZATION POTENTIALS IN RELATION WITH MATRIX EFFECTS OF INDUCTIVELY COUPLED PLASMA/MASS SPECTROMETER

S. Beaudet, J.P. Schmit and M. Chtaib; Université du Québec à Montréal, Dept. of Chemistry and GEOTOP, P.O.Box 8888 Stat. "A", Montreal H3C 3P8

INTRODUCTION

Inductively Coupled Plasma / Mass Spectrometer (ICP/MS), a relatively new instrument, is now gaining importance as a powerfull and very promising method for elemental analysis. This mainly results from a happy marriage between an atmospheric pressure plasma torch acting as an efficient ion source and a high sensitivity quadrupole mass spectrometer.

One of the greatest ICP/MS features arises from its capability in determining almost all the elements of the periodic table with excellent detection limits.

However, ion transmission between plasma torch and mass spectrometer has been found dependent upon the ion optic design. Moreover, under definite circumstances, multielement analysis can exhibit severe matrix effects.

In this work, the response of the instrument has been studied in relation with two different ion optics. Finally, some matrix effects closely dependent on the element ionization potentials have been described.

EXPERIMENTAL

The instrument used is the ICP/MS - ELAN from Sciex. Samples are introduced in the vapour phase inside the plasma torch by using a Meinhard Hi-Solids concentric nebulizer. 100 ppb sample solutions were prepared by disolving the elements of interest as nitrate salts in ultra pure HNO_3 2 N.

ION TRANSMISSION

A. First ion optic (Figure 1)

Figure 2 shows the ion transmission efficiency for a mixture of elements (C, N, Na, Cu, La, Cd, Ce, Pb) when varying the bias potential (V_R) of the ion extracting lens "Ring".

It is interesting to emphasize the presence, apparently independent on the ion mass, of particular optimum ion transmission ($V_R$max) for every type of ion.

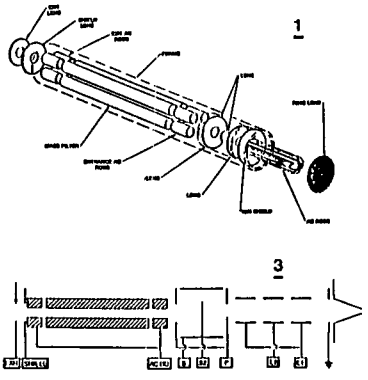

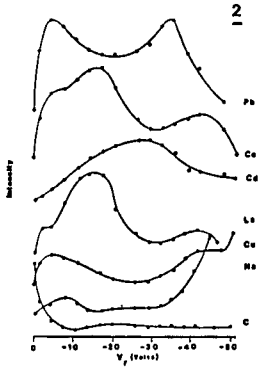

Approached $V_R max$ values for any element can be calculated by using the following semi-empirical equation:

$$V_R max = i - I_{Ar} - M_i / M_{Ar} \cdot E_{Ar}$$

where: i = ionization potential of the studied element
M_i = mass of the element
I_{Ar} = first Argon ionization potential (15.7 eV)
M_i = Argon atomic weight (40 uma)
E_{Ar} = 5/2 kT (T ~ 5000 to 7000 K)

B. Second ion optic (Figure 3)

Figures 4 and 5 show the optimum ion intensities obtained for a series of elements by varying the E_p lens and the V_e plate bias potentials, respectively.

It is evident that, by using the second ion optic, the optimum ion transmission is now mainly related to the mass of the considered element instead of the ionization potential.

However, although it can be seen that for masses higher than about 65 amu $V_e max$ is stable around -11.5 volts, the ion transmission for the lower masses (< 65 amu) is strongly dependent on the V_e plate potential (Figure 4). Moreover, by plotting $E_p max$ plate potential against the mass, we observe a potential drift (-14.5 up to -3.0 volts) necessiting along the same line to choose the "*best compromise*" when analyzing a multielement mixture (e.g. setting on Rh at 103 amu).

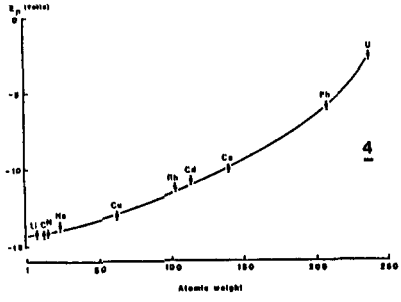

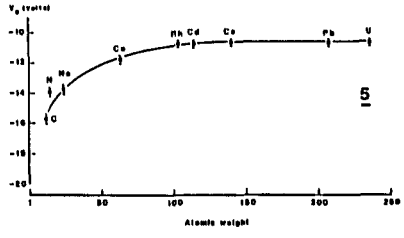

LOW CONCENTRATION MATRIX EFFECTS.

Matrix effects have been widely debated in ICP / MS litterature. This interelement interference is usually expected to occur when very different element concentrations are present in a sample mixture. However, as it can be seen on figure 6, matrix effect is also present at very low relative concentrations. This figure shows for 1 ppb of Y the influence of increasing concentrations of Ce. It can be seen that, even at low Ce concentration (100 ppb), depending on the plasma torch conditions (1400 W), matrix effects are detectable.

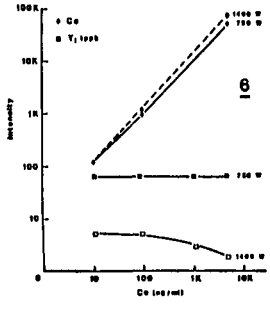

LASER MICROPROBE MASS ANALYSIS OF MICROCIRCUIT CONTAMINANTS

J.P. Schmit and S. Beaudet; Université du Québec à Montréal, Dept. of Chemistry and GEOTOP, P.O.Box 8888 Station "A", Montreal, H3C 3P8, and G. Madore; CANTHERM, 8415 Mountain Sights ave, Montreal H4P 2B8

INTRODUCTION

Everyday, microelectronic components are becoming smaller and more sophisticated. At the same time, the complexity of fabrication processes as well as fabrication rejects is dramatically increasing.

This unwanted correlation mainly arises from either the presence of unexpected impurities inside the bulk material as well as on the surface of the microcircuit components (1), or from the use of inapropriate conditions during some step of the fabrication process.

Whatever the origin of the problem, its solution almost necessarily involves a very systematic and spatially localised chemical analysis (chemical exploration) of the microcircuit components.

Laser Microprobe Mass Analysis, a relatively new developping technique, has been used in an attempt to solve three specific problems at the origin of important manufacture rejects.

1. Defective welding fingers on microcircuit substrates.

A critical step in manufacturing chip substrates lies in the proper deposition of solder on very small finger tips on ceramic subtrates. The purpose of this key step being to fix and enable getting good contact between the chip itself and the substrate, this later being the interface between the chip and the outside world. In such a context, it is evident that welding quality is of prime importance.

Rejects due to the absence of solder were studied within two different contexts:

a) the presence of a very thin black deposit on the defective fingers,
b) the presence of a uniform and extremely thin layer of unknown transparent material coating the whole substrate surface.

In both cases, visual examination through a microscope (250 x) have shown that no solder at all had been deposited on the defective fingers.

a) Comparison of spectra from normal and defective welding spots (spectra A and B) pint points the total absence of lead (M.W. 204 (1.5%), 206 (23.6%), 207 (22.6%), 208 (52.3%)) along with the absence of any other strong contamination. This observation showed that the use of a wrong welding bath temperature departing from the eutectic allowed micro-droplets of tin to exist inside the solder alloy.

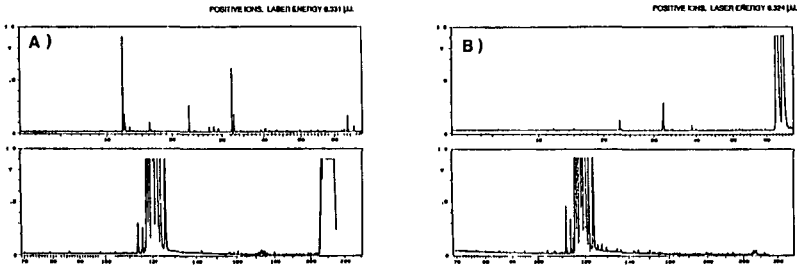

b) Spectra C and D show the presence of an unexpected organic compound at the surface of the defective welding spot. Laser microprobe analysis of this extremely thin film in both positive and negative ions modes, has shown that the presence of a photoresin residue was at the origin of the studied problem.

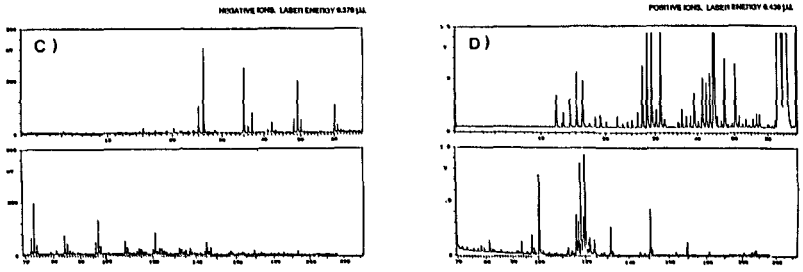

2. Unexpected transition temperature

Fabrication of semi-conductors having specific transition temperature requires controled R.F. sputtering of some particular metals from the transition group in Ar/O_2 atmosphere. This process is done inside a vacuum chamber under a total pressure ranging between 10^{-3} to 10^{-2} torr within a specific argon - oxygen gaz mixture.

Wafers and vacuum chamber (including all the inside accessories) are cleaned before R.F. sputtering by following a systematic and well known procedure involving different acids (HNO_3, HF) and organic solvants (acetone, methanol and trichloroethylene).

Despite these precautions, the five first runs were usually rejected because of their poor thermic performances. Only after these runs, the expected transition temperature was reached and reproducible.

The exponential chlorine concentration decrease concomitant to a transition temperature increase as shown on figure 1 indicated that the presence of chlorine (a known microcircuit poison) was the most probable source of the obtained poor thermal characteristics of the studied semiconductor films.

The simultaneous decrease of carbon and chlorine, run after run, allowed to conclude that the use of trichloroethylene in the vacuum system cleaning process was at the origin of this problem. The observed improvement of the transition temperature along with the number of decontamination runs has been attributed to the result of a progressive removal of trichloroethylene traces from the vacuum chamber. This assertion was confirmed by substituting trichloroethylene by a non-chlorinated solvent.

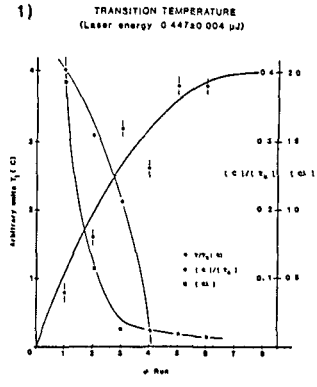

1. Circuit Board Contamination; T. Adams; Electroni.onics, 42-44, march 1986.

THE INFLUENCE OF SOURCE PARAMETERS ON INDUCTIVELY COUPLED PLASMA-MASS SPECTROMETRY

George H. Vickers, Daniel A. Wilson and Gary M. Hieftje, Department of Chemistry, Indiana University, Bloomington, IN 47405. Andrew T. Zander, Spectroscopy Division, Perkin-Elmer Corporation, 901 Ethan Allen Highway, Ridgefield, CT 06877.

Inductively Coupled Plasma-Mass Spectrometry (ICP-MS) has proven to be an extremely powerful technique for trace and multielement analysis. Several of its advantages include extremely low detection limits, minimal background, nearly simultaneous analysis, and isotope abundance information. However, as with all relatively new techniques, the full influence of the system operating parameters has yet to be assessed.

The development of ICP-MS has required the interfacing of two complex instruments, each of which is affected by a number of operating parameters. Therefore, it is necessary to understand the effects that each parameter has on the analytical performance. Limiting our studies to the ion source (the ICP), we have investigated the system response to many of its parameters. Recently, a similar study has been reported on a commercial instrument [1]; although there are similarities in the results, there are also several inconsistencies. The majority of these inconsistencies are probably due to fundamental differences in the two ICP-MS instruments.

The ICP-MS system that has been used for these experiments and its analytical figures of merit have been described in detail elsewhere [2]. Briefly, it incorporates a Plasma-Therm HFP-2500F ICP with a Balzers QMG 511 quadrupole mass spectrometer. The principal design features include analog and digital detection systems, positive and negative ion modes, and a three-dimensional translation stage for positioning the ICP with respect to the sampling orifice. These features provide the flexibility needed for both analytical and fundamental investigations. For the present work, the operating conditions are 1.25 kW forward radio-frequency (RF) power, 10.0 L/min Ar coolant flow rate, 0.0 L/min Ar auxiliary flow rate, 0.65 L/min Ar nebulizer flow rate, 0.1 mL/min solution uptake rate, and a sampling height of 10 mm above the load coil, unless stated otherwise.

Figure 1 shows the effect of nebulizer flow rate and RF power on the signal for a 10 ppm barium solution. At higher power, the greatest ion density occurs lower in the plasma; consequently, a greater nebulizer flow rate is required to move the ions into the sampling zone. The effect of power on the percentage of doubly-charged barium ions is shown in Figure 2. At all power levels, the percentage reaches a minimum at a nebulizer flow rate only slightly below that which yields the maximum analyte signal. However, this adjustment cannot be made without sacrificing an order of magnitude in Ba^+ sensitivity.

The effect of power and nebulizer flow rate on the signal for a 10 ppm cerium solution, shown in Figure 3, is similar to that which is obtained for barium and for the other elements studied (lead, lithium). Under the same conditions found to produce the greatest Ce^+ signal, the cerium oxide-ion percentage is extremely low, shown in Figure 4. However, lower nebulizer flow rates are found to produce a greatly increased oxide level.

At higher coolant flow rates, the maximum signal for all elements occurs at reduced nebulizer flow rates; Figure 5 displays the results for cerium. This behavior might be caused by a combination of temperature, pressure, and flow-pattern changes. However, the influence of the coolant flow rate is the least of all parameters investigated.

Finally, the effect of nebulizer flow rate and sampling height above the load coil on barium is shown in Figure 6. Several of the results discussed previously suggest a direct relationship between these parameters; the results of this experiment indicate otherwise.

Overall, the signals are extremely sensitive to the nebulizer flow rate; fluctuations as small as 0.01 L/min Ar can cause signal changes of approximately an order of magnitude. Obviously, extreme care must be taken in making this adjustment. Also, some of the results above contradict those from ICP-optical emission spectroscopy (OES), indicating that our mass spectrometer is not "passively" sampling ions from the ICP.

An hypothesis that can be drawn from this work is that a gas-flow-dependent secondary discharge exists in the interface of the ICP-MS. Such a discharge would increase the percentage of doubly-charged ions and decrease the oxide-ion percentage as the nebulizer flow rate is raised. Conveniently, a controlled discharge in the interface might help to reduce interferences caused by molecular species formed in the extraction process, without producing a high abundance of doubly-charged ions.

References:

[1]. G. Horlick, S. H. Tan, M. A. Vaughan and C. A. Rose; Spectrochim. Acta **40B**, 1555 (1985).
[2]. D. A. Wilson, G. H. Vickers, G. M. Hieftje and A. T. Zander; Spectrochim. Acta **42B**, in press.

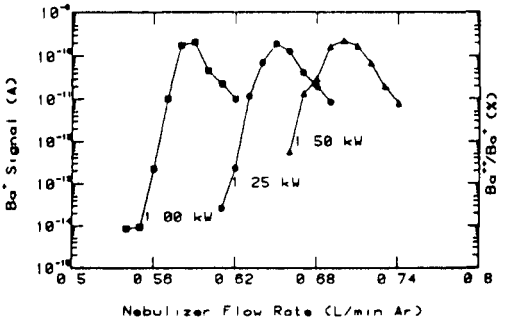

FIGURE 1

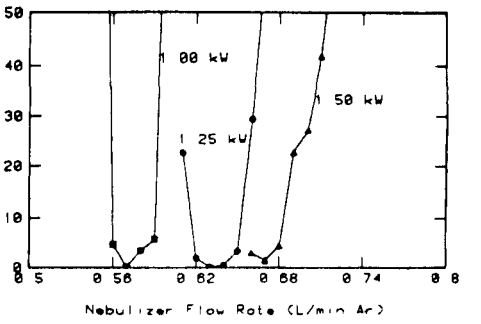

FIGURE 2

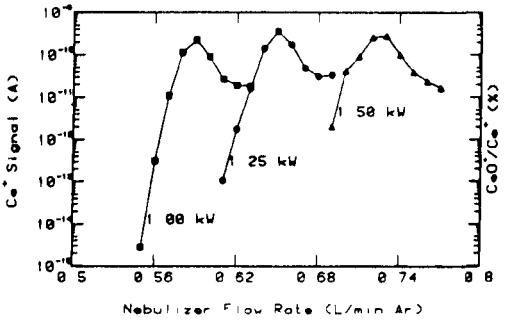

FIGURE 3

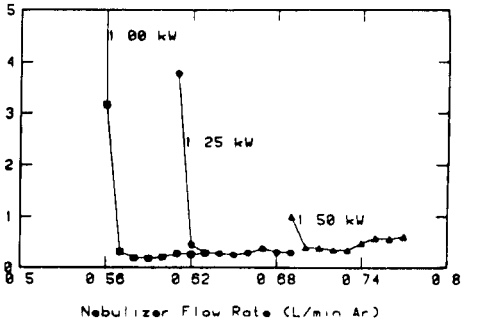

FIGURE 4

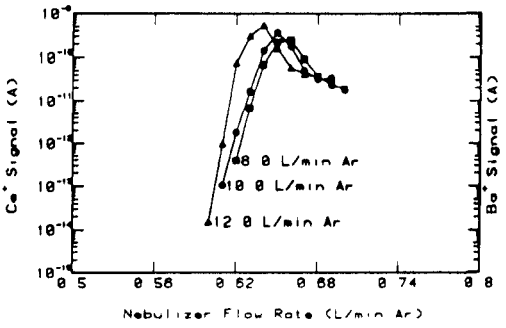

FIGURE 5

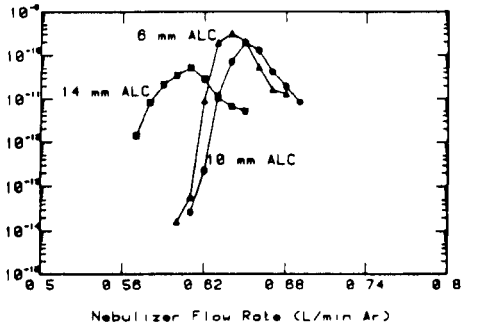

FIGURE 6

NONRESONANT MULTIPHOTON IONIZATION OF LASER-SPUTTERED NEUTRAL

Bruno Schueler* and Robert W. Odom, CHARLES EVANS & ASSOCIATES
301 Chesapeake Drive, Redwood City, CA 94063

Introduction: The laser microprobe has been demonstrated to be a powerful tool for the rapid, laterally resolved (~1 μm) survey microanalysis of inorganic and organic surfaces (1). In the analysis of semiconductors, metals and insulating materials most of the laser-ablated particles are neutrals (i.e., the charge to neutral ratio, Y^+/Y, is $< 10^{-4}$) and, hence, it is often desirable to enhance the detection sensitivity by increasing Y^+/Y. In addition, increasing the ionization efficiency in laser microprobe analysis could provide useful mass spectra from very small ablated volumes and thus provide more surface sensitive analysis. One potential method for enhancing the charge to neutral ratio in laser microprobe analysis is to ionize a portion of the ablated neutrals by non resonant multiphoton ionization (MPI) processes. This ionization can best be achieved by employing a second laser pulse which interacts with the plume of material vaporized by the ablating laser pulse.

Experimental: The instrumental configuration is comprised of a commercial reflection mode laser microprobe (Model LIMA 2A, Cambridge Mass Spectrometry, Cambridge, England) to which has been added a second quadrupled Nd:YAG laser along with beam focusing optics and position manipulators. The sample surface is irradiated by a pulse from the ablating laser which is focused to ~2 μm spot diameter. The neutral species produced by this ablating pulse are irradiated by the focused output from the second (ionizing) laser. This ionizing beam is focused to ~100 μm diameter at a distance of ~0.6 mm above the sample surface. The ions produced by this ionizing laser pulse are accelerated from the sample surface and injected into a time of flight (TOF) mass spectrometer equipped with an ion reflector. Discrimination against detection of the ions produced by the ablating laser is achieved by suitable setting of the sample voltage.

The ablating laser is generally operated at irradiances between 10^8 and 10^9 W/cm^2 while the irradiance of the ionizing laser can be as high as 10^{12} W/cm^2. The ionizing laser is operated at 266 nm while the ablating laser has been operated at both 266 and 532 nm. The delay between the firing of the ionizing laser is generally varied between 50 ns and 2.7 μs after the firing of the ablating laser pulse.

Results: The results obtained from a thorough study of GaAs are presented in this paper. Other targets such as $MoSi_{2.25}$, $WSi_{2.7}$, steel, and $Hg_{1-x}Cd_xTe$ exhibit a very similar general behavior.

The dependence of the post ionized As^+ signals from GaAs as a function of the delay time (Δt) between ablating and ionizing laser is shown in Figure 1. The Ga^+ signal intensities follow a similar time dependence. The data have been recorded for three different irradiances of the ablating laser ($E_0 \sim 5 \cdot 10^8$ W/cm^2). Each data point at a given delay time represents the average of seven analysis. Post-ionized As^+ signals can be detected as soon as ~200 ns after the ablating laser pulse and peak between 600 ns and 1.0 μs. At the highest ablating irradiance, a qualitative change in the time dependence of the As^+ signal can be observed, which is possibly due to contributions of molecular dissociation/ionization processes. Figure 2 illustrates the ratios of the post ionized Ga^+ and As^+ signals ($y(As^+)/y(Ga^+)$)

---

*also: Physics Department, University of Manitoba, Winnipeg, Manitoba R2N1L8, CANADA

vs. Δt. The post-ionized signals provide detectable levels for both ion signals in each analysis which should be contrasted with the ablation laser only analysis of this material in which the $y(Ga^+)/y(As^+) > 10^3$.

The total average post ionized signal can be estimated by integrating the ion signals over the complete time range. Table 1 summarizes the results of this integration.

Table 1: Integrated Ga^+ Post Ionization Signal Intensities and As^+/Ga^+ Ratios.

	ABLATING ENERGY		
	E_0	$3E_0$	$5.5E_0$
$Y(Ga^+)$	9×10^4	2×10^5	9×10^5
$Y(As^+)/Y(Ga^+)$	0.97	1.16	0.99

No visible craters were produced at E_0 or $3E_0$ ablation energies while small craters (diameter <0.5 μm) were observed at $5.5E_0$ ablation energies.

Conclusions: The above example demonstrates that laser microprobe analysis combined with laser post-ionization enhances the absolute sensitivity compared to the conventional (single laser) instrumental configuration by at least an order of magnitude, and provides more uniform ionization of the ablated neutrals. The enhanced sensitivity permits more sensitive surface analysis of the material while the uniform ionization efficiency can provide microanalytical determination of the stoichiometry of the samples composition.

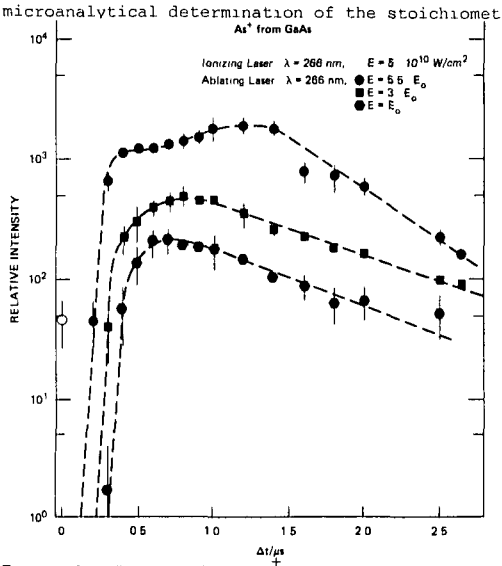

Figure 1. Post-Ionized As^+ signal as a function of Δt

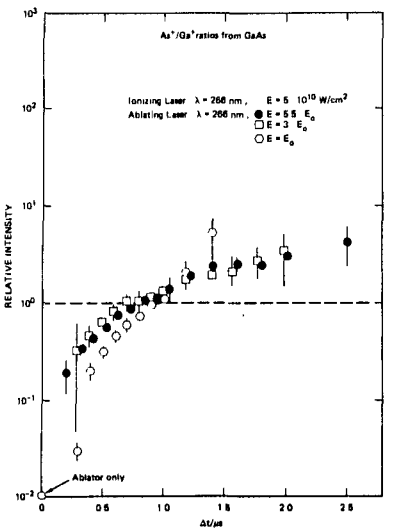

Figure 2. As^+/Ga^+ Ratios as a function of Δt

REFERENCES: 1. Fres. Zeit. Anal. Chem., 308, (1981)

ACKNOWLEDGEMENTS: Support for this work was provided by an NIH SBIR Grant (#1 R43 GM33123-01)

ANGAL: An Automated Laboratory for Noble Gas Isotope Dilution Mass Spectrometry

D. A. Leich, G. F. Hunt, G. McCrory, S. R. Stuckemeyer, and C. Velsko
Lawrence Livermore National Laboratory, Livermore, CA 94550

Isotope dilution mass spectrometry (IDMS) of noble gases has proven to be an important addition to the suite of analytical techniques applied to gas diagnostics of nuclear tests. The technique requires isotopic analyses of samples that have been spiked with a known amount of an enriched isotope. We use a standard mixture of ^{3}He-^{21}Ne-^{38}Ar-^{80}Kr-$^{124-129}$Xe as our IDMS spike to analyze all five noble gases in a single spiked-unspiked pair of aliquots from any given sample. Such an analysis requires 150 separate valve operations in a rigidly timed routine procedure. On our manually-operated sample-processing system, most of these valve operations involved all-metal ultra-high-vacuum (UHV) valves which required a wrench to open, and a torque wrench to achieve a specified closure. Thus, obtaining a complete noble-gas IDMS analysis was a tedious and demanding task that made automation very attractive.

Although automation is a key feature, the ANGAL (automated noble gas analysis laboratory) project actually sprang from an unrelated technical consideration: the problem of sample memory. Because we have been analyzing both spiked and unspiked samples in the same mass spectrometer, we have always observed a small residual of our spike in our unspiked sample analyses. This has severely limited our ability to measure isotopic abundances of the normally rare isotopes that constitute our spike. It is clearly preferable to analyze all spiked samples in one mass spectrometer and all unspiked samples in a second mass spectrometer. Thus the ANGAL project was conceived with the objective of redesigning our IDMS laboratory in order to add a second mass spectrometer and to automate the valve operations and other procedures as much as possible.

Overall Functional Design

The two mass spectrometers around which ANGAL is designed are commercial models built by Nuclide Corporation. GMS1 is a seven-year-old, six-inch-radius, 60°-magnetic-sector, static-mode gas mass spectrometer. GMS2 is a newer model, using a 6-in., 90°, double-directional focusing, double-dispersion geometry. As shown in Fig. 1, each GMS has its own gas sample purification (GASP) module attached to the mass spectrometer inlet. Like the GMSs, the GASP modules are designed to be baked to 300° C for thorough outgassing. A gas aliquotting manifold (GAM) functions as a common source of unprocessed gas samples to each GASP module. Calibrated 10-cm^3 volumes filled to 0.1-10 torr pressures (measured with a capacitance manometer) deliver accurately measured gas samples, each mixed with a metered amount of the noble gas spike, to GASP1. Smaller quantities (2.5-cm^3, at the same pressure) but without the spike, can be routed to GASP2. Separate crucibles (GEC) for on-line thermal extraction of gases from solid samples will be attached to each GASP module.

Since 1981, we have been using an LSI-11 microprocessor to control GMS1 in an automated data-aquisition mode, receive the raw data, and reduce them to analytical results. Currently, we are using the RSX-11M multi-user, multi-tasking operating system. We have now achieved a high degree of automation in the sample processing procedures by using pneumatically actuated Nupro SS-4BK valves (0.25-in. Vespel/stainless steel seal) on the GAM module, and Nupro SS-6BG valves (0.375-in. copper/stainless steel seal) on the GASP modules, and interfacing the valves and electronic controls to the LSI-11. We have also extended our computer control to operation of the GMS inlet and pump valves, using motor-driven ultrahigh vacuum valves of a new compact design, and to mechanical switching between Faraday-cup and electron-multiplier detectors in order to provide unattended operation.

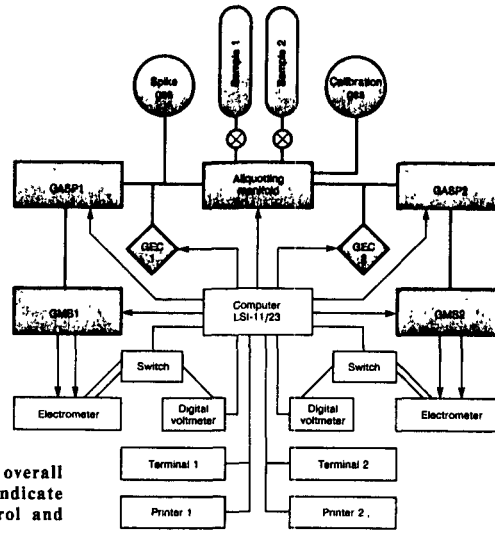

Figure 1. ANGAL block diagram illustrating overall functional design. Shaded blocks and bold lines indicate vacuum system components, while electronic control and monitoring components are unshaded.

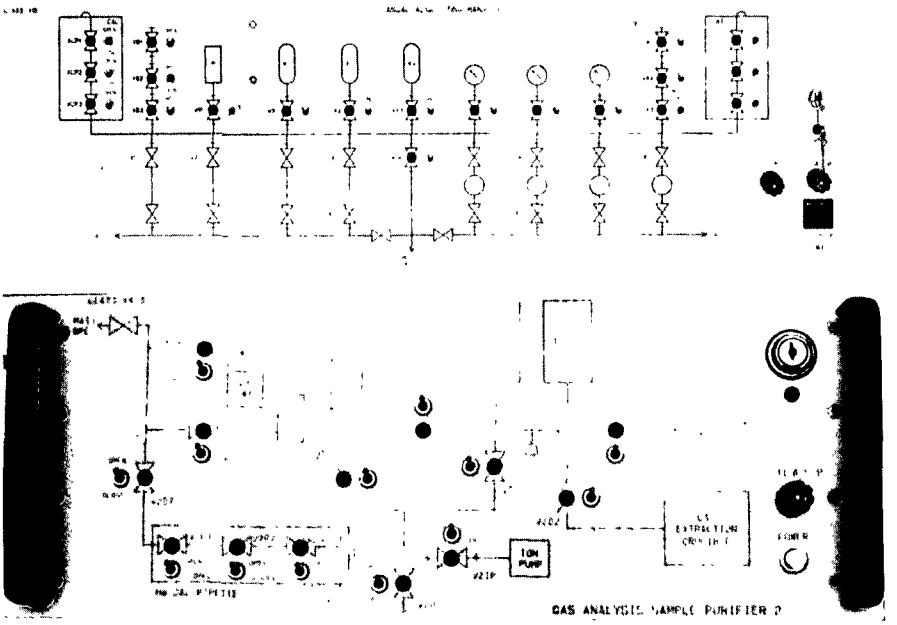

Figure 2. Valve control interface units for GAM (top) and GASP (bottom) modules.

Hardware Components

Three separate electronic units contain the valve-control interfacing for the three sample processing modules. Each interface unit has a plumbing schematic of the module it controls on the front panel (Fig. 2), with light-emitting diodes (LEDs) to show the open/closed status of each valve. The valves may be operated locally by toggle switches mounted adjacent to the schematic representation of each valve or remotely from the computer. GAM pressure measurements between 1 mtorr and 1000 torr are performed by three capacitance manometers in a multiplexer/signal-conditioner system that can be controlled by the computer. The temperatures of the getters and traps used in the GASP purification and separation procedures are controlled by commercial temperature controllers that are programmed by DAC outputs from the computer. The temperature controllers have deviation alarms that are used as flags to the computer to indicate when the programmed temperatures have been reached. We have modified ionization gauge controllers and other electronics units for more complete computer control. We have also added an IEEE 488 bus-controlled switch to select the Faraday or multiplier signal from the dual-channel electrometer for input to a 6 1/2 digit, 0.001%-accuracy digital voltmeter which transmits the measured signal intensity back to the computer via the IEEE 488 bus.

Control Software

Control of GAM, GASP and GMS modules and aquisition, storage and display of data are integrated into a single software package called MANGAL. MANGAL software and hardware have been designed to provide the operator with a continually updated visual display of system status as well as the option to assume manual control at any time. Sample processing software continually monitors getter temperatures and vacuum gauges to guarantee that they remain within acceptable limits. MANGAL records each process step or reading, along with the time it was executed, in a disk file for subsequent printout as a permanent record of the analytical procedure.

This work was performed under the auspices of the U.S. Department of Energy by Lawrence Livermore National Laboratory under contract No. W-7405-ENG-48.

NOVEL GASEOUS POLYATOMIC LANTHANIDE OXIDE SPECIES DETECTED BY FAST ATOM BOMBARDMENT MASS SPECTROMETRY

Ishenkumba A. Kahwa*, Thomas C.-Y. Hsieh+, Roger A. Laine# and Joel Selbin*
Departments of Chemistry* and Biochemistry# Louisiana State University and
Department of Food Science+, LSU Agricultural Center, Baton Rouge, LA 70803

Although solid single and multicomponent lanthanide oxides are extensively used in the laser [1], electronic [2], and catalytic [3] areas, their gas phase applications appear to have received little or no attention and knowledge of their gas phase chemistry is very limited. Previously known oxides are LnO, LnO_2, Ln_2O and Ln_2O_2 [4].

We have observed (Fig. 1 and 2) several novel binary and double component oxides in the source of a Fast Atom Bombardment Mass Spectrometer (FAB MS) namely, Ln_2O_3, Ln_3O_3, Ln_3O_4, Ln_4O_4, Ln_4O_5, Ln_4O_6, Ln_5O_6, Ln_5O_7, Ln_5O_8, Ln_6O_8, Ln_6O_9, Ln_7O_{10}, Ln_8O_{11}, Ln_8O_{12} and Ln_9O_{13}; and $CeEuO_2$, $CeEu_2O_3$, Ce_2EuO_4. The kind of gaseous oxides formed depends on the nature of the lanthanide element Ln as detailed elsewhere [5]. Where Ln is polyisotopic we have identified the oxides by their isotopic patterns and good agreement was generally found for oxides Ln_5O_7 and smaller. With monoisotopic elements such as yttrium and lanthanum many more oxides heavier than Ln_5O_7 were detected (Fig. 1). Closer proximity of the FAB gun enhanced the intensity of heavier forms of oxides of gadolinium showing poorly defined intensity patterns.

The double component oxides were observed by FAB MS analysis of a 1:1 molar powder mixture of off-white $Ce_2L(NO_3)_4$ and $Eu_2L(NO_3)_4 2H_2O$ [6], confirming that the formation of these oxides is a gas phase process and the following series of reductive condensations is proposed to illustrate the formation mechanism:

$$Ln_2L(NO_3)_4\ nH_2O_{(s)} \xrightarrow[\text{atoms}]{\text{Fast Xe}} Ln^+_{(g)} + LnO^+_{(g)} + [O]_{(g)}$$

$$2\ LnO^+_{(g)} + \bar{e}_{(g)} \longrightarrow Ln_2O^+_{2(g)} \xrightarrow[\bar{e}_{(g)}]{LnO^+_{(g)}} Ln_3O^+_{3(g)} \xrightarrow[\bar{e}_{(g)}]{LnO^+_{(g)}} Ln_4O^+_{4(g)}$$

Other oxides can be generated by condensation of suitable species.

The good possibility for formation of multicomponent oxides demonstrated here, the unusual Ln oxidation states associated with some of the oxides as well as the challenge of trapping and characterizing these oxides should stimulate increased investigative interest in the gaseous lanthanide oxide system.

Acknowledgements: I. A. Kahwa (on study leave from Chemistry Department, University of Dar es Salaam, P.O. Box 35061, Dar es Salaam TANZANIA) thanks the USA government (fulbright program) and L.S.U. for financial assistance. This work was supported in part by the Department of Chemistry and Biochemistry L.S.U., Baton Rouge, LA 70803.

References:

1. Weber, M. J., Lanthanide and Actinide Chemistry and Spectroscopy; Eldelstein, N.M. Ed. ACS Symposium series 131, 1980; pp. 275-311.
2. Nielsen, J. W., Industrial Applications of the Rare Earth Elements; Gshneidner, K. A. Ed. ACS Symposium series 164, 1981, pp. 219-222.
3. Wallace, D. W., Ref. 2 pp. 101-116 and Peters, A. W., ref. 2, pp. 117-131.
4. Kordis, J.; Gingerick, K. A. J. Chem. Phys. (1977), 66, 483-491.
5. Kahwa, I. A.; Hsieh, T.C.-Y.; Laine, R. A.; Selbin, J. Am. Chem. Soc. (1986) (submitted).
6. Kahwa, I. A.; Hsieh, T.C.-Y.; Laine, R. A.; Selbin, J. Inorg. Chim. Acta (1986) (in press).

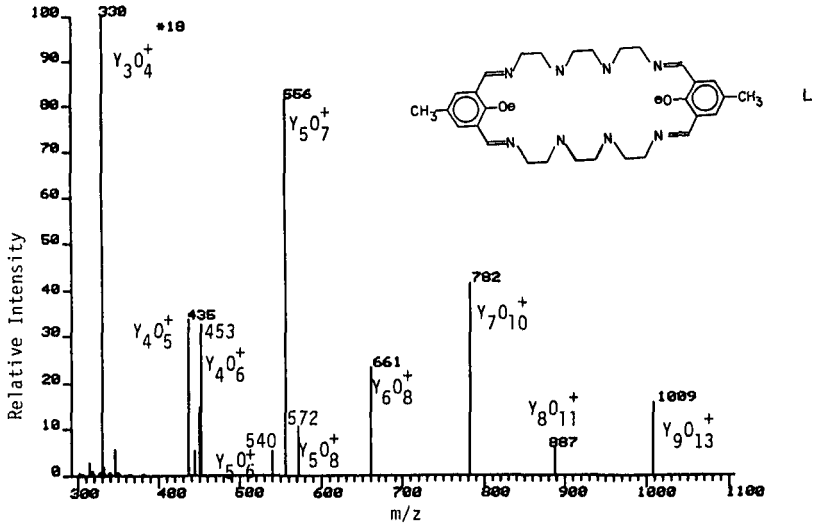

Fig. 1. The Fast Atom Bombardment mass spectrum of $Y_2L(NO_3)_3(OH)$ [6]. The species Y^+, YO^+, $Y_2O_2^+$, $Y_2O_3^+$ expected in the range 89 < m/z < 226 were not covered by the instrument's calibration range.

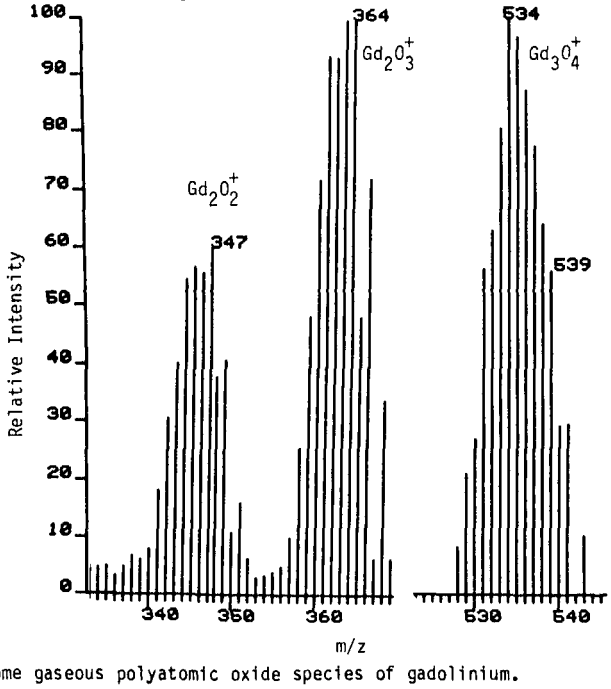

Fig. 2. Some gaseous polyatomic oxide species of gadolinium.

ACCURACY AND PRECISION OF HYDROGEN-2/HYDROGEN-1 ISOTOPE RATIO MEASUREMENTS BY ZINC REDUCTION OF WATER SAMPLES OF NATURAL ABUNDANCE AND BIOLOGICAL FLUIDS

William W. Wong, Lucinda S. Lee, and Peter D. Klein

USDA/ARS Children's Nutrition Research Center
Department of Pediatrics, Baylor College of Medicine
Houston, TX 77030

INTRODUCTION

Hydrogen is the gas required for $^2H/^1H$-ratio measurement by gas-isotope-ratio mass spectrometry (GIRMS). The general procedure for water samples is to reduce the water to hydrogen over uranium at 620°C. Because hydrogen is noncondensible at liquid nitrogen temperature, a mercury Toepler pump is used to transfer the hydrogen to a sample bulb before mass spectrometric analysis. Complete reduction of water to hydrogen and quantitative transfer of the hydrogen to the sample bulb are required to avoid isotope fractionation. Both processes are often time-consuming and the use of the same vacuum manifold and uranium reduction furnace for each sample often results in isotopic carry-over between samples with different deuterium contents.

Recently, Coleman et al. (1) and Kendall and Coplen (2) demonstrated the use of an AnalaR® zinc shot fraction (≤ 1-mm diameter) to reduce water samples to hydrogen at 450°C in individual reduction vessels. The zinc shot reduction technique has several attractive features: 1) no sample carry-over occurs, 2) many samples can be prepared at one time, and 3) the reduction vessels also serve as sample bulbs for direct introduction of the hydrogen gas into the mass spectrometer.

We have evaluated the accuracy and precision of the zinc reduction technique based on the measurements of $^2H/^1H$ ratios on 1) five international water standards and 2) four types of biological fluids (urine, plasma, saliva, breast milk) at enriched levels of deuterium.

EXPERIMENTAL

Preparation of the zinc shot. The AnalaR® zinc shot (Gallard-Schlesinger Chemical Manufacturing Co., Carle Place, NY) was sieved into sizes > 1 mm and ≤ 1 mm and washed with 3 M HNO_3 until the metal appeared shiny. After rinsing with deionized water, the zinc shot was lyophilyzed, degassed at 250°C under vacuum for 1 hr, and stored under vacuum until used.

Optimal sample size and best reduction vessel. Approximately 250 mg of the ≤ 1-mm diameter zinc shot was loaded into a borosilicate reduction vessel (Figure 1). The vessel was evacuated, filled with dry nitrogen, and 5- to 15-µL aliquots of a deionized water were introduced into the vessel with a Pencil-slim micropipet. With the water frozen at liquid nitrogen temperature, the vessel was again evacuated. The water was reduced to hydrogen by heating the zinc shot at 475°C for 30 min. The same experiment was repeated with quartz reduction vessels.

Accuracy and precision of the reduction technique. The accuracy and precision of $^2H/^1H$-ratio measurements for the reduction of water over the ≤ 1-mm zinc shot were determined on five international water standards: Vienna-Standard Mean Ocean Water, National Bureau of Standards water #1, National Bureau of Standards water #1A, Greenland Ice Sheet Precipitation, and Standard Light Antarctic Precipitation. 10-µL aliquots of each water standard were reduced with 250 mg of the ≤ 1-mm zinc shot at 475°C for 30 min. Ten samples each of urine, plasma, saliva, and human milk were tested after the addition of deuterium oxide. However, the human milk samples were defatted by centrifugation and the biological fluids (10µL) were placed in the vessel wall bubbles before reduction. The $^2H/^1H$-ratios were measured by GIRMS.

RESULTS

Optimal sample size and best reduction vessel. As shown in Figure 2, the best precision, 0.5 °/oo (SD, n = 20), was obtained with a 10-µL sample volume and a quartz reduction vessel.

Effect of particle size. The use of zinc shot ≤ 1 mm in diameter for the reduction of water to hydrogen yielded more precise $^2H/^1H$-ratios (SD = 0.5 °/oo, n = 20) than the coarser zinc particles (SD = 1.3 °/oo, n = 20).

Accuracy and precision of zinc reduction technique. An average accuracy of -2.0 ± 1.2 o/oo (mean ± SD, n = 58) and precision of 1.2 o/oo (SD) were obtained for the five international water standards with δ^2H values which ranged from 0 to -426.1 o/oo. At 580 o/oo enrichment levels of ^2H, the $^2H/^1H$ ratios measured from the urine, plasma, saliva, and breast milk samples were accurate to -4.6 ± 4.4 o/oo (mean ± SD, n = 200) and reproducible within 3.2 o/oo (SD).

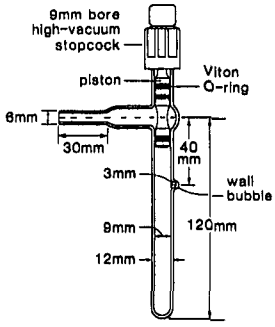

FIGURE 1: Reduction vessel.

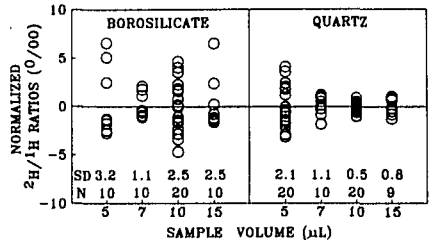

FIGURE 2: Effect of sample size and vessel composition on precision of $^2H/^1H$-ratio measurement

CONCLUSION

Our results indicate that the zinc reduction technique is well suited for $^2H/^1H$-ratio measurements of water samples at natural abundances of deuterium and biological fluids at enriched levels of deuterium. For accurate and precise $^2H/^1H$-ratio measurements, we recommend a 10-µL sample volume, 250 mg of AnalaR® zinc shot (≤ 1 mm in diameter), a quartz reaction vessel, and a reduction temperature of 475°C.

REFERENCES

(1) Coleman, M.L. et al. Anal. Chem. 1982, 54:993-995.

(2) Kendall, C. and Coplen, T.B. Anal. Chem. 1985, 57:1437-1440.

ACKNOWLEDGMENTS

This work is a publication of the USDA/ARS Children's Nutrition Research Center, Department of Pediatrics, Baylor College of Medicine and Texas Children's Hospital, Houston, TX. This project has been funded in part with federal funds from the U.S. Department of Agriculture, Agricultural Research Service under Cooperative Agreement number 58-7MNI-6-100. The contents of this publication do not necessarily reflect the views or policies of the U.S. Department of Agriculture, nor does mention of trade names, commercial products, or organizations imply endorsement by the U.S. Government.

RESONANCE IONIZATION MASS SPECTROMETRY OF La and Ba

L.W. Green, R.G. Macdonald and F. Sopchyshyn

Atomic Energy of Canada Limited
Chalk River Nuclear Laboratories
Chalk River, Ontario, Canada, K0J 1J0

Lanthanum-139 has most of the properties required for a fission monitor in nuclear fuels and is used as such by some laboratories. However, its determination by thermal ionization mass spectrometry is plagued by interference from Ba. Barium is a readily ionizable ubiquitous contaminant, especially in the rhenium filaments used for thermal ionization mass spectrometry, and its major isotope, ^{138}Ba, interferes with the only isotope of La available for spiking. A study of resonance ionization mass spectrometry of these two elements was undertaken because of the potential of this technique to selectively ionize La in the presence of Ba.

Two tunable dye lasers, pumped by a XeCl pulsed excimer laser, were temporally and spatially overdapped in the source region of a time-of-flight mass spectrometer. One of the dye lasers was typically charged with Coumarin 540A dye, and the other with Rhodamine 590 dye. Atomic vapours of Ba and La were generated by resistive heating of a Ta reservoir charged with either metal and located just below the ionization region of the mass spectrometer. Pulsed ion signals were detected with an electron multiplier and recorded with either a transient recorder-signal averager combination, for mass spectra, or a boxcar integrator, for optical spectra. Precise wavelength calibration was achieved by deflection of ~10% of a dye laser's output into a neon charged hollow cathode lamp and measurement of the optical galvanic signals for known neon transitions.

Some electric dipole allowed transitions for La are illustrated in Figure 1. As shown, there is a low-lying metastable state that is expected to be thermally populated at the temperatures used to volatilize La, 1150-1300°C, and there are a number of intermediate states for which there are electric dipole allowed transitions from the ground and metastable states. The electronic configurations for the higher lying states in La are not known but most of the J quantum numbers are.

The type of spectra obtained when one of the lasers was tuned to populate an intermediate state from either the ground or metastable state and the other was scanned, is illustrated in Figure 2. Each peak corresponds to excitation from an intermediate state, usually the $^4G_{5/2}$ 17947.13 cm^{-1} state, to an upper state followed by excitation to the ionization continuum by a photon from either laser. These are known as two colour-three photon ionizations and many such schemes were observed for both the ground and metastable states. In some cases (e.g. a') the intermediate state was populated by amplified spontaneous emission of the dyes.

Other types of transitions were also observed. One colour-two photon excitations from either the ground or metastable state to upper states were observed when the laser was tightly focussed. For these transitions there were no intermediate states. Two colour-two photon transitions slightly detuned (e.g. 1 A°) from an allowed transition were observed; most of these were eliminated when the λ_2 laser was delayed by ~10 ns with respect to the λ_1 laser. The remainder of these did not correspond to transitions expected from tabulated atomic energy levels, indicating that not all atomic energy levels in La have been identified.

The spectra for Ba were similar but less complex than those for La, there being only one resonance intermediate state (18060.26 cm^{-1}, 5535 A°) and no low lying metastable states. Scans over the range of the Coumarin dye, 5250 to 5900 A°, showed evidence of many one and two colour transitions, and that the resonance intermediate state was readily populated by amplified spontaneous emission of the dyes. This effect could be minimized by defocussing of the pump beam at the amplifier cell and defocussing of the dye beams at the ionization region.

Selective multiphoton ionization of La in the presence of Ba was demonstrated; a recommended excitation scheme is a two colour-two photon scheme with λ_1=5570.36 A° and λ_2=5558.8 or 5758.4 A°.

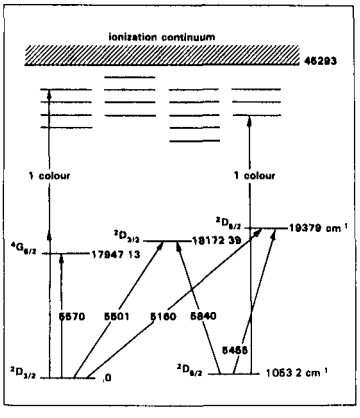

Figure 1. Some atomic transitions in La.

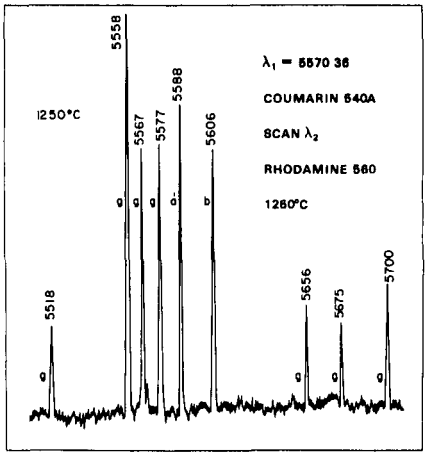

Figure 2. Optical spectrum of La with Rhodamine 560 dye. λ_1=5570 A°, Coumarin 540 A, to populate $^4G_{5/2}$ 17947.13 cm^{-1} state. Intermediate state g, $^4G_{5/2}$ 17947.13 cm^{-1}; a, 18172.39 cm^{-1}; b, 18156.97 cm^{-1}. 1250°C.

REMOVING METASTABLES FROM ANGLE-RESOLVED MASS SPECTROMETRY

C Moore, K R Jennings, S Evans
Kratos Analytical, Barton Dock Road, Urmston, Manchester M31 2LD, UK

In angle-resolved mass spectrometry an attempt is made to control the amount of energy transferred to an ion during collision activation by observing the yield of fragment ions as a function of angle relative to the direction of the primary ion beam. As previously described [1], a source capable of pivoting about a y-axis through the center of the collision cell has been built for use with the Kratos Analytical MS50 Mass Spectrometer. This swinging source has been used to produce ARMS data comparable to that obtained by other workers. One advantage of using a swinging source is that scattered ions which are detected by the mass spectrometer have travelled along its normal ion optical path and therefore any discrimination effects are independent of the scattering angle, θ .

Modifying the collision chamber so that it could have a voltage applied to it was expected to enhance the performance of the swinging source in the following ways:

(1) Allow one to study fragmentation occurring either inside (mainly collision induced) or outside (unimolecular) the collision cell.

(2) By limiting the collision region to the length of the collision cell (.4mm), the angular resolution of the source is improved.

The effect of the collision chamber voltage on the ion optics of the MS50 was investigated by studying the scattering of Ar^+ ions by Ar atoms. Kinetic energy loss spectra of the scattered ions were obtained at a number of different scattering angles, with and without a voltage on the collision chamber. Differences between the spectra were observed but did not significantly affect the angular dependence of the various peaks in the spectrum.

The collision chamber fitted to the swinging source is very short (.4mm) in the direction of the ion beams travel and therefore fragment ion intensities are strongly dependent upon collision gas pressure. As there are long field free regions either side of the cell, the number of fragment ions produced inside the cell (I_{IN}) compared with the number formed outside it (I_{OUT}) depends upon the system being studied.

For the reaction,

$$\underset{\text{methanol}}{[CH_3OH]^+} \longrightarrow [CH_3O]^+ + H$$

I_{IN} increases 100 fold when the collision gas pressure goes from 2.5 to 10 x 10^{-7} torr (measured on the source ball valve pumping line) whereas I_{OUT} only increases by a factor of 10 over the same pressure range. Quite different results were obtained when studying;

$$\underset{\text{Cyclohexane}}{[C_6H_{12}]^+} \longrightarrow [C_5H_9]^+ + CH_3$$

For this system, I_{OUT} is so large that it is attenuated by the addition of collision gas but I_{IN} does increase and therefore useful ARMS data can be obtained.

The 91/92 fragment ion ratio for n-butylbenzene has been studied by a number of different techniques[2]. It has been found to increase as the internal energy of the parent ions increase and can therefore be used as a calibrant. ARMS data which shows the ratio increases with scattering angle suggests that a correlation exists between the scattering angle and internal energy of the parent n-butylbenzene molecular ions. When n-butylbenzene molecular ions were produced in an electron impact ion source the angular dependence of the 91/92 fragment ion ratio depended upon the energy of the ionising electrons.

In Figure 1 the 91/92 ratio is plotted against θ using both the total fragment ion intensities (i.e. I_{IN} and I_{OUT}) and just fragment ion intensities from inside the cell (i.e. I_{IN}). Obviously, if one looks purely at collision induced dissociations the 91/92 ratio changes very little as the scattering angle is increased until ≈ 4° when it increases very rapidly. The differences between the 2 plots in Figure 1 are explained by the results in Figure 2 ($m^* = I_{OUT}$ and $CID = I_{IN}$). At low values of θ the detector signal for 92^+ ions is mainly due to unimolecular fragmentations occurring outside the collision cell (c.f. cyclohexane data), as θ increases this signal decreases because metastable ions are not scattered. However, as the 91^+ ion is produced mainly by collision induced reactions occurring inside the cell, the detector signal for this ion does not decrease as rapidly with increasing θ and therefore the 91/92 ratio increases i.e. if using (M* + CID) data, the rise in the 91/92 ratio with θ does not tell one anything about the internal energy of the n-butylbenzene molecular ions.

References

(1) Proceedings 32nd Annual Conference on Mass Spectrometry and Allied Topics (San Antonio) 1986, p562.

(2) R K Boyd, F M Harris, J H Beynon, Int. J. Mass Spectrom. Ion Processes., 66, 185 (1985).

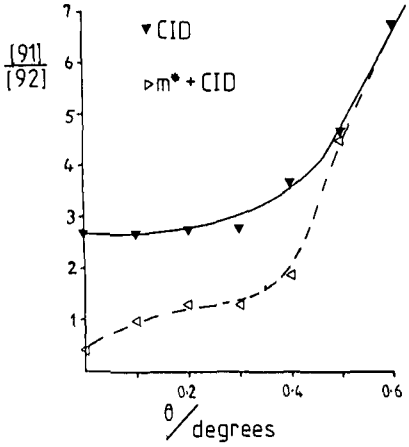

Figure 1

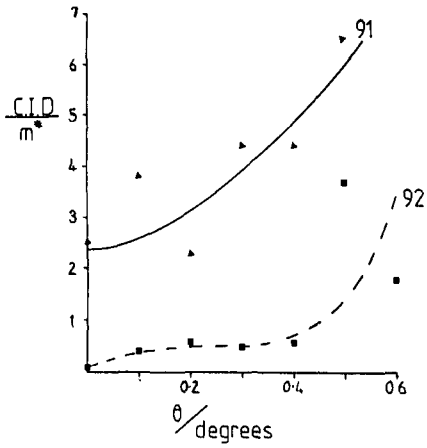

Figure 2

METHODOLOGY FOR THE DETERMINATION OF ABSOLUTE TOTAL CROSS-SECTIONS IN A QQQ INSTRUMENT AND ITS APPLICATION TO IN-SITU TARGET THICKNESS CALIBRATIONS

Richard I. Martinez
Center for Chemical Physics
National Bureau of Standards
Gaithersburg, MD 20899

and

Seksan Dheandhanoo
Department of Chemistry
Georgetown University
Washington, DC 20057

ABSTRACT

A methodology has been developed for the measurement of total reaction cross-sections $\sigma(E)$ in the range of collision energies E_{coll}=5-60 eV (LAB) used for collision-induced dissociation (CID) in triple-quadrupole (QQQ) tandem mass spectrometers. This methodology has been calibrated by making pseudo-first order kinetics measurements of the symmetric (resonant) charge transfer cross-sections $\sigma(E)$ for $Ne^+(Ne,Ne)Ne^+$. Our $\sigma(E)$, for E=5-60 eV and P=0.04-1 mtorr, agree with the Rapp-Francis theory to within 15%. We measured identical $\sigma(E)$ from both the rate of reactant decay and the rate of product formation. Hence, it should be possible to readily determine branching ratios $\alpha_i(E)$ for different reactive channels i. Our methodology provides a means whereby the absolute target thickness [(actual path length traversed by the ion) x (effective number density of the CID target)] of gas targets can be accurately calibrated in-situ for collision energies in the range of ca. 5-60 eV (LAB). Knowledge of target thicknesses is essential for the development of generic CID spectral libraries generated in different types of QQQ instruments [i.e., collision chamber vs. molecular beam targets]. An interlaboratory round robin test protocol is being proposed to assess the utility of our methodology for standardization of generic operating parameters. [**Letters of inquiry from prospective participants may be sent to NBS.**]

INTRODUCTION

The generation and interchange of reference libraries of CID spectra necessitates standardized operating conditions for the various types of QQQ instruments. A recent international round robin evaluation of the reproducibility of standard operating conditions indicated that CID gas target thickness was not a well-controlled parameter [1].

To provide a generic target thickness standard for Type A [1] (molecular beam target) and Type B [1] (collision chamber) QQQ instruments, we have developed a new kinetic methodology capable of providing in-situ calibration of target thickness.

Our kinetic methodology has been calibrated by measuring $\sigma(E)$ for $^{22}Ne^+(^{20}Ne,^{22}Ne)^{20}Ne^+$ for collision energies from ca. 5-60 eV. This reaction has been previously studied in the low-energy [2,3] (ca. 0.04-3 eV) and high-energy [4,5] (>50 eV) regimes. Our measurements complement the available data.

EXPERIMENTAL

Measurements were made in a specially designed QQQ instrument which can be configured as both a Type A or Type B MS/MS. The three mass filters Q1, Q2, and Q3 are completely nude (no housing). [For the Type A configuration, there is no collision chamber enclosure and a Lasertechnics LPV molecular beam valve is used for the CID gas inlet. For the Type B configuration, the collision chamber enclosure surrounds Q2.]

Ne^+ ions were generated by 70 eV electron impact, and the $^{22}Ne^+$ bullets were selected by Q1. The energy spread of the bullets entering Q2 was determined to be ≤1 eV for 90% of the ions [≤2eV for 99% of the ions; ≤4 eV for 99.9% of the ions] when measured by using the Q2 pole bias (rod offset) to generate a stopping potential curve. $E_{90\%}$ is the Q2 potential required to stop 90% of the ions. The collision energy E_{coll} was selected by setting the Q2 pole bias = $E_{90\%}$ - E_{coll}.

The $\sigma(E)$ shown as (○ , ●) in Fig. 2 for E_{coll}=5-60 eV [⊕ ion velocities v=0.9-2.3 ($\times10^6$) cm s^{-1}] were derived from the rate of decay of the bullet when measured as a function of the target pressure P_{Ne} (see Fig. 1). For E_{coll}= 6 and 36 eV, the $\sigma(E)$ determined from the rate of production of $^{20}Ne^+$ are shown in Fig. 2 as ▲ and were identical with the $\sigma(E)$ (○ in Fig. 2) determined from the rate of decay of the $^{22}Ne^+$ bullet.

RESULTS

Fig. 1 – Bullet decay experiments. Plots of Ln Y vs. P_{Ne} at fixed values of E_{coll}.
$Y = [^{22}Ne^+]_0/[^{22}Ne^+]$ and
$\ln Y = k\varepsilon L_{eff}(m/2E_{coll})^{1/2}\,[Ne]$
$= \sigma L_{eff}\,[Ne]$
$= \beta P_{Ne}$
L_{eff} = actual path length traversed by ion within Q2 collision chamber (corrected for rf effects).
m = mass of $^{22}Ne^+$ bullet.

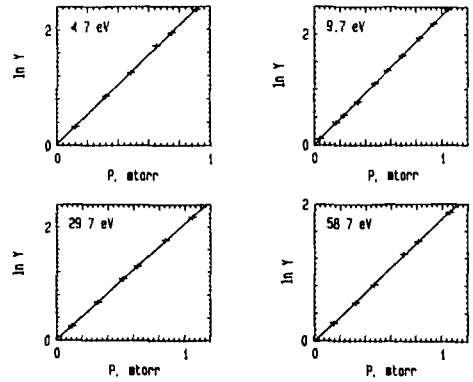

Fig. 2 – Plot of $\sigma^{1/2}$ vs. v. Comparison of our results with other workers and with the Rapp–Francis theory.
○,● – bullet decay experiments
▲ – product growth experiments

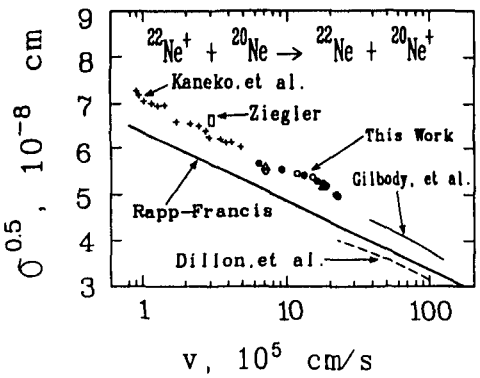

DISCUSSION

There are no literature values for $\sigma(E)$ for $Ne^+(Ne,Ne)Ne^+$ for E=5–60 eV, the range of energies used for CID. Our results (see Fig. 2) complement the work of others [2-5], and are within 15% of the Rapp–Francis theory [6]. Additional work is in progress to further refine our methodology and reduce known sources of error.

Our $\sigma(E)$ measurements indicate that our kinetic methodology provides a means whereby absolute target thicknesses can be accurately calibrated in-situ for E_{coll}=5–60 eV for any CID gas in Type A or Type B QQQ instruments. Since Ar and N_2 are commonly used as CID target gases, the measurement of $\sigma(E)$ for $Ne^+(N_2,Ne)N_2^+$ and $Ne^+(Ar,Ne)Ar^+$ should allow anyone to calibrate in-situ the target thickness of their N_2 or Ar gas targets.

Interlaboratory round-robin testing of our methodology in various types of QQQ instruments is essential to confirm its reliability as a generic standard.

REFERENCES

1. P.H. Dawson and W.-P. Sun, Int. J. Mass Spectrom. Ion Processes 55, 155 (1983/1984).
2. B. Ziegler, Z. Physik 136, 108 (1953)
3. Y. Kaneko, N. Kobayashi, and I. Kanomata, J. Phys. Soc. Japan 27, 992 (1969).
4. J.A. Dillon, Jr., W.F. Sheridan, H.D. Edwards, and S.N. Ghosh, J. Chem. Phys. 23, 776 (1955).
5. H.B. Gilbody and J.B. Hasted, Proc Roy. Soc. A238, 334 (1956).
6. D Rapp and W.E. Francis, J Chem. Phys. 37, 2631 (1962)

AN INTEGRATING TRANSIENT RECORDER FOR TIME ARRAY DETECTION

B. Newcome, E. Erickson, G. Yefchak, M. Davenport, and J. Holland

Departments of Chemistry and Biochemistry
Michigan State University
East Lansing, Michigan 48824

Many analytical problems require rapid collection of mass spectral data. Chromatographic peaks can elute from columns in times on the order of 1 s, requiring the collection of 10 to 50 spectra each second to preserve chromatographic resolution. Other transient samples with lifetimes of 1 s or less can require sampling rates of 1000 scans per second. The use of a GC inlet for tandem MS instrumentation can require scans in excess of 1000 per second. One of the few techniques capable of these high data collection rates is time-of-flight (TOF) MS in conjunction with time array detection.

In order to realize the potential of this method, an integrating transient recorder (ITR) capable of collecting all the information from each TOF transient (ion pulse) is being constructed. Design goals for the ITR include: summing 1 to 1000 transients per second; 5 ns sampling times (providing in excess of 16,000 samples per transient); continuous data collection at the maximum rate for at least an hour; and data reduction to mass/intensity pairs in real time prior to storage. Figures 1 - 3 are block, data flow, and logical representations of the system, respectively.

A 200 megasample/second ADC digitizes the signal from the spectrometer. The SUM AND STORE circuitry contains two banks of memory and adders which sum a preset number of digitized transients. While one bank of memory collects and sums successive transients, the other bank outputs the previous summed spectrum to the reduction hardware. The REDUCTION circuitry performs an operation in which data above a preset threshold value are stored in a FIFO buffer along with scan headers. These data are transferred to a 300 megabyte disk for later interpretation. The present instrumentation is capable of continuously producing up to 50 spectra each second with no loss of information from the TOF transients.

The present version utilizes post-processing for the reduction to mass/intensity pairs. This function will later be accomplished in real time with the use of digital signal processors. A small subset of the data will also be forwarded to a graphics processor to enable the operator to provide real time feedback. Future implementations are expected to increase the collection rate to 1000 spectra/s and meet all the design goals.

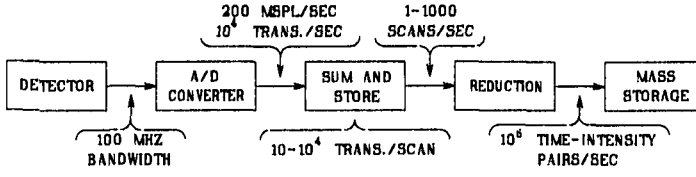

Figure 1

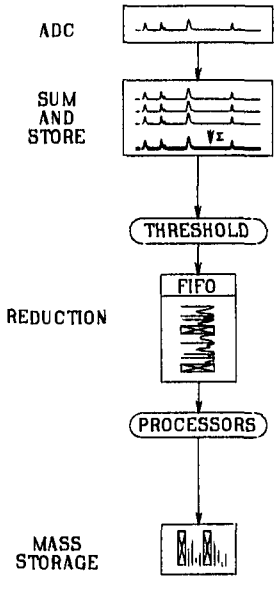

Figure 2

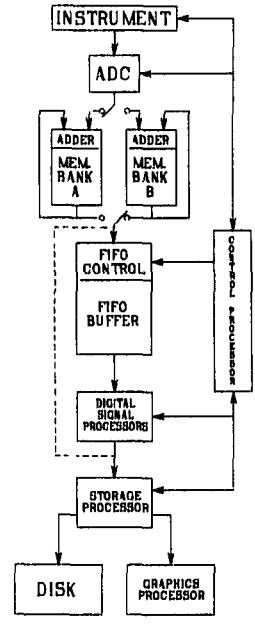

Figure 3

CALIFORNIUM-252 PLASMA DESORPTION FOURIER TRANSFORM ION CYCLOTRON RESONANCE MASS SPECTROMETRY

R.R. Weller[1], S.K. Viswanadham[2], M.A. Sheetz[3], C.S. Giam[1,2], D.M. Hercules[2]
Departments of Industrial Environmental Health Sciences[1], Chemistry[2], and Radiation Safety[3]
University of Pittsburgh, Pittsburgh, PA 15261

^{252}Cf plasma desorption mass spectrometry has provided a successful technique for the study of high mass molecules. The technique is ideally suited for TOF instruments, but has been hindered by the relatively low resolution in present TOF instruments. FT-ICR with its ability to detect a relatively low number of ions provides a method to obtain high resolution high mass spectra using ^{252}Cf plasma desorption techniques.

Samples adsorbed on aluminum foil or aluminized mylar, in front of a 100 µCi ^{252}Cf source are mounted on the end of a standard "solids" type probe and introduced to the high vacuum region of the Nicolet FTMS 1000 via an airlock. The sample-source assembly is located less than 2 cm from one trap plate. Ions are accumulated in the 5 cm cubic mesh cell until a sufficient number are obtained for detection (15-30 minutes, typically) and are subsequently detected by standard FTMS techniques.

Ions were obtained for CsI (Cs^+,m/z 133; I^-,m/z 127) (Fig. 1 and 2), N,N,N-trimethyl[D9]-p-aminophenolate iodide (cation, m/z 161), (Fig. 3) and gramicidin-S (M+H-Phe, m/z 994). The later peak was used as a reference for a study of the effect of the trapping potential on ion accumulation efficiency with best results obtained for a potential of 5.5v (Fig. 4). It should be noted that a higher trapping potentials the very large background peak at m/z 141 (+) and numerous smaller peaks are not observed. Ionic compounds were more readily desorbed than neutral compounds (as has been reported by other laboratories). The long ion accumulation times may lead to the problem of ion/molecule reactions or ion dissociation.

Future work must focus of the optimization of the parameters affecting ion accumulation and the determination of the source of the consistant background peaks. Once these items have been addressed then the full advantages of ^{252}Cf plasma desorption FT-ICR-MS may be realized.

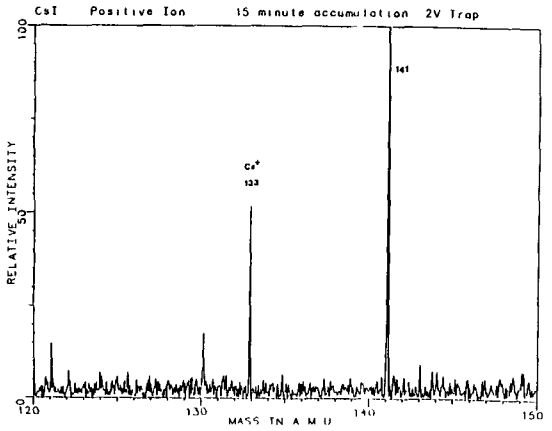

Figure 1

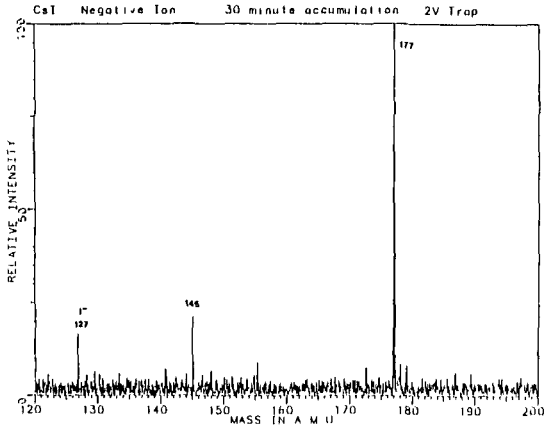

Figure 2

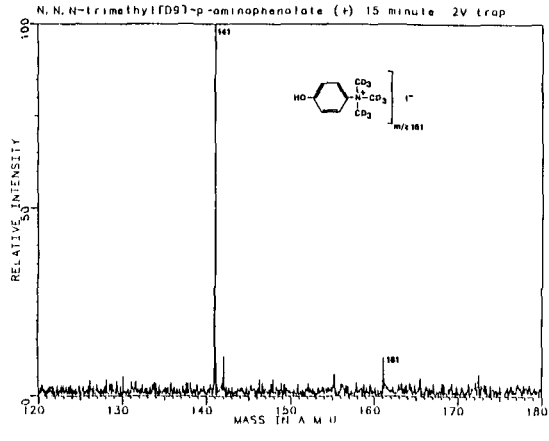

Figure 3

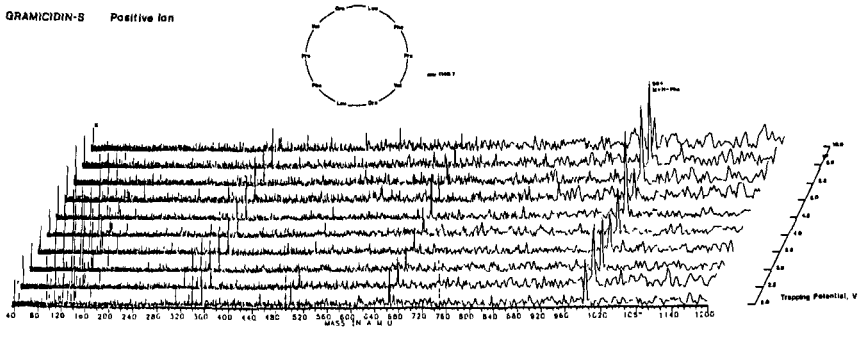

Figure 4

DESIGN AND ANALYTICAL APPLICATIONS OF A NEW HIGH MASS TANDEM MASS SPECTROMETER

P. A. Lyon, S. L. Hunt
3M Corporate Research 201BW09
Saint Paul, Minnesota 55144

S. Evans and H. Tudge
Kratos Analytical, Manchester, England.

The recent application of tandem mass spectrometry to separate components in complex mixtures and the discovery of fast atom bombardment (FAB) ionzation of nonvolatile samples make the combination of these techniques a logical choice for solving many of the difficult industrial analytical problems. Lacking these capabilities within our laboratories, we pursued the acquisition of an instrument which would incorporate these emerging technologies.

A new tandem mass spectrometer has been built and installed at 3M Corporate Research Laboratories possessing both high mass range and high resolution capabilities. The instrument uses an EBE configuration (Figure 1) and was designed to accept eventually a fourth sector (B).

An inhomogeneous high field fully laminated magnet was fitted to a standard double focussing MS-50 which functions as the first two analyzers. This magnet has a mass range in excess of 8,000 amu at full accelerating voltage (8 kV) at scan rates from 0.5 to 3000 sec/decade. Full scan calibrations (m/z >8,000) have been achieved in our laboratory using special nominal mass processing which stores data for every 1/16 amu. This speeds processing and permits mass ranges up to 32,000 amu. In recent work, ions of mass greater than 4,000 were observed for a series of cyclic perfluoroalkanesulfonates (1).

The first mass spectrometer of the tandem instrument is capable of defining a highly resolved ion beam (R= 100,000 in static mode, 10% valley definition) which can be sampled by an intermediate detector in the third field-free region or passed into a collision chamber. The excellent sensitivity of this instrument at a resolution of 10,000 is ideal for collision activation of higher molecular weight species now accessible using FAB.

A totally new collision cell has been constructed for the third field free region (Figure 2). The cell uses a row of thin capillary jets to form a narrow high pressure region where collision activation occurs. The cell is mounted on a removable flange which could easily be modified to accept alternate excitation modes (CAD, LD, EI, etc.). Lenses before and after the cell permit fragmentation products to be refocussed into the third analyzer (a 15" radius ESA) and when fitted, the fourth sector.

The instrument is operationally very flexible, capable of being operated manually or under full computer control. An autoconsole monitors and controls most system paramters and provides a real time output (comparable to a conventional oscilloscope trace) which is used for tuning. For each sweep the resolution and intensity of the most abundant peak in the window is displayed. The data system will control and acquire parent ion, daughter ion, constant neutral loss, and MIKES scans in addition to the metastable mapping feature.

Preliminary results indicate that MIKES spectra of typical ionic fluorochemicals are comparable to those obtained on the conventional MS-50 TA at the University of Nebraska (2). The instrument at 3M has also been used to successfully characterize commercial surfactants (FAB), dyes and colorants (FAB and DCI), fluorochemicals (HREI and FAB/MS/MS), and polyester film contaminants by HRGC/HRMS.

1. Hunt, S.L., Lyon, P.A., Behr, F.E., Winter, L.D., Cerny R.L. ; 34th Annual Conference on Mass Spectrometry and Allied Topics, Cincinnati, OH, June 8-13, paper TPD5.
2. Gross, M.L.; Chess, E.K.; Lyon, P.A.; Crow, F.W. Int. J. Mass Spectrom. Ion Phys. **1982**, 42, 243-254.

Figure 1

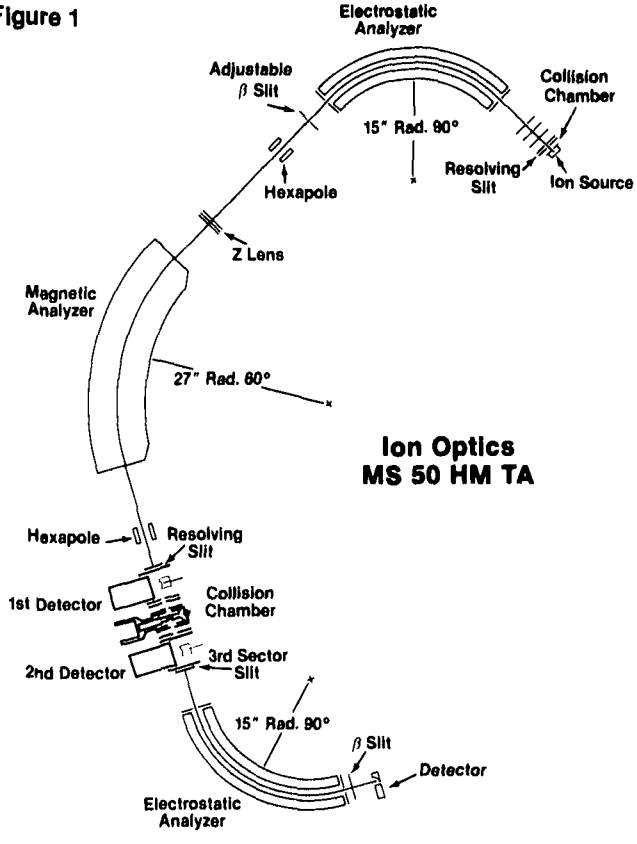

Figure 2

Collision Chamber Region

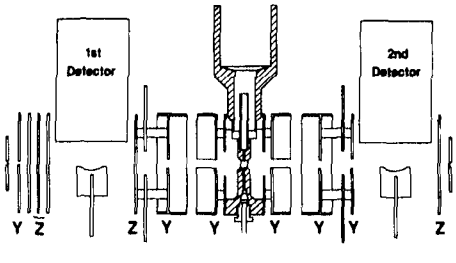

PARTICULATE ANALYSIS VIA SPUTTER ATOMIZATION/RESONANCE IONIZATION MASS SPECTROMETRY*

D. E. Goeringer, W. H. Christie, and H. S. McKown
Oak Ridge National Laboratory, Oak Ridge, TN 37831

Monitoring trace elements in small samples requires ultra-sensitive detection methods. Sputter atomization/resonance ionization mass spectrometry (SA/RIMS) is a highly sensitive technique for elemental and isotope ratio analyses. A conceptual diagram of the technique, which combines ion beam sputtering, resonance ionization, and mass spectrometry, is shown in Figure 1.

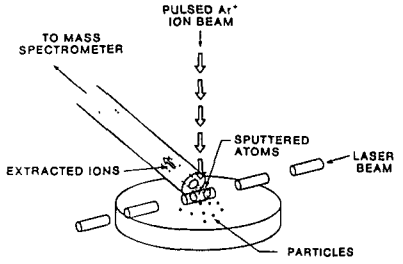

A pulsed beam of high-energy primary ions bombards the sample to produce a plume of neutral atoms. The cosine distribution of sputtered neutrals is intersected and ionized by a synchronized, pulsed laser beam tuned to a resonant transition in the sample atoms. Laser-generated ions are then extracted into a mass spectrometer for mass analysis. Use of a micro-focused primary beam enables small particles to be sampled individually; the pulsed nature of the beam allows its duty cycle to be matched with that of the laser resulting in efficient sample utilization. The pulsed laser generates the high power necessary to selectively ionize 100% of the intersected atoms. Mass analysis of the laser-generated ions provides the capability for isotope ratio measurements.

The SA/RIMS experiments were performed on modified ARL ion microprobe mass analyzer (IMMA). An optical port was added to the rear of the instrument for introduction of the laser beam, and an internal periscope assembly was located adjacent to the sputtering chamber for positioning the beam above the sample stage. The 532 nm output from a pulsed, frequency-doubled Nd:YAG laser was used to pump a dye laser using Rhodamine 610 dye. The dye laser output beam was contracted by a telescope assembly and directed into the optical port by a prism fixed to an adjustable mount. A diagram of the optical system is shown in Figure 2.

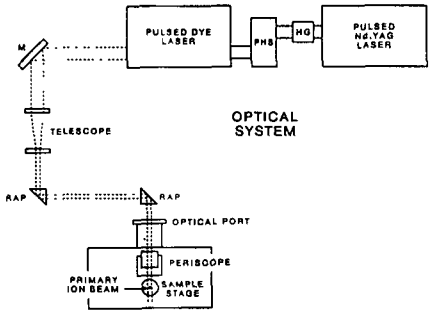

*Research sponsored by the U. S. Department of Energy, Office of Basic Energy Sciences, under Contract DE-AC05-84OR21400 with Martin Marietta Energy Systems, Inc.

By acceptance of this article, the publisher or recipient acknowledges the U S Government's right to retain a nonexclusive, royalty-free license in and to any copyright covering the article

Control/data acquisition was handled by an LSI-11/23-Plus microcomputer housing a Winchester hard disk, dual floppy disks, and parallel, analog-to-digital (ADC), and digital-to-analog (DAC) interfaces. Digital outputs from the parallel interface were used to select the dye laser wavelength via its scan control interface. The flashlamp sync output from the Nd:YAG laser triggered a gate/delay generator pair which set the delay and pulse duration for the primary beam. The Daly detector signal originating from packets of laser-generated ions was amplified and shaped by a fast current amplifier and sampled by a gated integrator. The integrator output was converted by the ADC and displayed in real-time on a scope via a DMA-controlled DAC.

SA/RIMS optical spectra can be obtained by monitoring the signal from laser-generated ions at a fixed mass while scanning the laser output wavelength; three such spectra are shown in Figure 3. These spectra compare signals from ^{238}U metal using different primary ions at a fixed energy of 16 keV and current of 10 nA. The energy density for the laser is also fixed at approximately 300 mJ/cm^2. The spectra suggest that Ar^+ is superior to N_2^+ and O_2^+ in generating gas phase neutral atoms from ^{238}U metal. The optical spectra show a strong signal at 591.54 nm (16900 cm^{-1}). Energy level tables for neutral atomic uranium show a transition at that wavelength originating from the ground electronic state. However, the ionization energy for uranium is 48800 cm^{-1}, suggesting that ionization is due to a single-color, three-photon transition from the ground state through two approximately equally spaced excited states.

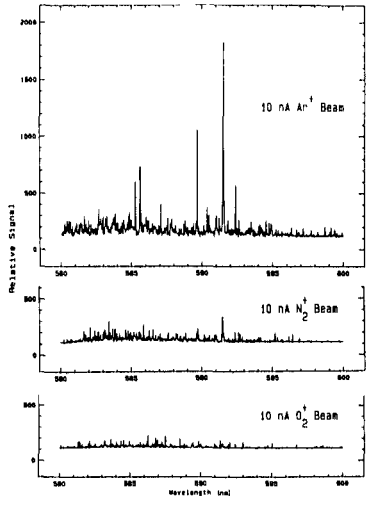

The table below compares relative signals for SA/RIMS and SIMS of ^{238}U metal. The data were obtained using a CW primary beam and a 6 μs integrator gate width. The SA/RIMS signal using an Ar^+ primary beam was much larger than that for an O_2^+ beam. The SA/RIMS signal with Ar^+ was also about two orders of magnitude greater than the SIMS signal using O_2^+ primary ions for sputter-ionization.

	SA/RIMS		SIMS
Primary Beam	10 nA; Ar^+	10 nA; O_2^+	10 nA; O_2^+
Net Signal	6.44	0.03	0.02
Relative Strength	320	1.5	1.0

FOURIER TRANSFORM ION CYCLOTRON RESONANCE MASS SPECTROMETRY AT LOW MAGNETIC FIELDS.

B. A. Hearn, G. Baykut, and J. R. Eyler, Department of Chemistry, University of Florida, Gainesville, Florida 32611.

With the thrust of instrument development for Fourier transform ion cyclotron resonance mass spectrometry toward higher resolution and extremely accurate mass determinations, a generation of instruments based primarily on superconducting magnets and electromagnets with high magnetic fields has become available commercially. The modern analytical laboratory, under increasing pressure to provide more information at lower cost, is many times limited in its choice of instruments by budgetary considerations. This has reduced the availability of Fourier transform ion cyclotron resonance mass spectrometry to many analytical chemistry laboratories. A Fourier transform ion cyclotron resonance mass spectrometer based on an inexpensive permanent magnet can be used as an alternative to the high magnetic field instruments currently available, allowing a more widespread utilization of the technique due to lower instrumentation costs.

Evaluation of several figures of merit for a Fourier transform ion cyclotron resonance mass spectrometer based on an inexpensive permanent magnet with a magnetic induction of 0.16 T showed that this instrument may be practical for use in the analytical chemistry laboratory. While the performance of the instrument was lower than that for instruments based on superconducting and electromagnets with higher magnetic fields, figures of merit that were measured indicated that the permanent magnet based mass spectrometer provides adequate performance. A reproducibility of about ± 4% (taken as the 95% confidence level for the average of 3 measurements) was obtained for a series of hourly measurements over a period of 6 hours. For a 10 day period, the reproducibility was ± 15% (using the same confidence level as above). The second figure of merit measured in this study was resolution values obtained with the permanent magnet. A comparison of resolution values measured for perdeuterated benzene with an electromagnet at 0.15 to 1.0 T and a superconducting magnet at 3 T with those obtained using a permanent magnet at 0.16 T showed that similar resolution values were found for all three magnets for a given number of data points and a given lower mass. As expected, the signal-to-noise ratio for the permanent magnet based mass spectrometer was low. Here, signal averaging can increase the signal-to-noise ratio, so a tradeoff exists between time and instrument cost. Overall, the permanent magnet based Fourier transform ion cyclotron resonance mass spectrometer shows promise in future analytical chemistry laboratories.

SOME RESULTS USING RF BURST EXCITATION AS A TOOL FOR INVESTIGATION OF PHENOMENA IN THE FTMS CUBIC ION TRAP

S.K. Huang and D.L. Rempel, Department of Chemistry, University of Nebraska, Lincoln, NE 68588-0304

Because the action of a low amplitude RF burst on an ion in a cubic trap is reasonably well understood and is selective in exciting only the cyclotron mode, RF burst waveforms can be used to gain information about the operation of the trapped ions in a FTMS experiment. Here, we focus on ion cloud shape information and double resonance limits.

RF burst waveforms can be used to infer information about the ion radial distribution by paying close attention to the signal as a function of cyclotron orbit size. To see how this might be done, consider a simplified model in which the excitation and detection fields are uniform. After excitation, the extreme radial displacement for each ion is the sum of the unknown magnetron, r_m, and known cyclotron, r_c, mode amplitudes. Ions are radially ejected as the excitation time is increased to give a signal, S, in equation 1. Here a is the length of the trap and ρ is the density of ions at r_m. The departure of the signal from a linear function of excitation time carries information about ρ. Experiments with ion distributions generated by electron beams, which are 10% and 50% of the trap size, show fair agreement between expected and actual results.

The spectral peak of ions excited to very large orbits is split into a doublet [1]. Comparison of experimental evidence and available theory support the conclusion that the high frequency peak is due to an ion population segment with low z-mode amplitudes, and the low frequency peak is due to a segment with high z-mode amplitudes. Since the RF burst excitation does not change the z-mode amplitudes, the relative intensities of the peaks carry information about the ion axial distribution just before excitation.

RF burst waveforms provide a convenient means for achieving an excitation spectral resolution high enough to test the limits of ejection performance due to effects intrinsic in the operation of the cubic trap. For low ion populations, an estimate of achievable ejection resolutions might be based on the frequency spread over the range of orbit radii through which the ions must pass to be ejected. For ions with low z-mode amplitudes, Dunbar's approximate expression for the average radial electric field strength [2] can be used to obtain equation 2, where m_c is the critical mass [3] and r/a is the maximum relative radius required for ejection. Measured resolutions are in the neighborhood of 2.4K for a 0.44 volt, 0.0254 cm trap operated at 1.2 Tesla. This compares with the calculated estimate of 2.69K.

It is proposed that the ejection performance of the cubic cell can be improved with formed excitation/detection plates and segmented trap electrodes. See Figure 1 for a representation.

Formed excitation and detection plates are one means of improving the uniformity of the excitation and detection fields. Such an idea was used by Clow and Futrell [4] to improve the uniformity of drift velocities in a drift cell ICR. For the cubic cell, this would be done by bringing all the edges of two nominally parallel plates closer together to compensate for their finite area and other electrode proximity. The same set of plates could be used at different times for both functions through the use of carefully designed switches [5].

Segmenting the trap electrodes by electrically isolating a disk-shaped region provides a means to minimize the trap electric field deviations from the linear ideal. This is similar to the use of segmented cylinders to reduce the anharmonicity of the trap potential along the z-axis in cylindrical traps [6].

Ejection would be accomplished by accelerating the selected ions to orbits a little larger than the disk and then grounding the outer trap segments to invert the trap-well for those ions with large cyclotron orbits.

References

[1] A.G. Marshall, J. Chem. Phys., 55(1971)1343.
[2] R.C. Dunbar et al., Int. J. Mass Spectrom. Ion Proc., 57(1984)39.
[3] E.B. Ledford et al. Anal. Chem., 56(1984)2744.
[4] R.P. Clow et al., Int. J. Mass Spectrom. Ion Proc., 8(1972)119.
[5] R.J. Doyle, Jr., et al. in "Ion Cyclotron Resonance Spectrometry II", H. Hartmann and K.-P. Warczek, eds., Springer-Verlag, Berlin, 1982, pp. 365-379.
[6] G. Gabrielse et al., Int. J. Mass Spectrom. Ion Proc., 57(1984)1.

Equation 1. $$S(r_c) = (2q/a) \int_0^{(a/2)-r_c} r_c \rho(r_m) dr_m$$

Equation 2. $$R = (\omega eff/\Delta\omega eff) \cong 1.429\,(m_c/m)(a/r\ )^3$$

Figure 1. Proposed modification of the cubic trap.

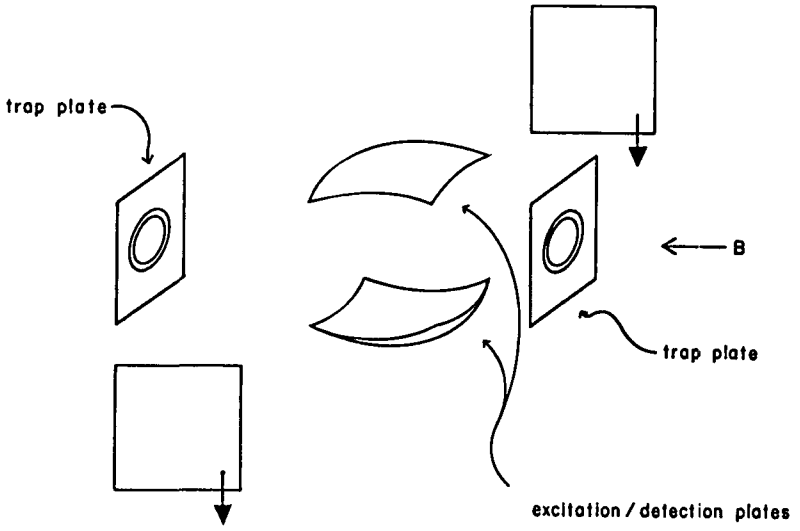

EFFECTIVENESS OF VELOCITY COMPACTION FOCUSING IN COMPENSATING FOR INITIAL TEMPERATURE DISTRIBUTION OF ION SOURCE PLASMA.*

M. L. Muga, TOFTEC, P.O. Box 12877, Gainesville, FL, 32604

The initial Boltzmann temperature distribution of ions is a main factor in limiting the attainable mass resolution in a Time-of-Flight (TOF) mass spectrometer (MS). Velocity compaction ion focusing applied to a straight path TOF MS is specifically designed to give all ions in a given mass group nearly equal velocities upon entering a final drift region. In this way, peak profiles remain 'frozen' even as adjacent mass peak-to-peak distances widen during the final drift period. Hence, for this ion focusing principle, the overall resolution is a measure of the effectiveness of velocity compaction in compensating for the initial temperature distribution of the ion source plasma.

Computer simulations have been performed for a two stage velocity compaction TOF MS in which deceleration of the ions at the end of a first stage separation is optimized for feeding the velocity compaction focusing second stage.

The derivation and flight time simulation programs are based on ion trajectories through a gridded system as shown in Figure 1 below consisting of an alternate deceleration/acceleration region, each followed by field-free drift regions. Ions begin at source on left and end flight by impacting on detector Dt.

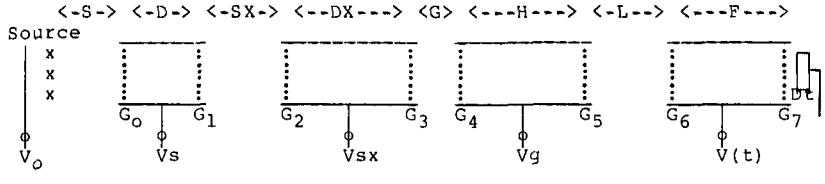

Fig. 1) Two-stage Velocity Compaction TOF Mass Spectrometer

The flight path consists of an extraction region, S, followed by a field free drift region, D, an acceleration region, SX, and drift region, DX, a deceleration region, G, with drift region, H, and a variable voltage acceleration region, L, followed by a final drift region, F. Any combination of regions can be used (or omitted) along with variations in applied voltages, including time-lag-focusing, for simulating flight times of ions of a given mass.

The ion plasma is given a Boltzmann distribution of velocities corresponding to a temperature in the range from 300°K to 5000°K. For most studies a temperature of 500°K was assumed as this temperature value has been shown to give simulation results consistent with an actual single stage working model used to demonstrate the velocity compaction principle. Resulting peak profiles over the range of 1000 - 8000 amu indicate mass resolutions are attainable in excess of 10,000 $[(M/\Delta M)|_{fwhm}]$.

The degree to which velocity compaction focusing compensates for flight time spread due to an initial Boltzmann velocity spread is shown in Figure 2a for temperature variations from 300°K to 1300°K. Over a spread of 1000°K little increase in peak width appears. The near constancy of peak width as a function of increasing temperature indicates the effectiveness of velocity compaction focusing in compensating for the initial Boltzmann

velocity distribution, a not surprising result since velocity compaction focusing is designed for this specific purpose.

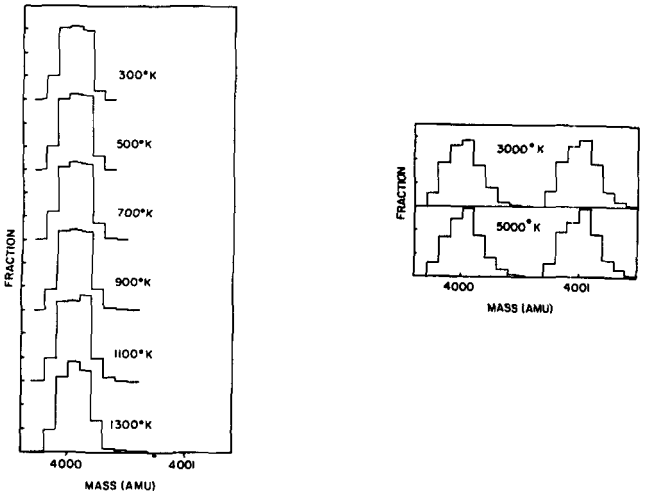

(a) (b)

Fig. 2) Effect of Initial Ion Temperature Distribution in Source Region.

Even at temperatures as high as 5000°K, by adjusting the time-lag-focusing period, effective separation is achieved as shown in Figure 2b. Thus velocity compaction focusing should work equally well for laser induced ionization from solid substrate for which higher effective temperature distributions are postulated.

* Supported by the Department of Health and Human Services Public Health Service Small Business Innovation Research (SBIR) Phase I Program, Project No. 1 R43 MH39422-01A1, National Institute of Mental Health.

A TIME-OF-FLIGHT MASS SPECTROMETER WITH AN ION MIRROR: IMPROVED RESOLUTION AND METASTABLE ION ANALYSIS

X. Tang, R. Beavis, W. Ens, B. Schueler, & K.G. Standing;
University of Manitoba, Winnipeg, CANADA R3T 2N2

A new time-of-flight (TOF) mass spectrometer has recently been constructed at the University of Manitoba. Like the Orsay 'Reflex' instrument [1] and the new Münster spectrometer [2], it compensates for the initial ion velocity spread by use of a plane ion mirror, as proposed by Mamyrin, et al. [3].

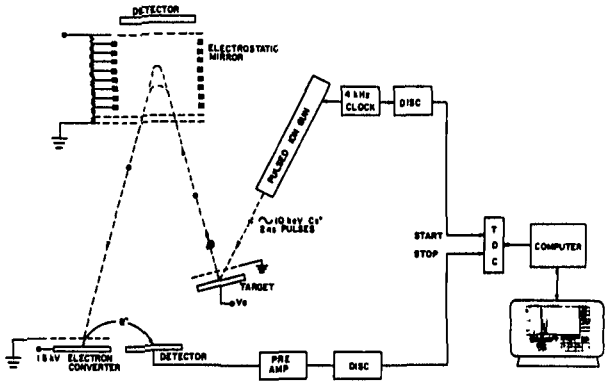

In our spectrometer, illustrated schematically in fig. 1, secondary ions produced by a pulsed ~10 keV Cs^+ beam are accelerated through ~10 keV, then pass down a flight tube into an ion mirror. After reflection by ~180°, the ions again traverse the flight tube and are detected by a microchannel plate detector beside the target. The total effective path length is ~2 m. Neutral fragments resulting from decay of parent ions in the first section of free flight are detected by a second detector behind the mirror.

Fig.#1 MANITOBA II: A time-of-flight spectrometer with an ion mirror

1. Mass Resolution

The ion mirror compensates for the initial velocity spread of the secondary ions to first order, and an improvement in resolution by $\gtrsim 2$ has been observed in preliminary measurements. Fig. 2 shows the best results obtained with our older spectrometer [4] (a conventional linear TOF instrument with a 1.6 m flight path) and with the new reflecting spectrometer. In the latter case, the peak width is about 4 ns (FWHM) at ~60 μs flight time, corresponding to a time resolution of $t/\Delta t$ = 13,000 or a mass resolution of $m/\Delta m$ = 7500. Part of the peak width is caused by the width of the primary ion pulse (~2 ns) but we believe that inhomogeneity of the electric field in the mirror accounts for much of the rest. We expect to reduce this effect by focusing the secondary ion beam to minimize the volume of the mirror used.

One of the advantages of using TOF is that high mass range is possible without sacrificing performance. The data shown in fig. 2 is a subset of the complete mass spectrum of CsBr.

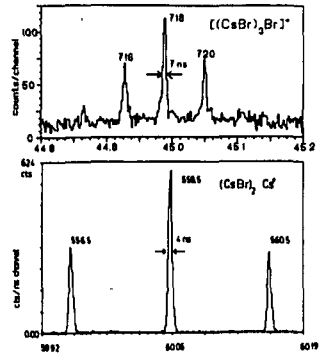

Fig. 2 The best resolution obtained with our linear TOF instrument (top) is about $m/\Delta m = t/2\Delta t$ = 3200 (FWHM). Resolution for the reflecting TOF spectrometer (bottom) is about 7000.

2. Reduction of Background

For organic compounds with $m/z \gtrsim 500$, a linear TOF instrument produces mass spectra that are characterized by broad peaks and a continuous background resulting from metastable decay during acceleration and in the field-free flight tube. Ions that decay in the drift region contribute to the parent ion peak because the centre-of-mass velocity remains constant, but the peak is broadened by the energy released. In the new instrument, neutral fragments from the decay in the first section of free flight pass through the mirror and do not contribute to the reflected spectrum. Charged fragments have less energy than the parents so less time is required to reflect them in the mirror and they appear

earlier in the mass spectrum. The broad metastable component of the peaks in the reflected spectrum (resulting only from decays after the mirror) is therefore greatly reduced and the smaller continuous background is compressed to lower time. With the velocity compensation for stable ions, the resulting resolution and signal-to-noise ratio near the molecular ion is significantly improved. Fig. 3 shows the mass spectrum of substance P near the molecular ions, taken with the linear instrument and with the reflecting instrument.

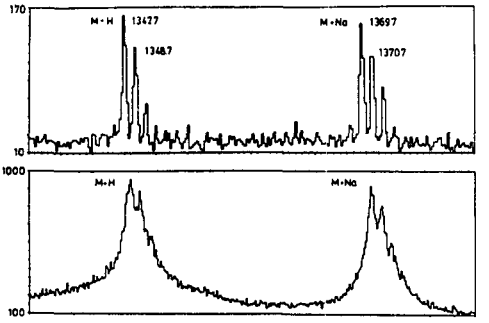

Fig. 3 Molecular ion peaks of substance P with the reflecting spectrometer (top) and the linear spectrometer (bottom)

3. Analysis of Metastable Ions

When a parent ion decays in the field-free region, its energy is shared between the fragments according to their mass. Since the time spent in the mirror depends on the energy, measuring the time separation between the parent and daughter ion peaks determines the mass of the daughter ions. To identify the metastable daughter ion peaks resulting from a selected parent, the reflected spectrum is taken in coincidence with neutral fragments which appear at the parent ion position in the 0° spectrum [1]. Thus a spectrum of daughter ions from any selected parent can be obtained. This is analagous to tandem mass spectrometry but here several such coincidence spectra as well as the normal charged and neutral spectrum can be recorded simultaneously. The number of coincidence spectra is currently limited to 4 by software and computer memory.

CsI is a good test case for metastable ion analysis because its decay pattern is well known. Fig. 4 shows the reflected spectrum between n = 7 & 16. The labelled decay paths have all been confirmed with coincidence spectra; examples are shown for n = 10 & 16. As expected, n = 13 is heavily favoured as a daughter ion while n = 14 & 15 daughters are an order of magnitude less intense. Ejected cluster ions with n = 13 do not exhibit anomalous stability.

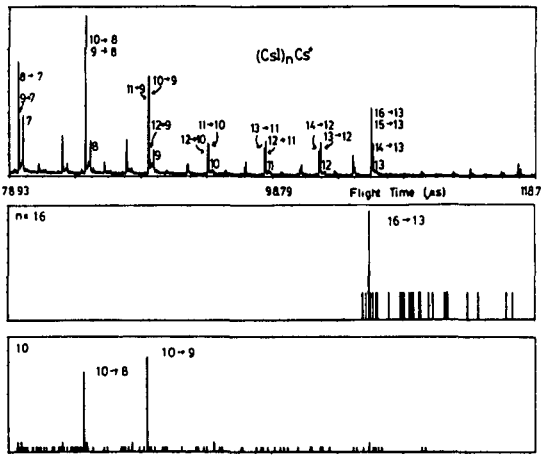

Fig. 4 Reflected spectrum of CsI between clusters n = 7 and n = 16. Peaks labelled with integers are the corresponding parent ions. Peaks labelled p -> q result from decay of cluster n = p to n = q in the first field-free region. The spectra below are the reflected spectra taken in coincidence with the neutral fragments from decay of n = 10 & 16.

1) S. Della-Negra and Y. LeBeyec, Int. J. Mass Spectrom. Ion Processes 61, 21(1984).
2) A. Benninghoven et al., IFOS III (1985) and SIMS V (1985).
3) Mamyrin et al., Sov. Phys. JETP 37, 45(1973).
4) B.T. Chait and K.G. Standing, Int. J. Mass Spectrom. Ion Phys., 40, 185(1981).

AN IMPROVED TIME OF FLIGHT MASS SPECTROMETER:

A.L. Rockwood; Department of Chemistry, University of Houston, Houston, Texas, 77004.

The spread in ion kinetic energy limits the resolution of conventional time of flight (TOF) mass analyzers. Mamyrin (1) and others have used electrostatic mirrors to correct flight time to first or second order against variations in kinetic energy. We have developed a method which gives infinite order correction against energy variations. We call this new type of mass analyzer a "perfectron" because it provides perfect correction and it is related to the reflectron.

In a perfectron, ions travel in a potential field of the form

$$\phi = kz^2/2 \tag{1}$$

(For the moment, only the one dimensional field and one dimensional ion motion are considered.) Ions start at z=0, travel up the flight tube, are reflected by the parabolic field, and recross the origin. The detector is placed at the origin and the flight time is

$$t = \pi/\omega \tag{2}$$

where

$$\omega = (kq/m)^{1/2} \tag{3}$$

The flight time is proportional to the square root of mass, but is completely independent of ion kinetic energy. Since the analyzer is perfectly corrected against energy variations, other factors will limit resolution, such as pulse response of the electronics, ion source imperfections, and metastable decompositions.

Requirements for high acceleration potential and long tube length are considerably relaxed, allowing flexible choice of operating conditions. Moderate (about 100 V) acceleration voltage may be desirable in many applications. It is also possible to operate the instrument as an ordinary reflectron, though little is to be gained by doing so. A number of variations on the perfectron were discussed, including the inverted perfectron, double pass reflectrons, magnetic confinement, combinations of these variations, and others.

Three dimensional fields and trajectories are easy to calculate. These results show that for instruments of equal flight times, the perfectron is $1/\pi$ the length of a conventional TOF, has about half the acceptance angle of conventional TOF (for cylindrical symmetry), is perfectly corrected against variations in source and detector positions (in the z=0 plane), and is perfectly corrected against variations in radial velocity.

The equation for lateral ion motion is

$$r = r_0\cosh(\omega t/2^{1/2}) + v_{0r}2^{1/2}\sinh(\omega t/2^{1/2})/\omega \tag{4}$$

where r_0 is the initial radial position and v_{0r} is the initial radial velocity.

A preliminary version of the instrument was built with 18 cm tube length and 17 V accelerating potential. Laser desorption using a

pulsed dye laser generated the ions to be analyzed. There were some deviations from the ideal parabolic field. This set of conditions provides a difficult test of the perfectron principle. A meshless design was chosen, mainly to avoid attenuating the ion beam, but also to avoid degrading optical quality of the ion beam.

At m/e=39, peak width was 160 nsec, which corresponds to a resolution of 125. The main factor limiting resolution in the present version is poor pulse response of the electronics, so prospects for better resolution are very good. More refined instruments using the perfectron principle should be capable of resolutions well over ten thousand, particularly since reflectrons, which are not as well corrected as perfectrons, already approach this performance.

Acknowledgements: I would like to thank Professor Marvin Vestal for stimulating discussions. William DeMaio's help with designing and building the vacuum system was invaluable. Shue Tze-Wen and Viswanatham Katta rendered other technical assistance. Funding was provided by National Institutes of Health, GM29151.

1) B.A. Mamyrin and D.V. Shmikk, J. Exp. Theor. Phys. 49, 762 (1979).

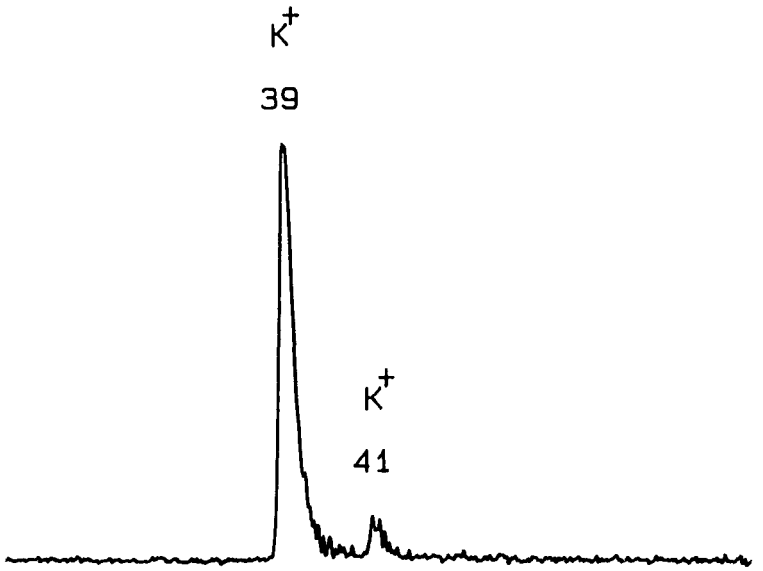

Figure 1) Blow-up of a TOF mass spectrum of potassium isotopes. Peak width is 160 nsec (fwhm) for a resolution of 125 at m/e=39. Peak width is presently limited by pulse response of electronics.

ABSORPTION-MODE FT/ICR MASS SPECTRA: SOLVING THE PHASE PROBLEM

Edward C. Craig,[a] Ivan Santos,[a] and Alan G. Marshall[a,b]

Department of Chemistry [a]
Department of Biochemistry [b]
The Ohio State University
140 West 18th Avenue
Columbus, OH 43210

Fourier transformation of a digitized time-domain ion cyclotron resonance (ICR) signal yields two frequency-domain spectra, $R(\omega)$ and $I(\omega)$, which are the real and imaginary parts of the complex spectrum (1). $R(\omega)$ and $I(\omega)$ are related to the desired absorption and dispersion spectra, $A(\omega)$ and $D(\omega)$, by a phase, ϕ, that can vary with frequency:

$$A(\omega) = \cos(\phi)\, R(\omega) - \sin(\phi)\, I(\omega) \qquad [1]$$
$$D(\omega) = \cos(\phi)\, R(\omega) + \sin(\phi)\, I(\omega)$$

The frequency-variation of ϕ arises principally from: (a) linear phase shift due to time delay between excitation and detection, (b) non-linear phase shift due to the excitation waveform (2), and (c) non-linear phase shifts from the detection electronics. Because of the difficulty in determining and correcting for the phase error, virtually all published FT/ICR spectra have been reported in magnitude-mode (1):

$$M(\omega) = [(A(\omega))^2 + (D(\omega))^2]^{1/2} \qquad [2]$$

Absorption-mode mass resolution can be up to twice as high as magnitude-mode mass resolution (3). Since mass resolution increases linearly with applied magnetic field strength, the phase correction of Eq. 1 potentially offers the same increase in mass resolution as the much more expensive alternative of doubling the magnetic field strength.

Phase correction in FT/ICR is much more difficult than for FT/NMR: (a) FT/NMR phase shifts are quite linear, whereas FT/ICR phase variation can be quite non-linear; and (b) the delay between excitation and detection amounts to many digitizer dwell periods in FT/ICR (compared to about 1/2 dwell period in FT/NMR), introducing a linear phase variation of many cycles across the FT/ICR spectrum. In this poster, we present a general method for phasing FT/ICR mass spectra, based upon a dispersion-vs.-absorption (DISPA)-based analysis for each major peak.

For a Lorentzian spectral peak, a DISPA plot gives a circle, whose center is rotated about the origin by the phase angle ϕ given in Eq. 1 (4). A rapid and convenient method for locating the center of the DISPA circle is to find the point of intersection of the perpendicular bisectors of two or more chords of the circle, as shown in Figure 1. The ratio of the ordinate to the abscissa at the center of the DISPA circle is equal to the tangent of the phase angle at the peak center. Once the phase at each peak center has been established (see Figure 2), a polynomial fit to a plot of ϕ vs. frequency gives the remaining phases needed to apply the phase correction of Eq. 1 to all of the peaks in the spectrum. A representative result is shown in Figure 3 for an experimental three-peak FT/ICR mass spectrum.

[This work was supported by N.I.H. 1R01 GM-31683, N.S.F. CHE-8218998, and The Ohio State University.]

1. Comisarow, M. B.; Marshall, A. G. (1974) Can. J. Chem. 52, 1997-1999.
2. Marshall, A.G.; Roe, D.C. (1980) J. Chem. Phys. 73, 1581-1590.
3. Marshall, A. G.; Comisarow, M. B.; Parisod, G. J. (1979) Chem. Phys. 71, 4434-4444.
4. Marshall, A.G. (1982) "Dispersion versus Absorption (DISPA): Hilbert Transforms in Spectral Line Shape Analysis," in Fourier, Hadamard, and Hilbert Transforms in Chemistry, ed. A.G. Marshall (Plenum, N.Y.), pp. 99-123.

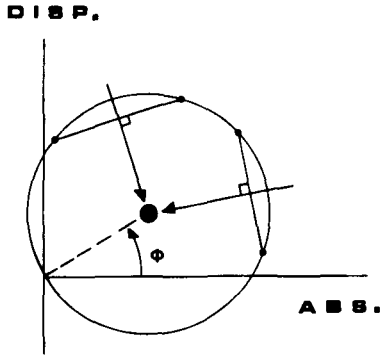

Figure 1.

Plot of dispersion vs. absorption (DISPA) for a Lorentzian spectral peak that is mis-phased by ϕ radians. $\phi \pm 2\pi n$, $n = 1,2,3,\cdots$, can be determined rapidly by finding the point of intersection of the perpendicular bisectors of two or more chords of the DISPA circle.

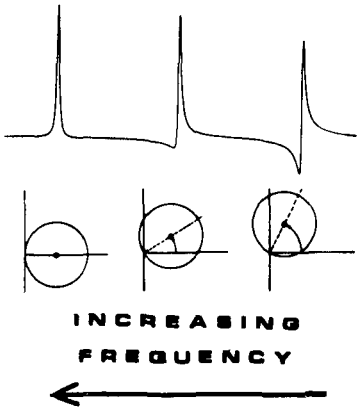

Figure 2.

Three Lorentzian spectral peaks, mis-phased by 0°, 31°, and 62° (top); their corresponding DISPA plots (bottom).

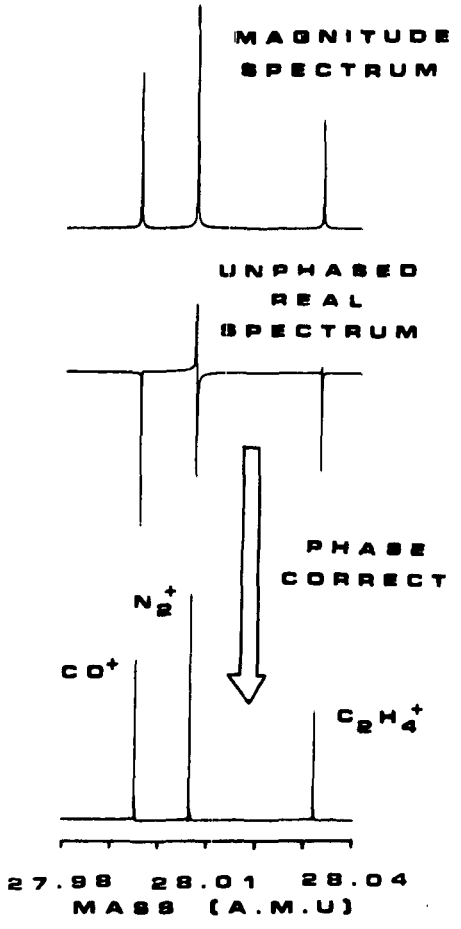

Figure 3. Effect of phase correction of experimental FT/ICR mass spectra of carbon monoxide, nitrogen, and ethylene. Note the improvement (by a factor of about $\sqrt{3}$ in this case) in mass resolution on proceeding from the magnitude-mode to the absorption-mode spectrum.

A TRAP AND PULSE TECHNIQUE FOR ENHANCING SIGNALS FROM ION/MOLECULE REACTIONS IN THE CENTER QUADRUPOLE OF A TRIPLE QUADRUPOLE MASS SPECTROMETER

G. G. Dolnikowski and M. Kristo
Department of Chemistry
Michigan State University
East Lansing, MI, 48824

The triple quadrupole mass spectrometer (TQMS) is a high performance tandem mass spectrometer that is most commonly used in conjunction with collision activated dissociation (CAD) for the production of daughter ions. In this research, collision activated reactions (CAR) are employed in the collision chamber of the TQMS to study ion-molecule reactions in an attempt to develop new analytical methods for structure analysis.

Unfortunately, the product ion yield for CAR appears to be 1-2 orders of magnitude less than that for CAD. This presents a major difficulty in using CAR as a tool for studying ion-molecule reactions or as an analytical technique. Therefore, a novel trap and pulse technique has been developed for improving the signal-to-noise ratio (S/N) for detection of CAR products.

CAD requires that the parent ion have a significant amount of kinetic energy (1-40 eV). Therefore, CAD daughter ions also have considerable kinetic energy and readily reach the detector. CAR requires that the parent ion be in thermal equilibrium with a stationary target gas. CAR products, therefore, have little kinetic energy and tend to remain in the collision chamber and may never reach the detector. This phenomenon causes CAR in the TQMS to generate artificially low yields of ionic products. In the trap and pulse technique, ions that are produced by ion-molecule reactions are trapped for a specified period of time in the central quadrupole region and then a pulsed potential on an extraction lens moves some of them toward the detector. The pulsed ions are mass-selected by the third quadrupole so that ions of only one nominal mass reach the detector for each pulse. Full range mass scans have been achieved by using the trap and pulse technique repetitively under software control.

When the center quadrupole's extraction lens potential is +100 V, positive ions are trapped in the center quadrupole region of the TQMS. Collisions with approximately 1×10^{-4} torr of a reactive collision gas thermalize the trapped ions. As the storage time increases, the number of trapped thermal ions increases since more parent ions are constantly arriving through the first quadrupole. The stored ions may react with the collision gas if the chemistry of the two species is appropriate. The stored product ions and residual parent ions are then extracted from the center quadrupole by dropping the voltage on the extraction lens to -100 V. This results in a pulse of ions toward the detector with a temporal profile like that shown in Figure 1.

CAR product ion abundances increase rapidly with storage time in the center quadrupole region until the number of ions reaches the space charge limit. Within 100 msec, CAR product ion abundance reaches 90% of its ultimate value, so an entire trap and pulse cycle can be accomplished relatively rapidly, allowing full range mass scans in a reasonable period of time (1-2 minutes).

Trap and pulse increases the signal intensity for all CAR products but does not increase noise in the system. Therefore, trap and pulse increases the S/N for CAR product ions. Figure 2 shows the increase in S/N for two CAR products over that achieved by conventional data acquisition.

Trap and pulse CAR also produces new CAR products that either are not produced without trapping or were present below the level of noise in the system using conventional data acquisition. Trap and pulse CAR yields results that correspond much more closely to chemical ionization data than is possible using CAR with conventional data acquisition.

FIGURE 1

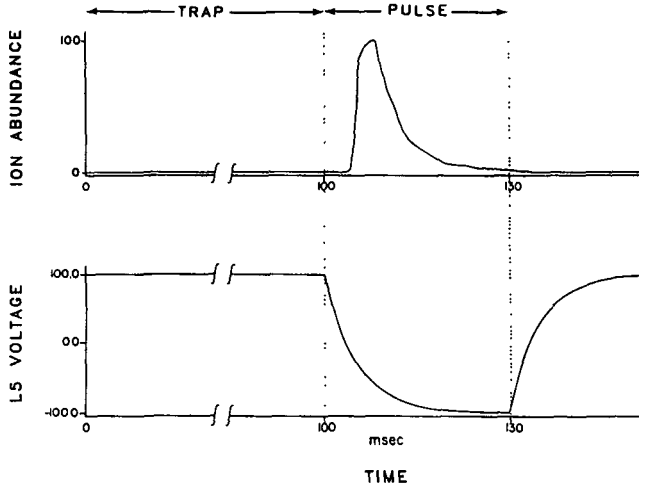

Fig. 1. Plots of ion abundance and lens 5 (Quadrupole drawout lens) potential versus time, showing one full trap and pulse cycle.

FIGURE 2

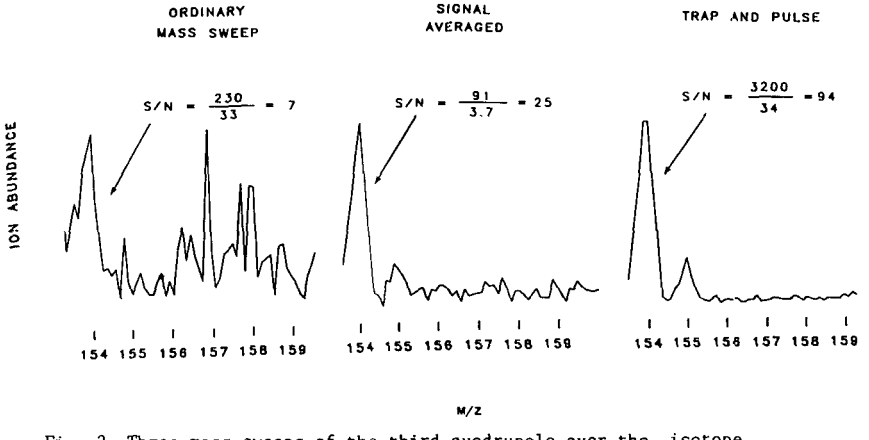

Fig. 2. Three mass-sweeps of the third quadrupole over the isotope peaks of the proton bound adduct of glycerol and acetic acid by conventional data collection (250 u/sec), by conventional data collection with real-time signal averaging (1 u/sec), and by trap and pulse data collection (1 u/sec).

Acknowledgement: This work was supported in part by a grant (RR-00480) from the Biotechnology Research Program, Division of Research Resources, National Institutes of Health.

MICROCOMPUTER-ASSISTED LINKED SCANNING WITH A KRATOS DS-55 DATA SYSTEM

Gilbert G. Jones and Glenn L. Nutter

Amoco Corporation
Amoco Research Center
P. O. Box 400
Naperville, IL 60566

Metastable ion spectra not only provide a valuable aid to the identification of compounds through the determination of ion fragmentation pathways, but also provide enhanced selectivity in the analysis of complex mixtures. The ability to obtain metastable ion spectra on a time scale compatible with GC/MS operation greatly expands the usefulness of metastable scanning in trace analysis.

Although computer-controlled linked metastable scan software and hardware are now available on most new magnetic sector instruments and also as a stand-alone unit(1), our objective was to add high speed (up to 0.5 sec/decade) metastable scanning to our existing commercial data system. A Rockwell AIM-65 single board microprocessor was interfaced to a Kratos DS-55M mass spectrometer data system and programmed to provide B/E, B^2/E, and constant-neutral-loss linked scans on a VG 7070HS double focusing forward-geometry mass spectrometer. Based on the technique pioneered by W. F. Haddon(2,3), the system uses a time-based calibration table and active computer control of the linked field to avoid tracking errors that may occur with analog function module-based systems.

A New Constant-Neutral-Loss Scan Function

A new constant-neutral-loss scan function, the $B^2(V-1)$ scan, was developed to eliminate the need for a special metastable mass scale or post-acquisition data manipulation. The mass of the detected ion, as calculated by the standard scan calibration table, is the daughter ion mass. The scan is implemented by controlling the accelerating voltage above the normal operating point (4 Kv for the 7070) so that it follows the magnetic field according to the relationship:

$$V = Vo \cdot \frac{M_1}{M_2}$$

where M_1 and M_2 are the parent and daughter ions, respectively. A maximum accelerating voltage of 6 Kv on the 7070 places a limit on the low mass end of the scan to a daughter mass equal to twice the neutral mass.

Experimental

Standard, unmodified data acquisition programs are used on the DS-55 data system to calibrate the mass scale and acquire metastable scan data. After normal low resolution calibration a FORTRAN program is invoked on the DS-55 Nova computer. The selected program (for B/E, B^2/E, $(B/E)\sqrt{1-E}$, or $B^2(V-1)$ scans) requests user input for the desired parent, daughter or neutral mass and proceeds to calculate and download a control table for the AIM-65 microcomputer. For B^2/E scans, anticipation of the voltage lag from the RC response time of the ESA power supply is included for the more precise tracking required by this scan mode. The programs for the B-E scans also create a modified calibrated reference file for use during metastable scan data acquisition. The correct masses of the daughter or precursor ions are automatically assigned during data acquisition. For B^2/E scans, metastable peak profile data may be collected using the raw data feature of DS-55 data acquisition. The raw data are displayed with a special graphics program developed from the DS-55 RESOL program.

Except for coordination of scan start times, the AIM-65 and DS-55 computers function independently during data acquisition. The information contained in the control table allows the AIM-65 to approximate the desired ESA or accelerating voltage scan function by a series of linear ramps between each nominal mass of the scan range. For metastable scans the ESA or accelerating voltage is controlled by an Analog Devices 16-bit digital-to-analog converter connected to a digital port on the AIM-65.

Results

Figure 1 is a single B^2/E scan of the $C_7H_{15}+$ ion in n-hexadecane, taken with a magnet scan rate of 0.5 second/decade and a spectrometer resolution of 1,000. The main beam mass 99 peak (actual intensity = 300,000 counts) is shown at its normal width, because the ESA voltage was kept at 100% until just after the peak passed the detector. The dish- topped peak from the decomposition of doubly-charged benzene molecular ions to mass 63 ions is shown in Figure 2. These data were taken at half the accelerating voltage used for calibration, so the precursor masses assigned by the calibration table are twice the actual values.

References

(1) M. Friedli, Org. Mass Spectrom. 19, 183(1984).
(2) W. F. Haddon, Anal. Chem. 51, 983(1979).
(3) W. F. Haddon, Org. Mass Spectrom. 15, 539(1980).

Figure 1

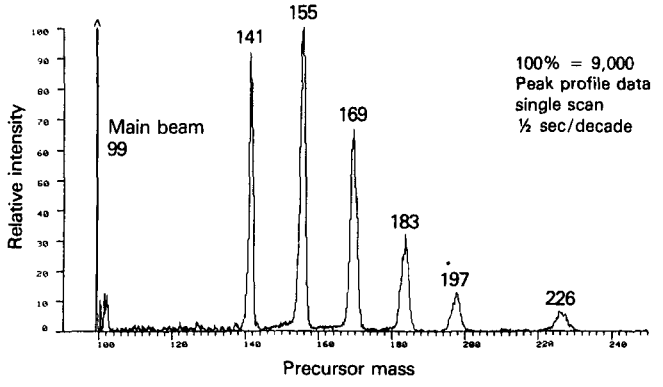

Figure 2

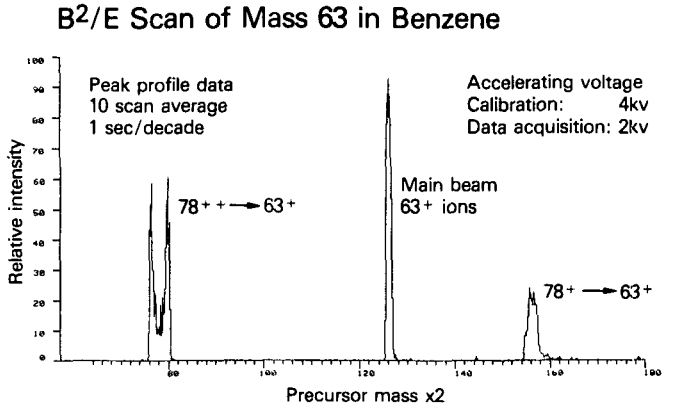

MULTI-PARALLEL MICRO-BORE COLUMNS FOR FAST GC AND GC/MS ANALYSIS":

Philip Epstein, Keith McKellop, Frank Hatch;
Boehringer Ingelheim Pharmaceuticals, Inc.,
90 East Ridge Road, Ridgefield, Connecticut 06877

Micro-bore fused silica columns of 100 µm I.D. or less have demonstrable potential for rapid high efficiency gas chromatographic analysis. Excellent descriptions of the theoretical considerations, technical problems and examples of high-resolution and high-speed analysis have been published by Schutjes et al.[1], Guiochon et al.[2] and Onuska[3]. Column efficiencies of 12,000 plates/meter have been achieved with 100 µm I.D. columns[2] and over 16,000 plates/meter with 50 µm I.D. columns[1]. These column efficiencies far out distance the maximum values of 4,500 plates/meter and 3,000 plates/meter achievable with 250 µm and 320 µm I.D. columns respectively.

Conventional gas chromatographic equipment can be employed for micro-bore column analysis; however, the requirements for highly sensitive detectors with rapid response times are increased compared with conventional capillary columns. Recently, Leclercq et al.[4] have published their work describing the application of 50 µm I.D. columns for faster and more sensitive GC/MS analysis. The major disadvantage of the micro-bore column is its limited sample capacity, typically in the range 1 to 5 ng.

In this report we present the technique of "multi-parallel" micro-bore gas chromatography as a method to overcome the sample capacity problems associated with single micro-bore columns. This technique was conceptualized previously[5] but never successfully carried out. The technique utilizes multiple columns of identical dimensions cut from a single 15 meter x 100 µm I.D. column, coated with a 0.25 µm film of metyl silicone (Quadrex Corporation, New Haven, CT). Column homogeneity or lack of homogeneity determines the fall off in achievable efficiency. The primary column characteristics studied included column efficiency, sample capacity indicated by a 10% decrease in resolution and sample discrimination effects on split injection. Hydrogen carrier gas was used for all experiments carried out on a HP-5880 gas chromatograph with flame ionization detection.

RESULTS

Van Deemter curves are plotted in Figure 1 for a single 2 m x 100 µm I.D. column and a parallel penta-column each 2 m x 100 µm I.D. Tetradecane was used as a test compound chromatographed isothermally at 85°C. The single column produced a maximum of 20,300 theoretical plates compared with 12,000 theoretical plates for the penta-column. A similar triple parallel column produced efficiencies up to 16,400 theoretical plates. The curves for both micro-bore columns exhibit broad minima in plate height and excellent efficiencies are obtainable at flow velocities of 150 cm/sec.

Column sample capacity determinations were carried out with tetradecane. A 10% increase in the peak width at 10% peak height was considered to be a sensitive indication of sample overload. The single, triple and penta columns exhibited sample capacities of 5 ng, 20 ng and 50 ng respectively.

Sampling discrimination effects were determined by six repeat split-injections of a mixture containing C_{15} to C_{36} hydrocarbons. No significant difference was observed between the single and penta columns.

CONCLUSION

Our initial results suggest that the multi-parallel column approach is a viable method for overcoming the limited sample capacity of micro-bore columns. The 40% drop in column efficiency, compared with the single column, is significant; however; 6,000 theoretical plates/meter is still a vast improvement over that achievable with conventional I.D. capillary columns. Multi-parallel columns of 4 to 5 meters in length would provide the ideal compromise of resolution (~ 30,000 plates) sample capacity and speed of analysis for quantitative GC/MS analysis.

Figure 1. Van Deemter Curve for (a) Single and (b) Parallel Penta Micro-Bore Columns

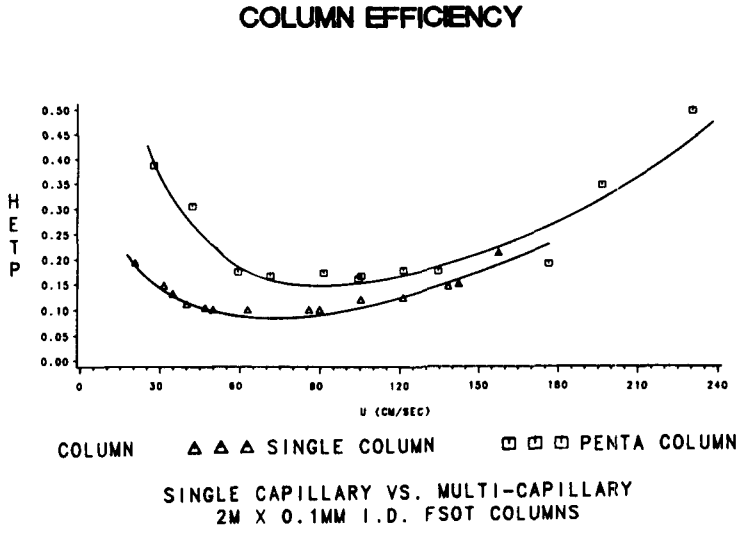

REFERENCES

1. Schutjes, Vermeer, Rijks, Cramers; J. Chrom. 253(1982)
2. Guiochon, Gonnord, Onuska; Analyt. Chem. 55(1983)
3. Onuska; J. Chrom. 289(1984)
4. Leclercq, Schutjes, Cramers; J. Chrom. Libr. 32(1985)
5. Pierce, Unrau, Oelhsclager, Hatch, Cutteridge; J. Chrom. Sci. 17(1979)

APPLICATION OF LIQUID IONIZATION MASS SPECTROMETRY TO ANALYSIS OF COAL TAR AND PITCH

Y. Fujioka; Nippon Steel Corp.
M. Tsuchiya; Department of Industrial Chemistry, The University of Tokyo, Hongo Bunkyo-ku, Tokyo 113 Japan.

This is a Preliminary study for characterization of coal tar and pitch by liquid ionization (LI) mass spectrometry[1]. It is important to measure the molecular weight distribution of components in tar and pitch in order to understand their chemical properties as industrial raw materials. In general, the LI method provides MH^+ peaks of organic compounds and makes it easy to determine their molecular weights. Standard compounds of polycyclic aromatic hydrocarbons (PAHs) and coal tar and pitches were measured by the LI method.

A sample is dissolved in chloroform to be measured directly or mixed with a matrix, according to the analytical procedure reported previously[1)2)]. Normal alkanes, cycloalkanes and halogenoaromatic hydrocarbons were examined as a matrix for the sample. The PAHs with a matrix such as cyclooctane and decahydronaphthalene, or the PAHs in chloroform solution without a matrix were measured with good results. therefore, chloroform solution without a matrix was mainly used in this paper.

As an example, LI mass spectrum of toluene-soluble components in a refind pitch is shown in Fig.1. MH^+ peaks from PAHs such as anthracene (m/z 179), pyrene (203), perylene (253) and so on were observed. This spectrum is similar to that measured by FD method. By FD, however, it is difficult to observe the low molecular weight compounds such as anthracene and pyrene, because the FD ion source is in a high vacuum. It is easy to measure the MH^+ ions of low molecular weight compounds by the LI method.

Selected ion profiles of PAH components extracted from a refined pitch with toluene are shown in Fig.2. Each component was observed at an optinum temperature, according to its molecular weight. The good correlation was found between the optimum temperatures and the molecular weights of the PAHs.

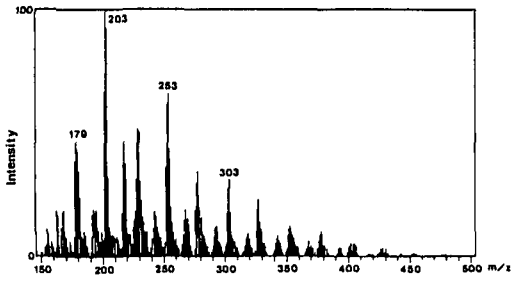

Fig.1. LI mass spectrum of toluene solubles from a refined pitch.

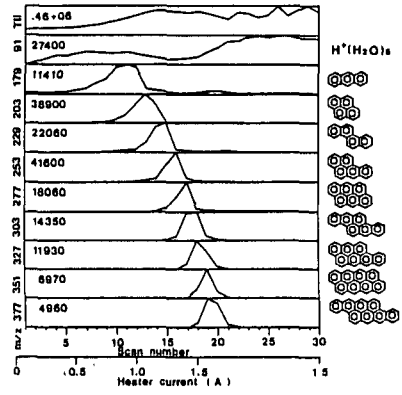

Fig.2 Selected ion profiles of toluene solubles from a refined pitch.

Molecular weights of larger PAHs than mass 350 were also measured easily by the LI method. The high molecular weight components were extracted from pitches with several solvents, considering solubilities of different PAHs. Figure 3 shows mass spectra of toluene-solubles, hexane-solubles, and toluene-solubles of hexane-insoluble components. The MH^+ peaks of high molecular weight PAHs are observed at m/z 379, 427, 453 and over 500 in Fig.3 and 4.

In conclusion, the LI method is very useful for analysing tar and pitches. It has following advantages over EI (GC/MS), FI and FD : those are rapidity of measurement, good stability and reproducibility of mass spectra and simplicity of analytical procedure.

References

1) M. Tsuchiya and H. Kuwabara, Anal. Chem., 56 14 (1984)
2) M. Tsuchiya, H. Kuwabara and K. Musha, Anal. Chem., 58 695 (1986)

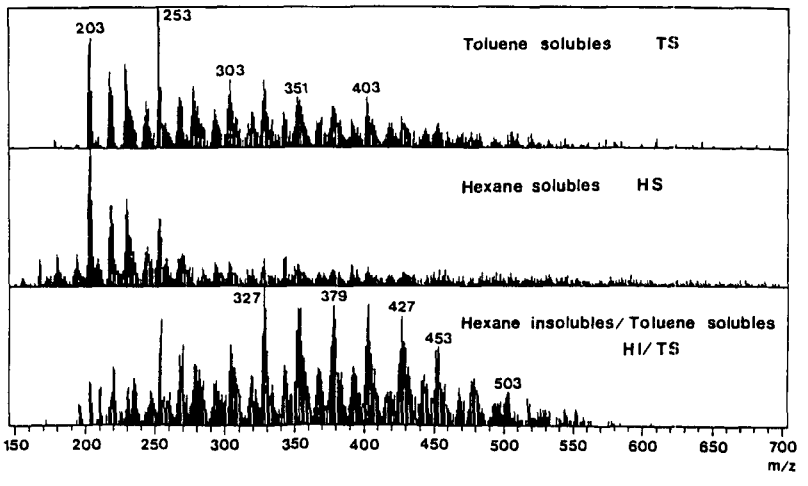

Fig.3 LI mass spectra of pitches separated by solvent extraction.

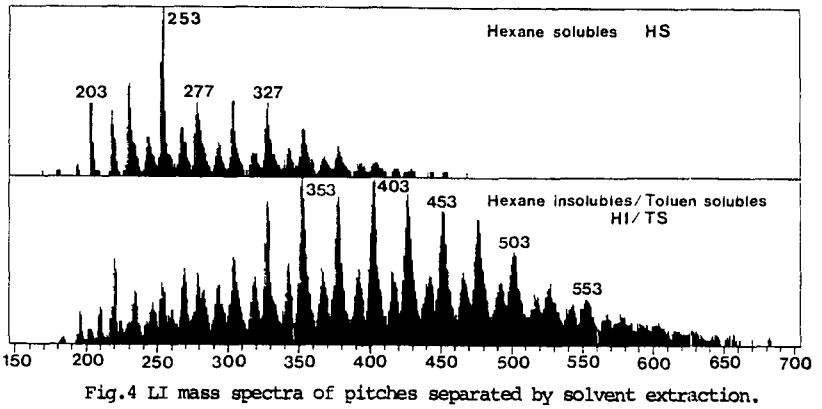

Fig.4 LI mass spectra of pitches separated by solvent extraction.

THERMOSPRAY LC/MS/MS ANALYSIS FOR AZO DYES SPIKED IN WASTEWATER

Leon D. Betowski and Steven M. Pyle, U.S. Environmental Protection Agency, Las Vegas, NV 89114; John M. Ballard, Lockheed Engineering and Management Services Co., Inc., Las Vegas, NV 89114; Glenn M. Shaul, U.S. Environmental Protection Agency, Cincinnati, OH 45268

The Water Engineering Research Laboratory of the U.S. Environmental Protection Agency is conducting research designed to develop techniques for predicting the fate of azo dyes in typical wastewater treatment systems which process wastewater contaminated with azo dyes. A part of this research involves bench scale investigations on the removal of water insoluble azo dyes by the activated sludge process. Azo dyes are of concern because some of the dyes, dye precursors or their degradation products such as aromatic amines, have been shown to be, or are suspected to be, carcinogenic. The results from this research are needed to aid in predicting the degree to which new azo dyes and/or their degradation products pass through the activated sludge process.

There has been a scarcity of standard analytical methods for specific dye compounds in wastewater and sludge samples. For this study a combination of HPLC and MS/MS was chosen to be evaluated as a potential method for disperse azo dyes. The method involved purifying the commercial dye for use as standards, developing an extraction procedure for recovering the dye from the wastewater and the use of HPLC and mass spectrometry to detect and quantify the recovered dye.

Preliminary studies included spiking a known amount of the purified dye into both organic-free water and wastewater, extracting the dye and comparing the results from HPLC/UV with those from thermospray MS/MS. Table I shows this comparison for Disperse Red 1. The mass spectrometric analysis was performed on a triple quadrupole mass spectrometer under three modes of acquisition - single quadrupole scanning (MS), daughter ion CAD experiments with quadrupole three scanned over a wide mass range, and selected reaction monitoring (SRM) with quadrupole three set to monitor a single ion. The limits of detection for these three modes of scanning via thermospray introduction for Disperse Red 1 are 600 pg, 2 ng, and 180 pg, respectively.

Primary effluent from a municipal wastewater treatment plant was used as the feed in bench scale activated sludge systems. These systems were spiked with disperse azo dyes at 1 mg/L and 5 mg/L levels and were sampled at various points in the process during a three or four week period. In addition, a control bench scale activated sludge system was operated in order to assess background contaminants. Mass spectrometric results were again compared with those obtained by HPLC/UV.

The investigation of the fate of disperse azo dyes in the activated sludge process was a major feature of this study. Two processes, adsorption and biodegradation, were considered as major routes of removal. Major degradation products have been identified by MS/MS analysis of these wastewaters. Single scan mass spectra followed by CAD daughter ion experiments showed ions from two reduction products in the samples from the activated sludge systems spiked with Disperse Red 1. CAD experiments on the actual standards confirmed these findings.

TABLE I

Recovery of Disperse Red 1 from Water Samples

	Recovery (%)			
Sample	HPLC/UV	MS	CAD	SRM
Organic-free water, 1	82.2 ± 0.3	92.5 ± 3.7	87.6 ± 4.6	95.5 ± 17.1
Organic-free water, 2	87.4 ± 0.6	90.2 ± 4.7	90.4 ± 9.9	90.0 ± 5.9
Wastewater, 1	93.4 ± 0.3	102 ± 31	82.7 ± 13	-
Wastewater, 2	96.2 ± 0.1	79.7 ± 15	83.7 ± 5.2	-

GC/MS ANANLYSIS OF ORGANIC POLLUTANTS IN PONCE AIR PARTICULATE. ASSESSMENT OF REGIONAL AND LOCAL INFLUENCES

Rafael Infante, Arnaldo Carrasquillo, Janice Irizarry,
José Lebrón, Noemi Negrón and Lourdes Peña.
Biomedical Research Program
Catholic University of Puerto Rico
Ponce, Puerto Rico 00732

Over the past decade, there have been increased interest in the development of receptor source-apportionment models to assists in defining control strategies for particulate pollution. Such model attempt to identify the principal sources of airborne particles and to determine their contributions to ambient aerosols mass concentrations using measurements made at the sampling (receptor) sites. These studies have examined temporal and geographical variations in the concentration and relative proportions of organic compounds classes and their possible source relationship. The existing data indicate that it may be possible to use polycyclic aromatic hydrocarbons, alkanes and certains apparently unique organic compounds to assist in distinguish among emissions from certain particulate pollution sources.

As part of our ongoing studies on particulate composition and its relationship to public health in Ponce, Puerto Rico, geographical and temporal variations in the composition and concentration of particulate extractable organic matter were investigated at five sites in Ponce during the 1984 year.

Sample of atmospheric particulate were collected over a 24-hour period using hi-volume samplers. Sampling sites were selected taking into account predominant wind pattern and known sources of air pollution. The filters containing the particulate were sequentially sonic probe extracted with cyclohexane, methylene chloride and acetone for 30 minutes. The solvent was then condensed to 1 mL using a Kuderna-Danish concentrator. GC/MS analysis was performed on a Hewlett-Packard 5995B GC/MS/COMPUTER system. A 30 meters fused silica capillary column coated with SE-54 stationary phase was used.

The identification of GC/MS peaks was based on library search (on-line data base of over 20,000 spectra), comparison of the observed spectra with the spectra of reference compounds and on fundamental interpretation. PAH's were identified by comparison of their relative retention times with reference compounds and confirmed by monitoring the ion characteristic of their molecular weights, in some cases other confirmatory ions were also monitored.

The saturated hydrocarbons were always present in the highest concentrations and were the most ubiquitous organic constituents in Ponce airborne particulate matter. The n-alkanes accounted for most of the extractable organic matter in all sampling sites and showed and odd to even carbon number preference indicating a substatial degree of contribution from natural sources. PAH's were present but at a much lower concentration. PAH's with 2- to 5- ring

structures were identified. PAH's with more than 5 rings could not be detected. Carboxylic acids were also observed and showed a even number preference. The biological origin of the acids indicate the predominat contributions of natural sources to the Ponce air particulate.

Variation in PAH's concentration are usually monitored to account for anthropogenic contributions to the particulate matter. Temporal and geographical variations in the abundances of both benzo[e]pyrene and benzo[a]pyrene are showed in figures 1 and 2. The maximun levels are observed for the Ponce east site during the February and March months. The Ponce east site is located close to sugar cane fields which are burned off between January and June to facilitate harvesting. These two months coincide with the sugar cane season were most of the agricultural burning activities are occuring.

In summary, the analysis of airborne particulate matter in the Ponce area showed the presence of saturated, aromatic, PAH's and carboxylic acids. Saturated hydrocarbons were found in greater abundance. The predominance of odd numbered n-alkanes and the predominant even numbered carboxylic acids indicate that the particulate matter in the Ponce area was dominated by natural sources. The variation in the abundances of benzo[e]pyrene and benzo[a]pyrene suggests that the agricultural burning of sugar cane is the most probable source for their occurence in the Ponce particulate matter.

Acknowledgement
Support of this work from MBRS-DRR-NIH Grant No. 0867 and GM-NIH Grant No. 07732 is gratefully acknowledge.

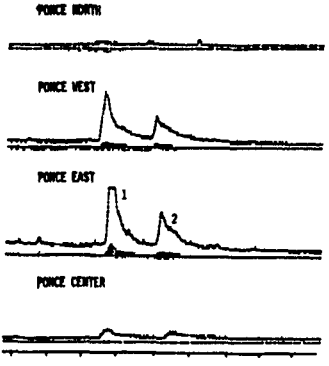

FIGURE 1. GEOGRAPHICAL VARIATIONS IN THE ABUNDANCE OF 1) BENZO[e]PYRENE AND 2) BENZO[a]PYRENE FOR THE 1984 YEAR.

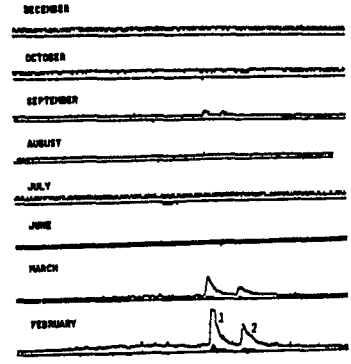

FIGURE 2. TEMPORAL VARIATIONS IN THE ABUNDANCE OF 1) BENZO[e]PYRENE AND BENZO[a]PYRENE FOR THE PONCE EAST REGION DURING 1984.

Enviromental Applications of the Thermospray LC/MS Interface
Part I: Dyes and Selected Pollutants

Donald A Flory and Matthew A. McLean
Department of Chemistry
University of Houston, Houston, TX 77004

Thermospray LC/MS has been used to analyze sulfonated azo dyes and selected Appendix VIII Hazardous Constituents. All samples were analyzed by directly injecting the sample into the LC mobile phase and ionizing them by thermospray ionization. The mobile phase used was 0.1 M ammonium acetate in water at pH 7.0. Certain parameters such as mobile phase pH, source block temperature and the use of external modes of ionization were investigated.

The best results were obtained at neutral pH in the negative ion mode. No external mode of ionization was necessary and the optimum ion source block temperature was determined to be between 300 to 330 C. For full scanning, from 150 to 450 amu, the sulfonated azo dyes investigated - acid orange 6 and 7 - gave signals of 10/1 (S/N) with as little as 150ng. Using SIM (of the deprotanated molecular ion) the same or better signal to noise ratios were obtained with sample sizes of 15 ng.

Other compounds investigated include pentachlorophenol(PCP) 4-nitrophenol and naphthaleneacetic acid. For both PCP and 4-nitrophenol good signal to noise ratios(S/N = 20) were obtained with as little as 5ng using full spectrum scanning(125 - 400 amu). Using SIM of the deprotanated anion for PCP a signal to noise ratio of four could be obtained with 440 pg injected.

NEW DEVELOPMENTS IN HERBICIDES ANALYSES BY THERMOSPRAY LIQUID CHROMATOGRAPHY-MASS SPECTROMETRY

L. M. Shalaby
Agricultural Products Department
E. I. du Pont de Nemours and Co., Inc.
Research Division, Experimental Station
Wilmington, Delaware 19898

The new thermospray studies for herbicides analyses included evaluation of two new ionization techniques, filament and discharge electrode, and an on-line radiochemical detector. Additional studies were carried out to optimize the molecular ions and fragmentation with thermospray ionization.

The filament-on mode generates ion signals for compounds which do not ionize efficiently with thermospray alone. Among these compounds are arylhalides and saccharin derivatives. With the filament-on mode ammonium acetate is not required for ionization and nonpolar solvents can be used. With this external ionization source the thermospray interface is amenable to normal phase LC.

Figure 1 shows both the methanol/thermospray ionization and cyclohexane/filament-on ionization spectra for chlorsulfuron herbicide. Using nonpolar solvents and filament ionization enhanced chlorsulfuron fragmentation and generated a new mass spectral pattern. This technique is useful for structure elucidation and confirmation.

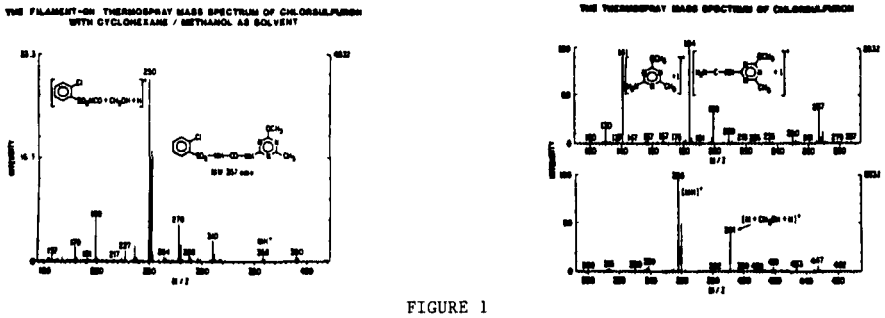

FIGURE 1

Discharge electrode offers an additional ionization mode and is more tolerant to LC solvents with high water content. Using water as the sample eluant and discharge ionization, the highest reagent ion is 73 amu and the mass scan range is extended by lowering the low mass scan to 74 amu. This new capability expands the LC-MS applications to low molecular weight compounds and fragment ions. Including the low mass fragment ions enhances total ion sensitivity and assists structural elucidation.

Study of the effect of gradient on the ion signal using the filament and discharge electrode indicated the ionization process is not dependent on temperature as is thermospray (1). No temperature programming is needed which simplifys the gradient elution LC-MS procedure. The inherent problem of ion signal decay (2) during a gradient still exists but to a lesser extent.

On-line LC-MS is used in our laboratory to analyze thermally labile 14C radiolabelled herbicides and metabolites. In spite of extensive purification to isolate individual radiolabelled metabolites, biological extracts still often contain impurities which complicate the mass spectral identification. To trace the radiolabelled metabolites, we split the lc effluent between a radiochemical detector and the mass spectrometer.

The radiochemical detector cannot be placed directly between the lc and the MS because the current detector cell will not tolerate the high back pressure of the thermosopray vaporization process. The system was optimized to give maximum radiochemical sensitivity and to minimize the time difference between the radiochemical peak and the ion peak.

We completed series of studies on sulfonylureas thermospray ionization. The results show the interface temperature is a critical parameter for molecular ion intensity and total ion sensitivity. As shown in Figure 2, the optimum temperature for detecting the molecular ion is lower (10-15^{0}C) than the optimum temperature for total ion sensitivity. For quantitation studies as residue and trace level analyses, we select higher temperature to maximize sensitivity. On the other hand, for structure elucidation studies we use lower temperature to enhance the molecular ions.

Investigation of the sulfonylureas thermospray spectra indicated monitoring both the positive and negative ion spectra is essential for structure elucidation. At the same time, the positive ion spectra for chlorsulfuron contains the triazine related ions, the negative ion spectrum contains the sulfonamide related ions. Both spectra contain the molecular ion which is detected as MH+ in the positive ion mode and M-H in the negative ion mode.

The new developments in thermospray ionization expanded the applications for herbicides analysis and improved sensitivity for trace level studies.

CHLORSULFURON TOTAL ION INTENSITY (—o—) AND ITS MOLECULAR ION INTENSITY (—▲—) AS A FUNCTION OF THE VAPORIZER CONTROL TEMPERATURE (T_1)

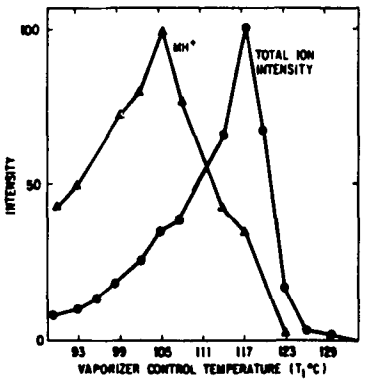

FIGURE 2

REFERENCES

1. D. A. Garteiz and M. L. Vestal, LC 3,4,334 (1985)

2. L. M. Shalaby, 33rd Annual Conference on Mass Sectrometry and Allied Topics, San Diego, California, May 26-31, 1986

COMPARISON OF THERMOSPRAY CONDITIONS FOR ORGANOPHOSHATE PESTICIDES

T.J.Francl, P.J.Kraske French and M.L.Thomson
American Cyanamid Company
Agricultural Research Division
P.O.Box 400
Princeton, New Jersey

The use of a filament for ionization in thermospray LC/MS has expanded the scope of compounds which can be examined. One class of compounds which do not ionize efficiently using NH_4OAc is organophosphates. By use of a filament for ionization, the sensitivity for these compounds is enhanced appreciably.

In this work, several aspects of thermospray ionization of organophosphates were investigated:

--- To what extent does a filament improve the performance of the thermospray LC/MS for organophosphates.
--- What are the effects of experimental parameters, ie. vaporizer temperature, mobile phase flow rate and composition.
--- What structural information can be obtained from collisionally activated dissociation of the protonated molecular ion.
--- How do the LC/MS/MS spectra compare to spectra obtained from other ionization techniques.

Thermospray ionization mass spectra for ABATE and malathion are shown in the figures below:

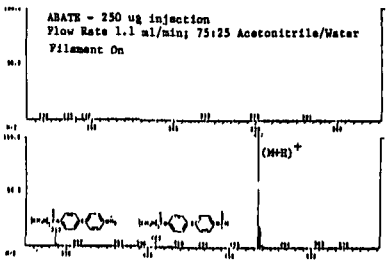

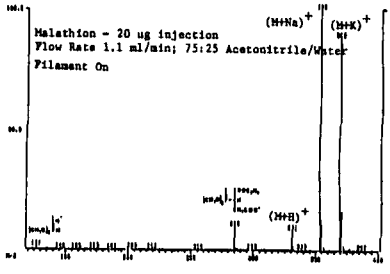

A comparison of the sensitivity using NH_4OAc and 'filament on' ionization modes is shown in Table 1.

Vaporizer Temperature

The effect of vaporizer temperature on the total ion intensity and on the ion intensity of the protonated molecular ion was investigated by dissolving ABATE in the mobile phase (75:25 acetonitrile/water). The vaporizer temperature was then programmed from 180°C to 120°C at about 5°C/min and a full scan obtained every 3 seconds. The resulting total ion and single ion chromatograms are shown in Figure 1.

Table 1.

CONDITIONS	SIGNAL/NOISE
200 ug ABATE - 'Filament Off'	10:1
20 ug ABATE - 'Filament On'	30:1
200 ng ABATE - 'Filament On' Single Ion Monitoring	800:1

Figure 1.

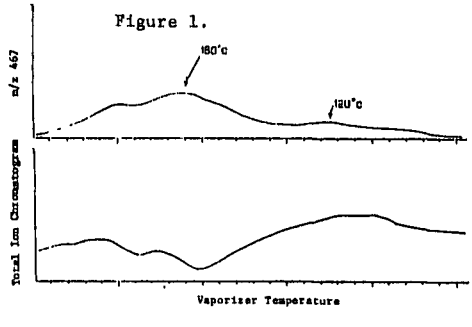

Mobile Phase Flow Rate

It has been proposed that the mobile phase flow rate affects the ability of the electrons to penetrate the solvent and ionize the analyte. A plot of total ion current of a 500 ug injection of ABATE vs. flow rate is shown in Figure2

Mobile Phase Composition

In the absence of a volatile buffer, the mobile phase is the source of protons in 'filament on' thermospray. Therefore, it is expected that as the concentration of water in the mobile phase is decreased, the ABATE intensity of the signal should also decrease.

Mobile phase compositions over the range from 50:50 acetonitrile/water to 100% acetonitrile, at constant vaporizer temperature (140°C), were investigated. The ABATE peak at the 50:50 composition was broad and low intensity and an accurate area for the total ion current could not be obtained. Normalized areas for 25%, 10% and 0% water are given in Figure3 .

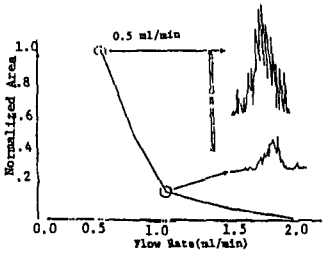

Figure 2.

Figure 3.

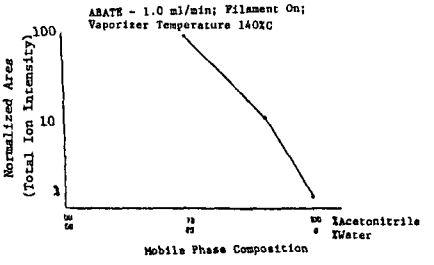

LC/MS/MS

MS/MS daughter ion spectra generated from protonated molecular ions formed in the thermospray show less fragmentation than the corresponding ions generated by FAB or chemical ionization. Figures 4,5 and 6 show LC/MS/MS daughter ion spectra for malathion generated using LC/MS/MS, chemical ionization and FAB, respectively. All experiments were performed with a collision energy -30 eV and collision pressures of 0.5-0.6 mTorr.

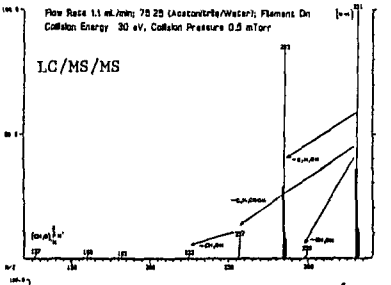

Figure 4.

Figure 5.

Figure 6.

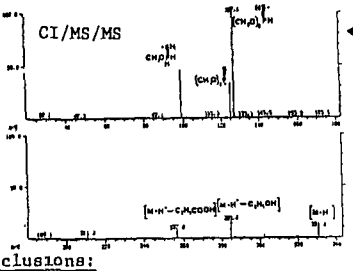

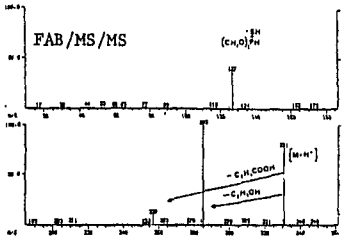

Conclusions:

- --- Sensitivity for thermospray LC/MS of organophosphates is increased using the 'filament on' mode of ionization.
- --- Using optimal conditions, the limit of detection of MS/MS experiments should be in the low nanogram region.
- --- An interactive relationship of vaporizer temperature, mobile phase composition and flow rate has been observed.
- --- MS/MS data generated from thermospray LC/MS show less fragmentation than ions generated under comparable conditions using FAB and chemical ionization.
- --- Other organophosphates, such as THIMET and COUNTER, produce 'filament on' thermospray spectra similar to malathion.

THE DETERMINATION OF ORGANOHALIDES IN WHIRLPOOL SPAS BY GC/MS

Frank M. Benoit, Health and Welfare Canada, Ottawa, Ontario, Canada and Ron Jackson, Barringer Magenta Ltd., Mississauga, Ontario, Canada.

The use of halogen (usually chlorine) for the disinfection of drinking water and public bathing water is widespread primarily because of the ease and effectiveness of application. However, the presence of organic materials in the raw water leads, upon treatment with halogen disinfectants, to the formation of halogenated products, of which the most abundant, the trihalomethanes, are observed at concentrations ca 1 to 15 μg/L in drinking water.

Halogen (chlorine and bromine) disinfectants are commonly used in whirlpool spas which are operated at temperatures ca 40°C with vigorous agitation and aeration of the water. High organic material concentrations of anthropogenic origin in the water of whirlpool spas can result from high bather load per volume of water and/or evaporation of the water assisted by the high temperature and agitation. The combined conditions of halogen, heat and high concentrations of organic materials are favourable to the acceleration of known halogenation reactions such as the production of haloforms and may be favourable to the initiation of new reaction pathways leading to hitherto unobserved halogenated products in the water.

Of particular concern is the possibility that during the use of thermal spas the occupants may be exposed to volatile organohalogen compounds emitted from the water into the air. In order to elucidate these concerns a survey of 25 whirlpool spa installations was conducted wherein the water and the surrounding air were examined for volatile organohalogen compounds.

The major contaminants in the air and in the water at all the spa sites tested was the trihalomethane ($CHCl_3$, $CHBr_3$) corresponding to the halogen (Cl_2, Br_2) used as the disinfectant. No other volatile organohalogen compounds attributable to reactions between the disinfectant and organic material in the water were detected in the water at a limit of detection of 1 μg/L or in the air at a limit of detection of 1 μg/m^3 at any of the sites tested. The concentrations of chloroform in the water of whirlpool spas treated with chlorine disinfectant determined in the present study were similar to the concentrations that have been reported previously in studies[1] of swimming pool water and both results were higher than the levels usually observed in drinking water treated with chlorine disinfectant.

Chloroform concentrations (μg/L) in water

Device	Range	Mean
Whirlpool	35 to 670	292
Swimming Pool[1]	83 to 665	271

High haloform levels in the water of whirlpool spas were generally associated with combined high halogen residual and high total dissolved solids in the water, spas that were constructed of wood and/or spas in which the water was replaced infrequently. Residential spa installations exhibited higher haloform concentrations in the water than commercial spa installations despite the heavier bather loads registered at the commercial spas.

When sampling the air using Tenax adsorbent, chloroform breakthrough occurred at low volumes (ca 15 L) but no bromoform breakthrough was observed. When sampling the air using Tenax adsorbent in the presence of chlorine, chlorinated artifacts (dichlorobenzene, chlorobenzene and tetrachloroethylene) were observed but when sampling in the presence of bromine no brominated artifacts were observed. No statistical relationship between the air and water concentrations of haloform was discernable when the results from the various spas were compared. We believe this was due to the depletion of haloform from the air at ventilation rates that varied from installation to installation. The average molar concentrations of bromoform in the water and in the air were ca two times that of chloroform.

Molar concentrations of haloforms in air and water

	Air ($\mu mol/m^3$) range	mean	Water ($\mu mol/L$) range	mean
$CHCl_3$	0.03 to 6.4	1.3	0.3 to 5.6	2.5
$CHBr_3$	0.004 to 7.6	3.0	0.1 to 14.4	5.0

The treatment of whirlpool spas with halogen disinfectants does lead to the production of haloforms in the water and the haloforms are transferred to the air during use of the spas. The heat, agitation and aeration of the water do not appear to produce higher haloform levels in whirlpool spas than are observed in swimming pools treated with similar levels ofhalogen disinfectants. Control of the haloform concentration in the water and hence in the air in the vicinity of whirlpool spas is best achieved by frequent water replacement to minimize the accumulation of bather detritus, maintenance of the disinfectant levels within the range recommended by the manufacturer, increased ventilation in the area of the spa and the avoidance of whirlpool spas constructed of wood.

[1]. Chambon, P., Taveau, M., Morin, M., Chambon, R., Vial, J., (1983) Water Res. 17, 65-69.

RAPID DETERMINATION OF VOLATILE POLLUTANTS IN AQUEOUS MATRICES VIA FLOW INJECTION MASS SPECTROMETRY

Patrick W. Langvardt, Kathy A. Brzak and Patrick E. Kastl
The Dow Chemical Company, Midland, MI

ABSTRACT

Analyses of aqueous samples for volatile organic pollutants have become an increasingly important task for environmental analytical chemists. Recently the scope of this task has been expanded through additional regulations. The methodology used for this work, purge-and-trap GC/MS, has proven to be accurate and reliable but is very time consuming. The objective of this work was to evaluate flow injection mass spectrometry (FIMS) as a means of rapidly and automatically screening aqueous samples, thus potentially reducing the overall workload.

The FIMS system tested (figure 1) included an LC pump and autosampler, a mass spectrometer (Finnigan 4610) and a silicone hollow-fiber interface device. The interface was constructed using a bundle of three Dow Corning silicone capillary tubes (0.006 in. I.D. x 0.015 in. O.D. x 4 in.) sealed into a stainless steel tee using Dow Corning Silastic® 732 RTV sealant. The tee was connected to the ion source with a hollow probe. Aqueous samples were injected (50 µL) into a water carrier stream flowing through the fibers. The volatile organics selectively permeate the fibers and were detected via selected ion monitoring.

All of the forty-five volatile organic compounds tested including the original purgeable priority pollutants were found to respond to FIMS. Limits of quantitation ranged from 1 ppb for benzene to 250 ppb for acrolein, with most in the 5 to 30 ppb range. The system was shown to have linear response for methylene chloride up to 1000 ppb and precision (peak height RSD) for six consecutive determinations of 25 ppb methyl chloride was approximately 6% (figure 2).

The proposed scheme for screening for priority pollutants entails sampling directly into autosampler vials. Six consecutive injections would allow screening for all of the above compounds in fifteen minutes. An internal standard such as difluorobenzene could be used. The analysis of chlorinated drinking water is presented as an example.

FIMS could be applied as a rapid screening and/or range-finding technique, particularly for samples expected to be "clean" as for drinking water or certain monitoring well water.

FIGURE 1

SCHEMATIC DIAGRAM OF FIMS SYSTEM

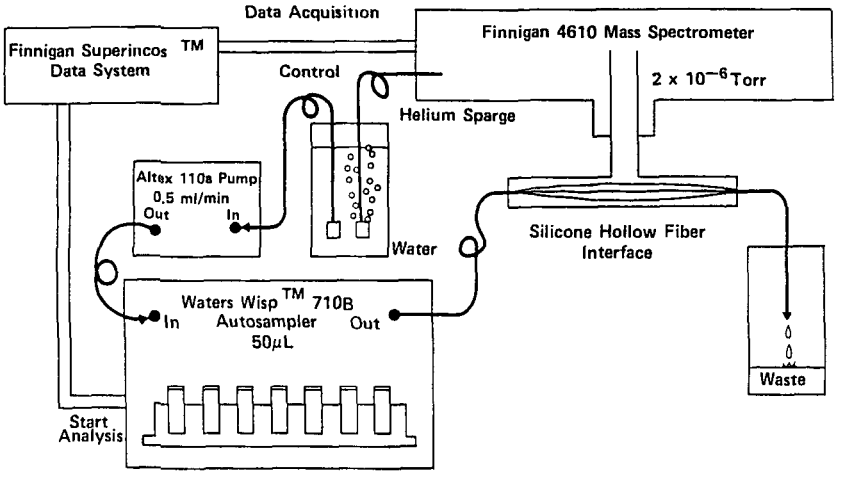

FIGURE 2

INJECTIONS FROM A SINGLE VIAL CONTAINING 25 PPB METHYL CHLORIDE

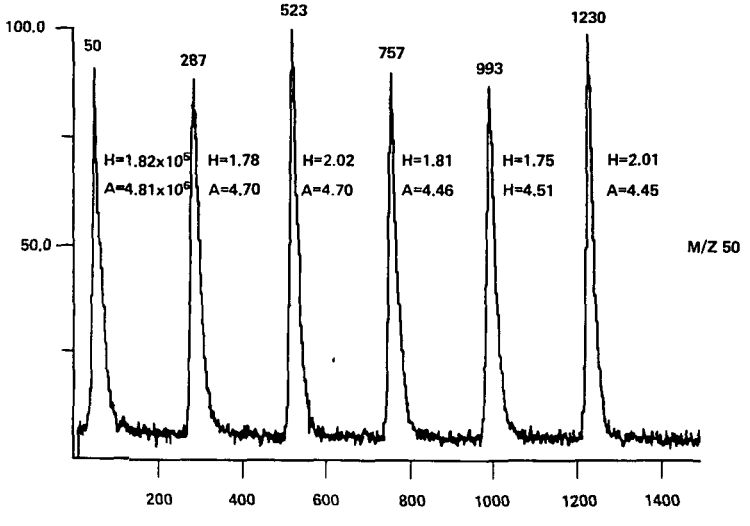

A GC/MS DESIGN FOR THE ANALYSIS OF VOLATILE AND EXTRACTABLE ORGANICS WITHOUT COLUMN CONVERSION

T. N. Ternes, Q. G. Grindstaff, and M. P. Jones

Plant Laboratory
Oak Ridge Y-12 Plant
Martin Marietta Energy Systems, Inc.
Oak Ridge, Tennessee 37831

M. F. Almond and M. Kearns

Kratos Analytical
Ramsey, New Jersey 07446

In laboratories where only one GC/MS is available for the two environmental analyses (Methods 624 and 625) or where an instrument has to provide back-up for either analysis, valuable time is wasted because the GC/MS has to be reconfigured between the two methods. For instance, the GC column has to be changed out and conditioned, which on some instruments means having to break the system vacuum to install or remove the columns thus increasing the conversion time. This arrangement is unsatisfactory for several reasons:

1) Rush samples which require 24 hour turnaround time are difficult to complete in that time frame

2) Possible methylene chloride contamination because it is a solvent for one method and a parameter of interest in the other

3) Increased instrument downtime from the "wear and tear" of converting between methods

Therefore, it would be desirable to find two temperature compatible columns, one suitable for each method, to be simultaneously installed in the GC so that either analysis can be readily performed.

At present, EPA specifies packed columns for the GC/MS methods, but fused silica capillary columns (FSCC) are now being utilized for the extractable organics since both the acid and base/neutral fractions can be analyzed on the same column with good separation. However, the packed columns used for the volatiles are not temperature compatible with the FSCC and the FSCC is not readily adaptable to purge-and-trap systems. As an alternative, we have investigated the application of a wide bore capillary column (WBCC) for the volatiles analysis and its compatibility with a FSCC. With the WBCC and FSCC installed, a lab could be prepared for either environmental analysis. The WBCC used is an SPB-1 loaded borosilicate glass capillary column, 60 meters long, 0.75 mm ID, and 1.0 μm film thickness.

The mass spectrometer was tuned to p-bromofluorobenzene (BFB) according to the ion abundance criteria established by EPA. Then a series of volatile standards was analyzed covering the range from 10 μg/L through 500 μg/L, and the response factors (RF) were calculated, according to the formula:

$$RF = \frac{(\text{Area Std.})\ (\text{Conc. Int. Std.})}{(\text{Area Int. Std.})\ (\text{Conc. Std.})}$$

ACKNOWLEDGEMENT

Operated for the U.S. Department of Energy, under contract DE-AC05-84OR21400.

In the EPA Contract Laboratory Program, a minimum RF of 0.300 is required for the volatiles. Also, the percent relative standard deviation (%RSD) was calculated using the response factors from the initial calibration curve. In order to use the average RF to calculate sample concentration, the %RSD must be less than 30%. Six compounds from throughout the chromatogram were chosen for comparison. Table 1 illustrates the RFs and the %RSDs for those six compounds on both the WBCC and the packed column. The WBCC performance meets EPA requirements.

TABLE 1

COMPOUND	RESPONSE FACTORS					
	WBCC			PACKED		
	MEAN	STD. DEV.	% RSD	MEAN	STD. DEV.	% RSD
1,1-DICHLOROETHENE	1.956	0.226	11.6	0.938	0.226	24.1
1,1,1-TRICHLOROETHANE	1.880	0.152	8.1	1.153	0.187	16.2
DIBROMOCHLOROMETHANE	0.855	0.120	14.0	1.689	0.456	27.0
TETRACHLOROETHYLENE	0.347	0.083	23.9	1.418	0.476	33.6
CHLOROBENZENE	0.924	0.209	22.6	2.350	1.005	42.8
1,1,2,2-TETRACHLOROETHANE	0.836	0.222	26.6	0.165	0.042	25.5

The WBCC stability was tested by repetitively cycling the oven from 50°C to 300°C. A flat, stable baseline with only a small bleed peak was observed. The packed column tends to degrade with use and the baseline will rise with an increase in temperature. Also, a column bleed peak interferes with the turning compound BFB. The WBCC bleed peak does not interfere with any of the target compound peaks or BFB. With the same temperature program as was used with the packed column, no more than two compounds co-elute on the WBCC. There are no interfering quantitating ions so automatic quantitation operates easily. The overall analysis time in only 15 minutes as compared to 21 minutes for the packed column.

This development work demonstrates the suitability of the WBCC for the analysis of the volatile organics and its compatibility with a FSCC which will satisfy our objective.

FAST, COST-EFFECTIVE IDENTIFICATION OF GROUND POLLUTION SOURCES.

J.S. Smith; Walter B. Satterthwaite Associates, Inc., 720 North Five Points Road, West Chester, Pennsylvania 19380.
M. Weiss; Bruker Instruments, Inc., Billreica, Massachusetts 01821.
D.A. Shepperd; Roy F. Weston, Inc., 256 Welsh Pool Road, Lionville, Pennsylvania.

There have been several field methods that have been developed to identify and assess relative concentrations of organic solvents in soil and groundwater. It is cost-effective to map an underground pollution plume using field techniques because field mobilization costs are minimized to one field visit and the laboratory costs are minimized due to the selection of the appropriate samples for verification and quantification.

It has been our good fortune to work with the new Bruker MM-1 mounted in a Chevy Blazer on various environmental problems. Utilizing this instrument in the field for qualitative analytical measurements has been successful. The unit is very mobile due to the four-wheel drive capabilities of the Blazer. It has been rugged. The operation was continuous during the survey of a landfill where four-wheel drive was a necessity. Approximately 10 hours of continuous operation was obtained during a hot (90°F) and dusty New Jersey day utilizing only the on-board 24 volt battery power supply. The mass spectrometer is a quadrapole instrument operating with unit resolution to mass 400. Its silica capillary G.C. column inlet system can respond to a sample vapor within 5 seconds. The computer control and software packages make the system easy to learn and use effectively. We have not yet started to find all of the uses and versatility that this system can produce to solve environmental problems.

This mass spectrometer has been used this spring to identify and measure (semi-quantitatively) soil gases for solvents in the groundwater, sanitary landfill gases, demolition landfill gases, headspace of groundwater monitoring wells, soil boring holes, and drums. The sensitivity to most organic solvents is in the low ppb v/v range. We were able to verify the presence of trichloroethylene (TCE) in the headspace of a home well containing 5 ppb TCE in the water that was 135 feet below ground level. This result has encouraged us to rely on the MM-1 to detect low levels of organic solvents in any matrix. Our experience is too limited at this time to understand the detection limits of the instrument for various compounds under an assortment of conditions.

One of the most useful features of this mass spectrometer inlet system is that you can backflush the entire inlet if you have over induled the system with sample. The backflush feature takes approximately 5 minutes, and the inlet is as clean as a freshly baked out system. There have been many times when this feature has saved hours if not the day. After placing this heated inlet system on a petroleum asphalt, we obtained a massive

response at every mass, making the instrument useless for further soil gas investigation. The backflush feature provided a "new" inlet sytsem in 5 minutes with the pushing of one button on the minicomputer console.

We have solved real problems with the MM-1 in the past year. One example concerns a demolition landfill in Pennsylvania. This landfill accepts and inspects loads of material coming from the demolition or repair of buildings. The trash includes wood, shingles, concrete, wallboard, etc. This landfill started in a stone quarry and presently contains 120 feet of fill. Six inches to one foot of dirt cover is used over every 10 feet of fill. A gas venting system is an integral part of the landfill design. The gas composition is mostly hydrocarbons with methane as the most abundant species. H_2S is present but the quantities are detectable by the human nose only. The gas flow cannot sustain combustion. Odor complaints by the township residents have spurred the Pennsylvania Department of Environmental Resources (PADER) into action. The action resulted in a request to contain the odors from the landfill by using a carbon adsorption tower. Testing an active (air pumped from the gas vent system through the carbon) carbon system and a passive propane flare for reduction of organic compounds was part of DER's program for odor control. Using the MM-1 in the landfill, a mass spectrum of the untreated and treated gases was obtained. The carbon treatment removed more than 99 percent of the compounds containing 6 carbon atoms or more, but did not remove all of the odor from the gas stream. The propane flare burned approximately 90 percent of all of the constituents of the gas. The odor was different than the untreated gas but was still noticeable. The MM-1 was used to look for any cracks in the fill surface and at the edge of the quarry walls that emitted appreciable quantities of landfill gas.

The final solution to the odor treatment system was to use a passive flare followed by an active carbon treatment system on the flare gases. This system eliminated the odors. Also, it was cost effective because the carbon remained active for a much longer period of time. [Active carbon adsorption tower became saturated with water within one day due to the heat (70°) and humidity of a landfill gas.] The MM-1 has provided an effective method to solve environmental problems in the field. Its main value has been to identify the unexpected organic chemicals within the sampling area.

A DETAILED MASS SPECTROMETRIC STUDY OF DFTPP

Yves Tondeur, Warren Niederhut, Kristi Bonaparte and Joseph E. Campana
Environmental Research Center
University of Nevada, Las Vegas, NV 89154

Decafluorotriphenylphosphine (DFTPP) was introduced as an ion abundance calibration compound for quadrupole GC/MS systems more than a decade ago. Its widespread use has facilitated the comparison of mass spectra from different instruments and the construction of universal mass spectral data bases. However, most sector mass spectrometers cannot meet the DFTPP ion abundance criteria, and many quadrupole GC/MS operators have difficulty in meeting the DFTPP criteria.

The elemental composition of the major ions in the 70 eV electron ionization mass spectrum of DFTPP and the ion filiations (Fig.1) were determined using a double-focusing mass spectrometer. The results show that DFTPP criteria ions originate from a variety of fragmentation pathways. They further emphasize the necessity to report the abundance of m/z 127 and m/z 51 relative to m/z 442 rather than to m/z 198 as it is presently done in the DFTPP tuning-criteria.

GC/MS data were acquired from a sector (ZAB-3F) and a quadrupole (Finnigan 4510) instrument. Figure 2 illustrates the seemingly anomalous evolution of two criteria ions (m/z 51 and m/z 198) abundances relative to the molecular ion (m/z 442) over the elution of the GC peak for different scan laws. Mass spectra collected during the evolution of the GC peak do not represent instantaneous ion abundances at single points on the total ion current profile. Faster scan rates (a minimum of 0.25 s/decade) are recommended with capillary columns to alleviate this expected (Fig.3) and undesirable behavior associated with rapid concentration changes of analyte with time. These data indicate that scan rate, scan law, chromatographic peak width, and the method used to extract ion abundance data can have a significant effect on the ability to meet the DFTPP ion abundance criteria.

Furthermore, ion abundances were studied from transit-time experiments performed on each type of instrument. The results (Fig.4) show that the discrepancies of DFTPP ion abundances observed between double-focusing and quadrupole instruments are due partly to differences in the time-of-flight of the ions (different geometries).

Finally, although less significantly, ion source temperature and sample concentration also contribute to the overall appearance of the DFTPP mass spectrum.

In conclusion, adapted tuning-criteria should be established under well-defined experimental conditions to reflect the use and introduction of modern instruments (GC and MS).

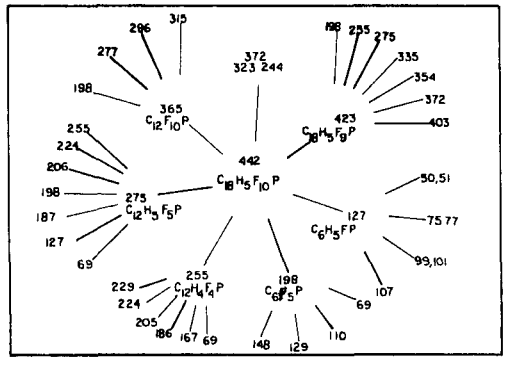

Figure 1: DFTPP ion filiations.

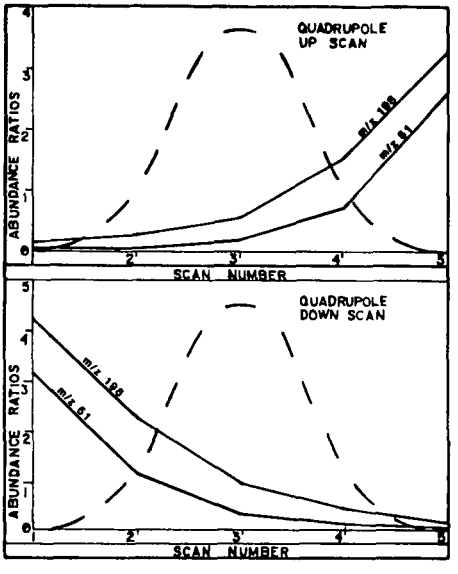

Figure 2: Abundance ratio profiles for two DFTPP criteria ions as a function of scan number for different scan functions. (scan rate = 465 amu/sec)

Figure 3: Three-dimensional representation for the rationalization of the abundance ratio profiles across a GC peak.

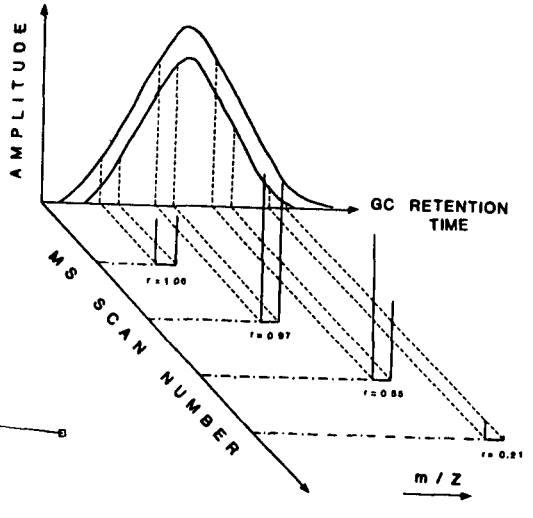

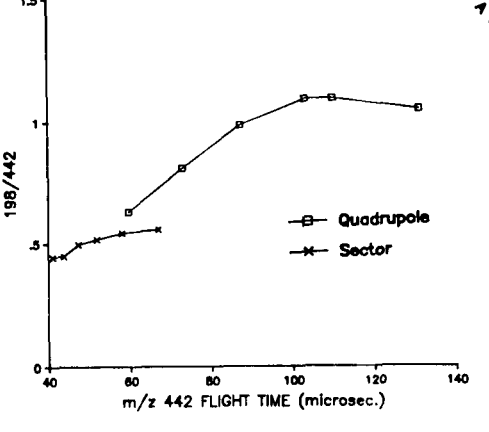

Figure 4: Abundance ratio of (m/z 198)/(m/z 442) as a function of the time-of-flight.

DEVELOPMENT OF ION ABUNDANCE CRITERIA FOR QUADRUPOLE GC/MS ANALYSIS

J.R. Donnelly, Y. Tondeur*, G.W. Sovocool**, and R.K. Mitchum** Lockheed-EMSCO and **U.S. Environmental Protection Agency, PO Box 15027, Las Vegas, NV 89114; *University of Nevada-Environmental Research Center, 4505 S. Maryland Parkway, Las Vegas, NV 89114

The use of decafluorotriphenylphosphine (DFTPP) as a reference compound to calibrate ion abundance measurements in GC/MS systems has been discussed[1] and subsequently applied by the U.S. Environmental Protection Agency (EPA) in connection with analysis of environmental samples. Criteria were based upon DFTPP mass spectral ion abundances obtained using available contemporary systems. Recently, problems with those criteria on a magnetic sector double-focusing instrument were presented,[2] in particular, the bias of low/high mass sensitivity. Since the instruments employed in the original study are no longer widely used for environmental measurements, it was felt that a reevaluation of these criteria was warranted due to new developments in GC/MS performance. Further, many environmentally significant compounds currently being monitored by GC/MS possess molecular weights well over 200 daltons. Therefore, instrument sensitivity at the higher masses has become an important consideration for EPA environmental monitoring efforts.

The chemistry of the ions formed in the mass spectrometer from DFTPP was examined using MS/MS on a VG ZAB-3F. It was found that m/z 198 was not related to many of the fragments used in the 1975 EPA criteria (Figure 1). Differences in ion abundance ratios, especially m/z 198/442, were observed with varying concentration (Table 1), source temperature (Table 2), and accelerating voltage (Figure 2). Ratios often varied considerably over the chromatographic peak (Figures 3 and 4). Many such variations can be explained based on concentration changes in the source from use of the capillary GC inlet system. DFTPP oxide (a contaminant in many DFTPP solutions) was prepared and its mass spectrum obtained (Figure 5).

An interlaboratory study was performed using modern instruments. Results, summarized in Table 3, were used to develop an updated set of criteria (Figure 6).

The EPA Contract Laboratory Program (CLP) data base was also searched and results from over 6500 DFTPP tunes were plotted using the IBM Model 3090 computer and Statistical Analysis Systems (SAS) software (Figure 7). While these data are obviously a subset of possible tunes, they are informative for they show where data tend to lie within the acceptance windows. For example, m/z 51/198 and m/z 442/198 showed broad data dispersion within the acceptance window while data for some other criteria showed approximately Gaussian distributions, allowing one to set updated criteria reflecting actual mass spectrometer performance. Excellent agreements were obtained between results from our interlaboratory survey and from distributions plotted using CLP data, extending Gaussian curves smoothly outside criteria acceptance windows where necessary to complete them.

This survey indicated that current instrumentation provides generally better high mass sensitivity than those surveyed previously, and that new ion abundance criteria to reflect this improvement can be justified. We propose the set of criteria shown in Table 4, which reflect sensitivity, resolution, and mass accuracy checks at the low, middle, and upper mass regions of interest for environmental monitoring by GC/MS. Modern instruments can meet these criteria, whereas the 1975 criteria (for example, the 127/198, 275/198, and 442/198 ratios) were often not met in this study.

The authors gratefully acknowledge participation in this study by: Diane Cho, Brady Englestead, Clinton Graden, Clyde Hedin, Tammy Jones, Jack Lay, Warren Niederhut, Steven Pyle, and David Speis.

REFERENCES

1. J. Eichelberger, L. Harris, and W. Budde, Anal. Chem. 47, 995 (1975).
2. J. McGuire, J. Craig, C. Thornton, ASMS 31st Annual Conference, 1983, p. 232.

NOTICE: This article has not been subjected to Agency policy review and therefore does not necessarily reflect the views of the Agency. Mention of trade names or commercial products does not constitute endorsement or recommendation for use.

Table 1

Concentration Effect on DFTPP Ion Abundances (300° C, 70 eV)

Concentrations (ng/uL)	Ion Abundance Ratios						
	441/442	422/442	366/442	275/442	198/442	127/442	51/442
5	0.17	0.06	0.02	0.20	0.73	0.08	0.31
50	0.17	0.06	0.02	0.20	0.69	0.08	0.34

Table 2

Source Temperature Effect on Ion Abundances (50ng, 70 eV)

Temperatures (° C)	Ion Abundance Ratios						
	441/442	422/442	366/442	275/442	198/442	127/442	51/442
110	0	0.06	0.02	0.13	0.42	0.15	0.14
300	0.17	0.06	0.02	0.20	0.63	0.20	0.24

Table 4

m/z	Recommendation	1975 Criteria
51, 127, 275	present: relative abundance ≥ 5%	30 60% of 198 40 60% of 198 10 30% of 198
198 or 442	base peak	198 base 442 > 40% of 198
68	≤ 2% of m/z 69	< 2% of 69
70	≤ 2% of m/z 69	< 2% of 69
197	≤ 1% of m/z 198	< 1% of 198
199	4 9% of m/z 198	5 9% of 198
443	15 24% of m/z 442	17 23% of 442
442	abundance ≥ 40% of m/z 198 if 198 is base peak	
198	≥ 15% of 442 if 442 is base peak	
365	delete criterion	> 1% of 198
441	delete criterion	present < 443

Bases of the art instrumentation can meet these criteria whereas the 1976 criteria (for examples the 127/198 275/198 and 442/198 ratios) were often not met in this study.

Table 3

	51/442	68/69	70/69	127/442	197/198	199/198	275/442	365/442	442	441	198/442	443/442	BASE PEAK	51/198	127/198	275/198
VG-ZAB-3F	23-33	66 (<1%)	3.8-5.9% of TO	20-31	197 (<1%)	6.2-8.3%	18 20	2 0 3.1	100	YES 8-10	42-73	17 4-20 7	442	46-55	50	33-38
KRATOS MS-50	NOT REPORTED	NOT REPORTED	NOT REPORTED	5 6-12 6%	NOT REPORTED	5.0-9.9% OUTLIERS 3.2-10	8 4-10.6%	.4-9%	100	YES 8-10	24 1-31 6	17 8-19 6	442		39	33-35
FINNIGAN-MAT 6230	NOT REPORTED			14 7-32 2		6 2-7 2	16.2-21.9	4.9-5 4	100	16.3-18 9 YES	55.4-61.2	23 3-27.5	442		15-32	22-28
FINNIGAN 1015	22 0			27 4		6.5	3 46	.8	100	NOT REPORTED	41.6	NOT REPORTED	442	52 9	65.9	8.3
EXTREL ELQ-400	46.1	NOT REPORTED	NOT REPORTED	47 2	59% (<1%)	6.2	15.3	1 7	94 7	YES	106%	17 3	198	44	45	15
EXTREL ELQ-400	27.1	NOT REPORTED	NOT REPORTED	31 5	NOT REPORTED	7 9%	15-18	.8%	100	YES 13 1	73 0	19 6	442	37	43	21
HP 5996	11 0-23.2	36%-2.75%	10%-9.15% 14.4%-8.12%	8 4-21 6	52-.95% (<1%)	5 1-7.0%	9.4-21.8%	1.6-3 6%	100	YES 11 4-15 2%	33.7-78.1	16.2-19.7	442	11-23	8-22	9-22
HP 5987A	22 8-28.7	0	0	72 8-77 9	0	6 5-7.0	25.9-32 0	2 2-2.4%	66.0-67 6	YES	148-152	18 1-20 5	198	15	50	18
HP 5985	12 6-12.8	0	0	42 4-43 7	0	7 0	66.8-69.5	2 8-2 9	66 8-69 5	YES	144-150	20 0-21 0	198	9	28	20
FINNIGAN 4023	60 0	0	77%	62 4	0	6 3	30.3	3 0	74 1	YES	135	17 9	198	44	46	24
FINNIGAN 4023	7.6-42.7	0	0	12 8-43 8	0	6 2	14.0-20 6	1.9-2 2	100	YES	42.5-92 7	17 0-18 0	442	18-46	30-47	22-33
FINNIGAN 4500	97.3	0	0	97 0	0	6.9	47 3	2 9	42 6	YES	229	19 6	198	41	41	20
FINNIGAN 705 ION TRAP	10 9-16 0	0	0	10 7-13 9	0	0	15 9-29.8	0-2 3	100	YES	12 8-19 4	15 0-16 6	442	56-140	85-103	97-232
VARIAN CH-5	NOT REPORTED			36	42	8.5	25.4	1 5	98 7	YES	101	25 6	198		37 5	25

Figure 1

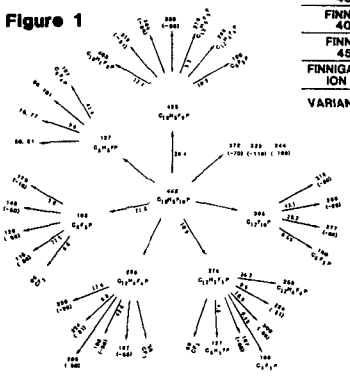

Figure 2

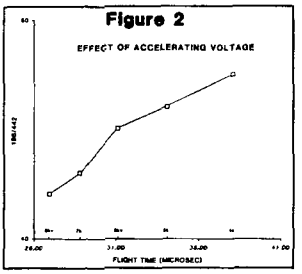

Figure 3

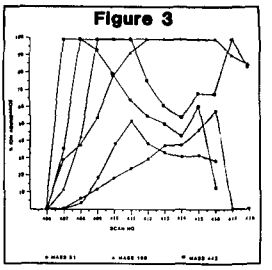

Figure 4

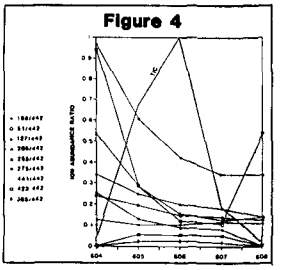

Figure 6

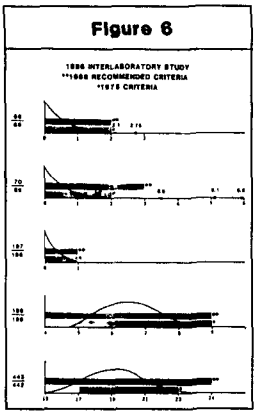

Figure 5

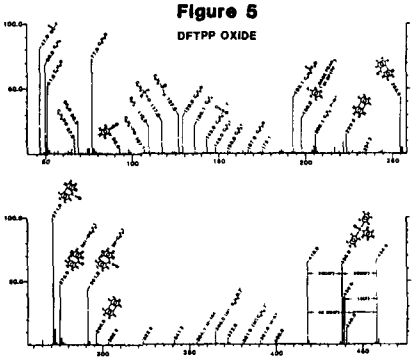

Figure 7

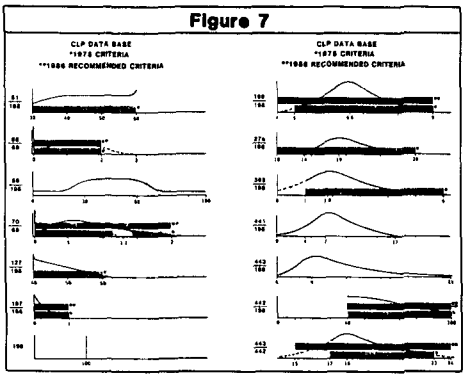

REVISED QUALITY INDEX FOR THE EPA/NBS MASS SPECTRAL DATA BASE

D. Thomas Terwilliger and John C. Ireland, Computer Sciences Corporation,
and William L. Budde, U.S. Environmental Protection Agency,
Cincinnati, Ohio 45268.

The EPA/NBS data base of reference EI mass spectra is widely used for compound identification in environmental monitoring and other applications of mass spectrometry. The purpose of this paper is to provide an update on the current status of the data base (1) and to describe recent improvements in the computerized evaluation of individual spectra. The EPA/NBS mass spectral data base is periodically reviewed, corrected, and updated with the goal of producing the highest possible quality collection of spectra. A major feature of the data base is the mandatory association of a unique Chemical Abstracts Service Registry Number (CASRN) with each spectrum. The CASRN is a key link to the published literature of substances including structure, nomenclature, chemical, and physical properties. Each compound also has associated with it a set of classification flags which categorizes the substance and allows data base developers to build subsets of the collection for specialized applications. Some limited information about each substance is provided within the data base depending on the distribution media. The NBS has plans to reprint the entire collection, including all available updates. The current distribution industry standard magnetic tape (2) contains 42,261 EI spectra, and is included as part of many mass spectrometry data systems.

A grand total of 74,582 spectra are presently available in an archive file that contains all spectra collected since the beginning of the project, including spectra of isotopically enriched compounds, multiple spectra of the same compound, non-EI spectra, and spectra that are not associated with a CASRN. As additional spectra are received they are always added to the archive file, flagged as appropriate, and the quality index (1) is computed. Whenever the data base is updated, spectra are selected according to the following rules: Spectra from isotopically enriched substances, non-EI spectra, or spectra without CASRN's are not selected. Where multiple spectra are associated with the same CASRN, the one with the highest quality index is selected. The Quality Index (QI) is thus the major tool used to evaluate individual spectra and to select a spectrum from multiple spectra of the same substance. The QI was originally defined by McLafferty (3) and modified as described previously (1). We have conducted a statistical assessment of the QI to determine the effectiveness of the algorithms. The QI is defined as 1000 times the product of several individual quality factors (QF's), which were designed to measure different properties of the mass spectrum. Each QF receives a value between zero and one, and the overall QI varies between 0 and 1000. The definition of each QF used to select the 1985 release of the data base along with the changes we have made will be published shortly and is available upon request.

The means and standard deviations of each quality factor using the entire data base were analyzed and a detailed examination of each definition was performed to determine the appropriateness of the individual formulas. Also a workshop (4) was organized to solicit comments on the quality of the data base and suggestions for improvement. This analysis resulted in the redefinition of 5 of the original 10 factors and the addition of 1 new factor. The table below lists the factors used throughout this study.

M	QF1 - Electron Energy	M	QF7 - Sample Purity
M	QF2 - Ions Above M+	N	QF8 - Calibration
N	QF3 - Illogical Losses	N	QF9 - DFTPP Reference
N	QF4 - Isotope Abundance	N	QF10 - Abundance of 28
M	QF5 - Number of Ions	A	QF11 - Saturation
M	QF6 - Low Mass Limit		

N - QF not modified M - QF modified A - QF added

An analysis of the means and standard deviations of the QF's calculated with the revised definitions was performed. Only QF5 is outside of the guidelines used to re-define the QF's, and it is only by a small amount. QF5 is different from the other quality factors in that there is a natural bias against fused aromatics whose spectra will always display fewer peaks. Even if these spectra are measured perfectly, QF5 will still be less than one, which will tend both to lower the mean and to raise the standard deviation. The number of spectra for which the overall QI is zero has been reduced by 65%. Most of these zeros come from QF3 and QF4 which relate directly to spectral quality. Saturated spectra are now being penalized. Since this property cannot be determined unambiguously for any given spectrum, its penalty was deliberately kept small.

Having arrived at a more satisfactory definition of the quality index, QI's were recalculated for the 74,582 spectra in the archive file. A new data base was selected using the previously described procedures. As a result, about 5% of the data base was replaced by alternative spectra which represent 47% of the multiple spectra eligible for exchange. This is a substantial number and should cause a noticeable overall improvement in spectral quality. An analysis of the QF's using this new data base shows that not all of the quality factors have an improvement in mean value, although the mean QI of the entire data base is 1.24 larger (23 larger if only those spectra actually exchanged are considered). The largest increase (.024 per exchanged spectrum) occurred for QF11, saturation, the new QF. The next largest change is for QF5, the number of ions, where the mean of the 2234 exchanged spectra decreased by .024. This is because the number of ions and saturation tend to work in opposite directions. Because QF5 counts only those peaks with a relative abundance greater than 1%, a badly saturated spectrum will tend to have a higher value of QF5 than a similar spectrum which is not saturated.

In conclusion, the definition of the Quality Index was modified to reflect actual spectrum quality more accurately. All entries in a new data base have a new QI, and 5.5% of the data base has been replaced by alternative and higher quality spectra. All users are urged to consider use of the QI in any application of this data base. We are continuing to solicit donations from the user community of any mass spectra available in machine readable form, preferably with the CASRN included. All new spectra will be evaluated as described, and if no spectrum is available, the spectrum will be added to the data base; if a spectrum is already available, the entry with the higher QI will be retained.

1. D.P. Martinsen et. al., Org. Mass Spectrom., 1982, 17, 547.
2. EPA-NIH Mass Spectral Database Magnetic Tape. National Bureau of Standards, Office of Standard Reference Data, Physics Building, Room A323, Gaithersburg, MD 20899.
3. F.W. McLafferty et. al., Org. Mass Spectrom., 1978, 13, 209.
4. ASMS, 33rd Conference, May 26-31, 1985, San Diego, Workshop on Mass Spectrometry Data Bases.

EXPANDED DATA BASE OF 130,000 MASS SPECTRA OF 110,000 COMPOUNDS

A. B. Twiss-Brooks, D. B. Stauffer, S. Loh, M.-Y. Zhang, and F. W. McLafferty

Chemistry Department, Cornell University, Ithaca, NY 14853-1301

Literally thousands of mass spectrometers world-wide are equipped with data systems capable of matching unknown mass spectra against a reference file. Obviously, major limiting factors in the success of such systems are the quality and quantity of reference mass spectra in the data base used. The Wiley/NBS reference file of electron-ionization mass spectra has been increased in size by >60% over the 1982 edition. Although the majority of spectra were retrieved from the primary literature, many donations from private collections are unusual in spectral quality and importance for specific applications. Approximately 140,000 spectra were collected, all of which were examined manually and by computer programs. This included checks for correct isotopic abundances, logical neutral losses, contaminant peaks, and errors in data transcription, eliminating redundant spectra and those of marginal quality. Spectra in the final collection were cross compared using the Probability Based Matching algorithm, eliminating those of the same compound which matched closely. However, spectra of the same compound showing greater differences are inspected for possible errors; if it is not possible to determine which is correct, or if the variations are due to varying experimental conditions, multiple spectra of the same compound are retained in the file to increase the matching probability.[1] A sophisticated program has been developed to assign Chemical Abstracts Registry numbers to these compounds using their name fragments, elemental compositions, and literature references, searching against "CAS On-Line". The final expanded data base contains approximately 130,000 different mass spectra of approximately 110,000 different compounds, by far the largest collection of its kind in the world.

In the conventional format this file requires ~90 megabytes of disk storage. To alleviate this problem all essential data have been compressed to require ~27 megabytes. Data calculable from other data, such as molecular weights, were eliminated. Storage requirements for names were reduced 67% by substituting single characters not otherwise appearing for recurring character strings (e.g., phenyl), using a Huffman code[2] to provide the shortest descriptions. For peak masses only the first is stored, with the remainder designated by mass differences similarly encoded.

To minimize storage requirements even further, specialty data bases covering common areas of application are being selected from the master file. Initial subsets are Biomedical, Toxicology, Environmental, Industrial, Flavors and Fragrances, and Academic (a maximum variety of compound types). Suggestions on types of compounds for these or other specialty tapes would be welcome.

Also in the planning stage is a set of bound volumes containing bar graph presentations of the best spectra of each compound in the expanded data base. Users of this data base owe a real debt of gratitude to the literally thousands of contributors that have made this possible. Collection activities continue at Cornell, and new spectra will be gratefully accepted from new as well as former contributors.

References:

(1) McLafferty, F. W.; Stauffer, D. B. Retrieval and Interpretive Computer Programs for Mass Spectrometry, J. Chem. Inf. Comp. Sci. **1985**, 25, 245-252.

(2) Standish, T. A. "Data Structure Techniques", Addison-Wesley: Reading, MA, 1980, p 295.

UTILIZATION OF A SECTOR MASS SPECTROMETER FOR PERFORMING ENVIRONMENTAL GAS CHROMATOGRAPHIC/MASS SPECTROMETRIC ANALYSES

Q. C. Grindstaff and T. N. Ternes

Plant Laboratory
Oak Ridge Y-12 Plant
Martin Marietta Energy Systems, Inc.
Oak Ridge, Tennessee 37831

M. F. Almond and M. Kearns

Kratos Analytical
Ramsey, New Jersey 07446

Historically, the magnetic sector mass spectrometer has not been used for routine Environmental Protection Agency (EPA) analyses. The main reason is that the sector instruments were not routinely tunable to the ion abundance criteria as established by EPA for gas chromatographic/mass spectrometric (GC/MS) performance compounds decafluorotriphenyl phosphine (DFTPP) and bromofluorobenzene (BFB). The tuning of a sector instrument to these ion abundance criteria meant considerable detuning of the ion source, which led to loss of both reproducibility and sensitivity. However, through a modification to the detector circuit, the sector instrument can be easily tuned to the DFTPP and BFB ion abundance criteria without significant loss of sensitivity.

The main problem that the detector circuit modifications overcomes is that the actual mass spectrum of DFTPP has mass 442 as the base mass, where EPA requires that mass 198 be the base mass. By use of the modified circuit, mass 442 can be attenuated to make mass 198 the base mass without affecting the rest of the mass spectrum. As previously mentioned, when the ion abundance criteria are met by detuning the ion source, the sensitivity is greatly affected. However, with the detector circuit modification, the sensitivity of the instrument is essentially the same whether the instrument is tuned for DFTPP ion abundance criteria or optimum performance. A signal-to-noise ratio of 63:1 for m/z 298 was demonstrated for 100 pg of methyl stearate under optimum tune while a ratio of 50:1 was shown for the DFTPP tune. Table 1 shows the accuracy and reproducibility of the MS-25 RFA to the EPA ion abundance criteria. The result for BFB ion abundance criteria is of equal accuracy and reproducibility.

The accuracy and precision of the response factors for Methods 624 and 625 for the MS-25 RFA were shown to be excellent. For Method 624, the largest relative standard deviation (RSD), which indicates accuracy, is 5.6% and the largest percentage difference from the actual value, which indicates precision, is 2.1%. For Method 625, the largest RSD reported is 7.7% and the largest percentage difference was found to be 5.3%.

The EPA check of the fitness of a GC/MS system for performing Method 625 is the calculation of the tailing factor of the RIC peaks for two compounds, benzidene and pentachlorophenol. EPA requires that the tailing factor for benzidene and pentachlorophenol be less than 3 and 5, respectively. The tailing factor determined for benzidene is 1.7 and for pentachlorophenol is 1.2.

In conclusion, the MS-25 RFA GC/MS with modified detector circuit has been demonstrated to be capable of performing EPA Methods 624 and 625. The data show that the MS-25 RFA meets or exceeds all EPA specifications for performance.

ACKNOWLEDGMENT

Operated by Martin Marietta Energy Systems, Inc., under contract DE-AC05-84OR21400 with the U.S. Department of Energy.

METHOD 625 ION ABUNDANCE CRITERIA

MASS	EPA CRITERIA	FIRST DAY	SECOND DAY	THIRD DAY	SEVENTH DAY
51	30–60% OF 198	42.9%	39.8%	38.6%	37.0%
68	< 2% OF 69	–	–	–	–
70	< 2% OF 69	–	–	–	–
127	40–60% OF 198	48.0%	47.9%	46.7%	46.6%
197	< 1% OF 198	–	–	–	–
198	BASE PEAK	100.0%	100.0%	100.0%	100.0%
199	5–9% OF 198	6.8%	6.7%	6.9%	6.7%
275	10–30% OF 198	29.3%	25.3%	25.1%	30.0%
365	> 1% OF 198	1.7%	1.8%	1.6%	1.8%
441	PRESENT < 443	12.6%	12.5%	11.7%	12.9%
442	< 40% OF 198	52.3%	51.9%	51.1%	56.3%
443	17–23% of 442	20.3%	19.5%	19.6%	19.9%

25 ng DFTPP, 1000 RESOLUTION, 0.3 sec/decade, NO RETUNE FOR SEVEN DAYS, NO BACKGROUND SUBTRACTION, 10^4 GAIN, MASS AXIS RECALIBRATION ON SEVENTH DAY.

AN EVALUATION OF CAPILLARY COLUMNS FOR THE GC/MS ANALYSIS OF POLYCHLORINATED DIBENZO-DIOXINS AND DIBENZOFURANS IN DIELECTRIC FLUIDS,

E.D. Hardin, P.B. Stewart, T.W. Campbell, D.A. Hayes A.W. Nichols and F.L. Shore, Radian Corporation, Austin, TX 78766

Analysis of polychlorinated dibenzodioxins and dibenzofurans (PCDD/PCDFs) for samples generated from the electric power industry is complicated by matrix interferences.[1,2] One of the most useful columns for PCDD/PCDF analysis is the J&W Scientific DB-5®.[3] The newly released Supelco SP-2331® column is a partially crosslinked version of the very useful SP-2330® column.[4] This project was funded by the Electric Power Research Institute (EPRI) to develop and validate analytical methodology for identification and quantitation of PCDD/PCDFs in dielectric fluids from electrical equipment. Specific evaluation of the methodology included high resolution capillary chromatography column evaluation, demonstration of linear GC/MS response over a wide range of analyte concentrations, and assessment of quantitative precision and accuracy of PCDD/PCDF determinations in several types of spiked samples and in-service dielectric fluids. Both in-service dielectric fluids and blind-spiked samples were extracted in triplicate and each extract was analyzed in triplicate to give a measurement of the precision and accuracy of the methodology.

The dielectric fluid extracts were analyzed by capillary GC/MS in the selected ion monitoring mode using a Hewlett-Packard 5985/87. A 60 m, J&W DB-5, 0.32 mm ID, 1 µm film thickness capillary column was used for quantitation of all PCDD/PCDF congeners, and a Supelco SP-2331, 0.32 mm ID, 0.32 mm ID, 0.2 µm film thickness capillary column was used for resolution of 2,3,7,8-TCDF and 2,3,4,8-TCDF. Hydrogen carrier gas and cool on-column injection was used in both cases. All dielectric fluids were extracted in triplicate and prepared for analysis using a tandem combination of modified Smith-Stallings[5] and EPA Region VII[6] extraction procedures.

Quantitation was performed versus five-point calibration curves generated in triplicate for eight of the most toxic PCDD/PCDF isomers. Radian, in conjunction with Cambridge Isotope Laboratories, Inc., synthesized carbon-13 labeled internal standards which were added before extraction so that PCDF congener classes could be quantitated from carbon-13 labeled PCDFs of the same chlorine number. In the case of HpCDF, no carbon-13 labeled analogue was available so quantitation was done versus ^{13}C-HxCDF.

A chromatographic test mixture containing the most toxic PCDD/PCDF isomers and coeluters was supplied by Battelle; Columbus Laboratories. The most difficult to resolve pair in the test mixture was 2,3,7,8-TCDF/2,3,4,8-TCDF. This pair could be separated at approximately 65% valley (see Figure 1) on SP-2331 but coeluted on DB-5. Another difficult pair to resolve was 1,2,3,7,8-PnCDF/1,2,3,4,8-PnCDF which could be separated at approximately 50% valley on DB-5 (see Figure 2) but coeluted on SP-2331. In analysis of extracts from the real samples, however, matrix interference often prevented resolutions to the extent possible in the test mixture.

Figure 1 2,3,7,8-TCDF/2,3,4,8-TCDF SEPARATION

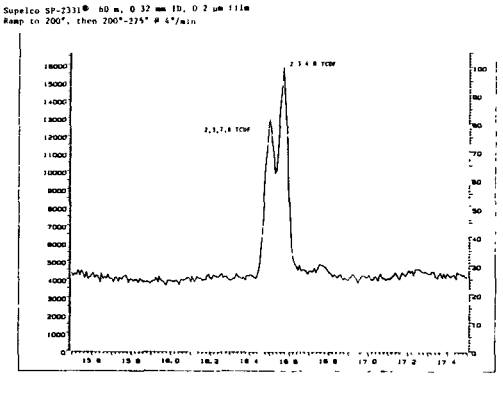

Figure 2 1,2,3,4,8-PnCDF/1,2,3,7,8-PnCDF

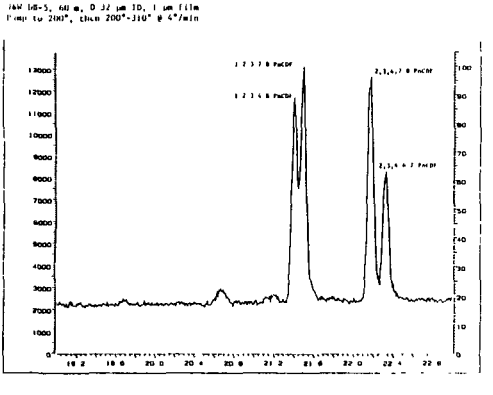

Resolution of 2,3,7,8-TCDD on DB-5 gave a maximum of 30% valley separation from the closest eluting TCDD isomer while SP-2331 gives nearly baseline resolution of 2,3,7,8-TCDD.

Both columns proved to be satisfactory for complete Cl_4 to Cl_8 PCDD/PCDF isomer group specific quantitation. For quantitation of individual congeners, a combination of both columns is necessary. The DB-5 column which utilizes a bonded methylphenylsilicone stationary phase proved to be more durable than the SP-2331 column which has a partially cross-linked cyanosilicone stationary phase. The SP-2331 column requires a deactivated fused silica pre-column and a relatively narrow range temperature program to extend the useful lifetime. On the other hand, DB-5 can be operated over a wider range temperature program and at a higher temperature (310° versus 275° on SP-2331). Also, DB-5 columns can be rejuvenated by backflushing with solvent. Backflushing is not recommended for the SP-2331 column.

Results from the dielectric fluid analyses show matrix interferences are still a problem with quantitation. On DB-5, the average multiple determination precision and the average multiple extraction precision for three blind-spiked samples was 4.0% and 4.2%, respectively. For the five most complex in-service liquids on DB-5, the average multiple determination precision and the average multiple extraction precision was 9.5% and 10.7%, respectively.

REFERENCES

1. Smith, L.M.; Johnson J.L.; In: "Chlorinated Dioxins and Dibenzofurans in the Total Environment"; Choudhary, G.; Keith L.H.; Rappe C.; Eds: Ann Arbor Science Publishers; Ann Arbor, MI, 1983; Part I, pp 321, 332.

2. Williams, C.H., Jr.; Prescott C.L.; Stewart P.B.; Choudhary, G. In: "Chlorinated Dioxins and Dibenzofurans in the Total Environment"; Choudhary, G.; Keith L.H.; Rappe C.; Eds: Ann Arbor Science Publishers; Ann Arbor, MI, 1985; Part II, pp 457, 468.

3. U.S. EPA, SW-846 "Test Methods for Evaluating Solid Waste". Method 8280.

4. Stallings, D.L.; Petty J.D.; Smith L.M.; Rappe C.; Buser H.R. In: "Chlorinated Dioxins in Related Compounds"; Huntzinger, O.; Eds: Pergamon Press:New York, 1982; pp 77-85.

5. Smith, L.M.; Stallings D.L.; Johnson J.L.; Anal. Chem. 1984, 56, 1830.

6. "Determination of 2,3,7,8-TCDD in Soil and Sediment", U.S. EPA Region VII Laboratory, Kansas City, KS 66115.

INCREMENTAL/DECREMENTAL HIGH RESOLUTION SELECTED ION MONITORING FOR EVALUATING INSTRUMENT PERFORMANCE.

John Roboz, Alexander Allan and Michael Chu.
Department of Neoplastic Diseases, Mount Sinai School of Medicine,
New York, NY 10029.

Peak matching with oscilloscope output or, less frequently, scanning over limited mass range with UV-oscillograph output have been commonly used to set and measure resolution in high resolution mass spectrometers. We have investigated an alternative approach which utilizes selected ion monitoring at high resolution. For example, with the VG Analytical Model ZAB-1F mass spectrometer it is possible to monitor the intensities of ion currents in up to twelve channels, each set at slightly different exact masses.

The principle of the technique can be illustrated in the documenting of a given resolution and corresponding peak shape using PFK. One channel is set at m/z=218.9856 and the others at masses corresponding to 5 mmu increments/decrements and the respective ion intensities are measured. When relative intensities are plotted as a function of mass a curve is obtained that should be symmetrical (checking peak shape) with its maximum at the exact mass of the m/z=219 peak of PFK. The resolution can simply be determined at, say, the 10% intensity points on the curve. Peak shapes and drift can also be checked by introducing, simultaneously or sequentially, benzene and pyridine and monitor peak intensities at their exact masses together with additional channels set at small (e.g., 2-5 mmu) incremental/decremental masses. The symmetry of the plotted curves provides information on the shape of the peaks. When the maximum of the curve is not at the exact mass of the compound used, instrumental drift is indicated which can be monitored both short and long term by this method.

To set resolution of approximately 10,000 one may monitor the exact masses of pyridine and benzene (C_5H_5N = 79.042 and $^{13}CC_5H_6$ = 79.050) and also the mass halfway between. As the collector slit is closed, the achievement of 10,000 resolution is signaled by a large decrease in the intensity of the ions in the halfway channel as the component peaks are resolved. This is accompanied by only a moderate decrease in the intensities in the other two channels representing the exact masses of pyridine and benzene. A resolution of nearly 13,000 can be achieved with butyl acetate by monitoring exact masses at m/z=57.0704 and 57.0659 ($^{13}CC_3H_8$ and C_4H_9) and at additional increments/decrements at 1 mmu intervals and constructing relative intensity versus mass plots. Additional potential doublets/pairs for documented resolution setting or testing include 1-octane ($^{13}CC_4H_{10}$-C_5H_{11}, R = 15,800), benzonitrile-styrene (C_7H_5N-C_8H_7, R=8,200), dimethyl formamide - n-butyl alcohol (C_3H_7NO-C_4H_9O, R=5,800) and (for the solid probe) 2,3,7,8-tetrachlorodibenzo-p-dioxin and chlorophenyldichloroethylene ($C_{14}H_8{}^{35}Cl_2{}^{37}Cl_2$-$C_{12}H_4O_2{}^{35}Cl_4$, R=9,000).

A useful application of this approach is the monitoring of the purity of GC or LC peaks in the analysis of small quantities of drugs or endogenous constituents in biological materials. For example, the exact mass of the trimethylsilylated derivative of glutamic acid was monitored (CI mode) at m/z=364.179 together with ten more channels at 3 mmu increments/decrements. The width of the window of increments/decrements was determined by considering the

elemental compositions of potential interferences corresponding to the exact masses monitored. When an internal standard is also available, such as was the case with the glutamic acid (deuterium enriched), the plots of the intensities of the incremental/decremental masses monitored against mass can be used to differentiate between instrumental drift and the presence of an interference. When there are equal deviations between the apices of the plots from the known exact masses for both analyte and internal standard, instrumental drift is the likely cause. When deviation occurs only with the analyte, the presence of interference is indicated.

The potential applications of incremental/decremental high resolution selected ion monitoring include: 1.) Setting and documenting resolution; 2.) Checking MS peak shape and stability; 3.) Determining or confirming GC/LC peak purity; 4.) Differentiating between drift and interference with the aid of internal standard.

(Supported by the T.J. Martell Memorial Foundation for Leukemia and Cancer Research).

Ion-Molecule Reactions in a Quadrupole Collision Cell of a BEQQ Mass Spectrometer

Alex Young, Ontario Regional Ion Chemistry Laboratory (ORICL),
Department of Chemistry, University of Toronto
Toronto, Canada, M5S 1A1

Ion-molecule reactions have long proven a fruitful field of investigation, moreover interest has recently been generated in the study of such reactions in quadrupole collision cells, be they attached to a triple quadrupole or a hybrid instrument. Recently, this laboratory acquired a ZAB-2FQ of BEQQ configuration and in an effort to characterize the capabilities of the instrument, exploratory studies were performed using the magnetic and electric sectors for reactant ion selection. The first quadrupole when pressurized with an appropriate reagent gas served as a reaction chamber; the second quadrupole identified the resultant products. The instrument is depicted diagrammatically in figure 1. The reactant ion collision energy may be varied in the quadrupole collision cell, in order to optimize adduct ion formation, or to perform experiments at identical centre of mass (C.M.) collision energies for differing partners.

The experiments to be described encompassed two areas of inquiry: the first dealt with isomer differentiation and subsequent questions as to the genesis of particular ion-molecule reaction products; the second was concerned with the question of the SN1 or SN2 mechanism in the gas phase.

Previous work by Jalonen[1] investigated low energy collisions in a triple quadrupole mass spectrometer using either 1,3-butadiene or benzene as a reagent to distinguish between $C_2H_5O^+$ isomers. Two isomers were examined: the 1-hydroxyethyl cation $(CH_3\overset{+}{C}HOH)$, and the methoxymethyl cation $(CH_3\ OCH_2)$. In figure 2 a similar experiment is shown wherein vinyl methyl ether was employed as the reagent. The left hand traces were obtained at identical c.m. energies and collision gas pressure and exhibit two major differences. The extent of reagent gas protonation to form an ion of m/z 59 is greater in the 1-hydroxyethyl cation experiment and an ion of m/z 73 is produced in the reaction with the methoxymethyl cation. This ion is not present in the upper trace. The isomeric ions may be readily distinguished; the results are rationalized by considering the reaction between CH_3OCH_2 and the ether as methyl cation addition to the latter to produce an ion of m/z 73. The reaction of $CH_3\overset{+}{C}HOH$ is initially that of proton transfer to the neutral ether to produce m/z 59, followed by solvolysis of the protonated ether. The right hand trace was obtained by reacting the protonated ether with the neutral in the quadrupole cell. Although the signal due to m/z 59 is saturated in this trace, the experimental result is almost identical to that of the upper left hand trace when the signal due to m/z 45- the proton transfer agent - is ignored.

The use of ammonia as a reagent for adduct ion formation has been investigated by Schmidt *et al.*[2] in a study employing protonated esters and ketones. In the upper trace of fig. 3 a similar experiment is shown wherein protonated methyl isobutyrate (m/z 103) was selected from the source and reacted with ammonia in the quadrupole cell. The reaction of interest is that of alcohol elimination/ammonia addition:

$$\underset{m/z\,103}{(CH_3)_2CH\overset{+}{C}(OH)OCH_3} + NH_3 \longrightarrow \underset{m/z\,88}{(CH_3)_2CHCO\overset{+}{N}H_3} + CH_3OH \quad (1)$$

The question as to an SN1 or SN2 mechanism was investigated by performing a second experiment depicted in the lower trace. The alcohol elimination product (m/z 71) was selected from the source and reacted with NH_3 at identical pressure and c.m energy; comparison of the upper and lower experiments indicates that the genesis of m/z 88 occurs via a SN1 mechanism. The ions of m/z 105 and 122 are due to one and two NH_3 molecules associated with m/z 88.

A similar study was performed using protonated cyclohexanol where the reaction of interest is dehydration/ammonia addition:

$$\underset{m/z\ 101}{\text{cyclo-}C_6H_{11}\overset{+}{O}H_2} + NH_3 \longrightarrow \underset{m/z\ 100}{\text{cyclo-}C_6H_{11}\overset{+}{N}H_3} + H_2O \quad (2)$$

In figure 4, the lower trace depicts the products of the reaction of the protonated alcohol. The dehydration product m/z 83 is the dominant ion; m/z 100 is the substitution product which may cluster with NH_3 to produce m/z 117. The ions of m/z 118 and 135 are produced by clustering NH_3 with the protonated alcohol. The upper trace was obtained at identical pressure and c.m. collision energy, but m/z 83 - the dehydration product - was selected from the source. The minor abundances of the ammonia addition products at m/z 100 and 117 are supportive of an SN2 mechanism for reaction 2, although clustering of the protonated alcohol with NH_3 followed by dehydration would also produce m/z 100. Evidence for the SN2 mechanism is given in reference 3.

References

1. J. Jalonen, J. Chem. Soc., Chem.Commun., 872 (1985)

2. J.P. Schmidt, P.H. Dawson and N. Beaulieu, Org. Mass Spectrom, 20, 269 (1985)

3. D.L. Hall, C. Gupta and T.H. Morton, J. Am. Chem. Soc., 103, 2416 (1981); J.C. Kleingeld and N.M.M. Nibbering, Org. Mass Spectrom., 17, 136 (1982); J.C. Tabet, Y. Tondeur, Y. Hirano, A. Wegmann, P. Tecon and C. Djerassi, Org. Mass Spectrom. 19, 473 (1984)

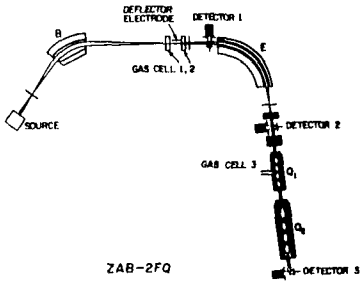

Fig. 1

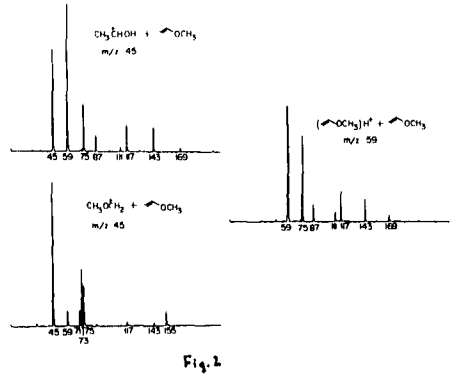

Fig. 2

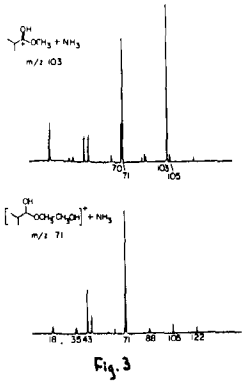

Fig. 3

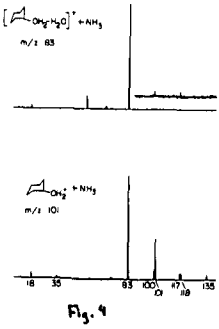

Fig. 4

QUANTITATIVE ELEMENTAL ANALYSIS BY LASER IONIZATION MASS SPECTROMETRY (LIMS)

Robert W. Odom and Ilsabe C. Niemeyer
Charles Evans & Associates
Redwood City, CA 94063

Laser ionization mass spectrometry (LIMS), which is also referred to laser microprobe mass spectrometry, employs a focused, high power density laser pulse to vaporize and ionize a microvolume of solid material (1). The ions produced from this laser photon/solid interaction are mass analyzed using a time-of-flight (TOF) mass spectrometer. The incorporation of a fast transient recorder (TR) into the TOF detection system enables one to acquire a complete mass spectrum of the ions produced from each laser irradiation.

A portion of our research with laser microprobe mass spectrometry has centered on the evaluation of the elemental detection capabilities of the technique in the analysis biological materials. In order to evaluate these elemental detection capabilities, we have developed a set of elemental standards. The development of suitable elemental standards in biological material analysis would ideally employ a matrix which has a composition quite similar to the actual tissue material of interest. In addition, since the laser microprobe is a microanalytical technique in which the sampling diameters can range from 0.5 to ~10.0 μm, the standards prepared for this technique must also be homogeneous both laterally and in-depth at micrometer dimensions. In order to meet these requirements, two approaches have generally been employed in the preparation of microanalytical elemental standards of biological tissues:

1. doping of organometallic compounds into protenaceous matrices such as aminoplastic, agar, albumin or gelatin (2), and
2. incorporating organometallic compounds into an epoxy or acrylic resin such as those employed in the preparation of tissue thin sections. (3)

Although protenaceous matrices have a composition which is similar to many forms of soft biological tissue, it is generally easier to microtome uniform thin sections (0.5 to 1.0 μm thick) from epoxy or acrylic resin material. We have prepared elemental standards using an epoxy embedding material (Spurrs Resin) primarily because of the ease in thin sectioning this material.

Since both the ablated volume and extent of ionization produced in laser microprobe analyses depend on a number a variables (e.g., sample absorbtivity, laser energy, and chemical composition of the vapor plume), the reproducibility of the detected ion signals can vary by an order of magnitude even under "controlled" experimental conditions. As a consequence, precise elemental analyses by this technique generally necessitates normalizing the analyte signal intensity to an ion signal whose intensity reproducibly correlates with these variable ionization conditions. Two potential normalization ion signals include a signal characteristic of the matrix material (e.g., C in epoxy resins or protenaceous matrices) or an internal standard. We have utilized Dy as an internal standard in the elemental standards we have prepared because we found that the low intensity of the detected C^+ ion signal produced from this epoxy did not provide sufficient precision as a matrix ion.

Standards were prepared over a concentration range from 0.1 to 1000 part per million by weight (ppmw) and the Dy concentration was 1000 ppmw. Samples have been prepared for Na, Al, Cr, Fe, Zn, Se, As, Cd, Sn, Hg and Pb. The homogeniety of these standards have been evaluated using secondary ion mass spectrometry (SIMS)/ion imaging. All standard samples for laser microprobe analysis were either 1.0 or 0.5 μm thick sections mounted on TEM grids. A Cambridge Mass Spectrometry, Ltd. (Cambridge, England) Model LIMA-2A reflection mode laser

microprobe was utilized in these analyses. Fifteen spectra at each elemental concentration were obtained in these analyses and the peak area intensity ratio of X^+/Dy^+ were evaluated from these spectra. Figure 1 is a typical response function obtained in the laser microprobe analysis of the Fe standard. This response function is a plot of the logarithm of the average $^{56}Fe^+/^{164}Dy^+$ ratio as a function of the logarithm of the Fe concentration. Although the slope of this line is 0.66 indicating that the detected Fe/Dy ion ratios are not a linear function of the Fe concentration, this response function curve is quite reproducible and can be considered a working curve for determining Fe concentrations in Dy doped specimens. The minimum detectable Fe concentration is approximately 60 ppmw.

An illustration of the use of this response function is given in Figure 2. This figure plots the X^+/Dy^+ (X= Ca, Fe) versus laser shot position in the analysis of human liver tissue containing high Fe levels. The tissue sample was prepared by embedding the fixed, dehydrated specimen in a Dy doped Spurrs resin and microtoming 1.0 µm thick sections for analysis. The peak Fe/Dy signal ratios correspond to high Fe containing regions (hemosiderin granules) in the tissue. The average Fe concentration in this liver tissue specimen was determined to be greater than 400 µmol/gm.

CONCLUSIONS: The preparation and analysis of homogeneous elemental standards represents the first step in developing quantitative analytical methods with the laser microprobe technique in the analysis of biological tissues. The response functions obtained provide a method for determining the elemental composition of these materials.

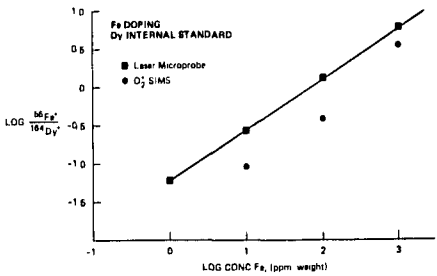

Figure 1. LIMS ^{56}Fe to ^{164}Dy ion signal ratios versus conc. Fe in Spurrs resin.

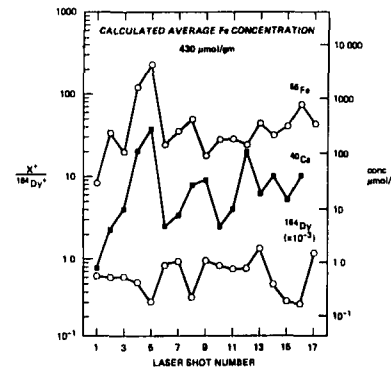

Figure 2. Fe and Ca to Dy ion signal ratio in the LIMS analysis of human liver tissue

REFERENCES: 1. Fres. Zeit Anal. Chem. 308 (1981)
2. N. Roos and T. Barnard, Ultramicroscopy 15, 277 (1984)
3. G.M. Roomans and H.L.M. Van Gaal, J. Microsc. 109, 235 (1977)

ACKNOWLEDGEMENTS: Support for this work was provided by an NIH SBIR Grant (#1 R43 GM33123-01). The assistance of Dr. Ronald H. Fleming in the preparation of the standard materials is gratefully acknowledged. Also, we would like to thank Drs. Bruce Scharzschmidt and Linda Ferril of the UCSF Medical Center for their assistance in the specimen preparation and evaluation of the liver tissue analysis.

IDENTIFICATION OF SECONDARY PARTICLES EMITTED FROM POST-ACCELERATION DETECTORS

G.H. Wang, C.F. Delwiche, W. Aberth and A.M. Falick
Department of Pharmaceutical Chemistry, University of California
San Francisco, California 94143-0446

Post-acceleration detectors (PAD) and conversion dynodes are widely used in organic mass spectrometry 1) to improve the sensitivity of detection of high mass and/or low energy ions and 2) to allow conventional electron multipliers to detect low-kinetic-energy negative ions. We have studied the secondary particles produced when positive or negative sample ions impinge on a PAD.

Initial experiments explored the effects of an applied electric or magnetic field on the secondary particles. No mass analysis of either primary or secondary ions was carried out in these experiments. It was found that 15-50% of the secondary charged particles formed from positive sample ions (from CsI or Ultramark 1621) are negative ions, with the remainder being electrons as expected. The secondary particles produced by negative sample ions and detected by the electron multiplier are positive ions. Full details of these measurements can be found in Ref. 1.

Subsequent experiments were aimed at specifically identifying the positive secondaries produced by negative ion impact on the PAD surface. The experimental set-up shown in Figure 1 was used. Negative sample ions were produced by directing a beam of Cs^+ ions (2) onto a sample stage held at a high negative potential. Either solid CsI or a mixture of fluorinated phosphazines (Ultramark 1621) were coated on the sample stage. The resulting negative ions were formed into a beam and focused onto a plane PAD electrode fabricated out of either stainless steel or aluminum. The PAD electrode was held at a few volts above ground potential to direct the positive secondary ions formed at the PAD surface towards the entrance of a quadrupole mass spectrometer (QMS). The QMS was equipped with a conventional conversion dynode and a channel electron multiplier (CEM).

Figure 2 shows the results obtained from a QMS scan of the positive secondary ions obtained from a beam of $(CsI)_nI^-$ ions. The $(CsI)_nI^-$ ions were not mass-analyzed prior to impinging on the stainless steel PAD electrode. Applied voltages were as indicated in Figure 1. The spectrum shown in Figure 2 strongly suggests that the major source of the positive ions is the layer of surface contamination present on the PAD electrode surface. The pressure in the vacuum system during this experiment was approximately $1x10^{-6}$ torr and the PAD electrode was exposed to the vacuum system for at least several hours after being cleaned before any spectra were obtained. At a pressure of $1x10^{-6}$ torr the time for deposition of a monolayer on a clean surface is approximately 1 sec. The sample beam current was about 10^{-14}A, which would be insufficient to clean the surface by sputtering.

Two further experiments were performed which tended to confirm that the ions observed came from surface contamination. First, the stainless steel PAD electrode was replaced with an aluminum electrode. The spectrum observed was virtually identical with Figure 2, indicating that under the experimental conditions used, ions from the electrode material itself are unimportant. Second, Ultramark 1621 was used as the sample in place of CsI. Again, no significant change was observed in the secondary ion spectrum, which implies that the sample ions are also not a major source of secondary ions.

References

1. G.H. Wang, W. Aberth and A.M. Falick, Int. J. Mass Spectrom. Ion Proc. (1986) 69, 233.

2. W. Aberth and A.L. Burlingame, in A. Benninghoven (Ed.), "Ion Formation in Organic Solids," Springer, Berlin, 1983, p. 167.

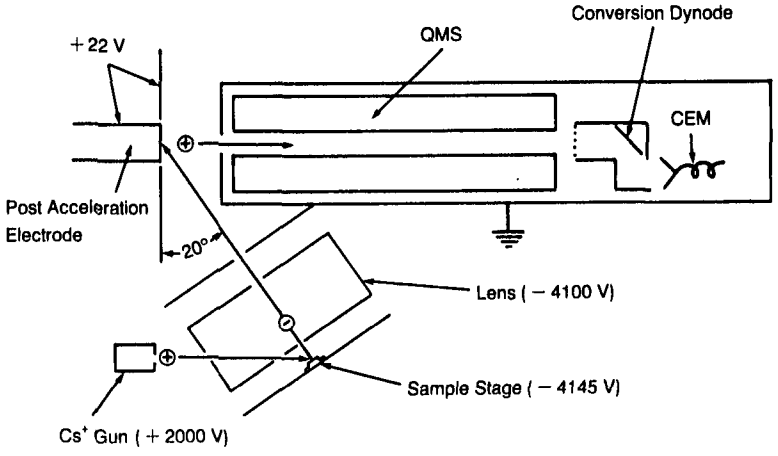

Figure 1. Experimental set-up used to analyze positive secondary ions formed at post-acceleration electrode.

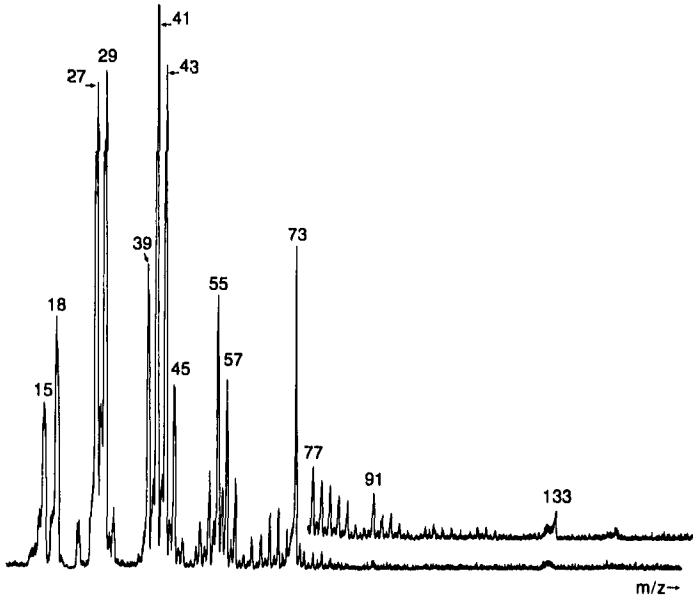

Figure 2. Mass spectrum of positive ions formed at post-acceleration electrode. Sample ions were negative $(CsI)_nI^-$ clusters.

ACKNOWLEDGEMENT. This work was supported by the NIH Division of Research Resources, Grant RR01614, (A.L. Burlingame, principal investigator)

A MULTIQUAD TRIPLE ANALYSER MS/MS/MS

C. BEAUGRAND, G. DEVANT, S.N. NERMAG, 49 Quai du Halage, F 92500 RUEIL-MALMAISON
C. ROLANDO, D. JAOUEN, Ecole Normale Supérieure, Département Chimie, 24 Rue Lhomond, F 75231 PARIS CEDEX 05

To investigate the MS/MS/MS technique, we chose to construct a Q/Q/Q instrument.
Compared to high energy collisions, low energy collisions offer the following advantages :
- Easier interpretation of spectra by analogy to wet chemistry in solution (less homolitic dissociation)
- More efficient reactive collisions.

Starting from a standard NERMAG R 30-10 MS/MS we have appended after the normal collision cell another analyzer followed by a new collision cell (1). This configuration is, in fact, a sextuple quadrupole which can be represented as follows :

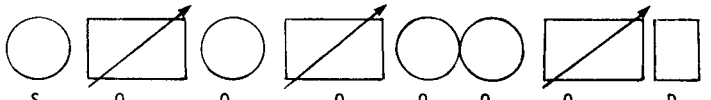

The analyzing quadrupoles Q_1, Q_3 and Q_6 provide unit resolution however for pratical applications a reduced resolution can be used on one of the first quadrupole Q_1 or Q_2. In this case sensitivity is about the same as a standard MS/MS.
We tested different MS/MS/MS modes and decided to classify them according to the function of each collision chamber. The interesting ones are the following :

Mode	Q_2	Q_4/Q_5	Application
1	CID	CID	Structure of a fragment formed during a first collision
2	Non dissociative collision	CID	Energy distribution of an activated molecule
3	Reaction	CID	Structure of a reaction product
4	Reaction	Reaction	Reactivity of new species

Only the first mode is common with high energy MS/MS/MS instruments. The others are specific to multiquad systems. To illustrate the possibilities of our instrument, an example in each mode is given :
Mode 1 CID of ion m/z = 242 from FAB ionization of Bu_4N^+, BF_4^- give an intense fragment at m/z = 142.
To identify the structure of this ion we recorded its CID spectra and compared it with CID spectra of various source ions.

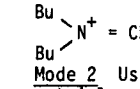

= CH_2 gives a very similar spectra
Mode 2 Using a high pressure in the first collision cell and retarding potetials, thermalisation or isomerisation of ions can be obtained. Looking at the intensity ratio of ions at m/z 91 and 92 coming from n-Butylbenzene while varying the first collision cell pressure, we find a reduction of 0,5 ev of internal energy.
Mode 3 The CID spectra of ion m/z = 114 coming from a reaction between 1-Hexane and a selected ion m/z = 58 of methyl vinyl ether is comparable to the CID spectra of the same ion obtained in the source under CI conditions.
Mode 4 New species can be generated by sequential reactions. A first reaction occurs between isobutane and a metal ion Ni^+ (m/z = 58) coming from a selection of ions generated by FAB ionisation of $NiCl_2$. A second reaction occurs between ammonia introduced in the second collision cell and an ion produced by the first reaction (m/z = 100). The produced ions are Ni^+, $Ni(NH_3)^+$ and $Ni(NH_3)_2^+$.

Triple sector quadrupole instrument offers specific advantages. Their are mainly due to the high efficiency of reactive collision and dissociative collisions obtained with quadrupole collision cell. More possibilities are offered by the various scanning modes available with such a machine and they will have to be investigated.

(1) A double collision cell ASMS San Diego p. 833 1985

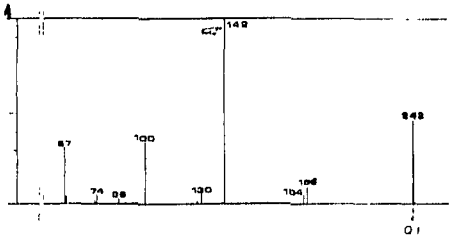

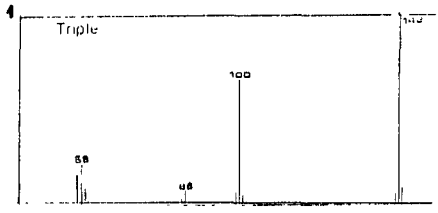

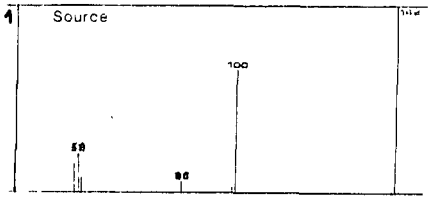

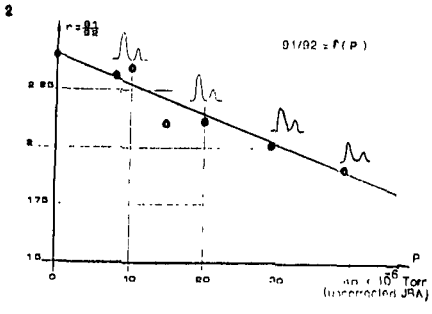

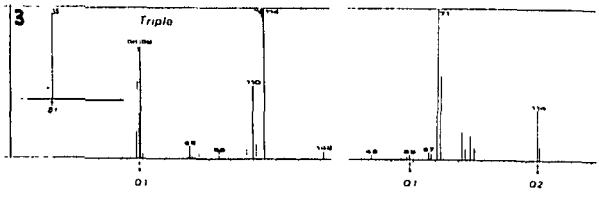

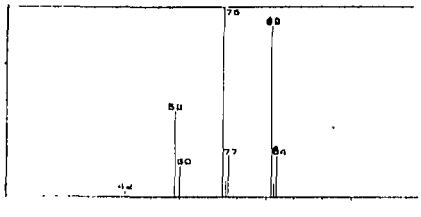

$$Ni^+ + C_3H_{10} \xrightarrow{CH_4} Ni(C_3H_8)^+ \xrightarrow{NH_3} Ni^+ + Ni(NH_3)^+ + Ni(NH_3)_2^+$$

The Design and Development of a Quinquequadrupole Mass Spectrometer

J.D. Morrison, K.A. Stanney, and J. Tedder
Chemistry Department, La Trobe University
Melbourne Australia and St. Andrews University, Scotland

The quadrupole mass filter is a simple and inexpensive solution to providing a mass spectrometer for chemical analysis and for energetic studies of ions. It is easy to attain modest mass resolution, but its main advantage has been the strong focussing property of the quadrupole lens, which makes it highly efficient, and very tolerant of poor vacuum, while resolution can be traded off against sensitivity by a simple voltage adjustment. It is also very easy to control the instrument digitally.

The triple quadrupole mass spectrometer, devised originally for ion photodissociation (IPD) studies, proved to have special advantages for analysis using the MS.MS technique, also could be used very successfully to study gas phase organic iron molecule reactions.

When ion photodissociation spectroscopy is used to study fragment ions, almost invariably the spectra obtained have no distinct threshold, and are almost featureless. This occurs because the fragment ions formed by electron impact are "hot", and populate a wide band of rovibrational states. It would be desirable to provide a drift space, where such ions could be relaxed, by collision with a suitable reagent gas.

The excellent transmission characteristics of the triple quadrupole encouraged us to extend the instrument by the addition of two more quadrupoles. This adds little in complexity, but enhances the scope of the instrument considerably. It not only provides drift spaces and collision regions for IPD work, but also make possible more complex ion reaction studies and MS.MS.MS.

Two such quinque- or penta-quadrupole instruments are under test, one in St. Andrews for ion chemistry the other at La Trobe for IPD work. Their basic design is shown in Figure 1.

Each quadrupole is driven by a separate supply, and can be operated either in mass filter or total, RF only, transmission mode. In mass filtering mode, at a resolution of 100, the transmission of each quad is ~18%, in RF only mode, ~30%.

There are many possible operating modes. The mass filters are usually operated with V_z = 9 ev, the RF only quads can be operated with V_z = 0.5 ev, to give longer residence times. Operation in the MS/MS/MS mode allows a unique and comprehensive study of both primary and secondary ion structure, derived from collisionally activated fragmentation and/or selective reactivity in ion molecule reactions brought about with a reactive collision gas.

$$\begin{array}{cccccccc} & & Q_1 & Q_2 & Q_3 & Q_4 & Q_5 \\ M + e & \text{———} & M^+ & \underline{\text{CID}} & F_1^+ & \underline{\text{CID}} & F_2^+ \end{array}$$

Combined with isotope labelling such reactions produce a very large amount of structural information. When charge transfer is occurring, we have obtained better transmission using segmented RF quadruples, giving a DC ramp (Figure 2).

MS/MS/MS can be carried out also by FTICR, but the maximum ion current which can be sustained is ~8000 ions. With the pentaquad, one can start with ~10^{-9} amp of primary ions, and still get ~10^{-12} amp at the final output. The equipment costs much less, data acquisition is much simpler, while the instrument can tolerate vacua of up to 10^{-4} torr.

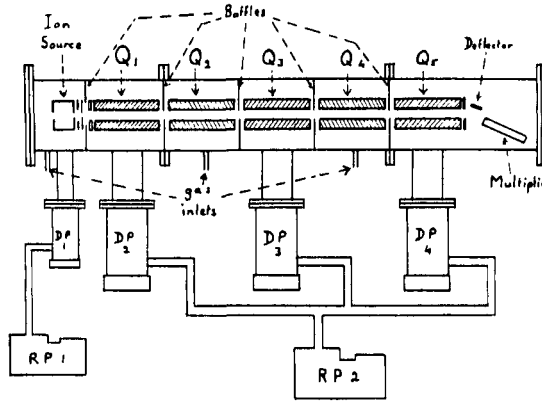

Figure 1 Schematic of quinque(penta)quadrupole MS.

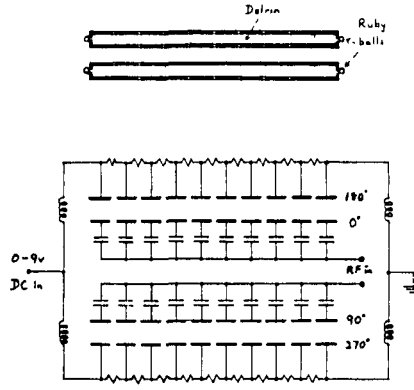

Figure 2

Segmented quadrupole used for charge transfer work, with method of supplying potentials.

SUPERCRITICAL FLUID CHROMATOGRAPHY-FOURIER TRANSFORM MASS SPECTROSCOPY, Jack Henion, and Edgar Lee, Drug Testing and Toxicology, New York State College of Veterinary Medicine, Cornell University, 925 Warren Drive, Ithaca, NY 14850; Robert Cody and James Kinsinger, Nicolet Analytical Instruments, 5225-1 Verona Road, Madison, WI 53711.

INTRODUCTION

The combination of supercritical fluid chromatography and Fourier transform mass spectrometry (SFC/FTMS) could offer some very useful analytical capability. SFC is well suited for the separation of components which exhibit low volatility or thermal instability in complex mixtures. Supercritical fluids possess properties which are intermediate between those of liquids and gases. Their higher diffusion coefficients and lower viscosities compared with liquids makes the analysis time for SFC separations shorter and the chromatographic efficiencies greater than those encountered in HPLC. The higher solvating power of supercritical fluids make SFC ideal for the separation of higher molecular weight and polyfunctional compounds which are not volatile enough for GC.

Fourier transform mass spectrometry (FTMS) has exciting analytical potential that could be utilized by its combination with either HPLC or SFC. However, the extremely demanding vacuum requirements of FTMS appear to preclude introduction of HPLC effluents as is done with modern LC/MS. The total effluent from capillary SFC, however, is not unlike that from capillary GC which has been successfully interfaced to FTMS. Therefore, if capillary SFC/FTMS could be accomplished, the accurate mass measurement and high molecular weight capability of FTMS could be available to on-line SFC. A SFC/FTMS system could be very useful to the analytical challenges of biotechnology and related areas. This work describes a preliminary investigation into the feasibility of capillary SFC/FTMS.

EXPERIMENTAL

The work was carried out as a collaborative effort between Cornell and Nicolet. The chromatographic system consisted of a Brownlee Laboratories dual-syringe Micro Pump charged with carbon dioxide and equipped with a Neslab Coolflow Model RTE 4 refrigerator for cooling the CO2 prior to entering the Micro Pump. A Valco micro-loop injector (Model A C14W) equipped with a digital volt interface and a SFC splitter was used to load samples onto the 0.050 i.d. x 5m fused silica capillary column housed in a Hewlett-Packard 5890 GC while the oven was maintained at 100 degrees. The stationary phase of the capillary column was 0.25 micron film thickness cross-linked SE-54 from Lee Scientific, Salt Lake City, UT. The exit of the analytical column was attached to a one meter "transfer line" capillary restrictor via a SGE mini union (MVSU/004). The fused-silica restrictor was deactivated by conventional methods and formed by drawing out the end of a 1 meter x 50 micron i.d. fused silica capillary in a micro flame to an inside diameter of approximately two microns. The capillary restrictor was inserted through a 0.200mm i.d. x 1m stainless steel capillary (Small Parts, Inc.) which was then "snaked" through the conventional GC/MS transfer line of the FTMS used in this work. The exit of the restrictor terminated at the entrance to the source cell inside the coil of the FTMS. All connections of the capillary tubing were made within the oven of the GC.

The FTMS instrument used in this work was a Nicolet FTMS-2000 equipped with a tandem source/analyzer cell positioned within the coil of the superconducting magnet. The system was operated in both the EI and CI modes with pressures maintained in the source (3-5 x 10 exp-5) and analyzer cells (1-4 x 10 exp-7) torr comparable to those experienced under equivalent GC/FTMS conditions. The transfer line between the GC and the vacuum inlet was heated crudely with heating tape while the remainder of the transfer line inside the vacuum system was not heated beyond that of its normal environment.

DISCUSSION

The initial goal of this work was to demonstrate that a working background pressure could be maintained in the FTMS vacuum system with continuous introduction of supercritical CO2. This was readily demonstrated although the analyzer pressure tended to remain on the high side of this range. However, by maintaining a suitably small capillary restrictor, a working pressure in the low 10 exp-7 torr could be maintained in the analyzer cell.

The next goal was to deliver a simple mixture through the system with the production of chromatographic profiles of the ion current and the corresponding mass spectra. This

was done using a mixture of methyl stearate and caffeine. The corresponding CI mass spectra for these compounds were consistent with that expected from conventional CI MS. Although one goal of this work was to successfully analyze a sample containing an involatile, high molecular weight compound, this was not achieved. This presumably resulted from difficulties encountered maintaining supercritical conditions in the one-meter capillary restrictor. Without careful heating of the entire length of the capillary path, it is difficult to maintain supercritical conditions necessary for chromatographing such materials.

Finally, the remaining goal of achieving accurate mass measurement under SFC/FTMS conditions was met. Under EI SFC/FTMS conditions accurate mass measurement of the molecular ion (m/z 194) from caffeine (25ng) gave an experimental value within 0.36 ppm of the calculated value in addition to measured values for the remainder of the major fragment ions observed in the EI SFC/FTMS mass spectrum of caffeine. The EI SFC/FTMS mass spectrum of caffeine was also obtained under low pressure conditions.

CONCLUSIONS

The feasibility of capillary SFC/FTMS is demonstrated by this work. Although the high mass range capability of FTMS was not accomplished here, it appears certain that improved delivery of the heated supercritical fluid could achieve this remaining goal. It remains a challenge, however, to carry out chromatography/FTMS experiments while maintaining optimum pressures in the FTMS vacuum system. The superior resolving power and high mass capability of FTMS can be seriously compromised by elevated pressures in the analytical source cell. When it becomes possible to routinely deliver components from a chromatographic effluent while maintaining very low pressures, SFC/FTMS could be a very powerful analytical technique.

THE EFFECTS OF RESIDUAL SPATIAL MAGNETIC FIELD INHOMOGENEITIES ON FOURIER TRANSFORM ION CYCLOTRON RESONANCE SPECTRA

Frank H. Laukien, Dep. of Chemical Physics, Harvard University, 12 Oxford St, Cambridge, MA 02138 (U.S.A.)

INTRODUCTION

Theoretical expressions for the shifts in the FTICR eigenfrequencies, and for the spectral broadening due to residual spatial magnetic field inhomogeneities are calculated. Modulation effects are analyzed, and upper limits for the mass resolving power $m/\Delta m$ in the presence of different types of residual field gradients are derived. Numerical estimates of all results are computed for a typical 4.7 Tesla cryo-shimmed supercon Spectrospin™ magnet. Finally, from these theoretical results more sensitive techniques for FTICR shimming, and for improved ultra-high resolution measurements are developped.

METHODS

A detailed analysis of the magnetic field strength variation reveals that transverse magnetic field components are of negligible importance in FTICR. It suffices to analyze the more important effects of residual spatial variations of the axial magnetic field component, B_z. In an orthogonal, scalar expansion of $B_z(\rho,\phi,z)$ the dominant field strength inhomogeneities are z-gradients, $g_z \equiv (\partial B_z/\partial z)$ = constant, x- and y-gradients, $g_x \equiv (\partial B_z/\partial x)$ = const., and radial gradients, $g_\rho \equiv (\partial B_z/\partial \rho) \propto \rho$; the shifts and spectral broadening effects of the dominant residual gradients are analyzed by introducing the forces associated with each gradient into the equations of motion and solving them.

Moreover, the effects of modulation and motional narrowing must be taken into account. From geometrical considerations it can be shown that in FTICR the spectral broadening due to g_z is motionally narrowed by the trapping motion at angular frequency ω_t; the spectral broadening due to g_x and g_y is modulated by ω_c and ω_m, but the field variation due to a spread in the cyclotron radii, $\Delta\rho_c$, in the presence of a radial gradient g_ρ is not motionally narrowed at all. Upper limits of the mass resolving power can be derived. When modulation does occur the resolution is given by $(m/\Delta m) \leq (B/\Delta B)^2 \cdot (\omega_{mod}/\omega_c)$.

RESULTS

1. Z-gradients

It is found that higher-order (non-constant) terms in g_z shift the angular trapping frequency ω_t by approximately (500/M) ppm, where M is the mass in amu. The cyclotron frequency ω_c is not shifted by g_z. Finally, the total field strength variation which thermal ions experience because of g_z are very small, and are rapidly modulated at ω_t. Even in cryo-shimmed magnets, the theoretical upper resolution limit given by g_z is of the order of 10^{12} - hardly a limitation.

2. X-and y-gradients

Higher-order terms introduce relative shifts in the cyclotron frequency of about 0.1 ppm, whose functional dependence is given by the proportionality $\Delta\omega_c(g_x) \propto (q/m)\rho_c^2$.

The force $\vec{F}$ on the ions' constant magnetic moment μ, which is associated with g_x, gives rise to constant drift velocity $\vec{v}$, given by $\vec{v} = (1/qB^2)\vec{F} \times \vec{B} = (q/2m)g_x\rho_c^2\hat{j}$. For accelerated ions, $\vec{v}$ can reduce the ion trapping (and observation) time to a few seconds, if $\vec{F}$ is not balanced by electrostatic "shimming" . Further, $\vec{v}$ reduces the trapping time of thermal ions below the value calculated from a random-walk type diffusion model, which is in qualitative agreement with experiment.

The upper limit of the mass resolving power $m/\Delta m$, as posed by the "slow" averaging at the magnetron frequncey ω_m of the smaller field variation $2g_x\rho_{gc}$, is typically about two orders of magnitude lower than the upper limit posed by the "fast" averaging at ω_c of the larger field variation $2g_x\rho_c$. Hence, the FTICR resolution in the presence of g_x is not determined by ω_c and ρ_c, but is ultimately limited by ω_m and ρ_{gc}, according to $m/\Delta m \leq (B/2g_x)^2 \cdot (\omega_m/\omega_c) \cdot (\rho_{gc})^{-2}$. Typical numerical values are 10^9 with cryo-shims only. Additional room-temperature shims improve the resolution by a factor between 500 and 10,000.

3. Radial gradients g_ρ

Radial gradients introduce relative shifts of the cyclotron frequency of about 0.5 ppm, according to $\Delta\omega_c = (q/2m)g_\rho\rho_c \propto \rho_c^2/m$. Unlike other shifts in FTICR, $\Delta\omega_c(g_\rho)$ is mass-dependent, and mass differences and calibrations consequently depend on absolute mass. The field variation due to g_ρ over an ensemble of ions with a spread $\Delta\rho_c$, which is not modulated, limits the resolution to $m/\Delta m \propto B/\{\rho_c \cdot \Delta\rho_c + \rho_{gc}^2\}$; for realistic values, the pressure-independent limit of $m/\Delta m$ in cryo-shimmed magnets is approximately 10^8. Additional room-temperature shims will increase the mass resloving power by a factor of 20 to 100. It is evident that $\Delta\rho_c$ and ρ_{gc} have to be minimized in ultra-high resolution experiments. $\Delta\rho_c$ can be minimized by accelerating slowly on the time scale of the magnetron motion, i.e. with $T_x \leq T_m$, and ρ_{gc} can be reduced by properly aligning a narrowly focussed electron beam with the axis of symmetry of $V(\rho,z)$.

IMPROVED SHIMMING AND HIGH-RESOLUTION MEASUREMENT TECHNIQUES

The general shimming philosophy is to atrificially accentuate the spectral broadening effect of the various gradients to be shimmed, in order to sensitively eliminate them. In all cases it turns out to be advantageous to shim with the smallest mass measurable (e.g. H_2^+), since inhomogeneity broadening for all gradient types is most pronounced for small masses.

Specifically, g_z should be reduced after deliberately increasing $\hat{z}$, the amplitude of the trapping motion, by accelerating the ions with a slight positive frequency offset $\Delta\omega \equiv \omega_{ac} - \omega_c > 0$; conversely, in high-resolution studies, the ions should be accelerated with a small negative frequency offset $\Delta\omega < 0$, in order to dampen $\hat{z}$.

The effective signal-decay time which can be associated with g_x has the functional dependence $\tau(g_\rho) \propto m^2/g_x^2\rho_{gc}^2$. Consequently, the guiding-center radius should be actively increased by temporarily biasing two sideplates asymmetrically by 0.1 Volts for 5 msec in order to increase ρ_{gc} to about 1cm. Afterwards the spectral broadening due to g_x will be much more pronounced, and can be shimmed sensitively for small masses. Obviously, in high-resolution experiments ρ_{gc} must be minimized.

The effective elimination of radial gradients is most critical , because g_ρ introduces both, measurable frequency shifts, and unmodulated spectral broadening. The effective signal-decay time for g_ρ is derived to be proportional to $\tau(g_\rho) \propto m/\{\rho_c \cdot \Delta\rho_c + \rho_{gc}^2\}$. Since $\Delta\rho_c$ is difficult to control experimentally, the same trick as in the g_x shimming technique can be employed to deliberately increase ρ_{gc}, while shimming g_ρ with the smallest measurable mass. For ultra-high resolution measurements both, ρ_{gc} and $\Delta\rho_c$ must be minimized.

TAILORED EXCITATION FOR FT/ICR MASS SPECTROMETRY

Alan G. Marshall,[a,b] Tao-Chin L. Wang,[a] Ling Chen,[a] and Tom L. Ricca[c]

Department of Chemistry[a]
Department of Biochemistry[b]
Chemical Instrument Center[c]
140 West 18th Avenue
Columbus, OH 43210

For a linear system (i.e., amplitude of the response is proportional to amplitude of the excitation), the time-domain and frequency-domain representations are related by a Fourier transformation. Because the ion cyclotron resonance experiment connects mass to frequency (1), one can construct ("tailor") any specifed mass spectral editing (e.g., flat power over a specifed mass range; flat power with windows or steps; non-linear power; or simultaneous power at several selected m/z-values only), by computing the inverse Fourier transform of the desired frequency-domain excitation to give the corresponding time-domain excitation waveform (2).

The large vertical dynamic range for the time-domain signal (top middle of Fig. 1) obtained by inverse FT of a constant-phase rectangular-magnitude frequency spectrum presents several practical difficulties: high transmitter power (because most of the excitation power is compressed into a small fraction of the excitation period); non-linearity in the transmitter electronics; and round-off errors from limited computer word length. These problems can be removed by frequency-domain phase modulation. Pseudo-random phase modulation (middle row of Figure 1) reduces the time-domain vertical dynamic range, but zero-filling reveals major irregularities in the final excitation magnitude spectrum. In contrast, quadratic ("chirp") phase modulation (bottom row of Figure 1) achieves the desired reduction in time-domain vertical dynamic range, and gives an optimally flat final excitation magnitude spectrum.

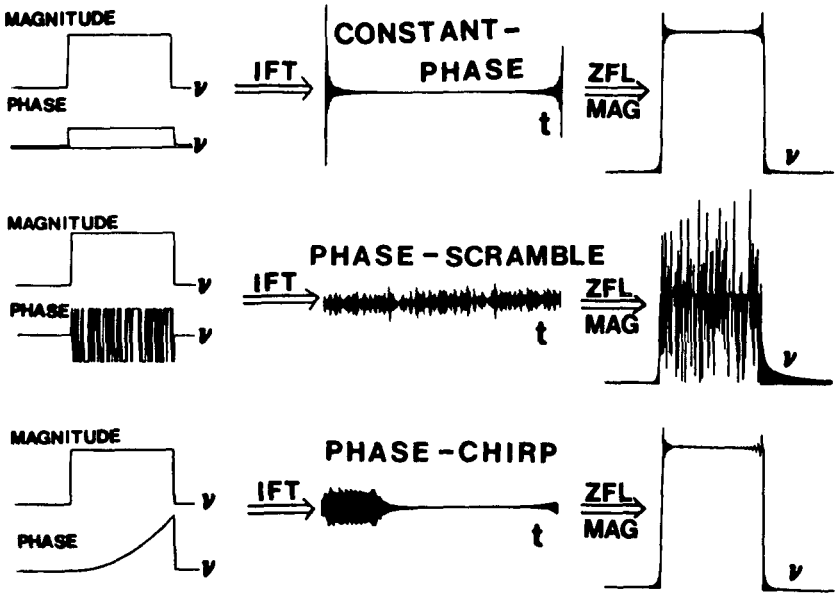

Figure 1. Frequency-domain excitation profiles (left), specified by their magnitude and phase spectra, were inverse Fourier transformed to give their corresponding time-domain waveforms (middle). The time-domain waveforms were then zero-filled and Fourier transformed to reveal the detailed magnitude-mode spectra (right) "at" and "between" the originally specified discrete frequencies.

The present Stored Waveform Inverse Fourier Transform (SWIFT) technique produces much more uniform excitation amplitude and better mass selectivity (see Figure 2c) than the frequency-sweep excitation (Figure 2a) used in all present FT/ICR spectrometers (3,4). Even better results are achieved when phase modulation (Figure 2d) and/or prior apodization of the time-domain waveform (Figure 2e) are introduced.

We have used SWIFT excitation for: improved precision in isotope-ratio measurements; high-resolution MS/MS; entension of FT/ICR mass spectral vertical dynamic range via selective multiple ejection of abundant ions of several m/z-values; simultaneous multiple-ion monitoring; multiple ejection of ions of selected m/z-values simultaneous with excitation of ions of other m/z-values; excitation with specified non-uniform power at different m/z-values; etc. Finally, although the above SWIFT experiments were conducted by applying the waveform to the transverse (to the applied magnetic field) plates of an ICR cell, the method can also be used to excite longitudinal motion in an ICR or Penning-type ion trap, to achieve simultaneous selective ejection of ions of one or more m/z-values.

[This work was supported by N.I.H. 1 R01 GM-31683, N.S.F. CHE-8218998 and the Ohio State University.]

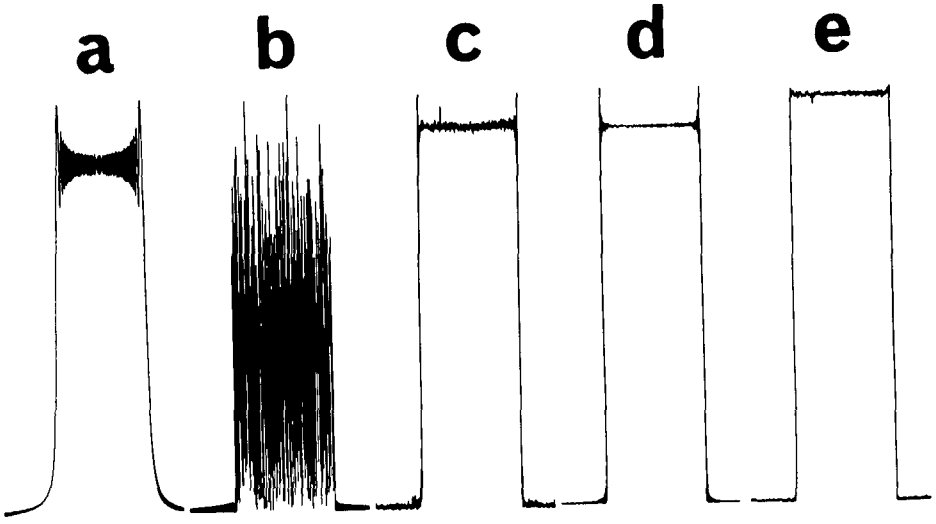

Figure 2. Experimental magnitude-mode FT/ICR excitation spectra, obtained via receive-during-transmit detection, with one zero-fill.

(a) Time-domain frequency-sweep
(b) Phase-scrambled SWIFT
(c) Constant-phase SWIFT
(d) Phase-chirp SWIFT
(e) Phase-chirp SWIFT, apodized by reducing the time-domain signal at both ends

References

1. Marshall, A. G. (1985) Acc. Chem. Res. 18, 316-322.
2. Marshall, A. G.; Wang, T.-C. L.; Ricca, T. L. (1985) J. Amer. Chem. Soc. 107, 7893-7897.
3. Comisarow, M. B.; Marshall, A. G. (1974) Chem. Phys. Lett. 26, 489-490.
4. Marshall, A. G.; Roe, D. C. (1980) J. Chem. Phys. 73, 1581-1590.

MAXIMUM ENTROPY METHOD IN FOURIER TRANSFORM MASS SPECTROMETRY

A.Rahbee
Air Force Geophysics Laboratory, Hanscom AFB, MA 01731

Fourier transform mass spectrometry is based upon simultaneous measurement of ions and subsequent analysis of a time domain signal by the FFT based techniques. The method has not proved very useful In some geophysical phenomena, in which the measured time signals are of such short duration that none of the traditional transform techniques yield satisfactory results. In 1967, J. P. Burg, recognizing shortcomings of the FFT based methods as applied to short duration signals, suggested a new method for spectral analysis based on the principle of maximum entropy (1). The method which is known as the maximum entropy method (MEM), basically avoids the zero-filling required by the FFT method and thus does not add any information to the data where it is not measured. The Burg MEM method, uses very few data points to project the existing data into the future and in the process, it calculates a set of coefficients that constitute a time domain filter. As it turns out the form of the spectral density derived by Burg is the same as that obtained in the auturegressive modelling of the time series (2). Basically the future values of the time series are predicted by a linear combination of the measured values and the "prediction error" is minimized to calculate the filter coefficients. The spectrum is then inversely proportional to the power response of the filter.

In a recent publication (3), Burg's algorithm was applied to time domain signals from a Nicolet FTMS-1000 in this laboratory and it was demonstrated that both the quality and resolution in the spectrum obtained by MEM were very much improved. The sidelobes were also absent. Application to single and two ion time signals with moderate resolution have been demonstrated. In most cases data length made up of as few as 100 points have provided superior results. More recently the method has been applied to the signals obtained in the heterodyne mode of the FTMS and resolutions (at 50% points) approaching 6 million have been recorded at a magnetic field value of 1.19 Tesla (4).

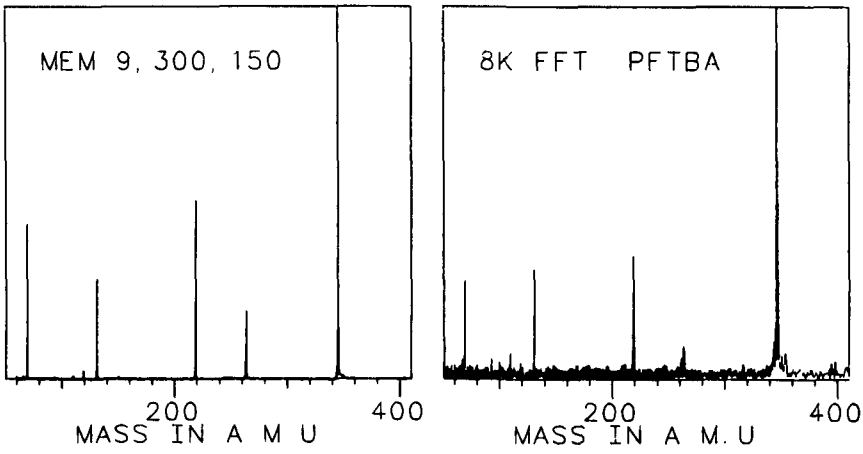

FIGURE 1. MASS SPECTRUM OF PFTBA BY MEM AND FFT METHODS

In addition to this work we have extended the technique to multi-ion signals by employing PFTBA in the spectrometer cell. Figure 1 shows the mass spectrum of this compound using both available methods. The MEM spectrum was obtained using 300 data points starting with point 9 and calculating 150 filter coefficients. The important implication of this new method of time series analysis is the fact that the relative amplitudes of the various sinusoids in the signal can be determined very early in the detection cycle and before the ions undergo appreciable decay due to collisions. This can be significant if ionic species have different collisional decay rates. To demonstrate this , a synthesized time signal made up of two sinusoids was employed in the analysis. One sinusoid had a constant amplitude in time while the other decayed exponentially. These two sinusoids were then added and used as a single time domain sugnal. Figure 2a shows the envelopes of these sinusoids. The initial amplitude of the decaying sinusoid was bigger by a factor of 2. Figure 2b is a plot of the amplitude ratios aganst the number of data points for the FFT. for MEM the first 100 points were used. It can be seen that erronenous ratios are obtained with FFT while MEM applied very early in the time signal provides the correct ratio. This result may have important implications for the chemical experiments done using FTMS.

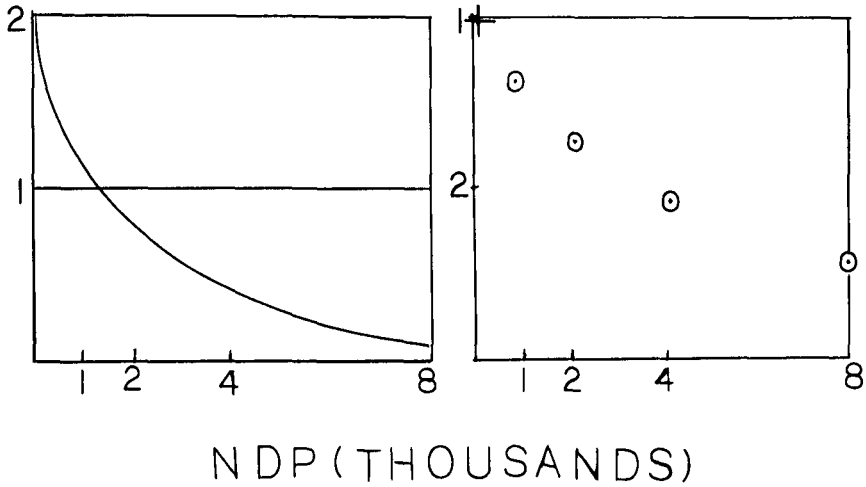

FIGURE 2. LEFT PANEL: ENVELOPES OF TWO SYNTHETIC SINUSOIDS
RIGHT PANEL: AMPLITUDE RATIOS BY (O) FFT, (+) MEM

(1) Burg, J.P., in "Modern Spectrum Analysis" D.G. Childers, ed. IEEE Press, New York. 1978, p.34.
(2) Ulrych, T.J. ; and Bishop, T.N. Rev Geophys., 13(1975)183
(3) Rahbee, A.,Chem.Phys. Letters, 117(1985)352.
(4) Rahbee, A., accepted for publication in IJMSIP.

ACCURATE MASS MEASUREMENTS MADE WITH SOFT IONISATION TECHNIQUES:-
A NEW APPROACH ALLOWED BY A UNIQUE ELECTROMAGNET DESIGN.

R.H. Bateman, R. Owen, V.C.Parr, D.Wood, VG ANALYTICAL FLOATS ROAD, WYTHENSHAWE, MANCHESTER M23 9LE, UK.

When mass measurements are made using conventional double focusing sector instruments fitted with solid core electromagnets a complex calibration procedure is required to fit the instrument scan law. This is due to the non-linearity of the magnet and the presence of hysteresis effects. This requires that a reference compound be present at the same time as the sample which in turn requires that the instrument be operated at a minimum of 3000 resolving power.

A new electromagnet has been developed and incorporated into a new instrument, the VG TS-250, using a non ferrous core which eliminates the non-linearity and hysteresis effects [1]. A summary of the ability to predict masses in a static manner is shown in table 1, where the instrument was tuned to the peak tops of the masses listed and the current through the coil was measured.

The consequence of the static results is that we can predict the mass focussed at the collector from the following equation.

$$M = K (I - dI)^2 \quad \text{- equation (1)}$$

where, I = the demanded current, K = a constant and dI = a small offset

When we scan the current to obtain a spectrum we do so by programming it as an exponentially decaying function of time.

$$\text{i.e.} \quad I_{demanded} = I_{start}\, e^{-t / T1}$$

where, I_{start} = the start current for the scan and T1 = the time constant.

In practice we must add a second exponential term to account for the dynamic characteristic of the current regulated power supply. Thus equation (1) becomes;

$$M(t) = K (I_{start}\, e^{-t / T1} + dI_1 e^{t / T2} - dI)^2$$

where dI_1 and T2 are the constants for the supply function.

This equation can be reduced to a form where there are five constants, thus a minimum of five points are needed to establish these values. Given five peaks the equation is solved by a numerical gradient search method [2].

Table 2 shows results obtained by using this method on a PFK scan taken at 1000 resolving power and 5s per decade scan rate. The rms error for the scan is 0.9 mmu, thus showing how well the theoretical model fits the real data.

Once the "shape" of the scan function has been determined in this way provision need only be made for one lock mass within a scan of a sample to correct I_{start} for any drift.

The effect of the second exponential term is isolated to the start of the scan so provision can be made to ignore this term in cases where the peaks of interest are removed from the start mass (say after the first 100 amu).

An example is shown in figure 1 for data acquired at 2s per mass decade with a start mass of 500, three points were used from the electron impact spectrum then exchanged for the chemical ionisation one and a spectrum of methyl stearate was acquired under ammonia CI conditions. A lock mass was used at m/z 148 from amyl acetate ($M+HNH_4$). A spectrum of the stearate is shown in figure 1(b) showing the elemental composition report for the pseudo molecular ion.

The ability to accurately define the instrument scan law from as few as three points greatly facilitates the procedures involved in carrying out accurate mass measurements. In particular the subsequent need for only one lock mass in the scans of interest facilitates this mode of operation when using soft ionisation techniques.

References

(1) Presented at IMSC 10, Swansea, UK, September 1985
"A novel general purpose double focusing mass spectrometer"
R.H. Bateman, P. Burns, R. Owen, V.C. Parr

(2) The Davidson - Fletcher - Powell method

Current (I)	Calculated Mass*	Accurate Mass	Error (mmu)
95 6924	252 8334	252 8354	-2 0
94 5526	246 8413	246 8443	-3 0
88 8356	217 8701	217 8666	3 5
87 6058	211 8743	211 8754	-1 1
80 0578	176 9071	176 9066	0 5
72 2206	143 9349	143 9348	0 1
71 4578	140 9071	140 9066	0 5
67 1524	124 4212	124 4207	0 5
65 3814	117 9375	117 9377	-0 2
61 9702	105 9378	105 9377	0 1
55 1758	83 9546	83 9534	1 2
42 1848	48 9845	48 9845	0 0
34 0896	31 9899	31 9898	0 1
31 9016	28 0082	28 0061	0 1
25 5982	18 0099	18 0106	-0 7

* Mass = $K(I-I_s)^2$ $K = 2\ 76569 \times 10^{-4}$ $I_s = 0\ 0798$

Table 1

TABLE OF MASS ERROR AGAINST MASS

1000 R.P. 5s/decade

NO	ACC.MASS	CAL. MASS	ERROR(MMU)
1	454.9728	454.9721	0.75
3	430.9728	430.9748	1.9
5	392.9760	392.9758	-0.2
7	354.9792	354.9793	0
9	330.9792	330.9803	1.0
11	292.9824	292.9813	-1.1
13	254.9856	254.9847	-0.9
15	230.9856	230.9862	-0.6
17	204.9888	204.9882	-0.6
19	180.9888	180.9887	0
21	161.9904	161.9897	-0.7
23	142.9920	142.9907	-1.3
25	118.9920	118.9912	-0.8
27	99.99360	99.99274	-0.9
29	80.99520	80.99633	-1.1
31	51.00460	51.00489	0.3

MEAN ERROR = -0.2769963 MMU
RMS ERROR = 0.9364488 MMU

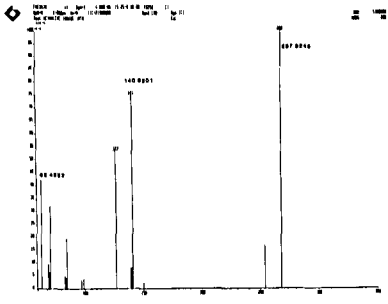

Fig 1a

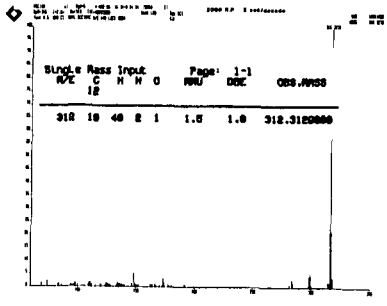

Fig 1b

INTERLABORATORY COMPARISON OF NEGATIVE CHEMICAL IONIZATION MASS SPECTRA: ELECTRON ENERGY DISTRIBUTION

Casey Grimm[a], Ralph Dougherty[b], William Budde[b], William Eichelberger[b], R. L. Foltz[c], C. Sakashita[c], Ronald Hites[d], and Elizabeth Stemmler[d].

a) Department of Chemistry, Florida State University, Tallahassee, Florida 32306; b) U. S. Environmental Protection Agency, EMSL, 24 West St. Clair Street, Cincinnati, Ohio 45268; c) Center for Human Toxicology, University of Utah, Skaggs Hall, Salt Lake City, Utah 84112; d) School of Public and Environmental Affairs, 410 H, Indiana University, Bloomington, Indiana 47405.

It has been known for many years that Negative Chemical Ionization (NCI) mass spectra have been subject to irreproducibility between laboratories and within the same laboratory. A number of factors have been identified which are known to contribute to this difficulty in reproducibility. These include: the concentration of oxygen in the ion source; the temperature of the ion source; the reagent gas within the ion source; the pressure of the reagent gas and the energy of the primary ionizing beam.

It is well known that in any interlaboratory comparison, the number of variables between laboratories is considerable. In spite of the fact that great effort is made on the part of all investigators to reproduce experimental conditions exactly from laboratory to laboratory, it is inevitable that some failure to reproduce specific details of the experiment will occur. This happened in this experiment, like all others. The remarkable feature of this experiment is the fact that the data from the participating laboratories was by and large constant. That is, the shape of the curves for detection limits of a series of specific electron capturing molecules was very similar from laboratory to laboratory (see Table 1 for the molecules and the specific disassociative and resonance capture reactions that were studied in this particular experiment).

There are many details featured in the data obtained from the participating laboratories which yield insights into the processes occurring in the individual mass spectrometers. For example, the sensitivity for NO_2^- in the Hewlett Packard instrument was unusually low as compared to the other instruments studied. This may reflect a more complete thermalization of the electron beam in that instrument. The sensitivity data for the compounds which capture electrons of lower energy, however, do not substantiate this.

Figure 1 illustrates a typical plot of log detection limit $^{-1}$ vs. the electron energy maximum for disassociative and resonance capture processes.

Figure 2 illustrates the relationship between the least squares fit of the log detection limit $^{-1}$ vs. the electron energy for the processes studied. This graph also contains a plot of the fit of the Boltzman distribution for a temperature for 150°C on the same plot. It is clear that the two energy distributions are not the same. The probable reason for this is the fact that equalibrium has not been established for the negative chemical ionization source of the Finnegan 4510 mass spectrometer used for this graphic. This is not surprising in that it has been known for 20 years that chemical ionization mass spectra represent quasi-equalibrium processes which are perturbed by the time dependents of the introduction and the exit of the reagent from the system.

REFERENCES

L. G. Christophorou, R. N. Compton, G. S. Hurst and P. W. Reichardt, J. Chem. Phys., 45, 536-547 (1966).

Ibid. 49, 1526-31 (1968).

TABLE 1

		ϵ_{max} (eV)
	$M^{-\cdot}$	0.0
	$M^{-\cdot}$	0.0
	Cl^-	0.36
$CHCl=CCl_2$	Cl^-	0.39
$CH_2ClCHCl_2$	Cl^-	0.42
	Br^-	0.84
	Cl^-	0.86
	Br^-	0.93
	Cl^-	1.1
	NO_2^-	3.5

FIGURE 1

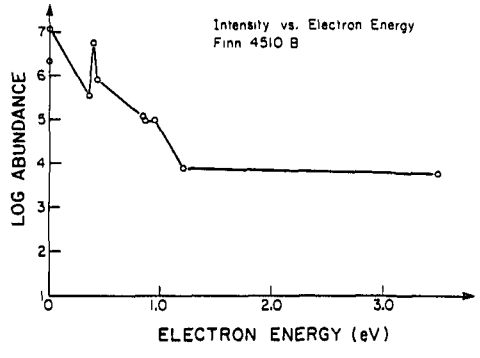

FIGURE 2

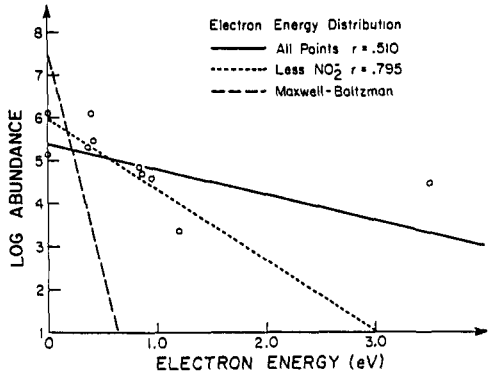

THE ROLE OF NEGATIVE ION MASS SPECTROMETRY IN THE DETECTION OF POLYCHLORINATED DIBENZOFURANS, BIPHENYLOLS AND DIPHENYL ETHERS IN MICHIGAN SPORT FISH: H.A. Price, R.H. Scheel, L.A. Warren and R.L. Welch, Center for Environmental Health Sciences, Michigan Deptment of Public Health, Lansing, Michigan 48909

Negative ion mass spectrometry (NI-MS) has become an important part of our analytical monitoring program of Michigan sport fish (both Great Lakes and inland waterways fish) and fisheaters for chlorinated pesticides, polchlorinated biphenyls (PCBs) and other environmentally related chemical contaminants.

Gas chromatography with electron capture detection (GC-ECD) is used for the quantitative analysis phase of the monitoring program. Confirmational analysis of these biological samples for the chemical compounds mentioned above is done by gas chromatography-mass spectrometry (GC/MS). Although these biological samples undergo extensive sample preparation prior to instrumental analysis (ref. 1), confirmational analysis by low resolution mass spectrometry in the electron impact ionization mode (EI-MS) yields disappointing results due to the interference of that portion of the sample matrix that comes through the sample cleanup procedure as well as the low levels of the chemical compounds themselves (figure 1). However, NI-MS because of its high sensitivity and selectivity for halogenated organic compounds even in the presence of biological tissue matrices, has now been incorporated into our analytical scheme as a confirmational tool.

Polychlorodibenzofurans (PCDFs) have been shown to be unintentional byproducts produced in the manufacturing of PCBs. The levels of PCDFs in PCBs can vary from 1 to 10 ppm with some samples reaching 33 ppm (ref. 2). The identification of PCDFs in biological tissues is made more difficult by the possible presence of polychlorinated diphenyl ethers (PCDPEs) and polychlorobiphenylols (PCBols). Using +EI-MS, PCDPEs yield intense ($M - Cl_2$) ion species with the same exact mass value and number of chlorines as a corresponding PCDF. Likewise, it was proposed that certain isomers of the PCBols would form ($M - Cl_2$) ion fragments again with the same exact mass and chlorine number as certain corresponding PCDFs.

It was hoped that the above problem of identifing PCDFs in the presence of PCDPEs and PCBols could be circumvented by the use of NI-MS to generate very stable parent molecular anions with little or no fragmentation (as noted above) and whose exact mass would be two mass units above those for the corresponding PCDFs. However, using NI-MS with methane as the reagent gas (ref. 3), *ortho*-chloro substituted PCDPEs were found to yield intense (M - HCl) anion fragments corresponding to certain PCDFs (figure 2). *ortho*-chloro-*ortho*-hydroxy substituted PCBols were also found to yield intense (M - HCl) anion fragments as well as (M + H - Cl) fragments. Without further sample preparation, resulting in the separation of the PCDPEs and PCBols from the PCDFs (ref. 4), the use of NI-MS appears to be of little value over +EI-MS in the identification of PCDFs in biological samples with the exception of its increased sensitivity for these compounds.

However, by generating single ion current (SIC) chromatographic tracings for the parent molecular anions of the PCDFs, PCDPEs and PCBols, one can quickly survey a biological extract for the possible presence of these compounds. One such survey scan for a Saginaw River fish pool (fraction III) extract is shown in figure 3 with SIC tracings for 304 and 306 (possible tetrachlorodibenzofurans) and for 340 (possible pentachlorodiphenyl ethers) along with the total ion current (TIC) chromatogram. The mass spectrum for the TIC chromatographic peak at 20.7 minutes (figure 4), which includes the 304, 306 and 340 mass ions, reveals a tetrachloro anion fragment at 304 amu, possibly corresponding to an isomer of a tetrachlorodibenzofuran. However, the pentachloro anion group at 340 amu suggests that this chromatographic peak is attributable to a pentachlorodiphenyl ether with its major fragment at 304 (M - HCl) and not to a PCDF.

Although we were not able to positively identify any PCDFs without further sample preparation, we were able to detect a number of PCDPEs in sport fish taken from various inland waterways throughout Michigan as well as fish taken from Lake Michigan by surveying each fish/fish pool extract with GC/NI-MS. As a result of these preliminary investigations, we intend to investigate the amounts of PCDPEs in Michigan sport fish in our future fish monitoring studies.

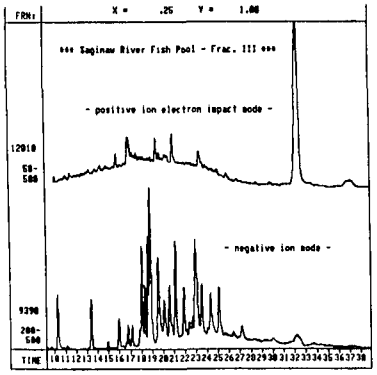

Figure 1. EI- and NI-TIC chromatograms for fish extract.

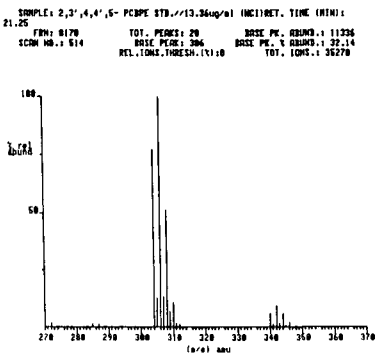

Figure 2. NI-mass spectrum for a pentachlorodiphenyl ether standard.

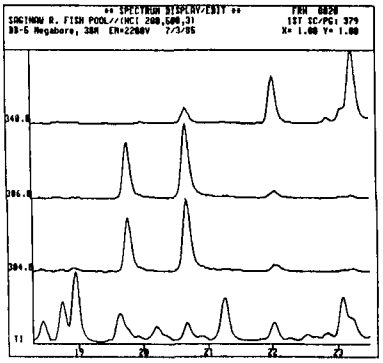

Figure 3. TIC and SIC chromatographic tracings for a fish extract.

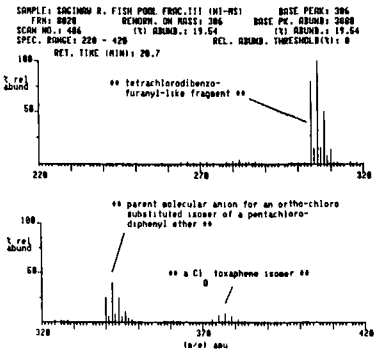

Figure 4. Mass spectrum of the chromatographic peak at 20.7 min.

References:

1.) H.A. Price, R.L. Welch, R.H. Scheel and L.A. Warren, Bull. Environ. Contam. Toxical., 37 (1), 1986

2.) R.D. Kimbrough, Ed., "Halogenated Biphenyls, Terphenyls, Naphthalenes, Dibenzodioxins and Related Products", Elsevier/North-Holland Biomedical Press, Amsterdam, New York, Oxford, 1980, p 7

3.) K.L. Busch, A. Norstrom, M.M. Bursey, J.R. Hass and C.A. Nilsson, Biomed. Mass Spectrom., 6 (4) 1979, 157-161

4.) H.R. Buser, J. Chromatogr., 107 (1975) 295-310
P.W. Albro and C.E. Parker, Ibid, 197 (1980) 155-169

THE QUANTITATION OF TOXAPHENE IN ENVIRONMENTAL SAMPLES USING NEGATIVE ION MASS SPECTROMETRY

Deborah L. Swackhamer, M. Judith Charles, and Ronald A. Hites
School of Public and Environmental Affairs and Department of Chemistry
Indiana University, Bloomington, Indiana

Toxaphene is a widely used pesticide consisting of a mixture of chlorinated camphenes. The primary components of this mixture are bornanes and bornenes having 6 to 10 chlorines. Used as an insecticide on cotton, soybean, and peanut crops and on cattle parasites, it was banned in the U.S. in 1982 due to its toxicological properties and environmental persistence.

Because of its complex nature and the fact that it is often found as a trace component among many other chlorinated contaminants such as PCBs and pesticides, toxaphene is very difficult to analyze. The purpose of our study was to develop an accurate method for quantitating toxaphene in environmental matrices. GC/MS provides selectivity compared to GC-ECD. A comparison of the EI, PCI, and NI spectra of toxaphene components revealed that the EI spectra were characterized by extensive fragmentation relative to the other methods. The NI spectra had the lowest degree of fragmentation and provided the greatest selectivity and sensitivity.

Our NI spectra were obtained at a source temperature of 100 C and pressure of 0.35 torr. Methane was the enhancement gas. GC conditions were as follows: initial temperature, 80 C, 10 deg/min to 200, 1.5 deg/min to 230, 10 deg/min to 280.

The NI spectra of the 6 chlorine compounds are characterized by a strong molecular ion cluster, while the components having 7 to 10 chlorines have a base peak in the M-35 cluster. We chose to selectively monitor ions from these clusters for each of the different levels of chlorination of the toxaphene components. Ions that are common to both bornenes and bornanes were chosen for quantitation and confirmation. The confirmation and quantitation ions for the 6 to 10 chlorine compounds were 340, 342, 341, 343, 375, 377, 411, 413, 447, 449. Four windows were chosen so that two or three chlorine classes are monitored at any given time. The four windows begin with the elution of the 6, 8, 9, and 10 chlorine compounds.

Our SIM program was modified to account for interferences posed by other common chlorinated pesticides. Heptachlor, octachlorostyrene (OCS), diphenyl ethers and technical chlordane, which contains a mixture of chlordane, chlordene, and nonachlor isomers and other related compounds, all contain ions that interfere with the monitored ions of toxaphene. In the case of chlordene, heptachor, and OCS, they elute in windows where the interfering ions are not being monitored and thus pose no interference in our program. Chlordane structures have a fragment cluster beginning at m/z 336 or 338 that interferes with the monitored ions 340 and 342. To correct for this interference we monitor m/z 336 and 338 and mathematically calculate and subtract out the contribution of chlordane to the area of the toxaphene quantitation ion. Nonachlors are accounted for by monitoring m/z 444. Nonachlors are resolved from toxaphene by our GC program and thus the area of m/z 342 is omitted from the quantitation at these retention times. Unfortunately the spectra of the diphenyl ethers have no distinguishing ions that we can monitor to correct for their interference.

Some compounds, although not having ions that interfere directly with toxaphene, have ions in their spectra that are one mass unit lighter than those being monitored for toxaphene so that, if present in sufficient quantity, the C-13 contribution of those ions would interfere with the toxaphene quantitation ions. Thus we also monitor ions one mass unit lighter than each of the quantitation ions and mathematically correct and subtract out the C-13 contribution to the area of the quantitation ion.

Our SIM program for quantitating toxaphene is presented below.

WINDOW

1	2		3		4	
338	336	371	* 375	* 411	* 411	* 447
338	338	373	376	412	412	448
* 340	* 340	* 375	* 377	* 413	* 413	* 449
* 341	* 341	376	* 428			
* 342	* 342	* 377	* 430			
* 343	* 343					
	444					

An inverted triangle and an x designate the quantitation and confirmation ions, respectively. Note the inclusion of the ions necessary to correct for technical chlordane and C-13 interferences. The area of each of the chlorine classes is summed for a total toxaphene area which is quantitated against a toxaphene standard relative to an internal standard. The internal standard, 2,2',3,4,4',5,6,6'-octachlorobiphenyl, elutes in the third window and is monitored by m/z 428 and 430. This PCB congener was chosen because it is not a natural Aroclor component and thus is not present in the environment.

We tested the ability of our program to accurately distinguish toxaphene in the presence of interferents. Three artificial mixtures of toxaphene and technical chlordane were prepared such that their NI response ratios were 2:3, 1:1, and 3:2. The concentrations and recoveries of toxaphene quantitated by our SIM program are shown below. The quantitation of toxaphene in the presence of technical chlordane was excellent and very reproducible.

Precision and Recovery

Toxaphene Conc., ppm	Chlordane Conc., ppm	Response Ratio	N	% Recovery (s.d.)
45	7	2:3	4	98 (15)
127	13	1:1	1	99
43	2.6	3:2	3	98 (16)
				mean: 98 (13)

The SIM method was applied to the quantitation of toxaphene in fish composites (see table below). While carp from Saginaw Bay in Lake Huron are generally orders of magnitude more contaminated than sport fish from Siskiwit Lake, their toxaphene levels were only twice as high. Thus our method was successful at identifying and quantitating a trace contaminant in a complex environmental matrix such as polluted carp. It is of interest to note how much the toxaphene has been weathered by chemical or biological processes causing a change in the relative distribution of toxaphene among the different chlorine classes. A comparison of the relative distribution between the Siskiwit fish and a toxaphene standard shows that the toxaphene is not weathered significantly in these fish. The toxaphene in the Saginaw Bay fish has been substantially weathered, however. Thus this method can be used to show the extent toxaphene has been weathered in an environmental matrix.

Toxaphene in Fish

	Total Toxaphene, ppb	% Distribution			
		6Cl	7Cl	8Cl	9+10Cl
Siskiwit Lake Trout	289	17	24	29	30
Siskiwit Whitefish	224	21	30	31	18
Saginaw Bay Carp	513	47	38	13	2
Toxaphene standard		20	33	33	14

In summary, we have developed a SIM program using NI GC/MS for quantitating toxaphene in environmental samples. This method has been shown effective for correcting the interferences posed by other chlorinated contaminants. Environmentally-induced changes in the relative toxaphene distribution among chlorine classes can be evaluated using this method.

THE METHANE ENHANCED NEGATIVE ION MASS SPECTRA OF DIPHENYL ETHANE DERIVATIVES SUCH AS DDT

Elizabeth A. Stemmler and Ronald A. Hites, School of Public and Environmental Affairs and Department of Chemistry, Indiana University, Bloomington, IN 47405

The mass spectra of twenty-three florinated, chlorinated, and brominated diphenylethane derivatives have been measured under methane, electron capture, negative ionization conditions. This class of compounds includes the pesticide DDT and it's metabolites. These compounds can be divided into three groups: diphenylethene derivatives, diphenylethane derivatives, and diphenylethanol derivatives (see below).

Diphenylethene Derivatives

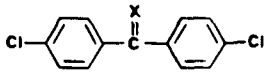

$X = CCl_2, CHCl$

Diphenylethane Derivatives

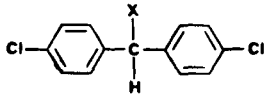

$X = CCl_3, CF_3, CHCl_2, CH_2OH$

Diphenylethanol Derivatives

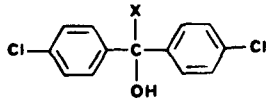

$X = CCl_3, CF_3, CO_2R$

In addition to the above compounds, in which the phenyl ring is substituted with a para chloro group, the mass spectra of compounds with an electron donating phenyl substituent were examined. These compounds included methoxychlor (substituted with para methoxy groups) and perthane (substituted with para ethyl groups). The response of these latter compounds under electron capture negative ion conditions was poor. Weak $(M-Cl)^-$ ions were observed, however, most of the ion current was carried by Cl^- ions.

In contrast, the diphenylethene derivatives, such as DDE, formed negative ions efficiently. Intense molecular ions were generated. Fragment ions due to the loss of Cl were also observed (see Figure 1A). The diphenylethane derivatives give more complex spectra. Although p,p'-DDD ($X=CHCl_2$) gave a weak molecular ion, p,p'-DDT gave no molecular ion. Losses of HCl, Cl_2, and HCl_2 were also observed (see Figure 2A). The loss of HCl is characteristic of the diphenylethanes and would result in production of the corresponding diphenylethene.

1A

1B

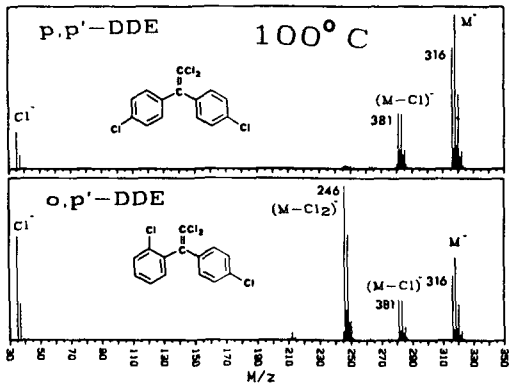

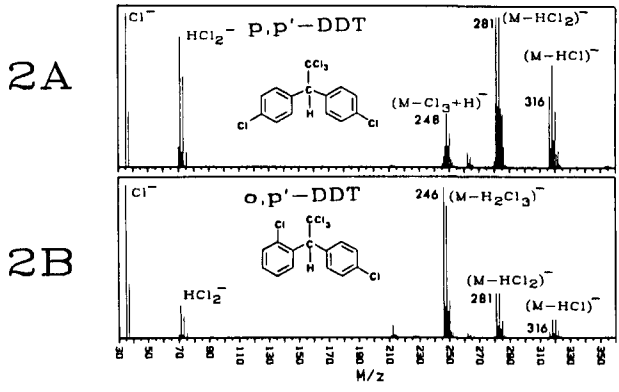

The diphenylethanols, such as Dicofol (see Figure 3), give a characteristic ion at m/z 250. This ion is generated from Dicofol by the loss of $HCCl_3$, resulting in formation of a dichlorobenzophenone anion. An ion at m/z 338 is generated when the ethanol is substituted with 4-bromophenyl groups.

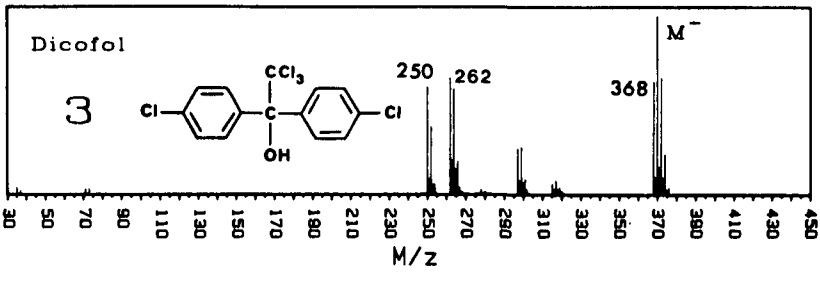

The p,p' and o,p' isomers of DDT, DDD, and DDE exhibit different fragmentation behavior. All the o,p' isomer give an ion at m/z 246 (see Figure 1B and 2B). This difference can be explained by the interaction of the ortho-phenyl chlorine with the substituents on the 2 carbon of the ethane molecule. In the case of DDE, this interaction results in the loss of Cl_2. The diphenylethanes, DDT and DDD, initially lose HCl, generating the diphenylethene, followed by the loss of Cl_2 and HCl respectively (see below).

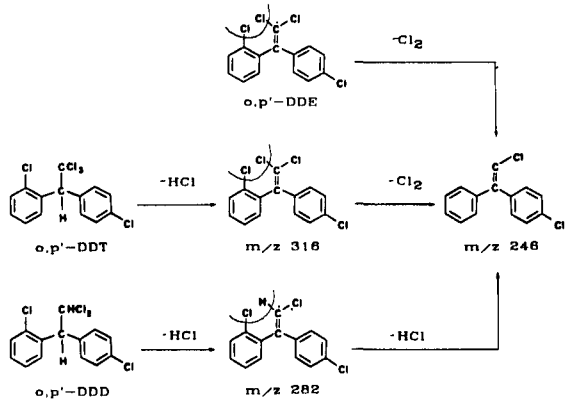

Negative Ion Chemical Ionization MS as an Environmental Enforcement Method — Residue Determination of Alachlor Metabolites in Edible Animal Products

R.G. Smith, S.A. Adams, J.M. Allan, L.M. Horner, R. Lauer, P.J. Nord, and A.J. Klein

Monsanto Company, Chesterfield, MO 63198.

Negative ion chemical ionization combined with capillary gas chromatography has been used in a recent study to determine residues of alachlor metabolites in edible animal products.

Alachlor is the active ingredient of Lasso® herbicide by Monsanto. It is used for the control of annual grasses and certain broadleaf weeds in corn, soybeans and other crops.

Alachlor has never been detected in plant metabolism or residue studies. Residues consist exclusively of alachlor metobolites. In corn forage, all of the major metabolites identified contain the 2,6-diethylaniline (DEA) moiety. More recently, an additional class of compounds containing the 2-(1-hydroxyethyl)-ethylaniline (HEEA) was identified in soybeans. A study was conducted to determine the concentration of alachlor metabolites in edible animal products after dosing the animals at high levels with synthetically prepared metabolites. A method was needed to determine to what extent these metabolites of alachlor are present in different products. The animal products examined were cows milk and hens eggs in addition to fat, kidney, liver, and muscle from cows, hens, and hogs.

The general methodology follows that of previous studies using other detectors. Samples are extracted, hydrolyzed it strong aqueous base, steam distilled, and extracted with methylene chloride. Alternate procedures require additional cleanup steps and separate determinations for DEA and HEEA. A GC-MS method was developed to determine both metabolite classes in a single sample as well as shortened the procedure. The greater selectivity of GC-MS enabled the validation range to be lowered by an order of magnitude.

This method uses the heptafluorobutyryl derivatives of DEA and HEEA which were found to give excellent responses under negative CI conditions. Another compound, 2,6-diethyl-4-fluoroaniline, was used for an internal standard. The mass spectra of the HFB derivatives of these compounds are shown in Figure 1. When used for selected ion monitoring the base ions of the DEA and 4-FDEA derivatives show high selectivity. However, the base ion for the HEEA derivative at m/z 213 is derived from the heptafluorobutyrate anion and has poor selectivity. Another ion, at m/z 343, was used for quantifying HEEA.

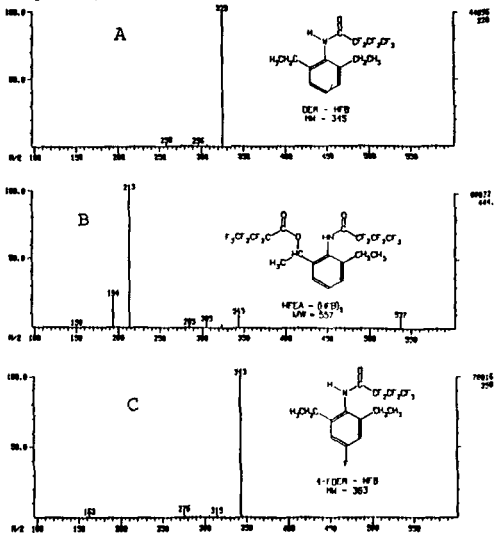

Figure 1.

Negative chemical ionization mass spectra of the HFBA derivatives of A) DEA, B) HEEA, and C) 4-FDEA.

The internal standard is added to each sample before derivatization. Excess derivatization reagent and solvent is evaporated and the residue taken up in 5% in isooctane. One microliter injections were made in the splitless mode on a 15 meter DB-5 caplillary column. Total analysis time is less than 10 minutes. Analyses were automated using an autosampler driven by the data system which also does the raw quantitation, generate response curves from standards, and uses the response curves to print quantitation reports.

The method was validated with each matrix, using fortified samples for the range 0.5–20 ppb. Validation requirements include recoveries average >70% over the validation range for both metabolites.

Typical selected ion chromatograms are shown for chicken muscle in figures 2 and 3. These represent control tissue and tissue fortified with 0.5 ppb of a mixture of alachlor metabolites.

Based on the advantages of time savings and selectivity demonstrated in this study mass spectrometry should be given due consideration in choosing environmental enforcement methods.

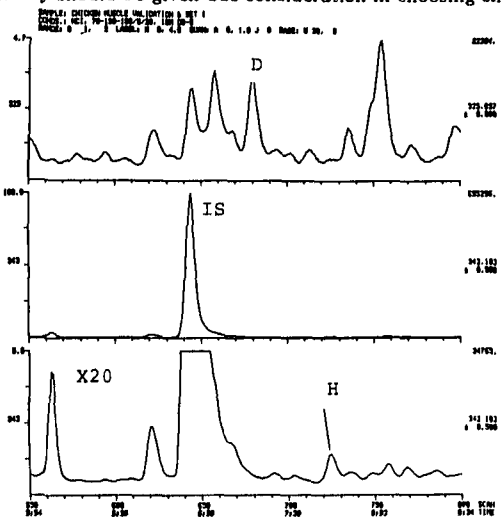

Figure 2. Selected ion chromatograms at m/z 325 (top), m/z 343 (middle), and m/z 343 magnified 20X (bottom) of control chicken muscle. HFBA derivatives are labelled D(DEA), H(HEEA) and IS(4-FDEA).

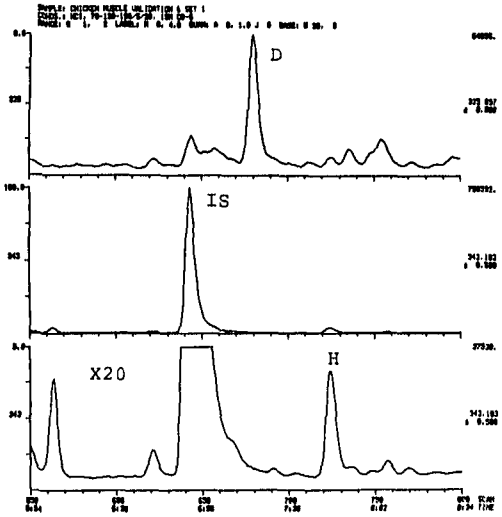

Figure 3. Selected ion chromatograms at m/z 325 (top), m/z 343 (middle), and m/z 343 magnified 20X (bottom) of chicken muscle fortified with 0.5 ppb each of DEA-generating metabolites and HEEA-generating metabolites. HFBA derivatives are labelled as in Figure 2.

INVESTIGATIONS OF THE MECHANISMS RESPONSIBLE FOR ISOMERIC DISCRIMINATION OF POLYCYCLIC AROMATIC USING NEGATIVE ION CHEMICAL IONIZATION*

M. V. Buchanan, M. B. Wise, and I. B. Rubin, Analytical Chemistry Division, Oak Ridge National Laboratory, Oak Ridge, Tennessee 37831

Previous studies have shown that a number of isomeric polycyclic aromatic hydrocarbons (PAH) may be distinguished by electron capture negative ion chemical ionization (NICI) using methane as a buffer gas. The basis for the differentiation appears to be related to the electron affinities (EA) of the various compounds. In general, compounds with EA values greater than 0.5 eV ionize to yield molecular anions, whereas those with lower EA values do not ionize. In addition, compounds containing a saturated five-membered ring and having EA values much lower than 0.5 eV, such as fluorene, yield anions at M+14 mass units. Studies have been conducted with both a conventional high pressure chemical ionization source with a quadrupole mass spectrometer and a Fourier transform mass spectrometer (FTMS) to investigate the mechanisms responsible for the different NICI responses of various PAH.

Initial studies centered on establishing whether the M+14 anion observed for fluorene was due to insertion of CH_2 (from the methane buffer gas) into the molecule or loss of two hydrogens and addition of an oxygen atom (from impurities). Using deuterium labelled analogues of fluorene, including d_{10}-fluorene and 9-d_2-fluorene, it was shown that oxygen was added at the C-9 carbon of fluorene, with the loss of the two hydrogens at that site. Comparison of collision induced dissociation spectra (MS/MS) obtained from fluorene, 9-methylfluorene and 9-fluorenone supported this conclusion.

Exact mass measurements made with the FTMS verified that the peak at m/z 180 was indeed due to insertion of oxygen into the molecule, as shown in Figure 1. In this experiment a mixture of fluorene (mw 166) and 9-methylfluorene (mw 180) were introduced into the FTMS via the direct insertion probe. Using argon as the buffer gas at a static pressure of about 2×10^{-6} torr, the resulting NICI spectra showed conclusively that the anions at m/z 180 from fluorene corresponded to a molecular formula of $C_{13}H_8O^-$. This spectrum illustrates another fact, as well. The formation of the m/z 180 anion was not dependent on the presence of methane as the buffer gas. Using longer delay times prior to detection of the ions, the M+14 anions have also been observed for fluorene when no buffer gas was used in the FTMS, suggesting that trace sources of oxygen in the instrument can participate in the reaction.

To elucidate which ions are participating in the formation of the observed product ions under NICI conditions, a swept double resonance experimental sequence which was written for use with the FTMS. In the double resonance experiment a product ion is monitored while a suspected reactant ion is continuously ejected from the cell. A decrease in the abundance of the product ion establishes that the ejected ion is a participant in the reaction. In the swept double resonance sequence, the frequency of the ejection pulse is automatically stepped in increments over a selected mass range to help elucidate the identity of the reactant ion. An example of the experiment is shown in Figure 2. Using oxygen-18 labelled water as the NICI buffer gas, d_{10}-fluorene (mw 176) yields an anion corresponding to loss of a deuterium at m/z 174. A swept double resonance experiment was conducted by monitoring this ion and sweeping frequencies corresponding to m/z 16 through 22 at 0.2 amu increments. A large decrease in the abundance of the product ion was observed at m/z 19 ($^{18}OH^-$), indicating that OH^- is the reactant ion responsible for the formation of

the M-D species. Decreases were also observed at m/z 17 ($^{16}OH^-$), as well as m/z 18 and 20, which correspond to $^{16}OD^-$ and $^{18}OD^-$, respectively, which arise due to H/D exchange of the buffer gas with the deuterium labelled fluorene.

At present, experiments are continuing to further the understanding of these NICI reactions in the hope that they could be tailored to differentiate between a wider variety of compounds.

*Research sponsored by the Office of Health and Environmental Research, U. S. Department of Energy under contract DE-AC05-84OR21400 with Martin Marietta Energy Systems, Inc.

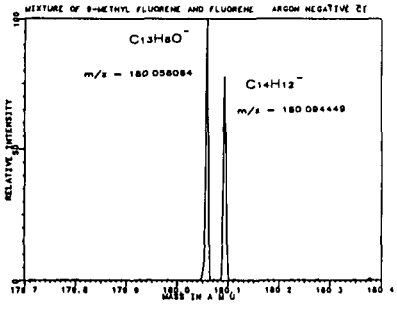

Figure 1. High Resolution FTMS NICI spectra of 9-methylfluorene and fluorene.

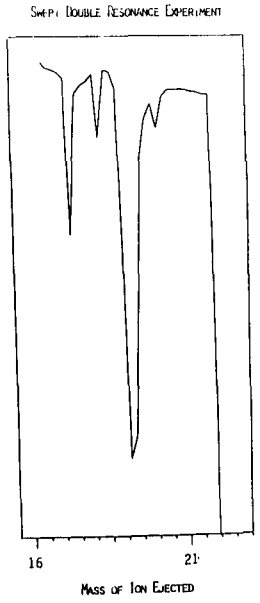

Figure 2. Swept Double Resonance Experiment: Abundance of m/z 174 from d_{10}-fluorene monitored as ions m/z 16-22 ejected.

ELECTRON CAPTURE PROCESSES AT REDUCED PRESSURES FOR SELECTIVE CHROMATOGRAPHIC DETECTION*

M. B. Wise and M. V. Buchanan, Analytical Chemistry Division, Oak Ridge National Laboratory, Oak Ridge, Tennessee 37831

Research in our laboratory has shown that electron capture negative ion chemical ionization mass spectrometry is a convenient means of distinguishing between certain isomeric polycyclic aromatic hydrocarbons (PAH). Experiments in which the CI reagent gas pressure was varied displayed a marked pressure dependence on the degree of isomeric discrimination observed, with the greatest selectivity achieved at lower pressures. Because of the similar nature of the processes that occur in an electron capture gas chromatographic detector (ECD), these experiments suggested that a similar degree of isomeric discrimination could be achieved by using a GC with an ECD operated at reduced pressures.

A block diagram of the experimental apparatus is shown in Figure 1. It consists of a DC mode cylindrical-planar ECD cell enclosed in a high vacuum chamber (Figure 2). Pressures in the cell can be varied from atmospheric to less than 1 torr. A gas mixing manifold is used to add reagent gas (typically argon with 10% methane) to the GC effluent prior to entering the detector cell.

Experiments with mixtures of PAH have shown that isomeric discrimination can indeed be achieved by operating this detector at reduced pressures. This is believed to be due to competition between capture of thermal electrons and electron emission (resulting from argon ionization) as compounds traverse the detector. The behavior of the detector is dramatically affected by the operating pressure, and the response for a particular compound is strongly related to its electron affinity value. This is demonstrated by Figure 3 which shows chromatograms of a 20 ug/ml mixture of anthracene, phenanthrene, fluoranthene, and pyrene. At atmospheric pressure, a conventional electron capture response is obtained giving a chromatogram of 3 peaks, Figure 3a. Phenanthrene has a low electron affinity (0.03 eV) and is not observed. When the operating pressure is reduced to ~200 torr, only fluoranthene, which has the highest electron affinity in the mixture, is observed to undergo electron capture, Figure 3b. Both pyrene and phenanthrene appear to undergo argon ionization (electron emission) at this pressure and are seen as negative peaks. Anthracene is not observed due to equilibrium between emission and capture of electrons. At approximately 1 torr of cell pressure, all compounds undergo argon ionization and all four compounds show up in the chromatogram with nearly equal intensity as shown in Figure 3c. By simply varying the cell pressure in the range of 10-300 torr, the selectivity of the detector can be continuously tuned enabling specific compounds to be determined. For instance, benzo(α)pyrene (EA=0.64 eV) can readily be distinguished from its isomer, benzo(e)pyrene (EA=0.35 eV) in a coal distillate sample (Figure 4).

*Research sponsored by the Office of Health and Environmental Research, U. S. Department of Energy under contract DE-AC05-84OR21400 with Martin Marietta Energy Systems Inc.

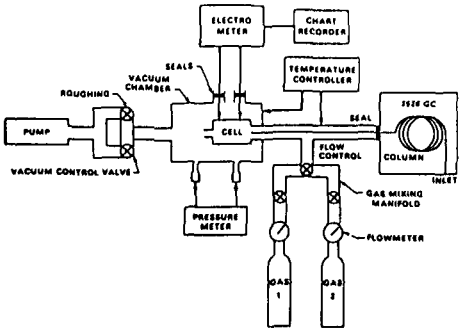

Figure 1. Block diagram of the instrument.

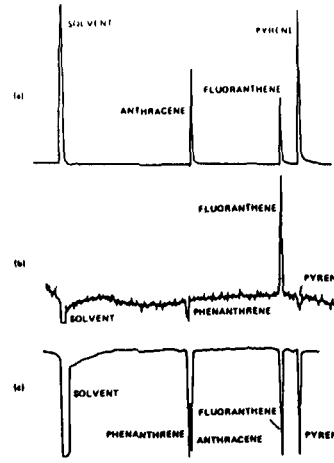

Figure 3. Mixture of anthracene, phenanthrene, fluoranthene, and pyrene at (a) 760 torr, (b) 200 torr, and (c) 1 torr cell pressure.

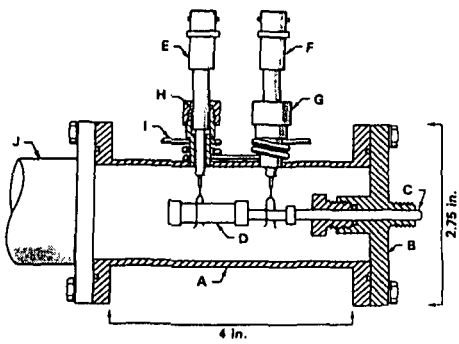

Figure 2. Expanded view of the vacuum chamber and cell.

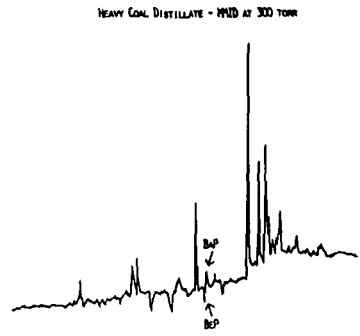

Figure 4. Heavy coal distillate sample at 300 torr cell pressure. Approximately 4 ppm of BaP in the injected sample.

DETERMINATION OF PAH AND ALKYLATED PAH IN PARTICULATE EXTRACTS USING NEGATIVE ION CHEMICAL IONIZATION MASS SPECTROMETRY

Laurence R. Hilpert
Center for Analytical Chemistry, National Bureau of Standards, Gaithersburg, MD 20899

An interesting aspect of the negative ion chemical ionization (NICI) mass spectrometry of polycyclic aromatic hydrocarbons (PAH) is the selectivity of detection observed for certain isomeric species. Two striking examples of this are the selectivity of detection observed for the molecular anion ($M^{-}\cdot$) of fluoranthene over pyrene, and the selectivity of detection of $M^{-}\cdot$ for benzo(a)pyrene over benzo(e)pyrene. Under optimized conditions of ion source pressure and temperature, the molecular anion for fluoranthene is more than 100x more abundant than that of pyrene, and the molecular anion for benzo(a)pyrene is more than 1000x more abundant than that of benzo(e)pyrene (1). In addition to the selectivity of detection observed for the parent PAH, similar selectivities are seen for their alkylated homologues. Using a combination of EI and NICI techniques, it is possible to differentiate individual isomeric PAH and alkylated PAH based on the selectivity of detection under NICI.

Two particulate samples which have been certified as Standard Reference Materials (SRMs) were analyzed by GC/MS using EI and NICI techniques. The first, SRM 1648, is an urban air particulate sample collected in the St. Louis, MO area. The material was collected over a period of approximately 12 months and therefore is a time-integrated sample which is representative of air particulate matter in an urban area. The second sample, SRM 1650, is a diesel particulate material collected from the heat exchangers of a dilution tube facility following 200 engine hours of particle accumulation. More than one heavy duty, direct injection diesel engine, operating under a variety of conditions, was used to generate the particulate sample. Both samples had been shown to contain a complex mixture of PAH and alkylated PAH at low (µg/g) levels. Analysis of these samples would therefore demonstrate the ability of NICI mass spectrometry to detect low levels of PAH species as well as discriminate between isomeric PAH and isomeric alkylated PAH.

Extracts of the particulate materials were prepared for GC/ MS analysis by Soxhlet extraction with methylene chloride for 24h followed by chromatography on a Florisil SepPak to remove polar and high molecular weight species. 2.0µL aliquots of the concentrated extracts were chromatographed on a 30m x 0.25mm i.d.

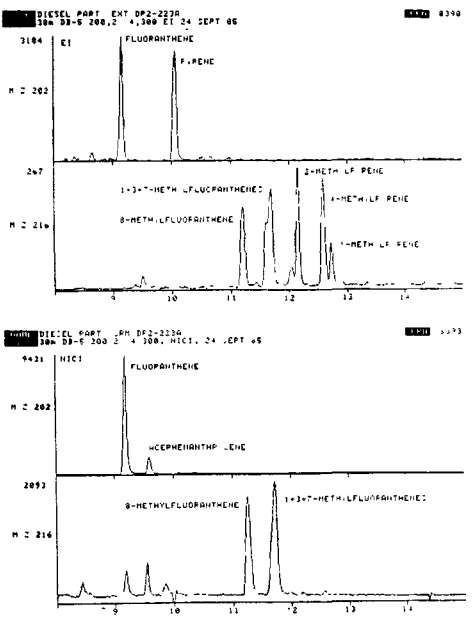

Figure 1

fused silica capillary column coated with a 0.25μ film of a non-polar liquid phase.The column was interfaced directly to the ion source of a quadrupole mass spectrometer which was operated in either the EI or NICI ionization modes. Methane was used as the reagent gas for the NICI measurements, and the operating presssure in the ion source manifold was 2.0 x 10^{-4} Torr corresponding to a pressure of approximately 0.3 Torr in the ion source itself.

Figure 1 shows mass chromatograms for m/z 202 (fluoranthene and pyrene) and m/z 216 (methylfluoranthenes/pyrenes) for a diesel particulate extract run in the EI (top) and NICI (bottom) ionization modes. Fluoranthene, pyrene, and the methylated fluoranthenes and pyrenes are all detected under EI conditions. There is no way to distinguish the methylfluoranthenes from the methylpyrenes, however, based on the EI analysis. Under NICI conditions, fluoranthene and the methylfluoranthenes are detected selectively. No peaks due to pyrene or methylpyrenes are observed. The NICI run also shows a small peak for acephenanthrylene which was barely visible in the EI run. Comparison of the EI and NICI data shows that the first two peaks in the EI m/z 216 mass chromatogram are due to the methylfluoranthenes. Individual peak identities were determined by analysis of authentic standards of the individual isomers.

Figure 2 shows mass chromatograms for m/z 252 (benzofluoranthenes, benzo(e)pyrene, benzo(a)pyrene, and perylene) and m/z 266 (methyl-substituted m/z 252) for an air particulate extract run in the EI and NICI modes. Once again, under EI there is no discrimination among any of the parent or alkylated-PAH species. It is impossible to tell whether the peaks in the m/z 266 mass chromatogram are due to methylated benzofluoranthenes, methyl-BePs, methyl-BaPs, or methyl-perylenes. Under NICI, the only species which are detected are the benzofluoranthenes, BaP and their methyl-homologues. Since methyl-BePs or methyl-perylenes do not respond under NICI, a comparison of the m/z 266 mass chromatograms from the EI and NICI runs enables identification of the methyl-BePs and/or methyl-perylenes. These peaks are identified by the * in the EI m/z 266 mass chromatogram.

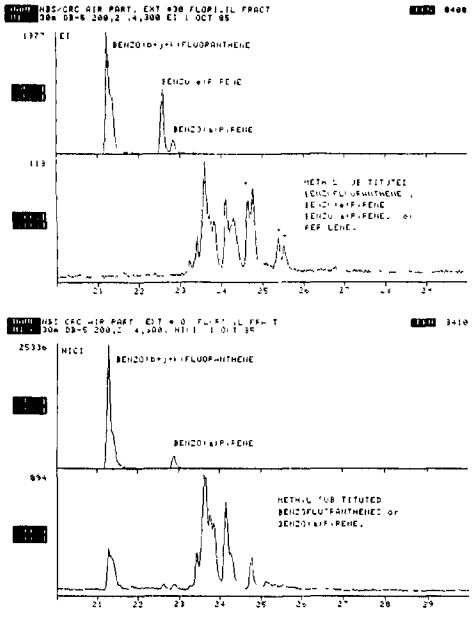

Figure 2

---

(1) Hilpert, L.R., Byrd, G.D., and Vogt, C.R. Anal. Chem. **56**, 1842 (1984).

GAS CHROMATOGRAPHIC/MASS SPECTROMETRIC ANALYSIS OF BIOLOGICALLY IMPORTANT AROMATIC AMINES. APPLICATIONS IN HUMAN DOSIMETRY.

W.G. Stillwell, Matthew S. Bryant, and John S. Wishnok, Department of Applied Biological Sciences, Massachusetts Institute of Technology, Cambridge, MA 02139.

The increased risk toward bladder cancer among smokers may be due in part to increased exposure to aromatic amines, such as 4-aminobiphenyl (4-ABP) and 2-naphthylamine, which are present in tobacco smoke. Compounds of this type require metabolic activation, via initial N-hydroxylation, in order to exert a carcinogenic effect. The resulting electrophilic metabolites bind in some cases to hemoglobin, and it has been possible, with 4-ABP, to utilize this reaction as an in vivo dosimeter to assess human exposure to the active metabolite. Hemoglobin from 10 ml of blood is hydrolyzed to release 4-ABP which is then derivatized and quantitated by GC/NICI/MS (1). The sequence is summarized in Scheme 1. We have extended this method to other aromatic amines present in cigarette smoke; our initial results are summarized below.

The mass spectra of the pentafluoropropionamide (PFP) derivatives of a series of aromatic amines have been recorded under various ionization conditions. With electron ionization, these derivatives typically give prominent molecular ions with fragmentation arising from elimination of C2F5 and COC2F5. Higher molecular weight polycyclic aromatic amines, e.g., 6-aminochrysene, give prominent molecular ions along with strong peaks corresponding to M-174 (loss of CNHCOC2F5). With positive chemical ionization using methane as the reagent gas the derivatives give intense protonated molecular ions along with the associated ions at M+29 and M+41. Negative ion chemical ionization yields, primarily, peaks corresponding to loss of HF from the molecular anions. The NICI, PCI, and EI mass spectra of ABP-PFP are shown in Figure 1. Negative ion chemical ionization, with selected-ion-monitoring, is generally more suitable than PCI or EI for the quantitative analysis of aromatic amines present in biological fluids at concentrations in the mid femtomolar range, although PCI and EI have been useful for providing additional structural information.

Blood samples were collected from smokers, nonsmokers, and ex-smokers. The red cells were isolated, lysed, and then dialyzed against distilled water for two days. An internal-standard solution, containing 2 ng aniline-d5, 1 ng 4'-F-ABP, and 0.5 ng 5-F-2-naphthylamine, was added and the dialysates were hydrolyzed for two hours with dilute base. The resulting solutions were extracted with methylene chloride and the extracts were dried over NA2SO4. The samples were derivatized with pentafluoropropionic anhydride and then concentrated to near dryness. The residues were dissolved in 20 ul EtOAc and analyzed on a Hewlett-Packard 5987 mass spectrometer in the NICI mode (the GC column was fused silica/Supelcowax; methane was the CI reagent gas).

Aromatic amines, including aniline, 4-ABP, 2-naphthylamine, and the three toluidines, have been detected via their hemoglobin adducts in humans (Figure 2). The levels of the adducts of 4-ABP, 2-naphthylamine, and o- and p-toluidine are higher in smokers than in nonsmokers. The level of the 4-ABP adduct decreases steadily to background levels during transition from smoking to nonsmoking (Figure 3). Levels of aniline adducts are higher than levels of 4-ABP adducts in both smokers and nonsmokers, and are apparently unrelated to smoking. Table 1 summarizes representative data for adduct levels in smokers and nonsmokers. This method appears to be useful for assessing exposure to active metabolites of potentially hazardous environmental substances. Qualitative evidence for exposure to many such chemicals already exists, and we are currently carrying out extensive quantitative studies of human exposure to environmentally significant aromatic amines. This research was supported by Grants from the American Cancer Society (SIG-10-I), N.I.H. (T32-ES07020), NIEHS (P01-ES00597), and the D.H.H.S. Shared Instrument Program (1 S10 RR01901).

1. M.S. Bryant, P.L. Skipper, S.R. Tannenbaum, and M. Maclure, Hemoglobin Adducts of 4-aminobiphenyl in Smokers and Nonsmokers. Cancer Res., Submitted.

SCHEME 1

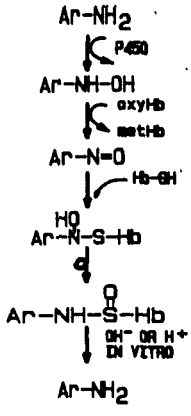

FIGURE 1

MASS SPECTRA OF ABP-PFP

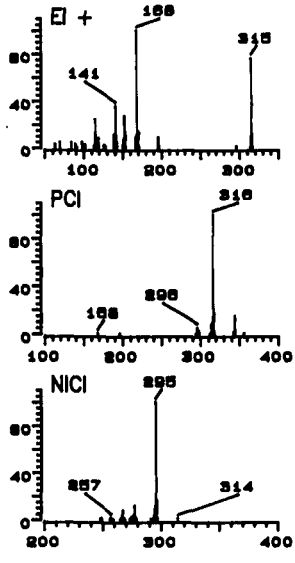

FIGURE 2

SIM TRACES FOR A SMOKER

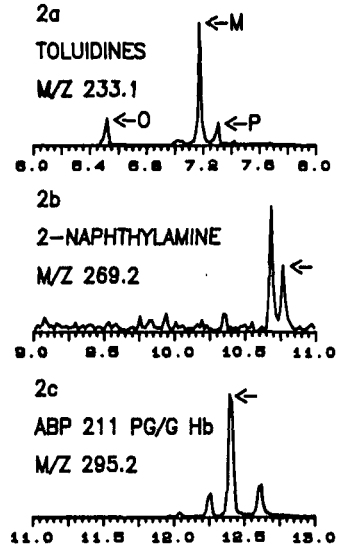

FIGURE 3

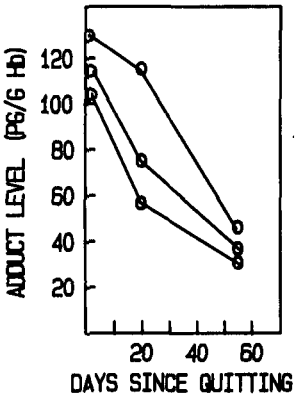

TABLE 1

ADDUCT LEVELS OF AROMATIC AMINES (ng/g Hb; MEAN, SD)

AMINE	SMOKERS (n=10)	NONSMOKERS (n=10)
4-ABP	0.17 (0.06)	0.03 (0.01)
2-NAPHTHYLAMINE	0.017 (0.006)	0.006 (0.003; n=9)
O-TOLUIDINE	0.097 (0.029)	0.034 (0.010)
M-TOLUIDINE	0.50 (0.2)	0.68 (0.2)
P-TOLUIDINE	0.13 (0.05)	0.07 (0.04)
ANILINE	4.9 (2.9)	3.8 (2.0)

Determination of Trace Levels of Aliphatic Amines in Air by Gas Chromatograph-Surface Ionization Mass Spectrometry

Toshihiro Fujii and Toshihumi Kitai
National Institute for Environmental Studies
Tsukuba, Ibaraki 305, Japan

The occurrence and determination of aliphatic amines has received a great deal of attention in recent years. The necessity of determining these compounds at low level in complex matrices has resulted in a number of analytical schemes. Usually concentration process prior to identification remains necessary. Solvent absorption and adsorption on porous polymers are well-known concentration techniques. The final analysis has been done with a FID or a nitrogen selective detector combined with GC. However, some drawbacks have been reported in terms of detection limit, identification, interference and peak tailing.

Surface ionization (SI) is defined as the ionizing process in which the chemical species ionize on the hot metal emitter, especially on refractory metal oxide emitters. Recent mass spectrometric studies of the SI of individual organics revealed that the SI gives greater output currents to certain kinds of organic compounds, demonstrating that SI mass spectrometry can be potentially useful as an analytical method.

This report describes the first demonstration of a GC/SIMS method. A newly-developed method based on the GC/SIMS with high detection capability can be very advantageous for the selective determination of volatile amines at low concentration in air. The present analytical procedure employs the direct gas sample inlet without the complicated sample preparation and the selective ion monitoring. It saves time and minimizes the risk of sample concentration and sample loss during manipulation procedures, such as solvent extraction, adsorption on the solid material or derivatization steps.

APPARATUS. The experiments were performed with a Finnigan 3300 gas chromatograph-mass spectrometer equipped with a home-built thermionic ion source (Figure 1). The design of the surface ionization source assembly (direct insertion probe) is such that the Re ribbon filament (6mm x 0.75 mm x 0.025 mm) can be placed in the center of the conventional electron ionization ion source chamber when the probe is inserted.

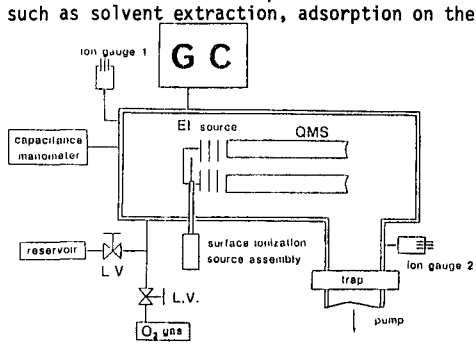

Fig.1 Schematic of GC-SIMS

PROCEDURE. A 1 ml sample was injected into a GC with a 1 ml glass syringe. The memory effect of the syringe from adsorption was reduced by washing with 10 % KOH in water and then with distilled water. Ambient air samples were collected in 1 L glass cylinders closed with valves and membranes through which the gas samples were taken by the syringe.

STANDARIZATION. For standarization, a water solution of methylamines whose composition was determined gas chromatographically beforehand, was used; monomethylamine (MMA) is 3 % water solution, dimethylamine (DMA), 24 % and trimethylamine (TMA), 11.5 %. Standard gases were made by vaporizing these amine solutions into the 1-L glass cylinder (treated with 10 % KOH solution) A series of standard concentrations from 0.85 to 48000 ppb (v/v) were made by further dilution. It was confirmed before the dilution process that the 1-L glass cylinder filled with air was free from methylamines. A plot of the peak area against the known standard concentrations gives a straight line over prepared concentration range with the uncertainty ± 12.8 %, demonstrating that the present procedure was sound. Quantitation of the amines was done by comparing the single ion chromatogram peak areas for sample of standards in similar concentration ranges.

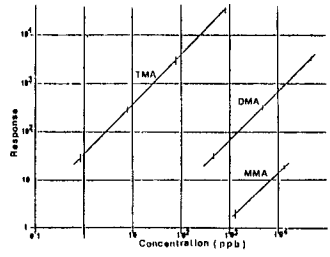

Fig.2 The calibration curve over the chosen range of standard gas sample for MMA, DMA and TMA.

SELECTED ION MONITORING (SIM) IN SI MODE. Since the present ion source is a combination type, it is very easy to compare the mass spectrometric sensitivity under SI mode and EI modes. Using the standard mixture of MMA, DMA and TMA, the effectiveness of the GC-MS in SI mode is demonstrated in the form of SIM chromatograms in comparison with that in conventional EI mode (Fig. 2). A SIM peak of high intensity $(M-H)^+$ ion was observed, particularly for TMA at the 230 pg/L level with the signal to noise ratio at 6, which is not detected at all in the EI mode. Table I summarizes ion species to be monitored, retention time, their detection limit of both EI and SI modes (concentration of each compound producing a peak three times higher than noise level as a 1 ml of standard air sample is injected), and SI/EI, the ratio of the detection capability obtained in the SI mode to that in the EI mode.

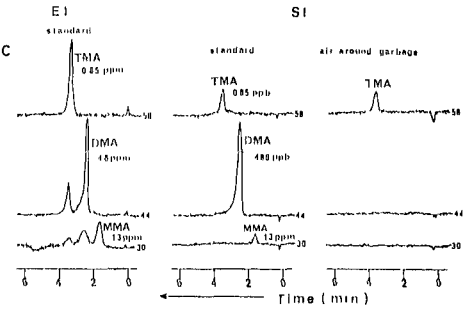

Fig.3. SIM chromatograms of aliphatic amines in a 1 mL air sample.

RECOVERY AND PRECISION. Under the condition that the KOH treatment of the packing material, the GC injector as well as gas syringe must be carried out correctly, the method of recovery after one day of storage was determined by making measurements on spiked samples at various concentrations of TMA (Table II). The percentage recovery of TMA standard fell in the range 102-91 %. The precision of the method was determined from replicate analyses of the standard sample at 8.5 ppb concentration of TMA, when the standard deviation was 0.24 and the coefficient of variation 6.8 % using peak height (mm).

APPLICATION TO AIR SAMPLE. The method was applied to determination of aliphatic amines in the air around cattle and poultry buildings, and garbage sites. Table III lists the results of these ambient sample measurements and Fig.2 shows a typical chromatogram from these sources in the extreme right-hand column. In air from the livestock house, TMA was successfully determined and neither DMA nor MMA was detected. Organic components did not interfere with these determinations because of the selectivity of the surface ionization. As can be seen, the level of TMA was highest for that air sample collected in the poultry house (i.e. site 1-1). Site 4-3 from a residential area gave no detectable TMA.

Table I. Aliphatic Amines examined in the air sample.

Compounds	Retention* Time (min)	Selected Ion (m/e)	Detection Limit** EI mode (ppm)	SI mode (ppb)	Detection Capability (SI/EI)
MMA	1.8	30	0.5	1300	0.38
DMA	2.6	44	0.62	51	12.2
TMA	3.7	58	0.14	0.42	333

* Column temperature 150 C with 55 ml/min at the He carrier flow rate
** At the signal to noise ratio of 3.

Table II. Recovery measurements on spiked air sample with varying amounts of TMA added.

TMA added (ppb)	TMA found (ppb)	TMA recovered (ppb)
0	4.2	0
4.2	8.5	4.3
8.5	12.1	7.9
12.7	16.1	11.9

Table III. Trimethylamine concentration levels in air sample*.

Sampling site	Date	TMA (ppb)
1-1 in poultry building	Feb.,1986	1.6 ± 0.1
1-2 around poultry building (5m away)		1.2 ± 0.1
2.1 in cattle building	Feb.,1986	0.6 ± 0.1
2-2 around cattle building (5m away)		tr
3-1 in swine building	March, 1986	0.8 ± 0.1
3-2 around swine building (5m away)		tr
4-1 garbage collection site (2 m^2)	March,1986	0.6 ± 0.1
4-2 1 m away from the above site		tr.
4-3 residence area 10 m away from 4-1 site		ND

tr.; trace, detectable but less than 3 times detection limit
ND, not detected.
*, storage time is less than one day.

CONCLUSION. This is the first study on surface ionization mass spectrometry coupled with gas chromatography, which is based upon the recent discovery that some organics are very efficiently surface ionized either in the molecular or radical form with the incandescent Re-filament. For the effectiveness of GC-SIMS, it has been applied to the trace analysis of aliphatic amines in ambient air. The presen study is a successful example of the GC-MS combined with the surface ionization method. We believe that the GC-SIMS method can be extended to analysis of other organic compounds in many environments which are able to be ionized efficiently on the SI emitter.

REFERENCES

(1) T.Fujii, Int.J.Mass Spectrom.Ion Phys. 1984, 57, 63-74.
(2) T.Fujii et al., J.Phys.Chem., 1985, 89, 4687-4690.
(3) T.Fujii et al., Int.J.Mass Spectrom. Ion Proc., in press.

DETECTION OF SUBSTITUTED POLYNUCLEAR AROMATIC HYDROCARBONS

C. P. Leibman and G. Mamantov
University of Tennessee, Knoxville, TN 37966

and

P. J. Todd
Oak Ridge National Laboratory, Oak Ridge, TN 37831

Intense secondary ions characteristic of substituted polynuclear aromatic hydrocarbons (PAH's) can be obtained if they are first dissolved in concentrated sulfuric acid (97%). Analysis of substituted PAH's is important since many are carcinogenic or mutagenic and they are often associated with fuel combustion. Thus, they pose a significant environmental hazard. Concentrated sulfuric acid is a novel matrix which significantly enhances the secondary ion emission of a variety of aromatic compound classes. Substituents for which abundant $M^{+\cdot}$ or $M+H^+$ secondary ions were detected include: nitriles (-C≡N), ketones (-CR=O), aldehydes (-CH=O), carboxylic acids (-COOH), phenols (-OH), ethers (-OR), alcohols (-ROH), halides (-X), hydrocarbons (-R), amino ($-NH_2$), nitro ($-NO_2$), carbonates ($-CO_3-$), and nitrogen containing heterocycles.

Many substituted PAH's are soluble in H_2SO_4 and are extensively ionized in solution. Aromatic ion formation occurs via protonation and single-electron oxidation in these solutions. Typically, abundant $M+H^+$ ions are observed in SIMS spectra of substituted PAH/H_2SO_4 solutions. The SIMS spectrum of a 5 wgt. % 9-phenylanthracene/ sulfuric acid solution, shown in Figure 1, is fairly representative of the substituted PAH's investigated. The base peak corresponds to the protonated molecular ion observed at m/z 255; abundant $M^{+\cdot}$ ions are also evident. A further feature of sulfuric acid is its low mass spectral background since it does not have a hydrocarbon backbone. Reduction of chemical noise improves the limits of detection that can be obtained for analytes dissolved in a sulfuric acid.

The low vapor pressure of sulfuric acid makes it amenable to the vacuum requirements of the secondary ion source. The vapor pressure of sulfuric acid (2.5×10^{-5} torr at 23°C)[1] is lower than that of glycerol (1.3×10^{-4} torr at 23°C)[2] by a factor of 5.

A 2 μL sample will yield stable secondary ions for over 1 h. Samples were deposited onto a platinum mesh (3 mm diameter) that had been spot-welded to the center of a stainless steel target (9.5 mm diameter). The sample was contained by the Pt mesh. Restriction of sample to the target and the low sample vapor pressure account for the lack of observable corrosion in the mass spectrometer. Since many of the analytes investigated are hazardous, all sample preparation was conducted in a drybox attached directly to the mass spectrometer. Restriction of sample to the target and the low sample vapor pressure account for the lack of observable corrosion in the mass spectrometer. Since many of the analytes investigated are hazardous, all sample preparation was conducted in a drybox attached to the mass spectrometer.

References

1. Roedel, W. J. Aerosol Sci. 1979, 10, 375-386.

2. Cammenga, H. K.; Schulze, F. W.; Theuerl, W. J. Chem. Eng. Data, 1977, 22, 131-134.

*Research sponsored by the U. S. Department of Energy, Office of Basic Energy Sciences, under Contract DE-AC05-84OR21400 with Martin Marietta Energy Systems, Inc.

By acceptance of this article, the publisher or recipient acknowledges the U.S. Government's right to retain a nonexclusive, royalty-free license in and to any copyright covering the article

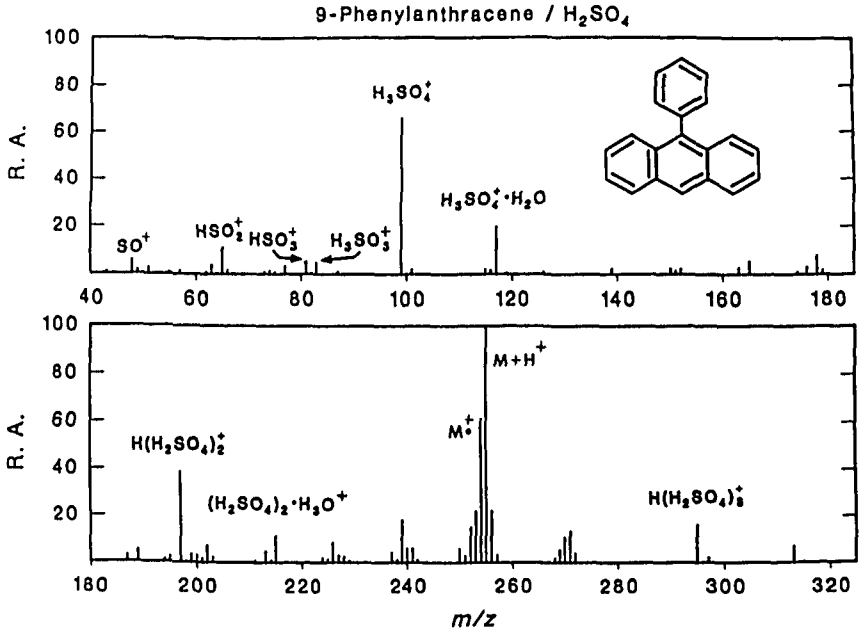

Fig. 1. SIMS spectrum of a 5 wgt. % 9-phenylanthracene/sulfuric acid solution

MASS SPECTROMETRIC CHARACTERIZATION OF PRODUCTS OF PYROLYSIS AND COMBUSTION OF UTILITY MATERIALS

Sueann Mazer, Wayne Rubey, and Barry Dellinger

University of Dayton Research Institute, 300 College Park, Dayton, OH 45469

Identification of trace by-products from high-temperature reactions of PCBs has prompted a search for alternative fluids which pose fewer health risks. A number of laboratories have since investigated formation of thermal decomposition products from proposed PCB substitutes. The research reported here concerns GC-MS identification of thermal decomposition products formed from other organic materials found in utility transmission and distribution equipment. These materials include wood, Kraft paper, Kraft paper treated for thermal stability with dicyandiamide (dicy), and Kraft-phenolic laminates.

These investigations were conducted using a specially constructed System for Thermal Diagnostic Studies (STDS). The STDS consists of a thermal instrumentation assembly interfaced to an HP 5890 GC and an HP 5970B MSD. The thermal assembly includes a modular control console and a modified HP 5890 GC which houses a furnace into which can be placed various test cells for conducting a range of thermal decomposition tests. A tubular flow reactor was used as the test cell for the experiments described herein. The GC chamber surrounding the reactor serves primarily as a temperature control device for transport of sample into and out of the reactor. The injection region of this chamber was fitted with a custom insert into which the CDS Pyroprobe was sealed.

Figure 1 shows a block diagram of the experiments which were conducted on the cellulose-based utility materials. The polymeric materials were initially degraded in a nitrogen atmosphere using the CDS Pyroprobe, which was programmed at 20°C/msec to 800°C. The gaseous degradation products were then passed into the reactor, where they were subjected to an 800°C decomposition temperature for two seconds in flowing nitrogen. The reactor effluent was analyzed using capillary GC-MS, with the mass selective detector being scanned from m/z 40 to 500.

Figure 2 shows the similarity of the product chromatograms obtained from maple wood, Kraft paper, and Kraft paper treated with dicyandiamide. The similarity of these chromatograms is not too surprising in light of the similar chemical structures of the materials. The major products are given in Table 1.

Figure 3 shows the similarity of the chromatograms obtained from two brands of Kraft-phenolic laminate, Herkolite™ and Spauldite™. The overall concentration of chromatographable products was considerably higher for the laminates than for the wood and paper. As Table 1 indicates, the major products from these laminates included the major products produced from wood and paper, as well as a host of additional products. Some of these are probably decomposition products from the phenolic resin, while others, such as the nitrogen-containing compounds, may have originated from an additive to the resin or laminate. Assessment of potential health risks from these thermal decomposition products is an ongoing project.

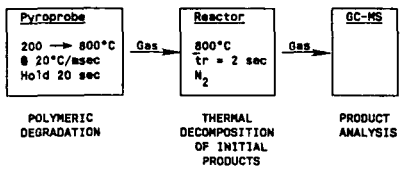

Figure 1. Thermal Decomposition Experimental Parameters.

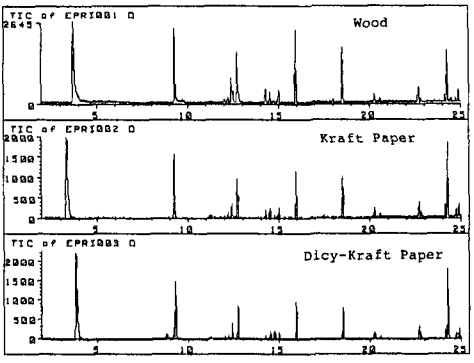

Figure 2. Chromatograms of Thermal Decomposition Products Obtained From Wood, Kraft Paper, and Dicy-Treated Kraft Paper.

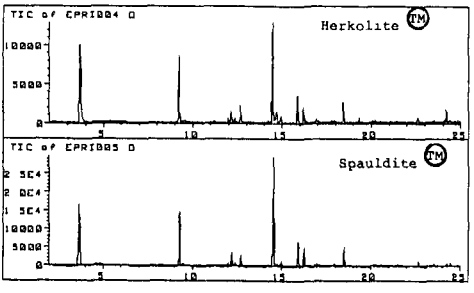

Figure 3. Chromatograms of Thermal Decomposition Products Obtained From Two Kraft-Phenolic Laminates.

Table 1. Major Thermal Decomposition Products from Cellulose Based Utility Materials at 800°C in Nitrogen.

Tentative Identification[a]	Maple Wood, Kraft Paper and Dicy-Kraft Paper	Kraft-Phenolic Laminates
Benzene	X	X
Toluene	X	X
Phenylacetylene	X	X
Styrene	X	X
1H-Indene or Propynylbenzene or Isomer	X	X
Benzaldehyde	X	X
Napthalene or Azulene or Isomer	X	X
Acenaphtylene or Biphenylene	X	X
Ethylbenzene		X
Xylene		X
9H-Fluorene		X
Phenol		X
Methylphenol		X
Benzofuran		X
Methylbenzofuran		X
Dibenzofuran		X
Aniline		X
Benzonitrile or Isocyanobenzene		X
Quinoline or Isoquinoline		X

[a]Other isomers possible.

DIFFERENTIATION OF POSITIONAL ISOMERS OF POLYCHLORINATED BIPHENYLS USING TRIPLE QUADRUPOLE MASS SPECTROMETRY AND AMMONIA AS THE COLLISION GAS: APPLICATION OF AN ION-MOLECULE REACTION STUDY.

Earl L. White* and Maurice M. Bursey†
Laboratory of Molecular Biophysics, National Institute of Environmental Health Sciences, P. O. Box 12233
Research Triangle Park, NC 27709

†Department of Chemistry, University of North Carolina at Chapel Hill, Chapel Hill, NC 27514

Polychlorinated biphenyls (PCBs) are major environmental pollutants and have been studied extensively during the last few years. These compounds exhibit varying levels of toxicity based on both the degree and position of chlorination. Most of the current methodology for PCB analysis involves quantification of these compounds as a class or congener group rather than as an isolated, specific isomer. Traditionally, results of PCB analyses were reported as an Arochlor type with four-digit numbers, where the last two digits indicated the level of chlorination. Identification of PCBs by class is relatively simple using capillary gas chromatography-mass spectrometry. However, differentiation and characterization of positional isomers is difficult if not impossible by conventional MS techniques. This study describes a method using triple quadrupole mass spectrometry and NH_3 as a reactive collision gas to differentiate between positional isomers.

An ion-molecule reaction study of benzoyl and p-substituted benzoyl ions showed that both nucleophilic substitution and addition occurred when NH_3 was used as the collision gas. Collisionally activated dissociation (CAD) and collisionally activated reaction (CAR) products were observed. Substituent effects were determined with p-halo-substituted benzoyl ions generated from protonated phenyl p-substituted benzoates. The pressure dependence and translational energy dependence of several reactions of these ions were studied. Conditions were chosen to maximize the information from product ions for qualitative analytical utility; therefore, no attempt was made to select single-collision conditions. In fact, the collision cell NH_3 pressure chosen was enough to attenuate the main beam by approximately 35% of its initial intensity, which is in the multiple-collision region. In this region, thermochemical information is of little value; however, both exothermic and endothermic processes were observed. Energetics for the reactions of the unsubstituted benzoyl ion with NH_3 showed that these processes ranged from -344 kJ mol^{-1} to +323 kJ mol^{-1} for the production of $[C_6H_5CO(NH_3)_4]^+$ and $[C_6H_4NH_3]^+$, respectively.

Application of these results to the reaction of NH_3 with a series of hexachlorinated biphenyl positional isomers using electron impact ionization suggests an energy dependence and consequently a difference in reactivity based upon relative positions of the chlorine atoms. The reaction of interest is given by the equation:

$$[C_{12}H_4Cl_6]^+ + NH_3 \longrightarrow [C_{12}H_4Cl_5NH_2]^+ + HCl$$

which indicate displacement of a Cl by NH_2 with loss of HCl. ND_3 was used to confirm reaction products. A plot of the fraction of total-ion-current vs. laboratory energy (eV) for a series of positional isomers showed a quantitative difference in production of this ion. The fraction of total-ion-current for this ion ranged from approximately 0.02 to 0.30 for 2,3,4,2',3',4'- and 2,3,5,2',3',5'-hexachlorobiphenyls, respectively. These differences demonstrate a characteristic difference in reactivity based on relative positions of the chlorine atoms.

*Present address: Applied Analytical Research Division, R. J. Reynolds Tobacco Company, Bowman Gray Technical Center, Winston-Salem, N. C. 27102

GAS CHROMATOGRAPHY-MASS SPECTROMETRY STUDIES ON BUTYLTINS AND THEIR ANALYSIS IN ENVIRONMENTAL SAMPLES. J. Greaves. Virginia Institute of Marine Science, College of William and Mary, Gloucester Point, VA 23062.

Tributyltin (TBT) is an antifouling agent that is added to some marine paints. It is currently used on merchant and recreational vessels and at the present time the U. S. Navy has expressed an intention of using it on naval vessels in order to reduce both fuel costs and maintenance time, thus improving fleet readiness. Environmental concerns have been raised because of the toxicity of TBT to invertebrates. Toxic effects in the sub parts per billion range have been reported. The use of TBT is considered to be particularly critical in areas such as the naval shipyards in Norfolk, Virginia because of the proximity of this area to the seed oyster production beds at the mouth of the James River.

Analytical procedures currently being used include tin hydride formation or derivatization for form tetraalkyltin which are then analyzed by gas chromatography with flame photometric detection (GC-FPD) or by atomic absorption spectrophotometry. The chromatographic advantages of using derivatization with hexyl magnesium bromide, to form hexylbutyltins, for the analysis of aqueous environmental samples has been reported (Unger, McIntrye, Greaves and Huggett; Chemosphere, 15:461-470, 1986).

Gas chromatography-mass spectrometry (GC-MS) has been used both in the full scanning and selected ion monitoring modes in order to provide confirmation of compounds tentatively identified by GC-FPD and to provide a second method of quantifying TBT and its degradation products in order to standardize laboratory results and in particular to be able to provide confirmation of quantifications made at the limit of detection of GC-FPD. An Hitachi GC coupled to an Extrel ELQ-400-2 quadrupole MS has been used for the analyses. The GC column was a 15m fused silica capillary coated with SE-54 which was run through the interface up to the source of the MS. The GC oven program was 70°C to 280°C at 10°C/min. The MS was operated in the positive chemical ionization (CI) mode with methane as the reagent gas. Comparison of methane with ammonia offered no advantage to using the latter. The alkyltins were derivatized with hexyl magnesium bromide to form the hexyl derivatives. The CI mass spectra obtained have no $[M+H]^+$ ions. The only major ion clusters corresponded to the loss of alkyl groups: i.e., tributyltin, hexyl derivative, gave m/z 319 and m/z 291 as the major peak in each cluster; dibutyltin, dihexyl derivative, gave m/z 317 and m/z 319; tripentyltin, hexyl derivative and internal standard, gave m/z 347 and m/z 333. Associated with each of these ions were ions corresponding to the isotope distribution of tin. This isotope pattern is very characteristic and it thus useful in recognizing compounds containing tin, in environmental samples. The fragmentation of the tetraalkyltins favors the loss of the heavier alkyl groups (hexyl for these compounds). This is most obvious for the dibutyltin (dihexyl derivative) where the base peak is the $[M\text{-hexyl}]^+$ ion at m/z 319. For TBT and monobutyltin the 3:1 ratio of alkyl groups masks this effect though it still can be seen if percentage intensities are calculated.

Analysis of water samples from the Elizabeth River and Sarah Creek (a tributary of the York River) area of Virginia have shown the presence of TBT and its breakdown products dibutyltin (DBT) and MBT. Confirmatory spectra were obtained in all cases. These water samples were obtained both from relatively open areas at the mouth of the Elizabeth River and from small boat marinas. Concentrations ranged from 5-150 ng/L of each compound.

Selected ion monitoring has been used for quantification. Calibration curves for each of the compounds (TBT, DBT and MBT) were straight for the 0-50 ppt range and gave correlation coefficient values of 0.99. A comparison study between GC-MS and GC-FPD using the same set of samples for analysis on each instrument gave excellent agreement between the two techniques with 13 of 18 determinations (6 each for TBT, DBT, and MBT) giving a concentration difference of ≤3 ng/L for concentrations in the 0-55 ng/L range. The maximum difference in concentration was 7 ng/L.

The results show the value of GC-MS both for the identification and confirmation of quantitative results obtained by GC-FPD. In addition the CI spectra obtained were characteristic, especially when the isotope distribution associated with tin is taken into account.

This research has been supported by the Virginia State Water Control Board and the Virginia Institute of Marine Science.

THERMAL IONIZATION MASS SPECTRAL ANALYSIS FOR STABLE ISOTOPE STUDIES OF MINERAL METABOLISM IN HUMANS

Judith R. Turnlund
USDA, Western Human Nutrition Research Center
Albany, CA 94710

Enriched stable isotopes of zinc, copper, iron, calcium, and magnesium were used as tracers in human experiments to determine their metabolic fate and gain a better understanding of mineral nutrition. Thermal ionization mass spectrometry (TIMS) was used to determine isotopic ratios of the minerals. The following isotopes were used in the studies:

$$^{67}Zn,\ ^{70}Zn,\ ^{65}Cu,\ ^{58}Fe,\ ^{54}Fe,\ ^{44}Ca,\ \text{and}\ ^{25}Mg$$

An automated, computer-controlled TIMS was used for measurement of iron and calcium isotopic ratios. Automated computer-controlled procedures have also been developed for isotope ratios of copper and zinc and are being developed for magnesium. These features increased speed of analysis and improved precision and accuracy of isotope ratio measurements. Measured natural ratios were within the range of established ratios for all ratios measured (1). Data from some of the experiments described were obtained with an older TIMS without automated, computer-controlled features.

Zinc, copper, and magnesium ratios were measured in purified samples using a single filament configuration. Silica gel was applied to the sample filament, followed by the sample, and H_3PO_4 to enhance ionization efficiency. Iron and calcium were determined using a double filament configuration.

A number of human studies were conducted in which mineral absorption was determined. Subjects of the studies were confined to a metabolic unit during the 84 to 92 day experiments (2). Enriched isotopes of Zn, Cu, and Fe were incorporated into diets fed to the subjects on selected days. Stable isotopes of Zn, Cu, Fe, Ca, and Mg were infused. Blood, urine, and fecal samples were collected. Minerals in the samples were separated and purified using ion exchange chromatography. To avoid mineral contamination, ultrapure reagents, distilled-deionized water, acid-washed glassware and plasticware, and thoroughly washed ion exchange resin were used for all of the sample preparation procedures. Isotopic ratios of the purified minerals were determined and used to calculate mineral absorption, excretion of endogenous minerals into the gastrointestinal tract, disappearance from the blood, and appearance in the urine. In addition to the stable isotope work, other data were collected which contributed to evaluation of mineral status and requirements. Data from the experiments have been used to gain a better understanding of mineral bioavailability, requirements, and status. Results of several of these studies are summarized below.

When normal healthy young men consumed recommended levels of all minerals, including 15 mg Zn, 3 mg Cu, and 10 mg Fe, Zn absorption averaged 31%, copper absorption averaged 26%, and Fe absorption averaged 8%. Copper and iron absorption were similar in elderly men, but zinc absorption was significantly lower and averaged only 17%. However, the elderly men were able to maintain zinc balance with absorption at this level. When the zinc content of the diets of young men was reduced, fractional absorption increased. Absorption averaged 24.7% with 16.5 mg Zn and 34.0% with 5.5 mg Zn. The increase in fractional absorption partially compensated for the lower amount of zinc in the diet. When sodium phytate was added to the diets of young men, zinc absorption fell from an average of 34.0% to 17.5% and resulted in negative zinc balance. Addition of the fiber source, α-cellulose, to the diet did not affect zinc absorption. Neither phytate nor α-cellulose impaired copper absorption.

Young women absorbed 24.6% of the ^{70}Zn added to food diets containing an average of 17 mg Zn. Copper absorption averaged 41% and 34% from diets with 1.44 and 2.53 mg of copper, respectively. Zinc absorption was not significantly different in pregnant women fed the same diets, but average absorption, 25.4%, was slightly higher in pregnant

women. Copper absorption was slightly but significantly higher in pregnant women than in non-pregnant women.

Zinc absorption was determined when a vitamin B-6 deficient diet containing 15 mg Zn was fed to young women. Average absorption was 40% and zinc balance was strongly positive, suggesting that zinc absorption and retention may be enhanced with vitamin B-6 deficient diets.

We injected five stable isotopes, ^{70}Zn, ^{65}Cu, ^{58}Fe, ^{25}Mg, and ^{44}Ca, simultaneously to evaluate the potential for using stable isotopes in mineral nutrition experiments. Experimental subjects were six healthy young men who were confined to a metabolic unit for a mineral absorption study. Five of the six received an infusion of the five isotopes and one subject received isotonic saline. Approximately 10% of circulating serum levels of the five minerals were infused, i.e., 350 µg each of ^{70}Zn, ^{65}Cu, and ^{58}Fe, 7 mg ^{25}Mg, and 35 mg ^{44}Ca. These levels were estimated to be the maximum amounts which could be used without markedly perturbing mineral metabolism. Blood was drawn at 15 minutes, 60 minutes, and 24 hours following isotope administration. Two 12-hour, then 24 hour urine collections and 6-day fecal collections were made. Zn, Cu, Fe, and Ca enrichments have been measured. Enrichments of zinc and calcium in plasma, urine, and feces were measured. It was possible to detect and measure enrichments in all the above samples by thermal ionization mass spectrometry.

Results of our absorption experiments suggest that a number of factors affect the availability of dietary zinc, and thus, the dietary zinc requirement. These factors include age, certain dietary components, levels of zinc, and levels of some other nutrients, as well as individual variability. Fewer of the variables studied to date appeared to alter copper availability, but results suggest that there are differences among individuals and that the level of dietary copper may affect copper availability.

Results of the isotope infusion experiments demonstrated that stable isotopes of five minerals can be infused simultaneously and enrichments measured in blood, urine, and feces. Therefore, mineral utilization and interactions can be evaluated in a number of minerals simultaneously using enriched stable isotopes.

Supported in part by USDA Competitive Grant CRCR-85-1-1581.

1. Holden, N.E., R.L. Martin, and I.L. Barnes. Pure and Applied Chemistry 55:1119-1136, 1983.
2. Turnlund, J.R. ACS Symposium Series 258:41-52, 1984.

Studies of Calcium Metabolism Using
Isotope Dilution - Thermal Ionization Mass Spectrometry

Alfred L. Yergey, David G. Covell, Nancy E. Vieira, Joseph Muenzer
National Institutes of Health, Bethesda, MD 20892

The five minor stable isotopes of Ca can all be used as in vivo tracers of Ca metabolism in humans. The particular isotopes that are used are selected based on considerations of saftey of experimental subjects as well as the price and availability. For long term kinetic studies, it is desired to perturb the rapidly circulating internal pool of Ca by 5 to 10-fold in the tracer isotope. For this reason ^{44}Ca cannot be used intravenously. On the other hand, ^{46}Ca is too expensive to use in any subjects other than newborns and infants. Stable isotopes are of course ideal tracers for their elements from physical and chemical standpoints,
and it is assumed that they mix rapidly and uniformly with the tracee. Stable isotopic tracers are generally not truly massless in the sense that radio tracers are, but careful choice of dose levels makes this assumption valid. We have been using a Finnigan MAT Thermoquad (thermal ionization/quadrupole) to measure Ca isotope ratios in human biological fluids for the past 18 months. The accuracy and reproducibility of this instrument for the measurement of Ca natural abundance ratios are shown in Table 1. It can be seen that the accuracy of a typical filament is excellent and that the reproducibility is quite satisfactory, although an order of magnitude improvement could be expected from a sector field analyzer. Initial experiments characterizing the instrument with respect to minimum detectable level of isotope above natural levels[1] showed that 2.5 delta % excess with a relative standard deviation of about 0.5% could be detected in serum and urine. While we are conducting a number of studies of the dynamics of whole body Ca metabolism, this presentation will focus on recent results from the dynamics of the absorption process. Figure 1 shows a schematic of absorption studies that employ two isotopic tracers, one orally and one intravenously. The pharmacokinetics of this model can be solved explicitly to yield an expression that shows that Ca absorption is the product of a number of rate constants and the tracer doses when sufficient time has elapsed from the start of the study. At sufficiently long times, Eq. 1 can be used to calculate reliable values of fractional absorption, "a":

$$\text{"a"} = \frac{(\text{n.a. oral tracer}) * (\text{delta \% excess oral tracer}) / (\text{oral tracer dose})}{(\text{n.a. iv tracer}) * (\text{delta \% excess iv tracer}) / (\text{iv tracer dose})}$$

where n.a. is the fractional natural abundance of the isotope used orally or intravenously. It is apparent that accurate determinations of fractiojnal absorption are very dependent upon accurate measurements of isotope ratios. We have applied this method to a number of subject populations including premature infants, children with end organ vitamin D resistance and normal adults. Results from the studies of prematures using ^{46}Ca (3 ug/kg) as the iv tracer and ^{44}Ca (1.2 mg/kg) as the oral tracer are shown in Figure 2. In contrast to the observation that absorption plateaus after about 24 hours for in normal adults, it is seen from the Figure that the value of fractional absorption for these two infants reached a plateau value after

about 12 hr. We have subsequently confirmed this much shorter time to plateau values in 4 other premature infants.

1. N.E. Vieira, M.P. Schmidt, A.L. Yergey, Proceeding of the 33rd Annual Meeting on Mass Spectrometry and Allied Topics, San Diego, CA, May 26-31, 1985, p. 615.

Table 1

Natural Abundance Ca

Isotope Ratios

Ratio	Observed*	NBS	Δ†
42/48	3.5197 ± 0.2%	3.5186	+0.03%
44/48	11.2695 ± 0.1%	11.2702	-0.006%
46/48	0.01754 ± 0.5%	0.01714	+2.33%

* Mean ± RSD - 3 sets of 10 scans each, 2 sec/amu
Fractionation corrections made using 43/48 for each 10 scan set

† Difference between Obs'd and NBS values

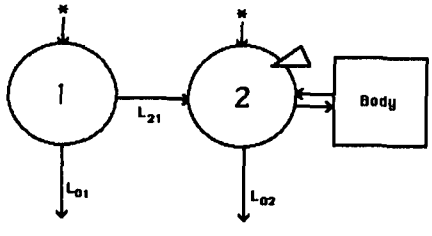

Figure 1. Compartmental Model for Absorption

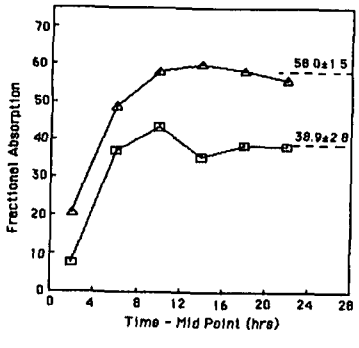

Figure 2. Absorption vs Time for 2 Premature Infants

ISOTOPE RATIOS BY INDUCTIVELY COUPLED PLASMA-MASS SPECTROMETRY FOR MINERAL BIOAVAILABILITY STUDIES: Robert E. Serfass, Joseph J. Thompson, and Robert S. Houk, Departments of Food and Nutrition, and Chemistry, Ames Laboratory - USDOE, Iowa State University, Ames, Iowa 50011.

Inductively coupled plasma-mass spectrometry (ICP-MS) is a relatively new instrumental method for elemental analysis and isotope ratio determination (1-3). The most common form of sample introduction is to nebulize an aqueous solution and inject the resulting aerosol into the ICP. Vaporization, atomization, and ionization of sample constituents are very efficient in the high temperature, inert gas atmosphere. By using the first ionization energies of each of the elements in the Saha equation, it is estimated that some 54 elements are expected to be ionized with an efficiency of 90% or more. Even metalloid or nonmetallic elements with high first ionization energies, such as Br, can be ionized with useful efficiency. Ionization reactions at atmospheric pressure are not extremely energetic so that analyte ions are present mainly as singly charged, monatomic positive ions with few (< 10%) molecular or multiply charged species. M^{2+} levels reaching 10% of total analyte ion density are expected only for elements with the lowest second ionization energies, in particular Ba and several rare earths. Most elements yield no significant M^{2+} or MO^+. Observed levels of MO^+ for elements that tend to form refractory oxide species, such as the rare earths, alkaline earths, Th, and U, can reach 0.8% relative to M^+. Oxide ion problems can be identified easily by obtaining m/z scans of actual samples and can be minimized by adjusting ICP operating parameters. Some oxide ions present in excess must be separated from trace analytes. For example, CaO^+ from large amounts of Ca in biological samples can interfere with determinations of nutritional trace analytes. The major ions in background spectra (Ar^+, ArH^+, O^+, H_2O^+) overlap directly with few analyte peaks of biological interest ($^{40}Ca^+$, $^{40}K^+$, $^{41}K^+$). Minor ions (O_2^+, ArO^+, Ar_2^+, etc.) must be anticipated and compensated for during determinations of S, Fe, Se, respectively.

Ions are sampled from the ICP into the mass spectrometer by allowing them to flow through a circular orifice (ca. 1 mm dia.) in a metal cone into a mechanically-pumped vacuum chamber at a pressure of approximately 1 torr. The central section of the expanding jet flows through a conical skimmer and into another high vacuum chamber where the ions are resolved by a quadrupole mass analyzer and detected by an electron multiplier in pulse counting mode. Sensitivity is greater than 10^5 $counts \cdot s^{-1} \cdot mg^{-1} \cdot L^{-1}$ for most elements so that detection limits are usually below 0.1 $\mu g \cdot L^{-1}$.

Isotope ratios are measured repetitively by signal averaging while either scanning the quadrupole continuously or jumping it sequentially between peaks of interest. Easily ionized elements that predominate in biological matrices (e.g., Na, Mg) can suppress analyte signal and alter isotope ratios (4). Sodium concentrations of solutions to be analyzed should be kept below 1mM for accurate ratio determinations of minor isotopes at total analyte concentrations between two and ten $mg \cdot L^{-1}$. Total ion current measurements at solute levels above 1% are complicated by orifice plugging and transport loss of analyte in the desolvation system for the ultrasonic nebulizer used. Accordingly results reported here for trace constituents of biological samples benefit from separation and/or preconcentration of the analytes of interest from the bulk of solute.

Solvent extraction of chelates of the analytes of interest, followed by a second extraction into dilute hydrochloric acid provides sufficient separation and preconcentration of elements such as zinc from ashed samples of bovine milk, infant formulas, blood plasma, red blood cells, feces, and urine. Double isotope ratios (e.g., ^{70}Zn and ^{67}Zn referenced to ^{68}Zn) are acquired on 10 µg of analyte in 5 ml of aqueous solution with relative standard deviations typically less than 1 percent. Differences between measured ratios and literature ratios for natural abundance samples are usually less than 2% and can be normalized by analysis of standards. Least squares analysis of $^{70}Zn/^{68}Zn$ ratios of spiked fecal solutions from natural abundance to 370 atom % excess of ^{70}Zn gives a correlation coefficient

of 0.99988. Recoveries of spikes of ^{70}Zn and ^{67}Zn in fecal solutions are within 1% of expected values, with reproducibilities (RSD) of 1% or less.

Rapid separation and preconcentration of analytes can be achieved by using ion pair-reversed phase liquid chromatography. Isotope ratios on eluting peaks of Cd and Pb were measured with precision better than 2%, demonstrating that LC-ICP-MS should facilitate the application of stable isotopic tracers to metal speciation studies in biological systems. Thus, ICP-MS can be useful for rapid isotope ratio determinations for many biological experimental designs where relative standard deviations of 0.3 to 2.0% are sufficient.

1. Douglas, D.J., Houk, R.S. Prog. Anal. Atomic Spectrosc. 1985, 8, 1-18.
2. Houk, R.S. Anal. Chem. 1986, 58, 97A-105A.
3. Gray A. L. Spectrochim. Acta 1985, 40B, 1525-1538.
4. Olivares, J.A., Houk, R.S. Anal. Chem. 1986, 58, 20-25.

QUANTITATION AND USE OF STABLE ISOTOPES OF CALCIUM IN CALCIUM NUTRITION STUDIES

X. Jiang, Y. Liu, D.L. Smith, I. Shu, and C. Weaver
Purdue University
West Lafayette, Indiana 47907

Bone fractures in the elderly are frequent, and are believed to be related to one's peak bone mass, which is usually attained between the ages of 30 and 40 years. Since peak bone mass may be determined, in part, by calcium intake during the growth years, it is important to know calcium bioavailability from calcium rich foods and frequently used supplements. We have used fast atom bombardment mass spectrometry (FABMS) and stable isotopic tracers of calcium to investigate the realationship between calcium intake, via diet or supplement, and calcium absorption.

Thermal ionization mass spectrometry is the reference method for determining isotopic abundances of metals and has been used extensively for this purpose. Despite its undisputed success, thermal ionization mass spectrometry has been used in few nutritional studies because of the necessity for extensive sample preparation, and because the appropriate instruments have not been readily available. FABMS, which could also be called particle induced desorption mass spectrometry, has been proposed as an alternative to thermal ionization (1,2). This method is attractive because it requires little sample preparation and may be performed with a conventional high resolution mass spectrometer normally used for organic analysis.

Calcium and magnesium isotopic tracers in urine are quantified by first making the oxalate/hydroxide precipitate, which is subsequently dissolved in hydrochloric acid and analyzed on a stainless steel probe tip. Metal ions, Ca^+ or Mg^+, are desorbed from the surface of the sample by a high energy xenon beam, and mass analyzed at a resolution of 4,000. A relatively simple data system, based on an IBM personal computer, directs the mass spectrometer to the isotopic beams of interest and records their intensities. Although calcium tracers may be analyzed directly in urine and plasma (1), higher accuracy is achieved with this sample preparation procedure.

The precision with which the Ca-40/Ca-44 ratio can be determined with the present mass spectrometer (Kratos MS-50) and custom data system is illustrated in Table 1. Each of the ten measurements is derived from the time averaged signals from ten cycles between the two isotopic peaks. Ion intensities from each cycle are used to calculate a value for the isotopic ratio; values for ten cycles are combined to give each of the values listed in Table 1. These data demonstrate that ion abundances of calcium can be determined from a single ten cycle measurement with an average RSD of 0.25%. When ten such measurements are combined, the RSD decreases to 0.07%. The average of the ion abundance ratios, 61.27, is greater than the accepted ratio of the isotopic abundances, 46.6, because these measurements are made with different ion accelerating voltages, and because there is a small isotope effect in the ion desorption process. This feature does not, of course, preclude using FABMS to determine <u>changes</u> in isotopic abundances (2). It is also important to note that there is no apparent change in the intensity ratio which may be attributed to isotopic enrichment during sputtering.

Experimental parameters used for acquiring these data are given in Table 2. Since the Ca-40 signal is much more intense than the Ca-44 signal, more time was spent monitoring the weaker signal, as indicated by the number of analog-to-digital (ADC) samples taken for each beam. The same ADC sampling frequency, 200 Hz, was used to record both beams. The actual time spent monitoring each of the beams in each cycle is determined by the number of samples and frequency of the ADC. Taking into account the electron multiplier gain, the rate at which ions reached the detector was also determined. These data were used to calculate the actual number of ions detected during a ten cycle measurement. Results in Table II show that ion statistics limit these measurements to approximately 0.12%. The difference between the theoretical and experimental RSD's (0.12% vs. 0.25%) may indicate presence of other sources of error, or may be due to uncertainty in determining the gain of the electron multiplier. The fact that the RSD for the ten measurements listed in Table 1 is a factor of approximately three less than the RSD for ten cycles, as would be expected if ion statistics were the limiting factor for high precision, suggests that the electron multiplier gain is likely incorrect.

Replicate analyses of enriched urine sample using FABMS showed tht enrichments of 10% can be determined with a precision of ±0.4%, which makes this a useful method for investigating calcium absorption in human subject.

Table 1

Results for ten, 10-cycle measurements of the Ca-40/Ca-44 ratio for a natural abundance calcium standard by high resolution FABMS.

	40/44	RSD% (10 cycles)
	61.33	0.18
	61.21	0.18
	61.24	0.29
	61.24	0.26
	61.26	0.16
	61.27	0.38
	61.26	0.25
	61.34	0.29
	61.25	0.28
	61.27	0.27
Ave.	61.27	0.25
RSD	0.07%	

Table 2

Experimental parameters used for acquiring results given in Table 1.

	Ca-40	Ca-44
Number of ADC Samples	30	390
ADC Sample Frequency (Hz)	200	200
Sampling Time/cycle (sec)	0.15	1.95
Ions Detected/sec	2.8×10^6	4.6×10^4
Ions Detected in 10 cycles	4.2×10^6	9.0×10^5

$$\text{RSD (Statistical Limit)} = 100\sqrt{1/N_1 + 1/N_2} = 0.12\%$$

References

1. D.L. Smith, Anal. Chem. 55, 2391 (1983).

2. G.O. Ramseyer, J.T. Brenna, G.H. Morrison, and R. Schwartz, Anal. Chem. 56, 402 (1984).

MASS DISCRIMINATION PHENOMENA IN FAST ATOM BOMBARDMENT MASS SPECTROMETRY OF METAL STABLE ISOTOPES: L.V. Miller, P. Peirce, C. Goss, K.M. Hambidge, and P.V. Fennessey; University of Colorado Health Sciences Center, Denver, Colorado 80262

Fast atom bombardment mass spectrometry (FAB-MS) of metals placed on a dry target has been shown to be a viable analytical tool since it's first description by Smith in 1983.[1] We have investigated and successfully applied this technique to isotope dilution studies of trace metal nutrition. However, we have been perplexed by the consistent presence of an isotope fractionation effect. Therefore, we have undertaken a systematic examination of this mass discrimination phenomenon in an effort to understand its source and nature.

We have examined a variety of metals, but used Molybdenum for a majority of our work because of its ease of use and its seven abundant isotopes. The work was performed on a VG 7070E double-focusing sector instrument and full scans of an element's isotopes were digitized and averaged with a Tracor Northern TN-1710 Digital Signal Analyzer.

A body of reference data of molybdenum isotope fractionation (Figure 1) was acquired under standard instrument operating conditions typical of all our FAB-MS of metals (Table 1). The data was plotted to show the deviation of measured abundances from theoretical abundance for all isotopes. Fractionation in %/AMU was derived from the regression line. The mean fractionation for all the standard data was 1.43 with a standard deviation of 0.076. One by one the various instrument conditions were adjusted to enhance any instrumental mass discrimination related to those conditions (Table 2). The only resulting fractionation values lying outside two S.D. significance limits were the voltage scan value, as expected, and the down scan value, which is probably a result of our sequential ion detection technique. A measurement of and subsequent recalculation for a 1.3% Molybdenum hydride interference proved insignificant, though a similar process proformed with the Tin data did produce a significant change in several isotope abundances and the resulting fractionation value. Hydride interference effects appear to vary from metal to metal as well as isotope to isotope.

When the source was changed and electron impact ionization of Xenon was performed under otherwise standard conditions, no isotope fractionation was observed. This points to the FAB sputtering/ionization process and/or the FAB source as the origin of the mass discrimination phenomenon.

A Molybdenum sample was placed in the FAB source and bombarded continuously for 8 hours (Figure 2). Observed average atomic weight values were calculated from the data acquired and plotted against time. The increase of the average atomic weight with time can be interpreted as demonstrating the existence of a preferential sputtering process as the origin of the mass discrimination effect observed with FAB-MS of metals. This would agree with theories proposed to explain the similar mass discrimination phenomenon attending secondary ion mass spectrometry of metal.[2]

We have also compared fractionation values determined for other metals. When this data is combined with additional data acquired using other primary atoms, we hope to be able to construct a hypothesis that will describe this phenomena in detail.

1. D.L. Smith, Anal. Chem., 55:2391,(1983).
2. R. Kelly, Nucl. Instr. Methods, 149:553, (1978).

TABLE 1
FAB - MS OF METAL ISOTOPES

STANDARD CONDITIONS

INSTRUMENT	
RESOLUTION	3000
ACCEL. VOLTAGE	6 kV
E. MULTIPLIER	2.2 kV
PEAK MULTIPLIER CURRENTS	1 TO 3 X 10^{-9}A
FAST ATOM GUN	8 kV/1 mA, XENON
SCANNING	MAGNETIC, LINEAR UP, 20 A M U /SEC
DIGITAL SAMPLE PTS/SCAN	8000
# SCANS DIGITALLY AVERAGED	200
SOURCE PRESSURE	1 TO 5 X 10^{-6} mB
ANALYZER PRESSURE	0.5 TO 2 X 10^{-9} mB
SAMPLE	8 TO 20 μg IN 3 TO 8 μl H_2O OR DILUTE ACID (A.A. STANDARDS) TAKEN TO DRYNESS
TARGET	DRY STAINLESS STEEL OR Au COATED

TABLE 2
MOLYBDENUM MASS DISCRIMINATION
ADJUSTMENT OF INSTRUMENT CONDITIONS

	%FRAC/AMU
E. MULTIPLIER TO 1.5 kV	1.53
E. MULTIPLIER TO 3.0 kV	1.43
CONV. DYNODE TO 3.0 kV	1.53
FARADAY DETECTOR	1.41
ACC. VOLTAGE TO 4.0 kV	1.47
VOLTAGE SCAN	3.97
ACC. VOLTAGE OFFSET +20 V	1.37
ACC. VOLTAGE OFFSET −20 V	1.48
FAST ATOM GUN TO 4.0 kV	1.38
EXPONENTIAL UP SCAN	1.48
LINEAR DOWN SCAN	1.11
1.3 % HYDRIDE RECALCULATION	1.45
STD. CONDITIONS MEAN ± 2 σ	1.43 ± 0.152

FIGURE 1

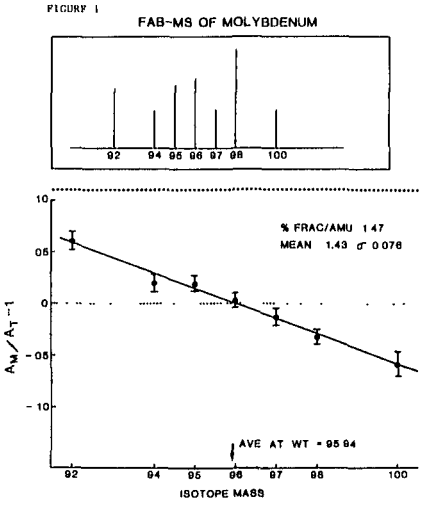

FIGURE 2

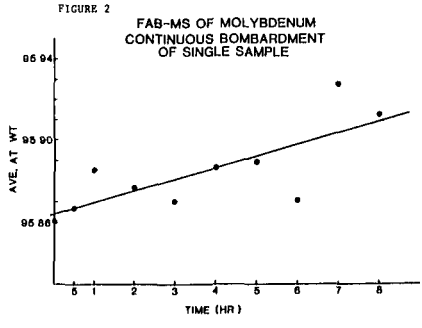

AN $^{18}O/^{16}O$ WATER-CARBON DIOXIDE EXCHANGE SYSTEM FOR ISOTOPE RATIO MEASUREMENTS OF MICROLITER-QUANTITIES OF WATER SAMPLES OF NATURAL ABUNDANCE AND BIOLOGICAL FLUIDS

William W. Wong, Lucinda S. Lee, and Peter D. Klein

USDA/ARS Children's Nutrition Research Center
Department of Pediatrics, Baylor College of Medicine
Houston, TX 77030

INTRODUCTION

The conventional technique for the measurement of $^{18}O/^{16}O$ isotope ratios in water and aqueous samples is to equilibrate 2 to 10 ml of sample with CO_2 of known ^{18}O content with constant shaking at 25°C for > 48 hr. The procedure is both time-consuming and labor-intensive because the water sample must be frozen before the CO_2 is added for equilibration or removed for isotope ratio measurements by gas-isotope-ratio mass spectrometry (GIRMS). In 1970, Roether (1) described a H_2O-CO_2 exchange system in which 10 ml of water was transferred to an equilibration vessel, after which the vessel was evacuated through a capillary. Because of the differential in pumping speeds between the water vapor and the atmospheric gases passing through the capillary, a negligible amount of water was pumped away. After evacuation, CO_2 was leaked into the vessel through the capillary and the H_2O/CO_2 mixture was allowed to equilibrate with constant shaking at 18°C for 2 hr. At the end of the equilibration, the CO_2 was expanded into a sample bulb for isotope ratio measurement. Nine water samples could be processed simultaneously.

A commercial version of the H_2O-CO_2 exchange system (ISOPREP-18, VG Instruments, Ltd., Cheshire, England) is now available. The system can accommodate 24 samples simultaneously. With the exception of sample introduction, the entire process of evacuation, CO_2 injection, shaking, CO_2 extraction, and isotope ratio measurement is controlled automatically with a computer. We have evaluated the accuracy and precision of the ISOPREP-18 H_2O-CO_2 exchange system for the analysis of 1) five international water standards and 2) microliter quantities of biological fluids at natural abundances and at enriched levels of ^{18}O.

EXPERIMENTAL

Effect of sample volume on equilibration time. Twenty-four 5-ml, 1-ml, 0.5-ml, and 0.1-ml aliquots of laboratory deionized water were introduced into the 16-ml equilibration vessels. The vessels were evacuated through the capillaries (0.015 mm id) for 180 sec and 300 mbar of CO_2 was admitted into each vessel. The H_2O-CO_2 mixtures were allowed to equilibrate for different durations at 25°C with constant shaking before the expansion of the CO_2 into the mass spectrometer for $^{18}O/^{16}O$ isotope ratio measurements.

Effect of vessel volume on equilibration time. The above experiment was repeated with 24 0.1-ml aliquots of water enriched with ^{18}O (502 °/oo vs V-SMOW/SLAP) using the 16-ml equilibration vessels and 1-ml flasks.

Memory effect. Memory effect was determined by measuring the $^{18}O/^{16}O$ ratios of 0.1-ml aliquots of ^{18}O-enriched urine, plasma, saliva, and breast milk repetitively after measurement of samples with natural abundances of ^{18}O.

Accuracy and precision. 100-µL aliquots of 5 international water standards (Vienna-Standard Mean Ocean Water [V-SMOW], National Bureau of Standards water #1 [NBS-1], National Bureau of Standards water #1A [NBS-1A], Greenland Ice Sheet Precipitation [GISP], and Standard Light Antarctic Precipitation [SLAP]) and 10 urine, plasma, saliva, and human milk samples with natural abundances of ^{18}O, and 10 of each enriched with $H_2{}^{18}O$ were introduced into the 1-ml equilibration flasks with an Eppendorf pipet. Five 100-µL aliquots of each biological fluid at natural abundance and after enrichment with ^{18}O were analyzed by GIRMS.

RESULTS

Effect of sample volume on equilibration time. The effect of sample volume on equilibration time is illustrated in Figure 1. A 5-ml water sample required approximately 4 hr for the oxygen atoms in the water and the CO_2 to reach 99.9% of the final isotope equilibrium. The time required for equilibration increased as the sample volume decreased; a 100-µl water sample required approximately 45 hr to attain 99.9% isotopic equilibrium.

Effect of vessel volume on equilibration time. Replacement of the 16-ml equilibration vessels with 1-ml flasks led to a drastic reduction in equilibration time (45 hr to 10 hr) for the 100-µl water sample.

Memory effect. As shown in Figure 2, the $^{18}O/^{16}O$ ratio of a spiked sample (approximately 254 o/oo over natural abundance) was within 99.6 ± .06% (mean ± SD, n = 4) of the final values after the third consecutive analysis.

Accuracy and precision. With a 1-ml sample volume, an average accuracy of 0.14 ± 0.40 o/oo (mean ± SD, n = 24) was obtained for the five international water standards with ^{18}O values which ranged from 0 to -55.5 o/oo vs V-SMOW/SLAP. These ratios were reproducible within 0.35 o/oo (SD). Similar accuracy (0.05 ± 0.44 o/oo, n = 111) and precision (0.33 o/oo, SD) were obtained on 100-µl aliquots of the same water standards with either the 16-ml or the 1-ml equilibration vessels. At 250 o/oo enrichment level of ^{18}O, the $^{18}O/^{16}O$ ratios measured from 0.1-ml aliquots of urine, plasma, saliva, and breast milk were accurate to -0.32 ± 0.87 o/oo (n = 200) and reproducible within 0.97 o/oo (SD, n = 200).

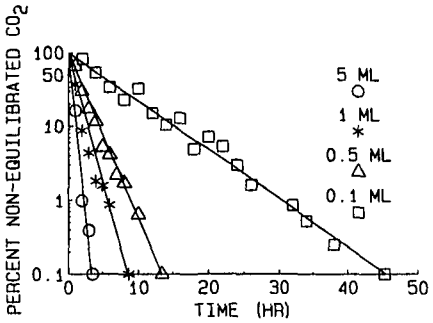

FIGURE 1: Effect of sample volume on equilibration time.

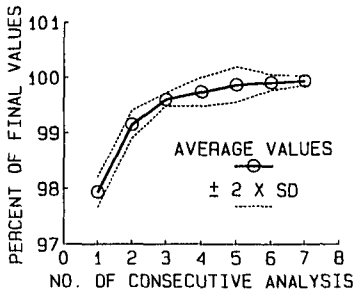

FIGURE 2: Memory effect.

CONCLUSION

With proper modifications and precautions, the ISOPREP-18 H_2O-CO_2 exchange system is capable of accurate and precise $^{18}O/^{16}O$ isotope ratio measurements on microsamples of water and biological fluids at natural abundances and at enriched levels of ^{18}O.

REFERENCES

(1) Roether, W. Int. J. Appl. Radiat. Isot. 1970, 21:379-387.

ACKNOWLEDGMENTS

This work is a publication of the USDA/ARS Children's Nutrition Research Center, Department of Pediatrics, Baylor College of Medicine and Texas Children's Hospital, Houston, TX. This project has been funded in part with federal funds from the U.S. Department of Agriculture, Agricultural Research Service under Cooperative Agreement number 58-7MNI-6-100. The contents of this publication do not necessarily reflect the views or policies of the U.S. Department of Agriculture, nor does mention of trade names, commercial products, or organizations imply endorsement by the U.S. Government.

IONIZATION MECHANISMS IN THE GLOW DISCHARGE ION SOURCE; K. R. Hess and W. W. Harrison, Department of Chemistry, University of Virginia, Charlottesville, Virginia, 22901

The pin glow discharge source has seen increasing use as an ion source for solids elemental analysis by mass spectrometry. The gaseous discharge produced by applying a large (1000 - 2000 V) negative potential between the cathode, formed from the sample material, and the ion exit orifice, which seves as the anode, is known to generate mass spectra representative of the sample composition. Two major mechanisms of ionization may occur in the discharge, electron impact and Penning ionization. Penning ionization involves an energy transfer from a metastable gas atom to a species with an ionization potential less than the energy of the metastable state, resulting in ionization. Although Penning ionization was thought to dominate in our discharge configuration, no conclusive evidence was available. Recent studies were undertaken to elucidate the ionization mechanisms occuring in our glow discharge source.

The experiments performed involved three areas; 1) measurement of the atomic densities of the sputtered species and the metastable argon species along with the corresponding ion signal magnitudes to determine if there is a correlation between the two, 2) investigations of the effect of laser depopulation of the metastable state on the ion signals from the discharge and the current/voltage properties of the discharge (opto-galvanic effect), and 3) studies of the effects of quenching agents and gas mixing on the discharge ion signals and current/voltage characteristics. The instrumentation used in these studies is diagramed in Figure 1. A Lumonics TE-860-4 excimer laser operating on XeCl pumps a Lumonics EPD-330 dye laser whose output is directed into a 6-way cross for interaction with the discharge plasma. The laser beam may be replaced by a hollow cathode lamp whose output traverses the discharge and is focused into a monochrometer for atomic absorption analysis. The ions formed in the discharge are extracted and focused by an einzel lens system, undergo energy filtering in a Bessel Box energy analyzer, and finally are mass filtered in a quadrupole. The ion signal may be detected in an analog mode or through ion counting using a Princeton Applied Research model #112 ion counter/processor. The mass spectrometer is controlled by DEC-MINC-11 computer. The discharge is operated at 0.3 -1.2 torr, 1- 5 mA, and voltages of 100 - 35000 V.

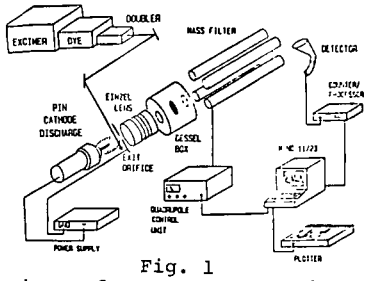

Fig. 1

The atomic density of copper was monitored as a function of pressure using the ground state 327.4 nm transition for atomic absorption. The atomic profile obtained is shown in Figure 2A. The metastable argon population vs. pressure was monitored by atomic absorption at the 696.54 nm transition, and the profile obtained is presented in Figure 2B. Figure 2C shows the copper ion signal profile vs. pressure plotted with product of the copper ground state population and the argon metastable state population. The two profiles show some correlation , indicating a copper ionization dependence on the argon metastable state as well as the copper atomic population. This is characteristic of Penning ionization.

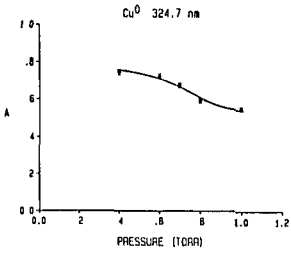

Fig. 2A

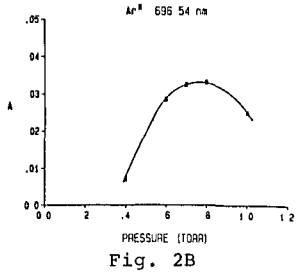

Fig. 2B

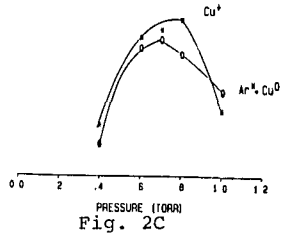

Fig. 2C

When the laser is tuned to a transition originating in the rare gas metastable state, a net depopulation of the state can occur through excitation out of the metastable level followed by relaxation to the ground state. With argon was used as the discharge gas and depopulated at 696.54 nm, the only ion signals showing decreases were Ar^+ and the species that can be Penning ionized. Species with ionization potentials higher than 11.55 eV, such as H_2O (I.P.=12.6) and N_2 (I.P.=15.6), do not show ion signal decreases upon laser irradiation. These species can be Penning ionized by neon (metastable level at 16.62 eV), and when using neon as the discharge gas with depopulation at 594.48 nm, all ion signals including H_2O and N_2 showed decreases during laser/discharge interaction. This, again, is indicative of a Penning ionization process. The decreases in Ar^+ and Ne^+ upon laser irradiation arise from less efficient electron impact ionization with metastable depopulation. Since there are more electrons with energies that can ionize the discharge gas from the metastable state, ionization from this state is more efficient than electron impact from the ground state and depopulation of the metastable state will result in a lower ionization rate of the rare gas.

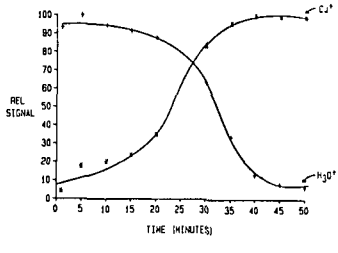

Fig. 3A

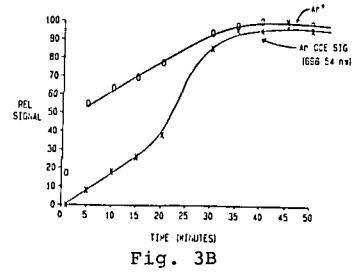

Fig. 3B

Mixtures of argon and neon result in the Penning ionization of argon by the neon, so increasing the amount of neon while reducing the amount of argon in the discharge actually increases the argon ion signal. Water is known to quench metastable states and is also known to be present in the discharge for some time after it is turned on. Magnitudes of discharge resistance changes and ion signals for several species were monitored vs. time after turning on the discharge. The results are plotted in Figure 3A and 3B. As the H_3O^+ decreases, all of the other ion species increase. The effect of laser depopulation of the metastable state (opto-galvanic effect) also increases as water decreases, since there is less quenching and higher metastable populations in the absence of water. These results again provide evidence that the metastable rare gas atoms serve a very important role in the ionization mechanisms present in the glow discharge.

PARAMETRIC EVALUATION OF THE HOLLOW CATHODE PLUME ATOMIZATION/IONIZATION SOURCE FOR SOLIDS ANALYSIS: F.L. King,Jr., R. Kenneth Marcus, and W.W. Harrison; Department of Chemistry, University of Virginia, Charlottesville, Virginia 22901.

Currently, the hollow cathode plume (HCP) glow discharge is being evaluated as a potential atomization/ionization source for solids mass spectrometry. Upon atomization, by means of cathodic sputtering, sample material diffuses out into an energetic plasma plume where ionization takes place. The effects of discharge parameters on ion signals observed can be related to ionization mechanisms in the plume.

EXPERIMENTAL

The HCP is mounted in a six way cross to allow for simultaneous study of metastable species by atomic absorption and ionic species by mass spectrometry. The plume is axially sampled by a quadrupole mass spectrometer through a skimmer cone with a 0.5 mm orifice, while being perpendicularly probed by atomic absorption as shown in Figure 1. Mass spectral scanning and ion energy profiling are controlled through a DEC MINC 11/23 which also stores the acquired data.

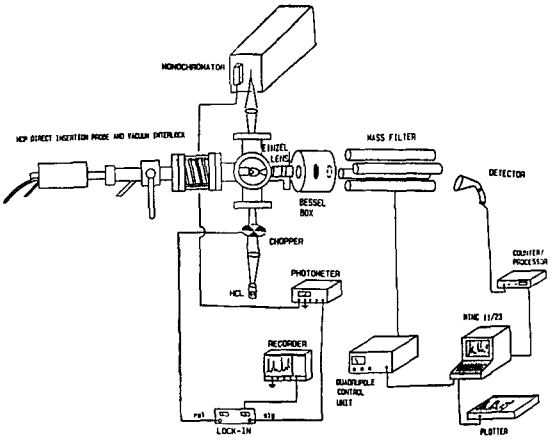

Figure 1. System for simultaneous atomic absorbtion mass spectrometric sampling of the HCP

Samples take the form of a disc 4 mm in diameter, 2 mm thick with a 1.5 mm orifice in the center where the discharge is localized. The disc is held in a disposable graphite cylinder which is then mounted in the tip of a direct insertion probe. Connections for discharge gas inlet and electrical current are made through the probe. The probe is mounted to the cross through a bellows which allows for the adjustment of the plume's position relative to the skimmer cone.

RESULTS AND DISCUSSION

It had previously been observed that a significant difference existed between the kinetic energies of discharge gas ions and sputtered sample ions, thus allowing spectral simplification by energy discrimination.[1] Studies of the effect of discharge pressure on this energy difference and argon metastable species were conducted to elucidate the nature of the ionization processes in the HCP and to determine the discharge conditions which yield the best sputtered ion signal. Atomic absorption studies show a decrease in the metastable argon population with increasing discharge pressure. Species in the plume undergo two primary mechanisms of ionization, electron impact and metastable collisions. The former mechanism would be expected to produce ions of lower kinetic energy than the latter, making it possible to discriminate energetically between species which are ionized by these different mechanisms. Ion energy profiling of sputtered and discharge gas ions at different pressures show that as pressure was decreased the energy profile of the discharge gas ions shifted towards that of the sputtered ions and split yielding two maxima, Figure 2.

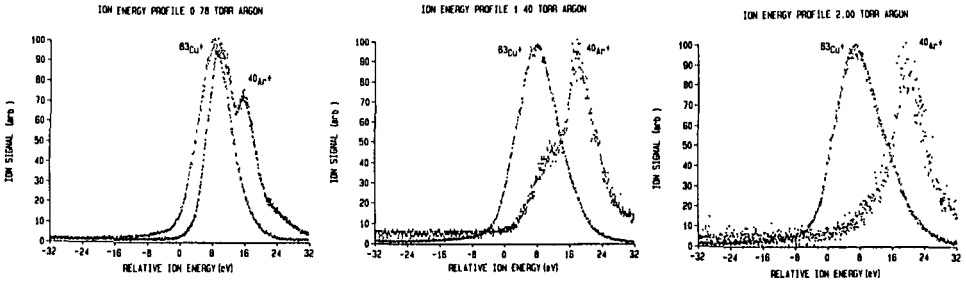

Figure 2. Ion energy profiles for $^{63}Cu^+$ and $^{40}Ar^+$ at .78 torr, 1.4 torr, and 2.0 torr (energy values not calibrated)

Penning ionization would be expected to be dominant when conditions provide the greatest metastable population, at lower pressures in the HCP. These data seem to indicate that sputtered species are ionized primarily through Penning (metastable collision) mechanisms at all pressures studied, while discharge gas species are primarily ionized by electron impact at higher pressures and metastable collisions at lower pressures. Optimal discharge pressure conditions for energy discrimination are found to exist at 1.4 torr where the sputtered ion signal also maximizes.

1. Marcus, R. Kenneth; King, Fred L. Jr.; Harrison, W. W. Anal. Chem. 1986, 58, 972.

THE EFFECT OF SMOOTHING ON THE PRECISION AND ACCURACY OF QUANTITATIVE GC-MS DATA.

Gareth C. Thorne* and Simon J. Gaskell
Tenovus Institute for Cancer Research, University of Wales College of Medicine, Cardiff, CF4 4XX, U.K.

(*Present address: Dept. of Medical Physics, Cardiff Royal Infirmary, Cardiff, U.K.).

Selected ion monitoring (SIM) techniques provide optimal sensitivities of MS analysis, permitting detection in the femtogramme range in favourable instances. Limits of detection are determined by the signal/background ratios achieved, the background being determined by both electronic noise and 'chemical noise'. The latter may be reduced or eliminated by an improvement in the selectivity of detection (by, for example, selected reaction monitoring). The electronic and statistical noise of ion detection then becomes limiting, dictating both the detection limit and the precision of quantitative analyses. Here we describe a rigorous evaluation of several approaches to the smoothing of GC-MS/dual SIM data and assess their influence on the precision and accuracy of isotope dilution data. Three smoothing routines have been used, each based on the moving average principle but differing in the weighting of data points: unweighted, weighting factors in the form of a symmetrical triangle, and weighting according to the Savitzky-Golay procedure (1). Each smoothing procedure led to a reduction in SIM peak height, though this was less severe for the weighted average methods. When the routines were applied to data obtained by analyses of oestradiol TMS ether and the [$^2H_3$]analogue (with S/N ratios for the raw data of 4:1 to 25:1), only minor improvements in the precision of peak height ratio determinations were observed. When S/N ratios were low and the molar ratio of analyte/labelled analogue differed significantly from unity, then application of data smoothing introduced significant bias to the peak height ratios (Figure 1). The sign of the bias reflected the proportionately greater reduction in peak height, following smoothing, which was observed for the weaker signal in dual SIM analyses.

Five series of analyses were also performed, with different quantities injected of a single standard mixture of oestradiol TMS and the [$^2H_3$]analogue (molar ratio 0.2). The signal/noise ratio for the analyte ranged from 10 to 80. Smoothing caused a more serious distortion in the peak height ratio when the observed signals were weaker (with correspondingly lower signal/noise ratios); the bias ranged from 1-4% when the Savitzky-Golay procedure was applied and was substantially greater for the other routines. The dependence of the bias caused by smoothing on the signal/noise ratio suggests a possible source of quantitative inaccuracy when different signal/noise ratios are observed during analyses of standard and unknown mixtures.

Table 1. Precision and accuracy of response ratio calculations[a].

	Peak height ratio calculations	Mean response ratio[b]	% CV	% bias
A.	Unsmoothed data	0.364	15.2	0
	Smoothed data[c]			
	Unweighted	0.342	12.4	6.0
	Symmetrical triangle weighting	0.344	13.3	5.5
	Savitzky-Golay	0.356	15.0	2.2
B.	Linear regression of response profiles	0.359	8.6	1.4

a. Analyses of oestradiol TMS and [$^2H_3$]analogue.
Unsmoothed data showed S/N ratios of 5:1 and 15:1, respectively.
b. n=18
c. 5-point filter widths.

Table 1 summarises precision and accuracy data from replicate analyses of a single standard mixture. Peak height ratio calculations from smoothed data are compared with the results of a previously-reported (2) approach, involving linear regression of the signals corresponding to analyte and labelled analogue; the latter approach is shown to be superior.

A full description of this work will appear in Biomedical and Environmental Mass Spectrometry.

1. Savitzky A, Golay ME. Anal Chem 1964; 36: 1627.
2. Thorne GC, Gaskell SJ, Payne PA. Biomed Mass Spectrom 1984; 11: 415.

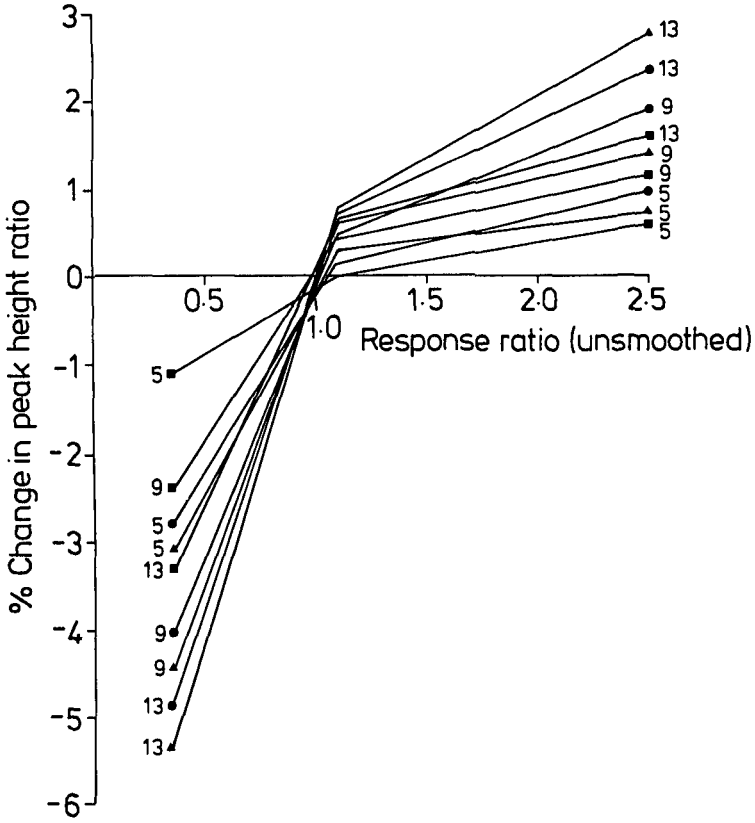

Figure 1. Changes in calculated peak height ratio following the application of three smoothing routines, each applied with three filter widths (5, 9 and 13 samples).
▲ : unweighted moving average. ● : symmetrical triangle weighting.
■ : Savitzky-Golay procedure

(GC-MS/dual SIM analyses of oestradiol TMS ether and the [$^2H_3$]analogue).

AN AUTOMATED PROCESS FOR THE IDENTIFICATION OF VOLATILE COMPOUNDS IN HUMAN ADIPOSE TISSUE - RESULTS OF AN NHATS STUDY

J. Onstot, J. Stanley; Midwest Research Institute
425 Volker Blvd., Kansas City, MO 64110
J. Remmers, J. Breen; U.S. EPA, Office of Toxic Substances,
401 M St., S.W., Washington, DC 20460

INTRODUCTION - One of the most routine tasks for which mass spectrometry is now utilized is the analysis of target compounds by GC/MS. This analysis is straightforward, capable of detecting very low levels of organic compounds in a variety of matrices, and can be used to screen large numbers of samples on a routine and relatively automatic basis. However, identification of non-target compound peaks observed in GC/MS analyses presents a number of unique problems which are not well addressed by automatic data processing techniques. Most commercial data systems provide some method of performing forward library searches using a reference mass spectral database and usually produce a report indicating which reference spectra most closely match the unknown spectra in a GC/MS run. However, it is often useful to know how frequently an unknown or non-target compound occurs within a given set of GC/MS analyses, regardless of whether it has been positively identified by a forward library search routine.

The work presented here was undertaken to attempt to modify the standard forward library search method so that frequency-of-occurrence information could be automatically maintained for both identified and unidentified peaks observed in a set of GC/MS data.

EXPERIMENTAL - The data set utilized for this study consisted of 46 composited human adipose tissue specimens obtained from the National Human Adipose Tissue Survey repository and analyzed for the U.S. Environmental Protection Agency, Office of Toxic Substances, as part of a broad-scan analysis study. The samples were analyzed by GC/MS in full scan mode on a Finnigan/MAT 4000 quadrupole GC/MS. Extraction of volatile components was accomplished using a modified dynamic headspace apparatus which was connected to the gas chromatograph inlet. Data was acquired onto a Finnigan/MAT Incos data system.

A program was written using both the Incos procedural language and FORTRAN to perform a modified automatic forward library search on unknown peaks in each of the 46 sample datafiles. Under the modified library search scheme, each unknown spectrum is compared against a mass spectral library of dynamic length, referred to hereafter as the seed library. If a suitable match cannot be found in the seed library, the search is repeated using the standard NBS library as the reference database. If a suitable match is found in the NBS library, the NBS reference spectrum is appended to the seed library. If a match cannot be found in either the seed or the NBS library, the unknown spectrum itself is appended to the seed library and assigned the name "Unidentified Peak." The appended spectrum is now available for future searches of unknown peaks. Since spectra are added to the seed library only on the condition that they have not yet been observed in the data set, the length of the seed library is determined by the number of unique mass spectra observed in the set to that point.

RESULTS AND DISCUSSION - Using the peak locating function in the standard Incos program MAP, an average of 60 peaks were found in each NHATS adipose GC/MS datafile. At the completion of the processing of each datafile in the set, a manual review was performed to check for misassignments by the program. It was found that an average of 13 misassignments were made for each processed datafile. Misassignments occurred most often for coeluting peaks and for peaks observed near the limit of detection of the mass spectrometer. It is presumed that these conditions were also responsible for the "Unidentified Peak" assignments.

In a number of instances, the program could not distinguish positional isomers whose spectra were practically identical. However, since GC retention information was included as an identification criterion in the program, identical spectra could be observed at different locations in the chromatogram and each would be assigned separate entries in the seed library.

The issue of misassignment to the seed library is particularly significant due to the logical design of the program. Since spectra appended to the library are available to all searches conducted after the addition, proliferation of errors throughout a sample set may occur if future matches are made to invalid reference spectra. For this reason, a manual review of all appended spectra must be made after each sample is processed. This is not a major task for samples with similar composition since few additions are typically made once

a few samples have been processed, thereby stocking the seed with the most commonly occurring compounds.

Analysis of the entire volatile data set using the peak identification program resulted in the identification of 220 unique entries to the seed library following correction for misassignment or duplication. Of these, 121 were identified by name from the NBS library and 99 remained unidentified.

CONCLUSIONS - The program described above can serve as a useful tool for extracting additional screening information from a set of GC/MS analyses. It provides a simple method for compiling a reference database tailored to a given sample type or analytical scheme. The program makes the task of compiling frequency-of-occurrence information very easy, and this information is available for both compound-identified and unidentified peaks. However, it was found that periodic manual review of the database was necessary to prevent proliferation of errors.

IDENTIFICATION OF ORGANIC COMPOUNDS USING AUTOMATED MS/MS SPECTRAL/SUBSTRUCTURE CORRELATION

K.J. Hart, A.P. Wade+, P.T. Palmer and C.G. Enke*

Department of Chemistry, Michigan State University, E. Lansing, MI 48824
+ Also of: The Information Technology Research Unit, British Petroleum Research Centre, Sunbury-on-Thames, Middlesex, TW16 7LN, U.K.

Tandem mass spectrometry provides a wealth of information useful for structure elucidation of organic compounds. This information is characterized by a greater dimensionality than that of conventional MS (as is evidenced by the availability of parent-daughter transitions, daughter scans and neutral loss information). An automated structure elucidation system which takes full advantage of these data is being developed in our laboratory. The system consists of a set of software tools which perform various tasks in the structure elucidation process. These software tools will be linked via a software controller to provide an intelligent system which has a TQMS instrument in its feedback loop.

The approach reported here differs from conventional spectral matching and from interpretive systems such as STIRS and Meta-DENDRAL. The automated procedure begins with the input of MS/MS data of known compounds (a training set) into a pattern recognition program (MAPS: Method for Analyzing Patterns in Spectra)[1]. This program correlates MS/MS spectral features with substructures present in known structures. From these correlations, MAPS then generates rules that can be applied to unknown compounds. An empirical formula generator (EFG) has been developed to provide the empirical formulae of unknowns based on their molecular weight and other data[2]. Data from MAPS may be used to constrain the number of possible empirical formulae that EFG generates for an unknown.

The empirical formulae and the substructures found in an unknown (by application of the MAPS rules) are used in conjunction with a structure generation program (GENOA)[3] to generate all the possible structures for the unknown. By inspecting the types of structures generated for a given unknown, the intelligent controller may be able to suggest new experiments to further resolve the structure elucidation problem. All programs are currently working with the exception of the IC. Its functions are currently being carried out by hand, and are still being discovered. One of the major considerations in this project at present is the integration of the software tools. The interaction of these software tools is shown in Figure 1. Also, a number of additional features are being considered for future incorporation into EFG and MAPS (eg. relevancy checks to reduce the number of possible sets of constraints before structure generation).

MAPS is written in InterLisp-D and runs on a Xerox 1108 AI Workstation. GENOA is written in VAX C and was obtained from Molecular Design LTD. The EFG is written in Fortran-77 and is currently being used on a DEC PDP-11/23+. The EFG will soon be ported to a DEC AI Vaxstation. The LISP, Fortran and C programming languages are all available for this workstation which will allow the EFG, GENOA and the IC to be run on a single computer. MAPS may be run over a network (DECNET or a serial interface using a protocol such as KERMIT). A TQMS instrument is used to acquire MS/MS data. Computer control of this instrument will be provided through an interface to a Novix FORTH processor board.

This system, while very limited at present, has been applied to a preliminary set of compounds with satisfactory results. A total of 10 empirical formulae were generated for N,N-dimethyl aniline by the EFG with

no constraints. When the constraints were applied only two empirical formulae were generated when constraints were applied from MAPS. These were $C_8H_{11}N$ and $C_6H_7N_3$. MAPS was able to identify the T-AMINE, XPHENYL and PHENYLAMINE substructures as present in the "unknown". Given no constraints, GENOA could not determine the number of structures for $C_8H_{11}N$ with any certainty, except that there were over 5000 (it fails to recognize duplicate structures above 5000). Only one structure was generated when the MAPS constraints were applied. Also, GENOA rejected the other empirical formula as being inconsistent with the constraints it was given.

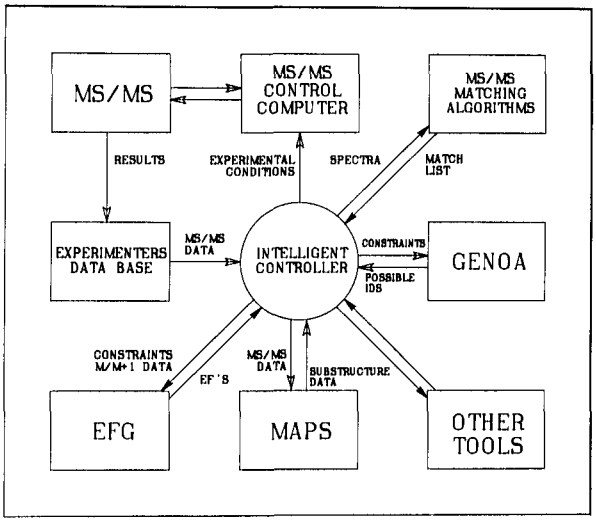

Fig. 1 - Schematic for the Automated Chemical Structure Elucidation System.

A variety of compounds with commonly encountered substructures will be examined using this system. Once rules for these substructures have been obtained, structure elucidation of more complex unknowns with only a few resulting candidate structures will become feasible.

Acknowledgement: This work was funded by NIH Grant # GM-28254. The authors thank Finnigan MAT for use of and support for the Xerox 1108 AI Workstation.

References:

1. P.T. Palmer and C.G. Enke, "Empirical Formula Determination by Triple Quadrupole Mass Spectrometry", 34th Annual ASMS Conference (Poster TPA7), Cincinnati, June 1986.
2. A.P. Wade, P.T. Palmer, K.J. Hart and C.G. Enke, "A Novel Approach for Automatic Elucidation of Spectral Substructure Relationships in MS^n Spectra", 34th Annual ASMS Conference (Poster TPD6), Cincinnati, June 1986.
3. R.E. Carhart, D.H. Smith, N.A.B. Gray, J.G. Nourse and C. Djerassi, "GENOA: A Computer Program for Structure Elucidation Utilizing Overlapping and Alternative Substructures", *J. Org. Chem.*, 46, (1981), 1708-1718.

USE OF AN ADVANCED GC/MS DATA PROCESSING ENVIRONMENT FOR THE COMPARISON OF CHROMATOGRAPHIC PATTERNS; B. Mason Hughes, Monsanto Company/Environmental Sciences Center, 800 N. Lingbergh Boulevard, St. Louis, Missouri 63167

A large number of environmental and other scientific studies require the processing of vast amounts of data which are acquired on capillary GC/EC, GC/FID, and GC/MS analytical instruments. One common step in data analysis involves the detailed comparison of chromatographic patterns. This presentation describes data processing approaches for the comparison of chromatographic patterns which can be implemented on a commercial GC/MS data processing system.

Figure 1 shows how mass spectra can be compared by placing the two mass spectral arrays into two RPN registers and performing the cross correlation coefficient (XCC) calculation described in the center of the figure. This coefficient approaches 1.000 as the two mass spectra become identical. An added feature of the XCC calculation is that the calculation can also be performed for only those mass spectral peaks which are present in either of the two arrays. As will be discussed later, this feature allows for patterns of a pure component to be compared with patterns of mixed components. This latter calculation is shown in Figure 1 as the XCC for only reference peaks.

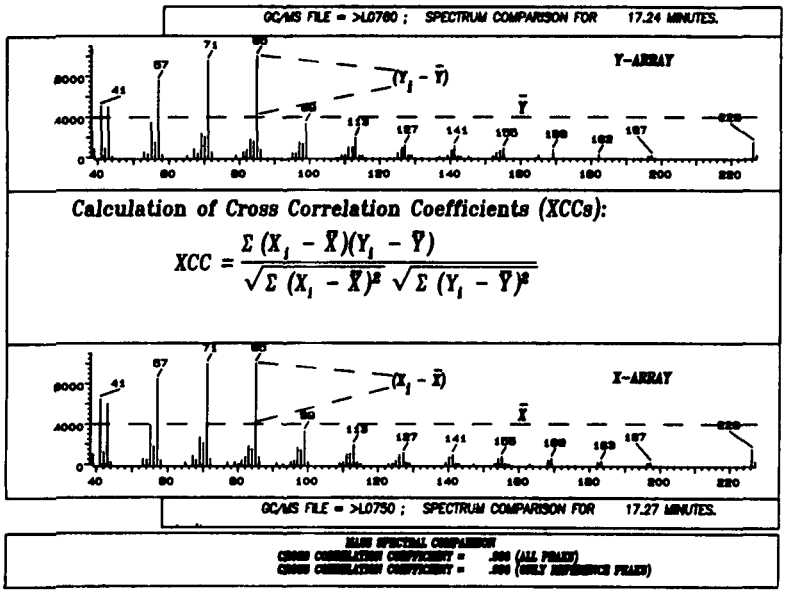

Figure 1. Description of the XCC calculation applied to mass spectra.

The Hewlett-Packard RPN system also allows such a calculation to be performed on arrays of chromatographic data. For this application, the reduced chromatogram array of two chromatograms are placed in two RPN registers and the XCC calculated. Figure 2 shows this calculation for chromatographic data.

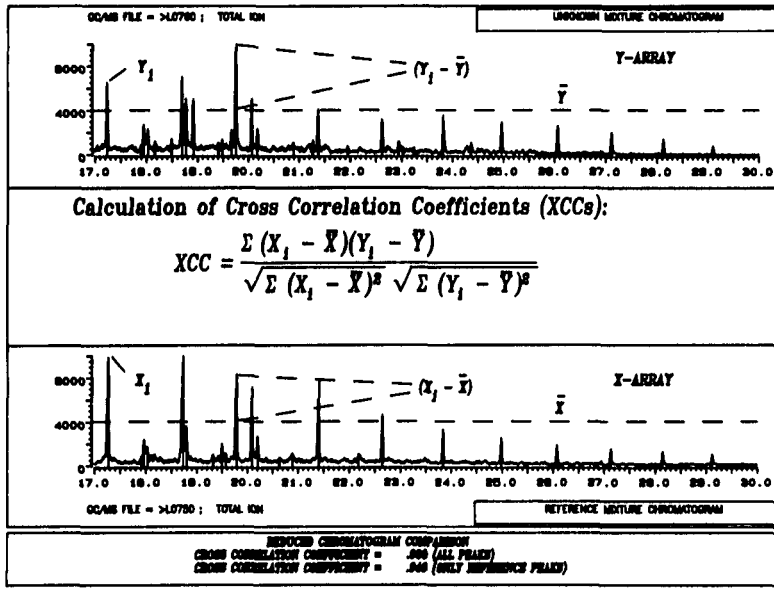

Figure 2. Description of the XCC calculation applied to chromatograms.

For this latter comparison, the reduced chromatograms are treated as the mass spectra in Figure 1. Several analogies apply to the comparisons of mass spectra and chromatographic data. The mass spectrum is analogous to the reduced chromatogram, the compound which produces the mass spectrum is analogous to the mixture or formulation which produces the reduced chromatogram, fragment ions in the mass spectrum are analogous to individual compounds in the reduced chromatogram, and metastable mass spectral peaks are analogous to poorly-resolved components in the mixture chromatogram.

The reduced chromatograms (shown as verticle lines, the lengths being proportional to the chromatographic peak areas and the positions occuring at chromatographic peak retention times) shown in Figure 2 are treated exactly as the mass spectra in Figure 1. However, only resolved chromatographic peaks will be included in this type of comparison. A second type of chromatographic display includes the subtraction of the chromatographic data shown in the X-array and Y-array in Figure 2. This subtracted array can easily be shown in the center of the figure, and gives information on the poorly-resolved components of mixtures which would not be seen from the reduced chromatogram comparison.

This approach has been used successfully in two important environmental applications. The first involves the determination of the identity of Aroclor formulations in environmental extracts, and the second involves the determination of the major sources of materials at a superfund site. Aroclor formulation identification used the reduced chromatogram comparison for capillary GC/EC chromatograms. Waste source identification involved the use of the reduced chromatogram comparison for capillary GC/MS chromatograms, followed by the mass spectral comparison (shown in Figure 1) for each component in the mixture. These two applications show that: 1) XCCs are very useful for comparing chromatographic and mass spectrometric patterns; 2) are cost effective, since all comparisons are computer generated, reducing the need for manual data interpretation; and, 3) require no detailed component identifications if samples of potential sources are available.

IMPROVEMENTS TO PBM/STIRS FOR THE IDENTIFICATION OF UNKNOWN MASS SPECTRA

D. B. Stauffer, S. Loh, and F. W. McLafferty
Chemistry Department, Cornell University, Ithaca, NY 14853-1301

R. B. Spencer
Nicolet Analytical Instruments, Madison, Wisconsin 53711

To utilize elemental composition information from high resolution MS in Exact Mass-Probability Based Matching (EM-PBM), elemental compositions have been assigned to many peaks in the unit-resolution reference file. For data weighting, a basic approach of PBM, the original "U value" reflects the uniqueness of peaks of a nominal mass value; each elemental composition at that nominal mass is now assigned a "U_x value" reflecting its occurrence probability among all compositions in the data base at that nominal mass.[1] U_x values assigned using logical neutral losses (Figure) agree surprisingly closely with those from "Mass Spectral Correlations",[2] and show relatively smooth changes with mass for homologous ion series. Preliminary results indicate that EM-PBM halves the number of incorrect spectra retrieved.

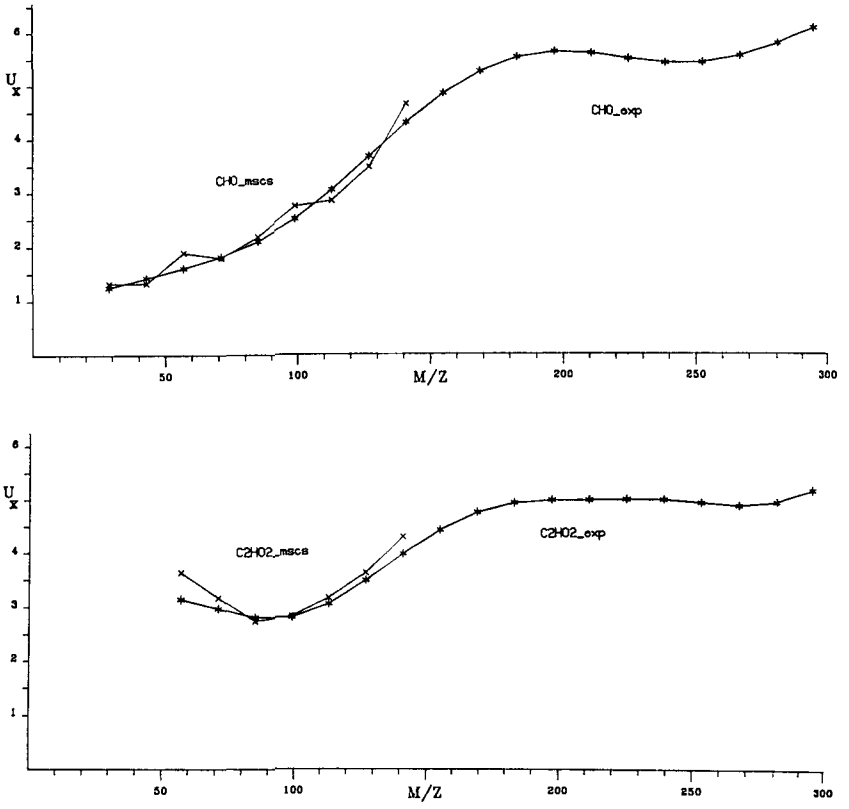

Figures. Exact mass "Uniqueness" values (U_x) for (top) $C_nH_{2n-1}O^+$ ions and (bottom) $C_nH_{2n-3}O_2^+$ ions derived from (crosses) reference 2 and (asterisks) using logical neutral losses.

The Self-Training Interpretative Retrieval System (STIRS) predicts the substructural units of the unknown molecule. Currently these are from a list of 587 chosen for their mass spectral utility. The occurrence in the best 15 matching reference compounds of a substructure is used, along with its occurrence in the whole database, to predict the substructure reliability.[3] In many cases, however, a substructure not in the 587 list is common among the best 15 reference compounds. An algorithm, developed previously here,[4] finds for any pair of compounds their maximal common substructures; this has been extended and made efficient for routine use. The original algorithm was developed on a DEC PDP-11/45; the use of a DEC MicroVAX-2 has reduced the computational time by a factor of 50. The algorithm requires connection-table descriptions of the structures of the reference compounds used. With the expanded mass spectral data base, discussed in another paper at this meeting, the number of compounds with such connection table descriptions has been more than doubled, greatly increasing the applicability of this algorithm.

References:

(1) Spencer, R. B.; Loh, S.; Stauffer, D. B.; McLafferty, F. W. Probability Based Matching of Unknown Mass Spectra with Exact Mass Data, Adv. Mass Spectrom., accepted.

(2) McLafferty, F. W.; Venkataraghavan, R. "Mass Spectral Correlations"; Second Edition, American Chemical Society, Washington, DC, 1982.

(3) Haraki, K. S.; Venkataraghavan, R.; McLafferty, F. W. Prediction of Substructures of Unknown Mass Spectra by the Self-Training Interpretive and Retrieval System, Anal. Chem. **1981**, 53, 386-392.

(4) Cone, M. M.; Venkataraghavan, R.; McLafferty, F. W. Molecular Structure Comparison Program for the Identification of Maximal Common Substructures, J. Am. Chem. Soc. **1977**, 99, 7668-7671.

PROCEDURE FOR REAL-TIME QUALITY CONTROL OF GAS CHROMATOGRAPHY/MASS SPECTROMETRY DATA

JOHN T. CODY
AIR FORCE DRUG TESTING LABORATORY
BROOKS AFB TX 78235-5000

JAMES BOURG
HEWLETT-PACKARD COMPANY
ST ROSE, LOUISIANA 70087

The application of quality control criteria to analytical results involves many decisions, most of which are simple to apply. Essentially all objective criteria used to determine the acceptability of analytical results can be incorporated into a computer program. These programs allow virtually real-time evaluation of the acceptability of the entire analytical run as well as the individual test results as soon as the data have been acquired by the system. All laboratories strive to maximize their computer resources and minimize operator intervention in their analytical procedures. Laboratories with a high volume of analyses have a need to process samples as efficiently as possible with minimal time spent on those which will ultimately have to be reanalyzed. When the analytical procedure produces data which may be used in litigation, the clarity and completeness of the data, presented in an understandable format is an extremely important factor.

A custom designed MACRO was written on a Hewlett-Packard (HP) Series 9000-236 WorkStation to analyze data obtained from 5890/5970 and 5790/5970 GC/MSD systems.

The software consists of two major programs. The first is responsible for sequencing the analytical procedure from data acquisition through the final report by calling standard HP program and custom designed MACROs. The second is responsible for the display of data and evaluation of quality control parameters.

Selection of the type of drug to be analyzed and choice of the sequence of injections is made by pressing custom designed soft keys developed for each specific assay.

Analysis begins by evaluation of a calibration standard containing the drug of interest along with an internal standard. Acceptable ranges for mass ion ratios and retention times are then computed based on this calibration standard. The data are presented in four sections, three of which are common to all printouts. The first two sections include header information from the data file and the ion chromatograms. Chromatograms consist of extracted ion current profiles for each drug ion of interest (313, 357 and 372 amu) with all ions superimposed to show their relative intensities. This is repeated for the ions of the internal standard and followed by a chromatogram of all ions (figure 1). Data from the calibration standard are then displayed and acceptable ranges calculated and printed (figure 2). This output format is unique to the calibration standard. The output format for all control and unknown samples include their respective data and an evaluation of the acceptability of the parameters. (figure 3). The final section for all analyses is an internal standard quantitation report (figure 4).

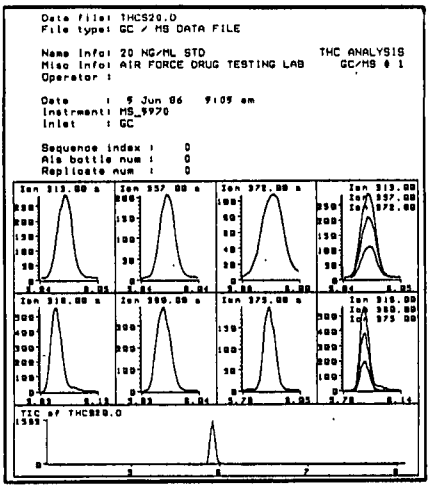

FIGURE 1

ION RETENTION TIMES
Mass 313 = 5.93
Mass 357 = 5.93
Mass 372 = 5.94
Mass 316 = 5.91
Mass 360 = 5.91
Mass 375 = 5.91

THC RETENTION TIME: 5.93
RELATIVE RETENTION TIME 313/316: 1.00

RETENTION TIME WINDOW: 5.87 - 5.99

MASS ION ABUNDANCES		MASS ION RATIOS		ACCEPTABLE RANGE
Mass 313:	10279.77	Mass 357/313 :	0.72	0.57 - 0.86
Mass 357:	7369.98	Mass 372/313 :	0.38	0.28 - 0.42
Mass 372:	3564.10	Mass 375/316 :	0.33	0.27 - 0.40
Mass 316:	22061.24	Mass 360/316 :	0.69	0.52 - 0.78
Mass 360:	14308.87			
Mass 375:	7371.80			

AIR FORCE DRUG TESTING LABORATORY

FIGURE 2

ION RETENTION TIMES
Mass 313 = 5.94
Mass 357 = 5.94
Mass 372 = 5.94
Mass 316 = 5.91
Mass 360 = 5.91
Mass 375 = 5.92

THC RETENTION TIME: 5.94
RELATIVE RETENTION TIME 313/316: 1.00

The Retention Time of THC is acceptable.

MASS ION ABUNDANCES		MASS ION RATIOS		ION RATIO STATUS
Mass 313:	96629.54	Mass 357/313 :	0.73	OK
Mass 357:	41143.75	Mass 372/313 :	0.34	OK
Mass 372:	19392.55	Mass 375/316 :	0.31	OK
Mass 316:	23056.57	Mass 360/316 :	0.64	OK
Mass 360:	15204.53			
Mass 375:	7378.73			

AIR FORCE DRUG TESTING LABORATORY

FIGURE 3

Operator:
Sample Info : 20 NG/ML STD
THC ANALYSIS
5 Jun 86 9:09 am

Peak Num	Type	Int Type	Ret Time	Signal Description		Compound Name	Area	Amount
1	*ISTD	1 BB	5.907	Mass	316.00 amu	DEUT.I.S.	22061	40.00 ng/ml
2		1 BB	5.932	Mass	313.00 amu	THC	10280	20.00 ng/ml

FIGURE 4

EMPIRICAL FORMULA DETERMINATION BY TRIPLE QUADRUPOLE MASS SPECTROMETRY

P. T. Palmer and C. G. Enke*
Department of Chemistry, Michigan State University, E. Lansing, MI 48824

The empirical formula of an unknown compound is often a crucial piece of information in elucidating the molecular structure. Empirical formula determination cannot be directly accomplished by Triple Quadrupole Mass Spectrometry due to the low mass resolution of quadrupoles. In this work, we describe a method that allows the indirect determination of empirical formulae on such an instrument. This method involves fragmentation of ^{13}C-containing isotopic ions to determine the number of carbon atoms in a compound. This number, along with the molecular weight of the compound, and other available constraints, is passed to an empirical formula generator program, which generates all possible empirical formulae consistent with those constraints. Although some of these formulae are highly unlikely, all obey the rules of valence. While this process does not always result in one empirical formula, once the number of carbon atoms in the compound is determined, the number of candidate formulae is substantially reduced. Furthur reduction is possible as more clues to the molecular composition are introduced.

The daughter spectrum of a ^{13}C-containing molecular ion contains peak pairs at adjacent masses which represent the loss or retention of the ^{13}C atom in the fragment ion. The ratio of the intensities of the daughter ions at masses m and m+1 is given by the equation $I_m/I_{m+1} = y/(x-y)$ <1>, where I_m and I_{m+1} represent the daughter ion intensities at m/z m and m+1 respectively, x is the number of carbon atoms in the compound, and y is the number of carbon atoms in the neutral fragment lost (1-4). From this ratio data, a factor of the number of carbon atoms in the compound may be determined.

As an example, the daughter spectrum of the ^{13}C-containing molecular ion of eicosane showed the ratio of the intensities at m/z 71/72, 85/86, and 99/100 to be 3.04, 2.30, and 1.89 respectively. To determine a factor of the number of carbon atoms in the compound from this data, the ratios were first converted to the nearest integer fractions; these ratios were found to be closest to the fractions 3/1, 7/3, and 13/7 respectively. Using these and equation <1>, the following equations were derived: $y_1=(3/4)x$, $y_2=(7/10)x$, and $y_3=(13/20)x$. Since y_1, y_2, and y_3 must be integers, the number of carbon atoms in the compound, x, must be a multiple of 20. The CI mass spectrum of this compound showed the molecular weight of this compound to be 220; therefore, the exact number of the carbon atoms had to be 20. Table 1 represents the partial output from the empirical formula generator, where the only constraints provided were the molecular weight of the compound, and that only carbon, hydrogen, and oxygen were present in the compound. Table 2 represents the output from the empirical formula generator when the additional constraint that the number of carbon atoms in the compound equals 20 was provided. When the number of carbon atoms in the compound was specified, the list of candidate empirical formulae was reduced from 34 to 3. The correct empirical formula was $C_{20}H_{42}$.

(1) M.H. Bozorgzadeh, R.P. Morgan, and J.H. Beynon, Analyst, 103(1978), 613.

(2) P.J. Todd, M.P. Barbalas, and F.W. McLafferty, Org. Mass Spectrom., 17(1982), 79.

(3) K.C. Cross, P.T. Palmer, A.B. Giordani, C.F. Beckner, P.A. Hoffman, H.R. Gregg, and C.G. Enke, in Artificial Intelligence Applications in Chemistry, T.H. Pierce and B.H. Hohne (Eds), American Chemical Society, Washington, DC, 1986, ACS Symposium Series 306, 321-336.

(4) K.E. Singleton, R.G. Cooks, and K.V. Wood, Anal. Chem., 55(1983), 762.

Table 1. PARTIAL OUTPUT FROM THE EMPIRICAL FORMULA GENERATOR FOR EICOSANE.

CONSTRAINTS:

SYMBOL	VALENCE	UPPER LIMIT	LOWER LIMIT	FACTOR	MASS
C	4	99	0	1	12.00000000
H	1	99	0	1	1.00782502
O	2	99	0	1	15.99491501

MASS = 282.00000000 +/- 0.500
LOWER LIMIT ON RINGS PLUS DOUBLE BONDS = 0.0
UPPER LIMIT ON RINGS PLUS DOUBLE BONDS = 20.0
NUMBER OF FORMULAE GENERATED = 34

CANDIDATE FORMULAE:

	MASS	DIFF	RDB	FORMULA
1)	281.934296	-0.06570	2.0	$C_2H_2O_{16}$
2)	281.970673	-0.02933	1.0	$C_3H_6O_{15}$
3)	282.007080	0.00708	0.0	$C_4H_{10}O_{14}$
	.	.	.	.
	.	.	.	.
	.	.	.	.
29)	282.328644	0.32864	0.0	$C_{20}H_{42}$
30)	282.198364	0.19836	8.0	$C_{20}H_{26}O$
31)	282.068085	0.06808	16.0	$C_{20}H_{10}O_2$
32)	282.234741	0.23474	7.0	$C_{21}H_{30}$
33)	282.104462	0.10446	15.0	$C_{21}H_{14}O$
34)	282.140839	0.14084	14.0	$C_{22}H_{18}$

Table 2. OUTPUT FROM THE EMPIRICAL FORMULA GENERATOR FOR EICOSANE WITH THE ADDITIONAL CONSTRAINT THAT THE NUMBER OF CARBONS EQUALS 20.

CONSTRAINTS:

SYMBOL	VALENCE	UPPER LIMIT	LOWER LIMIT	FACTOR	MASS
C	4	20	20	1	12.00000000
H	1	99	0	1	1.00782502
O	2	99	0	1	15.99491501

MASS = 282.00000000 +/- 0.500
LOWER LIMIT ON RINGS PLUS DOUBLE BONDS = 0.0
UPPER LIMIT ON RINGS PLUS DOUBLE BONDS = 20.0
NUMBER OF FORMULAE GENERATED = 3

CANDIDATE FORMULAE:

	MASS	DIFF	RDB	FORMULA
1)	282.328644	0.32864	0.0	$C_{20}H_{42}$
2)	282.198364	0.19836	8.0	$C_{20}H_{26}O$
3)	282.068085	0.06808	16.0	$C_{20}H_{10}O_2$

INTERACTIVE DATA ACQUISITION AND INSTRUMENT CONTROL FOR A SECONDARY ION MASS SPECTROMETER

Rick A. Flurer and Kenneth L. Busch
Department of Chemistry, Indiana University, Bloomington, IN 47405

We have designed and constructed a data system for a chromatography/SIMS instrument. Two dimensions of mass spectral information (m/z and relative abundance) are obtained for each x,y point in a planar array. Processing of the data is necessary for effective presentation of the data in axonometric and contour plots, and for spectral enhancement through data averaging and background subtraction. The data system is also used to control pertinent instrumental parameters, and to operate through a feedback mechanism in imaging analyses of chromatograms.

An IBM PC/AT microcomputer was chosen for its speed of operation and its large data storage capacity. The microcomputer is linked to an Extrel C-50 quadrupole mass spectrometer via a hardwire interface consisting of two Data Translation DT2801 general purpose data acquisition and control boards that plug into the expansion slots of the computer. Each board provides two 8-bit digital I/O ports (or one 16-bit port), two 12-bit digital-to-analog converters, and a 12-bit analog-to-digital converter with 16 multiplexed imputs. Each board also contains an on-board microprocessor to offload the host microcomputer and simplify programming. Two boards are required to provide all inputs and outputs necessary to control all instrument parameters amenable to computer control. The presently available converter resolution allows only three data points per dalton (1200 dalton mass range). However, to accurately define each maximum in a mass spectrum, a sampling rate on the order of 10 to 16 points per dalton is necessary. To achieve this accuracy, a stand alone 16-bit digital-to-analog converter will be added to control the quadrupole mass command. This converter will use one of the 16-bit digital I/O ports mentioned above. Additionally, a stand alone 16-bit analog-to-digital converter will be added to allow the quadrupole mass command to communicate its mass setting to the microcomputer, thus completing a feedback loop for control of the quadrupole mass setting. This converter will be interfaced to the microcomputer through a 24-bit parallel digital I/O port (model PIO-12, Metrabyte Corp.). The 24 I/O lines are divided into three 8-bit ports and are controlled by an Intel 8255 programmable peripheral interface chip. Two of the 8-bit ports will be combined to interface the 16-bit converter, and the third port will be used for handshaking signals.

The analytical value of the chromatography/SIMS experiment lies mainly in its ability to vary the effective spatial resolution of the mass spectrometric detection independent of the chromatographic separation. The algorithm used to vary the spatial resolution of the instrument is the step-back stop-down experiment (Figure 1), wherein the microcomputer directs the detection system to take a step backward, to narrow its field of view (analogous to reducing the f/stop on a camera), and then to reacquire the data at higher spatial resolution. The step-back stop-down experiment is implemented through a feedback mechanism which allows the microcomputer to access the incoming data before it is stored and make instrument control decisions affecting the spatial resolution, in real time, on the basis of changes in the acquired data. The effective spatial resolution of the instrument is altered through computer control of a sample stage driven by a pair of stepper motors, the beam rastering capability of the liquid metal gallium gun used as the primary ion source, and the primary beam diameter.

The ASYST scientific software is used to control all hardware. The ASYST software package is a complete programming language designed specifically for scientific and engineering applications. The system consists of three modules: 1) system/graphics/statistics, 2) analysis, and 3) data acquisition. The language consists of many words (subroutines) that are each designed to perform a specific task. To develop more sophisticated "turnkey" programs one merely links these words together. With the software written thus far, simple acquisition of data is straightforward (Figure 2), and contour plots of the distribution of a species on a thin layer chromatogram (Figure 3) are easily obtained on the basis of the abundance of a characteristic ion as a function of x,y position.

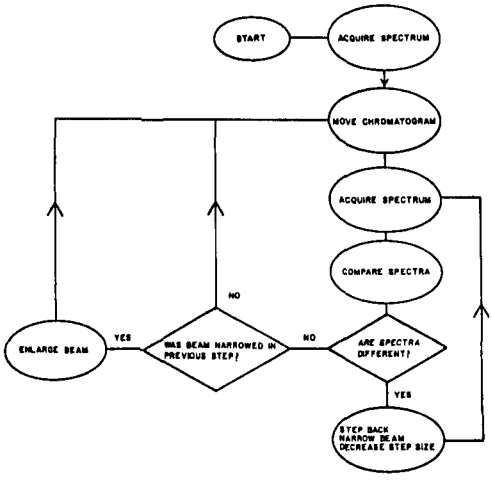

Figure 1

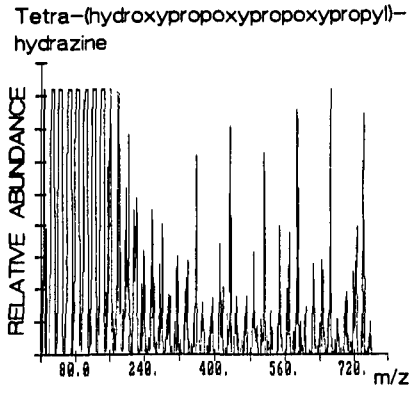

Figure 2

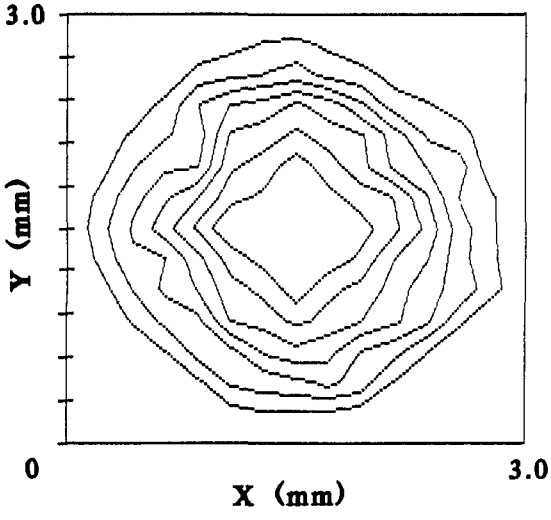

Corticosterone/
Girard's P
Silica TLC
m/z 480

Figure 3

USE OF CROSS-CORRELATION FOR RATIO MEASUREMENTS IN MASS SPECTROMETRY

A. Celikkaya and S. Süzer, Middle East Technical University
Department of Chemistry, Ankara, Turkey.

Cross correlation of two continious functions $F_1(x)$ and $F_2(x)$ is given by;

$$G(\tau)=\int_{-\infty}^{+\infty} F_1(x).F_2(x+\tau)\ dx \qquad \text{for } \tau = -\infty \text{ to } +\infty$$

Cross correlation of two spectra containing 2N+1 points taken at equal intervals, $F_1(I)$ and $F_2(I)$ where I is integer between -N and +N representing the spectral step, is given by;

$$G(\tau)=\sum_{-N}^{N} F_1(I).F_2(I+\tau) \qquad \tau = \text{integer between } -N \text{ and } N$$

and is most easily obtained by Fourier Transforming F_1 and F_2 into the frequency domain, multiplying the transformed functions and back transforming into the time domain. However, one is usually interested in the cross-correlation value at zero displacement i.e. $\tau=0$;

$$G(\tau=0)=\sum_{-N}^{N} F_1(I).F_2(I)$$

This is simply the product of two spectra, obtained by point-by-point multiplication and summing afterwards, and can be obtained without the use of Fourier Transformation. The cross-correlation value at zero displacement (τ=0) of the spectrum of a mixture with that of pure component, (i.e. multiplying the mixture spectrum with that of the pure component and adding them up), gives a measure of the content of that component in the mixture, and can be used for quantitative analysis. Mann et al. recently reported successful applications of this method for quantitative analysis in IR spectroscopy.[1]

Ratio measurements in the mass spectrum of a mixture is usually carried out by ratioing peak heights or areas of two or more representative peaks belonging to each component in the mixture. In this work, we investigate the applicability of the cross-correlation method for ratio measurements in the analysis of mixtures using mass spectrometry.

A quadrupole mass filter, Balzers QMS 311, interfaced to a DEC MINC 11/03 computer is used for recording the mass spectra. Ion currents, produced by a secondary electron multiplier, are coverted to voltages by a Keithley 419 picoammeter and are read into the computer via a 12 bit ADC.

Figure 1 displays the calibration lines obtained for calculated and prepeared ratios of different mixtures. Figure 1a is obtained by ratioing the peak area for the mass 32 (O_2^+ arising from O_2) and 30 (NO^+ from N_2O) for four different mixtures of O_2 and N_2O. Figure 1b is obtained by

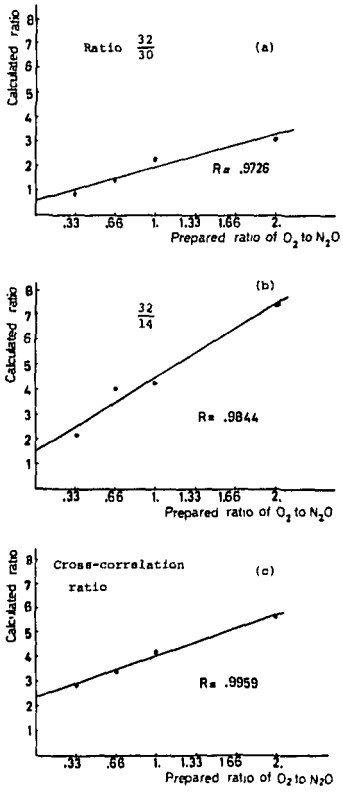

Figure 1.

ratioing peak areas for O_2^+ and N^+, and lc is obtained by using cross-correlation values at zero displacement for ratioing. Since the same set of data is used for computing ratios in all three graphs, it is meaningful to compare them. Correlation coefficient (R) of the calibration lines is one measure of the precision of the method and is seen to increase from .9726 for ratios using O_2^+ and NO^+ peaks to .9844 for O_2^+ and N^+ to finally .9959 when cross-correlation ratios are used. The increase from .9726 to .9844 is due to the fact that N^+ is more intense hence a more precise value is obtained when used. Further improvement to .9959 is due to the fact that in using cross-correlation values maximum information about data is utilized as opposed to only part of the data being used in simple ratios.

Figure 2.

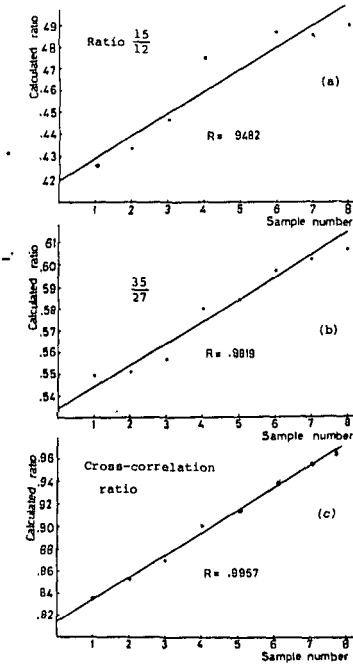

Application to liquid mixtures of CCl_4 and cyclohexane gives a more dramatic improvement in precision simply due to the fact that they contain a large number of peaks in thier spectra as shown in Figure 2 for 8 different mixtures.

We wish to acknowledge the Volkswagen Foundation of FR Germany for the generous grant which supplied the mass spectrometer.

References:

1-Tyson, L.L., Vickers, T.J. and Mann, C.K., Appl. Spectr. 1984, 38, 663-668.

Computer-Based System for Correlating Molecular Structures with Mass Spectral Data: Methods for Generating Molecular Substructures and for Incorporating Fragmentation Rules

Marshall M. Siegel*, Norman Bauman, Guy T. Carter
American Cyanamid Company, Medical Research Division,
Lederle Laboratories, Pearl River, NY 10965

Introduction

Superatoms are defined as sub-molecular units which do not undergo further fragmentation. Two types of superatoms are necessary to describe molecular structures and mass spectral processes: bonded superatoms and floating superatoms. Bonded superatoms are used to construct the proposed molecular structure and floating superatoms, which are found anywhere in the molecule, are used to describe structural rearrangements, adduct ions and neutral losses.

In principle, nearly all ions observed in mass spectra can be constructed from connected sets of bonded superatoms and floating superatoms having the masses of the observed ions. Since many solutions are possible, the most likely set of superatoms describing the ion is postulated to be that with the fewest bond cleavages between superatoms.

To solve this problem, all the connected sets of bonded superatoms which constitute possible answers must be determined and analyzed. Three methods for finding all the connected sets of superatoms were evaluated. These methods are referred to as: 1-The Brute Force Method, 2-The Bond Removal Method, and, 3-The Substructure Method.

Bond Removal Method:

The most efficient method is the Bond Removal Method which involves the following procedure:

a. For n superatom bonds, remove k of them at a time, where $k=0,\ldots,q$ and q is the maximum number of bond cleavages to be considered. As the superatom bonds are systematically removed, the molecule fragments into connected superatom pieces.

b. Compute the masses for all combinations of the molecular fragments and the floating superatoms. (Let p represent the maximum number of floating superatoms). All the computed ion masses equal to the observed masses are acceptable solutions.

The maximum possible number of combinations analyzed is relatively low because q is generally $\leqslant 4$ and p is generally $\leqslant 3$.

A feature of the Bond Removal Method is that duplicate solutions are possible since similar molecular fragments are generated from different combinations of superatom bonds removed from the molecule. Sorting routines are therefore used to remove duplicate solutions.

Fragmentation Rules

A further extension in the use of the mass spectral analysis algorithms is the incorporation of mass spectrometry fragmentation rules. Since the algorithms generate all the desired combinations of superatoms, the inclusion of fragmentation rules effectively suppresses the print-out of undesirable solutions.

The use of fragmentation rules is illustrated in the analyses of thermospray (TSP) mass spectral data for the oligomycin A, B,C and ω antibiotics, structures I-IV, respectively. (Structure I-IV are expressed as sets of superatoms. Each superatom is bracketed by wiggly lines and numbered for each structure.) The rules followed for computing and correlating the TSP data of the oligomycins, using the Bond Removal Method, are listed in Table I and the most significant ions observed in the TSP data are illustrated below as the H^+, Na^+ and/or NH_4^+ adduct ions of the decomposition ions (DI) and as the complement ions of the neutral losses (NL).

Table I

Rules Followed for Correlating the Thermospray Mass Spectra of Oligomycins

1. Application of "fragmentation" rules for: a) Retro-Aldol Reactions (Scheme I)
   b) Lactone Ester Reactions (Scheme II)
2. Only one floating superatom adduct (H^+, Na^+ or NH_4^+) per ion.
3. Multiple dehydration processes possible using - H_2O (- 18 daltons) as a floating superatom.
4. Structural differences used as functional group labels for correlating interspectral mass shifts.
5. Small intra-spectral mass shifts used for correlating presence of H^+, Na^+ and NH_4^+ adducts.
6. Even mass ions are NH_4^+ adduct ions.
7. Odd mass ions are H^+ or Na^+ ions.

Retro Aldol Reaction

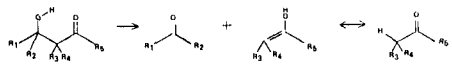

Scheme I

Lactone Ester Reactions

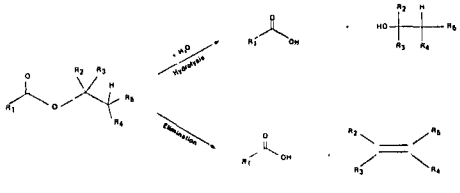

Scheme II

Observed Neutral Losses (NL) and Decomposition Ions (DI) in the TSP/MS of Oligomycins Related to Retro-Aldol and Lactone Ester Reactions

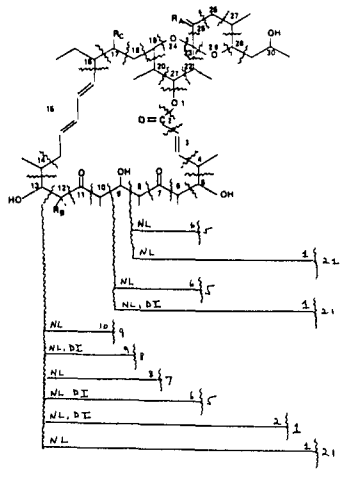

I - IV

Structure	Oligomycin	R_A	R_B	R_C
I	A	2H	OH	H
II	B	O	OH	H
III	C	2H	H	H
IV	ω	2H	OH	OH

AUTOMATIC PROCESSING OF QUANTITATIVE MULTIPLE-ION-DETECTION DATA

William K. Rohwedder and Darhal J. Wolf

Northern Regional Research Center, ARS-USDA, Peoria, Illinois 61604

A computer program has been developed to automatically process MID data, from the initial data acquisition to the final plots and tables of the combined data. The system quantitatively analyzes more than 20 components in each sample, and separates overlapping peaks from deuterium labeled compounds. The program automatically searches all GC peaks for the deuterium label which indicates elongation, desaturation, or chain shortening of the fed labeled fatty acids.

The method has been applied to a series of metabolism experiments (1,2,3) to determine the metabolic fate in humans of the unnatural fatty acids formed by hydrogenation of vegetable oils. Saturated, and mono- and di-unsaturated fatty acids were labeled with 2, 4, and 6 deuterium atoms, which were converted to triglycerides and fed to human subjects. The purpose of the experiment was to determine whether the subjects discriminated for or against cis and trans isomers and double-bond positional isomers.

The elaborate automatic processing program was necessary because of the large amount of data that had to be processed. The human subjects were fed deuterium labeled fatty acids as triglycerides as a single pulse. Blood was drawn at 9 intervals, and separated into 40 blood fractions. Each blood fraction contained about 20 fatty acids. Nine blood samples, times 40 blood fractions, times 20 fatty acids resulted in 7200 compounds analyzed per subject, which is an enormous amount of work for a small laboratory group.

The blood lipoprotein classes were separated by centrifugation, and each lipoprotein class was separated into phosopoholipids by thin-layer chromatography. The phospholipids were converted to methyl esters and analyzed by isobutane chemical ionization mass spectrometry.

The instrumentation consisted of a Finnigan 9600 GC equipped with 30m x .32mm fused silica columns coated with DB1, SP2330, and SP10 liquid phases. The GC was connected to a Finnigan model 4500 mass spectrometer. The mass spectrometer was connected to a Modcomp Classic II/25 data acquisition computer with a homemade interface card which included a hardware adder. The data acquisition computer was connected to a Modcomp Classic 7870 time-shared computer which did most of the data processing.

The MID data was acquired in 4 frames or sets of MID descriptors. Mass 269 to 279 were scanned to record the peaks of the 16 carbon fatty acids, 283 to 293 for 17 carbon fatty acids, 293 to 305 for the 18 carbon fatty acids, and 319 to 331 for the 20 carbon fatty acids. Only odd numbered masses were collected. The data acquisition computer controlled the mass digital-to-analog converter using a time and mass table, which included time for the electronics to settle on each mass peak. The measured intensity values were stored on the local disc, displayed on a Tektronics 4010 terminal, and sent to the time-shared computer.

The time-shared computer was programmed to operate as automatically as possible. The computer algorithm makes extensive use of standards. An 11-component mixture of methyl esters was run every day to determine GC elution time, isotope cluster patterns, and mass sensitivities. A known weight of a saturated 17 carbon fatty acid was added as an internal standard to all samples during sample workup. The analyzed weight of the 17:0 fatty acid was used to convert the final output of the other fatty acids to weights.

The computer program started the processing by determining the beginning and end of the mass chromatogram peaks using a 1st derivative calculation. The areas for each mass were stored separately for use in the simultaneous equation analysis of overlapping peaks. The GC peaks were identified by elution time using the 11 component standard. The areas from the identified peaks were grouped together according to chemical compound, including all isotope cluster and deuterium labeled peaks. All compound data sets were run through the simultaneous equation calculations using the isotope cluster patterns to determine isotopic composition of the compounds. This technique provided a search through all compounds for the deuterium label, which would indicate elongation, desaturation, or chain shortening of the fed labeled compounds. The raw data was adjusted for relative sensitivity of the mass spectrometer by the 11 compound external standard and converted to weights using the intensity of the 17:0 internal standard.

The weights for the compounds in each sample were stored in a relational data base management system which allowed the data to be formatted and combined in many different ways; such as, by subject, by hour, by blood fraction, and by fatty acid. Programming associated with the data base management system provided for reports, plots, and tables; such as percent of labeled materials, percent of total fat, selectivity, micrograms of sample, and micrograms of phospholipid per milliliter of blood.

REFERENCES

1. Rohwedder, W.K., Kwolek, W.F., Wolf, D.J., and Everhart, W.L. (1979) Biomedical Mass Spectrometry 6(2) 67-71.

2. Rohwedder, W.K., Emken, E.A., and Wolf, D.J., Lipids 1985, 20(5), 303-311.

3. Emken, E.A., Rohwedder, W.K., Adlof, R.O., DeJarlais, W.J., and Gulley, R.M., Biochimica et Biophysica Acta 836 (1985) 233-245.

SPECTRAL DATA INFORMATION SYSTEM

Gary A. McClusky, Stephen C. Werness, Dane E. DeJohn, and Marie H. Shih
Warner Lambert / Parke-Davis Pharmaceutical Research
Ann Arbor, Michigan 48105

A computer network of six spectrometer systems, three super-microcomputers, and a mainframe computer has been completed and is in full operation. The six systems are: (1) VG 7070E/HF mass spectrometer, (2) Finnigan 4500 mass spectrometer, (3) Varian XL300 NMR spectrometer, (4) Varian XL200 NMR spectrometer, (5) IBM WP100SY NMR spectrometer, and (6) Nicolet MX-1 IR spectrometer. These systems are interfaced to two super-microcomputers through serial communications lines (i.e., RS232). In turn, the microcomputers are interfaced to the IBM 3083 mainframe computer through remote job entry ports (i.e., 2780).

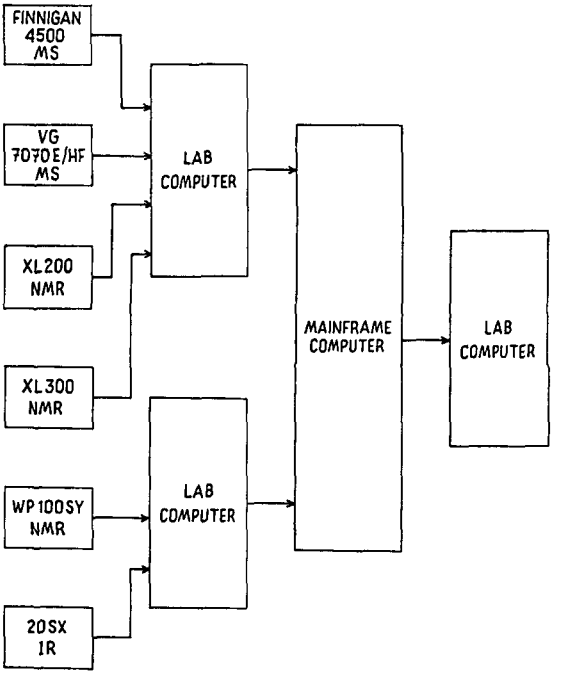

Communications programs were written for the six spectrometers to extract the desired information (i.e., data points and parameters) from the spectrometer data file. The Pascal or Fortran programs route the extracted information to a serial port and perform the necessary handshaking to allow transfer to the microcomputer. The data file is converted to a standard format depending upon spectrum type (i.e., MS, NMR, IR) prior to storage by the microcomputer.

Centralized data tracking, storage and retrieval takes place on the mainframe computer, which accommodates massive bulk storage requirements and links to associated information, such as molecular structure, physical properties, and compound status. The spectral information stored on the mainframe computer includes: (1) complete spectral dataset, (2) condensed version of spectra, and (3) experimental conditions and parameters relevant to data acquisition.

Libraries of condensed spectra for model compounds are updated on a continual basis. The reference libraries are composed of abbreviated spectra. These libraries are fully database searchable by spectral features, experimental conditions and parameters. They are also searchable in conjunction with physical properties and molecular structures stored in other databases.

Complete spectra are displayed by downloading to an intelligent graphics workstation. This distributed processing approach optimizes system performance by utilizing the mainframe for massive bulk storage and data organization and the microcomputer for specialized graphics capabilities. Thus, the intensive tasks of graphical manipulation can be performed off-line from the mainframe. The workstation is a supermicrocomputer interfaced to the mainframe by a remote job entry port.

Menu systems have been developed as the user interface on both the mainframe and workstation computers. An extensive help option is available to guide the user through the operations that need to be performed. The menus are used for retrieval of spectra and searching the spectral features in the condensed spectral databases.

An elaborate set of system management programs has been developed on the mainframe for: (1) loading databases, (2) establishing and checking data retention times, (3) tape archiving functions, (4) identifying data of interest to drug discovery process, (5) deleting expired data, (6) updating spectral libraries, and (7) system backups and regeneration.

This information system uniquely handles spectral data through a distributed computer network. A comprehensive approach to data storage allows the original spectra to be reconstructed on an intelligent graphics workstation. In addition, an abbreviated version of spectra are database searchable and can be linked to molecular structure.

AN INEXPENSIVE WAY TO ANALYZE THE OPTICS OF ELECTROSTATIC, SURFACE-IONIZATION ION-SOURCE CONFIGURATIONS

Silvio J. Balestrini, Los Alamos National Laboratory, Los Alamos, NM 87544, U.S.A.

The optical characteristics of surface ionization sources can often be studied in detail with the aid of a home computer. Sources with two-dimensional symmetry are considered. Ions are created on the surface of a hot filament. An accelerating voltage, V, is applied to the source and filament. The ions are accelerated and focused into a beam by a series of electrodes containing narrow axial slits. The ordering of elementary stages of acceleration that the electrodes form form is the optical stack. The focusing parameters are the fractions of the source voltage applied to the electrodes. A portion of the ions leaves the source through a beam-defining, collimating slit in the final electrode.

An ion trajectory at any point along the symmetry axis is described by a vector with two phase space components, which are treated as small quantities. The components at the filament are ω, the displacement from the symmetry axis, and ν, the velocity component of the ion parallel to the filament surface divided by its speed when it leaves the first stage. Elsewhere, the trajectory components are the displacement from the symmetry axis and the slope.

The vector of a trajectory at the end of an elementary stage is expressed as the vector at the beginning of the stage multiplied by the transfer matrix for that stage. An axial slit between stages will deflect a trajectory. It is possible to assign an equitable share of that deflection to the stages on either side of the slit as characteristics of those stages. The transfer matrix for the optical stack becomes the product of the transfer matrices of the constituent stages. The symbols for the transfer matrix elements of the stack and the vector elements for the position and slope at the collimator are given by

$$\begin{pmatrix} y_G \\ \theta_G \end{pmatrix} = \begin{pmatrix} \alpha & \beta \\ a & b \end{pmatrix} \begin{pmatrix} \omega \\ \nu \end{pmatrix}$$

An ion can arrive at y_G if it starts with the right combination of values for ω and ν, provided that it does not collide with an electrode on the way. The domain of possible values for ω and ν for successful trajectories defines the access area in the ω-ν-plane. The area is bounded in the ω-direction by the filament width and in the ν-direction by the slit widths between stages and the focusing parameters.

The probability density for a trajectory with an initial vector (ω,ν) is $P(\omega,\nu)$. In particular, those values of ω and ν for trajectories that can arrive at a given point, y_G, define the access line, a straight line of finite length within the access area. The summation of probabilities along the access line for y_G is the luminosity, or the probability density, $P(y_G)$, for successful trajectories at y_G.

Parallel expressions for the divergence, or the probability density for the slope, $P(\theta_G)$, will result by substituting a for α and b for β in the derivations.

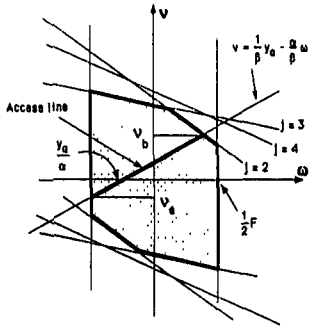

Typical access area (four stages)

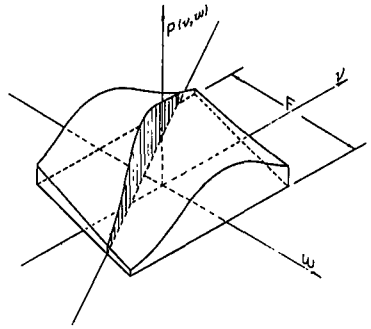

Typical probability density (two stages)

Ions leave the filament surface with a Maxwell-Bostzman distribution of tangential velocities in which the spread is characterized by the absolute temprature, T, of the filament. The luminosity profile at the collimator depends on the ratio T/V, the focusing parameters, and the contour of the access area. The final expression for $P(y_G)$ has the form of the difference between two error functions. This is a typical plot from an Apple II^+:

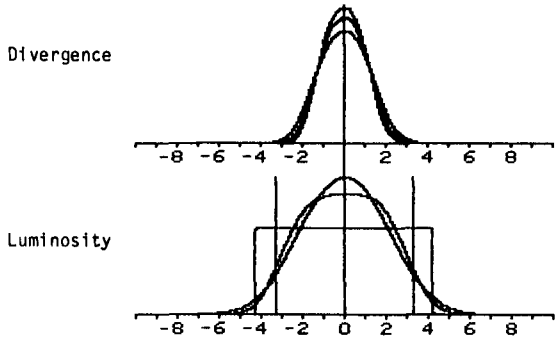

Integrations to evaluate efficiency and transmission at the collimator and at points upstream are possible by evaluating $P(y_G)$, or $P(\theta_G)$, at regular intervals and applying Simpson's rule.

The computer memory requirements are available in most popular home computers. Routines for matrix multiplication and the error function are easy to come by. The computer program used in this work has the added luxury of a library of matrices for elementary stages from which to compose optical stacks to study. Suitable focusing parameters can be found in order to design control circuitry.

HELPFUL REFERENCES:

1. S. J. Balestrini and B. G. Schuster, "A Computer-Based Method to Analyze Electrostatic, Surface-Ionization Ion-Source Configurations," In. J. Jass Spectrom. Ion Proc., 68 (1986) 265-286.

2. A. R. Miller, Basic Programs for Scientists and Engineers,(Sybex Inc., Berkeley, 1981).

AUTOMATED INTERPRETATION OF COMPLEX CAPILLARY GC/MS DATA

M. G. Legendre, R. H. Liu and R. J. Berni
USDA-ARS-SRRC, New Orleans, Louisiana, 70179.

Capillary gas chromatography technology is often needed and used in flavor related analyses, with the resulting chromatograms containing hundreds of unknown compounds (1). These constituents are often identified by manually going through each reconstructed ion chromatogram peak in a GC/MS data file.

In order to increase the efficiency of the data interpretation process, automatic procedures can be developed based on the "stringing" together of data system commands. An example of this is the vendor-contributed procedure, AUTOGC, which utilizes the INCOS data system to locate chromatographic peaks with a Biller-Bieman peak finder followed by searching the entire NBS library for the identification of the resulting peaks. When searching the entire NBS library, the INCOS routines may be saturated prematurely, in the pre-search step, with compounds having similar spectra and miss the actual compound. In 1985, Welch (2) reported on an improvement of this technique by incorporating Kovats' indices as an additional matching parameter in the searching process.

This report describes an alternate, somewhat simpler, approach in which each searching process is limited to a pre-determined narrow molecular weight (MW) window. The key feature of this procedure, as shown in Figure 1, involves the gradual moving of the MW window from lower weights to higher weights during the course of the data file interpretation process. Molecular weight windows are stored in a numeric list, IDSIL, and consist of a low MW limit, a higher MW limit and an associated cut-off scan. Each cut-off scan corresponds to the retention time up to which the current window is still applied in the searching process. Both the cut-off scan and the MW range for each window are based on expected compound retention characteristics as a function of molecular weight and boiling point, and these will vary with the selected column and temperature programming conditions.

Figure 1. Flow Diagram for IDQUAL

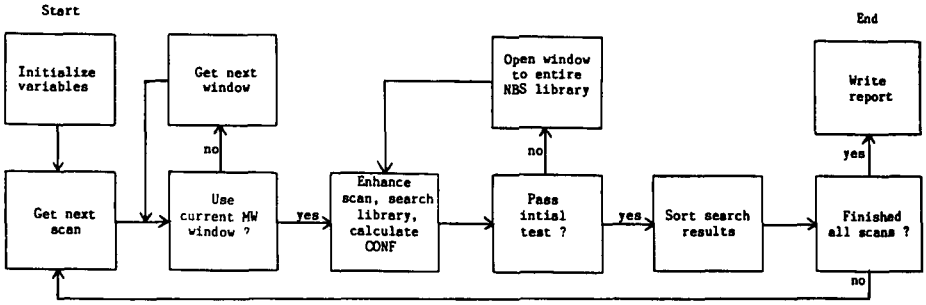

In an actual data file interpretation process, IDQUAL uses the data file, its scan list (generated by one of the built-in ALxx series routines) and the window information contained in IDSIL. First, the initial MW window and cut-off scan are put in MSDS variables !14, !15 and !3. A command (GW) developed in-house for the LIBR program, passes the window in !14 and !15 to the search algorithm and then a search is performed for the enhanced mass spectrum of the current entry in the scan list. The three best matches, as defined by FIT, are stored in a temporary library list. A "confidence" index (CONF) for each of these three matches is calculated using a weighted combination of FIT, RFIT and

PURITY. Each index is sequentially stored in !16 and immediately tested against a user-defined value for quality of match. Unless at least one of the three indices exceeds this value, IDQUAL will repeat the search process for the current scan list entry, this time using the entire NBS library. Results obtained from this repeated search are stored in place of the earlier ones. Since the elution characteristics of many compounds are affected by factors other than molecular weight and boiling point, the provision of the repeat search allows correct identification of analytes which do not conform to the expected elution patterns defined by the pre-set MW window. Before proceeding to the next scan list entry, the procedure determines whether to use the existing MW window or to proceed to the next one. The whole process is repeated until all chromatographic peaks have been completed. IDQUAL then produces a report including PURITY, FIT, RFIT, CONF and NAME for each three best matches associated with each scan list entry.

This approach has been tested on several food flavor GC/MS data files representing different degrees of complexity. These data files have been generated by a Finnigan-MAT 4500/INCOS system equipped with a 50-m SE-54 cross-linked fused silica capillary column. Results obtained by IDQUAL are compared with those obtained by manual interpretation and the conventional approach (CONVENTIONAL) that uses the entire NBS library for each search (Table 1). Assuming a 100% accuracy for the time-prohibitive manual interpretation, the IDQUAL approach results in 92%, 82%, 79%, 91% and 78% correct identifications. These identification rates are, in general, superior when compared to the corresponding results of 92%, 68%, 75%, 84% and 66% obtained with the CONVENTIONAL approach. Even though the match rate is somewhat lower than that of the manual approach, the CONF parameter provides an indication to warrant manual inspection on these doubtful identifications. It should be noted that the set-up time required for the execution of automatic procedures is normally minimal. Thus, the performance and the enormous amount of attended time saved with the use of IDQUAL should prove it a noteworthy approach.

Table 1. Comparison of Manual and Automatic Search Efficiencies

Data File	No. of Entries	No. Identified Manually	% Identified Correctly (100 for manual approach) IDQUAL	CONVENTIONAL	Time Used (Min.) Manual (w/o report)	IDQUAL (with report)	CONVENTIONAL (with report)
1	14	12	92	92	21	20	18
2	48	34	82	68	100	77	58
3	55	48	83	75	92	77	67
4	96	77	91	84	191	154	119
5	120	87	78	66	212	193	146

1. Dupuy, H. P., Flick, G. J., Bailey, M. E., St. Angelo, A. J., Legendre, M. G. and Sumrell, G.; J. Am. Oil Chem. Soc., 62 (1986), 1690.

2. Welch, K. J.; presented at the 33rd Annual Conference on Mass Spectrometry and Allied Topics; San Diego, Cal., 1985, p. 264.

AN ENHANCED PC VERSION OF THE SIMION ELECTROSTATIC LENS DESIGN PROGRAM

D.A.Dahl and J.E.Delmore

Idaho National Engineering Laboratory
EG&G Idaho, POB 1625 Idaho Falls, ID 83415

INTRODUCTION

Extensive modifications have been made to improve the performance, and ease of use of an IBM PC version of SIMION, an electrostatic lens design program originally developed by D. C. McGilvery[1]. In SIMION, an electrostatic lens is defined as a 2-dimensional electrostatic potential array containing both electrode and non-electrode points. The potential array is refined using over-relaxation methods allowing voltage contours and ion trajectories to be computed and plotted.

PERFORMANCE ENHANCEMENTS

Performance has been enhanced through several new features. The array refining process now employs dynamically self-adjusting over-relaxation. Non-electrodes within potential arrays can now be selectively preset with linear voltage gradients. These two features working together can speed refining by up to a factor of 10. Preset Z direction magnetic fields are now supported to give SIMION limited electrostatic/magnetic capabilities.

Trajectory computations now employ self-adjusting fixed distance integration intervals to help reduce errors. Trajectories can now originate outside the potential array, and focal points outside of the potential array are estimated to help reduce array sizes. Neutralizing ions are now supported. A new contouring option automatically picks voltage contours for display by examining the electrodes.

EASE OF USE ENHANCEMENTS

The user interface of SIMION has been extensively modified to take advantage of the interactive potential of an IBM PC/AT, a high resolution display, and a mouse. The user can view electrodes, trajectories, and contours on the display screen before plotting them (Figure 1). A 10 level zoom feature allows detailed inspection of contours, ion trajectories, and focal points.

Moreover, the mouse can be used to edit the potential array interactively (Figure 2). Electrodes can be inserted, deleted, moved, shaped, and adjusted for voltage via the mouse. Even non-electrodes can be inspected and modified to determine the effects of possible electrostatic field changes. A 10 level zoom capability with scrolling greatly facilitates editing large arrays.

USER EXPERIENCES

The improvements in performance and ease of use of this version of SIMION has significantly assisted our ion optics design efforts. For example, the program has been instrumental in the design of secondary ion extraction optics for a neutral beam SIMS. The performance of the as built ion extraction optics agrees well with SIMION predictions. Moreover, SIMION has been successfully used to identify the source of undesirable characteristics and subsequent modifications that have significantly improved the performance of this optics system.

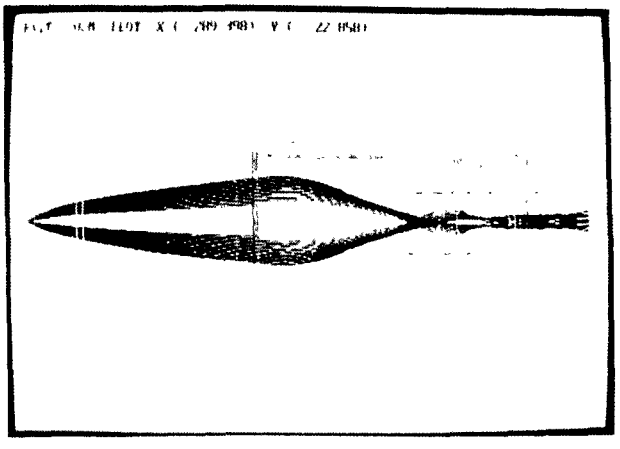

Figure 1. Screen view of an ion extraction lens.

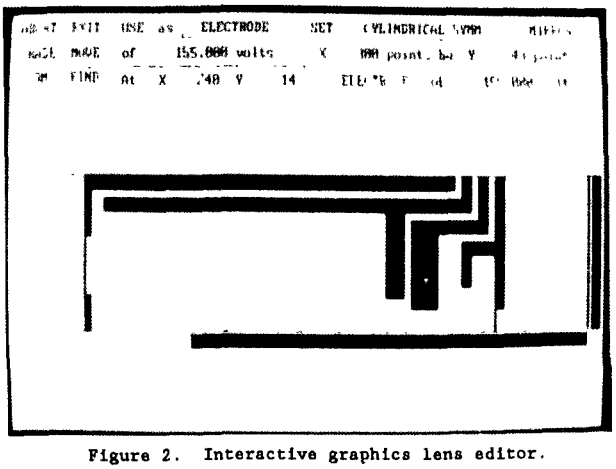

Figure 2. Interactive graphics lens editor.

REFERENCES

1. D.C. McGilvery, Ph.D. Dissertation, LaTrobe University, 1978.

ACKNOWLEDGEMENT

This work was supported in part by the Division of Chemical Sciences, Basic Energy Sciences, Office of Energy Research, Department of Energy under Contract 3ED102.

THE LKB-2091 CAPILLARY GAS CHROMATOGRAPH/MASS SPECTROMETER/DATA ANALYSIS SYSTEM USING THE IBM-AT.

Steven R. McGown, George R. Waller, Department of Biochemistry, Oklahoma Agricultural Experiment Station, Oklahoma State University, Stillwater, OK 74078.

An LKB-2091, a unit resolution, magnetic sector instrument was upgraded and computerized in a cost effective manner. The GC oven supplied by the manufacturer has been replaced with a Packard 438A CGC oven with subambient temperature capabilities. This CGC is microprocessor controlled and has 9 memory locations for the storage of particular run parameters. The oven lid can be lifted pneumatically for convenient column changing. The original jet separator assembly has been removed and the capillary column plumbed directly into the ion source. The original interface oven is still used and is heated to 265°C for normal operation. An on-column injector, manufactured by SGE, is utilized for trace analysis. Operating head pressures of around 5 psi give linear flow rates of approximately 25 cm/s at 300°C. With the oven temperature at 60°C, the internal pressure in the ion source is around 200 nanotorr, which is in part achieved by using a narrow bore column, 0.25mm in diameter and 30m long. A capillary column of these dimensions, with a 0.1 um film, gives rapid analysis, and good sensitivity. We are able to get full scan spectra on 10 ng samples injected in the split injector with the split at 1:5, but smaller sample sizes become difficult due to the narrowing of the CGC peak and the scan speed of the magnet is 1.3s for 20 u to 450 u. This is about 50 to 100 times greater than the original factory specifications. Direct probe work enables one to handle pure samples down to 500 pg and still get full spectral information. The data system, manufactured and installed by the Teknivent Corporation, is based on the IBM-AT. The IBM-AT is configured in the following manner: a 20 Mbyte hard drive, a 1.2 Mbyte floppy disk drive, an Intel 80287 math co-processor, 640 kbyte memory, a Hercules color/graphics card, an Amdek 300 monitor, a Hayes Smartcom II internal modem, and an Okidata 93 microline printer. An interface box, internal computer card, and all the necessary software for data acquisition and processing is supplied by Teknivent. The data system samples two inputs to the interface box at 30 MHz. One input is a Hall probe for magnetic field strength detection, and the other input is the electron multiplier. Standard compounds such as TRIS or PFK are used in order to calibrate the instrument daily. The computer associates a certain field strength with a certain mass which is done through a curve fitting routine. This feature allows non-linear scan functions, e.g. hyperbolic or log type functions, with the only constraint that the scans be reproducible. The actual mass peaks themselves must be at least 1 ms wide; with this in mind, the data system can scan 1000 peaks per second. Post-processing capabilities allow total and single ion chromatogram reconstruction scan averaging, and tabular listings. Most utilities found on larger data systems are available. The system has a library search routine which can search such data bases as the Wiley/NBS/EPA* library. The system also allows the user to construct their own library data base which is convenient for specialized work. In our case, we are constructing a library on allelochemicals to aid in our analysis. A salient feature of the libraries is that they contain full mass spectral information and are not truncated to 10 or 20 peak references. In conclusion, the LKB-2091, equipped with the Teknivent data system, can supply the state-of-the-art unit resolution mass spectra in the electron impact mode.

CGC INSERTED INTO
ION SOURCE

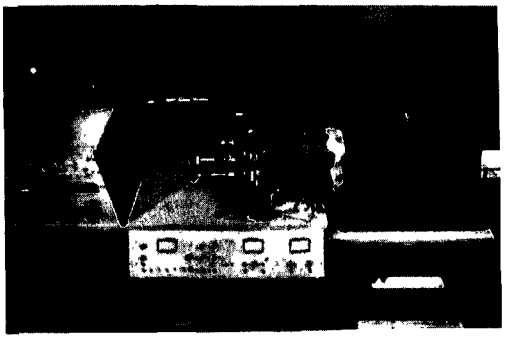

LKB 2091 MASS SPECTROMETER

TANDEM IBM-AT
DATA SYSTEM

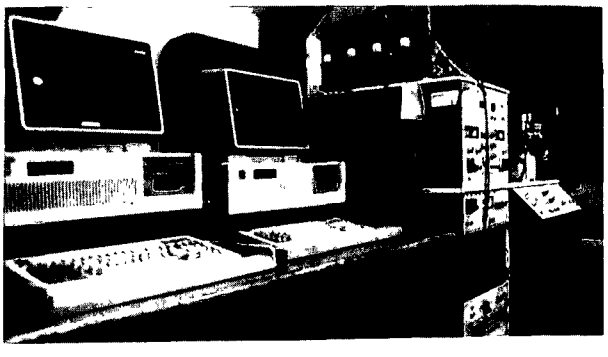

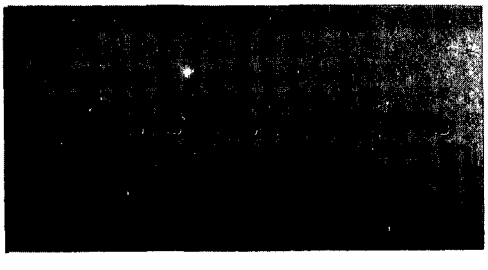

PRINTER OUTPUT
TOTAL ION CHROMATOGRAM

MASS SPECTRUM OF CODEINE

THE DETERMINATION OF THE LOCATION AND NATURE OF AMINO ACID SUBSTITUTIONS IN BIOSYNTHETIC BACTERIO-OPSIN

G. Allmaier, B.H. Chao, H.G. Khorana and K. Biemann, Departments of Chemistry and Biology, M. I. T., Cambridge, MA 02139.

Fast atom bombardment mass spectrometry (FAB-MS) of CNBr-peptides is an efficient method for structure determination of proteins, either for a check of the DNA-derived sequence of a biosynthetically modified protein or for the detection and characterization of posttranslational modifications or spontaneous mutations. This technique was employed to check the correctness of the structure of analogs of the membrane protein bacterio-opsin (NDBO) prepared by recombinant DNA technology. The protein serves as light driven proton pump in Halobacterium halobium. Modifications in certain regions of the protein such as replacement of amino acids or extensions of the N-terminus are necessary to an understanding of the mechanism of proton pumping. NDBO is extremely hydrophobic due to the presence of tracts of hydrophilic and hydrophobic amino acids (see Fig 1). This presents a major obstacle in the sequence determination with classical biochemical techniques (1,2).

The molecular weight of NDBO and the two analogs are too high for direct, accurate mass spectrometric analysis (NDBO MWt. 26000). The poor solubility precludes enzymatic digestion of the protein and CNBr cleavage had to be applied. The molecular weights of the ten CNBr cleavage products of unmodified NDBO are in the range accessible for our mass spectrometer (see Table 1). After CNBr cleavage separation of the mixture was necessary to reduce the complexity of the samples. A water/ethanol solvent system with TFA was used for the reversed phase HPLC of the large hydrophobic membrane fragments. All CNBr cleavage products were resolved by RP-HPLC.

The HPLC fractionated digest of NDBO revealed all of the CNBr-peptides at the correct values for their $(M+H)^+$ ions except CNBr-4. This very hydrophobic peptide was not detected, but could be found in combination with CNBr-3 as uncleaved product CNBr-3/4. The CNBr-peptides were mainly present as homoserine lactone. All $(M+H)^+$ ions were accompanied by $(M+28+H)^+$ ions indicating formylation by reaction with the formic acid used in the CNBr-cleavage. Further addition of 28 was detected in several cases (e.g., CNBr-7, $(M+H)^+$, $(M+56+H)^+$, and $(M+84+H)^+$). These formylations may be related not only to NH_2-groups but also to OH-groups.

One of the analogs produced by recombinant DNA-technique ($pPLBO_5$ BOTC-6) was modified at the N-terminus, pGlu—Ala— replaced by Met—Ala—. Since the N-terminal methionine is removed by CNBr, the resulting peptide thus would correspond to that of NDBO less pyroglutamic acid. The $(M+H)^+$ ion of these two peptides differed indeed by 111.1 daltons which confirms the correctness of the desired modification. All other CNBr-peptides were unchanged. The second analog ($pPLBO_5$ 219 F/L) had two modifications. The N-terminus was modified in the same way as $pPLBO_5$ BOTC-6 and was correct. Further, the codon for the amino acid Phe at position 219 had been replaced by that for Leu. This modification was verified by the shift found for the molecular weights of the CNBr cleavage products (CNBr-10) from the modified portion (see Table 1).

The methodology outlined in this work opens the way to a relatively fast comparison of proteins produced through recombinant DNA technology with that of the native type (NDBO). In this case all peptides produced by CNBr cleavage were small enough that this question can be answered by direct molecular weight determination by FAB-MS.

This work was supported by grants from the National Institutes of Health (RR00317 and GM05472).

REFERENCES

1. Gerber, G.E., Anderegg, R.J., Herlihy, W.C., Gray, C.P. Biemann, K. and Khorana, H.G., Proc. Natl. Acad. Sci., USA, 76, 227-231 (1979).
2. Khorana, H.G., Gerber, G.E., Herlihy, W.C., Gray, C.P., Anderegg, R.J., Nihei, K. and Biemann, K., Proc. Natl. Acad. Sci., USA, 76, 5046-5050 (1979).

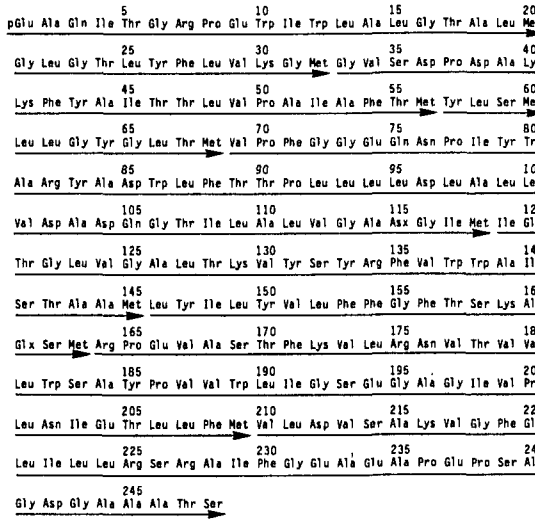

Figure 1. Primary structure of native delipidated bacterio-opsin (NDBO).

Table 1

Theoretical and observed $(M+H)^+$ values of CNBr-peptides.

Peptide	Position	Length	$[M + H]^+$ as homoserine lactone (theoret. mono-isotopic)	Most abundant observed peak in the $[M + H]^+$ region
CNBr - 1 NDBO	1	20	2190.2*	2191.3
CNBr - 2 NDBO	21	12	1250.7	1250.8
CNBr - 3 NDBO	33	24	2508.3	2509.4
CNBr - 4 NDBO	57	4	465.2	not observed
CNBr - 5 NDBO	61	8	819.5	819.5
CNBr - 6 NDBO	69	50	5397.9	5400.9
CNBr - 7 NDBO	119	27	2913.6	2913.9
CNBr - 8 NDBO	146	18	2081.1	2082.4
CNBr - 9 NDBO	164	46	5036.8	5068.9 $[M + 2B + H]^+$
CNBr - 10 NDBO	210	39	3843.0**	3845.1
CNBr 3/4 NDBO	33	28	3002.6	3003.7
pCNBr - 3 NDBO	37	20	2150.2	2151.5
CNBr - 1 $pPLBO_5$ BOTC-6	2	19	2079.1*	2080.2
CNBr - 1 $pPLBO_5$ 219 F/L	2	19	2079.1*	2080.2
CNBr - 10 $pPLBO_5$ 219 F/L	210	39	3809.1**	3811.8

* Δm = 111.1 (theoret. monoisotopic)
Δm = 111.1 (observed)

** Δm = 33.9 (theoret. monoisotopic)
Δm = 33.3 (observed)

HPLC/MS IN THE CLINICAL ANALYSIS OF POLAR CORTICOSTEROIDS AND STEROID CONJUGATES

D. Liberato, N. Esteban, H.-Y Kim and CHL. Shackleton. Laboratory of Theoretical and Physical Biology (NICHHD) and Laboratory of Clinical Studies (NIAAA) Bethesda MD 20892, Research Laboratory, Children's Hospital Medical Center, Oakland 94609

Thermospray HPLC/MS is a technique with obvious application in the study of hormonal steroids and their metabolites. However, use of a new technique, particularly one as complex as HPLC/MS, should be targeted to areas whose existing methodologies are weak. For example, little would be gained by use of HPLC/MS for the analysis of hydrolyzed steroid conjugates since the cumulative experience of 20 years of GC/MS has shown this to be a technique without peers for this type of analysis. However, there are fields where LC/MS could contribute greatly to clinical steroid analysis. One is the analysis of intact conjugates such as steroid glucuronides. Another is the analysis of the newly identified lipoidal estrogen conjugates which have extremely long retention time on GC, and a final example may be the analysis of polar unconjugated steroids which have problems associated with derivatization. This presentation addresses the analysis of these groups of steroids by LC/MS.

METHOD:

LC/MS was carried out on Biospect or Extrel Mass Spectrometers equipped with Vestec thermospray interfaces. Typical LC conditions and solvent systems were as follows:

1. Steroid glucuronides: 25 cm C_{18} column; Acetonitrile ammonium acetate (3:7 v/v); flow rate 1.25 ml/minute
2. Estradiol esters: 7.5 cm C_{18} column; methanol: hexane : 0.1 M ammonium acetate (25:1:1 v/v); 1 ml/minute
3. Unconjugated steroids: 25 cm C_{18} column; methanol: ammonium acetate (11:9, v/v); 1 ml/minute

RESULTS:

Steroid glucuronides:

Typical positive and negative mass spectra of a steroid glucuronide (11β-hydroxyandrosterone) are given in Fig. 1. In the positive ion mass spectrum the ammoniated molecular ion is at m/z 500 and sequential losses of water are seen at m/z 482, 464, 446 and 428. The alycone + NH_4^+ ion is at m/z 324 and losses of water give rise to ions at m/z 300, 288, 270 and 252. The negative ion mass spectrum is simple and dominated by the $M-H^-$ ion at m/z 481.

Estradiol esters:

Estradiol conjugated with fatty acids C 18:0 to C 20:4 can be separated within 11 minutes (Fig 2a). Typical positive ion mass spectra obtained are illustrated in Fig 2b. The base peak (m/z 255) of all the esters represents the aglycone. In the molecular ion region the following ions are important: MNa^+, MH^+ and $MNH_4^+-H_2O$. Only estradiol arachidonate (C 20:4) gave a significant fragment ion associated with the protonated fatty acid (m/z 305).

Unconjugated steroids:

Individual corticosteroid mass spectra gave valuable structural information and with the exception of of 6β-hydroxycortisol no corticosteroids exhibited ammoniated molecular ions, instead giving protonated ions $M+H^+$. The degree of fragmentation was associated with the number of hydroxyl groups, and particularly with the introduction of a 17α-hydroxyl which encouraged side-chain cleavage.

The supremacy of the HPLC/MS technique over GC/MS for the study of selected unconjugated steroids is illustrated by 18-hydroxycortisol, a steroid of current interest in the study of steroid hypertension. Fig. 3a illustrates the mass spectrum obtained by GC/MS of the methyloxime-trimethylsilyl ether. The molecular ion is not detectable. Add to this the fact that multiple derivatives are formed (due to partial existence of the compound as C-18-20 hemi-ketal and to the production of syn - and anti - forms of the oximes) and the disadvantages of GC/MS become substantial. In contrast liquid chromatography gives a single peak, the spectrum is structurally informative as well as giving a strong protonated molecular ion (Fig. 3b).

Supported in part by the NIH (AM34400)

Fig.1

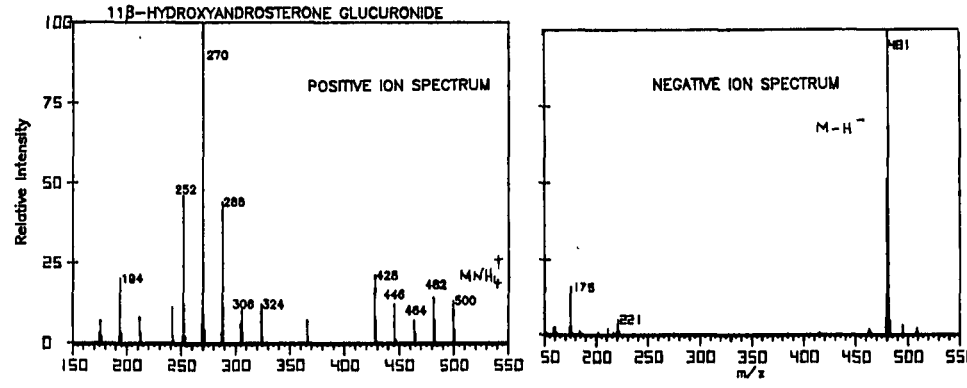

Fig.2a

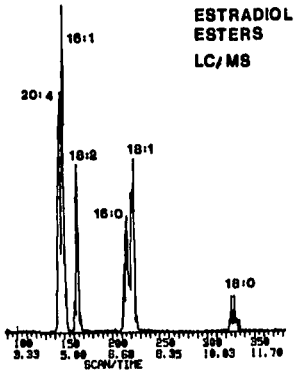

Fig.2b

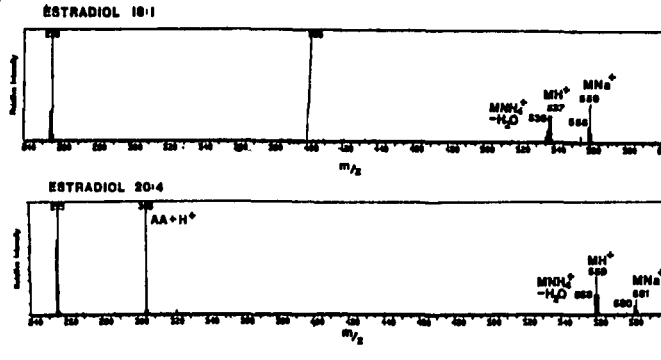

Fig.3a 18-HYDROXYCORTISOL

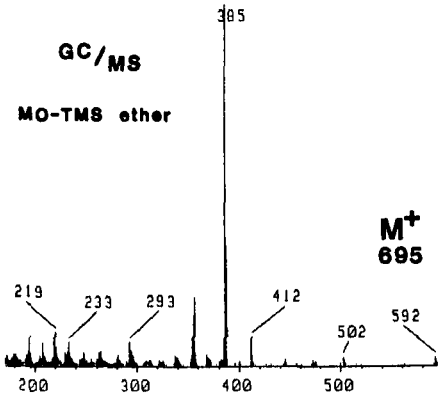

Fig.3b

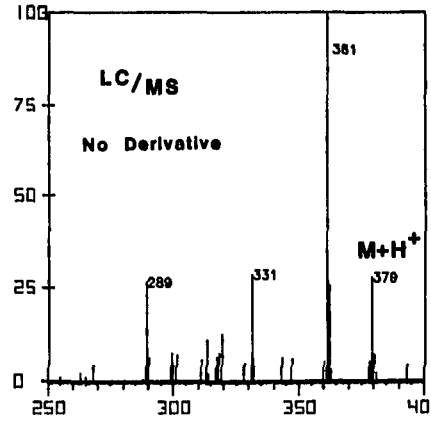

ANALYSIS OF FOLATES BY FAST ATOM BOMBARDMENT AND TANDEM MASS SPECTROMETRY

A. J. Clifford*, A. D. Jones**, and S. R. Missler***

*Department of Nutrition and **Facility for Advanced Instrumentation, University of California, Davis, CA 95616 and ***U.S. Army Med. Res. Inst. Infect. Diseases, Fort Detrick, MD 21701

Folacin is an essential nutrient that exists naturally in many different forms. The most widely used analytical method for this vitamin is still the microbiological assay with L. casei. New analytical approaches capable of accurately determining the minute levels of folate that are found in complex matrices of tissues and foods are clearly needed (1).

Because of the many forms of folates which occur naturally, tandem mass spectrometry was investigated with a view to developing an improved method of folate analysis. Three mass spectrometry (MS) studies were performed on the dimethyl esters of the following standard folates: folic acid (FA); tetrahydrofolic acid (THFA) formyltetrahydrofolic acid (FTHFA), and methyltetrahydrofolic acid (MTHFA) and pteroyltriglutamate (Pte Glu_3). In addition, a crude extract of rat liver was purified by cation and reversed phase chromatography and analyzed by FAB MS to obtain data on the feasibility of MS techniques for folate analysis in biological tissues.

First, the optimum conditions of fast atom bombardment (FAB) MS were determined to obtain mass spectra of each folate. Individual folate methyl esters (10-20 μg) dissolved in 2.5 μl MeOH:HCl (10/1:v/v) and 2.5 μl dithioerythritol:dithiothreitol (3/1::v/v) were loaded on the FAB target and full spectra were recorded with a VG 7070-EQ tandem mass spectrometer (Fig. 1A,2A,3A). Much smaller quantities of folate methyl esters could be detected than of the nonesterified forms. Still smaller quantities of the FA trimethylsilyl (TMS) derivative could be detected using methane chemical ionization. Results from these experiments showed that these soft ionization techniques yield mass spectra which exhibit strong pseudomolecular ions for these folates.

Secondly, daughter ion spectra of the $[M+H]^+$ ion of each folate methyl ester were produced by collisional activation following optimization of the collision parameters (Fig. 1B,2B,3B). Two or more intense daughter ions were obtained for each folate methyl ester as shown in the table below.

Folate	Parent Ion [M+H]+	Most abundant pair of Daughter ions	
FA	470	295	176
THFA	474	299	166
FTHFA	484	424	282
MTHFA	488	313	180
$PteGlu_3$ (40 eV)	756	295	444
$PteGlu_3$ (200 eV)	756	295	176

Except for FTHFA all folates gave a neutral loss of 174 (corresponding to loss of the glutamate moiety).

Thirdly selected reaction monitoring (SRM) of the decomposition of the $[M+H]^+$ ion of the standard folate esters to their dominant daughter ions (e.g. m/z 470 → 295 and 470 → 176 for the folic acid methy ester) showed that about 2.5 ng of each ester could be measured by MS/MS. Finally the mass spectrum of the partially purified extract of liver showed the expected pseudomolecular and adduct ions (Fig. 4). There was no evidence that interfering substances in the liver extract prevent ionization of folates by FAB.

The data demonstrate that tandem mass spectrometry is a promising approach to quantifying the multiple forms of folates that occur at low levels in foods and biological tissues. Application of this analytical methodology to foods and tissues will provide the needed data base to better identify the folate needs and status of humans.

---

1. S. A. Anderson and J. M. Talbot, 1981, LSRO Report #223-79-2275, Fed. Am. Soc. Exptl. Biol., Bethesda, MD.

FIGURE 1. A

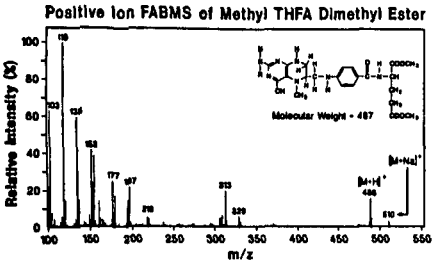

B

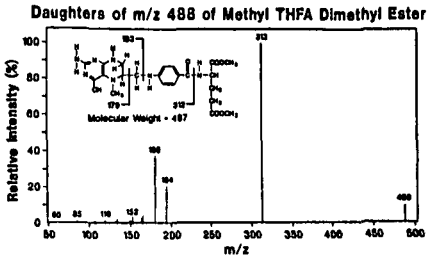

FIGURE 2. A

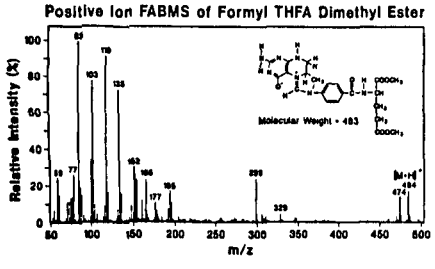

B

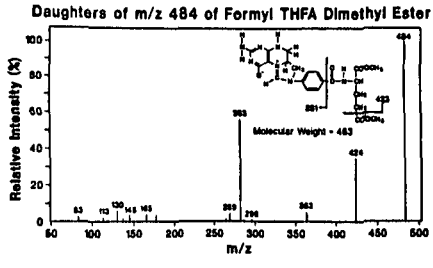

FIGURE 3. A

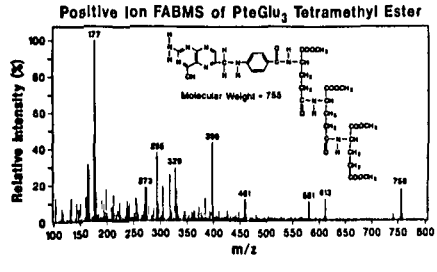

B

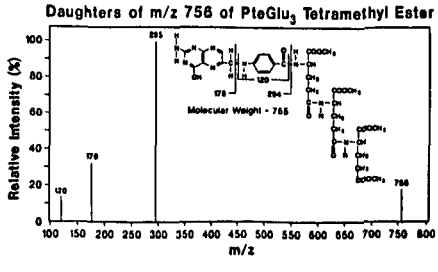

FIGURE 4.

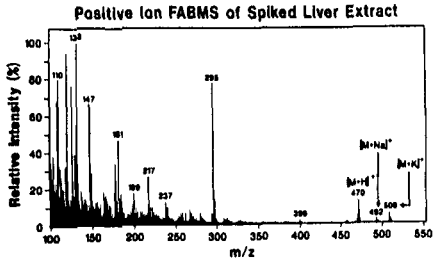

PICOLINYLDIMETHYLSILYL (PICSI) ETHERS: NEW DERIVATIVES FOR THE STRUCTURAL DETERMINATION OF FATTY ALCOHOLS BY GC/MS

D.J. Harvey

University Department of Pharmacology, South Parks Road, Oxford, OX1 3QT, UK.

Structural determination of fatty acids and alcohols by GC/MS requires the preparation of fragmention-directing derivatives to avoid such problems as double bond isomerisation. Nicotinates have been developed for fatty alcohols (1) and have been adapted for fatty acids by formation of the picolinyl esters (2). Preparation of the nicotinates involves reaction of the alcohol with fresh nicotinoyl chloride and extraction of the esters with an organic solvent, a disadvantage for examination of small samples. In order to combine the fragmentation-directing properties of the nicotinates and picolinyl esters with the ease of preparation of silyl ethers, picolinyldimethylsilyl (PICSI) ethers have been investigated.

Two methods were investigated for derivative preparation. In the first, the fatty alcohol was reacted for 5 min at 60°C with an excess of dichlorodimethylsilane in dimethylformamide containing 1% imidazole. A 30% solution of 3-pyridylcarbinol in acetonitrile was then added and heated at 60° for 5 min. Aliquots of the mixture were examined directly by GC/MS. In the second method, diethylaminodimethylsilyl-3-pyridylcarbinol was synthesized from 3-pyridylcarbinol and bis(diethylamino)dimethylsilane with distillation of the product (bp = 142 - 148°C/18 mm). This was then used as a conventional silylating reagent for preparation of the derivatives. GC/MS data were recorded with a VG Micromass 12B mass spectrometer interfaced to a VG 2050 data system and via a glass jet separator to a Varian 2440 gas chromatograph which was fitted with a 2 m x 2 mm glass column packed with 3% SE-30 on 100 - 120 mesh Gas Chrom Q. Spectra were recorded at 25 eV.

Both methods of sample preparation gave the required derivatives which fragmented in a similar manner to the nicotinates in that they produced a series of relatively abundant even-electron ions (series a) resulting from radical-induced cleavage at each carbon-carbon bond after random hydrogen abstraction from the chain by the charged pyridine group (Scheme 1).

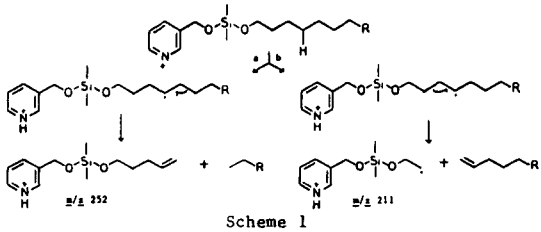

Scheme 1

These ions carried structural information such as double bond position. In addition, a series of odd-electron ions was present one mass unit higher (series b). These ions were formed by a related mechanism to the series a ions but with cleavage of the chain on the opposite side of the radical site. Molecular ions were the base peaks in all samples studied.

Fig. 1 shows the 25 eV mass spectrum of the PICSI derivative of octadecanol showing the abundant molecular ion and the ions of series a and b.

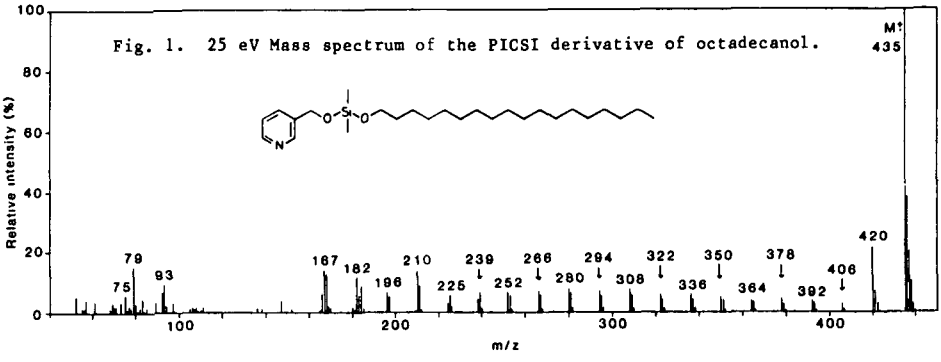

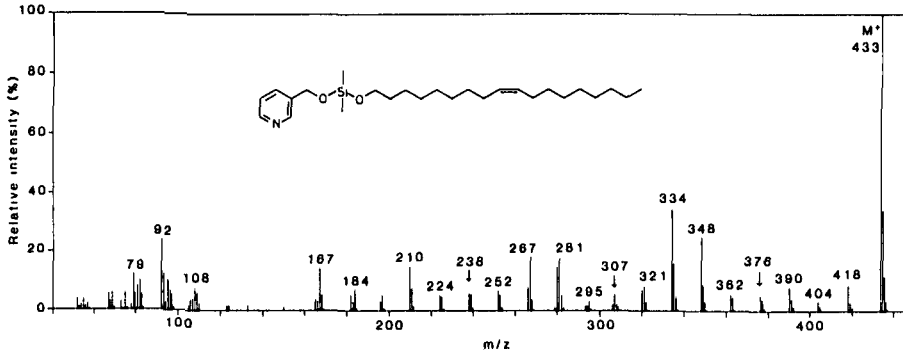

Fig. 2. 25 eV Mass spectrum of the PICSI derivative of cis-9-octadecenol.

The presence of a double bond in the aliphatic chain (Fig. 2) modified the masses and intensities of both the series a and b ions. The two mass unit deficit in mass in ions above m/z 294 localized the double bond at the delta-9-position. More prominent, however, were the increased abundancies of the series a ions at m/z 334 and 348 and the series b ions at m/z 267 and 281. Formation of these ions can be rationalised by abstraction of the two allylic hydrogen atoms with cleavages on either side of the double bond as shown in Schemes 2 and 3.

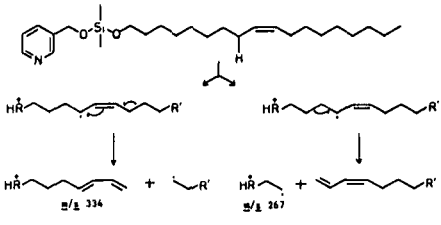

Scheme 2

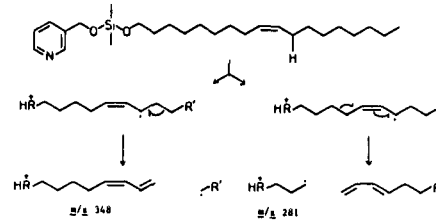

Scheme 3

More complex spectra were produced by alcohols having more double bonds as shown by the spectrum of arachidonic acid (Fig. 3). Abundant ions such as m/z 344 and 305 were the result of allylic hydrogen abstraction together with migration of a second allylic hydrogen atom to form conjugated ions and radicals. Full details of these fragmentations will be published later.

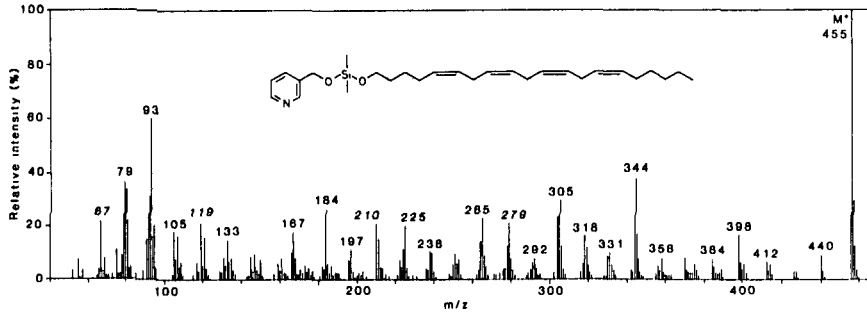

Fig. 3. 25 eV Mass spectrum of the PICSI derivative of arachidonic acid.

This work was supported by the Wellcome Trust.

1. W. Vetter and W. Meister, Org. Mass Spectrom., 1981, 16, 118.
2. D.J. Harvey, Biomed. Mass Spectrom., 1982, 9, 33.

RAPID INJECTION PORT DERIVATIZATION AND NEGATIVE ION GCMS DETECTION OF DEUTERIUM-LABELLED 4-PYRIDOXIC ACID. J. F. Gregory & J. P. Toth, Department of Food Science and Human Nutrition, University of Florida, Gainesville, FL.

Vitamin B-6, a group of seven substituted pyridine compounds, is an essential nutrient whose bioavailability in foods is imperfectly understood. The use of human subjects in bioavailability studies precludes the use of radioisotope-labelled compounds, but ^{15}N and ^{2}H-labelled B-6 compounds have been prepared and are suitable for such studies. We report here the development of a GCMS method for determining relative amounts of d_0, d_2 and d_5 forms of 4-pyridoxic acid (4-PA), the principal urinary metabolite of all B-6 compounds.

Positive CI, negative CI and EI analysis were performed using a Finnigan 4021 GCMS system with a 15 m x 0.32 mm DB-5 capillary GC column (J&W). Isobutane (ca. 0.2 torr) was the reagent gas for CI spectra. Co-injection of 4-PA with trifluoroacetic anhydride (TFAA), a method reported for the derivatization of amphetamine,[1] yielded a sharp GC peak with an intense negative ion electron capture mass spectrum. (Preliminary attempts at simultaneous acylation/esterification with TFAA and trifluoroethanol were unsuccessful, but their results suggested that a lactone was formed, obviating the need for esterification of the carboxyl group.)

The positive CI spectrum of the product indicates a molecular weight of 261, while the negative ion spectrum showed two mass peaks of roughly equal intensity at m/z 113 and m/z 164. These data suggest that the product is 3-trifluoroacetyl-4 PA lactone:

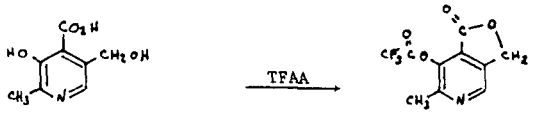

4PA

Formation of such a product is consistent with the known reactivity of TFAA[2] and is further supported by the positive and negative CI spectra of the homologous pentafluoropropionic anhydride (PFPA) derivative and the TFAA derivative of d_2-4-PA. These data also support the assignment of the m/z 113 and m/z 164 peaks to $CF_3CO_2^-$ and $[M-CF_3CO]^-$ respectively.

Selected ion monitoring in the PPINICI mode of m/z 262(+) and 164(-) permits detection of a 10-ng injection of derivative made from a urine extract containing 0.2 µg of 4-PA. Monitoring only m/z(-) permits detection of a 1-10 pg injection.

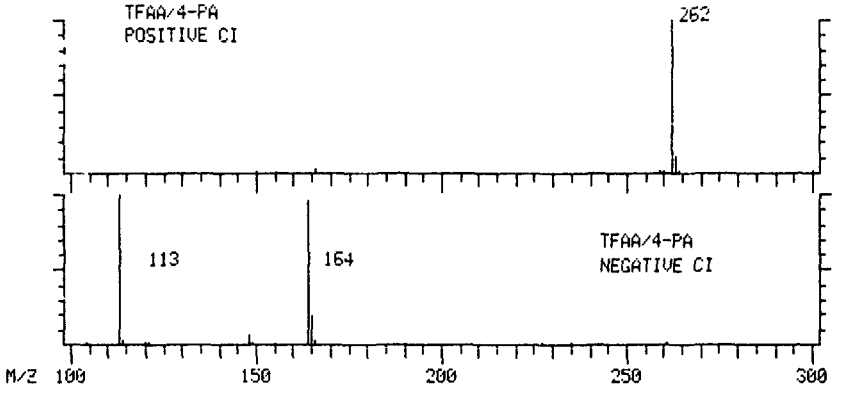

References

1. G.A. Eiceman, C.S. Leasure and S.L. Selim, J. Chrom. Sci., 1984, 22, 509.
2. E.J. Bourne, J.E.B. Randles, M. Stacey, J.C. Tatlow, J.M. Tedder, JACS, 1954, 76, 3602.

DETECTION OF FOLACIN BY TRIFLUOROACETIC ANHYDRIDE/TRIFLUOROETHANOL DERIVATIZATION AND NEGATIVE ION ELECTRON CAPTURE GCMS. J. F. Gregory & J. P. Toth, Department of Food Science and Human Nutrition, University of Florida, Gainesville, FL.

Folacins, e.g., folic acid (I), are essential nutrients whose dietary requirements in humans are incompletely understood due to a lack of information concerning folacin bioavailability in foods. Bioavailability studies in animals have used radioisotope tracers, but this approach is not possible with human subjects. Stable isotope labelled folacins, with deuterium labels on the benzene ring and/or glutamic acid side chains, have been prepared, and a GCMS assay for such compounds has been developed.

Simultaneous acylation/esterification of polyfunctional molecules with fluorinated reagents has been used to produce derivatives that are sufficiently volatile for GCMS analysis and highly sensitive to detection by negative ion electron capture mass spectrometry.[1] This approach was applied to the analysis of I, but to produce a derivative with a low enough molecular weight to be detected with a quadrupole instrument it is first necessary to cleave I to pABG, para-amino benzoyl glutamic acid (II).[2]

Derivatization of pABG standards was performed by incubation with trifluoroacetic anhydride (TFAA) and trifluoroethanol (TFE) for 1 hour at 90°C followed by evaporation of excess reagent and dissolving of the residue in ethyl acetate. Positive CI, negative CI and EI MS analyses were performed using a Finnigan 4021 GCMS system with a 30 m x 0.25 mm SE-30 capillary GC column (J&W). The reagent gas for CI spectra was methane at a pressure of ca. 0.2 torr.

Two derivatives of pABG were produced. Positive CI spectra of the minor product (ca. 10%) indicates a molecular weight of 526, corresponding to esterification of both carboxylic acid sites by TFE and acylation of the primary amine group by TFAA. The base peak in the negative ion spectrum of this compound corresponds to cleavage of the carbon-nitrogen bond on the glutamic acid moiety.

The major product (ca. 90%) has a molecular weight of 426 (Figure 1), and the base peak in its negative ion spectrum is due to the molecular anion (Figure 2). This molecular weight is consistent with the formation of a lactam (III) whose cyclic structure would stabilize the molecular anion. Formation of such a product is consistent with the known reactivity of TFAA.[3] Further support for the proposed structures was obtained by substituting pentafluoropropanol for TFE which yielded the expected homologs for both products.

Selected ion monitoring at m/z 426 in the negative ion mode permits detection of a 50 pg injection of derivative obtained from 1 ng of pABG. The m/z 462 anion retains deuterium labels on the benzene ring and/or glutamic acid side chain. This derivative thus possesses the sensitivity and selectivity needed for bioavailability studies.

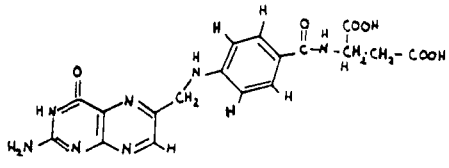

I

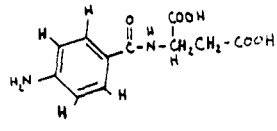

II

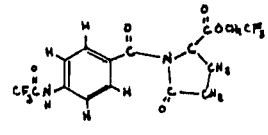

III

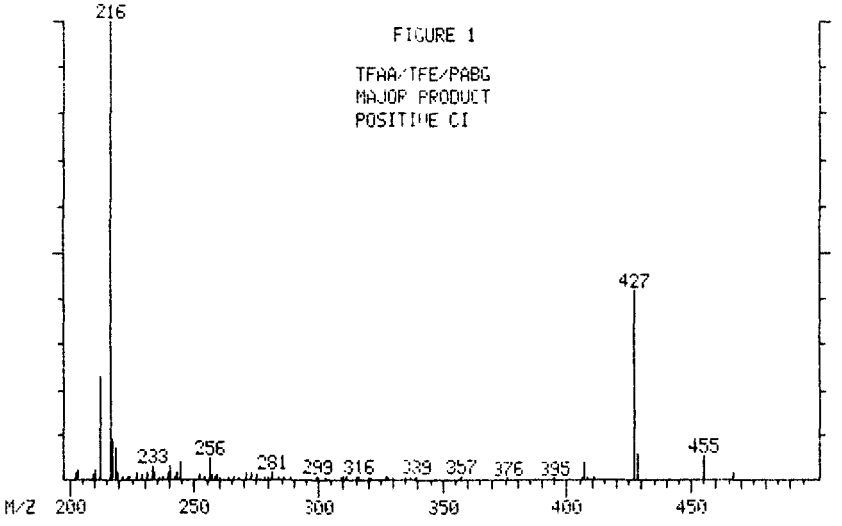

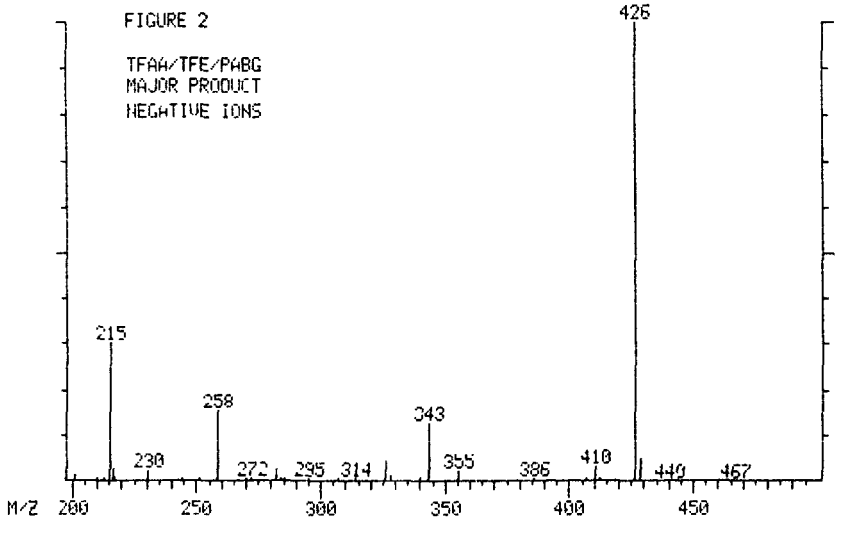

References

1. For example, C.L. Deyrup, S.-M. Chang, R.A. Weintraub and H.A. Moye, J. Agr. & Food Chem., 1985, 33, 944.
2. S.K. Foo, D.J. Cichowicz and B. Shane, Anal. Biochem., 1980, 107, 109.
3. E.J. Bourne, J.E.B. Randles, M. Stacey, J.C. Tatlow, J.M. Tedder, JACS, 1954, 76, 3206.

APPLICATION OF LASER DESORPTION-FOURIER TRANSFORM MASS SPECTROMETRY TO ANALYSIS OF POLYSACCHARIDES

Mildred L. Coates, Lydia M. Nuwaysir,
and Charles L. Wilkins
Department of Chemistry
University of California
Riverside, CA 92521

For large polar molecules, such as polysaccharides, mass spectral methods requiring the analyte to be soluble in a solvent or a liquid matrix are often inappropriate. Laser desorption(LD) is an alternative which allows examination of some compounds previously inaccessible by other methods. The mechanism of LD is not fully understood, but is believed to be a combination of processes, some thermal in nature. If thermal processes are important, then one would expect ions derived from these processes to appear in LD spectra and that such spectra would be similar to pyrolysis mass spectra.

The objective of this work is to evalute the use of laser desorption-Fourier transform mass spectrometry(LD-FTMS)(1.) for the characterization of underivatized polysaccharides. These compounds have high molecular weights and little or no solubility in neutral solvents, making them good candidates for LD-FTMS. Our earlier studies(2.,3.) indicated that characterization of these compounds by their fragmentation patterns might be possible.

This study was conducted with a Tachisto 215G pulsed TEA CO_2 gas laser interfaced to a Nicolet FT-1000 mass spectrometer. The FT mass spectrometer cubic ion cell is made from 2inX2in plates of 80% transmissive stainless steel. Desorption/ionization occurs when the laser beam is focussed onto the sample at the surface of a direct introduction probe. A delay of 15s after the laser pulse allows desorbed neutrals to be pumped away, while positive ions are trapped in the cell by a voltage of 0.7V on the trap plates. In the absence of external excitation, the ions move in cyclotron orbits, obeying the cyclotron equation, $\omega_c=(z/m)B$. Application of an rf frequency sweep, via the transmitter plates, causes the ions to increase their orbits and move closer to the receiver plates, inducing a flow of electrons. This image current is observed in the time domain and contains frequency information about all the ions in the cell, which can be retrieved by Fourier transformation of this signal to obtain a frequency/mass spectrum.

The polysaccharides examined in this study are six polyhexoses—locust bean gum, white dextrin, dextran, cellulose, starch, and xanthan gum—and three non-polyhexoses—chitin, agarose, and agar. Samples are ground together with KBr and affixed to the probe tip with double-sided-adhesive tape. The probe is inserted into the FT mass spectrometer until the tip comes up to the cell. A cone attached to the trap plate guides the insertion.

The laser beam perforates the sample layer, but not the tape itself. Ejection sweeps after the laser pulse are used to remove ions from the cell which come from the tape and the dopant. Turning the probe handle after each laser pulse to provide a fresh sample surface makes signal averaging possible. For each mass spectrum, 18, 24, or 36 transients, each containing 64K of data points, are co-added and augmented by one zero-fill. After baseline correction of the resulting signal and apodization using a sine-bell function, a fast Fourier transform is performed to obtain a magnitude mode spectrum.

Examination of the LD-FT mass spectra of the polyhexoses reveals the presence of series of K^+-attached ions, apparently resulting from cleavages within sugar rings, as well as between them. The general composition of these series ions is $[(162)_n+X+K]^+$, where 162 is the mass of the hexose repeating unit and X is some integer. The values of X seem to correspond to the masses of pyrolysis ions. The relative importance of these series and the mass distribution of the ions in the mass spectrum vary among the polyhexoses. Dextran, cellulose, and starch are all polyglucoses, differing only in the way in which the glucoses are linked. The observation that the

ion series in their mass spectra differ in relative importance indicates that linkage influences the fragmentations of these compounds.

Chitin is a naturally acetylated polyhexosamine. It resists grinding, so pieces are put directly onto the tape. Since no dopant is used, H^+- and Na^+-attached ions are observed in the mass spectrum, in addition to K^+-attached ions. Fewer ion series are observed than in the polyhexose spectra. The general composition of the series ions is $[(203)_n+X+C]^+$, where 203 is the mass of the acetylated hexosamine repeating unit, X is 0, 60, 74, or 185, and C is H, Na, or K.

Agarose is composed of chains of hexose rings alternating with anhydrohexose rings. Although agar consists of both agarose and agaropectin, the mass spectra of the two are similar. The major ions observed in these spectra reflect the alternating sugar sequence and appear to arise from cleavages between the sugar rings.

The LD-FT mass spectra of all the polysaccharides examined exhibit distinct fragmentation patterns. The variation between the fragmentation patterns of different polysaccharides suggests that these patterns could eventually be useful in characterizing these compounds. The regularity of these patterns implies an orderly cleavage process or processes. However, more investigation into the nature of these cleavages is necessary before the fragmentation patterns can be used to provide structural information.

1. Laude, D. A., Jr.; Johlman, C. L.; Brown, R. S.; Weil, D. A.; Wilkins, C. L. Mass Spectrom. Rev. 1986, 5, 107-166.

2. Coates, M. L.; Wilkins, C. L. Biomed. Mass Spectrom. 1985, 12, 424-428.

3. Coates, M. L.; Wilkins, C. L. Biomed. Environ. Mass Spectrom. 1986, 13, 199-204.

We gratefully acknowledge the National Institutes of Health, Grant GM-30604, and KELCO, Division of Merck & Co., for support of this research.

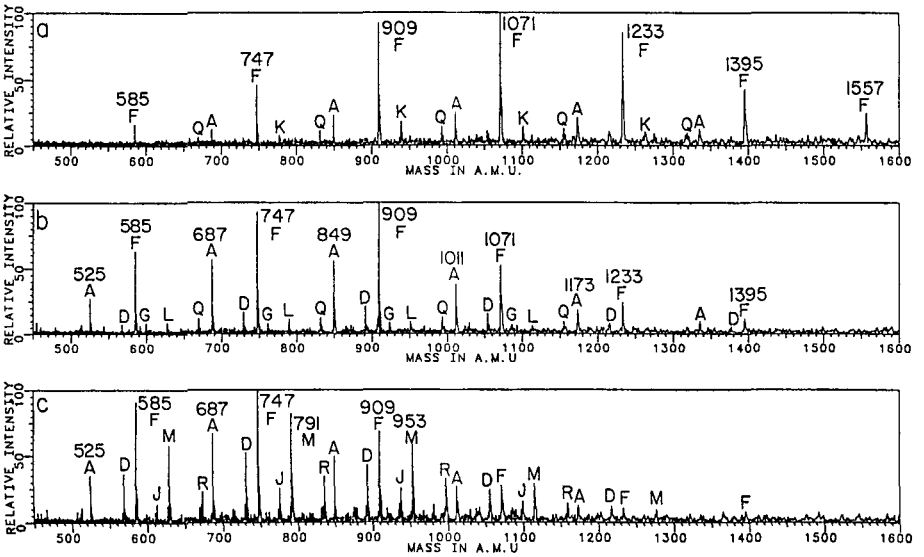

Figure: LD-FT mass spectra of KBr-doped a) dextran, b) cellulose, and c) starch.

STUDIES OF DEOXYNUCLEOSIDES BY FABMS

R. Chattopadhyaya, J. L. Wells, and D. K. Sen Sharma
Department of Chemistry and Biochemistry
University of California
Los Angeles, CA 90024

Biemann and McCloskey [1] showed for the first time the utility of mass spectrometry for the analysis of free nucleosides using the electron-ionization (EI) method. Since then results of several studies of both protected and unprotected nucleosides by EI mass spectrometry (MS) have been published [2]. Molecular weight determination of polar and thermally labile molecules such as nucleosides has been one of the most frustrating areas of mass spectrometry until the introduction of fast atom bombardment (FAB) technique. Recently this technique has been used for the study of some nucleosides [3].

In the present investigation two ribonucleosides and fifteen deoxynucleosides were studied by FABMS. They are: (1) 5-bromouridine, (2) 5-iodouridine, (3) 2'-A, (4) 2'-T, (5) 2'-G, (6) 2'-C, (7) 5-Br-2'-U, (8) 5-Br-2'-C, (9) 2-N-iBu-2'-G, (10) 4-N-Bz-5-Br-2'-C, (11) 5'-O-DMT-4-N-Bz-2'-C, (12) 5'-O-DMT-2-N-iBu-2'-G, (13) 5'-O-DMT-6-N-Bz-2'-A, (14) 5'-O-DMT-4-N-Bz-5-Br-2'-C, (15) 5'-O-DMT-4-N-Bz-2'-C(PT), (16) 5'-O-DMT-2-N-iBu-2'-G(PT), (17) 5'-O-DMT-6-N-Bz-2'-A(PT), where the abbreviations are: A-deoxyadenosine, T-deoxythymidine, G-deoxyguanosine, C-deoxycytidine, U-deoxyuridine, iBu-isobutyryl, Bz-benzoyl, DMT-4,4'-(dimethoxytrityl), and PT-cyanoethyl chlorophenyl phosphotriester. Compounds 9-17 were synthesized in our lab, whereas 1-8 were obtained from biochemical suppliers.

A modified MS-9 double focusing high resolution mass spectrometer was used for obtaining FAB mass spectra. Fast atom gun used was fabricated in our lab. Thioglycerol, glycerol, and m-nitrobenzyl alcohol (m-NOBA) were used as matrices. Concentration of the material analyzed was about 14μg/μl of matrix. About 0.3μl of the solution was spread on a stainless steel probe tip for exposure to impinging neutral xenon beam of 3-4 kV energy. Fig. 1 shows the mass spectrum of 5'-O-DMT-4-N-benzoyl-5-bromo-2'-deoxycytidine in which the protonated molecular ion MH^+ clearly confirms the identity of the molecular mass. Pseudo molecular ion MH^+ was detected for all the compounds studied, in addition to other diagnostically important ions due to base (B) and sugar (Su) portions of the molecules.

An interesting observation in this study was the reduction of halonucleosides producing dehalogenated analogs. Similar reaction was reported by Sethi et al [4]. The degree of dehalogenation was found to depend on the duration of irradiation of the matrix containing the solute by the xenon beam. Nakamura et al [5] noticed similar effect in arylhalides and N-hydroxy nitrogen compounds. Furthermore, the extent of hydrogenation was found to depend on the type of matrix used. Fig. 2 shows the results obtained in the case of 5-bromo-2'-deoxyuridine. No dehalogenation reaction was observed in the case of halodeoxynucleoside when m-NOBA was used as matrix. We are currently studying the origin of this effect.

REFERENCES:

1. K. Biemann and J. A. McCloskey, J. Am. Chem. Soc., 84, 2005 (1962).
2. C. Hignite, Biochemical Applications of Mass Spectrometry (First Supplementary Volume), Eds. G. R. Waller and O. C. Dermar, 1980, Wiley-Interscience, New York, N.Y.
3. F. W. Crow, K. B. Tomer, M. L. Gross, J. A. McCloskey, and D. E. Bergstrom, Anal. Biochem., 139, 243 (1984).
4. S. K. Sethi, C. C. Nelson, and J. A. McCloskey, Anal. Chem., 56, 1975 (1984).
5. T. Nakamura, H. Nagaki, and T. Kinoshika, Bull. Chem. Soc. Jpn., 58, 2798 (1985).

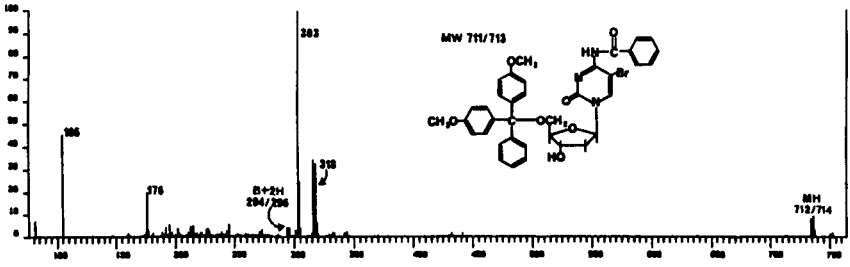

FIG.1. MASS SPECTRA OF 5'-O-DMT-4-N-BENZOYL-5-BROMO-2'-DEOXYCYTIDINE : FAB IN M-NOBA.

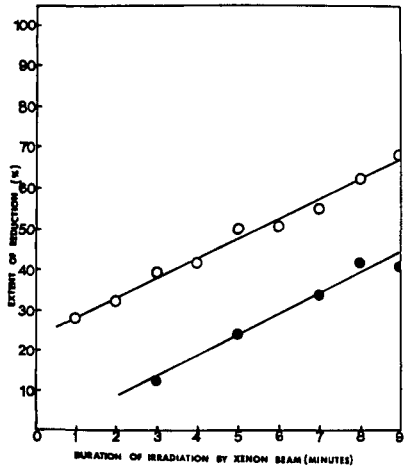

FIG.2. VARIATION IN THE EXTENT OF REDUCTION OF 5-BROMO-2'-DEOXYURIDINE WITH TIME OF IRRADIATION BY XENON BEAM : —○— IN GLYCEROL+WATER MATRIX
—●— IN THIOGLYCEROL MATRIX

QUANTITATIVE ANALYSIS OF ADENOSINE BY GAS CHROMATOGRAPHY-MASS SPECTROMETRY-SELECTED ION MONITORING AND STATISTICAL COMPARISON OF THE RESULTS WITH A RADIOIMMUNOASSAY.

Kevin D. Ballard, Rebecca G. Knapp[†], Thomas D. Eller, Jerry G. Webb, Walter H. Newman and Daniel R. Knapp, Departments of Pharmacology and [†]Biometry, Medical University of South Carolina, Charleston, SC 29425.

Analytical techniques involving quantitative mass spectrometry are frequently well suited for use as reference methods for determining the validity of other quantitative analytical methods. The basis for using quantitative mass spectrometric methods as reference or "standard" methods in such studies stems from the high specificity and sensitivity for the compounds of interest afforded by the mass spectrometer, particularly when combined with the specificity of high resolution chromatographic techniques such as capillary gas chromatography. We have developed a new capillary gas chromatography-mass spectrometry-selected ion monitoring (GC-MS-SIM) method for quantitating adenosine, and have used this method to evaluate a newly developed radioimmunoassay (RIA) for adenosine. The GC-MS-SIM method employs 5',5'-dideuteroadenosine as a stable isotope labeled internal standard, and uses the tetra-t-butyldimethylsilyl (tetra-TBDMS) derivatives of adenosine and its dideuterated analog, with selected ion monitoring of the M-57 ions characteristic of TBDMS derivatives under electron impact ionization conditions. This abstract presents details of the GC-MS-SIM method and the comparison of the results of this method with those obtained with the radioimmunoassay.

5',5'-Dideuteroadenosine (isotopic purity estimated at greater than 98%) was a generous gift from Karl H. Schram (University of Arizona, Tucson, AZ). Thirty-nine unknown samples were used for comparative measurements of adenosine concentration by RIA and GC-MS-SIM, including thirty-six coronary effluent samples from isolated, perfused guinea pig hearts, with Krebs-Henseleit solution (KHS) as the perfusing medium, and three left ventricular tissue extracts. Standard samples ranging in concentration from 1 to 100 ng/ml in adenosine concentration were prepared by serial dilution in KHS. Dideuteroadenosine (40 ng) was added to 1 ml aliquots of each standard and unknown sample. Adenosine was extracted from the sample matrix using ODS cartridge columns, desalted with a distilled water wash, and eluted into sealable ampules with 2.5 ml of 40% (v/v) aqueous methanol. The samples were dried and derivatized using 100 µl of N-methyl-N-t-butyldimethylsilyltrifluoroacetamide (MTBSTFA, containing 1% t-butyldimethylchlorosilane) and 400 µl of acetonitrile, with five hours heating in a 150 °C wax bath. The samples were then dried and redissolved with sonication in 20 µl n-dodecane. Quantitative GC-MS analyses were performed using a Varian 3700 gas chromatograph interfaced to a Finnigan MAT 212 mass spectrometer equipped with a Spectrosystem SS200 data system. The GC column was a narrow bore 30 m DB-5 (J & W Scientific) fused silica capillary column interfaced directly into the ion source of the mass spectrometer. A sample, typically 3 µl, was slowly injected on-column with the GC oven at 225 °C; the oven temperature was then rapidly ramped to 280 °C, and finally programmed to 300 °C at 3 °C/minute. The mass spectrometer was operated in electron-impact mode (70 eV ionization energy, 1 mA emission) under low resolution conditions (R = 700), and the ion intensities at m/z 666.4 and 668.4 were monitored by alternating the accelerating voltage. The areas under the GC ion intensity profiles were measured using the standard software with the SS200 data system. The 666/668 ion intensity ratio measurements were converted to idealized mole ratios (x/y, sample to internal standard) as recommended by Colby and McCaman.

Representative GC-MS-SIM traces at m/z 666.4 and 668.4 (corresponding to the M-57 ions of derivatized adenosine and dideuteroadenosine respectively) from a perfusate sample are presented in Figure 1. The tetra-TBDMS derivative of adenosine has excellent chromatographic properties on a fused silica DB-5 capillary column, and the SIM traces were entirely free of interference in this region of the chromatogram.

Figure 2 presents a linearly transformed standard curve from capillary GC-MS-SIM analysis. The solid line represents the estimated least squares regression line (correlation coefficient r = 0.9998), and the dashed lines represent the 95% inverse tolerance limits for the regression line, calculated as described by Williams. Inverse tolerance limits were employed similarly with the linearly transformed RIA standard curve, and, like those in Figure 2, were virtually parallel.

A plot of the quantitative measurements of adenosine concentration obtained by RIA versus those obtained by capillary GC-MS-SIM is presented in Figure 3. Vertical and horizontal bars represent 95% confidence limits for individual samples from RIA and GC-MS-SIM respectively. The solid line represents the estimated least squares regression line (correlation coefficient r=0.9888), and the dashed line represents the ideal line of identity. In order to test whether these two lines are significantly different, an

elliptical 95% joint confidence region for simultaneous estimation of the y-intercept and slope was constructed as described by Neter and Wasserman, and is presented in Figure 4. The ellipse is centered at the least squares regression estimates of the y-intercept and slope, shown as the point (9.3, 0.976). The conclusion that the y-intercept and slope are not significantly different from zero and one, respectively, is supported by the data since the point (0,1) is included within the boundaries of the ellipse. This suggests that the observed deviations of the y-intercept and slope from the ideal values are likely to be due to random chance.

The three major types of errors which may occur between the results of two analytical methods are constant, proportional, and random errors. Neither constant nor proportional error has been detected between the RIA and GC-MS-SIM methods in this study, since the y-intercept and slope in Figure 3 have been shown to be simultaneously not significantly different from zero and one, respectively. The major error detected statistically between these two methods is of the random type, usually measured from least squares analysis as the standard deviation of the residual error of regression (Syx). However, Syx is not a good estimator of random error when the Y data have nonconstant variance. It is evident in Figure 3 that the absolute magnitude of the uncertainty in the RIA data increases as the RIA value increases. Due to the virtually parallel nature of the 95% inverse tolerance limits associated with the RIA standard curve, the uncertainty in the RIA may be approximately described as incorporating a constant coefficient of variation, calculated to be 10% of the RIA value. For the data in Figure 3, the coefficient of variation serves as a more reasonable descriptor of the random error than Syx (110 ng/ml), which fails to indicate the nonconstant nature of the random error.

The statistical analysis supports the conclusion that the new RIA for adenosine will be useful in experiments where a random error of 10% can be tolerated. This work illustrates how GC-MS can be used to validate another analytical method with statistical comparison of the results leading to an objective numerical description of the agreement between the methods and an assessment of the types of error inherent in the methods.

Figure 1.

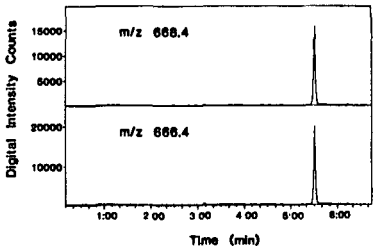

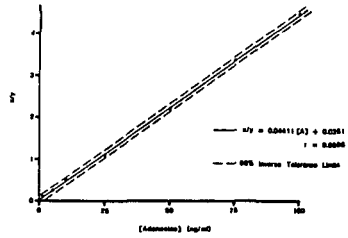

Figure 2.

Figure 3.

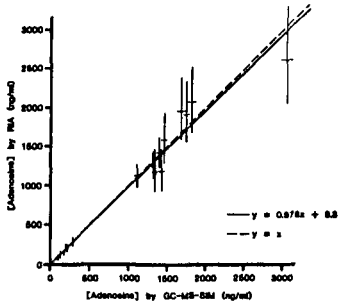

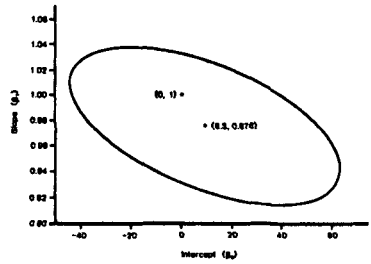

Figure 4.

Acknowledgement: This work was supported in part by NIH grants HL29566, RR01239 and HL33486.

REFERENCES

1. B.N. Colby and M.W. McCaman, Biomed. Mass Spectrom. 6, 225 (1979).
2. E.J. Williams, Regression Analysis, Wiley, New York (1959).
3. J. Neter and W. Wasserman, Applied Linear Statistical Models; Regression, Analysis of Variance and Experimental Designs, pp. 140-145, Irwin, Homewood, Illinois (1974).

ELEMENTAL ANALYSIS OF BIOLOGICAL MEMBRANES BY INDUCTIVELY COUPLED PLASMA / MASS SPECTROMETRY

J.P. Schmit, S. Neidhart, M. Chtaib, and R. Beliveau; Université du Québec à Montréal, Dept. of Chemistry and GEOTOP, P.O.Box 8888 Stat. A, Montreal H3C 3P8

INTRODUCTION

Characterization of cellular membrane structure and composition have stressed the importance of proteins and lipids which are the major biochemical constituents. The fluid mosaic model of Singer and Nicolson (1) has been adopted as a model being able to satisfy most of the data available. In this model, globular proteins are shown as floating icebergs on a sea of lipid bilayer. However, on the one hand, membrane proteins which represent 40 to 80 % of the total weight are well known as strong metallic ions binders, and on the other hand, ions being strong regulators of enzyme activity, local microenvironment in membrane can be expected to favor tight regulation by metals.

Surprisingly, no detailed study has been conducted on the elementary inorganic composition of biological membranes. The membrane system which has been chosen for investigation is the brush border membrane from rat kidney. Those membranes are located in the proximal tubule fraction of the nephron, where 80 to 98 % of nutriment reabsorption occurs. The transport and enzymatic activities of those membranes being very specific and intense, the regulation of those activities by inorganic ions can be expected to be of great significance in physiology. Thus, a detailed analysis of the inorganic content of those purified membranes has been undertaken.

BRUSH BORDER MEMBRANES PREPARATION

Brush-border membranes from rat kidney cortex were prepared as described by Booth & Kenny (2). The purified brush-border membrane vesicles were resuspended to a final protein concentration of 10 mg/ml 10 mM Tris/Hepes [4-(2-hydroxy-ethyl)-1-piperazine-ethanesulphonic acid] buffer pH 7.5, containing 300 mM mannitol. The enrichments in alkaline phosphatase and Na^+ + K^+ dependent ATPase were 12.2 + 0.3 and 0.41 + 0.1 fold (means + S.E.M.) respectively (3).

ICP / MS REQUIREMENTS

ICP / MS samples are usually introduced inside the plasma torch by nebulization. However, as stated above, membranes are composed of very complex macromolecules which are difficult to nebulize (actually they can plug the nebulizer) and big enough to be only partially burned by passing through the plasma torch. Thus, it was necessary to define an appropriate procedure to hydrolyse the membranes for ICP/MS inorganic analysis.

HYDROLYSIS PROCEDURE

Brush-border membrane hydrolysis has been performed under various temperature and time conditions. Figure 1 shows the variation of the intensities (normalized on the maximum Zirconium intensity) against hydrolysis time, while figure 2 shows the same intensities plotted against the hydrolysis temperature.

Figure 3 shows the relationship between the intensities of the major elements and the protein content of the initial solution.

As it can be seen, the response of the method has been found directly dependent on the hydrolysis conditions.

Moreover, it has been found that some elements exhibit particular behaviors. Among them, Zirconium seems especially independent. This latter observation could results from a particular geographic position of this element inside its host macromolecule requesting along the same line more drastic hydrolysis conditions to be extracted.

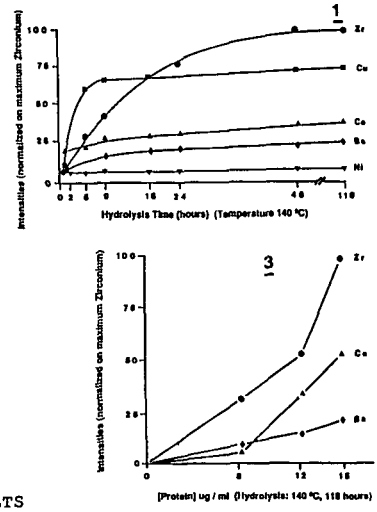

RESULTS

Spectrum 1 shows raw data (blank substracted) obtained after hydrolysis in HNO_3 2N at 140°C for 2 days. Thorium (m/z 234) (not present in membranes) is used as an internal standard. It shows the presence of some " exotic " elements (Zr, Ba, Ce) present in significant concentration in the studied membrane is clearly established.

CONCLUSION

ICP / MS has been found sensitive and selective enough to characterize minute amounts of inorganic element even deeply embedded inside biological membranes. As a consequence of this later observation, severe and controlled hydrolysis conditions must be performed before undertaking the ICP / MS elemental inorganic analysis. The response of the method for a given element being dependent on the hydrolysis conditions brings forward the hypothesis that some elements could be specifically localized inside their own biological matrices.

This is especially striking for Zirconium, a totally unexpected element, which lets open the question of its eventual physiological role in membrane transportation mechanism.

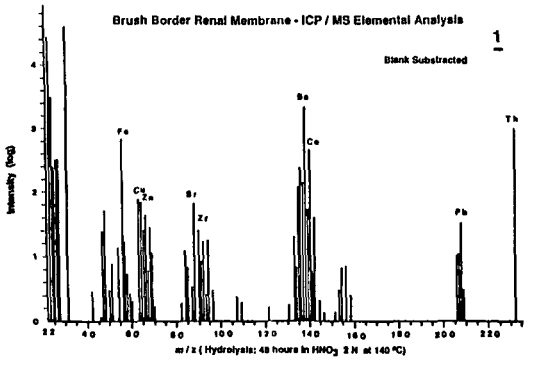

1. S.J. Singer and G.L. Nicolson, Science (1972) **175**, 720-731
2. A. Booth and A.J. Kenny; Biochem.J. (1974) **142**, 575-581
3. J. Strevey, M. Brunette and R. Béliveau; Biochem.J. (1984) **223**,793-802.

ASSESSMENT OF VITAMIN A STATUS OF HUMANS BY ISOTOPE DILUTION GC/MS

A. J. Clifford*, A. D. Jones**, Y. Tondeur***, H. C. Furr[+], H. R. Bergen, III[++], and J. A. Olson[+]

*Department of Nutrition and **Facility for Advanced Instrumentation, University of California, Davis, CA 95616, ***Environmental Research Center, University of Nevada, Las Vegas, NV 89154, and [+]Department of Biochemistry and Biophysics, Iowa State University, Ames, IA 50011

Recent epidemiological evidence linking vitamim A to cancer prevention (1,2) has stimulated interest in assessing the vitamin A status of humans. About 90% of the body's store of vitamin A is confined to the liver (mostly as fatty acid esters of retinol). Serum levels of retinol are relatively constant except in cases of acute deficiency or toxicity, and fail to serve as reliable indicators of vitamin A status (3).

A GC/MS procedure is described where picogram amounts of retinol (ROH) can be measured without derivatization. GC (4) was performed by on-column injection at room temperature using 15 meter X 0.25 mm ID open tubular column with a 0.1 μm thick film from J&W Scientific (Fig. 1). Cold on-column injection avoids dehydration and isomerization of retinol during the chromatographic separation. In GC/MS experiments the column was attached directly to a VG ZAB-HS mass spectrometer. Protonated retinol (H-ROH) was prepared by sodium borohydride reduction of retinol in MeOH followed by extraction in hexane. Deuterated retinol (D-ROH) was prepared by saponifying 10, 19, 19 19-$^2H_4$-retinyl acetate in MeOH containing 10% KOH (5). H-ROH and D-ROH were purified by reversed phase HPLC (6). The EI spectrum of the 10.1 min peak from H-ROH (Fig. 1) as well as that of D-ROH is shown in Fig. 2. Selected ion monitoring was performed on m/z 286 $[M^{+\cdot}]$ and m/z 268 $[M-H_2O]^+$ for H-ROH and on m/z 290 and m/z 272 for D-ROH. A calibration curve (Fig. 3) was generated by adding a fixed amount of D-ROH to varying amounts of H-ROH. Approximately 100 picograms total ROH and D-ROH/H-ROH ratios of 5 to 10% could be measured by these procedures.

Attempts to increase the yield of the molecular ion were limited by the persistent formation of the $[M-H_2O]^+$ ion in varying amounts. Chemical ionization invariably failed to produce significant amounts of pseudomolecular ion for retinol because of dehydration that occurred apparently in the ion source. EI spectra of retinol showed the $M^{+\cdot}$ ion at m/z 286, the $[M-H_2O]^+$ ion at m/z 268 and the $[M-CH_2OH]^+$ ion at m/z 255. Adduct ions were not apparent in the EI spectra. Positive ion FAB spectra also showed ions at m/z 286 and m/z 255. Only FAB spectra showed the $[M+H-H_2O]^+$ ion at m/z 269 and a thioglycerol adduct ion at m/z 393. The daughters of the $M^{+\cdot}$ ion of retinol were analyzed by acquiring constant B_1/E scans on a VG ZAB-2F instrument as well as unimolecular MIKE and EB_2 (constant B_2/E) scans on a VG ZAB-3F instrument (Fig. 4). The EB_2 scans gave better than unit resolution. In all cases, the $[M-H_2O]^+$ ion was only a minor peak in the daughter spectra. These findings suggest that dehydration of retinol is not a facile process and that it occurs prior to ionization.

Stable isotope dilution was used to assess total body vitamin A levels in a healthy adult male fed a known diet. Seventy-two mg $^2H_4$-retinyl acetate (approximately 20% of the total body content of vitamin A) was consumed at breakfast and blood samples were drawn at intervals for the following 28 days. Total ROH was extracted from EtOH-deproteinated serum and purified by reversed phase HPLC (6). The ratio of D-ROH to H-ROH in each serum sample was determined by GC/MS (Fig. 5). The expected rise, subsequent fall and final plateau in the ratio of D-ROH to H-ROH was observed (Fig. 5). At plateau (equilibrium) the D-ROH/H-ROH was approximately 0.2 corresponding to 20% of the total body vitamin A stores. These results demonstrate that stable isotope dilution is likely to be a valuable approach to assessing the vitamin A status of humans.

---

1. D. S. Goodman, New England J. Med., 1984, 310, 1023.
2. M. B. Sporn and A. B. Roberts, Cancer Res. 1983, 43, 3034.
3. J. A. Olson, J. Nat. Cancer Inst. 1984, 73, 1439.
4. A. J. Clifford, Y. Tondeur, R. Lautamo, W. Jennings, A. D. Jones, H. C. Furr, J. A. Olson and L. M. DeLuca, Fed. Proc. 1985, 44, 771.
5. H. R. Bergen III, Synthesis, analysis and characterization of deuterated analogues of vitamin A. Ph.D. Thesis, Iowa State University, Ames, IA.
6. H. C. Furr, O. Amedee-Manesme and J. A. Olson, J. Chromatogr. 1984, 309: 299.

FIGURE 1.

Chromatogram of *trans*-Retinol
Obtained with Cold On-column Injection

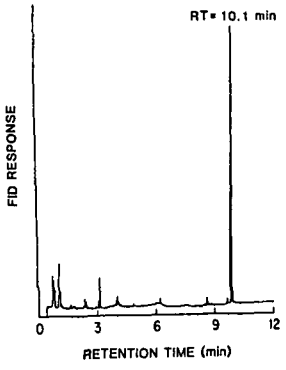

FIGURE 2.

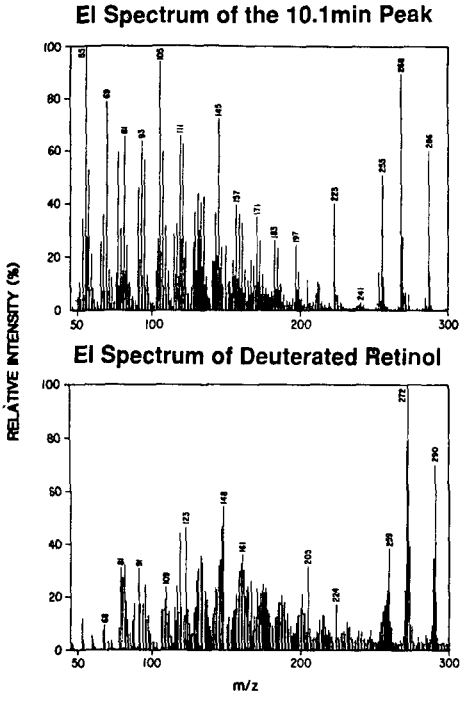

FIGURE 3.

Isotope Dilution Calibration Curve for Retinol

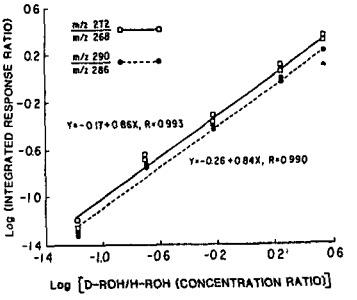

FIGURE 4.

Unimolecular MIKE Spectrum of Daughters of m/z 286 from Retinol

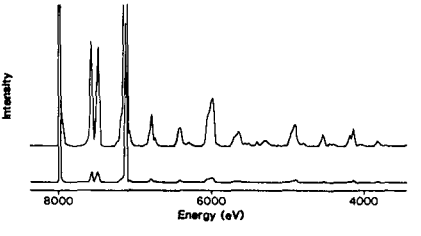

Unimolecular EB_2 Scan of Daughters of m/z 286 from Retinol

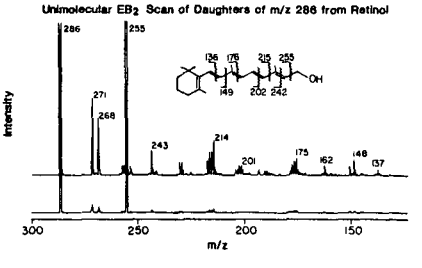

FIGURE 5.

D/H Ratio for Retinol in a Human Subject as a Function of Time

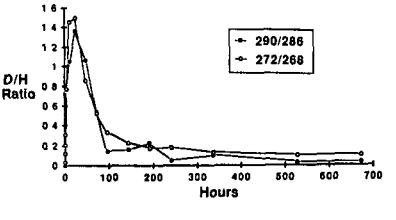

CHARACTERIZATION OF OLIGORIBONUCLEOTIDES UP TO 24 MER (M/Z 13726) BY SECTOR TYPE MASS SPECTROMETER

T. Matsuo, T. Sakurai, H. Matsuda, M. Matsugi, M. Ikehara
Osaka University, Toyonaka 560, Japan
T. Kobayashi, Y. Kammei, E. Kubota
JEOL Ltd., Akishima 196, Japan

INTRODUCTION

It is necessary to characterize quickly the synthetic oligonucleotides. Though the sequence analysis of oligonucleotides can be usually performed by chemical degradation method[1], the mass spectrometric method is simpler and less time consuming[2]. Furthermore, for the analysis of protected material, only mass spectrometric method can solve the problem. We have synthesised the 3'-half molecule of E. coli glycine t RNA_2 by the phosphotriester method and analysed each intermediate by mass spectrometer. The abbreviated scheme of synthesis is shown in Fig. 1. At first, trinucleotide intermediates were prepared and larger intermediates were synthesised by condensation of blocks. The intermediates shown in Fig. 1 with molecular weight were measured by mass spectrometer in order to check whether the requested materials were actually synthesised.

The objectives of the experiments are:

1) Detection of molecular ion and 3', 5' sequence ions of oligonucleotides.
2) Precise determination of molecular weight of middle molecule.
3) Detection of heavy molecular ions (M/Z > 10000).

EXPERIMENTAL

The FAB mass spectra were obtained by a modified JEOL HX100 mass spectrometer. The acceleration voltage was 5 KeV. JEOL DA5000 data system and UV recorder were used for data taking. Negative mass spectra were mainly taken because it was more effective than positive ones. Tioglycerol and $(CsI)_nI^-$ were used as matrix and calibrating compound, respectively.

RESULT AND DISCUSSION

The negative FAB mass spectrum of GAUGAUGCGG is shown in Fig. 2. The shorthand structure of this sample with nominal, exact and chemical masses is shown in the upper part of Fig. 2. The mass number expressed in the spectrum are integer number of chemical mass. When we measure the compound heavier than 5000, the data system is calibrated by using exact mass of $(CsI)_nCs^+$ or $(CsI)_nI^-$ and mass value based on chemical mass is used. The deprotonated molecular ion and the corresponding 3'- or 5' sequence ions are clearly observed. The purity as well as the composition of the sample can be conveniently verified by these mass spectra.

The precise molecular weight of this compound was determined by accumu-

lating several scans with an accuracy of 0.1 ~ 0.2 mass unit. We observed the molecular ion of 24 mer (nominal mass=13726) as shown in Fig. 3 though the mass resolution is poor. In future we must take the mass spectrum of such heavy compounds in high mass resolution.

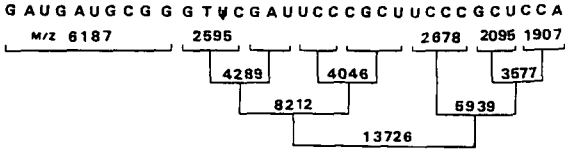

Fig. 1. The abbreviated scheme of synthesis.

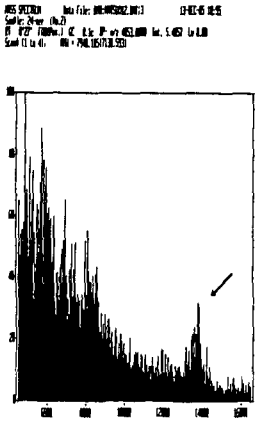

Fig. 3. Mass spectrum of 24 mer (nominal mass=13726).

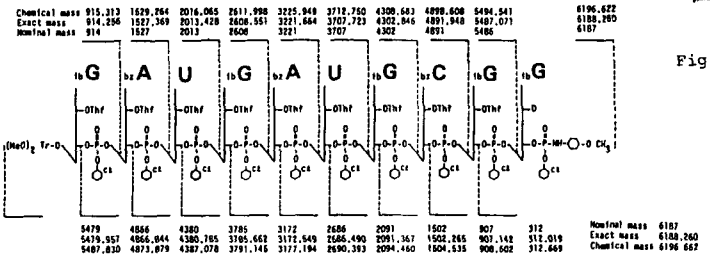

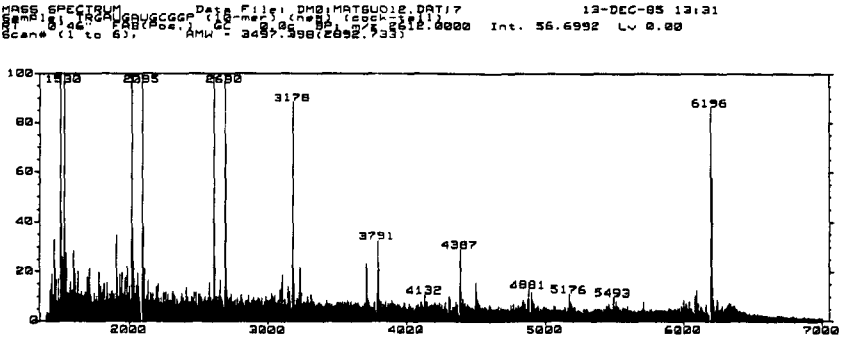

Fig. 2. Negative FAB mass spectrum of fully protected 10 mer (GAUGAUGCGG).

REFERENCES

1. A.M. Maxam and W. Gilbert, Proc. Natl. Acad. Sci. USA 74, 560 (1977).
2. L. Grotjahn, H. Blöcker and R. Frank, Biomed. Mass Spectrom. 12, 514 (1985).

CURIE-POINT PYROLYSIS OF SOME DIPEPTIDES CONTAINING AROMATIC AND HETEROCYCLIC AMINO ACID RESIDUES BY GC/MS.

Grant Gill Smith[1], Jaap J. Boon[2] and G. Sudhakar Reddy[1],

[1]Department of Chemistry & Biochemistry, Utah State University, Logan, UT 84322.

[2]FOM Institute for Atomic and Molecular Physics, Kruislaan, Amsterdam, The Netherlands.

Pyrolysis gas chromatography mass spectrometry (Py/GC/MS) has been successfully applied in analyzing thermally labile molecules including amino acids, peptides and proteins[1]. Even simple compounds, such as dipeptides give a complex mixture of products on pyrolysis which often indicate the original structure of the molecule. The purpose of this work is to study the pyrolysis of aromatic/heterocyclic dipeptides, tyr-tyr, ala-tyr, tyr-ala and his-his. Curie-point method was employed to affect the pyrolysis.

Aqueous solution containing 10 μg of dipeptide sample was coated onto a ferromagnetic wire, which was heated to 510° C for 10 seconds. Thus resulted pyrolysis fragments were swept onto a 25 m CP SIL-5 capillary column in a stream of helium for the analysis by GC/MS. The gas chromatograph oven was heated from 50° C to 300° C with an increment of 8° C min^{-1}. The chromatographic peaks were detected by a quadrupole mass spectrometer (MAT 44) operated under normal conditions in cyclic scan mode. About 800 to 1000 scans were stored in a data system for each analysis.

In each pyrogram five to six compounds were seen which characterize the aromatic/hetercyclic side chain of these dipetides. In contrast to the dipeptides containing aliphatic amino acids, these dipeptides did not show the evidence for the formation of diketopiperazines (DKP) on pyrolysis which clearly distinguishes these two sets of dipeptides from one another. Also, the products resulted from bimolecular condensations, which often represent strong peaks in the pyrograms of aliphatic amino acid dipeptides were absent in the pyrograms of these peptides.

Compounds identified in the pyrolysates of these peptides are given in Table. The identification and characterization of most of the pyrolysis products was done by comparison against the mass spectral data from the literature[2] or on the basis of their mass spectral fragmentation processes.

The pyrolysis of tyrosine containing dipeptides produced phenol, p-cresol, p-hydroxystyrene, ethylbenzene and benzyl alcohol as major pyrolysis products. These simple

Table. Compounds identified in the pyrolysates of tyr-tyr, tyr-ala, ala-tyr and his-his dipepties.

GC Peak	Compound	GC Peak	Compound
1	CO_2	10	Isomer of p-cresol
2	Phenol	13	Acetic Acid
3	p-Cresol	14	Imidazole
4	p-Hydroxybenzene	15	5-Methylimidazole
8	Ethylbenzene	18	5-Vinylimidazole
9	Benzyl Alcohol	19	5-β-Hydroxyethyl-imidazole

compounds provide structural information of the side chain moiety even when the tyrosine residue is present in the complex mixture. Similarly, imidazole and its derivatives were found in the pyrosylate of his-his dipeptide, which again point out its structural information. Formation of diketopiperazines and related products are of diagnostic value for dipeptides containing aliphatic amino acid residues, while the products characteristic of their side chain constitute key compounds in determining the aromatic or heterocyclic dipeptides.

ACKNOWLEDGMENTS: The authors are grateful to the Utah Agricultural Experiment Station and Utah State University for their financial support. Technical assistance from Mrs. A. Knoll and Dr. W. A. J. Schuyl, Delft University of Technology, The Netherlands is greatly appreciated.

REFERENCES:

1. W. J. Irwin, Analytical Pyrolysis, Marcel Dekker, New York, 1982.
2. 'Eight Peak Index of Mass Spectra', Mass Spectrometry Data Center, AWRE, Aldermaston, UK, 1974, Vol. 1-3.

MASS SPECTROMETRY OF THE 1,8-DINITROPYRENE-NUCLEOSIDE ADDUCT

M.A. Quilliam, P.J. Andrews, R.J. Gergely and R.W. Smith
Department of Chemistry, McMaster University,
Hamilton, Ontario, Canada, L8S 4M1

Nitrated polycyclic aromatic hydrocarbons have been observed in a variety of environmental samples, including diesel exhaust and urban airborne particulates. Dinitropyrenes are of particular interest because of their extremely potent direct-acting mutagenicity in Salmonella and their tumorigenicity in rats. It has been shown that nitropyrenes require enzymatic reduction in order to exert their mutagenic effects (1), that for 1,8-dinitropyrene a transacetylase enzyme is also necessary (2), and that the principal attack of the active intermediate (an N-hydroxylamino or N-acetoxyamino derivative) on DNA is at the C8 position of the guanine base (3). The structure of the 1,8-dinitropyrene adduct is given below. This paper examines the various ionization techniques for the mass spectrometry of dinitropyrene-nucleoside adducts and helps to further confirm the adduct structure.

Trimethylsilylation of the adduct to a TMS derivative with BSTFA allowed the acquisition of the EI spectrum on about 100 ng. It was necessary to use the DCI probe and rapid heating to get good sensitivity. The spectrum shows a strong molecular ion for the tetrakis-TMS derivative and a weak ion for the pentakis-TMS derivative. Fragment ions indicated the mass of the base unit.

FABMS was tried in a variety of matrices. Only glycerol and DMF saturated with ammonium chloride gave a spectrum, although it was very weak and short-lived. The major problem appears to be the very low solubility of the adduct.

When FAB with the LC/MS belt interface was attempted on a VG7070E, a very strong B+2H ion (m/z 412) and a very weak M+H ion (m/z 528) were observed. Combined LC/MS allowed the separation and detection of the adduct and an impurity, the acid decomposition product (loss of sugar), which gave an almost identical spectrum (M+H at m/z 412). We have had some problems reproducing these results lately on a new ZAB-E system. Further studies are proceeding.

Thermospray MS was attempted on two different systems (Finnigan 4500 and VG7070E) but was not successful. The thermospray was optimized for 2'-deoxyguanosine, which itself gave only a very weak M+H and a base peak of B+2H. Under these conditions, adenosine gave an intense M+H. The adduct gave no sensible spectra, the peaks that were observed being attributed to impurities.

Field desorption MS was successful at generating a spectrum for the acid decomposition product (M+H, M+Na, and M+K) but did not yield a spectrum for the adduct.

Electron ionization of the TMS derivative appears to be the most successful method, giving the best spectrum and sensitivity. LC/FABMS has good potential, but requires further study.

1. F.Messier, C.Lu, P.Andrews, B.E.McCarry, M.A.Quilliam, and D.R.McCalla, Carcinogenesis 2, 1007 (1981).
2. J.C.Orr, D.W.Bryant, M.A.Quilliam, and D.R.McCalla, Chem.-Biol. Interactions 54, 281 (1985).
3. P.J.Andrews, MA.Quilliam, B.E.McCarry, D.W.Bryant, and D.R.McCalla, Carcinogenesis 7, 105 (1986).

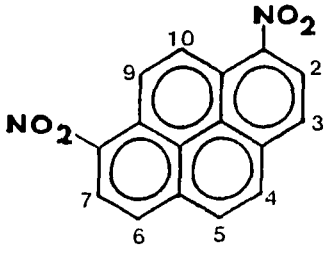

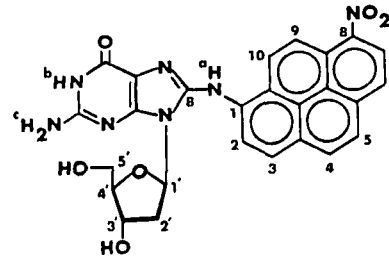

Figure 1: EI mass spectrum of TMS derivative of adduct.

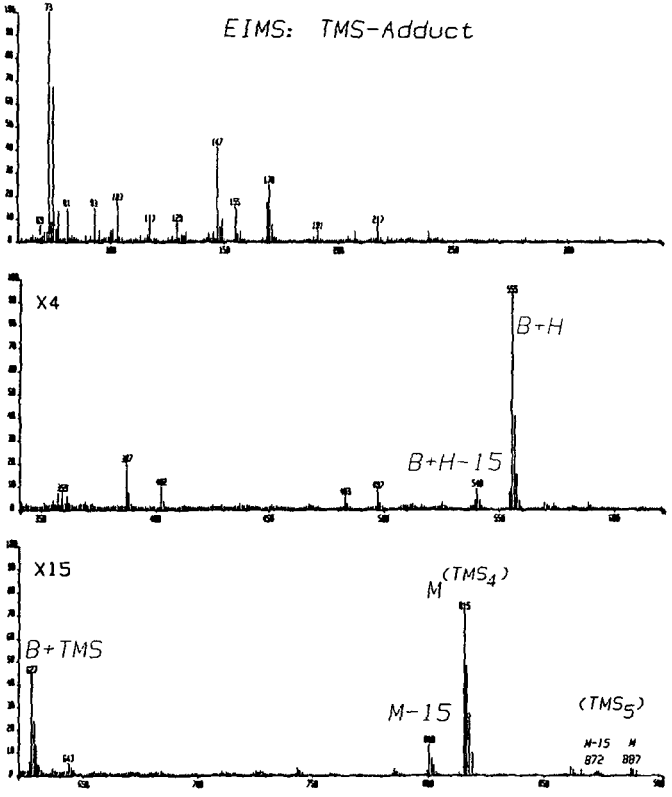

Figure 2: LC-FABMS of crude adduct.

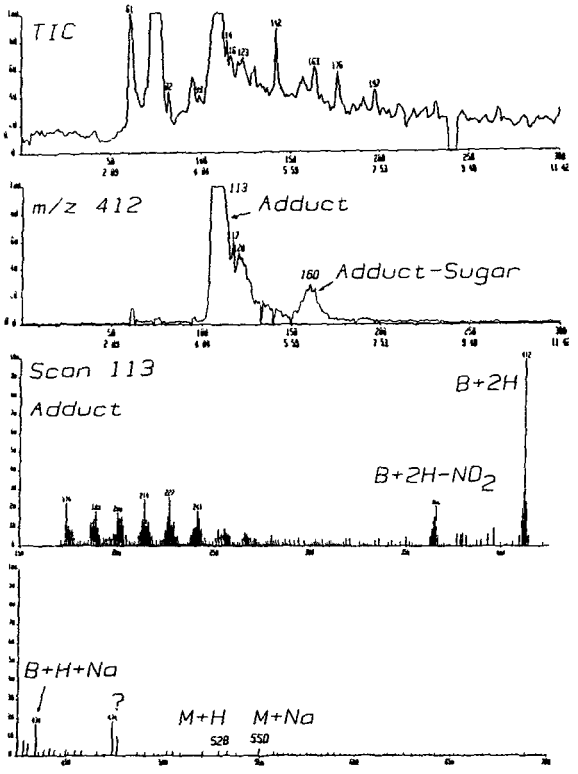

COMBINED LC/MS AS AN AID IN THE PREPARATIVE FRACTIONATION OF COMPLEX MIXTURES

M.A. Quilliam and K. Hoo, Department of Chemistry, McMaster University, Hamilton, Ontario, Canada, L8S4M1; and A.J. Berry and D.E. Games, Department of Chemistry, University College, Cardiff, Wales, U.K., CF11XL

The analysis of complex mixtures, such as environmental and petroleum samples, requires the combination of various fractionation methods. Normal phase and reverse phase HPLC with preparative columns are often used for fractionation by compound class or some other structural feature such as the number of aromatic rings. One of the major problems encountered in such work is that conventional detectors such as the UV absorption detector are not particularly useful for determining collection points. A complex mixture usually gives a broad envelope-type chromatogram without any indication of the position of individual compounds. Establishing collection points by previous analyses of standard compound mixtures relies on the availability of such standards and on the reproducibility of retention times. It is also difficult to determine if the column has been overloaded.

We have investigated the use of the mass spectrometer as a detector in such fractionation work. A split of 5% of the column effluent to a belt transport LC/MS interface (on a VG7070F) allows mass spectral detection, while 95% of the effluent is collected in a fraction collector. Examination of mass chromatograms allows decisions to be made on which fractions should be combined for the desired separation. This approach also provides a preliminary analysis of the sample.

As an illustration of the utility of the technique, we have studied the extract of a factory dust sample containing a variety of polycyclic aromatic hydrocarbons (PAH) and PAH derivatives. Using preparative normal phase LC (amino-cyano with a hexane-dichloromethane gradient) and mass chromatograms, it was possible to divide the sample into various fractions such as: (a) low molecular weight PAH ($\leqslant$278 amu), which was suitable for subsequent GC/MS work; (b) high mass PAH and nitro-PAH, which are best analyzed by reverse phase LC/MS; and (c) narrow PAH fractions according to the number of rings. Figure 1 illustrates the type of separation achieved by preparative normal phase LC and how the mass chromatograms can guide the pooling of fractions for very exact fractionations. Note that NPLC/MS provides a very good preliminary analysis of the sample, allowing detection of compounds such as 1-nitropyrene (m/z 247), anthraquinone (m/z 208) and xanthenone (m/z 196). Figure 2 shows the subsequent reversed phase LC/MS analysis of the PAH in the sample with 4 to "4.5" rings. These include such compounds as chrysene, benzo[a]pyrene and their alkyl derivatives. Such a very exact fractionation is not easy without mass spectrometry as a guide.

Figure 1a

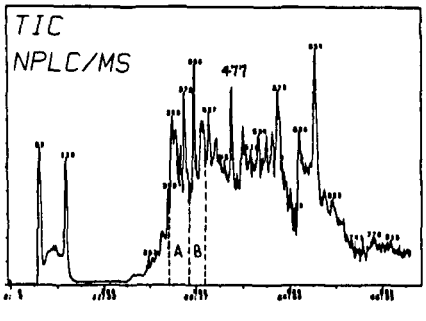

(continued)

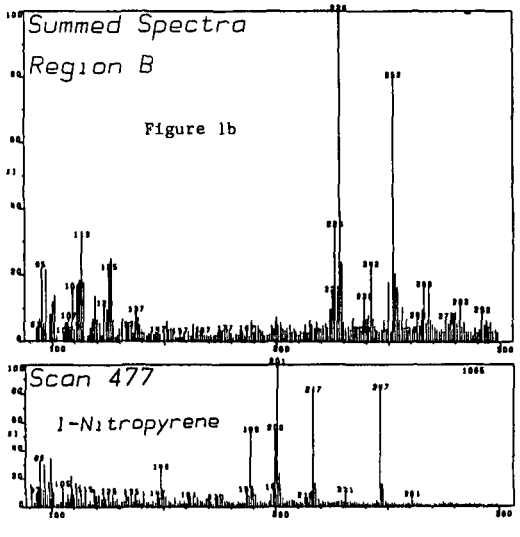

Figure 1b

Figure 1a (continued)

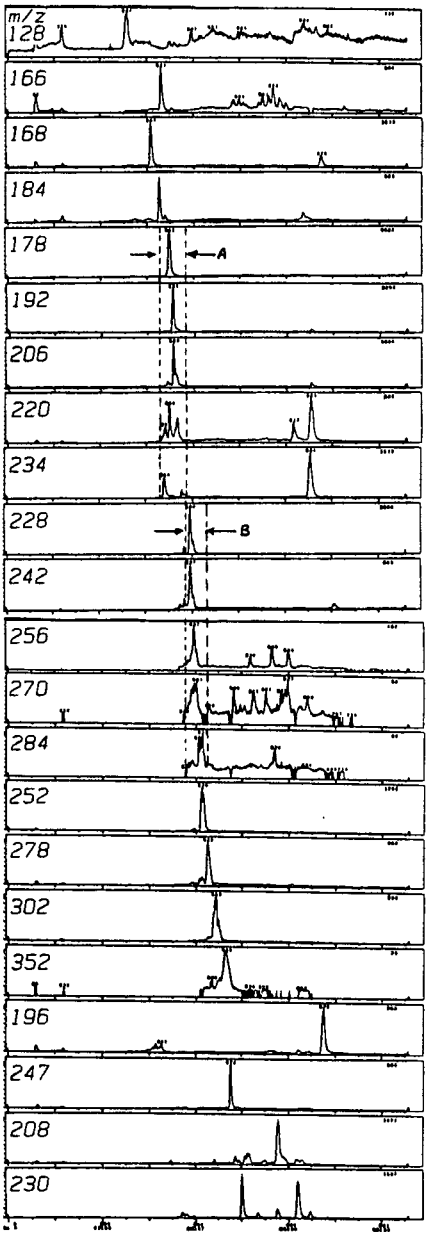

Figure 2

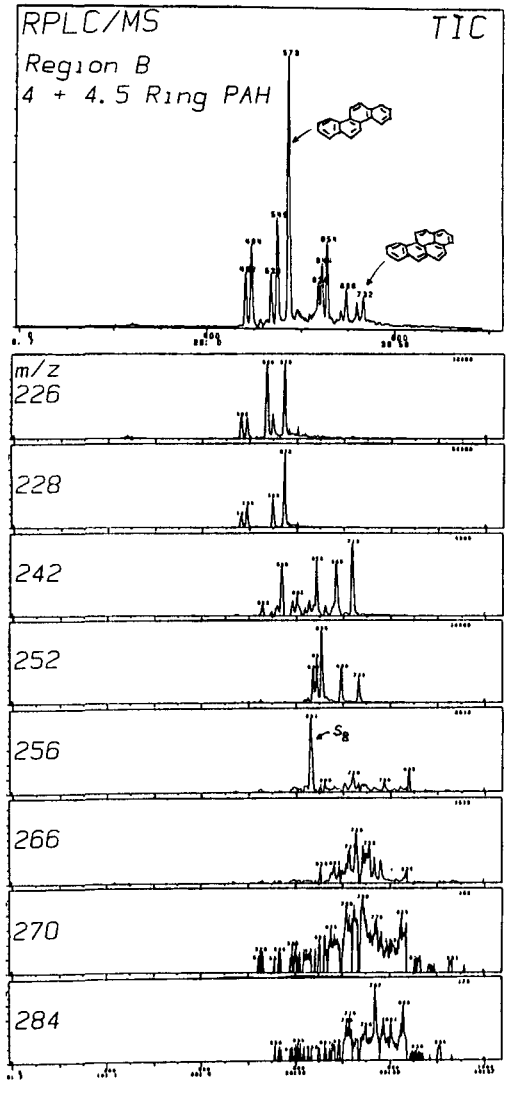

MASS SPECTROMETRY OF t-BUTYLDIMETHYLSILYL DERIVATIVES OF CYTOKININS

O.C. Wong, C.H. Hocart, D.S. Letham

Department of Developmental Biology, Research School of Biological Sciences, The Australian National University, Canberra, Australia

Cytokinins (purine plant hormones) occur in plants and microorganisms as free purine bases (zeatin, Z; cis-zeatin, cis-Z; dihydrozeatin, DZ; and isopentenyladenine, iP), purine ribosides, nucleotides, glucosides and alanine conjugates (lupinic and dihydrolupinic acid). However, it is likely that the free base is the functional or active form of the cytokinins, and hence quantification of the cytokinin bases is particularly important. When Z and related bases are subjected to GC as TMS derivatives, considerable losses and multiple peak formation have been observed. Poor recovery of Z is particularly acute during GC with some fused-silica capillary columns. While permethyl derivatives of cytokinin bases have been used for GC-MS, the preparation of the reagents and the derivatization procedure are both time consuming and inconvenient.

The above problems do not arise with t-butyldimethylsilyl (tBuDMS) derivatives of the bases. Initially attempts to make a tBuDMS derivative of Z used equal volumes of N-methyl-N-t-butyldimethylsilyltrifluoroacetamide (MTBSTFA) containing 1% t-butyldimethylchlorosilane (TBCS) and either acetonitrile or pyridine. This yielded mixtures of products. When 4-dimethylaminopyridine (DMAP) was included as a catalyst, quantitative yields of di-tBuDMS derivatives were obtained for Z, DZ and cis-Z and of N-9 mono derivatives for iP, adenine (Ade) and 6-benzylaminopurine (BAP). The silylation reagent finally used was dry pyridine (10 µl), 1 µl of DMAP solution (1 µg/µl in pyridine) and MTBSTFA-TBCS (10 µl); derivatization was at 90° for 15 min. The di-tBuDMS derivatives of Z, DZ and cis-Z are readily separable by GC and are rapidly hydrolyzed to mono-O-derivatives in aqueous solutions. The mono derivatives can be separated by TLC and HPLC.

The principal ions in the EI mass spectrum of di-tBuDMS-Z were: m/z 447 (M^+, 7%), 432 (9), 390 (28), 316 (53), 315 (90), 306 (i,26), 302 (100), 300 (bb,20), 299 (k,22), 274(36), 258 (23), 250 (20), 198 (g,26), 192 (21), 178 (10), 141 (g-57,41).

The tBuDMS derivatives of hydroxyl groups are, in general, characterized by a prominent loss of a t-butyl moiety (M-57). However, in the case of the bases with only a 9-tBuDMS group (BAP, iP, Ade), we observed the elimination of isobutene accompanied by hydrogen transfer (M-56) followed by the loss of a methyl radical (M-56-15). The M-56 and M-56-15 fragmentations are not evident in the spectra of mono-O-tBuDMS derivatives of Z, DZ or cis-Z and are characteristic of a 9-tBuDMS group. Di-tBuDMS-Z and di-TMS-Z, and also di-tBuDMS-DZ and di-TMS-DZ, showed significant differences in analogous ion intensity. In the spectrum of di-tBuDMS-Z, the unusual ion i (see below) was more intense, while ions bb and g were less intense, than in the spectrum of di-TMS-Z. The unusual ions j and n (see below) were present in the spectrum of di-tBuDMS-DZ but were absent in that of di-TMS-DZ.

Di-tBuDMS-Z and its cis isomer exhibit very similar spectra. However, the direct probe spectra of the mono-O-tBuDMS derivatives of Z and cis-Z differ markedly in relative

peak intensity. Thus in the cis-Z spectrum, ion i (base peak) is more intense than in the spectrum of Z (trans). The other main differences between the mass spectra of mono-O-tBuDMS-Z and its cis isomer appear to be largely a consequence of the facilitation of tBuDMS-OH elimination by the cis configuration.

Several unusual ions observed in the mass spectra of tBuDMS cytokinins merit comment. The unusual ion i has been assigned a structure derived from sidechain cleavage and transfer of the silyl moiety to position N-1, although transfer to other positions (N^6, N-7) cannot be excluded. Ion i is prominent in spectra of both the mono- and di-tBuDMS derivatives of Z and cis-Z (especially the mono) and also in the spectrum of mono-tBuDMS-DZ. Ions j and n occur only in the spectra of the mono- and di-tBuDMS-DZ and from high resolution mass measurements, represent the loss of C_5H_{13} and C_8H_{17} respectively. For ions bb and k we propose structures stabilized by cyclization. Corroborative evidence is provided by high resolution mass measurements and by the spectrum of di-tBuDMS-[$^2H_5$]-Z. Ions bb and k are most prominent in the spectra of compounds with an unsaturated sidechain.

tBuDMS derivatives have recently been used routinely for GC-MS analysis of cytokinin bases in diverse plant extracts down to the ng level (1,2,3,4). Structures proposed for the ions mentioned above are given below; the base peak in the spectrum of di-tBuDMS-Z is attributed to ion b.

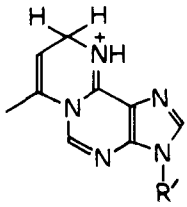

b

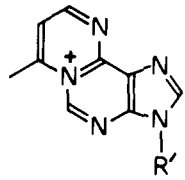

bb

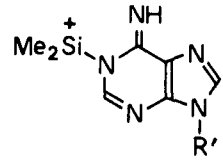

i

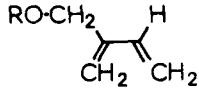

g

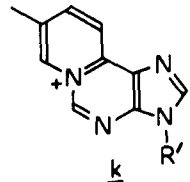

k

R and R' = tBuDMS

1. Palmer, M.V., and Wong, O.C. (1985) Plant Physiol. 79, 296-298.
2. Tay, S.A.B., MacLeod, J.K., Palni, L.M.S. and Letham, D.S. (1985) Phytochemistry 24, 2611-2614.
3. Palni, L.M.S., Tay, S.A.B., Nandi, S.K., Pianca, D.J., de Klerk, G.J.M., Wong, O.C., Letham, D.S. and MacLeod, J.K. (1985) Biol. Plant 27 195-203.
4. Hocart, C.H. (1985). PhD Thesis, The Australian National University, Canberra.

MASS SPECTROMETRIC STUDIES OF CYTOKININ METABOLITES IN RELATION TO RETARDATION OF LEAF SENESCENCE

O.C. Wong, R. Zhang, D.S. Letham

Department of Developmental Biology, Research School of Biological Sciences, The Australian National University, Canberra, Australia

Repeated application of 6-benzylaminopurine (BA), a synthetic cytokinin, is known to retard soybean leaf senescence. Prevention of this senescence is of both physiological and agronomic significance. Leaf senescence in soybean normally commences before seed development is completed and hence retardation of senescence could influence seed composition and yield. To assist in the design of more effective cytokinins, the metabolism of BA in soybean leaves has been studied.

The principal metabolite (Mt) was purified by sequential use of the following methods: partition between ethyl acetate and water, cellulose phosphate chromatography, preparative TLC, droplet counter-current chromatography, and HPLC. The desorption CI MS did not reveal a molecular ion, but the base peak (m/z 226) and an ion at m/z 136 (81%) were indicative of an intact benzylaminopurinyl moiety. However, the discharge ionization-secondary ion (DISI) spectrum (determined using glycerol as sample matrix) revealed a clear MH^+ at m/z 313. Mt was derivatized at 23° with pentafluorobenzyl bromide by an extractive alkylation method (solvents: $CHCl_3$ and aqueous Na_2CO_3 at pH 11) using tetrabutylammonium hydrogen sulphate as an ion-pairing reagent. This yielded two pentafluorobenzyl (pfBz) derivatives separable by TLC (silica gel, layer washed with EtOAc; $CHCl_3$:MeOH, 9:1) which were di-pfBz-Mt (R_f 0.78) and mono-pfBz-Mt (R_f 0.40). The former, the major product, was eluted with EtOAc for probe spectra. DCI (CH_4 gas)-<u>positive ion</u>: m/z 673 (MH^+, 1.5), 493 (3.9), 313 (1.8), 226 (47), 198 (22), 182 (50); <u>negative ion</u>: 491 (100), 472 (22), 311 (30), 247 (96), 224 (40), 196 (6), 181 (20). The DISI and the DCI spectra in conjunction provided unequivocal evidence that the mol wt of Mt was 312. Although the molecular ion was not evident in the negative ion spectra, for detection of other high mass ions (i.e. ions formed by loss of pfBz), the sensitivity of the negative ion spectrum was usually about 30 times that of the positive ion DCI mass spectrum. Hence, negative ion CI mass spectrometry may be particularly useful for quantitation of pfBz derivatives of compounds such as Mt.

The above results together with other data suggested that Mt was the 9-alanine conjugate of BA. Hence Mt and synthetic β-(6-benzylaminopurin-9-yl)alanine (I, 9Ala-BA) were compared critically. Like Mt, 9Ala-BA yielded mono- and di-pfBz derivatives (II and III, respectively). The two derivatives of 9Ala-BA could not be distinguished from those of Mt by TLC or mass spectra. Transesterification (heating at 70° with EtOH, diethoxypropane and HCl) converted the di-pfBz derivatives of Mt and 9Ala-BA into N-pfBz ethyl esters (IV) which also appeared to be identical. Hence Mt was concluded to be 9Ala-BA.

The pfBz derivative of 9Ala-BA used in the present study appears to have clear advantages for direct-probe mass spectra over per-trimethylsilyl and permethyl derivatives

and also other derivatives (e.g. N-perfluoroacyl esters) commonly used for derivatization of amino acids. pfBz derivatives are formed by a single step derivatization reaction, are stable during TLC and HPLC and can be detected with high sensitivity by negative-ion CI mass spectrometry. The EI mass spectrum of the di-pfBz derivative of 9Ala-BA revealed a number of fragmentations which are diagnostic for this and related compounds. These are rationalized below. The dominant feature of the EI mass spectrum is the cleavage of the derivatized amino acid moiety with hydrogen transfer to the charged purine fragment to yield an ion of m/z 225 (base peak).

Alanine conjugation at position 9 appears to be a form of BA inactivation in soybean leaves. This suggested that a 9-substituted BA might be more effective than BA in retarding soybean leaf senescence. Two more active compounds were found, namely, 9-tetrahydropyranyl-BA and 9-tetrahydrofuranyl-BA. Metabolites of these compounds were identified by mass spectrometry and included BA itself and the debenzylated products, 9-tetrahydropyranyladenine and 9-tetrahydrofuranyladenine. The high activity of the 9-substituted BA derivatives is probably due to slow release of free BA. Application of 9-tetrahydropyranyl-BA plus naphthaleneacetic acid as a spray to soybean plants markedly retarded leaf senescence and increased the protein content of the seed.

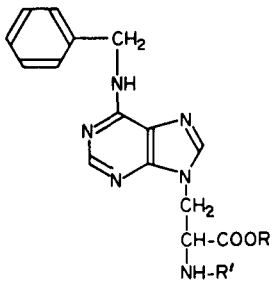

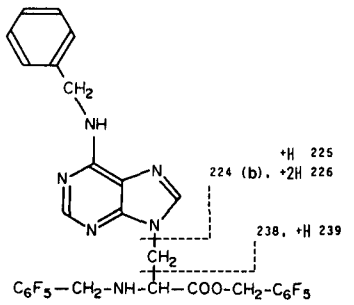

	R	R'
I	H	H
II	$-CH_2-C_6F_5$	H
III	$-CH_2-C_6F_5$	$-CH_2-C_6F_5$
IV	$-CH_2-CH_3$	$-CH_2-C_6F_5$

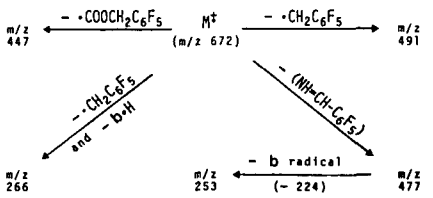

QUANTITATIVE ANALYSIS OF PGE_2 AND THE MAIN URINARY METABOLITES OF PGI_2 AND TXA_2, BY PACKED AND CAPILLARY COLUMN GC/NCI-MS, IN HUMAN AND IN RAT.

André Martineau[1] and Pierre Falardeau[2].

1- INRS-Santé, 7401 Hochelaga, Montréal (Québec), H1N 3M5, CANADA.

2- Clinical Research Institute of Montreal, 110 Pine ave W, Montreal, Quebec, H2W 1R7, CANADA.

INTRODUCTION:

Prostaglandin I_2 and thromboxane A_2 are the major prostaglandin endoperoxide metabolites synthesized by the blood vessels and the platelets respectively; they have potent vasoactive properties among others: PGI_2 is vasodilator and TXA_2 vasoconstrictor. The balance between the two opposing biological effects of thromboxane A_2 and prostaglandin I_2 is thought to be important for the homeostasis of the cardiovascular system. On the other hand, PGE_2, a vasodilator prostaglandin, is the major prostaglandin synthesized by the renal medulla and is involved in the modulation of the renal function, such as renal hemodynamics, water and solute excretion and liberation of hormones. Monitoring the level of those three prostaglandins (or their principal metabolites) constitutes a good evaluation of the prostaglandin system, mainly with regard to the physiological role of prostaglandins in the cardiovascular and renal system.

We have developped a method for the quantitative analysis of PGE_2 and the main urinary metabolites of PGI_2 and TXA_2, used as an index of their total or renal in vivo production in human and in rat. This method is based on GC-MS analysis in the electron capture negative chemical ionization mode, using either packed or capillary columns.

METHODS:

Each urinary sample (about 1/30 and 1/400 of the 24 hour urinary volume in rat and in human, respectively) is spiked with the following internal standards: 5 ng dinor-6-oxo-$PGF_{1\alpha}$-d_3, 10 ng 6-oxo-$PGF_{1\alpha}$-d_4 and TXB_2-d_4 and 20 ng PGE_2-d_4 and dinor-TXB_2-d_4.

After an overnight equilibration period at 4°C, the sample is acidified at pH 3 - 3.5 with HCl 4M and poured over a Clin Elut column (Analytichem). Prostaglandins are eluted using ethylacetate and further extracted in Tris buffer (pH8, 50 mM). Dinor-6-oxo-$PGF_{1\alpha}$, forming a lactone in acidic medium remains in the organic phase and is purified as previously described (1). The aqueous phase is acidified at pH 3 - 3.5 and applied over a C_{18}-Sep-pak previously washed with ethanol and water. The sample is transfered over the Sep-pak using a polypropylene syringe in order to minimize adsorption on glass. Prostaglandins are eluted with 7 ml ethylacetate-dicloromethane (75:25). The obtained solution is diluted by the addition of 13 ml CH_2Cl_2 and is applied over a Silica-Sep-pak prewashed with methanol, ethylacetate and hexane. 5 ml 50% AcOEt/CH_2Cl_2 are then passed through the Sep-pak and prostaglandins eluted with 5 ml MeOH - CH_2Cl_2 (60:40).

After evaporation of the solvent and transfer in a reacti vial, the prostaglandins are converted into their pentafluorobenzylester O-methyloxime derivatives. The derivatized sample is then transfered on the preconcentration zone of a 19 channel t.l.c. plate, preeluted twice with Acetonitrile. The plate is developped using the organic phase of the mixture AcOET/AcOH/hexane/H_2O (54:12:25:60). After elution, three zones are scrapped off the plate and extracted using ethylacetate: one zone containing dinor-6-oxo-$PGF_{1\alpha}$, another one containing 6-oxo-$PFG_{1\alpha}$ and the last one containing TXB_2, dinor-TXB_2 and PGE_2. After evaporation of the solvent, the samples are kept in pyridine in reacti-vials at -80°C. At the time of analysis, the samples are further converted into trimethylsilylether derivatives.

The samples are analysed by GC-MS, monitoring the $(M-PFB)^-$ ions. A 3% SP-2100 packed column (4 feet x 2 mm I.D.) was programmed from 270° (1 minute) up to 300° at a rate of 10°C per minute (Helium flow 30 ml/min). A 12 meter crosslinked methylsilicone (Hewlett-Packard: 0.2 mm I.D. x 0.33 micron film thickness) was programmed from 100° for 1 minute, then up to 290° at a rate of 15° per minute.

RESULTS:

The purification procedure was established using tritiated prostaglandin standards of extreme polarity (6-oxo-$PGF_{1\alpha}$ and PGE_2). The addition of those standards has permitted the optimization of prostaglandin recoveries (overall yield: 24%), along with the obtention of acceptable GC-MS traces. On the other hand the method was focused on the utilization of small columns (Clin Elut, Sep-pak) and thin layer chromatography in order to manipulate more samples at a time, with small volumes of solvent, in a relatively short period of time.

Figure 1, 2, 3, 4, show GC-MS traces obtained from rat and human urine using packed and capillary columns.

This method can provide the specificity and the sensitivity required to measure accuratly low picogram amounts of prostaglandins in biological fluids, along with a relatively short time of analysis.

(1) FALARDEAU, P., MARTINEAU, A.; Hypertension, 5: 701-705 (1983).

FIG 1

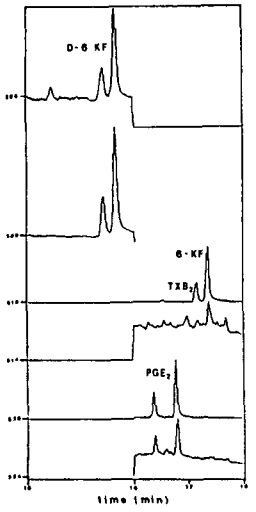

FIG 2

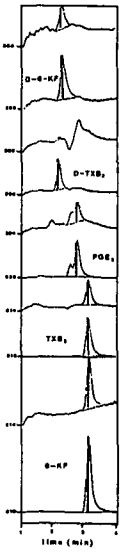

FIG 3

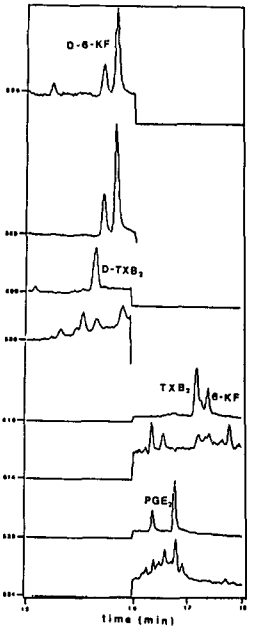

FIG 4

Selected ion chromatogram ($M-PFB^-$) of urinary dinor-6-oxo-$PFG_{1\alpha}$ (D-6-KF), dinor-TXB_2 (D-TXB_2), PGE_2, TXB_2 and 6-oxo-$PGF_{1\alpha}$ (6-KF), as pentafluorobenzylester-O-methyloxime-trimethylsilylether derivatives, obtained from rat (Fig 1, 2) and human (Fig 3, 4) urines, using packed (Fig 1, 3) and capillary (Fig 2, 4) columns.

ANALYSIS OF PROSTAGLANDINS IN CEREBROSPINAL FLUID BY CAPILLARY COLUMN GAS CHROMATOGRAPHY/ NEGATIVE ION CHEMICAL IONIZATION MASS SPECTROMETRY. James A. Yergey, Norman Salem, Jr.; Laboratory of Clinical Studies, National Institute on Alcohol Abuse and Alcoholism, DICBR, Room 3C-218, Building 10, Bethesda, MD 20892.

INTRODUCTION: The principal objective of this study is to apply state-of-the-art gas chromatographic/mass spectrometric methodologies to the analysis of fatty acid metabolites in an effort to elucidate the molecular alterations involved in various neuropathological states. Initial emphasis has been placed on characterizing the levels of prostaglandins in human cerebrospinal fluid (CSF). Prostaglandins are potent bioregulatory agents involved in modulating the activity of nearly every organ in the body, including the brain. Ethanol has the capability of interfering with their metabolism, thereby leading to a pathological state in many organ systems. Characterization of the prostaglandins in cerebrospinal fluid may lead to a better understanding of abnormal brain metabolism in alcoholics as well as in patients with other mental disorders. Preliminary investigations have suggested that prostaglandin levels in CSF drawn from patients with neurological impairment are markedly altered from those of normal volunteers. The levels are often near or below reported detection limits of 10-100 pg/ml of CSF.

METHODOLOGY OVERVIEW AND DISCUSSION: Cerebrospinal fluid samples were collected in tubes containing indomethicin to inhibit further prostaglandin formation, and internal standards (250 pg each of $^2H_4$-PGE_2, $^2H_4$-PGF_{2a}, and $^2H_4$-6-keto-PGF_{1a}), and frozen at -70°C. Thawed samples were brought to pH 3.5 with formic acid and extracted using Supelclean LC-18 extraction cartridges; sample was applied, rinsed with 2 ml 15% ethanol and 2 ml benzene, and the prostaglandins eluted in 2 ml ethyl acetate. Extraction recoveries were shown to be greater than 90% using tritiated standards. Samples were transfered to 1 ml Reacti-vial and derivitized to the methoxime, pentaflurobenzyl ester, trimethysilyl ether for GC/MS analysis. Tritiated standards were derivitized and analyzed by HPLC using a Radiomatic Flow-One detection system to determine reaction recoveries. The Beckman 450 HPLC system with Whatman Partisil-5 ODS-3 column was operated at a flow rate of 1 ml/min. A gradient elution from 70:30::H_3PO_4(pH3.5):acetonitrile to 20:80 over 20 min was used in order to observe both underivitized and derivatized standard. In addition to monitoring the ^3H label, an HP Model 8451A UV/Vis spectrophotometer with diode array detection was configured in-line for flow operation and a Basic program written to acquire/manipulate data at multiple wavelengths. Monitoring the UV simultaneously proved useful in reducing the chemical background for the GC/MS analysis. Although the samples appeared dry after several minutes following both the pentafluorobenzyl esterification and methoximation, the UV trace showed numerous peaks which were greatly reduced when drying times were increased. In addition, although esterification proceeded to completion for each of the standards, subsequent methoximation of ketone containing standards resulted in cleavage of the PFB group. As a result reaction order was reversed to make the methoxime derivative first. Recovery through the first two derivitization steps was greater than 85% for all standards. The trimethylsilyl derivative was not water stable and as such its recovery has not been assessed by this method. Derivatized samples were injected into a Carlo-Erba cold on-column injector at 80°C, and the column heated ballistically to 270°C. The Kratos MS-80 mass spectrometer was operated in negative chemical ionization mode and detection was by selected-ion-monitoring of the five sample and three deuterated internal standard masses.

GC/MS OF HUMAN CEREBROSPINAL FLUID SAMPLES: Recent analysis of 27 human CSF samples and appropriate standards, exemplified in Figures 1 and 2, yielded consistantly good signals for $^2H_4$-labelled internal standards. Detection limits for all 5 prostaglandins are now below 10 femtomole/ml CSF. This implies that extraction and derivitization are proceeding reproducibly. 6-keto-PGF_{2a} was quantifiable in 16 of the 27 samples (See Table 1). Patient information was not yet avaliable to generate any correlations with patient type. Chemical interference, in the form of broad peaks, continued to raise questions concerning measured levels of PGF_{1a} and PGF_{2a}. Standard runs did not contain these interfering peaks. Several chromatographic peaks were observed in samples that were not observed in any standard run. One such peak, eluting immediately prior to $^2H_4$-PGE_2, could easily be mistaken for PGE_2 in a poorly resolved chromatogram. No standards prepared the same day contained this peak, and an indomethicin blank showed no peaks on any SIM channel. No measurable amounts of PGE_1 or PGE_2 were observed, with one sample exception each. Again, no patient information is yet avaliable, and all patient types have probably not been well represented. The large "contaminant" peak mentioned above might easily have swamped any low level PGE_2 sample.

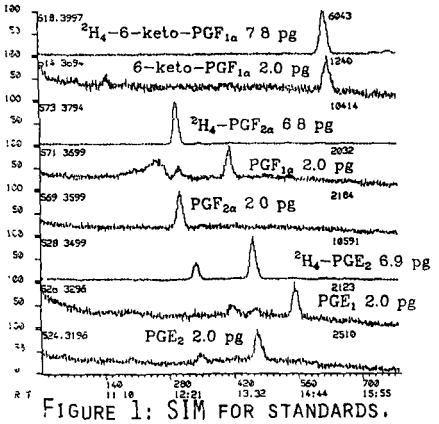

FIGURE 1: SIM FOR STANDARDS. QUANTITIES INJECTED ON-COLUMN.

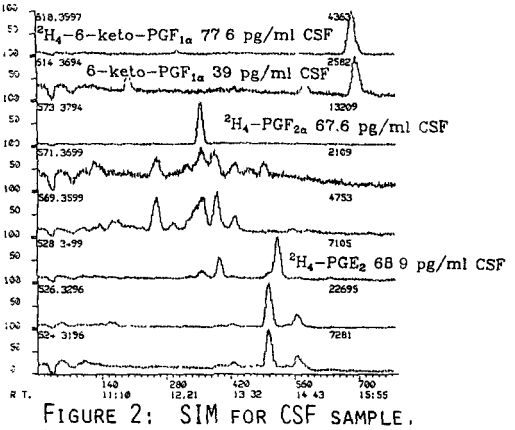

FIGURE 2: SIM FOR CSF SAMPLE. QUANTITIES ARE PG/ML CSF. 10% INJECTED.

TABLE 2: 6-keto-PGF$_{1\alpha}$ LEVELS IN HUMAN CEREBROSPINAL FLUID.

Sample	6-keto-PGF$_{1\alpha}$ (pg/ml CSF)
1	21
2	13,16
3	76,67
4	nd
5	nd
10	73
11	2
12	nd
13	nd
14	13
15	nd
16	nd
17	47
18	586
19	56
20	39
21	7
22	7
23	nd
24	36
25	18
26	3
27	6

DEUTERATED 4-AMINOBUTANAL DIETHYL ACETAL AS AN IN VIVO PRECURSOR OF THE NEUROTRANSMITTER, GABA.

D. Vicchio and P.S. Callery, Department of Medicinal Chemistry/ Pharmacognosy, University of Maryland, Baltimore 21201.

Cyclic acetals and aliphatic ethers are substrates for oxidations catalyzed by the Cyt-P450 system. Since 4-aminobutanal diethyl acetal (4-AMBDA) contains both an ether methylene and an acetal carbon, the possibility that it is enzymatically converted to the inhibitory neurotransmitter, 4-aminobutanoic acid (GABA) was investigated. In vitro incubation of 4-AMBDA with mouse or rat liver 10,000 x g supernatant yielded GABA. In vivo this GABA would be formed in the periphery, and thus should not penetrate the blood-brain barrier (BBB). However, one of the isolated oxidative metabolites of 4-AMBDA was 1-pyrroline, which can penetrate the BBB and then be converted to GABA. Thus, the possibility that 4-AMBDA can be used as a precursor of central GABA pools was investigated. However, the high concentrations of unlabeled endogenous GABA made this process difficult to study. This problem was circumvented by using deuterium labeled 4-AMBDA and determining by selected ion monitoring (SIM) GC/MS, the amount of GABA in the brain.

1-Pyrroline was shown to be an intermediate in vitro. 4-AMBDA was incubated with rat liver microsomes at 37°C for 10 minutes. After the incubation, 100 mg of $NaBH_4$ were added and the solution shaken for 30 minutes. Then 1.0 ml of a 10% toluene solution of pentafluorobenzoyl chloride was added, and the solution shaken at room temperature for 1 hour. The toluene was evaporated, the residue reconstituted in 100 uL of ethyl acetate, and analyzed by GC/MS. The results indicated that 4-AMBDA is converted to GABA through 1-pyrroline as an intermediate.

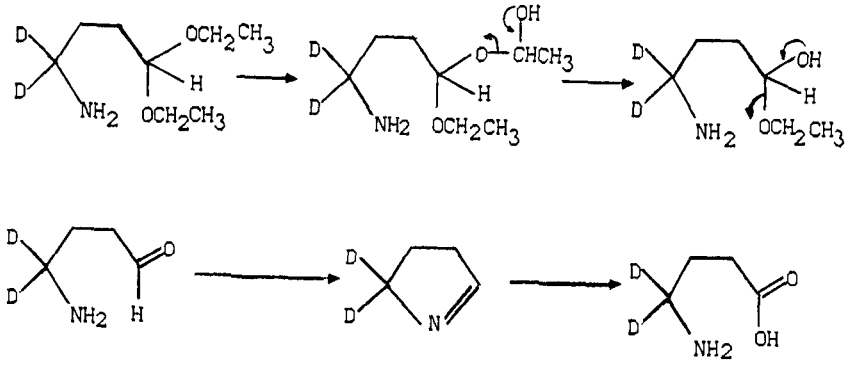

Scheme 1. Mechanism for the enzymatic oxidation of deuterated 4-aminobutanal diethyl acetal to deuterated GABA that is consistent with the data.

The substrate [4,4-$^2H_2$]4-AMBDA was synthesized by $LiAl^2H_4$ reduction of 3-cyanopropanal diethyl acetal. Male ICR mice were injected intravenously with 40 mg/kg aqueous solutions of [4,4-$^2H_2$]4-AMBDA. Controls were injected with 50 uL of distilled water. Fifteen minutes post injection, the mice were decapitated, their brains placed in trichloroacetic acid that contained 50 nmol of the homologue internal standard, 5-aminopentanoic acid (5-APA). The 12,000 x g supernatant was passed through a cation exchange column. The column was washed with 15 ml of water, followed by 15 ml of 1.0 N NH_4OH. The eluant from the basic fraction was evaporated to dryness, the residue derivatized with dimethylformamide dimethyl acetal:acetonitrile (2:1), and analyzed by GC/MS. Aliquots of the derivatized labeled GABA, [4,4-$^2H_2$] methyl 4-(N,N-dimethyl-N'-formamidino)butanoate, and 5-aminopentanoic acid, methyl 5-(N,N-dimethyl-N'-formamidino)pentanoate were analyzed on a gas chromatograph with a 30 m SE-54 column with helium as the carrier gas. The column was heated from 50 to 180°C at 30°C/min, and interfaced with a quadrupole mass spectrometer. In the SIM mode, the parent ions for GABA (m/z 172), [4,4-$^2H_2$]GABA (m/z 174), and 5-APA (m/z 186) were monitored for dwell times of 75 msec each, and the peak areas integrated by the data system. The relative areas of m/z 174 and 186 in the control and dosed animals were used to determine the amount of $^2H_2$-GABA in the brain. These data indicate that brain GABA pools become labeled when [4,4-$^2H_2$]4-AMBDA is administered, and that acetals may be used as precursors of central neurotransmitters.

THE USE OF SPECIFICALLY-LABELED ACYL-[^{18}O]-DIHYDROXYACETONE PHOSPHATE TO STUDY GLYCERYL ETHER BIOSYNTHESIS - QUANTITATION BY FAB AND GC-MS.

S.T. Weintraub, D.M. Peterson, and S.J. Friedberg, The Univ. of Tx. Health Science Center at San Antonio; San Antonio, Tx. 78284 and R.A. Martinez and P.L. Stotter, The Univ. of Tx. at San Antonio; San Antonio, Tx. 78285.

Although ether lipids are present in all animal tissues, their function is still largely unknown. They are found as structural components of cellular membranes and are abundant in conductive tissues. The finding of abnormally large quantities of O-alkyl lipids in the majority of tumors has prompted increased interest in elucidation of the biosynthesis of ether lipids. For the present study, specifically-labeled homologs of acyl-[^{18}O]-dihydroxyacetone phosphate (acyl DHAP) have been synthesized. This phospholipid has previously been shown to be a precursor in the formation of ether lipids. The original synthetic method incorporated ^{18}O into glycolic acid by reacting chloroacetic acid with $H_2{}^{18}O$. It was found that pre-equilibration of chloroacetic acid in $H_2{}^{18}O$ was essential to produce the >85% labeled product. No loss of ^{18}O was detected during the remainder of the synthesis which involved acylation, chain elongation with diazomethane and phosphorylation.

In the past, the evaluation of the results from in vitro enzyme experiments with acyl DHAP have been hampered by difficulty in analyzing this substance. Not only is the acyl group quite labile in the presence of mild base, but derivatization of the intact molecule to form a volatile product has been unsuccessful. Enzymatic removal of the phosphate followed by methoxime-TMS derivative formation has provided only limited information because of the extremely low product yield.

In order to analyze intact acyl DHAP, an investigation into the utilization of fast atom bombardment (FAB) mass spectrometry was initiated. FAB spectra (negative ion) were acquired on a Finnigan-MAT 212 mass spectrometer in combination with an INCOS 2200 data system. An Ion Tek saddle field atom gun was employed with xenon at 8 kV. Each sample was dissolved in chloroform:methanol (8:2) and applied in 2 μl to thioglycerol which was coated on the copper probe tip. The source temperature was 50 °C and the accelerating voltage was 3 kV. The contribution of the thioglycerol has been subtracted. After comparison with the pattern of relative intensities in the ion cluster around [M-H]$^-$ for numerous ^{16}O analogs, it was calculated that the ^{18}O content of the hexadecanoyl-[^{18}O]-DHAP (17:0-acyl-[^{18}O]-DHAP) was 88%.

By inclusion of a homolog of acyl DHAP as an internal standard, quantitative measurements were possible. Shown below is a FAB spectrum (negative ion) of an equimolar mixture of standard 14:0-acyl-[^{16}O]-DHAP and 17:0-acyl-[^{18}O]-DHAP along with a representative standard curve. As shown in the inset, it was also possible to estimate low levels of one species in a mixture. This is important for evaluation of small amounts of acyl exchange which can occur under certain enzymatic conditions.

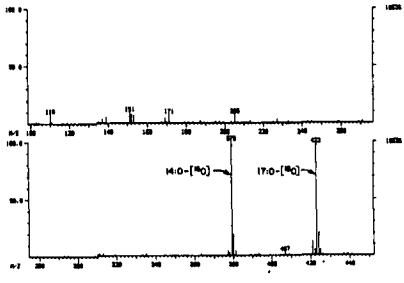

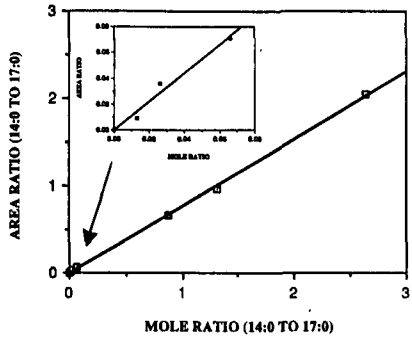

This technique is now being employed in the elucidation of the mechanism of an unusual enzymatic process involving acyl DHAP and the enzyme O-alkyl synthase. In this reaction, cleavage of acyl dihydroxy acetone phosphate occurs between carbon-1 and the adjacent oxygen instead of the "normal" mechanism which cleaves at the acyl carbon to oxygen bond. Fatty acid molecules produced from 17:0-acyl-[^{18}O]-DHAP by normal chemical hydrolysis will contain the natural abundance of ^{16}O, while those formed by the enzyme will be significantly enriched in ^{18}O. In the present study, both the acyl DHAP and fatty acid fractions were isolated from the in vitro enzyme experiment. The fatty acids were converted to methyl esters and evaluated for ^{18}O content by GC-MS. The pentadecanoic acid and 14:0-acyl-[^{16}O]-DHAP internal standards were added immediately after incubation and carried through the isolation procedure. Standard mixtures were treated in an analogous manner. A typical FAB spectrum before and after a 2 hour enzyme incubation of 17:0-acyl-[^{18}O]-DHAP is shown. The quantitative results are given below:

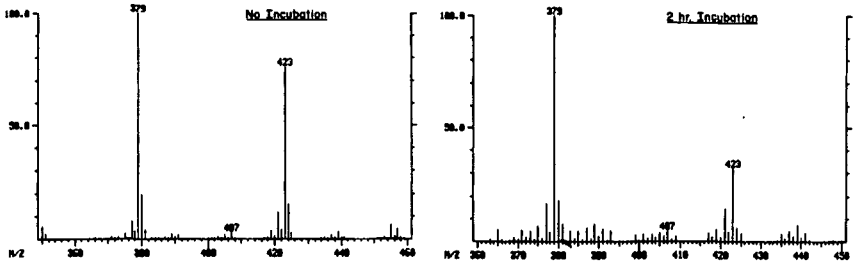

	17:0-ACYL-[^{18}O]-DHAP (NMOLE)	[^{18}O]-HEPTADENCANOIC ACID (NMOLE)
NO INCUBATION	138.8	1.7
2 HR INCUBATION	85.4	22.3
NET	-53.4	+20.6

Thus, a significant amount of the 17:0-acyl-[^{18}O]-DHAP was hydrolyzed by the "unusual" enzyme mechanism to yield [^{18}O]-heptadecanoic acid.

In order to obtain further information about the ^{18}O content of these compounds, current efforts are directed at the synthesis of acyl-[^{18}O]-DHAP with higher stable isotope enrichment. A new synthetic scheme has been devised which utilizes oxidative cleavage of acyl-2-butyne-[^{18}O]-1,4-diol and has several advantages over the previous method: 1) Higher ^{18}O content of the final product; 2) Re-cycling of the ^{18}O source to keep cost down; 3) Capability for larger scale synthesis with high yield steps; 4) Adaptation for incorporation of ^{2}H, ^{3}H, ^{13}C and/or ^{14}C at specific locations

Supported by grants 2RO1 CA15407 (NIH) to S. J. Friedberg and RR08194 (NIH) and F345 (Welch Foundation) to P. L. Stotter.

IDENTIFICATION OF LONG CHAIN BASES IN INOSITOL SPHINGOPHOSPHOLIPIDS FROM LEISHMANIA DONOVANI

Koka Jayasimhulu and Edna S. Kaneshiro
Departments of Environmental Health and, Department of Biological Sciences,
College of Medicine, University of Cincinnati, Cincinnati, OH 45267 & 45221

Introduction

Leishmania donovani, is the causative agent of visceral leishmaniasis or kala azar. In the human, these organisms are found with macrophage cells as the amastigote form. In the insect intermediate host, the protozoan is free-swimming and known as the promastigote form. Promastigotes can be readily grown axenically in cultures and biochemical analyses of these cells are feasible. We have recently identified inositol sphingophospholipids in the lipids of promastigotes. The presence of these inositol lipids is of interest because these compounds have previously been reported only from plant and fungal cells, but not from "animal" cells.

Methods

The inositol sphingolipids were purified by triethylaminoethyl cellulose column chromatography and thin-layer chromatography. Amide-linked fatty acids, long chain bases and water-soluble products from the InSL were released by acid hydrolysis in sealed ampoules using conc HCl:MeOH (1:5, v/v) for 48 hr or in MeOH:H_2O:HCl (11:2.6:1, v/v/v) overnight at 80°C as described by Carter & Gaver. Sphingolipids, fatty acids were quantified by GLC as above. Alternatively, fatty acid methyl esters (FAME) were identified and quantified by capillary column GLC-mass spectrometry analyses. A Carlo Erba series 4160 Fractovap gas chromatograph fitted with a fused silica column (60 m x 0.32 mm i.d.) coated with SE-54 (SPB-5, Supelco) and a cooled on-column injection system was used to separate the FAME. Material from the GLC system were introduced into a high resolution mass spectrometer (MS) system (Kratos, MS-80, Manchester, England) through a jet separator. Samples were injected into the GC at 60°C. Initial oven temperature was maintained for 2 min at 150°C to permit venting of the solvent after which the valve to the mass spectrometer was opened. The oven temperature was increased by 6°C/min to 280°C. Analyses were started 1 min after the opening of the valve, allowing material from the GLC to enter the MS. Electron impact mass spectra data were continuously collected and processed on a Data General NOVA/4C computer with a DS-55 data system (DS).

Long Chain Base The long chain bases (LCB) released by acid hydrolysis of the INSL, were converted to their N-trifluoracetyl derivatives by the addition of trifluoroacetylmethyl ester and adjustment of the pH to 8.4 with triethylamine. The reaction was allowed to proceed overnight at room temperature. The solvent was then evaporated under a stream of N_2 then samples were placed under a vacuum for 2-3 minutes to ensure complete removal of triethylamine. N,O-bis(trimethylsilyl)trifluoroacetamide (BSTFA) was then added to the N-trifluoroacetyl LCB and heated for 30 min at 60°C. Samples were dried under a stream of N_2 then dissolved in chloroform before analyses by GC-MS-DS.

Samples were injected into the GC at 60°C. After 1 minute, the oven temperature was raised to 220°C, then programmed to increased by 2°C/min to 260°C. The GC-MS data on the LDB derivatives were continuously collected 3 minutes after sample injection and 1 minute after opening of the GC to MS valve.

Fast atom bombardment MS (FABMS) analyses were done on free ceramides released from the InSL by phospholipase C digestion. Sorbital was applied to the tip of the FAB probe as described previously. One to two µl of the ceramides dissolved in chloroform was mixed in the sorbitol matrix. The FAB prove was introduced through the direct inlet system. The FAB gun and power supply employed were from Phrasor (Phrasor Scientific Inc., Duarte, CA).

Results

The major long chain bases were C_{18} and C_{16} sphingosines. The C_{18} long chain base gave ions at m/z 524 and 311, corresponding to $M^{+\cdot}$ -15 and the base peak. The elemental composition of these two ions were $C_{25}H_{49}Si_2F_3$ and C H OSi, respectively. The C_{16} long chain base derivative gave ions at m/z 496 ($C_{23}H_{45}NO_3Si_2F_3$) and 283 ($C_{17}H_{35}OSi$) corresponding to $M^{+\cdot}$ -15 and the base peak, respectively. Stearic acid was the major fatty acid found. The FAB mass spectra obtained on the mixture of ceramides showed loss of water from the $(M+H)^+$ ions.

Mass spectral analyses of the major long chain bases of the inositol sphingophospholipids of *Leishmania donovani* promastigotes

N-trifluoroacetyl, O-silyl sphingosines

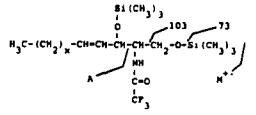

	m/z	Relative Intensity	Elemental Composition
x=12			
$(M^{+}-15)$	524	1.2	$C_{25}H_{49}NO_3Si_2F_3$
$(M^{+\cdot}-105)$	436	3.4	$C_{22}H_{39}NO_2SiF_3$
A	311	100 0	$C_{19}H_{39}OSi$
	301	2.9	$C_{10}H_{22}NO_2SiF_3$
	211	5.9	$C_7H_{12}NOSiF_3$
	129	22 6	$C_6H_{13}OSi$
	103	16.0	$C_4H_{11}OSi$
	73	28.6	C_3H_9Si
x=10			
$(M^{+}-15)$	496	1 3	$C_{23}H_{45}NO_3Si_2F_3$
$(M^{+}-105)$	406	3.8	$C_{20}H_{35}NO_2SiF_3$
A	283	100.0	$C_{17}H_{35}OSi$
	301	2.1	$C_{10}H_{22}NO_2SiF_3$
	211	4.6	$C_7H_{12}NOSiF_3$
	129	20.7	$C_6H_{13}OSi$
	103	7.7	$C_4H_{11}OSi$
	73	24.0	C_3H_9Si

N-trifluoroacetyl, O-silyl dihydrosphingosines

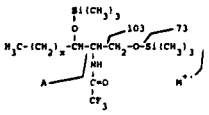

	m/z	Relative Intensity	Elemental Composition
x=14			
$(M^{+\cdot}-15)$	526	11.5	$C_{25}H_{51}NO_3Si_2F_3$
$(M^{+\cdot}-105)$	436	6.2	$C_{22}H_{41}NO_2SiF_3$
A	313	100.0	$C_{19}H_{41}OSi$
	301	18.5	$C_{10}H_{22}NO_2Si_2F_3$
	211	54.4	$C_7H_{12}NOSiF_3$
	129	20.8	$C_6H_{13}OSi$
	103	23.4	$C_4H_{11}OSi$
	73	44 1	C_3H_9Si
x=12			
$(M^{+\cdot}-15)$	498	9 2	$C_{23}H_{47}NO_3Si_2F_3$
$(M^{+\cdot}-105)$	408	6 3	$C_{20}H_{37}NOSiF_3$
A	285	100.0	$C_{17}H_{34}OSi$
	301	14 4	$C_{10}H_{22}NO_2SiF_3$
	211	46.9	$C_7H_{12}NOSiF_3$
	129	13.8	$C_6H_{13}OSi$
	103	18.7	$C_4H_{11}OSi$
	73	36.9	C_3H_9Si

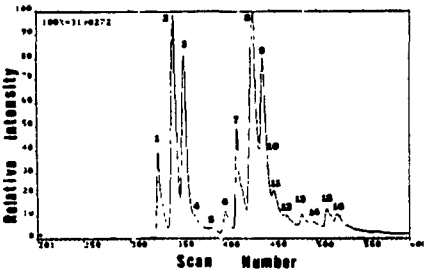

Tracing of the total ion chromatograph of the LCB derivatives of the InSL from *Leishmania* promastigotes separated by capillary column GC. Peaks 1 and 2 are C_{16} sphingosines, peak 3 is C_{16} dihydrosphingosine, peak 4 and 5 are C_{17} sphingosines, peak 7 and 8 are C_{18} sphingosines, peak 9 is C_{18} dihydrosphingosine, peaks 10 and 11 are C_{19} sphingosines, peak 12 is C_{19} dihydrosphingosine, peaks 14 and 15 are C_{20} sphingosines, and peak 16 is C_{20} dihydrosphingosine. Peaks 6 and 13 were not identified in this study.

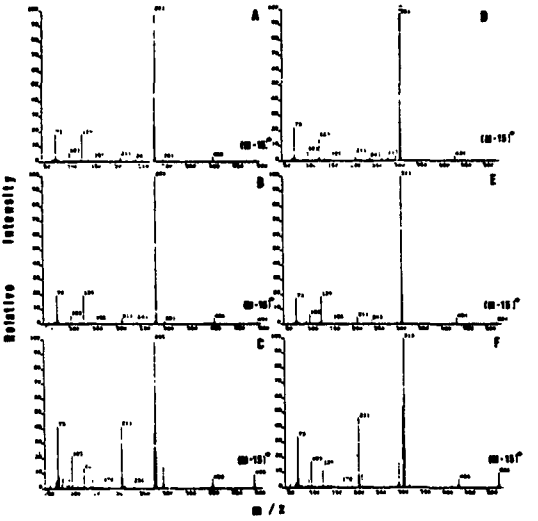

Mass spectra of the six major LCB in *Leishmania donovani* InSL A and B are spectra of C_{16} sphingosines (peaks 1 and 2 in TIC); C is C_{16} dihydrosphingosine (peak 3 in TIC) D and E are C_{18} sphingosines (peaks 7 and 8 in TIC), F is C_{18} dihydrosphingosine (peak 9 in TIC) Peaks indicated by $(M-15)^{+}$ represent the loss of a methyl group from the molecular ions which is commonly observed in silylated derivatives

METABOLISM OF PAF BY THE ISOLATED PERFUSED RAT LUNG

P.E. Haroldsen, N.F. Voelkel, and R.C. Murphy
Department of Pharmacology and Medicine
University of Colorado Health Sciences Center
Denver, CO 80262

Introduction

Platelet activating factor (PAF), identified as 1-0-alkyl-2-acetyl-sn-glycero-3-phosphocholine (1), is a unique phospholipid possessing profound biological activities and has been implicated as being an important mediator of various inflammatory reactions (2). PAF can be synthesized by numerous cells within the lung while profound effects upon pulmonary physiology including vasoconstriction, bronchoconstriction, and edema formation can result. There have been studies on the pulmonary metabolism of eicosanoids, but little is know about the metabolism of PAF by this organ. At the cellular level the metabolism of PAF has been well documented, where it is found to be rapidly inactivated by deacetylation followed by reacylation with long chain fatty acyl groups, in particular, arachidonic acid (3). However, the metabolic fate of PAF in an intact organ system such as the lung, remains unknown. In this study, the metabolic profile of PAF at the intact organ level was determined in the isolated perfused rat lung. Various techniques based on mass spectrometry were used to structurally identify the metabolites of PAF.

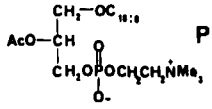

PAF

Methods

Lungs were isolated from Sprague-Dawley rats, ventilated (21% O_2, 5% CO_2, 74% N_2) and perfused with a physiological salt solution containing 3% albumin (fatty acid free). For administration of tritium labeled PAF (labeled in the alkyl mode) into the airways, a flexible polyethlyene catheter connected to a syringe containing 70 ml of PAF (100-1500 ng) saline/albumin solution, was advanced through the trachea into the peripheral region of the lower right lobe and injected as bolus. Following administration, the lung was ventilated and perfused for additional 15 min. Subsequently, the lung was homogenized and lipids extracted using chloroform/methanol and water. The lipid extract was separated into various components by TLC using silica gel plates and a solvent system chloroform/methanol/acetic acid/water (50/30/8/5). Three major bands of radioactivity were detected.

Band 1: Structure identification of this band which had the retention time of lyso-PAF was made by GC/MS of the isopropylidine derivative made by published techniques. Characteristic ions at m/z 101 and 341 were found for a major component of this TLC band which had the right retention time for 1-0-hexadecyl-monoglyceride isopropylidine derivatives (Table 1).

Band 2: Structure identification of this metabolite which had the retention time of authentic PAF was made by hydrolyzing the derivative with phospholipase C followed by reacting the resulting diglyceride with pentafluorobenzyl chloride for 1 1/2 hours at 100°. The derivatized sample was further purified on silica gel using benzene/hexane/ether (50/45/5), and reverse phase HPLC. The radioactive peak isolated from the HPLC was analyzed by negative ion chemical ionization. As seen in Table 1, the characteristic ion at m/z 552 revealed the presence of 1-0-hexadecyl-2-acetyl-diglyceride indicating that this peak corresponded to intact PAF.

Band 3: The retention time of this component, which was quite broad, corresponded to the elution characteristics of phosphatidylcholines. This material was hydrolyzed by phospholipase C followed by derivatization of the resulting diglycerides with 3,5-dinitrobenzoyl chloride. The mixture of DNB-diglycerides were separated by reverse phase HPLC and the radioactive peaks collected separately. These radioactive peaks were analyzed by negative ion desorption chemical ionization techniques using methane as the moderating gas. As listed in Table 3 the major radioactive molecular species of the phosphatidylcholines could be determined from the abundant molecular ions and corresponded to 1-0-hexadecyl-2-arachidonoyl-GPC and 1-0-hexadecyl-2-palmitoyl-GPC.

Table 1

Radioactive Metabolites of PAF Instilled Into the Isolated Rat Lung separated by TLC

Band	Identification	% Injected PAF	Derivative	Mass Spectrometry	Ions
I	Lyso-PAf	5.9 ± 2.7	Isopropylidene[1]	El(70eV)	101,341
II	PAF	11.2 ± 5.4%	Pentafluorobenzyl[2]	NCI(GC/MS)	552
III	16e/20:4-GPC	36.3 ± 1.3%	Dinitrobenzoyl[2]	DCI(-Ve)[2]	796
	16e/16:0a-GPC	17.8 ± 1.5%	Dinitrobenzoyl	DCI(-Ve)	748
	16e/18:0a-GPC	2.3 ± 0.4%	Dinitrobenzoyl	DCI(-Ve)	776
	16e/182a-GPC	5.4 ± 2.4%	Dinitrobenzoyl	DCI(-Ve)	772
	unknown	17.3 ± 1.5%	Dinitrobenzoyl	DCI(-Ve)	-

1. Hydrolyzed by HF prior to derivatization.
2. Hydrolyzed by phospholipase C prior to derivatization.

Discussion

The present study demonstrates that PAF is rapidly an extensively metabolized by the isolated perfused rat lung. It was found that by 15 min, 96% of the PAF instilled into the airways was retained by the lung with only 4% escaping into the vascular perfusate. Characterization of the metabolites of PAF indicated that phosphatidylcholine containing arachidonic acid was a major metabolite in the intact lung. Characterization of this molecule was carried out using a new technique of lipid analysis, namely formation of the dinitrobenzoyl derivative of diglycerides and negative ion desorption chemical ionization mass spectrometry (Figure 1).

The metabolism of PAF into lyso-PAF and long chain acyl-GPC molecular species by the lung indicates that this molecule undergoes a deacetylation/reacylation process. The specificity of the reacylation of this molecule is unique in that 46% of the reesterified fatty acid content was found to be arachidonate. This study further supports the relationship between PAF and arachidonate metabolism at the whole organ level.

Acknowledgements. This work was supported in part by grant from the National Institutes of Health AI20774 and HL34303.

References

1. C.A. Demopoulis, N. Pinckard, and D.J. Hanahan. J. Biol. Chem. 254:9355-9358 (1979).
2. R.C. Murphy and P.M. Henson. Ann. Inst. Pasteur/Immunol. 136B:219-221 (1985).
3. F.H. Chilton, et al. J. Biol. Chem. 257:5402-5410 (1982).

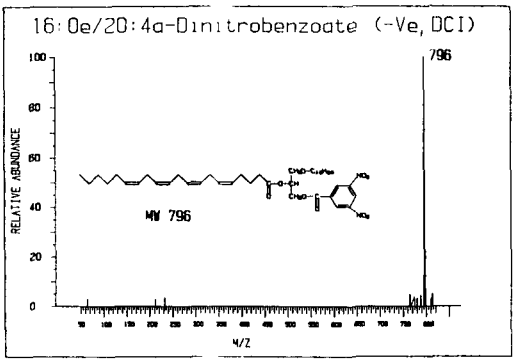

Figure 1. Desorption chemical ionization mass spectrum of the negative ions from the major PAF metabolite (as the DNB derivative) in the lung identified as 1-0-hexadecyl-2-arachidonoyl-3-dinitrobenzoate.

ANALYSIS OF COMPLEX CARBOHYDRATE MIXTURES BY HPLC-FABMS.

G. Her, S. Santikarn and V. N. Reinhold

Department of Nutrition,
Harvard School of Public Health, Boston, MA 02115.

High performance liquid chromatography (HPLC) is a widely used method for separation of biopolymers. In the pursuit of oligosaccharide structure, a biopolymer imbued with complex arrays of homopolymers, isomeric branching patterns and general microheterogeneity, the utilization of HPLC is cruital for successful component separation. Fast atom bombardment (FAB) mass spectrometry (MS) has proven to be a powerful technique for carbohydrate characterization. FAB spectra can provide molecular weight, and under selected conditions, sequence and branching information. The successful combination of these two techniques could provide great analytical assistance to a field greatly hampered by structural complexity. Moreover, due to limitations in HPLC sample detectability, pre- or post column derivatizations procedures are frequently necessary to maximize sensitivity. In an effort to maintain chromatographic efficiency and maximize sample detectability we have investigated the application of direct HPLC-MS coupling to problems in glycoconjugate and polysaccharide research.

Among the different approaches to LC-MS coupling, only the moving belt interface provides the capability for FAB ionization and this belt-type interface has proven successful for peptide studies[1].

First the FAB mass spectral characteristics of oligosaccharides desorbed from the moving belt was investigated. The following conclusions can be made: a.) the belt usually contributes less background ions (especially at low mass) than the liquid matrix; b.) carbohydrates with mass range of up to 4000 daltons can be desorbed intact from the moving belt, although the loss in sensitivity with increasing mass appears to be more noticable in the belt-FAB mass spectra than in the matrix-FAB spectra of the same material. Below 2000 daltons both techniques show comparable sensitivity; c.) belt-FAB mass spectra of oligosaccharides usually show sodiated molecular ions $(M + Na)^+$ and some fragment ions that can provide useful structural information. The absolute and relative abundances of these ions are sensitive to the belt speed. Figure 1. shows a positive ion belt-FAB mass spectrum of viridopentaose B which is used here to illustrate some of the above points.

When the moving belt is coupled to an HPLC the result is shown in Figure 2. The belt-FAB-MS provides a way to utilize gradient elution for underivatized oligosaccharides.

One of the main points with the moving belt interface is that the sample is not slways distributed evenly on the hydrophobic belt surface which results in an unstable ion flux.

1. Stroh, et. al., Anal. Chem., 57:985(1985).

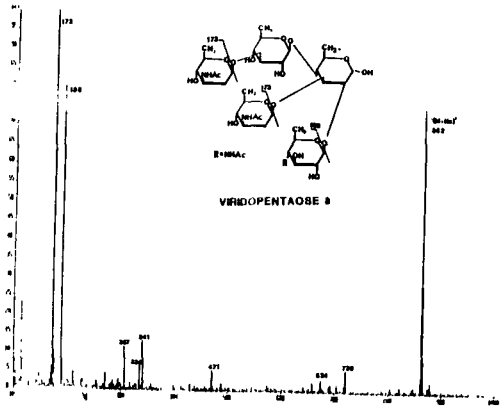

Figure 1: Positive ion Belt-FAB mass spectrum of viridopentaose

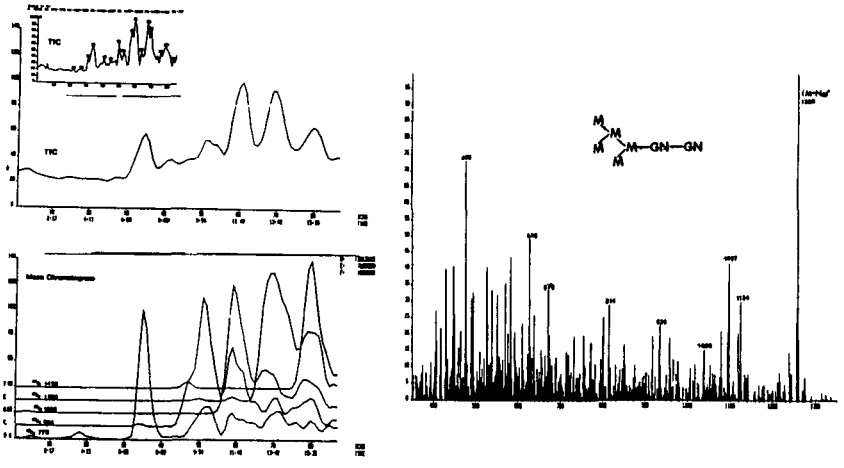

Figure 2.: Positive ion HPLC-FAB-MS of underivatized oligosaccharides isolated from urine of animals suffering from mannosidosis.

(a.) total-ion current; (b.) FAB mass spectrum of compound with retention time of 13:42 minutes. (HPLC conditions: 5 micron amino column; solvent: acetonitrile-water with a linear gradient of 25 to 55% water in 30 minutes; flow rate: 1.5 ml/min; split ratio 2:1).

CARBOHYDRATE MAPPING BY MASS SPECTROMETRY: A NOVEL METHOD FOR IDENTIFYING ATTACHMENT SITES OF ASN-LINKED SUGARS IN GLYCOPROTEINS

Steven A. Carr, Gerald D. Roberts and Walter Johnson, Department of Physical, Analytical and Structural Chemistry, SmithKline and French Laboratories, L-940, Swedeland, PA 19479

In the last ten years remarkable advances in the development of molecular synthesizers and recombinant DNA techniques have fostered a renewed interest in glycoproteins as drugs. Numerous glycoproteins are now being produced by recombinant techniques for possible therapeutic use. The carbohydrate chains of these molecules can play a significant role in the overall function of the glycoprotein including stablizing protein conformation, protecting against proteolytic degradation, targeting of the glycoprotein to specific tissues and controlling the lifetime of the molecules in the circulatory system.

Defining the sites of glycosylation and structures of carbohydrates at each site is of fundamental scientific interest and, furthermore, may be required by regulatory agencies for recombinant protein products. However, the task of unraveling the complete structure of a glycoprotein is extraordinarily complex. In addition to determining the sequences of the protein and carbohydrate, and the linkage and configuration of the saccharide monomers, the carbohydrate-protein link must also be ascertained and the specific amino acids to which carbohydrates are attached must be identified. The latter is arduous, particularly for multiply glycosylated proteins, and requires developing a unique strategy for each glycoprotein.

We have now developed a new mass spectrometric method for locating the specific sites of attachment of Asn-linked carbohydrates in glycoproteins (1). In favorable cases the composition of carbohydrates attached to specific glycosylation sites can also be determined. Only low nanomole amounts of protein are required which makes this method compatible with most microsequencing applications. The strategy (Scheme 1) is outlined below. The molecular weights of peptides released from the glycoprotein with proteases of known specificity are determined by FAB mass spectrometry and fitted to the known or DNA-derived sequence. Oligosaccharides attached to Asn are released either before or after proteolysis with a glycosidase, usually peptide:N-glycosidase F (Genzyme, Boston, MA). This enzyme cleaves the B-aspartylglycoslamine linkage of all known types of Asn-linked sugars and converts the attachment site Asn to Asp which weighs one dalton more. New peaks appearing in the mass spectra after treatment with the glycosidase correspond to formerly glycosylated peptides. Conversely, signals which disappear after glycosidase treatment correspond to glycopeptides. The differences in mass between these sets of signals often define a unique composition for the carbohydrate at each given site in terms of deoxyhexose, hexose, N-acetylhexosamine and sialic acid content.

We have applied this strategy in our structural studies of tissue plasminogen activator (tPA), a multiply glycosylated glycoprotein (2). Figure 1 shows partial FAB mass spectra of tryptic digests of reduced and carboxymethylated tPA before (top) and after (bottom) treatment with peptide:N-glycosidase F. The peak at m/z 1130 (bottom spectrum) corresponds to the MH^+ of the peptide (positions 441-449) that is produced by removal of the carbohydrate and conversion of the attachment site Asn to Asp. Absence of a peak at m/z 1129 in the tryptic digest prior to treatment with the glycosidase indicates that Asn 448 is fully glycosylated.

Glycopeptides ionize poorly compared to peptides and are generally not observed in the FAB mass spectra of proteolytic digests. However, if the complexity of the mixture is sufficiently reduced by subfractionation over reverse phase HPLC then glycopeptides can be directly observed. Comparison of the HPLC chromatograms of proteolytic digests of a glycoprotein before and after treatment with the glycosidase can be used to identify, isolate and purify unique glycopeptides for further analysis of structure. In this manner glycopeptides were purified from a complex digest of bovine ribonuclease B. The FAB mass spectra of these peaks indicate the presence of a family of related oligosaccharides differing in chain length, and yield their respective compositions in terms of hexose and N-acetylhexosamine (Figure 2).

In conclusion, the carbohydrate mapping technique should be a useful addition to the array of physiochemical methods used in the complete structural characterization of a glycoprotein and may be viewed as a simple extension of the FAB peptide mapping strategy, retaining all of the benefits ascribed to this method of verifying primary protein structure.

1. Carr, S.A. and Roberts, G.D. Anal. Biochem. 1986, (in press).

2. Pennica, D. et. al., Nature (London) 301, 214-221, 1983.

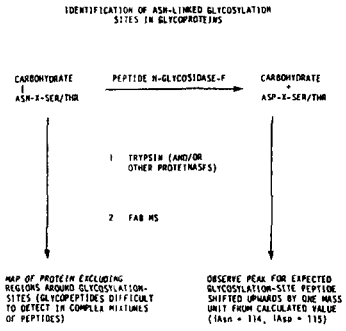

Scheme 1.

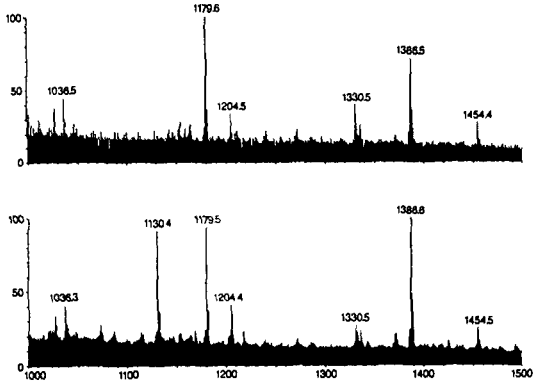

Figure 1. FAB mass spectrum of (top) a tryptic digest of reduced and carboxymethylated tPA and (bottom) after treatment with peptide:N-glycosidase F. Note the new peak at m/z 1130 (positions 441-449) in the bottom trace, and the absence of a peak at m/z 1129 in the top trace (see text).

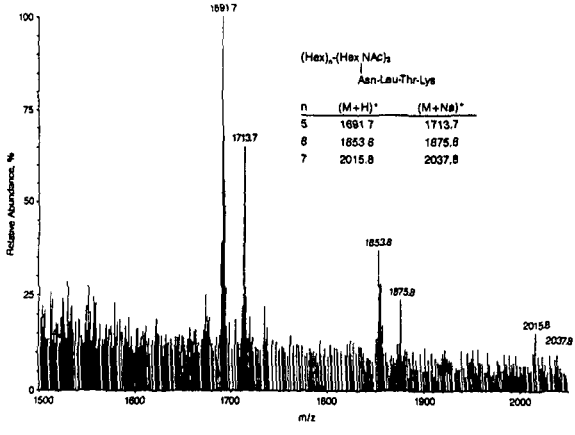

Figure 2. FAB mass spectrum of an HPLC subfraction of a tryptic digest of reduced and carboxymethylated ribonuclease B. Peaks correspond to the MH^+ and MNa^+ ions of the glycopeptides indicated.

STRUCTURAL STUDIES OF THE REPEATING OLIGOSACCHARIDE UNIT OF THE CAPSULAR POLYSACCHARIDE OF *STREPTOCOCCUS PNEUMONIA* TYPE 19B

Lawrence R. Phillips, William Egan and C.-J. Lee

Division of Biochemistry and Biophysics, and Division of Bacterial Products
Office of Biologics Research and Review, Food and Drug Administration
8800 Rockville Pike, Bethesda, MD 20892 USA

Abstract

The structure of the repeating oligosaccharide unit of the capsular polysaccharide of *Streptococcus pneumonia* Type 19B has been investigated. The repeating oligosaccharide, isolated from an aqueous hydrofluoric acid hydrolyzate of the polysaccharide, was shown, by fast atom bombardment mass spectrometry, to have a molecular weight of 1010 u. The repeating oligosaccharide was shown by traditional methods to be composed of 2-acetamido-2-deoxy-D-mannose, L-rhamnose, D-glucose, and D-ribose in the molar ratios of 2:2:1:1. Information about the sequence in the permethylated oligosaccharide was derived from electron-ionization and fast atom bombardment mass spectrometry. Additional data were obtained from methylation analysis and carbon magnetic resonance spectroscopy. These studies thus far have indicated that the polysaccharide consists of the following hexasaccharide repeating unit:

D-Man*p*NAc(1→4)-D-Glc*p*(1→4)-D-Man*p*NAc(1→4)-L-Rha*p*(1→)-D-Rib*f*(1→4)-L-Rha*p*(1→

Introduction

Pneumococcal group 19 includes types 19F, 19A(57), 19B(58), and 19C(59). The disease isolates of group 19 were the most frequent among 24 different pneumococcal types surveyed in Denmark during 1955-1970, whereas in the United States during 1967-1978, type 19 ranked 11th in frequency. However, the number of disease isolates due to types 19B(58) and 19C(59) were so few that these two types could be considered essentially non-pathogenic.

Even though there is great disparity in regards to pathogenicity, extensive cross antigenicity and immunogenicity have been observed among the group 19 polysaccharides. The unique property of non-pathogenic and other biological activities of types 19B(58) and 19C(59) pneumococci are considered to be closely related to the molecular structure and characteristics of their capsular polysaccharides. Hence, if another level of understanding of the disease is to be attained, such understanding may be derived, in part, from intimate knowledge of the chemical structure of these polysaccharides. Structures for types 19F and 19A(57) have been proposed, and herein we report some structural studies of the capsular polysaccharide of type 19B(58), and propose a structure for the repeating oligosaccharide unit thereof.

Isolation of the Repeating Oligosaccharide

Streptococcal pneumonia capsular polysaccharide type 19B was shown by ^{31}Pnmr to contain phosphorus, these results most probably indicating the presence of phosphoric diester linkages. Depolymerization of the polysaccharide by treatment with 60% aqueous hydroflouric acid was followed by chromatography on Bio-Gel P-2, to give a single, dephosphorylated oligosaccharide whose retention index indicated a molecular weight corresponding to six to eight sugar units.

Composition of the Repeating Oligosaccharide

^{13}Cnmr of the polysaccharide showed six signals in the region associated with anomeric carbon resonances (C_1), thereby indicating the presence of six sugar units. The isolated oligosaccharide was subjected to hydrolysis by hydrochloric acid and the hydrolyzate was analyzed for quantity and type of monosaccharides. The analysis was repeated using the pre-reduced oligosaccharide in order to determine the reducing terminus of the oligosaccharide. The isolated oligosaccharide was again subjected to hydrolysis by hydrochloric acid and the hydrolyzate was analyzed on an amino acid analyzer for the presence of amino sugars. Upon observation, the amino sugars were degraded by ninhydrin oxidation and the degradation products were analyzed by paper chromatography. The results of these experiments indicated that the oligosaccharide was composed of D-mannosamine, L-rhamnose, D-glucose and D-ribose (2:2:1:1).

Determination of Molecular Weight

Previously, the isolated oligosaccharide of type 19B(58) was shown to a hexasaccharide, composed of mannosamine, rhamnose, glucose, and ribose, in the ratio of 2:2:1:1. The oligosaccharide was then examined by fast atom bombardment (FAB) mass spectrometry to determine the molecular weight. The complementary nature of positive and negative FAB mass spectrometry allowed an assignment of 1010 u as the molecular weight of the oligosaccharide, which is consistent with the proposed monosaccharide composition. Further, this data allows speculation that a) the amino sugar components are most probably 2-acetamido-2-deoxy-D-mannose units, and b) there are no other moieties, e.g. -OMe or -OAc, present in the isolated oligosaccharide.

Monosaccharide Linkages and Ring Size

^{13}Cnmr indicated the presence of five pyranosides and one furanoside. Methylation analysis involves hydrolytic cleavage of differentially derivatived monosaccharides from the permethylated oligosaccharide, ultimately followed by GC/MS analysis to identify each of the original monosaccharides, their linkages with respect to their neighboring monosaccharides in the original oligosaccharide, and, with some limitations, an indication of the ring size. The results of the methylation analysis of the isolated oligosaccharide of Streptococcus pneumonia type 19B, in conjunction with the results of compositional analysis, indicated that there were three non-reducing termini (1-substituted L-rhamnose (pyranose); 1-substituted D-ribose (furanose); 1-substituted 2-acetamido-2-deoxy-D-mannose (pyranose)), and at least two substituted residues (1,4-substituted D-glucose (pyranose); 1,4-substituted L-rhamnose (pyranose, reducing terminus). The presence of many non-reducing termini and the absence of tri- or higher substituted monosaccharides would most probably indicate that the isolated oligosaccharide is actually a mixture of oligosaccharides.

Determination of the Monosaccharide Sequence

The oligosaccharide(s) was permethylated and analyzed directly by EIMS and FABMS. The "A" series of ions are shown below. In addition to the "A" series of ions, FABMS displayed the molecular species ($[M+H]^+$ m/z 1249) and two prominent elimination-type ions ("Elim" ions are indicated by asterisks):

Mass Spectra of the *N, O*-Permethylated Oligosaccharide Isolated from the Hydrolyzate (60% Aqueous Hydrofluoric Acid) of Pneumococcal Capsular Polysaccharide Type 19B

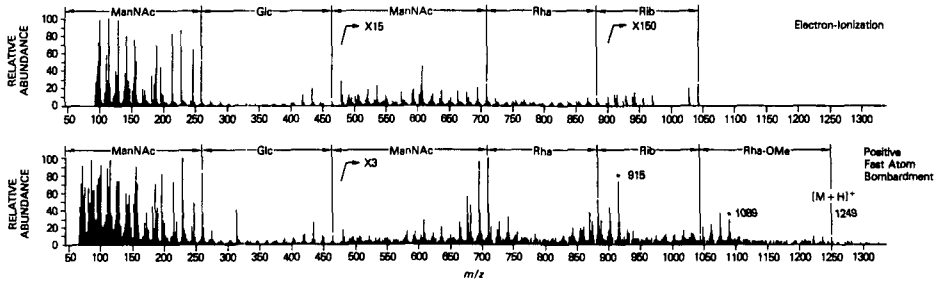

Another series of "A" ions are also evident, thus indicating the presence of another oligosaccharide. The results here and from methylation analysis would suggest that the isolated oligosaccharide is actually a mixture of oligosaccharides whose overlapping sequences might allow postulation of the chemical structure of the repeating oligosaccharide:

←Glc—ManNAc—Rha—Rib—Rha—ManNAc—Glc—ManNAc—Rha—Rib—Rha—ManNAc—Glc—ManNAc→

STRUCTURAL ELUCIDATION OF CONSTITUENT FATTY ACIDS AND ALCOHOLS FROM RAT MEIBOMIAN GLAND SECRETION USING GC/MS OF THEIR PICOLINYL AND NICOTINATE DERIVATIVES

D.J. Harvey, J.M. Tiffany and J.M. Duerden

University Department of Pharmacology, South Parks Road, Oxford, OX1 3QT,

and

Nuffield Department of Ophthalmology, University of Oxford, Walton Street, Oxford, UK.

The meibomian glands, which are found on the outer margins of the eyelid, produce an oily secretion over the surface of the eye to prevent evaporation of the tear film. The secretion consists of a complex mixture of wax and sterol esters, whose composition is both species and subject dependent. Structural elucidation of constituent fatty acids and alcohols by GC/MS can be accomplished using fragmentation-directing derivatives; this paper reports the use of nicotinate (1) and picolinyl esters (2) for studies of the alcohols and acids respectively from rat meibomian secretions.

The secretions were collected from male Wistar rats, hydrolysed with ethanolic KOH and converted into TMS, methyl ester/TMS, nicotinate/TMS and picolinyl/TMS derivatives. In addition, fractions were reduced with lithium aluminium deuteride and the resulting alcohols were examined as nicotinate/TMS derivatives. GLC data were recorded for TMS and Me/TMS derivatives with a Hewlett-Packard 5890A gas chromatograph fitted with a flame-ionization detector, a 50 m x 0.32 mm OV-1 bonded-phase fused silica capillary column and a Hewlett-Packard 3390A recording integrator.

GC/MS data of all derivatives were recorded at 25 eV with a VG Micromass 12B mass spectrometer interfaced to a VG 2050 data system and via a glass jet separator to a Varian 2440 gas chromatograph which was fitted with a 2 m x 2 mm glass column packed with 3% SE-30 on 100 - 120 mesh Gas Chrom Q.

Fig. 1 shows a gas chromatogram of constituent fatty acids and alcohols from rat meibomian secretions as TMS derivatives on the 50 m fused silica capillary column.

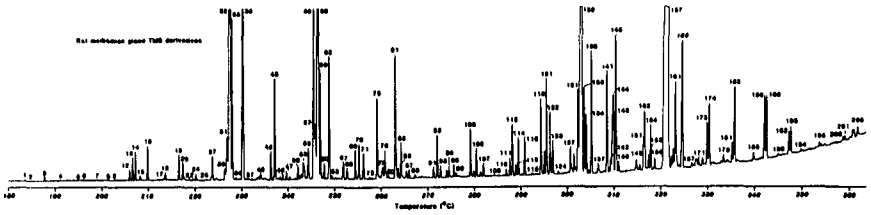

Fig. 1. Gas chromatogram of constituent fatty acids and alcohols from rat meibomian lipids separated on a 50 m bonded-phase OV-1 fused silica capillary column.

Both the nicotinate and picolinyl derivatives of the alcohols and acids respectively gave mass spectra consisting of a series of fragment ions produced by radical-induced cleavage of the aliphatic chains. These gave clear indication of the position of methyl branch-points and double bond position. This can be seen from Figs. 2 and 3 which show the 25 eV mass spectra of the picolinyl and nicotinate derivatives of iso-hexacosanoic acid and iso-hexacosanol respectively from the lipid extract.

A particularly useful technique was found to be reduction of the extract with lithium aluminium hydride and preparation of the nicotinate derivatives of the resulting alcohols. This produced a less complex chromatogram by removing peaks produced by fatty acids. Information on the fatty acid structure was not lost if lithium aluminium deuteride was used in place of the hydride; reduction of the acids proceeded with incorporation of two deuterium atoms.

By the use of these techniques, over 100 individual compounds, amounting to over 95% of the total constituents, were identified. The acids and alcohols had straight, branched (iso and anteiso) and unsaturated (omega-7 and omega-9) chains with lenghts from C_{12} to C_{34}. Cholesterol was the major steroid (Peak 157, 24.7%). Fatty acids showed a biphasic profile with major acids at C_{16} (Peaks 32, 33 and 35) and C_{18} (Peaks 56 - 62) with another group of acids in the C_{25} and C_{26} region (Peak 131 = anteiso-C_{25} and Peak 141 = iso-C_{26}). The major alcohol (Peak 132) was iso-C_{26}-OH (10.3%). Major compounds are listed in Table 1.

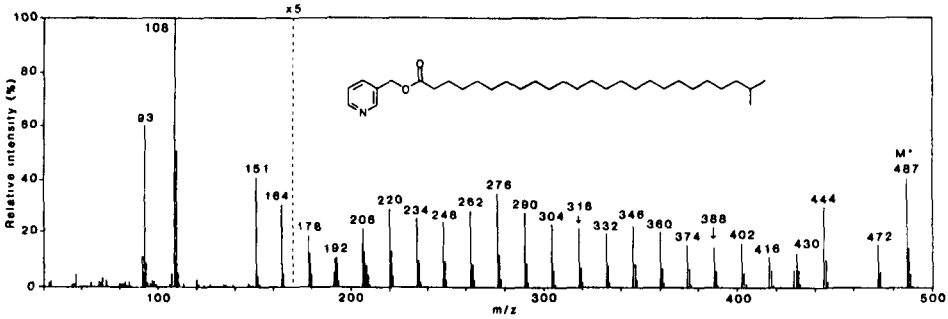

Fig. 2. 25 eV Mass spectrum of the picolinyl derivative of iso-hexacosanoic acid from rat meibomian gland hydrolysate.

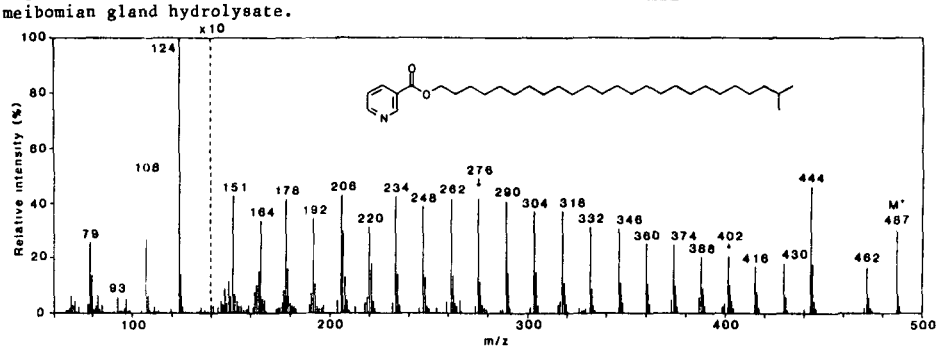

Fig. 3. 25 eV Mass spectrum of the nicotinate derivative of iso-hexacosanol from rat meibomian gland hydrolysate.

TABLE 1

Major acids and alcohols identified from hydrolysed rat meibomian gland lipid

Acids	Peak	%	Alcohols	Peak	%
n-16:1-delta-7	32	7.7	n-20:0	73	0.9
n-16:1-delta-9	33	1.5	i-24:0	112	0.6
n-16:0	35	4.0	n-24:1-delta-17	114	0.4
ai-17:0	43	1.1	n-24:0	116	0.4
i-18:0	56	2.7	i-25:0	121	1.1
n-18:1-delta-9	58	7.3	ai-25:0	122	0.7
n-18:1-delta-11	59	1.0	i-26:0	132	10.3
n-18:0	62	1.4	n-26:1-delta-17	133	0.9
i-20:0	81	1.5	n-26:1-delta-19	134	0.6
i-24:0	119	0.9	n-26:0	136	1.4
ai-25:0	131	1.1	ai-27:0	145	1.7
i-26:0	141	1.2	i-28:0	152	0.7
n-28:1-delta-21	161	1.2	n-28:0-delta-21	154	0.5
n-30:1-delta-23	182	1.0	n-30:0-delta-23	174	0.7
n-32:1-delta-23	192	0.8	n-32:0-delta-23	188	0.8
n-32:1-delta-25	193	0.3	n-32:0-delta-25	189	0.7

The profile was qualitatively similar to that from human meibomian secretion but with small differences in the relative concentrations of many of the individual constituents. Full details of the composition of both of these secretions will be published.

This work was supported by the Wellcome Trust.

1. W. Vetter and W. Meister, Org. Mass Spectrom., 1981, 16, 118.
2. D.J. Harvey, Biomed. Mass Spectrom., 1982, 9, 33.

QUANTITATIVE ANALYSIS OF PHOSPHOLIPID MOLECULAR SPECIES BY THEROMOSPRAY LC/MS.

Hee-Yong Kim and N. Salem, Jr.

Section of Analytical Chemistry, Laboratory of Clinical Studies, DICBR, NIAAA, Bethesda, MD 20892.

Phospholipids are one of the principal components of biological membrane and consists of several major classes each containing a variety of fatty acids. Since the physical and chemical properties of cell membranes are dependent upon the molecular species present, it is of great value to develop efficient analytical procedures for their quantitative analysis.

We have previously reported methods for separating and identifying phospholipid molecular species using thermospray LC/MS (1,2). Our current interest is focused on quantification of each molecular species in order to develop a fast and convenient method for compositional analysis of biological samples. Using LC conditions previously described (methanol-hexane-0.1M ammonium acetate 500:25:25), the linearity of the response was examined for various synthetic molecular species of phosphatidylcholines (PC). Since diglyceride ions were the base peaks in phospholipid spectra (an example is shown in Figure 1) quantification was performed based on these ions. This approach was particularly advantageous since it enables quantification even when the separation was not complete. Figure 2 shows the linear range of response using area measurement of di16:0-PC species with (2b) or without (2a) a column (4.6mm x 7.5cm, 3u, Altex Ultrasphere-ODS). The absolute amounts of phospholipids were determined by phosphorous assay (3). The response was reproducible when the vaporizer tip temperature and source temperature remained constant (148°C and 300°C, respectively; filament current was 0.2mA).

The linear range without a column was 0.04 to 8 nmoles, and with a column 0.1 to 10 nmoles. Above about 8-10 nmoles of phospholipid the slope of the response curve increased rapidly. This suggests that high phospholipid concentrations cause enhancement of ionization efficiency, although the enhanced response for large amount of sample is commonly observed in quadrupole instruments. When high concentrations (1M) of ammonium acetate are used in the mobile phase, the enhancement starts earlier in the curve (Figure 2a, line A) resulting in the narrowed linear range.

The calibration curves were prepared with a column using di-$^{2}H_{30}$-16:0-PC as an internal standard since its retention time was similar to those of the compounds of interest. As shown in Figure 3, between 1-10 nmoles the response was linear for various PC's. These calibration curves were employed to quantify the egg-PC and the results are shown in Table 1 along with the fatty acid composition by GC analysis after transmethylation. For quantification of the 18:0 18:2 species the calibration curve of the di18:1-PC was employed, since 16:0 20:4- and di18:2-PC (which have the same chain length and the number of double bonds) produced the same calibration curves. The calibration curve for the 18:0 20:4 species was very similar to that of the 16:0 20:4-PC. Since 16:0 18:2-PC was not available, the calibration curve of 16:0 18:1-PC was employed to quantity this species. The fatty acid composition was calculated from the LC/MS data and was compared to the GC data. The discrepancy between LC/MS and GC data was presumably due to the 18:1 18:2, 16:0 22:5, 18:0 22:5, 16:0 22:6 and 18:0 22:6 species. These could not be determined by this technique since the standards were not available, however, they were observed by the full scan mass spectrometric analysis.

1. H. Y. Kim and N. Salem, Jr. Anal. Chem. 1986, 58, 9-14.
2. H. Y. Kim and N. Salem, Jr. Presented at the 37th Pittsburgh Conference and Exposition on Analytical Chemistry and Applied Spectroscopy, Atlantic City, NJ, March 1986.
3. G. J. Nelson, In "Blood Lipids and Lipoproteins: Quantiation, Composition and Metabolism"; G. J. Nelson Ed.; Wiley-Interscience, New York, 1972.

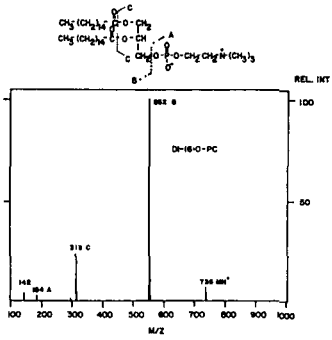

Figure 1. Thermospray mass spectrum of di16:0-PC. Diglyceride ion at m/z 522 is the base peak and monoglyceride ion is shown at m/z 313. Molecular ion was also detected at m/z 735 along with the ions from the head group at m/z 184 and 142.

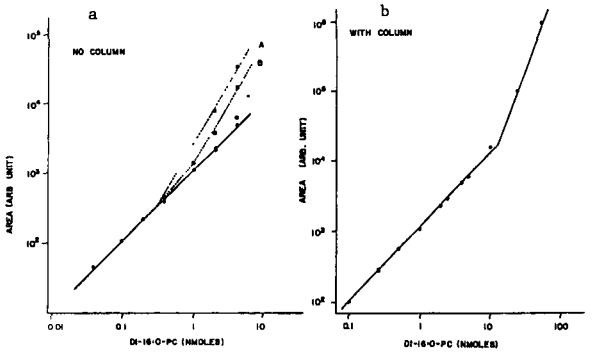

Figure 2. Response curves of di16:0-PC without (2a) or with (2b) a column (3u, Altex, Ultrasphere-ODS, 4.6 mm x 7.5 cm). The mobile phase was methanol: hexane:0.1M ammonium acetate (500:25:25). Data were obtained by selected ion monitoring of diglyceride ion (551.5 amu). Line A in 2a represents the response curve using 1M ammonium acetate in the mobile phase while Line B was obtained from the di16:0-PC diluted in the mobile phase containing 1M ammonium acetate.

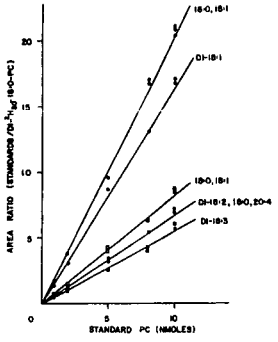

Figure 3. Calibration curves of various synthetic PC's obtained by selected ion monitoring using di-$^{2}H_{30}$-16:0-PC as an internal standard. The chromatographic conditions were the same as in Figure 2b.

Table 1. Molecular Species of Egg Phosphatidylcholines

Molecular Species (29 nmoles injected)		Fatty Acid Composition	LC/MS n/n%	GC w/w%	LC/MS Normalized w/w%	GC Normalized w/w%
16:0, 18:1	9.9 nmoles					
16:0, 18:2	4.0 nmoles					
18:0, 18:1	1.5 nmoles	16:0	25.2	23.9	34.3	31.2
di 18:1	1.3 nmoles	18:1	24.1	26.3	36.3	34.4
18:0, 18:2	1.5 nmoles	18:2	9.5	12.8	14.2	16.7
16:0, 20:4	0.7 nmoles	18:0	6.9	10.4	10.4	13.6
18:0, 20:4	1.0 nmoles	20:4	2.9	3.1	4.8	4.1
	19.9 nmoles (represented in the species quantified)					

PHOSPHOLIPID/ALKALI ION BINDING STUDIED BY FAB AND 252-Cf PD MASS SPECTROMETRY

Demirev P., Dept. Pharmacology, J.Hopkins Univ., Baltimore MD 21205

The interaction between phospholipids and monovalent alkali cations plays a significant role in bioenergetics, nerve impulse transmission, cell recognition, drug action, etc. It has been studied in recent years by a variety of physical techniques. On the other hand the formation of quasimolecular adduct ions by alkali cation attachment has been observed in all mass spectrometric desorption ionization methods including LSIMS/FAB, PD, FD and LD. LSIMS/FAB has been utilized not only for obtaining molecular weight and structural information but also for investigating properties of compounds in solution. These include dissociation constants of weak acids, enzyme kinetic constants, metal-ligand binding constants[1].

The ability of this mass spectrometric approach to assess the relative affinity of dipalmitoyl phosphatidylcholine (DPPC) towards different alkali cations (Li, Na, K, Rb, Cs) in forming M+Al adduct ions has been addressed in this study. The relative constants were estimated from the ratio of peak intensities of the corresponding protonated and cationized molecules. The results are shown in the table for two different matrices used (glycerol and diethanolamine). Within the limits of the reproducibility of the experiments (30%) there was found no correlation between the alkali cation radius and the relative binding constant, which had been reported by using other physical methods[2]. The dependence of the ratio of protonated versus cationized ions on the relative molar concentration of DPPC and CsI is shown on fig. 1. There is an increase in the Cs attachment with the increase in its relative concentration. The Cs attachment for three phosphatidylcholines with fatty acid substituents with different length - dilauroyl (12:0,12:0), dipalmitoyl (16:0,16:0) and dibehenoyl (22:0,22:0) - has been also examined, comparing FAB spectra of these compounds (run in glycerol, 2.5 nmoles PC : 35 nmoles CsI). The respective ratios are 2.2, 2.3 and 1.8. This suggests there is no substantial difference in the relative affinity of the three compounds towards Cs^+.

DPPC mixed with the corresponding alkali halides has been run on a 252-Cf PD mass spectrometer. The ratio of ion counts for the M+H/M+Al versus the alkali cation radius is plotted on fig. 2. This ratio changes with the increase of the alkali cation radius. The absolute increase of ion counts in the quasimolecular adduct ion peak with the decrease of the first ionization energy of the cation is shown on fig. 3. This is probably a phenomenon related to the desorption ionization process rather than to the nature of interaction between the alkali cation and phospholipid per se.

CATION (AI)	$R = \frac{M+H}{M+Al}$ (average of 4 FAB runs)	
	GLY	DEA
Li	3.5	2.0
Na	4.0	4.1
K	4.2	3.1
Rb	5.1	3.6
Cs	2.9	4.5

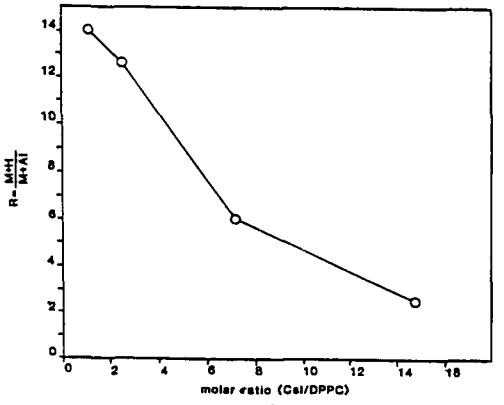

FIG. 1

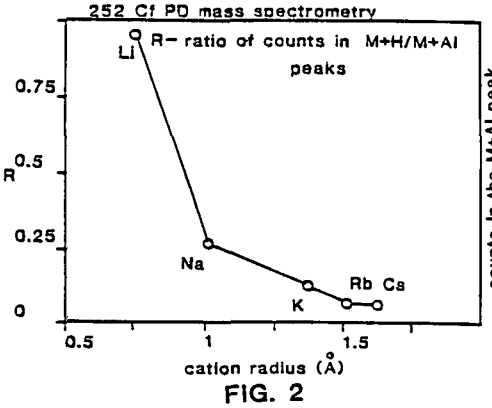

FIG. 2

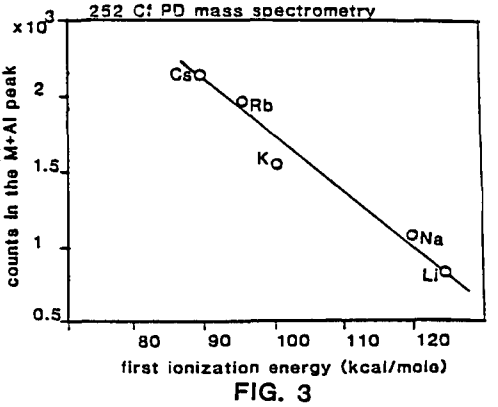

FIG. 3

Acknowledgements: This study has been supported by grants DMB-8515380 from the National Science Foundation and RR02727 from the National Institutes of Health.

References

1. Caprioli R., in "Desorption MS - are SIMS and FAB the same?" (ACS symp. ser. 292 , ed. Ph. Lyon), p. 209, 1985
2. Cserhati T., Szogyi M., Chem. and Phys. of Lipids, 34, p. 93 (1983).

NCI-GC-MS OF FLUORINATED IMINE AND IMIDE DERIVATIVES OF BIOGENIC PHENYLALKYL AND INDOLEALKYL AMINES

David A. Durden
Psychiatric Research Division, Saskatchewan Health,
CMR Building, University of Saskatchewan,
Saskatoon, Saskatchewan, Canada S7N 0W0

The trace amines phenylethylamine (PE), meta- and para-tyramine (mTA and pTA) and tryptamine (T) have been implicated in a variety of psychiatric and neurological disorders. Up to the present the amines have been quantified by high resolution mass spectrometry as their 1-dimethylaminonaphthalene-5-sulfonyl (dansyl) derivatives using deuterium labelled internal standards. The method gives a sensitivity of about 100 pg in physiological samples such as body fluids or (rat) brain regions. To be able to quantify the trace amines in brain subregions or in perfusates a more sensitive method is required and we are investigating the use of NCI-GC-MS.

Straight chain electron capturing derivatives such as pentafluoropropionyl (PFP) or heptafluorobutyryl (HFB) do not have sufficiently intense characteristic ions due to fragmentation. Compounds containing ring structures such as the melatonin spirocyclic PFP derivative (Lewy and Markey) or T as its acetyl-PFP derivative (P. Wood and this lab) exhibit extremely high sensitivity (e.g., T can be detected as low as 160 fg on column). We decided to investigate other electron capturing ring structures in the hope of finding a derivative suitable for analysis of all four trace amines. Ideally the product should have a high electron affinity and concentrate ionization in one ion. If this is the molecular ion discrimination against deuterium labelled internal standards due to isotope effects on fragmentation is avoided.

Equipment. VG 70-70F double focussing mass spectrometer. EI/CI ion source with modified CI slit (0.31 mm). Source temp 140. GC-HP5710 with 6' x 2mm i.d., 3% SP2100 on Supelcoport 80/100; He at 30 ml/min via jet separator. Capillary column, SGE 50m x 0.32 mm DB1, 1 micron bonded phase inserted into the ion source.

DERIVATIVES

Amine Derivatives
- N-pentafluoropropionyl (PFP)
- N,N-acetyl-pentafluoropropionyl (Ac-PFP)
- N-heptafluorobutyryl (HFB)
- N,N-acetyl-heptafluorobutyryl (Ac-HFB)
- N-pentafluorosuccinimide (PFS)
- N-pentafluorobenzylimine (PFBI)
- N-pentafluorobenzoyl amide (PFBzO)
- N-pentafluorobenzene sulfonyl ($PFBzSO_2$)

Phenol Derivatives
- O-trimethylsilyl (TMS)
- O-t-butyldimethylsilyl (TBDS)
- O-acetyl (O-Ac)
- O-pentafluoropropionyl (O-PFP)
- O-heptafluorobutyryl (O-HFB)

RESULTS

Perfluoroacyls. The straight chain PFP and HFB derivatives gave NCI spectra with prominent M-HF ions for PE and both M-HF and M-2HF ions for T. The spectra of mTA and pTA, however, contained ions of relatively low intensity due to extensive fragmentation.

Acetyl-PFP and acetyl-HFB. The NCI spectra of PA, mTA and pTA again contained several ions M-HF, M-2HF and M-HF-Ac all of relatively low intensity. Tryptamine is initially formed as the N-acetyl-N,N'-di-PFP (or HFB) derivative which cyclizes on column into the spirocyclic structure which exhibits a high electron affinity as the M-2HF ion. These latter appear to be the most sensitive derivatives for T.

Perfluorosuccinimides. Reaction of perfluorosuccinic anhydride with the amines is very rapid. PE produces a NCI spectrum with prominent M-HF and M-2HF ions. With mTA and pTA, however, further reaction occurs with the phenolic group and the perfluorosuccinate requires further derivatization. Silylation or t-butyldimethylsilylation failed to produce products with suitable spectra.

Pentafluorobenzenesulfonyl. Although the derivatives have been shown to have high electron affinities when used with electron capture GC detectors, they were totally unsuccessful

as the NCI spectra contained ions due only to the pentafluorobenzene-sulfonate fragment m/z 231.

Pentafluorobenzylimines. The pentafluorobenzylimine of PE appeared to be promising since the ionization is concentrated into the M^- ion. Similarly O-TMS-N-pentafluorobenzylimines of mTA and pTA produce M^- ions. Unfortunately the electron capture cross sections are comparatively low and both mTA and T form several products including cyclized dihydroisoquinolines and beta-carbolines.

Pentafluorobenzoyl. Pentafluorobenzoyl derivatives appear to have very high electron affinities with PE as the M-HF ion being the most sensitively detected compound even though several other fragment ions are formed. This derivative appears to be a suitable derivative for PE. T may be detected also as the M-HF ion. mTA and pTA may be detected as O-TMS or O-Ac derivatives.

N,O acetyl-N-pentafluorobenzoyl. Acetylation of the amino and phenolic functions prior to formation of the pentafluorobenzoyl derivative produces the apparently ideal derivatives for PE, mTA and pTA which exhibit intense M^- ions. The derivative of T, i.e. N-acetyl-N-pentafluorobenzoyl, has somewhat less desirable properties since several ions are formed including the M-HF ion. Attempts to form the spiro-cyclic derivative have failed so far.

Tissue examples. The use of NCI-GC-MS for the analysis of picogram levels of trace amines has been demonstrated through the quantitation of tryptamine as the spirocyclic-PFP derivative. These results are shown in Table 1.

TRYPTAMINE CONCENTRATIONS IN RAT BRAIN REGIONS

	tryptamine picograms	wt. mg	conc. ng/g	Previous values*
Caudate Nucleus	219 ±24	68.3 ±7.9	3.20 ±0.10	2.93 ±1.14
Hypothalamus	60 ±11	14.1 ±1.6	4.28 ±0.51	0.94 ±0.22

Values are means ± S.E.M. This work: NCI GCMS of the tryptamine PFP derivative. 1.28 ng T d_4 internal standard. Tissue from one rat. *Philips, S.R. et al.. 1974. Direct probe HRMS as the dansyl derivative. 25 ng T d_2 internal standard. Tissues from 10 rats were pooled.

CONCLUSION

Use of acetylation followed by pentafluorobenzoyation appears to provide the most sensitive derivatives for PE, mTA and pTA. Acetylation followed by perfluoroacylation appears to be better for T. The tissue values recorded using the latter method are in line with previous data.

REFERENCES

Lewy, A.J. and Markey, S.P. Science (1978) 201, 741-743.
Philips, S.R., Durden, D.A. and Boulton, A.A. Can. J. Biochem. (1974) 52, 447-451.

SELECTIVE ADSORPTION OF PEPTIDES IN PLASMA DESORPTION MASS SPECTROMETRY

P. F. Nielsen and P. Roepstorff
Department of Molecular Biology, Odense University 5230 Odense Denmark

A. G. Craig
Department of Immunology University of Uppsala Box 582 S-75723 Uppsala

The conventional sample application method in 252-CF plasma desorption mass spectrometry (PDMS) has been the electrospray method.[1] This involves dissolving the sample in a relatively volatile solvent followed by electrospraying the solution onto an aluminium foil. Using this technique, many proteins and peptides with molecular masses up to 23 k daltons have been measured[2]. However, many samples of biological origin containing impurities do not produce useful spectra.

Alternative sample preparation methods which increase the utility of PDMS have been developed, which involve adsorption of the sample molecules to a thin film of nitrocellulose[3] or naphion[4]. A similar effect is observed when reduced glutathione is added to the sample solution before spraying[5]. We have found the adsorption to nitrocellulose to be the method of choice for medium to high molecular mass biomolecules (1000 u).

In Figure 1 the different sample application methods are compared. The nitrocellulose adsorption allows an increase in sensitivity of two orders of magnitude. The saturation curves in Figure 2 show that the nitrocellulose is saturated when approximately 100 pmol of porcine insulin is applied to the target. It is also evident that the binding capacity of a nitrocellulose film prepared by dissolving a nitrocellulose membrane in acetone and electrospraying the solution is considerably greater than observed for a solution of nitrocellulose in amylacetate which is not electrosprayed. This presumably is due to a trans-esterification reaction resulting in the formation of cellulose acetate rather than cellulose nitrate.

The pH of the sample solution is of considerable importance for the quality of the mass spectrum. Generally basic peptides give the best PDMS spectra when applied to nitrocellulose and subsequently washed at high pH-valves. Acidic peptides give the best spectra when applied and washed at lower pH valves.

In conclusion the adsorption of larger biomolecules to selective backing materials like nitrocellulose offers several advantages compared to the conventional electrospray sample preparation:

- The removal of alkali metal ions and impurities results in a drastically improved molecular ion yield and thus considerably better sensitivity[3].

- Sample application from dilute solutions is possible simply by dipping the nitrocellulose target into the sample solution. This is a major advantage when using PDMS analysis in practical biochemical work.

- An increased abundance of multiply charged molecular ion species is observed, which facilitates molecular mass determination.

1 McNeal C J Anal Chem 57 (1979) 2036
2 Sundqvist B, Roepstorff P, Fohlman J, Hedin A, Hakansson P, Kamensky I, Lindberg M, Salehpour M and Save G Science 226 (1984) 696
3 Jonsson G, Hedin A, Hakansson P, Sundqvist B, Save G, Nielsen P, Roepstorff P, Johansson K. E, Kamensky I and Lindberg M Anal Chem 58 (1986) 1084
4 Jordan E A, MacFarlane R, Martin C R and McNeal C J Int J Mass Spec Ion Phys 53 (1983) 345
5 Alai M, Demirev P, Fenselau C and Cotter R J Anal Chem in press.

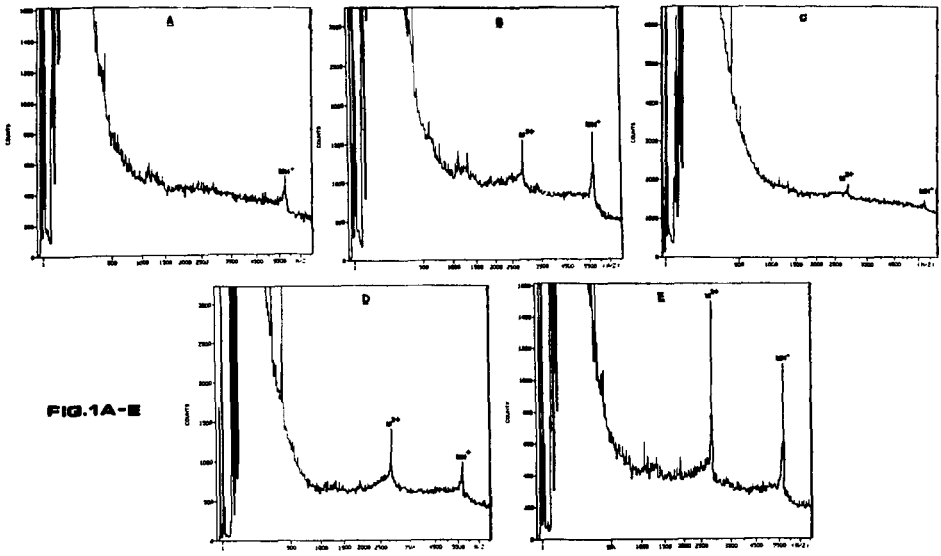

FIG.1A-E

Figure 1A-E PDMS spectra of porcine insulin obtained using different sample application techniques.

A: 10 nmol of porcine insulin applied by the conventional electrospray method
B: 4 nmol of porcine insulin and 25 mM reduced glutathione applied by the electrospray method.
C: 4 nmol of porcine insulin applied to a naphion film backing
D: 1 nmol of porcine insulin adsorbed to nitrocellulose at pH 2.0. Nitrocellulose in amylacetate was used.
E: 1 nmol of porcine insulin adsorbed to nitrocellulose at pH 2.0. Nitrocellulose at pH 2.0. Nitrocellulose in acetone was electrosprayed onto the foil.

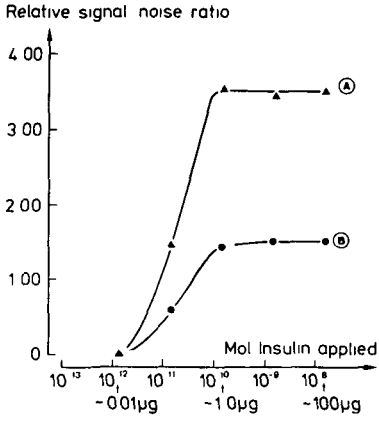

FIG.2

Figure 2 Plot of relative signal: noise ratio of porcine insulin molecule ion versus the amount of sample applied to a nitrocellulose film.

A: Nitrocellulose in acetone electrosprayed film.
B. Nitrocellulose in amylacetate evaporated film.

THE ROLE OF THE MS IN INDOOR AIR QUALITY ANALYSIS

Charlene W. Bayer* and Marilyn S. Black
Georgia Institute of Technology
GTRI/EDL/EHSD
Atlanta, Georgia 30332

Airborne contaminants are outgassed into the indoor environment from a variety of sources including tobacco smoke, carpeting, adhesives, paints, and vinyl flooring. The complexity of the volatile organic mixtures found in the airborne environment presents special difficulties in obtaining meaningful data. Mass spectral analysis is essential for the identification and quantitation of these intricate organic mixtures.

The means of introducing the sample into the GC/MS system can determine the sampling method of the air samples. Three modes of sample introduction are used including thermal desorption, solvent desorption and injection, and gaseous injection. Dynamic or passive sampling on solid sorbents are used for the first two modes. Collection in evacuated bottles such as Summa® polished canisters is the sampling method of choice for gaseous injection. Each sample introduction method has advantages and disadvantages. Thermal desorption requires no sample preparation, but special instrumentation is required. Solvent desorption does not require additional instrumentation and the sample can be repeatedly analyzed, but compounds of interest are diluted by the solvent addition. Gaseous introduction has the best chance of maintaining sample integrity, but requires sample concentration by a procedure such as cryofocusing.

Tobacco smoke is recognized as a contributor to indoor air pollution. Over three thousand compounds have been identified in cigarette smoke including nitrogenous compounds, polyaromatic hydrocarbons, terpenes, alkaloids, etc. Determination of the presence of volatile organic compounds resulting from environmental tobacco smoke, a combination of sidestream smoke and exhaled mainstream smoke, and differentiating it from the volatile organic compounds emitted from other contaminant sources is an ardous task. Dynamic air sampling on Tenax® with subsequent thermal desorption/gas chromatographic/mass spectrometric (TD/GC/MS) analysis was conducted in offices occupied by smokers and nonsmokers (Figure 1). These results were compared to those obtained by sampling sidestream cigarette smoke produced under controlled conditions in a specially designed chamber (Figure 2). Similar volatile organic compounds were detected in smokers' offices which are suspected to have originated from environmental tobacco smoke such as pyrrolidine and methylpyrroles.

Environmental chambers are used to study the emissions from consumer products such as carpeting, vinyl flooring, and room partition panels. Analysis by TD/GC/MS of these products in the chambers revealed parts-per-billion levels of various solvents being outgassed by these products. These solvents included benzene, toluene, 1,1,1-trichloroethane, tetrachloroethene, and xylenes. Contaminant sources are identified by first conducting dynamic sampling in a complaint area, then sampling the emissions from the suspected source in an environmental chamber under controlled conditions which simulate the conditions in the complaint area.

TABLE 1

COMPOUND	CONCENTRATION (PPBV) NONSMOKER	SMOKER 1	SMOKER 2
1,1,1-Trichloroethane	0.07	0.05	0.02
Benzene	0.05	nd	0.01
Trichloroethene	0.03	0.05	0.01
Toluene	0.24	0.19	0.16
o-Xylene	0.05	0.06	0.02
p-Xylene	0.02	0.02	0.01
Octane	0.01	0.01	0.01
Tetrachloroethene	0.01	0.02	0.02

FIGURE 1

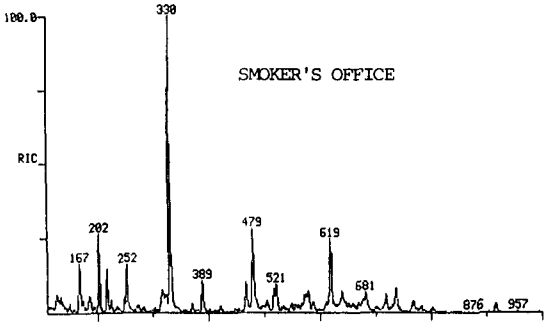
100.0
RIC
330
SMOKER'S OFFICE
202
167
252
389
479
521
619
681
876
957

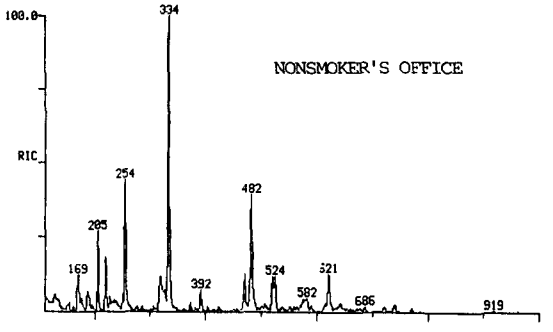
100.0
RIC
334
NONSMOKER'S OFFICE
254
205
169
392
482
524
582
621
686
919

APPLICATIONS OF LC/MS/MS TO THE DETERMINATION OF SULFONATED AZO DYES IN ENVIRONMENTAL SAMPLES: Jack Henion and Andries Bruins, Drug Testing and Toxicology, New York State College of Veterinary Medicine, Cornell University, 925 Warren Drive, Ithaca, NY 14850

Since the environmental ramifications of organic dyes appear to be an unknown, and in view of the current concern over the contamination of ground water, there is a need to develop analytical methodology for screening and characterizing these intractable compounds in addition to those compounds volatile enough for conventional GC/MS techniques. LC/MS and LC/MS/MS could offer the desirable combination of separation and identification.

Voyksner, and Betowski and Ballard, have aptly demonstrated the feasibility of thermospray ionization for LC/MS and LC/MS/MS of non sulfonated azo dyes. In our hands, however, positive and negative ion thermospray using 0.1 M ammonium acetate solutions did not appear to be well suited for mono- and disulfonated azo dyes.

Negative ion atmospheric ionization (API) LC/MS and LC/MS/MS using a heated pneumatic nebulizer, ion evaporation LC/MS, or electrospray LC/MS provided more encouraging results. The heated pneumatic nebulizer LC/MS interface allowed ionization and mass analysis of each of the organic sulfonated azo dyes, while ion evaporation and electrospray LC/MS have provided ionization of these dyes without the use of heat as part of the LC/MS interface. Molecular weight information is obtained in most cases, while in the LC/MS/MS mode structurally useful fragments are obtained which facilitate identification of these dyes. We have also found that in the parent ion LC/MS/MS mode one can monitor the parents of the m/z 80 ion ($SO_3^{-\cdot}$) and readily screen for a wide variety of sulfonated dyes which produce this common fragment ion.

The separation of the various dyes is readily accomplished by reversed-phase HPLC using a gradient of 20% to 60% acetonitrile in 0.1 M aqueous ammonium acetate. Each component is monitored on-line by the Sciex TAGA 6000E API triple quadrupole mass spectrometer.

An example of LC/MS ion current data for the gradient elution separation of five of the monosulfonated dyes is shown in Figure 1,together with an APCI spectrum of the third component. Significantly more structural information is available from LC/MS/MS experiments as shown in Figure 2. This full-scan negative ion LC/MS/MS mass spectrum shows abundant daughter ions from the m/z 377 parent ion including the abundant m/z 80 ion which is characteristic of these sulfonated dyes as noted above. Notice, too, that this LC/MS/MS spectrum includes important ions below m/z 200 which are not usually available from conventional forms of LC/MS.

Figure 3 shows the parent ion spectrum of m/z 80, revealing the $(M-Na)^-$ ion of acid red 88. Figure 4 shows LC/MS and LC/MS/MS by parent ion scanning of m/z 80 applied to a mixture of five monosulfonated azo dyes, isolated by solid phase extraction from Cayuga Lake water, fortified at the 100 ppb level. As expected, the LC/MS/MS experiment provides increased specificity for sulfonated compounds.

At the present time the limit of detection of a monosulfonated azo dye is approximately 100 ng for full scan APCI/LC/MS and 1 µg for full scan APCI/LC/MS/MS, using the heated pneumatic nebulizer interface and a standard 4.6 mm column. The sensitivity quoted is for a recognizable peak in the TIC trace.

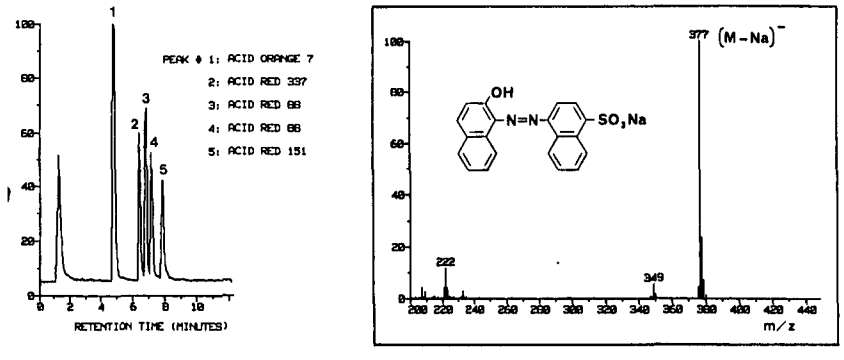

Figure 1

Electrospray combined with microbore LC (1 mm x 10 cm column, 3 μm, C18, Shandon) was significantly more sensitive. We have found that a high concentration of ammonium acetate dramatically reduces the sample ion current of mono and disulfonated azo dyes observed by electrospray, ion evaporation and thermospray in an API source.

This work was carried out under cooperative agreement with the Environmental Monitoring and Support Laboratory (EMSL, Cincinnati, Oh.) of the EPA, grant No. CR-S11661-10-0. We acknowledge the assistance of Dr. W.L. Budde during the course of these investigations.

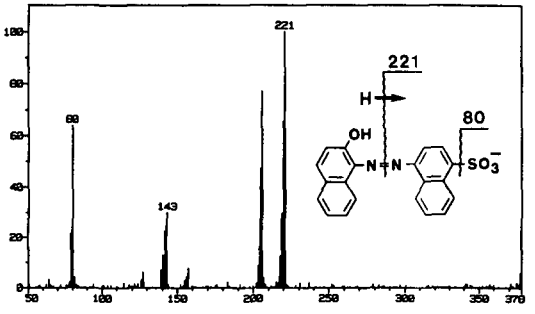

Figure 2

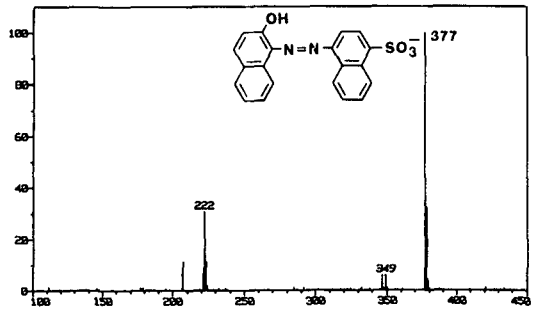

Figure 3

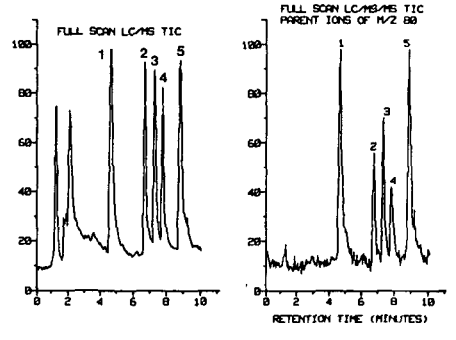

PEAK # 1: ACID ORANGE 7
2: ACID RED 337
3: ACID RED 88
4: ACID RED 88
5: ACID RED 151

Figure 4

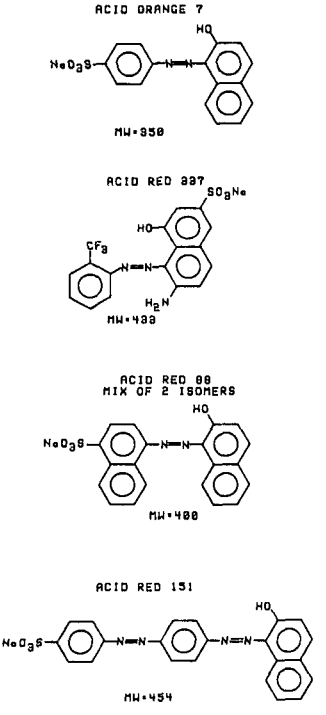

Evaluation of the Bioavailability of Chemicals to Fish Using GC/MS and LC/MS

Douglas W. Kuehl, Brian C. Butterworth, Lawrence P. Burkhard and Kenneth L. Johnson

U.S. Environmental Protection Agency
Environmental Research Laboratory-Duluth
6201 Congdon Boulevard
Duluth, Minnesota 55804

Abstract

During the past few years ERL-Duluth has been involved in research on the bioavailability potential of polyhalogenated chemicals from solid matrices, i.e., fly ash, sediment, and industrial sludge, to freshwater fish. The specific class of chemicals we are interested in are the planar aromatic chemicals, primarily because 2,3,7,8-TCDD is a member of this class. One of the most important parameters in the study of the uptake of chemicals by fish is the octanol-water partition coefficient (Kow). A linear relationship has been demonstrated between Log Kow and Log BCF (bioconcentration factor) for Log Kow 3 to 6. However, chemicals with Log Kow > 6 often deviate from this linearity to appear to have reduced uptake. This paper will discuss some of the mass spectral techniques developed at ERL-D for the study of bioavailability potential, and finally present some data from laboratory and environmental samples.

Reverse-phase high performance liquid chromatography has been used by many research groups to predict Log Kow. Generally a UV detector is used for these analyses. We have recently published a technique to estimate Log Kow using the mass spectrometer as a universal detector[1]. A belt drive interface was used which allowed electron impact ionization. Log Kow of a series of tetrachlorinated planar aromatics was estimated using this technique[2]. This information is being used to develop models to predict bioavailability potential.

There are two very important considerations for GC/MS analyses of PCDD/PCDF in bioavailability studies: 1) Instrumental QA requirements, and 2) Availability of analytical standards. Current analytical procedure/QA plans require the measurement of 6 parameters, 4 at the time of analyses, and 2, column performance and mass resolution, either after or before analyses. We have developed techniques to measure both of these parameters also during the analyses. A dual internal standard of $^{13}C_6$ 1,2,3,4-TCDD and $^{37}Cl_4$ 2,3,7,8-TCDD in a mixture of 21 TCDDs (not including 2,3,7,8-TCDD) is used to determine column performance and mass spectrometer resolution setting. The use of both internal standards spiked into each sample can then be used to evaluate these parameters during the analysis of each sample[3].

Another extremely important QA parameter is the determination of the mdL when 2,3,7,8-TCDD is not detected. We have previously demonstrated that fish accumulate only 2,3,7,8-TCDD, even when exposed to all 22 TCDDs[4]. We, therefore, add natural 1,2,3,4-TCDD to each sample at a level just above the target mdL, and using TCDD ions demonstrate that a natural TCDD can be detected at the mdL.

An analytical standard of all biosignificant PCDD/PCDF was developed at ERL-D by exposing carp (10 of 10 g each) to the organic solvent extract of municipal incinerator fly ash, and preparing an analytical standard extract from the PCDD/PCDF fraction of our sample cleanup procedure[5]. Characterization of the extract was done by a GC retention time comparison of fly ash extract, and literature values[6]. Additional fish exposed to fly ash (1000 mg) during a 60-day flow-through test, were then analyzed using the biosignificant standard. Results indicate that the Bioavailability Index (level of analyte in fish to level in solid) is nearly the same for PCDDs and PCDFs of the same degree of chlorination, and that the BI decreases with increasing degree of chlorination[7].

Laboratory fish exposed to Petenwell Reservoir, Wisconsin River, sediment (2,3,7,8-TCDD at 39 pg/g) accumulated 7.5 pg/g after 60 days, and subsequently depurated 32% after being held in clean water for 205 days. On a per gram of lipid basis the uptake represents 40% of the value seen in large Petenwell carp. The percent depurated is equivalent to that depurated from 3 Kg Petenwell carp held at ERL-D in 6000 gal. tanks for 1 year. Analysis for all PCDD/PCDF in the large depuration fish indicated that PCDFs are depurated faster than PCDDs and that the rate of depuration decreases with increasing degree of chlorination[8].

As a result of our analyses of nearly 600 fish samples for the U.S. EPA National Dioxin Study, we observed a correlation between TCDD contaminated fish and the location of pulp and paper plants on the rivers sampled for fish analyses, and predicted the pulp/paper, in particular the Kraft process plants, to be a major source of PCDD/PCDF in the aquatic environment. Analysis of pulp/paper mill sludge showed levels from 1-5 pg/g to over 400 pg/g (dry weight)[9]. These analyses were very difficult by GC/MS because of very high levels of contamination by tetrachloroxanthenes (1) which require > 18,000 to

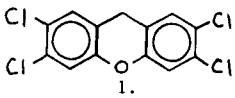

1.

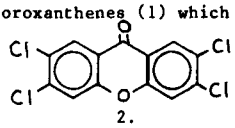

2.

mass resolve from TCDD, and tetrachloroxanthones (2) which require > 8,500 to mass resolve from $^{13}C_{12}$ TCDDs. TCX levels of contamination in sludge exceeded 40,000 pg/g, and they could be found in sediment and fish from rivers on which pulp/paper mills were located.

References

1. Burkhard, L.P., Veith, G.D. and Kuehl, D.W. Chemosphere 14(10):1551 (1985).
2. Burkhard, L.P. and Kuehl, D.W. Chemosphere 15(2):163 (1986).
3. Kuehl, D.W., Butterworth, B.C. and Johnson, K.L. Anal. Chem., July (1986).
4. Kuehl, D.W. et al. Chemosphere 14(5):427 (1985).
5. Kuehl, D.W. et al. Manuscript in preparation (Chemosphere).
6. Rappe, C. Environ. Sci. Technol. 18(3):78A (1984).
7. Kuehl, D.W. et al. Manuscript in preparation (Chemosphere).
8. Kuehl, D.W. et al. Manuscript in preparation (Chemosphere).
9. Kuehl, D.W. et al. Manuscript in preparation (Chemosphere).

TRACING GROUND WATER CONTAMINATION WITH A STATIC COLLECTION DEVICE AND MS

Kent J. Voorhees, Michael Malley, James Hickey,
Ronald W. Klusman and William W. Bath
Petrex and Colorado School of Mines, Golden, CO 80401
and Martin Marietta, Columbus, MD 21045

Conventional methods of measuring volatile organic compounds (VOC) in the vadose zone requires the collection of grab soil gas samples or soil samples. Grab soil samples have the disadvantage of being an instantaneous sample which cannot be easily corrected for changes in soil gas flux caused as a result of meteorological influences. Using the soil samples can reduce the effect of the meteorological parameters by the soil serving as an integration media for the gases. However, soil is a complex and highly variable material which can lead to differences in integrating ability based on soil type.

A new static collector, shown in Figure 1, has been designed to serve as an efficient integrator for VOC's (1). The device is placed in a shallow hole dug in the soil and left in place for about a week. Laboratory experiments have established 10^{-4} torr as the vapor pressure requirement for a compound to be efficiently trapped. After removal from the field, the VOC's are desorbed by placing the wire into a Curie-point mass spectrometer. Low-energy electron ionization (15eV) is used to minimize fragmentation. About 50 scans collected during the desorption process are summed together to represent a fingerprint of the soil gases. Mapping of specific ions representing a given compound is done by computer.

Over 20 surveys have been conducted using the static collection device. A variety of compounds, including phenols, chlorinated hydrocarbons, aromatic hydrocarbons, pesticides and aliphatic hydrocarbons have been trapped and analyzed using the static collector device with MS. As an example of a survey, the following case study concerning the location and extent of contamination of trichloroethylene (TCE) is presented. The study is on the extreme west flank of the Denver Basin near the base of the southern Rocky Mountain Front Range. The ground water in the area is at a depth of about 30 feet. Previous analysis from a limited number of wells established the TCE concentrations from 5ppb to 2000ppb.

Figure 2 shows the relative flux values of TCE vapors measured in the near surface using the static collector. The areas with high flux values corresponded to the water samples with the highest TCE concentrations. Based on the geology and well water analysis, Figure 3 was constructed to show the relationship of the ground water accumulations and the surface flux. This study shows that the static trapping MS method is useful in inferring the extent and apparent direction of contamination where hydrological data exists.

REFERENCES

1. Voorhees, K.J., Hickey, J.C. and Klusman, R.W., 1984, Analysis of Ground Water Contamination by a New Surface Static Trapping/Mass Spectrometry Technique, Analytical Chemistry, v. 56, pp. 2602-2604.

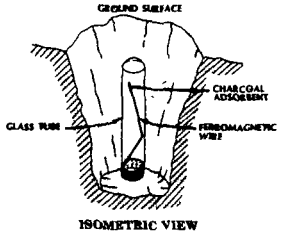

Figure 1 Schematic diagram of static collector used for trapping volatile organic compounds

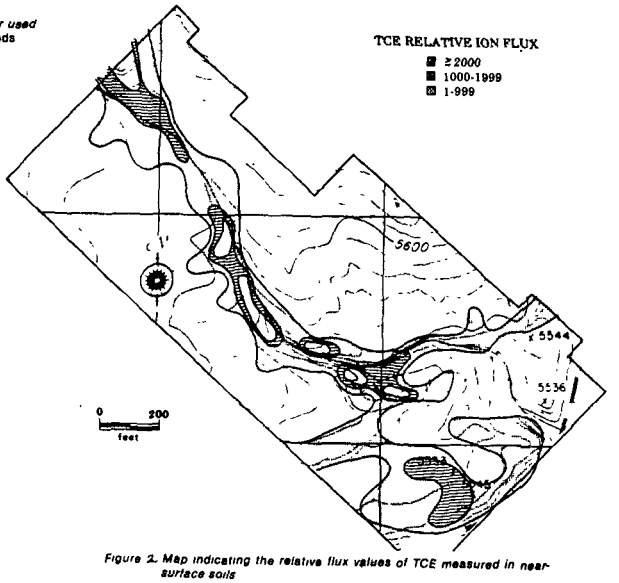

Figure 2. Map indicating the relative flux values of TCE measured in near-surface soils

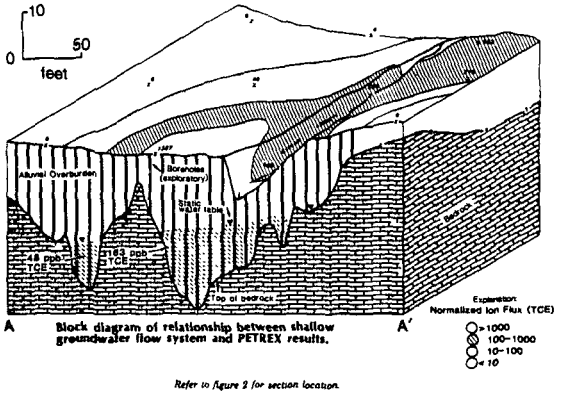

Refer to figure 2 for section location.

Figure 3. Block diagram along Section A-A' showing relationship between shallow ground water flow system and Petrex results

ENHANCED LSIMS PERFORMANCE USING A SUB-AMBIENT SAMPLE PROBE

A.M. Falick, F.C. Walls and R.A. Laine[a]
Mass Spectrometry Resource
Department of Pharmaceutical Chemistry, University of California
San Francisco, California 94143-0446

Recent advances in ion source technology for liquid secondary ionization mass spectrometry (LSIMS) have resulted in significant improvements both in sensitivity and sample lifetime (1,2). The most recent work (2) led to the conclusion that sample heating resulting in rapid matrix evaporation was a major cause of short sample lifetime, particularly with unfocused neutral fast atom primary beams. A new sample probe was therefore constructed to allow controlled cooling of the target during ionization.

The sample probe was fabricated according to the design shown in Figure 1. Although the probe was specifically designed for our mass spectrometer (MS-50) and ion source (2), only minor changes in the design would be required to adapt the probe to other mass spectrometers employing either neutral or ionic primary beams. The sample end of the hollow probe shaft is threaded to receive a polyimide (Vespel SP-1) insulator to which is attached a copper heat sink. The insulator serves to electrically isolate the sample tip from the probe shaft and also to reduce heat conduction from the shaft to the heat sink and tip. The joints between the heat sink, the insulator and the shaft are fitted with Viton O-ring seals. A small Teflon tube is inserted through the handle and shaft and terminates in a small chamber inside the heat sink. Freon coolant can be injected into the heat sink from a pressurized cannister as needed. The probe temperature is monitored by means of a thermocouple mounted on the ion source block. The probe tip can be maintained at any temperature between about -7°C and room temperature within about ± 2°C.

As an example of the performance of the cooled probe, Figure 2 is a graph of the intensity of the largest peak in the molecular ion cluster of peracetyl $[Glu(\beta 1\rightarrow 3)]_7$glucitol (PAG8) (m/z 2452.7) as a function of time, both with and without cooling. Approximately 20 μg of PAG8 were combined with tetraglyme on the probe tip and the molecular ion region was scanned repetitively. Occasional minor adjustments of probe position were carried out to maintain maximum total ion current (beam monitor). The probe tip temperature was kept at 9 ± 1°C when cooling was used; the tip temperature in the absence of cooling was 21.5 ± 0.5°C. The "background" signal is the average intensity of several peaks near the MH^+ peak but not related to it. The "chemical noise" or background in the entire spectrum was approximately proportional to the specific background peaks measured. A fuller discussion of this work will be published soon (3).

The most striking feature of Figure 2 is the greatly increased longevity of the sample spectrum when cooling was used. The cooling technique provides a long, relatively steady signal so that tune-up and acquisition of several long scans was easily possible with one sample loading. Alternatively, signal averaging could easily have been carried out over a large mass range. Such longevity is also essential for MS/MS experiments, where fragment ion scans may be desired for several ions in the primary spectrum. It should also be noted that sensitivity is substantially improved by the cooling technique. If sensitivity is calculated as the number of protonated molecule ions produced per microgram of sample placed on the probe tip, then a comparison of the areas under the two solid curves in Figure 2 shows that cooling results in approximately a ten-fold increase in sensitivity.

As a second example, we were able to obtain the spectrum of maltoheptaose using a matrix consisting of a 50/50 mixture of DMSO and water. The probe tip was maintained at a temperature of -4°C. At this temperature the spectrum lasted for several minutes. At room temperature, it was not possible to obtain any spectrum in this matrix.

[a]Department of Biochemistry, Louisiana State University, Baton Rouge, Louisiana 70803

In summary, the use of a cooled probe has two main advantages: First, in fairly volatile matrices such as thioglycerol, tetraglyme and sulfolane, the spectrum lifetime can be extended by a factor of 10. Second, matrix materials that are not possible to use at all at room temperature can now be routinely employed.

References

1. W. Aberth, K.M. Straub and A.L. Burlingame, Anal. Chem. (1982) 54, 2029.

2. a) A.M. Falick, G.H. Wang and F.C. Walls, presented at 33rd Ann. Conf. Mass Spectrom. and Allied Topics, San Diego, June, 1985. b) A.M. Falick, G.H. Wang and F.C. Walls, Anal. Chem., in press (June, 1986).

3. A.M. Falick, F.C. Walls and R.A. Laine, Anal. Biochem., submitted.

Acknowledgements

The sample of PAG8 was obtained from J. Rush and J. Kuc, Dept. of Plant Pathology, University of Kentucky. This work was supported by the NIH Division of Research Resources, Grant RR01614 (A.L. Burlingame, principal investigator) and NIH Grant GM25394 to R.A.L.

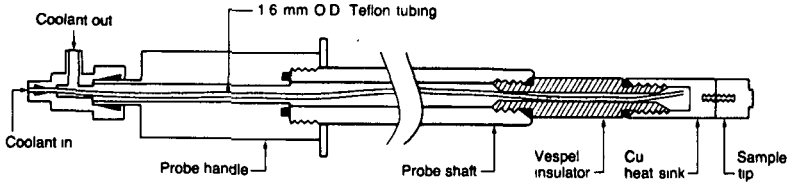

Figure 1. Diagram of coolable sample introduction probe.

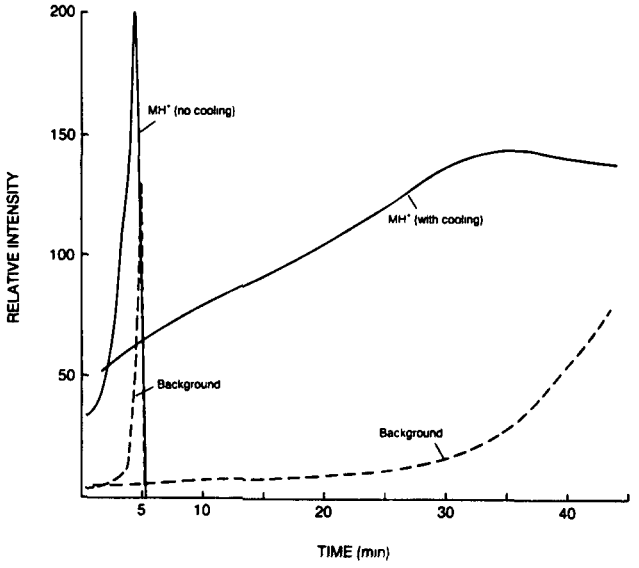

Figure 2. Intensity of the most intense ion in the MH^+ cluster in the mass spectrum of PAG8 as a function of time, with and without cooling (solid line). The corresponding background peak intensity is also shown (dashed lines).

COMPARISON BETWEEN GAS PHASE AND LIQUID PHASE IONIZATION FOR LC/MS/MS USING AN ATMOSPHERIC PRESSURE ION SOURCE, Andries Bruins, Thomas Covey and Jack Henion, Drug Testing and Toxicology, Cornell University, 925 Warren Drive, Ithaca, New York 14850.

One of the earliest reports on LC/MS demonstrated the use of an atmospheric pressure ionization (API) source (1). API has not been developed further for LC/MS since API sources have not been commercially available from the manufacturers of analytical mass spectrometers. One of the disadvantages of API mass spectrometers has been the extensive clustering of sample ions with polar molecules such as water, ammonia and others, which are the main components of a reversed-phase LC effluent. The Sciex TAGA 6000E is a triple quadrupole mass spectrometer equipped with an API source in which ions are drawn through a nitrogen curtain prior to being admitted into the ion sampling orifice. Clustering is prohibited for the most part, and final declustering takes place by acceleration and collisions during the free jet expansion into the vacuum system of the mass spectrometer.

Ionization of a sample dissolved in the eluent from an LC can take place either in the gas phase or in the liquid phase:

gas phase ionization	liquid phase ionization
solution	solution
↓	↓
droplets	charged droplets
↓	↓
desolvate	reduce size
↓	↓
dry sample	strong el. field
↓	↓
ionize by ion/molecule reactions	sample ions escape from liquid

Gas phase ionization is conveniently accomplished by the use of a heated pneumatic nebulizer combined with atmospheric pressure chemical ionization by a corona discharge. We have produced singly charged negative ions of mono and disulfonated azo dyes, corresponding with the molecular weight ($[M-H]^-$ of the free acid).

The crucial steps in liquid phase ionization are formation of a charged aerosol beam and the emission of ions from small droplets. We have produced charged droplets in air or nitrogen at atmospheric pressure by thermospray, by a pneumatic nebulizer plus induction electrode (2) (Sciex ion evaporation interface) and by a homemade electrospray LC/MS interface, (3) in which the electrospray process is assisted by pneumatic nebulization. In each case we were able to observe multiply charged ions, which could not be generated in the gas phase process. Thus, disulfonated azo dyes produced the $(M-2H)^{2-}$ ion of the free acid. Contrary to the gas phase process, liquid phase ionization of disulfonated azo dyes hardly produced singly charged negative ions.

An important observation in all three liquid phase ionization methods was the strong suppression of sample ion current of ionic samples (such as sulfonated azo dyes) when 0.1 M ammonium acetate is present in the LC eluent. The emission of sample ions from the liquid is apparently hindered by a high electrolyte concentration. In the case of sulfonated azo dyes we have found that 0.001 M ammonium acetate can sufficiently improve chromatographic peak shapes, without impairing the ionization process. Our findings support the recommendation that thermospray ionization of ionic samples in a low pressure ion source be carried out without the use of ammonium acetate (4).

This work was carried out under cooperative agreement with the Environmental Monitoring and Support Laboratory (EMSL, Cincinnati, Oh.) of the EPA, grant No. CR-S11661-10-0. We acknowledge the assistance of Dr. W.L. Budde during the course of these investigations.

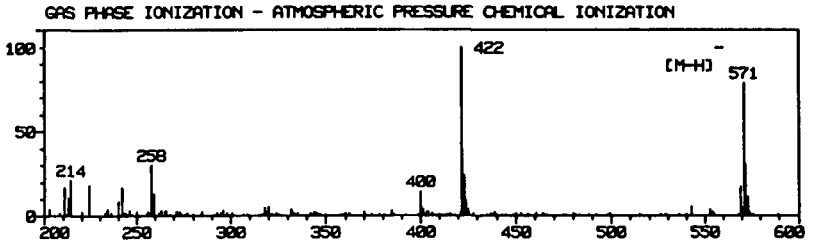

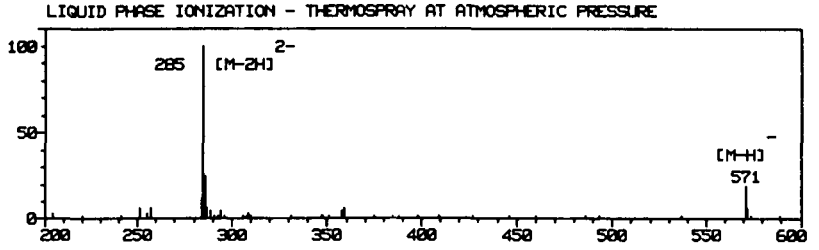

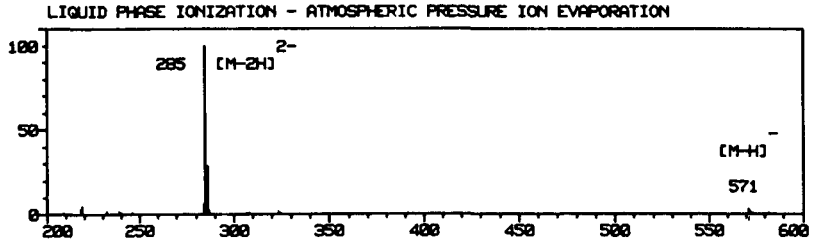

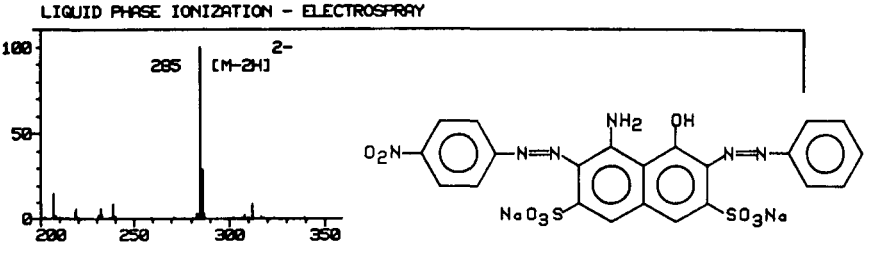

LC/MS of ACID BLACK 1, MW free acid = 572

References

1. D.I. Carroll, I. Dzidic, E.C. Horning and R.N. Stillwell, Appl. Spectrosc. Rev. 17, 337-406 (1981).
2. J.V. Iribarne, P.J. Dziedzic and B.A. Thomson, Int. J. Mass Spectrom Ion Phys., 50, 331-347 (1983).
3. A.P. Bruins, T.C. Covey and J.D. Henion, this conference, paper WPB 11.
4. G. Schmelzeisen-Redeker, U. Giessmann and F.W. Rollgen, Journal de Physique 45, C9 - 297 (1984).

A CONTINUOUS FLOW FAB PROBE FOR THE INTRODUCTION OF AQUEOUS SOLUTIONS,

Richard M. Caprioli and Terry Fan, University of Texas Medical School, Houston, Texas, 77030 and John Cottrell, Kratos Analytical, Manchester, U.K.

A continuous flow FAB probe has been described which allows aqueous solutions containing dilute buffers to be fed directly into the ion source. The device contains a 0.075 mm fused silica capillary column through which a solution is passed at a rate of 2-10 ul/min. At the probe tip inside the source, the solution is bombarded with xenon atoms and sample ions are sputtered and analyzed. Enzyme reactions as well as other aqueous solutions can be continuously monitored. The flow solution should contain at least 15-20% glycerol, although if it is not desirable to have glycerol in the reaction solution, it may be added at the probe tip from another capillary. An alternative mode of operation is to inject a small volume of sample in an aqueous medium into a stream of a solution containing 20% glycerol. Figure 1a shows the injection profile of 6.8 ng of the peptide substance P (MW 1347 daltons) contained in a 0.5 ul injection where the flow solution was water/glycerol (8/2) containing 0.2% TFA. The mass spectrum is shown in Figure 1b. The probe shows little memory as seen from only a slight tail on the chromatogram peak in Figure 1 and was shown to be linear in response from 0.3 - 500 ng for this peptide.

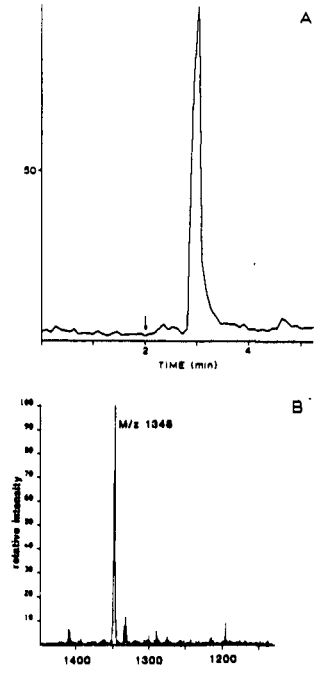

Figure 1 a) total ion chromatogram for injection of 6.8 ng of substance P in 0.5 ul onto the continuous flow probe.
b) FAB mass spectrum from this injection.

One particularly noteworthy consequence in using more aqueous solutions, with respect to normal FAB probes where 90% or more glycerol is used, is that the chemical noise so characteristic of standard FAB mass spectra is greatly reduced. Figure 2 shows the background region near the molecular ion of a peptide using the flow probe and a standard FAB probe. Background chemical noise coming from the glycerol mass on the standard probe is markedly decreased with the flow probe, leaving ions associated with the sample as prominent ions in the spectrum.

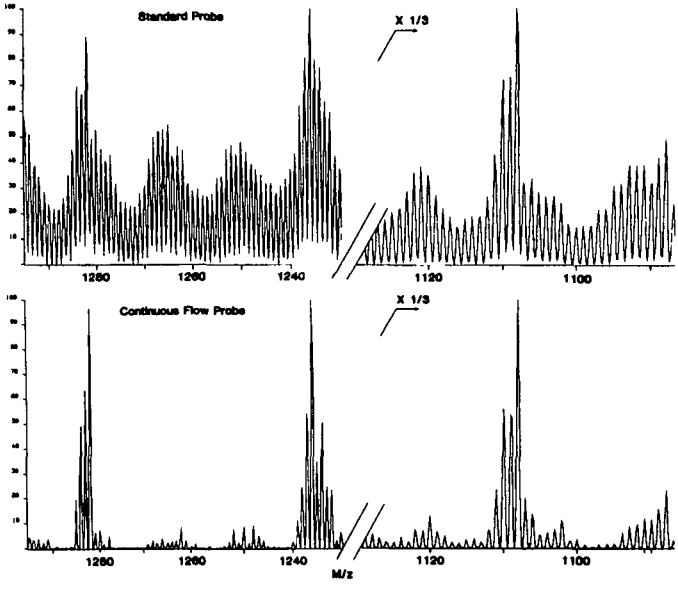

Fig. 2. Comparison of background spectra from a standard FAB analyses (using 90% glycerol) and the same compound injected onto the continuous flow probe, but in 20% glycerol.

Further, this reduced noise leads to an increase in sensitivity. The molecular ion species of substance P cannot be seen on the standard FAB probe at a level of 0.14 ng (100 femtomole), but is recorded with a signal-to-(chemical) noise of about 10:1 with the flow probe. This represents a sensitivity increase of about a factor of 200 in this case. An advantage of the FAB flow probe over other on-line systems is that it can be operated at full accelerating potential, 8 keV in the examples shown above, allowing the full sensitivity of the instrument to be utilized. This was demonstrated at high mass with the mass spectrum of the molecular ion species obtained from the injection of 1.5 ug of bovine insulin (MW 5730 daltons). An example of the use of this probe to monitor on-line proteolysis is the digestion of ribonuclease S peptide with carboxypeptidases Y and P. The reaction was done in 5 mM Tris (pH 6) buffer and this solution continuously fed into the FAB source. A second capillary was employed to deliver a 30% glycerol solution containing 0.3% TFA to the probe tip. The loss of 14 residues from the carboxy terminus of the truncated polypeptides was followed. Some time-course information can be obtained from these selected ion chromatograms and may be of value in cases where ions from other compounds in the sample interfere with ions of interest.

The advantages of the continuous flow probe include increased sensitivity through a decrease in the background chemical noise, and the capibility to directly analyze aqueous solutions continuous monitoring of batch reactions, and utilizing full sensitivity of the instrument by operating at high accelerating voltages. The disadvantages are that it must be operated in a stable made where flow and temperature are balanced and that source pressures are relatively high.

Lubman, D.M.; Sin, C.H.; Pang, H.M., Supercritical Fluid Injection of Nonvolatiles with Resonant Two Photon Ionization Detection in Supersonic Beam Mass Spectrometry. Department of Chemistry, The University of Michigan, Ann Arbor, MI 48109.

In our work resonant two-photon ionization (R2PI) in supersonic jets is used as a means of optically selecting ions for mass spectrometry. The use of supersonic beam injection provides internally ultracold molecules with sharp spectral features for chemical analysis for molecules whose spectra would otherwise exhibit broad, unresolvable contours at room temperature. High-powered tunable monochromatic laser sources can be used to probe this sharp structure by using a two photon ionization technique whereby the first photon excites a molecule to a real intermediate state and the second photon causes ionization. Thus, although ions are detected as the final product, the ionization cross-section reflects the $S_0 \rightarrow S_1$ transition of the molecule so that the ionization spectrum obtained serves to uniquely identify each mass peak in a time of flight mass spectrometer (TOFMS). This method has been used to provide enhanced selectivity in such difficult problems as isomer and isobar analysis, selective isotopic monitoring and trace discrimination of a contaminant in a large background matrix.

Our most recent work focuses on the use of this method for analysis of small biological species based upon the combination of wavelength selectivity and the high efficiency for producing molecular ions by the R2PI technique. One method investigated for use in solubilizing nonvolatile and thermally labile molecules involves expansions of supercritical fluids of CO_2 and N_2O at up to 400 atm backpressure into a mass spectrometer at 10^{-5} torr. Direct liquid introduction (DLI) techniques developed for HPLC/MS could also be used for introduction of nonvolatiles into vacuum. However, the much higher volatility of most gases that might be used in SFI (CO_2, N_2O, NH_3, etc.) provides a significant advantage over HPLC or liquid introduction into a mass spectrometer since the supercritical fluid immediately converts into a beam of molecules after introduction into vacuum, whereas DLI may require significant heating of the nozzle in order to prevent large clusters or crystals of material from condensing out upon expansion. In addition, SFI can utilize carrier gases to form a molecular beam which have a low enough number of internal modes so that significant cooling of the seed material can be achieved. The expansion of this ultradense jet can thus provide sharp spectral features for analysis of nonvolatiles in the reservoir at room temperature which would normally require significant heating for volatilization into the gas phase.

The experimental set-up is described elsewhere (1). It consists of a differentially pumped vacuum system with a TOF mass spectrometer sitting vertically on top of the chamber. The ultraviolet laser beam enters the chamber through quartz windows and R2PI is produced in the acceleration region of the TOFMS. The novel feature of this experiment is that a 150-200 μm orifice can be used to obtain high on-axis density in the jet even with 400 atm backpressure using a specially designed high pressure pulsed injection valve. Using this valve in conjunction with efficient LN_2 cryopumping, a pressure of ~10^{-5} torr can be maintained in the mass spec. The laser source is a Quanta-Ray Nd:YAG pumped dye laser which is frequency doubled in KD*P to produce tunable near-UV light. The supercritical fluid pressure of CO_2 and N_2O is provided by a Varian 8500 syringe pump.

In Figure 1a is shown a spectrum of the $S_0 \rightarrow S_1$ transition of carbazole expanded from supercritical CO_2 at 190 atm back pressure and 40°C. The melting point of carbazole is 245°C and at 40°C essentially no signal is observed from a 1 atm back pressure of Ar. In Figure 1b is a spectrum of carbazole obtained using 1 atm of CO_2 at 180°C. This spectrum was taken by use of a special pulsed solenoid valve capable of heating to at least 300°C. However, using supercritical fluid expansions of CO_2, a low temperature can be used to seed carbazole into a molecular beam, though it has a fairly high melting point.

Both spectra in figure 1 have absorptions that are broader than are observed with Ar since the rotational population is not as effectively cooled by CO_2 as by Ar. This result is expected since the terminal Mach number (M_T) depends on the heat capacity ratio, $\gamma = C_p/C_v$, which is larger for Ar than for CO_2. In essence, the monatomic gas has no vibrational and rotational degrees of freedom in which to store energy and thus reaches

its final translational temperature more quickly than in a polyatomic gas. This incomplete cooling of the beam leaves a significant number of molecules in excited rovibronic states, so that resonant ionization of these molecules make a substantial contribution to the signal seen as the laser is swept over a relatively broad spectral range which is why the background baseline never goes to zero.

The mass spectra obtained for the laser photoionization of various PNAH's in a time-of-flight mass spec are shown in Figure 2, which is a mass spectrum of acenaphthene, carbazole, phenanthrene, pyrene, and tetracene obtained from a supercritical expansion of 350 atm CO_2 at T=40°C using 266 nm as the ionization source. These compounds all dissolve strongly in the supercritical fluid even at 40°C even though tetracene has a melting point 300°C. We have also explored a number of small biologicals including tryptophan, tyramine, phenoxazine and benzimidazole which can be solubilized by supercritical CO_2 or N_2O at essentially room temperature and have obtained wavelength dependent spectra for benzimidazole.

1. Sin, C.H.; Pang, H.M.; Lubman, D.M.; Zorn, J. Anal. Chem. 1986, 58, 487.

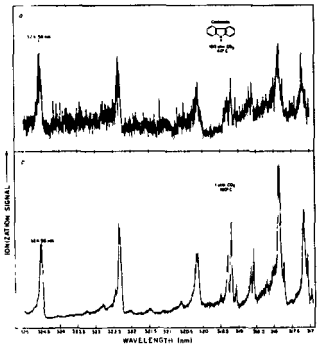

Fig.1 R2PI spectrum of carbazole expanded in a supersonic jet of (a)supercritical CO_2 at 190 atm and 40°C and (b) 1 atm CO_2 at 180°C.

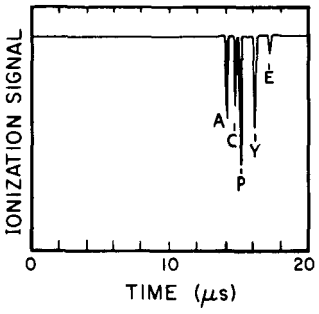

Fig.2 Time-of-Flight mass spectra of acenaphthene (A), carbazole (C), phenanthrene (P), pyrene (Y), and tetracene (E) expanded from a jet at 190 atm CO_2 and 70°C.

Tembreull, R.; Lubman, D.M., Pulsed Laser Desorption with Resonant Two-Photon Ionization Detection in Supersonic Beam Mass Spectrometry. Department of Chemistry, University of Michigan, Ann Arbor, MI 48109.

A classic problem in conventional mass spectrometry is the analysis of compounds which are difficult to vaporize, either due to low volatility or their susceptibility to pyrolysis. Significant progress has been made in this area with the advent of particle induced desorption methods such as FAB, SIMS, HIID and laser desorption. This particular work addresses the utility of laser desorption in the analysis of intractable species with special focus on the desorbed neutral fraction. Previous investigators have used relatively high laser power densities ($>10^7 W/cm^2$) to produce ionization during the desorption process. We believe a two step process involving separate desorption and ionization steps will ultimately prove to be more efficient and provide fundamental spectroscopic information on biolgical molecules.

The experimental apparatus is shown in figure 1. The desorbed molecular plume is entrained into a supersonic jet in one arrangement followed by ionization with a second laser in the acceleration region of the time-of-flight mass spectrometer (TOFMS). A second experiment involves a two step desorption-ionization process directly within the transmission region of the TOFMS. The latter experiment permitted differentiation between ions formed in the desorption process and ions formed via the absorption of a second ionizing laser. The desorption wavelength used in initial experiments was the second harmonic of a Nd:YAG laser at 532 nm. It was found, however, that a 10.6 μm beam provided for much greater efficiency producing ion currents at least an order of magnitude greater. Subsequent experiments were therefore performed with an infrared desorption laser. The ionizing wavelengths were 280, 266, 245 and 222 nm and were generated with a Quanta Ray Nd:YAG pumped dye laser system and a Quanta Ray WEX-1 wavelength extension device which was used for frequency doubling and wavelength mixing.

Figure 2 shows the spectra of several polynuclear aromatic hydrocarbons obtained by performing desorption with 10.6 μm radiation into a supersonic expansion of Ar. By carefully controlling the experimental parameters ion peaks of 15-20 ns FWHM could be observed. Notably no cationization occurred and only the radical parent molecular cation was detected in each case. "Soft ionization" can also be observed for many biomolecules. For example, the parent ion was selectively produced for catecholamines and related derivatives, e.g., DOPA and dopamine, for several tricyclic antidepressant drugs, such as chloropromazine and imipramine, and for a number of indole derivatives. Soft ionization was also observed for adenine, purine and niacin at 222 nm and pyridoxine at 266 nm. A few compounds underwent facile cleavage, and in these cases it does not appear to be possible to form the parent ion exclusively. Examples include the neurotransmitters epinephrine and norepinephrine, which fragment to give charged alkyl amine species, and the vitamins thiamine and riboflavin.

In conclusion, laser desorption coupled with resonant ionization detection has a tremendous potential for clinical applications. In most cases it is possible to softly ionize the molecule of interest. Conversely, the ionizing laser energy can be increased to yield diagnostic fragments for molecular identification. Cracking patterns obtained in this latter process are often much simpler than those observed in electron impact, however, fragmentation proceeds by similar mechanisms in both cases. It is also possible to produce exclusively ions of rather high appearance potential. Laser ionization, therefore, provides increased control over the fragmentation pattern obtained.

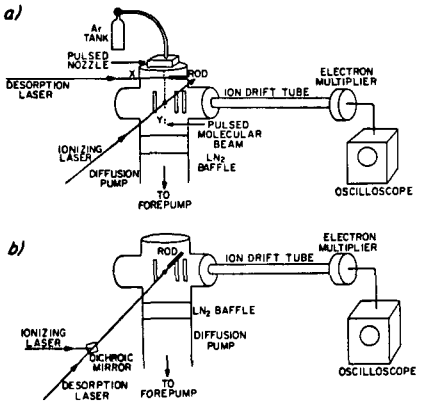

Figure 1. Schematic representation of the experimental setup in which laser desorption is performed (a) in the throat of a supersonic expansion or (b) in the acceleration region of a time-of-flight mass spectrometer. In configuration b a 532-nm laser beam was used for desorption to permit copropagation of the desorbing and ionizing laser beams by means of a dichroic mirror.

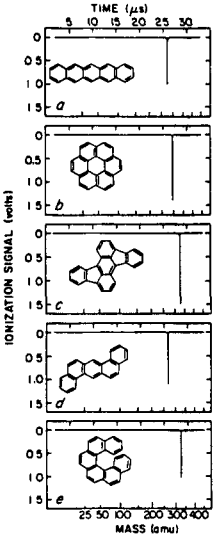

Figure 2. Time-of-flight mass spectra of (a) pentacene, (b) coronene, (c) rubicene, (d) 1,2:5,6-dibenzanthracene, and (e) phenanthro[3,4-c]phenanthrene obtained by using a 10.6 μm IR laser beam for desorption and a 266 nm laser beam for ionization of the desorbed neutral species. The background ionization induced by 266 nm alone has been subtracted from this figure.

THERMOSPRAY LIQUID CHROMATOGRAPHY/MASS SPECTROMETRY FOR THE IDENTIFICATION OF METABOLITES: COMPARISONS WITH OTHER DESORPTION IONIZATION METHODS

S.E. Unger, T.J. McCormick, B.M. Warrack, S.J. Lan, B. Swanson, D. Everett, and J. Mitroka, The Squibb Institute for Medical Research, P.O. Box 4000, Princeton, NJ 08543-4000

The disposition of pharmaceutical agents from biological media often results in the production of involatile, highly polar metabolites which until recent years have been difficult to directly characterize using mass spectrometry. The introduction of desorption ionization methods such as field desorption (FD), secondary ion mass spectrometry (SIMS) or fast atom bombardment (FAB), and most recently thermospray (TSP) ionization have allowed the analyst to directly determine the molecular weight, formula, and structure of metabolites when used in combination with high-resolution and collisional-activation MS/MS capabilities.

However, both FD and FAB-MS suffer from matrix effects which may suppress ionization of the metabolite in the presence of minute quantites of a co-isolate. These may be endogenous materials such as deoxytaurocholic acid isolated from bile or artifacts such as small quantities of surfactants carried through extensive isolation procedures.

Thermospray ionization offers the advantage of on-line LC/MS analysis of metabolites and therefore minimizes matrix effects by separation of components prior to mass spectral analysis. In combination with UV and radiochemical detection, analysis by thermospray LC/MS avoids time- and labor-intensive preparative chromatography and affords spectra of metabolites not amenable to direct analysis using FAB or FD-MS.

Thermospray LC/MS has aided in the identification of the metabolites of the steroid tipredane. Extensive oxidation is observed at both the sulfur of the 17-carbon thioether and at the 6-carbon of the B-ring. While the sulfoxide and sulfone of some tipredane-related steroids are amenable to fast-heating chemical ionization (DCI), tipredane and its more polar 6-beta-hydroxy analogs are not. These species yield both positive and negative thermospray-generated ions. The protonated molecule, $(M+H)^+$, is observed with ng detection sensitivity. The deprotonated molecule, $(M-H)^-$, along with the acetate addition ion is observed in the negative ion spectrum. Figure 1 illustrates this feature for the S-methyl sulfoxide of tipredane. Analysis of this species using DCI yielded only the ion at m/z 363 due to thermal elimination of CH_4SO, making characterization difficult as this species was also known to be a metabolite.

Figure 2 shows the negative thermospray mass spectrum of a metabolite of the ACE-inhibitor fosenopril. Loss of the ester side chain occurs releasing the active acid which is further metabolized by glucuonide attachment. The ion at m/z 610 is the $(M-H)^-$ parent for this species whose spectrum shows a diagnostic loss for glucuronide conjugates (176 amu). Some ammonium salt of the parent is also seen at m/z 627.

When insufficient fragmentation is observed in the thermospray mass spectrum, collisional activation with MS/MS analysis affords rich and informative spectra. Figure 3 illustrates the MS/MS spectrum (30eV; 1 mTorr Ar) of the steroid sulfoxide shown.

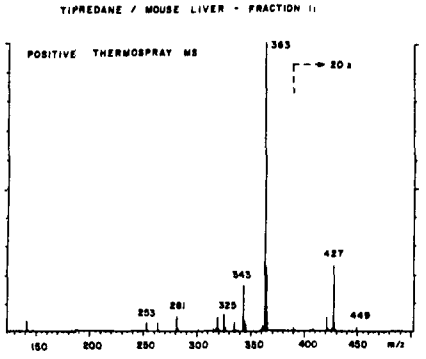

Figure 1

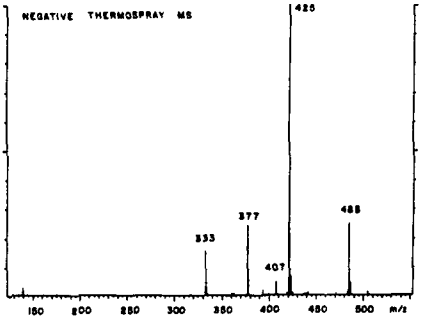

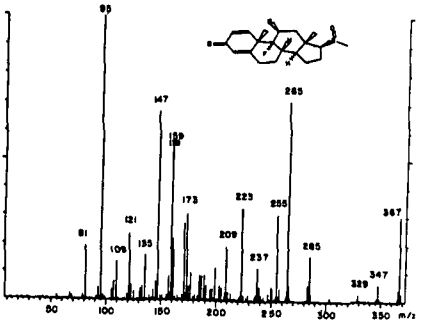

Figure 3

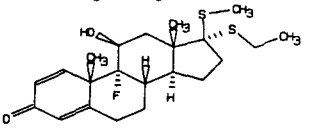

TIPREDANE

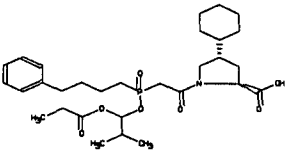

FOSENOPRIL

NEGATIVE THERMOSPRAY MASS SPECTRUM

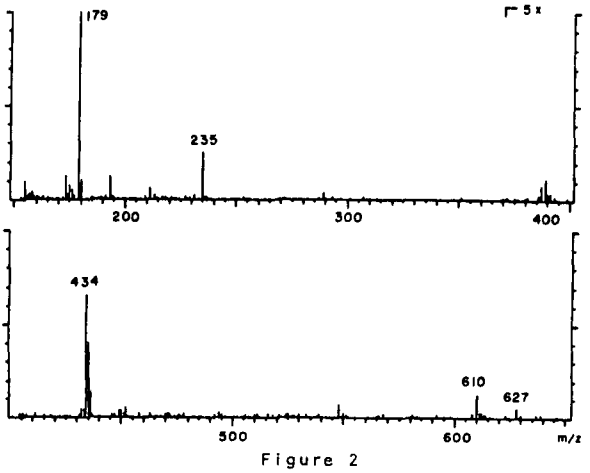

Figure 2

DEUTERIUM - LABELED CHOLESTEROL AS AN INTERNAL MONITOR OF THE FORMATION OF CHOLESTEROL OXIDES

B.A. Wasilchuk, P.W. LeQuesne, P. Vouros
Department of Chemistry, Northeastern University, Boston, MA 02115

One of the major problems encountered in the analysis of foods and biological samples for cholesterol oxidation products is the formation of artifacts arising from the autoxidation of cholesterol during sample preparation (1-3). Accurate determination of the origin of these oxidation products is therefore of paramount importance in order to avoid misinterpretation of the analytical results. In this work the utilization of deuterium - labeled cholesterol (d_9-cholesterol) as a means of monitoring for procedural oxidation is described.

The method involves the addition of d_9-cholesterol to the sample, then subjecting the labeled and unlabeled substrates to identical oxidation conditions during the analyte isolation process. Comparison of the ratios of deuterated to undeuterated oxides with those of labeled to unlabeled cholesterol provides a direct means of monitoring for procedural oxidation of cholesterol.

The mass spectrum (20eV) of the TMS derivative of the deuterium - labeled cholesterol synthesized for this study is shown in Figure 1. Side chain labeling of cholesterol was selected for two major reasons: First, since most of the cholesterol oxides of interest involve oxidative attack on the cholesterol ring system, deuterium labeling on the side chain should minimize the occurrence of isotope effects during the oxidation process. Secondly, since EI and CI mass spectra of the oxides of interest exhibit predominantly ring system fragmentations, deuterium labeling on the side chain should again minimize isotope effects occurring during mass spectral analysis. Isotopic enrichment calculations of the deuterated cholesterol show 2.3% d_6 incorporation, 6.8% d_7, 24.0% d_8 and 66.8% d_9 incorporation. The high isotopic enrichment of the synthesized deuterated cholesterol and the nine atomic mass unit difference between labeled and unlabeled analogs provide a mass spectral pattern free of interference which facilitates the quantitation by GC/MS. Moreover, the TMS derivatives of the labeled and unlabeled cholesterol and its oxides are resolved from each other using capillary GC/MS (see Figure 2).

The feasibility of the deuterated cholesterol internal monitor was demonstrated by mixing and oxidizing approximately equal quantities of labeled and unlabeled cholesterol. An aliquot of this mixture was withdrawn prior to oxidation to establish the initial D0/D9 cholesterol ratio. The final analysis was conducted on the TMS derivatives of the labeled and unlabeled oxides formed, by GC/MS using ammonia CI and selected ion monitoring. The results of this experiment are shown in Table 1. As can be seen, the initial D0/D9 cholesterol ratio before oxidation is in very good agreement with the D0/D9 oxide ratios obtained after oxidation. This serves to establish that both labeled and unlabeled cholesterol are oxidized at the same rate. In order to strengthen the feasibility of a strictly GC approach to the problem, the above experiment was repeated and GC/FID was used in the final analysis. As can be seen in Table 2, there is once again very good agreement between the initial D0/D9 cholesterol ratio and the final D0/D9 oxide ratios. Thus, the present investigation shows clearly the feasibility of using deuterium - labeled cholesterol as an internal monitor of the formation of cholesterol oxide artifacts arising from procedural oxidation. Due to the GC resolution of labeled and unlabeled species the final determination can be carried out using either GC or GC/MS. Presently, we are applying the deuterated cholesterol internal monitor to detect artifacts in the analysis of egg powders.

REFERENCES

1. J.R. Claude and J.L. Beaumont, J. Chromatog. 21 (1966)189
2. J.E. VanLier and L.L. Smith, Biochemistry 6,10 (1967)3269
3. S.R. Missler, B.A. Wasilchuk and C. Merritt, Jr., J. Food Sci. 50,3 (1985)595

Figure 1

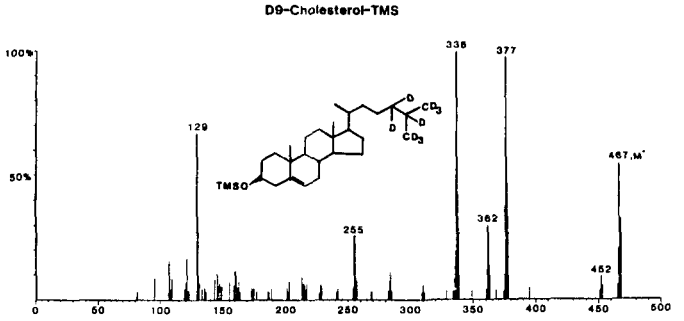

Figure 2

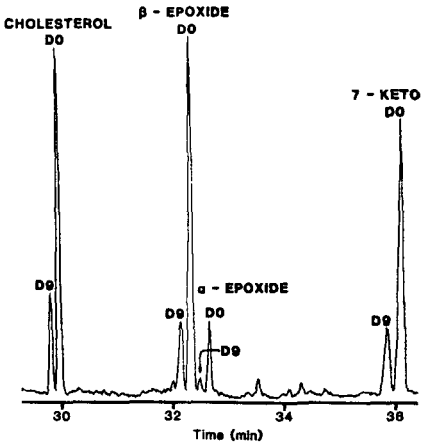

Table 1

D0/D9 GC/MS Ratio Comparisons

COMPOUND	D0/D9 PEAK AREA RATIO
Cholesterol	1.26 ± 0.04
β - Epoxide	1.29 ± 0.04
7 - Keto	1.26 ± 0.02

Table 2

D0/D9 GC Ratio Comparisons

COMPOUND	D0/D9 PEAK AREA RATIO
Cholesterol	1.07 ± 0.07
β - Epoxide	1.16 ± 0.07
7 - Keto	1.13 ± 0.06

High Sensitivity and High Resolution Probe Analysis of Indoleamines Using A Dual Cell FTMS

S.P. Markey, M.-C. Shih
Laboratory of Clinical Science, National Institute of Mental Health,
Bethesda, Maryland 20892

Significant advances in the commercial development of a dual cell Fourier transformation cyclotron resonance spectrometer attracted our laboratory to utilize this instrumentation for routine analysis of organic biomolecules. A Nicolet FTMS-2000 was used to study the parameters necessary to obtain both high sensitivity and high resolution. Initially, a series of indoleamines was chosen because of their reasonably well studied electron ionization and thermal desorption properties and their continuing interest as neurotransmitters or neurohormones. Due to results obtained with the first member of the series, melatonin (N-acetyl-5-methoxytryptamine), efforts to analyze the more polar and thermally labile indoleamines were halted.

In a conventional quadrupole spectrometer, melatonin evolves from a direct insertion probe at temperatures of 75 to 110°C, and exhibits a molecular ion (m/z 232, 10%) and two intense characteristic fragment ions (m/z 173, 90%; 160, 100%). Quantities as low as 1 to 10 μg are readily analyzed, and smaller quantities are probably lost due to chemical instability of melatonin on surfaces.

The analysis of 1 μg of melatonin using the standard probe assembly was unsatisfactory and revealed several major mechanical and thermal problems which are not easily resolved within a superconducting magnet environment. With 1 μg samples, indicated probe temperatures > 200°C were required to observe weak spectra which were dominated by probe background ions. The large probe size (1 m x 2.5 cm) required to insert a sample into the cell within the magnet bore exposes a large surface area to the vacuum system, introducing large amounts of adsorbed water and background contaminants. After completing a run and removing the probe, subsequent bake-out of the vacuum chamber demonstrated that the melatonin was present for hours, and very nice spectra could be recorded from sample evolved from the walls and cell plates. Operation of the instrument with the vacuum chamber heated to 150 or 200°C prior to probe insertion improved the rate and appearance of melatonin, but exacerbated the background problem, and failed to produce the expected enhancement of sensitivity. The instrument assembly drawings indicated a configuration of the probe assembly as shown schematically in Figure 1. The position of the probe shaft upon complete insertion placed the sample more than 60 mm away from the source cell, with an intervening 47 mm x 12 mm stainless steel source cylinder.

The purpose of the source cylinder is to confine neutrals coming from the GC (inlet not shown) or evolved from the probe surface by a laser beam focused from a parabolic mirror. For laser samples, a probe extension places the sample 1-3 mm away from the source cylinder; GC samples enter the cylinder directly from the side. The source cylinder is not independently heated, but like the source and analyzer cell is heated by radiation from the vacuum chamber. Confinement of neutrals within the source cylinder was intended to enhance electron ionization from the electron beam directed through the dual cell assembly.

Three experiments were used to improve instrument performance. First, variable lengths of silver probes were used to place the glass sample vial at closer intervals to the source cell. A series of spectra were obtained at each position and are plotted in Figure 2. As expected, when the sample was brought closer to the source cell, the signal for a fixed quantity of melatonin increased markedly. In these experiments, the probe was introduced stepwise into the heated vacuum chamber in order to reduce background, and the probe tip heater was programmed in a consistent manner. Secondly, the laser tip was used with a silver probe extension to place the sample closer and to control the voltage of

both the probe and the laser tip. A bias voltage applied to the probe surface was essential for obtaining spectra. Without a bias potential, at most probe positions the electron beam striking the laser probe surface produced a shower of secondary electrons which effectively recombined with positive ions and drastically reduced signal. At a potential of 5 V or more above the cell trapping potential, this effect was negligable as suggested by S. Ghaderi, Nicolet. Thirdly, the length of the source cylinder was shortened to a minimum of 17 mm in an effort to reduce its negative contribution to instrument performance. At the same time, probe contact was changed to bring the probe surface into flush contact with the remaining cylinder surface. The result was a probe sitting in a well rather than an open cylinder. The relatively high pressure of evolved neutrals had a negative rather than positive effect on signal. It is apparent that ions formed in a highly pumped region can be transmitted effectively into the source and analyzer cells for FTMS analysis; ions formed in a region of high density neutrals may create small plasmas in the intense magnetic field and not be useful for analysis.

There remains a techological challenge to introduce organic compounds into the FTMS cell with low background and high efficiency of sample utilization. Nevertheless, high resolution and high sensitivity spectra can be recorded as evidenced by the signal/noise ratio for 30 ng of melatonin recorded with an extended probe tip in heterodyne mode (mass range 160-180 daltons) as shown in Figure 3.

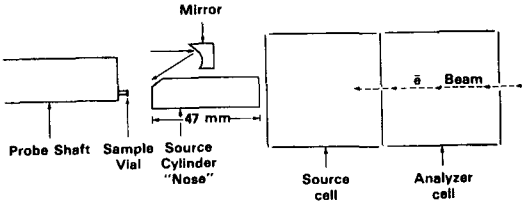

Figure 1

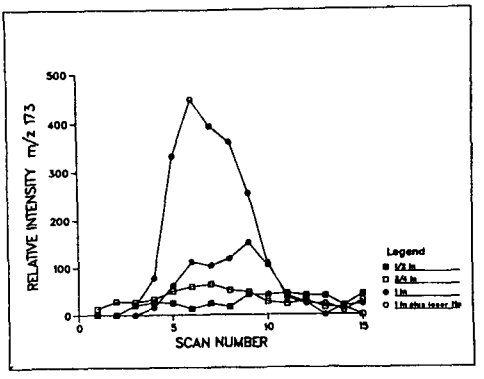

Figure 2

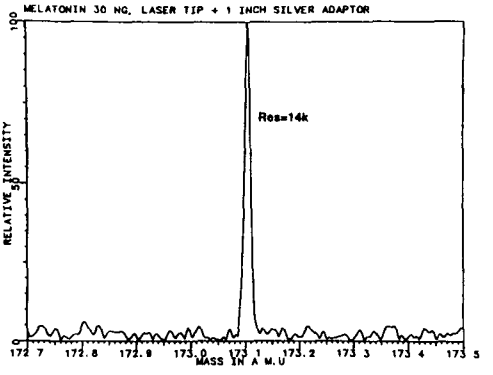

Figure 3

FAB MS-MS versus DCI MS-MS application towards polar molecules

G. DEVANT, F. De MAACK, S.N. NERMAG, 49 Quai du Halage - 92500 RUEIL-MALMAISON - FRANCE

Both fast atom bombardment (FAB) and chemical desorption ionization (DCI) have been successfully applied in the field of peptide analysis. The availability of mass spectrometry/mass spectrometry (MS/MS) has significantly extended the total amount of informations obtainable on this class of compounds by providing sequencing information.
In the case of DCI the choice of reagent gas permits acquisition of different kinds of spectra providing a variety of structural information.

Table 1 lists the most important considerations, together with their respectives advantages and disadvantages, of choosing between DCI and FAB.

TABLE 1

	DCI	FAB
CHARACTERISTICS	Soft ionization Poor fragmentation Fast phenomenon	Even softer Poor fragmentation Continuous phenomenon
ADVANTAGES	Choice of reagent gas More sensitive than FAB Easier to quantify than FAB	Choice of bombarding gas High mass ions production
DISADVANTAGES	Mass range limit Threshold Pyrolysis	Matrix Threshold Unpredictable sensitivity Cationization

In the case of N-acetyl aspartyl glutamic acid, it is possible to obtain the parent ion both with DCI and FAB. However, the MS/MS of the (M+1) ion provides surprisingly different spectra (fig. 1A,1B).

Figures 1A,1B

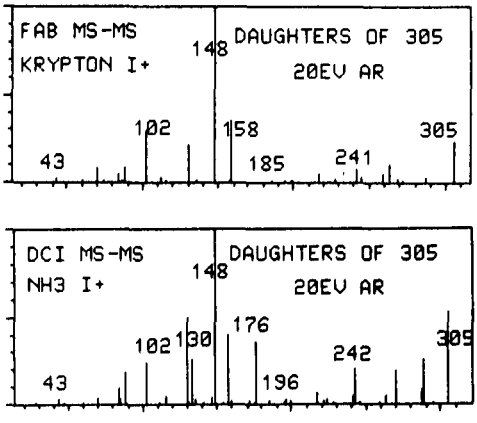

The FAB MS/MS of this dipeptide requires no special interpretation.

In contrast, the main action of ammonia as reagent gas in DCI is an aminolysis of the peptidic bond leading to a mixture of N-acetyl asparagine and glutamic acid. These two products undergo a kind of peptidic synthesis and combine with the original peptide to form a complex. This sequence has been postulated based on MS/MS information (in parent mode). Similar behaviour and potential problems in interpretation, may be expected for small peptides containing aspartic acid, glutamic acid, arginin .
A concurrent partial pyrolysis provides a dehydration of glutamic acid to pyroglutamic acid.

In some cases, for example anthelmycin, no DCI spectra can be obtained at all, and even FAB spectrum on single stage provides no structural information. The MS/MS spectrum of the (M + 1) ion (fig 2) shows significant and easy to interpret fragments.

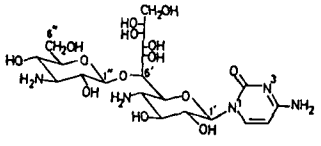

Figure 2

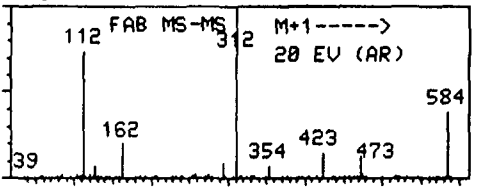

In conclusion, two major considerations should be made in choosing between DCI and FAB :
In the case of DCI, sensitivity is usually higher and quantification is often easier. However, one must make certain that the proper fragment ions are used because of the possibility of unexpected reactions. In FAB, the MS/MS spectra are usually easier to interpret and free of secondary reaction products.

PRACTICAL APPLICATIONS OF ON-LINE LIQUID CHROMATOGRAPHY/ FAST ATOM BOMBARDMENT MASS SPECTROMETRY

Justin G. Stroh, J. Carter Cook, Kenneth L. Rinehart, Jr., William C. Snyder
School of Chemical Sciences, University of Illinois at Urbana-Champaign, Urbana, IL 61801

Analysis of many biologically important compounds by mass spectrometry has become possible in recent years. Fast atom bombardment mass spectrometry has often been used with prior clean-up of the analyte by HPLC. We have recently described an on-line LC/FABMS system employing a moving belt with microbore columns in conjunction with a fritted contact depositor (1). This system has been used for the structural analysis of a mixture of leucinostatins (2,3).

One difficulty with FABMS is that the matrix sometimes interferes with the analyte signal. That is, at low mass, ions attributable to the matrix are often so intense that useful analyte ions in this region are obscured or obliterated. At higher mass, one often observes signals arising from addition of the matrix to the analyte. However, with the moving belt, no matrix is required as the surface exposed to the atom beam is continually replenished by rotation of the belt and, therefore, ions arising from the belt can be attributed to the analyte. This is exemplified by our experiments with the paulomycins (4). Figure 1 gives the solids probe FAB spectrum of pure paulomycin A in a matrix of dithiothreitol/dithioerythritol (5). Ions arising from M + Na are observed at m/z = 809, with other ions attributable to the matrix labeled with an MX. Figure 2 shows the spectrum of the same compound taken following an on-line separation of a mixture of paulomycins A and B by LC/FABMS. This spectrum shows an abundant M + Na ion with substantially more fragmentation, which aids in identifying the structure of the compound.

The data show that LC/FABMS is a practical technique for the analysis of mixtures of compounds and that the background normally associated with FABMS has been removed.

References

1. Stroh, J. G.; Cook, J. C.; Rinehart, Jr., K. L.; 10th Internatl. Mass Spectrom. Conf., September 9-13, 1985, Swansea, U.K.

2. Stroh, J. G.; Rinehart, Jr., K. L.; Cook, J. C.; Kihara, T.; Suzuki, M.; Arai, T. J. Am. Chem. Soc. 1986, 108, 858.

3. Fukushima, K.; Arai, T.; Mori, Y.; Tsuboi, M.; Suzuki, M. J. Antibiot. 1983, 36, 1606 and 1613.

4. Wiley, P. F. J. Antibiot. 1976, 29, 587.

5. Witten, J. L.; Schaffer, M. H.; O'Shea, M.; Cook, J. C.; Hemling, M. E.; Rinehart, Jr., K. L. Biochem. Biophys. Res. Commun. 1984, 124, 350.

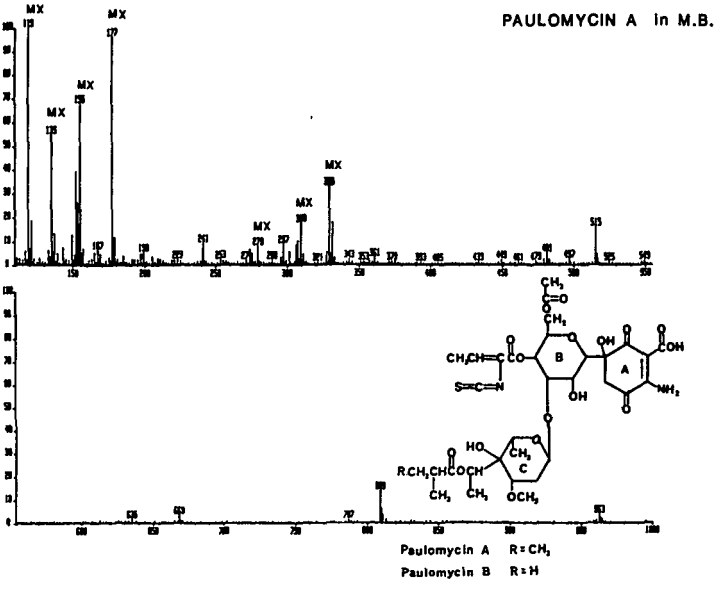

Figure 1

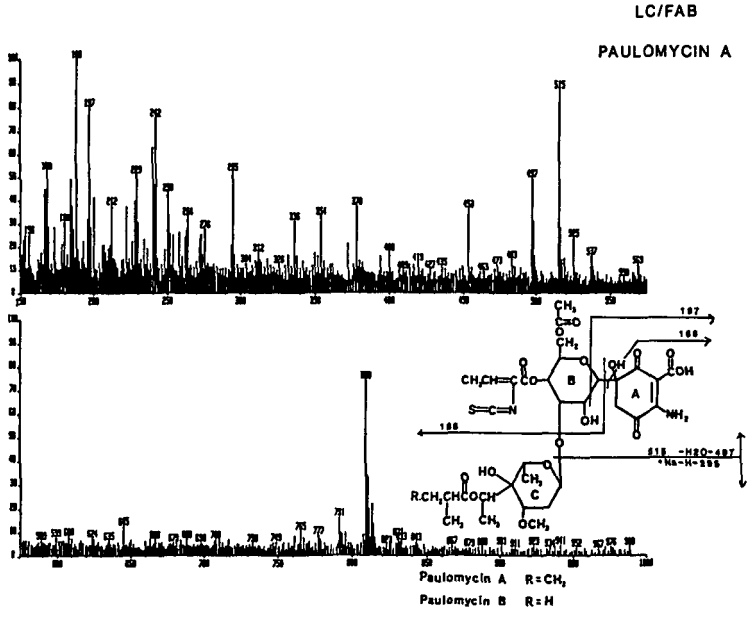

Figure 2

A NEW INSTRUMENT FOR CHROMATOGRAPHY/SIMS

Gerald C. DiDonato and Kenneth L. Busch
Indiana University
Department of Chemistry
Bloomington, IN 47405

We have designed and constructed a new instrument for the direct mass spectrometric analysis of thin-layer and paper chromatograms, and electrophoretograms. The instrument and the rationale for its design have been covered in detail elsewhere [1]. Briefly, chromatography/SIMS offers several advantages over presently developed forms of chromatography/mass spectrometry, namely, independence of access order, ease of sample storage, the ability to repetitively analyze a sample, and variable spatial resolution.

Initial efforts to sputter biochemical compounds from a thin-layer chromatogram yielded a weak and transient secondary ion flux. Most of the compound resides in the bulk of the chromatographic matrix and is inaccessible to the primary ion beam. At higher current densities necessary to sputter through the chromatogram, damage to the organic molecules can occur. A solution to this problem involves the use of a liquid matrix to extract compounds out of the bulk of the chromatogram, making them accessible to the primary ion beam and providing a stable flux of organic secondary ions. However, the spatial resolution of the chromatogram cannot be compromised. Extraction out of the bulk of the chromatogram without diffusion in the x and y planes is accomplished through the use of a phase-transition matrix which can be controllably cycled through the liquid-solid transition.

The matrix with which we have had the most success is threitol (1,2,3,4-butanetetrol). The threitol is overlayered onto the surface of the chromatogram by spray deposition. The intact chromatogram is then placed in the SIMS instrument for analysis. Threitol can be maintained in a liquid state by heat transfer from a heated metal support, or by melting from a high-density primary ion beam. Melting of the matrix occurs only at the point of analysis; while extraction occurs in the z direction, spatial resolution in x and y is maintained.

The pentapeptide methionine-enkephalin was used as a model compound to evaluate the efficiency of the extraction procedure. Figure 1 is the SIMS spectrum of 10 ug of the peptide extracted <u>in situ</u> from a 200 um thick silica TLC plate, showing the protonated molecular ion at m/z 574. This spectrum is similar to a spectrum obtained from a discrete sample. This amount of met-enkephalin provides a stable secondary ion signal for more than 30 minutes. Comparison of this spectrum with a similar extraction carried out by glycerol reveals that the glycerol is absorbed into the chromatogram to a greater degree than threitol and does not provide the necessary liquid reservoir of sample. Furthermore, sensitivity for discrete samples of met-enkephalin is a factor of 8 higher for threitol when compared with glycerol.

A spatially-resolved single ion monitoring spectrum of the $[M+H]^+$ of met-enkephalin is obtained in the following manner. The signal for the $[M+H]^+$ is recorded, the chromatogram moved 0.1 mm in the appropriate direction, and the signal recorded again. Movement of the chromatogram in both x and y yields a spatial profile of the compound as it resides in the chromatographic bed. Reconstruction of the ion intensities in x and y yields the axonometric plot shown in Figure 2.

We have employed this extraction and spatially resolved mass spectral analysis to paper electrophoresis as well. Electrophoresis requires that the molecule be in ionic form. This is achieved by derivatization of the steroid corticosterone with Girard's P [2]. Figure 3 is the SIMS spectrum of the derivatized steroid extracted <u>in situ</u> from Whatman 3MM electrophoresis paper. Once again the matrix is threitol. About 20 ug of sample is present. Spatially resolved spectra are also obtained for this compound. The signal for the intact cation at m/z 480 is recorded every 0.1 mm along each axis in the x and y direction, and the data is reassembled to produce the axonometric plot shown in Figure 4.

<u>References:</u>

1. John W. Fiola, Gerald C. DiDonato and Kenneth L. Busch, Rev. Sci. Instrum., in press.
2. *Gerald C. DiDonato and Kenneth L. Busch, Biomed. Mass Spectrom.*, <u>12</u> (1985) 354.

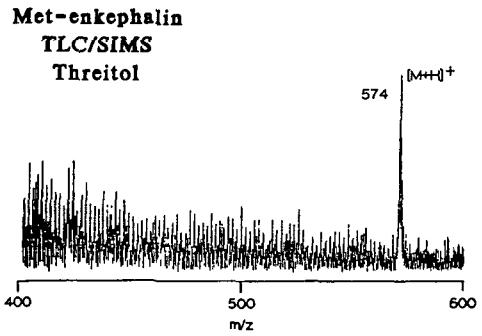

Figure 1

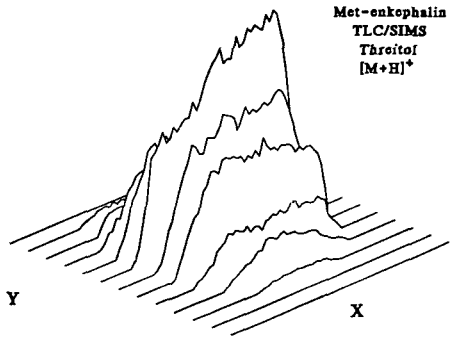

Figure 2

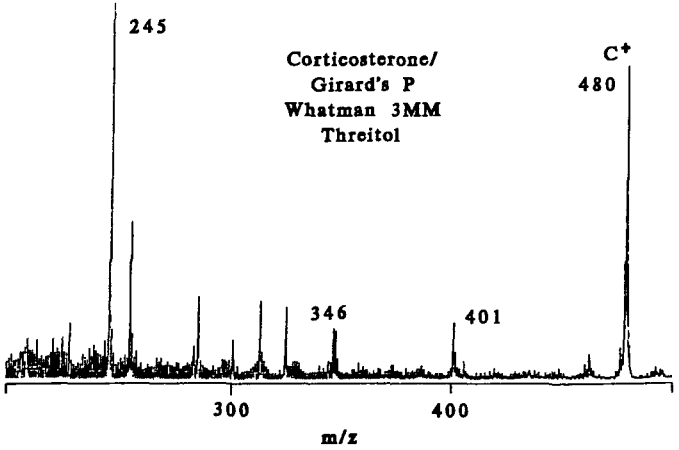

Figure 3

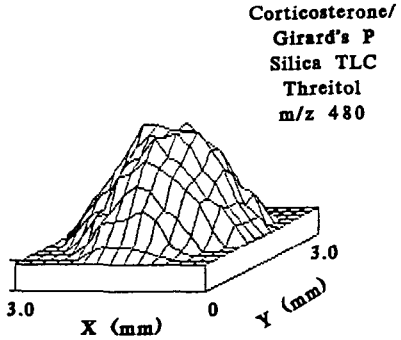

Figure 4

Biomolecules investigated by Multi-Photon-Ionization Mass Spectrometry

J. Grotemeyer, U. Boesl, K. Walter, E.W. Schlag

Institut fur Physikalische und Theoretische Chemie, Technische Universität München
Lichtenbergstr. 4, D-8046 Garching, Germany.

We demonstrate in this paper, that a "double-barelled" laser desorption and resonance enhanced multiphoton ionzation (REMPI) - mass spectrometry has several advantages over traditional single step desorption - ionization techniques, particularly if combined with a Reflectron-Time-of-Flight (RETOF) mass spectrometer. We demonstrate the effectiveness of this technique for large labile biomolecules.
The laser vaporization in the first stage of our instrument is analysed by multiphoton ionization mass spectra obtained in a second stage. This separation of the vaporizing and the ionizing process is one special feature of our technique, yielding intense signals of pure intact molecular ions in opposite to all other vaporization techniques. A second feature is the injection of the vaporized neutral molecules into a supersonic beam of a carrier gas which leads to intensive cooling of those molecules. This cooling provides small kinetic energy distributions and thus high mass resolutions in a time-of-flight mass spectrometer. A detailed description of the instrument is found in ref. /1/.

We present in this paper the resonance enhanced multiphoton ionization mass spectra of chlorophyll a, small protected tripeptides and angiotensin I.

In figure 1 the soft ionization mass spectrum of Chlorophyll a is shown. It shows in the high mass region three different molecular ion signals, namely the chlorophyll a at mass 892, the 10-Hydroxy-chlorophyll a at mass 908 and the Phaeophytin a at mass 870. The Phaeophytin a is a natural satellite of the Chlorophyll a, while the 10-Hydroxy-chlorophyll a is an extraction artefact.
Little loss of the phytyl side chain at mass 614 is observed. Structural informations can be obtained in the partial hard ionization mode as discussed in ref/2/.

Figure 2 shows the partial hard ionization mass spectrum of Angiotensin I. Note, that this coumpound has neither been protected at the N-terminal nor the C-terminal end. Besides the molecular ion, that gives rise to the basepeak at mass 1295, all sequence ions can be observed with high abundances. Together with the N-terminal degradation fragments the spectrum enables to deduce the sequence of the decapetide. Only little fragmentations in the side chains of the amino acids are observed.

In conclusion we believe, that our method of laser desorption and multiphoton ionization can open several new ways in mass spectrometry of larger molecules with low volatility.

/1/ Oral contribution on this conference, paper ROD 12; U. Boesl, J. Grotemeyer, K. Walter, E.W. Schlag.
J. Grotemeyer, U. Boesl, K. Walter, E.W. Schlag; accepted for publication by Org. Mass Spectrom.,publication date August 1986.
/2/ J. Grotemeyer, U. Boesl, K. Walter, E.W. Schlag; accepted for publication by J.Am.Chem.Soc., publication date June 1986.

Acknoledgment: This work has been supported by a grant from the Bundesministerium für Forschung und Technologie (13N5307) in collaboration with Bruker-Franzen Analytik, Bremen.

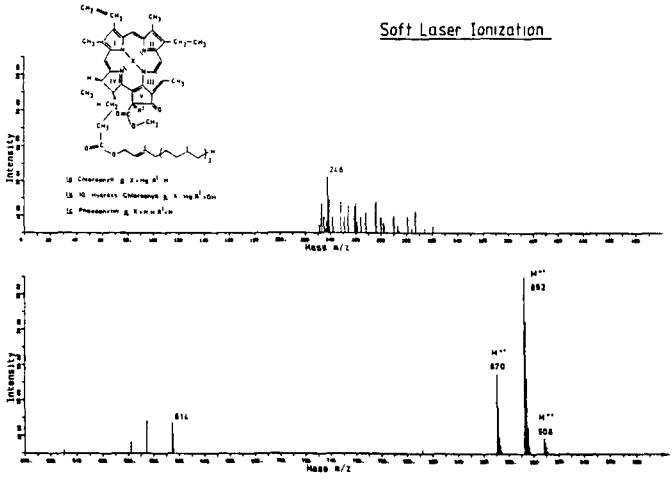

Figure 1 : Soft ionization mass spectrum of Chlorophyll a

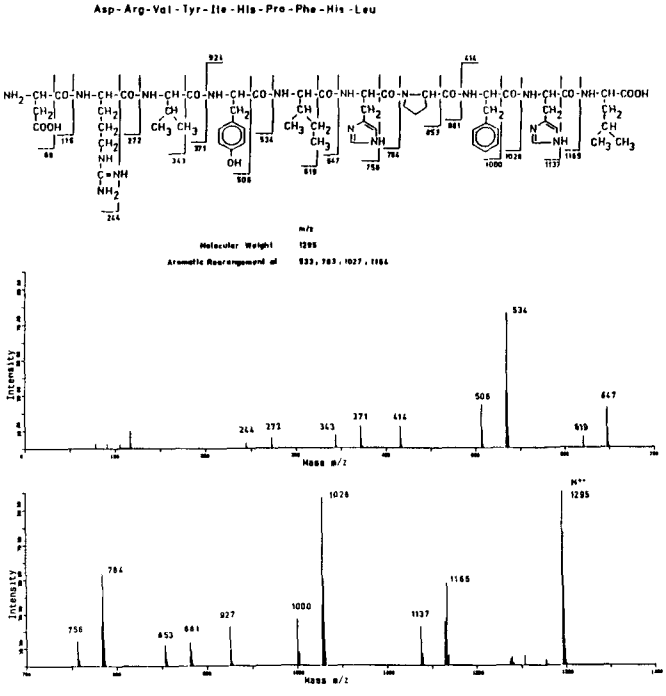

Figure 2 : Partial hard ionization mass spectrum of Angiotensin I

ABSOLUTE ISOTOPIC REFERENCE MATERIALS FOR SAFEGUARDS MEASUREMENTS

David W. Crawford, U.S. Department of Energy
New Brunswick Laboratory, Argonne, IL 60439

INTRODUCTION

The need for nuclear isotopic reference materials has been demonstrated for many years by both private industry and by the federal government. The private sector traditionally relies on such reference materials to insure that accurate measurements are maintained for criticality and process quality assurance purposes. The federal government through regulation also mandates reference materials use for safeguards purposes to assure that nuclear material accounting measurement practices are meeting essential reliability, accuracy, and compatibility criteria. Materials control and accountability (MC and A) information derived from reference materials is important to safeguards personnel in establishing limits of detection as applied to the potential diversion of nuclear materials. This information also indicates whether or not the instrumentation and measurement systems used to account for nuclear materials within a facility are functioning consistently within established limits.

The New Brunswick Laboratory (NBL) of the U.S. Department of Energy (DOE) has a major role in determining the validity of safeguards measurement systems used by DOE contractor facilities processing nuclear materials. This role is carried out by the conduct of site-specific assessments and the sponsorship of measurement evaluation programs. As part of its appraisal of the MC and A activities within the DOE facilities, NBL evaluates the internal measurement control information derived by the facilities' use of reference materials. This dependance on reference materials underscores another important role of NBL, that is, providing reference materials. To be effective, these reference materials must be suitable for the process being monitored, well-characterized in the properties of interest, and available in quantities and a form amenable to the measurements system providing safeguards accountability information.

Since 1981, NBL has had the sole responsibility within the federal government to provide special nuclear reference materials to the nuclear industry. In fulfilling this responsibility which is an integral part of the mission of NBL as the DOE Safeguards Analytical Laboratory, a number of reference materials specific to safeguards have been and are being produced. However, many more such reference materials are needed. NBL is using its unique combination of safeguards activities to identify and provide additional reference materials as well as technical assistance to assure their proper application to safeguards measurements.

Nearly three decades ago, the National Bureau of Standards (NBS) of the U. S. Department of Commerce certified a series of absolute uranium isotopic standards, which are widely used today in nuclear safeguards. Although several of these enrichments have been since replaced due to depletion of the inventories, the original suite is still the basis of all uranium and plutonium nuclear isotopic measurements performed today.

This paper will concentrate on the efforts of NBL to provide absolute isotopic reference materials for plutonium and americium measurement application. These particular reference materials are detailed here since NBL's work represents the first-of-its-kind technical effort to certify such materials on an absolute basis.

ABSOLUTE ISOTOPIC REFERENCE MATERIALS

Plutonium

In the late 1950's and early 1960's, NBS prepared a series of plutonium isotopic standards which have served as the national measurement base for the isotopic analysis of plutonium. Due to the unavailability of pure plutonium isotopes to prepare calibration mixtures for absolute isotope ratio bias corrections, these standards were certified based upon the NBS uranium isotopic reference materials. This basis for certification, coupled with high impurity levels due to ingrowing plutonium daughter products, packaging degradation due to radiation, and the large uncertainties commensurate with state-of-the-art mass spectrometric capabilities of 25 years ago, have now made these materials unsuitable for current state-of-the-practice safeguards measurements.

In 1972, the Atomic Energy Commission's Division of Nuclear Materials Security and Directorate of Regulatory Standards, participated in the formation of the Planning Committee on Nuclear Calibration and Test Reference Materials. The primary task of the Committee was to define and evaluate reference materials needs for national safeguards. The need for plutonium isotopic reference materials certified on an absolute basis was identified. A reappraisal of the Committee work through the U.S. DOE Office of Safeguards and Security in 1980 re-identified this need, and it was given highest priority by the U.S. and international nuclear organizations.

As the national certifying organization for special nuclear reference materials, NBL was tasked to make available plutonium absolute isotopic reference materials required to fulfill mass spectrometric and nondestructive assay safeguards measurement requirements of DOE and its contractors.

An equal atom ($^{242}Pu/^{239}Pu$ = 1:1) absolute isotopic reference material, NBL Certified Reference Material (CRM) No. 128, was the first absolute plutonium isotopic reference material produced and certified for U.S. safeguards and research activities. Its primary purpose is to calibrate mass spectrometers used to perform plutonium isotopic measurements. Since isotope dilution mass spectrometry (IDMS) is widely used in the plutonium production and processing industry, this reference material is extremely useful in providing instrument bias correction and measurement control information to the analysts as well as safeguards personnel. Also, precise measurements can be converted to accurate isotopic measurements using this material, which provide a high level of compatibility between mass spectrometric and other isotopic and assay techniques.

Table I summarizes the isotopic data and assay data used to calculate the certified value for CRM No. 128. The absolute $^{242}Pu/^{239}Pu$ ratio was determined mass spectrometrically through

intercomparisons between reference material samples and calibration mixtures with accurately known $^{242}Pu/^{239}Pu$ ratio values. The absolute $^{242}Pu/^{239}Pu$ ratio was also determined gravimetrically by the accurate blending of ^{239}Pu and ^{242}Pu isotopes with well-characterized isotopic and elemental composition. The unweighted mean of the mass spectrometric and gravimetric values was adopted as the certified value for CRM No. 128, as is shown Table II.

The production and certification of a series of four (4) ^{239}Pu absolute isotopic CRMs for both mass spectrometry and nondestructive assay (NDA) use are also currently underway at NBL. These CRMs will replace the existing NBS Plutonium Isotopic SRMs 946, 947, and 948, whose inventories are nearly depleted. Since the SRMs' certified isotopic values are not on an absolute basis, they are not sufficiently accurate to meet present-day safeguards requirements. The objectives of the new NBL CRMs will be: 1) to meet current state-of-the-practice mass spectrometric requirements, 2) to provide traceability for NDA measurements, and 3) to establish plutonium isotopic measurements on an absolute basis.
The four CRMs, consisting of 98%, 90%, 75%, and 55% ^{239}Pu, will bracket or resemble the isotopic ranges most often encountered by DOE contractors. The form, a chemically stable oxide powder, PuO_2, is similar to the chemical form of plutonium generated in industrial processes where accountability measurements are taken. These CRMs will permit better traceability of measurements performed on PuO_2 input or product materials.

The mass spectrometry units of PuO_2 will be packaged as 0.25 gram plutonium amounts, while NDA units are proposed to be in 5-10 gram plutonium amounts. Tests with PuO_2 materials at NBL indicate no difficulty in the dissolution of the oxide powder in nitric acid or aqua regia. Chemical purification to remove ^{241}Am and major impurities, as well as IDMS measurements using ^{244}Pu and ^{243}Am spike materials will provide precise minor ^{238}Pu and ^{241}Am values with a high degree of certainty to meet NDA needs. Using chemical purification dates, important daughter products, such as uranium and ^{241}Am, can be determined by decay models, using half-life and assay information, to extrapolate their values.

The advantages of the isotope dilution mass spectrometry technique to accurately determine the abundance values of minor isotopes at the part-per-million level has been demonstrated by other standards certifying organizations. More recently, NBL has used this technique to certify the minor isotopic composition of a ^{242}Pu Spike Assay and Isotopic Certified Reference Material, CRM No. 130. The samples were spiked with NBS SRM 996 (^{244}Pu) to approximate the ^{240}Pu concentration. By determining the assay of each minor isotope, the major ^{242}Pu could then be determined by difference. By measuring the isotope ratio of the sample isotope to high-purity ^{244}Pu and comparisons between this ratio with CRM No. 128, an absolute plutonium isotopic standard, absolute ratio values were used to gravimetrically determine the abundance value of each minor isotope.

Americium

A NBL project for the preparation and certification of an ^{243}Am Spike for NDA as well as IDMS determinations of ^{241}Am in plutonium-bearing materials is currently underway. Americium measurements are frequently performed using gamma-ray spectrometry for which there are no available reference materials. Therefore, the ^{243}Am CRM will provide a means for performing americium impurities corrections which have to be made in calorimetric measurements of plutonium. This CRM material will also provide a means for performing absolute americium measurements by IDMS, which has been demonstrated to be more precise and accurate than radiometric or NDA techniques. Ultimately, this CRM will provide traceability among all the various measurement techniques used for americium.

In addition to this spike CRM, a $^{241}Am/^{243}Am$ calibration standard will also be prepared so that systems used to perform americium measurements can be calibrated on an absolute basis.

High precision assay techniques (EDTA complexometric titration and "100% - Impurities" on the purified metal) will be used to characterize high-purity (99.9+%) ^{241}Am and ^{243}Am separated isotope solutions. Then aliquots of the ^{243}Am solution will be ampoulated and made available as the Spike. The ^{241}Am solution and remaining ^{243}Am solution will be quantitatively blended to produce the $^{241}Am/^{243}Am$ calibration standard. To establish the final isotopic ratio, calibration mixtures which bracket the standard's isotope ratio will be prepared and mass spectrometrically analyzed concurrently with the standard.

CONCLUSION

The use of absolute reference materials is an important part of any comprehensive safeguards measurements program. The availability of such materials in various physical forms is necessary to insure that not only accurate and reliable measurements are performed, but that process compatibility and traceability to a measurement basis exist.

The design effort required to produce and certify reference materials relies on input from both the private and public sector to insure that these materials are useful to measurement control. This input and NBL's responsiveness provide the means which enable reference materials to serve domestic safeguards needs.

Table 1
Absolute $^{239}Pu/^{242}Pu$ Ratio for CRM No 128
(all values decay-corrected to 10/1/84)

Calculation of Correction Factor				Absolute Ratio of CRM		
Calibration Mixture Number	Calculated	Observed	Correction Factor	CRM Sample Number	Observed	Corrected
1	0.99139	0.99522	0.99616	001	1.00130	0.99915
2	0.99666	0.99887	0.99779	144	1.00194	0.99979
3	1.00053	1.00303	0.99761	287	1.00162	0.99947
4	1.00573	1.00785	0.99790	494	1.00171	0.99956
5	1.01054	1.01267	0.99790	724	1.00138	0.99923
				855	1.00190	0.99975
				896	1.00155	0.99940
		Average:	0.99766		Average:	0.99948

Table 2
Certified $^{239}Pu/^{242}Pu$ Ratio for CRM No. 128
(all values decay-corrected to 10/1/84)

Measurement	Absolute $^{239}Pu/^{242}Pu$ Ratio	Standard Error	d.f.
Mass Spectrometry	0.99948	0.00020	19
Coulometry (mass)	0.99926	0.00009	5
Certified (unweighted mean)	0.99937	0.00013	21

Since t(95%,21) = 2.08, the 95% confidence interval for the certified value is ±0.00026

ISOTOPIC DILUTION MASS SPECTROMETRY MEASUREMENT OF PLUTONIUM INPUT SOLUTIONS TO THE HANFORD PLUTONIUM-URANIUM EXTRACTION FACILITY

E. S. Baker and C. R. Lagergren;
Rockwell Hanford Operations, Richland WA 99352

The Analytical Laboratories at Rockwell Hanford Operations are performing plutonium accountability measurements on the input solutions to the Hanford Plutonium-Uranium Extraction (PUREX) Facility. To satisfy the necessarily stringent nuclear material accountability requirements, plutonium isotopic dilution mass spectrometry (IDMS) is being used. To maintain high levels of accuracy and precision in a measurement process that has many critical steps and involves personnel in three (3) separate laboratory organizations, it is important that tight measurement controls be employed to monitor system performance.

Sampling of the input solution is performed in a hot cell. Duplicate samples are taken of each tankful and transferred to the PUREX Analytical Laboratory. An appropriate weight dilution is performed on the sample so that a portion transferred by weight to a vial containing a known quantity of dry plutonium-244 will have a $^{239}Pu/^{244}Pu$ atom ratio of approximately 10. Complete isotopic exchange between the spike and sample is achieved by fuming the sample with perchloric acid. The plutonium is then separated from fission products and transported to the mass spectrometer laboratory where final purification is performed. The sample is mounted on rhenium filaments together with platinum by an electrodeposition technique co-developed with R. E. Perrin, Los Alamos National Laboratory. A single analysis by triple filament thermal ionization mass spectrometry provides both sample plutonium isotopic composition and total plutonium concentration.

Measurement controls are provided by the analysis of (1) standard reference materials for determining method and instrument bias and relating measurements to a national data base, (2) duplicate and referee samples to monitor the overall method precision, and (3) mixtures of new standard and spike working solutions with older solutions to provide continuity and guard against errors in working solution preparation. The NBS Standard Reference Materials (SRMs) 946 and 947 isotopic standards are used to determine the mass spectrometer bias. The NBS SRM 949f plutonium metal, certified for its plutonium content, is used as the primary method standard. The NBS SRM 996 is used as the plutonium spike material. Although SRM 996 is certified as an assay and isotopic standard, the plutonium-244 concentration of the spike working solution from each SRM unit is measured relative to an SRM 949f standard solution using the same measurement system used to analyze samples. Utilization of the measured plutonium-244 working solution concentration nearly cancels the effect of the mass spectrometer bias calibration on the absolute accuracy of sample plutonium concentration measurements. Repeated analysis of the SRM 996/949f mixture allows for the continuous calibration of the spike solution through the life of the SRM unit and provides a sensitive indicator of changes in mass spectrometer bias. All of the standard working solutions are prepared in the Standards Laboratory.

The reduction of the effect of mass spectrometer bias on method accuracy is demonstrated by the following. Equation (1) gives the sample plutonium concentration (C_S) when the plutonium-244 spike working concentration (C_K) is derived from the SRM 996 unit certification.

$$C_S = W_S \frac{C_K \gamma^5}{M_7 R_7} \sum_{i=1}^{5} M_i \left[R_i \gamma^{(2-i)} - R_7 R_i \gamma^{-5} \right] \quad (1)$$

Where: W_S is the ratio of spike and sample weights with associated dilutions (W_F for 949/966 mix)

M_1, ..., M_5 and M_7 are the isotopic masses of ^{238}Pu, ..., ^{242}Pu and ^{244}Pu respectively

R_1, ..., R_5 and R_7 are the measured raw isotopic abundance ratios in the sample-spike mix of ^{238}Pu, ..., ^{242}Pu and ^{244}Pu relative to ^{239}Pu/ (R_1' for the 949f/966 mix)

$\mathcal{R}_1$ ...., $\mathcal{R}_5$ are the isotopic abundance ratios in the spike alone of ^{238}Pu ...., ^{242}Pu relative to ^{244}Pu.

γ is the per mass unit bias correction factor for measured isotopic abundance ratios in which the denominator contains the abundance of the isotope having the greater mass.

A similar equation exists giving the concentration of SRM 949f (C_F) from analyses of the working mix of SRM 949f/966. Combining the two equations to eliminate the spike concentration (C_K), one obtains Equation (2), where the atomic weight divided by the atomic fraction 239 (S for sample and F for 949f) has been substituted for the summation portions of both equations.

$$C_S = \frac{W_S}{W_F} \; C_F \; \frac{R_7'}{R_7} \; \frac{\left(\dfrac{\text{Atomic Weight}}{\text{Atomic Fraction 239}}\right)_S}{\left(\dfrac{\text{Atomic Weight}}{\text{Atomic Fraction 239}}\right)_F} \qquad (2)$$

The mass spectrometer bias correction factors cancel, except where they appear in the atomic weight and atomic fraction 239 portions of the equation.

A direct comparision of the accuracy obtainable in the analysis of typical material using the SRM 996 certified value and measured value for spike concentration is shown in the following table of component contributions at the 95% confidence level.

Component	Certified 996	Measured 996
W_S	.125	.125
W_F	----	.030
C_K	.150	----
γ	.689	.008
R_7	.174	.174
R_7'	----	.039
$\sum R_i$	.020	.020
$\sum R_i'$	----	.006

The obtainable accuracy of a single analysis using the measured 996 concentration is then 0.402% (at the 95% confidence level) plus the percent uncertainty of the unit of SRM 949f used (as provided on the certificate) as opposed to an accuracy of 1.158% using the 996 certified value.

Current operation of the plutonium IDMS procedure has demonstrated the following performance. Indicated precision is 0.30% from method standards, 0.27% from referee analyses and 0.47% from duplicate samples. The analytical precision of the method itself is 0.29% (combining method standards and referees) and is significantly different from that derived from duplicate samples. This suggests that the precision of sampling is 0.37%. The recovery on method standards is 100.10%. These performances represent the "state-of-the-practice" as IDMS is being performed at Hanford in a full-scale fuel reprocessing facility with non-professionals doing all of the work. They compare well with the "state-of-the-practice" target values of 0.5% relative standard deviation random error and 0.5% systematic error presented by DeBievre et al., "1983 Target Values for Uncertainty Components in Fissile Elements and Isotope Assay", ESARDA Bulletin, Number 6, April 1984.

ISOTOPIC ANALYSIS OF LITHIUM

L.W. Green, J.J. Leppinen and N.L. Elliot

Atomic Energy of Canada Limited
Chalk River Nuclear Laboratories
Chalk River, Ontario, Canada, K0J 1J0

One of the important uses of lithium is as a tritium breeder material in fusion reactors:

$$^{6}Li \xrightarrow{(n,\alpha)} {}^{3}H$$

$$^{7}Li \xrightarrow{(n,\alpha n)} {}^{3}H$$

The mass 6 isotope has a much greater neutron capture cross section than the mass 7 isotope, consequently enrichment of ^{6}Li from its natural abundance of 7.4% is advantageous. High precision isotopic analysis of Li is required for both determination of the degree of depletion of ^{6}Li in breeder material and for determination of the degree of separation of Li isotopes by isotope separation techniques.

Various procedures for isotopic analysis of Li have been reported (1-4); these involve deposition of Li on sample filaments as LiI, LiCl or $LiNO_3$ and measurement of the atomic ions at masses 6 and 7. Dual collector mass spectrometers designed for Li measurement were used in some cases. Our experience with these procedures showed high fractionation rates and severe irreproducibilities (± 10%) from one loading to the next. Although these irreproducibilities were due in part to the use of a large single-detector mass spectrometer designed for heavy elements, the high and fluctuating fractionation rate was likely the major cause.

To reduce the fractionation rate and other low-mass problems use of a molecular ion was investigated. After some experimentation and trials with various species, satisfactory signals were obtained for the Li_2F^+ species. Best results were obtained when LiOH and HF were mixed freshly in a 2/1 ratio and ~2 μg aliquots were gently evaporated on tantalum side filaments of a triple filament assembly. The side filaments were heated by radiant heat from the centre filament (1600°C) and Li_2F^+ ions were measured at masses 31, 32 and 33 (Figure 1). Replicate analyses of a series of standards ranging from 6 to 95% ^{6}Li yielded a mean of 0.9996 ± 0.0021 (1s) for the ratios of measured to known 6/7 ratios.

Reagents used in the isotope separation work or in sample preparation either suppressed the Li_2F^+ signal or caused severe isobaric interferences. These reagents were removed by ion exchange, first with a cation exchanger in the H^+ form then with an anion exchanger in the OH^- form, to yield LiOH. Initial work showed that considerable care was necessary to avoid contamination with natural lithium during this procedure. Also, the mass spectrometer source had to be cleaned routinely to avoid memory effect.

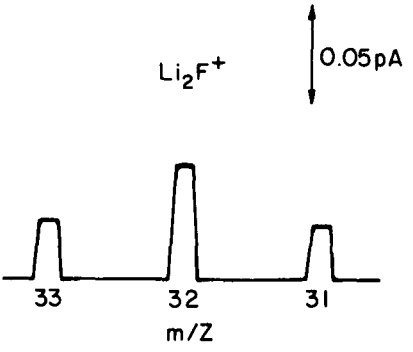

Figure 1. Mass spectrum of Li as Li_2F^+ ions. 50% enriched ^6Li.

REFERENCES

1. Svec, H.J.; Anderson, A.R. Geochem. Cosmochem. Acta, 1965, 29, 633-641.

2. Michiels, E.; De Bievre, P. Int. J. Mass Spec. Ion Phys., 1983, 48, 369-372.

3. Brown, H.L.; Biltz, C.; Anbar, M. Int. J. Mass Spec. Ion Phys., 1977, 25, 167-181.

4. Adriani, A.; Boniforti, R. Com. Naz. Energ. Nucl. Report RT-CHI (75)8, 1975.

APPLICATION OF ELECTRON ENERGY STUDIES TO RESONANCE IONIZATION MASS SPECTROMETRY

D. H. Smith, J. P Young, and D. L. Donohue
Analytical Chemistry Division
Oak Ridge National Laboratory
Oak Ridge, TN 37831

The goal of applying resonance ionization to isotope ratio mass spectrometry is to generate ions of one element of a mixture without ionizing other elements; this leads in principle to spectra that are free of isobaric interferences. In our early investigations of the lanthanide elements, several wavelengths were found that were relatively efficient at ionizing the element in question but whose optical processes were not readily understood (1-3). Application of known energy levels did not reveal likely ionization pathways. It was decided to investigate further by measuring the excess energy of the free electron created in the ionization process. An electron spectrometer was used to obtain electron spectra of Sm, Nd, and Pr. The spectra were complicated by the electronic structure of the singly--charged ion. For each of the elements studied, several low-lying ionic energy levels were populated during the ionization process; each of these led to a peak reflecting the difference in energy between the state of the ion and the final state of the atom. The electron of highest energy represented populating the ground state of the ion and was revealed by an abrupt high-energy cut-off in the spectra. The energy thus measured allowed calculation of the excited energy level of the atom from which the ion was created and also that of its initial state. Comparing spectra calculated by assuming equal probability of populating all accessible levels in the ion with those obtained experimentally yielded confirmation of these calculations. Comparison of the positions of the lines in the calculated spectra with those obtained experimentally allowed unambiguous assignment of starting levels: incorrect assignments led to spectra radically different in electron energies. The accompanying table lists the lines studied and some of the relevant parameters.

Lines Studied

Element	Wavelength, nm	Initial level, cm^{-1}
Nd	587.1	0
Pr	584.5	1376
Pr	598.0	0
Pr	611.7	0
Sm	593.7	1490
Sm	580.1	2273

Each of the transitions studied involved three photons: the ionization potentials of all three elements were about 45,000 cm^{-1}, and the energy of each photon was in the range of 16,000--17000 cm^{-1}; this absorption of three photons was necessary to remove an electron from the ground or low-lying state to the

ionization continuum. While we were able to identify unambiguously the starting energy level and the highest level occupied by the electron in the neutral atom on its ionization pathway, some uncertainty remained as to the identities of any intermediate levels involved. The power dependence of the three praseodymium transitions was measured and yielded a slope of one, indicating that only single-photon transitions were involved in the ionization process and that the rate-limiting transition was the ionization step.

We conclude from this work that electron spectroscopy is a valuable tool in elucidating ionization pathways and that transitions available to the RIMS practitioner are more than one would predict from direct application of energy level differences.

REFERENCES

1. J. P. Young and D. L. Donohue, Anal. Chem. 55, 88(1983).

2. J. P. Young, D. L. Donohue, and D. H. Smith, Int. J. Mass Spectrom. and Ion Phys. 56, 307 (1984).

3. D. L. Donohue, J. P Young, and D. H. Smith, Appl. Spectrosc. 39, 93 (1985).

Acknowledgment

This work was supported by the U. S. Department of Energy, Office of Basic Energy Sciences, through Contract DE-AC05-84OR21400 with Martin Marietta Energy Systems, Inc.

By acceptance of this article, the publisher or recipient acknowledges the U S Government's right to retain a nonexclusive, royalty-free license in and to any copyright covering the article.

INTERFACE PROPERTIES OF A QUADRUPOLE ICP/MS SYSTEM

Richard F. Browner and Guangxuan Zhu*

School of Chemistry
Georgia Institute of Technology
Atlanta, Georgia 30332

The advent of inductively coupled plasma/mass spectrometry (ICP/MS) has required the re-examination of many concepts well established in ICP optical emission studies. The initial approach to understanding and optimizing ICP/MS systems has been to study the effect of system variables on the plasma, and to consider the rest of the system including the plasma/mass spectrometer interface and the mass spectrometer itself, as a given. Studies of this type have demonstrated that certain variables, such as nebulizer gas flow and plasma operating power are key parameters which must be controlled in order to simultaneously optimize system response, while keeping interelement interferences within acceptable limits.

The ultimate success of ICP/MS as a routine analytical technique will depend on its ability to handle a wide range of sample types, at very low concentrations, while maintaining the type of interelement interference freedom that has typified ICPOES. To this end, it becomes clear that the ICP/MS system must be considered as a whole, and separate optimization of either the plasma or the mass spectrometer can lead to misleading trends.

The three main goals of this study were: (1) to make a general comparison of the properties of two commercial ICP/MS instruments (2) to examine the influence of high concentrations of elements such as of Na, which are known to affect ICP/MS signals, and to study the possible use of the mass spectrometer to control these (3) to determine the properties of the interface with respect to the production of doubly charged ions, and with respect to oxide and hydroxide species.

The work showed that a number of the trends that have been observed with other instruments may, in general terms, be transferred to the PlasmaQuad instrument. For instance, the nebulizer gas flow is a critically important parameter, and there is an optimum value of argon flow, which also varies with applied plasma RF power. The optimum nebulizer gas flow was found, however, to be significantly lower than for certain other instruments, peaking at 0.6 l/min, *vs.* typically 1.2 l/min. Also, the value for optimum gas flow did not vary much from element to element for those studied. This again contrasts with published studies for a different instrument.

Other interface parameters studied were: (1) the influence of sampling depth in the plasma on signal, at various plasma powers, for a number of elements (2) the influence of nebulizer gas flow on BaO^+ and $BaOH^+$, compared to Ba^+ (3) the influence of nebulizer gas flow on the ratio of Ba^{++} to Ba^+ ions. The optimum sampling height was found to be approximately 15 mm above the top of the plasma coil, rather lower than for some other systems. Furthermore, the trend was for the signal to peak at slightly *higher* gas flows as the sampling position was reduced. This again contrasts with some published data. The BaO^+ to Ba^+ ratio was found to be approximately 0.1%, and the Ba^{++} to Ba^+ ratio was found to be approximately 2%. The BaO^+ to Ba^+ ratio was rather lower than that reported previously, whereas the Ba^{++} to Ba^+ ratio was slightly higher.

As part of a preliminary study on the influence on the interactive nature of plasma and mass spectrometer parameters, the interference of high concentrations of Na on a low concentration Mg solution was studied. It has been stated that under these conditions enhancements are always observed. In our experiments, when conditions were set for greatest Mg response, negligible interference was observed. When the MS was detuned, however, reducing the overall response for Mg by up to a factor of 5, significant signal enhancements were found. Under certain conditions 500 ppm Na gave a greater enhancement than 1ppm Na, whereas under other conditions the order was reversed.

* On leave from Dalian Institute of Chemical Physics, Dalian, P.R. China.

ION KINETIC ENERGIES IN INDUCTIVELY COUPLED PLASMA MASS SPECTROMETRY (ICP/MS),

J.E. Fulford and D.J. Douglas, SCIEX®, 55 Glen Cameron Road, Thornhill, Ontario, L3T 1P2, Canada

Since the inception of ICP/MS in 1980 (1) the ion sampling interface has been a topic of considerable discussion and has been recognized as a critical part of any ICP/MS system. Some workers have reported that the ion kinetic energies measured at the quadrupole (i.e. in the vacuum system) were strongly dependent on the plasma operating parameters (2,3). Olivares and Houk[2] suggested that this behaviour was the result of a "secondary discharge" or "pinch" occurring in the sampling interface.

In this paper we report in more detail on the kinetic energies of ions sampled with an interface (4) which is designed to eliminate the secondary discharge. We show that the results are consistent with those expected from molecular beam sampling from a high temperature plasma and discuss the implications of these results for practical ICP/MS systems.

Ion kinetic energy distributions were measured by applying a retarding rod offset potential to the quadrupole mass filter and differentiating the resulting curve of ion signal vs. retarding potential. The most probable energy (MPE) was used as a measure of ion kinetic energy. The energies measured here are believed to be accurate to $\pm$1eV since the retarding curves are recorded in 1eV steps. All experiments were carried out with a distance of 16 mm between the sampler and load coil. All the species measured, showed similar shaped distributions in that the width of the energy distribution measured at half height was approximately equal to the MPE.

The MPE is plotted as a function of ion mass in Fig. 1 for the species Li^+, Mn^+, Ar_2^+, Rh^+, Pr^+ and U^+. It is seen that the energy increases monotonically with ion mass. The energies of the other singly charged ions, the oxide ions, and the doubly charged ions fit on the same curve. This implies that the oxide and doubly charged ions are formed in a collision dominated flow regime i.e. at or upstream of the skimmer rather than by ion molecule chemistry (MO^+) or secondary discharge effects (M^{+2}) downstream of the skimmer.

The energies of Fig. 1 are consistent with those expected from molecular beam sampling of an ICP. In the expansion, ions move at the speed of the argon neutrals. An ion of mass M will have an energy from the supersonic expansion given by the first term of equation 1.

$$E = \frac{M}{M_{Ar}} E_{Ar} + P \qquad (1)$$

where M_{Ar} is the mass of the neutral argon (40 amu) and E_{Ar} is the kinetic energy of the neutral argon. E_{Ar} can be calculated from a measurement of the gas kinetic temperature of the source (5). The first term of equation 1 predicts an energy for Li^+ less than 0.37eV. In fact 2eV was observed for Li. This higher energy likely derives from a plasma potential of approximately 2 V, or possibly space charge effects in the ion beam. This potential, P, apparently adds to the energy produced by the expansion.

The straight line in Fig. 2 was calculated assuming P = 2.0eV and a gas kinetic temperature T_0 = 4900°K. This value for T_0 lies in the midrange of gas kinetic temperatures measured optically in ICPs and is also consistent with the observed pressure in the first vacuum stage (5).

The variation of MPE as a function of aerosol flow rate is plotted for Li^+, Rh^+, PrO^+ and U^+ in Fig. 2. The most striking feature of this plot is that the MPE does not change appreciably ($\pm$1eV) over a large range (0.4 - 0.9 L/min) of aerosol flows. These observations are in contrast with the strong upward trend in MPE for increasing aerosol flow rate reported by Olivares and Houk[2]. With the interface used here, the analyte ion energies were found to be unchanged by the presence of 1000 ug/ml U or Na in solution.

The fact that ion energy is independent of changes in plasma parameters or sample composition is an important practical advantage. With the conventionally grounded ICP, slight changes in plasma conditions can produce large changes in ion energies, requiring

"retuning" of electrostatic ion optics and making optimization of the ICP and ion lens system interactive. With the interface used here the ICP parameters and ion optics can be optimized independently, greatly simplifying this process. This would appear to be an advantage both for fundamental ICP studies and for setting up the instrument for practical analysis.

REFERENCES

1. R. S. Houk, V. A. Fassel, G. D. Flesch, H. J. Svec, A. L. Gray and C. E. Taylor, Anal. Chem. 52, 2233 (1980).

2. J. A. Olivares and R. S. Houk, Appl. Spectrosc., 39, 1070 (1985).

3. A. L. Gray, presented at the Federation of Analytical Chemistry and Spectroscopy Societies 12th Annual Meeting, Philadelphia, October, 1985.

4. D. J. Douglas and J. B. French, Spectrochim. Acta B, 41B(3), 197 (1986).

5. J. E. Fulford and D. J. Douglas, Appl. Spectrosc., (in press).

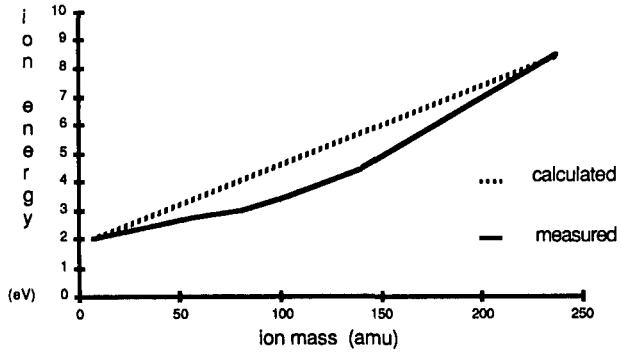

FIG. 1 DEPENDANCE OF MPE ON ION MASS
(Calculated line assumes a plasma potential (P) of 2eV and a temperature of 4900 K)

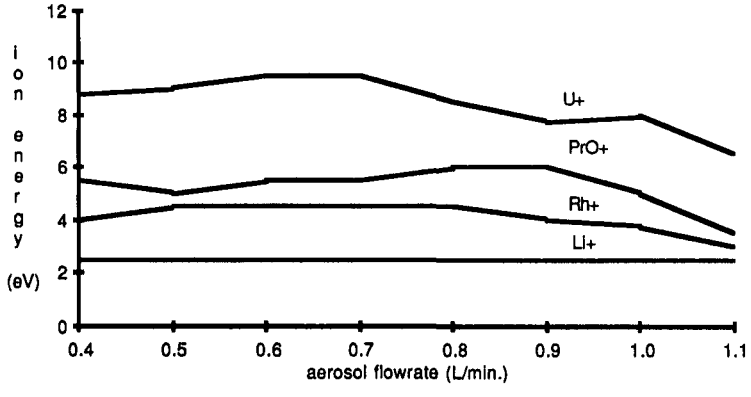

FIG. 2 EFFECT OF AEROSOL FLOWRATE ON MOST PROBABLE ION ENERGY

INTERFERENCES IN INDUCTIVELY COUPLED PLASMA-MASS SPECTROMETRY

Daniel A. Wilson, George H. Vickers, and Gary M. Hieftje, Department of Chemistry, Indiana University, Bloomington, IN 47405 and Andrew T. Zander, Spectroscopy Division, Perkin-Elmer Corp., 901 Ethan Allen Highway, Ridgefield, CT 06877.

Inductively Coupled Plasma-Mass Spectrometry (ICP-MS) has become a frequently used technique for elemental analysis in the years since it was introduced (1). The high sensitivity and low background of ICP-MS for most elements have been a major driving force for much of the work that has been done. However, even this low background can cause major spectral interferences on certain elements. An example is calcium, whose major isotope at 40 daltons suffers interference from argon.

In an effort to evaluate interferences in ICP-MS, we have examined spectral overlap of analyte species with background ions from the solvent and from acid species used in sample preparation. Spectral interferences caused by doubly charged and oxide ions from the analyte have been studied also. Such ions not only can interfere spectrally with other analytes but also decrease the sensitivity for the analyte by forming fewer singly charged ions. In addition, chemical or physical interferences in the plasma or sampling region caused by other species present in the sample matrix have been gauged.

The instrument used for the work reported here was assembled from a Plasma-Therm HFP 2500F ICP rf generator and impedance-matching unit and a Balzers QMG-511 quadrupole mass spectrometer. A description of the features of this instrument and an evaluation of its analytical characteristics have been reported (2).

The observed background mass spectrum when distilled, deionized water is used as the blank is similar to that obtained on commercial instruments and contains several regions with strong, complex features. These ranges are from 14-20 (nitrogen, oxygen, water, and hydroxide ions), 28-33 (molecular species of nitrogen, oxygen, and hydrogen), 36-41 (argon isotopes and argon-hydrogen dimers), 50-58 (molecular ions with argon, nitrogen, and oxygen), and 76-81 (argon-argon dimer isotopes and argon-argon-hydrogen species) amu. The rest of the mass spectrum is nearly free of background; however, many desired elements must be detected within the regions where there is significant background.

The background becomes even worse if the sample matrix contains 5% or more of certain acids often used for dissolution of solids or for stabilization of a solution. Conveniently, nitric acid gives approximately the same background as deionized water; however, sulfuric and hydrochloric acids generate many additional background ions. Ions observed from sulfuric acid interfere with the major isotopes of Ti (at 48 daltons), V (51), Zn (64), Ge (74,72), and As (75) while hydrochloric acid causes a strong interference for determination of As. The concentration of analyte equivalent to these background signals is roughly from 1 to 100 ng/mL.

Unfortunately, many elements efficiently form doubly charged analyte and analyte-oxide ions. These ions cause an interference on that analyte by decreasing the amount of singly charged analyte ions that are formed. They can also cause a spectral interference on other elements; this is particularly true for many oxide ions, which tend to overlap with other elements. Metal-hydroxide ions are also present at approximately 5% of the intensity of the metal-oxide peak. In the instrument used for the present work, oxide ion levels are unusually low, less than 0.3% of the singly charged ion signal for most elements. Doubly charged ion ratios are higher, but are less than 13% for all elements. The oxide and doubly charged ion ratios observed for several elements are shown in Table 1. Importantly, the reported ratios were taken under conditions that produced the maximum signal for the singly charged analyte ion in each case and not under conditions that yielded the lowest ratio. Changing the conditions over the range that is ordinarily used caused little change in the ratios listed in Table 1.

Several possible chemical or physical interferences were studied, including the kind frequently observed in flame and plasma atomic emission spectrometry. Ionization interference, caused by the presence of an easily ionized element, was studied by determining the effect of sodium on cadmium. Figure 1 shows that no significant ionization interference occurs, although the presence of the sodium increases signal instability. The same type of study is presented in Figure 2 for the vaporization interference of phosphate on cadmium; again, there is no significant concomitant effect.

Finally, we determined the effect of a number of elements on a single analyte. It has previously been reported that severe interferences in ICP-MS can be caused by almost any element at a sufficiently high concentration. Moreover, the severity of the interference appears to be partly dependent upon the mass of the interferent (3). In a preliminary study of this type of interference in the present instrument, three elements were used as interferents on cobalt. The interferents, their masses and the relative signals observed for cobalt are given in Table 2. The only significant interference is that caused by barium. There is as yet no clear dependence upon the mass of the interferent, although a more complete study is necessary.

References:

1. R.S. Houk, V.A. Fassel, G.D. Flesch, H.J. Svec, A.L. Gray, and C.E. Taylor, Anal. Chem., **52**, 2283 (1980).
2. D.A. Wilson, G.H. Vickers, G.M. Hieftje, and A.T. Zander, Spectrochim. Acta, **42B**, in press.
3. G. Horlick, S.H. Tan, M.A. Vaughan, Y. Shao, and J. Lam, Paper 1, Winter Conference on Plasma Spectrochemistry, Kailua-Kona, HI, January, 1986.

TABLE 1. *DOUBLY CHARGED AND OXIDE IONS OBSERVED IN ICP-MS*

Element	M^{++}/M^{+}(%)	MO^{+}/M^{+}(%)
Barium	12.5	0.0675
Cerium	4.91	0.263
Gold		0.00115
Lead	0.0525	not observed
Molybdenum	0.026	0.067
Strontium	6.07	0.014
Titanium		0.165
Uranium	11.8	0.377
Zirconium	0.374	0.239

TABLE 2. INTERFERENCES ON THE COBALT SIGNAL
Interferent Concentration = 100 ppm, Cobalt Concentration = 100 ppb

Interferent	Atomic Weight (g/mol)	Relative Signal
None		1.000 ± 0.039
Sodium	23	1.051 ± 0.039
Barium	138	0.834 ± 0.063
Gold	197	0.964 ± 0.037

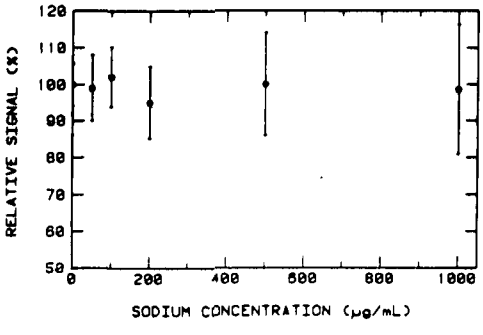

FIGURE 1
IONIZATION INTERFERENCE ON CADMIUM

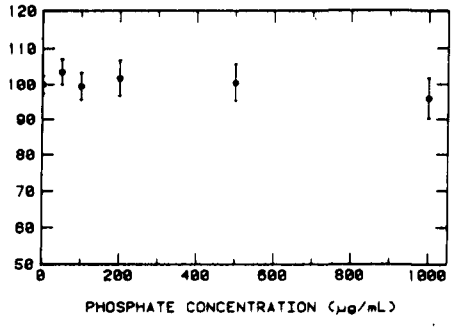

FIGURE 2
VAPORIZATION INTERFERENCE ON CADMIUM

GLOW DISCHARGE MASS SPECTROMETRY APPLIED TO THE DIRECT ANALYSIS OF SOLIDS

J E Cantle, N E Sanderson, R Nayler, P Jackson, P M Charalambous
VG Isotopes Limited, Winsford, Cheshire, CW7 3BX, UK

A glow discharge mass spectrometer (GDMS) is now in routine operation in a number of laboratories around the world. It consists of a DC glow discharge source coupled to a high resolution double-focussing mass spectrometer, with electronic recording and computer controlled data acquisition.

The spectrometer, operating at a mass resolution of 4000, typically delivers up to 1E-10 A of matrix beam current from a sample to the detector. The dual detector system has a dynamic range of eleven orders of magnitude, which enables all constituents of the sample (major, minor and trace) to be ratioed directly to the matrix in the same analytical cycle. The detector has a background of approximately 1E-19 A which enables detection limits below 10 ppb to be achieved in seconds of scanning.

The glow discharge source produces doubly charged ions at an equivalent concentration of about 100 ppm and molecular ions at equivalent concentrations that can also be up to a few hundred ppm. Therefore a high resolution analyser to resolve these interfering species is essential for meaningful trace analysis. With this capability however, the stability of the source, relatively uniform sensitivity for ionisation, and freedom from severe matrix effects lead to excellent precision and accuracy allied to full elemental coverage across the periodic table.

Detection Limits

Measurements of thorium and uranium at very low levels in various matrices have recently been carried out. The spectrum shows a peak at 0.9 ± 0.3 ppb from an aluminium matrix. The LOD, set by the background, is 0.2 ppb. Scan time was approximately 8 minutes.

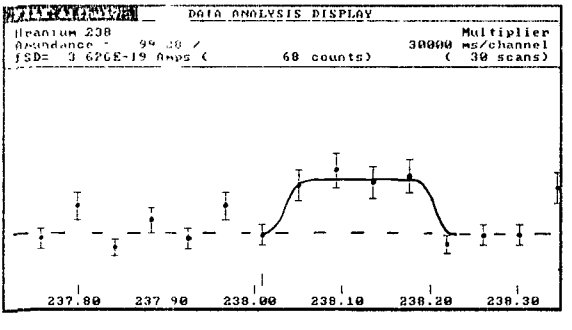

Uranium in aluminium at 0.9 ppb

Trace Analysis

Gallium has been analysed successfully for a range of some 30 trace elements. The spectrum illustrates a measurement of ^{56}Fe at 50 ppb achieved in 45 seconds. The resolution of the elemental peak from the molecular interference is clear.

GALLIUM MATRIX

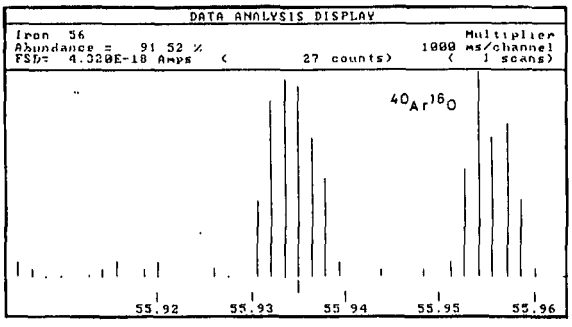

Iron at 50ppb

Quantitation

Analysis of a nickel based alloy has yielded precisions and accuracies approaching 1% for the major constituents, as illustrated in the table.

Ni-Alloy

Element	% RSD	Concentration found / Certified value
Al	1.02	0.9988
Ti	1.13	1.073
Cr	0.94	0.996
Co	0.52	1.001
Mo	0.82	1.011
Hf	1.20	1.015
Ta	1.30	1.004

Summary

GDMS based on a high resolution mass analyser now gives the capability for a full characterisation of solid materials by direct analysis of matrix, majors, minors and traces. The technique therefore offers several improvements on other established methods and can in fact perform analyses which would normally require a combination of these methods.

EFFECT OF EXPERIMENTAL CONDITIONS ON THE DAUGHTER ION SPECTRA OF STEROID GLUCURONIDES

Christian Guenat, Richard B. Cole and Simon J. Gaskell
NIEHS, P.O. Box 12233, Research Triangle Park, NC 27709

The principal advantages of collisional-activation/tandem mass spectrometry (MS) techniques over conventional MS relate to the improved facility for mixture analysis and the increased generation of structurally-diagnostic fragmentation. Successful application of these techniques to problems of biomedical interest, such as the differentiation of isomers, is dependent on the achievement of reproducible collisionally-activated decomposition (CAD) data. The ability to differentiate the steroid conjugates androsterone glucuronide (5α-androstan-3-ol-17-one-3-glucuronide) and etiocholanolone glucuronide (the 5β-isomer) is crucial to the diagnosis of 5α-reductase deficiency [1], a human enzyme disorder. These isomers may be distinguished under appropriate fast atom bombardment (FAB) / tandem mass spectrometry conditions on the basis of the relative abundances of daughter ions derived from CAD of $[M+H]^+$ (m/z 467) ions. The tandem double-focusing mass spectrometer used in these studies was a VG ZAB-4F of B1E1-E2B2 configuration. Daughter ions (m/z 250-460) produced in the third field-free region were monitored by performing a linked scan of B2 and E2.

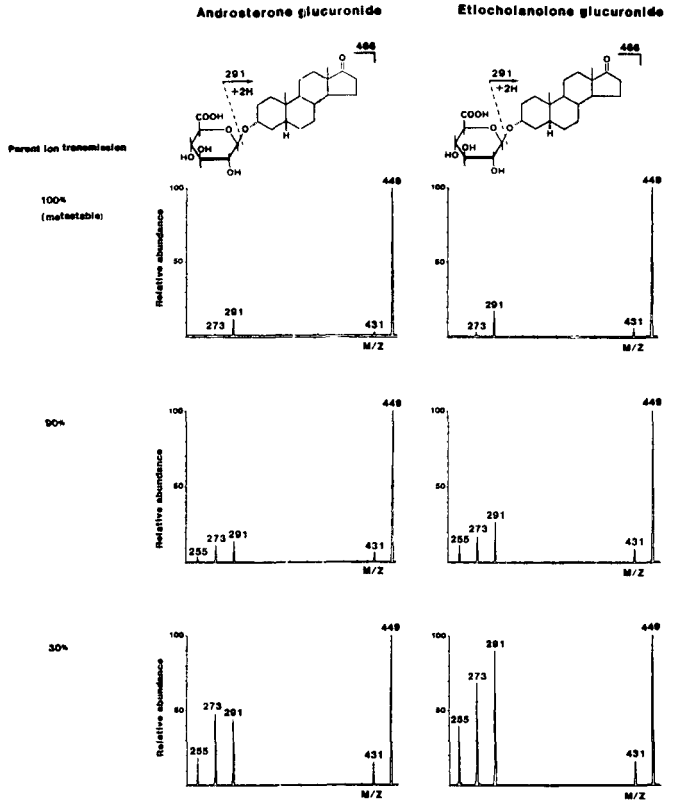

Figure 1.

Displayed in Figure 1 are the daughter ion spectra at different collision gas (helium) pressures (indicated as parent ion transmissions). As the collision gas pressure was incrementally increased, a steady increase in "aglycone" steroid fragments (those incorporating loss of the glucuronic acid moiety, i.e. m/z 291, 273, and 255) was observed. At high parent ion transmissions (100% and 90%), the daughter ion spectra of the two analytes were quite similar. At 30% parent ion transmission, however, two criteria can be used to distinguish between the isomers. For androsterone glucuronide (concentration < 7 mM in glycerol): 1) intensity of m/z 291 < m/z 273; 2) ratio of m/z 273:255 > 2. For the etiocholanolone isomer these inequality signs are reversed.

At very high androsterone glucuronide concentration (68 mM), a significant change occurred in the daughter ion spectrum, relative to lower concentrations. The intensity of m/z 291 was observed to be greater than m/z 273, hence, the first criterion for distinguishing between isomers was lost. Furthermore, the FAB source spectra at this highest concentration contained very weak glycerol cluster (m/z 185) and glycerol adduct (m/z 559) signals. Figure 2 (top) shows the time-dependent conversion of the daughter ion spectrum of an initially high concentration (68 mM) androsterone glucuronide sample, to that associated with the lower concentration condition, upon continual target sputtering. This conversion was correlated to a parallel time-dependent increase in the intensity of the source-formed m/z 559 ion detected at the indicated intervals. These results suggest that an enrichment of analyte at the sample surface (relative to the bulk) occurring above a critical concentration was responsible for the change in the daughter ion spectrum. This concentration-dependent variation may be attributable to either a change in the internal energy, or a shift in the distribution, of sputtered protonated molecular ion species.

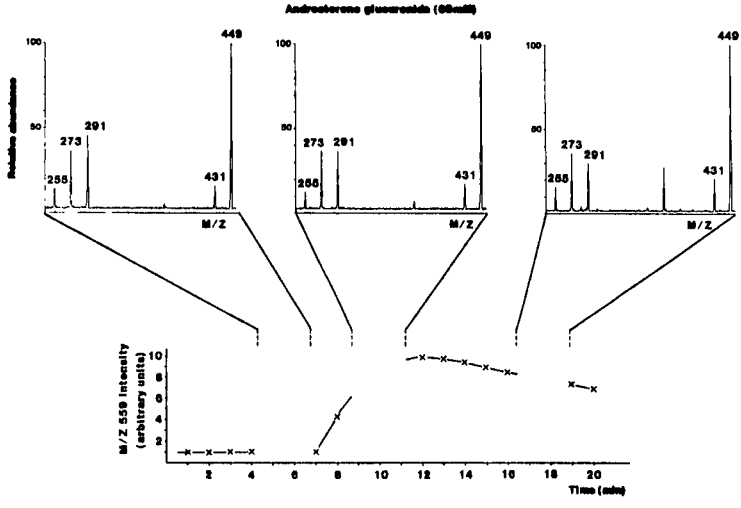

Figure 2.

1. Shackleton, C.H.L. Analysis of Steroids. In: Jaeger, H., ed. Glass Capillary Chromatography in Clinical Medicine and Pharmacology. Marcel Dekker, NY, 1985

OPTIMISATION OF ANALYTICAL PARAMETERS FOR THE TANDEM MASS SPECTROMETRY OF COMPOUNDS OF BIOCHEMICAL INTEREST USING A HYBRID SECTOR/QUADRUPOLE INSTRUMENT.

Simon J. Gaskell, Tenovus Institute for Cancer Research, University of Wales College of Medicine, Cardiff CF4 4XX, U.K.

Gareth C. Thorne, Department of Medical Physics and Bioengineering, Cardiff Royal Infirmary, Cardiff, U.K.

Christopher J. Porter, VG Analytical Ltd., Floats Road, Wythenshawe, Greater Manchester, M23 9LE, U.K.

We describe examples of two areas of application of tandem MS in biochemical problems:

(i) Characterisation of a peptide by collisionally-activated decomposition (CAD) of MH^+ ions, with particular reference to the choice of collision gas.

(ii) Quantification by multiple reaction monitoring of a steroid in a biological extract, using isotope dilution and conversion to an ionic derivative.

Analyses were performed using VG 7070EQ and 7070HSQ instruments (both of EBQQ configuration). Gaseous ion formation was by fast atom bombardment (FAB), using xenon as the primary beam and a glycerol matrix. CAD was studied in the first (R_f only) quadrupole; the collision gas was argon or xenon.

(i) CAD of a decapeptide

The generation of diagnostically-important fragment ions, following collisional activation, may be limited by the energy available for conversion to internal energy of the precursor ion. This is given by the collision energy in the centre-of-mass frame of reference,

$$E_{cm} = E_{lab} \cdot \frac{m_t}{m_p + m_t}$$

where E_{lab} = collision energy in the laboratory frame of reference; m_t = mass of target; m_p = mass of precursor. Thus, E_{cm} decreases with increasing mass of the precursor ion but may be increased by increasing the mass of the target.

CAD daughter ion spectra have been recorded for MH^+ ions (m/z 1193) derived from [D-Phe^{2,6}, Pro^3] luteinizing hormone-releasing hormone (a decapeptide). Significantly more sequence information was available from the xenon CAD (E_{cm} 3.5 eV) spectrum than from the argon CAD (E_{cm} 1.1 eV) spectrum. Thus, for example, the former spectrum included sequence ions B_6, B_7, B_8 (using the nomenclature of Roepstorff and Fohlman (1)) which were absent in the latter.

(ii) Quantification of cortisol in serum

Conversion of neutral analytes to ionic derivatives provides the potential for selective and sensitive analyses by FAB MS. Selectivity may be further enhanced by using tandem MS. Conversion of corticosteroids to ionic hydrazone derivatives prior to FAB MS analysis has been demonstrated previously by DiDonato and Busch (2). We have assessed the utility of derivatisation and FAB tandem MS for the quantification of cortisol in blood serum. Serum (1ml) was supplemented with [$^2H_3$] cortisol (200ng) and extracted with methylene chloride or with a Sepharose-coupled cortisol antiserum. The total extract was fractionated by preparative HPLC using an octadecylsilyl-silica column and methanol/water (60/40) as the mobile phase. After drying, the fraction was dissolved in 20µl ethanol/water/glacial acetic acid (50/50/0.1) containing Girard's P reagent (1µg/µl) and allowed to stand at 20° overnight. The structure of the derivative so prepared is shown in Figure 1.

FAB MS analysis of cortisol Girard's P derivative gave m/z 496 as the principal analyte-derived ion (Figure 2). CAD (argon; E_{lab} 8eV) of m/z 496 yielded a single prominent daughter ion of m/z 417, corresponding to loss of pyridine. Standard mixtures of cortisol (0-600ng) and [$^2H_3$] cortisol (200ng) were analysed by dual reaction monitoring of m/z 496 → 417, and m/z 499 → 420. Linear regression analysis of response ratio on amount of cortisol gave the equation y = 0.00609x + 0.038, with a correlation coefficient of 0.998. Cortisol was readily detected and quantified in serum extracts which had been fractionated by HPLC. Analyses of total serum extracts (following derivatisation), however, indicated suppression of the analyte signal by coextracted material.

1. Roepstorff P, Fohlman J, Biomed Mass Spectrom 1984; 11 : 601.

2. DiDonato GC, Busch KL, Biomed Mass Spectrom 1985; 12 : 364

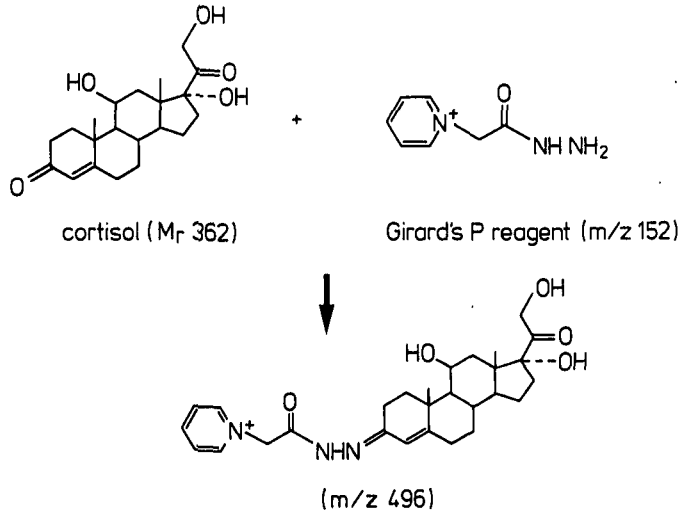

Figure 1. Conversion of cortisol to a derivative suitable for FAB/tandem MS.

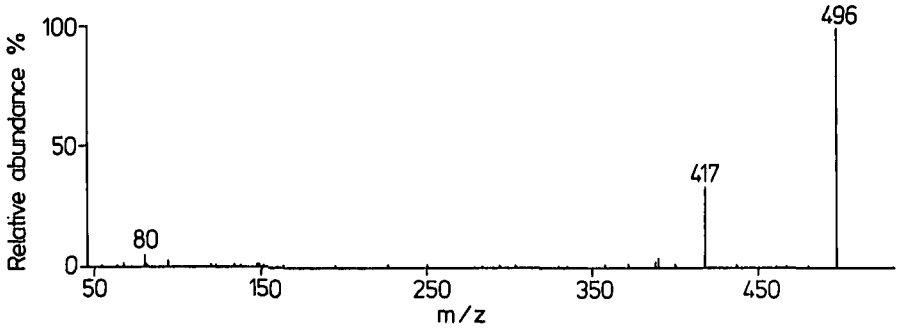

Figure 2. Daughter ion spectrum obtained following CAD of m/z 496 from cortisol Girard's P derivative.

COLLISIONALLY ACTIVATED DECOMPOSITION OF POLY(ETHYLENE GLYCOL)S: AN INVESTIGATION OF THE GENERAL UTILITY OF THE COLLISIONAL ACTIVATION TECHNIQUE WITH LARGE MOLECULES: Jeffrey P. Kiplinger and Maurice M. Bursey, Department of Chemistry, Venable and Kenan Laboratories 045A, University of North Carolina at Chapel Hill, Chapel Hill NC 27514 and National Institute of Environmental Health Sciences, P.O. Box 12233, Research Triangle Park NC 27709

The utility of the collisional activation dissociation (CAD) technique is limited by a falloff in daughter ion yield as parent ion mass increases from 1000 to 2000 amu. The apparent decrease in the efficiency of the collisional activation process has been thought of as a degree-of-freedom effect: as new rovibrational modes are added to the parent, its lifetime with respect to dissociation increases. We have investigated this effect using an easily characterized system of the poly(ethylene glycol) (PEG) homologues from the 15-mer to the 35-mer.

Spectra illustrated in Figures 1 and 2 show the CAD fragmentation patterns of $[M+H]^+$ and $[M-H]^-$ parent ions generated under fast atom bombardment conditions from a hexaethylene glycol matrix. Comparison of the yields of selected daughters as parent mass is increased is shown in Figures 3 and 4.

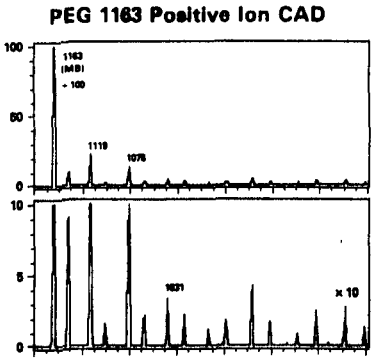

Figure 1.

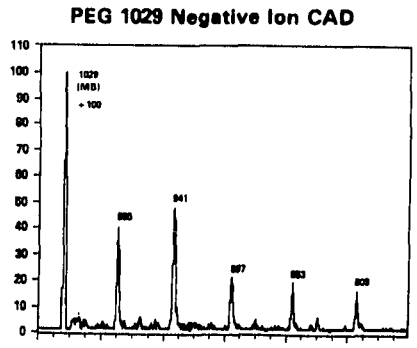

Figure 2.

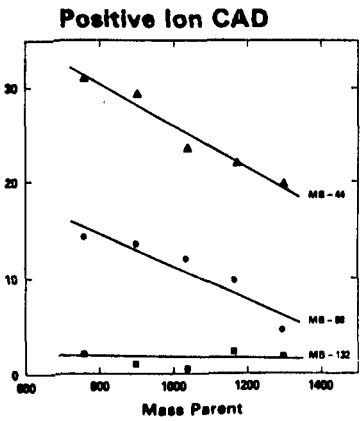

Figure 3.

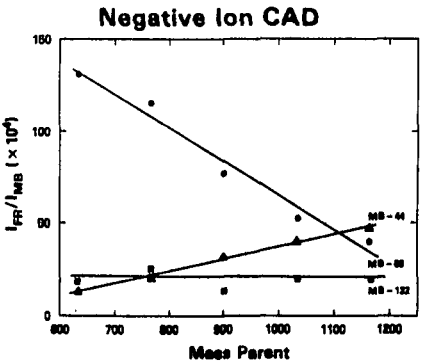

Figure 4.

Mechanisms of positive ion fragmentations are difficult to characterize, primarily because the structure of the parent ion is unknown. Since the majority of parents are unlikely to be protonate at a terminal hydroxyl group, successive loss of sequential C_2H_4O groups is an unlikely mechanism. It is probable that the majority of neutral fragments are larger than C_2H_4O. Trends in daughter ion yield as parent mass increases are difficult to evaluate, although the postulated degree-of-freedom effect is supported.

Negative ion fragmentations are more easily characterized mechanistically, and may be represented as internal displacement processes. The charge site must be at the end of the chain. No conclusions are made about structure of the neutral fragments, but the reactions must proceed through a cyclic transition state. Examination of these processes as parent mass is varied reveals a surprising increase in the intensity of the [MB-44] daughter, corresponding to the loss of a single chain unit. The difference between this process and the others lies in the 'tightness' of the predicted transition state. Figure 5 illustrates the differences in the energy surfaces for low vs. high-barrier fragmentations.

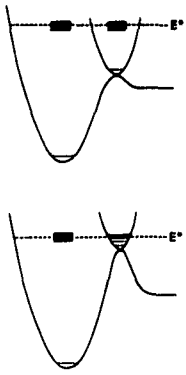

Figure 5.

In low barrier fragmentations, the reaction proceeds well above the transition state, and the increase in the density of states for the parent ion as mass increases is paralleled in the activated complex. With a high barrier, the rate of decomposition must be small when the energy of the complex is small, but will increase dramatically with a small increase in E* because the density of states for the complex increases dramatically. Since the enhancement for the collisionally activated transition state is proportionally greater than the enhancement for the parent ion, an increase in fragment yield on CAD of the parent is observed with increasing parent mass.

If the observation that high-barrier processes become more important as parent mass increases is fairly general, ultimately tight rearrangements will often become important in CAD spectra with high mass precursors. This could significantly affect the character of the CAD spectrum. Peaks which appear small and insignificant in lower mass homologues may supersede shrinking low-barrier daughter peaks as the parent ions grow larger, causing spectrometrists to reinterpret their assignments of 'structurally significant' peaks.

ANOTHER STRATEGY FOR PRODUCING REMOTE-CHARGE SITE FRAGMENTATIONS OF FATTY ACID POSITIVE IONS

L.J. Deterding, Midwest Center for Mass Spectrometry, Dept. of Chemistry, Univ. of Nebraska, Lincoln, Ne 68588.

It has been shown that certain closed-shell gas-phase ions undergo upon collisional activation a new type of decomposition called remote-charge site fragmentation. These reactions occur readily for FAB-desorbed carboxylate anions (1) and for lithiated species (2), but not for the corresponding protonated species. These reactions provide much more specific structural information than the EI mass spectra of earlier derivatives. Of the more recent derivatives, the pyrrolidides and picolinyl esters have been the most useful (3,4). These derivatives are commonly used in GCMS analysis. However, FAB MS-MS may provide more structurally specific information.

The picolinyl ester derivatives of common fatty acids can be readily desorbed as positive ions and collisionally activated. CA of the $(M + H)^+$ ion of the derivatized fatty acid reveals two types of fragmentation: (1) remote-charge site fragmentation that leads to parallel losses of C_nH_{2n+2} elements beginning at the alkyl terminus, and (2) fragmentation proximate to the charge. The latter produces such characteristic ions as those of m/z 93, 109, 152, and 164 (Fig. 1). Perturbation of the remote site fragmentation reveals a variety of fatty acid structural features, such as location of double bonds in mono- and poly-unsaturated acids, branching, hydroxy substituents, cyclopropane rings, and chlorinated acids. The fragmentation is perturbed in a highly specific manner for each type of modification. Hence, the location and the nature of the modification is readily apparent from the CAD spectrum.

Monounsaturated fatty acids fragment by losing C_nH_{2n+2} elements from the hydrocarbon terminus until the allyl bond is reached. Cleavage of the other allyl bond which is more proximate to the ester function is accompanied by the loss of C_nH_{2n}. Structurally isomeric unsaturated fatty acids can easily be determined in this manner. Location of double bonds in polyunsaturated fatty acids is possible for cases of two and three double bonds, but becomes more difficult for acids containing four or more sites of unsaturation (Fig. 2).

Other modified fatty acids reveal structural information upon collisional activation. Iso- and anteiso-branched acids can be easily distinguished (Fig. 3). Fragmentation at the methyl branch leads to a gap in the CAD spectrum, which permits locating the branch point. Hydroxy groups on fatty acids can be located at any position on the chain. For 2-hydroxy acids, three fragmentations are suppressed at the site of the hydroxy group with an enhanced fragment at m/z 166-168. Mid-chain hydroxy acids primarily show the loss of water, but remote-charge site fragmentation still occurs resulting in a gap in the CAD spectrum at the substituted carbon. Acids containing terminal hydroxy functions show an abundant loss of water and the loss of $C_nH_{2n+2}O$ fragments (Fig. 4). Location of a cyclopropane ring in a fatty acid is possible, but the location is not determined as readily as other substituents. Fragmentations at the site of the ring are of somewhat lower abundance than the other fragmentations (Fig. 5).

One minor caution of this method is that excess thionyl chloride may result in chlorination of the double bond in unsaturated fatty acids. Collisional activation of the dichlorinated acid results in the losses of one and two molecules of HCL. However, this problem is easily remedied by avoiding large excesses of the thionyl chloride.

Acknowledgment: This research was conducted under the direction of M.L. Gross.

References:

(1) Jensen, N.J.; Tomer, K.B.; Gross, M.L., J. Amer. Chem. Soc., 107, 1863, (1985).

(2) Adams, J.; Gross, M.L., J. Amer. Chem. Soc., Submitted.

(3) Anderson, B.A., Prog. Chem. Fats Other Lipids, 16, 279 (1978).

(4) Harvey, D.J., Biomed. Mass Spectrom., 9, No. 1, 33 (1982).

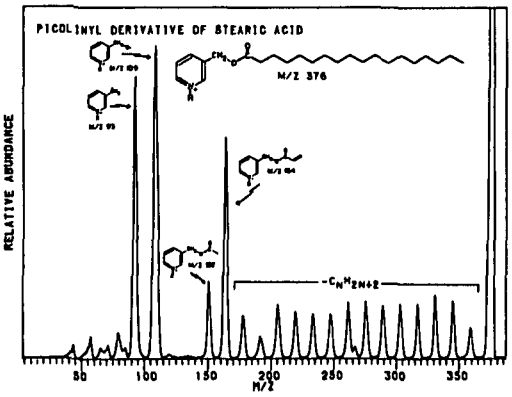

Figure 1

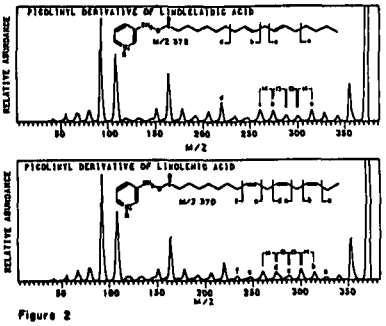

Figure 2

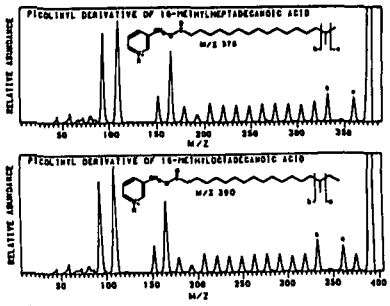

Figure 3

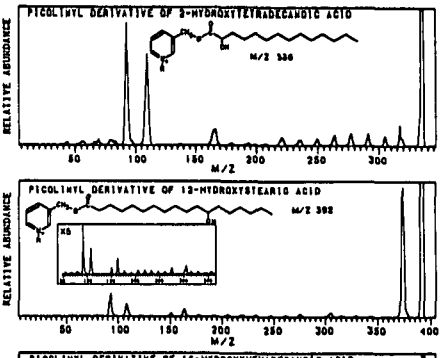

Figure 4

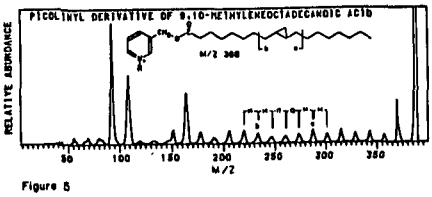

Figure 5

STRUCTURAL STUDIES OF SUBSTITUTED CYCLIC PERFLURORALKANESULFONATES USING FAST ATOM BOMBARDMENT COMBINED WITH TANDEM MASS SPECTROMETRY.

S.L.Hunt, P.A.Lyon, F.E.Behr, and L.D.Winter,
3M, 201-BW-09, St. Paul, MN 55144
R.L.Cerny, MCMS, University of Nebraska, Lincoln, NE 68588.

Fast atom bombardment has proved a useful ionization technique for analyzing both anionic and cationic surfactants. Straight chain perfluoroalkanesulfonates, a unique class of commercial surfactants, have been previously characterized using FAB and tandem mass spectrometry (1). In conjunction with that study, a series of cyclic perfluoroalkanesulfonates were investigated.

Both positive and negative spectra of FAB generated ions were obtained using either the Kratos MS50 TA at the University of Nebraska, or a new Kratos MS50 HM TA, the high mass tandem instrument installed in our laboratory (2). The negative ion spectrum of the model compound of the series (figure 1) is representative of the simple spectra given by the entire series. Clusters formed by the addition of LM neutrals to the L^- or LM_2^+ ions were found up to masses over 4000, $(LM)_8M$. Although this cluster series was the most abundant, several other ions were observed. The ion at m/z 323 (figure 1) may be an olefin impurity, or a fragment formed by a neutral F_2 loss. An F_2 loss is not observed in the CAD spectra of these compounds. The second anomalous ion, at 343 m/z, reflects the hydrocarbon starting materials and is a result of incomplete fluorination. Another impurity is seen at 399 m/z. This ion suggests the presence of open chain impurities, probably formed during electrofluorination. Since the FAB spectra showed little fragmentation, CAD was performed on the ions of interest.

The CAD spectrum of the perfluorocyclohexanesulfonate anion (figure 2) shows the simplicity of the fragmentation of most of these cyclic compounds. The major ion (281 m/z) results from an SO_3 loss and is prevalent in the CAD spectra of each compound in the series. This sulfonate loss is also seen unimolecularily in compounds containg a ring bound sulfonate. The straight chain compounds (1) also show fragmentation at the C-S bond, however in those compounds the sulfonate retained the charge.(figure 3A) Charge retention by the fluorocarbon portion of the cylic compounds indicates that the electron affinity of the ring is greater than 1.7 eV, the EA of SO_3 (m/z 80). Homologues with CF_2 groups between the ring and the sulfonate show an increase in charge retention by the sulfonate approaching that seen in the straight chain analogues.

From figures 3A and 3B it is obvious that the structure of the open chain impurity (3B) is more similar to the cyclic compound than the straight chain compound. This suggests that the ring has opened to form a tertiary carbon adjacent to the sulfonate.

The aromatic compounds, figures 3C and 3D, illustrate the effect of fluorination. The major fragmentation in both of the compounds again occurs at the C-S bond. However, in benzenesulfonate the sulfonate retains the charge, while in the perfluorinated compound the charge remains on the ring showing the ability of fluorocarbons to stabilize the negative charge. The hydrocarbon aromatic, and to a lesser extent the fluorocarbon, rearranges to loose SO_2 as an alternate fragmentation pathway.

1. Lyon, P.A.; Tomer, K.B.; Gross, M.L.; Anal. Chem. **1985**, 57, 2984-2989.
2. Lyon, P.A.; Hunt, S.L.; Evans, S.; and Tudge, H.; 34th Annual Conference on MS and Allied Topics, **June 8-13, 1986**, paper MPE5.

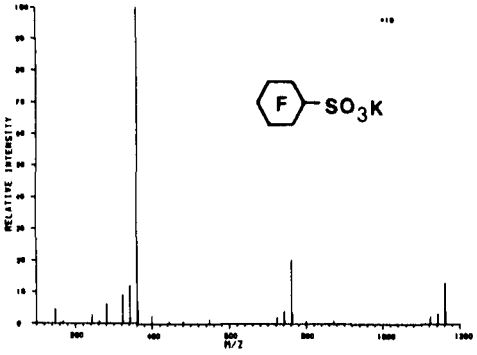

Figure 1 FAB spectrum of negative ions of perfluorocyclohexanesulfonate.

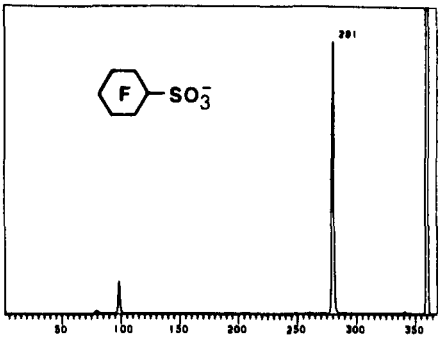

Figure 2 CAD spectrum of negative ion at 361 m/z, the molecular anion of perfluorocyclohexanesulfonate.

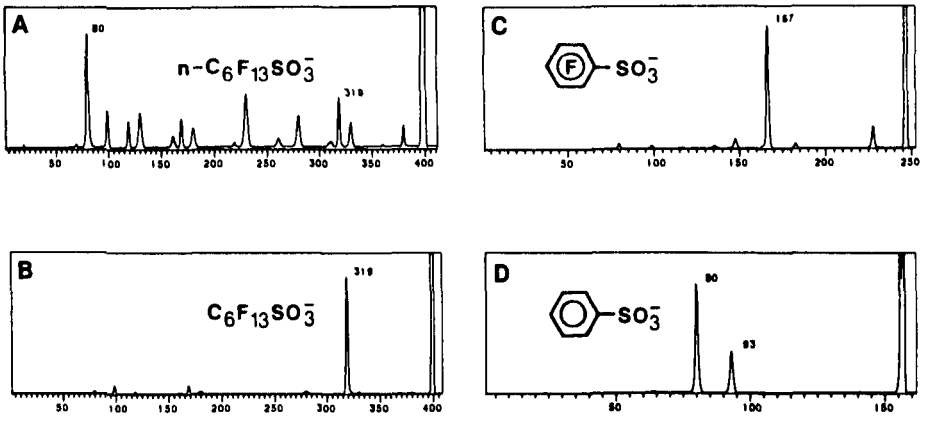

Figure 3 CAD spectrum of negative ions at
A: 399 m/z, the molecular anion of n-perfluorohexanesulfonate.
B: 399 m/z, the open chain species in perfluorocyclohexanesulfonate.
C: 247 m/z, the molecular anion of perfluorobenzenesulfonate.
D: 157 m/z, the molecular anion of benzenesulfonate.

A NOVEL APPROACH FOR AUTOMAIC ELUCIDATION OF SPECTRAL SUBSTRUCTURE RELATIONSHIPS IN MS^n SPECTRA

A.P. Wade+, P.T. Palmer, K.J. Hart and C.G. Enke*

Chemistry Department, Michigan State University, E. Lansing, MI 48824

+Also of: Information Technology Research Unit, British Petroleum Research Centre, Sunbury-on-Thames, Middlesex, TW16 7LN, UK.

Some molecules with common substructures show patterns of features in their MS/MS spectra which are indicative of those substructures. These patterns have previously been obtained "manually" from MS/MS spectra (1). The features characteristic of a particular substructure include not only the m/z values seen in primary and daughter scans, but also neutral losses, parent-to-daughter transitions and the presence (or absence) of a molecular ion. Conventional spectral matching programs do not explicitly use these last three, and thus do not take full advantage of the extra dimension of information that MS/MS affords.

This paper reports the development of an algorithm to:

1) Automatically identify spectral feature / substructure relationships from experimental spectra, and
2) Use these relationships (expressed as rules), along with other constraints, to determine the presence (or sometimes the absence) of these substructures in unknowns.

The advantages of carrying out this "pattern search" on a computer, rather than manually, include speed, completeness, lack of "personal bias" and statistical checking. The algorithm, henceforth referred to as MAPS (Method for Analysing Patterns in Spectra) is being developed in the InterLISP-D programming language on a Xerox 1108 AI Workstation. New types of features (e.g. multiplicity of daughters from parents, daughter spectra intensity values) and known substructures may readily be added into the software. While currently using MS/MS data, the MAPS approach (and much of the software) is equally well suited to MS^n data. It is hoped that by this methodology many currently unknown relationships may become readily identified, and that those relationships at present poorly characterized will become better defined. The problem of missing m/z values is dealt with, in part, by the use of rules known with various levels of certainty. Spurious m/z values will not correlate with particular substructures.

To facilitate the inference of spectral feature / substructure relationship rules, a "training set" of known compounds must be entered. The data required for each compound include its registry number, name, empirical formula, its MS/MS spectra and a list of the substructures which are present. This also requires the existence and updating of a library of known substructures. The MS/MS spectra are stored in a tree list structure which concisely indicates which ions are the daughters (or even granddaughters etc.) of which parent. Each line in either a parent or daughter scan is represented as a triplet consisting of its m/z value, the neutral loss which caused it, and its relative intensity. Currently the intensity values are not used, but will be incorporated in the future.

The features suggestive of particular substructures are identified by applying the algorithm to the training set of known compounds. These features are filtered to remove false correlations (due to artifacts of the training set) and then assembled into "IF (spectral feature A) AND (spectral feature B) (etc.) THEN (likely substructure)" rules. For example:

Rule 8:
IF [13/14] Line in neutral loss spectrum at m/z 28 CO
AND [6/14] Line in neutral loss spectrum at m/z 44 CO_2
THEN Functionality indicated is CARBOXYL

Each spectral feature in each rule has some level of correlation with the substructure. This is expressed as an [x/y] fraction, which indicates that x of the y training set compounds that had that substructure also had that feature. The lowest allowed certainty for a clause to be present in a rule may be defined by the user. Certain features that correlate almost exclusively with the presence of a substructure, but do not always occur when that substructure is present, are also allowed. Some 29 of these MS/MS rules have so far been identified.

"Expert" investigation of the substructures present in unknowns may be obtained by matching the substructure rules against their mass spectra. MS/MS spectra of unknowns may be entered into an "unknowns database". The MAPS software then looks for high (typically > 0.6) correlations between the empirically found substructure rules and features in the spectra of the unknowns. When such are found, it concludes that the corresponding substructures are likely to be present.

The number of spectra necessary in a library for meaningful subatructure / spectra relationships to be discovered can be relatively small, however the number of erroneous identifications should decrease as more examples are obtained.

Other features of the MAPS software include:-

* Analysis of predictive capability of rules by self-interpretation of knowns. As more known compounds are entered, predictive capabilities improve.
* Identification of rules with poor discriminating ability (i.e. those that cause errors). Cross correlation of rules indicates their degree of commonality and may suggest further experimentation to refine the rules base.
* Identification of the spectral features that are most indicative of the presence of known substructures.
* Analysis to show which compounds share which spectral features.

MAPS is one of a number of tools we are using in an attempt to obtain molecular structure information from low resolution MS/MS spectra. The list of substructures identified by MAPS greatly limits the number of possible molecular structures for the unknown. If sufficient overlapping substructures can be identified (and possibly the absence of other substructures ascertained) then the molecular structure of an unknown may be determined. MAPS also has potential application as an intelligent front end to a more conventional MS/MS library search, running on a large computer.

1. Cross, K.C., Palmer, P.T., Giordani, A.B., Beckner, C.F. Hoffman, P.A., Gregg, H.R. and Enke, C.G., in "**Artificial Intelligence Applications in Chemistry**", Pierce, T.H., Hohne, B.H., (Eds.), American Chemical Society, Washington, DC, (1986), ACS Symposium series 306, 321-336.

A Method to Determine the Elemental Compositions of Daughter Ions in MIKE Spectra.

M.H. Bozorgzadeh and R.L. Lapp; Midwest Center for Mass Spectrometry, University of Nebraska, Lincoln NE 68588-0304.

A method has been developed to determine the elemental composition of the daughter ions in either metastable or CAD spectra. The method is applicable to any type of MS/MS experiment, even to a MIKE spectrum for which the mass resolution is as low as 100. To employ the method it is necessary to take the daughter ion spectrum of the ion with the greatest natural abundance, M, and the ion at one mass unit higher, M+1. For each daughter ion produced from M, two daughter ions will be produced from M+1, one with the same isotopic composition and one containing a heavier isotope. Because the distribution of isotopes in the M+1 ion is homogeneous, and the isotope effect on fragmentation is negligible, the ratio of the abundances of these two daughter ions is equal to the ratio of the probability of finding the heavy isotope in the ion fragment to the probability of finding it in the neutral fragment(s). Since ions with the same mass but different elemental compositions have different "isotope ratios" the elemental composition of an unknown daughter ion can be determined by calculating the "isotope ratio" from the observed abundances.

Although this approach was suggested by the author in 1978, the method has not been generalized or applied to the complex situation of CAD spectra where many daughter ions are produced at unit mass intervals. In the case of an isolated peak, i.e. one with no peaks at ±1 mass unit, the "isotope ratio" may be calculated from:

$$X = \frac{A+1}{A+(A+1)} T$$

where A and A+1 are the abundances of the daughter ions at mass M and M+1, respectively, in the MIKE spectrum of M+1, and T is calculated from:

$$T = 1.11C + 0.015H + 0.37N + 0.037O$$

where C, H, N and O are the number of carbon, hydrogen, nitrogen and oxygen atoms in the parent ion. When peaks are present at adjacent masses the calculations are complicated by the overlap of the daughter ion containing the heavy isotope with the ion that is one mass unit higher but without the heavy isotope. In this case the equation is:

$$X = \left(\sum_{i=1}^{x} A_i \sum_{j=x+1}^{n+1} A'_j - \sum_{i=x+1}^{n} A_i \sum_{j=1}^{x} A'_j \right) T / A_x \sum_{j=1}^{n+1} A'_j$$

where A_x is the abundance of the daughter ion in the spectrum of M, A'_x is the abundance in M+1, $A_1 \ldots A_n$ and $A'_1 \ldots A'_{n+1}$ are the abundances of the other ions from M and M+1, respectively.

The method was tested first by applying it to compounds which produce daughter ions of known elemental composition. Then it was applied to several compounds which may produce daughter ions of more than one elemental composition.

A computer program, written in FORTRAN, was developed to perform these calculations. The required input for this program consists of the abundances of the ions in the M and M+1 spectra and the composition of the parent ion. The program then generates a list of possible compositions for each daughter ion and compares the "isotope ratio" for each possible composition to the ratio calculated from the abundances.

FOURIER TRANSFORM ION CYCLOTRON RESONANCE
MASS SPECTROMETRY OF ORGANOMETALLICS

Steven L. Mullen[a] and Alan G. Marshall[a,b]

Department of Chemistry[a]
Department of Biochemistry[b]
The Ohio State University
140 West 18th Avenue
Columbus, Ohio 43210

Organometallic compounds are often of low volatility (e.g., $<10^{-7}$ torr at temperatures below pyrolysis). Because an FT/ICR mass spectrometer operates at a source pressure approximately 1000 times lower than do other mass spectrometers, FT/ICR is well-suited for mass spectral analysis of organometallics (1). We have observed the molecular ion and the loss of the functional groups for several transition metal cluster carbonyls (from S. G. Shore) derived from the MOs_3 framework, in which M = Os, Ru, Rh, Fe, or C.

In many cases, transition metal complexes, particularly cations, are involatile. For these compounds, laser desorption FT/ICR mass spectrometry may be used (Figure 1). We have observed LD/FT/ICR spectra for iridium, iron, and tungsten complexes (from D. W. Meek and A. Wojcicki) and metal ions bound in vaulted macrocycles (from D. H. Busch). Although organic compounds generally show a molecular ion and little fragmentation under these conditions, organometallic compounds tend to exhibit several daughter ions.

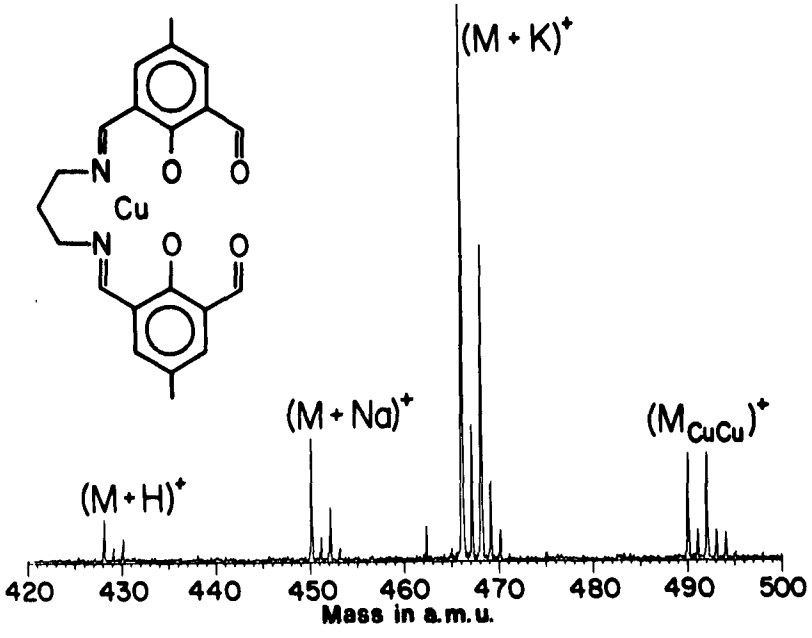

Figure 1. Laser desorption FT/ICR positive-ion mass spectrum of (1,6-Bis(2-hydroxy-5-methyl-3-carboxyphenyl)2,6-diaza-1,5-heptadiene)copper(II). Three pseudo-molecular ions ($(M+H)^+$, $(M+Na)^+$, and $(M+K)^+$) appear, along with the molecular ion of the dicopper impurity. This compound was furnished by D. H. Busch.

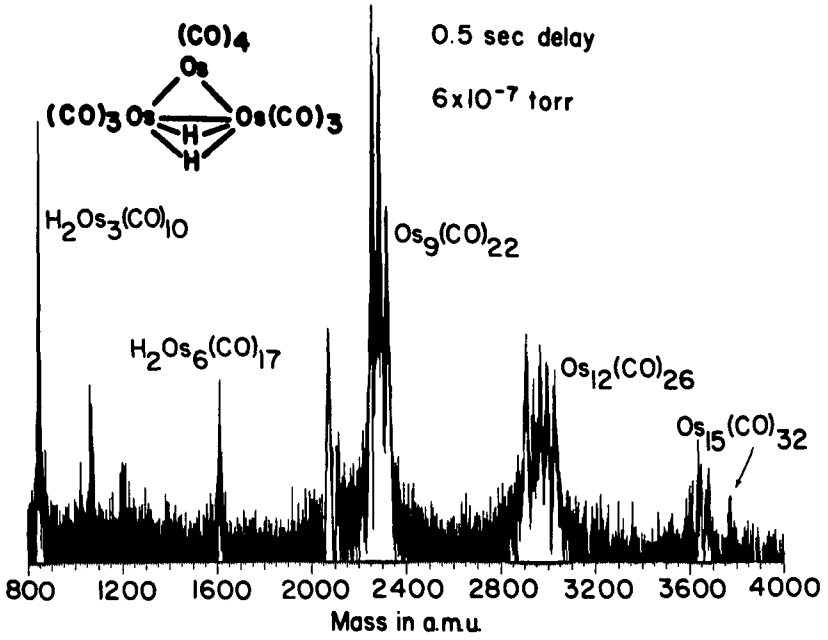

Figure 2. FT/ICR mass spectrum of $H_2Os_3(CO)_{10}$ at a pressure of 6 x 10^{-7} torr, acquired 0.5 s after electron ionization. The dimer possesses two hydrogens. The number of hydrogens on the trimer, tetramer, and pentamer has not been determined. This compound was provided by S. G. Shore.

FT/ICR mass spectrometers are widely used for the study of ion-molecule reactions. By allowing the molecular and daughter ions of $H_2Os_3(CO)_{10}$ to react with the neutral species, we have produced clusters containing up to fifteen osmium atoms (Figure 2). Milder conditions favor the production of dimer ions, $Os_6(CO)_7$ through $H_2Os_6(CO)_{18}$. Ion-molecule reactions that lead to the formation of dimer and larger clusters are typically accompanied by loss of H_2 and varying numbers of carbonyls. Under similar conditions, $Ru_3(CO)_{12}$ dimerizes to $Ru_6(CO)_{18}$, and $Fe_3(CO)_{12}$ condenses to give dimers and trimers. We have also observed addition products when neutral organic compounds (e.g., benzyl amine, methyl benzoate) react with $H_2Os_3(CO)_{10}$.

Finally, gas-phase basicities and proton affinities may be determined by observing proton transfer from a protonated compound of known basicity to a neutral organometallic compound. For the series, $M_3(CO)_{12}$, in which M = Fe, Ru, and Os, preliminary bracketing experiments suggest a gas-phase basicity order: $Fe_3(CO)_{12} > Ru_3(CO)_{12} > Os_3(CO)_{12}$.

This work was supported by NIH (1 R01 GM31683), The Standard Oil Company, and The Ohio State University. $Ru_3(CO)_{12}$ was kindly provided by the Engelhard Corporation.

References

1. Marshall, A. G. (1985) Acc. Chem. Res. 18, 316-322.

THE STRUCTURE OF THE IONS FORMED BY NO· LOSS FROM DINITROBENZENE AND DINITROTOLUENE ANIONS

G.L. Glish, S.A. McLuckey and D.H. Friar
Analytical Chemistry Division
Oak Ridge National Laboratory
Oak Ridge, TN 37831

The loss of NO· is a well known reaction for positively charged nitroaromatic compounds. We have found that this same reaction is also prominent for the complementary negative species.[1] The parallels extend even further in that the fragmentation occurs with a large kinetic energy release for both polarities. While suitable reference ions are not available for this $(M\text{-}NO\cdot)^+$ species, the $(M\text{-}H)^-$ ions from suitably substituted phenols provide ions with potentially the same structure as the $(M\text{-}NO\cdot)^-$ fragments of nitroaromatics.

We have studied a series of $(M\text{-}NO\cdot)^-$ ions from nitroaromatic compounds as well as possible reference structures formed by negative chemical ionization of the appropriate aromatic phenols. MS/MS spectra of the various ions were obtained on a modified ZAB mass spectrometer.

For the dinitrobenzenes, the results are straightforward. Figure 1 compares the MS/MS spectra of the $(M\text{-}NO)^-$ from meta-dinitrobenzene with the $(M\text{-}H)^-$ ion from meta-nitrophenol. The spectra are essentially identical thus indicating that the ions have the same structure. The spectra of the ortho and para isomers for dinitrobenzene are different from each other and from the meta isomer and they match very closely to the the corresponding nitrophenol isomer. From this we conclude that for the $(M\text{-}NO)^-$ ions formed in the ion source, the loss of NO· takes place via a three centered reaction mechanism. If this same reaction mechanism is responsible for the metastable loss of NO· from the nitrobenzene anions, which shows a large kinetic energy release, then it is quite similar to that that has been proposed as responsible for the large kinetic energy release for this reaction in the positive ion mode.

The case of the dinitrotoluenes (DNT) is more complex due to several factors. First, in most cases, a mixture of isomers will be formed unless one NO_2 group is exclusively responsible for the NO· elimination. Secondly, when deprotonating the reference compounds, i.e., methylnitrophenols, a mixture of isomers can be formed if proton abstraction occurs from the hydroxyl group and methyl group. Also, all of the isomers of the methylnitrophenols are not readily available.

For 2,6-DNT the first of these problems is avoided since elimination from either NO_2 group will give the identical ion. The second factor seems not to be a problem either in this particular case since the MS/MS spectrum of $(M\text{-}H)^-$ from 2-methyl-3-nitrophenol is identical to the $(M\text{-}NO)^-$ spectrum from 2,6-DNT.

For the other DNT isomers that we have studied (2,3-, 2,4- and 3,4-), the results are not as straightforward. The problem in determining the ion structures appears to be a result of the second factor discussed above, i.e., isomeric reference ions are formed from a single neutral species via competing proton abstraction from the hydroxyl and methyl groups. While the hydroxyl proton abstraction should be favored thermodynamically, the kinetics of chemical ionization make it possible to form ions by proton abstraction from the methyl group also. This is supported by the data where loss of OH· is the major ion observed whenever the nitro group is

Research sponsored by the U. S. Department of Energy, Office of Basic Energy Sciences, under Contract DE-AC05-840R21400 with Martin Marietta Energy Systems, Inc.

By acceptance of this article, the publisher or recipient acknowledges the U S Government's right to retain a nonexclusive, royalty-free license in and to any copyright covering the article

ortho to either of the other functionalities for all but one of the methylnitrophenols studied (3-methyl-4-nitrophenol).

Previous studies have shown that this reaction always occurs when there is an hydroxyl group ortho to a nitro group but only under certain conditions for ortho methyl groups.[2] This strongly suggests that some portion of the $(M-H)^-$ ions still have a proton on the oxygen which then can be transferred to the ortho nitro group with subsequent OH· loss. An example of this is shown in Figure 2a which is the partial spectrum of 5-methyl-2-nitrophenol. This can be compared with the same portion of the spectrum of 3,4-DNT (Figure 2b) which might be expected to give an ion corresponding to 5-methyl-2-nitrophenol deprotonated at the oxygen.

In conclusion, it has been shown that loss of NO· from dinitrobenzenes occurs to give an ion of the same structure as the corresponding positional isomer of deprotonated nitrophenol. 2,6-DNT also undergoes a similar reaction. However, the structure of the $(M-NO)^-$ ions from other DNTs can not be determined by comparison of MS/MS spectra with deprotonated methylnitrophenols. This is a result of the kinetics of deprotonation in the chemical ionization source. The deprotonation from of the methyl group gives an isomeric ion with different fragmentation routes than deprotonation of the hydroxyl and thus the MS/MS spectrum is a combination of both isomeric ions and does not match the MS/MS spectra derived from the $(M-NO)^-$ ions from the DNTs.

1. S.A. McLuckey and G.L. Glish, Proceeding of the 33rd Annual Conference on Mass Spectrometry and Allied Topics, San Diego, CA, 1985, p. 148.

2. S.A. McLuckey and G.L. Glish, Ibid., p. 591.

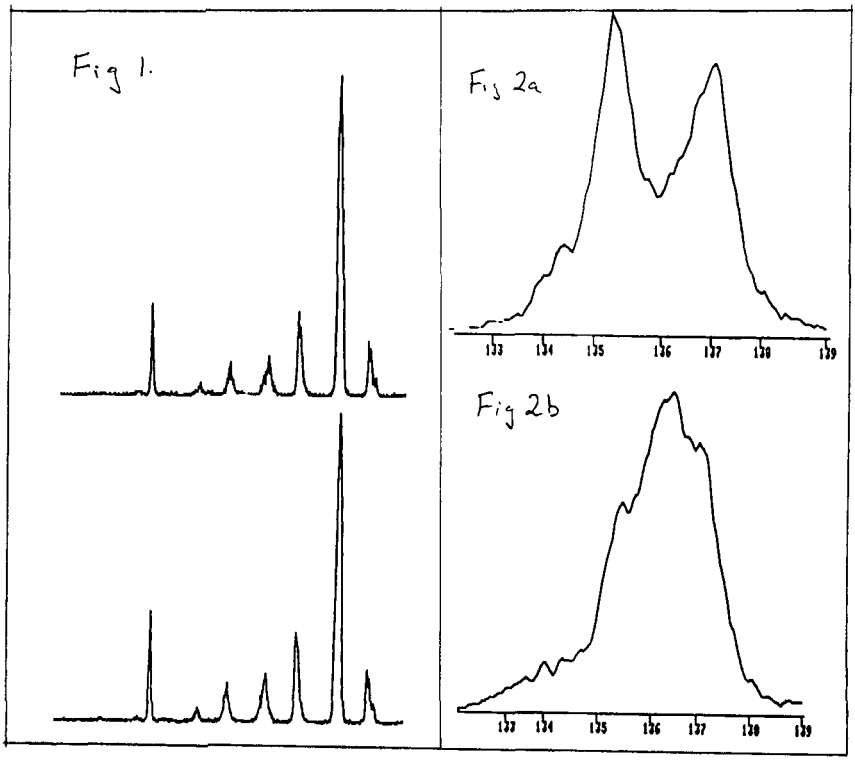

NEUTRALIZATION-REIONIZATION MASS SPECTROMETRY: CHARACTERIZATION OF NEUTRAL SPECIES BY SEPARATE COLLISIONAL DISSOCIATION

R. Feng, C. Wesdemiotis, and F. W. McLafferty

Chemistry Department, Cornell University, Ithaca, NY 14853-1301

In neutralization-reionization mass spectrometry (NRMS)[1] fast neutral species are formed from multikilovolt mass-selected ions by (a) electron exchange (charge exchange neutralization), (b) metastable ion dissociation or collisionally activated (CA) dissociation (dissociative neutralization), or (c) further dissociation of the primary neutrals resulting from these processes. The neutrals are characterized by reionization and mass analysis of the resulting ionic products.

NRMS can provide valuable information on the structures of both the prepared neutrals and their ionic precursors. Particularly promising for such structure elucidation is the fact that neutral species often dissociate by different pathways than the corresponding ions, e.g., the weakest bond in $H_3CCl^{+\cdot}$ is H-C, while that in neutral H_3CCl is C-Cl.[2] Further, the tendency for isomerization is often less pronounced in neutrals than in ions, e.g., the major dissociation of distonic $\cdot CH_2CH_2CH_2OH_2^+$ ions is H rearrangement followed by $C_2H_5\cdot$ loss, while the corresponding neutrals dissociate directly via H_2O elimination. Similarly, the EI mass spectra of 1- and 2-butene are almost identical because of a low interconversion barrier between the respective molecular ions compared to the dissociation thresholds. This easy equilibration is however frozen upon neutralization; the different reactivities of the resulting neutral molecules upon dissociation/reionization lead to significantly different NR spectra for 1- and 2-butene ions (Figure). Separate helium dissociation of the fast butene neutrals in a third collision region gives data on dissociations occuring before and after reionization.

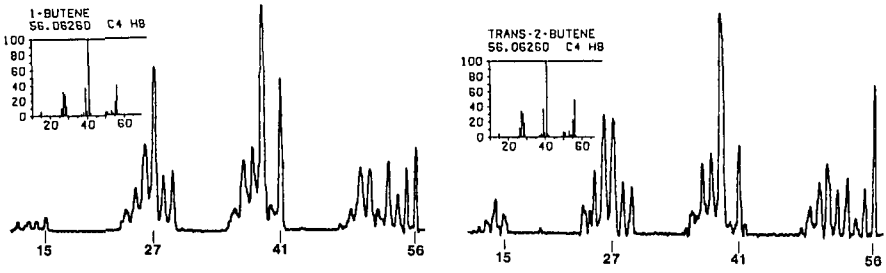

Figure. Hg/He (30% T) NR spectra of (A) $CH_2{=}CHC_2H_5^{+\cdot}$ and (B) t-$CH_3CH{=}CHCH_3^{+\cdot}$. Inserts are the corresponding EI spectra.

With NRMS the structure of the neutral product from an ion dissociation becomes accessible. If a mixture of more than one neutral species is formed, for their analysis the relative efficiency for reionizing each neutral must be determined; e.g., the O_2 reionization efficiency of $\cdot CH_2OH$ radicals is ~4 times greater than that of $CH_3O\cdot$.[3] This information and reference reionization spectra of $CH_3O\cdot$ (from $(CH_3)_2NCH(OCH_3)_2^{+\cdot}$) and $\cdot CH_2OH$ (from $(CH_3)_2NCH_2CH_2OH^{+\cdot}$) show that metastable or collisionally activated methyl acetate ions lose mainly $CH_3O\cdot$, not $\cdot CH_2OH$ as previously[4] reported. The newly-formed $CH_3O\cdot$ undergoes partial (~20%) isomerization to the more stable $\cdot CH_2OH$ in the 10^{-6} s before reionization.

The neutralization capability can be used to study hypervalent and other unstable species. The ylides H_2CYH (Y = Cl, F, OH, NH_2) have been prepared via charge exchange neutralization from the corresponding ylide ions and characterized by CAD and reionization.[2] They all are found to

represent local minima in the respective potential energy surfaces with finite barriers towards dissociation and isomerization, in contrast to theoretical predictions that only CH_2NH_3 is an equilibrium structure.[5] Similarly, neutralization of H_2Cl^+ ions leads to $H_2Cl\cdot$ radicals that survive for the time scale of the experiment. The unusual isotope effects observed for the NR spectra of deuterated H_2Cl^+ isotopomers suggest the structure HHCl for the stable chloronium radical.

References:

(1) Danis, P. O.; Wesdemiotis, C.; McLafferty, F. W. J. Am. Chem. Soc. **1983**, 105, 7454-7456. Danis, P. O.; Feng, R.; McLafferty, F. W. Anal. Chem. **1986**, 58, 348-354. Ibid. 355-358.

(2) Wesdemiotis, C.; Feng, R.; Danis, P. O.; Williams, E. R.; McLafferty, F. W. J. Am. Chem. Soc., accepted.

(3) Wesdemiotis, C.; Feng, R.; Williams, E. R. Org. Mass Spectrom., accepted.

(4) Terlouw, J. K.; Holmes, J. L.; Burgers, P. C. Int. J. Mass Spectrom. Ion Processes **1985**, 66, 239-243.

(5) Pople J. A.; Raghavachari, K.; Frisch, M. J.; Binkley, J. S.; Schleyer, P. v. R. J. Am. Chem. Soc. **1983**, 105, 6389-6398.

PHOTODISSOCIATION OF NEGATIVE IONS GENERATED BY LSIMS

M. J. Welch and E. White V
Center for Analytical Chemistry, National Bureau of Standards, Gaithersburg, Maryland, 20899

Photodissociation of negative ions has not received much study, partially, at least, because negative ions can lose an electron upon excitation and are neutralized. We have investigated the photodissociation by visible light of negative ions generated by LSIMS from a variety of substances. The experimental set-up, which has been described in detail elsewhere[1], is schematically shown in Figure 1. The system includes a Mattauch-Herzog geometry mass spectrometer equipped with a combination EI/FI/FD ion source, an argon ion laser which generates about 15 watts of visible light consisting of approximately 10 wavelengths ranging from 454 to 514 nm, and a pair of cylindrical lenses are used to focus the light in a narrow, slit-shaped image onto the source slit. The laser beam travels the same path as the ion beam from the center of the ion source through the first field-free region (FFFR). For this work all ionization was by cesium ion bombardment with the sample target positioned out of the path of the laser beam. This arrangement reduces the ion intensity but allows for the maximum ion beam-laser beam interaction. Ions which are formed by dissociations in the FFFR are detected by means of a linked scan at a constant ratio of B/E. The laser beam is chopped mechanically and a lock-in amplifier is employed to detect changes in ion intensity in-phase with the chopper.

Figure 1

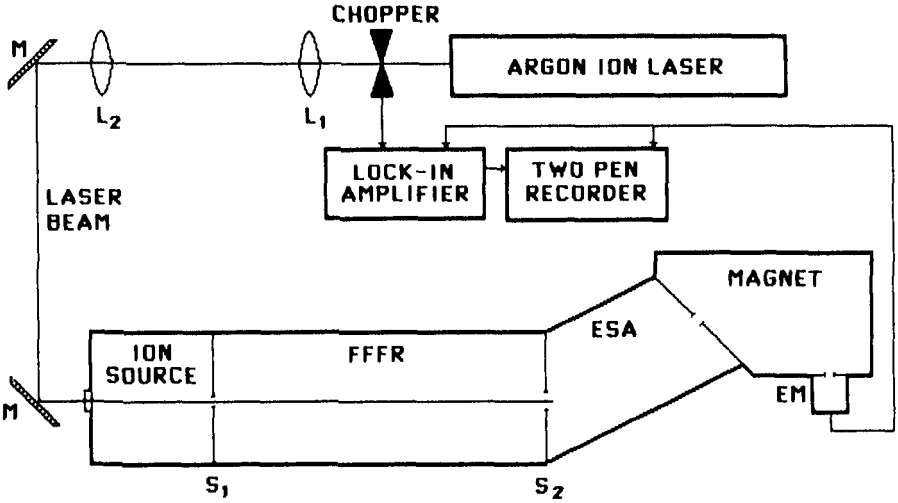

Results

A variety of compounds were tested for photodissociation activity and these are listed in Table 1. As was found with the photodissociation of positive ions generated by LSIMS[1], activity correlates with the presence of chromophores for the wavelengths of light used. Daughter ions formed by photodissociation generally involve losses of small neutrals and/or radicals for both positive and negative ions.

Table 1

Compounds Tested for Photodissociation Activity of Negative Ions

Compounds Exhibiting Activity [Parent Ion Tested]: Cresol Red $[M-H]^-$; Lichtgrun SF Gelbish $[M+2H-Na_2SO_4]^-$; Rhodamine B $[M-HCl]^-$; Crystal Violet $[M-HCl]^-$; Triethanolamine $[2M-CH_3OH]^-$; Methyl Red $[M-H]^-$, $M^{-\cdot}$; Folic Acid $[M-H]^-$; Ethyl Orange $[M-Na]^-$; Methyl Orange $[M-Na]^-$; Metanil Yellow $[M-Na]^-$; Bilirubin $[M-H]^-$; Bisbenzimide $[M-H]^-$; Riboflavin $[M+H]^-$, $M^{-\cdot}$, $[M-H]^-$; Fluorescein $[M-Na]^-$; Fluoresceinamine I-1 $[M-Na]^-$; Fluoresceinamine I-2 $[M-Na]^-$.
Compounds Not Exhibiting Activity [Parent Ion Tested]: Adenosine $[M-H]^-$; Tryptophan-TFA-Me ester $[M-H]^-$; Hexa-L-Tyrosine $[M-H]^-$; Glutathione $[M-H]^-$.

The competitive processes of photodissociation and electron photodetachment both contribute to the decrease in parent ion intensity observed for negative ions. For compounds such as methyl red and rhodamine B, for which the total positive ion current from photodissociation is much stronger than the corresponding negative ion current, the ratio of the total daughter ion intensity to the loss of parent ion intensity is 5 to 20 times greater for positive ions than for negative ions. The difference observed may be largely accounted for by electron detachment from the negative ions. For fluorescein, a compound for which the photodissociation of negative ions is much stronger than for positive ions, the ratio of daughters/parents is about equal for positive and negative. In this case the extent of electron detachment may be small compared to dissociation.

If photodissociation is to become a useful tool for obtaining structural information on large molecules longer interaction times, such as are available in FTMS instruments, are needed. The use of intense light sources in the ultraviolet would greatly expand the range of compounds for which photodissociation could be observed.

1. M. J. Welch, R. Sams, and E. White V, Analytical Chemistry, 58, pp.890-894 (1986).

INTERNAL ENERGY DISTRIBUTIONS OF ANIONS AND CATIONS ACTIVATED IN ION/ATOM AND ION/SURFACE COLLISIONS

V.H. Wysocki, H.I. Kenttämaa, and R.G. Cooks
Purdue University, West Lafayette, IN 47907

This paper focuses on internal energy distributions obtained for (i) electron ionization at various electron energies, and (ii) collisional activation in the gas phase (CID) and at a surface (surface-induced dissociation, SID).[1] Information on average and maximum energy deposition and on the shapes and widths of the corresponding energy distributions is obtained for these activation methods. This information is especially important for studies in which systematic variation of ion internal energy is desired.

The simple method used to estimate the internal energy distributions, P(E), of isolated ions is based on ion abundance data and known energetics of fragmentation and may be applied to different activation methods and to both positive and negative ions. In order to simplify the calculation of P(E), parent ions whose major fragmentation pathway consists of several consecutive reactions with known activation energies (E_i) and similar entropy requirements are used. The relative abundance of each fragment ion, $[F_i^+]$, divided by the energy interval $E_{i+1} - E_i$ gives the P(E) value which approximately corresponds to the average internal energy in this interval. All except the most obvious of kinetic factors are assumed to be negligible. Instrumental discrimination effects as well as other ion loss mechanisms have not been considered.

Internal energy distributions for $Fe(CO)_5^{+\cdot}$ generated (and activated) by electron ionization are presented in Figure 1. The distributions broaden as expected as the ionizing energy is increased. These distributions and other data (not shown) obtained for $(C_2H_5)_4Si$, $Cr(CO)_6$, $W(CO)_6$, and $(C_2H_5O)_3PO$ illustrate that P(E) associated with electron ionization are dependent on ion structure. The distributions show that multiple maxima and minima may occur in the energy distributions associated with electron ionization.

Internal energy distributions associated with collisional activation of $(C_2H_5)_4Si^{+\cdot}$ and $Fe(CO)_5^{+\cdot}$ are presented in Figure 2. The P(E) for low-energy (eV) gas-phase collisional activation, CID, (single-collision conditions) are seen to be smooth and are approximately independent of ion structure for $(C_2H_5)_4Si^{+\cdot}$, $Fe(CO)_5^{+\cdot}$, $W(CO)_6^{+\cdot}$, and $(C_2H_5O)_3PO^{+\cdot}$. Low-energy CID and low-energy (13 eV) electron ionization deposit similar amounts of energy. This suggests that low-energy electron ionization spectra may give a good approximation of low-energy (5-30 eV) collisional activation spectra in many cases. This has recently been illustrated for some phosphorus compounds.[3] The <u>average</u> amounts of energy deposited by high- and low-energy CID are similar (for $(C_2H_5)_4Si^{+\cdot}$: 1.7 eV at 28 eV collisions vs. 2 eV at 7 keV collisions) although the distributions for high-energy CID have a high-energy, low-probability tail which is absent for the low-energy distributions. In contrast to the distributions associated with gas-phase collisional activation, the curves for surface-induced dissociation (Figure 2c) are narrow and indicate that much higher average energy can be deposited (estimated average energy deposition in $(C_2H_5)_4Si^{+\cdot}$: 20 eV at 100 eV collisions with a stainless steel surface) than can be obtained by gas-phase collisions. Under multiple gas-phase collision conditions, it is possible to obtain average energy deposition of up to 6 eV, but the distributions are broader (see $Cr(CO)_5^{+\cdot}$ and $Fe(CO)_4^{+\cdot}$, Figure 3) than those obtained for SID.

Figure 3 contrasts internal energy distributions obtained for $Fe(CO)_4^{+\cdot}$ vs. $Fe(CO)_4^{-\cdot}$ and $Cr(CO)_5^{+\cdot}$ vs. $Cr(CO)_5^{-\cdot}$ under multiple gas-phase collision conditions. (The appearance energies for fragmentation of the negative ions are comparable to those for the positive ions.) The distributions obtained for the negative ions are strikingly narrow when compared to those of the positive ions. This suggests that collision-induced electron detachment is competing efficiently with collision-induced dissociation of the negative ions. This is further illustrated by the distributions obtained for single-collision CID of $Fe(CO)_4^{-\cdot}$ at 28 eV and 7 keV. The 7 keV distribution extends to only 6 eV - it does not have the high-energy tail which is present for curves obtained for positive ions.

References:

1) Md. A. Mabud, M.J. DeKrey, R.G. Cooks <u>Int. J. Mass Spectrom. Ion Processes</u> 1985, 67, 285.
2) H.I. Kenttämaa and R.G. Cooks, ibid., 1985, <u>64</u>, 79.
3) H.I. Kenttämaa <u>Org. Mass Spectrom.</u> 1985, <u>20</u>, 703.

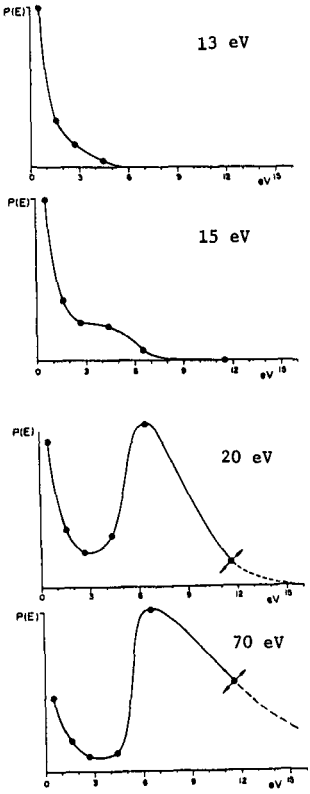

Figure 1. P(E) associated with electron ionization of $Fe(CO)_5^{+\cdot}$.

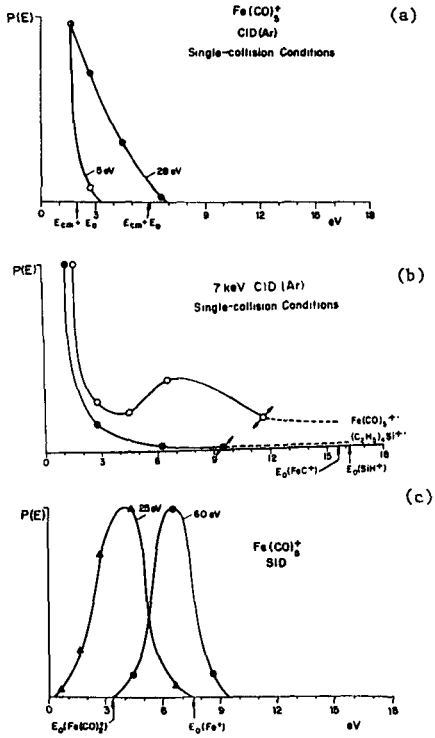

Figure 2. P(E) associated with gas-phase collisional activation of (a) $Fe(CO)_5^{+\cdot}$ at 5 and 28 eV ion kinetic energies and (b) $Fe(CO)_5^{+\cdot}$ and $(C_2H_5)_4Si^{+\cdot}$ at 7 keV. (c) P(E) associated with surface-induced dissociation of $Fe(CO)_5^{+\cdot}$ at 25 and 60 eV ion kinetic energy.

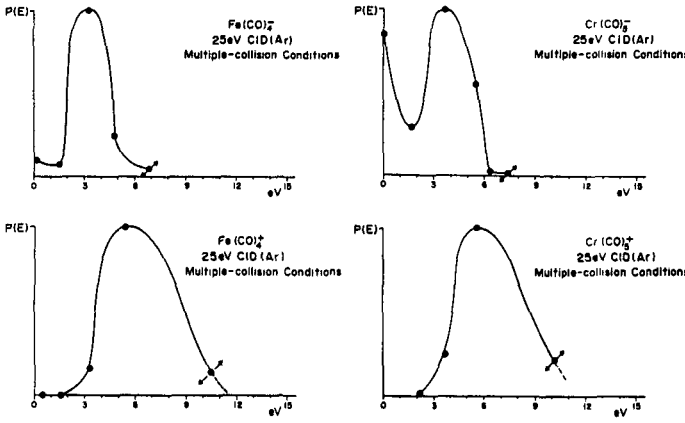

Figure 3. Comparison of P(E) of $Fe(CO)_4^{-\cdot}$ vs. $Fe(CO)_4^{+\cdot}$ and $Cr(CO)_5^{-\cdot}$ vs. $Cr(CO)_5^{+\cdot}$ (multiple-collision conditions).

SOME APPLICATIONS OF MS/MS TO STRUCTURE DETERMINATION

G. W. Becker, B. S. Briggs, M. Debono, J. M. Gilliam, R. M. Molloy, and J. L. Occolowitz; Lilly Research Laboratories, Indianapolis, IN 46285

This paper describes the use of MS/MS for the solution of three structure problems using a VG ZAB-3F (B_1EB_2) mass spectrometer.

i) The determination of the position of branching in a mixture of alkanoic carboxylate anions derived from the lipopeptolide antibiotics A21978C_1, C_2 and C_3 shown below. The negative CID spectrum of each anion; shown below, was used to determine the branching in the way described by Jensen.[1]

ii) Identification of amino sugar fragments in the FAB spectra of antibiotics. The CID spectra of four isomeric ($C_8H_{16}NO_2$) sugar fragments of known structure are shown on the bottom right of the next page, also shown is the CID spectrum of a $C_8H_{16}NO_2$ sugar fragment from a new antibiotic. The spectra show that the CID spectra can be used to differentiate the closely related sugar fragments of known structure and also that the sugar in the new antibiotic is not one of the four knowns. Subsequent NMR examination of the new antibiotic confirmed this conclusion. CID spectra were also used to differentiate methylvancosamine and methyl-3-epivancosamine.

iii) All of the tryptic peptides derived from biosynthetic human growth hormone were identified by FABMS, see scheme on left of next page. CID spectra of those peptides with MW<1000 were obtained by selecting (M+H) with B_1 and link scanning E and B_2. In this way all of the sequences of these peptides were confirmed and in some cases derived without knowledge of the primary sequence. The four spectra on the top right of the next page are representative. Mass calibration for B_2/E scans was achieved by transferring the attenuated E signal to the field probe port of the Varian-MAT SS-200 acquistion processor.

[1] Jensen, N. J., 33rd Annual Conference on Mass Spectrometry and Allied Topics. May 26-31, San Diego, CA. Abstracts, p. 917.

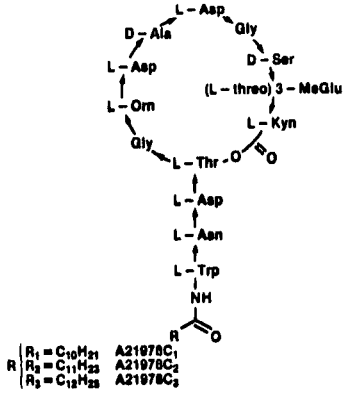

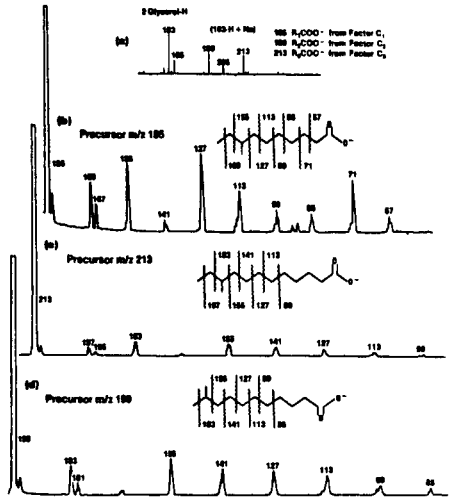

Above: Structures of A21978C_1, C_2, and C_3

Right: Negative CID spectra of the carboxylate anions derived by the hydrolysis of a mixture of the three antibiotics.

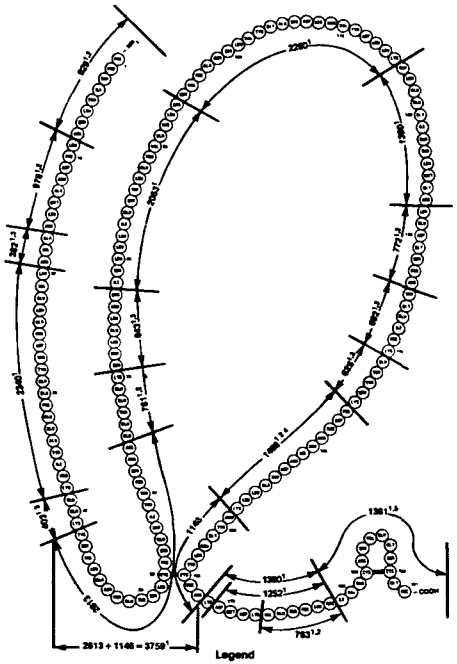

1. M + H observed in FAB spectrum
2. Confirmatory sequence information by MS/MS.
3. Sequence determined entirely by MS/MS and accurate mass measurement (Leu or Ile?).
4. MS/MS data courtesy of Prof. K. Biemann and Dr S Martin, MIT.
5. Ser-Arg bond opens to give peptide with MW 1399.

(Peptides examined were either completely or partially separated by HPLC)

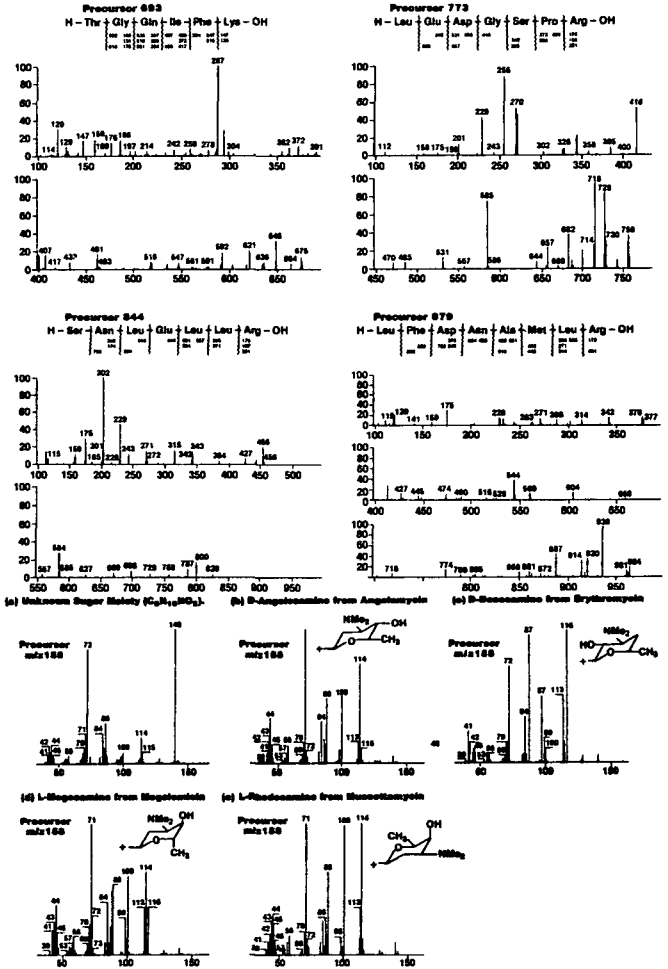

Above: Tryptic peptides derived from biosynthetic human growth hormone and a summary of information obtained by MS and MS/MS.

Right Top: CID spectra of some of the peptides shown above.

Right Bottom: (a) CID spectrum of a sugar fragment of unknown structure.
(b-e) CID spectra of four known sugar fragments.

CHARACTERISATION OF A PHYSALAEMIN-LIKE IMMUNOREACTIVE PEPTIDE BY TANDEM DOUBLE-FOCUSSING MASS SPECTROMETRY

D.J. Harvan, W.E. Wilson and C. Hamm, NIEHS, Research Triangle Park, NC 12733; R.K. Boyd, Department of Chemistry and Biochemistry, University of Guelph, Guelph, Ontario, Canada N1G 2W1.

The use of FAB/MS in determining molecular weights of peptides has been established since the inception of the technique.[1] If the peptide is present at sufficiently high concentration in the FAB matrix, useful sequence information can also be obtained.[2] Tandem mass spectrometry has also been used to characterise protonated molecular ions of peptides (see recent work[3-5] more complete references). Recently[6] a commercially available tandem double-focussing mass spectrometee was described, which permits high mass range and high resolving power for both precursor and fragment ions. The present work describes application of this instrument to a real-life problem, viz. identification of a physalaemin-like immunoreactive peptide (designated PHLIP-8) isolated[7] from stomachs of rabbits.

Anticipated advantages of tandem mass spectrometry over miniaturised sequenator technology[8] include less stringent requirements on peptide purity, and the expectation that modified or unusual amino-acid residues should provide no more difficult interpretative problems than more common residues. On the other hand, mechanisms of collision induced-dissociation (keV energies) of protonated peptides are not well established, so it was clear at the outset of this investigation that evidence for the internal consistency of the interpretation would be required.

Based upon evidence from accurate mass measurement of MH^+, amino acid analysis (2Glx:2Asx:Pro:Ile:Val:Ala) and a first fragment-ion spectrum of the MH^+ ion of PHLIP-8, the following sequence was proposed by a computer program written specially to aid interpretation of such spectra:

p-Glu-Val-Asp-Pro-Ile-Asn-Gln-Ala
(Synthetic peptide RSP-S1)

This peptide was synthesised, and its protonated molecular ion shown to yield a fragment ion spectrum which was in complete agreement with that predicted by the computer program. However, it showed no immunoreactivity, and thus RSP-S1 can not be identical with PHLIP-8. Moreover, the fragment ion spectrum of PHLIP-8 showed some puzzling discrepancies of 1 amu from that of RSP-S1.

At this point it was necessary to devise some tests of our interpretations of the fragment ion spectra. To this end, a peptide RSP-S2 was synthesised, which was identical to RSP-S1 in all respects except that the Asn residue was replaced by a second Asp residue (a mass difference of just 1 amu). Also, free carboxyl groups on each of the two synthetic peptides were converted to methyl esters to give shifts of multiples of 14 amu in the sequence peaks in the fragment ion spectra. Finally, both accuracy and precision of mass measurement of the fragment ion spectra were greatly improved through use of a new computer-based method.[9] An example of computer output of such a spectrum is shown in the figure.

As a result of these and other tests of the tandem mass spectrometry methodology, it finally become clear that a better structure for PHLIP-8 was similar to that of RSP-S1, but with the Asn and Ile residues interchanged. When this new peptide was synthesised, it was found to display

immunoreactivity similar to that of PHLIP-8. The fragment ion spectra of natural and synthetic PHLIP-8 were now in satisfactory agreement. The original confusion in the interpretation arose from intense peaks due to internal cleavage processes, leading for example to a $(Pro\text{-}Asn\text{-}H)^+$ fragment ion with m/z = 212.1, just 1 amu removed from the less intense sequence-ion $pGlu\text{-}Val^+$ at m/z = 211.1. A more detailed account of this work is in preparation.

Clearly, more background knowledge of CID reactions of peptides is required, before tandem mass spectrometry can be deemed a routine technique for sequencing. Nonetheless, as the success of the present work exemplifies, the technique holds great promise.

1. M. Barber, R.S. Bordoli, R.D. Sedgwick and A.N. Tyler, J. Chem. Soc. Chem. Commun. (1981) 325.
2. D.H. Williams, C.V. Bradley, S. Santikarn and G. Bojesen, Biochem. J. 201 (1982) 105.
3. I.J. Amster, M.A. Baldwin, M.T. Cheng, C.J. Proctor and F.W. McLafferty, J. Am. Chem. Soc. 105 (1983) 1654.
4. J.L. Witten, M.H. Schaffer, M. O'Shea, J.C. Cook, M.E. Hemling and K.L. Rinehart, Biochem. Biophys. Res. Commun. 124 (1984) 350.
5. K.B. Tomer, F.W. Crow, M.L. Gross and K.D. Kopple, Anal. Chem. 56 (1984) 880.
6. J.R. Hass, B.N. Green, R.H. Bateman and P.A. Bott, Proc. 32nd Conf. ASMS, San Antonio (1984), 380.
7. W.E. Wilson, D.J. Harvan, C. Hamm, L.H. Lazarus, D.G. Klapper, H. Yajima and Y. Hayashi, Int. J. Peptide Protein Res. (in press).
8. R.M. Hewick, M.W. Hunkapiller, L.E. Hood and W.J. Dreyer, J. Biol. Chem. 256 (1981) 7990.
9. R.K. Boyd, P.A. Bott, D.J. Harvan and J.R. Hass, Int. J. Mass Spectrom. Ion Proc. (in press).

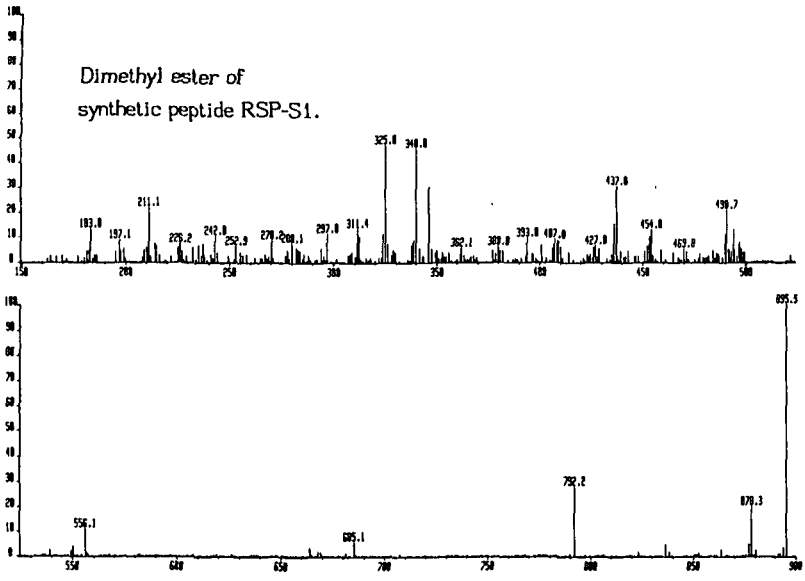

CALIFORNIUM-252 PLASMA DESORPTION MASS SPECTROMETRY OF SKIN LIPIDS

L.K. Pannell, Laboratory of Bioorganic Chemistry, NIADDK:NIH, Bethesda, MD. 20892.

Y-M. Yang, E.A. Sokoloski and H.M. Fales, Laboratory of Chemistry, NHLBI:NIH, Bethesda, MD. 20892.

Early in the application of the PDMS method, we and others (R.A. Macfarlane and C.J. McNeal, F. Field and B. Chait, personal communications) noted the occassional presence of ions at m/z 495, 523 and 551, usually increasing in that order. Their mass difference immediately suggested the acetate derived two-carbon homology of typical lipids. Fragment ions at m/z 211 and 239 further implicated myristoyl and palmitoyl groups, respectively. Further confirmation was obtained from the negative ion spectrum where the expected myristate and palmitate ions show clearly at m/z 227 and 255. The exact nature and source of these fatty acid moieties was not obvious to us, however, until we noticed that one sample foil exhibited a distinct fingerprint on the surface. At this point, the phenomenon could be repeated at will, merely by lightly applying a finger to a clean foil. To establish the identity of these compounds, representative members of the major classes of known skin lipids and related compounds were examined by PDMS.

1. Fatty Acid Anhydrides.

Stearic anhydride might be expected to show an $[M+H]^+$ ion at m/z 551 but actually showed only a weak peak at m/z 550 and a larger peak at m/z 533 corresponding to $[M-OH]^+$. The base peak was the stearoyl ion at m/z 267, and an ion at m/z 817 disclosed that it is capable of attachment to a molecule of stearic anhydride to form the symmetrical ion $[(RCO)_3O]^+$. The negative ion spectrum of stearic anhydride showed an analogous spectrum with the intense stearoyl ion replaced by the stearate ion at m/z 283. This ion also attaches to the anhydride molecule to produce the ion at m/z 833. Such attachment ions have been reported in negative ion PDMS, but the occurrence in positive ion PDMS seems not to have been described.

2. Fatty Acids.

Stearic acid itself shows a more usual type of PD mass spectrum with an abundant $[M+H]^+$ ion that loses water to form, once again, the stable acyl ion at m/z 267. However, there is no attachment of this ion to the acid (another possible source of the m/z 551 peak). Instead, rather abundant $[2M+H]^+$ and $[3M+H]^+$ ions are seen at m/z 569 and 853.

3. Skin Waxes.

Stearyl palmitate, a typical skin wax, shows an abundant $[M+H]^+$ ion at m/z 509 as well as some $[2M+H]^+$ at m/z 1017. The expected acyl ion is present

as well as its attachment ion to stearyl palmitate (m/z 748).

4. Glycerides

Major constituents of the skin lipids are of course the glycerides, and they were considered early in this problem although their high molecular weights seemed to militate against their involvement in a peak at m/z 551. The spectra of mono-, di- and tripalmitin were acquired. The monoglyceride showed an entirely satisfactory $[M+H]^+$ ion along with the usual acyl ion at m/z 239 resulting from loss of the elements of glycerol. The acyl ion reattaches to a monoglyceride molecule, accounting for a small peak at m/z 569, but the most abundant ion in this region was the $[2M+H]^+$ion at m/z 661.

In spite of its diol nature, the monoglyceride showed only a slight water loss peak from the $[M+H]^+$ ion at m/z 313. In some contrast, the ion representing water loss from the $[M+H]^+$ ion of the diglyceride (m/z 551) was much more abundant. An important peak, similar to the one seen in the anhydrides representing loss of one of the acid moities, was present at m/z 313. The water loss ion at m/z 551 does not suggest this diglyceride as the sought-after fingerprint substance, however, since the $[M+H]^+$ ion at m/z 569 was not seen in the spectrum of the latter substance.

The triglyceride, although it is a simple ester, showed only a small peak for its $[M+H]^+$ion at m/z 807. Instead , it easily loses a molecule of palmitic acid, forming the fingerprint ion peak at m/z 551 as its most abundant ion. The acyl ion at m/z 239 was also abundant. A peak at m/z 1045 could be assigned to attachment of the acyl ion to the triglyceride.

It is apparent that the ion at m/z 551 in the fingerprint-related spectrum might have as its source either tripalmitin or any of the other triglycerides containing at least two palmitoyl groups. A similar argument involving one palmitate and one myristate or two myrisitates applies to the ions at m/z 523 and 495, respectively.

Conclusions

The PD mass spectra of these simple lipids are often characterized by intense peaks for the stable fatty acid acyl or, in the negative ion mode, carboxylate ions. These ions are sometimes found reattached to neutral molecules of the same substance. The fingerprint spectra were assignable to triglycerides of palmitic and myristic acids.

(This paper is currently in press with Biomedical and Environmental Mass Spectrometry).

ANALYSIS OF SOME SUBSTITUTED PYRIDINE C-NUCLEOSIDES BY MICROBORE DLI/LCMS.

E.L. Esmans, M. Belmans, Y. Vrijens, Y. Luyten,
F.C. Alderweireldt, L.L. Wotring* and L.B. Townsend*.
University of Antwerp (R.U.C.A.), Lab. for Organic Chemistry,
Groenenborgerlaan 171, B-2020 Antwerp (Belgium).
* University of Michigan, College of Pharmacy,
Ann Arbor, Michigan (U.S.A.)

Within the framework of a programme aiming at the development of anti-tumour and/or anti-viral drugs, DLI/LC-MS has been used as a sensitive technique for the analysis of some original pyridine-C-nucleosides I to XI.

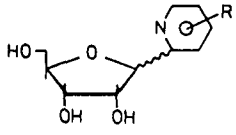

I=R=H ; II=R=3-Me ; III=R=4-Me ; IV=R=5-Me ; V=R=6-Me

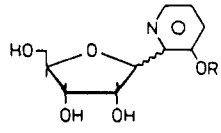

VI=R=Me ; VII=R=C_2H_5 ; VIII=R=C_3H_7 ; IX=R=C_4H_9

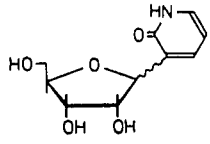

X

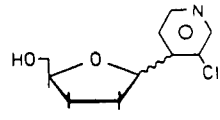

XI

It is evident that reliable data, obtained from the biological evaluation of synthetic nucleosides against L-1210 mouse leukemia, Coxsackie virus, polio virus, Rhinovirus, etc. are highly dependent upon the quality of the compounds submitted. Therefore, in order to obtain rapidly data on both criteria of purity and structure, crude reaction mixtures of I to XI were analyzed using microbore DLI/LC-MS.

The source temperature was 190°C and the temperature of the desolvation chamber was maintained constant at 210°C.

Compounds I to V were analyzed using 85% 0.01 M NH_4OOCH/15% CH_3OH as the eluant. A chromatogram which can be considered representative for this set of compounds is depicted in Fig.1 showing the DLI/LC-MS analysis of V.

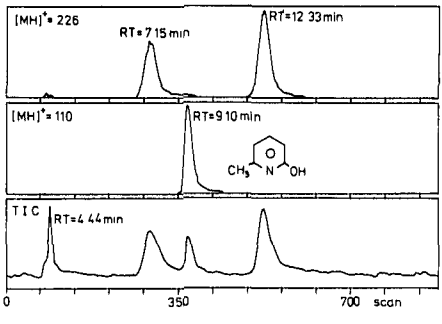

Fig. 1.

6-Methyl-2-(D-ribofuranosyl)-pyridine (V) was located by aid of the reconstructed ion chromatogram for the protonated molecular ion $[MH]^+$. Because it was observed, two chromatographic peaks (RT = 7.15 min and 12.3 min) to respond at m/z = 226, it was concluded that the separation of the α- from the β-anomer had been accomplished. However, due to the observation of similar mass spectra, the absolute configuration (α or β) at C_1' could not be assigned. Therefore an experiment was set up, separating a mixture of α- and β-adenosine under analogous conditions, followed by the injection of pure β-adenosine. From these results it could be concluded α-adenosine to have the lowest k'-value. The conclusion was confirmed by comparison of the corresponding peak areas calculated from the LC-MS runs with the ^{13}C-NMR integration data.
Together with the C-nucleosides described above, impurities were found at 4.44 min and 9.10 min respectively. These compounds were identified as methane sulfonic acid and 6-methyl-2-pyridone.
The 2-(D-ribofuranosyl)-3-alkoxypyridines (VI to IX) behaved chromatographically somewhat different and were eluted by using 60% 0.01 M NH_4OOCH/40% CH_3OH. Under these conditions the α- and the β-anomer of VI were not resolved. The DLI/LC-MS investigation of a mixture aiming at the synthesis of 2-fluoro-3-(D-ribofuranosyl)-pyridine gave however unexpected results. The mass spectra of the compounds eluting at respectively 2.50 min and 3.23 min were characterized by m/z = 228 ($[MH]^+$), 124 ($[B+30]^+$) and 138 ($[B+44]^+$). These values differ 2 amu from the expected values for the fluoro-compound. From this observation it was concluded the compound to be 3-(D-ribofuranosyl)-2-pyridone (X). This means that during the last step of the general synthetic procedure[1] the fluorine-atom was replaced by a hydroxyl function.
Since the impurities identified by LC-MS were quite different in structure from the C-nucleosides, a purification procedure of the latter was elaborated based upon affinity chromatography (Affigel 601).
Finally, in order to get information on the biological properties of some pure anomeric forms and to study the conformation of the ribofuranosyl ring by 360 MHz ^{1}H-NMR, some nucleoside mixtures were separated on a semi-preparative scale using reverse phase chromatography (LICHROSORB 10RP8 25 cm x 9 mm I.D.) using appropriate mixtures of 0.01 M NH_4OOCH/CH_3OH.
The C-nucleosides were screened against L-1210 mouse leukemia and a number of virusses, but no significant inhibitory effects have been observed at concentrations up to 400 µg/ml.

REFERENCES

1. M. Belmans, E.L. Esmans, R. Dommisse, J. Lepoivre, F.C. Alderweireldt, J. Balzarini and E. De Clerq: Nucleos. & Nucleot. 4, 523 (1985).

ACKNOWLEDGEMENTS

We thank Prof. Dr. M. Anteunis for the 360 MHz ^{1}H-NMR facilities. This work is supported by NATO-grant 424/84 and aided by grant CH-321 from the American Cancer Society.

MECHANISM OF CATIONIZATION OF OLIGOSACCHARIDES AND NUCLEOSIDES IN LASER DESORPTION FOURIER TRANSFORM MASS SPECTROMETRY

M.P. Chiarelli, Department of Chemistry, University of Nebraska, Lincoln, NE 68588-0362

The combination of laser desorption and Fourier transform mass spectrometry may provide a means of analysis for high mass molecules. Work in this laboratory with disaccharides (1) has shown that no $(M - H)^-$ ions are formed in the negative ion mode. Observation of a molecular ion complex requires cationization. An understanding of the cationization mechanism is essential for maximizing analytical sensitivity.

Direct evidence for gas-phase formation of sodium sucrose was obtained at a power density of 200 w/cm^2 (2). Thermal desorption of spatially separate reagents yielded potassium sucrose adducts (3). At higher power densities (10^7 w/cm^2) kinetic energy distributions have been used to support two mechanisms. Amino acid and nucleoside alkali-adducts were generated from larger clusters (4). A selvedge-formation mechanism was inferred for sodium sucrose in another study (5). The purpose of this study is to compare the extent of gas-phase sodium ion cationization of sucrose at two power densities. Sodium chloride and sucrose are loaded on separate substrates as part of a split probe.

All spectra were obtained with a home-built Nicolet 1000 data system. Solutions were electrosprayed to give a coverage of 8 $\mu g/cm^2$. Single-shot spectra were acquired at power densities of 10^5 and 10^9 w/cm^2.

A number of control experiments were performed to establish the dynamic range. The intensities of the ions presented in the Tables are 3-point peak areas referenced against m/z 365 desorbed from the mixed solid. Sucrose was desorbed off the probe and the mesh independently to estimate the background (Table I). It was observed that the ions from the mesh exceeded that of the reference. These results prompted the final control, sucrose on the Cu probe with the mesh present, to check for contamination of the sucrose. A small amount of m/z 365 was observed. These Figures represent the low end of the dynamic range. In terms of sensitivity, high-melting, thin mesh such as W is analytically superior to bulk Cu.

Table II contains results of the experiments in which the mixed solid is under the mesh and when the reagents are separate. The former experiment estimates the upper limit of the study because mixing of the reagents will occur mainly in the sections of the mesh transparent to the Cu.

The results show that gas-phase cationization is more extensive at the low power density. The data suggest that complexation may continue outside 100 μm at 10^5 w/cm^2. At the high power density, the data may indicate that cationization takes place within the spatial resolution of this experiment.

One explanation is that gas-phase cationization parallels the pulse length. The shorter pulse deposits the energy in a shorter time and generates a higher temperature than the long pulse. More material is desorbed in a shorter period of time and the selvedge is more compact, more dense, and shorter-lived than at the low power density.

We wish to extend our modus operandi to another system under conditions of resonant absorption (6). Uridine is a compound that does not give an intense $(M + H)^+$, and the abundance of $(M + Na)^+$ in the positive ion mode is much greater than the abundance of $(M - H)^-$ in the negative ion mode. The onset of m/z 243 is four times greater at 1064 nm than at 266 nm.

References

(1) D.A. McCrery and M.L. Gross, Anal. Chim. Acta, 178, 91-103 (1985).
(2) R. Stoll and F. Rollgen, Z. Naturforsch., 37a, 9-14 (1982).
(3) G.J.Q. van der Peyl, et al., Org. Mass Spectrom., 16, 416-420 (1981).
(4) E.D. Hardin and M. Vestal, Anal. Chem., 53, 1492-1497.
(5) G.J.Q. van der Peyl, et al., Int. J. Mass Spectrom. Ion Proc., 62, 51-71 (1984).
(6) M. Karas, et al., Anal. Chem., 57, 2935-2939 (1985).

I. SUCROSE CONTROLS							
POWER DENSITY	2×10^5 W/CM^2				2×10^9 W/CM^2		
PROBE	NaCl SUCROSE	SUCROSE	UNLOADED	SUCROSE	NaCl SUCROSE	SUCROSE	SUCROSE
MESH	NOT PRESENT	NOT PRESENT	SUCROSE	UNLOADED	NOT PRESENT	NOT PRESENT	UNLOADED
DIST	30 UM	30 UM	30 UM	30 UM	30 UM	30 UM	30 UM
M/Z 365 RI	10 ± 2	13 ± 03	17 ± 2	04 ± 02	10 ± 15	09 ± 01	—
ALL IONS	18 ± 3	29 ± 05	31 ± 4	13 ± 05	—	—	—

Na Sucrose, Cu probe, unloaded mesh flush to probe, P= 2x10+5 w/sm

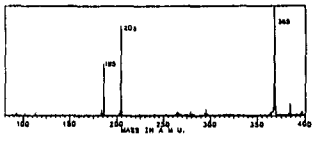

Sucrose W mesh, P=2x10+5 w/sm2

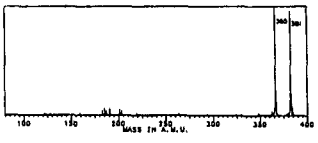

II SODIUM SUCROSE EXPERIMENTS									
POWER DENSITY	2×10^5 W/CM^2			2×10^7 W/CM^2			2×10^9 W/CM^2		
PROBE	NaCl Sucrose	NaCl Sucrose	Sucrose	NaCl Sucrose	NaCl Sucrose	Sucrose	NaCl Sucrose	NaCl Sucrose	Sucrose
MESH	not present	unloaded	NaCl	not present	unloaded	NaCl	not present	unloaded	NaCl
DIST	30 μm			100 - 150 μm			30 μm		
M/Z 365 RI	10±.2	56±.8	33±.06	10±.3	06±.03	.13±.03	10±.15	56±.08	09±.02
ALL IONS	18±.3	43±.25	70±.15	19±.6	.34±.09	.56±.11	—	—	—

Na on W mesh/ Sucrose on Cu probe, P=2x10+5 w/sm2

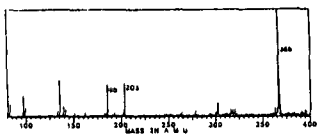

Na Sucrose Cu probe, P=2x10+5 w/sm2

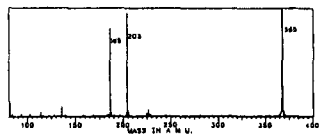

Na Sucrose, Cu probe, P=2x10+5 w/sm2

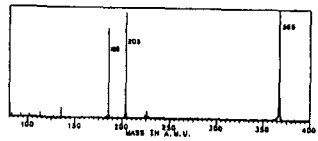

Sucrose on Cu probe only, P=2x10+5 w/sm2

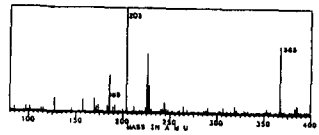

Na Sucrose Cu probe, P=2x10+5 w/sm2

Na on W mesh / Sucrose on Cu probe P=2x10+5 w/sm2

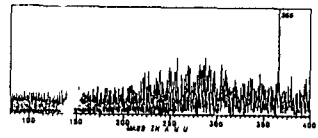

Uridine Negative Ion Mode, 266 nm, P=1x10+5 w/sm2

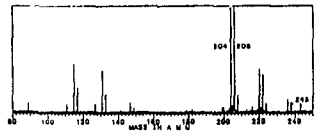

Uridine Negative Ion Mode, 1064 nm, P=1x10+5 w/sm2

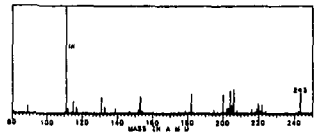

MASS SPECTROMETRY OF ELECTROPHORE LABELLED DNA BASES AND NUCLEOSIDES. PENTAFLUOROBENZYL AND CINNAMOYL DERIVATIVES.

T.M. Trainor, D.H. Fisher, J. Adams, R.W. Giese, and Paul Vouros. Barnett Institute of Chemical Analysis, Northeastern University, Boston, MA 02115.

Mass spectrometry is particularly useful in the characterization of DNA structure by analysis of the component bases, nucleosides, and nucleotides. We have been interested in developing analytical methodology for the trace level detection of chemically modified DNA bases and nucleosides in physiological samples. This requires detection limits not normally associated with the desorbtion ionization techniques (FAB, FD, or SIMS) usually applied to the underivatized species. Electron capture negative ion chemical ionization mass spectrometry is known to provide exceptional sensitivity for compounds with electron capturing properties. Our approach has been to take advantage of the sensitivity of both GC-ECD and GC-SIM-MS in the NCI mode by preparing suitable electrophoric derivatives of the target compounds. In this study we examined the methane NCI and PCI mass spectra of several model bases and nucleosides labelled with pentafluorobenzyl and cinnamoyl electrophores.

All mass spectra were obtained on a Finnigan 4023 GC/MS equipped with a fused silica capillary column (Hewlett-Packard Ultra-2, 20 m) inserted directly into the ion source. Methane was used as reagent gas (0.30 torr), helium as carrier gas, and the ion source temperature was maintained at 200°C. The derivatives were prepared as described previously (1,2), diluted in toluene, and introduced into the MS via the GC or by the direct insertion probe.

For the nucleosides studied, the cinnamoyl esters are distinguished by the production of the molecular anion M^- as the base peak under NCI conditions. In contrast, the pentafluorobenzyl ethers ionize via a dissociative process to give varying abundances of the $(m-181)^-$ ion and a base peak at m/z 178 $(CH_2C_6F_4O)^-$. The corresponding PCI mass spectra of these derivatives provide both molecular weight confirmation via the MH^+ ion and details of structural features through the presence of several abundant fragment ions.

The pentafluorobenzyl electrophore has been utilized in the trace level determination of the modified base 5-methylcytosine in DNA. The NCI mass spectra of the mixed derivative N^4-trimethylacetyl-1-pentafluorobenzyl-5-methylcytosine, Figure I, reveals only the $(m-181)^-$ ion at m/z 208. The analytical method utilizes GC-SIM-MS, monitoring the $(m-181)^-$ ion for both the analyte and an added tetrafluorobenzyl derivative that serves as an internal standard, Figure II.

References

1. Adams, J.; David, M.; Giese, R.W. Anal. Chem. 1986, 58, 345-348.
2. Adams, J.; Giese, R.W. J. Chromatogr. 1985, 347, 99-107.

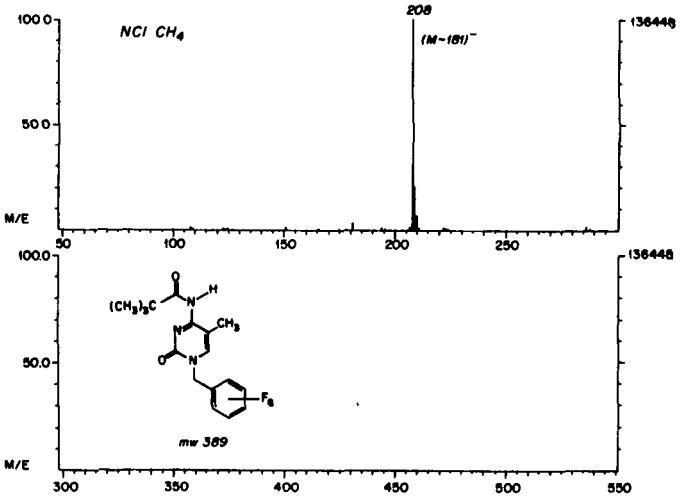
NCI CH4
208
(M-181)⁻
136448
100.0
50.0
M/E
50
100
150
200
250
136448
100.0
50.0
M/E
300
350
400
450
500
550
mw 389

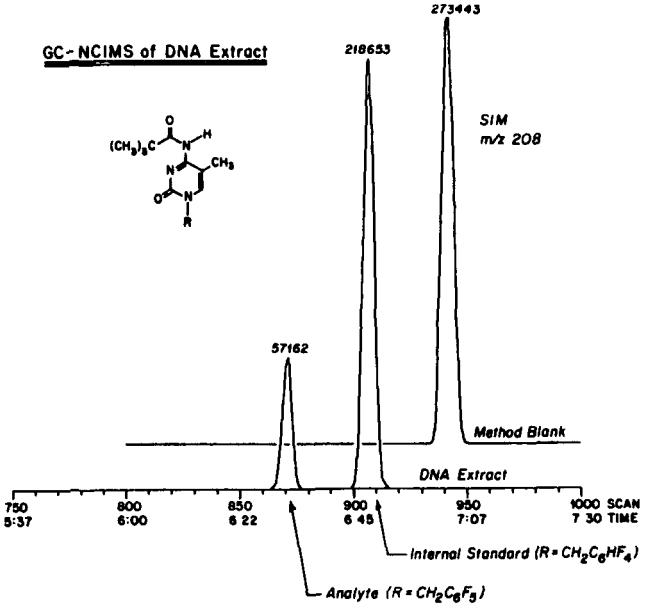
GC-NCIMS of DNA Extract
273443
218653
SIM
m/z 208
57162
Method Blank
DNA Extract
750
5:37
800
6:00
850
6 22
900
6 45
950
7:07
1000 SCAN
7 30 TIME
Internal Standard (R = CH2C6HF4)
Analyte (R = CH2C6F5)

IDENTIFICATION OF BACTERIA BY ANALYSIS OF THE GROWTH MEDIUM VIA MS WITH CI

D. C. Conway and Humberto Lopez, Department of Chemistry, and
J. M. Quarles, Jr., Department of Medical Microbiology and Immunology,
Texas A&M University, College Station, TX. 77843

The object of this research is to develop a rapid method for the identification of bacteria by MS using CI to reduce ion fragmentation. The growth media were analyzed by the procedure described previously[1] with the following changes: (1) The distance between the repeller plate and the MS window was increased to 7.5 cm. This results in increased reaction times and sensitivity. (2) The resistance at the probe heater contacts was not constant, which resulted in variation in the sample heating rate. This problem was alleviated by using connectors with Au coated pins. (3) The CI gas was 0.36 Torr CH_4 with a trace of H_2O and C_6H_6, so the CI reagent ion was $C_6H_7^+$. (4) The 4A-Molecular Sieve (NH_3 absorber) was removed from the ion chamber.

The bacteria were separated from the growth medium and sufficient solution placed in a 0.04 ml stainless steel cup to provide 0.5 mg of solid. After a low temperature drying cycle, the cup was heated in the inlet probe to 170-270°C, and a mass spectrum, taken for 140 sec.

"Unknown" mass spectra were processed by a microcomputer and compared to the "known" spectra stored in a file. Each spectrum was represented by a vector in hyperspace, so the match was determined by the smallest angle θ between the unknown and known vectors. Certain larger mass peaks characteristic of benzene (78, 79, 107, 119, and 156) and the growth media[1] were excluded. A set of masses was chosen to define a unique hyperspace to test for each type bacteria. This is to optimize the test hyperspace for each type bacteria to increase the angles between the vector for that type bacteria and the vectors for the other types. Previously,[1] a common hyperspace was used for all bacteria. It is easier to separate each of the known vectors from the n-1 other known vectors in n hyperspaces than to separate n known vectors from each other in one hyperspace. The unique hyperspace approach makes the identification procedure more reliable.

Seven types of bacteria were separated from their growth media as described[1] and stored in 62.5% alcohol. During a 7 week period 49 spectra were taken for these solutions. The average of the first, middle, and last spectra was used as each standard; the rest, as unknowns. The average values obtained for $\cos^2(\theta)$ between the unknown and known vectors are given in Table I. The

underlined values lie within the standard deviation range of the largest value. It can be seen that the mass spectrometry is reasonably reproducible.

Table I. $\cos^2(\theta)$

Knowns	1	2	3	4	5	6	7
Unknowns							
1	0.932	0.361	0.408	0.265	0.283	0.263	0.204
2	0.144	0.964	0.649	0.516	0.721	0.714	0.415
3	0.025	0.291	0.986	0.960	0.682	0.779	0.870
4	0.020	0.271	0.975	0.993	0.659	0.754	0.941
5	0.117	0.653	0.653	0.520	0.892	0.855	0.388
6	0.097	0.506	0.874	0.797	0.923	0.947	0.722
7	0.020	0.272	0.879	0.942	0.648	0.756	0.978

Code: (1) Escherichia coli, (2) Staphyloccus aureus (3) Listeria monocytogenes (1703) = LM-1703, (4) LM-1709, (5) LM-1706, (6) LM-1707, (7) LM-1710

The same types of bacteria were grown again, killed in 64% C_2H_5OH, and separated by centrifugation. The set of mass spectra for these growth media did not match the previous set. For example, Listeria monocytogenes (1703) = LM-1703 had large peaks at m/e = 108 and 198 with I(198)> I(108) for the first batch. However, in the second batch these peaks were much smaller and the relative intensities reversed with I(198)<<I(108). One problem is that many of the lines used to characterize most bacteria in the present study came from cluster ions. Thus the important 108 and 198 lines are derived from a neutral species of mass 90 as 108 = 90 + NH_4^+ and 198 = 2(90) + NH_4^+. It is presumed that the yield of the mass 90 product was less in the second batch of LM-1703 bacteria. The factors that determine the bacterial product concentrations in the growth media will be investigated.

We wish to thank Kathleen Conway for growing the second batches of Listeria monocytogenes bacteria.

[1] D.C. Conway and J. M. Quarles, Jr., Proc. 33rd Annual Conf., Amer. Soc. Mass Spectrom., 955.

QUANTITATION OF POLYOLS IN SERUM AND TISSUES FOR DIAGNOSIS OF FUNGAL INFECTIONS

KOKA JAYASIMHULU AND BRIAN WONG

Departments of Environmental Health and Internal Medicine
University of Cincinnati College of Medicine, Cincinnati, Ohio 45267

Introduction

Several medically important fungi produce large amounts of acyclic polyols in vitro. Past studies have shown: 1) that Candida produce large amounts of D-arabinitol both in vitro and in vivo; 2) that animals and humans with invasive candidiasis have elevated serum arabinitol concentrations and arabinitol/creatinine ratios; and 3) that arabinitol is produced in vivo in amounts that are directly proportional to the size of the metabolically active fungal population in infected tissues. Arabinitol is thus a quantitative diagnostic marker for candidiasis. It has also long been known that D-mannitol is a major metabolic product of the Aspergillus species, and we are currently studying D-mannitol as a potential quantitative diagnostic marker for experimental and human aspergillosis.

Sensitive and accurate methods for measuring these polyols in complex biologic samples (serum, urine, tissues, etc.) are required for these studies, and we have developed methods for measuring arabinitol and mannitol in serum and homogenized tissues by GC/MS.

Methods

Sample preparation: Alpha-methylmannoside is added as an internal standard to 0.2 ml of serum or 0.2 ml of homogenized tissue (1:9 w/v in 0.9% NaCl). The proteins in serum or in the homogenized tissue supernatant (1500g x 15 min after heating to 100° x 10 min to release intracellular solutes) are precipitated with 0.8 ml acetone, and the supernatant after centrifugation at 1500g x 5 min at 4° is dried in a nitrogen stream at 50°. Peracetate derivatives are prepared by adding 0.1 ml of a 2:1 (v/v) mixture of acetic anhydride:pyridine and then by heating to 80° for 30 min. 1.0 ml water and 1.0 ml chloroform are added, and the chloroform layer is washed twice more with 1.0 ml water and dried with granular anhydrous sodium sulfate. The chloroform is evaporated in a nitrogen stream, the sample is redissolved in 20 µl of methylene chloride, and 1.0-2.0 µl of final sample is analyzed by GC/MS.

GC separation: The GC separation is with a 1.8 m x 2.0 mm glass column packed with SP2340 (Supelco) with helium (30 ml/min) as the carrier gas. The oven temperature is 230° for the first 3 min and then is increased at 6° per min to 260°. The injector and the connecting oven containing the jet separator are maintained at 260°.

MS analysis: The Kratos MS80 mass spectrometer is tuned for maximum sensitivity at a resolution of 1000, and isobutane is introduced as the CI reagent. The m-59 ions of peracetylated arabinitol (m/e+ = 303.1080) and mannitol (m/e+ = 375.1291) and the m-31 ion of the peracetylated internal standard (m/e+ = 331.1029) are monitored by multiple peak monitoring or by selected ion monitoring. The m/e+ = 267.8171 ion of iodoform is the continuous mass marker. Quantitation is by comparison of the areas of the arabinitol, mannitol and internal standard peaks.

Results

In standard solutions of D-arabinitol, D-mannitol and the internal standard, 0.01 µg of polyol per ml could be quantified by multiple peak monitoring.

Representative analyses of the serum of a patient with sustained Candida tropicalis fungemia and of the livers of a normal rat and a rat with disseminated Aspergillus fumigatus infection are shown in figures 1 and 2, respectively.

Conclusions

The methods described here will facilitate further studies of fungal polyols as diagnostic markers for experimental and human fungal infections.

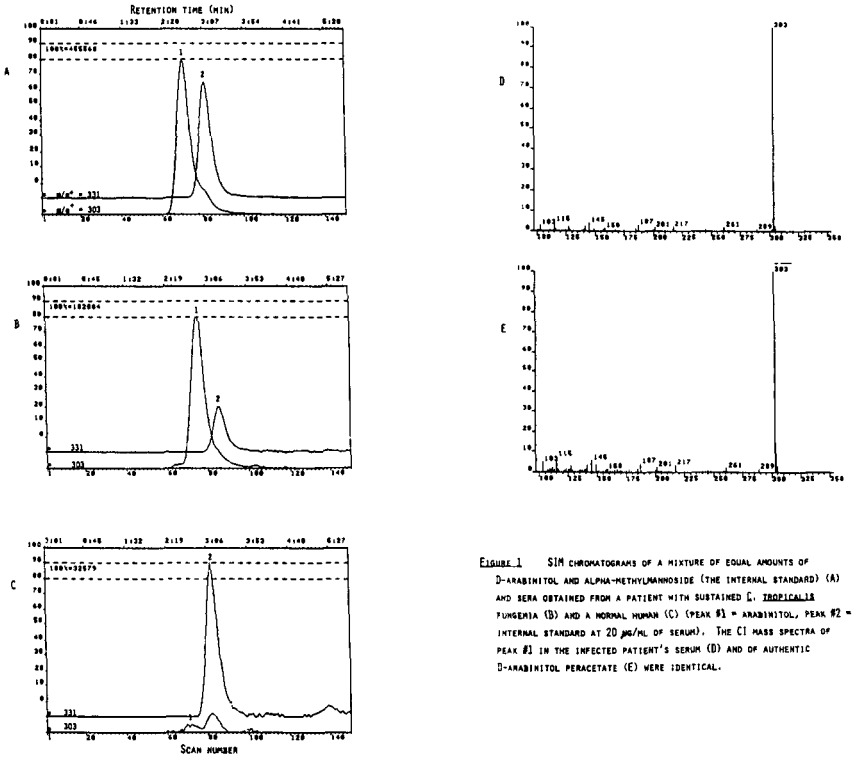

FIGURE 1 SIM CHROMATOGRAMS OF A MIXTURE OF EQUAL AMOUNTS OF D-ARABINITOL AND ALPHA-METHYLMANNOSIDE (THE INTERNAL STANDARD) (A) AND SERA OBTAINED FROM A PATIENT WITH SUBTAINED C. TROPICALIS FUNGEMIA (B) AND A NORMAL HUMAN (C) (PEAK #1 = ARABINITOL, PEAK #2 = INTERNAL STANDARD AT 20 µG/ML OF SERUM). THE CI MASS SPECTRA OF PEAK #1 IN THE INFECTED PATIENT'S SERUM (D) AND OF AUTHENTIC D-ARABINITOL PERACETATE (E) WERE IDENTICAL.

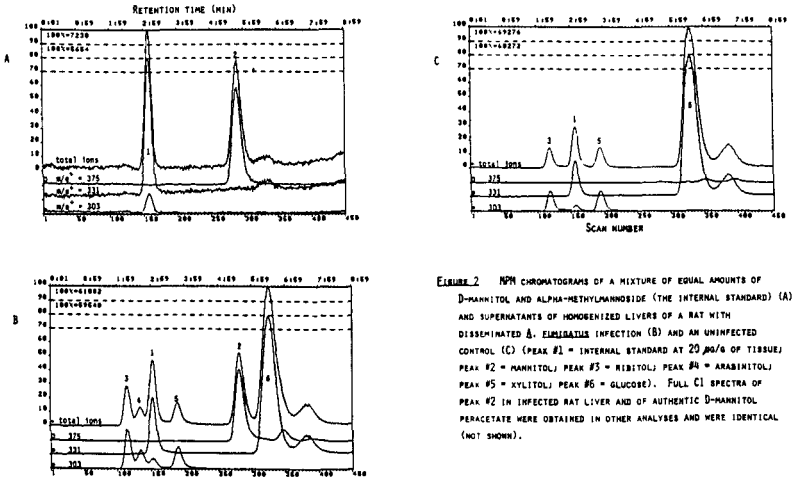

FIGURE 2 NPM CHROMATOGRAMS OF A MIXTURE OF EQUAL AMOUNTS OF D-MANNITOL AND ALPHA-METHYLMANNOSIDE (THE INTERNAL STANDARD) (A) AND SUPERNATANTS OF HOMOGENIZED LIVERS OF A RAT WITH DISSEMINATED A. FUMIGATUS INFECTION (B) AND AN UNINFECTED CONTROL (C) (PEAK #1 = INTERNAL STANDARD AT 20 µG/G OF TISSUE; PEAK #2 = MANNITOL; PEAK #3 = RIBITOL; PEAK #4 = ARABINITOL; PEAK #5 = XYLITOL; PEAK #6 = GLUCOSE). FULL CI SPECTRA OF PEAK #2 IN INFECTED RAT LIVER AND OF AUTHENTIC D-MANNITOL PERACETATE WERE OBTAINED IN OTHER ANALYSES AND WERE IDENTICAL (NOT SHOWN).

IDENTIFICATION OF THERMAL DEGRADATION PRODUCTS OF COMPOUNDS COSYNTHESIZED IN THE PRODUCTION OF PHENCYCLIDINE (PCP)

C. A. Haney and L. A. Jones

GC/MS Facility, North Carolina State University, Raleigh, NC 27695-7003.

The synthesis of phencyclidine (PCP) yields, in addition to the compound of interest, 13 additional nitrogen-containing compounds.[1] The three components identified thus far are 1-(1,1' biphen-4-yl cyclohexyl) piperidine (biphenyl PCP), 1,1'-(1,4-phenylenedicyclohexylidene) bis piperidine (bis PCP) and 1-[1-phenylethyl) cyclohexyl] piperidine (ethyl PCP). Preliminary investigations suggest that one or more of these compounds metabolizes to form a compound of extreme toxicity.[2] The analysis of these cosynthetics by gas chromatography is complicated by apparent thermal degradation products. Thermal degradation in the GC analysis of PCP has been reported.[3-7] The purpose of this paper is to identify the thermal decomposition products of the identified PCP cosynthetics by mass spectrometry.

For this study the injection port temperatures were 140°C, 200°C, 230°C, 260°C and 290°C; the transfer line temperatures were 200°C, 200°C, 230°C, 260°C and 290°C, respectively. None of the cosynthetics show any thermal decomposition with an injection port temperature of 140°C. At 200°C, ethyl PCP shows one thermal decomposition product identified as piperidinocyclohexene (I), biphenyl PCP shows one thermal decomposition product identified as biphenyl cyclohexene (II), and bis PCP shows two thermal decomposition products identified as 1,4 dicyclohexylbenzene (III) and 1(1-phenyl-4-cyclohexyl) piperidine (IV). As the injection port temperatures are increased, the degree of thermal decompositions increases with a concurrent decrease in the amount of parent compound. Interestingly, an injection port temperature of 290°C produces only 1,4 dicyclohexylbenzene from bis PCP. At an injection port temperature of 260°C, ethyl PCP shows three additional thermal decomposition products; 1-cyclohexyl-1-phenyl-ethane (V), 1-cyclohexyl-2-phenyl ethane (VI) and 1-[1-(phenylethyl)-cyclohexene] piperidine (VII).

1. Jones, L. A., Beaver, R. W., Schmoeger, T. L. J. Org. Chem. 46(1981) 3330-3.

2. Leander, J. D., Ort, J. F., Jones, L. A. Res. Commun. Subst Abuse, 2(2) 1981.

3. Wong, L. K., Biemann, K. Biomed. Mass Spectrom., 173-185, 2(1975) 204-5.

4. Lindgren, J. E., Holmstedt B. Arch. Toxicol. Suppl., 66(5), (1983) 1186-95.

5. Helisten, C., Shulgin, A. J. Chromatogr., 117(1976) 232-35.

6. Lin, C. K., Fentiman, A. F., Foltz, R. L., Forney, R. D. Sunshine I, Biomed. Mass Spectrom. 2(1975) 206-14.

7. Legault, D. J. Chromatog. Sci., 20(1982) 228-230.

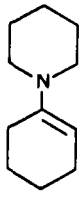

(I) Piperidino-cyclohexene

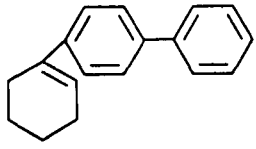

(II) Biphenylcyclohexene

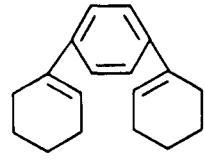

(III) 1,4 dicyclohexyl-benzene

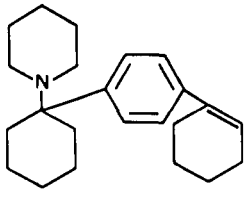

(IV) 1-(1-phenyl-4-cyclohexyl) piperidine

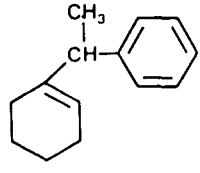

(V) 1-cyclohexyl-1-phenyl-ethane

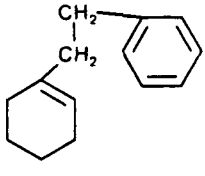

(VI) 1-cyclohexyl-2-phenyl-ethane

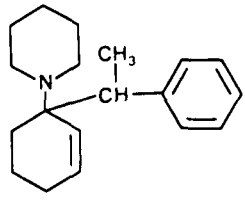

(VII) 1-[1-(phenylethyl)-2-cyclohexene] piperidine

A COMPARISON OF IONIZATION METHODS FOR THE ANALYSIS OF TECHNETIUM RADIOPHARMACEUTICALS

T.J. McCormick, B.M. Warrack, and S.E. Unger, The Squibb Institute for Medical Research, P.O Box 4000, Princeton, NJ 08543-4000
A.N. Nunn and E.N. Treher, The Squibb Institute for Medical Research, P.O. Box 191, New Brunswick, NJ 08903

Charged (cationic and anionic) complexes of technetium have been used as organ imaging agents and are amenable to field desorption (FD) and fast atom bombardment (FAB) mass spectrometry. Neutral Tc complexes are currently under investigation as imaging agents due to their ability to pass biological barriers and represent a new challange to the analyst.

We investigated the use of desorption ionization mass spectrometry for the characterization of both cationic octahedral and neutral seven-coordinate Tc complexes. This included FD and FAB-MS as well as fast-heating chemical ionization (DCI) and thermospray (TSP) ionization. Neutral complexes containing propylene amine oxime, PnAO, and analogs of glyoxime were examined. Those containing glyoxime (GLY), dimethylglyoxime (DMG), and cyclohexanedione dioxime (CDO) also incorporated boronate esters as shown. These seven-coordinate Tc radiopharmaceuticals represent a new class of imaging agents whose mass spectrometry has not previously been described. Cationic complexes included those containing phosphorous and arsenic ligands such as DIPHOS, DMPE, and DIARS.

Cationic complexes were most amenable to FD and FAB-MS with detection sensitivity favoring FD-MS (10-20 ng). Thermospray ionization was useful in generating positive parent ions of some cationic complexes, however, extensive oxidation of phosphorous destablizes the complex. Figure 1 illustrates this for $Tc(DMPE)_2Cl$ (top) whose MS/MS spectrum is also shown (bottom). Field desorption spectra of cationic Tc complexes exhibit the intact cation and may be obtained from either activated or unactivated emitters, serving to distinguish cationic from neutral complexes.

Neutral seven-coordinate complexes also yield both FD and FAB-MS (see Figure 2), however, matrix effects and a relative insensitivity make these techniques less attractive. Both DCI and TSP are amenable to these complexes as their boronate esters and yield positive and negative ions with ng detection sensitivity.

Thermospray ionization offers the advantage of on-line LC/MS which is best accomplished using a column with an inert support such as polystyrene. Reverse phase chromatography using isocratic or binary gradients which employ 0-20% water (0.1M ammonium acetate) and acetonitrile as mobile phase yielded best results. Either the electron filament or discharge was used to enhance detection sensitivity.

Table 1 compares the positive ion mass spectra of five related neutral seven-coordinate Tc complexes generated using four desorption ionization methods. Both positive and negative ions were observed with all ionization methods, save FD-MS which was operated only in the positive mode. Signal intensity was sufficient to yield MS/MS spectra of either cationic or neutral complexes (Figure 3).

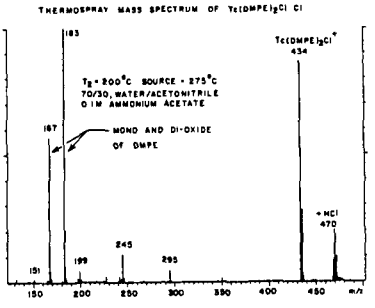

Figure 1

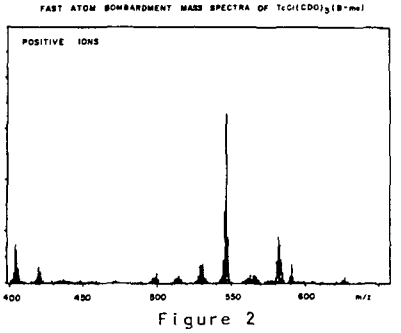

Figure 2

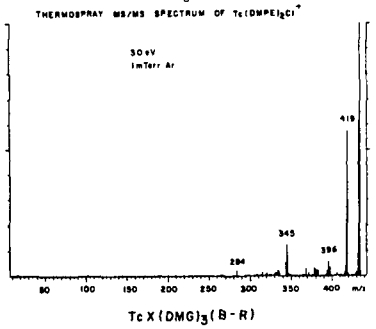

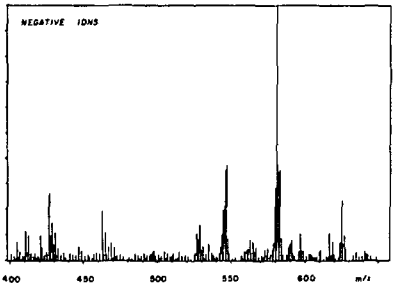

$TcX(DMG)_3(B-R)$

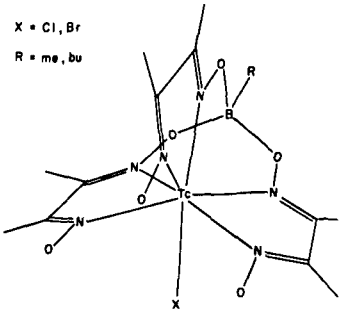

Table 1 *

Positive Ions in Mass Spectra of Seven-Coordinate Tc(III) Compounds

Compound	FD-MS	FAB-MS	TSP-MS	DCI-MS
A	590/592(100) 295/296(22)	590/592(19) 591/593(23) 511(100)	591/593(100) 511(23)	591/593(100) 511(32)
B	546/548(100)	546/548(15) 547/549(13) 511(100)	547/549(100) 511(33)	547/549(100) 511(54)
C	626/628(100)	626/628(22) 627/629(28) 547(100)	649/651(100)Na 547(22)	627/629(100) 547(89)
D	582/584(100)	582/584(24) 583/585(18) 547(100)	583/585(100) 547(21)	583/585(100) 547(44)
E	668/670(100)	668/670(23) 669/671(26) 589(100)	691/693(100)Na 589(89)	669/671(100) 589(55)

A = $TcBr(DMG)_3(B-bu)$ B = $TcCl(DMG)_3(B-bu)$ C = $TcBr(CDO)_3(B-me)$
D = $TcCl(CDO)_3(B-me)$ E = $TcBr(CDO)_3(B-bu)$

* For Br and Cl containing compounds, intensity is given as the first isotope only.

Figure 3

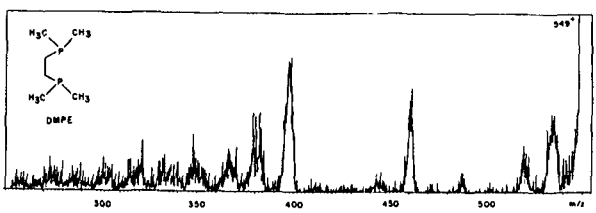

FAST ATOM BOMBARDMENT MASS SPECTRA OF 4-HYDROPEROXY-CYCLOPHOSPHAMIDE DERIVATIVES

Lawrence R. Phillips[1], Victoria L. Boyd[2], William M. Bone[2], and Gerald Zon[1]

[1]Division of Biochemistry and Biophysics, Office of Biologics Research and Review
Food and Drug Administration, 8800 Rockville Pike, Bethesda, MD 20892 USA, and
[2]Division of Biochemistry, Walter Reed Army Institute of Research, Washington, D.C. 20307

Abstract

The positive and negative fast atom bombardment (FAB) mass spectra of several 5-substituted 4-hydroperoxy-cyclophosphamides were recorded and examined. Features found to be shared among the FAB mass spectra of these compounds yielded important information regarding the molecular weight, exocyclic mustard moiety, and with limitations, the oxazaphosphorine ring system.

Introduction

Selected derivatives of 4-hydroperoxy-cyclophosphamide (Figure 1) were synthesized and the solution chemistry of each was studied by ^{31}P NMR spectroscopy under a standard set of reaction conditions at physiological pH (7.4) and temperature (37°C). The relative ratios of the tautomeric species, 4-hydroxy-cyclophosphamide and aldophosphamide, and their half-lives were measured by ^{31}P NMR spectroscopy following the in situ deoxygenation of the 4-hydroperoxy-cyclophosphamide analogues or dissolution of the aldophosphamide derivatives.

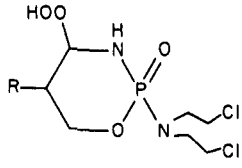

Compound	R=
Ia	H,H
Ib	H,Br
Ic	H,Cl
Id	H,OMe
Ie	H,Me
If	Me,Me

Figure 1. The structure of 4-hydroperoxy-cyclophosphamide (Ia), and derivatives studied.

As a prerequisite necessary to this study, the synthesized materials required verification of the correctness of chemical structure. Proposed structures were consistent with other analytical data obtained from NMR spectroscopy (^{1}H, ^{13}C, and ^{31}P). The mass spectra of these compounds were then examined. In particular, the 4-hydroperoxy-cyclophosphamide derivatives gave distinctive electron-ionization mass spectra, but failed to show a molecular species[1-4]. It was therefore decided to subject these compounds to analysis by fast atom bombardment mass spectrometry.

Experimental

Positive and negative fast atom bombardment mass spectra were recorded with a Kratos MS-50 mass spectrometer equipped with a Kratos DS-55 data system (Data General Nova 4X minicomputer employing the RDOS operating system). Glycerol (0.3 uL) was deposited on a copper sample probe-tip, and to this samples were directly added and dissolved as completely as possible. Bombardment was achieved with a 25-uA beam of 7 keV xenon atoms generated in a Saddle-Field neutral-beam gun (Ion Tech, Ltd., Teddington, England). Linked scanning FAB mass spectra were obtained under either unimolecular decomposition conditions or collisionally activated conditions at constant B/E. Collisionally activated decomposition (CAD) spectra were obtained by colliding 6 keV ions with air in the first field-free region of the mass spectrometer. The collision cell was operated at a pressure so as to reduce the main ion beam intensity to about one-half of its usual value.

Results and Discussion

There are several features found to be common to the FAB mass spectra of the 5-substituted, 4-hydroperoxy-cyclophosphamides (representative spectra are shown in Figure 2). First, and

perhaps most importantly, all compounds gave prominent molecular species in both positive and negative FAB, thus permitting easy verification of the molecular weight. Preliminarily, lower or higher sample concentration in the glycerol matrix did not result in the observation of any additional cluster or polymeric species than was observed for 5,5-dimethyl-4-hydroperoxy-cyclophosphamide (compound If, Figure 1), as shown in Figure 2.

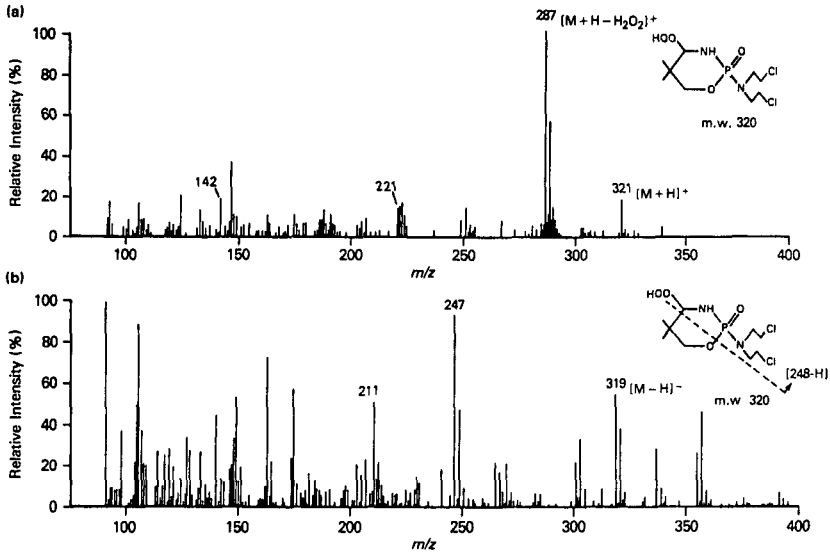

Figure 2. (a) Positive and (b) negative FAB mass spectra of 5,5-dimethyl-4-hydroperoxy-cyclophosphamide.

The positive FAB mass spectra showed simple loss of water or hydrogen peroxide from the molecular species, the former usually possessing a low intensity while the latter usually represented the base peak of the spectrum. Always present was a characteristic "clump" of ions at m/z 221 to m/z 225 which could be explained, in part, by fragmentation of the oxazaphosphorine ring. Another ion common to all the spectra was found at m/z 142, which is most probably due to the addition of two hydrogen atoms to the nitrogen mustard moiety subsequently followed by cleavage of the exocyclic phosphorus-nitrogen bond.

The negative FAB mass spectra showed intense $[M-H]^-$ ions as well as what appeared to be simple cluster ions of the molecular species together with either H_2O or HCl. Simple loss of water from the molecular species, and sometimes from the clustered species, was generally observed. The base peak of the negative FAB mass spectra was usually m/z 247, which could be rationalized by fragmentation of the oxazaphosphorine ring. Subsequent loss of HCl would lead to the ion observed at m/z 211. Upon closer examination of 5,5-dimethyl-4-hydroperoxy-cyclophosphamide, linked scanning FAB mass spectra at constant B/E under either unimolecular decomposition conditions or under collisionally activated conditions helped to confirm simple loss of water from the molecular species, but did not provide the means to establish an obvious inter-relationship between m/z 247 and m/z 211, or between either of these two ions and the molecular species or any of the clusters of the molecular species.

References

1. H. I. Kenttamaa, P. Savolahti and J. Koskikallio, Int. J. Mass Spectrom. Ion Phys. 47 (1983) 463.
2. M. N. Mruzek and I. C. Shaw, Biomed. Mass Spectrom. 11 (1984) 360.
3. M. Przybyski, H. Ringsdorf, U. Levssen, G. Peter, G. Voelcker, T. Wagner and H. J. Hohorst, Biomed. Mass Spectrom. 4 (1977) 209.
4. V. T. Boyd, Ph.D. Dissertation, 1985, The Catholic University of America, Washington, D.C.

CHARACTERIZATION OF ANTHRACYLCINES BY USING FAST ATOM BOMBARDMENT MASS SPECTROMETRY

Chhabil Dass, R. Seshadri, M. Israel, and D.M. Desiderio

University of Tennessee, Memphis, Memphis, Tennessee 38163

This study was undertaken to understand correlation between the mass spectral data and the structural features of the anthracyclines. Anthracyclines are important class of compounds because of their putative antitumor properties. Structurally, they are composed of two moieties: the anthraquinonic aglycone and the aminosugar. The anthracyclines (Table I) are thermally labile compounds. Therefore, the research was accomplished by utilizing FAB-MS, "a soft ionization" technique, in the positive and negative ionization modes. The fragmentation pattern was also confirmed by using MS/MS in the B/E-linked-field scan mode.

The negative ions FAB spectra of the anthracyclines are shown in the Table II. The radical anion ($M^{\cdot-}$) is the most abundant in the molecular ion cluster region. Spectra of the antibiotics are weak when glycerol is used as a matrix. However, a relatively abundant $M^{\cdot-}$ is observed by using a mixture of glycerol and sulfolane as solvent. Sulfolane alone did not stay longer on the probe tip.

The major fragmentation, as shown in the Table II and Scheme I, is cleavage of the bond between anthracycline and sugar moieties with the charge retention by the aglycone yielding mainly d type ions. The e and f ions are also formed but of lower intensity. The charge retention by the sugar moiety is also observed if the amino group is substituted by electronegative group (CF_3CO). For example, the compounds 4-8 all yield an abundant m/z 242 ion due to sugar moiety. The ions $NHCF_3CO^-$ (m/z 112) and CF_3CO^- (m/z 97) are also observed in the spectra of these (4-8) compounds. We also observed loss of H_2O and amino group from the $M^{\cdot-}$ (a and b ions, respectively). The loss of side chain from d as well as from the $M^{\cdot-}$ yields d_1 and c ions. The fragmentations initiated in the side chain (not shown) are also observed and their importance increases with the length of the side chain. As a consequence, relatively less abundant $M^{\cdot-}$ is observed in the spectra of 5-8. Fragmentations in the anthracyclinone ring are also seen in the spectra of the antibiotics.

The positive ion FAB yields less abundant molecular ion [$(M+H)^+$] than the corresponding $M^{\cdot-}$ in the negative ion mode. The major fragmentations are similar except that the masses of the ions are shifted. The fragments containing the fluoroacetyl group are not seen. The fragments related to the sugar moiety are seen only when R_2 = H or $C_6H_5CH_2$ (ions e, e_1, and e_2 in Table III).

We also studied the corresponding anthracyclinone molecules (Table IV). These compounds having the anthraquinonoid structure are undetectable in the positive ion mode. However, an abundant $M^{\cdot-}$ was observed in the negative ion mode. The major fragmentation observed were the loss of water and side chain (Table V).

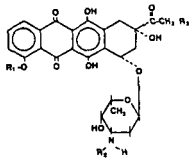

	R_1	R_2	R_3	Formula	Mol. Wt.
1 ▲	CH_3	H	H	$C_{27}H_{29}NO_{10}$	527.18
2 ■	CH_3	H	OH	$C_{27}H_{29}NO_{11}$	543.17
3 ○	H	H	H	$C_{26}H_{27}NO_{10}$	513.18
4	CH_3	CF_3CO	OH	$C_{29}H_{28}F_3NO_{12}$	639.16
5	CH_3	CF_3CO	$OCO(CH_2)$	$C_{31}H_{30}F_3NO_{13}$	681.17
6	CH_3	CF_3CO	$OCO(CH_2)CH_3$	$C_{32}H_{32}F_3NO_{13}$	695.18
7	CH_3	CF_3CO	$OCO(CH_2)_2CH_3$	$C_{33}H_{34}F_3NO_{13}$	765.28
8	CH_3	CF_3CO	$OCO(CH_2)_4COOH$	$C_{35}H_{38}F_3NO_{15}$	787.20
9	CH_3	$C_6H_5CH_2$	$OCO(CH_2)_2CH_3$	$C_{39}H_{43}NO_{12}$	717.26
10	CH_3	$C_6H_5CH_2$	OH	$C_{34}H_{33}NO_{11}$	633.22

▲ daunorubicin , ■ adriamycin ,
○ carminomycin

TABLE I

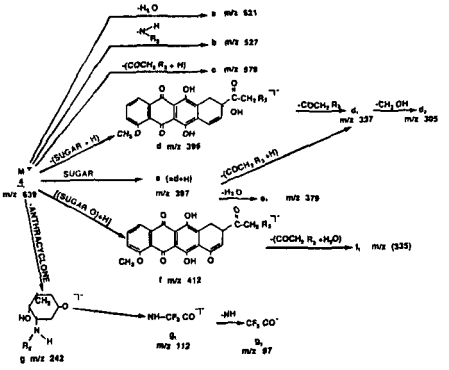

SCHEME I

PARTIAL NEGATIVE ION FAB SPECTRA OF ANTHRACYCLINES

COMPOUND	M^{-}	a	b	c	d	e	f	d_1	d_2	e_1	f_1	g	g_1
1	527	-	-	483	380	381	396	337	305	363	335	-	-
2	543	525	527	483	396	397	412	337	305	379	335	-	-
3	513	485	497	469	366	367	382	323	305	349	321	-	-
4	639	621	527	579	396	397	412	337	305	379	335	242	112
5	681	663	-	579	436	439	454	337	305	421	335	242	112
6	695	-	-	-	452	453	-	337	305	-	335	242	112
7	765	747	-	579	522	523	538	337	305	505	335	242	112
8	787	749	655	579	524	525	540	337	305	507	335	242	112
9	633	615	528	573	396	397	412	337	305	379	335	-	-
10	717	-	-	573	480	481	496	337	305	-	335	-	-

TABLE II

PARTIAL POSITIVE ION FAB SPECTRA OF ANTHRACYCLINES

COMPOUND	$(M+H)^{+}$	a	a_1	b	c	d	e	e_1	e_2
1	528	383	365	339	321	307	148	130	113
2	544	399	381	339	321	307	148	130	113
3	514	369	351	325	307	307	148	130	113
4	640	399	381	339	321	307	-	-	-
5	682	441	423	339	321	307	-	-	-
6	696	455	437	339	321	-	-	-	-
7	766	525	-	339	321	307	-	-	-
8	768	527	-	339	321	307	-	-	-
9	634	399	381	339	321	307	238	220	113
10	718	483	465	339	321	307	238	220	113

TABLE III

B. Aglycones

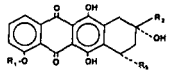

		R_1	R_2	R_3	Formula	Mol. Wt.
1	Daunorubicinone	CH_3	OH	$COCH_3$	$C_{21}H_{18}O_9$	398.10
2	Adriamycinone	CH_2	OH	$COCH_2OH$	$C_{21}H_{18}O_9$	414.10
3	Carminomycinone	H	OH	$COCH_3$	$C_{20}H_{16}O_8$	384.09
4	4-O Desmethyl-adriamycinone	H	OH	$COCH_2OH$	$C_{20}H_{16}O_9$	400.08
5	7 Deoxyadria-mycinone	CH_3	H	$COCH_2OH$	$C_{21}H_{18}O_8$	398.10
6	7-Deoxy 13-dihydro-adriamycinone	CH_3	H	$CH(OH)CH_2OH$	$C_{21}H_{20}O_8$	400.12

TABLE IV

PARTIAL NEGATIVE ION FAB OF AGLYCONES

COMPOUND	M^{+}	a	b	b_1	b_2	b_3	c	c_1	c_2	c_3
1	398	380	354	337	321	305	311	297	283	269
2	414	396	354	337	321	305	311	297	283	269
3	384	366	340	323	-	305	297	283	269	255
4	400	382	340	323	307	305	297	283	269	255
5	398	-	339	-	321	305	311	297	283	269
6	400	-	339	-	321	305	311	-	283	269

TABLE V

MATRIX-ASSISTED MOLECULAR SIMS OF QUINONE ANTIBIOTIC, SAFRAMYCIN Y SERIES

Makoto Suzuki, Ken-ichi Harada, Katsuyoshi Masuda, Akira Tatematsu and Tadashi Arai*

Faculty of Pharmacy, Meijo University, Tempaku, Nagoya 468, Japan
Research Institute for Chemodynamics, Chia University, Inohana, Chiba 280, Japan*

Antitumor antibiotic, saframycins contain unique isoquinoline-quinone structure. FABMS of saframycins has been studied by several research groups, and reported that the spectrum taken in glycerol showed MH^+ and $(M+2nH)H^+$ ions, corresponding to the reduction of quinone ring by the hydrogen donating liquid matrix materials.[1] The production of these molecular ion species of unreduced (quinone) and reduced (hydroquinone) forms is influenced by choice of matrix material, length of analysis and quinone structure.[2]

Recently, we have developed the matrix systems which can regulate the reduction process from quinone to hydroquinone in the study of molecular SIMS of saframycin Y series produced by directed biosynthesis with the resting cell of Streptomyces lavendulae 314.[3]

As shown in Fig. 1, SI mass spectrum in same length of analysis (scan number 11) of saframycin Yd-1 using glycerol matrix (a) shows MH^+, $(M+2H)H^+$ and $(M+4H)H^+$, and we can recognize predominant $(M+4H)H^+$ ion formation in the spectrum (b) taken in glycerol + thio-

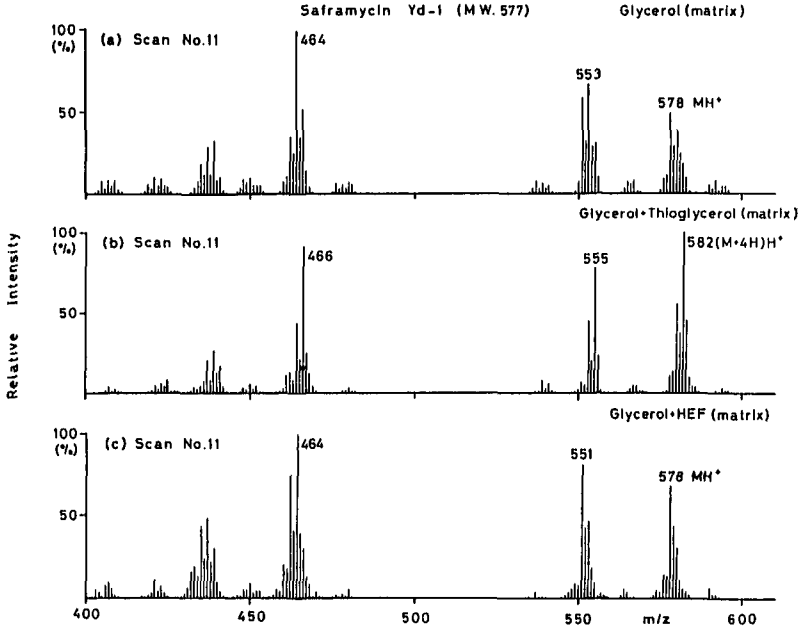

Fig. 1, SI mass spectra of saframycin Yd-1 with various matrix systems

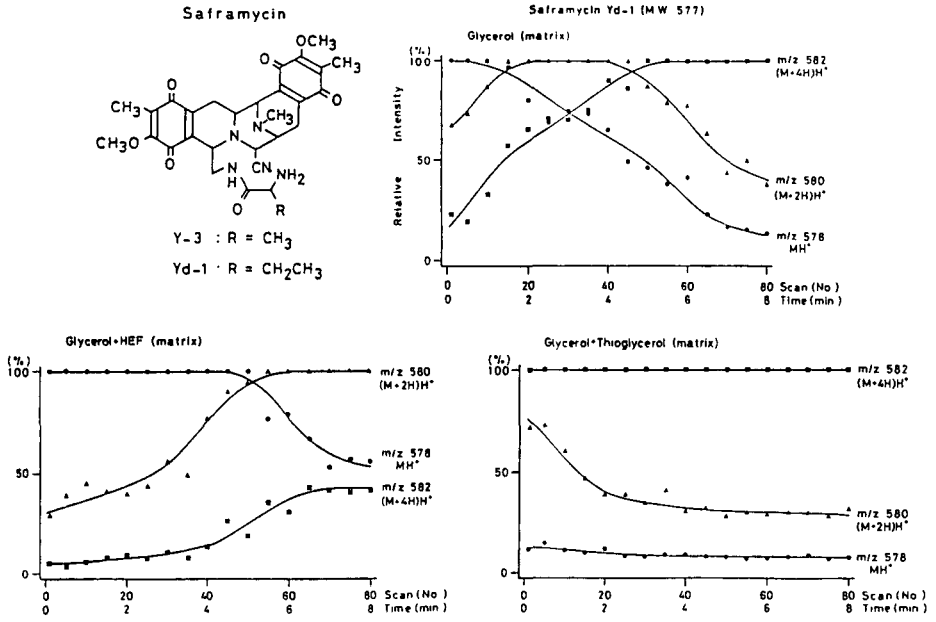

Fig. 2. The process of molecular ion species formation of saframycin Yd-1

glycerol matrix. Such phenomenon is also observed in the case using other thiol matrix system, dithioerythritol + dithiothreitol mixture (magic bullet). On the other hand, we can observe clear MH^+ ion retaining in the spectrum (c), which is measured by glycerol + 2-hydroxyethylformamide (HEF) matrix, and similar behavior is characterized in the spectrum with other amide matrix system.

Fig. 2 shows the process of molecular ion species formation of saframycin Yd-1 using glycerol, thiol and amide as the matrix materials. Moreover, saframycin Y-3, Y-2b and Y-2b-d also indicate similar processes.

These experimental results suggest the possibility about precise anlysis of molecular weight and extensive application of B/E linked scanning or MS/MS technique to two kinds of precursor ions, MH^+ and $(M+2nH)H^+$ of novel antibiotics belonging to saframycin Y series.

References

1) K. Fukushima, T. Arai, K. Takahashi, Mass Spectroscopy (Tokyo), 32, 137 (1984).
2) R. Cooper, S. Unger, J. Antibiotics, 38, 24 (1985).
3) T. Arai, K. Yazawa, K. Takahashi, A. Maeda, Y. Mikami, Antimicrob. Agents Chemother., 28, 5 (1985).

ANALYSIS OF AMPICILLIN BY THERMOSPRAY LC/MS IN BIOLOGICAL FLUIDS

Somchai Suwanrumpha and Marvin L. Vestal
Department of Chemistry,
University of Houston-University Park,
Houston, TX 77004

A reversed-phase high-performance liquid chromatography system for the separation of ampicillin and its metabolite, penicilloic acid, has been developed for use in thermospray LC/MS. The quantitation of ampicillin in urine sample by LC/MS was compared to the results from UV detector. On-line sample clean-up is used to minimize the sample preparation time and to prolong the analytical column life time. The cleaning system consisted of a tandem injection valves with double LC pumps and C-18 3 cm. pre-column which was modified from Koch and Kissinger (1). The only preparation for the sample was to freeze the urine sample in order to precipitate the protein and then filter the melt sample. The appropriate dilution of the filtrate were subjected to the HPLC analysis.

By using the UV detector, the time for a single analysis was 18 minutes (13 minutes for sample clean-up time and 5 minutes for the chromatographic analysis). The linear regression was 0.99469 for the calibration curve of ampicillin with a detection limit of 200 ng per injection. However, the penicilloic acid cannot be determined.

The time for a single analysis by using thermospray/MS was 13 minutes (8 minutes for sample clean-up time and 5 minutes for chromatogarphic analysis). The thermospray vaporizer probe temperature was adjusted to maximize solvent and ampicillin molecular ion intensities. The tip and source block temperature were 178-180 C and 278-280 C, respectively. The mass spectrometer was employed in the selected ion monitoring mode at the fragment and molecular ions of ampicillin. The linear regression analyses of the calibration curve were 0.9956 for the total ions chromatogram and 0.9982 for ion monitored at M/Z = 191, a fragment ion.

Samples of urine collected from a subject given an oral dose of 500 mg of ampicillin were analyzed. The rate constant for excretion of ampicillin was estimated using a one-compartment model (2). The half life in the body was found to be 1.2 hours, in agreement with earlier studies(2,3).

CONCLUSION

1. Using MS as a detector for LC analysis can minimize the sample preparation and analysis time. The average time for each sample analysis time by LC/MS was 10 minutes compared to using UV detector which was 15 minutes

2. The detection limit of ampicillin in LC/MS is a magnitude lower than 40 ng per injection by using selected ion monitoring mode for the fragment peak. The detection limit of ampicillin by UV detector was 200 ng per injection. In addition, the metabolite of ampicillin can be determined by LC/MS and the detection limit is also at the 40 ng per injection range. Positive identification of ampicillin metabolites will be investigated in the future study.

3. Linear regression analyses of the calibration curve from both techniques are comparable. However, the detection in MS is more selective by utilizing the M/Z of the fragment and molecular ions.

4. With a short reversed phase pre-column and suitable mobile phase. The tandem injector valves can be used as a on-line sample clean-up which minimizes the sample preparation time.

1. D. Koch and P. T. Kissinger, Anal. Chem. 52, 27 (1980)
2. T. Uno, M. Masada, K. Yamaoka and T. Nagawa, Chem. Pharm. Bull., 29(7), 1957 (1980)
3. Remington's Pharmaceutical Sciences, 16th ed., Mack Publishing Co., Easton, PA., 1980, 1137

THE APPLICATION OF THERMOSPRAY TO THE STUDY OF THE MECHANISM OF THE CONVERSION OF MODIFIED ACV - TRIPEPTIDES TO PENICILLINS AND CEPHAMS BY CELL-FREE ENZYMES.

R.T. APLIN. THE DYSON PERRINS LABORATORY, OXFORD UNIVERSITY, OXFORD. OX1 3QY., M. McDOWELL AND K. ROLLINS, V.G. MASSLAB LTD., TUDOR ROAD, ALTRINCHAM, CHESHIRE, W14 5RZ, U.K.

Thermospray has been shown to be applicable to the analysis of the mass spectrometrically difficult α-aminoadipyl penicillins and cephams. Examples of the improved spectra obtained by using acidified Acetonitrile: water (0.1M NH_4 OAc; pH 5.5 HOAc) as the mobile phase were presented for the compounds involved in the cell free enzyme conversion of the tripeptide LLD-ACV into Cephalosporin C (Scheme 1) and for ampacilin. The molecular ions are easily detected at the 100 μg level but quasi molecular ion abundances are ca., +50% greater than the calculated values even at the 1 μg level. Overall sensitivity for enzymically derived samples is much greater (at least x50) than that obtained with +ve ion FAB analysis, due to the lack of matrix effects associated with the relatively high levels of sodium ions present in these samples. Accurate isotope ratios, essential for the study of enzyme kinetics of the conversion shown in Scheme 1, either on the molecular ion, the β-lactam cleavage fragment or the pseudo molecular ion, required in our hands the IBEI or DCI analysis of derivatised material (N-carboxy ethyl, O-methyl esters).[1]

Scheme 1. BIOSYNTHESIS of Penicillin N and Cephalosporin C

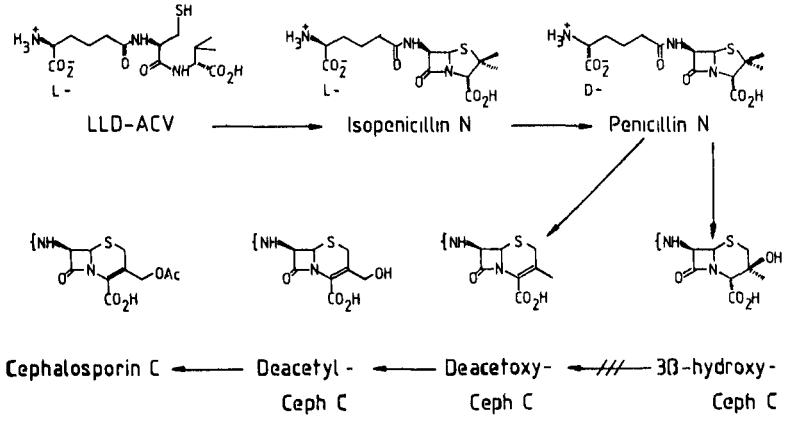

1. J.E. Baldwin, E.P. Abraham, R.M. Adlington, R.T. Aplin, B. Chakravarti, L.D. Field, E-M,M, John, and R.L. White Tetrahedron, 39, 1061.

ANALYSIS OF THE CURIE-POINT PYROLYSIS PRODUCTS OF SOME DIPEPTIDES AND THEIR DIKETO-PIPERAZINES BY GC/MS.

Grant Gill Smith[1], Jaap J. Boon[2] and G. Sudhakar Reddy[1],

[1]Department of Chemistry & Biochemistry, Utah State University, Logan, UT 84322.

[2]FOM Institute for Atomic and Molecular Physics, Kruislaan, Amsterdam, The Netherlands.

Pyrolysis gas chromatography in combination with mass spectrometry (Py/GC/MS) has been shown to be a powerful technique in analyzing thermally labile molecules including amino acids, peptides and proteins[1]. In this work, Curie-point pyrolysis method was employed to study the pyrolysis of val-pro, pro-val, ala-pro, pro-ala, gly-ala, ala-gly and their diketopiperazines (DKPs).

Ten μg of the dipeptide sample, dissolved in water was coated onto a ferromagnetic wire, which was inductively heated to 510° C for 10 seconds. Thus formed pyrolysis products were swept onto a 25 m CP SIL-5 fused silica capillary column in a stream of helium. The gas chromatograph oven was heated from 50° C to 300° C at a rate of 8° C min^{-1}. The peaks were detected by quadrupole (MAT 44) mass spectrometer operated under normal conditions in a cyclic scan mode. Approximately 800 to 1000 scans were collected in a data system for each analysis.

In each case five to six major compounds were formed which represent approximately 90% of total yield. Dipeptides readily expelled a water molecule to form the corresponding diketopiperazines. Expulsion of CO_2 was also noted from all the dipeptides studied. Once the diketopiperazine is formed, it looses simple molecules such as H_2, CO and propene in a single or two steps to give a series of primary products. Condensation products, for example, the presence of N-methyl DKP and val-val DKP was also seen. Only two major products were formed in the pyrolysis of ala-gly, gly-ala and their diketopiperazine. Proline containing dipeptides, on the other hand, formed more products due to the presence of proline moiety. It is interesting to note that DKPs yielded more number of products than their corresponding dipeptide molecules. Most of the pyrolysis products formed were identified by a careful comparison against the mass spectral data from the literature[2] or on the basis of their mass spectral fragmentations. Following scheme shows the formation of primary pyrolysis products from the dipeptides val-pro, pro-val and their diketo-piperazines.

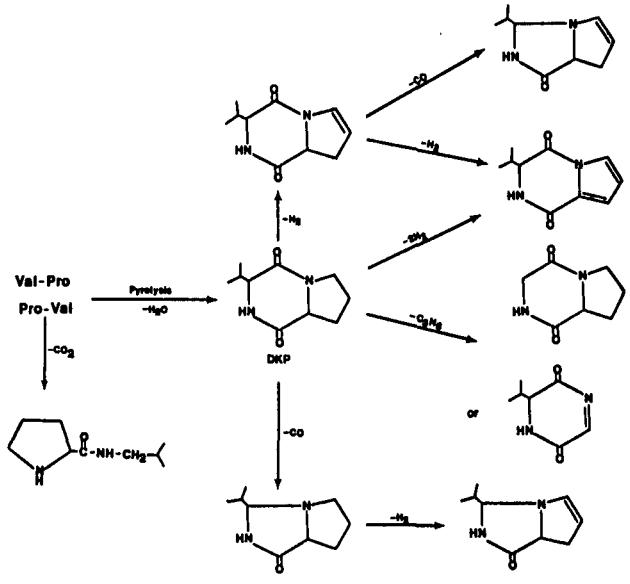

Scheme

The products formed in low or trace amounts constitute secondary pyrolysis products, which are formed by multi-step processes. Many workers investigated the pyrolysis of proline and proline containing peptides which represent an area of controversy. For example, Giacobbo and Simon[3] reported the formation of 1-pyrroline in the pyrolysis of proline in large amounts. On the contrary, Smith et. al[4] noted that the pyrolysis of proline afforded only pyrrole. 1-Pyrroline was seen as a major product in the pyrolysis of peptides with proline at carboxyl terminal. Our study demonstrated that 1-pyrroline is formed only in pro-val and pro-ala dipeptides while pyrrole was seen in the pyrograms of all the proline dipeptides studied. In contrast to the previous reports, we noted that pyrrole and 1-pyrroline were formed only in trace amounts. Acetone, isobutyramide, pyrrolid-2-one and cyanopyrrole represent other secondary products in the pyrolysates of these compounds.

The formation of DKP and the related primary products in large amounts suggest the practical utility of this method for rapidly determining these peptide residues in complex materials when present in low levels.

References:

1. W. J. Irwin, Analytical Pyrolysis, Marcel Dekker, New York, 1982.
2. 'Eight Peak Index of Mass Spectra', Mass Spectrometry Data Center, AWRE, Aldermaston, UK, 1974, Vol. 1-3.
3. H. Giacobbo and W. Simon, Pharm. Acta Helv., 39, 162 (1969).
4. R.M. Smith, S. A. K. Shawkat and W. P. Hayes, Analyst (London), 105, 1176 (1980).

Development of a New Definitive Method for Uric Acid

P. Ellerbe, S. Meiselman, A. Cohen, R. Schaffer, M.J. Welch and E. White V
Center for Analytical Chemistry, National Bureau of Standards, Gaithersburg, Maryland 20899

As part of a program for developing definitive methods for organic serum constituents, we are developing an isotope dilution mass spectrometry (IDMS) method for the measurement of uric acid in human serum. Other IDMS methods for uric acid require complex sample work-up, are less precise, or have not been tested for column memory effects or measurement bias.

In our method a known weight of serum is spiked with a known weight of uric acid-[1,3-$^{15}N_2$] dissolved in ammonium hydroxide and is passed over an AG1-X2 acetate resin to remove possible interferences. The uric acid is eluted with acetic acid and the eluent is freeze-dried. Standards are prepared by weight from solutions of unlabelled and labelled uric acid, and are freeze-dried. The uric acid is derivatized with N-methyl-N(t-butyldimethylsilyl)trifluoroacetamide containing 1% imidazole in acetonitrile at a molar ratio of 390:1 reagent:uric acid by heating at 60°C for 48 h.

The GC column used is a 15 m 0.25 mm id DB-1 FSOT at 270°C. The amount injected is about 3 ug of derivative in 1 ul of solution, with the splitter set at 4:1 vent to column. The retention time is about 4 min, with a peak width at the base of about 14 sec. The ionization mode is EI, with a source temperature of 200°C. Measurement of the unlabelled/labelled ratio is made by monitoring the intensities of the $(M-57)^+$ ions at m/z 567 and 569.

To accurately and precisely measure this ratio, at least 30 measurement cycles must be acquired across the GC peak. Magnetic switching is too slow for the narrow GC peaks (5-25 seconds) typical of capillary columns, and accelerating voltage switching is too imprecise. We therefore have devised a switching system using beam deflection plates located in front of the collector slit.

Samples are analyzed according to a strict protocol. Each sample is run with standards bracketing it in both time and ratio. The weight ratio of sample is calculated by linear interpolation between the two standards The measurement is repeated on a second day, with the standards in reverse order, and the average of the two days' results is defined as one valid measurement.

Since silyl groups on nitrogen are easily lost or exchanged, underivatized uric acid left over from one injection could rederivatize with the next injection, and then elute from the GC with the uric acid of that injection. This could cause a column memory effect: the value of the ratio of one injection would be affected by a previous injection. There is no evidence of column memory effects.

With this system, repeated measurements of a given mixture of uric acid-1,3-$^{15}N_2$ and SRM uric acid typically have CVs of under 0.1%.

We prepared three independent sets of standards and tested them for within-set and between-set consistency. The members of each set were used as standards to measure the weight ratios of the members of the other sets as if they were samples, according to the measurement protocol. The difference within each set between the measured and weighed weight ratios is calculated as a percent difference, which is a measure of internal consistency. As an example, this is the comparison between sets A and B. All of the percent differences in this set are acceptably low, so we consider this set as consistent within itself.

Sample Set A #	Bracketed by Set B #	Weight Ratios (m/z 567/569) IDMS	weighed	Percent Difference
2	1,2	.9153	.9179	-0.28
3	3,4	.9886	.9895	-0.09
4	3,5	.9938	.9934	+0.04
5	5,6	1.0415	1.0415	0.0
6	5,6	1.0725	1.0765	-0.37

The mean percent difference was calculated for each comparison between sets, and was then averaged to calculate a mean bias between sets to check for between-set consistency.

Set used as: Standard	Sample	Mean % Difference	Mean Bias
A	B	+0.16%	
B	A	-0.14%	0.15%
A	C	-0.09%	
C	A	+0.12%	0.10%
B	C	-0.21%	
C	B	-0.23%	0.22%

Each set of standards is consistent with the other sets.

To test for the presence of measurement bias, for example from a previously undetected interference, we can confirm results by measurement under different conditions. Our first test of measurement bias was run using the only other high mass ions in the EI spectrum with enough intensity for precise measurements: the molecular ions at m/z 624 and 626. A serum sample was measured according to the protocol at m/z 567 and 569 and m/z 624 and 626. The percent difference between the weight ratios obtained from each set of ions was 0.11%, which is less than the precision of the measurements; therefore, no measurement bias was observed.

This uric acid method requires only minimal sample preparation, shows no GC column memory effect, gives excellent precision on repeated measurements of individual samples, shows acceptably low bias within and among sets of independently prepared standards, and shows no measurement bias for serum in a preliminary test. We will develop this method into a candidate definitive method and use it to certify uric acid concentrations in reference serum pools.

ISOTOPE DILUTION MASS SPECTROMETRY UTILIZING ELECTRIC DEFLECTION PLATE SWITCHING

S. Meiselman, P. Ellerbe, M.J. Welch, and E. White V
Center for Analytical Chemistry
National Bureau of Standards
Gaithersburg, MD 20899

ID/MS can give accurate and precise results and therefore we have used it in the development of high accuracy "definitive methods" for organic serum analytes. Methods have been developed for cholesterol, glucose, uric acid, urea and creatinine using an instrument system consisting of a gas chromatograph/single focusing, magnetic sector mass spectrometer with a custom built data system which controls certain instrument functions and acquires and processes data. This system has been described in detail elsewhere (1).

This system had serious limitations when applied to the measurement of analytes eluting from GC capillary columns. The dead time due to magnet switching and the real time display, allowed too few measurements of the intensities of the ions to obtain results of acceptable precision, for these peaks, which are typically 5 to 20 seconds wide.

Modifications were made to the system and procedure to ease these limitations. An alternate means of switching masses was devised which eliminates that portion of the dead time due to magnet settling time. This was accomplished by selecting the masses of interest by use of deflection plates located after the magnet and before the collector slit as shown in the figure. The magnet is set to the lower mass (or between the masses) of interest. Both a square wave signal which selects the mass and a triangular wave signal to sweep the selected ion beam across the slit are applied to the summing point of an amplifier which drives the deflection plate. The square wave voltage from a 16 bit DAC under computer control alternately switches the ion beams through the collector slit and a triangular wave from a 12 bit DAC sweeps about one mass unit across the slit. The real time display and it's inherent dead time were eliminated.

Measurements of the ratio of unlabeled to labeled analyte are made by selected ion monitoring. Deflection plate voltages are set such that the unlabeled and labeled ion beams will alternately be switched to the collector slit. Before elution of the GC peak of interest, the program controlling data acquisition is started. The acquisition is a series of repeated cycles. The following describes one measurement cycle: The square wave voltage is switched to select the mass of the unlabeled analyte. Acquisition of ion intensity data is started. During acquisition, the triangular wave applied to the deflection plate sweeps the ion beam back and forth across the collector slit. Upon completion of a present number of sweeps, data acquisition is interrupted. The square wave is switched to select the mass of the labeled analyte and acquisition started again for the same number of deflection plate sweeps. Acquisition is interrupted again and the next measurement cycle begins.

The cycle is repeated continuously before and during elution of the GC peak until the ion intensity signal drops below a preset level, at which time data acquisition is stopped. A baseline is calculated, subtracted from the intensities measured across the peak, and results are displayed and printed. The total dead time was reduced from about 640 milliseconds to 80 milliseconds. Coefficient of variation for measurements of the ratio of the ion intensities at two masses on peaks approximately 10 seconds wide were less than 0.1%.

The use of deflection plate switching has enabled the SIM analysis of narrow GC peaks with the same level of precision obtained by magnetic switching on much wider peaks.

References

1. Michael J. Welch, Alex Cohen, Harry S. Hertz, Fillmer C. Ruegg, Robert Schaffer, Lorna T. Sniegoski, and Edward White V, Anal. Chem. 56, 713 (1984).

IDMS USING ELECTRIC SWITCHING

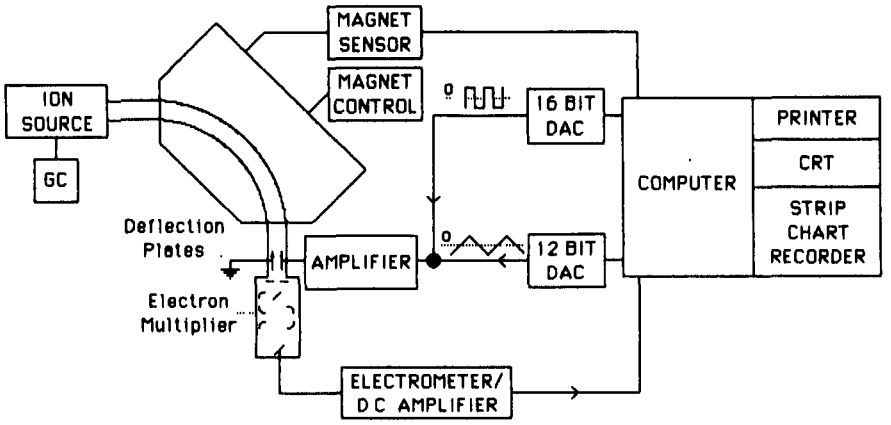

Distinction of Isomeric α- and ß-Aspartame by Thermospray LC/MS

J.A. Stamp, D.A. Garteiz*, and T.P. Labuza.
Department of Food Science, University of Minnesota
1354 Eckles Ave., St. Paul, MN. 55108.
*Vestec Corporation, Houston, TX. 77054.

Aspartame (N-L-α-aspartyl-L-phenylalanine-1-methyl ester), an FDA regulated dipeptide sweetener, has begun to appear in a wide variety of commonly consumed food products. The widespread usuage of aspartame, has surfaced a number of concerns regarding its stability in aqueous systems and the nature of its degradation products (1).

The polar nature and thermal instability of both aspartame and its decomposition products, provides a challenge when attempting to volatilize samples for mass spectrometric analysis. Uncontrolled decomposition during the ionization process, often results in a mass spectrum, which is representative of pyrolysis products of the parent molecule. Attempts to identify aspartame decomposition products by GC/MS of the corresponding TMS derivatives, produced no molecular ion and identification of four decomposition products was made by analysis of thermal decomposition products produced during the technique (2). We have studied the stability of aspartame in liquid model systems and identified six decomposition products by GC/MS analysis of the corresponding N-α-trifluoroethyl-O-trimethylsilyl polyamino alcohol derivatives, using a modified version of the method of Carr and Biemann (3). One of the interesting decomposition products that we proposed in that study, was the ß-isomer of aspartame (4). As shown in figure 1, the ß-isomer is hypothesized to form from α-aspartame under acidic conditions via a succinimide intermediate, leading to the exchange of the position of the peptide bond to the ß-carboxyl of the aspartyl moiety. However, the differences in the mass spectral behaviors of the α- and ß-isomers seen using GC/MS techniques made unequivocal identificaltion of the ß-isomer difficult.

The emergence of the thermospray interface for LC/MS, has produced a useful technique by which to obtain molecular weight and structural information for a variety of polar and thermally labile compounds. Its soft ionization process produces very intense protonated molecular ions and a limited number of fragment ions. Since the mechanism by which fragmentation occurs to produce the spectra of the isomers of aspartame by LC/MS, differs from traditional electron impact (EI) fragmentation, thermospray provides an excellent complementary technique by which to obtain the additional information needed to confirm structure.

A simple model system consisting of aspartame (The NutraSweet Co.,Skokie,Il.), at 2mM in 0.1 M ammonium acetate adjusted to pH 3 with formic acid, was thermally treated at 100°C for up to eight hours to induce thermal decomposition. A HP 5982 quadrupole mass spectrometer was used in this study which was coupled to a thermospray LC/MS interface operated in the "filament-off" mode. The optimal thermospray conditions were found to be a vaporizer tip temperature of 215°C, a source temperature of 300°C, and a vapor temperature of 240°C. The separation of the aspartame decomposition products was accomplished with an isocratic mobile phase of 15:85 acetonitrile/0.1M ammonium acetate, adjusted to pH 3 with formic acid on a Waters Nova-Pak C_{18} column at a flow rate of 1ml/min and a 20µl injection size.

Figure 2, shows the UV and total ion current (TIC) traces from analysis of a mixture of aspartame decomposition products, with the α-isomer eluting as peak G and the ß-isomer as peak F. No baseline drift or excessive noise was observed during thermospray analysis. The thermospray LC/MS spectra collected for the α- and ß-isomers are shown in figure 3, and are characterized by the protonated molecular ion at m/z 295 and a variety of fragment ions whose structural identities are rationalized in figure 4. The structures of the two isomers can be readily distinguished by comparing the ratio of intensities for both protonated molecular ions and fragment ions as summarized in Table 1. The ratio of α/ß intensities for the MH^+ ion was 0.25 and proved to be a reproducible and distinquishing feature. The fragment ions of m/z 263 and 180 also showed consistant α/ß ratios of 0.25 and 3 respectively, with additional fragment ions being produced that were unique to each isomer.

In effect, it is seen that thermospray ionization and fragmentation resembles ammonia CI type spectra. Peptides being amines, are ideal analytes for thermospray since they have proton affinities higher than ammonia, formed from the volatile electrolyte buffer in the

mobile phase. Thus greater structural information is produced from resultant protonated molecular ions due to higher internal energy available for fragmentation. Whereas, compounds analized by thermospray with lower proton affinities than ammonia will produce predominately MH^+ and $M+NH_4^+$ adduct ions with few fragment ions seen, that would likely occur with high probability at those sites of low critical internal energy for fragmentation. Results of this work support the ability of thermospray LC/MS to provide adequate structural information to unambiguously characterize the identity of the α- and ß-isomers of aspartame.

1. Homler,B. (1984). *Food Tech.*, **39**, 50.
2. Furda,I. et al. (1975). *J. Agr. Food Chem.*, **23**, 340.
3. Carr,S., Herlihy,W., and Biemann,K. (1981). *Biomed. Mass Spectrom.*, **8**, 51.
4. Stamp,J.A., and Labuza,T.P. (1986). in preparation.

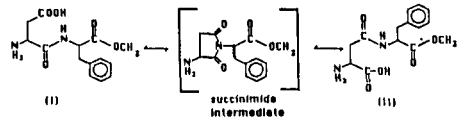

Figure 1: Formation of β-aspartame (II) from α-aspartame

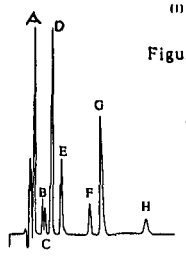

PEAK	COMPOUND
A	phenylalanine
B	ß-aspartyl-phenylalanine
C	α-aspartyl-phenylalanine
D	diketopiperazine
E	phenylalanine-methyl ester
F	ß-aspartame
G	α-aspartame
H	? unknown

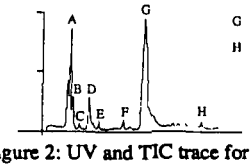

Principle Ions Formed from Aspartame Isomers †

m/z	180	190	196	202	217	219	222	235	249	263	277	295
α-Aspartame	100	-*	9 8	5	5	-	-	7	7	5	30	25
β-Aspartame	33	5	-	5	-	3 5	21	-	-	20	52	100

† Values includes all fragments which have a ≥2% intensity for both isomers.

* Particular mass not present in spectra.

Figure 2: UV and TIC trace for aspartame decomposition products 100°C for 8 hours.

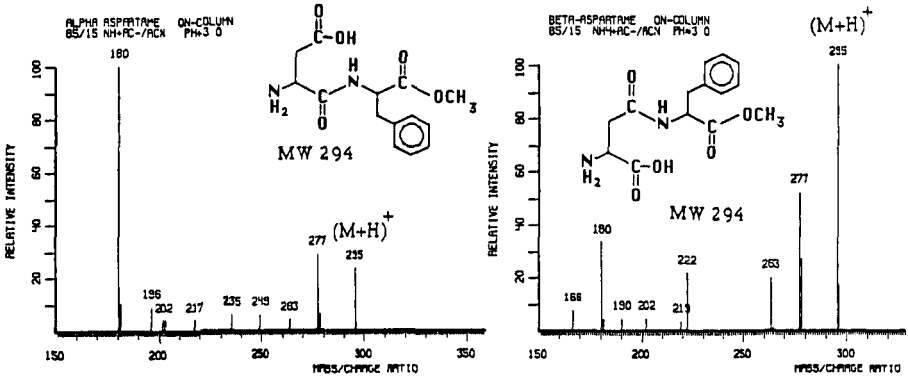

Figure 3: Thermospray LC/MS spectra for (I) α-aspartame and (II) ß-aspartame.

SURVEY OF THE "ORTHO EFFECT" IN PCB MASS SPECTRA

G. W. Sovocool and J. R. Donnelly*
U.S. Environmental Protection Agency and *Lockheed-EMSCO
P.O. Box 15027, Las Vegas, NV 89114

The "ortho effect" as applied to chlorinated biphenyl (PCB) and brominated biphenyl (PBB) electron ionization mass spectra refers to the enhancement of the ion intensity resulting from the loss of a halogen atom $(M-X)^+$ relative to the molecular ion $(M^{+\cdot})$. This increased intensity of the halogen loss fragment ion occurs in those chlorinated and brominated biphenyls having the requisite number and placement of halogen atoms ortho (2,2′) to the ring juncture (1,1′). Thus, 2,2′-; 2,2′,6-; 2,2′,6,6′- substituted biphenyls will exhibit an ortho effect. Previous studies in the chloro series emphasized this effect for three (2,2′,6) ortho chlorines but indicated an effect for two ortho chlorines[1]. Studies in the bromo case clearly showed an effect for two (2,2′) bromines (See Fig.1 and Fig. 2)[2]. The purpose of this study was to extend, as a tool for structure identification, the limited cases of observed ortho effects to all currently available congeners. This would further validate the mass spectral ortho effect for use with the GC retention index[3]. This combination would permit the structural assignment of all 209 congeners of the chlorinated biphenyls from GC and mass spectral data alone. It should then be possible to make distinctions among isomers using fewer (1-2) GC columns than would be required on the basis of 2-5 GC columns needed by the retention index method alone. The method chosen to achieve this goal was to survey the spectra present in the NIH/EPA mass spectral data base[4]. An example showing an ortho effect in the simplest possible case of 2,2′-dichlorobiphenyl is shown in Figure 3. The magnitude of the ortho effect was measured by using the largest component of the isotopic clusters. Certain of these library spectra appeared to be inconsistent with predictions based on the previous studies of the ortho effect (See Table 1). Authentic standards of these compounds were obtained and the spectra were found to be in agreement with the predictions (See Table 2).

Of 95 congeners found in the NIH/EPA library, 43 showed large ortho effects (greater than 15% magnitude) for one ortho chlorine per ring (2,2′- substitution) or three ortho chlorines (2,2′,6- substitution). For four ortho chlorines (2,2′,6,6′- substitution) a reduced (generally < 7%) ortho effect was observed. Depending on threshold (zero) settings and individual spectral quality, this small effect may be difficult to detect. The magnitude of the ortho effect appeared to show a gradual reduction with increasing total number of chlorines. The remaining congeners found in the library and lacking ortho substitution on both rings yielded results consistent with the prediction that they would show no ortho effect. The spectra were carefully evaluated to exclude the $(M-HCl)^{+\cdot}$ fragment and attendant ^{13}C isotopic contribution.

The results are consistent with formation of a bridging halonium ion upon halogen elimination (See Fig. 4). Neighboring group (ortho halogen on the other ring) assistance in the elimination of the ortho halogen requires 2,2′- substitution. Thus, isomers having two or three ortho halogens can eliminate one halogen and form the planar, bridging halonium ion. However, with loss of one halogen from isomers having four ortho halogens, formation of this planar, bridged ion is hindered due to steric hindrance involving the 6,6' halogens, explaining the reduced ortho effect for these isomers. Halogen substitution (beyond 2,2′) in the 3,3′ positions appears to lead to enhanced fragmentation, attributed in the past to steric buttressing[1]. However, a similar enhancement is also seen with 5,5′ substitution. Halogens in the 4 and 4′ positions appear to reduce the ortho effect. Because the substituents enhancing the effect are ortho and para to the presumed ortho site of positive charge, while the position reducing the effect is meta to the site of positive charge, these effects are analogous to the effects of chlorine in aromatic electrophilic substitution reactions. This suggests that the ortho effect may be primarily electronic in nature, once the basic requirement of 2,2′ substitution is fulfilled.

In conclusion, the presence or absence of an ortho effect has been validated for 95 individual PCBs. The ortho effect in the 2,2′,6,6′- substituted biphenyls was found to be significantly less and may be due to steric hindrance associated with formation of the $(M - Cl^+)$ charged species. The ortho effect was found to be predictable and consistently present or absent in all halogenated biphenyls tested, according to a simple rule. That rule is: each ring must contain one or two halogens ortho to the ring juncture.

The authors gratefully acknowledge the generous gift of PCB standards from Prof. Stephen Safe of Texas A & M University; the assistance of Dr. Yves Tondeur of the University of Nevada Enviromental Research Center in obtaining mass spectra on the standards and the help of Mr. Brady Englestead in the preparation of the text.

REFERENCES

1. L.A. Levy, and E.O. Oswald, Biomed. Mass Spectrom. 3, 88 (1976).
2. G.W. Sovocool, and N.K. Wilson, J. Org. Chem. 47, 4032 (1982).
3. P.W. Albro, J.K. Haseman, T.A. Clemmer, and B.J. Corbett, J. Chrom. 136, 147 (1977).
4. S.R. Heller, and G.W.A. Milne, EPA/NIH Mass Spectral Data Base, NSRDS-NBS63. Supt. of Docs., U.S. Govt. Printing Office. 1978. First Supplement 1980. Second Supplement (with L.H. Gevantman) 1983.

NOTICE: This article has not been subjected to Agency policy review and therefore does not necessarily reflect the views of the Agency. Menton of trade names or commercial products does not constitute endorsement or recommendation for use.

Figure 1

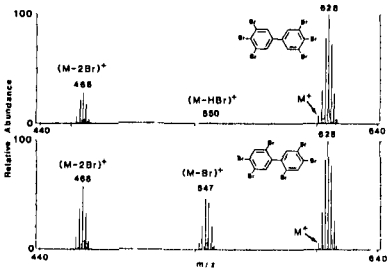

Top Spectrum has no 2,2' substitution and NO Ortho Effect
Contrast with lower Spectrum (2,2')

Figure 2

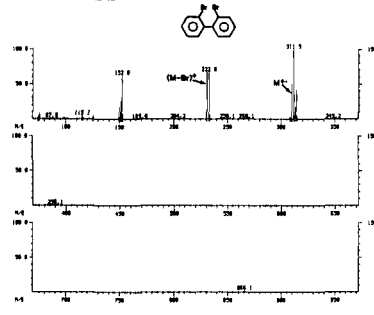

Figure 3

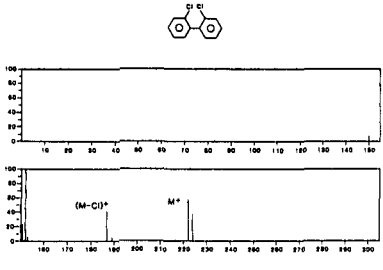

Table 1

NUMBER Cl CONGENER	NUMBER IN LIBRARY EPA/NIH	NUMBER IN LIBRARY WITH ORTHO EFFECT (2 or 3 Cl) PREDICTED	FOUND	EMBL-LV RESULTS
1	2	0	0	
2	5	1	1	
3	12	2	1	BECAME 2
4	23	9	6	BECAME 9
5	16	12	12	
6	18	10	9	BECAME 10
7	13	10	10	
8	6	3	3	
9	1	1	1	
10	1*		0	2% EFFECT

* LIBRARY SPECTRUM WAS AN OCTACHLOROBIPHENYL

Table 2

ISOMER	(M-Cl)+/M+ (%) IN LIBRARY	EMBL-LV RESULTS (%)
2,6,2'	6	46
2,3,5'3'	20,86	42 ± 8 85-SATURATED
2,4,2'	NOT IN LIBRARY	29,36
2,3,4,2'3'4'	9	23
2,5,2	52	47
2,3,4,5'	59	25
DECA	14*	2

* SPECTRUM OF AN OCTACHLOROBIPHENYL-ERROR IN LIBRARY VOLUME

Figure 4

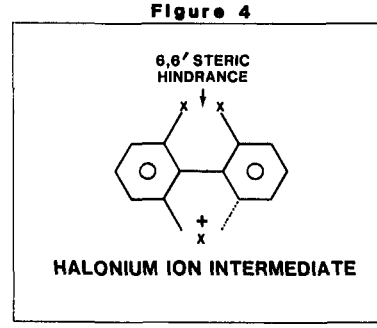

DETERMINATION OF PCB CONTENT IN HAZARDOUS WASTE FROM SPECIFIC CONGENERS

Carol S. Chow and *John M. Krecisz
Chemical Waste Management
150 W. 137th St., Riverdale, IL 60627

Traditionally, hazardous waste samples have been analyzed for PCB by GC/ECD, with PCB content expressed in terms of Aroclor concentration. This technique is very straightforward since waste samples, unlike environmental or biological samples, generally contain relatively intact Aroclor patterns. Thus problems with fractionated or degraded Aroclor patterns are seldom encountered when determining PCB in hazardous waste. In addition, most permittors and regulators are more comfortable in dealing with PCB content in terms of Aroclors.

However, the challenge encountered in PCB analysis of hazardous waste lies in separating the PCB from the numerous analytical interferences present in the material, particularly when the interferents are chemically stable organochlorine compounds. In this case, more sophisticated techniques, such as HRGC/MS/SIM, may be required to determine the presence of PCB.

This situation arises when analyzing for PCB in waste samples of mixed organochlorine materials slated for incineration in Europe. These waste materials are essentially a soup of polychlorinated solvents, containing percent levels of typical chlorinated solvents, as well as other constituents such as polychlorinated propanes, propenes, butadienes, and benzenes. The complexity of these sample matrices makes PCB determination by HRGC/MS/SIM a necessity.

PCB content in waste samples regulated by European authorities is determined by the sum of the following eleven PCB congeners[1]:

PCB-15	(4,4'-Dichlorobiphenyl)
PCB-28	(2,4,4'-Trichlorobiphenyl)
PCB-52	(2,2',5,5'-Tetrachlorobiphenyl)
PCB-49	(2,2',4,5'-Tetrachlorobiphenyl)
PCB-44	(2,2',3,5'-Tetrachlorobiphenyl)
PCB-70	(2,3',4',5-Tetrachlorobiphenyl)
PCB-101	(2,2',4,5,5'-Pentachlorobiphenyl)
PCB-87	(2,2',3,4,5'-Pentachlorobiphenyl)
PCB-153	(2,2',4,4',5,5'-Hexachlorobiphenyl)
PCB-138	(2,2',3,4,4',5'-Hexachlorobiphenyl)
PCB-180	(2,2',3,4,4',5,5'-Heptachlorobiphenyl)

Therefore, GC/MS procedures were developed for these waste samples with the following objectives in mind, 1) determination of the eleven PCB congeners for European permitting, 2) correlation of these specific congeners to Aroclor patterns for American permitting, and 3) determination of a limited number of PCB congeners to be used for rapid screening of PCB in mixed organochlorine waste.

Samples were prepared for analysis by vigorously vortexing several grams of the waste material with 10% acetone/hexane to form a 10 to 1 dilution. The diluted samples were then cleaned using a KOH wash, followed by an acid wash, followed by microcolumn cleanup. D10-Phenanthrene and D12-Benzo(a)anthracene were added as internal standards.

The diluted samples were then injected onto a 30M DB-5 fused silica capillary column, and detection of the PCB congeners was achieved by select ion monitoring of the parent ion (M), M+2, and M+4 ions using an HP 5985B GC/MS. Concentrations were calculated using all three ions in order to check against any erroneous results due to interfering ions.

Ten of the eleven PCB congeners were adequately determined using these GC/MS procedures. The exception was PCB-15, which was difficult to determine due to numerous interferences at its low molecular weight region. This congener, however, is not likely to be significant in waste samples.

In order to use this technique on waste materials for routine disposal permitting, it was necessary to correlate these eleven congeners to Aroclor concentration. These congeners proved to form an excellent cross-section of major Aroclor components, and correlation factors were determined in order to express the concentrations of individual congeners in terms of total PCB as Aroclors. These factors indicated that the specified congeners account for approximately 40% of the PCB concentration when expressed in terms of the major Aroclors (1242, 1254, and 1260). In addition, the presence of Aroclors may be rapidly determined by screening for a limited number of PCB congeners, in particular PCB-28, PCB-52, PCB-70, PCB-153, and PCB-138.

Thus the total PCB concentration in a hazardous waste sample could be determined by select ion monitoring of several key PCB congeners.

1) PCB numbering system developed by Ballschmiter and Zell, "Fresenius Z. Anal. Chem.", 1985, 57, 2452.

* Present address: SCA Chemical Services, 11700 S. Stony Island, Chicago, IL 60617.

ANALYSIS OF MULTIPLE SOURCE FEED MATERIALS FOR DIOXIN PRECURSORS

J.T. Bursey, D.E. Wagoner, J.F. McGaughey, E.E. Messer, A.J. Miles, M.A. Palazzolo
Radian Corporation, Research Triangle Park, North Carolina 27709 and
D.F. Oberacker and J.H. Southerland, U.S. Environmental Protection Agency, Research Triangle Park, North Carolina 27711

The Air Management Technology Branch of EPA's Office of Air Quality Planning and Standards (OAQPS) was responsible for implementing Tier 4 of the National Dioxin Study. The intent of Tier 4 was to study combustion processes as potential sources of dioxin emissions and to address the questions: do combustion sources emit dioxins? If so, how much? Are these emissions significant?

Based on a literature review, the following factors appear to affect dioxin emissions: polychlorinated dibenzodioxin content of feed, precursor content of the feed, combustion temperature, residence time, oxygen availability, feed processing, and supplemental fuel. Thirteen source tests, testing nine different types of combustion units, were conducted during 1984 and 1985. The units included three sewage sludge incinerators, three black liquor boilers, one wire reclamation incinerator, one industrial solid waste incinerator, one carbon regeneration furnace, and one wood stove. Three Modified Method 5 (MM5) test runs were performed at each test site (except for the wire reclamation incinerator site, where six runs were performed) at the outlet of the air pollution control device and at the inlet to the control device (if feasible). MM5 sample components were analyzed for PCDD and PCDF content using high resolution gas chromatography/high resolution mass spectrometry by EPA's Troika Laboratories. Combustion gases at each site were continuously monitored for oxygen, carbon monoxide, carbon dioxide, total hydrocarbons, oxides of nitrogen, and sulfur dioxide to document the stability of combustion conditions. Also, the following types of sampling were conducted at all or some of the sites: feed sampling, hydrochloric acid emissions sampling, ambient air sampling, combustion ash sampling, soil sampling, and auxiliary process sampling.

Results of the sampling and analysis showed that all combustion sources tested under Tier 4 emit PCDD/PCDF, varying over four orders of magnitude between the test sites. Emissions of 2,3,7,8-TCDD generally account for less than 1% of total PCDD, with furan emissions generally on the same level as dioxin emissions. Highest PCDD emissions appear to be associated with low temperature resource recovery processes. There is also an association between total organic halide (TOX) content of the feed and maximum PCDD and PCDF emissions. Data also indicated a wide range of measured removal efficiencies for the seven different air pollution control devices tested. Based on the data obtained, dioxin and furan emissions appear to be more difficult to control than conventional particulate emissions, possibly due to the occurrence of gas phase reactions.

Analytical efforts in the Radian Research Triangle Park Laboratory focused on the analysis of feed material for dioxin precursors, including chlorinated benzenes, polychlorinated biphenyls, and polychlorinated phenols. Media analyzed for these compounds included sludge feed, ambient air, paint sludge, wood/plastic/dust, cardboard/paper/wood, strong black liquors, wire insulation feed, transformer feed, wood feed, spent carbon feed coke, circuit boards, electrical switching gear, telephone parts/wire, drum coating, drum residue, oak feed, and pine feed. The highest concentrations of chlorinated phenols were observed in wood/plastic/dust, with the highest concentrations of the base/neutral component being observed in the drum residue. Sample preparation procedures were developed for this study, since no procedures were available from the literature. Large sample sizes (50 g) were used in order to compensate as far as possible for lack of homogeneity in the sample media and to lower detection limits for the overall method as far as possible. Sample extracts were analyzed by capillary gas chromatography/mass spectrometry, using selected ion monitoring techniques both to enhance the sensitivity of the technique and to increase the specificity by filtering information from the plentiful extraneous compounds present. The Total Organic Halogen (TOX) procedure was applied to several samples which could not be analyzed successfully by GC/MS techniques as well as other media. Sample media analyzed by the TOX technique include transformer feed, wire insulation feed, spent carbon feed, wood/plastic/dust, drum coating, electrical switching gear, and circuit boards. Direct correlation between TOX and GC/MS results is difficult, however. The two values correlate directly when the compounds of interest (PCBs, chlorinated benzenes, and chlorinated phenols) are the only halogenated species present. The correlation of "precursor" compounds observed in the feed and dioxins in the emissions is also not

straightforward, since conversion of the precursors to dioxins/furans depends upon operating parameters used in the combustion sources. Table 1 shows a list of factors affecting dioxin emissions and the Tier 4 surrogate measurements for those factors. Of the entire list of factors, only residence time and PCDD in feed were not studied in the Tier 4 program.

Speciation of the organic compounds identified as dioxin precursors in the range of sampling media required an extensive effort both in the area of sample preparation and quantitative analysis. Surrogate recoveries tended to be low because of the multiplicity of column chromatographies, washings, and rinses which were required in order to obtain a sample extract which could be analyzed successfully. Based on analytical standards, the instrumental detection limit for the dioxin precursors on the GC/MS system ranged between 100-500 pg, injected onto the GC column. To deliver 100-500 pg to the GC column, the sample extract must contain 100-500 ng/mL of precursor. If this 1 mL of extract represents a 50 g sample with 100% recovery of compounds of interest, the original sample must contain 100-500 ng of analyte. However, if the recovery is only 10%, then the original 50 g sample must contain 1000-5000 ng of analyte. When samples of small size (1 g) were extracted and analyzed, recoveries of surrogate compounds increased to 80-100%; however, with markedly inhomogeneous media, obtaining a representative 1 g sample is very difficult indeed. Even after extensive purification, samples proved difficult to analyze by GC/MS. The TOX procedure afforded a substantially simpler method for sample preparation and analysis and provided extremely useful information. Since concentrations of speciated organics could not be related easily to the presence of dioxin, perhaps the TOX procedure provides a more cost-effective alternative to the extensive preparation and GC/MS analysis. No matter what the operating conditions of the combustion source, if there are no chlorinated organics in the feed, no dioxin will be formed. If the feed material contains chlorinated organic compounds, the system has a potential for producing dioxins/furans, depending upon the exact operating conditions of the combustion source.

TABLE 1. TIER 4 SURROGATE MEASUREMENTS FOR FACTORS AFFECTING DIOXIN EMISSIONS

Factors Affecting Dioxin Emissions	Variable or Surrogate Variable Measured in the Tier 4 Program
PCDD in feed	None (some feed samples archived for potential PCDD analysis)
Precursors in feed	Chlorobenzenes, chlorophenols, PCBs and TOX in feed
Chlorine in feed	Chlorine in feed and HCl emissions
Combustion temperature	Combustion chamber temperature or flue gas temperature
Residence time	Not measured, no surrogate
Oxygen availability	O_2 content of stack gas, CO emissions, THC emissions
Feed processing	Broad characterization of feed types, moisture content of feeds (if appropriate), feed rate
Supplemental fuel	Fuel flow and heat input recorded, if available

NOTE: TOX = total organic halogen content of feed
THC = total hydrocarbon concentration in flue gas

This work was supported by the Environmental Protection Agency under Contract No. 68-03-3148, Work Assignment No. 12.

NEGATIVE CHEMICAL IONIZATION MS/MS FOR IDENTIFICATION OF CHLORINATED COMPOUNDS IN NORTHERN SHARK LIVER

R. Guevremont[1,2], R.A. Yost[1], W.D. Jamieson[3], and P.G. Sim[3]
[1]Department of Chemistry, University of Florida, Gainesville, FL 32611
[2]on leave from National Research Council of Canada, Halifax, Nova Scotia
[3]Marine Analytical Standards Program, National Research Council of Canada, Halifax, Nova Scotia B3H 3Z1

The Marine Analytical Standards Program of the National Research Council of Canada, in its program to develop reference materials based on marine biota, is investigating preparation and analysis of several tissues of the Northern Shark (Dogfish). We report here GC/NCI/MS/MS investigations for identification of polychlorinated biphenyls (PCB's) in Northern Shark liver oil.

Ambiguities of two types occur in the usual methane electron capture spectra of PCB's, those resulting from chromatographically unresolved congeners of the same chlorination, and those from unresolved congeners of two or more levels of chlorination. The latter is a problem if the $(M-Cl)^-$ ions from the more highly chlorinated congeners interfere with, or add uncertainty with regard to identity (or existence) of the less chlorinated congeners.

Evidence suggests that the oxygen-enhanced negative chemical ionization of PCB's results in the formation of a $(M-Cl+O)^-$ ion without apparent ambiguity regarding the degree of chlorination of the original congener. If, in addition, the CAD spectra of these $(M-Cl+O)^-$ ions reflect structural features of the original congener, then problems with chromatographically unresolved mixtures could be largely overcome.

MS/MS experiments were carried out on a Finnigan TSQ 45 triple quadrupole mass spectrometer. Oxygen at a pressure of 0.4 torr was used for oxygen enhanced NCI. A high-voltage Townsend discharge (Finnigan DISIMS control module) was used for ionization. The ion source temperature was 110°C. Collision gas (Xe) pressure was adjusted for 30% transmission of the 633^- ion of perfluorotributylamine. Collision energy was 30 eV.

Reference mixtures of pure synthetic PCB congeners were used without dilution (CLB-1, Marine Analytical Standards Program, NRC, Halifax, Canada). CAD daughter spectra for 40 congeners from penta to nonachlorobiphenyl were studied in this work. (The IUPAC numbering and structures of PCB congeners appear in Ref (1)). A 10g sample of Northern Shark liver oil was dissolved in hexane. Sulfur compounds were removed with copper amalgam, and the sample "cleaned up" with separations on Florisil and silica gel columns. Final volume of the concentrate was 2 ml.

Source temperature has been shown to modify the relative abundances of parent and daughter ions. At the collision gas pressure used here, the ratio of daughters of $(M-Cl+O)^-$, to the parent ion, was an order of magnitude higher at 130°C than at 70°C, but CAD formation of Cl^- was increased. For IUPAC 121 the ratio of parent to Cl^- was 4.4, 2.5, 2.4 and 2.2 at 70°C, 90°C, 110°C and 130°C, respectively.

Daughter spectra of $(M-Cl+O)^-$ ions of many of the PCB's were unique: several are shown in Figs 1-2. Based on a preliminary study of the results, "scrambling" of structural information does not occur. The gas phase reaction to form $(M-Cl+O)^-$ is complete and is site-specific (although the site has not yet been deduced). The identity and relative intensity of CAD composition products seem to be indicative of the original structure of the congener.

The CAD spectra of the available congeners suggest many simple qualitative patterns describing the ease of loss of neutrals including (HCl), $(HCl)_n$ and what appears to be $[(HCl)_n+CO]$ (n=1,2 for most congeners). However, a quantitative procedure for predicting the CAD spectrum based only on structure has not yet been deduced.

NRCC No. 25651

Daughter spectra of the $(M-Cl+O)^-$ ions from several chromatographic peaks of the extract of Northern Shark liver oil, along with the CAD spectrum of the PCB congener in reference material CLB-1 which elutes at the same retention time (separated on DB-5 capillary column, J&W Scientific), are shown in Fig 2. The daughter spectra of IUPAC 105 and that from the GC/MS/MS experiment with Northern Shark liver oil, for example, are very similar and strongly suggest that 105 is indeed found in this sample. However, as reported by Safe, et al. (2), IUPAC 127 may have a similar chromatographic retention time. Since the relationship between the daughter spectrum of $(M-Cl+O)^-$ ion and the structure of the congener is not easily defined, the unequivocal identification can only be complete once the daughter spectrum of the $(M-Cl+O)^-$ ion of IUPAC 127 is obtained.

The CAD spectrum of the $(M-Cl+O)^-$ ion may be useful for identification of PCB congeners in environmental samples. Several limitations are apparent. Collection of useful CAD spectra requires higher analyte concentration than is necessary for CH_4 NCI spectra. In Fig 2 the concentration of IUPAC 105 in CLB-1 was 4.2 µg/ml, and in the Northern Shark liver extract was about 0.17 µg/ml. The CAD spectra of many congeners show simple loss of (HCl) and $(HCl)_2$. There will be spectra too similar for unambiguous identification. Finally, the daughter spectra of $(M-Cl+O)^-$ of known congeners must be available for the most reliable identification.

References

(1) K. Ballschmiter and M. Zell, Fresenius Z Anal. Chem. 302, 20-31(1980).
(2) M.D. Mullin, C.M. Pochini, S. McCrindle, M. Romkes, S.H. Safe, and L.M. Safe, Environ. Sci. Technol. 18, 468-476(1984).

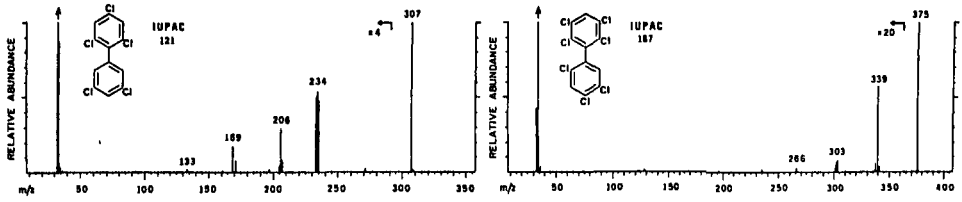

Figure 1. Daughter spectra of $(M-Cl+O)^-$ ions from PCB congeners IUPAC 121 and 187.

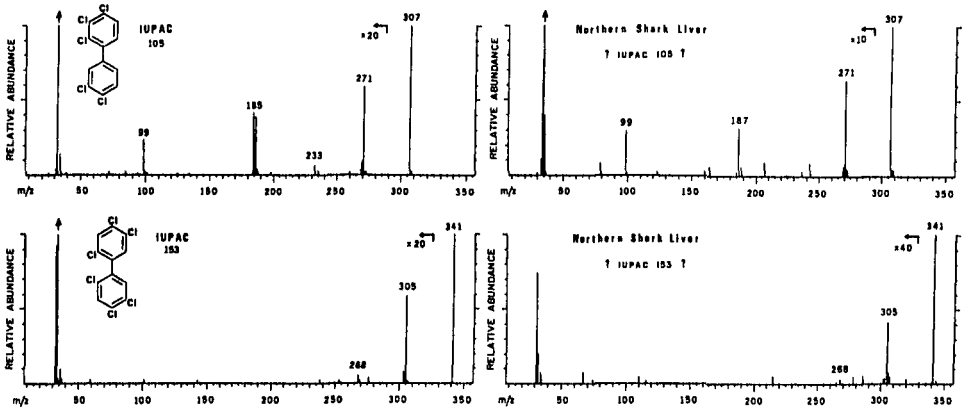

Figure 2. Daughter spectra of the $(M-Cl+O)^-$ ions from known PCB congeners (left) and from PCB's in extract of Northern Shark liver (right).

THE IDENTIFICATION OF A POTENTIAL INTERFERENT IN THE ANALYSIS OF CHLORINATED DIBENZO-P-DIOXINS AND DIBENZOFURANS

R. Orth, J. Fuhrmann, J. Wuebbels, R. Noble, S. Gibson, J. Wehler and F. Hileman

Monsanto Company
St. Louis, Missouri 63167

The GC/MS analysis of environmental samples for trace levels of polychlorinated dibenzo-p-dioxins and dibenzofurans has the potential for interference by co-eluting compounds which give rise to the same nominal masses and similar isotopic ratios. Such interferents were observed in the analysis of a contaminated soil sample analyzed for 2,3,7,8-tetrachlorodibenzo-p-dioxin (TCDD) at a detection limit of 0.1 ppb. To assist in devising methods for removing the interferents, the determination of chemical structure of the interferents was undertaken.

The initial soil workup procedure began with spiking 25 grams of sample with ^{13}C labeled TCDD followed by extraction with hexane/MeOH. After decanting the extract from the soil, the extract was washed with water to remove the methanol. The hexane was chromatographed on silica and then alumina to remove interferents. The eluant was initially screened for TCDD on a 30 meter DB-5 column with LRMS-SIM detection.

As can be seen in Figure 1, serious interferents appeared in the GC/LRMS-SIM analysis. These compounds not only interfered with the native TCDD but also with the labeled ^{13}C-TCDD. A full scan GC/MS analysis showed that there were three chromatographically resolvable interferents all having identical mass spectra, an example of which is shown in Figure 2. The mass spectrum indicates that in addition to interfering with TCDDs in the m/z 320 range, the interferents have masses in the m/z 304 and m/z 354 ranges which can interfere with the analysis of tetrachlorodibenzofuran and pentachlorodibenzo-p-dioxin respectively.

Additional workup methods were attempted to remove the interferents. These included the partitioning of the initial hexane extract against concentrated sulfuric acid or concentrated base. These approaches, however, did not effectively remove the interfering components. Another approach was to take the final extract from the initial column chromatography and chromatograph this on a carbon column using the technique outlined by EPA (1). This was successful in lowering the interferents so that the ^{13}C-labeled TCDD was discernable when analyzed on the DB-5 column but the interferences were still observed for the native TCDD. A highly polar SP-2330 capilliary column, which gives 2,3,7,8-TCDD specific analysis, was then used to try to resolve the interferences from the TCDD. This did not occur and in fact the interferences were more poorly resolved from TCDD on a SP-2330 column as compared to a DB-5 column. Since the carbon column improved the analysis for TCDD, the eluant from the first carbon column was chromatographed a second time on another carbon column. This was found to be successful in permitting the analyses to be carried out even on a SP-2330 column as shown in Figure 3.

The interferents were then isolated and concentrated so that a mass spectrum and elemental composition could be obtained. The high resolution mass spectrum was very similar to that shown in Figure 2. The spectrum shows that the interferents contain five chlorines and a methyl group. Also, the lower mass range suggests an aromatic hydrocarbon. Mass spectral analysis at resolution of 8,000 indicates the elemental composition of the parent peak at 354 is $C_{14}H_9Cl_5$. The elemental composition of 303 is $C_{13}H_5Cl_4$ indicating a loss of CH_3 and HCl. This was verified using MS/MS where 303 was found to be the daughter of 339 which arises by loss of CH_3. This supports the methyl substitution of the aromatic system and suggests that there are two possible structures, methylpentachlorodiphenyl methane or a pentachloro-dimethyl biphenyl.

Since the mass spectral data was ambiguous in the structural assignment of the interferents, additional sample was collected using the carbon columns and analyzed by NMR. The proton NMR shows chemical shifts of 2.35 ppm (methyl substitution on an aromatic ring) 4.36 ppm (methylene protons of diphenyl methane), 6.31 ppm (an aromatic proton ortho to the methylene bridge) and 7.10 ppm (other aromatic protons). These NMR results along with the mass spectral data give the structure as various isomers of methylpentachlorodiphenyl methane.

These interferences can be removed using the carbon column techniques described. In addition, the elemental composition of the m/z 320-324 fragments indicates that the mass spectrometer can be used to resolve the interferent from 2,3,7,8-TCDD. For example, the contribution to m/z 322 is from $^{13}C_1C_{13}H_8Cl_2{}^{37}Cl_2$ which contributes 88% to the interfering m/z. The use of HRMS will resolve this interfering peak if set to a resolution of 6000 or better. In addition, a second peak contributing to m/z 332 is from $C_{14}H_8Cl^{37}Cl_3$ which has a contribution of 12%. This can be resolved with a resolution greater than 9000. Thus the original clean up method would be satisfactory if combined with GC HRMS-SIM with a resolution of 10,000. Another technique that might also be used is the $KMnO_4$/NaOH column of Nestrick and Lamparski (2). It is believed that this reagent could oxidize the methyl group on the aromatic rings and permit the removal of these interferences.

References

1) U.S. Environmental Protection Agency, Region VII, "Determination of 2,3,7,8-TCDD in Soil and Sediments", September 1983.

2) T. Nestrick and L. Lamparski, Anal. Chem. 1982, 54, 2292-2299.

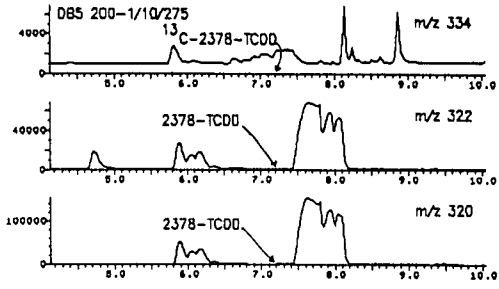

Figure 1. GC/LRMS-SIM Analysis of Original Extract

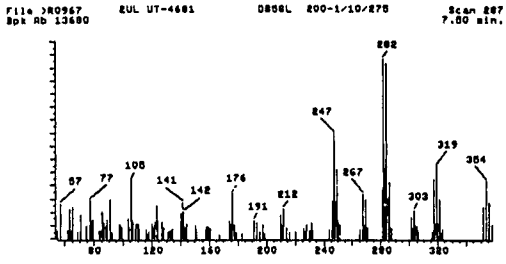

Figure 2. LRMS of Interfering Compound

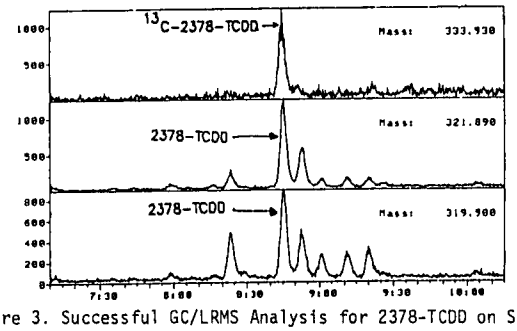

Figure 3. Successful GC/LRMS Analysis for 2378-TCDD on SP2330 Column

IDENTIFICATION OF CHLORINATED BIPHENYLENES AND OTHER POLYCYCLIC AROMATIC COMPOUNDS FORMED FROM THE INCINERATION OF PCB-DIELECTRIC FLUIDS AT A CAPACITOR PLANT'S DISPOSAL SITE

Paul H. Peterman, Lawrence M. Smith, David L. Stalling, and Jimmie D. Petty
Columbia National Fisheries Research Laboratory
US Fish & Wildlife Service, Route 1
Columbia, MO 65201

Polychlorinated dibenzofurans (PCDF), dibenzo-p-dioxins (PCDDs), biphenylenes (PCBP) and other polycyclic aromatic compounds (PCPAC) have been reported in investigations of Polychlorinated Biphenyls (PCB) pyrolysis in capacitor and transformer fires (1-3). Generally, these compounds are planar and very toxic. Their relative amounts and composition vary considerably, depending upon the conditions of the fire and upon the variety of organics present in the dielectric fluids. The period of time is another factor involving our investigation, since open burning was routinely done prior to ca. 1980.

From 1947-1979, a capacitor plant manufactured a variety of capacitors containing PCB, primarily as Aroclor 1242 and 1254. The plant was located in a wildlife refuge. Waste (defective) capacitors were routinely burned with supplemental fuel (e.g. Diesel or Fuel Oil and sometimes old tires) in open bonfires. The residual ash was apparently covered each time with a layer of soil.

An environmental investigation began in 1984 to measure the concentration of PCB and suspected chlorinated polycyclic aromatic compounds (PCPAC). Based on isomer specific PCB analysis, the total PCB was 0.3% in replicate soil samples.

For the PCPAC compounds, a slightly modified Smith et al. (1984) procedure (4) was used. Fourteen grams of air-dried soil was Soxhlet extracted with 60/40 benzene/methanol and subsequently with dichloromethane. The procedure included a carbon on glass fibers column separation to isolate the PCPAC from the PCB. About 0.1 g equivalent of the extract was initially injected. Using selected ion monitoring, a Finnigan 4023 GC/MS monitored six groups of 12 ions. Not only were the PCDF and PCDD compounds detected but also other planar PCPAC, e.g. PCBP and Polychlorinated Naphthalenes (PCN).

Subsequently, the GC/MS acquired full-scan (45-520 d) EI mass spectra at 1 sec/scan. A 30 m x 0.25 mm i.d. DB-5 (0.25 um) capillary column was temp. programmed from 120 °C (1 min)- 210 °C @ 20 °C/min, 210 °C - 280 °C @ 4 °C/min, and 280 °C - 300 °C @ 4.5 °C/min. Quantitative estimates were made based on m/z 470, 472 ion responses of $^{13}C_{12}$-Cl_8- PCDD. Detected compounds were either confirmed with standards, tentatively identified or characterized as unknowns. Dozens of different closely-eluting PCPAC congeners complicated the analysis.

Total concentrations (ng/g) in the soil extract were the following: PCDF, 571 (2,3,7,8- ca. 32); PCDD, 43 (2,3,7,8- <0.1); PCN, 64;

PCBP, 9; plus Polychlorinated Phenanthrene/Anthracenes (PCPh/An) at 68 and Dibenzothiophenes (PCDBT) at 67. The carbon column effectively isolated these various compounds apart from all but non-ortho substituted PCBs.

The PCPh/An and PCDBT compounds were tentatively identified. Their congener distribution and concentrations are similar but contrast with those of other PCPAC. Apparently, nonchlorinated precursors present in the supplemental fuel became chlorinated during the open burning of PCB material. Mass spectra of these compounds show very abundant molecular ion clusters and typical $(M-70)^+$ fragment ions. The $(M-CSCl)^+$ or $(M-79)^+$ fragment ions of PCDBT were not very abundant, in contrast to the $(M-COCl)^+$ in PCDD mass spectra. The added $(M+2)^+$ ion abundance from a sulfur atom was barely discernable. The PCDBT elute several minutes later than PCDD using a 30 m DB-5 column, but may interfere in some dioxin analyses.

The PCBP consisted mainly of Cl_4- congeners. Their chromatographic pattern was similar to that in an analysis of an air duct filter from a multi-building facility near an incinerator in Arkansas. Total PCBP concentration is relatively low compared to other reported PCB fires (3).

---

1. Buser, H., Environ. Health Persp. 60:259-268 (1985).
2. Stalling, D.L. Preliminary Report to NY Dept. of Health (1981).
3. Williams, C.H. Jr., C.L. Prescott, and P.B. Stewart in Chlorinated Dioxins and Dibenzofurans in the Total Environment II. L.H. Keith, C. Rappe and G. Choudhary, Ed., pp. 457-468 (1985).
4. Smith, L.M., D.L. Stalling, and J.L. Johnson, Anal Chem 56: 1830-1842.

MINIMIZING INTERFERENCES IN GC/MS ANALYSIS FOR TETRACHLORODIBENZO-P-DIOXINS

J.R. Donnelly, Y. Tondeur*, W.J. Niederhut*, and G.W. Sovocool**
Lockheed-EMSCO, P.O Box 15027, Las Vegas, NV 89114 and **U.S. Environmental Protection Agency, P.O. Box 15027, Las Vegas, NV 89114; *University of Nevada Environmental Research Center, 4505 Maryland Parkway, Las Vegas, NV 89154

The U.S. Environmental Protection Agency (EPA) utilizes both low resolution and high resolution mass spectrometric (HRMS) methods for ppb (ng/g) to ppt (pg/g) level analysis of tetrachlorodibenzo-p-dioxins (TCDDs) in environmental samples. Two of these methods are presented in IFB-WA84-A002 and EPA 600/4-865-004. Refinement of the HRMS method has included a study of potential analytical interferences and of the means to eliminate or minimize these interferences, including silica, alumina, and charcoal partitioning columns.

Calculations showed that hexa- and hepta-chlorobiphenyls would interfere at m/z 257, 259, and 322 in the determination of TCDDs. Hexachloronaphthalene (HxCN) isomers present in Halowax 1014 would interfere at m/z 332, and 334. If perfluorokerosene (PFK) calibrant is chosen over perfluorotributylamine (FC43, PFTBA), interferences could become significant at m/z 259, 320, 322, 332, and 334.

Relative to the m/z monitored (Table 1), potential interferences were tested from Aroclor 1260 (Figure 1 and Table 2), Halowax 1014 (Figure 2 and Table 3), and PFK mass accuracy calibrant (Figure 3 and Table 4). Sample processing ("cleanup") efficiency was tested (Table 5) using Aroclor 1260, a commonly encountered high concentration interference for TCDD analysis, which if coelution occurs requires high mass spectrometric resolution to separate from the TCDD peaks (Figure 2 and Table 2).

In summary, interferences from Aroclor 1260 occurred at the retention times of 1,3,6,8; 1,3,7,9; 1,4,7,8; 2,3,7,8; and 1,2,6,7-TCDDs. Interference at the m/z values monitored for $^{13}C_{12}$-TCDD internal standards was noted at the retention time of the 1,2,3,4-TCDD isomer chosen as recovery internal standard. These results are shown in Figures 1 and 2.

To minimize false positive results, the criteria shown in Table 6 were chosen for confirmation of TCDD presence in environmental samples. Interferences may be minimized by the following:

(1) efficient sample preparation (chromatography);
(2) selection of m/z less subject to interference from environmentally occurring contaminants (m/z 259 instead of 257);
(3) use of FC43 (PFTBA) calibrant rather than PFK;
(4) use of at least 10,000 mass resolution.

NOTICE: This article has not been subjected to Agency policy review and therefore does not necessarily reflect the views of the Agency. Mention of trade names or commercial products does not constitute endorsement or recommendation for use.

Table 1

m/z Monitored for TCDD Analysis

257 or 259	$M^{\cdot +}$ - COCl or (M+2) $^+$ - COCl
320	M $^+$
322	(M+2) $^+$
332	M $^+$ ($^{13}C_{12}$ -TCDD internal standard)
334	(M+2) $^+$ ($^{13}C_{12}$-TCDD internal standard)

Other Relevant m/z

328	M $^+$ ($^{37}Cl_4$ -TCDD)
318	M $^+$ (tetrachloroxanthenes)

Table 2

Potential Interferences from PCBs Near m/z 257,259

TCDD ($M^{\cdot +}$ - COCl)$^+$ 257 = $C_{11}H_5O^{35}Cl_4$ = 256.9326
259 = $C_{11}H_5O^{35}Cl_3{}^{37}Cl_1$ = 258.9296

Assignment of Fragment Ion	Accurate Mass	Required Resolution	Relative Abundance
Tetrachlorobiphenyls (M-Cl)*			
$C_{12}H_6{}^{35}Cl_3{}^{37}Cl_1$	256.9506	14,400	1.00
$C_{12}H_6{}^{35}Cl_2{}^{37}Cl_2$	258.9476	14,500	0.33
Pentachlorobiphenyls* (M-2Cl)$^+$, ^{13}C			
$^{13}C_{11}{}^{12}C_1H_5{}^{35}Cl_3{}^{37}Cl_1$	256.9461	19,200	1.00
$^{13}C_{11}{}^{12}C_1H_5{}^{35}Cl_2{}^{37}Cl_2$	258.9432	19,300	0.33
Hexachlorobiphenyls (M-3Cl)*			
$C_{12}H_4{}^{35}Cl^{37}Cl_3$	256.9320	321,100	1.00
$C_{12}H_4{}^{35}Cl_2{}^{37}Cl_2$	258.9290	323,600	0.11
Heptachlorobiphenyls (M-4Cl)$^+$, ^{13}C			
$^{13}C_{11}{}^{12}C_1H_3{}^{35}Cl_3{}^{37}Cl_2$	256.9275	48,700	1.00
$^{13}C_{11}{}^{12}C_1H_3{}^{35}Cl_2{}^{37}Cl_3$	258.9245	48,800	0.11
Octachlorobiphenyls (M-5Cl)*			
$C_{12}H_2{}^{37}Cl_3$	258.9134	13,200	(no 259)
$C_{11}{}^{13}C_1H{}^{37}Cl$	258.9089	10,800	(no 259)

*PCBs most likely to coelute with TCDDs

Table 3

Interferences from Halowax 1014

m/z from Halowax	m/z from TCDD	mmu	Required Resolution
331.829	331.937	108	3,070
333.826	333.934	108	3,070

Table 4

Interferences from PFK,a

m/z from PFK	m/z from TCDD	mmu	Required Resolution
258.9805	258.9298	50.7	5,100
256.9586	258.9296	28.8	9,000
319.9845	319.8965	88.0	3,600
321.9869	321.8936	93.3	3,500
331.9844	331.9368	47.6	7,000
333.9891	333.9339	55.2	6,000

aTwo batches, peak match at 10,000 resolution

Table 5

SAMPLE PROCESSING EFFICIENCY

10 ppb Aroclor 1260 (100 ng) on carbon column (Carbopack/Celite)

m/z	% in TCDD Fraction
257	0.5–0.6%
322	0.3–0.5%

10 ppm Aroclor 1260 (100 ug) using entire sample processing scheme (silica, alumina, carbon columns)

m/z	% in TCDD Fraction
257	.001–.006%
322	.007–.008%

Overall column efficiency for Aroclor 1260 99.992 – 99.999%

Figure 1

10 ng AROCLOR 1260

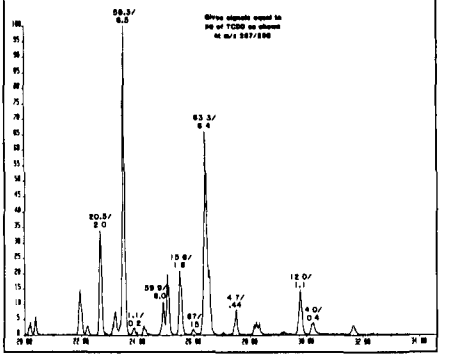

Figure 2

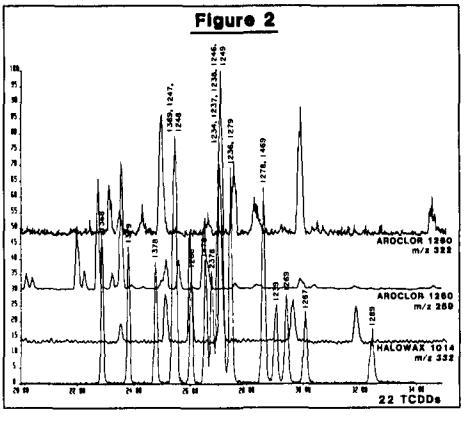

Figure 3

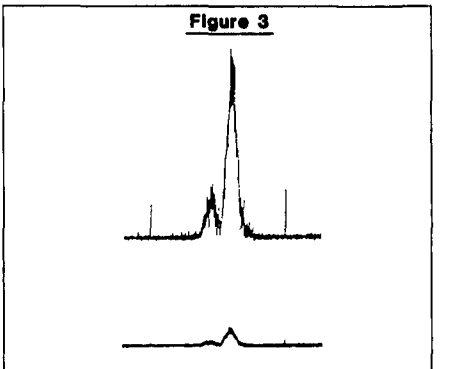

PFK Interferences near m/z 259, 70 eV, 10,000 resolution

LABORATORY STUDIES AT CDC INVOLVING DIOXINS

Donald G. Patterson, Jr., Larry L. Needham, and Eric J. Sampson
Division of Environmental Health Laboratory Sciences, Center for Environmental Health
Centers for Disease Control, Public Health Service
U.S. Department of Health and Human Services, Atlanta, Georgia 30333

INTRODUCTION: Environmental contamination by chlorinated dibenzo-p-dioxins (PCDDs) and dibenzofurans (PCDFs) continues to be a major public health concern. It is of particular interest whether environmental exposure is translated into elevated body burden. Human adipose tissue samples, collected at autopsy from persons with no known exposure to environmental contamination, have been found to contain between 3 and 19 parts-per-trillion (ppt) of 2,3,7,8-tetrachlorodibenzo-p-dioxin (TCDD) in several recent studies (1a-e). These studies also found other dioxins and furans (all laterally 2,3,7,8-chlorinated) at levels up to hundreds of ppt for octachlorodibenzo-p-dioxin. These findings indicate a background level of dioxins and furans in the adipose tissue of the general population within the U.S.A. and several other countries.

We have recently developed and applied a HRGC/HRMS method for analyzing human adipose tissue for TCDDs (1d,2,3). This ability to accurately measure dioxin in adipose tissue in the ppt range has significantly improved our ability to assess exposure and to validate exposure modeling. Additional studies are needed in order to better interpret the results of recent studies involving dioxins and furans in human adipose tissue: 1) Expanded studies of the general U.S. population; 2) Studies of the pharmacokinetics of dioxins and furans in humans; 3) Studies of the anatomical distribution of dioxins and furans within human tissues.

National Reference Value Range for 2,3,7,8-TCDD in a Characterized U.S. Population

Objectives: 1) To determine a "reference value range" for 2,3,7,8-TCDD in human adipose tissue; 2) To investigate associations between concentration of TCDD and personal characteristics such as age group, sex, exposure and medical history; 3) To determine concentrations of other 2,3,7,8-chlorine substituted dioxins and furans; 4) To determine a "reference value range" for total PCBs, selected PCB congeners, and chlorinated hydrocarbon pesticides in adipose tissue and serum; and, 5) If and when the limit of detection is reduced sufficiently by future technological developments, serum "reference value range" will be determined.

Current Status: Because of recent advances in a serum method, considering a change to serum instead of adipose tissue.

Half-Life of TCDD in Humans

The half-life of TCDD in primates has been estimated to be about one year (4). Recently, an investigator in Switzerland voluntarily ingested radiolabeled TCDD, and from subsequent measurements on urine and feces, he estimated the half-life to be 4.95 years (5). TCDD was measured in the adipose tissue of a man 31 years after he was exposed in an industrial accident and found a TCDD level of 100 ppt (6). Assuming first-order kinetics and a one year half-life, the original level of TCDD would have been 200,000,000,000 ppt, or 20% of his fat mass -- clearly impossible.

We have measured TCDD levels of 122 ppt, 166 ppt, and 745 ppt in individuals who gave a history of last exposure from 12 to 14 years before their biopsy. A one-year half-life leads to unacceptably high estimates of original TCDD levels in these individuals. These data are consistent with a 5 to 8 year half-life in humans.

Distribution of Dioxins and Furans in Different Anatomical Sites

To appropriately assess potential health effects in humans associated with exposure to 2,3,7,8-TCDD, a valid estimate of exposure is required. Measurement of body burden of TCDD is more direct and valid than estimates of exposure from epidemiological modeling. In human studies, adipose has been the tissue of choice for measuring TCDD and has been obtained from the abdominal wall, buttocks and intestinal omentum. Additionally, TCDD can be measured in other organs when samples are available (e.g. autopsies). It is expected that TCDD is distributed uniformly in adipose without preference for a particular anatomic site. But this has been tested in only one study in two individuals (7). Since different adipose sites and organs are being sampled in human studies, quantitative measurements determining intersite differences are needed.

We have collected tissues at autopsy from ten females and ten males. We collected adiopse tissue from the heart, kidney, omentum, abdominal wall, buttock, breast, and organ tissue from the heart, kidney, and liver. The samples were processed through our semiautomated sample cleanup method (2) and analyzed on a Vg 70/70 E (SP 2330 column, EI) and Finnigan 4500(DB-5 column, NCI).

The adipose from five individuals was analyzed only for 2,3,7,8-TCDD and the results are shown in Table 1. The data have been corrected to reflect the lipid content of each sample and indicate that 2,3,7,8-TCDD is uniformly distributed on a lipid basis in the fat stores of the body.

The adipose from eleven other individuals was analyzed for all of the dioxins and furans. The results of the analyses on a lipid basis are shown in Table 2. A statistical analysis of the data indicates that most of these dioxins and furans are uniformly distributed in the fat stores of the body.

Table 1. Concentration (ppt) of 2,3,7,8-TCDD on a Lipid Basis in Adipose Tissue From Various Anatomical Sites

Sex	Age	Race	Heart	Kidney	Omental	Abdominal	Buttock	Breast
M	28	W	3.0	2.9	3.1	2.6	3.4	--
F	59	W	5.8	6.1	5.7	4.6	5.9	5.2
M	27	W	4.2	3.4	3.4	3.2	3.3	--
F	30	W	12.6	8.7	9.4	9.2	9.0	8.2
M	51	B	6.2	5.4	6.5	6.8	4.9	--

Table 2 Concentration (ppt) of All Dioxins and Furans on a Lipid Basis in Adipose Tissue From Various Anatomical Sites

Sex/Age/Race	Compound	Heart	Kidney	Omental	Abdominal	Buttock	Breast
F/37/B	2378-TCDD	7.6	6.7	6.6	7.2	6.4	5.4
	2378-TCDF	0.8	0.7	0.7	0.5	0.5	0.5
	23478-PCDF	5.5	4.3	3.7	4.2	4.5	4.7
	12378-PCDD	30	19	19	25	25	22
	123478-HxCDF	7.1	6.0	5.9	6.6	7.8	6.6
	123678-HxCDF	9.2	6.8	5.2	10		8.4
	123478-HxCDD	8.7		6.5		8.2	
	123678-HxCDD	140	141	134	158	142	145
	123789-HxCDD	25	21	17	25	25	29
	1234678-HpCDF						
	1234678-HpCDD						
	OCDD						
M/17/B	2378-TCDD		3.3	3.1	3.6		
	2378-TCDF	3.9	0.9	0.9	1.0		
	23478-PCDF		3.8	3.3	3.7		
	12378-PCDD	47	23	26	38	15	
	123478-HxCDF		4.9	5.2	12		
	123678-HxCDF		17	8.4		8.2	
	123478-HxCDD						
	123678-HxCDD	205	136	133	162	167	
	123789-HxCDD			32		25	
	1234678-HpCDF						
	1234678-HpCDD						
	OCDD						
F/74/B	2378-TCDD	34	37	40	38	38	36
	2378-TCDF	1.0	0.9	1.6	0.8	0.8	1.2
	23478-PCDF	12	11	13	13	12	12
	12378-PCDD	42	32	42	38	27	31
	123478-HxCDF	13	14	15	12	11	12
	123678-HxCDF	22	22	12	24	16	13
	123478-HxCDD		11		18	19	16
	123678-HxCDD	213	245	213	246	235	245
	123789-HxCDD	33	45		36	34	35
	1234678-HpCDF						
	1234678-HpCDD						
	OCDD						
F/29/B	2378-TCDD	8.5	3.2	3.6	2.3	2.6	3.1
	2378-TCDF	5.7	1.2	0.8	0.7	0.7	0.9
	23478-PCDF	24	2.1	2.1	1.8	1.9	
	12378-PCDD	56	7.7	7.8	6.9	6.9	7.0
	123478-HxCDF	21	3.3	3.2	3.1	2.7	3.3
	123678-HxCDF	19	4.3	5.0	3.4	6.3	4.8
	123478-HxCDD	22	3.8	4.4	4.6	6.2	6.6
	123678-HxCDD	462	54	48	52	47	49
	123789-HxCDD	69				18	
	1234678-HpCDF						
	1234678-HpCDD						
	OCDD						
M/19/B	2378-TCDD	6.0	2.7	3.0	3.0	3.7	
	2378-TCDF		1.1	0.8	1.1	0.8	
	23478-PCDF		4.0		3.9	4.0	
	12378-PCDD	30	15	15	16	14	
	123478-HxCDF	8.6	5.0	4.3	4.1	4.0	
	123678-HxCDF	15	7.6	7.0	8.3	6.9	
	123478-HxCDD	17	9.6	8.5		5.5	
	123678-HxCDD	204	114	106	121	116	
	123789-HxCDD				22	20	
	1234678-HpCDF						
	1234678-HpCDD						
	OCDD						
F/35/W	2378-TCDD	4.1	4.4	4.5	4.6	4.3	4.1
	2378-TCDF	0.7	0.6	0.7	0.7	0.6	0.7
	23478-PCDF	3.7	3.2	3.3	3.3	3.1	3.1
	12378-PCDD	13	9.6	9.2	8.5	8.4	9.7
	123478-HxCDF	3.9	3.4	3.1	3.4	3.1	3.1
	123678-HxCDF	5.5	5.7	4.1	4.0	5.5	4.2
	123478-HxCDD	4.7			3.7		4.6
	123678-HxCDD	87	84	79	84	82	77
	123789-HxCDD	21	16	14	15	16	15
	1234678-HpCDF						
	1234678-HpCDD						
	OCDD						
M/43/B	2378-TCDD	4.8	5.2		5.3	5.6	
	2378-TCDF	0.6	0.6		0.7	0.8	
	23478-PCDF	4.6	4.7		4.2	4.6	
	12378-PCDD	11	12	10	11	12	
	123478-HxCDF	4.1	3.7		3.9	4.5	
	123678-HxCDF	5.5	5.2		5.2	5.4	
	123478-HxCDD	5.8	5.0		5.2	6.2	
	123678-HxCDD	113	97	89	102	101	
	123789-HxCDD	14	14		16	18	
	1234678-HpCDF						
	1234678-HpCDD						
	OCDD						
F/55/W	2378-TCDD	8.8	8.9	8.8	8.3	3.1	8.3
	2378-TCDF	1.5	1.4	1.8	1.8	1.5	1.5
	23478-PCDF	5.0	4.8	4.6	4.3	4.3	4.6
	12378-PCDD	12	15	14	12	13	13
	123478-HxCDF	3.4	3.0	3.0	3.2	3.0	
	123678-HxCDF	7.1	4.4	5.6	5.8	3.4	
	123478-HxCDD	5.9	11	10	5.3	5.5	5.0
	123678-HxCDD	104	89	99	91	88	84
	123789-HxCDD	17	18	16	18	17	17
	1234678-HpCDF				8.9		
	1234678-HpCDD				48		
	OCDD				398		
M/23/B	2378-TCDD	1.7	1.7	2.0	1.6	1.7	
	2378-TCDF	1.3	0.9	0.8	0.7	1.0	
	23478-PCDF	3.8	3.0	3.2	3.4	3.2	
	12378-PCDD	12	9.5	15	10	13	
	123478-HxCDF	4.5	3.4	4.8	3.9	5.5	
	123678-HxCDF	7.1	4.0	7.2	5.1	7.7	
	123478-HxCDD						
	123678-HxCDD	92	81	110		89	
	123789-HxCDD	18	17	19			
	1234678-HpCDF		24	22			
	1234678-HpCDD		45	55			
	OCDD		536	526			
F/45/B	2378-TCDD	4.7	4.3	4.1	4.8		
	2378-TCDF	1.6	1.0	0.8	0.9		
	23478-PCDF	4.4	3.9	4.1	3.9		
	12378-PCDD	13	12	12	12		
	123478-HxCDF	3.1	5.0	4.7	4.7		
	123678-HxCDF	8.2	7.3	6.3	8.9		
	123478-HxCDD	7.1	7.9	6.2	13		
	123678-HxCDD	115	99	88	105		
	123789-HxCDD	22	19	14	17		
	1234678-HpCDF						
	1234678-HpCDD						
	OCDD						
M/48/W	2378-TCDD	5.8	5.8	3.8	4.1	3.1	
	2378-TCDF	1.0	0.9	0.8	0.8	1.0	
	23478-PCDF	4.7	4.2	4.1	4.1	4.0	
	12378-PCDD	16	13	13	13	14	
	123478-HxCDF	6.0	4.2	3.6	3.6	3.8	
	123678-HxCDF	9.6	4.9	5.0	6.3	5.5	
	123478-HxCDD				9.1		
	123678-HxCDD	143	109	97	92	100	
	123789-HxCDD		14	14	13	13	
	1234678-HpCDF						
	1234678-HpCDD						
	OCDD						

(1)(a) Ryan JJ, et al.: 186th ACS, Washington D.C., 1983, No. 55: 157; (b) Graham M, et al.: Dioxin-84; Ottawa, Canada; October 16-18; (c) Graham M, et al.: Dioxin-85; Bayreuth, FRG; September 16-19; (d) Patterson DG, et al.: Dioxin-85; Bayreuth, FRG; September 16-19; (e) Gross ML, et al.: Environ Res 1984;33:261-268; (2) Lapeza, CR; Patterson, DG; Liddle, JA; Anal. Chem., 1986, 58, 713-716; (3) Patterson, DG; et al.: Anal. Chem., 1986, 58, 705-713; (4) McNulty WP, et al.: Persistence of 2,3,7,8-Tetrachlorodibenzo-p-Dioxin in fat of a rhesus monkey (Macaca mulatta) Food Chem; (in press); (5) Poiger H, et al.: Dioxin-85; Bayreuth, FRG; September 16-19; (6) Nygren M, et al.; 189th ACS, 1985; Miami, Florida; April 29-May 3; (7) Ryan JJ, et al; 189th ACS 1985; Miami, Florida; April 29-May 3.

PERSISTENCE OF 2,3,7,8-TCDD IN RHESUS MONKEYS: ANALYTICAL METHODOLOGY AND PRELIMINARY RESULTS

J.C. PAN, N.C.A. Weerasinghe and J.L. Meehan,
Midwest Center for Mass Spectrometry,
Univ. of Nebraska-Lincoln, Lincoln, NE 68588
and
R.E. Bowman,
Primate Laboratory,
Univ. of Wisconsin-Madison, WI 53715

Studies on long term, low-dose exposure of 2,3,7,8-tetrachlorodibenzo-p-dioxin(TCDD) to rhesus monkey are important in the context of extrapolating the results to man because of similarities of the former species to the latter. However, difficulties arise in the determination of TCDD when the size of tissue biopsy samples is limited to only a few hundred milligrams.

To achieve the sensitivity required for these studies, we have recently coupled a Carlo-Erba capillary GC with a Kratos MS-50 high resolution MS by using a capillary column sample inlet to perform trace analysis in HRGC/HRMS mode. The use of the capillary column with the adaption of an on-column injection technique not only increases instrument sensitivity but also eliminates carryover problems often seen with packed columns. Data acquisition using a newly installed integrating amplifier gives an improvement of the signal/noise ratio by a factor of four over the previously-used standard Kratos Daly detector and preamplifier. Use of a carbon-on-silica column in addition to previously-used silica and alumina columns gives much cleaner sample extracts which increase signal/noise ratio by decreasing chemical noise[1]. With the improvements in instrumentation and sample clean-up techniques, we can easily detect 2,3,7,8-TCDD at 0.5-5 ppt levels for sample size of about one gram utilizing no more than 20% of the sample extract for analysis.

In this paper, we present preliminary results of a study on monkeys recovering from four years of daily exposure to low levels of TCDD. The two main goals of the projects are: 1. to establish the TCDD levels at the end of exposure period (putative steady state level), the half-life and average amount retained in the body fat after ingestion, and 2. to assess the amount of TCDD transferred by a nursing mother to its infant.

TCDD clearance from the body has been already reported to have an apparent half-life of one year in an acute one-time exposure study[2]. In the present study, TCDD levels were measured in adipose tissues of four rhesus monkeys following four years of exposure at 25 ppt TCDD containing diet. TCDD was measured in subcutaneous and/or mesenteric fat samples taken the day the diet was terminated. More fat samples were taken and analyzed for TCDD at 6 months and every 3 months thereafter up to 33 months (see Table 1). Half-lives of TCDD (assuming 1st-order kinetics) in these monkeys range from 8 months to 18 months with a mean $\pm$ SD of 14 $\pm$ 4 months which is in agreement with the previous finding.

In the study of TCDD transfer during lactation, three female monkeys were exposed at 25 ppt levels of TCDD in their daily diet for four years. Sixteen months after the diet was terminated, each monkey gave birth to a viable infant. The mothers were allowed to nurse the infants for 4 months. Fat biopsy samples of the mothers were taken at parturition. More samples of the mothers and the infants were taken at weaning which was four months after parturition. Concentrations of TCDD detected in infants' fat samples are in the range of 400 ppt to 1400 ppt (see Table 2). At least in two cases, concentrations of TCDD measured in the mesenteric fats of infants are approximately 5-fold higher than those of mothers at weaning. These results are in agreement with previous finding of 5-fold biomagnification of PCB in infants over nursing mothers during lactation[3]. Furthermore, the absence of detectable levels of TCDD in a chronically exposed mother (at 50

ppt for 3 year) after nursing its infant may be attributed to the transfer during lactation[4].

REFERENCES:

1. Gross, M.L., Sun, T., Lyon, P.A., Wojinski, S.F., Hilker, D.R., Dupuy, A.E. and Heath, R.G., Anal. Chem. 1981, 53, 1902-1906
2. McNulty, W.P., Nielson-Smith, K.A., Lay, J.O., Lippstreu, D.L., Kangas, N.L., Lyon, P.A. and Gross, M.L., Food Cosmetic Toxicol., 1982, 20, 985-986
3. Bailey, J., Knaff, V., Mueller, W. and Hobson, W., Environ. Toxicol., 1980, 21, 190-196
4. Weerasinghe, N.C.A., Meehan, J.L. and Bowman, R.E., 33rd Annual Conf. of Amer. Soc. for Mass Spec., 1985, 654-655

TABLE 1

MONTH \ ANIMAL ID	PP91		PP100		PP104		PP110	
	Mes	SubQ	Mes	SubQ	Mes	SubQ	Mes	SubQ
0	-	250	-	930	-	600	-	990
6	ND(120)	-	530	520	665	640	770	615
9	ND(120)	130	950	900	570	400	-	-
12	ND(40)	50	620	510	320	300	502	540
15	ND(30)	ND(8)	610	250	680	430	-	-
18	ND(30)	ND(50)	730	730	ND(350)	540	-	360
21	20	ND(8)	280	650	-	540	-	-
24	-	-	-	-	-	-	330	340
27	30	20	400	400	260	305	145	300
30	Died of TCDD unrelated renal failure		280	300	265	260	250	160
33			320	290	250	260	225	70

TABLE 2

MONTH \ ANIMAL ID	PP94			PP95			PP98		
	Mother		Infant	Mother		Infant	Mother		Infant
	Mes	SubQ	Mes	Mes	SubQ	Mes	Mes	SubQ	Mes
0	-	35	-	-	310	-	-	165	-
4	70	40	380 365	290	370	1400 1300	1200	ND	760

Note: 1) Concentrations are in ppt on wet weight basis.

2) Mes = Mesenteric fat, SubQ = subcutaneous fat.

THE QUANTITATION OF PCB'S, PCDF'S AND PCDD'S BY ELECTRON IMPACT GC/MS USING RESPONSE FACTOR ESTIMATION

A. D. Sauter and J. J. Downs, A. D. Sauter Consulting, 2356 Aqua Vista, Henderson, NV 89015 and J. D. Buchner and V. A. Pizzitola, Extrel Corporation, 240 Alpha Drive, Pittsburgh, PA 15238.

U.S. EPA methods for the determination of polychlorinated dibenzofurans (PCDF's) and polychlorinated dibenzodioxins (PCDD's) in hazardous wastes (1) and for the determination of polychlorinated biphenyls (PCB's) in samples originating at Superfund hazardous waste sites (2) require the determination of the concentration of all isomers of a given compound class. For technical, practical, and economic reasons, it is effectively impossible to standardize a GC/MS system for all analytes of interest in such applications of GC/MS. Therefore, response factor estimation procedures are required for the quantitation of these important environmental pollutants when various isomers are identified in samples, but standards are not available. The approach currently proposed for the quantitation of PCB's in Superfund analyses utilizes the concept of "isomer group" quantitation. This procedure employs a mean response factor for congeners of the various degrees of chlorination to quantitate "unknown" species. Likewise, the RCRA method for the quantitation of PCDD's and PCDF's also employs mean response factors for quantitation of various tetra, penta, hexa, hepta and octa species. Obviously, the accuracy of "statistical" approaches to RF value estimation depends on how well the RF value distributions of the analytes identified in samples match the distribution of the RF values utilized to establish the mean values. Clearly, a formalism which could provide RF value estimates for the quantitation of various "unknowns" would be preferred from a technical accuracy and a QA/QC standpoint, as "The object of all science, whether natural science or psychology, is to co-ordinate our experiences and to bring them into a logical system" (3).

Recently, we have published a model for the estimation of electron impact GC/MS RF values (4). In this work, we have applied our model to estimating RF values for various PCB's, PCDF's and PCDD's with good results. For the thirty compounds listed in Table 1, the average estimated/observed response factor was found at 1.07 ± 0.114. These data included 25 RF values determined using full scan data at nanogram levels and 5 RF values determined at picogram levels in the selected ion monitoring mode. While the application of the model is limited to situations where mass and/or chromatographic discrimination are not severe, properly applied, our model provides a formalism which can yield estimated RF values with an average accuracy of approximately $\pm$ 10 percent at one standard deviation. Within a proper QA/QC context, we assert that similar accuracy can be expected for quantitation of various PCB's, PCDD's and PCDF's for which standards are not available. We show how our model can be employed to this effect, and we demonstrate how our model could unify the environmental Quality Control and Quality Assurance of the GC/MS determination of PCB's, PCDD's and PCDF's.

---

(1) RCRA Method 8280, Draft, May 12, 1986.
(2) Proposed Analytical Method for Pesticides and PCB's, Exhibit D, presented at CLP Method Review Conference, Atlanta, GA, March 1985.
(3) Einstein, A., The Meaning of Relativity, Princeton University Press, Princeton, N.J.
(4) Sauter, A. D., Downs, J. J., Buchner, J. D., Ringo, N. T., Shaw, D. L., and Dulak, J. G., Model for the Estimation of Electron Impact Gas Chromatography/Mass Spectrometry Response Factors for Quadrupole Mass Spectrometers, Analytical Chemistry, in press.

Table 1

Estimated/Observed Response Factors for Selected PCB's, PCDD's and PCDF's

PCB's	Estimated/Observed
2	1.13
3,3'	1.02
2,4,5	1.09
2,2',4,4'	0.974
2,3',4,5',6	0.961
a pentachlorobiphenyl	0.866
2,2',3,4,5,5',6	1.08
2,2',3,3',4,4',5,5'	1.10
2,2',3,3',4,4',5,5',6	1.10
2,2',3,3',4,4',5,5',6,6'	1.13
PCDD's[a]	
2,3,7,8	0.950
1,2,3,7,8	0.925
1,2,3,4,7,8	1.00
1,2,3,4,6,7,8	1.19
1,2,3,4,5,6,7,8	1.08
PCDD's	
2,3,7,8	1.10
1,2,3,7,8	1.10
1,2,3,6,7,8	1.04
1,2,3,4,6,7,8	0.975
1,2,3,4,5,6,7,8	0.925
TCDD's	
2,3,7,8	1.25
1,2,3,8	0.983
1,2,3,4	0.953
1,2,7,8	1.16
1,2,8,9	1.29
PCDF's	
2,3,7,8	1.14
1,2,3,7,8	1.09
1,2,3,4,7,8	1.01
1,2,3,4,6,7,8	1.32
1,2,3,4,5,6,7,8	1.29
	$\overline{E/O} = 1.07 \pm 0.114$

[a] SIM RF values provided by D. Catalano, IT Corp., Knoxville, TN.

GC/MS CHARACTERISTICS OF THE THIRTY-EIGHT ISOMERS OF TETRACHLORODIBENZOFURAN

B.G. Chittim, Wellington Environmental Consultants, P.O. Box 1261, Guelph, Ontario, Canada N1G 6N6; S. Safe and L. Safe, Department of Veterinary Physiology and Pharmacology, Texas A&M University, College Station, Texas 77843; H.S. McKinnon, D.S. Waddell and R.K. Boyd, Department of Chemistry and Biochemistry, University of Guelph, Guelph, Ontario N1G 2W1.

The toxicity of polychlorodibenzofurans (PCDF's) is remarkably dependent on their structure. Therefore it is important to develop methodologies leading to isomer-specific analysis of PCDF mixtures. The present work represents one essential step in such a development, in which all isomers of tetrachlorodibenzofuran (TCDF) have been prepared by unambiguous synthetic routes described previously.[1] Structures of some of these reaction products have been confirmed using proton nmr spectroscopy. It is important to note that in those cases where the synthesis is not wholly specific, only a small number of isomers (typically two) can be formed, with well-established mechanistic preferences for one product. The purified isomers all have purities greater than 94%.

Previously, the best available work on GC/MS characteristics of PCDF's was that due to Hileman and his collaborators[2-4], who synthesised the PCDF's by the much less specific means of pyrolysis of individual congeners of polychlorinated biphenyls. In order to confirm tentative assignments of isomeric structures, Hileman et al. devised an ingenious mathematical model for the GC behaviour of these compounds. The structure/retention characteristics thus obtained clearly depend on a somewhat circular argument. Also, since pure isomers were not available, no quantitative information could be obtained.[2-4] The present work was devoted to checking the structure/retention assignments of Hileman et al.[2-4], and to investigating relative response factors relevant to mass spectrometric quantitation. Some preliminary work was reported previously.[5]

The GC characteristics reported by Hileman et al.[2-4] are generally well supported by the present work. (Currently the single isomer 1,2,8,9-TCDF is missing from our collection of confirmed isomers). The figure shows the present results for Kovats retention indices, obtained using a 30m DB5 column, plotted vs. those reported previously by Mazer et al.[2] who used a very similar SE-54 column. The agreement is excellent. (Note corrections subsequently published by the original authors[2]). Results of a subsequent investigation[4] by the same authors, using a DB5 column, showed similar agreement with the present data. Excellent agreement was also obtained between the present work and the results of Hileman et al.[4], for a 60m highly polar column (SP-2330[4] vs. SP-2331 used here).

Systematic investigation of mass spectral characteristics of these TCDF isomers showed that absolute intensities of molecular ions maximised in the 60-70 eV range, while that of the $(M-COCl)^+$ ions also maximised in this range though perhaps at slightly lower electron energy. This is in contrast to the situation with the related tetrachlorodibenzodioxins (TCDD's), for which absolute intensities of molecular ions are maximised at around 30-40eV. Relative response factors for TCDF isomers were determined for both molecular ions and $(M-COCl)^+$ fragments, at 70eV. Relative to that for 2,3,7,8-TCDF defined as unity, mass spectral sensitivities for molecular ions ranged from 0.4 to 2.9. No analytically useful information is obtainable from the small differences observed in the cracking patterns of different isomers.

This work is currently being completed and prepared for more detailed publication. Further details are available from the authors.

1. S.H. Safe and L. Safe, J. Agric. Food Chem. 32 (1984) 68.
2. T. Mazer, F.D. Hileman, R.W. Noble and J.J. Brooks, Anal. Chem. 55 (1983) 104; ibid. 55 (1983) 1648.
3. F.D. Hileman, M.D. Hale, T. Mazer and R.W. Noble, Chemosphere 14 (1985) 601.
4. M.D. Hale, F.D. Hileman, T. Mazer, T.L. Shell, R.W. Noble and J.J. Brooks, Anal. Chem. 57 (1985) 641.
5. D. Fung, R.K. Boyd, S. Safe and B.G. Chittim, Biomed. Mass Spectrom. 12 (1985) 247.

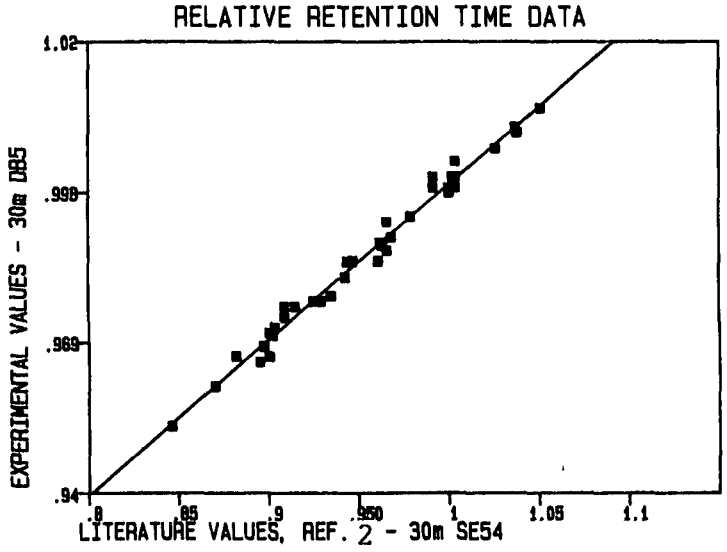

ANALYSIS FOR POLYCHLORINATED BIPHENYLENES IN HUMAN ADIPOSE TISSUE BY NEGATIVE CHEMICAL IONIZATION

Donald G. Patterson, Jr., Cynthia C. Alley, and Elizabeth R. Barnhart

Division of Environmental Health Laboratory Sciences, Center for Environmental Health
Centers for Disease Control, Public Health Service
U.S. Department of Health and Human Services, Atlanta, Georgia 30333

INTRODUCTION

Polychlorinated dibenzo-p-dioxins (PCDDS) and dibenzofurans (PCDFS) are well known environmental contaminants which have been found on flyash of municipal incinerators in many countries. These toxicants have been found in human tissues in a range of a few parts per trillion (PPT) up to hundreds of PPT for the higher chlorinated congeners.

Polychlorinated biphenylenes (PCBPS) are closely related to PCDDs and PCDFs. The 2,3,6,7-TCBP isomer was found to be equipotent with 2,3,7,8-TCDD in microsomal enzyme induction (1). PCBPS have been found as products from capacitor fires in Sweden (2). Four PCB fires were investigated in which the PCBPS were present at concentrations 10 times higher than PCDFS (3). A large number of PCBPS were produced during an electrical accident (Pyrolysis of PCBS) in a New York State office building (4). In these fires the presence of PCBPS could not be confirmed due to a total lack of analytical standards.

OBJECTIVES

Since one of the major sources of PCDDs/PCDFs in humans is probably municipal waste incinerators where organic waste containing chlorine is burned (2,5), it was of interest to: 1) synthesize qualitative standards of chlorinated biphenylenes for method development; and 2) examine human adipose tissue for the chlorinated biphenylenes.

EXPERIMENTAL

Biphenylene Standards: The best yield of the lower chlorinated biphenylenes was achieved by reacting Biphenylene with Sulfuryl chloride for 2 h at less than 70°C. Longer reaction times and higher temperature gave non-biphenylene products (6). Photodechlorination of octachlorobiphenylene was used to generate the higher chlorinated biphenylenes (6).

Human Adipose Sample Preparation and analysis: Omental adipose samples were collected at autopsy from males, females, blacks and whites from Atlanta, Georgia. Ten gram portions of these samples were extracted and cleaned up by our semiautomated method (7). A portion of the extract was analyzed for tetrachlorodioxins (TCDDs) by HRGC/HRMS on our ZAB-2F(8) and the results have been reported elsewhere (9). The remaining extracts from 23 adipose samples were combined and analyzed for PCDDs, PCDFs, and PCBps by negative chemical ionization under the following conditions: 60-m DB-5, 0.25-mm I.D., 0.25 μm film thickness fused silica capillary column; 100°C, 2 min isothermal, 20°C/min to 260°C, 1°C/min to 300°C, 30 min isothermal at 300°C.

RESULTS

The Reconstructed Ion Chromatogram (RIC) for the standard mixture of biphenylenes used in this study is shown in Figure 1. Carbon-13 labeled TCDF and OCDD were added to rovide references for relative retention times (RRT).

Figure 2 depicts the RIC' for the composite human adipose extract analyzed for PCDDs and PCDFs. The ions monitored for HxCDDs (M/z 392,394) also monitor the HpCBPs and the ions used to monitor HpCDDs also monitor the OCBP. We have identified the peak just after 123789-HxCDD as a HpCBP. The MID descriptor monitoring the heptachlorodioxins changed just prior to the OCBP peak.

To confirm the presence of these two biphenylenes in human adipose, we ran the composite extract under a new MID descriptor which contained one ion for each tetra, penta, hexa, hepta, and octa dioxin/furan. We also included three ions each to monitor tetra through octabiphenylene. The results of the analysis are shown in Figure 3. The peaks for HpCBP and OCBP are at RRTs 1.528 and 1.943, respectively. The isotope ratio for the three ions monitored match the theoretical values for both biphenylenes and the RRTs are the same as those of the analytical standards run under the same column conditions.

CONCLUSIONS

We have found two compounds in a composite adipose sample from 23 individuals which meet all of our criteria for a heptachlorobiphenylene and octachlorobiphenylene (correct isotope ratios for three ions, correct masses, and the same retention times as synthetic standards).

We cannot rule out the possibility that one or more of the 23 individuals may have had a unique point source exposure to biphenylenes.

Because of the potential high toxicity of this type of compound, analyses of individual fat samples will be conducted to see if there is a background level of biphenylenes in humans similar to dioxins and furans.

Figure 1. Octachlorobiphenylene Photolysis Mixture

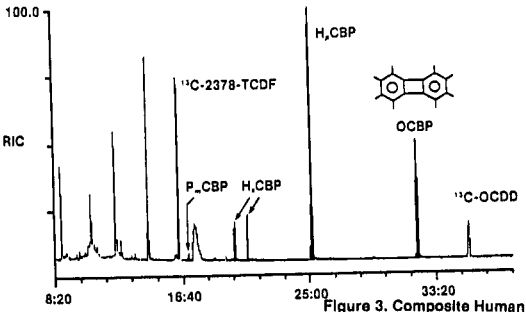

Figure 2. Composite Human Adipose Sample Analyzed for Dioxins and Furans

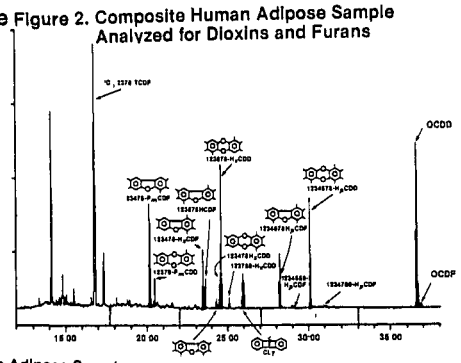

Figure 3. Composite Human Adipose Sample Analyzed for PCDDs; PCDFs; and PCBPs

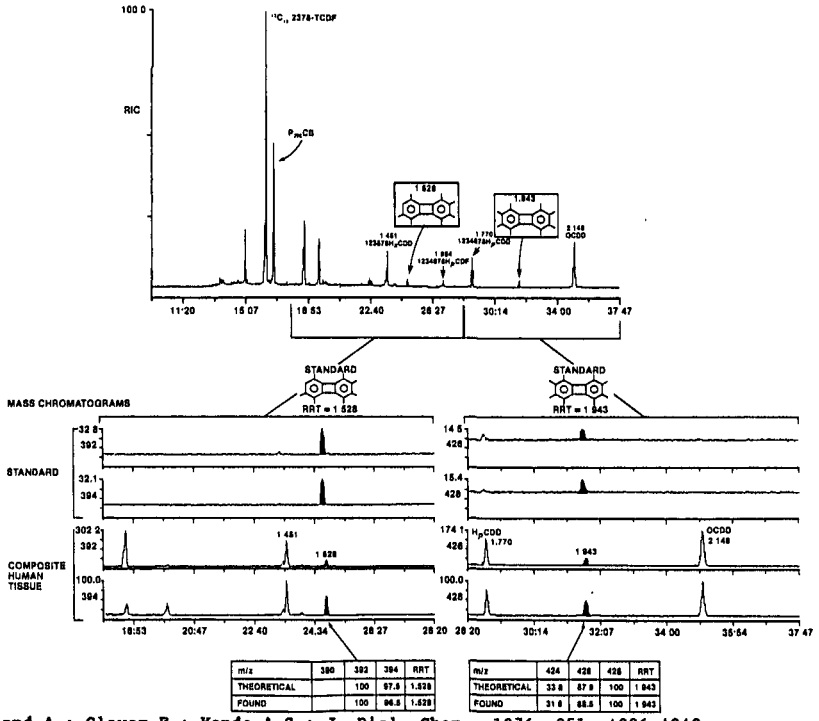

m/z	380	382	384	RRT
THEORETICAL		100	97.8	1.528
FOUND		100	96.5	1.528

m/z	424	426	428	RRT
THEORETICAL	33.8	87.9	100	1 943
FOUND	31.8	88.5	100	1 943

1. Poland A.; Glover E.; Kende A.S.; J. Biol. Chem., 1976, 251, 4936-4940.
2. Rappe C., et al., "Chlorinated Dioxins and Dibenzofurans in the Total Environment," Choudhary G.; Keith L.H.; Rappe C. (Eds) Butterworth, Stoneham, MA, 1983, Chapter 7.
3. Williams CH, et al. "Chlorinated Dioxins and Dibenzofurans in the Total Environment II," (Keith LH; Rappe C; Choudhary G; Eds.) Butterworth, Stoneham, MA, 1985, Chapter 32.
4. Smith L; Stalling DL; Johnson L; Anal. Chem., 1984, 56, 1830-1834.
5. Karasek FW; Hutzinger O; Anal. Chem., 1986, 58, 633A-642A.
6. Barnhart ER, et al., "Chlorinated Dioxins and Dibenzofurans in the Total Environment III," (Rappe C; Choudhary G; Keith LH; Eds.), Lewis, Chelsea, MI, 1986, Chapter 33.
7. Lapeza CR; Patterson DG; Liddle JA; Anal. Chem., 1986, 58, 713-716.
8. Patterson DG, et al., Anal. Chem., 1986, 58, 705-713.
9. Patterson DG; Holler JS; Smith SJ; Liddle JA; Sampson EJ; and Needham LL; In Press in Chemosphere, 1986, June.

GAS CHROMATOGRAPHY/MASS SPECTROMETRY STUDIES IN SUPPORT OF SYNTHESIS OF STANDARD REFERENCE MATERIAL FOR DETERMINING THE CHLORINATED PYRENE CONTENT OF BIOLOGICAL SPECIMENS

Cynthia C. Alley, Elizabeth R. Barnhart, Donald G. Patterson, Jr., Vincent L. Maggio, and David L. Ashley
Division of Environmental Health Laboratory Sciences, Center for Environmental Health
Centers for Disease Control, Public Health Service
U.S. Department of Health and Human Services, Atlanta, Georgia 30333

INTRODUCTION

Polychlorinated pyrenes (PCPYs) have been reported in the soot from polychlorobiphenyl fires and in the condensate from municipal waste incinerators (1-4). As such, they could be expected to accumulate in animal or human tissue. PCPYs have the same nominal molecular mass as polychlorodibenzofurans (PCDFs) with one more chlorine atom per molecule and could possibly be interferents in the mass spectral determination of PCDFs. Analytical standards for the development of methods using mass spectrometry are not available commercially.

OBJECTIVES

Our objectives were to: 1) Synthesize standards of PCPYs for method development; and 2) Determine if PCPYs could interfere in the GC/MS analysis for PCDFs.

EXPERIMENTAL

Synthesis: Polychloropyrenes were prepared by chlorinating pyrene with sulfuryl chloride reagent (Reagent C, Perchlorination Kit, Analabs, Inc., New Haven, CT). As is usual with sulfuryl chloride reagent, a mixture of PCPYs was produced. These mixtures were fractionated on a semi-preparative ODS column (5). The fractions were analyzed by GLC, GC/MS, and NMR.

GC/MS Conditions: A Finnigan 4500 GC/MS/DS with a 60m DB-5, 0.25mm, 0.25μm fused silica capillary column was operated in the Negative Chemical Ionization mode. The reagent gas was methane. The column was temperature programmed as follows: 100C (2 min) to 260C at 20C/min, then to 300C at 1C/min and held at 300C for 40 min. Each sample injection was piggybacked with 13C-2378-TCDF so RRTs could be compared. The ionizer temperature was 100C and the injector temperature was 300C. The electron energy was 70 eV.

NMR Conditions: A Varian XL300 NMR spectrometer with a 7.0 Telsa superconducting magnet was used. The samples were analyzed at ambient temperature using a 5mm probe and a 90 degree pulse.

RESULTS

The PCDFs are separated into discrete groups. The PCPYs, on the other hand, overlap severely and interfere with each other because of abundant fragment ions from sequential chlorine losses. The PCPYs did not interfere with the tetra-, penta-, or hexa- chlorofurans but did not interfere with the hepta- and octa- chlorofurans.

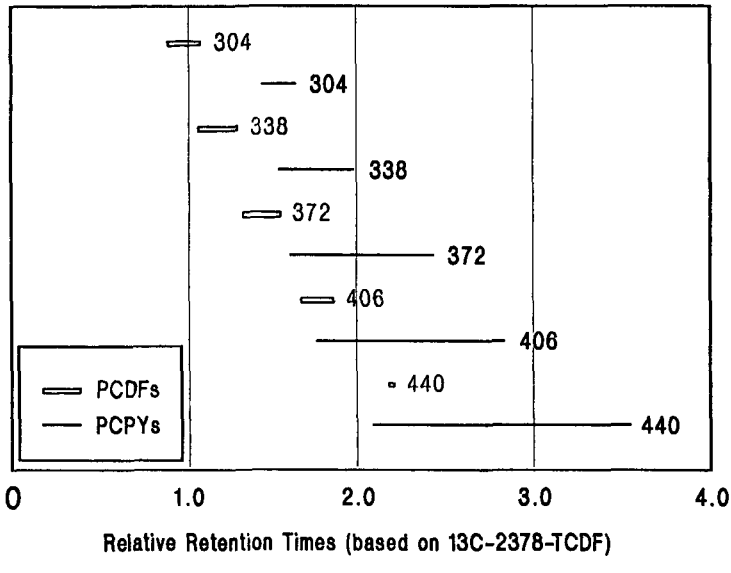

Our synthetic mixtures contained only a small fraction of the 291 possible PCPY congeners, and, therefore, the potential interference problem could be more severe. As of this date, we have isolated and purified five PCPYs for use as quantitative analytical standards and have obtained their NMRs, FTIRs, and RRTs. The NCI mass spectra for three of these congeners are shown below along with a representative PCDF.

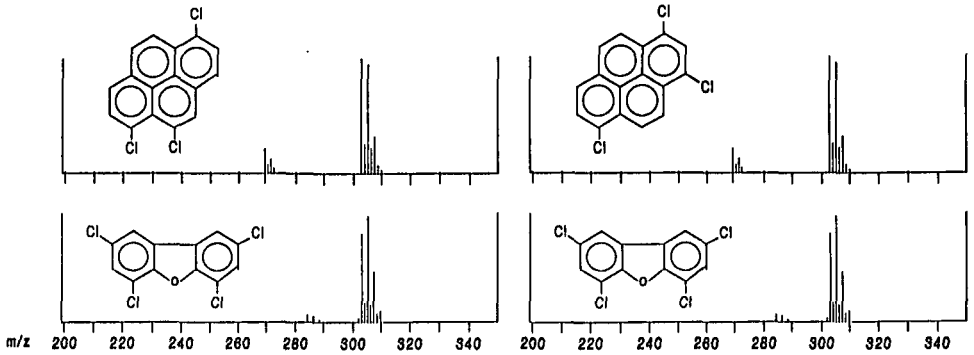

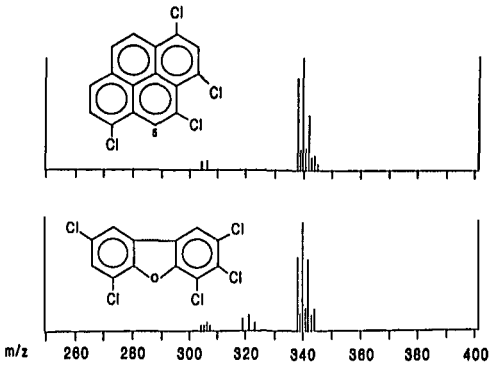

PCDF AND PCPY ISOMERS

	PCDFs	PCPYs
Mono-	4	3
Di-	16	15
Tri-	28	34
Tetra-	38	60
Penta-	28	66
Hexa-	16	60
Hepta-	4	34
Octa-	1	15

REFERENCES

1. A. R. Oyler, R. J. Liukkonen, M. K. Lukasewycz, O. A. Cox, D. A. Peake, and R. M. Carlson. Implications of Treating Water Containing Polynuclear Aromatic Hydrocarbons with Chlorine: A Gas Chromatographic Mass Spectrometric Study. Environmental Health Perspectives, 46,73-86 (1982).
2. C. Rappe, S. Marklund, P.-A. Bergqvist and M. Hansson. Polychlorinated Dioxins (PCDDs), Dibenzofurans (PCDFs) and Other Polynuclear Aromatics (PCPNAs) Formed During PCB Fires. Chemica Scripta 20, 56-61 (1982).
3. C. Rappe, S. Marklund, P.-A. Bergqvist and M. Hansson. Polychlorinated Dibenzo-p-dioxins, Dibenzofurans and Other Polynuclear Aromatics Formed During Incineration and Polychlorinated Biphenyl Fires. In "Chlorinated Dioxins and Dibenzofurans in the Total Environment", vol. 1, G. Choudhary, L. Keith, C. Rappe, eds., Boston:Butterworth-Ann Arbor Science, pp. 99-124 (1983).
4. C. H. Williams, Jr., C. L. Prescott and P. B. Stewart. Formation of Polychlorinated Dibenzofurans and Other Potentially Toxic Chlorinated Pyrolysis Products in PCB Fires. In "Chlorinated Dioxins and Dibenzofurans in the Total Environment II," L. H. Keith, C. Rappe, G. Choudhary, eds., Boston:Butterworth-Ann Arbor Science, pp. 457-468 (1985).
5. E. R. Barnhart, D. G. Patterson, Jr., J. A. H. MacBride, L. R. Alexander, C. C. Alley, and W. A. Turner. In "Chlorinated Dioxins and Dibenzofurans in Perspective," G. Choudhary, L. H. Keith, E. Rappe, eds., Chelsea: John Lewis Publisher, pp 501-510 (1986).

LEUKOTRIENES AND PLATELET ACTIVATING FACTOR:
LIPID MEDIATORS OF THE ACUTE HYPERSENSITIVTY REACTION

R.C. Murphy, K.L. Clay, and F.H. Chilton
Department of Pharmacology
University of Colorado Health Sciences Center
Denver, CO 80262

Mass spectrometry has played a critically important role in the structure elucidation of numerous lipid substances suspected of being involved or synthesized by cells undergoing an immunological reaction. In addition, mass spectrometry continues to play an important role not only in the elucidation of novel lipid substances which have biological activity, but also as a means by which metabolites of these lipids can be structurally characterized and serving as a basis for highly sensitive methods whereby these lipid substances can be quanitated in various biological fluids. In addition to the impact that mass spectrometry has played in our biochemical understanding of these lipid substances, investigators who had been involved in these studies have made substantial contribution to the field of mass spectrometry itself. For example, one of the early uses of stable isotope dilution in mass spectrometry was carried out in an attempt to quanitate prostaglandins in biological fluids (1).

One of the compounds suspected to be an important mediator of the inflammatory response as well as being involved in producing profound bronchoconstriction in humans was known for many years as slow reacting substance of anaphylaxis (SRS-A) (2). Earlier structural studies of this molecule suggested that it had a molecular weight between 400 and 600 daltons (3) contain sulphur (4) as well as having activity in vivo in picomolar quantities. Since this molecule was so potent it was difficult to obtain sufficient quantities of this sample for more traditional means of structural elucidation. In the late 1970's there are some suggestions that arachidonic acid might play a precursor role in the biosynthesis of this molecule. In 1979 the structure of SRS-A was elucidated and renamed as leukotriene C_4 which was a novel metabolite of arachidonic acid by the 5-lipoxygenase pathway (5). This molecule was found to originate from the condensation of glutathione with a reactive conjugated triene epoxide, leukotriene A_4, in various cells including the mast cell, eosinophil, macrophage, and basophil. One of the critical pieces of information which led to the elucidation of the structure of this molecule was a Raney nickel desulphurization of the active substance SRS-A into a product which could be characterized as 5-hydroxyeicosanoic acid, thus establishing the carbon backbone as well as the position of the oxygen atom at carbon-5.

Mass spectrometry played a critical role in the structure elucidation of another series of novel metabolites of arachidonic acid also rising from this reactive triene opoxide leukotriene A_4. This molecule is now known as leukotriene B_4 and is a 5,12-dihydroxyeicosatetraenoic acid product of the enzymatic addition of water to carbon-12 of leukotriene A_4 (6). Leukotriene B_4 is a potent chemotactic and chemokinetic molecule which may be responsible for the accumulation of neutrophils at the site of a inflammatory response.

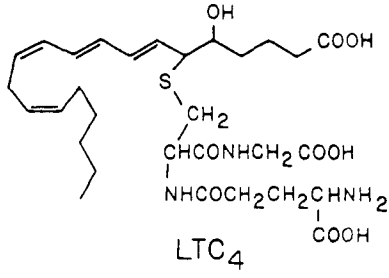

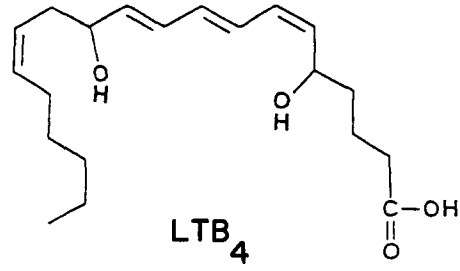

Platelet activating factor (PAF) was first discovered in 1969 as a substance synthesized in basophils in the response to immunological stimulus (7). It was known to be a lipid substance, but it was not until 1979 that the structure of this molecule was characterized as 1-0-alkyl-2-acetyl-sn-glycero-3-phosphocholine as a unique phospholipid possessing profound biological activity. The structure of this molecule was obtained following some degradative studies as well as through chemical synthesis from a semi-synthetic starting material (8). We now know that this molecule can be synthesized by cells such as the basophil, neutrophil, eosinophil, mast cell, and macrophage following various inflammatory stimuli. In studies of the molecular species of PAF generated from the human neutrophil following a phagocytic stimulus, we found that a single unique molecular species of PAF was produced suggesting a high degree of specificity in biosynthesis of this molecule (9). Mass spectrometry continues to play an important role in the measurement of this molecule and sensitive techniques based upon fast atom bomdardment mass spectrometry as well as degradation of PAF into the diglyceride followed by derivatization to trimethylsilyl (9), tert-butyldimethylsilyl derivative (10), or pentafluorobenzoyl ester (11). Since bioassay and radiolabel incorporation of acetate are the only other means by which one can quanitate this molecule, mass spectrometry should enjoy a unique position in being able to sensitively and specifically measure platelet activating factor in various biochemical and clinical studies.

In studies of the metabolism of platelet activating factor in the isolated lung (12), as well as in purified human neutrophils (13), platelet activating factor has been found to be rapidly metabolized to a unique phosphatidlycholine which contains arachidonic acid at the sn-2 position. This unique metabolism of platelet activating factor suggest that there is a biochemical link between arachidonic acid (the precursor of eicosanoids, such as prostaglandins, leukotrienes, and thromboxanes) as well as platelet activating factor (a molecule that has profound physiological influence upon many biochemical steps within a cell). Thus, there is increasing evidence to suggest that the biochemical events leading to the synthesis of a 1-0-hexadecyl-2-arachidonoyl-glycero-phophoscholine serves to generate a common precursor for the three potent lipid mediators discussed above (platelet activating factor, prostaglandins, and leukotrienes). Since these molecules are not stored within cells but rather are only synthesized following the immunological stimulus, a central role for phospholipase A_2 can be invisioned for this process. Upon activation of phospholipase A_2, the precursor phosphatidylcholine can be split into the two immediate precursors of these lipid mediators, these precursors being lyso-platelet activating factor and free arachidonic acid. This hypothesis further implies that there may exist a complex network of mediator biosynthesis within cells and that interuption of the more distal sites of the biosynthesis of these mediators may not completely attenuate the immunological stimulus which results from the activation of phospholipase A_2.

Acknowledgement. This work was supported in part by a grant from the National Institutes of Health HL25785, HL34303, and AI20774.

References

1. C.C. Sweeley, W. Elliott, I. Fries, and R. Ryhage. Anal. Chem. 38:1549 (1966).
2. R.P. Orange and K.F. Austen. Adv. Immunol. 10:105 (1969).
3. R.P. Orange, R.C. Murphy, M.L. Karnovsky, and K.F. Austen. J. Immunol. 110:760 (1973).
4. R.P. Orange, R.C. Murphy, and K.F. Austen. J. Immunol. 113:316 (1974).
5. R.C. Murphy, S. Hammarstrom, and B. Samuelsson. Proc. Nat. Acad. Sci. 76:4275 (1979).
6. P. Borgeat and B. Samuelsson. J. Biol. Chem. 254:2643 (1979).
7. P.M. Henson. J. Exp. Med. 131:297 (1970).
8. C.A. Demopoulos, R.N. Pinckard, and D.J. Hanahan. J. Biol. Chem. 254:9355 (1979).
9. K.L. Clay, R.C. Murphy, J.L. Andres, J. Lynch, and P. Henson. Biochem. Biophys. Res. Commun. 121:815 (1984).
10. K. Satouchi, R.N. Pinckard, and D.J. Hanahan. Arch. Biochem. Biophys. 211:683 (1981).
11. C.S. Ramesha and W.C. Pickett. Biomed. Env. Mass Spectrom. 13:107 (1986).
12. P. Haroldsen, N. Voelkel, and R.C. Murphy. this volume.
13. F.H. Chilton, et al. J. Biol. Chem. 257:5402 (1982).

Pharmacology of the Parkinsonian Syndrome Producing Neurotoxin MPTP - The Role of Mass Spectrometry

S.P. Markey, J.N. Johannessen, S.-C. Yang, C.J. Markey, J.P. Bacon, J.M. Savitt, and D.S. Hanselman
Laboratory of Clinical Science, National Institute of Mental Health, Bethesda, Maryland 20892

Problems brought into a mass spectrometry laboratory sometimes have fascinating prior history and thus mass spectrometric identification leads to even more interesting results. Such has been the case with MPTP (1-methyl-4-phenyl-1,2,3,6-tetrahydropyridine). MPTP is a potent neurotoxin which produces an irreversible parkinsonian syndrome in man. The story began in our laboratory in 1977, when a 23 year old college student and drug abuser was referred to the National Institute of Mental Health because of a severe parkinsonian condition. He had a nine year history of drug abuse, and had been synthesizing his own compounds for over one year. He preferred meperidine analogs, and in the older chemical literature he had found a simple synthesis for 1-methyl-4-phenyl-4-propionoxypiperidine, MPPP, which is a potent narcotic analgesic that was never commercially developed. He injected preparations intravenously of the hydrochloride salt of MPPP, growing increasingly careless in his product purification with each preparation. After injecting his last batch, he had bad side-effects, and within a week, he grew rigid and was unable to speak. Upon admission to an emergency room, he was diagnosed initially as catatonic schizophrenic, but was eventually seen by a neurologist, who recognized the parkinsonian symptoms. His symptoms could be reversed for hours at a time with L-DOPA therapy, and he was referred to NIMH for further study. Reversible drug-induced parkinsonism is a well described phenomenon, but the permanent nature of this case warranted further study. Unfortunately, the patient's basement laboratory had been thoroughly cleaned. Later the patient wrote detailed instructions for us regarding his laboratory procedures and his reactions were duplicated in our laboratories. Following his procedures, we invariably identified MPPP, MPTP, and synthetic precursors in his crude product (Figure 1). A trace of his synthetic product was found in the grease of a vacuum dessicator cover and revealed the same product mixture. Pure MPPP and mixtures of the crude drug were tested in rats and failed to produce any permanent movement disorder. When this patient died due to a drug overdose, autopsy of his brain revealed that he had selectively damaged the cells in the substantia nigra region, resulting in brain pathology similar to Parkinson's disease (1). Our failure to produce a similar condition in laboratory rats led us to shelve this research project.

In July, 1982, four young drug abusers came to the attention of Stanford University neurologists because of the similarity of their severe parkinsonian conditions. All of the drug abusers had injected a "synthetic heroin" and within a few days became rigid. Recognizing the similarity between these patients and the Bethesda case, drug samples were collected and analyzed mass spectrometrically (Figure 2). MPPP and MPTP were found in the powders which had been synthesized in a clandestine laboratory on a kilogram scale. The samples used by the most severely affected patients contained almost pure MPTP. Based upon these findings, Langston and colleagues concluded that MPTP was the likely neurotoxin (2). This was confirmed by Burns et al. who produced a parkinsonian condition in monkeys (3). Interestingly, pure MPTP does not produce analogous brain cell death in rats, confirming the earlier observations.

Mass spectrometric investigations of drugs are well proven both for qualitative identifications of compounds and their metabolites and for quantitative analyses. Radio- and stable isotope labeled isotopomers of MPTP were synthesized, and the major brain metabolites of MPTP in the primate were determined mass spectrometrically to be its oxidation product, 1-methyl-4-phenylpyridinium ion (MPP^+) (4). The occurrence and storage of MPP^+ correlates with species susceptibility to MPTP neurotoxicity.

Most recently, MPTP analogues have been synthesized in order to test compounds which could be bound to protein (diazo or aldehyde coupling) to form antigens or bound to cellular components in in vivo animal studies. Mass spectrometric methods have been used to characterize these compounds (MPC 12).

A $^{14}C_6$-MPTP isotopomer has been synthesized for metabolic studies. High performance liquid chromatography of ^{14}C-labeled brain extracts tentatively identified two metabolites which have been confirmed to be 4-phenyl-1,2,3,6-tetrahydropyridine and 1-methyl-4-phenyl-2-pyridone by GC-MS.

References

1. G.C. Davis, A.C. Williams, S.P. Markey, M.H. Ebert, E.D. Caine, C.M. Reichert, and I.J. Kopin, Psychiatry Res. 1, 249 (1979).
2. J.W. Langston, P. Ballard, J.W. Tetrud, and I. Irwin, Science 219, 979 (1983).
3. R.S. Burns, C.C. Chiueh, S.P. Markey, M.H. Ebert, D.M. Jacobowitz, and I.J. Kopin, Proc. Natl. Acad. Sci. USA 80, 4546 (1983).
4. S.P. Markey, J.N. Johannessen, C.C. Chiueh, R.S. Burns, and M.A. Herkenham, Nature (London) 311, 464 (1984).

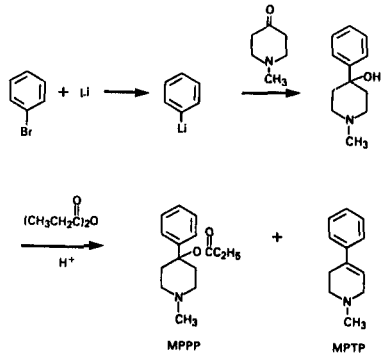

Figure 1

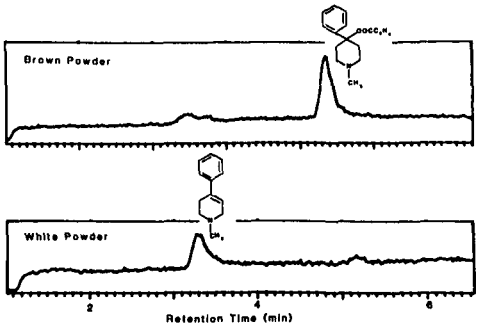

Figure 2

ROLE OF FAB-MS IN STRUCTURAL ANALYSIS OF PEPTIDES

Blair A. Fraser

Division of Biochemistry and Biophysics, Center for Drugs and Biologics, FDA, Bethesda, Maryland 20892

Since its commercial introduction in 1981, fast atom bombardment (FAB) has become a popular ionization method for analyzing peptides by mass spectrometry. Used with other contemporary methods of protein chemistry, FAB plays a useful role in peptide structural analysis.

Structural analysis of peptides requires three sequential interdependent processes: purification, characterization, and application. During purification of the peptide, suitable assays, appropriate extraction schemes, and selective chromatogaphic conditions are essential for obtaining pure peptides of high specific activity in high yield.

Once purified, a portion of the peptide can be characterized by amino acid analysis and FAB-MS. Employing a sensitive method of amino acid analysis, a portion of the peptide is hydrolyzed. Amino acids in the hydrolyzate are then identified and quantified. Amino acid analysis not only establishes that the material is a peptide but is used to calculate the protonated molecular weight of the peptide. An appropriate portion of the peptide is then analyzed by FAB-MS. Comparison of the protonated molecular weight deduced from the amino acid composition with that measured by FAB-MS is used to infer additional information about the peptide.

The molecular ion region may reveal additional information. Disulfide bonds in particular peptides undergo reduction under FAB conditions and this reduction changes the appearance of the protonated molecular ion envelope [1]. Other peptides may show preference for particular cations. Amino acids in some peptides may undergo oxidation during purification [2].

Since this initial characterization requires picomoles of sample, the remainder of the peptide is available for sequential Edman degradation and bioassay. If the peptide has a free amino terminus, Edman degradation will directly determine the amino acid sequence. If the peptide has a blocked amino terminus or is too long for a single Edman degradation, enzymatic fragmentation may be necessary. In particular situations, exopeptidase digestion followed by FAB-MS analysis of the resulting peptide mixtures may also provide information about the amino acid sequence.

Once the data from amino acid analysis, FAB-MS, Edman degradation, and exopeptidase digestion are available, a structure for the peptide can be deduced. The data needs to be consistent. The proposed structure will then be applied to the biological problem. Synthesis, either chemical or biological, or upscaled isolation will provide suitable quantities of the peptide for functional studies. During chemical synthesis of peptides, FAB-MS is a valuable tool.

We have employed this general strategy for several projects including characterization of a gonadotropin releasing hormone from lamprey [2], an adipokinetic hormone from the corn ear worm [3], and the acetylated amino terminal peptide of a growth factor from brain.

References

1. Buko, A.M. and Fraser, B.A., Biomedical Mass Spectrometry 11:577 (1985).

2. Sherwood, N.A., Sower, S.A., Marshak, D.R., Fraser, B.A., and Brownstein, M.J., The Journal of Biological Chemistry 261:4812 (1986).

3. Jaffe, H., Raina, A.K., Riley, C.T., Fraser, B.A., Holman, G.M., Wagner, R.M., Ridgway, R.L., and Hayes D.K., Biochemical and Biophysical Research Communications 135:622 (1986).

FURTHER ADVENTURES WITH AN ELECTROSPRAY ION SOURCE

C. M. Whitehouse, F. Levin, C. K. Meng, and J. B. Fenn
Department of Chemical Engineering
Yale University
New Haven, CT 06520-2159

We present some observations on four facets of Electrospray Ionization (ESPI) that have not yet received much attention. The original short abstract identified the first three as the main subjects for discussion in this longer report but in keeping with the usual unpredictability of experiments, results on a fourth topic turned out to be more interesting and will emphasized.

1. Bath Gas Contamination. On several occasions strange peaks in observed ESPI mass spectra have been traced to contaminants in the nitrogen bath gas. To elucidate these observations we have effected deliberate contamination of the bath gas by injecting small quantities of such species as acetone, dioxane, methyl amine and tri-ethylene glycol. Strong peaks comprising protonated parent molecules were obtained even at a concentration level estimated at ppb on the basis that the injection point was far enough upstream to provide uniform distribution of the measured amount of injected species in the known flow rate of bath gas. When we introduced even greater amounts of the same materials by adding them to the methanol-water mixture comprising the electrosprayed liquid, no corresponding peaks were found in the resulting spectra. We conclude that the ionization mechanism must involve charge exchange or chemi-ionization interactions between the gas phase molecules and charged species produced in the electrospray process.

2. Negative Ion Formation. In its earlier configuration ESPI has shown that it could produce negative as well as positive ions from solute species in liquids.(1) We can now report satisfactory production of negative ions with the present apparatus which incorporates a conversion dynode and replaces with a length of glass capillary the simple orifice that passes ions from the atmospheric pressure electrospray chamber into the vacuum system. In this capillary viscous drag can raise product ions to virtually any desired voltage, e.g. for injection into a magnetic sector analyzer.(2) The most interesting particular observation was the appearance of negative ion clusters containing up to three molecules of solute analyte when the electrosprayed liquid comprised one ug/µl of adenosine monophosphate in 1:1 methanol-water. Such cluster formation or "fractional charging" will be discussed below.

3. Discharge Fragmentation. In some early experiments we had found that when the voltage applied to the incoming liquid exceeded a critical value there occurred marked changes in the observed spectra charaterized by the appearance of solute fragments and new species most readily associated with discharge reactions in the corona that could be observed in bench experiments when the room was darkened. In the hope that such a discharge might bring about fragmentation that would be useful in determining the identity and structure of large analyte species we have carried out experiments with several peptide solutes. No fragmentation has yet been found. The large species ions appear intact, or not at all if the discharge becomes strong enough to abort the electrospray dispersion of the liquid. We conclude that solute ions are not desorbed into the bath gas until the droplets are far enough downstream to escape any discharge effects.

4. Multiple and Fractional Charging. The spectra obtained with relatively large solute species frequently show peaks corresponding to multiply charged ions. We have been trying to determine the conditions that favor such multiple charging because it is an attractive means of extending the mass range of an analyzer. For example, the mass of Renin Substrate is 1757 daltons, well above the 1500 limit of our quadrupole. At a concentrations of 4 ng/µl in 1:1 methanol-water ESPI provided large well defined peaks for doubly and triply charged ions such that I^{+++}/I^{++} was about 0.2. It seems to emerge, as one might expect, that the ratio of analyte molecules to available charge plays a governing role. Decreasing the Renin Substrate concentration tenfold to 0.4 ng/µl decreased I^{++} to 0.15 of its original value but I^{+++} decreased only 25 per cent so that I^{+++}/I^{++} increased to nearly unity.

Similarly, we found with Cyclosporin-A in 1:1 methanol water that as the solute

concentration decreased from 1000 ng/μl to 0.5 ng/μl the ratio I^{++}/I^{+} increased from about 0.04 to nearly unity. In the case of polyethylene glycol (Carbowax 1000), at a concentration of 1000 ng/μl in 1:1 methanol-water I^{++}/I^{+} ratios were only about 0.02. As the solute concentration decreased I^{++} increased in relative magnitude until at 1.0 ng/μl the I^{+} peaks were barely visible above the noise. Incidentally, the peak height distributions in all cases were close to the advertised values of molecular weight distribution. We also found that in a solvent comprising 0.99 acetonitrile, 0.005 methanol and 0.005 water, Cyclosporin at 10 ng/μl gave rise to no discernible doubly charged ions. At the same concentration in 1:1 methanol water I^{++}/I^{+} was about 0.66. In the latter case the solvent provided a much greater abundance of cations so that it was much easier for a solute molecule to acquire more than one charge.

If this competition-for-charge picture embodies any truth, at very high solute concentrations one might expect to find several solute molecules sharing one charge to give what we have dubbed "fractional charging" or clustering. Indeed, as we pointed out earlier, with adenosine monophosphate the spectrum obtained with ESPI in the negative ion mode showed peaks corresponding to singly charged dimers and trimers as well as monomers. A more dramatic case involves arginine. At 5.7×10^{-3} M in 1:1 methanol water the positive ion spectrum showed well defined peaks for clusters containing up to seven arginine molecules per charge. When the solution contained acetic acid at 10^{-4} M the cation concentration was not greatly increased and the spectrum was very similar. However, when the acetic acid concentration was increased to 10^{-3} M, the fractionally charged peaks nearly disappeared into the noise. It seems reasonable to attribute this disappearance to the greatly increased abundance of protons in the solution.

There remains the question of whether the observed clustering could have occurred in the gas phase after a monomeric ion had been desorbed from a microdroplet. In view of the minimal volatility of these solutes, their very low concentration in the electrosprayed solution and the large molar flux of bath gas relative to liquid, it seems very unlikely that gas phase concentrations of solute species could have been high enough to account for clustering after a monomer ion had been desorbed into the gas phase. Consequently, we believe that the observed clustering relates to the liquid phase. Implicit in this speculation, and almost self evident from all of our experience thus far, is a conclusion that ESPI Mass Spectrometry should be a powerful tool in the study of solution chemistry.

References

1. Yamashita, M.; Fenn, J. B.; J. Phys. Chem. 1984, 88, 4671.

2. Whitehouse, C. M., Dreyer, R. N., Yamashita, M., and Fenn, J. B.; Anal. Chem. 1985, 57, 675.

Laser Mass Spectra of Solutions at Ambient Pressure

John J. Morelli, Kenneth J. Rosnack Jr., and David M. Hercules,
Department of Chemistry, University of Pittsburgh, Pittsburgh, PA 15260 U.S.A.

FAB mass spectrometry and liquid SIMS are at the forefront of chemical and biological mass spectrometric studies involving substances in polar condensed phases, conditions resembling the natural aqueous environment of living organisms (1). Direct investigation of predominently aqueous systems have not been made due to the vacuum requirements of particle bombardment techniques. The development of Atmospheric Pressure Ionization (2) and Liquid Ion Evaporation (3) are exceptional in that the analysis of volatile solutions is possible; however, both techniques require nebulization or volatilization prior to ionization. The direct analysis of cellular matter at ambient pressure remains an elusive accomplishment for mass spectrometrists.

Recently, developments allowing direct laser mass spectrometric investigations at ambient pressure were reported (4) - (6). Ambient pressure laser mass spectrometry (LMS) is advantageous since ionization occurs while the sample remains in its natural physical state (referring to temperature and pressure). A thin polymer (Formvar) film is used to isolate samples from the vacuum of a laser mass spectrometer. Ambient pressure LMS was used in the direct analysis of pesticides on plant tissue (4), pure organic liquids having moderate to high volatility (5), and vacuum sensitive condensed matter (6). The present report demonstrates ambient pressure LMS as a technique capable of analyzing aqueous and nonaqueous solutions of both high and low volatility.

Figures 1a - 1c show the positive ion laser mass spectra of glycerol (Fig. 1a), CsI in glycerol (Fig. 1b), and benzoic acid in glycerol (Fig. 1c). While the operating vacuum (2×10^{-5} torr) of the laser mass spectrometer (LAMMA-1000) allows direct analysis of glycerol matrices without the presence of Formvar films, advantages exist for using polymer seals. Formvar seals allow two primary advantages: 1) much of the volatile material that normally degasses during chamber evacuation remains entrapped under the seal; 2) the droplet of glycerol remains stationary despite the vertical orientation required by the mass spectrometer. The most significant observation regarding the spectra in Figure 1 is the absence of glycerol cluster peaks which are prominent interferences in FAB and liquid SIMS.

Figures 2a - 2d show the positive and negative ion laser mass spectra of retinoic acid in MeOH (Figs. 2a and 2c) and toluene (Figs. 2b and 2d). These spectra indicate that aromatic matrices can form cluster ions analogous to glycerol fragments found in FAB spectra. Matrice clusters do not form when MeOH or glycerol are employed in ambient pressure LMS. Also note that less fragmentation occurs in the positive ion laser mass spectra of retinoic acid solvated in toluene compared to that obtained from the MeOH solution.

Figures 3a and 3b show the spectra obtained from aqueous glycine under ambient conditions (Fig. 3a) and glycine deposited on silver foil obtained under vacuum conditions (Fig. 3b). Figure 3 demonstrates that the laser mass spectra obtained from solutions can differ from those obtained under vacuum.

References

1. Burlingame, A. L.; Baillie, T. A.; Derrick, P. J., Anal. Chem., 1986, 58, 165R-211R.
2. Dzidic, I.; Caroll, I.; Stillwell, R. N.; Horning, E. C., Anal. Chem., 1975, 47, 1308.
3. Thomson, B. A.; Iribne, J. V.; Dziedzic, P. J., Anal. Chem., 1982, 54, 2219-2224.
4. Morelli, J. J.; Hercules, D. M., 1986, Anal. Chem., in press.
5. Morelli, J. J.; Novak, F. P.; Hercules, D. M., "Comparison of LMS Obtained at Ambient Conditions vs. Sample Freezing" in: Secondary Ion Mass Spectrometry SIMS V, Benninghoven, A.; Colton, R. J.; Simons, D. S.; Werner, H. W., Ed., 1986, Springer-Verlag, New York, 551-554.
6. Holm, R.; Kampf, G.; Kirchner, D.; Heinen, H. J.; Meier, S., Anal. Chem., 1984, 56(4), 690-692.

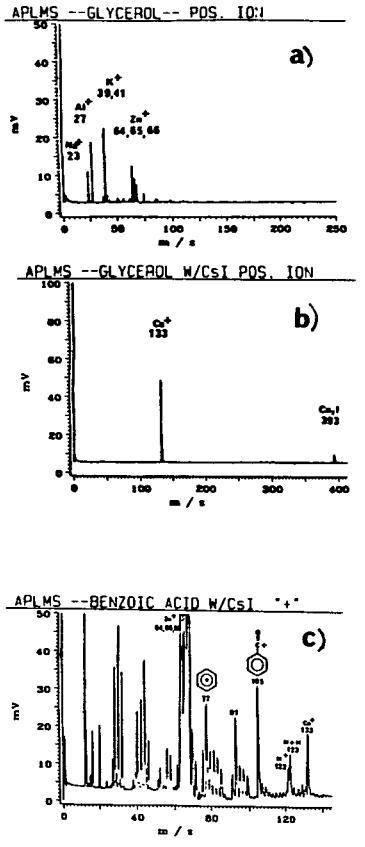

Figure 1:

APLMS Obtained from Glycerol Matrices

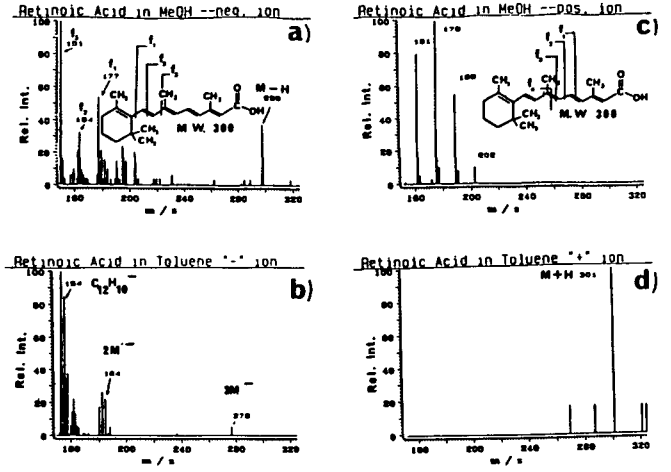

Figure 2: APLMS of Retinoic Acid in MeOH and Toluene

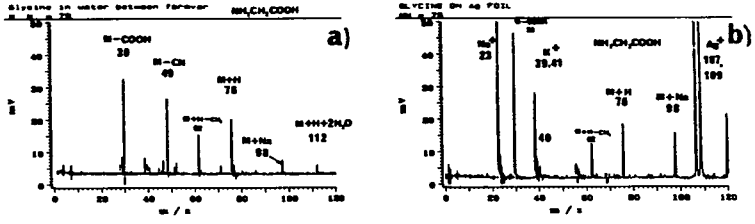

Figure 3: LMS of Glycine at Atmospheric Pressure vs. Vacuum Condition

UV Laser Induced Desorption-Ionization Studied with Prism Internal Reflection and Time-Of-Flight Mass Spectrometry

M. Yang, J. R. Millard, and J. P. Reilly
Department of Chemistry, Indiana University
Bloomington, IN 47405

Pulsed UV laser radiation has been used to ionize aromatic molecules adsorbed to thin metal films. In the prism internal reflection geometry the laser beam is refracted through a quartz prism and is incident on the metal film at the quartz-thin film interface. This ionization geometry eliminates gas phase ionization, thereby enabling the study of surface bound species and increasing the TOFMS mass resolution (1).

We have investigated laser ionization of benzene, phenol, and aniline adsorbed on gold, silver, and aluminum surfaces. At the wavelengths employed in this work, ionization of these aromatic species in the gas phase is a two-photon process. For molecules adsorbed on a metal surface, ionization may be a multiphoton process, but thermal ionization resulting from laser heating also becomes a possibility. To elucidate the mechanism of internal reflection surface ionization we have measured the ionization thresholds. In all cases these thresholds correspond to the two-photon ionization potentials, demonstrating that ion formation with this geometry is indeed a two-photon process. Results are shown in Figure 1 for aniline adsorbed on gold. Surface and gas phase ionization are both nonthermal, two-photon processes.

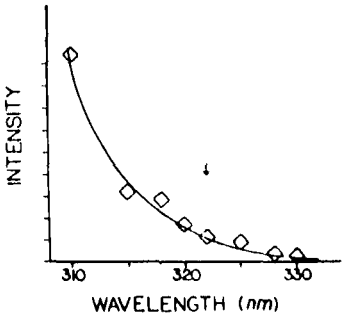

Figure 1: Threshold measurement for aniline on gold with surface ionization. The two photon I.P. indicated [2].

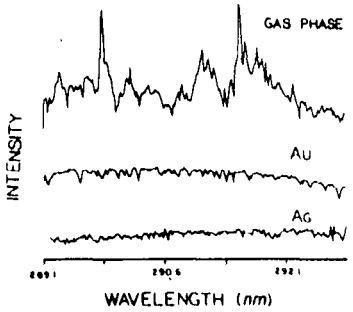

Figure 2: Wavelength dependence of aniline for gas phase and surface ionization from Au and Ag.

The multiphoton ionization cross section is greatly increased if resonant excitation of a real intermediate state is possible. Thus the wavelength dependence of ionization provides information on the energy levels of the molecule. Figure 2 compares the wavelength dependence of gas phase ionization to internal reflection surface ionization for aniline on silver and gold. The gas phase spectrum is in agreement with previously published results (3). However, no reproducible structure is found in the surface ionization spectra from either substrate metal. (The noise in the spectra is primarily due to laser power fluctuations.) This result indicates that the density of intermediate states is nearly constant over this wavelength region. The most probable explanation is that mixing of the molecular states with metal bands results in very broad, essentially continuous intermediate states. Although both ionization methods are multiphoton processes, surface ionization lacks the selectivity of gas phase ionization because of the broad intermediate states involved.

Ion flight times may be calculated for a given mass from the grid spacings and electric fields in the TOFMS. Measured ion flight times are in excellent agreement with the calculated values for gas phase ionization and external reflection surface ionization (reflection from the gas metal interface.) However, the flight times of ions created by internal reflection ionization are shorter than predicted.

From the observed shift in ion flight times we conclude that the ions have appreciable

initial kinetic energies. Analysis of the ion kinetic energies yields important information on the desorption mechanism. A series of mass spectral peaks have been converted to energy distributions and plotted in Figure 3. The resulting kinetic energy distributions are clearly nonthermal, and therefore the distribution is a function of applied potential in the acceleration region. This unexpected result may open new avenues in the study of surface-ion interactions and the kinetics of desorption. Possible desorption mechanisms accounting for the observed kinetic energy distribution and its dependence on acceleration potential will be discussed in a forthcoming publication (4).

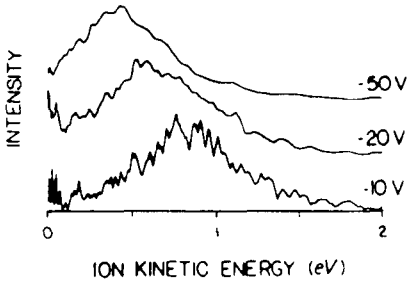

Figure 3. Kinetic energy distributions of aniline on gold in the internal reflection geometry. The FWHM is constant, but the mean varies with acceleration potential.

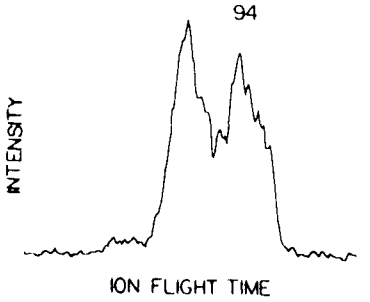

Figure 4. Ionization of phenol on a gold film with the external reflection geometry. Two distinct ion populations are evident. These may arise from different ion formation mechanisms.

When the laser is tuned to a wavelength just above the two photon ionization threshold, no gas phase ionization occurs. However, if the beam strikes the surface in the external reflection geometry two distinct surface ion peaks are observed at flight times corresponding to internal and external reflection ionization. A mass spectrum of phenol on gold taken under these conditions is shown in Figure 4. We postulate that these two populations of desorbed ion are formed by different mechanisms (4). The "fast" ions are formed on the surface and then desorbed. The "slow" ions arise from neutrals that are desorbed and then ionized above the surface. Because the beam intensity above the surface is extremely low, this mechanism is not possible with internal reflection ionization. Both mechanisms can occur simultaneously for external reflection, however, and hence two different peaks are observed. At higher photon energies where gas phase ionization can occur the desorption-ionization mechanism may predominate and essentially only one external peak is seen. Because neutral surface ions on metals is a rapid and efficient process, fewer "fast" ions are expected with external reflection ionization.

Surface ionization by prism internal reflection has been shown to be a two-photon process. The wavelength dependence exhibits no strong resonances, indicating that the intermediate states involved are broad and nearly continuous. Two mechanisms by which ions are formed and desorbed are postulated for external reflection. Only one of these mechanisms is possible in the internal reflection geometry. Ions formed by internal reflection ionization desorb from the surface by a nonthermal mechanism with kinetic energies that are a function of the applied field in the drawout region. In addition to being a useful ionization technique in mass spectrometry, this method is a potentially powerful method of probing the interactions of molecular species with surfaces.

References

1. M. Yang, J. R. Millard, and J. P. Reilly, Optics Communications, 55 (1985) 41.
2. Ionization potentials are from CRC Handbook of Chemistry and Physics, 60 (1980) E75.
3. J. C. D. Brand, D. R. Williams, and T. J. Cool, J. Molec. Spectrosc. 20 (1966) 359.
4. M. Yang, M. R. Millard, and J. P. Reilly, manuscript in preparation.

ALKALI SPECIFIC CATION ATTACHMENT AND FRAGMENTATION IN LDMS

B.Lindner, H.-W. Wollenweber, E.Th. Rietschel, and U.Seydel

Forschungsinstitut Borstel, D-2061 Borstel, W. Germany

Laser desorption mass spectrometry, even when utilized in a microprobe instrument like the LAMMA 500, has proven to be a valuable technique for obtaining information on molecular weight and chemical structure of complex thermolabile biomolecules /1/. With the LAMMA 500 instrument the pattern of a spectrum of a compound depends strongly on sample preparation, e.g. thickness, on laser irradiance and focussing conditions. Thus, from the same compound very simple spectra, containing mainly the abundant quasimolecular peak - representing soft ionization conditions - or highly complex spectra due to extreme fragmentation can be produced /2/.

Furthermore, the admixture of different cation species, which are normally added to enhance ionization via cation attachment, may influence the fragmentation behavior and the relative quasimolecular ion yield significantly.

As an example in fig.1 the positive ion LD mass spectra of dephosphorylated free lipid A from Salmonella.minnesota RE (R595) lipopolysaccharide mixed with equimolar amounts of CsI (top) or NaI (bottom) is given. The included chemical structure /1/ shows the inherent biological heterogeneity originating from the presence (M) or absence (M*) of a palmitic fatty acid residue at the reducing end.

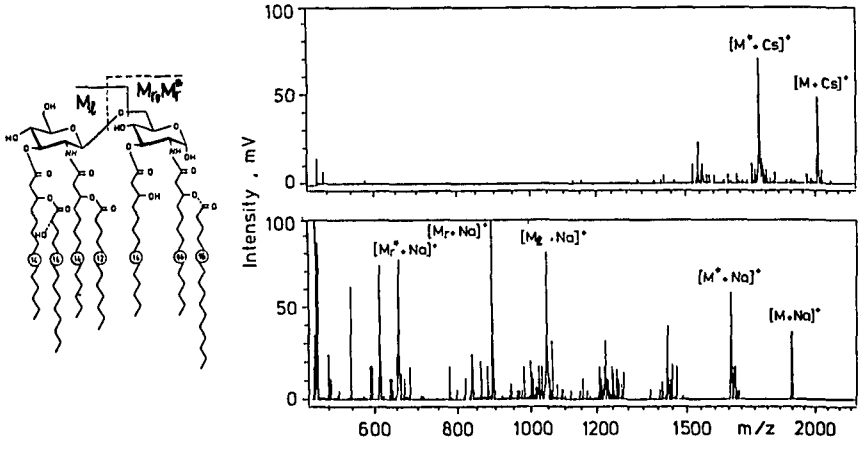

Fig.1: Positive ion LD mass spectra of dephosphorylated free lipid A from S.min. RE (R595) equimolarly mixed with CsI (top) and NaI (bottom)

In the upper spectrum (CsI) only the intense peaks of the two molecular species and low intensity peaks from the cleavage of an additional fatty acid residue are seen. The lower spectrum (NaI) is much more complex exhibiting additional prominent peaks which originate from the cleavage of the glycosidic bond. For the investigated classes of compounds (lipids and oligosaccharides) the highest ratios of quasimolecular to fragment ion intensities were obtained from mixtures with CsI, decreasing in the sequence CsI, RbI, KI, NaI, LiI.

It must be pointed out, however, that this cation specific fragmentation can not be generalized for all classes of compounds. Thus, for instance, the admixture of NaI to gramicidin yields only the quasimolecular peak.

Another effect concerning the cation induced fragmentation is depicted in fig.2 showing, for stachyose, the influence of the amount of alkali salt added. Higher salt concentrations obviously lead to increased fragmentation.

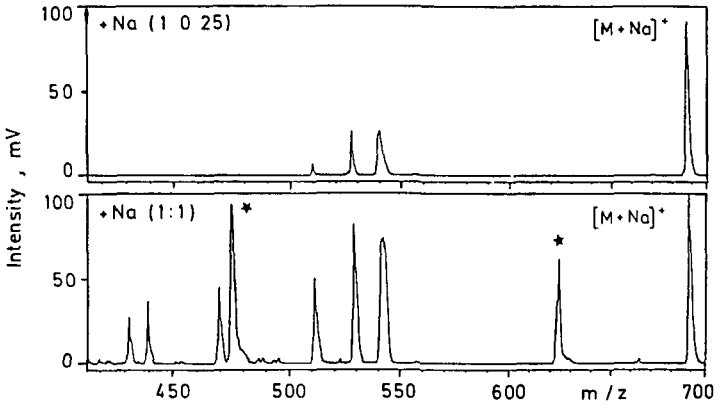

Fig.2: Positive ion LD mass spectra of stachyose mixed with NaI at different molar ratios; 1 : 0.25 (top) , 1 : 2 (bottom). * ; cluster ions of the type $[(NaI)_nNa]^+$

These findings emphasize the importance of a consideration of the possible influence of cation specific fragmentation for the interpretation of mass spectra, particularly from natural isolates.

1. U. Seydel, B. Lindner, H.-W. Wollenweber, E.Th. Rietschel, Eur. J. Biochem.145,505(1984)
2. B.Lindner and U.Seydel, Anal. Chem.57,895(1985)

A high resolution time-of-flight mass spectrometer using laser vaporization and resonance-enhanced multi-photon ionisation

R.Frey, G.Weiß, H.Kaminski and M.Weiß

Bruker-Franzen Analytik GmbH,
Kattenturmer Heerstraße 122
D-2800 Bremen 61

Bruker Analytische Meßtechnik GmbH
Siberstreifen
D-7512 Rheinstetten 4/Fo.

U.Boesl, J.Grotemeyer, K.Walter and E.W.Schlag

Inst. f. Physikal. Chemie, Technische Universität München
Lichtenbergstr.4
D-8046 Garching

The combination of a time-of-flight mass spectrometer with an ion source based on resonance-enhanced multi-photon ionization has been demontrated to be a very efficient tool for the analysis of volatile substances (1).

Our instrument consists of a laser ion source including a tunable laser system for resonant laser ionization, direct inlet systems for gases, liquids and solids, a high resolution time-of-flight mass analyzer with its new gridless ion reflector, a fast data acquisition hardware and a data system for data processing and instrument control (2). For the vaporization of solid samples presented below a small IR-laser was added.

The following features make the system interesting for many applications.

* complete mass spectrum with a single ionization pulse
* many mass spectra per second
* in principle unlimited mass range
* mass resolution > 5000
* selective ionization of a single component of a complex mixture
* soft ionization for simple molecular weight determination
* hard ionization for structure analysis

The high mass resolution of our instrument is due to a new gridless ion reflector and to the laser ion source with its well defined place and time of ionization. The resolution is limited mainly by the laser pulse duration of 5 nsec. Recently a mass resolution of 10,000 has been achieved with the same time-of-flight analyzer using 1.5 nsec laser pulses and a cold supersonic beam sample inlet (3).

With the wavelength selectivity of the resonance-enhanced multi-photon ionization the system offers quasi a two-dimensional analysis method. In fig.1 sections of mass spectra of a mixture of fluorobenzene (F, M=96.038) and 2,5- dimethyl-furane (D, M=96.058) are shown which demonstrate the high mass resolution and the selective ionization. The two compounds of the same nominal mass 96 can be separated due to the mass resolution of 6500 (a.) using 5 nsec laser pulses. In addition selective ionization of one or the other compound can be achieved by choice of the wavelength (b.,c.).

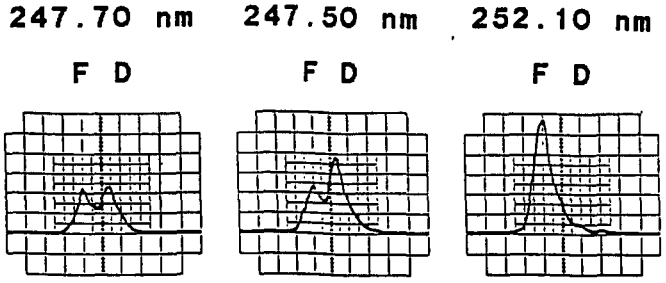

Fig.1

To extend the applicability of the system to solid samples these must be vaporized non-destructively before analysis.
Adequate to the pulsed ionization is a pulsed desorption. Thus we irradiate the sample in the ion source by IR-laser pulses. In the case of atoms the pulsed desorption by means of fast ions or laser pulses followed by resonant or non-resonant laser ionization has already proved in the literature to be a highly sensitive analytical tool.
In order to detect intact molecular ions we use laser pulses of moderate power for the desorption (10^4 - 10^5 W/cm^2) as well as for the following resonant ionization (10^9 - 10^6 W/cm^2).
As an example mass spectra of butyl-PBD (M=354 amu) are shown in fig.2, with soft (a.) and hard (b.) ionization.

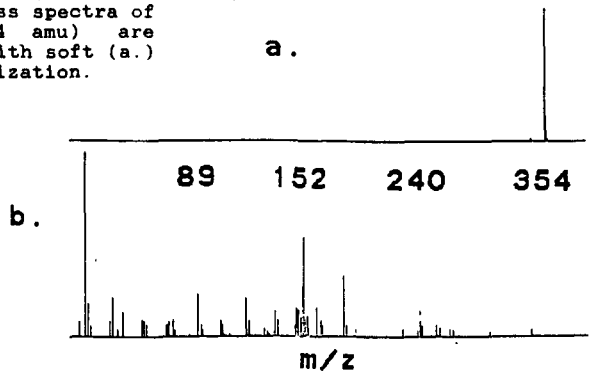

Fig.2

Due to the pulsed vaporization only small amounts of sample are needed for analysis. The process is of thermal nature, but reduced thermal degradation and less damage of the sample can be achieved. Whereas the selectivity of the ionization is limited due to broader spectral structures at higher temperatures the capability to soft or hard ionization is still maintained. This method may be appropriate for a large number of solids.
In order to analyse very labile molecules a further step will be included namely a cooling process after the pulsed desorption and before the resonant laser ionization, such that any thermal destruction will be prohibited (4).

References

1. H.J.Neusser, U.Boesl, R.Weinkauf and E.W.Schlag, I.J.Mass Spectrom. Ion Proc. 60, 147 (1984)
2. R.Frey, G.Weiss, H.Kamiński and E.W.Schlag Z.f.Naturf.40, 1349 (1985)
3. U.Boesl, K.Walter, J.Grotemeyer and E.W.Schlag, I.J.Mass Spectr. Ion Proc.submitted
4. J.Grotemeyer, U.Boesl, K.Walter and E.W.Schlag , Org.Mass Spectrom. submitted

"ELECTRON CAPTURE AGENTS AS MODIFIERS FOR INCREASED CIMS SENSITIVITY":

Frank Hatch, Gordon Hansen, Keith McKellop, Philip Epstein;
Boehringer Ingelheim Pharmaceuticals, Inc.
90 East Ridge Road, Ridgefield, CT 06877

In 1984 B. Munson et al.[1] reported the observation that small amounts of electron capture agents added to chemical ionization reagent gas systems could increase the extent of conversion of ion/molecule reactions and increase CIMS sensitivity. Further, in 1983 M. Siegel[2] published a theoretical treatment of the rate equations governing the formation and elimination of positive and negative ions under conventional CIMS operation. Siegel concluded that in order to maximize positive ion sensitivity negative ion sensitivity must be minimized. Both publications have significant consequences for increased sensitivity in positive ion CIMS analysis.

Addition of electron capture agents to the CI reagent gas effectively converts the free thermal electron population to large negative ions. These electron capture modifiers compete with sample compounds which may undergo resonance or dissociative electron capture. The observed increase in positive ion CIMS sensitivity, may occur by three mechanisms: 1) a decrease in the positive ion/negative ion ambipolar diffusion rate increasing the residence time of ions in the source, 2) minimized positive ion/e^- recombination rates and 3) elimination of competitive ionization paths especially for compounds with significant electron affinities. What is generally not appreciated is the fact that many non-halogenated compounds have significant electron affinities.[3]

Experimental

All experiments were carried out on a Finnigan 4023 GC/MS/DS which has been modified for CIMS operation at 2.0 torr by reduction of the electron entrance and ion exit aperture to 1 mm. The Finnigan 9610 GC was replaced with a Carlo Erba 5300 gas chromatograph. Normal CIMS parameters include: electron multiplier 1400 v, dynode 3000 v, electron energy 190 v, emission current 0.1 ma, source pressure 2.0 torr, temperature 300°C. Electron capture agents were introduced through the calibration inlet.

Results

Decanoic acid methyl ester (1 pg) exhibits a 4 fold increase in signal/noise (S/N) when 1% perfluorotributylamine (PFTBA) is added to methane at 1.5 torr. This compound has a minimal electron affinity so mechanism 3 can be ignored. It is difficult to distinguish between the contributions of mechanisms 1 and 2 but they should affect all compounds equally.

Several phenoxyaminopropane-TMS derivatives were observed to undergo an 8-10 fold increase in positive ion sensitivity with 10% perfluorohexane (PFH) in ammonia at 2.0 torr. This increase was observed for both proton transfer reaction and NH_4^+ adduct ion formation. These compounds were observed to have some electron capture negative ion response which decrease on addition of the PFH.

Compounds with a strong electrophore should exhibit the largest increase in positive ion sensitivity when electron capture modifiers are added to the CI plasma. Also, modifiers with high electron attachment rate constants should be most effective in providing a minimum e^- population in the CI plasma. This theory was investigated by the injection of 20 pg amounts of a tetrafluorobenzyl-dichloroanilino derivative, Figure 1, which has both a high proton affinity to ensure reaction with NH_4^+ and a strong electron capture efficiency. The relative response observed for this compound by GC/CIMS with (a) NH_3 2.0 torr, (b) NH_3 + 5% PFTBA 2.0 torr and (c) NH_3 + 2% octafluorotoluene (OFT) are given in Figure 1. The sensitivity (S/N) increases by a factor of 4 and 20 for PFTBA and OFT respectively. The electron attachment rate constant for OFT is 2.2×10^{-7} cm/sec, essentially identical to CCl_4.

Electron capture responses in general are well known to be dependent on the thermal electron population and easily saturable at the nanogram level. Therefore any observed positive ion CIMS increase in sensitivity will be dependent on sample size. In Table 1 we show the normalized responses for injections of the tetrafluorobenzyl-dichloroanilino derivative at the 0.5 ng through 10 ng level. The observed increase in sensitivity varies greatly with sample size, clearly demonstrating the saturation of the electron capture response. The normalized values for the 0.5-10 ng injections demonstrate that we are not in effect increasing sensitivity as much as we are preventing a decrease in sensitivity through "sample depletion" as concluded by Siegel. Similar patterns were observed for the other compounds discussed in this presentation. One final note concerns the description of the well known "carrier effect" observed in quantitative GC/MS analysis. It is very possible that 10-100 fold excess of "carrier" or labelled internal standard may be saturating the free electron population and preventing a decrease in positive ion CIMS sensitivity. This mechanism may be more significant than the assumed adsorption losses on the well deactivated chromatographic columns available today.

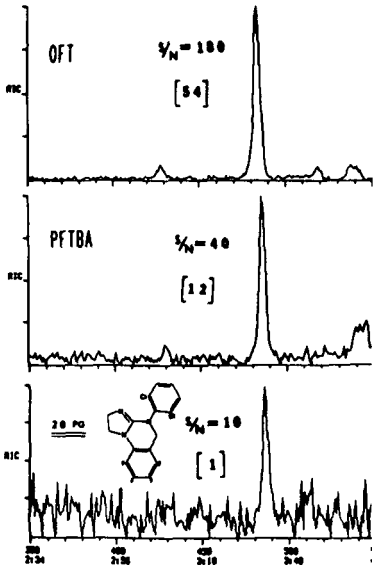

Clonidine-PFB Injected (ng)	Normalized Response(10ng)		EC Related Increase
	NH3	+PFTBA	
10	10.0	10.0	3.7X
5	4.0	4.9	6.7X
1	0.25	1.1	23X
0.5	0.01	0.6	26X

Table 1. Normalized (10 ng) response for the tetrafluorobenzyl-dichloroanilino derivative, with and without PFTBA.

Figure 1. Relative SIM response S/N [Peak Area] for 20 pg injections; NH_3 at 2.0 torr and NH_3 at 2.0 torr plus PFTBA or OFT

1) P. Rudewicz, Ta-min Fing, K. Blom and B. Munson; Anal. Chem. 1984, 56, 2610.
2) M. Siegel, Inter. J. of Mass Spectrom. and Ion Physics, 1983, 46, 325.
3) J. Vessman, J. of Chromatography 1980, 184, 313.

UNUSUAL HIGH PRESSURE ELECTRON CAPTURE MASS SPECTRA OF FLUORANIL AND CHLORANIL

L. J. Sears and E. P. Grimsrud
Montana State University
Bozeman, Montana 59717.

The technique of chemical ionization mass spectrometry, where positive or negative reagent ions are used for the ionization of analyte molecules in about one torr of buffer gas, has undergone continuous use and development since its conception about twenty years ago. Generally, the spectra produced by CI has been explainable in terms of the primary ion-molecule reactions which occur between the set of reagent ions present and the sample molecule. On the other hand, when negative ion spectra are produced by the reactions of thermalized electrons under ordinary CH_4/CI conditions, observations are often not explainable in terms of the primary electron capture reaction which might have been expected. We describe here a model of the high pressure electron capture mass spectrometry (HPECMS) ion source which suggests that unusual ions, produced by processes other than the primary EC reactions, are to be expected in the HPEC mass spectra of certain compounds. What are thought to be examples of the qualitative (spectra) and quantitative (relative sensitivities) implications of this model will then be described.

A model showing the most important reactions of ions, electrons, and the analyte expected to occur in a HPECMS ion source are shown in Figure 1. In a common CH_4/CI source ($I_{E\ beam} \simeq 100\ \mu A$, P = 1 torr), the density of reagent positive ions (CH_5^+ and $C_2H_5^+$) and that of thermal electrons will be about 10^{10} particles/cc.(1) Therefore, in addition to the primary reactions of CH_5^+ (and $C_2H_5^+$) and electrons with the analytes, MX, recombination reactions between position ions and electrons and between positive ions and negative ions will also occur as shown. Because of the high ion and electron densities, the rates of the recombination reactions are exceedingly fast as shown. In Figure 1 the lifetimes of various species against the processes indicated have been calculated assuming the following approximate rate coefficients: k(EC) $\simeq 1 \times 10^{-6}$ cc/s, k (ion-molecule) = 1×10^{-9} cc/s, k (electron recombination) = 3×10^{-6} cc/s and k (negative ion recombination) = 1×10^{-6}.

In Figure 1 the formation of positive and negative unusual ions, Z_i^+ and Z_i^-, is shown to be possible through continued reactions of the neutrals formed by earlier recombination reactions. However, the formation of unusual ions, Z_i^+, through the ion-molecule reaction route is not likely to generate ions of major intensity because their formation requires much more time (60 ms) than the residence time (10 ms) of neutrals, including MX, in the source. For this reason, CIMS spectra generated by ion-molecule reactions have been interpretable largely by consideration of the primary reactions of the reagent ions, only.

Figure 1 indicates that if electrons are the ionizing reagent, the further EC reactions of recombination-generated neutrals can become much more important. Due to the fact that electron capture can be about two orders of magnitude faster than ion-molecule reactions, only about 0.6 ms may be required to form unusual ion, Z_i^-. Even ions Z_j^- and Z_k^- can be formed very rapidly provided the intermediate recombination-generated neutrals retain high electron capture capabilities. In our studies of HPECMS we have made several experimental observations which seem to be most readily explained in terms of the model in Figure 1.

The HPECMS spectra of chloranil and fluoranil are shown in Figure 2. Unexpected ions, due to $(M+H-X)^-$ and $(M-2X)^-$ where X = F or Cl are observed. Similar ions of the type $(M + H_n\text{-}Cl_n)^-$ in the HPECMS spectra of polychlorinated molecules have also been reported by Stemmler and Hites (2). Separate experiments(3) using a high pressure source with $I_{E\ beam} = 10^{-11}$ A produced only the M^- ion of fluoranil and chloranil in methane. The predominance of the unusual ions shown in Figure 2 is not removed by changes in source temperature between 100 and 300°C. No change in spectra was also caused by coverage of the source walls with aluminum foil. Figure 3 shows the normalized single ion reconstructed chromatograms of a GC-HPECMS analysis of fluoranil. It is seen that the two unusual ions tend to persist in time after fluoranil has passed through the cell. These observations are consistent with the reaction sequence shown in Figure 4.

Another observation of a quantitative nature concerns the relative sensitivity of HPECMS to the two compounds, perfluoromethylcyclohexane (C_7F_{14}) and para fluoronitrobenzene (FNB). The ratio of electron capture rate constants of C_7F_{14} and FNB is known to be 4:1.(3) In

Figure 5, the relative HPECMS responses to C_7F_{14}, FNB and fluoranil are shown. The sensitivity to C_7F_{14} is almost two orders of magnitude greater than to FNB. For both of these, the only ion observed is the parent molecular negative ion. We suggest that the explanation for these observations is the following: after electron capture by C_7F_{14}, the same original molecule is regenerated by the recombination of $C_7F_{14}^-$ with positive ions. Thus, a cyclic process occurs in which C_7F_{14} is not consumed. The recombination of the M^- ion of FNB, on the other hand, appears to produce neutrals which are no longer EC-active and FNB is destroyed by electron capture. Our conclusion concerning C_7F_{14} is also supported by studies in our laboratory using electron capture detectors of various designs which operate at atmospheric pressure. In these experiments, a "hyper-coulometric" response to C_7F_{14} is observed - that is, many electrons per molecule of C_7F_{14} are lost as C_7F_{14} passes through the detector. Yet, the only negative ion observed is $C_7F_{14}^-$.

The theoretical points illustrated in Figure 1 were generated from basic considerations of gas phase ion dynamics. Some support for the model has been provided here from two sets of observations by HPECMS. It seems likely that other observations by HPECMS might also be explainable in terms of this model. Unfortunately, relatively little is known concerning recombination reactions between positive and negative ions. Nevertheless, this study suggests that they can be very important in causing both detrimental and beneficial effects in HPECMS.

(1) Siegel, Practical Spectroscopy Series, Vol. 3, Merrit and McEwen, Eds., Marcel Dekker, 1980, p. 297.
(2) Stemmler and Hites, Anal. Chem., 57 (1985) 684.
(3) Grimsrud, Caldwell, Chowdhury, and Kebarle, J. Am. Chem. Soc., 107 (1985) 4627.

Figure 1. Model

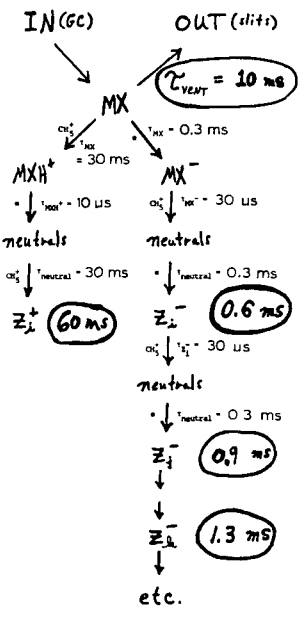

Figure 2. HPECMS, 150° C, 0.3 torr CH_4

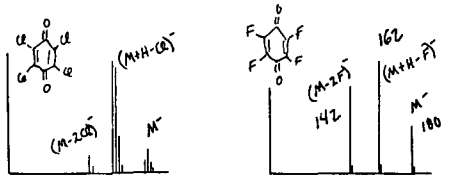

Figure 3. Fluoranil

Single ion reconstructed GC's.

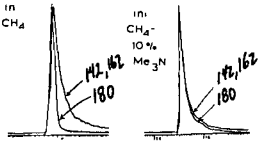

Figure 4. Explanation

Fluoranil and Chloranil

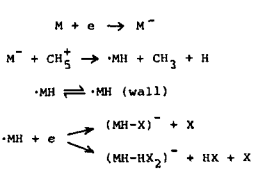

Figure 5. HPECMS Total Ion Responses

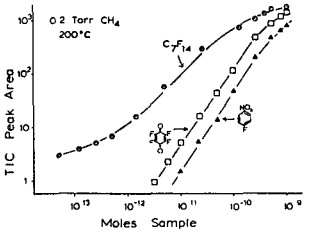

ELECTROPHILIC MODIFIER GASES IN CI: ENHANCEMENT OF THE POSITIVE CI RESPONSES OF ANALYTES IN TRACE ANALYSIS

J.V. Johnson and R.A. Yost
Chemistry Department, University of Florida, Gainesville, FL 32611

The capability to modify the gas-phase chemistry occurring in a chemical ionization (CI) source permits a mass spectrometrist to tailor the ionization to his needs. With the introduction of a relatively small but constant level of an electrophilic compound, e.g. perfluorotributylamine, PFTBA, and CCl_4 (the electrophilic modifier gas), into a methane or ammonia CI source, it has been possible to enhance the $(M+H)^+$ positive CI (PCI) response of some analytes by one or two orders of magnitude [1-3]. Thus, it should be possible to exploit this phenomenon in trace analysis to lower the limit of detection for an analyte. The specific objectives were: (1) to determine the mechanism by which the enhancement of the PCI signal occurs, (2) to examine the generality of the use of electrophilic modifier gases with different CI reagent gases, and (3) to exploit this PCI enhancing effect to lower the limit of detection for the determination of lysergic acid, diethylamide (LSD).

All data were collected with a Finnigan MAT TSQ45 GC/MS/MS. Samples were introduced either via solids probe, a 15" packed column [2], a 15-meter, 0.25 mm i.d. SE-54 fused silica open tubular (FSOT) column introduced directly into the ion source, or a 0.53 mm i.d. DB-5 Megabore FSOT column. In order to reduce the flow rate, the Megabore column was interfaced to a 1-meter piece of 0.25 mm i.d. DB-5 FSOT column which was then introduced directly into the ion source. When performing methane CI with the Megabore and packed columns, methane was used as a carrier gas and the column headpressure was adjusted to give an indicated ion source pressure between 0.6 and 1.0 torr. With the 15-meter FSOT column, helium was always used as the carrier gas with flow rates of ca. 50 cm/s, giving an ion source pressure of ca. 0.03 torr. Methane or ammonia was then added as a makeup gas to give indicated ion source pressures of ca. 1.0 and 0.4 torr, respectively. The modifier gases PFTBA and CCl_4 were introduced directly into the ion source via a solenoid-actuated needle valve.

In the determination of the heptafluorobutyryl (HFB) derivative of tryptoline (TLN-HFB), we had obtained limits of detection of 0.11 and 430 picograms for methane electron capture negative chemical ionization (ECNCI) and methane postive CI (PCI) selected reaction monitoring (SRM), respectively, with sample introduction via a 15" packed column (retention time was ca. 45 s) [2]. However, with the analysis of crude brain extracts which had been derivatized with heptafluorobutyryl imidazole, quenching of the ECNCI-SRM ion signal by a factor of 6 and enhancement of the PCI-SRM signal by a factor of 23 occured. We attributed the quenching of the ECNCI signal to the competition for and depletion of the limited thermal electron population by other compounds which were coeluting with TLN-HFB. The enhancement of the PCI signal was then attributed to the increased abundance of neutral TLN-HFB molecules which could then react with the methane positive reagent ions. As the enhancement of the PCI signal by the components of the brain extracts was not very reproducible, a constant amount of the highly electrophilic PFTBA was admitted directly into the source (no observable change in the ion source pressure was noted). This permitted the PCI-SRM limit of detection for the TLN-HFB to be lowered by a factor of ca. 15 as compared to without having the PFTBA in the source.

Munson et al. [3] attribute the enhancement effect of electrophilic substances to an increased resident time and thus reaction time due to the presence of negative ions. Upon reexamining their work, but observing both the PCI and ECNCI signals, it was determined that in all cases, the ECNCI signal of these compounds was reduced by a factor of 1-10 times and, with the exception of iodobenzene, the PCI signal was enhanced, usually by a factor of 6-10 times with the addition of PFTBA (we are currently unsure why the reduction in the PCI signal of iodobenzene occured) (Table 1). When the absolute changes in the intensities of the negative and positive ions are considered and assuming equal electron multiplier response for negative and positive ions, the enhanment of the PCI signal cannot be solely attributed to the change in abundance of neutral molecules resulting from the quenching of the negative ion production.

Table 1. Effect of PFTBA on Positive and Negative CI of Various Compounds

Compound	PCI (w)/(w/o)	ECNCI (w/o)/(w)	|Δ PCI|/|Δ NCI|	PCI/NCI (w)	PCI/NCI (w/o)
$CH_3-C_6H_5$	10	8.5	17	1.7	143
$F-C_6H_5$	6.3	4.4	12	1.8	49
$Cl-C_6H_5$	6.9	6.8	12	1.8	83
$Br-C_6H_5$	5.9	7.0	8.9	1.6	64
$I-C_6H_5$	0.48	1.3	0.70	0.28	0.17
LSD (10 ng)	6.0	3.9	20	3.0	75
LSD (100 ng)	7.3	4.1	24	2.9	86
TLN-HFB	17	9.4	0.018	0.00098	0.16

Siegel and Fite [4] have shown that the major losses of ions in the ion source occurs mainly via recombination of positive and negative ions, recombination of positive ions and electrons, and diffusion of all ions to the source walls. As the recombination rates of positive ion and negative ions are within an order of magnitude slower than those of positive ions and electrons, and as the ambipolar diffusion constant of a positive ion-negative ion-dominated population is less than that for a positive ion-electron-dominated population, an increase in the positive ion abundance would be expected with an increase in negative ions. When PFTBA was gradually admitted into the ion source via a needle valve, the abundance of all the reagent ions in both NH_3 and CH_4 PCI were found to increase by 2-5 times. As the enhancement of the PCI ions of most of the examined compounds was equivalent to this observed increase in the PCI reagent ions, we then concur with Munson et al. in concluding that the major enhancement of the PCI signal by the presence of electrophilic compounds appears to be due to the reduction in the ion losses by recombinations and diffusion to the ion source walls. However, the quenching of the ECNCI of the analyte molecules to cause an increase in their ionization via PCI, may contribute to a substanial degree for some compounds, e.g. TLN-HFB.

In the trace analysis of TLN-HFB via PFTBA-modified CH_4 PCI-SRM, it was observed that the degree of enhancement which occurs is not constant but decreases with decreasing concentration. This mandated the use of internal standards and more specifically, the use of deuterated internal standards. We evaluated this technique for the determination of LSD standards with d_{10}-LSD as an internal standard and were able to reduce the limit of detection from ca. 80 pg to ca. 40 pg (amount injected on the Megabore column, described above). The calibration curve for the area ratio (A0/A10) versus the amount ratio (d0/d10) was linear from the limit of detection to 50 ng d_0-LSD injected on column.

Although PFTBA has been used in the studies above, preliminary investigations showed that CCl_4 may offer additional advantages in being more electrophilic than PFTBA and thus produces a greater enhancing effect on the PCI signal. In addition, it offers the advantage of forming only $(M+H-HCl)^+$ ions of low abundance and of low mass in the PCI and thus should be less likely to interfere with any analyte ions.

[1] Foltz, R.L. Paper presented at the 31st Annual Conference on Mass Spectrometry and Allied Topics, Boston, MA, May 8-13, 1983.

[2] Johnson, J.V.; Yost, R.A.; Faull, K.F. Anal. Chem. 1984, 56, 1655-1661.

[3] Rudewicz, P.; Feng, T.; Blom, K.; Munson, B. Anal. Chem. 1984, 56, 2610-2611.

[4] Siegel, M.W.; Fite, W.L. J. Phys. Chem. 1976, 80, 2871.

DETECTION OF $(M+Cl)^-$ IONS UNDER CONDITIONS FOR
ELECTRON CAPTURE NEGATIVE CHEMICAL IONIZATION (EC-NCI) MASS SPECTROMETRY

Kassel, D. B.*, Kayganich, K. A.*, and Watson, J. T.**
Departments of Chemistry* and Biochemistry*
Michigan State University
East Lansing, MI, 48824

Substantial enhancement of negative ions consisting of either $(M-H)^-$ or $(M+Cl)^-$ of several classes of analyte molecules (M) has been observed following pretreatment of the ion source of an HP/5985 quadrupole GC/MS with CCl_4. A short-lived (5 minutes or less) introduction of CCl_4 is used for the purpose of generating low mass anions for proper tuning of the mass spectrometer for the analysis of negative ions. Once this tuning procedure has been completed, the CCl_4 is pumped away and the conditions employed for EC-NCI are those conventionally used; methane at 1 torr. Subsequent introduction of any of several different types of analyte results in the observation of a mass spectrum containing a substantial, if not predominant, $(M+Cl)^-$ peak. The two spectra shown in Figure 1 (a) and (b) obtained for Aspartic Acid-trifluoroacyl-n-butyl ester (TAB) prior to, and after exposure of the ion source to CCl_4 illustrate the phenomenon.

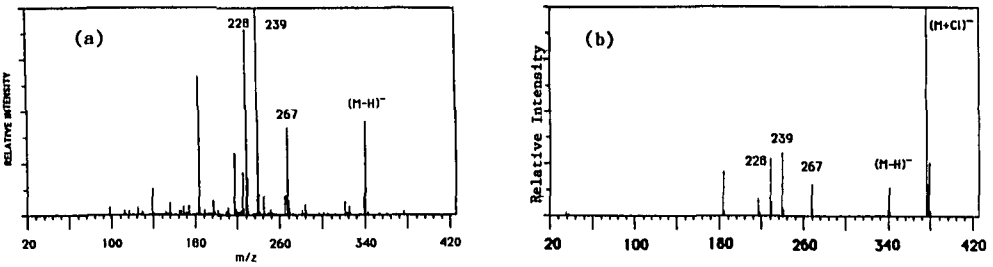

Figure 1 (a). Conventional EC-NCI (CCl_4 pressure = 300 mtorr) mass spectrum of Aspartic Acid-TAB. (b). Mass spectrum of the same compound following exposure of the ion source to CCl_4 (1×10^{-4} torr) for approximately 5 minutes prior to introduction of the sample on column.

In addition to an intense $(M+Cl)^-$ ion, an overall signal enhancement of all analyte ions in the mass spectrum following pretreatment of the ion source with CCl_4 is observed relative to the conventional EC-NCI mass spectrum, shown in Figure 1 (a). A 5- to 10-fold increase in relative response has been observed for a wide range of compounds, including amino acid-TAB derivatives, the trimethylsilyl (TMS) derivatives of organic acids, and others. The formation of $(M+Cl)^-$ may be observed up to several hours following pretreatment of the ion source. However, the intensity of this anion diminishes over time; furthermore, this diminution increases with ion source temperature.

The EC-NCI conditions described here are significantly different from those employed by Dougherty (1), and others (2), in which $(M+Cl^-)$ adducts of organic compounds are formed. Unlike the Dougherty mass spectra, we observe only very low levels of Cl^- ions. Furthermore, no dependency on the formation of analyte anions from the Cl^- species is observed. In addition, the mass spectrum (Figure 2) of Aspartic Acid-TAB by CCl_4-NCI in which CCl_4 is used as the reagent gas (similar to Dougherty's use of CH_2Cl_2) is significantly different from the one (Figure 1 b) obtained by our CCl_4-pretreatment method .

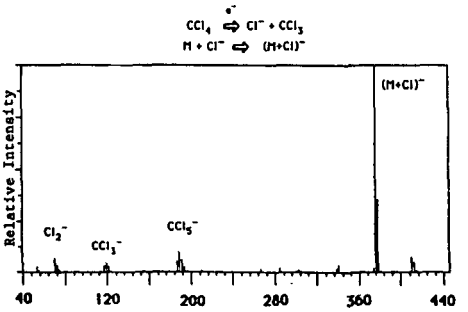

Figure 2. CCl_4-NCI mass spectrum of Aspartic Acid-TAB (CCl_4 pressure = 1 torr).

We propose that the $(M+Cl)^-$ ion formed following pretreatment of the ion source with low levels of CCl_4 arises from formation of an $(M+Cl)\cdot$ radical, followed by thermal electron capture. Since only very low levels of gas phase Cl^- ions are observed by this method, we suggest that $Cl\cdot$ radicals bound to the ion source walls are the source of Cl in the production of intense $(M+Cl)^-$ ions. Jones, et al. (3) have reported the presence of Cl radicals on Fe surfaces, following treatment with CCl_4. For unsaturated organic compounds, there appears to be sufficient interaction between analyte, $Cl\cdot$ radicals and the source volume surface for production of very intense $(M+Cl)^-$ ions. This interaction not only provides a convenient mass marker for rapid molecular weight determinations, but our preliminary results indicate that a several-fold increase in analyte response by EC-NCI-MS may be obtained.

Acknowledgement: This work was supported in part by a grant (RR-00480) from the Biotechnology Research Program, Division of Research Resources, National Institutes of Health.

1. Dougherty, R. C., Roberts, J. D., and Biros, F. J. Anal. Chem., 47: 54, (1975).

2. Tannebaum, H. P., Roberts, J. D., and Dougherty, R. C. Anal. Chem., 47: 49, (1975).

3. Jones, R. G. Surface Science, 88: 367, (1979).

MATRIXLESS FAST ATOM BOMBARDMENT MASS SPECTRAL CHARACTERIZATION OF DIAZENIUM AND HYDRAZONIUM CATIONIC COMPOUNDS[1]

Clifton G. Sanders, Thomas R. Sharp and Evan L. Allred
Department of Chemistry, The University of Utah, Salt Lake City, Utah 84112, U.S.A.

FAB-MS of compounds dispersed in a suitable matrix has become an important technique for structure elucidation of large molecular weight (>300) organic and organometallic compounds. However, the observation that FAB mass spectra of inorganic salts - e.g. the alkali metal halides - can be observed from dry, matrixless preparations suggested to us that this procedure might prove suitable for the study of small molecular weight organic cations. In connection with our research on the synthesis and chemistry of acyclic[6] and small ring trialkyl diazenium salts, we attempted to record the mass spectra of the structures shown in the accompanying figures. Our observations suggest this technique is a direct and simple spectroscopic method for not only generating mass spectra for structural characterization, but also for differentiating between isomers.

Compounds were synthesized by procedures reported elsewhere[2,3]. A sample of each compound was dissolved in a small amount of acetone, and applied to a clean FAB target. Solvent was evaporated in air. Final traces were pumped away as the FAB probe was inserted into the mass spectrometer -- a VG Analytical 7070-E operating at +5 KV, resolving power 1000, scanning over m/z 10-300 at 20 sec/decade. Samples were bombarded with 6.0 - 7.0 KeV Ar^{o} from an Ion Tech gun operated at appx. 1.0 - 1.5 mAmp. Repetitive scan spectra were recorded by a VG DS2050 datasystem, mass calibrated with the cluster ion spectrum of H_2SO_4[4,5].

In the spectra of cations of 1 and 2, the "molecular ions" (m/z 155) are easily recognized. The primary fragmentation consists of neutral loss of C_4H_8, resulting from rearrangement of hydrogen from the t-butyl group onto the ring. The spectrum of ring-deuterated 2 (not shown) supports this conclusion. The primary difference in the spectra of 1 and 2 is the total ion current percentage of the "molecular ion" (m/z 155) and first fragment ion (m/z 99) signals. Structure 1 is much more stable towards desorption and mass analysis than structure 2, although solution chemistry indicates that 2 is more stable than 1 in condensed phase.

Additional structures 3, 4 and 5 were examined. All produce readily interpretable spectra consistent with the indicated structures. Acyclic structure 3 (mol. wt. 171) shows notable stability as well as what appears to be a characteristic C_4H_8 neutral loss. Bicyclic structure 4 (mol. wt. 153) shows the least stability toward the FAB experiment of all, indicated by the low molecular ion signal. Structure 5 is a reduced form of structures 1 and 2, having a cation m.w. of 157. The mass spectrum shows the appropriate m/z 157 molecular ion, but the principal fragmentation is loss of H_2 to generate the double bond-containing compound. Comparison of the spectral details for 5 with those of 1 and 2 indicates that H_2 loss produces the N-N double bond isomer, consistent with the fact that 1 is mass spectrometrically more stable than 2.

Overall signal intensities observed from samples prepared in this manner were significantly less, by at least one order of magnitude, than those typically observed for a matrix-dispersed sample. However, the signals owing to the compounds of interest were easily and reproducibly observed, and the spectra were relatively free of background mass peaks because of the absence of a matrix. A qualitative evaluation of the "signal to noise" ratio and the ability to distinguish sample mass peaks from background can be seen in the figures. The spectra shown have not been subjected to background subtraction or any other spectral enhancement technique.

Comparison of spectra of the perchlorate and iodide salts indicated that there were no major differences, within the limits of normal relative intensity variations expected of repetitively scanned mass spectra. An important point to note is that the samples have never been exposed to extremes of temperature. Evaporation of the deposition solvent took place at room temperature, and the FAB ion source is operated at ambient temperatures, in contrast to the typical electron impact or chemical ionization source which operates at 150°C and above. This is an important consideration when dealing with compounds such as these, which are thermally unstable or prone to thermally induced rearrangements.

These observation make clear the fact that FAB mass spectral observations on small molecular weight organic cations, utilizing the matrixless sample preparation technique, can be invaluable in making structure assignments of these types of compounds, and should become a standard technique in the organic cation chemist's repertoire. It is further evident that isomeric structure differentiation can be done very simply and straightforwardly.

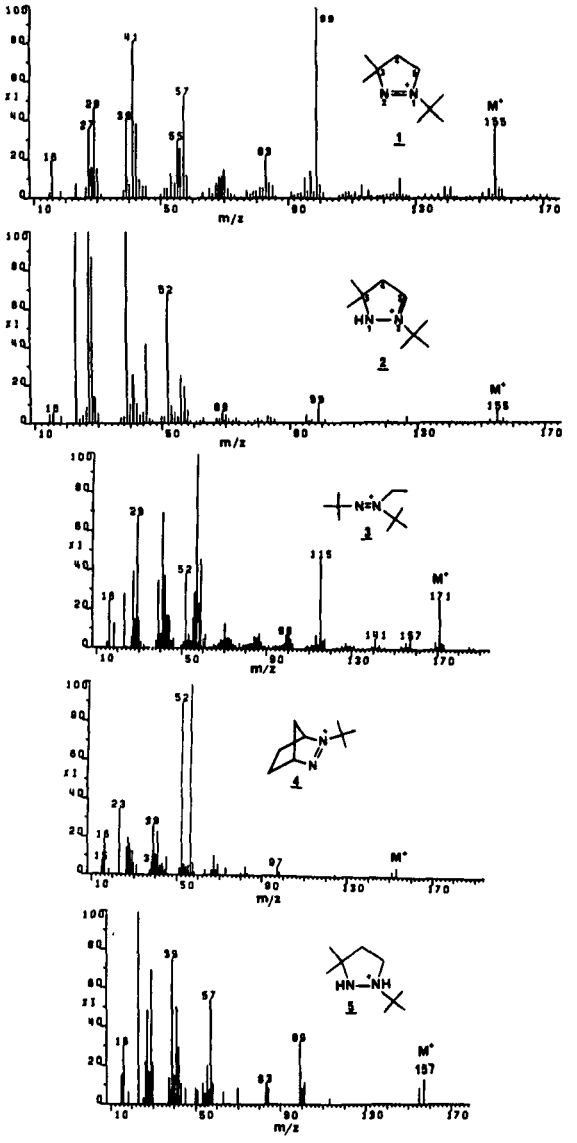

---

1. Supported by National Science Foundation grant CHE-7913781. Instrumentation obtained with National Science Foundation grants CHE-8100424 and CHE-8310031.
2. C.G. Sanders, T.R. Sharp, E.L. Allred (1986). **Tetrahedron Letters** (in press).
3. C.G. Sanders, T.R. Sharp, E.L. Allred (1986). in preparation.
4. T.R. Sharp, H.K. Jones (1986). **These Proceedings.**
5. T.R. Sharp (1986). **Org. Mass Spectrom.** 21, (in press).

IRON(I) CHEMICAL IONIZATION AND GC/FTMS FOR LOCATING DOUBLE BONDS.

D.A. Peake and S.K. Huang,
Department of Chemistry, University of Nebraska,
Lincoln, NE 68588.

Locating double bonds by using transition-metal ions as CI reagents was demonstrated recently for pure olefin samples (1). In that study, metal ions were generated by using EI of iron pentacarbonyl. The main limitation of this approach is the need for high-resolution or MS/MS analysis of adducts formed by reactions of metal carbonyl ions with the olefin in a high-pressure ion source. HRMS is needed to separate isobars of the general formulae $Fe(CO)_x^+$ and $Fe(C_2H_4)_x^+$.

Production of atomic metal ions is easily accomplished by using a pulsed laser coupled with a Fourier transform mass spectrometer. Atomic iron ions were produced by multiphoton dissociation and ionization of iron pentacarbonyl (2). The combination of pulsed-GC/FTMS (3) and iron(I) CI is demonstrated for the analysis of olefin mixtures. This new approach simplifies the CI spectrum and obviates the requirements of high resolution and MS/MS.

Mixtures of heptene and octyne isomers were separated by using capillary GC, and each component in turn reacts with iron(I) in the cell of the FT mass spectrometer. The position of the double or triple bond is located from the products formed by oxidative addition of the metal ion to the allylic or propargylic C—C bond (Scheme I). After allylic insertion of the metal ion, a β-H atom is transferred from the metal to the π-allyl ligand to produce a bis(olefin) complex which dissociates by loss of the smaller alkene ligand.

The reactions of isomeric heptenes illustrate the method for locating double bonds. Figure 1 is the $FeC_7H_{14}^+$ (m/z 154) chromatogram and demonstrates that there are three heptene isomers present. The 1- and 2-heptene isomers both react with Fe^+ to eliminate propene, whereas 3-heptene reacts by loss of ethylene. Although MS/MS spectra of the 1- and 2-heptene adducts can differentiate these isomers (1), the ion/molecule reactions observed in the FTMS do not allow differentiation since rearrangement leads to the same products. Nevertheless, the GC retention times allow assignment of the lower-boiling 1-heptene as peak 1 and 2-heptene as peak 2.

Figure 2 demonstrates that 20 ng of 1-heptene injected on column produces a detectable ion chromatogram and a spectrum with sufficient S/N for locating the double bond. The instrument detection limit is less than 0.6 ng, since greater than 95% of the column effluent is diverted to a rough pump during the time when the pulsed-valve is closed.

A homologous series of 1-alkenes (C10—C14) was studied to test the effect of longer chain alkenes on the allylic insertion mechanism. As illustrated in Figure 3, 1-decene reacts to eliminate C_3H_6 (m/z 154) and C_6H_{12} (m/z 112). In the Fe(I) CI spectrum of 1-tetradecene, only the second loss of propene (m/z 168) is observed. Thus, one limitation of the metal ion chemistry is a tendency for two consecutive allylic insertions to occur for alkenes C12 or longer. However, locating the double bond in longer-chain olefins is possible provided standards are available.

In a high-energy MS/MS experiment, Fe(1-tetradecene)$^+$ loses propene preferentially, in contrast to the FTMS results. Although stable adducts formed from $FeCO^+$ and stablized in a high-pressure source dissociate less readily upon CA, the relative abundance of two consecutive propene losses does increase with chain length (Figure 4). This suggests that in the FTMS, the excess internal energy of the adduct is dissipated by a second rearrangement which results in the apparent loss of C_6H_{12}.

REFERENCES

(1) D. A. Peake and M. L. Gross, Anal. Chem. 1985, 57, 115-120.
(2) S. K. Huang and M. L. Gross, J. Phys. Chem. 1985, 89, 4422-4423.
(3) T. M. Sack, D. A. McCrery and M. L. Gross, Anal. Chem. 1985, 57, 1290-1295.

Scheme I.

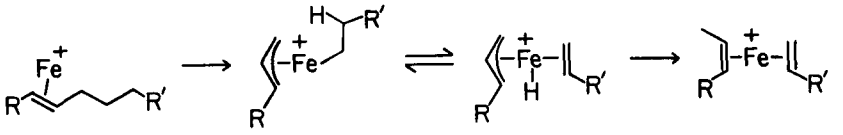

Figure 1. Iron(I) CI Chromatogram of Heptenes; 1, 1-heptene; 2, 2-heptene; 3, 3-heptene.

Figure 2. Fe^+ and 1-heptene, 20 ng on Column, one scan.

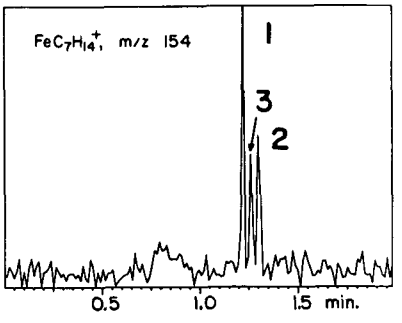

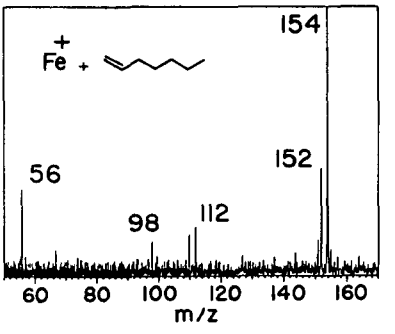

Figure 3. FTMS Spectra of Fe^+ and (a) 1-Decene and (b) 1-Tetradecene.

Figure 4. Collisionally Activated Loss of Propene vs. Two Propenes From Fe(1-alkene)$^+$ Complexes.

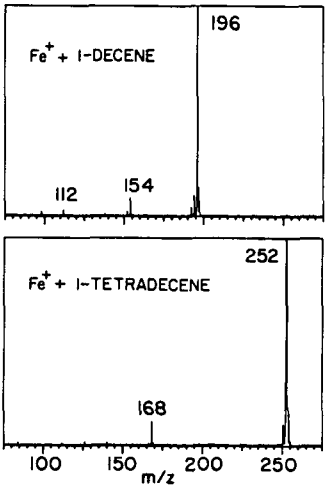

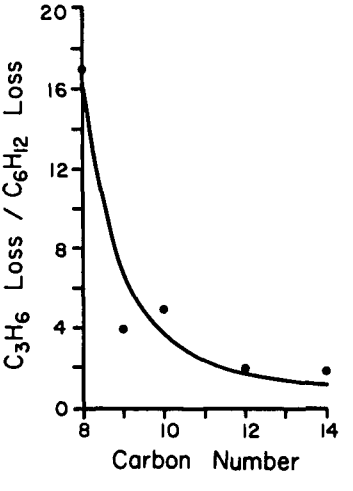

Collision-Induced and Unimolecular Dissociation of Carbon Dioxide Clusters, Studied with a Tandem Molecular Beam Quistor-Quadrupole Instrument

G. Romanowski, R.-H. Gabling and K. P. Wanczek,
Inorganic Chemistry, NW 2,
University of Bremen, D-28 Bremen 33, West Germany

Unimolecular and bimolecular reactions of ionized clusters are of great interest because they lead to an understanding of the structural properties of such agglomerates and of weak intermolecular interactions in general. After formation of cluster ions by electron impact ionization normally a large amount of energy is transferred to the cluster, leading to evaporation reactions by dissociation of van der Waals bonds and to fragmentation of covalent bonds in the molecules forming the cluster (1,2). Fragmentation and evaporation reactions are also important in the generation of mass spectra of clusters after electron impact ionization. The observation of fragmentation in the mass spectra of clusters shows that the transfer of energy from the ionized molecule to the residual cluster is slow and has low efficiency. Cluster ions which fragment do not have a statistical energy distribution. Otherwise they would evaporate completely after ionization as predicted by RRKM theory. It is therefore of great interest to study slow dissociation reactions of clusters after electron impact.
We have constructed a tandem molecular beam Quistor quadrupole instrument for the study of slow cluster ion decompositions (3). The clusters are generated in a supersonic beam instrument at a stagnation pressure of 1 bar and a stagnation temperature of 293 K. The cluster source chamber, the skimmer and the nozzle chamber are all differentially pumped with a total pumping speed of 5,000 l/s. The diameter of the convergent nozzle is 0.3 mm. A cylindrical Quistor is modified to allow passage of the supersonic beam through the cyclindrical electrode. The ion trap is located at the intersection of the beam and quadrupole axes. In the trap the clusters are ionized by a pulsed axial electron beam of 90 eV energy. The storage time of the ions in the Quistor can be changed between 0 and 50 ms. After the end of storage time the ions are ejected by a pulse of 60 V peak hight into the quadrupole for mass analysis. The Quistor can be operated in the RF only mode or with an additional DC voltage to reduce the stored mass range. For the study of cluster ion dissociation kinetics, the storage range was limited to the cluster ion under investigation and to its dissociation products. All clusters with higher masses are not stored. In this way the dissociation of each single cluster ion can be investigated by measuring the calibrated ion intensities as a function of storage time. The rate constants of nonreactive loss of ions are estimated for the ions X^+ (X = Ar, Xe, and CO_2) in their corresponding neutral gases with the same technique. The following values are obtained (in units of $10^{-17}m^3$ /molecule s): CO_2^+/CO_2 :3.8; Ar^+/Ar:6.8; Xe^+/Xe:6.7.

The time dependence of the intensities for the cluster ions $(CO_2)_N^+$ (N = 2,3,4) were investigated for the reactions

$$(CO_2)_N^+ \rightarrow (CO_2)_{N-1}^+ + CO_2$$

The total loss rate constants of the cluster ions were plotted as a functions of pressure. From the plots the unimolecular k_u^N and bimolecular rate constants k_{bi}^N shown in Table 1 are obtained.

Table 1. Rate constants k_u^N and k_{bi}^N for the disappearance of cluster ions.

N	k_u^N /s^{-1}	k_{bi}^N/$m^3 molecule^{-1} s^{-1}$
2	≅0	3.6×10^{-17}
3	≤31	2.1×10^{-16}
4	≤60	2.5×10^{-16}

The values for unimolecular dissociation are only upper limits because we were not able to measure the exact pressure in the Quistor. We could only determine the background pressure. These rate constants are very low. For the dimer $(CO_2)_2^+$ this rate constant is zero within the uncertainty of measurement. For the other cluster ions the rate constants are surprisingly small.
The difference for the rate constants of the trimer and tetramer ions is much larger then the uncertainty of measurement. The larger rate constant for the tetramer may be due to the smaller binding energy per molecule in the larger cluster.
The bimolecular rate constants are the sum of a rate constant of non-reactive loss from the Quistor and of a rate constant of collision-induced dissiation. It can be concluded comparing the rate constants of nonreactive loss for ions X with the values in Table 1 that the trimer and tetramer ions react away mainly by CID, while the dimer ion disappears chiefly by non-reactive loss.
The results show that cluster ions with lifetimes of 50 ms are formed after electron impact ionization of neutral clusters. These cluster ions show very slow energy dissipation.

References

1. G. Romanowski and K. P. Wanczek, Int. J. Mass Spectrom. Ion Processes, 62 (1984) 277.
2. A. J. Stace, Chem. Phys. Lett., 99 (1983) 470.
3. R.-H. Gabling, G. Romanowski and K. P. Wanczek, Int. J. Mass Spectrom. Ion Processes, 69 (1986) 153.

CARBON CLUSTERS OF HIGH MASS DURING INFRARED LASER DESORPTION OF AROMATIC POLYMERS

Charles Eric Brown
Department of Biochemistry
Medical College of Wisconsin
Milwaukee, WI 53226

Peter Kovacic
Department of Chemistry
University of Wisconsin-Milwaukee
Milwaukee, WI 53201

Charles A. Wilkie
Department of Chemistry
Marquette University
Milwaukee, WI 53233

INTRODUCTION

While recording laser desorption/Fourier transform (LD/FT) mass spectra of benzenoid and heterocyclic aromatic polymers, which are of interest because of their electrical conductivities, populations of peaks separated by 24 amu were observed. These populations of peaks are very similar to mass spectra that have been reported with laser vaporization of carbon species from the surface of graphite.[1-3] In agreement with these studies on the vaporization of carbon, we observe peaks at masses that correspond to clusters with only an even number of carbon atoms. In contrast with the previous work, we used only a pulsed CO_2 laser [10.6μm], and clusters with masses at least as high as 5,000 amu were observed in some cases. Both positive and negative ion species have been detected.

EXPERIMENTAL

Laser desorption/Fourier transform mass spectra of solid polymer samples deposited on a stainless steel probe were recorded with a Nicolet FTMS-1000 spectrometer equipped with a Nicolet laser desorption interface and a Tachisto Tac-II pulsed CO_2 laser [10.6μm]. Samples were deposited onto the probe tip by the procedure of Brown et al.[4,5] with a 10 pound sledge hammer and Scotch double stick tape.

RESULTS AND DISCUSSION

The negative ion LD/FT mass spectrum of the product from polymerization of terphenyl exhibits peaks between about 500 and 1,500 amu that are separated by 24 amu (Fig. 1). Each of these peaks is accompanied by a ^{13}C isotope peak of the appropriate intensity. Similar populations of peaks, but at masses above about 1,500 amu, are observed in the positive ion LD/FT mass spectra in the products from polymerization of pyrene (Fig. 2A) and the synthesis of poly(2,5-thienylene).[6,7] Material from bromination of poly(p-phenylene) yields both positive and negative ions of oligomers that differ by 24 amu, but the positive ions are in a much higher mass range (i.e. above about 1,500 amu) than the negative ions (i.e. between about 500 and 1,500 amu) (Fig. 2B and C). In each case, these clusters are seen in addition to the polymer that was being synthesized. By way of contrast, no clusters were observed with pulsed infrared irradiation of samples of amorphous and flake graphites.

Thermal degradation of poly(2,5-thienylene) with loss of sulfur occurs at temperatures above 600°K, and the remaining carbon backbone might be expected to yield polynuclear material.[8] Thus, the possibility exists that pulsed infrared laser irradiation might produce such thermal degradation within the mass spectrometer. However, this seems less likely with the benzenoid aromatic polymers.

These polymers are ionized by pulsed infrared laser irradiation with little apparent fragmentation, usually just loss of one electron.[4,5] Since infrared radiation does not have sufficient energy per quantum to eject electrons, we have suggested that ionization of conjugated aromatic polymers occurs by multiphoton excitation of higher energy levels.[9] Nonlinear optical properties of thick layers of these materials, which are analogous in structure to laser dyes such as p-terphenyl and p-quaterphenyl, may produce higher order harmonics of the laser radiation.

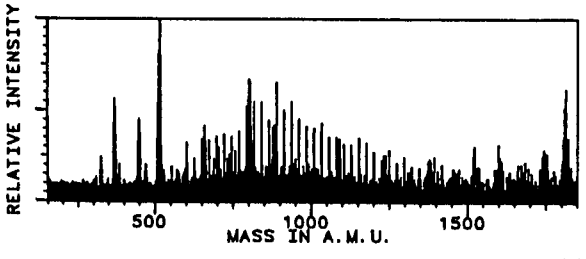

Figure 1. Negative ion LD/FTMS of the products from reacting terphenyl with $AlCl_3$-$CuCl_2$.

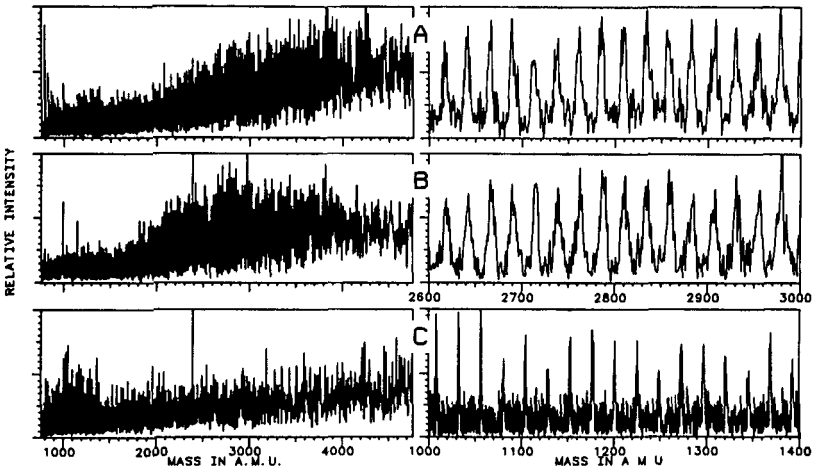

Figure 2. LD/FTMS of high-molecular-weight materials observed in reaction products from (A) dehydrocoupling of pyrene, and (B,C) bromination of poly(p-phenylene). Positive ions are presented in (A) and (B), and negative ions in (C). Spectral expansions are given on the right.

Synthesis of poly(p-phenylene) (PPP) by dehydrocoupling of benzene with $AlCl_3$-$CuCl_2$ has been demonstrated by LD/FTMS to yield a complex mixture of polymeric materials. PPP is the primary product, but there are varying levels of contamination by polynuclear material, and monochlorinated and polychlorinated material.[4,5] The composition of this mixture can be altered by a number of minor changes in the reaction conditions during dehydrocoupling. For example, raising the reaction temperature or substituting $FeCl_3$ for $AlCl_3$-$CuCl_2$ leads to increased chain termination by chlorine and a concomitant decrease in the concentration of polynuclear contaminants when benzene is polymerized.[4,5] Substitution of benzene-d_6 or biphenyl for benzene favors the formation of polynuclear species.[4,5]

Our current working hypothesis is that graphite-like polynuclear structures within the samples which provided Figs. 1 and 2 may have given rise to the observed carbon clusters during vaporization and multiphoton ionization of the benzenoid aromatic polymers. Rohlfing et al.[1] demonstrated previously that a low order power law ionization process is involved in the production of carbon clusters by laser vaporization of graphite.

ACKNOWLEDGEMENTS

We thank James A. Kinsinger, R.E. Hein and Robert B. Cody, Jr. of Nicolet Analytical Instruments for their assistance.

REFERENCES

1. E.A. Rohlfing, D.M. Cox, and A. Kaldor, J. Chem. Phys., 81, 3322 (1984).
2. H.W. Kroto, J.R. Heath, S.C. O'Brien, R.F. Curl, and R.E. Smalley, Nature, 318, 162 (1985).
3. L.A. Bloomfield, M.E. Geusic, R.R. Freeman, and W.L. Brown, Chem. Phys. Lett., 121, 33 (1985).
4. C.E. Brown, P. Kovacic, C.A. Wilkie, R.B. Cody, Jr., and J.A. Kinsinger, J. Polym. Sci. Polym. Lett. Ed., 23, 453 (1985).
5. C.E. Brown, P. Kovacic, C.A. Wilkie, J.A. Kinsinger, R.E. Hein, S.I. Yaniger, and R.B. Cody, Jr., J. Polym. Sci. Polym. Chem. Ed., 24, 255 (1986).
6. See "Laser Desorption/Fourier Transform Mass Spectral Analysis of Heterocyclic Aromatic Polymers" by C.E. Brown, and P. Kovacic in this volume.
7. C.E. Brown, P. Kovacic, R.B. Cody, Jr., R.E. Hein, and J.A. Kinsinger, J. Polym. Sci. Polym. Lett. Ed., in press (1986).
8. W.K. Kobel, H. Kiess, M. Egli, and R. Keller, "Polythiophene Conductive Polymers," Workshop on Conductive Polymers, Brookhaven National Laboratory, October 7-9, 1985.
9. C.E. Brown, P. Kovacic, C.A. Wilkie, R.B. Cody, R.E. Hein, and J.A. Kinsinger, ACS Polym. Materials Sci. Eng., 54, 307 (1986).

GAS PHASE REACTIONS OF SILICON CATION CLUSTERS

William R. Creasy, Steven W. McElvany, and Anthony O'Keefe

Naval Research Laboratory
Washington, D. C. 20375-5000

Several studies have been done recently of the structure and energetics of neutral and ionic silicon clusters Si_n^+, due to the importance of silicon as a semiconductor. A number of experimental and theoretical methods have been used. One method of studying silicon cation clusters is through their reactivity with neutral molecules. A study of the reactions of silicon cation clusters with methylsilane was recently done by Bondybey and co-workers,[1] using an experimental technique similar to that in this study.

The present study uses the technique of laser vaporization to form small silicon cluster ions, which are then trapped in a Fourier transform ion cyclotron resonance mass spectrometer (FTMS). The vaporization is done using pulses from a frequency-doubled Nd:YAG laser (532 nm, 5-10 mJ/pulse), which are focussed on a piece of single crystal silicon located flush with the bottom plate of the FTMS cell. A distribution of cluster ions Si_n^+ from n=1 to 6 are produced. One ion is isolated by resonant frequency ejection of the other ions, and it is allowed to react with a reagent gas at 1-5 X 10^{-7} torr for 0.1 to 5 s. The mass spectrum is then taken to detect reactant and product ions. By varying the reaction time, rate constants can be measured which are in the range of 10^{-9} to 10^{-12} cm^3/s.

The rate constants for the reactions of Si_n^+ with some neutral molecules are plotted in Figure 1, relative to the rate constant of Si^+, as a function of cluster size n. The rate constants for methylsilane[1] are also included. Several trends are apparent from the plot. Rates tend to decrease monotonically as the clusters get larger, with a few exceptions for methanol and methylsilane at n=3 and 5. The largest decrease for all the reactions is the transition from n=3 to n=4, for which the rate constants decrease by a factor of five to ten. For the reactants H_2O, N_2O, and NH_3, no reactions are observed for n>3. The decrease is consistent with theoretical calculations[2] which suggest that Si_4^+ is more stable, and less likely to react, than Si_3^+ or Si_5^+.

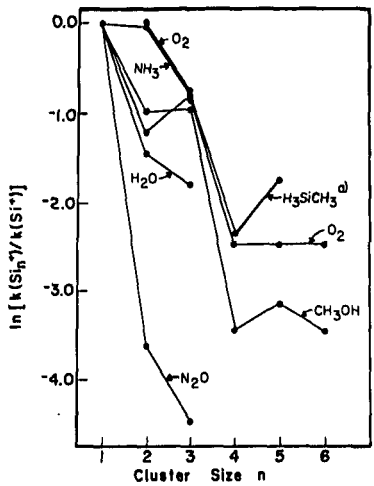

Figure 1: Relative reaction rates of Si_n^+ with the molecules shown, relative to the rate of Si^+ reaction. The absence of a data point means that no reaction was observed, or the rate constant was slower than 10^{-12} cm^3/s. a) Taken from Ref. 1.

The reactions which were studied can be separated into two types. The first type includes the reactions of H_2O, NH_3, C_2H_2, and CH_3OH, which react via a dehydrogenation of the neutral followed by production of a variety of products. The products may or may not involve breaking up the cluster ion. For example, the reaction rates and product branching ratios of the methanol reaction are listed in Table I. The ion $SiOCH_3^+$ is formed from all the cluster ions, but a variety of other products are also formed. No products of the type $Si_xH_y^+$ are observed for any of the reactions of the neutrals, which is consistent with the facts that the Si-H bond is quite weak and that no reaction is observed of the cluster ions with H_2.

Table I: Reaction rates and branching ratios for $Si_n^+ + CH_3OH$.

	n = 1	2	3	4	5	6
rate of loss of Si_n^+ (cm^3/s)	1(-9)[a]	5(-10)	5(-10)	4(-11)	6(-11)	4(-11)
Product ratios						
$SiOCH_3^+$	.1	.8	.9	1.0	1.0	.1
$SiOH^+$	.9	.1				
Si_2OH^+		.1	.1			
$Si_6OCH_3^+$						.6
$Si_5OCH_2^+$						.3

$SiOH^+ + CH_3OH$ ----> $SiOCH_3^+$ k = 9(-10)

a) Numbers in parentheses are exponents.

The other type of reaction studied, which includes O_2 and N_2O, oxidize and usually fragment the cluster ions. For the example, reaction of all Si_n^+ with O_2 produces smaller ions. These reactions are very exothermic due to the formation of strong SiO bonds, but they are slow. The rate constant for Si_2^+ is 7×10^{-11} cm^3/s. The rates and product ratios of these reactions, and their relationship to a general reaction coordinate, will be discussed in a forthcoming publication.

Reactions on the silicon surface were also studied using the same experimental technique. On vaporizing ions from the silicon, it was observed that unusual ions were produced in addition to the usual Si_n^+ distribution after extended exposure to some reagent gases. For example, vaporization from a surface exposed to NH_3 produced the ions Si_2N^+ and $SiNH_2^+$, from one exposed to C_2H_2 produced $Si_nC_2H^+$, for n=1 to 3, and from one exposed to H_2O produced $SiOH^+$. Several tests were used to confirm that the ions were vaporizing from the surface, and were not due to gas phase reactions or to surface heating by multiple laser pulses. It was also shown that the surface which is struck by the laser is cleaned by each laser pulse. Therefore, the amount of exposure of the surface to reagent gases was varied simply by varying the time between laser pulses. The relative intensity of the ion Si_2N^+ to the cluster ions was measured as a function of exposure to NH_3. This measurement gives a method of determining the sticking coefficient of ammonia on the silicon surface, which is approximately 1.0, and can be used to measure surface reaction rates. This type of experimental probe of surface reactions and surface diffusion rates is complementary to other techniques.

REFERENCES

1. M. L. Mandich, W. D. Reents, Jr., and V. E. Bondybey, J. Phys. Chem., 90 2315 (1986).
2. K. Raghavachari and V. Logovinsky, Phys. Rev. Lett. 55 2853 (1985).

POSITIVE AND NEGATIVE CLUSTER IONS OF PHOSPHORIC AND SULFURIC ACIDS[1]

Thomas R. Sharp and Harlan K. Jones
Department of Chemistry, The University of Utah, Salt Lake City, Utah 84112, U.S.A.

Series of cluster ions have been observed in both the positive ion and the negative ion FAB mass spectra of neat sulfuric acid and neat phosphoric acid.

Observations were made with a VG Analytical 7070-E mass spectrometer, operating at +5 KV accelerating potential, resolving power 1000, scanning over m/z 10-1400 at 20 sec/decade. Samples were bombarded with 6.0-7.0 KeV Ar^o produced by an Ion Tech saddle field source operated at 1.0-1.5 mAmp. Repetitive scan spectra were recorded by a VG DS2050 datasystem.

The positive ion spectrum of sulfuric acid consists principally of a series of protonated molecular cluster ions of formula $(H_2SO_4)_nH^+$. Very little fragmentation occurs, the only significant ion signals which can be attributed to fragmentation of a sulfuric acid molecule appearing below m/z 99. The principal additional feature is that water absorbed because of the very hygroscopic nature of concentrated sulfuric acid causes the appearance of a series of cluster ions of formula $(H_2SO_4)_nH_3O^+$. By contrast, the negative ion spectrum shows almost exclusively a series of clusters of formula $(H_2SO_4)_nHSO_4^-$. Only at very high water contents *do a low intensity water adduct series start to appear. Clusters containing as many as 16* acid molecules have been observed in both positive ion and negative ion spectra.

The spectra of phosphoric acid show significantly more detail. In the positive ion spectrum, the primary feature is the $(H_3PO_4)_nH^+$ molecular cluster series. Fragment ion series, resulting from loss of multiple H_2O molecules are also present. The negative ion spectrum shows a molecular cluster ion series of formula $(H_3PO_4)_nH_2PO_4^-$, and series resulting from H_2O losses. The primary difference between the positive ion and negative ion spectra are that, in the positive ion spectrum, the most intense ion series is the cluster molecular ion series, while in the negative ion spectrum the most intense series corresponds to loss of two H_2O molecules from the cluster molecular ion.

Two analytical uses of these cluster ion spectra have been evaluated. One is to use the spectra for either positive ion or negative ion datasystem mass calibrants[2]. H_2SO_4 reference peaks which have been successfully used for this purpose are given in Table 1. Another has been utilization of the relative intensities of the $(H_2SO_4)_nH^+$ and $(H_2SO_4)_nH_3O^+$ clusters of equal n for evaluating the water content of concentrated sulfuric acid.

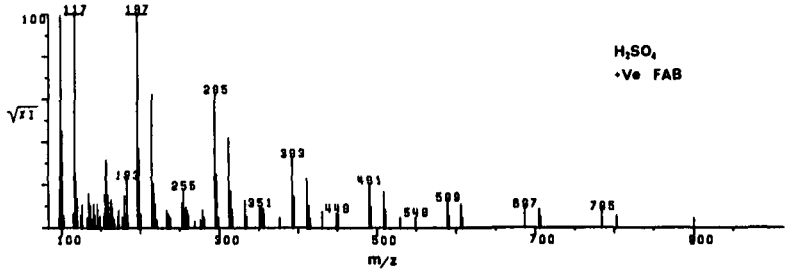

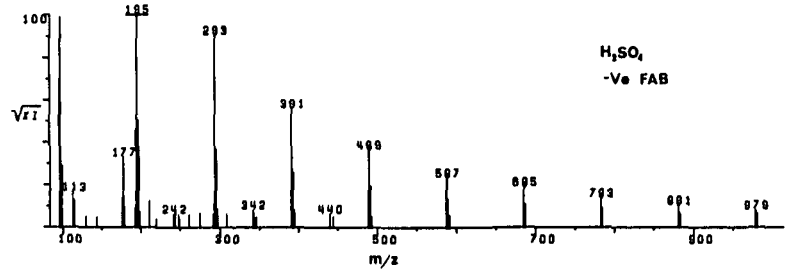

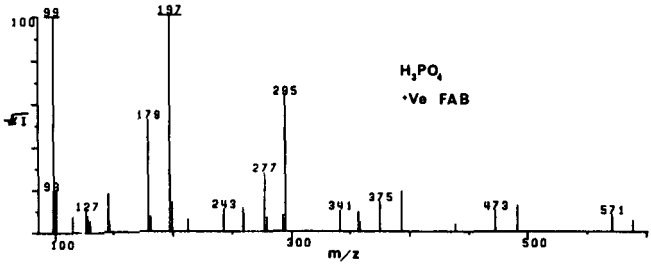

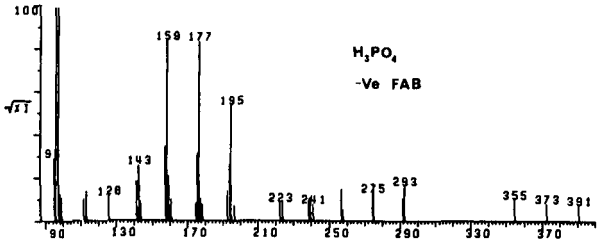

TABLE 1:
Sulfuric Acid Reference Masses for +Ve and -Ve FAB Ionization

n	Positive Ion			Negative Ion		
	Accurate Mass[a]	Intensity	Cluster Formula	Accurate Mass[a]	Intensity	Cluster Formula
1	98.97520	100.0	$(H_2SO_4)_1H^+$	96.95955	70.0	$(HSO_4)^-$
	116.98680	b	$(H_2SO_4)_1H_3O^+$			
2	196.94257	37.5	$(H_2SO_4)_2H^+$	194.92693	100.0	$(H_2SO_4)_1(HSO_4)^-$
	214.95320	b	$(H_2SO_4)_2H_3O^+$			
3	294.90995	10.5	$(H_2SO_4)_3H^+$	292.89430	34.0	$(H_2SO_4)_2(HSO_4)^-$
	312.92050	b	$(H_2SO_4)_3H_3O^+$			
4	392.87733	3.8	$(H_2SO_4)_4H^+$	390.86168	12.5	$(H_2SO_4)_3(HSO_4)^-$
	410.88790	b	$(H_2SO_4)_4H_3O^+$			
5	490.84471	1.5	$(H_2SO_4)_5H^+$	488.82906	5.0	$(H_2SO_4)_4(HSO_4)^-$
	508.85530	b	$(H_2SO_4)_5H_3O^+$			
6	588.81208	0.4	$(H_2SO_4)_6H^+$	586.79643	1.9	$(H_2SO_4)_5(HSO_4)^-$
	606.82260	b	$(H_2SO_4)_6H_3O^+$			
7	686.77946	0.14	$(H_2SO_4)_7H^+$	684.76381	1.5	$(H_2SO_4)_6(HSO_4)^-$
	704.79000	b	$(H_2SO_4)_7H_3O^+$			
8	784.74684	0.05	$(H_2SO_4)_8H^+$	782.73119	0.8	$(H_2SO_4)_7(HSO_4)^-$
	802.75740	b	$(H_2SO_4)_8H_3O^+$			
9	882.71421	0.02	$(H_2SO_4)_9H^+$	880.69857	0.4	$(H_2SO_4)_8(HSO_4)^-$
	900.72480	b	$(H_2SO_4)_9H_3O^+$			
10	980.68159	5×10^{-3}	$(H_2SO_4)_{10}H^+$	978.66594	0.1	$(H_2SO_4)_9(HSO_4)^-$
	998.69210	b	$(H_2SO_4)_{10}H_3O^+$			
11	1078.6489	1.8×10^{-3}	$(H_2SO_4)_{11}H^+$	1076.6333	0.05	$(H_2SO_4)_{10}(HSO_4)^-$
	1096.6595	b	$(H_2SO_4)_{11}H_3O^+$			
12	1176.6163	6×10^{-4}	$(H_2SO_4)_{12}H^+$	1174.6007	0.02	$(H_2SO_4)_{11}(HSO_4)^-$
	1194.6269	b	$(H_2SO_4)_{12}H_3O^+$			

a. Accurate masses were calculated using the following monoisotopic masses: ^{1}H, 1.0078246; ^{32}S, 31.97207; ^{16}O, 15.99491.

b. Intensities for $(H_2SO_4)_nH_3O^+$ ion series not given, as they vary with the amount of water present in the H_2SO_4 sample used.

---

1. Instrumentation obtained with funds from National Science Foundantion grants CHE-8100424 and CHE-8310031.

2. T.R. Sharp (1986). **Org. Mass Spectrom.** 21, (in press).

EFFECT OF GAS PHASE ION MOLECULE REACTIONS ON THERMOSPRAY SPECTRA

A. J. Alexander and P. Kebarle,
Chemistry Department,
University of Alberta,
Edmonton, Alberta
Canada T6G 2G2

Gas phase ion molecule reactions have a strong influence on the relative ion intensities in thermospray mass spectra. The relative intensities of the positive ions in the TSP spectra of 0.1 M ammonium acetate solution follow a pattern that can be predicted on basis of gas phase ion molecule equilibria. Analyte ions form clusters with gas phase solvent, NH_3 and CH_3COOH molecules. The cluster ratios follow gas phase ion-cluster equilibria predictions. With volatile and moderately volatile analytes B in ammonium acetate solution, the BH^+ ions are formed by gas phase protonation of gaseous molecules B by the ammonium reagent ions. Typical results for 4-methylpyridine are shown below. At $[B]_{aq} < 10^{-3}$M, the gas phase protonation in slow (kinetic control) and the BH^+ signals are linear with B. At $[B]_{aq} > 10^{-3}$M the protonation becomes progressively faster, proton transfer equilibria conditions are approached and the BH^+ response is nonlinear. For a mixture of bases, the one with the highest proton affinity will dominate the TSP spectrum. Gas-phase ion/molecule kinetic expressions can be used to predict the observed ion intensity changes as a function of $[B]_{aq}$. The average effective reaction time of the ions is ≈300 μs.

Experiments with a pulsed electron beam entering the thermospray source 4 mm ahead of the ion exit leak were used to determine the residence time of the ions in the thermospray jet. Results so far obtained indicate that the transport from electron beam to ion exit slit is determined by the thermospray flow velocity. It was found that relative to the electron beam pulse width the residence time distribution was broadened by ~65 μs. Under these conditions the proton transfer reaction:

$$H_3O^+(H_2O)_n + B \longrightarrow BH^+ + (H_2O)_{n+1}$$

does not attain equilibrium and both reactant and product ion decays as a function of time are very similar. Results for $[B]_{aq} = 10^{-2}$ M pyridine are shown.

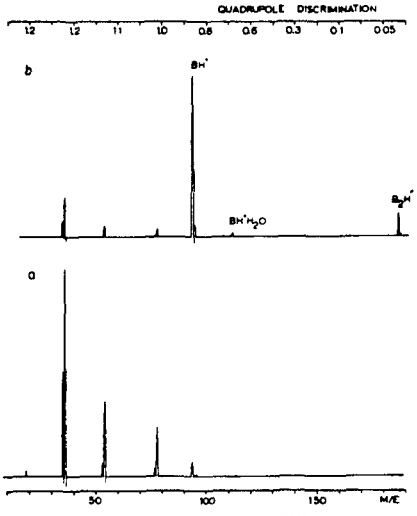

Figure 4. TSP mass spectra observed with 4-MePy (B) aqueous solutions containing 0 1 M ammonium acetate: (a) $[B]_{aq} = 10^{-4}$ M; (b) $[B]_{aq} = 5 \times 10^{-3}$ M

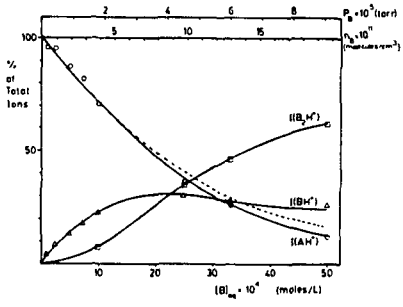

Figure 5. Observed TSP ion intensities in percent of total ion intensity; aqueous solutions 0.1 M ammonium acetate. B = 4-MePy $I(AH^+)$ is the combined intensity of the ammonium ions. AH^+ is involved in the gas-phase protonation of B. Dashed curve shown for $I(AH^+)$ is calculated with first-order kinetics equation

$$I(AH^+) = 100e^{-k_{gp}n_B t}$$

n_B is concentration of B in gas phase

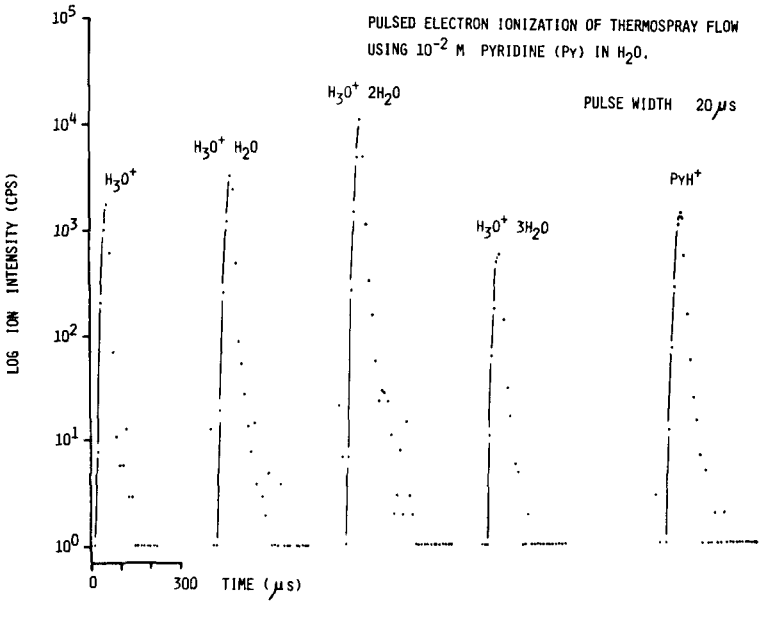

PHOTOELECTRON SPECTROSCOPY OF NEGATIVE CLUSTER IONS; J. T. Snodgrass, J. V. Coe, C. B. Freidhoff, K. M. McHugh, and K. H. Bowen; Johns Hopkins University, Department of Chemistry, Baltimore, Maryland 21218.

Photodetachment studies on negative cluster ions have been performed using the technique of negative ion photoelectron spectroscopy. The experiments were conducted by crossing a mass selected beam of negative cluster ions with a fixed frequency photon beam and energy analyzing the resulting photodetached electrons. By applying this method to negative cluster ions, we have measured neutral cluster electron affinities as a function of cluster size and composition, bond dissociation energies for negative cluster ions, and have gained insight into a descriptive understanding of the bonding in negative cluster ions.

Systems which have been investigated to date include: $NO^-(N_2O)_{n=1,2}$, $NO^-(Ar)$, $NO^-(Kr)$, $NO^-(Xe)$, $H^-(NH_3)_{n=1,2}$, $NH_2^-(NH_3)_{n=1,2}$, $(N_2O)_2^-$, $(CO_2)^-_{n=2-5}$, $(SO_2)_2^-$, $(H_2O)^-_{n=11-19}$, $(CS_2)_2^-$, $(NO)_2^-$, $Se^-_{n=2-4}$, $Te^-_{n=2,3}$, and $P^-_{n=2,3}$. The photoelectron spectra of the $NO^-(N_2O)_n$ cluster ion series are shown below. The peaks in the well-known spectrum of free NO^- arise from transitions between the ground vibrational state of NO^- and the first few vibrational states of neutral NO. The highest electron kinetic energy peak contains the transition between the NO^- vibrational and rotational ground states and the NO neutral vibrational and rotational ground states. The energy for this transition, which is equal to the electron affinity of NO, is approximately obtained by subtracting the electron kinetic energy of this peak from the fixed photon energy. This yeilds an electron affinity of 0.024 eV. The photoelectron spectra of the clustered ions, $NO^-(N_2O)$, and $NO^-(N_2O)_2$ exhibit the characteristic spectral pattern of free NO^-, shifted to lower electron energies and somewhat broadened. The presence of the NO^- spectral pattern strongly implies that largely intact NO^- ions exist within these cluster ions, and serve as chromophores for photodetachment. This conclusion is perhaps somewhat unexpected since the electron affinity of NO is nearly an order of magnitude less than the electron affinity of N_2O. Based on this interpretation we obtain electron affinities of ~0.25 eV for $NO(N_2O)_1$ and ~0.5 eV for $NO(N_2O)_2$. The electron kinetic energy shifts in the photoelectron spectra are interpreted as a consequence of the stabilization of largely intact NO^- ions due to complexation with N_2O to form cluster ions. The magnitudes of these shifts are approximately equal to stepwise ion-solvation enthalpies, or equivalently, bond dissocation energies in the cluster ions. We find a shift of ~0.2 eV between the spectrum of NO^- and of $NO^-(N_2O)_1$ and an approximately equal shift between the spectrum of $NO^-(N_2O)_1$ and $NO^-(N_2O)_2$.

The photoelectron spectra of $NO^-(Ar)$, $NO^-(Kr)$, and $NO^-(Xe)$ also exhibit the spectral pattern of free NO^-, indicating localization of the excess negative charge on the NO moiety in these cluster-ions. Spectral shifts observed were ~0.06 eV for $NO^-(Ar)$, ~0.09 eV for $NO^-(Kr)$ and ~0.17 eV for $NO^-(Xe)$. When these spectral shifts are plotted against the polarizability of the rare gas, we find a very linear relationship. The spectral shift for $NO^-(N_2O)$ plotted at the polarizability of N_2O however falls well above this line, indicating perhaps some chemical contributions to the bonding.

The photoelectron spectra of $H^-(NH_3)_1$, $H^-(NH_3)_2$, $NH_2^-(NH_3)_1$ and $NH_2^-(NH_3)_2$ all indicate that a localized charge description of bonding is accurate for these cluster ions. We find that the NH_2^- ion interacts more strongly with NH_3

than the H^- ion. Energetic information from these spectra are in excellent agreement with theoretical calculations.

The photoelectron spectra of CO_2^- and N_2O^- are similar as might be expected since these species are isoelectronic. The spectra of the dimeric negative cluster ions however indicate much stronger interactions in $(CO_2)_2^-$ than in $(N_2O)_2^-$. Data on $(SO_2)_2^-$ are in good agreement with thermochemical measurements from high pressure mass spectrometry.

Although the water molecule does not have a positive electron affinity, it has ofter been suggested that gas phase negative cluster ions, $(H_2O)_n^-$, ought to exist and that some of these might be counterparts to solvated electrons. We have recently recorded the photoelectron spectra for a number of these species in the size range of n=11 through 19. We find electron binding energies smoothly increasing from ~0.75 eV for $(H_2O)_{11}^-$ to ~1.1 eV for $(H_2O)_{19}^-$.

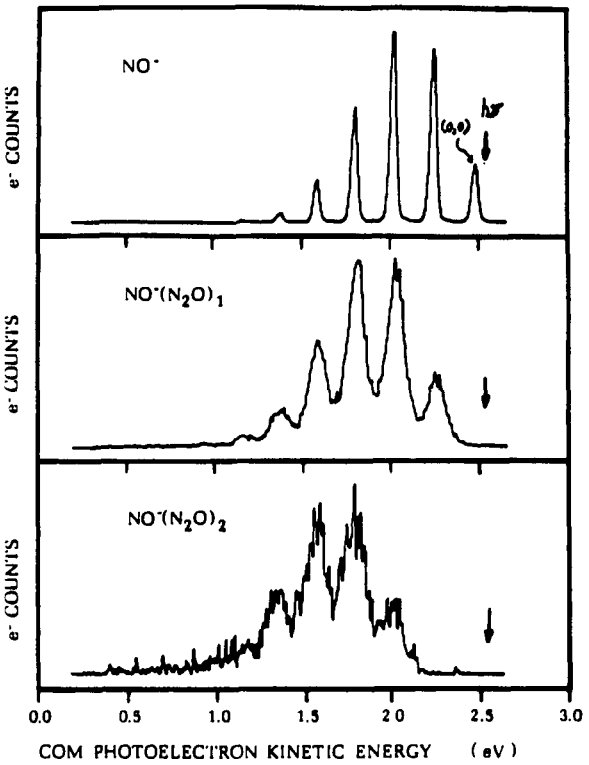

SPECTROSCOPIC AND THERMODYNAMIC INVESTIGATIONS OF TRANSITION METAL CLUSTER IONS IN THE GAS PHASE: PHOTODISSOCIATION OF MFe^+.

Robert L. Hettich and Ben S. Freiser

Department of Chemistry
Purdue University
West Lafayette, Indiana 47907

Heteronuclear metal dimer ions, MFe^+ (M=Sc,Ti,V,Cr,Fe,Co,Ni,Cu,Nb,Ta) were generated and isolated in the gas phase using Fourier transform mass spectrometry, equation 1. Observation of these ionic species in a ligand-

$$M^+ + Fe(CO)_5 \longrightarrow MFe(CO)_x^+ \xrightarrow{CID} MFe^+ \qquad (1)$$

free environment provides a method of probing the fundamental bonding nature between two bare transition metal atoms. The photodissociation spectra of MFe^+, obtained by monitoring the fragmentation of MFe^+ as a function of wavelength, provide both spectroscopic and thermodynamic information. Both M^+ and Fe^+ are observed as photoproducts, with the metal having the lowest ionization potential predominating, equation 2. The photodis-

$$MFe^+ \xrightarrow{h\nu} M^+ \text{ or } Fe^+ \qquad (2)$$

sociation spectra reveal broad absorption in the ultraviolet and visible spectral regions with a range of cross sections from 0.06 A^2 for VFe^+ to 0.62 A^2 for $CrFe^+$. Bond energies obtained by observing photoappearance onsets are in the range of 48 kcal/mol for $ScFe^+$ to 75 kcal/mol for VFe^+ and show good agreement with values obtained by ion-molecule bracketing techniques, suggesting that the observed thresholds are thermodynamic and not spectroscopic. The metal cluster ions are found in general to be bound more strongly than their neutral metal dimer counterparts. The ionization potentials for MFe can be calculated from $D^o(M\text{-}Fe)$ and $D^o(M^+\text{-}Fe)$ and are found to be in the range of 5.4 eV for VFe to 7.4 eV for TaFe. Based on the results obtained in this study, MFe^+ for M=Sc-Fe (and for M= Nb, Ta) are postulated to involve both s and d electron bonding whereas MFe^+ for M=Co-Cu may be bound predominantly by s electron density.

Table I. Thermodynamic Data for Metal Clusters.

AB	$D^o(A-B)$[a] (kcal/mol)	IP(AB)[b] (eV)	PDS[c] $D^o(A^+-B)$ (kcal/mol)	I-M[d] $D^o(A^+-B)$ (kcal/mol)	PDS[e] $D^o(B^+-A)$ (kcal/mol)
ScFe	55	6.8	48 ± 5	49 ± 6	79 ± 5
TiFe	42	6.0	60 ± 6	49	84 ± 6
VFe	44	5.4	75 ± 5	62	101 ± 5
CrFe	32	6.0	50 ± 7	f	75 ± 7
Fe_2	18	6.0	62 ± 5	58 ± 7	62 ± 5
CoFe	30	6.5	62 ± 5	62 ± 6	62 ± 5
NiFe	39	6.6	64 ± 5	68 ± 5	69 ± 5
CuFe	30	6.7	53 ± 7	52	56 ± 7
NbFe	59	6.5	68 ± 5	60	91 ± 5
TaFe	60	7.4	72 ± 5	60	72 ± 5

a) Weltner, W. Jr.; Van Zee, R.J. Ann. Rev. Phys. Chem. (1984) 35, 291.

b) Calculated from $D^o(A^+-B)$, $D^o(A-B)$, and IP(A).

c) Photodissociation results.

d) Ion-molecule reaction results.

e) Calculated from $D^o(A^+-B)$, IP(A), and IP(B).

f) Indeterminate.

RELATIONSHIP BETWEEN STRUCTURE AND REACTIVITY FOR METAL CLUSTERS FORMED IN ION-MOLECULE REACTIONS IN GROUPS 6 AND 7 METAL CARBONYLS

W. D. Reents, Jr., AT&T Bell Laboratories, Murray Hill, NJ 07974,
W. K. Meckstroth, and D. P. Ridge, Department of Chemistry,
University of Delaware, Newark, DE 19716

We have previously reported ion-molecule reaction studies for gas phase cationic clustering reactions in the Group 7 metal carbonyls, $Re_2(CO)_{10}$[1], $Mn_2(CO)_{10}$[2], and $ReMn(CO)_{10}$.[2] From these studies we concluded that it was possible to infer structural information about the cluster ions from their kinetic behavior. We have now extended these studies to include the Group 6 metal carbonyls. The cations derived from electron impact on $Cr(CO)_6$ and $W(CO)_6$ were reacted with their respective neutral precursor in the ion source of a Nicolet FT/MS-1000 Fourier transform mass spectrometer. A 1"x1"x3" rectangular cell was utilized. Conditions were similar to those reported previously.[1,2] The products of the ion-molecule reactions were dimetal clusters, $M_2(CO)_m^+$, where m is 2 to 11. These products reacted further forming clusters as large as $M_5(CO)_{17}^+$.

Rate constants for the cluster ions can be determined from plots showing the variation of ion abundance with time. Typically an ion abundance increases to a maximum and then levels off or diminishes depending on its reactivity. All reactions are pseudo-first order, since the neutral concentration is much larger than the ion concentration. Rate constants for reactive ions were obtained from the decay portion of the curves. These decays could be fit with single exponential functions with deviations less than the noise level in all cases. For less reactive ions, an upper limit on the rate constant was derived from the flat or slightly increasing portion of the curves.

To establish a quantitative relationship between structure and reactivity, we calculated the electron deficiency of the cluster ions based on the effective atomic number rule with modifications suggested by Teo.[3] For a cluster ion, $M_n(CO)_m^+$, with b metal-metal bonds and E valence electrons the electron deficiency, D, is

$$D = \frac{18n - (En + 2m + 2b - 1)}{n} + \frac{2X}{n} \qquad (1)$$

The value X varies from 0 to 3 based on Teo's rules[3] and accounts for the possibility of delocalized bonding. In order to determine b we need to make some assumptions about the structures. It was assumed in the cases of the Group 7 metal carbonyls that the clusters had closed polyhedral structures with metal-metal bonds along the edges. It was found that this led to a correlation between structure and electron deficiency consistent with the simplest possible model. That is, the rate constants for the clustering reactions were large if the electron deficiency was two per metal atom or greater, and the rate constants decreased rapidly as the electron deficiency decreased below two. Thus, it would appear that in these cases the only requirement for reaction is that the neutral have access to a metal atom with a two electron deficiency in its valence shell. This model is consistent with the general behavior of transition-metal complexes. Coordination complexes with a full two electron vacancy in their coordination shell tend to react very efficiently, whereas complexes with a full coordination shell or even a one electron deficiency tend to be more stable. Previous work by Wronka and Ridge on reactions of negative ions formed from $Fe(CO)_5$ showed that their reactivity with the parent neutral followed this model.[4]

The regular behavior shown in Fig. 1 by the Group 7 metal carbonyl cluster ions supports the closed polyhedral structural assignments. Out of 76 clusters observed for these three systems only 10 were exceptional. Four with high electron deficiencies were less reactive than expected, and six with low electron deficiencies were more reactive than expected. Possible explanations of these exceptions were suggested in terms of delocalized bonding ($X>0$ in eq. 1), stabilization via multiple bonds, and ligand crowding effects.[2] The possibility of dissociation of CO or η-4 CO in the clusters was also suggested.[3]

An examination of the $Cr(CO)_6$ and $W(CO)_6$ systems based on the same treatment is shown in Fig. 2. There are two marked deviations from the behavior shown by the Group 7 cluster ions.

First, a correlation between rate and electron deficiency is not clearly evident. Second, all of the rate constants are substantially less than the rate constants for electron deficient Group 7 cluster ions. The explanations used for the 10 exceptional ions in the Group 7 cluster ions could be invoked for the Group 6 cluster ions. Fredeen and Russell reported relative rate constants for several reactions in $Cr(CO)_6$ and $Fe(CO)_5$ and in discussing their results they adopted the reactivity vs coordinative unsaturation theory.[5] They suggested that η-4 carbonyl bonding and multiple metal-metal bonds may play a role in the Cr clusters. One possible explanation of the larger set of rate constants plotted in Fig. 2 is that as a result of such effects all the Cr and W clusters are nearly coordinatively saturated. Another possibility is that there is some difference in the mechanisms of the Group 6 and Group 7 clustering reactions. Freedeen and Russell report that the reactivity of some of the Cr clusters varies with the way in which they are formed.[5] This suggests the possibility of isomeric structures or a dependence of reactivity on internal energy. Such effects could show up as nonexponential decays in experiments of the kind reported here. Our failure to detect nonexponential decay, however, may simply reflect relatively small populations of isomeric or excited clusters rather than their absence.

Although the differences between the Group 6 and Group 7 cluster ions are remarkable, it is striking that metals belonging to the same group behave similarly. This is not the case for metal surfaces. In metal surfaces CO dissociates readily on W, Cr, and Mn surfaces, whereas CO does not dissociate on a Re surface.[6] Thus, it would appear that these transition metal clusters are yet too small to behave in the same fashion as metal surfaces. It should also be noted that the degree of ligand substitution for the cluster ions is generally much greater than is possible for metal surfaces. This could also account for the differences observed between the cluster ions and metal surfaces.

---

1 Meckstroth, W. K.; Ridge, D. P.; Reents, W. D., Jr. J. Chem. Phys. 1985, 89, 612-617.
2 Meckstroth, W.K.; Freas, R. B.; Reents, W. D., Jr.; Ridge, D. P. Inorg. Chem. 1985, 24, 3139-3146.
3 a) Teo, B.K. Inorg. Chem. 1984, 23, 1251-1256; b) Teo, B.K.; Longoni, G.; Chung, F. R. K. Inorg. Chem. 1984, 23, 1257-1266.
4 Wronka, J.; Ridge, D. P. J. Am Chem. Soc. 1984, 106, 67-71.
5 Fredeen, D. J. A.; Russell, D. H. J. Am. Chem. Soc. 1985, 107, 3762-3768.
6 Brodin, G.; Rhodin, T. N.; Brucker, C.; Benbow, R.; Hurych, Z. Surface Science, 1976, 59, 593-603.

Figure 1. ABSOLUTE RATE CONSTANTS vs. ELECTRON DEFICIENCY

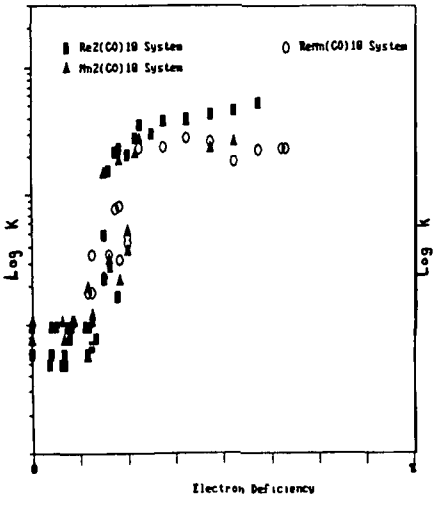

Figure 2. ABSOLUTE RATE CONSTANTS vs. ELECTRON DEFICIENCY

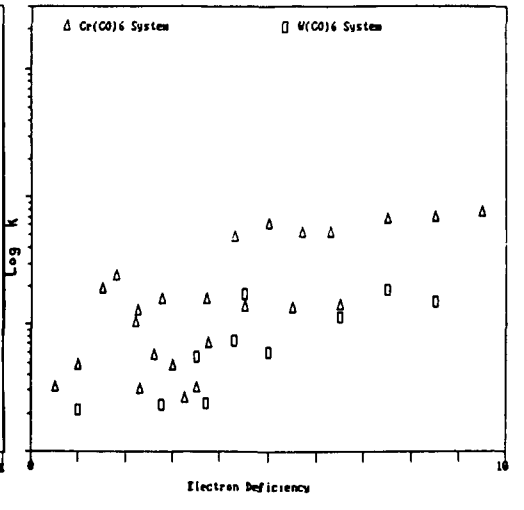

DISSOCIATIONS OF METAL CARBONYL CLUSTER IONS

Royal B. Freas and Mark M. Ross
Chemistry Division, Naval Research Laboratory, Washington, DC 20375-5000

Joseph E. Campana
Environmental Research Center, University of Nevada, Las Vegas, NV 89154

Douglas P. Ridge
Department of Chemistry, University of Delaware, Newark, DE 19716

INTRODUCTION

We are using various mass spectrometric techniques to study fundamental properties of metal cluster ions. These properties include the formation and fragmentation of cluster ions and the relationship between structure and reactivity of charged metal clusters. One of the issues that we address concerns the role that cluster ion structure plays in the reactivity and fragmentation of these species.

APPROACH

The cluster ions being studied in this report were formed by ionization-induced fragmentation of metal carbonyls. The fragment ions thus produced undergo reaction with neutral metal carbonyl to form cluster ions. For several systems, the clustering reactions of metal carbonyl fragment ions have been elucidated using ion cyclotron resonance (ICR) mass spectrometry[1].

The metal carbonyl cluster ions were also formed in the electron and chemical ionization source of a reverse-geometry, double-focusing VG ZAB-2F mass spectrometer, capable of mass-analyzed ion kinetic energy (MIKE) spectrometry. This capability was used to study the collision-induced dissociation (CID) and the photodissociation of mass-selected cluster ions in the second field-free region of the mass spectrometer. Helium was used as the collision gas in the CID experiments. An argon ion laser was used in the photodissociation studies, and the laser beam was aligned to be collinear with the ion beam.

RESULTS

Collision-Induced Dissociation of Manganese Carbonyl Cluster Ions

Manganese carbonyl fragment ions, produced by ionization-induced dissociation, react with $Mn_2(CO)_{10}$ to form trimanganese and tetramanganese cluster ions. In general, the reactions proceed via carbonyl ligand displacement as shown in equations 1 and 2. The reaction products were identified unambiguously using double-resonance ICR techniques[1].

$$[Mn(CO)_y]^+ \ (y=0\text{-}5) + Mn_2(CO)_{10} \rightarrow [Mn_3(CO)_{y'}]^+ \ (y'=8\text{-}15) + zCO \ (z=0\text{-}3) \quad (1)$$

$$[Mn_2(CO)_y]^{\cdot+} \ (y=0\text{-}5,10) + Mn_2(CO)_{10} \rightarrow [Mn_4(CO)_{y'}]^{\cdot+} \ (y'=8\text{-}15) + zCO \ (z=0\text{-}3) \quad (2)$$

The trimanganese and tetramanganese cluster ions undergo further reactions with additional $Mn_2(CO)_{10}$ to produce larger cluster ions. It was observed that the relative rate constants for clustering decrease with coordinative saturation of the cluster ions[1]. That is, coordinatively saturated manganese carbonyl cluster ions react slowly, and conversely, coordinatively unsaturated manganese carbonyl cluster ions react rapidly. In addition, relative rate constants for clustering increase with electron deficiency of the cluster ion[1]. The electron deficiency is the difference between 18 and the average number of valence electrons per metal atom in the cluster ion. Cluster ions that are coordinatively unsaturated generally have large electron deficiencies

The collision-induced fragmentation patterns of $[Mn_3(CO)_y]^+$ and $[Mn_4(CO)_y]^{\cdot+}$ clusters show a correlation with clustering reaction rates and electron deficiencies. That is, cluster ions with large rate constants dissociate primarily by the loss of 1-CO or 2-CO. Cluster ions with small rate constants dissociate principally by the cleavage of Mn-Mn bonds to lose $\cdot Mn(CO)_5$, or to form $[Mn_2(CO)_5]^{\cdot+}$. This correlation is shown in the data in Table I, where the relative rate constants and electron deficiencies can be compared with the most abundant CID fragmentation and percentage of Mn-CO bond cleavages (the sum of all the fragments due to carbonyl ligand losses). As a rule, cluster ions with large rate constants or large electron deficiencies (and hence a large reactivity) exhibit between 60 to 100 percent Mn-CO bond dissociations.

There are several exceptions to the correlation of reaction rates with electron deficiencies. Two of these include the $[Mn_3(CO)_{10}]^+$ cluster and the $[Mn_4(CO)_{15}]^+$ cluster[1]. The $[Mn_3(CO)_{10}]^+$ cluster is less reactive than expected for a cluster with a large electron deficiency, perhaps because of stabilization by electronic effects or the formation of a fourth Mn-Mn bond[1]. The $[Mn_4(CO)_{15}]^{\cdot+}$ cluster is more reactive than expected, based upon a small electron deficiency, possibly because of an open structure due to ligand crowding[1]. However, for both of these cluster ions, the correlation between reactivity and fragmentation is observed. That is, the $[Mn_3(CO)_{10}]^+$ cluster is less reactive and this correlates with the low abundance (35%) of Mn-CO bond fragmentations and the loss of $\cdot Mn(CO)_5$ as the most abundant dissociation. Additionally, the $[Mn_4(CO)_{15}]^+$ cluster exhibits abundant Mn-CO bond cleavages, indicative of a more reactive cluster.

TABLE I. Correlation Between Fragmentation Patterns and Cluster Reactivity

Cluster Ion	Rate Constant[1]	Electron Deficiency[1]	M-M Bonds[1]	% M-CO Dissociation	Major CID Fragment(s)
$[Mn_2(CO)_{10}]^{\cdot+}$	<0.15	1/2	1	42	$\cdot Mn(CO)_5$
$[Mn_3(CO)_9]^+$	-	3-1/3	3	94	CO
$[Mn_3(CO)_{10}]^+$	1.4	2	4	35	$\cdot Mn(CO)_5$
$[Mn_3(CO)_{11}]^+$	-	2	3	70	$\cdot Mn(CO)_5$; CO
$[Mn_3(CO)_{12}]^+$	-	1-1/3	3	95	CO
$[Mn_3(CO)_{15}]^+$	<0.20	0	2	20	$Mn_2(CO)_{10}$
$[Mn_4(CO)_8]^{\cdot+}$	6.9	4-1/4	6	63	$Mn_2(CO)_2$; CO
$[Mn_4(CO)_9]^{\cdot+}$	6.1	3-3/4	6	60	$\cdot Mn(CO)_5$; CO
$[Mn_4(CO)_{10}]^{\cdot+}$	10.0	3-1/4	6	75	CO
$[Mn_4(CO)_{11}]^{\cdot+}$	9.9	2-3/4	6	98	CO
$[Mn_4(CO)_{12}]^{\cdot+}$	7.3	2-1/4	6	96	2CO
$[Mn_4(CO)_{15}]^{\cdot+}$	0.32	1-1/4	5	57	$Mn_2(CO)_{10}$

We postulate that the correlation between CID fragmentation patterns and cluster reactivity exists because cleavages of Mn-CO bonds are facile for the reactive cluster ions. The loss of a carbonyl ligand leaves an empty metal orbital or bonding site available to form Mn-Mn bonds yielding larger clusters. Thus, CID probes labile CO ligands in the cluster ions via vibrational dissociation.

Photodissociation of Manganese Carbonyl Cluster Ions

We have performed also preliminary studies of the photodissociation of cluster ions. Some concerns of these studies include (1) what are the types of photofragments of the cluster ions, (2) what are the dynamics of the photodissociation (cross-sections, absorption maxima, etc.), and (3) what are differences between collision-induced dissociation and photodissociation?

Photodissociation of the manganese carbonyl fragment and cluster ions at λ = 514 nm shows that the odd-electron positive ions photodissociate readily, and primarily by the loss of three to five carbonyl ligands. Also, the number of carbonyl ligands lost increases with increasing photon energy (shorter wavelengths). In contrast, the even-electron positive ions do not photodissociate readily at λ = 514 nm, with the exception of $[Mn_3(CO)_{10}]^+$, an ion that was noted to be exceptional in the discussion above. Plots of the log of the photofragment ion abundance versus the log of the laser power for several of the cluster ions were linear and corresponded to single photon processes.

Photodissociation of Chromium Carbonyl Fragment Ions

Photodissociation of the even-electron dichromium cluster ions was not observed, analogous to the lack of photodissociation of the mono- and trimanganese cluster ions noted above. The monochromium carbonyl fragment positive and negative ions are odd-electron species and were observed to undergo photodissociation. The photofragment ions vary for different parent ions as shown in Table II.

TABLE II. Photofragment Ions from the Reaction:
$[Cr(CO)_x]^{\cdot\pm} + h\nu \rightarrow [Cr(CO)_{x-y}]^{\cdot\pm} + yCO$

X	Positive Ions	Negative Ions
x = odd	y = (x + 1)/2	y = 1 and 2
x = even	y = x/2 and (x/2)+1	y = 1 and 2

As was observed for the manganese ions, the relative abundances of the photofragment ions depends upon the photon energy. In contrast to some of the manganese carbonyl ions, the photodissociation cross-section of the chromium carbonyl ions increases with increasing photon energy indicating that different ions have different absorption curves.

The major differences between photodissociation and collision-induced dissociation of the cluster ions were the types of photofragments that were observed. Photodissociation produced abundant Mn-CO bond cleavages; only two manganese carbonyl cluster ions $[Mn_2(CO)_{10}]^{\cdot+}$ and $[Mn_3(CO)_{10}]^+$ were observed to cleave Mn-Mn bonds (forming $[Mn_2(CO)_5]^{\cdot+}$). In contrast, CID of several of the less reactive manganese cluster ions produced abundant Mn-Mn bond cleavages (Table I).

ACKNOWLEDGEMENTS

We thank J.R. Wyatt (NRL), A. O'Keefe (NRL), and A.P. Baronavski (NRL) for helpful discussions. R.B. Freas acknowledges support from the National Research Council as a Cooperative Research Associate at NRL.

REFERENCES

1. Meckstroth, W.K.; Freas, R.B.; Reents, Jr., W.D.; Ridge, D.P. *Inorg. Chem.*, **1985**, *24*, 3137-3146.

METAL ACETYLACETONATES REVISITED: NEW MASS SPECTRAL EVIDENCE FOR POLYMERIC CHEMISTRY

Kenneth L. Busch and Gerald C. DiDonato
Department of Chemistry, Indiana University, Bloomington, IN 47405

The relatively high volatility of metal acetylacetonates makes it possible to introduce these compounds to an electron ionization source via a direct insertion probe. Changes in the valency of the metal is a key concept in the interpretation of the fragmentation. An equally satisfactory explanation has not been provided for the presence of polymeric ions containing two or more metal ions. Polymeric ions of various compositions and widely varying abundances have been reported by the many workers who have recorded the electron ionization mass spectra of these compounds. The last thorough study of the mass spectra of these compounds is over a decade old, despite the persistence of unresolved questions of ion identity and origin. We have used a high resolution, high mass range, hybrid geometry MS/MS instrument equipped with electron ionization, chemical ionization, and a direct exposure probe to investigate the gas phase ion chemistry of the metal acetylacetonates (acacs). Many new higher molecular weight polymeric ions have been identified. The chemical ionization reactivity of the metal acacs differs, with only a few organometallic ions participating in proton transfer reactions. Differences between the electron ionization and the direct exposure probe electron ionization mass spectra are substantial, with more complex polymeric ions noted in the latter. Simple physical mixture of the metal acacs on the probe results in the formation of mixed metal polymeric ions. The daughter ion MS/MS spectra of these mixed metal ions provide information about the relative strength of the metal-ligand interaction. The daughter ion MS/MS spectra of the same mixed metal ion generated by different ionization methods differ in the relative abundances of the daughter ions observed.

Figure 1 contains the electron ionization, chemical ionization, direct exposure electron ionization, and direct exposure chemical ionization mass spectra of $Zn(acac)_2$. Many ions are common to the spectra, but there are some important differences. The molecular ion at m/z 262 is accompanied in the chemical ionization mass spectra by a more abundant protonated molecular ion at m/z 263. A careful examination of the isotopic envelope reveals that the ion $Zn(acac)_2H_2^+$ is also formed. None of the other ions in the spectrum are protonated by the chemical ionization reagent gas. A second difference between the electron ionization and the chemical ionization mass spectra is the higher relative abundances of the higher mass polymeric ions in the latter. For instance, the polymeric ion $Zn_2acac_3^+$ is twice as abundant in the chemical ionization mass spectrum as in the electron ionization mass spectrum. The direct exposure probe mass spectra also contain increased abundances of the higher mass ions, or in the case of DCI, new ions such as $Zn_3(acac)_5^+$.

Figure 2 contains the electron ionization and direct exposure electron ionization mass spectra of vanadium acetylacetonate. The direct exposure electron ionization mass spectrum contains the higher mass polymeric ions in greater relative abundances. The polymeric ion at m/z 597 $V_2acac_5^+$ is about 17 times more abundant in the DEI spectrum. The ion at m/z 763 $V_3Oacac_6^+$ is observed exclusively in the DEI spectrum. The ions above m/z 597 have not been previously observed. In general, the direct exposure electron ionization mass spectra contain more abundant high mass ions for all of the transition metal acetylacetonates studied.

Figure 3 compares the daughter ion MS/MS spectra of a mixed metal polymeric ion formed by the electron ionization and direct exposure probe electron ionization mass spectra of a 1:1 stoichiometric mixture of two metal acacs. Most of the daughter ions are themselves bimetallic. The acetylacetonate ligands dissociate, generating losses of 43, 59, 82, and 99 daltons. The bis acac ion loses 18 daltons (presumably water) in each case. Metal atoms are lost as $Me(acac)_2$ to form the daughter ions $Me(acac)^+$. The ratios shown are reproducible for each ionization method. The increased relative abundance of the $Me(acac)^+$ ion in the DEI spectrum suggests a difference in the nature of the parent ion selected. The ratio of the $Cr(acac)^+$ to $Mn(acac)^+$ ion also varies with the collision energy in the rf-only quadrupole.

Figure 1

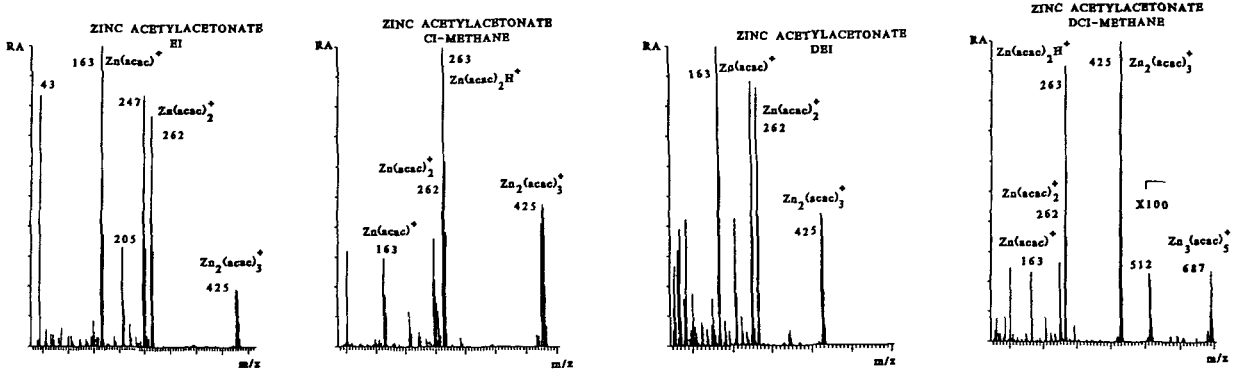

Figure 2

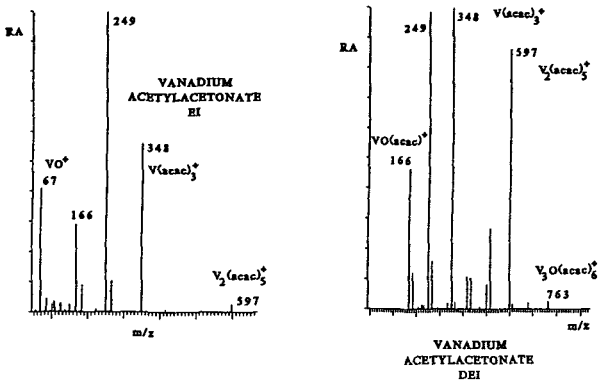

Figure 3

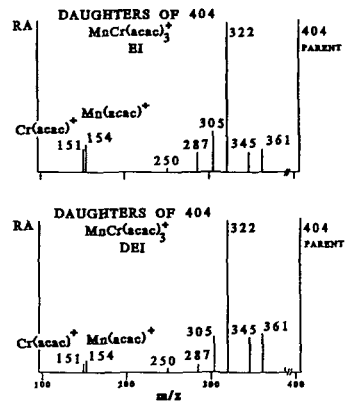

THE ANION-STABILIZING EFFECT OF THE TRIMETHYLSILYL GROUP

John E. Bartmess and Deborah A. Thomas
Department of Chemistry, University of Tennessee, Knoxville, TN 37996

The objective of this project is to determine both the stabilizing effect of a trimethylsilyl group on an adjacent anion, and the stability of the trimethylsilyl anion itself. It is expected that both polarizability interactions and polar effects should play a role. This work was conducted using a pulsed ICR spectrometer.

When alkylsilanes are reacted with various anions in the gas phase, the Lewis acid/base chemistry tends to predominate over the Bronsted chemistry. Addition to give a pentavalent intermediate, followed by fragmentation involving loss of some of the attached groups, is common. It is also difficult to obtain some of these in pure form. Trace amounts of Me_3SiCl give copious Cl^- signals, and trace $(Me_3Si)_2NH$ in Me_3SiNH_2 interferes with establishment of the equilibrium.

The ΔG^o_{acid} for Me_3SiH was determined experimentally by bracketing methods in the ICR instrument. It was necessary to bracket the Me_3SiH acidity since, as reported by the groups of both Bowie and DePuy, silanes undergo an addition/elimination process rather than the desired Brønsted acid-base equilibrium. The Me_3Si^- was produced by fluorodesilylation of hexamethyldisilane. The acidity of Me_3SiH was bracketed between that of pivaldoxime and acetoxime, giving ΔG^o_{acid} = 358.8±4 kcal/mole and ΔH^o_{acid} = 366.7±4 kcal/mole. Similarly, the ΔG^o_{acid} for trimethlysilylamine and trimethylsilanol were determined experimentally by bracketing methods. The anions were produced by fluorodesilylation of hexamethyldisilazane and hexamethyl-siloxane. The amine is not protonated by methanol, but is protonated by t-butyl alcohol and $(Me_3Si)_2NH$, for ΔG^o_{acid} = 371.0±3 kcal/mole and ΔH^o_{acid} = 378.9 kcal/mole. ΔG^o_{acid} for the trimethylsilanol (Me_3SiOH) is between that of pivaldoxime and acetoxime, giving ΔG^o_{acid} = 358.8±4 kcal/mole, and thus ΔH^o_{acid} = 365.5 kcal/mole.

ΔG^o_{acid} for hexamethyldisilazane [$(Me_3Si)_2NH$] was determined by the standard equilibrium method. $(Me_3Si)_2N^-$ was produced by proton abstraction using either isoamyl alkoxide or fluoride. ΔG^o_{acid} = 352.9 kcal/mole, relative to m-chloroaniline and pyrrole. With ΔS^o_{acid}=24.6eu, ΔH^o_{acid}=360.3 kcal/mole.

By the bracketing experiments of Depuy and coworkers in the flowing afterglow spectrometer, ΔG^o_{acid} for $(C\Delta H_3)_3SiCH_3$ is 390±6 kcal/mole, between ammonia and water. While equilibrium studies should be viable for this acid, the gas phase acidity scale is currently poorly developed in this region. This result gives ΔH^o_{acid} = 399±6 kcal/mole.

Thus, for ΔH^o_{acid}, the trimethylsilyl group increases the acidity of methane by 18±7 kcal/mole, of ammonia by 24.7±4 kcal/mole, and of water by 24.7±4 kcal/mole. The second trimethylsilyl group on ammonia shows a saturation effect, increasing the acidity over the first substitution by only 18.6±4 kcal/mole.

The ΔH^o_{acid} for silane is known to be 371.5±2.3 kcal/mole. Therefore, Me_3SiH is more acidic than silane by about 5 kcal/mole. In contrast to the silanes, the analogous carbon acids CH_4 and Me_3CH differ by less than a kcal/mole, based on the kinetic technique of DePuy and coworkers. ΔH^o_{acid} for methane is 416.6 kcal/mole while the ΔH^o_{acid} for isobutane is estimated to be 416.0 kcal/mole. The electronegativities are in the order Si<H<C, so methyl should be inductively more electron accepting on silicon than hydrogen. Thus methyl stabilizes silanions, relative to hydrogen, while hydrogen should destabilize carbanions, relative to methyl.

NEW SOURCES OF ELECTRON IMPACT PRODUCED ANIONS

John E. Bartmess and Cathy Crowder
Department of Chemistry, University of Tennessee, Knoxville TN 37996-1600

The objective of this project is to design a method by which desired anions can be produced in the gas phase by the dissociative attachment process with a large cross section. A rational scheme for the structure of precursor molecules is sought. To produce low energy anions in the gas phase it is proposed that the following conditions should be met:

1. The lowest unoccupied molecular orbital must be bound.
2. There must be a suitable low energy dissociative channel.
3. The excited state $[AB^-]^*$, must live long enough to dissociate.

A proposed molecule is $Ar-N=N-CR_2-G$. In this system G is a good electron accepting group such as nitro or acetyl. The π system of the arylazo moiety captures the electron and the azo bonds form a weak link which can dissociate. The result is the $R_2C=G^-$ carbanion, plus $PhN=N^\cdot$ or $Ph^\cdot$ and N_2. The structures tested here were synthesized by adding the dry salt $BF_4^-PhN_2^+$ to an aqueous solution of the carbanion of interest $[Me_2C=NO_2^-, MeC(COCH_3)_2^-]$. Attempts at acylation of the lithio anion of acetone phenylhydrazone gave only N-acylated product, not the desired C-acylation.

Pulsed ion cyclotron resonance spectrometry was used to generate and detect the anions at pressures ranging from 1 to 10 microtorr, depending on the volatility of the sample.

For R=Me, $G=NO_2$, for $R=CF_3$, $G=CF_2CF_2CF_3$, and for PhN=NNHPh, copious amounts of anions were seen. These are structures, however, where the -G group is capable of dissociative attachment itself. In these cases, the phenylazo group provides the dissociative ability, but not necessarily the electron capture aspect. For R=COMe, G=Me, no anions were seen with Ar=phenyl, but for Ar=p-nitrophenyl, the desired reactivity was observed. We can thus "tune" the structure as needed with ring substituents, to vary the lifetime of the radical anion before electron detachment and increase the probability of dissociation before electron detachment occurs.

In contrast, azobisisobutyronitrile does not give anions under these conditions, though it is known to thermally dissociate to N_2 and $Me_2CCN^\cdot$. It lacks the bound π system to capture the electron long enough for dissociation. $PhN=NSO_2Ph$ also does not give the expected anion; the dissociative channel may not be low enough in energy.

Dissociative attachment data were also reported for a number of CH_3COX and PhCOX structures.

ACKNOWLEDGEMENT: We thank Dr. Bruce Smart of DuPont for the sample of phenylazo-perfluoro-tert-hexane.

SUBSTITUENT EFFECTS ON GAS PHASE ELIMINATION PROCESSES

John E. Bartmess and Terry Sumpter
Department of Chemistry, University of Tennessee, Knoxville TN 37996-1600

The anionic β-elimination reaction has been shown to occur in the gas phase for a number of leaving groups, but only limited studies have been done of the E_1cb-E_2-E_1 spectrum as a whole. We are studying the effect of structural variation on the substrate, so as to determine the effect of solvent on this reaction, by comparing the gas phase and solution phase data. In the gas phase, if the overall elimination reaction is exothermic, then only the free anionic leaving group is observed. If the reaction is endothermic, but less so than the hydrogen bond strength of the conjugate acid of the attacking base forming a cluster ion with the leaving group, then the cluster ion is observed. The groups of Depuy, Jennings and Beauchamp have observed this E_2 vs. cluster formation pattern of reactivity. The thermochemical threshold for the changeover is not well defined, however. DePuy and coworkers have clamined that structural effects on eliminations in dialkyl ethers imply an E_1cb mechanism, with carbanionic development in the transition state. Here we have investigated cases where there should be unambiguous anionic contribution to the mechanism.

The reactivity of a prototypical E_1cb system, $PhCH_2CH_2Y$, undergoing elimination of Y^- upon attack by anionic bases, has been investigated using ICR spectrometry. A value for the stability of the benzylic carbanion $PhCHCH_2Y^-$ is needed, in order to examine the nature of the reaction coordinate. By the usual gas phase equilibrium acidity methods, $PhCH_2OCH_3$ has ΔH^o_{acid} = 376.4 kcal/mole, and $PhCH_2CH_3$ is 378.2 kcal/mole. Thus, $PhCH_2CH_2OR$ should be ca. 377 kcal/mole; leaving groups such as acetate and chloride should increase this by 2-3 kcal/mole at most. $PhCH_2CH_2OH$ has ΔH^o_{acid} = 371.5 kcal/mole.

For $PhCH_2CH_2OCH_2CH_3$, there is the possibility of E_2 elimination across the ethyl group to give $PhCH_2CH_2O^-$ or its cluster ion. Neither product is observed on reaction with methoxide; only the E_1cb product $MeOH\cdot\cdot{}^-OEt$.

KINETICS - Efficiencies relative to k_{ADO}

LG	Base= MeO^-	ΔH^o_{rxn}	Base = $iAmO^-$	ΔH^o_{rxn}
OMe	-	+11	0.00 free	+19
		-11	0.77 cluster	-4
OEt	0.0	+8	- free	+16
	0.40	-12	cluster	-2
$OCH_2CH{=}CH_2$	0.75	+5	0.76 free	+13
	0.48	-15	0.41 cluster	-8
OAc	0.05	-27	0.13 free	-19
	0.00		0.00 cluster	

PROBLEMS

The trifluoroacetate group gives copious amounts of $CF_3CO_2^-$ on electron impact; we have not yet done double resonance ejection studies to get clean kinetics. The trifluoroethanol group undergoes elimination of HF with clustering, in preference to elimination of the trifluoroethoxide.

Thermochemically, acetate should be a much better leaving group than the alkoxides studied here. The low efficiency can be attributed to side reactions such as transesterification and subsequent deprotonation of the acetete esters; the appropriate ions are seen for all attacking alkoxides.

For both alkoxide bases with allyl alkoxide as the leaving group, only cluster ions should be accessible thermochemically, yet we see appreciable amounts of $CH_2{=}CHCH_2O^-$. We believe this arises from production of the cluster ion with sufficient internal energy to cause fragmentation of part of the population; $CH_2{=}CHCH_2O^-\cdot\cdot HOMe$ production is ca. 15 kcal/mole exothermic.

OBSERVATION OF CARBON-HELIUM IONS

S. E. Young and M. J. Coggiola
Mass Spectrometry Group
SRI International, Menlo Park CA 94025

Stable cations containing helium are well known, however, none of these ions involves a helium-carbon bond. Recently, a number of ions containing both carbon and helium have been theoretically predicted to exist as stable species [1,2], including $C_2He_2^{2+}$, $COHe^{2+}$, $CNHe^{2+}$, and C_2He^+. Of these, $C_2He_2^{2+}$ is calculated to be the most stable dication species, requiring 80 kcal/mole to lose a neutral helium atom, and 113 kcal/mole to lose a helium ion. The calculated bond lengths in $C_2He_2^{2+}$ are very nearly the same as for the isoelectronic acetylene molecule. Despite this predicted stability, the $C_2He_2^{2+}$ ion has not been previously observed.

Motivated by these predictions, we have carefully examined the ion species formed in a low-pressure helium discharge having a graphite cathode. The source was formed from a 0.5" diameter quartz tube fitted with a brass tip having a 0.014" diameter extraction aperture. The cathode consisted of a 0.125" diameter spectroscopic grade graphite rod with a 0.078" diameter hole drilled 0.125" deep to form a hollow cathode. A voltage of 2-3 kV was applied between the probe tip and the cathode. Helium at a pressure of approximately 1 Torr was admitted into the source, causing a discharge to form spontaneously. The cathode to anode spacing was 0.5-0.75". Ions were extracted from the source at 6 kV and focussed using a dual quadrupole electrostatic lense before being mass analyzed by an MS-9 double focussing spectrometer. Resolution of the MS-9 was approximately 6000. A narrow mass range of 0.1 AMU was repetitively swept by a multichannel scaler that drove the magnet and accumulated the ion counts. Integration times of 30 minutes or more were required to obtain the spectra shown below.

Figure 1 shows a mass spectrum taken at a nominal m/z of 16. Six peaks are clearly distinguishable above the background. The three largest peaks (a,c,f) were identified by accurate peak matching as $^{12}CH_4^+$, $^{14}NH_2^+$, and O^+, respectively. Peaks (b) and (d) were calculated to have exact masses corresponding to $^{13}CH_3^+$ and $^{15}NH^+$. The remaining peak (e) was found to have an exact mass of 16.00251, in excellent agreement with the expected mass of $C_2He_2^{2+}$ or CHe^+ of 16.00260.

As further confirmation of the formation of a carbon-helium ion, isotopic substitution studies were undertaken using ^3He. Figure 2 shows a narrow mass region in the vicinity of the $C_2{}^3He_2^{2+}$ ion. The two largest peaks are due to NH^+ (15.0109) and CH_3^+ (15.0235). The high mass shoulder peak at 15.019 corresponds to $^{13}CH_2^+$, while the low mass shoulder peak at 15.016 corresponds very well with the expected position of $C_2{}^3He_2^{2+}$ or C^3He^+. A corresponding spectrum taken with only ^4He in the ion source showed the peak at 15.016 to be completely absent.

Using a $^3He/^4He$ mixture in the discharge ion source, it should be possible to determine if the observed ion is CHe^+ or $C_2He_2^{2+}$. The former will give rise to peaks at nominal m/z of 15 and 16, while the latter will produce peaks at m/z 15, 15.5, and 16. A preliminary search in the region of m/z 15.5 showed no evidence of a peak. However, the lack of nearby accurate calibration masses makes this search difficult,

and further work is needed to confirm the composition and charge of the observed ion species.

These observations represent the first experimental evidence of the existance of ion species containing a carbon-helium bond. These ions exist as either stable species, or with metastable lifetimes exceeding 10 μs.

[1] W. Koch and G. Frenking, submitted to J. Chem. Phys.
[2] D. L. Cooper and S. Wilson, Molec. Phys. 44, 161 (1981).

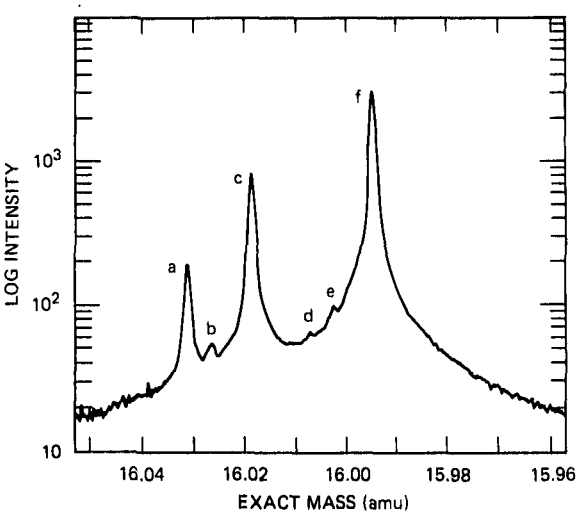

Figure 1. High resolution mass spectrum of ions formed in a low-pressure carbon-helium discharge. The peaks are identified as: (a) CH_4^+; (b) $^{13}CH_3^+$; (c) NH_2^+; (d) $^{15}NH^+$; (e) $C_2He_2^{2+}$ or CHe^+; (f) O^+.

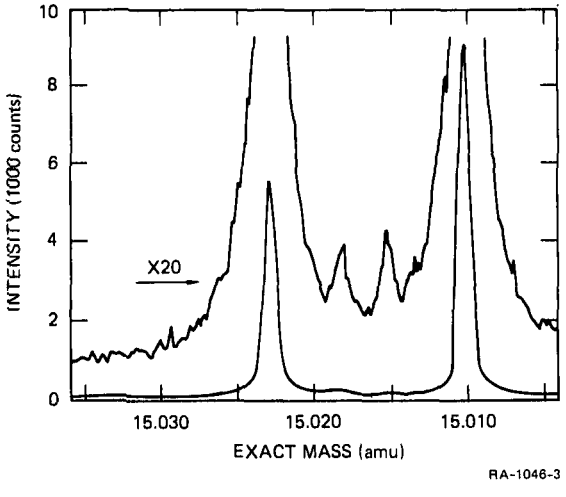

Figure 2. Mass spectrum of ions formed using ^3He in the discharge. The peaks are identified as CH_3^+ (15.0235), $^{13}CH_2^+$ (15.0190), $C_2He_2^{2+}$ or CHe^+ (15.0160), and NH^+ (15.0109).

UNIMOLECULAR DECOMPOSITION OF HEPTYL IONS IN THE MICROSECOND TIME SCALE

C. Guenat*, D. Stahl and T. Gäumann
Institut de Chimie-Physique, EPFL-Ecublens, CH-1015 Lausanne, Switzerland
* Present address: NIEHS, P.O. Box 12233, Research Triangle Park, NC 27709

Heptyl ions are the first in the homolog series of alkyl cations which do not experience complete randomization of the carbon atoms prior to metastable decomposition. Instead, the ions seem to follow specific rearrangement schemes through protonated cyclopropane intermediates. In the work presented here, the unique metastable fragmentation pathway of heptyl ions [reaction (1)] has been monitored for over fifty carbon-13 mono- and

$$C_7H_{15}^{+} \text{ ------> } C_4H_9^{+} + C_3H_6 \qquad (1)$$

multi-labeled compounds having three initial isomeric structures. This study enabled us to propose a new model for the fragmentation of heptyl ions which have undergone extensive rearrangement, prior to propene loss. This model allows the calculation of probabilities for one or any combination of carbon atoms to be part of this fragment and applies to the fragmentation of any heptyl ion isomer. Two cases are considered, depending on whether the initial heptyl ions are branched or linear.

BRANCHED HEPTYL IONS

Experimental observations:
- Each primary carbon atom has approximately the same probability of being contained in the propene neutral fragment.
- The same observation is true for the internal carbon atoms.
- The probability to simultaneously lose three primary carbon atoms is nearly equal to zero (i.e., each propene fragment contains at least one carbon atom arising from an internal position of the initial structure).

From these results, the model presented in scheme 1 has been deduced. The key is to postulate a structure before fragmentation, which has two types of carbon atoms, all being equivalent within a category. The first category contains three carbon atoms from which two are being lost. The second one has four carbon atoms with one being lost as part of the propene fragment. A suitable structure could be a protonated cyclopropane substituted with four methyl groups, each being able to migrate from one corner to another (structure c). The carbon atoms labeled (★) originate from the position labeled (•) in the original structures.

Scheme 1.

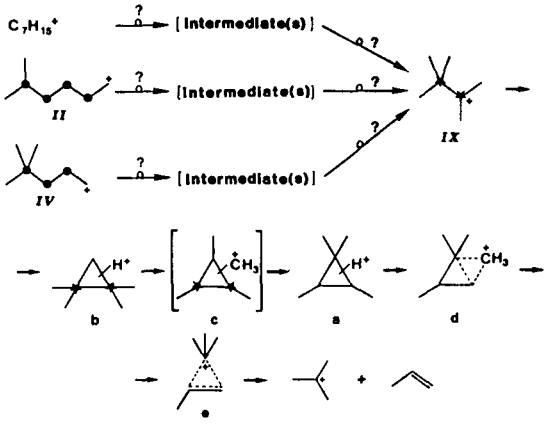

The probabilities for losing different combinations of carbon atoms as predicted by the model, are given in table 1, along with experimental data ("A∩B" means that carbon atoms A and B are lost together). No labeled precursors were available for the t-butyldimethylcarbenium ion (structure IX).

LINEAR HEPTYL IONS

Experimental observations:
- The two primary carbon atoms have almost an equal probability of being lost with the propene fragment.
- The internal carbon atoms are no longer equivalent as was the case for the branched isomers. There is, nevertheless, a symmetry with respect to carbon atom 4.

The model presented in scheme 1 still applies in this case, but further consideration is also required. By isomerization towards a branched isomer, some internal carbon atoms of the n-heptyl ions must become situated at a terminal position. Carbon atom 4 can only occupy an internal position in structure IX (*) if the other internal position is occupied by carbon atoms 2 or 6. In other words, carbon atom 4 behaves either as a primary or as an internal carbon atom. Consequences are that some possibilities for structure IX are not allowed and some combinations for structure c may have statistical weights equal to 1, 2 or 3.

Table 2 presents the results predicted by the model as well as the experimental data ("A∩B" means that carbon atoms A and B are lost together). The numbers in parentheses are the values for the symmetrical positions.

The model presented here allows one to calculate the probabilities for the loss of any combination of carbon atoms as part of the propene fragment. Results are in very good agreement with the experimental data obtained for the three isomers studied. This model takes into account the final phase of the rearrangement and subsequent fragmentation. The first steps, however, are unknown at this point and may involve a mixture of tertiary structures and protonated cyclopropanes.

C-atom(s)	II		IV		IX
	calc.	exp.	calc.	exp.	calc.
1	33,3	32,7	33,3	32,8	33,3
2	50,0	48,8	55,6	54,9	66,6
3	50,0	50,6	55,6	55,3	66,6
6	33,3	30,5	33,3	32,5	33,3
1∩2	13,3	12,6	15,6	14,5	20,0
1∩3	13,3	13,5	15,6	15,4	20,0
1∩6	6,7	5,7	6,7	5,6	6,7
2∩3	20,0	20,2	24,4	24,9	33,3
1∩2∩3	3,3	-	4,4	5,2	6,7
4∩6∩7	1,7	-	2,2	1,5	0,0
1∩6∩7	0,0	0,6	0,0	0,5	0,0
2∩3∩4	5,0	-	6,7	-	6,7
1∩2∩4	3,3	-	4,4	-	3,3

Table 1.

C-atom(s)	I		
	calc.	exp.	
1	33,3	32,6	(29,9)
2	50,0	49,7	(51,2)
3	45,8	46,3	(46,9)
4	41,7	40,4	
1∩2	13,3	12,3	(11,7)
1∩3	11,7	11,6	(10,8)
1∩4	10,0	-	
1∩7	6,7	5,2	
2∩3	18,3	18,1	
2∩4	16,7	-	(16,9)
2∩6	20,0	19,9	
3∩4	15,0	14,6	(14,5)
3∩5	16,7	-	
1∩2∩3	2,9	3,3	
1∩4∩7	0,8	-	
2∩4∩6	4,2	-	
3∩4∩5	3,3	-	

Table 2.

SOLVENT AND CONCENTRATION EFFECTS ON THE FORMATION AND STABILITY OF POSITIVE AND NEGATIVE CLUSTER IONS OF TETRA-ALKYLAMMONIUM HALIDE SALTS

Emirgül Tolun* and John F.J. Todd, Chemical Laboratory, University of Kent, Canterbury, Kent, CT2 7NH, U.K. *Present address, UTCHS, Stout Neuroscience Mass Spectrometry Laboratory, Memphis, TN 38163, U.S.A.

Introduction: Fast atom bombardment mass spectrometry (FABMS) of tetra-alkylammonium halide salts (NR_4X where X = Cl, Br, I and NR_4 = NMe_4, NEt_4) show positive and negative cluster ions of the type $[(NR_4)_{n+1}X_n]^+$ and $[(NR_4)_nX_{n+1}]^-$, extending at least up to n = 14. Ion intensity enhancements observed at particular n-values (n = 4, 7, 8, 13 or n = 6, 12) are related to the formation of certain stable structures and also to the cation and anion size (1). However, both the anomalous ion intensity regions and occurrence of larger cluster ions (n<5) gradually disappear as the salt + glyerol solution is diluted. The objective of this study is to investigate the effect of concentration on the stabilities and on the degree of fragmentation of cluster ions. The collision induced dissociation (CID) spectra recorded from different concentrations of salt solutions are compared for the cluster ions of both glycerol soluble and "glycerol insoluble" salts.

Experimental: The mass spectra of the salts which are readily soluble in glycerol (NEt_4Cl, NEt_4Br and NMe_4Cl) are obtained from 0.1M - 1M salt + glycerol solutions. In the case of the partially soluble salts NEt_4I and NMe_4Br, an ionizing solvent is added to the salt + glycerol mixture in order to achieve a mixed solvent matrix with composition ranging from 30% solvent + 70% glycerol to 80% solvent + 20% glycerol. The FAB mass spectra are obtained on an AEI MS9 double focusing mass spectrometer updated by VG Analytical Ltd., using fast Xe atoms (2mA - 8kV). The CID spectra are obtained with Argon as the target gas using B/E linked scanning.

Results: The anomalous ion intensity regions are observed only when the spectra are acquired from concentrated salt + glycerol solutions (approximately 0.5 -1.0M). As the solution is diluted, the abundance of n<3 cluster ions and ion intensity enhancement at n = 4 decrease, and finally for very dilute solutions n<5 cluster ions are not detected.

The FABMS of the partially soluble salts do not show any ion intensity enhancements when the spectra are recorded from a glycerol-only matrix. However, the addition of an ionizing solvent such as formic acid, formamide or demthylformamide to the salt + glycerol mixture promotes occurrence of both larger cluster ions and anomalous ion intensity regions. This is probably due to the increased solubility and dissociation of the otherwise insoluble salt in the glycerol matrix. Surprisingly, addition of an ionizing solvent to the glycerol soluble salt + glycerol solution has the opposite effect, i.e. a decrease in the cluster ion formation and stabilities observed (2).

The positive and negative CID spectra of the n = 1-5 cluster ions show simultaneous losses of up to four neutral molecules depending on the cluster size (eq. 1, 2).

$$[NR_4(NR_4X)_n]^+ \xrightarrow{-m(NR_4X)} [NR_4(NR_4X)_{n-m}]^+ \qquad (1)$$

$$[X(NR_4X)_n]^- \xrightarrow{-m(NR_4X)} [X(NR_4X)_{n-m})^- \qquad (2)$$

(n = 1-5 and m = 1-4).

Both n = 4, n = 3 and n = 2 positive cluster ions observed from the spectra of concentrated solutions of NR_4X salts preferentially decay to the most intense $[NR_4)_2X]^+$ (n = 1) cluster ion.

A comparison between the CID of $[(NR_4)_{n+1}X_n]^+$ cluster ions recorded from dilute and concentrated salt solutions shows distinct differences in relative intensities and fragmentation pathways, the major difference being the overall decrease in the fragment ion abundances as the salt concentration is lowered. This is clearly illustrated when

the ratio of normalized total fragment ion abundances observed from the FAB-CID of cluster ions formed in concentrated salt solutions (1M) (I_{tc}) to those formed in dilute salt solutions (0.1 - 0.2M) (I_{td}) are plotted against precursor cluster number (n) (i.e. I_{tc}/I_{td} vs. n plots) (Figure 1). The difference in the extent of fragmentation of $[(NEt_4)_{n+1}Br_n]^+$, $[(NEt_4)_{n+1}Cl_n]^+$ and $[(NMe_4)_{n+1}Cl_n]^+$ as shown in Figure 1 are related to ionic size effects.

Conclusions: This study has demonstrated that the solubility and salt concentration in the liquid matrices used are critical factors in determining cluster formation and stabilities. It is argued that the decrease in fragmentation is related to the decrease in internal energies of the cluster ions sputtered from dilute solutions since the matrix molecules may absorb some of the energy deposited by the fast atom beam. The CID results obtained from different salt concentrations in glycerol or glyerol + solvent matrices suggest that the physical and chemical properties of different solvents might be important in dissipating the energy of the primary atom beam.

References

1. E. Tolun, J.F.J. Todd, Org. Mass Spectrom. submitted (or accepted) for publication.

2. E. Tolun, PhD Thesis, University of Kent, U.K., 1986.

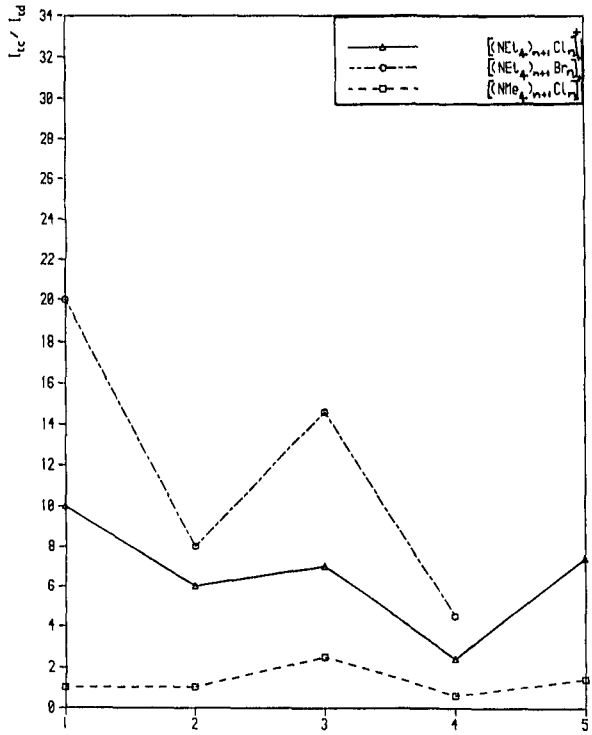

Figure 1. Relative increases in CID fragmentation of $[(NR_4)_{n+1}Xn]^+$ (n = 1-5) with concentration for glycerol "insoluble" salts.

RADIATIVE RELAXATION of PHOTOEXCITED C_6H6^+ AND $C_6D_6^+$ IONS:

Hun Youg So, Robert C. Dunbar
Department of Chemistry, Case Western Reserve University, Ohio 44106 USA

Two-photon dissociation of $C_6H_6^+$ and $C_6D_6^+$ ions is measured at low pressure to investigate the mechanism of the collisionless energy dissipation channel for photoexcited ions. The radiative relaxation rates of these ions are measured using a chopped laser at 488 nm and are compared with calculated radiative internal energy dissipation rates for neutral counterparts.

The two-photon dissociation process is a successful approach to determining the rates and mechanism of the dissipation of internal excitation by infrared fluorescence. The focus of the present study is on the observation of an isotope effect for the title ions to clarify the factors underlying the faster relaxation rates of polyatomic ions compared with those of neutral counterparts. The mechanism itself and the factors determining the relaxation rate are not fully understood yet.

To raise the internal energy of $C_6H_6^+$ and $C_6D_6^+$ ions above the dissociation threshold, more than 4 eV of energy is required. Following absorption of a first photon (488 nm, 2.53 eV), dissociation by a second photon can be observed only if the second photon is absorbed before the ion dissipates sufficient energy to relax it below its one-photon threshold. Study of several polyatomic ions has shown that timescales of tens to hund-reds of milliseconds are required to dissipate 1-2 eV of internal energy. The repetitively pulsed laser scheme was adopted in this work for the best combination of sensitivity and accuracy. Variations in observed photodissociation with chopping rate are due to the varying extent of relaxation of the ions between successive pulses. For relaxation rate determination, computer simulation of two-photon kinetics is used to fit the chopper rate dependence.

These relaxation rates were compared with the calculated values for neutral counterparts. The infrared radiative properties of the neutrals can be calculated with confidence fron the known ifrared absorption intensities via the Einstein transition coefficients and statistical considerations.

Table I Radiative Relaxation Rates, s^{-1}

	Ion	Neutral
C_6H_6	11±2	3.2
C_6D_6	11±2	1.2
Ratio(H/D)	1±0.05	2.7

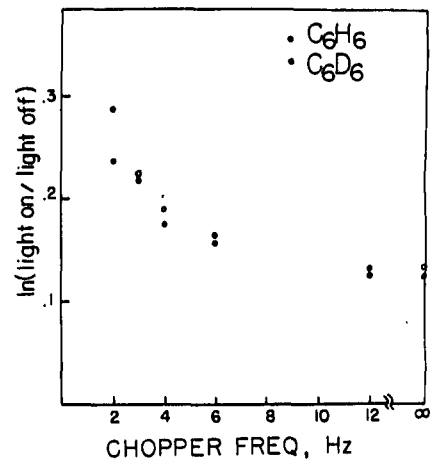

Fig. 1. Chopper rate dependence of photodissociation

The chopper-rate dependence for the benzene and deuterated benzene ions are shown in Fig. 1. The kinetic scheme is used for the simulation. Table 1 shows the observed radiative relaxation rates of the ions and the calculated ones of neutrals. A strong isotope effect on radiative relaxation rate is clearly expected because mode frequencies and intensities are decreased for deuterated benzene. Under the assumption that ions radiate infrared photons like neutrals, we can expect an isotope effect of a factor of 2 to 4. The absence of a noticeable isotope effect and the surprisingly high relaxation rate are unexpected. The observed relaxation rates imply that infrared fluorescence in the ions may be dominated by an extremely strong infrared active mode involving little C-H(C-D) motion. The asymmetric ring deformation and stretching mode is the most probable active mode when C-H or C-D modes are excluded.

Conclusions

1) No isotope effect is noticeable.
2) Infrared radiative intensities are much greater in the ions.
3) The ring deformation mode could be predominent
4) Possible charge displacement could be the major contribution for vibrational radiative relaxation.

References

1) R. C. Dunbar, Chem. Phys. Lett., 125 (1986) 543
2) J. P. Hanovich, R. C. Dunbar, T. Lehman; J. Phys. Chem., 89 (1985) 2513

THERMOCHEMICAL PROPERTIES OF POTASSIUM CATIONS

D. H. Evans, R. G. Keesee, and A. W. Castleman, Jr., Department of Chemistry, The Pennsylvania State University, University Park, PA 16802 USA.

Using a variable temperature high pressure mass spectrometer, the thermodynamics of the $K^+(CH_3OH)_n(H_2O)_m$ mixed cluster system was measured. The basic apparatus and general procedure to conduct these experiments has been described previously (1). Potassium ions are produced via thermionic emission from a platinum filament coated with a matrix containing a potassium salt. The ions are directed into a reaction cell of well defined temperature containing a mixture of methanol and water diluted with carbon dioxide to desired levels. The pressure is maintained sufficiently high (1-10 torr) such that ions reside in the reaction cell for a time adequate to ensure the attainment of equilibrium. After exiting a 75 micron diameter orifice the ions are mass analyzed with a quadrupole mass spectrometer and counted. The equilibrium constant is calculated (1) from the measured ion intensities and known partial pressure of the clustering neutral, By determining the equilibrium constant as a function of temperature, the enthalpy and entropy changes of the reaction can be found using standard thermodynamic equations. Measurements were taken over the range of 0°C to 200°C and clusters with up to four attached neutral ligands were studied.

The measured thermodynamic quantities for the $K^+/CH_3OH/H_2O$ system are listed in Table I along with relevant values determined previously. For the association reaction of H_2O onto K^+CH_3OH and $K^+(CH_3OH)(H_2O)$, the water vapor pressure was inferred by simultaneously monitoring the $K^+(H_2O)_n$ intensities and using well known equilibrium constants for K^+ hydration. Enthalpy and entropy changes were determined through closure of thermodynamic cycles for the ligand exchange reactions and for association reactions not measured directly. Alternatively, consistency of the data can be verified where the thermochemical properties of the formation of a cluster can be traced via two routes. For example, experimental data for the formation of $K^+(CH_3OH)_2(H_2O)$ from $K^+(CH_3OH) + CH_3OH + H_2O$ can be obtained from two different routes:

$$K^+(CH_3OH) \xrightarrow{CH_3OH} K^+(CH_3OH)_2 \xrightarrow{H_2O} K^+(CH_3OH)_2(H_2O)$$

giving -29.3 kcal/mole and -53.0 cal/K mole, respectively, for the $\Delta H°$ and $\Delta S°$. These values compare well with the respective ones of -29.1 kcal/mole and -49.8 cal/K mole for the route:

$$K^+(CH_3OH) \xrightarrow{H_2O} K^+(CH_3OH)(H_2O) \xrightarrow{CH_3OH} K^+(CH_3OH)_2(H_2O)$$

This indicates that the consistency of the data is good.

Regarding these data on the mixed clusters, some general trends in the enthalpy and free energy changes are evident. First, the successive addition reactions exhibit the usual decreasing trend with increasing size for $-\Delta G^o_{298}$. Second, and most importantly, the enthalpy of association of methanol onto a specific ion is consistently greater than the enthalpy of association of water onto that ion. This cannot be explained on the basis of the dipole of the molecules since the dipole of water is slightly larger than that of methanol, 1.85 debye for water compared with 1.70 debye for methanol. However, the averaged polarizability of methanol is noticeably stronger than that of water, 3.3 $Å^3$ for methanol compared with 1.45 $Å^3$ for water. The larger polarizability of methanol apparently more than compensates for the effect of the stronger dipole of water, thereby leading to a greater bond energy and hence larger enthalpy of association for methanol compared with water.

Acknowledgments:

Support by The National Science Foundation, Grant No. ATM-82-04010, and the Army Research Office, Grant No. DAAG29-84-K-0087, is gratefully acknowledged.

References:

1. A. W. Catleman, Jr., P. M. Holland, D. M. Lindsay and K.I. Peterson, J. Am. Chem. Soc., 100, 6039 (1978).

2. W. R. Davidson and P. Kebarle, J. Am. Chem. Soc. 98, 6125 (1976).

3. S. K. Searles and P. Kebarle, Can. J. Chem. 47, 2619 (1969).

Table 1

The Thermodynamic Quantities for the Association Reaction
$I + B \rightarrow I(B)$ in the $K^+/CH_3OH/H_2O$ System

I	B	$-\Delta H^\circ$ (kcal/mol)	$-\Delta S^\circ$ (cal/K mol)	$-\Delta G^\circ_{298}$ (kcal/mol)	Ref
K^+	H_2O	16.9	19.9	11.0	[2]
$K^+(CH_3OH)$	CH_3OH	18.0	35	7.6	*
$K^+(CH_3OH)$	H_2O	15.6	22.5	8.9	*
$K^+(H_2O)$	CH_3OH	19.6	32.5	9.9	*
$K^+(H_2O$	H_2O	16.1	24.2	8.9	[3]
$K^+(CH_3OH)_2$	CH_3OH	14.5	28	6.2	*
$K^+(CH_3OH)_2$	H_2O	11.3	18.0	5.9	*
$K^+(CH_3OH)(H_2O$	CH_3OH	13.5	27.31	5.4	*
$K^+(CH_3OH)(H_2O)$	H_2O	13.1	22.6	6.4	*
$K^+(H_2O)_2$	H_2O	13.2	23.0	6.3	[3]
$K^+(CH_3OH)_3$	CH_3OH	12.5	29	3.9	*
$K^+(CH_3OH)_2(H_2O)$	CH_3OH	12.5	25.6	4.9	*
$K^+(H_2O)_3$	H_2O	11.8	24.7	4.4	[3]

*Present Work

TUNING THE EFFECTIVE AUTONEUTRALIZATION LIFETIME OF SF_6^-

J.E.Delmore and A.D.Appelhans

Idaho National Engineering Laboratory
EG&G Idaho, POB 1625 Idaho Falls, ID 83415

There have been many measurements of electron autodetachment lifetimes reported for the unimolecular reaction

$$SF_6 + e^- \text{--->} \quad SF_6^- \text{--}^k\text{-->} \quad SF_6 + e^-. \qquad 1$$

This process is termed "autoneutralization", analogous to the term autoionization, whereby an excited molecule autodetaches an electron to give a positive ion. SF_6^- autoneutralization mean lifetimes (1/k) ranging from 10 uS (1) up to milliseconds (2,3) with many intermediate values have been reported (c.f. 4,5). These studies have employed time-of-flight mass spectrometry (1,4), ion cyclotron resonance (2,3), and pulsed-source magnetic-sector mass spectrometry (5) to measure ion-to-neutral ratios, free electron production, and the change in ion intensity with time. It has been proposed (3) that the wide range of reported lifetimes is a result of multiple states of SF_6^- autoneutralizing at different rates (lifetimes), and that the observed mean lifetime is a function of the time frame (from the point of ion formation) in which the observation was made. If this is the case the various techniques previously applied would be expected to produce differing results. Although the multiple-state hypothesis appears reasonable, the mechanism(s) controlling the hypothesized distribution of states (and thus mean lifetime) has not previously been clearly demonstrated

The present study was undertaken to clarify some of these issues by applying an alternate experimental approach: the direct measurement of the SF6 neutrals produced in a beam of SF6- ions under a variety of source temperatures, pressures, and acceleration voltages. The beam was sharply focused, and the ion and neutral components were separated at various points along the flight path via electrostatic or magnetic fields. The neutral beam intensity was measured utilizing a multichannel plate array detector and photometer. There were no significant effects on the measured lifetimes due to pressure or acceleration, however the mean lifetime increased from 15 to 20 uS as the ion source temperature was reduced. Although the individual data sets exhibited a near single exponential behavior, composite analysis indicated multiple states (lifetimes) were active and that the process must involve a mixture of at least three short lived and 1 or more long lived or stable states (6). Thus the rate equation describing the neutral intensity is

$$N(t) = I_1(1 - e^{-k1t}) + I_2(1 - e^{-k2t}) + \ldots + I_n(1 - e^{-knt}). \qquad 2$$

This was determined by examination of the residuals of the exponential fit to the data. Data were collected for several different time windows (from the point of ion formation) and compared with simulated data. The simulated data were produced using a 3-component exponential and then fit assuming a single component exponential to determine the mean lifetime. The agreement of the measured and simulated mean lifetimes and residuals indicated that there were multiple lifetimes. By changing the temperature of the SF_6 gas within the ion source the population distribution (I_n's) of the lifetimes could be varied, higher temperature pumping the molecules into shorter lived states. Figure 1 shows the change in mean lifetime (assuming a single exponential) as a function of ion source (gas) temperature. The results indicate that the distribution of energy states can be controlled to vary the composite autoneutralization rate. Thus the wide variation in previously published lifetimes is most probably due to the different energy state distributions for the different experimental conditions. The major parameter controlling the distribution and thus mean lifetime appears to be the SF_6 gas temperature prior to electron capture.

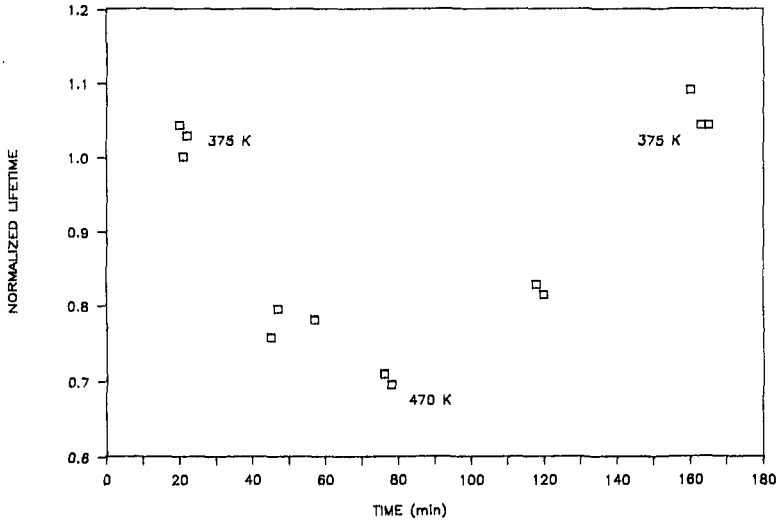

Figure 1. Measured change in the mean lifetime of SF_6^- as a function of the ion source housing (SF_6 gas) temperature normalized to the mean lifetime at 375 K. The SF_6^- ion production was held constant as the source housing (gas) temperature was varied (using resistive heating of Re filaments operated below the electron ejection threshold). The lifetime was measured at several times (temperatures) as the source was heated and cooled. The slow change in the mean lifetime indicates that it is the SF_6 gas temperature, controlled by the source housing temperature that is changing the distribution of energy states and thus the mean lifetime.

REFERENCES

1. D.Edelson, J.E.Griffiths, and K.B.McAfee,Jr. J.Chem.Phys. 37,917-18(1962).
2. M.S.Foster and J.L.Beauchamp Chem.Phys.Ltr. 31,3, 482-486(1975)
3. R.W.Odom,D.L.Smith, and J.H.Futrell J.Phys.B. 8,1349-1366(1975).
4. P.W.Harland and J.C.Thynne J.Phys.Chem. 75,23,3517-23(1971).
5. C.Lifshitz J.Phys.Chem 87,3474-79(1983).
6. J.E.Delmore and A.D.Appelhans J.Chem.Phys., in press.

ACKNOWLEDGMENT

This work was supported by the Division of Chemical Sciences, Basic Energy Sciences, Office of Energy Research, Department of Energy under contract 3ED102.

A TPEPICO-MS STUDY OF THE FRAGMENTATION OF DIMETHYL SULFOXIDE

Zha, Qingmei; Nishimura, T. and Meisels, G. G.
Department of Chemistry University of Nebraska, Lincoln NE 68588

Threshold Photoelectron Photoion Coincidence (TPEPICO) mass spectrometry is a powerful technique for the study of the dynamics of the dissociation of ions because it allows determination of breakdown graph of kinetic energy release distributions, and of fragmentation rate constants of narrowly energy selected ions. This technique therefore has been employed for tests of theories of unimolecular ion dissociation. Most studies have reported excellent agreement between statistical theory and experiment.

Dimethyl Sulfoxide (DMSO) has been chosen for this study because it is a commonly used organic compound, but few appearance potential data have been reported and the mechanism of its fragmentation is not well understood. DMSO also represents an organic molecule containing Sulphur as the heteroatom, a compound class which has not been studied extensively to date by TPEPICO. This study represents another aspect of our attempts to understand better the role of heteroatoms in unimolecular fragmentation of ions.

The experimental breakdown graph (Fig. 1) shows that, in the energy range of 9.0-17.5 eV, the major fragment ions are m/z 63, 61, 47(46,45) and 35(34,33). Five small ions, m/z 31,29,27,18 and 15 (not containing S atom) were detected also; because of their higher appearance potentials and lower relative abundance they were not included in the breakdown graph corrected for the transmission of energetic electrons through the collimated hole structure (Fig. 2). The onset of m/z 63, 61 and 47(46,45) ions occurs at 10.64 eV, 10.55 eV and 10.69 eV respectively where the PES (Fig.3) intensity almost drops to zero. The two-step behavior of the breakdown curve for CH_3S^+ (m/z 47, also 46 and 45) suggests that this ion may be formed by two different pathways: at lower energy directly from m/z 78 parent ion and at higher energy (more than 14 eV) via the CH_3SO^+ ion (m/z 63). The formation of m/z 35(34,33) ion begins at about 13.5 eV, and requires considerable rearrangement of its precursor(s). The appearance potentials of those five small ions coincide with the fourth, fifth and sixth bands in the PES which have π(S=O) and $\pi(CH_3)$ characters.

All of our appearance potential data are lower than those previously reported by other authors using electron impact methods.[1,2] The better accuracy of photoionization reactions is well established, and results to a substantial extent from narrower energy distributions and different threshold behavior. Fig. 4 summarizes the fragmentation pathways.

Fig. 5 is the breakdown graph calculated using the statiatical theory[3,4] in the energy range of 9.0-13.5eV. The curves reflect F factors[5] (indicating lightness of the transition shell) of 0.85, 0.95 and 1.00 for m/z 63, 61 and 47(46,45) ions respectively. Also shown are corrected experimental data points. Even though there are small differences between the experimental and the calculated results, the latter predicting onsets at slightly lower energies, there is generally good agreement, and we conclude that the fragmentation behavior of DMSO can be described adequately in terms of RRKM-QET theory

Acknowledgment: we thank the Department of Energy for support under contract number DE-AS02-76-ER02576.

1. J.C.Blais et al, J.Chim.Phys.Physiochim.Biol. 67, 1457(1970).
2. P.Potzinger et al, Z.Naturforsch. 30A, 340(1975).
3. C.Klots, J.Chem.Phys. 75, 1526(1971).
4. G.Z.Whitten et al, J.Chem.Phys. 38, 2466(19630.
5. R.Bombach et al, Int.J.Mass Spectrom.Ion.Proc. 58, 217(1984).

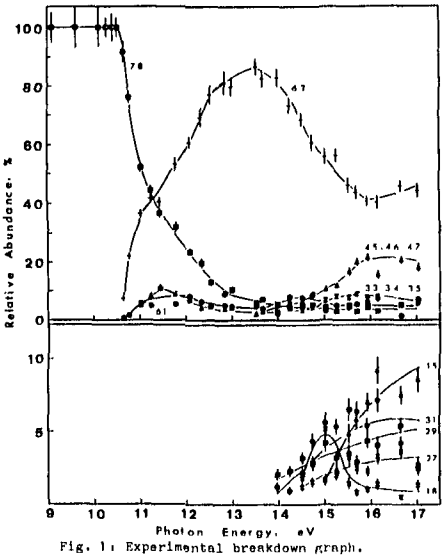

Fig. 1: Experimental breakdown graph.

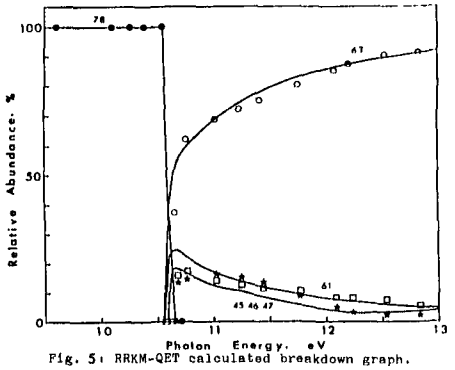

Fig. 5: RRKM-QET calculated breakdown graph.

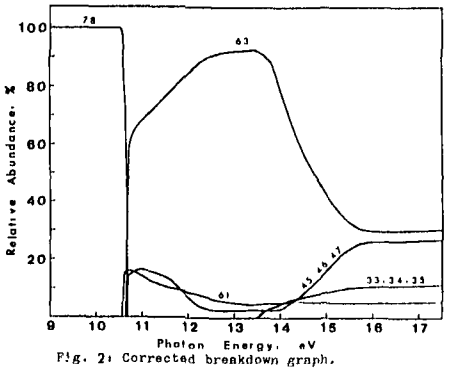

Fig. 2: Corrected breakdown graph.

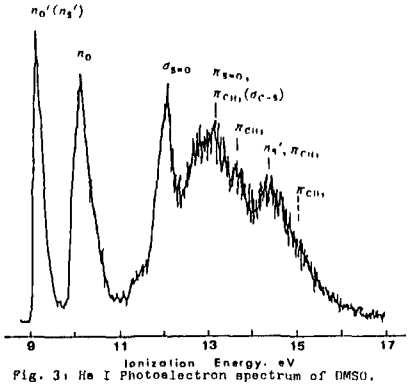

Fig. 3: He I Photoelectron spectrum of DMSO.

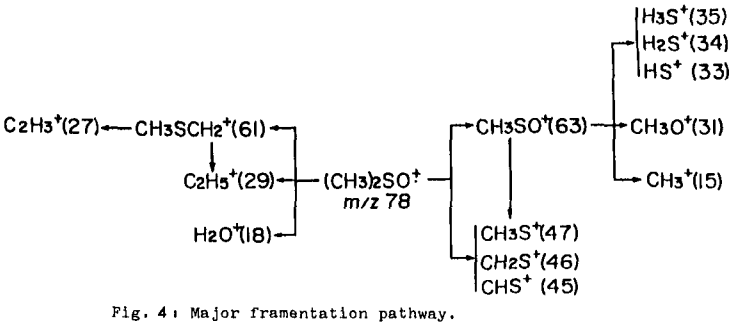

Fig. 4: Major framentation pathway.

THE USE OF A THERMOSPRAY INTERFACE TO A MASS SPECTROMETER AS A FLOW REACTOR FOR IN-SITU THERMAL DEGRADATION STUDIES : APPLICATIONS TO BETA-LACTAM ANTIBIOTICS

Marshall M. Siegel*
American Cyanamid Company, Medical Research Division, Lederle Laboratories
Pearl River, NY 10965

Robert K. Isensee, Debra J. Beck
Oneida Research Services, Inc., Whitesboro, NY 13492

Introduction The ions observed in TSP mass spectra could arise from both condensed-phase and gas-phase reactions. Recently, Bursey, et al. [1] demonstrated that the ionization of neutral analytes arose during TSP/MS studies as a result of gas-phase chemical ionization processes in the TSP source. However, no systematic studies have been reported evaluating the effect of thermal energies on the condensed-phase chemistry occuring in the TSP vaporizer.

Summary Cefixime (a third generation cephalosporin), ampicillin and penicillin V, representative beta-lactam containing antibiotics, were studied via direct injection into a thermospray (TSP) system interfaced to a triple quadrupole mass spectrometer. The temperature of the thermospray vaporizer was varied so as to study in a systematic way the region where the vaporizer temperature was in excess of that necessary for vaporization and degradation. Under such conditions, the molecules decompose producing ions consistant with the condensed-phase chemistry of beta-lactams. These results are correlated with degradation products observed during accelerated stability studies. From the TSP/MS and TSP/MS/MS data, the mechanism for the condensed-phase decomposition reactions of beta-lactams can be deduced. Under the thermal conditions used for these studies, the thermospray interface behaves as a flow reactor and the mass spectrometer as an in-situ detector for condensed-phase thermal degradation studies.

Discussion The TSP/MS spectra of cefixime were obtained at different vaporizer exit temperatures (t2) and block temperatures (t5). Dramatic changes in ion abundances with temperature were observed. As illustrated in Figure 1, the abundance of the $(M+H)^+$ ion optimized at a t2 of about 216° C and increased with t5 over the temperature range of 270 to 325° C. Figure 2 illustrates that the ratios of the ion abundances of a variety of "fragment" ions relative to the $(M+H)^+$ of cefixime increase exponentially as t2 is raised (with t5 held constant). Since the only parameter varied in these temperature profile studies was t2, it must be concluded that the spectral changes were thermally induced.

Many of the observed cefixime "fragment" ions are proton adduct molecular ions of thermally induced degradation products synthesized in the vaporizer probe. Evidence for this thermal mechanism can be garnered from the abundant ions appearing in the cefixime TSP spectrum at m/z 428 $[(M+H-26)^+]$, 287 $[M+H-167)^+]$ and 472 $[(M+H+18)^+]$. TSP/MS/MS of these ions were identical to that of cefixime degradation products 3, 5 and 2, respectively. In the negative TSP mode, an ion at m/z 426, corresponding to deg. 3, $[(M-H-26)^-]$, is observed.

TSP/MS spectra of cefixime and degradation products 1, 2, 3 and 5 were obtained. Among the abundant ions observed in the TSP spectrum of deg. 2 are ions originating from deg. 3 and deg. 4 while the TSP spectrum of deg. 3 does not contain ions arising from deg. 4. This demonstrates that deg. 3 and deg. 4 are both primary degradation products of deg. 2. The formation of deg. 4 is rationalized as arising from deg. 2 via a Meyers type reaction [2,3] for the synthesis of C+1 aldehydes, forming the unobserved intermediate structure 6 which readily undergoes decarboxylation. Deg. 5, a 1,1-diol (hydrated aldehyde), is isolated at room temperature from solution and not deg. 4 . However, when deg. 5 is studied at elevated temperatures by TSP/MS, its equilibrium shifts so as to dehydrate and behave like deg. 4. These primary degradation processes, observed in the temperature profile data for cefixime, are summarized in Scheme i. Scheme i corresponds to the proposed primary degradation scheme of cefixime based upon accelerated stability studies and to similar degradation schemes proposed for cephlosporins and penicillins [4,5].

Ampicillin and penicillin V were directly injected into the TSP interface at temperatures above their degradation temperatures. The outstanding feature of each spectrum is the appearance of the abundant $(M+H-26)^+$ ions. Apparently, the primary degradation processes for these penicillins are similar to the cephaloporins (Scheme i).

The TSP temperature profile study demonstrates that compounds with degradation temperatures in the temperature regime where TSP data can be obtained tend to produce degradation ions. Under these conditions, the TSP vaporizer probe behaves as a heated flow reactor and the mass spectrometer serves to detect and analyze the product ions in-situ.

References

1. M. M. Bursey, C. E. Parker, R. W. Smith, S. J. Gaskell, Anal. Chem. 57, 2597 (1985).
2. J. L. Altman, S. L. Richheimer, Tetrahedron Lett. 4709 (1971).
3. A. I. Meyers, J. L. Durandetta, J. Org. Chem. 40, 2021 (1975).
4. E. H. Flynn, Ed., "Cephalosporins and Penicillins", Academic Press, NY (1972). Chpts. 3 and 5.
5. J. M. Indelicato, D. E. Dorman, G. L. Engel, J. Pharm. Pharmacol. 33, 119 (1981).

Figure 1

TSP Temperature Profile of Cefixime (M + H)$^+$ Ion (m/z 454)

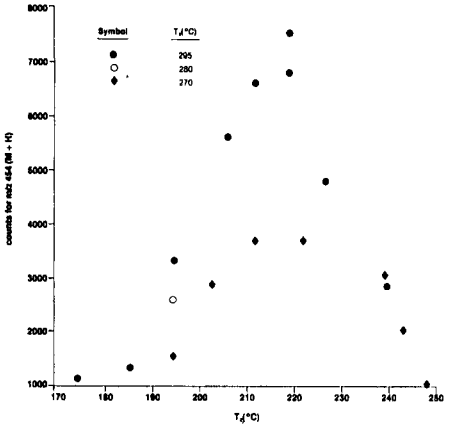

Figure 2

TSP Temperature Profile of Decomposition Ions Relative To (M + H) Ion

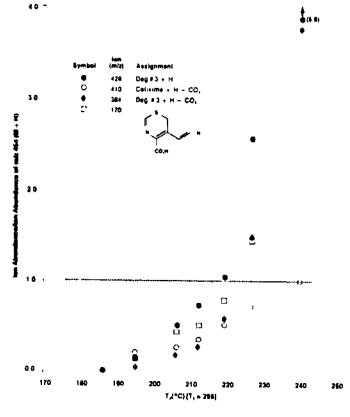

PRIMARY DEGRADATION SCHEME FOR CEFIXIME

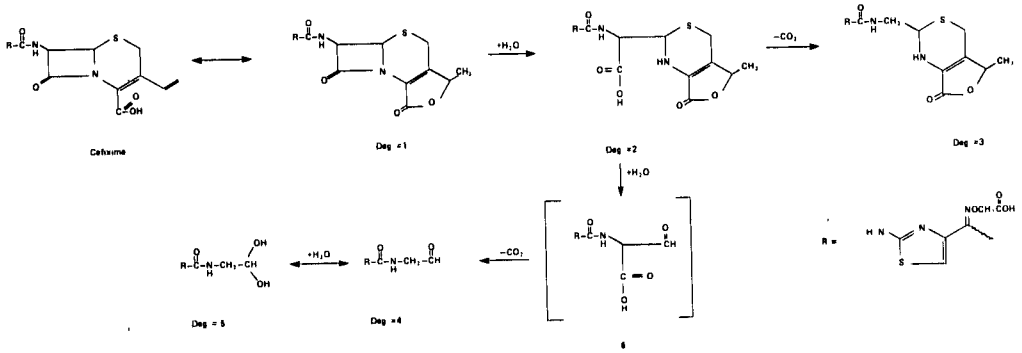

SCHEME I

ANALYSIS OF NAPHTHENES BY NORMAL PHASE LIQUID CHROMATOGRAPHY/THERMOSPRAY MASS SPECTROMETRY

T. H. Wang, Pennzoil Products Company, P.O. Box 7569, The Woodlands, Texas 77387; M. McLean, Department of Chemistry, University of Houston 77004; C. H. Vestal, Vestec Corporation, Houston, Texas 77054.

Introduction:

Thermospray mass spectrometry (MS) has shown great potential for the analysis of non-volatile, thermally labile samples in reverse-phase liquid chromatography using an aqueous buffer solution as a mobile phase[1-2]. A few studies have been conducted in the area of normal phase liquid chromatography. The objective of this research is to expand the thermospray MS technique in conjunction with normal phase liquid chromatography. We have applied this method with a filament-on technique to analyze a class of naphthenic compounds.

Experimental:

The mobile phase for the liquid chromatography was hexane with a flow rate of 0.8 ml/min. The thermospray was interfaced with the HP-5970 mass selective detector and also with the HP-5982 mass spectrometer. Samples were dissolved in hexane and injected directly into the mass spectrometer using a filament-on technique.

Results and Discussion:

The analysis of sixteen naphthenic standards and various naphthenic mixtures by normal phase liquid chromatography/thermospray MS was carried out. Hexane was used as the mobile phase. The spectrum of hexane gave a base peak at m/e 85 which was produced by the $(M-1)^+$ ion. The percent ion intensities of mass spectra of the naphthenic standards by thermospray MS analysis are listed in Table I. The results indicate that the thermospray MS spectrum is represented by a combination of EI and CI spectra. It shows M^+, $(M+1)^+$, $(M-1)^+$, $(M-2)^+$, etc., adducts. It also produces $(M+CH_3+1)^+$, $(M+CH_3)^+$, $(M+CH_3-1)^+$ and $(M+CH_3-2)^+$ adducts by ion-molecular reaction[3].

The naphthenic mixture I contains $C_{35}H_{70}$, $C_{45}H_{90}$ and $C_{55}H_{110}$ with molecular weights of 490, 630 and 770 respectively. The naphthenic mixture II contains $C_{41}H_{82}$, $C_{53}H_{106}$ and $C_{65}H_{130}$ with molecular weights of 574, 742, and 910 respectively. The naphthenic mixtures I and II were analyzed by thermospray MS. The spectra (Figures I & II) reveal intensely abundant molecular ion species $(M-1)^+$ and $(M+CH_3-1)^+$. This technique was particularly useful for compounds having molecular weights greater than 500. In contrast, solid probe EI analysis gave more fragmented ions and very little parent ion information. Semi-quantitation of naphthenic mixtures can also be achieved by comparing the relative intensities of the base peaks $(M-1)^+$.

Conclusions:

The normal phase liquid chromatography/thermospray MS method provides a powerful time-saving procedure for analyzing naphthenic compounds. Comparison of the relative intensities of the base peaks $(M-1)^+$ results in a quick overview of the semi-quantitative content of the samples.

Acknowledgements:

The authors are grateful to Drs. G. P. Sturm, Jr. and S.-Y. Tang of the National Institute for Petroleum and Energy Research for providing the naphthenic standards.

References:

[1] M. L. Vestal, "High-Performance Liquid Chromatography/Mass Spectrometry," Science, 226 (1984) 275.
[2] D. A. Garteiz and L. Vestal, "Thermospray LC/MS Interface--Principles and Applications," Liquid Chromatography, 3, 4 (1985), 335.
[3] J. L. Franklin, Ion-Molecule Reactions, Vol. I & II, Plenum Press (1972).

TABLE I. PERCENT ION INTENSITIES OF MASS SPECTRA OF NAPHTHENIC STANDARDS BY THERMOSPRAY MS ANALYSIS

Compound Name	Chemical Formula	M. W.*	Relative Sensitivity	% Ion Intensity										Fragment Ions
				$(M+1)^+$	M^+	$(M-1)^+$	$(M-2)^+$	$(M-3)^+$ etc.	$(M+CH_3+1)^+$	$(M+CH_3)^+$	$(M+CH_3-1)^+$	$(M+CH_3-2)^+$		
1-(1-n-Hexadecyl)-4-(1-n-Pentadecyl)cyclohexane	$C_{37}H_{74}$	518	1	0	0	0	50	0	0	0	0	0		50
n-Eicosylcyclohexane	$C_{26}H_{52}$	364	20	0	0	0	13	0	15	54	0	0		18
n-Pentadecylcyclohexane	$C_{21}H_{42}$	294	17	0	0	0	30	0	4	11	0	0		55
5-n-decylhydrindan	$C_{19}H_{36}$	264	108	0	3	10	17	10	5	28	0	0		27
5-n-Tetradecylhydrindan	$C_{23}H_{44}$	320	73	0	2	16	31	7	1	18	0	0		25
5-n-Octadecylhydrindan	$C_{27}H_{52}$	376	92	0	0	8	17	43	0	6	0	0		26
2-n-Octadecyldecalin	$C_{28}H_{54}$	390	42	0	0	13	30	3	0	3	0	0		47
2-n-Pentadecyldecaline	$C_{25}H_{48}$	348	298	0	0	6	16	15	4	17	6	35		0
2-(1-n-Hexadecyl)-7-(1-n-Pentadecyl)decalin	$C_{41}H_{80}$	572	59	0	2	14	26	0	0	0	0	0		58
2-n-Octadecylperhydrophenanthrene	$C_{32}H_{60}$	444	175	0	6	10	10	14	4	8	0	2		46
2-n-Tetradecylperhydrophenanthrene	$C_{28}H_{52}$	388	106	3	14	14	5	4	0	5	0	0		55
2-n-Decylperhydrophenanthrene	$C_{24}H_{44}$	332	134	1	11	15	7	7	2	14	0	1		42
Perhydroacenaphthene	$C_{12}H_{20}$	164	1000	0	8	37	9	21	3	17	0	2		3
1-n-Tetradecylperhydropyrene	$C_{30}H_{54}$	414	607	0	12	37	0	0	0	0	0	0		51
1-n-Decylperhydropyrene	$C_{26}H_{46}$	358	307	7	27	12	0	3	1	2	0	0		48
1-n-Hexylperhydropyrene	$C_{22}H_{38}$	302	465	3	18	14	1	43	0	0	0	0		21

*Molecular Weight

FIGURE I. NORMAL PHASE LIQUID CHROMATOGRAPHY/THERMOSPRAY MASS SPECTROMETRIC ANALYSIS OF NAPHTHENIC MIXTURE I

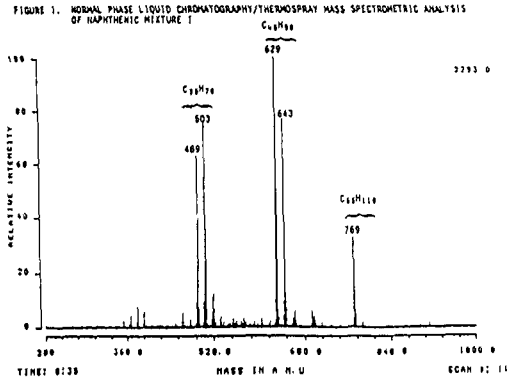

FIGURE II. NORMAL PHASE LIQUID CHROMATOGRAPHY/THERMOSPRAY MASS SPECTROMETRIC ANALYSIS OF NAPHTHENIC MIXTURE II

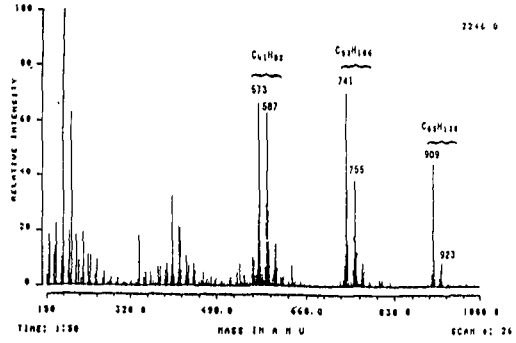

CRITICAL PARAMETERS EFFECTING THERMOSPRAY PERFORMANCE,

R.H. Robins and F.W. Crow, Spectroscopy Development, Product Control, The Upjohn Co., Kalamazoo Michigan

Introduction: Thermospray ionization (TSP) has found its place in mass spectrometry as a routine ionization method and as an interface for HPLC systems. TSP has proven to be a very useful adjunct to conventional ionization methods for the analysis labile, nonvolatile, and inisolable analytes. With an understanding of several basic source parameters, a wide variety of compounds can be analyzed by TSP on a routine basis in the R&D laboratory. Purpose: To introduce Thermospray LC/MS techniques to a pharmaceutical Quality Control laboratory as a routine method for: 1. The analysis of thermally labile, nonvolatile, or inisolable species not amenable to conventional methods. 2. The development of macromolecular, protein based pharmaceutical agents. Goals: 1. To provide TSP capabilities with little or no interference to existing capabilities. 2. To understand critical TSP parameters to allow rapid analysis of a wide variety of compounds on a routine basis. 3. To demonstrate the utility of the technique through the analysis of difficult samples. Instrumentation: Basic components of the TSP LC/MS system include a Varian Vista 5500 gradient LC pump with high back pressure UV detector, a Finnigan rev. A TSP interface and controller, and a Finnigan 4600 quadrupole GC/MS spectrometer with SuperIncos data system. Optimization experiments were performed using a 70:30 H2O:MeOH 0.1M NH4OAc mobile phase, and flow injection at 1-2 ml/min. Vaporizer Tip: The most critical parameter is the quality of the vaporizer tip from which the TSP aerosol is produced. The diameter of the tip and its position relative to the sampling cone have a pronounced effect on sensitivity, stability, and the ability to observe high mass ions. At right the effect of vaporizer tip internal diameter on the spectrum PEG 1000 is illustrated. Vaporizer Temperature: Proper choice of the vaporizer temperature is important if the information desired is to be obtained. Some compounds provide abundant molecular ions over a large temperature range (ca. 50+C) while others do not. Often the formation of molecular ions occurs at lower temperatures than required for maximum sensitivity with respect to the RIC. Increasing the vaporizer temp often promotes fragmentation yielding structurally significant ions. The nature of the analysis determines the most effective operating temperature. Repeller Voltage: To enhance the transverse ejection of ions from the TSP source through the sampling cone, a repeller lens is employed. The potential of the repeller lens influences the spectrum. At higher potential, high mass transmission is enhanced with reduced stability of low mass ions. At low potential, low mass sensitivity is adequate and high mass sensitivity is poor. High Mass Transmission: Because ion sampling in the TSP source is 90 degrees to the flow of mass through the source block, high mass ions are discriminated against. Any parameter which serves to increase the transverse diffusion of material from the flow axis generally serves to improve high mass transmission. Such factors as increasing the flow rate, the repeller voltage, and restricting the vaporizer serve to enhance high mass transmission.

Calibration: Because TSP produces primarily molecular ions, oligomeric mixtures such as the PEGs are typically used as calibrants. We have found that mobile phase solutions of NaOAC are also useful and eliminate some of the problems associated with ghosting and isotopic "clutter" found with the PEGs. The calibrant is used to asses system performance and optimization as well as calibration prior to sample analysis.

Conclusion: Commercially available interface systems have allowed TSP to be easily incorporated into existing MS system with little modification or interference to existing capabilities. With an understanding of critical TSP parameters a wide variety of compounds can be efficiently analyzed especially where convention methods are ineffective and thus greatly increase analytical capability of the R&D laboratory.

TSP SYSTEM

TSP INTERFACE

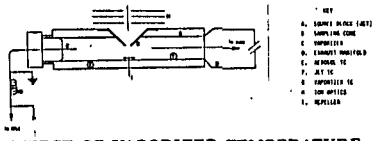

EFFECT OF VAPORIZER TEMPERATURE ON SPECTRUM OF CEFOTAXIME (MW=455)

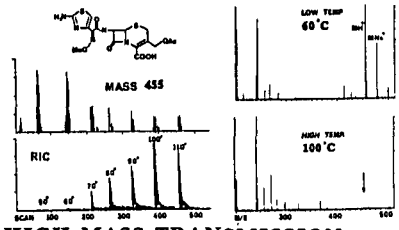

HIGH MASS TRANSMISSION:

Schematic representation of the effect of operator controllable parameters on the appearance of the spectrum of PEG-1000.

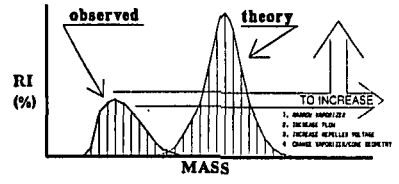

EI, CI, FAB, AND TSP SPECTRA OF CEFPIMAZOLE (MW=670)

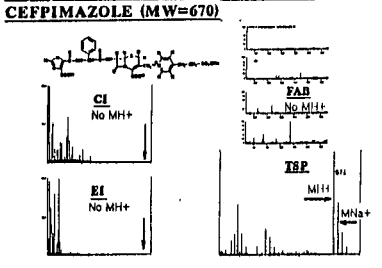

SIMPLIFIED TSP-MS PEPTIDE SEQUENCING SCHEME

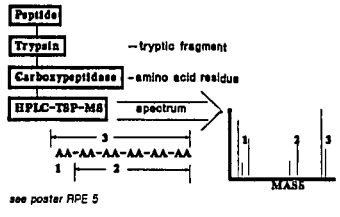

see poster RPE 5

EFFECT OF VAPORIZER DIAMETER ON THE SPECTRUM OF PEG-1000

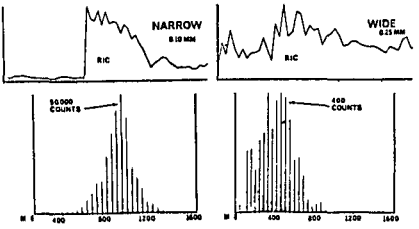

EFFECT OF REPELLER VOLTAGE:

LOW MASS (PROPYL PARABEN MW=180) vs HIGH MASS (PEG-1000) SENSITIVITY

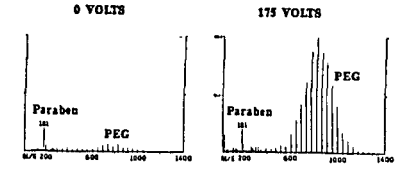

OPTIMIZED SPECTRA OF PEG-1000 AND SODIUM ACETATE CALIBRANTS

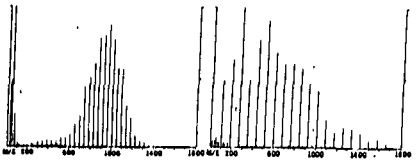

GRADIENT HPLC CHROMATOGRAM OF LHRH ANALOGS WITH TSP SPECTRA

(LHRH= LUTEINIZING HORMONE RELEASING HORMONE)

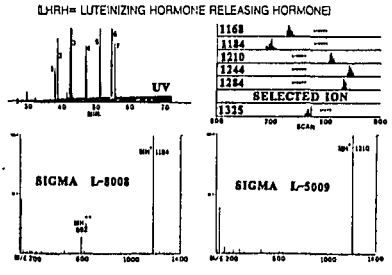

ELUENT pH AND THERMOSPRAY SPECTRA: DOES THE CHARGE ON THE ION IN SOLUTION INFLUENCE THE SPECTRUM?

R.W. Smith[1], C.E. Parker[1], D.M. Johnson[2], and M.M. Bursey[2].

[1]Laboratory of Molecular Biophysics, NIEHS, Research Triangle Park, NC 27709.
[2]Department of Chemistry, UNC-Chapel Hill, Chapel Hill, NC 27514.

If the ions observed in "filament off" thermospray (TSP) LC/MS are formed directly from solution, adjustments of pH through the pK_a value should affect ion yield and appearance of the spectrum. If ions are formed in the gas phase, little pH effect would be expected.

As the solution pH is varied through the pK_a value, the dominant solute species changes.

$$H_2A^+ \longrightarrow HA + H^+ \longrightarrow A^- + 2H^+$$
$$(\text{increasing pH} \longrightarrow)$$

If the primary sample thermospray ions are formed directly from solution, a significant change in the thermospray spectra should be observed. Conversely, if gas phase ionization predominates, changes in the pH should have little effect on the spectra. Moreover, decreases in gas-phase reagent ion intensities should be observed when the sample peak elutes (1,2).

A series of nine compounds was selected where the dominant species would bear a charge under the thermospray conditions used, and where the charge on the dominant species would change across the range of pH values studied (pH 4.4 to pH 11). These compounds included carboxylic acids, amino acids, sulfates, and phosphates. One compound, HEPES, has been studied by FAB; its FAB spectrum is dependent upon the solution pH (3). Dramatic changes in the organic SIMS spectrum of tris(hydroxymethyl)methylaminopropanesulfonate as a function of pH have been reported (4).

A VG 12-250 LC/MS (VG Masslab, Altrincham, UK; quadrupole mass spectrometer) was used in the thermospray mode: vaporizer temperature, 290°C; desolvation chamber temperature, 250°C; source temperature, 200°C; VG "focus 4" electrode, 200V. A Gilson HPLC system consisting of two Model 302 pumps, a Model 811 dynamic mixer, and a Model 802B manometric module (Gilson Medical Electronics, Middleton, WI) was used. Samples were injected into a Rheodyne, Inc. (Cotati, CA), Model 7010 injector fitted with a 50 µl loop. The pH measurements were made with a Fisher Digital, Model 107, pH meter (Fisher Scientific, Fair Lawn, NJ).

The water (HPLC grade), ammonium acetate, glacial acetic acid (HPLC grade), and ammonium hydroxide used in the mobile phase solutions, and the glycine were from Fisher Scientific. The histidine used was from Aldrich (Aldrich Chemical Co., Milwaukee, WI). All other compounds studied were obtained from Sigma Chemical Co., St. Louis, MO.

The compounds were dissolved in and injected into a mobile phase consisting of 0.1 M ammonium acetate, adjusted to the desired pH values with acetic acid or ammonium hydroxide. The flowrate used was 0.9 ml/min.

The experiments indicate that the pH of the solution has little effect on the ion yield and nature of ions observed. It has previously been observed (3,4) that for FAB and SIMS the ion intensities are relatively constant until the pH of the solution nears the pK_a. At (or near) the pK_a, there is a rapid decrease in certain ion intensities. The lack of this spectral feature in thermospray suggests that the ionization mechanisms may be different in FAB and

thermospray. From the thermospray data presented above, gas-phase ionization appears to be predominant, even when the solutes are highly ionized in solution. Thus, even for these compounds, where solution-phase ionization should be an important mechanism, the only significant method of ionization appears to a gas-phase process.

1. Bursey, M.M., Parker, C.E., Smith, R.W., and Gaskell, S.J.; Anal. Chem., 1985, 57, 2597-2599.
2. Alexander, A.J. and Kebarle, P.; Anal. Chem., 1986, 58, 471-478.
3. Caprioli, R.M.; Anal. Chem., 1983, 55, 2387-2391.
4. Inchaouh, J., Blais, J.C., Bolbach, G., and Brunot, A.: Int. J. Mass Spec. Ion Proc., 1984, 61, 153-156.

GLUTAMIC ACID -- POSITIVE THERMOSPRAY

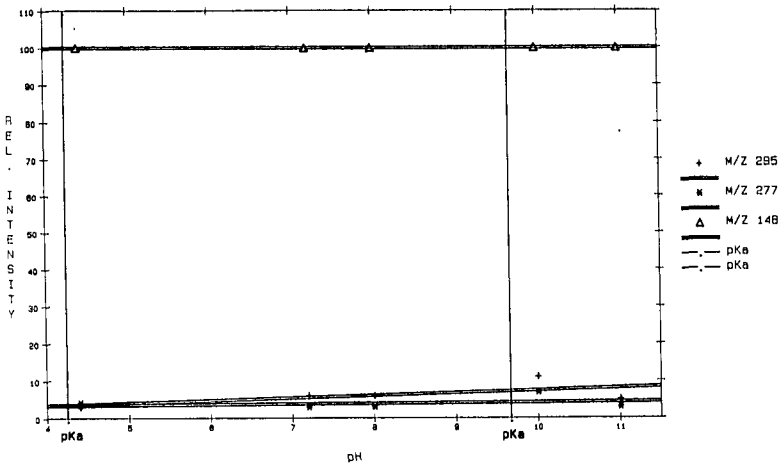

GLUTAMIC ACID -- NEGATIVE THERMOSPRAY

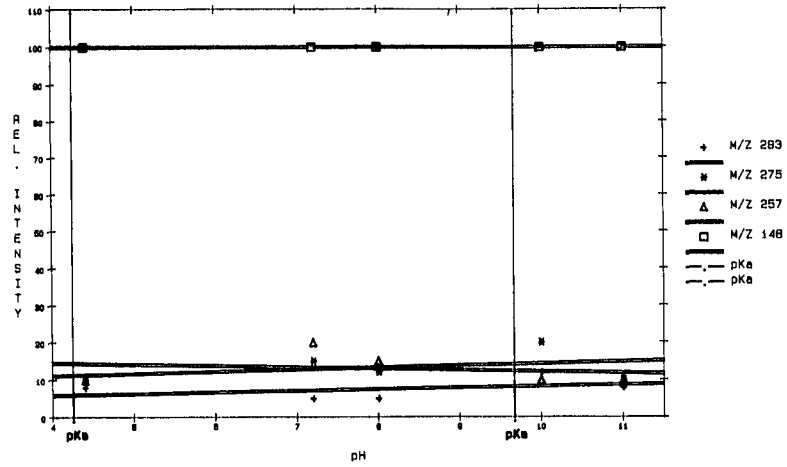

Mixed-Mode Column Thermospray LC/MS

J.R. Lloyd, M.L. Cotter, D. Ohori and A. Oyler

Research Laboratories
Ortho Pharmaceutical Corporation
Raritan, New Jersey 08869-0602

Although the number of applications of thermospray LC/MS (TSP) to the analysis of complex mixtures is increasing rapidly,[1] several limitations to the technique remain. One frequently encountered problem is the incompatability of the TSP ion source with HPLC methods utilizing nonvolatile buffers or ion-pairing reagents since these buffers are deposited on the ion source and other parts of the mass spectrometer and/or they form intense cluster ions which mask the ions of interest. This incompatibility is a severe limitation since reversed-phase ion-pair HPLC methods can achieve efficient separations of complex mixtures containing both neutral and ionic components.[2]

We have developed a unique method which achieves separations similar to reversed-phase ion-pair HPLC, but is completely compatible with TSP since volatile buffers are added to the mobile phase. The method utilizes a commercially available mixed-mode RP-SCX column,[3] which incorporates both reversed and strong cation exchange phases on a silica support[4] and a mobile phase consisting of ammonium trifluoroacetate modified with methanol.

To demonstrate the utility of this LC/MS method, we have chosen a mixture of some common constitutents of cold remedies, which under the conditions of our separation, would be present as neutral and ionic species. In acidic aqueous solution, p-acetophenetidide (1) and 3-(2-methoxyphenoxy)-1,2-propanediol (2) would be present as neutrals, while the amines (R)-(-)-phenylephrine (3), (1S,2R)-(+)-norphedrine (4) and (1S,2R)-(+)ephedrine (5) would be ionic. An ion-pair reversed-phase separation of a similar mixture has been published, but the method involved the addition of the nonvolatile reagent sodium pentanesulfonate to the mobile phase.[5]

Good separation of compounds 1-5 was achieved by isocratic elution from the mixed-mode RP-SCX column with a mobile phase consisting of 75:25 1M ammonium trifluoroacetate:methanol at a flow rate of 0.5 mL/min. The high concentration of ammonium trifluoroacetate was found to greatly improve the chromatographic peak shapes of the ionic components. At lower buffer concentrations, the peaks were very broad and considerable tailing was evident. The high concentration of buffer did limit the flow rate to 0.5 mL/min, since at higher flow, buffer would be deposited in the source vacuum line resulting in a restriction and increased source pressure after approximately an hour of operation.

Utilizing discharge ionization, we obtained intense $(M+H)^+$ ions for each component and very little fragmentation was observed. The RIC for this mixture is shown in figure 1. Each component is present at the 1 μg level. Discharge ionization increased the sensitivity by a factor of approximately five compared to pure thermospray ionization. The low flow rate employed was not the optimum flow rate for thermospray ionization, but the external source of ionization provided by the discharge electrode was able to compensate for the low flow rate. The separating capabilities of the mixed-mode RP-SCX HPLC method coupled with thermospray LC/MS detection should prove to be a powerful tool for the analysis of complex mixtures.

The TSP data was obtained with a Finnigan 3000 quadrupole mass spectrometer retrofitted with a Vestec thermospray LC/MS interface. Data reduction was accomplished with an INCOS data system.

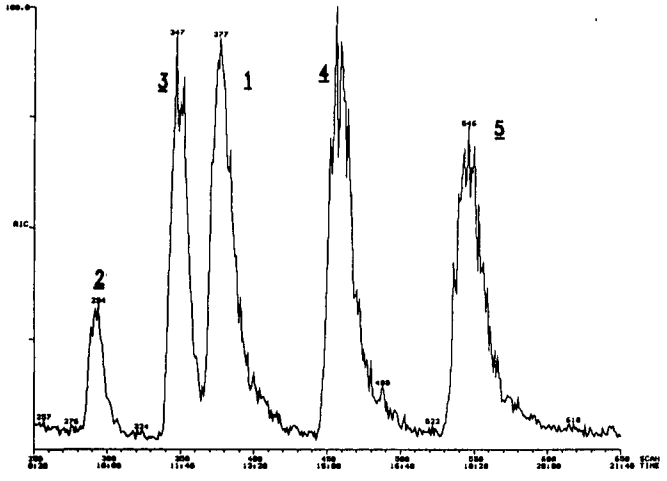

Figure 1: Mixed-mode RP-SCX HPLC Separation of Compound 1-5 with Discharge Ionization Thermospray LC/MS Detection

References:

1. Vestal, M.L.; Anal. Chem. Symp. Ser., 1985, 24, 99-118 and references sited within.

2. Hearn, M.T.W., Ed. "Ion-Pair Chromatography: Theory and Biological and Pharmaceutical Application"; Marcel Dekker: New York, 1985.

3. E.S. Industries, Marlton, N.J. 08053.

4. Crowther, J.B. and Hartwick, R.A.; Chromatographia, 1982, 16, 349-353.

5. Bidlingmeyer, B.A.; J. Chromatogr. Sci., 1980, 18, 537.

THE DEVELOPMENT OF NOVEL SAMPLE INTRODUCTION TECHNIQUE FOR FAB MEASUREMENT

T. Mizuno and Y. Itagaki, JEOL LTD., Tokyo 196, Japan
Y. Ito, T. Takeuchi, D. Ishii and M. Goto, Nagoya University, Nagoya 464, Japan

1. Introduction

LC/MS is considered to be the most suitable analysis method for non-volatile compound mixtures. The combination of FAB with LC/MS will allow a simple and reliable interface to be developed, since FAB does not require sample evaporation prior to ionization.

A moving belt LC/MS interface with an FAB ion source seems to be useful, but there are still some problems of memory effect in addition to its instrumental complexity.

We have designed a novel interface having a simpler construction so as to eliminate memory effect.[1)~3)]

In this system, all effluents from a micro HPLC is directly introduced into the FAB ion source through a capillary tube-connected frit Therefore, it is also possible to use this interface as a sequential and effective sample introduction system.

2. Experimental

The schematic diagram of the sequential sample introduction system is shown in Fig. 1. Samples are introduced and dispersed on the frit, which is placed at the center position of the FAB ion source and used as a target.

10% glycerol is added to the mobile phase [$CH_3CN:H_2O$(50/50)] in advance The samples are bombarded with a neutral Xe beam on the frit and FAB-ionized. A line filter (3 μm) is placed between the HPLC pump and injector in order to filter the mobile phase.

The position of the target can be changed in the X, Y, Z directions using an adjusting probe to give a maximum FAB ion intensity. The flow rate of HPLC was controlled as low as 2 $\mu\ell$/min.

A Milton Roy Micrometric pump equipped with a micro injector Rheodyn 7520 and JEOL's JMS-DX300 mass spectrometer with an additional vacuum pump were used. The operating conditions were as follows: ion accelerating voltage +3 kV SEM voltage 1 4 kV ion source temperature 150°C.

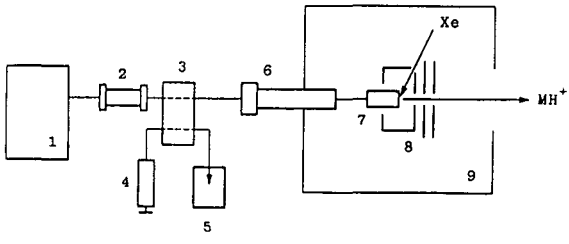

Fig.1; Block diagram of LC/MS. 1= Micro LC ; 2=line filter
3= sample injector ; 4= syringe; 5=waste reservoir
6= adjusting probe ; 7= target ; 8=FAB ion source
9= mass spectrometer

3. Results and discussion

Figure 2 shows mass chromatograms of cephalexin (500ng) repeatedly injected at 1.5-minute intervals. It can be seen from the profiles of the chromatograms that the samples were completely consumed through the ionization and solvent evaporation. The standard deviation of the peak intensity was approximately 7%, which was a little larger than the value derived from a UV chromatogram.

Figure 3 shows mass spectra obtained with the same run. Mass spectra (A) and (B) correspond to the sample and the background part respectively, while (C) is a subtracted spectrum ((A)-(B)) in which the background due to the matrix is clearly removed.

The peak at m/z348 is assigned to the molecular ion and the peak at m/z440 is due to the glycerol adduct ion.

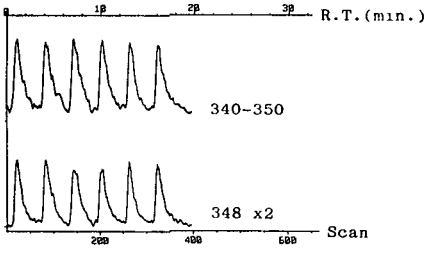

Fig.2, Mass chromatograms of cephalexin(500 ng).
Mobile phase; CH_3CN/H_2O(50/50):Glycerol(9 1)
Flow rate, 2 ul/min.

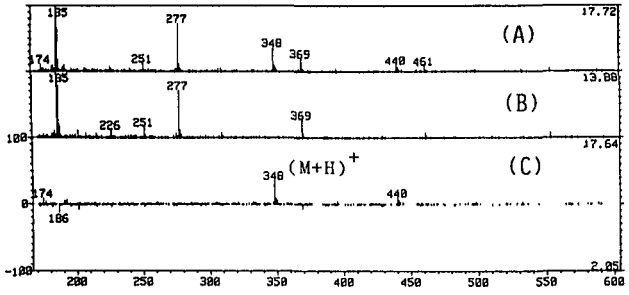

Fig.3; Mass spectra of cephalexin.
(A) and (B) correspond to the sample and the background part of the chromatogram respectively. (C) is the subtracted spectrum (A)-(B).

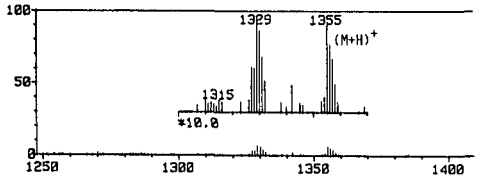

Fig.4; Mass spectrum of vitamin B_{12}

Figure 4 shows the mass spectrum of vitamin B12 obtained using this introduction system. The ratio of the protonated molecular ion [m/z1355] intensity to the fragment ion [m/z1329] intensity was almost the same as that obtained by the conventional FAB method.

4. Conclusion

This newly developed sequential sample introduction system is quite simpler in construction than the moving belt system and, moreover, has no memory effect as shown in the experiment.

Furthermore, by way of FAB, this system can be used for non-volatile and/or high molecular weight compounds. These features can be realized in the LC/MS system which was shown previously.[1)~3)]

5. References

1) Y. Ito, T Takeuchi, D Ishii and M. Goto, J. Chromatogr., 346 (1985) 161.
2) Y. Ito, T. Takeuchi, D. Ishii, M. Goto and T. Mizuno, J. Chromatogr., (in press).
3) D. Ishii, Y. Ito, T. Takeuchi, M. Goto and T. Mizuno, 7th International Symposium on Capillary Chromatography, May 11-14, 1986, Gifu, Japan.

DEVELOPMENT AND PERFORMANCE OF A DISPOSABLE MOVING BELT LC-MS INTERFACE

William DeMaio and M.L. Vestal, University of Houston, Dept. of Chemistry, Houston, Texas 77004

This work was undertaken to develop practical on-line LC-MS techniques for the analysis of large nonvolatile biomolecules. To help achieve this goal, a moving belt LC-MS interface suitable for laser desorption (LD) mass spectrometry was developed. This moving belt interface has an 80% sample transfer efficiency and provides a reproducible surface suitable for LDMS.

The interface is based on the single pass concept. A thermospray vaporizer operating at atmospheric pressure deposits samples onto a darkened aluminum ribbon. A capstan belt drive unit pulls the ribbon at constant speed underneath the thermospray vaporizer and through a series of four differentially pumped chambers. A set of slits 0.018 cm (0.007") wide machined into an aluminum plate separate each chamber. The slits are positioned so that the top surface of the ribbon does not touch any other surface. The first three chambers are pumped by 1000 l/min, 300 l/min, and 400 l/min mechanical pumps respectively. The fourth chamber is pumped by a 150 l/sec 2 inch diffusion pump and the source chamber is pumped by a 1200 l/sec 4 inch diffusion pump. Under typical operating conditions, the source pressure is approximately 1 - 2 x 10^{-6} torr. No type of belt clean-up system is necessary because the surface is used only once.

Darkening of the low cost aluminum ribbon was achieved by passing the ribbon through a hot bath of Na_2CO_3/Na_2CrO_4 solution. The darkened surface absorbs laser radiation more efficiently than the highly reflective untreated aluminum surface. In addition, the darkened surface enhances Na^+ cation attachment during laser desorption.

The sample deposition efficiency of the thermospray vaporizer was determined by comparison of the absorbance (at 487 nm) of a 250 ul solution of 1.8x10^{-3} M acid orange 7 dissolved in 6 ml H_2O with the absorbance of 250 ul acid orange 7 solution thermosprayed onto an aluminum ribbon. The orange dye was

recovered by washing the ribbon in 6 ml H_2O. A deposition efficiency of approximately 80% was obtained.

A study of the effects of laser pulse repetition rate and focussing of the laser beam on the LD mass spectrum of histidine was performed. At laser pulse repetition rates where multiple laser pulses strike the same section of the ribbon surface, the $M+Na^+$ ion was the main characteristic ion present in the mass spectrum. At laser pulse repetition rates where each laser pulse strikes a new section of the ribbon surface, characteristic fragment ions as well as the Na^+ attached pseudomolecular ion were present. These results are consistent with results of previous studies.[1]

Representative LD mass spectra of some ribonucleosides, sugars, amino acids, and antibiotics were obtained using the interface. Most of the mass spectra exhibited $M+Na^+$ pseudomolecular ions and some characteristic fragment ions. Future work with interface will involve obtaining actual chromatograms of biological compounds.

(1) T.P. Fan, E.D. Hardin, M.L. Vestal Anal. Chem. 1984, 56, 1870.

COMPARISON OF RESULTS FROM PACKED AND OPEN TUBULAR CAPILLARY COLUMN SFC/MS[a]

Udseth, H. R. and Smith, R. D.

Chemical Methods andSeparations Group, Chemical Technology Department
Pacific Northwest Laboratory[b], Richland, Washington 99352

Supercritical fluid chromatography has been practiced on both packed and capillary columns. The two techniques have provided complimentary abilities, with packed columns being preferred for speed of separation and quantitation, while capillary columns provide superior resolution. When coupled to a mass spectrometer, another factor, the flow rate, must be considered. The flow from a capillary column is ideally suited to use with a mass spectrometer while packed column flows are at least an order of magnitude higher. Thus, most SFC/MS to date has been done with capillary columns. In order to explore the use of packed columns with SFC/MS, we modified the chemical ionization source of our mass spectrometer to provide direct source pumping on an expansion chamber adjacent to the inoization region. Figure 1 shows a schematic of the current configuration. Under typical operating conditions approximately 96% of the gas load is handled by the direct pumping line, and the pressure in the source is reduced sufficiently so that CI reagents (methane, isobutane or ammonia) can be added and good CI spectra obtained. In addition, the probe tip heater (a direct current heated stainless steel tube) was transferred to the expansion region. This removes an unwanted heat load from the probe and allows better temperature control of the column (or passivated transfer line for packed columns) down the length of the probe.

This added pumping capability allows a packed column to be substituted for the capillary without further modification. We evaluated this configuration with several test solutions (coal tar extract, a polarity test mixture of C_{10}, C_{15}, naphthalene, acetophenone, N-ethylaniline, 1-decanol, and p-chlorophenol; and a mixture of pesticides and herbicides containing alachlor, BPMC, propachlor, propoxur, linuron, carbofuran, carbaryl, and diuron) using both pure CO_2 and CO_2/MeOH as the supercritical fluid. The high pumping speed of this configuration was then exploited to operate a long capillary column at high flow velocities and evaluate its performance.

We used a microbore column from Brownlee for these studies. We operated it isobarically at pressures from 320 bar to 450 bar and isothermally at 50C. The dead time could be varied by changing the restrictor and was typically two minutes. The performance was similar to that seen by other users with FID detectors. For apolar materials (coal tar extract and some of the other test compounds) moderate resolution with good peak shape and reasonable retention times were obtained with pure CO_2 as the fluid. For the more polar compounds the peak shapes degraded badly and the retention times became excessively long. The addition of a small amount of MeOH (1% v/v) changed the situation dramatically. Figure 2 shows a comparison of the results for the mixture of herbicides and pesticides separated on the microbore column. The conditions are as indicated on the figure. In the upper chromatogram pure CO_2 was used as the fluid. All of the compounds have reasonable retention times but the large amount of tailing present in most of the peaks results in a poor overall chromatogram. The bottom chromatogram was generated from the same mixture using a CO_2/MeOH (1% v/v) fluid . The change in peak shapes is dramatic and the overall quality of the chromatogram is greatly improved. It is interesting to note the selective changes in k' for these compounds. Most of them show a greatly reduced capacity factor but carbaryl and diuron are unaffected.

The microbore column was replaced by a 100 μm x 30m capillary column which was coated with a relatively thick stationary phase (~1μm). It was expected that the combination of high flow rate and thick stationary phase would allow us to use much larger sample loadings without splitting the injection while maintaining low analysis times and moderately high resolution. When the polarity test mixture was chromatographed, CO_2 was used as the fluid and 0.6 μg per component were injected. Under these conditions the microbore column had shown long retention times and excess tailing for the more polar components. Exploiting the flexibility inherent in capillary columns to ramp the pressure at 12.5 bar/min all of the compounds eluted with a k' less than 2, with minimal tailing, no signs of overloading and with greatly increased resolution.

The capabilities of this system were more fully demonstrated by work done on the polymeric surfactant triton X-100. Working at high flow rates and a pressure ramp of 12.5 bar/min, the entire sample (19-mer at m/z=1060) can be eluted in less than 10 minutes. The separation is not baseline beyond n=3, but the oligomers up to n=13 can be distinguished on the TIC. By reducing the pressure ramp to 2.5 bar/min much better resolution can be obtained. Figure 3 shows the results of such a separation. The conditions are as shown

on the figure. Near beaseline separation has been achieved for all of the oligomers out to n=19, the highest mass scanned and the total analysis has been done in 25 minutes.

This source configuration offers a practical means of coupling a packed column SFC to a mass spectrometer. Both pure and modified supercirtical fluids can be used. The use of modifiers with packed columns is clearly desireable, but until the production of usable gradients is routinely achieved, the full potential of packed columns will not be realized in SFC. Working with high flow rates also permits an extension of the range of application of capillary columns. The use of a thick stationary phase permits sample injection without splitting and shows no evidence of peak overloading at moderate sample size. This is obtained at a cost in chromatographic efficiency and the application must determine which is more important. The two techniques still provide complimentary abilities but we believe that the advantages provided by capillary columns will make them the choice when sensitivity, resolution or flexibility are the primary requirements.

a Prepared for the U. S. Department of Energy under Contract DE-AC06-76RLO-1830
b Operated by Battelle Memorial Institute

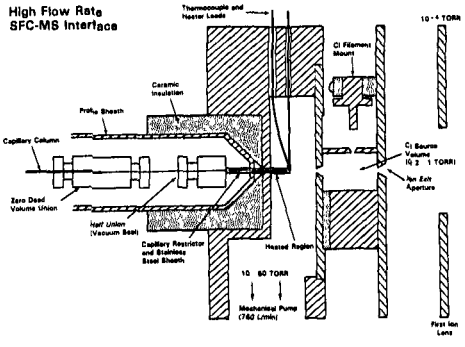

Figure 1

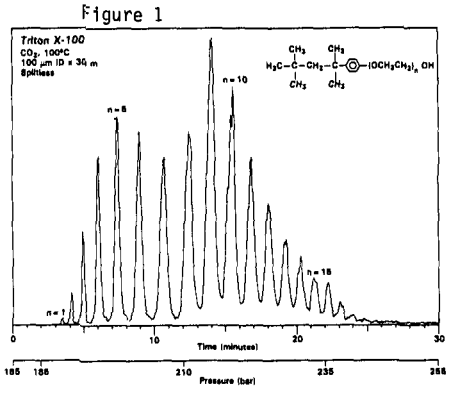

Figure 3

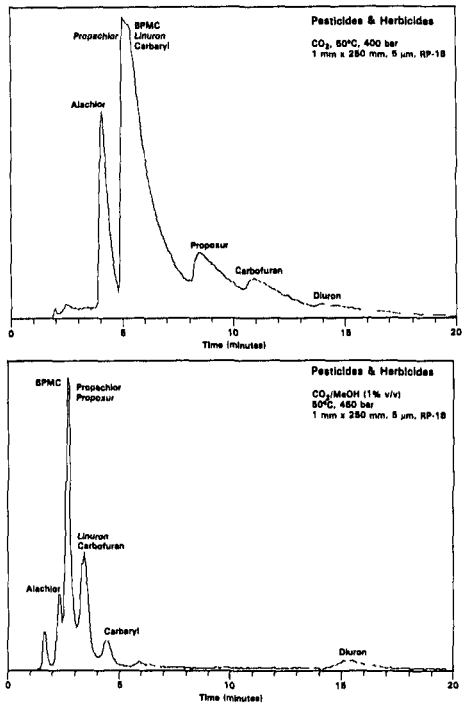

Figure 2

Gradient Elution LC/MS Using A MAGIC Interface

L. E. Abbey, D. E. Bostwick, P. C. Winkler,
D. D. Perkins, and R. F. Browner

School of Chemistry
Georgia Institute of Technology
Atlanta, Georgia 30332

An improved monodispersed aerosol generation interface (MAGIC) has been constructed and applied to analyses using binary gradient elution of normal and reverse phase solvent systems, and using both standard analytical and narrow bore (2.1 mm) columns. Several labile and involatile samples were analyzed to demonstrate the usefulness of the MAGIC interface in problems requiring non-thermal sample enrichment and transfer.

The MAGIC interface design includes the following distinctive features:

1. Monodispersed aerosol generation of the HPLC solvent and solute.
2. Near-atmospheric pressure desolvation of the aerosol.
3. A two-stage supersonic flow separator to remove solvent vapor and helium dispersion gas from the particle beam.
4. Because desolvation takes place at near-atmospheric pressure, no heating of the sample is required to achieve solvent evaporation.

Analyses were run on polyaromatic hydrocarbons, a mixture of chloro- substituted phenyl ureas, and a mixture of industrial grade fatty acids. All spectra were obtained using a Finnigan MAT 112S mass spectrometer and a Finnigan MAT SS200 data system. The ion source was heated to 250 °C. The spectra were full scan spectra, taken at 1 second/mass-decade. In each case the scan was started immediately above the solvent mass. Both electron impact and chemical ionization (isobutane) spectra were obtained on each sample. The liquid chromatograph was a Hewlett Packard model 1090A.

The PAH mixture was obtained by passing a sample of coal tar dissolved in hexane through a silica gel Sep-Pak (Waters Assoc., Milford, MA) and eluting the PAH fraction with a wash of hexane. The fraction was separated using a 4.6 mm x 60 mm (3 μm particles) C18 column. The separation was achieved by using a solvent system of 70% methanol/water programmed to 100% methanol in 15 minutes, with a flow of 0.5 mL/min.

The fatty acid mixture was separated using the same column with the following solvent system: 70% acetonitrile/water programmed to 100% acetonitrile in 15 minutes, with a solvent flow of 0.5 mL/min. The water contained 2% acetic acid.

The phenyl urea mixture was separated using a C18 column (2.1 mm x 25 cm, 5 μm particles) and a reverse phase solvent system consisting of 40% methanol/water, programmed to 100% methanol in 8 minutes, with a flow of 0.5 mL/min.

As previously noted, no heat is added to the sample during transport, so the only heat available for sample vaporization is contributed by the ion source body. Electron impact or chemical ionization spectra may be obtained in conjunction with the MAGIC interface, provided the compound gives an adequate vapor pressure at an obtainable ion source temperature. Labile compounds may be easily handled using the MAGIC interface with the ion source temperature maintained at an appropriate temperature. For further data on the role of ion source temperature in the MAGIC system, see the poster in this session by Perkins, et al.

Future work will center on applications of the MAGIC system on a wide range of analytical problems, and the use of FAB as an ionization method with the MAGIC system.

FATTY ACIDS

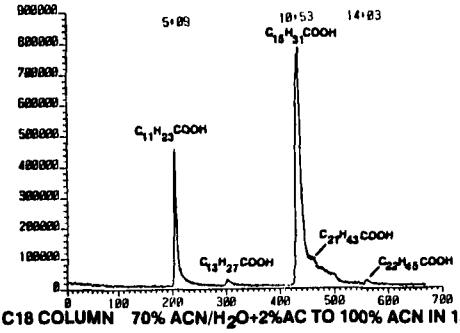

C18 COLUMN 70% ACN/H_2O+2%AC TO 100% ACN IN 13 MIN

POLYAROMATIC HYDROCARBONS

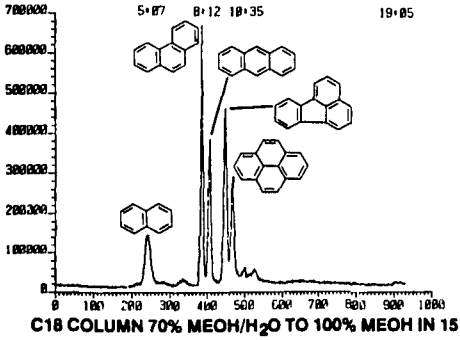

C18 COLUMN 70% MEOH/H_2O TO 100% MEOH IN 15 MIN

PHENYLUREAS

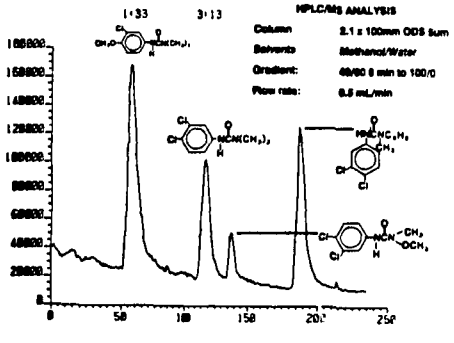

AN INVESTIGATION OF OPERATIONAL PARAMETERS AND REPRODUCIBILITY OF THE MONODISPERSED AEROSOL GENERATION LC/MS INTERFACE

Deborah D. Perkins, Paul C. Winkler, Lawrence E. Abbey and Richard F. Browner

School of Chemistry
Georgia Institute of Technology
Atlanta, Georgia 30332

The monodispersed aerosol generation interface for combining liquid chromatography with mass spectrometry (MAGIC LC/MS) has been successfully applied to both normal and reversed-phase separations. Basically, the nebulizer forms an aerosol from the total column effluent. The aerosol then passes through an evaporation chamber where desolvation occurs. The dispersion gas and mobile phase vapor are pumped away in the aerosol beam separator leaving the analyte to travel through the line-of-sight into the mass spectrometer. The objective of this study is to evaluate some of the operational parameters affecting the performance of the interface such as flow rate, ion source temperature, and mobile phase composition. A profile of short term reproducibility shows only small fluctuations of signal with time.

Typically, the MAGIC LC/MS interface is operated at flow rates ranging from 0.3 to 1.2 mL/min. The lower boundary is largely determined by adequate formation of the liquid jet. The upper limit is determined largely by transport effects. For the mobile phase methanol, the peak response for a 4ug injection of the test compound methyl stearate occurs at 0.6 mL/min when there is a constant helium pressure of 15 psi. The optimal flow rate is expected to be somewhat mobile phase dependent.

A common technique in liquid chromatography is gradient elution. It is important to know how the changes in mobile phase composition are influencing the response of the analyte. We have found that under conditions involving mobile phases such as hexane and ethyl acetate, the change in response with varying composition is negligible. For separations involving reversed-phases, however, we see a 2.5 fold increase in sensitivity as we proceed from a 50% water/ 50% methanol mixture to 100% methanol. This is for the most part due to water condensation on the walls of the chamber.

An investigation into the effect of ion source temperature on the intensity of response for the compound methyl stearate was performed. The ion source temperature changes the intensity very little from 140° C to 230°C. Although a total ion chromatogram at lower ion source temperatures reveals a decreased intensity, the peaks are broader and the area is relatively the same as that obtained at higher ion source temperatures.

Thermally labile compounds which are not amenable to gas chromatography are perfect candidates for LC/MS. The processes which occur in the MAGIC LC/MS interface as the analyte of interest is nebulized, desolvated, separated from the helium dispersion gas and mobile phase, and subsequently introduced into the ion source do not decompose a thermally labile compound. One such compound is aldicarb, the carbamate pesticide. An EI spectrum for aldicarb at a source temperature of 82° C reveals the M+ ion at 190. Decomposition of thermally labile compounds will only occur as a result of ion source temperature.

ELECTROSPRAY LC/MS WITH AN ATMOSPHERIC PRESSURE IONIZATION TANDEM QUADRUPOLE MASS SPECTROMETER, Andries Bruins, Thomas Covey, and Jack Henion, Drug Testing and Toxicology, NYS College of Veterinary Medicine, Cornell University, 925 Warren Drive, Ithaca, New York 14850.

Dispersion of liquids into a charged aerosol beam by electrospray was first demonstrated by Zeleny (1). The emission of sample ions from charged droplets offers a mild ionization technique for polar and ionic analytes. This process, which has been called ion evaporation (2) not only takes place at atmospheric pressure, but is also considered one of the ionization mechanisms in the low pressure thermospray ion source. Electrospray combined with an atmospheric pressure ion source takes advantage of the mild ionization conditions in which no heat is applied.

Electrospray LC/MS has been claimed in patents and has recently been reported in the literature (3). The instruments used were home made or extensively modified commercial mass spectrometers. The major problem in electrospray LC/MS is the sampling of ions from atmospheric pressure into the vacuum of the mass spectrometer, without the extensive clustering with water and other polar molecules during the free jet expansion stage (3). The Sciex TAGA 6000E is a triple quadrupole mass spectrometer equipped with an API source in which ions are drawn through a dry nitrogen gas curtain prior to being admitted into the ion sampling orifice. Clustering is minimized for the most part, and final declustering takes place by accelerating clusters and collision induced dissociation during the free-jet expansion. It is essential however, that the electrospray interface is not directed straight towards the ion sampling orifice, but is positioned approximately 5 to 10 mm off-axis, to prevent penetration of droplets and clusters through the gas curtain. The electrospray process is dependent on solvent composition, the high voltage applied to the sprayer, the distance between the sprayer and a counter electrode and the flow rate of the LC effluent. Electrospray LC/MS is compatible with low flow rates as used in microbore LC (10 ul/min). We have had difficulties obtaining a stable spray if the concentration of water in acetonitrile was raised and/or the flow rate was increased. Electrospray could be improved by increasing the spray voltage. This, however, initiated a corona discharge and suppressed the sample ion current.

The supply of a stream of nitrogen around the spray capillary assists the nebulization process and has allowed us to use a high percentage of water, higher flow rates (tested up to 100 ul/min) and a moderate voltage on the sprayer (plus or minus 3.0kV). Also, the position of the sprayer could easily be increased to 3-4 cm from the counter electrode without affecting the charged aerosol beam generation. In short, the assistance of pneumatic nebulization has made the electrospray LC/MS more rugged and reliable and simpler to set up.

We have used our electrospray interface mainly for the generation of negative ions. Most samples were introduced via a 1 mm x 10 cm hypersil 3 um C_{18} column (Shandon) using an eluent composed of acetonitrile and 0.001 M ammonium acetate in water, at 40 ul/min.

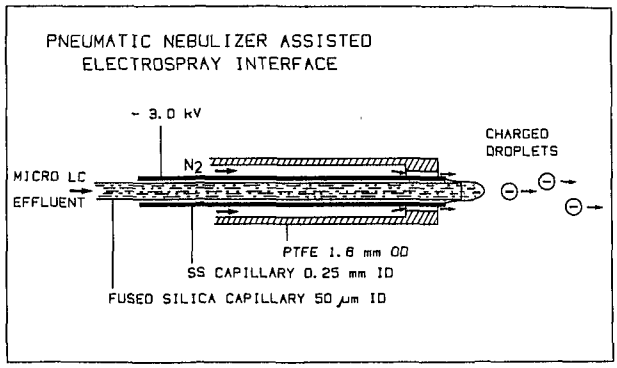

A few samples were analyzed without the use of a column. Ammonium acetate was added to improve chromatographic peak shapes. It is important to note that a high concentration (0.1M) of ammonium acetate strongly suppressed the ion currents of ionic samples.

Mono-sulfonated azo dyes show the $[M-H]^-$ ion of the free acid. Di-sulfonated azo dyes give doubly charged negative ions $[M-2H]^{2-}$ of the free acid. Estrioltrisulfate shows the triply charged $[M-3H]^{3-}$ ion as the base peak, together with $[m-2H]^{2-}$ and a very weak $[M-H]^-$ ion. As an example of a neutral sample, digitoxin shows both the (singly charged $M+CH_3COO^-$ (m/z 823) and the doubly charged $M + 2\ CH_3COO^-$ m/z 441) ions.

Almost no fragment ions are observed, but fragments can easily be generated by collision induced dissociation either in the free jet expansion region, or in the second quadrupole of the triple quadrupole mass spectrometer.

This work was carried out under a Cooperative Agreement with the Environmental Monitoring and Support Laboratory (EMSL, Cincinnati, OH) of the EPA, grant No. CR-S11661-10-1. We acknowledge the assistance of Dr. W.L. Budde during the course of these investigations.

References

1. J. Zeleny, Phys. Rev. 10, 1 (1917)
2. J.V. Iribarne, P.J. Dziedzic and B.A. Thomson, Int. J. Mass Spectrom Ion Phys., 50, 331-347 (1983)
3. C.M. Whitehouse, R.N. Dreyer, M. Yamashita and Y.B. Fenn, Anal. Chem. 57, 675 (1985).

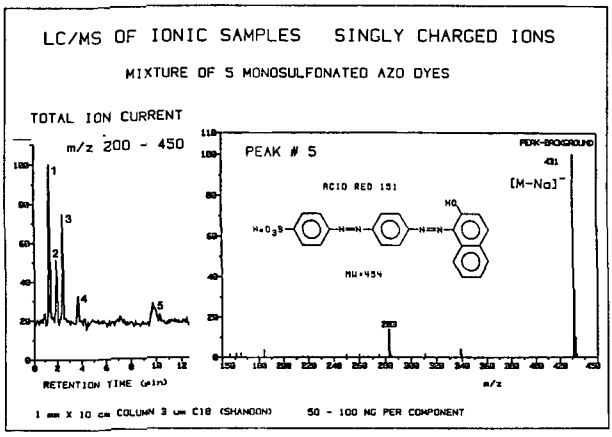

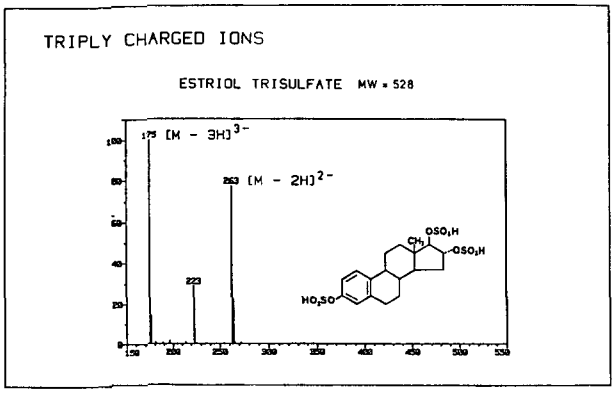

THERMOSPRAY LIQUID CHROMATOGRAPHY - MASS SPECTROMETRY USING A DOUBLE FOCUSING MAGNETIC SECTOR INSTRUMENT

R J Greathead, R J Parillo, J R Chapman, J A E Pratt and M R Clench
Kratos Analytical, 170 Williams Drive, Ramsey, NJ 07446, USA

F Mellon
ARC, Norwich, USA

Introduction

Thermospray liquid chromatography - mass spectrometry using an interface designed for a magnetic sector instrument offers the benefits associated with double focusing mass spectrometers. These benefits include elemental composition determinations and MS-MS type experiments as well as an inherent high sensitivity and high mass performance. These techniques have been successfully applied to a number of problems particularly in the food and drug industry. Presented here are data obtained on Kratos Analytical MS25RFA and MS80RFA Mass Spectrometers which illustrate these techniques.

Methods and Results

The interface can be used with both isocratic and gradient elution conditions to obtain the desired separations and is compatible with a wide range of buffer systems. Chromatographic integrity is maintained. Experimental conditions such as the composition of mobile phase and source and vaporiser temperatures can be adjusted to optimise the fragmentation and sensitivity on analyte species, allowing low level detection of target compounds. An important example in the detection of drugs of abuse is illustrated in Figure 1.

Using post column addition of a reference material such as polyethylene glycol, it is possible to obtain accurate mass data when operating in the high resolution mode. The data shown in Figure 2 is a high resolution spectrum of a methylated salt together with a calculated elemental composition.

The use of MS-MS provides a further aid to structural interpretation. The methylated salt shown in Figure 2 has been further characterised by fragment ion scans, the spectrum from this experiment is shown in Figure 3. The high mass capability of magnetic sector instruments provides the analyst with excellent performance in the LC-MS of biomolecules and drugs. Figure 4 illustrates this with a full spectrum of the drug cyclosporin A.

Conclusions

Thermospray LC-MS on a sector mass spectrometer provides the benefits of high sensitivity, elemental analysis and structural elucidation by MS-MS with an on-line chromatographic technique.

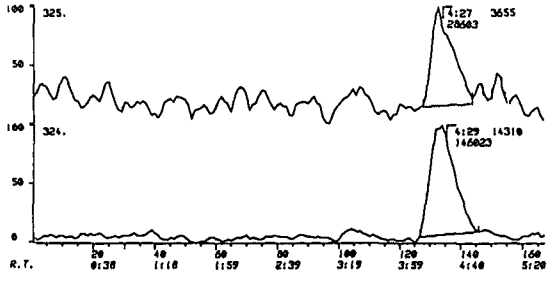

Figure 1 10pg of LSD

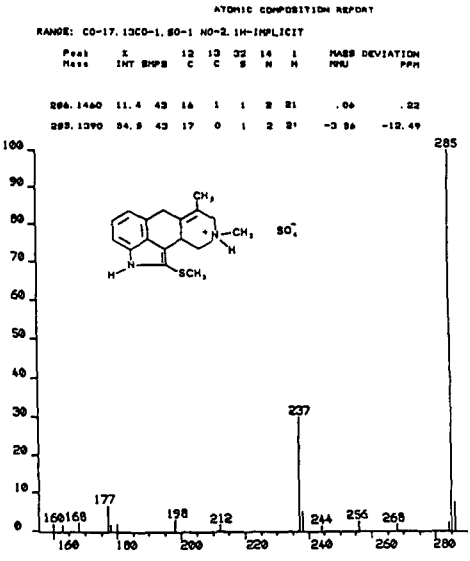

Figure 2 Accurate mass spectrum of a methylated salt

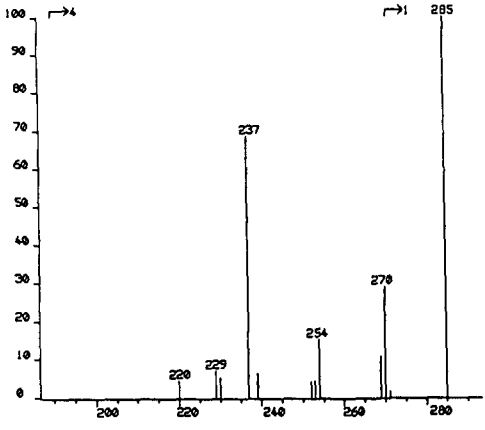

Figure 3 Fragment Ion scan of a methylated salt

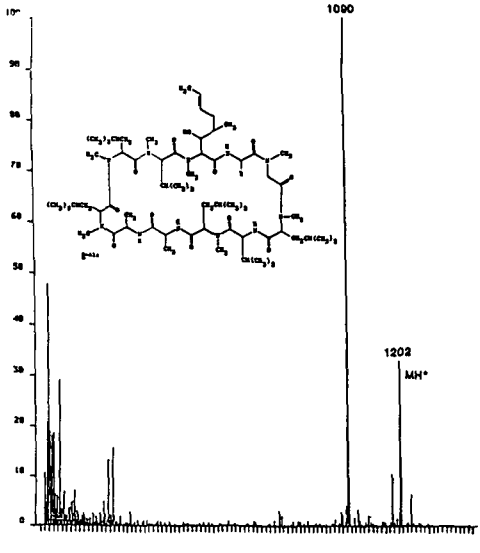

Figure 4 TSP spectrum of cyclosporin A

ANTIBIOTICS: LOW LEVEL DETECTION USING THERMOSPRAY LIQUID CHROMATOGRAPHY-MASS SPECTROMETRY

Paul C. Goodley, Hewlett-Packard Company, 1601 California Avenue, Palo Alto, CA 94304

Antibiotics play an important part in the health treatment against pathogenic bacteria in both humans and animals. Recent studies indicate that more than 40% of the antibiotics produced in the U.S. (2.45 million kilograms) were administered to animals. Analytical chemical detection and characterization of many of these molecules via traditional techniques of culture media and UV-VIS detection is slow and/or lacks specificity. The molecular structures of some classes of antibiotics resemble sugars, amino acids, and other natural products compounding the complexity of the analysis. Thermospray LC/MS has been used to enhance the specificity and to detect the antibiotics lincomycin, erythromycin, puromycin, chloramphenicol, and sulfamethazine. The minimum detection limits are at the 100 to 150 picogram level for lincomycin.

Figure 1 shows three rapid injections of 250 pg of lincomycin using the Selective Ion Mode (SIM). Table 1 gives a list of the antibiotics examined by TS/LC/MS and their minimum detection limit for both the SCAN mode and SIM mode. Figure 2 shows the Total Ion Chromatogram (TIC) and mass spectra of two injections of 50 ng quantities of lincomycin.

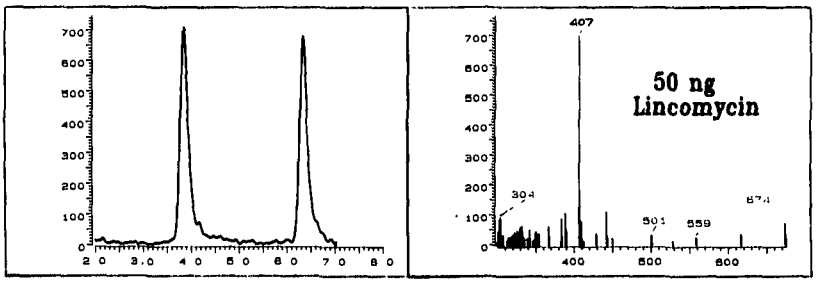

Figure 1: 50 ng Lincomycin Thermospray LC/MS

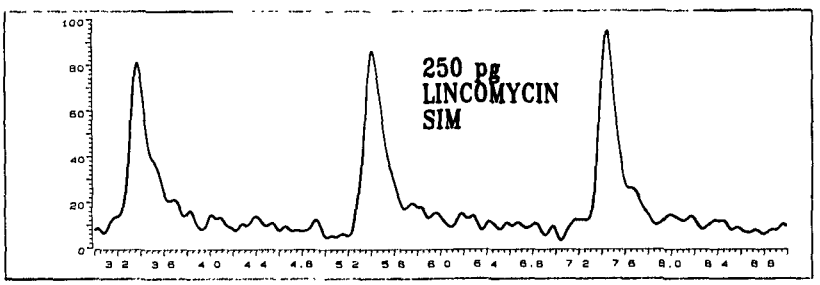

Figure 2: 250 pg Lincomycin Thermospray LC/MS SIM Mode

TABLE I

ANTIBIOTIC	MDL/ SCAN	MDL/SIM
ERYTHROMYCIN	9ng	---
NOVOBICION	176ng	---
LINCOMYCIN	3ng	100pg
HYGROMYCIN	156ng	---
BACTERICIN	168ng	---
PUROMYCIN	8ng	128pg
KANAMYCIN	80ng	---
GENTICIN	210ng	---
RIFAMYCIN	110ng	---
GRAMICIDIN S	60ng	---
CHLORAMPHENICOL	4ng	120pg
SULFAMETHAZINE	3ng	110pg

References:

1. Blakley, C. R., M. J. McAdams, and M. L. Vestal, J. Chromatog., 158, 261 (1978).
2. Blakley, C. R., J. J. Carmody, and M. L. Vestal, J. Am. Chem. Soc., 102, 5931 (1980).
3. Blakley, C. R. and M. L. Vestal, Anal. Chem. 55, 75 (1983).
4. Vestal, M. L., Int. J. Mass Spectrom. Ion Phys., 46, 193 (1983).
5. Vestal, M. L., "Ionization Techniques for Non-Volatile Molecules," Mass Spectrometry Reviews, 2, (1983), 449-80, John Wiley & Sons, Inc.

THERMOSPRAY LC/MS ANALYSIS USING AMMONIA GAS CHEMICAL IONIZATION: Daniel A. Garteiz, Calvin R. Blakley, and Rebecca M. Osterman, Vestec Corporation, Houston, Texas, 77054

Thermospray LC/MS is a soft ionization technique. In order to generate directly evaporating "reagent ions" which then undergo CI type ion/molecule reactions with analytes, ammonium acetate is added to the mobile phase. But the usefulness in non-aqueous systems is limited by the insolubility of that salt (or similar volatile buffers). In acetonitrile and less polar solvents, one must look to other means of producing reagent ions. Also, the presence of ammonium acetate may be undesirable for chromatographic separations.

We have found an alternative solution which is a step beyond the already reported and well accepted use of a Thermospray filament or discharge electrode. We have made a retrofit modification of a Vestec Thermospray ion source by using a special stainless fitting to introduce NH3 as a CI gas. The filament or discharge electrode is used to create ions.

In our experiment, solvent spectra were acquired from water, methanol, acetonitrile, and 50/50 mixtures of these. Each solvent system was studied with the filament on, with ammonium acetate, and with NH3 gas. Three compounds were selected to be representative of different levels of ease in becoming protonated: Cyanazine (easy), Allethrin (moderately easy), and Fructose (not easy).

The results showed that with the proper flow rate of NH3, NH4+ adducts and ammonia clusters appear in the solvent spectra and the spectra resemble those obtained from ammonium acetate. The compounds were effectively ionized in all cases but Fructose is an application where an ammonium adduct particularly enhances the spectrum. Allethrin shows a stronger molecular ion and a weaker ammonium adduct. Cyanazine forms no ammonium adduct.

Ammonia gas can be successfully used as a CI reagent in Thermospray LC/MS analysis. The spectrum of acetonitrile shows the potential for the use of NH3 with non-polar solvents. The possibility of having the ammonium ion present across solvent gradients is another application of this new method.

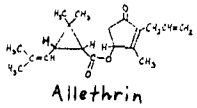

Allethrin

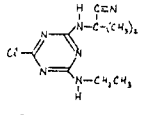

Cyanazine

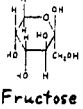

Fructose

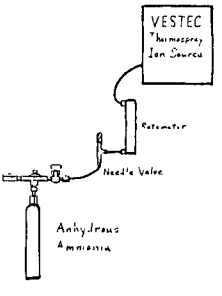

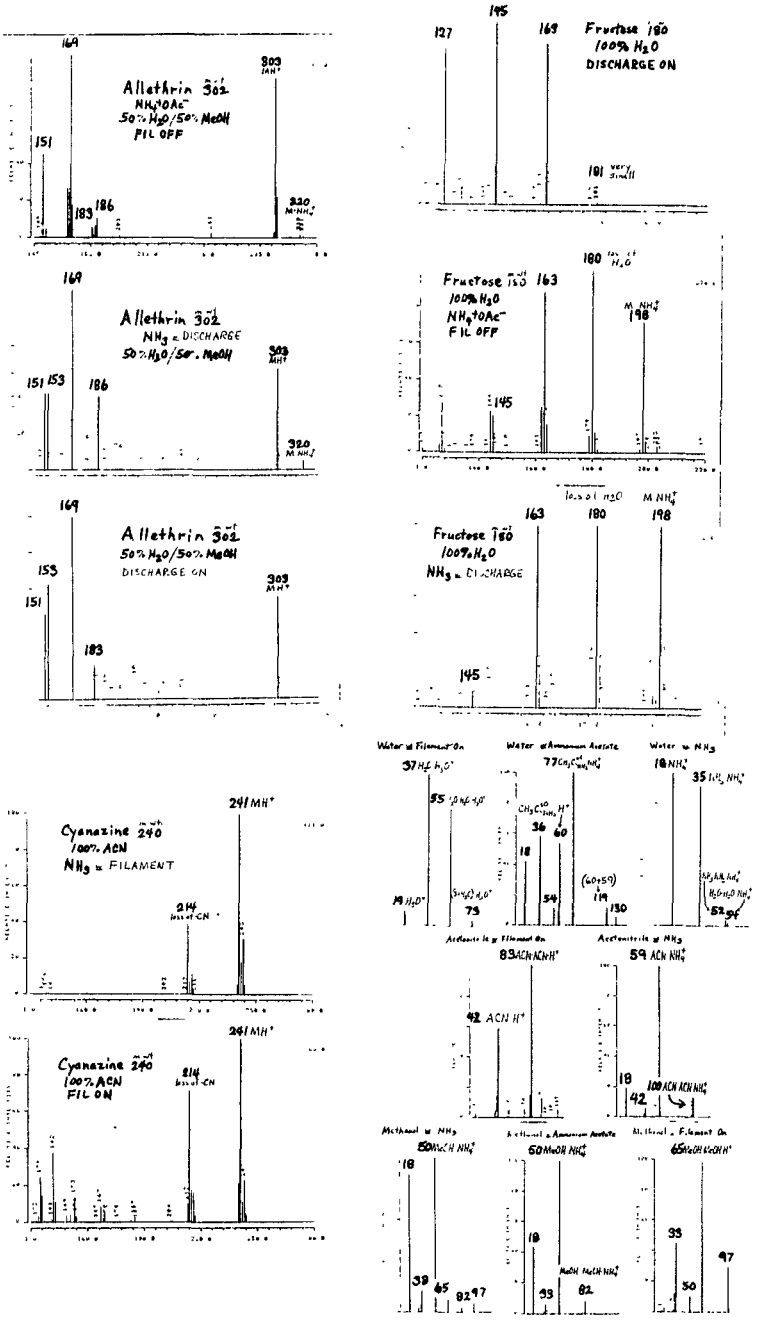
Allethrin 302
NH4+OAc−
50% H2O/50% MeOH
FIL OFF
169
151
183
186
303 MH+
320 M+NH4+
Allethrin 302
NH3 = DISCHARGE
50% H2O/50% MeOH
169
151 153
186
303 MH+
320 M NH4+
Allethrin 302
50% H2O/50% MeOH
DISCHARGE ON
169
153
151
183
303 MH+
Cyanazine 240
100% ACN
NH3 = FILAMENT
241 MH+
214 loss of CN
Cyanazine 240
100% ACN
FIL ON
241 MH+
214 loss of CN
Fructose 180
100% H2O
DISCHARGE ON
127
145
169
181 very small
Fructose 180
100% H2O
NH4+OAc−
FIL OFF
163
180 loss of H2O
M NH4+ 198
145
Fructose 180
100% H2O
NH3 = DISCHARGE
163
180
198
145
Water w Filament On
37 H+ H2O+
55 H2O H+ H2O+
19 H3O+
73
Water w Ammonium Acetate
77 CH3CO2NH4 NH4+
36
60
18
54
(60+59)
119
130
Water w NH3
18 NH4+
35 H2O NH4+
52
Acetonitrile w Filament On
83 ACN ACN H+
42 ACN H+
Acetonitrile w NH3
59 ACN NH4+
18
42
100 ACN ACN NH4+
Methanol w NH3
50 MeOH NH4+
18
39
45
82 97
Methanol w Ammonium Acetate
60 MeOH NH4+
18
33
MeOH MeOH NH4+
82
Methanol w Filament On
65 MeOH MeOH H+
33
50
97

ENVIRONMENTAL APPLICATIONS OF A NEW THERMOSPRAY LC/MS INTERFACE FOR BENCHTOP MASS SPECTROMETERS

S. Michael McCown and Christina Hsieh Vestal
Vestec Corporation, 9299 Kirby Drive, Houston, Texas 77054

The bench-top mass spectrometers have received wide acceptance as GC detectors. These small mass spectrometers are being widely used to monitor a variety of environmental pollutants. Many of these compounds are not amenable to GC analysis. Although LC procedures are available for some of these compounds, the complexity of the mixtures combined with the non-specificity of the LC detectors makes this approach less than ideal.

Thermospray LC/MS provides soft ionization techniques which work best with polar non-volatile compounds.(1) For these reasons, thermospray LC/MS can be the technique of choice to handle some of these difficult environmental analyses. One drawback to the technique has been that thermospray interfaces have been limited to more expensive mass spectrometers equipped for chemical ionization. We now report on the use of a new thermospray interface that can be readily coupled to an inexpensive benchtop mass spectrometer. Figure 1 shows a schematic of the thermospray ion source for a Hewlett Packard Model 5970 Benchtop Mass Selective Detector and Figure 2 shows a schematic of the differentially pumped automatic vacuum system.

This inexpensive Thermospray LC/MS was used to analyze mixtures of 18 herbicides on column using water/acetonitrile gradient elution and discharge ionization. The spectra of these herbicides consisted of the base peak at $(M+H)^+$ with few fragments. The SIM detection limits for all of these compounds were in 100pg - 10ng range as summarized in Table I. Most of these herbicides showed an excellent signal-to-noise ratio at the 10ng level under full-scan conditions (scanning m/z 150-300 in 1 second). Detection limits obtained in this work appear to be about an order of magnitude lower than those reported previously using thermospray LC-MS without an external ionizaion source.(2,3)

A series of pesticides including pyrethrins, amitrole, thiourea, methomyl, thiram, 2-imidazolidinethione, warfarin, cycloheximide, brucine, rotenone, and reserpine have also been used to evaluate the performance of this low cost thermospray LC/MS system. Results obtained using the thermospray "discharge" mode of ionization are presented in Tables II, III, and IV. In all cases $M+H^+$ is the base peak and most show little fragmentation.

These results show that the inexpensive thermospray LC-MS system yields results competitive with those obtainable from more expensive systems. In the selected ion monitoring mode most of these compounds can be detected at levels of a few nanograms or less on column, even when present in relatively

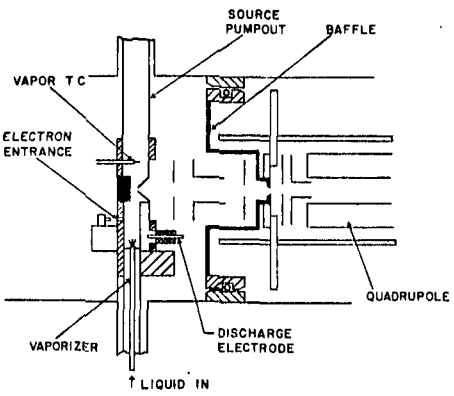

Figure 1. Schematic diagram of Thermospray(tm) ion source for benchtop mass spectrometers

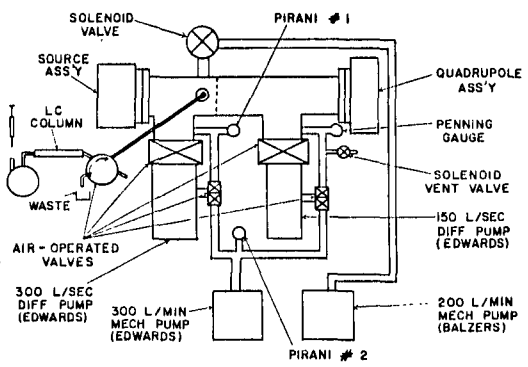

Figure 2. Schematic diagram of vacuum system

On ALTEX Ultrasphere-ODS (4.6mmx25cm) 5u C18 Column

Acetonitrile/Water 30/70(1 min.)-40/60(1 min Gradient)-40/60(10 min.)-95/5(10 min. Gradient)-95/5(2 min.)

Discharge

Compound		M W	Retention Time(min.)	Relative Sensitivity $(M+1)^+$	$\frac{(M+3)^+}{(M+1)^+}$ (%)	Detection Limit(SIM)(ng)
1 Metoxuron	$C_{10}H_{13}ClN_2O_2$	228	7.944	100	23	0.2
2. Monuron	$C_9H_{11}ClN_2O$	198	9.166	107	35	0 2
3. Simazine	$C_7H_{12}ClN_5$	201	9.194	191	23	0.5
4. Cyanazine	$C_9H_{13}ClN_6$	240	9.661	79	26	0.2
5 Metribuzine	$C_8H_{14}N_4OS$	214	10.552	87	4	0.4
6. Fluometuron	$C_{10}H_{11}F_3N_2O$	232	13.716	169	0.1	0.2
7 Cyprazine	$C_9H_{14}ClN_5$	227	13.967	83	33	0.4
8. Atrazine	$C_8H_{14}ClN_5$	215	14.030	103	36	0.4
9. Diuron	$C_9H_{10}Cl_2N_2O$	232	15.831	67	76	0.3
10. Prometon	$C_{10}H_{19}N_5O$	225	16.209	158	0.8	0.3
11. Metobromuron	$C_9H_{11}BrN_2O_2$	258	17.634	68	96	0.3
12. Ametryn	$C_9H_{17}N_5S$	227	18.952	121	4	0.2
13. Propazine	$C_9H_{16}ClN_5$	229	19.130	97	28	0.1
14. Siduron	$C_{14}H_{20}N_2O$	232	19.619	82	0.3	0.4
15. Anilazine	$C_9H_5Cl_3N_4$	274	21.080	10	100	3.0
16. Prometryn	$C_{10}H_{19}N_5S$	241	21.249	120	3	0.2
17. Neburon	$C_{12}H_{16}Cl_2N_2O$	274	22.546	52	78	0.2
18. Dipropetryn	$C_{11}H_{21}N_5S$	255	22.796	107	3	0.3

Table I. Analysis of 18 herbicides

100' Acetonitrile

Discharge

Compound		M.W	Retention Time(min.)	Relative Intensity
Pyrethrin II	$C_{22}H_{28}O_5$	372	2.463	33
Cinerin II	$C_{21}H_{28}O_5$	360	2.509	7
Jasmolin II	$C_{21}H_{30}O_5$	374	2.662	1
Pyrethrin I	$C_{21}H_{28}O_3$	328	3.053	100
Cinerin I	$C_{20}H_{28}O_3$	316	3.130	31
Jasmolin I	$C_{21}H_{30}O_3$	330	3.444	5

Table II. Analysis of pyrethrins

50/50 Acetonitrile/0 1 M Ammonium Acetate

Discharge

Compound		M.W.	Retention Time(min.)	Relative Sensitivity	Detection Limit(SIM)
Amitrole	$C_2H_4N_4$	84	1.597	47	2.0
Thiourea	CH_4N_2S	76	1.680	42	2.0
2-Imidazolidinethione	$C_3H_6N_2S$	102	1.799	100	0.1
Methomyl	$(C_5H_{10}N_2)_2S$	162	2.273	31	0.5
Thiram	$C_6H_{12}N_2S_4$	240	4.915	2	1.0

Table III. Analysis of 4 pesticides (M.W. 70 - 250)

50/50 Acetonitrile/0 1 M Ammonium Acetate

Discharge

Compound		M.W.	Retention Time(min.)	Relative Sensitivity	Detection Limit(SIM)(ng)
Warfarin	$C_{19}H_{16}O_4$	308	2.087	68	2.0
Cyclohexamide	$C_{15}H_{23}NO_4$	281	2.486	10	1.0
Brucine	$C_{23}H_{26}N_2O_4$	394	4.280	100	1.0
Rotenone	$C_{23}H_{22}O_6$	394	11.257	91	0.5
Reserpine	$C_{33}H_{40}N_2O_9$	608	11.411	10	4.0

Table IV. Analysis of 4 pesticides (M.W. 200 - 650)

complex mixtures. It appears that thermospray LC-MS using a benchtop mass spectrometer may provide the basis for a useful method for determining these difficult pesticides in real environmental samples.

Acknowledgement: The authors thank Dr. Daniel A. Garteiz for his help.

References:

1. Vestal, M.L.; Fergusson, G.J., Anal. Chem. 56, 2632 (1984).
2. Voyksner, R.D.; Haney, C.A., Anal. Chem. 57, 991 (1985).
3. Voyksner, R.D.; Bursey, J.T.;Pellizzari, E.D., Anal. Chem. 56, 1507(1984)

STUDIES ON SIZE AND CHARGE DISTRIBUTION OF DROPLETS FORMED IN THERMOSPRAY

Viswanatham Katta and Marvin L. Vestal
Department of Chemistry, University of Houston,
Houston, Texas-77004.

OBJECTIVE: In thermospray interface for LC-MS, ionization is caused by ion evaporation from charged droplets formed by a symmetric charging mechanism. The aim of this work is to study the size and charge distribution of these droplets by ion mobility spectrometry under various conditions of probe temperatures, nitrogen flow rate and electric field. The charge to size ratios obtained from mobility studies will be useful in understanding ion evaporation rates.

INTRODUCTION: Models for ion evaporation [ref 1] differ in the limits predicted for charge to size ratio required for the process. There is not enough experimental data for these quantities. The initial thermospray droplets have very high velocities, charges and masses, thus they are not amenable to analysis by MS directly. Ion mobility spectrometry was chosen as it can give charge/radius ratio and does not have any mass limitation. Whether the droplet should be considered as molecular ion ($r \ll$ mean free path λ) or macro ion ($r \approx \lambda$) [ref 2] depends on experimental conditions.

EXPERIMENTAL: A variable length (0.5-13.5 cm) drift tube was built. As the droplets were expected to reach gas(vapor) flow velocities within a short time and also lose some charge, a Tyndall type ion gate was built for pulsing them. The gated ions enter the drift tube and travel along the drift field to reach a biased collector. Signal is preamplified and observed on a digital oscilloscope. The gating pulse also starts the acquisition and scans are averaged to get better S/N ratio. The drift tube and nitrogen were heated to 70-80 C. Drift times were measured as a function of probe temperature Tl, drift field E, gating pulse height and width, and nitrogen flow rates. 0.5 M ammonium acetate at a flow rate of 1.5 ml/min was used.

RESULTS AND DISCUSSION: Even after a few hundred scans no definite peaks could be identified in the region (10-100 mS) expected for droplets. Early peaks (1-3 mS) did not change their position as the probe temperature was raised. This broad peak could be attributed to solvent/cluster ions. As a check, PEG 1450 in ammonium acetate was used, and a broad peak at 4.8 mS was observed. The mass ratio calculated from drift times also suggest that the early peak is from solvent/cluster ions. Low drift fields and high gas flow rates have broadened the peak but still not resolved in individual components. Long scan times required to observe the droplets were severely affected by noise due to 60 Hz from thermospray heating and LC pump fluctuations.

CONCLUSIONS: It is hard to detect droplets, unless thermospray and LC pump noise are decoupled from the signal. From the observed signal levels it is doubtful whether droplets could be gated successfully. If the droplets are not slowed down and lose some of their charge, the pulses (> 1000 V) required to electrically gate them are impractical. Mechanical chopping of the spray may be the way to gate these "massive" ions.

ACKNOWLEDGEMENTS: We thank Dr. Alan L. Rockwood for interesting discussions, National Science Foundation (grant CHE 8311354) and the Robert A. Welch Foundation for financial support. REFERENCES: 1. Vestal M. L., Ion emission from liquids, in Ion formation from organic solids, Ed. A. Benninghoven (1983). 2. E. A. Mason, in Plasma Chromatography, ed T.W.Carr(1984).

STUDIES WITH THERMOSPRAY LIQUID CHROMATOGRAPHY - MASS SPECTROMETRY

R. Willoughby, F. Poeppel, J. Buchner, V. Pizzitola, Extrel Corporation, Pittsburgh, Pa.

INTRODUCTION:

Thermospray LC/MS has gained wide acceptance in recent years. One observed limitation to the technique has been the lack of sensitivity (low nanogram) for most compounds when compared to GC/MS. Typical ion currents generated with currently available source designs are in the high picoamp to low nanoamp range. It was felt that current source designs could be modified to improve ion collection efficiency.

OBJECTIVES:

1. Study the faraday current generated by the TSY probe as a function of temperature and flow rate.
2. Develop a TSY source with enhanced ion sampling efficiency.

EXPERIMENTAL:

Phase I- A simple test vacuum chamber was constructed to allow the measurement of faraday current from the TSY probe. The chamber contained a focussing electrode and a faraday cup oriented on axis with the TSY probe introduction. The composition of the mobile phase was 50/50 ACN/H_2O (0.1M ammonium acetate). Temperatures and flow rates were varied. The current generated in the primary aerosol was measured. Since these measurements were taken outside the mass spectrometer, no information about the nature of the charge was obtained (i.e. charged particle or gas phase ions).

Phase II- A standard TSY source block was modified to include a focussing lens. Adenosine and PEG 600 were used to evaluate the performance of the interface. Lens voltage and tuning parameters were varied in an effort to enhance collection efficiency of the source.

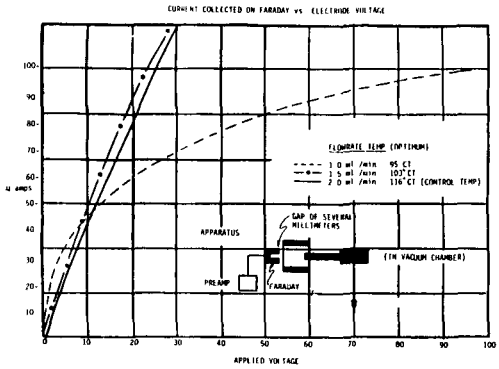

Figure 1. Probe current experiments.

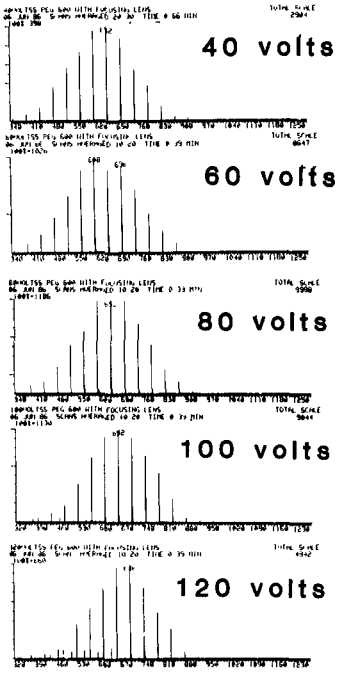

Figure 2. PEG600 spectra.

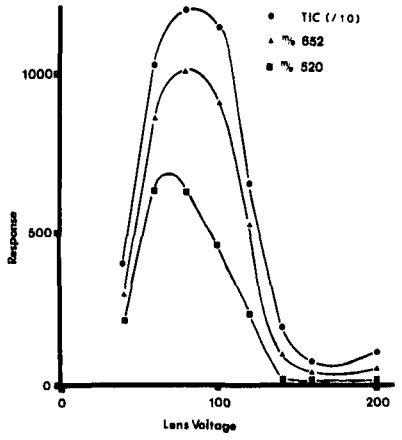

Figure 3. Focussing effects.

RESULTS:

Phase I- Figure one shows the plot of electrode voltage versus faraday current at several flow rates. These measurements were taken at the optimum temperature for T1. Two conclusions were drawn from these data. The current generated by the thermospray aerosol was significantly larger than the signal reaching the detector of the mass spectrometer and a focussing lens was effective in concentrating the charged species on a relatively small collector cup. Consequently, the same approach could be implemented in designing an improved source with the hope of concentrating the ions in the source at the skimmer aperture.

Phase II- Figure two shows spectra obtained with PEG 600 at various lens voltages in the modified source. An optimum lens voltage was observed at approximately 80 volts. Ion ratios did not significantly change as a function of lens voltage between 40 and 120 volts. Sodium adducts increased at higher lens voltages. Figure three shows the total ion and selected ion currents for several ions as a function of lens voltage.

CONCLUSION:

The use of a source focussing lens is a possible means of improving the sampling efficiency and sensitivity of the thermospray interface. The lens produces higher collection efficiency while showing no significant change in ion ratios.

A NEW SOURCE AND PROBE FOR THERMOSPRAY APPLICATIONS:

D.S. Jones, R.H. Bateman, M. Lancaster, T. Liszka, S.T. Krolik, V.C. Parr,
VG ANALYTICAL LTD., FLOATS ROAD, WYTHENSHAWE, MANCHESTER, M23 9LE, UK.

The use of thermospray in combined LCMS is well established for quadrupole mass spectrometers. However, thermospray in conjunction with a magnetic sector instrument offers the potential benefits of high resolution, accurate mass measurement, linked scan experiments and high mass capability.

A number of technical problems which were initially encountered, have been solved. This has resulted in;

a) design of a convenient and efficient pumping system for the thermospray source which eliminates the need for cryotrapping of solvents.

b) an optimised ion source lens arrangement to improve ion extraction and to reduce the excessive fragmentation observed from previous high voltage sources.

c) development of a very fast response thermospray probe, driven by a high power, high precision controller.

d) an overall thermospray system capable of handling 2ml/min of solvent and stable at full accelerating voltage.

Pumping

Cryotrapping systems suffer from the universal problem that solvent must eventually be removed from the vacuum system by venting, thawing and draining. This process is both disruptive and potentially dangerous in the hands of the inexperienced. We have found that a far more convenient arrangement is to pump reverse phase solvent vapours directly through a corrosion resistant, high temperature rotary pump with partial gas ballast. The anticipated problem of discharge between the ion source at high voltage to the thermospray rotary pump at earth potential was not encountered. This is presumably due to suppression by the relatively high (> 1 millibar) pressure in the pumping line.

Lenses

Initial experiments revealed that thermospray spectra from magnetic instruments suffered from the problem of excessive fragmentation. This is attributable to dramatic acceleration of ions through the high pressure region immediately outside the sampling cone of the ion source. The ion source, in this situation, is acting as a high energy collision cell. By "drifting" ions through the high pressure region, fragmentation has been substantially reduced.

Probe & Controller

The thermospray probe has been designed around precision 0.5mm. o.d. needle tubing heated directly by current. Narrow diameter tubing has the advantages of faster temperature response time and more reproducible performance from probe to probe.

Methanolic Thermospray

Recently, our laboratory has produced some surprising spectra by thermospray in 100% methanol without buffer and without any form of "assisted" ionisation. This is contrary to a recent report by Liberato & Yergey [1]. Our general observations from the limited number of compound examined are:

(1) A number of "intractable" thermospray compound have yielded far superior spectra in 100% methanol. Examples are vitamin B12 (shown below), riboflavin and ristocetin (Mwt 2066). Many organic compounds, such as saccharides, exhibit predominant $M+Na^+$ and $M+K^+$ ions with surprising absence of strong low mass solvent ion clusters. Formation of $2M+Na^+$ and $2M+K^+$ from large injections is fairly common.

(2) Inorganic salts such as NaI, RbI and especially CsI in 100% methanol yield much more intense spectra than in aqueous solutions with buffers. Clusters, identical to those observed in FAB, are formed to above mass 2000 with relative ease in both positive and negative ion mode.

One obvious application is a calibrant for the mass spectrometer in thermospray mode, a role which in the past, has been performed by either polypropylene or polyethylene glycol. The considerable advantages of methanolic salts such as NaI and CsI are:

a) Calibration with monoisotopic element clusters is relatively simple not requiring high resolution at high mass.

b) The salts give spectra only for the short period during which they enter the ion source. Their residual background contribution is insignificant due to their low volatility.

c) Halide salts are considerably mass deficient and generally are easily resolved from organic ions in the mass spectrometer.

d) Spectra are very simple, unlike the complex and variable ratios of MH^+ and MNH_4^+ observed in glycol thermospray. This is well-suited to the recognition algorithms employed by data system calibration programs. Reference files conventionally used for CsI positive and negative FAB calibration can be used for thermospray without modification.

Reference

(1) Liberato, D,J. Yergey, A.L; Anal. Chem. 1986, 58, 9-14.

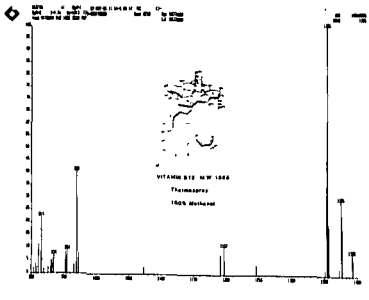

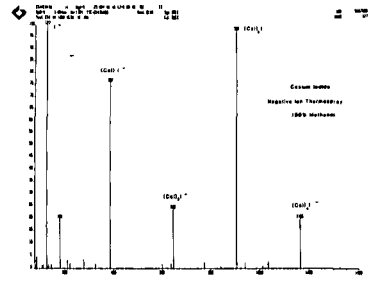

PHOTOELECTRON SPECTROSCOPY OF SeO^-, TeO^-, SeO_2^-, Se_2^-, Te_2^-, Te_3^-, AND P_2^-; J. T. Snodgrass, J. V. Coe, C. B. Freidhoff, K. M. McHugh, and K. H. Bowen; Johns Hopkins University, Department of Chemistry, Baltimore, Maryland 21218.

The photoelectron (photodetachment) spectra of SeO^-, TeO^-, SeO_2^-, Se_2^-, Te_2^-, Te_3^-, and P_2^- were recorded using 2.540 eV photons. Analyses of these spectra provide adiabatic electron affinities (EA's) for the corresponding neutral molecules. A hot-cathode discharge ion source was used to produce SeO^-, TeO^-, SeO_2^-, and Se_2^- ions by heating elemental selenium or tellurium in N_2O. Te_2^-, Te_3^- and P_2^- ions were produced using a cold-cathode discharge ion source by heating elemental tellurium or phosphorus in argon.

The photoelectron spectrum of SeO^- contains peaks arising from transitions between the lower vibrational levels of the SeO^- $^2\Pi$ ground state and the first few vibrational levels in the X $^3\Sigma^-_{0+}$ and a $^1\Delta$ states of SeO. From this spectrum we have determined the electron affinity of SeO [EA = 1.456±0.020 eV], the singlet-triplet splitting in SeO [ν_{00} (a $^1\Delta$ - X$^3\Sigma^-_{0+}$) = 5530±200 cm^{-1}], vibrational frequencies for the a$^1\Delta$ state of SeO [$\Delta G_{1/2}$ = 916±35 cm^{-1}] and the $^2\Pi$ ground state of SeO^- [ω_e = 730±25 cm^{-1}, $\omega_e x_e$ = 2±4 cm^{-1}], and the equilibrium bond length and bond dissociation energy of the SeO^- $^2\Pi$ ground state [r_e = 1.726±0.010Å, D_o = 3.84±0.09 eV]. The photoelectron spectrum of TeO^- contains peaks arising from transitions between the lower vibrational levels of the TeO^- electronic ground state and the first few vibrational levels in the XO^+ and $X1^\pm$ states of TeO. From this spectrum we have determined the electron affinity of TeO [EA = 1.697±0.022 eV], and the vibrational frequency, equilibrium internuclear separation, and bond dissociation energy for the ground electronic state of TeO^- [ω_e = 690±80 cm^{-1}, r_e = 1.884±0.028Å, and D_o = 3.63±0.15 eV]. The photoelectron spectrum of SeO_2^- contains a series of peaks which make up a vibrational progression in the symmetric stretching mode of the ground electronic state of SeO_2, originating in the ground vibrational and electronic state of SeO_2^-. Transitions which originate in vibrationally excited states of SeO_2^- are also observed (hot band transitions). Analysis of this spectrum yeilds the electron affinity of SeO_2 [EA = 1.823±0.040 eV] and an approximate measure of the symmetric stretching frequency of SeO_2^- [ω_e = 810±80 cm^{-1}]. The photoelectron spectrum of Se_2^- contains peaks arising from transitions between the lower vibrational levels of the Se_2^- electronic ground state and the first few vibrational levels in the XO_g^+ and $X1_g^\pm$ states of Se_2. The electron affinity of Se_2 [EA = 1.94±0.07 eV] was determined by modeling this spectrum. The photoelectron spectrum of Te_2^- consists of a single broad peak which contains several unresolved transitions between the lower vibrational levels of ground state Te_2^- and the first few vibrational levels of the XO_g^+ state of Te_2. The electron affinity of Te_2 [EA = 1.92±0.07 eV] was determined by modeling. The photoelectron spectrum of Te_3^- is dominated by the photodetachment transitions of Te^-. This indicates that Te_3^- has a propensity to photodissociate into Te^- and Te_2 when irradiated by 2.540 eV photons, and that some of the nascent Te^- ions are then photodetached. The observation of this photodissociation process with 2.540 eV photons implies an upper limit of 2.7 eV for the electron affinity of Te_3.

The electron affinities for SeO, TeO, Se_2, and Te_2 reported here, together with previously determined electron affinities for O_2, SO, S_2, allow an examination of the systematic variations in the electron affinities of Group VIB monoxides and homonuclear diatomics. We find that the electron affinities of these molecules approach the electron affinities of their Group VIB atoms more

closely as one proceeds down the VIB column toward the heavier species. Insight into the significance of these trends can be gained by considering the energetic relationships between the electron affinities of the Group VIB atoms and the electron affinities of molecules containing the corresponding Group VIB atoms. We illustrate this approach by considering the relationship between the electron affinities (EA's) of the homonuclear diatomics, X_2, and their parent atoms, X:

$$EA(X) - EA(X_2) = D_o(X_2) - D_o(X_2^-)$$

where $D_o(X_2)$ and $D_o(X_2^-)$ denote the bond dissociation energies of X_2 and X_2^-. The decreasing differences between the electron affinities of X and X_2 through the sequence X=O, S, Se, and Te (see table below), implies an increasing similarity between the bond dissociation energies of neutral X_2 and its negative ion, X_2^-. This increasing chemical similarity between the neutral molecules and their negative ions is perhaps due to the increasing diffuseness of the molecular orbitals in which the negative ions' excess electrons reside, and the decreasing influence of such electrons on the bonding in these negative ions. This observation is also supported by the fact that the vibrational frequencies of X_2 and X_2^- become increasingly similar through the sequence, O_2, S_2 and Se_2. Analogous considerations for the electron affinities of the Group VIB monoxides lead to similar conclusions.

Electron Affinities of Group VIB Atoms and Homonuclear Diatomics (All values in eV).

X	EA(X)	$EA(X_2)$	$EA(X) - EA(X_2)$
O	1.462	0.440	1.02
S	2.077	1.663	0.41
Se	2.021	1.94	0.08
Te	1.971	1.92	0.05

The photoelectron spectrum of P_2^- contains peaks arising from transitions between the lower vibrational levels of the P_2^- X $^2\Pi_g$ ground state and the first few vibrational levels of the P_2 X Σ_g^+ ground state. From this spectrum we have determined the electron affinity of P_2 [EA = 0.589±0.025 eV] and the vibrational frequency, equilibrium internuclear separation, and bond dissociation energy for the X $^2\Pi_g$ state of P_2^- [ω_e = 640±50, r_e = 1.979±0.010Å, and D_o = 4.88±0.06 eV]. The positive electron affinity of P_2 compared to the non-positive electron affinity of N_2 emphasizes the often noted electronic differences between phosphorus and nitrogen.

MEASUREMENT OF THE RADIATIVE RELAXATION RATE OF PHOTO-EXCITED IODOBENZENE USING TWO-LIGHT-PULSE PHOTODISSOCIATION: EVIDENCE FOR AN INFRARED MULTIPHOTON MODEL FOR RELAXATION

Bruce Asamoto and Robert C. Dunbar
The Standard Oil Company and
Case Western Reserve University
Cleveland, Ohio

The two-light-pulse photodissociation experiment provides a means of measuring the relaxation of excited state ions. Thermal energy ions are trapped within an ICR cell. The first light pulse is used to excite the ions to a specific internal energy. After a delay time, the second pulse is used as a probe to measure the fraction of ions still above a given threshold. By comparing the observed temporal profiles of relaxation with calculations based on models of the process, we can arrive at a model for the relaxation of photo-excited ions. A value for the relaxation rate of ions can also be determined.

The amount of internal energy required to dissociate iodobenzene is 2.3 eV. Using a photon energy of 590 nm (2.1 eV), iodobenzene will require two photons to dissociate. In the two-light-pulse experiment, the first light pulse raises the internal energy of a population of iodobenzene ions to 2.1 eV A delay period follows during which the ions relax towards the ground state ion. If the ions relax to below 0.2 eV, it will again require two photons to dissociate. Those ions which have not relaxed below the threshold will require only a single additional photon. This means at very short pulse separation times, there will be excess dissociation over the limit of long separation times, where the dissociation will be equivalent to that of two isolated light pulses.

Two models for relaxation can be envisioned (Figure 1). In a rate-process model, the relaxation would follow a simple first order rate constant. This kinetic behavior would be expected if the relaxation occurs via emission of a single visible photon. Another model referred to as the cascade model, assumes relaxation through emission of multiple infrared photons. The results would reflect these processes as follows: with the rate-process model, the amount of dissociation would decrease exponentially with increasing delay time; with the cascade model, initially, there would be no decrease in dissociation as all relaxation occurs to states above the one-photon threshold. This would be followed by a period where dissociation would rapidly decrease with increasing delay time. The "induction" time during which no ions relax below the one-photon threshold is the most characteristic feature of the cascade model.

The results of the amount of dissociation versus delay time are shown in Figure 2. Also shown are best fit computer simulations using the rate-process model and the cascade model. The rate-process fit assumed a relaxation rate of 2.8/sec. The cascade model simulation assumed an infrared fluorescent photon energy of 1000 cm^{-1} and an initial emission rate of 68 photons/sec. The overall relaxation rate to below the one-photon threshold is 1.4/sec. A correction to account for nonhomogeneous irradiation was used in the cascade fit. This correction changed the amount of dissociation at the high and low limits but not the characteristic shape of the curve.

The results clearly support a cascade model. The salient feature in the data is the initial period where no quenching of excess dissociation occurs. The rate-process predicts the most rapid relaxation during this period. Figure 3 shows a set of data taken at very short delay times which more clearly illustrates the induction period.

The rate of relaxation of the iodobenzene neutral was calculated from theory, using the infrared absorption intensities of neutral iodobenzene for absolute numerical calibration. This yields an ir photon emission rate of 23 photons/sec (again assuming a photon energy of 1000 cm^{-1}). The overall relaxation rate is 0.4/sec. The relaxation of the ion is 2.3 times faster than it would be if the ion had the same infrared properties as neutral iodobenzene.

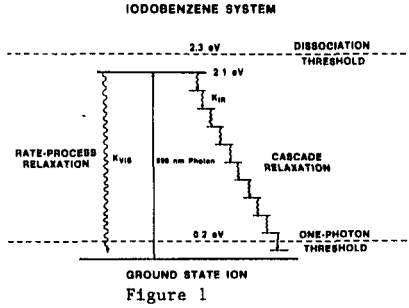

Figure 1

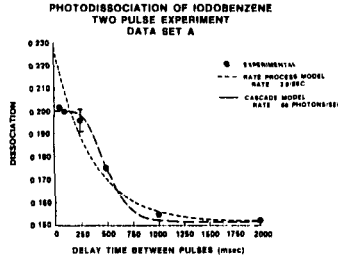

Figure 2

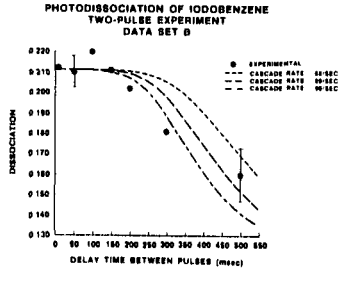

Figure 3

COLLISIONAL QUENCHING OF PHOTO-EXCITED BROMOBENZENE IONS

M. S. Ahmed and R. C. Dunbar
Department of Chemistry
Case Western Reserve University
Cleveland, Ohio 44106

Introduction:

Intermolecular energy transfer in collisions as a common activation or deactivation process of excited molecules, plays important roles in many gas phase reactions. In spite of this only little is known of the details of energy transfer between highly excited polyatomic molecular ions and their collision partners. In the present paper, we report data on energy transfer involving excited bromobenzene radical cation and thirty-five different collision partners. Our goals are to determine collision efficiencies of these cool neutral molecules and to correlate several molecular parameters such as dipole moment, polarizabilities, boiling point, molecular weight, internal degrees of freedom and specific chemical interaction.

Bromobenzene radical cation undergoes photodissociation by a sequential two-photon process (1). The dissociation threshold is 2.76 eV. The collisional relaxation of the sequential two-photon process can be understood as follows: After absorption of the first photon, a well known quantity of internal energy in the form of vibrational excitation is deposited in the ion. If the excited ion loses sufficient energy in colliding with cool neutral molecules to drop the ion internal energy below the one photon threshold, it can no longer be dissociated by the second photon. By observing the variation in the observed extent of photodissociation with neutral pressure, the quenching rate constant can be determined. Comparing the quenching rate constant with the orbiting collision rate constant yields the number of collisions needed to quench the excited ion (see Table 1).

Experimental:

The experiment has been done with a pulsed Ion Cyclotron Resonance Spectrometer. The cell used was cubical of 2.54 cm dimension. Bromobenzene ions are formed by a 200 ms pulse of an 11 eV electron beam. The ions are sampled by a detect pulse of 4 ms duration after irradiation by the Coherent Radiation CR-12 argon ion laser at 514.5 nm. Bromobenzene ions were trapped for 1 sec. The pressure of bromobenzene was maintained at $1\text{-}2\times10^{-8}$ torr while the pressure of the quench gas varied up to 2×10^{-5} torr. The pressure was measured by the ion-pump current gauge which was converted into absolute pressure by dividing by the ion gauge sensitivity factor.

Conclusions

1. For monoatomic gases, the collision efficiency increases with increasing atomic mass.

2. Deuteration does not change the quenching rate although the collision efficiency per collision changes. This is in agreement with similar recent findings for iodobenzene (2).

3. Unsaturated hydrocarbons are observed to be better quenchers than the corresponding saturated ones. Ion-quench-gas chemical interaction may be responsible for the increased collision efficiency.

4. The rapidly rising quenching efficiency with molecular complexity indicates the participation of a number of internal degrees of freedom.

5. Modelling the results by a complete equilibration model is poor. It gives 42 collisions for He and 26 collisions for D_2 (compared with the observed 150 and 110, respectively). Complete equilibrium among all vibrational, rotational and translational degrees of freedom is not achieved in each collision.

Table 1. Bromobenzene Ion Quenching

Collision partner	Collision number	Collision partner	Collision number
^3He	182.3	CH_3F	29
^4He	151.5	CH_3Br	23
Ne	100.2	C_2H_4	12.4
Ar	76.8		20.6
Kr	30.4	C_2H_6	23.7
Xe	23.6	C_2H_5Cl	21.8
H_2	163.3	C_2H_5F	26.5
D_2	110	C_3H_6	6.5
O_2	30.3	c-C_3H_6	16.5
N_2	70.3	n-C_3H_8	18
NO	32.4	C_3H_7Cl(1-chloro)	20.4
CO	36	C_3H_7Cl(2-chloro)	20.2
CO_2	18	i-C_4H_8	9.2
OCS	8.2	n-C_4H_{10}	9.6
H_2O	22	C_6F_5I	3.5
C_2H_2	9.3	c-C_6H_{10}	4.5
CH_4	39.5	c-C_6H_{12}	6.5
CH_3Cl	27.4		

References

1. R. C. Dunbar and E. W. Fu, J. Phys. Chem. 81, 1531 (1977).

2. R. C. Dunbar and J. Ferrara, J. Chem. Phys., 83, 6229 (1985).

DIAGNOSTIC STUDIES OF THE FLOW DYNAMIC EFFECT ON RATE COEFFIENTS OTAINED WITH A SELECTED ION FLOW TUBE (SIFT)

R. J. Shul, R. Passarella, B. L. Upschulte, R. G. Keesee, and A. W. Castleman, Jr., The Pennsylvania State University, University Park, PA 16802 USA

In making system-to-system comparisons, rate coefficients obtained for ion-molecule reactions using flow techniques are often reported to vary by approximately ±30%. An extensive systematic study has been conducted in our laboratory using a Selected Ion Flow Tube technique (SIFT) to determine the dependence of the rate coefficient on a number of system parameters. These include: pressure, buffer gas flow rate, ion velocity, separation between the flow tube and the sampling orifice, end correction, reaction distance, style of reactant gas inlet and flow tube diameter. The bimolecular charge transfer of Ar^+ with O_2 was used as the standard test reaction in this diagnostic study.

Five different reactant gas inlets were used and are shown schematically in Figure 1. The two finger inlets studied were 1/8" and 1/4" O.D. stainless steel tubing in which the neutral reactant gas was introduced in the direction of the carrier gas. The remaining three inlets were all constructed of 1/16" O.D. stainless steel tubing containing six equally spaced 1/64" diameter holes. Neutral reactant gas was introduced against the carrier gas flow for both the ring and the spiral inlets. Three of the holes were directed radially inward and three radially outward for the introduction of reactant gas with the radial inlet. The inlets were studied in four different flow tubes with diameters of 10.16 cm, 7.62 cm, 6.16 cm and 5.54 cm. Measurements were made at two reaction distances; namely, 45.9 cm and 7.13 cm, under a variety of conditions of flow tube pressures and carrier gas flow rates.

Literature values reported for the rate coefficient of the $Ar^+ + O_2$ reaction range from 4.3 to 7.0×10^{-11} cm^3/s (1). In our studies we observe a range of 2.8 to 8.0×10^{-11} cm^3/s depending on the experimental parameters used. The flow tube pressure and the distance separating the flow tube and the sampling orifice showed no effect. Variation of the buffer gas flow rate introduced curvature into the semilogarithmic plots of ion intensity versus neutral reactant gas concentration which has been attributed to high buffer gas flow rates and can be eliminated by a decrease of this flow. Excessive carrier gas flow rates cause an ion concentration distortion at the point of reactant gas introduction resulting in improper mixing of the reactant gas with the ions throughout the reaction region. It has also been observed that accurate measurement of the ion velocity at all possible flow tube conditions is necessary. Calculation of the ion velocity may introduce as much as 12% error in the determination of a rate coefficient.

Table I shows the range of rate coefficients obtained under a variety of experimental conditions and the evaluation of an end correction using "standard" methods suggested in the literature (2). The end correction has been used to correct for the inability of a gas inlet to instantaneously introduce the reactant gas uniformly over the full cross section of the flow tube. The inconsistency of the rate coefficients determined with the end correction ($k_{(\varepsilon)}$) and the large range of end correction values (ε) obtained in this study indicate that the end correction concept is oversimplified. Proper correction must account for reactive and diffusive loss processes, distortion of ion concentration due to reactant gas addition and ion concentration profiles.

Table II shows that the spread in rate coefficients as a function of inlet design decreases toward longer reaction distances and larger flow tube diameters. We also observe that larger flow tubes do not appear to require an end correction since the rate coefficients are experimentally reproducible independent of reaction distance, pressure and buffer gas flow rates. This indicates that longer reaction times help reduce the effect of non-uniform reactant gas addition, distortion of the ion concentration, and coupling of the diffusive and reactive loss of ions for all inlet styles. This is further verified by pre-mixing the O_2 with the carrier gas to maximize the reaction time and efficient mixing. The rate coefficients obtained under such conditions at varying flow tube diameters are within experimental reproducibility.

Acknowledgments:

Support by the Department of Energy, Grant No. DE-AC02-ER-60055, is gratefully acknowledged.

Reference:

1. N. G. Adams and D. Smith, Int. J. Mass Spectrom. Ion Phys. 21, 349 (1976).

2. D. K. Bohme, R. S. Hemsworth, H. W. Rundle, and H. I. Schiff, J. Chem. Phys. 58, 3504 (1973).

Table I

Variation in the Measured Rate Constant For the Reaction

$$Ar^+ + O_2 \xrightarrow[He]{} O_2^+ + Ar \qquad (300°K)$$

Inlet	$\times 10^{-3}$ Q(sccm)	$\bar{P}$ (torr)	Z (cm)	k	$\times 10^{11}$ (cm^3/sec) k_{avg}	k(ε)	ε (cm)
1/8" Finger	8.5	0.30	46.9	8.0	7.7	1.2	26.4
(pointed with	12.0	0.41	46.9	7.3			
buffer flow)	8.5	0.32	71.3	5.4	5.4		
	12.0	0.43	71.3	5.4			
1/4" Finger	8.5	0.31	46.9	5.8	5.8		
(pointed with	12.0	0.42	46.9	5.7		2.4	62.1
buffer flow)	8.5	0.31	71.3	4.6	4.6		
	12.0	0.43	71.3	4.6			
Radial	8.5	0.31	45.9	5.1	5.2		
	12.0	0.42	45.9	5.3		2.8	38.8
	8.5	0.32	71.3	4.4	4.4		
	12.0	0.43	71.3	4.3			
Ring	8.5	0.31	46.9	4.6	4.4		
(pointed	12.0	0.42	46.9	4.3		0.19	1.01
against	8.5	0.32	72.3	3.0	2.9		
buffer flow)	12.0	0.44	72.3	2.8			

Table II

The Inlet, Flow Tube Size Dependence of the Rate Constant for

$$Ar^+ + O_2 \xrightarrow{He} O_2^+ + Ar$$

Inlet	R(cm)	$kx10^{11}$ (cc/s) Z = 71.3 cm Q_{He}(8500 sccm)	Q_{He}(12000sccm)	Avg k	$kx10^{11}$ (cc/s) Z = 45.9 cm Q_{He}(8500 sccm)	Q_{He}(12000 sccm)	Avg k
Ring	3.08	3.0	2.8	2.9	4.6	4.3	4.4
Radial	3.08	4.4	4.3	4.4	5.1	5.3	5.2
1/4" Finger	3.08	4.6	4.6	4.6	5.8	5.7	5.8
1/8" Finger	3.08	5.4	5.4	5.41	6.1	7.3	6.7
Ring	3.81	4.0	4.0	4.0	4.0	3.8	3.9
Radial	3.81	4.2	4.4	4.3	4.8	4.8	4.8
1/4" Finger	3.81	4.4	4.0	4.2	3.9	3.7	3.8
1/8" Finger	3.81	4.5	4.6	4.6	4.8	4.9	4.8
Spiral	3.81	4.2	3.9	4.0	4.4	4.6	4.5
Ring	5.08	3.7	3.6	3.6	3.1	3.3	3.2
Radial	5.08	4.0	3.8	3.9	3.9	3.8	3.8
1/4" Finger	5.08	3.8	3.9	3.8	4.0	3.7	3.8
1/8" Finger	5.08	3.6	----	3.6	3.9	3.7	3.8

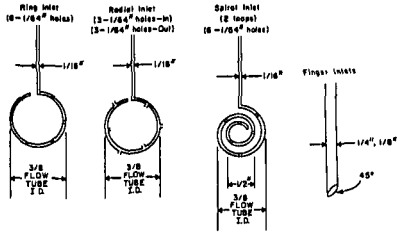

FIGURE 1

Introduction and Detection of Cluster Ions
in a Fourier Transform Mass Spectrometer

W. D. Reents, Jr., V. E. Bondybey, and M. L. Mandich

Direct laser vaporization of materials provides a simple method to form small ionic silicon clusters.[1] These clusters may be kept in the ion trap of a Fourier transform mass spectrometer (FTMS) for several seconds. The capabilities of the FTMS are then used to determine bimolecular rate constants, identify reaction products, and evaluate product distributions of the ionic silicon clusters.

The chemistry of positive and negative silicon clusters, containing up to seven atoms, with methylsilane and tungsten hexafluoride have been examined. Significant differences in reaction rates and products as a function of cluster size are evident as shown in Tables 1-3. The reactions with methylsilane lead to growth of the cluster by incorporation of the silicon. The reaction rate constants decrease with increasing cluster size (Table 1). The lowest energy products predominate for Si_{1-4}^+. However, high energy products appear for Si_5^+. This indicates that the slow rate observed is not due to lack of internal energy since there is sufficient energy to cause bond scission. The decreasing reaction rate is believed to be due to a charge which is increasingly delocalized with increasing cluster size. This coupled with the poor basicity of methylsilane makes it more difficult to access the requisite transition state. The acidic nature of methylsilane is also poor since no reactions of the anionic silicon clusters with methylsilane are observed.

A mechanism must utilize the radical or silylene nature of these clusters.[2] The radical would result in hydrogen abstraction[3] whereas the silylene group would yield insertion into the silicon-hydrogen bond.[4] Only the latter mechanism explains the formation of H_2. A second H_2 would be lost following a second insertion reaction. Loss of H or CH_3 would occur from the methylsilane silicon immediately following insertion if sufficient energy in the transition state is present. Therefore, the transition state has stronger bonds for Si_5^+ than the smaller clusters had. This correlates with theoretical calculations which predict stronger silicon-silicon bonds with increasing cluster size.[2]

Both the anionic and cationic silicon clusters react with WF_6 by fluorine transfer (Tables 2 and 3). The reaction is sufficiently exothermic that the smaller clusters are broken apart. For the cationic clusters this simplifies to only monofluorination with a concurrent reduction in reaction rate at Si_4^+. A change to only monofluorination also occurs for the anions (at Si_6^-) but a similar reduction in reaction rate is not observed because of the charge transfer reaction which is present as well. A mechanism involving both the radical and the silylene groups is warranted. The radical is involved as an abstractor of fluorine[3] whereas silylene groups are involved in insertion into tungsten-silicon bonds.[4] As with methylsilane, a reduction in reaction rate for the cationic clusters occurs. This is most likely due to the inability to open the closed ring silicon structure which would create additional radical sites for further reaction. Unlike methylsilane, a radical reaction is present for all of the clusters examined.

REFERENCES

1. W. D. Reents and V. E. Bondybey, Chem. Phys. Lett., 125, 324-327 (1986).
2. K. Ragavachari and V. Logovinsky, Phys. Rev. Lett., 55, 2853-2856 (1985).
3. J. W. Wilt, "Reactive Intermediates", R. A. Abramovitch, ed., v. 3, 1983, pp. 113-197.
4. Y. Tang, "Reactive Intermediates", R. A. Abramovitch, ed., v. 2, 1982, pp. 297-366.

TABLE 1

Si_n^+ REACTIONS WITH CH_3SiH_3

Reaction	Product Fraction (%)	Rate Constant ($\times 10^{11}$) (cm^3 molecule^{-1} sec^{-1})
$Si^+ + CH_3SiH_3 \rightarrow Si_2CH_4^+ + H_2$	53	17
$SiCH_3^+ + SiH_3$	47	
$Si_2^+ + CH_3SiH_3 \rightarrow Si_2CH_4^+ + H_2$	28	5 ± 1
$Si_2CH_2^+ + 2H_2$	40	
$Si_2CH_3^+ + SiH_3$	13	
$Si_2CH_5^+ + SiH_4$	16	
$Si_2CH^+ + SiH_3 + H_2$	3	
$Si_3^+ + CH_3SiH_3 \rightarrow Si_3CH_4^+ + H_2$	76	7.6 ± 0.7
$Si_3CH_2^+ + 2H_2$	24	
$Si_4^+ + CH_3SiH_3 \rightarrow Si_4CH_4^+ + H_2$	70	1.8 ± 0.2
$Si_4CH_2^+ + 2H_2$	30	
$Si_5^+ + CH_3SiH_3 \rightarrow Si_5CH_5^+ + H$	81	3.0 ± 0.3
$Si_5H_3^+ + CH_3$	19	
$Si_6^+ + CH_3SiH_3 \rightarrow$ N.R.		< .012
$Si_7^+ + CH_3SiH_3 \rightarrow$ N.R.		< .073

TABLE 2

Si_n^- REACTIONS WITH WF_6

REACTION[a]	PRODUCT FRACTION (%) excl WF_6^-		RATE CONSTANT ($\times 10^{11}$) (cm^3 molec^{-1} sec^{-1})
$Si^- + WF_6 \rightarrow SiF^- + WF_5$	2.0	15	41
$WF_4^- + SiF_2$	2.5	19	
$WF_5^- + SiF$	9.0	67	
$WF_6^- + Si$	86.5	-	
$Si_2^- + WF_6 \rightarrow Si_2F_3^- + WF_4$	0.4	2	110
$SiF_3^- + WF_2 + SiF$	0.1	1	
$WF_2^- + 2SiF_2$	16.4	77	
$WF_3^- + SiF_2 + SiF$	0.4	2	
$WF_4^- + SiF_2^- + Si$	1.9	9	
$WF_5^- + Si_2F$	2.2	10	
$WF_6^- + Si_2$	76.6	-	
$Si_3^- + WF_6 \rightarrow Si_3F^- + WF_4$	0.1	2	47
$WF_2^- + SiF_2 + Si_2F_2$	2.3	40	
$WF_5^- + Si_3$	94.3	-	
$WSiF_2^- + 2SiF_2$	3.3	58	
$Si_4^- + WF_6 \rightarrow Si_4F^- + WF_5$	0.2	3	55
$WSiF_2^- + 2SiF_2$	1.9	30	
$WF_2^- + SiF_2 + Si_3F_2$	2.1	34	
$WF_5^- + Si_4F$	2.1	34	
$WF_6^- + Si_4$	93.7	-	
$Si_5^- + WF_6 \rightarrow Si_5F^- + WF_5$	6.23	38.44	44
$WSiF_2^- + 2SiF_2$	9.94	61.56	
$WF_6^- + Si_5$	83.86	-	
$Si_6^- + WF_6 \rightarrow WF_5^- + Si_6F$	1.7	100	63
$WF_6^- + Si_6$	98.3	-	

[a] Most stable neutral products are shown.

TABLE 3

Si_n^+ REACTIONS WITH WF_6

REACTION[a]	PRODUCT FRACTION (%)	RATE CONSTANT ($\times 10^{11}$) (cm^3 MOLECULE^{-1} SEC^{-1})
$Si^+ + WF_6 \rightarrow SiF^+ + WF_5$	14	66
$WF_3^+ + SiF_3$	1	
$WF_4^+ + SiF_2$	67	
$WF_5^+ + SiF$	18	
$Si_2^+ + WF_6 \rightarrow Si_2F^+ + SiF + WF_4$	7	21
$Si_2F^+ + WF_5$	8	
$Si_2F_2^+ + WF_4$	8	
$WF_2^+ + 2SiF_2$	27	
$WF_3^+ + SiF_2 + SiF$	15	
$WF_4^+ + Si_2F_2$	22	
$WF_5^+ + Si_2F$	13	
$Si_3^+ + WF_6 \rightarrow Si_3F^+ + WF_5$	7	16
$Si_3F_2^+ + WF_4$	4	
$WF_2^+ + SiF_2 + SiF_2 + Si_2F$	2	
$WF_3^+ + SiF_2 + Si_2F$	5	
$WF_4^+ + Si_3F_2$	17	
$WSiF_2^+ + 2SiF_2$	55	
$WSiF_3^+ + SiF_2 + SiF$	5	
$WSiF_4^+ + Si_2F_2$	5	
$Si_4^+ + WF_6 \rightarrow Si_4F^+ + WF_5$	100	0.9
$Si_5^+ + WF_6 \rightarrow Si_5F^+ + WF_5$	100	0.[illegible]
$Si_6^+ + WF_6 \rightarrow Si_6F^+ + WF_5$	100	0.[illegible]

[a] Most stable neutral products are shown

CHAINLENGTH EFFECTS IN THE GAS PHASE CHEMISTRY OF TRANSITION METAL- AND METAL CONTAINING-IONS WITH UNSATURATED ORGANIC MOLECULES.

R.M. Stepnowski, J. Allison, Michigan State University, Department of Chemistry, East Lansing, Michigan 48824

The chemistry of transition metal and metal containing ions has been studied for molecules containing a variety of functional groups[1,2]. While examining molecules with long alkyl chains, such as 1-heptanol, it became apparent that while the functional group still "controlled" the reaction, the metal inserted into C-C bonds remote from the functional group. This result was termed the "chain length effect", because the length of the carbon chain influences which bonds are attacked. The chain length effect has been reported for the 1-n-chloroalkanes and the 1-n-alcohols[3].

This study involves the reactions of aldehydes and nitriles. The C_{2-7} straight chain aldehydes and the C_{2-9} nitriles were reacted with metal and metal containing ions produced by 70 eV electron impact on $Fe(CO)_5$, $Ni(PF_3)_4$, $Co(CO)_3NO$, $Cr(CO)_6$, and $Mn_2(CO)_{10}$. Reaction products and pathways were determined using Ion Cyclotron Resonance (ICR) Mass Spectrometry. The preferred sites of insertion of Co^+ with heptanal, heptanitrile, and other molecules with an $n\text{-}C_6H_{13}$ alkyl chain are shown in Fig. 1.

Nitriles react with transition metal ions via the same mechanisms as alcohols and 1-chloroalkanes. There are some important differences in the chain length effect, however. For the nitriles, the R-CN bond is not attacked, due to two factors. The first is, if we assume that the $R\text{-}CN\text{-}M^+$ complex is linear (along the C-CN-M), the C-CN bond is mechanistically inaccessible to the metal. Secondly, the C-CN bond is relatively strong. For example, $D(CH_3\text{-}OH)$ = 91 kcal/mol, $D(CH_3\text{-}CN)$ = 123.9 kcal/mol. Possible conformation of the complex initially formed are such that the metal ion may interact with parts of the alkyl chain much farther from the functional group than it would in the corresponding alcohol. The reactivity of the ions of Fe, Co, Ni, Cr and Mn with nitriles affirm the concept of promotional energy[4]; that thos metal ions which require **more** energy to promote 2 electrons from d to s or p orbitals will be **less** reactive.

Ligand effects were also observed. Ligand substitution reactions were observed for the usually unreactive $CoNO^+$ ion, suggesting that the $RCN\text{-}Co^+$ bond is strong. Nitriles have high proton affinities, and the strength of metal ion-ligand interactions can be correlated to proton affinities. Reaction of MCO^+ is mainly through C-H insertion or C-C insertion near the end of the alkyl chain, where steric effects will be minimized.

The reactions of aldehydes are more specific than in the corresponding alcohols, with fewer bonds being attacked. Ni^+ appears to form five membered ring intermediates, while Fe^+ and Co^+ form six membered rings.

The aldehydes differ from the nitriles in that the MCO^+ ions react with the aldehydes to form a variety of products. By contrast, the MCO^+ ions form very few products with the nitriles, and then only with those with the longest alkyl chains.

1. R.R. Corderman and J.L. Beauchamp, J. Am. Chem. Soc., **98**, 5700 (1976).
2. M. Lombarski and J. Allison, Int. J. of Mass Spec. and Ion Phys., **65**, 31 (1985).
3. A. Tsarbopoulos and J. Allison, J. Am. Chem. Soc., **107**, 5085, (1985).
4. S.J. Babinec and J. Allison, J. Am. Chem. Soc., **106**, 7718, (1984).

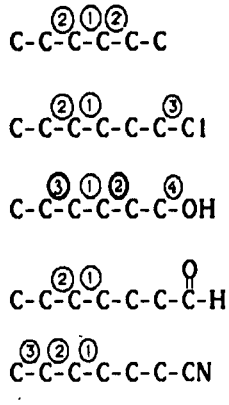

Figure 1 Insertion sites of Co^+ into molecules containing an n-hexyl alkyl chain.

In this figure, the bond into which Co^+ insertion occurs most often is labeled 1 . The bond yielding the next largest fraction is marked 2 . The ordering of bond insertion for alcohols assumes that the product $CoC_4H_6^+$ is formed by H_2 loss from $CoC_4H_8^+$. If $CoC_4H_6^+$ is formed by dehydration of $CoC_4H_8O^+$, the numbers in **bold circles** will switch.

Reactivities of Heterodinuclear Transition Metal Cluster Ions with small hydrocarbons in the gas phase using Fourier Transform Mass Spectrometry

Y. Huang, E.C. Tews, S.W. Buckner and B.S. Freiser
Department of Chemistry
Purdue University

The reactivity of several heterodinuclear transition metal ions is discussed. The preparation of the clusters is carried out in a Fourier Transform Mass Spectrometer (FTMS) equipped with a laser ionization source for production of metal ions. The metal ions are reacted with a metal carbonyl introduced into the cell via a pulsed valve with the following general reactions occuring (1)

$$M^+ + M'(CO)_n \text{ ---- } MM'(CO)_3^+ + n\text{-}3\ CO \qquad (1)$$

The $MM'(CO)_3^+$ then undergoes collision-induced dissociation to produce the bare metal cluster ion via sequential loss of carbonyl ligands.

The clusters compared were $NbFe^+$, $CuFe^+$, $LaFe^+$, $RhFe^+$, $RhCo^+$, VFe^+, $CoFe^+$ and $ScFe^+$.

Only $LaFe^+$, $RhFe^+$, and $RhCo^+$ are observed to react with alkanes. All three cluster ions react with alkanes larger than methane mainly via dehydrogenation. C-C cleavage occurs for small cyclic alkanes with weak C-C bonds. $RhFe^+$ and $RhCo^+$ show similar patterns of reactivity with multiple dehydrogenation of alkanes larger than ethane. Interestingly, n-pentane and cyclopentane react with $RhFe^+$ and $RhCo^+$ to split the cluster and form $RhC_5H_6^+$ and $RhC_5H_5^+$, presumably the cyclopentadiene- and cyclopentadienyl-rhodium cations. This is interesting as Rh^+ does not react with either n-pentane or cyclopentane to produce Rh-cyclopentadienyl$^+$. The loss of a stable FeH probably facilitates the formation of the cyclopentadienyl ligand. The hexanes react with the Rh^+ cluster via multiple dehydrogenation with no cluster splitting occuring. $LaFe^+$ shows less extensive dehydrogenation than either $RhCo^+$ or $RhFe^+$. The reactivity of $RhFe^+$, $RhCo^+$ and $LaFe^+$ is more similar to that of Rh^+ [1] and La^+ [2] than Fe^+ [3] and Co^+. Dehydrogenation is the preferred pathway in the reactions of $LaFe^+$ with 1,3-dehydrogenation occuring in reaction with neo-pentane whereas the rhodium cluster ions react via loss of methane and hydrogen. Both $RhFe^+$ and $RhCo^+$ react with O_2 as in reaction (2)

$$RhM^+ + O_2 \text{ ---- } Rh^+ + MO_2 \qquad (2)$$

$LaFe^+$ reacts with O_2 as in reaction (3)

$$LaFe^+ + O_2 \text{ ---- } LaO^+ + FeO \qquad (3)$$

The Rhodium clusters react with ethylene oxide to abstract an oxygen and form the cluster oxide ions. This implies 85 kcal/mol$<D^o(RhM^+\text{-}O)<$119 kcal/mol (M= Fe,Co).

The other clusters discussed are unreactive with alkanes. This is in contrast to the reactivity of the constituent atomic metal ions which are reactive with alkanes via both C-H and C-C bond activation.

$NbFe^+$ is the most reactive of the other clusters, reacting with alkenes larger than ethene. C-H bond cleavage is the preferred reaction pathway. This indicates insertion into an allylic C-H bond may be the rate limiting step as opposed to formation of a metal-pi bond. More extensive dehydrogenation occurs with $NbFe^+$ than with $CuFe^+$, $CoFe^+$, VFe^+ or $ScFe^+$. Cluster splitting occurs with C_5 and C_6 linear alkenes and large cyclic alkenes to produce tha Nb(cycloalkene)$^+$ species. This indicates dehydrocyclization is a prevalent reaction pathway in reactions

with larger linear alkenes. Formation of NbFe(cycloalkene)$^+$ and NbFe(bis-cycloalkene)$^+$ species also occurs, though. The formation of NbFe(bis-cycloheptatriene)$^+$ from cycloheptene is the largest cluster-sandwich ion species observed to date.

$CuFe^+$, $ScFe^+$ [4] and $CoFe^+$ [5] all exhibit similar reactivity. All three clusters react with alkenes larger than propene. Multiple dehydrogenation is observed for reactions of 1-hexene with $CuFe^+$ and $CoFe^+$. Splitting of the cluster occurs in reactions of cyclohexene with $CoFe^+$ and $ScFe^+$.

VFe^+ [6] is the least reactive of the clusters discussed. VFe^+ only reacts with C_6 and C_7 cycloalkenes.

The secondary reactions of the clusters which react with alkanes are similar but slower and involve less extensive neutral loss than the primary reactions. For the clusters which were unreactive with alkanes, their secondary reactions with alkenes were more rapid and involved more extensive neutral loss than their primary reactions with alkenes.

The ordering of reactivity of the cluster ions discussed, based upon extent of neutral loss, is

$$RhFe^+ \; RhCo^+ > LaFe^+ > NbFe^+ > CuFe^+ \; CoFe^+ \; ScFe^+ > VFe^+$$

The reactivity of the metal cluster ions is very different from the reactivity of the atomic metal ions with the clusters being, in general, less reactive.

The enhanced reactivity of $RhFe^+$, $RhCo^+$ and $LaFe^+$ is clearly related to the fact that they involve a first row metal bound to a second or third row metal. Although $NbFe^+$ does not react with alkanes it also follows this trend in so much as its reactivity with alkenes is much greater than that of VFe^+. The combination of a first row and a second or third row metal may involve decreased orbital overlap due to differences in constituent orbital energy and size and thus, atoms in the cluster would behave more like the individual atomic metal ions.

ACKNOWLEDGMENT

Acknowledgment is made to the Division of Chemical Sciences in the Office of Basic Energy Sciences in the United States Department of Energy (DE-AC02-80ER10689) for supporting the metal ion studies and to the National Science Foundation (CHE-8310039) for providing funds for FTMS methodology. S.W. Buckner gratefully acknowledges the Purdue Research Foundation for fellowship support. E.C. Tews gratefully acknowledges American Cyanamid for fellowship support.

REFERENCES

1) Byrd,G.D. and Freiser,B.S; J. Am. Chem. Soc., 104, 5944, (1982)
2) Wise,M.B., Jacobson,D.B., Huang,Y. and Freiser,B.S.; Organometallics, submitted
3) Byrd,G.D., Burnier,R.C. and Freiser,B.S.; J. Am. Chem. Soc., 104, 3565, (1982)
4) Lech,L.M. and Freiser,B.S.; unpublished results
5) Jacobson,D.B. and Freiser,B.S.; J. Am. Chem. Soc., 107, 1581, (1985)
6) Hettich,R.L. and Freiser,B.S.; J. Am. Chem. Soc., 107, 6222, (1985)

HIGH ENERGY COLLISION EFFECT ON ACTIVATION OF UNIVALENT METAL-ION/ALCOHOL COMPLEXES

S.K. Huang and R.W. Holman, Department of Chemistry, University of Nebraska, Lincoln, NE 68588-0304

High energy collisionally activated decomposition (CAD) mass spectrometry has proven to be a powerful technique for structure elucidation of gas phase ions. High energy CAD has been shown to be less prone to precursor ion internal energy effects, and less energy randomization occurs during the course of collisions than is the case in low energy CAD. Moreover, skeletal rearrangements which can be problematic in low energy CAD are not a problem, and hence high energy CAD spectra are more reflective of the ion's initial structure than are low energy CAD spectra.

Recent high energy CAD studies of univalent metal ion-organic complexes include the Fe^+ complexes with alkanes [1] and alkenes [2]. In their study of Fe^+-alkane complexes, Larsen and Ridge [2] concluded that the potential surface on which thermal ion-molecule reactions take place is the same as that for high energy CAD. This was based on the similar fragmentation patterns seen in each case.

In the present study, Fe^+ and Cr^+ reactions with alcohols are investigated. The high energy CAD spectra of these complexes are compared with those of metastable decompositions, low energy CAD, and thermal ion-molecule reactions (IMR). The goal, then, is to establish differences in the product distribution of the same complex under the above differing modes of mass spectral analysis, so as to ascribe the role that the collisional activation process plays.

A striking difference in the formation of $CrOH^+$ and $FeOH^+$ is seen in going from unimolecular dissociation to high energy CAD of the same complex. Low energy CAD yields a small amount of $FeOH^+$ and no $CrOH^+$ at all, while thermal IMR yields none of either. This can be interpreted as follows: $FeOH^+$ (0.8 eV above ground state) can be formed upon high energy collisions with the target gas via either an adiabatic electronic exitation followed by rapid relaxation to an excited vibrational state on the electronic ground state surface, or by direct vibrational/rotational exitation. In contrast, $CrOH^+$ can be formed only by an initial exitation to an electronic excited state followed by rapid relaxation.

Other differences in product distribution can be seen in Table I. The ion molecule reactions and low energy CAD tabulated below were conducted in the cell of an FTMS. In FTMS, multiple collisions between the metal-ion/alcohol complex and neutrals take place to a great extent. These multiple collisions lead to multiple neutral losses from the complex that are either small or absent in either the unimolecular dissociation or high energy CAD of the same complex.

The high energy CAD experiments were performed by using a tandem mass spectrometer. Under high energy CAD conditions, multiple collisions play a much smaller role than in FTMS, and hence multiple neutral losses are less prominent. The degree of multiple collisions in high energy CAD decreases with increasing collision cross section and/or mass of the organic moiety.

To further probe the effect that the collisional activation process has on the metal-ion/alcohol complex product distribution, experiments were performed whereby the percentages of ion suppression were varied. In addition, the target gas in one experiment was changed from He to N_2.

The results from these experiments yielded several conclusions. It can be concluded that MOH^+ is a high energy fragment, as the ratio of MOH^+/MH_2O^+ increases with increasing beam suppression. The slight decrease of $FeOH^+/FeH_2O^+$ ratio at greater than 60% beam suppression could be due to the concurrent increase of $FeC_4H_6^+$. Also, the lack of dependence of the $CrOH^+/CrH_2O^+$ ratio on beam suppression, and the decrease seen in the $FeOH^+/FeH_2O^+$ ratio when N_2 was employed as a target gas, clearly supports the exitation mechanism proposed above.

It is clear that the collisional activation process plays several key roles in the analysis of metal-ion/alcohol complexes. Firstly, the complex may be excited to an electronic excited energy surface with a subsequent crossing over to a ground state energy surface which supplies the energy to form high energy products. Such products would not be seen in the absense of high energy collisions. Secondly, the degree of multiple collisions that a metal-ion/alcohol complex experiences is a function of both the organic moiety and the degree of beam suppression. The formation of MOH^+ can be used as a fingerprint for assisting structure determination in metal-ion/alcohol complexes. An example for this is given for $FeC_4H_8O^+$ formed from the reaction of $FeCO^+$ with 1-butanol. The high energy CAD spectrum of the above adduct is compared to that of a model complex ion, the Fe^+ adduct with 3-butene-1-ol, in Figure 2. A reasonable match can be seen in

both Figure 2 and Table II. This indicates that the dehydrogenated product from the Fe^+ reaction with 1-butanol has structure (I), derived from C-H insertion into the alcohol, and not structure (II) which arises from an initial O-H insertion. Hence, the formation of high energy products, in this case MOH^+, can be informative in both structure determinations and in elucidating mechanistic detail.

References

(1) Peake, D.A.; Gross, M.L.; Ridge, D.P. J. Am. Chem. Soc. 1984, 106, 4307.
(2) Larsen, B.S.; Ridge, D.P. J. Am. Chem. Soc. 1984, 106, 1912.

Figure 1.

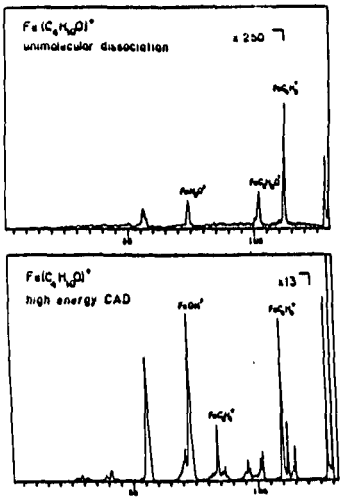

TABLE I

		Ins	High E CAD	Unimolecular Dissociation	Low E CAD
Fe^+	2-Propanol	H_2, H_2O C_3H_6	H_2O, C_3H_6 C_3H_7	H_2O, C_3H_6	$H_2, H_2O,$ C_3H_6, C_3H_7
	1-Butanol	$H_2, H_2O,$ $H_2 + H_2O, C_2H_6O$ C_4H_8	H_2, CH_3, CH_4 $H_2O, H_2 + H_2O$ $C_2H_4, C_2H_5,$ CH_3O, CH_5O C_2H_6O, C_4H_8 C_4H_9	H_2, H_2O $C_2H_6O,$ C_4H_8	$H_2, H_2 + H_2O,$ C_4H_9
Co^+	2-Propanol	H_2, H_2O C_3H_6	H_2, CH_3, CH_4 H_2O, H_2O C_2H_4, C_3H_5 C_3H_7	H_2, CH_3 H_2O, C_3H_6 C_3H_7	H_2, H_2O C_3H_6
	1-butanol	H_2, CH_4 $H_2 + H_2O$	$H_2, H_2O + H_2,$ $C_2H_5, CH_3O,$ C_3H_7, C_3H_8 C_4H_8		None

TABLE II

CAD Spectra of $FeC_4H_8O^+$

	fragment ions					
	$FeC_4H_6^+$	$FeC_2H_4O^+$	$FeC_3H_5^+$	$FeC_2H_2^+$	$FeOH^+$	Fe^+
1-butanol	100	1.31	1.67	2.46	7.98	8.3
3-butene-1-ol	100	3.0	1.03	2.42	6.70	5.8

Figure 2.

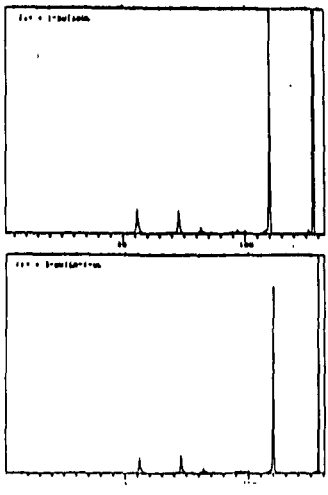

Figure 3.

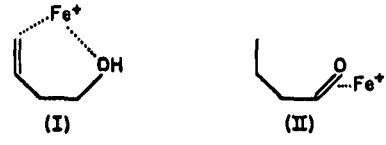

(I) (II)

A STUDY OF THE DISTONIC RADICAL CATION ADDUCTS OF BENZENE WITH OLEFINS

R.W. HOLMAN, C.D. WARNER, AND M.L. GROSS, UNIVERSITY OF NEBRASKA, LINCOLN, NE 68588

The gas-phase reactions of the benzene radical cation with neutral ethylene and propylene were investigated for two reasons: firstly, to gain a better understanding of distonic radical cation adducts, and secondly, to further test the range of reactivity of the benzene radical cation.

The initially formed bimolecular adduct from the reaction of the benzene radical cation with any monofunctional olefin must necessarily be in the form of a distonic species, a radical cation, whose charge and radical sites are separated (Figure 1). Little is known of the general chemical properties of bimolecularly formed distonic radical cation adducts. It is of fundamental interest, then, to gain an understanding of how these radical cations differ from their proximate (charge and radical sites not separate) radical cation analogues.

The use of tandem mass spectrometry to form bimolecular adduct ions of varied and controllable degrees of internal energy has facilitated the mechanistic understanding of gas-phase reactions (1,2). The alteration of source pressure allows for differential collisional stabilization, and this permits the study of both high and low internal energy species. This energy-resolved technique was utilized in the study of the reactions of the benzene radical cation with neutral ethylene and propylene.

The initial distonic radical cation adducts formed in these reactions were found to rearrange as a function of internal energy as evidenced by their energy-dependent CAD spectra (Figure 2 and Table I).

The proposed mechanism for the reaction of the benzene radical cation with ethylene is presented in Figure 3. The mechanism for the reaction between the benzene radical cation and propylene is quite similar and will be omitted for purposes of clarity.

The initially-formed distonic adduct does not undergo an energetically difficult 1,3-hydrogen shift to form the ethyl benzene radical cation (evidence supporting this is from comparative CAD spectra, which is not shown), but instead rearranges to a [4.2.0] bicyclic radical cation **I**. This species can ring-open in one of two ways: via route a to yield the distonic species **II**, or via route b to yield the cyclooctatriene radical cation **III**. The fate of species **II** is to either undergo a H-shift (carbocation mediated) to the o-xylene-like radical cation **IV**, or to ring-open to an acyclic polyene **V**. The fate of species **III** at high energies is to ring-open to **V**.

The lowest energy adduct that could be isolated for collisional activation existed as a mixture of three species: species **III**, species **IV**, and species **V** (the ring-opened form of species **III**).

The highest energy adduct isolated at minimal collisional stabilization is only species **V**, the acyclic polyene radical cation. At this energy all of species **III** has ring-opened to **V** as has all of species **IV** (via route d).

It is clear, then, that distonic radical cation adducts are subject to unique rearrangements that are quite energy-dependent. Distonic radical cations, therefore, must be considered as distinct chemical species whose properties differ from those of their proximate radical cation analogues. In addition, the benzene radical cation has been shown to be reactive with monofunctional olefins. This can be added to the range of reactivity of the benzene radical cation which inclues $2^{\bullet}$- and $3^{\bullet}$-alkyl iodides, bifunctional olefins, alkynes, and strained ring cyclic hydrocarbons.

References

(1) Groenewald, G.S.; Gross, M.L. J. Am. Chem. Soc. 1984, 106, 6569.
(2) Groenewald, G.S.; Gross, M.L. J. Am. Chem. Soc. 1984, 106, 6575

Figure 1.

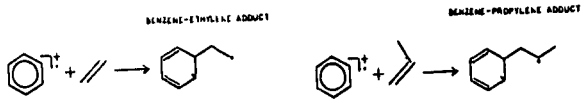

Figure 2.

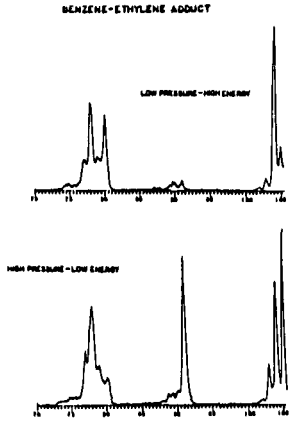

TABLE I.

Benzene + Ethylene Partial CAD

SOURCE	INTERNAL	M/Z									
PRESSURE	ENERGY	105	104	103	102	91	89	80	79	78	77
$2X10^{-5}$	HIGHEST	8.6	31.6	3.1	.7	2.6	.7	16.2	7.2	18.6	6.6
$3X10^{-5}$	↓	15.5	28.7	4.2	.6	5.6	.1	10.2	7.3	19.8	8.5
$1X10^{-4}$	↓	17.2	25.3	4.1	.8	6.8	.7	9.9	6.8	18.7	9.9
$4X10^{-4}$	LOWEST	20.1	16.9	5.8	.5	20.2	20	3.7	5.8	14.4	7.6

Figure 3.

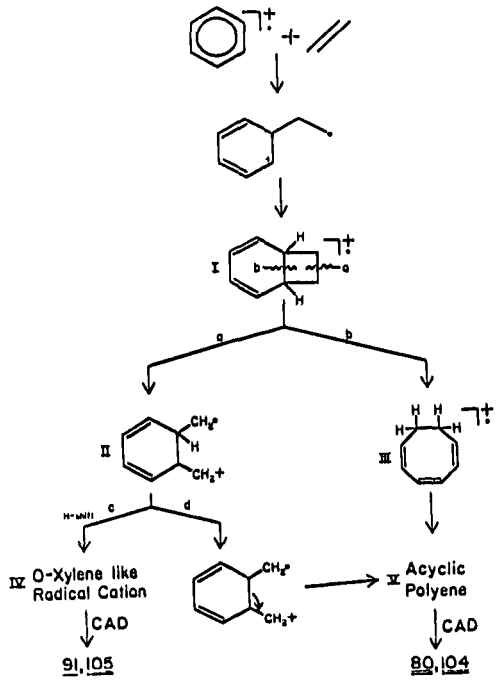

FORMATION AND REACTIONS OF SiH_5^- IN THE GAS PHASE

David J. Hajdasz and Robert R. Squires
Purdue University Department of Chemistry
West Lafayette, IN 47907

Using the flowing afterglow technique, we have investigated the formation, properties and reactivities of the silylhydride anions, $Et_3SiH_2^-$, $n\text{-}C_5H_{11}SiH_4^-$ and SiH_5^-. We have observed that direct addition of hydride to alkylsilanes results in the formation of the stable pentavalent hydride adduct.

$$H^- + Et_3SiH \longrightarrow Et_3SiH_2^-$$

These reactions are believed to be saturated termolecular processes because of their large bimolecular rate coefficients ($k^{II} = 4.5 \times 10^{-9}$ cc/molecule-sec) and their pressure independent product distributions from 0.3 to 0.9 torr.

In addition to having large bimolecular rate coefficients for adduct formation, silanes have relatively low hydride affinities (<25 kcal/mole). These two characteristics combine to make silanes ideal candidates for hydride transfer studies. Indeed, these silylhydride ions can be used to reduce a wide range of substrates ($Fe(CO)_5$, CO_2, Et_3B), but of special significance is their ability to transfer hydride to other silanes. We have taken advantage of this reaction to form the simplest hydride adduct of silane, SiH_5^-, via the bimolecular H^- transfer shown below:

$$H^- + Et_3SiH \longrightarrow Et_3SiH_2^- \xrightarrow{SiH_4} SiH_5^-$$

A typical bracketing approach could not be used to obtain the relative hydride affinities of the silanes because suitable reference species with appropriate hydride affinities are unavailable. Therefore, a thermochemical cycle was used to obtain the limits for the hydride affinities.

$$\begin{array}{ccc} R_4SiH^- + HX & \longrightarrow & R_4Si + H_2 + X^- \\ \downarrow HA(R_4Si) & & \uparrow -\Delta H_{acid}(H_2) \\ R_4Si + H^- + HX & \xrightarrow{\Delta H_{acid}(HX)} & R_4Si + X^- + H^- + H^+ \end{array}$$

This general protolytic reaction between the silylhydride and a reference Bronsted acid can be used to derive the limits for the hydride affinities since the $\Delta H_{acid}(H_2)$ and $\Delta H_{acid}(HX)$ are known quantities. For example:

$$SiH_5^- + CH_3OH \longrightarrow SiH_4 + H_2 + CH_3O^-$$

The occurrence of this reaction implies:

$$D[SiH_4 — H^-] = 408.3 - \Delta H_{acid}(CH_3OH)$$

By monitoring the occurrence or non-occurrence of protonolysis using a series of reference acids, the limits for the hydride affinities can be calculated. Experiments using NH_3, D_2O, H_2O and simple alcohols provided the following results: $18.0 \leq D[SiH_4 — H^-] \leq 26.9$, $5.3 \leq D[C_5H_{11}SiH_3 — H^-] \leq 16.3$, $4.7 \leq D[Et_3SiH — H^-] \leq 15.6$ (values in kcal/mole).

In addition, we have made attempts to investigate the structures of these ions. Two important possibilities are: an electrostatically bound adduct (Fig A), or symmetrical trigonal bipyramidal (TBP) structure (Fig B).

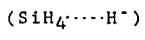

Fig A

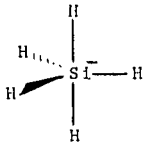

Fig B

In order to distinguish between these two forms, we have performed deuterium labelling experiments. In these experiments, the monodeutero adduct ion , formed by reaction with D^-, is allowed to react with a suitable substrate (CO_2), and the product distribution of H^- vs D^- transfer is determined. Since these silylhydride ions are expected to have low barriers to Berry pseudorotation (3 kcal/mole),complete scrambling of all ligands would occur in a TBP structure, and a statistical ratio of H^- vs D^- transfer would result. Exclusive D^- transfer would imply an electrostatically bound adduct.

$$Et_3SiH + D^- \longrightarrow Et_3SiHD^- \xrightarrow{CO_2} \begin{cases} HCOO^- \\ DCOO^- \end{cases}$$

$$n\text{-}C_5H_{11}SiH_3 + D^- \longrightarrow n\text{-}C_5H_{11}SiH_3D^- \xrightarrow{CO_2} \begin{cases} HCOO^- \\ DCOO^- \end{cases}$$

The expected 1:1 and 3:1 $HCOO^-:DCOO^-$ ratios were not observed, however the deviations were a constant $k_H/k_D = 2.1$. This indicates an isotope effect, but also complete scrambling of the ligands prior to the probe reaction with CO_2. Therefore, we have assigned a symmetrical TBP structure to the ions.

A Multidisciplinary Approach to Molecular Neurobiology

Daniel R. Marshak

Cold Spring Harbor Laboratory
Cold Spring Harbor, New York 11724

Proteins and peptides are essential to the normal growth, differentiation, and function of cells in the nervous system. Three central problems of function in the nervous system involve proteins and peptides, including (i) signal transduction, (ii) cellular differentiation, and (iii) cell recognition. Signal transduction refers to the transmssion of chemical or electrical stimuli between cells or within a cell. Cellular differentiation refers to the morphological and physiological changes of a cell as directed by the gene products of that cell or neighboring cells. Cell recognition refers to the surface interactions between cells that serve to establish specific cellular contacts. In each area, the structural analysis of the proteins involved contributes immensely to our understanding of the function of the nervous system[1].

Such structural analysis requires a multidisciplinary approach[2]. Investigators must employ all available methodologies to elucidate the relationships between the structure and function of proteins. During the past decade, the revolutions in molecular biology and computer science have been accompanied by a technological upheaval in protein biochemistry. The analysis of a protein now involves biological assays, chemical analyses, nucleic acid cloning methods and physical measurements of natural products. In addition, synthetic proteins are now available from chemical or biological sources. Among the newest methods of protein analysis is fast atom bombardment-mass spectrometry (FAB-MS). The structural analysis of proteins and peptides by FAB-MS in conjunction with other existing methods has been essential to several recent discoveries in this laboratory[2-6].

For the purpose of a structural analysis, it is useful to classify proteins according to their masses[1]. General strategies can be adopted for proteins within each class. Class I, mass 200-10,000, includes neuropeptides, hormones, and certain growth factors. These proteins can be analyzed directly by FAB-MS, restricted only by the mass limits of the mass spectrometer. Class II, mass 10,000-60,000, includes certain enzymes, regulatory proteins, peptide precursors, and receptor proteins. These proteins are usually cleaved by chemical or enzymatic techniques in order to generate peptide fragments for analysis. These fragments can be analyzed by FAB-MS for primary structure as well as for post-translational modifications. Class III, mass greater than 60,000, includes large enzymes, structural proteins, certain receptors, ion channels, and cell surface recognition molecules. These proteins are frequently insoluble under standard aqueous conditions and require special methods for purification including affinity chromatography. Often, complete primary sequence is obtained at the DNA level. Mass spectrometry is extremely useful for characterizing modifications of functional domains of these proteins and for analysis of synthetic peptides based on these structures. In each class of proteins, investigations in this laboratory have made use of FAB-MS for the structural analysis of proteins important to neurobiology.

In class I, gonadotropin releasing hormone, a decapeptide, was isolated from the brains of lampreys, a primitive vertebrate species of fish[3]. The complete structure of this hormone was determined by FAB-MS of 200 pmol of the natural product. The observed mass of the molecular ion, $(M+H)^+$ was less than 0.05 amu from the calculated mass. Four amino acid residues at each end of the molecule were identified by intensities corresponding to ions of the ammonium series and the acylium series. In addition, fragments of the peptide were obtained by digestion with chymotrypsin, and the structure of each fragment was determined by chemical sequence analysis and FAB-MS.

In class II, two new growth factors have been identified that are important to brain tissue development. Neurite extension factor is a molecule of 21,000 molecular weight that stimulates embryonic neurons of the cerebral cortex to extend neural processes[4]. The acetylated amino-terminus of this protein was assigned by FAB-MS. The disulfide-bonding pattern is currently under investigation by classical chemical methods and FAB-MS analysis. Another factor, endothelial cell growth factor β, is thought to be involved in arteriogenesis in the brain[5]. The N-acetylation and the primary sequence of the amino terminus were determined by FAB-MS in conjunction with chemical techniques.

In class III, the neural cell adhesion molecules have been studied[6]. These molecules are large, cell surface glycoproteins involved in cell recognition during embryogenesis. The amino terminal domain was analyzed by chemical sequencing methods, and the corresponding synthetic peptide was synthesized by solid phase methods. The synthetic product was evaluated by FAB-MS, and several anisole-peptide adducts were removed as contaminants. These adducts were separated from the desired product by high performance liquid chromatography and were identified by FAB-MS. These analyses indicated a loss of either water or ammonia during the formation of the adduct by condensation. The resulting synthetic peptide was used as an antigen, and the anti-peptide antibody was quite useful for radioimmunoassays, immunoblotting procedures, and immunocytochemistry.

Thus, FAB-MS has been an important tool in a multidisciplinary approach to molecular neurobiology.

References

1. Marshak, D.R. 1986. Structural analysis of proteins in the nervous system. *In* **Modern Methods of Protein Chemistry** (J. L'Italien, editor) Plenum Press, New York, in press.

2. Marshak, D.R. and Fraser, B.A. 1986. Structural analysis of peptides. *In* **Brain Peptides**, second edition (D.T. Krieger, M.J. Brownstein and J.B. Martin, editors) John Wiley & Sons, New York, in press.

3. Sherwood, N.M., Sower, S.A., Marshak, D.R., Fraser, B.A. and Brownstein, M.J. 1986. Structure and function of gonadotropin releasing hormone from lamprey brain. **J. Biol. Chem.** *261*, 4812-4819.

4. Kligman, D. and Marshak, D.R. 1985. Isolation and characterization of a neurite extension factor from bovine brain. **Proc. Natl. Acad. Sci. USA** *82*, 7136-7139.

5. Burgess, W.H., Mehlman, T., Marshak, D.R., Fraser, B.A. and Maciag, T. 1986. **Proc. Natl. Acad. Sci. USA**, in press.

6. Rougon, G. and Marshak, D.R. 1986. Structural and immunological characterization of the amino-terminal domain of mammalian neural cell adhesion molecules. **J. Biol. Chem.** *261*, 3396-3401.

MOLECULAR BIOLOGICAL APPLICATIONS OF FAB-MS

L. GROTJAHN AND H. STEINERT

GBF (Gesellschaft für Biotechnologische Forschung mbH), Mascheroder Weg 1,
D - 3300 Braunschweig (Germany)

Molecular biology is a modern aspect of the biological sciences and concerns the investigation of biological structures and functions on the molecular level. A great deal of progress has been made in molecular biology since 1958 when the reduplication mechanism of deoxyribonucleic acid (DNA) was established. A further milestone was the elucidation of the correspondence between protein biosynthesis and the genetic code. In brief this knowledge shows us the way from DNA via RNA to protein, the main principle in molecular biology. This molecular biological research has led to important developments in the areas of gene technology and biotechnology.

In the last decade we have also had impressive developments in sector field mass spectrometry. In particular Barbers investigations on the new soft ionization method fast atom bombardment and the improvement of magnet systems (for example the introduction of inhomogenous magnet systems) allows the use of this analytical method in areas, where it was unthinkable a few years ago.

Negative ion FAB-MS is a well proven method for the mass spectroscopic sequence analysis of modified and unmodified oligonucleotides up to the decamer or for the fully deprotected end products up to 13 base units in length (1). For modified oligonucleotides, particularly for those where the phosphate group has been altered (eg. oxygen against sulphur or CH_2) and rendered resistent to nucleases, this method can be succesfully applied and is the only method for such sequence analyses, as all classical methods have so far failed. Protected oligonucleotides with a negative charge at the terminal phosphate, produced either by initial chemical degradation of the terminal phosphate protecting group or by reaction in the matrix, generally yield the sequence information by consideration of the 3'-phosphate sequence ions. The fragmentation behaviour of the fully deprotected oligonucleotide allows a bidirectional sequence analysis.

Modified nucleotides and oligonucleotides were used to determine the stereochemical course of the Eco R1 catalysed reaction (2). First the modified synthesized octanucleotide d(GGsAATTCC) containing the recognition sequence of the Eco R1 restriction endonuclease with a phosphorothioate internucleotidic linkage at the cleavage site was characterized by FAB-MS bidirectional sequence analysis. After characterization, this phosphorothioate octamer was used for the determination of the mechanism of the biomolecular process. The Eco R1 catalysed reaction occurred in the presence of $H_2{}^{18}O$. After further enzymatic reactions the final endproduct ATPαS could also be characterized by FAB-MS. The incorporated ^{18}O was in the α,β bridging position. Thus, the stereochemical course of Eco R1 catalysed reactions occur with inversion of the configuration at the phosphorous atom.

Positive and negative ion FAB-MS were applied to clarify the phosphorylation position in ribosomes. Of the 30 ribosomal proteins only S6 is phosphorylated when the cell system is stimulated for example by either insulin, growth hormones, progesterone or other substances. After phosphorylation cellular protein biosynthesis is greatly increased. ARG ARG LEU SER SER LEU ARG ALA is the C-terminal fragment of the ribosomal protein S6 and occurs in the small subunit 40S of the ribosome. With biochemical and mass spectroscopic methods we could characterize the point of phosphorylation in this small peptide. The naturally occurring phosphorylated C-terminal fragment of S6 and the synthesized phosphorylated peptide were both investigated with cyclo AMP dependent proteinkinase. These in vivo investigations showed, that the synthesized and naturally phosphorylated peptides were equivalent. As we had only enough sample of the synthesized phosphorylated peptide we performed FAB-MS measurements only with this compound and compared the results with the nonphosphorylated peptide of the same sequence. For the phosphorylated peptide we could see a mass shift of 80 compared with the nonphosphorylated one for the sequence ions from the first serine onwards. So we could establish, that only one serine had been phosphorylated and this one was the first one from the N-terminus.

Positive ion FAB-MS shows great promise for investigating biosynthesized proteins and also enzymatically or synthetic proteins, especially for characterizing posttranslational modifications. Repetative scanning of the molecular ion mass region at high resolution in a mass window between 20 and 200 and accumulation of the ion signals with a multichannel analyzer allows mass measurements with an accuracy of 5-10 ppm by using a suitable reference material (eg. cesium iodide). The molecular ions in the higher mass range gave complex cluster pictures, which can be reconstructed by simulation programs. Hence the nature of a designed protein can be determined from a comparison of the measured and simulated results.

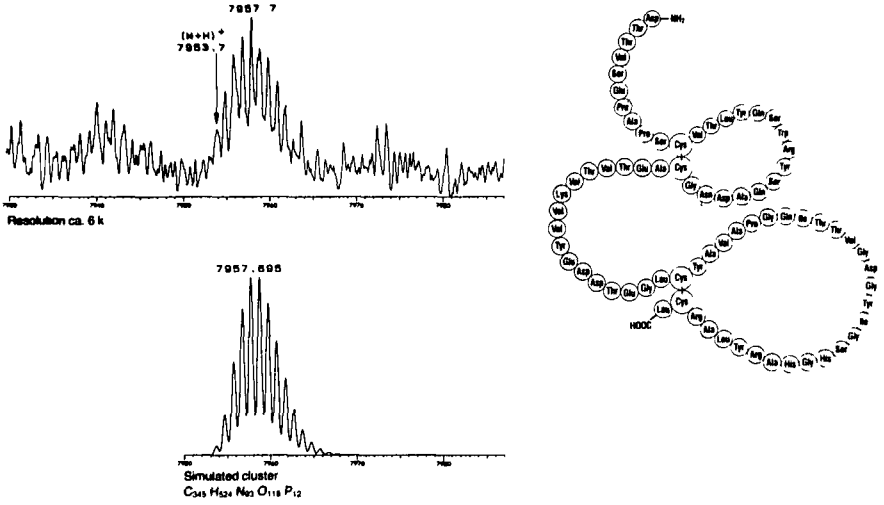

Fig. 1. Molecular ion region of the positive ion FAB mass spectrum of Tendamistat HOE 467 Hoechst (KRATOS MS 50 RF).

Fig. 1 shows the molecular ion region of Tendamistat, a naturally occurring alpha-amylase inhibitor from culture fluids of streptomyces tendae 4158 (3). Tendamistat inhibits the alpha-amylase and prevents glucose formation from carbohydrates. Currently a specific change of amino acids is being investigated in order to make the Tendamistat more acceptable for humans. The resolved molecular ion isotope cluster shows the protonated molecular ion with only carbon 12 at m/z 7953.7, the most intense single envelope has the mean exact mass 7957.7. Hence it is possible to investigate a designed Tendamistat in the same manner.

(1) L. Grotjahn, H. Blöcker and R. Frank, Biomed. Mass Spectrom. 12, 514 (1985)

(2) B.A. Conolly, F. Eckstein and L. Grotjahn, Biochemistry 23, 2026 (1984)

(3) L. Vertesy, V. Oeding, R. Bender, K. Zepf and G. Nesemann, Eur. J. Biochem. 141, 505 (1984)

STRUCTURAL STUDIES OF INTACT COMPLEX CARBOHYDRATES OBTAINED FROM HEPATITIS B SURFACE ANTIGEN GLYCOPROTEIN USING CESIUM ION LIQUID SECONDARY ION MASS SPECTROMETRY

Beth Gillece-Castro, Susan A. Fisher and A.L. Burlingame
Mass Spectrometry Resource, The Liver Center and
Department of Pharmaceutical Chemistry, University of California
San Francisco, California 94143-0446

In this laboratory work is underway to develop liquid matrix secondary ion mass spectrometry for structural investigation of intact complex carbohydrates obtained from glycoproteins and glycolipids by enzymic and chemical cleavage methods. In this report we will illustrate our research strategy using N-linked asparagine glycosylation of glycoproteins in which the oligosaccharides are liberated by PNGaseF (1) and derivatized with p-aminobenzoic acid ethyl ester (ABEE) to form a secondary amine derivative from the liberated oligosaccharide reducing terminus. This permits introduction of this chromophore into the oligomer for HPLC detection as well as a preferred sight of protonation and deprotonation in order to facilitate obtaining positive and negative secondary ion mass spectra by sputtering from liquid matrices using a primary cesium ion beam (2,3). Our initial investigations follow the work of Sweeley and co-workers (4) using maltotetraose and maltoheptaose as linear oligomer standards, and have then proceeded to study a series of branched high mannose oligomers obtained from the glycoprotein IgM, isolated from myologenous leukemia liberated by Endo F or PNGaseF in collaboration with A.L. Tarentino (5) and selected other high mannose carbohydrates isolated from yeast mannan by Ballou (16). In contrast to the results of Wang et al (4) and Carr, et al (7) using the 2-aminopyridine analog in the protonated form, the ABEE derivative permits the production of negative secondary ion mass spectra characterized by an unusually advantageous signal to chemical noise ratio showing a smooth envelope of relative fragment abundance characterized by rearrangement losses of sequentially larger "anhydro residue" moieties (8) from the non-reducing terminus. See Figure 1. Results from a series of branched high mannose oligomers (9) give rise to an additional series of negatively charged ion species 14 mass units higher which appear to occur only in connection with the presence of branched residues. The previously reported (8) anhydro non-reducing terminal losses thus appear to be associated with linear unbranched hexose sequences. The envelope of relative abundances of fragment ions observed would appear to be eventually useful in aiding structural assignment of the size and nature of the branching at particular backbone residues, especially in a high mannose core oligosaccharide from yeast.

Finally, to illustrate usage of this strategy for an unknown material, a carbohydrate oligomer was isolated after PNGase digestion from the denatured glycoprotein obtained from the Hepatitis B surface antigen (HbsAg) viral particle isolated from human serum by D.L.Peterson (10). Progress of the enzymatic cleavage was monitored using SDS-PAGE and the oligosaccharide portion was isolated using gel chromatography on Sephadex G-50 and Bio-Gel P-4. The underivatized oligosaccharide mixture gave intense pseudomolecular ions in negative ion mode at m/e 1931 (M-H) and 2222 (M-H plus 2244 $M-H_2+Na$). The difference in molecular weight can be accounted for by one N-acetyl neuraminic (sialic) acid, and the molecular weights are consistent with complex biantennary structures comparable to the oligosaccharide of transferrin. The oligosaccharide was then desialated and reacted to form the ABEE derivative. Following HPLC, the negative ion LSIMS spectrum in Figure 2 was obtained. The molecular weight of 1789 and fragments for losses of sequential hexose, N-acetyl hexosamine, and hexose support the proposed biantennary structure shown. In addition, another molecular ion species of 8% intensity relative is observed which suggests the presence of a deoxyhexose such as fucose on a fraction of the oligosaccharides. These results from the HBsAg demonstrate the usefullness of the strategy in determining structures of complex carbohydrates.

References.

1. A.L. Tarentino, C.M. Gomez and T.H. Plummer Jr., Biochem., 24, 4665-4671 (1985).
2. W. Aberth, K.M. Straub and A.L. Burlingame, Anal. Chem., 54, 2029-2034 (1982)
3. A.M. Falick, G.H. Wang and F.C. Walls, Anal. Chem., 28, 1308-1311 (1986).
4. W.T. Wang, N.C. LeDonne, B. Ackerman and C.C. Sweeley, Anal. Biochem., 141, 366-381 (1984).
5. A.L. Tarentino, C.M. Gomez and T.H. Plummer Jr., Biochem., 24, 4665-4671 (1985).
6. P.-K. Tsai, J. Frevert, and C.E. Ballou, J. Biol. Chem., 259, 3805-3811 (1984).

7. S.A. Carr, V.N. Reinhold, B.N. Green and J.R. Haas, Biomed. Mass Spectrom., 12, 288 (1985).
8a. J.P. Kammerling, W. Heerma, J.F.G. Vliegenthart, B.N. Green, I.A.S. Lewis, G. Strecker and G. Spik, Biomed. Mass Spectrom, 10, 420-425 (1983).
8b. J.W. Webb, B.L. Gillece-Castro, J. Ke, A.L. Burlingame (in preparation).
9. A.L. Tarentino, B.L. Gillece-Castro, S.J. Fisher, A.L. Burlingame (in preparation).
10. D.L. Peterson, J. Biol. Chem., 256, 6975-6983 (1981).

Acknowledgement.

Financial support was provided by NIH Grants RR 01614 (to A.L.B.) and AM 26743 (to A.L.B).

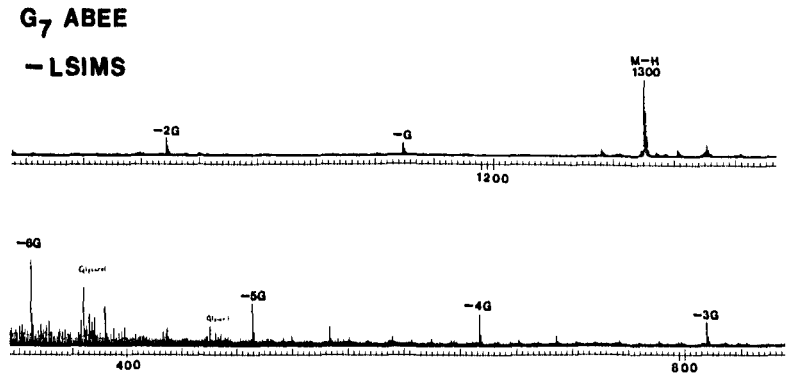

FIGURE 1

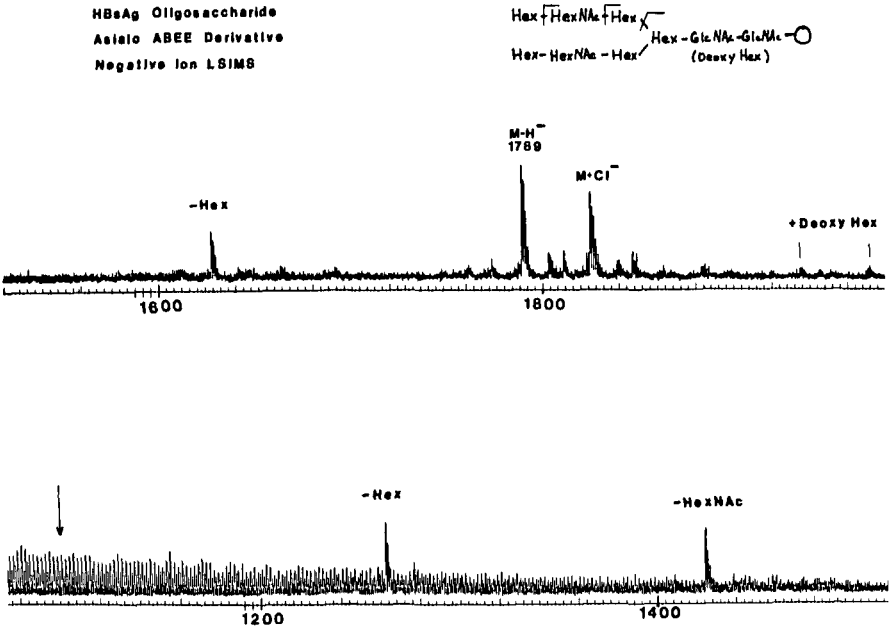

FIGURE 2

MASS SPECTROMETRIC MEASUREMENT OF OPIOID BRAIN PEPTIDES

D.M. Desiderio
Departments of Neurology and Biochemistry
and Charles B. Stout Neuroscience
Mass Spectrometry Laboratory
University of Tennessee, Memphis, Tennessee 38163

Mass spectrometry is being used to quantitate endogenous opioid peptides with a very high level of molecular specificity attached to that analytical measurement (1). Fast atom bombardment produces the protonated molecular ion of enkephalins, and, in an effort to optimize the molecular specificity of that measurement, mass spectrometry-mass spectrometry (MS/MS) provides the product-ion spectrum of that protonated molecular ion (2,3). A forward geometry (B,E; B = magnetic field; E = electric field) mass spectrometer (Finnigan MAT 731 or VG 7070E-HF) is used in the B/E linked-field selected reaction monitoring (SRM) mode to obtain those data. A synthetic peptide internal standard with a chemically incorporated stable isotope (^{18}O) is added early in the extraction scheme to maximize analytical accuracy (4). In the MS/MS spectrum, a unique C-terminus containing amino acid sequence-determining fragment ion, such as -GFL or -GFM from leucine enkephalin (LE = YGGFL) and methionine enkephalin (ME = YGGFM), respectively, is chosen for measurement. In addition, more recent results use an N-terminus containing ion such as YGGF-. With this latter methodology, 40 pg of synthetic leucine enkephalin corresponding to 72 femtomoles are quantified (5).

The experimental hypothesis being tested physiologically is that the tachykinin and the three known opioid peptidergic pathways participate in several clinical and physiological processes, and that those pathways are altered in deranged physiological states such as during pain, stress, and tumor formation versus control states. Mass spectrometry/mass spectrometry is a very effective method to minimize the chemical and matrix noise associated with FAB-MS processes, and the structural resolution in the MS/MS mode is increased significantly, especially when two different fragment ions from a peptide are monitored. Radioimmunoassay (RIA) and radioreceptorassay (RRA) data are obtained to corroborate the corresponding immunoactivity and receptoractivity, respectively, of the HPLC-purified peptide (6). In addition, the combination of reversed phase HPLC gradients with RRA provides an extraordinarily effective screen to determine the metabolic profile of several opioid peptidergic pathways and their resulting products.

The following types of biological tissue have been studied in the human and dog: CSF, pituitary, tooth pulp, caudate nucleus, thalamus, and hypothalamus. In the case of the human tooth pulp, RIA results demonstrate our ability to effective mobilize the methionine enkephalinergic and substance P-ergic pathways following application of orthodontic stress (7).

ACKNOWLEDGEMENTS

The authors gratefully acknowledge financial assistance from NIH (GM-26666, RR-01651) and the typing assistance of Dianne Cubbins.

REFERENCES

1. D.M. Desiderio, Analysis of Neuropeptides by Liquid Chromatography and Mass Spectrometry, Elsevier, Amsterdam (1984) 235 pp.
2. I. Katakuse and D.M. Desiderio, Int. J. Mass Spectrom. Ion Phys. 54, (1983) 15.
3. D.M. Desiderio and I. Katakuse, Anal. Biochem. 129 (1983) 425.
4. D.M. Desiderio and M. Kai, Int. J. Mass Spectrom. Ion Phys. 48 (1983) 261.
5. D.M. Desiderio and C. Dass, Anal. Chem., submitted.
6. D.M. Desiderio, H. Takeshita, H. Onishi, F.S. Tanzer, C. Wakelyn, and C. Dass, NIDA Monograph, in press.
7. J.A. Walker, Jr., F. S. Tanzer, E.F. Harris, C. Wakelyn, and D.M. Desiderio, Amer. J. Orthodon., submitted.

ENZYMES AND MASS SPECTROMETRY: A NATURAL COMBINATION

Richard M. Caprioli, The University of Texas Medical School, Houston, TX 77030

The direct analysis of components in enzymic reactions using mass spectrometry as the primary analytical tool has seen a great deal of activity in recent years, especially since the advent of desorption ionization techniques. The interest in enzymes in these applications generally fall into two classes. The first are those where the enzyme is used as a tool for the analysis of some aspect of the substrate, as for example, in the use of proteases for the digestion of large proteins and polypeptides for the purpose of sequencing by mass spectrometry. The second are those were some function of the enzyme itself is being studied, such as a reaction mechanism or kinetic parameters of a particular reaction.

I. UTILIZING ENZYMES TO AID ANALYTICAL TASKS

One of the major uses of enzymes in mass spectrometry in recent years is the utilization of proteases to give specific clips of proteins and polypeptides with analysis of the molecular ions of the fragments by mass spectrometry. Basically, two approaches are used. In the first, endopeptidases such as trypsin or chymotrypsin are used to reduce the size of the protein to peptide fragments which are amenable to mass spectrometric analysis. These fragments may be analyzed directly by mass spectrometry to obtain the sequence or they can be further degraded by chemical or enzymic methods before sequencing. In the second approach, isolated peptides usually containing fifteen or twenty residues are sequentially degraded by exopeptidases such as aminopeptidase and carboxypeptidase with mass spectrometry being used to either identify the residue removed or the molecular weight of the remaining polypeptide chain.

The hydrolytic properties of the particular enzyme used may be of considerable help in establishing the amino acid sequence since the terminal residue of the polypeptide fragment at the site of cleavage of the original protein is determined by enzyme specificity, although it may be one of several possible residues. Enzymes used commonly for this purpose include trypsin, chymotrypsin, S. aureus V8 protease, thermolysin, and carboxypeptidase Y, among others. It should be recalled however, that other factors such as the nature of neighboring residues in the peptide, the pH and type of buffer used, the presence of secondary or higher structure of the sample, etc., all may affect enzyme action and cause deviations from the generally acknowledged activities.

In most applications where polypeptides of unknown sequence are being analyzed, a variety of methods are utilized in obtaining the sequence. These can include automated Edman degradation, enzyme hydrolysis, purification of fragments by gel permeation or HPLC, GC/MS methods with derivatized peptides, and fast atom bombardment mass spectrometry (FABMS) or other desorption ionization techniques for underivatized peptides. The effective use of mass spectrometry for the analysis of enzyme digests in which relatively large peptide fragments (1500-4000 daltons) are produced has seen considerable use over the past five years. Similar approaches are also used in applications where the identification and position of modified amino acid residues are of interest, or where the sequence of a particular protein which has been deduced from the corresponding DNA is being confirmed or verified. Hydrolytic enzymes are also beginning to see wider use in the structure elucidation of oligonucleotides and oligosaccharides.

II. DETERMINATION OF ENZYMIC REACTION PARAMETERS

The kinetics of the trypsin catalyzed hydrolysis of several small peptides has been studied using FABMS (1). Reactions were followed with time by removing aliquots of the reaction mixture at specific intervals and after addition of an equal volume of glycerol containing a small amount of acid, the sample was analyzed. Quantitative data was obtained using internal standards. A series of rates were determined by varying amount of substrate while holding the enzyme

concentration constant. A double-reciprocal plot (1/[substrate] versus 1/rate) gave a y-intercept equal to 1/Vmax and an x-intercept to -1/Km. Values for kcat and kcat/Km, a ratio which is a measure of the activity of the enzyme for a given substrate, were then calculated. Current work involves similar studies with larger peptides, containing 20-30 residues and multiple cleavage sites.

The mass specificity and ability to directly analyze polar and charged molecules of mass spectrometry permits the assay of an extremely broad range of molecules not easily amenable to more classical analytical methods. A number of reports have described applications which involve details of the mechanism, specificity, and biological activity of enzymes where mass spectrometry has played major role.

Several approaches have been devised over the past several years to allow aqueous solutions to be analyzed directly by mass spectrometry, with the desorption ionization methods being of particular interest. Thermospray mass spectrometry has shown a great deal of potential and success in allowing aqueous solutions to be analyzed. Recently, it has been used to directly monitor the reaction products of the tryptic digestion of several peptide substrates (2). Further, the investigators placed two immobilized enzyme/HPLC columns in series, the first containing trypsin and the second containing carboxypeptidase Y. They demonstrated that partial sequence information can be obtained in this manner in an automated on-line procedure.

Early experiments involving direct introduction of enzymes on the probe tip inside the mass spectrometer demonstrated that reactions could occur and be monitored in real-time during the first few minutes. In order to provide a continuous flow of solution into the mass spectrometer, a special FAB probe has been described which allows 2-10 ul of an aqueous solution, containing 20% glycerol, to be continuously fed into the instrument (3). Solutions of compounds or aliquots from reaction mixtures can be injected directly into the flow stream by use of a microinjector or the reaction mixture continuously fed into the instrument, as the application demands. The probe shows a remarkably low memory effect, showing little tailing of the peak as monitored by the mass spectrometer. Of particular significance is the fact that the background chemical noise associated with standard FAB spectra is greatly reduced when using the continuous flow probe, giving considerable improvement in signal to noise. Further, since the probe allows the mass spectrometer to operate at full accelerating potential, its high mass performance is excellent as demonstrated with the well resolved molecular ion cluster of bovine insulin at 5730 daltons from the injection of 1.5 ug of sample. For applications in monitoring enzyme reactions, however, the device is used in the mode where the reaction mixture is continuously fed into the instrument. This has been demonstrated using carboxypeptidase Y and P for the hydrolysis of ribonuclease S peptide.

CONCLUSION

Mass spectrometry has made great strides in the past 5 years which now allow it to play central and direct role in the methods available to the biochemist for the analysis of cellular constituents. Further, it brings to this research arena the mass selectivity of mass spectrometry with the capability for direct and on-line applications. There is little doubt that as research and development continue to grow in the fields of biochemistry and molecular biology, both qualitative and quantitative aspects of molecular analysis as determined by mass spectrometry will be of utmost importance.

1. Caprioli, R.M.; Fan, T. Anal. Biochem. 1986, 155, (IN PRESS)
2. Kim, H.Y.; Pilosof, D.; Dyckes, D.F.; Vestal, M.L. J. Am. Chem. Soc. 1984, 106, 24.
3. Caprioli, R.M.; Fan, T.; Cottrell, J.S.; Anal. Chem. (Submitted).

RECENT STUDIES IN THE ANALYSIS OF BIOPHARMACEUTICALS BY MASS SPECTROMETRY

Steven A. Carr, Gerald D. Roberts, Mark E. Hemling, Lewis B. Killmer, Walter Johnson and Mary Mentzer, L-940, SmithKline and French Laboratories, Swedeland, PA 19479

Physiologically active proteins, glycoproteins and polypeptides are the subject of intensive research in academic laboratories and in the applied molecular biology industry. This interest stems from a desire to understand the molecular relationship between structure and function and the potential use of many of these substances as biopharmaceuticals.

From an analytical perspective, the principle milestones that need to be achieved in the analysis of protein biopharmaceuticals include verifying the amino acid sequence of the protein or synthetic polypeptide, demonstrating that miscoding has not occurred, identifying and quantitating trace impurities such as other proteins, nucleic acids, antibiotics, surfactants and protease inhibitors, and, establishing the presence and nature of blocking groups and other posttranslational modifications such as carbohydrates. The latter is particularly important since covalent posttranslational modification (PTM) is often essential for proteins to achieve their full physiological activity.

Mass spectrometry together with specific chemical and biochemical manipulations are used to assess qualitative purity and to establish sequence fidelity. FAB MS is particularly well suited for these tasks since good coverage of even large proteins (> 500 amino acids) can be achieved. MS is also unquestionably the method of choice for identifying PTM's since MS relies on an intrinsic physical property of the modification, its mass, rather than a nonspecific change such as a shift in chromatographic retention. A recent example from our laboratory involved the development of a general strategy for determining the sites of attachment of Asn-linked sugars in glycoproteins. This new procedure and its application to tissue plasminogen activator, a glycoprotein of pharmaceutical interest, are described elsewhere in this volume (1).

The problems associated with the analysis of recombinant hepatitis B surface antigen illustrate the need for MS in the analysis of biopharmaceuticals. The recombinant protein is expressed as a 22 nm particle with a molecular mass of approximately 4×10^6 daltons which consists of 70% protein, 25% lipid and 5% carbohydrate. The DNA-derived sequence of the major protein is 226 aa in length consisting predominantly of hydrophobic residues. This protein is repeated approximately 40 times in the particle. Attempts to provide direct confirmation of the primary sequence by conventional approaches were thwarted by the total insolubility of the protein following removal of lipids. Partial Edman sequence data confirming the first 8 residues were ultimately obtained by resolubilization with surfactants, but it required using large amounts of protein indicating that the NH_2-terminus was at least partially blocked. Under specific denaturing conditions the protein could be readily digested with chymotrypsin, but the resulting fragments were far to small and hydrophobic to be sequenced by Edman degradation. In contrast, direct analysis of the chymotryptic digests (and HPLC subfractions derived therefrom) by FAB MS was not inhibited by the size or hydrophobicity of the chymotryptic peptides. These experiments confirmed 85% of the primary sequence and established the presence of an acetyl block on the NH_2-terminus. Clearly this is a case where the use of MS was not only desireable, but essential for obtaining the desired structural information.

Tandem mass spectrometry, particularly in conjunction with FAB ionization, holds great promise for providing detailed structural information on polar, involatile compounds which may yield only MW information in their "normal" FAB mass spectra. With the acquisition of the VG ZAB-SE 4F we have begun to explore the utility of these techniques in addressing difficult structural questions such as determining the sequence of the first four residues of a blocked NH_2-terminal tryptic tetradecapeptide from an epithelial cell growth factor protein. FAB MS^2 of 1/3 of the total sample (500 pmol) yielded the MW which clarified the aa composition and established the presence of an acetyl blocking group. Unfortunately the spectrum was devoid of fragments. In a subsequent experiment the parent ion cluster at m/z 1541.6 from 500 pmol of the peptide was fragmented in the field free region between MS1 and MS2 and the resulting daughter ion spectrum recorded and mass assigned by computer. The observed fragments (Fig. 1) define the sequence of the first twelve residues. These assignments were corroborated by computer-aided analysis of the data which ruled out all but one of the twelve possible arrangements of the first four residues. Finally, preliminary results obtained on high MW peptides indicate that analytically useful structural information can be obtained by FAB MS/MS on peptides with masses of up to 4200 daltons (2). These data are encouraging and suggest that MS/MS will play an increasingly important role in the analysis of biopharmaceuticals.

1. See papers TPC 8 and RPE 7, this volume.
2. See paper FOB 14, this volume.

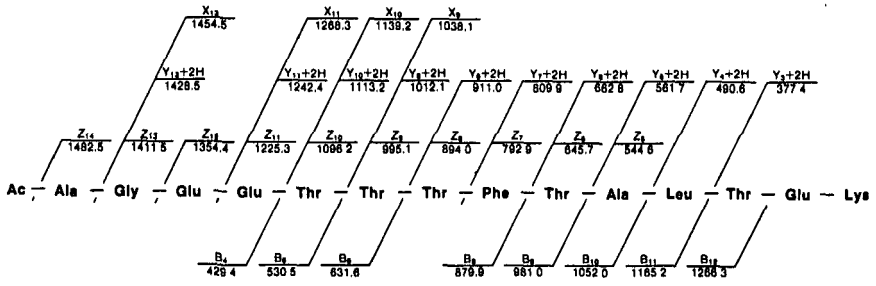

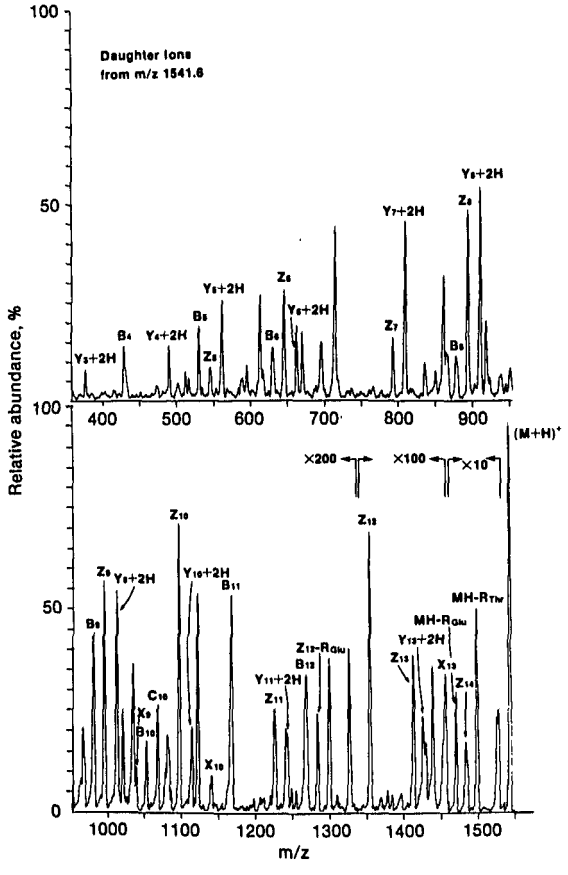

Figure 1. Daughter ion mass spectrum of m/z 1541.6, the protonated molecular ion cluster of the acetyltetradecapeptide; collision energy = 10 kV; res. MS1=MS2=600. Spectra were recorded with the VG 11-250 data system and represent the sum of 8 scans on a total of 500 pmol of peptide in thioglycerol. Fragment ion nomenclature is according to P. Roepstorff and J. Fohlman, Biomed. Mass Spectrom. 11, 569 (1985).

A NEW TECHNIQUE FOR THE MASS SPECTROMETRIC ANALYSIS OF THERMALLY LABILE COMPOUNDS. D. Bombick, D. Kassel and J. Allison, Department of Chemistry, Michigan State University, East Lansing, MI 48824

Presently a number of desorption/ionization (DI) methods are available for the analysis of thermally labile compounds. No single ionization technique can be used to analyze every thermally labile compound. Often these DI methods are costly and may involve modifications to the mass spectrometer. The analytical utility of alkali ion adducts in these DI methods is well known. Often, an alkali salt is added to the analyte to promote the formation of these adducts. Here we use an inexpensive thermionic potassium ion emitter probe which fits into the direct insertion probe inlet of a mass spectrometer. The design is described elsewhere (1). When a thermally labile compound is deposited onto the potassium thermionic emitter and heated rapidly within the source of the mass spectrometer, ions representative of the compound are generated. A spectrum is obtained for every compound studied to date; in almost all cases the ions are potassium adducts.

In Figures 1 and 2 some typical results for sucrose and hexaglycine are shown. From the spectrum of hexaglycine, potassium adducts appear from cleavage of the polar peptide bond with a concurrent hydrogen shift. The potassium adducts at m/z 219 and 201 in the sucrose spectrum can be generated in a similar fashion. These species can be explained using familiar low energy decomposition pathways such as 1,2-eliminations. Our current understanding of the mechanism of this technique is as follows:

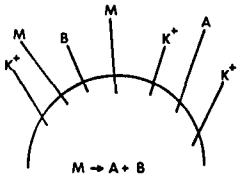

K^+IDS Potassium Ionization Of Desorbed Species

Via low energy processes a molecule M can decompose to species A and B. Desorption of M,A, and B results in a high pressure (selvedge) region above the surface of the potassium thermionic emitter. Through a termolecular process with emitted potassium ions, potassium adducts are formed which would result in the observed ions $(M+K)^+$, $(A+K)^+$, and $(B+K)^+$. We call this ionization technique K^+IDS (Potassium Ionization of Desorbed Species).

An important factor in K^+IDS is rapid heating. Beuhler and co-workers (2) found that at low temperatures decomposition processes were favored. At higher temperatures, vaporization of intact molecules is favored. It is therefore useful to rapidly heat the analyte to favor vaporization of intact species over the formation of possible decomposition products. This behavior can be seen in the insert of Figure 2. In this case a faster heating rate was used to favor the formation of the cationized molecular ion $(M+K)^+$ at m/z 399. An increase in $(M+K)^+$, however, is at the expense of decomposition adduct ions in the spectrum which are used for structural information. We can adjust the heating rate so that molecular weight and structural information is available, as shown in the enlarged spectrum in Figure 2.

K^+IDS has shown potential for mixture analysis. In analyzing polymers (mixtures of oligomers) it was found the oligomer-potassium adducts produce a spectrum which parallels the molecular weight of the polymer. This observation suggests that the relative concentrations of desorbed species parallel that of the original mixture. This would be a useful characteristic of K^+IDS for mixture analysis.

These studies have shown that K^+IDS may be a viable low cost alternative for the analysis of thermally labile compounds.

(1) Bombick, D.; Pinkston, J.D.; Allison, J. Anal. Chem., **1984**, 56, 396.
(2) Beuhler, R.J.; Flanigan, E.; Green, L.J.; Friedman, L. J. Am. Chem. Soc., **1974**, 96, 3990.

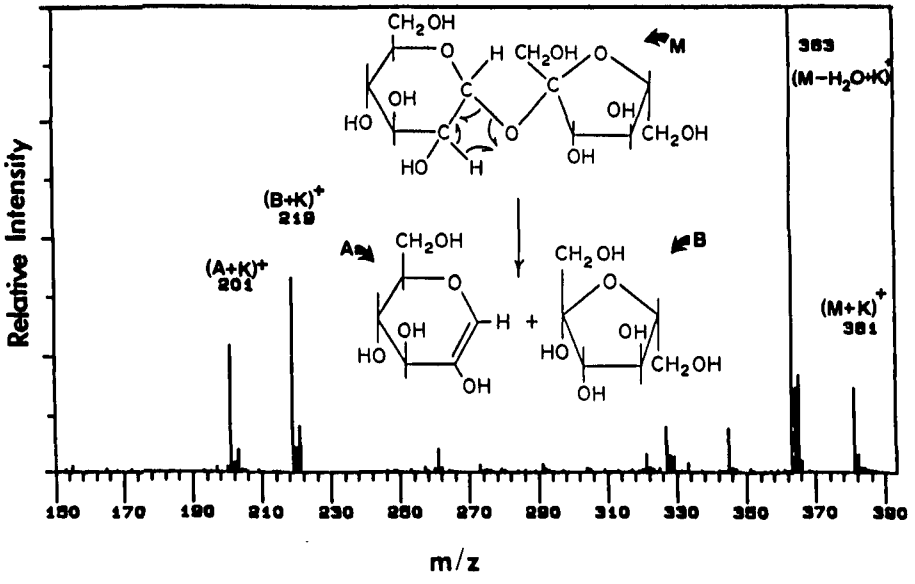

Figure 1. K^+IDS Spectrum of Sucrose

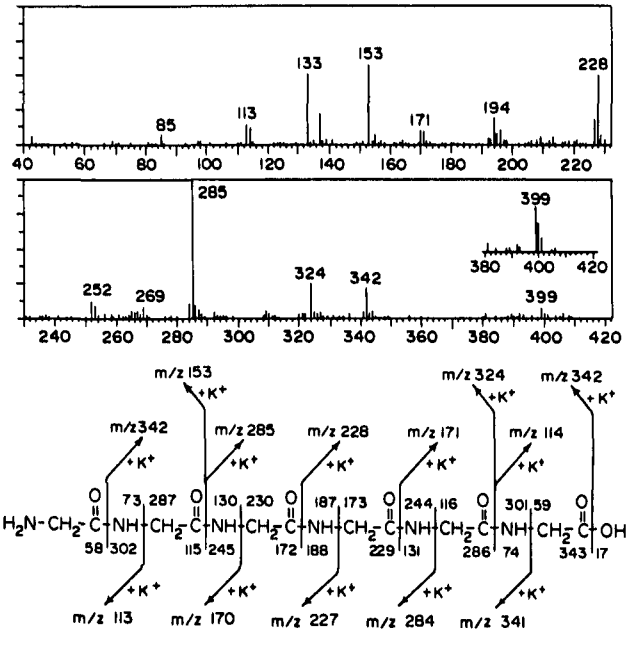

Figure 2. K^+IDS Spectrum of Hexaglycine. Scheme Shows How Ions are Formed.

NEW DEVELOPMENTS IN ELECTROCHEMICAL/FAST ATOM BOMBARDMENT MASS SPECTROMETRY

John E. Bartmess and Lawrence R. Phillips
Department of Chemistry, University of Tennessee, Knoxville TN 37996-1600 and Center for Drugs and Biologics, Food and Drug Administration, Bethesda MD 20205

We have continued the development of the electrochemical/fast atom bombardment (EFAB) technique first reported at ASMS last year, as a method for obtaining FAB spectra of the non-polar species resistant to normal FAB. We have addressed several problems of the original technique, involving (1) optimizing cell design to increase the electrochemically produced ions while reducing the repeller effect of the electrochemical voltages in the source, (2) the origin of the observed ions (are they direct redox or from subsequent chemical reaction?), and (3) finding a matrix both amenable to electrochemistry but of low enough polarity to solubilize the non-polar species. The work has been performed on both a Kratos MS-50, at the Walter Reed Army Institute of Research, with a FAB Xenon beam (7kV, 25 μa) and the EFAB probe of a Cu ring/Brass disk, ca. 5.5 mm dia., and on a MAT 731 at the National Bureau of Standards, Gaithersburg, MD, Center for Analytical Chemistry, with a FAB Cesium Ion beam (5 kV) and the EFAB Probe of stainless steel, ca. 3.3 mm dia. On both instruments, using the open ring-disk electrode and tuning the signal at an electrochemical voltage (V_e) of 0 V results in a falloff of TIC by two orders of magnitude as V_e is varied either to -16V or +16V. We believe this to be a tuning effect of the disk voltage acting as a repeller in the source. The cesium ion beam gives a smaller analyte/matrix ion ratio (0.03) for the $(M-H)^+$ of n-$C_{16}H_{33}Br$, than does the Xe beam (ca. 1:1), but this may be due to the EFAB probe in the Cs^+ experiment being smaller in diameter than for the Xe beam.

To cure the repeller problem, a nickel 150 mesh screen was attached over the ring electrode. This reduced the TIC variation to 20% as V_e is varied -16 to +16V, but no V_e dependent ions were observed. We have probably trapped these below the electrode, inaccessible to the FAB beam. Lack of convection may also be a factor. A three wire grid was constructed for the MS-50 probe, as a compromise between the two cases above. This gave a decrease in TIC of a factor of two as V_e was varied away from the tuning point, but also gave up to eightfold increase in the $(M-H)^+$ ion for n-$C_{16}H_{33}Br$, at 3 V oxidising, relative to no signal for this at 0V.

We believe than the principal charge carriers for electrochemistry in glycerol are hydroxide and hydronium ions, from the 0.1% water present in hygroscopic glycerol. All anion chemistry observed - ester hydrolysis, acid deprotonation, and electron transfer - is consistent with the presence of hydroxide or glycerol alkoxide. Addition of water in 50 mM steps to the glycerol resulted in a 3-5 fold increase in TIC, but no apparent effect on ion ratios or intensities.

Other matrices tried included sulfolane and 1,2-hexanediol; both were too volatile. A 1:1 glycerol/1,2-decanediol mixture gave no 93^+ ions, but many alkane-like decanediol ions.

ANALYTE, MATRIX, AND SOLVENT EFFECTS ON ION CURRENT PROFILES OBSERVED IN THERMALLY-ASSISTED FAB (TA-FAB)

B. L. Ackermann*, J. F. Holland*, C. E. Heine*, and J. T. Watson**
Departments of Chemistry* and Biochemistry*
Michigan State University
East Lansing, MI, 48824

A new method for the production of matrices for FAB known as thermally-assisted FAB (TA-FAB) has been introduced (1). Under TA-FAB, substances which are inherently too immobile to serve as FAB matrices are heated to a fluid state by resistively heating the probe tip during bombardment. While several substances have been proposed as candidates for this method, initial success has been attained using aqueous solutions of saccharides, such as fructose or glucose. When heated, these solutions function similarly to glycerol except a significant decrease in matrix interference occurs. This has been attributed to the tendency for saccharides to resist cluster formation, and to a discrimination for analyte over matrix ions which occurs as the matrix temperature is elevated (1). This behavior has been documented for several classes of biomolecules showing comparable sensitivity to FAB (1). In a recently completed study, TA-FAB gave superior results to FAB for a series of cyclic tetrapeptide mycotoxins isolated from the fungus Helminthosporium carbonum (2). The current investigation seeks to clarify the factors involved in the TA-FAB phenomenon and to propose a model consistent with experimental observations.

To illustrate the nature of the data obtained by TA-FAB, Figure 1 shows two desorption profiles for the analysis of 3μg thiamine hydrochloride (Vit. B_1) in 0.5μl aqueous glucose. The upper profile (m/z 265) displays the behavior observed for the molecular cation and is representative of analyte. The lower profile (m/z 73) is for the prominent glucose fragment $(C_3H_6O_2)^+$ and depicts matrix desorption. The experimental profile may be divided into three regions of behavior, which may be differentiated according to matrix fluidity as confirmed by visual inspection and viscosity measurements. In the first region (scan 1-4), data were acquired with no heating (FAB only). Under these conditions (10^{-8} torr), TA-FAB matrices are much more viscous than glycerol. Therefore, insufficient mass transport effectively prohibits analyte DI in this region. The ions observed are primarily fragments from the saccharide matrix.

The second region is distinguished by the desorption of analyte ions in direct response to heating the matrix. Beginning at scan 5 (Figure 1), a ramp in probe current was initiated at 0.90A and allowed to proceed at 100 mA/min to a final value of 1.54A at scan 18. During this interval a differentiation between analyte and background is apparent from the profiles shown. The selection was most dramatic at scan 13 (1.29A), a point known as the best matrix temperature (BMT). The differential desorption of analyte and background leads to a valid subtraction of matrix-related background in favorable cases (1).

The experimental observations in the second region can be accounted for by two differing explanations. Either the conditions in region 2 greatly favor desorption-ionization of analyte or a preferential extraction of analyte occurs toward the surface in response to heating. Both of these possibilities are being considered. Although the DI efficiency of the analyte may be larger than that for the matrix for factors such as pre-ionization, experimental evidence suggests that a mechanism which embodies the second possibility may be operative.

A model known as ternary perculation (TP) is being investigated with regard to the second possibility. The word ternary emphasizes an important distinction about TA-FAB matrices, namely that they consist of three components: analyte, substrate, and water, where the substrates used are usually small saccharides. Perculation, on the other hand describes the migration of water which occurs during TA-FAB. According to the TP hypothesis, escaping water molecules, released from the matrix by heating, have the capacity to preferentially transport the analyte to the surface during TA-FAB. Hence water, which is necessary to sustain analyte signals, might also participate in the observed selection for analyte relative to background. Another factor included in the TP hypothesis is the possibility that an ordered exclusion of analyte occurs, in response to heating which is analogous to the process of zone refinement. In other words, a thermodynamically favorable situation (eg., maximum fructose-fructose interaction) is made kinetically viable by heating. A pictorial representation of the TP mechanism is shown in Figure 2. Evidence for the substantial ordering of saturated aqueous fructose solutions was obtained from x-ray and

Raman studies by Mathlouthi et al. (3, 4), and is of critical importance to an understanding of the TA-FAB phenomenon.

The third stage in the experimental profile is identified by the decline of analyte ion current to a level indistinguishable from background past the BMT. Experimental evidence confirms that this effect is due to the removal of water and hence mobility from the matrix, and not due to a depletion of analyte.

Acknowledgement: This work was supported in part by a grant (RR-00480) from the Biotechnology Research Program, Division of Research Resources, National Institutes of Health.

1. Ackermann, B. L., Watson, J. T., Holland, J. R. Anal. Chem, 57: 2656, (1985).

2. Ackermann, B. L., Watson, J. T., Holland, J. R. Submitted for publication in Biomed. Environ. Mass Spectrom.

3. Mathlouthi, M. Carbohydr. Res., 91: 113, (1981).

4. Mathlouthi, M., Meffroy-Biget, A. M., Luu, C., Luu, D. V. Carbohydr. Res., 81: 213, (1980).

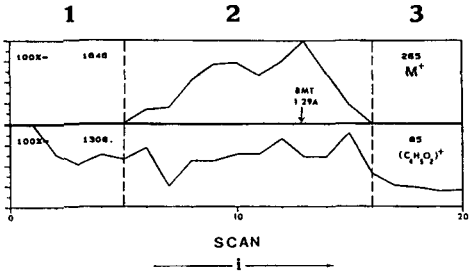

Stage	Heat	Desorption of Analyte	Matrix Behavior
1	No	Little or None	Unlike Glycerol
2	Yes	Strong	Like Glycerol
3	Yes	None	Unlike Glycerol

Figure 1 Desorption profiles for 3 µg thiamine hydrochloride showing the three regions of desorption behavior for analyte (m/z 265) and matrix (m/z 73) which are differentiated according to matrix fluidity

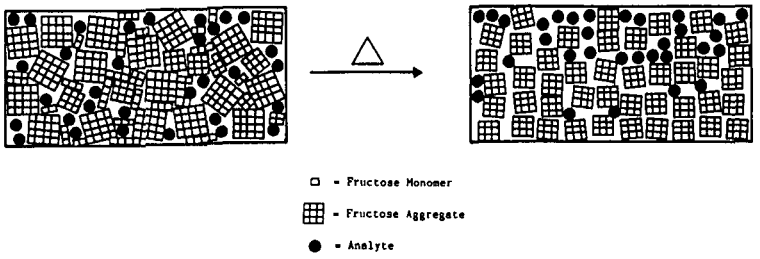

Figure 2 An artist's conception of the ternary percolation model before and after heating.

ORGANIC SECONDARY ION EMISSION FROM SULFURIC ACID SOLUTIONS*

C. P. Leibman and G. Mamantov
University of Tennessee, Knoxville, TN 37966

and

P. J. Todd
Oak Ridge National Laboratory, Oak Ridge, TN 37831

Enhanced secondary ion emission is observed from substituted aromatic/H_2SO_4 solutions. Further, the chemistry of aromatic compounds in sulfuric acid solutions has been studied extensively. We have been able to correlate many of the ions observed in the secondary ion mass spectra of organic/sulfuric acid solutions with ions known to exist in such solutions.

As a matrix material, concentrated sulfuric acid (97%) is unequivocally acidic and most of the compounds investigated are extensively protonated in solution. Not surprisingly, SIMS spectra of the organic/H_2SO_4 solutions studied generally show abundant $M+H^+$ ions. Studies using electron spin resonance and UV spectroscopy indicate that radical cations ($M^{\ddagger}$) are also formed when aromatic hydrocarbons are dissolved in sulfuric acid. Molecular radical cations ($M^{\ddagger}$) are apparent in SIMS spectra of many of the compounds investigated.

It has been suggested that radical cation formation is subsequent to protonation. A mechanism proposed for this single electron oxidation follows:

$$A + H_3SO_4^+ \rightleftharpoons AH^+ + H_2SO_4 \qquad (1)$$

$$A + AH^+ \rightleftharpoons AH\cdot + A^{\ddagger} \qquad (2)$$

$$AH\cdot + 2H_2SO_4 \rightleftharpoons A^{\ddagger} + 2H_2O + SO_2 + HSO_4^- \qquad (3)$$

where A represents the aromatic hydrocarbon. The proposed mechanism is attractive since it has been shown that the ease of oxidation parallels the basicity of the aromatic and not the ionization energy or oxidation potential.[2]

Sulfonation product ions were frequently detected with abundant $M^{\ddagger}$ ions. These products are evident in SIMS spectra as both sulfonated radical cations ($M+SO_3^{\ddagger}$) and protonated sulfonic acids. For some of the compounds undergoing sulfonation reactions, temporal variation in their SIMS spectra was observed. This time-dependent behavior is observed in the SIMS spectrum of 9-aminophenanthrene shown in Figure 1. As the time since preparation of the 9-aminophenanthrene/H_2SO_4 solution increases, there is a change in the base peak from $M^{\ddagger}$ to the sulfonation product $(M+SO_3)^{\ddagger}$. Also significant is the increase in the $(M^{\ddagger}/M+H)^+$ ratio. Thus protonation, oxidation, and sulfonation reactions compete to form ionic aromatic species. The product energetics and formation kinetics of these reactions is reflected in the secondary ion emission from organic/H_2SO_4 solutions.

References:

1. Carrington, A.; Dravieko, F.; Symons, M. C. R.; J. Chem. Soc. (1959), 947.

2. Kijenski, J.; Wojtkowska, B.; Benbenek, S.; Malinowski, S.; Bull. Acad. Pol. Sci., Chim. (1978) 26(7), 519-522.

*Research sponsored by the U. S. Department of Energy, Office of Basic Energy Sciences, under Contract DE-AC05-84OR21400 with Martin Marietta Energy Systems, Inc.

By acceptance of this article, the publisher or recipient acknowledges the U S Government's right to retain a nonexclusive, royalty free license in and to any copyright covering the article

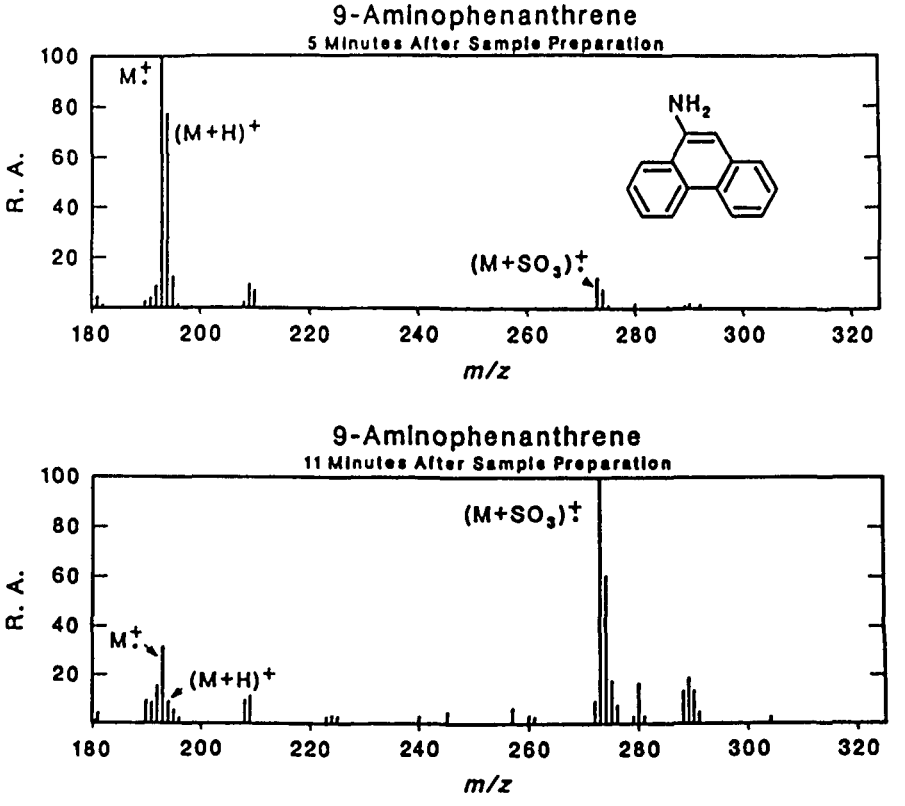

Fig. 1. SIMS spectra of 9-aminophenanthrene obtained 5 minutes and 11 minutes after sample preparation.

ROLE OF GAS-PHASE BASICITIES IN FABMS

J. Sunner, R. Kulatunga and P. Kebarle
University of Alberta
Edmonton, Alberta
Canada T6G 2G2

FAB mass spectra were obtained for neutral mixtures of compounds with a range of gas phase basicities (1). The compounds were frequently used FAB matrices: triethanolamine,, diethanolamine, 4-octylaniline, 1,2,4-butanetriol, glycerol and 4-nitrobenzyl alcohol.

The proton affinities, PA, and gas phase basicities, GB, of the FAB matrix compounds were determined using pulsed high ion source pressure mass spectrometry (2). The results are given in Table 1. The proton affinities of both glycerol and of butanetriol were found to be considerably higher than expected for alcohols. There is also a large internal entropy loss upon protonation. It is concluded that the protonated glycerol and butanetriol molecules are cyclized as a result of the proton being dicoordinated to two hydroxyl groups. Because of the large entropy change, the gas phase basicity of glycerol and of butanetriol, relative to most other compounds, decreases with increasing temperature.

FAB mass spectra were obtained for all combinations of binary mixtures of the compounds in Table 1 using one compound as analyte and the other as matarix. The result can be summarized as follows: When

$$6B(\text{analyte}) < 6B(\text{matrix})$$

the analyte made a small or insignificant contribution to the mass spectrum. However, when

$$GB(\text{analyte}) > GB(\text{matrix})$$

the analyte peaks, mainly the protonated molecular ion, were intense and the matrix peaks were suppressed, Fig. 1. The analyte peaks dominated over the matrix peaks already with an analyte concentration of ca. 2 mole percent. The preference found for high GB analytes can be expressed as a "preference factor":

$$\text{"preference factor"} = \frac{\text{Int(analyte peaks)}}{\text{Int(matrix peaks)}} \times \frac{x(\text{matrix})}{x(\text{analyte})} \qquad (1)$$

where x = mole fraction. Many analytes, in addition to those in Table 1, when dissolved at a low concentration in a matrix with a lower GB, were found to have preference factors in the range of 20 to 50. It was also found, that not only will a high GB analyte suppress the matrix peaks, but it will also suppress, to about the same extent, the peaks due to other analytes with lower GB's.

The intensity of cluster ions in FAB mass spectra is determined by:

1) The thermodynamic stability of the cluster.
2) The propensity of the cluster to undergo unimolecular reactions.
3) Competition with other reactions (proton transfer).

The results favour a "gas collision model" (3,4). Every ion initially formed as a result of the collision cascade undergoes collisions with ca 20 different molecules in the matrix during the expulsion into the vacuum. Some of these collisions will result in proton transfer:

$$MH^+ + An = AnH^+ + M \qquad (2)$$

M = matrix and An = analyte molecule. The direction of this reaction is determined by the gas-phase basicities.

References

1) J. Sunner, R. Kulatunga and P. Kebarle, Anal. Chem. in print.

2) P. Kebarle, Ann. Rev. Phys. Chem. **28**, 445 (1977).

3) J. Michl, Int. J. Mass Spectrom. Ion Phys. **53**, 255 (1982).

4) J. Sunner, R. Kulatunga and P. Kebarle, Anal. Chem. accepted.

Table 1.

	PA /kcal·mol^{-1}	GB /kcal·mol^{-1}	ΔS^o_{int} /cal·K^{-1}·mol^{-1}
Triethanolamine	233	225	0
Diethanolamine	228	220	0
4-Octylaniline	214	206	0
1,2,4 Butanetriol	216	201	-26
Glycerol	209	196	-18
p-Nitrobenzylalcohol	194	186	0

PA = proton affinity, GB = gas phase basicity at 300K, ΔS^o_{int} = internal entropy change upon protonation.

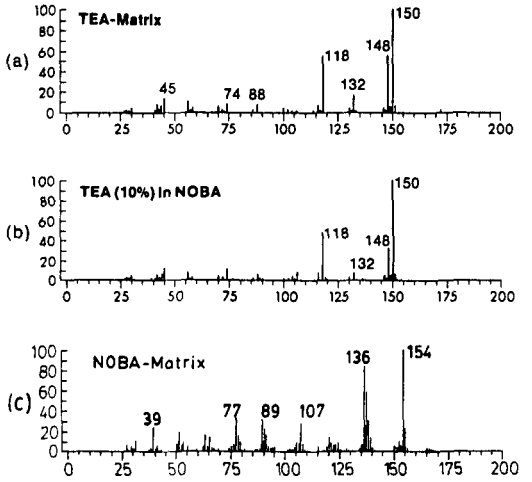

FIG 1

THE STUDY OF PEPTIDE-COLLOIDAL GOLD CONJUGATES BY TIME-OF-FLIGHT SIMS

D.E. Main, R. Beavis, W. Ens, and K.G. Standing
Physics Dept, Univ. of Manitoba, Winnipeg, Canada R3T 2N2

INTRODUCTION The analysis of small quantities of materials from biological sources presents several problems: loss of sample by sorption and dilution; introduction of contaminates; and difficulty in manipulating such small quantities. These effects become particularly critical in the analysis of solid deposits by particle induced desorption ionization mass spectrometry (e.g. SIMS) where contaminates may dominate or suppress the spectrum of a minute sample. Thin sample films, particularly upon gold or silver, offer increased sensitivity, but do not circumvent all of these problems. Stable, near monomolecular films of macromolecules may be formed by sorption upon colloidal gold particles(1). Such conjugates are of great value in histochemistry and theoretically allow small quantities (p-fmol) of material to be sampled, isolated and manipulated with little loss. We have examined the suitability of using colloidal gold for the sampling and subsequent analysis of biological molecules. Colloidal gold conjugates for a variety of small peptides and one antibiotic were prepared and subsequently analyzed by time-of-flight SIMS. Factors affecting sensitivity and adsorption were noted. Renin substrate(1758 u), dynorphin A fragment 1-10(1234 u), proenkephalin(889 u), substance P(1347 u) and its oxidative degredation products, valinomycin(1111 u), and several mixtures were studied.

EXPERIMENTAL Stable and reproducible preparations of colloid were prepared by citrate reduction of Au(III) to give $\sim 10^{12}$ particles/mL, 20 nm in diameter. No attempts were made to minimize sample quantities in this survey, hence commonly 6-9 nmol of sample was used for conjugation. Conjugates were prepared by incubation of sample at either pH 5 or 10 and isolated by repeated centrifugation and washing(3-4 x). Total incubation and washing volumes were $\leq$ 1.0 mL. Washed sample($\leq$ 5uL) was used in the analysis. Positive and negative secondary ion spectra were taken under static conditions on the Manitoba time-of-flight spectrometer(2).

CONJUGATE PREPARATION Stable dispersions were characterized by a clean absorption maximum at ca. 522 nm with an insensitivity to addition of NaCl to 90mM. Retaining these characteristics after washing assured no retention of aqueous contaminates. Stability and hence adsorption completeness was found to depend strongly upon sample structure and solution conditions (viz pH and ionic strength). Assuming efficient and complete "monolayer" coverage of 50 molecules per particle, a maximum 80 pmol of sample should be retained. However, evidence of less than efficient adsorption and conjugate recovery suggests that this value may be overestimated.

SECONDARY ION SPECTRA Isolated conjugates exhibited easily detectable and stable positive molecular ions. No fragments or negative molecular ions were noted. In general the molecular ion peaks were more stable than for electrosprayed material. For the cyclic antibiotic valinomycin, the intact molecule did not appear to be sampled. Rather, the ring cleaved hydrolysis product was easily seen(Fig. 2). For all peptide samples, $[M+H]^+$, and $[M+Na]^+$ were observed. For renin substrate, the N-acetylated contaminate in the commercially "96% pure(HPLC)" was noted as well(e.g. see protonated and sodiated ions in Fig. 3A). In general conjugates of small peptides with colloidal gold may be analyzed by TOF SIMS with sensitivity ($\leq$ ca. 80 pmol) much better than electrospray and approaching that of using etched silver. A precise comparison and quantification of detection limits, extension of utility and study of solution conditions is in progress.

1) M. Horisberger, Scanning Electron Microscopy II,9(1981).
2) W. Ens, R. Beavis, G. Bolbach, D. Main, B. Schueler and K.G. Standing, Nucl. Instr. Meth. A245,146(1986) and references therein.

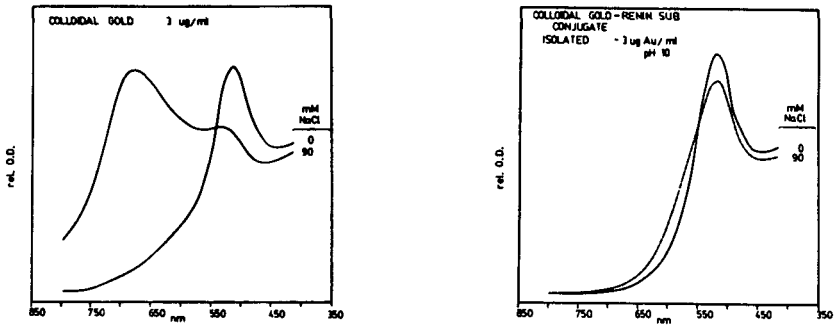

FIGURE 1: Visible absorption spectra of colloidal gold: A) unconjugated; and B) conjugated with renin substrate(excess).

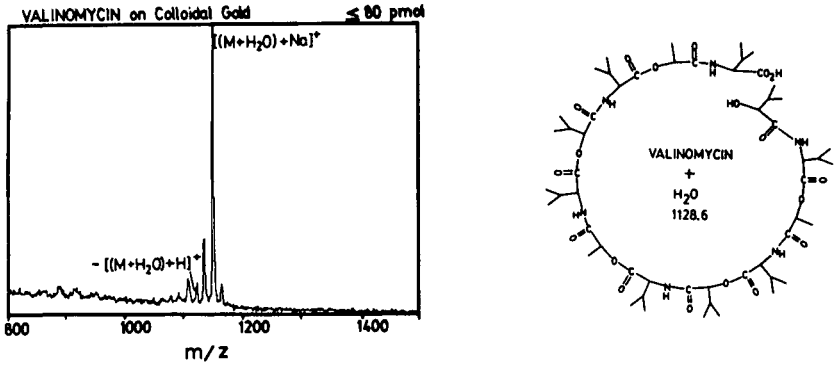

FIGURE 2: Positive SIMS spectrum of isolated valinomycin colloidal gold conjugate (from 45 nmol).

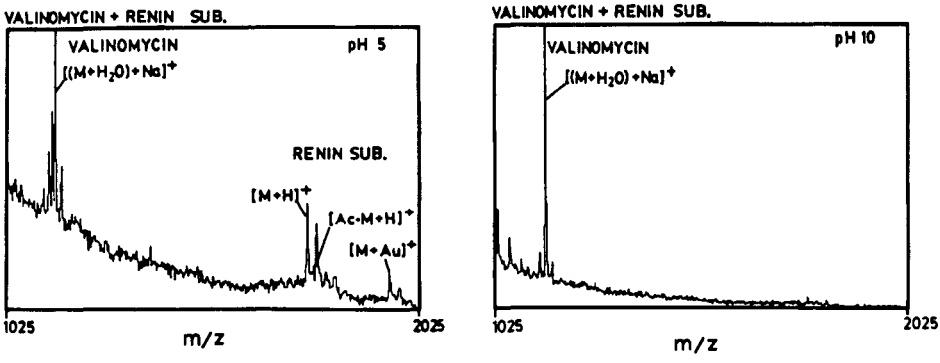

FIGURE 3: Positive SIMS spectra of conjugate prepared from a mixture of valinomycin and renin substrate (from 9 and 6 nmol respectively): A) pH 5, B) pH 10.

COMPARISON OF MOLECULAR ION YIELDS FOR keV ION AND 252 Cf FISSION FRAGMENT BOMBARDMENT

W. Ens[1], B.T. Chait[2], R. Beavis[1], D. Main[1], & X. Tang[1]
1 Physics Dept. Univ. of Manitoba, Winnipeg, Canada R3T 2N2
2 The Rockefeller University, New York, New York 10021

In general, the yield of molecular ions ejected from a solid surface by particle bombardment decreases as the sample molecular weight increases. The rate of decrease for positive molecular ions from a series of peptides was compared using 8 keV Cs^+ ions and 252Cf fission fragments. The samples (leu enkephalin (556u), ACTH (1-10) (1300u), substance P (1348) alpha endorphin (1746u), renin substrate (1760u), dynorphin (2148u), ACTH (1-24) (2933u), beta endorphin (3465u), and insulin (5733u)) were electrosprayed onto aluminized polyester film and the same target was used in both measurements. In both cases, mass spectra were taken with a linear time-of-flight spectrometer: secondary ions were accelerated to 10 kV across 4mm and detected by microchannel plates with no post-acceleration. The length of the flight tube was 1.5m for the keV Cs^+ and 3 m for the fission fragments; an electrostatic particle guide was used for the latter.

As in our previous comparison [1], we found the spectra to be remarkably similar. As illustrated in figs. 1 and 2 for leu enkephalin and alpha endorphin, the shape and relative intensities of the molecular ion peaks and the shape of the metastable continuum are almost identical.

To obtain the molecular ion yields, similar background subtractions were performed and the same integration limits were used. A reliable method of measuring the primary ion flux in the pulsed ion experiment was not available so the intensity of the m/z 29 peak (C_2H_5) was taken for normalization. The decision was made empirically: In the fission fragment experiment, an accurate measure of the primary flux is the run time and the intensity of m/z 29 was found to scale with run time to within 20%. Since the spectra are very similar it seems justified to assume the same is true for incident keV ions.

Fig. 3 shows the yield of of molecular ions vs. mass for incident fission fragments and 8 keV Cs^+ ions. The curves are normalized at leu enkephalin. The detector efficiency falls off with mass, especially when post acceleration is used so the actual yield in both cases may drop off more slowly than indicated but the comparison is still valid. The yield of molecular ions ejected by 8 keV Cs^+ was found to drop off more steeply than for fission fragments. Normalized to leu enkephalin, the yield of ACTH (1-24) is approximately 10 times lower for 8 keV Cs^+. This difference is smaller than a previous comparison between 3 keV Cs^+ ions and 54 MeV $^{63}Cu^{9+}$ ions [2] but may still have important implications on the upper mass limit for the two techniques.

The yields for beta endorphin and bovine insulin are not plotted in fig. 3 because molecular ions for these compounds were not detected using 8 keV Cs^+ without post-acceleration, although both gave molecular ions using fission fragments. We estimate the normalized insulin yield with fission fragments to be <u>at least</u> 70 times greater than with 8 keV Cs^+ ions. Measurements using post-acceleration are in progress and recently molecular ions for beta endorphin were detected using 8 keV Cs^+ but the same target has not yet been analyzed with fission fragments. Preliminary results indicate the curves continue to diverge.

In fig. 4 the yields are also compared to those from targets prepared with the same solution deposited onto etched Ag foil and analyzed with 8 keV Cs^+. In this case the mass spectra are considerably different (see figs. 1 and 2), and in favourable cases the yield is much higher than for electrosprayed targets. However, the reproducibility is still too poor to determine whether there is a difference in the slope of the yield curves. The data indicate an advantage of a Ag substrate, at least for some compounds, and also the danger in using different target preparation techniques when comparing particle desorption methods.

1) W. Ens, K.G. Standing, B.T. Chait and F.H. Field, Anal. Chem. 53(1981)1241.
2) I. Kamensky, P. Hokansson, B. Sundqvist, C.J. McNeal and R. MacFarlane, Nucl. Instrum. Methods 198(1982)65.

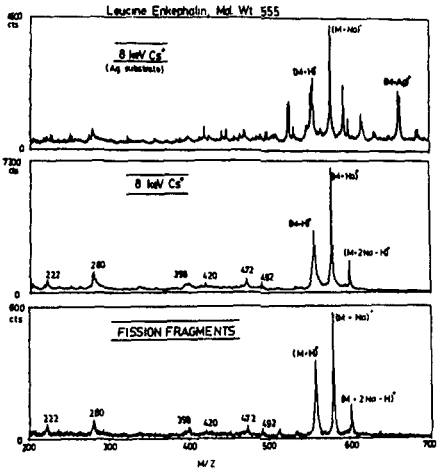

Fig. 1 TOF mass spectra of leu enkephalin. The bottom two spectra used the same electrosprayed target. For the top spectrum the solution was deposited onto etched Ag with a micropipette.

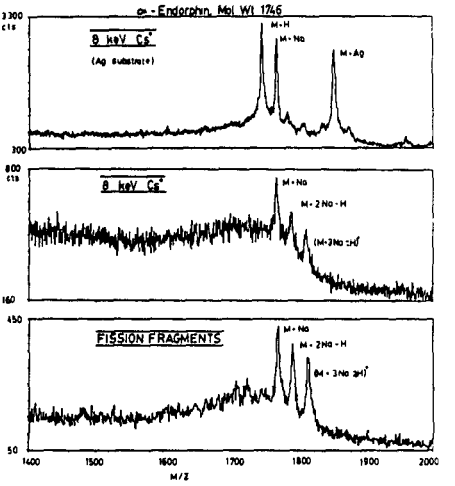

Fig. 2 TOF mars spectra of d endorphin. The bottom two spectra used the same electrosprayed target. For the top spectrum the solution was deposited onto etched Ag with a micropipette.

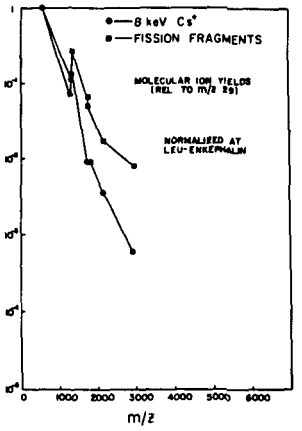

Fig. 3 Total molecular ion intensities (relative to m/z 29) for fission fragments and 8 keV Cs^+ incident on the same electrosprayed target. The peptides used are listed in the text.

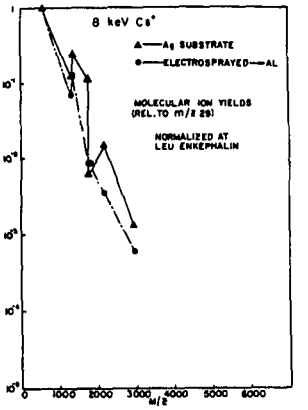

Fig. 4 Total molecular ion intensities (relative to m/z 29) for 8 keV Cs^+ incident on electrosprayed targets with etched Ag substrate . The peptides are listed in the text.

Presented at The 34th Annual Conference on Mass Spectrometry and Allied Topics.
Cincinnati, Ohio, June 1986.

(ROB8) The Role of Surface Chemistry in the Secondary Ion Mass Spectrometry of Liquid Surfaces.

Woodfin V. Ligon, Jr. and Steven B. Dorn, General Electric Company, Corporate Research and Development, P. O. Box 8, Schenectady, N. Y. 12301

It is well established that primary beams with a flux on the order of 10^{12} ions cm^{2} sec^{-1} sample only about the first 80 A of a liquid surface. It is obvious therefore that we cannot hope to understand the distribution of secondary ions obtained in a given experiment unless we understand the processes which determine the composition of the uppermost layers of the liquid surface. For solvents like glycerol with unusually high surface tensions, this means understanding classical surface chemistry because a knowledge of the bulk composition does not, by itself, provide a knowledge of the surface composition. Surfactant-like solutes which can lower the surface tension may be thousands of times more abundant at the surface of the solution than they are in the bulk.

This phenomenon of surface enrichment as a function of solute structure is largely responsible for the dramatic differences in sensitivity observed for otherwise quite similar analytes. Perhaps the best example involves the comparison of the tetramethylammonium ion with the cetyltrimethylammonium ion. The tetramethyl species is barely detectable at the 0.01 M level in glycerol whereas the long chain species is readily detectable at 10^{-6} M. It is also important to recognize that materials with high surface activity can suppress the sensitivity of less surface active materials. This is because the less surface active materials can be physically excluded from the surface. If a substance is not at the surface, it cannot be observed in the SIMS experiment. It is for this reason that tiny traces of lipid related impurities can completely obscure less surface active analytes such as peptides.

Once we appreciate the crucial role played by surface chemistry, we can design our experiments to take advantage of these effects. In the simplest case we can derivatize analytes to enhance their surface activity. Derivatization to introduce a formal charge has already been shown to be useful but as is clear from the case of the tetramethylammonium ion, it is not sufficient. For many uncharged analytes both charge and surface activity must be introduced. In general, surface activity is most easily obtained by introducing an alkyl chain of at least 10 carbons in length. As an example, Ligon has described the use of dodecanal to derivatize peptides by formation of a Schiff's base (1).

We also report (2) that 2-dodecen-1-ylsuccinic anhydride is a useful reagent to introduce both charge and surface activity into primary and secondary amines. Such derivatives are readily detected at 10^{-5} M in glycerol. Figure 1 shows the analysis of a selection of amines using this strategy.

Kidwell et al.(3) have described use of Girard's reagent T to obtain charged derivatives of ketones. We now report the synthesis and use of a new Girard's type reagent in which one methyl group on the quaternary ammonium function has been replaced by a 12 carbon aliphatic chain. The reagent was synthesized in the usual way except that N,N-dimethyldodecylamine was used instead of trimethylamine. Figure 2 shows the use of this reagent to study a variety of aliphatic ketones. The ketones are present (in the bulk) in equimolar quantities but show different response because of the surface active effects of the hydrocarbon chains associated with the ketones themselves. For small ketones like acetone the derivatives obtained are orders of magnitude more sensitive than the corresponding derivative obtained with Girard's reagent T. In both of these cases, (ketones and amines) it is important to realize that these relatively hydrophobic derivatives are far more likely to compete effectively for the surface in the presence of lipid derived impurities (interferences) because they are readily miscible with other hydrophobic substances and can, in effect, share the surface.

It is also possible to employ classical surfactants to modify the surface in useful ways. Figure 3 shows the effect of adding stearate anion to the solution of ketone derivatives shown in Figure 2. Here the surface is dominated by stearate because of its high surface activity (C-18 chain). The ketone derivatives now serve only to provide charge neutrality at the surface and their inherent differences in surface activity are entirely overwhelmed by the effect of stearate. Accordingly, the SIMS spectrum reflects the concentration in the bulk where the materials are present in equimolar amounts. Stearate is not observed at all in the positive ion spectrum.

Another very useful application of surfactants is to remove matrix interference from the spectrum. For this application, tetramethylammonium stearate may be used in positive ion mode and cetyltrimethylammonium acetate may be used in negative ion mode. In both cases the reagent should be used at about 0.001 M.

References:

(1) W. V. Ligon, Anal. Chem., 1986 , 58, 485

(2) W. V. Ligon and S. B. Dorn, Anal. Chem., 1986 (in press for August)

(3) D. A. Kidwell, M. M. Ross, and Colton, R. J. Biomed. Mass Spectrom. 1985 , 12, 254.

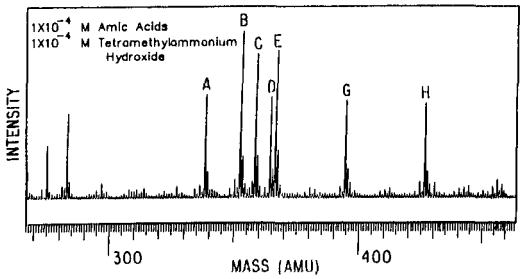

Fig. 1. Amic acid derivatives of the following amines: A. diethylamine, B. n-pentylamine, C. aniline, D. 4-methylpiperidine, E. n-hexylamine, F. dibutylamine, G. bis(2-ethoxyethyl)-amine. Glycerol solution 0.0001 M in each derivative. Negative ion SIMS spectrum.

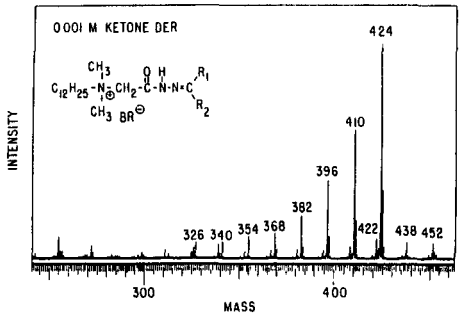

Fig. 2. Ketone derivatives using C-12 Girard's type reagent. Straight chain 2-ones from acetone (m/z 326) thru 2-decanone (m/z 424). Glycerol solution, 0.001 M in each derivative. Positive ion SIMS spectrum.

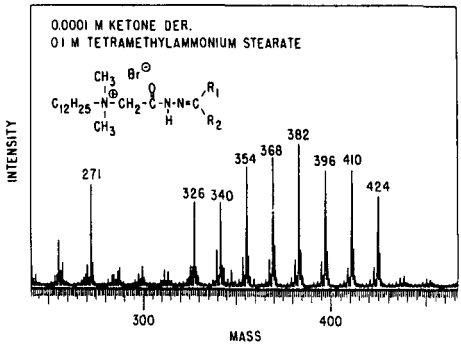

Fig. 3. Ketone derivatives as per fig. 2. except tetramethylammonium stearate added to suppress differences in surface activity among the derivatives

SURFACE SUPPLY OF SAMPLE MOLECULES BY ION MIGRATION IN FAB MS

K.P. Wirth, S.S. Wong and F.W. Röllgen

Institute of Physical Chemistry, University of Bonn, Wegelerstr. 12, D-5300 Bonn 1, FRG

In fast atom bombardment mass spectrometry (FAB MS) molecular ions are formed during continuous erosion of a liquid sample/matrix layer by a high incident atom flux. The supply of molecules from the bulk to the surface of the liquid is not a prerequisite of this ionization technique but it can contribute to the emission current of molecular ions and in particular affects the decrease of the molecular ion intensity as function of time.

The transport of molecules from the bulk to the surface of the liquid sample solution can arise from the following mechanisms:

1. Diffusion of molecules resulting from a gradient in the chemical potential of the solute between the surface and the bulk.
2. Ion migration of charged molecules in the field imposed by secondary emission of ions. The current flowing through the liquid and compensating surface charges is of the same order of magnitude as that equivalent to the flux of the incident particles which typically lies in the range of $\mu A/s\ cm^2$.
3. Convection of the liquid caused for example by gas evolution and bubble formation in the liquid. Gas evolution can result from electrochemical reactions at the liquid/metal support interface and has been frequently observed through viewing windows of the ion source of our mass spectrometer.

In recent experiments studying the decrease of molecular ion intensities as function of time during the erosion of thick sample/glycerol layers of about 0.5 mm (deposited on a horizontal metal support) a strong drop in intensity was observed for a basic protective peptide (PZ-Pro-Leu-Gly-Pro-Arg) while in the same time interval the abundance of molecular ions of oligosaccharides remained nearly constant /1/. The decrease in intensity of the protonated peptide cannot be explained by diffusion only but was attributed to the supply of sample molecules from the bulk to the surface of the layer by ion migration /2/. This electrophoretic effect and the resulting depletion of the peptide in the layer during sputtering is supported by the following observations:

a) A steeper intensity drop was found for basic peptides than for Glu-Glu-Glu and Ala-Ala-Ala-Ala-Ala.
b) The addition of HCl to the peptide/glycerol solution leads to a steeper drop of the molecular ion intensity than a HCl free solution (Fig. 1). This is in accordance with an increase of the contribution of protonated peptide molecules as charge carries by the HCl added. For NaOAc a reverse effect i.e. a less steep decrease of the molecular ion intensity was observed because Na^+ ions are mobile charge carriers in the solution.
c) The residue of the layer at the time the molecular ion signal of the peptide disappears into the chemical noise is still a liquid containing enough glycerol for molecular ion formation.
d) Since the peptide has a yellow color according to the azo dye protective group the effect of ion migration of the peptide in an imposed field could be visualized by an independent electrochemical experiment. In this experiment a pure glycerol solution was placed above the peptide/glycerole layer in an electrochemical cell, and the migration of the peptide was monitored by the moving boundary of the colored part of the liquid applying a current density of about 1 $\mu A/cm^2$. A migration effect of several tenth of mm/min was observed

while the effect of diffusion was more than an order of magnitude less.

Although the contribution of ion migration to the supply of molecules from the bulk to the surface is established by these experiments further observations allow to draw the conclusion that still other effects are involved in the decrease of the molecular ion intensity of peptides. For example the rather steep decay of the molecular ion signal of non-basic peptides compared to that of saccharides and a fast intensity decrease for the basic peptide even in the presence of mobile anions suggests the contribution of migration of anions to this decay effect. We suppose that reactive anions generated by the FAB induced radiation chemistry migrate into the bulk of the solution and cause chemical modifications and degradation of sample molecules. Further experiments have to elucidate these and other FAB induced migration and chemical effects.

/1/ S.S. Wong and F.W. Röllgen, Nucl. Instrum. and Meth. B14, 436 (1986)
/2/ S.S. Wong, K.P. Wirth and F.W. Röllgen in IFOS 3, Ed. A. Benninghoven, Springer Proc. in Physics, Vol 9, 1986.

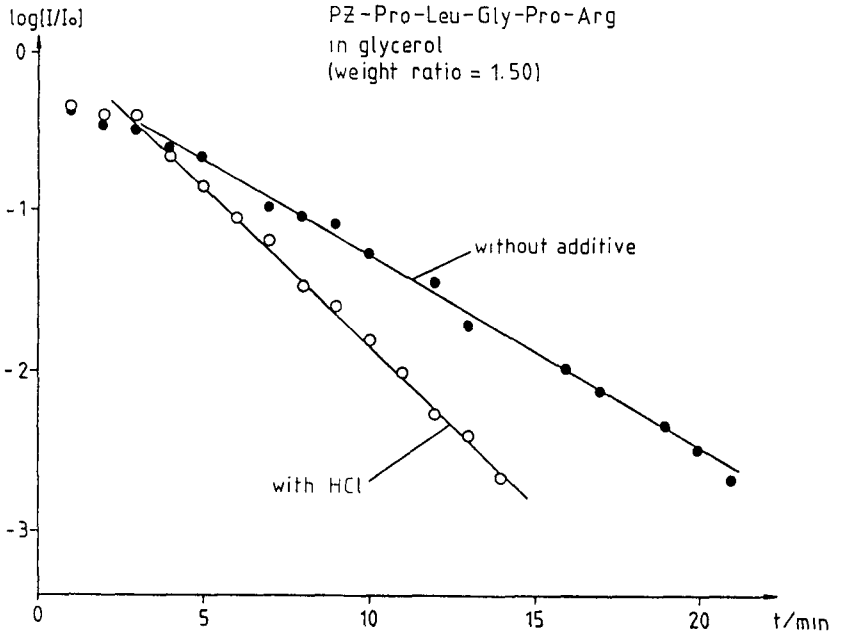

Fig. 1

ON THE VALIDITY OF THE PREFORMED ION MODEL IN FABMS.

J. Sunner, R. Kulatunga and P. Kebarle
University of Alberta
Edmonton, Alberta
Canada, T6G 2G2

The total positive secondary ion current emitted during fast atom bombardment, FAB, of glycerol (matrix) solutions of alkali chlorides (MCl), HCl, and pyridine hydrochloride (analytes) was measured, as a function of the concentration of the analyte (1). Whereas the spectra changed drastically upon addition of small amounts of salts, it was found that the total secondary ion current changed very litte, Fig. 1. This result is in apparent contradiction to the "preformed" model of ion formation. However, it can be understood within a gas phase collision model (2,3).

In the track of the fast atom, a high temperature, high density and high pressure "gas" is formed in a surface cavity. The "gas" subsequently expands into the vacuum. Ions are formed in the energetic collisions between the bombarding fast atoms and molecules in the matrix.

$$\overline{Xe} + Gly_{(\ell)} = F_I^+ \text{ (fragment ions)} \qquad (1)$$

Reactions between the fragment ions and neutral matrix molecules result mainly in protonated matrix ions:

$$F_I^+ + Gly = F_{II}^+ + \text{neutral fragments} \qquad (2)$$

$$F_{II}^+ + Gly = GlyH^+ + \text{neutral fragments} \qquad (3)$$

The protonated matrix ions cluster with matrix molecules:

$$GlyH^+ + Gly = (Gly)_2H^+ \qquad (4)$$

Collisions of the ions with gasified analyte molecules lead via ion molecule reactions to the dominant analyte ions:

$$GlyH^+ + An = AnH^+ + Gly \qquad (5)$$

The above mechanism occurs also when alkali chlorides are the analyte. In this case, the ion molecule reactions involve neutral gasified ion pairs, f.ex.:

$$GlyH^+ + KCl_{(g)} = K^+ + Gly + HCl \qquad \Delta G^o = -46 \text{ kcal/mol} \qquad (6)$$

Cationized molecules are formed by:

$$GlyH^+ + KCl_{(g)} = K^+(Gly) + HCl \qquad \Delta G^o \approx -40 \text{ kcal/mol} \qquad (7)$$

It was found, that there is a strong correlation between the intensity of alkali cation clusters (cationized molecules) in the FAB spectra and the gas phase stability of these clusters. This is illustrated in Fig. 2. In the figure, $M^+(H_2O)_2$ was used as a model compound to estimate the stability of the corresponding clusters with glycerol

The cavity initially contains, in addition to ca 1000 glycerol molecules, neutral fragments, ions preformed in the liquid and ions formed by the collision cascade. An increase in the concentration of preformed ions would be expected to result in an increase in the secondary ion current. That this is not the case can be understood as a result of extensive recombination between positive and negative ions, f.ex.:

$$K^+_{(\ell)} + Cl^-_{(\ell)} = (K^+Cl^-)_{(g)} \qquad \Delta H^o \simeq 50 \text{ kcal/mol} \qquad (8)$$

The formation of free ions in the gas requires much more energy, ca. 170 kcal/mol. The recombination reaction (8) is of the second order, and the concentration of a reactant at time t is given by:

$$[A^+]_t = \frac{1}{k_r t + 1/[A^+]_o} \qquad (9)$$

where k = rate constant and $[A^+]_o$ is the initial ion concentration. When only maybe 1 ion out of 100 survives the recombination process, it follows that $k_r t >> 1/[A^+]_o$ and $[A^+]_t$ is almost independent of $[A^+]_o$. Therefore, if the initial concentration of the ions increase, there is only a negligible increase in the numbers of surviving ions.

References

1. J. Sunner, R. Kulatunga and P. Kebarle, Anal. Chem., in print
2. J. Sunner, R. Kulatunga and P. Kebarle, Anal. Chem., accepted.
3. J. Michl, Int. J. Mass Spectrom. Ion Phys., 53, 255, 1983.

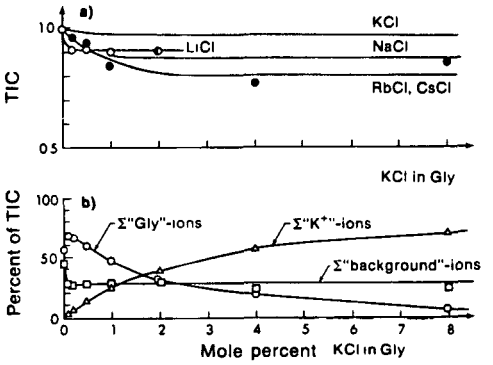

FIG 1

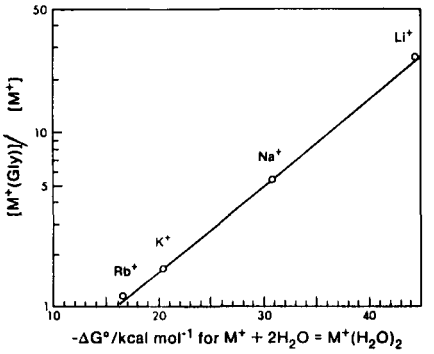

FIG 2

MATRIX PHYSICAL PROPERTIES AND THEIR EFFECTS ON ANALYTE SURFACE CONCENTRATION

Peter J. Todd
Oak Ridge National Laboratory, Oak Ridge, TN 37831

A sensible view of the role of liquid matrices in organic SIMS is that they act as reservoirs for dissolved analytes. During the course of a SIMS experiment, these analytes are pictured as diffusing to the surface, being drawn toward it by surface action or simply remaining stationary as the matrix evaporates and is sputtered away. Each of these mass transfer mechanisms can be described explicitly, and by using measured, reported, or estimated physical constants, the separate and cumulative effects of each mechanism can be estimated. The physical constants of interest are diffusion constants, analyte surface activity, matrix evaporation, and sputtering rates.

In general, diffusion constants of species in glycerol solution are about 10^{-8} cm^2/sec - 10^{-9} cm^2/sec. These values are used as limiting diffusion constants in a numerical[1] solution of Fick's Law, namely:

$$\frac{\partial c}{\partial t} = -D^2 \frac{\partial C}{\partial X^2} \qquad (1)$$

Modification to the numerical solution to account for sputtering is simple coordinate transfer (2), where S is the

$$\frac{dx}{dt} = S \qquad (2)$$

sputtering rate measured as $\sim$40 Å/sec/μA/cm^2 of 5 keV Ar^+. Evaporation is accounted for by surface volume reduction (3), where E is the evaporative rate

$$\frac{dC_s}{dt} = \frac{Cs}{1-E} \qquad (3)$$

of the matrix for pure glycerol, evaporation erodes the surface at $\sim$300 Å/sec. Surface activity is considered as a force which acts only at the surface, forcing for a concentration gradient specified by the (measured) surface activity of the analyte.

Results of these calculations are summarized in Figs. 1 and 2, which show the relative surface concentration as a function of time for surfactants and non surfactants, respectively, during sputtering by 5 μA/cm^2 Ar^+. Noteworthy is the fact that surfactant concentration necessarily decreases during an experiment, whereas non-surfactant concentration may increase, decrease, or remain constant, depending upon primary ion current density and diffusion constant.

*Research sponsored by the U. S. Department of Energy, Office of Basic Energy Sciences, under Contract DE-AC05-84OR21400 with Martin Marietta Energy Systems, Inc.

By acceptance of this article, the publisher or recipient acknowledges the U S Government's right to retain a nonexclusive, royalty-free license in and to any copyright covering the article

Figure 1 (right). Surface concentration for a surfactant dissolved in glycerol during sputtering. Surface concentration decreases rapidly, a result of the concentration gradient imposed by surface activity.

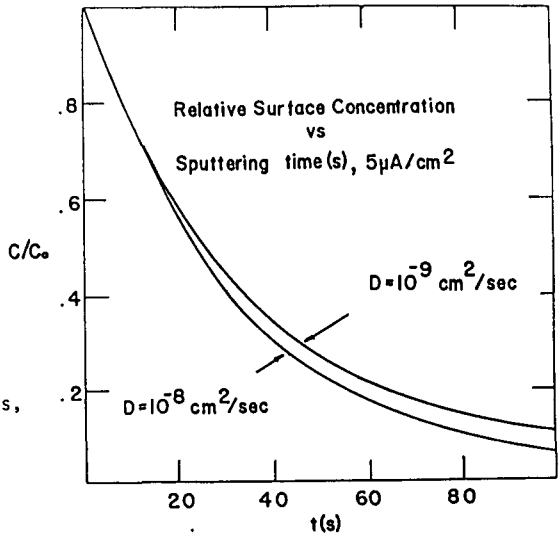

Figure 2 (below). Evaporation of matrix alone competes with sputtering of both matrix and analyte to control surface concentration of analyte in cases of surface-inactive analytes. Depending upon which feature dominates, surface concentration may increase, decrease, or remain unchanged.

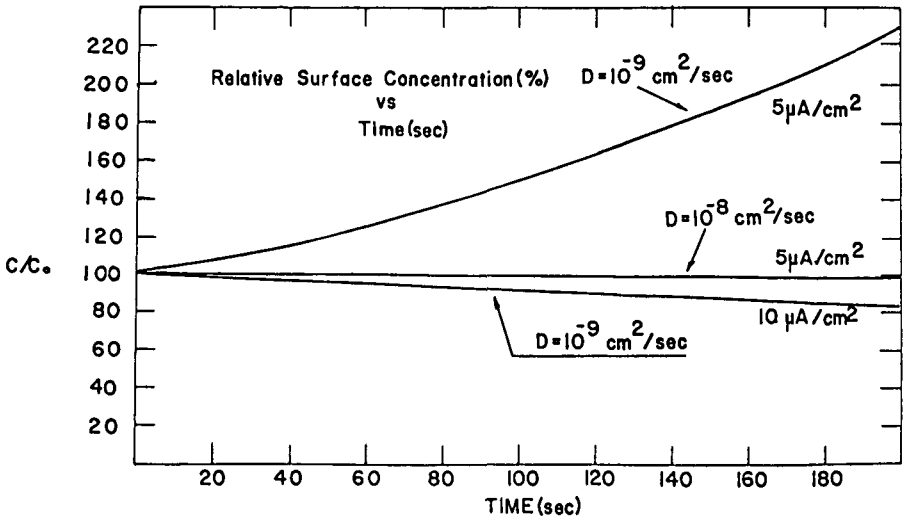

Reference:

1. Crank, J., "Mathematics of Diffusion," Clarendon Press, Oxford, England, 1975.

LOW TEMPERATURE PARTICLE BOMBARDMENT (FAB/SIMS) OF METHANOL

R.N. Katz, Tanuja Chaudhary, and F.H. Field
The Rockefeller University
New York, N.Y. 10021

Temperature as a parameter influencing fragmentation and ionization has yielded information valuable to mass spectrometry for twenty years. We have begun an investigation of temperature effects in particle bombardment mass spectrometry (FAB/SIMS), and we report here the results obtained when methanol is bombarded at temperatures ranging from -173 C to -94 C. The work was done on a single focusing magnetic sector instrument, modified to permit cooling of the ion source with liquid nitrogen. The sample was bombarded with a 40-50 μamp beam of Ar atoms and ions accelerated by 8.0 keV.

The spectrum of glycerol was studied initially because it is a typical FAB matrix. It was found that the number of distinct ions increased dramatically as the temperature went down. The low temperature spectrum was complex and bore no resemblance to the usual FAB spectrum of glycerol; therefore, experiments were done using methanol, a chemically simpler alcohol. Methanol behaved like glycerol in that the TIC remained sensibly constant while the number of peaks increased as the temperature declined. The spectrum of methanol at high temperatures was dominated by an envelope of methanol cluster ions $H(CH_3OH)_n^+$ and also contained primary ions at m/z 15, 29 and 31. The spectrum of liquid methanol at -94 C (Figure 1) was virtually the same as the spectrum of solid methanol at -104 C. At -173 C the spectrum is characterized by a non-descript distribution of ions whose intensities decreased essentially monotonically as the mass increased (Figure 2). At the intermediate temperature of -136 C, the spectrum contains the cluster ion envelope superimposed on the non-descript distribution of ions, and is a composite of the spectra shown in Figures 1 and 2.

A plot of the sum of the methanol cluster ion intensity divided by the total ion current versus temperature (Figure 3) shows that this change occurs between -120 C and -140 C, well below the melting point of methanol (m.p. -98 C). Melting of the solid by the bombarding beam did not occur since lowering the beam intensity (TIC decreased by a factor of twenty) did not significantly alter the behavior of the methanol or change the form of the curve, which was similar to that of Figure 3. Surface charging of the solid methanol is not responsible for the change in the spectrum of methanol with temperature because deflecting the argon ions out of the bombardment beam, and bombarding the sample with argon atoms only produces the same types of spectra. A plot of the $\sum_n H(CH_3OH)_n^+/TIC$ versus temperature forms a curve which is essentially the same as that shown in Figure 3. We have no explanation for this phenomena, and we are continuing to work on this problem.

Acknowledgement

This work was supported in part by the Division of Research Resource, National Institues of Health.

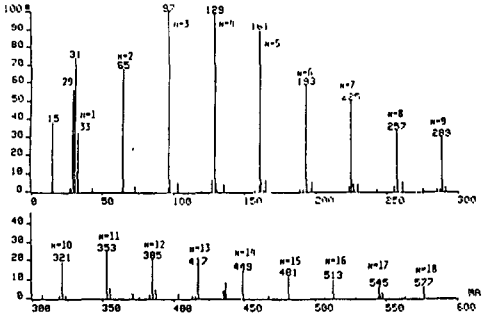

Fig. 1

Spectrum of liquid methanol at -94C
Peaks are annotated with the value of
n in $H(CH_3OH)_n^+$

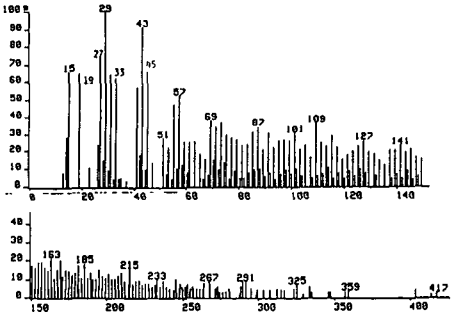

Fig. 2

Spectrum of CH_3OH at -173C

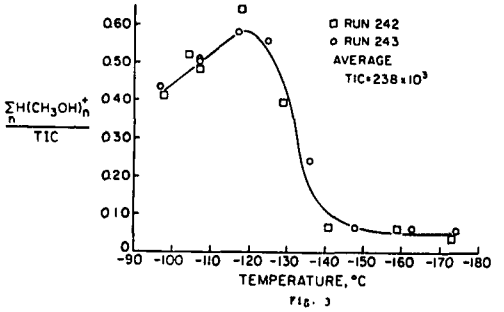

Fig. 3

Plot of $\sum_n H(CH_3OH)_n^+/TIC$ vs. T at normal bombarding intensity. Points for duplicate runs shown.

Laser Desorption Fourier Transform Mass Spectrometry of Porphyrins

Robert S. Brown and Charles L. Wilkins, Department of Chemistry, University of California, Riverside, CA 92521

Porphyrins and metalloporphyrins have been the subject of numerous studies involving a wide range of mass spectrometric techniques for structural characterization, the most widely employed being chemical ionization (CI)[1,2] and more recently fast atom bombardment (FAB)[3,4] mass spectrometry. The importance of this compound class, both in natural products and to the petroleum industry, has resulted in many new compounds being synthesized or isolated with a concomitant need for improved methods for structural characterization. While CI methods have been quite useful in identifying substituents, they are generally limited to lower mass samples. FAB works well on higher mass, nonvolatile samples but can suffer from matrix solubility problems and gives little or no fragmentation in many cases.

Laser Desorption Fourier Transform Mass Spectrometry (LD-FTMS) is a promising new technique for the analysis of non-volatile compounds and has been applied to a number of both naturally occuring and synthetic porphyrins. LD-FTMS spectra of chlorophyll a and chlorophyll b are dominated by intense pseudomolecular ions which have lifetimes in excess of several seconds. This is in sharp contrast to earlier studies with ^{252}Cf fission fragment ionization[5] which had concluded that the molecular ions of Chlorophyll a were metastable and underwent unimolecular decomposition in less than 67 microseconds. These results are important with regard to the application of LD-FTMS to the study of large labile molecules due to its inherently longer measurement time scale (> 10 mS)

In addition to the naturally occurring chlorophylls, a large number of synthetic porphyrins and metalloporphyrins have been studied. LD-FTMS spectra of these porphyrins typically exhibit intense molecular or pseudomolecular ions. In addition, lower intensity ions due to substituent losses are sometimes observed. Figure 1 is the positive ion spectrum of a ferrocene modified tetra phenyl porphyrin. Although little fragmentation is observed, calibration and accurate mass measurement produced a 1.1 ppm error for the mass 1373 ion, sufficient to establish its molecular formula. Figure 2 is the spectrum of μ-oxy-bis-tetra(4-methoxy phenyl)porphinato iron(III) chloride. This spectrum is dominated by a $(M-Cl)^+$ ion along with fragments due to cleavage at the bridging oxygen (m/z 787 and 803).

Laser power has an important effect on the porphyrin spectra. Low power spectra are dominated by cation attachment species with little fragmentation while higher laser power densities produce spectra which are dominated by M^+ ions and more fragmentation. This observation may aid in understanding the desorption/ionization mechanism in LD-FTMS.

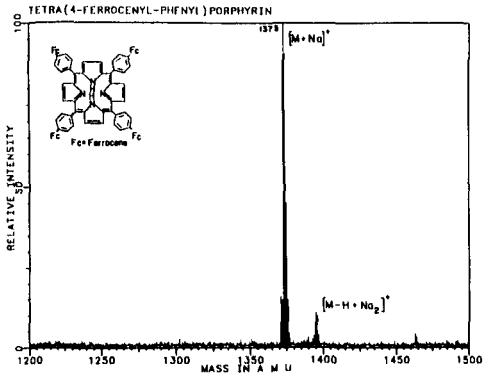

Figure 1

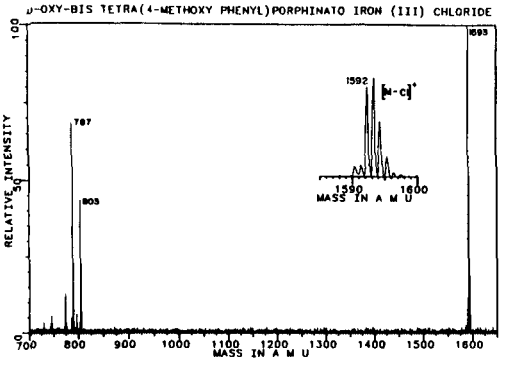

Figure 2

While some fragmentation is apparent in most of the porphyrin spectra, detailed structural characterization would be greatly aided by MS/MS experiments. In this regard, photodissociation would appear to be an ideal candidate. Photodissociation of porphyrins has been demonstrated[4] with FAB ionization and a double sector mass spectrometer. FTMS offers the potential for much higher daughter ion resolution as well as multi-stage MS/MS experiments. Figure 3 shows the results of a preliminary two color laser desorption(CO_2 laser) photodissociation(excimer laser) experiment on the molecular ions, $(M+K)^+$, $(M+Na)^+$ and $(M+H)^+$, of tetra(4-N,N-dimethyl anilinium)porphyrin. Significant additional fragmentation is evident with little or no loss in resolution.

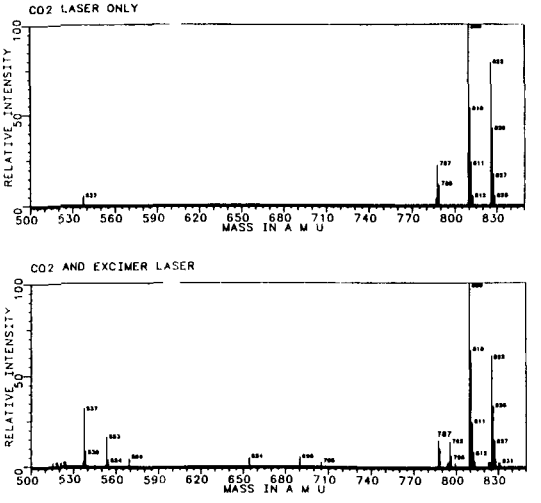

Figure 3

REFERENCES:
1. Bo-Ragnar Tolf, Xiang-Yu Jiang, Annemarie Wegmann-Szente, Lisa A. Kehres, Edward Bunnenberg and Carl Djerassi, JACS, 1986, 108, 1363-1374.
2. Padmanabhan Sundararaman, E.J. Gallegos, E.W. Baker, J.R.B. Slayback and M.R. Johnston, Anal. Chem., 1984, 56, 2552-2556.
3. Mei-Yi Zhang, Xi-Yun Liang, Yu-Yi Chen and Xiao-Guang Liang, Anal. Chem., 1984, 56, 2288-2290.
4. Elaine K. Fukuda and Joseph E. Campana, Anal. Chem., 1985, 57, 949-952.
5. B.T. Chait and F.H. Field, JACS, 1984, 106, 1931-1938.

Fast Atom Bombardment Induced Adduct Ion Formation in the Mass Spectra of Alkyl Pyridinium Chlorides: T. Keough, The Procter & Gamble Co., Miami Valley Laboratories, P.O. Box 39175, Cincinnati, OH 45247.

In 1982, Field[1] observed adduct ion formation during FAB of glycerol, the most commonly used FAB matrix. Subsequently, it has become well-recognized that beam induced chemical reactions can occur in FAB[2-10], as well as in static SIMS and plasma desorption. During the analysis of cetyl pyridinium chloride (Fig. 1) we observed a series of abundant adduct ions, indicated by arrows, whose intensity approximately equaled that of the intact molecular cation at M/Z 304. We have used this compound to systematically explore mechanisms of adduct ion formation and elimination under FAB conditions.

Thermal reduction of alkyl pyridiniums has been observed[11-13] under electron ionization and field desorption conditions (Fig. 2). Radical-radical recombination processes, involving $H^{\bullet}$ loss followed by $CH_3^{\bullet}$ addition to the ring, are thought to produce the indicated intermediate. Upon heating, it eliminates HCl producing the volatile material that is subsequently ionized and detected. The same basic mechanism may also occur under FAB conditions, however, several C-centered radicals are available for reaction if glycerol is used as the FAB matrix.[1,14] MS/MS of some of these adduct ions confirms that substitution does, in fact, occur on the ring. Furthermore, the adduct having a mass of 14 Daltons greater than that of the molecular cation was shown to arise via substitution of the 4-position of the ring. Thus, for this system, the adduct formation processes exhibit considerable site specificity.

We attempted to eliminate FAB-induced adduct ion formation by varying bulk analyte concentration[15], addition of a free radical scavenger[16], and by varying the FAB matrix. Changing the matrix from glycerol to thioglycerol (TG) reduced the relative abundance of adduct ions by a factor of 100.

Several reasons might account for the reduction of adduct ions when using the TG matrix. We are investigating the possibility that TG suppresses the radical-radical recombination processes that lead to adduct ion formation. It is well-known that thiols function as protectors for organic molecules exposed to conventional ionizing radiation.[17] Possible mechanisms of protection include ionic and radical processes (Fig. 3). Ionic mechanisms involve charge transfer of the ionized analyte (2) thereby suppressing the ion/molecule reaction leading to radical formation (1). This process does not necessarily require that the sulfur compound contain the thiol functionality. Alternatively, radical processes such as (3) or (4) might be important under FAB conditions. Both of these latter processes involve loss of the thiol hydrogen. We note that other sulfur containing matrices such as 2,2'-thiodiethanol and 3-methylthio-1,2-propanediol show minimal adduct ion reduction relative to glycerol. Therefore, suppression by the ionic route apparently does not account for the bulk of the adduct ion reduction in the TG matrix. Furthermore, we observe only slight deuterium incorporation into the molecular cation when TG-D_3 is used as the FAB matrix (Fig. 4). We would have anticipated extensive D incorporation into the analyte if (3) was a major route of adduct ion suppression. Of the radical mechanisms, (4) seems more likely. Of course, this process requires the presence of S-centered (TG-$H^{\bullet}$) radicals which is supported by two observations: (1) The proton-bound dimer region of the TG FAB spectrum exhibits an abundant disulfide ion (M/Z 215) and (2) an adduct ion is observed 108 Daltons above the molecular cation when TG-D_3 is used as the matrix. This is consistent with recombination of an S-centered (D_3-TG-$D^{\bullet}$) radical with the (analyte-$H^{\bullet}$) radical rather than recombination of a carbon-centered (D_3-TG-$H^{\bullet}$) radical. Obviously, a suitable thiol, deuterium labeled on the carbon α to the sulfur atom, would be a useful matrix to critically test whether radical process (4) accounts for the observed adduct ion reduction in the TG matrix. Unfortunately, we have not yet obtained such a matrix.

The abundance of FAB-induced adduct ions decreased dramatically, for this particular analysis, in the thioglycerol matrix. This should not be interpreted as a general effect. Some of the beam induced adduct formation processes previously reported[7,9,10] occur readily in the thioglycerol matrix.

References

1. F. H. Field, J. Phys. Chem., 86, (1982) 515.
2. M. E. Rose, et al, Biomed. Mass Spectrom., 10, (1983) 512.
3. S. K. Sethi, et al, Anal. Chem., 56, (1984) 1975.
4. J. Meili, et al, Org. Mass Spectrom., 19, (1984) 581.
5. W. D. Lehmann, et al, Biomed. Mass Spectrom., 11, (1984) 217.
6. H.-M. Schiebel, et al, Biomed. Mass Spectrom., 12, (1985) 170.
7. B. Divisia-Blohorn, et al, Org. Mass Spectrom., 20, (1985) 463.
8. G. Pelzer, et al, J. Phys. Chem., 88, (1984) 5065.
9. L. Kurlansik, et al, Biochem. Biophys. Res. Commun., 111, (1983) 478.
10. M. A. Baldwin, et al, Org. Mass Spectrom., 21, (1986) 235.
11. E. Larsen, et al, Org. Mass Spectrom., 13, (1978) 417.
12. P. Ellingsen, et al, Org. Mass Spectrom., 13, (1978) 455.
13. T. D. Lee, et al, Anal. Chem., 53, (1981) 304.
14. T. Keough, et al, 33rd ASMS, (1985) 964.
15. H. Pang, et al, 32nd ASMS, (1984) 751.
16. K. L. Busch, et al, Fifth International Conference on SIMS, Washington, D.C., 1985.
17. H. M. Nanobashvili, et al, Fifth Symposium on Radiation Chemistry, (1982) 581.

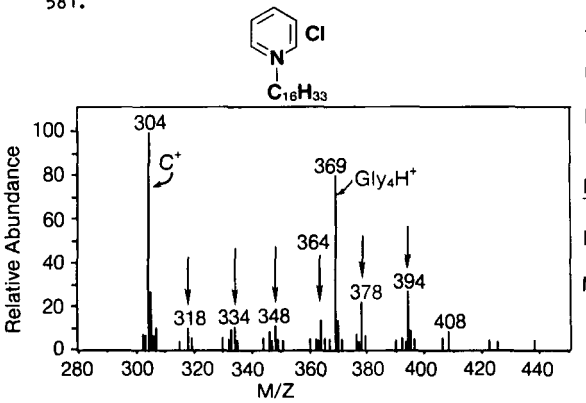

Figure 1

Ionic Mechanism

$$MH^{+\bullet} + MH \rightarrow MH_2^+ + M^\bullet \quad (1)$$

$$MH^{+\bullet} + RSH \rightarrow MH + RSH^{+\bullet} \quad (2)$$

Radical Mechanisms

$$M^\bullet + RSH \rightarrow MH + RS^\bullet \quad (3)$$

$$M^\bullet + R'CH_2S^\bullet \rightarrow MH + RCH{=}S \quad (4)$$

Figure 3

Thermal Reduction of Alkyl Pyridinums

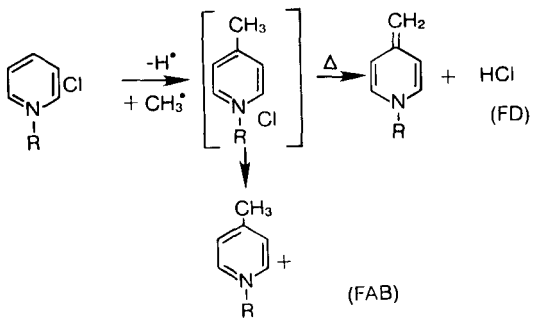

Figure 2

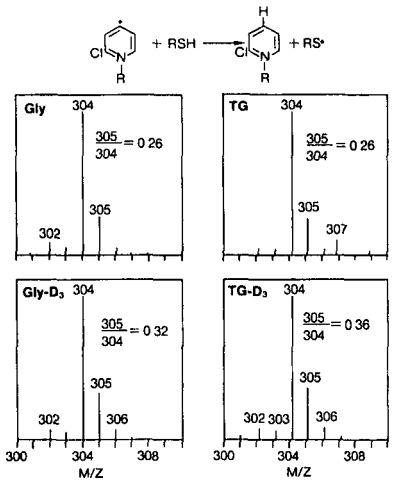

Figure 4

OBSERVATION OF $(M+nH)^+$ ION SPECIES WHERE n = 2, 3, AND 4 IN FAST ATOM BOMBARDMENT MASS SPECTROMETRY.

Brian D. Musselman
Department of Biochemistry
Michigan State University
East Lansing, MI, 48824

During the analysis of a series of substituted porphyrins using fast atom bombardment (FAB) mass spectrometry, it was observed that the intensities of the isotopic peaks in the cluster representing $(M+H)^+$ did not match the predicted abundances. The $(M+H)^+$ cluster appeared to contain significant contributions above normal at $(M+2)^+$, and $(M+3)^+$. Cerny and Gross (1) previously reported on similar observations which were attributed largely to the low energy unoccupied molecular orbitals (LUMOs) available in the nucleotide bases being analyzed. Since porphyrins have similar functional groups to those in nucleosides an examination of these compounds was undertaken in order to determine the basis of the observed distortions in the ratio of isotope peak intensities during FAB-MS. A series of *mono-, di-, and tetra-substituted porphyrins was analyzed by FAB. The addition of* electrophilic functional groups such as napthalene and anthracene to the porphyrin was observed to increase the abundances of ions representative of a molecule which has been reduced through addition of hydrogen.

Using this background information, a review of the FAB literature was completed in order to assess the extent to which these ions are formed in other types of compounds. Examples of the appearance of these ions in a variety of molecules, particularly polypeptides, were found. Moreover, the peak intensity at M+2, M+3 and M+4 also appeared to be dependent upon the solvent matrix used for the FAB analysis. As an example of the solvent effect, Table 1 illustrates the data obtained from FAB analysis of Met-enkephalin in two different solvents, glycerol and thioglycerol. Analysis in thioglycerol yielded a distribution of ions identical to that expected for the protonated molecule ion. Analysis in glycerol yielded an excess ion abundance above those expected at $(M+2)^+$, $(M+3)^+$ and possibly $(M+4)^+$, although determination of the contribution to the latter ion is beyond the limits of confidence for these measurements. Using the excess ion abundance present at $(M+2)^+$ as a measure of $MH_2^{+\cdot}$ generated during fast atom bombardment, subtraction of the contribution which the stable isotopes of this molecular adduct ion was completed. This subtraction eliminated the excess ion abundance at $(M+3)^+$, and $(M+4)^+$ leaving no significant excess ion abundance at $(M+3)^+$ or $(M+4)^+$ for this compound. It is apparent from the analysis of a number of polypeptides that this phenomenon is not an isolated observation, but rather common in both positive and negative ion spectra of samples analyzed in glycerol.

Table 1. *Percent $(M+n)^+$ relative to $(M+H)^+$ Met-enkephalin in different solvents*

	n = 1	2	3	4
Calculated isotope distribution	100	33.7	11.4	2.5
Experimental Results				
Glycerol	100	39	14	3
Thioglycerol	100	33	11	2

1. Cerny, R., and Gross, M., Anal. Chem. 57, 1150, (1985).

2. Pelzer, G., DePauw, E., Viet Dong, D., Marien, J., J. Phys. Chem., 88, 5065, (1984).

3. Gale, P., Bentz, B., Chait, B., Field, F., and Cotter, R., Anal. Chem., 58: 1070, (1986).

Pelzer, et al. (2), demonstrated that for a series of organic dyestuffs significant formation of $(M+2)^+$ and other reduced ion species could be related to the magnitude of the polarographic half-wave reduction potential. The more negative the potential the less abundant the ion intensity of the reduced ion. Gale, et al. (3) subsequently analyzed a more extensive number of dyes with reduction potentials varying from -0.605 to -0.205V. The potential at which the formation of $(M+2H)^+$ increased significantly was between -0.335 and -0.395V. A gradual increase in formation of $(M+2H)^+$, and $(M+3H)^+$ was not observed over the range of potentials, but rather, between these two values the production of $(M+2H)^+$ and $(M+3H)^+$ rose significantly as shown in Figure 1. In this case there seems to be a specific potential range in which significant changes in the rate of formation of the reduced ion species is apparent. It is important to note that these organic dyes are highly aromatic in nature, like our porphyrins, and thus we attempted to relate this data to our findings for porphyrin analyses completed using a thioglycerol matrix. Previous experiments indicate that thioglycerol can inhibit formation of MH_2^+. These studies indicate that indicate that formation of reduced species can be observed in the thioglycerol therefore either a different form of reduction must be operational during the ionization of these porphyrins or they must have physical chemical properties which enhance formation of the reduced species. As an example, using the compounds in Table II in the case of the etioporphyrin, increased ion abundance at $(M+2)^+$ and beyond was not observed until the phenyl, napthyl, and anthracenyl functional groups were added to the molecule. Trends in the proton affinities, electron affinities, and $E^{red}_{1/2}$ potentials of these functional groups can all be related to the increasing abundance of ions at M+2, M+3, and M+4 observed in the FAB mass spectrum. Further analyses must be completed to determine, if possible, the contribution of each factor to the formation of these ions.

Table II.

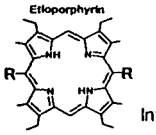

Intensity at $(M+n)^+$ relative to $(M+H)^+$

R	n	2	3	4	5
	Obs.	62	25	8	
	Theory	51	13	2	
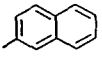	Obs.	74	34	12	6
	Theory	60	18	4	0
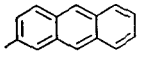	Obs.	84	50	22	12
	Theory	70	24	5	

Figure 1 Polarographic half-wave reduction potentials vs. abundance of $(M+2H)^+$ and $(M+3H)^+$ for 7 dyes

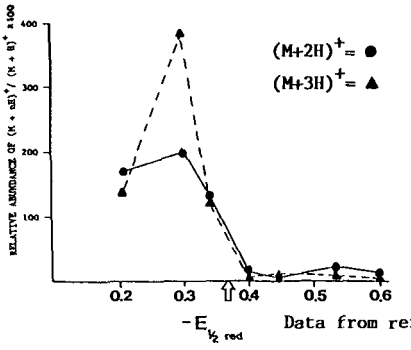

Data from ref. 3

The observations described in this work indicate that the solvent utilized for the FAB analysis affects the formation of (M+2H) and (M+3H) ions during the experiment. Evidence that these molecules are reduced in solution is not available since to this date we have not observed any increase in the abundance of $(M+2H)^+$ or $(M+3H)^+$ relative to $(M+H)^+$ for spectra collected at different time intervals during the FAB analysis. Thus the suggestion that these reactions occur in the gas phase or selvedge region where factors such as proton affinity, electron affinity, and desolvation of the analyte must be considered. Finally, and most significantly, keeping in mind that formation of $(M+nH)^+$ for n=2, and 4, and $(M+3H)^{\cdot+}$ are observed in FAB mass spectra, caution must be exercised in the use of the distribution of isotope peak intensities to determine the molecular formula of an unknown compound using FAB ionization.

Acknowledgement: This work was supported in part by a grant (RR-00480) from the Biotechnology Research Program, Division of Research Resources, National Institutes of Health.

COLLISIONAL MASS SPECTROMETRY OF GASEOUS PROTONATED AMINES

E.J. REINER AND A.G. HARRISON
Department of Chemistry
University of Toronto
Toronto, Canada M5S 1A1

The collision-induced dissociation (CID) mass spectra of C_3 to C_6 alkyl amines have been determined at both high (8KeV) and low (5-100eV) collision energy using a hybrid BEQQ mass spectrometer. For protonated monoalkylamines, $R_1R_2CHNH_3^+$, in high energy collisions three main reaction channels are observed (Scheme 1), loss of ammonia forming an alkyl ion, elimination of alkene forming the ammonium ion and elimination of an alkane forming on immonium ion; in the latter reaction, which provides information on the branching at the α-carbon, the largest possible alkane is lost in preference to smaller alkanes. The low energy (100ev) CID mass spectra show the same reactions with reduced intensity for the alkane elimination reaction and an increased extent of further fragmentation of the alkyl ions. The first observation is consistent with the conclusion that alkane elimination has a high critical reaction energy and occurs only for those ions in the high energy tail of the energy distribution function arising from the high-energy collisional activation process. This high-energy tail is largely missing in the low energy collisional activation process, although judging from the extent of fragmentation of the alkyl ions the average energy transferred is greater than for high energy collisions.

For protonated polyalkylamines in high energy collisions the same reactions are observed (Scheme 2). However, a new alkane elimination reaction, with the alkane incorporating an alkyl group bonded to N and an alkyl group bonded to the α-carbon, is observed. Following low energy collisional activation the first alkane elimination reaction is not observed, however the second alkane elimination reaction does occur. As the Figure shows this reaction (forming m/z 44 from protonated dimethyl butylamine) becomes significant only above 30eV collision energy.

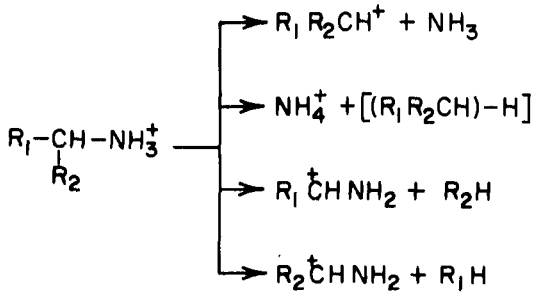

SCHEME 1

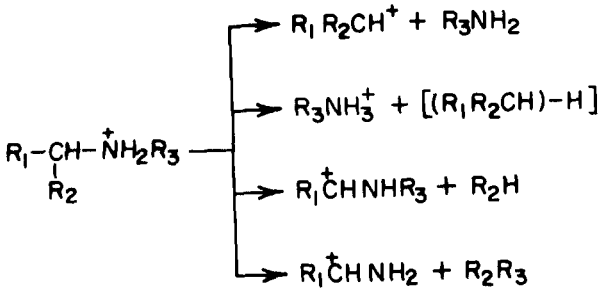
R1-CH-N+H2R3
R2
R1 R2CH+ + R3NH2
R3NH3+ + [(R1R2CH)-H]
R1CH+NHR3 + R2H
R1CH+NH2 + R2R3

SCHEME 2

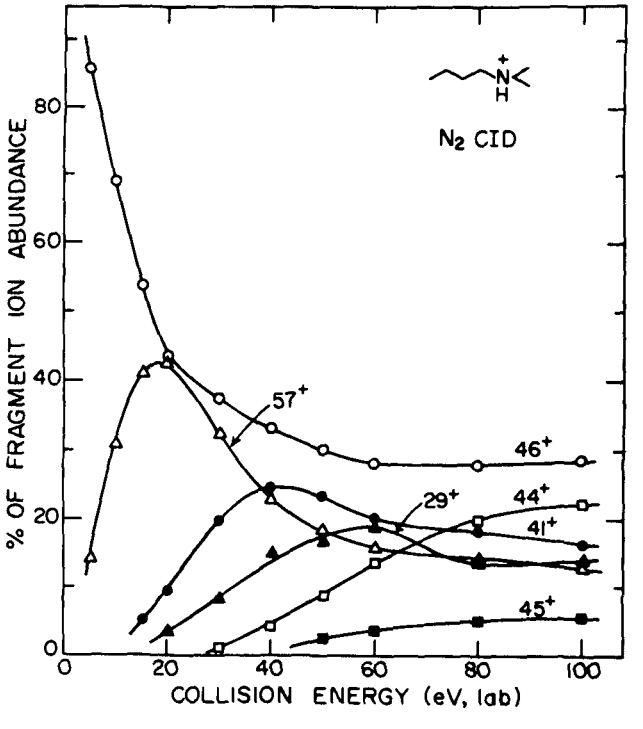
N2 CID
% OF FRAGMENT ION ABUNDANCE
COLLISION ENERGY (eV, lab)
57+
46+
29+
44+
41+
45+
0
20
40
60
80
100

Structure of Ions in the Ion Chemistry of $(CF_3)_2NO$ and $(CF_3)_2NONO$ Studied by Collision-Induced Dissociation in a Broad Energy Range with High Magnetic Field FT ICR Spectrometer

J.-W. Park and K. P. Wanczek,
Inorganic Chemistry, NW 2, University of Bremen,
D-28 Bremen 33, West Germany

The ion-molecule reactions of the stable radical $(CF_3)_2NO$ and of $(CF_3)_2NONO$ have been studied with an FT ICR spectrometer employing a high field superconducting magnet with 7.02 Tesla field strength. The spectrometer is equipped with a cylindrical ICR cell of 2.5 cm radius and 5 cm length. For broad band Fourier transform experiments a fast ADC of 20 MHz maximum sampling rate and 128 K buffer memory is employed. A base pressure of less than 10^{-9} mbar can be reached with a high speed diffusion pump with liquid nitrogen cooled baffle. The purity of the samples was determined additionally with sector field mass spectrometry.
The ion chemistry of the positive and negative ions of bis-trifluoromethylnitroxide is shown in Schemes 1 and 2.

Scheme 1

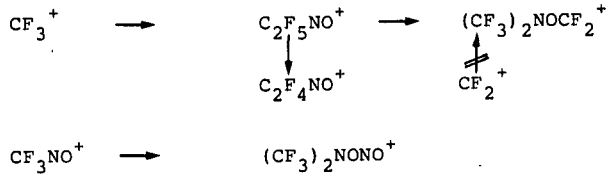

Scheme 2

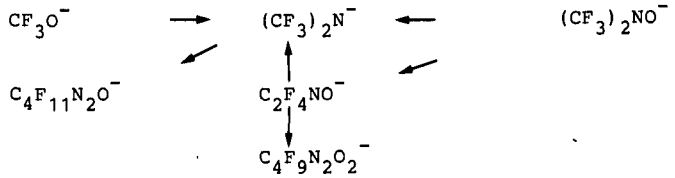

The chemistry is dominated by displacement reactions.

In the ion chemistry of $(CF_3)_2NONO$ only one major reaction of the molecular ion with the neutral molecule has been observed to yield $(CF_3)_2NONONO^+$.

For structural studies CID experiments of the major ions have been performed. First all unwanted ions are ejected from the ICR cell. Then the kinetic energy of the ion under consideration is increased by irradiation with its resonance frequency. From the dependence of the ion number on the pressure it is shown that only at pressures below 10^{-8} mbar a kinetic energy corresponding to a radius of gyration of approximately 2.5 cm can be reached. At higher pressures the kinetic energy of the ions is lower than calculated.

The CID spectum of $(CF_3)_2NONONO^+$ is shown in Fig. 1. The primary ion loses NO (m/q 198) already at low collision energies, at intermediate energies NO^+ loss (m/q 30) becomes important. CF_3^+ (m/q 69) is lost at higher energies. From $(CF_3)_2NONO^+$ NO is lost at higher collision energies then the first NO of $(CF_3)_2NONONO^+$.

Fig. 1

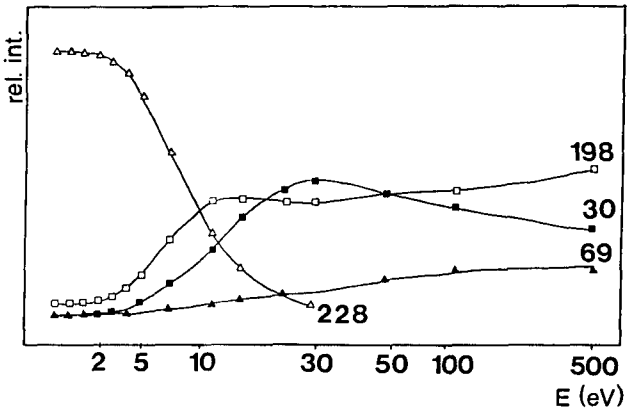

The CID spectra of $C_3F_8NO^+$ proves the structure $(CF_3)_2NO{=}CF_2^+$. For the $C_2F_4NO^+$ ion, a product of the CID, the structure $CF_3NO{=}CF_2^+$ is shown.

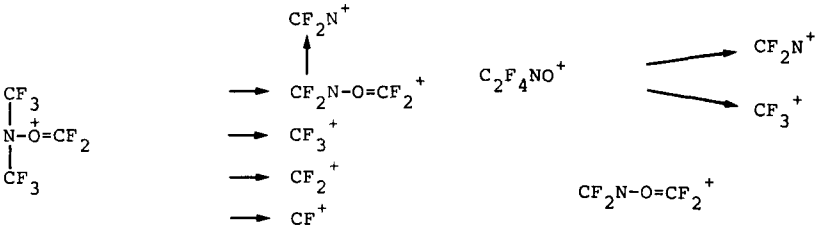

The positive molecular ion of $(CF_3)_2NO$ shows no N-O bond dissociation in the CID experiment, however the negative molecular ions does. This proves a different N-O bond strengths in the two ions.

CHARGE INVERSION AND NEUTRALIZATION - REIONIZATION MASS SPECTRA OF ALKOXIDE ANIONS

R.S. MERCER AND A.G. HARRISON
DEPARTMENT OF CHEMISTRY
UNIVERSITY OF TORONTO
TORONTO, CANADA M5S 1A1

The charge inversion and neutralization reionization (NRMS) mass spectra of the C_1 to C_3 alkoxide anions have been determined using a reversed geometry (B/E) mass spectrometer with dual collision cells in the field-free region between the magnetic and electric sectors. The effect of the identity of the collision gas on the charge inversion spectra and the effect of the identity of the two collision gases on the NRMS spectra have been investigated. In addition isotopic labelling has been employed to elucidate fragmentation mechanisms.

The present brief summary will focus on the isopropoxide anion as a typical example. Figure 1 shows the charge inversion spectra obtained using He, N_2 and O_2 as collision gases. The spectra are similar although there is an increase in yield of a product of m/z 44 with N_2 and, particularly, O_2 as collision gas. The origin of this product, which is first order in pressure, is uncertain but may involve formation of a superexcited alkoxy radical which autoionizes after loss of a methyl radical. Figure 2 shows the charge inversion spectra of labelled isopropoxide ions. It is clear that the major fragmentation reactions of the unstable isopropoxy cation involve loss of alkanes (CH_4 and C_2H_6) by 1,1- elimination reactions. (In addition anions of the formula RCH_2O^- form R^+ by loss of CH_2O on charge inversion). Figure 3 shows the NRMS spectra observed using He as the reionization gas and He, Xe, N_2 and O_2 as neutralization gases. The O_2/He combination gives a spectrum most similar to the one-step charge inversion spectrum. The other NRMS spectra show enhanced signals, particularly at m/z 28 and m/z 42 presumably due to the reionization of additional neutral species formed in the neutralization step.

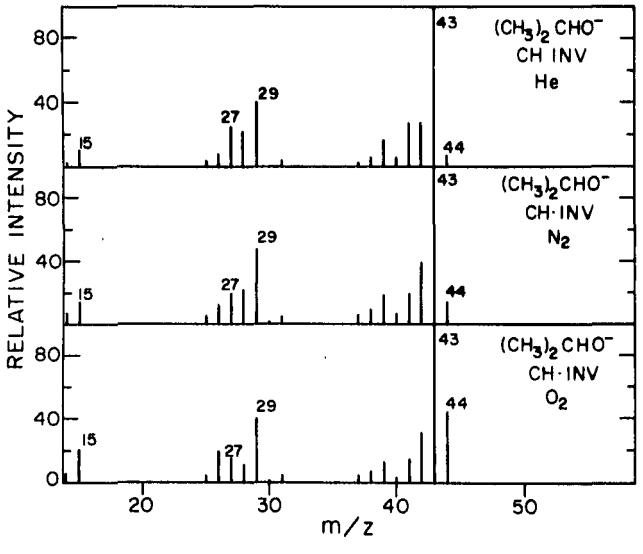

FIGURE 1

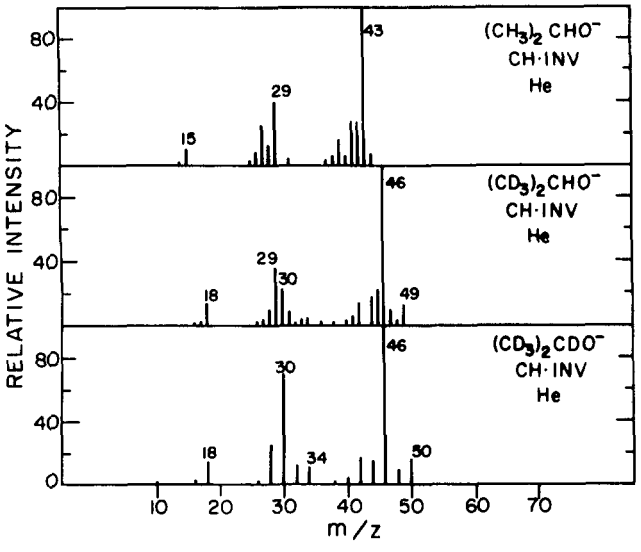

FIGURE 2

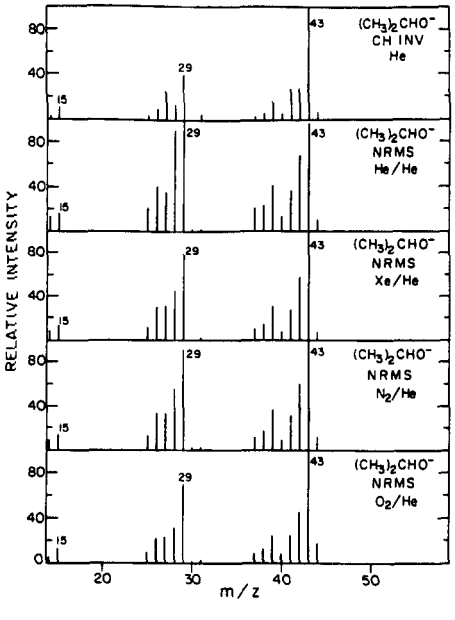

FIGURE 3

MS/MS BY ION - ELECTRON COLLISIONS IN FTMS

Robert B. Cody
Nicolet Analytical Instruments, 5225-1 Verona Road, Madison, WI 53711

Ben S. Freiser
Dept. of Chemistry, Purdue University, W. Lafayette, IN 47907

In 1979, we reported the use of low energy ion-electron collisions to induce fragmentation of organic ions, in a technique referred to as "electron impact excitation of ions from organics (EIEIO)" (1). The technique was initially employed to obtain breakdown curves (2,3) and to observe the production of multiply-charged argon ions (4). However, several obstacles prevented its application to MS/MS and mixture analysis experiments. The major difficulty resulted from our inability to successfully employ ion ejection techniques to select a parent ion. This was attributed to the "shielding effect" of the electron beam against the irradiating RF.

Recent experiments involving a Fourier transform mass spectrometer employing a superconducting magnet and a dual-cell geometry (5) have shown that it is possible to employ ion ejection techniques by gating off the electron beam for a short time during ion ejection, and then turning the electron beam on again to permit electron impact excitation of the ions. The high magnetic field (3 Tesla) assists in confining the ions in the electron beam, and the dual-cell design permits daughter ions produced by the electron impact process to be isolated from reactive neutrals.

Since no collision gas is employed, it is possible to obtain high daughter ion resolution (Fig. 1). Unlike FTMS CID experiments (6), the method does not increase the orbital radius of ions, and may be useful in multistage (MS)n experiments in which daughter ions are transferred back-and-forth between the source and analyzer cells. The method is fast (about 100 msec), and may have application in experiments such as GC-FTMS/MS where time is a factor.

1. Cody, R. B.; Freiser, B. S. Analytical Chemistry 1979, 51, 547-551.

2. Fedor, D. M.; Cody, R. B.; Burinsky, D. J.; Freiser, B. S.; Cooks, R. G. Int J. Mass Spec. Ion Proc. 1981, 39, 55-64.

3. McLuckey, S. A.; Sallans, L.; Cody, R. B.; Burnier, R. C.; Verma, S.; Freiser, B. S.; Cooks, R. G. Int. J. Mass Spec. Ion Proc. 1982, 44, 215-229.

4. Freiser, B. S. Int. J. Mass Spec. Ion Proc. 1980, 33, 263-267.

5. U.S. Patent Application, Serial No. 610502

6. Cody, R. B.; Burnier, R. C.; Freiser, B. S. Anal. Chem. 1982, 54, 96.

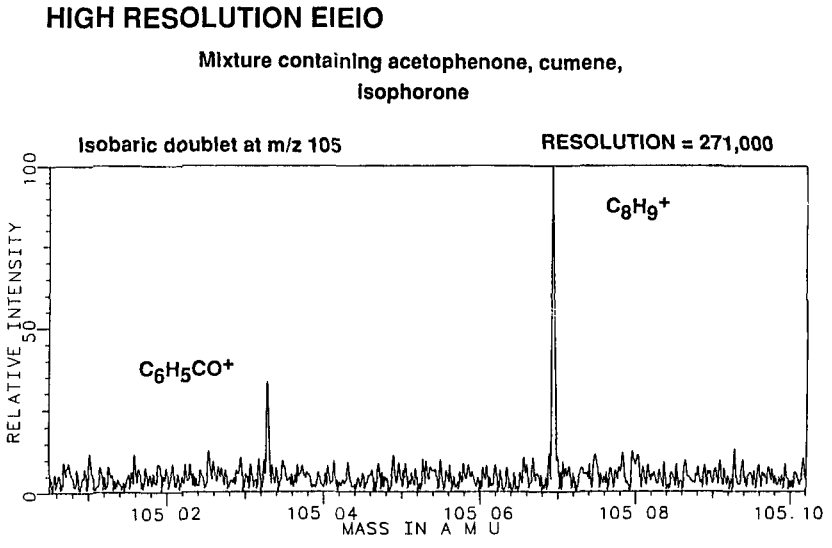

Fig. 1. High-resolution spectrum of isobaric doublet produced by electron impact excitation of the molecular ions of acetophenone and cumene in a three-component mixture.

DISSOCIATIVE AND REACTIVE COLLISIONS BETWEEN MOLECULAR IONS AND SURFACES

Md. A. Mabud and R.G. Cooks, Purdue University, Chemistry Department, West Lafayette, IN 47907.

Gaseous ions can be characterized by inducing dissociation via ion/surface interactions (1). Three different aspects of surface-induced dissociation (SID), viz. (i) the internal energy deposition (ii) the ability to characterize isomeric ions and (iii) dissociation following charge exchange of doubly-charged ions at the surface, have been investigated.

SID was found to be an efficient method of excitation of polyatomic ions. As shown in Table 1, collision of the $Si(C_2H_5)_4^{+\cdot}$ ion with a stainless steel surface at 60 eV (laboratory) deposits approximately 7 eV average internal energy, an extremely large quantity compared to gas phase excitation processes. The amount to energy deposited, and hence the extent of fragmentation, can be easily controlled by selection of the impact energy and both very low or high energy deposition can be obtained.

Table 1

Internal energy deposition in $Si(Et)_4^{+\cdot}$ during collision with a stainless steel surface

Collision energy (eV) (lab.)	Average energy deposited (eV)	Maximum energy deposited (eV)	Avg. Int. Ener. / Lab. kE %
22	3.7	7	17
25	5.1		20
30	5.8	8	19
40	5.9		15
50	6.8	11	14
60	7.0		12
65	8.5	16	13
75	8.9		12
85	10.2		12
100	12.8		13
115	13.3		12

Dissociation of polyatomic ions in ion/surface collisions is also accompanied by chemical reactions. These processes include pick-up of H, H_2 and CH_3 from the surface by the incident ion. Reactive collisions have been found useful in distinguishing closely related isomeric ions. The $C_2H_4O^{+\cdot}$ ion from acetaldehyde, 1,3-dioxolane and ethylene oxide was studied and the isomeric ions were readily distinguishable based on the extent of hydrogen abstraction and fragmentation induced by collision. This is illustrated in Figure 1. Structural information obtained in the SID daughter spectra allows one to assign structure to these ions. The power of ion/surface interactions in ion characterization lies in the fact that (i) highly excited ions fragment by easily interpreted bond cleavage reactions and (ii) reactive collisions accompany dissociative collisions and so add to the information in the daughter ion spectra.

Charge exchange of polyatomic ions upon collision with metal surfaces was investigated for doubly-charged organic ions (2). Although simple charge exchange is observed, dissociative charge exchange is far more prominant. The following sequence os events seem to occur in course of doubly-charged ion/surface interaction: (i) Doubly-charged ions approach the surface and may accept an electron to become singly-charged and internally energized. (ii) These singly-charged ions then collide inelastically with the surface and become further internally excited. (iii) These excited species leave the surface region and subsequently dissociate unimolecularly to give fragment ions.

The signal-to-noise characteristics of the SID daughter spectra are excellent even for the study of multiply-charged ions, which are formed in very low abundance in the ion source. Unlike CID, where precise pressure control of the target gas is necessary, the SID experiment is very simple and gives highly reproducible results. Typically it requires about 10 minutes to obtain high quality daughter ion spectra.

The aspects of ion/surface interactions that have been touched upon in this discussion cover only a fraction of the phenomena that offer analytical utility. We expect rapid exploitation of this subject.

References:

1) Md. A. Mabud, et al. Int. J. Mass Spectrom. Ion Proc. 67 285 (1985)
2) Md. A. Mabud, et al. Int. J. Mass Spectrom. Ion Proc. in press

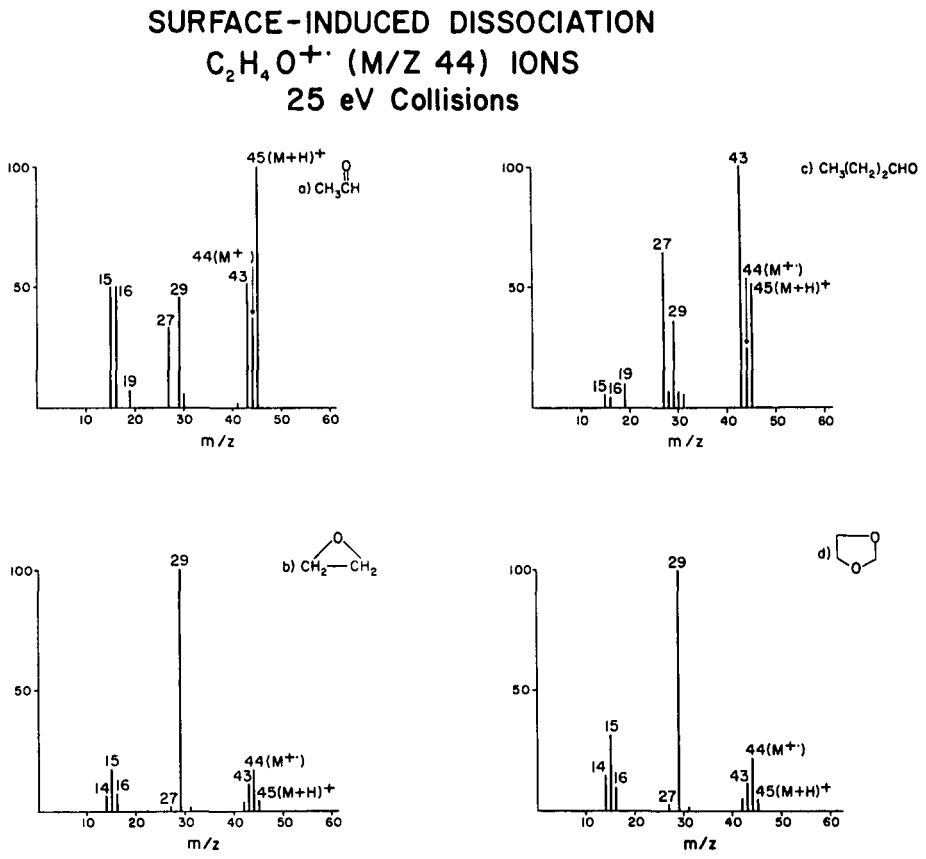

Figure 1. Comparison of daughter spectra, produced by collision at a stainless steel surface, at a laboratory kinetic energy of 25 eV, for $C_2H_4O^{+\cdot}$ ion from precursors (a) acetaldehyde (b) ethylene oxide (c) butyraldehyde (d) 1,3-dioxolane.

ISOTOPIC LABELLING STUDIES IN THE NON-RESONANT MULTIPHOTON IONIZATION/FRAGMENTATION OF ANILINE

Jeffrey A. Zimmerman and Rebecca M. O'Malley,
Chemistry Department, University of South Florida
Tampa, Florida 33620.

A major obstacle to the development of multiphoton ionization (MPI) as an analytical tool is that the mechanism of the ionization/fragmentation process is not well understood. Contrary to the fairly standard electron impact spectra obtained using 70 eV electrons, MPI fragmentation patterns reported both in the literature and recorded in this laboratory have been found to vary tremendously, depending on laser wavelength, laser pulse energy and the focusing conditions used in a particular experiment. This study of the non-resonant MPI/fragmentation patterns of aniline, aniline N15 and aniline-2,3,4,5,6-d_5 was undertaken in an attempt to identify the characteristics of the processes involved. The data presented here were obtained using a laser/time-of-flight mass spectrometer combination of equipment at laser wavelengths of 532 nm and 355 nm.

From the spectra obtained for the unlabeled aniline it is clear that the ionization process initiated by multiphoton absorption is quite different from electron impact. In the electron impact spectrum a large percentage of the ionization is observed as the molecular ion at m/z=93. The most intense fragment ion, $C_5H_6^{+\cdot}$ (m/z=66) corresponds to the loss of the neutral entity CNH from the molecular ion. In contrast, the majority of the ionization observed in both the multiphoton initiated spectra corresponds to small fragment ions, the most intense ones being observed at m/z = 12,24,26,28,38,39, and 52. In this system it is apparent that some of these ions could be N-containing. For example m/z=28 could be $C_2H_4^{+\cdot}$ or CNH_2^+ and m/z=38 could be $C_3H_2^{+\cdot}$ or C_2N^+. To identify the N-containing ions analogous data for aniline N15 were obtained. These spectra allowed the positive identification of a number of N-containing ions; the most important ones being CNH_2^+, C_2N^+, $C_3NH_2^+$ and $C_3NH_4^+$. Analysis of the spectra showed that N-containing ions formed a much larger percentage of the ions detected in the laser initiated spectra than in the electron impact spectra.

Plots of fragment ion intensity dependence on laser pulse energy showed mixed behaviour according to the classification scheme of Gedanken et al.[1], changes in relative ion intensities being observed at lower laser pulse energies, but constant fragment ion ratios at higher laser pulse energies. This seems to indicate class A behaviour (ionic ladder switching) at low laser pulse energies and class C behaviour (typical non-resonant behaviour) at higher energies. The ionic ladder switching part of the mechanism was considered further by the comparison of CAD decomposition data acquired for the N and N15 systems. This shows several ionic routes to $C_3H_3^+$, but there are no direct ionic routes to the other major ions observed: $C^{+\cdot}$, $C_2^{+\cdot}$, $C_2H_2^+$, $CNH_2^{+\cdot}$, C_2N^+, $C_3NH_2^+$. One possibility is that the neutrals eliminated in the ionic fragmentation reactions could be ionized in the laser pulse. This would give sources for CNH_2^+, $C_2H_2^{+\cdot}$, $C^{+\cdot}$ and $C_2^{+\cdot}$ (Neutral acetylene undergoes non-resonant MPI at these wavelengths to produce C^+ and $C_2^{+\cdot}$ in addition to $C_2H_2^{+\cdot}$). However, this does not account for the C_2N^+ and $C_3NH_2^+$ ions. These possibly arise from some neutral fragmentation of the aniline molecule, prior to ionization (class B behavior).

MPI data for aniline 2,3,4,5,6-d_5 show that CNH_2^+ is observed both as CNH_2^+ and CNHD and $C_2H_3^+$ is observed both as $C_2HD_2^+$ and $C_2D_3^+$, indicating that rearrangement between the H atoms initially attached to the N atom and those on the ring is an important part of the overall process.

---

1. A. Gedanken, M.B. Robin and N.A. Keubler, J. Phys. Chem., 86, 4906 (1982).

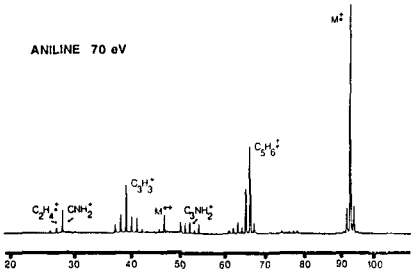

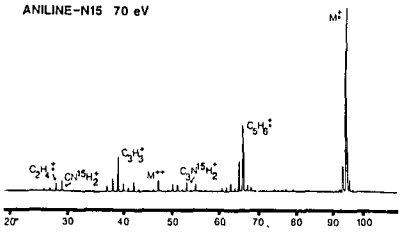

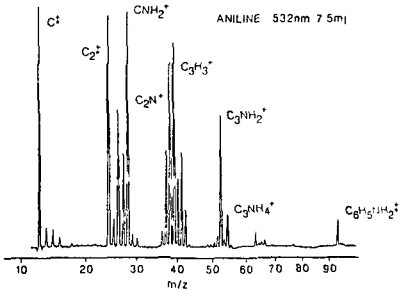

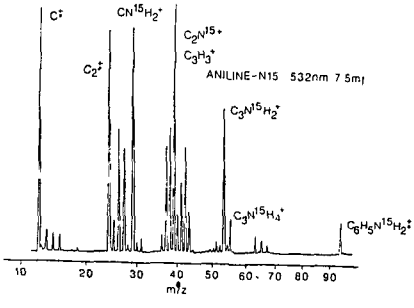

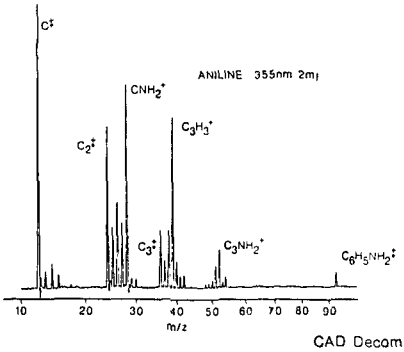

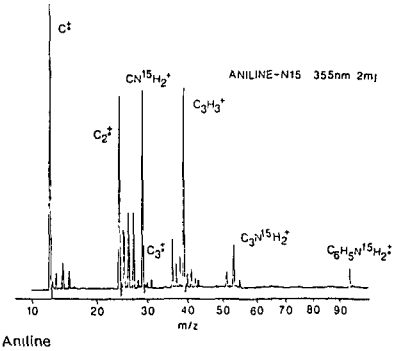

CAD Decompositions in Aniline

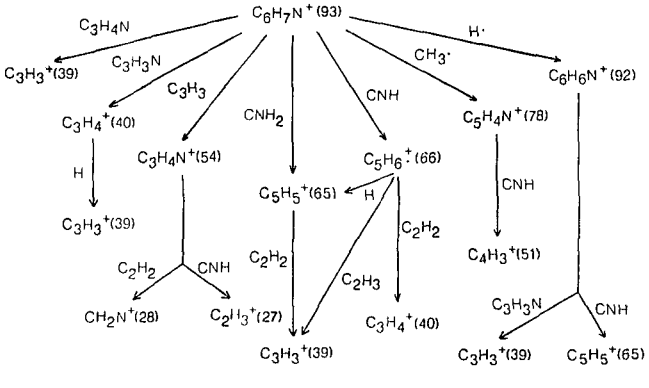

STRUCTURE ELUCIDATION OF ISOMERS BY MULTIPHOTON IONIZATION. T.C. Chang and M.V. Johnston, Department of Chemistry and Biochemistry, University of Colorado, Boulder, CO 80309-0215

A wide variety of soft ionization techniques have been developed over the past decade. By definition, these methods induce little fragmentation and therefore provide only limited structural information of molecules. When applications to structure elucidation are pursued, they must be combined with collisionally induced dissociation or laser photodissociation in a tandem experiment. On the other hand, resonant two photon ionization is a soft ionization method that can naturally incorporate a photodissociation step. At low laser powers, the parent ion alone is efficiently produced by the absorption of two ultraviolet photons through an intermediate excited electronic state. As the laser power is increased, parent ions created by two photon ionization can absorb additional photons to cause fragmentation. In principle, the degree of fragmentation can be "tuned" to meet the requirements of the experiment at hand by simply varying the laser power. We have undertaken a systematic study of C_7H_8O and $C_8H_{10}O$ isomers to illustrate the ability of parent ion photodissociation within the multiphoton ionization/fragmentation (MPI) process to extract structural information. These results are also pertinent to any photodissociation experiment using ultraviolet photons regardless of the manner in which the parent ion is formed.

Illustrative MPI mass spectra for the C_7H_8O isomers anisole, benzyl alcohol, o-cresol, and p-cresol and for the $C_8H_{10}O$ isomers phenethyl alcohol (PEA), sec-phenethyl alcohol (s-PEA), 2-methylbenzyl alcohol (2-MBA) and 4-methylbenzyl alcohol (4-MBA) are shown in Figure 1. These spectra were taken at 266 nm with a laser intensity of ca. 10 MW/cm^2. 266 nm is a convenient wavelength to compare MPI spectra since all of these compounds can be ionized by a resonance enhanced two photon ionization. The laser intensity was chosen to induce only minor fragmentation of the parent ion. With the exception of o-cresol and p-cresol, the MPI generated fragmentation patterns are sufficiently different to allow selective discrimination and identification of these structural isomers.

In the extreme statistical limit as defined by Silberstein and Levine (1), MPI fragmentation patterns are governed by the mean energy deposited into the molecule and the molecular empirical formula. Deviations from this limit are due to ion dynamical effects. Figure 1 shows that dynamical effects play an important role in the fragmentation of these isomers since the mass spectra are different.

The fragment ions observed in Figure 1 are also found in 70 eV electron impact ionization mass spectra and in daughter ion scans of the parent ions undergoing collisional activation. However, many high m/z fragments which are prominent in EI and CAD spectra are weak in relative abundance or missing entirely from the corresponding MPI spectrum regardless of laser power. For example, m/z 107 fragments of benzyl alcohol and s-PEA are not observed in the respective MPI mass spectra even at very low laser power. In order to illustrate this point more clearly, 70 eV EI and MPI mass spectra of s-PEA are compared in Figure 2. No laser power can be found where m/z 107 is efficiently produced in the MPI mass spectrum.

The bias of parent ion fragmentation in MPI toward low mass, high energy species can be rationalized by the parent ion internal energy produced by the absorption of one ultraviolet photon. Photon absorption leads to a narrow energy distribution of the excited parent ions at the photon energy (4.66 eV for 266 nm radiation). Thus, all parent ions dissociate from the same high energy point on the breakdown curve. The high average internal energy for an ensemble of ions promotes fragmentation to smaller mass species while the narrow energy distribution discriminates against lower energy processes. This effect has been recently demonstrated in calculations of branching ratios for the unimolecular dissociation of energy selected benzene ions (2).

References:

1. J. Silberstein and R.D. Levine, J. Chem. Phys. (1981) 75, 5735.

2. J. Silberstein, I. Salman, R.D. Levine, J. Phys. Chem. (1985) 89, 5573.

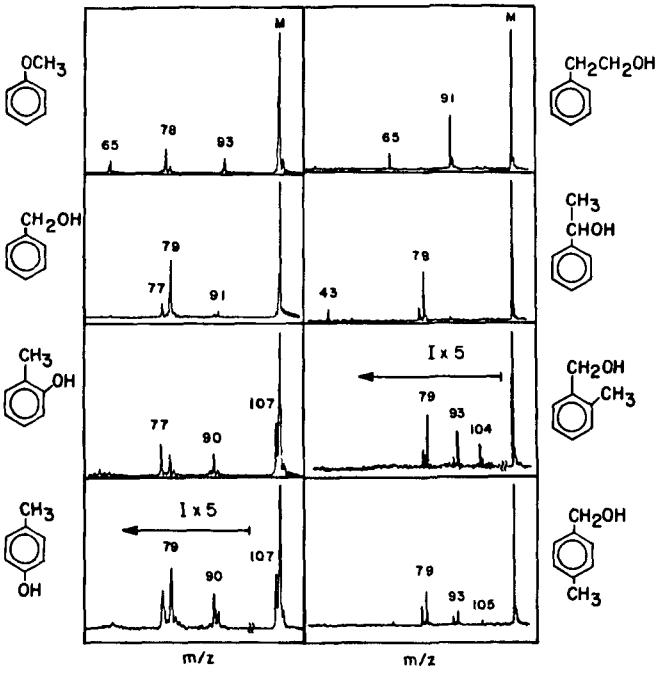

Figure 1: MPI mass spectra of C_7H_8O and $C_8H_{10}O$ isomers using radiation at 266 nm.

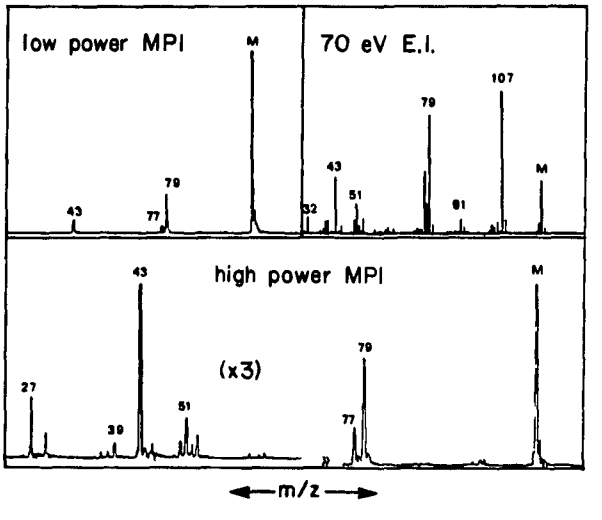

Figure 2: EI and MPI mass spectra of sec-phenethyl alcohol.

Paper Number ROC 10

Simplification of Ion Photodissociation Spectra

S.P. Goss and J.D. Morrison
Chemistry Department, La Trobe University, Melbourne, Australia

It was originally believed that while electron impact could produce ions in various excited electronic states, after analysis, ~30μS later, all of these would have reverted to their ground states. Ion photodissociation experiments showed that this was not the case, and that significant populations of excited states are formed in many ions which survive mass analysis, and can be detected in subsequent photo-fragmentation. This is the case even where the deexcitation process involves an allowed transition as, for example, in the halogen cations, and would have been expected to have occurred in 10^{-8} second.

When photofragmentation occurs by a predissociation mechanism very detailed absorption spectra can be observed for the precursor ion by this means. When the precursor ion is formed populating only a few sharply defined rovibronic states, as occurs for example with CH_3I^+, it is a relatively simple matter to assign it.

For SO_2^+, photodissociation with visible light can take place only from excited states of the parent ion, and the photoelectron spectrum, PES, indicates that transitions are occurring from the $\tilde{A}$ and $\tilde{B}$ electronic states of the ion, to the $\tilde{C}$ and less probably to the $\tilde{D}$ and $\tilde{E}$ states. The Franck Condon intersections for the latter all lie above the first dissociation limit for the $\tilde{X}$ ground state of the ion leading to $SO_2^+ \rightarrow SO^+ + O$, and predissociation occurs. All of these states show extended rovibrational progressions, so that a most complex IPD spectrum is obtained, consisting of very many shaded bands.

At first sight, it would seem an easy matter using the vibrational information from the PES, to interpret the IPD spectrum in terms of $\tilde{C} \leftarrow \tilde{A}$ and $\tilde{C} \leftarrow \tilde{B}$ transitions. As it turns out, the resolution of the PES data is around 20 meV, while the resolution of the IPD data is ~10μeV, and it is a matter of great difficulty to make this assignation. We believe our spectrum is due mainly to $\tilde{C} \leftarrow \tilde{B}$ transitions, Paulson and co-workers believe it is due to $\tilde{C} \leftarrow \tilde{A}$.

Further progress is possible only if the IPD spectrum can be simplified. We have achieved this recently, using resonant charge transfer in the ion source from the $^2P_{1/2}$ level of Xe^+ to excite selectively what we believe to be the $\tilde{B}$ (030) level (Figure 1).

We are also exploring other methods for achieving such spectral simplification. Varying the ionizing electron energy in the source has proved successful in the cases of O_2^+ and the halogen cations, where the precursor states are separated by several ev. It does not give conclusive evidence for SO_2^+. Since the IPD spectrum is essentially the convolution of two comb functions, the population distribution for the precursor state and that for the product state, if one had data for one or other of these states, it might be possible to simplify the IPD spectrum by a deconvolution process.

A synthetic IPD spectrum was generated, noise added, and the effect of deconvoluting this by the iterative and Fourier Transform methods tested. The iterative method failed, but using the Fourier Transform method, with stick functions for the precursor state, even when significant

distortion was introduced in the spacings and intensities of the vibrational lines in this, the correct positions and numbers of the lines in the product state could be obtained (Figure 2). We are presently applying this method to the SO_2^+ data.

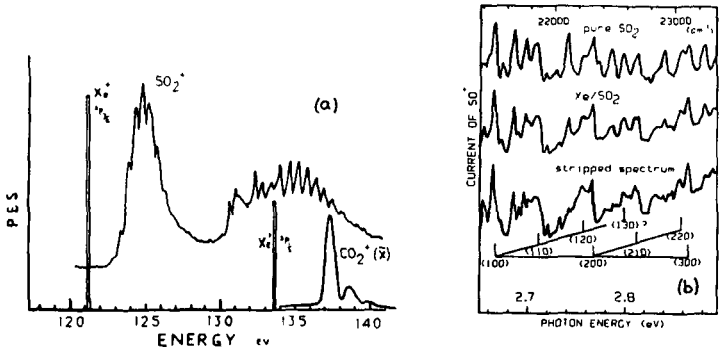

Fig 1 (a) PES for SO_2, Xe, and CO_2 showing possibilities for resonant charge transfer
(b) SO_2 photodissociation spectra, pure and selectively excited with Xe $^2P_{1/2}^+$

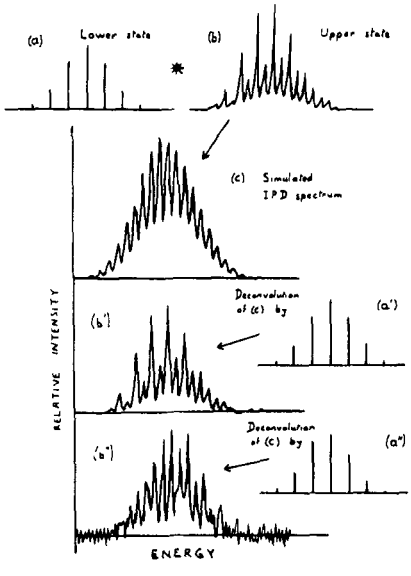

Fig 2 Deconvolution as a means of simplifying a simulated IPD spectrum

Laser-Ion Beam Photodissociation Studies: The Dissociation Reactions of $Fe_3(CO)_x^+$ and $Co_4(CO)_x^+$.

R.E. Tecklenburg, Jr., and D.H. Russell

Texas A&M University
Department of Chemistry
College Station, TX 77843

The study of gas phase transition metal compounds and clusters has been the focus of a large number of research groups in recent years.[1,2,3] One of the major thrusts behind this research has been to gain a better understanding of the reactive and intrinsic properties of these transition metal compounds. Laser-ion beam photodissociation techniques have recently been used to study the unimolecular dissociations and excited states of transition metal cluster fragment ions.[4] Most of these ions photodissociate readily at visible wavelengths due to their large visible absorption cross-sections and relative weak metal-metal and metal-ligand bond strengths (< 50 kcal/mole). Studies on the photodissociation reactions of transition metal cluster carbonyl fragments should provide structural information on these systems, as well as estimates of bond dissociation energies, D(M-CO), and D(M-M), derived from photodissociation thresholds.

The present work investigates the visible wavelength photodissociation of transition metal fragment ions formed the 70 eV electron impact of $Fe_3(CO)_{12}$, and $Co_4(CO)_{12}$. The photodissociation apparatus consists of a Kratos MS-50TA mass spectrometer, Coherent CR-18 argon-ion, and CR-599 dye lasers. Presently we are studying the dissociation reactions of $Fe_3(CO)_x^+$, (x=4-12) and $Co_4(CO)_x^+$, (x=0-12), as well as the bare metal cluster fragment ions e.g. Co_4^+, Co_3^+, Co_2^+. Two wavelength ranges are used to examine photodissociation reactions occurring in the first field free region of the mass spectrometer; 458-514.5 nm and 581-651 nm, which vary in power from 10W to 100mW. Relative photodissociation cross-sections are measured and plotted against laser wavelength for each photodissociating ion. The photodissociation cross-sections are normalized for variations in laser power at each wavelength, total ion current, photofragment peak intensities, and signal averager gains. Metal-metal and metal-ligand binding energies can be estimated for those ions whose photodissociation cross-sections tend toward zero above some critical threshold wavelength. Tables I and II list the measured metal-metal and metal-carbonyl bond energies for iron and cobalt cluster fragment ions, respectively. The measured bond dissociation energies, however, are found to lie substantially below, (20-35%), the average bond energies determined by thermochemical methods for neutral $Fe_3(CO)_{12}$ and $Co_4(CO)_{12}$.[5] To explain these results, one has to assume that electron impact ionization produces ions with substantial amounts of internal energy. In our laboratory, studies are underway to investigate the excess internal energy distributions of these ions, and what effect this has on the appearance of the photodissociation spectra, as well as the measured bond dissociation energies (D(M-CO), and D(M-M)). To probe this question, the transition metal cluster fragment ions are collisionally stabilized using argon bath gas in a high pressure chemical ionization source. As can be seen in Figure 1, loss of three carbonyl ligands from the molecular ion of $Fe_3(CO)_{12}$ is preferred over loss of two by electron impact ionization. When this same ion is collisionally stabilized prior to a cross-beam photodissociation experiment in the third field free region of the mass spectrometer, loss of two carbonyl ligands is found to be the dominant fragmentation pathway. This result suggests that accurate measurements of bond dissociations derived electron impact photodissociation studies, requires that the hot ions be cooled prior to photoactivation.

1. Armentrout, P. B.; Beauchamp, J. L. *J. Am. Chem. Soc.* **1981**, *103*, 6628.
2. Byrd, G. D.; Frieser, B. S. *J. Am. Chem. Soc.* **1982**, *104*, 1238.
3. Anderson Fredeen, D. J.; Russell, D. H. *J. Am. Chem. Soc.* **1985**, *107*, 3762.
4. Jarrold, M. F.; Misev, L.; Bowers, M. T. *J. Phys. Chem.* **1984**, *88*, 3928.
5. Connor, J. A.; Skinner, H. A.; Virmani, Y. *Faraday Symp. Chem. Soc.*, **1984**, *8*, 18.

Table I. The measured metal-carbonyl bond energies for iron cluster fragment ions.

TRANSITION	THRESHOLD (nm)	THRESHOLD (kcal/mol)	THRESHOLD ENERGY ÷ BONDS BROKEN (kcal/mol)
$Fe_3(CO)_6^+ \rightarrow Fe_3(CO)_4^+$	627.7	45.5	45.5
$Fe_3(CO)_6^+ \rightarrow Fe_3(CO)_4^+$	627.7	45.5	22.8
$Fe_3(CO)_7^+ \rightarrow Fe_3(CO)_4^+$	616	46.4	15.5
$Fe_3(CO)_7^+ \rightarrow Fe_3(CO)_6^+$	640	44.7	22.3
$Fe_3(CO)_8^+ \rightarrow Fe_3(CO)_6^+$	616	46.4	23.2
$Fe_3(CO)_9^+ \rightarrow Fe_3(CO)_7^+$	627.7	45.5	22.8
$Fe_3(CO)_{10}^+ \rightarrow Fe_3(CO)_8^+$	640	44.7	22.3
$Fe_3(CO)_{12}^+ \rightarrow Fe_3(CO)_{10}^+$	640	44.7	22.3

Table II. The measured metal-metal and metal-carbonyl bond energies for cobalt cluster fragment ions.

TRANSITION	THRESHOLD (nm)	THRESHOLD (kcal/mol)	THRESHOLD ENERGY ÷ BONDS BROKEN (kcal/mol)
$Co_2^+ \rightarrow Co_2^+$	>514.5	<55.6	<37.8
$Co_4^+ \rightarrow Co_2^+$	>514.5	<55.6	<11.1
$Co_4^+ \rightarrow Co_3^+$	604	47.3	15.8
$Co_4(CO)_7^+ \rightarrow Co_4^+$	627.7	45.5	22.8
$Co_4(CO)_8^+ \rightarrow Co_4(CO)^+$	640	44.7	22.3
$Co_4(CO)_8^+ \rightarrow Co_4(CO)_6^+$	640	44.7	22.3
$Co_4(CO)_9^+ \rightarrow Co_4(CO)_6^+$	>640	<44.7	<22.3
$Co_4(CO)_7^+ \rightarrow Co_4(CO)_5^+$	>651	<43.9	<21.9
$Co_4(CO)_8^+ \rightarrow Co_4(CO)_6^+$	627.7	45.5	22.8
$Co_4(CO)_{11}^+ \rightarrow Co_4(CO)_9^+$	616	46.4	23.2
$Co_4(CO)_{12}^+ \rightarrow Co_4(CO)_{10}^+$	640	44.7	22.3

Figure 1 (a) Photodissociation spectra for $Fe_3(CO)_{12}^+$ when the ions are produced by 70 eV electron impact, and (b) when $Fe_3(CO)_{12}^+$ is collisionally stabilized prior to photoactivation.

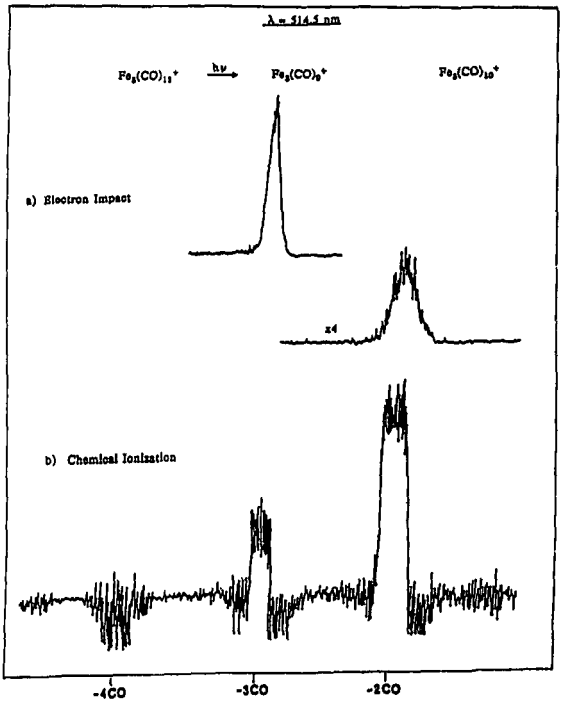

INFRARED MULTIPHOTON DISSOCIATION OF SOME PROTONATED OXYGEN-CONTAINING HYDROCARBONS. COMPETITIVE PHOTODISSOCIATION CHANNELS AND THEIR RELATIONSHIP TO MULTIPLE PROTONATION SITES.

G. Baykut, C. H. Watson and J. R. Eyler, Department of Chemistry, University of Florida, Gainesville, FL 32611

Infrared multiphoton dissociation of protonated 1,2-dimethoxyethane, bis(2-methoxyethyl)ether, 1,2-bis(2-methoxyethoxy)ethane, bis[2-(2-methoxyethoxy)ethyl]ether, 3-butoxyethanol, 2-(2-methoxyethoxy)ethanol, 2-(2-ethoxyethoxy)ethanol 2-(2-butoxyethoxy)ethanol and 2-phenoxyethanol has been studied using a Fourier transform ion cyclotron resonance mass spectrometer (FTICR) and a continuous wave CO_2 laser, gated by a trigger pulse from the FTICR.

Since protonation lowers the C-O bond dissociation energy, cleavage of C-O bonds has been observed following laser irradiation of the protonated molecules. Water loss from protonated alcohols and loss of alcohol as neutral photofragment were the common dissociation pathways:

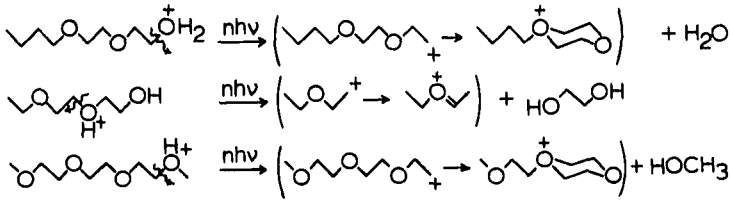

In some cases the mechanism of the photodissociation could be explained with a rearrangement process:

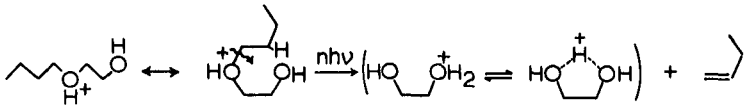

In those dissociations the photofragment appeared to be a protonated alcohol.

The infrared multiphoton dissociation of the protonated alcohols and polyethers gave information about the site of protonation. The further photodissociation of primary dissociation products was also observed quite often:

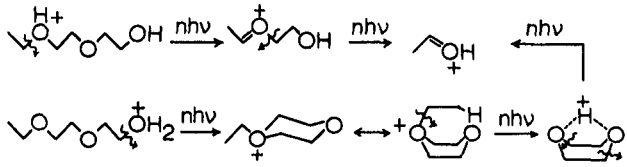

A variable time period inserted between the protonation of molecules and the photodissociation changed the photodissociation pattern. For example protonated bis(2-methoxyethyl)ether, m/z 135, photodissociates to produce m/z 103 and 59,[1]

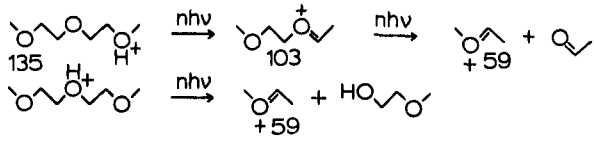

Ejection of the m/z 103 ion permits the direct photodissociation pathway m/z 135 → m/z 59 to be observed. The peak intensity of the m/z 59 product decreases with the increasing time delay before photodissociation, which can be related to the formation of a more stable intramolecular proton bond involving the two methoxy oxygens[2] since the ion loses its energy by nonreactive collisions during the "waiting" time. Intermolecular proton exchange can also be considered as an alternative relaxation process.

References

1 G. Baykut, C. H. Watson, R. R. Weller and J. R. Eyler, J. Am. Chem. Soc. 107 (1985) 8036.
2 M. Meot-Ner (Mautner), J. Am. Chem. Soc. 105 (1983) 4906.

INFRARED MULTIPHOTON DISSOCIATION OF LASER DESORBED IONS

C. H. Watson, G. Baykut, and J. R. Eyler, University of Florida, Department of Chemistry, Gainesville, Florida 32611

The technique of laser desorption (ld) has been widely used in mass spectrometry to desorb and ionize high molecular weight or other nonvolatile samples and it has the great advantage that abundant molecular or pseudomolecular ions are produced. Positive pseudomolecular ions are most often formed by attachment of a cation, typically a proton or potassium or sodium cation, to the parent molecule. Negative pseudomolecular ions can also be formed by laser desorption, usually by loss of a proton. Often little fragmentation occurs and a strong molecular ion signal (M^+, $(M + H)^+$, $(M + Na)^+$, $(M + K)^+$, M^-, or $(M - H)^-$) provides molecular weight information.

Fragmentation is also often desirable in mass spectrometry to characterize and identify molecular structure. One active line of research in our lab has been the use of infrared lasers to photodissociate gaseous ions to obtain both structural and energetic information. We have found that irradiation of moderately large ions by continous and pulsed infrared lasers often results in photodissociation. Thus, large molecular or pseudomolecular ions of high mass-to-charge ratio produced by laser desorption can be fragmented by an infrared laser pulse.

Light from a Lumonics TE 860 CO_2 grating-tuned pulsed infrared laser enters the vacuum chamber of our Nicolet FTMS 1000 mass spectrometer (Fticr) through a ZnSe window and is focussed by a 0.5 inch ZnSe lens onto a solids probe containing the analyte (see Figure 1a). The pulsed laser produces a 2.6 joule pulse of one microsecond duration at 10.61 micrometers and has a 2 X 3 cm. rectangular beam shape. The ions formed by laser desorption are trapped inside the modified analyzer cell of our mass spectrometer. An unfocussed laser pulse from either the pulsed laser or an Apollo 570 continous wave (cw) laser irradiates the ions, causing them to dissociate (see Figure 1b and 1c). The cw laser has a maximum output power at 10.61 micrometers of 50 watts and a beam diameter of 6 millimeters.

In the two laser experiment the conventional solids probe was replaced by a NaCl window mounted on a hollow tube which extended into the vacuum chamber to within a few millimeters of the Fticr cell. The analyte was dissolved in either acetone or ethanol and placed on the end of the tube opposite the window and nearest the cell with a micropipette. This assembly served as both sample support and as a second window for laser irradiation of the ions.

The sucrose negative ion mass spectrum following laser desorption revealed a $(M - 1)^-$ ion at m/z 341. When irradiated with the cw laser this ion dissociated with production of ions at m/z 251, 249, 179 and 161.

With hesperidin, the negative ion ld mass spectrum of this compound indicated that an ion of m/z 612 was produced. This ion was observed to dissociate by loss of the attached sugar, and produced an ion at m/z 301 when irradiated by the cw laser.

In the 2-ethyl-(5,5-diphenyl-2,4-imidazolidinedione)-7-acetoxy-1-naphthyl sulfonamide negative ion ld mass spectrum an ion at m/z 500 originating from loss of C_2H_3O was observed. This ion photodissociated when irradiated by the cw laser to produce an ion at m/z 251. High resolution mass analysis of the ion at m/z 251 indicated that it has the empirical formula $C_{15}H_{11}N_2O_2$.

In the tertbutylpyridinium perchlorate positive ion mass spectrum the parent cation at m/z 136 was observed. When it was irradiated with a second unfocussed laser pulse from the pulsed laser a fragment ion, $C_5H_6N^+$, at m/z 80 was observed.

The feasibility of using infrared laser photodissociation to further fragment ions produced by laser desorption has been demonstrated for moderate molecular weight compounds. This technique should work equally well for both positive and negative ions formed by laser desorption. However, for the compounds studied to date negative ion laser desorption usually produced much higher intensities of molecular or pseudo-molecular ions than the corresponding positive ion mode.

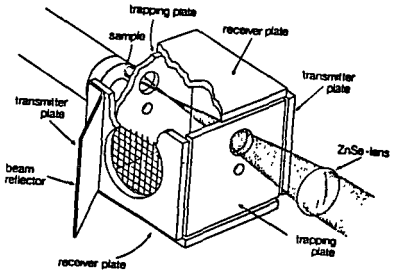

Figure 1a.
Focussed light from a pulsed infrared laser forms ions by laser desorption.

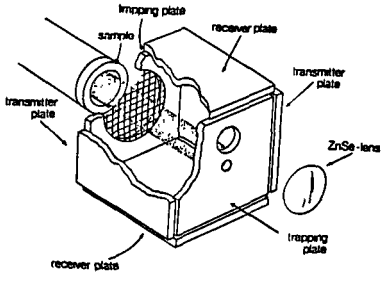

Figure 1b.
Light from a continuous wave infrared laser enters the cell through a salt window and tube assembly to dissociate trapped ions.

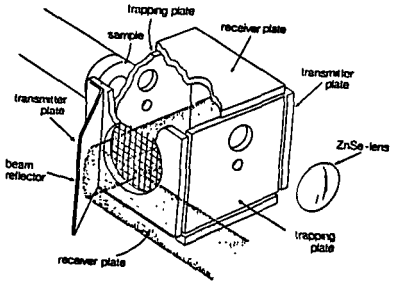

Figure 1c.
Alternatively an unfocussed pulse of light from the pulsed laser can be reflected into the analyzer cell to dissociate trapped ions.

THE PHOTOFRAGMENTATION OF METHYLHEXENES IN A FT-ICR MASS SPECTROMETER

M.Bensimon, T.Gäumann and J.Rapin*

Institut of Physical Chemistry
Federal School of Technology
CH-1015 Lausanne, Switzerland

The unimolecular dissociation of olefinic molecular ions is complicated to describe because the double bond can shift through the molecule. This means that the charge is not localized and that the original position of the neutral fragments lost may not be evident. The combination of a FT-ICR mass spectrometer and a CO_2 laser gives the possibility to trap a specific ion and to energize it very softly inducing photofragmentation at the fragmentation threshold. The infrared spectrum of molecular ions, i.e. the rate constant for photofragmentation as a function of the laser wavelength for a specific fluence, is studied for three different methylhexenes: 2-methyl-1-hexene, 2-methyl-2-hexene and 5-methyl-2-hexene and some of their ^{13}C and D labelled isotopomeres. The intensity of the molecular ion of 2-methyl-3-hexene is too small to give reasonable results with photofragmentation.

The loss of ethylene as a neutral fragment which is a minor pathway within the ion source, becomes the major reaction for metastable decay within a classical instrument and the only fragmentation for photofragmentation. The origin of this loss is compared for reactions within the source, the metastable decay and the photofragmentation.

The apparatus and mode of operation is the same as described in a previous publication [1]. The working pressure is below 10^{-8}torr; the molecular ions suffer no collision during the measuring period.

Infrared spectrum: The infrared spectra of the three isomeric neutrals differe in absorbance or in position and structure of the lines. The infrared spectrum of the ions are also different from one another; however they show a similarity to the neutrals in terms of absorbance and structure. They are shifted by about 60 wavenumbers in the same direction. This consideration allows us to assume that the molecular ion keeps the information about the original structure of the neutral.

^{13}C Labelling: Although the loss of ethylene seems to be a simple reaction, it can be shown with ^{13}C labelling that most of the ethylene is lost from three carbon positions, the ratio of their participation changes from one isomer to the other. One explanation is that this reaction goes through three different transitions states of nearly the same energy but that the probability for each transition state is different from one isomer to the other. There is no evidence for carbon scrambling in this fragmentation

^{13}C and D Labelling: Measurements with 2-methyl-1-hexene-3-D_2-4-^{13}C shows a partial randomisation of the hydrogen in the fragment lost. The randomisation of H can only be observed with a shift of the double bond or of the charge, that means with the loss of the information about the structure of the original molecular ion which is inconsistent with the previous observation One explanation may be that the randomisation is accomplished at the transition state.

Litterature:

[1] Advances in Mass Spectrometry X, Swansea Conference, 1986
John Wiley and Son Ltd.

INTERNAL ENERGY DEPOSITION IN ION TRAP MASS SPECTROMETRY

John N. Louris, Jenny Brodbelt and R. Graham Cooks, Purdue University, West Lafayette, IN 47907; George Stafford and John Syka, Finnigan MAT, San Jose, CA 95134.

Quadrupole ion trap ms/ms, the newest method of performing tandem spectrometry, shares with ICR ms/ms the characteristic that the parent and daughter ions are separated in time, rather than in space. The ion trap technique has been described earlier, and preliminary results have been reported [1]. Briefly, ions are produced and trapped in the RF-only mode, and then ions of a particular m/z are excited into trajectories of larger amplitude by the application of a supplementary RF voltage across the two end-electrodes of the trap. The increased velocity of the ions promotes the production of daughter ions through CID processes.

Figure 1 shows the effect of applying a supplementary RF voltage when recording the daughter spectrum of nitrobenzene, with and without the relatively high pressure of He usually used in the trap [2]. Figure 1a shows that in the absence of the supplementary RF voltage and without added He, little fragmentation occurs. Surprisingly, the addition of He, Figure 1b, actually inhibits fragmentation. Presumably, collisional damping decreases the velocity of the parent ion, thereby reducing fragmentation. We have observed similar inhibitions of fragmentation by the addition of He to ions derived from a variety of compounds. Figure 1c shows the effect of applying the supplementary RF voltage in the absence of added He; the parent ion peak is broadened, but little fragmentation is induced. Lastly, Figure 1d shows the result of application of the supplementary RF voltage in the presence of added He; the parent ion is very efficiently converted to fragment ions. The efficiency of conversion and detection of fragment ions in ion trap ms/ms can be quite remarkable.

We have studied the fragmentation of the molecular ion of tetraethylsilane, whose major fragmentation pathway consists of several consecutive reactions with known activation energy, as a probe of internal energy deposition in ion trap ms/ms:

$$\underset{\text{m/z 144}}{(C_2H_5)_4Si^{+\cdot}} \xrightarrow[\mathcal{E} = 0.5\ \text{V}]{} \underset{\text{m/z 115}}{(C_2H_5)_3Si^{+}} \xrightarrow[\mathcal{E} = 2\ \text{V}]{} \underset{\text{m/z 87}}{(C_2H_5)_2SiH^{+}} \xrightarrow[\mathcal{E} = 3.5\ \text{V}]{} \underset{\text{m/z 59}}{(C_2H_5)SiH_2^{+}}$$

Figures 2 through 8 illustrate the effect of various operating parameters on the daughter spectrum. Figure 2 shows that in the absence of a supplementary RF voltage but with a trapping time of up to 1000 ms, the molecular ion disappears and is replaced by an ion of m/z 133. This reaction may be rationalized as the substitution of water for one of the ethyl groups, or the addition of water to the m/z 115 fragment. Such ion-molecule reactions are conveniently promoted and studied in the trap, and the use of ms/ms in conjunction with the use and study of ion-molecule reactions is developing rapidly (for example, CI followed by ms/ms).

Figure 3 shows the effect of varying the trapping parameter q, while leaving the supplementary RF voltage and trapping time constant. At very low q values the parent ion is ejected without forming fragments. At higher q values, the parent is efficiently converted into m/z 115 and at higher q values still, m/z 87 and m/z 59 appear. However, as q is raised the mass range that can be trapped is decreased so that the lower mass fragments can not be trapped at higher q values.

Figure 4 shows the result of varying the excitation voltage at constant q and trapping time. At lower voltages m/z 115 is produced exclusively, and at the highest voltages all peaks are of low intensity because most of the parent ion is ejected without producing trapped fragments.

Figures 5-8 show the time course of the fragmentation reaction at different voltage levels. At the lowest voltage levels, about 10 ms are required for complete conversion of the parent ion, but at higher voltage levels the reaction is complete within 1 ms. Also, an apparent energy deposition of at least 3 eV is achieved at the highest voltage.

In summary, the conversion of parent ion to daughter ions can be very efficient in ion trap ms/ms. Appropriate manipulation of the excitation voltage, frequency, and duration allows control of energy deposition over a wide range. Ion/molecule reactions as well as collision-activated dissociation are accessible for investigation.

References

1. Kelley, et al., Thirty-third Annual Conference on Mass Spectrometry and Allied Topics, p. 707.
2. Stafford et al., International Journal of Mass Spectrometry and Ion Processes, 60 (1984) 85-98.

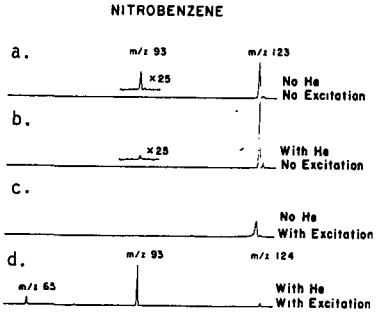

Figure 1

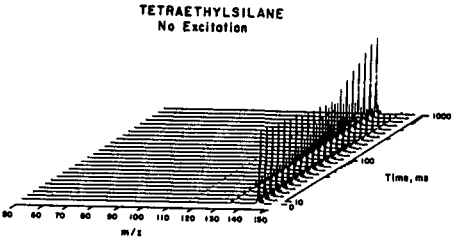

Figure 2

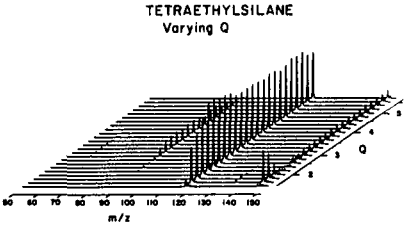

Figure 3

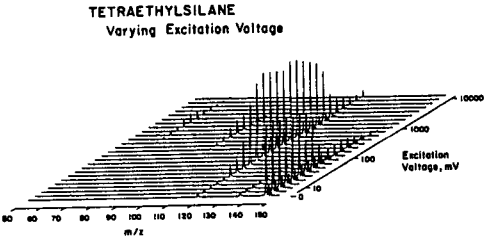

Figure 4

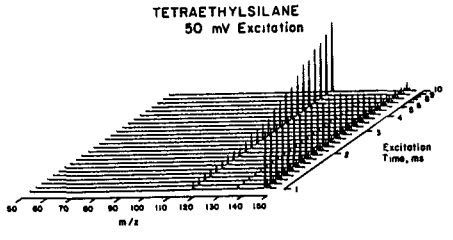

Figure 5

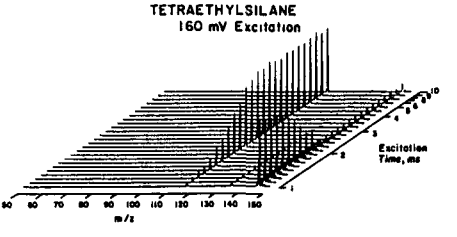

Figure 6

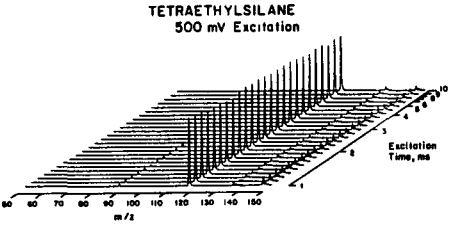

Figure 7

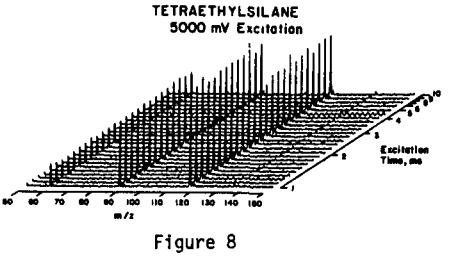

Figure 8

FAST ATOM BOMBARDMENT MASS SPECTROMETRY OF POLAR COMPOUNDS IN VEGETABLE OILS, R. A. Sanders, B. A. Charpentier, T. Keough; The Procter & Gamble Company, Winton Hill Technical Center, 6071 Center Hill Road, Cincinnati, OH 45224.

INTRODUCTION: Polar components in vegetable oils have not been particularly well characterized because of the difficulty of obtaining quality spectral information on complex mixtures of compounds which are not amenable to gas chromatography. This paper presents fast atom bombardment (FAB) conditions and results for several representatives of a class of polar compounds found in vegetable oils: flavonols and flavonol-glycosides[1-4]. The results presented here were obtained from standards, and demonstrate that FAB can provide valuable identification information for these compounds which have traditionally required derivatization. Preparative liquid chromatographic procedures for isolating these compounds from vegetable oils have been developed, and FAB offers complementary structural information to be used with IR and NMR information on the isolated fractions.

EXPERIMENTAL: All of the flavonoids analyzed dissolved readily in thioglycerol and yielded $(M+H)^+$ ions. Some of them (e.g., rutin and naringin) also worked in glycerol, but thioglycerol was more generally successful and produced fewer interferences in the mass range of interest.

Samples were analyzed on each of the following instruments: VG-ZAB2f and Kratos MS-30. Both were equipped with Ion Tech saddle field guns and were operated in the positive ion mode. The ZAB was operated at 8kV accelerating potential; the MS-30 at 4kV. MS/MS spectra were achieved with an electric sector scan of the ZAB (MIKES).

RESULTS & DISCUSSION: Table I lists the flavonoids analyzed along with their molecular weights and the aglycone molecular weights. Figure 1 shows the FAB spectrum of the aglycone quercitin in thioglycerol. The protonated molecule at m/z 303 also occurs in the flavonol-glycosides which have quercitin (or an isomer) as the aglycone. Figure 2 is the FAB spectrum of rutin (in thioglycerol) -- a rhamnosyl-glucose derivative of quercitin. The molecular weight (610) is clearly delineated with ions at m/z 611 and a sodium adduct ion at m/z 633. The aglycone molecular weight (302) is indicated with the fragment at m/z 303. Figure 3 is a FAB spectrum of naringin with glycerol as the matrix. Again, $(M+H)^+$ is clearly present (m/Z 581) along with the aglycone fragment at m/z 273. In addition, an ion at m/z 673 corresponds to the naringin-glycerol protonated complex. Prunin, with the same aglycone, also yields an ion at m/z 273 along with the protonated molecule at m/z 435, as shown in Figure 4. Rhiofolin (FAB spectrum in Figure 5) differs from naringin only by the presence of a double bond in ring 2 of the aglycone. The corresponding ion mass shifts to m/z 579 and m/z 271 are observed. Figure 6 shows the thioglycerol FAB spectrum of poncirin with $(M+H)^+$ at m/z 595 and protonated aglycone at m/z 287.

It is clear that fast atom bombardment provides information valuable for identifying flavonol-glycosides in the form of aglycone and intact molecular weight determinations. It is also desirable to be able to distinguish between flavonoid isomers such as hesperidin and rutin. Their normal FAB spectra are very similar and any minor differences are obscured by matrix ions. However, by observing the collision-induced-dissociation spectra of the protonated aglycones (m/z 303), the two isomers are readily distinguished as shown in Figure 7. Large fragments at m/z 177 and 195 are characteristic of the aglycone of hesperidin but are completely missing in the aglycone of rutin.

CONCLUSION: Flavonols and flavonol-glycosides may be identified without derivatization using positive ion fast atom bombardment mass spectrometry. Thioglycerol was an acceptable matrix and the protonated molecular ions and protonated aglycone ions were observed for all flavonoids studied here. MS/MS provides the additional capability of distinguishing between isomeric aglycones.

1. DeKoster, Heerma and Nieman, "Fast Atom Bombardment of Flavonols", Biomed. Mass Spectrom., 12, 596, 1985.
2. Domon and Hostettmann, "Mass Spectrometric Studies of Underivatized Polyphenolic Glycosides", Phytochemistry, 24, 575, 1985.
3. Nawwar, El-Sissi and Barakat, "Flavonoid Constituents of Ephedra Alata", Phytochemistry, 23, 2937, 1984.
4. Sakushima, West and Brandenberger, "Positive and Negative Ion Mass Spectrometry of Some Flavonoid Glycosides and Glucuronides", Iyo Masur Kenkyukai Koenshu, 9, 217, 1984.

TABLE I

Molecular Weights

Flavonoid	MW	Aglycone MW
Quercitin	302	302
Rutin	610	302
Hesperidin	610	302
Naringin	580	272
Prunin	434	272
Rhiofolin	578	270
Poncirin	594	286

1

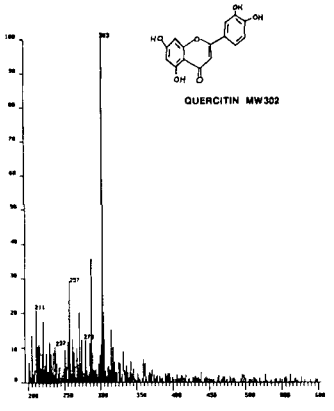

2

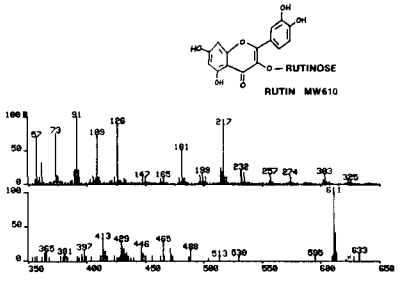

3

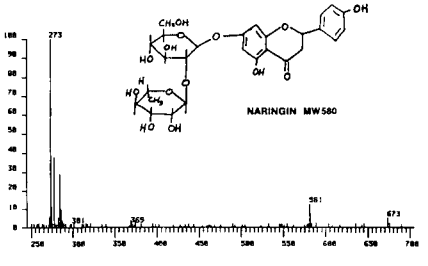

4

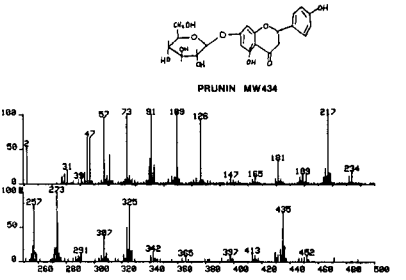

5

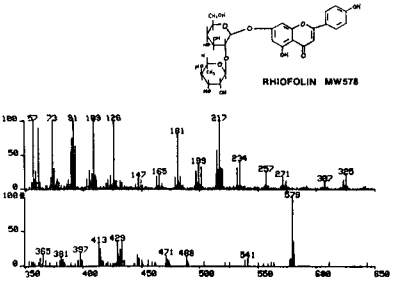

6

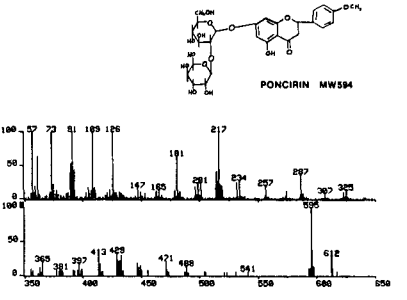

7

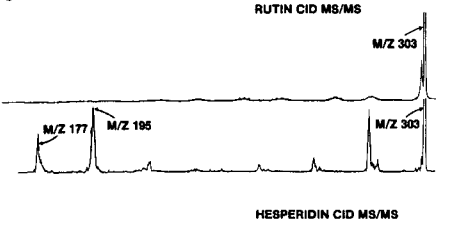

APPLICATION OF PATTERN RECOGNITION TO METAL ION CHEMICAL IONIZATION MASS SPECTROMETRY FOR TEN TRANSITION METAL IONS WITH KETONES, ALDEHYDES AND ETHERS

R. A. Forbes, E. C. Tews, Y. Huang, and B. S. Freiser*
Chemistry Department, Purdue University
S. P. Perone
Lawrence Livermore National Laboratory

I. Introduction.

Transition metal ions hold promise as selective chemical ionization (CI) reagents for mass spectrometry, since a wide variety of metals with differing reactivities may be used. Pattern recognition techniques have been used to analyze the data from this new and emerging ionization method with two basic objectives. First, pattern recognition accuracies provide a quantitative measure of the ability to discriminate classes of compounds using metal ion chemical ionization (MICI) data. Second, feature selection provides a means for finding the chemical basis for the discrimination by extracting just the relevant mass peaks from the set of all observed masses.

II. Experimental.

The data for the pattern recognition analysis were obtained using a Fourier transform mass spectrometer (FTMS) equipped with a laser ionization source (1). Metal ions were formed by focusing the beam of a Quanta-Ray Nd-YAG laser onto pure metal rods located on the cell plates of the spectrometer. The chemical ionization mass spectra for 10 different transition metal ions with 27 organics (of the three classes ketone, aldehyde, and ether) were collected (along with the 70 eV electron impact data) and the primary products determined.

III. Pattern recognition method.

Pattern recognition computations were performed using an IBM 9000 laboratory computer. All software was written in our laboratory using IBM

version FORTRAN 77. The feature selection and prediction programs employ the k-nearest neighbor algorithm with a novel feature weighting and the leave-one-out method for generating total recognition accuracies for data sets (2). Interpretation of the results of feature selection is aided by a number of routines which visually display the class separations.

IV. Results.

A 100% recognition accuracy for the 27 compounds is possible using Sc^+, EI, and Cu^+ data, requiring 8, 10, and 12 features respectively. From an examination of visual displays, however, and the fact that Sc^+ requires the fewest features, it can be concluded that Sc^+ provides the best separation of the three classes. In addition to discriminating the chemical classes, the data can be used to examine similarities and differences among the metal ions, by assigning classes according to metal ions used. In this way, trends in reactivity for the group IIIB, group VB, and first row transition metal ions were examined.

V. Conclusion.

In conclusion, the metal ions exhibit a wide variety of reactivities, from simple condensation (Cr^+) to extensive fragmentation (Sc^+, Nb^+). Thus it is possible to select metal ion reagents which will provide either molecular weight or structural information. In addition, the pattern recognition methods used provide an easy means for handling and analyzing the emerging MICI database.

References.

(1) Burnier, R. C.; Byrd, G. D.; Freiser, B. S. J. Am. Chem. Soc. 1981, 103, 4360.

(2) Forbes, R. A.; Tews, E. C.; Wise, M. B.; Freiser, B. S.; and Perone, S. P. J. Chem. Inf. Comput. Sci. In press.

ION/MOLECULE POLYMERIZATION OF BENZYL ESTERS CHARACTERIZED USING FOURIER TRANSFORM ION CYCLOTRON RESONANCE MASS SPECTROMETRY

R.R. Weller, Y. Fang and C.S. Giam
Department of Industrial Environmental Health Sciences
University of Pittsburgh
Pittsburgh, PA 15261

Fourier transform ion cyclotron resonance mass spectrometry provides a unique method for the study of ion/molecule reactions. In examining the reactions of benzyl esters, it was found that polymers of the form $C_6H_5CH_2(C_6H_4CH_2)_n$ (where n= 1,2,3) are formed. This is analagous to that observed by Cameron and Cooks[1] for benzyl acetate.

Five benzyl esters were examined of the form $C_6H_5CH_2OCOR$: benzyl acetate ($R=CH_3$); benzyl carbamate ($R=NH_2$); benzyl chloroformate (R=Cl); benzyl benzoate ($R=C_6H_5$); and benzyl 2-bromacetate ($R=CH_2Br$). Samples were purified with several freeze-pump-thaw cycles and introduced to the Nicolet FTMS-1000 through a precision leak valve.

Parent ions were observed for all compounds, but at very low intensities. Under self-CI conditions, $M+1^+$ was observed as a major peak, along with peaks at m/z 181, 271, and 361. High resolution studies confirmed that these peaks corresponded to the polymer formula mentioned above (with the largest error being 4.7 ppm).

Multiple resonance experiments, either isolating m/z 91 or selectively ejecting m/z 91 prove that it is the reactant ion producing 181. Similarly, m/z 181 produces 271 and 271 produces 361 (see Figure 1 and 2). The probable reaction pathway is:

$$C_6H_5CH_2^+ + C_6H_5CH_2OCOR \longrightarrow [C_6H_5CH_2(C_6H_4CH_2)_1]^+ + \text{neutrals}$$

m/z 91 m/z 181

$$[C_6H_5CH_2(C_6H_4CH_2)_n]^+ + C_6H_5CH_2OCOR \longrightarrow [C_6H_5CH_2(C_6H_4CH_2)_{n+1}]^+ + \text{neutrals}$$

m/z 181 (n=1) m/z 271 (n=1)
m/z 271 (n=2) m/z 361 (n=2)

FT-ICR-MS provides a means of easily studying ion/molecule reaction pathways. Future work will involve obtaining accurate pressure measurements enabling the determination of rate constants for the polymerization reaction. Studies of other compounds, hopefully will provide information on the mechanism for polymerization.

1) D. Cameron, R.G. Cooks, JACS, 101, 3162 (1979).

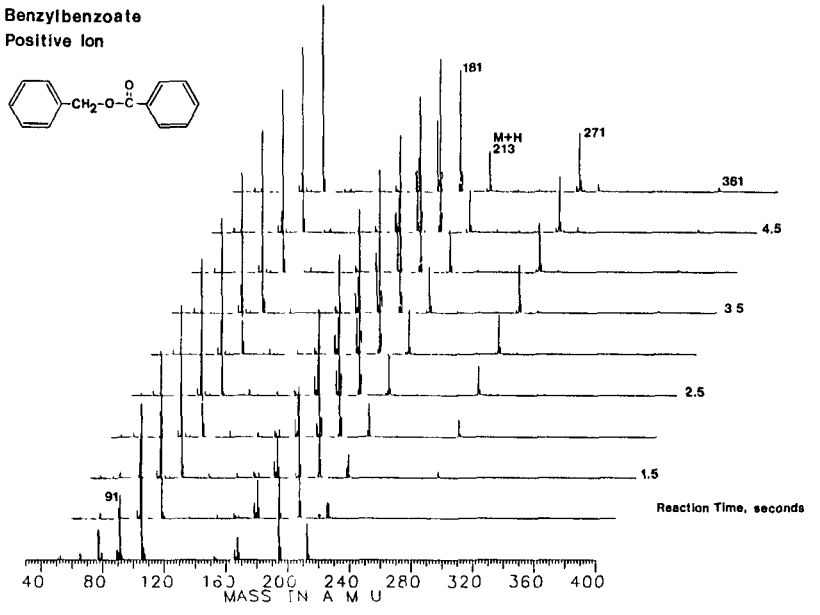

Figure 1

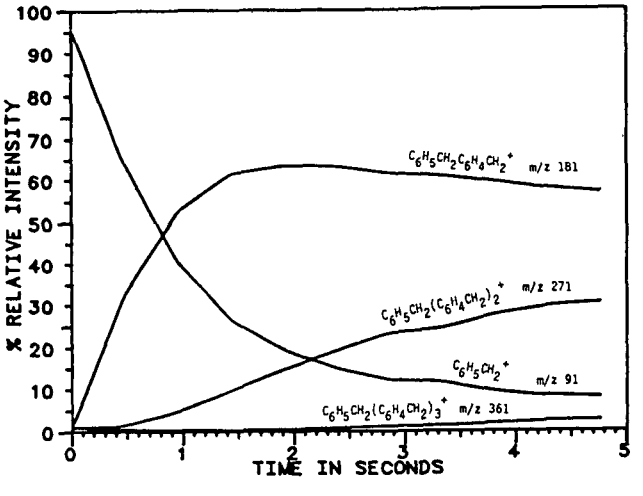

Ion kinetics of m/z: 91, 181, 271, 361 from benzyl benzoate self-CI

Figure 2

LIMITS OF DETECTION IN MASS SPECTROMETRY:AN ATTEMPT TO BRING ORDER OUT OF CHAOS:S.T. Krolik and B.J. Millard, VG ANALYTICAL LTD., FLOATS ROAD, WYTHENSHAWE, MANCHESTER, M23 9LE UK.

Introduction

There are many different definitions in the mass spectrometry literature of limit of detection. These fall mainly into two categories:

1. Definitions based on signal to noise (S/N) ratios.
2. Definitions based on statistical differences between replicate blanks and replicate samples.

It is suggested that a better definition for limit of detection is one in which confidence limits are determined from a well designed calibration curve.

Discussion

Signal to Noise Measurements

Definitions of limit of detection (LOD) based on S/N measurements usually quote a level at which the S/N ratio is some multiple of the S/N ratio obtained on blank samples. Some definitions use a factor of two, while others use a factor of three. As can be seen from Figure 1, a major difficulty with this method is in taking a measurement of the noise level. Decisions as to which noise spikes may be considered to be outliers are often difficult. This makes S/N ratios subject to considerable errors. There might also be chemical interference at the point where the noise is measured, leading to over-estimation of noise levels.

Statistical Differences

Another definition of LOD is based on statistical differences between replicate measurements on blanks and samples containing the compound being measured. The measurements on blanks will give responses whose distribution has a mean of Y and standard deviation s, as shown in Figure 2. The limit of detectable response is then considered to be those samples whose mean (Y_L) is 3s higher than the mean of the blanks. It is considered that the lowest limit of quantifiable response (Y_Q) as opposed to detectable response is at the higher level of 10s above the mean of the blanks. The responses are converted into sample quantities by substitution into the calibration curve equation. We suggest that this equation is obtained by regression calculations on samples where the mean response (Y_C) is at least 50s higher than the response of the blanks in order to improve the reliability of the regression line.

Confidence Bands

We suggest that a method which is superior to both of the above is one which is based upon a calculation of confidence bands on either side of the regression line. The bands, such as those shown in Figure 3, represent the limits within which there is a 95% or 90% probability that the sample quantity lies for a particular measured response. The determination of the limit of detection is shown in Figure 3 for measurements on TCDD at 10,000 resolving power. This gives a LOD of 18 fg (P=0.95) and 11 fg (P=0.90).

By contrast, the S/N method, shown in Figure 4, gives values of 28 fg at S/N = 3, while the replicate sample method gives a value of 8 fg.

Conclusion

The advantage of calculating the LOD from the confidence bands about the regression line is that all measurements at all sample levels make a contribution to the final result. The replicate sample method is based only on measurements on blanks, while the S/N method suffers from the difficulty of making reliable measurements of noise.

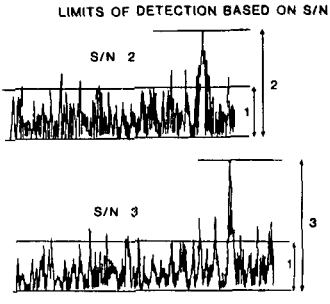

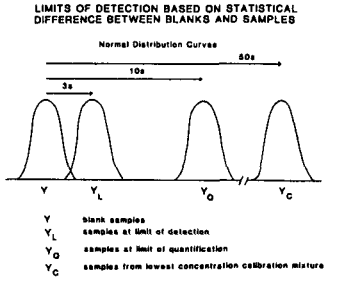

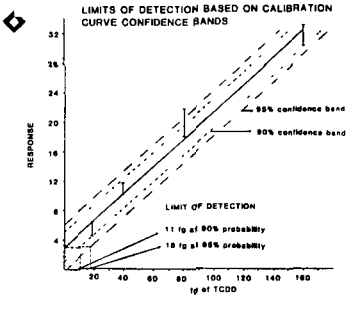

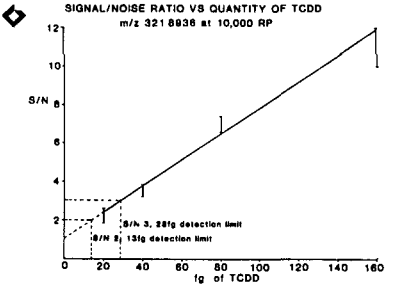

Field Ionization Mass Spectra of Bifenthrin-a Synthetic Pyrethroid, H.C. Hu, FMC Corporation, Princeton, NJ and R.T. Rosen, Center for Advanced Food Technology, Cook College, Rutgers University, New Brunswick, NJ

Extended Abstract

Synthetic pyrethroids are an important class of insecticide possessing powerful insecticidal properties, but having low toxicity to mammals. Many of these compounds contain substituted benzyl moieties whose resonance-stabilized tropylium ion is so dominant, when mass spectra are obtained in both EI and CI ionization modes, that the molecular ion is not observed, and no useful fragmentation pattern is discernible.

Bifenthrin (manufactured by FMC Corporation) has a structure of

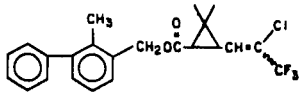

The molecular ion of the compound (m/z = 422) was not observed in neither EI or CI spectrum, as shown in Figures 1 and 2. In the EI spectrum, it fragments and gives a tropylium ion of $R\text{-}C_7H_7^+$ (m/z = 181) while in the CI spectrum, its shows a tropylium ion, a tropylium dimer ion minus a hydrogen (m/z = 361) and a tropylium trimer ion minus a hydrogen (m/z = 542).

On the other hand, field ionization (FI) spectrum as shown in Figure 3, gives a much simpler spectrum with a strong molecular ion which, in complement with EI- and CI-MS data, can be used to elucidate the structure of the compound.

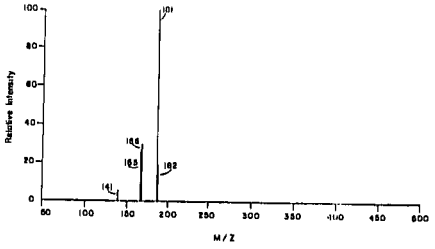

FIGURE 1. EI-MS OF BIFENTHRIN INSECTICIDE

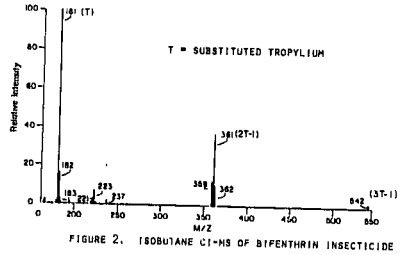

FIGURE 2. ISOBUTANE CI-MS OF BIFENTHRIN INSECTICIDE

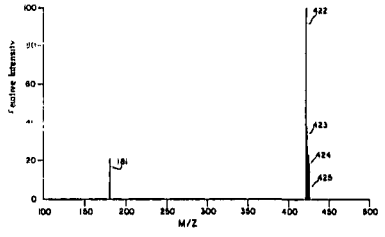

FIGURE 3. FI-MS OF BIFENTHRIN INSECTICIDE

CHARGE EXCHANGE FAB-MS OF LOW MOLECULAR WEIGHT ALCOHOLS. APPLICATION TO THE ANALYSIS OF GINGEROLS AND SHOGOALS.

**Robert T. Rosen, Chi-Tang Ho, Chu-Chin Chen and Thomas G. Hartman, Center for Advanced Food Technology and Food Science Department, Cook College, Rutgers University, New Brunswick, New Jersey 08903.*

FAB-MS was used to determine the molecular weights of a series of gingerols and shogaols, compounds responsible for the pungent properties of ginger. As the compounds are thermally labile, EI and CI (including DCI) techniques failed, even at low sources temperatures. Positive FAB-MS gave large M^+ and M^+-OH ions for straight chained alcohols but only M^+ for the branched analogs. Cationization was also observed, confirming the molecular weights. In these cases, proton transfer was not the primary mechanism of ion formation, rather charge exchange from the glycerol matrix resulted in usable spectra.

Figure A shows the general structures of gingerols and several related compounds and thermal reaction products. Figures B through E are the FAB Mass spectra of various straight chain gingerols. These illustrate the usefulness of FAB-MS for the characterization of thermally labile components.

FIGURE A

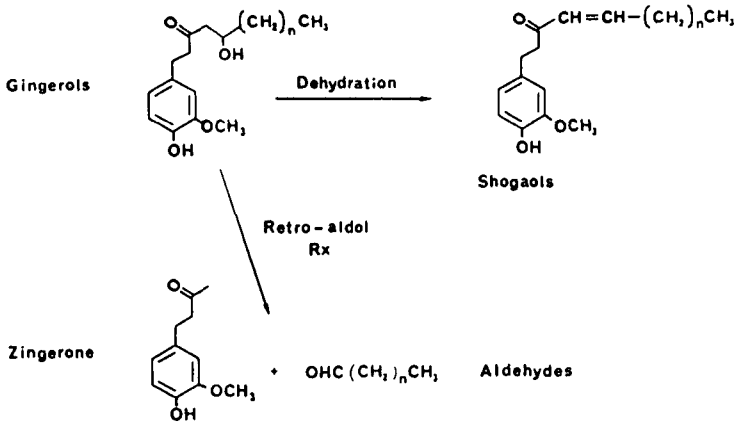

FIGURE B

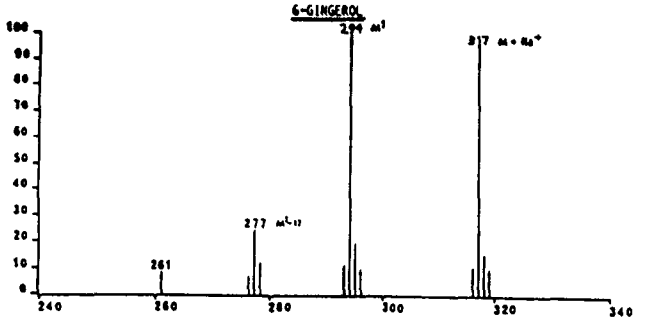

FIGURE C

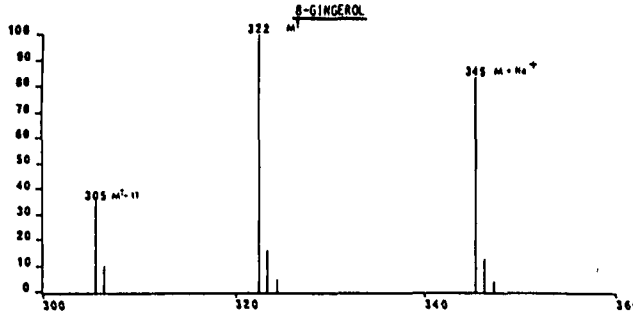

FIGURE D

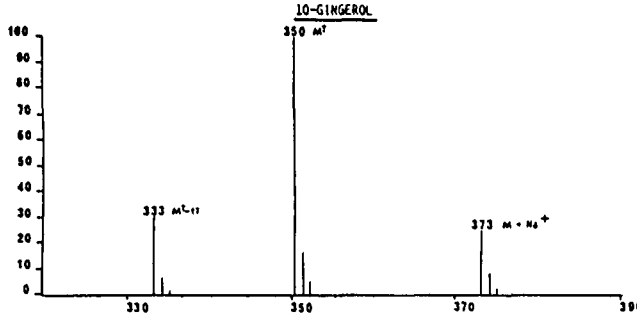

FIGURE E

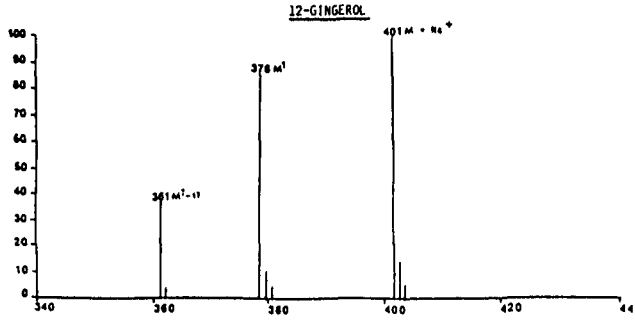

THE APPLICATION OF CI/MS ANALYSIS FOR NONIONIC SURFACTANTS AND THE LOTUS 1-2-3.

Jia-shen Wang, Avelina Qua, and Ira E. Rosenberg
Clairol Inc., Stamford, Connecticut 06922

Nonionic surfactants are an important raw material used in cosmetic products. The degree of ethoxylation (EO) as well as the alkyl chain length (R) are criteria which can effect formulation parameters. Rapid analysis for this class of raw materials is often requested in conjuction with formulation problems.

The approach we have employed uses conventional solid probe, methane chemical ionization MS along with an electronic worksheet (Lotus 1-2-3) for data handling. CI/MS provides informations on the distribution of the molecular species encountered in this class of raw materials. The worksheet which has been designed uses the data collected from the mass spectrum to perform the calculation for the average R and EO.

The worksheet is divided into thirteen sections. One section is used for entering the CI-mass spectrum data. A second section is used to construct a list of ions of interest. A built-in function (@VLOOKUP) reads the intensities of the interested ions in the spectrum. The ion intensities are forwarded to other sections to perform the calculations necessary to determine the average alkyl chain length and the average degree of ethoxylation. The calculations are based on the equation

$$\text{Average EO (or R)} = \sum I_i \times EO_i \text{ (or } R_i)/\sum I_i$$

In this calculation, it is assumed that the intensity of an ion is proportional to the concentration of a given molecular species. No other factors were considered.

The average R obtained from MS analysis is consistent with the information obtained by NMR analysis, however, the average EO obtained is less than that obtained by NMR. One explanation for this result is that the species with larger EO units have a tendency to produce more fragment ions and fewer M+1 ions. As a result, the average EO which has been calculated based on M+1 ions only is less than the actual value. To compensate for this discrepancy, the values obtained for the samples are ratioed to their respective standards. The average EO and R of a sample, therefore, one reported as a relative value to a standard.

Types of samples which have been analyzed by this method are polyethylene nonyl phenyl ethers and polyethylene alkyl ethers. The methodology has strong ramifications for rapid QC/QA analysis in the cosmetic industry.

4-Phenyl-1,2,4-triazole-3,5-dione in the Analysis of Conjugated Dienes

David C. Young and Paul Vouros
Northeastern University, Barnett Institute and Department of Chemistry,
360 Huntington Ave., Boston, MA 02115

Brian Decosta and Michael F. Holick
Human Nutrition Research Center on Aging at Tufts University,
711 Washington St., Boston, MA 02111

One of the most powerful dienophiles known, 4-phenyl-1,2,4-triazole-3,5-dione (PTAD) is important as a protecting group for 5,7 dienes in steroid synthesis (1,2). In this study its analytical utility is investigated with respect to the mass spectrometric determination of diene location in a chain. In addition, the usefulness of PTAD derivatization as part of a separation scheme is demonstrated.

Of primary importance is the 1,4 cycloaddition reaction with dienes which results in the formation of a six membered heterocyclic ring. In the case of certain highly hindered dienes, an alternate reaction, the "ene" reaction, occurs in which PTAD adds to the diene at one end and abstracts an allylic proton at the other (see scheme 1).

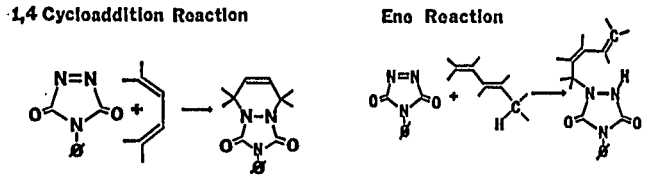

Scheme 1. Two modes in which PTAD reacted with conjugated dienes.

The mass spectra of the cycloadducts were very simple. The ring system dominated the fragmentation with loss of alkyl groups attached to the ring accounting for the major ions. Ions arising from secondary loss of phenylisocyanate were also important. (Scheme 2)

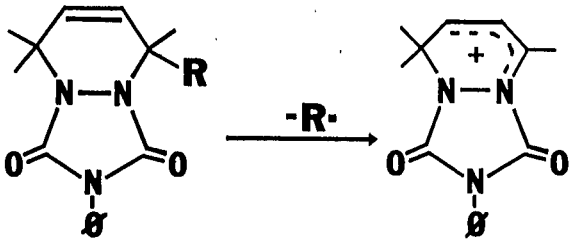

Scheme 2. Fragmentation of cycloadduct

These ions make the determination of the diene's position in the chain a simple matter especially since they are the larger ions in a relatively simple spectrum. The molecular ion is usually abundant and always present (Figure 1).

Of the compounds examined, only 2,5-dimethyl-2,4-hexadiene gave the "ene" reaction product. The spectrum resulting from this type of adduct was less useful than that of the cyclic adducts. The base peak corresponded to loss of the protonated PTAD moity. The rest of the spectrum was of low

abundance with the molecular ion and M-15 peaks having intensities of less than 1%.

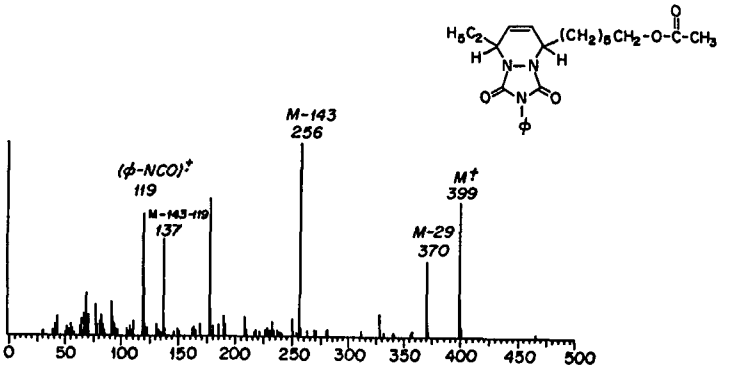

Figure 1. Mass spectrum of the PTAD adduct of 7,9-dodecadienylacetate

Because of the polarity of the PTAD molecule as well as the polarizability of the phenyl ring contained therein, the derivatized dienes are usually more strongly retained on silica gel than the underivatized molecules. This was taken advantage of in the separation of steroids with a 5,7 diene from the total lipid extract of brine shrimp. First the total lipid extract was subjected to normal phase HPLC on a preparative silica gel column and a fraction collected containing the 5,7 steroidal dienes which were identifiable by the U.V. spectrum. This fraction was then reacted with PTAD in methylene chloride derivatizing any dienes present and leaving the bulk of the lipids unchanged. The fraction was then subjected to normal phase chromatography again separating the derivatized dienes from compounds with which they had previously coeluted. The resulting fraction was then analyzed by reversed phase HPLC separating the various forms of 5,7 diene present. Original dienes could at this point be regenerated using any of a number of techniques which have been developed for the removal of PTAD from steroids containing the 5,7 diene.

Clearly,due both to the information contained in the mass spectra and to the chromatographic qualities, PTAD derivatization can be useful in the analysis of conjugated dienes.

1. R.C.Cookson, S.S.H.Gilani, and I.D.R.Stevens; J.Chem.Soc.(C),1967, pp1905-1909
2. D.H.R.Barton,X.Lusinchi,and J.S.Ramirez; Tetrahedron Lett.,1983,Vol.24, pp2995-2998

RPA 10 A Mass Spectrometric Study of the Vaporization of bis(4-dimethylaminophenyl) squaraine and its Derivatives.

Law, K.Y., Bluett, L.J., Bailey, F.C.; Xerox Corporation, Webster, N.Y.

Bis(4-dimethylaminophenyl) squaraine and its derivatives consistently give a mass spectrum under electron impact ionization that contain ions at a higher mass than the expected molecular ion. These ions can be assigned the overall formula of M + CH_2R+ and M + H_2+, where CH_2R corresponds to the alkyl group of the N,N-dialkylanilino moiety of the squaraine. This observation suggests that intermolecular alkyl-transfer and H-transfer reactions are occuring in the mass spectrometer.

To determine whether the reactions are caused by ion-molecule reactions in the ion source, a cross-over experiment was done. This experiment consisted of making a physical mixture of propyl and butyl substituted squaraines and analyzing by solid probe mass spectrometry. Table I shows the cross-over ions observed.

Table I. Cross-over Experiment.

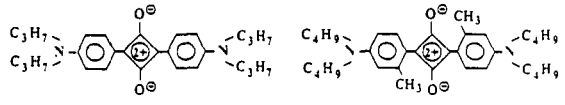

	3	7
	m/z	
	Pr_2SQ	Bu_2SQ
M^+	432	516
(M+CHR) Ion	474	572
Cross-over Ion	488	558

A second experiment was done where these same squaraines were analyzed simultaneously (without being physically mixed). In this experiment the cross over ions were not observed, indicating that the higher molecular weight ions are not the result of ion-molecule reactions.

Analysis of the bis(4-dimethylaminophenyl) squaraine by negative chemical ionization using N2O shows the presence of the dimer and trimer. An parent/daughter MS/MS experiment, where the trimer was selected as the parent, shows that the dimer was actually a fragment ion of the trimer. Figure 1 shows the MS/MS experiment using argon as the collision gas.

Figure 1. MS/MS Parent/Daughter Experiment.

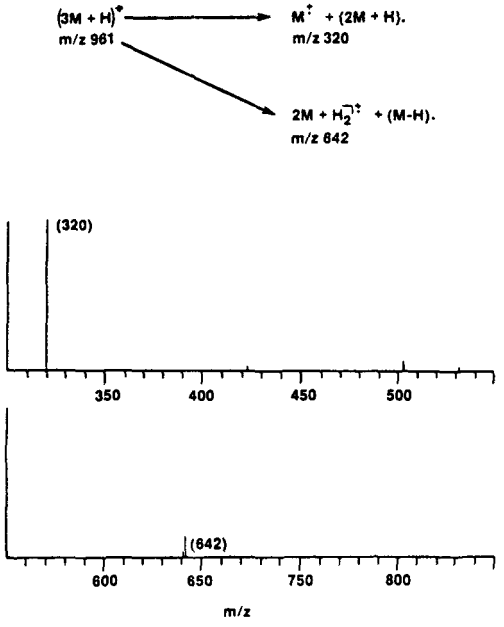

Metastable ions were evaluated and found to support the trimer fragmenting to the M+ CH_2R+ and the M + H_2+.

In conclusion, it was found that the anomolous mass spectrum obtained from bis(4-dimethylaminophenyl) squaraine and its derivatives is due to the vaporization of the squaraine as the trimer with subsequent fragmentation and re-arrangement.

NEGATIVE CHEMICAL IONIZATION MASS SPECTROMETRY OF SOME NITRO COMPOUNDS.

Pradip R. Das and Birendra N. Pramanik, Research Division, Schering-Plough Corporation, Bloomfield, New Jersey 07003, U.S.A.

Negative chemical ionization (NCI) mass spectrometry is suitable for the analysis of organic compounds containing electronegative groups because of its high sensitivity and selectivity. This stems from the fact that NCI involves low energy processes for producing negative ions, consequently fragmentation is minimal and the intensities of molecular or pseudomolecular ions, characteristic of the molecules being studied, are high.

NCI studies of polyhalogenated insectides showing self-ionization (Reference 1) have been extensively reported. This type of process has not been applied to other classes of compounds, viz. nitrocompounds. In this report we studied classes of nitrocompounds, viz. nitrosugars, aliphatic and aromatic nitrocompounds. The NCI studies were also extended to halogenated compounds and nitrocompounds containing halogens.

An Extrel 400-1 EI/CI quadrupole mass spectrometer was used for these NCI studies. The pressure in the ion source region with CI reagent gas (Ammonia, Methane or Isobutane) was maintained at 1.5 - 2.0 x 10^{-4} torr. The source block temperature was maintained at 125° - 150°C, while the solid probe was independently temperature controlled from ambient temperature to about 300°C in most cases.

The nitrocompounds studied gave $(M + NO_2)^-$ adduct ions and M^- in general and $(M + NO)^-$ and $(M - H)^-$ in a few cases. Intense $(M + NO_2)^-$ ions were observed for aliphatic nitrocompounds (as compared to aromatic nitrocompounds). Nitrosugar (aliphatic nitrocompound with multifunctional groups) displayed $(M + NO_2)^-$ as the base peak (Figure 1).

The $(M + NO_2)^-/(M + NO)^-$ ratio decreased with increasing probe temperature (Figure 2) indicating that at elevated temperatures $(NO_2)^-$ dissociates to produce more $(NO)^-$ which then forms the $(M + NO)^-$ adduct ion.

Nitrocompounds containing halogen provided $(M + X)^-$ and $(M + NO_2)^-$ in most cases; $(M + X)^-$ being the predominant of the two ions in the spectrum (Figure 3). A chlorine containing steroid, beclomethasone dipropionate, displayed strong $(M + Cl)^-$ in the mass spectrum.

A mixture of two different compounds, one containing a nitro group and the other without a nitro function, was analyzed under NCI conditions. Both compounds displayed $(M + NO_2)^-$ adduct ions corresponding to their respective molecular weights (Figure 4).

It appears that $(NO_2)^-$ is generated from the nitrocompound by a dissociative resonance capture process. The $(NO_2)^-$ produced then ionizes the neutral molecule by a self-ionization process to form $(M + NO_2)^-$.

Reference

1. R.C. Dougherty and J. Dalton, Org. Mass Spectrom. 6, 1171 (1972).

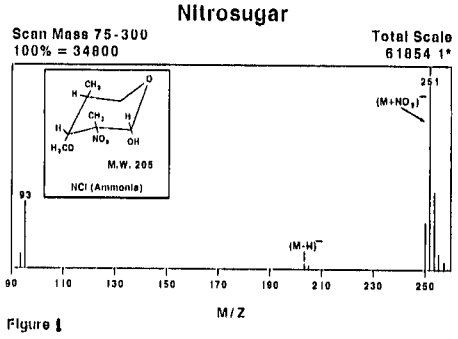

Figure 1

Effect Of Temperature On $(M+NO_2)^-$

2-Methyl-2-Nitro-1-Propanol

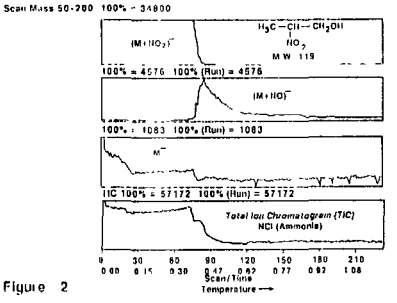

Figure 2

4-Chloro-3-Nitroaniline

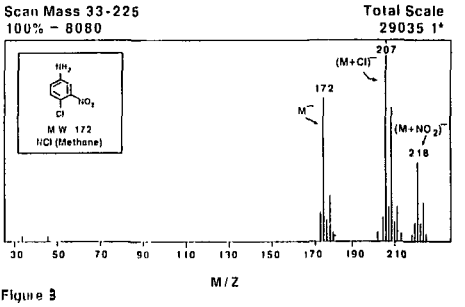

Figure 3

NCI (Ammonia) Spectrum Of A Mixture Of Benzoic Acid & Nitrosugar

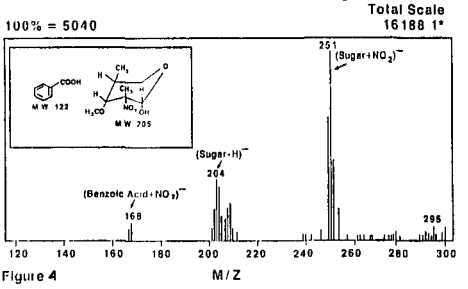

Figure 4

Analysis of Resin Acids in Pulp and Paper Industry Effluents by Fused Silica Capillary Column Gas Chromatography/Mass Spectrometry. François Messier, André Fouquet, Gilbert Gravel and Donald Colgan. Ministère de l'Environnement du Québec, Laboratoire de Montréal, 850 boul. Vanier, St-Vincent-de-Paul (Laval), H7C 2M7, Québec Canada.

Resin acids are one of the many constituents of softwood and are found in the pulp and paper effluents. They count up to 60-90% of overall toxicity in the mechanical pulping effluents. Total resin acid concentrations in mechanical pulping effluents can range up to 62 mg/L, whereas median lethal concentrations (96 hr LC (50) of these acids for juvenile rainbow trout are between 0.4-1.1 mg/L in static bioassays [1]. Because of their toxicity, resin acid analysis is important to monitoring the effeciency of a pulp mill's biobasin. Previously developped analytical procedures for trace level determination of resin acids in kraft mill process samples consisted of four major steps: (a) isolation and concentration by solvant extraction or porous polymer resin adsorption/desorption (b) methylation of resin acids with diazomethane (c) removal of neutral interfering substances by silica gel column chromatography, and (d) identification and determination of the resin acids present. The objective of the present work is to replace the methylation with diazomethane by an easier derivatization process the trimethylsilylation with N,O, Bis (trimethylsylil) trifluoroacetamide (BSTFA), and also the utilisation of the GC/MS in the selective ion monitoring for the identification and determination of these resin acids. The various resin acids studied are: sandaricopimaric (1), isopimaric (2), palustric (3), levopimaric (4), dehydroabietic (5), abietic (6), and neoabietic (7) acids.

The sample is first acidified to convert resin acid salts to their free form, wich are then extracted with dichloromethane. The extract is evaporated and an aliquot of the resulting residue containing the resin acids and other dichloromethane soluble organic compounds is transferred to a reacti-vial, BSTFA is added to lead to the trimethylsilyl ester (TMS) derivative. This silylated solution is then injected onto the GC/MS. A Hewlett Packard MSD 5970 was used with a 30 m x 0.25 mm ID DB-1 capillary column. The GC/MS parameters are: injection mode: splitless; injector temperature: 250°C; column temperature: 100°C hold for 1 min, programming rate 1, 10°/min to 180°C, rate 2, 3°/min to 245°C, rate 3, 15°/min to 300°C. The chosen ions for the different resin acids are:

Sandaricopimaric	1 :	m/z	121,359,374
Isopimaric	2 :	m/z	241,256,359
Palustric	3 :	m/z	241,359,374
Levopimaric	4 :	m/z	121,359,374
Dehydroabietic	5 :	m/z	239,357,372
Abietic	6 :	m/z	256,359,374
Neoabietic	7 :	m/z	135,359,374

The mass spectra of each TMS derivative contained the following fragments: the molecular ion ($M^{+\cdot}$) and the characteristic ion $(M-15)^+$. These ions are used to identify and quantify the resin acids. Although the levopimaric acid is not separated from the dehydroabietic acid with the GC conditions used, it is possible to identify and quantify these two compounds using different mass in the mass spectrum monitoring. The yields of the procedure for these seven resin acids are up to 80 % with a relative standard deviation of 12 %. This methodology can be used to determine the amount of resin acids in wastewaters in ug/L concentrations.

1- J.M. Leach and A.N. Thakore, Tappi 59, 129 (1976)

HIGH SENSITIVITY FAB/EI USING A DIP GUN ON A MAGNETIC SECTOR

Julius Perel and John F. Mahoney, Phrasor Scientific, Inc.
Duarte, California 91010
Roger Greathead, Kratos Analytical, Ramsey, New Jersey 07446

The Direct Insertion Probe (DIP) Gun configuration has produced FAB data on various magnetic sector mass spectrometers, (Ref. 1). Originally developed for use on quadrupole mass spectrometers, in which the ionization source is at ground potential, the DIP Gun was extended to magnetic sectors through the development of an insulated target tip. This tip allows the FAB sample target to enter the ionization source and attain its high voltage level while being attached to a grounded probe. The target tip, capable of withstanding 10kV, contains a narrow beam cylinder and target which enters into the center of the ionization source. The beam cylinder designed for the Kratos MS80 has a diameter of 2.11mm to fit the source block aperture and the target area is about $3mm^2$. This is mounted on a cylindrical insulator and attached to the end of the probe. The FAB gun is at the end of the probe and the beam passes through the tip cylinder to bombard the sample at the target. Sample ions are desorbed in the center of the mass spectrometer ionization source and analyzed by the mass spectrometer.

The advantages of the DIP Gun include excellent alignment and high sensitivity afforded by mounting the target tip on the gun probe shaft and by maintaining a short distance between target and ion/atom emitter. In particular, FAB data was obtained with the standard EI/CI source. Performing FAB does not require a source change which then allows for alternate or even simultaneous FAB/EI data acquisition. Thus, calibration can be performed at any time.

FAB spectra was obtained on a Kratos MD80RFA, using the DIP Gun with the standard EI/CI source. Low sample level peptides, methionine enkephalin, eledoisin and melittin along with cesium iodide, were measured. The FAB spectrum of methionine enkephalin, made using a sample of 250ng at a scan speed of 10sec/decade, is shown in Figure 1. The eledoisin spectrum seen in Figure 2 was made using a sample of 425ng and also run at a scan speed of 10sec/decade. The cesium iodide spectrum, seen in Figure 3, contains mass peaks above 6628 m/z, which is $(CsI)_{25}Cs^+$.

The Dip gun configuration has, with limited testing, already demonstrated good sensitivity and greater convenience when compared to the standard FAB installation on the Kratos MS80RFA. The data shows that the Dip Gun performs well on a high voltage magnetic sector sector instrument, and that strong spectra can be obtained from low sample levels of peptides. High mass spectra was measured using both cesium iodide and organic compounds (melittin). Thus, tests of the DIP Gun on a magnetic sector instrument demonstrate no inherent limitations in the capabilities of the gun to perform sensitive high mass measurements.

REFERENCES:

1. J. Perel, J. F. Mahoney and C. J. Metral, "FAB Spectra Taken With a DIP Gun On A Magnetic Sector", Paper 861, Pittsburgh Conference and Exposition, Atlantic City (10-14 March 1986).

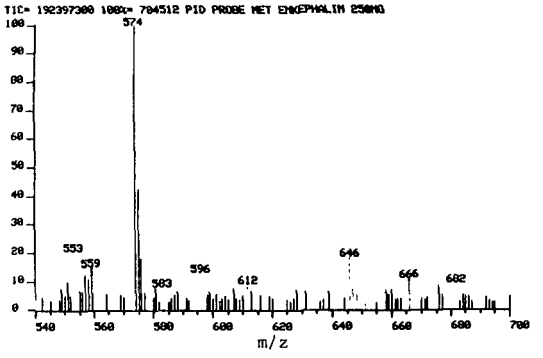

Figure 1. DIP Gun FAB Spectrum of Methionine Enkephalin Taken on a Kratos MS80RFA

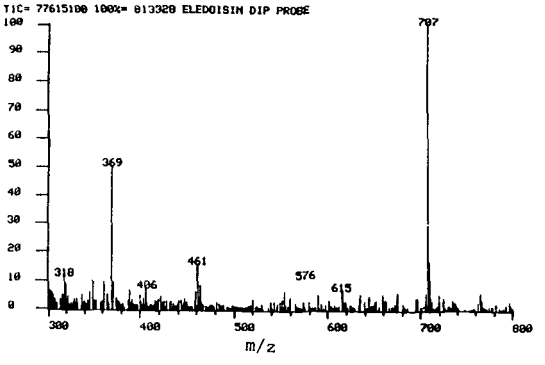

Figure 2. FAB Spectrum of Eledoisin

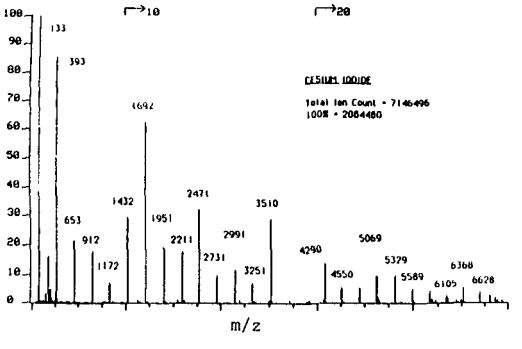

Figure 3. FAB Spectrum of Cesium Iodide Ranging Up to a Mass of 6628 m/z (25 clusters).

HARDWARE PEAK-FINDING FOR RELIABILITY AND INCREASED SCAN RATES

M. J. Kristo and B. H. Newcome, Departments of Chemistry and Biochemistry, Michigan State University, East Lansing, MI 48824.

Reducing sequential intensity data to mass/intensity pairs for all peaks in the mass spectrum can occupy most of the control processor's time. "Peak-finding" can thus limit the maximum speeds to less than that possible for the mass filter employed. Also, since the processor spends so much time on this task, a substantial fraction of the ion current goes unsampled. Therefore, it is desirable to reduce the amount of time necessary to perform peak-finding and to make it a task which can be performed in parallel with other functions.

We have developed an electronic peak-finding accelerator for quick reduction of raw intensity versus mass data to mass-intensity pairs for all peaks in the spectrum. The accelerator accepts sequential intensity data from the control system processor and returns peak positions and intensities for storage. The peak-finder achieves the speed of a dedicated data acquisition peripheral, yet retains programmability through downloadable software sequencing of the hardware functions.

A block diagram of the hardware peak-finder is found in Figure 1. Letters in parantheses in the following paragraphs refer to sections on the diagram. The heart of the hardware peak-finder is a RAM-based state machine. The desired peak-finding algorithm is downloaded from the host processor to the peak-finder's RAM (B). The algorithm is a control sequence program and directs the processing of incoming data. The sequence of instructions in the program is controlled by the next-address latch (C). A 16:1 multiplexer (D) provides the ability to branch in the program on any one of 16 conditions. These conditions (E) are generated by the status of the comparators and flags in the peak-finder. Incoming data is manipulated on a 32-bit bus, which connects the input latches, the output latches, latches for a threshold value, and two banks of comparators with registers. Additional counters and flipflops track the occurence of certain events. Thus, many useful hardware functions can be performed, which parallel functions used in software algorithms. Furthermore, it is simple to add further arithmetic elements without extensive redesign.

Acquired data are written into the input latches of the accelerator (A) and peak data are read from the output latches (B). The host processor can monitor the status of the peak-finder (whether the current datum has been processed and whether or not a peak was found) by reading the user status byte (F). With this type of handshaking, the peak-finder can process data simultaneously with the host processor, thus freeing the processor to attend to other tasks.

The accelerator's peak-finding program is written in horizontal microcode (64-bits wide), which is tedious to write by hand. Therefore, a microcode compiler, based on the programming language FORTH (1), has been written to facilitate the development of code for new peak-finding algorithms. The compiler retains the programming style of FORTH. Individual control fields are predefined as dictated by the hardware itself. These fields are then linked together into 64-bit microcode instructions. Finally, instructions are linked, either sequentially or through an IF . . . THEN control structure into

the complete algorithm which is stored on disk for later downloading into the peak-finder. This compiler relieves users from the need to understand the accelerator's program code when implementing new algorithms.

The hardware peak-finder achieves this programmability with no cost in speed. The peak-finder can process 10 million microcode instructions per second. With a typical algorithm, it will handle data rates up to 1,000,000 data points per second or 100,000 AMU per second at 10 points per AMU.

1. polyFORTH, FORTH Inc., Hermosa Beach, CA.

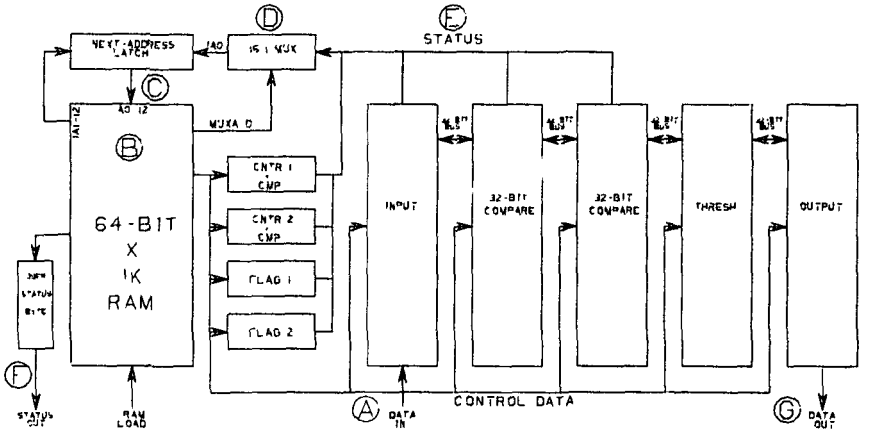

Figure 1. Functional Diagram of the Hardware Peak-Finder.

AN ADAPTOR FOR CONSTANT-NEUTRAL-LOSS SCANS ON A KRATOS MS-50TA

D.E. Giblin and R.L. Lapp, Midwest Center for Mass Spectrometry, Dept. of Chemistry, University of Nebraska, Lincoln, NE 68588-0304.

Many classes of ions exhibit losses of characteristic neutral species when collisionally activated. Collisionally activated decomposition (CAD) coupled with constant-neutral-loss linked scanning would, therefore, provide a means of detecting certain classes of compounds in complex mixtures.

A design goal was to implement the linked scan for constant-neutral-loss on a Kratos MS-50TA and to take advantage of the main collision cell which is in the third field-free region between the magnetic analyzer and the second ESA. An advantage of this instrumental geometry, which is effectively reverse Nier-Johnson, is that the generation of the required scan function is much less difficult than that which uses the first field-free region in a convention Nier-Johnson instrument. Also, transparency to all other modes of operation when not in use was considered necessary.

To meet the design goals, an add-on circuit card for the metastable control unit was constructed. The circuitry on the card synthesizes the necessary scan function: $B^2(E_{2,0}-E_2)$=constant. $E_{2,0}$ is the potential of the second ESA required for transmission of the main beam, E_2 is the potential for the scan function, and B is the magnetic field strength. The card can also synthesize the scan function for parent-ion linked scan: B^2E_2=constant. Both scan functions are capable of producing high resolution (~10K) spectra[1]. However, selection of the mass of the neutral loss or daughter ion has low selectivity (~100).

The linked scans for constant-neutral-loss and parent-ion are implemented as variants of the already existing B/E_2=constant scan. The three scan types are selected by a switch and are active only when B/E_2 is activated on the metastable control unit. Transparency of operation is achieved since the add-on unit functions, when inactive, as a unity gain amplifier in the intercepted E_2 reference chain.

The Coarse and Fine helipots on the metastable unit are used to select the mass of the neutral loss or daughter ion. These controls determine the gain of the reference chain from the Hall probe to the second ESA power supplies.

The collection and processing of data from constant-neutral-loss scans is performed in two different ways. For low resolution scans (<3K), the data are digitized at a constant rate across each scan, and successive scans are added together for signal averaging. For high resolution (~10K) the digitized data are usually converted to peak data (time centroid, height, and width) by the DS-55 preprocessor. The data for each scan are stored separately. Signal averaging is then accomplished by adding together peaks that occur within a time window. This adjustment is necessary because of variability of successive magnetic field scans.

Approximate mass assignments are made by converting the time data to mass data using the regular magnetic field scan function along with the start and stop masses derived from the mass marker. Accurate masses can then be assigned by using peaks of known composition and adjusting the scan function accordingly.

References

[1]R.K. Boyd, C.J. Parker and J.H. Beynon, Int. J. Mass Spectrom. Ion Physics, 44 (1982), 199.

POSITIVE/NEGATIVE ION SOURCE ELECTRONICS CONVERSION

FOR THE FINNIGAN 4000/4500

J. L. Stauffer, Center for Human Toxicology, University of Utah, Salt Lake City, Utah

The source electronics of the Finnigan 4000 and 4500 series of instruments that are designed for positive ion analysis only, can be modified to provide source potentials for both positive and negative ion analysis at low cost, and with relative simplicity provided that fast switching between the two modes is not required. The modification described here provides for switching between positive and negative ion analysis via front panel toggle switches, with a changeover time of a second or so. (Complete conversion to negative ion analysis requires the addition of a conversion dynode in front of the electron multiplier, not described here.)

The output polarity of the -150 volt regulator on the Finnigan ion source control PCB is not reversible. In order to overcome this difficulty a separate +150 volt regulator was constructed that is electrically a mirror image of the -150 volt regulator. The new regulator was assembled on a small, separate board that was mounted on the inside wall of the QEM electronics drawer, next to the ion source PCB. The new +150 volt regulator shares the same power source and the same output filtering as the original -150 volt regulator. Only one of the regulators is active in the circuit at any given time--the appropriate regulator is switched into the circuit as the other is switched out. The output of the active regulator is at its design voltage, while the output of the other regulator (and it's input) is grounded. The output of the active regulator is distributed to the ion source lenses via a modification of the original potential distribution and control network. The overall scheme is illustrated in Figure 1. The narrow lined portions of the figure represent original circuitry, the wide lined that which has been added or modified, and the dashed part original connections that were removed.

The output for L5, the quad entrance, is obtained with a simple modification. Since the L5 potential is set by a purely resistive divider, it is necessary only that the input to the divider be switched to connect to the output of the active voltage regulator. The outputs for L3 and L4, the extractor and lens, are buffered by transistors. The polarity on these transistors must be preserved when the polarity of the output is reversed. This is accomplished by tying the -150 volt-or-ground side of the voltage regulators to the emitter resistors, and the +150 volt-or-ground side to the collectors. The base bias resistors for the two transistors are simply switched to the output of the active voltage regulator exactly as for L5. In order to preserve the bipolar range of L3 in the negative ion mode, it is necessary to utilize the -15V supply of the original circuit in a manner complimentary to the original use of the +15V supply in the positive ion mode. The switching for this is illustrated in Figure 1.

For proper operation of the modified circuit it is necessary that at least two of the added front panel switches, S2 and S3, be set to the same position. However, no circuit damage will result if they are inadvertently set to opposite positions. A more elaborate scheme might be to provide a bank of relays to accomplish the switchover, all of which could be controlled by a single front panel switch, or by software.

In addition to the changeover of the lens potentials, it is necessary to also switch the polarity of the quad offset and the offset program potentials, and to ground the electron trap. In the modification described here, the quad offset and offset program polarity change is accomplished by reversal of the input leads, via S3C and S3D, to the summing of amp 8B on the RF/DC PCB (note that it is necessary to preserve the integrity of the feedback connections). This simple electrical reversal of the leads result in an increased gain factor for 8B and correspondingly faster acting front panel quad offset and offset program controls, but this has been entirely satisfactory in use. S3B provides the necessary grounding for the source electron trap in the negative ion mode.

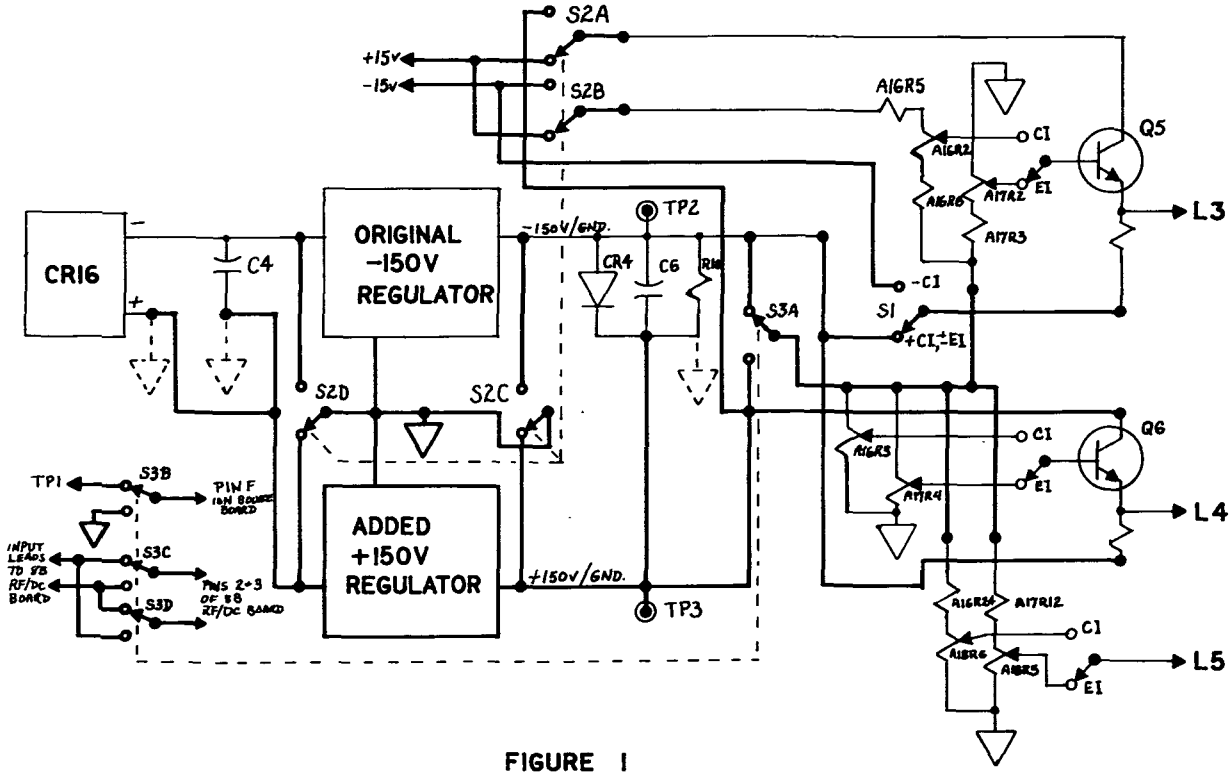
S2A
+15v
-15v
S2B
A1GR5
C1
A1GR2
Q5
A1GR6
A17R2
E1
L3
A17R3
CR16
C4
ORIGINAL
-150V
REGULATOR
-150V/GND.
TP2
CR4
C6
R16
-C1
S3A
S1
+C1,-E1
S2D
S2C
C1
Q6
A1GR3
E1
A17R4
L4
TP1
S3B
PIN F
IN BOARD
BOARD
INPUT
LEADS
TO S8
RF/DC
BOARD
S3C
PINS 2+3
OF S8
RF/DC BOARD
S3D
ADDED
+150V
REGULATOR
+150V/GND.
TP3
A1GR4
A17R12
C1
A1GR6
A1GR5
E1
L5

FIGURE 1

MODIFICATIONS TO THE FIELD CONTROL AND SCAN CIRCUITRY OF A CEC 21-110B MASS SPECTROMETER FOR IMPROVED LINEAR MASS SCANS AND HIGH RESOLUTION DATA ACQUISITION*

L. Ramaley**, F.G. Mason, T.E. Dalton and W.D. Jamieson
Atlantic Research Laboratory, National Research Council
1411 Oxford St., Halifax, N.S. CANADA B3H 3Z1

In the original magnet power supply for the 21-110B mass spectrometer, the current through the magnet was controlled and two scanning mechanisms were provided: a forty-turn, motor driven potentiometer produced slow scans and capacitor discharge produced fast scans. Greenwood *et al.* (1) improved the stability of the supply by replacing the power output stage with a Hewlett-Packard 6274B power supply and also rewired the capacitor discharge circuitry for computer interfacing. The INCOS data system in our laboratory was difficult to use in conjunction with the capacitor discharge scan, so further modifications were made to the magnet scan circuit.

The H-P 6274B power supply and the forty-turn potentiometer were retained, but a stepper-motor drive for the potentiometer was provided for more exact speed control. In addition an analog square root module (Burr Brown #4302) was inserted in the circuit between the potentiometer and the power stage and the Hall probe provided with the instrument was wired so that it could be placed in the feedback loop of the power supply for magnetic field control (see Fig. 1). The ability to sense magnet current was retained so that the power supply could control either the current or the field depending on the setting of a single switch. A scan function linear in time at the input of the square root module thus forces either the magnetic field or the magnet current to vary as the one-half power of time, and provides a mass-scan-function linear in time. The capacitor charge/discharge circuit, not shown in the figures, is not wired through the square root module, but is connected directly to the power supply input. The capacitor can be either charged or discharged, providing both up and down scanning in this mode. The forty-turn potentiometer is used to establish the starting mass in a down scan or the final mass in an up scan.

For linear manual scanning, the forty-turn potentiometer (Fig. 2) is connected to the input of the square root module. For computer controlled scanning, the circuitry of Fig. 3 replaces the potentiometer. In this arrangement a 12-bit analog-to-digital converter (ADC) in a standard Finnigan Mat #2010 interface converts the signal from the ion current amplifier for transmission to the INCOS data system. Two 16-bit digital-to-analog converters (DAC's) with differential outputs are used to provide the scan function. For normal scanning (2 to 950 u at 8 kV accelerating potential) only the DAC whose signal is not attenuated is used. The resolution in this mode is about 70 DAC steps/u. For high resolution scanning the normal scan DAC provides the initial mass setting and a second DAC, whose signal is attenuated by a factor of ten, is used for the scan. The resolution in this mode is thus 700 DAC steps/u but the mass range which can be scanned is reduced to 90 u.

The current control mode provides the highest measurement stability but the field control mode gives the best linearity and convenience of use, both for manual and computer controlled scans. In the manual, field controlled mode the average deviation from linearity over a mass range of 70 to 720 u is 5.5 u and the average relative deviation from linearity is 1.8 %. Scan rates vary from 0.15 to 4.75 u/s up or down. In the exponential scan mode, rates of 9 to 300 s/decade are provided, either up or down.

For computer interfaced scans, normal scanning is most easily done in the field controlled mode. For a resolution of 3000 over a mass range of 60 to 720 u, internal calibration (use of an internal standard) provides an average error of 50 ppm in mass assignment. The error for external calibration depends on the circumstances. The error is 200 ppm if the calibration directly preceeds the scan and the same scan parameters are used. If a calibration from a previous day is used, the error grows to about 1 ppt. If the scan rate or mass range changes between calibration and scan, the error also increases. For example, the error is 0.8 ppt if the calibration is done at 0.15 s/u and the scan done at 0.075 s/u and the error is 0.6 ppt if the calibration is run from 60 to 720 u while the scan ranges from 100 to 400 u. In the field control mode there

* NRCC #25899

** On leave from the Department of Chemistry, Dalhousie University, Halifax, N.S. CANADA B3H 4J3.

is no need to have the magnet cycle for a long period of time to reach a stable condition.

For accurate mass scans any 90 u region from 2 to 860 u can be scanned and internal calibration must be used. At a resolution of 7000 and a scan rate of 1 u/s, current control gives an average error of 10 ppm in mass assignment with a standard deviation of 5.3 ppm and field control provides an error of 30 ppm with a 21 ppm standard deviation. Peaks of interest should be toward the middle of the scan range.

The circuit changes described above greatly enhance the convenience of use of the instrument, especially when computer-interfaced.

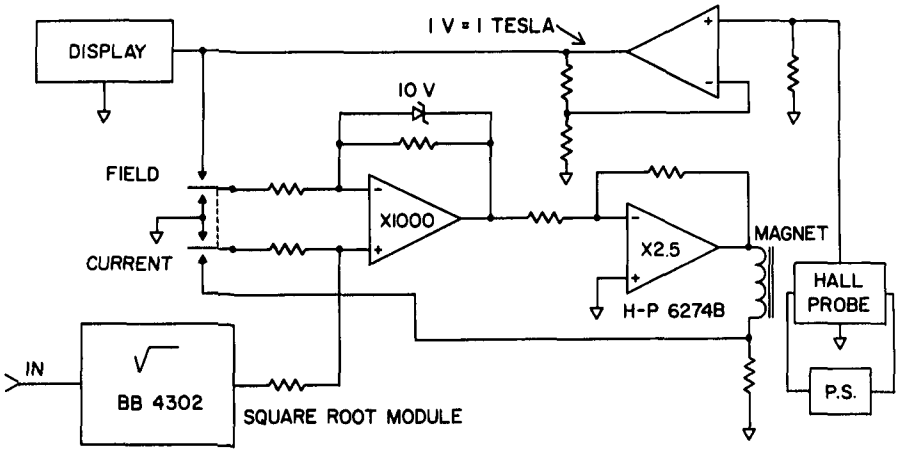

MAGNET CONTROL CIRCUIT

Figure 1.

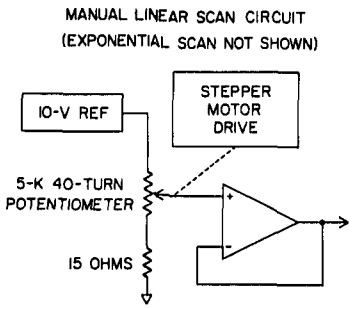

Figure 2.

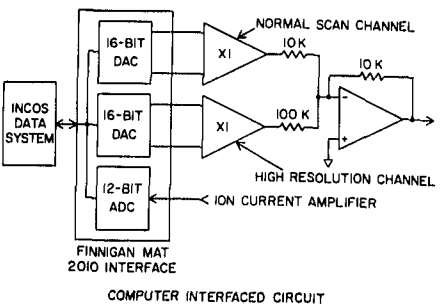

Figure 3.

References

1. G.J. Greenwood, J.F. Stewart, and D.M. Cantor, *Rev. Sci. Instrum.*, *51*, 146 (1980).

MOBILE MASS SPECTROMETRY -- THE INSTRUMENT COMES TO THE PROBLEM

Kenneth L. Gallaher, James H. Gibson, Joseph Kosman,
Don G. Rosenhammer, Raymond Teller
Standard Oil Research and Development
4440 Warrenville Center Road, Cleveland, Ohio 44128

During the past few years, a new kind of mass spectrometer has become commercially available, the bench top GC/MS. The Hewlett Packard HP5970B is a classical quadrupole, while the Finnigan ion trap is a new mass spectrometer design. Our primary interest in these systems was their use as a portable MS. A portable MS makes it easy to perform analyses where the sample cannot be carried to a mass spectrometry facility. We have used our system for the analysis of: the products from a micro reactor; effluent from a pyrolysis gas chromatograph; and reactive products from a chemicals plant.

These instruments are relatively inexpensive; they are designed to be user friendly; and they are small. They consist of a personal computer; a GC; and the mass spectrometer (which is physically smaller than a GC). Overall, a system requires about six linear feet of laboratory bench space. Both allow control of the instrument through the data system and have extensive data analysis capabilities including spectral search using the full NBS library. They are designed for capillary column, 70 ev, EI only operation. The only utility requirement is 110 volt power, plus helium for the gas chromatograph.

Our Hewlett Packard system is installed permanently on two carts. A heavy duty 24x36 inch cart for the GC, transfer line control, and MS; and a smaller cart for the computer, terminal, disk drive, and printer. This arrangment allows easy transportation through doors and hallways and is narrow enough to operate in a laboratory aisle way.

The only "custom" part of our system is the heated transfer line which is a two foot long one-fourth inch OD transfer line from CDS of Oxford, PA. The large diameter allows use of an inner tube, either eighth inch OD stainless steel or deactivated fused silica capillary, for the actual transfer line.

PROCESS ANALYSIS. Although small mass spectrometers are designed as GC/MS systems, they may also be suitable for some "process" type applications where the time variant sample source might be a chemical reactor or a thermal gravimetric analyzer (TGA) rather than a GC. Experimental considerations for this application are fairly simple: (1) A heated transfer line will be needed if the sample stream is condensable; (2) A knockout trap will be required if heavy products are produced; (3) The ion source may experience a substantially higher amount of average sample flux than it would in a GC/MS mode. This can mean that the source will be contaminated at a very rapid rate; (4) An ion gauge for pressure measurement is particuarly important since there is not the normal pressure protection that a GC column provides.

The reactor effluent was split to reduce the flow to the one cc/minute capacity of the instrument. If rapidly time variant phenomena are to be monitored, the whole gas mixing, reactor, and interface system must be designed to minimize dead volume. We tested our splitter system by switching rapidly from helium to methane. The methane rise time was about 15 seconds. Most of this rise time is due to the sampling system since the mass spectrometer itself can routinely demonstrate better than 1 second resolution for capillary GC/MS analysis.

MICRO REACTOR MONITORING. In this experiment, products of a micro reactor operated in the "slug" mode were monitored. The reactor was periodially switched between an oxygen stream and a feed stream. Figure 1 shows a single ion trace at mass 78 for benzene for several pulses.

This data gave several pieces of new information:
(1) Benzene was being formed. Previous GC analyses had not detected benzene.
(2) There was a significant improvement in benzene yield with higher catalyst temperature.
(3) Benezene yield was time variant. Although this phenomenon was not unexpected, it had not previously been observed because the earlier analysis method consisted

of analyzing a single cut from the middle of each pulse by gas chromatography.

QUANTITATIVE PROCESS ANALYSIS. The HP instrument was also evaluated as a possible process instrument in the more classical sense, i.e., as a high precision quantitative instrument for slowly varying streams where an analysis time of 30 seconds to many minutes is desirable. To do this, a standard test mixture consisting of 2% each O_2, CO_2, and Argon, 1% CO and 0.5% each propane and propylene was used. Not surprisingly, performance was not nearly as good as for dedicated process mass spectrometrs such as the Extrel EL-150 or the VG MM8-80. Absolute intensities measured on the EL-150 had better standard deviations (typically less than .1% relative) than intensity ratios on the HP (7-17%)!

NYLON PYROLYSIS. In order to use a specialized pyrolysis GC, the portable mass spectrometer and data system was wheeled to the pyrolysis unit. The capillary column from the pyrolysis GC was run through a spare injection port of the GC, through the heated transfer line, and connected directly to the mass spectrometer. Thermal desorption/GC/MS analysis of an extract from a commercial Nylon 6,6 polymer was then run. In particular, it was of interest to verify that a large GC peak was "cyclic monomer" $(-CO-(CH_2)_4-CO)-NH-(CH_2)_6-NH-)$. A commercial source of the monomer to determine retention time was not available. The extract was volatilized with a CDS Pyroprobe at 290°C. The volatiles were cryofocused at the head of the capillary column which was maintained at -80°C. Figure 2 shows a mass spectrum of the unknown peak, which was confirmed to be the monomer.

REACTIVE SAMPLE ANALYSIS. In order to discover if chemical plant samples were changing before analysis, the portable mass spectrometer was taken to the plant. The instrument was disassembled, packed into a standard size station wagon, and driven to the plant. The instrument required only one hour for reassembly. It was allowed to pump down over night. The next morning, computer diagnostics and mass calibration were successfully run and analyses began. Analyses showed that the samples were indeed degrading with time, even if refrigerated at 4°C.

CONCLUSION. These results have demonstrated that a small bench top GC/MS unit can be realistically transported and used at a site out of the analytical laboratory. Interfacing has been shown to be a fairly simple matter. The instrument has never sustained any serious damage that can be attributed to moving it. Most importantly, it has allowed us to obtain data that otherwise would have been obtained only at the cost of substantially more effort or perhaps not at all.

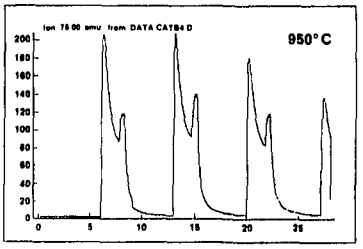

Figure 1

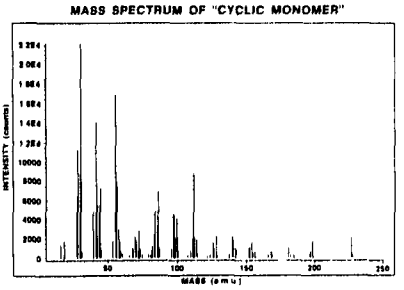

Figure 2

NOVEL QUADRUPOLE GEOMETRY FOR REDUCTION OF IONIZATION RELATED NOISE

J.E.P. Syka, A.E. Schoen, P.C. Ceja; Finnigan MAT, San Jose, CA 95134. R.M. Smith; Finnigan Corporation, Evergreen, CO 80439

The ionization methods of choice for high mass compounds, FAB and liquid SIMS, produce an abundance of excited neutrals. These particles transmit from the ion source region down the length of the anlyzer in a line-of-sight fashion and impinge upon surfaces in the vicinity of the detector. Secondary charged particles of both polarities are emitted which reach the detector and produce substantial levels of incoherent signal. This neutral noise determines the detection limits of the analysis.

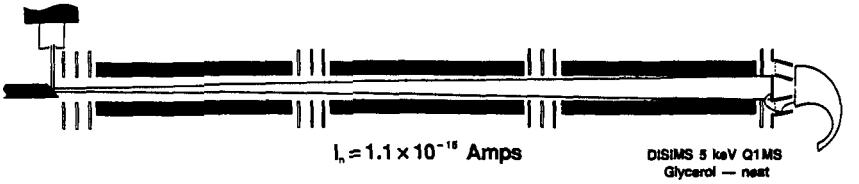

The transmission of excited neutrals to the detector region can be greatly reduced by using a RF only quadrupole collision cell with a non-linear or curved axis (patent applied for). Ions travel through such a device substantially like they do through the straight version. The excited neutrals, because of the curvature of the analyzer axis, can only travel as far as the exit of the collision cell without striking an electrode. Most of the secondary charged particles emitted can not pass through the mass analyzing electric field of the Q3 filter and do not reach the detector to produce neutral noise.

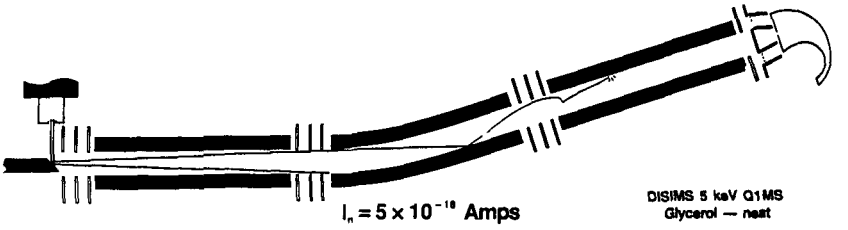

Observation of the ion mass peak with current I_s in the presence of neutral noise is limited by the magnitude of i_n, the shot noise (AC) component of the neutral noise current. The signal to noise ratio, S/N, is therefore related to I_s and i_n by the proportionality:

$$S/N \propto I_s/i_N$$

Substitution of the square root relationship between I_n, the average noise current, and i_n yields the proportionality:

$$S/N \propto I_s/\sqrt{I_N}$$

The linear triple quadrupole geometry exhibits 1.1 X 10^{-15} Amps of noise when neat glycerol is bombarded with 5 keV Argon ions. The non-linear geometry has 5 X 10^{-18} Amps of noise under identical conditions. This factor of 220 reduction in DC noise indicates an expected S/N improvement greater than ten. The elimination of baseline liftoff also simplifies data acquisition and improves the reliability of centroid algorithms on small peaks.

RF Only Quadrupole

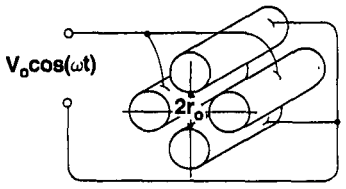

Curved RF Only Quadrupole

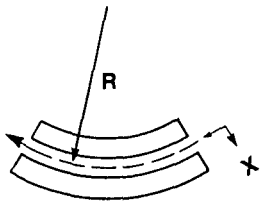

An ion's motion will be constrained about the axis of a RF only quadrupole if the operating point (Mathieu stability parameter), q, for that ion is less than 0.91. Such ions travel through the quadrupole as if they were guided by a potential trough. For an ion with a low q, the transverse motion is approximately sinusoidal.

$$(1) \quad q = \frac{4e\,V_0}{(m/z)\,\omega^2\,r_0^2}$$

When the axis of the quadrupole is curved, ions are subject to an outward or "centrifugal" force in the plane of the curve. The effect of this force is to cause the ion to ride up on the side of the pseudo-potential trough created by the RF quadrupole field. The amount of this induced transverse displacement can be approximated by equation (2). Since this displacement is time variant, there is an average induced transverse velocity associated with it as in equation (3).

$$(2) \quad \Delta X = \frac{16\,KE_{AXIAL}}{m\,q^2\omega^2\,R}\left(1 - \cos\frac{q\omega}{2\sqrt{2}}\cdot t\right)$$

If $q < .4$

$$(3) \quad \overline{\Delta \dot{X}} = \frac{8\sqrt{2}}{\pi}\cdot\frac{KE_{AXIAL}}{m\,q\,\omega\,R}$$

From these expressions, it can be shown that the higher the axial kinetic energy, KE_{axial}, and the smaller the radius of curvature, R, the larger induced transverse displacement and velocity. However, these induced displacements and velocities are also strongly affected by the choice of the operating point, q, and RF drive frequency. Proper choice of q, , and R to minimize induced transverse displacement and velocity will allow a curved quadrupole collision cell to operate as well as a straight one for a desired range of kinetic or collision energies.

NEW METHODS AND CONCEPTS IN DIGITAL CONTROL
OF A QUADRUPOLE MS/MS INSTRUMENT

U. Steiner, S. Sokolow; Finnigan MAT, San Jose, CA 95134

Advanced digital control techniques have been implemented in a quadrupole MS/MS instrument that overcome the complexities inherent to the rapid scanning of non-linear parameters. For example, conventional MS/MS instruments require detailed analog/digital electronics to correct for the variation in ion energy distribution between parent, daughter, and neutral loss operating modes.

The new digital control circuitry of the Finnigan MAT TSQ R 70 overcomes these difficulties via the use of mass-linked look-up tables which are accessed by a scan generator. All ion-path parameters can be maximized for each mass without loss of speed or performance. Now, the non-linearities inherent to MS and the difficult energy relationships in MS/MS analyses are completely corrected for by the scan generator.

The uniqueness of this design are multi-fold:

- o Instrument parameters can be set independently at each mass
- o Each mode of MS/MS operation can be optimized separately
- o Mass calibration for all modes is done during acquisition, eliminating problems of inherent non-linear relationships in multi-analyzer instruments.
- o Mass calibration, peak normalization, etc. ...., are done in real-time, allowing interpretation of the analyses on a scan-by-scan basis.
- o The pre-computed relationships stored within the instrument control system and accessed by the scan generator enhance your results.

Figure 1. Conventional TSQ instrument control block diagram showing tunable analog pots.

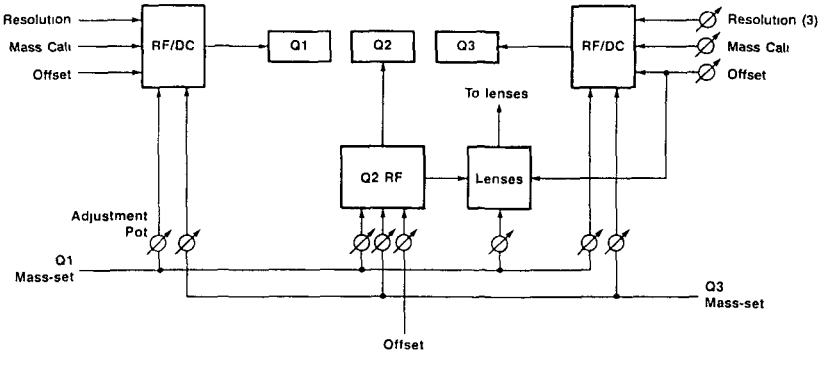

Figure 2. TSQ 70 scan generator block diagram showing digital control via slave DACs and look-up tables.

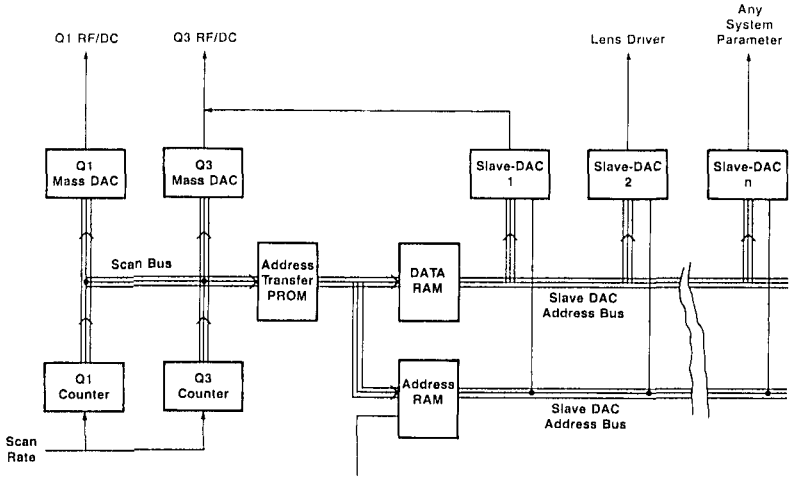

ION TRANSMISSION CONSIDERATIONS FOR TANDEM QUADRUPOLE MASS SPECTROMETRY

A.E. SCHOEN, J.E.P. SYKA; Finnigan MAT, 355 River Oaks Parkway, San Jose, CA 95134.

A common misconception is that the Rf only quadrupole, in a triple quadrupole mass spectrometer, is capable of passing all masses simultaneously. In fact, many parameters affect the transmission of this device. The trajectory of an ion is influenced by the RF amplitude, ion mass, kinetic energy, and entrance and exit conditions of Q2. Plots of ion transmission versus RF amplitude or kinetic energy show abundant fine structure which clearly indicate an opportunity for irreproducible results if not considered.

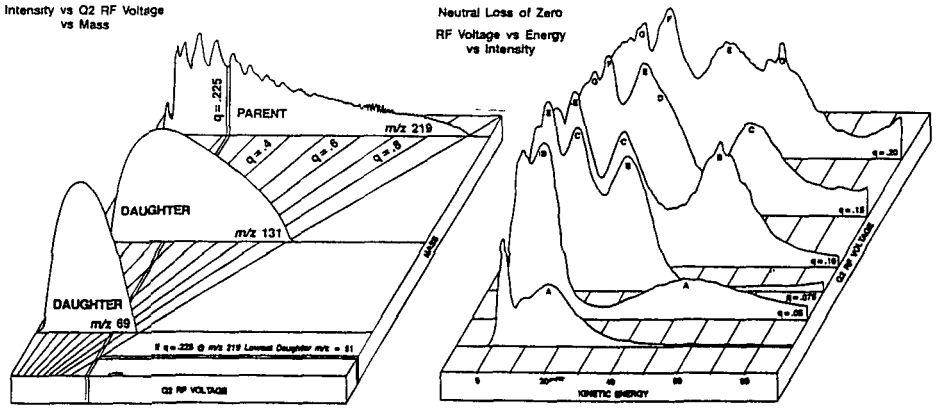

In a Rf only quadrupole, ion motion transverse to the quadrupole axis is periodic. Parent ions in a RF only quadrupole collision cell typically have an operating point (Mathieu stability parameter), q, of less than 0.4. Such ions have approximately sinusoidal motion transverse to the quadrupole axis. The frequency of this secular motion is:

$$\omega_c \cong \frac{q}{2\sqrt{2}}\,\omega \qquad \text{where} \qquad q = \frac{4\,eV_o}{(m/z)\,\omega^2 r_o^2}$$

Parent ions typically enter the collision cell close to the device axis. At every half cycle of their secular motion they return close to the axis. If the axial kinetic energy, KE axial, is well defined, the beam of parent ions travelling through the collision cell will return close to the device axis at regular intervals. The length, λ, of these beam node intervals is given as:

$$\lambda = \frac{4\pi}{q\omega} \cdot \sqrt{\frac{KE_{AXIAL}}{m}}$$

When the length of the collison cell corresponds to an integer number of beam node lengths, one observes a maximum in parent ion transmission. If the parent ion beam exits the collision cell at a midpoint between beam nodes a minimum in parent ion transmission is observed. The entrance and exit conditions of a Rf only quadrupole determine the degree to which its transmission characteristics are observed. In Q1MS mode, Q3 is operating as a Rf only ion transmission device. The lensing between Q2 and Q3 determine any trajectory descrimination. In Q3MS mode, the DC component of Q3 causes severe entrance conditions which restricts ion acceptance thereby accentuating the transmission characteristics of Q2. Therefore, better and more reproducible results will be obtained if all single MS experiments are done in Q1MS mode.

For MS/MS modes, different considerations are important. Parent ions are randomly converted to daughter ions throughout the length of the collision quadrupole. Therefore, all trajectories possible for a daughter ion are populated and daughter transmission is smooth and uniform. However, discrimination against daughter ions can occur if the Q3 offset is not programmed to compensate for kinetic energy partitioning during fragmentation. The offset for Q3 and all ion optical elements following the collision region must scan with mass to maintain uniform kinetic energy for all daughters as each is sequentially observed.

To obtain the 196 eV daughter spectrum of Pyrene, the Rf amplitude in Q2 must be set to pass from mass 202 to below 27. The frequency must be sufficient to contain a 196 eV ion of mass 202 through the curvature of a non-linear TSQ® 70 collision cell. The offset of Q3 must scan with its mass to decelerate each daughter ion to the proper kinetic energy for mass analysis. Most of the fragmentation processes shown do not appear below 100 eV CID. Even at this kinetic energy, the unfragmented parent ion dominates the spectrum and is not shown.

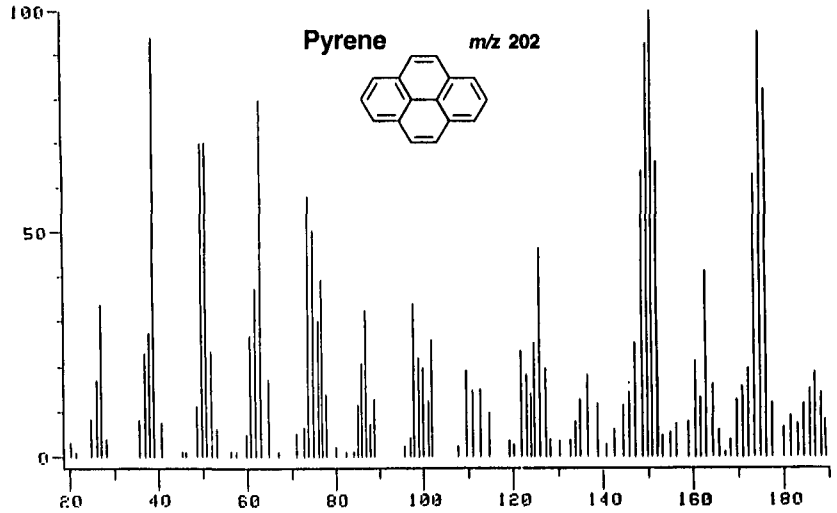

CEHT: 196 EV PYRENE

THE DESIGN OF A NEW DOUBLE FOCUSING MASS SPECTROMETER

C. Brunnée, U. Markwardt, K. Brachmann, P. Dobberstein, G. Jung, and R. Pesch

Finnigan MAT GmbH, Bremen, Federal Republic of Germany

With the advent of FAB ionization on one side and the increasing demand on ultra-sensitive, ultra-specific trace analysis on the other, the performance requirements for organic mass spectrometers have changed significantly in the last few years. A new double focusing mass spectrometer is described that has been designed specifically for these applications.

The performance of the analyzer can be characterized by the figures related to mass range, sensitivity, and resolution. Since the mass range depends on the square of the magnetic deflection radius r_m, a relatively large value of 35 cm has been chosen, resulting in a mass range of 3500 Daltons at full acceleration voltage (5 kV) and maximum field strength (about 1.7 Tesla).

Sensitivity and resolution of a sector-type mass spectrometer are interrelated and therefore have to be considered together. Theory (1) predicts that in a system with no image aberrations the product of sensitivity x resolution for a given magnetic deflection radius r_m depends linearly on the ion beam area A in the magnet (Fig. 1). Therefore all ion optical considerations were aimed at maximizing A while keeping image errors small. Second and third order calculations (2) and extensive experimental work led to the final system (Fig. 2).

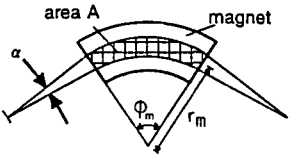

Fig. 1

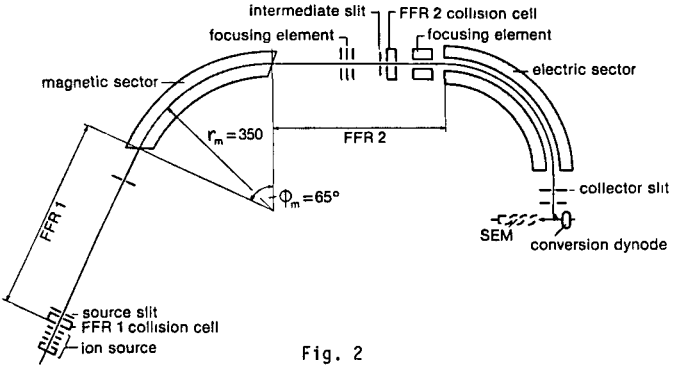

Fig. 2

Special care has been taken to minimize the α^2 (α = divergence angle in deflection plane) and $\alpha\delta$ (δ= relative initial energy spread) errors because these limit the usable beam aperture and thus directly affect the usable beam area A. Aberrations related to y (beam height) and β (divergence angle perpendicular to the plane of deflection) are also very small. The errors that depend on the initial energy spread of the ions ($\delta^2 + \alpha\delta$) have been minimized to virtually Ø ("perfect double focusing") (Fig.3).

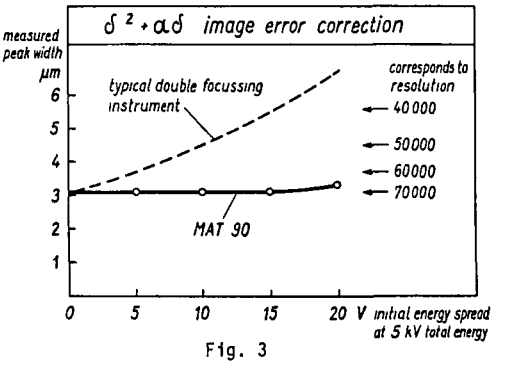

Fig. 3

This is of particular importance for techniques like FAB that deal with ions exhibiting a large initial kinetic energy spread.

The choice of a relatively large magnetic deflection angle Φ_m again relates to maximizing the beam area A. The overall dimensions of the instrument have been kept small by using non-normal magnetic field entrance and exit.

The routinely achieved mass resolution of well above 50 000 demonstrates the quality of the optical system. The sensitivity of 1×10^{-7} C/µg at R = 1 000 (methylstearate, EI, m/z 298) and 5×10^{-9} C/µg at R = 10 000 prove the validity of the beam area considerations.

The technical realization of the analyzer is based completely on newly designed components. Special emphasis has been put on ease of operation and reliable performance. As an example the ionization region of the ion source can be exchanged and reconfigured without breaking vacuum through the introduction of separate so-called ionization volumes. This technique (3) allows optimum adaptation of the ion source for various ionization techniques. Since the ionization region is the part most susceptible to contamination by sample, reagent gas or matrix, the simple exchange or replacement of ionization volumes also significantly increases the productivity of the instrument due to reduced need of source cleaning.

The instrument is controlled and operated by an integrated multi-processor arrangement consisting of five independent 16-bit processors and a PDP 11/73 host computer (Fig. 4).

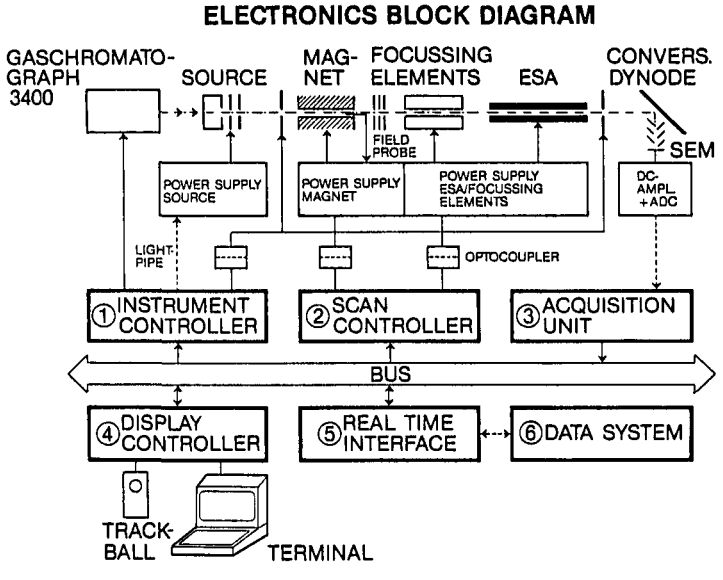

Fig. 4

Connections between digital and analog electronics are completely optically decoupled for maximum reliability. The system fully supports interactive operation as well as automated data-dependent procedures for complete experiment series. System status information and results can be displayed simultaneously and independently using up to eight windows on the central control terminal.

(1) H. Wollnik, Nucl. Instr. and Meth. 95 (1971) 453

(2) "GIOS" a Program for the Design of Ion Optical Systems, H. Wollnik, I. Brezina, E. Kasseckert, K. Becker and T. Matsuo, unpublished

3) U.S. patent 4,388,531

Effects of Windowing Upon FTMS Signals

by D. Alan Hanna and Seth Goodman
Nicolet Analytical Instruments
Madison, Wisconsin, 53711-0508

Introduction

It is generally desirable to apply a window function to an FTMS transient before it is Fourier transformed to yield a spectrum. The main purpose of this is to suppress baseline ringing caused by the abrupt onset and termination of the transient. Use of a window function on transients with moderate or severe decay rates also reduces the size of the broad "skirts" at the base of peaks. The improvements to peak shape are especially important if automated peak finding is required.

These improvements to peak shape come at the expense of both peak center lobe width and signal to noise ratio (S/N). The deterioration in the latter two quantities depends on the particular window function used and the decay rate of the transient. An adjustable window function allows the spectroscopist to make an appropriate tradeoff between peak shape, peak center lobe width and S/N. One such window family that can be adjusted by a single parameter, α, is:

$$\begin{array}{ccccc} \dfrac{1-\cos\left(\frac{\pi t}{\alpha}\right)}{2} & , & 1 & , & \dfrac{1-\cos\left(\frac{\pi(1-t)}{\alpha}\right)}{2} \\ 0 \le t \le \alpha & & \alpha \le t \le 1-\alpha & & 1-\alpha \le t \le 1 \end{array} \qquad 0 \le \alpha < .5$$

$$\frac{1-\cos(2\pi t)}{2} - (.2\alpha - .1)(1 - \cos(4\pi t)) \qquad .5 \le \alpha < .95$$

The window function is used by multiplying it by the original FTMS transient, point by point, and then using the modified transient for all further processing. The particular value for α which is chosen will determine the extent to which the original transient is modified. An α value of 0 represents no change to the original whatsoever, a value of .95 represents the greatest modification within this family of window functions.

Effect of window functions on baseline peak shape

The effect of varying the window parameter, α, on baseline peak shape is shown for various transient decay rates (see figure 1). The plot is normalized to the peak width at 1% height for $\alpha = 0$, which corresponds to no window function. The total width of a peak, including baseline ringing, at 1% of its maximum height is an indicator of its suitability for automated peak finding methods and its distinguishability from nearby peaks with greatly different intensities. Improvement to peak shapes of lightly decayed transients by windowing results mostly from removing baseline ringing. Peak shapes of heavily decayed transients are improved by reducing the broad "skirts" at the base of Lorentzian peaks.

Effect of window functions on peak center lobe width

The effect of varying the window parameter, α, on peak center lobe width is shown for various transient decay rates (see figure 2). Center lobe width is important for achieving high resolution of peaks of nearly equal intensity. For a lightly decayed transient, applying a window function always increases the center lobe width of the peak. The "stronger" the window function used (larger α) to improve peak shape near the baseline, the more the widening of the center lobe. Exactly the opposite happens for heavily decayed transients. "Stronger" windows which improve peak shape near the baseline also decrease center lobe width.

Effect of window functions on S/N

The effect of varying the window parameter, α, on S/N is shown for various transient decay rates (see figure 3). S/N is defined here as the ratio of peak height to RMS noise amplitude in the white noise portion of the spectrum. Because using a window function on lightly decayed transients increases the center lobe width, the peak height can be expected to decrease. Noise is reduced by the window function, too, but not as much as peak height so the S/N decreases. Heavily decayed transients have decreased peak widths after using window functions, but so much of their energy falls under the initial low part of the window that the peak height is reduced, decreasing S/N. Apparently, this series of window functions reduces S/N for a transient of any decay rate.

Conclusions

Applying a window function to an FTMS transient before Fourier transformation can make a significant improvement in the baseline peak shape. For highly decayed transients, center lobe width is also improved. However, in all cases S/N suffers. A series of curves characterizing an adjustable window function allows making a rational tradeoff between baseline peak shape, center lobe width and S/N for a transient of a given decay rate.

References

1] Geckinli, N. C. and Davras, Y., *IEEE Trans. on Acoustics, Speech and Signal Processing*, "Some novel windows and a concise tutorial comparison of window families",vol ASSP-26, Dec 1978, pp. 501-507.

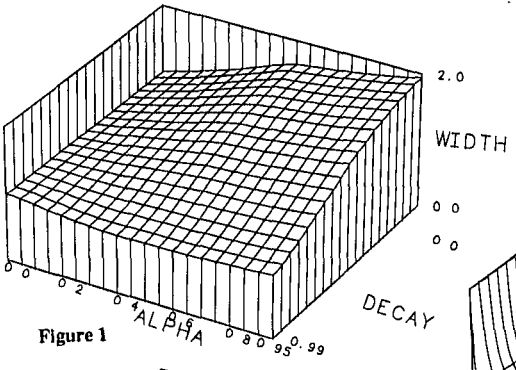

Figure 1

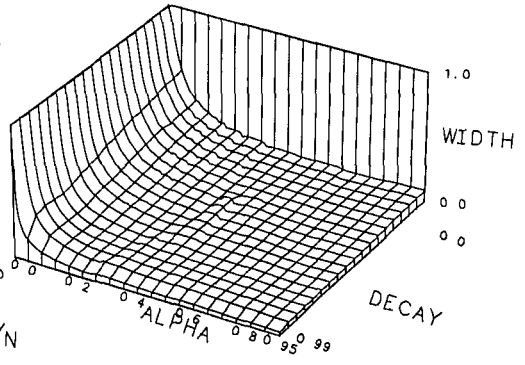

Figure 2

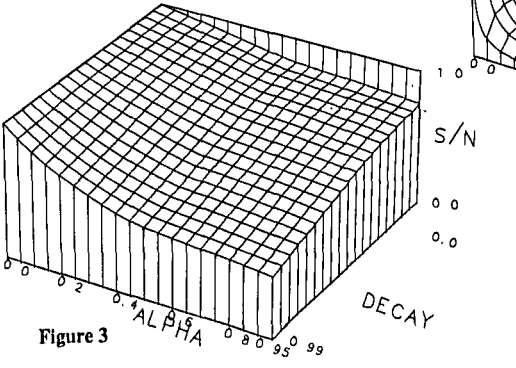

Figure 3

NEW SOFTWARE FOR THE CONTROL AND ANALYSIS OF SELECTED ION MONITORING EXPERIMENTS

G A Warburton, C Moore, S Kennerley and P A Ryan
Kratos Analytical, Barton Dock Road, Urmston, Manchester M31 2LD, UK

Introduction

It has become increasingly important in recent years to be able to detect extremely low concentrations of toxic substances such as TCDD's and PCB's. Low concentrations of certain materials have been shown to exhibit toxic and/or carcinogenic effects in test animals.

DS90 incorporates a quantitation processing package which allows accurate calculation of target compound concentration levels. Acquisition has the ability to alter the magnetic field during voltage generated SIM experiments to permit maximum sensitivity to be maintained, yet retain the precision needed to acquire unambiguous data at 10,000 resolution.

The Component File

The component file is the control unit from which SIM experiments and quantitation routines are created. It is essentially a library of target compounds. The component file contains information on:

- Compound name
- Up to 6 characteristic ions per compound
- Ion intensities for the 6 ions
- Expected retention time, retention index and retention window
- Concentration information for quantitative calibrations
- Internal standard information
- Peak width parameters for automatic detection

Up to 200 components can be stored in a file and any number of files may be created.

Quantitation

Quantitation routines utilise component files for their information. Two basic options are available - **Calibration**, in which data from known standards are processed and stored and **Analysis** in which unknown samples can be automatically quantified. Three types of calibration routine, linear, quadratic and average response factor are available.

The program utilises internal or external standards, 1 or 2 internal standards may be used. Calibration and hence analysis can be performed on up to six ions from each component against six ions in each internal standard. Up to five concentration levels may be used in a calibration with up to six injections at each level.

The data shown in Figure 1 shows a calibration curve obtained from injections of 1000, 100 and 10 femtograms of PCB's in the negative ion mode.

Analysis uses a relevant calibration, the component file and peak detection routines to locate, identify and quantify GC peaks automatically. The report gives data on the average result together with the standard deviation.

SIM Operation

Selected Ion Monitoring (SIM) experiments are performed from a SIM experiment file. This experiment file is created from a component file. Individual groups are created according to retention times and windows. Any component with overlapping windows will be combined in the same group.

The SIM experiment is performed by ESA switching but different magnet positions are allowed for each group. During a single analysis many different components may be monitored over widely differing mass ranges. Electric sector voltage switching provides the most accurate method of mass selection yet has the disadvantage of lowering sensitivity over large mass ranges. By combining magnet switching between groups with ESA switching between masses, maximum sensitivity and accuracy can be obtained. Other facilities include a sweep, cycle time (total) and relative or fixed dwell times. If relative dwell times are specified the peak intensity information supplied in the component file is utilised. Calibration is performed automatically for each group including the magnet position changes.

This complete experiment file can be stored on disk together with any calibrations for immediate use in future analyses.

Figure 2 illustrates the detection levels possible using the SIM program with an MS50FS. In this case 10 femtograms each of three PCB isomers have been detected in the negative ion mode.

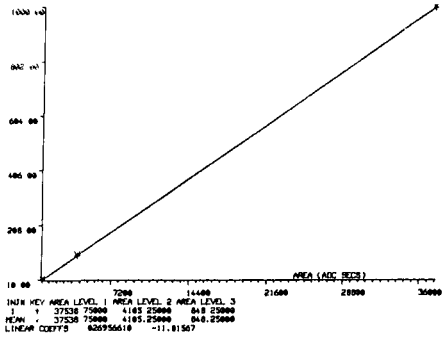

Figure 1 **Calibration graph for 1000, 100 and 10fg injections of PCB's in the negative ion mode**

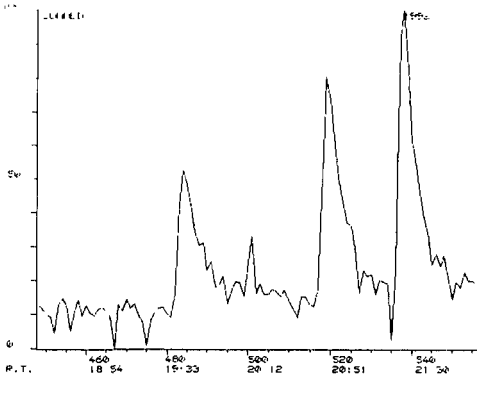

Figure 2 **Total ion current for three PCB isomers analysed at the 10fg level**

LOW MASS DETECTION IN FTMS BY AUTOMATIC UNFOLDING OF ALIASED PEAKS

Robert B. Cody, James A. Kinsinger, and Seth D. Goodman
Nicolet Analytical Instruments, 5225-1 Verona Road, Madison, WI 53711

The increasing use of higher magnetic fields in FTMS brings about a need for fast digitizer rates in order to detect low mass ions, which have high resonant frequencies. This requirement may be overcome by deliberately exciting low mass ions into coherence, while operating the digitizer at a reduced rate. Low mass ions having resonant frequencies greater than one-half the digitization rate will appear at predictable lower frequencies in the spectrum (1). An automatic routine has been developed which locates and identifies these low mass ions as they occur in the spectrum. The method is based upon a low mass lookup table, which may also be useful as an adjunct to elemental composition calculations for spectral interpretation.

The low mass lookup table is based upon the fact that a limited number of elemental compositions are possible for low mass ions in organic EI spectra. The table is an extension of Mass Spectral Correlations (2), with added isotopic information and molecular ion compositions. The presence of a low mass ion is determined by calculating the apparent frequency for each ion in the table, and checking for its presence in the spectrum. An ion with resonant frequency f, greater than one-half the sampling frequency fs, will have an apparent frequency fapp, according to the relation:

$$fapp = /f-nfs/$$

where n is an integer (0,1,2...) that satisfies the condition:

$$0 \leq fapp \leq fs/2$$

The inherent high-resolution and mass accuracy of FTMS make it practical to separate folded-back peaks from ions of the same nominal mass.

The method is limited by the lookup table to ions which are normally encountered in EI spectra of organic compounds. Resolution and mass accuracy should be sufficient to separate masses that are at least 0.01 amu apart. Under these constraints only a small number of masses cannot be distinguished on the basis of mass alone, and other criteria must be applied (e.g. the presence of isotope peaks for chlorine-containing ions).

This procedure provides methods for detection of lower masses without increasing the digitizer rate, increasing resolution by increasing the observation time for a fixed number of data points (without losing low mass information), and rapidly determining elemental compositions of the low mass ions in the spectrum.

1. Cody, R. B.; Kinsinger, J. A. Analytical Chemistry 1986, 58, 670-671.

2. McLafferty, F W.; Venkataraghaven, R. "Mass Spectral Correlations", 2nd edition; ACS: Wash. D.C., 1982.

CYCLOHEXANONE

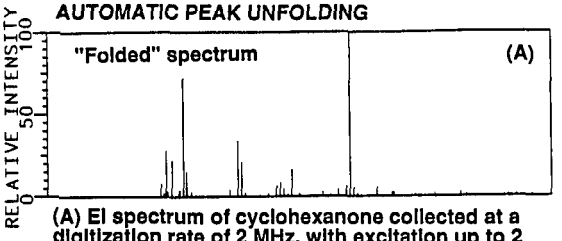

(A) EI spectrum of cyclohexanone collected at a digitization rate of 2 MHz, with excitation up to 2 MHz.

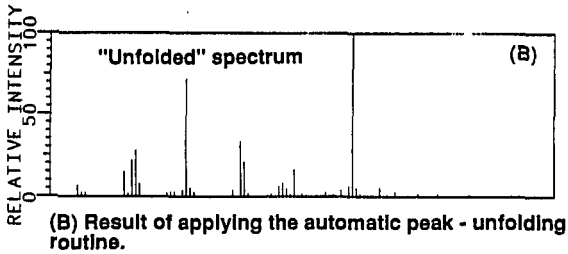

(B) Result of applying the automatic peak - unfolding routine.

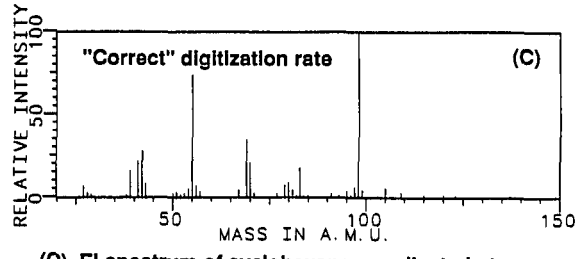

(C) EI spectrum of cyclohexanone collected at a digitization rate of 4 MHz, with excitation up to 2 MHz.

AN EI SOURCE OPTIMISED FOR LOW LEVEL POLLUTANT ANALYSIS BY GC-HRSIR

B.N. Green. B.W. Gray, S.A. Guyan and S.T. Krolik, VG Analytical Ltd, Floats Road, Wythenshawe, Manchester M23 9LE. UK.

Introduction

In the analysis of low levels of pollutants by gas chromatography - high resolution selected ion recording (GC-HRSIR), one of the major factors which limits the detection level and reproducibility is the basic sensitivity of the ion source. Over the last 2 years or so, improvements to the ion optics of medium performance instruments together with the development of ion sources has substantially improved the sensitivity, particularly whilst operating at the high ion chamber pressures inevitably present when coupled to a capillary GC. Nevertheless, even at 1000 resolution, only a fraction of a percent of the molecules entering the ion chamber are registered as ions at the collector. This low efficiency of converting molecules to detectable ions occurs mainly in the source. A new EI source has been developed in which the conversion of molecules to ions has been improved, essentially by increasing the probability that a molecule will be ionized whilst it is in the source. Moreover, by operating the source at 30-35 eV electron energy, its sensitivity is only marginally reduced by the large helium pressures encountered when coupled to the GC.

Source Characteristics

The basic sensitivity of the new source when fitted to a medium performance instrument (VG 70-S) was measured at 1000 resolution to be over 2×10^{-7} c/ug of methyl stearate introduced by the direct insertion probe.

To simulate its performance under GC conditions, the molecular ion of m-xylene was monitored as various flow rates of helium were admitted into the ion chamber. Figure 1 shows the way in which the relative sensitivity varied with helium flow rate at several electron energies, with the source controls initially optimised at 1 ml/min. As expected, at 70 eV electron energy, the sensitivity rapidly dropped as the flow rate of helium was increased, so that at 1 ml/min, the sensitivity had dropped to less than 30%. However, when the space charge effects caused by the helium ions was reduced by operating at 30-35 eV electron energy, the sensitivity was only marginally less with 1 ml/min flowing than at 70 eV with no helium flowing. Moreover, provided the source is optimised at a flow rate in the middle of the range over which it is desired to operate, a fairly flat plateau is obtained. For example, at around 34 eV electron energy, with initial optimisation at 1 ml/min, flow rates from 0.5 - 1.5 ml/min were accommodated with a change of about 10% in sensitivity.

High Resolution - Selected Ion Recording Performance

To illustrate the performance of the source under GC-HRSIR conditions, a standard solution containing nominally 60 fg of 2,3,7,8-TCDD and 10 pg of ^{13}C-2,3,7,8-TCDD was injected onto a 0.2 mm diameter 30 metre long OV-1 fused silica capillary column. The mass spectrometer was operated at 10,000 resolution and the m/z 319.8965, 321.8936, 331.9368 and 333.9339 ions were monitored using the standard SIR routine on the VG 11-250 data system. Each mass was monitored for 80 ms in each cycle (440 ms). A lock mass from PFK at m/z 316.9824 was also monitored once during each cycle and used to keep the instrument accurately positioned on the selected masses. This facility is essential to maintain maximum sensitivity and to ensure reproducibility in the area and isotope ratio measurements since, at 10,000 resolution, a drift of only 10 ppm in the mass position will cause a loss of about 20% in sensitivity whilst a 50 ppm drift will reduce the response to only 5%.

Figure 2 shows typical raw (unsmoothed) data from 60 fg of the natural 2,3,7,8-TCDD. In order to show the noise level more clearly, part of the base line on traces B and C has been magnified by a factor of 5. It can be seen that the signal to noise ratio in the response from the 60 fg of natural TCDD is over 10:1. This and similar data, after adjustment for GC peak width indicates that better than 10 to 1 signal to noise ratio can be expected from 100 fg of 2,3,7,8-TCDD when the GC peak width at half height is 2 seconds.

To assess the reproducibility, 8 injections of a standard containing 1 pg of 2,3,7,8-TCDD and 5 pg of ^{13}C-2,3,7,8-TCDD were made and the m/z 320/322 and 332/334 ratios calculated automatically from the areas under the peaks. These ratios are listed in the Table together with the standard deviation and coefficient of variation. Thus a coefficient of variation of better than 5% in the ratio can be expected from 1 pg of TCDD injected.

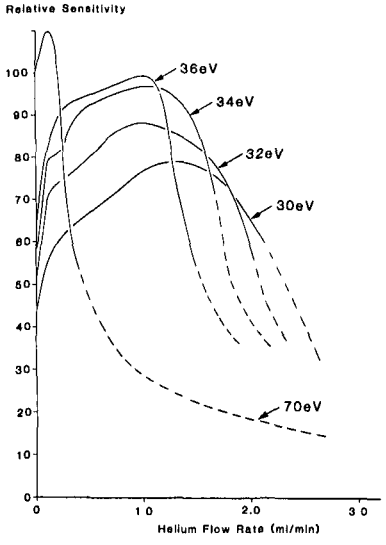

Figure 1. Source characteristics.

Run Number	m/z 320/322 Ratio	m/z 332/334 Ratio
1	0.812	0.786
2	0.788	0.798
3	0.786	0.795
4	0.773	0.781
5	0.739	0.773
6	0.763	0.779
7	0.734	0.807
8	0.795	0.795
Mean Ratio	0.774	0.789
Standard Deviation	±0.027	±0.011
Coeff. of Variation	±3.5%	±1.5%

Table. Isotope ratio reproducibility from 1pg and 5pg of natural and ^{13}C labelled TCDD resp.

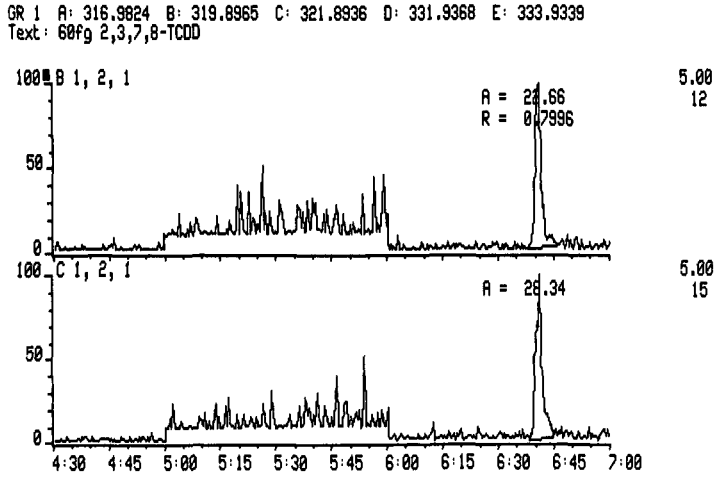

Figure 2. Responses at m/z 319.8965 and 321.8936 from 60fg of 2,3,7,8-TCDD. Resolution = 10,000.

"A CALIBRANT FOR ACCURATE MASS MEASUREMENT IN HIGH RESOLUTION CIMS"

M.J.EVANS, L.MALTAIS AND M.J. BERTRAND
REGIONAL CENTER FOR MASS SPECTROMETRY
DEPARTMENT OF CHEMISTRY
UNIVERSITY OF MONTREAL
P.O.BOX 6128, STATION A, MONTREAL, QUEBEC, CANADA H3C 3J7

INTRODUCTION

A number of compounds and substances have been reported and used as mass reference standards in analytical mass spectrometry. In electron impact ionization perfluoroalkanes and perfluorotributylamine are widely used and can provide evenly spaced and relatively intense ions up to m/z 800. Perfluorotriheptyltriazine is also a useful calibrant for masses above 600 daltons and Fomblin oil can be utilized up to mass 2300. For other ionization techniques, compounds such as phosphazenes have been reported for mass calibration in field desorption and metal halides are frequently used in fast atom bombardment. In electron capture chemical ionization compounds such as phosphazenes and perfluorotriazines have been studied and it has been reported that Fomblin oil can be used to calibrate a data system up to 3500 daltons. However, for accurate mass determination in high resolution positive chemical ionization few compounds can be used on a routine basis. Perfluorokerosene and perdeuterated alkanes have been suggested (1) but the former was found not to yield ions with isobutane, to generate background ions at every mass with methane and the latter are difficult to use in a heated inlet system because they lack volatility. In order to find a calibrant for routine accurate mass determination of common organic compounds under general CI conditions, polydimethylsiloxanes have been studied and results indicate that they possess most of the characteristics of a mass calibrant.

EXPERIMENTAL

The mixture of polydimethylmethylsiloxanes (average M.W.770) used in this study was obtained from Polysciences (Warrington PA). All mass spectral analyses were conducted on a Kratos MS-50 TCTA mass spectrometer using a Kratos Mark IV EI/CI source. For accurate mass determination the reference compounds were introduced through a heated inlet reservoir maintained at 200° and the analytes using the direct insertion probe. The reagent gas (CH_4 or $i\text{-}C_4H_{10}$) was admitted into the ion source through the inlet reservoir to reduce pressure differentials in between the ion source and the reservoir.

RESULTS AND DISCUSSION

Polydimethylsiloxanes are readily available from commercial sources because of their extensive use in chemistry and their volatility is compatible with conditions usually encountered in a mass spectrometer. The volatility of small oligomers (m/Z 1000) is such that the volatility of the mixture can be adjusted to operating conditions by varying the relative concentrations of the individual constituents. These compounds exhibit periodicity in there structure which should ensure the presence of evenly spaced ions throughout the mass range of interest. Eventhough the $(CH_3)_2S_1\text{-}O$ units of the backbone are not mass deficient (74.0188 daltons) the mass excess is small and the ion peaks should be easily separated at moderate resolutions from those of common organic compounds.

The chemical ionization spectra of the mixture have been obtained using methane and isobutane as reagent gases and part of the spectrum obtained with methane is shown in figure 1. The spectrum consists of a major sequence of ions at 73,147,221, 295 and every 74 daltons up to masses 1035 resulting from the cleavage of the S_1O bonds. Other ions in the spectrum belong to three other minor overlapping sequences that result in the presence of ions at every 14,14,16 and 30 daltons. Although of weak relative intensities above m/z 800 ions peaks are seen up to m/z 1051 with this mixture. The weak intensities of the peaks above mass 800 are partly explained by the low concentrations of higher oligomers (n 10) in the mixture. Using isobutane as a reagent gas the features of the spectrum are essentially the same but the absolute intensities of the ions peaks were found to be lower. The accurate masses and

compositions of the sequence peaks have been determined by peak matching and the exact masses of the ions observed are given in Table I. Values indicated by an (R) in Table I are used for computer interpolation whereas all the other peaks can be used for manual peak matching. Using a data system the useful mass range for calibration was found to be from 73 to 739 using this mixture. In order to verify the usefulness of the mixture of polydimethylsiloxanes as a mass reference standard for routine exact mass determination of common organic compounds, several samples have been analyzed at 10,000 resolving power and a few examples are given in Table II. It can be seen from the results that the deviations observed are all within the usual errors for these types of measurements under these conditions. The presenceof heteroatomes such as Br or Si on these molecules or the low H/C ratio as in $C_{18}H_{21}O_6N_3$ did not create any interference with the peaks of the calibrant. In most cases a reference peak can be found within 15% of any mass value except at the lower end where the ionic intensities in between m/z 73 and 147 are rather weak.

(1) I. Dzidic, D.M. Desiderio, M.S. Wilson, P.F. Crain, J.A. McCloskey. Anal. CHem. (1971), 43,77.

FIG 1

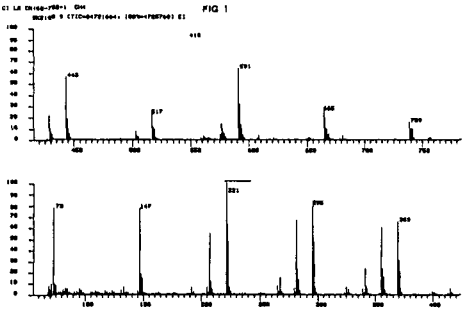

TABLE I

EXACT MASSES OF IONS IN THE CI/CH_4 SPECTRUM OF THE MIXTURE

MASS	FORMULA		MASS	FORMULA		MASS	FORMULA	
73.0473	C_3H_9Si	(R)	415.0372	$C_8H_{27}Si_4O_7$	(R)	739.2165	$C_{21}H_{43}Si_{12}O_6$	(R)
89.0423	C_3H_5SiO		429.0893	$C_{11}H_{33}Si_4O_6$	(R)	755.2114	$C_{21}H_{53}Si_{12}O_{10}$	
118.9621	$C_3H_3Si_2O_3$		443.1413	$C_{12}H_{35}Si_4O_6$	(R)	785.1312	$C_{18}H_{57}Si_{13}O_{12}$	
135.0141	$C_3H_5Si_2O_3$	(R)	459.1362	$C_{12}H_{35}Si_4O_7$	(R)	799.1832	$C_{21}H_{43}Si_{11}O_{11}$	
147.0661	$C_5H_{15}Si_2O$	(R)	489.0560	$C_{11}H_{33}Si_5O_8$	(R)	813.2353	$C_{22}H_{45}Si_{11}O_{11}$	
163.0610	$C_5H_{15}Si_2O_2$		503.1080	$C_{12}H_{35}Si_5O_7$	(R)	829.2302	$C_{22}H_{45}Si_{11}O_{12}$	
192.9809	$C_4H_3Si_2O_4$		517.1600	$C_{12}H_{35}Si_5O_8$	(R)	859.1500	$C_{19}H_{53}Si_{12}O_{13}$	
207.0329	$C_4H_{13}Si_2O_3$	(R)	533.1550	$C_{12}H_{35}Si_5O_9$	(R)	873.2020	$C_{20}H_{55}Si_{12}O_{12}$	
221.0849	$C_5H_{21}Si_2O_3$	(R)	563.0748	$C_{11}H_{33}Si_6O_9$	(R)	887.2520	$C_{20}H_{55}Si_{12}O_{11}$	
237.0798	$C_5H_{21}Si_2O_4$		577.1268	$C_{12}H_{35}Si_6O_8$	(R)	903.2490	$C_{19}H_{53}Si_{12}O_{12}$	
266.9997	$C_4H_{13}Si_3O_3$	(R)	591.1789	$C_{12}H_{35}Si_6O_9$	(R)	933.1688	$C_{19}H_{55}Si_{12}O_{14}$	
281.0517	$C_5H_{21}Si_3O_4$	(R)	607.1738	$C_{12}H_{35}Si_6O_{10}$	(R)	947.2208	$C_{20}H_{55}Si_{12}O_{13}$	
295.1037	$C_6H_{27}Si_3O_3$	(R)	637.0936	$C_{11}H_{33}Si_7O_{10}$		961.2728	$C_{21}H_{57}Si_{12}O_{12}$	
311.0986	$C_6H_{27}Si_3O_4$		651.1456	$C_{12}H_{35}Si_7O_9$	(R)	977.2677	$C_{21}H_{57}Si_{12}O_{13}$	
341.0184	$C_5H_{21}Si_4O_4$	(R)	665.1977	$C_{12}H_{35}Si_7O_{10}$	(R)	1007.1876	$C_{18}H_{55}Si_{12}O_{15}$	
355.0705	$C_6H_{27}Si_4O_3$	(R)	681.1926	$C_{12}H_{35}Si_7O_{11}$		1021.2396	$C_{19}H_{57}Si_{12}O_{14}$	
369.1225	$C_{11}H_{33}Si_4O_4$	(R)	711.1124	$C_{11}H_{33}Si_8O_{11}$		1035.2916	$C_{20}H_{57}Si_{12}O_{13}$	
385.1174	$C_{11}H_{33}Si_4O_5$		725.1644	$C_{12}H_{35}Si_8O_{10}$		1051.2865	$C_{20}H_{57}Si_{12}O_{14}$	

TABLE II

EXAMPLES OF EXACT MASS DETERMINATION OF (M+H) IONS USING POLYDIMETHYLSILOXANES AS A MASS REFERENCE STANDARD.

COMPOUND	THEORETICAL	MEASURED[1]	ERROR(ppm)
$C_{16}H_{38}O_2$	299.2950	299.2945	1.5
$C_{12}H_{13}O_2SiBr$	273.0315	273.0315	0
$C_{18}H_{21}O_6N_3$	376.1508	376.1509	0.2
$C_{22}H_{19}SiN$	342.2617	342.2634	3

[1] Mean of three measurements.

ADVANTAGES AND LIMITATIONS OF "BATCH" MASS SPECTROMETRIC METHODS FOR MIXTURE ANALYSIS.

Daniel B. Kassel, Daniel D. Bombick, Karen J. Light, John Allison, Department of Chemistry, Michigan State University, East Lansing, MI 48824

A most useful method for analyzing mixtures of volatile compounds is in the combination of gas chromatography and mass spectrometry (GC/MS). Mixtures of non-volatile compounds require extensive work-up procedures involving derivatization to enhance their volatility for GC/MS analysis. These procedures are often time-consuming; frequently a portion of the sample is easily lost in the isolation and derivatization procedures. Furthermore, mass spectra are frequently found to be dominated by fragment ions indicative of the derivatizing agent.

An alternative to the GC/MS approach is to characterize mixtures by "batch" methods which do not utilize a chromatographic step. "Batch" methods such as Fast Atom Bombardment (FAB) may eliminate the need for derivatization and excessive sample handling. Furthermore, analysis times may be significantly shortened by these "batch" approaches. We have investigated the utility of available and novel "batch" ionization methods in the context of their ability to characterize simple model mixtures both qualitatively and quantitatively.

Direct insertion EI- and CI-MS analysis of mixtures suffers from spatial overlap of species distilling off of the probe, marking characterization, both quantitatively and qualitatively, difficult. An alternative direct method for mixture analysis which eliminates the problem of the temporal distribution of species by DIP-MS is that of FAB. Components of the mixture are ionized simultaneously; typically, only a few ions representative of a particular compound are formed. However, FAB-MS is hindered, and characterization of mixtures is complicated, by severe matrix effects (a well documented phenomenon). Negative ion FAB spectra of these mixtures, though, are not as prone to the matrix effects observed in the positive ion mode. A major problem with the FAB technique for mixture analysis is in the choice of an appropriate solvent.

A new ionization technique has been developed in our laboratory for the analysis of thermally labile compounds. The analyte is deposited on a potassium thermionic emitter probe and heated rapidly within the mass spectrometer's source. Potassium ion adducts are generated which are representative of the analyte. Our results suggest that potassium adducts are formed in the high pressure region above the surface of the thermionic material. We call this technique K^+IDS (potassium ionization of desorbed species). Similarly if a sodium thermionic material is used the technique is called Na^+IDS (sodium ionization of desorbed species).

One of the first mixtures analyzed using this new technique was a polymer. A polyethylene glycol polymer of known average molecular weight was used. Consider such a polymer as a mixture of oligomer species containing the monomeric unit characteristic of that polymer. Initial results showed that the average molecular weight could be obtained using K^+IDS. This would suggest that the relative concentration of desorbed species above the surface of the emitter parallels that of the original mixture. In addition, since the mixture is rapidly heated, little or no decomposition products are formed.

Based on these results, K^+IDS may have potential for routine mixture analysis, in which all components are (essentially) simultaneously desorbed from the surface of the alkali emitter. Furthermore, this method is solvent independent. Results by K^+IDS and Na^+IDS of our model fatty acid mixtures, and others, are encouraging for quantitative determinations. No matrix effects are present and only molecular weight information is obtained, thereby providing a true molecular weight profile of the mixtures. Shown in figure 1a and 1b are the mass spectra of fatty acid mixture analyzed by both negative ion FAB and Na^+IDS. A correlation between molecular weight and ion intensity is observed. This behavior is also shown for K^+IDS mass spectra.

Similar behavior is observed for other model mixture systems, when homologous series are involved. This technique, therefore, appears to be useful as a "batch" method for quantitative analysis of mixtures. Molecular weight, "fingerprint" profiles of complex mixtures, such as urine samples, may be available by this method. We are currently investigating the possibility of combining this technique with the strengths of MS/MS for more complete characterization of complex mixtures.

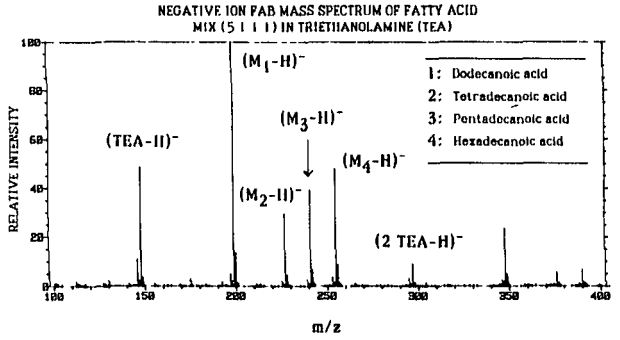

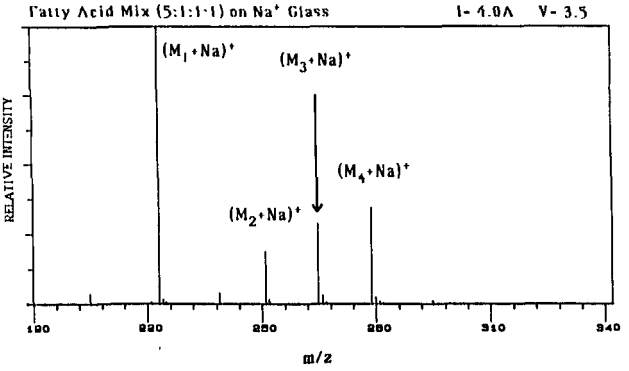

Figure 1 (a) 5:1:1:1 molar mixture of fatty acids C_{12}, C_{14}, C_{15}, and C_{16} by negative ion-FAB in triethanolamine.

(b) Same fatty acid mixture by Na^+IDS.

COMPARISON OF CI AND EI DIRECT INJECTION CAPILLARY GC/MS METHODS FOR THE ANALYSIS OF SELECTED MEAT FLAVOR PRINCIPLES USING A PURGE-AND-TRAP TECHNIQUE

R. H. Liu, M. G. Legendre, R. J. Berni, J. W. Kuan and J. R. Vercellotti
USDA, ARS, SRRC, P. O. Box 19687, New Orleans, LA 70179
and
H. P. Dupuy
Virginia Polytechnic Institute and State University, Blacksburg, VA 24601

Heteroatomic compounds containing oxygen, nitrogen and sulfur, mostly Maillard reaction products with cyclic structures (1), have been previously established (2) as the principal constituents contributing to meat flavors and aromas. In cooked meat and related samples, these compounds usually occur at parts per billion levels in the presence of massive numbers of lipid oxidation products at parts per million or higher concentrations. Conventional approaches used for the analysis of these compounds usually involve the laborious extraction of kilograms of sample, concentration of large volumes of the combined extracts followed by GC or GC/MS analysis of the resulting concentrates. In this report, an efficient purge-and-trap approach is discussed that uses a commonly available rotary evaporator device. The analytes, entrapped in Tenax packed in a glass liner, are then purged, with an external inlet device (3), into a GC/MS system for analysis. Results obtained from complimentary EI and CI approaches are compared.

Figure 1A represents a typical reconstructed total ion chromatogram obtained under 70 eV EI conditions. Since the compounds of interest are presented in relatively low concentrations, selected ion displays (Fig. 1B-1G) are used to alert their possible presence. Using these displays as a guide, identifiable spectra are obtained with

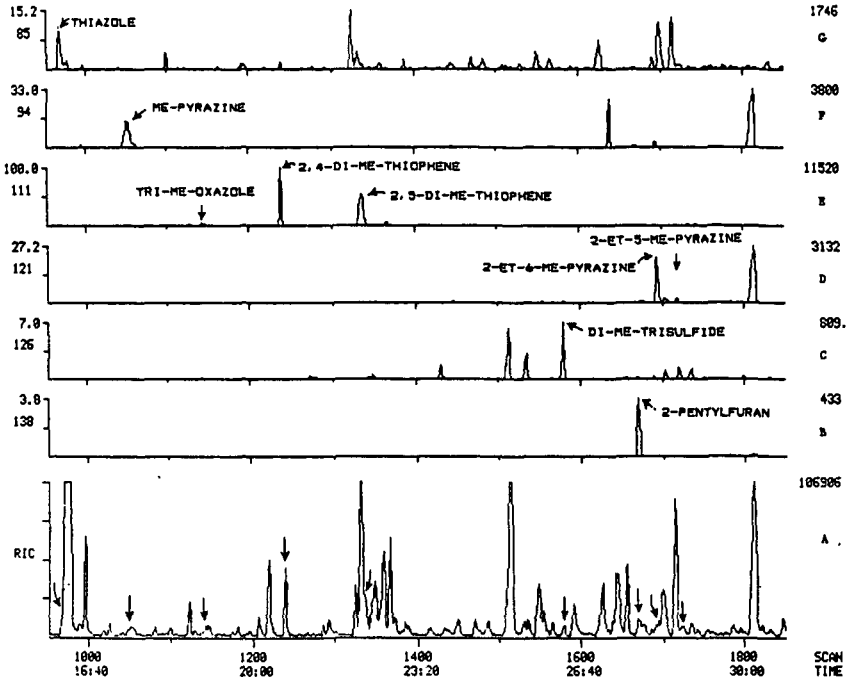

FIGURE 1. TOTAL ION (A) AND SINGLE ION (B - G) DISPLAYS OF A TYPICAL CHROMATOGRAM

proper background subtraction and then interpreted. With this simple approach, more than fifty heteroatomic compounds are identified in a single analysis. Relative retention characteristics under a set of experimental conditions are then used as one of the parameters for the identification of these compounds in the ion chromatograms obtained under CI conditions.

Chemical ionization experiments include the use of helium as the carrier gas with methane or ammonia as the CI reagent gas, and the use of methane as the carrier gas with or without ammonia as the reagent gas. Identifications of the compounds of interest are based on the relative retention times established by EI experiments and the ion intensity ratio of protonated and adduct ions. Realizing that protonated and adduct ion intensity ratios are affected by reagent gas pressure, the latter parameter is closely controlled by monitoring the relative intensities of selected ions produced by the reagent gas used (4). Protonated and adduct ion intensity ratios of selected heteroatomic compounds of interest are shown in Table 1.

Data summarized in Table 2 compare the responses of the most intense ions derived from selected heteroatomic compounds under EI and various CI conditions. Since chromatographic patterns of these compounds vary with the carrier gas conditions used in CI experiments, peak areas, rather than peak scan intensities, are used for comparison. Data obtained from the adopted conditions indicate that CI experiments with methane as the carrier gas provide the most intense responses for most of the heteroatomic compounds. However, the use of ammonia as the CI reagent gas provides better distinction of protonated to adduct ion intensity ratios. These compounds are also slightly better resolved with helium as the carrier gas.

TABLE 1
PROTONATED TO ADDUCT ION INTENSITY RATIO

Compound	He/CH_4 MC_2H_5/MH	CH_4 MC_2H_5/MH	He/NH_3 MNH_4/MH	CH_4/NH_3 MNH_4/MH
2-Acetylthiazole	1.9	0.8	310	90
Thiazole	13	11	54	33
4-Methylthiazole	15	13	21	11
4,5-Dimethylthiazole	17	18	8.5	3.4
Benzothiazole	6.3	8.7	7.5	0
2-Methylpyrazine	13	13	52	15
2-Methylthiopyrazine	9.3	20	39	15
2-Ethylpyrazine	14	16	34	*
2,5-Dimethylpyrazine	14	12	17	12
2-Ethyl-6-methylpyrazine	14	15	14	3.1
Pyrazine	12	9.8	8.0	0
2-Ethyl-3-methylpyrazine	16	16	7.0	1.9
2-Ethyl-5-methylpyrazine	13	11	5.6	0
2-Acetyl-3-ethylpyrazine	3.4	6.0	3.2	0

TABLE 2
INTENSITIES OF MOST PROMINENT IONS

Compound	He/CH_4	CH_4	He/NH_3	CH_4/NH_3	EI
2-Acetylthiazole	1324	3735	326	312	391
Thiazole	20630	61651	17873	5436	14495
4-Methylthiazole	20465	55332	27404	9919	14549
4,5-Dimethylthiazole	25302	41720	24062	9692	10383
Benzothiazole	396	888	589	503	650
2-Methylpyrazine	1901	4504	1355	202	1756
2-Methylthiopyrazine	450	2156	462	287	478
2-Ethylpyrazine	1036	15179	5167	*	3745
2,5-Dimethylpyrazine	1630	1903	2479	3061	1869
2-Ethyl-6-methylpyrazine	1158	3848	2067	1013	1548
Pyrazine	2861	3694	600	56	2848
2-Ethyl-3-methylpyrazine	2572	9795	5153	2339	1871
2-Ethyl-5-methylpyrazine	568	2442	1033	478	737
2-Acetyl-3-ethylpyrazine	426	1740	440	373	20

---

1. M. E. Bailey. In "The Maillard Reaction in Food and Nutrition", G. R. Waller and M. S. Feather, eds. Amer. Chem. Soc., Washington, 1983, p. 169.
2. S. Fors. In "The Maillard Reaction in Food and Nutrition", G. R. Waller and M. S. Feather, eds. Amer. Chem. Soc., Washington, 1983, p. 185.
3. M. G. Legendre, G. S. Fisher, W. H. Schuller, H. P. Dupuy and E. T. Rayner. J. Amer. Oil Chem. Soc., **56** (1979), 552.
4. R. H. Liu, I A. Low, F. P. Smith, E. G. Piotrowski and A.-F. Hsu. Organic Mass Spectrom., **20** (1985), 511.

GC/MS OF FLUORINATED REFERENCE MATERIALS

R. W. King
University of Florida, Department of Chemistry
Gainesville Florida 32611

FC 43, from the electrochemical fluorination of tri(n-butyl)amine, has long been used as a mass spectral reference material. FC 75, "perfluoro-2-butyltetrahydrofuran", is much less common.

The EI mass spectrum of FC 43 has peaks at m/z 614 and 576 which formally correspond to the loss of three and five atoms of fluorine from the molecular ion. Lytle and Siegel[1] reported that FC 43 is separable by low-temperature GC; lower and higher homologs of $C_{12}F_{27}N$ were found.

GC/EIMS on a poly(perfluoropropene oxide) packed column shows that FC 43[2] consists mainly of C_{12} compounds with traces of lower homologs. A very good separation is obtained on Carbopack-C/0.1% SP-1000[3]; there is one symmetrical major peak comprising about 80% of the whole, with at least twelve earlier, smaller peaks.

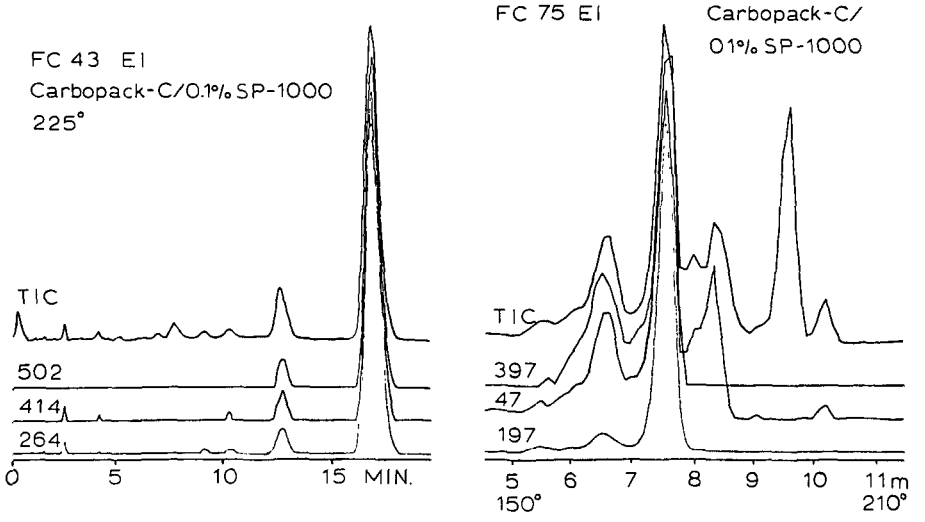

GC/EIMS Traces of FC 43 and FC 75 on Carbopack-C/0.1% SP-1000

Methane PCI[4] reveals a pattern: the 4-8 m. group of peaks has a highest mass of m/z 614 and the 8-20 m. group m/z 652, the M-F peaks of $C_{12}F_{25}N$ and $C_{12}F_{27}N$. Because of the large range of retention times on this packing compared to the fluoroether, the separation is on the basis of molecular shape as well as weight. Qualitatively similar, but chromatographically inferior, results are obtained on uncoated Carbopack-C; no appreciable amounts of higher homologs are detected at temperatures up to 350 degrees. Coated Carbopack is limited to 225 degrees. This is therefore gas/solid chromatography, via the pores of the graphitized carbon solid phase. Since linear molecules fit such pores best, a decrease in retention time should correspond to chain branching or ring formation.

The mass spectrum of the major component is quite simple. It differs from that of FC 43: m/z 614 and 576, which were hard to rationalize on the basis of a $C_{12}F_{27}N$ formula, are absent, along with m/z 464 and 376. The highest mass seen is m/z 502, which corresponds to a beta-cleavage loss of C_3F_7 from a n-C_4F_9 group. This component is probably pure $(n\text{-}C_4F_9)_3N$.

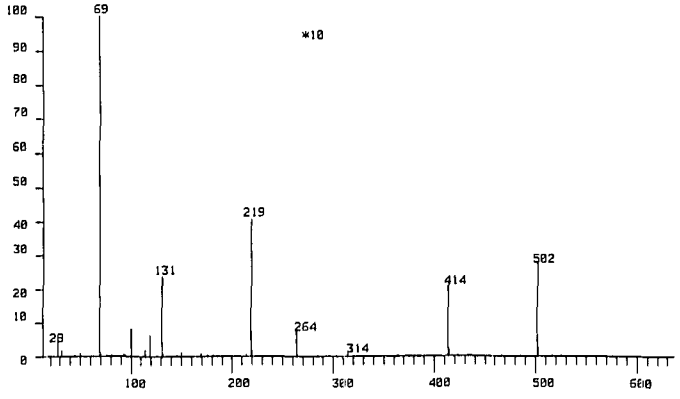

EI Mass Spectrum of the Major Component of FC 43

In contrast, FC 75 is a more complex mixture, with the major peak on Carbopack-C/0.1% SP-1000 comprising less than half of the total. The trace of m/z 397, M-F of $C_8F_{16}O$, shows a similar pattern to the F_{27} compounds in FC 43, with its major peak corresponding to the major peak in the total ion current trace. The trace of m/z 197, which would arise from beta-cleavage loss of C_4F_9 from the ring, follows that of m/z 397. However, the trace of m/z 47, CF_2O, which should indicate the presence of oxygen, shows some oxygenated compounds with no m/z 197 or 397 and longer retention times than the major peak, also some peaks without oxygen. The spectrum of the peak at 9.6 m. shows only fluorocarbon ions. The fluorination reaction yielding FC 75 appears to be more destructive than that producing FC 43. The major component may be perfluoro-2-n-butyltetrahydrofuran.

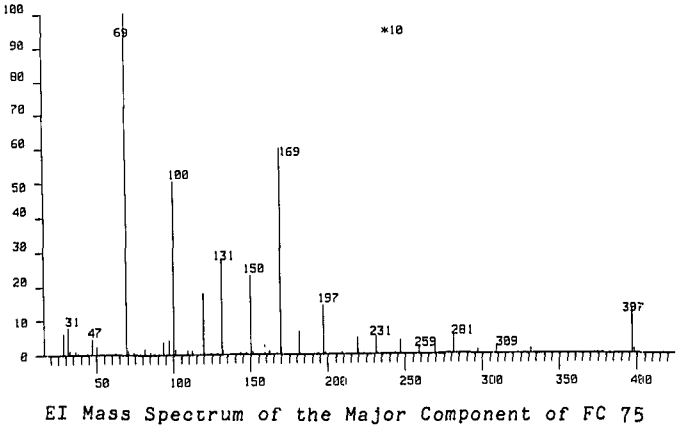

EI Mass Spectrum of the Major Component of FC 75

1. L. T. Lytle and M. W. Siegel, 33rd Pittsburgh Conference, Atlantic City, N.J., March 1982, Paper 99.
2. Samples of MS-grade FC 43 and FC 75 were obtained from SCM Specialty Chemicals, Gainesville, Florida.
3. Supelco, Inc., Bellefonte, Pennsylvania.
4. Courtesy of Dr. J. V. Johnson.

ANOMALOUS MASS SPECTRA IN THE GC/MS CHARACTERIZATION OF SOLVENTS AND VOLATILE COMPOUNDS

T. M. Seck and L. Timmons
Midwest Research Institute
425 Volker Boulevard
Kansas City, MO 64110

During the GC/MS analyses of trace impurites, the elution of the solvent or the overloaded major component causes a significant pressure surge in the ion source of the mass spectrometer. This pressure surge is normally of no consequence and results only in saturated mass spectra for that particular component. However, in instruments equipped with combined EI/CI ion sources, the pressure surge can cause ion-molecule reactions to occur, even without the presence of a reagent gas. The pressure of the eluting compound becomes so high that self ion-molecule chemistry has a significant effect on the appearance of the mass spectrum. Of particular interest is the fact that the resultant mass spectra can be far different from the compound eluting and may be misinterpreted by the analyst and computer.

The problem outlined above was encountered in this laboratory during the GC/MS analysis of minor impurities in methylene chloride. A series of experiments confirmed that ion-molecule reactions in the combined EI/CI source were responsible for the "anomalous" spectra as no anomalies were observed when an EI only ion source was used. This work was undertaken to determine the extent of self ion-molecule chemistry that may occur during the GC/MS characterization of volatile compounds and common solvents and to evaluate the consequences of the routine interpretation of mass spectra contaminated by ion-molecule reaction products.

EXPERIMENTAL. Several low boiling compounds were analyzed by GC/MS using both EI-only and the combined EI/CI source, operating in EI mode. In all cases, the GC effluent was not vented and the filament remained on throughout the analysis. Similar results were obtained from two instruments, a Kratos MS50TC and a Finnigan 4000.

The static high pressure experiments were carried out by admitting the analyte to the EI/CI source of the MS50TC via the reagent gas system and acquiring representative mass spectra at various source housing pressures.

RESULTS. Nearly all of the compounds studied yielded fairly abundant ion-molecule reaction products when analyzed by GC/MS using the EI/CI source (see Table 1). A typical result is illustrated for methylene chloride in Figure 1. It appears as if an "impurity", having characteristic ions at m/z 83,97 and 133 is co-eluting with the methylene chloride. The mass spectrum of the "impurity and pure mehtylene chlortide are shown in Figure 2 for comparison. It is clear that the spectrum of the ion-molecule reaction products is different enough from that of methylene chloride that one could make the erroneous interpretation that the spectrum represents a compound of molecular weight greater than 133 and containing at least 3 chlorines Proof that the observed "anolamous" ions observed for methylene chloride are indeed ion-molecule reaction products comes from the high pressure experiments (see Figure 3). From this plot, the increase in abundance of the ions at m/z 83, 97, and 133 with increases in source pressure is clear evidence that they are reaction products, while the concomitant decrease in m/z 84 indicates its role as a reactant in the self ion-molecule reactions.

CONCLUSION The routine use of combined EI/CI ion sources for the routine characterization of volatile compounds has been shown to produce "anomalous" spectra due to self ion-molecule reactions of the compounds of interest under certain conditions. The resultant spectra are quite different from the spectra of the pure compounds and can lead to misinterpretation and erroneous library search results unless the analyst is aware of the consequences of the use of the relatively gas-tight combined EI/CI source.

TABLE 1 OBSERVED PRODUCT IONS

NAME	MASS	PRODUCT IONS TENT. ID.	REL. ABND.
Methylene chloride	83	$CHCl_2$	50
	97	$C_2H_2Cl_2$	10
	117	CCl_3	3
	133	$C_2H_4Cl_3$	6
Pentane	71	C_5H_{11}	94
Methanol	33	CH_5O	100
	47	C_2H_7O	3
Ethanol	47	C_2H_7O	100
	75	$C_4H_{11}O$	9
	93	$C_4H_{13}O_2$	11
Ethyl acetate	89	$C_4H_9O_2$	100
	131	$C_6H_{11}O_3$	2
	177	$C_8H_{17}O_4$	12
1,1-Dichloroethylene	85	C_2H_2Cl	7
	97	$C_2H_3Cl_2$	35
	121	$C_2H_3Cl_2$	53
Trichloroethylene	119	-	6
	154	C_2HCl_3	4
	189	C_2HCl_4	19
Tetrachloroethylene	188	-	5
	211	C_3Cl_5	2
	258	C_4Cl_6	4
Acetone	59	C_3H_7O	100
	101	$C_5H_9O_2$	13
	117	$C_6H_{13}O_2$	14

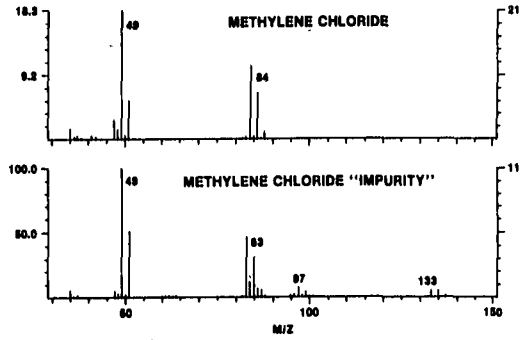

FIGURE 1. Mass spectra of pure methylene chloride and co-eluting "impurity".

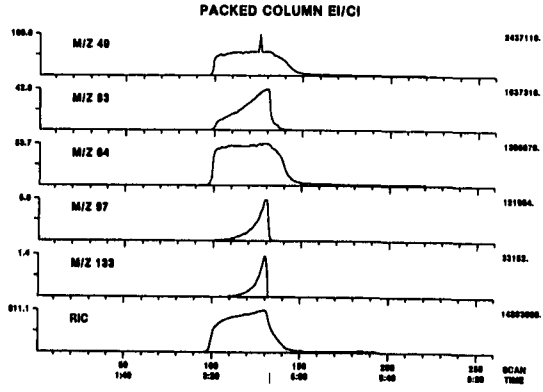

FIGURE 2. Mass chromatograms for EI/CI analysis of methylene chloride by GC/MS.

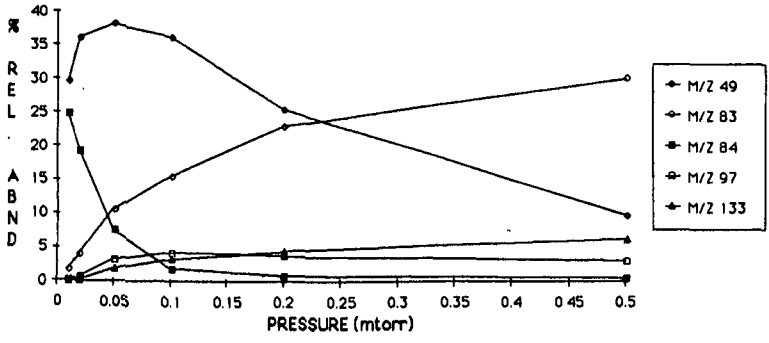

FIGURE 3. Pressure dependence of methylene chloride ions.

ANALYTICAL APPLICATIONS OF HEADSPACE GC/MS/IR

R. Citerin, K. L. Gallaher, R. G. Kollar, and M. Markelov
The Standard Oil Co.
4440 Warrensville Center Road
Cleveland, Ohio 44128

The technique of Headspace sampling is useful for analysis of volatile materials in difficult matrices. Depending on the problem, the need for specific analysis or detection encouraged investigations in our laboratory to couple mass spectrometry and infrared spectroscopy to the analysis.

Sensitivity enhancement has been obtained through Headspace sampling of volatile compounds since a larger volume of vapor can be injected on a G.C. column than with a liquid sample. The larger sample capacity of microbore columns (0.53mm I.D.) over conventional capillary systems also enhances sensitivity.

An example of the need for specific detection in complex materials is the determination of alcohols in gasoline. The sample is 0.2 volume per cent methanol in gasoline. Figure (1) shows the reconstructed ion chromatogram of a 200 ul volume Headspace injection onto a 25M x 0.20mm I.D. 5% phenyl methyl silicon capillary column split 75/1. The sample is 0.2 volume percent methanol in gasoline. The response is best seen from the selected ion chromatogram for M/Z 31. The background subtracted spectrum is shown in Figure 2. The alcohol spectrum remained heavily interfered with by light hydrocarbons.

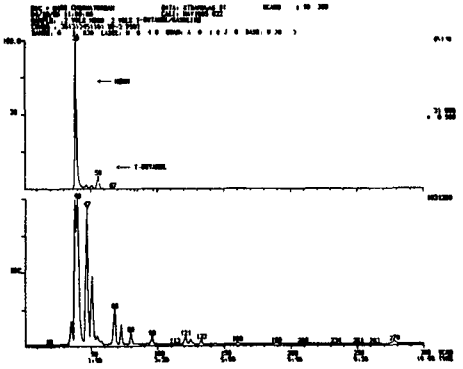

Figure 1

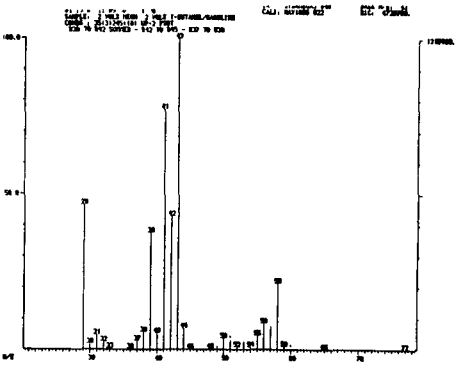

Figure 2

A similar GC/IR experiment was done with a 50M x 0.53mm 5% phenyl methyl silicon microbore column. Two hundred ul of the same 0.2 volume percent methanol in gasoline was used, but with no splitting. A Nicolet 60 SX FT/IR and standard GC/IR light pipe accessory (1.5mm x 15 cm) was used with Nicolet software that provided 8 wavenumber (cm^{-1}) resolution and 16 co-added scans per file. Figure 3 is the "chemigram" or integrated intensity of the vibrational region 1300 - 1000 cm^{-1} which is characteristic of the C-O-H stretching region for alcohols. The lower trace of Figure 3 is the carbon- hydrogen stretching frequency (2930 - 2985 cm^{-1}) which resembles a F.I.D. response. Figure 4 is the background subtracted spectrum of the largest peak seen in the C-O-H chemigram and is a good spectrum of methanol. Comparing the Headspace methanol infrared spectrum to that of a 0.2ul liquid injection, the Headspace data showed a 13X increase in signal from the most intense files in the respective GC/IR peaks.

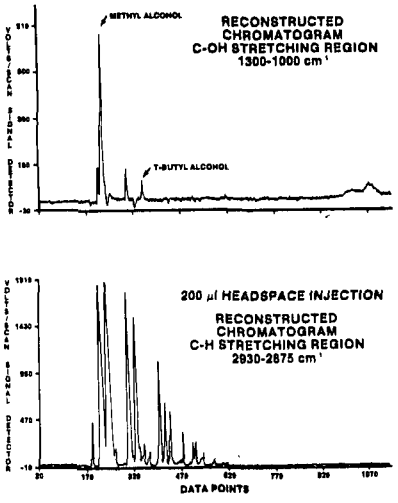

Figure 3

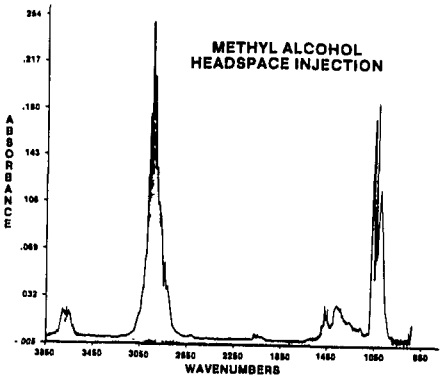

Figure 4

Contaminated soil is a difficult sample matrix with which to work. Headspace sampling eliminates the need for sample extractions required by most other methods. Combining both Headspace GC/MS and Headspace GC/IR, complimentary information is obtained and the results more confidently reported when both are used together. MS is the method of choice for determining molecular weight and a wide variety of homologous series. However, infrared spectroscopy is much better for distinguishing between isomers and screening for specific functionalities -- especially polar functions. Figure 5 is the reconstructed ion chromatogram of a 300 ul contaminated soil Headspace injection. Selected ion chromatographs of M/Z 35,49 and 77 are intended to screen alkyl chlorides and aromatics. Figure 6 is the analogous GC/IR experiment.

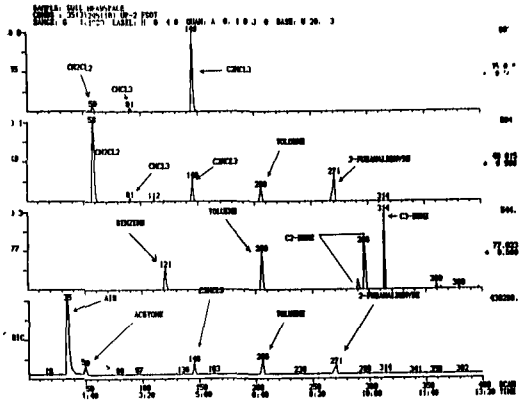

Figure 5

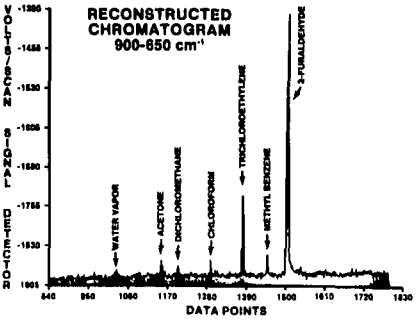

Figure 6

MASS SPECTRAL IDENTIFICATION OF ARTIFACTS FORMED IN SILYLATION REACTIONS

J. L. Little, J. L. Crawford

Physical and Analytical Chemistry Research Division

Eastman Chemicals Division

Kingsport, TN 37662

Trimethysilyl (TMS) derivatives are routinely employed in gas chromatography to increase the volatility and stability of organic compounds containing active hydrogens. Normally, only the desired derivative is formed when organic compounds are derivatized with silylation reagents such as BSA [N,O-bis(trimethylsilyl)acetamide] and BSTFA [N,O-bis(trimethylsilyl)trifluoroacetamide]. However, some functional groups such as aldehydes, amides, acids, ketones, and phenols under certain conditions form additional unexpected derivatives we refer to as silylation artifacts. Furthermore, even the derivatization reagent can react with itself, inorganic reagents, or organic solvents to yield artifacts. This extended abstract includes some of the artifacts that have been identified by mass spectral data in our laboratory and others. A supplementary text available from the authors includes a more extensive list of artifacts, their electron impact mass spectra, references to artifacts noted in the chemical literature, and means to avoid formation of some classes of artifacts.

Aldehydes

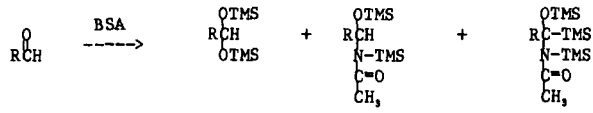

Acids

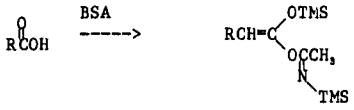

Ketones

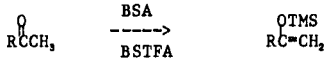

Amide

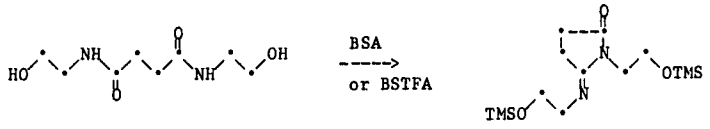

Solvents

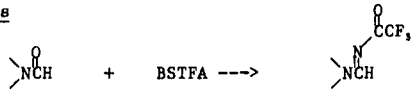

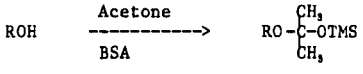

MS/MS FOR THE DETERMINATION OF TRACE LEVELS OF LSD IN HUMAN URINE

J.V. Johnson, M.R. Lee, M.S. Lee, J.C. Anders, and R.A. Yost
Chemistry Department, University of Florida, Gainesville, FL 32611

Lysergic acid diethylamide (LSD, MW =323) is one of the most potent hallucinogenic drugs of abuse. From an analytical standpoint, the determination of LSD in human urine represents a challenging problem. LSD has a low psychoactive oral dose of ca. 1 µg/Kg. It is rapidly metabolized with a half-life in humans of ca. 3 hours. In addition, none of the metabolites of LSD have as yet been identified in humans. Thus, an analytical technique is required which is selective and sensitive enough to determine the trace levels of LSD present in users' urine and which is rapid enough to screen large numbers of samples in a cost-effective manner. Tandem mass spectrometry (MS/MS) has been shown to have these capabilities [1]. Here we demonstrate the sensitivity and selectivity of EI-, CH_4 and NH_3 CI-MS/MS for the determination of LSD and the increased speed of analysis possible with sample introduction via short (< 2 meters) GC columns and solids probe.

All data were collected on a Finnigan MAT TSQ45 triple quadrupole tandem mass spectrometer. Ionization of LSD was accomplished by EI (70 eV, 0.3 mA), CH_4 and NH_3 PCI and ECNCI (100 eV, both at indicated ion source pressures of 1.0 torr), and thermospray (Vestec Corp., Houston, TX, temp. T1 =163°C, temp. T2 = 270°C, temp. ion source = 240°C, 1.5 mL 0.1 M ammonium acetate/min). The ion source was maintained between 180°C and 190°C for EI and CI. Samples were introduced via a 2 m, 0.25 mm i.d. DB-5 fused silica capillary (FSOT) column (1.0 µL splitless, 100°C to 275°C @ 20°C/min), a 15 in, 0.75 mm i.d. 3% OV101 packed column (1.0 µL, 270°C isothermal), a 2 m, 0.53 mm i.d. DB-5 Megabore FSOT column (1.8 µL, 275°C isothermal), a direct insertion solids probe (1.0 and 5.0 µL, 50°C to 400°C either ballistically or at 100°C/min), and directly injected with thermospray (25 µL, 1.5 mL ammonium acetate/min). The packed and Megabore columns were connected to a 1 m, 0.25 mm i.d. DB-5 FSOT column which was introduced directly into the ion source. For sample introduction via GC, the injection port and interface oven were maintained in the range of 275 to 320°C. Helium was used as a carrier gas for the GC experiments except for the CH_4 CI experiments, in which case, CH_4 was used as the carrier gas and the column headpressure was set to give an ion source pressure of 1.0 torr CH_4. For the NH_3 experiments, NH_3 was added as a makeup-gas to give an indicated ion source pressure of 1.0 torr.

The EI M^+ ion, m/z 323, the PCI $(M+H)^+$ ion, m/z 324, and the NCI $(M-H)^-$ ion, m/z 322, all fragmented extensively under collisionally activated dissociation (CAD) to give the daughter spectra in Figure 1. The ionization mode which generated the $(M+H)^+$ ion did not appear to have any significant effect upon the relative intensities of its daughter ions. Collision gas pressures between 2.8 and 3.4 mtorr N_2 and collision energies between 25 and 28 eV were found to be optimal for maximizing the sensitivity for the selected reaction monitoring (SRM) of each parent ion to its most abundant daughter ion, i.e. EI-SRM ($323^+ \rightarrow 207^+$), PCI-SRM ($324^+ \rightarrow 223^+$), and NCI-SRM ($322^- \rightarrow 195^-$).

Having characterized and optimized its MS/MS behavior, LSD was quantitated in methanol standards to determine the relative sensitivities of the different ionization methods and sample introductions (Table 1). With gas chromatographic introduction of samples, the lower limits of detection (LODs, defined as the amount of sample giving a signal three times higher than the blank) obtained with the 2m DB-5 FSOT column can be attributed to its greater inertness and to its significantly narrower peak width, increasing the signal-to-noise ratio, as compared to the short packed column. The lower LODs of PCI-SRM compared with NCI-SRM can be directly attributed to the lower efficiency of production of $(M-H)^-$ ions as compared to the production of $(M+H)^+$ ions, indicated by the LODs obtained with the selected ion monitoring (SIM) of these ions. However, some of the reduced sensitivity can be attributed to the lower efficiency of converting the $(M-H)^-$ parent ion to its daughter ions as compared to that of the conversion of the $(M+H)^+$ ion to its daughter ions (Figure 1). The lowest LOD for the determination of LSD in solvents was obtained with thermospray-SIM of the $(M+H)^+$. As the LODs for CI-SRM and the respective CI-SIM quantitations are similar (Table 1), thermospray should behave similarly and thus should provide the lowest LOD, at least with LSD standards. Experiments are proceeding in our laboratory to further evaluate the potential of thermospray-MS/MS for trace analysis. Although EI-SRM provided a LOD comparable to some of the CI-SRM LODs, it was not considered further for experiments due to the interference expected in the analysis of actual urine samples. Although the quantitation of LSD with the 2-m DB-5 FSOT column and

CH_4 PCI-SRM provided the next lowest LOD, for maximum sensitivity it required splitless injections and temperature programming of the GC oven. This resulted in relatively long analysis times of ca. 15 minutes per sample; whereas with the packed column GC and solids probe, analysis times of 1-3 minutes per sample were possible. In addition, there would need to be some sample preparation prior to actual urine samples being injected onto the GC. This would not be the case for sample introduction with the solids probe, as will be described below.

Solids probe/CH_4 PCI-SRM quantitation of LSD in spiked urine and in methanol were compared. For the quantitation of LSD with the solids probe, d_{10}-LSD (compliments of Naval Research Laboratory, Washington, DC, PCI-SRM: $324^+ \rightarrow 223^+$) was added to each of the solutions at the 5 ppm level. Five µL of each solutions containing different concentrations of d_0-LSD in methanol and in urine were allowed to dry in untreated glass solids probe vials at 80°C for ca. 45 minutes in the dark. Subsequently, the samples were introduced into the ion source by vaporization from the solids probe while it was heated from 50 to 400°C, ballistically. This resulted in an actual data acquisition time of 30 seconds and analysis times of 3 minutes per sample. The LODs for the solids probe/PCI-SRM of LSD in urine and in methanol were 80 and 178 pg of LSD on the probe, respectively, their calibration curves were linear over several orders of magnitude. Although it was found that the PCI-SRM response from LSD in the urine was ca. 13 times the response of the LSD in the methanol standards, the LOD was only lowered by a factor of 2. We attribute the enhanced response to the "carrier effect" of other urine components competitively inhibiting the adsorption of LSD onto active sites on the glassware and other apparatus. That the LOD in urine was not lower than was expected based upon its enhanced response, can be attributed to the thermal decomposition of other components in the urine causing an increase in the chemical noise and background.

Normally one uses a different, more sensitive analytical technique to cofirm the presence of any positives detected in the initial screening step. However, with MS/MS it is possible to use the same instrument for screening and for confirmation of any positives. Analogous to the limit of detection, the limit of identification can be defined as the necessary spectral features which must be present in order to positively identify the component of interest. The limit of identification of LSD in urine was ascertained by a visual inspection of PCI-CAD daughter mass spectrum of the m/z 324 ion generated from urine containing different levels of LSD. Figure 2 shows that the limit of identification is ca. 1 ng of LSD on the probe (in 5 µL of urine). Note that unlike other screening techniques, sensitivity was sacrificed in going from the screening step (SRM) to the confirmation step (full mass range PCI-CAD daughter mass spectra). However, the advantage comes from being able to perform both steps with a single instrument and often on the same sample.

In conclusion, it has been determined that solids probe CH_4 PCI-SRM is the preferred MS/MS method of choice, of those evaluated, for the determination of trace levels of LSD in urine. With this technique a limit of detection and a limit of identification for LSD in urine of 0.08 and 1 ng, respectively, of LSD on the probe were obtained.

[1] Johnson, J.V.; Yost, R.A. Anal. Chem. 1985, 758A-768A.

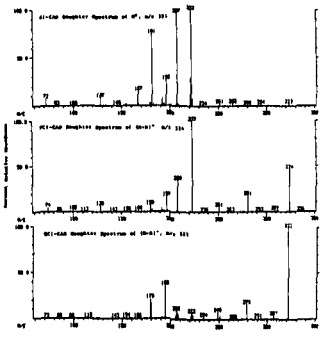

QUANTITATION OF LSD IN METHANOL

Introduction / Ionization	SRM LOD (ng)	SIM LOD (ng)
GC/EI	3	-
GC/CH_4 PCI	1 - 8	8
GC/NH_3 PCI	5 - 14	10
GC/CH_4 NCI	14 - 17	18
GC/NH_3 NCI	7 - 34	27
Thermospray PCI	-	0.25
DP/CH_4 PCI	3	-

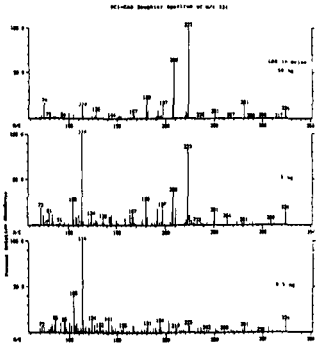

DETERMINATION OF 2,4,6- TRINITROTOLUENE AND ITS METABOLITES IN URINE OF MUNITION WORKERS BY MICRO-LC/MS

J. Yinon and D.-G. Hwang

Department of Isotope Research
Weizmann Institute of Science
76100 Rehovot, Israel

2,4,6-Trinitrotoluene (TNT) has been the most commonly used explosive since World War I. Occupational exposure to TNT has been reported to occur by inhalation, ingestion and skin absorption.[1] The toxic action of TNT in humans may lead to toxic hepatitis and aplastic anemia and to less serious medical problems such as gastritis, dermatitis and anemia.

As a result of our study on the metabolism of TNT in laboratory animals[2-4], we have developed an analytical method based on micro-LC/MS for the determination of metabolites of TNT in urine. The analytical system consists of a micro-HPLC interfaced to a magnetic sector mass spectrometer by a direct liquid introduction probe and is described elsewhere.[5] The HPLC column used was a RP-8 reversed-phase microcolumn 2.1 mm I.D. x 10 cm. Mobile phases were acetonitrile:water (37:63) and methanol:acetonitrile:water (20:18:62) at a flow rate of 120 µl/min.

Seven urine samples of TNT workers were analyzed. As a blank reference a urine sample of one of the authors was analyzed. Quantitation of the metabolites was obtained by plotting HPLC chromatogram peak heights vs. amount of standard metabolite injected, and thus obtaining standard curves which were used for quantitation of sample metabolites. Extraction was done with toluene.[3]

Figure 1 shows the micro-HPLC chromatogram of a urine sample. 2,6-Diamino-4-nitrotoluene (2,6-DA) and 2,4-diamino-6-nitrotoluene (2,4-DA) were separated in a different run (not shown) where the mobile phase was methanol:acetonitrile:water (20:18:62). A LC/MS mass spectrum of a separated 4-amino-2,6-dinitrotoluene (4-A) fraction is shown in Figure 2. Table 1 shows the detected quantities of TNT and its metabolites in the urine samples of the TNT workers.

The results indicate that the main metabolic pathways of TNT in humans are reduction processes and are therefore similar to those in rats and rabbits.[3-5] The detection limit of the metabolites in urine was 1 ng/10 ml.

ACKNOWLEDGEMENT

We would like to thank Dr. R. Ashkenazi from the Institute of Occupational Health at the University of Tel-Aviv for supplying the munition workers' urine samples.

REFERENCES

1. J.A. Hathaway, J. Occ. Med. 19, 341 (1977).
2. J. Yinon and D.-G. Hwang, J. Chromatogr. Biom. Appl. 339, 127(1985).
3. J. Yinon and D.-G. Hwang, Toxicology Lett. 26, 205(1985).
4. J. Yinon and D.-G. Hwang, J. Chromatogr. Biom. Appl. 375, 154(1986).
5. J. Yinon and D.-G. Hwang, Adv. Mass Spectr. (in press).

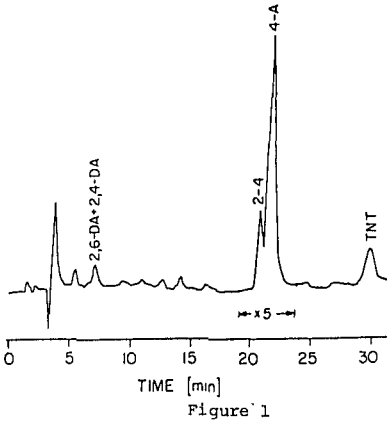

COLUMN: RP-8 MICROCOLUMN 2.1mm I D × 10cm
MOBILE PHASE: ACETONITRILE-WATER (37:63)
FLOW RATE: 120μl/min
UV WAVELENGTH: 214nm

Figure 1

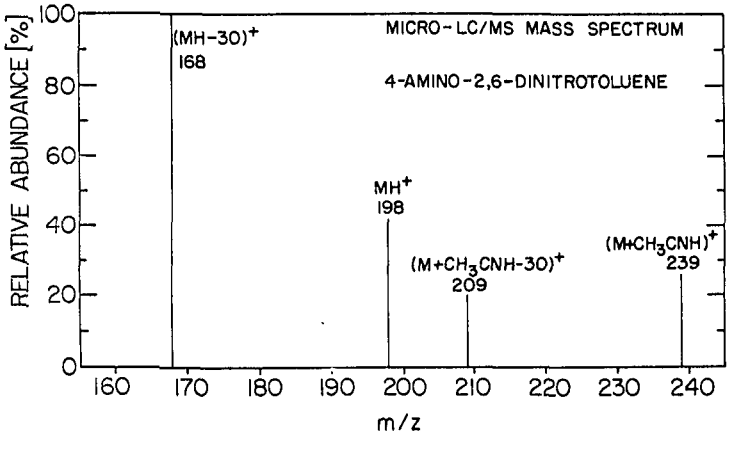

Figure 2

Table 1. TNT METABOLITES FOUND IN URINE OF MUNITION WORKERS

Metabolite	Amount of metabolite found in urine [μg/20 ml]						
	Sample No. 6	Sample No. 1	Sample No. 3	Sample No. 7	Sample No. 8	Sample No. 4	Sample No. 5
2,6 - DA	0.13	0.29	0.17	0.20	0.73	1.33	1.67
2,4 - DA	0.63	0.48	0.67	0.83	2.43	5.83	6.0
2 - A	0.11	0.07	1.67	2.89	5 78	40.0	54.4
4 - A	0.56	0.47	4.78	24.6	28.7	133	193
TNT	0.22	0.33	0.56	1.44	0.33	5.56	4.44

DEVELOPMENT OF A CONFIRMATORY TEST FOR EXPOSURE TO 3-QUINUCLIDINYL BENZILATE (BZ), G. D. Byrd, L T. Sniegoski, L C. Sander, and E. White V, Center for Analytical Chemistry, National Bureau of Standards, Gaithersburg, MD 20899.

The current military stockpiles of the incapacitating agent 3-quinuclidinyl benzilate (BZ) in the U. S. are scheduled for demilitarization in the near future. This process will create the potential for worker exposure to this material. Consequently, there is a need for a confirmatory test for human exposure to BZ prior to the commencement of the demilitarization process. The work described here concerns the development of a specific confirmatory test for human exposure to BZ using isotope dilution GC/MS analysis of urine sample extracts.

BZ is a relatively nonvolatile ester that affects the brain and nervous system. It is a specific binding antagonist for the muscarinic class of receptors and is capable of producing incapacitation at very small doses (1-5 $\mu g/kg$)[1]. Of the BZ that enters the body, 50 to 90% is excreted via the kidneys with most in the form of the metabolites benzilic acid (BA) and 3-quinuclidinol (Q) which are shown in Figure 1. The exact relationship between BZ dose and levels of BZ, BA, and Q in the urine is not well understood. However, based on the known no-effect level, the required detection limits of these analytes in urine have been set at 0.5 ng/mL for BZ and 5 ng/mL for BA and Q. Confirmation of specific exposure to BZ requires that the analysis be for intact BZ or for both BA and Q. A method for quantifying all three analytes is desirable. Initial work on this project has focused on the metabolites BA and Q. Isotope dilution GC/MS was selected as the analytical method because of the need for high sensitivity and selectivity for these analytes in a complex matrix.

BA was extracted directly from urine with chloroform. Q, on the other hand, proved difficult to extract from urine into organic solvents due to its polar and hydrophilic properties. A method using a Florisil SepPak cartridge was developed to remove the Q from urine The Q was eluted from the cartridge with concentrated NH_4OH. The extracts from both samples were dried and derivatization reagent was added to each to form the trimethylsilyl derivatives of the analytes (BA-TMS and Q-TMS). The recovery of each analyte from urine is approximately 50%.

The GC/MS instrument used was equipped with a 30 meter DB-17 fused silica capillary column directly interfaced to the source of a quadrupole mass spectrometer. Analyses were carried out by single ion monitoring (SIM) using the most intense ions above m/z 100. The fragment ion $(C_6H_5)_2COTMS^+$ at m/z 255 was monitored for BA-TMS and the molecular ion at m/z 199 was monitored for Q-TMS. Figure 2 shows the selected ion chromatogram obtained from urine samples spiked with the metabolites at approximately 5 ng/mL. Labeled analogs of BZ, BA, and Q were synthesized in order to do the isotope dilution measurements.

This work demonstrates that the BZ metabolites BA and Q can be determined at the 5 ng/mL level in urine. Future work will involve the development of a method for detecting BZ itself in urine.

References

[1]Ketchum, J. S., CRDL Technical Memorandum 20-29, Human Investigations Facility, Directorate of Medical Research, U. S. Army Chemical Research and Development Laboratories, Edgewood Arsenal, MD (Sept. 1963).

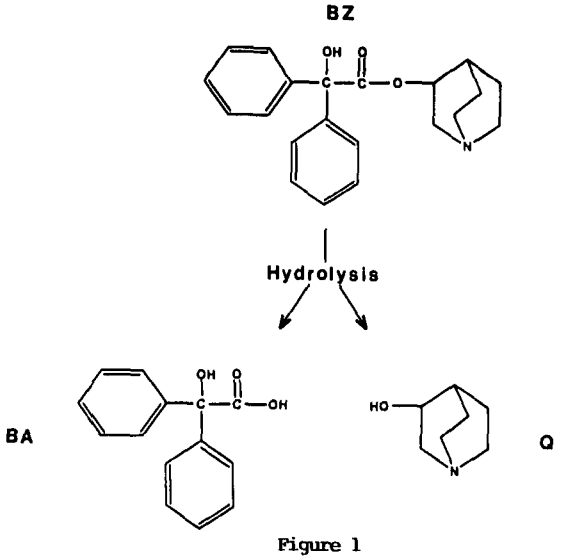

Figure 1

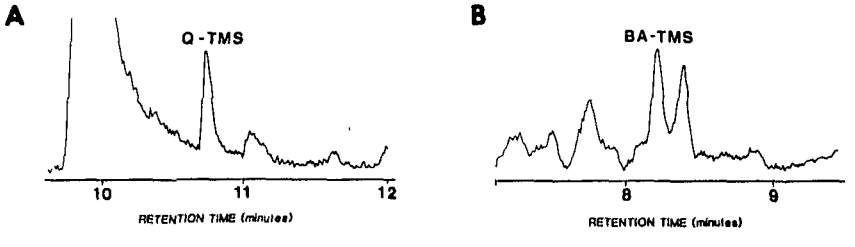

Figure 2: SIM of A) m/z 199 and B) m/z 255 for derivatized extract from urine containing 5 ng/mL of Q and BA.

Volatile Organic Compound Analysis by Gas Chromatography with the Ion Trap Detector

Eric Johnson, Ernie Petit, Eric Melanson
Finnigan MAT, 355 River Oaks Parkway, San Jose, CA 95134

Recent legislation has brought much attention to the present techniques used for the analysis of volatile organic compounds (VOC) in drinking water. This new emphasis will likely place the burden for primary water testing with state and local municipalities and an expansion to the list of targeted compounds seems eminent. Current analytical methods to survey for VOCs in water require packed column gas chromatography (GC) with mass spectrometric detection (MS). Given the relative low resolution of packed column GC and the high cost of full GC/MS systems, both technical and financial considerations must now play an equal role in the direction of new methods development.

In late 1985, the United States Environmental Protection Agency (EPA) proposed a new GC/MS method (Method 524.1) for the determination of VOCs in drinking water. In that notice (see FR 46908-46909) EPA requested comments on the proposed method regarding detection and quantitation limits, precision, accuracy and analysis costs.

We have evaluated a modifed version of Method 524.1 for these parameters and applicability of the method for drinking water monitoring. The method, as proposed, requires the use of a packed column containing 1% SP1000 on Carbopack B. Unfortunately, several of the compounds in the method do not elute from this column in a reasonable time, and the maximum temperature of the liquid phase must be exceeded. We, therefore, modified the method by replacing the packed column with a recently developed bonded phase fused silica capillary of large internal diameter (DB624, 0.53mm I.D.; J & W Scientific) specifically optimized for the analysis of volatile constituents. For this evaluation, we used the Finnigan MAT Model 710 Ion Trap Detector (ITD™) because of its high sensitivity, ease of operation and low cost.

A Typical Chromatogram of VOC Standards by Purge and Trap Capillary GC/ITD

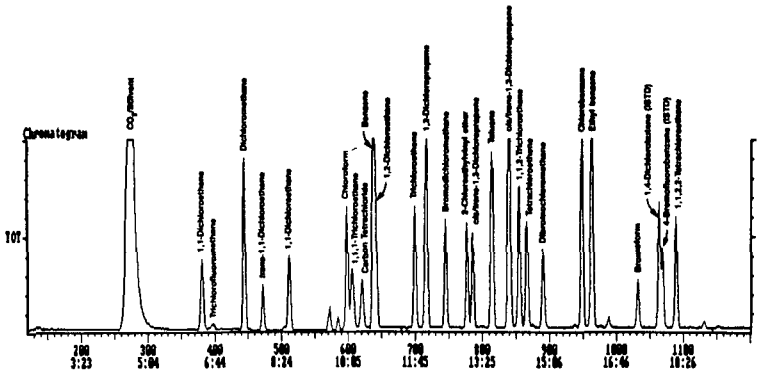

Reagent water was spiked with standards for some of the purgeable organics obtained commercially along with surrogate standards and 4-bromofluorobenzene. Five mL samples were analyzed using an automated purge and trap device with the heated transfer line coupled directly to a 30m, 0.53 mm I.D. J & W Megabore DB624 column with a three micron film thickness. Samples were purged for 10 minutes at 30°C, including a two minute dry purge period, followed by a three minute desorption at 200°C and terminated by trap bakeout at 250°C for five minutes. The analytical column was operated with a subambient equipped, temperature programmable gas chromatograph and interfaced to the open split transfer line of the ITD. At a flow rate of 5 mL/min through the analytical column and the open split flow restrictor at 1 ml/min, an effective 5:1 split ratio was achieved.

A series of standards injected directly into the capillary column and a series of purge and trap experiments using reagent water indicate a 1-5 ppb detection limit under the current configuration and the ability to routinely meet specifications for 4-bromofluorobenzene added directly to the purge vessel at a 10 ppb level. Linear behavior was exhibited for many compounds in a 2-160 ppb range under the high throughput capabilities of the ITD.

A modification of Method 524.1, used in conjunction with an ITD, may be an alternate method of meeting EPA objectives with suitable precision and accuracy and merits further study. The novel phase DB624 column exhibits much improved resolution performance for many of the analytes of interest in comparison with packed column chromatography. Furthermore, because the ITD is a low cost, easy-to-operate instrument with analytical capabilities of much higher priced systems, the per analysis cost is expected to be lower than estimated by EPA.

THE DEVELOPMENT OF THERMOSPRAY MASS SPECTROMETY COMBINED WITH ELECTROCHEMICAL REDOX PROCESSES

T. A. Getek
Department of Chemistry
University of Houston
University Park
Houston, TX 77004

OVERVIEW:

The exponential increase in usage and success of Thermospray mass spectrometry (TMS) has made it a popular favorite for performing liquid chromatography followed by mass spectrometry (LCMS). Several TMS advantages include the accommodation of 1 to 2 ml/min flow rates, soft ionization for determining the base molecular weight of a compound, and the capability for handling polar solutes and solvents with high dielectric constants. It is this latter advantage that triggered the development of combining mass spectrometry (MS) with electrochemistry (EC). The concepts of performing EC in solutions followed by MS led to the appropriate acronym, Solution ElectroChemistrY Mass Spectrometry (SECYMS).

EXPERIMENTAL SECYMS:

The criteria for an EC cell in SECYMS are two-fold. 1) The cell should be capable of withstanding 1000 PSI due to the narrow bore of TMS capillary. 2) The coulometric efficiency should be approximately 100%. A block diagram is depicted in Fig. 1.

Acetaminophen (APAP) was used as a test sample for SECYMS. APAP (MW=151) is easily oxidized at 0.4V. The before and after electrolysis is shown in Fig. 2. One of the products of oxidized APAP is quinone (QU) which has a MW=108.

Caffeine (MW=194) was next tested by SECYMS. Injections of 0.04 mg/ml were made at various potentials. When the potential was increased, the caffeine was oxidized and the caffeine ion (MW=195) decreases (Fig. 3).

ENHANCED TMS WITH SECYMS:

It was found that hydroquinone (HQ) when tested with TMS in the positive ion mode did not produce any major discernible m/z peaks. In order to "see" HQ (MW=110), a sample was oxidized at 0.4V. On oxidation, signals at m/z 110 and 124 were observed which correspond to quinone's TMS. Quinone (MW=108) is the expected product of HQ oxidation. This is an example of enhancing a TMS signal by electrochemically transforming the compound of interest to one more favorably "seen" by TMS.

SUMMARY

SECYMS is a simple and powerful technique capable of evaluating the products and mechanisms of EC reactions. Mass spectroscopists may find SECYMS as a novel and invaluable tool for assisting in the determination of intractible compounds by TMS.

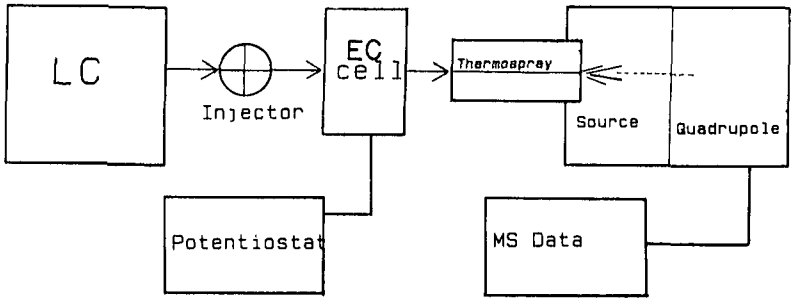

Fig. 1

BLOCK DIAGRAM OF SECYMS

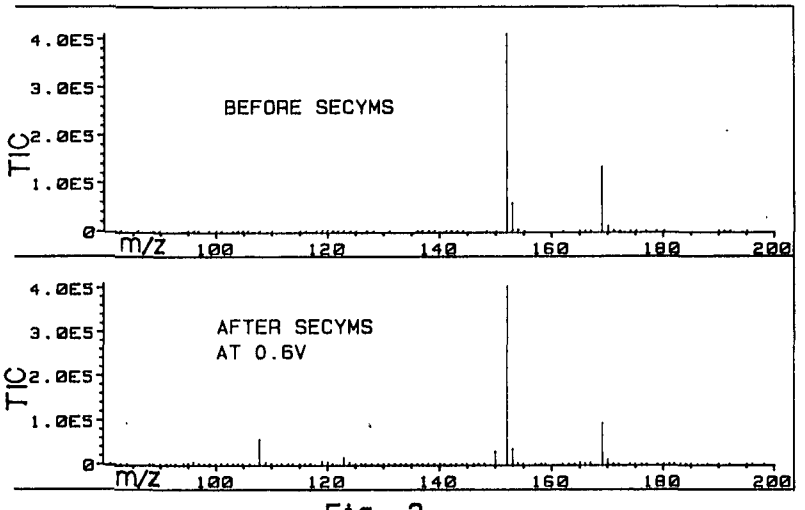

Fig. 2

ACETAMINOPHEN BEFORE AND AFTER ELECTROLYSIS AT 0.6V

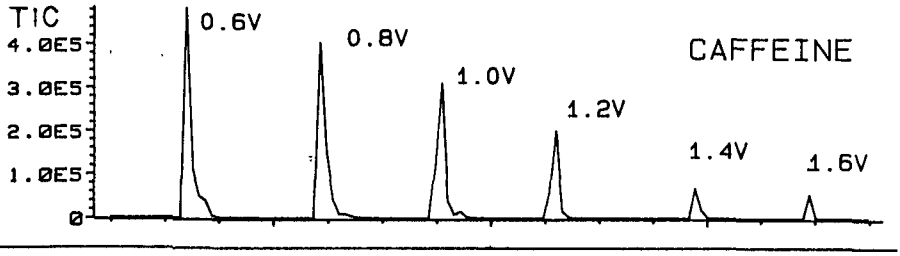

Fig. 3

DIRECT ION EVAPORATION OF IONIC ORGANIC AND INORGANIC COMPOUNDS IN THERMOSPRAY HPLC/MS

Robert D.Voyksner, Research Triangle Institute, Analytical and Chemical Sciences, P. O. Box 12194, Research Triangle Park, North Carolina 27709.

Thermospray HPLC/MS has proven successful for the analysis of a variety of polar and nonpolar organics in complex matrices. In most cases, ionization of these compounds occurs through ion evaporation in the presence of an ionic buffer or through a chemical ionization process induced by reagent ions originating from a filament or discharge. The ions detected are usually influenced by ion/molecule reactions in the source due to the high pressures of buffer and HPLC solvent present. It is difficult to decouple thermospray ionization (ion evaporation) from these ion/molecules reactions so that the various steps in ionization can be examined.

Thermospray without buffer or an auxillary ionization was evaluated to better understand the ionization processes and to analyze organics and inorganics. These spectra should show less dependence on gas phase reactions with buffer and solvent. Also the absence of buffer will remove the low mass solvent/buffer ions which can interfere with low mass analysis of inorganic cations and anions (m/z 10-200).

Inorganics

Numerous inorganic anions and cations could be detected individually by thermospray in the absence of buffer (Table 1). The ions detected in the mass range from 10 to 300 were from direct ionization ($[M]^-$ or $[M]^+$), ion/molecule reactions ($[M+H_2O]^+$ $[M+H]^+$) and clusters ($[2M+H]^+$ $[2M+H_2O]^+$). The absence of buffer removed the numerous solvent/buffer ion interferences normally observed in thermospray with buffer or a filament. It was observed that for the halogen anions and alkali metal cations that $[M+H_2O]^+$ is favored for anions as follows: F>Cl>Br>I and for metals Na>K>Rb>Cs. This corresponds to water clusters being favored for the most electronegative halogens and the highest ionization potential alkali metals. The list of cations detected is rather short since most metals (transition metals such as Cr, Ag, Cu, Ni, V, Zr, and Pt) did not produce a cation. Only cations in the +1 valance state were detected.

Organics

The spectra for nucleotides (monophosphates of adenosine cytidine, guanosine, inosine, and uridine) in 100% water were similar to those acquired with buffer or filament CI. However, the molecular cation $[M+Na]^+$ was more intense for thermospray without buffer. The relative total ion current areas for the techniques were 1 vs. 3 vs. 5 for thermospray (no buffer) vs. thermospray with buffer vs. filament CI. The molecular ion of a dinucleotide (Adenylyl 3'- 5' cytidine) exhibited a factor of ten better molecular ion intensity in water ($[M+H]^+$ at m/z 573) than with buffer. Filament CI only resulted in adenyl and cytidine fragments (m/z 268 and 244). Also, no buffer clusters and better $[M+Na]^+$ ion intensity are observed for the dinucleotide when analyzed in 100% water.

Ionization Process

Nucleotides in the presence of alkali metals exhibited weak $[M+Metal]^+$ ions under non-buffer operaton (Table 2). The intensity of the cationized molecular ion followed the stability of the ionic complex formed (Li > Na > K > Rb > Cs), analogous to results for alkali metal addition in FAB (1). The plot for concentration vs. intensity for the $[M+H]^+$ and $[M+Na]^+$ ion for both buffer and non-buffer thermospray indicates that the formation kinetics are different for the protonated molecular ion and the cationized molecular ion (indicated by the different slopes). The difference between the ion intensities for $[M+H]^+$ with and without buffer is proportional to the square root of total ion concentration. Since the ammonium acetate (0.1M) is at a much greater concentration the sample ($1x10^{-7}$M), a difference of 3-4 orders in magnitude in intensity is expected. However, the cationized molecular ion is favored in the absence of buffer and exhibits a better signal to noise ratio than the $[M+H]^+$ ion (with buffer) near detection limits (< 700 ng). These observations seem to indicate that different mechanisms are involved. The $[M+H]^+$ formation is primarily a gas phase reaction through interactions with the solvent buffer, based on proton affinity. The cationized ions could be ionic complexes in solution that are desolvated, with a minimal interaction in the gas phase, to produce the $[M+Metal]^+$ ion.

The absolute intensity of the catonized molecular ion does not increase as NaCl is added to the solution. The residual Na in solution and Na from the mono-phosphate nucleotide salt appears to bind to the free nucleotide to form the cationized molecular ion. The intensity of $[M+H]^+$ and the cationized molecular ion $[M+Na]^+$ is dependent on the pH of the water solution in non-buffer operation (Figure 1). At low pH's the $[M+H]^+$

is favored (pH < 3) while pH > 4 favors the $[M+Na]^+$ ions. This dependence is not noted in an ammonum acetate (0.1M) solution since gas phase reaction with the buffers enables $[M+H]^+$ formation at various pH's. Adenosine has 2 amine protons which can act as Bronsted acids or bases (pKa'=3.63 and pKa" 12.6). The relationship between ion intensities for $[M+H]^+$ and $[M+Na]^+$, in the absence of buffer, correlates well with the various protonated forms of adenosine in solution ($[H_2$ adenosine], [H adenosine]$^-$, and [adenosine]$^{-2}$) in the pH range studied (Figure 2). The fully protonated molecule $[H_2$ adenosine] curve in Figure 2 matches the $[M+H]^+$ ion intensity curve in Figure 1. Likewise the [H adenosine]$^-$ curve (Figure 2) correlates well with the $[M+Na]^+$ ion intensity curve in Figure 1. Thermospray ions detected and their relative intensities seem dependent on the solution chemistry. The protonated molecular ions are favored for fully protontated species and cationization is favored when one proton is donated, enabling the formation of an alkali metal complex. Furthermore, the pKa' of adenosine can be calculated from the curve for $[M+H]^+$ ion intensity in Figure 1. The calculated value of 3.47 is in close agreement with the literature value of 3.63. It appears that thermospray (without buffer) can be used to calculate pKa values analogous to pKa calculations made by FAB techniques(2).

References

(1) L. Mallis, D. Russell, Anal. Chem. 58, 1076 (1986).

(2) R. Caprioli, Anal. Chem. 55, 2387 (1983).

TABLE 1. INORGANICS ANALYZED BY THERMOSPRAY ION 100% WATER

Anion	Base Peak	m/z
F^-	$[F+2H_2O]^-$	55
Cl^-	$[Cl+H_2O]^-$	53
Br^-	$[Br]^-$	79
I^-	$[I]^-$	127
NO_3^-	$[2NO_3+H]^-$	125
SO_4^-	$[2HSO_4+H]^-$	195
PO_4^-	$[2H_2PO_4+H]^-$	195
CO_3^-	$[2CO_3+H]^-$	121
CN^-	$[2CN+H]^-$	53
MnO_4^-	$[2MnO_4+Na]^-$	261
$Cr_2O_7^-$	$[Cr_2O_7Na+H_2O]^-$	257
$S_2O_3^-$	$[NaS_2O_3]^-$	135
Cations		
Cs^+	$[Cs]^+$	133
Rb^+	$[Rb+H_2O]^+$	103
K^+	$[K+H_2O]^+$	57

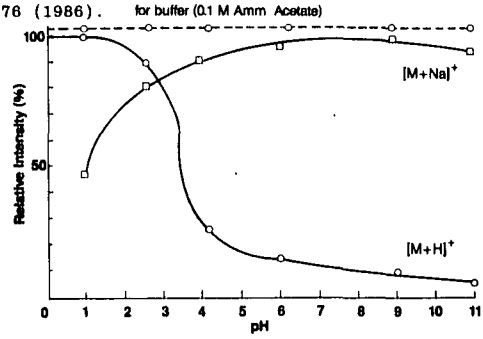

Figure 1

The dependence of the $[M+H]^+$ and $[M+Na]^+$ ions of adenosine on the pH of the solution analyzed by thermospray.

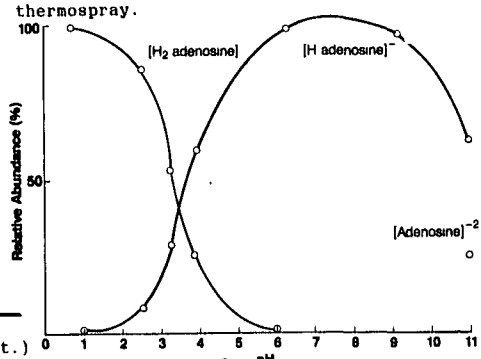

Figure 2

Relative concentrations of the various protonated species of adenosine with pH. Note that the relative abundance of the fully protonated adenosine (H_2 adenosine) species matches the $[M+H]^+$ ion intensity in Figure 1, enabling the determination of pKa for adenosine.

TABLE 2. CATIONIZED MOLECULAR IONS FORMED WITH VARIOUS ALKALI METALS AND ADENOSINE

Metal	Cat. Mol. Ion	m/z	(%Rel. Int.)
Li	$[M+Li]^+$	274	(7)
Na	$[M+Na]^+$	290	(6)
K	$[M+K]^+$	306	(4)
Rb	$[M+Rb]^+$	352	(1)
Cs	$[M+Cs]^+$	400	(0.2)

FORMATION OF $(M-1)^-$ or $(M+OAc)^-$ IONS IN NEGATIVE ION THERMOSPRAY MASS SPECTROMETRY.

C.E. Parker[1], R.W. Smith[1], S.J. Gaskell[2] and M.M. Bursey[3].

[1]Laboratory of Molecular Biophysics, NIEHS, Research Triangle Park, NC 27709.
[2]Tenovus Institute for Cancer Research, University of Wales College of Medicine, Cardiff, UK.
[3]Department of Chemistry, UNC-Chapel Hill, Chapel Hill, NC 27514.

We assume that the molecule to be studied by LC/MS contains hydrogen and we will call it HA; we call the anion of the additive B^-. When HA and B^- collide, there are two competitive processes that can lead to products, eq. 1 and 2.

$$HA + B^- \longrightarrow AHB^- \quad (1)$$
$$HA + B^- \longrightarrow A^- + HB \quad (2)$$

For almost all polar molecules studied by TSP LC/MS, eq. 1 is the formation of a hydrogen bond. Thermochemically, this reaction is always favorable: ΔH_r^o is the value of the strength of the hydrogen bonds and has been found to be 41-77 kJ mol^{-1} for bonding to chloride (1), 97-139 kJ mol^{-1} for bonding to fluoride (2), 123-128 kJ mol^{-1} for bonding to acetate (3), and 80-92 kJ mol^{-1} for bonding to alkoxide (4).

If the ionization process in TSP is gas phase, then the additive B will form A^- from HA by proton abstraction when HB has a numerically higher gas-phase acidity (eq. 2).

The principle then is as follows: (i) When eq. 2 is endothermic, HA forms AHB^- only. (ii) When eq. 2 is exothermic, HA forms A^-; A^- will be much more abundant than AHB^- if AHB^- fragments by rearrangement or if the pressure is inadequate to stabilize it collisionally.

A VG 12-250 LC/MS (VG Masslab, Altrincham, UK; quadrupole mass spectrometer) was used in the thermospray mode: vaporizer temperature, 390°C; desolvation chamber temperature, 270°C; source temperature, 200°C; VG "focus 4" electrode, 300V. A Gilson HPLC system consisting of two Model 802B manometric module (Gilson Medical Electronics, Middleton, WI) was used. Samples were injected into a Rheodyne, Inc. (Cotati, CA), Model 7010 injector fitted with a 50 µl loop.

Water and methanol were HPLC grade (Fisher Scientific Co., Fair Lawn, NJ). Sources of other compounds were as follows: trifluoroacetic acid, Fairfield Chemical Co., Blythewood, SC; trichloracetic acid and ammonium acetate, Fisher; hydrochloric acid, J.T. Baker Chemical Co., Phillipsburg, NJ. The solutions used were prepared from equal volumes of methanol and 0.1 M aqueous ammonium acetate; methanol, 0.1 M aqueous ammonium acetate, and 0.1 M hydrochloric acid. The hexestrol and E-diethylstilbestrol were purchased from Sigma Chemical Co., St. Louis, MO; the other stilbestrol analogues were gifts from Manfred Metzler, University of Wurzburg, FRG. The metribuzin metabolites were obtained from Mobay Chemical Co., Kansas City, MO. The hydrocortisone and corticosterone were obtained from Sigma Chemical Co., St. Louis, MO. The chloramphenicol propionate was a service sample from Karen Demby, School of Pharmacy, University of North Carolina at Chapel Hill.

From a table of gas-phase acidities of various functional groups (5), it should be possible to estimate gaseous acidities of many kinds of molecules typically analyzed by TSP LC/MS (or any other process dependent on gas-phase chemical ionization so that the

nature of their negative-ion spectra can be predicted from comparison with the gas-phase properties of other anions present, using the examples above as paradigm. Then, whether the peak at highest mass is the $[M-1]^-$ peak or the $[M+B]^-$ peak can be controlled by suitable choice of B^- as an additive (Figure 1). Similarly, the question of identification of an unknown peak as $[M-1]^-$ or $[M+B]^-$ can be addressed. Practically all organic compounds with ionizable hydrogen can be made to form easily identifiable $[M+B]^-$ ions (for example, by using trichloroacetate as a postcolumn additive); and the formation of $[M-1]^-$ or $[M+B]^-$ with different additives will provide information on the functionality of the unknown.

1. Larson, J.W., McMahon, T.B., J. Am. Chem. Soc., 1984, 106, 517-521.
2. Larson, J.W., McMahon, T.B., J. Am. Chem. Soc., 1983, 105, 2944-2950.
3. Clair, R.L., McMahon, T.B., Can. J. Chem., 1979, 57, 473-479.
4. Caldwell, G., Rozeboom, M.D., Kiplinger, J.P., Bartmess, J.E., J. Am. Chem. Soc., 1984, 106, 4460-4667.
5. Bartmess, J.E., J. Phys. Chem. Ref. Data, in press.

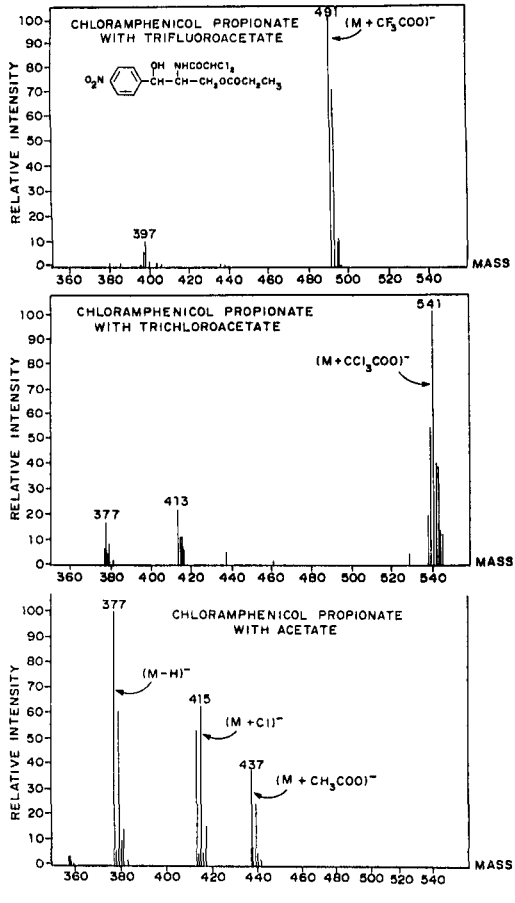

DEVELOPMENT AND PERFORMANCE OF TIME-OF-FLIGHT SECONDARY ION MASS SPECTROMETERS

E. Niehuis, T. Heller, H. Feld and A. Benninghoven
Phys. Inst., Universität Münster, Domagkstr. 75, D4400 Münster, FRG

Optimum sample utilization is crucial for trace analysis of nonvolatile bio-organic compounds by desorption techniques, in particular for applications in life sciences. In many cases only very small amounts of purified sample can be isolated from biological tissue or body fluids.
Time-of-flight mass analyzers are characterized by high transmission and simultaneous detection of all masses. The primary beam intensity of a TOF-SIMS designed for high sensitivity must be high enough to consume the sample molecules in the bombarded target area in a relatively short time.

TOF-SIMS I

In 1982 we developed a high performance time-of-flight secondary ion mass spectrometer [1] that meets these requirements for optimum sensitivity . It consists of a pulsed primary ion source with a magnetic sector field for mass separation and bunching, a multiple focusing electrostatic sector analyzer ("Poschenrieder") and a detection system that provides postacceleration to 20 keV energy for positive and negative secondary ions.

pulsed ion source	- Ar^+,	12 keV
	- pulse width	10 ns
	- max.intensity	50,000 ions/pulse
	- beam diameter	0.7 mm
TOF analyzer	- resolution	M/dM = 500 - 1000 (FWHM)
	- transmission	50 %
detection system	- postacceleration	up to 20 keV
	- efficiency >50%	up to mass 5000
registration system	- signal averager	in ion counting mode
	- time resolution	10 ns
	- no limitation	in number of stop events

We investigated different classes of molecules such as aminoacids, PTH-aminoacids, pharmaceuticals, biopolymers (peptides, oligonucleotides, oligosaccharides) and synthetic polymers (polyethylene, polystyrenes, nylons).
Absolute sensitivities and detection limits were determined for a variety of biomolecules, for example:

Bradykinin	sensitivity	2 C/mol
	detection limit	1 fmol

TOF-SIMS II

We have designed and tested a new TOF-SIMS instrument that combines high sensitivity and high mass resolution [2].

Primary beam system:

A pulsed 90 degree deflection provides an electrodynamical mass separation. The same momentum, defined by the time integral of the high voltage deflection pulse is added to primary ions of different mass but same energy. Therefore their final momenta have different directions. The diverging angle is drastically reduced after the 90 degree deflection, because radial velocity differences are transformed into axial ones. Different masses are separated by a slit at the end of an appropiate drift path. The primary ion mass can be selected by the pulse width of the deflection pulse. We have tested the mass resolution of this method with Xe and achieved a mass resolution of 500.

Due to axial velocity differences the ion bunch spreads resulting in a pulse width of about 20 ns at the exit of the deflector. These velocity differences can be reversed by axial bunching. A second HV pulse is switched on when the ion bunch reaches the center of the buncher. The ions gain energy according to their positions. The distance of the time focus is determined by the pulse amplitude. The pulse width at the target depends on the entrance slit width of the deflector and the diverging angle of the incident ion beam. We achieved a width of 1.5 ns for Ar^+ at 10 keV with a slit of 0.5 mm, a width of 800 ps with a slit of 0.25 mm.
The diameter of the primary ion beam is about 50 µm, the maximum intensity is 10,000 ions/pulse.

Mass analyzer:

A two stage reflector of Mamyrin type [3] is used with a reflection angle of 177 degrees. The mirror consists of a retarding gap (30 mm) and a reflecting gap (60 mm) defined by grids of 90% transparency. The total path length is 2.0 m. To improve transmission an Einzel-lens is used for the beam transport. This lens provides a large acceptance angle of 3 degrees in both directions at a magnification of 50. Therefore the calculated transmission is about 50%.
The resolution of the analyzer is limited by the time dispersion in the acceleration gap. By an appropiate choice of the reflector voltages this time dispersion can be reduced for a certain energy width. A resolution of 15,000 can be expected for an acceleration gap of 2 mm at an energy width of 0.4 %.
The resolution was tested with a time-to-analog converter combined with a multichannel analyzer. The base peak of Crystal Violet (MW=372.24) has a total flight time of 72.50 µs at an acceleration voltage of 2.0 kV. The peak width at half maximum (2.8 ns) corresponds to a mass resolution of 13,000, the width at tenth maximum (5.4 ns) to 6700.

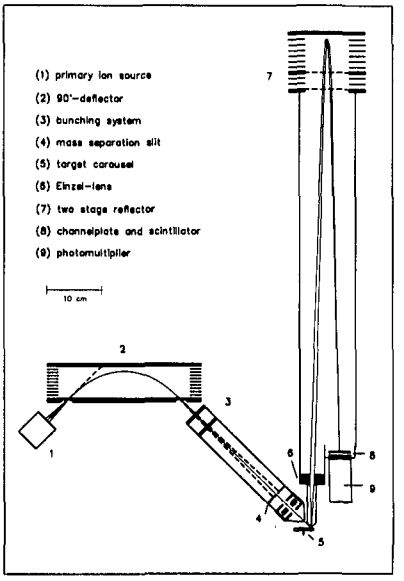

schematic of the instrument

Detection and registration:

The detection system provides postacceleration of the secondary ions up to 20 keV for both polarities to achieve a high detection efficiency even for large molecules. A single channel plate is used for the ion-electron conversion and preamplification. The signal is coupled to ground and amplified by a fast scintillator and a photomultiplier. A new registration system with a time resolution of 1.25 ns is under construction. It consists of a triggerable time-to-digital converter with 256 stops and a special hardware for the fast accumulation of the data. Count rates of more than 1E6 c/s can be processed.

[1] P. Steffens, E. Niehuis, T. Friese, D. Greifendorf and A. Benninghoven
J.Vac.Sci.Technol. A 3 (1985) 1322

[2] E. Niehuis, T. Heller, H. Feld and A. Benninghoven
Proc. Third Int. Conf. on "Ion Formation from Organic Solids (IFOS III)", to be published in Springer Series in Chemical Physics, 1986

[3] V.I. Karataev, B.A. Mamyrin and D.V. Shmikk
Sov. Phys.-Tech. Phys., 16 (1972) 1177

SECONDARY ION TIME-OF-FLIGHT MASS SPECTROMETRY AT MANITOBA

K.G. Standing*, R. Beavis, G. Bolbach**, W. Ens, F. Lafortune, D. Main, B. Schueler, X. Tang and J.B. Westmore

Physics and Chemistry Departments,
University of Manitoba, Winnipeg, Canada R3T2N2

Several years ago a time-of-flight mass spectrometer (Manitoba I) was constructed at the University of Manitoba (1). This instrument, shown schematically in Figure 1, is similar to the spectrometer of Macfarlane and Torgerson (2), but produces secondary ions by bombardment with a pulsed beam of low energy primary ions (normally ~ 10 keV Cs+), instead of fission fragments.

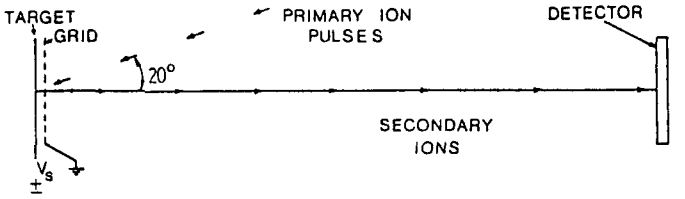

Fig. 1 : "Manitoba I" TOF mass spectrometer (1,3)

Linear TOF spectrometers like this one have a very simple geometry. After acceleration the secondary ions travel in straight lines to the detector. Consequently, the transmission is high and is determined simply by the accelerating voltage and the size of the detector. Measurements of ion yields are thus relatively easy to interpret (4-6).

In this type of instrument, the products of metastable decay in the flight tube continue on to the detector with little change in velocity. They appear in the mass spectrum as a broadened peak at the position of the parent ion (1,7). If these fragments are included in the parent peak, the mass spectrum is measured at an effective time immediately after acceleration (typically $\lesssim$ 200 ns after emission). In sector-field spectrometers or in TOF instruments with a curved optic axis (8), the time between emission and measurement is typically longer by a factor $\gtrsim 10^3$. The mass spectrum measured in linear TOF spectrometers is therefore much closer to the mass spectrum actually emitted than the spectrum measured in those instruments which operate on a longer time scale. Striking effects of such differences have been observed (9).

Observation of the unimolecular decay products increases the spectrometer efficiency and shortens the time scale, but the broad peaks often act as an undesirable background. Considerable improvement may be obtained by the use of an small electrostatic ion mirror, as illustrated in Figure 2. Parent ions and charged fragments are deflected into the detector at 90°, while the neutral fragments continue into the 0° detector. The parent ions are thus separated from the fragments and it is possible to investigate correlations between neutral and charged fragments (10).

TOF measurements put stringent demands on any data system. For optimum efficiency, high speed and large memory are required. Until fairly

* 1985-86 at Institut de Physique Nucléaire, Orsay, France.
**Permanent address : Institut Curie, Paris, France.

recently suitable systems had to be custom built, but they can now be assembled from commercially available components. We have recently introduced such a system, which has given us significant improvements in both data collection and resolution (11).

An intrinsic limitation on the resolution of simple linear spectrometers is given by the axial velocity spread of the secondary ions ejected from the target. Perhaps the simplest solution to this problem is the introduction of a (relatively long) ion mirror, as proposed some years ago by Mamyrin (12), and as applied recently at Orsay (13) and Münster (14). Considerably improved resolution has been obtained in a new spectrometer (Manitoba II) incorporating such a device (15).

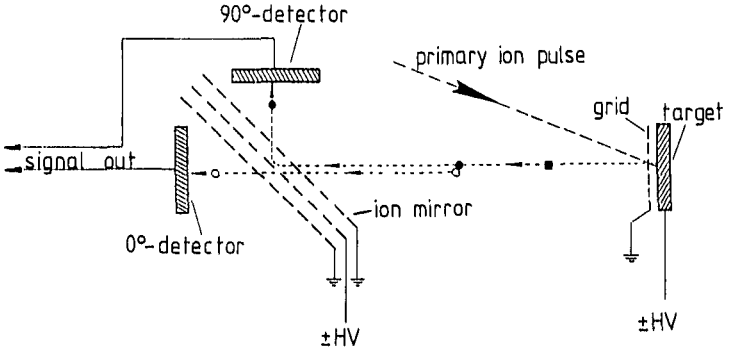

Fig. 2 : Electrostatic mirror with detectors at 0° and at 90°.

REFERENCES

1. B.T. Chait and K.G. Standing, Int. J. Mass Spectrom. Ion Phys. 40, 185 (1981).
2. R.D. Macfarlane and D.F. Torgerson, Int. J. Mass Spectrom. Ion Phys. 21, 81 (1976).
3. K.G. Standing, R. Beavis, W. Ens and B. Schueler, Int. J. Mass Spectrom. Ion Phys. 53, 125 (1983).
4. K.G. Standing, B.T. Chait, W. Ens, G. McIntosh and R. Beavis, Nucl. Instr. and Meth. 198, 33 (1982).
5. B. Schueler, R. Beavis, W. Ens, D.E. Main and K.G. Standing, Surface Science 160, 571 (1985).
6. W. Ens, K.G. Standing, B.T. Chait and F.H. Field, Anal. Chem. 53, 1241 (1981) ; W. Ens et al, these proceedings.
7. B.T. Chait and F.H. Field, Int. J. Mass Spectrom. Ion Phys. 41,17 (1981); B.T. Chait, ibid 53, 227 (1983).
8. P. Steffens, E. Niehuis, T. Friese, D. Greifendorf and A. Benninghoven, J. Vac. Sci. Technol. A3, 1322 (1985) and references therein.
9. W. Ens, R. Beavis and K.G. Standing, Phys. Rev. Letters 50, 27 (1983) ; K.G. Standing, W. Ens and R. Beavis in : Ion Formation from Organic Solids, Springer Series in Chemical Physics 25, Ed. A. Benninghoven (Springer, Berlin, 1983) p. 107.
10. W. Ens et al and B. Schueler et al, in Proc. SIMS V (Springer 1985) and in these proceedings ; K.G. Standing et al, Proc. IFOS III (Springer 1986).
11. W. Ens, R. Beavis, G. Bolbach, D. Main, B. Schueler and K.G. Standing, Nucl. Instr. and Meth. A245, 146 (1986).
12. B.A. Mamyrin, V.I. Karataev, D.V. Schmikk and V.A. Zagulin, Sov. Phys. JETP 37, 45 (1973).
13. S. Della-Negra and Y. Le Beyec, Int. J. Mass Spectrom. Ion Processes 61, 21 (1984).
14. A. Benninghoven et al, SIMS V 1985, IFOS III 1986 and these proceedings.
15. X. Tang et al, these proceedings.

VELOCITY COMPACTION - THEORY AND PERFORMANCE.*

M. L. Muga, TOFTEC, P.O. Box 12877, Gainesville, FL, 32604

Velocity compaction (VC) is an ion focusing principle applicable to pulsed ion source time-of-flight (TOF) mass spectrometers (MS) and is designed for achieving improved mass resolution. This novel focusing scheme selectively accelerates the ions in an iso-mass ion packet in such a manner as to give all ions a nearly equal final drift velocity. In this way the spatial distribution of ions within the iso-mass ion packet is 'frozen' and peak-to-peak adjacent-mass ion packets continue to separate during the final drift period with minimal overlap, unlike the case with the conventional TOF mass spectrometer for which increasing overlap occurs during the final drift period.

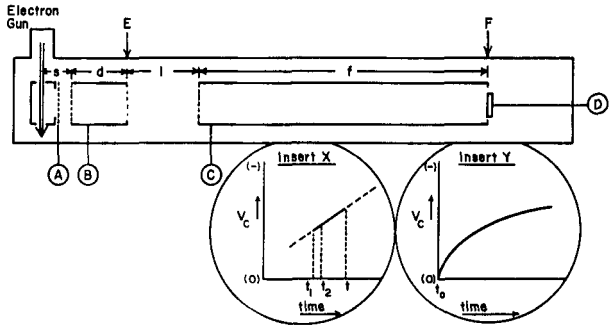

Figure 1

Consider a single cycle of operation in which a bunch of ions is formed in pulsed ion source of Figure 1 and extracted from the ion source region by the application of a constant low value extraction voltage V_x (ca negative ten volts) applied to the extraction grid A, and accelerated into drift region d. After initial partial separation into different iso-mass ion packets the ions enter varying acceleration region l. Further, consider two ions of identical mass entering region l at the same time but with different velocities, v_1 and v_2. Upon entering region l these ions experience a constantly increasing acceleration field due to the changing voltage V(t) applied to grid C (see insert X of Figure 1). The lower velocity ion will receive the larger acceleration over region l since the voltage will be larger by the time it arrives at grid C. The general relation for which velocity equalization will be attained for equal charge-to-mass ions entering region l at the same time, independent of the mode of ion extraction, is

$$\Delta V/\Delta t = 2mvl/q\tau^2 \qquad 1)$$

where $\Delta V/\Delta t$ is the absolute rate of change of voltage with time over the acceleration interval flight-time τ for ions of charge-to-mass ratio q/m and with mean velocity v entering acceleration region of length l.

For ions extracted under constant momentum conditions, 'momentum extraction', the general relation becomes

$$\Delta V/\Delta t = 2E\Delta t' l/\tau 2 \qquad 2)$$

where E is the electric field applied for a short time duration $\Delta t'$ over the extraction region of the ion source.

For ions extracted under constant energy conditions, 'energy extraction', the general relation becomes

$$\Delta V/\Delta t = \sqrt{8Vm/q}\; l/\tau^2 \qquad 3)$$

where V is the instantaneous voltage and other parameters have been previously defined. For constant energy extraction, the specific condition, using practical parameters, for which the slower ion of a given mass will attain the same velocity as the faster one is given by the relation

$$\Delta V(t)/\Delta t = (V/l)\sqrt{2qV_x/m} \qquad 4)$$

provided V_x is negligible compared to V. Here $\Delta V/\Delta t$ is the time rate at which the voltage is to be increased on grid C relative to second grid B during the passage of ions of mass m and charge q over the acceleration region of length l.

Moreover, if the voltage V(t) is varied according to the relation (see insert Y of Figure 1)

$$V = (V_o/c)\; t^r \qquad 5)$$

then velocity compaction surprisingly will apply equally to all mass groups. Here, V_o is the voltage applied at the time ions of mass 1 amu enter the accelerating region 1, and c and r are adjustable constants which depend on the extraction voltage V_x and the distance between center of ion formation and extraction grid A and the lengths of the first drift region d and acceleration region l. Under these conditions all ions of a given mass, simultaneously entering region l, will have the same velocity upon leaving region l and optimum velocity compaction will have been effected. Consequently, neglecting space focusing effects, the ion packet size for a given mass is maintained for the length of drift region f until impact with detector D.

The results of computer simulations based on these equations are compared with the experimental demonstration of velocity compaction ion focusing in Figure 2. The similarity confirms the general validity of this novel focusing technique.

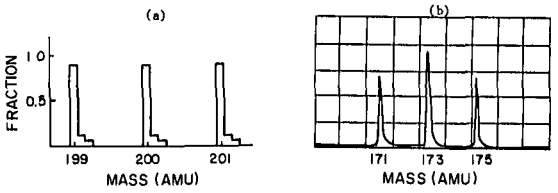

Figure 2

(a) Computer simulated mass spectrum based on Velocity Compaction ion focusing in a single stage Velocity Compaction TOF MS.

(b) A portion of the mass spectrum of $CHBr_3$ showing the isotopic peaks of the species $CHBr_2^+$ taken with a single stage Velocity Compaction TOF MS of like design.

*Supported in part by the Department of Health and Human Services Public Health Service Small Business Innovation Research (SBIR) Phase I Program, Project No. 1 R43 MH39422-01A1, National Institute of Mental Health.

IMPROVED PERFORMANCE OF A TANDEM QUADRUPOLE/TIME-OF-FLIGHT MASS SPECTROMETER

G.L. Glish, S.A. McLuckey and H.S. McKown
Analytical Chemistry Division
Oak Ridge National Laboratory
Oak Ridge, TN 37831.

There is a general need today for instruments that can determine trace organic compounds in ambient air. Desirable characteristics of such an instrument include: high sensitivity, high speed, high selectivity, capability to detect a wide variety of different compounds, small size, and low cost. Mass spectrometry in general and mass spectrometry/mass spectrometry (MS/MS) in particular provides the first four of these characteristics. However, commercial MS/MS systems are neither small nor inexpensive. Therefore we have built a tandem quadrupole time-of-flight mass spectrometer in order to decrease the size and cost of an instrument for the above mentioned application.[1] The key to this instrument is the TOF portion of it.

Time-of-flight (TOF) mass spectrometers were quite popular many years ago and are now seeing a resurgence in popularity. Much of this resurgence in popularity is a result of the high mass capability of TOF mass spectrometers. In addition, newer designs have greatly improved the mass resolution. However, our reasons for using TOF are for the other basic characteristics that it has always had: high sensitivity ,high speed,low cost, small size and simple operation.

While TOF provides the complete mass spectrum in each pulse, for low level signals the typical mode of detection involves using a boxcar integrator to successively sample across the time window of the mass spectrum. This then is the same as scanning and the advantage of having the whole spectrum present at once is lost. In our first model of this instrument,[1] we used a used a time-to-digital converter with the TOF gate pulse as the start pulse and a ion pulse from the detector as the stop pulse. This system works well for very low level signals where the probability of having more than 1 ion per TOF gate is small. However, for larger signals, only the first ion to reach the detector is detected and thus higher mass ions are discriminated against. In addition, a background count precludes the detection of any actual ions for that TOF pulse which reduces the sensitivity. To minimize overcome these problems to a certain extent, we have designed and implemented a new data acquisition system.

The new data acquisition system is controlled by an IBM-XT and based around a LeCroy 4208 8-hit time-to-digital converter and a LeCroy 4802 CAMAC crate controller. Up to eight ions per TOF pulse can be detected with a time resolution of the electronics of 1 nanosecond. With this system signal averaging of TOF spectra at a rate of 20-30 kHz can be achieved.

Figure 1 shows a comparison of the MS/MS spectra of 181^+ from perfluorokerosene (PFK) obtained with the old data acquisition system and the new one. The improvement in signal to noise is readily visible. For the largest peak 6 times more counts were obtained in 1/10 the time in using the new data system.

Figure 2 shows an example of the speed of the system. This MS/MS spectrum of 56^+ from cis-2-butene was obtained in less than 0.5 seconds with a parent ion current of $\approx 7 \times 10^{-14}$ amps.

Research sponsored by the U. S. Department of Energy, Office of Safeguards and Security, under Contract DE-AC05-840R21400 with Martin Marietta Energy Systems, Inc.

By acceptance of this article, the publisher or recipient acknowledges the U.S. Government's right to retain a nonexclusive, royalty-free license in and to any copyright covering the article

This system can also be used to obtain data on extremely low parent ion signals. Figure 3 shows an example of this where the MS/MS spectrum of 150^+ from PFK, at a parent ion current of $\approx 5 \times 10^{-17}$ amps, was obtained in 25 minutes. This spectrum shows quite good signal-to-noise and actually could have been acquired in substantially less time.

While this instrument has the advantageous characteristics described above it does have certain disadvantages. First, there is poor daughter ion mass resolution relative to quadrupole MS/MS instruments, although it is similar to that of most sector MS/MS instruments. Secondly, the appearance of the spectrum depends upon the parameters of the TOF deflection pulse, which is somewhat analogous to the problems that can occur with quadrupoles if they are not properly tuned. The last major disadvantage with this system is that it is still limited to relatively small ion currents. High mass discrimination will occur if there are more than 8 ions per TOF pulse. Discrimination will also occur if two ions are spaced apart in time less than the dead time of the detector.

1. G.L. Glish and D.E. Goeringer, Anal. Chem., 56, 2291 (1984).

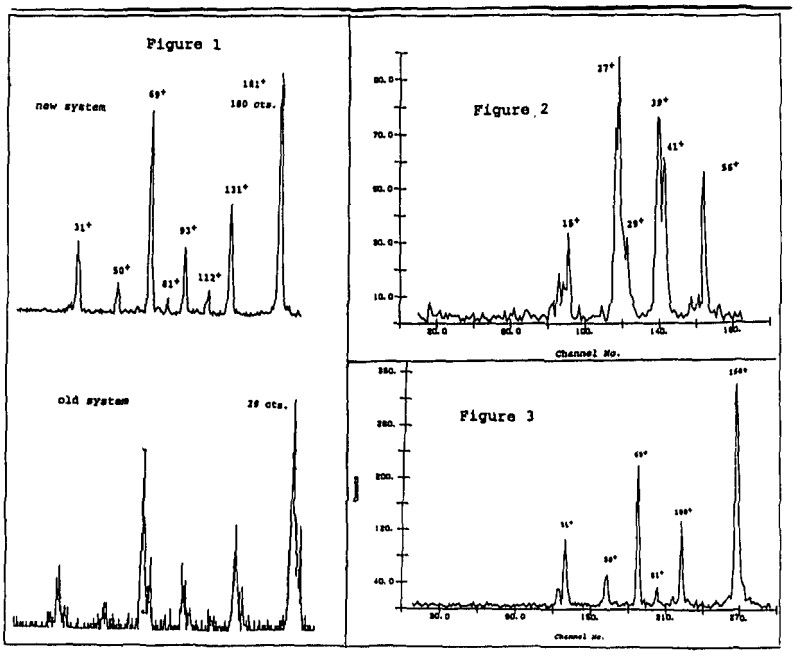

A NEW HIGH RESOLUTION MASS SPECTROMETER

M. Yang, J. P. Reilly
Chemistry Department, Indiana University
Bloomington, IN 47405

Mass resolution in conventional Time-of-Flight mass spectrometers is basically limited by time-broadening due to the spacial width of the ionizing region and the initial kinetic energy distribution of ionizing molecules. However, uv laser induced surface desorption ionization with prism internal reflection essentially eliminates the spacial distribution and a reflectron mass spectrometer can focus the time-broadening due to the initial velocity distribution. Consequently, the combination of this new ionization system with a reflectron mass spectrometer can in principle lead to mass resolution of over one million.

Fig. 1 shows the geometry of the new mass spectrometer. For mass 93 with drift energy of 100 eV, the flight time shifts resulting from the initial kinetic energy at the position a) just before the reflecting electric field, b) after the field, and c) where the MCP detector is located, are plotted in Fig. 2. From this result and assuming the initial kinetic energy distribution of 1 ± 0.5 eV [1], the computer calculates the mass peak widths as 48.2 ps and 2.275 ns for laser temporal widths of 20 ps and 2 ns, respectively. These values correspond to mass resolution 1,593,000 and 33,700.

In the TOF mass spectrometer, the time interval for next mass is inverse by proportional to the square root of the mass and the mass peak width is proportional to the square root of the mass. Thus, if the mass peak width is determined mainly by external parameters, for example, laser temporal width, then the mass resolution increases with the square root of the mass.

In the case of mass 1 million amu, the flight time will be 16 ms and the next mass (1,000,001 amu) is shifted by 7.99 ns. The peak width due to the initial kinetic energy of 1 ± 0.5 eV is calculated to be 4.59 ns. This means that these ions can be resolved even with a 2 ns laser. In practice the high mass limit will be determined not by the mass spectrometer but by limitations on extracting very high mass ions from the surface.

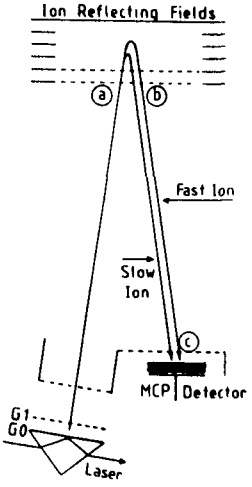

Figure 1

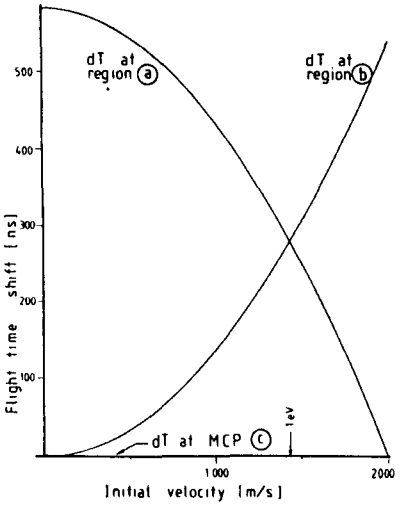

Figure 2

Figure 3 shows the experimental mass spectrum for aniline, mass 93. The uv laser pulse width was about 2 ns. The time for the next mass is 830 ns, the peak width is 7 ns, so the mass resolution is calculated as 11,000. Theoretically the mass peak width of 3 ns was expected, however the 4 ns more broadening apparently results from other effects. For example, the flatness of the grid mesh was not perfect, and the electric fields were not absolutely constant.

The features of this new mass spectrometer can be summarized as follows:

1. Mass resolution: theoretically over 1 million is possible, experimentally 11,000 at mass 93 amu has been achieved.
2. High mass limit: limited only by the ion extraction.
3. No fragmentation is evident [2].
4. Complete mass spectrum in one flash.
5. Fast scanning.
6. High sensitivity.
7. Nonvolatile and thermally sensitive molecule can be ionized.
8. 'Pure desorbing ion' provides a new method for studying the desorption.
9. High resolution without fragmentation enables isotope pattern analysis studies, through which we can count the number of atoms of every element in an unknown heavy molecule.

References

1. M. Yang, J. R. Millard, J. P. Reilly, to be published.
2. M. Yang, J. R. Millard, J. P. Reilly, Optics Communications, 55, 41 (1985).

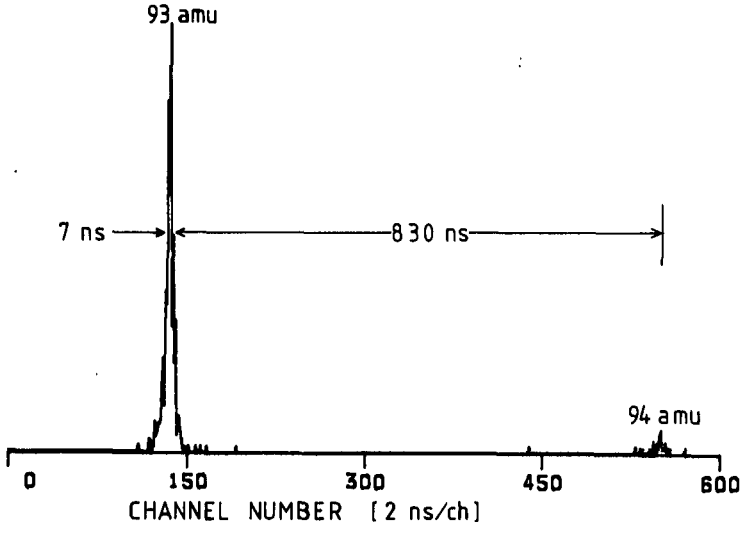

Figure 3

HIGH-RESOLUTION TIME-OF-FLIGHT MASS SPECTROMETRY WITH LASER DESORPTION AND LASER IONIZATION SOURCE

U. Boesl, J.Grotemeyer, K.Walter, E.W.Schlag
Institut für Physikalische und Theoretische Chemie, Technische Universität Munchen
Lichtenbergstr.4, D-8046 Garching, Germany

We present here a new mass spectrometric method with the following new features :

1.) Separation of the vaporizing and ionizing process
2.) cooling of the evaporized neutral molecules
3.) ionizing by resonance enhanced multiphoton ionization (REMPI)
4.) detection by a high mass resolution reflectron time-of-flight mass spectrometer

The advantages of these new features are: a.) mass spectra with intensive pure molecular ion signals without transfer, abstraction or addition species like hydrogen, sodium etc.; b.) controllable fragmentation from very soft (base peak = molecular ion) to very strong fragmentation; c.) high yield of metastable ions; d.) high mass resolution of the TOF-spectrum; e.) high sensitivity

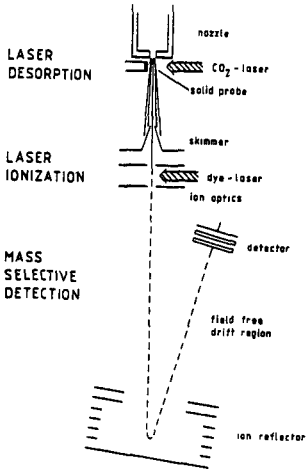

In the following we shall describe our technique and in more detail the four stages mentioned above. As in the scheme of our instrument to be seen this is build up by three separated vaccuum chambers, the laser desorption-, the laser ionization- and the mass spectrometer chamber. A solid probe is mounted near the nozzle of a pulsed valve. A low powered CO_2 laser desorbs ions as well as neutrals, which suffer many collisions in the nearby supersonic beam and then are cooled and transported to the skimmer. A clean molecular beam of argon and desorbed molecules enters the ionization region, while due to the construction of the ion source the desorbed ions are rejected. The ionization takes place by multiphoton absorption within a frequency doubled dye laser pulse. The so formed ions are accelerated into the field free drift region, corrected for energy differences in an ion-reflector and detected by a tandem-channelplate detector. For more experimental details see ref /1/.

1.) Laser Desorption of neutral molecules

Most desorption techniques are used as an ion source of non volatile molecules. However, it is well known that in these techniques neutrals are emitted in greater abundance than ions. We use the emission of neutrals by laser desorption in our technique and thus are able to seperate desorption and ionization process. One major advantage is the possibility of cooling the desorbed molecules before ionization.

2.) Cooling of the desorbed neutral molecules in a supersonic beam

A very efficient way of cooling is the cooling in a supersonic molecular beam. Best cooling can be reached for the translational degrees of freedom, in comparison to rotational and vibrational motions. Translational temperatures of 10 K and better can be reached in our molecular beam. The advantages of cooling are:

1.)low rotational and vibrational excitation lead very often to simplified structured optical spectra and enables state-selective and species-selective excitation by REMPI.
2.)low translational temperatures include narrow initial velocity distribution and make high mass resolution in a time-of-flight mass spectrometer possible.

Even in a RETOF the so called turn around times, due to initial velocities may spoil the mass resolution. Especially for desorption like SIMS, FAB and laser desorption the final

kinetic energy distribution of the desorbed particles is typically in the 1eV region, which would lead in our instrument to mass resolutions of 1000 or less. With kinetic energy distributions in the 1meV region (= 10 K) we get a mass resolution of better than 10 000.

3.) Resonance enhanced Multiphoton Ionization (REMPI)

The third step after desorption and cooling is the REMPI. For fragile compounds and large molecules REMPI has many fascinating advantages. With dye lasers, an ideal light source is available; resonance enhancement results in high ion yields at fairly low laser power; state selective and species selective ionization are possible as well as soft ionization, ionization combined with tuneable fragmentation and enhanced production of metastables /2/. As for the fragmentation, in opposite to other ionization techniques like electron impact, REMPI is a multistep process. This process is dependent on the n-th power of the intensity with n the step number. This leads to a drastic change of the mass spectra with changing the laser intensity. For mass spectra of large fragile compounds measured with our experimental setup see ref /1,3,4/.

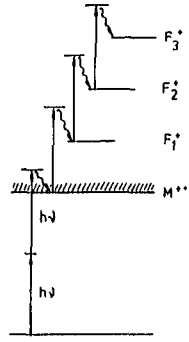

Resonant enhanced Multiphoton Ionisation

4.) Detection by a high resolution Reflectron-TOF mass spectrometer

The ideal mass spectrometer to be combined with a REMPI ion source is a TOF instrument. Both are pulsed techniques. The advantages of a TOF are unlimited mass range, high transmission and registration of all ions formed with one laser pulse. The advantage of a laser ion source are beneath those mentioned above short time and small spatial characteristics. With a Reflectron-TOF considerable mass resolutions can be achieved. However, even for a Reflectron instrument exist some limitations. Below the main contributions to the total width of a time-of-flight peak are listed:

Δt(laser)	5 - 8 nsec	commercial dye laser
Δt(turn around)	5 nsec	for room temp.; 700 V/cm extraction field
Δt(Coulomb)	3 nsec	10^4 ions within $(0.15)^2$ * 0.6 mm^3 laser focus

By using a pulse cutting system for the laser, cooling within a supersonic molecular beam and a special focus size for minimizing Coulomb repulsion Δt(laser) could be reduced to 1.5 nsec, Δt(turn around) and Δt(Coulomb) to less then 1 nsec. This results in mass resolution of better than 10000 (50% valley) measured for p-Xylene /5/.

/1/ J. Grotemeyer, U. Boesl, K. Walter, E.W. Schlag; accepted for publication by Org. Mass Spectrom.; publication date August 1986.
/2/ U. Boesl, H.J. Neusser, E.W. Schlag; Chem. Phys. Lett. 87 (1982), 1.
U. Boesl, H.J.Neusser, R. Weinkauf, E.W. Schlag; J. Phys. Chem. 86 (1982), 4857.
/3/ Oral contribution on this conference, paper TOE 12, J. Grotemeyer, U. Boesl, K. Walter, E.W. Schlag.
/4/ J. Grotemeyer, U. Boesl, K. Walter, E.W. Schlag; accepted for publication by J. Am. Chem. Soc.; publication date June 1986.
/5/ K. Walter, U. Boesl, E.W. Schlag; accepted for publication by Int.J.Mass Spectrom. Ion Proc. 1986.

Acknoledgement: This work has been supported by a grant from the Bundesministerium fur Forschung und Technologie (13N5307) in collaboration with Bruker-Franzen Analytik, Bremen.

Application of FAB/MS to the Charcterization of Mammalian Peptide Hormones.

K.F. Faull, O. Beck[1], A.N. Tyler[2], K.A. Roth[3], R.G. Lorenz[4] and J.D. Barchas.
Department of Psychiatry and Behavioral Sciences, Stanford University Medical Center, Stanford, CA 94305. Current addresses: [1]Department of Toxicology, Karolinska Institute, Stockholm, Sweden; [2]Metabolism Division Unit, [3]Department of Pathology, and, [4]Department of Anatomy and Neurobiology, Washington University School of Medicine, St. Louis, MO 63110.

The ability of FAB/MS to provide accurate molecular weight data of peptides down to the low pmol level and thus substantially contribute to the characterization of peptide hormones is demonstrated with two recent examples of work from our laboratory.

The tachykinins represent a family of biologically-active amidated peptides which possess a common COOH-terminal amino acid sequence. Using a COOH-terminal directed antisera which had full cross-reactivity with known tachykinins, Dr. Kevin Roth sought to characterize the immunoreactivity present in ileal carcinoid tissue[1]. Four immunoreactive peaks (approximately 1-2 nmol ea.) accounting for the bulk of the immunoreactive material in the original extract, were purified to apparent homogeneity from 15 gm of tissue using Sephadex G50 column chromatography and RP-HPLC. Characterization of the components was achieved with a combination of gas phase Edman sequencing, ninhydrin amino acid analysis, and M.W. determination by FAB/MS. Mass spectrometry was completed on a ZABSE (VG) instrument with 8 kV accelerating voltage and xenon atom bombardment (8 kV, 0.1 mA) using monothioglycerol matrix. Resolution of approximately 1000 was used and a window of 150-400 D covering the region of the suspected molecular weights was repetively scanned at a rate of 2-5 s/scan. Data was summed using a multichannel analyzer. Mass assignments were made by reference to CsRbI. Quantitation was based on results from the radioimmunoassay.

The analysis of Peaks I and II was routine. Edman sequencing of Peak I on 600 pmol was incomplete but yielded 8 residues which was identical to the first 8 residues of substance K (total of 10 residues). The amino acid composition of Peak I on 588 pmol was consistent with substance K, and FAB/MS on 10 pmol demonstrated a prominent ion at m/z 1133.4 which was in close agreement with the M.W. of substance K (1132.5 D). Edman sequencing of Peak II (600 pmol) was also incomplete, but yielded 6 residues which were identical to the first 6 residues of substance P (total of 11 residues). The amino acid composition of Peak II (340 pmol) was consistent with substance P, and FAB/MS (10 pmol) demonstrated a prominent ion at m/z 1347.4 which was in close agreement with the M.W. of authentic substance P (1346.7 D).

The analysis of Peaks III and IV was more complicated. Edman sequencing (600 pmol) of these peaks was unsuccessful, suggesting blocked N-terminii, and although the peaks had identical amino acid compositions (360 and 660 pmol, respectively) which were consistent with substance P(5-11), their HPLC retention times excluded this possibility. FAB/MS of Peak IV (250 pmol) revealed an ion at m/z 852.3 which with the amino acid data was consistent with pyro-glu-substance P(5-11) (M.W. 851.4). FAB/MS of Peak III (100 pmol) revealed a weak ion 16.2 D higher which was consistent with oxidized pyro-glu-substance P(5-11). These identifications were confirmed by co-chromatography with authentic pyro-glu and oxidized pyro-glu substance P(5-11).

The endorphins represent another family of biologically-active peptides derived from the parent peptide proopiomelanocortin. Robin Lorenz attempted to characterize the opioid-like immunoreactivity in extracts of shark pituitary[2]. Data was collected on a total of 4 peptides which were purified to apparent homogeneity on the basis of antibody recognition of the N-terminal sequence Ac-YGGFX-, using RP-HPLC. Again complete characterization of the peptides was achieved by a combination of sequencing, amino acid analysis and FAB/MS. Between 500-1500 pmol of each fraction (as determined by RIA quantitation) was used for Edman sequencing. Each FAB/MS experiment used between 4-20 pmol of material and amino acid analysis on one fraction used 500 pmol of material. The FAB/MS experiments were carried out with instrument settings the same as described earlier, which for 3 of the fractions produced unresolved molecular ion clusters.

The results (Table 1) showed that incomplete data was obtained from sequencing, but the combination with molecular weight determination by FAB/MS and amino acid analysis completely characterized the fractions as shark β-endorphin (1-30) and three structural variants.

Table 1: Molecular Weights of Shark Endorphins

Fraction	Sequencing MW	FAB/MS	Δ	Structure
VIII and X	3255.8	3521.8	266 (glu-his)	Shark β-endorphin 1-30
IX	3083.7	3197.7	144 (asp-NH_2)	Shark β-endorphin 1-27
VII	2851.0	2955.0	99 (val)	Shark β-endorphin 1-25
II	not done	1219.3		Shark β-endorphin 1-10

The carboxy terminal residues 29 and 30 of Fractions VIII and X, residue 27 of Fraction IX and residue 25 of Fraction VII were not detected by Edman degradation and were assigned on the basis of the molecular weight determined by FAB/MS. Residues 29 and 30 of Fraction VIII were confirmed by amino acid analysis. The sequence of Fraction II is assigned only on the basis of FAB/MS results.

The method employed for molecular weight determination by FAB/MS which involved centroiding the unresolved molecular ion cluster generally showed an accuracy of ± 0.5 D (Table 2), and for two fractions showed differences between the masses of the ions, in the positive and negative mode of 1.8 and 1.9 D, confirming the $(M+H)^+$ and $(M-H)^-$ structures respectively.

Table 2: Errors Observed in Mass Measurement of Shark Endorphins

Fraction	Calc. M. Wt.	Measured MH^+	Δ_p	$(M-H)^-$	Δ_n	Δ_{p-n}
X	3522.1	3522.8	-0.3	3521.0	+0.1	1.8
IX	3197.8	3198.7	-0.1	3196.8	0	1.9
VII	2955.5	2955.9	-0.6			
II	1218.5	1219.3	-0.2			

In conclusion, the results from these two examples showed that molecular weight determination by FAB/MS is a powerful complement to the conventional techniques used in peptide sequencing. For molecular weight measurement, the sensitivity limit for FAB/MS is generally equivalent to the requirements for amino acid analysis and gas phase micro sequencing. The peptide molecular weight provides and absolute value to which sequence data and amino acid composition must conform.

References

[1]K.A.Roth et al. Regulatory Peptides 12:185-199 (1985).
[2]R.G. Lorenz et al. Peptides 7(1), in press (1986).

MULTIPLE REACTION MONITORING OF LEUCINE ENKEPHALIN FOR QUANTIFICATION AT THE FEMTOMOLE LEVEL

CHHABIL DASS AND DOMINIC M. DESIDERIO
UNIVERSITY OF TENNESSEE, MEMPHIS, TENNESSEE 38163

There is an increasing demand in several branches of the neurosciences and other fields to quantify neuropeptides in extracts of biologic tissues and fluids with high level of molecular specificity and a very high sensitivity at the femtomole level. Many laboratories currently utilize radioimmunoassay, radio receptorassay, either alone or in combination with HPLC, for peptide measurement. However, these techniques lack the utmost molecular specificity and the data derived from those measurements can best relate only to secondary structural characteristics such as immunoreactivity, receptor binding, hydrophobicity etc. MS/MS, on the other hand, is a novel technique that can select a specific and unique daughter ion from the mass spectrum of a parent ion, thereby enhancing the molecular specificity of the measurement because of the unique and important precursor-product relationship. This particular precursor-product pair can be used to quantify the precursor. This unique advantage is very important for the analysis of a biological extract because of the fact that n amino acids could produce a large number (n!) of peptide, a number simply to large to be readily resolved chromatographically or with limited MS data. We report here a MS/MS method for the quantification of leucine enkaphalin (YGGFL; see Figure 1 for its structure). The strategy is to form a quasimolecular ion $(M+H)^+$ of the neuropeptide by positive ion FAB, monitor the daughter ions formed by metastable transitions (1) and (2) (scheme 1) occuring in the first field free region of the forward geometry (E-B, where E and B are electric and magnetic sectors, respectively) instrument by using B/E-linked-field scans. The transistions utilized for quantification of LE are 556→336 and 556→425 that are due to the C-terminus-containing tripeptide fragment -GFL and the N-terminus-containing tetrapeptide fragment YGGF-, respectively.

Scheme 1

LE (YGGFL) + m/z 556 → **-GFL]$^+$ m/z 336 (1)**
LE (YGGFL) + m/z 556 → **YGGF-]$^+$ m/z 425 (2)**

The mass spectrometer utilized for these studies is a VG 70E-HF instrument fitted with an Ion Tech saddle field FAB Gun. Xe (at 7keV) is used as the bombarding atom. A VG 11-250 M+ data system was used to record the data in the selected reaction monitoring (SRM) mode. The data at the two transitions are recorded for two minutes and the solution (1μg μL^{-1}) of the synthetic peptide in methanol was diluted sequentially to provide solutions in 40-2000 μg mL^{-1}. Glycerol (0.2 μL) was used as liquid matrix.

Figure 2 plots the MS/MS signal measured as area under the signals (left axis in arbitrary A/D units) from the two transitions versus the amount of LE deposited on the FAB probe tip. The straight line statistics for these data are y=34x+166 for the transition 556→425, and y=2.5x-17.2 for 556→336. The signal due to the daughter ions at m/z 425 is more abundant than the signal at m/z 336. However, the two peptide fragment desorption profiles parallel each other. The level of detection sensitivity is 40 pg (72 fmol) with a signal to noise ratio of 3-to-1.

The data presented here shows that the multiple reaction monitoring of two transitions provides a sensitive method for the

estimation of LE. The MS technique is more comparable and competitive with RIA methodology. Lastly, our level of confidence has increased significantly by monitoring the two unique transistions from the same precursor.

Figure 1

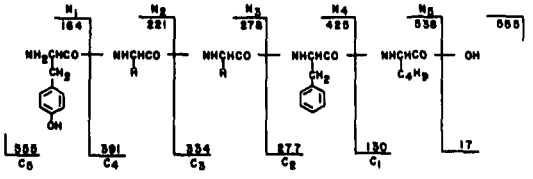

Figure 2

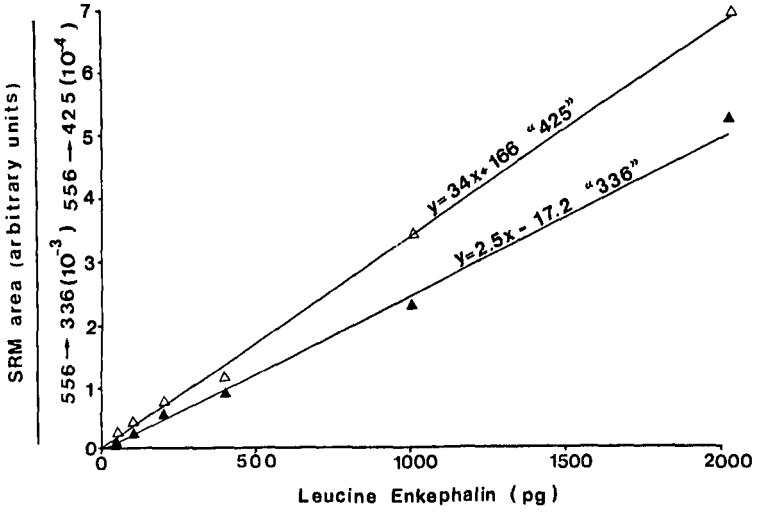

USING FAB MASS SPECTROMETRY AS A MASS ASSAY FOR PEPTIDE IDENTIFICATION

B.W. Gibson, D.H. Williams, L. Poulter, S. Naylor and A.F. Findeis
University Chemical Laboratory
Lensfield Road, Cambridge, CB2 1EW, U.K.

The South African frog, Xenopus laevis, secretes a complex mixture of biogenic amines and peptides from its dorsal skin upon stimulation (1). During the last fifteen years, three peptides have been isolated and identified from these secretions using classical bio-assay procedures; xenopsin, caerulein and TRH. However, it is clear from the HPLC chromatograms (Figure 1) that there are as many as 50 or more components present in these secretions that elute in a hydrophobic range expected for peptides. We have attempted to characterize these components by FAB mass spectrometry in a type of 'mass-assay' procedure, since the bio-assay techniques used previously may not be appropriate for their detection.

The preliminary screening of numerous HPLC fractions by FAB mass spectrometry produced over 30 molecular ions. Using a combination of FAB-MS peptide sequencing, Edman degradation and amino acid analysis, we have been able to identify those components as peptides, originating from additional post-translational processing of regions of the precursors to the peptides xenopsin, caerulein and PGL[a] (2). Recent bio-activity studies have shown that the larger of these peptides are hemolytic and can be predicted to have an α-helical structure in interfacial environments due to their amphiphilic nature. It is interesting to note that most of these peptides ran exceedingly well by FAB-MS, even at high mass (Figure 2). We now think this is due to the high surface activity of these peptides, since they would be expected to form α-helices at the glycerol-vacuum interface as well as on membrane surfaces.

In order to apply FAB-MS as a 'mass-assay' technique in a general sense, it is essential that certain peptides be made more 'surface-active', such that they will not be discriminated against if they happen to be hydrophilic. In a first step to realize this goal, we have used a hydrophobicity index based on the surface tension measurements of Bull and Breese (3) to predict the relative surface activities and thus ionization efficiencies of peptides in mixtures (4). Our preliminary results obtained from the analysis of tryptic digests of horse heart cytochrome C and myoglobin indicate that we can accurately predict whether or not a peptide will be observed. This predictive scheme is based on the additive values of the free energies of transfer to the surface of the constituent amino acids (see Figure 3). More recently, we have observed the effects of isopropyl ester formation on these ionization yields and have found that virtually all peptides, once made reasonably hydrophobic, can be observed in complex mixtures (5). This result has important applications in the analysis of tryptic digests of large proteins for sequence confirmation as well as in a 'mass-assay' procedure for the identification of novel peptides (6).

References.

1. Evspamer, V. and Melchiorri, P., TIPS, Oct.: 391-395 (1980).
2. Gibson, B.W., Poulter, L., Williams, D.H. and Maggio, J., J. Biol. Chem., 261, 5341-5349 (1986).
3. Bull, H.B. and Breese, K., Arch. Biochem. Biophys., 161, 665-670 (1974).
4. Findeis, A.F., Naylor, S., Gibson, B.W. and Williams, D.H., manuscript in preparation.
5. Naylor, S., Findeis, A.F., Gibson, B.W. and Williams, D.H., J. Am. Chem. Soc.: in press.
6. Gibson, B.W., Poulter, L. and Williams, D.H., Peptides, 6, 23-27 (1985).

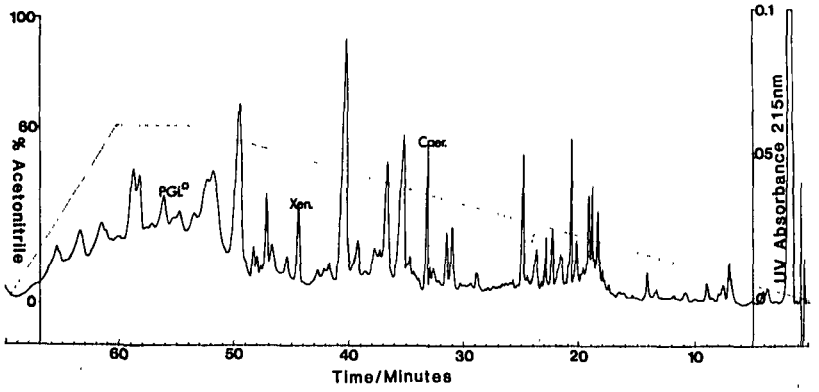

Figure 1. HPLC of Xenopus laevis skin secretions:

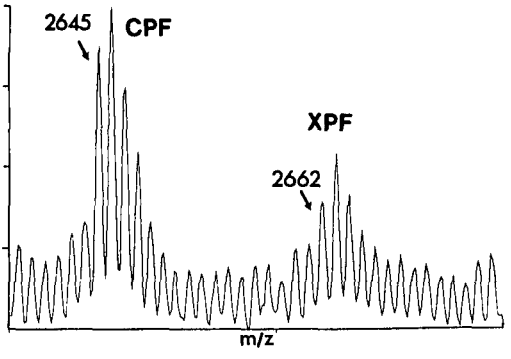

Figure 2. Caerulein precursor fragment (CPF) and xenopsin precursor fragment (XPF) FAB/MS spectrum taken on Kratos MS-50 high field inhomogeneous magnet.

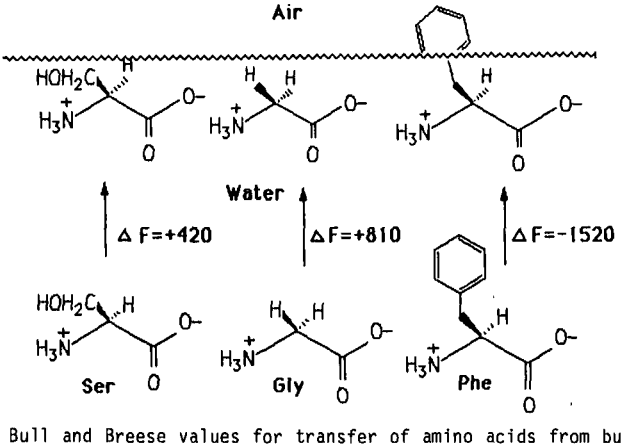

Figure 3. Bull and Breese values for transfer of amino acids from bulk to surface (in cal/mole).

FAST ATOM BOMBARDMENT MASS SPECTROMETRY OF DISULFIDE-CONTAINING PEPTIDES AND PROTEINS

Razieh Yazdanparast*, D.L. Smith*, P. Andrews#, and J.E. Dixon#

*Department of Medicinal Chemistry and Pharmacognosy
and
#Department of Biochemistry
Purdue University
West Lafayette, Indiana 47907

One of the challenging steps in complete structure elucidation of cystine-containing peptides and proteins is the location of disulfide crosslinks. Existing methods of assignment identify peptides by a combination of their chromatographic properties and amino acid sequence.

In a previous report (1), we described the general behavior of intra- and interchain disulfide bonds in peptides exposed to the high energy xenon atom beam used for anlayses with fast atom bombardment mass spectrometry (FABMS). These data showed that disulfide bonds undergo gradual reduction during the course of FABMS analysis. In addition, no evidence for disulfide bond rearrangements in interchain disulfide-containing peptides was found during the course of FABMS analysis. These observations suggested that FABMS may be an ideal method for assigning disulfide crosslinks in proteins.

We have now used a combination of specific and nonspecific degradation reactions with FABMS to assign the four disulfide bonds of hen egg-white lysozyme and bovine ribonuclease A. Peptides produced by tryptic digestion of CNBr-treated lysozyme and ribonuclease A, illustrated in Figure 1, were identified by FABMS analysis of either the crude digest or chromatographically separated fraction of the digest. Protonated molecule ions were distinguished from fragment ions by the presence of a second peak 22 mu higher than the MH^+ ions corresponding to MNa^+ ions. Peptide identification was confirmed by the change in molecular weight after removal of one N-terminal amino acid by a one-step manual Edman degradation.

The FAB mass spectrum of the tryptic digest of CNBr-treated lysozyme contained three peaks at m/z 3269, 1516, and 992, which were assigned to the three disulfide-containing peptides: 62-68/74-96, 22-33/115-116, and 6-12/126-128, respectively. Chemical reduction of an aliquot of the tryptic digest of CNBr-treated lysozyme with dithiothereitol/dithioerythritol mixture resulted in the replacement of peaks at m/z 992 and 1516 with two new sets of peaks at m/z (660,335) and (1269,250), respectively. From these observations and the primary structure of lysozyme, it is evident that disulfide bonds are located between cysteines 6 and 127, and cysteines 30 and 115. However, no assignments could be made among the remaining cysteines because of the presence of three cysteine residues in the same peptide chain (74 to 96). Peptide fragments suitable for determining the remaining two disulfide linkages were produced by mild acid hydrolysis of the peptide 62-68/74-96, which had been purified by HPLC. Ions corresponding to disulfide bonded peptide pairs were identified by changes in the mass spectra of the hydrolysate recorded before and after chemical reduction with thiol reagents. Masses of molecular ions of peptides diagnostic of disulfide linkages, as well as their assignments to the original protein, are illustrated in Figure 2.

Unlike lysozyme, none of the disulfide bonds of ribonuclease A could be assigned from the FAB mass spectrum of the tryptic digest of CNBr-treated ribonuclease A. However, two disulfide bonds between cysteines 26 and 84, and cysteines 65 and 72 were assigned by mass spectral analysis of peptides isolated from the digest by HPLC. The disulfide crosslink between residues 65 and 72 was established by a peak at m/z 1979 (see Fig. 1b) and its disappearance from the FAB mass spectrum of the chemically reduced sample. Similarly, the peak at m/z 2296 was assigned to a peptide which has the disulfide bond between residues 26 and 127. The remaining disulfide bonds could not be located because unique peptides were not formed by the CNBr and tryptic cleavage reactions. Suitable peptides were, however, formed when a second enzyme, Staphylococcus aureus V-8 was added to the digest. The FAB mass spectrum of this digest had peaks at m/z 1644 and 2029, which correspond to peptides 54-61/105-111 and 40-49/92-98, respectively.

The results presented here indicate that disulfide bond linkages in a protein can be located using 1-2 nmoles of the protein fragmented by chemical or proteolytic methods. Although peptides diagnostic of disulfide linkages may often be detected by FABMS in the crude digest, some peptides must first be isolated by HPLC. This capability of FAB mass spectrometry provides a sensitive and reliable method for assigning disulfide linkages in a variety of biologically active peptides and proteins.

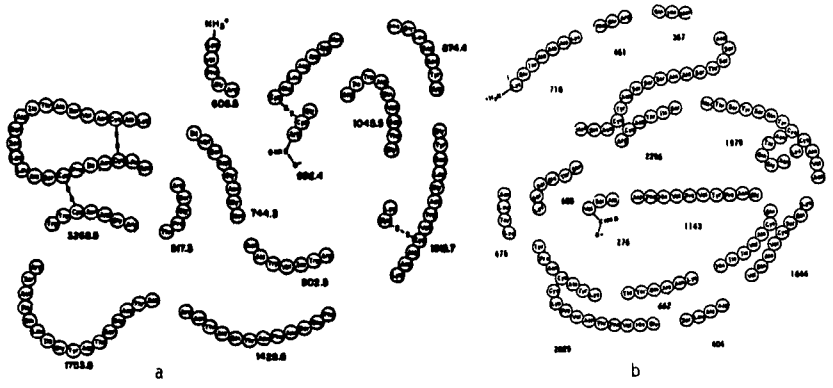

Fig. 1. Peptide fragments produced by tryptic digestion of CNBr-treated hen egg-white lysozyme (a) and bovine ribonuclease A (b). The masses of the protonated molecule ions are as indicated.

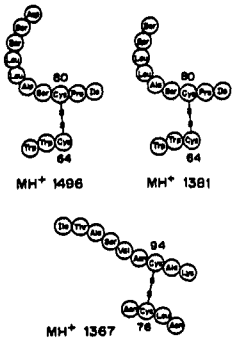

Fig. 2. Three of the disulfide-containing peptides from partial acid hydrolysis of 62-68/74-96 tryptic peptide of hen egg-white lysozyme.

References

1. Yazdanparast, R., Andrews, P., Smith, D.L., and Dixon, J.E., Anal. Biochem. 153, 348-353 (1986).

ANALYSIS OF LYSOZYME DERIVED PEPTIDES BY FAST ATOM BOMBARDMENT AND TANDEM MASS SPECTROMETRY.

Hartman, T.G., *Rosen, R.T., Govindarajan, S., Ho., C.-T. and Rosen, J.D., Department of Food Science and Center for Advanced Food Technology, Rutgers University, New Brunswick, New Jersey 08903

Fast atom bombardment (FAB) and tandem mass spectrometric techniques (MS/MS) were employed in a study of protein-carbohydrate interaction. These methods were used to determine the formation of high molecular weight glycosylation products in a glucose-lysozyme model system. Peptide maps of the tryptic and chymotryptic hydrolysis products of egg white lysozyme and its glycosylated reaction products were obtained using FAB mass spectrometry. The peptide mixtures were also separated and fractionated using reverse phase high performance liquid chromatography (HPLC) and components were isolated in pure form or as simple enriched mixtures. A combination of FAB and MS/MS were employed to obtain collisionally activated dissociation (CAD) spectra for several peptides.

Peptide maps of native and glycosylated lysozyme provided information on the intensity and site specificity of the glycosylation reaction. The protonated molecular ion species of select individual peptides containing lysine or arginine residues were observed to increase in molecular weight by 162 mass units. This increase corresponds to the presence of 1-deoxy-D-fructos-1-yl residues formed in the glycosylation reaction.

Figure A is the total FAB tryptic peptide map of lysozyme obtained by direct mixture analysis of the tryptic digest. Trypsin cleaves peptide linkages on the carboxyl side of lysine and arginine residues. The protonated molecular ion species corresponding to the individual peptides are listed in the order of tryptic cleavage beginning at the N-terminus of the protein (T-1 → T-18). Similarly Figure B shows the low mass (<1000) FAB chymotryptic peptide map of lysozyme (C-1 → C13). Chymotrypsin cleaves peptide bonds primarily on the carboxyl side of aromatic amino acid residues. Figure C is a region of the FAB tryptic peptide map obtained from lysozyme glycosylated by a 72 hour incubation with glucose at 50°C and 65% relative humidity. Mass increases of 162 (+G) or 324 (+2G) corresponding to the formation of 1-deoxy-D-fructos-1-yl residues on individual peptides are indicated. Figure D shows a region of the FAB chymotryptic peptide map derived from the same glycosylated protein. The combined tryptic and chymotryptic data indicate that, under the given reaction conditions glycosylation of lysozyme occurs primarily at the N- and C-terminal region of the protein. These results demonstrate the usefulness of FAB/MS for the characterization of glycosylated proteins and peptides. NJAES #K-10535-1-86.

FIGURE A FAB TRYPTIC PEPTIDE MAP OF LYSOZYME

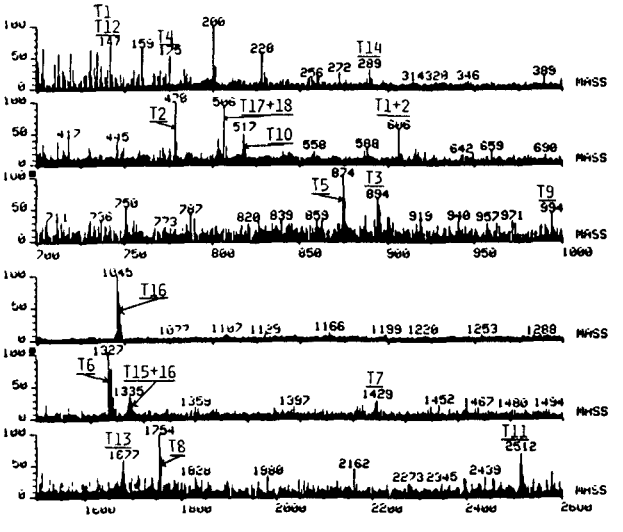

FIGURE B FAB CHYMOTRYPTIC PEPTIDE MAP OF LYSOZYME

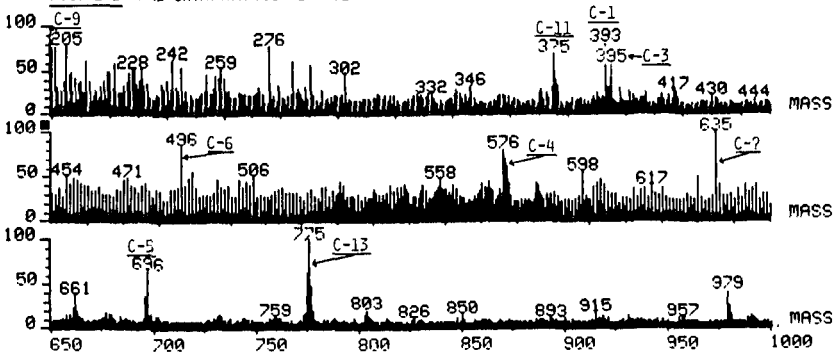

FIGURE C EXPANDED REGION OF THE FAB TRYPTIC PEPTIDE MAP OF GLYCOSYLATED LYSOZYME

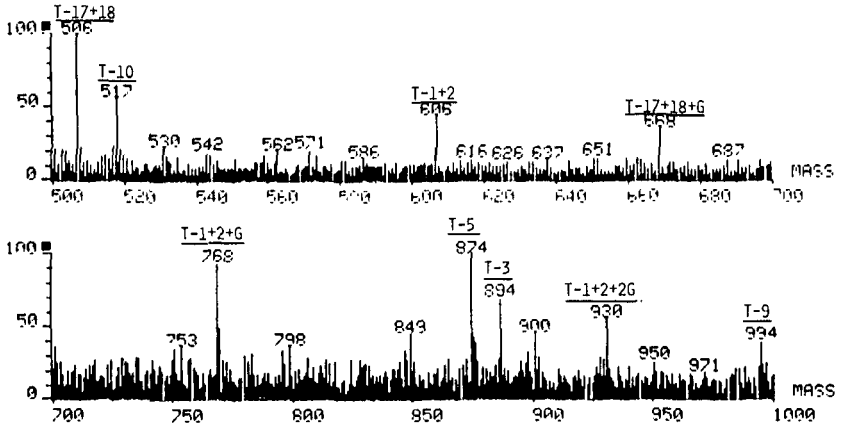

FIGURE D EXPANDED REGION OF THE FAB CHYMOTRYPTIC PEPTIDE MAP OF GLYCOSYLATED LYSOZYME

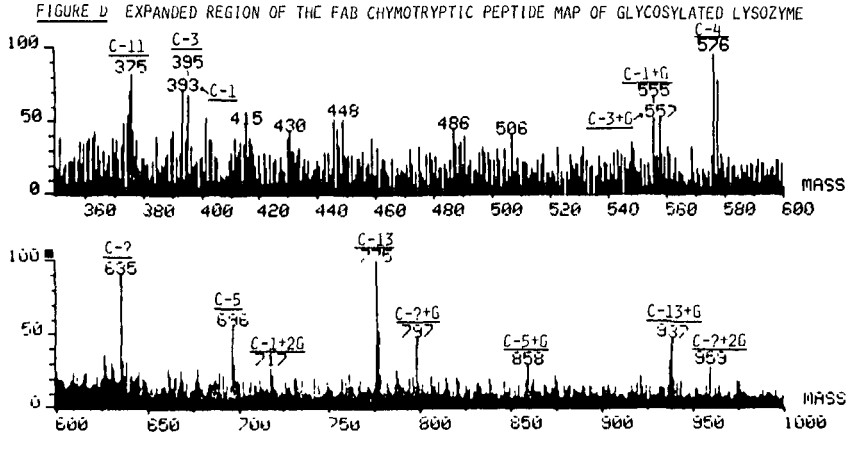

FAB-MS OF PROTEINS - ENZYME-AIDED SEQUENCE DETERMINATION OF PEPTIDES AND IDENTIFICATION OF PARTICULAR AMINO ACIDS

Ch.HAFOK, I.Maurer-Fogy and E.R.Schmid*

Ernst Boehringer Institut, Dr.Boehringer Gasse 5-11,A-1121 Vienna and

*Institute for Analytical Chemistry, Währingerstr.38,A-1090 Vienna, Austria

FAB-MS is used in addition to Edman degradation for controlling the primary structure of recombinant proteins, e.g. Interferonα2 and Interferonγ. Elaboration of new methods was carried out with standard peptides as insulin, glucagon, serum thymic factor and/or melittin. The proteins are cleaved enzymatically with endopeptidases as trypsin or staphylococcus aureus V_8-protease. The resulting peptides are separated by reverse phase high performance liquid chromatography (HPLC) and analysed by FAB-MS. All spectra were recorded with a Finnigan MAT 8230 mass spectrometer. Positive and negative spectra were scanned from high to low mass at a scan rate of 30 sec per decade using a xenon fast atom beam. The matrix material is glycerol. 0.25 µl 5N HCl is added to reaction mixtures containing basic buffers just before inserting them in the mass spectrometer.

I. Peptides originating from a protein by an enzymatic cleavage show in nearly all cases a molecular ion. To confirm the molecular weight an additional enzymatic cleavage is performed. The enzymes used are staphylococcus aureus V_8- protease, trypsin,and chymotrypsin, according to the structure expected. They are dissolved in water and simply added to the sample on the target which remains from the molecular ion determination. The temperature is increased to about 40°C. Using trypsin or chymotrypsin, ammonium bicarbonate buffer, pH 8, is put on the probe tip additionally. Two to ten minutes later the spectrum is recorded. In fig.1 the upper spectrum shows an interferon-γ-staph.a.-peptide with its molecular ion, doubly charged molecular ion, and some small fragment ions. The lower spectrum is recorded after addition of trypsin and ammonium bicarbonate (reaction time two minutes at room temperature). Six new molecular ions indicate the six peptides arising from cleavage at the basic amino acids. With this short and easy procedure the occurence of a different peptide with the same molecular weight is practically excluded.

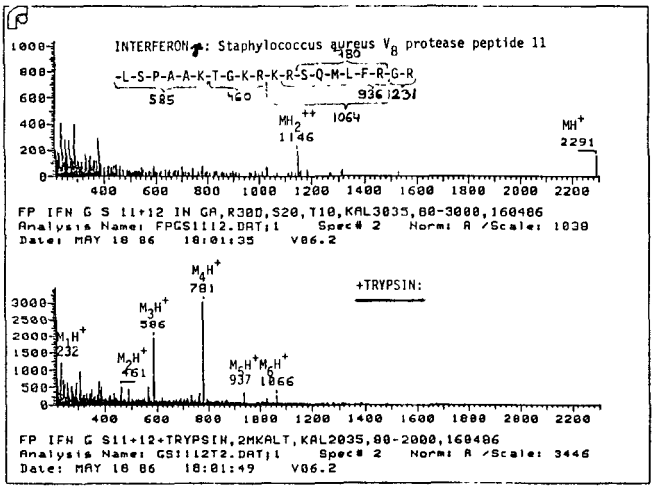

Fig.1: Interferon-staph.a.peptide (upper spectrum)compared with the tryptic peptides of this peptide after 2 min cleavage directly on the target (lower spectrum).

II. If the sequence of an unknown peptide is determined, fragment ions would be very useful. Unfortunately they show too low abundance in our spectra and furthermore there are too many combinations to ascertain a particular sequence. For unequivocal sequence determination we use exopeptidases, carboxypeptidase Y for determination of the C-terminus, and leucine aminopeptidase for the N-terminus. These reactions are performed in a water bath at 37°C, and samples are taken after one and two hours. The mass spectra of the incubation mixtures show several new molecular ions with lower mass values according to the loss of successive amino acids. In fig.2 the mass spectrum of the incubation mixture of a tryptic peptide of melittin is presented. Leucine aminopeptidase and ammonium bicarbonate buffer, pH 8, were added. The spectrum was recorded after one hour at 40°C. Seven sequential amino acids from the N-terminus are detected.

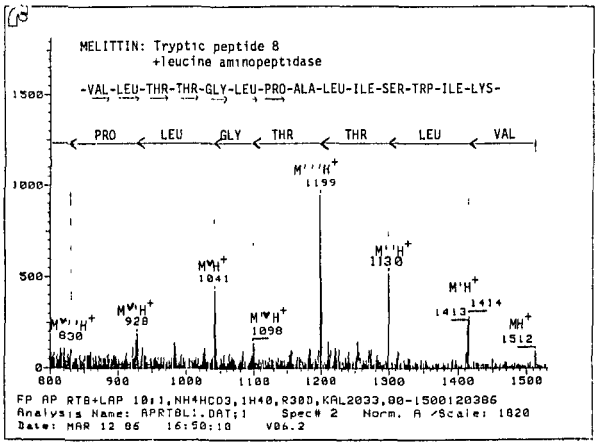

Fig.2: Molecular ions in a reaction mixture of a tryptic melittin-peptide and leucine aminopeptidase showing the N-terminal amino acid sequence.

III. Blocked N-termini are a difficult analytical problem in protein sequencing. Sometimes blocking is due to the amino acid pyroglutamic acid (pGLU). In this case leucine aminopeptidase does not cleave the N-terminal amino acid. The enzyme pyroglutamate aminopeptidase is used to confirm the presence of pGLU as blocked N-terminus. The peptide is dissolved in ammonium bicarbonate buffer, pH 8, and incubated with pyroglutamate aminopeptidase for several hours in a water bath at 39°C. Afterwards FAB mass spectra are successfully recorded. They clearly show the loss of pGLU.

IV. Two pairs of amino acids have the same molecular weight. Leucine and isoleucine cannot be distinguished directly. Glutamine and lysine are the second pair. The presence of lysine in a peptide can be proven by adding methylisothiocyanate (MITC) to the peptide dissolved in triethylamine, pH 10. Incubation is performed in a water bath at 60°C for one hour. Each free NH_2-group adds one molecule of MITC, irrespective of its origin, whether it is the N-terminus or in the side chain of a lysine.

In conclusion FAB mass spectrometry can give useful information for special questions in peptide sequencing. Especially the addition of enzymes to the sample directly on the target is a very simple and helpful procedure to cleave peptides and to determine amino acids.

ENZYMATIC HYDROLYSIS AND ELECTROHYDRODYNAMIC IONIZATION: AN APPROACH TO KINETICS AND STRUCTURE

Kelsey D. Cook and Sandra L. Murawski
Department of Chemistry, University of Tennessee, Knoxville, TN 37996

The exceptional "softness" of electrohydrodynamic ionization mass spectrometry (EHMS), while an asset for characterization of complex mixtures of homologous compounds of known structure (e.g., synthetic polymers) generally results in spectra devoid of structural information. This seriously limits the information available from spectra of reasonably pure peptide samples. While MS/MS could provide one approach to circumventing this limitation, a simpler possibility arises from the fact that EH spectra appear to reflect solution chemistry. By incorporating an enzyme as a reagent in the liquid matrix for a peptide sample, it should be possible to obtain sequence and rate information from the time dependence of the EH spectrum. A similar approach has been employed with FABMS (liquid SIMS) [e.g. ref. 1 and 2]. However, while a glycerol/water mixture provides a suitable liquid matrix for FAB, enzyme activity is lost if the proportion of glycerol becomes too high. Thus, *in situ* FAB analysis of enzyme kinetics has been limited by the fractional distillation of water from FAB samples. There is also some possibility of bombardment-induced sample damage, although this is apparently not the limiting factor.

By contrast, the relatively large sample reservoir (typically 0.5 ml) used in EHMS, and the low sample consumption rates (ca. 5 µl/hr for glycerol to ca. 5 µl/min for water) [3] suggest that EH could provide a means for *in situ* real time characterization of enzymatic reactions over relatively long time periods, enabling biochemical control of "fragmentation" with virtually no increase in ion internal energy. As a test of this possibility, EH spectra of carbobenzoxyphenylalanylleucine (Cbz-Phe-Leu) were obtained from buffered solutions of the protected dipeptide and carboxypeptidase Y (En).

Table 1 summarizes the key ions in a series of spectra obtained from a solution prepared by combining 700 µl of glycerol (containing 30 µmol Cbz-Phe-Leu and 0.3 mmol NaI) with 300 µl of water (containing 25 nmol En, buffered to pH 7.1 with 50 µmol Tris and HCl). (The aqueous solution had been incubated at 5°C for 24 hr to restore enzyme activity prior to mixing with glycerol.) Each entry in Table 1 represents a sum of intensities of bare and solvated quasimolecular ions (protonated or sodiated) of the species indicated (typically 1 to 5 ions each). All intensities are relative to the sum of detected buffer ions ($[Tris+H+G_n]^+$, where G denotes solvating glycerol molecules). Only glycerol solvation was observed, consistent with earlier mixed solvent EH studies [3]. Although there is appreciable scatter in the data from this single experiment, the abundance of hydrolysis products (first Leu and Cbz-Phe, then Phe) generally increased with time, as expected. The slow appearance of Phe is consistent with rates reported elsewhere [4]. Enzymatic catalysis was confirmed by repetition with no En, in which case no analyte ions were detected. This experiment also confirmed that intact substrate was undetected in the spectra of Table 1 due to low sampling efficiency, rather than rapid initial hydrolysis. Even the more basic unprotected dipeptide Phe-Leu could be sampled from aqueous glycerol only with low intensity. Acidification of this matrix (increasing HCl concentration to 1 M) neither induced hydrolysis nor increased sensitivity to Cbz-Phe-Leu. Use of more acidic matrices similar to those that have been useful as FAB matrices for peptides (thioglycerol or 1.3 M aqueous dithiothreitol with ammonium iodide supporting electrolyte) increased the sampling efficiency for Phe-Leu, but did not enable detection of a signal from the protected substrate. These matrices impeded enzymatic hydrolysis, probably by denaturation of the enzyme through reduction of disulfide bonds [5].

In conclusion, the results of this preliminary study suggest that EHMS may prove to be a valuable complement to FAB for *in situ* real-time analysis of peptide hydrolysis, and as an aid to sequencing. Further studies are necessary to identify an optimum matrix and/or appropriate analyte base strength to facilitate sampling of the intact substrate.

REFERENCES

1. L.A. Smith and R.M. Caprioli, Biomed. Mass Spectrom. 11, 392-395 (1984).
2. M. Przybylski, Fres. Z. Anal. Chem. 315, 402-421 (1983).
3. S.L. Murawski and K.D. Cook, Anal. Chem. 56, 1015-1020 (1984).
4. R. Hayashi, Y. Bai, and T. Hata, J. Biochem. 77, 69-79 (1975).
5. E. Scoffone and A. Fontana, in "Protein Sequence Determination", 2nd Ed.; S.B. Needleman, Ed., Springer-Verlag: New York, 1975, pp. 192-193.

TABLE 1

Hydrolysis Time (min)	Intensity			
	Cbz-Phe-Leu	Cbz-Phe	Leu	Phe
40	0.0	0.0	5.0	0.0
62	0.0	1.8	5.5	0.0
72	0.0	2.3	5.1	0.0
79	0.0	1.4	11	0.7
236	0.0	15	31	6.5
240	0.0	14	21	24

PROTEIN SEQUENCING BY TANDEM MASS SPECTROMETRY

J. YATES, III, D. F. HUNT, AND J. SHABANOWITZ, Department of Chemistry, University of Virginia, Charlottesville, Virginia 22901

Methodology for the sequence analysis of proteins based on tandem mass spectrometry has been developed. Proteins at the 10 nmol level are converted to a complex mixture of oligopeptides by using site specific proteases or chemical reagents. Reverse phase HPLC is then employed to fractionate the products of these reactions. The molecular weights of peptides in each fraction are then determined by conventional liquid secondary ion mass spectrometry using thioglycerol as the matrix and 8 kV cesium ions as projectiles. Tandem mass spectrometry is employed to determine the amino acid sequence of all peptides detected in each HPLC fraction.

Peptide $(M+H)^+$ ions in a particular HPLC fraction are selected one after another by quadrupole 1 of a triple quadrupole mass spectrometer/data system and transmitted to quadrupole 2 where they impact on argon atoms and undergo collision activated dissociation. Fragmentation occurs predominately at the amide linkages during this process. The resulting collection of fragment ions is then mass analyzed in quadrupole 3 to produce a spectrum containing the necessary peptide sequence information. Interpretation of the resulting CAD mass spectra is generally straight forward and can be checked by performing one or more additional experiments. Formation of methyl esters shifts the C-terminal sequence ions by at least 14 mass units and facilitates identification of these ions in the spectra. Acidic residues in the sequence add an additional 14 mass units. Gln and Lys are differentiated by treating the sample with either phenyl isothiocyanate or N,N-dimethylaminopropyl isothiocyanate and by observing a shift of 135 or 144 mass units, respectively for Lys containing peptides. Confirmation of the N-terminal amino acid in the CAD sequence can be obtained by carrying out a single cycle of the Edman degradation and, if necessary, by performing CAD on the resulting peptide.

The tandem MS methodology has been used for the sequence analysis of the 38 kDa purple acid phosphatase isolated from bovine spleen. This glycoprotein contains a novel binuclear iron center and catalyzes the cleavage of phosphate groups from proteins. It is one of only a few examples of iron containing proteins that catalyze nonredox reactions and may play a vital role in cellular regulation within the reticuloendothelial system. Purple acid phosphatase, as isolated, contains 16 kDa and 20 kDa subunits linked by a disulfide bond. A 2 kDa piece is lost in the isolation procedure. Sequencing efforts to date have concentrated on the 16 kDa subunit. Peptides covering 95% of the subunit have been sequenced. Overlaps for ca. 81% of the primary structure have been obtained (Fig. 1). Preliminary results have also been obtained on another protein of unknown sequence, the spectroscopically related iron containing protein, uteroferrin. Uteroferrin is a glycoprotein isolated from the uterus of pregnant sows and appears to be involved in iron transport between mother and conceptus. Phosphatase activity is of secondary importance (1). A trypsin/ S. aureus protease digestion on uteroferrin produced several peptides also observed in the 16 kDa subunit from purple phosphatase. A high degree of homology between these two proteins seems likely.

Studies on the acetylcholine receptor protein have been conducted to delineate the transmembane disposition of the protein. The receptor protein was affininty purified and reconstituted in a lipid membrane. Orientation of the receptor was shown to be 85-90% right-side out (synapse out). The membrane bound protein was digested with trypsin for 6 hr and pelleted by centrifugation. The supernatant was collected and the peptides present were sequenced by tandem mass spectrometry. Since only that part of the protein protruding into the extracellular medium should be accessible to trypsin, identification of the peptides present in the supernatant helps define the transmembrane disposition of the protein. Preliminary results are presented in Table 1. This approach would seem to have tremendous potential for probing the topography of membrane associated proteins.

(1) Buhi, W. C.; Ducsay, C. A.; Bazer, F. W.; and Roberts, R. M.; J. Biol. Chem., (1982), 257, 1712-1723.

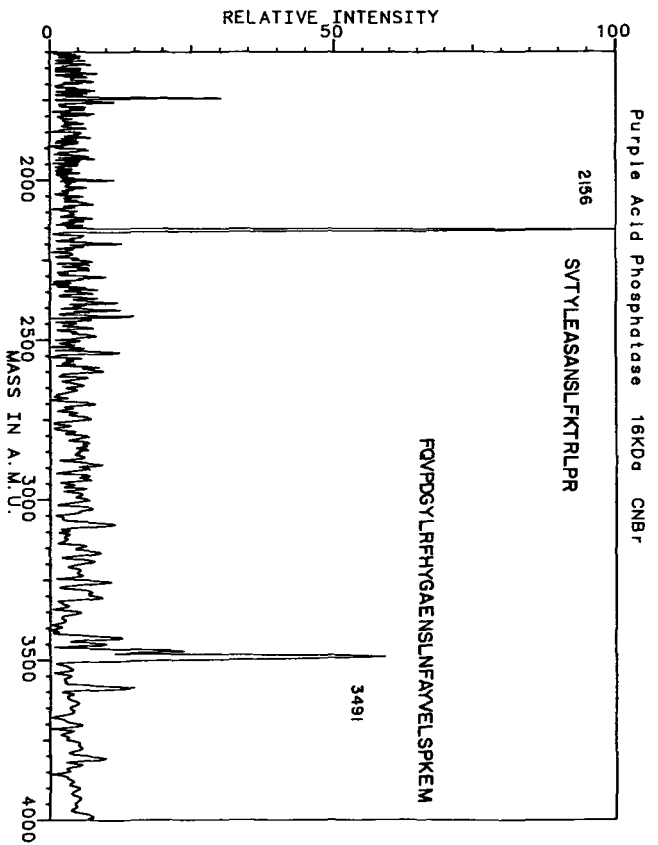

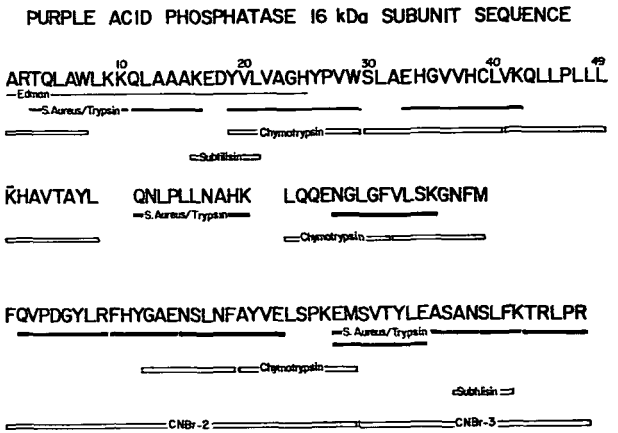

Figure 1

Sequence	Subunit	Topographical Location(Lindstrom Model)
LLLDYTGK	alpha	extracellular
IFADDIDISDISGK	alpha	cytoplasm
EAVEAIK	beta	cytoplasm
DLANFAPEIK	gamma	cytoplasm
AEEYILK	gamma	cytoplasm
QIFLEK	delta	cytoplasm
ILHMSR	delta	cytoplasm
YIAEHMK	alpha	cytoplasm
VAVQPER	beta	cytoplasm
SAIEGVK	alpha	cytoplasm
HGLVPR	delta	cytoplasm
LVANLLENYNK	alpha	extracellular
HLFLGFLPK	gamma	cytoplasm

Table 1

THE ROLE OF A MATRIX IN PEPTIDE MAPPING BY PLASMA DESORPTION MASS SPECTROMETRY

A G Craig[1], Å Engström[1], H Bennich[1], I Kamensky[2], P Roepstorff[3], R Self[4], W J Richter[5], F Raschdorf[5], M Salehpour[6] and B U R Sundqvist[6].

[1]Department of Immunology, Biomedical Center, Uppsala University, Box 582, S-751 23 Uppsala, Sweden.
[2]Bio-Ion Nordic AB, Box 15045, S-750 15 Uppsala, Sweden.
[3]Department of Molecular Biology, Odense University, Campusvej 55, DK 5230 Odense M, Denmark.
[4]Agricultural Food Research Council, Institute of Food Research, Norwich Laboratory, Colney Lane, Norwich, NR4 7UA, UK.
[5]Central Function Research, Ciba-Geigy Ltd., CH-4002 Basel, Switzerland.
[6]Tandem Accelerator Laboratory, Uppsala University, Box 533, S-75121 Uppsala, Sweden.

Recent developments of the plasma desorption (PD) ionisation technique involve depositing a nitrocellulose film to the aluminium foil, and then adsorbing the sample to the film [1]. This technique has enabled studies of biomolecules such as the intact eglin-c molecule. In the spectrum of these large molecules peaks due to the singly, doubly and triply charged species are present.

Using the normal electrospray sample preparation technique the PD spectrum of the tryptic digest of eglin-C [2] shows clearly discernable peaks which include the complete tryptic map of the sequence except for the segment 23-48. Figure 1 shows the low mass portion of this spectrum. Application of the nitrocellulose adsorption technique to the same digest reveals an increased sensitivity to some fragments. The spectrum shown in Figure 2 has an intense peak at m/z 3164 corresponding to the missing segment 23-48. The two peaks at m/z 1445 and 1850 were both present also in the spectrum of the electrosprayed sample. The peak at m/z 1740 is proposed to correspond to the segment 23-35. The fast atom bombardment ionisation technique was not sensitive to this segment and some of the low mass fragments. We beleive that the nitrocellulose technique enables measurement of fragments which otherwise could not compete efficiently for ionisation against salts, impurities and other species.

In the case of the tryptic digest of papaya mosaic virus protein both the fast atom bombardment (FAB) and PD detect many of the fragments. However both ionisation techniques fail to detect the same fragments. We suggest that the FAB technique is not insensitive to these fragments due solely to a liquid matrix effect. The low solubility of some fragments may not allow these species to be introduced into the mass spectrometer.

The insensitivity of FAB to one of the tryptic fragments of glucagon has been reported [3]. Amino acid analysis of the purified fragments indicate that nonspecific cleavage can occur during tryptic digestion of glucagon. PD is sensative not only to the fragments detected by FAB but also other fragments which amino acid analysis indicates are present in the sample. We therefore suggest that selectivity of the liquid matrix may in this case enhibit the ionisation of certain species.

We conclude that nitrocellulose adsorption significantly extends the sensitivity of the PD technique. Liquid matrix effects can influence the sensitivity of FAB, however, the specificity of the enzyme and the solubility of the fragments can also be responsible for the absence of particular fragments in a digest.

(1) G P Jonsson, A B Hedin, P L Håkansson, B U R Sundqvist, B G S Säve, P F Nielsen, P Roepstorff, K-E Johansson, I Kamensky and M S L Lindberg, Anal Chem 58 (1986) 1084
(2) W J Richter, F Raschdorf and W Maerk, Mass Spectrom in Health and Life Sciences (1985) 193
(3) M R Clench, G V Garner, D B Gordon and M Barber, Biomed Mass Spectrom 12 (1985) 355.

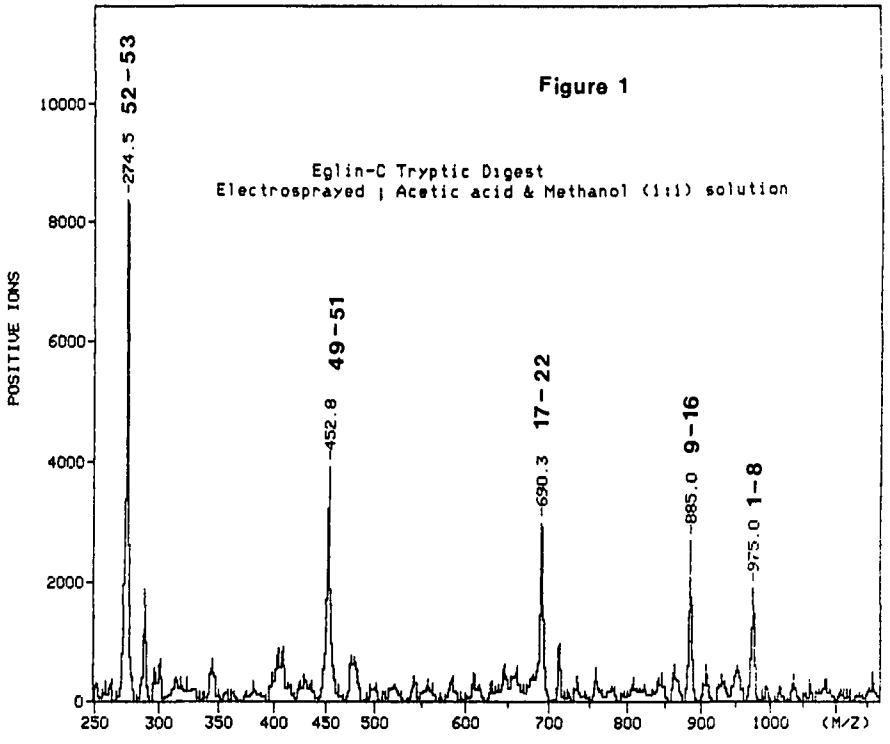

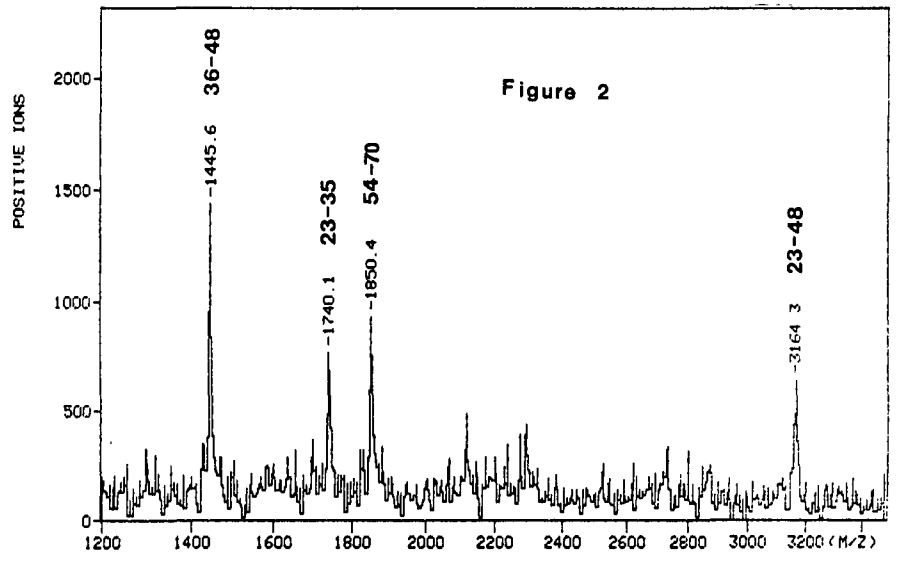

Eglin-C Tryptic Digest
Nitrocellulose ; 0.1 % TFA solution ; washed with 0.1 % TFA

AMINO ACID SEQUENCE OF A PARAMECIUM CALMODULIN USING FAB/MASS SPECTROMETRY WITH CONVENTIONAL SEQUENCING TECHNIQUES. W.H. Schaefer, T.J. Lukas and I.A. Blair, Department of Pharmacology and Howard Hughes Medical Institute, Vanderbilt University, Nashville, Tennessee 37232.

Calmodulin is a calcium modulated regulatory protein found in all eukaryotic organisms examined to date, including plants, animals, and protozoans. Calmodulins are characteristically very acidic proteins (pI 4) with molecular weights about 17k daltons. The primary structure of calmodulin is quite highly conserved, even among such a diverse range of species. Slight differences in structure due to a few amino acid substitutions or post-translational modifications can result in great differences in its multiple biochemical activities *in vitro*. The structural features of calmodulin that are important for the various activities have not been clearly defined.

The unicellular *Paramecium* species was chosen as a model system for conducting structure/function studies because of the possibility of obtaining mutants. Hinrichsen and his colleagues (*Science* 232 (1986) 503) have identified a mutant *Paramecium* that exhibited exaggerated locomotor responses to stimuli. Normal responses were temporarily restored by microinjection of purified wild-type calmodulin into the mutant *Paramecium*. This suggested that the mutation had affected the structure of the calmodulin.

We have begun to address this problem by determining the amino acid sequence of the wild-type *Paramecium* calmodulin. Conventional Edman chemistry was used in conjunction with FAB/MS in order to obtain unambiguous structural information. Because it was a relatively large protein, in addition to being N-blocked, the calmodulin was first cleaved into smaller peptides for structural analyses. Digestion with *S. aureus* V8 protease produced all component calmodulin peptides in high yield. Furthermore, the peptides were of sizes amenable to FAB/MS analyses and automated Edman sequencing. After separating the peptides by HPLC, each purified peptide was subjected to amino acid composition analysis, automated Edman sequence analysis, and FAB/MS to determine the molecular weight of the peptide. Some peptides required a second HPLC purification step to clean them sufficiently for FAB/MS. This approach provided unambiguous structures for each of the peptides, except the blocked amino terminal peptide. The actual organization of these peptides within the calmodulin was determined from overlapping peptides produced from digesting the calmodulin with trypsin, cyanogen bromide, and arginine protease.

(1) We found that the utility of FAB/MS was dependent on the properties of the peptides and the amounts of the peptides available. About 1nmol of peptide was used for each FAB/MS analysis. Molecular weight data with nominal mass accuracy was usually obtainable for peptides up to ca. 2500 daltons. Sample purity was extremely important. The peptides had to be freed from metal cations, as well as other non-peptide contaminants to insure proper ionization. The importance of having cation-free samples is shown in Figure 1. The top panel shows the spectrum obtained after initial HPLC purification of the peptide that spans residues 48-54 of the calmodulin. The peptide exhibited an MH^+ at *m/z* 862, but the spectrum was dominated by Na^+ and K^+ attachment products at *m/z* 884, 900, 922 and 938. The water used for HPLC was found to be the source of cation contamination. The spectrum obtained after a second HPLC step using pure water is shown in the bottom panel. The MH^+ peak at *m/z* 862 was now predominant; however, the potassium attachment ion at *m/z* 900 was still relatively intense. The high affinity for potassium of this acidic peptide was observed in a number of other V8 cleavage products of calmodulin.

(2) The FAB/MS data enhanced our confidence in the structures determined from the amino acid composition and Edman sequencing results. Figure 2 shows the structure of the peptide spanning residues 32-47 of the calmodulin. The specificity of the V8 protease would predict cleavage after Glu-45. The structure determined by Edman chemistry indicated an additional Ala-Glu after Glu-45. An MH^+ at *m/z* 1703 confirmed this structure, and showed that no post-translational modifications of the peptide had occurred.

(3) Finally, the FAB/MS data facilitated the positive identification of post translational modifications of the *Paramecium* calmodulin. Two methylated lysine residues, including the trimethyllysine at Lys-115, were found. The amino terminus of the calmodulin was shown to contain an N-acetyl blocking group.

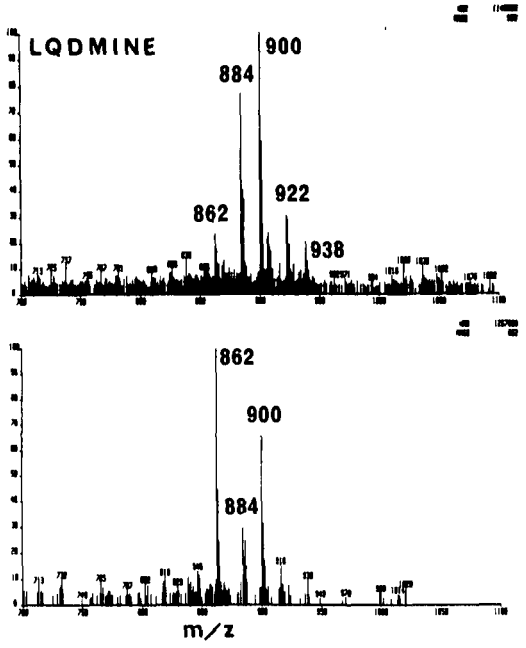

Fig. 1. Positive FAB mass spectrum of peptide containing amino acids 48-54 of Paramecium calmodulin. Upper panel shows spectrum after initial separation. Lower panel shows spectrum after second HPLC separation.

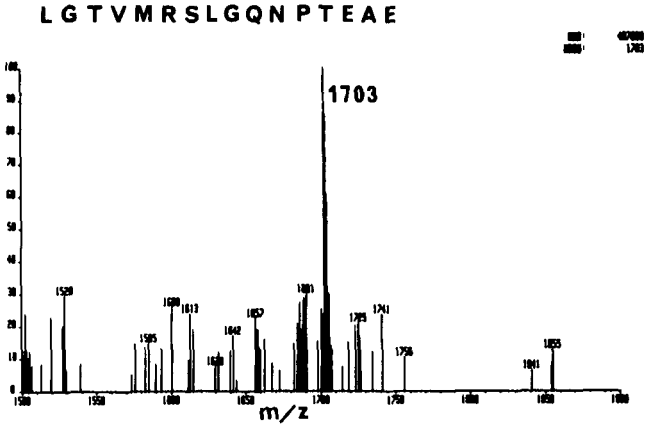

Figure 2. Positive FAB mass spectrum of peptide containing amino acids 32-47 of Paramecium calmodulin.

Supported by NIH grants GM30861 and RR-01688.

THE ELECTRONIC AND GEOMETRIC STRUCTURE OF THE TRANSITION METAL CARBYNE CATIONS $ScCH^+$, $TiCH^+$, VCH^+ and $CrCH^+$.

A. Mavridis, A.E. Alvarado-Swaisgood, and J.F. Harrison, Department of Chemistry, Michigan State University, E. Lansing, MI 48824-1322 USA.

The electronic and geometric structures of several transition metal carbyne cations have been studied by *ab initio* methods (MCSCF and MCSCF+1+2). We conclude the following:

1. $CrCH^+(^3\Sigma^-)$, $VCH^+(^2\Delta)$ and $TiCH^+(^1\Sigma^+)$ are all characterized by a metal-carbon triple bond of similar length (1.772, 1.745 and 1.758 Å respectively).
2. The calculated M≡C bond strengths for Cr, V and Ti are 70.8, 108.0 and 113.0 kcal/mol relative to the $^4\Sigma^-$ state of CH and 53.7, 90.8 and 95.9 kcal/mol relative to the $^2\Pi$ state. (We use the experimental $^2\Pi$-$^4\Sigma^-$ separation of 17 kcal/mol rather than our calculated splitting of 11 kcal/mol.)
3. There seems to be an approximate intrinsic metal-carbon bond energy for these species given by the sum of the exchange energy loss suffered by the metal ion in anticipation of bond formation and the calculated bond energy. Relative to the $^4\Sigma^-$ state of CH this is 148, 152 and 139 kcal/mol for $CrCH^+$, VCH^+ and $TiCH^+$ for an average of 146 kcal/mol.
4. The $^2\Pi$ state of $ScCH^+$ is characterized by a double bond between Sc and C with a bond length of 1.940 Å and a bond energy of 96.3/79.2 kcal/mol relative to the $^4\Sigma^-$ state of CH.
5. The electron distribution in $CrCH^+$, VCH^+ and $TiCH^+$ is remarkably similar. The $3d_\sigma$ orbital on the metal contains ~0.5 electrons while each d_π orbital hosts ~1.10 electrons with the 4s, $4p_\sigma$ occupancy varying from 0.1 to 0.2 electrons.
6. The MCSCF+1+2 calculations used to determine D_e's are size consistent.

THEORETICAL STUDY OF THE EFFECT OF A PERMANENT DIPOLE MOMENT ON THE KINETIC ENERGY RELEASE IN THE DISSOCIATION OF ION-MOLECULE CLUSTERS

Lewis M. Bass, University of South Carolina at Aiken

The effect of the dipole moment of water on the KERD (kinetic energy release distribution) for the reaction

$$H_2O \cdot H_3O^+ \longrightarrow H_2O + H_3O^+ + KE \tag{1}$$

has been investigated theoretically by incorporating the ion-dipole interaction into the statistical phase space model of kinetic energy release. According to the phase space model the KERD is calculated from the equation

$$P(E_t) = \frac{\iint_{E,J} F(E,J,t)\rho(E_t;E,J)}{\iint_{E,J} F(E,J,t)\,G(E,J)} \tag{2}$$

where F(E,J,t) is the probability of dissociation with energy E and angular momentum J during the timeframe , t, of the experiment, $\rho(E_t;E,J)$ is the density of states for the fragment pair with total energy E and total angular momentum J and relative kinetic energy E_t, and G(E,J) is the sum of states for the fragment pair with total energy E and total angular momentum J. The interaction potential is important in that it determines the range of angular momentum states accessible to the fragment pair in the evaluation of $\rho(E_t;E,J)$ and G(E,J).

In the standard phase space approach, which has been applied to reaction (1) previously[1], the ion-neutral interaction is represented by the Langevin potential,

$$V_{LANG}(r) = -\frac{q^2\alpha}{2r^4} \tag{3}$$

which yields the effective potential

$$V_{eff}(r) = \frac{L^2}{2ur^2} - \frac{q^2\alpha}{2r^4} \tag{4}$$

In the above equations q is the unit charge, α is the polarizability, r is the center of mass separation of the fragment pair, L is their orbital angular momentum and u is their reduced mass. For a given relative kinetic energy, E_t, the maximum value of L for which the fragment pair can overcome the centrifugal barrier (the maximum in the effective potential) is

$$L^*(E_t) = (\lambda E_t)^{1/4} \tag{5}$$

where

$$\lambda = \frac{8q^2\alpha u^2}{\hbar^4} \tag{6}$$

When the ion-dipole term is included the interaction potential becomes

$$V_D(r,\theta) = -\frac{q^2\alpha}{2r^4} - \frac{q\mu_D}{r^2}\cos\theta \tag{7}$$

where μ_D is the dipole moment of the neutral fragment. This two-dimensional potential does not lead to an analytical expression for $L^*(E_t)$. However, in the locked dipole limit θ remains fixed at 0, and the effective potential can be written as

$$V_{eff}(r) = \frac{(L^2 - 2uq\mu_D)}{2ur^2} - \frac{q^2\alpha}{2r^4} \tag{8}$$

which has the same r-dependence as the Langevin potential and can be treated similarly to obtain

$$L^*(E_t) = [\sqrt{\lambda E_t} + 2uq\mu_D]^{1/2} \tag{9}$$

Eq. (9) can readily be substituted for eq.(5) when carrying out the phase space calculations. The result is shown by the dashed line in Figure 1. Note that an "effective" dipole moment (the product of the ADO locking constant and the actual dipole moment) was used in this calculation.

Phase space calculations can also be carried out using a more detailed treatment of the ion-dipole interaction, such as the ADO theory[2]. First, note that the ADO theory can be used to estimate an "effective" dipole moment as described above. Also, the ADO result can be used to estimate an "effective" polarizability as discussed elsewhere[1]. Use of the effective μ_D or α in eq. (9) or (6), respectively, provides a simple means of accounting (albeit roughly) for the ion-dipole potential in an average sense. The result obtained when the effective α is used with eq.(6) has been presented elsewhere[1] and is shown here by the dot/dashed line in Figure 1 for comparison. A more detailed incorporation of the ADO theory can be carried out by using the available parametric equations[2] to obtain a set of (L^*,E_t) values, which then provide the basis for estimating $L^*(E_t)$ for any E_t by linear extrapolation. In this manner, the $L^*(E_t)$ values from ADO theory are incorporated directly into the phase space model. The calculations reported here have been carried out using this approach for the calculation of $\rho(E_t;E,J)$, but using the simpler, average-treatment described above for the evaluation of $G(E,J)$. This is a reasonable initial approach since the former is an E_t-dependent quantity whereas the latter represents a sum over all E_t values and should not be affected greatly by treating the dipole interaction in an average sense. The results of these calculations are shown by the solid lines in Figure 1. For the curve labeled "LD" eq.(9) was used (with the "effective" dipole moment) in computing $G(E,J)$ values; for the curve labeled "LANG" eqs. (5) and (6) were used (with the "effective" polarizability). In both cases $\rho(E_t;E,J)$ values were evaluated using $L^*(E_t)$ obtained from ADO theory.

Clearly, the inclusion of $L^*(E_t)$ values directly from ADO theory leads to improved agreement with experimental results. Furthermore, the Langevin-type potential (with an "effective" α) provides a better description of this system than the locked dipole-type potential (with an "effective" μ_D). We are in the process of studying other systems similar to reaction (1) to determine if the observations made here are general in nature, or if the comparisons between theory and experiment will vary with different systems.

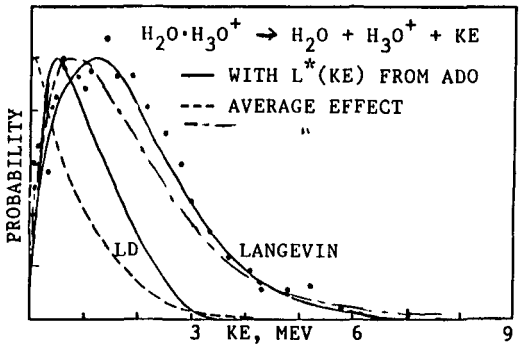

FIGURE 1

REFERENCES:

[1] A.J. Illies, M.F. Jarrold, L.M. Bass and M.T. Bowers, J. Am. Chem. Soc., 105, 5777 (1983).

[2] T. Su and M.T. Bowers, J. Chem. Phys., 58, 3027 (1973).

ACKNOWLEDGEMENTS:

1. Initial work on this project began in Professor Bowers' lab at the University of California at Santa Barbara.

2. Acknowledgement is made to the Petroleum Research Fund for partial support of this research under grant #16955-GB6.

KINETICS OF GAS PHASE METAL IONS

S. Sigsworth, L. DiFazio, R. Leuchtner, R. G. Keesee, and A. W. Castleman, Jr., The Pennsylvania State University, University Park, PA 16802 USA

Studies of metal ions contribute to a further understanding of catalysis, ion implantation (doping of semiconductors), the reactions of the products of meteoritic ablation, and the energetics and lifetimes of complexes in termolecular reactions. Atomic silver, copper and lead are the ions of interest in the present study.

Experiments were done using a metal ion flow tube. This apparatus consists of a flow tube pumped by a fast roots pump, an ion sampling region, and a differentially pumped detection region. Ions are produced by thermionic emission, allowed to react with neutrals released from a downstream port, sampled with a 1.0 mm sampling orifice, mass filtered with a quadrupole, and detected with a channeltron electron multiplier.

Rate constants, as a function of pressure, were determined for Ag^+ with NH_3, CH_4, CH_3F, CH_3Cl, and CH_3Br. Atomic lead ions were similarly studied with four ligands, and copper ions were studied with three small molecules, including dimethylamine (DMA). Silver and lead ions demonstrated low pressure termolecular kinetics for all cases except for the methyl-substituted amines. The methyl amines, with available beta-hydrogens, give transition kinetics in all cases studied, i.e., kinetic behavior midway between that for low pressure termolecular and high pressure saturated termolecular. The reaction of copper ion with NH_3 is in the low pressure regime, while its reaction with CH_3Cl and dimethylamine (DMA) certainly are cases of transiton kinetics.

In cases which are establishd to be solely termolecular, the kinetics are assumed to follow the simple Lindemann mechanism. The ion of interest collides with the reactant neutral to give a metastable collision complex, which can either dissociate back to the original reactants or alternatively become stabilized by collision with a third-body. At the low pressure limit, this yields a rate proportional to the product of the number densities of the ion, the neutral reactant, and the background gas. Thus we have a third-order rate coefficient that is constant with pressure. The slope, $d(\ell nI)/d(B)$, of a plot of the natural log of metal ion intensity versus reactant neutral concentration, is used to determine the effective second-order rate constant, $K_o^3(M)$, and the third-order rate constant, K_o^3, via the following straightforward equation:

$$K_o^3(M) = -\frac{d(\ell nI)}{d(B)}\frac{V_p}{Z}$$

where, K_o^3 ≡ third-order rate constant
(M) ≡ third-body number density
I ≡ metal ion intensity
(B) ≡ reactant neutral number density
V_p ≡ ion velocity determined via ion pulsing
Z ≡ reaction distance

The third-order rate coefficients, K_o^3, for both Li^+ and Ag^+ show very large increases in rate from CH_4 to CH_3F (refer to Table I). However, of these two ions, only Ag^+ demonstrates an additional rate increase (factor of seven) from CH_3F to CH_3Cl. Copper ion is the most reactive, while Pb^+ is the least reactive of the four ions studied. Apparent anomalous behavior is demonstrated by Li^+ with CH_3F. The value of 8.4×10^{-28} cm^6 sec^{-1} (verified in our laboratory to within 2%) is the only lithium ion rate constant larger than its silver ion counterpart. This high value led Spears and Ferguson (1) to infer that there is no correlation between both the polarizability and the lowest vibrational frequency of the methyl halogens and the corresponding lithium ion rate coefficients. As can be seen in Table I, the Li^+/CH_3F value interrupts what otherwise are very nice correlations. However, for silver ion there is a good correlation between the rate coefficients and the trends of both the ligand vibrational frequencies and polarizabilies. Polarizability is seen to increase, while vibrational frequency decreases with reaction rate. These correlations for silver, thus far, appear to be independent of ligand type. The strong apparent relationship between vibrational frequency coupled with the long lifetimes of these complexes, calculated from the third-order rate coefficient, ADO, and Langevin theory, have led us to infer that there is probably significant rotational-vibrational energy conversion in these silver ion complexes. The

energy being redistributed in this fashion, is expected to lead to a longer lifetime of the intermediate complex through the coupling of angular momentum (2,3). These longer lifetimes would lead to increased rate constants, as observed. In addition, the vibrational frequency for the methyl halogens being for a carbon-halogen stretch, along with the sudden increase in reactivity from CH_3F to CH_3Cl leads us to suspect metal insertion, at least for CH_3Cl and CH_3Br. If insertion occurs, it would be via reverse methyl migration from the halogen to the metal. Weaker bonds, i.e., those having lower vibrational frequencies, should assist this process. Methyl fluoride may also participate in this mechanistic scheme, but not as readily as CH_3Cl and CH_3Br. Insertion requires the halogen to lose electron density. Fluorine is highly electronegative and would be expected to resist this. The high vibrational frequency and strong C-F bond in MeF are just manifestations of this very high electronegativity. With insertion, the identity of the complex changes from a simple collision complex to a complex having less in common with and a lower probability to reconvert to the initial reactants. Slower decay rates, i.e., longer lifetimes, automatically imply faster overall rates.

Studies of methyl amines with various metal ions reveal that non-transition metal ions, e.g., Na^+, K^+, In^+, and Pb^+ react to give only the associated product, while the transition metal ions, Cu^+ and Ag^+, apparently insert into the methyl substituted amines via oxidative addition and beta-hydrogen shift. All the methyl amine/metal ion reactions are fast. Trimethylamine (TMA) with Cu^+ and DMA with all metal ions studied react with an effective bimolecular rate constant of circa 10^{-9} cc/sec (10^{-10} cc/sec for non-transition metals). For TMA, the only product channel with Cu^+ is formation of $[H_2C = N(CH_3)_2]^+$ at one amu below TMA and, apparently, neutral CuH. Monomethylamine (MMA) and dimethylamine (DMA) react with silver ion to give both an associated adduct and, peculiarly, the protonated amine. From our studies, it seems that the formation of protonated DMA and MMA must involve two amine molecules, with the first step after oxidative addition being metal insertion into one of the molecules via beta-hydride shift. It is interesting to note that increasing the methyl substitution stepwise from NH_3 to $(CH_3)_3N$, i.e., TMA, gives the following distributions of apparent simple cluster product and metal insertion product: 100:0, 70:30, 5:95, and 100:0 for reaction of Ag^+ with NH_3, MMA, DMA, and TMA, respectively. Thus it seems that as the methyl substitution of these ammonia analogs increases, metal insertion becomes a more probable process. This is consistent with the fact that each methyl group provides three beta-hydrogens, one of which can be shifted in beta-hydrogen transfer. Thus the probability of one such shift occurring is increased.

Acknowledgments:

The authors thank Professor Konrad Weil for helpful discussions during the course of this work. Support by the National Science Foundation, Grant No. ATM-82-04010, the Army Research Office, Grant No. DAAG29-84-K-0087, and the Department of Energy, Grant No. DE-AC02-82-ER60055, is gratefully acknowledged.

References:

1. K. G. Spears and E. E. Ferguson, J. Chem. Phys. 59, 4174 (1973).
2. F. J. Schelling and A. W. Castleman, Jr., Chem. Phys. Lett. 111, 47 (1984).
3. E. E. Ferguson, J. Phys. Chem. 90, 731 (1986).

Table I
Association Rate Coefficients as a Function of Ligand Properties

Ligand Properties			Metal Ion Rate Coefficients (K_o^3/cm^6sec^{-1}			
Polariz. ($\alpha \cdot 10^{24}cm^3$)	Vib. Freq. (ν, cm^{-1})	Ligand	Cu^+	Ag^+	Pb^+	Li^+
1.95	2170	CO	---	0.19	---	---
2.60	1520	CH_4	---	0.30	N.R.	0.05
2.97	1049	CH_3F	---	2.9	---	8.4
2.26	933	NH_3	18.0	3.7	0.2	2.1
4.56	732	CH_3Cl	111.0	21.0	0.83	6.7
5.55	610	CH_3Br	---	42.0	1.8	8.0

Li^+ Data from: K. G. Spears and E. E. Ferguson, J. Chem. Phys. 59, 4174 (1973).

IDENTIFICATION AND ELECTROPHILIC REACTIVITY OF PRODUCTS FROM 2-METHYLPROPANE AND FIRST ROW TRANSITION METAL CATIONS USING A MS/MS/MS QUADRUPOLE TRIPLE SECTOR

Hélène MESTDAGH, Nicole MORIN and Christian ROLANDO, Ecole Normale Supérieure, Département de Chimie, UA 1110, Laboratoire de l'Activation Moléculaire, 24 rue Lhomond, F 75231 PARIS CEDEX 05 FRANCE ; Claude BEAUGRAND and Frédéric de Maack, NERMAG, 49 Quai du Halage, F 92500 RUEIL MALMAISON, FRANCE.

The reaction of transition metal cations with isobutane has been investigated using many different instruments : FTMS, sectors instruments, ion beam (1). Nevertheless, the high pressure (up to .01 torr) useable in the quadrupole collision cell of quadrupole sectors instrument allowed to obtain new results by stabilizing the primary adduct of the reaction. Metal cations were produced from the nitrate salts using a FAB source ; the versatility of this ionisation allowed the study of the complete first row of transition metals (2). The ions produced by the FAB source are not excited : colliding the metal cation with argon in the first collision cell of our MS/MS/MS triple quadrupole (3) does not alter the reaction with isobutane in the second collision cell. Under these conditions (isobutane pressure 5 mtorr, 12 cm pathway in the collision cell) all the metals are reactive.

The structure of the adducts was investigated by further collision activated dissociation using our quadrupole triple sector MS/MS/MS : $Cu(C_4H_{10})_2^+$ which gave mainly $Cu(C_4H_{10})^+$, and $Cu(C_4H_{10})^+$ which gave mainly Cu^+ are likely Van der Waals complexes (Figure 1a) ; on the other hand $V(C_8H_{14})^+$ which gave $V(C_4H_7)^+$ and V^+ is likely a bis π -allyl complex (figure 1b).

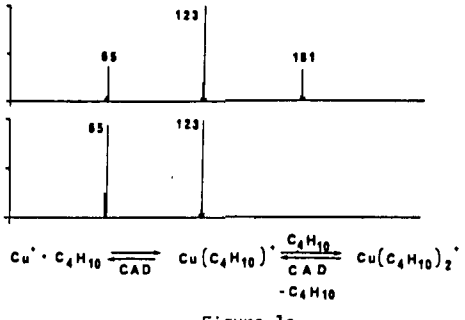

Figure 1a

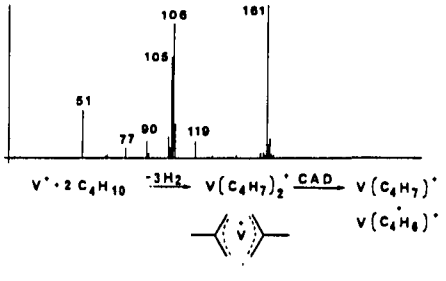

Figure 1b

Using the double collision cell the kinetic energies of parent and fragments issued from CAD could be measured. From these values, the energy of dissociation of the Van der Waals complexes between cuprous ion and isobutane could be estimated to .6 + .2 eV.

The influence of pressure was investigated using a constant pressure of isobutane and a variable pressure of argon. As shown in figure 2 the reaction of Cu^+ with isobutane has about the same efficiency when using .5 millitorr of isobutane and 5 millitorr of argon as when using 2 millitorr of pure isobutane. This emphasizes the double role of the reagent gas : reaction and desexcitation of the energy-rich intermediate . In the case of the Van der Waals complex the desexcitation is the rate determining step as shown by a linear relationship between

$$\log \frac{Cu^+}{TIC}$$

and the argon pressure (figure 3).

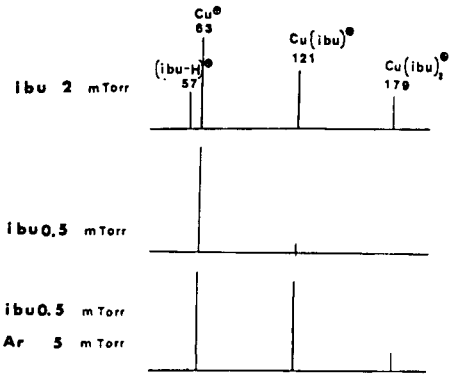

Figure 2

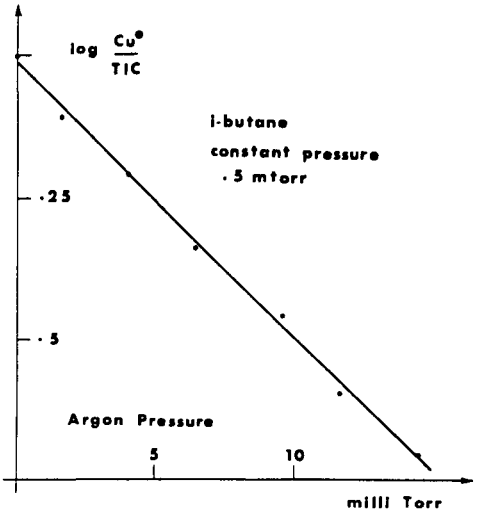

Figure 3

The reactivity of Fe^+, Co^+ and Ni^+ with isobutane is characterized by cleavage of both C-H and C-C bonds. With Ni^+ the major product ion is $Ni(C_3H_6)^+$: its CAD indicates a Ni^+(propene) structure, which is in agreement with reported results using other instruments. $Ni(C_3H_6)^+$ reacts with ammonia giving $Ni(NH_3)^+$ and $Ni(NH_3)_2^+$, whereas with cyclopentene the exchange reaction is incomplete, and some dehydrogenation to cyclopentadiene occurs.

(1) R.H. CRABTREE, The organometallic Chemistry of alkanes, Chem. Rev, 1985, 85, 245-269.
(2) H. MESTDAGH, N. MORIN and C. ROLANDO, Tetrahedron Letters, 1986,33.
(3) A Double Collision Cell for Quadripole MS/MS instrument, C. BEAUGRAND, G. DEVANT and C. ROLANDO, Abstract of the 33th ASMS meeting, 1985 26-31 mai, San Diego, p.833.
(4) A Multiquad Triple Analyser MS/MS/MS C. BEAUGRAND, G. DEVANT , C. ROLANDO, D. JAOUEN, 34th AMSM meeting.

THE INTERACTION OF GAS PHASE TRANSITION METAL IONS WITH ALKANES: IS BUTANE MORE STRONGLY BOUND TO Cr^+ THAN CO?

John Allison, Deborah J. Hankinson, James F. Harrison, Paul M. Hunt, Organometallic Dynamics and Structure Group, Department of Chemistry, Michigan State University, East Lansing, MI 48824

Gas phase transition metal and metal-containing ions have a rich chemistry with organic molecules. Among the reactions reported to date, the reactions of ions such as Fe^+ with alkanes have received considerable attention. When ligands are attached to the metal, ligand substitution reactions are frequently observed such as

$$NiCO^+ + C_3H_7Cl \rightarrow NiC_3H_7Cl^+ + CO \quad (1)$$

It has been suggested that metal ion affinities parallel proton affinities for ligands which are simple π - and n-donor bases. In this context, it is interesting to note that alkanes also act as good ligands in the gas phase, and compete with (what organometallic chemists traditionally consider to be) "good" ligands such as CO. For example:

$$CoCO^+ + C_4H_{10} \rightarrow CoC_4H_{10}^+ + CO \quad (2)$$

This type of reaction prompts a number of questions. Are alkanes better ligands than CO for gas phase transition metal ions? That is, is reaction (2) a ligand substitution reaction, or must it be more complex? Perhaps the metal (of $CoCO^+$) first inserts into a C-C bond before the CO is lost - that is the ionic product in reaction (2) may not be a simple metal-alkane adduct, but may exist as a metal-insertion product such as C_2H_5-Co^+-C_2H_5.

A program has been developed for calculating the interaction energy for a metal ion with a molecule as a function of the spatial configuration of the molecule and the position of the ion relative to the molecule. The interaction between the ion and the molecule consists of three components in this model: 1) Charge/induced-dipole interactions; 2) Charge/permanent multipole interactions; and 3) Repulsive interactions. The charge/induced-dipole interactions are approximated by using bond polarizabilities. The charge/permanent multipole interactions are approximated by calculating the interaction of the ion's charge with estimated partial charges on the various atoms in the molecule. The repulsive interactions are of the form $A(B/r)^{12}$, similar to the repulsive term of the Lennard-Jones 6-12 potential. The A and B terms are derived from potentials obtained from ab-initio calculations on the species Cr^+-H and Cr^+-C.

Using the chosen variables for the calculation, the maximum interaction energy for Cr^+ and butane was calculated to be 66 kcal/mol. We are not suggesting that this level of calculation will provide the correct interaction energy, however it is useful to compare relative values determined in this way. This energy is due mainly to the interaction of the ion with four polarizable C-H bonds, and is seen for a particular configuration of the butane in which all of these bonds are in close proximity with the metal.

As an example of the output of this program, Figure 1 shows the points at which Cr^+ may be located for which the interaction energy is 10 kcal/mol - for the XY and YZ planes for the configuration shown.

In comparison, the highest interaction energy which was obtained for the Cr^+-CO system was 27 kcal/mol. Thus, based on this level of calculation, we would predict that alkanes could displace CO, since alkanes are very polarizable molecules, and can interact strongly with univalent cations.

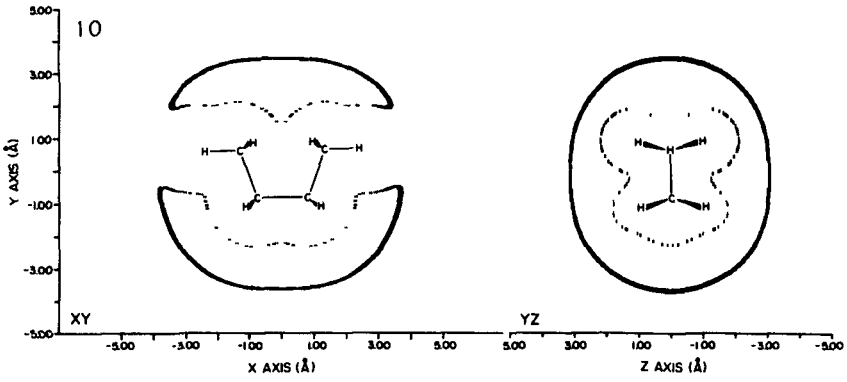

Figure 1. This figure shows locations at which Cr^+ could be placed to give an interaction energy of 10 kcal/mol with this conformation of butane. Points are shown for two planes, with the origin being at the center of mass of the molecule. Note that there are points a few angstroms from the atoms, and other points much closer. The inner points are found on the repulsive wall, i.e. those on the rising part of the potential. The potential dips in at the "top" of the molecule. It is in this region where the highest potential is found.

FTMS STUDIES OF Sc^+-LIGAND COMPLEXES: ISOMER DIFFERENTIATION AND BOND ENERGY DETERMINATION

Leo M. Lech and Ben S. Freiser

Department of Chemistry
Purdue University
West Lafayette, IN 47907

This work, performed on a prototype Fourier transform mass spectrometer (FTMS), was aimed at differentiating a variety of isomeric Sc^+-ligand complexes in the gas-phase. Collision-induced dissociation (CID), ion/molecule reactions, and deuterium exchange reactions revealed some subtle and some not so subtle differences when applied to two $ScC_4H_6^+$ ions, three $ScC_4H_4^+$ ions, and two $ScC_5H_6^+$ ions.

$ScC_4H_6^+$ can be generated by dehydrogenation of the linear butenes or isobutene. Although there are subtle differences in the CID spectra of the two ions (same products with different relative intensities), there is a striking difference between the reactivity of these two ions with benzene, reactions 1 and 2. Similar reactivity is observed in ion/molecule reactions with acetonitrile. Again, the $ScC_4H_6^+$ ions generated from the linear butenes show only a condensation product, whereas $ScC_4H_6^+$ generated from isobutene shows both condensation and dehydrogenation of acetonitrile.

	Linear Butenes	Isobutene	
$ScC_4H_6^+ + C_6H_6 \rightarrow Sc(C_{10}H_{12})^+$	100%	52%	(1)
$ScC_4H_6^+ + C_6H_6 \rightarrow Sc(C_{10}H_{10})^+ + H_2$		48%	(2)

$ScC_4H_4^+$ can be generated by reactions of Sc^+ with 1,3-butadiene, cyclobutane, and secondary reactions with ethene. CID on $ScC_4H_4^+$ generated from ethene and 1,3-butadiene both give three products, reactions 3-5,

$$ScC_4H_4^+ \xrightarrow{CID} ScC_4H_2^+ + H_2 \quad (3)$$

$$ScC_4H_4^+ \xrightarrow{CID} ScC_2H_2^+ + C_2H_2 \quad (4)$$

$$ScC_4H_4^+ \xrightarrow{CID} Sc^+ + C_4H_4 \quad (5)$$

with similar product distributions. CID of $ScC_4H_4^+$ from cyclobutane, however, shows no loss of H_2, reaction 3. Displacement of acetylene by benzene, reaction 6, is observed for $ScC_4H_4^+$ from 1,3-butadiene but not from ethene, providing a means for differentiating these two species.

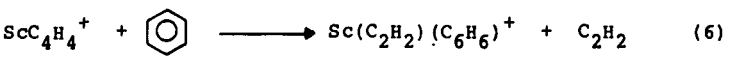

The $ScC_5H_6^+$ isomers can be differentiated by both CID and deuterium exchange experiments. CID of $ScC_5H_6^+$ generated from cyclopentene yields Sc^+ as the major product with some additional fragmentation at high CID energies. Deuterium exchange experiments reveal one fast exchange followed by five slower exchanges which is characterstic of the cyclopentadienyl species (1). In contrast, CID of $ScC_5H_6^+$ generated from various branched alkenes show much more fragmentation and deuterium exchange reveals six very slow exchanges.

The Sc^+-benzene bond strength was bracketed by modifying the FTMS experiment which characteristically monitors exothermic reactions. By exciting Sc^+ into ethane, Sc^+-H, an endothermic product, was formed and isolated. Benzene was then pulsed into the ICR cell and displacement of the hydride by benzene was not observed. This suggests that the Sc^+-benzene bond strength is between 49 kcal/mol, obtained from thermodynamic calculations, and 54 kcal/mol, the previously determined value for $D^o(Sc^+\text{-}H)$ (2). To further corroborate this result, photodissociation experiments using cutoff filters were performed. The results of these experiments gave a Sc^+-benzene bond strength between 52 and 55 kcal/mol, which is in excellent agreement with the value obtained by reacting Sc^+-H with benzene.

References

1. Jacobson, D.B.; Freiser, B.S. J. Am. Chem. Soc. (1983) 105, 7492.
2. Tolbert, M.A.; Beauchamp, J.L. J. Am. Chem. Soc. (1984) 106, 8117.

GAS PHASE ION-MOLECULE REACTIONS OF Fe^- AND Co^- WITH THIOLS, SULFIDES AND DISULFIDES USING FOURIER TRANSFORM MASS SPECTROMETRY; Larry Sallans, Kelley R. Lane and Ben S. Freiser; Purdue Univeristy, Dept. of Chemistry, W. Lafayette, IN. 47907

INTRODUCTION

The ion-molecule chemistry of atomic and coordinated metal ions has proven to be a very rich and active area of research over the past decade. A major factor in rationalizing the considerable effort dedicated to gas phase metal ion chemistry is to provide thermochemical information that is essential to the understanding of catalytic reaction mechanisms. Information that has been already obtained includes homolytic and heterolytic metal-hydrogen, metal-carbon and metal-oxygen bond strengths; relative ligand binding energies; gas phase Lewis basicities; hydride affinities; electron affinities; and ionization potentials for neutral transition metal complexes.

The majority of gas phase metal ion chemistry has involved metal cations, primarily due to the ease of their formation. Although research involving metal complexes has grown rapidly within the last few years, ion-molecule reactions involving atomic metal anions have only recently been introduced through a novel technique utilizing the collision-induced dissociation of metal carbonyl anions.[1]

Previously, we published the first gas phase reactions involving metal anions with organics. These reactions were primarily proton abstraction reactions used to bracket the gas phase acidity of the metal anions. This paper extends that study by demonstrating that metal anions do react with organic molecules in a context other than proton abstraction, charge transfer or dissociative charge transfer.

EXPERIMENTAL

This study centers predominately upon the reactions of Fe^- and Co^- with thiols, sulfides and disulfides. All experiments were performed using a Nicolet prototype FTMS-1000 Fourier transform mass spectrometer. The instrument has been equipped with a 5.2 cm cubic trapping cell situated between the poles of a Varian 15 inch electromagnet maintained at 0.9 T.

Generation of the bare metal anions was accomplished by collision-induced dissociation of the dissociative electron attachment product from the corresponding metal carbonyls (eq 1 and eq 2). The bare metal anion was isolated from the parent and other daughter

(1) $Fe(CO)_5 + e^- \longrightarrow Fe(CO)_4^- \xrightarrow{CID} Fe^-$

(2) $Co_2(CO)_8 + e^- \longrightarrow Co(CO)_4^- \xrightarrow{CID} Co^-$

ions through double resonance ejection. Reactions with background organosulfur compounds were then monitored.

RESULTS AND DISCUSSION

The primary reaction products formed from metal anions and thiols, MS^-, MSH^- and $HMSH^-$ (where M is the metal), can be entirely ascribed in terms of oxidative addition to the weak C-S bond. Mechanistic pathways include reductive elimination, direct cleavage and ß-hydrogen shift to the metal followed by alkene loss. Direct cleavage becomes more favorable as the stability of the alkyl radical increases and although it is a somewhat unussual pathway, it is observed in reactions between metal cations and thiols.

A comparison between the ion-molecule products of anions and cations with thiols shows similar mechanisms. Both reactions involving cations and anions show oxidative insertions into the C-S bond; however, the cationic system can form a stable [alkene-M^+-H_2S] complex via hydrogen transfer from the metal to the thiol functionality. In the anion, immediate alkene loss occurs upon hydrogen transfer to the metal without subsequent transfer to the thiol portion.

Collision-induced dissociation, CID, is used to support proposed structures for the primary products, H-Fe-SH$^-$ and Fe-SH$^-$. These ions undergo secondary reactions involving direct cleavage and dehydrogenation. Provided that a statistical charge distribution is rapidly established within the ion-molecule complex, CID may be used to elicit a fragment's electron affinity. This and other thermochemical information is given in Table 1.

TABLE 1. Summary of Derived Thermochemical Data*

	Fe	Co
$D^o[M^-\text{-}S]$	>103	>103
$D^o[M^-\text{-}SH]$	75-92	75-92
$\Delta H_f^o[MS^-]$	<68	<58
$\Delta H_f^o[MSH^-]$	39-56	29-46
$\Delta H_f^o[HMSH^-]$	<72	<62
$EA[MSCH_3^-]$	~43	~43

* All values are in kcal/mol; M = Fe or Co

Both Fe$^-$ and Co$^-$ react readily with dimethyl disulfide and diethyl disulfide showing a distinct preference (approx. 3:1) for cleaving the C-S bond as opposed to the S-S bond. Reaction products include CH_3S^-, $MSCH_3^-$, MSS^- and $MSSCH_3^-$ for reactions with CH_3SSCH_3, and $CH_3CH_2S^-$, $HMSS^-$, $MSSC_2H_3^-$ and $MSSC_2H_5^-$ for reactions with $CH_3CH_2SSCH_2CH_3$. Reactions involving diethyl disulfide show a greater extent of dehydrogenation for the iron system relative to the cobalt.

In contrast to thiols and disulfides, sulfides exhibit a reluctance to undergo reactions with either Fe$^-$ or Co$^-$ and show only limited reactivity for larger acyclic and smaller cyclic sulfides. The lack of observable reactions with small acyclic sulfides is unexpected and difficult to rationalize. Reaction products for the sulfides are similar to those observed for the thiols.

A brief survey involving other metal anions was also performed. Reactants used in this survey include: benzenethiol, ethanethiol, diethyl disulfide and carbon disulfide. The relative reactivity of the atomic metal anions (V$^-$, Cr$^-$, Fe$^-$, Co$^-$ and Mo$^-$) with the various organosulfur compounds vary immensely. From this brief survey, it appears that the anions of iron and cobalt generally react rapidly with the divalent sulfur compounds with the exception of the sulfides. Reactions of molybdenium and chromium are relatively slow, and in some cases, it appears that chromium is unreactive. Their inability to undergo facile reactions may be due to the stable d^5s^2 electronic configuration. Vanadium falls between the two extremes in reactivity but is slightly more unussual in product type and relative distribution. To some extent this can be related to Vanadium's larger electron deficiency.

[1] Sallans, L.; Lane, K.R.; Squires, R.R.; Freiser, B.S. **J. Am. Chem. Soc.**, **1985**, 107, 4379-4385.

THE EFFECT OF ION KINETIC ENERGY IN ION/MOLECULE REACTIONS USING FTMS

Stephen W. McElvany, Anthony O'Keefe, and J.R. McDonald
Naval Research Laboratory, Chemistry Division, Washington, DC 20375

The changes in the observed ion/molecule reaction products and their branching ratios as the kinetic energy of the reactant ion is varied (e.g. from thermal to 100 eV) can provide both mechanistic and thermodynamic information on a particular reaction system. Previous studies have utilized tandem mass spectrometers in various configurations (1,2), and more recently guided beam and crossed beam techniques (3,4), to study the effect of added kinetic energy to the reactant ion. In this study, a Fourier Transform Mass Spectrometer (FTMS) was used to study the effect of reactant ion kinetic energy on ion/molecule reactions by performing mass isolation, ion excitation, ion/molecule reactions, and product ion detection entirely within the ICR cell.

The reactions of C^+ (thermal to 30 eV) with small hydrocarbons (CH_4,C_2H_4, and C_2H_6) were studied in the FTMS to determine the viability of performing these type of studies in the FTMS. The C^+ ions were formed either by electron impact on CO or by charge exchange from He^+ to CO. Although it has been suggested that both ground state (^2P) and metastable (^4P) C^+ ions are formed in the electron impact process (5), charge exchange products in reactions with N_2, O_2, and Kr to probe for metastable C^+ were not observed in the FTMS. This lack of evidence for the presence of C^+ (^4P) may suggest that the lifetime of the metastable state is less than the timescale of the FTMS experiment (10 msec). Once the C^+ ions are formed, they are mass isolated using resonant ejection techniques. At this point, kinetic energy may be added to the C^+ ions by applying an Rf potential at the cyclotron frequency of C^+ across the cell for a pre-determined time. The translational energy of the ion can be calculated using classical equations (6) and is dependent upon the amplitude of the Rf potential, the mass of the ion, and the length of time the ion is irradiated. The calculated energies may be experimentally verified simply by observing the length of excitation time which is required before the ions are ejected from the cell. The C^+ ions are then allowed to react with the background gas and the ion/molecule reaction products determined using typical ion detection techniques.

The reaction of C^+ with methane as a function of the reactant ion kinetic energy has been studied extensively using other techniques (1-4) and provides a well characterized system to compare with the FTMS results. A plot of the C^+ with CH_4 product ion branching ratios as a function of the C^+ translational energy is shown in Figure 1.

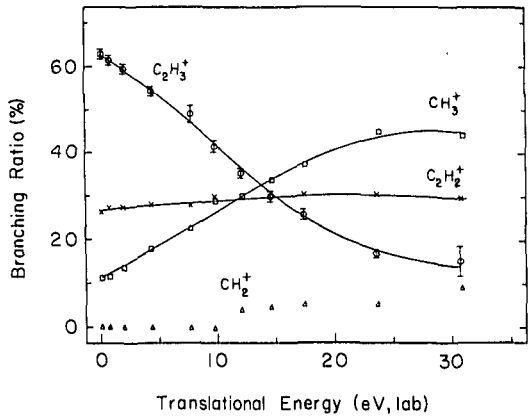

Figure 1. Changes observed in the reaction of C^+ with CH_4 as a function of the reactant ion kinetic energy.

The changes observed in Figure 1 correlate well with the previous studies. The product ions which result from complex formation ($C_2H_3^+$) decrease in intensity, whereas those which result from direct processes such as hydride abstraction or charge exchange ($CH_3^+$and CH_2^+) increase as the C^+ kinetic energy is increased. The $C_2H_2^+$ product ion remains constant over this energy range as a result of two competing exothermic and endothermic channels (loss of H_2 or 2H). Qualitative mechanistic information was also obtained in the reactions of C^+ with C_2H_6 and C_2H_4 by performing kinetic energy studies. The difference between the FTMS results and the previous studies occurs in the apparent energy range over which the changes in branching ratios are observed. The changes which are seen over ≈ 30 eV in the FTMS experiment (Figure 1) are observed over ≈10 eV in the other techniques. The difference in energy scales may result from non-reactive collisions of the reactant ion with the background gas which results in a "cooling" of the reactant ions in the FTMS experiment. Changes which were observed in the curves shown in Figure 1 as a function of the background pressure (i.e. the changes occurred over larger energy ranges at higher pressures) and simple hard sphere calculations support this hypothesis.

The information which may be obtained by varying the reactant ion kinetic energy in the FTMS has also been applied to more complex systems. One such system which is currently under investigation is the reaction of carbon cluster ions (C_n^+;n=3-25), formed by laser vaporization of graphite, with H_2, O_2, and small hydrocarbons. Mechanistic information obtained from kinetic energy studies has been helpful in elucidating the mechanisms which occur in the carbon cluster ion reactions.

References

1. P.S. Wilson, R.W. Rozett, and W.S Koski, J. Chem. Phys. 52, 5321 (1970).
2. R.D. Smith, J.J. DeCorpo, W.N. Allen, and F.W. Lampe, J. Chem. Phys. 65, 3665 (1976).
3. P. Armentrout (private communication).
4. R.A. Curtis and J.M. Farrar, J. Chem. Phys. 83, 2224 (1985).
5. R.C.C. Lao, R.W. Rozett, and W.S. Koski, J. Chem. Phys. 49, 4202 (1968).
6. W.T. Huntress, M.M. Mosesman, and D.D. Elleman, J. Chem. Phys. 54, 843 (1971).

SLOW CHARGE TRANSFER REACTIONS IN THE GAS PHASE - EXPERIMENTS AND INTERPRETATION

D. E. Richardson, C. S. Christ, Jr., P. Sharpe and J. R. Eyler, Department of Chemistry, University of Florida, Gainesville, FL 32611

Electron transfer reactions are central to many inorganic and bioinorganic processes and have been studied extensively, although primarily in aqueous solution. As part of a wide-ranging investigation of inorganic ion/molecule reactions with direct analogies in solution, we have carried out FTICR experiments involving various metallocenes (ferrocene, ruthenocene, manganocene, cobaltocene) and other inorganic compounds such as SF_6. Table I shows the results obtained for metallocene self-charge exchange rate constants[1], and the efficiencies of these reactions, defined as the observed rate constant divided by the calculated Langevin-Giomousis-Stevenson rate. Most reactions are seen to proceed at efficiencies near the expected value of 0.5 (50% chance of electron transfer for each orbiting encounter), but a very low rate is found for the manganocene/manganocenium system.

Table I. Gas Phase Self-Exchange Rates for Metallocenes
$M(Cp)_2 + M(Cp)_2^+$

M	k_{et} ($cm^3 molec^{-1} s^{-1}$)	EFF (k_{et}/k_{coll})
Cr	2.3×10^{-10}	0.22
Mn	6.3×10^{-12}	0.006
Fe	1.3×10^{-10}	0.12
Co	3.7×10^{-10}	0.36
Ni	3.1×10^{-10}	0.30
Ru	1.2×10^{-10}	0.13

The observed results can be interpreted[2] in terms of a double-well potential surface, with a central barrier arising from bond length and force constant changes necessitated in passing from neutral to ion, or vice versa. Marcus theory[3] has been quite successful in estimating kinetic barriers such as these in solution, and we have applied it to provide a semi-quantitative prediction of barriers and charge transfer rates for the systems studied. Table II gives the measured efficiencies and predicted barriers for some metallocene and other inorganic charge transfer reactions.

Table II. Estimated Reorganizational Barriers For Self-Exchange Reactions

SYSTEM	EFF	ΔR_{0+}(Å)	f(avg.)(mdyn/Å)	ΔE^*_{in}(kcal/mol)
$Cp_2Co^{+/0}$	0.36	0.11	2.8	2.4
$Cp_2Fe^{+/0}$	0.12	0.04	3.0	0.34
$(Me_5Cp)_2Mn^{+/0}$	0.15	0.04	2.8	0.32
$Cp_2Mn^{+/0}$	0.006	0.25	1.95	8.7
$SF_6^{-/0}$	$< 5 \times 10^{-5}$	0.145	4.88	22.0

$$\Delta E^*_{in} = \frac{f_0 f_+ (\Delta R_{0+})^2}{f_0 + f_+}$$

Electron transfer reactions involving different species (cross-reactions) have also been studied in some detail. Table III shows the results for various metallocene cross-reactions, with near thermoneutral reactions involving manganocene once again being quite inefficient.

Table III. Rates of Gas Phase Cross Reactions

M	M'	E_o (est,eV)	k_{et} cm^3 $molec^{-1}s^{-1}$)	EFF (k_{et}/k_{coll})
Cr	Fe	-0.98	4.2×10^{-10}	0.42
Cr	Ru	-	4.7×10^{-10}	0.50
Cr	Ni	-0.48	5.7×10^{-10}	0.57
Mn	Fe	-0.45	2.4×10^{-10}	0.23
Mn	Ni	-0.05	1.5×10^{-11}	0.015
Ni	Mn	0.05	6.3×10^{-12}	0.006

In an attempt to assess the importance of energy defects and Franck-Condon factors, electron transfer to atomic and small molecular ions from certain metallocenes was examined. No significant correlation between energy matching of initial and final states and the rates of charge transfer could be seen. Two factors which contribute to this poor correlation are the strong ion-induced dipole interaction which changes the energy defect in the "precursor" and "successor" states, and the importance of chemical activation in providing energy to overcome energy defects.

[1] J. R. Eyler and D. E. Richardson, J. Am. Chem. Soc. 107, 6130 (1985).
[2] D. E. Richardson, J. Phys. Chem., in press.
[3] R. A. Marcus, Ann. Rev. Phys. Chem. 15, 155 (1964).

GAS PHASE CHEMISTRY OF THE BENZENE RADICAL CATION: REACTION WITH 1,3-BUTADIENE

C. D. Werner, Department of Chemistry, Hastings College, Hastings, NE.
Robert W. Holman, Midwest Center for Mass Spectrometry, U. of Nebraska, Lincoln, NE

Earlier work on the ion-molecule reaction chemistry of various C_6H_6 radical cations[1] showed that in the ICR cell at ~1×10^{-5} torr ionized benzene did not react with 1,3-butadiene. We have reinvestigated the reaction of ionized benzene with 1,3-butadiene at higher pressures in a tandem mass spectrometer by acquiring the collisionally activated decomposition (CAD) spectrum of the distonic adduct ion. Additional work using FTMS has shown that the radical cation responsible for the reaction in the tandem mass spectrometer is the benzene radical cation. These results are interpreted in terms of an initially formed distonic adduct (I) which resembles 2-phenyl-2-butene. A ring closed product resembling ionized 1-methyl indan is formed if the adduct has sufficient internal energy.

Reaction in a 1:1 mixture of benzene and 1,3-butadiene ionized by an electron beam gives an adduct $[C_{10}H_{12}]^{+\cdot}$ at approximately 0.7 torr (eq. 1). The $C_{10}H_{12}$ adduct is

$$1)\qquad [C_6H_6]^{+\cdot} + C_4H_6 \longrightarrow \underset{\textbf{(I)}}{[C_{10}H_{12}]^{+\cdot}} \quad (m/z\ 132)$$

about equal in abundance to the benzene radical cation at m/z 78 (m/z 132 is 102% of m/z 78). Because this indicates that the benzene radical cation and butadiene are quite reactive, it is appropriate to compare its reactivity to that of two other alkenes. The data show that butadiene is one to two orders of magnitude more reactive than ethene and also that its reactivity is a function of internal energy. Furthermore, collisional activation of the adduct produces little benzene radical cation indicating that the adduct is highly covalent. In addition to showing little return to

RELATIVE REACTIVITY OF BENZENE RADICAL CATION WITH ALKENES

$P(CS_2)$torr	P(TOTAL)torr	ETHENE	PROPENE	BUTADIENE
0.0	2.0×10^{-5}	0.7	1.0	81.0
1.0×10^{-5}	3.0×10^{-5}	1.2	2.3	84.0
8.0×10^{-5}	10.0×10^{-5}	2.2	4.2	90.0
38.0×10^{-5}	40.0×10^{-5}	3.9	9.8	102.0

starting material, the CAD spectrum of the distonic adduct, **I**, shows that loss of CH_3 is predominant in the adduct. Many structures were considered as candidates for the adduct including tetralin and 2-phenyl-2-butene. The CAD spectra of these two models and six

CAD SPECTRA OF $C_{10}H_{12}$ (m/z 132) IONS

	Fragment ions						
m/z	117	115	105	104	91	77	51
Adduct	100	43	7	<2	24	7	5
Tetralin	100	122	<2	451	231	53	23
2-phenyl-2-butene	100	49	3	<2	25	9	4

others were acquired using charge exchange with toluene. The resulting collisionally stabilized low energy ions could be expected to closely resemble the low energy distonic adduct obtained at 0.7 torr. Neither the CAD spectrum of tetralin, the model of the product ion of a [4+2] cycloaddition, nor that of 1-phenyl-3-butene, the model for reaction of benzene radical cation at carbon one of 1,3-butadiene, resemble the CAD spectrum of the adduct at either energy extreme. The model which resembles the adduct

formed by reaction at carbon two is 2-phenyl-2-butene and its CAD spectrum resembles that of the adduct more than any other model

The reaction was conducted at four different source pressures to determine whether the collisional stabilization would alter the reaction path as observed in other systems[3,4]. The adduct CAD spectra do change as a function of internal energy Differences in the CAD spectra of the model compound, 2-phenyl-2-butene, using CS_2 charge exchange, 70eV EI, and toluene charge exchange were also noted as a function of internal energy. The parallel changes in the spectra as the internal energy is changed are clearly seen when the ratios of abundances for the m/z 91/117 ions and for the m/z 115/117 ions are tabulated. At higher energies, both the adduct and the radical cation

ION ABUNDANCE RATIOS OF ADDUCT AND 2-PHENYL-2-BUTENE

ADDUCT		2-PHENYL-2-BUTENE	
91/117	115/117	91/117	115/117
.09	.11	.13	.17
.11	17		
		.19	.41
20	.38		
		.25	.5
.23	.49		

undergo ring closure and hydrogen shifts to achieve the structure of 1-methyl indan. Further evidence for this cyclization is that other high energy acyclic $C_{10}H_{12}$ species cyclize to the more thermodynamically stable 1-methyl indan[2].

When 1,3-butadiene-d_6 reacts with ionized benzene, the loss of methyl is 80% as CD_2H for the low energy intermediate and 88% for the high energy ring-closed intermediate. In order for the ring open intermediate to lose methyl, a 1,3 hydrogen shift must take place. The resultant CD_2H group accounts for the CD_2H loss from the labeled adduct. Likewise, a 1,3 hydrogen shift in the cyclic species explainsthe predominant loss of CD_2H at high energy.

Attempts to observe a reaction in the FTMS between benzene and 1,3-butadiene at 10^{-7} torr using electron ionization gave no detectable signal. When a 1:1 mixture of toluene and 1,3-butadiene is irradiated at 266nm with a laser pulse only toluene is ionized. The ionized toluene and 1,3-butadiene form the adduct, $[C_{11}H_{14}]^{+\cdot}$, verifying that the aromatic radical cation reacts with the neutral. In a pulsed valve experiment, 1,3-butadiene is admitted to the cell, and ionized by electron impact. After the electron beam is turned off and toluene admitted, no adduct is observed. These observations support the conclusion that the reactive species is the benzene radical cation.

The results obtained by tandem mass spectrometry and FTMS support a two-step mechanism. In the initial step, benzene radical cation reacts at carbon two of 1,3-butadiene to give the distonic adduct, **I** If the adduct is formed at low energy, the adduct undergoes hydrogen shifts to give a product ion which resembles 2-phenyl-2-butene. In the absence of stabilizing collisions the initially formed adduct cyclizes to give the ring-closed ion Collisional activation of the ion gives the same fragments as does 1-methyl indan.

1. Gross, M L , Russell, D. H. , Aerni, R J. ; Bronczyk, S. B., J. Am Chem. Soc **1977**, 99, 3603
2. Dass, C. , Gross, M. L., Org. Mass Spectrom. **1983**, 12, 542.
3. Groenewald, G S. ; Gross, M. L , J Am Chem Soc. **1984**, 106, 6569.
4. Groenewald, G. S. ; Gross, M L., J. Am. Chem Soc. **1984**, 106, 6575.

HYDROXIDE INITIATED GAS-PHASE CHEMISTRY OF QUINONES

Carolyn L. Johlman and Charles L. Wilkins
Department of Chemistry
University of California
Riverside, CA 92521

The reactions of OH^- (produced from H_2O at 4 x 10^{-7} torr) with anthraquinone (AQ), napthaquinone (NQ), benzoquinone (BQ), and various alkyl-substituted analogues have been studied by using Fourier transform mass spectrometry. The major product of these reactions is $(M-H)^-$. For reaction times greater than 300 ms in the $OH^-/H_2O/Q$ system (Q=AQ, NQ, BQ), products that correspond to $(M+17)^-$ and $(M-H+M)^-$ (M=AQ and NQ) become dominant. The relative abundances of $(M+17)^-$ and $(M-H+M)^-$ are dependent upon the relative concentration of water and neutral quinone. The $(M+17)^-$ and $(M-H+M)^-$ comprise less than 8% of the total production distribution for the reactions of hydroxide with alkyl-substituted quinones.

Possible reaction pathways for formation of the $(M+17)^-$ ions include nucleophilic addition of hydroxide to the carbonyl carbon or a secondary reaction of $(M-H)^-$ with water. The following experimental observations support the latter pathway for formation of $(M+17)^-$: (a) $(M+17)^-$ is not formed when anhydrous hydroxide is used as a reagent; (b) the abundance of $(M+17)^-$ is enhanced by an increase in the concentration of H_2O; (c) an $(M+19)^-$ ion is produced when D_2O is present; (d) an $(M+19)^-$ ion is produced when $H_2{}^{18}O$ is the reagent; (e) $(M+17)^-$ is absent if $(M-H)^-$ is ejected; and (f) $(M+17)^-$ appears when $(M-H)^-$ reacts with neutrals. The fact that the $(M+17)^-$ results from an H_2O adduct of $(M-H)^-$ is surprising because formation of such ions by non-reactive collisions in the 10^{-8}-10^{-4} torr pressure range is rare.

A $(M-H+M)^-$ product from the reaction of $(M-H)^-$ and neutral quinone is supported by CAD, ion-ejection, ion-decay-and-growth, and isotopic-labeling results. Also, isotope incorporation in $(Aq-H+AQ)^-$ follows the pattern for $(AQ-H)^-$.

Alkyl-substituted quinones exhibit little tendency to dimerize in the gas phase and the dimers that are produced do not involve the $R-CH_2^-$ site but the aromatic ring. The tendency of AQ and NQ in the gas phase to form adducts with their $(M-H)^-$ ions (compared with minimal adduct formation for alkyl-substituted quinones) confirms that the negative charge on the aromatic ring favors adduct formation. The low abundances of $(M-H+M)^-$ are due to slower proton abstraction at aryl sites. Neutral BQ readily forms adducts with M-1 carbanions other than $(BQ-H)^-$; repulsion of the oxygens may hinder formation of an adduct between BQ and $(BQ-H)^-$. The $(M-H+M)^-$ ions are either cluster ions that share a hydrogen atom between the two molecules, or they result from nucleophilic attack of a carbanion upon a carbonyl carbon.

In the presence of D_2O, $(AQ-H)^-$ exchanges all seven of its hydrogens at essentially the same rate indicating that they have similar acidities (Fig 1a). If OD^- is ejected, the reaction of $(AQ-H)^-$ with D_2O regenerates OD^-, which suggests that the acidities of AQ and H_2O are similar. Exchange data for $(NQ-H)^-$ establish that one hydrogen atom is more acidic than that other four, which is consistent with more rapid proton abstraction from the quinone ring (Fig 1b). Comparison of the reaction profiles for $\underline{d}_3$-methylnaphthaquinone with D_2O and H_2O demonstrates that exchange of the aryl hydrogens occurs, but at a much slower rate than the alkyl exchange. $(BQ-H)^-$ rapidly exchanges one hydrogen for deuterium with minor incorporation of a second and third deuterium.

Oxygen-16/oxygen-18 exchange of both oxygens of $(AQ-H)^-$ is observed in the presence of $^{18}OH^-/H_2{}^{18}O$. Possible mechanisms for oxygen-16/oxygen-18 exchange include attack by $^{18}OH^-$ at the carbonyl carbon and exchange between $(M-H)^-$ and $H_2{}^{18}O$. The data indicate that the latter mechanism is predominant; an increase in the $H_2{}^{18}O$ pressure enhances exchange, while increases in the abundance of $^{18}OH^-$ have no affect upon the relative abundances of the exchanged $(M-H)^-$. Furthermore, when $^{18}OH^-$ is ejected during the entire reaction, exchange still occurs. Considerably less exchange is observed when anhydrous $^{18}OH^-$ is used, and the exchange that is observed for $(AQ-H)^-$ may result from reaction with $^{18}O_2$ or $^{18}O^-$ rather than $^{18}OH^-$. The

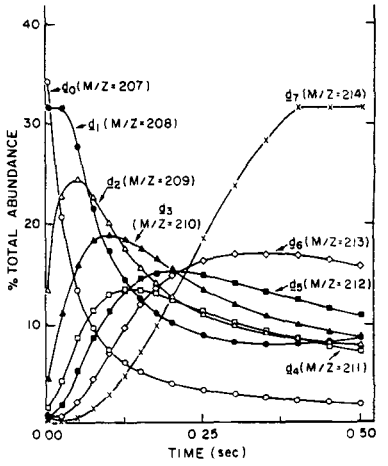

Figure 1a

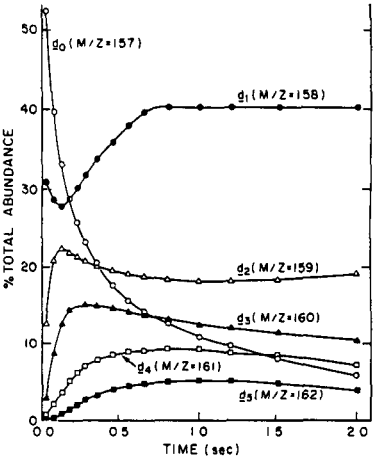

Figure 1b

$(AQ+17)^-$ ion is not the reaction intermediate for the exchange because its continuous ejection does not prevent $^{16}O/^{18}O$ exchange or formation of $(AQ-H)^-$. Apparently $(AQ-H)^-$ attacks $H_2{}^{18}O$ to form an intermediate too short-lived to be observed, with $H_2{}^{18}O$ attached to the carbonyl carbon. The presence of aromatic rings stabilizes the intermediate, and exchange occurs more rapidly for AQ than for NQ with its single aromatic ring.

The reactions of hydroxide with tetrachlorobenzoquinone and tetrafluorobenzoquinone also have been studied. The major reaction pathway is charge exchange to produce abundant $M^{-\bullet}$; however, the observation of F^-, Cl^-, $(M-HF+O)^-$ and $(M-HCl+O)^-$ (Table I) indicates that nucleophilic displacement also occurs. The greater abundance of Cl^- relative to F^- is consistent with it being a better leaving group in nucleophilic displacement reactions. Because F^- is a stronger gas-phase base than Cl^-, loss of HF with formation of $C_6F_3O_3^-$ is dominant in the OH^-/H_2O/tetrafluorobenzoquinone system. Loss of CO from $M^{-\bullet}$ and loss of CO and F from the $(M-HF+O)^-$ anions is also observed.

In summary, the major reaction pathway for the quinone-hydroxide ion interaction in the gas phase is proton transfer to form the quinone carbanion and water. Such a reaction pathway is consistent with both the strong base properties and high electron affinity of "unsolvated" hydroxide ion in the gas phase. Less basic anions, with lower electron affinities than hydroxide, such as $O_2^{-\bullet}$, $O^{-\bullet}$ and t-BuO$^-$ are expected to undergo electron transfer rather than proton transfer. For example, $O_2^{-\bullet}$ reacts to produce abundant molecular ions of $AQ^{-\bullet}$, $BQ^{-\bullet}$, and $NQ^{-\bullet}$ analogous to reactions in solution. In addition, $O^{-\bullet}$ (a strong gas-phase base with a lower electron affinity than OH^-) reacts by both proton abstraction and charge transfer with NQ to produce NQ^- and $(NQ-H)^-$.

Table I. Product Distribution for the Reaction of OH^- and $C_6X_4O_2$ (X=F,Cl).

Compound	$M^{-\bullet}$	$(M-HX+O)^-$	% Total Product Abundance $(M-HX+O-CO)^-$	$C_5X_3O_2^-$	X^-
Tetrafluorobenzoquinone	53.1	17.8	26.7	2.0	0.5
Tetrachlorobenzoquinone	82.3	1.6	9.8	0.8	5.5

Ion/Molecule Reactions of Protonated Alcohols with Acetic Acid in the Triple Quadrupole Mass Spectrometer

G.G. Dolnikowski*, J.T. Watson*+

Departments of Chemistry* and Biochemistry+
Michigan State University, East Lansing, MI 48824

The triple quadrupole mass spectrometer (TQMS) used in this research has two zones in which ion-molecule reactions may take place: the chemical ionization (CI) source and the central quadrupole region. Collision-activated reactions (CAR) are generated in the central quadrupole region (1-3). CAR is an MS/MS technique which allows the user to select a particular parent ion with the first quadrupole mass filter, and to select reaction products with the third quadrupole. CAR does not allow subsequent characterization of product ions by CAD (unless the instrument contains two more quadrupoles). On the other hand, performing ion-molecule reactions in the CI source produces ions that can be analyzed by CAD in the central quadrupole. In CI, however, one cannot select a particular parent ion for the reaction one wishes to study. In this way CI and CAR are complementary techniques for studying ion-molecule reactions.

A number of ion-molecule reactions have been studied in the TQMS using CI and CAR. This report cosists of preliminary results from a study of the chemistry of protonated alcohols, diols, and phenols with acetic acid and reactions of methanol with the $(M-1)^+$ ions of aromatic compounds. All of the data were collected with a data system employing a "trap and pulse" technique (4) which enhances the signal intensity of CAR products and provides CAR spectra that more closely resemble CI spectra.

When one protonates ethanol by CI and reacts this species with acetic acid in the central quadrupole, one obtains the CAR product spectrum shown in Figure 1A, in which MH^+ represents the protonated molecule of ethanol, and $(MH + AA)^+$ represents the proton-bound adduct of ethanol and acetic acid. These two species represent only ions of minor intensity in the Figure 1A. The major ions in Figure 1A are due to proton transfer from the protonated ethanol to the acetic acid, followed by numerous reactions of the protonated acetic acid with the neutral acetic acid molecules in the central quadrupole region. The reactions of protonated acetic acid with acetic acid neutrals are a chemical background that can easily be subtracted out of the spectrum. Figure 1B shows the background subtracted spectrum of protonated ethanol reacting with acetic acid in the central quadrupole. The peak of m/z 89 has been shown by CI/CAD to be the protonated molecule of ethyl acetate. This evidence indictates that protonated alcohols and acids can react in the gas phase to form protonated esters. This is a reaction which is strongly reminiscent of solution chemistry. More complicated protonated alcohols such as phenol and glycerol react with acetic acid in the central quadrupole to form other ionic products whose structures have not yet been determined.

In Figure 1, the alcohol was ionized and reacted with a neutral molecule in the center quadrupole. One can also inject the a neutral alcohol into the central quadrupole and react it with a selected ion from the ion source. Figure 2 shows a reaction of the $(M-1)^+$ ion of benzene $(C_6H_5^+)$ with methanol in the central quadrupole. The adduct of $C_6H_5^+$ and methanol is not observed. Instead one observes an ion of m/z 94 which has been shown by CI/CAD to be the molecular ion of phenol. One also observes an ion of m/z 91 whose formula in $C_7H_7^+$. The formation of the phenolic ion has been determined to be a general reaction for $(M-1)^+$ ions of unsubstituted aromatic compounds including pyridine and polycyclic aromatic hydrocarbons.

FIGURE 1

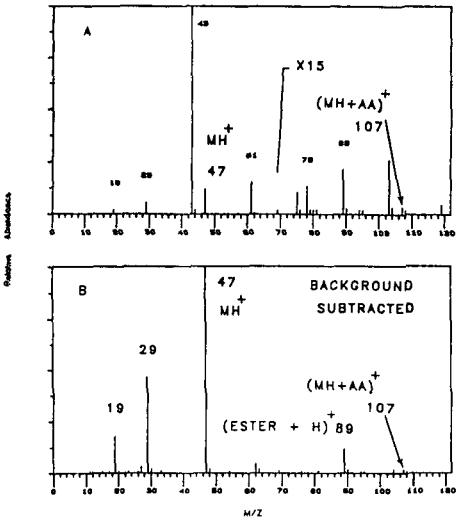

FIGURE 2

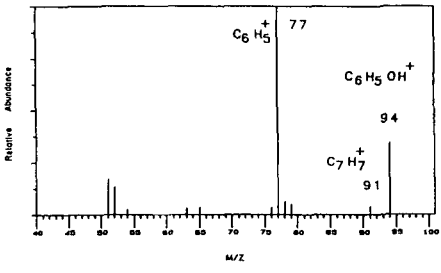

1. Schmit, J. P., Dawson, P. H., Beaulieu, N. Org. Mass Spectrom., 4: 269-275, (1985).

2. Fetterolf, D. D., Yost, R. A. Int. J. Mass Spectrom. Ion Proc., 62: 33-49, (1984).

3. Morrison, J. D., Stanney, K., Tedder, J. M. J. Chem. Soc. Perkin, Trans. II, 967-969, (1981).

4. Dolnikowski, G. G., Kristo, M. See MPE-13, this conference.

Acknowledgement: This work was supported in part by a grant (RR-00480) from the Biotechnology Research Program, Division of Research Resources, National Institutes of Health.

DIRECT QUALITATIVE AND QUANTITATIVE CHARACTERIZATION OF SOLID RUBBER SAMPLES BY LASER PYROLYSIS MASS SPECTROMETRY (PY-MS)

William H. McClennen, Joseph M. Richards, Henk L.C. Meuzelaar
Biomaterials Profiling Center, University of Utah
391 S. Chipeta Way, Suite F, Research Park
Salt Lake City, Utah 84108

Jerry B. Pausch, Robert P. Lattimer
BFGoodrich Research and Development Center
Brecksville, Ohio 44141

Modern commercial rubbers are complex mixtures of highly cross-linked polymers, organic and inorganic fillers, and a variety of preservatives and other organic additives. Conventional methods of analysis involve a number of steps taking hours or even days to complete. Mass spectrometric techniques have been used to analyze the organic components [1], but most have still required significant sample preparation such as cryo-grinding [2] or solvent extraction. They have also seldom given complete results on both the polymer and additive composition. The objective of this research is to develop and evaluate direct methods of vulcanized rubber analysis requiring minimal time and sample preparation.

In this work a tunable 5 watt CO_2 laser was used to flash vaporize additives and pyrolyze polymers directly into the low voltage (14 eV) electron ionization source of the quadrupole mass spectrometer. The laser beam was shutter pulsed (10-500 ms) and could be rapidly scanned across the sample surface to vary pyrolysis conditions. Qualitative evaluation was made on a series of samples containing styrene butadiene rubber (SBR), cis-polybutadiene rubber (BR) and natural (polyisoprene) rubber (NR) as the main polymeric components and a variety of additives. The additives included three or more antioxidants, antiozonants and crosslinking accelerators as well as varying amounts of carbon black filler, processing oil, sulfur, zinc oxide and stearic acid. Both fragment and molecular ions were observed for most of the organic additives and for monomers and small oligomers from all of the polymers.

A major challenge in this technique is to reproducibly pyrolyze the surface of a bulk sample to give consistent ratios of the various components. In pulsed spot pyrolysis, the polymers tend to depolymerize with exponential rates causing peak product concentrations which are critically dependent on the laser power and pulse duration. However, by scanning the laser beam across the rubber surface, there is a prolonged, more constant evolution of products which is much more efficient for repetitive MS scanning.

To examine reproducibility, butadiene rubber (BR) and natural rubber (NR) samples and three mixtures of the two were pyrolyzed using the laser beam scanning technique. Factor and discriminant analysis were performed on the replicate spectra of these five samples and the scores of the main discriminant function are plotted versus their relative composition. The non-linearity of the bivariate plots is apparently due largely to the lower decomposition temperature for the polyisoprene (NR) than the polybutadiene.

These results have confirmed that laser pyrolysis mass spectrometry can indicate the presence of most of the typical polymeric and organic additive components. Although the technique requires minimal sample preparation, precise pyrolytic conditions (e.g., laser power and scanning) are crucial to good reproducibility. Also, relative responses of different polymers in mixtures appear to be somewhat matrix dependent when they have rather different decomposition temperatures. However, standard deviations of <20% have been attained in these preliminary analyses and good quantitative accuracies should be possible with further refinement and proper calibration.

REFERENCES:

1. J.B. Pausch, R.P. Lattimer and H.L.C. Meuzelaar *Rubber Chem. Technol.* 56, 1031 (1983).

2. R.P. Lattimer, K.M. Schur, W. Windig and H.L.C. Meuzelaar, *J. Anal. Appl. Pyrol.*, 8, 95 (1985).

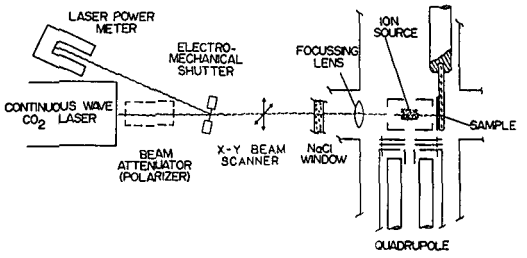

Figure 1. Schematic diagram of the experimental setup for direct pyrolysis of solid rubber samples next to the ion source. Note the polarizer attenuated beam is reflected off the shutter and constantly read by the power meter between pyrolysis experiments. The beam scanner is able to move the focussed beam through a 2.5 mm diameter area on the sample.

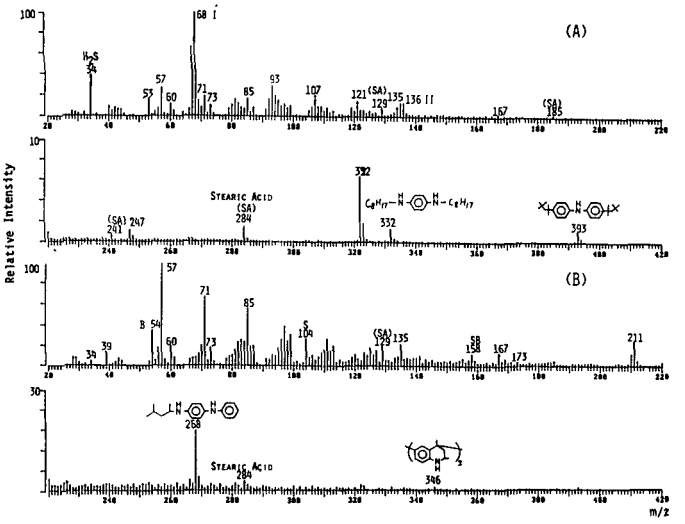

Figure 2. Pyrolysis mass spectra of a) a natural rubber (NR) compound and b) a styrene butadiene rubber (SBR). Note the monomer ions indicated by I (isoprene), S, and B. The molecular ions of antioxidants and antiozonants are labelled with their structures.

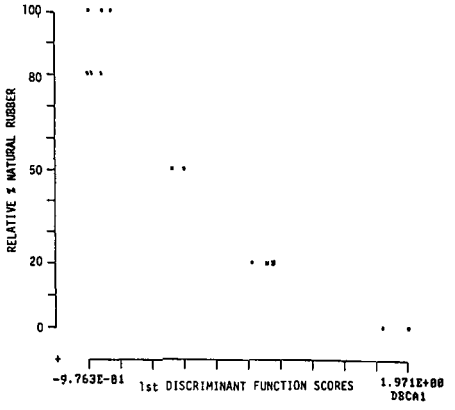

Figure 3. Plot of discriminant function scores versus %NR composition. Two or three spectra were run for each of the 5 samples. The lack of discrimination of the 80 and 100% NR samples seems to be predominantly due to the lower decomposition temperature of the NR than the BR.

CHEMICAL AGING AND THERMAL STABILITY OF POLY(ARYLETHERETHERKETONE) [PEEK]

M. A. GRAYSON AND CLARENCE J. WOLF, McDonnell Douglas Research Laboratory, St Louis, MO 63166

Poly(arylethereterketone) [PEEK] has potential as a thermoplastic resin for carbon-based composites in aerospace systems. However, little is known about the long term chemical stability of this resin in the aerospace environment. Wet-dry cycling of neat PEEK in water shows no change in water transport in the resin over two complete cycles in excess of $8x10^3$ h. [1]. However, wet-dry cycling of neat PEEK in dichloromethane shows a large change in the transport of this solvent in a single cycle. Furthermore, the resin undergoes swelling and a loss of mechanical properties [2]. It is of interest to determine if such changes are due to physical aging or chemical aging. Tandem mass spectrometry (MS/MS) and evolved-gas analysis mass spectrometry (EGAMS) were used to investigate chemical aging in neat PEEK.

EXPERIMENT: Neat PEEK injection-molded placques 1.8 mm-thick were obtained from RTP Co. (Winona MN) and aging specimens 10 by 20 mm were cut from the placques and dried to constant weight. Specimens were exposed to two aging environments: (1) immersion in water at 95°C for $16x10^3$ h, and (2) immersion in dichloromethane at 35°C for $7.2x10^3$ h. Samples of 500 to 1000 µg were cut from the edge of the specimens and analyzed by EGAMS. They were heated to 570°C at 12°C/min and continuously scanned with the mass spectrometer from 10 to 1000 daltons at 20 seconds per decade. Accurate mass measurements and tandem MS experiments were performed to elucidate the elemental composition and structure of selected ions in the mixture of compounds released from the sample during heating. Modified selected-ion recording techniques were used to quantify the amount of solvent trapped in the PEEK during synthesis.

RESULTS: Physical Aging. The equilibrium concentration of solvent in the aged samples was reached in less than 500 h. For water aging, final weight gain at saturation was approximately 0.5 wt%; no swelling was observed in the sample; water transport was Case I Fickian. For aging in dichloromethane, the final weight gain at saturation was on the order of 24 wt%; swelling of nearly 12 % occurred; the transport was Case II Fickian.

Characterization of Unaged PEEK. From EGAMS analysis of the unaged PEEK it was determined that the compounds evolved from the sample can be classified into three categories: (1) trapped solvent and side-reaction products from synthesis; (2) trapped thermal degradation products from processing; and (3) pyrolysis products formed during the EGAMS experiment. The compounds found in category (1) evolve as a peak during the initial portion of the temperature program prior to thermal degradation of the polymer chain. The major compounds in this category include a solvent, diphenylsulfone [3], and a psuedo-monomer with molecular weight 506, elemental composition $C_{32}H_{20}O_4F_2$, and structure as shown in I.

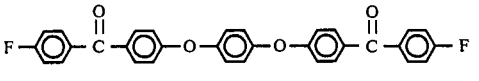

I

Less than 0.1 wt% of the diphenylsulfone solvent was measured in the sample by selected-ion recording. The compounds in category (2) evolve as a peak during initial sample heating and then evolve again as the sample undergoes pyrolysis. The major compounds in this category are phenol and a dimer in which one of the phenyl-ether-phenyl chain portions has formed a dibenzofuran moiety. This material has a molecular weight of 576, an elemental composition of $C_{38}H_{24}O_6$, and a structure as shown in II. Hay and Kemmish [4] propose pyrolysis products containing the dibenzofuran structure in their study on the thermal decomposition of PEEK.

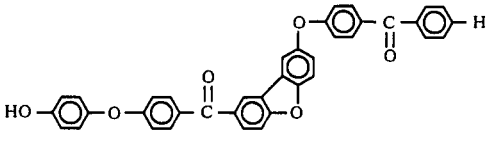

II

Most of the compounds in this category contain the dibenzofuran structure in their chain, thus indicating that they are formed as the result of thermal rearrangement and not as side reaction products from synthesis. The last category of compounds evolves only after the sample has reached pyrolysis temperatures. The most abundant compounds from pyrolysis of PEEK, other than phenol, are a psuedo-monomer of 382 daltons and elemental composition $C_{25}H_{18}O_4$, and the dibenzofuran analog of the previous product of 380 daltons and elemental composition $C_{25}H_{16}O_4$. The structure proposed for the compound at mass 382 is shown in III:

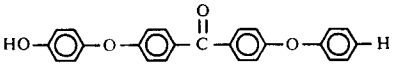

III

It is interesting to note that there are a number of fluorine containing compounds evolved from PEEK both before and during pyrolysis. PEEK is prepared by the condensation of near stoichiometric quantities of 4, 4'-difluorodiphenylether and the hydrated potassium salt of bis-4-hydroxyphenylketone [5]. Even though a small amount of end-capping agent is used to control molecular weight, a fraction of the polymer chains terminate with 4-fluorophenylether groups. Two "difluoro" compounds were found at mass 506 and 794 with proposed molecular formulas of $C_{32}H_{20}O_4F_2$ and $C_{51}H_{32}O_7F_2$ respectively. Both of these materials represent short PEEK chains terminated with fluorine atoms. In addition, during thermal degradation, there are a number of "monofluoro" compounds that represent cleavage of the chain end along different parts of the polymer chain as pyrolysis commences.

Characterization of PEEK aged in water: The majority of compounds trapped in PEEK as solvents, side-reaction products and thermal degradation products of processing remain trapped in the resin despite long-term immersion in water. There are no changes in the identity of the compounds evolved during pyrolysis indicating that no detectable chemical changes in the polymer chain have occurred as the result of aging in water at 95°C for 1.6×10^3 h. This is in agreement with our previous work on the transport of water in PEEK [1].

Characterization of PEEK aged in dichloromethane: Nearly all of the indigenous compounds trapped in the PEEK are leached out during immersion in dichloromethane. As in the case of aging in water, there are no discernible changes in the identity of compounds evolved during thermal degradation. This implies that changes observed in the polymer in our previous work on the transport of dichloromethane in neat PEEK [2] are all due to physical aging and not chemical aging.

SUMMARY: Neither aging in water nor in dichloromethane for long periods of time appears to cause chemical aging in the PEEK resin. There are over a dozen compounds trapped in the PEEK resin from the synthesis and processing. There are over 40 different compounds observed during pyrolysis of the neat PEEK resin with molecular weights as high as 864. Diphenylsulfone is the most abundant indigenous compound and phenol is the most abundant pyrolysis product.

ACKNOWLEDGMENTS:

The authors thank Jack Bornmann for his consultations on the structure of pyrolysis products.

This work was performed under the McDonnell Douglas Independent Research and Development Program.

REFERENCES:

1. M. A. Grayson and C. J. Wolf, Journal of Polymer Science, (accepted).
2. M. A. Grayson, C. J. Wolf, and P. S. Pao, Journal of Polymer Science (accepted).
3. R. O. Yelton, T. L. Shell, D. M. Colman, presented at the 33rd Annual Conference on Mass Spectrometry and Allied Topics; San Diego, CA 1985.
4. J. N. Hay, D. J. Kemmish (in press).
5. T. E. Attwood, P. C. Dawson, J. L. Freeman, L. R. J. Hoy J. B. Rose, and P. A. Staniland, Polymer, 22, p 1096, 1981.

ANALYSIS OF CHLORINE-CONTAINING POLYMERS BY DIRECT PYROLYSIS MASS SPECTROMETRY

Jeffrey M. McGuire and Charles C. Bryden
Hercules Incorporated
Research Center
Wilmington, DE 19894

Determining the identity and composition of carbon-black filled, cross-linked elastomers is a difficult problem. The most common techniques employed are pyrolysis gas chromatography (Py-GC/MS). However, when chlorine-containing polymers are pyrolyzed, hydrochloric acid is often produced, which can degrade capillary columns. We have found that pyrolysis of poly(epichlorohydrin) and poly(epichlorohydrin-co-ethylene oxide) damages capillary columns sufficiently that aliphatic alcohols are totally absorbed. Py-GC on such a column often yields irreproducible results.

A technique which avoids the column degradation problem is direct pyrolysis mass spectrometry (Py-MS). Through the use of rapid pyrolysis techniques, such as Curie-point or filament pyrolyzers, or temperature-programmed pyrolysis performed with the direct insertion probe, Py-MS offers a rapid, sensitive and specific technique for polymer identification.

We have found that Py-MS can be performed on a Hewlett-Packard mass selective detector using the gas chromatograph as an interface for the pyrolysis unit. By substituting a length of uncoated fused-silica tubing for the fused-silica capillary column normally installed in the gas chromatograph, mass pyrograms were obtained that are quite similar to those acquired using instruments with direct probe inlet systems. The method is rapid and reproducible, and can be employed for quantitative analysis as well as for fingerprint identification.

A similar approach was taken previously (1), but instrumental modifications were required. The present approach requires no modifications. A Hewlett-Packard 5970B mass selective detector interfaced to a HP 5890A gas chromatograph was used to obtain the mass spectra. The mass spectrometer was scanned from m/z 20 to 800 in 1.5 seconds at a source temperature of 200°C, and electron impact (70 - e.v.) spectra were acquired using the HP 59970A work station supplied with the instrument. The polymers (0.2 to 0.3-mg) were pyrolyzed using a Chemical Data Systems Model 120 Pyroprobe with a coil filament, and quartz tube sample holders.

A 5-m x 0.20-mm uncoated polysiloxane-deactivated fused silica capillary tube, maintained at 250°C (in the GC oven) was used to couple the pyrolysis unit and the mass spectrometer through a direct interface. All samples were preheated in the pyrolysis unit interface for 5 minutes at 250°C with continuous helium gas flushing. The samples were then pyrolyzed by heating from 250°C to 500°C at 100°C/s, and holding the final temperature (500°C) for 17.5 seconds.

Owing to the absence of any coating on the 5-m capillary tube, the pyrolyzate is swept essentially unretained into the mass spectrometer. Figure 1 shows a typical trace of the total ion current obtained. Pyrolysis was performed at 5.0 minutes after an initial heating at 250°C. It was found that single spectra, recorded at the point of maximum elution were more reproducible than a spectrum averaged over the entire peak.

The reproducibility of this technique was investigated by pyrolyzing a sample of poly(vinyl chloride) over a period of several weeks. Ten different samples were used and the average of the ten major peaks from a single scan of each pyrolysis run was recorded. These results are summarized in Table 1.

This technique was also employed in the compositional analysis of several poly(epichlorohydrin-co-ethylene oxide) gum stocks. Using principal component analysis for several of the major peaks in the spectra, the following equation was developed to estimate the mole percent of epichlorohydrin present in the copolymers:

$$\% \text{ Epi} = 50.853 + 30.352 \ln (\Sigma_{EPI}/\Sigma_{EO})$$

where Σ_{EPI} = the sum of the intensities of m/z 36, 39, 41, 42, 55, and 57, and Σ_{EO} = the sum of the intensities of m/z 31, 44, 45, 59, 72 and 73. Figure 2 shows a plot of the results obtained from the analysis of four different copolymer compositions using direct pyrolysis mass spectrometry and ^{13}C NMR. Each of the four points represents an average of five pyrolysis runs with a relative standard deviation of 2.3%.

The feasibility of direct pyrolysis-mass spectrometry using a low cost mass selective detector has been demonstrated for several chlorine-containing polymers. The technique shows promise for qualitative identifications, particularly of intractable samples, and for quantitative analyses of copolymers. The technique is superior to Py-GC, because capillary columns can be damaged by the pyrolozate of some chlorinated polymers.

(1) Hughes, J. C.; Wheals, B. B.; Whitehours, M. J., Analyst, 1977, 102, 143-144.

- - - - - - - - - - - - - - - -

Table I. Direct Pyrolysis-Mass Spectrometry of Poly(vinyl chloride)

Ion (m/z)	35	36	37	38	39	50	51	52	77	78
Mean Intensity [a]	22.9	100	10.1	34.8	7.8	9.5	10.2	8.6	10.6	37.8
Relative standard deviation, %[a]	2.2	---	6.5	2.8	17	14	14	17	17	16

[a] For ten mass spectra.

Figure 1

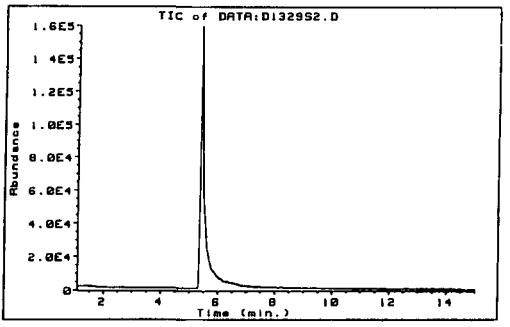

Figure 2

Mole % Epichlorohydrin

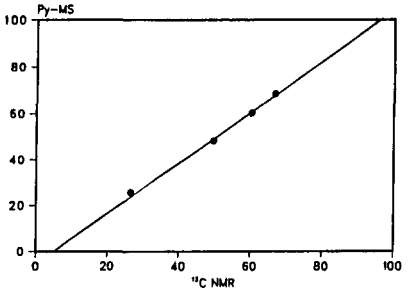

Identification of Organic Additives in Rubber Vulcanizates Using Mass Spectrometry

R. P. Lattimer, R. E. Harris, C. K. Rhee
The BFGoodrich Research and Development Center
Brecksville, Ohio 44141 (USA)

H.-R. Schulten
Fachhochschule Fresenius
6200 Wiesbaden (FRG)

The identification of additives in compounded polymers is complex because many compound classes are used, many additives are labile, and additive concentrations may be quite low. Thus most methods of rubber compound analysis involve some separation of the ingredients into different fractions prior to chromatographic or spectroscopic analysis. Since crosslinked rubbers are insoluble, a fairly complex extraction scheme is often employed. Of particular interest are direct methods, i.e., analysis of the polymer with no or minimal pretreatment (1,2). In this study, direct thermal desorption has been used with three different ionization methods (EI, CI, FI). The vulcanizates were also examined by direct FAB-MS as a means for surface desorption /ionization.

Extracts containing the organic additives were examined directly by four ionization methods (EI, CI, FD, FAB). FD-MS is particularly effective for mixture analysis since molecular ion abundances are high with minimal fragmentation (3).

Experimental: Three rubber compounds were prepared. Chemical structures for the additives are provided. Rubber extract analysis: The cured rubbers were cut into small pieces and solvent extracted for 24 hours. A concentrated solution was used for FD analyses and residues for EI, CI and FAB. Direct rubber analysis: Small pieces of rubber were cut and placed in crucibles for EI, CI, and FI analyses. For FAB, the the vulcanizates were cut into strips and attached to the probe with Scotch® 924 transfer tape.

Results/Discussion

Vaporization/ionization methods. Mass spectra which follow illustrate the differences in the various methods. The isobutane CI spectrum of the rubber heated in the direct probe includes ions from HPPD (m/z 211, 268, 269), poly TMDQ (m/z 174, 291, 307, 331, 346, 347, 371, 386, 387, 504, 519, 520, 559), stearic acid (m/z 285), and DODPA (m/z 393, 394). An interesting feature is the m/z 88 ion, which is $(M+H)^+$ for morpholine, a decomposition product from the accelerator OBTS. Sulfenamide accelerators decompose during vulcanization to yield, among other products, an amine plus benzothiazole. The FI and extract FD spectra include molecular ions for these same species. Molecular ions for paraffin wax oligomers (m/z 282, 296, 310 et al) are prominent in the extract FD spectrum. The FAB spectrum was obtained from the neat, oily extract. Of the various vaporization /ionization methods, it appears that field desorption/ionization (FD/FI) is the most efficient for identifying typical organic additives in rubber vulcanizates. Other ionization methods may be required, however, for detection of specific types of additives.
In this study, there was no clear advantage for direct analysis as compared to extract analysis. Both approaches gave comparable results. Direct analysis is a little faster, but extraction methods are more versatile.

References:
(1) Pausch, J. B.; Lattimer, R. P.; Meuzelaar, H. L. C., Rubber Chem. Technol., 1984, 56, 1031-1044.
(2) Lattimer, R. P.; Harris, R. E., Mass Spectrom. Rev., 1985, 4, 369-390.
(3) Lattimer, R. P.; Welch, K. R., Rubber Chem. Technol., 1980, 53, 151-159.

Chemical Structures of Organic Additives.

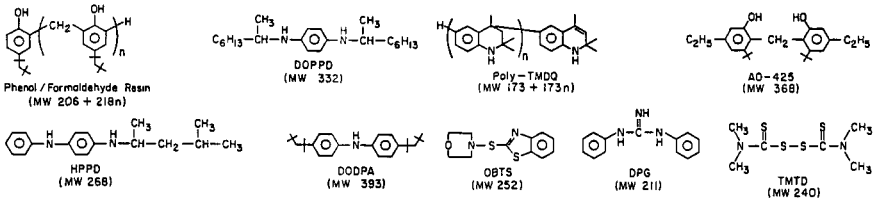

Chemical Ionization (Isobutane) Mass Spectrum of Vulcanizate B (Direct Analysis)

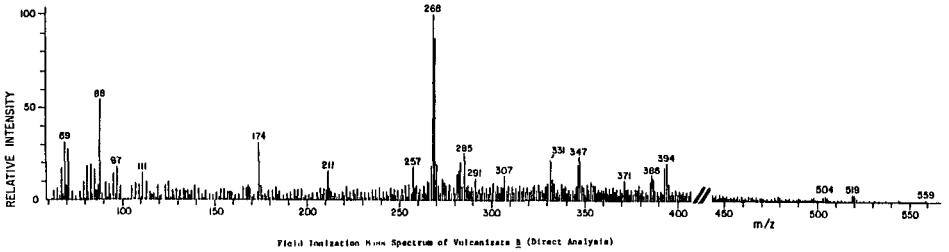

Field Ionization Mass Spectrum of Vulcanizate B (Direct Analysis)

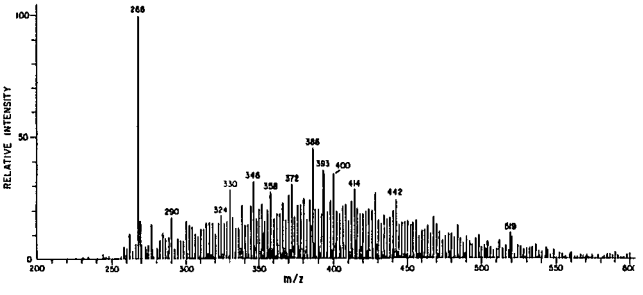

Field Desorption Mass Spectrum of Vulcanizate B (Acetone Extract).

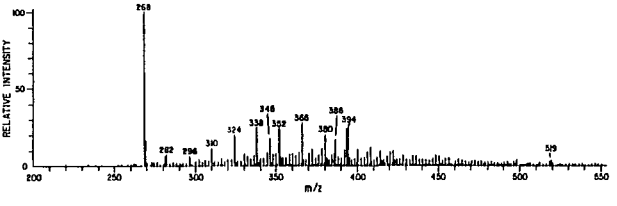

Fast Atom Bombardment Mass Spectrum of Vulcanizate B (Acetone Extract).

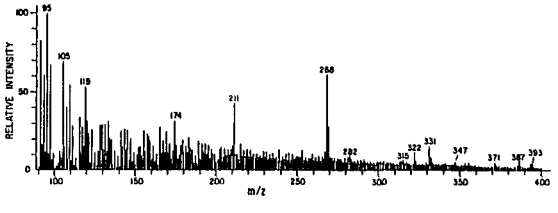

FIELD DESORPTION MASS SPECTRAL ANALYSIS OF HIGH MOLECULAR WEIGHT POLYMERS

S. D. Maleknia and C. E. Costello, Department of Chemistry, M. I. T., Cambridge, MA 02139.

Introduction. Although the driving force for the construction of the new generation of high field mass spectrometers was the development of fast atom bombardment (FAB) ionization, it seemed quite likely that this type of instrument would also offer improved performance for field desorption (FD) studies, particularly for those classes of compounds for which promising FD results had already been obtained by operation of lower field mass spectrometers at reduced accelerating voltage. We have now obtained FDMS (at 10 kV accelerating voltage) for several synthetic polymers · polyperfluoropropylene oxide; polystyrenes of M_r 5500, 7500 and 12000; polyethylene glycols and polypropylene glycols, nylon 6 and nylon 6/6 and present this data below. We found that polystyrene sulfonate underwent thermal decomposition without providing a useful FD mass spectrum. Results for FDMS of biopolymers will be reported elsewhere.

Materials and Methods. Krytox^r 16140, manufactured by Dupont, was obtained as a gift from C. L. Wilkins. Polystyrenes, nylons and polyethylene glycol were purchased from Scientific Polymer Products, Inc. (Ontario, NY). For FDMS analysis, solutions of the samples (1μg/μl) were applied to the emitter from a syringe, except for the Krytox^r which was applied by dipping the emitter into a chloroform solution of the polymer. Benzonitrile-activated carbon emitters were used. FDMS were obtained with a JEOL HX110/HX110 tandem mass spectrometer, operated at 10 kV accelerating voltage, with −1.5 to −2.5 kV counter electrode voltage and −18.5 kV post-acceleration. Ion source temperature was 70 – 85 °C. Resolution was 1:1000, unless noted. The mass scale was calibrated in the FAB mode, using $Cs(CsI)^+$ clusters. Data was acquired and processed with the DA5000 data system. For most experiments, the emitter current was raised quickly (8 mA/min) to a value just below the optimum current, then programmed slowly (1/4 to 1/2 mA/min) while the polymer desorbed. Mass spectra were acquired in the profile mode, and scans were added together after data acquisition, so that the low temperature spectra of volatile impurities and high temperature spectra of decomposition products, if any, could be excluded from the sum.

Results and Discussion. Fig 1 shows the FDMS obtained for 0.5 ug of polystyrene 579 (M_r 7500). Fig 2 shows the M^{++} region of the FDMS obtained for 0.5 ug of polystyrene 540 (M_r 12000). For those polymers for which molecular-weight related ions were observed (Krytox^r, polyethylene glycol, polystyrene), the sensitivity was sufficient to obtain good signals from a few nanograms of each component – in the MW range of 5000-10000, this represents a few picomoles of each. For these samples, calculations of molecular weight distributions appear in the Table, together with values determined by other methods as provided by the manufacturer. Structures that correspond to cleavages along the backbone could be assigned to the fragment ions observed in the FDMS of Krytox^r and of the nylon6/6. These appear in Schemes 1 and 2.

Conclusions. These experiments demonstrate that FDMS is appropriate for the analysis of some classes of polymers to the same high mass range reported for FABMS of biopolymers, around 14000 daltons. Peak widths are approximately those anticipated for the calculated isotopic distribution. For polymers which are desorbed without extensive thermal degradation, the sensitivity of the technique for the determination of MW is remarkable – in the few picomole range, with sufficient mass assignment accuracy to specify the polymer structural components. Values measured by FDMS are consistent with those obtained by other techniques.

Although the major high mass ion series in the spectra of Krytox^r are fragment ions, they apparently represent the loss of only a small fragment, since their masses are close to the expected MW. For the polystyrenes, the abundance of the doubly-charged ions is so great that this series may also be used for MW profiling, thus extending the effective MW range at full accelerating voltage. Thermal decomposition at high emitter currents limits the MW range for which FDMS analysis is useful for profiling polyethylene glycol. The spectra determined for nylons depend on both the solvent and the emitter temperature.

Acknowledgements. This study was prompted by earlier work reported by others: Matsuda, Schulten, Lattimer, Derrick and Hercules, in particular, and the compounds selected for this project were largely in response to the suggestions provided by their results. Presentation of this work was furthered by data reduction and spectra plotting programs written by J. E. Biller. The M. I. T. Mass Spectrometry Facility is supported by Grant No. RR00317 from the NIH Division of Research Resources (to K. Biemann).

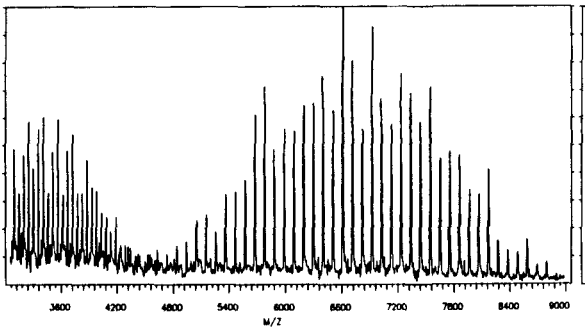

Fig 1. FDMS of 0.5 µg polystyrene 579 in benzene. Amount of each observed component was therefore 5-25 ng (0.7-3.5 pmol). Plot shows avg/6u for sum of 5 scans.

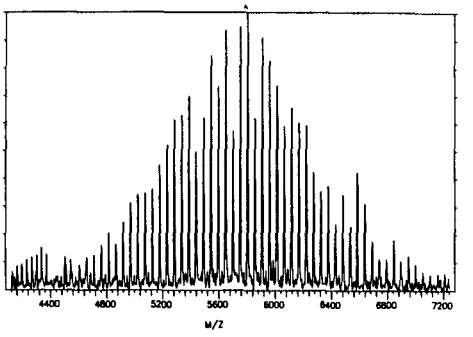

Fig 2. FDMS of 0.5 µg polystyrene 540 in benzene. Amount of each observed component was therefore 2-25 ng (0.2-2 pmol). $M^{+++\cdot}$ and M^{++} region scanned in this experiment. Plot shows avg/4u for sum of 5 scans.

TABLE

POLYMER	$\bar{M}_n$	$\bar{M}_w$	$\bar{M}_w/\bar{M}_n$	COMMENTS
Polystyrene 578	5200(VPO) 5320(FDMS) 5412(FDMS)	5480(LS) 5479(FDMS) 5565(FDMS)	1.12(GPC) 1.03(FDMS) 1.03(FDMS)	 (Z=1,H) (Z=1,A)
Polystyrene 579	7400(VPO) 6766(FDMS)	7820(LS) 6883(FDMS)	1.19(GPC) 1.02(FDMS)	 (Z=1,H)
Polystyrene 540	12000(MO) 11400(GPC) 11467(FDMS) 11352(FDMS)	12200(LS) 12800(GPC) 11580(FDMS) 11434(FDMS)	 1.12 (GPC) 1.01(FDMS) 1.01(FDMS)	 (Z=2,H) (Z=1,H)
Krytox J6140	6710(FDMS)	6915(FDMS)	1.03(FDMS)	(Z=1,H)
PEG 677	3336(GPC) 3030(FDMS)	3662(GPC) 3110(FDMS)	1.10(GPC) 1.03(FDMS)	 (Z=1,H)

Molecular weight data for vapor phase osmometry (VPO), laser scattering (LS), gel permeation chromatography (GPC) and membrane osmometry (MO) provided by manufacturer. Field desorption values are shown for singly (Z=1) and doubly (Z=2) charged ions calculated for peak heights (H) or areas (A). Krytox FDMS values are for C series fragment ions. Polyethylene glycol FDMS values are for $(M+Na)^+$ series ions.

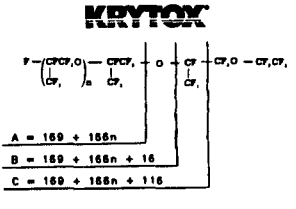

Scheme 1

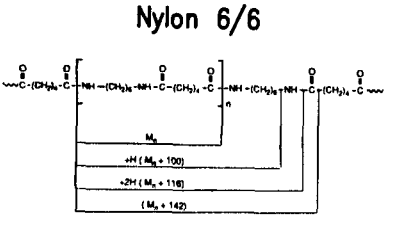

Scheme 2

POLYMETHYLENE LINKAGES IN TANDEM MASS SPECTRAL ANALYSIS OF COAL REDUCTION PRODUCTS

K.V. Wood, R.R. Pachuta; Engine/Fuels Laboratory, Purdue University, West Lafayette, IN 47907; R. Narayan, Laboratory of Renewable Resource Engineering, Purdue University, West Lafayette, IN 47907.

Detailed characterization of the components in complex coal products often necessitate multiple separation schemes prior to analysis. The amount of prior separation can be alleviated somewhat with the use of tandem mass spectrometry (MS/MS) which is ideally suited for the analysis of complex mixtures. The three principal scanning modes of MS/MS - daughter, parent and neutral loss all provide insight for characterizing complex mixtures. Daughter spectra are used for identification and confirmation of specific components. Parent spectra are valuable for characterizing a given mixture for those components having a specific chemical substructure. Neutral loss spectra are useful for characterizing complex mixtures for compounds containing selected functional groups. Analysis of the results from MS/MS studies of specifically degraded coal products can then be used to relate the identified components to their origin in the coal. In this study the tetrahydrofuran (THF) extract of a potassium/crown ether coal reduction of an Illinois No. 6 coal was analyzed by MS/MS because the NMR analysis indicated an abundance of polymethylenes in this extract. The potassium/crown ether reduction is a powerful yet selective reagent which is carried out at room temperature and room pressure. The potassium/crown ether reagent generates a stable solution of electrons which, because of their size and reactivity, diffuse into the macromolecular coal network and transfer onto the aromatic substrates. This results in the formation of aromatic radical anions and dianions which undergo cleavage at diaryl ether or alkane linkages. In addition reduction of aromatic rings to dihydro- and tetrahydro- products can occur.

A Finnigan MAT triple stage quadrupole mass spectrometer was used for this study. The THF extract from the coal-reduction was introduced into the mass spectrometer via the solids probe, volatilized by heating and ionized using isobutane chemical ionization (source pressure at 0.4 torr). To obtain a daughter spectrum the ion of interest was selected with the first mass analyzer and passed into the collision quadrupole for collision induced dissociation (CID). The resulting fragment ions were then mass analyzed with the second mass analyzer. Argon was the collision gas, present at a pressure of 2.0 mtorr. The collision energy was set at 20 eV.

The THF extract was volatilized over a temperature range up to 350° C. The mass range of ions detected at the upper temperature limit extended beyond m/z 700. The sample was run in triplicate in order to determine the volatility of the sample and was found to be 55% volatile over this temperature range. At the upper temperatures an envelope of ions were present at every mass, peaking in the m/z 400 range. At the lower temperatures on the other hand, (see Figure 1), a very distinctive pattern of sets of three ions (beginning at m/z 129, 131, 133) was observed extending well over m/z 250. These three series represent protonated alkyl naphthalenes (m/z 129, 143, ...), alkyl dihydronaphthalenes (m/z 131, 145, ...) and tetrahydronaphthalenes (m/z 133, 147 ...). Figure 2 is the parent spectrum of m/z 131 which characterizes the entire series of alkyl dihydronaphthalenes in the coal sample. Similar parent spectra (m/z 129 and 133) were obtained for the other two series as well. These identifications were confirmed through daughter spectra. The daughter spectrum of the first member of each series were compared with and matched authentic naphthalene, dihydronaphthalene and tetralin. The higher homologs of each series were identified through comparison of the fragmentations of their daughter spectra with the previous (lower) series member. These three series of ions account for 25% of the ion current over the temperature range studied. Identification of these three series are consistent with the significant polymethylene character observed in the NMR. Considering the reactive nature of the potassium/crown ether reagent these series probably all represent the presence of alkylnaphthalenes in the original coal. (The dihydro- and tetrahydro- compounds probably represent reduced alkylnaphthalenes). The reduction products identified are indicative of polymethylene linkages in hydrocarbon rich pockets in the original coal sample which must be accounted for in the processing of coal.

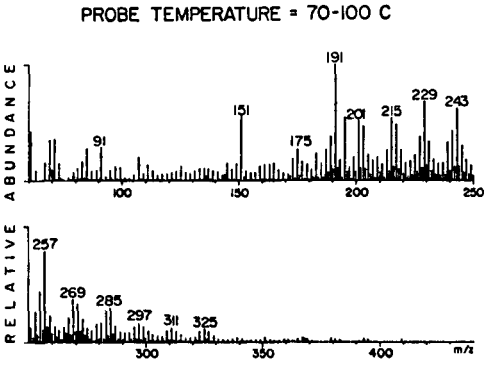

Figure 1

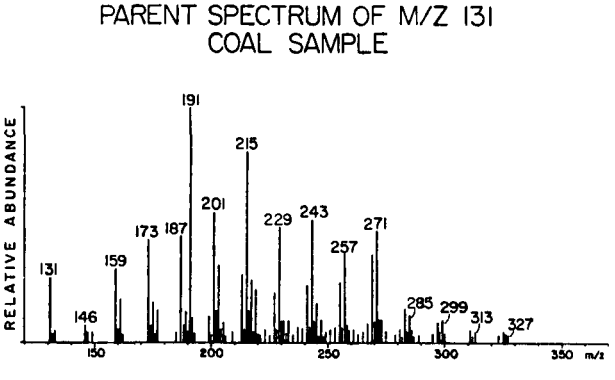

Figure 2

ANALYSIS OF POLYCYCLIC TERPANES AND AROMATIC STEROIDS BY MS/MS

F.M. Bockhoff, A.J. Barwise, R.J. Drozd, and M.A. Kruge
Standard Oil Research Center
4440 Warrensville Rd., Warrensville Hts., Ohio 44128

The distribution of biological marker compounds in sediments and petroleums is indicative of thermal maturity and depositional conditions. Geological samples are routinely analyzed for these compounds by GC/MS. Mass chromatograms of the m/z 191 and m/z 217 ions are especially useful for profiling the triterpane and sterane distributions, respectively. However GC/MS is limited by overlapping components and by the inability of high MW components to elute from the column. Additional information on components of interest may be obtained by the use of direct probe/MS/MS.

Samples of saturate and aromatic hydrocarbon fractions were derived from Thornton bitumen, which was obtained from the Silurian Niagara dolomite of Illinois. Each fraction was analyzed by direct probe/MS/MS on a Finnigan TSQ mass spectrometer. The probe temperature was ramped up to 400 deg C and electron impact ionization was used. Argon collision gas was used with a collision region pressure of about 1 millitorr. The saturate fraction was analyzed for pentacyclic triterpanes and the aromatic fraction was analyzed for monoaromatic and triaromatic steroids.

Pentacyclic triterpanes have the general structure shown in Figure 1. Their EI spectra exhibit a prominent ion at m/z 191 with structurally relevant ions at m/z 369 and at an additional mass containing the portion of the molecule with the alkyl chain group. These three fragments can be used to characterize this general structure and are also found in the daughter ion MS/MS spectra of molecular ion species. The MS/MS experiment measuring the parents of m/z 191 can be used to profile the pentacyclic triterpane molecular ion distribution in the saturate fraction. Figure 2 shows the parents of m/z 191 with molecular ions observed up to m/z 902. This corresponds to a formula of C65 H122. This is a significant improvement over GC/MS, which can detect this series up to only C40. Figures 3 and 4 show the daughter ion spectra of two members of the series. M/z 482 corresponds to C35 H62 and m/z 777 corresponds to C56 H108. Both of the daughter spectra exhibit the three characteristic ions of pentacyclic triterpanes.

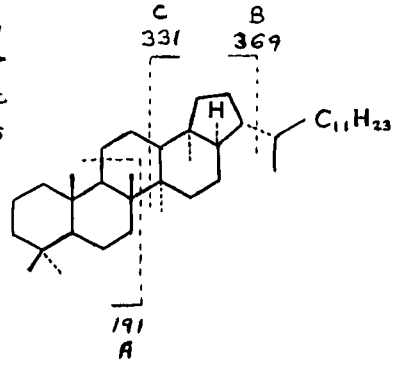

Figure 1
Pentacyclic Triterpanes

Figure 2

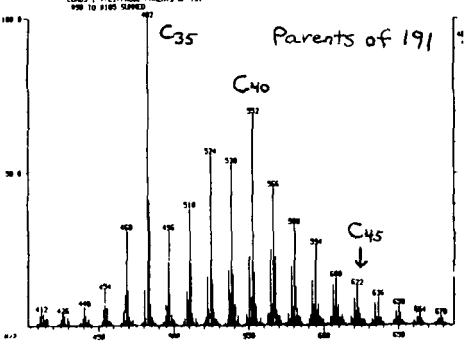

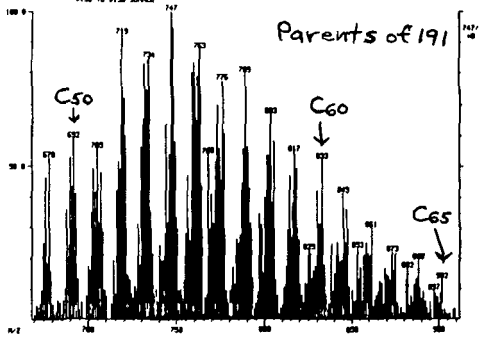

Figure 3

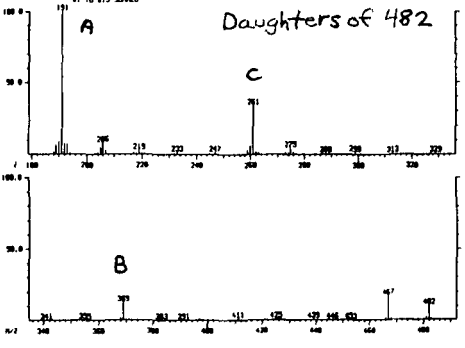

Figure 4

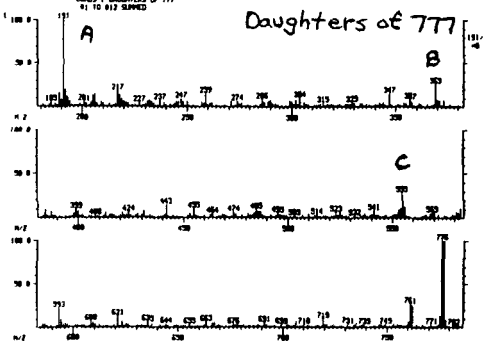

The EI spectra of monoaromatic steroids and triaromatic steroids contain characteristic ions at m/z 253 and m/z 231 respectively. The aromatic fraction was analyzed for parents of m/z 253 and parents of m/z 231. The resulting spectra indicate that the molecular ions in each case could extend up to at least C45. The daughter ions of a typical monoaromatic steroid at m/z 394 and a typical triaromatic steroid at m/z 372 do not appear to have ions that could be used to easily characterize either steroid class. Even the m/z 253 and 231 ions do not stand out from the large number of fragment ions observed.

In conclusion, the presence of pentacyclic triterpanes up to C65 H122 is indicated in the saturate fraction by MS/MS. Structural features are present in their daughter spectra. Monoaromatic and triaromatic steroids appear to be present in the aromatic fraction up to at least C45. However, their daughter spectra do not contain many distinct structural features.

NEGATIVE ION CHEMICAL IONIZATION MASS SPECTROMETRY FOR ISOMER DIFFERENTIATION OF NITROGEN HETEROCYCLIC, SULFUR HETEROCYCLIC AND MIXED NITROGEN-SULFUR HETEROCYCLIC COMPOUNDS

J. A. Campbell, G. Kallos, E. Hermann, D. Patrick, M. LaPack, M. L. Lee, and R. N. Castle
Dow Chemical U.S.A., Midland, MI

In many instances, the biological activity of many substituted organic compounds is isomer dependent. In view of this fact, techniques that can assist in distinguishing isomers become extremely important. Typical electron impact and positive ion chemical ionization mass spectrometry, in most cases, provide little or no additional information in terms of isomer differentiation. The major strengths of negative ion chemical ionization (NICI) mass spectrometry are (1) higher sensitivity for the detection of specific molecules as compared to other ionization processes and (2) higher selectivity for isomer differentiation for some examples (1).

We have utilized the Finnigan 4600 GC/MS with PPINICI (pulsed positive ion negative ion chemical ionization) to study isomers of the following type using methane and 5% oxygen/methane mixtures (with Townsend Discharge).

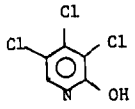

A

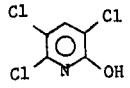

B

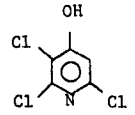

C

The experimental conditions were as follows:

Column:	DB-5, 15 m x 0.25 mm, 1 μm film thickness
Temperatures:	injector - 250°C
	source - 150°C
	transfer line - 275°C
Pressures:	ionizer 0.29 torr
	high vacuum 1.2 x 10^{-5} torr

With the oxygen/methane mixture, the Townsend Discharge conditions were: ionizer 0.68 torr, high vacuum 4.2 x 10^{-5} torr, source temperature 150°C, discharge current 70 μA, discharge voltage 1.3 kV.

Figure 1 illustrates the NICI (methane) spectra for these three compounds. The electron impact mass spectra are virtually identical, as well as the positive ion chemical ionization mass spectra. The NICI spectra show some interesting ions corresponding to $(M+CH_2)^-$. It has been postulated that these unusual ions reflect the participation of free radicals in the overall negative ionization process as has been described in other NCI studies of high electron affinity, double bond containing molecules (1,2). The major ion observed for molecule A is m/z 181 $(M-HCl)^-$ and for C m/z 162 $(M-Cl)^-$. The results seem to indicate that when a substituent is para to the nitrogen as in A & C, the intensity of $(M+CH_2)^-$ is very low. For molecule B, on the other hand, the major ion observed is the $(M+CH_2)^-$ adduct ion. We have also observed this in the study of various dichloropyridinols as well. The NICI spectra (oxygen/methane) indicate intense ions at m/z 192 $(M+CH_2-Cl+O)^-$

Other compounds we have examined include the following:

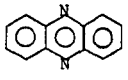

D

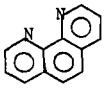

E

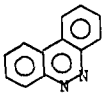

F

For compound F, the major ion observed is m/z 180 (M^-). In contrast, the major ions for E are m/z 179 $(M-1)^-$ (100) and 180 (M^-) (30) and for D the ions are m/z 180 (M^-) (100) and m/z 179 $(M-1)^-$ (70).

Compounds containing a single nitrogen were also examined. The major peak in the NICI spectrum for acridine is m/z 179 (M^-) and for 5,6-benzoisoquinoline, the major ion observed is m/z 178 $(M-1)^-$.

Other novel structures containing both sulfur and nitrogen were studied also.

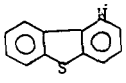

G

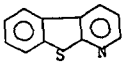

H

A 5% oxygen/methane mixture was utilized and compound H actually shows oxygen incorporation at m/z 200 $(M+O)^-$, whereas molecule G does not. The NICI (methane) spectra are practically identical.

Negative ion chemical ionization mass spectrometry has proven to be quite useful for isomer differentiation for nitrogen heterocyclic, sulfur heterocyclic, and mixed nitrogen-sulfur heterocyclic compounds.

REFERENCES

1. L. J. Sears, J. A. Campbell, and E. P. Grimsrud, ASMS Meeting, San Diego, CA, 1985, p. 89.

2. C. N. McEwen and M. A. Rudot, JACS, 103, 4343, 1981.

Figure 1. Negative Ion Chemical Ionization(Methane) Mass Spectra For The Trichloropyridinols.

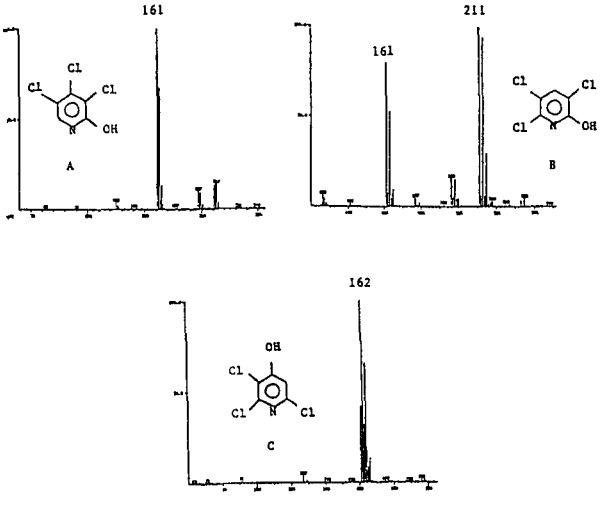

MASS SPECTROMETRIC STUDIES OF THE PUMPING OF METHANE BY THERMAL CRACKING AND GETTERING

EDWARD K. PANG
GTE ELECTRICAL PRODUCTS
LIGHTING RESEARCH AND ENGINEERING
DANVERS, MA 01923

The objective of this work is to study a method by which methane can be pumped efficiently. It is interesting to study such a mechanism because methane can be problematic in many vacuum systems, for example, the vacuum system in a fusion reactor device.

EXPERIMENTAL

The experimental system is shown schematically in Figure 1. A well-degassed, high-purity tungsten coil at about 2300°C and a well-activated zirconium/aluminum alloy getter are used for cracking and pumping, respectively. Deuteriated-methane is used for the experiment in order to distinguish the reaction products from gases evolved from the system. A non-bakeable all-glass inlet system connected to a quadrupole mass spectrometer is constructed for analysis. The system is coupled with a quartz reaction chamber and a quartz lamp envelope in which a high-purity tungsten coil is housed.

RESULTS

1. Degassing of tungsten coils reveals that hydrogen and carbon monoxide are the main constituents to be evolved from the coils.
2. Degassing of Zr/Al alloy getter shows that hydrogen and carbon monoxide are the major gases given off by the getter. The degassing curve (Figure 2) shows a maximum around 410°C, at which the getter begins to sorb the evolved gases.
3. Temperatures of the tungsten coil rise continuously with increasing voltages (Figure 3). Tungsten starts to evaporate significantly in vacuum at operating voltage of 115 volts.
4. With the tungsten coils at about 2300°C, CD_4 is converted into D_2, using the quadrupole mass spectrometer to monitor CD_4 and D_2 partial pressures. The CD_4 partial pressure clearly drops while D_2 partial pressure rises simultaneously (Figure 4).
5. The tungsten coils are operated at about 2300°C and the getter at about 400°C while exposing to a known quantity of CD_4. CD_4 and D_2 are monitored simultaneously. CD_4 partial pressure drops continuously, but D_2 partial pressure does not rise appreciably (Figure 5).

CONCLUSIONS

1. A tungsten coil operating at high temperatures can effectively crack methane into hydrogen.
2. A tungsten coil/alloy bulk getter combination provides a practical means to pump methane. Methane is cracked into hydrogen which is subsequently sorbed by the Zr/Al alloy bulk getter.

REFERENCES

1. J.L. Cecchi and R.J. Knize, *J. Vac. Sci. Technol.A*, 2, 1214(1984).
2. M.H. Mendelsohn and D.M. Gruen, *J. Less-Common Met.*, 74, 449(1980).
3. E.K. Pang, P.L. Fortucci, and V.D. Meyer, *Anal. Chem.*, 57, 2995(1985).

4. E.K. Pang and W.M. Keeffe, Proceedings of the 33rd Annual Conference on Mass Spectrometry and Allied Topics,pp.802-803(1985).
5. H. Winters, *J. Chem. Phys.*, 62, 2454(1975).
6 H. Winters, *J. Chem. Phys.*, 64, 3495(1976).
7 M.P. Lopez and J.M.L. Sancho, *Surface Science*, 77, L167(1978).

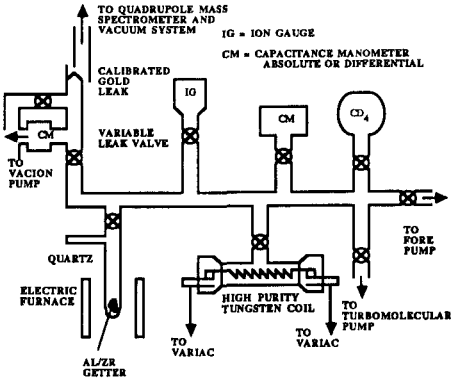

FIGURE 1 SCHEMATICS OF EXPERIMENTAL SYSTEM

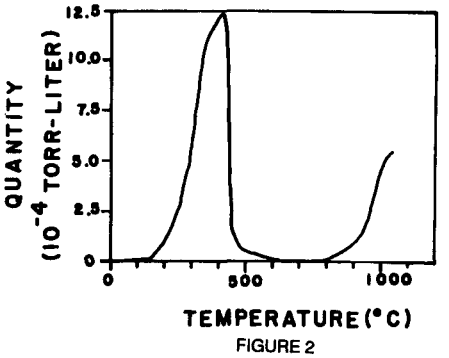

FIGURE 2

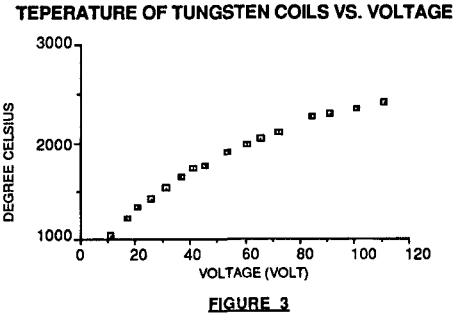

FIGURE 3

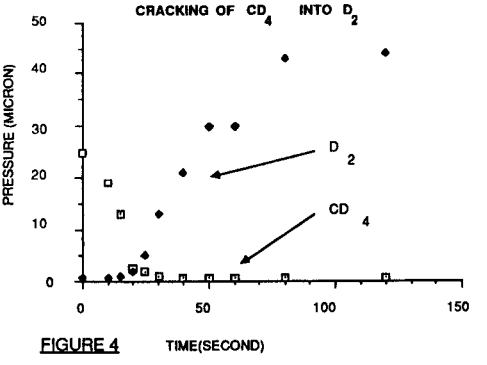

FIGURE 4

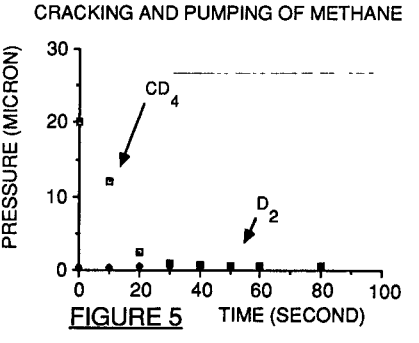

FIGURE 5

ANALYSIS OF A DIESEL FUEL SEDIMENT BY HIGH RESOLUTION MASS SPECTROMETRY:

R. D. Grigsby, S.-Y. Tang, and G. P. Sturm, Jr.; National Institute for Petroleum and Energy Research, P. O. Box 2128, Bartlesville, OK 74005

The formation of sediments in fuels has deleterious consequences in the operation of diesel and turbine engines, particularly in military applications where long storage periods may be required. In this investigation, a sediment from a marine diesel fuel was analyzed by high resolution mass spectrometry.

Low-energy electron impact (ca. 10 eV) was used for ion formation, and two methods of sample introduction were employed. In the first, the sediment was heated to 300 deg C, and the volatiles were evaporated into a 300 deg C all-glass expansion volume inlet. Approximately 37 % by weight of the sample was vaporized. Spectra were recorded at a resolution of 40,000 and peaks were detected at least to m/z 300. Molecular ions containing various combinations of C, H, O, N, and S could be identified.

In the second method, the sediment was introduced by probe microdistillation from a cooled/heated quartz probe (1). Linear programming at 10 deg C/min was used over a temperature range from -40 to +600 deg C. About 70 % of the sample by weight was vaporized. A resolution of 10,000 was used. Molecular ions containing C, H, O, N, and S could be identified in a mass range extending to approximately m/z 700. A spectrum recorded at a probe temperature of 490 deg C is shown in Figure 1.

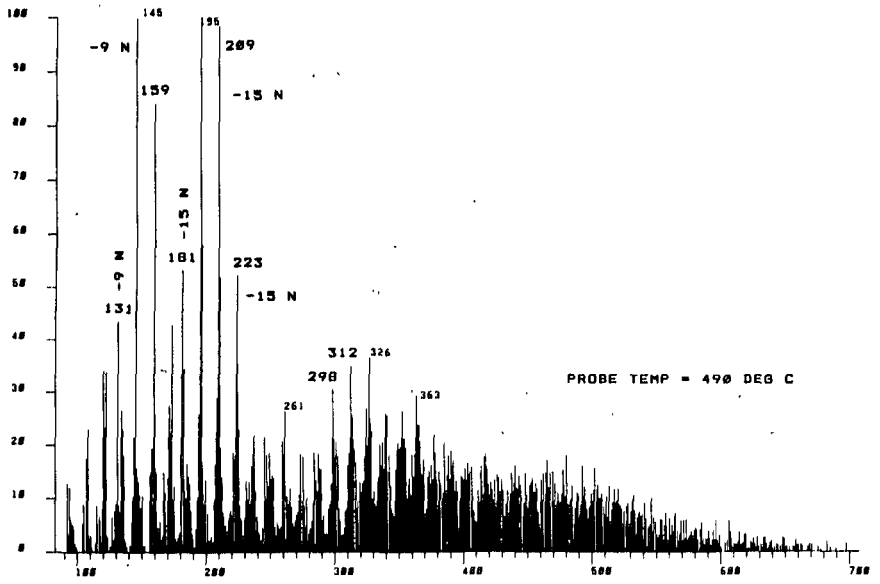

Figure 1. Spectrum of a diesel fuel sediment recorded at a probe temperature of 490 deg C.

Intense peaks in the spectrum are identified with C(n)H(2n+z)N homologs with z numbers of -9 and -15. At a temperature of 490 deg C, these compounds probably arise from thermal decomposition of the sediment.

By plotting the ion current vs. temperature for molecular ions detected in the probe microdistillation spectra, it is possible to estimate which compounds are desorbed at the lower probe temperatures and which are formed by pyrolysis at the higher temperatures. Figure 2 shows the ion current plots for m/z 184 (-16 S) in the series C(n)H(2n+z)S and m/z 108 (-6 O) in the series C(n)H(2n+z)O. The fact that m/z 184 appears in the spectra recorded at probe temperatures below 175 deg C indicates that the corresponding compound is weakly bound to the sediment. On the other hand, m/z 108 is a predominant ion in the spectra recorded between 300 and 600 deg C, indicating that the corresponding compound is much more tightly bound in the sediment.

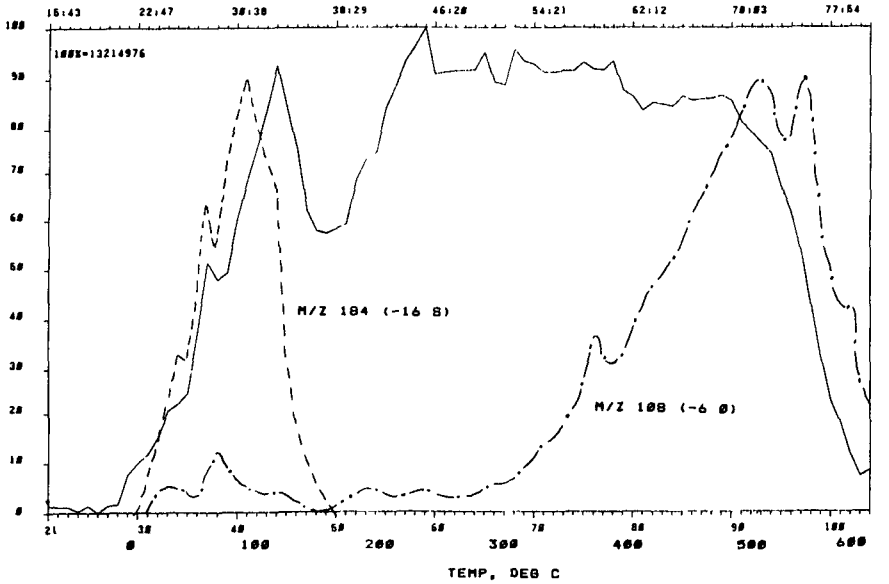

Figure 2. Plot of ion current vs. temperature for m/z 184 and m/z 108 in the spectra of a diesel fuel sediment.

Both sets of data are consistent with the presence of a polymer having monomers and other low molecular weight molecules adsorbed on its surface. Compounds such as C(12)H(8)S, MW = 184, desorb from the surface at the lower probe temperatures, but other compounds, such as C(7)H(8)O, MW = 108, desorb at the higher probe temperatures because they are covalently bonded in the polymer itself.

Appreciation is expressed to the Defense Fuel Supply Center, DFSC-TB, Cameron Station, Alexandria, VA and the Mobility and Fuels Research and Development Program, Navy Energy Office, Office of the Chief of Naval Research through the Defense Logistics Agency, Contract No. DLA600-84-5050, for support of this work.

1. Schronk, L. R.; Grigsby, R. D.; Scheppele, S. E., Anal. Chem., 1982, 54, 748-755.

MASS SPECTROMETRIC ANALYSIS OF COAL EXTRACTS BEFORE AND AFTER TREATMENT WITH MOLTEN CAUSTIC

Charles E. Schmidt, Louise J. Douglas, and Bruce R. Utz, DOE/PETC, P.O. Box 10940, Pittsburgh, PA 15236

The sulfur and ash content of coal can be reduced by treatment with molten caustic (KOH/NaOH).[1] To date, development of chemical coal-cleaning concepts based on alkali treatment have proceeded on the basis of limited fundamental knowledge of the chemistry involved. The objective of this research is to develop a better understanding of the chemical interaction of molten alkali with coals, and the nature of the sulfur species before and after alkali treatment.

A high-sulfur Iowa coal (Bevier seam) was extracted with pyridine. A sulfur-rich concentrate was obtained from the aromatic portion of the extract by ligand exchange chromatography.[2] This sulfur-rich fraction of the Bevier coal extract was analyzed by low-voltage, high-resolution mass spectrometry (LVHRMS); high-resolution gas chromatography employing a sulfur-specific flame photometric detector; and combined gas chromatography-mass spectrometry (GC/MS). Fifteen heterocyclic sulfur compounds were positively identified by GC/MS and by matching retention times in co-chromatography determinations with authentic standards. All of the sulfur compounds identified in the Bevier extract by gas chromatography contained a thiophenic ring. The results of the LVHRMS analysis of the sulfur-rich fraction from the Bevier coal extract indicated the possible presence of non-thiophenic sulfur compounds, such as thiols, sulfides, and disulfides, in addition to the aforementioned thiophenic organosulfur species.

Model compound studies[3] have shown the desulfurization of benzothiophene by molten hydroxide occurs in two steps (as shown below). First, initial cleavage of the thiophene ring results in the loss of a one-carbon fragment, leaving an aromatic thiol (or salt of an aromatic thiol). Subsequently, sulfur is lost from the aromatic thiol, resulting in the formation of toluene.

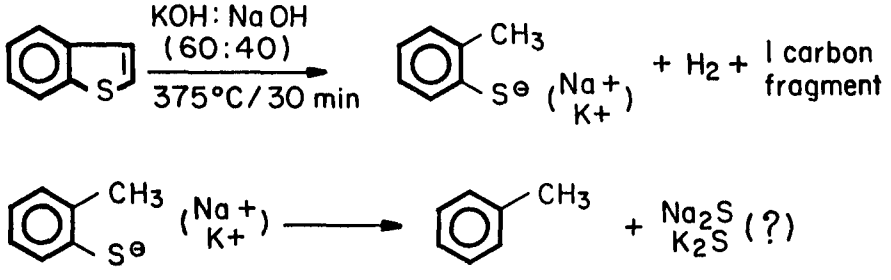

Portions of the pyridine extract from the Bevier coal were treated with molten caustic to remove organosulfur compounds. In one experiment, a 60/40 wt% mixture of KOH/NaOH was reacted with the pyridine extract at 375°C for 30 minutes. The pyridine extract was also treated with 100% molten KOH at 400°C for 3 hours. The two chemically treated Bevier extracts, as well as the untreated pyridine extract, were analyzed by LVHRMS employing direct-insertion probe techniques to facilitate the analysis of the high-molecular-weight components in the extracts.

Ten chemical classes were determined by LVHRMS techniques for the two caustic-treated extracts and for the original pyridine extract (Table 1). The sulfur-containing components, having the general formula C_xH_yS, decreased from 16% for the raw-coal extract to 5.5% for the extract treated with a 60/40 wt% mixture of molten KOH/NaOH at 375°C. The C_xH_yS species, shown by GC/MS to be composed mainly of thiophenic structural types, were further reduced to 2.7% in the extract chemically cleaned with 100% KOH at 400°C for 3 hours. The amount of hydrocarbons (C_xH_y) decreased from 32% in the untreated pyridine extract to 16% for the extract treated with the 60/40 wt% mixture of molten hydroxide. This decrease was contrasted by a

large increase in the level of hydrocarbons (58%) for the extract treated solely with KOH at 400°C. The amount of single-oxygenated compounds (C_xH_yO) also varied considerably upon treatment of the Bevier coal pyridine extract with caustic under different conditions. The reaction of the extract with the 60/40 melt at 375°C resulted in a doubling of the C_xH_yO class, from 21% for the untreated extract to 44% for the treated extract. The concentration of oxygenates (C_xH_yO) remained about the same for the reaction of 100% KOH with the pyridine extract at 400°C for 3 hours.

In this study of chemically treating a coal extract at two different conditions with molten hydroxide, thiophene sulfur compounds were shown to decrease, corroborating model compound studies involving benzothiophene treatment with molten caustic. For the two reaction conditions employed, side reactions forming oxygenated compounds seemed more prevalent in the treatment of the extract with 60/40 wt% mixture of molten KOH/NaOH at 375°C. In general, the levels of the sulfur-containing classes all decreased upon caustic treatment with a 60/40 mixture of KOH/NaOH at 375°C for 30 minutes, while those of the non sulfur-containing oxygenates all increased. The lower levels of organosulfur compounds in the extract treated with only KOH at 400°C for 3 hours are a result of the more severe reaction conditions. Additionally, the increase in the amount of hydrocarbons for the 3-hour treatment is in accordance with the model compound product distribution.

Table 1. Comparison of Chemical Class Distributions for the Bevier Coal Extract and Molten-Caustic-Treated Bevier Coal Extracts as Determined by LVHRMS

Chemical Class	Coal Extract	Treated Coal Extract	
		KOH/NaOH (60/40)	KOH
C_xH_y	32	16	58
C_xH_yO	21	45	23
$C_xH_yO_2$	7.6	14	3.3
$C_xH_yO_3$	2.3	0.92	0.16
C_xH_yS	16	5.6	2.7
C_xH_yOS	9.4	6.0	1.2
$C_xH_yO_2S$	3.6	3.8	0.95
C_xH_yN	3.9	3.7	9.6
C_xH_yNO	2.8	4.9	1.6
$C_xH_yNO_2$	1.1	0.53	---

REFERENCES

1. Masciantonio, P.X., Fuel 1965, 44, 269.

2. Nishioka, M.; Campbell, R.M.; Lee, M.L.; Castle, R.M. Fuel 1986, 65, 390.

3. Utz, B.R.; Soboczenski, S.K.; Friedman, S. Preprint, Am. Chem. Soc. Div. Fuel Chem. 1985, 30(2), 35.

MOLECULAR BEAM MASS SPECTROMETRIC STUDIES OF COAL DUST-AIR FLAMES

Frank T. Greene and J. Eugene O'Donnell
Midwest Research Institute
Kansas City, Missouri 64110

This research was undertaken to determine the behavior of alkali metal and other species implicated in ash fouling and slagging problems during low rank coal combustion. These studies are conducted in premixed laminar coal dust-air flames. Coordinated vapor phase, coal/ash and temperature measurements permit the determination of the behavior of the various species during the combustion process in both the vapor and condensed phases. The gaseous species are identified and their partial pressures measured as a function of distance along the flame axis using molecular beam mass spectrometry (MBMS). Coal/ash samples are also collected as function of distance along the flame axis and analyzed by SEM/EDX, ESCA, and other techniques. Flame temperatures are measured using a thermocouple technique.

Profiles of a number of gaseous species have been obtained for lean pulverized Decker-N_2-O_2 and Beulah-N_2-O_2 flames. These flames had measured temperatures which ranged from about 1500°C just above the "reaction zone" to less than 800°C at large distances from the burner. For the alkali metals the only significant gaseous species observed to date are sodium and sodium hydroxide. Profiles of these two vapors indicate that a very large excess of Na(g) is produced early in the combustion of both Beulah and Decker, and that this excess is very short lived and decays either by reactions to form undetected gaseous sodium species or by conversion into a condensed phase, but not by reaction with O_2 and H_2O to form NaOH(g). Downstream of the Na(g) "spike" the partial pressures of Na(g) and NaOH(g) are relatively constant. This is consistent with existing thermochemical data. Samples of Beulah lignite were ion exchanged with acetic acid and calcium acetate. When ion exchanged coal was burned, the sodium spike was reduced by more than a factor of 100. This suggests that the spike is produced from organically bound sodium, and probably accompanies the decarboxylation of the low rank coal.

* This work was supported by the U.S. Department of Energy, Grand Forks Project Office, under Contract No. DE-AC18-81FC10287.

THE APPLICATION OF THERMOSPRAY LC/MS AND THERMOSPRAY LC/MS/MS TO THE ANALYSIS OF EPOXY COMPOSITE MATERIALS

J. F. Litton, S. J. Selover, M. R. Wakefield, and T. M. Tuell
Lockheed Missiles & Space Co., Inc., Sunnyvale, CA 94088-3504

INTRODUCTION:

Epoxy composites have found widespread use in aerospace and other industries. Composite materials have the strength, weight, and thermal properties necessary to be of use in aircraft and other applications. For many years, high performance liquid chromatography (HPLC) has been used as a quality control tool to monitor the composition of the resin portion of these composite materials. A great number of components that elute from the liquid chromatograph remain unidentified. The identity of adducts, reaction products, and additives would aid in evaluation of resin properties and processing variables.

Thermospray liquid chromatography/mass spectrometry (TSPLC/MS) is an appropriate method for characterizing epoxy resin portions of composite materials. The liquid chromatographic eluent can be identified by mass spectrometry, enabling characterization of the components. Thermospray liquid chromatography/mass spectrometry/mass spectrometry (TSPLC/MS/MS) provides additional structural information on the components of epoxy composite materials. We have used TSPLC/MS and TSPLC/MS/MS to characterize two different types of epoxy composites.

EXPERIMENTAL:

All experiments were performed on a Finnigan MAT TSQ mass spectrometer fitted with a thermospray LC/MS interface. An Altex gradient liquid chromatograph was used for the liquid chromatographic separations. A 5m Altex Ultrasphere-ODS column and acetonitrile-water gradients were utilized at a flow rate of 0.8 m L/min. A 0.1M solution of ammonium acetate was added to the eluate at a flow rate of 0.8 m L/min. The thermospray vaporizer temperature was ramped from 145°C to 120°C during the liquid chromatography gradient. The mass spectrometer was operated in the scanning mode for TSPLC/MS experiments and in the daughter ion mode for TSPLC/MS/MS experiments.

RESULTS AND DISCUSSION:

Epoxy composites of two different types (shown below) were examined.

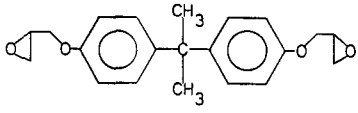

Diglycidyl Bisphenol A (DGBA)

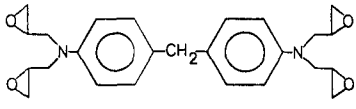

Tetraglycidyl Methylene Dianiline (TGMDA)

TSPLC/MS of DGBA based epoxy resins show the major component to correspond to DGBA, molecular weight 340. The predominant mass peak occurs at $(M + NH_4)^+$, m/z 358. Other components observed included isomers of DGBA as well as hydrolyzed forms and chlorohydrin forms of DGBA. An adduct of DGBA with the catalyst dicyandiamide was also observed.

TSPLC/MS of TGMDA based epoxy resins show the major components to be TGMDA, molecular weight 422, and diamino diphenyl sulfone (DDS), molecular weight 248. The predominant mass peaks occur at $(M + 1)^+$. Other components observed include isomers of TGMDA, hydrolyzed forms and chlorohydrin forms of TGMDA, and monoamino diphenyl sulfone.

TSPLC/MS/MS was used to obtain additional structural information about the components of epoxy composites. TSPLC/MS/MS was applied to TGMDA based epoxy resins to confirm the structure of the components and to differentiate between isomers.

One difficulty with the TSPLC/MS as presently set up lies with the inability to detect later eluting peaks. The thermospray buffer (0.1M ammonium acetate) is added after the column and mixes with the eluate. The components, soluble in 100% acetonitrile, come out of solution in this new mixture and are not detected.

Future work will involve the characterization of other composite systems. In addition, other ionization methods will be investigated to analyze later eluting components.

PEPTIDE SEQUENCING BY COMPUTERIZED INTERPRETATION OF FAB MASS SPECTRA

Terry D. Lee, Vickie Spayth and Kassu Legesse

Beckman Research Institute of the City of Hope
Division of Immunology, Duarte, CA 91010

The objective of this research was to determine the extent that peptide primary structure can be determined from amino acid composition and FAB mass spectral data. A necessary tool for our approach to this problem was a computer program which derives possible amino acid sequences from mass spectral fragment ions. The basic operation of the program was described previously (33rd Conf. ASMS p. 266). Since then, certain additions have been made to the program and it has been tested on a variety of known and unknown peptide spectra.

In a number of instances, the computer interpretation program failed to yield a unique most probable sequence. The capability was added to calculate for each, user selected sequence on the list, all the members for each of the twelve even electron fragment ion series. These are then compared with the prominent ions in the spectrum and all matches are listed. This provides a convienient means of evaluating the degree to which a given sequence fits a spectrum and greatly reduces the number of spectra that have ambiguous interpretations.

The interpretation program has been used to evaluate a number of data acquisition parameters inclucing: sample amount, purity, matrix compound, and scan type. Generally, sample amounts in the range of 1-20 nmole yield directly interpretable spectra. At lower sample levels, background subtraction or B/E linked scans are needed to reduce interference from the matrix. Daughter ion spectra obtained with as little as 150 pmole have been successfully sequenced using the interpretation program. A glycerol matrix is generally preferred for nmole amounts of sample. Dithiothreitol : dithioerythritol is preferred for B/E linked scan spectra in the 100 to 500 pmole range. The use of this method to sequence an unknown peptide is illustrated on the opposite page.

In conclusion, peptides can be sequenced by a combination of amino acid analysis and FAB mass spectrometry using sample amounts comparable to those required by most automated Edman microsequencers. Presently, the length of a peptide which can be accomidated by the interpretation program is limited to ten residues by the size of the computer (HP1000, 128K memory, 10 Mbyte disk storage). This method should be applicable to peptides up to twenty residues.

Sample: Tryptic fragment of Fibronectin

Purification: Sephadex G25
HPLC Vydac C18, TFA buffer

Amino Acid Analysis (0.1 of Sample):

Glx	150.6 pmole
Tyr	143.0
His	86.9
Arg	147.0

Mass Spectrum (0.1 of Sample):
Matrix - DTT:DTE (5:1), CSA (6 mM)
MH+ = 603
MW = 602
Glx = Gln

Composition: QYHR

B/E Link Scan Spectrum (0.1 of Sample):
Matrix - DTT:DTE (5:1), CSA (6 mM)
Accumulation - 40 Scans
Cycle Time - 25 s

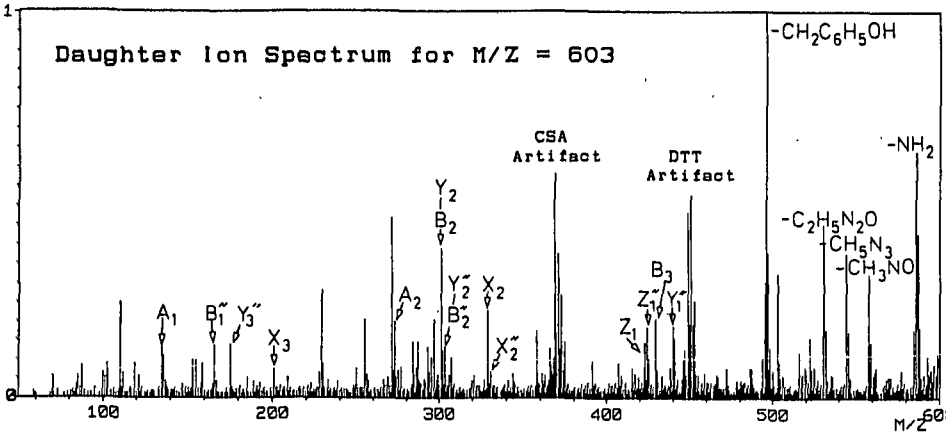

Prominent Ions in Spectrum:

559	495	407	303	230	135
558	453	391	301	229	121
557	451	375	297	228	119
544	450	373	295	209	112
532	449	371	293	201	110
531	441	369	287	185	103
530	440	366	284	175	102
522	429	358	273	166	101
516	425	331	271	159	100
503	424	329	255	155	87
497	423	321	250	153	85
496	415	307	233	136	70

Computer Derived Sequences:

Sequence	Score	Matches
*YHQR	33	15
HYQR	27	16
YHRQ	17	14
HYRQ	14	15
HRYQ	11	10
YRHQ	10	8

Matches With Predicted Fragments:

Sequence	A	A"	B	B"	C	C"	Z	Z"	Y	Y"	X	X"
YHQR	XX			XX			XX	XX		XX		
15	XX		XX	XX					XX	XX	XX	XX
			XX							XX	XX	
HYQR	XX	XX			XX	XX	XX	XX				
16	XX		XX	XX					XX	XX	XX	XX
			XX							XX	XX	
YHRQ	XX			XX			XX	XX		XX		
14	XX		XX	XX					XX	XX	XX	XX
	XX											XX
HYRQ	XX	XX			XX	XX	XX	XX				
15	XX		XX	XX					XX	XX	XX	XX
	XX											XX
HRYQ	XX	XX			XX	XX	XX	XX				
10							XX	XX				
	XX											XX
YRHQ	XX			XX			XX	XX		XX		
8										XX		
	XX											XX

Studies on the Kinetics of Hydrolysis of Large Polypeptides by Endopeptidases Using FABMS

William E. Seifert, Jr. and Richard M. Caprioli
Department of Biochemistry and Molecular Biology
and the Analytical Chemistry Center
The University of Texas Medical School at Houston
Houston, Texas 77030

Historically, the kinetics of action of endopeptidases have been studied using a number of analytical methods, primarily spectrophotometric techniques in which a substrate analog or small, chemically-modified peptide is used in order to provide a compound which can be easily followed with time during the incubation with the enzyme. These substrate analogs usually allow the reaction to be followed with a high degree of specificity and high sensitivity. For example, a routine method for assaying trypsin is to use tosylarginine methyl ester (TAME) or benzoylarginine ethyl ester as the substrate and to follow the hydrolysis of the ester by UV spectrophotometry. Although, these substrate analogs provide for a convenient assay for endo-peptidases, the kinetic constants which can be obtained using these assays may not truly represent the kinetic parameters which would be obtained using natural polypeptide substrates.

The development of fast atom bombardment mass spectrometry has provided a powerful analytical tool for biomolecular analysis in studies involving peptides, as well as many other ionic constituents in aqueous solutions. FABMS provides the biochemist a high degree of molecular specificity, high sensitivity, and analyses of peptide mixtures without chemical derivatization. Previous work from this laboratory (1) has shown that FABMS can be used to determine the kinetic constants for the hydrolysis of small peptides by trypsin. The purpose of the present study is to determine whether these same techniques can be used to determine the kinetic constants for the hydrolysis of large polypeptides (8 - 30 amino acid residues), and whether kinetic data can be obtained from peptides with multiple sites of cleavage.

Three peptides were investigated as substrates for trypsin, angiotensin II, insulin B-chain, and glucagon. Angiotensin II is a relatively small polypeptide having 8 amino acid residues and a molecular weight of 1046 daltons. It has one tryptic site of cleavage, between Arg(2) and Leu(3). Insulin B-chain and glucagon are large polypeptides having 30 and 29 residues and molecular weights of 3495 and 3481, respectively. Each has more than one possible site of cleavage by trypsin. Each of these peptides were incubated with TPCK-treated trypsin at pH 8.1 in the presence of Ca++. The concentration of enzyme ranged from 0.2 - 8 uM, depending on the substrate. Substrate concentrations were varied from 0.25 - 8.0 mM. Aliquots were removed with time, quenched with oxalic acid, and kept frozen until analyzed by FABMS.

FABMS analyses were performed on the aliquots using a Kratos MS-50RF mass spectrometer equipped with a FAB. Data acquisition was accomplished using the multi-channel analysis mode of the DS90 data system. The enzymatic reaction was followed by monitoring the intensities of the ions corresponding to the M+H ions of the tryptic fragments. Ion intensities were measured from the average of 8-10 mass spectra. Kinetic constants were determined from the initial rates determined from the decrease in the relative intensity of the M+H ion of the native peptide.

Insulin B-chain has two possible sites of cleavage, between Lys(29)-Ala(30) and Arg(22)-Gly(23). The rate of hydrolysis of the Arg(22)-Gly(23) bond was found to be much greater than the Lys(29)-Ala(30) bond, therefore, kinetic constants were determined for the hydrolysis of the Arg-Gly bond. The ratio kcat/Km, a measure of the affinity of the enzyme for the substrate, was found to be much greater for insulin B-chain Arg-Gly bond than for the Arg-Leu bond of angiotensin II. Kinetic studies using glucagon as substrate were precluded due to

incomplete solubility of the polypeptide at the pH required for trypsin. However, analysis of the time course of the reaction indicated that a relative rate of hydrolysis could be determined: Arg(17)-Arg(18)$\gg$Lys(12)-Tyr(13)$>$Arg(18)-Ala(19).

Table I. Kinetic Constants for the Tryptic Hydrolysis of Peptides

Peptide		Km, mM	k_{cat}, s^{-1}	k_{cat}/K_m, $M^{-1}\ s^{-1}$
Angiotensin II		1.83	0.83	455
Insulin B-chain (R-G)		0.65	37.6	57492
M-R-F-A	(1)	1.9	7.1	3622
F-M-R-F(NH_2)	(1)	5.9	69.0	11600
F-R-S-V	(1)	4.8	99.2	20667
G-G-R-G(NH_2)	(2)			3500
A-V-R-G(NH_2)	(2)			18000
L-V-R-G(NH_2)	(2)			21600
G-V-R-A(NH_2)	(2)			25900
Ac-G-R-V-OMe	(3)	3.6	20	5600
Ac-G-P-R-V-OMe	(3)	4.7	290	62000

(1) Caprioli and Smith, Anal. Chem., 1986, 58, 1080-1083.
(2) Liem and Sheraga, Arch. Biochem. Biophys., 1974, 160, 333-339.
(3) Lobo et al., Arch. Biochem. Biophys., 1976, 177, 235-244.

ASSIGNMENT OF DISULFIDE BOND LINKAGES IN SYNTHETIC N-POMC (1-28) BY FAB-MASS SPECTROMETRY:

J.A. Chakel and J. Ramachandran, Genentech, Inc., 460 Point San Bruno Blvd., South San Francisco, CA 94080

M. Nixon, Univ. of California, San Francisco, CA 94143.

G. Feistner, J.D. Barchas and K.F. Faull, Dept. of Psyciatry and Behavioral Sciences, Stanford University Medical Center, Stanford, CA 94305.

Proopiomelanocortin (POMC) is a 267 amino acid precursor from which corticotropin (ACTH) and lipotropin (LPH) are generated by proteolytic processing in the anterior pituitary gland. ACTH is preceeded by a sequence of 103 amino acid residues which forms the amino terminal segment of POMC. Estivariz et al. [Nature 297: 419-422 (1982)] reported that an N-terminal peptide of the POMC molecule corresponding to the first 28 residues [N-POMC (1-28)] isolated from human pituitaries may be involved in regulating adrenal growth. In order to investigate the role of this peptide in adrenal physiology, we have synthesized N-POMC (1-28) by solid phase peptide synthesis. N-POMC (1-28) contains four cysteine residues at positions 2, 8, 20 and 24 which can generate three different pairs of disulfide bridges upon oxidation.

Earlier work has shown that FAB-MS is useful for the structure elucidation of disulfide bonded peptides [1-4]. Digestions of synthetic N-POMC (1-28) were performed first with S. aureus V8 protease and then trypsin to cleave the peptide between the cysteine residues as shown in the sequence below:

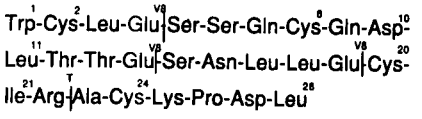

Three different sets of disulfide linked peptides are possible (Table 1). A FAB-MS spectrum of 10 µg of the crude enzymatic digest in thioglycerol (Figure 1) yielded strong protonated molecular ions at mass 1193.6 and 1500.2. This established the disulfide bond linkage in the oxidized synthetic N-POMC (1-28) as cysteines 2 to 24 and cysteines 8 to 20. All of the reduced peptide fragments (Table 2) also exhibited protonated molecular ions, with the exception of the tripeptide (20-22) which was below the mass range used. The cleavage by V8 protease at the Glu-Cys bond (19-20) is incomplete as evidenced by the peak at mass 947.5 which corresponds to the peptide (15-22). Covalently linked dimer ions for the cysteine containing peptides (1-4) and (23-28) are observed at 1097.5 and 1289.7 dalton, respectively. Also covalent attachment ions of thioglycerol to the cysteine containing peptide fragments (1-4), (5-14) and (23-28) are seen at 656.2, 1217.6 and 752.3 dalton, respectively. No dimer ion or thioglycerol adduct ion was observed for the non-cysteine containing peptide fragment (15-19). The strong signal in Figure 1 at 1149.6 dalton represents a loss of carbon dioxide from the 1193.6 ion (verified by high resolution measurement).

In summary, FAB-MS provided a rapid means of elucidating the disulfide bond arrangement in oxidized synthetic N-POMC (1-28) and these results confirm the disulfide arrangement in the natural N-POMC peptides.

This work was supported in part by CA-16417 (J.R.) and N.I.D.A. DA-01207 (J.D.B.)

1) A.M. Buko and B.A. Fraser, Biomed. Mass Spectrom. 12, 577 (1985).
2) H.R. Morris and P. Pucci, Biochem. Biophys. Res. Commun. 126, 1122 (1985).
3) F.W. Crow and W.K. Duholke, 33rd Ann. Conf. on Mass Spectrometry and Allied Topics, San Diego, California (1985).
4) R. Yazdanparast, P.C. Andrews, D.L. Smith and J.E. Dixon, Anal. Biochem. 153, 348 (1986).

Table 1. Disulfide Linked Peptides

S-S Bond Linkage	Expected Peptide	MH^+ (daltons)
2 - 24	(1-4) + (23-28)	1193.5
8 - 20	(5-14) + (20-22)	1499.6
2 - 8	(1-4) + (5-14)	1658.6
20 - 24	(20-22) + (23-28)	1034.5
2 - 20	(1-4) + (20-22)	938.4
8 - 24	(5-14) + (23-28)	1754.8

Table 2. Reduced Peptides

Peptide	MH^+ (daltons)
(1-4)	550.2
(5-14)	1111.4
(15-19)	575.3
(20-22)	391.2
(23-28)	646.3

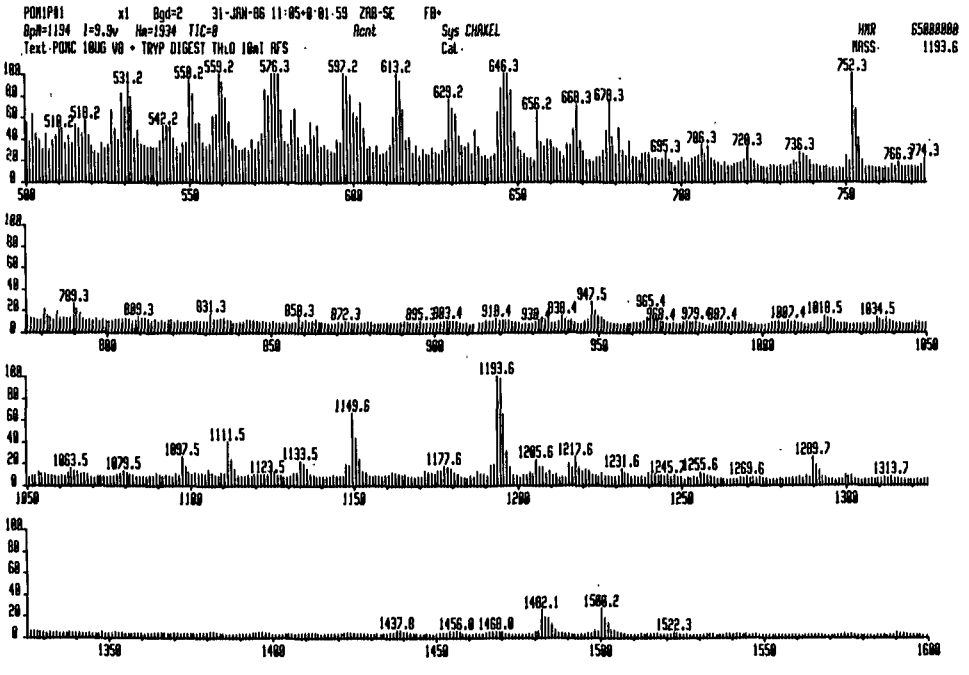

Figure 1.

ANALYSIS OF PEPTIDE MIXTURES AND TRYPTIC DIGESTS BY GRADIENT LIQUID CHROMATOGRAPHY/THERMOSPRAY MASS SPECTROMETRY, F.W. Crow and R.H. Robins, Spectroscopy Development, Product Control, The Upjohn Co., Kalamazoo, Mich.

OBJECTIVES: Characterize protein digests by Thermospray(TSP) LC/MS. A common method to determine or verify protein structure is enzymatic cleavage followed by analysis by LC. The TSP/MS interface can provide the researcher with rapid molecular weight information for each LC peak. For TSP to be applicable it must provide this information over a large LC gradient range.

EXPERIMENTAL: rBSt(fig.1) + trypsin incubated over night @ R.T. Column = BakerBond C-4 on Varian 5560 LC. Gradient: 100% to 55% A @ 0.5%/min. where A = 0.1% TFA/water, B = 0.1% TFA/ACN. Quench at this point with TFA to obtain data on oxidized form (fig.2). React with dithiothreitol prior to quenching for reduced form data. On line UV detection acquired using high pressure cell. Thermospray interface by Finnigan on Finnigan 4600.

TSP/MID DATA (fig 3-4): Multiple ion detection is sensitive and selective for those ions which are monitored, in this case fragments from oxidized rBSt. The crowded region near the void volume is clarified by use of TSP. 5 early eluting peaks are detected. Later in the chromatogram where the UV trace shows one peak, 3 peaks are detected. Unknown, unexpected peaks or peaks arising from incomplete digestion are, of course, not detected.

TSP/FULL SCAN DATA (fig. 5-6): In full scan the S/N is less than in MID, but the information content is higher. By using the UV retention information one can locate useful data about LC peaks where the peak is not obvious from inspection of the TIC. Peptides having a molecular weight greater than the instrument mass range (1700amu), can be detected by the presence of their doubly protonated (double charged) ions. Note the sodium adduct at +11 amu.

TEMPERATURE EFFECTS : The temperature of the TSP vaporizer tip has been found to be critical in optimizing for analysis of peptides. The figure compares the total ion current and molecular ion current from a peptide as a function of vaporizer temperature. Sensitivity goes up but molecular weight information drops and vanishes. The ions at high temp. do not contain much structural information.

DISULFIDE BRIDGED PEPTIDES (7-8): In proteins such as rBSt, where there are more than two cysteines, detection of disulfide bridged compounds provides significant data about protein folding. The MID data indicates the presence of a disulfide bridged peptide T-23+25. Incomplete digestion is common and is seen in the full scan data by the occurrence of two partly cleaved products: T-23+24,25 and T-23,24+25.

CONCLUSIONS: We have shown that Thermospray LC/MS: 1. is effective over a wide gradient range, 2. shows full scan sensitivity <2nmoles of injected peptide, 3. with MID is ca. 100 times more sensitive, 4. shows no evidence of signal suppression when analyzing mixtures, 5. disulfide bridged peptides remain intact under TSP conditions, allowing one to probe protein secondary structure.

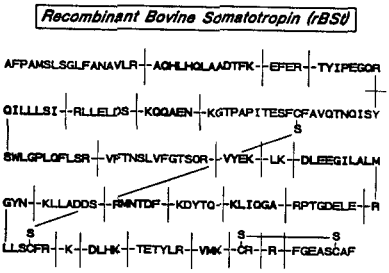

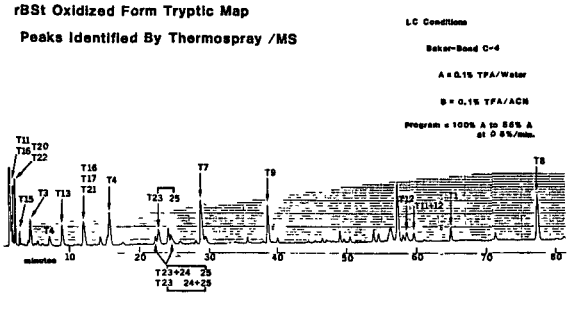

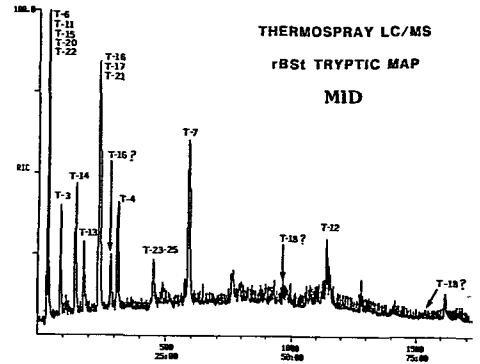
THERMOSPRAY LC/MS
rBSt TRYPTIC MAP
MID
RIC
T-6
T-11
T-15
T-20
T-22
T-16
T-17
T-21
T-7
T-16 ?
T-14
T-3
T-4
T-13
T-23-25
T-18 ?
T-12
T-18 ?

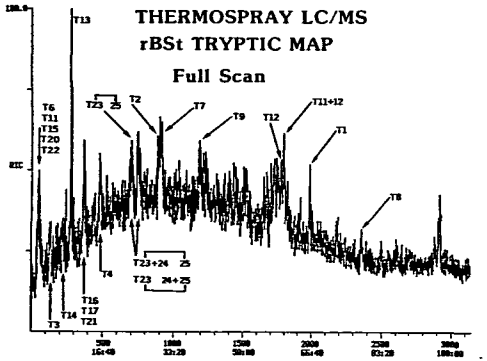
THERMOSPRAY LC/MS
rBSt TRYPTIC MAP
Full Scan
RIC
T13
T6
T11
T15
T20
T22
T23 25
T2
T7
T9
T12
T11+12
T1
T8
T4
T3
T14
T16
T17
T21
T23+24 25
T23 24+25

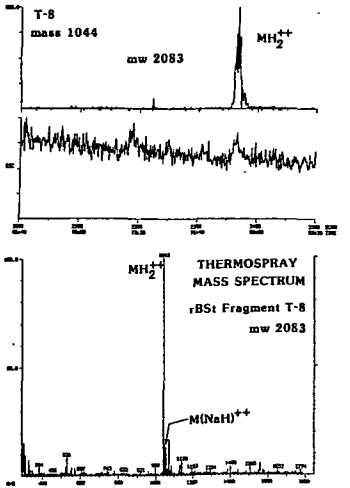
T-8
mass 1044
mw 2083
MH_2^{++}
THERMOSPRAY
MASS SPECTRUM
rBSt Fragment T-8
mw 2083
$M(NaH)^{++}$

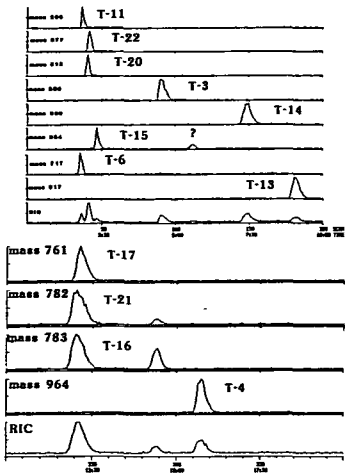
T-11
T-22
T-20
T-3
T-14
T-15
?
T-6
T-13
mass 761
T-17
mass 782
T-21
mass 783
T-16
mass 964
T-4
RIC

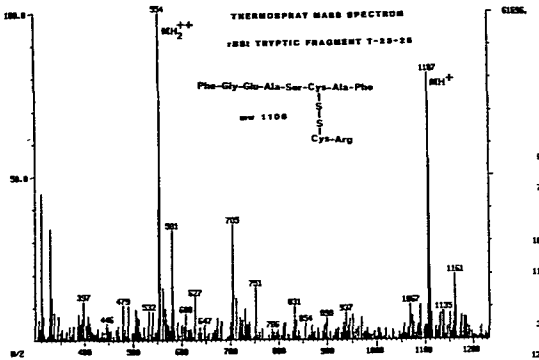
THERMOSPRAY MASS SPECTRUM
rBSt TRYPTIC FRAGMENT T-23-25
Phe-Gly-Glu-Ala-Ser-Cys-Ala-Phe
mw 1106
Cys-Arg
MH_2^{++}
MH^+
m/z

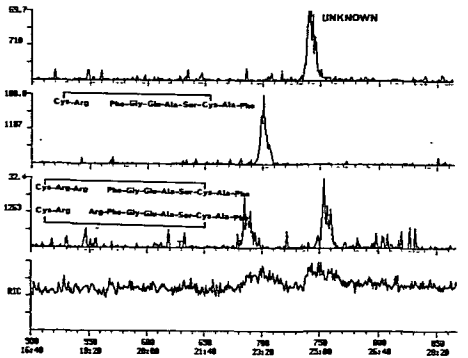
UNKNOWN
Cys-Arg
Phe-Gly-Glu-Ala-Ser-Cys-Ala-Phe
Cys-Arg-Arg
Phe-Gly-Glu-Ala-Ser-Cys-Ala-Phe
Cys-Arg
Arg-Phe-Gly-Glu-Ala-Ser-Cys-Ala-Phe
RIC

STRUCTURAL ANALYSIS OF TISSUE PLASMINOGEN ACTIVATOR GLYCOPROTEIN BY MASS SPECTROMETRY,

Steven A. Carr, Gerald D. Roberts and Walter Johnson, Department of Analytical, Physical and Structural Chemistry, L-940, SmithKline and French Laboratories, Swedeland, PA 19479

Cardiovascular and cerebrovascular disease resulting in fibrin clot formation is the leading cause of death in industrialized countries. Plasmin, the body's natural fibrin clot dissolving substance, is released from the inactive proenzyme plasminogen by specific enzymes termed plasminogen activators which effect the cleavage of a single peptide bond in this molecule. The best known activators of plasminogen are streptokinase, urokinase and tissue plasminogen activator (tPA). The former two proteins either induce systemic bleeding or are immunogenic and, therefore, are of limited therapeutic value. In contrast, full activation of tPA is achieved only upon binding to fibrin and thus activation of plasminogen occurs only at the clot. Studies of the clinical usefulness of tPA are now being made possible by the production of this protein using recombinant methods.

The primary structure of tPA has been deduced by sequencing of the gene and partially confirmed by conventional protein sequence analysis. tPA consists of 527 amino acids and possesses four potential sites of attachment of sugar to Asn (Fig. 1). Using the FAB peptide mapping strategy developed by Biemann and others we have now verified the structure of recombinant tPA produced in mammalian cell culture (1). Our specific goals were to establish that miscoding had not occurred, to determine the nature and location of posttranslational modifications such as carbohydrates and to compare our protein with standards of tPA obtained from a human Bowes melanoma cell line.

Several nanomoles of tPA was reduced and carboxymethylated and then digested (in separate experiments) with a variety of proteolytic enzymes including trypsin, chymotrypsin and Staph. V8. The peptides and their sequence locations were identified by FAB MS and computerized analysis of the data. The mixtures were also subjected to three cycles of manual Edman degradation and the resulting mixtures of attenuated peptides were analyzed by FAB MS after each cycle. This provides additional confirmation of the identity and sequence location of many of the "mapped" peptides. In addition a number of previously unidentified, major peptide-related signals were unambiguously assigned to the sequence of tPA in this manner.

The ability to acquire and sum raw data over wide mass ranges, with a sufficient number of points across each peak, (often more than 32,000 pts across the spectrum) is essential to obtain good coverage of the primary sequences of large proteins such as tPA, (for example, see Fig. 2). Two factors mitigate for this need; first, total ion yields for peptides generally decrease with mass and second, peptide signals in mixtures may be competitively suppressed. In the present study signal averaging was used to acquire all data above mass 3000, and to confirm scan data obtained from m/z 2500-3000.

Using the strategies outlined above, 76% of the primary sequence of tPA was rapidly confirmed. All peaks observed in the FAB MS data for two batches of tPA produced under different conditions could be mapped to the deduced primary sequence. No unmatched peptide signals indicative of miscoding errors were detected. Comparison of our recombinant protein with standards of human Bowes melanoma cell tPA by FAB MS strongly indicates that they have identical primary structures.

Total coverage of the protein was increased to 89% using a new procedure for locating sites of Asn-linked carbohydrates in glycoproteins by MS (2). The strategy involves treatment of the glycoprotein with peptide:N-glycosidase F (before or after denaturation and proteolytic digestion) which releases Asn-linked sugars and converts the Asn at the former attachment site to an Asp. The released peptide encompassing the former glycosylation site is mass spectrometrically unique from the nonglycosylated counterpart since it weighs one mass unit more (iAsn = 114, iAsp = 115). Thus, new peaks observed in the FAB mass spectra of the glycosidase treated samples correspond to specific sites of glycosylation. Using this procedure we have established that three of the four potential glycosylation sites in tPA (Asn 117, 184 and 448) have sugar attached, while the fourth site (Asn 218) does not (Fig. 1).

In summary we have demonstrated that the primary structures of glycoproteins may be readily confirmed and sites of attachment of carbohydrate rapidly identified using peptide and carbohydrate mapping by FAB MS. Using this new procedure for locating sites of Asn-linked carbohydrates in glycoproteins by MS, we have found that three of the four potential glycosylation sites in tPA have sugar attached while the fourth site does not. Removal of the sugars also enables observation of peptides from the glycosylation sites, thereby further increasing the percentage of the primary sequence that is mapped.

1. Carr, S.A. manuscript in preparation.
2. Carr, S.A. and Roberts, G.D. Anal. Biochem. 1986 (in press).

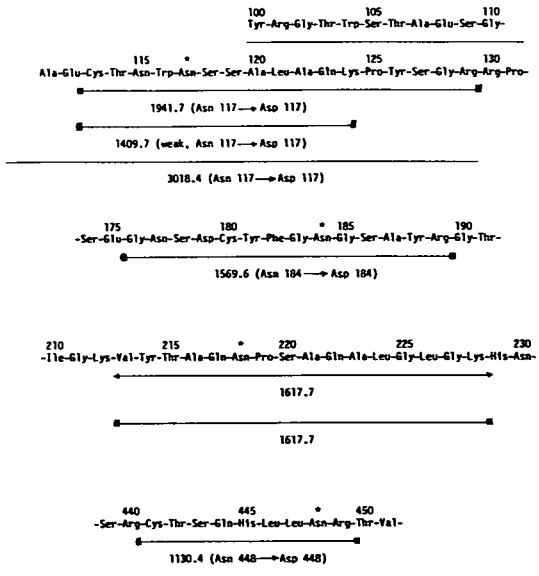

Figure 1. Partial sequences around the four potential Asn-linked glycosylation sites of tPA. Peptides identified in the FAB MS experiments are indicated as follows: —— = trypsin, ←——→ = trypsin/Staph. V8 and ■——■ = peptide:N-glycosidase F digestion of the trypsin/Staph. V8 digest. Masses correspond to the observed (M+H)+.

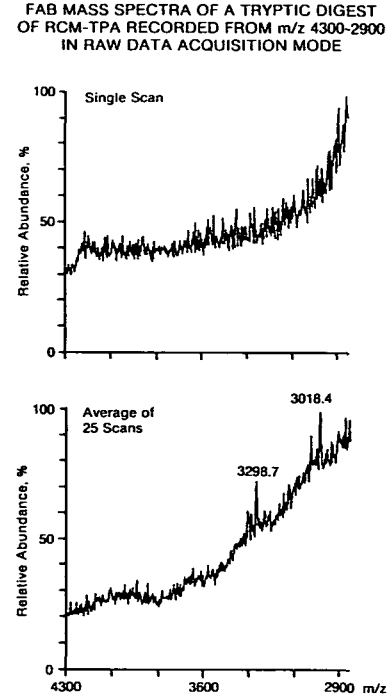

Figure 2.

MS AND MS/MS IN THE STRUCTURAL ANALYSIS OF THIOREDOXINS AND INVERTASE

R.S. Johnson, W.R. Mathews, and K. Biemann, Department of Chemistry, Massachusetts Institute of Technology, Cambridge, MA 02139

Thioredoxins are hydrogen carrier proteins that are involved in a number of oxidation-reduction reactions (1). They have been found in organisms ranging from archaebacteria, bacteria, and plants to mammalian systems; therefore, structural studies may provide some insight into evolutionary relationships. In this study, the primary structure of the thioredoxins isolated from Chlorobium thiosulfatophilum has been determined using a combination of methods involving Edman degradations, FABMS, and MS/MS. After enzymatic or chemical cleavage of this protein, the molecular weights of the resulting mixtures of peptides were determined by FABMS. Sequence information for these peptides was obtained via Edman degradations followed by molecular weight determinations of the truncated peptides; the difference in molecular weight of each peptide in the mixture before and after each Edman step indicates the successive N-terminal amino acids in each peptide. As sequence information accumulated, homology between Chlorobium and E. coli thioredoxins began to appear and was of use in positioning individual peptides within the protein sequence. Recent acquisition of a tandem high resolution mass spectrometer, the JEOL HX110/HX110 (2), has made it possible to obtain B/E linked scans of mass selected, collisionally activated peptide ions. Thus, it became possible to confirm or correct the sequence deduced from the Edman/FABMS data. The methodology employed was not able to distinguish between leucine and isoleucine. In only one position was this ambiguity resolved, where an ion was observed 28 amu below the A_6 ion in Fig. 1, indicating the prescence of isoleucine at the sixth amino acid from the N-terminus of that peptide, which corresponds to position 107 of the intact thioredoxin. No other tryptic peptides gave suitable A series ions from which this differentiation could be made, hence methods for inducing the formation of A ions are currently underway.

Invertase from yeast (Saccharomyces cerevisiae) is a sucrose cleaving enzyme that exists in extracellular (external) and intracellular (internal) forms. The known DNA sequence codes for both forms, the difference being that external invertase is glycosylated whereas internal invertase is not (3). Edman/FABMS techniques, as used for Chlorobium thioredoxin, were used on internal invertase to confirm the DNA sequence. From the DNA sequence, fourteen potential glycosylation sites containing the sequence -Asn-Xxx-Ser(or Thr)- can be deduced for external invertase. It remained to be determined which of these potential glycosylation sites are actually glycosylated.
Endo- -N-acetylglucosaminidase H (Endo H) treatment of external invertase removes all of the sugar moieties except for single N-acetylglucosamines (NAcGlc), which remain attached to the protein, thus marking the glycosylation sites. These sites can then be located by comparing the MH^+ ions of tryptic digests of internal and Endo H treated external invertase. Peptides from Endo H treated external invertase with an attached NAcGlc will have MH^+ ions 203 amu higher than the corresponding peptide ions from internal invertase. In one case, an ion was observed to have a mass that corresponded to a tryptic peptide, as deduced from the DNA sequence, plus 3 X 203; ie, three NAcGlc. Since this peptide contains four potential glycosylation sites, it was further cleaved with chymotrypsin to produce smaller peptides containing single glycosylation sites, which were then examined using FABMS.

1. A. Holmgren, Ann. Rev. Biochem., 54, 237 (1985)
2. Y. Kammei, Y. Itagaki, E. Kubota, H. Kunigiro, and M. Ishihara, 33rd Ann. Conf. on Mass. Spect. and Allied Topics, May 26-31, 1985, San Diego, CA, p. 855
3. R. Taussig, M. Carlson, Nucleic Acids Res., 11, 1943 (1983)

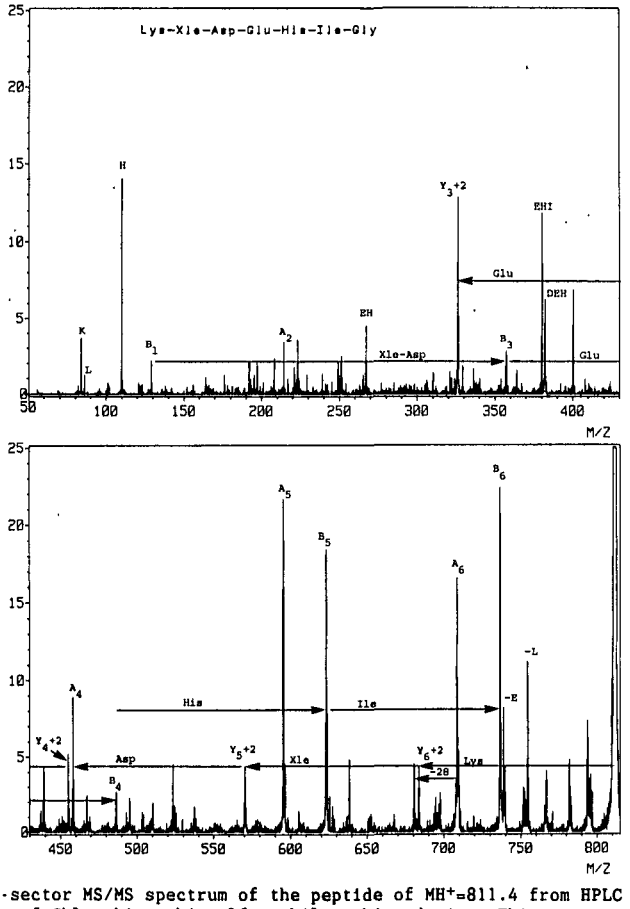

Figure 1: Four-sector MS/MS spectrum of the peptide of MH^+=811.4 from HPLC fraction 2 of a tryptic digest of Chlorobium thiosulfatophilum thioredoxin. This mass spectrum was recorded at 30 Hz filtering and 50% parent ion reduction with helium as a collision gas. MS1 and MS2 resolution was 1:1000 with a scan time from m/z 50 to 811.4 of 1.4 minutes. The sample matrix consisted of glycerol/DTT/DTE/HOAc. Ions marked L and H are immonium ions of leucine/isoleucine and histidine; the ion marked K is due to cyclization and loss of ammonia from lysine immonium ions; the ions -E and -L are due to losses of glutamic acid and leucine/isoleucine side chains from the parent ion; EH, EHI, and DEH are internal cleavage ions; and the remaining nomenclature is that of Roepstorff and Fohlman.

Acknowledgments - This work was supported by NIH Division of Research Resources grant GM05472 (to K. Biemann). The MIT Mass Spectrometry Facility is supported by NIH Division of Research Resources grant RR00317 (to K. Biemann). We thank Dr. Bob B. Buchanan, University of California, Berkeley for the thioredoxin sample, and Dr. Frank Maley, New York State Department of Health, Albany, NY for the invertase samples.

Tandem Mass Spectrometry of Oligopeptides

S.A. Martin and K. Biemann
Department of Chemistry, Massachusetts Institute of Technology
Cambridge, MA 02139 U.S.A.

The advent of soft ionization techniques such as fast atom bombardment (FAB) made it possible to characterize underivatized polar, polyfunctional molecules by mass spectrometry. The characteristic features of this technique are: the very abundant yield of ions associated with the molecular weight, ions at every mass asssociated with the matrix and depending on several factors including amino acid composition fragment ions of much lower abundance which are related to the sequence of the peptide. In an effort to better understand the relationship between the peptide desorbed and the fragment ions produced, and thus increase the ability to determine the correct sequence of unknown peptides, we had previously reported a detailed interpretation of the mass spectra of more than 30 known peptides. This investigation has now been extended to a study of their daughter ions employing tandem mass spectrometry. In addition to examining the fragmentation resulting from ion dissociation the relationship of various fragment ions has been clarified. This is possible because all ions observed in a linked scan must be associated with the parent ion which has been selected at greater than unit resolution. A JEOL HX110/HX110 tandem high resolution four sector mass spectrometer of EBEB geometry is being employed in this work.

The type and extent of peptide fragmentation in the MSMS mode and the effect of various amino acids on the fragmentation series observed is illustrated by a comparison of Fibrinopeptide A Human, M_r 1535.7 and [des-Arg^{16}]-Fibrinopeptide A, M_r 1379.6 (Figure 1). The MSMS spectrum of Fibrinopeptide A (Fig 1A) is dominated by C-terminal fragments, however, this shifts to the ion series associated with the N-terminal when the C-terminal arginine is removed (Fig 1B). Both spectra exhibit strong immonium ions for Leu, Glu and Phe and in the spectrum of Fibrinopeptide A an abundant series of ions (W) corresponding to the Y series minus the N-terminal side chain are observed. To date, the largest peptide run in the MSMS mode for which almost complete sequence information was obtained is Adrenocorticotropic Hormone (ACTH) Human Clip (18-39) M_r 2464.2. In this example the entire A series with the exception of A_{39}(Gly) was observed. Examination of the fragmentation patterns of peptides in the MSMS mode, such as those shown in Figure 1, has resulted in several general observations concerning the characterization of peptides in this mode. These include:

1. Increase coverage of the sequence and signal to noise in the MSMS mode
2. Enhancementment of particular ion series based on the position of basic amino acids in the sequence.
   i. A series if N-terminal basic amino acid i.e. Arg.
   ii. B series if no basic site at or near the N-terminus.
   iii. Y series if basic amino acid at or near C-terminus.
3. Characterization of Leu/Ile based on the side chain losses from the corresponding A series ion, A_n-42 for Leu and A_n-28 for Ile. In addition, characteristic side chain losses for A series ions are observed for Glu/Gln (A_n-58/A_n-57) and Asp/Asn (A_n-44/A_n-43).
4. Observation of a strong ion series in the MSMS mode which corresponds to the Y series in which the N-terminal R group has been lost. This is referred to as the W series.
5. Predominant ion series in MSMS mode are A, B and Y compared to C, Y and Z in the MS mode.

These data demonstrate that peptides of relatively high molecular weight, 2500 daltons, will undergo collision induced dissociation yielding complete or almost complete sequence information. Furthermore, the molecular ion of interest can be selected at unit resolution or better and the resulting daughter ion spectrum mass assignments will be accurate to within 0.3 daltons of the calculated value over the entire mass range for peptides below mass 2200 with slightly greater errors at higher mass.

Acknowledgement. The M.I.T. Mass Spectrometry Facility is supported by Grant No RR00317 from the NIH Division of Research Resources.

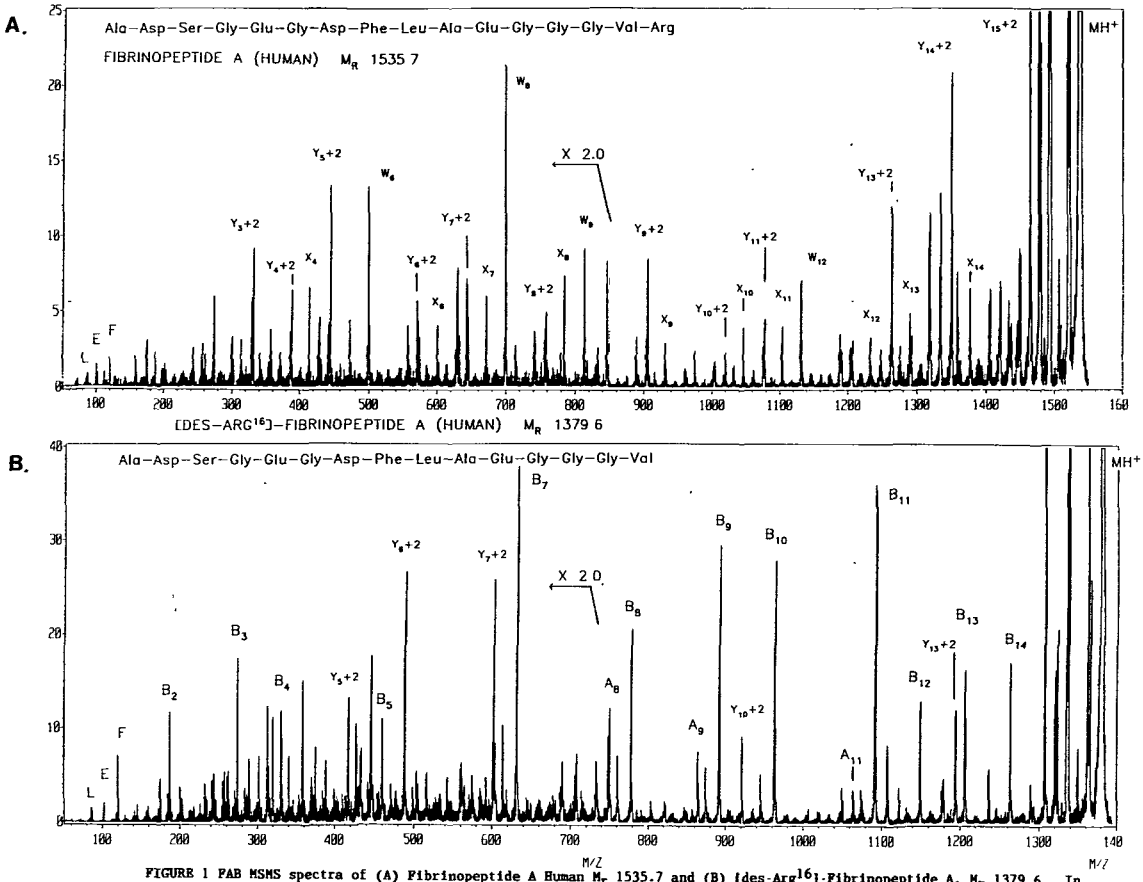

FIGURE 1 FAB MSMS spectra of (A) Fibrinopeptide A Human M_r 1535.7 and (B) [des-Arg16]-Fibrinopeptide A, M_r 1379.6. In the MSMS spectrum of Fibrinopeptide A (A) all the abundant ions are associated with the C-terminus. In addition to a strong Y series, another series labeled W is observed. This series consist of the Y series ion in which the side chain of the N-terminal amino acid has been lost. Removal of the C-terminal basic amino acid, Arg, produces the MSMS spectrum (B) in which the majority of the abundant ions are associated with the N-terminus. Both (A) and (B) show strong immonium ions for Leu, Glu and Phe.

ACCURATE MASS MEASUREMENTS IN FAB-MS OF AN UNKNOWN, SECRETIN-LIKE PEPTIDE (MW3110).

G. J. Feistner, B. N. Green*, K. F. Faull, K. Tatemoto, and J. D. Barchas; Department of Psychiatry and Behavioral Sciences, Stanford Medical Center, Stanford, CA 94305, and VG Analytical Ltd, Manchester M23 9LE, England.

Precise mass measurements of peptides in FAB-MS with an accuracy of better than 5 ppm have been obtained up to mass 2680 [1, 2]. Encouraged by these reports we tried to elucidate the elemental composition of a variant of secretin, a 27 amino acid containing peptide of MW 3110, previously isolated from porcine intestinal extracts [3]. Since the variant is N-blocked and its amino acid composition (and sequence) is identical to that of secretin except for a missing histidine, the modification is thought to involve the N-terminal histidine of secretin (MW 3054). A partial liberation of histidine from the variant can be achieved under vigorous hydrolysis conditions. Such a modified histidine does not appear to have been described in the literature [4]. An accurate mass measurement with a standard deviation of 5 ppm or 15 mmu would allow us to distinguish, for example, between C_3H_4O (56.026 u) and C_2O_2 (55.990 u; equivalent to 2 formyl groups) as the modifying group(s).

To achieve this goal, we have tried to secure the precise mass of the variant by three different methods: 1) manual peak matching, 2) electrical scans in the multichannel analyzer mode over a narrow mass range ("software peak matching") using CsI and secretin as external and internal standards, respectively, and 3) software peak matching using two authentic peptides as internal standards, thereby eliminating the need for an external standard and allowing to scan over a smaller window.

1) Manual peak matching was performed on a mixture of secretin and the variant (7.5 µg each) in thioglycerol. The corresponding $[M+H]^+$- and the first C-13 isotope peaks were matched against each other yielding values of 55.9857 u and 55.9888 u, respectively.

2) The VG software peakmatching procedure was applied to the same peptide mixture. Centroiding was achieved at 50% peak height. The systematic error resulting from external calibration with CsI appeared to be about 100 mmu, however, this does not effect the mass difference between corresponding isotope peaks of the two peptides. The values found for the M+1, M+2, and M+3 peaks were 56.0225 u, 55.9858 u, and 55.9646 u, respectively, which corresponds to a mean value of 55.9909 u and a standard deviation of 29 mmu.

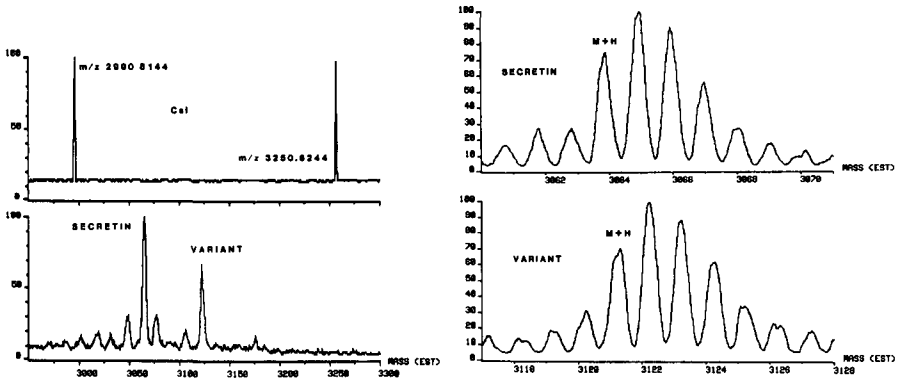

3) To run the software peakmatching program with two internal standards, a second reference compound had to be found. In this mass range this was not trivial, and we are grateful to Ding Chan (Peninsula Lab. Inc., Belmont, CA) for generously providing a sample of somatostatin 8010 (MW 3129). Close in molecular weight to the secretin variant, it allowed us to scan over a narrow mass range. However, somatostatin contains a cystine bridge, which becomes partly reduced during the FAB-measurement resulting in loss of intensity for any single quasimolecular isotope peak of this peptide. Another problem encountered during this approach was the different hydrophobicity of the three peptides. Since somatostatin is less surface-active than secretin (calculated according to [5]), it tended to be suppressed

unless an excess of somatostatin was used; we were successful with a mixture of 6 µg each of the secretins and 40 µg somatostatin. The M+1 and M+2 peaks of each reference compound in the four possible combinations were used to mass measure the M+n (n=1-4) peaks of the variant, thus yielding a set of 16 accurate mass values for the unknown and subsequently 16 values for the histidine modification. The mean value was calculated to 55.9735 u with a standard deviation of 21 mmu. Calculated accurate masses for the isotope peaks of the reference compounds were kindly provided by L. Tokes and K. Chan (Syntex, Palo Alto, CA).

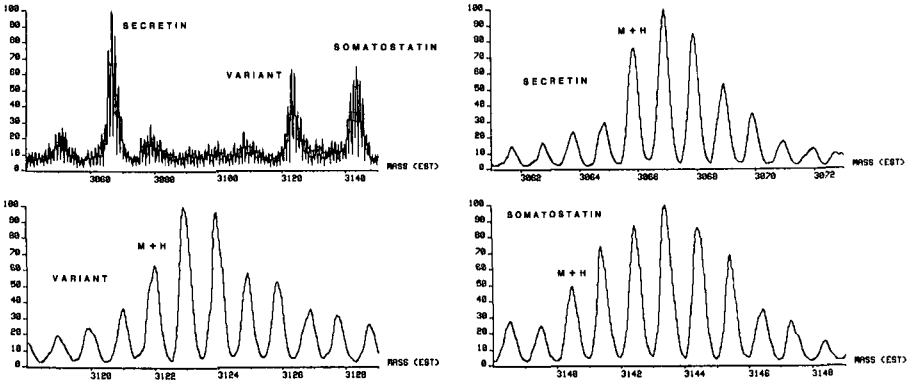

Although the standard deviation found with software peakmatching is not quite as good as was hoped for, results obtained by the three different methods consistently point to a hetero atom rich modification of secretin. As a whole, the data suggest that the true value may be found within 55.987 +/- 0.030 u. The elemental composition which comes closest to this value is C_2O_2 (-3 mmu). However, such a modification would be expected to be acid labile which is not observed for the secretin variant. Other possibilities consistent with the mass measurements include C_2S (+14 mmu), CON_2 (-14 mmu), C_2H_2ON (-27 mmu), none of which leads immediately to a structure proposal. Thus our conclusion is that a smaller fragment or the modified histidine itself needs to be isolated for further structure elucidation.

Since the standard error for the two different software peakmatching methods employed was found to be essentially the same, the hassle involved in optimizing the analysis for a mixture of three peptides does not seem to pay off. A calculation for the base peak in method 3 (secretin M+2) revealed that it consisted of approximately 80 ions. For a resolution of 4000 one may thus expect a standard deviation of 6 ppm [6] and correspondingly more for the smaller peaks. In contrast, the standard deviation for the intense CsI peaks should be less. Another disadvantage of using two authentic peptides as internal standards is the increased contribution of M, M-1 and M-2 ions in the upper mass range [7] as well as overlapping of peaks due to fragmentation and impurities. There appears to be a tradeoff between the gain in accuracy due to a smaller scan window and the above mentioned factors.

[1] Rinehart, K. L. Jr., and Bieman, K. et al. 1985, in: Burlingame, A. L. and Castagnoli, N. Jr. (eds) Mass spectrometry in the health and life sciences, Elsevier, Amsterdam, p. 119 and 239, resp.; [2] Rapp, U. et al., Int. J. Mass Spectrom. Ion Phys. 46, 371 (1983); [3] Tatemoto, K. 1980, in: Glass, G. (ed.) Gastrointestinal hormones, Raven Press, New York, p. 975; [4] Wold, F. and Moldave, K. 1984. Posttranslational modifications (Meth. Enzymol. Vol. 106) Academic Pree, New York; [5] Bull, H. B. and Breese, K., Arch Biochem. Biophys. 161, 665 (1974); [6] Chapman, J. R. 1978. Computers in mass spectrometry, Academic Press, New York, p. 57; [7] Fujita, Y. et al., Int. J. Mass Spectrom. Ion Phys. 63, 231 (1985).

STUDIES OF PROTEIN SEQUENCING BY ON-LINE ENZYMATIC HYDROLYSIS, LIQUID CHROMATOGRAPHY, AND THERMOSPRAY MASS SPECTROMETRY

L. Yang, K. Stachowiak, and D. F. Dyckes, Department of Chemistry, University of Houston, Houston, TX 77004

Studies of protein sequencing to develop a general method for sequencing unknown proteins have employed many different methods. Among these, on-line peptides sequecing using enzymatic hydrolysis, liqud chromatography, and thermospray mass spectrometry has been demonstrated to be a promising method for generation of useful peptide sequence information with great speed and reliability (1). This method couples enzymatic hydrolysis, LC separation, with on-line thermospray MS (Fig. 1). Thermospray MS is a soft ionization technique (2) generally producing only molecular ions for peptides (3). As is well known, enzymatic hydrolysis only cleaves peptide bonds in proteins and peptides. This combination provides useful information which is easy to interpret for sequencing proteins. By coupling with immobilized carboxypeptidase Y (CPY), thermospray MS produces an extremely useful technique for sequence determination for peptides (1). In the present research this method was applied to sequencing a protein with more then 50 amino acid residues.

The target protein studied was trypsin inhibitor. Its amino acid sequence is shown in figure 2, and its tryptic peptides and possible peptides in the peptide mixture in figure 3. Trypsin inhibitor was reduced and S-carboxy-methylated before digestion by immobilized trypsin column. The tryptic peptide mixture from the trypsin column was separated with a variety of LC columns and identified by thermospray MS. Figure 4 illustrates the results from 5 nanomole of trypsin inhibitor. The inhibitor was completely digested and the peptides fragments identified with thermospray MS following the trypsin column on-line. The Ultrasil-NH_2 separation of the peptide mixture was not compatible with the CPY column. Figure 5 shows the results obtained from 10 nanomole of trypsin inhibitor with separation on a C_4 column. Reasonable separation was obtained for further sequencing the peptides by thermospray MS coupled to the CPY column. Some useful sequence information was obtained. This information also indicated that the optimum conditions for LC separation are not favorable for either trypsin or CPY digestion.

Results discribed above further show that on-line coupling of enzymatic hydrolysis, LC separation, with thermospray MS is a promising method for generation of sequence information of proteins. This most serious problem remaining involves finding operating conditions which are simultaneously compatible with the enzyme columns, the LC separation and the thermospray mass spectrumeter.

REFERENCES

1. Kim,H.Y.;Pilosof,D.;Dyckes,D.F.;Vestal,M.L.,J. Am. Chem. Soc. 1984, 106, 7304.
2. Blakley,C.R.;Carmody,J.J.;Vestal,M.L.,J.Am.Chem.Soc.1980, 26, 1467.
3. Pilosof,D.;Kim,H.Y.;Dyckes,D.F.;Vestal,M.L.,Anal.Chem.,1984, 56, 1236.

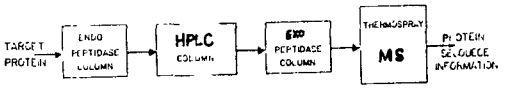

Fig 1 Schematic diagram of the method coupling of enzymatic hydrolysis, LC separation, with on-line thermospray MS.

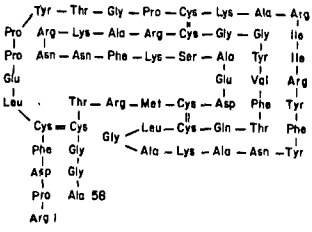

Fig 2 Amino acid sequence of trypsin inhibitor

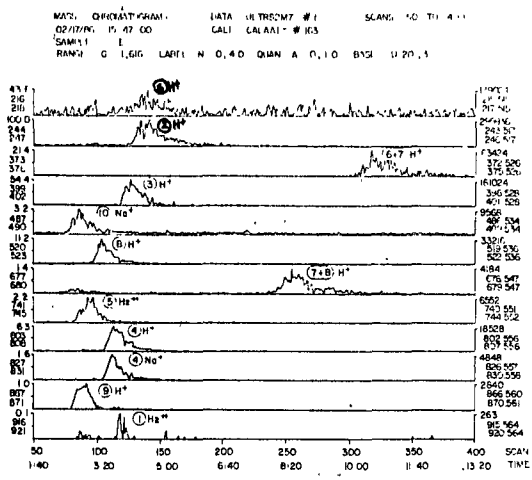

Fig. 4. Mass chromatograms obtained from 5 nmole of trypsin inhibitor by thermospray MS following the trypsin column and Ultrasil-NH_2 column on-line. Solvent was 0.1M NH_4OAC (pH=8 4) at 1.25mL/min.

(M.W.)

① Arg-Pro-Asp-Phe-Cys-Leu-Glu-Pro-Pro-Tyr (1837)
Lys-Cys-Pro-Gly-Thr

② Ala-Arg (245)

③ Ile-Ile-Arg (400)

④ Tyr-Phe-Tyr-Asn-Ala-Lys (804)

⑤ Ala-Gly-Leu-Cys-Gln-Thr-Phe-Vla-Tyr-Gly (1489)
Arg-Cys-Gly

⑥ Ala-Lys (217)

⑦ Arg (174)

⑧ Asn-Asn-Phe-Lys (521)

⑨ Ser-Ala-Glu-Asp-Cys-Met-Arg (868)

⑩ Thr-Cys-Gly-Gly-Ala (466)

(1+2) (2064)
(2+3) (627)
(3+4) (1186)
(2+3+4) (1413)
(6+7) (373)
(7+8) (677)
(8+9) (1371)

Fig. 3. Possible tryptic peptides of the inhibitor.

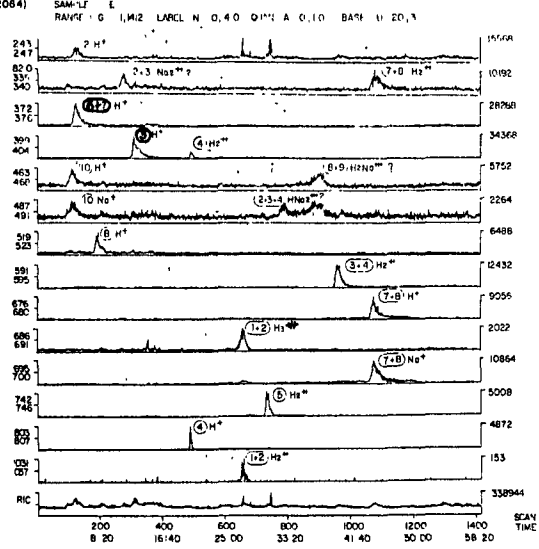

Fig. 5. Mass chromatograms obtained form 10 nmole of trypsin inhibitor by thermospray MS following the trypsin column and C_4 separation on-line. Solvent system is as follows.

Solvent A. 0.5% n-propanol + 0.1M NH_4OAC(pH=7 0)
Solvent B. 2% n-propanol + 98% 0.1M NH_4 OAC(pH=7 0)
Solvent C : 15% n-propanol + 85% 0.1M NH_4OAC(pH=7.0)

Gradient elution program.

Solvent	Time(min)	Tv(°C)	Flow Rate(mL/min)
100. A	1.0	158	
100° A - 100. B	5.0	156	
100/ - 50% B + 50% C	7.0	155	1 0
50 B + 50% C - 100% C	15 0	153	
100 C	10.0	152	

MOLECULAR WEIGHT DETERMINATION OF ENDOGENOUS AND CLONED EPIDERMAL GROWTH FACTORS AT THE PICOMOLE LEVEL BY WIEN LSIMS

William Aberth, Bradford W. Gibson and A.L. Burlingame
Mass Spectrometry Facility
Department of Pharmaceutical Chemistry
University of California, San Francisco, CA 94143-0446
and Richard P. DiAugustine and Michael P. Walker
National Institutes of Environmental Health Sciences
Research Triangle Park, North Carolina 27709

A prototype Wien mass spectrometer has been constructed and recently applied to the analysis of both cloned and endogenous forms of epidermal growth factor (EGF). The discovery of multiple forms of EGF and the interest of biotechnology companies in cloning EGF demanded that a rapid and sensitive analytical method be developed for EGF characterization. A prime advantage of the Wien instrument for such analyses is its high sensitivity at high mass (see Fig. 1) coupled with a short analysis time per sample of 5 minutes or less. This is partly due to the ability of Wien analyzers to select high masses at high accelerating voltages (1) and the use of a position computing signal accumulation system (2). A channel electron multiplier array detector intercepts a segment of the mass spectrum which contains the mass of interest and these ion pulses are accumulated by a multichannel analyzer (2). At 40 kV accelerating voltage and maximum magnetic field, this amounts to a mass range of ± 400 amu at 6000d (see Fig. 1), with a resolution of 500 (FW 1/2M) and ± 1800 amu at 16,500d with a resolution of 200 (see Fig. 2).

The analysis of recombinant peptide and protein products is necessary to insure that the proper product has been produced by the host organism. We have mass analyzed a cloned human EGF (Chiron, Emeryville, CA) and compared it to a native mouse α-EGF and found that the cloned EGF had the correct average mass (MH^+ (experimental) = 6060 ± 3, MH^+ (predicted) = 6061). In another study, we have found that commercial preparations of α-EGF have a number of unidentified components (3). These components were separated by HPLC and approximately 10-50 picomoles of material were analyzed directly by the Wien mass spectrometer. A component that elutes just prior to α-EGF ("pre α-EGF") was found to have a mass essentially identical to α-EGF at 6040 ± 3d (see Fig. 3). In a subsequent experiment using gas phase Edman sequencing, we were able to identify this component as Asp^1-EGF, where the N-terminal Asn^1 had undergone alkaline deamidation to Asp^1. A second component termed α-EGF was found to be 200d lower in mass, and it appears to be a truncated version of α-EGF involving loss of N-terminal Asp^1 and Ser^2 (-201d). Both the Asp^1-EGF and the α-EGF appear to have similar activities to α-EGF, indicating that these N-terminal modifications are not important for bioactivity and should not invalidate studies where these commercially impure preparations were used. This study has demonstrated the importance of the Wien mass spectrometer sensitivity when only subnanomolar amounts of sample are available for analysis.

Acknowledgments. This work was supported in part by NIH Grant GM 32315.

References.

1. W. Aberth, Biomed. Mass Spectrom. (1980) 7, 367.

2. W. Aberth, Int. J. Mass Spectrom. Ion Phys. (1981) 37, 379.

3. R.P.DiAugustine, M.P. Walker, W. Aberth, B.W. Gibson and A.L. Burlingame, manuscript in preparation.

Fig. 1.

CEMA spectrum of Bovine insulin demonstrating sensitivity resolution and calibration of analysis. Sample was added to .5 µl matrix of 1:1 glycerol/monothioglycerol with .25 µl of 0.1N HCl. Spectrum was accumulated for about 3 minutes.

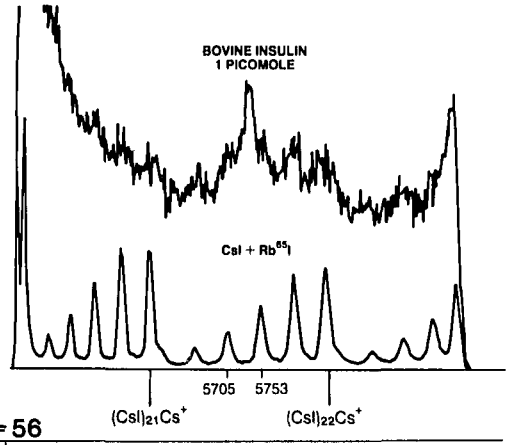

Fig. 2.

Demonstration of the high mass survey capability of the WMS using the position sensitive CEMA detector. A comparison with Fig. 1 shows the relative increase in mass range with increasing mass while the CsI cluster peak width remains approximately constant.

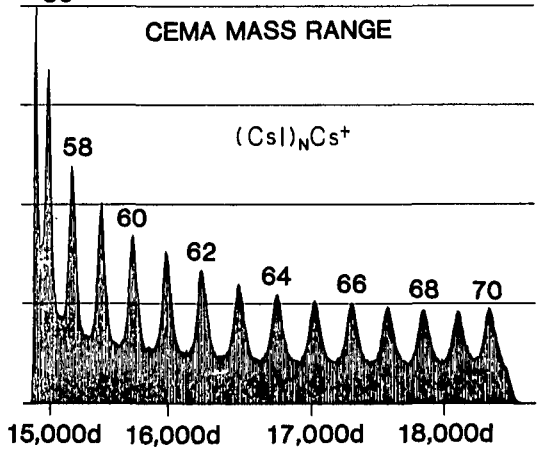

Fig. 3.

CEMA spectra of mouse α-EGF and pre α-EGF ("Asp^1-EGF") taken with 40 picomoles of sample. EGF was added to 0.1% TFA and mixed with 0.5 µl of 1:1 glycerol/monothioglycerol. Spectra were accumulated over a 3-4 minute period.

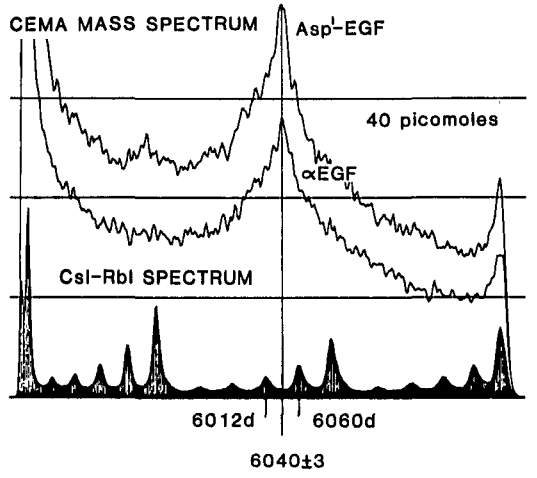

MASS SPECTROMETRIC ANALYSIS OF THE MIXED DISULFIDE DERIVATIVES OF PEPTIDES

M.ALAI, C.FENSELAU, Johns Hopkins University, Baltimore, MD 21205

The tripeptide glutathione (γ-glutamyl cysteinyl glycine) is the major free thiol in most living cells and participates in a number of biological processes such as the detoxification of xenobiotics. There is increasing evidence that the formation of disulfides between glutathione and the cysteine residues in functional proteins affects the biological activity of the latter. However, due to the lack of a satisfactory analytical technique quantification and characterization of mixed disulfides of this type has been very difficult.

In this study using Cf-252 plasma dsorption and fast atom bombardment mass spectrometry in conjunction with reversed phase HPLC a number of glutathione-peptide hormone derivatives are examined. Products of both enzymatic and chemical reactions (pH 7.0) are analyzed. RP-HPLC separates the isomeric mixed disulfide derivatives. Plasma desorption mass spectrometry allows rapid analysis of the reaction product mixtures. FAB mass spectra provide molecular weight and fragment ions which allow distinction between the isomeric disulfide derivatives, purified by HPLC. B/E linked scan of the daughter ions of the GS-peptide peak permits selective analysis of components of the reaction mixture and provides information on the gas phase decomposition of the parent ion. Glycerol was the matrix of choice for FAB-MS analysis, since thioglycerol is known to reduce the S-S linkage.

Comparison of the enzymatic vs. the chemical formation of the mixed disulfide derivatives of peptides indicate that the product specificity is increased by enzyme catalysis, however, more total product is formed in the chemical reaction.

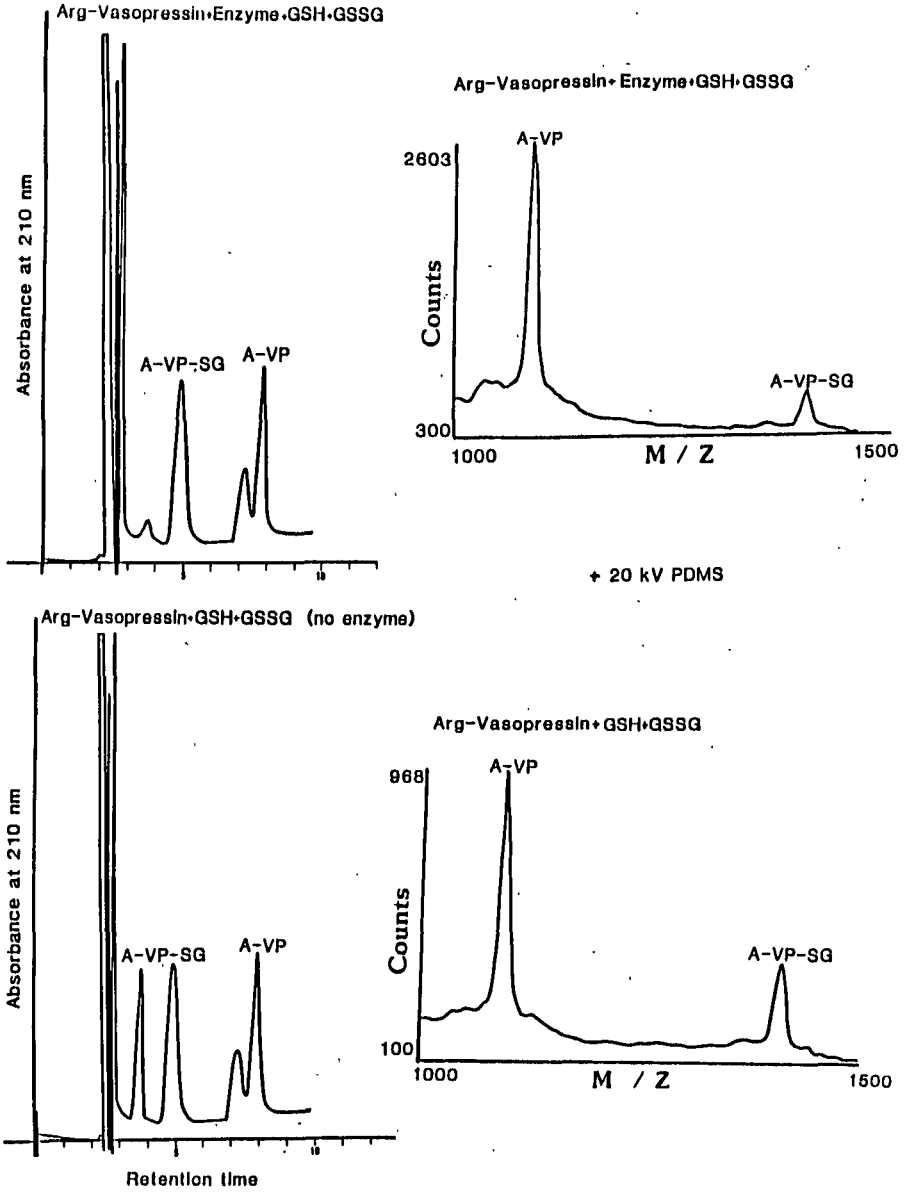

RP-HPLC and plasma desorption mass spectrometric analysis of the reaction products.

THE USE OF FAB-LCMS FOR THE ANALYSIS OF HIGH MOLECULAR WEIGHT PEPTIDES:

R.S. Bordoli, A.E. Fairbrother, S.T. Krolik and H.J. Wright, VG ANALYTICAL LTD., FLOATS ROAD, WYTHENSHAWE, MANCHESTER M23 9LE,UK.

Introduction

Liquid chromatography is the method of choice for separating polar and thermally labile compounds and FAB-MS has proved to be a powerful tool in the analysis of such compounds.

However analysis of high molecular weight peptides (>10,000 daltons) is very difficult, if not impossible, by FAB-MS.

The use of classical methods to cleave these into residues of <3,000 amu facilitates ease of analysis by FAB-MS[1] and is extremely useful in peptide mapping for amino acid sequence determination. The complete analysis of peptide residue mixtures by direct FAB probe is not always possible as will be demonstrated but the use of a moving belt LC interface in conjunction with FAB-MS has proven to be a powerful technique in the sequencing of peptides [2].

The application of these techniques to the qualitative analysis of a complex tryptic digest mixture of wide ranging molecular weight is shown.

Experimental

The sample studied was an oligopeptide (Mwt >20,000) which was cleaved specifically by a proteolytic enzyme. The mixture of underivatised peptides being obtained by partial hydrolysis of 500ug of oligopeptide in an incubation medium of ammonium carbonate plus trypsin.

The mass spectral analysis was performed on a VG 70-SE mass spectrometer with a mass range of 3000 amu at 8keV ion energy, operating in the FAB ionisation mode and interfaced to a VG 11-250J+ data system. The instrument was fitted with a VG moving belt LC interface and spray depositor (Fig 1).

Results & Discussion

Trypsin cleaves peptides at the C terminal end of arginine and lysine except in the case where proline is the contiguous amino acid residue. Fig. 2 shows the oligopeptide structure with all the expected points of cleavage. The table Fig. 3 lists the peptide residues with their corresponding $(M+H)^+$ and gives a comparison of the tryptic digest residues observed from the direct FAB probe and the FAB LC-MS.

FAB Probe

It can be seen from the spectrum (Fig. 4) that the proteolytic digest subjected to FAB without separating the individual peptides gave intense pseudo-molecular ions with few signals from fragment ions. We were unable to detect the low molecular weight peptides partly due to interference from matrix peaks but it has also been shown [3] that not all of

the pseudo molecular ions in a tryptic digest are observed, possibly due to a variation in the surface activity of the fragments. Neither of the peptide residues containing cysteine bridges were likely to have been reduced to thiols in the acid solution.

FAB LC-MS

The LC-UV trace and chromatographic conditions appear in Fig. 5 and the TIC and a selection of mass chromatograms of the expected residues are shown in Fig. 6. It will be seen from the comparison table (Fig. 3) that we were able to detect eleven of the expected peptide residues by LC-MS including all the low molecular weight peptides since there is no matrix on the belt and no suppression of signal due to fragments of differing surface activity eluting together. A selection of the FAB LC-MS spectra appear in Fig. 7.

Strong pseudo-molecular ions for all the peptide residues below mass 2000 were observed apart from the residue containing the disulphide linkage which may have been reduced.

Conclusion

These data show that FAB-MS can be used to provide a rapid approach to the molecular weight identity of enzyme digest fragments of large oligopeptides.

When FAB is used in conjunction with on line LC separation fragments which were previously undetected are now detected, but more importantly the molecular weights observed can be correlated with the LC eluent peaks. Where the LC eluents do not give good FAB mass spectra, particularly at high (>2000) mass, fraction collection and concentration may be required.

Whilst the technique does not presently give sufficient information to enable the peptide sequence to be determined, its potential usefulness in locating modifications to previously known structures, or in the identification of post translational modifications in structures deduced by reading gene sequences, is readily apparent.

References

1. Fukuhara, K., Tsuji, T., Toi, K., Takao, T., Shimonishi, Y., J. Biol. Chem. 1985, 260, 10487 - 10494

2. Stroh, J.G., Cook, J.C., Milberg, R.M., Brayton, L., Kihara, T., Huang, Z., Rinehart Jr., K.L., Anal. Chem. 1985, 57, 985 - 991

3. Clench, M.R., Gamer, G.V., Gordon, D.B., Barber, M. Biomed. Mass. Spectrom. 1985, 12, No. 7, 355 - 357

FAB MS/MS - EXPERIMENTS FOR SEQUENCING OF PEPTIDES

Uwe Rapp, Monika Hoehn and Gerd Dielmann
Finnigan MAT GmbH, Barkhausenstr. 2, D-2800 Bremen, FRG

Fast Atom Bombardment Mass Spectrometry (FAB MS) has been extensively used for the analysis of peptides. In most cases molecular weight information can be obtained. However, depending on the amount of sample available, the purity of the sample and the matrix used, the determination of the sequence appears to be cumbersome in many cases, even when using positive and negative ionization complementarily. This is due to the mixture of all the components present which may all be ionized by FAB.

For this type of analytical problem the MS/MS technique acts as an excellent filter for removing all matrix and background signals, leaving the sequence-specific ions only. Here a hybrid MS/MS system of BEQQ geometry can be used as follows: the BE-section is focussed on the $(M+H)^+$, $(M-H)^-$ peak, or a significant fragment ion, and a daughter ion scan is performed with the Q-section.

Fig. 1 shows a low resolution FAB spectrum of a hexapeptide using positive ionization and thioglycerol as matrix. Besides the M+H, the dominating peaks are due to the thioglycerol-cluster (m/z 109, 217, 325). Suspected sequence ions are indicated under the mass scale; however, they are, if present, hidden in the "background".

Fig. 2 depicts the MS/MS daughter scan when m/z 605 $(M+H)^+$ is selected as parent ion. All interfering ions are removed, only decays from the $(M+H)^+$ are recorded, resulting in a significant enhancement of sequence information.

Fig. 3 shows an MS/MS daughter ion spectrum of the fragment ion m/z 490. Although it is very small a characteristic spectrum is obtained.

Fig. 4 displays the MS/MS daughter ion spectrum of an octapeptide with molecular weight 862 u. The sequence is nicely "readable" and not interfered by peaks which are different to explain.

The MS/MS technique adds another dimension towards the sequencing capabilities of a mass spectrometer. The most significant feature is the removal of background ions by applying the second MS as an appropriate "filter". Another gain in selectivity can be achieved in using the high resolution capability of the BE-section of the hybrid instrument.

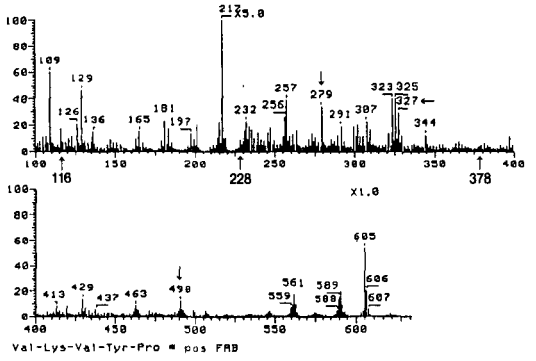

Figure 1

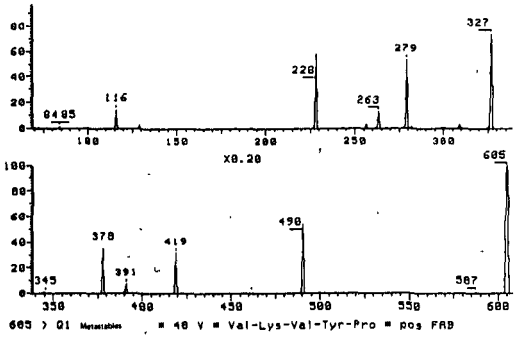

Figure 2

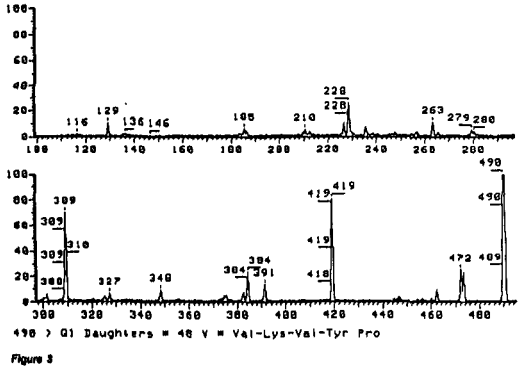

Figure 3

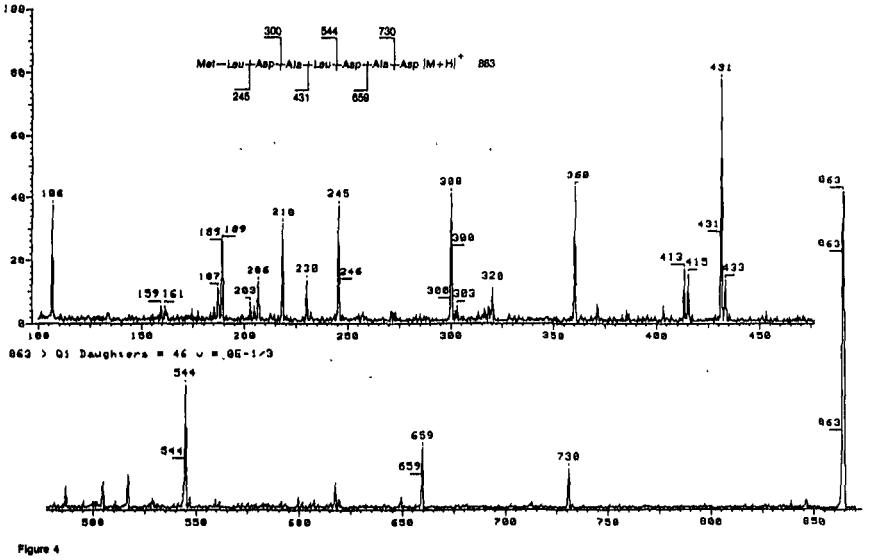

Figure 4

BIOMEDICAL MASS SPECTROMETRY TO M/Z 3000 WITH A QUADRUPOLE SYSTEM,

I. Jardine, C. A. Lisek, A. Tsarbopoulos and G. S. Scanlan, Department of Pharmacology, Mayo Clinic, Rochester, MN 55905 and D. C. Smith, VG Mass Lab, Manchester, UK

Many biomedical applications of mass spectrometry involve the analysis of compounds with masses greater than 2,000 daltons. Analysis of such compounds by quadrupole mass spectrometry was previously not feasible because of the limited mass range of commercially available instruments. A quadrupole mass spectrometer (VG 30-253) has now been built which has a mass range of 2-3000 amu. Examples of FAB analysis (8 KeV Xe; magic bullet matrix) of compounds to m/z 3000 are presented to illustrate the capabilities of this instrument.

Presented were the analysis of salt clusters (CsI and CsCl) demonstrating full mass range unit resolution capabilities (e.g. Fig. 1); demonstrated sensitivity of analysis of various peptides (γ-endorphin, MW 1859.4; a dynorphin analog, MW 2128.5; and melittin, MW 2846.5) (e.g. Figs. 2-4); FAB-MS analysis of tryptic digestion products of CNBr-treated peptides (human calcitonin, MW 3418.4; and chicken egg white lysozyme, MW ~14,000); and the determination of the presence of disulfide linkages in peptides by observing the reduction of S-S bonds with time in a 30% acetic acid/magic bullet matrix.

In conclusion, a new high mass quadrupole mass spectrometer has been successfully built and applied to biomedical analytical problems demonstrating both good sensitivity and resolution throughout the mass range of 2-3000 amu.

FIG. 1

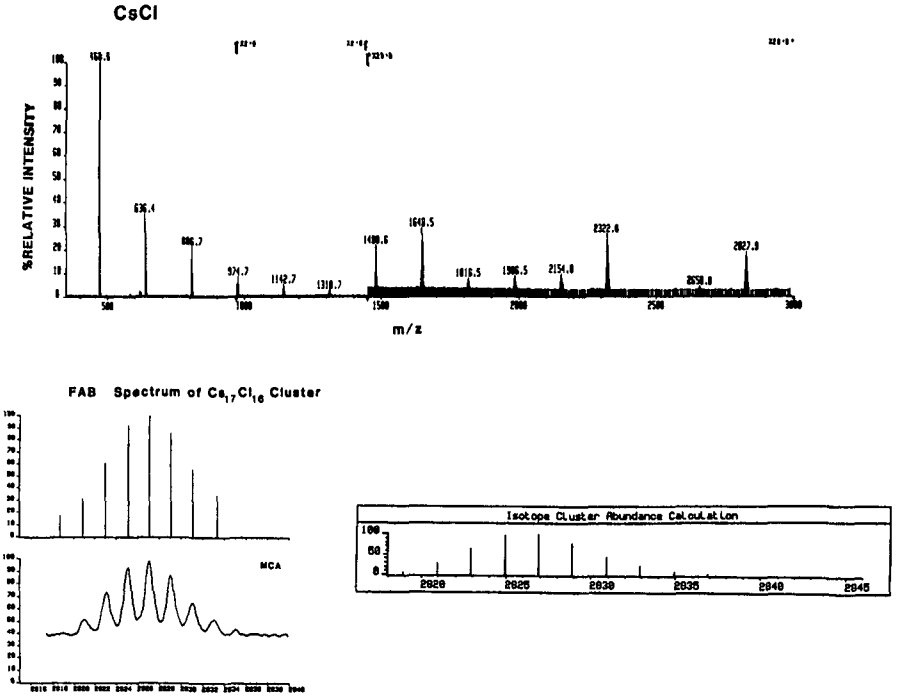

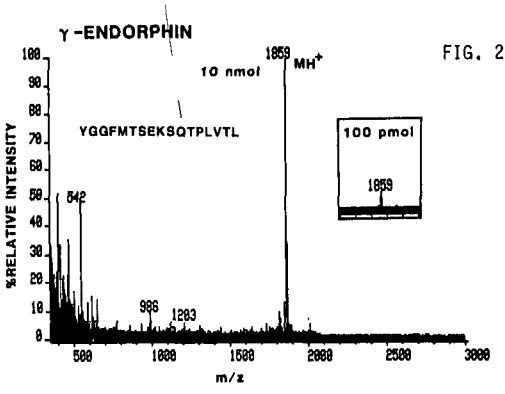

FIG. 2

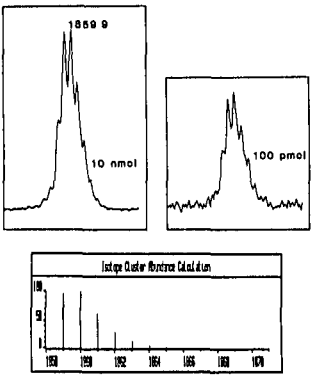

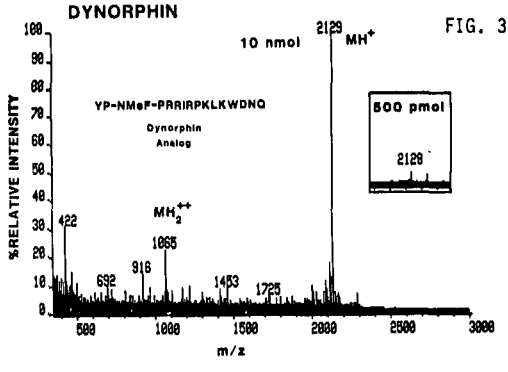

FIG. 3

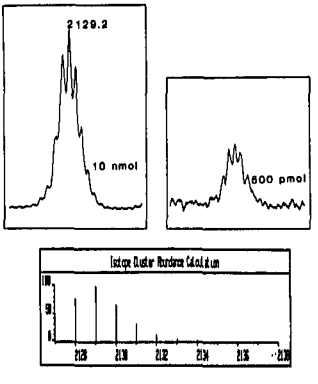

FIG. 4

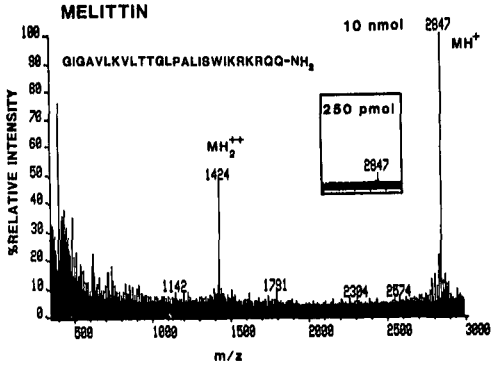

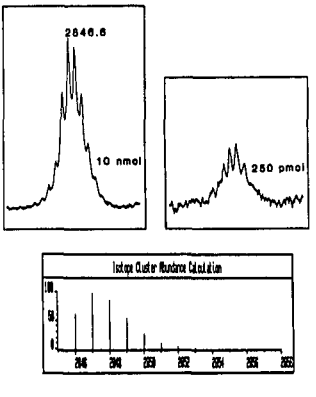

DI-ISOPROPYL ETHER AS A SELECTIVE CI REAGENT GAS

by Regina Barry and Burnaby Munson
University of Delaware
Newark, DE 19716

A major advantage of chemical ionization (CI) mass spectrometry lies in the flexibility to choose a reagent gas system for the specific type of analysis desired. NH_3 as a CI reagent gas produces spectra with very little fragmentation, and provides selectivity for basic compounds. Di-isopropyl ether has approximately the same proton affinity (206 kcal/mol) as NH_3 (204 kcal/mol). The major reactant ion in dilute mixtures of nitrogen, helium or methane with di-isopropyl ether is $(i\text{-}C_3H_7)_2OH^+$. The extent of the solvation reaction,

$$R_2OH^+ + R_2O \longrightarrow H(R_2O)_2^+ \qquad (1)$$

is significantly less for di-isopropyl ether than for other symmetric ethers or NH_3 under comparable conditions. It is expected that isopropyl ether will show less solvation with samples than NH_3.

The reactions of isopropyl ether in a 5% mixture with methane were studied by high pressure mass spectrometry. Primary ionization of the bulk gas produces ions which then react with isopropyl ether to produce the major ions at low pressures: 41^+, 43^+, 59^+, 61^+ and 87^+. As the total source pressure increases, these ions (with the exception of 87^+) react with the neutral isopropyl ether to produce $(M+H)^+$ at $m/z = 103^+$. The formation of the protonated dimer at $m/z = 205^+$ is strongly affected by temperature and source pressure. ICR double resonance experiments confirm that all the ions (except 87^+) react to produce $m/z = 103^+$. In addition, it is observed that $m/z = 61^+$ is produced by the collisionally induced decomposition of 103^+.

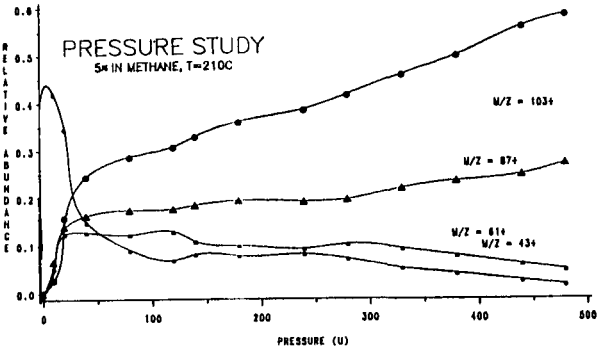

A plot of the relative sensitivities of samples with isopropyl ether vs. their proton affinities shows a "step-function" increase, similar to ammonia. Di-isopropyl ether mixtures show virtually no sensitivity with compounds that have proton affinities below ca. 195 kcal/mol. For compounds with proton affinities of 200 kcal/mol < PA < 206 kcal/mol, isopropyl ether will form small amounts of solvated ions; however, the sensitivity for these compounds is much lower than with NH_3:

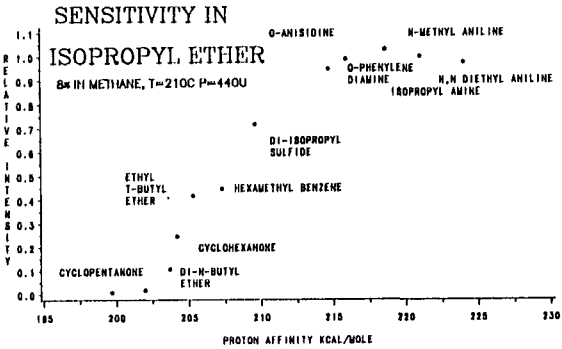

A number of compounds have been observed to undergo substitution reactions with ammonia to produce ions of apparent mass, M^+. Consequently, in the absence of information about the type of molecule being analyzed, it is difficult to assign molecular weight, since the characteristic ions may be $(M+NH_4)^+$, $(M+NH_4 - H_2O)^+$, or $(M+H)^+$. Several of these compounds were studied with isopropyl ether/methane mixtures. Anisole, which does not undergo the substitution reaction with NH_3, but instead produces low intensity M^+, yields low intensity $(M + H)^+$ with an isopropyl ether mixture. Benzyl alcohol, known to undergo substitution with ammonia, gives the typical result of a low intensity ion at mass $(M + H - H_2O)^+$, with little, if any, of the protonated species present.

Highly stabilized complexes are formed in the gas phase by multiple hydrogen bonds between the crown ethers and ammonium ions. Therefore, the predominant ion in the NH_3 CI spectra of crown ethers is the $(M+18)^+$ species, although the proton affinities of the larger ethers are approximately 220 kcal/mol. The geometry of R_2OH^+ from isopropyl ether precludes the formation of complexes with the crown ethers and other polyethers. The spectra contain primarily $(M+1)^+$ with a small (<5% of base peak) amount of $(M+19)^+$ due to solvation of water. Polyethers with proton affinities < ca. 208 kcal/mol have very low sensitivities with isopropyl ether.

Certain compounds display markedly low sensitivities in ammonia CI. An ion trace of the protonated ammonia dimer at m/z = 35^+ in GC/CIMS experiments reveals that this ion is produced by the reaction of ammonia with these samples. There is a "switching" reaction between ammonium adduct ions and NH_3 which reduces the NH_3 sensitivities for many compounds:

$$(M+NH_4)^+ + NH_3 \longrightarrow NH_4(NH_3)^+ + M \qquad (2)$$

A trace of m/z = 205^+ in GC/CIMS experiments shows that this ion is not produced by analogous reactions with isopropyl ether.

Dilute mixtures of isopropyl ether in nitrogen or methane can serve as useful reagent gases for analytical problems where relatively gentle ionization is desired, but for which NH_3 does not give a simple result. Isopropyl ether shows minimal solvation for most species, and gives higher sensitivities than ammonia for compounds which undergo the base-switching reaction. The intense reagent ions of isopropyl ether at m/z 103^+, 87^+ and 61^+ may interfere with the analysis of samples which give molecular ions at these masses.

Mass Spectral Analysis of Membranes and Cell Walls: Comparative Selectivity in Desorption Techniques

D. N. Heller, C. Fenselau, R. J. Cotter, P. Demirev, J. Olthoff, and J. Honovich, Pharmacology Dept., Johns Hopkins University School of Medicine, Baltimore MD 21205;

M. Uy, Johns Hopkins University Applied Physics Laboratory, Laurel, MD 20707;

T. Tanaka, Y. Kishimoto; Neurology Dept., Kennedy Institute, Baltimore, MD 21205.

Three desorption ionization techniques--laser desorption, plasma desorption and liquid secondary ion mass spectrometry--have been applied to intact cells, membranes, and various samples and extracts of lysed cells. It has been shown that intact compounds can be desorbed from biological membranes to provide mass spectral "fingerprints" which reflect each sample's unique biochemical composition. In addition, these complex mixtures and biochemical systems have been used to compare the performance of the desorption techniques themselves. Of significance for the understanding of desorption techniques is the observation that particular compounds are selectively desorbed and ionized for mass spectral analysis.

All measurements were carried out on time-of-flight instruments to allow direct comparison of spectra. Plasma desorption (PDMS) measurements were obtained on a BIO-ION 10K mass spectrometer, with a 10 μCi Cf-252 source. Laser desorption and liquid SIMS measurements were carried out using a Tachisto 215G carbon dioxide laser or Minibeam I ion gun, respectively, interfaced to a CVC-2000 time-of-flight mass spectrometer. Accumulated spectra were recorded and processed using a LeCroy 3500SA signal averaging system. Samples for liquid SIMS were dissolved in glycerol or thioglycerol.

The lipids of cell membranes (phospholipids, glycolipids or neutral lipids) are selectively desorbed relative to other cell components, such as proteins, nucleic acids, and carbohydrates. Also, depending on the lipid content of each sample, some lipids are selectively desorbed over others, based upon a comparison of the spectra to literature reports on lipid content. Lipids with preformed charges (or those which can be given a charge in a liquid matrix) are preferentially desorbed over other lipids. However, selectivity for different classes of lipids results (in some cases) in completely different mass spectra for the same sample using different desorption modes. Thus lyophillized rat brain myelin shows only cationized cerebrosides (glycolipid) in laser desorption, phosphatidylcholine (a quaternized phospholipid) in positive ion PDMS and liquid SIMS, and sulfatides (sulfated cerebrosides) in negative ion PDMS. All these compounds are known to be present in myelin, a multilayered membrane which surrounds the axons of nerve cells.

In some cases lipids can be ionized directly from lyophillized cells. Laser desorption consistently detects phosphatidylethanolamine (PE), the dominant phospholipid of lyophillized E. coli cells. The limit of detection is 2 μg cells, of which only about 5% is PE (based on dry weight). Laser desorption typically produces cationized molecules following desorption of neutrals; potassium is added to the probe, resulting in MK+ ions (Figure 1). Plasma desorption did not yield any ions from either E. coli or Bacillus subtilis cells which were dried on the sample foil from water suspension. Liquid SIMS ionizes lipids from B. subtilis cells dispersed in a liquid matrix (Figure 2). Presumably the primary ion beam ruptures cells and spills membrane lipids into the matrix, from which point ionization takes place.

In a comparison of cell preparations carried out with negative ion FAB on a magnetic sector instrument, it was shown that disruption of the cells can increase phospholipid signals. Either lysing the cells with solvent or agitating them with glass beads beforehand increased the PE signal intensity by about three- to five-fold. Interestingly, the PE signal intensity from a total lipid extract (about 9% of the cell's dry weight) was only about 10% greater than PE intensity from solvent-lysed cells. The selectivity advantage of phospholipids over other cells components is particularly large, for the liquid SIMS/FAB case.

Disrupting bacteria cells prior to analysis increases the information content of all the desorption mass spectra. This is especially true for PDMS, where some type of lysing technique had to be used to observe phospholipid ions. Applying a $CHCl_3$/MeOH lipid extract to the sample foil improved the quality of the PDMS spectra even further.

We undertook to determine if specific compounds can be detected from intact membranes and cells. Having shown that membrane lipids can be selectively desorbed as molecular ions, we are attempting to understand the mechanisms of such selectivity and the possibilities for characterizing and distinguishing bacterial and mammalian cells.

Figure 1.
Laser desorption mass spectrum

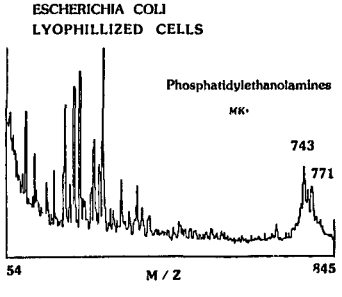

Figure 2.
Liquid SIMS mass spectrum

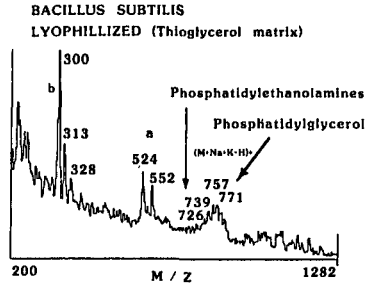

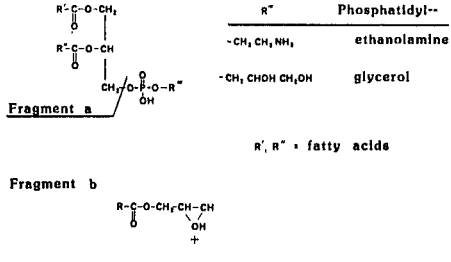

LASER DESORPTION/FOURIER TRANSFORM MASS SPECTRAL ANALYSIS OF HETEROCYCLIC AROMATIC POLYMERS

Charles Eric Brown
Department of Biochemistry
Medical College of Wisconsin
Milwaukee, WI 53226

Peter Kovacic
Department of Chemistry
University of Wisconsin-Milwaukee
Milwaukee, WI 53201

INTRODUCTION

The electrical conductivity of aromatic polymers (both benzenoid and heterocyclic) has become a topic of intense interest in recent years. Previously, the authors showed that laser desorption/Fourier transform mass spectrometry yields detailed information about the chain lengths, end group structures and halogen contents of benzenoid aromatic polymers[1,2]. The work presented here demonstrates that laser desorption/Fourier transform mass spectrometry (LD/FTMS) also is useful for the characterization of conducting heterocyclic polymers such as poly(1-methyl-2,5-pyrrolylene) [Ia], poly(1-phenyl-2,5-pyrrolylene) [Ib], poly(2,5-thienylene) [II], and poly(2,5-selenienylene) [III].

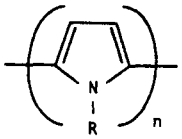

Ia: R=CH_3
Ib: R=C_6H_5

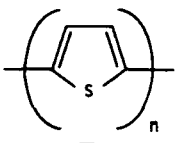

II

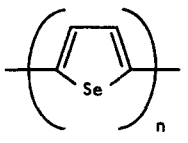

III

EXPERIMENTAL

Laser desorption/Fourier transform mass spectra of solid polymer samples deposited on a stainless steel probe were recorded with a Nicolet FTMS-1000 spectrometer equipped with a Nicolet laser desorption interface and a Tachisto Tac-II pulsed CO_2 laser. Samples were deposited onto the probe tip by the procedure of Brown et al.[1,2] with a 10 pound sledge hammer and Scotch double stick tape.

RESULTS AND DISCUSSION

Poly(2,5-selenienylene) yields only a negative ion LD/FT mass spectrum of low intensity

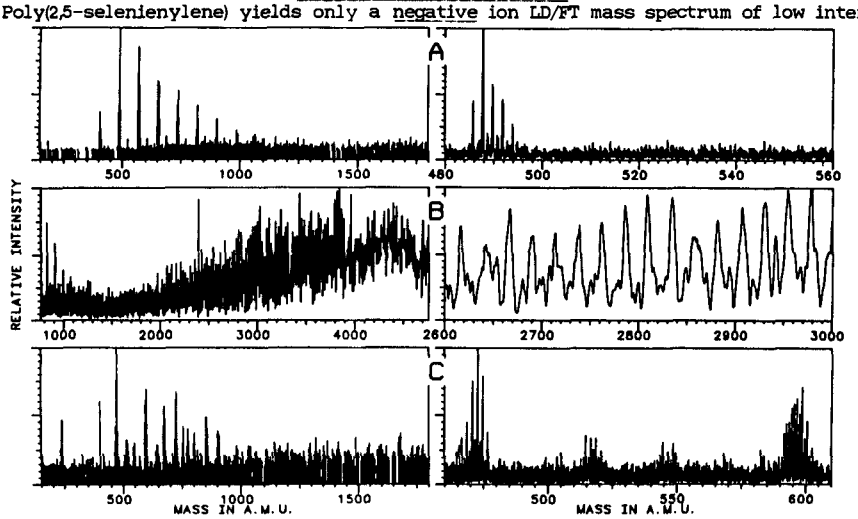

Figure 1. (A,B) Positive ion LD/FT mass spectrum of poly(2,5-thienylene), and (C) the negative ion LD/FT mass spectrum of poly(2,5-selenienylene). Spectral expansions are given on the right.

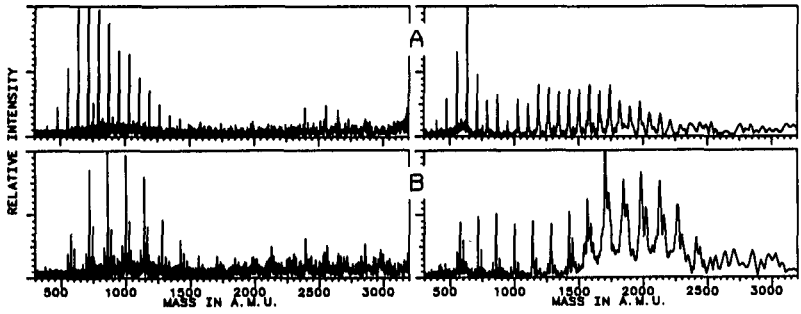

Figure 2. Positive ion LD/FTMS of (A) poly(1-methyl-2,5-pyrrolylene) and (B) poly(1-phenyl-2,5-pyrrolylene). Of the 64K data points of the digitized time domain signal, only the initial 32K were Fourier transformed to obtain the spectra on the left, and only the initial 4K for those on the right.

(Fig. 1C), unlike the other heterocyclic polymers reported here and the majority of benzenoid polymers,[1,2] which yield predominantly positive ion spectra. This may be an indication that selenium affects the manner in which the heterocyclic polymer backbone stabilizes charge, which could, in turn, underlie its poor conductivity upon doping.

The heterocyclic aromatic polymers exhibit somewhat more complex patterns of halogenation than was observed with the benzenoid polymers.[1,2] Poly(1-methyl-2,5-pyrrolylene) (Fig. 2A) has mainly hydrogen at the terminal 2- and 5-positions. The identity of end groups of poly(2,5-thienylene) (Fig. 1A) varies with chain length of the oligomers. Short oligomers contain primarily one or two bromines, whereas oligomers larger than 700 amu tend to have hydrogens at both terminal positions. Poly(1-pheny-2,5-pyrrolylene) (Fig. 2B) and poly(2,5-selenienylene) (Fig. 1C) were found to have high bromine contents, and both underwent rearrangement/fragmentation reactions during LD/FTMS at least to some extent. Explanations of the conductivities of heterocyclic aromatic polymers that ignore such variability in halogen content may be incomplete.

The LD/FT mass spectrum of poly(2,5-thienylene) exhibits a substantial population of carbon clusters (Fig. 1B) of the type observed with laser vaporization of graphite.[3] Thus the question arises of whether poly(2,5-thienylene), when synthesized by catalyzed condensation of the Grignard, contains graphite-like polynuclear contaminants. Thermal degradation with loss of sulfur occurs at temperatures above 600°K, and the remaining carbon backbone might be expected to yield polynuclear material.[4] Thus, the possibility exists that pulsed infrared laser irradiation might produce such thermal degradation within the mass spectrometer. However, contamination by polynuclear species should be considered as a factor that might contribute to the electrical conductivity of poly(2,5-thienylene).

Since the mass spectrum of poly(2,5-thienylene) (Fig. 1A and B) and its carbon clusters covers a continuous mass range of 5000 amu, the instrumentation should be capable of detecting oligomers over at least this mass range if there were no other effects that interfered. We have found, however, that drastically decreasing the acquisition time for the time domain signal increases the apparent mass range of the oligomers of poly(1-methyl-2,5-pyrrolylene) and poly(1-phenyl-2,5-pyrrolylene) by about 1000 amu (Fig. 2A and B, respectively). Reducing the acquisition time has no effect on the apparent mass range of the oligomers of poly(2,5-thienylene) and poly(2,5-selenienylene). A possible, though untested, explanation for this observation is that steric constraints might cause the poly(1-substituted-2,5-pyrrolylenes) to exist as extended rods. High mass oligomers of such molecules could experience a high rate of collision with other species in the detector cell of the mass spectrometer and thereby lose coherence of motion during detection.

REFERENCES

1. C.E. Brown, P. Kovacic, C.A. Wilkie, R.B. Cody, Jr., and J.A. Kinsinger, J. Polym. Sci. Polym. Lett. Ed., 23, 453 (1985).
2. C.E. Brown, P. Kovacic, C.A. Wilkie, J.A. Kinsinger, R.E. Hein, S.I. Yaniger, and R.B. Cody, Jr., J. Polym. Sci. Polym. Chem. Ed., 24, 255 (1986).
3. E.A. Rohlfing, D.M. Cox, and A. Kaldor, J. Chem. Phys., 81, 3322 (1984).
4. W.K. Kobel, H. Kiess, M. Egli, and R. Keller, "Polythiophene Conductive Polymers," Workshop on Conductive Polymers, Brookhaven National Laboratory, October 7-9, 1985.

FORMATION OF $(CsI)_X(NaI)_Y$ CLUSTERS IN A LIQUID MATRIX. AN EXACT MASS AIDE FOR FAB.

INTRODUCTION

The FAB spectrum of a solid mixture of CsI/NaI appears mostly as a superposition of the separate CsI and NaI spectra with predominance of the CsI spectrum at equimolar concentration. By contrast, the spectra of NaI/CsI mixtures in a polar liquid matrix show the appearance of (CsI) (NaI) clusters. The relative intensity of a specific cluster agrees qualitatively with a statistical model based on the randomization of the cluster formation process. The transition from the random clustering characteristic of the liquid matrix to the selective clusters observed in the solid mixtures can be observed by selecting an appropriate temperature.

The presence of $(CsI)_X(NaI)_Y$ adducts in a liquid matrix can be of help in accurate mass work due to the additional reference peaks introduced throughout the mass range. By properly selecting the molar ratio, NaI/(CsI + NaI), it is possible to maximize a specific cluster nearest an unknown peak of interest, improving the accuracy of the exact mass measurements.

EXPERIMENTAL

Stock solutions of CsI and NaI were prepared by dissolving 520 mg and 300 mg respectively in 4 ml of H_2O in two separate vials. These solutions were used to prepare ten solutions with molar ratios, NaI/(NaI + CsI), of 0 to 1. Each solution was analyzed by FAB using a VG-70EQ double focusing mass spectrometer. Analysis was carried out by depositing 2 µl of sample on to the FAB target and acquiring 3 or 4 spectra of the solid followed by addition of 1 µl magic bullet, 4/1:DTE/DTT, and collection of a large set of spectra. To minimize the effect of evaporation of the matrix the source block and all reentrant ports were kept cold. Absolute intensities of all $(NaI)_X(CsI)_Y$ - I, X + Y<6, were collected and separated according to cluster size, X+Y, normalized and plotted as shown in Fig. 1a,b,c. Additional experiments include a high temperature run to illustrate the effect of matrix evaporation, Fig. 2; and an exact mass measurement using a selected cluster, Fig. 3.

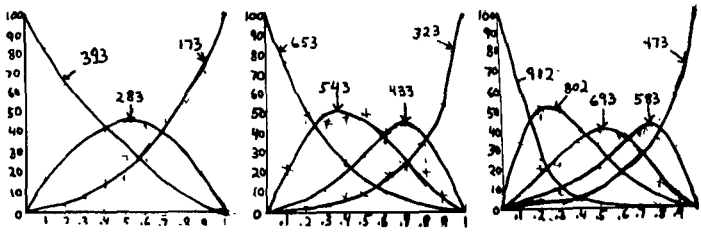

Fig. 1 Relative intensities of $(CsI)_X(NaI)_Y$ - I as a function of molar ratio X = NaI/(CsI + NaI) for some values of X+Y. a) X+Y = 2; b) X+Y = 3; c) X+Y= 4

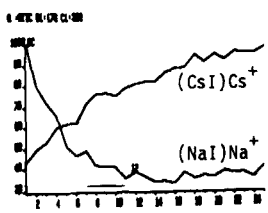

Fig. 2 Ion traces for m/z = 173, 283, 393 of a mixture of NaI/CsI in magic bullet at 70°.

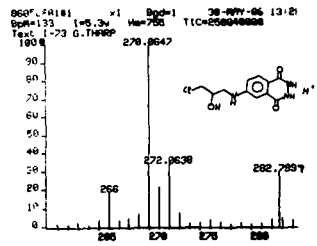

Fig. 3 Exact mass measurement using m/z = 282.7997 of CsNaI cluster maximized at molar ratio x = .5.

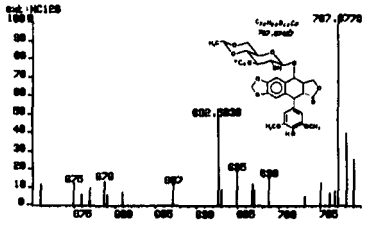

Fig. 4 Exact mass measurement of Etoposide Antitumor Agent using m/z = 692.5038 Cs Na I cluster.

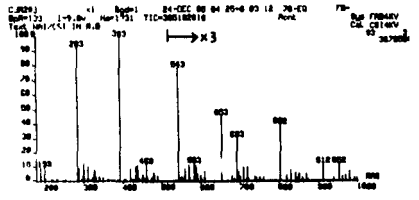

Fig. 5 Spectrum of a CsI/NaI mixture in Magic Bullet at a molar ratio of .3.

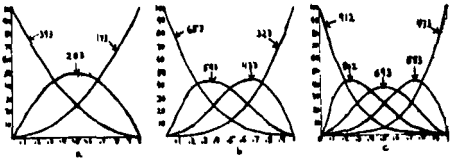

Fig. 7 Plot of the expected relative intensities of $Cs_XNa_YI_{X+Y-1}$ clusters as a function of molar ratio of NaI. a) X+Y = 2; b) X+Y = 3; c) X+Y = 4. Terms follow weight given by binomial terms of $(Z + (1-Z))^{X+Y}$ where Z = molar ratio.

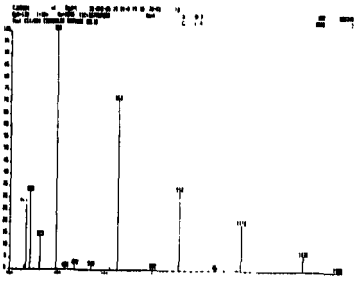

Fig. 6 Spectrum of an equimolar mixture of CsI/NaI in the solid phase.

RESULTS AND DISCUSSION

Previous studies of the FAB spectra of alkali halides in glycerol have revealed a time dependent behavior of the spectra and many explanations have been offered for the appearance of these spectra. The results obtained here, however, can be explained rather simply, but not exclusively, by assuming that all CsI, NaI molecules in a matrix are free to dissociate and associate with any other molecule in the matrix; that is, that the probability of formation of a cluster $(NaI)_X(CsI)_Y - I$, and therefore, its ion intensity, is determined solely by the statistical weight of the X, Y combination relative to others. This assumption is found to be at least qualitatively valid for a given cluster number, X+Y, as can be readily seen by comparing Fig. 1a - 1c with the statistical curves of Fig. 7a - 7c. For solid mixtures, however, the assumption is no longer valid as can be concluded from Figs. 5 and 6. In order to reconcile the contrast shown in Figs. 5 and 6 we must conclude that the formation of the crystal lattice must introduce restrictions, perhaps steric and energetic, on cluster formation. All these restrictions, however, are removed once the alkali halide molecules enter the solvent and the crystal lattice is destroyed. In such case, the time variation of the spectra as the matrix evaporates is not only the result of increase in concentration of the alkali halide, but a competition between crystallization and solution. Because of the solubility limits of the alkali halides in most matrices the transition region should evidence pronounced variations in the spectrum instead of the more gradual variations implied by a concentration increase. Experiments to verify the latter point are complicated by the difficulty in maintaining a homogenous distribution of material on the FAB target. Nevertheless, the results seem to indicate that the explanation is valid.

REFERENCES

1. J. Miller; R. Theberge; Org. Mass Spectrom. 10, 600 (1985)
2. F.M. Devienne; R. Combarieu; J.C. Roustan; Int. J. Mass Spectrom. Ion Proc. 65, 159 (1985)
3. M.M. Bursey; G.D. Marbury; J.R. Haas; Biomed. Mass Spectrom. 11, 522 (1984)
4. T. Keough; Anal. Chem. 57, 2027 (1985)

POST SPUTTERING EI FAB MS

J. P. Lehman, G. Gillen, Dept. of Chemistry
Arizona State University, Tempe, AZ 85287

A Finnigan-MAT 312 EI-FD ion source was modified to incorporate a built-in fast atom source of the capillaritron type as shown below. The fast atom source was mounted in place of one of the extraction plate support insulators and the extraction plate slit was lengthened to the maximum. The conventional EI electron beam can be applied to the sputtered or evaporated species for ionization or further excitation. The effect of this post sputtering EI type excitation on the observed spectra of typical FAB matrices and analytes with respect to sensitivity, fragmentation, and cluster formation is reported.

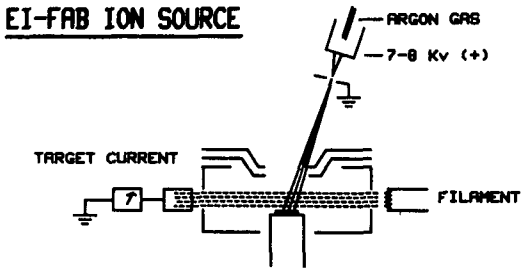

Typical operating conditions were; 5 micro A Ar^+ at 7-8 kV, 1 mA e^- at 70 ev. The FAB probe was positioned just out of the main e^- beam by noting the change in target current at the added, isolated target current meter.

SENSITIVITY:

Sucrose

m/z	ION	FAB	EIFAB	EIFAB/FAB
343	MH^+	.056	2.8	50
325	MH^+-H_2O	100	100	1.0
255	MH^+-92	1.5	14.7	10
93	GH^+	59	100	1.7
185	G_2H^+	.011	1.1	100

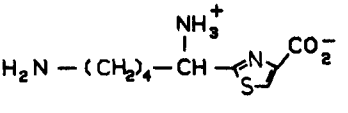

230	MH^+	5.0	45	9.0
185	G_2H^+	7.0	100	14.3

CLUSTER IONS:

m/z	ION	FAB	EIFAB	EIFAB/FAB
		Glycerol		
92	$G^{+\cdot}$	.009	1.7	200
93	GH^+	20.0	100	5.0
185	G_2H^+	8.9	.09	.01
277	G_3H^+	5.8	.058	.01
369	G_4H^+	1.06	.01	.01
		CsI		
127	I^+	---	35.2	$> 10^3$
133	Cs^+	100	24.6	.246
254	I_2^+	---	.22	$> 10^3$
392	Cs_2I^+	36.2	1.23	.034
652	$Cs_3I_2^+$	16.1	---	$< 10^3$
902	$Cs_4I_3^+$	4.63	---	$< 10^3$

FRAGMENTATION:

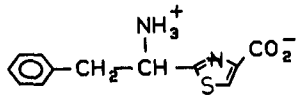

m/z	ION	FAB	EIFAB	EIFAB/FAB
249	MH^+	85.5	27.7	.32
232	MH^+-NH_3	26.6	24.5	.92
188	$MH^+-NH_3-CO_2$	5.4	100	18.5
		GLY-LEU-ALA		
260	MH^+	38.4	40.1	1.04
216	MH^+-CO_2	13.4	22.5	1.68
203	MH^+-GLY	16.1	14.2	.88
185	$203-H_2O$	13.5	14.9	1.10
171	MH^+-ALA	100	100	1.00
159	$203-CO_2$	21.3	31.1	1.46
143	171-C=O	99.2	90.5	.912

Investigation of sputtered matrices and analytes in addition to those presented here including such analytes as disaccharides, amines, hydrazines, amino acids, and salt clusters demonstrate that enhanced sensitivity is obtained for some analytes, no significant effect on sensitivity is shown for others, and that sensitivity for some analytes such as salt clusters is actually reduced.

Importantly, chemical ionization type fragmentation is induced in some analytes adding to the structural information available from typical mass spectra which frequently yield molecular weight information but insufficient fragmentation information for structure elucidation. When the MH^+ of the analyte is significantly enhanced, the G_2H^+ of glycerol is similarly enhanced, suggesting that large neutral clusters of analyte and glycerol are being sputtered which are subsequently ionized by electron ionization.

A COMPARISON OF 8KEV FAB AND 30KEV CAESIUM ION BOMBARDMENT FOR THE DESORPTION OF LARGE BIOMOLECULES

G J Elliott, J S Cottrell and S Evans
Kratos Analytical, 170 Williams Drive, Ramsey, NJ 07446, USA

Introduction

Desorption ionisation of large biomolecules is generally achieved by FAB at an impact energy of 8 to 10keV. There is evidence to suggest that molecular ions may be produced with greater efficiency by increasing either the mass or energy of the primary beam particles. The improvement in desorption efficiency resulting from the use of Xenon atoms rather than Argon is well known, but the effect of going to higher impact energies is not so readily investigated using commercially available FAB guns.

To study the effect of increasing the impact energy, we have used a Caesium ion gun. An ion gun was chosen in preference to a neutral gun because the impact energy depends only on the potential difference between the anode and the sample stage. Examples from the mass spectra of large biomolecules are presented to illustrate the effect of increasing the primary beam energy from 8keV to 30keV.

The Caesium Gun and LSIMS Source

The Caesium gun used in this work was provided by Dr W A Aberth of the University of California, San Francisco, and manufactured by Antek Inc. The use of this gun has a number of advantages over the conventional neutral beam gun.

1. Because of its small size, it can be mounted directly on the ion source.
2. As no gas is required, source pressure is improved.
3. Source contamination is greatly reduced.
4. The area of sample bombarded is reduced. This means sample waste is minimised.
5. The primary beam energy can be varied over a wider range, as the ion gun can be floated to a high potential relative to the target.

The new LSIMS source closely follows the design described by Falick, Wang and Walls, (1,2). The source was fitted to a Kratos Analytical MS50RF double focusing mass spectrometer.

Results

In the majority of our experiments, the Caesium ion current incident on the sample surface was estimated to be ca. 1μA. This is considerably lower than the 40 to 50μA typically measured on the monitor electrode of a saddle-field FAB gun. However, it is difficult to relate this monitor current to the flux of neutrals actually illuminating the sample surface. Another factor which complicates the comparison between Cs SIMS and FAB is the difference in the source geometries. The Cs SIMS source incorporates an additional electrode which provides an adjustable ion extraction field. For these two reasons, we have only attempted a qualitative comparison of the two techniques.

As can be seen from the data in the accompanying table, ion currents from the Cs SIMS source were usually a factor of 3 to 5 times higher than those obtained by FAB. This enabled a resolved spectrum of bovine proinsulin to be obtained from a single sample loading, whereas three sample loadings were required to obtain a similar result by FAB.

Results - continued

The most remarkable result obtained from the new source is the spectrum of intact human lysozyme (mol.wt. 14,701u). The resolution was estimated from the CsI calibration spectrum to be ca. 1,000. The primary beam was 1 μA of Cs ions at an impact energy of 30keV. It was not possible to obtain any useful signal from this sample under FAB.

References

1. Falick, A.M., Wang, G.H. and Walls, F.C., Anal. Chem., In Press
2. Falick, A.M., Wang, G.H. and Walls, F.C. and Aberth, W., paper presented at the 33rd Ann. Conf. in Mass Spec. and Allied Topics, San Diego, 1985.

Material	Mass	Resolution	FAB ion current/A	Cs SIMS ion current/A
CsI	5849	1500	9×10^{-14}	3×10^{-13}
CsI	8187	1500	9×10^{-15}	7×10^{-14}
Bovine Insulin	5735	1500	2×10^{-14}	1×10^{-13}
		7500	5×10^{-16}	3×10^{-15}
Bovine Proinsulin	8680	1500		3×10^{-15}
		10000		1×10^{-16}

Table 1 **Comparison of ion currents produced by LSIMS and FAB**

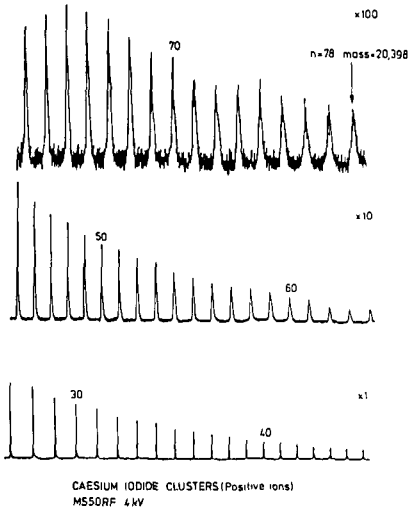

Figure 1

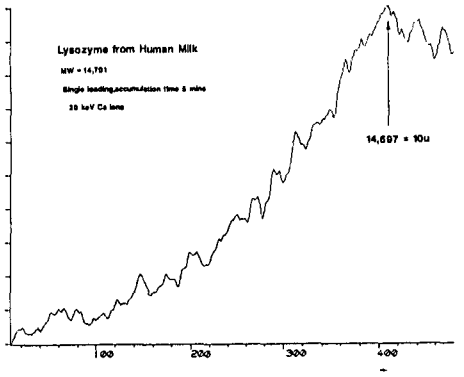

Figure 2

Surface Ionization Mass Spectrometry of Organics;
I. N-containing aliphatic organic compounds

Toshihiro Fujii and Toshihumi Kitai
Division of Chemistry and Physics,
National Institute for Environmental Studies,
Tsukuba, Ibaraki 305, Japan

We commenced the study of surface ionization organic mass spectrometry (SIOMS) under the experimental conditions that organic molecules are supplied from the gas phase onto a heated emitter SI ion source, two years ago. Interaction of organic molecules with the hot emitter surface leads to the thermionic emission. The previous studies indicate that depending on their nature, one of three basically different processes occurs.
(1) Molecular Surface Ionization (MSI). M^+ ions are observed only for M having not too high a molecular ionization energy (IE). Aniline is the typical molecule. MSI is easier in the case where the dissociative surface reaction takes place very slowly since the ionization process competes with the pyrolytic surface reaction.
(2) Dissociative Surface Ionization (DSI). $(M-H)^+$, $(M-CH_3)^+$, or $(M-OH)^+$ ions are often observed for many organics. The following consecutive process is very likely the mechanism: the formation of surface dissociative reaction product with a low IE followed by the SI.

$$M \longrightarrow (M-X) + X \qquad X = H, CH_3, OH$$
$$(M-X) \longrightarrow (M-X)^+ + e$$

(3) Associative Surface Ionization (ASI). Some basic compounds such as the pyridine molecule, generate the protonated (associated) molecule on the hot emitter surface. It was found that a bimolecular surface reaction of the proton complex is the most probable mechanism of formation.

In this paper studies have been made of surface ionization on the oxidized hot Re emitter for various types of N-containing aliphatic organics, with the objectives of investigating quantitatively what kinds of ions are formed efficiently from these compounds and assigning the observed ions to the mode of the ion formation mechanism mentioned above.

All work was performed on a Finnigan model 3300 gas chromatograph-mass spectrometer equipped with the home-built thermionic ion source. The constant admission of liquid organic sample was accomplished by using a variable leak valve. All the solid samples were admitted to the mass spectrometer either through the gas chromatograph or by the solid probe with a heated quartz ampoule.

For the 30 N-containing aliphatic organic organic compounds, Table I summarizes the predominant ions in the SI spectrum, the optimum emitter temperature which gives the maximum ion signal to each of them, the relative sensitivity (A/torr) and SI/EI, the ratio of the highest intensity in the SI mode to that in the EI mode. The SI mass spectra obtained are discussed with reference to simple N-containing aliphatic organic compounds, which are classified by the functional group.

AMINES The SI spectra of primary, secondary and tertiary methylamine molecules are characterized by ions of the efficient DSI process: very intense $(M-H)^+$ ions, which are directly characteristic of the molecular weight, and other relative strong ion peaks.
QUATERNARY AMMONIUM SALT The present result demonstrates some of potential applications of this method even toward the quaternary nonvolatile salts.
DIAMINES $(M-3H)^+$ is base peak, carrying 34 % of the total ion current for diaminobutane and 9 % for diaminopropane.
AMINOALCOHOLS As a rule, the mass spectrum in the SIOMS has a simple pattern. However, triethanolamine forms as many as fifteen peaks of significant intensity.
NITRO-AND CYANO-COMPOUNDS, OXIMES, AMIDES Most compounds are not amenable to SI analysis; generally the SI spectrum shows few, if any, peaks of very low intensity.
HYDRAZINES In the ionization of methylhydrazine and dimethylhydrazine both invariably exhibit M^+ ions and diagnostic DSI ions of $(M-H)^+$ with great efficiency, but lines of the $(M+H)^+$ ions derived from the associated species are absent.
NITROSAMINES N-nitrosodimethylamine generates $(M-16)^+$ and m/z 45,44,43 peaks while N-nitrosophenylamine gives $(M-16)^+$ and $(M-29)^+$. Presumably $(M-16)^+$ ions correspond to loss of oxygen.

(1) T. Fujii, *Int. J. Mass Spectrom. Ion Phys.*, 1984, 57, 63-74.
(2) T. Fujii et al., J.Phys. Chem., 1985, 89, 4687-4690.
(3) T. Fujii, J. Phys. Chem., 1984, 88, 5228-5232.

The present study, together with previous ones (1-3), reveals some principle schemes for the SI spectra of N-containing aliphatic compounds. Generally the spectrum has a simple pattern and a high peak of $(M-nH)^+$ ions, where n is an odd number. For most compounds the $(M-H)^+$ intensity is highest and the electronic-chemical properties of the radical substituent in the molecule affect the ionization efficiency of $(M-H)^+$ ions. M^+ ions are formed when the molecular IE is small. $(M+H)^+$ ions with great intensity can be formed by a protonation process in cases where the recombination energy of $(M+H)^+$ ions is small.

Under the experimental conditions used, the SI mass spectrum is clearly selective, being suitable for the qualitative and quantitative analysis of alkylamines, quaternary ammonium salts, diamines, aminoalcohols, hydrazines and nitrosamines, but not for nitro compounds, cyano compounds, oximes and amides. Particularly alkylamines and hydrazines can be seen to have SI sensitivities which are significantly higher than for EI. This should stimulate the development of the SIOMS method for the high sensitivity analysis of these compounds.

Table I. Surface ionization mass spectrum and relative sensitivity of N-containing organics

Compound (m/e, IP)	Intense Peak (m/e)	Emitter Temp.(K)	Relative Sens.(A/torr)	SI/EI(n)	Remarks
AMINE					
1 methylamine (31, 8.97)	32, $(M+H)^+$	600	4.2×10^{-4}		AP(8.25 eV)
	30, $(M-H)^+$	960	4.2×10^{-3}	0.66(30)*	IP(8.72 eV)
2 dimethylamine (45, 8.24)	46, $(M+H)^+$	600	0.28		AP(7.94 eV)
	44, $(M-H)^+$	960	2.8	61(44)	IP(8.0 eV)
	42, $(M-3H)^+$	960	1.9×10^{-3}		
3 trimethylamine (59, 7.8)	58, $(M-H)^+$	960	$5.6\times10^{+1}$	650(58)	
	42,	960	2×10^{-3}		
	30,	1100	2.5×10^{-2}		
QUATERNARY AMMONIUM SALT					
4 tetramethylammonium** chloride (109)	74, $(CH_3)_4N^+$	960	100	19(74)	Ts=210C***
	58	960	6.0		
DIAMINE					
5 diaminoethane (60, 7)	59, $(M-H)^+$	960	1.6×10^{-2}	0.23(30)	
	44,	960	1.4×10^{-2}		
	42,	960	1.2×10^{-2}		
	30,	960	9.4×10^{-2}		
	61, $(M+H)^+$	600	trace		
6 diaminopropane (74, 7)	71, $(M-3H)^+$	960	3.8×10^{-1}		
	58,	960	3.3×10^{-1}		
	56,	960	1.6×10^{-2}	0.9(30)	
	44,	960	1.4×10^{-1}		
	30,	960	5.3×10^{-2}		
7 diaminobutane (88, 7)	85, $(M-3H)^+$	960	2.1×10^{-1}	1.1(30)	
	72,	960	1.2×10^{-1}		
	44,	960	8.0×10^{-2}		
	30,	960	2×10^{-1}		
AMINOALCOHOL					
8 ethanolamine** (61, 7)	62, $(M+H)^+$	600	3.3		Tc=160C****
	60, $(M-H)^+$	960	7.9		
	58, $(M-3H)^+$	960	3.6		
	56,	960	6.9		
	44,	960	100	0.57(30)	
	30,	960	24		
9 diethanolamine** (105, 7)	98,	960	100	1.0(74)	Tc=160C
	88,	960	15		
	86,	960	32		
	74,	960	35		
	72,	960	11		
	70,	960	22		
	56,	960	33		
	106, $(M+H)^+$	600	trace		
	100,84,42,	960	trace		
10 triethanolamine** (149, 7)	130,	960	11		Tc=200C
	118,	960	15		
	100,	960	100	1.5(118)	
	98,	960	88		
	96,	960	11		
	72,	960	31		
	70,	960	13		
	58,	960	11		
	144,116,114,	960	< 10		
	112,94,88,86,	960	< 10		
NITRO COMPOUND, NITRITE & CYAN COMPOUND					
11 nitromethane (61,11.08)			no response		
12 nitroethane (75,10.88)			———		
13 2-nitropropane (89,10.71)			———		
14 t-butylnitrite (103, 7)			———		
15 acetonitrile (41,12.2)			———		
16 n-valeronitrile (83, 7)			———		
17 methylisocyanate (57, 7)			———		
18 ethylisocyanate (71, 7)			———		
OXIME					
19 acetaldoxime (59, 10.65)	44,42,	960	trace		
20 butyraldoxime (87, 7)	70,	960	2.7×10^{-3}	0.26(41)	
	56,53,	960	trace		
AMIDE					
21 formamide (45, 10.24)			———		
22 acetamide (59, 9.77)	43,	960	trace		Tc=140C
23 acrylamide (71, 7)			———		Tc=150C
24 dimethylformamide (73, 7)	74, $(M+H)^+$	600	trace		
	44,	960	trace		
25 carbamide** (60, 10.27)	61, $(M+H)^+$	600	100	0.001(46)	Ts=120C
	43,	960	33		
	41,	960	50		
	18,	960	50		
26 guanidine** (59, 9.10)	60, $(M+H)^+$	600	100	0.04(18)	Ts=200C
	45,	960	9.1		
	18,	960	12		
HYDRAZINE					
27 methylhydrazine (46, 7.67)	46, M^+	960	5.2×10^{-1}	1.4(28)	
	45, $(M-H)^+$	960	5.4×10^{-3}		IP(7.3eV)
	32,	960	7.0×10^{-3}		
28 dimethylhydrazine (60, 7.46)	60, M^+	960	1.1×10^{-1}		
	59, $(M-H)^+$	960	2.1	4.1(28)	IP(6.4eV)
	44,	960	2.0×10^{-2}		
	42,	960	1.4×10^{-3}		
	32,	960	1.3×10^{-3}		
	30,	960	1.0×10^{-2}		
	18,	960	2.1×10^{-2}		
NITROSAMINE					
29 N-nitrosodimethylamine** (74, 7)	58,	960	6.4		Tc=80C
	45,	960	2.5		
	44,	960	100	0.1(42)	
	43,	960	7.5		
30 N-nitrosodiphenylamine** (189, 7)	182,	960	23		Tc=180C
	169,	960	100	0.05(169)	

*) (n) in the SI/EI column indicates the mass number, n, of the base peak in the EI spectrum for comparison.
**) The spectrum of the compound marked by ** is expressed in the pattern coefficient in the column of Relative Sensitivity.
***) The quartz ampule temperature. Ts, is given in the column of Remark.

SELECTIVE REACTANT IONS IN CHEMICAL IONIZATION MASS SPECTROMETRY: TRIMETHYLSILYL IONS

Ron Orlando and Burnaby Munson
Department of Chemistry
University of Delaware
Newark, DE 19716

The most abundant species in the tetramethylsilane/helium CI reagent gas system is the trimethylsilyl ion at m/z 73. Other ions are observed as products of reaction of trimethylsilyl ions with tetramethylsilane, $(CH_3)_7Si_2^+$ at m/z 161 and less abundant ions with major isotopes at m/z 145 and 131. The other abundant product ion in this system is the hydrated trimethylsilyl ion at m/z 91, which is formed by reactions of the trimethylsilyl ion with traces of water. The relative abundances of these ions are dependent on both the temperature and pressure. As the temperature decreases and as the pressure increases, the relative abundances of the higher mass ions increase.

The trimethylsilyl ion reacts rapidly with aliphatic alcohols to form three major product ions:

- alkyl ions $(M - OH)^+$, by hydroxide abstraction from the alcohols
- the hydrated trimethylsilyl ion, $(CH_3)_3SiOH_2^+$, by water abstraction from the alcohols
- adduct ions, $(M + 73)^+$.

Both the alkyl and adduct ions provide molecular weight information about the parent alcohol and the hydrated trimethylsilyl ion can be used as a diagnostic ion for alcohols.

Ion ejection experiments under ICR conditions on mixtures of alcohols and tetramethylsilane showed that the adduct ions were formed by reactions of the hydrated trimethylsilyl ions with the neutral alcohol. This reaction scheme was verified by trapped drift experiments in which the ions were allowed to react for different amounts of time before they were detected. Kinetic plots clearly showed that the trimethylsilyl ion reacted with the alcohols to form the hydrated trimethylsilyl ion which then reacted with the alcohols to form the adduct ion.

$$73^+ + M \longrightarrow (M - OH)^+ + (CH_3)_3SiOH \qquad (1)$$

$$73^+ + M \longrightarrow (CH_3)_3SiOH_2^+ + C_nH_{2n} \qquad (2)$$

$$(CH_3)_3SiOH_2^+ + M \longrightarrow (M + 73)^+ + H_2O \qquad (3)$$

The alternative method of formation of the $(M + 73)^+$ adduct ions which might occur under CI conditions is a collisionally stabilized addition,

$$(CH_3)_3Si^+ + M \longrightarrow [M + 73]^+_* \longrightarrow (M + 73)^+ \qquad (4)$$

If the consecutive reactions (2) and (3) are responsible for the formation of the $(M + 73)^+$ ions under CI conditions, then the ratio, $(M + 73)^+/91^+$, will increase with increasing concentration of alcohol. If the collisionally stabilized addition reaction (4) is dominant under CI conditions, then the ratio, $(M + 73)^+/91^+$, will be independent of alcohol concentration. GC/CIMS experiments showed that this ratio increased linearly with increasing alcohol concentration and that the intercept was nearly zero. Consequently, even at the high pressures of the CI experiments, the adduct ions were formed predominantly by the two consecutive reactions, (2) and (3). The extent of formation of $(M + 73)^+$ adduct ions also decreased with increasing temperature. Consequently, the ratio of adduct ions to fragment ions in CIMS with tetramethylsilane will be very strongly dependent on the experimental conditions and not easily reproduced from one laboratory to another.

The trimethylsilyl ions react with alcohols to form either alkyl ions by reaction (1) or the hydrated trimethylsilyl ion by reaction (2). The latter ion can react further to form adduct ions. The ratio of rate constants for reactions (1) and (2), the branching ratio, can be obtained as the ratio of ion currents, $R^+/[91^+ + (M + 73)^+]$. This ratio should be a function of the structure of the alcohols and should increase as the stability

of the alkyl ion increases. However, this ratio must be independent of experimental conditions for this ratio to be useful for differentiation among isomeric alcohols. Experiments under CI conditions showed that this branching ratio was independent of temperature. Essentially the same value was observed for the branching ratios for these two compounds under CI conditions and under ICR conditions at room temperature. The agreement of branching ratios under ICR and CI conditions indicates that there is virtually no collisionally stabilized formation of the $(M + 73)^+$ ions under CI conditions.

The branching ratios for a few isomeric aliphatic alcohols are sufficiently different that one may differentiate among the isomers. The primary alcohols give a much smaller $R^+/[91^+ = (M + 73)^+]$ ratio than secondary or tertiary alcohols.

Laser Desorption ICR with an External Ion Source

P. Kofel, M. Allemann, P. Grossmann
Spectrospin AG, Industriestr. 26, CH-8117 Fällanden

An ICR spectrometer with an external ion source has important advantages compared to a conventional ICR instrument [1,2]. The access to the source is much improved and differential pumping between the ion source and the analyzer cell can be introduced. In this poster we would like to discuss some results which have been achieved with an external laser desorption ion source.

The external ion source is evacuated by a 330 l/s turbo molecular pump. The source can easily be removed for cleaning or maintainance without breaking down the ultra high vacuum. Therefore long deadtimes are avoided.

The ions are formed from the surface of a copper or a silver target. A Nd:YAG laser was used for our experiments, which delivers a pulse of 8 n sec length with an energy of approximately 150 mJ. The achieved power density was in the order of 10^9 W/cm^2. The pulsed nature of the LD ionisation harmonizes especially well with the pulsed ICR spectrometer.

After formation, the ions are accelerated towards a system of lenses. These lenses allow collimation and deflection of the ion beam in order to optimize the conditions for the transfer of the ions. The ions are transfered with very low energy (few eV) to the cell. This is only possible because of the strong stray field of the 4.7 T superconducting magnet which helps to collimate the ion beam. As soon as the ion bunch reaches the cell, the trap is closed by switching the appropriate trapping plate from zero to trap potential. The flight time of the ions can be used for preseparation of ions [3]. Fig. 1 shows the influence of the time between the laser pulse and the trapping pulse on the mass spectrum of Euroshift FOD. The experiment allows calculation of an average transfer energy from the measured flight time. The energy is in the order of 1 eV.
Broad band spectra can be measured if the transfer energy is chosen higher and therefore the flight time effects become very small. Fig. 2 shows an overview LD spectrum of Euroshift FOD, the insert illustrates that the high resolution capability of the instrument is fully conserved if external ionization is used. At mass 1038 a resolution of 250'000 (FWHH) could be achieved. The high resolution spectrum was acquired with one scan.

References:

[1] R.T. McIver, R.L. Hunter, and W.D. Bowers, Int. J. Mass Spectrom. Ion Proc. 64 (1985) 67

[2] P. Kofel, M. Allemann, Hp. Kellerhals, K.P. Wanczek, Int. J. Mass Spectrom. Ion Proc. 65 (1985) 97

[3] P. Kofel, M. Allemann, Hp. Kellerhals, K.P. Wanczek, Int. J. Mass Spectrom. Ion Proc., accepted

Fig. 1

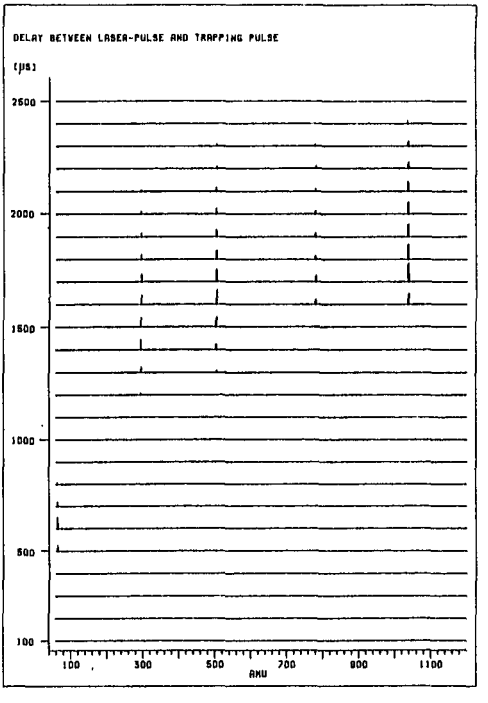
DELAY BETWEEN LASER-PULSE AND TRAPPING PULSE
[µs]
2500
2000
1500
1000
500
100
100
300
500
700
900
1100
AMU

Fig. 2

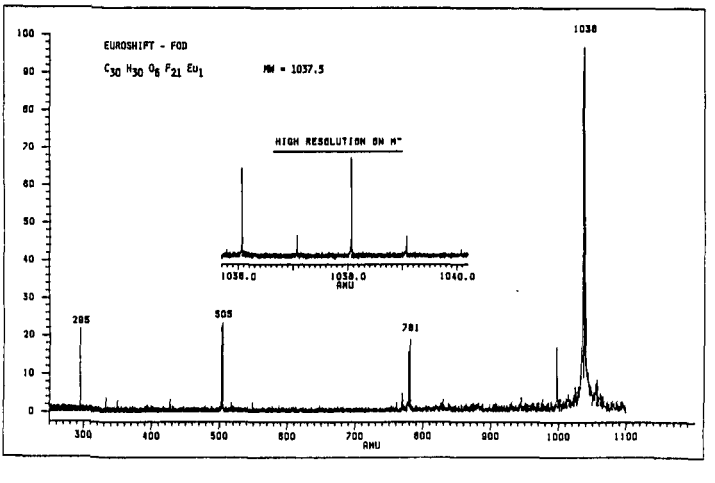
EUROSHIFT - FOD
$C_{30}H_{30}O_6F_{21}Eu_1$
MW = 1037.5
HIGH RESOLUTION ON M+
1036.0
1038.0
1040.0
AMU
1038
285
505
781
100
90
80
70
60
50
40
30
20
10
0
300
400
500
600
700
800
900
1000
1100
AMU

DESIGN OF A PULSED NOZZLE FOR SUPERCRITICAL FLUID/MASS SPECTROMETRY:

Ho Ming Pang, Chung Hang Sin, David M. Lubman; Department of Chemistry University of Michigan, Ann Arbor, MI 48109 and Jens Zorn, Department of Physics, University of Michigan, Ann Arbor, MI 48109.

Supercritical fluids have been successfully used in chromatography for the analysis of nonvolatile or thermally labile compounds because of their high dissolving power with low viscosity at low operating temperatures. Upon expansion into vacuum, they become gases again and thus can be converted into a supersonic expansion jet so that supercritical fluids can be conveniently interfaced to mass spectrometer as the detector. When injected continuously into a mass spectrometer, these supercritical fluids under high pressure, e.g. several hundred atmospheres, require the use of a small orifice, about 10 microns, to limit the high gas throughput. Since the on axis molecular beam density is proportional to the square of the orifice diameter, using a small orifice provided a low on axis density thus limiting the sensitivity of this technique; however, using a large orifice requires higher pumping capacity to handle the large gas load. We have therefore designed a high pressure pulsed nozzle[1] or molecular beam modular for interfacing supercritical fluid injection to a mass spectrometer in order to increase the on axis molecular beam density and thus the sensitivity.

The major component of the pulsed nozzle is a modified Bosch fuel injector which is mounted inside a stainless steel house. The nozzle can pulse inject the supercritical fluids of CO_2 and N_2O up to a pressure of 380 atm and up to a 200°C operating temperature. The use of short pulses can reduce the duty cycle necessary for pumping this large gas load. With the use of differential pumping and liquid N_2 cryopumping, a 150 micron orifice can be used to increase the on axis density by a factor of 225X compared to a continuous expansion through a 10 mircon orifice without overloading the vacuum system. A special teflon o-ring or a copper gasket is used to seal the front plate and the main body; therefore, there is no leak problem under the high pressure and temperature conditions. Since the nozzle can be disassembled, cleaning and changing the orifice to a different size is easy. A liquid nitrogen cooled skimmer is used to sample the coldest part of the supersonic beam from the nozzle and to reduce the shock waves. The detection chamber pressure is maintained at about 1×10^{-5} torr when the nozzle is operating at 10 Hz. The experimental setup has been described previously[2]. Supercritical fluids of CO_2 and N_2O are produced by a Varian 8500 syringe and dissolves a solid compound in a high pressure reservoir which is then carried into the pulsed nozzle for injection. the molecules are ionized by resonant 2-photon ionization using an ultraviolet laser beam 266nm generated by a frequency quadrupled Nd:YAG laser The ions produced are then analyzed by a time-of-flight mass spectrometer.

Several non-volatile polynuclear aromatic hydrocarbons (PNAH) compounds, biological compounds and drugs have been detected by using the supercritical fluid injection into a supersonic beam mass spectrometer. For example, carbazole which has a melting point of 245°C can be detected at 60°C under 350 atm backpressure of N_2O. Tryptophan which has a melting point of 290°C can be detected by using supercritical fluid of CO_2 at 40°C and 380 atm. The unique features of these mass spectra are 1) operating temperature only slightly higher than room temperature can be used to dissolve the non-volatile or thermally labile compounds; 2) with using laser ionization, molecular ions are produced without fragmentation.

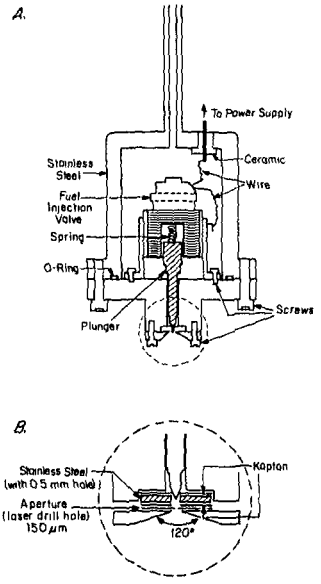

Figure: (A) Ultra-high pressure pulsed nozzle assembly.
(b) Close-up of nozzle aperture.

1) Ho Ming Pang, Chung Hang Sin, David M. Lubman, Jens Zorn; Anal. Chem., 1986, 58, 1581
2) Chung Hang Sin, Ho Ming Pang, David M. Lubman, Jens Zorn; Anal. Chem., 1986, 58, 487

Kolaitis, L.; Lubman, D.M., Detection of Nonvolatile Species by Laser Desorption-Atmospheric Pressure Mass Spectrometry. Department of Chemistry, University of Michigan, Ann Arbor, MI 48109.

We are using laser desorption as a means of volatilizing thermally labile compounds into the gas phase for detection in atmospheric pressure mass spectrometry. Such compounds include amino acids, purine and pyrimidine bases and their nucleosides, vitamins, drugs and catecholamines. The main advantage of this method is that desorption of neutrals using the 2nd harmonic of a Nd:YAG laser (532 nm) and the atmospheric pressure ionization process using a ^{63}Ni β source, occur in two separate steps as compared to LDMS where desorption and ionization occurs in one step. Complete desorption of the sample can be achieved with mainly production of neutrals and almost 100% ionization efficiency due to the large number of collisions under atmospheric pressure and high proton affinities of most of the compounds examined which result in detection limits of ~0.3 ng.

The experimental apparatus consists of an atmospheric pressure source chamber, interfaced to a Spectra EL Extranuclear Quadrupole mass spectrometer and has been described previously (1). The laser beam enters the chamber through a quartz window and impinges on a ceramic rod from which the sample is desorbed. The ceramic rod enters from the opposite side of the chamber and extends into the guard ring structure where the desorption and subsequent ionization occurs. The sample is prepared by dissolving it in toluene solvent and applying the resultant paste on the end of the rod. The sample is allowed to dry so that a coat which probably consists of several hundred monolayers is formed on the surface.

In our work using LD-APIMS with the Ni β source the key result is that only the molecular ion M^+ or the protonated molecular ion MH^+ is obtained, with little or no fragmentation. Thus the desorption process produces intact neutrals and the CI API method softly ionizes these species. Purines and pyrimidines produce only an MH^+ peak (2), except in the cases of thymine, cytosine and creatinine, where also strong dimer peaks appear after desorption since these compounds are known to dimerize readily, although the dimer peak will decrease as the concentration becomes lower. All nucleosides examined herein (2) produce only an MH^+ peak (see figure 1) and the same is observed with a number of amino acids studied (2). Further, there are examples such as pyridoxine and riboflavin, where small molecule elimination cannot be avoided, although it is not clear whether this is due to the desorption or ionization step. In addition the compounds that are in the M·HCl form are detected without the HCl which must be detached in either the desorption or ionization step. Catecholamines and their metabolites are a particularly important group. Tyrosine produces a strong MH^+ with no fragmentation. DL-Dopa exhibited an intense peak of mass 193 which corresponds to MH^+ where Dopamine.HCl was found to have a peak at 153 which corresponds to (MH^+-HCl). Norepinephrine.HCl gave a simple characteristic peak at mass 154 which appears to be (MH^+-HCl-NH_2), and epinephrine and tyramine gave single peaks corresponding to the protonated molecular ion MH^+.

The key to the results is the desorption process. In LD generally a high-powered (0.5-1 J) pulsed laser is used to rapidly desorb a thin coat of material from a surface to produce ions for examination in a mass spectrometer. In the desorption process used herein a low-powered laser (<100 mJ/pulse) is used. A similar method has been used for laser desorption under vacuum conditions in our previous work (4) and although the initial desorption occurs from the surface this desorption sends a shock wave through a solid causing material to desorb from the sample into the gas phase. Thus, depending on the laser power, a small amount of material can be desorbed on each laser pulse so that the sample may last up to several minutes even at a laser repetition of 10 Hz. The slow desorption method is preferable for sensitive detection since rapid desorption may saturate the reactant ions from the Ni β API source and much of the sample lost for sensitivity measurements.

1. Kolaitis, L.; Lubman, D.M. Anal. Chem., in press, August 1986.
2. Kolaitis, L.; Lubman, D.M. Anal. Chem., 1986, submitted, April 1986.
3. Stryer, L. Biochemistry, W.H. Freeman and Co., San Francisco, 1975.
4. Tembreull, R.; Lubman, D.M. Anal. Chem., 1986, in press, June 1986.

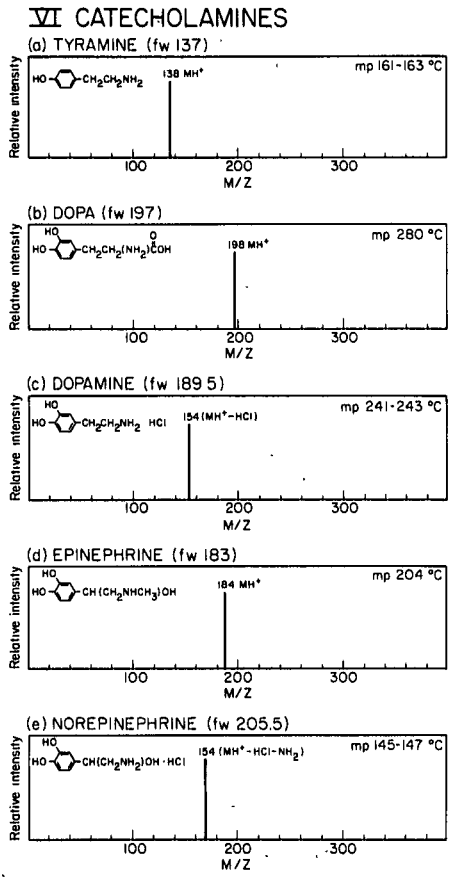

Figure 1. Laser Desorption-Atmospheric Pressure Ionization Mass Spectrometry of Catecholamines.

CLUSTERS OF WATER UNDER ATMOSPHERIC PRESSURE STUDIED BY

FIELD IONIZATION AND LIQUID IONIZATION MASS SPECTROMETRY

M. Tsuchiya and E. Aoki; Dept. of Industrial Chem., The University of Tokyo, Hongo, Bunkyo-ku, Tokyo 113 Japan
K. Otsuka; MS Group, JEOL LTD., Nakagami, Akishima, Tokyo

Studies of clusters involving water molecules are particulary important since they provide insight into the nature of hydrogen-bonded systems. Liquid ionization (LI) mass spectrometry[1,2] was applied to study on the behavior of water clusters at atmospheric pressure.

A schematic diagram of an ion source is shown in Fig.1. A needle emitter (sample holder) is made of gold. A simple stainless steel tube grounded was used for producing metastable argon atoms (Ar^*) by corona discharge. Water is introduced through a teflon pipe with a piece of paper as shown in Fig.1, or through the side tube in which a lump of tissue paper wet with distilled water is installed. It was found that field ionization of water can occur even at atmospheric pressure by simply increasing a voltage (V_E) of the needle up to 2.0 - 2.2 kV without corona discharge. Abundant cluster ions appear suddenly to give a mass spectrum similar to that obtained with Ar^* (LI).

Cluster ions of water, $H^+(H_2O)_n$, are usually observed as a background of the instrument under ordinary conditions for organic compounds (n: 2 - 8). When vapor pressure of water is high and the V_E is increased, larger cluster ions of water appear and increase their abundances significantly with the V_E as shown in Fig.2A (V_E = 2.0 kV).[2]

When the temperature of the needle is increased (22 °C → 130 °C) by a wire heater, the cluster ion distribution shifts toward smaller n-values. When sample water was introduced from the upper side tube using a lump of tissue paper (upside down of Fig.1), the needle temperature has small effect on the cluster ion distribution. The base peaks are all at m/z 379 (n = 21) corresponding to the well known stable cluster ion. In contrast, when the tissue paper was placed inside the lower side tube (similar to Fig.1), the needle temperature show significant effect on the cluster ion distribution. The m/z value of the base peak shifts toward smaller one such as 307, 181 and 73 by increasing the needle temperature.

Mass spectra shown in Fig.2 were obtained by FI at the needle temperature of 100 °C using the teflon pipe just as shown in Fig.1. When the edge of tissue paper was placed close to the needle (distances a and b in Fig.1 were 1.5 and 4 mm, respectively), Fig.2A was obtained. In Fig.2B, the distances a and b were 5 and 6 mm, and in Fig.2C were 10 and 8 mm, respectively. The cluster ion distribution changes significantly with the distance a. Figure 3 shows some relationships between the sum of cluster ion abundances (ΣI, I: each peak intensity) and each average cluster ion size N ($N = \Sigma nI/\Sigma I$, n: number of water molecules in each cluster ion) for each mass spectrum.

Water vapor in atmospheric Ar may condense easily on the needle tip and any surfaces in the ion source. By heating the needle, the rate of condensation may decrease. A higher V_E promotes desorption of larger cluster ions from the liquid surface. When average vapor pressure of water in Ar gas, P_W, is low, both of average cluster size (N) and total ionization (ΣI) increase with the P_W, but when P_W is high, ΣI values show a maximum at the value N = about 21 (Fig.3) that coincides with a size of the 21st cluster ions. For instance, ΣI value of Fig.2B (data No.31) is the highest, instead of Fig.2A (No.30). The widest distribution was obtained at room temperature by FI, that is data No.15 in which peaks apppeared at m/z from 37 to 797 (I = 50 %), in spite of having a N value similar to that of No.33 (that resembles Figure 2A). These results clearly indicate that sample introduction from a short distance or from upper side result in large N values, but ΣI shows a maximum, regardless of the P_W. It is interesting to note that Fig.3 resembles Fig.2B.

Only one possible explanation for these differences in mass spectra, is that primary ions produced on the needle tip already have some distributions which would be similar to those observed by this method. And these results strongly suggest that clusters of water molecules exist in the gas phase as well as at the surface of liquid water, and clusters with n = around 21 would vaporize most easily from the liquid water.

References

1) M.Tsuchiya and H.Kuwabara, Anal. Chem., 56, 14 (1984).
2) M.Tsuchiya, K.Otsuka and H.Kuwabara, Chem. Letters, (1985) 709.

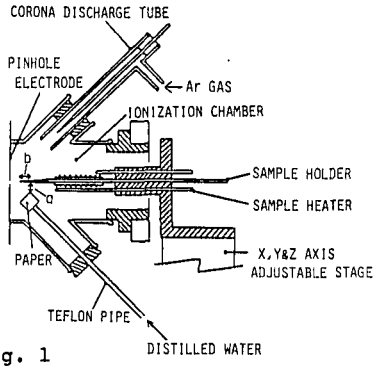

Fig. 1

SCHMATIC DIAGRAM OF LIQUID-IONIZATION ION SOURCE

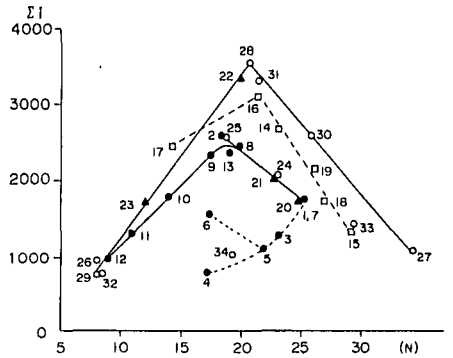

Fig.3 Correlation between Total ion abundances (ΣI) and Average sizes of cluster ions (ΣnI/ ΣI)

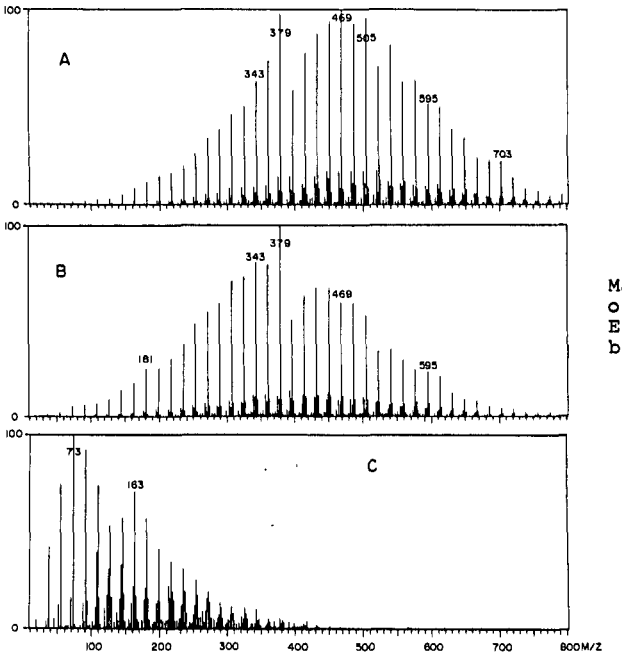

Fig. 2

Mass spectra of clusters of water --
Effect of distances a and b.

A; a: 1.5 mm, b: 4 mm
B; a: 5 mm, b: 6 mm
C; a: 10 mm, b: 8 mm

DEVELOPMENTS IN HIGH FIELD IONIZATION MASS SPECTROMETRY.

W.M. Lagna *, P.S. Callery, S.M. Musser and R.C. Robbins *.
* Chemical Research and Development Center, Aberdeen Proving Grounds, MD 21010.
University of Maryland School of Pharmacy, 20 North Pine Street, Baltimore, MD 21201.

High field ionization was originally designed as a non-thermal method of interfacing a liquid chromatograph to a quadrupole mass spectrometer. The method has been extended to aerosol and gas analyses with minimal change in the source assembly. Charge transfer from an electrode held at very high potential occurs di rectly to gases. Non-thermally induced volatilization of a liquid occurs when the charge imparted to a droplet of the nebulized effluent exceeds the critical charge to radius ratio. HFI demonstrated high ionization efficiencies independent of the nature of the solvent. An earlier limitation of periodic electrostatic discharge has been overcome by elimination of metallic components and the use of very high density, high dielectric materials in the source region. Stable ion currents are obtained when the high field potential exceeds the critical breakdown potential of the gas in the ion source region. On introduction of a nebulized liquid, the continuous current discharge potential is observed to be inversely proportional to the dielectric constant of the solvent. This is consistent with earlier theories which predict the characteristics of the field are constrained by the activity and dielectric properties of the droplets in the vapor, not by the components of the gas phase. However, the conditions necessary for continuous ion currents are sensitive to the source geometry and the operating source pressure.

In the high potential negative polarity mode, the field electrode acts as an electron emitter. The mechanisms of ion formation appear similar to those of electron impact, and fragmentaion is observed to increase with increasing electrode potential. It is uncertain whether fragmentation arises from mechanical transfer of energy or from electronic instability resulting from a multiply charged parent. Ion formation appears to be under kinetic control, and multiply charged species are observed.

The LC effluent is nebulized at ambient pressure and temperature outside of the source region. This eliminates the need for cartridge heaters in the nebulizer. A direct inlet into the differentially pumped source volume reduces the wetting of the source walls which minimizes electrostatic discharge. The eluent and entire source assembly are at ambient temperature.

An in-beam electron impact source has been integrated into the lens assembly of the HFI source. The EI filament can be operated with the HFI source or independently for generation of conventional EI spectra.

The HFI source has been fitted to Extrel and Finnigan quadrupole mass spectrometers with few modifications. The ability to directly analyze liquids, aerosols and gases permits application of the source to metabolic and environmental sampling. The high inherent sensitivity makes the source suited for continuous air monitoring. However, the possibility of electrical discharge from the ionizing electrode or source region presents a hazard to the MS operator and the associated equipment.

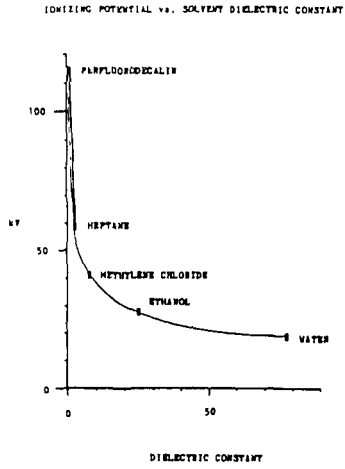

Figure 1. The HFI continuous current electrical discharge potentials are plotted against the dielectric constant of the nebulized solvent. Liquid flow rates were 1 ml per minute at a source volume pressure of approximately 0.4 torr.

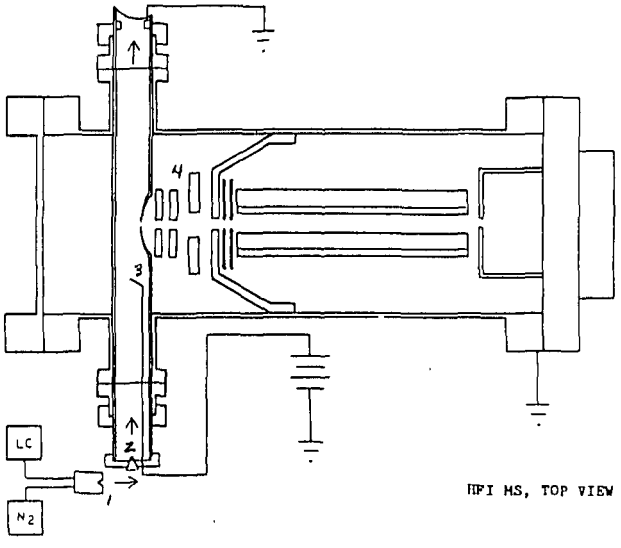

Figure 2. Diagrammatic representation of the top view of a quadrupole based high field ionization mass spectrometer. Nebulized solvent (1) or vapors enter the source region through inlet (2). Ions are formed at the electrode (3) and are focused in the lens region (4) into the quadrupole mass filter

THE ROLE OF LC/MS IN THE CHARACTERIZATION OF NEW NUCLEOSIDES FROM TRANSFER RNA. C.G. Edmonds, T. Hashizume and J.A. McCloskey, Departments of Medicinal Chemistry and Biochemistry, University of Utah, Salt Lake City, UT 84112; R. Gupta, Southern Illinois University, Carbondale, IL 62901; K.O. Stetter, University of Regensburg, Federal Republic of Germany.

Combined liquid chromatography-thermospray mass spectrometry has proven to be an individually powerful and, in relation to other methods, highly complementary tool in the investigation of nucleosides occurring in the enzymatic hydrolysates of transfer RNAs from a variety of sources. Among the 76 to 92 nucleotide units comprising an isoaccepting tRNA as many as 13 may be post-transcriptionally modified residues, with the range of 10-15 being typical. More than 60 such modified structures are known in nature. In unfractionated tRNA more than 60 such isoaccepting species may be present. The success of characterization of new modified nucleosides in complex mixtures depends initially on the quantity of nucleic acid available. The preparation of pure isoaccepting tRNAs requires multiple chromatographies and is expensive of time and sample. Except in a few exceptionally straightforward cases only a few tens of micrograms are generally obtainable. On the other hand, unfractionated tRNA is available in quantities limited principally by the ease of cultivation and harvest of the organism with, in favorable cases, multi-milligram quantities being straightforwardly obtainable. Thus in the progression on isoacceptor to partially purified to bulk tRNA there is a decreasing scale of biochemical effort in preparation, and an accompanying increasing difficulty of analysis as a single modified residue in an isoaccepting tRNA proceeds from about the 1% level downwards, in a mixture of increasing complexity. The attractions of combined LC/MS for a wide ranging multicomponent analysis increase with decreasing availability of sample. This is a consequence of the amount and diversity of qualitative information which pertains in the correspondence among chromatographic retention, uv absorbance behavior and thermospray mass spectra for each component of the mixture. The features of thermospray mass spectra of nucleosides and the method for such qualitative experiments have been outlined in a previous contribution to this meeting (1).

An example of the utility of LC/thermospray MS in a screening experiment which quickly identifies the constituents of known structure and focuses attention on less familiar entities is the analysis of the nucleosides derived from enzymatic hydrolysis of the bulk tRNAs of the thermophilic archaebacterum Thermoproteus neutrophilus (growth optimum 88°C). In a single LC/MS experiment the known nucleosides present were identified and several candidate unknown peaks were revealed. Two of these could be identified from their chromatographic and uv absorbance behavior, thermospray mass spectra and correspondence with synthetic materials: previously unknown N^4-methyl-2'-O-methylcytidine and N^4-acetyl-2'-O-methylcytidine. Thermospray mass spectrum and reconstructed ion current profiles for the latter is shown in Fig. 1.

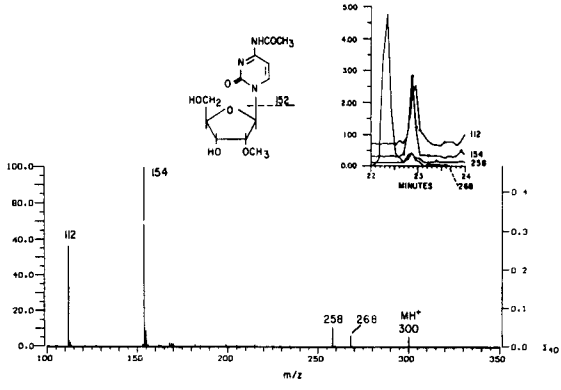

Figure 1. Thermospray mass spectrum and ion current profiles for the modified nucleoside from T. neutrophilus assigned as N^4-acetyl-2'-O-methylcytidine.

Profiles maximizing at 22.85 min corresponding to MH^+ (m/z 300) and BH_2^+ (m/z 154) are seen with accompanying losses of 42 amu from these (m/z 258 and m/z 112 resp.). A response at m/z 268 is seen for t^6A (22.3 min) and also co-eluting with the unknown. This latter response is presently unassigned and does not appear in the synthetic ac^4Cm which conforms to the unknown in all other respects.

Structure assignments were based on 40 ng-levels of individual nucleosides measured directly from crude mixtures: 50 times lower than the smallest quantity previously characterized by other mass spectrometric techniques. The identification of modifications in tRNA is the first step in a broader consideration of their relationship to structure and function in the intact nucleic acid, which is particularly intriguing in the case of archaebacteria which grow at temperatures near the boiling point of water.

Acknowledgment:

The authors are indebted to P.F. Crain for work on characterization of N^4-methyl-2'-O-methyl-cytidine.

References:

(1) C.G. Edmonds, T.C. McKee and J.A. McCloskey, 33rd Ann. Conf. on Mass Spectrom. and Allied Topics, 1985, pp.514-515.
(2) D.W. Phillipson, C.G. Edmonds, P.F. Crain, D.L. Smith and J.A. McCloskey, 34th Ann. Conf. on Mass Spectrom. and Allied Topics, 1986, paper FOA 4.

FAST ATOM BOMBARDMENT COMBINED WITH TANDEM MASS SPECTROMETRY FOR MODIFIED NUCLEOSIDES AND NUCLEOTIDES

K.B. Tomer, R.L. Cerny, Midwest Center for Mass Spectrometry, Department of Chemistry, University of Nebraska, Lincoln, NE 68588; M. Deinzer, Oregon State University, Corvallis, OR; E. Cavalieri and A. Eastman, Eppley Cancer Inst., Omaha, NE

The nature of the products of reactions of mutagenic and/or carcinogenic electrophiles with nucleosides and nucleotides are of great interest to cancer researchers. The combination of fast atom bombardment with tandem mass spectrometry yields structural information that may not be present in the full scan spectrum of these compounds or that may be obscured by mixture or background ions.

Modified nucleosides or nucleotides, upon collisional activation, fragment into ions representative of the subunits of the parent, e.g. the sugar, the modified base, the modifying group and the parent base. The identity of the modified base in carcinogen-oligonucleotide adducts can be elucidated on the basis of the MS-MS spectra of the modified oligonucleotide.

Two examples come from the FAB/MS/MS spectra of a series of twelve nucleosides and nucleotides which were modified by covalent bonding to dehydroretronecine and dihydropyrrolizinol. The MS/MS spectrum of the $(M+K)^+$ ion illustrates how the compound fragments into its building blocks (Fig. 1). Ions for the unmodified nucleoside, BSK^+, the unmodified base, BHK^+, the modified base, RBK^+, and the modifying group, R^+, are all observed.

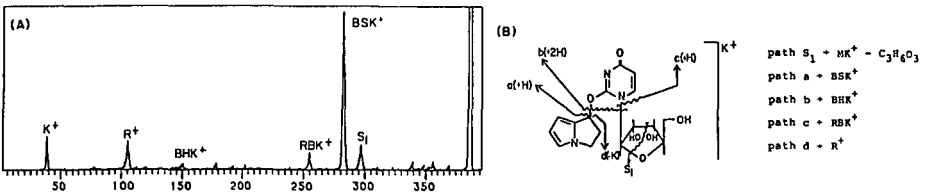

Fig. 1. A) MS/MS spectrum of the $(M+K)^+$ ion of the dihydropyrrolizidinol adduct of uridine.
B) Fragmentation scheme of the MS/MS spectrum of the $(M+K)^+$ ion of the dihydropyrrolizidinol adduct of uridine.

Similarly, the MS/MS spectrum of the $(M+K)^+$ ion of the dehydroretronecine adduct with thymidine-5′-monophosphate shows ions due to the modifying group, R^+, the sugar phosphate, $(S-2)PO_3H_2K^+$, the modified base, RBK^+, and the unmodified nucleotide, $B(S-1)PO_3H_2K^+$, (Fig. 2).

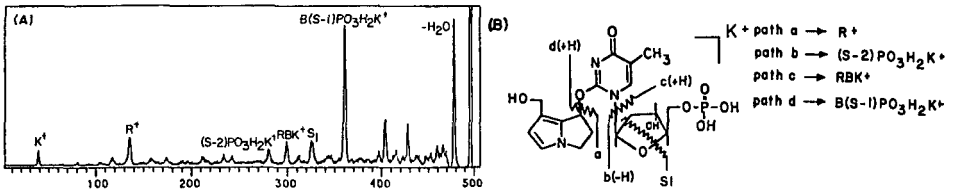

Fig. 2. A) MS/MS spectrum of the $(M+K)^+$ ion of the dehydroretronecine adduct with thymidine-5′-monophosphate.
B) Fragmentation scheme of the MS/MS spectrum of the $(M+K)^+$ ion of the dehydroretronecine adduct with thymidine-5′-monophosphate.

The FAB/MS/MS spectra of the $(M+H)^+$ ions of two benzo[a]pyrene modified guanine isomers readily distinguish the sites of modification (Fig. 3)

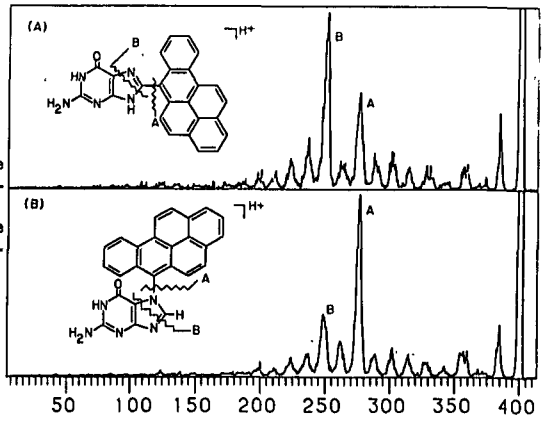

Fig. 3. A) MS/MS spectrum of the C-8 adduct of benzo-[a]pyrene and guanine.
B) MS/MS spectrum of the N-7 adduct of benzo-[a]pyrene and guanine.

It is possibly significant to the understanding of the action of carcinogens such as benzo[a]pyrene that reaction at nitrogen results in elimination of the sugar while reaction at carbon yields an intact modified nucleoside.

The MS/MS spectrum of the $(M-H)^-$ anions of the N-acetylaminofluorene modified dCdG dinucleotide (Fig. 4) (provided by Dr. F. Kadlubar of NCTR) clearly shows sequence ions and unequivocally locates the base modified by reaction with N-acetylaminofluorene.

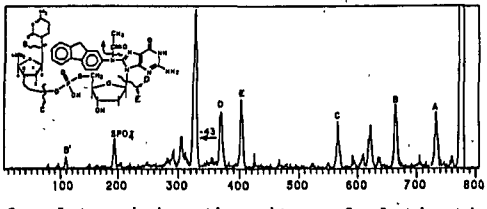

Fig. 4. MS/MS spectrum of the (M-H) anion of N-acetylamino-fluorene modified dCdG.

MS/MS spectra are also useful for determining the sites of platination in DNA upon reaction with the cancer therapeutic drug cis-diammine-dichloroplatinum (11). Adducts formed by both adjacent interaction (Fig. 5a) and DNA-interstrand cross-links (Fig. 5b) can be distinguished.

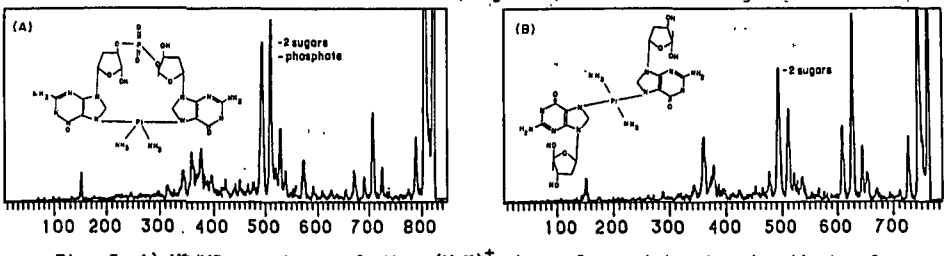

Fig. 5. A) MS/MS spectrum of the $(M+H)^+$ ion of an intrastrand adduct of cis-diamminedichloroplatinum 1t and DNA.
B) MS/MS spectrum of the $(M+H)^+$ ion of an interstrand adduct of cis-diamminedichloroplatinum 1t and DNA.

ISOLATION AND STRUCTURE ELUCIDATION OF A UNIQUE HYPERMODIFIED NUCLEOSIDE FROM *E. COLI* TRANSFER RNA. D. W. Phillipson, C. G. Edmonds, P. F. Crain, D. L. Smith and J. A. McCloskey. Departments of Medicinal Chemistry and Biochemistry, University of Utah, Salt Lake City, UT 84112.

There are over 60 naturally occurring modified nucleosides presently known to occur in transfer RNA. Some of the more extensively modified nucleosides are usually found in the anticodon region of isoaccepting tRNAs, a leading example being queuosine (Q), 1.[1]

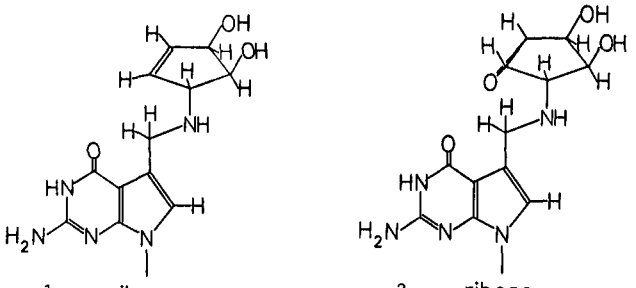

The examination by HPLC, of an isoaccepting $tRNA^{Tyr}$ from *E. coli* MRE-600 which was expected to contain Q, showed peaks for all of the expected nucleosides except Q. An unidentified peak was also observed, and when examined by thermospray LC/MS showed many similarities with the thermospray spectrum of Q. Specifically, the m/z 163, 180 and 295 ions which have been assigned to the base (minus the cyclopentenediol side chain) or base plus ribose portions of Q were also observed in the spectrum of the unknown. Other ions in the unknown were shifted 16 amu to higher mass relative to the Q spectrum. The shifted ions included the base peak ion in the Q spectrum at m/z 116 which was assigned as the side chain $C_5H_8NO_2$ portion of the molecule. This ion was found in the spectrum of the unknown at m/z 132. The $M+H^+$ and $M+Na^+$ ions were also found 16 amu higher in the unknown spectrum. The thermospray spectrum of the unknown was strongly suggestive of the unknown being a Q-like compound with an extra oxygen atom incorporated into the C_5 moiety of Q.

The low resolution EI spectrum of a heptasylil derivative of the unknown showed intense ions at m/z 655 and 656 which were also observed in the Q-TMS EI spectrum[1] and represent the 7-deazaguanosine moiety. The formula $C_{38}H_{79}N_5O_8Si_7$ was established by exact mass measurement, showing that the molecular formula for the unknown corresponds to Q + oxygen.

The data given above required the unknown be assigned as a 7-deazaguanosine derivative with an isolated methylene attached to the base at the 7 position and bound in turn to a $C_5H_8NO_3$ unit containing two double bond equivalents. Additional material was isolated for NMR from *E. coli* MRE-600 or *E. coli* W following hydrolysis in 0.3N KOH. The resulting nucleoside mixture was chromatographed by HPLC, with the unknown and a related compound produced by the alkaline hydrolysis eluting shortly before the unknown. The isolates were evaporated from D_2O and subjected to ^1H NMR at 500 MHz. The compounds were named Q'1 and Q'2, corresponding to their elution order under the HPLC conditions used.

The ^1H NMR spectrum of Q'2 (the natural product), while yielding some useful information such as a down-field resonance assignable as H-8 of a deazaguanosine as well as a doublet assigned as the anomeric proton resonance and an absence of other signals attributable to olefinic resonances, showed that most resonances upfield of the HOD peak at 4.6 ppm were not well enough resolved to be assigned. Therefore efforts were concentrated on assigning the spectrum of the alkaline conversion product, Q'1. The most downfield resonance, a singlet at 7.11 ppm, is in the correct region to be assigned as H-8 of a deazaguanosine. Homonuclear decoupling allowed the unambiguous assignment of all of the proton resonances of the ribose moiety. The absence of resonances assignable to olefinic protons and the lack of a methyl doublet or triplet in the spectrum demonstrated that all of the carbons in the C_5 side-chain were part of a

cyclic structure. A singlet integrating for two protons at 4.23 ppm was assigned as the isolated methylene group. Decoupling also showed that the methine proton assigned as a proton bond to a carbon which is bound to nitrogen resonating at 3.10 ppm was flanked by two other methine protons which by their chemical shifts 4.45 and 4.48 ppm must reside on carbons bound to hydroxyl groups. The two remaining proton resonances, which appeared as broad singlets at 3.73 and 3.77 ppm, were assigned as epoxy protons. The lack of coupling was explained in light of a paper by Tori et al. in which epoxide protons on the D ring of steroids showed no coupling to their vicinal neighbors and less than 3 Hz coupling between the epoxy protons themselves.[2] The chemical shifts of the epoxide protons are downfield of the normal epoxide shift range but not out of the range of cis-epoxide protons having electronegative groups attached.

Other evidence for an epoxide group came from an interpretation of the observed reversible isomerization of the compounds in base (the Payne reaction) in which an alpha hydroxy epoxide of the correct stereochemistry forms an equilibrium mixture of isomeric epoxides in aqueous base.[3] Other chemistry established the relative stereochemistry of 4 of the 5 centers of the carbocyclic ring as follows. Treatment of Q'1 or Q'2 with 2,2-dimethoxypropane/acetone with camphorsulfonic acid yielded a diisopropylidene derivative in the case of Q'2 while Q'1 formed a monoisopropylidene derivative. This established that the hydroxyls of the carbocyclic ring of Q'2 were vicinal and cis. Because of the stereochemical requirements of the Payne reaction, the alpha hydroxyl must also be trans to the epoxide. Therefore the stereochemistry of the ring must be as drawn as in 2 for Q'2. In an additional confirmation of the epoxide function, the diisopropylidene derivative of Q'2 was treated with 1-propanethiol in aqueous base and the formation of an addition product was observed. Thermospray mass spectra of these derivatives as well as peak matching their $M+H^+$ ions from FAB ionization supported their assigned structures.

From the evidence presented above and other arguments, we conclude that the unknown nucleoside possesses the structure shown as 2. From a biological standpoint this result raises interesting questions concerning the only presently known epoxide in nucleic acids. From a chemical perspective this study illustrates the complementarity of LC/MS with other techniques for microscale structural analysis.

References

1. H. Kasai, Z. Ohashi, F. Harada, S. Nishimura, N. J. Oppenheimer, P. F. Crain, J. G. Liehr, D. L. von Minden, J. A. McCloskey, Biochemistry 14, 4189-4208 (1975).
2. K. Tori, T. Komeno, T. Nakagawa, J. Org. Chem. 29, 1136-1141 (1964).
3. G. B. Payne, J. Org. Chem. 27, 3819-3822 (1962).

DETERMINATION OF THE 2-HYDROXY- AND 2-KETO-ACID METABOLITES OF VAL, LEU AND iLEU IN SERUM: A STABLE ISOTOPE DILUTION ASSAY.

O. A. Mamer, The Biomedical Mass Spectrometry Unit, McGill University, 1130 Pine Ave. West, Montreal, Canada H3A 1A3. N. S. Laschic and C.R. Scriver, The Montreal Children's Hospital, 2300 Tupper Ave. Montreal, Canada H3H 1P3.

Methods for measuring serum and urine concentrations of 2-hydroxyisovaleric, 2-hydroxyisocaproic, 2-hydroxy-3-methylvaleric, 2-ketoisovaleric, 2-ketoisocaproic, and 2-keto-3-methylvaleric acids (HIVA, HICA, HMVA, KIVA, KICA, and KMVA, respectively) in a single analysis are few. The oximation method (1) is one, but it is subject to variable extraction losses, E and Z isomerism in the ketoximes, variable and incomplete chemical yield in the derivatization step and other errors. Other methods such as those based on the quinoxalinol derivatives of the ketoacids (2,3) and the pentafluorobenzyl esters (4) not only suffer from many of these same problems but do not permit the determination of the corresponding hydroxyacids. Since each keto- hydroxyacid pair is in an enzyme-mediated equilibrium and all 6 accumulate in Maple Syrup Urine Disease, the concentrations of all 6 are important in monitoring metabolic homeostasis of affected patients.

A stable isotope dilution assay has been developed for serum that permits these determinations in a single GC-MS run. It is insensitive to extraction and handling losses, chemical yield and other problems of earlier methods.

A 10 ul aliquot of an ethyl acetate solution containing 10 ug each of 2-hydroxy-2,3-$^2H_2$-isovaleric, 2-hydroxy-2,3,3-$^2H_3$-isocaproic, and 2-hydroxy-2,3-$^2H_2$-3-methylvaleric acids is added to a 1 ml aliquot of serum. The serum is then deproteinized with 3 drops of saturated aqueous sulfosalicylic acid. The supernatent is made basic (pH 12-14) with 2N NaOH and the ketoacids are reduced in situ with 1 mg of sodium borodeuteride (heating at 60°, 15 min). The ether extract is made (discarded) and the aqueous phase is acidified with 5N HCl (caution: vigorous hydrogen evolution!). The acidified mixture is again extracted with ether, and the extract is dried over anhydrous sodium sulfate, evaporated to dryness and silylated. The silylate is analyzed in selected ion monitoring with GC inlet (170° isothermal, 4m x 2mm i.d. glass column packed with 15% OV-101). The HIVA set has a retention time of 6.2 min, HICA 7.8 min, and HMVA 8.2 min. Ions selected for the HIVA set are the $[M - Me]^+$ fragments m/z 247, 248, and 249 for unlabelled endogenous HIVA, once-labelled HIVA derived fron the borodeuteride reduction of endogenous KIVA, and the twice-labelled internal standard, respectively (Rel. Int. 35%). Ions monitored for the HICA set are m/z 159, 160, and 162 which are the $[M - COOTMS]^+$ fragments for unlabelled HICA, once-labelled HICA reduced from KICA, and thrice-labelled HICA internal standard (Rel. Int. 100%). Similar fragments are monitored for the HMVA set at m/z 159, 160 and 161 (Rel. Int. 100%). Areas measured for these fragments are entered into a computer program used to correct measured areas for natural abundance isotope inclusion and isotopic impurities in the standard mixture and borodeuteride. Concentrations are calculated from these corrected data.

Normal serum concentrations of these 6 acids found here in 14 children are listed below:

	KIVA	HIVA	KICA	HICA	KMVA	HMVA
Mean (n=14)	9.03	3.84	20.85	0.71	14.54	0.39
Std. Dev.	4.55	1.55	10.14	0.51	6.65	0.27
Reported (1)*	5.56		27.8		9.0	
(2)¶	19.2		47.8		23.1	
(4)§	11.3/13.3		24.5/37.4		19.0/23.3	

* sera of 4 fasting healthy adults. ¶ plasma of 7 fasting healthy adults.
§ sera of 20 females and 20 males, ages not specified.

Correction of the measured peak areas is essential; it may be done manually with a calculator with high probability of error. A program to make these corrections and calculate concentrations is written in 'Basic' and may be used with an International Business Machines PC personal computer. A listing of this program and instructions for its use are available to those interested and may be obtained from one of us (O.A.M).

1. G. Lancaster, P. Lamm, C.R. Scriver, S.S. Tjoa and O.A. Mamer, Clin. Chim. Acta, 48, 279 (1973).
2. U. Langenbeck, U. Wendel, A. Mench-Hoinowski, D. Kuschel, K. Becker, H. Przyrembel and H.J. Bremer, Clin. Chim. Acta, 88, 283 (1978).
3. U. Langenbeck, H. Luthe and G. Schaper, Biomed. Mass Spectrom., 12, 507 (1985).
4. I. Penttila, A. Huhtikangas, J. Herranen and O. Moilanen, J. Chromatogr. Biomed. Appl., 338, 265 (1985).

STRUCTURE DETERMINATION OF SCH 13384 COMPONENTS 1 & V BY FAST ATOM BOMBARDMENT (FAB) MASS SPECTROMETRY

B.N. Pramanik, A.K. Ganguly, J.B. Morton, T.M. Chan, O. Sarre, Peter Bartner, and V.M. Girijavallabhan, Pharmaceutical Research and Development Division, Schering-Plough Corp., Bloomfield, NJ 07003, USA.

Sch 13384 Components 1 & V represent oligosaccharide group of antibiotics everninomicins and are produced[1] by Micromonospora carbonaceae. Everninomicins are highly active against Gram-positive bacteria. Structural elucidation of everninomicins B, C and D were carried out in our laboratories[2-4] using chemical degradation, NMR and MS. The fast atom bombardment (FAB) mass spectrometry[5] of everninomicin D, N-acetyl everninomicin D and their degradation products were also reported. The structures of antibiotics 13384-I & V remained unknown for a long period of time.

Recently we have carried out extensive studies involving FABMS, chemical degradation, CMR and NMR to determine the structures of 13384-I & V. FABMS studies provided important structural features which lead to the structure elucidation of Sch 13384 components I & V. We wish to report the results of our FABMS studies.

In our present investigation FABMS data were recorded on Finnigan MAT312 and VGZAB-SE mass spectrometers employing xenon fast atoms. The quality of the spectra depended on the solvents used for dissolving the compounds and also the liquid used as a matrix. The best results were obtained using glycerolthioglycerol as a matrix[5] and dimethyl sulfoxide as a solvent. Sch 13384-I & V displayed ion peaks $(M+H)^+$ and $(M+Na)^+$ of moderate intensity and exhibited fragmentation pattern which afforded valuable structural informations.

Diethanolamine is a useful matrix for the determination of molecular weights of oligosaccharide antibiotics. Sch 13384-I & V showed intense adduct ions corresponding to $(M+DEAH)^+$; limited fragment ions were observed in the spectra.

The molecular weights of (1) and (2) were established as 1629 and 1599, respectively from FAB data. Each FAB spectrum contained two sets of fragment ions generated by the cleavage of the center orthoester and were easy to recognize; one set showed chlorine isotopes and the other set of ions contained no chlorine. Sugar sequencing information were obtained from such spectra data. High resolution FABMS studies of important fragment ions were carried out for confirmation of our structural assignments. For further details see Fig. A & B.

Chemical degradation studies[2-4] followed by spectral analysis were performed to establish these structures (13384-I & V), see Fig. C & D.

References

1. Weinstein, M.J., Luedemann, G.M., Oden, E.M., Wagman, G.H., Antimicrob. Agents Chemother. 1965, 1964, 24.
2. Ganguly, A.K., Sarre, O.Z., Greeves, D., Morton, J., J. Am. Chem. Soc. 1975, 97, 1982.
3. Ganguly, A.K., Szmulewicz, S., J. Antibiotics 1975, 28, 710.
4. Ganguly, A.K., Saksena, A.K., J. Antibiotics 1975, 28, 707.
5. Ganguly, A.K., Pramanik, B.N. Girijavallabhan, V.M., Sarre, O., Bartner, P.L., J. Antibiotics 1985, 38, 808.

Figure A: FAB(+VE) - Mass Spectrum of SCH 13-384-I

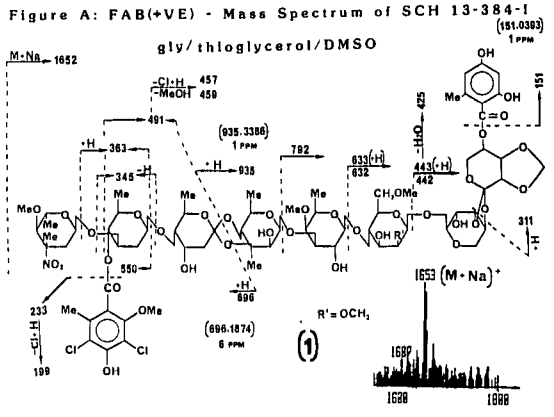

Figure B· FAB(+VE) · Mass Spectrum of SCH 13-384-5 in thioglycerol/DMSO

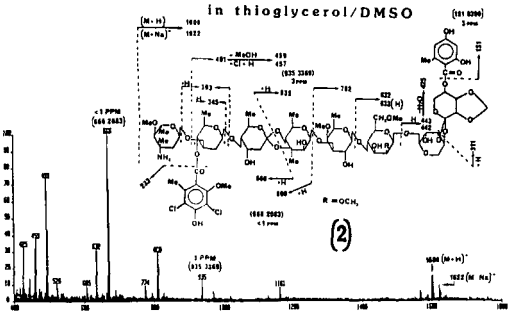

Figure C· FABMS of OLGOSE 13384-I in gly/thioglycerol (Isolated by chemical degration)

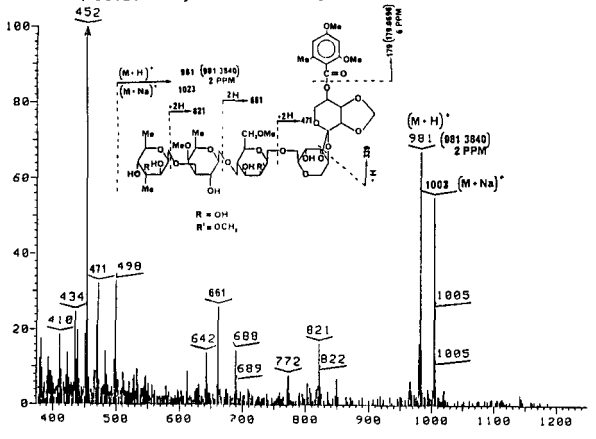

Figure D1: (Lactone from chemical degration)

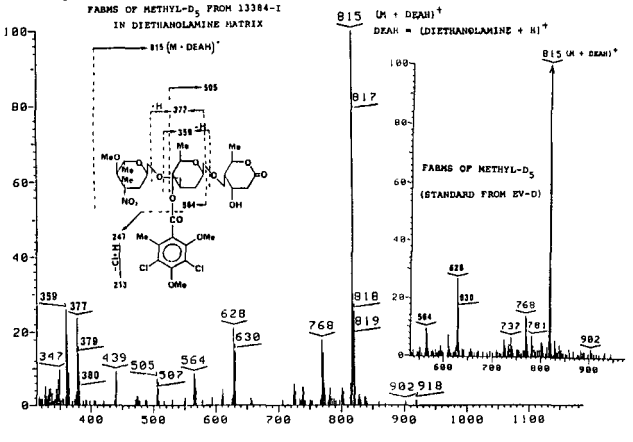

Figure D2: (Isolated by chemical degradation)

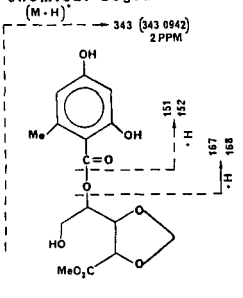

NEGATIVE ION CHEMICAL IONIZATION MASS SPECTROMETRY OF 2,4-DINITROPHENYL PEPTIDES

Todd D. William and Robert J. Anderegg

Department of Chemistry
University of Maine, Orono, Maine 04469

We recently reported that 2,4-dinitrophenyl (DNP) amino acid derivatives could be selectively and sensitively analyzed by negative ion chemical ionization mass spectrometry (NICIMS)(1). The components in a mixture of amino acid derivatives can be determined from direct insertion probe samples, no chromatography is required. The mass spectrum of each DNP amino acid shows virtually no fragmentation; the ion current is carried in the molecular ion. N-terminal amino acid analysis was demonstrated using both proteins and the primary degradation products of proteins treated with trypsin or cyanogen bromide.

With small model di and tripeptides, similar spectra are obtained. Peptide derivatives, as DNP methyl esters, appear as molecular anions without fragmentation. We are taking advantage of this effect to develop a method of sequencing peptides. Rather than rely on mass spectrometric fragmentation to produce ions characteristic of the amino acid sequence, we generate our fragments chemically and measure the molecular weights of each peptide in the resulting mixture. As an example, the tripeptide Met-Leu-Phe, when derivatized to the DNP-peptide-methyl ester, gives an abundant M^-, with no fragmentation. When the DNP peptide is treated briefly with aqueous acid, a mixture of peptides is formed from cleavage of the peptide bonds. Mass spectrometry, by methane NICI, of this mixture generates the spectrum shown in Figure 1. The prominent ions are the molecular anions of the N terminal DNP amino acid, dipeptide, and tripeptide. Other peptides in the mixture (i.e. those from the C-terminus of the peptide) are not observed, because they do not carry the electrophilic DNP group and so are not ionized.

Our strategy of observing molecular ions from chemically generated peptides is similar to that described by others (2 - 5); however, because of the selectivity of the negative ionization, clean spectra are observed with little sample preparation. Chemical or enzymatic methods can be used to generate the peptide mixture.

We have analyzed a number of peptides, representing nearly every common protein acid functionality. Fragmentation is observed in several situations. Serine peptides frequently lose H_2O, giving rise to a M^- and $(M-18)^-$ doublet. This water loss is probably thermally induced dehydration from heating of the direct insertion probe. Histidine peptides show a significant loss of 30 amu, presumably the loss of NO by dissociative capture. As peptides become larger, thermal decomposition competes with evaporation, leading to increased fragmentation. This is noted for peptides containing lysine, tyrosine, and histidine. Ions corresponding to the loss of methanol and other rearrangements are observed late in the heating cycle of their DNP peptide methyl esters. Direct chemical ionization (DCI) in the negative ion mode seems to decrease the fragmentation due to pyrolysis.

References

1. T.D. Williams, L. Vachon, and R.J. Anderegg, Anal. Biochem. 153, 372-379 (1986).
2. R.M. Capriolí and T. Fan Anal. Biochem. 154, 596-603, (1986).
3. D. Pilosof, H.-Y. Kim, M.L. Vestal and D.F. Dyckes, BMS 11, 403-7 (1984).
4. T.J. Yu, H.A. Schwartz, S.A. Cohen, P Vouros and B.L. Karger, J. Chrom. 301, 425-440, (1984).
5. D.A. Kidwell, M.M. Ross and R.J. Colton, J. Am. Chem. Soc. 106, 2219, (1984).

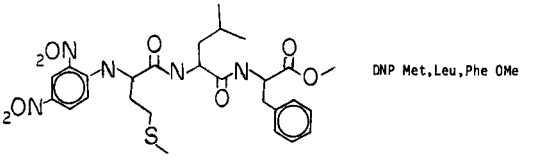

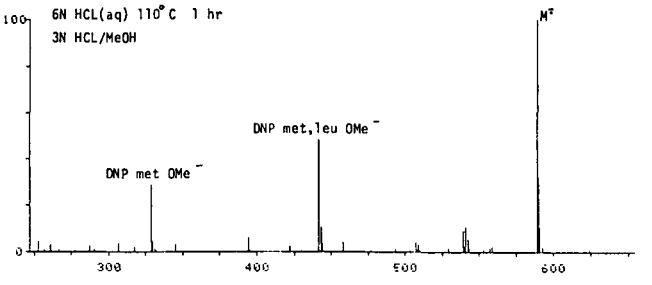

Figure 1. NICI spectrum of peptide mixture generated by acid hydrolysis of DNP Met-Leu-Phe

THERMOSPRAY MASS SPECTROMETRY OF AMINOGLYCOSIDE ANTIBIOTICS

Timothy A. Getek, Department of Chemistry, University of Houston Houston, TX 77004

Thomas G. Alexander, Food and Drug Administration, Center for Drugs and Biologics, Washington, DC 20204

OVERVIEW: The assay of aminoglycoside antibiotics, in particular gentamicin (see Fig. 1), is made difficult by its multicomponent nature and the lack of a chromophore for easy UV detection after liquid chromatographic (LC) separation. Detection schemes involving refractive index, fluorescence after chemical derivatization, and electrochemical oxidation have been employed. Gentamicin and similar aminoglycosides are excellent candidates for LC Thermospray mass spectrometry (TMS).

EXPERIMENTAL: Gentamicin samples were prepared at 1 mg/mL concentrations. An initial use of a pentane sulfonic acid ion pair mobile phase developed by Anhalt and coworkers (1) gave good separation but prolonged use resulted in white solids adhering to the TMS ion source. An alternate trifluoroacetic acid mobile phase was developed based on the work of Inchauspé and Samain (2). By adding ammonium acetate buffer, which aids in TMS ionization, a suitable mobile phase was optimized using a simplex method. The final LC mobile phase consisted of 0.13 M ammonium acetate, 0.09 M acetic acid, and 0.047 M trifluoroacetic acid which was brought to a pH 3.5 with ammonium hydroxide. An example separation is shown in Fig. 2.

The TMS units utilized were two. One unit was a Biospect quadrupole with Incos data system equipped with a home-made thermospray wand. The other unit was a Hewett-Packard 5988 MS with a Vestec Thermospray and HP-9000 data system. TMS spectra were taken without the LC column using 0.1 M ammonium acetate at a pH 4.5. The gentamicin fragmented extensively with very little parent ion remaining intact. The low mass scan is shown in Fig. 3 and the high mass scan encompassing the base MW of gentamicin components is seen in Fig. 4. In terms of identifying the component with the base molecular weight ion, it was not a confident determination. However a low mass fragment is associated with each component. For C1a there is a m/z 129, C2 m/z 143, and C1 has a m/z of 157. These m/z peaks agree well with the fact that the MW of the components are separated by 14 amu. By utilizing these masses, the components were readily identified and two unknown chromatographic peaks were seen (U1 and U2 in Fig. 2). These unknown peaks have similar fragmentation to C2 and may represent the C2a and C2b compounds.

GENTAMICIN	C1a	MW = 449
	C2	MW = 463
	C1	MW = 477
	C2a	MW = 463
	C2b	MW = 463

1) J. Anhalt, F. Sancilo, and T.McCorkle, J. Chromatogr., 153, 489(1978).
2) G. Inchauspé and D. Samain, J. Chromatogr., 303, 277(1984).

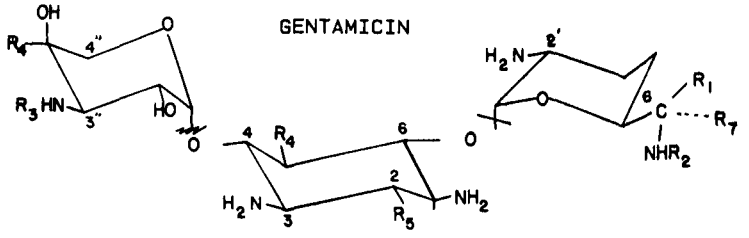

FOR GENTAMICIN: $R_3=CH_3$; $R_4=CH_3$; $R_5=H$; $R_6=OH$

COMPONENT	R_1	R_2	R_7
C1	CH_3	CH_3	H
C2	CH_3	H	H
C1a	H	H	H
C2a	H	H	CH_3
C2b	H	CH_3	H

FIG. 1

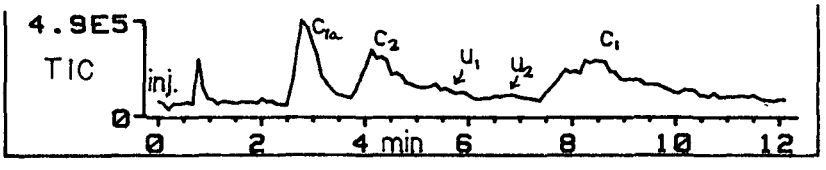

FIG. 2

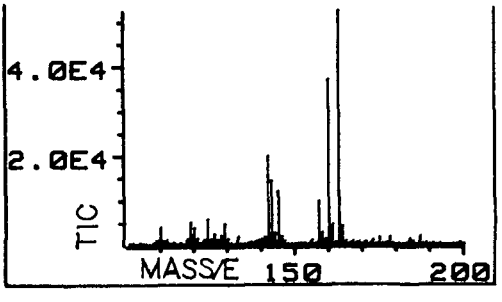

FIG. 3

FIG. 4

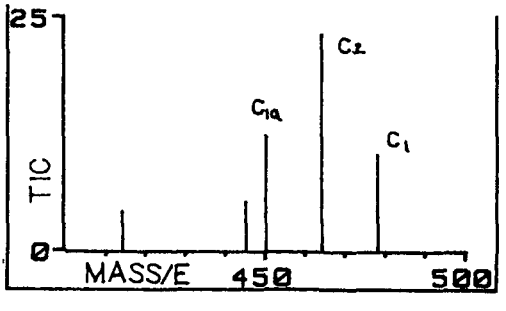

STRUCTURAL DETERMINATION OF LIPID A FROM GRAM NEGATIVE BACTERIA USING LASER DESORPTION MASS SPECTROMETRY

J.P.HONOVICH and ROBERT J. COTTER
The Johns Hopkins School of Medicine
Baltimore, MD 21205 USA

NILOFER QURESHI and KUNI TAKAYAMA
Veterans Administration Hospital
Madison, WI 53705 USA

Lipid A is a hetergeneous mixture of phoshorylated (1'-6 linked glucosamine) disaccharides containing up to seven fatty acid chains attached to the 2 and 2' positions by amide linkages and the 3 and 3' positions by acyl linkages. It should be noted that the phosphate groups require methylation for both chromatographic separation and mass spectral analysis. Lipid A is part of a larger lipopolysaccharide (LPS) found on the outer surface of the outer membrane of gram negative bacteria.

While the distribution of fatty acids can be determined following their hydrolysis from the disaccharide backbone, mass spectral analysis of intact lipid A from N. Gonnorrhoeae by laser desorption (1) has been used to determine the location of specific fatty acids on the disaccharide. Quasi-molecular ions corresponding to K^+ adducts were readily observed. The fragment ions seen correspond to losses of the acyl-linked fatty acids at the 3 and 3' position while no losses were seen for the amide linked fatty acids. Three two-bond cleavages of the reducing sugar then allowed the determination the fatty acids at position 3, the fatty acid at position 2, and the total mass of the distal portion.

This fragmentation scheme has been used to elucidate the structures of lipid A from N. Gonorrhoeae, E.Coli and R. Sphaeroides, as well as component continuing additional saccharide units. The figure on the next page shows the structure and spectrum of the intact LPS of the Re-mutant of E.Coli which contains two additional KDO (2-keto-3-deoxyoctonate). The largest ions observed correspond to loss of the di-phosphate groups from the quasi-molecular ion. The phosphate can cleave on either side of the oxygen along with a hydrogen or methyl transfer to produce the even electron ions which are almost always observed with this technique. Losses of three types of fatty acids (C_{12} = 200 amu, C_{14} = 228 amu, and $C_{14}OH$ = 244 amu) are seen in various combinations in addition to the loss of the remaining monophosphate group (126 amu). The ions around 1700 amu are the result of a 2-bond ring cleavage where the C_1 to C_4 ring carbons are lost from the diphosphate end of the molecule. Additional losses of fatty acids and the phosphate group from this "distal ion" are seen. No fragmentation, involving the KDO group were observed. Work on a di-phosphate, single KDO substituted Lipid A showed these same general fragmentation feature.

(1) Takayama, K., Qureshi, N., Hyver, K., Honovich, J., Cotter, R.J., Mascagni, P, and Schneider, H., (1986) J. Biol. Chem., (in press).

Research was supported in part by grant CHE-8410506 from the National Science Foundation.

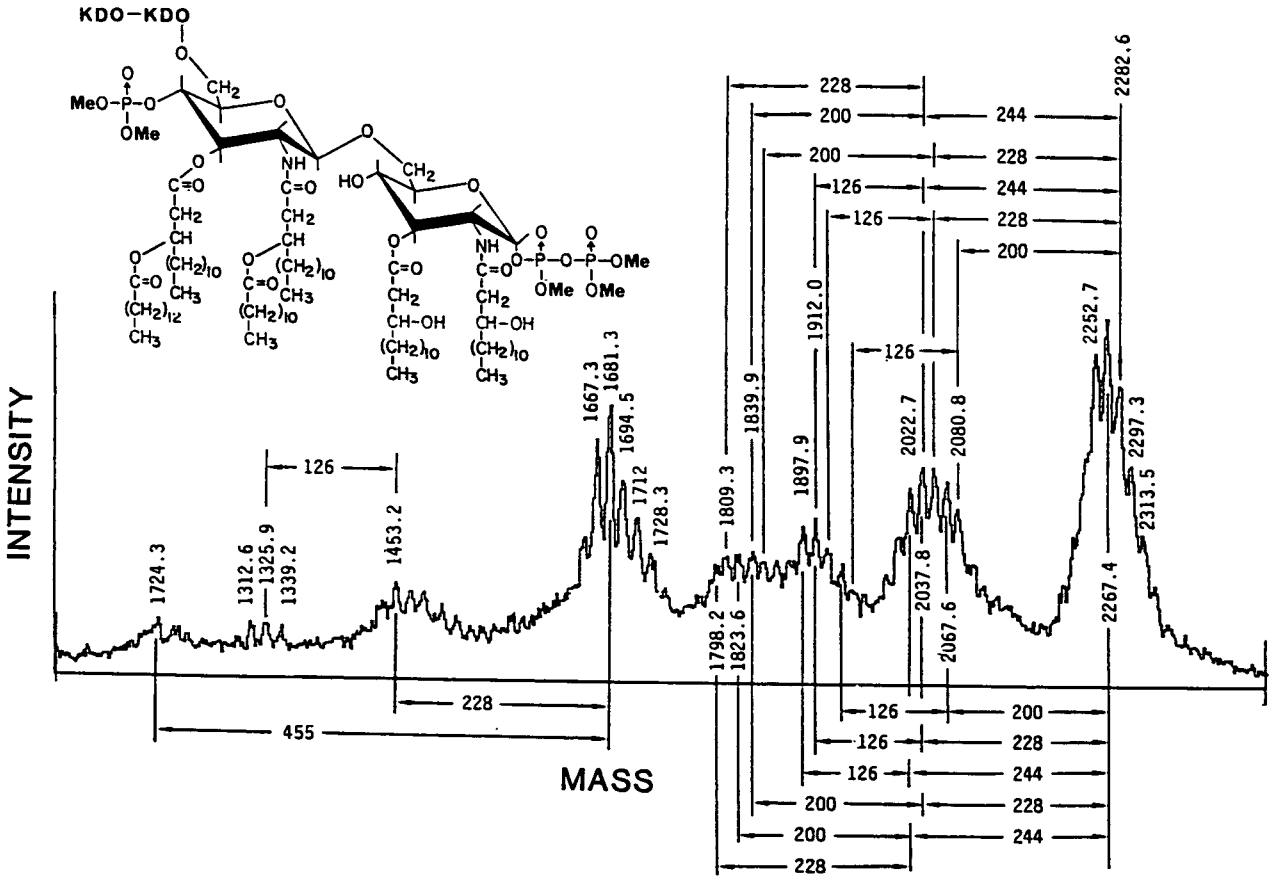
KDO—KDO
INTENSITY
MASS
1724.3
1312.6
1325.9
1339.2
1453.2
1667.3
1681.3
1694.5
1712
1728.3
1798.2
1809.3
1823.6
1839.9
1897.9
1912.0
2022.7
2037.8
2067.6
2080.8
2252.7
2267.4
2282.6
2297.3
2313.5
126
228
455
200
244

STRUCTURE ELUCIDATION OF THE OLIGOSACCHARIDE ISOLATED FROM CELL WALL POLYSACCHARIDE OF STREPTOCOCCUS SANGUIS (MITIS) Ss 34: Floyd C. McIntire, C. Allen Bush, Su-Chen Li, Michael McNeil, Susan S. Tjoa, Shing-Shing Wu and Paul V. Fennessey.

Coaggregation between Actinomyces viscosus T14V and Streptococcus Sanguis (mitis) Ss 34 depends upon the interaction between a lectin on T14V and a specific carbohydrate on Ss 34. This coaggregation is inhibited by β-galactosides such as lactose and β-N-acetylgalactos- aminides. This type of interaction may be important in the build-up of dental plaque.

When Ss 34 cell walls were autoclaved, a water soluble polysaccharide was obtained which, after purification by column chromatography, was a potent inhibitor of coaggregation, 17 times more potent than lactose on a weight basis. This polysaccharide consists of oligosaccharides held together by phosphodiester bridges. Hydrolysis and reduction of this polysaccharide with NaOH-$NaBH_4$ followed by alkaline phophatase removed most of the phosphate. Separation by HPLC yielded a major hexasaccharide alditol(O-6), which showed coaggregation inhibitory activity. On a molar basis, O-6 has a potency approximately equal to lactose and 5 times the potency of free GALNAc.

O-6 was analyzed by hydrolizing the oligosaccharide and forming the acetates. Analysis by capillary GC/MS showed 4 major components identified as Rhamnose (Rha), Glucose (Glc), Galactose (Gal) and N-Acetylgalactosamine (GalNAc) in the ratios of 1:1:2:2. Identification was based on comparison of their gas chromatographic methylene units (MU) and confirmation was made by mass spectrometry (MS).

In order to locate the reducing terminal sugar, O-6 (containing H at the reduced terminal) was hydrolyzed, then reduced with $NaBD_4$ and acetylated. This experiment introduced deuterium at C-1 of the other alditol acetates. A review of the mass spectra showed deuterium in rhamnose, glucose and galactosamine. However, the galactitol acetate peak contained a mixture of hydrogen and deuterium and, therefore, the reducing terminal of the oligosaccharide was galactose.

By preparing the trimethylsilylated R(-) and S(+) 2-butyl glycosides, all monomers were found to have a D configuration except that Rha was L.

The FAB mass spectra of the underivatized O-6 (HexNAc - Rha - Hex - Hex - HexNAc - Hexitol) gave a molecular ion and confirmed that O-6 is a hexasaccharide alditol. The major ions were at m/z 1059 and 1081 being $(M + H)^+$ and $(M + Na)^+$ respectively. One other ion seen in the FAB/MS of the underivatized unknown was at m/z 877 and represents the loss of the hexitol (galol) from the reducing end. The peracetylated derivative gave a more complete FAB mass spectrum in which m/z 1815, 1423, 848, 560, 330 and m/z 950,662, 375 represent sequence fragmentations with charge retention at the nonreducing and reducing ends respectively. These ions could be interpreted on the basis of the sequence given above. No assignment could be made to the positions of glucose and galactose in the sequence.

Establishment of the points of linkage of the monomers were done by comparing the gas chromatographic retention indices and MS of the permethylated alditol acetates to those of authentic compounds. The 3(or 4)-mono-OAc-1,2,4,5,6-penta-OMe- galactitol confirms the galol at the reducing end of O-6 with a 1→3(or 1→4) link to GalNAc. The 1,5-di-OAc-3,4,6-tri-OMe-2-acetylamino-2- deoxygalactitol confirms that this moiety was that of the nonreducing terminal GalNAc. The 1,4,6-tri-OAc-2,3,5-tri-OMe-galactitol indicates that the internal gal is in the furanoside conformation. 1,3,5-tri-OAc-6-deoxy-2,4-di-OMe- rhamnitol, 1,4,5-tri-OAc -2,3,6-tri- OMe -glucitol and 1,5,6-tri-OAc -3,4-di-OMe -2-acetylamino -2-deoxygalactitol represent derivatives of the internal components of O-6. Treatment of O-6 with 48% HF, followed by reduction, yielded a tetrasaccharide alditol O-4, which gave important information concerning the sequence of glucose and galactose. The isolation of 6-mono-O-Ac-penta-OMe-galactitol confirms that the reducing end of O-4 is a galactitol rather than a glucitol. Furthermore, O-4 was found to have an identical sequence as that found in O-6 from the non-reducing end to the internal Gal.

Because the 3- and 4-mono-O-Ac-penta-OMe derivatives are identical isomers, (confirmed by their identical MU's and MS) we prepared their deutero derivatives. The incorporation of deuterium at C-1 yielded two compounds that are no longer identical. Comparing the two deuterium containing spectra, we found shifts of fragments m/z 89 to

90, 157 to 158, and 205 to 206, for the 3-OAc derivative and shifts of 133 to 134, 185 to 186, and 249 to 250 for the 4-OAc derivative. The MS of the C-1 deutero acetate of O-6 was identical to that of the 3-isomer, and we, therefore, confirmed that the terminal galol of O-6 is a 1→3 link to GalNAc rather than a 1→4 link.

All sugars were found to have a pyranoside conformation, except for the internal Gal, which is a furanoside.

The NMR indicated that all the linkages are β, except that the non-reducing terminal GalNAc has an α-link to Rha.

The above analyses are all in agreement that the complete structures of O-6 and O-4 are:

D-GalNAcpβ1→3L-Rhapβ1→4D-Glcpβ1→6D-Galfβ1→6D-GalNAcpβ1→3D-Galol; and
D-GalNAcpα1→3L-Rhapβ1→4D-Glcpβ1→6D-Galol.

ANALYSIS OF SOME FUSARIUM MYCOTOXIN METABOLITES BY THERMOSPRAY HPLC/MS

Robert D. Voyksner[1], Carol A. Haney[2], Winston M. Hagler[2], and Steven P. Swanson[3]; (1) Analytical and Chemical Sciences, Research Triangle Institute, P. O. Box 12194, Research Triangle Park, NC 27709; (2) North Carolina State University, Raleigh, NC 27695; (3) University of Illinois, Urbana, IL 61801.

Mycotoxins, secondary metabolites of fungi, cause serious losses to agriculture. Animals consuming mycotoxin-contaminated feedstuffs are adversely affected and grain marketing is disrupted. Mycotoxin contamination was thought to be a post-harvest phenonmenon caused by spoilage due to fungal growth in improperly handled commodities. With the discovery that half or more of the mycotoxin contamination in grain occurs before harvest because of plant disease, a vigorous effort evolved in the plant sciences to eliminate pre-harvest contamination as well as detoxification/decontamination of grain.

The concept of analyzing the animal for mycotoxin residues to diagnose exposure to mycotoxins has long been recognized as preferable to the analysis of feeds (1). While considerable progress in this direction has been made, only in the last few years have the patterns of metabolism and excretion of the major mycotoxins been elucidated.

HPLC/MS techniques for the analysis of the metabolites are preferred since derivatization is avoided and less sample preparation is required than the corresponding GC/MS analysis. Many of the toxic metabolites are believed to be conjugates, making HPLC/MS the only technique available for their specific detection. HPLC/MS methods are presented which detect and confirm mycotoxins metabolites and their conjugates in animal urine and fecal extracts.

Mycotoxin standards were analyzed using thermospray ionization in the presence of a buffer in positive and negative ion detection and filment chemical ionization (CI) for both positive and negative ion detection. In most cases, positive ion detection resulted in more structural information about the toxin. Generally, the toxins showed an $[M+H]^+$ and/or $[M+NH_4]$ with loss of OH, H_2O, CH_3COOH and CH_2O. These losses are primarily from alkyl or functional groups attached to the parent ring. The negative ion spectra of the toxins resulted in similar information showing $[M+OAc]^-$ and $[M-H]^-$ anions, with little fragmentation.

The spectra acquired in filament CI are nearly identical to those obtained under thermospray conditions for both negative and positive ion detection. However, filament CI proved to be at least 15 to 40 times more sensitive than thermospray ionization. Negative ion detection using filament CI proved to be 2-3 orders of magnitude more sensitive than negative ion thermospray. Negative ion detection was still slightly less sensitive (a factor of 2-5) than positive ion under filament CI conditions. Filament CI was clearly the best mode of operation.

Instrumental detection limits using HPLC/MS were estimated for all mycotoxin standards in positive ion detection filament CI mode to verify the method's capability to detect toxins at the expected low ng to high pg level. The HPLC separation used a Zorbax ODS (DuPont, Wilmington, DE) 25 cm x 4.6 mm column with a mobile phase initially of 40% methanol in water (0.1 M ammonium acetate). The mobile phase was programed linearly to 90% methanol in water containing 0.1 M ammonium acetate in 15 min. and held for 5 min. at the final conditions. The flow rate was 1.5 mL/min. Estimated detection limits using full scan data acquision, for most metabolites of deoxynivalenol (DON) and T-2 were from 200 pg to 10 ng. Multiple ion detection (monitoring the $[M+NH_4]^+$ and one fragment ion) enabled detection for T-2 metabolites down to 10 to 200 pg (Figure 1).

Analysis of Animal Urine and Fecal Extracts

Fecal samples from rats fed T-2 were analyzed to identify the various metabolites formed. The selected ion chromatogram (Figure 2) indicated the presence of 3'OH HT-2 and HT-2, the expected metabolites of T-2. Also a weak signal for T-2 triol and a broad peak for Neosulaniol (Neo) was detected. However, after analysis of reference standards and examination of spectra, the peak at m/z 400, thought to be Neo, was found to be an interference. The other metabolities identified in the sample matched reference spectra and reference retention times.

Thermospray HPLC/MS analysis of a series of fecal extracts from hens fed grain contaminated with DON was performed to determine the presence of DON and its de-expoxy metabolite (DOM-1) and the relative quantities of each. Figure 3A shows the selected ion chromatograms for the $[M+H]^+$ ion for DON and DOM-1. While the peaks cannot be seen in HPLC/UV, they can be seen easily using MS detection. Figure 3B shows the selected ion chromatogram for a 60 ng injection of a reference standard containing DON and DOM-1. The hen fecal sample spectra and retention times are identical to that of the standard. It appears that nearly half of the DON excreted from hens is in the form of DOM-1.

Urine from cows fed grain contaminated with DON was analyzed by HPLC/MS to detect free and glucuronide conjugates of DON and DOM-1. Normally, this analysis is performed by GC or GC/MS in a multi-stage process. First, the free toxins from the samples are derivatized and analyzed, then the glucuronide toxins are cleaved with β-glucuronidase, extracted, derivatized, and analyzed. The difference between the total toxin and the free toxin determined in the first step yields the amount of conjugated toxin present. HPLC/MS can detect both the free and conjugate toxins in a single analysis without derivatization. The positive and negative ion spectra of the peak identified as the glucuronide of DOM-1 (Figure 4) are consistent with the expected molecular weight and fragment ions for the conjugate. It is estimated that about 80% of the DON in grain is excreated as the glucuronide of DOM-1. Monitoring this would be the most sensitive indicator of cattle contaminated with DON.

References

(1) C. Mirocha "Applied Mycology of Fusarium" ed. M. Moss, J. Smith, Cambridge Univ. Press Cambridge, UK (1984).

(2) R. Corley, S. Swanson, W. Buck, J. Agric. Food Chem. 33, 1085 (1985).

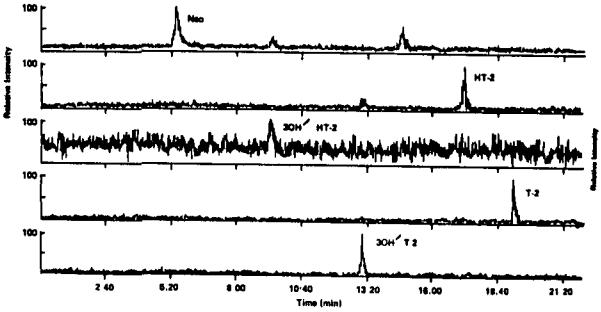

Figure 1. HPLC/MS selected ion chromatograms for the $[M+NH_4]^+$ ion of T-2 toxin and its metabolites for 250 pg injected under multiple ion detection. (Each ion was observed 0.2 seconds in a 0.5 mass window centered at the mass of the $[M+NH_4]^+$ ion.)

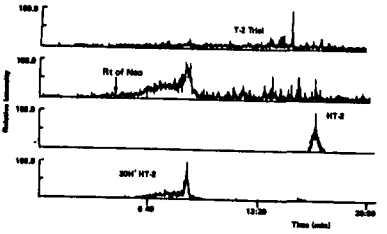

Figure 2. HPLC/MS selected ion chromatograms for the analysis of the rat fecal sample. This sample was determined to contain HT-2 and 3'OH HT-2, and a trace of T-2 triol.

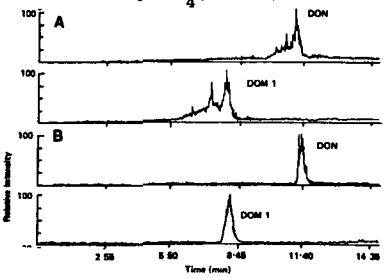

Figure 3. Analysis of a hen fecal extract for DON and DOM-1. HPLC/MS selected ion chromatograms for the analysis of the hen fecal sample, showing the presence of DON and DOM-1 (A). HPLC/MS chromatograms for the analysis of a reference standard (60 ng) of each toxin (B).

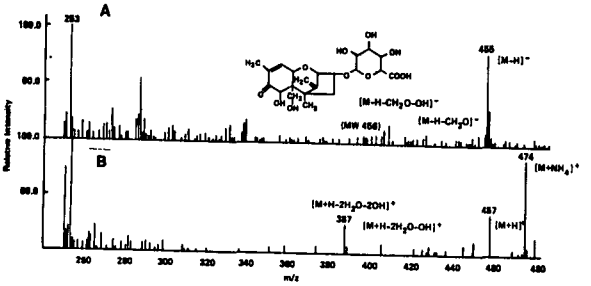

Figure 4. Thermospray HPLC/MS negative ion (A) and positive ion (B) spectra of a peak identified as the glucuronide conjugate of DOM-1 (MW 456) in the cow urine sample.

THE IMPACT OF TAMOXIFEN, AN ANTI-TUMOR AGENT, ON STEROID METABOLISM IN THE TUMOR-BEARING RAT AS ASSESSED BY METABOLIC PROFILING

J. J. Leary* and C. W. Welsch+
Departments of Chemistry* and Anatomy+
Michigan State University
East Lansing, MI, 48824

Tamoxifen (ICI 46,476) is a widely used and effective drug for the endocrine management of advanced breast cancer in postmenopausal women (1, 2). While Tamoxifen therapy effectively causes tumor regression, researchers have shown that the drug also triggers changes in the level of circulating steroids and peptide hormones. Because modulation of the endocrine system by this nonsteroidal antiestrogen may explicate some of the drug's adverse effects (nausea, edema, hypercalcemia, etc.), it is important to assess the impact of this drug on overall steroid hormone secretion and metabolism in the normal (2) and tumor-bearing animal model for breast cancer.

The Sprague-Dawley rat is frequently used as an animal model for human mammary carcinoma because breast tumors induced by dimethylbenzanthracene in this rat are morphologically similar to those occurring in humans. In this study, two groups of six female Sprague-Dawley rats were housed in standard stainless steel individual metabolism cages designed for daily feces and urine collection, as previously described (2). At 50 days of age, 7,12-dimethylbenzanthracene (DMBA) (Eastman Kodak, Rochester, NY) was administered i.v. to both groups of female rats at a dose of 2mg/100g body weight. This dose of DMBA induces multiple hormone-responsive mammary carcinomas in 100% of the treated rats by 2 months post-carcinogen treatment. When all rats were bearing palpable tumors, both groups received daily saline injections. Twenty-four hour urines were collected from all twelve rats for ten days. During the next ten-day period, the control group continued to receive daily saline injections. The other group of six rats were injected daily with Tamoxifen citrate (ICI Americas, Inc., Wilmington, Delaware) at a dose of 75µg/100g body weight. The rats treated with Tamoxifen displayed an average decrease of 26% in the diameter of the mammary carcinomas. Twenty-four hour urines were collected from both groups for ten days. Daily vaginal swabs were obtained for all rats in order to characterize each phase of the estrous cycle (specifically: proestrus, estrus, and diestrus). Methoxime-trimethylsilyl derivatives were prepared by the method of Vrbanac et al. (3).

The urinary steroid metabolic profiles of tumor-bearing controls and Tamoxifen-treated tumor-bearing rats were generated with gas chromatography and gas chromatography/mass spectrometry, as previously described (2). Steroid components were identified using mass spectral information obtained from an LKB 2091 GC/MS/DS with a 15 meter DB-1 fused silica capillary column (0.53mm i.d., 1.5µm film thickness) (J&W Scientific). The Helix Pomatia ß-glucuronidase-sulfatase used for the hydrolysis of steroid conjugates predominantly liberates corticosteroid metabolites of adrenal origin, which elute in the retention index range from 2900 to 3200 (4). The urinary steroid metabolic profiles of tumor-bearing rats treated with Tamoxifen were compared with those obtained from the control tumor-bearing animals.

Cycling normal female rats not bearing tumors display a cyclic excretion behavior of a tetrahydroxy-pregnan-one eluting at retention index of 3117 (Figure 1). The excretion is usually at a minimum during the diestrus phase (approximately 3µg per mg creatinine) and reaches a maximum during the proestrus or estrus phase (approximately 8µg per mg). This normal estrous cycle is disrupted in the tumor-bearing rat, possibly due to hormone secretion by the carcinomas. The excretion of this tetrahydroxy-pregnan-one from two tumor-bearing rats is displayed in Figure 2. Tumor-bearing rat #6 is a control receiving only saline injections for the first and second ten-day periods. Tumor-bearing rat #8 received saline injections for the first ten-day period, and Tamoxifen for the second ten-day period. Both rats show an erratic excretion of this tetrahydroxy-pregnan-one for the first ten days. When tumor-bearing rat #8 is treated with Tamoxifen, this excretion drops to zero. This Tamoxifen-suppressed excretion behavior also is displayed for three other major corticosteroid metabolites: trihydroxy-pregnan-one; tetrahydroxy-pregnen-one; and another isomer of tetrahydroxy-pregnan-one. The rat is "locked" into the diestrus phase of the estrous cycle. Tumor-bearing rat #6 continues with its erratic cycling behavior during the second ten-day period.

In conclusion, preliminary results indicate that the excretion of corticosteroid metabolites from tumor-bearing rats treated with Tamoxifen is suppressed when compared with tumor-bearing rats receiving only saline. This behavior is similar to that observed when normal, cycling female rats are treated with Tamoxifen.

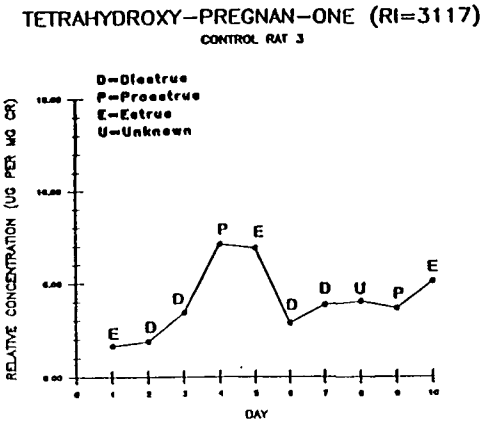

Figure 1. Excretion of an isomer of tetrahydroxy-pregnan-one from a normal, cycling female rat.

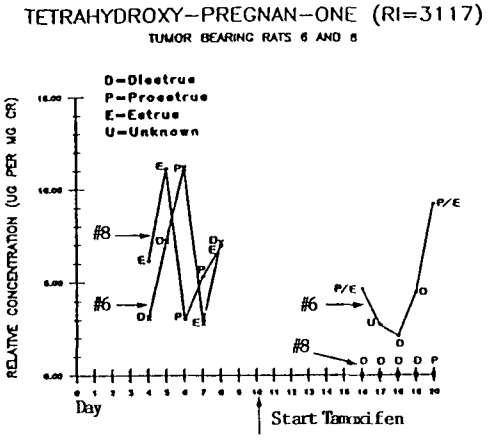

Figure 2. Excretion of an isomer of tetrahydroxy-pregnan-one from two tumor-bearing rats. Rat #6 receives only saline injections, days 1-20. Rat #8 receives saline on days 1-10, Tamoxifen on days 11-20.

Acknowledgement: This work was supported in part by a grant (RR-00480) from the Biotechnology Research Program, Division of Research Resources, National Institutes of Health.

1. Furr, B. J. A., and Jordan, V. D. Pharm. Ther., 25: 127, (1984).

2. Leary, J. J., Watson, J. T., and Welsch, C. W. The Influence of the Anti-tumor Agent, Tamoxifen, on Normal Steroid Metabolism in the Rat as Assessed by Metabolic Profiling," presented at the 33rd Annual Conf. on Mass Spectrom. and Allied Topics, San Diego, CA, pp. 214-215 (1986).

3. Vrbanac, J. J., Pinkston, J. D., and Sweeley, C. C. Biomed. Mass Spectrom., 10: 155, (1983).

4. Gustafsson, J. A., and Pousette, A. Biochim. Biophys. Acta, 280: 182, (1972).

12-HYDROXYEICOSATETRAENOIC ACID METABOLISM IN PSORIATIC SKIN: GC-MS ANALYSIS. A.I.Mallet, Institute of Dermatology, United Medical and Dental Schools, University of London, Homerton Grove, London E9 6BX, England.

The lipoxygenase products of arachidonic acid (AA) are of especial interest to research into the inflammatory and proliferative disease, psoriasis. The major AA metabolite is 12-hydroxyeicosatetraenoic acid (12HETE) and this is present in raised concentrations in lesional skin (1). In vivo administration of 12HETE into human skin causes a typical inflammatory response and an inflitrate of polymorphonuclear leukocytes (PMNs) (2). 12HETE is usually associated with platelets and a recent report (3) has demonstrated the ability of PMNs to oxidise platelet produced 12HETE to the omega-oxidation product 12,20-dihydroxyeicosatetraenoic acid (12,20diHETE). We were interested to see if this process occurred in vivo with our 12HETE and to determine if it could affect significantly the levels of 12HETE we have been measuring in human skin. We describe here the methods we have adopted to analyse 12,20diHETE in skin derived samples and the results of a preliminary study in psoriatic lesions.

Psoriatic lesional skin scale was obtained by gentle abrasion while chamber fluids were collected by bathing an abraded area of skin for 30 min with phosphate buffered saline (1ml) contained in a plastic chamber affixed to the skin with cyanoacrylate adhesive. The hydroxyfatty acids were extracted at pH 3.5 into ethyl acetate and were partitioned between phosphate buffer pH 8.3 and 1-chlorobutane which extracted the free fatty acids and monohydroxyacids. The aqueous phase was then acidified to pH 3.5 and re-extracted with ethyl acetate to obtain the dihydroxy acids (4). Further purification by straight phase HPLC was followed by derivatisation and GC-MS analysis. Hydrogenation was carried out essentially as described by Murphy (5) and silylation reagents were obtained from the ususal sources, with the exception of tert-butylphenylmethoxylsilyl (tBPMS) bromide, which was synthesised by ourselves (6). GC-MS analysis was performed on capillary quartz columns (SE30 stationary phase) interfaced directly to a VG Analytical Ltd. 305 mass spectrometer operating in EI mode at 40 ev. Authentic 12,20diHETE was a generous gift from Merck Frosst Inc., Canada.

Our initial experiments on psoriatic scale showed that an appropriate fraction from the HPLC system contained material which could be the expected metabolite. Our chosen method for the analysis of 12HETE employs hydrogenation (to improved GC stability) and tert-butyldimethylsilylation of both alcohol and acid moieties (to provide high MS sensitivities at m/z $[M-57]^+$); this procedure, applied to the above fraction, showed that a diHETE was present, but no information was visible in the spectrum to confirm the presence of an hydroxyl group on C-20. We therefore treated the reduced material, after esterification with diazomethane, wih tBPMS-bromide in solution in methylene choride- triethylamine. This reagent is specific for the silylation of primary hydroxyl groups and fails to react, under these conditions, with secondary or tertiary groups (6). As a control, 5,12diHETE, which has only secondary hydroxyl groups, was treated in the same way. Any unreacted hydroxyl groups were then derivatised with BSTFA to give the trimethylsilyl ethers. The expected product (tBPMS ether, TMS ether, Me Ester) was formed (Figure 1). Quantitative anlysis was then performed using 5(S),12(S)diHETE as an internal standard and the hydrogenated tris-tBDMS derivative as the derivative; the 5,15 and 12,20 dihyroxyacids separate well on the GC column used (Figure 2). We have analysed psoriatic scale, chamber fluid from lesional areas and chamber fluid from uninvolved skin and in all these samples the omega oxidation product appears to be present at a concentration of some 10% of the parent 12HETE .

FIGURE1. MASS SPECTRUM OF 12,20DIHETE tBPMS, TMS ETHER, ME ESTER.

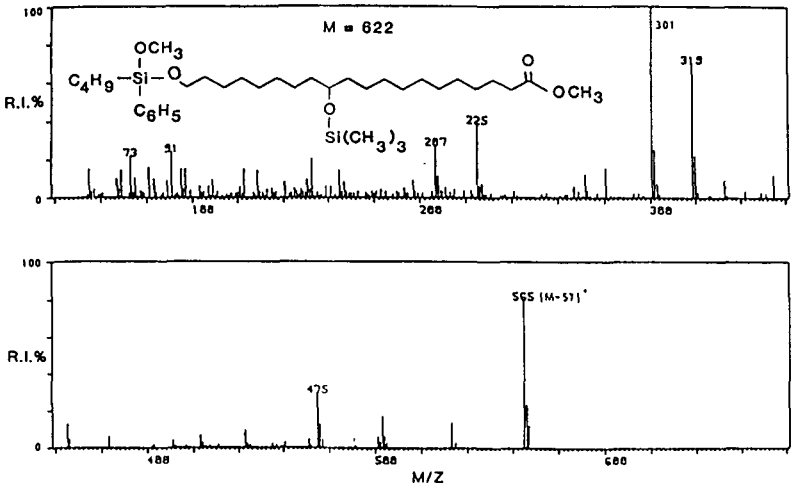

FIGURE 2. SIM TRACES FOR 12,20DIHETE TRI-tBDMS DERIVATIVE AT THREE CHARACTERISTIC IONS. 5,12DIHETE INTERNAL STANDARD.

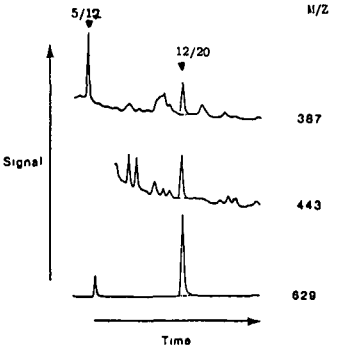

We conclude that an enzyme system for this metabolite exists in human skin (probably a P-450 system) and that the extent of oxidation, though not negligible, is not such as to invalidate our published work on the variation of 12HETE concentrations in inflamed skin.

References:

1. R.D.R.Camp, A.I.Mallet, P.M.Woollard, S.D.Brain, A.K.Black and M.W.Greaves, Prostaglandins, 26 1983 431.
2. P.M.Dowd, P.M.Woollard, A.K.Black, R.D.R.Camp and M.W.Greaves, Br. J. Dermatol., 109 1983 703.
3, P.Y-K.Wong, P.Westlund, M.Hamberg, E.Granstrom, P.H-W. Chao and B.Samuelsson, J. Biol. Chem., 259 1984 2683.
4. R.M.Barr, E.Wong, A.I.Mallet, L.A.Olins and M.W.Greaves, Prostaglandins, 28 1984 57.
5. R.C.Murphy, Prostaglandins, 28 1984 597.
6. Y.Guindon, R.Fortin, C.Yoakim and J.W.Gillard, Tet. Lett., 25 1984 4717.

THERMOSPRAY LIQUID CHROMATOGRAPHY-MASS SPECTROMETRY OF CARBOHYDRATES.

F. F. Hsu, C. G. Edmonds and J. A. McCloskey. Departments of Medicinal Chemistry and Biochemistry, University of Utah, Salt Lake City, UT 84112.

Structural studies of carbohydrates and glycoconjugates rely heavily on high performance liquid chromatography, but microscale work suffers from inadequate detector sensitivity. An initial study has been made of the thermospray mass spectra of 23 mono- through tetra-saccharides, and some of their 1-O-methyl and O-permethyl derivatives, in 0.1M NH_4CO_2H, pH 5.6, and to establish sensitivity parameters for LC/MS under reversed-phase HPLC conditions with the above mobile phase (1). In typical thermospray spectra of monosaccharides and 1-O-methylmonosaccharides, MNH_4^+ ions are of greatest abundance. Other major ions for 1-O-methylmonosaccharides are MNH_4^+-CH_3OH and those from consecutive losses of H_2O. Ions derived from consecutive loss of H_2O from MNH_4^+ are also abundant in monosaccharides. Structure assignments for fragment ions based on LC/MS experiments using D_2O mobile phase indicate that anhydro ions are formed through loss of D_2O from MND_4^+.

For disaccharides, molecular species ranged from 0.8-5% relative intensity, with m/z 240 (MNH_4^+-$C_4H_8O_4$) usually the prevalent ion for dihexopyranoses. Ion species corresponding to monosaccharides indicate that hydrolysis and thermolysis may play an important role in thermospray ionization of carbohydrates. Spectral differences between maltose and trehalose imply that the thermospray ionization technique may be applied in isomer differentiation.

The thermospray mass spectrum of permethylmaltose is shown in Figure 1, where MNH_4^+ ion is of high abundance. This enhancement of parent ion intensity was found in every case, including the tetrasaccharide stachyose. The principal assignments as schematically illustrated for permethylmaltose (Scheme 1), are in accord with analogous assignments from earlier studies employing other ionization methods (2-6).

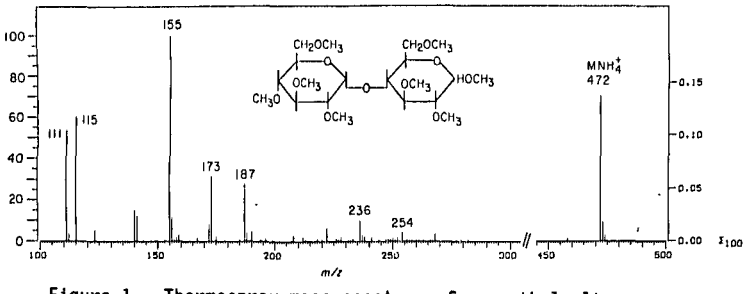

Figure 1. Thermospray mass spectrum of permethylmaltose.

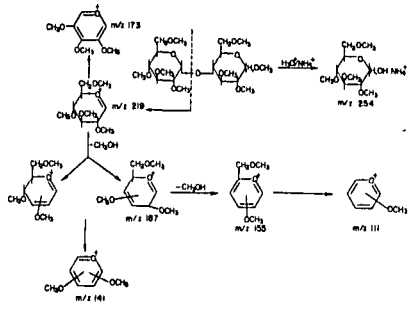

Scheme 1. Fragmentation pathways of permethylmaltose by thermospray ionization.

LC/MS sensitivity levels of 100pg for 1-O-methylglycopyranoside with S/N >15 (Figure 2) were obtained by selected ion monitoring, which is 10^5 more sensitive than commonly used refractive index detection, and >10-10^3 better than with post-column reaction methods. Responses similar to Figure 3 in terms of signal/noise ratio were obtained for 2ng injections of underivatized monosaccharides. These results suggest that LC/MS can play an useful role in structural and analytical studies of glycoconjugates, in particular when sensitivity is an important concern.

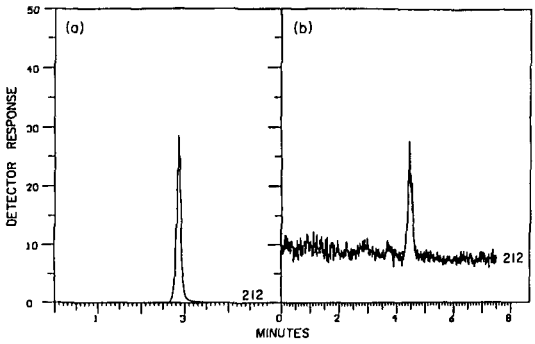

Figure 2. Selected ion recording (m/z 212) from LC/MS of
(a) 100 ng of α-1-O-methylglucopyranoside;
(b) 100 pg of α-1-O-methylmannopyranoside.

References:

1. Hsu, F.F.; Edmonds, C.G.; McCloskey, J.A. Anal. Lett. (1986) in press.
2. von Minden, D.L.; McCloskey, J.A. J. Am. Chem. Soc. (1973) 95, 7480.
3. Chizhov, O.S.; Kadentsev, V.I.; Solov'yov, A.A.; Levonowich, P.F.; Dougherty, R.C. J. Org. Chem. (1976) 41, 3425.
4. Kambara, H.; Hishida, S. Anal. Chem. (1981) 53, 2340.
5. Kambara, H.; Hishida, S. Org. Mass Spectrom. (1981) 16, 167.
6. Kochetkov, N.K.; Wulfson, N.S.; Chizhov, O.S.; Zolotarev, B.M. Tetrahedron (1963) 19, 2209.

MASS SPECTRAL MEASUREMENTS OF INDIVIDUAL BACTERIA PARTICLES IN AIR

M. P. Sinha, Jet Propulsion Laboratory, California Institute of Technology, Pasadena, California 91109

INTRODUCTION: A novel method for determining the chemical composition of individual aerosol particles on a continuous, real-time basis has been developed in our laboratory. The method known as particle analysis by mass spectrometry (PAMS)[1] involves a combination of the technique of particle beam generation with mass spectrometry. The application of PAMS to the characterization of biological particles in air is described in this paper. Bacteria particles suspended in air (aerosol) are directly introduced one at a time into the ion source of a mass spectrograph and complete spectra from individual particles are measured. PAMS is uniquely suited for the detection and identification of airborne microoganisms in both field and protected environments. Measurement of mass spectrum of individual particles would eliminate the interferences arising from the background particles present in most environments.

EXPERIMENTAL: A particle beam generator and a miniaturized focal plane mass spectrograph (Mattauch-Herzog type) constitute the two main components of the PAMS system. Introduction of aerosol particles directly into the ion source is accomplished by using a particle beam generator. The details of the beam generator and its characteristics have been described earlier.[1] Briefly, it consists of a capillary nozzle (100 μm in diameter) and a set of two skimmers (350 and 500 μm orifice diameters). The regions between the capillary and the first skimmer, and between the skimmers are differentially pumped. A beam of particles is produced by an aerosol expanding into a vacuum through the capillary nozzle. The particles, being much heavier than the carrier gas molecules, remain concentrated along the central axis. The skimmers allow an efficient transmission of the particles into the mass spectrometer chamber. The particle beam is directed into a V-shaped zone refined rhenium filament located in the ion source of the mass spectrograph. The filament is heated resistively. A particle striking the filament produces a plume of vapor molecules which are then ionized by electron impaction. Each particle thus produces a pulse of ions after its volatilization and ionization. The ion pulse width is found to be about 1 ms. Figure 1 shows the schematic of the PAMS system. The different mass ions present in a pulse are separated spatially along the focal plane of the magnetic sector. The spectrograph has a 5" long focal plane and covers a mass range of 25-500 amu. The uniqueness of the mass spectrograph lies in its electro-optical ion detector which enables the simultaneous measurement of all the ions along the focal plane. The ions exiting out of the magnet impinge on the active surface of a two dimensional electron multiplier array (MCA). An electron cascading process is initiated along the channel length of the MCA. The electrons coming out of the other end of the multiplier array are accelerated to a phosphor coated fiber optic window, whereby photon images are generated for the different mass ions. The positions of these ion images are proportional to their masses and their intensities are proportional to the total number of ions. The position and intensity of these ion images are measured with a self-scanned photodiode array (PDA). The photodiodes are integrating detectors.

In the measurement of the particle mass spectra, the PDA's are interfaced to a data system based on a TI 990/10 computer system. The signal is integrated for a period of 50 or 100 ms and is read by the computer. The process is repeated continuously. Each read-out is called a scan. In this mode of data acquisition, each scan constitutes a mass spectrum of all ions that are accumulated during the integration period. Aerosols of different bacteria particles were generated by the nebulization of their suspensions in alcohol, and introduced into the source in the form of a beam. For a low number density of aerosol particles each scan consequently contains either the mass spectrum of a bacterial particle or of the background gases only.

RESULTS AND DISCUSSIONS: Figure 2a shows the mass spectrum of a single particle of *bacillus cereus*. The background gas spectrum is shown in figure 2b. This is a scan for which no particle was present in the ion source. The background spectrum needs to be subtracted from figure 2a spectrum in order to get the true particle spectrum. The particle mass spectrum extend up to the mass 300 amu. This is in contrast to the pyrolysis mass spectrum of bulk sample of bacteria particles and may be attributed to the differences in pyrolysis conditions. The higher mass fragments are expected to possess more information content about their parents and will be helpful in the differentiation of bacterial cells.

We have thus demonstrated that using the PAMS method, mass spectra of single biological aerosol particles can be measured on a continuous, real-time basis. We also find that the mass spectra from different bacteria particles possess some distinguishing features. Further work on the application of PAMS for the characterization of bioparticles is in progress.

ACKNOWLEDGMENTS: The author wishes to thank the late Mr. Charles Giffin for his help in the design of the mass spectrograph and the detector and Mr. James Hill for his important role in the construction of the PAMS system. The work was supported in part by the U.S. Army Chemical Research Development and Engineering Center.

REFERENCE: 1. Sinha, M.P., Giffin, C.E., Norris, D.D., Estes, T.J., Vilker, V.J. and Friedlander, S.K. (1981) J. Colloid Interf. Sci. 87, 140.

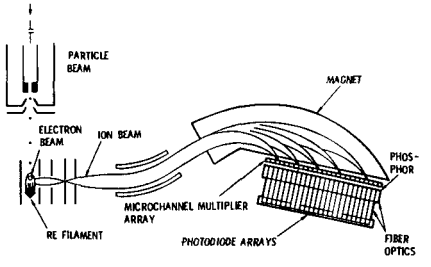

Fig. 1: Schematic of PAMS System

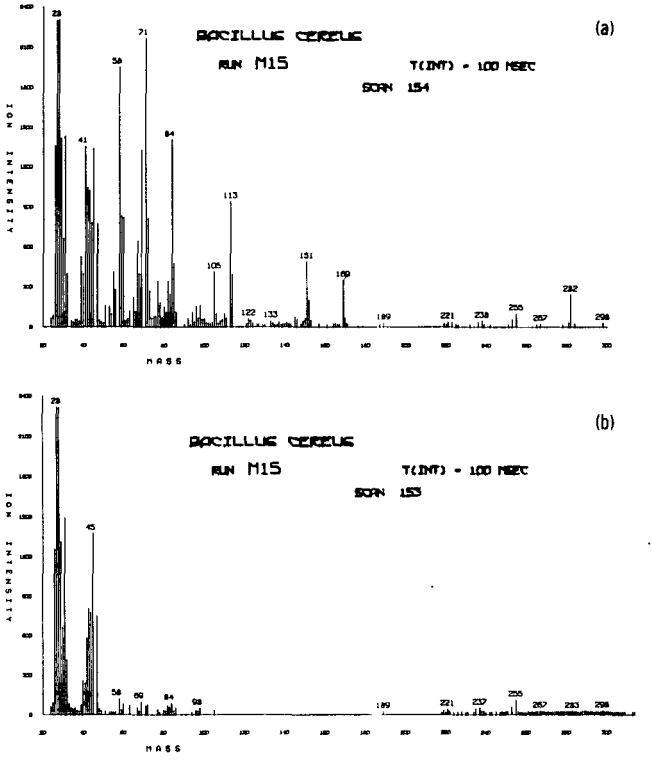

Fig. 2:
(a) Mass spectrum of a single bacillus cereus bacteria particle;
b) Mass spectrum of background gases from a scan containing no bacteria particle.

THERMOSPRAY LC/MS IN STUDIES OF BIOMEDICAL AND CLINICAL IMPORTANCE

D.J. Liberato, N.V. Esteban and A.L. Yergey

Lab. of Theoretical and Physical Biology, NICHD, NIH, Bethesda, MD 20892

The thermospray LC/MS technique has been employed in the separation and analysis of many non-volatile, polar compounds encountered in studies of pharmacological and clinical interest. We report here on selected topics of our work which includes both metabolite identification and utilization of stable isotope labelled compounds as tracers.

The development of a sensitive method for the qualitative and quantitative analysis of glucose is reported. This isotope dilution-mass spectrometry method, using U-13C-Glucose as tracer, allows accurate determination at low isotopic enrichments 0.1%-1% (Figure 1), in very small serum samples (200ul). This technique has the advantage of allowing simultaneous separation and structural identification of both glucose and other monosaccharides, with a detection limit of 50 pmoles. Application of the described method to the determination of low isotopic enrichment in human serum (1%) after constant intravenous infusion of U-13C-Glucose in a child with glycogen storage disease confirmed the validity of this technique for clinical investigation (Figure 2).

The feasability of an isotope dilution-thermospray LC/MS method, using either D3-Cortisol or 13C2-Testosterone as non-radioactive tracers, for studies of production and utilization rates were also explored. Preliminary studies with both cortisol and testosterone indicate that a precision of 5% is obtained in the 1-10% enrichment range and sensitivities under selected ion monitoring (SIM) better than 20pmoles could be obtained on column.

Lastly, studies were undertaken to explore the utility of thermospray in the analysis of alkylated DNA species. Separation and identification of adenine, 7-methylguanine and O6-methylguanine were accomplished using a mobile phase consisting of 2% acetonitrile, 98% 0.1M aqueous ammonium acetate modified with 10mM triethylamine and formic acid to pH 3.5 on a C-18 column (Figure 3). Sensitivities for each compound under SIM was better than 10ng on column. The spectra of each base were characterized exclusively by protonated molecules. Figure 4 illustrates the spectum obtained for 1nmole of 7-methylguanine on column. Thus, this method appears promising for use in identifying adducts of biological origin

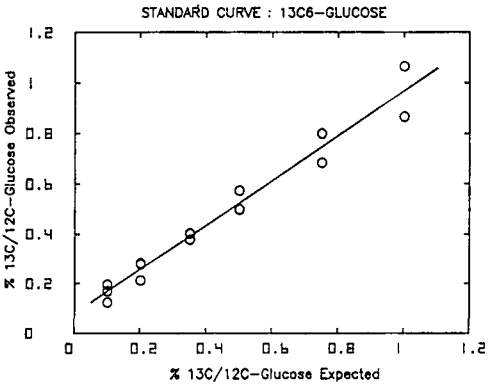

Figure 1. Glucose standard curve.
(.1%-1% enrichment,7% precision)

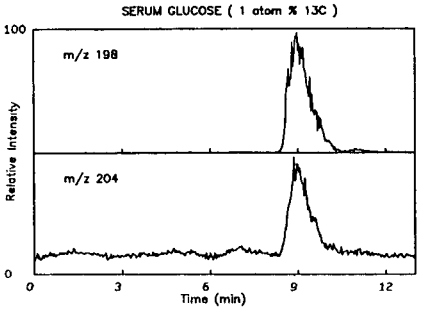

Figure 2 Glucose from serum.
(1% infusion)

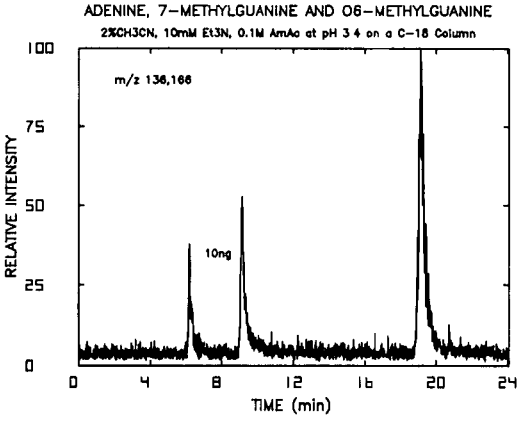

Figure 3 Alkylated base chromatogram

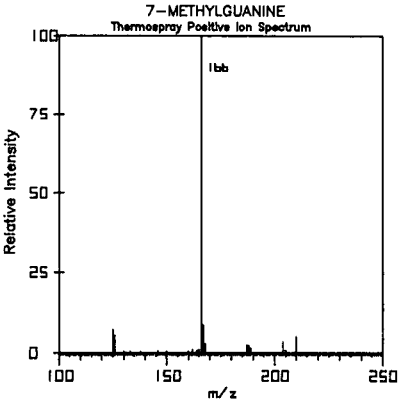

Figure 4. Spectrum of 7-Methylguanine.

DIFFERENTIAL DIAGNOSIS FOR HEPATOPATHY IN FIVE PATIENTS WITH VALPROATE THERAPY

I. Matsumoto, T. Kuhara, Y. Inoue, M. Matsumoto and T. Ohkura

Department of Biochemistry, Institute of Human Genetics
Kanazawa Medical University, Uchinada, Kahoku, Ishikawa 920-02, Japan

Summary: Urinary organic acid profiles of five patients who exhibited hyperammonemia and hepatopathy associated with valproate therapy have been studied by using GC/MS and mass chromatography. In a patient with fulminant hepatitis, large amounts of the end product of ω-oxidation of valproate was found but neither β-oxidation intermediates nor glucuronide of valproate was detectable. In contrast, in a patient with Reye's syndrome, only β-oxidation intermediates disappeared, valproate glucuronide was detectable, and 2-propylglutarate was greatly enhanced. In the rest of three patients, several abnormal metabolites which were characteristic of each inherited metabolic disease were detected in their urine. Although organic acid profiles in these patients were complicated, they could be chemically diagnosed as having ornithine transcarbamylase deficiency, citrullinemia and propionic acidemia, respectively, by GC/MS and amino acid analysis.

Introduction: Sodium valproate, sodium 2-n-propylvalerate (VPA), is an effective and widely used anticonvulsant particularly useful in the management of several seizure disorders. Although VPA is accepted to be relatively safe, it has been reported that the administration of VPA for a long time causes severe liver disease or malformation in some patients. As its frequency is very low (1/20,000) most of these patients had been suspected to be idiosyncratic. However, the nature of their specific idiosyncracy has not been studied yet. Minor elevations in serum levels of liver enzymes are observed fairly frequently, but they do not appear to be related to serious hepatic dysfunction. The recent reports of fatal hepatic dysfunction are of concern, however, although the causative role of VPA is not always clear cut. Several fatal cases of hepatotoxity in patients receiving VPA has only relatively recently been recognized as an adverse effect of the drug. It seems to be due to an idiosyncratic response to the drug rather than dose related and it has been postulated that VPA is not normally toxic, but in the presence of a metabolic abnormality (e.g., an inborn error of metabolism) it may be. Also VPA causes various metabolic disturbances because it inhibits several enzymes involved in intermediary cell metabolism. Thus hyperammonemia may be induced as well as hyperglycinemia. Hyperammonemia is fairly common and usually asymptomatic. The elevation of blood ammonia has been related to the occasional occurrence of stupor. In view of the possibility of fatal hepatotoxity in patients receiving VPA, it is of vital importance to detect this serious reaction early. We have studied the urinary metabolic profiles of VPA and endogenous acids in five patients who exhibited hyperammonemia and hepatopathy by using GC/MS, mass chromatography and an automatic amino acid analyzer in order to investigate biochemical mechanism of the adverse effects of VPA.

Five Cases with Liver Disease and Hyperammonemia Associated with VPA Therapy: Case 1. 3-year-old male; age of onset, 1 Y 8 M; died of fulminant hepatitis at 3 Y 4 M. Case 2. 6-year-old female; normal development until 6 Y; developed Reye's syndrome at 6 Y; term of VPA and other antiepileptic drug, 4 days. Case 3. 1-year-old female; developmental retardation; age of onset (grand mal), 6 M; term of VPA plus PB therapy, 4 M. Case 4. 2-year and 7-month-old female; coma, convulsion, Cheye-Stokes breathing, hyperammonemia (1,400 μg/dl). Case 5. 1-year-old female; developmental retardation; age of onset (recurrent convulsions), 11 M; term of VPA therapy, 2 M; hyperammonemia, Reye-like syndrome.

Experimental: Urine specimens from the patients during episodes or fresh morning urine specimen in a remittance were collected, frozen immediately and stored at -20°C until analysis. Organic acids were extracted three times with diethylether. After extracted organic solvent layer was evaporated to dryness under nitrogen stream, and N, O-bis-trimetylsilyl-trifuloroacetamine was added to the residue to convert trimethylsilyl (TMS) derivatives for GC/MS analysis. Gas chromatographic separation was performed with 3 m long, glass column packed with 4% OV-17 coated on Uniport HP. The oven temperature was kept initially at 100°C for 4 min. and then raised by temperature programmiing at 8°C/min to 290°C. GC/MS analysis was performed with a JEOL model JMS DX300 on-lined JMA 3500 data system. Two minutes after injection, repetitive scan was started from m/z 50 to 600 every 5 sec. The mass spectrometer was operated in the electron impact (EI) mode with an electron energy of 70 eV and an ion source temperature of 200°C.

Results & Discussion: All five patients were examined for their urinary organic acid profiles. Normally VPA undergoes glucuronic acid conjugation, β-oxidation and ω, and ω-1 oxidation. The most important urinary metabolite in all species is glucuronide. Approximately 70% of the administered dose is eliminated by this route in 24 hours and the rest are excreted as β-, ω- or ω-1 oxidation products.

In patient 1 who died of fulminant hepatitis, significant amounts of 2-n-propylglutaric acid (PGA), the end product of ω-oxidation of VPA, was found but neither 2-n-propyl-3-oxopentanoic acid and 2-n-propyl-3-hydroxypentanoic acid, the β-oxidation intermediates, nor glucuronides of VPA was detectable. As this patient had been simultaneously receiving phenobarbital, a P-450-inducing agent, it is suggested that ω-oxidation was greatly enhanced in the patient. This patient appears to have an error in the metabolism of VPA.

Patient 2 was confirmed to have Reye's syndrome. In her urine, only β-oxidation intermediates completely disappeared, VPA glucuronide was detectable, and PGA was significantly increased.

The urinary VPA-metabolite profile in patient 3 was normal. In addition, a series of metabolites characteristic of propionic acidemia were detected. Propionic acidemia causes hyperammonemia secondarily and hyperammonemia causes convulsion. In patients with propionic acidemia, propionyl CoA undergoes altered metabolism which facilitates the transport from the mitochondria, and thus several metabolites characteristic of this disorder can be detected. Even after VPA medication was discontinued, and VPA metabolites disappeared, propionyl CoA metabolites were still detected. Thus she was chemically diagnosed as having propionic acidemia.

Patient 4 and 5 developed severe hyperammonemia. Uracil is a reliable index for the chemical diagnosis of urea cycle enzymopathy except for carbamoyl phosphate synthase deficiency. Uracil is extracted with ethylether at acidic pH and thus can be analyzed by single GC/MS run simultaneously. In both patient 4 and 5, increased urinary excretion of uracil as well as orotic acid was confirmed by mass chromatography. In patient 4, only glutamine was elevated in both urine and serum and in patient 5, citrulline and glutamine were markedly elevated. Therefore patient 4 was chemically diagnosed as having ornithine carbamoyl transferase deficiency, and patient 5 citrullinemia, both are primary hyperammonemia. After the chemical diagnoses, these three patients were treated correctly and did not exhibit seizure thereafter.

It was shown that GC/MS studies of urinary acid profiles are very important for the patients with severe side effects associated with VPA therapy.

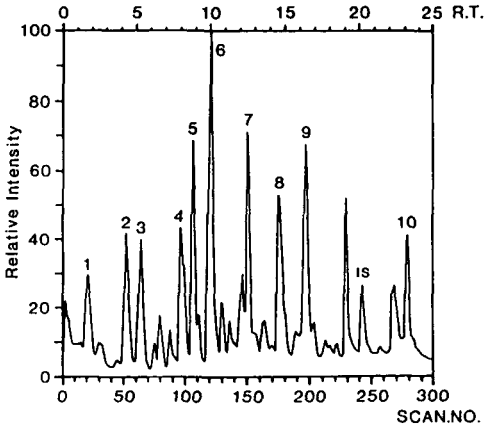

Fig. 1. RIC chromatogram of trimethylsilyl derivatives of urinary acids from case 3 under VPA therapy; 1. lactate 2. 3-hydroxypropionate, 3-hydroxybutyrate & 3-hydroxyisobutyrate 3. 3-hydroxyisovalerate 4. 3-ketovalerate 5. 2-methyl-3-oxovalerate (trans) & 2-propyl-3-hydroxyvalerate 6. 2-propyl-3-oxovalerate 7. 2-propylglutarate 8. tiglylglycine & p-hydroxyphenylacetate 9. methylcitrate 10. VPA-glucuronide.

MASS SPECTRAL DETERMINATION OF THE EMPIRICAL FORMULAS AND COMPOSITIONS OF PEPTIDES BY FABMS.

M.J. BERTRAND, P.THIBAULT, M.J.EVANS AND Z.ZIDAROV
Regional Center for Mass Spectrometry, Department of Chemistry,
University of Montreal
P.O. Box 6128, Montreal, Québec, CANADA, H3C 3J7

INTRODUCTION

In recent years, the introduction of desorption ionization techniques which permit the analysis of polar compounds in their underivatized form, has opened new avenues in this field of chemical analysis. Peptides have been analyzed by FAB and studies have focussed on the development of strategies to characterize their amino acid compositions ans sequences. The FAB spectra of peptides reveal a substantial amount of information that can be used for identification and structure determination. The mass spectra are usually characterized by the presence of molecular ion clusters of good relative intensities, of sequence fragments and ions at the lower mass end of the spectra related to the radicals of the amino acids present in the peptide. Several attempts have been made to use computer interpretation to generate amino acid sequences from the mass spectra of peptides (1,2) but sequence analysis is still difficult and tedious without prior knowledge of the amino acid content of the peptide. An approach using mass spectral data to generate the empirical formulas, the amino acid compositions and the sequences of small peptides (m/z 1500) is described and its usefullness is discussed using model compounds.

EXPERIMENTAL

All mass spectral data were obtained on a Kratos MS-50 TCTA mass spectrometer equiped with a Kratos FAB source an Iontech B-11N atom gun and a post-acceleration detector. Exact masses and isotopic abundances were measured in the negative ion mode using the narrow accelerating voltage scan technique (3) and a Kratos DS-55 data system. Negative ion spectra were generated from an alkaline water-glycerol (1:2) matrix and positive ion spectra from an acidic water-glycerol (1:2) mixture. Computations of empirical formulas, amino acid compositions and sequences were performed on a CDC-Cyber 835 computer using the program "PEPTIDES" written (Fortran V) in this laboratory.

RESULTS AND DISCUSSION

In order to evaluate the feasibility to determine the amino acid composition and sequence of peptides from mass spectral data obtained by FABMS, calculations were conducted using a series of model peptides. A computer program was written to obtain empirical formulas from the exact masses and isotopic abundances. The algorithm uses the mass of the peptide and initial approximations to evaluate the minimum and maximum chain length N_{min} and N_{max}. It then uses the elemental compositions of homologuous peptides to calculate extreme compositions of the type $C_{max}H_{max}O_{min}N_{min}S_{min}$ and $C_{min}H_{min}O_{max}N_{max}S_{max}$ and generates all possible elemental compositions in between those formulas. Among the resulting formulas only those that respect the nitrogen rule the number of unsaturated sites and have masses and isotopic ratios within a given range of the real values are retained. The number of empirical formulas that are obtained using such an approach are given, for three ranges of masses and isotopic abundances, by the values in paranthesis in Table 1. It can be seen in most cases that the number of solutions obtained are too numerous for practical use. This is partly due to the fact that within the empirical formulas retained some do not correspond to actual peptides. In order to eliminate these pseudo-peptide formulas each formula is mathematically treated by a Diophantin equation system that is constructed from the structure of a peptide. Each formula that has one or many solutions in the Diophantin system is a true peptide and the exact solutions to the equation system constitute amino acid compositions. The number of empirical formulas corresponding to real peptides as calculated for the model compounds are given in Table I. It can be seen that the number of solutions obtained under the ranges of errors corresponding to E_2 and E_3 is approching tractable values.

Experimental measurements were conducted to verify if the error ranges used in the calculations could be achieved on a routine basis for actual samples. The experimental results obtained for typical peptides are given in Table II. It can be seen that the errors in mass are all within 15 ppm and that the errors on the isotopic abundances are within 10% of the actual values which indicates that the algorithm can be used successfully to obtain the empirical formulas and compositions of small peptides up to m/z 1500. Furthermore the computer program can use as input other information contained in the mass spetrum such as low mass ions corresponding to amino acids and sequence fragments. A typical result of composition analysis from the mass spectra of Met-Enkephalin is shown on figure 1. It can be seen that, from the data, the program finds only two compositions corresponding to a tetra and a penta-peptide and that the actual composition of Met-Enkephalin is one of the solutions. As a further development the program can also generate possible sequences if fragmentations ions are entered as data.

REFERENCES

(1) Biemann K., Cone C., Webster B.R., Arsenault G.P. J. Am. Chem. Soc. 88, 5598 (1966).

(2) Matsuo T., Sakurai T., Matsuda H., Wollnik H., Katakuse I. Biomed. Mass Spectrom. 10, 57 (1983).

(3) Grotjahn L., Taylor L.C.E. Org. Mass Spectrom. 20, 146 (1985).

TABLE I

PEPTIDE FORMULAE CALCULATED USING THE EXACT MASSES AND ISOTOPIC RATIOS

COMPOUNDS	MASS	M+1/M	M+2/M	M+3/M	FORMULAE		
					E1	E2	E3
LEU-ENKEPHALINE	555 2692	33.0	6.7	-	2 (5)	1 (1)	1 (1)
MET-ENKEPHALINE	573.2256	32.7	10.8	-	2 (6)	1 (2)	1 (1)
PENTA-PHENYLALANINE	753.3526	51 9	14.1	-	1 (3)	1 (1)	1 (1)
BRADYKININE	1059.5613	61.4	20.7	5.0	14 (35)	9 (22)	3 (6)
SUBSTANCE-P	1346 7121	77 4	36.6	12.8	31 (116)	19 (71)	6 (13)

E1 ΔM=±25ppm, E1=±10%, E2=±10%, E3=±10%
E2: ΔM=±15ppm, E1=±10%, E2=±10%, E3=±10%
E3: ΔM=±10ppm, E1=± 5%, E2=± 5%, E3=± 5%

Values between parenthesis show the number of empirical formulas before Diophantine resolution.

FIGURE 1

INPUT-OUTPUT FOR MET-ENKEPHALIN

PROGRAM INPUT

Monoisotopic mass? 573 220 — range on M (ppm)? 15
M+1/M (%) ? 32 3 — range on M+1/M ? 10
M+2/M (%) ? 11 0 — range on M+2/M ? 10
Radicals observed ? Pha,Met, Tyr
Radicals excluded ? Lys,Pro,Trp,His

PROGRAM OUTPUT

PEPTIDE FORMULAS FOUND

C	H	O	N	S	Exact mass	M+1/M	M+2/M
27	35	7	5	1	573 225696	32 67	10 78

AMINO ACID CONTENT

N_L=5

PRO	PHE	HIS	ARG	TRP	GLU	TYR	ASP	ASN	GLN	GLY	ALA	VAL	LEU	LYS	SER	THR	CYS	MET
0	1	0	0	0	0	1	0	0	0	2	0	0	0	0	0	0	0	1

N_L=4

PRO	PHE	HIS	ARG	TRP	GLU	TYR	ASP	ASN	GLN	GLY	ALA	VAL	LEU	LYS	SER	THR	CYS	MET
0	1	0	0	0	0	1	0	1	0	0	0	0	0	0	0	0	0	1

TABLE II

CALCULATED AND EXPERIMENTAL VALUES FOR ACCURATE MASSES AND ISOTOPIC PEAK RATIOS

	Mass			M+1/M			M+2/M		
Compound	calc.	obs.	ppm	calc.	obs.	%	calc.	obs.	%
Leu-Enkephaline	555.2684	555.274	+11	33.0	33.7	+2.1	6.7	6.4	-4.4
Met-Enkephaline	573.2256	573.220	-10	32.7	32.3	-1.2	10.7	11.0	+2.8
Gastrine related	596.2361	596.242	+ 7	35.2	35.6	+1.1	11.4	11.1	-2.6
Tetra-Phenylalanine	606.2842	606.280	- 7	41.2	43.4	+5.4	9.3	10.1	+8.6
Penta-Phenylalanine	753.3526	753.345	- 7	51.5	55.1	+7.0	14.2	15.5	+9.2
Bradykinine	1059.5613	1059.550	-10	61.4	64.1	+4.4	20.7	22.0	+6.2
Substance-P	1346.7121	1346.722	+ 7	77.4	77.8	-0.4	36.6	38.4	+5.0

CAPABILITIES AND LIMITATIONS OF TANDEM MASS SPECTROMETRY FOR THE IDENTIFICATION OF DRUG METABOLITES

Mike S. Lee, Richard A. Yost; Department of Chemistry, University of Florida, Gainesville, FL 32611.
Robert J. Perchalski; Pharmatec Inc., Alachua, FL 32615.

A rapid and systematic method for the identification of drug metabolite structures with tandem mass spectrometry (MS/MS) without prior separation has been developed in our laboratory. Early results with this MS/MS method were obtained with methane positive chemical ionization (CI). We have now completed systematic studies on a variety of drug types to determine the capabilities and limitations of this method. We have also evaluated variations of the MS/MS method, including alternate CI gases, negative CI, electron ionization (EI), derivatization, and thermospray ionization.

The MS/MS method involves the coordinated use of the normal, daughter, parent and neutral loss modes of a triple quadrupole mass spectrometer. The method is based on the fact that drug metabolites usually retain much of the original parent drug structure, or at least retain some substructures of the drug. Therefore, metabolites would be expected to undergo similar collisionally activated dissociations (CAD) to those of the pure drug. Specifically, both should lose some of the same neutral fragments and form some of the same daughter ions. The neutral loss and parent scans of the instrument are used to selectively screen a physiological sample for those species which contain the characteristic functionalities or substructures of the pure drug, without separation of the mixture components. Ions contained in the neutral loss and parent spectra correspond to possible metabolites, and their daughter spectra are obtained.

Four metabolites of a new antiepileptic drug, zonisamide (Figure 1), were postulated directly from an enzyme-hydrolyzed urine extract. These metabolites are shown in Figure 2, along with their molecular weights (M.W.) and the major CAD fragmentations observed in their daughter spectra. The metabolites A and B were inferred by use of the neutral loss scan-daughter scan sequence. This was possible because the metabolites retained the intact unmetabolized sulfonamide portion of the parent drug, which was easily lost under CAD conditions (neutral loss of 81). Thus, metabolism occurred on the ring portion of the drug. The metabolites C and D were inferred by the use of the parent scan-daughter scan sequence. These metabolites were the result of metabolism occurring on the sulfonamide portion of the drug, and thus retained the ring substructure of the parent drug. Under CAD conditions, metabolites C and D formed an abundant daughter ion at m/z 132, corresponding to the ring substructure of the parent drug.

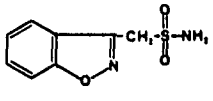

Figure 1. Structure of zonisamide (M.W. 212).

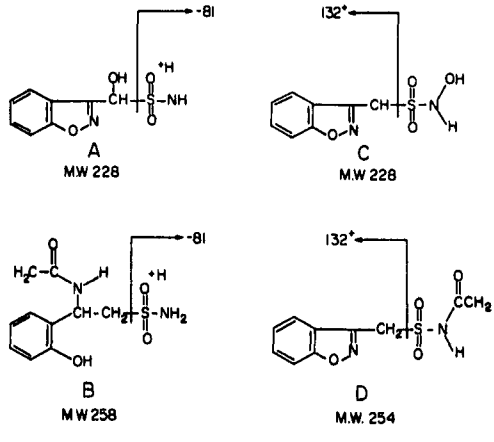

Figure 2. Metabolites of zonisamide identified by the MS/MS technique and their characteristic fragmentations observed in the daughter spectrum of their $(M+H)^+$ ions.

In this MS/MS method the neutral loss and parent scans complement each other. In the case of zonisamide, the neutral loss scan was essentially used to screen for all metabolites which retained the sulfonamide portion of the drug, while the parent scan was used to screen for all metabolites which retained the unmetabolized ring portion of the pure drug. Therefore, if metabolism occurs on either portion of the drug molecule (ring or sulfonamide), and if the other portion remains unmetabolized, all metabolites will be detected by either the neutral loss scan or parent scan. However, if both of the substructures were metabolized, the metabolites would remain undetected. To determine whether this did actually occur, new neutral losses and daughter ions observed from the daughter spectra of the metabolites were selected for their respective neutral loss and parent experiments. This allowed for the identification of further metabolites with similar substructures present in the previously identified metabolites, but not necessarily present in the parent drug. No metabolites of this type (metabolism occurring on both portions) were identified.

The MS/MS method was also performed with an alternate CI reagent gas, isobutane. The isobutane CI spectra are generally characterized by an abundant protonated molecular ion $(M+H)^+$ with less fragmentation and less intense adduct ions compared to those obtained by methane CI. Relative sensitivities of various compounds were observed to be different than those observed by methane CI. The isobutane daughter spectra of the $(M+H)^+$ ions contained the same daughter ions with approximately the same relative abundances as the methane CI daughter spectra.

The EI mode was used with this MS/MS method to attempt to identify metabolites in urine. However, no metabolites were identified. This was probably due to the high background produced from the extensive fragmentation of the variety of components of urine in the EI mode, with abundant ions at every mass which may essentially mask the ion current of a possible metabolite. The lack of success may also be attributed to the low abundance of the molecular ion of the drug (and probably of its metabolites, as well) produced by EI. A low abundance of molecular ion peaks and high abundance of daughter ions may lead to complicated neutral loss and parent spectra which contain mostly metabolite fragment ions rather than metabolite molecular ions.

Simultaneous positive/negative CI spectra were generated with the use of a 1:1 N_2O/CH_4 mixture at a total source pressure of 0.9 torr. The negative ion CI daughter spectra of the $(M-H)^-$ ions obtained with this MS/MS method showed less fragmentation than observed in the positive ion CI daughter spectra of $(M+H)^+$, and thus, less structural information was obtained. Although the exclusive use of negative ion spectra may not be as useful as the positive ion spectra for the identification of drug metabolites with this method, it may be used to provide structural information complementary to the positive ion spectra.

A derivatization technique was employed to create simple and predictable CAD fragmentations characteristic of the derivatized structure. The strategy was to derivatize the pure drug and characterize its CAD fragmentations (neutral losses and daughter ions). A urine sample was then derivatized in the same way, so that the derivatized functional group could serve as a marker to selectively screen for all components which contain this targeted substructure. Dimethylformamide dimethylacetal (DMF-DMA) was used to derivatize a pure carbamazepine sample and the carbamazepine metabolites present in a urine sample. Only one metabolite of carbamazepine, the epoxide metabolite, was identified with this method.

Studies were performed with a Vestec thermospray LC/MS interface to determine the feasibility of thermospray ionization with this MS/MS method for the identification of polar conjugated metabolites in urine. Our preliminary studies involved the use of model glucuronides, p-nitrophenyl glucuronide and menthol glucuronic acid. To date thermospray ionization has been too erratic and unstable to permit the reliable identification of drug metabolites with this method. Improvements in sensitivity and spectral reproducibility must be made with thermospray if it is to be used with this MS/MS method.

FRAGMENTATION BEHAVIOR OF HIGH MASS MOLECULES

Demirev P., Fenselau C., Olthoff J. and Cotter R.
Dept. Pharmacology, J. Hopkins Univ., Baltimore MD 21205

The introduction of desorption ionization techniques - PD and LSIMS in particular - in conjunction with mass analyzers capable of handling ions above 3000 D has greatly expanded the range of accessible compounds for study by mass spectrometry. The observed spectra of these compounds (mainly peptides) have some features in common which have already been discussed [1]. Among them are: sufficiently intense singly and multiply charged molecular ions, decreased amount of prompt fragmentation carrying sequence/structural information, loss of small neutral groups from the molecular ion, leading to extended envelopes on its low mass side, exponentially decreasing continuous background as mass increases. The quasi-equilibrium theory (QET), which has been widely accepted to rationalize the fragmentation of lower molecular weight compounds, could also be applied to the unimolecular behaviour of these heavy ions. For example, the change in the fragmentation rates for an end-bond versus centre-bond cleavage in a chain type molecule as the number of atoms increase, has been predicted on the basis of QET, as we have represented in Fig. 1, following the ideas of Bunker [2]. For the case of (bio)polymers this would lead to preferential small group losses from the ends, rather than consecutive cleavages along the backbone of the molecule, which together with charge delocalization [3] could explain the observed fragmentation patterns [1,4].

The overall decrease of the rate for a particular fragmentation with increase in molecular size ("degrees of freedom" effect) is known for low molecular weight compounds [5]. The change in rate constant with increasing number of atoms in the molecule provided that v-frequency factor, Eo-activation energy, E-internal energy are constant, is illustrated in Fig. 2. In the case of higher mass compounds it could be illustrated by comparing the intensities of peaks resulting from the loss of F and their precursors for different number of monomers in the precursors in the negative ion PD spectrum of a polymer - Krytox. Comparing ratios of molecular versus fragment ions for three phosphazenes with different massses (2121, 2828 and 3628 D) leads to the same observation - the decrease of the rate constant with the increase in molecular size which results in less prompt fragmentation observed in that time frame.

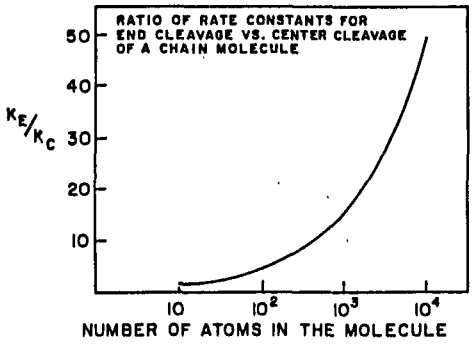

Fig. 1

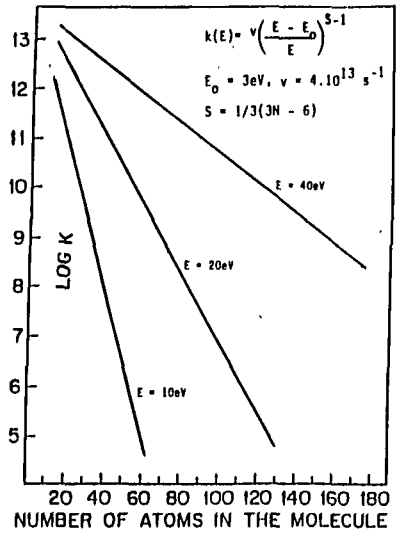

Fig. 2

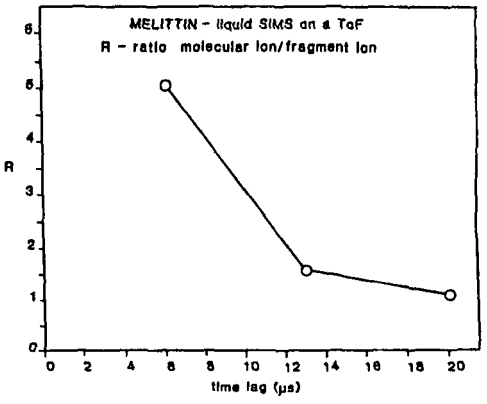

Fig. 3

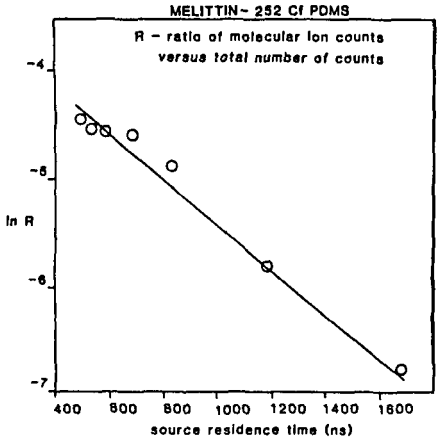

Fig. 4

The effect of the source residence time is studied in two experiments - a dynamic (draw out pulse) ToF with a LSIMS ion source [5] and a static ToF PD mass spectrometer. There is elevated abundance of fragment ions (corresponding to the sequence) in the spectrum of melittin (mw 2850) when the time lag of the draw-out pulse is changed from 5 to 20 us - Fig. 3. The ratio of total fragment to molecular ion counts versus source residence time (varied by changing the accelerating voltage) is plotted on Fig. 4 for the same compound run on the PD spectrometer. There is a decrease in that ratio with the increase of the source residence time. These experiments suggest that fragmentations with rates in the metastable (us) time scale become increasingly important and are predominant with the increase of molecular size. Finally we note that presence of non-covalent interactions in peptides might lead to additional stabilization of the resulting molecular ions in the gas-phase which in effect increases the activation energy for fragmentation.

Acknowledgements: This study has been supported by grants: DMB-8515390 from the National Science Foundation and RR02727 from the National Institutes of Health.

References

[1] P. Demirev, M. Alai, R. van Breemen, R. Cotter, C. Fenselau, in "SIMS V" (Springer Series in Chem. Physics, v.47) Springer-Verlag, 1986, p.527.
[2] D. Bunker, F. Wang. J. Am. Chem. Soc., 99, 7457 (1977).
[3] A. Craig, P. Derrick, J. Am. Chem. Soc., 107, 6707 (1985).
[4] R. Cotter, B. Larsen, D. Heller, J. Campana, C. Fenselau, Anal. Chem. 57, 1943 (1985).
[5] F. McLafferty, W. Pike, J. Am. Chem. Soc., 89, 5351 (1967).
[6] R. Cotter, Anal. Chem. 56, 2534 (1984).

A COMPARISON OF OLIGOSACCHARIDE FRAGMENTS GENERATED BY DIFFERENT METHODS OF SAMPLE DESORPTION

V. N. Reinhold, S. Santikarn and G. R. Her
Harvard School of Public Health, Boston, MA 02115

Desorption spectra of biopolymers are replete with ions that do not contribute structural insight. Many of these ions can be directly related to the FAB matrix or sample contaminants, the latter of which may contribute complex surface effects and even repress sample desorption. For the structurally relevant ions generated in each process, we have compared direct chemical ionization (DCI), collision induced dissociation (CID), and fast atom bombardment (FAB) with and without a matrix, (the non-matrix study carried out with a belt HPLC interface).

With linear biopolymers sequence and a determination of molecular weight, provides an adequate solution to many structural problems. For oligosaccharides sugar linkage and chain branching must also be understood. The problems of isomeric moieties (e.g., mannose, galactose, glucose) adds further complexity in the analysis of carbohydrate materials. Under selected conditions, branching information can be detected in all of the above ionization processes and it has been our goal to determine those factors responsible while maintaining sensitivity.

Branching detail is dependent on a simple premis--that molecular fragments are a consequence of single cleavage only. Most fragment ions can be rationalized on this basis. Unfortunately, the broad energy spread (high energy tail) of many ionization processes results in some double cleavage, thereby destroying this structural detail. For permethylated oligosaccharides ammonia DCI has worked exceptionally well for the determination of molecular weight and linear sequence. Because this technique requires heat to initiate desorption, pyrolysis becomes a problem and branching information is lost for late desorbing materials, (e.g., polar and higher molecular weight samples). From a study with known compounds, branching details are observed in spectra desorbed early from the probe while subsequent spectra exhibit double cleavage ions and extensive pyrolysis. At somewhat higher concentrations, FAB-MS can provide comparable structural detail on underivatized oligosaccharides. Unfortunately, close scrutiny of all spectra indicates that even with this "soft ionization" process, ions are present that can be accounted for as double cleavage fragments. Thus, definitive branching assignment for unknown materials becomes very tenuous. We have previously shown that high energy collision spectra (BE-CID-EB) with a four sector instrument can provide branching information. MIKES analysis (BE) under the same collision conditions has proven equally successful.

Among other things, FAB sensitivity is a function of the sample and matrix, and, diminished by any technique that causes dispersal of ion signal. In light of this, we have compared FAB desorption from different matricies and substrates. In Figure 1 is a comparison of conventional matrix FAB-MS to belt FAB-MS. The top two spectra (taken with equal concentrations of a mixture of viridopentaose A, B and C) demonstrates the spreading of molecular-weight related ions due to the matrix. In addition, the second spectrum shows excessive non-informative fragmentation (loss of m/z 42 from the amino sugar components) and a series of matrix ions, $[(\text{glycerol})_{7-9} + H]^+$. The spectrum in the third panel (identical concentration) was obtained by FAB desorption from a moving belt interface and clearly indicates the three materials and their molecular weights, (e.g., 799, 815, and 840 daltons, ions at m/z 821, 837, and 862; $(M + Na)^+$). An important additional factor is the low background observed in the belt FAB

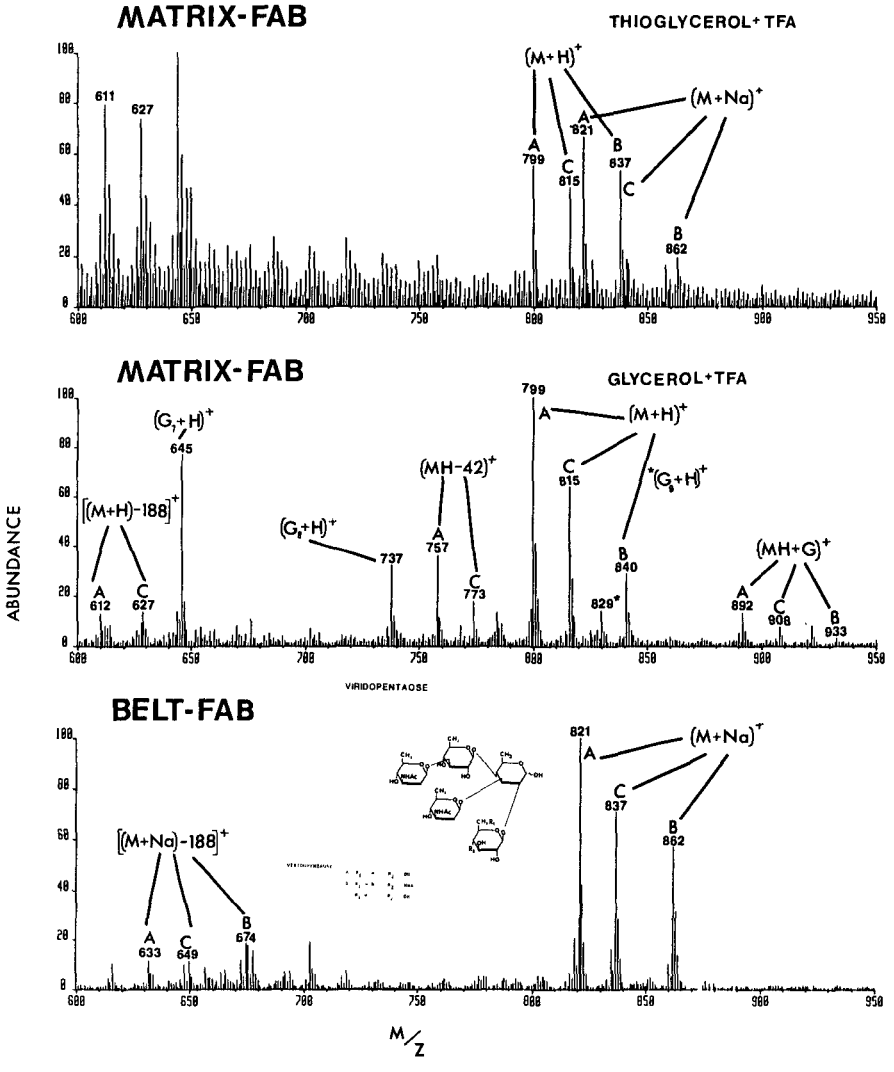

spectrum allowing a study at very low masses. These characteristics of belt FAB desorption have been extremely important, especially when concerned with sensitivity. Finally, belt FAB desorption has proven to be a "softer" ionization process and we have not detected double cleavage fragments for branched oligosaccharides. This has been a most important observation which we hope to exploit extensively.

* We wish to acknowledge Professor Makoto Suzuki, Meijo University, Nagoya, Japan for his generous gifts of viridopentaose A, B, and C. This work was supported, in part, by NIH, NSF and USAMRIID.

Characterization of Carbohydrate-Insulin Conjugates Using Fast Atom Bombardment Mass Spectrometry: D. V. Myhre, T. Keough, and M. S. McCracken; The Procter & Gamble Co., Miami Valley Laboratories, P.O. Box 39175, Cincinnati, OH 45247.

Morell and coworkers previously reported[1] that blood glycoproteins containing terminal non-reducing D-galactosyl groups are rapidly cleared from the circulation of animals by interaction at the asialoglycoprotein receptor of the hepatocytes. In this study, we prepared several carbohydrate-insulin conjugates containing one or more terminal D-galactosyl residues to study their binding to the asialoglycoprotein receptor.

The synthetic method (Fig. 1) using N-hydroxysuccinimide amino acid esters is a well-known method for peptide synthesis.[2] The reaction of these activated esters, which occur at free anime groups, yields a mixture of lactobionyl insulins which were separated and characterized primarily by FAB/MS. The bulk of our efforts centered on the characterization of the dilactobionyl insulin (DLI) shown. Most of our FAB results were obtained on our low field ZAB-2F mass spectrometer operated at 2 or 3 kV. For sensitivity reasons, some analyses were also conducted on a high-field ZAB at the University of Illinois.

DLI consistently yielded poorer sensitivity than porcine insulin in the molecular ion region of the FAB spectrum. We therefore decided to characterize the molecule by chemically cleaving the disulfide bridges and separately analysing each chain. Low resolution survey scans (Fig. 2), such as that for the B-chain region for porcine insulin (upper) and those for two separate DLI preparations (middle, lower), indicated that both chains had been modified. However, the A- and B-chains did not exhibit the expected upward mass shift of 340 Daltons relative to insulin. Instead, an additional mass increment of approximately 116±2 Daltons was contained in each chain. Similar results were obtained by the ^{252}Cf plasma desorption method (Fig. 3). The observed molecular ion at M/Z 6692 is approximately 233 Daltons greater than the anticipated mass assuming the coupling reaction proceeded according to Figure 1.

Higher resolution experiments were conducted on the modified A- and B-chains using FAB/MS. The measured nominal masses of both chains actually turned out to be 115 Daltons greater than originally anticipated.

The lactobionyl coupling reaction was repeated on a lower molecular weight substrate, Gly-Val, to produce a more readily characterizable molecule containing the additional mass increment. FAB/MS of a crude reaction mixture and a HPLC cleaned up sample (Fig. 4) revealed that the desired product had been produced (MH^+=630, MNa^+=652). Incidentally, we propose that the additional mass increment results because the amine group of the dipeptide does not react at the ester as originally anticipated. Rather, reaction occurs at the succinimide carbonyl. Ring opening followed by intramolecular proton transfer yields a species containing an additional $C_4H_5NO_3$ group between the N-terminus of the dipeptide and the lactobionyl group (Fig. 4). This type of process has been previously reported[3] as a <u>minor side reaction</u> produced during the coupling of the N-hydroxysuccinimide ester of proline with free proline.

Exact mass (peak matching) measurements on the MH^+ and MNa^+ ions of the modified dipeptide initially failed due to a lack of sensitivity. We therefore developed a computerized peak matching technique that allows signal averaging prior to mass assignment. The technique is similar to that previously reported by Murphy and coworkers[4] with the exception that, for convenience, we used linear sweeps of the magnet over narrow mass windows (0.1 to 0.2 Daltons) to obtain the data. Typical results are given in Fig. 5. The upper traces contain the refocussed reference ions that were used to calibrate the mass scales and the lower traces are actual data. Based on the average of five determinations, we conclude that the exact mass of the modified dipeptide is 629.225 Daltons. Subtracting the dipeptide and lactobionyl portions of the molecule yields an exact mass for the additional increment. This value, 115.024, agrees reasonably well with that expected for $C_4H_5NO_3$ (115.027). Furthermore, MS/MS (Fig. 6) of the M/Z 272 ion, formed by loss of lactobionic acid from the MH^+ ion, is completely consistent with the proposed structure.

References

1. A. G. Morell, et al, J. Biol. Chem., 246, (1977) 1461.
2. G. W. Anderson, et al, J. Am. Chem. Soc., 86, (1964) 1839.
3. J. Savrda, J. Org. Chem., 42, (1977) 3199.
4. K. L. Clay, et al, Int. J. Mass Spectrom. Ion Phys., 53, (1983) 327.

Acknowledgements

We would like to thank Mr. J. C. Hill and Dr. R. D. MacFarlane (Texas A&M University) for the ^{252}Cf PDMS results and Mr. J. C. Cook (University of Illinois) for use of the high ZAB in his laboratory.

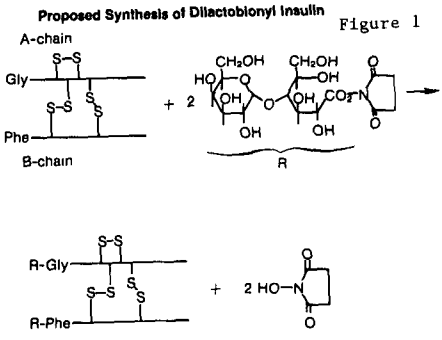

Figure 1

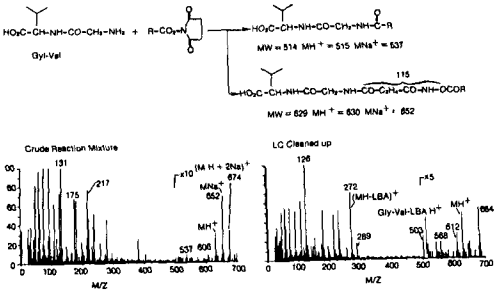

Figure 4

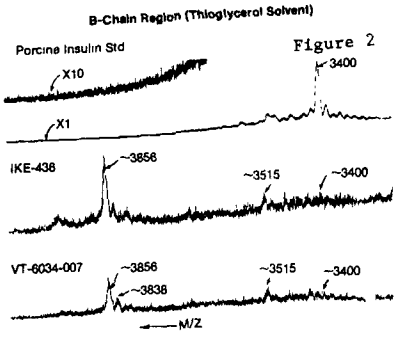

Figure 2

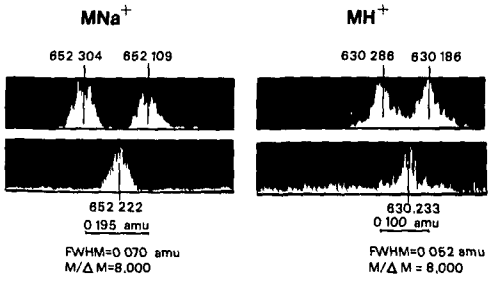

Figure 5

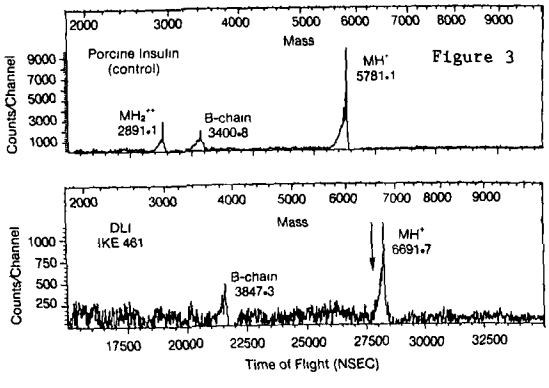

Figure 3

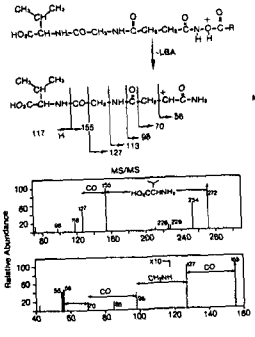

Figure 6

HIGH FLUX PARTICLE BOMBARDMENT TOF MASS SPECTROMETRY II.

J.K. Olthoff, J.P. Honovich, and R.J. Cotter, Dept. of Pharmacology,
The Johns Hopkins University, Baltimore MD 21205

Two years ago we introduced a different approach to the design of a SIMS-TOF mass spectrometer (1,2). The primary ion flux was high enough to produce secondary ion currents observed as analog signals, rather than single ion counts. Fast analog-to-digital conversion (waveform recording) and signal averaging was used rather than time-to-digital (TDC) conversion. The field-free ion source and pulsed extraction voltage enabled the use of liquid matrices, such as glycerol. The purpose of this approach, therefore, was to take advantage of the solution chemistry available in the FAB technique along with the high transmission and ion collection efficiency of a non-scanning instrument.

A Kratos Minibeam I ion gun is interfaced to a CVC-2000 TOF mass spectrometer. The primary beam is a 1-5 microamp, 1-10 microsecond pulse of Xe ions. Secondary ions are extracted 10-20 microseconds after the primary ion pulse. In the current version, a dual channel plate post-acceleration detector has been added and ions in each cycle are recorded and added to preceding cycles using a LeCroy 3500 SA signal averager with a 100 MHz waveform recorder.

Average and instantaneous primary ion currents may be varied over a wide flux range with and without a matrix. Spectra obtained with a glycerol/thioglycerol matrix exhibit enhanced protonated molecular ion peaks and longer sample lifetimes. Changing the delayed ion extration time varies the fragmentation patterns observed for many compounds. For Melittin, longer delay times allow more time for metastable fragmentation and therefore increases the size of fragment peaks. Finally, the high flux particle bombardment TOF produces spectra similar to those obtained by FAB for peptides over a wide range of masses. A spectrum of Oxytocin is shown as an example.

(1) R.J. Cotter, "High Flux Particle Bombardment TOF Mass Spectrometry", Proceedings of the 31st Annual Meeting of the American Society for Mass Spectrometry, 1983, p. 538.

(2) R.J. Cotter, "Liquid Secondary Ion Time-of-Flight Mass Spectrometry", Anal. Chem., 56, 2594 (1984).

Research was supported in part by grant 1-RO1-GM-33967-01A1 from the National Institutes of Health.

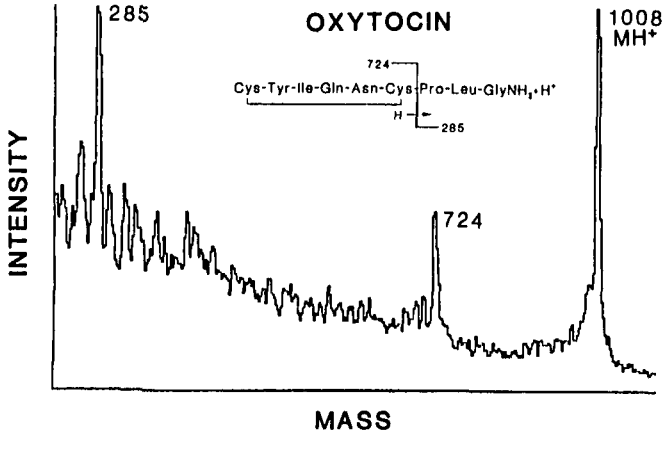

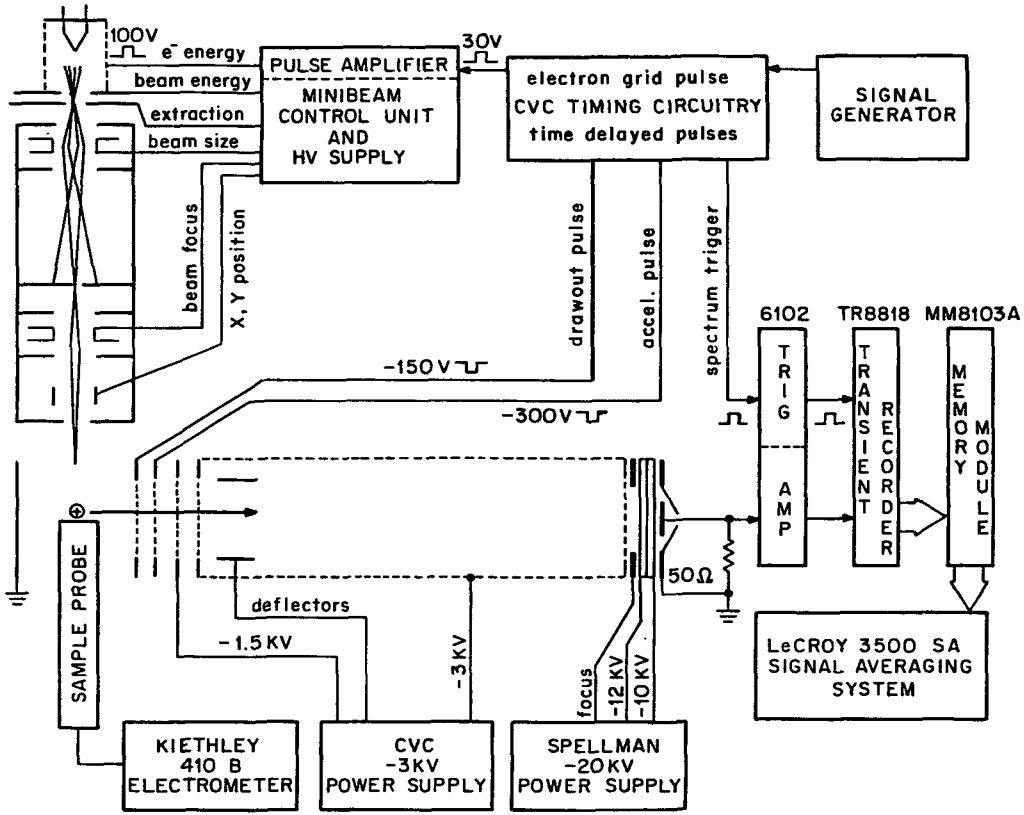
100V
e⁻ energy
beam energy
extraction
beam size
PULSE AMPLIFIER
MINIBEAM
CONTROL UNIT
AND
HV SUPPLY
30V
electron grid pulse
CVC TIMING CIRCUITRY
time delayed pulses
SIGNAL
GENERATOR
beam focus
X, Y position
drawout pulse
accel. pulse
spectrum trigger
-150V
-300V
6102
TRIG
AMP
TR8818
TRANSIENT
RECORDER
MM8103A
MEMORY
MODULE
50Ω
SAMPLE PROBE
deflectors
-1.5 KV
-3 KV
focus
-12 KV
-10 KV
LeCROY 3500 SA
SIGNAL AVERAGING
SYSTEM
KIETHLEY
410 B
ELECTROMETER
CVC
-3KV
POWER SUPPLY
SPELLMAN
-20KV
POWER SUPPLY

ANALYSIS OF BIO-ORGANIC MOLECULES BY PLASMA DESORPTION MASS SPECTROMETRY

I Kamensky[1], Å Engström[2], A G Craig[2], H Bennich[2], P F Nielsen[3], P Roepstorff[3], G Jonsson[4], P Håkansson[4] and B U R Sundqvist[4].

[1]Bio-Ion Nordic AB, Box 15045, S-750 15 Uppsala, Sweden.
[2]Department of Immunology, Biomedical Center, Uppsala University, Box 582, S-751 23 Uppsala, Sweden.
[3]Department of Molecular Biology, Odense University, Campusvej 55, DK-5230 Odense M, Denmark.
[4]Tandem Accelerator Laboratory, Uppsala University, Box 533, S-751 21 Uppsala, Sweden.

Plasma desorption mass spectrometry has an impressive record of achievements in the determination of high mass compounds. The time-of-flight mass analysis with its virtually unlimited mass range has been largely responsible for this success. However a second equally important reason is the use of high energy primary particles such as fission fragments from Cf-252. In the Bio-Ion instrument, a 10 uCi source is used providing about 2000 primary particles/sec. Each primary particle desorbs several secondary ions which are detected at the stop detector at the end of the flight tube. The low flux of primary ions is one reason why the technique is so gentle. As a consequence, the sample survives in the ion source for long times, and only a small fraction of the sample is really consumed. It is also possible to recover a large part of the sample applied.

Two sample preparation techniques are mainly used:
The electrospray technique has been described earlier [1]. A more recent development is the nitrocellulose (NC) adsorption technique [2] for peptides, proteins and nucleotides. In summary, a layer of NC is deposited on the normal metal foil (e.g. by electrospray). Sample is subsequently dropped on the surface and left to adsorb for a few minutes. Finally, the foil is washed with a solvent thus removing salts and other low molecular weight impurities from the surface. After drying, the sample is introduced to the ion source.

It has been found that the pH of the solvent plays an important role in this process. By varying the pH of the solvent, yields of molecular ions can be enhanced or completely quenched. The sensitivity has been improved drastically as compared to the electrospray method. It is possible to analyse a mono-layer of molecules providing sensitivity down to pmole amounts. Most importantly, using this method, it has been possible to achieve molecular ions of a number of hitherto intractable molecules.

As an example, the sequence of an Insect Cuticle Protein from locusta migratoria was confirmed by plasma desorption. During sequence determination a discrepancy was found between the molecular weight determined by SDS-gel electrophoresis (21,600 daltons) and the weight calculated from the sequence (15,323 daltons). The protein has a highly unusual composition as 4 amino acids constitute more than 70% of the total sequence. Several identical fragments could be repeated. This might indicate that one or more fragments were missed in assembling the sequence. After adsorption on NC paper, a PDMS spectrum was acquired and the molecular weight assigned to 15,329 daltons confirming the determined sequence [3].

Another example of the improvement is illustrated by Porcine Trypsin, MW 23,463, a spectrum of which has been measured [4] using the electrospray technique. The error in the assignment was +-140 daltons. The result shown in Fig. 1 is the same compound on NC. Calculation based on both the 2+ and 3+ molecular ions, allows in this case an assignment of 23,450+-20 daltons. The main reason for the increased precision is due to the much narrower peak shapes. It is envisaged that the internal energy of the secondary ions formed from NC is lower as compared to electrosprayed samples.

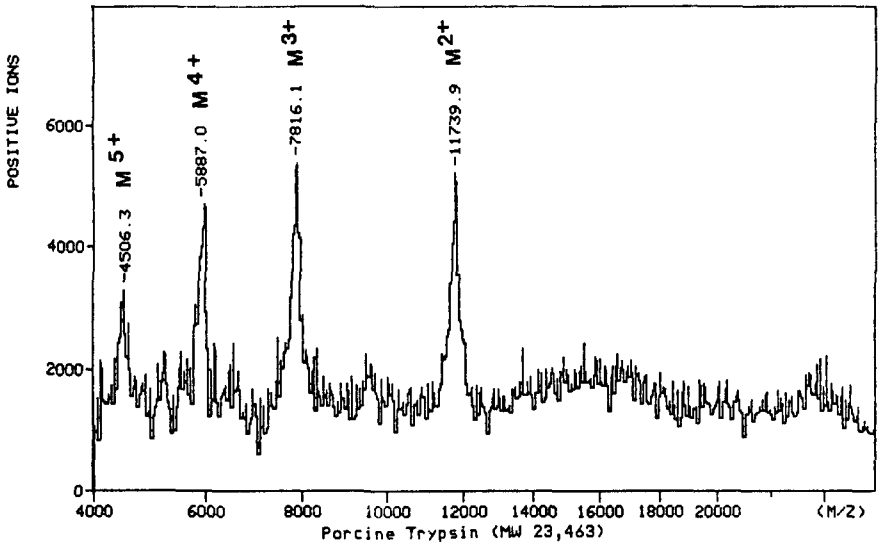

When structural information is desired, the electrospray technique is preferable since samples prepared by NC adsorption almost exclusively give molecular weight information. This is illustrated by the polypeptide Nisin MW 3354, used in many countries as food preservative. The structure of Nisin can be monitored by the PDMS technique. The spectrum contains the sodium cationized molecular ions and some of the major fragments.

An example showing how mass determination can assist in peptide sequencing is given by an antibacterial peptide, Cecropin B. The first 32 amino acids of Cecropin B from the Chinese oak silk moth (Antherea pernyi) have been sequenced by Edman degradation. The molecular weight has been determined using PDMS as 3817.4 daltons. Comparing the partially sequenced Cecropin B with the known complete sequence of Cecropin B (35 amino acids) from giant silk moth (Hyalophora cecropia), it is apparent that the molecules are very similar. If we assume that the last three amino acids are the same in both cecropins, the molecular weight of Cecropin B from A. pernyi would be 3817.7 daltons which corresponds to the measured value within 0.3 daltons. From this result, the last three amino acids in the sequence of Cecropin B from A. pernyi are postulated.

Other examples of high mass determinations using NC technique are given by:

Beta-2-microglobulin MW 11,729

RNase, MW 13,612

Retinol Binding Protein, MW 21,230

Protected oligonucleotide (AAGGGU), MW 5336.3

(1) B Sundqvist, I Kamensky, P Håkansson, J Kjellberg, M Salehpour, S Widdiyasekera, J Fohlman, P A Peterson and P Roepstorff
Biomed Mass Spectrom 11 (1984) 242-257
(2) B Sundqvist, P Roepstorff, J Fohlman, A Hedin, P Håkansson, I Kamensky, M Lindberg, M Salehpour and G Säve, Science 226 (1984) 696-698
(3) G P Jonsson, A B Hedin, P L Håkansson, B U R Sundqvist, B G S Säve, P F Nielsen, P Roepstorff, K-E Johansson, I Kamensky and M S L Lindberg, Anal Chem 58 (1986) 1084
(4) P Roepstorff, B U R Sundqvist, P Höjrup, G Jonsson, P Håkansson S O Andersson and K E Johansson, submitted Biomed. Mass Spectrom.

A RAPID, SENSITIVE MASS SPECTROMETRIC METHOD FOR INVESTIGATING MICROSCALE CHEMICAL REACTIONS OF SURFACE ADSORBED PEPTIDES AND PROTEINS

B.T. Chait and F.H. Field
The Rockefeller University
New York, N.Y. 10021

We have recently demonstrated (1) a new mass spectrometric method for investigating microscale gas-solid chemical reactions. In the present paper we report an extension of this technique to the investigation of the chemical reactions of small quantities of surface bound peptides and proteins with condensed phase reagents (2). The technique involves ^{252}Cf mass spectrometric analysis of noncovalently surface bound molecules prior to and after chemical modification.

The general procedure for carrying out the new technique involves the following steps:

(a) The sample insertion probe of our ^{252}Cf fission fragment mass spectrometer is coated with a thin film of nitrocellulose (NC). The NC is in turn coated with a solution containing a small quantity (10^{-9}-10^{-12} mol) of peptide or protein to be reacted. The solvent is evaporated leaving a bare layer of the peptide or protein bound to the NC. This sample preparation procedure follows closely that described by Sundqvist, Roepstorff, and co-workers(3), but with some differences (2). (b) The NC-sample covered sample insertion probe is inserted into the mass spectrometer and a spectrum of the compound is obtained, essentially nondestructively. (c) The probe is removed from the mass spectrometer and a small quantity of reagent is applied to the surface to effect the desired reaction with the sample under controlled conditions. (d) The reagent is removed, and the probe with the chemically modified material is reinserted into the mass spectrometer and a new spectrum is obtained. (e) Finally the spectra of the unmodified and the modified compounds are compared.

Our first tests of this procedure involved an investigation of cleavage reactions of the disulfide bonds in bovine insulin, cyclic somatostatin and conotoxin G1 utilizing the reducing reagent 1,4 dithiothreotol (DTT). The results of this reductive cleavage on bovine insulin are given in the Fig. 1. The high mass portion of the ^{252}Cf ionization time-of-flight mass spectrum from 5×10^{-10} mol of insulin deposited or NC prior to treatment is shown in Fig. 1(A). Fig. 1(B) shows the mass spectrum obtained from the same sample foil after DTT treatment for 5.0 min. The disappearance of the protonated molecular ion peaks and the appearance of protonated A- and B-chain product peaks indicates that the reduction reaction has progressed almost to completion. Fig. 1(C) shows the spectrum from the same foil after the surface was thoroughly washed with water. The peaks corresponding to the A-chain ions have disappeared indicating that the A-chain products are not strongly bound to the NC and are removed by the washing. Similar experiments performed with smaller amounts of insulin showed that the reduction reaction can be successfully effected as the surface concentration is lowered (Figs. 1(D-F)). Reaction of DTT under similar conditions with surface bound cyclic somatostatin and conotoxin G1 yielded respectively linear somatostatin with MW 2u higher than the cyclic reactant and linear conotoxin with MW 4u higher than the bicyclic starting material.

From this initial study we can summarize the general properties of the new mass spectrometric reaction probe as follows: Sensitivity is high (10^{-11} mol of peptide or protein required) and further increase in sensitivity by reducing the area of the sample probe (presently 1.1 cm^2) has been obtained. Low yields of product (<10%) can be detected reliably. The analyses are rapid and convenient since the chemical operations are easily performed and since the mass spectra described here required a measurement time of only 3-30 min. The mass spectrometric analyses are essentially nondestructive so that sequential reactions can be conveniently carried out and monitored, e.g., we have methylated the sulfhydryl groups of reduced somatostatin utilizing p-nitrobenzenesulfonic acid methyl ester.

We have applied the new technique to a determination of the extent of S-S bond formation following oxidation of reduced synthetically produced human transforming growth factor (TGF_{α}) (4) which contains 50 amino acid residues and 6 half-cystine residues. The measured MW after reduction was determined to increase by 6u confirming the presence of 3 intact disulfide linkages in the synthetic material.

In addition to the disulfide cleavage reactions described above we have also carried out and monitored a range of other chemical reactions utilizing condensed phase reagents. These reactions are summarized in Table I and details of the enzyme catalyzed surface reactions are given elsewhere in these proceedings.

Acknowledgements

This work was supported in part by the Division of Research Resources, National Institutes of Health.

References

1. B.T. Chait and F.H. Field, J. Am. Chem. Soc. 107, 6743-6744 (1985)
2. B.T. Chait and F.H. Field, Biochem. Biophys. Res. Comm. 134, 420-426 (1986).
3. G.P. Jonsson, A.B. Hedin, P.L. Hakansson, B.U.R. Sundqvist, B.G.S. Save, P.F. Nielsen, P. Roepstorff, K.E. Johansson, I. Kamensky, M.S.L. Lindberg, Anal. Chem. 58, 1084-1087 (1986).
4. TGF$_{\alpha}$ was supplied by Stephen Kent, Division of Biology, California Institute of Technology.

Table 1

SUMMARY OF CONDENSED PHASE REAGENT REACTIONS INVESTIGATED WITH THE MICROSCALE REACTION MS PROBE.

Reactions of	To Obtain
Edman degradation reagents	Cleavage of N-terminal residues of bradykinin, bovine insulin B-chain.
Dithiothreotol	Reduction of S-S bonds in bovine insulin, cyclic somatostatin, conotoxin G1, human transforming growth factor, enzymatic cleavage products of neurophysin II.
Carboxypeptidase A	Cleavage of bovine insulin.
Carboxypeptidase B	Cleavage of bradykinin.
Carboxypeptidase Y	Cleavage of angiotensin, bradykinin, β-endorphin, bovine insulin B-chain, bovine insulin.
Trypsin	Cleavage of bovine insulin B-chain, vasoactive intestinal peptide, dynorphin, porcine proinsulin.
Trypsin and leucine methyl ester	Trypsin catalyzed condensation reaction of leucine methyl ester with dynorphin tryptic fragments, leucine-enkephalin arginine and bradykinin.

Fig. 1

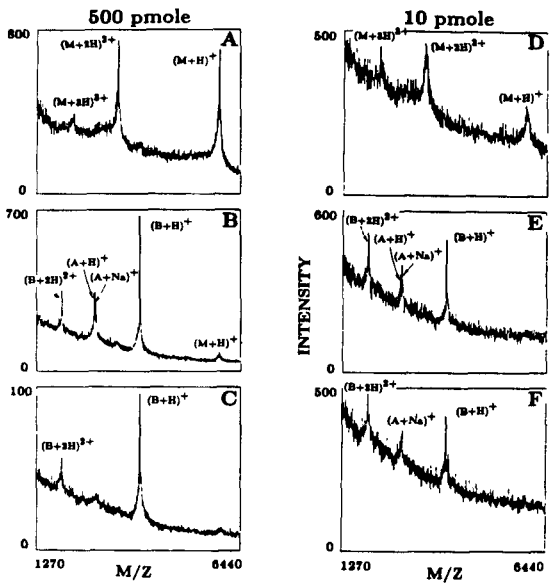

A NEW MASS SPECTROMETRIC TECHNIQUE FOR INVESTIGATING MICROSCALE ENZYME CATALYZED CHEMICAL REACTIONS OF SURFACE BOUND PEPTIDES AND PROTEINS.

B.T. Chait, Tanuja Chaudhary, and F.H. Field
The Rockefeller University
New York, N.Y. 10021

We have recently demonstrated a new mass spectrometric method for investigating the reactions of surface bound organic compounds with gas-phase (1) and condensed-phase (2) reagents. In the present study we demonstrate the utility of the new mass spectrometric method for the investigation of enzyme catalyzed reactions on small (submonolayer) quantities of surface bound peptides and proteins. The technique involves ^{252}Cf fission fragment ionization mass spectrometric analysis of noncovalently surface bound molecules prior to and after enzyme catalyzed chemical modification. The peptide and protein samples are prepared by adsorption to a thin layer of nitrocellulose (NC) using the procedure described by Sundqvist, Roepstorff, and co-workers (3), but with some differences (2).

Carboxypeptidases are enzymes that remove amino acids one residue at a time from the C-termini of polypeptide chains. We have used the new technique with carboxypeptidase Y, A and B for obtaining information on the C-terminal sequence of surface bound angiotensin II, bradykinin, β-endorphin, insulin B-chain and insulin. The high mass portion of the ^{252}Cf ionization mass spectrum obtained from 10^{-9} mol of bradykinin deposited on NC, prior to enzyme digestion, is shown in Fig. 1 (top panel). The bottom panel of Fig. 1 shows the mass spectrum obtained from the same sample foil after digestion with 10^{-11} mol carboxypeptidase Y for 5 min at 41°C. The identities of several of the C-terminal amino acid residues can be directly read off the spectrum.

Fig. 2 illustrates the sensitivity attainable with the technique and shows the spectrum of 10^{-12} mol of bradykinin taken prior to and after reaction with carboxypeptidase B for 1 min. For this reaction we were able to demonstrate that the peptide remains attached to the NC surface throughout the hydrolysis reaction. We have also demonstrated the feasibility of carrying out and observing reactions on surface immobolized enzymes.

The endopeptidase trypsin hydrolyses peptides on the C-terminal side of basic amino acid residues. We have demonstrated the use of the new technique to identify the resulting tryptic fragments from vasoactive intestinal peptide, dynorphin, insulin B-chain and proinsulin. The production of des-ala-insulin and the excised C-peptide from porcine proinsulin was clearly observed mass spectrometrically (see Fig. 3). In other experiments, trypsin digests performed in the presence of ^{18}O labelled water allowed unambiguous identification of the C-terminal tryptic fragments, since the C-terminal fragment(s) do not incorporate the ^{18}O.

We have also used the new technique for rapidly optomizing the conditions required for enzyme catalyzed semi-synthetic condensation reactions on polypeptides.

Acknowledgement

This work was supported in part by the Division of Research Resources, National Institutes of Health

References

1. B.T. Chait and F.H. Field, J. Am. Chem. Soc. 107, 6743-6744 (1985).
2. B.T. Chait and F.H. Field, Biochem. Biophys. Res. Comm. 134, 420-426 (1986).
3. G.P. Jonsson, A.B. Hedin, P.L. Hakansson, B.U.R. Sundqvist, B.G.S. Save, P.F. Nielsen, P. Roepstorff, K.E. Johansson, I. Kamensky, Anal. Chem. 58, 1084-1087 (1986).

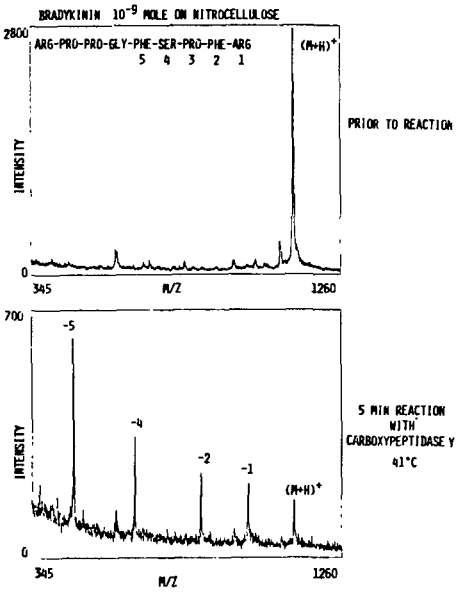

Fig. 1

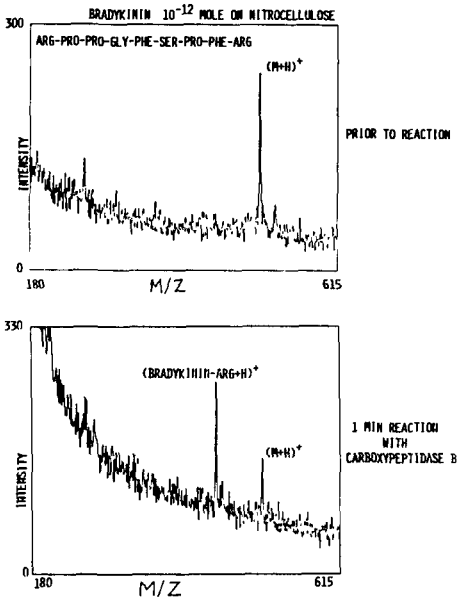

Fig. 2

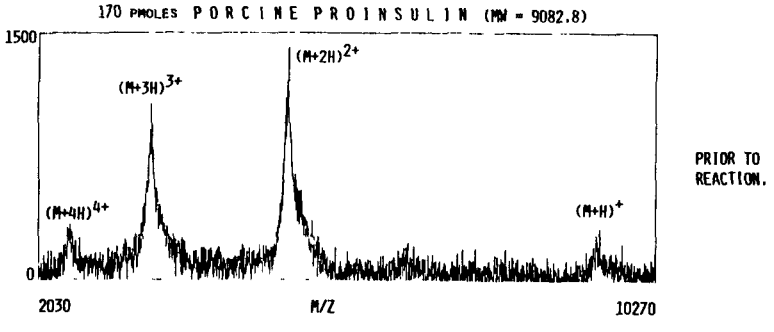

Fig. 3

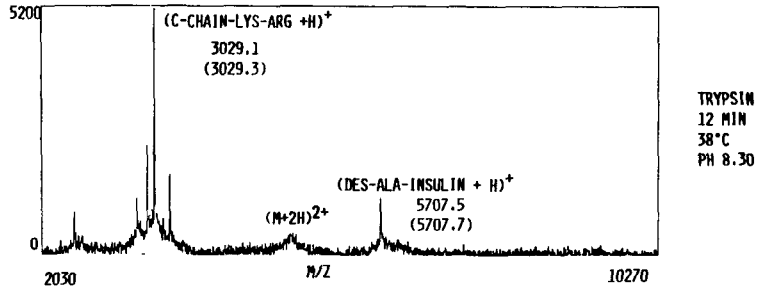

TANDEM QUADRUPOLE-FOURIER TRANSFORM MASS SPECTROMETRY: NEW DEVELOPMENTS

J. SHABANOWITZ and D. F. HUNT, Dept. of Chemistry, U. of Virginia, Charlottesville, VA, 22901; M. CASTRO and D. H. RUSSELL, Dept. of Chemistry, Texas A&M U., College Station, TX,

Determination of oligopeptides in the mass range, 1,000 to 3,000, by L-SIMS on a tandem quadrupole-Fourier transform mass spectrometer has been described previously (1). Sample at the 10-100 pmol level is dissolved in a 1/1 thioglycerol/glycerol matrix and subjected to particle bombardment by a beam of 6-10 keV cesium ions in a conventional differentially pumped Finnigan-MAT quadrupole ion source. Two sets of rf-only quadrupole rods are employed to transmit the desorbed ions with high efficiency through the fringing fields of an Oxford 7-T superconducting magnet and into an ion cyclotron resonance cell. Mass analysis of the trapped ions is accomplished by Fourier transform mass spectrometry using a Model 2,000 data system from Nicolet Analytical Instruments.

Here we describe our research to extend the mass range of the tandem quadrupole-Fourier transform instrument. Our earlier results (1) indicated that (M+H)+ ions for glucagon, melittin, insulin B-chain and either bovine or porcine insulin itself, peptides in the 2,800-5,800 dalton range, could be observed albeit with poor resolution and low S/N. During the last 8 months a number of experiments and instrument modifications have been undertaken to facilitate analysis of (M+H)+ ions above m/z 3,000. These include, improvements in the vacuum system, optimization of quadrupole transmission, reduction of electronic noise, changes in the configuration and dimensions of the ICR cell, movement of the ion source off axis, and redesign of the ion source.

Figures 1 and 3 illustrate typical spectra observed for renin and glucagon, respectively, under the "old" conditions tabulated below. The insert in Fig. 1 is typical of spectra obtained by employing a low mass cutoff on the rf only quadrupoles and no sweep out of low mass ions in the ICR cell. Use of both a high mass cutoff and a low mass sweep out were necessary to produce the spectra shown in Figs. 1 and 3. The far superior spectra shown in Figs. 2 and 4 of renin and glucagon, respectively, were obtained by using the "new" conditions tabulated below. New operating parameters include reduced sample quantity, greatly reduced ionization time, use of a mass cutoff below 400 amu, no low mass sweep out in the cell, and use of a pulsed trapping voltage on the entrance aperture to the cell. Changes most responsible for the improved spectral quality involved milling out most of the ion source block to lower the gas pressure in the vicinity of the sample probe and pulsing trapping plate 1 to zero volts during the ionization event. The new instrument parameters and configuration now allow routine acquisition of spectra for oligopeptides up to 6,000 daltons, including the insulins (Fig. 5). Spectra similar in quality to that for cytochrome-C in Fig. 6 are obtained for small proteins in the 10-13 kDa range.

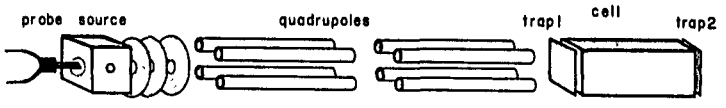

	SAMPLE	PROBE	Cs^+ BEAM	SOURCE BLOCK	QUAD MASS CUTOFF	TRAP#1	TOTAL IONIZATION TIME (20scans)
OLD	100-1000 pmol	+1.9V	1000 ms	normal 4500	400-2000 amu	+2V	20000ms
NEW	10-100 pmol	+1.5V	4ms	milled out	400 amu	+3V pulsed	80ms

	ION BEAM	TRAP#1	DELAY	SWEEP OUT	DELAY	EXCITE	DETECT	TRAP#2	TOTAL EXP TIME
OLD	1000 ms	+2V	100ms	yes	100ms	2.5ms 35Vp-p	8or16 ms	+2V	1300 ms
NEW	4ms	+3V pulsed	5ms	no	5ms	same	same	+3V	30ms

(1) Hunt, D. F. , Shabanowitz, J., Yates, J. R., III, McIver, R. T., Jr., Hunter, R. L., Syka, J. E. P., Amy, J., Anal. Chem., 57, 2728-2733 (1985).

(FIGURE 1)

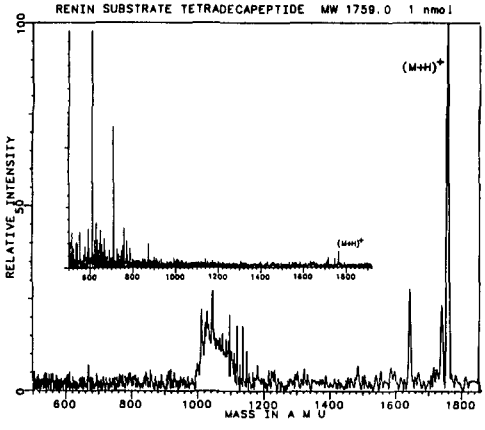

(FIGURE 2)

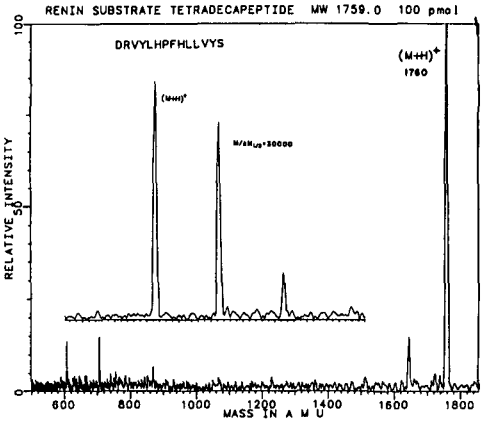

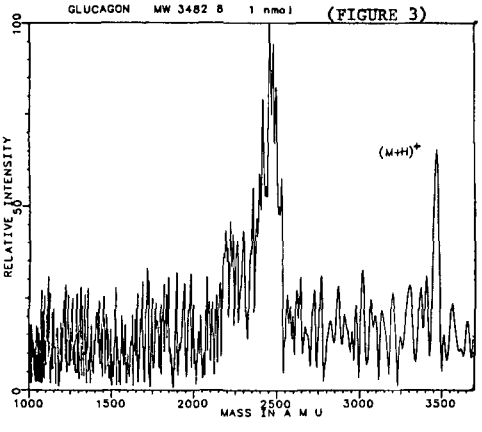

(FIGURE 3)

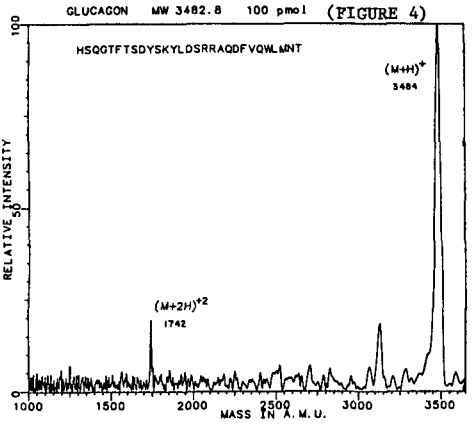

(FIGURE 4)

(FIGURE 5)

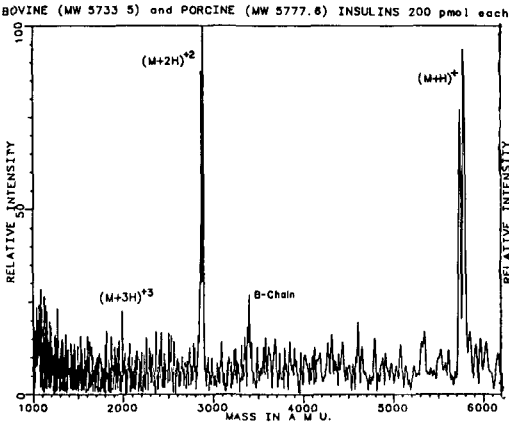

(FIGURE 6)

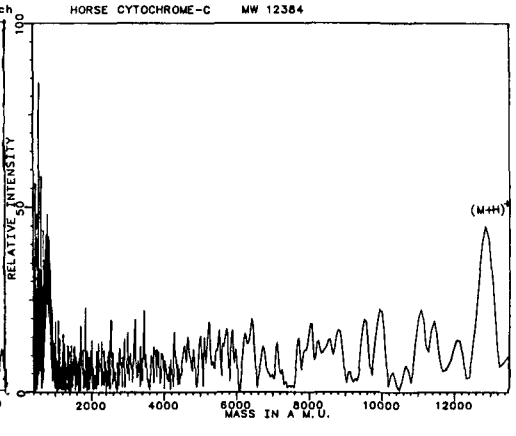

SOLID-STATE SIMS FOURIER-TRANSFORM MASS SPECTROMETRY OF HIGHER MOLECULAR WEIGHT COMPOUNDS

I. J. Amster, J. A. Loo, J. Furlong, B. H. Wang, E. R. Williams, and F. W. McLafferty

Chemistry Department, Cornell University, Ithaca, NY 14853-1301

For high molecular weight analysis, Fourier-transform mas spectrometry (FTMS) has several advantages, such as ultrahigh resolution, mass range, sensitivity, and a capability for MS/MS. "Static" SIMS is a proven method for the production of molecular ion species from nonvolatile organic compounds; its low background pressures, capability for pulsed operation, and high sensitivity are a few reasons for excellent compatability with FTMS. Our experiments are performed with a pulsed cesium ion gun interfaced to a Nicolet Fourier-transform mass spectrometer with a 3 T magnet and a single ion cell. All spectra are obtained from solid state samples. Careful control of several experimental conditions is necessary in order to obtain a SIMS/FTMS spectrum. The sample must be evenly dispersed and at a low surface concentration (<1 nmole/cm^2) to avoid sample charging which interferes with the trapping of ions. Codeposition of an alkali halide with the sample can enhance the formation of cationized molecular ions. The abundance of the molecular ion species of peptides is increased even more dramatically by the codeposition of glutathione, a peptide that has found similar use in plasma desorption experiments.[1] The substrate has a marked effect on the appearance of an SIMS/FTMS spectrum. A comparison of gold, silver, and copper targets shows that a gold substrate produces the greatest yield of molecular ion species, while copper produces the most fragmentation; silver is intermediate in behavior. This is in line with the early SIMS work of Benninghoven.[2] Nitrocellulose, which has been used as a substrate for peptide samples in plasma desorption experiments,[3] was tested as substrate for SIMS/FTMS. Gramicidin S adsorbed onto nitrocellulose produces abundant molecular ion species, but shows more fragmentation than for the sample deposited on a gold target. The abundance of the molecular ion species (m/z 1904) of gramicidin D relative to the abundance of fragment ions is found to increase in a linear fashion with increasing primary ion acceleration energy over the range of energies tested (1.5 keV to 11 keV). By optimizing the parameters mentioned, several peptides (gramicidin S, gramicidin D, substance P, bradykinin potentiator B, somatastatin), saccharides (maltooctaitol, maltoheptaitol), organic polymers (polystyrene, polyethylene glycol), and an organometallic compound (vitamin B_{12}) are found to produce abundant molecular ion species as well as fragment ions useful for structural elucidation. The CAD spectrum (Figure, next page) of the sodium attached molecular ion of gramicidin S produced by SIMS/FTMS is found to be remarkably similar to the reported CAD spectrum of the $(M + K)^+$ ion of this compound produced by laser desorption FTMS.[4] The sensitivity of SIMS/FTMS is promising; 100 femtamoles of gramicidin S produces a molecular ion species of signal:noise 3:1.

References:

(1) Alai, M.; Demirev, P.; Fenselau, C.; Cotter, R. J. Anal. Chem., submitted.

(2) Benninghoven, A. Springer Ser. Chem. Phys. **1983**, 25, 64.

(3) Jonsson, G. P.; Heddin, A. B.; Hakansson, P. L.; Sundqvist, B. U. R.; Save, B. G. S.; Nielson, P. F.; Roepstorff, P.; Johansson, K. E.; Kamensky, I.; Lundberg, M. S. L. Anal. Chem. **1986**, 58, 1084.

(4) Cody, R. B.; Amster, I. J.; McLafferty, F. W. Proc. Nat. Acad. Sci. U.S.A. **1985**, 82, 6367.

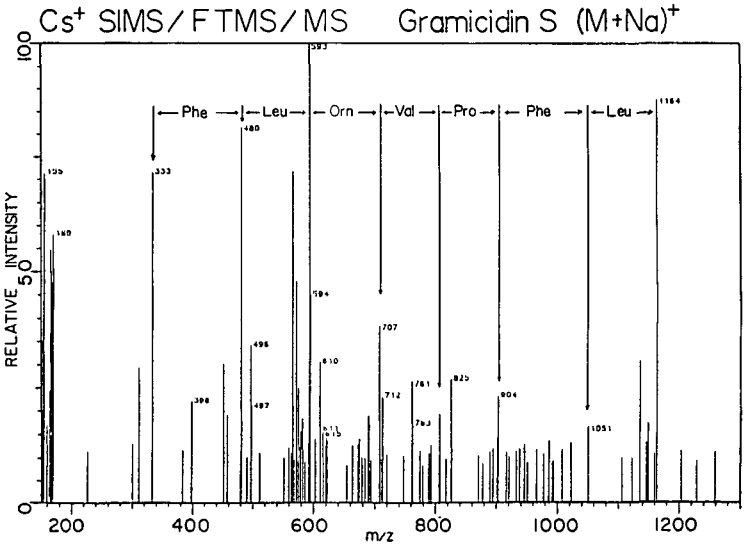

Figure. FT mass spectrum from the collisional dissociation of $(M + Na)^+$ produced by Cs^+ SIMS ionization of Gramicidin S.

MOLECULAR WEIGHT DETERMINATION AT HIGH MASS BY QUADRUPOLE MASS SPECTROMETRY

M.A. McDowall, D.C. Smith, N. Lynaugh.
VG Masslab Limited, Altrincham, WA14 5RZ, UK.

Biochemists have a requirement to determine the average molecular weights of protein fragments and other large biochemicals within Ca 100 ppm, as an adjunct to their investigations by classical methods. Hitherto measurements of this precision at high mass have only been possible with medium and high performance magnetic sector instruments configured for FAB ionization. Sector instruments with their inherent capability for high resolution and tandem mass spectrometry are in several respects over specified for simple molecular weight determinations. We have therefore investigated the potential of quadrupole mass spectrometry for molecular weight determinations up to m/z 4000. Thermospray ionization (TSP) is ideally suited to the analysis of protein fragments and other biomolecules which commonly occur in aqueous media in the presence of buffer salts. The potential of TSP ionization for high mass analysis has not been determined to date, their is a paucity of thermospray data showing molecular ionic species in excess of m/z 2000 although Vestal et al have shown that peptides of Ca 3500 daltons molecular weight can be successfully volatilized in a thermospray and be detected as triply or quadruply protonated molecular ions.

We have constructed a quadrupole instrument in which the rod size, resolution and RF operating frequency have been selected to facilitate FAB and TSP mass spectrometry up to 4000 daltons.

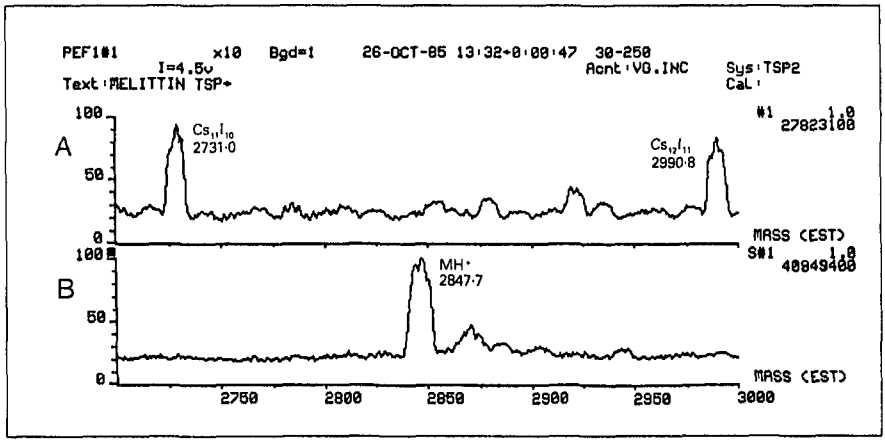

Figure 1. Thermospray continuum mass spectra:
Spectrum A, caesium iodide reference.
Spectrum B, molecular ion region of melittin.

In our experimental procedure a molecular ion cluster is produced by FAB or TSP ionization. The resultant peak is recorded by the data system in the form of a continuum mass spectrum. The molecular peak is centroided to determine its mean value in units of time and mass measured by comparison with two centroided reference peaks. In preliminary experiments using this technique we have been able to determine the protonated molecular weight of the known peptide Melittin at m/z 2847.5 to within 110 ppm (±0.3 daltons) in both FAB and TSP (Fig 1) ionization modes.

In further studies in the FAB mode we have successfully observed the protonated molecular ions of two larger peptides; Oxidised Bovine Insulin B Chain (MW = 3496) and Glucagon (MW = 3483). The positive ion FAB spectrum of the protonated molecular ion cluster of Oxidised Bovine Insulin B Chain is shown in Figure 2 compared to a reference spectrum of Caesium and Rubidium Iodide cluster ions. From this single experiment in the FAB mode we have been able to determine the protonated molecular weight of Oxidised Bovine Insulin B Chain at m/z 3496.9 to within 140 ppm (±0.5 daltons). The protonated molecular weight of Glucagon was determined with a similar degree of precision.

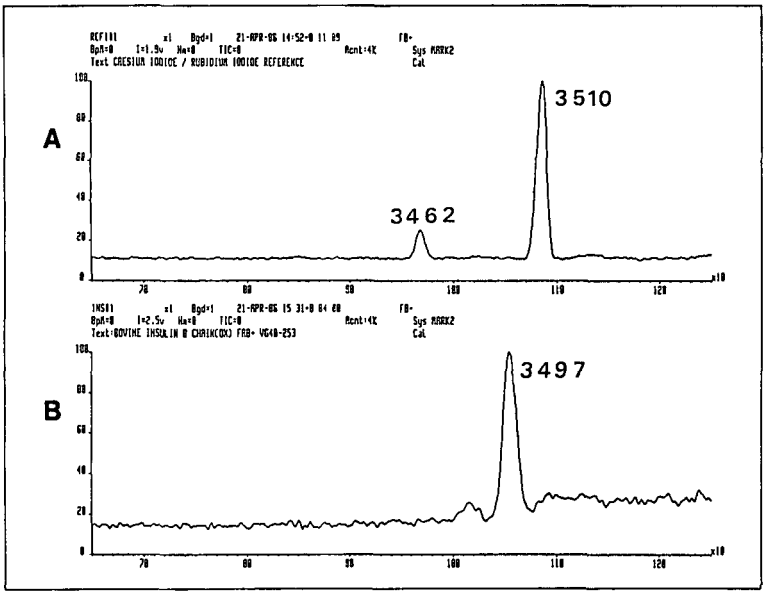

Figure 2. FAB continuum mass spectra:
Spectrum A, Caesium/Rubidium Iodide reference.
Spectrum B, molecular ion region of Oxidised Bovine Insulin B Chain.

Time-of-Flight Secondary Ion Mass Spectrometry of Polyurethanes

Ioannis V. Bletsos and David M. Hercules
Department of Chemistry, University of Pittsburgh, Pittsburgh, PA 15260 U.S.A.

Dieter van Leyen and Alfred Benninghoven
Physikalisches Institut der Universität Münster, D-4400 Münster, FRG

Polyurethanes (PUR) present a special challenge for characterization by mass spectrometry (MS). Pyrolysis coupled to MS has been used to characterize PUR, but the degradative nature of the technique has restricted the study of PUR to the low mass range ($m/z \leq 500$) (1). Time-of-flight secondary ion mass spectrometry (TOF-SIMS) studies of nylons (2) and other polymers (e.g., polystyrenes, polysiloxanes, etc.) (3) indicated that the technique might be used successfully to characterize PUR. The primary objective in the characterization of PUR is the identification of the R_1, R_2, and R_3 groups in the general PUR formula shown below:

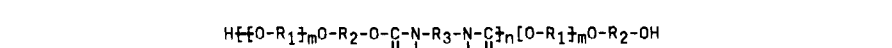

We present here a brief report of our studies of PUR using TOF-SIMS.

The PUR samples (Mobay Chemical Inc., Pittsburgh, PA) were dissolved in dimethylformamide (DMF) and tetrahydrofuran (THF). The concentrations of the solutions were approximately 1×10^{-3} M with respect to the repeat unit. A 1 µL of solution was deposited on 100 mm^2 of a silver substrate which had been cleaned by etching in HNO_3 (20% vol.). Approximately 1-5 µg of each polymer were deposited on the silver substrate for analysis. The spectra of the PUR were obtained by a TOF-SIMS equipped with a mass selected primary ion source, an angle and time focusing TOF analyzer, and a single ion counting detector (4).

A section of the TOF-SIMS spectrum of a polyurethane in the range m/z = 650-1650 is shown in Figure 1. The formula of the PUR used in this example is given below:

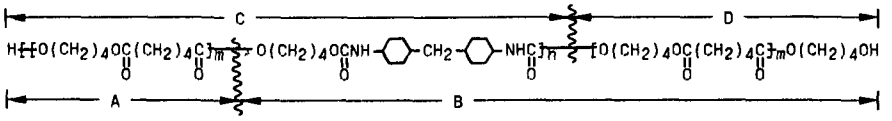

Bond cleavage produces four different kinds of fragments (labeled A through D above) cationized with Ag^+ or Na^+ and observed in the range m/z = 400-3000. Ag^+ is produced by sputtering the substrate, and Na^+ is present from contamination from the solvent (DMF). Fragmentation patterns are consistent throughout the detectable mass range and correspond to four well-defined series of peaks: $(xA+M)^+$, $(xB+M)^+$, $(xC+M)^+$, and $(xD+M)^+$, where M = Ag, Na, and x = 1,2,3,... . The peaks of the spectrum of Figure 1 are identified by the letter of the series to which they correspond. From the position of a peak and the spacing between consecutive peaks of the same series, the structures of the PUR repeat unit and terminal groups can be determined. For example, the peaks at m/z = 707, 709 correspond to $[(O(CH_2)_4OC(=O)(CH_2)_4C(=O))_3 + Ag]^+$, and the peak at m/z = 864 corresponds to

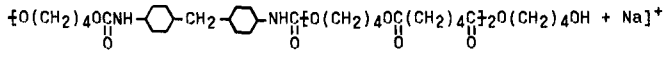

The fragmentation pattern observed in the TOF-SIMS spectrum of the PUR example presented here is characteristic of all PUR samples studied. Therefore, the major fragments of the PUR under Ar^+ bombardment can be generalized as follows:

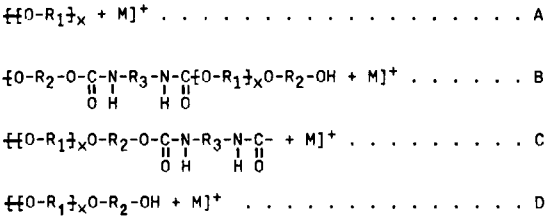

From such well defined fragmentation patterns the structures of the diols, esters, and isocyanates used in the synthesis of PUR can be identified, and their sequence in the repeat unit and terminal groups can be determined.

References

1. Marshal, G. L., Eur. Polym. J. 1983, 19, 439.

2. Bletsos, I. V.; Hercules, D. M.; Greifendord, D.; Benninghoven, A., Anal. Chem. 1985, 57, 2384.

3. Beltsos, I. V.; Hercules, D. M.; vanLeyen, D.; Benninghoven, A., submitted to Macromolecules.

4. Steffens, P.; Niehuis, E.; Friese, T.; Greifendorf, D.; Benninghoven, A., J. Vac. Sci. Technol. A 1985, 3, 1322.

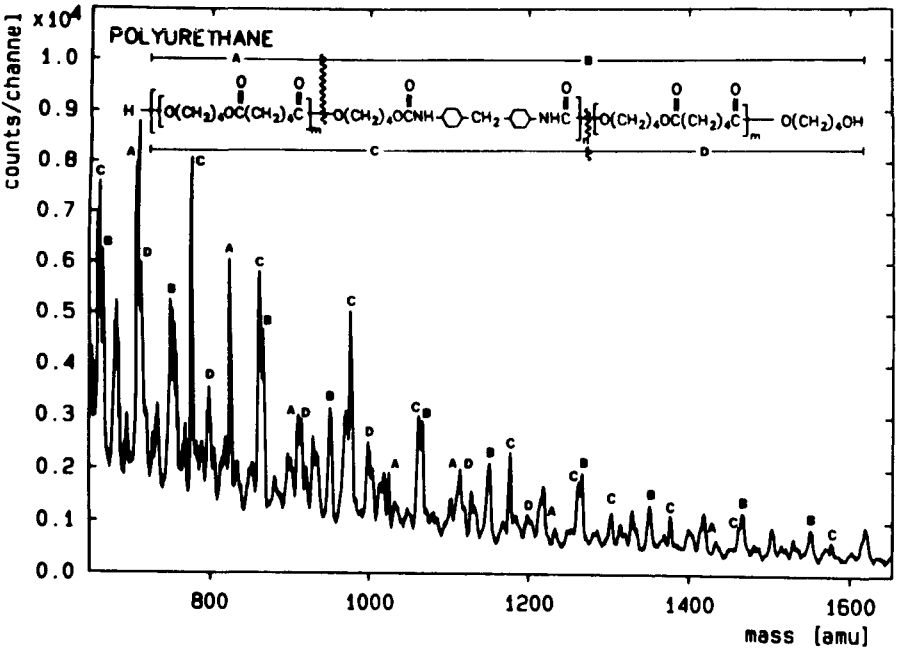

Figure 1: TOF-SIMS Spectrum of a Polyurethane in the Range m/z = 650-1650.

Nitrocellulose as a Matrix for the Adsorption-Desorption of Bovine Insulin

J.C. Hill, R.G. Phelps, and R.D. Macfarlane
Department of Chemistry
Texas A&M University
College Station, TX. 77843

An active area of research in the 252-Cf-plasma desorption mass spectrometric analysis of high molecular weight peptides and proteins is the use of polymers as sample matrices. Jordan et al first opened up the field by studying the ion-exchange polymer, Nafion, showing its potential use as an ion-selective matrix for the adsorption of solvated cations [1]. This was later extended to include peptides such as insulin [2]. Macfarlane et al have studied the polymers polypropylene and poly(ethylene terephthalate) developing the concept that polymer surfaces in general can be used to produce a more well defined matrix for the production of molecular ions [3]. Recently, Sundqvist et al have reported the use of nitrocellulose as a matrix allowing for the selective adsorption of proteins and peptides and giving remarkably enhanced molecular ion yields for small proteins. They have suggested that the adsorbed peptide is attracted to the nitrocellulose by the polarized nitrate ester groups that have their "negative" oxygens directed away from the surface into the liquid phase [4]. If the nitrate is indeed the active site, the function of the nitrocellulose as an effective adsorption-desorption medium would be dependent on the concentration of surface nitrate ester groups. This paper reports on our current research into the function of the nitrocellulose matrix, discussing the optimum conditions for the preparation of the nitrocellulose matrix and the nature of the analyte-nitrocellulose bond formed in the adsorption process.

Optimum conditions for the use of the nitrocellulose matrix, defined in terms of molecular ion yield for insulin, were elucidated by studying both the negative and positive secondary ions of nitrocellulose and the positive secondary ions of bovine insulin. Experiments included a study of methods used to prepare the matrix, and a study of the influence of the thickness of the nitrocellulose matrix. The results of this analysis indicate that the optimum nitrocellulose matrix is prepared by electrospraying 50 uL of 1 ug/uL nitrocellulose, dissolved in acetone, and deposited over 1 cm^2 of the target surface.

In the course of this research, we have found that it is possible to de-nitrate the surface of nitrocellulose by exposing it to UV irradiation in air. The amount of de-nitration is dependent on the irradiation time. Analysis of the irradiated nitrocellulose by ESCA (Electron Spectroscopy for Chemical Analysis) shows that after 5 min irradiation the mildly-hydrophobic nitrocellulose surface (11.7% nitrogen) has been converted to a highly hydrophilic surface with a reduction in nitrogen to less that 2% (figure 1). This result suggests that the nitrate ester groups have been replaced by a more hydrophilic moiety as a result of the UV-air irradiation. We believe that the nitrocellulose has been converted to cellulose in the process. Fig. 2 shows the ESCA result for the oxygen region.

We then adsorbed insulin on the nitrocellulose and de-nitrated cellulose and obtained 252-Cf-PD spectra for the two samples. The results are shown in Fig. 3. Except for a 15% decrease in overall intensity of the insulin peak for the cellulose matrix there were no differences in the mass spectra. However, both spectra exhibit a greatly enhanced intensity relative to that for a multilayer sample or for insulin adsorbed on a highly hydrophobic surface such as poly(ethylene terephthalate).

We conclude from these results the following. The enhanced desorption yield for nitrocellulose cannot be attributed to the nitrate ester group although it does enhance the adsorption yield. The fact that a pure cellulose matrix also gives superior desorption yields for insulin suggests that the hydrophilic nature of the substrate may be the important feature in the enhanced molecular ion yields for small proteins.

REFERENCES

1. Jordan, EA.; Macfarlane, R.D.; Martin, C.R.; McNeal, C.J. Int. J. Mass Spectrom. Ion Phys., 1983, 53, 345.
2. Macfarlane, R.D. Mass Spectrometry in the Health and Life Sciences, Burlingame, A.L.; Castignoli, N., ed. (Elsevier, Amsterdam, 1985), p. 85.
3. Macfarlane, R.D.; McNeal, C.J.; Martin, C.R. Anal. Chem. 1986, 58, 1091.
4. Johnson, G.P.; Hedin, A.B.; Hakansson, P.L.; Sundqvist, B.U.R.; Save, B.G.; Nielsen, Roepstorff, P.; Johansson, K.E.; Kamensky, I.; Lindberg, S.L. Anal. Chem. 1986, 58, 1084.

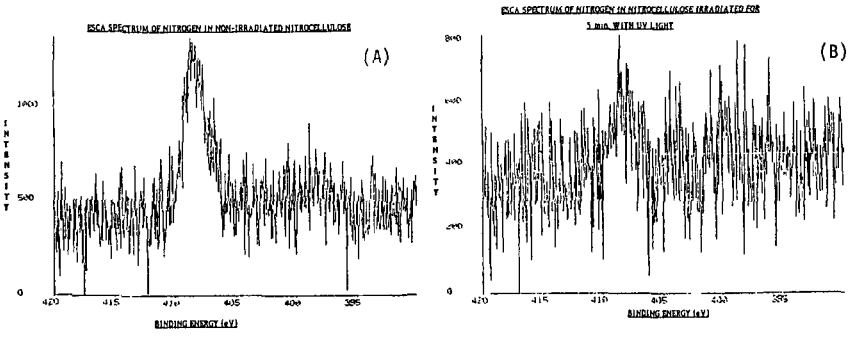

Figure 1. ESCA analysis of nitrogen in a) non-irradiated nitrocellulose and b) nitrocellulose irradiated for 5 minutes with UV light.

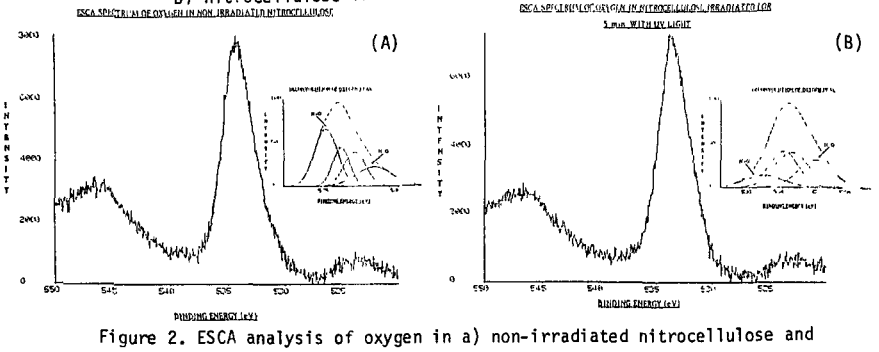

Figure 2. ESCA analysis of oxygen in a) non-irradiated nitrocellulose and b) nitrocellulose irradiated for 5 minutes with UV light.

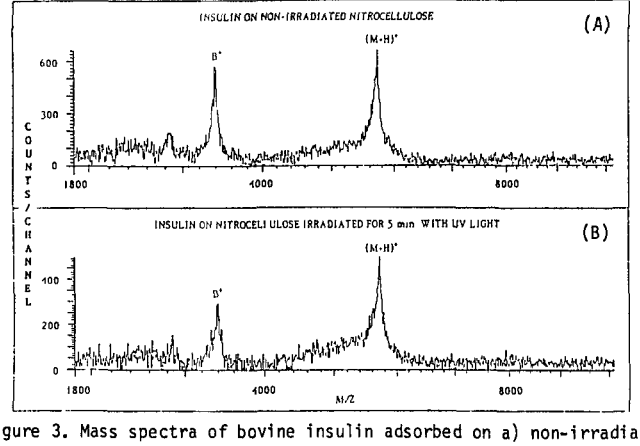

Figure 3. Mass spectra of bovine insulin adsorbed on a) non-irradiated nitrocellulose and b) nitrocellulose irradiated for 5 minutes with UV light.

We wish to acknowledge the support of this research by the National Institutes of Health (GM-26096), the National Science Foundation (CHE-82-06030), and the Robert A. Welch Foundation (Grant A-258).

THE PERFORMANCE OF A NEW TANDEM HIGH MASS INSTRUMENT FOR BIO-ORGANIC MS-MS APPLICATIONS.

R.H. Bateman, R.S. Bordoli, B.N. Green, G.W. Lee, and B.J. Millard. VG ANALYTICAL LTD, FLOATS ROAD, WYTHENSHAWE, MANCHESTER M23 9LE UK.

Description

A high mass tandem mass spectrometer has been developed for the analysis of bio-organic compounds. This new instrument is based on the VG ZAB-SE, which has a magnetic sector radius of 660mm and a mass range of 12,000 at 10keV ion energy. It consists essentially of two ZAB-SEs (MSI and MSII) combined in a B_1E_1 - E_2B_2 configuration. Precursor ions, selected by MSI, are focused in a collision cell located between MSI and MSII and the fragments produced by collision induced dissociation (CID) in the cell are analysed by the double focusing arrangement MSII.

The collision cell may be operated either at ground potential or at elevated potentials. With the cell grounded, the parent ions enter the cell at the full energy (10keV) and the daughter ions then have a range of energies 10,000 m_2/m_1 where m_1 and m_2 are the precursor and fragment ion masses respectively. A daughter spectrum is produced by scanning E_2 and B_2 together in a linked scan, so that B_2/E_2 is constant.

With the cell at an elevated potential the precursor ions are retarded on entering the cell and the fragment ions produced therein accelerated on leaving it. In this way, the daughter ions enter MSII with a higher energy than with the cell grounded and thus higher daughter ion resolution and sensitivity can be achieved, particularly with the lower mass fragments.

Performance

The mass range of both MSI and MSII is 12,000 at 10keV ion energy. MSI has a resolution capability of 125,000 although as a precursor ion selector for MSII the practically useful resolution is substantially lower due to the relatively weak ion currents produced by existing sources at the higher masses. Fragment ion resolutions up to 2500 m_2/m_1 are achieved when collisions are made at 10keV energy (collision cell grounded). This is illustrated in Figure 1 where the $^{85}Rb_5{}^{87}Rb_2I_6$ ion (m/z 1359.8) was selected by MSI, induced to dissociate in the cell by helium, and the fragments produced by the loss of RbI analysed by MSII. The daughter ion resolution was 2500. By operating the cell at elevated potentials so that the precursor ions are retarded on entering the cell, resolutions up to 7500 m_2/m_1 are achievable.

At 1000 resolution, parent ions are transmitted from the exit of MSI and through MSII, with an efficiency of about 70%. CID efficiences (sum of the daughter ion intensities at the final collector divided by the parent ion intensity leaving MSI) depend on the sample, but values of 1 -10% are typical at 1000 resolution. Examples include 3, 6 and 6% for the daughters of the CsI clusters at m/z 912, 1172 and 1432 respectively. For substance P (MW 1347), the daughter ion efficiency was 1.4%, and for the oxidised B chain of bovine insulin (MW 3496) 2%.

Applications at High Mass

So far, the MH^+ ions of about 10 peptides with molecular weights in the range 3000-4200 have yielded daughter ion spectra containing sequence information. Included in the list are the C peptide (MW 3019), glucagon (MW 3481) and human parathyroid hormone (1-34) (MW 4115). These spectra were obtained at relatively low resolution for both parent and daughter ions (1000 and 500 respectively). Generally, spectra were recorded with the data system operating in an MCA mode and several scans were summed.

Figure 2 shows the daughter ion spectrum of the MH^+ ion of the oxidised bovine insulin B chain as raw data. In this case 9 scans were summed over a total acquisition time of 5 minutes. 16,000 channels were used to record the data. Figure 3 shows the data after peak centroiding and mass assignment using the daughter ion spectrum of the cesium iodide cluster ($Cs_{13}I_{12}$) for calibration. Two partial sequences, one from each end of the molecule are tentatively indicated in the spectrum.

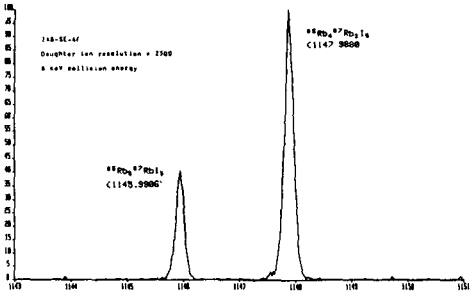

Figure 1. Daughters produced by loss of RbI from $^{85}Rb_5{}^{87}Rb_2I_6$ showing 2500 resolution.

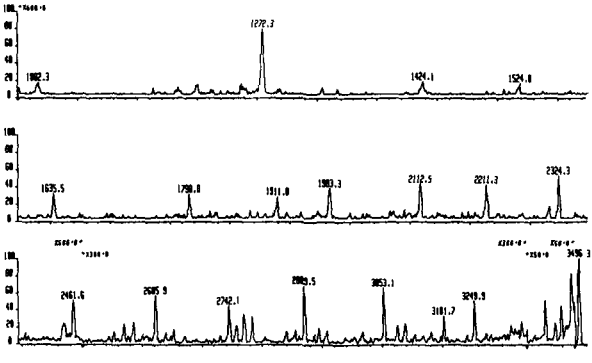

Figure 2. Daughter ion spectrum of oxidised bovine insulin B chain. Raw MCA data.

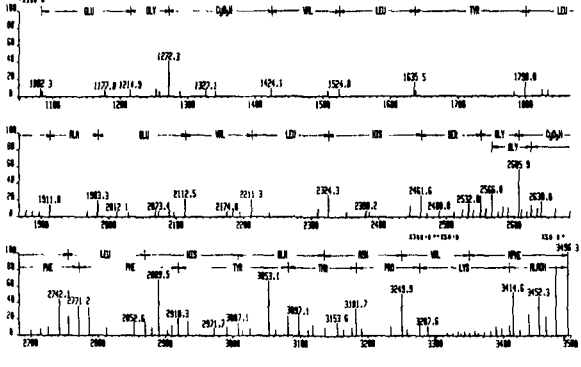

Figure 3. Daughter ion spectrum of oxidised bovine insulin B chain after centroiding.

A MODIFIED DOUBLE-FOCUSING MASS SPECTROMETER WITH SIMULTANOUS ION DETECTION FOR HIGH-MOLECULAR WEIGHT COMPOUNDS

C.E.D. Ouwerkerk and A.J.H. Boerboom
FOM-Institute for Atomic and Molecular Physics,
Kruislaan 407, 1098 SJ Amsterdam, The Netherlands

Mass analysis of high-molecular weight compounds demands a reexamination of the ion optical design of mass spectrometers. In this contribution we describe two innovations applied to a conventional Nier-Johnson mass spectrometer in order to increase the sensitivity at masses up to 10,000 amu.

Instead of extending the mass range with expensive high-field magnets with large radii we chose to diminish the accelerating voltage of our mass spectrometer. As the ion extraction is determined by fields and not by potentials is must be possible to design a source where directly low-energy ions are obtained in sufficient intensity. A circular (Pierce-)geometry is used to provide the proper extraction fields. Three quadrupole lenses shape and focus the ion beam independently for both the x- and y-directions. Optimization of the electrode voltages is aided by computer calculation of the fields and trajectories in the source [1]. Fig. 1 shows schematically the design for the low-voltage desorption source.

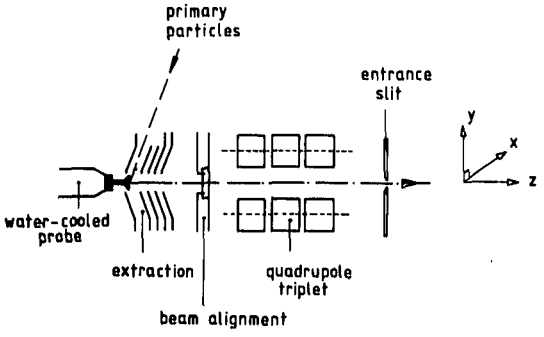

Fig. 1. The design for the low-voltage desorption ion source.

Secondly, the magnet of the mass spectrometer was redesigned to enable the simultaneous detection of ions over a mass range Δ m/m of 11% with a micro-channelplate detector. This increases the measuring time per mass peak and thus the sensitivity with several orders of magnitude. It was emphasized to obtain a focal plane perpendicular to the main trajectory and as flat as possible by shaping the exit plane of the magnetic sector. Furthermore, the angular aberration coefficient was minimized using a specially shaped entrance plane of the magnetic sector. In the design stage the position of the focal plane of the mass spectrometer was determined by first order trajectory calculations. The exit plane is defined by a fourth order polynomial, and the entrance plane by a second order polynomial.

By third order matrix calculation (TRIO-program) the fringing fields were taken into account and the double focusing condition was proved to hold over the considered mass range. A position-sensitive micro-channelplate (MCP) detector with high spatial resolution was used [2]. In this detection method a multi-anode array detects the center of gravity of the electron cloud coming from the MCP's, which yields the position of the incoming ion. With this socalled dissection method a FWHM resolution of 0.1% of the total detector length can be reached with an overall linearity of 0.1%. Up to now a mass resolution of 3000-3500 (FWHM) has been obtained over a range of 30 mm at the plane of detection. Fig. 2 shows the spectrum obtained from the desorption of the nona-peptide bradykinin from a glycerol matrix with 3 keV Xe^+ primary ions and a source voltage of 3 keV.

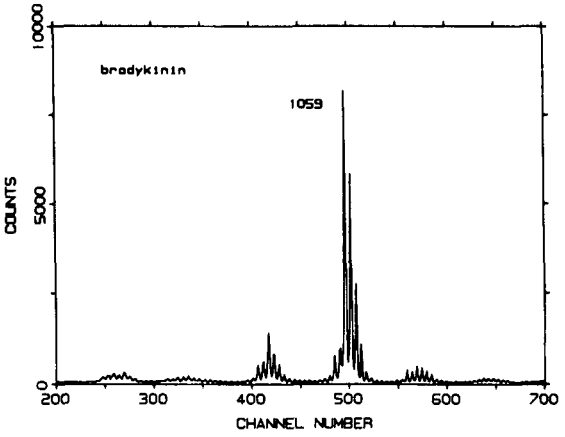

Fig. 2. Simultaneous detected spectrum of the molecular ion of the nona-peptide bradykinin desorbed from a glycerol matrix.

Concluding, the ion optics of a double-focusing mass spectrometer has been improved and a position-sensitive electronic detection system has been implemented, resulting in an increase in sensitivity of two orders of magnitude [3].

1. C.E.D. Ouwerkerk and A.J.H. Boerboom, Int. J. Mass Spectrom. Ion Proc., submitted

2. D.P. de Bruijn and J. Los, Rev. Sci. Instrum. 53, 1020 (1982)

3. C.E.D. Ouwerkerk, A.J.H. Boerboom, T. Matsuo and T. Sakurai, Int. J. Mass Spectrom. Ion Proc., in press

Operational Characteristics of Two Channel Electron Multipliers Commmonly used in Mass Spectromety

Peter F. Somssich
GTE Electrical Products
Lighting Research and Engineering
Danvers,MA. 01923

Abstract

In many applications, particularly those involving the use of mass spectrometers, a channel electron multiplier(CEM) is often used as a detector which can provide high sensitivity. Approximately 10 years ago when these devices were not as commonplace as today, many of the users were well acquainted with both the positive features as well as the limitations of these devices. The information that many users today have about the operational characteristics of their CEM is often inadequate, in particular when changes in the gain of the device are critical for the specific application. Since no two devices and in particular no two CEMs function identically, it is very unwise to rely exclusively on the manufacturers specifications. Because the application involved (analysis of the stratosphere using a rocket launched mass spectrometer with a CEM) was very dependent on stabile operating conditions of the CEM the Max Planck Institute of Nuclear Physics in Heidelberg,West Germany, conducted extensive testing of two types of Bendix CEMs (now marketed by Galileo): 4028 and 4700. Since those tests newer and slightly improved versions of these CEMs are on the market, the basic results of our testing are still applicable .

Description of the Testing Procedures

The testing of the CEMs utilized a mass spectrometer tuned to specific ion species to provide the CEM with a variable input flux. Both the mass spectrometer and the CEM were operated in a vacuum chamber at pressures of 10^{-7} and lower. For some of the testing even this input flux had to be reduced using a combination of orifices and grids so that a large dynamic range was available during the studies. Fig.1 shows output signal versus CEM-potential characteristic for the 4028 device when detecting N2+ ions. Three values of input current are included showing in general a linear increase of output current with increasing input current. Fig. 2 shows the same type of measurement in the pulse counting mode. This shows the device to possess a plateau for counting between approx. 2300V and 2600V. Fig.3 shows the output current as a function of the CEM-potential at three values of input current for the 4700 device. Fig.4 shows the results for the pulse counting mode using the same device. The pulse counting plateau for this device is much broader extending from about 2100V to 2900V. As can be observed from Figs.1 and 3 the 4700 device is normally operated at an output current that is 3 magnitudes higher than that of the 4028 model. This is an important feature that the user must keep in mind in light of the fact that if a CEM is operated at an input current and gain setting that results in an output current of 1/10 of the CEM bias current or even higher, the resulting output signals will not change linearly with changes in the input signal. This can result in data that is totally useless. Fig.5 shows the output current/count rate as a function of the input current for the 4028 device whereas Fig.6 show the same for the model 4700. The measurements were done while both were operating in the plateau region. The results indicate that a deviation from the linear dependency on the input signal can be observed at $2x10^{-8}$ A for the 4028 and at $1.8x10^{-5}$ A for the 4700. Figs.7 and 8 show the measurement of the electron gain as the function of CEM-potential for different ion species using both CEMs. The curve labelled V_D plots the function as given by the manufacturer. As can be observed the measured curves sometimes differ extremely from that of the manufacturer. The detection efficiency for both devices for the four species used He+,Ne+,N2+ and Ar+ was approximately 35%.

Bibliography

1) Somssich P., Diplomarbeit, University of Heidelberg,FRG (1976)
2) Kurz E., Channel Electron Multipliers, American Lab., March 1979 3) Rosenbauer H., unpublished, (1978)
4) McComas D.J. and Bame S.J.,Rev. Sci.Instr. 55(4)1984
5) Galileo Electro-Optics Corp.

My thanks to the Max Planck Institute in Heidelberg,FRG, in particular to Dr.R.Nord and Dr.D.Krankowsky for their assistance in this work. I would also like to thank GTE Sylvania ,in particular Dr.V.Meyer, Connie Gean and Bob Haggerty.

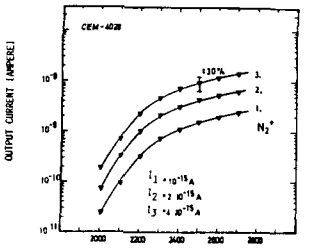

FIG. 1

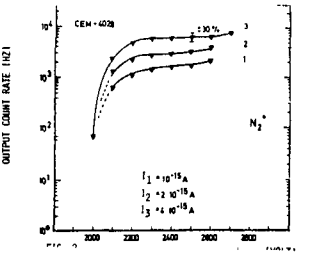

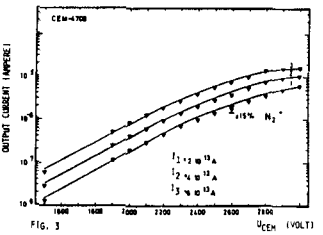

FIG. 3

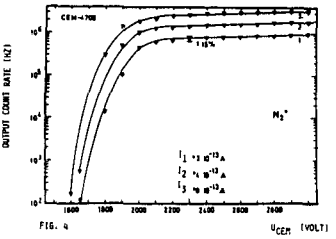

FIG. 4

OUTPUT CURRENT/ COUNT RATE - LOADING

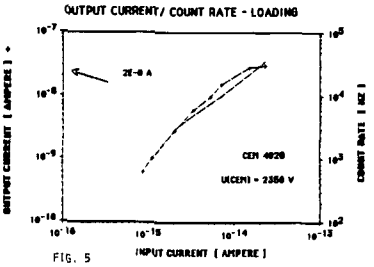

FIG. 5

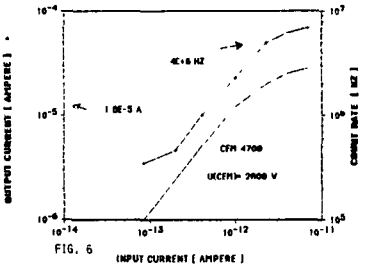

FIG. 6

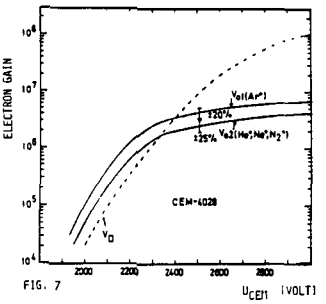

FIG. 7

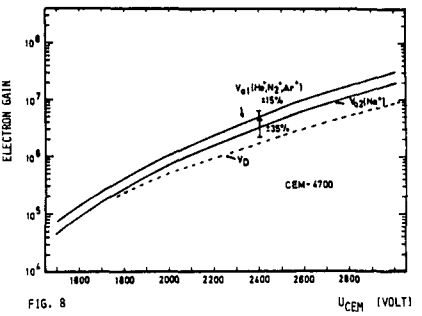

FIG. 8

DUAL-MODE DETECTION FOR EXTENDED DYNAMIC RANGE IN MS/MS

M. J. Kristo and C. G. Enke, Chemistry Department, Michigan State University, East Lansing, MI 48824

We have developed a microprocessor-based control system for the Galileo Dual-Mode Channeltron (1) capable of collecting analog and ion-counting information in the same scan. At low ion currents, the processor can obtain ion-counting information; at high currents, a high-gain protection circuit disables the ion counting section of the detector and only analog information is available. Kondrat and Cooks (2) described the large decrease in chemical noise obtained with two stages of mass filtering, but very little has been done to capitalize on the resulting extension of the dynamic range. The dual-mode detection system can measure ion currents from the limits of chemical noise in the system (1 count per second) to the saturation point of the low-gain section of the Dual-Output Channeltron (around 10E+9 counts per second). There are four parts to the dual-mode control system: 1) the analog processing circuitry, 2) the ion-counting circuitry, 3) the protection grid logic, and 4) the algorithm for normalizing the analog and ion-counting data.

The analog information is processed by previously-designed multiamp and data acquisition boards (3). The multiamp provides the analog signal from the detector at five different gains (ranges) simultaneously. The data acquisition circuit converts the largest, nonsaturated signal, together with the range of the signal, to a 20-bit integer value. In comparison, typical mass spectrometric data systems give 12 or 16-bit intensities before summing. The analog subsystem produces an averaged value at 4 microseconds per average.

A pulse amplifier discriminator (PAR Model 1182) transforms the detector current pulses from the high-gain section of the Dual-Output Channeltron into digital logic pulses. These pulses are then counted by a versatile pulse-counter/timer circuit. The circuit can accumulate pulses for constant periods of time (constant scan rate) or determine the time required to achieve a preset count (constant precision). The count rate is also checked after a short time into the count interval. This feature can quickly sense a below-threshold level (user-defined) and signal the processor to continue scanning. Studies have shown that as much of 70% of the time in data acquisition is spent in gathering data where no useful information is present (4).

The protection grid logic is implemented totally in hardware for minimum response time. The circuit continually monitors the X16 signal from the multiamp board. If that signal exceeds a certain preset threshold, the protection grid logic holds the grid at -350 Volts, preventing electrons from entering the high-gain section. If the signal does not exceed threshold, then the grid is held at 0 Volts and the ion-counting section is enabled. The grid logic also clears a flipflop to indicate that the protection grid is enabled. The processor can set or read this flipflop to determine the state of the protection grid, that is, whether to acquire analog or ion-counting information.

Ion-counting and analog data are scaled in software, providing consistent ion intensities at both outputs. Analog data is shifted to

occupy, roughly, the upper five bits of the 32-bit datum. Since a known fraction of the ion current pulses will fail to be counted due to the fixed resolution of the counting system and the random arrival of ions (% LOST = 100 * Res * Pulse Flux), acquired experimental flux rates can be reverse-fitted to obtain the actual input count rate. This data extends the linear response of the ion current versus analog intensities to 8 MHz as shown in Figure 1, providing easy correlation between analog and ion current data.

This data collection system maximizes the data collection rate and extends the useful dynamic range to 8 orders of magnitude. This wide range of detection for single scans is particularly useful in MS/MS applications.

1) Galileo Corp., Sturbridge, MA 01518.
2) R. W. Kondrat and R. G. Cooks, Anal. Chem., 50, 81A-92A (1978).
3) B. H. Newcome, private communication.
4) E. J. Darland, G. E. Leroi, and C. G. Enke, Anal. Chem., 52, 714 (1980).

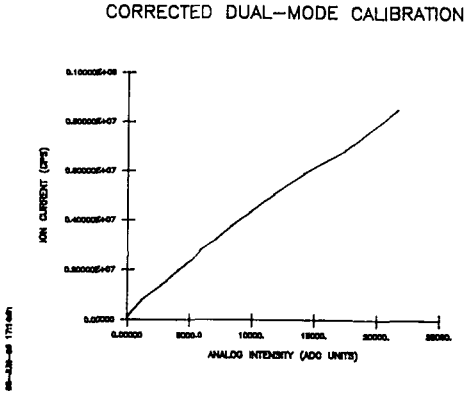

Figure 1. Ion current, corrected for errors due to the fixed resolution of the counting system and random ion arrival times, versus analog intensity.

CONTINUING DEVELOPMENTS OF ADVANCED ION TRAP INSTRUMENTATION

P.E. Kelley, J.E.P. Syka, P.C. Ceja, G.C. Stafford, Jr.; Finnigan MAT, San Jose, CA 95134. J.N. Louris; Purdue University, Dept. of Chemistry, West Lafayette, IN 47907. H.F. Grutzmacher, D. Kuck; Fakultat fur Chemie der Universitat Bielefeld, Bielefeld, FRG. J.F.J. Todd; University of Kent, Chemical Laboratory, Canterbury, Kent, UK.

The advent of mass selective instability high pressure operation of the ion trap (1) has led to increased sensitivity and improved mass resolution, particularly at high mass (>200u). In this mode, the ion trap is operated only on the q-axis of the stability diagram (i.e. RF-only potentials). Also, a background pressure of helium is maintained at 10^{-3} torr. Variations to this scan scheme, with some instrument modifications, allow for electron ionization (EI) MS/MS daughter experiments and "notch" filter operation (2).

Research has continued to develop new scanning modes and we now report positive chemical ionization (CI) and its integration into MS/MS daughter experiments. Additionally, we are now able to store selected ions for several seconds in the ion trap. This allows for the study of certain intramolecular processes or intermolecular ion-molecule interactions.

Positive chemical ionization within an ion trap is made possible by adding a low pressure of reagent gas (e.g. 10^{-3} torr methane), whereupon the long residence time (up to 100ms) permits the build-up of species such as CH_5^+ and $C_2H_5^+$. These in turn react with the analyte molecules (M) present at approximately 10^{-7} torr to yield ions such as MH^+ and fragmentation products. To achieve this, the scan cycle of the RF drive voltage is set so that initially only reagent ions (e.g. m/z's 17 and 29) are stored. This is followed by a reaction period when ions formed from the analyte are trapped, these being subsequently scanned out of the trap to give a mass spectrum. Additionally, EI spectra can be obtained with the continuous presence of CI reagent gas by simply changing the scan function.

Figure 1 depicts the general scanning techniques to produce EI or CI spectra using the ion trap with the continuous presence of reagent gas. The EI scan function is represented by the solid line and the CI scan function is represented by the dashed line. EI spectra are produced by setting the initial RF voltage (A), during ionization, at a level such that all m/z's up to and including the molecular weight of the CI reagent gas are not stored. This does not allow for the formation of the CI reagent ions. All other ions with masses greater that the initial RF voltage level (i.e. those formed from the electron ionization of the sample) have stable trajectories and remain trapped in the device. Scanning the RF voltage (C) then results in an EI mass spectrum of the sample.

An example of EI or CI spectra obtained from the ion trap is shown in Figure 2. The top spectrum is the EI mass spectrum of nicotine obtained without methane reagent gas present in the device. The middle and bottom data were acquired with the continuous presence of methane reagent gas and represent the EI and CI mass spectra, respectively. Integration of this scan function with the MS/MS scan function (Reference 2) allows for the aquisition of CI MS/MS data

We have also developed a method that utilizes only AC fields to isolate a particular mass of interest. This is accomplished as follows: In the first step, during ionization, a RF voltage at fixed amplitude is applied to the ring electrode of the ion trap and the end cap electrodes are held at ground potential. This allows for a wide mass range of ions to be created and stored in the device. These m/z's have distinct and unique natural frequencies of oscillation in the ion trap.

Next, with the electron gun turned off, the m/z's below the parent mass of interest can be eliminated by simply ramping the amplitude of the RF voltage applied to the ring electrode. As long as the q of the parent remains less than 0.908, it will remain trapped in the device. The elimination of m/z's greater than the parent mass can be accomplished simultaneously by incorporation of a frequency synthesizer connected to the end cap electrodes. The scan function to isolate a single mass with only AC fields is shown in Figure 3. At point B, the frequency synthesizer is adjusted and turned ON to the frequency of oscillation of the parent + 1 mass, and sufficient time and voltage at this frequency are applied to resonate the parent + 1 mass out of the ion trap.

As the RF voltage applied to the ring electrode is ramped at a suitable rate, masses higher than the parent come sequentially in resonance with the superimposed AC field and are ejected from the ion trap. At point D on the scan diagram, all m/z's below the parent have been expelled from the ion trap and m/z's greater than the parent mass (PM) have been expelled to an upper mass limit (UML) expressed as:

$$UML = \frac{0.908 \times PM}{q_{FSO}}$$

where q_{FSO} is the q of the parent mass when the frequency synthesizer is first turned ON. Now, what remains in the ion trap is the parent mass of interest and m/z's greater than the upper mass limit. The experiment, from here on in, depends on whatever is appropriate for the *measurement being taken.*

An example of isolating a single mass in the ion trap with only AC fields is shown in Figure 4. In this example, m/z's 79 or 85 can be isolated from a mixture of protonated benzene and d_6-benzene. In this case, isolation of a single mass is very important to study the hydrogen/deuterium exchange in the gas phase ion-molecule reactions between protonated benzene and neutral d_6-benzene as shown in Figure 5.

References:

(1) G.C. Stafford, Jr., P.E. Kelley and D.R. Stephens, U.S. Patent 4,540,884 (1985).

(2) P.E. Kelley, G.C. Stafford, Jr., J.E.P. Syka, W.E. Reynolds, J.N. Louris, J.W. Amy and J.F.J. Todd, 33rd Annual Conf. on Mass Spectrom. and Allied Topics, San Diego, CA (1985) 707.

Ion Trap EI or CI Scan
With Reagent Gas Present

Fig 1

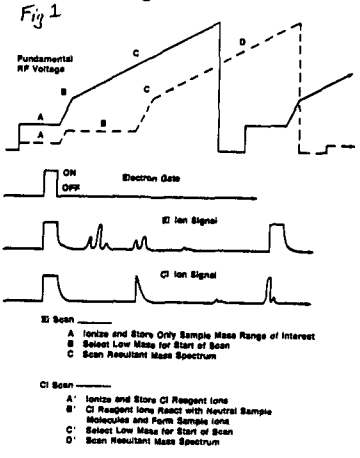

Electron Ionization Mass Spectrum of Nicotine

Fig 2

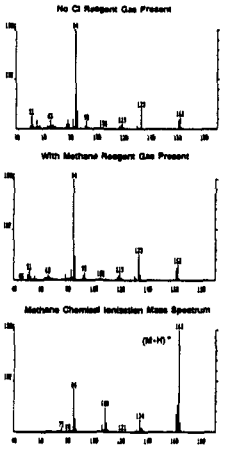

Fig 3

Isolation of a
Single Mass in the Ion Trap

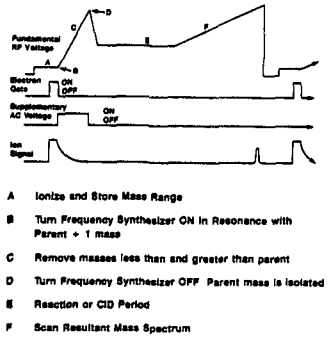

ITMS
Methane CI of a Mixture of
Benzene and Perdeuterobenzene

Fig 4

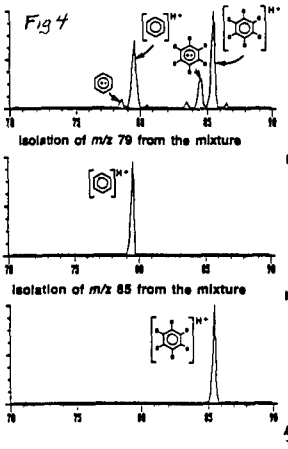

ITMS
Intermolecular Reaction of $C_6H_6^+$ and C_6D_6 as a
Function of Time

Fig 5

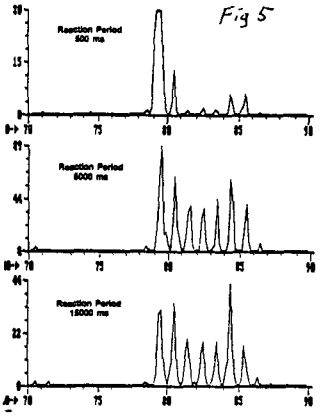

EXTENSIONS TO COMBINED CHROMATOGRAPHY - MASS SPECTROMETRY ON A DOUBLE FOCUSING SECTOR INSTRUMENT

J R Chapman, E D Ramsey and J A E Pratt
Kratos Analytical, Barton Dock Road, Urmston, Manchester M31 2LD, UK

There are now a number of chromatographic techniques whose compatibility with on-line mass spectrometry has been established and which should therefore be available on any instrument intended for the analysis of complex mixtures. Recent modifications to the Kratos Analytical MS25 RFA and MS890 double focusing mass spectrometers have been directed towards the provision of facilities for capillary supercritical fluid chromatography-MS (SFC-MS) and improvement of the existing thermospray LCMS interface.

Chromatography with a supercritical fluid as the mobile phase offers the opportunity of carrying out analyses in a much shorter time than with equivalent LC techniques. In addition, supercritical fluids are excellent solvents for higher molecular weight materials. Implementation of SFC using a capillary column provides fluid flow rates that are suitable for direct coupling to the mass spectrometer without any intervening enrichment device. Accordingly, a new inlet has been developed for the MS25 and MS890 which accepts SFC or GC capillary columns whilst providing the temperature control needed to maintain chromatographic integrity. In addition, the inlet is fully demountable.

Modifications to the dedicated thermospray LCMS ion source have resulted in a significant improvement in LCMS sensitivity on the MS25 and MS890 with a particular improvement in performance with higher molecular weight solutes. The modifications lie in the areas of improved source gas tightness, redesign of the source internal geometry to minimise thermal decomposition and improvements in ion extraction and focusing from the source.

Alternative forms of ionization offer the user greater scope for LCMS analysis when the solvent system used results in poor sensitivity with thermospray ionization or will not support the electrolyte concentration needed for thermospray ionization. The addition of a discharge ionization facility together with the existing filament assembly make Kratos Analytical LCMS systems very versatile in this respect.

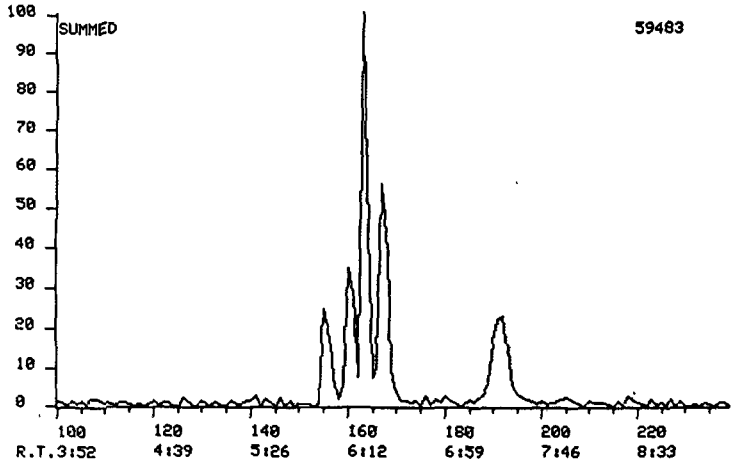

Figure 1 Typical SFC-MS chromatogram obtained from a mixture of hydrocarbons

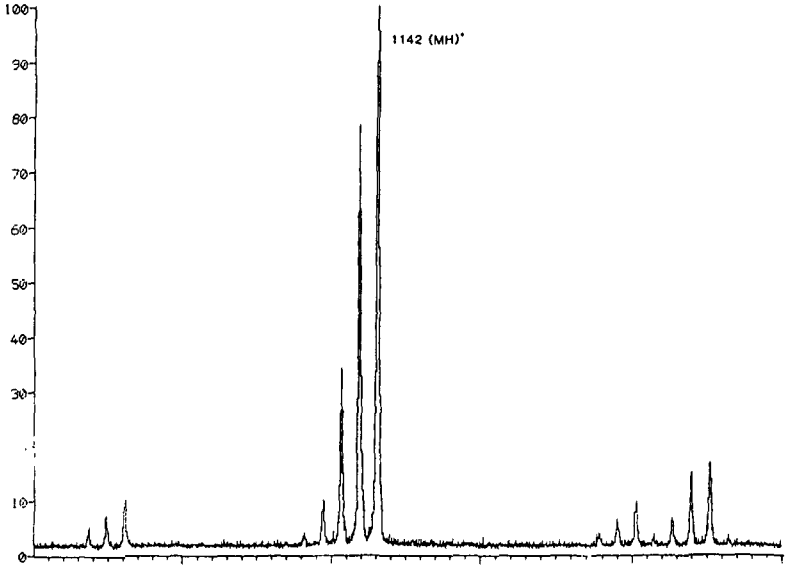

Figure 2 Raw data profile obtained from TSP ionization of Gramicidin S

THE USE OF HIGH RESOLUTION AND ACCURATE MASS MEASUREMENT IN GC/MS USING FOURIER TRANSFORM MASS SPECTROMETRY, James A. Kinsinger, Nicolet Instrument Corporation, 5225-1 Verona Road, Madison, WI 53711

The use of the dual-cell differentially pumped Fourier transform mass spectrometer (FTMS) as a gas chromatographic detector has enhanced the amount of useful information one can obtain from complex mixtures. Accurate mass measurements, easily obtainable from FTMS instrumentation, can assist in confirmation of the presence of a suspected compound or help identify an unknown compound, either by library searching or by structure determination from the fragmentation pattern.

The advantages of FTMS for GC/MS applications are threefold.

1) All ions are detected simultaneously. The recorded mass spectra are not distorted as sample concentration changes, only the signal/noise is affected. As a result, fewer "scans" need to be acquired to obtain the correct picture of the GC effluent, both for compound identification and quantitation.

2) High-resolution mass spectra can be easily obtained. No slits are required to provide resolution, only that ion motion remain coherent for a sufficient time to accurately measure the frequency, typically 20 to 1000 milliseconds to provide resolution of 3000 to 150,000. This time is provided by the detection of ions in the low pressure side (analyzer side) of the dual-cell FTMS-2000 Fourier transform mass spectrometer.

3) With the high-resolution capability comes the ability to measure the mass of ions accurately. The use of stable superconducting magnets and frequency detection enable operational modes that do not require calibrant to be present during the GC run to measure masses to within 5 to 10 ppm.

Application of these advantages to samples have been demonstrated by the ability to detect cocaine in an urine extract. Not only do the peak intensities match with a drug standard of comparable level (10ng), but the mass assignments agree to within 20 ppm or less.

In a sample of pepperment flavor extract, mass measurements were sufficiently accurate to provide only one possible formula based on the presence of carbon, hydrogen and oxygen using a 25 ppm tolerance. The use of this accurate mass data produced three unique mass chromatograms at m/z 139 due to the presence of $C_{11}H_7$, $C_9H_{15}O$ and $C_{10}H_{19}$ ions in various components of the mixture. A resolution of 6,000 FWHH was sufficient to resolve these three components.

High-resolution GC/MS analysis is possible due to the differential pressures in the dual-cell instrument. The figure shows a partial mass spectrum of naphthalene with 186,000 resolution (FWHH). During this particular GC run, ions from dimethylphenol, dimethylaniline and naphthalene were all analyzed. After adjusting the calibration using the m/z 128 ion from naphthalene, mass measurement differed from the theoretical values by an average of less than 1 ppm (see Table).

Table

Mass Measurement Accuracy from High-Resolution GC Run

Compound	Measured Mass (amu)	Deviation (ppm)
2,6 - dimethylphenol	122.072674	-0.5
2,4 - dimethylaniline	120.080819	-0.4
	121.088539	0.5
naphthalene	126.046572	-1.4
	127.054382	-1.2
	128.062054	-0.02
Average		-0.7

Figure

Naphthalene

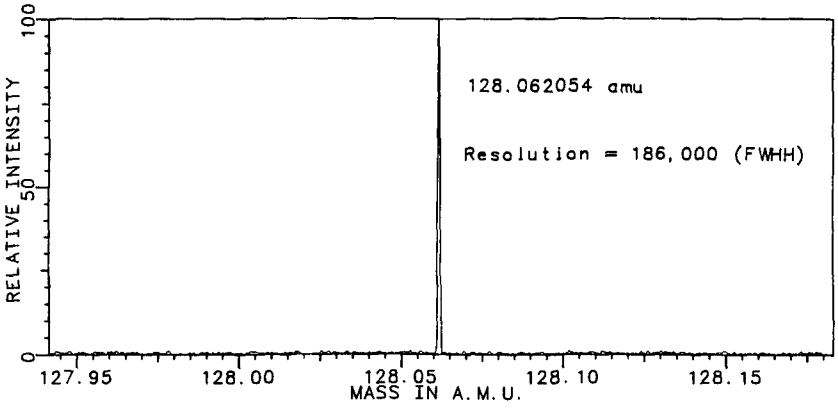

ISSUES REGARDING THE ROLES OF ION-NEUTRAL COMPLEXES AS INTERMEDIATES IN UNIMOLECULAR DISSOCIATIONS

David J. McAdoo, Marine Biomedical Institute, University of Texas Medical Branch, Galveston, Texas 77550

For the purpose of this presentation, an ion-neutral complex is defined as an associated ion-neutral pair held together in the gas phase by electrostatic attractions. Experiments by Longevialle and Botter[1] on steroidal ions demonstrate that the two fragments can adopt any configuration relative to each other, a picture supported in more detail by recent computations by Postma et al. on the ethylene ion-H_2O complex.[2] Several years have passed since information regarding ion-neutral complex mediated unimolecular decompositions in the gas phase has been systematically reviewed.[3] In that review, Thomas Morton made the point that in ionic rearrangements bond breaking to form a complex sometimes precedes hydrogen transfers or isomerizations, in contrast to "conventional" mechanisms of ionic rearrangement and dissociation, in which isomerization precedes bond scission. Issues that currently need addressed are (1) under what conditions are such complexes formed and how does formation depend on the properties of the partners, (2) what configurations can they assume, (3) what are the criteria for recognizing the intermediacy of such complexes, and (4) what is the relationship between ion-neutral complex mediated reactions and current theoretical descriptions of ion-molecule reactions and unimolecular decompositions?[4]

Reactions Occurring Through Ion-Neutral Complexes. Ion-neutral complexes are formed when a bond in an ion is stretched to the point that covalent forces become insignificant, the incipient fragments being held together by electrostatic attractions. This happens even for neutral fragments as nonpolar and nonpolarizable as methyl, so complex formation should be a general occurrence just below the threshold for bond breaking. This is supported by computations.[4b,c] Evidence demonstrating that the energy range over which complex formation is significant depends on both the polarizability of the neutral and the nature of the ion is presented elsewhere in this Proceedings.[5]

Many unimolecular dissociations display no evidence of complex formation. This is attributable to the need for a reaction other than simple dissociation be available to the complex to reveal its presence. Ion-neutral complex-mediated reactions must be competitive with other possible reactions to be observed. As with all unimolecular reactions, their competitiveness is determined by their critical energies and dependence of their rates on energy. Evidence to date suggests that ion-neutral complex-mediated reactions other than simple dissociations may only occur when they have activation energies at or below those of competing processes,[5] even though the initial pair may sometimes be formed at energies below those at which they can react further. Also many of these reactions quickly disappear with increasing energy due to being overwhelmed by simple dissociation.

The number of reactions proposed to be ion-neutral complex mediated is now fairly extensive, so criteria need to be established for recognizing when an ion-neutral complex intermediate is involved in a reaction. The following are suggested as a start to developing such criteria, although not all will be applicable to any specific instance.

1. The products of simple dissociation of the complex will be observed at sufficiently high energies.
2. Appearance energy measurements will place the threshold for the complex mediated reaction at or below those of competing processes.
3. Ion-neutral complex-mediated reactions will have slower rises of rates with energy than competing simple cleavages.
4. Occurrence of extensive and nonspecific hydrogen migration.
5. Isomerization below the threshold for simple dissociation.
6. Requirement of a non-classical transition state if an ion-neutral complex intermediate is not invoked.
7. Results of molecular orbital calculations.[2]

Applicability to and Tests of Theories of Reaction Rates. According to present beliefs regarding ionic dissociations, two bottlenecks that can act as transition states are passed in the course of an ionic dissociation.[4] The first, the tight or "locked rotor" transition state occurs when the two fragments start to rotate relative to each other, causing the density of states, which has been decreasing during bond stretching as rotational and vibrational energy is being converted into potential energy, to increase. The second occurs at the centrifugal barrier.[4b] Available data[6] support computational predictions[4b,c] that the first bottleneck usually occurs at energies below the threshold for simple dissociations. According to theory, complexes correspond to the system being between the two bottlenecks.[4b] We equate ion-neutral complexes with the theoretical complex. This description of unimolecular dissociations correlates with phase space theory, which assumes

that a statistical distribution of internal energy is maintained as the system passes between the two bottlenecks. This is to be expected when the incipient fragments part slowly i.e., go through a complex in which they can collide and exchange energy, but not if dissociation is extremely rapid. Theory predicts that as excess energy decreases, rate control will be transferred from the second to the first transition state due to a very rapid increase in flux through the second transition state.[4a,b] Rapid changes from alkane eliminations to alkyl losses also supports this view of ionic dissociations.[5,6] A computational description of ion-neutral complex-mediated dissociations needs to be developed, as RRKM theory fails drastically to predict the relative rates of methyl and methane loss from the isopropyl methyl ether ion.[7] Especially intriguing is the hypothesis that very close to its threshold for decomposition, the $CH_3CO^+...CH_3$ complex may preferentially lose methyl from low rotational states and methane from high rotational states.[8] This suggestion is based on the observations that (1) at very short times this ion has a slight preference for methyl loss very close to threshold, (2) at long times this ion loses methane at least 100 times as often as methane, and (3) the frequency of methane loss increases drastically at long times with increasing temperature, but only slightly if at all at short lifetimes.

1. P. Longevialle and R. Botter, J. Chem. Soc. Chem. Comm. 823 (1980).
2. R. Postma, P.J.A. Ruttink, B. Van Baar, J.K. Terlouw, J.L. Holmes, and P.C. Burgers, Chem. Phys. Lett. 123, 409 (1986).
3. T.H. Morton, Tetrahedron 38, 3195 (1982).

4a. W.H. Miller, J. Chem. Phys. 65, 2216 (1976). b. M.T. Bowers, M.F. Jarrold, W. Wagner-Redeker, P.R. Kemper and L.M. Bass, Faraday Discuss. Chem. Soc. 75, 57 (1983). c. J.A. Dodd, D.M. Golden and J.I. Brauman, J. Chem. Phys. 80, 1894 (1984).

5. J.C. Traeger, C.E. Hudson and D.J. McAdoo, This Conference, presentation FOC9.
6. C.E. Hudson and D.J. McAdoo, Int. J. Mass Spectrom. Ion Proc. 59, 325 (1984).
7. D.J. McAdoo, J.C. Traeger, C.E. Hudson and L.L. Griffin, submitted.
8. J.C. Traeger, C.E. Hudson and D.J. McAdoo, submitted.

CHEMICAL IONIZATION OF 2-FLUORO-1-ALKENES: EVIDENCE FOR A LONG-LIVED ION-MOLECULE COMPLEX IN THE GAS PHASE.

Jörg Moenig, Kamalesh K. Johri, Douglas Bond, and Thomas Hellman Morton
Department of Chemistry, University of California, Riverside, CA 92521

The gas phase ion chemistry of 2-fluoro-1-alkenes, $CH_2{=}CFCH_2R$, has been investigated using a B-E double-focussing instrument. Under conditions of methane chemical ionization, these compounds exhibit prominent $[M-F]^+$ ions. Examination of the MIKE spectra of these ions and comparision with the MIKES of chemically ionized acetylenes and dienes suggest that the $[M-F]^+$ ions are vinyl (rather than allyl) cations. For instance, a comparision of the $[M-F]^+$ metastable decompositions from CI of 2-fluoro-1-heptene with the $[M+H]^+$ metastable decompositions of 1,3-heptadiene and the heptynes (Table I) suggests that the $[M-F]^+$ ions have the structure $H_2C{=}\overset{+}{C}CH_2CH_2CH_2CH_3$.

Table I. MIKE spectra of $M^{\prime}$= m/z 97 from chemical ionization of C_7 precursors.

Source	$[M^{\prime}-42]$	$[M^{\prime}-30]$	$[M^{\prime}-29]$	$[M^{\prime}-28]$	$[M^{\prime}-16]$	$[M^{\prime}-15]$
CD_4 CI of $CH_2{=}CFCH_2C_4H_9$	100	--	--	74.0	0.4	1.0
CH_4 CI of 1-heptyne	100	--	--	64.5	0.8	1.6
CH_4 CI of 2-heptyne	100	1.5	4.9	84.6	2.6	14.2
CH_4 CI of 3-heptyne	100	3.0	8.7	78.9	2.3	13.2
CH_4 CI of 1,3-heptadiene	100	--	--	61.3	2.4	10.5

One probable source of the $[M-F]^+$ is fluoride abstraction by methyl and ethyl cations. Another possibility is protonation of the fluorine atom followed by HF loss (as distinguished from protonation of carbon, which with CD_4 chemical ionization gives rise primarily to $[M+D-HF]^+$ ions). This possibility is intriguing because <u>ab initio</u> molecular orbital calculations (at the 3-21G level) show the C-F bond of F-protonated vinyl fluorides to be dissociative. The optimized geometry of the C-protonated 2-fluoropropene has a calculated heat of formation of 140 kcal/mol, while that of the unprotonated precursor, $CH_3CF{=}CH_2$, has a calculated heat of formation of -35 kcal/mol. The optimized geometry of the F-protonated tautomer, $CH_3\underset{\underset{+FH}{|}}{C}{=}CH_2$, *has a calculated heat of formation of 175 kcal/mol, 10 kcal/mol higher* than the heat of formation of $CH_3\overset{+}{C}{=}CH_2$ plus HF. Moreover, the C-F bond distance in the unprotonated vinyl fluoride is calculated to be 1.35 Å, while that of the F-protonated molecule is calculated to be 1.53 Å. These

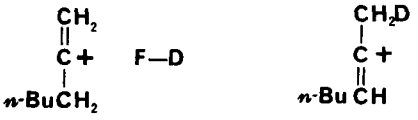

I II

calculational results suggest that if evidence for a metastable F-protonated vinyl fluoride should be adduced, the structure is likely to the that of an ion-dipole complex (as represented by species I above) rather than a covalently bound molecule.

Chemical ionization of 2-fluoro-1-heptene with CD_4 yields a metastable $[M+2]^+$ ion, which ejects HF 60 times more readily than DF. Chemical ionization of monodeuterated 2-fluoro-1-heptene, $CHD{=}CFCH_2CH_2CH_2CH_2CH_3$, with CH_4 yields a metastable $[M+2]^+$ ion, which ejects HF 140 times more readily than DF. The predominant pathway must be deposition of the proton (or deuteron) on carbon, followed by 2,3-elimination of HF to give a product ion with the structure II. The minor product from DF loss would have been expected to occur to the same extent from both reactions, if CI on carbon were the only pathway. But as more DF loss results from the CD_4 chemical ionization, we infer that two isomers of the $[M+2]^+$ are formed, one of which loses DF exclusively. If the calculational results hold true for the higher homologues, then this suggests that there are ion-molecule complexes with lifetimes in the $> 10^{-7}$ sec range between ions and neutrals that, like HF, have large permanent dipole moments and small polarizabilities.

ION-MOLECULE COMPLEXES IN FIRST & SECOND-ORDER REACTIONS. CONNECTING THE TWO KINETIC REGIMES IN THE GAS PHASE.

Thomas Hellman Morton, Dion Stams, and Eric W. Redman
Department of Chemistry, University of California, Riverside 92521

An ion-molecule complex is an electrostatically bound aggregate in the gas phase whose bonding lacks directional character. In order to be kinetically significant, the complex must live long enough for the charged and uncharged partners to sample a large number of relative orientiations. Ion-molecule complexes can be contrasted with hydrogen bonded complexes in terms of the internal degrees of freedom that each type of complex possesses. In both types, the complex has six degrees of freedom not possessed by the separated ion and neutral. In a hydrogen-bonded complex, only one of these is an internal rotor, as represented by the curved arrow below for $A\text{-}H^{+}\cdots B$. An ion-molecule complex $[R^{+}\ Y]$ has at least three internal rotor degrees of freedom, as the curved arrows depict.

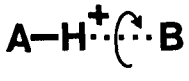

HYDROGEN-BONDED COMPLEX

ION-MOLECULE COMPLEX

How long can an ion-molecule complex live before dissociating into R^{+} and Y? The following RRKM calculation provides a lower limit for R^{+} = 1-methylcyclopentyl cation and Y = trimethylamine. Treating the ion as a point charge and neglecting the permanent dipole of trimethylamine altogether, the electrostatic well is 0.12 eV deep at a separation $r_{\perp} = 5$ Å (chosen to be outside covalent or hydrogen-bonding distance). At this separation, the maximum contribution from the ion-permanent dipole interaction would be 0.07 eV. Thus it is energetically possible for the trimethylamine molecule to explore all orientations relative to the ion, and the ion-molecule complex is portrayed as having five internal rotors, as shown by the curved arrows below.

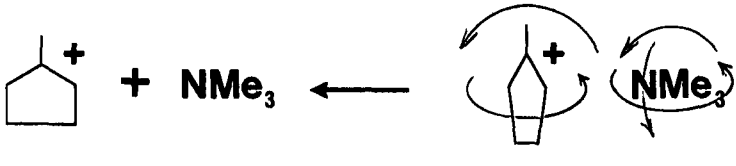

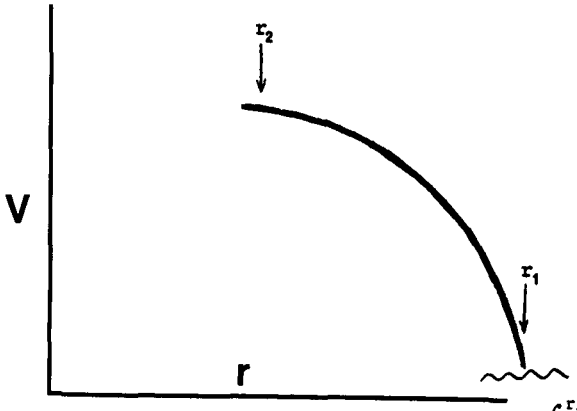

$$V = -\frac{\alpha e^2}{2r^2(r^2-\alpha^{2/3})} - \frac{J(J+1)}{2\mu r^2}$$

$$\text{Number of states} = \frac{\sqrt{2\mu}}{2\pi}\int_{r_2}^{r_1}\sqrt{V}\ dr$$

To perform an RRKM calculation, the sixth internal degree of freedom was chosen to be the quantized motion of a polarizable neutral in the field of a point dipole, a central force potential V for which the formula is given in the figure above. Obviously, such a potential is grossly inaccurate when the separation, r, is much shorter than 5 Å, and the short-range interactions are neglected (as represented by the squiggly line in the figure above). But for separations between $r_1 = 5$ Å and the Langevin potential energy maximum at r_2, and estimate of the number of states can be made using the WKBJ approximation, for which the formula is given in the figure above. Using this expression to compute a semiclassical density of states for the ion-induced dipole interaction and performing a Laplace convolution with the density of states for the remaining degrees of freedom, the RRKM calculation predicts a lifetime on the order of 20 picoseconds.

This kind of calculation shows that an ion-molecule complex that has more than enough energy to dissociate can still persist for a substantial length of time before dissociating, if we assume that all internal degrees of freedom exchange energy freely. If alternative dissociation pathways are available, then the ion-molecule complex can last long enough to explore them. Similar ion-molecule complexes intervene in bimolecular reactions (i.e. where the arrow at the bottom of the previous page goes from left to right instead of right to left).

Site specificity of a H rearrangement cancelled by subsequent H exchanges in ion-neutral complexes

Pierre A. Longevialle
ICSN CNRS 91190 Gif sur Yvette, FRANCE

Amides derived from 3-aminosteroids lose their functional group (enol tautomer of the amide) under EI with rearrangement of an H from C_2 or C_4 (γ position to the carbonyl) but also C_5, C_1 and other sites to a lesser extent (1). Concomitantly the protonated amide appears in the spectrum, the proton originating also from several sites. In the case of benzoylamides, these fragmentations are competing with loss of an aromatic H (D labeling) and loss of 106 m.u. (possibly benzaldehyde) in the μs time frame (Scheme 1). These latter decompositions are made competitive by the delocalisation of the charge over the aromatic ring after the initial exothermic H transfer to the carbonyl which is the common first step. Interestingly, by D labeling at C_2 and C_4 M-106 becomes entirely M-107. This shows that the first step H transfer is indeed site specific (C_2 and C_4) as a true McLafferty rearrangement. The non site specificity observed in the loss of amide results from H-D exchanges in ion-neutral complexes (2) as shown on scheme 2 concerning an N-methyl acetamide. For ions within a certain energy range below the AE of M-amide ions (hatched area) the neutral enolamide (3) associates with the ionized olefin in a long lived complex. The PA of the amide is larger than the PA of the olefinic radical by 30 to 40 kcal/mole. Therefore a proton, preferentially allylic, may be transferred from ion to neutral leading to a new complex of lower enthalpy. The same proton may go back to the steroid leading either to the original olefin or an isomer. The hydroxylic H may also be transferred to the steroid leaving the acetamide (more stable than its enol tautomer by about 10 kcal/mole). Again, this neutral amide may be protonated, and so on, the system exploring a potential surface whose minima correspond to ion dipole stabilized complexes in which ionic partners are either the protonated amide or a variety of ionized steroidal olefin isomers. Any of these complexes may, eventually, decompose, leading to M-amide ions (M-73) or protonated amide (74). The initial site specificity is cancelled because the H which is transferred on the carbonyl in the first step (hydroxylic H of the enolamide) is very prone to go back to the steroid leading to the more stable amide and to be replaced with another H. By contrast, in the loss of 106 m.u. the H transferred to the carbonyl in the first step probably rearranges in a position of the neutral (possibly aldehydic) from where it cannot exchange later. Therefore, even if benzaldehyde (μ=2.9 D) gives also a complex with M-106 ion and becomes protonated (protonated benzaldehyde does not appear significantly in the spectrum, though) the original H is not involved subsequently in eventual proton exchanges and the initial site specificity is conserved in this fragmentation.

In conclusion, ion dipole stabilized complexes are found again to play an important role in the fragmentation of amides (4).

1. Z. Pelah, M.A. Kielczewski, J.M. Wilson, M. Ohashi, H. Budzikiewicz and C. Djerassi, J. Amer. Chem. Soc (1963) 85 2470
2. T.H. Morton Tetrahedron 38 3195 (1982)
3. Dipole moments of formamide and acetamide are 2.6 and 4.2 D and their enol tautomers 3.55 and 3.9 D respectively (G. Bouchoux and Y. Hopilliard, Ecole Polytechnique, Palaiseau, France).
4. P. Longevialle Org. Mass Spectrom. 20, 644 (1985).

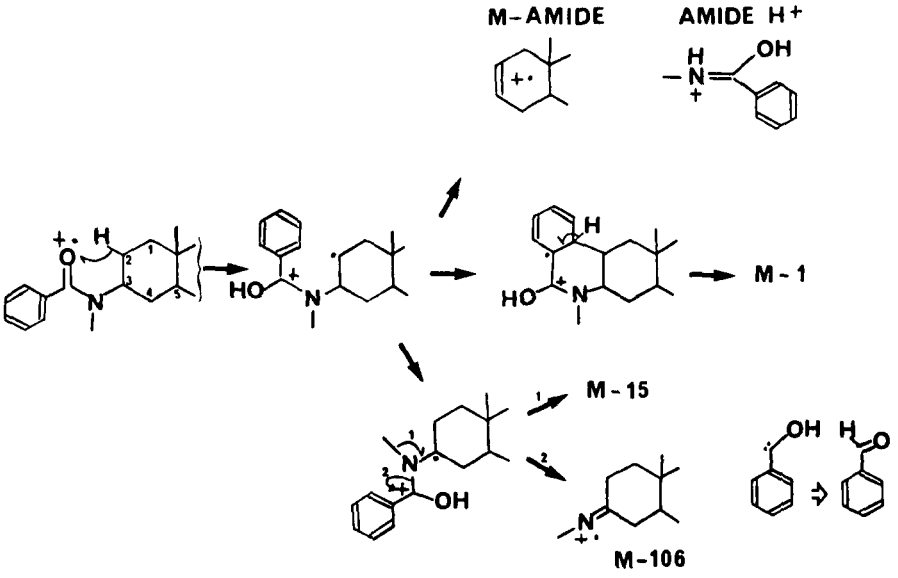

Scheme 1. Fragmentation pattern of a steroidal N-methyl benzoylamide.

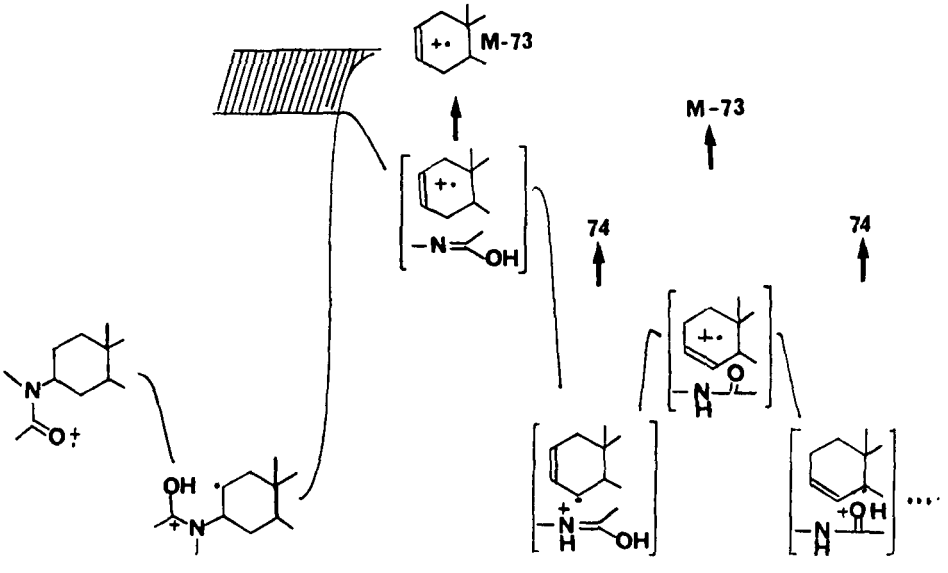

Scheme 2. Qualitative potential energy profile for the decomposition of a steroidal acetamide under electron impact.

PHOTOELECTRON SPECTROSCOPY OF THE NEGATIVE IONS TeH^- AND TeO^-

C. B. Freidhoff, J. V. Coe, J. T. Snodgrass, K. M. McHugh, and K. H. Bowen
Johns Hopkins University, Department of Chemistry, Baltimore, MD 21218

We have employed a negative ion photoelectron spectrometer to record the spectrum of TeH^- and TeO^-. Negative ion photoelectron spectroscopy is conducted by crossing a mass-selected beam of negative ions with a fixed-frequency, intracavity beam from an argon ion laser and energy analyzing the resulting photodetached electrons. Both spectra were recorded with 2.540 eV photons.

TeH^- was produced in a cold-cathode discharge source using an oven at ~500°C to vaporize Te into the anode and Ar or H_2 as a discharge support gas. The photoelectron spectrum is shown in Figure 1. The three peaks are due to the simultaneous photodetachment of both Te^- and TeH^-. Both ions are present in the mass-selected beam due to the wide isotopic pattern of Te and the available resolution of our mass filter. Peaks A and B arise from the well-known transitions of Te^-:[1] $Te(^3P_{0,1}) \longleftarrow Te^-(^2P_{3/2})$ and $Te(^3P_{0,1}) \longleftarrow Te^-(^2P_{1/2})$, respectively. Peak C is a transition not seen before and is not attributable to Te^- and is assigned to TeH^-. The use of H_2, instead of Ar, as the discharge support gas increases the ratio of the intensities of peak C to B by a factor of two, while the ratio of peak B to A was unaffected. The extra electron in TeH^- is believed to occupy a non-bonding orbital, as has been found in OH^-, SH^-, and SeH^-.[2-4] The electron affinity of TeH was determined to be 2.102±0.015 eV and the dissociation of TeH^- into Te^- and H was estimated to be 2.0 eV. The electron affinities of the Group VIB atoms, hydrides, and halogens are presented in Table 1. In each case, the electron affinity (EA) of the hydrides more closely resemble the EA of its Group VIB atom than it does the EA of the isoelectronic halogen, as predicted by Cade.[5] In addition, the EA of the hydrides are found to approach the EA of their Group VIB atom more closely as one proceeds down the VIB column of the periodic table.

TeO^- was produced in a hot-cathode discharge source which employed two filaments-one to produce a plasma from the support gas and oxygen source N_2O, and the other to vaporize Te into the plasma. The photoelectron spectrum of TeO^- is presented in Figure 2. The analysis of this spectrum was complicated by the large triplet splitting found in the neutral TeO. This splitting was measured to be 789 cm^{-1} by Winters, et. al.,[6] and is very close to the $\Delta G_{1/2} \cong 790$ cm^{-1} for both states. This causes the vibrational level 'v' of the upper state to lie within a few wavenumbers of the vibrational level 'v+1' of the lower state. Since our analyzer's resolution is 30 meV(240 cm^{-1}), the transitions are unresolved. The two split states are also not equally degenerate, so that transitions to the upper($X1^{\pm}$) state are twice as strong as those to the lower($X0^+$) state. Because of these complications, a computer modeling was used to analyze the spectrum. This analysis assigned peak C as containing the transition $TeO(X0^+(v=0)) \longleftarrow TeO^-(X3/2(v=0))$. The EA of TeO was determined to be 1.697±0.022 eV. The following negative parameters were determined: $\omega_e''(TeO^-)$= 690±80 cm^{-1}, $r_e''(TeO^-)$= 1.884±0.028 Å, and $D_0(TeO^-)$= 3.63±0.15 eV. The EA of the Group VIB monoxides, atoms and hydrides are presented in Table 1. Like the hydrides, the

electron affinity of the monoxides EA(XO) approaches the electron affinity of the heavier VIB atom EA(X) as one proceeds down the Group VIB column. This reflects, in both diatomic series, the decreasing influence of the extra electron on the bonding of these diatomic negative ions.

Table 1. ELECTRON AFFINITIES
(All values in eV.)

Group VIB monoxides[8]	Group VIB atoms[9]	Group VIB hydrides[8]	Group VIIB atoms[9]
O_2(0.440)	O(1.462)	OH(1.828)	F(3.399)
SO(1.126)	S(2.077)	SH(2.317)	Cl(3.615)
SeO(1.456)[10]	Se(2.021)	SeH(2.21)	Br(3.364)
TeO(1.697)[11]	Te(1.971)	TeH(2.102)[11]	I(3.059)

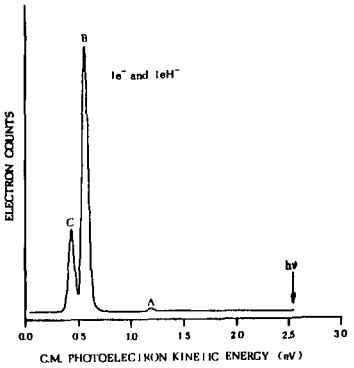

FIGURE 1

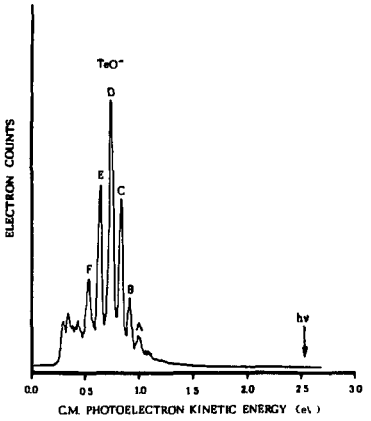

FIGURE 2

1. J. Slater and W.C. Lineberger, Phys. Rev. A 15, 2277(1977).
2. P.A. Shulz, R.D. Mead, P.L. Jones and W.C. Lineberger, J. Chem. Phys. 77, 1153(1982).
3. F. Breyer, P. Frey and H. Hotop, Z. Phys. A 300, 7(1981).
4. K.C. Smyth and J.I. Brauman, J. Chem. Phys. 56, 5993(1972).
5. P.E. Cade, Proc. Phys. Soc. 91, 872(1967).
6. R. Winter, I. Barnes, E.H. Fink, J. Wildt and F. Zabel, J. Mol. Struct. 80, 75(1982).
7. K.P. Huber and G. Herzberg, Molecular spectra and molecular structure. IV. Constants of diatomic molecules(Van Nostrand Reinhold, New York, 1979).
8. P.S. Drzaic, J. Marks and J.I. Brauman, in Gas-Phase Ion Chemistry, edited by M.T. Bowers (Academic, New York, 1984), Vol.3.
9. R.D. Mead, A.E. Stevens and W.C. Lineberger, in Gas-Phase Ion Chemistry, edited by M.T. Bowers (Academic, New York, 1984), Vol. 3.
10. J.V. Coe, J.T. Snodgrass, C.B. Freidhoff, K.M. McHugh and K.H. Bowen, J. Chem. Phys. 84, 618(1986).
11. Values determines in this work.

EXPERIMENTAL AND THEORETICAL CHARACTERIZATION OF AN ION-NEUTRAL COMPLEX-MEDIATED REACTION, CH_4 ELIMINATION FROM $CH_3OCH(CH_3)_2$

Larry L. Griffin,[a] John C. Traeger,[b] Charles E. Hudson and David J. McAdoo
[a]Texas A&M University, Galveston, Texas, [b]Chemistry Department, LaTrobe University, Bundoora, Victoria 3083, Australia and [c]Marine Biomedical Institute, University of Texas Medical Branch, Galveston, TX. 77550

Competition between methane elimination and methyl loss from ionized isopropyl methyl ether (1) were characterized to improve our understanding of the dynamics of ion-neutral complex-mediated dissociations. The suggested decomposition mechanism of $CH_3\overset{+}{O}CH(CD_3)CH_3$ is given in Scheme I.

Scheme I

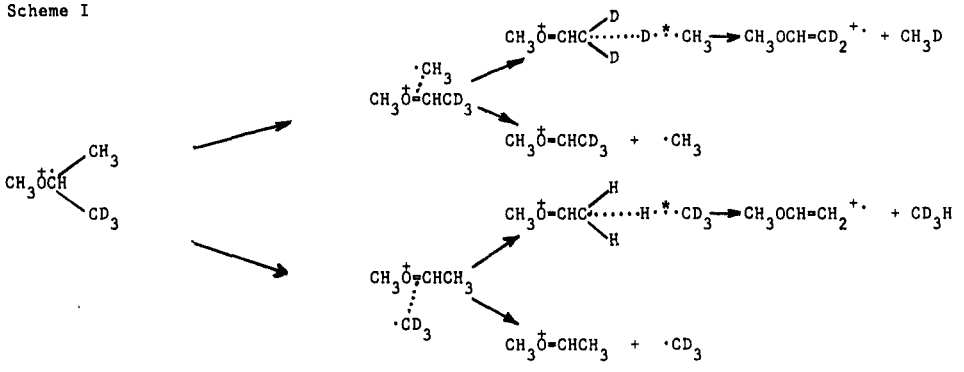

Metastable and collision-induced decomposition spectra of 1 and several labeled forms thereof are given in Table 1.

Table 1. Metastable Spectra of Ionized Methyl Isopropyl Ether

Ion	mode	Species Lost						
		CH_3	CH_4	CH_3D	CHD_2	CH_2D_2	CD_3	CHD_3
$CH_3\overset{+}{O}CH(CH_3)_2$ (1)	U	3[a]	97					
$CD_3\overset{+}{O}CH(CH_3)_2$ (1a)	U	4[a]	96					
	C	100	<0.3[b]					
$CH_3\overset{+}{O}CH(CD_3)CH_3$ (1b)	U	23[a]		16				61
	C	70	<0.07[b]	<0.04[b]			30	0.03[b]
$CH_3\overset{+}{O}CH(CHD_2)$ (1c)	U				6	91		3
	C				100	<0.6[b]		

Data are based on peak areas. U - unimolecular, C - collision induced.
[a]Corrected for a collision-induced contribution. [b]Corrected for unimolecular contributions.

The unimolecular CD_3 loss was at most 2% of the unimolecular CH_3 loss, demonstrating a very strong secondary isotope effect on methyl loss. This effect persisted to fairly high energies, as 1b lost more than twice as much CH_3 as CD_3 upon collision, and $-CH_3$ was 2.2 times more intense than $-CD_3$ at a photon energy 1.0 eV above threshold. However, the photon impact derived thresholds for $-CH_3$ and $-CD_3$ from 1b were identical (Table 2). Differences in angular momentum in the transition state, predicted densities of states of the products, or cross sections for the two decompositions were rejected as possible sources of this isotope effect. Thus it appears to defy conventional explanation. The ratio $-CH_2D_2/-CH_3D$

= 30 for 1b, demonstrating the additional presence of a strong primary isotope effect. According to previous interpretations,[1] the presence of both types of isotope effects indicates that the transition states for bond scission and hydrogen abstraction are very close in energy.

Table 2. Photoionization Appearance Energies from Methyl Isopropyl Ethers.

	IE (eV)	Neutral Fragments			
		CH_3	CH_4	CD_3	CD_3H
1	9.50	9.71	9.69		
1a	9.49	9.68	9.66		
1b	9.49	9.68		9.68	ca 9.7[a]

[a]It was impossible to obtain precise onsets for the CH_3D and CD_3H losses from 1b due to a poor signal to noise ratio.

The difference between the thresholds for the methyl and methane losses was only 0.02 eV, validating the conclusion drawn from the isotope effects that transition state energies for bond cleavage and hydrogen abstraction are very close. This is also consistent with the hypothesis that C-C bond cleavage is common to both. The PI curves for methane loss plateau 0.2-0.3 eV above threshold, confirming that methane elimination from 1 occurs over a limited energy range.

Ion molecule reactions change from complex-mediated to direct dynamics with increasing relative translational energy of the reactants. Dynamics are considered to be direct when the reactants are in close proximity for less than one rotational period.[2] Adapting this criterion to the present situation by assuming that methane loss requires partial rotation of $CH_3O{=}CHCH_3^+$ in the complex leads to the conclusion that the methane loss diminishes as dissociation becomes direct, i.e. within 0.2 to 0.3 eV of threshold.

According to theory, a complex can be defined as a region of high probability from which the system can either return to reactants through a flux bottleneck, or can proceed to products.[3] In ionic fragmentations, flux bottlenecks occur when the incipient fragments begin to rotate freely, and at the centrifugal barrier.[4] We believe that the complexes we are studying exist between these two bottlenecks.[5]

1. C.E. Hudson and D.J. McAdoo, Int. J. Mass Spectrom. Ion Proc. 59, 325 (1984).
2. B.H.Mahan, Acc. Chem. Res. 1, 217 (1968).
3. W.H. Miller, J. Chem. Phys. 65, 2216 (1976).
4a. M.T. Bowers, M.F. Jarrold, W. Wagner-REdeker, P.R. Kemper and L.M. Bass, Faraday Disc. Chem. Soc. 75, 57 (1983. b. J.A. Dodd, D.M. Golden and J.I. BRauman, J. Chem. Phys. 80, 1894 (1984).
5. C.E. Hudson and D.J. McAdoo, Proceedings of the Annual Conference on Mass Spectrometry and Allied Topics, San Diego, CA., 1985m p. 928.

ENERGY RANGES OF ION-NEUTRAL COMPLEX FORMATION: ALKANE ELIMINATIONS FROM IONIZED KETONES

John C. Traeger, Charles E. Hudson and David J. McAdoo, Department of Chemistry, LaTrobe University, Bundoora, Victoria, 3083 Australia and Marine Biomedical Institute, University of Texas Medical Branch, Galveston, Texas 77550

Low energy alkane eliminations from gaseous ions appear to take place through ion-neutral complexes.[1] Non-polar neutrals would be held in such complexes by ion-induced dipole attractions, so complex stability should vary with the polarizability of the neutral and the way charge is distributed in the ion. We characterized alkane eliminations from ketone ions,[2] proposed to occur as follows, to test this prediction.

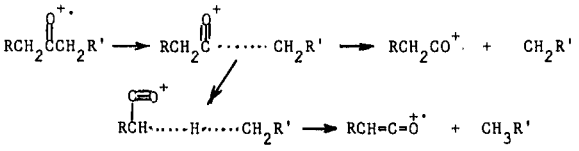

Ketone metastable spectra are given in Table 1. Each spectrum is dominated by loss of an alkyl by α-cleavage or the corresponding alkane. Photoionization efficiency curves

Table 1. Metastable Decomposition Patterns of Ionized Ketones

RC(=O)R'	-R	-RH
$CH_3C(=O)CH_3$	9[a,b]	100
$CH_3C(=O)CH_2CH_3$	100	6
$CH_3C(=O)CH(CH_3)_2$	100	1
$CH_3CH_2C(=O)CH_2CH_3$	17[a]	100
$CH_3CH_2C(=O)CH(CH_3)_2$	4[a]	14
$(CH_3)_2CHC(=O)CH_2CH_3$	3[a]	100
$(CH_3)_2CHC(=O)CH(CH_3)_2$	4[a]	100
$CH_3CH_2C(=O)C(CH_3)_3$	100	<0.5

a. Largely collision induced b. Run on a Kratos MS 50DA mass spectrometer

were determined to define the energy ranges over which ion-neutral complex formation is important. Results and pertinent thermochemical data are given in Table 2.

Table 2. Thermochemical Data (kJ mol^{-1}, 298 K)

RC(=O)R[1]	Predicted Threshold -R	Predicted Threshold -RH	Observed Threshold -R	Observed Threshold -RH
$CH_3C(=O)CH_3$	1002.2	1006.6	1001.5	1001.5
$CH_3C(=O)CH_2CH_3$	957.2	926.6	955.2	
$CH_3C(=O)CH(CH_3)_2$	953.3	853.5	953.3	
$CH_3CH_2C(=O)CH_2CH_3$	945.1	933.0	946.5	933.0
$CH_3CH_2C(=O)CH(CH_3)_2$	947.4	866.0	947.5	927.2
$(CH_3)_2CHC(=O)CH_2CH_3$	929.1	937.5	931.1	930.1
$(CH_3)_2CHC(=O)CH(CH_3)_2$	928.8	868.0	930.1	895.4

Curves for alkyl losses rise steadily over the energy range examined, whereas the curves for the alkane eliminations reach a plateau a few tenths of an eV above threshold. The difference between the onsets of the plateaus and crossover points and the threshold for the R loss are given in Table 3. These serve as measures of the competition between the two fragmentations.

Table 3. Energies (kJ mol^{-1}) Required to Reach the -R/-RH Crossover Points and Plateaus in the -RH Curves

RC(=O)R'	Crossover Point	Plateau Onset
$CH_3C(=O)CH_3$	0	15
$CH_3CH_2C(=O)CH_2CH_3$	60	50
$CH_3CH_2C(=O)CH(CH_3)_2$	25	50
$(CH_3)_2CHC(=O)CH_2CH_3$	120	70
$(CH_3)_2CHC(=O)CH(CH_3)_2$	110	70

Comparison of the values in Table 3 for ionized acetone, 3-pentanone and 2,4-dimethyl-3-pentanone shows that the energy range over which alkane elimination takes place and its ability to compete with the corresponding alkyl loss increases with the size of the neutrals lost. Polarizabilities of free radicals should increas with size, the energy range over which alkane elimination is significant increases with the polarizability of the radical in the complex. When the size of the ion accompanying a given radical increases, the energy range over which complex formation takes place decreases. We attribute this to an increasing distance between the charge center and the neutral in the complex and/or to the distribution of charge over more atoms in the ion. We believe the decreasing ability to form complexes with increasing size of the ion accounts for the dominant elimination of methane from ionized acetone, and very weak methane elimination the 2-butanone and 3-methyl-2-butanone ions. There is no other apparent reason why the missing alkyl eliminations do not occur.

1. C.E. Hudson and D.J. McAdoo, Int. J. Mass Spectrom. Ion Proc. 59, 325 (1984).
2. R.G. Cooks, A.N.H. Yeo and D.H. Williams, Org. Mass Spectrom. 2, 985 (1969). S.Hammerum, K. Donchi and P.J. Derrick, Int. J. Mass Spectrom. Ion Phys. 47, 347 (1983).

ION NEUTRAL COMPLEXES AS INTERMEDIATES IN FORMATION OF "MCLAFFERTY +1" ($CH_3CO_2H_2^+$) IONS FROM $C_5H_{10}O_2^{+\cdot}$ ISOMERS

Charles E. Hudson[a], Lawrence L. Griffin[b], Ellen Broido[a], Mark D. Skyiepal[b] and David J. McAdoo[a] a. University of Texas Medical Branch, Galveston, Texas 77550 b. Texas A&M University, Galveston, Texas 77553

"McLafferty +1 ions" (one mass unit heavier than the ion formed by McLafferty rearrangement) are a common feature of spectra of higher carbonyl compounds, but despite extensive investigation, their formation has never been adequately explained. The metastable ion spectra of several $C_5H_{10}O_2^{+\cdot}$ ions (Table I) shows that the "McLafferty +1 ion" (C_3H_5 loss) is exhibited in those ions that also show a C_2H_4 loss

Table I. Metastable Ion Spectra of $C_5H_{10}O_2^{+\cdot}$

Ion	$-C_3H_5$	$-C_2H_5$	$-C_2H_4$	$-CH_3$
$(CH_3)_2CHCH_2CO_2H^{+\cdot}$	60	1	27	11
$CH_3CH_2CH_2CH_2CO_2H^{+\cdot}$	14	26	5	55
$\dot{C}H_2C(=OH)OCH(CH_3)_2^{+\cdot}$	86	1	12	1
$C_2H_5CH(CH_3)CO_2H^{+\cdot}$	<2	26	<2	74
$(CH_3)_3CCO_2H^{+\cdot}$	<1	2	<1	98
$C_2H_5\dot{C}(CH_3)CO_2H_2^{+\cdot}$	2	33	2	67
$(CH_3)_2CH\dot{C}HCO_2H_2$	<1	8	<1	92

This suggests that the C_2H_4 and C_3H_5 losses stem from common intermediates.

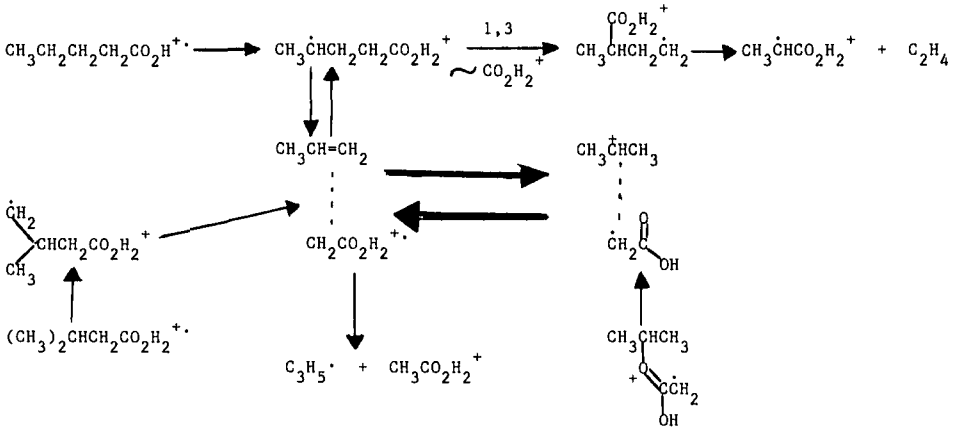

Where the dashed line indicates an ion neutral complex held together by ion dipole and ion induced dipole forces. This scheme is consistent with the finding that 3-methyl-butanoic acid 2,2-d_2 loses $C_2H_2D_2$ in 99% of its ethylene losses and that the other two hydrogens in the ethylene lost stem from the carboxyl and methyl hydrogens in nearly statistical proportions. Table II compares the predictions of the scheme to the observed ethylene losses from ^{13}C labelled pentanoic acids.

Fraction of $^{13}CCH_4$ Lost From Pentanoic Acids

C	1	2	3	4	5
Prediction	0	100	50	0	50
Observed	0[2]	97[2]	52,38[2]	3	

The predictions of the scheme are compared with the observed fragmentations for isotopically labelled forms of the isopropyl acetate enol ion

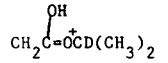

	$-C_3H_5$	$-C_3H_4D$	$-C_2H_4$	$-C_2H_3D$
Observed	2	98	97	3
Predicted	0	100	100	0

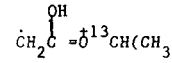

	$-C_3H_5$	$-^{13}CC_2H_5$	$-C_2H_4$	$-^{13}CCH_4$
Observed	2	98	94	6
Predicted	0	100	100	0

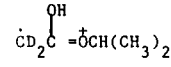

	$-C_3H_5$	$-C_3H_4D$	$-C_3H_3D_2$	$-C_2H_4$	$-C_2H_3D$	$-C_2H_2D_2$
Observed	99	1	-	10	6	85
Predicted	100	0	0	0	0	100

The substantial agreement between the predicted and observed ion abundances lends credence to the notion of ion dipole and ion induced dipole complexes reacting in well understood ways such as by Markovkikov addition or allylic abstraction from an alkene.

(1) H.E. Audier and G. Sozzi, Org. Mass Spectrom. 19, 150 (1984).
(2) H.E. Audier and G. Sozzi, unpublished results.

Acknowledgements. We are grateful to the Midwest Center for Mass Spectrometry for use of their instruments and to H.E. Audier and G. Sozzi for sharing their data with us prior to publication.

ION/MOLECULE COMPLEXES AS INTERMEDIATES OF THE FRAGMENTATION OF PROTONATED ARYL KETONES

Hans-Fr. Grützmacher and Ulrich Filges
Fakultät für Chemie, Universität Bielefeld
D-4800 BIELEFELD, Universitätsstraße, West Germany

Protonated aryl aldehydes (1-4, R=H) and aryl ketones (1-4, R=CH_3) are formed by EI-induced fragmentations of appropriately substituted aryl alcohols. This ensures that the proton resides initially at the carbonyl group. These protonated aromatic carbonyl compounds decompose as metastable ions (2nd FFR of a VG ZAB 2F mass spectrometer) mainly via three reactions shown in scheme 1.

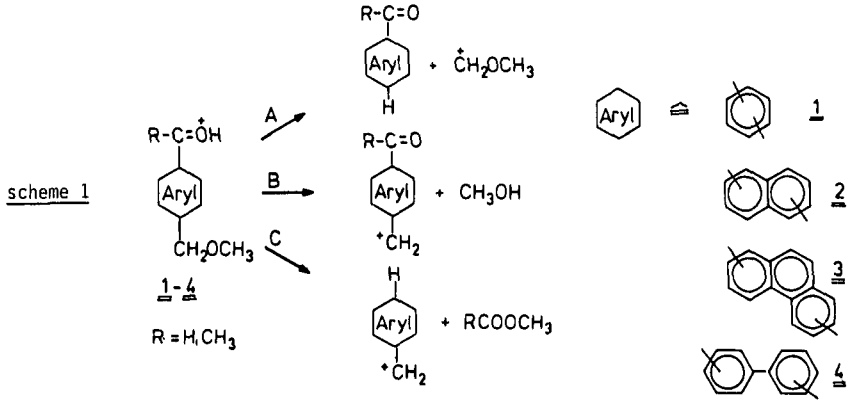

Reactions A and B can be understood by a "conventional" fragmentation mechanism via proton migration from the carbonyl group onto the aromatic ring(s) and across the aromatic system to the ether O-atom of the methoxymethyl side chain (scheme 2). This latter intermediate leads to elimination of CH_3OH (reaction B) while protonation of the aromatic ring at the ipso-position of the side chains results in the formation of the $CH_3\overset{+}{O}=CH_2$ ions (reaction A) and in some cases to the formation of RCO^+ ions.

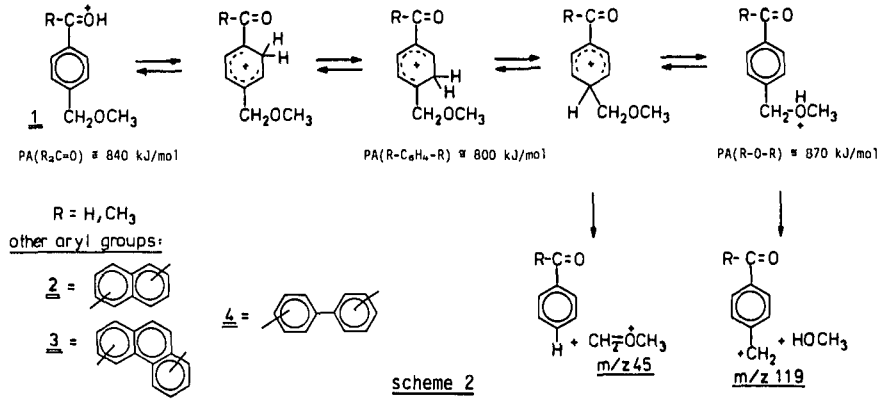

These mechanisms are proven by H/D exchange preceding the elimination of $CH_3O(H,D)$ via reaction B in deuterated analogues of 1 and 2. It is shown that the H- and D-atoms bound to the O-atom of the carbonyl group and to the aromatic ring(s), respectively, participate specifically in the exchange reactions. However, no complete H/D-scrambling involving these positions is observed but preferential loss of the H-atom originally bound to the carbonyl group. Thus, proton migration across the aromatic rings takes place not only by 1.2-H-shifts of σ-complexes but also by π-complexes.

Reaction C involves specifically the groups RCO and OCH_3, respectively, of the two distal side chains as shown by the decompositions of deuterated derivatives although some exchange between R = H,D and H- or D-atoms at the aromatic system is observed. The only mechanism in agreement with the experimental results is the formation of an acylium ion/aromatic ether complex formed by a collapse of the σ- or π-complex (scheme 3).

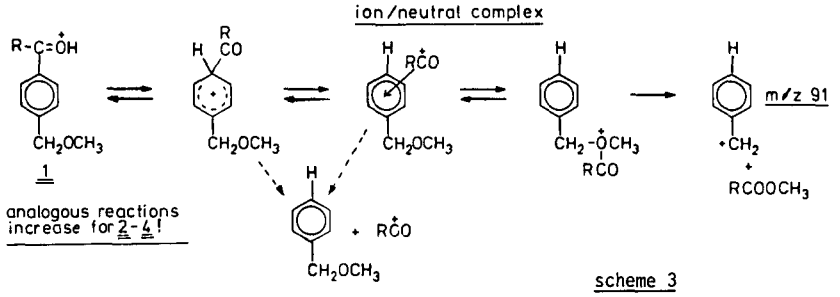

scheme 3

Stabilisation energy E_s = 186 kJ/mol (benzene derivative, r = 3 A)
230 kJ/mol (naphthalene derivative, r = 3 A)
290 kJ/mol (phenanthrene derivative , r = 3 A)

The acylium ion $RC\overset{+}{O}$ can obviously move rather easily and migrate from one benzene ring to the other in 2 and 3 (planar systems) or in 4 (non-planar system). It is directed towards the methoxy group of the side chain by the ion/dipol attractions of the polar C-O bonds and eventually eliminated as an ester molecule. The relative abundance of reaction C increases in the series 1 - 3 as does the stabilization energy of the corresponding ion/neutral complex.

The reactions of the protonated aryl aldehydes and ketone show clearly that intermediate ion/neutral complexes are very important for the unimolecular fragmentations of metastable ions and that the reactions within these complexes can determine the fate of the low energy ions.

HEAT OF FORMATION FOR THE 1-METHYLALLYL CATION BY PHOTOIONIZATION MASS SPECTROMETRY

John C. Traeger

Department of Chemistry, La Trobe University,
Bundoora, Victoria 3083, AUSTRALIA.

The $C_4H_7^+$ cation is known to have a number of stable isomeric structures in the gas phase,[1] the lowest energy form being the trans-1-methylallyl structure. A number of thermochemical studies have been made of this ion, with recent experimental heats of formation ranging from 876 kJ mol^{-1} to 833 kJ mol^{-1}.[2,3] Ionization studies of the free radical provide a heat of formation near 850 kJ mol^{-1}, although this is dependent on the value assumed for the radical heat of formation.[4,5]

In this work, $C_4H_7^+$ appearance energies have been measured by dissociative photoionization mass spectrometry for a series of organic compounds. For the process $C_4H_7X + h\nu \rightarrow C_4H_7^+ + X + e^-$ the 298 K cationic heat of formation is given by the thermochemical expression[6]

$$\Delta H^\circ_{f_{298}}([C_4H_7]^+) = AE_{298} + \Delta H^\circ_{f_{298}}(C_4H_7X) - \Delta H^\circ_{f_{298}}(X) + \Delta H_{corr}$$

where the stationary electron convention for cationic heats of formation has been adopted.[6]

The thermal energy correction term, ΔH_{corr}, is derived from statistical mechanical calculations and depends on a knowledge of the vibrational frequencies for the photoionization products. Although such experimental information is readily available for the neutral products formed in this study, it was necessary to make an estimation for the 1-methylallyl cation. This was done by an ab initio molecular orbital calculation using the GAUSSIAN 82 suite of programs,[7] which included a geometry optimization at the 3-21G level.

From the AE's and associated thermochemical data for the nine unimolecular reactions studied an average $\Delta H_f(C_4H_7^+)$ of 870.5±2.9 kJ mol^{-1} is calculated. For all reactions there is a competing fragmentation process at or near the $C_4H_7^+$ AE; the C_4H_8 isomers readily lose CH_3 whereas the C_5H_{10} isomers all undergo loss of C_2H_4. When the observed AE's for these processes are compared with the known thermochemistry for $C_3H_5^+$ and $C_3H_6^{+\cdot}$ formation it is apparent that a significant proportion of the above 2.9 kJ mol^{-1} error is associated with the neutral precursor heats of formation. If these are modified so that the calculated $C_3H_5^+$ and $C_3H_6^{+\cdot}$ heats of formation agree with the literature values[8] a revised

set of $C_4H_7^+$ heats of formation may be calculated (Table I). From this, a value of 870.0±0.5 kJ mol^{-1} is obtained for the 1-methylallyl cation heat of formation at 298 K. This may be used in conjunction with the radical adiabatic ionization energy of 7.49 eV[5] (a value substantiated by the present vibrational frequency calculations) to derive a 298 K heat of formation of 148.3±2.4 kJ mol^{-1} for the 1-methylallyl radical.

Table I. Thermochemistry for the gas-phase reaction at 298 K

$$C_4H_7X + h\nu \rightarrow C_4H_7^+ + X + e^-$$

C_4H_7X	X	IE (eV)	AE (eV)	ΔH_{corr} (kJ/mol)	$\Delta H^\circ_{f_{298}}$ (kJ/mol)		
					C_4H_7X	X	$C_4H_7^+$
1-butene	H	9.57	11.13	16.4	-2.7	218.0	869.6
2-methyl propene	H	9.19	11.26	16.4	-15.2	218.0	869.6
cis-2-butene	H	9.13	11.19	16.4	-7.5	218.0	870.6
trans-2-butene	H	9.09	11.24	16.4	-12.3	218.0	870.6
cyclopentane	CH_3	10.35	11.08	20.6	-75.6	143.9	870.2
2-methyl-1-butene	CH_3	9.10	10.66	20.6	-35.1	143.9	870.2
2-methyl-2-butene	CH_3	8.69	10.80	20.6	-48.6	143.9	870.2
cis-2-pentene	CH_3	9.02	10.62	20.6	-31.2	143.9	870.2
1-pentene	CH_3	9.50	10.50	20.6	-20.6	143.9	869.2

References

(1) Schleyer, P.v.R.; Dill, J.D.; Pople, J.A.; Hehre, W.J. Tetrahedron **1977**, 33, 2497-2501.

(2) Brand, W.A.; Baer, T. J. Am. Chem. Soc. **1984**, 106, 3154-3160.

(3) Aue, D.H.; Bowers, M.T. In 'Gas Phase Ion Chemistry'; Bowers, M.T., Ed., Academic Press: New York, 1979; Vol. II, Chapter 9.

(4) Lossing, F.P. Can. J. Chem. **1972**, 50, 3973-3981.

(5) Schultz, J.C.; Houle, F.A.; Beauchamp, J.L. J. Am. Chem. Soc. **1984**, 106, 7336-7347.

(6) Traeger, J.C.; McLoughlin, R.G. J. Am. Chem. Soc. **1981**, 103, 3647-3652.

(7) Binkley, J.S.; Frisch, M.J.; DeFrees, D.J.; Raghavachari, K.; Whiteside, R.A.; Schlegel, H.B.; Fluder, E.M.; Pople, J.A. Carnegie-Mellon University, Pittsburgh, PA, 15213.

(8) Traeger, J.C. Int. J. Mass Spectrom. Ion Processes **1984**, 58, 259-271.

ELECTRON AFFINITIES OF COMPOUNDS M AND PRESENCE OF M^- AND CLUSTERS OF M^- IN NEGATIVE ION CHEMICAL IONIZATION

S. Chowdhury and P. Kebarle,
Department of Chemistry,
University of Alberta,
Edmonton, Alberta,
Canada T6G 2G2

A fundamental property of a negative ion is the lowest energy required to remove an electron. Thus for the reaction $M^- \rightarrow M + e$, ΔH^o = electron affinity, EA of M. The ion molecule equilibrium method was applied for the determination of electron affinities using the electron transfer equilibria (1)

$$M_1^- + M_2 \rightleftharpoons M_1 + M_2^- \qquad (1)$$

Determinations of equilibrium constants K_1 at different temperatures provide, via van't Hoff plots, ΔH_1^o and ΔS_1^o, where ΔH_1^o is given by equation (2)

$$\Delta H^o{}_1 = EA(M_1) - EA(M_2) \qquad (2)$$

An interconnecting scale of ΔH_1^o for different M can thus be constructed and electron affinities of all compounds in the scale can be obtained by anchoring to the known electron affinity of a standard. Electron affinities of about 100 molecules were obtained [1-3]

Stable negative ions observed at 150°C for compounds having EA > 0.5 eV. For lower electron affinity compounds rapid thermal electron detachment destroys the ions. The thermal electron detachment rate and its temperature dependence could also be measured [4].

At lower temperature the ions M^- were found to form clusters, $M^-{\bullet}M$ with M or $M^-{\bullet}Sl$ with solvent molecules. The equilibria (3) involving substituted nitrobenzenes and quinones as M and CH_3OH, CH_3CN,

$$M^- + Sl = M^-{\bullet}Sl \qquad (3)$$

$(CH_3)_2SO$, $(CH_3)_2NCOH$, and THF as solvent molecules Sl, were measured in a pulsed electron beam mass spectrometer in chemical ionization condition with time resolved analysis. The bond energy was found to decrease with increasing electron affinity of M. Since higher EA of M is achieved through conjugation of the charge in M^-, bond energy decreases with increasing EA of M. This is an expected effect (Fig. 1). The decrease of bond energy is more rapid for the protic solvent, CH_3OH than for the dipolar aprotic solvent, CH_3CN. This is atttributed to the different location of the dipoles on the protic and aprotic Sl molecules.

However the bond energies obtained for $M^-{\bullet}M$ is found to have no apparent relationship with the EA(M) (Fig. 2). In general the bond energy in $M^-{\bullet}M$ is higher for compounds M with higher dipole moments. A comparison was also made with the $-\Delta H^o(NO_2^-{\bullet}M)$ and $-\Delta H^o(2\text{-}NO_2NB^-{\bullet}M)$ where NB = nitrobenzene and a linear relationship was obtained which shows that these bondings are similar, however the latter is weaker. This is probably due to the more charge delocalization in $2\text{-}NO_2NB^-$ than in NO_2^-.

[1] E. P. Grimsrud, G. Caldwell, S. Chowdhury and P. Kebarle, J. Am. Chem. Soc., **107** (1985) 4627.

[2] E. P. Grimsrud, S. Chowdhury and P. Kebarle, J. Chem. Phys. **83** (1985) 1059.

[3] S. Chowdhury, E. P. Grimsrud, T. Heinis and P. Kebarle, J. Am. Chem. Soc. (in press).

[4] E. P. Grimsrud, S. Chowdhury and P. Kebarle, J. Chem. Phys. **83** (1985) 3983.

Figure Captions

Figure 1 Plot of ΔG^o at 70°C and ΔH^o for reaction $M^- + Sl = M^- \cdot Sl$ versus electron affinity of M. The three plots are for Sl: Me_2SO ; MeCN ; MeOH The actual M^- are identified by the number. All M^- used in the plot were substituted nitrobenzenes XNB; substituent X is; 2,3-diCH_3 (#1), 3-OCH_3 (#2); 4-OCH_3(#3); 2-CH_3 (#4); 3-CH_3 (#5); 4-CH_3 (#6); H (#7); 2-F (#8); 3-F (#9); 4-F (#10); 2-Cl (#11); 3-Cl (#12); 4-Cl (#13); 3-CF_3 (#14); 2-CN (#15); 3-CN (#16); 4-CN (#17); 2-NO_2 (#18); 3-NO_2 (#19); 4-NO_2 (#20). The ΔH^o values are approximate and were obtained by assuming that ΔS^o = -25 cal/mol degree, which is an average value for ΔS^o, obtained from van't Hoff plots.

Figure 2 Plot of ΔG^o at 70°C for reaction $M^- + M = M^- \cdot M$ vrsus electron affinity of M. The substituents, X of XNB are shown by the side of the point.

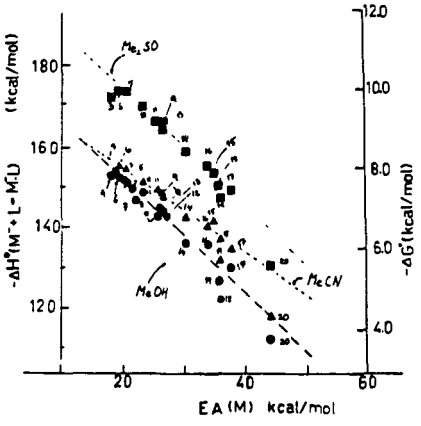

FIGURE 1

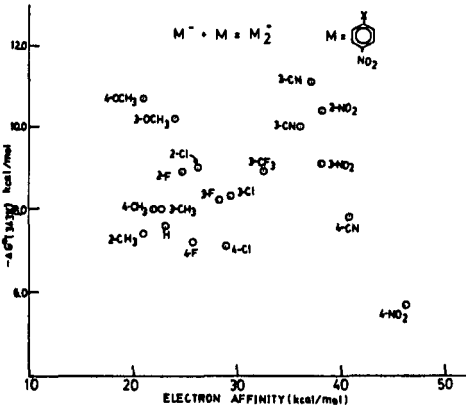

FIGURE 2

TIME-OF-FLIGHT STUDIES OF METASTABLE SECONDARY ION DECAYS

B. Schueler*, W. Ens, D.E. Main, and X. Tang
UNIVERSITY OF MANITOBA, PHYSICS DEPARTMENT, WINNIPEG, MANITOBA R3T 2N2, CANADA

The bombardment of samples by keV primary particles causes the emission of atomic and molecular secondary ions and neutrals. After the secondary molecular ions leave the primary interaction region, they may undergo metastable decays due to the energy transferred to them during the production process. We have studied the metastable ion decays of p(X)-phenylalanine derivatives (X= H, halides, OH, OCH_3) and determined the (approximate) decay pathways as well as the corresponding rate constants of some typical secondary ions.

1. Experimental

The experiments were performed with the Manitoba time-of-flight SIMS instrument [1]. A pulsed primary ion beam (t~3ns f.w.h.m.; 3-20 keV Cs+) hits the target. Secondary ions of a selected polarity are electrostatically accelerated and enter a drift region. At the end of the drift region charged parent and daughter ions are deflected by 90° by means of an electrostatic mirror into one detector. Neutral particles pass through the mirror and hit a second detector. Both detectors and mirror are mounted on a linear motion feedthrough so that the distance between target and mirror (drift path:d) can be continuously varied from 0.45m to 1.45m. An externally adjustable iris in front of the mirror assures a constant acceptance angle for different target-mirror distances.

2. Fragment ions

If a secondary ion undergoes fragmentation in the drift path, the centre-of-mass velocity remains unchanged. The kinetic energy, however is shared between the fragments according to their masses. Due to its reduced kinetic energy a fragment ion will penetrate the mirror less deeply and therefore reach the detector earlier than its parent ion. This allows for the approximate determination of the fragment ion mass.

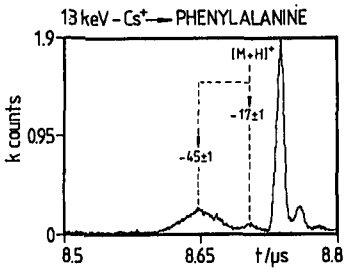

Fig. 1: Parent $[M+H]^+$ and its metastable decay signals in phenylalanine.

The secondary ion fragmentation pathways have been determined for the quasimolecular ions $[M+H]^+$, $[M-45]^+$ and the cluster ions $[2M+H]^+$ of the above compounds. For $[M+H]^+$ ions from phenylalanine (Fig. 1) and its halogenated derivatives the major decay paths are due to loss of $[45\pm1]$u accompanied by a weaker signal due to loss of $[17\pm1]$u. The intensities are reversed for tyrosine and methoxy-phenylalanine. All $[2M+H]^+$ cluster ions were found to decay by loss of one neutral molecular unit[M]. The $[M-45]^+$ secondary ions of the halogenated compounds and methoxyphenylalanine were observed to decay by loss of the p(X) - substituent. The corresponding pathways for phenylalanine and tyrosine could not be unambiguously identified.

3. Rate constants

A secondary ion(p) can only be detected at its original mass if it survives until after the deflection period in the mirror. The experimental evaluation of the relative parent ion yields for different target-mirror distances d and hence different survival time t(d) enables the determination of the first order rate constant k_1 since the above ratio is $\sim\exp(-k_1 t)$.

Fig. 2 shows the dependence of $y(t)/y(Na^+)$ on the survival time of the parent ions (as measured for different d) emitted from methoxyphenlalanine. Fig. 3 shows the evaluated rate constants of some secondary ions from same p(X)-phenylalanine derivatives (X=I,H,OH, OCH_3). The experimental error is ~±20%.

*also: Charles Evans & Associates, 301 Chesapeake Dr., Redwood City, CA 94063

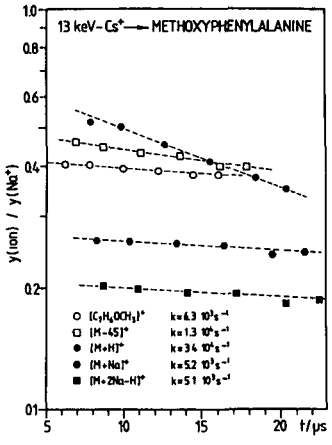

Fig. 2: Parent ion yields (y(ion)) vs. survival time as given by the target-mirror distance for methoxyphenylalanine. All yields are normalized to the sodium ion yield $y(Na^+)$.

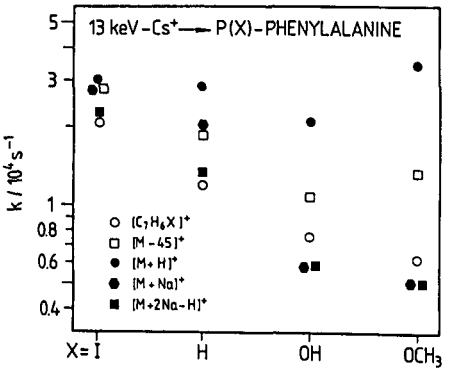

Fig. 3: First order rate constants k for some metastable secondary ions from p(X)-phenylalanine derivatives.

4. Dependence of the rate constants on the primary ion energy loss

The rate constants for the decays of $[M+H]^+$, $[M+Na]^+$, $[M+2Na-H]^+$ $[M-45^+]$ and the tropylium ion from phenylalanine were measured using E_p 3, 8 and 13 keV-Cs^+ primary ions. The corresponding primary ion energy losses are ~ 53, 81 and 97 eV/Å, respectively. Although the secondary ion yields increased by factors ~ 5 and the ratios of quasimolecular / fragment ions (e.g. $[M+H]^+$ / $[M-45]^+$ etc.) decreased for increasing E_p the measured rate constants were found to be constant within experimental error[Fig. 4,5].

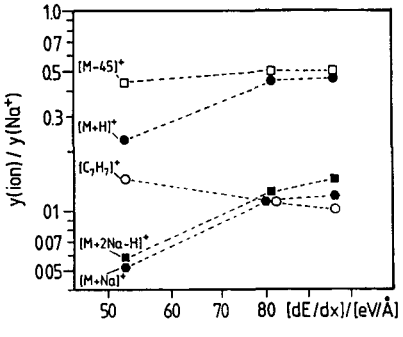

Fig. 4: Dependence of some relative secondary ion intensities from phenylalanine on the primary ion energy.

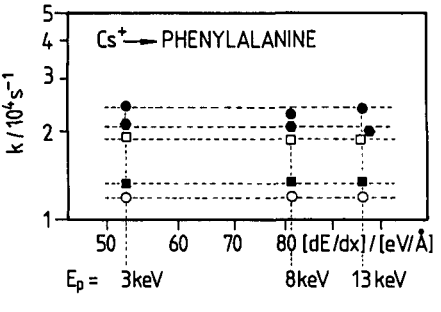

Fig. 5: Rate constants vs. energy loss of the primary ion for some secondary ions from phenylalanine (symbols as in Fig. 4).

Reference

[1] B. Schueler et.al.; Secondary Ion Mass Spectrometry SIMS-V, Springer Ser. Chem. Phys. 44, p.57 (1986)

THERMAL ENERGY CHARGE TRANSFER REACTIONS OF Ar^+ AND Ar_2^+

R. Passarella, R.J. Shul, B.L. Upschulte, R.G. Keesee, and A.W. Castleman, Jr., Department of Chemistry, The Pennsylvania State University, University Park, PA 16802, USA

Charge transfer reactions of Ar^+ and Ar_2^+ with a variety of neutrals were measured for the purpose of obtaining data to compare the rates of reactions of these monomer and dimer ions. The work was motivated by interest in attempting to further elucidate the important factors responsible for the rate of charge transfer reactions. Two basic theories have been proposed which include a non-adiabatic electron jump mechanism which is invisioned to occur over a relatively large distance, or a charge transfer reaction which occurs via a collision complex where the ion and neutral are in close proximity.

Experiments were performed in our laboratory with a selected ion flow tube (SIFT). This is a modification of a flowing afterglow which has a quadrupole mass filter to select a single ionic species from a remote ion source which are then injected into a flowing inert carrier gas. The ions thermalize via collision and thereafter react with a neutral gas added at an appropriate region downstream. Ions on the flow tube axis are sampled through an orifice where they are mass analyzed with a second quadrupole mass spectrometer and detected in the pulse counting mode. Rate coefficients are derived under experimental conditions where the neutral is in excess and the intensity of ion is directly proportional to concentration of the ion. Thereupon the reaction is pseudo first order and requisite rate coefficients are obtained from the slope of a semilogarithmic plot of the ion intensity versus the concentration of the neutral reactant.

In the present series of reactions the ion reacts with the neutral species which transfers an electron with a rate coefficient of k. Reactions of the monomer and dimer argon ions were investigated with the following neutrals: H_2O, SO_2, H_2S, CO_2, CH_4, SF_6, N_2O, NH_3, CS_2, NO_2, NO, CO, and O_2. No trends were found between the observed rate coefficient and the calculated coefficient in terms of the ionization potential, energy difference between the recombination energy of reactant ion and adiabatic ionization potential of product ion, dipole moment or polarizability (see Table I).

When comparing the rate coefficient of monomer and dimer, three general categories are observed as seen in Table II. These are cases where: the dimer rate is approximately 1.5 to 3 times faster than that of the monomer, the monomer rate is about 2 times faster than the dimer one, and the monomer and dimer rates are about equal. Most of the reactions studied are considered fast, i.e., $k_{obs} > 0.1$ kcal and some are even faster than the calculated collision rate based on Langevin (1) or ADO (2) theory.

In an attempt to further elucidate the mechanism for these thermal energy charge transfer reactions, the photoelectron spectra (3) for the neutral molecules are considered to determine if any energy resonance with favorable Franck-Condon factors exists at the recombination energy of Ar^+ (15.7 eV) and Ar_2^+ (14.4 eV). The consideration of these spectra led to the observation that energy resonance and Franck-Condon factors are not necessary for a fast thermal energy charge transfer reaction. However, the relative proximity of Ar^+ and Ar_2^+ recombination energy to the bands of photoelectron spectra does explain the relative rates of monomer and dimer reactions with a specific neutral. In each case, however, it was observed that the proximity of the well was the governing factor, i.e., the ionic species which lies closer to a vibrational state of the electronic well as indicated by the spectra has a faster reaction rate.

Acknowledgments:

Support by the National Science Foundation, Grant No. ATM-82-04010, is gratefully acknowledged.

Reference:

1. E. W. McDaniel, V. Cermak, A. Dalgarno, E. E. Ferguson, and L. Friedman, "Ion-Molecule Reactions," Wiley, New York (1970).

2. T. Su and M. T. Bowers, Int. J. Mass Spectrom. Ion Phys. 12, 347 (1973).

3. D. W. Turner, C. Baker, A. D. Baker, and C. R. Brundle "Molecular Photoelectron Spectroscopy," Wiley-Intersciences (1970).

Table I

Charge Transfer Reactions	k_{obs} (cc/s)	k_{cal} (cc/s)	IP(eV)	Δ energy (eV)	Dipole Moment(D)	$\bar{\alpha}(A^3)$
$Ar_2^+ + H_2O \rightarrow$ Products	1.6×10^{-9}	1.8×10^{-9}	12.6	-1.8	1.85	1.44
$Ar_2^+ + SO_2 \rightarrow SO_2^+ + 2Ar$	1.4×10^{-9}	1.3×10^{-9}	12.3	-2.1	1.63	3.70
$Ar_2^+ + H_2S \rightarrow H_2S^+ + Ar$	1.3×10^{-9}	1.4×10^{-9}	10.5	-5.2	0.97	3.83
$Ar_2^+ + CO_2 \rightarrow CO_2^+ + 2Ar$	1.3×10^{-9}	7.2×10^{-10}	13.7	-0.7	0.00	2.65
$Ar_2^+ + H_2S \rightarrow H_2S^+ + 2Ar$	1.2×10^{-9}	1.2×10^{-9}	10.5	-3.9	0.97	3.83
$Ar_2^+ + CH_4 \rightarrow$ Products	1.1×10^{-9}	1.0×10^{-9}	12.6	-1.8	0.00	2.56
$Ar^+ + H_2O \rightarrow$ Products	1.0×10^{-9}	2.0×10^{-9}	12.6	-3.1	1.85	1.44
$Ar^+ + CH_4 \rightarrow$ Products	9.5×10^{-10}	1.1×10^{-9}	12.6	-3.1	0.00	2.56
$Ar^+ + SF_6 \rightarrow SF_5^+ + F + Ar$	9.3×10^{-10}	1.1×10^{-9}	14.6	-1.1	0.00	6.54
$Ar_2^+ + N_2O \rightarrow N_2O^+ + 2Ar$	8.2×10^{-10}	7.6×10^{-10}	12.9	-1.5	1.167	2.92
$Ar^+ + NH_3 \rightarrow NH_3^+ + Ar$	8.0×10^{-10}	1.9×10^{-9}	10.2	-5.5	1.47	2.20
$Ar^+ + CO_2 \rightarrow CO_2^+ + Ar$	7.1×10^{-10}	8.3×10^{-10}	13.7	-2.0	0.00	2.65
$Ar^+ + SO_2 \rightarrow SO_2^+ + Ar$	5.4×10^{-10}	1.5×10^{-9}	12.3	-3.4	1.63	3.70
$Ar_2^+ + NH_3 \rightarrow NH_3^+ + 2Ar$	4.5×10^{-10}	1.7×10^{-9}	10.2	-4.2	1.47	2.20
$Ar_2^+ + SF_6 \rightarrow SF_5^+ + F + 2Ar$	4.2×10^{-10}	8.3×10^{-10}	14.6	+0.2	0.00	6.54
$Ar^+ + N_2O \rightarrow N_2O^+ + Ar$	3.3×10^{-10}	8.8×10^{-10}	12.9	-2.8	0.167	2.92
$Ar_2^+ + CS_2 \rightarrow CS_2^+ + 2Ar$	3.1×10^{-10}	1.1×10^{-9}	10.1	-4.3	0.00	8.73
$Ar_2^+ + NO_2 \rightarrow NO_2^+ + 2Ar$	2.8×10^{-10}	7.6×10^{-10}	9.8	-4.6	0.316	3.02
$\rightarrow NO^+ + O + 2Ar$						
$Ar^+ + NO \rightarrow NO^+ + Ar$	2.7×10^{-10}	6.6×10^{-10}	9.3	-6.4	0.153	1.70
$Ar^+ + CS_2 \rightarrow CS_2^+ + Ar$	1.6×10^{-10}	1.4×10^{-9}	10.1	-5.6	0.00	8.73
$Ar_2^+ + CO \rightarrow CO^+ + 2Ar$	1.4×10^{-10}	7.2×10^{-10}	11.4	-3.0	0.112	1.95
$Ar^+ + NO_2 \rightarrow NO_2^+ + Ar$	1.3×10^{-10}	8.9×10^{-10}	9.8	-5.9	0.316	3.02
$\rightarrow NO^+ + O + Ar$						
$Ar_2^+ + O_2 \rightarrow O_2^+ + 2Ar$	7.5×10^{-11}	6.2×10^{-10}	12.1	-2.3	0.00	1.59
$Ar_2^+ + NO \rightarrow NO^+ + 2Ar$	4.4×10^{-11}	7.4×10^{-10}	9.3	-5.1	0.153	1.70
$Ar^+ + CO \rightarrow CO^+ + Ar$	4.0×10^{-11}	8.1×10^{-10}	11.4	-4.3	0.112	1.95
$Ar^+ + O_2 \rightarrow O_2^+ + Ar$	3.9×10^{-11}	7.0×10^{-10}	12.1	-3.6	0.00	1.59

Table II

Charge Transfer Reactions	$k_{monomer}/k_{dimer}$	$k_{monomer}/k_{cal}$	k_{dimer}/k_{cal}
$Ar_n^+ + H_2O \rightarrow$ Products	0.63	0.50	0.89
$Ar_n^+ + SO_2 \rightarrow SO_2^+ + nAr$	0.39	0.38	1.1
$Ar_n^+ + CO_2 \rightarrow CO_2^+ + nAr$	0.55	0.85	1.8
$Ar_n^+ + O_2 \rightarrow O_2^+ + nAr$	0.52	0.056	0.12
$Ar_n^+ + NO \rightarrow NO^+ + nAr$	0.59	0.059	0.11
$Ar_n^+ + CS_2 \rightarrow CS_2^+ + nAr$	0.52	0.11	0.28
$Ar_n^+ + N_2O \rightarrow N_2O^+ + nAr$	0.40	0.38	1.1
$Ar_n^+ + CO \rightarrow CO^+ + nAr$	0.28	0.049	0.19
$Ar_n^+ + NO_2 \rightarrow NO_2^+ + nAr$	0.46	0.15	0.37
$\rightarrow NO^+ + O + nAr$			
$Ar_n^+ + SF_6 \rightarrow SF_5^+ + F + nAr$	2.2	0.85	0.51
$Ar_n^+ + NH_3 \rightarrow NH_3^+ + nAr$	1.8	0.42	0.26
$Ar_n^+ + H_2S \rightarrow H_2S^+ + nAr$	1.1	0.93	1.0
$Ar_n^+ + CH_4 \rightarrow$ Products	0.86	0.86	1.1

THEORETICAL AND EXPERIMENTAL STUDIES OF THE

DICATION OF NITRIC OXIDE

R.W. Wetmore (University of Waterloo) and R.K. Boyd (University of Guelph), Guelph-Waterloo Centre for Graduate Work in Chemistry, University of Guelph, Guelph, Ontario, Canada, N1G 2W1.

The fact that diatomic dications can be stable on the microsecond timsescale, despite the coulombic repulsion between the atomic ion fragments, has been known to mass spectrometrists for more than 50 years.[1] As well as the obvious fundamental interest in these species, their potential importance for the chemistry of the ionosphere has been emphasised.[2] The present work represents part of a program to understand more about these species through a combination of experiment and high-level ab initio calculations of potential surfaces; recent work[3,4] on CO^{2+} and N_2^{2+} exemplifies the approach. Briefly, the theoretical procedure employs a large basis set plus a full singles-and-doubles excitation configuration interaction calculation. This is achieved, using (by modern standards) relatively modest computational resources, via a procedure[5] in which physically significant aspects of the interaction are identified and given a full treatment, with remaining terms taken into account as an effective potential using perturbation theory.

The present report deals briefly only with the interplay of these theoretical esults with experimental data, obtained by mass spectrometry, on dissociative processes of NO^{2+}. A full account of the interpretation of all available experimental information on NO^{2+} has been submitted for publication.

The first modern investigation[6] of dissociation of NO^{2+} measured a kinetic energy release of 6.1eV. This investigation[6] observed dissociations occurring in the first field-free region of a double-focussing mass spectrometer, and attributed the observed transition to a unimolecular process. Subsequent work[7], using similar techniques, confirmed the previous finding[6] but it was unclear whether or not the 6.1eV process was truly unimolecular. In addition, a second process with a kinetic energy release of 8.1eV was observed[7] to be excited through collisions, especially with helium.

For NO^{2+} ions to survive the flight to the field-free region[6,7] requires that they have lifetimes, with respect to both predissociation (tunnelling or curve-crossing) and to radiation, which are at least several μs. The present theoretical calculations indicate that the only states of NO^{2+} which can thus qualify are the v=0 level of the $A^2\Pi$ states. None of these levels is perturbed by curve crossings, and their tunnelling lifetimes were presently calculated to be effectively infinite with respect to the experimental timescale.[6,7]. Theory thus clearly predicts that no unimolecular dissociation processes should be observable for NO^{2+} ions which have survived for a few μs. It thus became important to test this prediction experimentally, in view of the uncertainty in the earlier work.[6,7]

The ion kinetic energy spectra for the process $NO^{2+} \rightarrow O^+(+N^+)$ were recorded using a VG Analytical ZAB-2F double-focussing mass spectrometer of reversed configuration. By studying fragmentations occurring in the second field-free region of this instrument, the pressure of collision gas could be controlled independently of the pressure of NO in the ion source, the main cause of uncertainty in the earlier work.[6,7] The figure shows partial spectra at different pressures indicated on the ion gauge situated near the throat of one of the diffusion pumps located on either side of the gas collision cell. The broad peak at low energy corresponds to dissociative

electron capture, $NO^{2+} \xrightarrow{M} NO^{+} \dashrightarrow O^{+}(+N)$. The two sharper peaks at higher energy are the residual high-energy "horns" of two peaks distorted by severe z-discrimination due to high values of kinetic energy release. The first of these corresponds to an energy release of 6.1eV, and that at higher kinetic energy to 8.1eV energy release.

The variations of these peaks, with pressure of added helium collision gas, are very different. The direct dissociation of NO^{2+}, with energy release of 8.1eV, appears to occur only with helium as collision gas. With zero helium in the collision cell, i.e. only the background gas acting over the entire length (~1m) of the field-free region, both the dissociative charge-transfer and direct-dissociation peaks are still clearly visible. (This spectrum is the accumulation of 400 scans). Extrapolation of intensity vs. pressure plots to zero pressure suggest that both of these processes are wholly collision-induced. (The dissociative electron capture process, of course, must be so). Thus, these experimental findings are in accord with the theoretical predictions described above.

1. E. Friedlander, H. Kallman, W. Lasereff and B. Rosen, Z. Phys. 76 (1932) 60.
2. S.S. Prasad and D.R. Furman, J. Geophys. Res. 80 (1975) 1360.
3. R.W. Wetmore, R.J. LeRoy and R.K. Boyd, J. Phys. Chem. 88 (1984) 6318.
4. R.W. Wetmore and R.K. Boyd, J. Phys. Chem. (in press).
5. J.J. Diamond, G.A. Segal and R.W. Wetmore, J. Phys. Chem. 88 (1984) 3532.
6. J.H. Beynon, R.M. Caprioli and J.W. Richardson, J. Am. Chem. Soc. 93 (1971) 1852.
7. J.M. Curtis and R.K. Boyd, J. Chem. Phys. 81 (1984) 2991.

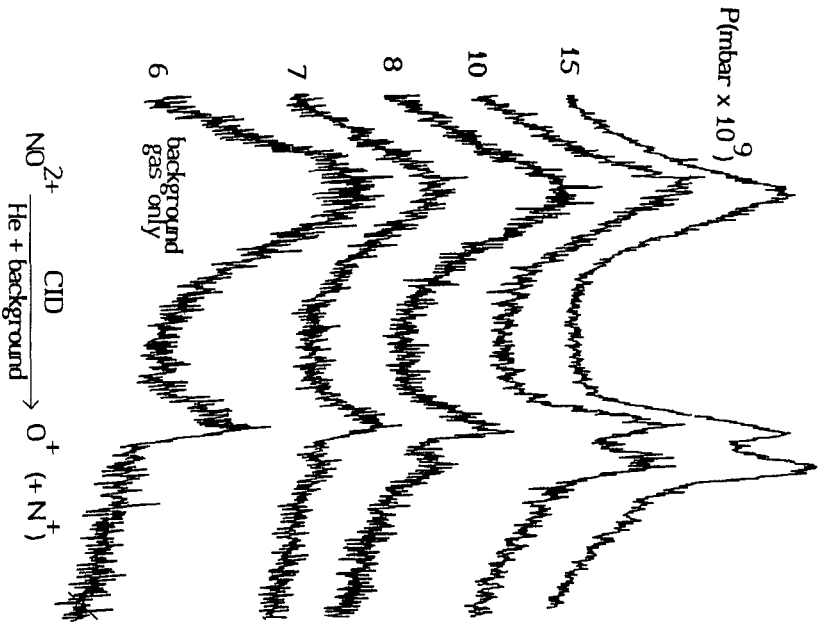

Kinetic Isotope Effects In The Fragmentation Of Energy-Selected Methyl Formate Ions.

Nishimura, T. and Meisels, G. G., Department of Chemistry, University of Nebraska, Lincoln, Nebraska 68588-0312

Previous results have established, from mass spectra and appearance potentials obtained for normal and isotopically labelled methyl formate, that the unimolecular dissociations of this ion are characterized by the migration of a formyl hydrogen. King and Long [1] have pointed out several difficulties in their attempts to calculate the mass spectra of methyl formate using the quasi-equilibrium theory (QET).

It is possible that kinetic isotope effects may be sensitive to quantum mechanical effects on the potential energy surface of the reaction, especially when hydrogen atom transfer is involved. Therefore, we have studied kinetic isotope effects in the dissociation of methyl formate ion as a possible probe of reaction dynamics using threshold photoelectron-photoion coincidence (TPEPICO) mass spectrometry.

The experimental breakdown diagrams were constructed from ion abundances obtained from peak areas. Complete shift of the m/z 32 ion inthe normal breakdown curve to the m/z 33 ion in the d-labelled breakdown curve confirms this hydrogen atom shift and simultaneous ejection of a carbon monoxide which lead to the formation of methanol ion with the appearance potential of 11.28 ± 0.07 eV. The m/z 31 ions in unlabelled methyl formate can be produced via the following reaction pathways:

$$CH_3OC(H)O^{+\cdot} \rightarrow CH_3OH^{+\cdot} + CO \quad (1)$$

$$CH_3OH^{+\cdot} \rightarrow CH_2OH^{+} + {}^{\cdot}H \quad (2)$$

or

$$CH_3OC(H)O^{+\cdot} \rightarrow CH_3O^{+} + {}^{\cdot}HCO \quad (3)$$

These two reaction pathways were clearly distinguished in the breakdown graph of the $CH_3OC(D)O^{+\cdot}$ ion (Fig. 1). The appearance potentials of the CH_3O^+ ion (m/z 31) and CH_2OD^+ ion (m/z 32) were found to be 12.1 ± 0.3 eV and 11.77 ± 0.07 eV, respectively. These values lead to $\Delta H_f(CH_3O^+)$ = 200 ± 7 kcal/mol and $\Delta H_f(CH_2OH^+)$ = 162 ± 2 kcal/mol, respectively. The heat-of-formation of CH_3O^+ can be compared with the value, 204 ± 5 kcal/mol, obtained from the TPEPICO experiments of the dimethyl ether [2], and that of CH_2OH^+ is consistent with the value, 167 kcal/mol, derived from the photoionization study of methanol [3].

The observed appearance potential, 12.91 ± 0.07 eV, of the m/z 29 ion produced from normal formate ions suggests that this ion seems to be formed through the direct dissociation

$$CH_3OC(H)O^{+\cdot} \rightarrow HCO^{+} + CH_3O^{\cdot} \quad (4)$$

At higher ionization energies, HCO^+ (or COH^+) is likely to be produced by a successive fragmentation probably involving CH_2OH^+.

Since the reaction (4) involves only a secondary isotope effect, which is usually small, an ion at the m/z 29 should be observed in the TPEPICO mass spectra of the d-labelled methyl formate. Contrary to our expectation, the production of m/z 29 ions was not detectable and only m/z 30 ions were observed; this ion is produced by the loss of a hydrogen molecule not from two centers (C ans O) but from one center (the C atom)

$$CH_2{=}OD^{+} \rightarrow COD^{+} + H_2 . \quad (5)$$

The appearance potential of 14.14 ± 0.16 eV for the m/z 30 ion is almost identical to the value of 14.11 eV calculated thermochemically, confirming the occurrence of this process.

These results may suggest a remarkably large secondary isotope effects for the reaction (4) and (5). Major fragmentation pathways are summarized in Fig. 2.

Average kinetic energies of product ions were extracted from their TOF distributions. The m/z 29 ions produced from $CH_3OC(H)O^+$ demonstrated large ion kinetic energies while those of m/z 30 ions from $CH_3OC(D)O^+$ was small in the vicinity of fragmentation onset. Since the m/z 29 ions near the onset seem to be mainly HCO^+ ions resulting from the reaction (4), the large KE obseved may reflect direct dissociation. For the formations of CH_3O^+ and CH_3^+ kinetic energy releases were extracted and compared with the RRKM/QET calculations.

Asymmetric time-of-flight distributions due to metastable dissociation were observed for the formation of the methanol ion, and were found to be well fitted with a two-component decay rate. The RRKM/QET rates rapidly increase to 10^9 s^{-1} even the very onset. The statistical theory , thus, does not predict metastable decomposition. These disagreements could result from nonstatistical fragmentation and/or a fragmentation process involving an intermediate isomerization process. Although it is currently difficult to specify a reaction mechanism for this process, it does not appear possible to explain the overall feature of the dissociation of the methyl formate ion by statistical theory involving any single state or isomer.

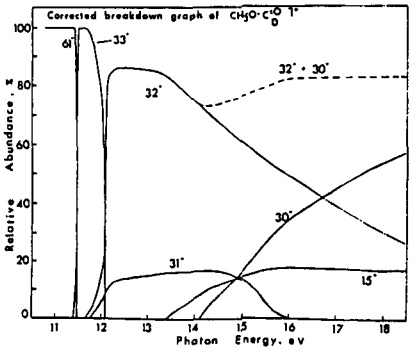

Figure 1.

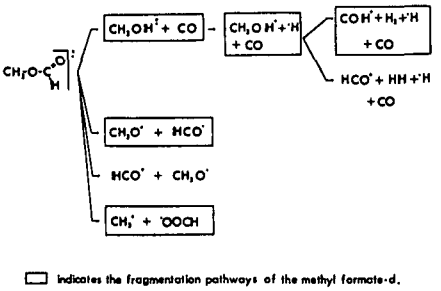

Figure 2.

[1] A. B. King and F. A. Long, J. Chem. Phys., 29, 374 (1958); [2] P.R. Das, T. Nishimura and G.G. Meisels, 32nd Annual Conference on Mass Spectrometry and Allied Topics, San Antonio, Texas (1984); [3] P. Warneck, Z. Naturforsch., 26a, 2047 (1971).

ACKNOWLEDGEMENTS

We thank the Department of Energy for support under Contract No. DE-AS02-76-ER02567, and TN thanks to Professor Gordon A. Gallup and Dr. D. Chen for helpful discussions.

CHARACTERIZATION OF ENCAINIDE METABOLITES BY FAB/MS: B.J. Sweetman, R.F. Mayol*, J.A. Labudde* and I.A. Blair. Department of Pharmacology, Vanderbilt University, Nashville, TN 37232. *Pharmaceutical Research and Development division, Bristol-Myers Company, Evansville, IN 47721.

Encainide hydrochloride (E) is a new antiarrhythmic agent developed in the laboratories of the Mead Johnson Company (Division of Bristol-Myers). It is currently undergoing Phase III clinical trials. Chemically, E is 4-methoxy -N-(2-(2-(1-methyll-(1-methyl 1- 2-piperidinyl) ethyl) phenyl) benzamide hydrochloride.

Following administration of ^{14}C-labelled E in man, approximately 45% of the oral radioactivity was excreted in the urine (2% as unchanged drug) and 40% in the feces. The majority of patients convert E to O-desethyl E (ODE) and 3-methoxy-O-desethyl E (MODE). Both of these metabolites show antiarrhythmic activity in animals. Clearance of these metabolites appears to be slower than that of E. Half life of the parent drug is 1-2hrs., that of ODE is 2.5-4 hrs., and that of MODE 6-14 hrs. Approximately 10% of the population does not metabolize encainide as extensively as the majority. In these non-extensive metabolizers the elimination half-life of E ranges from 6-10 hrs. In these patients lower levels of ODE and no MODE are observed in plasma and an additional metabolite, N-desmethyl E (NDE) is present. (Wang, T., Roden, D.M., Wolfenden, H.T., Woosley, R.L., Wood, A.J.J., and Wilkinson, G.R. J. Pharm. Exper. Ther. 1984, 228, 605; Kates, R.E., Harrison, D.C., Winkle, R.A., (Clin. Pharm. Ther. 1982, 31, 427).

Infusion of ^{14}C-E in man showed more total radiolabel in plasma and urine than could be accounted for by the sum of ODE, MODE and NDE. In plasma, these metabolites represent only from one-third to one-half of the infused radioactivity. Liquid chromatography and other techniques indicates that the balance of the infused radioactivity could be accounted for by the presence of some very polar metabolites, some of which could be converted to E, ODE and MODE on hydrolysis. The objective of this work was therefore to attempt to identify these polar compounds.

Encainide derivatives E, ODE, MODE and N-O-dimethyl encainide were synthetic products which were supplied by Mr. D.L. Elliott of Bristol Myers. Human subjects were given encainide labelled with carbonyl-^{14}C and benzylic methylene $^{12}C/^{13}C$ (50:50) as indicated in the structure below.

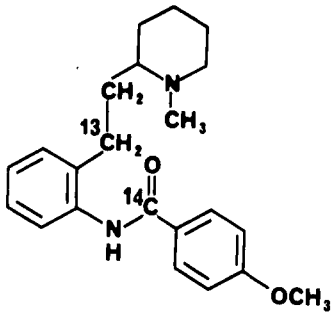

Fast atom bombardment mass spectrometry was carried out using a VG 70-250 double focussing instrument equipped with a high field magnet and manufacturer provided probe and ion source. Mass spectra were obtained using xenon atoms of 8 Kev energy from an Ion Tech saddle field gun. The accelerating voltage was held at 6kv and glycerol was employed as the matrix. Spectra were obtained in the alternating positive/negative ion modes. Spectra were averaged and matrix subtracted. Electron impact spectra were run at 70ev and samples were introduced via the direct introduction probe.

EI mass spectra of the encainide derivative revealed four major routes of fragmentation-loss of an N-methyl group, cleavage of the peptide bond, cleavage of the piperidinyl moiety and in the N-demethylated series cleavage between the benzylic carbon and the adjacent methylene group. The FAB spectra provided complementary data with molecular species dominating the spectra in both negative and positive modes. The positive ion spectra revealed structurally significant fragments ions

corresponding to cleavage of the peptide bond and cleavage adjacent to the piperidine ring. The negative ion spectra were rather simple with essentially only one ion present corresponding to $(M-H)^-$. Pooled 0-24hr urine (4 subjects), (220ml) was chromatographed on a C-18 Sep-Pak column using CH_3CN (5-35%) after acetone precipitation. The eluate was chromatographed on a C18 μ Bondapack column using methanol/0.01M ammonium acetate (pH 5.0), using Waters gradient #6, 20-35% MeOH for 20 min at 4 ml/min. This gave three major fractions A,B and C as designated which were subjected to further HPLC purification steps.

Fraction C Consisted of known non-polar compounds such as E, ODE and MODE.
Fraction B Consisted of at least four sulfate conjugates which will be the subject of a presentation elsewhere.
Fraction A Was the most polar fraction and was re-chromatographed on a Phenyl column using a mobile phase of CH_3CN/NH_4OAc using a gradient of 15%-45% CH_3CN over 5 min followed by a gradient to 85% CH_3CN over a further 10 min. This resolved fraction A into 3 sub-fractions designated A1, A2 and A3 in order of polarity. A1 was re-chromatographed on a silica column using a mobile phase of CH_3CN on pump A and CH_3CN: 0.01MNH_4OAc (70:30) on pump B. Initial conditions were 20% B at 1ml/min and then Waters gradient #3-up to 100% B for 10 min. This yielded three fractions designated A1A, A1B and A1C. Under these conditions, A1A eluted first, A1B was a minor component at 9.4 min and was discarded, and A1C eluted at 10.3 min and was subjected to FAB-MS without any further purification. A2 was re-chromatographed on an analytical C-18 μ-Bondapack column using a mobile phase containing 20% CH_3CN and gave a total of ca. 25μg product.

Metabolite A1A

The negative FAB mass spectrum showed a $^{12}C/^{13}C$ doublet at m/z 494/493 suggesting the molecular weight of the metabolite was 495/494. This corresponds to a dihydroxy derivative of MODE-lactam sulphate. In keeping with this proposed structure a doublet was observed at m/z 464/463 - a fragmentation that was found to be unique for the MODE-lactam sulphate. The compound failed to give an EI spectrum so no confirmation of the proposed structure could be made.

Under positive FAB conditions, metabolite A1A gave no structurally significant ions and the spectrum was dominated by cationized matrix peaks and no ions could be observed that were derived from the analyte molecule. We have previously observed a number of examples where ionization of the analyte molecule in the FAB mode is suppressed by cations present in the matrix.

Metabolite A1C

The cation contamination present in this very polar series of samples was highlighted in metabolite A1C where after a number of attempts only a very weak positive ion FAB spectrum was obtained. It showed the presence of both mono- (m/z 551/552) and di-cationized (m/z 573/574) molecular species. The relatively high molecular weight of the metabolite suggested that it may be a glucuronide conjugate rather than being sulphated as was found for other metabolites. The structure that fitted best with the observed protonated molecular ion corresponded to an ODE-lactam derivative. This structural assignment is extremely tentative and other possible structures include N-demethyl MODE-glucuronide. The assignment of the molecular weight was confirmed by the negative FAB spectrum which shows a doublet at m/z 527/528 together with sodium cationized ions at m/z 549/550.

Metabolite A2

The negative ion FAB spectrum of A2 showed an intense $^{12}C/^{13}C$ doublet at m/z 477/478 indicating a molecular weight of 478/479. In addition, doublets at 499/500 and 521/522 were attributed to M-2H+Na-and M-3H+2Na, respectively. The doublet at 447/448 was attributed to loss CH_2O from M-H, analogous to that seen for MODE lactam sulfate. Doublets at m/z 397/398 and 367/368 may be due to loss of sulfate and sulfate together with CH_2O, respectively. The positive ion spectra appeared to corroborate these assignments showing MNa_2-H at m/z 522/523, together with the doublet for the loss of CH_2O. There appears to be at least one additional compound present which is contributing to the mass spectra. Attempts to obtain electron impact spectra gave negative results.

These results highlight the difficulties associated with removing interfering cations from small quantities of very polar drug metabolite fractions despite extensive and careful chromatographic purification procedures. there is a distinct need for the development of new methods for the complete removal of cations from polar metabolite fractions destined for analysis by FAB-MS.

Supported by USPHS Grant EHS521085, NIH grants, RR-01688 and a program grant from Bristol-Myers.

A CAPILLARY COLUMN GC/NEGATIVE ION CHEMICAL IONIZATION METHOD FOR DETERMINATION OF CHLORAMPHENICOL IN BOVINE AND SWINE MUSCLE:

Michael K. Hoffman, Roger T. Wilson and Terry N. Chamberlain, USDA, FSIS, SCI-Chemistry, Cotton Annex Building, 300 12th St., SW, Washington, D.C.,20250

INTRODUCTION - Chloramphenicol (D(-)-threo-2-dichloroacetamido-1-p-nitrophenyl-1,3-propanediol) is an effective and inexpensive antibiotic permitted for use in humans under limited circumstances because deaths from aplastic anemia have been reported to follow even short therapeutic treatments. In the United States, chloramphenicol is not permitted for use in animals raised for food. In fact, the Code of Federal Regulations requires that labels bear the statement, "the product is not to be used in animals which are raised for food production."(1) Nevertheless, there is evidence that misuse of the drug has occurred within the United States, primarily in calves. FDA withdrew approval of the liquid formulation of the drug in early 1986. Canada permitted use of the drug to control respiratory and enteric diseases in swine until a temporary ban was issued on June 12, 1985 which has since been made permanent. The drug has been widely used in Europe.(2)

To detect illegal use of chloramphenicol in food-producing animals requires a highly specific and sensitive test because the drug is metabolized rapidly and only very low levels remain in animal tissues just a few hours after a therapeutic dose has been injected. Pickering et al compared a single ion monitoring GC/MS method using an internal standard for quantitation with radioenzymatic and gas chromatographic assays.(3) Although good sensitivity was reported, the specificity provided by single ion monitoring would not be sufficient for a regulatory method.

The object of this work was to develop a GC/MS method to confirm the identity of apparent residues of chloramphenicol in bovine or swine muscle tissues for a monitoring program conducted by the Food Safety and Inspection Service, U. S. Department of Agriculture. The method was expected to complement the FSIS-developed extraction procedure used for the GC-EC quantitation of the drug from muscle tissue. In actuality, the GC/MS method proved to be reliable for confirming the presence of chloramphenicol at levels substantially below that at which the GC-EC quantitation could be used.

RESULTS AND DISCUSSION - Chloramphenicol was extracted from bovine or swine muscle tissue and derivatized with Sylon HTP to form the trimethylsilyl ether. Electron impact (EI), positive ion and negative ion chemical ionization (PICI, NICI) spectra were obtained under conditions which maximized the high mass end of the spectrum. The PICI and NICI mass spectra were obtained using methane and exhibit ions expected under such conditions. The presence of both the electron-withdrawing p-nitrophenyl and the dichloroacetamido groupings in chloramphenicol make it approximately 100 times more sensitive to NICI analysis than that observed under PICI conditions. Both NICI and PICI spectra provide a sufficient number of ions of structural significance to characterize the entire molecule and provide a basis for the development of a confirmatory method. Major decomposition pathways of the protonated molecular ion (m/z 467) under PICI conditions lead to fragment ions at m/z 451 (MH - CH_4), 431 (MH - HCl), 377 (MH - HOTMS), 347 (MH - HOTMS - NO), 254 (MH - HOTMS - $NHCOCHCl_2$) and 225 (MH - $Cl_2CHCONHCHCH_2$-OTMS). While the NICI spectrum exhibits significantly less fragmentation (and less structural detail), sufficient structural information is found in fragments related to the molecular weight (i.e. the molecule anion at m/z 466), the presence of two chlorines is shown in the molecular anion cluster;, the loss of Cl and TMS to form the species corresponding to the small peaks at m/z 358 and 360; m/z 322 representing the loss of one TMS group, Cl and HCl; and m/z 304 corresponding to loss of water from m/z 322. The composition of the ion at m/z 232 is not known.

NICI was chosen because of its greater ultimate sensitivity and the absence of any mass spectral response in blank (control) tissue extracts from the ions that would be monitored for chloramphenicol. Multiple ion detection (MID) analyses were performed by monitoring six ions which had been previously selected from the NICI spectra. These ions were at m/z 304, 322, 358, 360, 466, and 468. In the MID mode, linearity of response of the molecular anion and all fragment ions range from less than 200 pg to greater than 3.0 ng, as shown in Figure 1. These data were obtained from samples submitted blind to two analysts who used mass spectrometers from different manufacturers as part of certification studies. As little as 10 picograms (pg) of derivatized chloramphenicol (standard) produced a response at the mass of the molecular anion (m/z 466) with a S:N of greater than 5:1. Figure 2 presents the molecular anion responses taken from the MID analyses of a standard solution, a control tissue sample, a fortified tissue extract and an incurred tissue sample.

The seriousness of the misuse of chloramphenicol in veal calves during the period from July, 1981 to December, 1983 is documented by the high levels found by the FSIS Monitoring Program. The information in Table 1 shows the high levels (greater than 10 ppb) found in the FSIS monitoring program samples. The findings also provide evidence of the wide-spread geographic misuse of the drug.

CONCLUSION - A sensitive screening procedure has been developed for chloramphenicol residues in bovine muscle tissue for use at or below the 10 ppb level. Extracts prepared for quantitation by GC-EC may be directly analyzed by the GC/MS procedure without additional sample clean-up.

REFERENCES

1. Code of Federal Regulations: Title 21,part 555.110a(c)(iii)(d).
2. Bories, G. S. F., Peleran, J-C., and Wal, J-M., J. Assoc. Off. Anal.Chem., 66, 1521 (1983).
3. Pickering. L.K., Hoecker, J.L., Kramer, W.G., Liehr, J.G., and Caprioli, R. M., Clin. Chem., 25, 300 (1979).

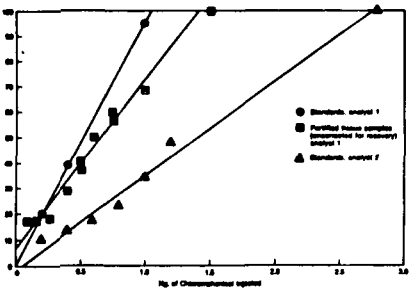

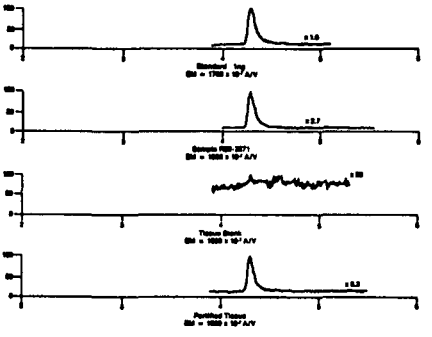

TABLE 1 - Distribution of Confirmed Chloramphenicol Violative Samples

State	Date	Level
Massachusetts	July, 1981	37.5 ppb
Wisconsin	July, 1981	337 ppb
Pennsylvania	August, 1981	12.7 ppm
Washington	August, 1981	773 ppb
California	February, 1982	5.77 ppm
California	March, 1982	8.30 ppm
California	June, 1982	23.0 ppb
Wisconsin	September, 1982	130 ppb
Massachusetts	January,1983	5.96 ppm
Connecticut	February, 1983	1.71 ppm
Connecticut	February, 1983	4.32 ppm
Wisconsin	July, 1983	46.0 ppm
California	July, 1983	4.0 ppm
Wisconsin	July, 1983	380 ppb
Connecticut	December, 1983	348 ppm
California	December, 1983	4.75 ppm
California	December, 1983	22 ppb

Quantitative Determination of Rimantadine by GC-MS

E.K. Fukuda, L.C. Rodriguez, N. Choma, N. Keigher, F. De Grazia and W.A. Garland,
Department of Drug Metabolism, Hoffmann-La Roche Inc., Nutley, NJ 07110

A GC-MS procedure has been developed for the quantitation of Rimantadine, an antiviral drug effective against Type A influenza. The procedure, which has been used for the analysis of plasma samples from humans, rats and mice given rimantadine, utilizes selective ion monitoring (SIM), methane negative ion chemical ionization (NCI) and stable isotope dilution.

Samples are prepared using a modification of the CN Bond-Elut R column extraction procedure previously reported for the analysis of Rimantadine by EC/GC [1]. The reconstituted residue of the column eluents are treated with pentafluorobenzoyl chloride and the resulting derivatized Rimantadine, and its $[^2H]_4$-stable isotope analog internal standard, are analyzed by GC-MS. The mass spectrometer (Kratos MS-50) is operated under methane NCI conditions using SIM techniques to monitor the $[M-HF]^-$ (m/z 353) ion of the derivatized analyte, and the $[M-^2HF]^-$ (m/z 356) ion of the derivatized internal standard.

Figure 1 shows a selected ion current profile from the analysis of a calibration standard containing 5 ng/ml of analyte and 100 ng/ml of internal standard. The following GC conditions were used: methane carrier gas with the flow rate set to about 1 ml/min, Chrompack CP Sil 8 CB capillary column, column temperature of 260°C, interface and injector temperatures of 300°C.

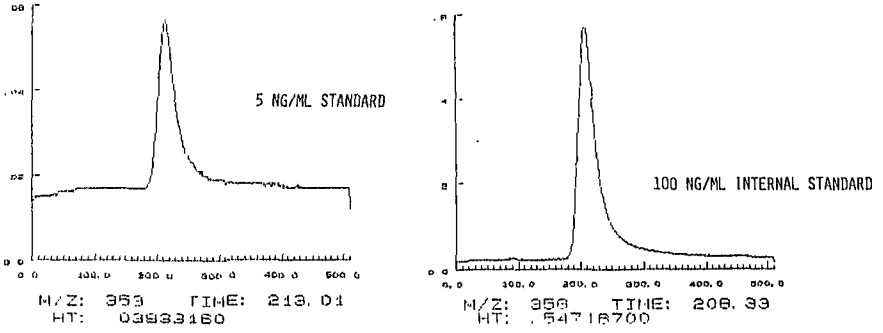

FIGURE 1

The retention times (given in scan numbers in the figure) are about 2.8 min.

Figure 2 shows a linear calibration curve relating the ratio of the $[M-HF]^-$ to $[M-^2HF]^-$ ions to the amount of analyte added to drug-free plasma. The calibration range is from 5 ng/ml to 500 ng/ml. Each calibration concentration was run in duplicate.

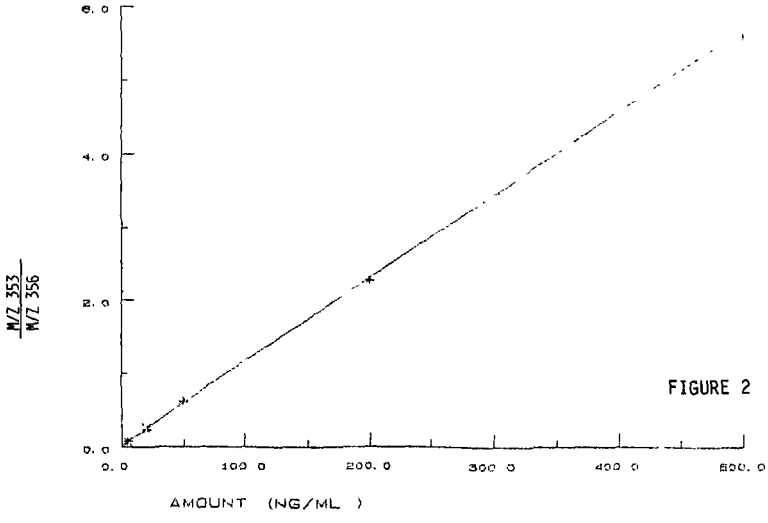

FIGURE 2

This assay represents an improvement to the previous EC-GC method, both in terms of sensitivity (down to 5 ng/ml) and speed (sample analysis time on the order of 5 min). Currently, this assay is being applied to study the pharmacokinetics of Rimantadine in humans, and toxicity experiments in rat, mouse and dog.

[1] F.G. Hayden, H.E. Hoffman and D.A. Spyker, Antimicrob. Agents Chemother., 23, 458-464 (1983).

APPLICATION OF Cf-252 PLASMA DESORPTION MASS SPECTROMETRY TO THE ANALYSIS OF SULFATE, GLUCURONIDE AND GLUTATHIONE CONJUGATES

Alai M., Dulik D., Pallante-Morelli S.
Johns Hopkins University, Baltimore MD 21205

Cf-252 Plasma Desorption mass spectrometry has been evaluated for the routine analysis of polar low molecular weight conjugated drug metabolites. 20-50 nmoles of these compounds provide good quality spectra with less chemical noise than what is seen with the larger molecules. The average molecular weight accuracy is ±0.5 amu. Positive and negative ion modes can be switched rapidly and in one operation information from both modes can be obtained. Glutathione conjugates often formed multiple sodium adducts. These strong adducts were even seen in the negative ion mode, but to a lesser extent. Fragment ions formed by the loss of the glutathione moiety $(MH-307)^+$ were observed throughout. Glucuronide conjugates had a simpler pattern of molecular ion species. Sodium attachment was not as prominent as in the case of glutathiones. The only major fragmentation observed was that formed by the loss of glucuronic acid moiety $(MH-176)^+$. However, the presence of such intense fragment ions may in part be due to the hydrolysis during the electrospray process.

The negative ion spectra of sulfate conjugates provided more conclusive structural information than the positive ion spectra and were simpler to interpret. Although the sulfates were prepared as alkali metal salts, adducts were not detected in the negative ion mode.

Sample preparation for analysis by PDMS is critical in reducing hydrolysis of the drug conjugates and minimizing the extent of the sodium attachment.

Amitriptyline glucuronide, m.wt. 454

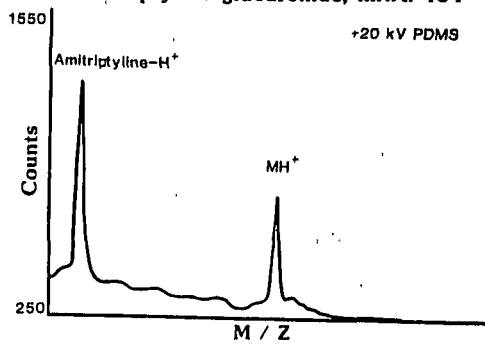

p-Nitro-phenyl sulfate, potassium salt , m.wt. 257

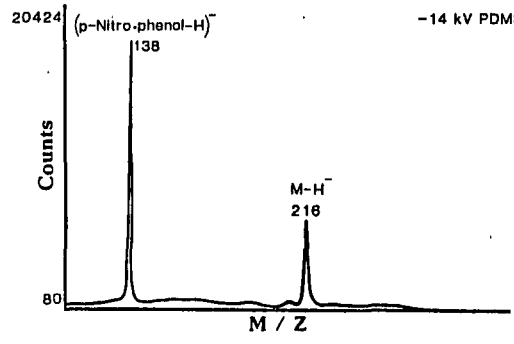

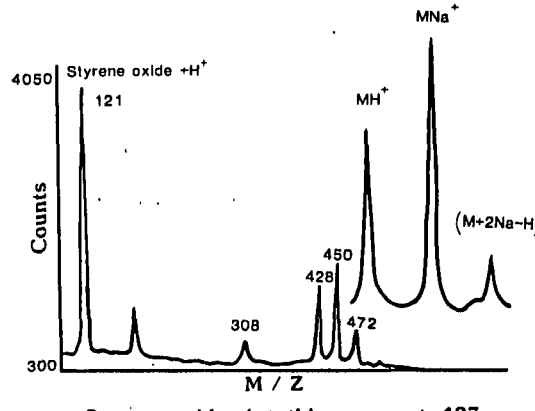

Styrene oxide-glutathione , m.wt. 427

20 kV PDMS

CHARACTERIZATION OF MANDELIC ACID AND PHENYLGLYCINE sec-BUTYL ESTER DIASTEREOISOMERS FROM DIAZOTIZED AMPICILLIN AND β-LACTAMASE I. C. Bouziane and R. A. Day, University of Cincinnati, Cincinnati, Ohio 45221; A. Kornel, Environmental Protection Agency, HWERL, Cincinnati, Ohio 45268.

The resolution of D- and L-mandelic acid is an important step toward elucidating the mechanism of inhibition of β-lactamase I by diazotized ampicillin (DAMP). This will answer the question whether a chiral center is induced in the process of enzyme inhibition.

The separation and analysis of the diastereoisomers is done by GC/MS using a DB-5 capillary column (30 m long with 0.25 mm ID). Both EI and CI modes were used. One milligram of the enzyme was inhibited by DAMP as described by Patil and Day (1). The inhibited, covalently modified enzyme, and the dialysate were hydrolyzed in 6N HCl at 110 °C for 16 hours, then the HCl is evaporated under vacuum. Mandelic acid from the inhibited enzyme was first extracted from the acidified protein hydrolyzate in CH_2Cl_2; then the methylene chloride phase is evaporated under nitrogen. The derivatization of the sample is done along with other samples from the hydrolyzed dialysate and the D- and L-pairs of the standards, phenylglycine (PHG) and mandelic acid (MA). The diastereoisomeric derivatives were obtained first by esterification with D-2-butanol/7N HCl and then by acylation with heptafluorobutyric anhydride according to the method described by Tunlid and Odham (2).

Preliminary results from PICI using isobutane as reagent gas gave *quasi*-molecular ions (MH^+ of m/z = 404) for either D- or L-PHG. In addition, it gave a base peak of m/z = 348 which corresponds to fragment resulting from the loss of butene from the protonated PHG molecule ($M+H-C_4H_8^+$) (Fig. 1). However, when the EI mode was used, similar fragments ($M-OCOC_4H_9^+$) corresponding to m/z = 302 and m/z = 303 were obtained from the spectra of PHG and MA respectively (Fig. 1). So far, based on their fragmentation pattern, spectra from either pair of diastereomers are similar. Results from the ampicillin sample gave a similar spectrum to the one of PHG. Similarly, sample from the DAMP and the dialysate gave spectra that are characteristic of MA (Fig. 2). These results confirm previous ones obtained not only with EI/MS of the hydrolysed, silylated samples (AMP, DAMP, and dialysate) but with FAB/MS as well. In addition, the results from the GC/MS suggest that one of the diastereomers of MA is the major end-product of the dialysate. Furthermore, both of the MA diastereomers seem to be present at different levels in the acid hydrolysate from the DAMP suggesting that in the absence of penicillinase, the substrate appears to hydrolyze preferentially to a given diastereomer and in its presence, through an enzyme mediated process, to the other diastereomer. Results obtained from the inhibited hydrolysed, derivatized enzyme are not conclusive whether MA is definitely the end-product.

Further experiments are needed not only to confirm these results but to establish that indeed a given diastereomer of MA is the end-product resulting mainly from the inhibited enzyme when DAMP is used as substrate for β-lactamase I.

References

1. Patil, G. V. and R. A. Day (1972) Biochim. Biophys. Acta 293, 490-6.

2. Tunlid, A. and G. Odham (1984) Biomed. Mass. Spectrom. 11(8), 428-34.

Figures

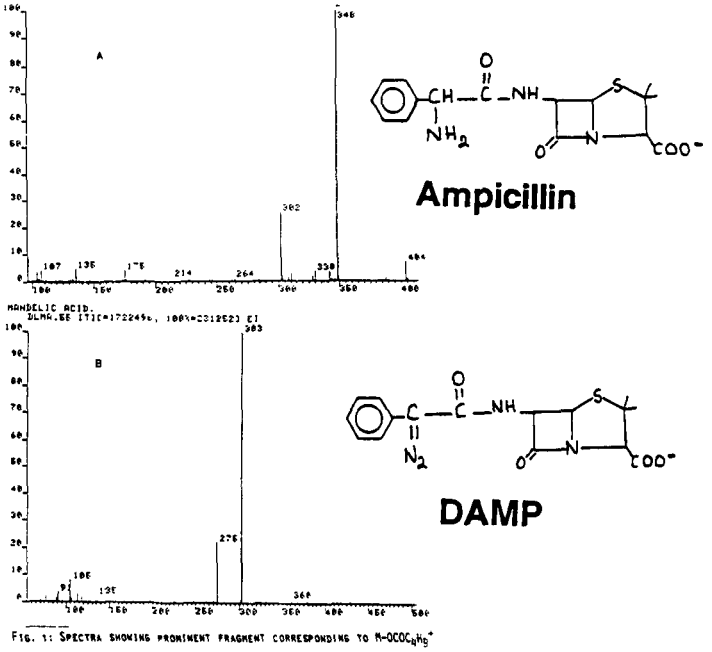

FIG. 1: SPECTRA SHOWING PROMINENT FRAGMENT CORRESPONDING TO M-OCOC$_6$H$_5$$^+$ FROM:

(A) D- OR L-PHENYLGLYCINE (M/Z = 302)

(B) D- OR L-MANDELIC ACID (M/Z = 303)

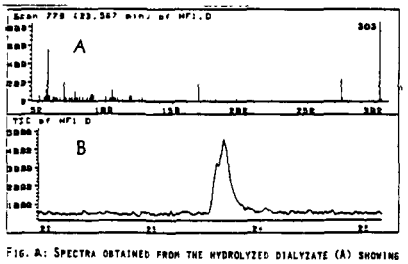

FIG. A: SPECTRA OBTAINED FROM THE HYDROLYZED DIALYZATE (A) SHOWING THE SAME PATTERN SEEN WITH THE DAMP SAMPLE (B), WHERE ONE OF THE DIASTEREOMERS SEEMS TO BE PROMINENT(m/z 303)

QUANTITATIVE ANALYSIS OF TERBUTALINE BY THERMOSPRAY LC/MS

M. HAYES, M. BAX, D. ALKALAY

DEVELOPMENT DEPARTMENT, PHARMACEUTICALS DIV.,
CIBA-GEIGY CORP., ARDSLEY NY, 10502

Terbutaline, widely used in the treatment of bronchial asthma and reversible bronchiospasm, has been extensively studied using GC/MS and, more recently, LC/electrochemical detection methods. We have found that thermospray LC/MS can be utilized for rapid, sensitive and reproducible quantitative analysis of terbutaline.

This approach does not require derivatization and is simple to use. The LC/MS interface is reproducible and allows automated operation of the system. Our data shows that the method is useful for plasma determinations in the range of 1 to 600 ng/ml and is suitable for both human and animal pharmacokinetic studies.

All work was performed using a Nermag 10-10C mass spectrometer with a Vestec Thermospray interface. The ionization mode was positive ion thermospray. The chromatographic system utilized Waters pumps and a WISP autosampler. A 3 micron x 5 cm C18 column was used. The mobile phase was 10% acetonitrile in 0.15 M ammonium acetete.

Following optimization of the chromatographic and mass spectrometric conditions, the LC/MS system was evaluated to determine its suitability for performing extended analyses. An automated run was set up containing 165 standards, QC samples and blanks in buffer. The analysis was done over a 15 hour time span.

Table 1 shows the results for the quality control samples in the extended analysis. The accuracy and reproducibility remain constant over the full 15 hours of the analysis.

TABLE 1

Precision and Accuracy of QC Samples
During Extended Analysis

ADDED (NG/ML)	FOUND (NG/ML)	% STD. DEV FIRST 10	LAST 10	ALL 94
2	1.97	11.1	9.0	8.4
20	19.9	4.5	4.9	4.3

The sensitivity remained high throughout the run and was 75% of the initial value after 15 hours. Short term fluctuations appear to be due to changes in vaporizer temperature.

Table 2 lists the results of the analysis of terbutaline spiked into human plasma. The mean deviation of the found concentration from the added values was 4.9%. The chromatogram in Figure 1 is of a sample of human plasma spiked with 1.2 ng/ml of terbutaline.

Table 2

Linear Regression of Determinations of Terbutaline in Spiked Plasma

CONCENTRATION (ng/ml)	% DEVIATION
1.23	-3.2
1.23	-4.3
6.16	-0.6
12.3	4.9
61.6	7.9
123	4.4
246	-9.4
616	-4.3
Mean of Absolute Error	4.9%

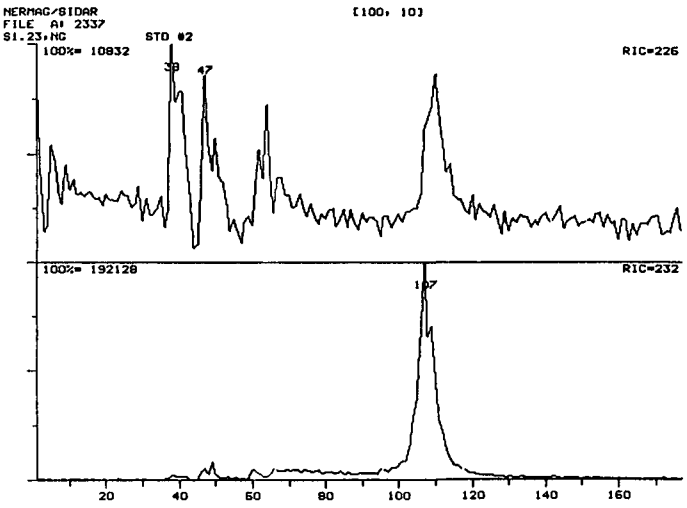

Figure 1

THE METABOLISM OF CYCLOSPORINE IN LIVER TRANSPLANT PATIENTS

L. K. Wong, H. Hashem and R. Venkataramanan
University of Pittsburgh School of Pharmacy
Pittsburgh, PA 15261

J. Buchner and R. Willoughby
Extrel Corporation
240 Alpha Drive, Pittsburgh, PA 15238

Cyclosporine is a potent immunosuppressant used to prevent rejection of transplanted organs. Cyclosporine is eliminated from the body primarily by hepatic metabolism. Previous studies indicated that most of the drug and its metabolites were excreted in the bile and that a very low percentage is eliminated in the urine. Reports also indicated that suppression of the metabolism of cyclosporine reduced its toxicity. The objective of this study is to identify cyclosporine metabolites in the bile of transplant patients.

Extraction:

Bile samples were obtained from liver transplant patients via a t-tube inserted into the common bile duct. The samples were extracted with ether and the ether was evaporated under nitrogen. The residue was dissolved in methanol and acidified using HCl, then washed twice with hexane. The aqueous solution was neutralized with sodium hydroxide and extracted with ether. The ether layer was then evaporated under nitrogen reconstituted in methanol and introduced onto a HPLC column.

HPLC:

The column description, the solvent system and the HPLC program used are described in Table 1.

TABLE 1

COLUMN: 15 cm x 4.6 mm I.D. C_{18} Column, particle size 5 um. Flow rate 1.7 ml/min. Column oven temperature 73°C, run time 60 min.

Time	Acetonitrile %	Water %
0	43	57
17	47	53
18	47	53
36	52	48
46	66	34
49	73	27
60	73	29

HPLC chromatogram is depicted in Figure 1.

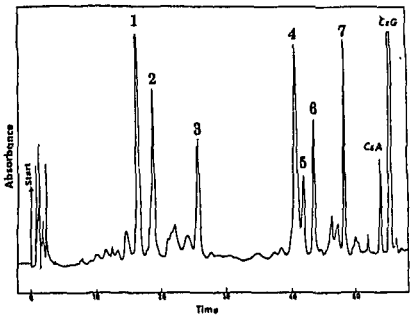

Figure 1: The HPLC chromatogram of Cyclosporine and ether extractable metabolites.

Mass Spectrometry:

The individual metabolite peaks were collected from HPLC. The organic layer was removed under nitrogen and the aqueous layer was freeze dried. The residue obtained was reconstituted in ether and was analysed by desorption chemical ionization mass spectrometry using methane. The mass spectrometer is an Extrel Model 400-2D instrument.

Cyclosporine and its metabolites showed a characteristic fragmentation pattern under methane chemical ionization conditions. All four metabolites and cyclosporine showed a quasi-molecular ion and a M+29 adduct ion. They all showed a loss of a C_7 fragment from amino acid number 1 which corresponds to loss of 112 amu in the case of cyclosporine and for metabolites which do not have a substitution in this moiety. However, peak 1 (dihydroxy cyclosporine) and peak 6 (hydroxy cyclosporine) both show a loss of 128 fragment instead of 112 indicating an OH substitution at that position.

Peak 1 showed a M+1 at 1235 indicating two hydroxy substitutions. Peak 3 showed an M+1 at 1205. This increase of 2 amu indicates metabolic loss of a methyl group and the addition of a hydroxy substitution. Peaks 5 and 6 showed a M+1 at 1219 indicating a substitution with a hydroxy group.

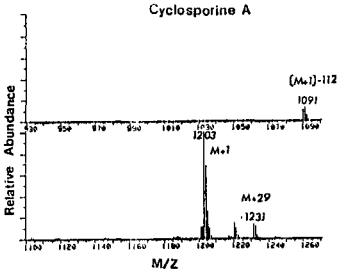

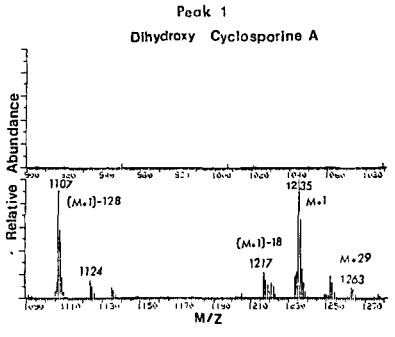

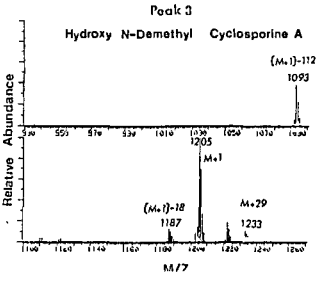

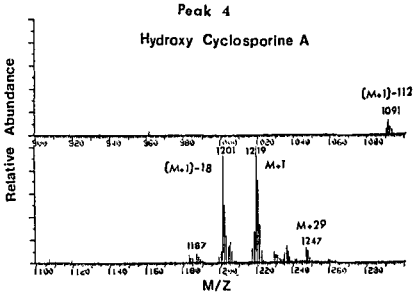

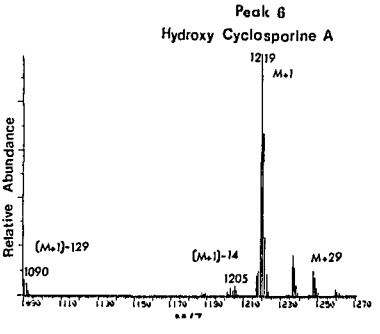

Summary:

The mass spectrometric data obtained from five biliary cyclosporine metabolites indicate that the major metabolic changes of the drug are hydroxylation, giving rise to mono- and dihydroxy cyclosporine A, and hydroxylation and N-demethylation giving rise to monohydroxy-N-demethyl cyclosporine A. Similar metabolites of cyclosporine have been detected in urine.

ACCURATE HPLC-MS ANALYSIS OF A PHOTOAFFINITY DERIVATIVE OF COLCHICINE.

S. T. Weintraub, L. J. Floyd and L. D. Barnes, The Univ. of Tx. Health Science Center at San Antonio; San Antonio, Tx. 78284 and R. F. Williams, The Univ. of Tx. at San Antonio; San Antonio, Tx. 78284

Colchicine has been shown to exhibit specific, high affinity binding to tubulin, resulting in depolymerization of microtubules. In order to investigate tubulin-microtubule interconversion, a photoaffinity analog of colchicine, 2-nitro-4-azidophenyl-deacetylcolchicine (NAP-DAC), was synthesized. Photolysis of the azido compound leads to release of nitrogen and yields a highly reactive nitrene which can form a covalent bond with tubulin, near the colchicine binding site. During the HPLC purification of NAP-DAC it was observed that two products had been formed. After isolation of each component, however, it was apparent that an equilibrium process was occurring because a mixture was again present a few hours after the initial isolation. Colchicine binding studies, performed after HPLC separation of the two isomers, revealed that the compound which eluted as peak 1 exhibited negligible incorporation into tubulin. For peak 2, equal photolabeling of the alpha and beta chains was observed, with the total representing 85% of the added photoaffinity analog. The present study was undertaken to elucidate the nature of the two products.

For UV/VIS detection, approximately 0.2 μg of NAP-DAC was chromatographed by two 5 μ Ultrasphere C18 columns (15 cm and 25 cm, each 4.6 mm i.d.). The mobile phase was methanol:water (80:20). Isomers of NAP-DAC were purified by HPLC and immediately after collection, the UV/VIS absorption spectrum of each was recorded. The tropolone ring absorption at 354 nm remained the same for both isomers, but the longer wavelength absorption from the nitrophenylazide group was found at approximately 465 nm in peak 1 and 450 nm in peak 2.

HPLC-mass spectrometry was performed on a Finnigan-MAT 212 mass spectrometer in combination with an INCOS 2200 data system. The HPLC was connected to the mass spectrometer by means of a moving belt interface. The effluent from an Ultrasphere C18 column was deposited directly onto the belt after passage through a capillary glass transfer line. The belt was maintained at a speed of 2.5 cm/sec, with 5 watts being supplied to the tip heater. The solvent evaporation region was heated to approximately 125 °C. The mobile phase was methanol:water (90:10). The mass spectrometer was operated under electron impact conditions at 70 eV, with an accelerating voltage of 3 kV, an ion source temperature of 250 °C and resolution of either 1000 or 4000, as specified. Perfluorokerosene-H was utilized as the reference compound.

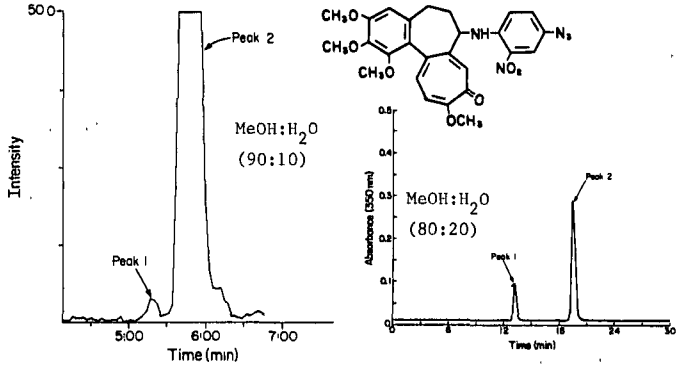

Shown on the previous page is a reconstructed total ion current chromatogram (RIC) of HPLC-MS (1000 resolution) of NAP-DAC. Approx. 20 μg. of the isomer mixture was utilized so that the sample eluting as peak 1 would be easily detected. The relative amount of peak 1, as compared to peak 2, was much less in the RIC than after UV/VIS detection.

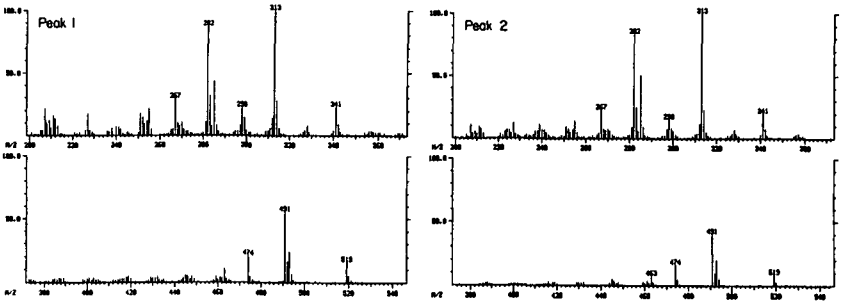

EI mass spectra (1000 resolution) of NAP-DAC isomers (above) and accurate mass measurement (4000 resolution, below).

Observed Mass (Δ, mmu)		Formula	Assignment*
Peak 1	Peak 2		
519.1768 (1.4)	519.1704 (4.9)	$C_{26}H_{25}N_5O_7$	$[M]^+$
491.1786 (9.3)	491.1731 (3.8)	$C_{26}H_{25}N_3O_7$	$[M - N_2]^+$
(1.6)	(7.3)	$C_{25}H_{25}N_5O_6$	$[M - CO]^+$
341.1274 (11.5)	341.1388 (7.5)	$C_{20}H_{21}O_5$	$[M - NH\text{-}NPA]^+$
(1.1)	(5.1)	$C_{19}H_{19}NO_5$	$[M - (NPA + CH_3)]^+$
313.1404 (3.5)	313.1294 (14.5)	$C_{19}H_{21}O_4$	$[M - (NH\text{-}NPA + CO)]^+$
(9.0)	(1.9)	$C_{18}H_{19}NO_4$	$[M - (NPA + CH_3 + CO)]^+$
282.1348 (9.1)	282.1254 (0.2)	$C_{18}H_{18}O_3$	$[M - (NH\text{-}NPA + CO + OCH_3)]^+$
(21.8)	(12.3)	$C_{17}H_{16}NO_3$	$[M - (NPA + CH_3 + CO + OCH_3)]^+$

*NPA = NITROPHENYLAZIDE

Based on the available evidence, and after a comparison with model compounds, one explanation for the two NAP-DAC species is the existence of *syn* and *anti* isomers which are the result of quinoid resonance forms of the nitrophenylazide moiety. Support for this proposal is as follows: 1) Significant differences between the mass spectrum of NAP-DAC and that of N-methyl-deacetylcolchicine imply the existence of double bond character between the NH and the nitrophenylazide; 2) The close similarity in the mass spectra of the two species is consistent with *syn* and *anti* isomers; 3) *Syn* and *anti* isomers often exhibit differences in chromatographic retention times; 4) The shift in the long wavelength absorption maximum between the two species can reflect hydrogen bonding between the nitro group and the colchicine moiety. This may be possible in one isomer and not in the other

Supported in part by NIH grant GM 30665 to R. F. Williams.

MASS SPECTRAL ANALYSIS OF PHENOTHIAZINE N-OXIDES

G. McKay, R. Edom, E. M. Hawes, J. W. Hubbard and K. K. Midha
College of Pharmacy, University of Saskatchewan,
Saskatoon, Saskatchewan, Canada S7N 0W0

The positive identification of tertiary amine N-oxides has been an analytical challenge for a variety of reasons. Their thermal lability has precluded their direct analysis using either gas chromatography or conventional mass spectrometry. Both techniques give rise to the rapid and near complete decomposition of the N-oxide to various compounds which include such products as the parent 3° amine, 2° amine and products formed by Cope elimination. Thus these results, which may be partly due to the thermal lability of the N-oxides, can confound and confuse their EI mass spectra for positive identification of these compounds.

In the case of phenothiazine N-oxides, the situation is even more complex because of extremely low levels encountered in plasma from patients and because phenothiazine antipsychotics are subject to biological oxidation at several positions in the molecule, including the formation of hydroxy and sulfoxide metabolites. In an attempt to develop a sufficiently sensitive and reliable technique to positively identify phenothiazine N-oxides, a series of mass spectroscopic studies were undertaken using six representative phenothiazine N-oxides listed in Table I below:

Table I: Structures of Various Phenothiazine N-Oxides

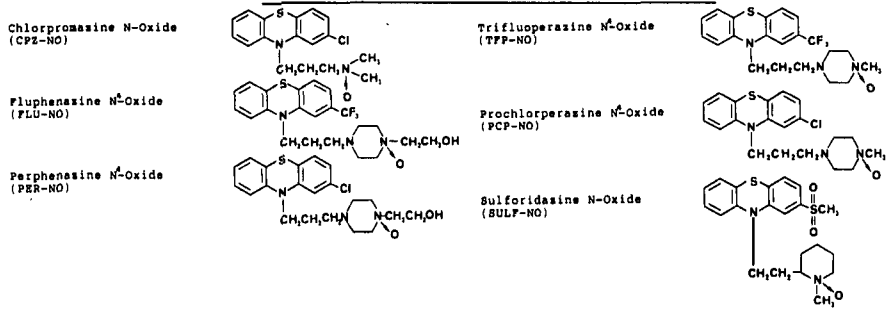

Samples were analyzed under three different modes of ionization; EI, CI(AMM) and FAB on VG analytical mass spectrometers MM16F (CI), 7070HE (EI, FAB). All samples were analyzed as the free base except prochlorperazine dimaleate. Samples (5-10 μg) were loaded into disposable capillary probe tips for EI and CI spectra and introduced via the solid direct probe inlet system. FAB spectra were obtained by first dissolving the sample (5-10 μg) in a matrix of glycerol which was then applied to the FAB stainless steel target (3 x 8 mm).

Typical spectra are shown in Figure 1 of CPZ-NO run under the three different modes of ionization.

Characteristic ions of the various phenothiazine N-oxides are listed in Tables I-III. In all cases the molecular ion is either missing (FLU-NO, TFP-NO, PCP-NO, SULF-NO) or is very weak in intensity (3% or less, CPZ-NO and PER-NO) during EI mass spectrometry. Diagnostic, N-oxide intact, side chain ions are listed in Tables I-III. Abundant pseudo-molecular ions during FAB analysis are listed in Table III.

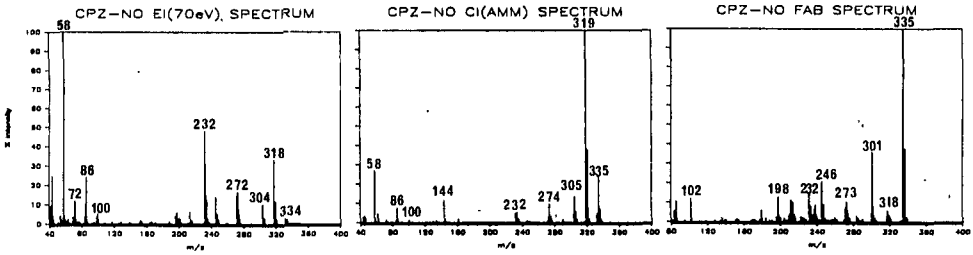

FIGURE 1 - Mass Spectra of CPZ-NO analyzed by EI, CI and FAB mass spectrometry.

TABLE I Intensities of Characteristic Ions in the EI Spectra of Some Phenothiazine N-Oxides

Phenothiazine N-Oxide	Mol. Wt.	Characteristic Ions m/z (% Rel.Int.)
CPZ-NO	334	334(3), 332(3), 318(34), 304(10), 273(17), 100(5)*
FLU-NO	453	451(3), 437(37), 435(49), 393(19), 363(4), 350(2),185(1)*
PER-NO	419	419(2), 417(3), 403(85), 359(18), 329(4), 316(3), 185(2)*
TFP-NO	423	421(4), 407(85), 393(16),363(2), 350(4), 155(4)*
PCP-NO	389	373(79), 359(13), 316(3)
SULF-NO	418	416(4), 402(11), 400(7), 388(2), 140(9)*

TABLE II Intensities of Characteristic Ions in the CI Spectra of Some Phenothiazine N-Oxides.

Phenothiazine N-Oxide	Mol. Wt.	Characteristic Ions m/z (% Rel.Int.)
CPZ-NO	334	335(24), 319(100), 305(14), 274(10), 100(2)*
FLU-NO	453	454(9), 437(100), 410(60), 394(42)
PER-NO	419	420(22), 404(100), 185(1)*
TFP-NO	423	424(20), 407(100), 394(17)
PCP-NO	389	390(21), 374(100), 360(11), 317(1), 155(1)*
SULF-NO	418	419(100), 403(28), 389(5), 140(2)*

TABLE III Intensities of Characteristic Ions in the FAB Spectra of Some Phenothiazine N-Oxides

Phenothiazine N-Oxide	Mol. Wt.	Characteristic Ions m/z (% Rel. Int.)
CPZ-NO	334	335(100), 318(6), 304(2), 273(10), 102(12)*
FLU-NO	453	454(100), 437(3)
PER-NO	419	420(100), 403(5), 185(4)*
TFP-NO	423	424(76.3), 407(3)
PCP-NO	389	390(100), 373(4)
SULF-NO	418	419(70), 402(2), 388(3), 140(2)*

*Indicates diagnostic N-oxide intact side chain ions.

The comparison of spectra obtained under different modes of ionization can help to distinguish between thermal decomposition and fragmentation induced by ionization. In the case of phenothiazine N-oxides conventional EI spectra yield in all cases, spectra with little or no molecular ion information. Like other N-oxides thermal decomposition either via direct deoxygenation, Cope elimination, or dealkylation accounts for most of the reduction in relative intensity of molecular ions. The CI spectra show the presence of quasi $[MH]^+$ and $[MH-16]^+$ ions which demonstrate that deoxygenation occurs prior to ionization. Other temperature dependent decompositions can be identified by observance of quasi M+1 ions in CI spectra versus EI spectra such as the loss of $-CH_2O$ and $HO-N(CH_3)_2$ (Cope elimination) from CPZ-NO. The absence of these ions in FAB spectra supports the concept that they are generated by thermal decomposition. The three modes of ionization used in this study are complementary. EI versus CI spectra are useful for studying thermal decomposition. The CI spectra also yield some information concerning the molecular weight of the N-oxide while FAB generated spectra yield long-lived intense molecular ions. Together these three techniques aid in the positive identification of phenothiazine N-oxides.

ACKNOWLEDGEMENT

Supported by the Medical Research Council of Canada, PG-34.

IDENTIFICATION OF NAFIDIMIDE METABOLITES
IN CANCER PATIENTS BY THERMOSPRAY LC/MS

M.A. McLean and M.L. Vestal, Univ. of Houston, Dept. of Chemistry, Houston, TX 77004. D.A. Garteiz, Finnigan Mat Corp., San Jose, CA 95134. R.A. Newman, M.D. Anderson Hosp. and Tumor Inst., Houston, TX 77030

Thermospray LC/MS has been used to separate and identify urinary metabolites of nafidimide (I) in both dogs and cancer patients. Mass spectral data presented indicates the major metabolites from the two species are significantly different.

A total of six metabolites in cancer patients have been identified. These include the N'-acetylated, N-oxide, N'acetylated-N-Oxide, N'-acetylated-N-desmethyl and two N'-acetylated-hydroxy nafidimides. The mass spectra of the N-oxide maetabolites both show characteristic fragmentation patterns of M-16, M-30 and M-45 correponding to loss of oxygen, fomaldehyde and dimethylamine respectively. Other metabolites were identified on the basis of their retention times and/or their protanated molecular ions $(MH)^+$ which in all cases represented the base peak in the mass spectrum.

The major metabolites in dogs were also determined by the thermospray LC/MS technique. These metabolites were identified as the N-oxide and N-desmethyl nafidimides. The N-desmethyl metabolite was identified by its mass spectrum which consisted predominantly of the protanated molecular ion at m/e 270. The N-oxide metabolite was identified from its mass spectrum containing characteristic fragment ions and an ion at m/e 300 corresponding to the protanated molecular ion. In both man and dog the assignment of the N-oxide metabolite was confirmed by matching both the mass spectra and LC retention time of a synthesized N-oxide to that of the metabolite.

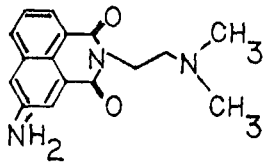

Confirmation of the N-acetylated nafidimide metabolite in man was also confirmed by matching retention time and mass spectra of the metabolite to an authentic sample

Summary of mass spectral data and metabolite assignments

RETENTION TIME (min.)	m/e	METABOLITE ASSIGNMENT
4.2	342	N-acetylated-hydroxy
4.6	328,312,297	N-acetylated-N-oxide
4.8	284,270,255,239	N-oxide
6.1	328	
7.2	342	N-acetylate-hydroxy
7.4	312	N-acetylated-N-desmethyl
9.0	326	N-acetylated
9.5	284	Parent

QUANTITATION OF NOVEL AMINO ACIDS
AND SUGARS BY THERMOSPRAY LC/MS/MS
AND LC/MS IN BIOLOGICAL SAMPLES

John E. Coutant and Kenneth Y. Chan
Merrell Dow Research Institute
Cincinnati, OH 45215

The purpose of this study was to evaluate LC/MS and LC/MS/MS for the quantitation in serum of compounds that are polar and water-soluble. Novel amino acids and sugars are two such classes of compounds that are difficult to extract and analyze by other techniques.

MDL 25,637 is a novel sugar which was designed as an intestinal α-glucohydrolase inhibitor. DL-α-difluoromethylorginine (DFMA) is an arginine decarboxylase inhibitor which interrupts polyamine synthesis in cells which possess these enzymes.

MDL 25,637

DFMA

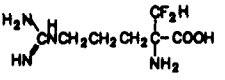

Serum samples were prepared by deproteinizing with an equal volume of 0.4N perchloric acid. The supernatant was injected directly into the HPLC. A Finnigan MAT TSQ-46 equipped with a Vestec thermospray source and interface was used for all samples.

Samples of the sugar, MDL 25,637, were run both by LC/MS and LC/MS/MS. The HPLC system consisted of a Zorbax NH_2 analytical column (4.6 mm ID x 25 cm) with a mobile phase of 60/40 acetonitrile/water at 1.0 ml/min. A make-up buffer of 0.1M ammonium acetate was added post column at 0.3 ml/min. LC/MS experiments were run in the selected ion monitoring (SIM) mode using the protonated molecular ion of MDL 25,637 (m/z 356). LC/MS/MS experiments were run in the selected reaction monitoring (SRM) mode following the collisional activated decomposition (20eV, 1 millitorr) of m/z 356 to m/z 194.

The comparison of LC/MS with LC/MS/MS of a 25 ug/ml plasma standard of MDL 25,637 is shown in Figure 1. As expected, MS/MS gives an increase in selectivity and sensitivity with direct injections of deproteinized serum. However a lower response relative to standards in water was observed for both LC/MS and LC/MS/MS due to matrix effects in the thermospray ion source.

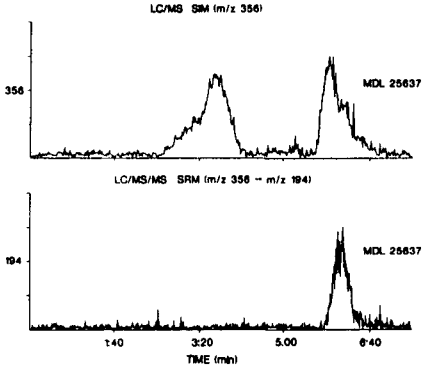

Figure 1

The concentration of α-difluoromethylarginine in the sera of mice dosed orally at 500 mg/kg of DFMA was determined by LC/MS. SIM monitoring of the protonated molecular ions (MH+) and ions due to the loss of water from the protonated molecular ions (MH-18+) was done both for DFMA and an internal standard, α-methylarginine (MA).

The HPLC was a gradient system with mobile phases of (A) 0.2M acetic acid and (B) 0.2M ammonium acetate pH 4.5 at a flow of 1.3 ml/min. The gradient program was linear from 95%A (after 5 min) to 20%A in 15 min. The analytical column was a 4.6 mm ID x 25 cm. Partisil SCX. A high pressure switching valve was added post column so that the analytical column effluent could be diverted from the LC/MS while the flow of a dilute buffer delivered by a third pump was maintained through the thermospray interface. This protected the thermospray probe from plugging due to silica stripping of the HPLC column and components eluted in the solvent front. The use of the switching valve also maintains thermospray probe temperatures as constant as possible to reproduce DFMA response.

The LC/MS response for DFMA in mouse sera was linear from 5 to 500 ug/ml but was often non-linear at higher concentrations. LC/MS analysis of mouse serum showed that DFMA was rapidly absorbed from solution given orally and eliminated with an initial half-life of approximately 20 min.

Use of Ion/Molecule Reactions for Selected Reaction Monitoring in GC/MS/MS Analyses.

Michael T. Kinter [1,2,3] and Maurice M. Bursey[2]

[1]Laboratory of Molecular Biophysics, National Institute of Environmental Health Sciences, P.O. Box 12233, Research Triangle Park, North Carolina, 27709 and [2]William Rand Kenan, Jr., Laboratories of Chemistry, The University of North Carolina at Chapel Hill, Chapel Hill, North Carolina 27514.
[3]Present Address: Department of Pathology, University of Virginia Medical Center, Charlottesville, Virginia 22908.

We have observed that some ion/molecule reactions in a triple quadrupole have high product ion yields. In the few systems studied thus far, ion/molecule reaction product yields (under conditions favoring ion/molecule reaction) have been as much as 20 times greater than the yield for collisionally activated decomposition (CAD) products (under conditions favoring CAD). These high yield ion/molecule reactions should lead to improved sensitivity and perhaps lower limits of detection in reaction monitoring mass spectrometry experiments. In addition, ion/molecule reactions might provide a transition unique to the target analyte in a complex system. This unique transition would then lead to increased selectivity in the analysis.

Two model compounds were studied, ethylene glycol monomethyl ether (EGME) and chlorobenzene, in simple extracts of human urine. For each compound, comparisons were made between GC/MS analyses using selected ion monitoring (SIM), CAD SRM and ion/molecule reaction SRM.

Figure 1 contains the daughter ion spectra of M/Z 59 from the CI spectrum of EGME at 1 eV and 30 eV using ammonia as the collision gas. Since it has been shown that ion/molecule reactions predominate at low ion kinetic energy and collisionally activated decompositions predominate at high ion kinetic energy, these spectra can be used to determine the major products of each process (Reactions 1 and 2).

$$\underset{m/z\ 59}{CH_3OCH_2CH_2^+} \text{ --- } \underset{m/z\ 29}{C_2H_5^+} + H_2CO \qquad (1)$$

$$\underset{m/z\ 59}{CH_3OCH_2CH_2^+} + NH_3 \text{ --- } \underset{m/z\ 44}{H_2NCH_2CH_2^+} + CH_3OH \qquad (2)$$

The ion yield for each reaction as a function of ion kinetic energy at a series of collision cell pressures is shown in Figure 2. As can be seen in this figure, the yield for the ion/molecule reaction product (m/z 44) is approximately 5 times greater than the yield for the CAD product (m/z 29) under the respective optimum conditions. This higher yield for the ion/molecule reaction is reflected in the sensitivity of the SRM analyses as shown in the calibration curves (Figure 3). GC/MS analysis of a urine extract is then shown in Figure 4 using a) SIM, b) CAD SRM, and c) ion/molecule

reaction SRM. In this example, EGME was not detected using CAD SRM, although a signal was observed for a compound eluting prior to EGME. Using ion/molecule reaction SRM, not only was EGME detected, illustrating the increased sensitivity, but the peak due to the compound eluting prior to EGME was eliminated, illustrating the increased selectivity. Similar results were obtained for the chlorobenzene analysis in which ion/molecule reaction SRM and CAD SRM were of comparable sensitivity, but the ion/molecule reaction SRM analysis was more selective (Figure 5).

These examples illustrate that ion/molecule reaction SRM can provide both greater sensitivity and selectivity than SRM as it is now practiced, that is, using CAD. That a truly unique transition can be found in every case using an ion/molecule reaction cannot, of course, be guaranteed, but the fact that different reactive collision gasses can be used adds a dimension beyond those of simple CAD SRM.

Figure 1

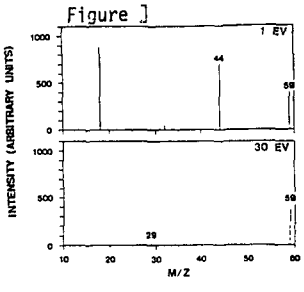

Figure 2

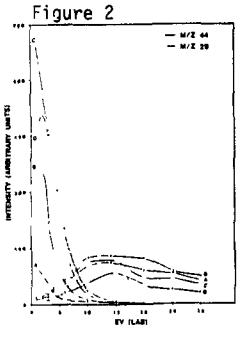

Figure 3

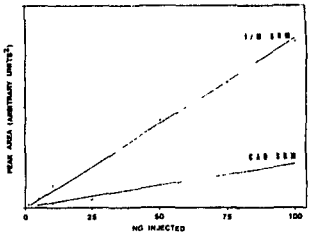

Figure 4

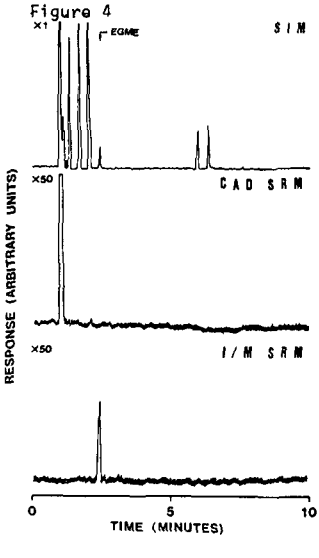

Figure 5

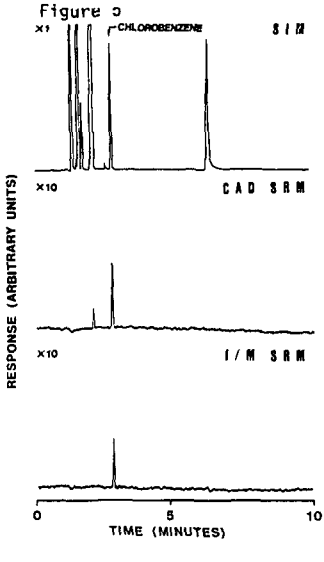

BENCHTOP SUPERCRITICAL FLUID CHROMATOGRAPHY/MASS SPECTROMETRY DETERMINATION OF STEROIDS;

Edgar D. Lee and Jack D. Henion; Drug Testing and Toxicology, NYS College of Veterinary Medicine, Cornell University, 925 Warren Drive, Ithaca, New York 14850.

INTRODUCTION

Supercritical fluid chromatography (SFC) is growing rapidly due to recent advances in column technology and instrument design. The main features which make SFC desirable for certain analyses over high pressure liquid chromatography (HPLC) and gas chromatography (GC) are that supercritical fluids have higher solute diffusivities than liquids, lower viscosities than liquids, and better solvating properties than gases. These features make possible higher chromatographic efficiences and faster analysis times than in liquid chromatography, and the ability to separate compounds which are thermally labile or beyond the volatility range of gas chromatography. Both temperature programming and gradient elution programming can be applied in SFC along with density programming which is unique to SFC.

SFC is amenable to most common HPLC and GC detectors. This is best evidenced by the ease in which packed-column supercritical fluid chromatography/mass spectrometry (SFC/MS) has been demonstrated using direct fluid introduction with the diaphragm probe interface (1). Although packed-column SFC/MS is suitable for many applications, the pressure drop across the column limits the length and hence the total number of theoretical plates obtainable. Because the permeability of an open tubular capillary column is higher than a packed column, long column lengths can be used and higher chromatographic efficiencies obtained. The low flow of the fluid from the exit of the small diameter capillary columns makes it possible to interface SFC with an inexpensive mass spectrometer such as the mass selective detector (MSD) (2). Our efforts have focused on implementing SFC on a benchtop mass spectrometer so that SFC/MS may be available at a low cost to analysts.

EXPERIMENTAL

The chromatographic system (Figure 1) consisted of a Brownlee Labs Micropump equipped with a Neslab cool flow model RTE4 for cooling the fluid prior to entering the dual syringe pump, a Hewlett-Packard 5890 gas chromatograph oven, and a Valco Model AC14W injector equipped with a 0.2 ul sample loop and a sample splitter (SGE Austin, TX). The column used was a 0.050 mm i.d. x 10 m fused-silica capillary coated with a 0.5 um film of SE-33 (Lee Scientific, Provo UT) and housed in the chromatographic oven which was maintained at a temperature of 100°C. The supercritical fluid used was SFC grade carbon dioxide (Scott Specialty Gases, Plumsteadville, PA). Pressure and flow restriction at the exit of the column was accomplished with a tapered restriction similar to what has been described by Gunthrie (3).

The mass spectrometer used was a modified Hewlett-Packard 5970 MSD equipped with a HP5995 chemical ionization source. The vacuum housing was altered to accommodate a 330 L/sec turbomolecular pump in place of the standard 50 L/sec turbomolecular pump and built into the side of the chromatographic oven to minimize the length of the transfer line. A potentiometer was inserted into the filament regulation circuit so that the electron energy is variable from 0-250V. The chemical ionization reagent gas was methane and 150V was used for the electron energy.

RESULTS AND DISCUSSION

The total ion current chromatogram of 75ng each of five related steroids is shown in Figure 2A. The first and second peaks contain two components each, testosterone acetate and methyl-1-dehydrotestosterone, and testosterone and 1-dehydrotestosterone in peaks 1 and 2 respectively. The third peak is testosterone propionate. The components in the first two peaks may be resolved with a longer column length at the expense of analysis time.

Figure 2B is the mass spectrum obtained from the third peak in Figure 2A. This spectrum has an abundant $(M+1)^+$ ion and the loss of the propionic acid group as would expected from methane chemical ionization of testosterone propionate. Chemical ionization gives little structural information and electron ionization would be preferable. At slightly lower flows and with the increased pumping of the modified MSD electron impact ionization should be possible. We are presently focusing our efforts in this area.

ACKNOWLEDGMENTS

We thank Brownlee Labs for the genrous gift of the Micropump, Hewlett-Packard Co. for the loan of the complete 5890/5970 Mass Selective Detector system, and Dr. Jean Luc Truche for invaluable assistance during the course of this work also Harry M. Zweig Memorial Fund.

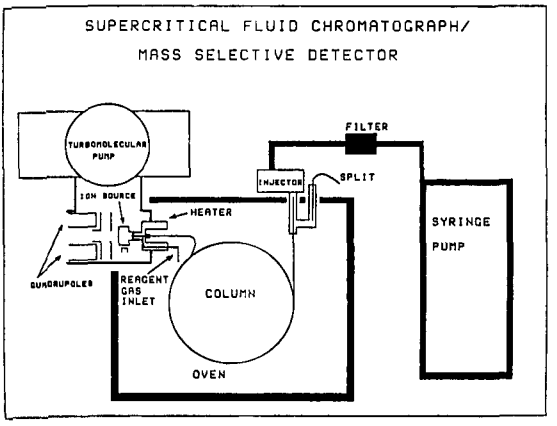

Figure 1. Schematic diagram of SFC/MSD system.

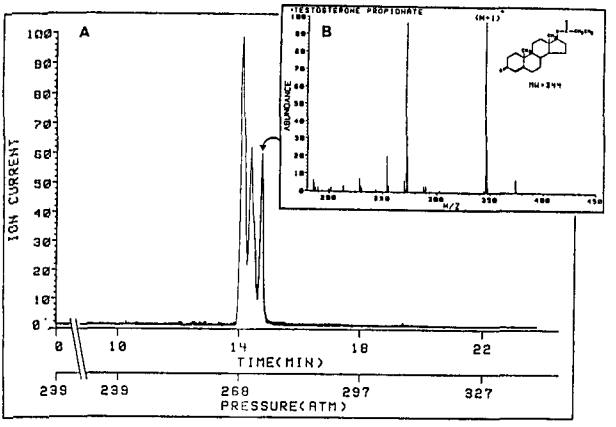

Figure 2. (A) TIC chromatogram of testosterone acetate, methyl 1-dehydrotestoserone, testosterone, 1-dehychotestosterone, and testosterone propionate. (B) spectrum of testosterone propionate.

REFERENCES

1. J.B. Crowther and J.D. Henion, Anal. Chem., 1985, 57, 2711-2716.
2. E.D. Lee and J.D. Henion, Jr. High Resolut. Chromatogr. and Chromatogr. Commun., 1986, 9, 172-174.
3. H.E. Schwartz, R.G. Brownlee, and E.J. Guthrie, Jr. Chromatogr., In Press.

QUANTITATION OF THE ARYLEICOSANOID, ALPHA-PENTYL-3-(2-QUINOLINYLMETHOXY)-BENZENEMETHANOL, IN HUMAN PLASMA BY SIM GC/MS.

S.Y. BROWN AND R.L. CHOI. Drug Disposition Department, Rorer Group, Inc., Tuckahoe, NY.

INTRODUCTION

The aryleicosanoid, alpha-pentyl-3-(2-quinolinylmethoxy)benzenemethanol (I) (a 5-lipoxygenase inhibitor and leukotriene D_4 antagonist), is now under clinical investigation for potential use in treatment of diseases such as asthma, allergy and psoriasis - diseases in which the involvement of leukotrienes is implicated. Because I is extensively metabolized after oral administration, a sensitive method able to assay low plasma levels of I was required. A specific and sensitive gas chromatographic/selected ion monitoring mass spectrometric assay for the determination of I in human plasma is described.

METHODS

The assay involves hexane extraction of plasma, followed by derivatization with N-methyl-N-trimethylsilyltrifluoroacetamide (MSTFA) to form the trimethylsilyl (TMS) ethers of I and the butyl analog of I (II), the internal standard. The derivatized extracts were chromatographed on a 3% OV-101 column, isothermally at 260° (Finnigan model 9600 GC) and were analyzed on a Finnigan 4500 mass spectrometer. Figure 1 shows representative EI mass spectra of I-TMS and II-TMS obtained with the mass spectrometer scanning from 45-650 amu in 2 sec. For selected ion monitoring, the mass spectrometer was set to scan m/z 142 (the methylquinoline ion, which was the base peak for the TMS ethers of both I and II; used for quantitation of I), as well as m/z 115 and 336 (used for confirmation of compound identity). The fragment ion at m/z 115 corresponds to the indenyl ion obtained following elimination of HCN from the methylquinoline ion. The ion at m/z 336 was formed following the loss of the pentyl side chain from I-TMS and the butyl side chain from II-TMS. Figure 2 shows m/z 142 chromatograms of human plasma sample extracts, each spiked with II (internal standard; 40 ng/ml).

RESULTS AND DISCUSSION

Linearity of response, as a function of concentration, was demonstrated in five standard curve determinations with correlation coefficients ranging from 0.99941 to 0.99997. Coefficients of variation for day-to-day m/z 142 peak height ratios (I-TMS to II-TMS) ranged from a low of 4.3% at 40 ng I/ml to a high of 18.9% at 5 ng I/ml, with an average of 8.0 ± 5.4%. The accuracy data, expressed as mean relative error, varied from 0.6 ± 0.5% at 160 ng/ml to 11.8 ± 6.9% at 5 ng/ml. The efficiency of the extraction of I and II from plasma averaged 86% for both compounds with standard deviations of 4% and 8%, respectively. The assay was specific for I in that no interfering peak was present at the retention time of I in the chromatograms of control human plasma extracts. The utility of the assay was demonstrated with the analysis of plasma samples from human subjects administered a 1000 mg oral dose of I.

CONCLUSION

The GC/MS assay for I was shown to be specific, sensitive, reproducible and accurate in the concentration range of 5-160 ng/ml plasma. This assay is particularly useful for assaying plasma with low concentrations of I.

Figure 1

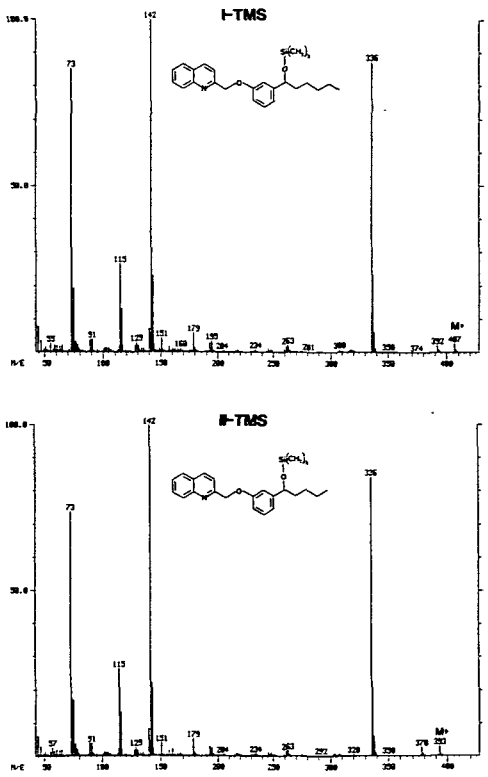

Figure 2

m/z 142 CHROMATOGRAMS OF HUMAN PLASMA SAMPLE EXTRACTS, EACH SPIKED WITH II (40 ng/ml); (A) CONTROL PLASMA (B) VALIDATION PLASMA STANDARD EXTRACT CONTAINING I (40 ng/ml) AND (C) EXTRACT OF PLASMA FROM HUMAN SUBJECT OBTAINED 2 HR POST-DOSE OF I (1000 mg)

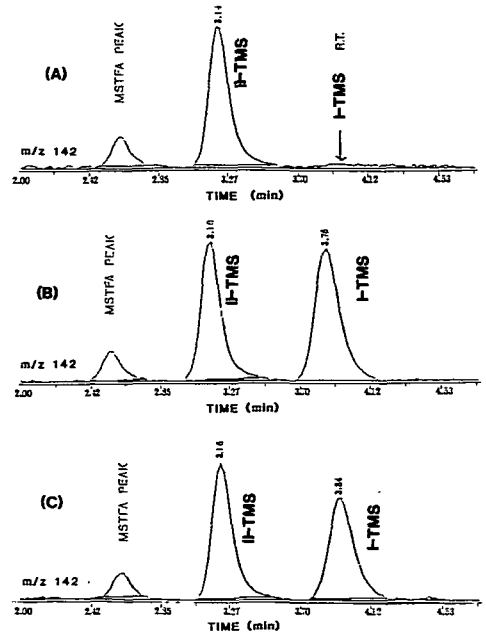

THE USE OF MS AND MS/MS IN DRUG-RELATED STUDIES

Alison E Ashcroft, Roger J Greathead, Malcolm L Kimber
Kratos Analytical, Barton Dock Road, Urmston, Manchester M31 2LD, UK

Summary

The detection and analysis of drugs is an important technique in areas such as horse-racing, athletics, pharmaceuticals and medicine.

Data are presented here with reference to LC-MS, Selected Ion Monitoring, High Resolution Selected Ion Monitoring, MS-MS and linked scanning MS.

Experimental

All the work described was performed on a Kratos Analytical MS890MS hybrid mass spectrometer of EBQQ geometry. The first stage comprises a high performance double focussing mass spectrometer with a mass range of 16,000u and resolving power of 50,000, and has an off-axis detector which allows standard EB operation to be carried out. For MS-MS studies, this detector is by-passed and the ion beam decelerated into a dual quadrupole (Extranuclear Corp) collision and analysis stage.

Results and Discussion

A frequently encountered problem in sporting events is the detection of the presence of illegal drugs, such as caffeine in horse urine. A selective technique such as MS-MS must be used and the fragment ion spectrum of 800pg of caffeine is shown in Figure 1. When this is compared to the reference MS-MS spectrum of caffeine, unambiguous identification is rapidly achieved.

Figure 1 : The MS-MS fragment ion spectrum of caffeine (800pg).

MS-MS studies prove useful also in the area of peptide identification and sequencing. The protonated molecular ion from FAB provides molecular weight information, while the MS-MS fragment ion spectrum of the protonated molecular ion generates sequence information. For the latter type of scan, the nature and pressure of the collision gas and collision energy in the first quadrupole are important parameters. The type of collision cell used permits fragment ion collection efficiencies of > 90%, and many peptides have been successfully studied.

Often sub ppb and ppt detection of toxic substances is required, and Selected Ion Monitoring is the most sensitive method available. This technique has been used to monitor a PFB-cytosine derivative, and Figure 2 shows the signal detected from 40fg of sample, achieved by negative ion chemical ionization at 1000 resolution (10% valley).

Figure 2 : SIM - NICI - PFB derivative cytosine (40fg).

Target compound detection can be hindered by the coexistence of impurities and compounds closely related to the sample of interest. Higher resolutions are then required to increase the specificity of the technique. 25,000 resolution (10% valley) was required to detect a Thromboxane B_2 derivative unambiguously.

Linked scanning (B/E) LC-MS has proved to be a useful technique for studying the ionophore antibiotic erythromycin. The thermospray spectrum of erythromycin shows a protonated molecular ion, but little fragmentation information. A collision gas was introduced into the first field free region in order to fragment the protonated molecular ion. The fragments thus produced were detected by a B/E scan, and loss of the desosamine sugar moiety from the molecular ion confirmed the identification.

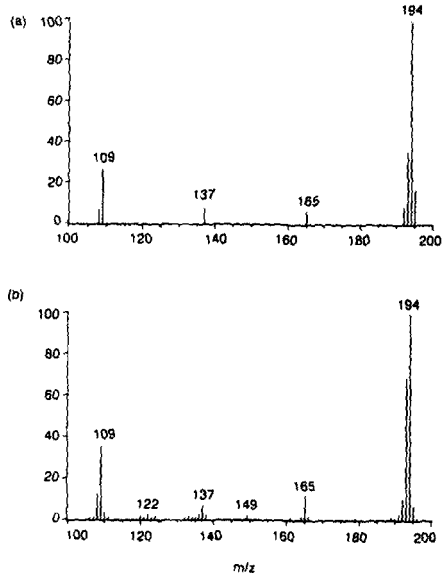

Figure 1 Fragment ion scan of 800pg of caffeine (top) compared to caffeine reference spectrum (bottom)

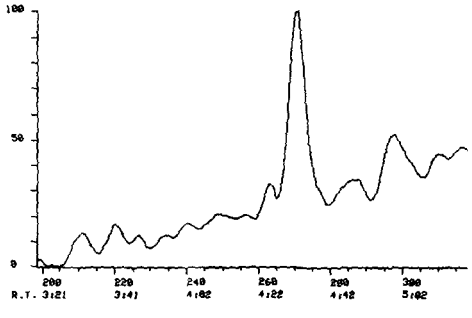

Figure 2 Selected Ion Monitoring trace obtained from an injection of 40 femtograms of PFB-cytosine in the negative ion mode

LASER MICROPROBE MASS ANALYSIS OF INDUSTRIAL ATMOSPHERIC DUST PARTICLES

S. Beaudet and J.P.Schmit; Université du Québec à Montréal, Dept. of Chemistry and GEOTOP, P.O. Box 8888 Stat. A, Montreal H3C 3P8, and J. Lesage; IRSST, 505 Blv. Maisonneuve W, Montreal H3A 3C2.

Assesment of potential environmental and toxicological consequences of airborne microparticles requires detailed physical and chemical characterization of individual microparticles as well as possible adsorbed materials. This is of prime importance if we consider that physiological effects resulting from ingestion of airborne microparticles often originate from combination of the physico-chemical nature of the microparticle itself and the nature of the organic poisons adsorbed on its surface.

In this context any approach to the study of this synergetic effect must involve along with the study of microparticulate morphology a direct characterisation of the chemical elemental composition of individual microparticles as well as adsorbed organics.

This problem is especially important in industrial environment where high concentration of airborne toxic microparticles can be found. Laser microprobe mass analysis has been used in an attempt to correlate chemical analysis of individual airborne microparticle and specific industrial environment.

SAMPLING

a) Benzo-a-pyrene standard sample was prepared by filtering through a PVC membrane a known volume of air containing a density of 5 ug / m^3 of benzo-a-pyrene dry airborne microcrystals.
Actual atmospheric benzo-a-pyrene sample was prepared by disolving 5 ug of benzo-a-pyrene in dichloromethane. The solution was mixed with 5 mg of graphite microparticles and evaporated to dryness. The resulting powder was suspended in air and filtered through a PVC membrane.
b) On site Airborne microparticles have been collected by filtering a known volume (960 liters) of air through polyvinylchloride (PVC) or Teflon membranes.
c) Sampling was done at the welding site in close vicinity of a worker using M.I.G. (Metal Inert Gas CO_2 atmosphere) procedure. The welding electrode was of the E70-S-3 type. The welded stainless steel were of the SAE-1010 and 44W types. Table I shows the elemental composition of these materials.

RESULTS AND DISCUSSION

a) Benzo-a-pyrene (M.W. 252) can be easily analysed by ionization of a pure microcrystal at low laser energy directly on the PVC mechanical substrate. However, very few fragments were obtained. On the actual sample, by using approximately the same laser energy, benzo-a-pyrene molecular ion can be detected at m/z 252 besides of the twelve sequence resulting from ionization of the graphite microparticulate substrate.
b) Actual industrial airborne microparticulate samples.
Spectrum A shows the elemental composition of a collected unknown fiber. Besides of Ca (m/z 40), V (m/z 51), and Zn (m/z 64, 66, 68) the presence of Na (m/z 23), Al (m/z 27), Si (m/z 28), K (m/z 39, 41), Cr (m/z 52) and Fe (m/z 56) suggest the presence of a glass fiber. This hypothesis is supported by the fact that sampling was done close to an industrial oven in which the inner walls were coated with a material containing glass fibers.

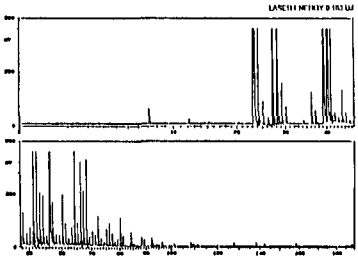

c) Spectrum B yields the elemental composition of a black airborne particle collected in close vicinity of a welding station. Comparison with the elemental composition of the material used (Table I) demonstrates that this particle originates from the welding atmosphere itself.

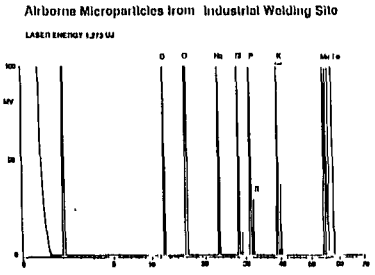

TABLE I : ELEMENTAL COMPOSITION OF THE USED MATERIAL (IN %).

Product	C	Mn	Si	P	S
E70-S-3	0.06 to 0.15	0.90 to 1.40	0.45 to 0.70	0.025	0.035
SAE-1010	0.08 to 0.13	0.30 to 0.60	----	0.040	0.50
44W	----	1.50	----	------	-----

CONCLUSION

Although used as a microprobe analyser in a wide variety of environmental problems, the versatility as well as the power of this technique seem to be especially appropriate in such circomstances.

However, its main advantage lies in its capability of very selective analysis directly on the raw microparticulate material. Moreover, by modulating the laser power energy, although it seems not easy to completely characterise an unknown adsorbed organic, it is possible to detect "*expected*" organics adsorbed on selected microparticles. This is especially important in associating morphology, elemental composition, and adsorbed organics for synergetic study. An approach which has been proved of crucial importance for human health.

Finally, it is evident that this method can clearly relate the very nature and the origin of airborne microparticles as well as adsorbed organics breathed by workers in specific industry.

SEPARATION AND IDENTIFICATION OF THE OPTICAL ISOMERS OF 17-METHYLMORPHINAN-3-OL IN URINE SAMPLES AS (-) MENTHYL CARBAMATE DERIVATIVES BY CAPILLARY COLUMN GC/MS.

R.L. Wilson*, Division of Pharmaceutics, College of Pharmacy, The Ohio State University, Columbus, Ohio 43210 and R.A. Sams, College of Veterinary Medicine, The Ohio State University, Columbus, Ohio 43210.

The separation and identification of drugs of abuse has always been of primary interest to forensic chemists. Now, an extra burden has been added in that laboratories are often required to prove conclusively which optical isomer of a substance is present in a sample[1] since pharmacologic effects may be produced by only one isomer or the effects produced by the two isomers may differ greatly. This laboratory has been concerned with identifying drugs in the presence of inactive isomers of these drugs.

As an example, dextromethorphan[(+) 3-hydroxy-17-methyl morphinan] is metabolized in horses by O-demethylation to dextrophanol [(+)17-methyl morphinan-3-ol], which is the stereo-isomer of the narcotic levorphanol. Current techniques, such as radio-immunoassay, are not stereo-specific and may not resolve the stereoisomers present.

We have developed a faster and more reliable method for the resolution of dextrorphanol and levorphanol.

Following hydrolysis with B-glucuronidase, the samples are extracted with methylene chloride. An aliquot of the extract is spotted on a silica gel thin-layer chromatographic plate. After development, the region corresponding to the analytes is removed by scraping. The analytes are then derivatized by extractive alkylation[2] with ethyl iodide using tetrabutyl ammonium sulfate as an ion pair reagent.

(-) Menthyl carbamates are then formed using (-) menthyl chloroformate in toluene. The resulting diastereomers are separated by capillary gas chromatography using a 30 M x 0.25mm ID DB-5 fused silica column and identified by mass spectrometry.

Figure 1 shows the structure of the final derivative.

A typical separation is shown in Figure 2. Here, the ions at m/z 233 and m/z 320 are due to the internal standard levoethorphan-D5. The ions at m/z 228 and m/z 315 are due to derivatized levorphanol and dextrorphanol. Levorphanol elutes before dextrorphanol.

FIG. 1: **STRUCTURE OF THE FINAL DERIVATIZATION PRODUCT**

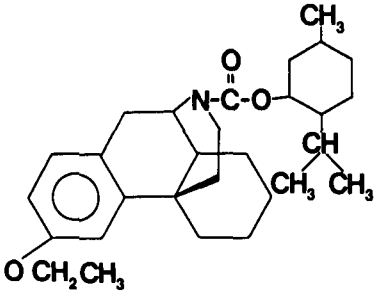

FIG. 2: **MASS CHROMATOGRAM OF A DERIVATIZED STANDARD CONTAINING LEVORPHANOL, DEXTROPHANOL AND THE INTERNAL STANDARD**

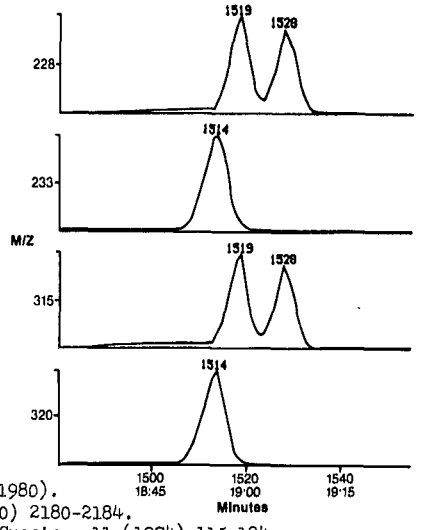

REFERENCES:
1) State vs McNeal, 288 N.W. 2d 874 (Wis.App 1980).
2) J.H. Liu and W.W. Ku, Anal. Chem., 53 (1980) 2180-2184.
3) P. Hartvig and J. Vessman, J. Acta Pharm. Suecica, 11 (1974) 115-124.
4) R.A. Olofson, et. al., Tetrahedron Lett., 18 (1977) 1567-1570.

ACKNOWLEDGEMENT:
This work was supported in part by funds provided by the Ohio State Racing Commission, the Ohio Thoroughbred Fund, and the National Association of State Racing Commissioners Uniform Drug Testing and Quality Assurance Program.

* Present address: Battelle Columbus Laboratories, 505 King Ave., Columbus, OH 43201

STUDIES OF BETA-ADRENERGIC BLOCKER DRUGS WITH LIQUID CHROMATOGRAPHY - MASS SPECTROMETRY

R. Willoughby, F. Poeppel, J. Buchner, V. Pizzitola, Extrel Corporation, Pittsburgh PA
A. Pirone and S. Assenza, ICI Americas, Wilmington DE.

INTRODUCTION:

LC/MS provides an ideal combination of chromatographic separation and specificity for the analysis of labile drugs and metabolites. Unfortunately, most currently used techniques lack the structural information available with the use of electron impact ionization. MAGIC-LC-MS (Monodisperse Aerosol Generation Interface for Combining Liquid Chromatography with Mass Spectrometry) is reportedly capable of generating conventional EI spectra. However, a wider variety of applications data are required to fully characterize this technique.

OBJECTIVE:

Evaluate the MAGIC-LC-MS technique for the analysis of beta-blocker drugs.

EXPERIMENTAL:

A prototype interface was inserted into a model EL 400-3 mass spectrometer. A series of beta blockers were separated on a C-18 column, 50/50 ACN/H_2O, pH = 3 with acetic acid.

CONCLUSIONS:

MAGIC-LC-MS is capable of generating library searchable EI spectra for the series of beta blockers in this study.

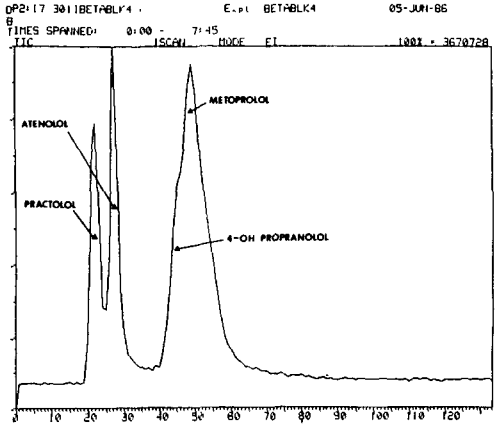

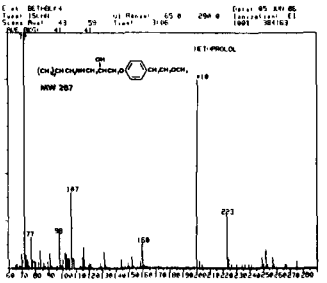

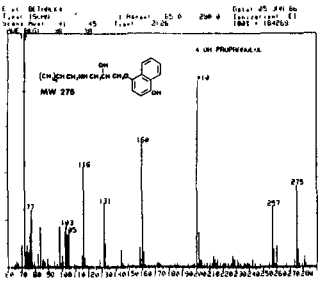

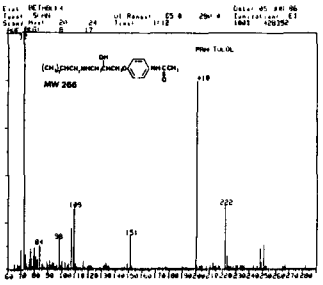

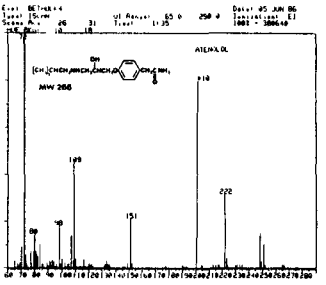

A Comparison of FAB-MS/MS and HPLC-MS/MS for the Analysis of Catecholamine Metabolites. Patrick Rudewicz and Kenneth Straub. Smith Kline and French Laboratories; Dept. of Drug Metabolism, 709 Swedeland Road, Swedeland, PA 19479.

Introduction

The combination of FAB-MS/MS and thermospray (TSP)-MS/MS provides a unique tool for the rapid structure elucidation of metabolites, in that many classes of polar, thermally labile compounds can be efficiently ionized to yield molecular ions which can subsequently be collisionally dissociated to yield structurally informative fragment ions. Previous efforts in this laboratory have been aimed at designing specific MS/MS scan sequences that can be used to characterize common classes of drug conjugates. Neutral loss scans give high specificity for the detection of O-glucuronides (+/- 176 amu) and aryl sulfate esters (+/- 80 amu). By combining neutral loss scans that are specific for the conjugating species together with precursor ion scans that are specific for substructural features of the drug, both primary and secondary metabolites of a drug can be rapidly identified within a complex sample matrix.

The catecholamine drug ibopamine (SK&F 100188; epinine diiso-butyric ester), is a positive inotropic agent currently under investigation for treatment of patients with congestive heart failure. Studies have shown that when ibopamine is administered, the isobutryl groups are rapidly hydrolyzed and epinine (N-methyldopamine) is released into the circulation (1). The major urinary metabolites of ibopamine in both the rat and the dog have been identified in previous studies (1) using conventional methodologies and are shown in Figure 1. Studies with monkeys indicated the possible presence of novel metabolic pathways, prompting us to explore the use of MS/MS methodologies for the characterization of the metabolites of ibopamine in this species.

Experimental

Mass Spectrometry. MS/MS experiments were carried out on a tandem quadrupole mass spectrometer, ("TSQ-15", Finnigan-MAT, San Jose, CA), equipped with a 4500-series ion source. Fast atom bombardment (FAB) mass spectra were obtained using a saddle field-type discharge source (Ion Tech model 11NF, Ion Tech Ltd., Teddington, UK). HPLC-MS spectra were obtained using a Finnigan thermospray ion source and controller. Typical operating temperatures were: vaporizer 140 °C; jet 190-200°C; aerosol 220-240°C. An electron filament was not employed. A Beckman "Ultrasphere" octadecyl-silane column (4.6mm x 25cm, 5 µm particle size) was used for all separations. Linear gradients of 50 mM ammonium acetate, pH 4.0 and methanol were used [2% organic --> 30% organic in 20 min] at a flow rate of 1.2 ml/min. Analysis of metabolites by FAB-MS/MS was carried out directly on a 0.5 µl sample of urine obtained from male Cynomolgus monkeys which had received 35 or 350 mg/kg of SK&F 100188-A-^{14}C (ibopamine; "A" refers to the hydrochloride salt). TSP-MS/MS analyses were carried out on 10-20 µl samples of filtered urine obtained from the same monkeys, injected directly onto the HPLC column.

Results and Discussion

FAB-MS/MS: Since ibopamine is known to undergo rapid hydrolysis *in vivo* to epinine (N-methyldopamine), a search for metabolites of the parent drug can be conducted using ions characteristic of epinine. A daughter ion CAD spectrum of the protonated molecular ion of epinine (MH^+, m/z 168) formed under FAB conditions shows a major fragment ion at m/z 137, corresponding to loss of the elements of methylamine (Figure 2a). The initial search for the metabolites of epinine in monkey urine, therefore, was a parent ion scan of m/z 137 (this fragment ion is also formed from ibopamine). Figure 2b shows the parent ion spectrum of all the ions that fragment to give m/z 137 when 0.5 ul of urine (obtained from a Cynomolgus monkey given a 350 mg/kg dose of SK&F 100188-A) was analyzed by FABMS. Prominent ions appear at m/z 168, 182, 197, 229, 248, and 344. Except for m/z 229, these ions are not observed at comparable intensities in urine obtained from animals that did not receive the drug, and are therefore putative metabolite parent ions. Subsequent neutral loss scans of +176 amu and +80 amu combined with a comparison of CAD spectra with synthetic standards confirm that the ions at m/z 344 and m/z 248 are the protonated molecular ions of epinine glucuronide and epinine sulfate, respectively. Similarly, a neutral loss scan of 45 amu and comparison of CAD spectra with standards confirm that the ions at m/z 168 and m/z 182 are the molecular ions of dihydroxyphenylacetic acid (DOPAC) and homovanillic acid (HVA), or its isomer 3-hydroxy-4-methoxyphenylacetic acid, respectively.

LC-MS/MS: Analysis of a 20 µl urine sample by thermospray HPLC-MS (scanning Q1 only) results in the relatively complex total ionization chromatogram (TIC) shown in figure 3a. The individual epinine metabolites that were identified in the FAB-MS/MS experiments give TSP mass spectra consisting of either MH^+ or $(M+NH4)^+$, along with some fragment ions. The metabolites, however, are difficult to distinguish from either endogenous compounds or eluent background without an exhaustive search of each scan. The use of MS/MS scans that are specific for each type of conjugate can result in a dramatic simplification of the ion chromatogram. For example, figure 3b shows the TIC obtained with a scan that is diagnostic for O-glucuronides, a neutral loss scan of +176 amu. The TIC indicates the presence of a major component with a retention time similar to that of epinine glucuronide, as well as a number of additional components. The mass spectrum of the major component consists primarily of two ions, m/z 168 and m/z 18. The precursor ion to m/z 168 is (168 + 176)= m/z 344, which corresponds to protonated epinine glucuronide. The ion at m/z 18 (NH_4^+)is derived from (18 + 176)= m/z 194, which corresponds to an ammoniated glucuronic acid fragment ion. The peak in Figure 3b with a retention time of 13 min. has a neutral loss spectrum which consists primarily of two ions at m/z 18 and m/z 200. This is consistent with a glucuronide of HVA or its isomer, and the full scan (Q1) mass spectrum of this component confirms the presence of an ion corresponding to $(M+NH_4)^+$ for this conjugate at m/z 376.

The reults of a neutral loss scan that is diagnostic for carboxylic acids (-44 amu) has two major peaks at m/z 123 and m/z 137, derived from precursor ions at m/z 167 and m/z 181. These correspond to the expected molecular anions of DOPAC and HVA, and a comparison of thier CAD spectra with synthetic standards confirms thier identification. Reconstructed ion chromatograms (RIC) of daughter ion spectra of m/z 248 (MH^+ for epinine sulfate) reveal the presence of two major components that give identical CAD spectra, both of which are identical to those obtained for epinine-3-O-sulfate and epinine-4-O-sulfate. Comparison of LC retention time data confirm the presence of both isomers in urine. Using FAB-MS/MS and TSP-MS/MS, greater than 95% of the radiolabel present in an HPLC (flow scintillation detector) trace of a urine sample containing ^{14}C-ibopamine metabolites is accounted for.

1.Hwang, B.Y-H.; Kuo, G.Y.; Lynn, R.L. IUPHAR 9th Internatl. Congress of Pharmacology; London, 1984, Abstract No. 523P.

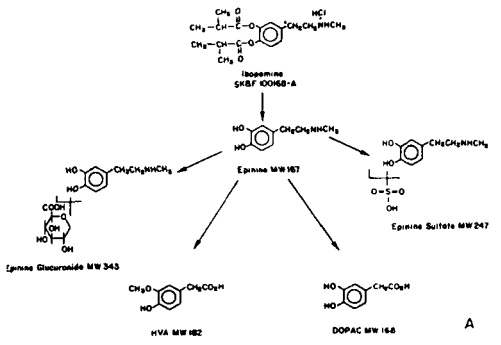

Fig. 2

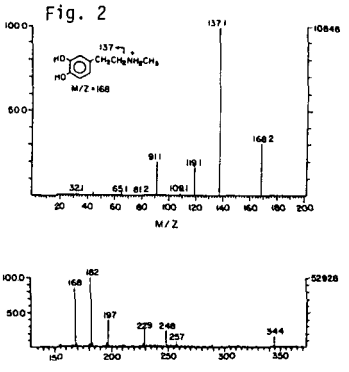

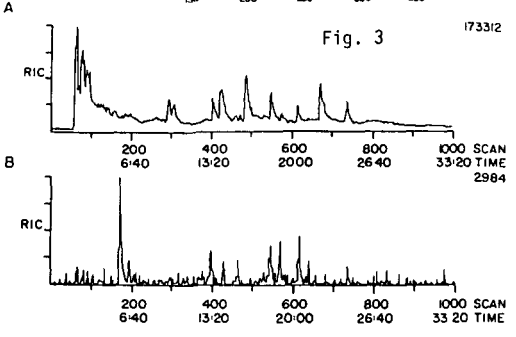

Fig. 3

A Pharmacokinetic Comparison of Triclopyr and its Butoxyethyl Ester in Fischer 344 Rats. Patrick E. Kastl, Gauke E. Veenstra and Emile A. Hermann The Dow Chemical Company Midland,MI 48674

Triclopyr,[(3,5,6-trichloro-2-pyridinyloxy)acetic acid], as the butoxyethyl ester (EB ester) is used in many herbicide formulations as the active ingredient. Triclopyr is an auxin type herbicide that provides control of woody plants and broadleaf weeds.

Metabolism studies were designed to investigate the pharmacokinetic fate of triclopyr and its EB ester in Fischer 344 rats. In this work sensitive analytical methods were developed for determining these materials in whole rat blood. These methods utilized electron impact(EI) ionization GC/MS with multiple ion detection(MID) for quantitative determinations. Analysis of blood following oral administration of radiolabeled EBester showed only the acid(triclopyr) present using these methods. No EB ester was found 0-8 hours post-dosing in blood. Following administration of equimolar doses of either radiolabeled triclopyr or its EB ester the radioactivity-time profiles of blood-plasma were nearly identical. The majority of radioactivity (approximately 80%) was excreted rapidly in the urine 0-12 hours post-dosing of either material. These radiolabeled urine samples were profiled by high performance liquid chromatography(HPLC) and detected with an in-line radioactivity monitor. Selected fractions were collected and identified by direct probe CI MS. The HPLC radioactivity profiles from animals dosed with triclopyr or its EB ester were nearly identical and showed five radiolabeled peaks present. One radiolabeled peak contained approximately 90% of the radioactivity present in the urine samples and was identified as the acid(triclopyr). Three other radiolabeled peaks contained approximately 8% of the radioactivity present in urine and were identified as 3,5,6-trichloro-2-pyridinol or as acid labile conjugates thereof.

In summary the data indicates that the EB ester of triclopyr is rapidly hydrolyzed in vivo to the acid(triclopyr), thus demonstrating that both materials result in the same chemical entities within the body. Therefore equimolar doses of these two materials should produce equivalent toxic effects since the biological fate of these materials is similar.

DETECTION OF SUFENTANIL ADMINISTRATION TO HORSES BY CAPILLARY GAS CHROMATOGRAPHY/MASS SPECTROMETRY WITH NEGATIVE CHEMICAL IONIZATION OF A HEPTAFLUOROBUTYRYL DERIVATIVE

James S. Noonan and Richard A. Sams, College of Veterinary Medicine, The Ohio State University, Columbus, Ohio, 43210

INTRODUCTION

Sufentanil, a synthetic opioid related to the phenylpiperidines, is approved for use in humans as an adjunct to inhalation anesthesia. Its analgesic potency is 5 to 7 times that of fentanyl and 400 to 1000 times that of morphine.(1,2) Since narcotics produce dose-dependent increases in spontaneous locomotor activity in horses, they are sometimes administered to horses in an attempt to affect their racing performance. An analogue of sufentanil, fentanyl, has been detected in urine samples collected from horses racing in the United States. We suspect that sufentanil may be similarly used.

Fentanyl is metabolised by oxidation of the propionamide group to a malonanilinic acid derivative in horses with at least 65% of the total dose eliminated in the urine as the acid metabolite.(3) This metabolite is isolated from urine by a liquid/liquid extraction procedure and hydrolyzed to despropionylfentanyl, which is detected and identified by GC/MS.(4)

In a preliminary study, apparent sufentanil concentrations determined by sufentanil radioimmunoassay of urine samples collected from horses given a 250 ug intravenous dose of sufentanil did not exceed 4 ng/ml. Therefore, in order to reliably detect sufentanil administration to horses, we developed a highly sensitive mass spectral identification method. High sensitivity and specificity were achieved by capillary gas chromatography, sample derivatization, and ammonia negative chemical ionization mass spectrometry.

MATERIALS AND METHODS

Four horses were administered 250 ug of sufentanil intravenously. Urine samples were collected from the horses at various times after dosing and were analyzed in two groups. The first group consisted of 4 urine samples collected from one horse before and at 2, 4, and 6 hours after sufentanil administration. Urine was collected from the other three horses before and at 2, 4, 8, and 24 hours after sufentanil administration, and the samples from each collection period were combined.

A 50 ml portion of each urine sample was adjusted to pH 2 with 4 N HCl and saturated with NaCl. The sample was divided into two equal portions. One portion was extracted with 100 ml of dichloromethane/isopropanol (90:10). The organic solvent was separated and used to extract the second portion. The solvent was separated and evaporated on a rotary evaporator to near dryness. The residue was dissolved in 30 ml of 4 N HCl and autoclaved for 1 hour a 121°C and 15 psi. The solution was then washed twice with 25 ml of cyclohexane, which was discarded. The aqueous solution was placed in an ice bath and adjusted to pH 10 with 50% NaOH, and extracted twice with 25 ml of dichloromethane. The dichloromethane extracts were combined in a round bottom flask and taken to dryness on a rotating evaporator. The flask was rinsed twice with 2 ml of 2 N HCl. The combined HCl solutions were washed twice with 3 ml of cyclohexane, which was discarded. After cooling in crushed ice, the solution was adjusted to pH 10 with 50% NaOH and extracted twice with 5 ml of petroleum ether. The combined extracts were taken to dryness under a stream of nitrogen at room temperature. To the dry residue in the tubes were added 40 ul of ethyl acetate and 20 ul of heptafluorobutyric anhydride. The capped tubes were placed in a heating block for 90 minutes at 65°C. Solvent and excess reagent were removed under a stream of nitrogen at room temperature.

Derivatized samples were analyzed by capillary gas chromatography/mass spectrometry with on-column injection with a retention gap (5) before the analytical column (30 m x 0.257 mm i.d., DB-1 coating, 0.25 um thick). Column performance deteriorated after 8 to 10 samples had been analyzed, but was restored by removing a meter of the retention gap column at the inlet end.

The mass spectrometer was calibrated with perfluorotributylamine (PFTBA) in the electron impact (EI) mode and EI spectra were acquired with 30 milliamperes emission current and 70 electron volts. For negative chemical ionization (NCI) spectra, the mass spectrometer was switched to NCI mode and ammonia was admitted to the source. In the NCI mode, the mass spectrometer was adjusted for maximum sensitivity by admitting PFTBA and then varying the lens potentials and ammonia pressure in the source until the greatest amplitude of the ion at m/z 433 was obtained.

RESULTS AND DISCUSSION

Selective mass spectral detection of the derivative in an area of the chromatogram free of interfering peaks enabled us to use a high gain on the electron multiplier. Use of ammonia as a reagent gas resulted in lower background noise. A molecular mass of 526 for the derivative was indicated by the pseudo-molecular ion at m/z 527 and the M+29 adduct ion at m/z 555 in a spectrum obtained under positive chemical ionization conditions with methane as the reagent gas. The mass spectrum of the derivative under EI conditons was characterized by a base peak at m/z 429, which was attributed to the ion resulting from the loss of neutral 2-methylene thiophene from the molecular ion. The mass spectrum of the derivative uder ammonia NCI conditions was characterized by a base peak at m/z 269, which was attributed to a rearrangement of the heptafluorobutyrlanilide ion with a loss of fluorine. Under full scan NCI conditions with ammonia as the reagent gas, 500 pg of the derivative injected produced spectra with at least a 10:1 signal to noise ratio.

Electron impact and NCI spectra of the sufentanil derivative were obtained from the extracts of the 2, 4, and 6 hour urines from the first horse. NCI spectra were obtained from the 2, 4, and 8 hour combined urine samples from the second group of horses. No EI spectra were taken from the extracts of these three samples. The 24 hour urine sample extract contained one ion (m/z 269) in the NCI mass spectrum, and one ion (m/z 429) in the EI mass spectrum, and both of these appeared at the retention time of an authentic standard of the derivative.

REFERENCES

1. E.R. Barnhart, Physicians Desk Reference, 1985, 1040-42.

2. T.J. Gillespie, A.J. Gandolfi, R.M. Malorino, and R.W. Vaughan, "J. Anal. Toxicology", 1981, 5:133-37.

3. J.M. Frinche, and G.L. Henderson, "Drug Metab. Dispos.", 1980, 8:425-7.

4. F. Ozog, Industrial Laboratories Co., Denver, CO, 1979, personal comm.

5. K. Grob, Jr., and H.P. Neukom, "Jour. of Chromatogr." 1985, 323:237-46.

ACKNOWLEDGEMENTS

This research was supported by the National Association of State Racing Commissioners Uniform Drug Testing and Quality Assurance Program and the Ohio State Racing Commission.

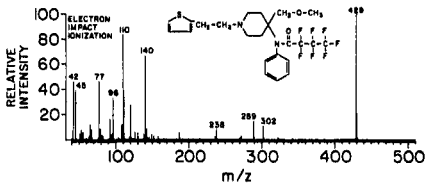

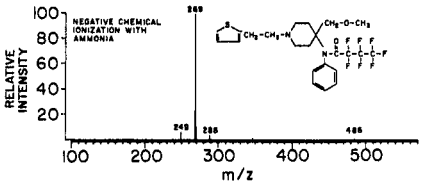

FAST ATOM BOMBARDMENT MASS SPECTROMETRY AND FAST ATOM BOMBARDMENT MASS SPECTROMETRY/MASS SPECTROMETRY OF THREE GLUTATHIONE CONJUGATES OF ACETAMINOPHEN; J. O. Lay, Jr., D. W. Potter, and J. A. Hinson, National Center for Toxicological Research, Jefferson, AR, 72079.

ABSTRACT

Three synthetic glutathione conjugates of acetaminophen were examined by fast atom bombardment/mass spectrometry (FAB/MS) and fast atom bombardment/mass spectrometry/mass spectrometry (FAB/MS/MS). The conjugates 3-(glutathion-S-yl)acetaminophen (GS-A), 3-(glutathion-S-yl)diacetaminophen ($GS-A_2$), and 3-(diglutathion-S-yl)diacetaminophen (GS_2-A_2) were examined by FAB/MS and showed intense $[MH]^+$ ions at m/z 457, 606, and 911 respectively. Fragmentation was not observed in any compound except GS-A. However, collisional activation at high energy (8KeV) of the intense $[M+H]^+$ ions produced numerous fragments which were examined by FAB/MS/MS and shown to be characteristic of the parent compound. For example, several characteristic cleavages were observed indicating the presence of a glutathione moiety in all three compounds. These included losses of 44, 75, 129, and 275 daltons. Furthermore, the diglutathione conjugate showed losses corresponding to combinations of up to two of these masses indicating cleavage within both of the glutathione moieties.

INTRODUCTION

Characteristic cleavages within the glutathione moiety of GS-A have been observed when the protonated, FD produced, quasimolecular ion was collisionally activated and its daughter ions examined in a linked scan (1). GS-A has also been examined by FAB/MS, but no characteristic fragment ions were observed (2). In this paper we report several characteristic cleavages, especially within the glutathione moiety, from the conjugates GS-A, $GS-A_2$, and GS_2-A_2 by FAB/MS and FAB/MS/MS.

EXPERIMENTAL

FAB mass spectra were obtained with a Kratos MS-50 equipped with an M-Scan fast atom source and gun. FAB ionization employed 10KeV xenon atoms. Spectra were recorded in 30 sec. scans downfield.

FAB/MS/MS data was acquired using an MS-50 triple analyzer instrument equipped with an Ion Tech fast atom gun. Measurements were obtained by mass selecting the $[MH]^+$ ion for "MIKES" scans with collisional activation.

Samples were dissolved in methanol (1ug/ul) and 1 ul was applied to the target after about 1 ul of thioglycerol.

RESULTS AND DISCUSSION

FAB/MS: With GS-A a protonated molecular ion was observed at m/z 457. Other ions at m/z 382 and 328 corresponded to characteristic cleavages within the glutathione moiety, namely loss of the glycine (GLY) and glutamic acid (GLU) groups respectively. The FAB mass spectra of the larger conjugates, $GS-A_2$, and GS_2-A_2, also gave protonated molecular ions at m/z 606 and 911 respectively, but showed no fragmentation.

FAB/MS/MS: The FAB/MS/MS spectrum of GS-A showed a significant number of fragment ions corresponding to the same cleavages previously reported using FD/MS/MS(1). Fragment ions observed at m/z 413, 382 and 328 correspond to loss of CO_2, GLY, and GLU. Additional fragments at m/z 182 and 139 correspond to cleavage within the cystine moiety adjacent to sulfur (G*), followed by further loss of a $COCH_3$ group. Some significant loss of water to give the ion at m/z 439 was also observed. The fragmentation observed with $GS-A_2$ was identical except that the masses of the fragment ions were shifted higher in mass by 149 daltons.

The fragmentation behavior of collisionally activated GS_2-A_2 appears somewhat more complicated, but was actually consistent with the proposed structure. The ions observed at m/z 867, 836, 782, and 636 correspond to the losses of 44, 75, 129, and 275 daltons. These are the same losses observed previously. The masses are shifted higher by 305 daltons (relative to $GS-A_2$) reflecting the addition of the second glutathione substituient. Three other ions were observed which are attributed to multiple losses from one or more of the glutathione moieties. An ion at m/z 707 suggests loss of both GLY and GLU. The ions at m/z 653 and 561 can only be interpreted based on losses from both glutathione moieties. The ion at m/z 653 represents loss of two GLU, while m/z 561 appears to correspond to loss of G* and GLY.

CONCLUSION

The FAB mass spectrum of GS-A showed a prominent $[MH]^+$ ion as well as loss of GLY and GLU, confirming the presence of a glutathione moiety. The larger conjugates GS-A_2 and GS_2-A_2 also showed large protonated molecular ions by FAB/MS, but did not show significant fragmentation. Fragmentation of collisionally activated $[MH]^+$ ions from all three conjugates occured via characteristic cleavages within the glutathione moiety. Cleavages occuring through both glutathione moieties were also observed with GS_2-A_2. These results show that FAB/MS/MS with collisional activation leads to structurally characteristic cleavages from within the glutathione moiety which are not observed via normal FAB/MS, for these conjugates. Similar results are expected with other glutathione conjugates.

REFERENCES

(1) S. D. Nelson, Y. Vaishnav, H. Kambara, and T. A. Baillie, Biomed. Mass Spectrom. 8 244 (1981).

(2) B. L. Ackermann, J. T. Watson, J. F. Newton, Jr., J. B. Hook, and W. E. Braselton, Jr., Biomed. Mass Spectrom. 11 502 (1984).

Characteristic Cleavages from the Glutathione Moiety in the FAB/MS/MS Spectra of GS-A, GS-A_2, and GS_2-A_2.

	FAB/MS/MS Mass Lost						
PARENT COMPOUND	44	75	129	275	204	258	350
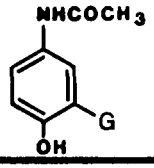	413	382	328	182	—	—	—
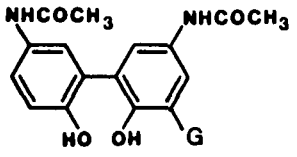	562	531	477	331	—	—	—
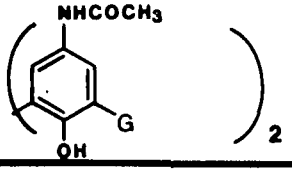	867	836	782	636	707	653	561
(G-glutathione)	CO_2	GLY	GLU	G*	GLY, GLU	GLY, GLY	GLY, G*
	Fragment lost						

DESORPTION CHEMICAL IONIZATION AND FAST ATOM BOMBARDMENT MASS SPECTROMETRY STUDIES OF THREE GLUCURONIDE METABOLITES OF DOXYLAMINE:

J. O. Lay Jr., W. A. Korfmacher, D. W. Miller, P. Siitonen, C. L. Holder, and A. B. Gosnell*; National Center for Toxicological Research and Henderson State University*, Jefferson Arkansas, 72079.

ABSTRACT

Three glucuronide metabolites of doxylamine succinate were isolated by high performance liquid chromatography (HPLC) from male Fischer 344 rats. The metabolites were then further separated by an additional HPLC step into fractions containing predominately a single glucuronide metabolite. Analysis of metabolites by methane and ammonia desorption chemical ionization (DCI), with and without derivatization, revealed fragment ions suggestive of a hydroxylated doxylamine moiety, but little else. Identification of the metabolites as glucuronides of doxylamine, desmethyldoxylamine, and didesmethyldoxylamine was accomplished based on determination of the molecular weight and exact mass of the components using fast atom bombardment (FAB) ionization. This assignment was confirmed by the fragmentation observed in FAB/MS and FAB/MS/MS experiments. Para substitution of the glucuronide on the phenyl moiety was observed by 500 MHz NMR spectrometry. Subsequently, the fraction containing all three glucuronide metabolites, after a single stage of HPLC separation, was analyzed by FAB/MS, and the proton and potassium containing quasimolecular ions for all three metabolites were observed.

INTRODUCTION

The antihistimine doxylamine succinate, N,N-dimethyl-2-[phenyl-1-(2-pyridinyl)ethoxylethanamine succinate, is a component in a widely used drug, Bendectin. Several urinary metabolites of doxylamine and related compounds have been examined by CI/MS (1-3). In this paper we describe the characterization of three previously unidentified glucuronide metabolites of doxylamine by both CI/MS and FAB/MS as well as by NMR spectrometry.

EXPERIMENTAL

Fischer 344 male rats were dosed by gavage with 50 mg of doxylamine succinate in one ml of aqueous solution. Isolation of a glucuronide-containing fraction from urine employed a Supelco 5u CN column with an isocratic system consisting of 70% methanol/30% 0.01M potassium phosphate- 0.02M trimethylamine (PP-TMA) buffer with an adjusted pH of 7.5 and a flow rate of 1 ml/min. The three glucuronides were then separated in a second step using 5% methanol/ 95% PP-TMA.

DCI/MS: Samples were introduced into a Finnigan MAT 4023 via a heated platinum filament (50 mA/sec for 60 sec). The reagent gas (methane or 10% ammonia/nitrogen) was set to an uncorrected source pressure of 0.25 torr. The source tempperature was 200 C for methane and 270 C for ammonia DCI/MS experiments.

FAB/MS: Low and high resolution FAB mass spectra were obtained using a Kratos MS-50 equipped with an M-Scan fast atom source and gun. FAB ionization employed 10KeV xenon atoms. High resolution measurements were obtained by peak matching one of the metabolites' quasi-molecular ions against the prominent m/z 429 ion, ($C_{12}H_{29}O_8S_4$) from the thioglycerol matrix. FAB/MS/MS data was acquired using an MS-50 triple analyzer equipped with an Ion Tech fast atom gun. 'MIKES' scans were obtained by mass selecting the protonated quasi-molecular ion for collisional activation.

NMR: Proton NMR measurements were made using a Bruker WM-500 spectrometer operated at 500 MHz, in methanol-d4.

RESULTS AND DISCUSSION

DCI/MS: Initial analyses of all three metabolite-containing fractions (I-III) with either methane or ammonia reagent showed a base peak at m/z 198 and essentially no other fragment ions. The methane DCI mass spectrum of II after acetylation (acetic acid in pyridine),

showed a large peak at m/z 557 attributed to [MH-CH3COOH]+ from a tetraacetylated monodesmethyldoxylamine glucuronide. Acetylated I and III gave DCI mass spectra (with methane) which were nearly identical with II except that the ions attributed to acetic acid loss were observed 14 and 28 amu lower than with II. This observation was consistent with the assignment of acetylated metabolites I and III as the tetraacetylated didesmethyldoxylamine and triacetylated doxylamine glucuronides. Similar results were obtained with ammonia DCI/MS of acetylated I-III.

FAB/MS: Analysis of the unseparated glucuronide fraction showed peaks at m/z 435, 449, and 463 corresponding to the protonated molecular ions for metabolites I, II, and III. Signals at 473,487, and 501 indicated potassium adduct-molecular ions. A second HPLC cleanup followed by a C18 SEP-PAK resulted in a significant improvement in the FAB spectra. For example, for the HPLC fraction containing II, ions at m/z 449, 471, and 487 corresponding to the proton, sodium and potassium adduct-ions, were readily observed. Fragment ions at m/z 374 and 198 were also observed with II (and also with I and III). The elemental compositions of the quasi-molecular ions of I-III were determined by high resolution peak matching to have the correct exact masses for assignment as glucuronides, with elemental compositions given by C21H24N2O8R2X, where R=H and/or methyl and X=H or Na.

FAB/MS/MS of the [MH]+ from II showed prominent ions at m/z 374 and 198 (also observed in the FAB/MS spectra) which likely have structures a and b from sequential loss of the ethanolamine and glucuronide moieties. Loss of ethanolamine has been observed previously in the DCI/MS spectra of doxylamine and some related compounds (2). Loss of the sugar moiety has also been reported in the FAB spectra for many glucuronides, although generally by direct cleavage from the quasimolecular ion (4). I and III gave identical fragment ions and differed only in the mass of the parent protonated quasimolecular ions.

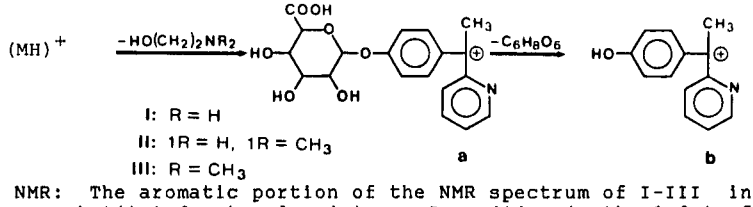

NMR: The aromatic portion of the NMR spectrum of I-III indicated a para-substituted phenyl moiety. Impurities in the 1.0 to 5.5 ppm region obscured the aliphatic and glucuronide moieties. The aromatic region of III was also obscured. These data suggest that the glucuronides I and II are substituted on the para position of the phenyl moiety and we have assumed, but not proven, that III is also.

CONCLUSION

Three new rat urine metabolites of doxylamine succinate were identified after HPLC separation as p-benzyl glucuronides of doxylamine and the mono- and didesmethyl derivatives.

REFERENCES

1. C. L. Holder, W. A. Korfmacher, W. Slikker, Jr., H. C. Thompson, Jr., and A. B. Gosnell, Biomed. Mass Spectrom. 12, 151 (1985).
2. W. A. Korfmacher, C. L. Holder, J. P. Freeman, R. K. Mitchum and A. B. Gosnell, Org. Mass Spectrom. 20, 435 (1985).
3. W. Slikker Jr., C. L. Holder, J. R. Bailey, J. F. Young and H. C. Thompson, Jr., Teratology 27,77A (1983).
4. C. Fenselau, L. Yelle, M Stogniew, D. Liberato, J. Lehman, P. Feng, and M. Colvin Jr., Int. J. Mass Spectrom. Ion Phys. 46,411 (1983).

IDENTIFICATION OF METABOLITES OF 3,4-DICHLOROBENZYLOXYACETIC ACID (3,4-DCBAA) BY HPLC, EI-MS, AND LC-MS

R. C. Peffer, M. A. Zemaitis, L. K. Wong and J. A. Alvin
University of Pittsburgh School of Pharmacy
Pittsburgh, PA 15261

J. Buchner
Extrel Corporation
240 Alpha Drive, Pittsburgh, PA 15238

The metabolism of 3,4-DCBAA has been characterized in rats to provide a preliminary estimate of how the drug would be handled in humans. Five male Wistar rats were given single intraperitoneal injections of (2-^{14}C)-3',4'-DCBAA (100 mg/kg). The majority of the radioactive dose was excreted in the urine (77.4 $\pm$ 4.6%), while a lesser amount appeared in the feces (3.2 $\pm$ 0.5%).

The urinary metabolites were isolated by reverse-phase HPLC and identified by EI-MS. Figure 1 shows a typical HPLC profile of the major urinary metabolites and the amount of radioactivity present in each one-minute fraction of the eluent. Peaks 2 and 3 were easily identified from their EI spectra as 3,4-dichlorohippurate (M^+ at m/z 247; b.p. at m/z 173) and unchanged 3,4-DCBAA, respectively. Peaks 4 and 5 were tentatively identified from their EI spectra as the glycine conjugate and the taurine conjugate of 3,4-DCBAA (Figure 2). However, the lack of significant molecular ions for these conjugates required the use of a softer ionization technique to confirm these proposed structures.

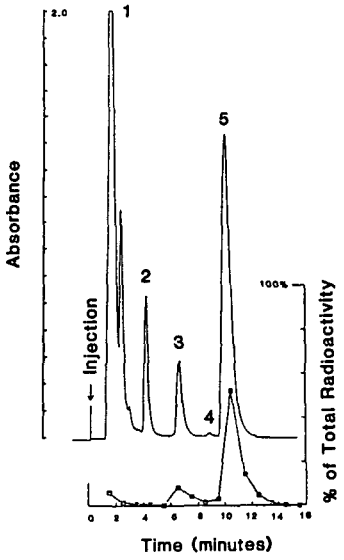

Figure 1. HPLC Profile of Urinary Metabolites

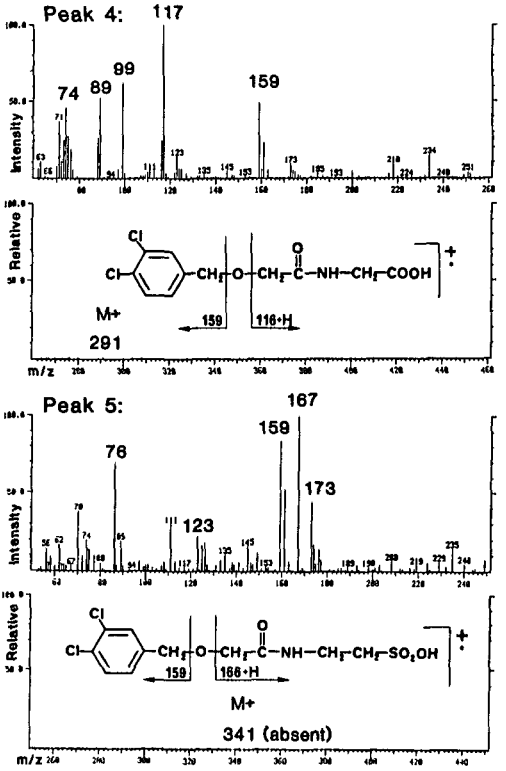

Figure 2. EI-MS Spectra of Conjugates

A thermospray LC-MS system (Extrel Corp., Model 400-2D) was utilized to simultaneously separate and identify the glycine and taurine conjugates of 3,4-DCBAA. Using an ammonium acetate buffer system, abundant $M+H^+$ and $M+NH_4^+$ ions were obtained for both conjugates (Figure 3). These ions displayed the isotope ratio for two chlorines and maximized at the appropriate point on the HPLC profile.

Quantitation of the urinary metabolites revealed that the taurine conjugate represented 60.1 ± 4.4% of the radioactive dose. Lesser percentages were excreted as unchanged drug (12.5 ± 1.2%), glycine conjugate (2.2 ± 0.2%), and a polar unknown (1.8 ± 0.4%). Approximately 11.1 ± 4.4% of the dose was converted to the non-radioactive 3,4-dichlorohippurate. With one exception (2-naphthylacetic acid), only trace (<5%) levels of taurine conjugates have been reported previously for rat metabolism studies with other aryl carboxylic acids. The high percentage of 3,4-DCBAA that is converted to a taurine conjugate (60.1% of the dose) is an unprecedented finding in rats. These results could give new insight into the structure-metabolism relationships of conjugation reactions.

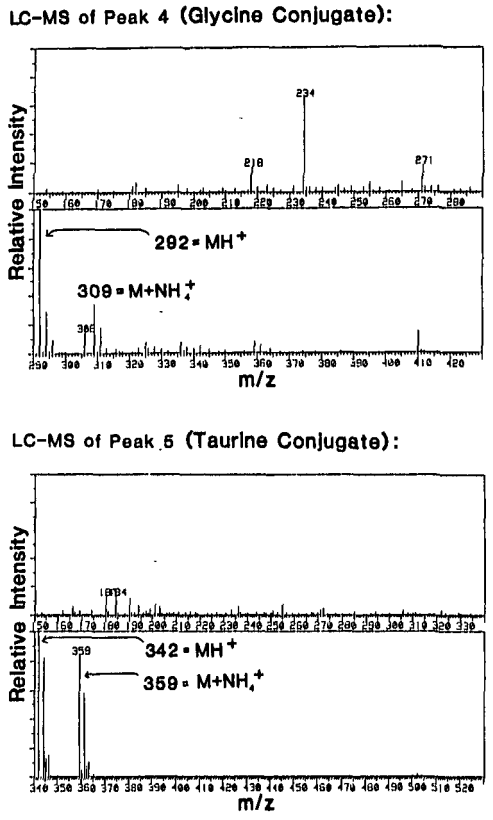

Figure 3. LC-MS Spectra of Conjugates

Thermospray HPLC-MS/MS for Rapid Profiling of Drug Metabolites

K Straub, P Rudewicz, L. Gutzait, and B Mico, Department of Drug Metabolism, Smith Kline & French Laboratories, Swedeland, PA 19479

The complete characterization of the routes of biotransformation of a drug is a difficult, labor-intensive analytical task. Tandem mass spectrometry offers an alternative method of analysis to traditional techniques, in that scanning modes that are specific for different structural features can be used to establish the presence of particular components in a complex sample matrix This approach is uniquely suited to metabolite analysis since (1) the structure of the parent drug is known, and a fragmentation 'map' of its substructural elements can therefore be constructed[1]; and (2) a relatively restricted set of metabolite classes is commonly observed (glucuronides, sulfate esters, etc.). By designing an appropriate set of MS/MS scan sequences to search for these two types of metabolites ---those that retain substructures in common with the parent drug, and components that correspond to common classes of metabolites--- a relatively complete characterization of the major routes of metabolism can be achieved from a limited series of MS/MS experiments Previous efforts in our laboratory have been aimed at designing specific MS/MS scan sequences that can be used to characterize common classes of drug metabolites[2], while much of this initial work was based on particle-induced desorption ionization (FAB or liquid SIMS), recent results show that these same scanning techniques can be used to characterize ions formed by 'thermospray' (TSP) ionization.

The application of these techniques for total metabolite analysis was investigated with a novel drug, 4-[di-n-propylaminoethyl]-2-(3H)-indolone (SK&F 101468; **1**). This material is a selective, potent dopamine-2 agonist, and is currently being evaluated as an antianginal and antihypertensive agent. The structure of the drug is characterized by the presence of distinctive alkylamino and aryl substituents that undergo fragmentation with retention of charge. The combination of these structural features together with the possibility of conversion to a number of different types of secondary conjugates makes the use of HPLC in combination with MS/MS particularly appropriate.

HPLC-MS/MS spectra were obtained with a triple quadrupole (Finnigan TSQ-15) mass spectrometer, using a TSP ion source interfaced to a Beckman 320 gradient HPLC Separations were carried out on a 'deactivated' ODS column (15cm x 4.2mm, 1.2 ml/min) using linear gradients of 100 mM NH_4OAc (pH 3 8)/acetonitrile. A number of different MS/MS scans could be carried out in a repetitive fashion as part of a single experiment, since the chromatographic peak widths under these conditions were on the order of 30-60 sec. Male Sprague-Dawley rats received 20 mg/kg of drug p.o , urine samples were then collected and analyzed directly (100µl on-column), or as crude fractions from a C18 solid phase extraction cartridge Fragment ions characteristic of the drug were identified by first carrying out a CAD experiment on the parent compound (fig 1). Under TSP ionization conditions, a prominent fragment ion corresponding to cleavage of the bond alpha to the nitrogen is observed at m/z 114, cleavage adjacent to the nitrogen with retention of charge by the indolone yields m/z 160 and (via loss of CO) m/z 132 A precursor ion scan for m/z 114, then, will serve to identify all components that retain the characteristic aminoalkyl substituent. The occurrence of N-dealkylated metabolites can be anticipated and screened for by an analogous precursor ion scan for m/z (114- 42)= 72

Reconstructed ion chromatograms from the analysis of a 100 µl urine sample by these two precursor scans, and by a neutral loss scan specific for O-glucuronides (NL +/-176 amu) are shown in fig. 2, and confirm the presence of one despropyl (peak 'B') and three dipropyl ('A', 'C', and 'D') substituted components, one ('A') of which contains a glucuronide substructure The apparent masses corresponding to $(M+H)^+$ identified by the parent scans for these four components are 453 ('A'), 219 ('B'), 277 ('C'), and 261 ('D') No additional metabolites were detected using other conjugate-specific MS/MS scans.

Peak 'D' was identified as parent drug by comparison of its CAD mass spectrum and retention time with SK&F 101468, while 'C' was shown to have a CAD spectrum consistent with a phenolic metabolite, fragment ions at m/z 176 and 148 analogous to the ions at m/z 160 and 132 in the parent structure confirm the presence of the hydroxyl in the indolone substituent The site of substitution was shown to be *para* to the alkylamino group by comparison with a synthetic standard Peak 'B' (identified by the PA 72 scan) gave a CAD spectrum that was identical to that of the parent drug, except that m/z 114 was shifted to

m/z 72. Comparison with standards confirmed the identity of this metabolite as that of the N-despropyl analogue. The CAD spectrum of the remaining metabolite, peak 'A', is shown in fig. 3; a fragmentation sequence corresponding to loss of the glucuronyl gives m/z 277, which has a CAD spectrum identical to that observed for peak 'C'. The position of substitution was confirmed on isolated material in a subsequent ^{1}H-NMR experiment.

In addition to the three major metabolites and parent drug, a minor component was evident at scan 677 in the NL176 and PA114 scans. The NL176 experiment gives a signal at mass 293, corresponding to a precursor mass of 467; this minor component (ca. 3% of total drug-related material) most likely corresponds to the O-glucuronide of an isotin derivative of 'A'. This component co-elutes with peak 'B' under the chromatographic conditions used here, and its presence was overlooked in initial HPLC analyses of ^{14}C-labeled samples using liquid scintillation detection.

These five components were shown to account for >95% of the drug-related material present in urine through the use of ^{14}C-labeled drug. All of the major metabolites were therefore characterized in two HPLC-MS/MS experiments: the first to identify likely precursor ions of components that contain structural features characteristic of the parent drug and of common conjugating species, and the second to obtain structural information by daughter ion analysis of the molecular species identified by the first experiment. A relatively complete characterization of the metabolic profile of a drug substance can therefore be obtained directly on either unextracted biological samples or on a crude extract through the use of carefully designed precursor ion and class-specific MS/MS scans. Tandem mass spectrometry in combination with TSP ionization is thus an extremely powerful tool for the characterization of drug metabolites. An extension of these techniques to the study of the metabolism of endogenous compounds is under investigation.

1. Perchalski, R.J.; Yost, R.A.; Wilder, B.J.; Anal. Chem. (1982) **54**, 1466.
2. Straub, K.; Garvie, C.; 33rd ASMS Conf. (1985) pp. 472-473.
3. Straub, K.; Rudewicz, P.; Garvie, C.; Xenobiotica (1986) in press.

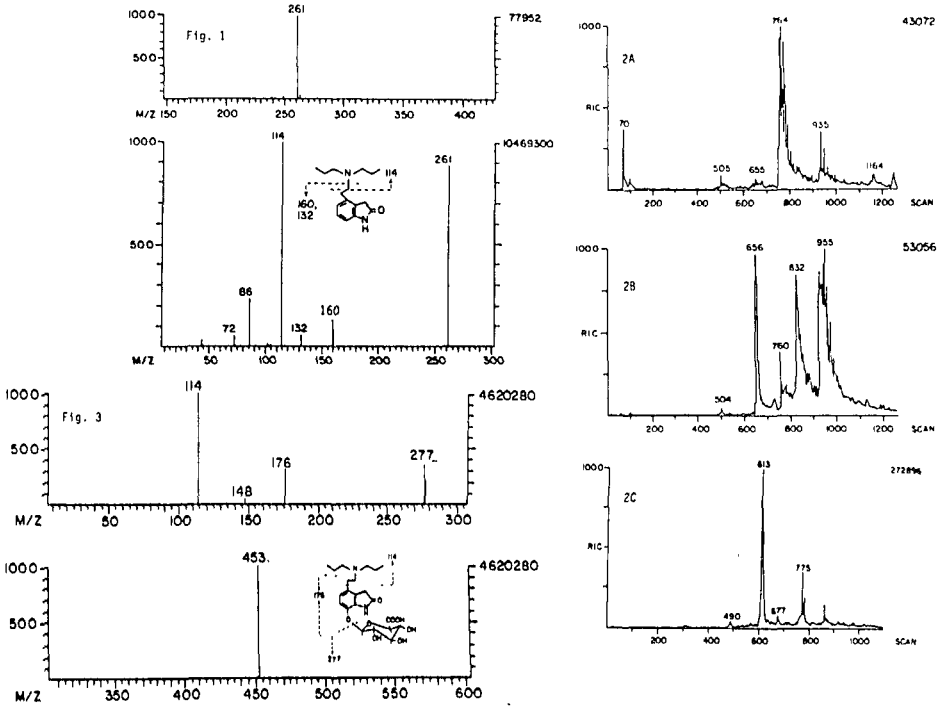

APPLICATION OF SIR AND DEFOCUSSING METASTABLE SIR TO THE IDENTIFICATION OF FLUPHENAZINE 5-SULFOXIDE IN MAN AFTER INTRAMUSCULAR ADMINISTRATION OF FLUPHENAZINE DECANOATE

R. W. Edom, G. McKay, P. W. Brooks, J. W. Hubbard and K. K. Midha
College of Pharmacy, University of Saskatchewan
Saskatoon, Saskatchewan, Canada S7N 0W0

Fluphenazine (FLU), a piperazine-type phenothiazine, is a commonly used drug in the therapy of schizophrenia. The 5-oxide (sulfoxide) metabolites of phenothiazine antipsychotic drugs are generally believed to be devoid of beneficial neuroleptic activity. In certain patients, the formation of high levels of 5-oxide metabolites of phenothiazine drugs such as chlorpromazine and thioridazine appears to sequester the therapeutic activity of the drug. By analogy, the possibility exists that patients non-responsive to therapy with FLU may have relatively high plasma levels of FLU-sulfoxide compared with patients who respond well to FLU. In man, FLU-sulfoxide has been shown to be a major metabolite of FLU after oral administration, and it is excreted in the urine both as free metabolite and as the hydroxyethyl glucuronide conjugate. However, there are no reports of the metabolic formation of FLU-sulfoxide following intramuscular (IM) administration of FLU decanoate. The IM administration of FLU decanoate is known to provide sustained plasma levels of FLU which are usually less than 5 ng/mL plasma. Therefore, the greatest difficulty in the detection and characterization of metabolites has been that the plasma levels are extremely low.

To investigate the formation of FLU-sulfoxide following IM FLU decanoate, urine and plasma samples were obtained from intramuscularly treated patients who had not received oral FLU for at least six months prior to this investigation. The samples were prepared using selective solvent extraction at basic pH and were analyzed by capillary GC/MS. Electron impact mass spectra (Figure 1), and GC retention times, for the TMS derivatives of FLU and FLU-sulfoxide were determined using authentic standard compounds. However, the levels of FLU and its metabolites were sufficiently low in both plasma and urine of intramuscularly treated patients to preclude their analysis by conventional full mass scanning.

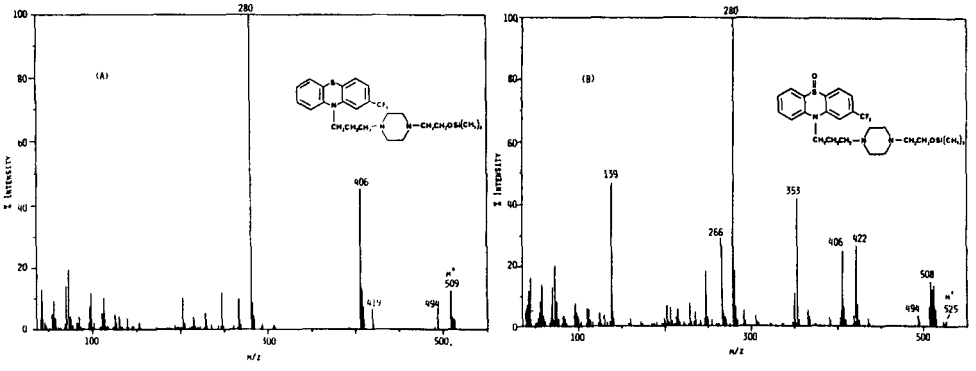

Figure 1: 70 eV EI mass spectra of the TMS derivatives of (A) FLU and (B) FLU-sulfoxide.

The detection and identification of FLU-sulfoxide in patient urine was achieved on the basis of its GC retention time, and by selected ion recording (SIR) of 3 fragment ions. These ions include:

m/z 509.2144 ($M^{+\cdot}$-16) formed due to loss of oxygen from the molecular ion.
m/z 494.1909 ($M^{+\cdot}$-31) formed due to loss of a methyl radical from m/z 509.
m/z 422.1514 ($M^{+\cdot}$-103) formed due to loss of $^{\cdot}CH_2OSi(CH_3)_3$ from the molecular ion.

Note in the above mass spectrum that m/z 422 is a diagnostic ion of FLU-sulfoxide. Monitoring the molecular ion at m/z 525.2093 was not possible due to its weak intensity. Figure 2 shows a typical SIR report for the analysis of a 2 mL urine sample from an individual patient. Responses are observed at the correct retention time for all the 3 ions monitored, proving the existence of FLU-sulfoxide in the urine.

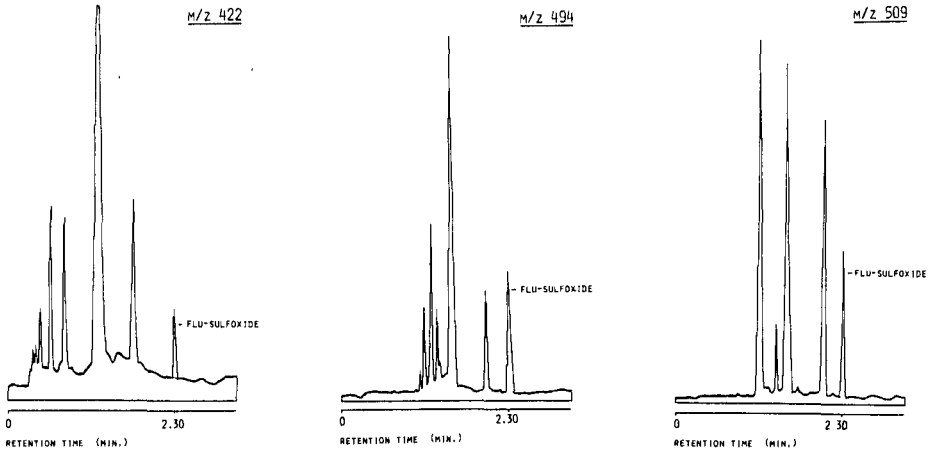

Figure 2

To identify FLU-sulfoxide in patient plasma the more selective and sensitive technique of defocusing metastable SIR was used. In this procedure, two first field free region metastable transitions to a common ion diagnostic of FLU-sulfoxide were monitored. This diagnostic ion at m/z 353.0935 arises from:

1) m/z 525.2093 ($M^{+\cdot}$)——————————*——————————>m/z 353.0935
2) m/z 525.2093 ($M^{+\cdot}$)————————m/z 422.1514——————*——————>m/z 353.0935

m/z 422.1514 ——————*——————> m/z 353.0935

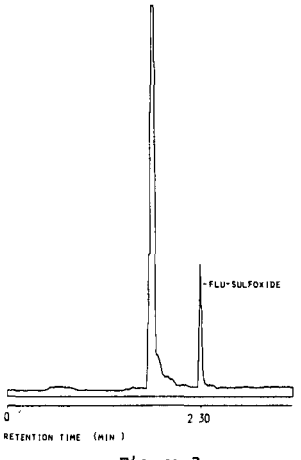

Figure 3

Figure 3 shows a typical defocussing metastable SIR report for the analysis of a 2 mL plasma sample, where the metastable transition for m/z 422.1514 to m/z 353.0935 is observed at the correct retention time. It demonstrates the existence of FLU-sulfoxide in the plasma. The large peak in the spectrum is due to an endogenous compound, presumably the TMS derivative of cholesterol. Unfortunately, the transition from m/z 525.2093 to m/z 353.0935 did not have adequate sensitivity to provide a response.

The results of these studies based on SIR and defocussing metastable SIR confirm the presence of FLU-sulfoxide in urine and plasma samples from schizophrenic patients treated intramuscularly with FLU decanoate.

Acknowledgement: Medical Research Council of Canada (P.G. 34).

GAS CHROMATOGRAPHY--FAST ATOM BOMBARDMENT--MASS SPECTROMETRY OF CARBOXYLIC ACIDS

By E. J. Gallegos
Chevron Research Company, Richmond, California

This paper describes the unique use of GC/FAB/MS in the analysis of carboxylic acids in oil well production water.

This work was done using 5700A Hewlett-Packard GC coupled to a VG 7070E mass spectrometer configured as shown in Figure 1.

Both FAB positive- and FAB negative-ion detection methods were used in this study.

Figure 2 shows the mass spectrum of isobutyric-TEA-Ca complex taken using GC/FAB+/MS methods. The acids elute from the column, condense into the FAB plate selvedge composed of triethanolamine, TEA, and CA++, and are desorbed by the neutral Kr atoms as the positive ion carboxylic acid-calcium-TEA complex and are subsequently analyzed conventionally by the mass spectrometer. Although at least six different acid-Ca++-TEA complexes are formed, the RCO_2-Ca-TEA complex is the dominant, by far, in the FAB+ experiments.

Figure 3 shows a MAP display if the $HC_nH_{2n}CO_2H$ acids in a weathered oil, well water extract. These peaks are due to the Ca++-TEA complex of the acids from C_4 through C_{12}. This is a direct determination of molecular weight and isomer distribution of acids with in situ derivatization.

This GC/FAB+/MS run also yielded data on the $C_nH_{2n-2}CO_2H$ acids and on low levels of benzoic acids.

Figure 4 shows the mass spectrum of isobutanoic and butanoic acid anions using GC/FAB-/MS methods.

The acids elute from the column, condense on a clean stainless steel FAB plate, and are desorbed as the anions by the neutral Kr atoms. Note that, in this case, the mass spectra show the molecular M- anion as the largest peak but also show some fragmentation which is useful in structure elucidation. This is not the case in FAB+ methods described above.

Figure 5 shows a MAP display of the $HC_nH_{2n}CO_2H$ acid anions from C_2 to C_{10} in a fresh oil, well water extract. The GC/FAB-/MS method also gives molecular weight and isomer distribution information without in situ derivatization. The GC/FAB-/MS run also yielded data on the $HC_nH_{2n-2}CO_2H$ acids and on low levels of benzoic acids also present.

Conclusions

GC/FAB+/MS is feasible. The conversion of the carboxylic acids to the Ca-TEA complex is quantitative and the selvedge composition appears to be specific to carboxylic acids.

GC/FAB-/MS is also feasible. The method is specific to carboxylic acids. Structural information is available from the mass spectra.

Encl. -

FIGURE 1

GC/FAB/MS SOURCE CONFIGURATION

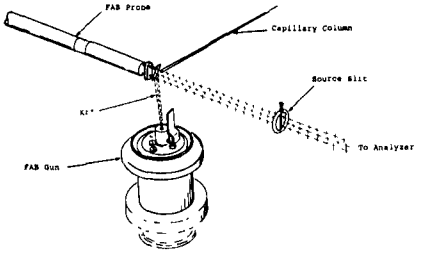

FIGURE 2

ISO BUTYRIC-TEA-CA GC/FAB+/MS MASS SPECTRUM

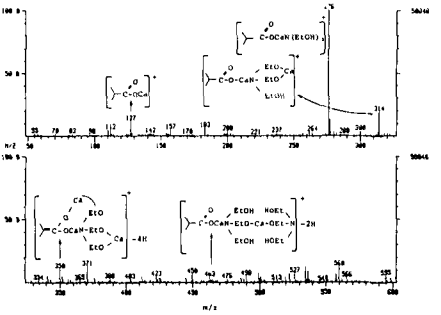

FIGURE 3

MAP DISPLAY OF $HCnH_{2n}CO_2H_2$ ACIDS IN A WEATHERED OIL WELL WATER EXTRACT BY GC/FAB+/MS

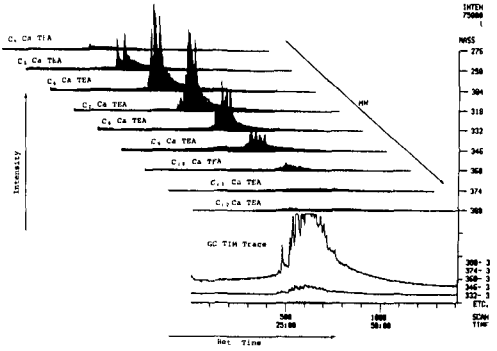

FIGURE 4

GC/FAB+/MS MASS SPECTRA OF ISO BUTANOIC AND BUTANOIC ACIDS

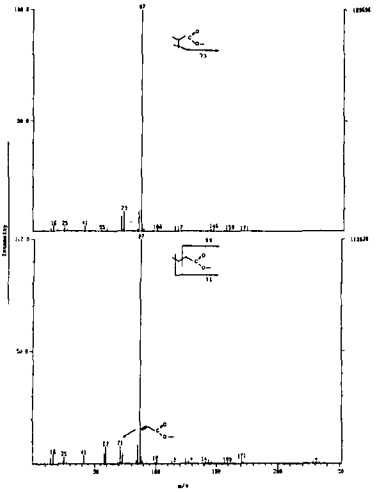

FIGURE 5

MAP DISPLAY OF $HCnH_{2n}CO_2H$ ACIDS IN A FRESH OIL WELL WATER EXTRACT BY GC/FAB+/MS

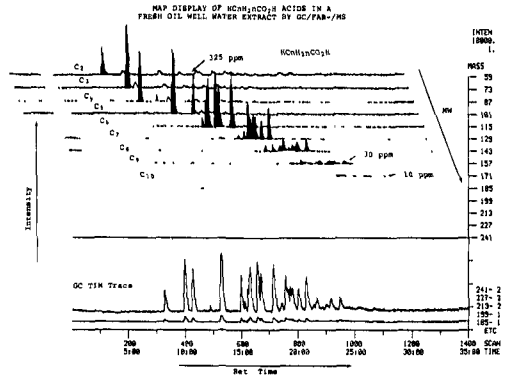

CORRELATION OF DEGRADATION PRODUCT PROFILES FROM AQUATIC HUMIC SUBSTANCES AS DETERMINED BY GC/MS WITH C-13 NMR SPECTRAL CHARACTERISTICS.

Daniel L. Norwood,[1,2] Russell F. Christman,[1] and Patrick G. Hatcher[3]; (1) University of North Carolina, Department of Environmental Sciences and Engineering, Chapel Hill, NC 27514; (2) Research Triangle Institute, Analytical and Chemical Sciences, P.O. Box 12194, Research Triangle Park, NC 27709; (3) United States Geological Survey, Reston, VA 22092.

INTRODUCTION

Structural studies on complex, polydisperse natural product organic materials such as humic substances have traditionally employed chemical degradation coupled with GC/MS analysis of degradation products. The gas chromatograph, however, limits the observable molecular weight range and precludes analysis of humic substances or their macromolecular degradation products directly. It is therefore desirable to investigate alternative techniques which will complement and enhance the information derived from chemical degradation/GC/MS. Solid-state ^{13}C-NMR employing cross polarization (CP), magic-angle spinning (MAS) and high power proton decoupling, is a relatively new technique capable of determining carbon distribution, both qualitative and quantitative, in macromolecular substances.

This report describes the use of oxidative chemical degradation/GC/MS in combination with solid-state ^{13}C-NMR techniques for analysis of the lignin-derived phenolic sub-structure of an isolated aquatic fulvic acid. The profile of carbon distribution of the fulvic acid provided by the ^{13}C-NMR is shown to enhance the interpretation of GC/MS product distributions derived from aqueous chlorination and CuO oxidation.

METHODS

Fulvic acid was obtained from Singletary Lake, Bladen County, NC, by methods previously described (1). Aqueous chlorination and the extraction of chlorination products have also been documented (1). CuO oxidation of fulvic acid was accomplished by the procedure of Hedges and Ertel (2). GC/MS analysis of fulvic acid degradation products was carried out on a VG 7070F system with appropriate capillary columns. For the chlorination products accurate mass measured EI, positive CI (isobutane), and negative CI (isobutane) spectra were obtained. For CuO products only nominal EI spectra were required. CP/MAS ^{13}C-NMR spectra were recorded at 100 MHz on a CMC 100 spectrometer.

RESULTS

Aqueous chlorination of Singletary Lake fulvic acid produced a number of organohalides indicative of phenolic ring-rupture reactions. Such compounds include chloroform, di- and trichloroacetic acids, dichlorosuccinic acid, and dichloromaleic acid. It was hypothesized that attack by aqueous chlorine on the lignin-derived phenolic sub-structure of the fulvic acid macromolecule was responsible for the generation of these organohalides.

A series of CP/MAS ^{13}C-NMR experiments was performed in order to determine the overall carbon distribution in the fulvic acid and to identify oxygen substituted (potentially phenolic) aromatic carbon. A typical CP/MAS spectrum is shown in Figure 1. Oxygen substituted aromatic carbons resonate in the 150-160 ppm range, where a broad shoulder may be observed. Other experiments involving selective relaxation of protonated carbons removed much of the peak overlap in this region and revealed a small but definite signal for potentially phenolic carbon.

Based on these results, CuO oxidation of the fulvic acid was performed in order to determine individual phenolic components in the sub-structure. GC/MS analysis of the resulting products revealed the presence of many phenolic structures. Some of these were unambiguously lignin-derived and included vanillyl, syringyl and cinnamyl phenols. Other phenolic substances, including 3,5-dihydroxybenzoic acid which is particularly reactive with

aqueous chlorine, were also detected. Yields of phenolic compounds were found to be small, agreeing with the CP/MAS ^{13}C-NMR results.

CONCLUSIONS

(1) Singletary Lake fulvic acid contains a relatively minor partially lignin-derived phenolic sub-structure.
(2) The reactivity of this phenolic sub-structure with aqueous chlorine may produce the observed chlorination products.
(3) The use of ^{13}C-NMR enhances the interpretation of GC/MS product distributions.

REFERENCES

1. R.F. Christman, D.L. Norwood, D.S. Millington, J.D. Johnson, A.A. Stevens, Environ. Sci. Technol., 17, 625 (1983).
2. J.I. Hedges and J.R. Ertel, Anal.Chem., 54, 174 (1982).

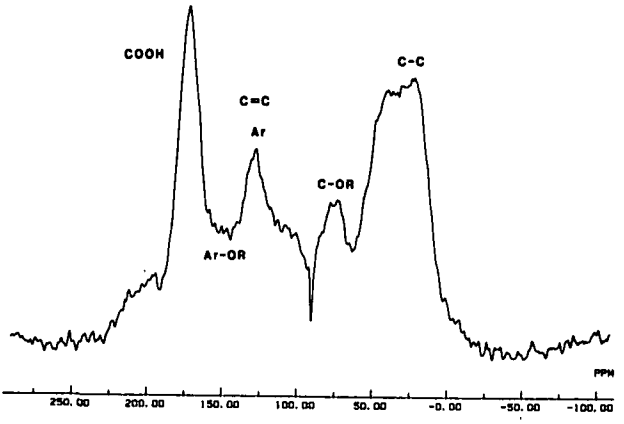

Figure 1. CP/MAS ^{13}C-NMR spectrum of Singletary Lake fulvic acid.

Chemical Ionization Studies of t-Butyldimethylsilyl Derivatives of Environmental Organic Contaminants.

J. V. Headley. Alberta Environmental Centre, Vegreville, Alberta, CANADA, T0B 4L0.

The presence of resin acids, fatty acids and phenolics in biodegraded treated kraft pulp mill effluents (BTKME) is of environmental concern due to their toxicity and resistance to biological and chemical degradation. Specific detection methods employing gas chromatography with electron capture detection (GC/ECD) have been developed[1]. Complimentary GC/MS methods have also been used where appropriate for confirming the identification of these contaminants[2].

In a study of a colour removal process for BTKME, a sensitive GC/MS method was required for confirmations at trace levels (low ppb or ppt). As part of this investigation, studies were initiated on the chemical ionization mass spectrometry (CIMS) of the t-butyldimethylsilyl (MTBS) derivatives of the compounds listed in Table 1.

Table 1 Organic contaminants investigated

PHENOLICS	RESIN ACIDS	OTHER
guaiacol	dehydroabietic	benzoic acid
vanillin	levopimaric	abienol
4,5-dichloroguaiacol	sandaracopimaric	manool
3,4,5-trichloroguaiacol	dichlorodehydroabietic	
4,5,6-trichloroguaiacol	FATTY ACIDS	
tetrachloroguaiacol	oleic	
4-chlorocatechol	palmitic	
4,5-dichlorocatechol	stearic	
tetrachlorocatechol		

The silylation reaction is given below.

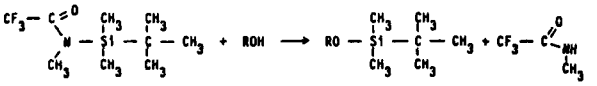

This work was performed using an HP5987 GC/MS equipped with HP1000 RTE 6 V/M software and the AQUARIUS package. Tuning of the ion-source and calibration of the mass axis was performed using perfluorotributylamine (PFTBA). The background pressures in the source chamber were held at 3.2 and 1.8 x 10^{-4} torr for the methane and ammonia chemical ionization (CIMS) studies respectively. These pressures corresponded to the optimum sensitivity for ions at m/z 414, 219 and the abundance of $NH_4^+(NH_3)$ falling within the range 40-80% abundance of NH_4^+. Likewise the selection of the electron energy was based on optimising the sensitivity of ions at m/z 219, 414 and 452, 633 for the positive ion (PI) and negative ion (NI) CIMS respectively. The temperature dependence of the CIMS was studied in the range 105-200°C. Effluent samples were extracted with methylene chloride, the extracts (100 µL) of which were silylated with t-butyldimethylsilyltrifluoroacetimide containing 1% t-butyldimethylsilane (10 µL) and acetonitrile (10 µL). This mixture was heated at 60°C for 2.5 hr.

The major ions in the EI, methane PICI, ammonia PICI and ammonia NICI mass spectra of the MTBS derivatives are summarised in schemes 1-4 respectively. Apart from the interference of $NH_4^+(NH_3)_n$ ions in the low temperature ammonia PICIMS of the phenolic compounds, the mass spectra of the MTBS derivatives obtained at 105°C contain informative, high mass, abundant ions. The extent of fragmentation is strongly temperature dependent and is illustrated in Figure 1, in which the temperature dependences of the MH^+ and (MH^+-115) ions of tetrachloroguaiacol (MTBS) are given.

The enhanced sensitivity of NICI for the chlorinated contaminants compared to the other ionization modes employed is illustrated in Figure 2, in which the reconstructed chromatograms for tetrachlorocatechol $(MTBS)_2$ are given. Trace impurities present in the standard are observed in the NICI mode.

For the optimum precision and accuracy of the quantitative analysis, the silylation step is required to be quantitative and the mass spectra of the derivatives must be reproducible. Incomplete silylation occurred when the silylation mixture was heated at 60°C for only 1 hr. Under the conditions employed, quantitative silylation was attained with a relative standard deviation of 20 percent. Incomplete silylation was still observed for the neutral alcohols and the technique may therefore be limited to acidic compounds. The MTBS derivatives of the resin acids, fatty acids and phenolics are well suited for SIM quantitative analysis and confirmations at trace levels.

References

1. R. H. Voss. Environ. Sci. Technol. 17, 530 (1983).

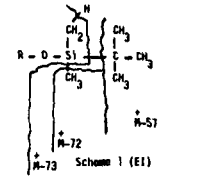

Scheme 1 (EI)

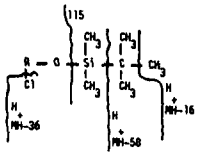

Scheme 2 (CH_4 PICI)

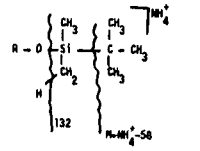

Scheme 3 (NH_3 PICI)

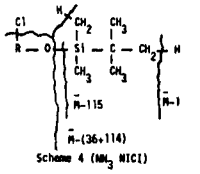

Scheme 4 (NH_3 NICI)

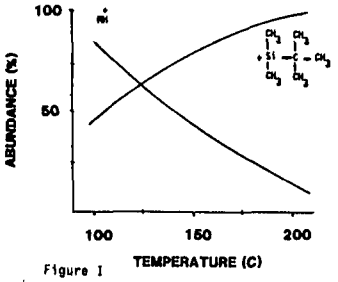

Figure I

TEMPERATURE DEPENDENCE OF MH^+ AND (MH^+-115) IONS IN METHANE PICIMS OF TETRACHLOROGUAIACOL AT CONSTANT PRESSURE

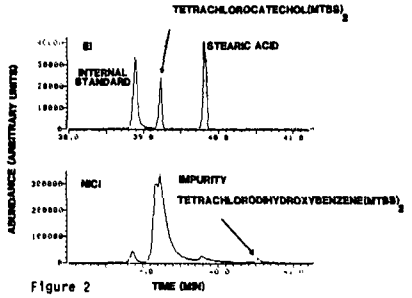

Figure 2

Reconstructed GC/MS profiles of 90ng tetrachlorocatechol$(MTBS)_2$

THE USE OF COMBINED SUPERCRITICAL FLUID CHROMATOGRAPHY-MASS SPECTROMETRY TO CHARACTERIZE CAROTENOID PIGMENTS

Nelson M. Frew and Carl G. Johnson
The Woods Hole Oceanographic Institution, Woods Hole, MA 02543

Richard H. Bromund
The College of Wooster, Wooster, OH 44691

INTRODUCTION

The carotenoids (carotenes and xanthophylls) are isoprenoid pigments which are widely distributed in both photosynthetic and non-photosynthetic organisms. We are specifically interested in marine carotenoids as model indicators of the fate of labile organic matter which is produced in the surface ocean and is subject to various biological and chemical degradative processes. The carotenoids are tetraterpenoids, each consisting of a conjugated polyene backbone commonly terminated at each end by six-membered rings of varying unsaturation. The terminal rings (as well as the backbone) are typically substituted with various polar functional groups, including hydroxyl, methoxy, keto, acetyl and epoxy groups, among others. The highly reactive nature of these compounds not only makes them attractive as indicators of short-term degradative processes but also makes their isolation and mass spectral characterization difficult, particularly at trace levels (< 100 ng). We have investigated the possibility of structurally characterizing carotenoids using capillary supercritical fluid chromatography-mass spectrometry. In view of their lability, polarity and molecular weight range, the carotenoids present an interesting test of the current capabilities of capillary SFC-MS.

EXPERIMENTAL

The supercritical fluid chromatograph consisted of a Brownlee Micropump, a Rheodyne 7520 injector and a Carlo Erba 4160 gas chromatograph equipped with a standard flame ionization detector. Chromatography was carried out on DB-5, DB-17, DB-225 and DB-WAX stationary phases (J & W Scientific) using 50 and 100 micron ID fused silica capillary columns between 2 and 20 meters in length. Columns were connected either directly to the injector through a splitter tee or indirectly using a short retention gap of uncoated capillary. CO_2 was used as the carrier fluid at 40-80°C with linear flow velocities of 2-5 cm/sec. Underivatized carotenoid standards were dissolved in methylene chloride to give concentrations of 400-4000 ng/µl and injected using a 0.2 µl rotor volume and split ratios in the range of 2-10:1. The chromatograph was interfaced to a Finnigan 4500 quadrupole mass spectrometer using an electrically-heated interface mounted so that the column effluent entered the ion source normal to the quadrupole axis. The restrictor end of the column was positioned 0.5 mm back from the column entrance hole in the ion volume. The interface was maintained at the column oven temperature and no additional heat was supplied to the restrictor other than that from the source block. Methane chemical ionization spectra were obtained under the following conditions: CH_4 pressure, 0.5 torr; electron energy, 130 eV; source temperature, 100°C. Data were acquired over the mass range 400-800 daltons using two-second scans. Desorption chemical ionization was carried out under similar conditions using the standard insertion probe fitted with a copper tip which extended approximately 2 mm into the ion volume. The probe heating rate was 120°C/min.

RESULTS AND DISCUSSION

All of the carotenoids studied were sufficiently soluble in supercritical CO_2 to allow elution and chromatographic separation on the stationary phases tested. Due to their polarity and molecular weight, the successful elution of these compounds was crucially dependent on the flow restrictors used. Best results were obtained for tapered jet-type restrictors formed directly on the column. Significant advantages of restrictors integral with the column are the ease of interfacing to the spectrometer, the absence of connecting dead volumes and active surfaces and the fact that the stationary phase extends virtually to the point of detection.

In general, selectivities for the carotenoids on the stationary phases studied were rather limited when compared with selectivities observed for high pressure liquid chromatography using, for example, n-propyl amino columns. Useful separations were obtained only on moderately polar to polar stationary phases. Separation of several carotenoids on a 20 m x 100 μm DB-17 (50% methyl, phenyl-50% dimethyl-polysiloxane) is illustrated in Figure A. The highest selectivity was obtained with DB-WAX (a bonded Carbowax 20M type). Strong retention of the more polar carotenoids on this phase necessitated the use of very short columns, high linear flow velocities and very high fluid densities (> 0.9 gm/ml) to elute these compounds. The high selectivity of DB-WAX makes it the most promising phase for the SFC separation of carotenoids and affords the possibility of using polar modifier gradients to enhance the quality of the chromatography.

Supercritical CO_2 was a convenient, efficient mobile phase for transferring these thermolabile compounds to the ion source. Modifications to the Finnigan 4500 were minimal and fully compatible with GC/MS operation. Adequate sensitivities (50-100 ng) were obtained using column effluent introduction normal to the quadrupole axis, although we did not attempt to maximize sensitivity.

In comparison with in-beam desorption chemical ionization techniques, which frequently result in dehydration and thermal degradation, the SFC/MS method produces spectra of superior quality for very labile pigments such as fucoxanthin and its derivatives (Figure B). The lower temperatures prevalent in the ion source due to the cooling effect of CO_2 expansion from the restrictor appear to result in extremely mild ionization conditions. With the exception of the fucopigments, CI-CH_4 fragmentation of the carotenoids studied, including carotenes, keto-carotenoids and carotenoid diols, was minimal. The simplicity of the spectra obtained may be advantageous in determining trace distributions of these pigments using their molecular ion abundances. Further structural characterization would require more energetic ionization conditions or tandem mass spectrometry in combination with collision-induced dissociation.

ACKNOWLEDGEMENT

This research was supported by the Oceanic Chemistry Program, Office of Naval Research, under contract N00014-85-C-001.

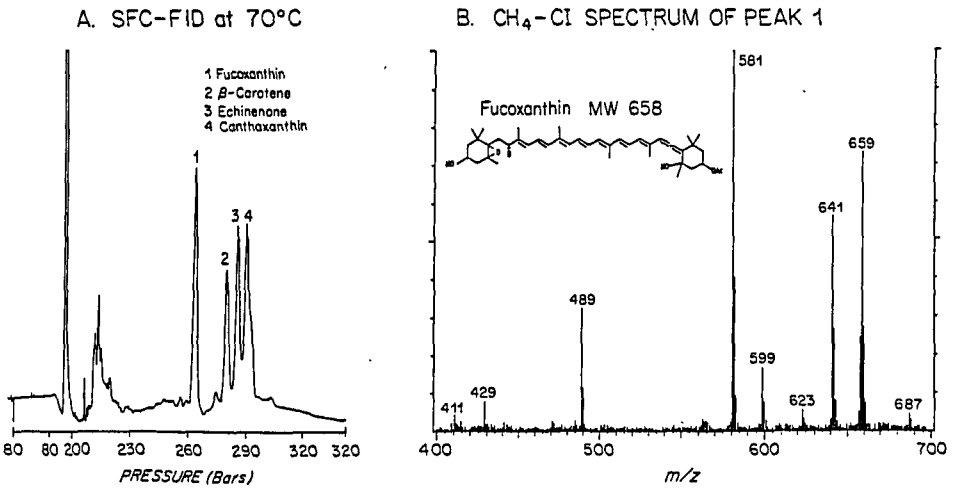

THE IMPACT OF SAMPLE COLLECTION TECHNIQUES AND SOURCES OF BACKGROUND CONTAMINATION ON GC/MS DATA FOR ENVIRONMENTAL SAMPLES

A.E. Rosecrance, J.M. Schreiber
JTC Environmental Consultants, Inc., Rockville, Maryland 20850
C.A. Rathbun
Martin Marietta Environmental Systems, Columbia, Maryland 21045

Background contamination is a problem frequently encountered by a GC/MS laboratory performing environmental analyses. Contamination sources are frequently outside of the laboratory's control, resulting from the field contractor. Sources of contamination include sample collection containers, sample collection techniques, preparation and analysis procedures, and instrumental background. The usability and significance of environmental sample data is directly related to the techniques used for sample collection and the considerations that are given to avoiding contamination in the field and the laboratory.

This paper investigates two sources of contamination that were introduced during separate sample collection episodes. The first source of contamination was found to be vials obtained from a supplier that utilized 1,1,1-trichloroethane for final treatment of vial caps during manufacture. The second source of contamination was found to be the cleaning procedure used for decontamination of sampling equipment. Several cleaning procedures for decontamination of sample collection containers were evaluated to determine the levels of contamination introduced by various cleaning procedures. GC/MS analyses were performed according to U.S. Environmental Protection Agency methods (1).

One contamination situation occurred in groundwater samples. Trichloroethylene (TCE) and 1,1,1-trichloroethane were found in a water source not previously shown to contain these compounds. Over several collection episodes of the groundwater samples in question, it was found that 55% contained TCE and 90% contained 1,1,1-trichloroethane, at levels of 2-50 ppb and 4-100 ppb, respectively. The source of contamination was determined to be the sample containers. TCE and 1,1,1-trichloroethane were also found in the trip and field blanks, but not in the laboratory blanks. The contaminants were found to result from a vial supplier that used 1,1,1-trichloroethane for final treatment of the caps during manufacture.

Another contamination incident was the random occurrance of acetone in groundwater samples. Groundwater samples were found to contain acetone levels ranging from 20-4000 ppb. Trip blanks and laboratory controls did not contain acetone, but water quality modeling on the aquifer indicated the unlikelihood that acetone was truly present in groundwater. The source of contamination was determined to be the procedure used for decontamination of sample collection equipment by the field contractor. JTC collected samples of the contractors decontamination wash and rinse waters. Analysis of these waters confirmed the acetone source. A study on the efficiency by several cleaning procedures was undertaken to develop a procedure that reduced sample contamination potential.

Several documents provide recommendations on cleaning of field sampling equipment (2,3). For proper cleaning and decontamination of samplers and sample containers, they recommended that the cleaning procedure include the use of a detergent wash, an acid rinse and a solvent rinse, each followed by a rinse with organic-free water. The following procedures for cleaning a 1 liter glass sample container were evaluated, with each cleaning solution used in order of sequence listed:

Cleaning Procedures		Results
A	B	B/A
Detergent Water Acetone Water	Detergent Water Acetone 10% HNO_3 Water	40% reduction in acetone with nitric acid rinse
C	D	D/C
Detergent Water Acetone Water 10% HNO_3 Water	Acetone Water Detergent Water 10% HNO_3 Water	95% reduction in acetone with acetone prior to detergent
E	F	F/E
Detergent Water CH_2Cl_2 Water 10% HNO_3 Water	CH_2Cl_2 Water Detergent Water 10% HNO_3 Water	97% reduction in CH_2Cl_2 with CH_2Cl_2 prior to detergent

Blank water samples and spiked water samples were prepared in 40 ml vials following each cleaning procedure to test for removal of cleaning solvents by each procedure.

A significant reduction in acetone and methylene chloride was observed for the cleaning procedures that utilized solvent rinse prior to detergent and acid cleaning steps. These results indicate that the solvent rinse step for decontamination of sample containers should be placed before the detergent wash and acid rinse steps. This procedure has been applied for use in the field cleaning of the sample collection equipment. During several subsequent groundwater sample collection episodes, little or no acetone contamination has been observed. Additional studies have illustrated that acetone is not needed in the cleaning sequence and the elimination of an organic solvent has significantly reduced field contamination of samples.

---

1. U.S. Environmental Protection Agency, "Test Methods for Organic Chemical Analysis of Municipal and Industrial Wastewater," EPA 600/4-8-057, Purgeables -- Method 624, July, 1982.

2. U.S. Environmental Protection Agency, "Handbook for Sampling and Sample Preservation of Water and Wastewater," EPA 600/4-82-029, September, 1982.

3. New Jersey Department of Environmental Protection, Department of Waste Management, "Field Sampling Procedures Manual," November, 1985.

On the Examination of Surface Films by Cf-252 PDMS

J.S. Showell
National Science Foundation, Washington, D.C. 20550
H.M. Fales, Y-M. Yang, E.A. Sokoloski
Laboratory of Chemistry, NHLBI:NIH, Bethesda, Md. 20892
L.K. Pannell
Laboratory of Bioorganic Chemistry, NIADDK:NIH, Bethesda, Md. 20892

During a recent investigation of skin lipids by Cf-252 PDMS, we noted that under certain conditions several lipid mixtures failed to show quasimolecular or fragment ion intensities appropriate for their composition. Thus, although a 1:1 mixture of tripalmitin and tristearin showed a nearly 1:1 response for the $(M+H-RCOOH)^+$ ions when very lightly electrosprayed on the aluminized mylar sample holder, the same mixture brushed on the mylar film in a heavier layer showed a response of 1.39 (tripalmitin/tristearin).

Furthermore, when a similar sample was annealed below its m.pt. at atmospheric pressure and allowed to cool, the ratio changed to 4.60! Samples prepared by solvent evaporation on the foils also change in relation to these intensities as they are allowed to remain under vacuum in the instrument. Similiar effects had been noted earlier with samples of palmitic and stearic anhydrides, but these were initially discounted as being due to the reactive nature of these substances.

Triglycerides, although known to be very stable chemically, do exhibit certain unusual physical properties. Thus, individually they undergo at least 3 crystalline phase transitions and when mixed with each other show complex phase properties. The crystalline nature of such mixtures therefore depends on the past history of the sample and metastable forms have been observed. The source of these transitions are the many possible alignments of the long hydrocarbon chains. It has been established (see D. Chapman "The Structure of Lipids". Mathsen & Co., Ltd, London) that the major interactions in the crystal state are due to van der Wall's forces between alternating methylene groups of adjacent chains (because of their zig-zag alignment) and this amounts to about 1-2 kcal/mole per CH_2CH_2 unit. This energy is surely sufficient to cause molecules deficient in methylene units (tripalmitin in tristearin) to be forced into the surface from regions near the surface in accord with Le Chatelier's principle. Since Cf-252 PDMS is a desorption process wherein ions are derived mainly from the outermost layers of the sample (R.D. Macfarlane and D.F. Torgerson, Science 191 920-925 (1976)), the apparent excess of tripalmitin observed in most spectra is understandable. Ratios closer to 1:1 are achieved only from very dilute solutions of electrosprayed samples where the particles must be extremely small as they are formed through rapid evaporation during the spray process. Presumably, a metastable condition exists within such particles wherein insufficient time has been provided for migration of the tripalmitin to the surface.

It is noteworthy that all of these observed phenomena are indeed due to the crystalline nature of the material and disappear entirely when samples of triglycerides such as 2:1 tricaprylin and tridecanoin are chosen that liquify on admixture at room temperature.

Further studies are being conducted with samples of waxes such as behenyl arachidate/ arachadyl behenate (showing similar effects) and perdeuterated lipids to determine whether the effect can discriminate even at this level.

ANALYSIS BY SIMS AND ESCA OF BIOMOLECULES ATTACHED TO SURFACES

David A. Kidwell and Richard J. Colton
Naval Research Laboratory, Washington, DC 20375

NRL is developing techniques to mass screen urine samples for drugs of abuse. These techniques simultaneously must detect multiple drugs in urine. One approach that we are investigating is based on the optrode technique.

In an optrode, a beam of light, filtered with a dichroic filter, is passed into an optical fiber. Coated on the fiber are covalently-bound derivatives of drugs. The incident light has some penetration into the medium, the depth of which is controlled by the angle of incidence and the refractive indices of the medium and the fiber. The light excites fluorescently-labeled antibodies that have bound to the attached drug. The light emitted by the fluorophore is coupled back into the fiber and is detected at the fiber end.

Figure 1 shows the steps involved in covalently coupling the drug to the fiber. Each step must be optimized. Classical methodologies rely upon weight gain, incorporation of radioactive materials or use of immunological techniques to determine the amount of material attached to the support. These classical techniques are not suited for the analysis of the optical fibers because: 1) The weight gain is small due to the low surface area of the fiber. Less than a microgram of drug is attached. 2) Radiolabeling is expensive. Each derivative must be synthesized and is unique. 3) Antibody affinity only measures the incorporation of the end product. It does not indicate what step needs to be optimized. For these reasons, surface sensitive techniques were applied to this analysis.

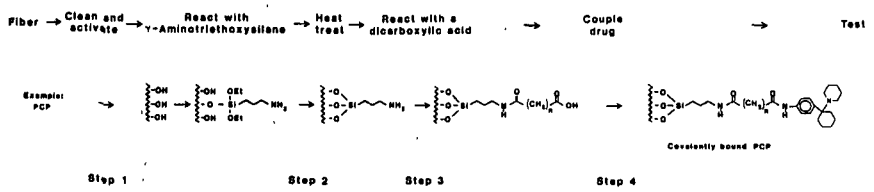

Figure 1 - Surface Derivatization Chemistry

ESCA analysis was performed on the product (see the table below) for each of the steps shown in Figure 1. These analyses showed that: 1) In step 2 incomplete attachment occurred which was deduced from the high C:N ratios. This high C:N ratio suggests that several different attachments of the aminopropyl group have occurred. 2) In step 3 there was incomplete reaction of the amine groups, even under extended conditions. This was explored by trifluoroacylation of the surface using trifluoroacetic anhydride. ESCA analyses of these surfaces showed that in most cases less than 50% of the covalently bound amines reacted. Steric hinderance of several of the amine species is the most likely explaination.

ESCA Analyses of Derivatization Chemistry

Step	C/N Ratio Expected	C/N Ratio Observed	Interpretation
1	0:0	no N 6 at% C	Clean surface
2	3:1	6-8:1	Incomplete attachment
3	7:1	6-15:1	Partial reaction
4 (PCP)	8:1		Drug attachment
(BzE)	9.5:1	12-17:1	
Commercial controlled pore glass	3:1	13:1	Dirty

Since ESCA provides the carbon and nitrogen content of the surface but *not the structures of the molecular species* attached to the surface, static SIMS was used. Figure 2 shows the SIMS spectra of a blank rod, PCP on acid-etched silver, PCP coated on a blank rod non-covalently, and the covalently-bound drug. In all cases with covalently-bound materials, there were no distinguishable molecular species observed. Immunoassays (modified EMIT and modified ELISA) confirmed the attachment of drugs. On the average, 30ng/cm^2 of PCP were attached.

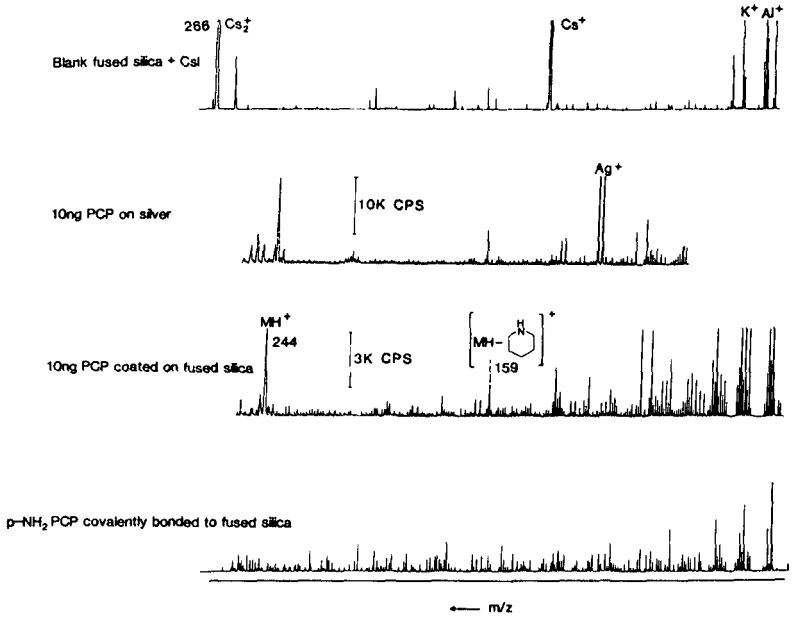

Figure 2 - SIMS of PCP Preparations

In conclusion, ESCA is very useful for examining species covalently bonded to surfaces. ESCA does not indicate the nature of the molecular species on the surface. ESCA analysis coupled with selected chemistry indicates that several types of surface bonding occurs. SIMS was unable to characterize the types of molecules covalently attached to the surface. Only nonspecific fragments are produced.

EFFECTS OF PRIMARY ION BEAM PARAMETERS ON THE SECONDARY ION MASS SPECTROMETRY OF AN EXEMPLARY BIOMOLECULE: Richard B. Cole [1,2], Christian Guenat [1], J. Ronald Hass [3], and Richard W. Linton [2]; 1) Laboratory of Molecular Biophysics, National Institute of Environmental Health Sciences, P.O. Box 12233, RTP, NC 27709; 2) Department of Chemistry, University of North Carolina, Chapel Hill, NC 27514; 3) Triangle Laboratories Inc., P.O. Box 13485, RTP, NC 27709.

Intrinsic to ion microprobe imaging experiments is a high primary ion current density (e.g., 10^{17} ions cm^{-2} sec^{-1}, for a 500 pA current striking a 2 to 3 micron spot). Damage effects attributable to these high primary beam densities have encumbered the ability to observe high mass molecular ions from fragile organic species such as biomolecules.

A microfocusing liquid metal ion (Ga^+) source coupled to a double-focusing mass spectrometer (VG ZAB-2F) has been used to probe the effects of primary beam parameters on the detection of secondary ions from methionine enkephalin suspended in a butanetetrol matrix. Changes in both the protonated molecular ion signal at m/z 574, and the fragment ion signal at m/z 120, were monitored as a function of primary ion current density (controlled by the primary beam focus), and local primary ion dose (controlled by the rastering speed using a focused primary beam).

The m/z 120 signal vs. time profiles obtained under four current density conditions are plotted in Fig. 1 (current densities for A-D are defined in Fig. 2). The signals were observed to level off at "steady state" intensities of varying magnitude, determined by the severity of beam damage effects and the relative availability of fresh sample diffusing through the liquid matrix into the impacting beam region. Curve "D" (dashed line) represents the "static" SIMS condition where the sputtered area is the largest, and the primary beam damage effects are minimized.

Superimposed upon these secondary ion production considerations are instrumental factors such as variability in collection efficiency which can account for the decrease in observed "steady state" signal at low primary current densities. Collection of secondary ions from the beam edges is postulated to become increasingly inefficient above a critical spot size.

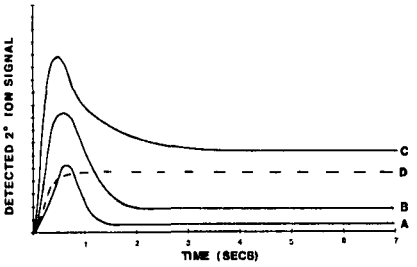

Figure 1

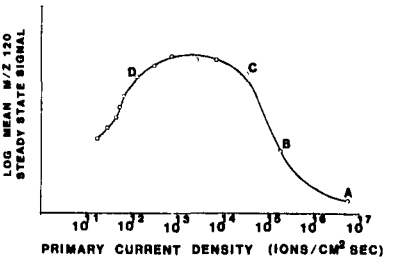

Figure 2

The effect on the detected signal is shown graphically in Fig. 2, a plot of log m/z 120 "steady state" signal vs. log primary current density. The drop-off in detected signal at high primary current densities is primarily attributed to a relatively slow rate of analyte diffusion, compared to the increasing rate of arrival of primary ions impacting in a given sputtered area. The current density where the incoming diffusion rate is just sufficient to compensate for the sample consumption rate can be defined as the upper limit to an extended definition of "static" SIMS for liquid matrices which accommodates the notion of sample renewal via diffusion. This critical primary beam dose rate was experimentally determined to be ca. 10^{12} ions cm^{-2} s^{-1}.

The ratio of the m/z 120 signal to the m/z 574 signal was monitored as a function of rastering speed, and consequent change in local primary ion dose, using a focused primary beam. The 120/574 ratio was shown to maximize at intermediate ion doses, ca. 10^{15} ions cm^{-2} (Fig. 3). This behavior was rationalized on the basis of an initial increase in the formation of surface damage products (with increasing primary ion dose) favoring the sputtering of the fragment m/z 120 molecule. This was followed by a further increase in beam damage effects which resulted in discrimination against the formation of both product ions, relative to ions of lower mass. Included in Fig. 3 are two reference points, one acquired with a focused beam at rastering speed = 0 (a hypothetically infinite dose) computed using the ratio of the "steady state" signals; the other is the secondary ion ratio obtained under the "static" SIMS condition using a defocused primary beam. An experimental implication is that the means of achieving the highest signal-to-noise ratio image of an intact fragile molecular species is via signal averaging of repeated low dose (high rastering speed) images.

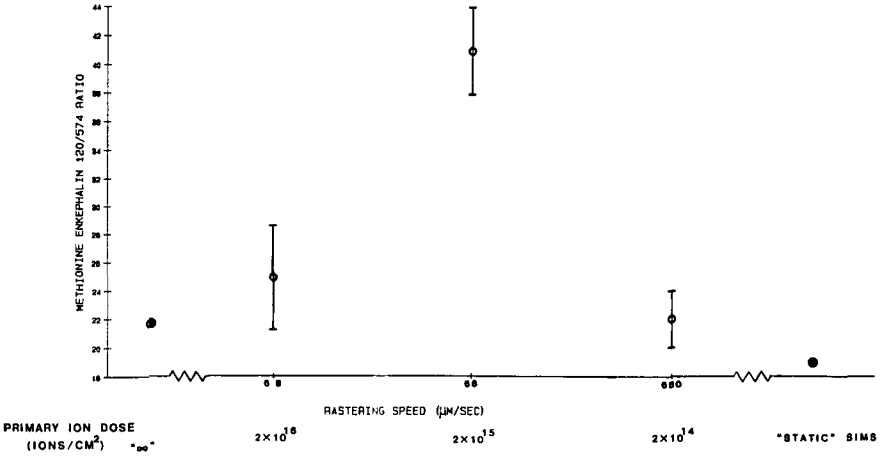

Figure 3

NEUTRAL SIMS OF GALLIUM ARSENIDE

David M. Hindenlang and R. Donald Sedgwick, Allied-Signal Inc., Morristown, NJ 07960

Introduction

Information on sputtering from liquid surfaces by neutral bombarding particles, as in FAB ionization, is complicated by surface dynamics and a lack of detailed knowledge of the actual structure of the surface phase. Hence conclusions about ionization in FAB sources have focused on mechanisms which emphasize surface dynamics and equilibrium adsorption models. The mechanisms of sputtering by neutral bombardment can best be studied using a well characterized sample system. We report here measurements on the sputtering from a relatively simple solid binary system, gallium arsenide (GaAs), where surface dynamics and adsorption effects can be considered minimal. GaAs is widely employed as a substrate for semiconductor microelectronics applications and has been extensively characterized by a variety of spectroscopic techniques.

Summary

Sputtering of GaAs using 7 keV xenon atoms with positive ion and negative ion analysis by a high mass range mass spectrometer has been studied. Cluster ion series of Ga_nAs_m from n+m=1 to n+m>10 have been observed and characterized. The cluster patterns are complex because of the Ga isotope distributions and mixtures of varying values of n for the same value of n+m. Anion spectra are generally more representative of a 1:1 stoichiometry for GaAs. The observed ion intensities, especially for single metal cations (n+m=1), have more to do with ion chemistry and ion stabilities than with quantitation in the sample. Clusters (especially anions) for values of n+m~3-5 show more nearly equivalent levels of Ga and As (values of n≈m). For values of n+m from 5 to >10 gallium content is dominant in both positive and negative ion clusters. The highest value of As observed in clusters at a significant intensity is m<4.

Experimental

The instrumentation for this examination of GaAs wafers was a VG Analytical ZAB-HF reverse geometry high resolution double focusing mass spectrometer with FAB source using 7 keV xenon atoms. Both positive ion and negative ion spectra were recorded on the VG Analytical 11-250 instrument control and data collection system, with magnetic scanning using field control and an ion energy of 8 keV. Signal averaging of spectra was accomplished using the MCA facilities of the 11-250 data system.

Isotopes and Physical Data

Gallium (Z = 31)

Symbol	Mass	Abundance
Ga^{69}	68.9256	60.2%
Ga^{71}	70.9247	39.8%

Electron structure (Ar) $3d^{10}\ 4s^2\ 4p^1$
Common oxidation state +3
First ionization potential 6.0 eV

Arsenic (z = 33)

Symbol	Mass	Abundance
As^{75}	74.9216	100%

Electron structure (Ar) $3d^{10}\ 4s^2\ 4p^3$
Common oxidation state -3 (+3, +5)
First ionization potential 10.5 eV

Positive Ion Spectra

At low mass positive ion spectra are dominated by Ga species. For example at n+m=1 the intensity of m/z 75^+ (Ar^+) is about 1% of the combined m/z 69, 71 (Ga^+) intensity. The low relative abundance of As^+ is consistent with the high ionization potential (10.5 eV) of arsenic compared with gallium (6.0 eV). Somewhat higher mass clusters are more representative of sample composition and structure, showing more contribution from As to the complex patterns. For example for n+m=3 there is a significant contribution from $AsGa_2$ and some As_2Ga, while at n+m=4 and 5 the dominant ionic species have one As constituent. Even higher mass clusters (n+m=5 to 20) continue to show substantial As content but the ratio never approaches the theoretical 1:1. The m/z width of the cluster patterns does not continue to increase since only a few (3 or 4) species are observed within each cluster pattern. The value for the As contribution is always observed to be m<4 with the remainder Ga_n where n can be as high as 20. There is an interesting alternation in the observed intensities of cluster patterns with the series of odd values of n+m more intense than the even series.

Negative Ion Spectra

The negative ion spectra indicate overall more nearly equivalent intensities for Ga and As contributins. Essentially no Ga^- is observed, but substantial As^- (m/z 75^-) is observed. At n+m=2 again essentially no Ga_2^- is observed but $GaAs^-$(144^-, 146^-) is significant along with As_2^- (150^-). For values of n+m from 3 to 5 the general contribution of Ga and As to cluster patterns is generally around the theoretical stoichiometric 1:1. A slight dominance of As is observed at n+m=3 (no Ga_3^-) while a slight dominance of Ga is observed at n+m=5. At even higher mass (n+m>5) the Ga contributions to observed clusters become dominant, similar to the positive ion spectra. The value for the As contribution again is always observed to be m<4, with the remainder Ga_n. Hence the m/z width of the cluster patterns does not continue to increase since only a few species are observed within each cluster pattern. Negative ion spectra show the same interesting oscillation in observed intensities of cluster patterns, with the series of odd values of n+m more intense than the even series. Negative ion spectra are observed to be less intense and statistics on isotope patterns are not as good as for positive ion spectra.

Conclusions

Neutral particle sputtering of clusters from this "simple", rather well defined binary solid surface is still rather complex, giving rise to some intriguing observations. The complex series of cluster patterns of GaAs are not readily or uniformly explainable by sample stoichiometry or combinations of cations and anions of common oxidation states. The dominance of Ga^+ over As^+ at low mass is explainable in terms of relative ionization potentials. The relative contribution of As to positive ion clusters begins to increase (through n+m~5) but then reaches a plateau level (m<4). The observed high mass species simply show increasing Ga_n levels. Negative ion spectra show a relative preponderance of As contribution at low mass, which decreases through the theoretical stoichiometric ratio of Ga:As of 1:1 around n+m=4. Again the contribution of As to high mass clusters reaches a plateau at m<4 while increasing Ga_n accounts for the higher mass clusters observed. Both positive ion and negative ion spectra indicate greater intensities for cluster patterns of odd values of n+m versus even values.

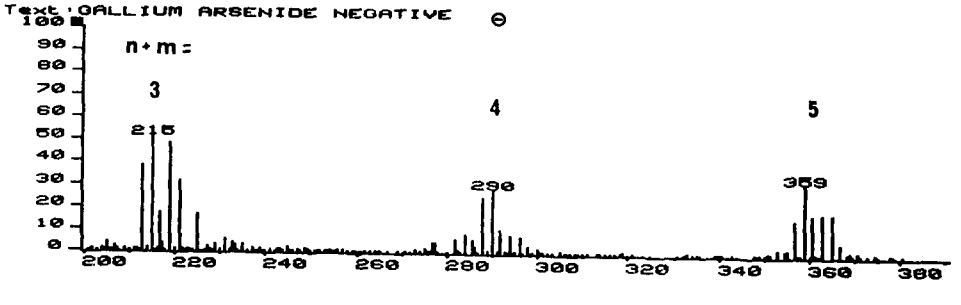

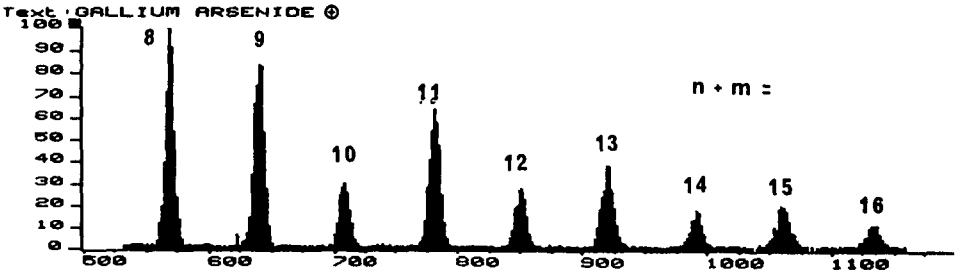

ENHANCED DETECTION OF POSITIVE OR NEGATIVE IONS
UNDER SELECTIVE ILLUMINATION OF O_2 OR Cs
AND COINCIDENT MEASUREMENT OF PHOTOEMISSION
ACCOMPANIED BY SPUTTERING DUE TO ION BOMBARDMENT

M.Ohshima, T.Shinomiya, H.Tamura*,
Y.Sugiyama, A.Namiki, S.Nishigaki, and T.Noda;
Toyohashi University of Technology, Toyohashi, 440 Japan
*Hitachi Central Research Lab., Kokubunji, Tokyo, 185 Japan

In these years, microprobe SIMS has become very important in analyses of semiconductors and the like, and higher sensitivity has been seriously demanded. Authors tried to enhance signals of secondary ions from electropositive or negative elements in solid specimens by flooding O_2 or Cs onto the specimen, while retaining the same ion gun in use. In order to search a clue of sputtering phenomenon which is not well known, photoemission spectra were also measured in coincidence with the secondary ion emission.

Configuration of the apparatus used is shown in Fig. 1. The primary ion probe and the secondary ion analyzer are the same as those of Hitachi IMA-2, but its specimen chamber was modified to mount a variable leak valve unit for O_2 introduction and a Cs vapor gun for deposition, and to evacuate with a turbo molecular pump of 2000 l/s. The ion gun was selectively employed between a modified duoplasmatron and a liquid metal source we developed.

Photoemission from the specimen was lead to a Nikon 250 mm monochromater through a vacuum window and an f 100 mm lens, both made of quartz. Charge pulses from a cooled photomultiplier were converted into voltage pulses and discriminated at the input of a pulse counter to reduce the noise below I cps.

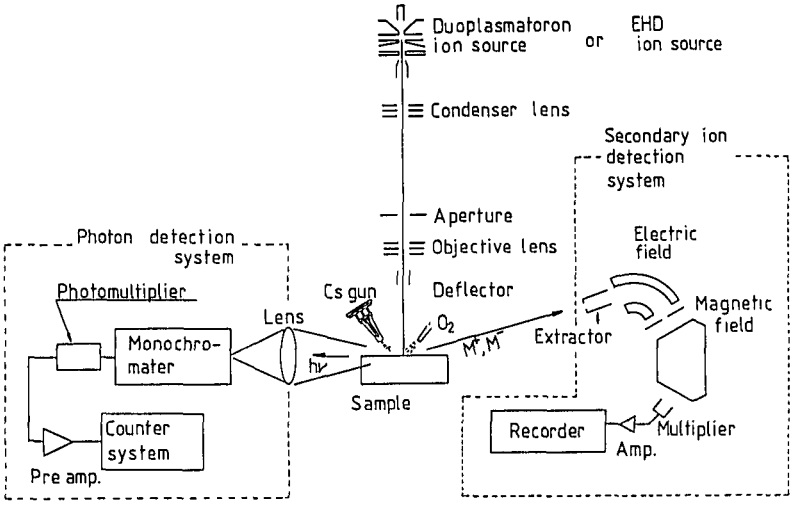

Fig. 1. Schematic diagram of the apparatus

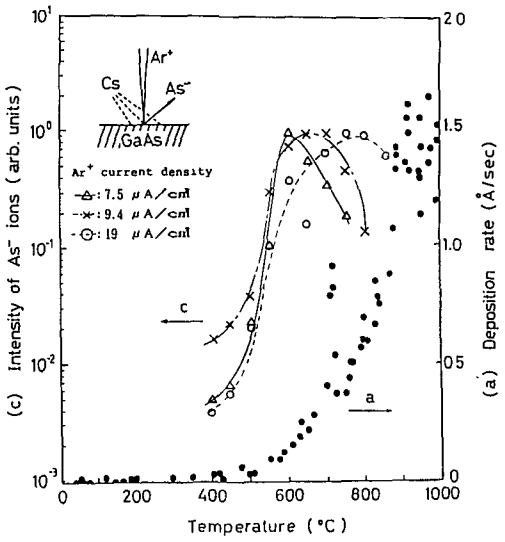

As shown in Fig. 2, intensity of As^- ions from GaAs under Ar^+ impact was dramatically increased with the rate of Cs deposition on the specimen surface, and reached a maximum, which appeared at higher deposition rate for increased current of the primary Ar^+ beam. The fact means that there is an optimum coverage of Cs on the surface.

Fig. 2. Enhancement of As secondary ions with Cs flooding

Coincident measurements of secondary ions and photons as a function of specimen surface coverage showed good correlations for Si^+/Si I from Si and As^-/As I from GaAs as seen in Fig. 3.

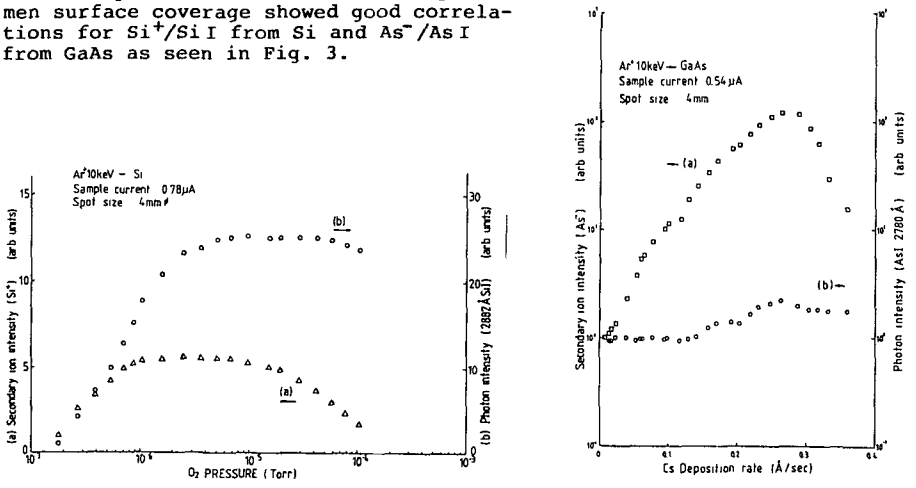

Fig. 3. Coincident measurements of secondary ions and photons.
(a) Si^+ and Si I(288.2nm) from Si under O_2 introduction
(b) As^- and As I(278.0nm) from GaAs under Cs flooding

FLUORINE ANALYSIS BY TIME-RESOLVED MASS SPECTROMETRY

P. H. Hemberger, R. J. Beckman, and R. C. Heaton
Los Alamos National Laboratory
Los Alamos, NM 87545

Fluorine analysis by mass spectrometry is hindered by the high reactivity of fluorine with the gas sampling system and the mass spectrometer. Although instrument passivation is a traditional approach to reducing sample reactions during analysis, we have found it to be an unreliable method of assuring consistent results. The primary objective of this project was to develop assay methods for excimer laser gas mixtures. A secondary objective was to survey each sample cylinder for volatile impurities.

In the first two series of analyses, a quadrupole mass spectrometer was passivated with a 5% fluorine in argon mixture and evacuated to base pressure. Peak heights in the sample mass spectrum were corrected for background contributions and instrument discrimination. Poor reproducibility of the analytical results with this method was demonstrated by duplicate analyses of the samples (Figure 1). A time-resolved method of analysis was developed to use the temporal variations in instrument response. In this method, instrument responses to fluorine, krypton, and argon were recorded as a function of time. Well-characterized standards, which were similar in composition to the samples, were analyzed in the same fashion after every two samples. The intensity versus time data for all samples and standards which were analyzed in one day's run were reduced by least-squares methods (Figure 2). Using the standards as calibration points, an equation which relates concentration to time can be derived. From the time of analysis of each sample, the concentration of fluorine and krypton in each mixture was calculated. Selected results for both mass spectrometric methods are shown and compared to gas chromatographic analyses in Figure 3. The precision of measurement for months 1 and 2 is 30% relative to the mean based on replicate analyses. The precision of the time-resolved method is 8% relative to the mean.

The time-resolved methods described here can improve the reliability of analysis of reactive species. However, this methodology requires standards which are similar in composition to the samples. Impurity analysis was difficult as sample impurities could not easily be differentiated from fluorine reaction products formed within the system. Minor impurities consisted of hydrocarbons and fluorinated silanes. Hydrogen fluoride was the major product of fluorine reactions in the system and was difficult to quantify as an impurity.

Figure 1.

SAMPLE	MONTH 1 %F_2	MONTH 1 %Kr	MONTH 2 %F_2	MONTH 2 %Kr
1	0.52	8.5	0.37	12.8
2	0.41	10.8	0.22	12.1
3	0.32	12.4	0.31	13.8
4	0.37	11.4	0.17	13.7
5	0.34	10.3	0.08	10.8
7	0.31	11.9	0.36	14.5
8	0.34	11.8	0.35	14.1
24	--	--	0.32	13.2

Figure 2. Ratio of F^+ to Ar^+ vs. time of analysis. The data are best described by a second order polynomial.

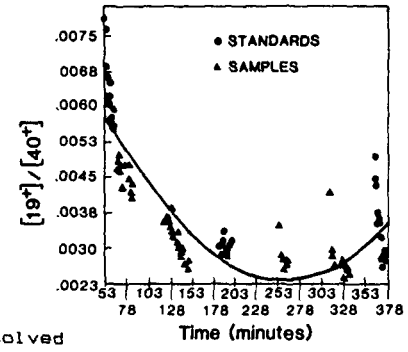

Figure 3. Results of time-resolved and gas chromatographic analyses.

SAMPLE	MONTH 1 %F_2	MONTH 1 %Kr	MONTH 2 %F_2	MONTH 2 %Kr	TIME-RES %F_2	TIME-RES %Kr	G.C. %F_2	G.C. %Kr
5	0.34	10.3	0.08	10.8	0.41	10.1	0.33	10.1
7	0.31	11.9	0.36	14.5	0.42	10.1	0.37	10.2
24			0.32	13.2	0.43	10.2	0.39	10.1
41					0.41		0.38	
42					0.34		0.36	
43					0.43		0.41	
44					0.40		0.39	
46					0.40		0.40	

PYROLYSIS MASS SPECTROMETRY OF ANTIMONY OXIDE-ORGANOHALOGEN FLAME RETARDANTS IN PLASTICS

P. Jane Gale, Bryan L. Bentz and Wendell M. Lee
RCA Laboratories, Princeton, NJ 08540

The combination of halogenated organics and antimony trioxide is known to be an effective flame retardant system for organic polymers. A synergism is thought to develop when the two classes of compound are used concert, although the chemistry of the interaction is not well understood. It has been suggested that the halides react with Sb_2O_3 near the pyrolysis temperature of the polymer to produce antimony trihalides, which then act as dehydrating agents for the flammable substrate and perhaps, also, as radical traps [1]. The formation of antimony chlorides and bromides has been demonstrated in the pyrolysis of mixtures of antimony oxide and HCl or HBr [2]. Antimony chlorides have also been shown to form in the pyrolysis of poly(vinyl chloride), PVC, doped with antimony trioxide. By analogy, it has been assumed that brominated organics produce antimony bromides when pyrolyzed in the presence of antimony trioxide, although a recent finding calls this into question: no antimony bromides were observed in pyrolysis of antimony oxide mixed with a common organo-bromine flame retardant, decabromodiphenyl oxide [3]. Is this difference attributable to a difference in reactivity of the two halogens or is it related to the form in which the halogens were presented?

Pyrolysis of poly(vinyl bromide), PVB, doped with antimony trioxide forms antimony bromides in abundance, as can be seen in Figure 1, suggesting equivalence in reactivity of chlorine and bromine if their chemical form is equivalent. It should also be noted that pyrolysis of the undoped PVB produces a substantial amount of HBr, analogous to the well-known formation of HCl in the pyrolysis of PVC. Pyrolysis mass spectral analyses of a number of compounds were carried out, both in the presence of antimony trioxide and in its absence. As shown in Table 1, all the compounds which evolved HX on pyrolysis produced SbX_3 when pyrolyzed in the presence of Sb_2O_3. A look at the structures of the compounds involved shows that compounds which react all have hydrogen on a carbon vicinal to the halogenated carbon, whether the compound is a polymer or a flame retardant additive. Conversely, compounds without hydrogen vicinal to the halogen do not form a hydrogen halide or an antimony halide during pyrolysis. This finding is illustrated with pyrolysis spectra from aliphatic hexabromocyclododecane and aromatic tetrachlorophthalic anhydride mixed with antimony trioxide, shown in Figure 2. Pyrolysis of the former mixed with antimony trioxide produces a large amount of antimony bromide, while a similar analysis of the latter produced none. The result obtained from this analysis of 70% chlorinated paraffin provides an interesting intermediate case which proves the point: since, in a 70% chlorinated compound, many of the hydrogens have been replaced by halogens, only a small amount of HCl can be formed during its pyrolysis. Correspondingly, a small amount of antimony chloride is observed in the pyrolysis of the polymer mixed with antimony trioxide.

1. James J. Pitts in Flame Retardancy of Polymeric Materials, vol. 1, W. C. Kuryla and A. J. Papa, eds.(New York: Marcel Dekker, 1973).
2. J. W. Hastie, Combust. Flame, 21, (1973), 49.
3. J. Simon, T. Kantor, T. Kozma, and E. Pungor, J. Thermal Anal. 1982, 25, 55-77.

MASS SPECTRA FROM PYROLYSIS OF POLY(VINYL BROMIDE)
FIGURE 1

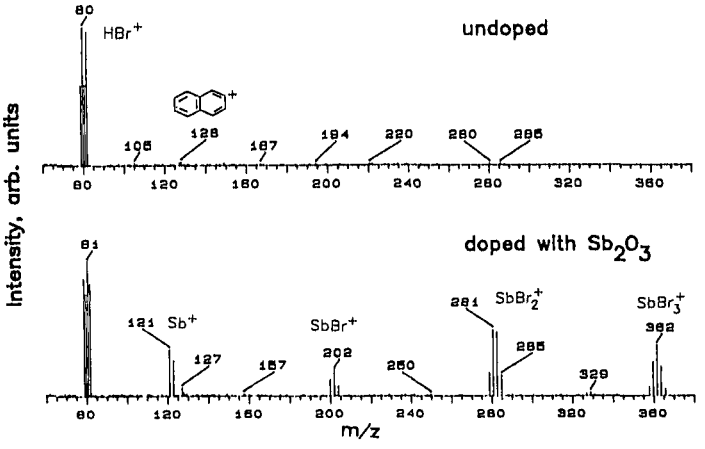

TABLE I
RESULTS OF PYROLYSIS IN ABSENCE AND PRESENCE OF Sb_2O_3

Name	Structure	Forms HX	Forms SbX_3
Dibromoethyldibromocyclohexane	Br_2-(cyclohexane)-$CH(Br)CH_2Br$	yes	yes
Hexabromocyclododecane	Br, Br, Br, Br, Br, Br	yes	yes
Octabromodiphenyl oxide	Br_4-(C6H4)-O-(C6H4)-Br_4	no	no
Decabromodiphenyl oxide	Br_5-(C6H4)-O-(C6H4)-Br_5	no	no
Tetrachlorophthallicanhydride	Cl_4-(benzene)-(C=O)$_2$O	no	no
Chloroparaffin, 70%	$CY_3(CY_2)_nCY_3$ Y = H,Cl	some	some
Chlorinated polyethylene, 25%	$[CY_2-CY_2]_n$ Y = H,Cl	yes	yes

FIGURE 2
MASS SPECTRA FROM PYROLYSIS OF HEXABROMOCYCLODODECANE

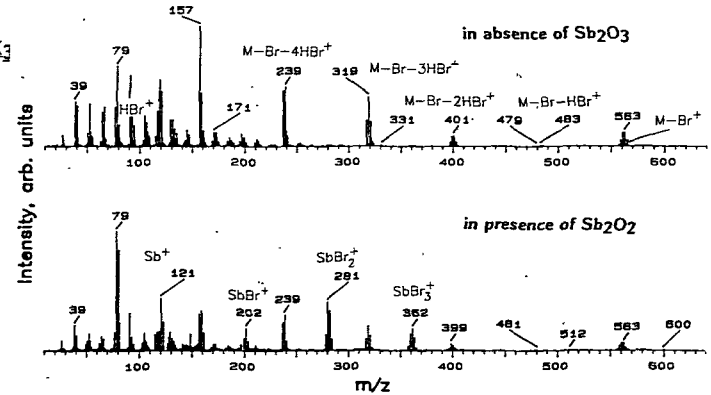

MASS SPECTRA FROM PYROLYSIS OF TETRACHLOROPHTHALLIC ANHYDRIDE

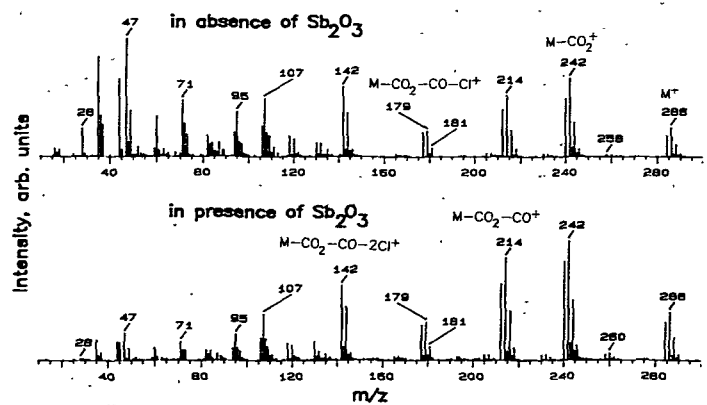

DEVELOPMENT AND TESTING OF A CURIE-POINT PYROLYSIS INLET FOR THE FINNIGAN ION TRAP DETECTOR

Joseph M. Richards, Henk T. Stolk, William H. McClennen and Henk L.C. Meuzelaar
Biomaterials Profiling Center, University of Utah
391 S. Chipeta Way, Suite F, Research Park
Salt Lake City, Utah 84108

Donald C. Bradford
Finnigan MAT
355 River Oaks Parkway
San Jose, California 95134

Though the Finnigan Ion Trap Detector (ITD) is designed and used primarily as a detector system for gas chromatography, it has several features which make it attractive for development as a stand alone MS, e.g., for pyrolysis mass spectrometry (Py-MS) studies. Among the attractive features are its ease of operation, high scanning speed, ability to detect all ions produced in a single, transient event (e.g., flash pyrolysis), and possibilities for CI and tandem MS (MS/MS) operation modes. Moreover, the ITD's small size, low price and its user friendly operating software make it well suited for environmental monitoring (i.e., pollutants or aerosols), industrial process monitoring, biomedical and forensic applications. By interfacing a Curie-point pyrolysis inlet to the ITD, a bench top Py-MS system can be developed which can analyze nonvolatile organic materials in several different Py-MS modes including Py-EIMS, Py-CIMS and Py-MS/MS.

Initial experiments involved connecting a Curie-point pyrolysis inlet directly to the heated, open-split GC interface of the ITD. Pyrolysis in this configuration was carried out in an inert (He) atmosphere, and the products of pyrolysis were swept into the ITD by the He carrier gas. Analyses of synthetic polymers: poly(α-methylstyrene), nitrocellulose, and poly(methylmethacrylate) gave spectra with characteristic molecular and fragment ions of the respective monomers and other pyrolysis products. The time information about the relative thermal stabilities of these polymers was also preserved. However, the elution of the pyrolysis products into the ITD was accompanied by extensive peak broadening and tailing. This resulted in the pyrolysis products from a ca. 2 s heating profile (temperature rise time ca. 2 s, total heating time 10 s, equilibrium temperature of the filament 610°C) giving a total ion current curve that was approximately 12 s wide at half maximum. Analysis of biopolymers (deoxyribonucleic acid DNA, bovine serum albumin BSA, and glycogen), however, resulted in the loss of polar pyrolysis prdoucts. These losses are apparently due to condensation in the transfer line or the pyrolysis inlet. Moreover, the long residence time of the pyrolyzate in the hot (250°C) transfer line may lead to undesireable rearrangements or secondary reactions among the pyrolysis products [1].

To overcome these difficulties, the pyrolysis reactor was modified in order to connect directly to the ITD via a 3 inch glass lined tube. This configuration is shown in Figure 1 (Py-ITD). Analysis of a polymer mixture of nitrocellulose, poly(styrene) and poly(α-methylstyrene) showed significant reduction in peak broadening and tailing and preservation of time (temperature) resolved information. The direct interface also resulted in improved sensitivity as was seen in the analysis of 5 ng of a poly(ether urethane urea) (Biomer [2]) under standard ionization conditions. Analysis of Biomer yielded spectra which contain peaks characteristic of the diisocyanate and polyol components [3] and reflect the temperature-dependent nature of the pyrolysis process (Figure 2). Analysis of DNA, BSA, and glycogen produced spectra which compare favorably with low voltage (12 eV) Py-EIMS and with Py-APCIMS. However, for both the Biomer and the biopolymer spectra, there are many spectral features which differ significantly from either low voltage Py-EIMS and Py-APCIMS. These differences are apparently due to the different ionization and mass analysis techniques used in the ITD and are not clearly understood at this time.

Future studies on this system will investigate the sensitivity and reproducibility of the system using Py-EIMS and Py-CIMS. Also the information content of the spectra will be studied.

1. S.C. Israel, W.C. Yang, and M. Bechard, *J. Macr. Sci. Chem.*, 1985, 22(5-7), 779-801.

2. Biomer is a trademark of Ethicon Inc.

3. J.M. Richards, W.H. McClennen, H.L.C. Meuzelaar, D.E. Gregonis, W.M. Reichert and M.A. Helle, *Macromolecules*, 1985, 18, 496-500.

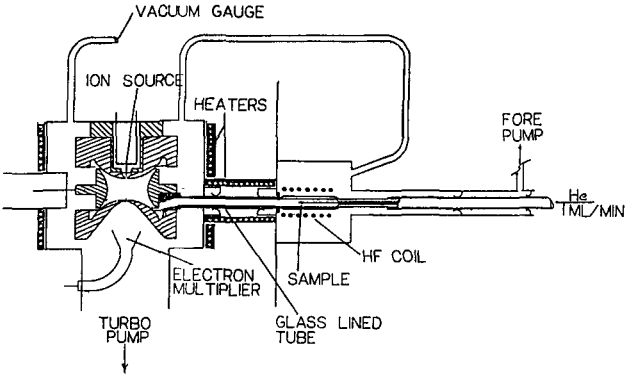

Figure 1. Schematic of the Curie-point pyrolysis Ion Trap system (Py-ITD). Sample is coated onto the tip of a ferromagnetic filament which is inductively heated to its Curie-point by the high frequency coil. Helium is introduced through the sample probe at a rate of 1 m/min.

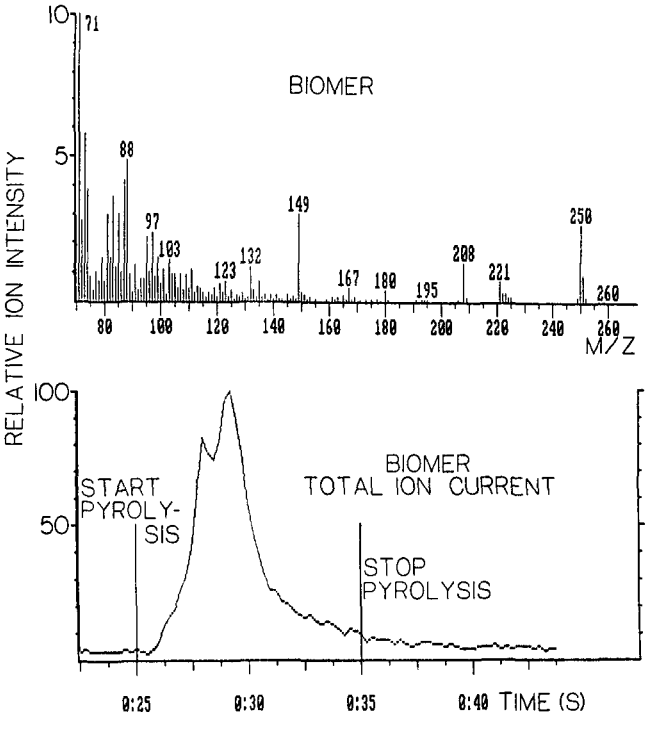

Figure 2. Spectrum and total ion current curve from the analysis of 5 ng of Biomer. In the mass spectrum, note the peaks which are characteristic of the diisocyanate (m/z 208, 221, and 250) and polyol (m/z 71 and 73) components. The peaks which are characteristic of the diamine chain extender (m/z 86) and the polyol dimer fragment (m/z 143 and 145), however are not seen. The total ion current curve shows two maxima which have been attributed to the degradation of the diisocyanate followed by polyol decomposition.

LASER DESORPTION FT/ICR MASS SPECTROMETRY:
ANALYSIS OF POLYMERS AND ELECTRODE SURFACES

Ronald E. Shomo, II,[a] Annjia T. Hsu,[a] Alan G. Marshall,[a,b] and David G. Westmoreland,[c]

Department of Chemistry[a]
Department of Biochemistry[b]
The Ohio State University
140 West 18th Avenue
Columbus, OH 43210.

Rohm and Haas Company[c]
Research Laboratories
727 Norristown Road
Spring House, PA 19477

Laser desorption Fourier transform ion cyclotron resonance mass spectrometry (LD/FT/ICR) performed with a Tachisto 215G pulsed CO_2 laser (10.6 μm) typically produces a prominent pseudomolecular ion (e.g., $(M+K)^+$) for a wide variety of large involatile organic molecules (1,2). We have extended our studies to several new molecular classes, many never before seen by mass spectrometry.

For a series of polymers of varying size distribution (e.g., Triton® X100 and X165 surfactants), we have compared LD/FT/ICR mass spectra with profiles obtained via liquid chromatography with either UV or quadrupole mass spectrometry total ion current detection. The LD/FT/ICR peak distribution agrees well with both the LC/UV and LC/MS profiles, but is achieved in about 1 sec from a single laser pulse without prior chromatographic separation. The apparent LD/FT/ICR relative peak intensities, distorted by limited digital vertical resolution, can be improved by curve-fitting procedures. Moreover, accurate-mass measurements (300 < m/z < 1400) from the LD/FT/ICR mass spectra confirm the chemical formulas for each oligomer (see Figure 1).

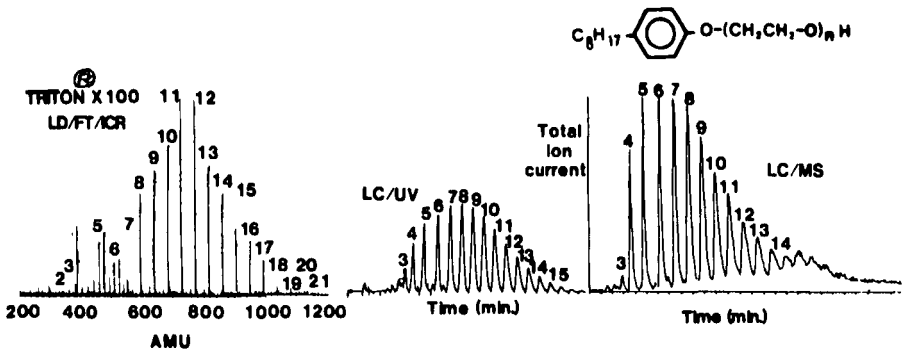

Figure 1. Triton® X100 surfactant oligomer distribution.

Left: FT/ICR detection of ions formed by a single CO_2 laser pulse.
Middle: UV absorbance detection of eluent from a liquid chromatograph.
Right: Total ion current LC/MS profile obtained from a quadrupole mass spectrometer.

We have also studied the surface chemistry of glassy carbon electrodes. The different electrochemical behavior of a freshly polished electrode and an electrochemically pretreated electrode has been noted previously (3,4). In all cases, the pretreatment included application of relatively large positive potentials (e.g., 1.8 V) and/or negative potentials to the working electrode. It has been conjectured that electrochemical pretreatment may introduce or alter the nature of functional groups on the electrode surface. Our LD/FT/ICR results (see Figure 2) show clear differences in surface composition for pretreated and the freshly polished electrodes. From the chemical formulas determined via accurate-mass measurements, the ions at m/z = 465, 639, and 735 appear to be potassium adducts of fused aromatic rings. An exciting new prospect, currently under investigation, is depth-profiling of the electrode surface, based on comparison of LD/FT/ICR mass spectra obtained from successive laser shots at the same spot on the electrode. We have also observed carbon cluster ions, C_n^+, $4 \leq n \leq 26$, from a glassy carbon electrode via pulsed CO_2 (10.6 μm) and from graphite via Nd/YAG (1.06 μm or 532 nm) irradiation.

[This work was supported by N.I.H. 1 R01 GM31683, N.S.F. CHE-8218998 and The Ohio State University.]

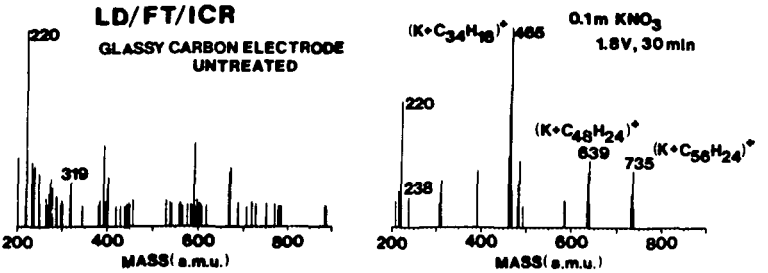

Figure 2. *Mass spectra of glassy carbon electrodes, obtained by Fourier transformation of the time-domain ICR signal accumulated from five pulses of a CO_2 laser.*

Left: Freshly polished electrode without further pretreatment.

Right: Polished electrode which had been electrochemically pretreated by applying 1.8 V vs. SCE in 0.1 M KNO_3 electrolyte for 30 min. The electrodes were kindly provided by R. L. McCreery.

References

1. Shomo, R. E., II; Marshall, A. G.; Weisenberger, C.R.; (1985) Anal. Chem. 57, 2940-2944.
2. Shomo, R. E., II; Marshall, A. G.; Lattimer R. P. (1986) Int. J. Mass Spectrom. Ion Proc., in press.
3. Engstrom, R. C.; Strasser, V. A. (1984) Anal. Chem. 56, 136-141.
4. Van der Linden, W. E.; Dieker, J. W. (1980) Anal. Chim. Acta 119, 1-24.

MODIFICATION OF A FINNIGAN-MAT TRIPLE STAGE QUADRUPOLE FOR ORGANIC SIMS OF SOLID SURFACES

Bryan L. Bentz, P. Jane Gale and Richard E. Honig
RCA Laboratories, Princeton, NJ 08540

The need to determine the surface composition of organic solids has stimulated much scientific activity in recent years. Bombardment of surfaces with keV particles, MeV particles, or photons has been explored. To maximize the desorption of intact organic molecules adsorbed on a solid substrate, the "static SIMS" approach, as defined by Benninghoven [1] for surface analysis, appears most suitable [2-5]. This method limits the primary particle dose to about 10^{13} particles/cm^2, so that less than 10% of the sample surface is damaged during the time of analysis. This so-called dose limitation assures that most molecules are not fragmented by multiple primary particle impact. It also limits the secondary ion signal per unit area that can be obtained. To compensate, it is desirable to collect ions sputtered from relatively large sample areas. Static SIMS spectra are frequently dominated by molecular ions, giving few clues to the structure of desorbed species. To determine not only molecular ion masses but also the structure of desorbed molecules, it is a logical step to combine static SIMS with a Triple Stage Quadrupole (TSQ) mass spectrometer. The collisional dissociation capability on our TSQ should provide a powerful tool for desorbed ion structural studies.

With the expanding interest in the electronics industry for the utilization of novel organic materials systems, the need has arisen in our mass spectrometry laboratory to characterize intact solid organic surfaces. Instrumentation is at our disposal for organics analysis by Liquid SIMS and SIMS survey analyses of many conducting inorganic solid materials. That required for low dose, organic solid surface analysis is not available. Accordingly, we are modifying our TSQ to form a UHV static SIMS spectrometer. The new instrument will provide added capabilities, as well as allow convenient, rapid change-over to the standard modes of TSQ operation: GC/MS, EI, CI, and Liquid SIMS.

Figure 1 shows the spectrometer system under development. A homebuilt 15-port vessel serves as the SIMS UHV sample chamber. The cylindrical chamber (6" in diameter, 14" in height) couples to the TSQ vacuum manifold via a 6" OD doublesided Conflat flange. The flange is machined to supply 12 electrical feedthroughs and to support a portion of the secondary ion optics developed in-house. Pumping is provided by a 500 l/sec turbopump fitted with a LN_2 trap and Ti sublimator. A homemade transfer lock, pumped by a 50 l/sec turbopump, is used for sample exchange.

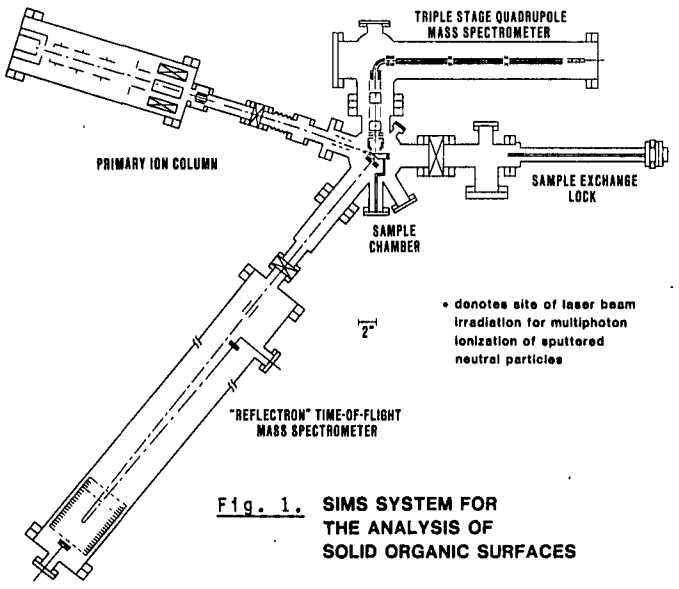

Fig. 1. SIMS SYSTEM FOR THE ANALYSIS OF SOLID ORGANIC SURFACES

A Colutron G-2 ion source with ExB filter will be used to produce keV primary ions (Ar, Xe, or Cs, 1-10 keV). The primary column is differentially pumped and contains two lenses for adjusting beam current and probe size. Raster capabilities are provided by plate condensers. The fluence condition for static SIMS can be met by either forming a defocused static beam or scanning a focused probe over a relatively large sample area. The ion beam will operate in static or rastered, dc or pulsed modes.

The secondary ion optics to extract and transport ions for TSQ mass analysis consist of a cathode immersion lens, dynamic emittance deflection plates, and a 90° spherical electrostatic analyzer (ESA) with input/output lenses (see Figure 1). The design of an immersion lens for wide area ion extraction (~1 cm^2) is being aided by computer calculations of ion trajectories. Dynamic emittance matching, developed by Liebl [6], is used to optimize secondary ion transmission and system sensitivity. This deflection system, synchronized with the primary beam raster, continuously directs secondary ions produced from a rastered area onto their optical axis. This has the effect of increasing the acceptance angle of the mass spectrometer. To avoid a line-of-sight path from the sample to the detector, we have constructed a 90° spherical ESA and inserted it in the secondary ion beam line. This device can select an energy bandpass of secondary ions and prevents high energy particles and photons from creating a signal at the detector. Aperture-type deceleration and focus lenses preceed and follow the ESA to adjust beam energies. Standard Finnigan-MAT quadrupole rods are used (4-1000 amu) and no modifications to the rf/dc electronics have been undertaken. A pulse counting electron multiplier is used as the detector. Figure 2 shows the axis potential of the overall SIMS/TSQ system.

As shown in Figure 1, the overall spectrometer system will consist of a quadrupole mass analyzer and a time-of-flight (TOF) spectrometer. These two spectrometers will be used separately for static SIMS, not in tandem or simultaneously. The TOF offers unlimited mass range and high, uniform transmission. Use of an ion mirror can improve mass resolution. Additionally, the TOF is the spectrometer best suited for laser multiphoton ionization studies of desorbed neutral particles, which we plan to pursue.

SUMMARY OF MAJOR INSTRUMENT MODIFICATIONS TO THE TSQ

1. Homebuilt SIMS vacuum chamber with pumping stack coupled to TSQ vacuum manifold at a 6" OD flange available in "source" chamber.
2. Standard EI/CI source flange removed and replaced with a 6" OD flange onto which is mounted a home-built 90° spherical ESA with input/output lenses.
3. Triple quadrupole mass filter assembly with pumping cone retracted by 1.6" using Conflat flange insert which entends the standard vacuum manifold.
4. Interlink system developed to protect the combined vacuum systems against electrical/vacuum failure, venting automatically the 3 turbopumps with dry N_2 after a preset delay period.
5. GC/MS interface oven module removed; the available 2.75" OD flange fitted with a viewport.
6. Analog electron multiplier replaced with a pulse counting version.

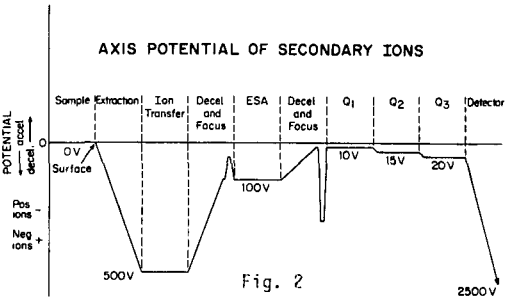

Fig. 2

REFERENCES

1. A. Benninghoven, D. Jaspers, and W. Sichtermann, Appl. Phys. 11, 35 (1976).
2. A. Benninghoven, J. Vac. Sci. Technol. A3, 451 (1985).
3. D. Briggs and M. Hearn, Spectrochim. Acta 40B, 707 (1985).
4. J. Gardella, Jr. and D. Hercules, Anal. Chem. 52, 226 (1980).
5. J. Campana, M. Ross, S. Rose, J. Wyatt, and R. Colton, in "Ion Formation from Organic Solids", A. Benninghoven, ed. (Springer Verlag, Berlin, 1983), p. 144.
6. H. Liebl, in Inst. Phys. Conf. Ser. No. 38, "Low Energy Ion Beams", K. G. Stephens, I. H. Wilson, and J. L. Maruzzi, eds. (Institute of Physics, London, 1978), p. 266.

THE GROWING ROLE OF MASS SPECTROMETRY IN MOLECULAR BIOLOGY

Klaus Biemann
Department of Chemistry, Massachusetts Institute of Technology
Cambridge, MA 02139.

Introduction

Since the discovery and deciphering of the genetic code our understanding of biological processes on the molecular level has incresed rapidly. The more recent development of methods to modify the structure of genes by manipulating DNA in cells, even in those of entirely different (and simple to grow) organisms, has opened a fast moving field of enormous scientific and commercial importance. Commonly called "genetic engineering" the biological or synthetic production of modified or custom-designed genes is often undertaken to generate the biologically active gene products, namely the proteins synthesized in the ribosomes along the messenger RNA's which in turn represent the image of the self-replicating parental DNA.

Thus, over the past decade it has become possible to not to only produce rare, biologically very interesting proteins in larger quantities, but also to prepare specific modifications in their primary structure. These modified proteins are used to study the details of their biological activity and mechanism of action, or may be designed to have more desirable therapeutic properties.

This sudden burst of new and modified proteins has led to a renaissance of protein chemistry, particularly protein structure determination, which seemed to have reached a high point in the late 1970's but appeared from then on to become obsolete (1) by the newly developed methods for the very rapid determination of the base sequence of the DNA coded for the synthesis of the protein. The structure of the latter can then be simply deduced using the genetic code.

Although in vivo protein synthesis and their biological action, mostly as enzymes, is only one part of the fast moving area of biology today, it is the one where mass spectrometry presently is beginning to have the greatest impact. There are a number of reasons for this: (1) There is only one chemical method in general use for the determination of the amino acid sequence of proteins, namely the Edman degradation (2). While it has been greatly improved and automated over the last two decades, as a sequential technique it is limited in the number of consecutive amino acids that can be determined starting at the N-terminus and it is rendered useless if there is an acylated or tertiary N-terminal amino acid present. (2) Mass spectrometry is particularly suited for the determination of linear molecules with repeating building blocks, such as peptides. (3) Mass spectrometry is applicable to a great variety of structures and thus can detect structural ("posttranslational") modifications a protein has undergone after its synthesis along the messenger RNA which codes only for the original, unmodified amino acids. (4) Mass spectrometry is the only structural specific technique that comes close to the sensitivity required in the determination of the structure of proteins, many of which are available only in very small quantities (nanomoles or less).

The Structure of Bacterio-opsin and Synthetic Analogs.

A spectacular example of the level of sophistication which bio-synthetic generation of a family of closely related proteins has achieved was discussed in Professor H. Gobind Khorana's preceding plenary lecture entitled "Two Light-Transmitting Systems: Rhodopsin and Bacteriorhodopsin" (the major part of which will soon appear elsewhere (3)). The determination of the primary structure of bacterio-opsin (bacteriorhodopsin from which the retinal chromophore has been removed) isolated from *Halobacterium halobium* is an example of the complementarity of the Edman degradation carried out in H.G. Khorana's research group and mass spectrometric peptide sequencing by GCMS developed in our laboratory (4). The nature of this membrane protein which exhibits very unusual solubility characteristics (very hydrophobic) and is, therefore, difficult to digest by proteolytic enzymes precluded the use of a single technique. The protein turned out to consist of a single chain of 248 amino acids which transverses the cell wall seven times as shown in Figure 1. For the determination of the primary structure, bacterio-opsin was treated first with chymotrypsin which attacks only one single peptide bond, between Phe-71 and Gly-72 which are exposed on the outside of the membrane.

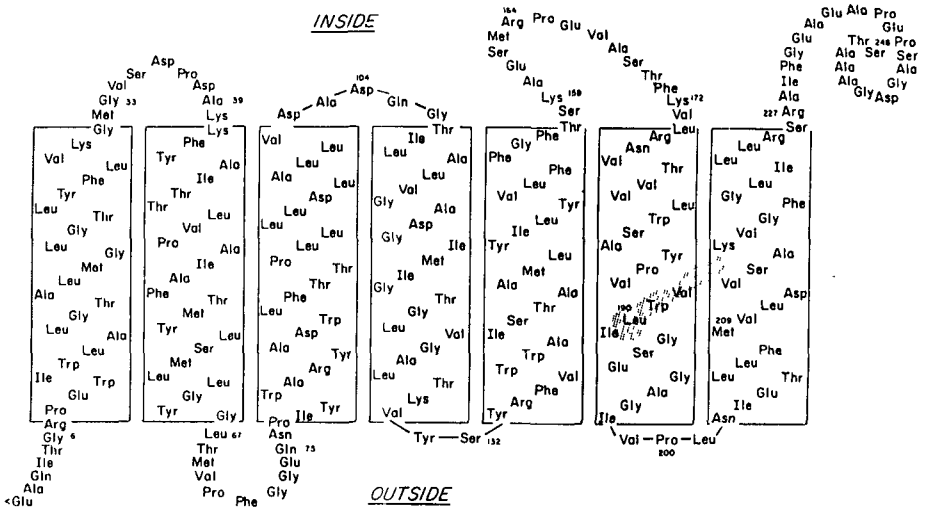

Fig. 1. The amino acid sequence of bacteriorhodopsin showing how the polypeptide chain transverses the cell wall (from ref. 3). The shaded area depicts the location of the retinal molecule which is attached to Lys-216.

After removal from the membrane each of the resulting two peptides which were not soluble in aqueous media under conditions required for digestion with proteolytic enzymes were chemically cleaved with cyanogen bromide at the ten methionines and their individual sequence determined (5). In addition to providing sequence information for almost 90% of the molecule, mass spectrometric data permitted the proper ordering of all the cyanogen bromide peptides by searching a very complex partial hydrolyzate of the two segments (1-71, 72-248) of the protein for small methionine containing peptides, using our GCMS method (6).

In retrospect, this work represented the most complex protein to which GCMS technology was applied, surpassed only by its use in the verification and correction of the structures predicted for alanyl-tRNA synthetase (7) and glutaminyl-tRNA synthetase (8) (from *E. coli*) deduced from the DNA sequence of their corresponding genes. Since then, fast atom bombardment mass spectrometry (FAB-MS) (9) has further revolutionized the field of protein structure and chemistry. An example is further work carried out in Prof. Khorana's laboratory, where specific single amino acid substitutions in the bacterio-opsin molecule are generated, using what amounts to modified totally synthetic genes coding for this protein (3). In view of the novelty of this approach it was desirable to verify that the desired change had actually been accomplished and that the gene product (the modified bacterio-opsin) had not undergone further processing or conversion in the cells producing it.

For this purpose, the intact bacterio-opsin molecule is cleaved with cyanogen bromide into ten peptides ranging in length from 4 to 46 amino acids (Fig. 2). Determination of their molecular weights which should remain the same except for those which encompass the site of single amino acid substitution and thus exhibit the appropriate shift. The $(M+H)^+$ ions of all these peptides (which had been at least partially separated by HPLC) were observed. However, the ease with which this could be accomplished differed widely for each of these ten peptides, not only because of their widely differing molecular weight but even more because of the stretches of high hydrophobicity in some of them (the shaded regions in Fig. 2 represent hydrophobic amino acids).

CNBr-1 1-20 <Glu Ala Gln Ile Thr Gly Arg Pro Glu Trp Ile Trp Leu Ala Leu Gly Thr Ala Leu Hse

CNBr-2 21-32 Gly Leu Gly Thr Leu Tyr Phe Leu Val Lys Gly Hse

CNBr-3 33-56 Gly Val Ser Asp Pro Asp Ala Lys Lys Phe Tyr Ala Ile Thr Thr Leu Val Pro Ala Ile Ala Phe Thr Hse

CNBr-4 57-60 Tyr Leu Ser Hse

CNBr-5 61-68 Leu Leu Gly Tyr Gly Leu Thr Hse

CNBr-6 69-118 Val Pro Phe Gly Gly Glu Gln Asn Pro Ile Tyr Trp Ala Arg Trp Ala Asp Trp Leu Phe Thr Thr Pro Leu Leu Leu Leu Asp Leu Ala Leu Leu Val Asp Ala Asp Gln Gly Thr Ile Leu Ala Leu Val Gly Ala Asp Gly Ile Hse

CNBr-7 119-145 Ile Gly Thr Gly Leu Val Gly Ala Leu Thr Lys Val Tyr Ser Tyr Arg Phe Val Trp Trp Ala Ile Ser Thr Ala Ala Hse

CNBr-8 146-163 Leu Tyr Ile Leu Trp Val Leu Phe Phe Gly Phe Thr Ser Lys Ala Glu Ser Hse

CNBr-9 164-209 Arg Pro Glu Val Ala Ser Thr Phe Lys Val Leu Arg Asn Val Thr Val Val Leu Trp Ser Ala Tyr Pro Val Val Trp Leu Ile Gly Ser Glu Gly Ala Gly Ile Val Pro Leu Asn Ile Glu Thr Leu Leu Phe Hse

CNBr-10 210-248 Val Leu Asp Val Ser Ala Lys Val Gly Phe Gly Leu Ile Leu Leu Arg Ser Arg Ala Ile Phe Gly Glu Ala Glu Ala Pro Glu Pro Ser Ala Gly Asp Gly Ala Ala Ala Thr Ser

Fig. 2. The amino acid sequences of the ten peptides generated from bacterio-opsin by cleavage with CNBr. The shaded areas indicate strongly hydrophobic amino acids.

Of the more than a dozen such synthetic, site-specific mutants of bacterio-opsin molecules that have been prepared (3), two have been examined by FABMS to date (10). Both have an N-terminal Met-Ala instead of the expected Met-Gln-Ala as evidenced by a $(M+H)^+$ ion at m/z 2080.2 of the CNBr peptide #1 (the N-terminal methionine is removed in the cleavage reaction) (Fig. 3). In one of the two, Phe-219 had been replaced with Leu and its CNBr peptide #10 shows an average $(M+H)^+$ ion at m/z 3811.8, as compared to m/z 3845.1 for the corresponding peptide from the unmodified protein (Fig. 4). The molecular weight of the other eight peptides remained the same indicating that no unexpected changes had taken place elsewhere.

The apparently poor sensitivity and resolution evident in Figure 4 (compared to many other peptides of this molecular weight range which we have examined) is probably due to the high abundance of hydrophobic amino acids occurring in several stretches in this peptide. Another feature of Figures 3 and 4 should be pointed out, namely the peaks 28 (and sometimes 56 or even 84) mass units above the $(M+H)^+$ ion. These seem to be due to partial formylation occurring during the CNBr-cleavage reaction which is carried out in 70% formic acid over an extended period of time. While these peaks confirm the molecular weight, the formation of the by-products reduce the yield of unmodified cleavage peptide and thus the abundance of the corresponding $(M+H)^+$ ion.

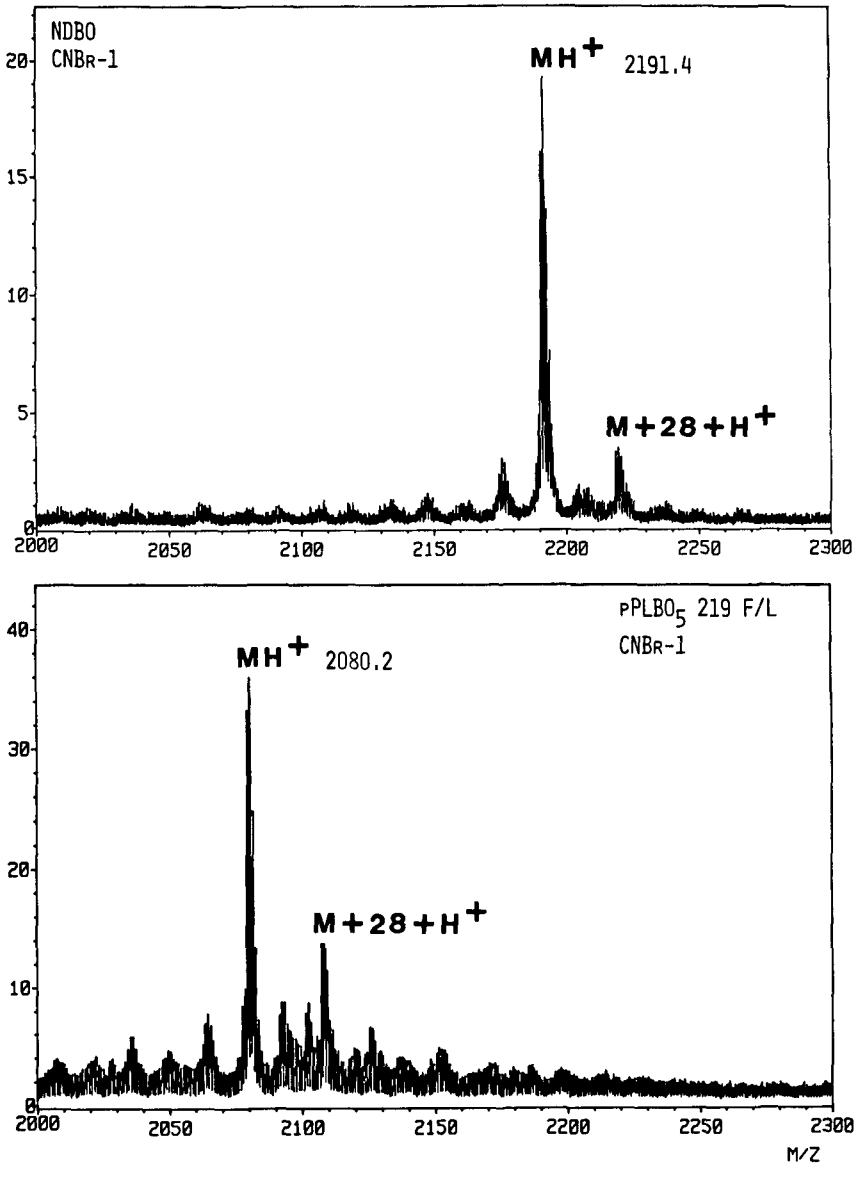

Fig. 3. FAB mass spectrum of CNBr peptide 1 from native bacterio-opsin (top) and from a modified analog (bottom). Single scan. Raw data points for the region from m/z 2000 to 2300 plotted by JEOL DA 5000 data system.

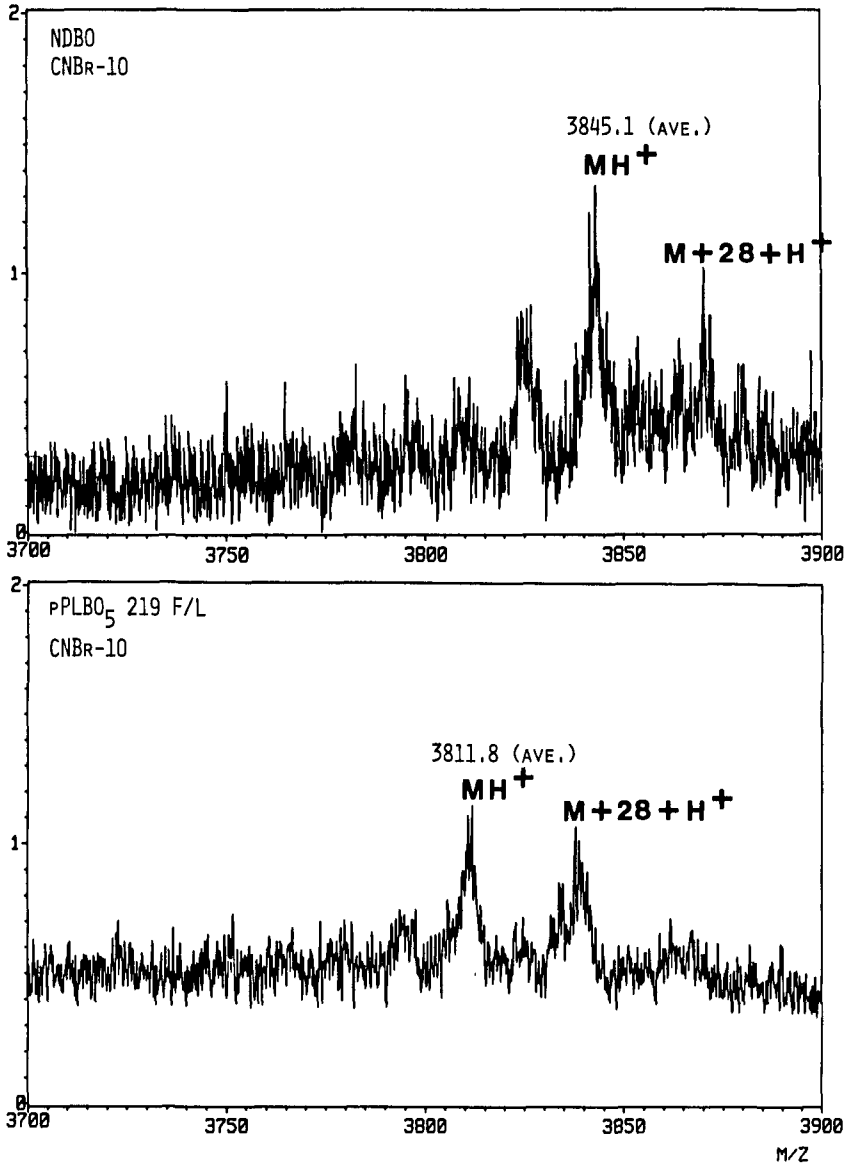

Fig. 4. FAB mass spectrum of CNBr peptide 10 from native bacterio-opsin (top) and from a modified analog (bottom) in which Phe-219 had been replaced by Leu. Single scan. Raw data points plotted by DA 5000 data system. This peptide is very hydrophobic (see Fig. 2) and thus gives poor FAB sensitivity (see text).

Correlation of DNA Sequence and Protein Structure.

Another area in which the capability of FABMS to provide reliable molecular weight determination of peptides, even when present as a mixture, is very useful is the verification and correction of DNA sequences determined for the purpose of defining the amino acid sequence of the corresponding protein (11). A comparison of the experimentally determined molecular weights of the peptides produced by tryptic digestion of the protein with those predicted for the hypothetic amino acid sequence derived from the DNA sequence allows one to identify the correct reading frame (out of the three possible ones); to detect and identify any error in the DNA sequence which causes a shift in the reading frame and thus a stretch of incorrect amino acid sequence; to identify errors that lead to an incorrect amino acid; to define the correct initiation and termination codons; and to recognize posttranslational modifications. Examples of all of these cases have been encountered in this laboratory over the past six years in the work on DNA-protein correlations involving relatively large proteins ranging from 271 to 875 amino acids in length (Table 1).

Table 1

Confirmations and corrections of DNA sequences
by mass spectrometric check of corresponding protein.

Name of Protein	# of Amino Acids	DNA-Sequence Collaborator	Ref.	Yr. of Public.
Alanyl-tRNA synthetase[a]	875	P. Schimmel	7[e]	1981
Glutaminyl-tRNA synthetase[a]	550	D. Söll	8[e] 12[f]	1982
Glycyl-tRNA synthetase[a]	α:303 β:687	P. Schimmel	13[f]	1983
Methionine-tRNA synthetase[b]	751	Y. Boulanger	11[f]	1984
Endo-β-N-acetylglucosaminidase[c]	271	P.W. Robbins	14[f]	1984
Histidine-tRNA synthetase[a]	424	P. Schimmel	15[f]	1985
Rabbit Muscle Creatine Phosphokinase	380	P. Schimmel	16[f]	1984
Rabbit Brain Creatine Kinase	380	P. Schimmel	17[f]	1985
Cytos. Phosphoenolypyruvate Carboxykinase[d]	626	D.K. Granner	18[f]	1985
Glutamyl-tRNA synthetase[a]	471	J. Lapointe	19[f]	1986

[a] *E. coli*
[b] yeast
[c] *Streptomyces*
[d] rat
[e] by GCMS
[f] by FABMS

The simplicity, speed and reliability of present DNA sequencing methodology (20,21) is far superior to any existing amino acid sequencing technique (Edman degradation or mass spectrometry). For this reason, it is more efficient to determine the primary structure of large proteins *via* the DNA sequence. However, since the major experimental effort lies in the identification, isolation and cloning of the proper gene which is just as difficult for those coding for small proteins as it is for large ones, direct sequencing of smaller proteins is preferable. This, in addition to the determination of posttranslational modification is, therefore, the most promising area of mass spectrometry.

Direct Mass Spectrometric Sequencing of Proteins.

While the FAB mass spectra determined with relatively large samples of pure peptides of reasonable size (5-15 amino acids) do often exhibit considerable sequence information, it is rarely possible to deduce the sequence of an unknown peptide present in or isolated from a proteolytic digest with any degree of reliability. We have, therefore, developed a strategy that involves tandem mass spectrometry (MS/MS) (22) on partially separated (by HPLC) fractions of enzymatic or chemical cleavage products of proteins (Fig. 5).

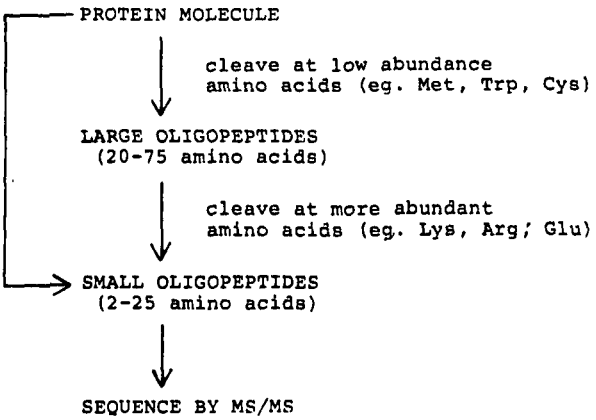

Fig. 5. Strategy for the sequencing of proteins by FAB-MS and FAB-MS/MS.

A new four-sector tandem mass spectrometer of EBEB configuration (JEOL HX110/HX110, Fig. 6) (23) installed in our laboratory in August 1985 is used for this purpose. It has a mass range of 14,500 at full accelerating voltage (10 KV), collision cells in the first (after ion source #1) and third field free region, off-axis electron multipliers after B_1, E_2 and B_2 which are operated with -18 KV post-acceleration. Most importantly, there is a complete ion source with direct probe (FAB/EI) for MS-2 (located in the interface between the collector slit of MS-1 and entrance slit of MS-2) which facilitates direct calibration of MS-2 in the normal scan mode. This calibration is used to determine the software controlled linked-scan mode, making it unnecessary to compile a calibration in the linked scan mode.

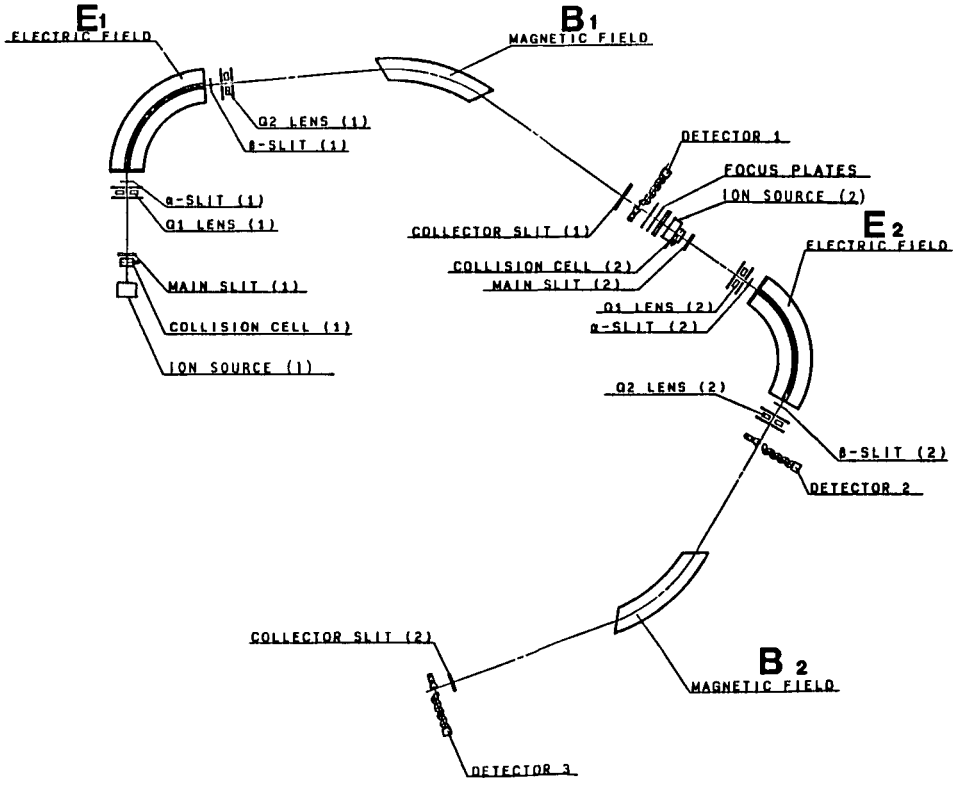

Fig. 6. Schematic of JEOL HX110/HX110 four sector tandem mass spectrometer.

As an example, the MS/MS spectrum obtained from a 22 amino acid long segment (positions 18-39) of human adrenocorticotropic hormone (hACTH) after collisional activation (He) in the third field free region (between B_1 and E_2) is shown in Figure 7. This peptide exhibits predominantly N-terminal ions due to cleavage of the -CH-CO- bond (type A, according to Roepstorff and Fohlman (24)). This set of data permits the determination of the entire sequence of this peptide, including the identification of leucine rather than isoleucine in position 20 because of the peak 42 amu below ion A_{20} and the absence of an ion 28 amu below A_{20}, a characteristic feature that permits distinguishing these two isomeric amino acids (25). It should be noted that the appearance of an extended A ion series is more an exception than the rule and may be due to the presence of two basic amino acids (Arg, Lys) at and near the N-terminus (25).

Digestion of proteins with enzymes of high specificity for reasonably abundant amino acids (such as trypsin for Arg and Lys or *Staphylococcus aureus* V8 protease for glutamic acid) usually generates peptides less than about 25 amino acids long, just right for the MS/MS approach.

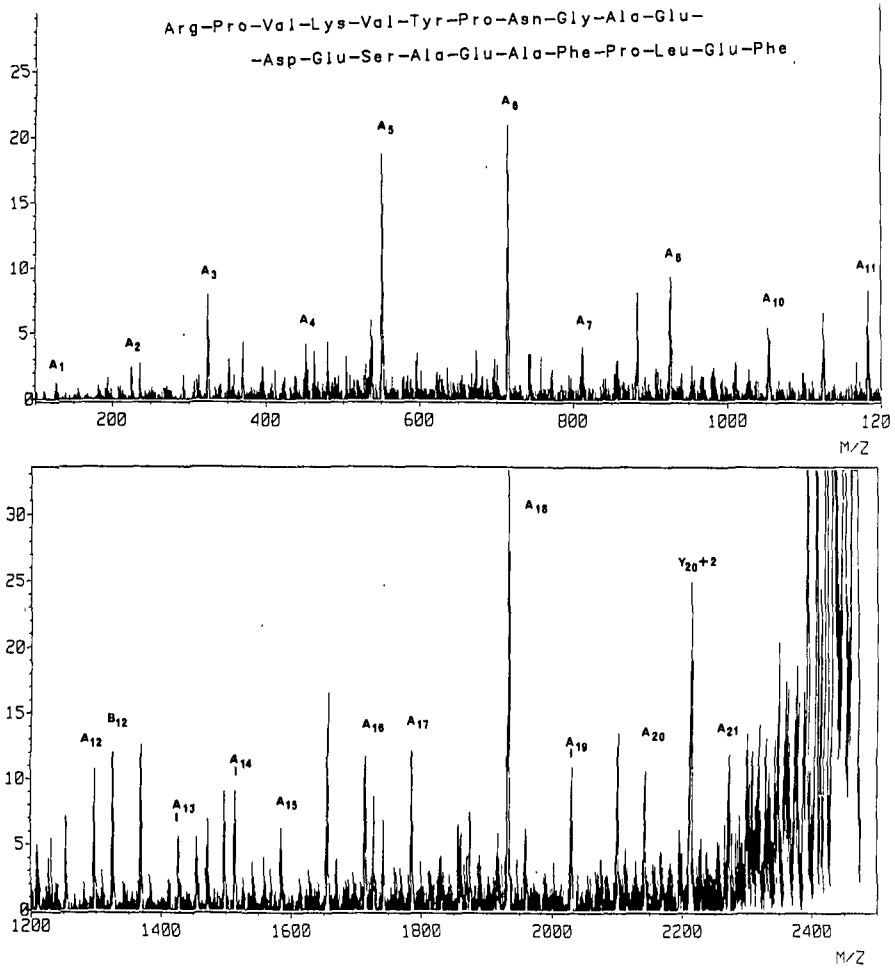

Fig. 7. Daughter ion mass spectrum obtained after collision (He) of $(M+H)^+$ of a 22 amino acid segment of ACTH (m/z 2465.2). For discussion see text. Precursor ion energy: 10 KV; collision cell potential 0 V; MS-1 resolution set to transmit monoisotopic $(M+H)^+$ ion; MS-2 resolution 1000. Single scan (3.2 min). Raw data points plotted by DA 5000 data system. Mass assignments within 0.3 amu.

We are presently involved in the determination of the primary structure of a number of thioredoxins from a variety of sources. Thioredoxins are ubiquitous, biologically active proteins that exist and carry out similar functions in all organisms, from single cell bacteria to mammalian systems. They participate in biological redox reactions such as reduction of sulfates and methionine sulfoxides, hydrogen donor for ribonucleotide reductase, subunit for T_7 induced DNA polymerase, reduction of protein disulfides and regulation of enzyme activity (26). Thioredoxins are usually 100-110 amino acids long and a few of them are of known structure, among them that produced by *E. coli* (27). We have previously determined the structure of the thioredoxin from *Chlorobium thiosulfatophilum*, chiefly by FAB-MS using the subtractive Edman approach and some MS/MS data (28). Now we are in the process of determining the primary structure of the thioredoxin from *Rhodospirillum rubrum* by the strategy outlined in Figure 5. This involves, of course, the interpretation of the MS/MS spectrum in terms of an unknown amino acid sequence which demands a higher degree of spectral quality and information content than the rationalization of a spectrum with a known structure.

Figure 8 shows the daughter ion spectrum of a tryptic peptide of $(M+H)^+$ 1318.6. The interpretation of the data involves three regions. At the low mass end one can identify signals due to the immonium ions, $(H_2N{=}CHR)^+$, typical for some of the amino acids present (m/z 70, 72, 86, 120 and 159 for Pro, Val, Leu/Ile, Phe and Trp respectively, labeled in Fig. 8 by the single letter codes of these amino acids). Further information concerning amino acids present can be deduced from the region just below the precursor ion $(M+H)^+$ which often contains ions due to the loss of the side chain of an amino acid (such as Val and Glu, labeled -V and -E in Fig. 8). The sequence itself is deduced from the middle part of the spectrum by identifying consecutive relatively abundant peaks differing in mass by the molecular weight of an amino acid minus 18 daltons. Three such series (A, B and Y+2) are present in this spectrum which altogether uniquely define the sequence as shown at the top of the figure. Again the presence of a peak 42 amu and absence of a peak 28 amu below the ion A_6 indicate that the sixth amino acid must be leucine and not isoleucine. Similar data from other peptides derived from this protein have allowed us to determine about 85% of its primary structure and the remainder will soon be in hand (29). Because the intepretation of such MS/MS spectra is not trivial and can be tedious, we have developed an interactive computer program to aid in this process (30).

Collisionally induced daughter ion spectra of proteolytic peptides from large proteins of unknown structure will also be very useful in the identification of unique, short amino acid sequences that can be used to synthesize oligonucleotides needed in the search for the gene coding for the synthesis of the protein (31). For this purpose, it is not necessary to obtain the complete sequence of all peptides generated but only partial ones, as long as they contain chiefly amino acids that have a unique codon, such as Met or Trp, or are represented by very few codons (Tyr, His, Glu, Gln, Asp, Asn and Cys have two codons). Searching for spectra for peaks with the mass difference corresponding to these amino acids pinpoint peptides with a high probability of containing such unique stretches which then can be further examined. We have used this approach earlier (16) using our GCMS method, but FABMS/MS should be more efficient.

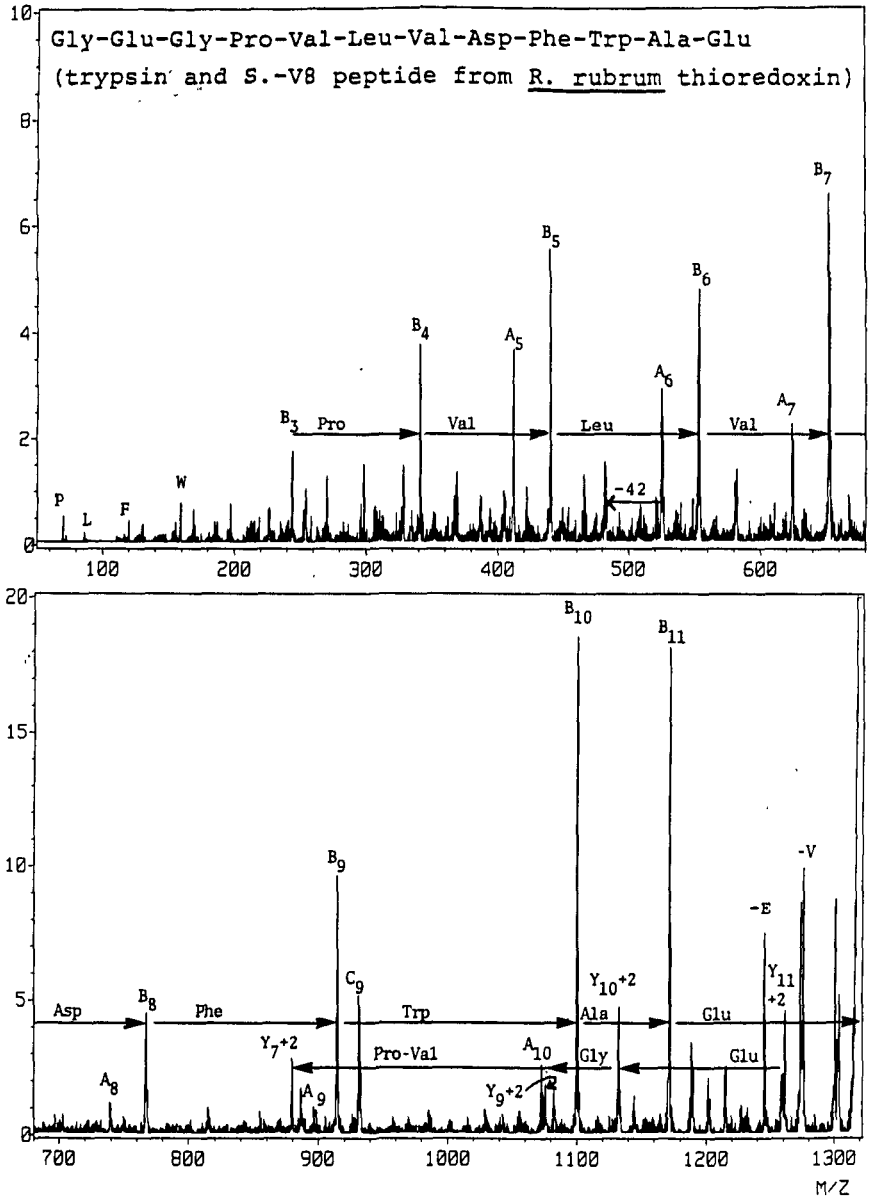

Fig. 8. Daughter ion mass spectrum of one of the peptides derived from thioredoxin (*Rhodospirillum rubrum*) and its interpretation. For details see text. Experimental conditions as for Fig. 7.

Recognition of Post-translational or chemical modifications.

N-acylation (mostly at the N-terminal amino acid), glycosylation, phosphorylation, sulfonation, etc. are common modifications important for the biological function of proteins. Special methods are available for their identification (32) but they are often tedious and not generally applicable. Over the past two decades, mass spectrometry has played a prominent role in this area (33) and FABMS, as such, or in conjunction with MS/MS further increases this potential.

For example, the identification of the location of attachment of oligosaccharide chains to a protein (which always occurs on asparagine present in an Asn-X-Ser/Thr environment) can be accomplished by FABMS in various ways. In those cases where both the glycosylated and unglycosylated protein can be isolated, one merely needs to compare the molecular weight differences of the tryptic (or other) digests of the unglycosylated form and the glycosylated one from which the sugar moieties, with the exception of the first one (N-acetylglucosamine) were removed with endo- -N-acetylglucosaminidase. A mass difference of $n \times 302$ daltons indicates the presence of n acetylglucosamines which must be attached to Asn as mentioned above. Usually $n = 1$ and there is only one suitable Asn in the peptide and this is thus the point of attachment (28). If n is smaller (but not zero) than the number of suitably located asparagines, one must take recourse to MS/MS and look for mass differences corresponding to Asn + 203. The same is necessary if the unglycosylated protein is not available. This can also be overcome by the approach developed by Carr (34) based on enzymatic removal of the entire glycosidic side chain, including the N-acetylglucosamine, which liberates an Asp in this position. Thus, a new peptide appears in the FAB mass spectrum of a tryptic hydrolyzate because of the dramatic decrease in molecular weight of the peptide upon removal of the carbohydrate portion.

Proteins or peptides with an acyl group on the N-terminal amino acid are a notorious problem in conventional protein chemistry because they are not amenable to the Edman degradation (and can not be deduced from a DNA sequence). Mass spectrometry is the ideal, perhaps only direct method to answer such questions (11,33). As a related problem, we have discovered a potentially troublesome side reaction in the CNBr-cleavage of proteins which is carried out in 70% formic acid during prolonged periods of time (12-24 h). Apparently, partial formylation takes place giving rise to peaks $n \times 28$ daltons above the $(M+H)^+$. This may not only be confusing but also has the deleterious effect of splitting molecular ion signals and thus reducing the abundance of the unmodified $(M+H)^+$. This side reaction seems to occur not only at the N-terminal amino group but also on lysine side chains and even as O-formyl groups on serine (30). These reactions were probably previously overlooked because these side products would either not be amenable to the Edman degradation or their phenylthiohydantoins would lose the formyl group (if present as an ester) in the course of the analysis or would merely cause an extraneous peak (for formyl-lysine).

Summary

The foregoing discussion outlines the contribution which mass spectrometry can make to the field of protein structure determination. High mass mass spectrometry and tandem mass spectrometry of relatively large and complex molecules are just at the beginning of its development. Rapid further progress will surely be made, both in the application of existing methodology and with respect to new experimental developments in the area of ion production, efficient dissociation of large molecules, ion detection, etc.

This paper stressed the work done and ongoing in our own laboratory and centered on the sequencing of peptides and proteins. However, there are many other important areas of biology where mass spectrometry has made substantial contributions. Some of these were covered by symposia held during this conference. For example, other aspects of protein chemistry were discussed by Morris and Dell (35), the potential utility of high mass mass spectrometry in the carbohydrate field were illustrated by Burlingame (36) and Reinhold (37), the information obtainable from synthetic nucleotides by Grotjahn (38) and some typical problems in biotechnologically oriented pharmaceutical laboratories, where modern mass spectrometry can be of great utility, were reported by Carr (39). All these and other presentations and topics attest to the fact that mass spectrometry is going to play a more and more important role in molecular biology and biochemistry.

Acknowledgement

Work done at M.I.T. was supported by grants from the National Institutes of Health (GM05472 and RR00317).

REFERENCES

1. A.D.B. Malcolm, *Nature 275*, 90-91 (1978).
2. For a review, see H.D. Niall, *Methods Enzymol. 27*, 942-1010 (1973).
3. H.G. Khorana, *Ann. N.Y. Acad. Sci.*, 1986, in press.
4. S.A. Carr, W.C. Herlihy and K. Biemann, *Biomed. Mass Spectrom. 8*, 51-61 (1981).
5. a) G.E. Gerber, R.J. Anderegg, W.C. Herlihy, C.P. Gray, K. Biemann and H.G. Khorana, *Proc. Natl. Acad. Sci. USA 76*, 227-231 (1979).
   b) H.G. Khorana, G.E. Gerber, W.C. Herlihy, C. Gray, R.J. Anderegg, K. Nihei and K. Biemann, *Proc. Natl. Acad. Sci. USA 76*, 5046-5050 (1979).
6. W.C. Herlihy, R.J. Anderegg and K. Biemann, *Biomed. Mass Spectrom. 8*, 62-69 (1981).
7. S.D. Putney, N.J. Royal, H. Neuman de Vegvar, W.C. Herlihy, K. Biemann and P.R. Schimmel, *Science 213*, 1497-1501 (1981).
8. P. Hoben, N. Royal, A. Cheung, F. Yamao, K. Biemann and D. Soll, *J. Biol. Chem. 257*, 11644-11650 (1982).
9. M. Barber, R.S. Bordoli, R.D. Sedgwick and A.N. Tyler, *J. Chem. Soc. Chem. Commun. 7*, 325-327 (1981).
10. G. Allmaier, B.H. Chao, H.G. Khorana and K. Biemann, 34th Annual Conf. on Mass Spectrometry and Allied Topics, Cincinnati, OH, June 1986, paper TPB 11.
11. B.W. Gibson and K. Biemann, *Proc. Natl. Acad. Sci. USA 81*, 1956-1960 (1984).
12. K. Biemann, *Int. J. Mass Spectrom. Ion Phys. 45*, 183-194 (1982).
13. T.A. Webster, B.W. Gibson, T. Keng, K. Biemann and P. Schimmel, *J. Biol. Chem. 258*, 10637-10641 (1983).
14. P.W. Robbins, R.B. Trimble, D.F. Wirth, C. Hering, F. Maley, G.F. Maley, R. Das, B.W. Gibson, N. Royal and K. Biemann, *J. Biol. Chem. 259*, 7577-7583 (1984).
15. R. Freedman, B. Gibson, D. Donovan, K. Biemann, S. Eisenbeis, J. Parker and P. Schimmel, *J. Biol. Chem. 260*, 10063-10068 (1985).
16. S. Putney, W. Herlihy, N. Royal, H. Pang, H.V. Aposhian, L. Pickering, R. Belagaje, K. Biemann, D. Page, S. Kuby and P. Schimmel, *J. Biol. Chem. 259*, 14317-14320 (1984).
17. L. Pickering, H. Pang, K. Biemann, H. Munro and P. Schimmel, *Proc. Natl. Acad. of Sci. USA 82*, 2310-2314 (1985).
18. E.G. Beale, N.B. Chrapkiewicz, H.A. Scoble, R.J. Metz, D.P. Quick, R.L. Noble, J.E. Donelson, K. Biemann and D.K. Granner, *J. Biol. Chem. 260*, 10748-10760 (1985).
19. R. Breton, H. Sanfacon, I. Papayannopoulos, K. Biemann and J. Lapointe, *J. Biol. Chem.*, in press.
20. F. Sanger, A.R. Coulson, *J. Mol. Biol. 94*, 441-448 (1975).
21. A.M Maxam and W. Gilbert, *Proc. Natl. Acad. Sci. USA 74*, 560-564 (1977).
22. Tandem Mass Spectrometry, F.W. McLafferty (ed.), John Wiley & Sons, NY, 1983.
23. Y. Kammei, Y. Itagaki, E. Kubota, H. Kunihiro and M. Ishihara, 33rd Annual Conf. on Mass Spectrometry and Allied Topics, San Diego, CA, May 1985, p. 855.
24. P. Roepstorff and J. Fohlman, *Biomed. Mass Spectrom. 11*, 601 (1984).
25. S.A. Martin and K. Biemann, 34th Annual Conf. on Mass Spectrometry and Allied Topics, Cincinnati, OH, June 1986, paper RPE 9.
26. Thioredoxin and Glutaredoxin Systems. Structure and Function. A. Holmgren, C-I. Branden, H. Jornvall, B-M. Sjoberg (eds.), Raven Press, NY, 1986.
27. J.-O. Hoog, H. Von Bahr-Lindstrom, S. Josephson, B.J. Wallace, S.R. Kushner, H. Jornvall and A. Holmgren, *Biosci. Reports 4*, 917-923 (1984).
28. R.S. Johnson, W.R. Mathews and K. Biemann, 34th Annual Conf. on Mass Spectrometry and Allied Topics, Cincinnati, OH, June 1986, paper RPE 8.
29. R.S. Johnson and K. Biemann, to be published.
30. H.A. Scoble, C.E. Costello and K. Biemann, 34th Annual Conf. on Mass Spectrometry and Allied Topics, Cincinnati, OH, June 1986, paper MOD 7.
31. R.B. Wallace, M.J. Johnson, T. Hirose, T. Miyake, E.H. Kawahima and K. Itakura, *Nucl. Acids Res. 9*, 879-894 (1981).
32. Methods in Enzymology. Posttranslational Modifications *106*, K. Moldave and F. Wold (eds.), Academic Press, Orlando, FL, 1984.
33. S.A. Carr and K. Biemann, pp. 29-58 in ref. 32.
34. S.A. Carr and G.D. Roberts, *Anal. Biochem.*, 1986, in press.
35. H.R. Morris, 34th Annual Conf. on Mass Spectrometry and Allied Topcis, Cincinnati, OH, June 1986, paper WOD 9.
36. A.L. Burlingame, *ibid.*, paper ROA 8.
37. V.N. Reinhold et al., *ibid.*, paper FOB 3
38. L. Grotjahn and H. Steinert, *ibid.*, paper ROA 6.
39. S.A. Carr et al., *ibid.*, paper ROA 14.

Introductory Lecture

Tandem Mass Spectrometry: Coming of Age

Richard A. Yost
University of Florida
Department of Chemistry
Gainesville, FL 32611

Tandem mass spectrometry (MS/MS), with its roots in early studies of ion-molecule reactions (1), has gained widespread acceptance since its introduction as an analytical tool for structure elucidation (2) and mixture analysis (3) in the 1970's. This "coming of age" of MS/MS is evidenced by the appearance of the first book on the subject (4), as well as the publication of reviews on instrumentation (5), structure elucidation (6), and trace mixture analysis (7).

This introductory lecture on MS/MS will present the concepts, instrumentation, capabilities, and applications of the technique. It will aim to educate the uninitiated, as well as to stimulate the practitioner and to content the devotee.

In tracing the growth of any analytical method, one may identify a common set of seven phases, as detailed in a 1965 editorial in Analytical Chemistry (Figure 1). These seven ages of an analytical method are analogous to the seven ages of man set forth by William Shakespeare in his play "As You Like It" (Figures 2 and 3). It is intriguing to trace the growth of MS/MS in the context of these seven ages.

The Seven Ages of an Analytical Method

1. **Conception** of fundamental principles
2. Experimental **validation** of analytical potential
3. Instrumental developments/**availability**
4. Establishment of a solid fundamental **foundation**
5. Widened scope of **application**
6. **Acceptance** as a routine, standard method
7. **Senescence**, overtaken by newer methods

ANALYTICAL CHEMISTRY, VOL. 45, NO. 14, DECEMBER 1973 • 2305

Figure 1.

Figure 2.

All the world's a stage,
And all the men and women merely players.
They have their exits and their entrances,
And one man in his time plays many parts,
His acts being seven ages. At first the infant,
Mewling and puking in the nurse's arms.
Then, the whining school-boy with his satchel
And shining morning face, creeping like snail
Unwillingly to school. And then the lover,
Sighing like furnace, with a woeful ballad
Made to his mistress' eyebrow. Then, a soldier,
Full of strange oaths, and bearded like the pard,
Jealous in honour, sudden, and quick in quarrel,
Seeking the bubble reputation
Even in the cannon's mouth. And then, the justice,
In fair round belly, with good capon lin'd,
With eyes severe, and beard of formal cut,
Full of wise saws, and modern instances,
And so he plays his part. The sixth age shifts
Into the lean and slipper'd pantaloon,
With spectacles on nose, and pouch on side,
His youthful hose well sav'd, a world too wide
For his shrunk shank, and his big manly voice,
Turning again toward childish treble, pipes
And whistles in his sound. Last scene of all,
That ends this strange eventful history,
Is second childishness and mere oblivion,
Sans teeth, sans eyes, sans taste, sans everything.

AS YOU LIKE IT [ACT II SC. VII]

Figure 3.

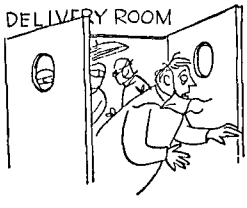

Figure 4.

1. Conception of fundamental principles of MS/MS (Figure 4). The first age of MS/MS dates back to the observation of "Aston Bands" in 1919 (8), arising from ion-molecule reactions in the rather poor vacuum of Aston's mass spectrograph. The desire to more carefully study ion-molecule reactions inspired physicists and physical chemists in the 1960's to design tandem mass spectrometers such as that shown in Figure 5 (9). (Note that this five-sector instrument is similar to modern four-sector MS/MS instruments.) These early days of tandem mass spectrometry were reviewed at the 1985 ASMS Conference by Fred Lampe in a lecture entitled "Ion-Molecule Reactions: The Roots to the Branches" (10). To reach the second age of MS/MS required that individuals recognize the analytical potential of these principles (Figure 6).

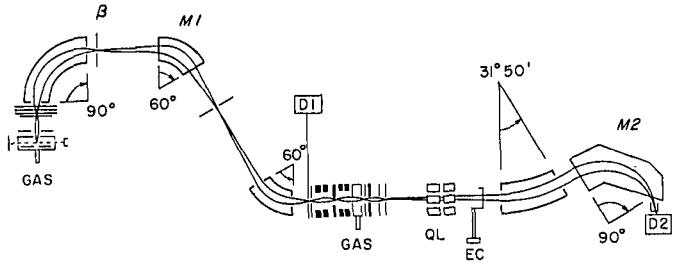

Figure 5. Tandem Mass Spectrometer for Study of Ion-Molecule Reactions

Figure 6.

2. Experimental validation of the analytical potential of MS/MS. The potential of tandem mass spectrometry for the elucidation of ionic (and molecular) structure was first recognized in the mid 1960's (11,12). The utility of MS/MS as a "complete chemical laboratory" in which new species can be synthesized, purified, reacted, and the products analyzed, was neatly demonstrated in a publication (13) from John Beynon's laboratory (Figure 7). Not long after tandem mass spectrometry's potential for structure elucidation was demonstrated, the possibilities for mixture analysis were first shown (14). Research in Graham Cooks' laboratory (15) establishing the ability of MS/MS to analyze complex mixtures without prior separation (Figure 8) caught the attention of analysts near and far. As Kondrat and Cooks pointed out in 1978 (2):

> Perhaps the single most exciting feature of the MIKES methodology is the ability to identify components of complex mixtures...without any prior chemical separation whatsoever.

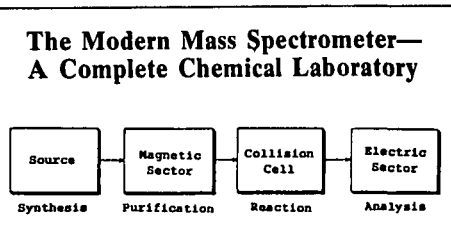

Figure 7.

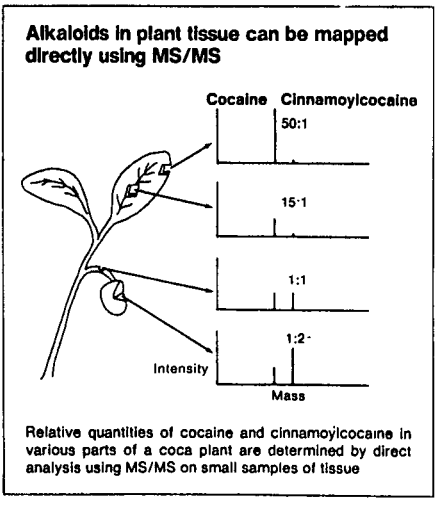

Figure 8.

The enthusiasm which is characteristic of this age of any analytical method (Figure 9) has been discussed by Dai Games (16):

> In the euphoria of discovering a new way of putting a mass spectrometer together, the advantages are typically highlighted, and drawbacks which can cause considerable problems in using the instrumentation in a routine manner tend to be overlooked or deemphasized.

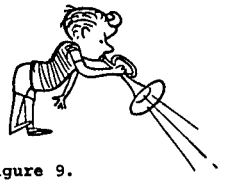

Figure 9.

Hand-in-hand with the enthusiasm, however, comes criticism (Figure 10). In his lecture upon receiving the 1984 Instrumentation Award of the ACS Analytical Division, Graham Cooks gave an example (17):

> An early criticism of tandem mass spectrometry was that because mass spectroscopists do not understand simple mass spectra, they are ill-advised to add to their difficulties.

Cooks further pointed out the general nature of such criticism when a new analytical method is first proposed (17):

> When people are given something they manifestly did not ask for and certainly do not appreciate, they tend to react unkindly. Especially so if they are experts whose own work is about to be encompassed within the emerging work.

While these criticisms may not dampen enthusiasm, the requirement during this second age of an analytical method to "build your own" instrumentation restricts the new method to those laboratories willing (and able) to design and construct complex instrumental systems (Figure 11). The third age of MS/MS, then, is ushered in by the development of instrumentation and its widespread (commercial) availability.

Figure 10.

Figure 11.

3. Instrumental developments/availability. The earliest MS/MS instruments (Figure 12) used for analysis were double focusing (two-sector) mass spectrometers of normal geometry (electric sector E before the magnetic sector B). It was realized early on that a reversed geometry (magnet first, BE) could provide the most useful MS/MS scan (daughters of a selected parent ion) more easily under manual control (18). In the late 1970's we first demonstrated the analytical capabilities of a new instrument, the triple quadrupole mass spectrometer (19). A major limitation of the two-sector instruments (both EB and BE) is the limited mass resolution which results from the kinetic energy released upon fragmentation and the dependence on ion velocity in both magnetic (momentum) and electric (energy) analyzers. This led to the development of three- and four-sector instruments, as well as hybrid sector/quadrupole systems (Figures 13, 14).

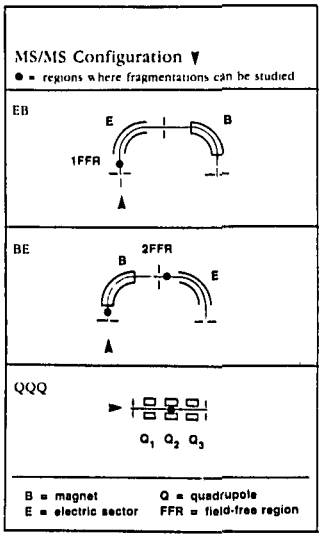

Figure 12.

Kratos MS50
VG 7070
JEOL JMS-HX110

VG ZAB2F
Finnigan MAT 90

Finnigan MAT TSQ70
Sciex TAGA 6000
Extrel ELTQ 400-3
Nermag R30-10
VG 30-253T

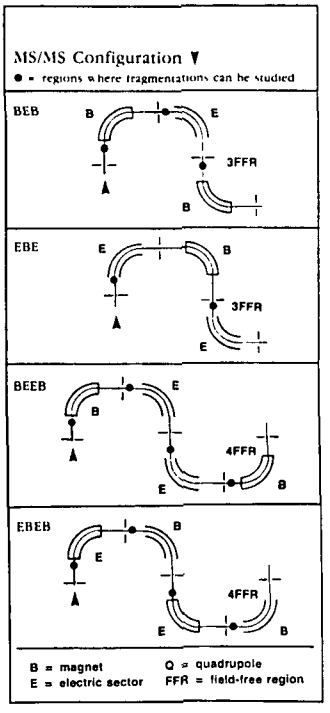

VG ZAB-3HF

Kratos MS50TA

VG ZAB-4HF

JEOL JMS-HX110-HX110
Kratos
VG 70-S4F

Figure 13.

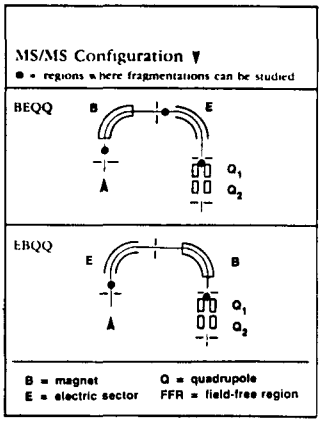

Finnigan MAT HSQ
VG ZAB-HSQ

VG 70-SQ
Kratos MS80RFAQ

Figure 14.

Each of the instruments above consists of two (or more) analyzers in series; that is, they are tandem-in-space instruments. More recently, MS/MS instruments have been developed which consist of a single ion region which sequentially serves as ion source, MS I, collision region, and MS II; that is, they are tandem-in-time instruments (Figure 15). Two instruments, the Fourier transform and ion trap systems, are tandem-in-time systems (Figure 16).

Tandem-in-space

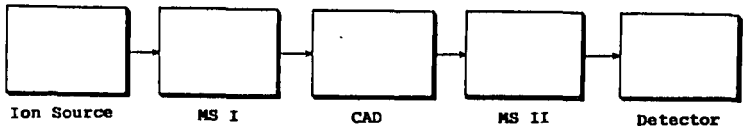

Tandem-in-time

Ion Source
MS I
CAD
MS II
Detector

Figure 15.

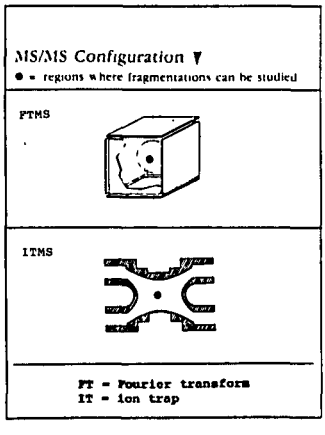

Nicolet FT2000
Spectrospin CMS47

Finnigan MAT ITMS

Figure 16.

It is interesting to note that instruments of each of these types (Figures 12-16) were first constructed for fundamental studies in physics and physical chemistry; however, it was the analytical capabilities of each instrument - often discovered several years later - which led to the commercial development listed in each figure. The commercial availability of these systems (Figure 17) made possible widespread analytical studies in an increasing number of laboratories.

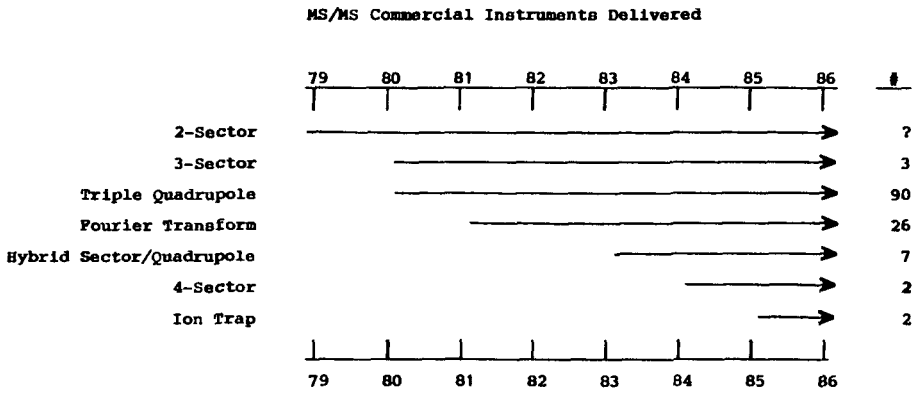

Figure 17.

The availability of commercial instruments provided for the first time the capability to generate enormous amounts of MS/MS data (Figure 18). With early (manually controlled) instruments, acquisition of MS/MS data could be very time consuming, as pointed out by Huang and Kiser in 1978 (20):

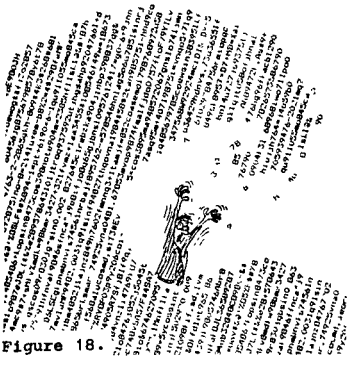

Figure 18.

> The many weeks needed to locate and study systematically all the observable metastable transitions in a mass spectrum is clearly a serious drawback to the ready use of this technique in defining the ionic fragmentation pathways of a molecule.

While the need for computer control of so complex an analytical instrument seems obvious today, it was not necessarily widely appreciated in the early days of instrumental development. Reviewers of the first proposal for development of the computer-controlled triple quadrupole instrument pointed out that (21):

> Experience with tandem mass spectrometers indicates that computer control is usually impractical.

Today nearly every commercial MS/MS instrument is computer controlled, and includes extensive capabilities for processing complex MS/MS data. This trend is most apparent in the first wave of "second generation" MS/MS instruments. The new Finnigan MAT TSQ70 triple quadrupole instrument, for example, is completely computer-controlled (no knobs, dials, or meters) and includes capabilities for real-time optimization, and expert system control. The effect of computers on MS instrumentation is reflected in a recent comment in Chemical and Engineering News (22):

> Twenty years ago, mass spectrometers were considered unfriendly beasts, tamable only by experts. Today, mass spectrometers are more sophisticated than ever, but they're also easier to use.

These instrumental developments, and the commercial availability of instruments, has brought us to the fourth age of MS/MS and its "coming of age" (Figure 19). This progress has occured quite rapidly, as pointed out by Fred McLafferty (23):

> I must confess that the remarkable growth of tandem mass spectrometry (MS/MS) in the last few years caught me by surprise.

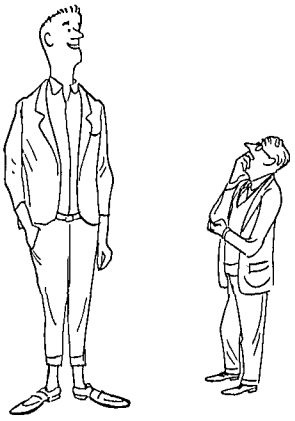

Figure 19.

4. Establishment of a solid fundamental foundation, and 5. Widened scope of application (Figure 19). One indication of our arrival at this age is the publication of the first book devoted solely to MS/MS, containing 26 chapters representing research from 33 laboratories world-wide (4). If we plot the number of papers and posters on "analytical" MS/MS presented at ASMS conferences over the past ten years, this trend is even more apparent (Figure 20).

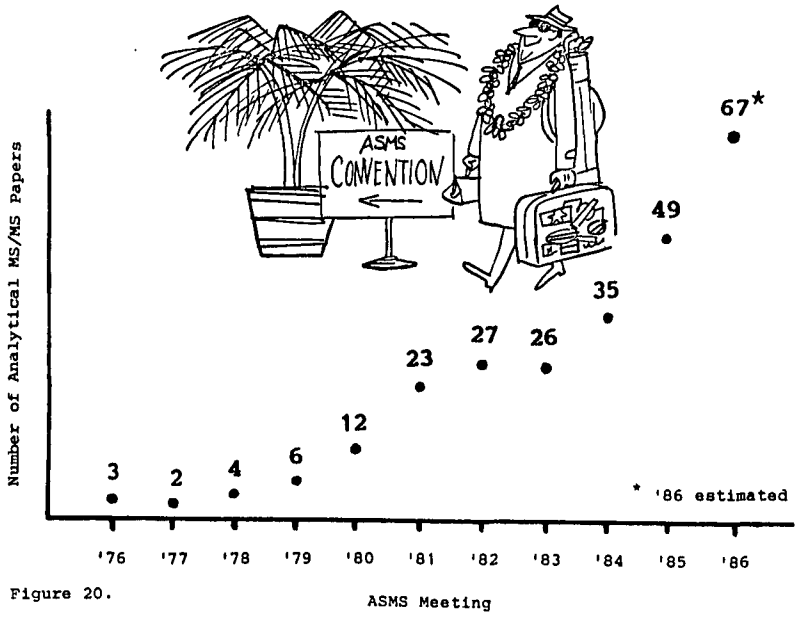

Figure 20.

One element of the maturing of MS/MS has been the increased appreciation of the analytical potential of additional "resolution elements" (24). Although these approaches to increasing the information content of MS/MS methods can include variations in sample introduction and ionization, perhaps the most interesting approaches have involved the ion activation process (Table 1). Variation of the collision energy in low energy collisionally activated dissociation (or of the scattering angle in high-energy CAD), for example, provides information which is extremely useful for elucidation of ion and molecular structure, as well as for optimization of CAD conditions (25). The ability to obtain such data in only a few minutes under computer control (5) has made this a practical approach for routine analysis (Figure 21).

Table 1. Ion activation processes in MS/MS

Unimolecular (metastable)	$m_1^+ \rightarrow m_2^+ + m_3$
Collisionally activated dissociation (CAD)*	$m_1^+ \xrightarrow{N} m_2^+ + m_3$
Photodissociation	$m_1^+ \xrightarrow{h\nu} m_2^+ + m_3$
Electron excitation	$m_1^+ \xrightarrow{e^-} m_2^+ + m_3$
Charge stripping	$m_1^+ \xrightarrow{N} m_1^{2+} + e^-$
Charge inversion	$m_1^- \xrightarrow{N} m_1^+ + 2e^-$
Charge exchange	$m_1^+ \xrightarrow{N} m_1 + N^+$
Associative ion/molecule reactions	$m_1^+ \xrightarrow{N} m_1N^+$

*Often called collision-induced dissociation (CID)

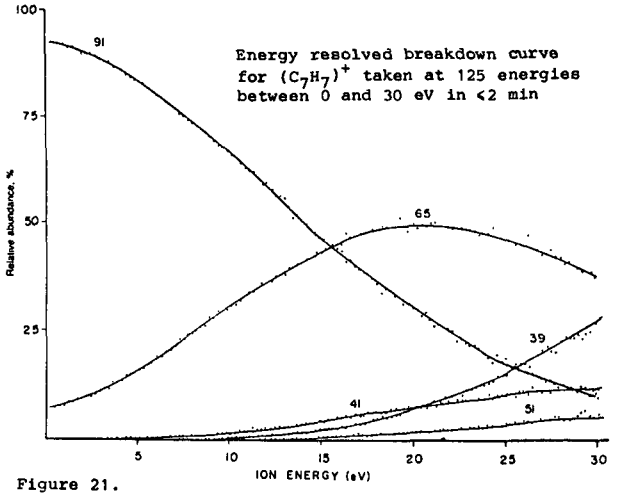

Figure 21.

Another approach which can help distinguish isomers or selectively detect compound classes is collisionally activated reaction (CAR) using associative ion/molecule reactions at low collision energies (24). For example, the linear and cyclic $C_5H_6^+$ ions produce nearly identical CAD daughter spectra (Figure 22), but are easily distinguished by CAR with isobutane (Figure 23).

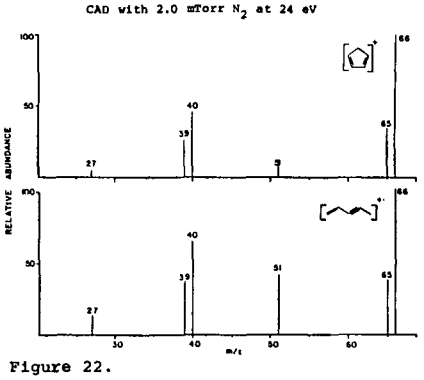

Figure 22.

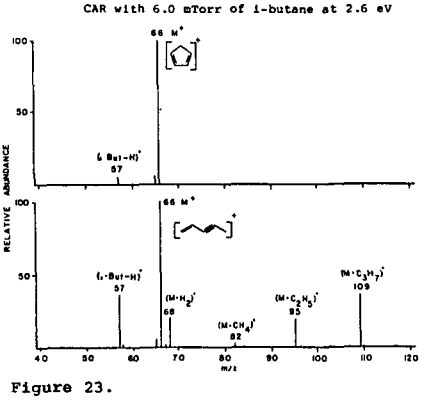

Figure 23.

Perhaps the most promising use of MS/MS for structure elucidation, however, is in conjunction with the new desorption ionization methods, including thermospray LC/MS. Tandem mass spectrometry can potentially provide informative daughter ion fragmentation from the molecular ions produced by these methods, and can furthermore eliminate interference from the matrix background which inevitably results. While applications of MS/MS for structure elucidation are becoming increasingly important, it is mixture analysis applications which have been the driving force behind the rapid growth of MS/MS (Figure 24).

Figure 24.

While early applications of MS/MS emphasized direct mixture analysis without sample preparation, there has been a trend towards incorporating appropriate cleanup into MS/MS methods. We recently pointed out that (7):

> Recent applications of MS/MS... have shown the wisdom of not giving up everything we have learned about sample extractions and chromatography, but rather making sensible trade-offs between the selectivity of MS/MS and the selectivity of sample preparation and separation.

A particularly powerful approach for trace analysis in complex mixtures is combined GC/MS/MS (Figure 25), especially with short packed or capillary GC columns (25). As an example (26), a 20 cm long packed column (0.1 cm id) provides retention times of <20s for trichlorophenol and hexachlorabenzene, while electron-capture negative CI selected reaction monitoring provides detection limits in the femtogram range (Table 2). This GC/MS/MS method permits the analysis of samples at a rate of 100 injections/hr (Figure 26).

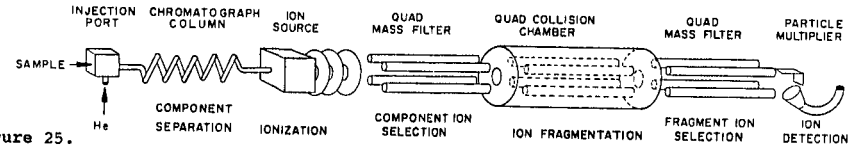

Figure 25.

Table 2. MS/MS Limits of Detection

	conc [a]	mass [b]	moles [c]	molecules
Hexachlorobenzene				
	50 ppt	50 fg	180 amol	1.1×10^8
Trichlorophenol				
	250 ppt	250 fg	1.3 fmol	7.7×10^8

[a] concentration in 1 µL samples
[b] mass in femtograms (10^{-15}g)
[c] mol in femtomol and attomol (10^{-18}mol)

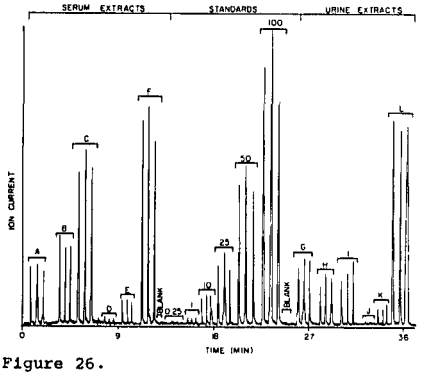

Figure 26.

The example above clearly demonstrates the power of short-column GC in conjunction with MS/MS. Is there a need for MS/MS when "good" GC with conventional columns is employed? This question was addressed in a study comparing GC/MS and GC/MS/MS for the detection of trace levels of tryptolines in crude extracts of brain tissue (27). Figure 27 compares typical chromatograms produced by GC/MS (selected ion monitoring) and GC/MS/MS (selected reaction monitoring). The analyte (arrow) is not visible in the GC/MS case, but is clearly indicated by GC/MS/MS.

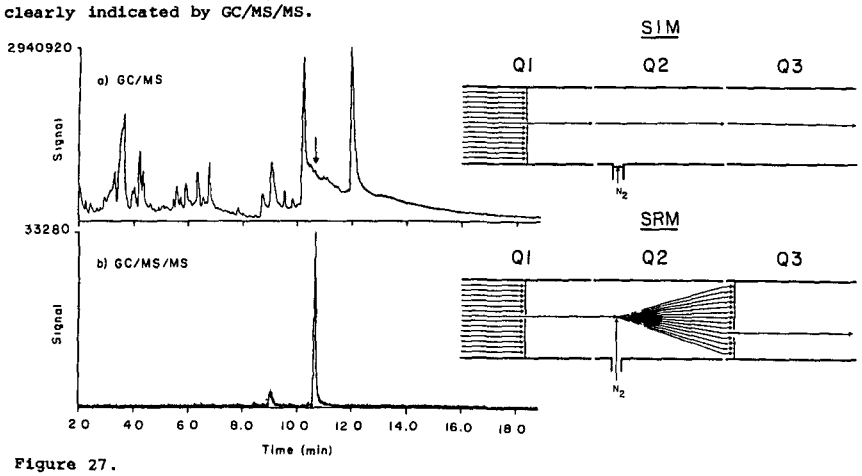

Figure 27.

What does the future hold for MS/MS? Recall that the **sixth** age of an analytical method is **acceptance as a routine, standard method.** Achieving that level of maturity will require continued instrumental evolution. Fred McLafferty has suggested that (28):

> Demand will bring the price of computerized MS/MS instruments down to $50,000; the present price appears to be the major deterrant to MS/MS growth rivaling that of GC/MS and LC/MS.

One of the most promising approaches for a low cost tandem mass spectrometer for routine analyses is that ion trap MS/MS system developed recently by Finnigan MAT. We have performed some preliminary experiments comparing the MS/MS efficiency of the ion trap system with that of the triple quadrupole instrument (Table 3). The ion trap demonstrates more efficient CAD (i.e., ability to fragment the selected parent ion and collect the resultant daughter ions) and a much more efficient second stage of mass analysis (i.e., transmission through MS II). Thus, the ion trap has the potential to become the most sensitive MS/MS instrument ever, as well as the least expensive.

Table 3. Comparison of MS/MS efficiencies.

	MS/MS Efficiency[a]		
	CAD	MS II	Overall
Triple Quadrupole	16%	10%	1.6%
Ion Trap	58%	93%	54%

[a]Averages for the following reactions of $(C_2H_5O)_2P(O)C_2H_5$:

$$M^+ \rightarrow (HO)_2P(OH)C_2H_5^+$$
$$(M+H)^+ \rightarrow (HO)_2P(OH)C_2H_5^+$$
$$(M-C_2H_3)^+ \rightarrow (HO)_2P(OH)C_2H_5^+$$

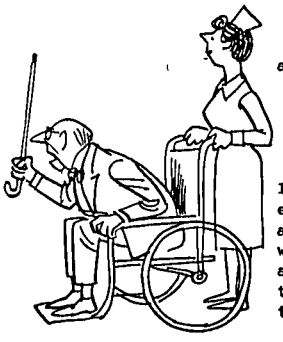

Figure 28.

The widespread acceptance of MS/MS was predicted in Science as we entered this decade (29):

> If the current trends are any indication, MS/MS should become one of the most widely used instrumental techniques of the 1980's.

I, for one, am happy to see MS/MS remain a little longer in the exciting period of research into fundamentals and new applications (the fourth and fifth ages). I would predict that widespread acceptance of MS/MS as a routine method (the sixth age) will come to pass; however it is sobering to realize that this is inevitably followed by the **seventh** age (**senescence, as the technique is overtaken by newer methods**) (Figure 28).

Acknowledgments

Adaption of illustrations from a series of books by Richard Armour illustrated by Leo Hershfield is acknowledged ["Going Around in Academic Circles" (1965), "The Medical Muse" (1963), "Light Armour" (1954), and "Nights with Armour" (1956)], all published by McGraw-Hill, New York. Dr Richard Armour is Professor Emeritus of English at Scripps College in Claremont, CA. Dr. Armour points out that "he wrote impressive volumes of biography and literary criticism until he became a full professor with tenure and found that sort of thing no longer necessary." Leo Hershfield was a Floridian who served as a graphic reporter for television (from the McCarthy hearings to the Calley trial) when not illustrating Dr. Armour's work.

Diagrams of the various MS/MS instrumental configurations are adapted from Reinhold Pesch's illustrations (Spectra **1983**, 9 (4), 13-17).

Finally, I would like to gratefully acknowledge my colleagues, graduate students, and post docs, past and present, for their immeasurable contributions to this work and for making it fun as well.

References

1. Franklin, J.L., Ed. "Ion-Molecule Reactions"; Plenum: New York, NY, 1972.
2. Bozorgzodeh, M.H.; Morgan, R.P.; Benyon, J.H. Analyst **1978**, 103, 613-622.
3. Kondrat, R.W.; Cooks, R.G. Anal. Chem. **1978** 50, 81A-92A.
4. McLafferty, F.W., Ed. "Tandem Mass Spectrometry"; John Wiley & Sons: New York, NY, 1983.
5. Yost, R.A.; Fetterolf, D.D. Mass Spectrom. Rev. **1983**, 2, 1-45.
6. McLafferty, F.W. Philos. Trans. R. Soc. London Ser. A. **1979**, 293, 93.
7. Johnson, J.V.; Yost, R.A. Anal. Chem. **1985**, 57, 758A-768A.
8. Aston, F.W. Proc. Chem. Phil. Soc. **1919**, 19, 317.
9. Futrell, J.H.; Miller, C.D. Rev. Sci, Instr. **1966**, 37, 1521-1526.
10. Lampe, F.W., Presented at the 33rd Annual Conference on Mass Spectrometry and Allied Topics, San Diego, May 1985.
11. Shannon, T.W.; McLafferty, F.W. J. Amer. Chem. Soc. **1966**, 88, 5021.
12. Jennings, K.P. Int. J. Mass Spectrom. Ion Phys. **1968**, 1, 227.
13. Porter, C.J.; Beynon, J.H.; Ast, T. Org. Mass Spectrom. **1981**, 16, 101.
14. Wanless, G.G.; Glock, G.A., Jr. Anal. Chem.**1967**, 39, 2-13.
15. Cooks, R.G.; Glish, G.L. Chem. Eng. News, Nov. 30, 1981, 40-52.
16. Games, D.E. Spectra **1983**, 9 (1), 2.
17. Cooks, R.G. Anal. Chem. **1985**, 57, 823A.
18. Beynon, J.H.; Cooks, R.G.; Amy, J.W.; Baitinger, W.E.; Ridley, T.Y. Anal. Chem. **1973**, 45, 1023A.
19. Yost, R.A.; Enke, C.G. Anal. Chem. **1979**, 51, 1251A-1264A.
20. Huang, C.-S.; Kiser, R.W. Int. J. Mass Spectrom. Ion Phys. **1978**, 27, 209.
21. Review of first proposal for triple quadrupole MS/MS, 1976.
22. Chem. Eng. News, March 24, 1986, 70.
23. McLafferty, F.W. Trends Anal. Chem. **1982**, 1, 298.
24. Fetterolf, D.D.; Yost, R.A. Int. J. Mass Spectrom. Ion Process. **1984**, 62, 33-49.
25. Trehy, M.L.; Yost, R.A.; Dorsey J.G. Anal. Chem. **1986**, 58, 14-19.
26. Yost, R.A.; Fetterolf, D.D.; Hass, J.R.; Harvan, D.J.; Weston, A.F.; Skotnicki, P.A.; Simon, N.A. Anal. Chem. **1984**, 56, 2223-2228.
27. Johnson, J.V.; Yost, R.A.; Faull, K.F. Anal. Chem. **1984**, 56, 1655-1661.
28. McLafferty, F.W. Science **1981**, 214, 286.
29. Maugh, T.H., III Science **1980**, 207, 677.

Twenty Years of Chemical Ionization

A. G. Harrison
Department of Chemistry
University of Toronto
Toronto, Canada

Twenty years ago, in June 1966, Munson and Field (1) published the first paper on chemical ionization mass spectrometry. They noted in their introduction that

> "The purpose of this paper is to present a new technique of generating mass spectra, chemical ionization mass spectrometry, in which the characteristic ionization of the materials in question is produced by ionic reactions rather than electron impact. These chemical ionization mass spectra probably will be of particular interest for analytical mass spectrometry."

This latter prediction has been amply demonstrated over the past twenty years since the technique has become one of the most widely used ionization methods when dealing with structural elucidation and quantitation problems in many branches of chemistry and biochemistry and in medical and environmental studies.

As Lampe has pointed out in a lecture to this society in 1985 (2), the history of gas-phase ionic reactions dates from the beginnings of mass spectrometry and the work of Thompson (3) and Dempster (4) who identified H_3^+ in the mass spectrum of H_2 and to the work of Hogness and Lunn (5) who showed that it originated by the reaction

$$H_2^+ + H_2 \rightarrow H_3^+ + H \quad (1)$$

However, the modern era of gaseous ionic reactions dates from the 1950's when Tal'roze and Lyubimova (6), Stevenson and Schissler (7) and Field, Franklin and Lampe (8) independently discovered the reaction

$$CH_4^+ + CH_4 \rightarrow CH_5^+ + CH_3 \quad (2)$$

and showed that it occurred rapidly. This early work, which was carried out on conventional analytical mass spectrometers at low pressures and, therefore, low conversions, excited the interest of radiation chemists, in particular, and there was an immediate move to develop instruments capable of working at higher source pressures more closely approaching those used in radiation chemical studies.

With these higher pressure instruments conflicting results began to appear. Some workers reported that CH_5^+ and $C_2H_5^+$, the product of reaction (3),

$$CH_3^+ + CH_4 \rightarrow C_2H_5^+ + H_2 \quad (3)$$

were unreactive with methane while others reported that these ions reacted further with methane. To further complicate the situation different workers reported different reaction products. This budding controversy was resolved by Munson and Field (9, 10) in the early 1960's when they reported that CH_5^+ and $C_2H_5^+$ were unreactive with carefully purified methane but that when impurities (<1%) were deliberately added to the methane CH_5^+ and $C_2H_5^+$ showed a reactivity and, more importantly, gave products which depended on the identity of the additive. It was this latter observation which led to the development of chemical ionization using methane reagent gas as introduced by Munson and Field in 1966 (1).

The major reactions occurring in CH_4 CI were noted by Munson and Field to be proton transfer from CH_5^+ and $C_2H_5^+$ to the additive M (reactions (4) and (5)) as well as hydride ion abstraction by $C_2H_5^+$ (reaction (6)). In addition $M \cdot C_2H_5^+$ and $M \cdot C_3H_5^+$ adduct ions are sometimes observed. The MH^+ ions may undergo fragmentation (reaction (7))

$$CH_5^+ + M \rightarrow MH^+ + CH_4 \quad (4)$$

$$C_2H_5^+ + M \rightarrow MH^+ + C_2H_4 \quad (5)$$

$$\rightarrow (M-H)^+ + C_2H_6 \quad (6)$$

$$MH^+ \rightarrow A_i^+ + N_i \quad (7)$$

The utility of the CI method is that, in many cases, not only is molecular weight information abtained from the MH^+ ion signal but also structural information is obtained from the fragment ions observed. As shown in Figure 1 fragmentation of the even-electron MH^+ species usually involves elimination of stable even-electron neutral molecules

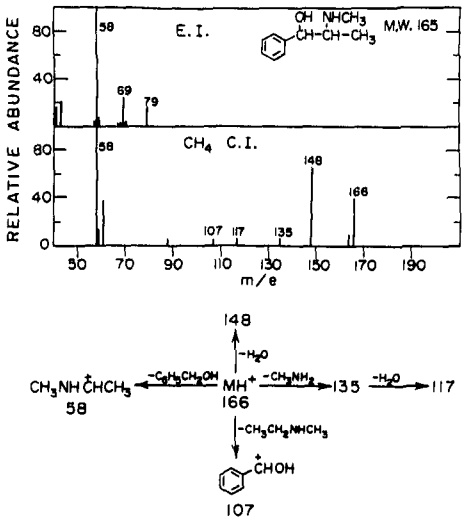

Fig 1. EI and CH_4 CI Mass Spectra of Ephidrine (11)

incorporating functional groups present in the molecule; the method frequently provides structural information complementary to that obtained by EI.

Instrumentation

The instrumental modifications to an EI instrument necessary for chemical ionization operation have been discussed in detail elsewhere (12). In brief, to achieve the necessary ion source pressure (0.2 to 1.0 torr), while keeping the pressure in the source housing and analyzer low, the ion source is made as gas tight as possible (usually involving a decrease in size of the electron beam entrance aperture and the ion exit aperture) and high speed pumping is provided for the source region. At the elevated source pressures in magnetic sector instruments with the source at high potential there may be some problem with electrical discharges along the lines used to introduce samples and reagent gases unless precautions are taken; this problem does not arise in quadrupole instruments. An alternative approach is taken in the atmospheric pressure chemical ionization (APCI) instrument developed by Horning and colleagues (13) and shown schematically in Figure 2. Here ionization

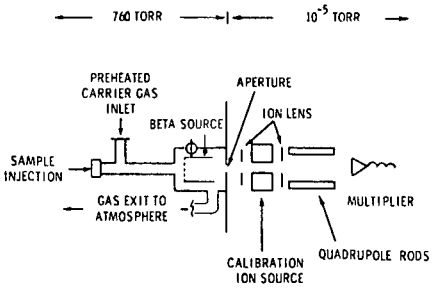

Fig 2. Schematic of APCI Instrument

is initiated by a radioactive source or an electrical discharge in a carrier gas at atmospheric pressure containing the sample at low partial pressure. The final ions in the system are sampled through an aperture into a differentially-pumped quadrupole mass analyzer. This type of instrument, which is commercially available, provides excellent sensitivity for trace analysis because of the long reaction times and high pressures. However, these parameters usually mean that the ionization ends up residing with the most stable ionic species which may not be the species of analytical interest unless the chemistry of the API source is modified.

Positive Ion Chemical Ionization

A. Brønsted Acid Reactions

The reactions of CH_5^+ and $C_2H_5^+$ (reactions (4) and (5)) are examples of the general Brønsted acid proton transfer reaction

$$BH^+ + M \rightarrow MH^+ + B \quad (8)$$

for which the enthalpy change is given by

$$\Delta H_{react} = PA(B) - PA(M) \quad (9)$$

If PA(M)>PA(B) (PA=proton affinity) the reaction is exothermic and normally occurs rapidly. It appears that most of the reaction exothermicity resides in the MH^+ ion formed. Thus, by choosing Bs of different proton affinities the excitation of MH^+ and, consequently the extent of fragmentation of MH^+ can be varied. Table 1 lists Brønsted acid reagent systems which have seen appreciable use. Since the PAs of

most organic molecules are in the range 180-230 kcal mol^{-1} (14), this array of reagent ions provides the opportunity to vary the protonation exothermicity over a substantial range. Figure 3 presents an

TABLE 1

Brønsted Acid Reagents

Reagent Gas	BH^+	PA(B)[14] (kcal mol^{-1})
H_2	H_3^+	101
CH_4	CH_5^+	131
	$C_2H_5^+$	164
H_2O	$H^+(H_2O)_n$	173*
i-C_4H_{10}	$C_4H_9^+$	197
NH_3	$H^+(NH_3)_n$	205*

* Data for monosolvated ion.

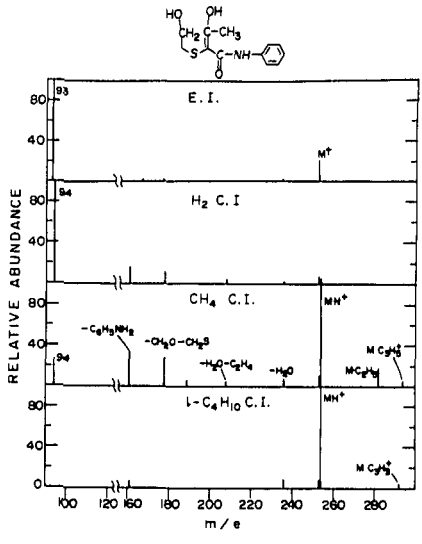

Fig 3. Effect of ΔH_{prot} on CI Mass Spectra

example of the effect of varying the protonating agent on the spectrum observed; in many cases the CH_4 reagent system yields the best combination of molecular weight and structural information. When proton transfer is endothermic, clustering may occur; for example, the

formation of M NH_4^+ in the NH_3 CI of saccharides has proven to be particularly useful for molecular weight determination (15, 16).

In APCI using ambient air or nitrogen carrier gas the dominant positive ion reagent species is the solvated proton $H^+(H_2O)_n$ which has been shown (17) to arise by the reaction sequence,

$$e + N_2 \rightarrow N_2^+ + 2e \quad (10)$$

$$N_2^+ + 2N_2 \rightarrow N_4^+ + N_2 \quad (11)$$

$$N_4^+ + H_2O \rightarrow H_2O^+ + 2N_2 \quad (12)$$

$$H_2O^+ + H_2O \rightarrow H_3O^+ + OH \quad (13)$$

$$H_3O^+ \rightsquigarrow H^+ (H_2O)_n \quad (14)$$

The protonating agent can be modified by adding bases of higher proton affinity to the gas stream.

B. Charge Exchange Ionization

An alternative to proton transfer is charge exchange ionization. Here the reagent gas is chosen to produce in the initial ionization step a species $R^{+\cdot}$ which subsequently reacts with the substrate M by charge exchange (reaction(16)) to produce $M^{+\cdot}$, which may subsequently fragment.

$$e + R \rightsquigarrow R^{+\cdot} + 2e \quad (15)$$

$$R^{+\cdot} + M \rightarrow M^{+\cdot} + R \quad (16)$$

$$M^{+\cdot} \rightarrow A_i^+ + N_i \quad (17)$$

The odd-electron $M^{+\cdot}$ species produced in reaction (16) fragments by the same pathways as the $M^{+\cdot}$ species produced in electron impact ionization; the major difference is that the $M^{+\cdot}$ produced by electron impact have a range of excitation energies while the $M^{+\cdot}$ produced by charge exchange have an excitation energy given approximately by

$$E(M^{+\cdot}) = RE(R^{+\cdot}) - IE(M) \quad (18)$$

Where $RE(R^{+\cdot})$ is defined by

$$R^{+\cdot} + e \rightarrow R, \ -\Delta H = RE(R^{+\cdot}) \quad (19)$$

Table 2 lists charge exchange reagent systems covering species with recombination energies from 9.3 eV to 16 eV (18)

TABLE 2

Charge Exchange Reagent Systems

Reagent Gas	Reactant Ion	RE($R^{+\cdot}$)(eV)
C_6H_6	$C_6H_6^{+\cdot}$	9.3
N_2/CS_2	$CS_2^{+\cdot}$	10.2
CO/COS	$COS^{+\cdot}$	11.2
Xe	$Xe^{+\cdot}$	12.1, 13.4
CO_2	$CO_2^{+\cdot}$	13.8
CO	$CO^{+\cdot}$	14.0
N_2	$N_2^{+\cdot}$	15.3
Ar	$Ar^{+\cdot}$	15.8, 15.9

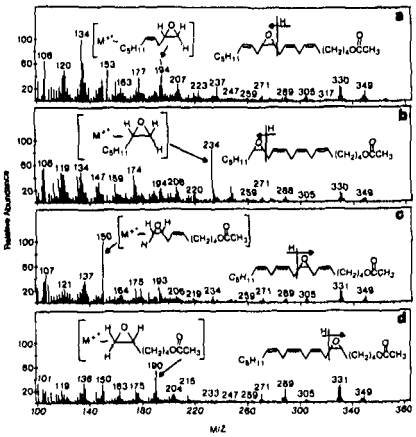

Fig 4. $CS_2^{+\cdot}$CE Mass Spectra of Monoepoxide Isomers of Arachidonyl Acetate (20)

The major analytical uses of charge exchange ionization are to enhance differences, relative to EI, in the mass spectra of isomeric compounds (19-21) or to achieve selective ionization of components of mixtures (22-25). The former use is illustrated in Fig. 4 which shows the $CS_2^{+\cdot}$CE mass spectra of isomeric epoxides. Significant differences are observed despite the fact that the 70 eV EI mass spectra are essentially identical (20). In the latter area, charge exchange from

$C_6H_6^{+\cdot}$ has been used to ionize selectively unsaturated fatty acid esters in the presence of saturated fatty acid esters (22) and PCBs in atmospheric samples (23) while both $C_6H_{12}^{+\cdot}$ (cyclohexane) (24) and $C_6H_5Cl^{+\cdot}$ (25) have been used to ionize selectively aromatic hydrocarbons in petroleum products.

Although NO^+ (produced in NO or N_2/NO mixtures) reacts in part by charge exchange with species of low IE (<8.5 eV) it also reacts by H^- abstraction and adduct ion formation depending on the substrate. The reactions of NO^+ have been reviewed in detail (12).

Negative Ion Chemical Ionization

Although the original work of Munson and Field (1) was concerned only with positive ion CI, they did note that the techniques described would be applicable for the production of negative ions; this prediction also has proven to be true. The field of negative ion CI is less well developed than positive ion CI, in part, because, until recently, many commercial mass spectrometers were not equipped to operate in the negative ion mode. In recent years negative ion CI has seen increased use in analytical applications although fundamental and mechanistic studies still are rather limited.

C. Electron Capture Ionization

Electron capture by neutral molecules is a resonant process which normally requires near-thermal energy electrons. In practice these quasi-thermal electrons are produced by using a buffer gas, which does not produce stable negative ions, to thermalize the electrons by inelastic scattering and dissociative ionization processes. Typical buffer gases which have been used (26) include Ar, N_2, CH_4, i-C_4H_{10}, NH_3 and CO_2, with CH_4 probably being the most popular. The quasi-thermal electrons attach to the substrate molecule to produce molecular anions or fragments derived therefrom

$$e + R \rightsquigarrow e_{therm} + R \quad (20)$$

$$e_{therm} + M \rightarrow M^- \quad (21)$$

$$M^- \rightarrow A_i^- + N \quad (22)$$

The rate constants for the electron capture reaction (21) depend strongly on the structure of M and may vary from $10^{-13} cm^3 mol^{-1} s^{-1}$ to 10^{-7} $cm^3 mol^{-1} s^{-1}$ (27). By contrast, ion/molecule reactions involving particle transfer (such as proton transfer) have maximum rate constants of $2x10^{-9}$ $cm^3 mol^{-1} s^{-1}$. Hence, in suitable cases, electron capture ionization may be much more sensitive than either Brønsted acid or Brønsted base ionization reactions; thus accounting for the popularity of electron capture ionization when high sensitivity is required. To achieve such a high sensitivity may require derivatization of the molecule (28). Since nitroaromatic and perfluoro compounds normally have large electron capture rate constants the typical procedure is to make perfluoracyl, perfluorobenzyl or nitroaromatic derivatives. The high rate constants for electron capture arise from the high mobility of the electron.

However, there are a number of problems with electron capture ionization since the spectra tend to be rather irreproducible. This arises, in part, because of varying electron energy distributions and, in part, because of the presence of impurities. For example, trace levels of O_2 or H_2O lead to the formation of O^-, O_2^- or OH^- which will give different products on reaction with the substrate. To counter this problem some workers (29) have added small amounts of O_2 to the methane moderating gas. It also appears that electron capture mass spectra may vary with sample size (30).

D. Brønsted Base Reagents

In negative ion CIMS Brønsted bases, reacting primarily by reaction (23), play a role analogous to the role of Brønsted acids

$$B^- + M \rightarrow (M-H)^- + BH \quad (23)$$

in positive ion CIMS. Reaction (23) will be exothermic, and occur efficiently, if the proton affinity of B^- is greater than the proton affinity of $(M-H)^-$. Table 3 records the proton affinities (31) and electron affinities of a variety of Brønsted bases. Of these, OH^- (produced in a N_2O/CH_4 or a $N_2O/i\text{-}C_4H_{10}$ mixture) O^- (produced in a

N_2O/N_2 mixture) and Cl^- (produced by electron capture by CH_2Cl_2, $CHCl_3$ or CF_2Cl_2) have seen the most use. Both OH^- and CH_3O^- are strong bases and react with most substrates by proton abstraction to produce $(M-H)^-$ which usually shows little further fragmentation. Thus, this mode of

TABLE 3

Brønsted Base Reagents

B^-	$PA(B^-)$*	$EA(B)$*
H^-	400	17.4
NH_2^-	400	18.0
OH^-	382	42.2
O^-	382	33.7
CH_3O^-	379	36.2
F^-	372	78.4
O_2^-	351	10.1
Cl^-	333	83.4

* kcal mol^{-1}

ionization is useful for molecular weight determination. Weaker Brønsted bases, such as Cl^-, react by adduct ion (MB^-) formation when proton abstraction is endothermic. These adducts have found use in molecular weight determination in a variety of situations (for a review see (26)). The competition between proton abstraction and adduct ion formation can be strongly dependent on molecular architecture and, for example, cis and trans cycloalkane diols show quite different spectra with F^- as reagent ion (32).

Solvated O_2^- ions are the dominant species in APCI using air as carrier gas; it also may be prepared in a medium pressure instrument by a Townsend discharge in pure O_2 (33). O_2^- has a relatively low proton affinity and will abstract only very acidic hydrogens. Because of the low electron affinity of O_2 it also may react by charge exchange. It also has been observed to cluster and to displace H and Cl.

$$O_2^- + M \rightarrow (M-H)^- + HO_2 \qquad (24)$$

$$\rightarrow M^- + O_2 \qquad (25)$$

$\rightarrow MO_2^-$ (26)

$\rightarrow (M-H+O)^- + OH$ (27)

$\rightarrow (M-Cl+O)^- + ClO$ (28)

The radical anion O^- reacts, in part, by proton abstraction but also reacts by H_2^+ abstraction from suitably activated CH_2 groups, by H-atom displacement and by alkyl-group displacement (34, 35). All of these reaction channels are shown in the O^- CI mass spectra of the carbonyl compounds shown in Figure 5 (36). A complication is that O^- also reacts with some substrates by H^- atom abstraction to form OH^- which may react further with the substrate to form $(M-H)^-$. Thus, the O^- CI mass spectrum observed may depend on sample size.

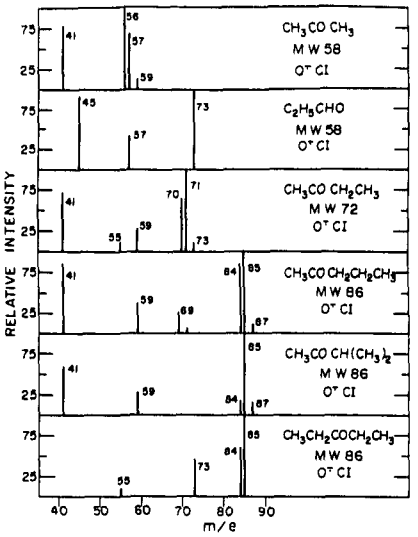

Fig 5. O^- CI Mass Spectra of Some Carbonyl Compounds

Pulsed Positive Ion Negative Ion Chemical Ionization

Since both positive ion and negative ion chemical ionization are useful and, fequently, provide complementary information, there is an obvious advantage in obtaining both types of spectra on the same sample. The quadrupole mass filter transmits positive ions and negative ions with equal facility and Hunt et al (37) have developed a pulsing mode of operation of a quadrupole, illustrated schematically in Figure 6, which

permits simultaneous measurement of both types of spectra. They also have described a variety of reagent systems which may be used in such a mode of operation. For example, the use of CH_4 as reagent gas gives Brønsted acid reactions in the positve ion mode and electron capture reactions in the negative mode while addition of CH_3ONO to the methane gives CH_3O^- as a Brønsted base reactant in the negative mode. This pulsed mode of operation of quadrupole is available on a commercial instrument.

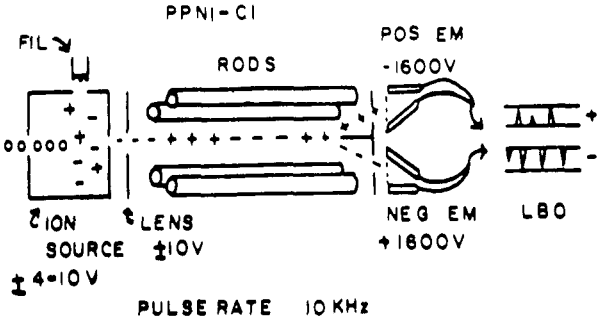

Fig 6. Pulsed Positive Negative Ion CI

The Future in CIMS

The number of papers presented at this conference which involve chemical ionization show clearly that the field is thriving and is likely to continue to do so. In this brief review I have been able to present only briefly a biased view of the major developments in the field; it is perhaps well to finish briefly with a gaze into the crystal ball to see what the future holds for the field. An obvious objective of chemical ionization is to develop reagents which react specifically with individual functional groups and thus signal the presence of that functional group. Thus one example is the determination of double bond position using vinyl methyl ether as reagent gas (38). Clearly progress will continue to be made in this area, in part, involving the reactions of metal ions (39). This latter work has been carried out largely using Fourier Transform mass spectrometry (FTMS) and there is no doubt that the future will see much more development and use of FTMS in the chemical ionization mode (40). A major use of chemical ionization,

illustrated amply at this conference, is as a soft ionization technique to prepare ions for collison-induced dissociation of MS/MS experiments. Here there is much work to be done to determine which mode of chemical ionization yields the most or best information when the CID experiment is done. For example, we have noted that CID on the MH^+ ion of alkenyl acetates provides no information on double bond location while CID on the $(M-H)^-$ ion does provide such information (41). Clearly much work remains to be done and when CIMS is reviewed on the fortieth anniversary the reviewer will have even more difficulty than I had in covering all the interesting work.

References

1. M. S. B. Munson and F. H. Field, J. Am. Chem. Soc., 88, 2621 (1966).
2. F. W. Lampe, 33RD Annual Conference on Mass Spectrometry, San Diego, (1985).
3. J. J. Thompson, Phil. Mag., 24, 209 (1912).
4. A. J. Dempster, Phil. Mag, 31, 438 (1916).
5. T. R. Hogness and E. G. Lunn, Phys. Rev., 26, 44 (1925).
6. V. L. Tal'roze and A. K. Lyubimova, Dokl. Akad. Nauk. SSSR, 86, 969 (1952).
7. D. P. Stevenson and D. O. Schissler, J. Chem. Phys., 23, 1353 (1955).
8. F. H. Field, J. L. Franklin and F. W. Lampe, J. Am. Chem. Soc., 79, 2419 (1957).
9. F. H. Field and M. S. B. Munson, J. Am. Chem. Soc., 87, 3289 (1965).
10. M. S. B. Munson and F. H. Field, J. Am. Chem. Soc., 87, 3294, 4242 (1965).
11. H. M. Fales, H. A. Lloyd and G. W. A. Milne, J. Am. Chem. Soc., 92, 1590 (1970).
12. A. G. Harrison, Chemical Ionization Mass Spectrometry, CRC Press, Boca Raton, (1983).
13. E. C. Horning, M. G. Horning, D. I. Carroll, I Dzidic and R. N. Stillwell, Anal. Chem., 45, 936 (1973).
14. D. H. Aue and M. T. Bowers, in Gas Phase Ion Chemistry (M. T. Bowers, Ed.), Academic Press, N. Y., (1979).
15. A. M. Hogg and T. L. Nagabhusan, Tetrahedron Letts., 4827 (1972).
16. D. B. Horton, J. D. Wander and R. L. Foltz, Carbohyd. Res., 36, 75 (2974).

17. A. Good, D. Durden and P. Kebarle, J. Chem. Phys., 52, 212, 222 (1970).

18. A. G. Harrison, in Ionic Processes in the Gas Phase (M. A. Almoster Ferreira, Ed.) Reidel, Dordrecht, (1984).

19. A. G. Harrison and M. S. Lin, Org. Mass Spectrom., 19, 67 (1984).

20. T. Keough, E. D. Mihelich and D. A. Eickhoff., Anal Chem., 56, 1849 (1984).

21. J. A. Abbatt and A. G. Harrison, Org. Mass Spectrom., in press.

22. S. C. Subba Rao and C. Fenselau, Anal. Chem., 50, 511 (1978).

23. B. A. Thompson, T. Sakuma, J. Fulford, D. A. Lane, N. Reid and J. B. French, Adv. Mass Spectrom., 8, 1422 (1980).

24. L. W. Sieck, Anal. Chem., 51, 128 (1979).

25. L. W. Sieck, Anal. Chem., 55, 38 (1983).

26. H. Budzikiewicz, Mass Spectrom. Rev., in press

27. L. G. Christophoru, Adv. Electronics and Electron Phys., 46, 55 (1978).

28. D. F. Hunt and F. W. Crow, Anal. Chem., 50, 1781 (1978).

29. J. R. Hass, M. D. Friesen, D. J. Harvan and C. E. Parker, Anal. Chem., 50, 1474 (1978).

30. E. A. Stemmler and R. A. Hites, Anal Chem., 57, 684 (1983).

31. J. E. Bartmess and R. T. McIver, in Gas Phase Ion Chemistry (M.T. Bowers, Ed.) Academic Press, N. Y., (1979).

32. F. J. Winkler and D. Stahl, J. Am. Chem. Soc., 101, 3685 (1979).

33. D. F. Hunt, C. N. McEwen and T. M. Harvey, Anal. Chem., 47, 1730 (1975).

34. K. R. Jennings, in Gas Phase Ion Chemistry (M. T. Bowers, Ed.) Academic Press, N. Y., (1979).

35. A. P. Bruins, A. J. Ferrer-Correia, A. G. Harrison, K. R. Jennings and R. K. Mitchum, Adv. Mass Spectrom, 7, 355 (1978).

36. A. G. Harrsion and K. R. Jennings, J. C. S. Faraday Trans II, 72, 1601 (1976).

37. D. F. Hunt, G. C. Stafford, F. W. Crow and J. W. Russell, Anal. Chem., 48, 2098 (1976).

38. A. J. Ferrer-Correia, K. R. Jennings and D. K. Sen Sharma, Org. Mass Spectrom., 11, 867 (1976).

39. R. A. Forbes, E. C. Tews, B. S. Freiser, M. B. Wise and S. P. Perone, Anal. Chem., 58, 684 (1986).

40. C. L. Johlman, R. L. White and C. L. Wilkins, Mass Spectrom. Rev., 2, 389 (1983).

41. G. Takeuchi and A. G. Harrison, unpublished results.

ABBEY,L E 584
ABBEY,L E 582
ABDEL-MAKSOUD,H M 120
ABERTH,W 860
ABERTH,W 218
ACKERMANN,B L 635
ADAMS,J 101
ADAMS,J 449
AHMED,M S 604
ALAI,M 1005
ALAI,M 862
ALDERWEIRELDT,F C 445
ALEXANDER,A J 537
ALEXANDER,T G 907
ALKALAY,D 1009
ALLAN,A 212
ALLAN,J M 242
ALLEMANN,M 886
ALLEY,C C 498
ALLEY,C C 500
ALLISON, J 736
ALLISON,J 801
ALLISON,J 610
ALLISON,J 632
ALLMAIER,G 308
ALLRED,E L 525
ALMOND,M F 208
ALVARADO-SWAISGOOD,A 794
ALVIN,J A 1042
AMSTER,I J 947
ANDEREGG,R J 905
ANDREWS,P J 333
AOKI,E 892
APLIN,R T 467
APPELHANS,A D 562
ARAI,T 463
ARMENTROUT,P B 19
ARROWSMITH,P 136
ASAMOTO,B 602
ASHCROFT,A E 1027
ASHLEY,D L 500
ASSENZA,S P 1032
BACON,J P 504
BAILEY,F C 701
BAKER,E S 403
BAKER,R H 110
BALESTRINI,S J 300
BALLARD,J M 185
BALLARD,K D 323
BARBUCH,R J 40
BARCHAS,J B 846
BARCHAS,J D 774
BARCHAS,J D 856
BARNES,L D 1013
BARNHART,E R 500
BARNHART,E R 498
BARRY,R 870
BARTMESS,J E 551
BARTMESS,J E 634
BARTMESS,J E 549
BARTMESS,J E 550
BARTNER,P L 903
BARTNER,P L 122
BARWISE,A J 829
BASS,L 795
BATEMAN,R H 232
BATEMAN,R H 955
BATH,W W 375
BAUMAN,N 294
BAX,M 1009
BAYER,C W 369
BAYKUT,G 166
BAYKUT,G 681
BAYKUT,G 679
BEAN,R M 76
BEAUDET,S 1029
BEAUDET,S 140
BEAUDET,S 138
BEAUGRAD,C 220
BEAUGRAND,C 393
BEAUGRAND,C 799
BEAVIS,R 641
BEAVIS,R 764
BEAVIS,R 643
BEAVIS,R 171
BECK,D J 566
BECK,D J 105
BECK,O 774
BECKER,G W 439
BECKMAN,R J 1067
BEHR,F E 424
BELIVEAU,R 325
BELMANS,M 445
BENCSATH,F A 5
BENNICH,H 790
BENNICH,H 939
BENNINGHOVEN,A 951
BENOIT,F M 193
BENSIMON,M 683
BENTZ,B L 1069
BENTZ,B L 1075
BERNI,R J 738
BERNI,R J 302
BERRY,A J 11
BERRY,T 335
BERTRAND,M J 734
BERTRAND,M J 927
BETOWSKI,L D 185
BIEMANN,K 852
BIEMANN,K 97
BIEMANN,K 854
BIEMANN,K 1077
BIEMANN,K 308
BLACK,M S 369
BLAIR,I A 116
BLAIR,I A 112
BLAIR,I A 999
BLAIR,I A 792
BLAKLEY,C R 591
BLETSOS,I V 951
BLUETT,L J 701
BOCKHOFF,F M 829
BOCKHOFF,F M 744
BOERBOOM,A J H 957
BOESL,U 772
BOESL,U 399
BOLBACH,G 764
BOMBICK,D D 632
BOMBICK,D D 736
BONAPARTE,K 201

BONAR,J 62
BONDYBEY,V E 608
BONE,W M 459
BOON,J J 468
BOON,J J 331
BORDOLI,R S 864
BORDOLI,R S 955
BORNSTEIN,D 95
BOSTWICK,D E 582
BOUZIANE,C 1007
BOWEN,K H 600
BOWEN,K H 539
BOWEN,K H 977
BOWMAN,R E 492
BOYD,R K 441
BOYD,R K 995
BOYD,R K 496
BOYD,V L 459
BOZORGZADEH,M H 428
BRACHMANN,K 724
BRAND,H R 56
BREEN,J 278
BRIGGS,B S 439
BRIGHT,D S 124
BRODBELT,J 685
BROIDA,E 983
BROMUND,R H 1054
BROOKS,P W 1046
BROWN,C E 531
BROWN,C E 874
BROWN,N K 74
BROWN,R S 655
BROWN.S Y 1025
BROWNER,R F 582
BROWNER,R F 584
BROWNER,R F 409
BRUINS,A 585
BRUINS,A 371
BRUINS,A 379
BRUNNEE,C 724
BRYAN,S R 128
BRYANT,D W 333
BRYANT,M S 250
BRYDEN,C C 821
BRZAK,K A 195
BUCHANAN,M V 244
BUCHANAN,M V 246
BUCHNER,J 1011
BUCHNER,J D 1032
BUCHNER,J D 596
BUCKNER,S W 612
BUDDE,W L 205
BUDDE,W L 234
BURKHARD,L 373
BURLINGAME,A L 624
BURLINGAME,A L 860
BURSEY,J T 480
BURSEY,M M 572
BURSEY,M M 258
BURSEY,M M 1021
BURSEY,M M 420
BURSEY,M M 760
BUSCH,K L 290
BUSCH,K L 397
BUSCH,K L 21
BUSCH,K L 547
BUSH,A 911
BUSH,E D 114
BUTFERING,L 15
BUTTERWORTH,B C 373
BYRD,G D 752
CALLERY,P S 894
CALLERY,P S 345
CAMPANA,J E 545
CAMPANA,J E 201
CAMPANA,J E 23
CAMPBELL,J A 831
CAMPBELL,T W 210
CANTLE,J E 414
CAO,Z-M 28
CAPPIS,J H 0
CAPRIOLI,R M 628
CAPRIOLI,R M 381
CAPRIOLI,R M 844
CARMICHAEL,W C 93
CARR,S A 850
CARR,S A 630
CARR,S A 355
CARRASQUILLO,A 186
CARTER,G T 294
CASTLE,R 831
CASTLEMAN,A W 797
CASTLEMAN,A W 560
CASTLEMAN,A W 606
CASTLEMAN,A W 993
CAVALIERI,E 898
CEJA,P C 963
CEJA,P C 718
CELIKKAYA,A 292
CERNY,R L 424
CERNY,R L 99
CERNY,R L 898
CHAIT,B T 941
CHAIT,B T 943
CHAIT,B T 643
CHAKEL,J A 846
CHAMBERLAIN,T N 1001
CHAN,K Y 1019
CHAN,T M 903
CHANG,T C 673
CHAO,B 308
CHAPMAN,J R 587
CHAPMAN,J R 965
CHARALAMBOUS,P 414
CHARLES,M J 238
CHARPENTIER,B A 687
CHATTOPADHYAYA,R 321
CHAUDHARY,T 653
CHAUDHARY,T 943
CHEN,C-C 696
CHENG,M T 45
CHESS,E K 76
CHIARELLI,M P 447
CHILTON,F H 502
CHITTIM,B G 496
CHOI,R L 1025
CHOMA,N 1003
CHOU,F E 1
CHOW,C S 478
CHOWDHURY,S 989

CHRIST,C S 809
CHRISTIE,W H 164
CHRISTMAN,R F 1050
CHTAIB,M 138
CHTAIB,M 325
CHU,M 212
CITERIN,R 744
CLAY,K L 502
CLENCH,M R 587
CLIFFORD,A J 312
CLIFFORD,A J 327
COATES,M L 319
CODY,J T 286
CODY,R 224
CODY,R B 730
CODY,R B 667
COE,J V 977
COE,J V 539
COE,J V 600
COGGIOLA,M J 552
COLE,R B 1061
COLE,R B 416
COLGAN,D 705
COLTON,R J 1059
COMEZOGLU,F T 66
CONWAY,D C 451
COOK,J C 395
COOK,K D 786
COOKS,R G 17
COOKS,R G 437
COOKS,R G 685
COOKS,R G 669
COSTELLO,C E 97
COSTELLO,C E 825
COTTER,M L 574
COTTER,R J 931
COTTER,R J 937
COTTER,R J 909
COTTER,R J 872
COTTRELL,J 381
COTTRELL,J S 880
COUTANT,J E 1019
COVELL,D G 262
COVEY,T 107
COVEY,T 585
CRAIG,A G 790
CRAIG,A G 367
CRAIG,A G 367
CRAIG,A G 939
CRAIG,E C 175
CRAIN,P F 900
CRAWFORD,D W 401
CRAWFORD,J L 746
CREASY,W R 533
CROW,F W 848
CROW,F W 570
CROWDER,C 550
CUNNINGHAM,R 62
CURRY,B 60
CUTIE,S S 7
D'AGOSTINO,P A 70
DAHL,D A 304
DALTON,T E 714
DAS,C 461
DAS,C 776
DAS,P R 703
DAS,P R 122
DAVENPORT,M 158
DAY,R A 1007
DAY,R A 36
DEBONO,M 439
DECOSTA,B 699
DEINZER,M 898
DEJOHN,D E 298
DELLINGER,B 256
DELMORE,J E 304
DELMORE,J E 562
DEMAIO,W 578
DEMIREV,P 363
DEMIREV,P 872
DEMIREV,P 931
DESIDERIO,D M 776
DESIDERIO,D M 461
DESIDERIO,D M 626
DETERDING,L 422
DEVANT,G 220
DEVANT,G 393
DHEANDHANOO,S 156
DIAUGUSTINE,R P 860
DIDONATO,G C 21
DIDONATO,G C 397
DIDONATO,G C 547
DIELMANN,G 866
DIETRICH,A M 78
DIFAZIO,L 797
DINO,J J 80
DIXON,J E 780
DOLNIKOWSKI,G G 815
DOLNIKOWSKI,G G 177
DOMON,B 95
DONG,Z-W 28
DONNELLY,J R 488
DONNELLY,J R 476
DONNELLY,J R 203
DONOHUE,D L 407
DORN,S B 645
DOUGHERTY,R C 234
DOUGLAS,D J 410
DOUGLAS,L J 837
DOWNS,J J 494
DROVER,D R 70
DROZD,R J 829
DUERDEN,J M 359
DULIK,D 1005
DUNBAR,R C 604
DUNBAR,R C 602
DUNBAR,R C 558
DUPUY,H P 738
DURDEN,D A 365
DYCKES,D F 858
EASTMAN,A 898
EDMONDS,C G 896
EDMONDS,C G 900
EDMONDS,C G 919
EDOM,R 1015
EDOM,R W 1046
EFURD,D W 0
EGAN,W 357
EICHELBERGER,J 234
ELLER,T D 110

ELLER,T D 323
ELLERBE,P 470
ELLERBE,P 472
ELLESTAD,G A 32
ELLIOTT,G 880
ELLIOTT,N L 405
ENGSTROM,A 790
ENGSTROM,A 939
ENKE,C G 54
ENKE,C G 288
ENKE,C G 280
ENKE,C G 426
ENKE,C G 961
ENS,W 991
ENS,W 641
ENS,W 764
ENS,W 643
ENS,W 171
EPSTEIN,P 181
EPSTEIN,P 517
ERICKSON,E 158
ESMANS,E L 445
ESTEBAN,N 310
ESTEBAN,N V 923
EVANS,D H 560
EVANS,J E 120
EVANS,M J 927
EVANS,M J 734
EVANS,S 162
EVANS,S 880
EVANS,S 154
EVERETT,D 387
EYLER,J R 166
EYLER,J R 809
EYLER,J R 681
EYLER,J R 679
FAIRBROTHER,A E 864
FALARDEAU,P 341
FALES,H M 1058
FALES,H M 443
FALICK,A M 218
FALICK,A M 377
FAN,T 381
FANG,Y 691
FARCASIU,D 43
FAULL,K F 774
FAULL,K F 856
FAULL,K F 846
FEISTNER,G 846
FEISTNER,G J 856
FENG,R 433
FENN,J B 507
FENNESSEY,K 109
FENNESSEY,P 109
FENNESSEY,P 911
FENNESSEY,P V 268
FENSELAU,C 931
FENSELAU,C 872
FENSELAU,C 862
FIELD,F H 943
FIELD,F H 941
FIELD,F H 653
FIELD,F H 5
FILGES,U 985
FINDEIS,A F 778
FISHER,D H 449
FLORY,D A 188
FLOYD,L J 1013
FLURER,R A 290
FOERST,D 72
FORBES,R A 689
FOUQUET,A 705
FRANCL,T J 191
FRASER,B A 506
FREAS,R B 23
FREAS,R B 545
FREIDHOFF,C B 539
FREIDHOFF,C B 977
FREIDHOFF,C B 600
FREISER,B S 689
FREISER,B S 612
FREISER,B S 667
FREISER,B S 803
FREISER,B S 805
FREISER,B S 541
FREW,N M 1054
FREY,R 515
FRIAR,D L 431
FRIEDBERG,S J 347
FUHRMANN,J 484
FUJII,T 882
FUJII,T 252
FUJIOKA,Y 183
FUKUDA,E K 1003
FULFORD,J E 410
FURLONG,J 947
FURR,H C 327
GABLING,R -H 529
GALE,P J 1069
GALE,P J 1075
GALLAHER,K L 716
GALLAHER,K L 744
GALLEGOS,E J 1048
GAMES,D E 11
GAMES,D E 335
GANGULY,A K 903
GARLAND,W A 1003
GARRELL,J 58
GARTEIZ,D A 591
GARTEIZ,D A 474
GARTEIZ,D A 1017
GARTEIZ,D A 593
GASKELL,S J 418
GASKELL,S J 276
GASKELL,S J 416
GASKELL,S J 80
GAUMANN,T 683
GAUMANN,T 554
GEISE,U 134
GERGELY,R J 333
GETEK,T A 907
GETEK,T A 756
GIAM,C S 160
GIAM,C S 691
GIBBS,P H 66
GIBLIN,D E 711
GIBLIN,D E 99
GIBSON,B W 778
GIBSON,B W 860
GIBSON,J H 716

GIESE,R W 449
GILLEN,G 878
GILLIAM,J M 439
GIRIJAVALLABHAN,V M 903
GLISH,G L 25
GLISH,G L 768
GLISH,G L 431
GOERINGER,D E 164
GOODLEY,P C 589
GOODMAN,S 726
GOODMAN,S 730
GOSNELL,A B 1040
GOSS,C 268
GOSS,S P 675
GOTLIN,R 109
GOTO,M 576
GOVINDARAJIN,S 782
GRAVEL,G 705
GRAY,B W 732
GRAYSON,M A 819
GREATHEAD,R 707
GREATHEAD,R J 1027
GREATHEAD,R J 587
GREAVES,J 259
GREEN,B N 955
GREEN,B N 732
GREEN,B N 856
GREEN,L W 152
GREEN,L W 405
GREENE,F T 839
GREGG,H 56
GREGORY,J F 316
GREGORY,J F 317
GRIFFIN,L 979
GRIFFIN,L L 983
GRIFFIS,D P 128
GRIGSBY,R D 835
GRIMSRUD,E P 234
GRIMSRUD,E P 519
GRINDSTAFF,Q G 208
GRINDSTAFF,Q G 197
GROSS,M C 91
GROSS,M L 89
GROSS,M L 101
GROSS,M L 616
GROSSMANN,P 886
GROTEMEYER,J 399
GROTEMEYER,J 772
GROTJAHN,L 622
GROTZMACHER,H-F 985
GRUTZMACHER,H F 963
GUENAT,C 554
GUENAT,C 416
GUENAT,C 1061
GUENAT,C R 80
GUEVREMONT,R 482
GUPTA,R 896
GUTZAIT,L 1044
GUYAN,S A 732
HAFOK,CH 784
HAGLER,W M 68
HAGLER,W M 913
HAJDASZ,D 618
HAKANSSON,P 939
HALUSHKA,P V 110
HAMBIDGE,K M 268
HAMBIDGE,S 109
HANEY,C A 68
HANEY,C A 455
HANEY,C A 913
HANKINSON,D J 801
HANNA,D A 726
HANSELMAN,D S 504
HANSEN,G 85
HANSEN,G 517
HARADA,K -I 463
HARDIN,E D 210
HAROLDSEN,P E 351
HARRIS,R E 823
HARRISON,A G 665
HARRISON,A G 27
HARRISON,A G 1103
HARRISON,A G 661
HARRISON,J F 794
HARRISON,J F 801
HARRISON,W W 272
HARRISON,W W 274
HART,K J 280
HART,K J 54
HART,K J 426
HARTMAN,T G 696
HARTMAN,T G 782
HARVAN,D S 441
HARVEY,D J 74
HARVEY,D J 314
HARVEY,D J 359
HARVEY,T M 78
HASHEM,H 1011
HASHIZUME,T 896
HASS,J R 78
HASS,J R 1061
HATCH,F 517
HATCH,F 85
HATCH,F 181
HATCHER,P G 1050
HAWES,E M 1015
HAYES,D A 210
HAYES,M 1009
HEADLEY,J V 1052
HEARN,B A 166
HEATON,R C 1067
HEIDHART, S 325
HEINE,C E 635
HELLER,D N 872
HEMBERGER,P H 1067
HEMLING,M E 630
HENION,J 379
HENION,J 371
HENION,J 224
HENION,J 107
HENION,J D 1023
HER,G 353
HER,G R 933
HERCULES,D M 509
HERCULES,D M 160
HERCULES,D M 951
HERMANN,E 831
HERMANN,E A 1035
HESS,K R 272
HETTICH,R L 541

HICKEY,J C 375
HIEFTJE,G M 142
HIEFTJE,G M 412
HILBERT,L R 248
HILEMAN,F 484
HILL,J C 953
HINDENLANG,D M 1063
HINSON,J A 1038
HITES,R A 238
HITES,R A 240
HITES,R A 234
HO,C -T 782
HO,C-T 696
HOCART,C H 337
HOFFMAN,M K 1001
HOFFMANN,E 34
HOLDER,C L 1040
HOLICK,M F 699
HOLLAND,J 158
HOLLAND,J F 635
HOLMAN,R W 811
HOLMAN,R W 616
HOLMAN,R W 614
HOLTZCLAW,J R 30
HONIG,R E 1075
HONOVICH,J 937
HONOVICH,J 909
HONOVICH,J 872
HOO,K 335
HORAN,A C 122
HORNER,L M 242
HOUK,R S 264
HSIEH,T C 148
HSU,A T 1073
HSU,C S 43
HSU,F F 919
HU,H C 695
HUANG,S K 167
HUANG,S K 527
HUANG,S K 614
HUANG,Y 612
HUANG,Y 689
HUBBARD,H L 110
HUBBARD,J W 1015
HUBBARD,J W 1046
HUDSON,C 979
HUDSON,C E 983
HUGHES,B M 282
HUNT,D F 945
HUNT,D F 93
HUNT,D F 788
HUNT,G F 146
HUNT,P M 801
HUNT,S L 162
HUNT,S L 424
HWANG,D -G 750
IKEHARA,M 329
INFANTE,R 186
INOUE,I 925
IRELAND,J C 205
IRIZARRY,J 186
ISENSEE,R K 566
ISHII,D 576
ISRAEL,M 461
ITAGAKI,Y 576
ITO,Y 576
JACKSON,P 414
JACKSON,R 193
JAKUBOWSKI,E M 1
JAMIESON,W D 714
JAMIESON,W D 482
JAOUEN,D 220
JARDINE,I 868
JARVIS,B B 66
JAYASIMHULU,K 453
JAYASIMHULU,K 349
JENNINGS,K R 154
JENSEN,N J 89
JENSEN,N J 91
JIANG,X 266
JOHANNESSEN,J N 504
JOHNSON,C G 1054
JOHNSON,C L 813
JOHNSON,D M 572
JOHNSON,E 754
JOHNSON,J V 748
JOHNSON,J V 521
JOHNSON,R S 852
JOHNSON,W 850
JOHNSON,W 630
JOHNSON,W 355
JOHNSTON,M V 673
JONES,A D 327
JONES,A D 312
JONES,D S 598
JONES,G G 179
JONES,H K 535
JONES,L A 455
JONES,M P 197
JONSSON,G 790
JONSSON,G 939
JUNG,G 724
JUNGALWALA,F B 120
KABAY,M C 210
KAHWA,I A 148
KALINOSKY,H T 13
KALLOS,G 831
KALLOS,G J 3
KALLOS,G J 7
KAMENSKY,I 939
KAMENSKY,I 790
KAMINSKI,H 515
KANESHIRO,E S 349
KAPUSCINSKI,M M 38
KARRICK,G L 40
KASSEL,D 523
KASSEL,D B 736
KASSEL,D B 632
KASTL,P E 1035
KASTL,P E 195
KATTA,V 595
KATZ,R N 653
KAUFMAN,D G 80
KAYGANICH,K 523
KEBARLE,P 537
KEBARLE,P 649
KEBARLE,P 989
KEBARLE,P 639
KEESEE,R G 993
KEESEE,R G 560

KEESEE,R G 797
KEESEE,R G 606
KELLEY,P E 963
KENAN,W R 258
KENNERLEY,S 728
KENTTAMAA,H I 437
KEOUGH,T 657
KEOUGH,T 687
KEOUGH,T 935
KHORANA,H G 308
KIDWELL,D A 1059
KILLMER,L B 630
KIM,H-Y 361
KIMBER,M L 1027
KING,F L 274
KING,R W 740
KINSINGER,J 224
KINSINGER,J A 730
KINSINGER,J A 967
KINTER,M T 1021
KIPLINGER,J P 420
KISHIMOTO,Y 872
KITAI,T 882
KITAI,T 252
KLEIN,A J 242
KLEIN,P D 150
KLEIN,P D 270
KLUSMAN,R W 375
KNAPP,D R 110
KNAPP,D R 323
KNAPP,R G 323
KNOBELOCH,G W 0
KOFEL,P 886
KOLAITIS,L 890
KOLLAR,R G 744
KORFMACHER,W A 1040
KOSMAN,J 716
KOVACIC,P 874
KOVACIC,P 531
KOWALSKI,M 49
KRASKE,P J 191
KRECISZ,J M 478
KRISHNAMURTHY,T 93
KRISHNAMURTHY,T 105
KRISTO,M 177
KRISTO,M J 961
KRISTO,M J 709
KROLIK,S T 693
KROLIK,S T 598
KROLIK,S T 732
KROLIK,S T 864
KRUGE,M A 829
KUAN,J W 738
KUCK,D 963
KUEHL,D W 373
KUHARA,T 925
KULATUNGA,R 649
KULATUNGA,R 639
LAASASENAHO,K 72
LABUDDE,J A 999
LABUZA,T P 474
LAFORTUNE,F 764
LAGERGREN,C R 403
LAGNA,W M 894
LAINE,R A 148
LAINE,R A 377
LAN,S J 387
LANE,K R 805
LANGVARDT,P W 195
LAPP,R L 711
LAPP,R L 428
LASCHIC,N S 902
LASER,B 134
LATTIMER,R P 817
LATTIMER,R P 823
LAUER,R 242
LAUKIEN,F H 226
LAY,J O 1040
LAY,J O 1038
LAY,K Y 701
LE QUESNE,P W 389
LEARY,J J 915
LEBRON,J 186
LECH,L M 803
LEE,C -J 357
LEE,E 224
LEE,E D 1023
LEE,G W 955
LEE,L S 150
LEE,L S 270
LEE,M 831
LEE,M R 748
LEE,M S 748
LEE,M S 929
LEE,T D 842
LEE,W M 1069
LEGENDRE,M G 302
LEGENDRE,M G 738
LEHMAN,J P 878
LEIBMAN,C P 254
LEIBMAN,C P 637
LEICH,D A 146
LEPPINEN,J J 405
LESAGE,J 1029
LETHAM,D S 339
LETHAM,D S 337
LEUCHTNER,R 797
LEVI-SETTI,R 132
LEVIN,F 507
LIBERATO,D 310
LIBERATO,D J 923
LIGON,W V 645
LIMBIRD,L E 116
LINDBERG,M S L 939
LINDBERG,M S L 790
LINDNER,B 513
LINTON,R W 128
LINTON,R W 1061
LISEK,C A 868
LITTLE,J L 746
LITTON,J F 840
LIU,R H 302
LIU,R H 738
LLEWELLYN,B M 83
LLOYD,J R 574
LOH,S 284
LOH,S 207
LONGEVIALLE,P A 975
LOO,J A 947
LOPEZ,H 451

LORENZ,R G 774
LOURIS,J 685
LOURIS,J N 963
LU,Y-M 266
LUBMAN,D M 888
LUBMAN,D M 890
LUBMAN,D M 385
LUBMAN,D M 383
LUKAS,T J 792
LUYTEN,Y 445
LYNAUGH,N 949
LYON,P A 424
LYON,P A 162
MAACK,F 799
MAACK,F 393
MABUD,M A 669
MACDONALD,R G 152
MACFARLANE,R D 953
MACMAHON,T 612
MADORE,G 140
MAGGIO,V L 500
MAHONEY,J F 707
MAIN,D 764
MAIN,D 643
MAIN,D E 641
MAIN,D E 991
MALEKNIA,S D 825
MALLET,A I 917
MALLEY,M J 375
MALLIS,L M 87
MALLIS,L M 103
MALTAIS,L 734
MAMANTOV,G 637
MAMANTOV,G 254
MAMER,O A 902
MANDELBAUM,A 95
MANDICH,M L 608
MARKELOV,M 744
MARKEY,C J 504
MARKEY,S P 81
MARKEY,S P 391
MARKEY,S P 504
MARKWARDT,U 724
MARSHAK,D R 620
MARSHALL,A G 175
MARSHALL,A G 1073
MARSHALL,A G 228
MARSHALL,A G 429
MARTIN,S A 854
MARTINEAU,A 341
MARTINEZ,R A 347
MARTINEZ,R T 156
MASON,F G 714
MASUDA,K 463
MATHEWS,W R 852
MATSUDA,H 329
MATSUGI,M 329
MATSUMOTO,I 925
MATSUMOTO,M 925
MATSUO,T 329
MAURER-FOGY,I 784
MAVRIDIS,A 794
MAYOL,R F 999
MAZER,S 256
MCADOO,D 979
MCADOO,D J 969
MCADOO,D J 983
MCADOO,D J 981
MCCALLA,D R 333
MCCARRAHER,L C 118
MCCARRY,B E 333
MCCLENNEN,W H 1071
MCCLENNEN,W H 817
MCCLOSKEY,J A 896
MCCLOSKEY,J A 919
MCCLOSKEY,J A 900
MCCLUER,R H 120
MCCLUSKY,G A 298
MCCORMICK,T J 387
MCCORMICK,T J 457
MCCRACKEN,M S 935
MCCRORY,G 146
MCDONALD,J R 807
MCDOWALL,M A 949
MCDOWELL,M 467
MCELVANEY,S W 533
MCELVANY,S W 807
MCGAHREN,W J 32
MCGAUGHEY,J F 480
MCGOWN,S R 306
MCGUIRE,J M 821
MCHUGH,K M 600
MCHUGH,K M 977
MCHUGH,K M 539
MCINTIRE,F 911
MCKAY,G 1015
MCKAY,G 1046
MCKELLOP,K 181
MCKELLOP,K 517
MCKINNON,H S 496
MCKOWN,H S 164
MCKOWN,H S 768
MCLAFFERTY,F W 284
MCLAFFERTY,F W 947
MCLAFFERTY,F W 207
MCLAFFERTY,F W 433
MCLEAN,M 568
MCLEAN,M A 188
MCLEAN,M A 1017
MCLUCKEY,S A 25
MCLUCKEY,S A 431
MCLUCKEY,S A 768
MECKSTROTH,W K 543
MEEHAN,J L 492
MEISELMAN,S 472
MEISELMAN,S 470
MEISELS,G G 997
MEISELS,G G 564
MELANSON,E 754
MELLON,F A 587
MENG,C K 507
MENTZER,M 630
MERCER,R S 665
MESSER,E E 480
MESSIER,F 705
MESTAGH,H 799
METRAL,C J 876
METZ,S 41
MEUZELAAR,H L C 817
MEUZELAAR,H L C 1071

MEUZELAAR,H L C 957
MEUZELAAR,L C 64
MICO,B 1044
MIDHA,K K 1046
MIDHA,K K 1015
MILES,A J 480
MILLARD,B J 955
MILLARD,B J 693
MILLARD,J R 511
MILLER,D W 1040
MILLER,L V 268
MISSLER,S 93
MISSLER,S R 312
MISSLER,S R 23
MISSLER,S R 66
MITCHUM,R K 203
MITROKA,J 387
MIZUNO,T 576
MOLLOY,R M 439
MOORE,C 728
MOORE,C 154
MORAN,M G 126
MORELLI,J J 509
MORIN,N 799
MORRISON,G H 126
MORRISON,J D 222
MORRISON,J D 675
MORTON,J B 122
MORTON,J B 903
MORTON,T H 971
MORTON,T H 973
MOTHERSOLE,S 36
MUELLER,D 95
MUENZER,J 262
MUGA,L 766
MUGA,M L 169
MULLEN,S L 429
MUNSON,B 884
MUNSON,B 870
MURAWSKI,S L 786
MURPHY,R C 351
MURPHY,R C 502
MUSSELMAN,B D 659
MUSSER,S M 894
MYHRE,D V 935
NAMIKI,A 1065
NARAYAN,R 827
NAYLER,R 414
NAYLOR,S 778
NEEDHAM,L L 490
NEGRON,N 186
NERO,V P 38
NEWBURY,D E 130
NEWCOME,B 158
NEWCOME,B H 709
NEWMAN,R A 1017
NEWMAN,W H 323
NIEDERHUT,W 201
NIEDERHUT,W J 488
NIELSON,P F 939
NIELSON,P F 367
NIEMEYER,I C 216
NISHIGAKI,S 1065
NISHIMURA,T 564
NISHIMURA,T 997
NIXON,M 846
NOBLE,R 484
NODA,T 1065
NOONAN,J S 1036
NORD,P J 242
NORWOOD,D L 1050
NUNN,A 457
NUTTER,G L 179
NUWAY-SIR,L 319
O'DONNELL,J E 839
O'KEEFE,A 533
O'KEEFE,A 807
O'LEAR,J D 17
O'MALLEY,R 671
OBERACKER,D F 480
OCCOLOWITZ,J L 439
ODOM,R W 144
ODOM,R W 216
OHKURA,T 925
OHORI,D 574
OHSHIMA,M 1065
OLSON,C T 83
OLSON,J A 327
OLTHOFF,J 872
OLTHOFF,J 931
OLTHOFF,J 937
ONSTOT,J 278
ORLANDO,R 884
ORTH,R 484
OSTERMAN,R M 591
OTSUKA,K 892
OWEN,R 232
OYLER,A 574
PACHUTA,R R 827
PADMANABHAN,G 41
PALAZZOLO,M A 480
PALLANTE-MORELL,S 1005
PALMER,P T 288
PALMER,P T 54
PALMER,P T 280
PALMER,P T 426
PAN,J C 492
PANG,E K 833
PANG,H M 888
PANNELL,L K 443
PANNELL,L K 1058
PARILLO,R J 587
PARK,J -W 663
PARKER,C E 760
PARKER,C E 572
PARR,V C 598
PARR,V C 232
PASSARELLA,R 993
PASSARELLA,R 606
PATRICK,D 831
PATTERSON,D G 490
PATTERSON,D G 498
PATTERSON,D G 500
PAUSCH,J B 817
PEAKE,D A 527
PEET,N P 40
PEFFER,R C 1042
PEIRCE,P 268
PENA,L 186
PERCHALSKI,R J 929

PEREL,J 707
PERKINS,D D 584
PERKINS,D D 582
PERKINS,J R 11
PERONE,S P 689
PERRIN,R E 0
PESCH,R 724
PESCH,R 866
PETERMAN,P H 486
PETERSON,D M 347
PETIT,E 754
PETTY,J D 486
PHELPS,R G 953
PHILLIPS,L R 357
PHILLIPS,L R 634
PHILLIPS,L R 459
PHILLIPSON,D W 900
PIKE,A 109
PIRONE,A J 1032
PORTER,C J 418
POTTER,D W 1038
POULTER,W L 778
PRAKASH,C 112
PRAMANIK,B N 903
PRAMANIK,B N 703
PRAMANIK,B N 122
PRATT,J A E 587
PRATT,J A E 965
PRICE,H A 236
PROVOST,L R 70
PYLE,S M 185
QUA,A 698
QUARLES,J M 451
QUILLIAM,M A 333
QUILLIAM,M A 335
QURESHI,N 909
RAHBEE,A 230
RAJAKYLA,E 72
RAMACHANDRAN,J 846
RAMALEY,L 714
RAMSEY,E D 965
RAPIN,J 683
RAPP,U 866
RATHBUN,C A 1056
RAUSHEL,F M 87
REDDY,K 116
REDDY,S G 331
REDDY,S G 468
REDMAN,E W 971
REDMAN,E W 973
REENTS,W D 543
REENTS,W D 608
REILLY,J P 770
REILLY,J P 511
REINER,E J 661
REINHOLD,V N 353
REINHOLD,V N 933
REMMERS,J 278
REMPEL,D L 167
RHEE,C K 823
RICCA,T L 228
RICHARDS,J M 817
RICHARDS,J M 1071
RICHARDSON,D E 809
RICHTER,W J 95
RIDGE,D P 545
RIDGE,D P 543
RINEHART,K L 395
ROBBINS,R C 894
ROBERTS,G D 630
ROBERTS,G D 850
ROBERTS,G D 355
ROBERTS,L J 112
ROBINS,R H 570
ROBINS,R H 848
ROBOZ,J 212
ROCKWOOD,A L 173
RODRIGUEZ,L C 1003
ROENSCH,F R 0
ROEPSTORFF,P 939
ROEPSTORFF,P 790
ROEPSTORFF,P 367
ROHWEDDER,W K 296
ROLAND,C 220
ROLANDO,C 799
ROLLGEN,F W 15
ROLLGEN,F W 647
ROLLINS,K 467
ROMANOWSKI,G 529
ROSECRANCE,A E 1056
ROSEN,J D 782
ROSEN,R T 695
ROSEN,R T 782
ROSEN,R T 696
ROSENBERG,I 698
ROSENHAMMER,D G 716
ROSNACK,K J 509
ROSS,M M 545
ROTH,K A 774
RUBEY,W 256
RUBIN,I B 244
RUDEWICZ,P 1044
RUDEWICZ,P 1033
RUDEWICZ,P 9
RUSSELL,D H 945
RUSSELL,D H 103
RUSSELL,D H 677
RUSSELL,D H 87
RYAN,P A 728
SACK,T M 742
SAFE,S 496
SAKKERS,P 72
SAKURAI,T 329
SALEHPOUR,M 790
SALEM,N 343
SALEM,N 361
SALLANS,L 805
SAMPSON,E J 490
SAMS,R A 1031
SAMS,R A 1036
SANDERS,C G 525
SANDERS,R A 687
SANDERSON,N E 414
SANTIKARN,S 353
SANTIKARN,S 933
SANTOS,I 175
SARRE,O 903
SARVER,E W 105
SARVER,E W 93
SAUTER,A D 494

SAVICKAS,P J 3
SAVITT,J M 504
SCANLAN,G S 868
SCHAEFER,W H 792
SCHAFER,W 866
SCHEEL,R H 236
SCHLAG,E W 772
SCHLAG,E W 399
SCHLUNEGGER,U P 47
SCHMELZEISEN-REDEKER,G 15
SCHMID,E R 784
SCHMIDT,C E 837
SCHMIDT,W 134
SCHMIT,J P 140
SCHMIT,J P 138
SCHMIT,J P 325
SCHMIT,J P 1029
SCHOEN,A E 722
SCHOEN,A E 718
SCHREIBER,J M 1056
SCHUELER,B 144
SCHUELER,B 641
SCHUELER,B 764
SCHUELER,B 171
SCHUELER,B 991
SCHULTEN,H -R 823
SCHULTZ,J 62
SCOBLE,H A 97
SCRIVER,C R 902
SEARS,J 234
SEARS,L J 519
SEDGWICK,R D 1063
SEIFERT,W E 844
SELBIN,J 148
SELF,R 939
SELF,R 790
SELOVER,S J 840
SENSHARMA,D K 321
SERFASS,R E 264
SERVE,M P 83
SESHADIRI,R 461
SEYDEL,U 513
SHABANAWITZ,J 93
SHABANOWITZ,J 945
SHABANOWITZ,J 788
SHACKLETON,C H L 310
SHALABY,L M 189
SHARP,T R 49
SHARP,T R 535
SHARP,T R 525
SHARPE,P 809
SHAUL,G M 185
SHEPPERD,D A 199
SHIH,M -C 391
SHIH,M -C 81
SHIH,M H 298
SHINOMIYA,T 1065
SHOMO,R E 1073
SHORE,F L 210
SHOWELL,J S 1058
SHU,I 266
SHUL,R J 606
SHUL,R J 993
SIEGEL,M M 32
SIEGEL,M M 566
SIEGEL,M M 294
SIGSWORTH,S 797
SIITONEN,P 1040
SIM,P G 482
SIN,C H 888
SINHA,M P 921
SMITH,D C 949
SMITH,D C 868
SMITH,D H 407
SMITH,D L 780
SMITH,D L 900
SMITH,D L 266
SMITH,G G 331
SMITH,G G 468
SMITH,J R 1
SMITH,J S 199
SMITH,L M 486
SMITH,R D 13
SMITH,R D 580
SMITH,R G 242
SMITH,R M 718
SMITH,R W 572
SMITH,R W 760
SNIEGOSKI,L T 752
SNODGRASS,J T 600
SNODGRASS,J T 539
SNODGRASS,J T 977
SNYDER,W C 395
SO,H Y 558
SOKOLOSKI,E A 1058
SOKOLOSKI,E A 443
SOKOLOW,S 720
SOMSSICH,P F 959
SOPCHYSHYN,F 152
SOUTHERLAND,J H 480
SOVOCOOL,G W 488
SOVOCOOL,G W 476
SOVOCOOL,G W 203
SPAYTH,V 842
SQUIRES,R R 618
STACHOWIAK,K 858
STAFFORD,G 437
STAFFORD,G 685
STAFFORD,G C 963
STAHL,D 554
STALLING,D L 486
STAMP,J A 474
STAMS,D A 973
STANDING,K G 764
STANDING,K G 641
STANDING,K G 171
STANG,P J 49
STANLEY,J 278
STANNEY,K A 222
STAUFFER,D B 284
STAUFFER,D B 207
STAUFFER,J L 712
STEINAUER,R 47
STEINER,U 720
STEINERT,H 622
STEMMLER,E A 240
STEPNOWSKI,R M 610
STETTER,K O 896
STEWART,P B 210
STILLWELL,W G 250

STIMLER,E 234
STOGNIEW,M 41
STOLK,H T 1071
STOOTER,P L 347
STRAUB,K 9
STRAUB,K 1044
STRAUB,K 1033
STROH,J G 395
STUCKEMEYER,S R 146
STURM,G P 835
SUGIYAMA,Y 1065
SUMPTER,T 551
SUN,Z-L 28
SUNDQVIST,B U R 790
SUNDQVIST,B U R 939
SUNNER,J 649
SUNNER,J 639
SUTER,M 47
SUWANRUMPHA,S 465
SUZER,S 292
SUZUKI,M 463
SWACKHAMER,D L 238
SWANSON,B 387
SWANSON,S P 913
SWANSON,S P 68
SWEATT,J D 116
SWEETMAN,B J 999
SWEETMAN,B J 112
SYKA,J 437
SYKA,J E P 718
SYKA,J E P 963
SYKA,J E P 722
SZAFRANIEC,L 93
TABET,J C 23
TAKAYAMA,K 909
TAKEUCHI,T 576
TAMURA,H 1065
TANAKA,T 872
TANG,S -Y 835
TANG,X 171
TANG,X 991
TANG,X 643
TANG,X 764
TATEMATSU,A 463
TATEMOTO,K 856
TECKLENBURG,R E 677
TEDDER,J 222
TELLER,R 716
TEMBREULL,R 385
TERNES,T N 197
TERNES,T N 208
TERWILLIGER,D T 205
TEWS,E C 612
TEWS,E C 689
THIBAULT,P 927
THOMAS,B 76
THOMAS,D 549
THOMPSON,J J 264
THOMSON,M L 191
THORNE,G C 418
THORNE,G C 276
TIFFANY,J M 359
TIMMONS,L 742
TJOA,S 911
TODD,J F J 556
TODD,J F J 963
TODD,P J 254
TODD,P J 651
TODD,P J 637
TOLUN,E 556
TOMER,K B 89
TOMER,K B 898
TOMER,K B 99
TOMER,K B 91
TONDEUR,Y 488
TONDEUR,Y 327
TONDEUR,Y 203
TONDEUR,Y 201
TONDEUR,Y 23
TOTH,J P 316
TOTH,J P 317
TOWNSEND,L B 445
TRAEGER,J 979
TRAEGER,J C 987
TRAEGER,J C 981
TRAINOR,T M 449
TREHER,E 457
TSARBOPOULOS,A 868
TSUCHIYA,M 183
TSUCHIYA,M 892
TUDGE,H 162
TUELL,T M 840
TURNLAND,J R 260
TWISS-BROOKS,A B 207
TYLER,A N 774
UDSETH,H R 13
UDSETH,H R 580
UNGER,S E 457
UNGER,S E 387
UPSCHULTE,B L 993
UPSCHULTE,B L 606
UTZ,B R 837
UY,M 872
VANLEYEN,D 951
VARGHESE,P 58
VEENSTRA,G E 1035
VELSKO,C 146
VENKATARAMANAN,R 1011
VERCELLOTTI,J R 738
VESTAL,C H 593
VESTAL,C H 568
VESTAL,M L 465
VESTAL,M L 595
VESTAL,M L 578
VICCHIO,D 345
VICKERS,G H 412
VICKERS,G H 142
VIEIRA,N E 262
VISWANADHAM,S K 160
VISWANADHAN,S K 160
VOELKEL,N F 351
VOORHEES,K J 375
VOUROS,P 389
VOUROS,P 699
VOUROS,P 449
VOYKSNER,R D 758
VOYKSNER,R D 913
VOYKSNER,R D 114
VRBANAC,J J 110
VRIJENS,Y 445

WADDELL,D S 496
WADE,A P 280
WADE,A P 426
WADE,A P 54
WAGNER,G 134
WAGONER,D E 480
WAKEFIELD,M R 840
WALKER,M P 860
WALLER,G R 306
WALLS,F C 377
WALTER,K 399
WALTER,K 772
WANCZEK,K P 663
WANCZEK,K P 529
WANG,B H 947
WANG,G H 218
WANG,J-S 698
WANG,T H 568
WANG,T-C L 228
WARBURTON,G A 728
WARNER,C D 616
WARNER,C D 811
WARRACK,B M 387
WARREN,L 236
WASILCHUK,B A 389
WATSON,C H 681
WATSON,C H 679
WATSON,J T 815
WATSON,J T 635
WATSON,J T 523
WATSON,J T 118
WEAVER,C M 266
WEBB,J G 323
WEERASINGHE,N C A 492
WEINTRAUB,S T 347
WEINTRAUB,S T 1013
WEISS,G 515
WEISS,M 199
WEISS,M 515
WEISZ,A 81
WELCH,M J 472
WELCH,M J 435
WELCH,M J 470
WELCH,R L 236
WELLER,R R 691
WELLER,R R 160
WELLS,J L 321
WELLS,K 66
WELSCH,C W 915
WENCLAWIAK,B 51
WERNESS,S C 298
WESDEMIOTIS,C 433
WESTMORE,J B 764
WESTON,R F 199
WETMORE,R W 995
WHITE,E 470
WHITE,E 472
WHITE,E 752
WHITE,E 435
WHITE,E L 258
WHITEHOUSE,C M 507
WILKIE,C A 531
WILKINS,C L 813
WILKINS,C L 319
WILKINS,C L 655
WILLIAMS,D H 778
WILLIAMS,E R 947
WILLIAMS,R F 1013
WILLIAMS,T D 905
WILLOUGHBY,R 1011
WILLOUGHBY,R C 596
WILLOUGHBY,R C 1032
WILSON,D A 142
WILSON,D A 412
WILSON,R L 1031
WILSON,W E 441
WINDIG,W 64
WINKLER,I 47
WINKLER,P C 582
WINKLER,P C 584
WINTER,L D 424
WIRTH,K P 647
WISE,M B 244
WISE,M B 246
WISHNOK,J S 250
WOLF,C J 819
WOLF,D J 296
WOLFF,B 234
WOLLNIK,H 762
WONG,B 453
WONG,C 52
WONG,C M 56
WONG,D C 337
WONG,L K 1042
WONG,L K 1011
WONG,O C 339
WONG,S S 647
WONG,W W 150
WONG,W W 270
WOOD,D 232
WOOD,K V 827
WOTRING,L L 445
WRIGHT,B W 13
WRIGHT,H J 864
WRIGHT,L G 17
WUEBBELS,J 484
WYATT,J R 30
WYSOCKI,V H 437
YANG,L 858
YANG,M 770
YANG,M 511
YANG,Y-M 443
YANG,Y-M 1058
YATES,J 788
YAZDANPARAST,R 780
YEFCHAK,G 158
YERGEY,A L 262
YERGEY,A L 923
YERGEY,J 343
YINON,J 750
YOST,R A 929
YOST,R A 482
YOST,R A 748
YOST,R A 1090
YOST,R A 521
YOUNG,A B 214
YOUNG,A B 27
YOUNG,D 699
YOUNG,J P 407
YOUNG,S E 552

YU,K O 83
ZAKETT,D 3
ZANDER,A T 412
ZANDER,A T 142
ZECHMAN,J 122
ZEMAITIS,M A 1042
ZHA,Q 564
ZHANG,M -Y 207
ZHANG,R 339
ZHANG,X-M 28
ZHU,G 409
ZIDAROV,D 927
ZIMMERMAN,J A 671
ZON,G 459
ZORN,J 888

WORKSHOP ON ACADEMIC MASS SPECTROMETRY LABORATORIES

The purpose of this workshop was to increase communications between spectroscopists located in an academic service facility. The results of an informal survey of such facilities were presented and discussed. As expected a wide range of experiences were reported. The workshop attempted to address the common needs expressed in the survey. The topics discussed included: instrument maintenance, student use of instrumentation, service charges, and communication between these facilities and the users. A panel was organized to put together a more comprehensive survey of such facilities. Also, a mailing list was initiated in order to maintain communications within this group and to serve as another source of information, similar to the newsletter approach currently implemented by a few laboratories. One such item to be sent to attendees is the insurance policy approach to instrument repair discussed by Dan Jones from U.C. Davis.

The general conclusions of the workshop were: formation of an interest group - a nearly unanimous vote of the 90 - 100 attendees, a need to provide education and training for students, and a general statement of purpose - to aid the scientific community in solving problems using mass spectrometry.

Respectfully submitted,

Karl V. Wood
Department of Chemistry
Purdue University
West Lafayette, IN 47907

Rich Kondrat
Department of Chemistry
Rm. 1132
Pierce Hall
University of California
Riverside, CA 92521

ASMS INTEREST GROUP ON SOLIDS AND SURFACE ANALYSIS

WORKSHOP REPORT

"Emerging Instrumental Techniques for the Imaging of Surfaces"

The workshop was held on Monday evening, 9 June, from 8-10:15 p.m.. About forty people attended. The purpose of the workshop was to discuss t e instrumental methods and techniques used to collect, process, and analyze the ion images of surfaces. The workshop also acted as an extended discussion period for the symposium on "Ion Image Processing and Analysis in SIMS" held earlier that day.

The format of the workshop consisted of informal discussion of specific topics that were introduced and outlined by R. Colton, the organizer of the workshop. The main topics included goals and problems, instrumentation, and applications. The goal of ion image processing and analysis in SIMS is to quantitatively map the distribution of elemental and molecular surface species on the sub-micron scale with high sensitivity and specificity. While the earlier symposium dealt primarily with the emission of elemental species, the workshop wanted to address the prospect for chemical or molecular ion imaging.

The problems were outlined in terms of the limited spatial resolution of the primary ion source and the secondary ion detection system, the difficulty of quantitative analysis (particularly of heterogeneous materials), beam-induced artifacts, and the handling/processing/storage of "tons" of data.

Most of the discussion focussed, however, on instrumentation. The main topics included the source (liquid metal ion (LMI) and neutral beam), the detector (microchannel plate/phosphor, video cameca, framestore datasystem), and the analyzer (quadrupole, magnetic sector, and time-of-flight (TOF)).

In addition to the invited symposium speakers (D. Bright, M. Moran, S. Bryan, D. Newbury, and R. Levi-Setti), Z. Wilk (U. of Pittsburgh) and K. Busch (Indiana U.) were asked (in advance) to prepare some materials for the workshop. The workshop attendees were also invited to speak and many did.

R. Levi-Setti (U. Chicago) presented a detailed discussion of the limitation of current instrumental techniques for ion imaging and presented the design of a new instrument that couples a LMI source and TOF analyzer with a non-resonance postionization technique for sputtered neutrals. Z. Wilk (U. of Pittsburgh) presented some unpublished molecular ion maps of organic dyes obtained with a LAMMA 1000 (TOF) instrument. The spatial distribution of the molecular cation was imaged.

R. Colton (NRL) presented a schematic diagram of a scanned microfocused neutral beam developed by A. Brown and coworkers (U. Manchester). The source was designed to overcome charging problems associated with the analysis of insulators. S. Bryan (No. Carolina U.) described a modified CAMECA 3f ion source that includes a neutralization collision cell.

A. Patkin (Perkin-Elmer) gave a brief retrospective discussion of early work in image processing and analysis in SIMS. He also pointed out the need to use at least 512X512 pixels and to improve the graphic display of images. D. Griffis (No. Carolina State U.) described the digital ion imaging system developed in his lab using a CID digital camera and microcomputer. B. Buttrell (Evans & Assoc.) described the dual microchannel plate detection system and resistive anode encoder (RAE) developed and marketed by their laboratory. The RAE provides an alternative method of digital ion imaging. J. Brenna (Cornell U.) described their video tape system for ion imaging.

Two essential components include a time base corrector and video controller. J. Brenna discussed the video system developed by D. Leta (Exxon) that uses a 512X512X8 video digitizer and a laser disk recorder. D. Newbury (NBS) described the hard copy camera station used on the NBS system.

In the area of applications, K. Busch (Indiana U.) described work on a spatially resolved SIMS technique to analyze chromatograms (TLC, paper, electrophoresis). The use of a phase transition matrix (threitol) to extract the analyte from the chromatogram was also enclosed.

WORKSHOP ON HOW TO MANAGE AN ENVIRONMENTAL LABORATORY

Environmental Interest Group

This workshop was concerned with the technical issues of managing a laboratory that uses mass spectrometry for environmental sample analyses. The workshop was held between 1:00 - 2:15 PM on Tuesday June 10, 1986 and approximately 180 participants were present.

The workshop began with the introduction of the following panelists:

B. F. Dudenbostel	New Jersey Department of Environmental Protection
John Logsdon	Rocky Mountain Analytical
Ron Mitchum	U. S. Environmental Protection Agency
Ron Hass	Triangle Laboratories
Bruce Colby	Pacific Analytical
Fred Hileman	Monsanto Research

Each panelist made a brief introductory statement concerning an important specific technical issue involved in managing an environmental laboratory None of the panelists used the overhead projector. After these statements the workshop was opened to an active give-and-take discussion among the panelists and participants from the audience Many in the audience made statements and expressed opinions. The subjects discussed included quality assurance, day-to-day motivation of analysts doing repetitive analyses, need for software expertise in the laboratory, what to look for in selecting equipment, and many other related subjects. Judging from the participation and the number of persons remaining at the end of the workshop (about 180), the event was a success.

Submitted on June 23, 1986 by. William L Budde
U. S. Environmental Protection Agency
26 W. St Clair St.
Cincinnati, OH 45268

Discussion on Availability of Metal Stable Isotopes

An ad hoc discussion of concerns based on the increasing unavailability of stable isotopes of metals was held following the symposium "Tracers in Mineral Nutrition". Joe Tracy from the isotope separation and productiona facility at Oak Ridge National Laboratory made introductory remarks and answered questions. In summary.

1. The equipment at Oak Ridge, while old is quite capable of producing more than enough stable isotopes to meet the needs for all isotopes for all users of these materials. The facility's diffusion pumping systems are presently being modernized, but the power supplies, sources, magnets, etc. are all completly adequate.

2. The units of operating time for the calutron separators are "tank hours". Although the production facility has a total annual capacity of about 366k tank hours, only 91k tank hours annually are required to maintain 3-5 year inventory supply.

3. Total operating time for FY'86 will be about 48k tank hours and this number is expected to increase only slightly in FY'87 to about 54k tank hours. It is clear that with this trend the isotope supply will continue to diminish. Any level of operation below the 90k level will affect only the date at which inventories will be completly depleted.

4. The annual budget is about $1 million for full production. Funding of the production facility is a combination of appropriations from the Department of Energy and income from isotope sales. The level of the DOE appropriation is determined at least partially by anticipated sales and production expectations. Severe oscillations in funding have occurred when production has been increased to respond to over optimistic predictions of high demand generated by potential users and partially by ORNL.

WHAT TO DO-

1. Write to·

Mr. Joseph A. Setaro, Head Isotopes Section
P O. Box X
Oak Ridge, TN 37831
(615) 574-5903.

Give him you isotope needs, <u>realistic needs!</u>, for the next four years.

2. Ask Mr. Setaro to add your name to the mailing list of the Isotope Users Committee.

Alfred Yergey

Alfred L. Yergey
Discussion Organizer

A Report on:

MULTI COLLECTORS IN THE REAL WORLD

A Workshop Sponsored by the Isotope Ratios Interest Group

This workshop was organized primarily to discuss and review current applications of multicollectors for measuring isotope ratios from hydrogen to uranium. An additional goal was to provide a forum for describing the advances now being made and future directions in the field of multicollectors. Four presentations, two by manufacturers and two by users were made followed by questions and answers and a lively discussion among the 60 attendees.

This workshop is in a sense a followup to a workshop held in 1984 when multicollectors were first being commercialized. At that time there was very little field experience. Now, though the technology is still rapidly evolving, there is a body of practical experience that allows the mass spectrometry community to determine the usefulness of multicollectors.

The first speaker, Patrick Turner of V. G. Instruments described some of the recent advances in instrumentation. In particular, he emphasized the benefits of a mass focal plane that is at a right angle to the ion beam as well as multicollectors that are motorized and computer controlled. He also showed a system where the Daly detector can still be used together with the multicollector. Mr. Turner then presented detailed results showing the improved precision and accuracy of multicollectors applied to isotope analysis of various elements.

Mr. Guenter Wagner of Finnigan-MAT described his company's recent instrumental developments. He emphasized the use of up to nine Faraday Cups together with the simultaneous use of a secondary electron multiplier to measure isotopes with a wide abundance range. Computer controlled detector positioning to 0.001 mm allows change of the element analyzed in a few minutes. He also presented data showing high precision and accuracy for strontium, neodymium, lead and uranium.

Two users, Jim Satkowski from Savannah River Plant and Clint Sulfridge from Oak Ridge National Laboratory described their application of multicollectors in a production type facility. Both use Finnigan-MAT mass spectrometers with fixed collectors in the automatic mode. Their laboratories emphasize sample throughput and use relatively large samples. They run a limited number of elements and do not change elements in the automatic mode. Both appear satisfied that in the real world multicollectors offer a significant and useful improvement over single collectors.

The conclusion of existing users is that multicollectors are desirable not only because they offer increased sensitivity and improved precision, but also because they increase sample throughput and simplify automatic instrument operation. Many laboratories are now looking forward to using multiple detectors with wider dynamic range and increased sensitivity as well as automated detector positioning.

Respectfully submitted:

John D. Stein

QUANTITATIVE ORGANIC ANALYSIS WORKSHOP REPORT

QUANTITATIVE ANALYSIS BY LC/MS

This year's workshop considered the use of combined high performance liquid chromatography/mass spectrometry for quantitative analysis. This topic is of considerable interest in analytical chemistry because of the possibility of avoiding extensive work-up and derivatization procedures that are required for GC/MS. The further possibility of analyzing highly polar molecules that are not amenable to GC also exists. The advent of Thermospray LC/MS has provided a facile means to generate CI-like spectra for complex bioorganic molecules. The molecular ion species are normally relatively intense and this suggests the possibility of devising highly specific assays. The interest in the topic was evidenced by the large audience of 400 people who attended the workshop.

Dr. J. Henion presented some of his experiences in devising technology to allow the coupling of HPLC to the mass spectrometer. Drawing on experience garnered in the field of qualitative analysis he described in detail the problems he had encountered with a variety of techniques. He left the impression that an ideal solution was yet to be found but that his preference was the atmospheric pressure ionization source. He described how this technology was facilitating a number of complex analyses in his laboratory.

Dr. D. Gartiez focussed his remarks on quantitative analysis using the Thermospray technique. He described how Thermospray LC/MS had been used in quantitative analysis and showed how it added to other methodologies that were available. He stated that it was impossible to predict exactly what compounds it would be useful for in the future. He suggested that it was one of the techniques that could potentially be useful for specific applications and should be available to analytical chemists as part of their instrumental capability.

Dr. A. Yergey stressed the potential use of LC/MS for the analysis of highly polar molecules such as acetyl choline. Compounds such as this are not amenable to GC/MS analysis and he suggested that LC/MS provides a powerful method for such molecules that are intractible to other MS techniques. He made the point that Thermospray LC/MS is currently being used in his laboratory for quantification of a number of molecules. He further suggested that as with GC/MS there was a requirement for heavy isotope labelled standards to obtain the desired precision and accuracy of analysis.

Dr. S. Gaskell focussed on the use of data reduction techniques for handling LC/MS chromatograms. He showed that there were techniques available to handle the relatively ragged peaks that are often obtained with LC/MS. He demonstrated the use of a method based on response ratio determinations using a linear regression calculation of signal intensities.

In summary, although LC/MS appears to provide an attractive alternative to GC/MS for quantitative analysis the real applications to date are relatively few. The major applicability for quantitative analysis appears to be for analyte molecules that are intractible to GC/MS analysis. The workshop highlighted the necessity for further development before it can provide a real alternative to GC/MS for quantitative analysis on a routine basis.

Ian Blair

Ian A. Blair
Department of Pharmacology
Vanderbilt University
Nashville, TN 37232

YOUNG MASS SPECTROMETRISTS WORKSHOP

The Young Mass Spectrometrists (YMS) Workshop was attended by approximately 200 conference participants. The workshop was opened with a brief introduction and overview by Joe Campana. It was emphasized that a YMS was a mass spectrometrist in the early stages of their career and that age was inconsequential in this definition.

Gary Glish introduced the first segment of the workshop where mass spectrometrists from academia and industry addressed issues of interest to YMS. The first speaker, Professor Gerry Meisels discussed, from an administrative point of view, topics important to those considering or early in an academic career. This included: advantages of postdoctoral work; how to write a letter of application; the interview, start-up funding; and tenure considerations. He emphasized that the job of an Assistant Professor at a major university is a three-legged stool -- Teaching, Research and Service. He made the point that all universities are teaching institutions and therefore, teaching is a high priority. As far as tenure is considered, he believe that the quality of research publications was more important than the quantity. Also, outside support, especially demonstrated by grant renewal, is important in the tenure decision.

The second speaker, Professor Kelsey Cook addressed the same issues as Professor Meisels except from the view point of a person who is early in his academic career. First, he reemphasized the importance of excelling in teaching. He then pointed out that an advantage of academia is self-directed research and independence. He discussed how to succeed and most importantly, how to get tenure. He addressed the importance of new ideas and creativity in research, the significance of the research, research results, communication, international recognition, quality of teaching publications and research proposals. In the discussion of quality versus quantity, with respect to publications, it was stressed that while quality was most important, there are some tenure committee members who count publications. Finally, the importance of persistence and determination to succeed in any career was discussed. There is no substitute for these two qualities and 60-70 hours of work per week.

Dr. Don Zakett was the next speaker and he discussed some areas of interest to people in or going into the industrial laboratory. He felt that during an interview, that the interviewee should let the interviewer do as much of the talking as possible. However, it was pointed out that the interviewee must make sure that his/her capabilities and qualifications for the job are recognized. It was also pointed out that the interviewee should be, in a sense, interviewing the prospective employer to make sure it is a place where the interviewee would enjoy working. Another topic that was discussed was the ability to do independent research. Fred McLafferty pointed out that there should be no time problem in doing personal independent research in off-hours if one is willing to work the 60-70 hours per week that Prof. Cook mentioned. This led into a discussion of publishing research results. It was generally agreed that this was something that varied from company to company. Dr. Zakett offered some advice on how to facilitate being able to publish research results. As one example he said he always runs two sets of compounds, one of interest to the company and one not of interest so that he can publish the results on the latter set with out any worry of proprietary information being involved.

After this portion of the workshop, a little time was spent discussing whether a YMS interest group should be formed in ASMS. Mark Ross presented some possible objectives of such a group. The most

important of these objectives are: to improve communication between individual YMS and between YMS and ASMS; to provide YMS with information on career planning and professional development; and to increase the level of activity of YMS in ASMS. There was some discussion of this and of possible future YMS workshops. Some suggestions for future workshops included presentations on careers in government, with instrument manufacturers and discussing in more detail industrial careers.

A questionnaire was distributed that solicited opinions on whether or not a YMS interest group should be formed and, if so, what purposes should the group serve. The results of the questionnaire were as follows. Support for forming a YMS interest group was overwhelming, 101 for, 2 against. The reasons for forming such a group received support as follows: I want to get to know my peer group - 80; I want to become active in the ASMS - 59; would help my career - 57; other - 6. Possible objectives of a YMS interest group received the following support: Increase the participation and activity of YMS in the ASMS - 77; enhance professional development within the ASMS - 71; educate YMS with regard to career opportunities - 65; advise the ASMS Board on topics/programs of interest to YMS - 48.

Submitted by:

Joe Campana, Mark Ross & Gary Glish

Report of Biomedical Applications
Interest Group

A major discussion topic involved the consideration of means by which ASMS members could become more familiar with fundamentals, nomenclature, and the basic tools and techniques used in molecular biology. The majority of attendees supported the suggestion that a series of lectures, or a poster-type session, or an extended workshop, be presented in Denver to address this need. The presentations, if given orally, should be made by an individual who not only understands the subject, but is also able to communicate with the audience. Several candidates were suggested. These presentations would be tutorial in nature, not advanced research seminars by these individuals.

Several symposium topics were suggested which encompassed well-defined area of biomedical applications, ie, toxicology, clinical, enzymic techniques, nucleic acids, carbohydrates, proteins, etc. An important part of this symposium would involve a discussion the approaches and details of the techniques used. At least two main speakers should be from outside ASMS. One way to interest other scientists in the annual meeting is to have them as major symposium speakers. Although this was attempted in Cincinnati, the ASMS meeting, unfortunately, coincided with major biochemistry and molecular biology meetings.

With respect to the meeting in Cincinnati, the interest group felt overall that it went quite well. However, some problems were identified. Generally, the quality of the slides, especially when shown in a very large auditorium were poor; they were very difficult to read except by those in the first few rows. The projection system was not good on the whole - screens were too small, images not enlarged when possible, speakers continually asked for focusing, etc. A suggestion was made to use giant screen TV monitors in the larger lecture halls, or a duplicate slide screen on the side half way back in the hall.

The poster sessions were excellent and should be further supported. Posters should not be scheduled concurrently with symposia on the same topic. Larger rooms should be used to avoid crowding, more poster sessions added, especially in evenings, and posters should be allowed to stay up longer.

Other general comments included providing low cost lunches (eg, such as at the San Diego meeting), and reactivation of the nomenclature committee with placement of accepted nomenclature in the proceedings. The lack of a Friday lunch break was generally acceptable. Overall, members thought the intensity of the meeting was too great. Ways should be found to decrease this, ie, more poster sessions and less oral presentations.

Submitted by
Richard Caprioli
Chairman

ASMS Education Committee Report

ASMS, once again, sponsored a series of short courses on the weekend preceding the Annual Conference. As in prior years, course evaluations received from the students indicated that the courses were very successful with most students achieving their goals. This year's short courses and organizers were as follows:

Interpretation of Mass Spectra - James Kelley
Quantitative Mass Spectrometry - Alfred Yergey
Ion Optics - Wade Fite
Fourier Transform Mass Spectrometry - Robert McIver, Jr.

To better understand the needs of ASMS membership in education as well as to explore the continuing role ASMS should play in educating non-specialists on the problems which mass spectrometry can solve, a workshop was held on "ASMS as an Educator." Discussion was lively and will help steer the course for future educational activities of the Society. A summary of the workshop, addressing each of the major subjects covered, follows:

Itinerant Short Courses

The topic of presenting short courses to Local Discussion Groups has often been raised by the Discussion Group Leaders. Several options were discussed: contracting with a professional educational group, using Local Discussion Group members, asking members of the ASMS Education Committee to conduct a course, or using Local Discussion Group members to conduct the course put on by the ASMS Education Committee. The majority of the discussion focussed on the last option. It was decided to explore interest of Local Discussion Group leaders in being trained to put on the current ASMS Interpretation and Quantitation introductory courses. If response is positive, a workshop will be arranged for next year's Annual Conference to train representatives.

Introductory Lectures

Much of the discussion on the advisability and desirability of introductory lectures in the ASMS Annual Conference program revolved around the topic of "introductory" vs. "review of field" lectures. Interest was expressed in both areas. It was suggested that ASMS interest group coordinators be involved in selection of potential speakers for introductory or review-type lectures. It was recommended that truly introductory lectures be scheduled in parallel to other sessions and not as plenary lectures.

Educational Symposia

It was suggested that a symposium be held on a regular basis (though not necessarily each year), with one speaker from each interest group charged with presenting a lecture on-current state-of-the-art research in that technical area. The lectures should be at a level appropriate to the educated mass spectrometrist, but nonspecialist in the particular field. There was broad interest in arranging such a symposium and it will be proposed for next year's conference.

Advanced Topic Short Courses

The attendees at the workshop agreed that advanced topic short courses were of interest to the membership of the Society. There were several recommendations for possible topics, as well as recommendations and volunteers for coordinating these courses. Possible topics and coordinators are: FTMS and Ion Optics (both courses currently offered), SFC/MS, Practical CI (Burnaby Munson as Coordinator), FAB (as a short course or evening workshop), MS/MS (Graham Cooks as Coordinator), and Electronics (Chris Enke as Coordinator).

It was recommended that next year's course offerings brochure be more detailed with a more comprehensive description of each course.

Mass Spectrometry Introductory Brochure

It was agreed that an introductory brochure on mass spectrometry containing the benefits the technique can offer for solving problems in other disciplines would be a worthwhile Education Committee activity. Research physicians, in particular, were recommended as one target audience. Volunteers to work on such a brochure included Rich Kondrat, Al Yergey and Harry Hertz. It was also recommended that ASMS explore the feasibility of preparing a video tape introduction to mass spectrometry for the same audiences as above. Finally, it was suggested that ASMS look into the preparation of video tapes on the operation of mass spectrometers for use in locations such as multi-user mass spectrometry service laboratories.

General Discussion

Several other suggestions dealing with educational activities were made. ASMS should seek invitations to lecture at meetings of other professional societies. This is yet another mechanism to make non-practitioners aware of the benefits mass spectrometry offers.

It was recommended that ASMS short courses emphasize a team approach to problem solution. This is frequently a very successful mechanism for students to help each other learn and thereby gain a better grasp of the material themselves.

The "ASMS as an Educator" workshop triggered ongoing discussion throughout the conference week. Additional suggestions for future activities included an introductory symposium on pharmacokinetics, a short course on lasers in mass spectrometry, and workshops on teaching mass spectrometry to undergraduate/graduate students, and teaching mass spectrometer operation in the multi-user academic or industrial laboratory.

The Education Committee appreciates the many fine suggestions made this year, looks forward to continuing input in the future and plans to implement many of these suggestions to serve the ASMS membership and scientific community.

Respectfully submitted,

Harry S. Hertz

ENVIRONMENTAL INTEREST GROUP REPORT, 1986

1986 Meeting

The Environmental Interest Group sponsored one symposium and one workshop. The symposium was titled "Environmental Applications of Mass Spectrometry." It featured the following talks:

The role of the MS in Indoor Air Quality Analysis
Bayer, C.W. and Black, M.S.
Georgia Institute of Technology

Applications of LC/MS/MS to the Determination of Azo Dyes in Environmental Samples
Henion, J. and Bruins, A.
Cornell University

Impact of Niagara Falls Dumpsites on Lake Ontario
Hites, R.A. and Jaffe, R.
Indiana University

Bioavailability Studies of High Log Kow Chemicals by Gas and Liquid Chromatography-Mass Spectrometry
Kuehl, D.W., Butterworth, B.C. and Burkhard, L.
US EPA

Tracing Groundwater Contamination with a Static Collection Device and MS
Voorhees, D.J., Malley, M.J., Hickey, J.C., Klusman, R.W. and Bath, W.W.
Colorado School of Mines

The sumposium was attended by up to 250 people. The environmental workshop was titled "How to Manage an Environmental Laboratory," and it was organized by Bill Budde whose report on this workshop is included in this volume.

1987 Meeting

Suggestions for symposia for next year's meeting included:

-Supercritical fluid chromatography and its applications

-Human dosimetry

-Risk assessment and MS

-The interaction of MS and toxicology

-High through-put MS techniques

There was a general concern that future symposia focus on the problem and the science not just on the mass spectrometry.

Submitted by:
Ronald A. Hites
Indiana University

GOOD LABORATORY PRACTICES INTEREST GROUP REPORT

A symposium on Science and the Law was sponsored which featured three lawyers and a judge. The talks were on "Science and Law: Marriagable or Irreconcilable Differences", "Preparing a Scientist to Testify", "The Generation of Legally Defensible Data", and "The Expert Witness in the Courtroom". The symposium was well received based on the number of favorable comments.

The interest group meeting was well attended, and discussion centered around suggestions for next year's annual conference program.

SUGGESTIONS FOR PLENARY LECTURES

1. A government agency (eg EPA) laboratory auditor or examiner, or the manager of an auditing group on criteria for acceptable performance.
2. A 'Devil's Advocate' on how to choose the best analytical scheme for the determination of target compounds.

SUGGESTIONS FOR WORKSHOPS OR SYMPOSIA

1. GLP standards for government, university, industry, pharmaceutical, data systems, DEA, etc. Perhaps this could be joint with Environmental or Quantitative interest groups.
2. Computer notebook. Have computer people as well as ASMS address us.
3. Education and GLP are we well prepared?
4. Decision making based on MS data. What is done with it? How should it be reported in the literature? Perhaps joint with Quantitative interest group.

A suggestion was made as to how ASMS can be of help to the interest group. A poll of the members to determine the impact of GLP on their operation with questions to find out how many have been audited and whether there are specific GLP guidelines. This could be implemented through Spectaker or piggybacked on a ballot as well as at the annual meeting.

Concerning drawing-in participation from other disciplines, it was suggested that people who belong to other organizations can work to bring awareness of MS to that group. Also it was suggested that a notice of the annual meeting should appear in general interest journals such as C&E News or Science. Another suggestion was to provide instrument manufacturers with ASMS brochures to be included with new spectrometers.

Finally it was suggested that it would be appropriate to form a Pharma Interest Group based on the number of papers presented at the annual meeting.

Lewis A. Shadoff, Coordinator

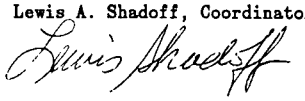

REPORT ON THE HISTORY INTEREST GROUP MEETING

The history interest group meeting was held on Monday afternoon, June 9, 1986. Approximately 30-40 people attended part or all of the meeting. The meeting began with a report on the progress in identifying and cataloging historical artifacts that was initiated as a result of the interest group meeting held last year. Announcements of this effort were published in Int. J. Mass Spectrom. Ion Processes, Org. Mass Spectrom., Biomed. Mass Spectrom., C&E News, Anal. Chem., CHOC News, and The Spectaker. Thus far the response has been very limited. Therefore an extended discussion took place on how to best proceed to find out where historical mass spectrometry artifacts are located. It was decided that we should request that the ASMS board of directors allow another historical exhibit like the one held during the San Antonio meeting. A lot of positive feedback was generated from that exhibit and it is hoped that interest generated by another such exhibit would get people more directly involved in identifying historical artifacts.

Discussion proceeded as to what the longer range goals of the interest group should be. Suggestions included: establishment of a photographic catalog with narrative describing the items; a small display of smaller hardware that could be exhibited at every third or fourth annual meeting; and a large permanent exhibit at an appropriate museum or similar facility. While all these were deemed as good ideas, the general consensus was that we needed to walk before we run and that the smaller scale goals were more appropriate at this time. It was also suggested that we should try to get our European counterparts involved in our efforts.

The next topic discussed was that of retrospective lectures. Several names and topics were proposed as possibilities. The proposal that received the most support was to invite Professor Baldeschwieler to give a plenary/retrospective lecture concerning the development of ICR. This proposal has been forwarded on to the ASMS board with a request that there be an annual retrospective lecture and that these lectures be videotaped and kept with those of the San Antonio meeting. It was noted that these videotapes are available on a loan basis to ASMS members.

Two possible topics for workshops for the meeting next year were then discussed. The first suggestion was that we should have another workshop dealing with the history of some of the instrument companies in sort of a continuation of the workshop held in San Antonio. Another suggestion was for a workshop where academicians from different generations would describe the expectation of graduate students and how these have changed through the years.

The meeting ended with a brief discussion about what ASMS can do to better support the interest group and what the interest group can do to help build bridges to other groups outside of ASMS. In the first area it was felt that provision for an annual retrospective lecture (videotaped) was one immediate thing that could be done and that future financial support for the development of a historical display would also greatly help the interest group meet its goals. For the second area, it was felt that this interest group could interact with other groups and organizations interested in the history of science. This would help to ensure that mass spectrometry history is represented in larger scale history projects involving science in general.

At this point our meeting time had run out and we adjourned.

Submitted by:

Gary L. Glish, Coordinator

ION PHYSICS AND INSTRUMENTATION INTEREST GROUP MEETING

The Interest Group Meeting commenced following the symposium, "Advances in Time-of-Flight Mass Spectrometry", sponsored by the interest group; and it was attended by over 50 members. The Interest Group sponsored two symposia this year, the one given above and one on Hybrid MS/MS; both were well attended and received by the Conference participants.

The group addressed two questions at the meeting, the first, "What can the Interest Group do for ASMS?" and the second was "What can ASMS and the Conference do for the Interest Group?" The responses to these two questions primarily reflected an emphasis on the ASMS programs. There also was some discussion related to attracting new members from related disciplines and there was mention of services that the Interest Group could provide to ASMS members.

The participants provided a number of excellent topics for future programs: FTMS, particle detectors, ion storage techniques, particle physics, abandoned (or resurrected) techniques, atmospheric ion/molecule reactions, lasers and mass spectrometry, atmospheric pressure ionization, mechanisms in fast-atom bombardment, mechanisms in thermospray, and beam techniques in mass spectrometry. There was extended discussion among the participants on lasers and molecular beams in mass spectrometry. From the discussion, the interest, and the enthusiasm of the group, a coherent mini-program evolved, which centered around a theme on lasers and mass spectrometry.

The group generally agreed that the 1987 program contain the following elements:

1. A short course (weekend prior to the meeting) on fundamentals of lasers.

2. An Introductory Lecture on Laser Spectroscopy with an emphasis on ion spectroscopy.

3. A symposium on ion spectroscopy with the opening lecture devoted to an introduction to the use of molecular beams with mass spectrometers.

4. A workshop on the do's and don'ts of molecular beams in mass spectrometry.

5. A contributed session on lasers and mass spectrometry.

This program will offer an extraordinary opportunity to educate the ASMS membership on laser and ion spectroscopy and molecular beams. Furthermore, it could (if publicized) draw into ASMS many spectroscopists who depend on mass spectrometry in their discipline but who do not associate themselves with the mass spectrometry community.

The other symposia topics that were supported enthusiastically are "Ion Storage Techniques" and "Fourier Transform Mass Spectrometry". A plenary lecture covering the Abandoned Techniques or Resurrected Techniques now in vogue also had much interest. An introductory lecture on particle physics especially one that would exemplify the importance of mass spectrometric measurements in that field is also supported by the Interest Group; such a lecture could be followed by a symposium on that topic. In addition, the Interest Group supports, through co-sponsorship, a symposium on "Sputtered Neutral Mass Spectrometry" as recommended by the Solids and Surfaces Interest Group.

The group encourages the Board to continue offering an Ion Optics short course. Short courses on surface science and on MO calculations were also recommended. Another alternative to the later suggestions is Introductory Lectures on the two subjects.

The Group called out a need for and encourages the ASMS board to allocate a sufficient budget for travel, honorariums, and registration fees for plenary, introductory and symposium speakers. This is a necessity that will help organizers (who are not ASMS board members) attract the best speakers from related and outside disciplines, and it will demonstrate the professional attitude of the society. In this regard, it is recommended that the society prepare a general letter for symposium organizers in order to formalize a policy on honorariums, registration, etc.

The board should support strengthening the stature, awareness, and recognition of each interest group within the society. This could be accomplished by involving the interest group (represented by the coordinator) in other programs and activities related to the group interests and by clearly associating the Interest groups with such programs and activities.

It was suggested that the Interest Group could serve as a source on the location of computer programs on ion and particle optics. Anyone who has access to such programs or knows of such programs should send information to the Interest Group Coordinator. In the future this information could be incorporated into a ASMS Electronic Bulletin Board.

Respectfully submitted,

Joseph E. Campana

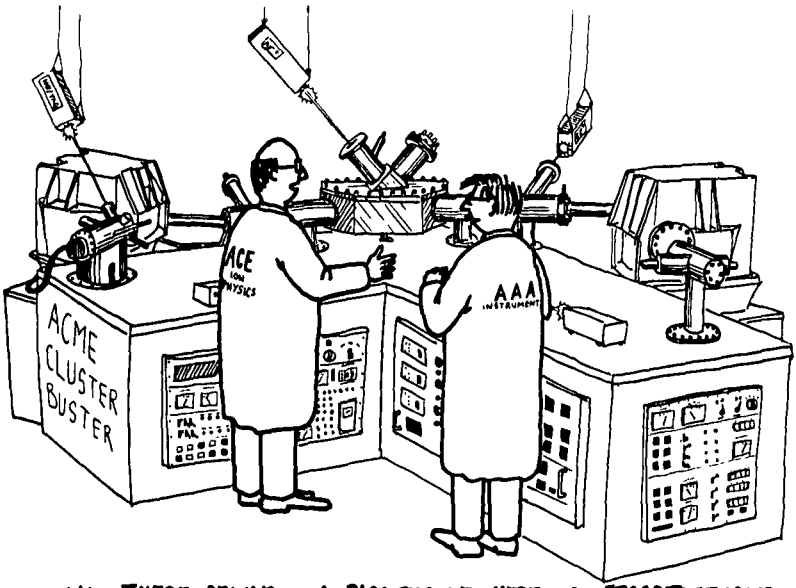

ALL THESE DELAYS— A PICOSECOND HERE, A FEMPTOSECOND THERE — WE'LL HAVE TO GET THE DARN THING FIXED!

ISOTOPE RATIO INTEREST GROUP REPORT

This year's interest group meeting followed a workshop on "Multi-collectors in the Real World," convening at 9 PM on Tuesday, June 10. It was attended by about fifty people.

The highlight of this year's meeting was a symposium on application of isotope ratio mass spectrometry to nutrition studies. It was organized by David L. Smith and represented a relatively new area, one in which few papers had been presented at previous meetings.

Two workshops affiliated with this group were held: the one mentioned above on multi-collectors organized by John Stein, and one on stable isotopes organized by Al Yergey. Each served its function admirably, adding considerably to the value of the conference.

The Group felt that ASMS was reasonably responsive to the needs of what is by now only a small fraction of the total membership of the Society. Attracting attendees from areas under-represented at previous conferences presents problems that need to be addressed on a broad front. As an example, last year I arranged to have a symposium on geological applications of isotope ratios; this year, without the spur of a dedicated symposium, no geological papers were presented. One possible explanation is that geologists look on mass spectrometers as black boxes and have only tepid interest in the raison d'etre of our Society. There are, in addition, numerous conferences dedicated to geological concerns and limited budgets and time for the people concerned. I assume that a similar situation exists in numerous other areas. Thus, in addition to attracting people from such disciplines to one meeting, we need to consider how to attract them on a regular basis to future meetings without the stimulus of a dedicated symposium. This year, as I mentioned, a symposium on nutritional applications was held. This brought several respected investigators to our meeting; I hope that other aspects of our conference were valuable enough to them to stimulate their participation at future ASMS conferences.

David H. Smith
Isotope Ratio Interest
Group Chairman

QUALITATIVE ORGANIC STUDIES COMMITTEE MEETING

Approximately twenty people attended the meeting on June 9, 1986. There was a lively one-hour discussion of possible lectures, symposia, and workshops covering a surprisingly broad range of interests. There was near unanimity on the importance of ionization methods for larger molecules, with special attention on mechanisms, applications to a variety of biomolecules and polymers, and a "how-to-do-it" workshop to emphasize experimental details and collection of reference spectra. More reports on pyrolysis/MS for even larger molecules were requested. Interest also was expressed in derivation of stereochemical information and the structural utility of negative ions.

Suggested topics outside the field of mass spectrometry included Insect Chemical Communication, 2-D NMR, and Research Funding from Federal Agencies.

Respectfully submitted,

F. W. McLafferty

Acting Chairman,
replacing J. L. Holmes

BUSINESS MEETING OF THE AMERICAN SOCIETY FOR MASS SPECTROMETRY

Hyatt Regency Hotel
Cincinnati, Ohio
June 11, 1986

The meeting was called to order at 10:59 a.m. by President Cooks. He welcomed the officers of foreign mass spectrometry societies. Henry M. Fales was appointed as parliamentarian for the meeting.

Robert McIver presented the Secretary's report. The minutes of last year's Business Meeting are contained in the Proceeding's of the 33rd Annual Conference. It was moved, seconded and approved by those in attendance that the minutes of the meeting be accepted as printed. The Secretary then announced the results of the 1986 ASMS elections. The next Vice President for Programs is Ronald A. Hites, the Treasurer is Kelsey D. Cook, and Christie G. Enke is the new Member-at-Large with responsibility for educational affairs. The other candidates - Fred E. Saalfeld, Paul C. Goodley, and Rodger L. Foltz - were acknowledged and applauded by the members.

The winners of the ASMS Conference Travel Awards for 1986 were announced by McIver. They were Mildred Coates, Gerald DiDonato, Rong Feng, John C. Hill, Fong F. Hsu, Nancy J. Jensen, Jodie V. Johnson, Richard C. Peffer, Eric J. Reiner, Joseph T. Snodgrass, Roger Tembreull, and Todd D. Williams. The total amount for travel awards was $4865.

The Secretary then reviewed several revisions to the ASMS Bylaws made last year by the Board of Directors. A major change was in section 4 concerning the committee structure of the Society. There are now two standing committees, the Nominating Committee and the Education Committee, and the committee members are appointed by the President. The Society shall also have Interest Groups which are responsible for advising the Board of Directors and especially the Vice President for Programs on particular subject areas and serve as a resource in the development of the program for the Annual Conference. The President appoints Interest Group coordinators who chair meetings of participants at the Annual Conference.

McIver concluded his report by stating that it was his sad duty to inform the membership of the Society of the passing away of Deborah Slowikowski.

Treasurer James DeCorpo began his report by stating that ASMS membership now stands at 2042, a growth of 5.4% over last year. The Annual Conference in San Diego last year came out ahead by $1800. The assets of the Society as of 12/31/85 were $201,866 compared with $154,616 a year earlier. DeCorpo commented that these reserves were needed to maintain the Society's credit rating because our annual cash flow is approximately $200,000. It was moved, seconded and approved by the membership that the Treasurer's financial report be accepted.

Gerry Meisels, Vice President for Programs, acknowledged the work of this year's Program Review group (R. Caprioli, R. Hites, R. Minard, L. Shadoff, M. Gross, G. Meisels, R. Cooks, and P. Eisenberg). More than 500 abstracts were reviewed and grouped into sessions. He described the objectives of the review process and the criteria for selection. Meisels announced that the topic for the ASMS Fall Workshop is Time-of-Flight Mass Spectrometry. A one-day meeting with oral presentations and posters will be held on November 10, 1986, in Washington, D.C. He concluded his remarks by acknowledging the outstanding contributions of Judith Watson to the general administration of the Society and to planning the Annual Conference, the Short Courses, and the Fall Workshop.

The Vice President for Arrangements, Catherine Costello, explained that delays in the construction of the Cincinnati Convention Center forced the Board to change the site and date of this year's Annual Conference. We were indeed lucky that the excellent facilities at the Hyatt were available. Concerning future meeting sites, the 1987 Annual Conference will be held in Denver, May 24-29, at the Marriott Hotel. The San Francisco meeting in 1988 will be June 5-10 at the Hilton Hotel. And the Royal York Hotel in Toronto will be the site in 1989 from May 21-26.

Member-at-Large Charles McEwen asked that the extended abstracts be turned in as early as possible so the bound volume can be prepared.

Gordon Wood, Member-at-Large, reported the enrollment figures for this year's Short Courses: Interpretation of Mass Spectra (19), Quantitative Mass Spectrometry (19), Ion Optics (36), and Fourier Transform Mass Spectrometry (24).

In the President's Report, Graham Cooks recognized the contributions of Terry Ashe, who has returned to the Board as the E-14 representative. President Cooks then addressed the membership on matters of importance to the health and growth of the Society. The text of the address will appear in the bound volume.

President Cooks then announced that two ASMS Research Awards would be presented this year. W. Alan Wolstenholme came forward to present the VG Instruments Research Award to Joseph J. Grabowski, Assistant Professor of Chemistry at Harvard University. Robert E. Finnigan then came forward to present the Finnigan MAT Research Award to Gregory I. Gellene, Assistant Professor of Chemistry at the University of Notre Dame. Each of the awardees received $25,000 to support their research.

Consideration of the proposed amendment to Article IV of the ASMS constitution was begun by Robert McIver. In April the text of the proposed amendment was mailed to all members. McIver showed a slide that compared the old and new versions of Article IV. Graham Cooks turned the chair over to Catherine Costello, and it was moved by Cooks and seconded that the proposed amendment be submitted to the membership. Cooks then described the historical relationship between ASMS and committee E-14 of ASTM and the inequities he perceived with the present Board structure. Cooks closed by urging the members to accept the proposed amendment. Catherine Costello opened the floor for discussion and recognized Thomas Aczel. Dr. Aczel thanked Graham Cooks for his fair statement and then proposed an amendment to the amendment which stated that the Board of Directors would consist of the Officers and "three elected members-at-large, the immediate Past-President, and the Chairman of ASTM Committee E-14 on Mass Spectrometry." The Parliamentarian ruled that this proposed amendment was not appropriate. The Chair recognized Fred McLafferty who spoke in support of the proposed amendment and emphasized that a group which represents only a small percentage of ASMS membership should not have a special seat on the Board. Wade Fite asked what the responsibilities of the third member-at-large would be, and Graham Cooks said that it was the intent of the Board that this member have responsibility for measurements and standards. Terry Ashe commented that the issue of E-14 representation on the Board has been discussed for the last four years and he felt it needed to be resolved. After further discussion, the question was moved, seconded, and by voice vote the membership approved the wording of the proposed amendment. A letter ballot on the proposed amendment will be prepared by the Secretary.

In Other Business, John M. McCrea moved that "The members of ASMS assembled in the meeting recommended to the Board of Directors that stipulation of ASMS membership be removed from the list of qualifications for any research awards sponsored or administered by the Society." The motion was seconded by Fred McLafferty and passed by a show of hands. James J. Stoffels of the Pacific Northwest Laboratory read a statement that described the difficulties he encounted in getting clearance for his paper on isotope dilution analysis of iodine-129. Thomas Aczel moved that ASMS write a letter to express concern about this situation and ask why clearance was not granted. After discussion the motion was withdrawn.

Graham Cooks called Bill Budde to the podium and presented him with a plaque that recognized his many contributions to the arrangements for the Annual Conference in Cincinnati. Finally, President Cooks expressed his appreciation to retiring Board members Gordon Wood, James DeCorpo, Ed Emery and Catherine Fenselau for their work on behalf of ASMS. The meeting was adjourned at 12:38 p.m.

Respectfully submitted,

Robert T. McIver, Jr.
Secretary

MINUTES OF THE 1986 MEETING OF ASTM COMMITTEE E-14 ON MASS SPECTROMETRY

Tuesday, June 10, 1986
1:00 pm
Hyatt Regency Hotel
Cincinnati, Ohio

The meeting was opened by Terry Ashe, Chairman, who announced the other new E-14 officers: Ron Grigsby, Vice-Chairman, and Steve Reynolds, Secretary. He then introduced Hans Greene, the ASTM Staff Manager, who gave his staff report. The main points were: Standard E 304-81 is overdue for review and Standards E 137-82 and E 899-82 are due for review by the end of 1986. As of January, 1986, there were 50 members of E-14.

Thomas Aczel then gave a brief report on the D-2 Committee meeting. A proposal for molecular weight calibration from Ron Grigsby was accepted, some typos were found in Method 2786, Terry Ashe reported on the evaluation of replacements for the CEC-103's, and publication of Thomas Aczel's book on characterization of shale oil was announced.

Maynard Hamming has resigned as Chairman of Subcommittee E-14.04, and anyone interested in succeeding him should contact Hans Greene.

Phil Price gave a report on the activities in E-14.10 on Definitions and Terms. They have compiled a list of about 500 mass spec definitions and are working on converting them to ASTM format. Other organizations have published some terms; Hans Greene said we might use them if they are not copyrighted and we have an agreement with the publishers.

Terry Ashe called for volunteers for Chairman of Subcommittee E-14.15 on New Instrumentation and Techniques. Anyone interested should contact Hans Greene.

Dave Parees gave a report on the activities of Subcommittee E-14.13 on GC/MS. Work has proceeded on the standard for evaluation of new GC/MS instruments, but he needs some help from people with expertise in the following areas: statistical analysis, detection limits, and S/N ratios. Dave asked anyone who had not received a copy of the report and wanted one to indicate this on the attendance list.

At this point, Hans Greene mentioned that only members of the committee are on the committee permanent mailing list and non-members who attend the business meeting will be on the list for that year only.

Terry Ashe discussed our status within ASMS. We need to become more involved with ASMS interest groups, with the CAG, and with the Good Lab Practices Committee. One of our primary functions is to promote knowledge of mass spectrometry.

Terry Ashe called for a discussion of old business, there was none; then new business. Thomas Aczel asked people to contact him if they wished to join a CEC-103 users group. Tom also suggested we might sponsor a course on MS and offered to conduct it. Terry Ashe pointed out that this should be coordinated with ASMS so as not to interfere with or overlap their efforts. Dave and Phil both requested again that anyone who would like to work with them on their respective committees should contact them.

Terry Ashe announced the locations of the next three ASMS meetings: Denver in '87, San Francisco in '88, and Toronto in '89.

Terry Ashe discussed the proposed amendment to Article 4 of the ASMS constitution, removing the ASTM E-14 chairman from the ASMS board. The general consensus of attendees was that this was a bad idea. Terry urged all members to attend the ASMS business meeting and vote against it. If the amendment goes to a ballot, we should encourage our fellow members to vote against it. Tom Aczel volunteered to write a letter to be distributed to ASMS members explaining our position.

Terry Ashe discussed briefly the possibility of merging E-14 with either E-13 or E-19. There was no interest indicated in this by attendees.

The meeting was adjourned at 2:02 pm.

Respectfully Submitted,

STEPHEN D. REYNOLDS
Secretary

LIST OF ATTENDEES

Name	Affiliation	Phone #
Adam Schubert	ARCO	213-548-8000
Rod Page	ARCO	213-548-8000
Chuck Polley	ARCO Chemical	215-359-2440
C. Sam Hsu	ER&E	201-730-2228
James C. Tou	Dow Chemical	517-636-2551
Ben M. Evans	Conoco Inc.	405-767-4736
Ron Grigsby	NIPER	918-337-4376
S. Y. Tang	NIPER	918-337-4484
Lawson E. Sherman	Texaco	914-831-3400
Michael Pastel	American Cyanamid	914-735-5000
Carol Chow (for M. Marcus)	Chemical Waste Management	312-841-8360
Archie M. LeGrand	Westinghouse NFD	803-776-2610
Michael J. Dekrey	Conoco Inc.	405-767-2945
James L. Little	Tennessee Eastman Co.	615-229-5651
Steve Berger	Hewlett-packard	415-857-7890
A. G. Sharkey	University of Pittsburgh	412-624-7990
David M. Parees	Air Products & Chem. Inc.	215-481-5794
Gilbert G. Jones	Amoco Research	312-420-5773
Daniel W. Phelps	Amoco Production Co.	918-660-3129
Timothy J. Carlin	Mobil R&D Corp.	609-423-1040
Nancy E. H. Wright	Sun Refining & Marketing Co.	215-447-1814
Thomas Aczel	ER&E	713-425-5131
David P. Wesley (for Donald Woods)	Ashland Petroleum Co.	606-329-3333
Phil Price	Union Carbide	304-747-5594
Paul Shearer	Hennler Inc.	302-995-3258

REPORT OF ASTM COMMITTEE D-2, RES. DIV., IV SECTION M ON MASS SPECTROMETRY

The annual meeting of the Section was held on Monday, June 9, 1986, at the Hyatt Regency Hotel in Cincinnati, Ohio. The meeting was attended by 21 members and was chaired by Thomas Aczel of Exxon Research and Engineering Company.

The agenda of the meeting is given below:

- Introduction — Thomas Aczel
- Task force report on recalibration of ASTM methods — Ron Grigsby
- Correction of typographical errors in ASTM D-2786 — Thomas Aczel
- Report on the performance of a Hewlett-Packard MSD Instrument — Terry Ashe
- New business — All

A summary of the above reports and related discussions is given below.

Introduction The chairman welcomed all attendees and invited them to participate both in the meeting and in the cooperative efforts sponsored by the Section. He emphasized that participation in the Section's activities is open to all interested parties and does not require membership in ASTM.

Proposal on Recalibration of ASTM Methods Ron Grigsby summarized the background and status of this effort. ASTM methods dealing with mass spectrometry were developed using Consolidated Electrodynamics Co. Model 21-103 and 21-104 instruments manufactured in the 1950s and early 1960s. These instruments are now increasingly difficult to maintain; hence, a need to transfer the methodology to a newer generation of low resolution, quantitative mass spectrometers. At the same time, there is also a need to reexamine the accuracy of these highly precise methods as deviations between data obtained on the old and newer instruments could be very well due to increased accuracy of the newer instruments.

A detailed proposal to implement this effort was presented by Ron Grigsby (copies are available either from him or the Chairman). The magnitude of the effort required for implementation, including collection of pure compounds, separation of petroleum fractions of interest, analysis, and data evaluation, is, however, beyond the capabilities of voluntary efforts. It is believed that execution of the project could be best carried out by assigning the bulk of the effort to a non-profit institution with financing to be sought from government and industrial sources, such as API, ASTM, NSF, The Petroleum Research Foundation, individual oil companies (Amoco and Conoco already expressed willingness to contribute $5,000 each), etc. Total needs are $60,000 for the first year; responsibility of the effort is to be assigned to NIPER, Bartlesville, OK, (Ron Grigsby is willing to carry it out).

All members were explicitly comfortable with this arrangement. The Chairman will try to obtain the necessary funds at the earliest possible date.

R. Grigsby also offered to the group computer programs that execute the calculations required by ASTM D-2786, 2789, and 3239. These will be given free of charge to interested parties who request them (hard copy or disk if a blank is sent to Ron; direct arrangements with him are advised).

Correction of Typographical Errors in ASTM D-2786 Three typographical errors in the inverses published were pointed out by Thomas Aczel. They are the following:

- n-C_{21} inverse: The term in column 7, row 7, is +0.4123, not -0.4123.
- i-C_{23} inverse: The term in column 1, row 7, is -0.0019, not -0.0190.
- n-C_{27} inverse: The term in column 1, row 2, is -0.1219, not -0.2119.

A complete set of corrected inverses for D-2786 is also available from Dick Teeter of Chevron. These contain additional corrections as well as a set of graphs that illustrate continuities/discontinuities in the inverses.

Performance of the Hewlett-Packard MSD Instrument Terry Ashe reported on this item. His experience at Sarnia with the above instrument was quite satisfactory, both in high and low voltage applications. Other instruments might perform just as well; we solicit data on any that are in actual use.

New Business Formation of a CEC 103 Users Group is being considered. Interested parties should contact Thomas Aczel at Exxon Research, P. O. Box 4255, Baytown, TX 77522, Phone: (713)425-5131.

Miscellaneous Questions and/or comments on overall D-2, Res. Div. IV, Section M activities should be directed to Thomas Aczel at the above address.

Respectfully Submitted,

Thomas Aczel, esq.

THOMAS ACZEL
Chairman

On the evening of June 11, 1986 an event pitting the cunning and strength of the Younger Mass Spectrometrists (YMS) against that of the middle-aged-turks (MAT) took place. While the better portion of the events that took place that evening can be more appropriately past on from generation to generation by raconteurs, some of the occurrences deserve to be written into this volume to ensure their accuracy through the ages. As an aside, let it be remembered that the challenge was made by the MAT group and that they made up the events; nonetheless, YMS group handily out scored the MAT group 8 to 4, as determined by the distinguished (at least in mass spectrometry) judges.

The event of most note during the competition was the limerick contest. Below are the limericks presented by the YMS side and several others that were not presented due to time constraints. It should be pointed out that these limericks passed the test of time, i.e. written late at night around a keg of beer, they still sounded okay the next morning. Most were written by committee, some by individuals. Authors names have been deleted to protect the guilty.

There once was a group of old turks
Who had a few middle-aged quirks
    To their surprise
    without the young guys
No mass spectrometer works

There once was a MAT from Purdue
Who took only a spectrum or two
    He said with a grin
    As he tugged at his chin
"This is about all I can do."

There once was from MAMS a madam
Who didn't know ions from atoms
    She said with a smile
    As she twiddled the dial
"I need a new postdoc to add'em."

There once was a maestro from Lincoln
Whose head overheated from thinkin
    His skull is now bare
    Cause he lost all his hair
And now he just watches lights blinkin.

There once was an MIT lass
With four sectors she measured her mass
    She used in her lab
    A strange matrix for FAB
Called Ex-Lax, cause all things must pass.

Do teachers of mass spectrometry
Producing their academic progeny
    For their procreation
    And intimate relations
Employ forward or reverse geometry?

There was a man from the windy city
Who thought he was oh so witty
    But being a MAT
    Is not where it's at
So we look upon him with pity.

Then there's Big Al from Frisco
Who Porsches in from Sausalito
And he says with a smile
As he drives those long miles
"I'll write my review at the disco."

In Urbana there lives Carter Cook
Wrote the VG mass spectrometry book
As a turk he is older
With red slacks that are bolder
For the well dressed Urbana man look.

There was a middle-aged turk named Harry
Who once was our secretary
He once did mass spec
But said "oh what the heck
Lab work is just too damn scary."

There once was a wizard named Fred
Who's four sector rolled over dead
As he wrote the big paper
It turned into vapor
So he switched to FT instead.

There once was a middle-aged board
Who mistakingly challenged the young hoard
They spent oodles of time
Making those ridiculous signs
Time, the young couldn't afford.

In addition to the limericks, a highlight of the evening was the YMS fight song. This again was written by committee and passed the test of time.

YMS FIGHT SONG
(sung to the tune of "The Caissons Keep Rolling Along")

Over beer, over ale
As we seek the ion trail
We will always go chugging along.
Over wine, over booze
We will work while they will snooze
We will always be righting their wrongs.

For it's hi, hi, hee - WE are mass spectrometry
Count out your masses loud and strong!
For where e'er we go, you will always know
We are dragging the old farts along.

Society Office
Post Office Box 1508
East Lansing, MI 48823
(517) 337-2548

President
R. Graham Cooks
Department of Chemistry
Purdue University
West Lafayette, IN 47907

Vice President for Programs
G. G. Meisels
College of Arts & Sciences
1223 Oldfather Hall
University of Nebraska
Lincoln, NE 68588-0365

Vice President for Arrangements
Catherine E. Costello
Massachusetts Institute of Technology
Chemistry 56-029
Cambridge, MA 02139

Secretary
Robert T. McIver, Jr.
Department of Chemistry
University of California
Irvine, CA 92717

Treasurer
James J. DeCorpo
Naval Sea System Command
Code 05R32
Washington, DC 20362

ASTM Committee E-14
Ed Emery
NY Environmental, Inc.
75 Urban Avenue
Westbury, NY 11590

Member at Large
Charles N. McEwen
E.I. DuPont de Nemours
Central Research Department
Wilmington, DE 19898

Member at Large
Gordon W. Wood
Graduate Studies & Research
University of Windsor
Windsor, Ontario N9B 3P4

Past President
Catherine C. Fenselau
Department of Pharmacology
Johns Hopkins University
725 N. Wolfe Street
Baltimore, MD 21205

CHALLENGE EVENTS

Arm Wrestling - each side enters one champion.

Wildest Beard Contest

Wildest Garb Contest

Highest Mass in a Single Mass Spectrometrist

Lowest Mass in a Single Mass Spectrometrist

Largest Radius of Curvature Contest

Smallest Radius of Curvature Contest

MS Trivia Contest:
Submit 10 questions
Other side pulls 5 out of a hat.

Write & sing an MS Fight Song

Limerick Contest - open to all members of both sides.

Charade an Eminent Mass Spectrometrist

Create a Human Slide

Most Creative Shadow Projection with Overhead Projector:
Max 3 people, no props - only human parts.

Do the quadrupole dance
4 people to be joined by ensemble at the end.

Provide one of each mass spectrometrist:

1. Highly charged
2. Neutral
3. Positive
4. Negative
5. Ground State
6. Most excited

YOUNG MASS SPECTROMETRISTS FIGHT SONG 1986
(sung to the tune of "The Caissons Keep Rolling Along")

Over beer, over ale,
As we seek the ion trail
We will always go chugging along.
Over wine, over booze,
We will work while they will snooze--
We will always be righting their wrongs.

For it's hi, hi, hee -- WE are mass spectrometry;
Count out your masses loud and strong!
For where e'er we go, you will always know
We are dragging the old f...s along.

MIDDLE AGE TURKS FIGHT SONG 1986

Over beer, over ale
As they lose the ion trail
They will never go chugging alone
Over wine over booze,
They will constantly snooze--
They can never be righting their wrongs.

For it's hi, hi, hee -- WE are mass spectrometry;
Count out your masses loud and strong!
For where e'er they go, everyone will know
We are dragging the young turks along.

LIMERICKS (YMS vs MAT)

Hugh Heffner is into MS
His interest is due, I guess
To the exploitation
Without explaination
of daughters without parents, no less.

There was an ion named Mabel
Whose virtue was quite metastable
She said to the pole
My virginity you stole
Hence Ion no longer able

Did you hear about young turks from ASMS
Having party'd, were trying to get rest
When the fire bell sounded
Down the stairs they bounded
How exciting to see how they dressed!

Ohio nio
kawa ni ukaberu
ASMS kana

It means:

Great ASMS
is floating
on Ohio River

REPORT OF THE PRESIDENT
by
R. Graham Cooks

It would be pleasant to accentuate the positive - and I am immensely proud of the achievements of the Board over the past few years and the active role in the Society played by so many members. One could point to the healthy state of the membership and finances of the Society, the compelling program at the annual conference, as well as new ventures in continuing the mass spectrometry education of members and of the community-at-large. Vitality is also evident in the vigor of the Local Discussion Groups, the emerging service laboratory group, the Research Awards, member services such as employment assistance, communication through the Spectaker, and stronger international ties, including the 1988 meeting in San Francisco which will have elements of a Pacific rim conference. One might even mention the new-found vigor of the Middle-Aged Turks.

My main message, however, is not one of achievement but one of concern for the future. Why do I speak of concern at a time of unprecedented interest in mass spectrometry, when the Society is vigorous and growing, healthy fiscally and programmatically? Concern arises because mass spectrometry is a 'coalition discipline' and it is precisely under such circumstances that coalitions weaken. Our coalition embraces the spectrum from theory to applications. For many years the resulting cross-fertilization has been more stimulating than irritating to both groups. As we grow, we will ned to work harder to maintain this situation. I am disturbed when some members refuse the label spectroscopist fearing some stigma.

Given free reign to reorganize science, few would stick to the classical divisions. Indeed, an almost ideal module from which to grow vigorously would today be centered upon instrumental methodology, loosely defined to allow flexibility for growth and blessed with an abundance of applications. Such is precisely the situation of mass spectrometry, yet we cringe at our identification with a technique.

Another feature which can be damaging to a 'coalition discipline' is a lush underbrush of smaller meetings. ASMS is a goose - for many years it has been a goose - that has been delivering golden eggs annually. We have something uniquely valuable in these annual conferences, and it would be a terrible waste if this ceased. Many of us feel strongly about this, and I am urging the Board as I step down from my office to take strong measures to protect and improve the quality of our program. We cannot allow ancillary activities to weigh down the annual program. Nor can we abandon the newest and most exciting topics in mass spectrometry to smaller meetings, thereby impoverishing the ASMS conference. In this respect there needs to be cooperation in coordinating activities for the sake of all who week to advance our discipline.

We face another issue where quality must be improved. The number of people engaged full-time in operating mass spectrometers and in interpreting mass spectra is growing rapidly with the introduction of

low-cost, high performance instruments. We will all suffer if we don't make an effort to raise the level of practice of mass spectrometry by all practitioners. There is a great opportunity here to contribute to the infrastructure of American science while fulfilling the ASMS charter; "to promote and disseminate knowledge of mass spectrometry". So important does the Board believe this task to be that in its streamlining of Society governance, an Education Committee was recently established. We look forward to a vigorous program under Harry Hertz's direction.

It is axiomatic that science is ternational in character and that cooperation with other groups which foster mass spectrometry is in the interest of mass spectrometry and the members of ASMS. The Board is determined that ASMS exercise appropriate leadership in this area and do so in as constructive a manner as possible. For this reason, our 1988 San Francisco conference will provide a particular opportunity for intereactions with Pacific rim countries. Furthermore, in an effort to avoid a conflict with the Triennial meetings in Europe, we are attempting to align the ASMS calendar so that our West Coast meeting does not coincide with this event. We are also inviting interested members to inquire about participation in the 2nd Japan/China Symposium on Mass Spectrometry in Osaka in September 1987.

Let me conclude by admitting that some of us on the Board were once young and impatient with ASMS. In so doing I urge our younger members to put their backs to the wheel and to work for ASMS. A magnificent step towards securing that future we seek for our society and our science is being inaugurated at this meeting. I refer to the ASMS Research Awards sponsored by Finnigan MAT and VG Instruments. These awards are designed to assist young investigators at critical stages in their careers. We are indebted to the sponsoring companies and particularly to Bob Finnigan and Alan Wolstenholme for their parts in making these awards possible.

LAWRENCE E ABBEY
GEORGIA TECH
CHEMISTRY DEPT

ATLANTA GA 30332
PHONE: 404 894 4061

LINDA D ABRAMS
7306 ORCHARDHILL DR

RICHMOND VA 23234
PHONE. 804 359 1900

JEANETTE ADAMS
1732 SOUTH 42ND

LINCOLN NE 68506
PHONE: 402 472 3507

M S AHMED
DEPT OF CHEMISTRY
CASE WESTERN RESERVE UNIV

CLEVELAND OH 44106
PHONE

KENNETH M ALDOUS
NY STATE HEALTH DEPT
WADSWORTH CENTER
TOWER BLDG
ALBANY NY 12201
PHONE. 518 473 0030

ANN ALFORD-STEVENS
US EPA
26 WEST ST CLAIR STREET

CINCINNATI OH 45268
PHONE

RAY H ALLEN
R H ALLEN CO
PO BOX 27

BOULDER CO 80306
PHONE: 303 442 2141

GUNTER ALLMAIER
M I T
DEPT OF CHEMISTRY
56-012
CAMBRIDGE MA 02139
PHONE: 617 253 7237

HAMDY ABDEL-MAKSOUD
KENNEDY SHRIVER CTR
200 TRAPELO ROAD

WALTHAM MA 02254
PHONE: 617 642 0188

FRED P ABRAMSON
GEORGE WASHINGTON UNIV
PHARMACOLOGY DEPT

WASHINGTON DC 20037
PHONE: 202 676 2946

R A ADAMS
3480 TANBARK CT NE

ATLANTA GA 30319
PHONE: 404 255 4817

MEHRSHID ALAI
JOHNS HOPKINS SCH OF MED
B-7 BIOPHYSICS
725 N WOLFE STREET
BALTIMORE MD 21205
PHONE 301 955 3022

JERRY W ALEXANDER
CA DEPT OF FOOD & AG
3292 MEADOWVIEW RD

SACRAMENTO CA 95832
PHONE: 916 427 4989

CHUCK ALGOOD
DEPT OF CHEMISTRY
UNIV OF DELAWARE

NEWARK DE 19716
PHONE 302 451 2917

CYNTHIA C ALLEY
CTRS FOR DIS CONTROL
TOXICOLOGY C17-1814

ATLANTA GA 30333
PHONE 404 452 4144

NICK ALMASY
MI DEPT OF AGRICULTURE
1615 S HARRISON ROAD

EAST LANSING MI 48823
PHONE: 517 373 6410

ROBERT M ABERNATHEY
LOS ALAMOS NAT'L LAB
M/S 1663

LOS ALAMOS NM 87544
PHONE 505 667 9810

BRADLEY L ACKERMANN
BIOCHEM RM 11
MICHIGAN STATE UNIV

EAST LANSING MI 48824
PHONE 517 355 0612

ROBERT C ADAMS
SOUTHERN RESEARCH INST
2000 NINTH AVE SOUTH
PO BOX 55305
BIRMINGHAM AL 35255-5305
PHONE: 205 323 6592

MARK ALASANDRO
E I DUPONT
BIOMEDICAL PRODUCTS DEPT
EXPER STN BLDG 353/234
WILMINGTON DE 19808
PHONE.

N E ALEXANDER
NIH
BLDG 13 ROOM 3W13

BETHESDA MD 20892
PHONE:

DAVID ALKALAY
CIBA-GEIGY CORP
444 SAWMILL RIVER RD

ARDSLEY NY 10502
PHONE:

JOHN ALLISON
MICHIGAN STATE UNIV
CHEMISTRY DEPT

EAST LANSING MI 48824
PHONE: 517 353 4513

MICHAEL F ALMOND
KRATOS ANALYTICAL
170 WILLIAMS DR

RAMSEY NJ 07446
PHONE: 201 934 9000

WILLIAM H ABERTH
UC SAN FRANCISCO
PHARMACEUTICAL CHEM

SAN FRANCISCO CA 94143-0446
PHONE: 415 476 4893

THOMAS ACZEL
EXXON R/E
PO BOX 4255

BAYTOWN TX 77522
PHONE: 713 425 5131

JOSEPH B ADDISON
GOVERNORS STATE UNIV
COLL OF ARTS & SCI

UNIVERSITY PK IL 60466
PHONE: 312 534 5000

RICHARD ALBERT
ETC CORP
47 ANSTICE STREET

OYSTER BAY NY 11791
PHONE

E D ALFORD
BROWN & WILLIAMSON
PO BOX 35090

LOUISVILLE KY 40232
PHONE: 502 568 7680

ALEX R ALLAN
MT SINAI HOSPITAL
BOX 156
306 E 96TH STREET
NEW YORK NY 10128
PHONE

LAURA A ALLISON
CONOCO INC
R&D EAST
PO BOX 1267
PONCA CITY OK 74603
PHONE 405 767 2761

V O ALTEMOSE
CORNING GLASS WORKS
SP-FR-1-8

[illegible]NING NY 14830
[illegible]ONE. 607 974 3364

JON AMSTER
CORNELL UNIV
BOX 165
BAKER LAB
ITHACA NY 14853
PHONE: 607 255 3731

M M ANBAR
181 HALWILL DR

SNYDER NY 14226
PHONE. 716 831 2328

ROBERT J ANDEREGG
UNIV OF MAINE
273 AUBERT HALL

ORONO ME 04469
PHONE: 207 581 1171

BRIAN K ANDERSON
1061-A BRIDGEWAY CIRCLE

COLUMBUS OH 43220-3324
PHONE. 614 459 2355

DAVID J ANDERSON
GEOLOGY 541
INDIANA UNIV

BLOOMINGTON IN 47405
PHONE: 812 335 1005

SCOTTY ANDERSON
CHEMISTRY DEPT
SUNY

STONY BROOK NY 11794-3400
PHONE: 516 246 6556

STEPHEN ANDERSON
116 UNIVERSITY VILLAGE

SALT LAKE CTY UT 84108
PHONE:

WILLIAM R ANDERSON
LEHIGH UNIV
MUDD BLDG 6

BETHLEHEM PA 18015
PHONE: 215 861 3465

D A ANDRZEJEWSKI
FDA
200 C STREET SW HFF-426

WASHINGTON DC 20204
PHONE. 202 245 1371

VINCENT ANICICH
8036 GRAYSTONE

SUNLAND CA 91040
PHONE:

ALEX APFFEL
HEWLETT-PACKARD
1601 CALIFORNIA AVE

PALO ALTO CA 94304
PHONE:

ANTHONY D APPELHANS
EG&G IDAHO INC
PO BOX 1625

IDAHO FALLS ID 83415
PHONE: 208 526 0862

GEORGES M ARGOUD
DEPT OF MEDICINE
UNIV OF NEW MEXICO HOSPITAL
2211 LOMAS AVENUE NE
ALBUQUERQUE NM 87131
PHONE: 505 277 4657

PETER B ARMENTROUT
DEPT OF CHEMISTRY
UNIV OF CALIFORNIA

BERKELEY CA 94720
PHONE. 415 642 4428

KENNETH ARMOCK
MI DEPT OF AGRICULTURE
1615 S HARRISON ROAD

EAST LANSING MI 48823
PHONE· 517 373 6410

RUSSELL ARNONE
169 SYCAMORE AVENUE

SHREWSBURY NJ 07701
PHONE: 201 741 8273

BRUCE K ASAMOTO
STANDARD OIL RESEARCH
4440 WARRENSVILLE CTR ROAD

CLEVELAND OH 44128
PHONE: 216 581 5776

KEIJI G ASANO
DEPT OF CHEMISTRY
MICHIGAN STATE UNIV

EAST LANSING MI 48824
PHONE· 517 353 5215

ROBERT W ASHMORE
DEPT OF PHARMACOLOGY
EXPERIMENTAL THERAPEUTICS
WALTER REED AIR
WASHINGTON DC 20307-5100
PHONE.

JAWEED ASHRAF
DELSI INSTRUMENTS
10 KINGSBRIDGE ROAD

FAIRFIELD NJ 07006
PHONE: 201 227 7690

JOHN W AULD
37748 SUNNYDALE

LIVONIA MI 48154
PHONE· 313 897 1395

PIERRE J AUSLOOS
NAT'L BUR OF STAN
CTR FOR CHEM PHYSICS

WASHINGTON DC 20234
PHONE: 301 921 2711

BARRY M AUSTERN
US ENVIRON PROT AGENCY
26 W ST CLAIR STREET

CINCINNATI OH 45268
PHONE: 513 684 7638

E R AUSTIN
IFDC
PO BOX 2040

MUSCLE SHOALS AL 35660
PHONE: 205 381 6600

ROBERT P AUTY
BETH ISRAEL HOSPITAL
330 BROOKLINE AVENUE

BOSTON MA 02215
PHONE: 617 735 4302

MICHAEL J AVERY
IOWA STATE UNIV
9 GILMAN

AMES IA 50011
PHONE: 515 294 6615

RUSSELL J AYERS
FOOD & DRUG ADMINISTRATION
1560 E JEFFERSON

DETROIT MI 48207
PHONE: 313 226 6129

JUNE AYLING
DEPT OF PHARMACOLOGY
UNIV OF SOUTH ALABAMA

MOBILE AL 36688
PHONE:

LUCIA M BABCOCK
CHEMISTRY DEPT
CHOPPIN HALL
LOUISIANA STATE UNIV
BATON ROUGE LA 70803
PHONE 504 388 4694

LUBO BACZYNSKYJ
THE UPJOHN CO
301 HENRIETTA

KALAMAZOO MI 49001
PHONE 616 385 7401

JOHN C BAENZIGER
ROOM A-20
702 BARNHILL DR

INDIANAPOLIS IN 46223
PHONE: 317 264 4345

TOMAS BAER
UNIV NORTH CAROLINA
CHEMISTRY DEPT

CHAPEL HILL NC 27514
PHONE: 919 966 5433

DONALD A BAFUS
4114 CLOVERNOOK LANE

SEABROOK TX 77586
PHONE: 713 483 4641

G L BAFUS
1504 S 23RD

BLUE SPRINGS MO 64015
PHONE. 816 966 5000

ALFRED BAHNSON
414 MAIN BLVD

PITTSBURGH PA 15237
PHONE. 412 624 3115

THOMAS A BAILLIE
UNIV OF WASHINGTON
MEDICINAL CHEMISTRY
BG-20
SEATTLE WA 98195
PHONE: 206 545 2468

MICHAEL A BAIM
PROCTER & GAMBLE
HB BLDG
11511 REED HARTMAN HWY
CINCINNATI OH 45241
PHONE 513 530 2658

E S BAKER
ROCKWELL HANFORD
200 WEST 234-5

RICHLAND WA 99352
PHONE 509 373 3872

TERRIE S BAKER
COMPUCHEM LABORATORIES
PO BOX 12652

RES TRI PK NC 27709
PHONE 919 549 8263

TIMOTHY R BAKER
71 EUSTON ROAD #1

BRIGHTON MA 02135
PHONE 617 254 0428

MICHAL BALAZY
DEPT OF PHARMACOLOGY
UNIV OF COLORADO
4200 EAST 9TH AVE
DENVER CO 80262
PHONE 303 394 8961

C R BALDOCK
114 OGONTZ LANE

OAK RIDGE TN 37830
PHONE: 615 483 6779

SILVIO J BALESTRINI
LOS ALAMOS NAT'L LAB
GROUP INC-11 MS-G7776

LOS ALAMOS NM 87545
PHONE 505 667 4151

GWENDOLYN L BALL
2315 LANCASHIRE 2A

ANN ARBOR MI 48105
PHONE: 313 769 8010

JOHN M BALLARD
CELANESE RESEARCH
86 MORRIS AVE

SUMMIT NJ 07901
PHONE 702 798 2230

KEVIN D BALLARD
MED UNIV OF SC
PHARMACOLOGY DEPT
176 ASHLEY AVENUE
CHARLESTON SC 29401
PHONE 803 792 2471

JOE BANAR
LOS ALAMOS NAT'L LAB
MS J514
BOX 1663
LOS ALAMOS NM 87544
PHONE.

L J BARABAS
POLYMER INDUSTRIES
PO BOX 2184

GREENVILLE SC 29602
PHONE 803 244 5351

WAYNE M BARAN
100 E STREAMWOOD BLVD

STREAMWOOD IL 60103
PHONE 391 3380

MICHAEL P BARBALAS
523 BLOOMFIELD AVE

NUTLEY NJ 07110
PHONE 201 661 3123

ROBERT J BARBUCH
MERRELL DOW PHARMACEUTICAL
PO BOX 68470

INDIANAPOLIS IN 46268
PHONE 317 873 7194

ROBERT M BARKLEY
CHEMISTRY DEPT
CAMPUS BOX 215
UNIV OF COLORADO
BOULDER CO 80309-0215
PHONE: 303 492 1158

T M BARLAK
7400 VERNON SQ DR
APT 303

ALEXANDRIA VA 22306
PHONE 202 487 0056

I L BARNES
NBS
A-23 PHYSICS

GAITHERSBURG MD 20899
PHONE: 301 921 2781

RAMON M BARNES
CHEMISTRY DEPT
GRC TOWERS
UNIV OF MASSACHUSETT
AMHERST MA 01003-0035
PHONE: 413 545 2294

DOUGLAS F BAROFSKY
DEPT OF AGRICULTURAL CHEM
OREGON STATE UNIV

CORVALLIS OR 97331
PHONE 503 754 2906

ELISABETH BAROFSKY
DEPT OF AG CHEMISTRY
OREGON STATE UNIV

CORVALLIS OR 97331
PHONE. 503 754 2906

ANDREW BARONAUSKI
NAVAL RESEARCH LAB
CODE 6110

WASHINGTON DC 20375
PHONE

W B BARRETT
15 LOVETON CIRCLE

SPARKS MD 21152
PHONE: 301 771 4950

V M BARRINGER
4604 EMMACYN DR

SUMMERFIELD NC 27358
PHONE.

ROBERT P BARRON
FDA-CTR DRUGS & BIOLOGICS
HFN-88S/OFF BIOLOGICS
8800 ROCKVILLE PIKE
BETHESDA MD 20892
PHONE: 301 496 9020

REGINA M BARRY
2805 NORMANDY CT

NEWARK DE 19713
PHONE: 302 451 2917

T L BARRY
FDA
850 3RD AVE

BROOKLYN NY 11232
PHONE 718 965 5722

MICHAEL J BARTELS
TOXICOLOGY LAB
1803 BLDG
DOW CHEMICAL CO
MIDLAND MI 48674
PHONE 517 636 9057

GREG J BARTLING
1014 RIVERVIEW TERRACE

NEW MRTNSVLL WV 26155
PHONE: 304 455 4400

AMOS BARTOLI
US STEEL CORP TECH CTR
ONE TECH CENTER DR

MONROEVILLE PA 15146
PHONE. 412 372 7458

LEWIS M BASS
DIV OF NATURAL SCI
UNIV OF S CAROLINA

AIKEN SC 29801
PHONE: 803 648 6851

MARK F BEAN
DEPT OF PHARMACOLOGY
JOHNS HOPKINS SCH OF MED
725 N WOLFE STREET
BALTIMORE MD 21205
PHONE 301 955 6961

DEBRA J BECK
ONEIDA RESEARCH
ONE HALSEY ROAD

WHITESBORO NY 13492
PHONE 315 736 3050

CARL F BECKNER
FINNIGAN MAT
355 RIVER OAKS PKWY

SAN JOSE CA 95134
PHONE 408 433 4800

JON L BEIHOFFER
QUALITY ASSURANCE LAB
UNIV OF NEVADA
4505 MARYLAND PWY
LAS VEGAS NV 89154
PHONE. 702 739 3142

V E BELL
HOFFMANN-LAROCHE INC

NUTLEY NJ 07110
PHONE: 201 235 2852

CANDACE D BARTMAN
EXTREL CORP
PO BOX 11512

PITTSBURGH PA 15238
PHONE· 412 782 3884

LOUISETTE J BASA
GENENTECH INC
460 PT SAN BRUNO BLVD

S SAN FRAN CA 94080
PHONE

MARK R BAUER
MICHIGAN STATE UNIV
CHEMISTRY DEPT

EAST LANSING MI 48824
PHONE. 517 353 5215

ELLYN S BEARY
NAT'L BUR OF STAN
BLDG 222 RM A 353

GAITHERSBURG MD 20899
PHONE. 301 921 3674

DONALD D BECK
GENERAL MOTORS RESEARCH
PHYSICAL CHEMISTRY DEPT

WARREN MI 48098
PHONE· 313 575 2286

A A BEDNARCZYK
NAARDEN INTERNATL
10 PAINTERS MILL RD

OWINGS MILLS MD 21117-3686
PHONE: 301 363 2550

ROBERT G BEIMER
S-CUBED
3398 CARMEL MTN ROAD

SAN DIEGO CA 92121
PHONE:

THOMAS A BELLAR
US EPA
26 W ST CLAIR

CINCINNATI OH 45268
PHONE·

JOHN BARTMESS
CHEMISTRY DEPT
UNIV OF TENNESSEE

KNOXVILLE TN 37996
PHONE: 615 974 6578

B B BASCHKIN
2 CAPTAINS LANE

RYE NY 10580
PHONE:

CHARLENE W BAYER
6276 ROSECOMMON DRIVE

NORCROSS GA 30092
PHONE· 404 894 3825

BRIAN DAVID BEATO
3751 SW 20TH AVENUE
APT 132

GAINESVILLE FL 32607
PHONE· 904 392 0515

MARY D BECK
1252 QUARRY LANE

PLEASANTON CA 94566
PHONE. 415 426 2600

THOMAS D BEHYMER
INDIANA UNIV
541 GEOLOGY BLDG

BLOOMINGTON IN 47405
PHONE 812 335 1217

RONALD L BELANGER
1899 MAPLE HILL ST

YORKTWN HGHTS NY 10598
PHONE· 914 335 6208

THOMAS H BELLUS
UNIV OF WASHINGTON
CHEMISTRY DEPT BG-10

SEATTLE WA 98195
PHONE· 543 6144

P L BARTNER
SCHERING CORP
60 ORANGE

BLOOMFIELD NJ 07003
PHONE: 201 429 3989

BRENDA P BASILE

18314 ELMDON

HOUSTON TX 77084
PHONE: 713 492 2510

M GOKHAN BAYKUT
CHEMISTRY DEPT
UNIV OF FLORIDA

GAINESVILLE FL 32611
PHONE: 904 392 0536

ALFRED J BEATTIE
E I DUPONT
EXPERIMENTAL STA
PPD BLDG 269
WILMINGTON DE 19898
PHONE: 302 772 2240

CHRISTOPHER H BECKER
SRI INTERNATIONAL
M S PS091
CHEMICAL PHYSICS LAB
MENLO PARK CA 94025
PHONE: 415 859 5130

ROSS C BEIER
VTERL, USDA

COLL STN TX 77841
PHONE: 409 260 9411

BRUCE BELL
DOW CHEMICAL CO
BLDG 574

MIDLAND MI 48667
PHONE. 517 636 9646

F A BENCSATH
THE ROCKEFELLER UNIV
1230 YORK AVENUE

NEW YORK NY 10021
PHONE: 212 570 8795

J G BENDORAITIS
MOBIL RESEARCH & DEV

PAULSBORO NJ 08066
PHONE. 609 423 1040

BRIAN D BENNETT
CHEMISTRY DEPT
UNIV OF CINCINNATI

CINCINNATI OH 45220
PHONE·

LINDA BENSON
MAYO CLINIC/FOUNDATION
200 SW 1ST STREET

ROCHESTER MN 55905
PHONE: 507 284 4212

BRYAN L BENTZ
RCA LABS
SARNOFF RES CTR

PRINCETON NJ 08540
PHONE: 609 734 2015

WOLFGANG BENZ
HOFFMANN-LAROCHE INC
KINGSLAND ST

NUTLEY NJ 07110
PHONE. 201 235 3786

PETER J BERG
MAYO ENDOCRINE RES
5-164 W JOSEPH
200 1ST STREET SW
ROCHESTER MN 55905
PHONE. 507 285 5097

PHILIP S BERGER
TEKNIVENT CORP
10774 TRENTON CORP

ST LOUIS MO 63132
PHONE. 314 429 7272

STEVEN R BERGER
HEWLETT-PACKARD CO
1601 CALIFORNIA AVENUE

PALO ALTO CA 94304
PHONE.

ALICE M BERGMANN
SUNY @ BUFFALO
DEPT OF CHEMISTRY
18 ACHESON HALL
BUFFALO NY 14214
PHONE 716 831 3016

LYLE E BERGQUIST
2676 EAST OTERO PLACE No 11

LITTLETON CO 80122
PHONE·

R E BERKLEY
133 MONTCLAIR CIRCLE

DURHAM NC 27713
PHONE: 919 541 2439

DOROTHY BERTINO
227 N ROBERSON ST

CHAPEL HILL NC 27514
PHONE: 919 541 2964

PATRICIA BETHEL
2433 BYRON STREET

BERKELEY CA 94702
PHONE·

LEON D BETOWSKI
EPA-EMSL
QUAL ASSURANCE DIV
PO BOX 15027
LAS VEGAS NV 89114
PHONE: 702 456 8165

ROBERT J BEUHLER
BROOKHAVEN NAT'L LAB
CHEM DEPT BLDG 555

UPTON NY 11973
PHONE 516 282 4326

JOSEPH R BIANCHINE
VP MEDICAL AFFAIRS
AMERICAN CRITICAL CARE
1600 WAUKEGAN ROAD
MCGRAW PARK IL 60085
PHONE 312 473 3000

KLAUS BIEMANN
MIT
CHEMISTRY 56-010

CAMBRIDGE MA 02139
PHONE 617 253 7221

D M BIER
WASHINGTON UNIV
METABOLISM
SCHOOL OF MEDICINE
ST LOUIS MO 63110
PHONE: 314 362 6923

MARK E BIER
CHEMISTRY BLDG
BOX 333
PURDUE UNIV
W LAFAYETTE IN 47907
PHONE 317 494 5262

VERONICA M BIERBAUM
UNIV OF COLORADO
CHEMISTRY DEPT
CAMPUS BOX 215
BOULDER CO 80309-0215
PHONE 303 492 7081

J E BILLER
MIT
CHEMISTRY 56-025
77 MASS AVE
CAMBRIDGE MA 02139
PHONE 617 253 7232

STEPHEN S BILLETS
US EPA EMSL-QAD
PO BOX 15027

LAS VEGAS NV 89114-5027
PHONE· 702 798 2232

DANIEL BINDER
WATER RESEARCH LABORATORY
910 DUBLIN ROAD

COLUMBUS OH 43215
PHONE:

ROBERT C BINIAKEWITZ
CHAMPION INT'L CORP
WEST NYACK ROAD

WEST NYACK NY 10994
PHONE 914 578 7208

GEORGE M BIRD
SUN CHEMICAL CORP
631 CENTRAL AVE

CARLSTADT NJ 07072
PHONE· 201 933 4500

IONA BLACK
305 N SALISBURY STREET
2N

W LAFAYETTE IN 47906
PHONE

SADOR S BLACK
E R SQUIBB & SONS
PO BOX 191

NEW BRUNSWICK NJ 08903
PHONE· 201 545 1300

IAN A BLAIR
PHARMACOLOGY DEPT
VANDERBILT UNIV

NASHVILLE TN 37232
PHONE 615 322 2094

CALVIN R BLAKLEY
2007 WILDERNESS PT DR

KINGWOOD TX 77339
PHONE· 713 796 9677

JULIE A BLANCKAERT
6103 E LONG CIRCLE N

ENGLEWOOD CO 80112
PHONE. 303 796 7504

JEFFREY D BLANK
152 DAVEY LABORATORY
PENN STATE UNIV

UNIV PARK PA 16802
PHONE 814 865 2202

IOANNIS V BLETSOS
DEPT OF CHEMISTRY
UNIV OF PITTSBURGH

PITTSBURGH PA 15260
PHONE: 412 624 2799

KARL BLOM
2805 NORMANDY CT

NEWARK DE 19713
PHONE. 302 451 2917

KEVIN B BOLGER
US EPA
CENTRAL REGIONAL LAB
536 S CLARK ST, 10TH FL
CHICAGO IL 60605
PHONE 312 353 9085

E J BONELLI
HP SCIENTIFIC INSTR
1601 CALIFORNIA AVE

PALO ALTO CA 94304
PHONE 415 857 6028

SCOTT BOUCHER
XEROX AI SYSTEMS
450 ALGONQUIN ROAD

ARLINGTON HTS IL 60005
PHONE 312 981 7447

MOHAMMED BOZORGZADEH
DEPT OF CHEMISTRY
UNIV OF NEBRASKA

LINCOLN NE 68588-0304
PHONE: 402 472 3507

JOEL C BRADLEY
CAMBRIDGE ISOTOPES
20 COMMERCE WAY

WOBURN MA 01801
PHONE 617 938 0067

L L BRAYTON
PO BOX 5075, STN A

CHAMPAIGN IL 61820
PHONE 217 333 2545

FRED W BRILL
105 N MARION DRIVE

GOLDSBORO NC 27530
PHONE 919 731 5200

LYNN J BLUETT
154 BIRCHWOOD DR

ROCHESTER NY 14622
PHONE 716 422 3179

DANIEL D BOMBICK
DEPT OF CHEMISTRY
MICHIGAN STATE UNIV

EAST LANSING MI 48824
PHONE 517 353 6495

JEANNE BONURA
ANALYTICAL TECHNOLOGIES
2113 S 48TH STREET #110

TEMPE AZ 85282
PHONE 602 438 1530

WILLIAM J BOULDIN
DOW CHEMICAL CO
OCD-ENV SER-SOUTH

FREEPORT TX 77541
PHONE

DONALD E BRACKEN
NJ STATE DEPT OF HEALTH
PUB HEAL & ENVIR LABS
CN 360
TRENTON NJ 08625
PHONE 609 984 0646

D K BRAIN
PROCTER & GAMBLE
IVORYDALE TECH CENTR

CINCINNATI OH 45217
PHONE 513 627 5661

J THOMAS BRENNA
IBM
DEPT T43/014-2
1701 NORTH STREET
ENDICOTT NY 13760
PHONE: 607 755 1363

JENNIFER S BRODBELT
BOX 335, CHEMISTRY BLDG
PURDUE UNIV

W LAFAYETTE IN 47906
PHONE 317 494 5264

JAMES R BOAL
THE UPJOHN CO
301 HENRIETTA STREET

KALAMAZOO MI 49001
PHONE

HENRY A BONDAROVICH
C/O IFF
1515 HWY 36

UNION BEACH NJ 07735
PHONE 201 264 4500

JULIET H BORTHWICK
2416 RAINTREE COURT

PLANO TX 75074
PHONE:

MICHAEL T BOWERS
UNIV OF CALIFORNIA
CHEMISTRY DEPT

SANTA BARBARA CA 93106
PHONE 805 961 2893

RICHARD T BRACKMANN
EXTREL CORP
PO BOX 11512

PITTSBURGH PA 15238
PHONE 412 782 3884

VERNON O BRANDT
ETHYL TECHNICAL CENTER
BOX 14799

BATON ROUGE LA 70898
PHONE: 504 768 5837

DAVID BRENT
BURROUGHS WELLCOME
3030 CORNWALLS

RES TRI PK NC 27709
PHONE 919 248 4235

JAMES MARK BROGE
GENERAL MILLS
9000 PLYMOUTH AVE N

GOLDEN VALLEY MN 55427
PHONE: 612 540 3410

FRANK M BOCKHOFF
STANDARD OIL CO
4440 WARRENSVILLE CTR ROAD

CLEVELAND OH 44128
PHONE 216 581 5838

WILLIAM BONE
WRAIR
ATTN BIOCHEMISTRY
WALT REED ARMY MED
WASHINGTON DC 20307
PHONE: 202 576 4108

DAVID BOSTWICK
GEORGIA INST OF TECH
CHEMISTRY DEPT

ATLANTA GA 30332
PHONE 404 894 4061

WILLIAM D BOWERS
CHEMISTRY DEPT
UNIV OF CALIFORNIA

IRVINE CA 92717
PHONE: 714 856 6780

JAMES G BRADLEY
JET PROPULSION LAB
MS 11-116
4800 OAK GROVE DR
PASADENA CA 91109
PHONE. 818 354 2328

W E BRASELTON
MICHIGAN STATE UNIV
PHARMACOLOGY DEPT

EAST LANSING MI 48824
PHONE 517 355 7441

PHILIP R BRIGGS
HARVARD UNIVERSITY
CHEMISTRY DEPT
12 OXFORD ST
CAMBRIDGE MA 02138
PHONE 617 495 1903

GEORGE E BRONSON
THE UPJOHN CO
301 HENRIETTA STREET

KALAMAZOO MI 49009
PHONE.

HARRY O BROTHERTON
CHEMISTRY DEPT
NORTHEAST LOUISIANA UNIV

MONROE LA 71209
PHONE. 318 342 4136

SUSAN A BROTHERTON
EMS LABORATORIES
7901 W MORRIS

INDIANAPOLIS IN 46231
PHONE: 317 243 8304

ROBERT P BROUGHAM
DELSI INSTRUMENTS
10 KINGSBRIDGE ROAD

FAIRFIELD NJ 07006
PHONE· 201 227 7690

C L BROWN
CALIFORNIA STATE UN
CHEMISTRY DEPT

LOS ANGELES CA 90032
PHONE· 213 224 3613

CHARLES E BROWN
DEPT OF BIOCHEMISTRY
MED COLL OF WISCONSIN
8701 WATERTOWN PLANK RD
MIKWAUKEE WI 53226
PHONE. 414 257 8436

JOHNIE C BROWN
CHEMISTRY DEPT
UNIV OF WISCONSIN
1101 UNIVERSITY AVENUE
MADISON WI 53706
PHONE 608 262 3449

ROBERT D BROWN
110 WINDBRIDGE DRIVE

WEST CHESTER PA 19380-3940
PHONE

ROBERT S BROWN
950 LINDEN ST APT B-22

RIVERSIDE CA 92507
PHONE. 714 787 4740

SHARON BROWN
23 NASSAU ROAD

VERONA NJ 07044
PHONE

SHARON M BROWN
IFF R&D
1515 HWY 36

UNION BEACH NJ 07735
PHONE: 201 264 4500

TIMOTHY C BROWN
EASTMAN KODAK
BLDG 82 ROOM C-230
66 EASTMAN AVENUE
ROCHESTER NY 14650
PHONE· 716 477 6733

MARILYN L BROWNAWELL
320 ROBERTS LN

SCOTCH PLAINS NJ 07076
PHONE. 201 463 0003

RICHARD F BROWNER
SCH OF CHEMISTRY
GEORGIA INST OF TECH

ATLANTA GA 30332
PHONE. 404 894 4020

A P BRUINS
CORNELL UNIV
EQUINE DRUG TESTING
925 WARREN DRIVE
ITHACA NY 14850
PHONE· 607 255 6555

DOMINIQUE BRUMENT
DELSI INSTRUMENTS
10 KINGSBRIDGE ROAD

FAIRFIELD NJ 07006
PHONE 201 227 7690

ROBERT J BRUNFELDT
R J BRUNFELDT CO
PO BOX 2066

BARTLESVILLE OK 74005
PHONE· 918 336 4467

R J BRUNI
ARTHUR D LITTLE INC
ACORN PARK

CAMBRIDGE MA 02140
PHONE 617 864 5770

JOHN MICHAEL BUCHANAN
8319 GARFIELD COURT

SPRINGFIELD VA 22152
PHONE. 703 451 0392

MICHELLE V BUCHANAN
OAK RIDGE NAT'L LAB
BOX X 4500S E160

OAK RIDGE TN 37831
PHONE· 615 576 6690

JOHN P BUCK
900 PARKVIEW LANE

MUKWONAGO WI 53149
PHONE 414 363 3475

THOMAS J BUCKLEY
11388 CANARY DRIVE

IJAMSVILLE MD 21754
PHONE 301 921 2784

WILLIAM L BUDDE
EPA
26 W ST CLAIR ST

CINCINNATI OH 45268
PHONE· 513 684 7309

S S BULUSU
US ARMY ARDC
ENERG MAT DIV
BLDG 3028
DOVER NJ 07801
PHONE· 201 724 2818

ZORA E BUNN
PO BOX 12313
2 TRIANGLE DRIVE

RES TRI PK NC 27709
PHONE 919 549 0611

DAVID J BURINSKY
ROHM & HAAS CO
727 NORRISTOWN RD

SPRING HOUSE PA 19477
PHONE 215 641 2141

RICHARD BURKE
IT CORPORATION
5103 OLD WILLIAM PENN HWY

EXPORT PA 15632
PHONE. 412 731 8806

W H BURKE
3226 TOWER TRAIL

DALLAS TX 75229
PHONE· 214 247 8327

LEISA BURKES
PROCTER & GAMBLE
MIAMI VALLEY LABS
11810 EAST MIAMI RIVER RD
ROSS OH 45061
PHONE. 513 245 2325

A L BURLINGAME
UNIV OF CALIFORNIA
PHARMCEUTICAL CHEM

SAN FRANCISCO CA 94143-0446
PHONE 415 666 5641

ROBERT BURPEE
PPG IND INC
PO BOX 31

BARBERTON OH 41203
PHONE·

D G BURROWS
NORTHWEST & ALASKA
FISHERIES CENTER
2725 MONTLAKE BLVD E
SEATTLE WA 98112
PHONE. 206 442 5660

JOAN T BURSEY
RADIAN CORPORATION
PO BOX 13000

RES TRI PK NC 27709
PHONE 919 481 0212

MAURICE M BURSEY
UNIV NORTH CAROLINA
CHEMISTRY DEPT 045A

CHAPEL HILL NC 27514
PHONE 919 962 4403

PETER C BUSCEMI
ATF-NATL LAB CENTER
1401 RESEARCH BLVD

ROCKVILLE MD 20850
PHONE: 301 294 0410

KENNETH L BUSCH
CHEMISTRY DEPT
INDIANA UNIV

BLOOMINGTON IN 47401
PHONE: 812 335 2081

ERNIE D BUSH
20 COTSWOLD PLACE

DURHAM NC 27707
PHONE. 919 248 3218

GORDON F BUTLER
554 RED ROCK

WADSWORTH OH 44281
PHONE. 216 336 9675

GERRY W BUTTLER
MONSANTO CO
MAIL CODE U4C
800 N LINDBERGH BLVD
ST LOUIS MO 63167
PHONE 314 694 4213

S E BUTTRILL
CHAS EVANS & ASSOC
301 CHESAPEAKE DRIVE

REDWOOD CITY CA 94063-4723
PHONE 415 572 1601

W H BUTTRILL
1616 MEETING HOUSE

ANNAPOLIS MD 21401
PHONE: 301 757 1854

JOHN T BYCHOWSKI
FIREMAN'S FUND
ENVIRONMENTAL LAB
3700 LAKEVILLE HWY
PETALUMA CA 94952
PHONE: 707 778 4193

GARY D BYRD
NAT'L BUR OF STAN
A 113 CHEMISTRY

GAITHERSBURG MD 20899
PHONE 301 921 2153

DAVID CAIN
MONSANTO RESEARCH CORP
MOUND FACILITY
PO BOX 32
MIAMISBURG OH 45342
PHONE

GARY CALDWELL
MCNEIL PHARMACEUTICAL

SPRING HOUSE PA 19477
PHONE 215 628 5537

JOHN B CALLAGHAN
680 FRANKLIN STREET

DENVER CO 80218
PHONE 303 399 3747

PATRICK S CALLERY
UNIV OF MARYLAND
20 N PINE ST

BALTIMORE MD 21201
PHONE 301 528 2980

E L CALLIS
LOS ALAMOS NATIONAL LAB
MAIL STOP G740

LOS ALAMOS NM 87545
PHONE.

DOUGLAS CAMERON
UNOCAL
SCI & TECH DIV

BREA CA 92621
PHONE: 714 528 7201

JOSEPH E CAMPANA
QUALITY ASSURANCE LAB
UNIV OF NEVADA
4505 MARYLAND PKWY
LAS VEGAS NV 89154
PHONE 702 739 3142

CLAY S CAMPBELL
FINNIGAN MAT
355 RIVER OAKS PKWY

SAN JOSE CA 95134-9990
PHONE 408 433 4800

JAMES A CAMPBELL
574 BUILDING
DOW CHEMICAL CO

MIDLAND MI 48640
PHONE 517 636 5253

SCOTT CAMPBELL
SHELL DEV CO
PO BOX 4248

MODESTO CA 95352
PHONE. 209 545 8105

THOMAS W CAMPBELL
8009 HILLRISE DRIVE

AUSTIN TX 78759
PHONE 512 474 5547

DAVID C CANADA
MARTIN MARIETTA CORP
PO BOX P K10048

OAK RIDGE TN 37831
PHONE. 615 574 9764

RICHARD J CAPP
3038 PITCHFORK LN

MCKEES ROCKS PA 15136
PHONE 412 777 8372

JOHN H CAPPIS
LOS ALAMOS SCI LAB
INC-7 MS-J514

LOS ALAMOS NM 87544
PHONE: 505 667 4498

RICHARD M CAPRIOLI
UNIV OF TEXAS HSC
ANALTYICAL CHEM CTR
PO BOX 20708
HOUSTON TX 77225
PHONE

H S CARDEN
5361 BIGGER RD

KETTERING OH 45440
PHONE 513 865 3789

DANIEL B CARDIN
UNION OIL RESEARCH
376 S VALENCIA ROOM M-104

BREA CA 92621
PHONE: 714 528 7201

JO CARLIN
MERCK SHARP & DOHME
RESEARCH LABORATORY
PO BOX 2000
RAHWAY NJ 07065
PHONE: 201 574 5920

TIMOTHY J CARLIN
MOBIL RES & DEV CORP
RESEARCH DEPT

PAULSBORO NJ 08066
PHONE. 609 423 1040

STEPHEN F CARLSEN
CIBA-GEIGY
444 SAW MILL RIVER ROAD

ARDSLEY NY 10502
PHONE: 914 478 3131

STEVEN A CARR
SMITHKLINE & FRENCH
AP&S CHEMISTRY F-90
1500 SPRING GARDEN ST
PHILADELPHIA PA 19101
PHONE 215 751 5743

JOHN E CARROLL
MATTSON INSTRUMENTS
6333 ODANA ROAD

MADISON WI 53719
PHONE 608 273 2370

GUY T CARTER
AMERICAN CYANAMID CO
MED RESEARCH DIV
LEDERLE LABORATORIES
PEARL RIVER NY 10965
PHONE. 914 735 5000

JOEL A CARTER
RT 7
BOX 487-C
CLINTON TN 37716
PHONE. 615 574 2447

ALLEN M CARY
FINNIGAN MAT
355 RIVER OAKS PKWY
SAN JOSE CA 95134
PHONE. 408 483 4800

L F CASABONA
TELEDYNE-ISOTOPES
50 VAN BUREN AVE
WESTWOOD NJ 07675
PHONE: 201 664 7070

CAROLYN J CASSADY
216 VALLEY STREAM LANE
WAYNE PA 09187
PHONE: 215 359 2411

P M CASTLE
778 CEDARWOOD DR
PITTSBURGH PA 15235
PHONE 412 256 2090

ALBERT W CASTLEMAN
PENNSYLVANIA STATE UNIV
CHEMISTRY DEPT
152 DAVEY LAB
UNIVERSITY PK PA 16802
PHONE: 814 865 7242

MAURO E CASTRO
DEPT OF CHEMISTRY
TEXAS A&M UNIV
COLLEGE STN TX 77843
PHONE: 409 845 0614

DENNIS CATALANO
IT CORP
312 DIRECTORS DRIVE
KNOXVILLE TN 37923
PHONE·

LARRY C CATTRAN
HEWLETT PACKARD
1601 CALIFORNIA AVE
PALO ALTO CA 94304
PHONE: 415 857 6118

AHMET CELIKKAYA
110 ENGINEERING ANNEX
IOWA STATE UNIV
AMES IA 50010
PHONE· 515 294 1214

STEVEN P CEPA
ABBOTT LABS
D 417 AP-9
ABBOTT PARK IL 60064
PHONE. 312 932 2081

RONALD L CERNY
CHEMISTRY DEPT
MCMS
UNIV OF NEBRASKA
LINCOLN NE 68588
PHONE 402 472 3507

JAN CHABALA
UNIV OF CHICAGO
5640 S ELLIS AVENUE
CHICAGO IL 60637
PHONE:

JOHN CHAFFIN
CITY OF SAN DIEGO
4077 N HARBOR DRIVE
SAN DIEGO CA 92101
PHONE 619 225 9367

J W CHAI
DEPT OF PHARMACOLOGY
MED UNIV OF S CAROLINA
CHARLESTON SC 29425
PHONE. 803 792 2471

BRIAN CHAIT
ROCKEFELLER UNIV
1230 YORK AVE
NEW YORK NY 10021
PHONE· 212 570 8849

JOHN A CHAKEL
GENENTECH INC
460 PT SAN BRUNO
SO SAN FRAN CA 94080
PHONE. 415 266 1239

WALTER S CHAMBERLIN
1001 CEDRO CT
LOS ALAMOS NM 87544
PHONE 505 667 2054

C L CHAN
E LOS ANGELES COLLEGE
CHEMISTRY DEPT
1301 E BROOKLYN AVE
MONTEREY PARK CA 91754
PHONE 213 265 8650

CONNIE K CHAN
40-22 77 STREET
ELMHURST NY 11373
PHONE 212 367 7879

DANIEL Y K CHAN
METPATH LABORATORY
1300 E TOUHY AVENUE
DES PLAINES IL 60018
PHONE· 312 635 4700

KELVIN W CHAN
SYNTEX RESEARCH
3401 HILLVIEW AVE
PALO ALTO CA 94304
PHONE 415 855 5660

KENNETH Y CHAN
MERRELL-DOW
2110 E GALBRAITH ROAD
CINCINNATI OH 45215
PHONE

PISAL CHANDRASURIN
BURROUGHS WELLCOME
RES TRI PK NC 27709
PHONE·

CHERNG CHANG
WRIGHT STATE UNIV
BREHM LAB
DAYTON OH 45435
PHONE· 513 873 3123

S Y CHANG
MERRELL DOW RESEARCH INST
PO BOX 68470
INDIANAPOLIS IN 46268
PHONE. 317 873 7197

TED T CHANG
AMERICAN CYANAMID
1937 W MAIN ST
STAMFORD CT 06904
PHONE· 203 248 7331

PETER J CHANTRY
WESTINGHOUSE
RES & DEV
1310 BEULAH RD
PITTSBURGH PA 15235
PHONE. 412 256 1001

RICHARD CHAPMAN
FINNIGAN MAT
355 RIVER OAKS PKWY
SAN JOSE CA 95134
PHONE. 408 433 4800

DENNIS M CHARKOWSKI
UNIV OF IOWA
PHARMACOLOGY DEPT
B S B
IOWA CITY IA 52242
PHONE. 319 353 4718

JUDI CHARLES
HAZARDOUS MATERIALS LAB
2151 BERKELEY WAY
BERKELEY CA 94704
PHONE: 415 525 2486

BONNIE A CHARPENTIER
PROCTER & GAMBLE CO
6071 CENTER HILL RD
FOODS F1B26
CINCINNATI OH 45224
PHONE: 513 542 1951

PHILIPPE CHASTAGNER
E I DUPONT
SAVANNAH RIVER LAB
MS/735A D106
AIKEN SC 29808-0001
PHONE: 803 725 3293

DALE A CHATFIELD
SAN DIEGO STATE UNIV
CHEMISTRY DEPT

SAN DIEGO CA 92182
PHONE: 619 265 5806

CHIA T CHEN
11616 FLINTS GRV LN

GAITHERSBURG MD 20878
PHONE 202 523 7174

LING CHEN
CHEMISTRY DEPT
OHIO STATE UNIV
140 W 18TH AVENUE
COLUMBUS OH 43210
PHONE: 614 422 0480

NANCY WU CHEN
COOK CTY OFF OF THE
MEDICAL EXAMINER
2121 W HARRISON ST
CHICAGO IL 60612
PHONE: 312 666 0500

PAUL H CHEN
ENVIRONMENTAL SCI & ENGIN
PO BOX ESE

GAINESVILLE FL 32602
PHONE: 904 332 3318

YA-CHI CHEN
2507 CREEK MEADOW DR

HOUSTON TX 77084
PHONE:

MICHAEL T CHENG
STAUFFER CHEMICAL CO
1200 SOUTH 47TH ST

RICHMOND CA 94804
PHONE: 415 231 1062

EDWARD K CHESS
BATTELLE NWST LABS
PO BOX 999

RICHLAND WA 99352
PHONE: 509 376 2234

T L CHESTER
PROCTER & GAMBLE CO
PO BOX 39175

CINCINNATI OH 45247
PHONE: 513 245 2450

G B CHHEDA
ROSWELL PARK INSTITUTE
666 ELM STREET

BUFFALO NY 14263
PHONE

GIRISH B CHHEDA
ROSWELL PAK MEM INST
666 ELM ST

BUFFALO NY 14263
PHONE: 716 845 2388

MICHAEL P CHIARELLI
2205 S 10TH STREET
NO 107

LINCOLN NE 68502
PHONE: 402 472 3507

D M CHINN
FINNIGAN MAT
355 RIVER OAKS PKWY

SAN JOSE CA 95134
PHONE: 408 433 4800

JOHN W CHINN
CHEMISTRY DEPT
UNIV OF TEXAS

AUSTIN TX 78712
PHONE: 512 471 7344

GARY R CHIPMAN

AMOCO RES CTR
PO BOX 400
NAPERVILLE IL 60566
PHONE: 312 420 5248

DIANE CHO
FINNIGAN MAT
355 RIVER OAKS PKWY

SAN JOSE CA 95134
PHONE: 408 433 4800

CHIH-CONG CHOU
US ARMY
CRDEC SMCCR-RSB

ABER PROV GRD MD 21010-5423
PHONE:

F E CHOU
334 OVERBROOK RD

BALTIMORE MD 21212
PHONE: 301 391 9116

CAROL S CHOW
CHEMICAL WASTE MNGMT
150 WEST 137TH STREET

RIVERDALE IL 60627
PHONE 312 841 8360

JEFF CHRISTENSON
NICOLET INSTRUMENTS
5225-1 VERONA ROAD

MADISON WI 53711
PHONE: 608 271 3333

PETER CHRISTIANSEN
FINNIGAN MAT
355 RIVER OAKS PKWY

SAN JOSE CA 95134
PHONE: 408 433 4800

W H CHRISTIE
OAK RIDGE NAT'L LAB
PO BOX Y BLDG 9735

OAK RIDGE TN 37831
PHONE: 615 574 2455

RAY CHRISTOPHER
4415 NORWALK DR #18

SAN JOSE CA 95129
PHONE: 408 946 4848

T Z CHU
FINNIGAN CORP
355 RIVER OAKS PKWY

SAN JOSE CA 95134-9990
PHONE: 408 433 4800

HENRY CHUNG
R J REYNOLDS TOBACCO
BOWMAN GRAY TECH CTR
BLDG 611-13E/002
WINSTON-SALEM NC 27102
PHONE: 919 773 4939

LILLIAN CHURCHILL
SIGNAL RESEARCH CTR
50 EAST ALGONQUIN ROAD
BOX 5016
DES PLAINES IL 60017-5016
PHONE: 312 391 3170

ROBERT CITERIN
4440 WARRENSVILLE CTR RD

CLEVELAND OH 44128
PHONE

JAMES D CIUPEK
UNIV OF CHICAGO
DEPT OF CHEMISTRY
5735 S ELLIS AVE
CHICAGO IL 60637
PHONE:

KEITH L CLAY
UNIV OF COLORADO
PHARMACOLOGY DEPT
4200 E 9TH AVE
DENVER CO 80262
PHONE: 303 394 8961

MICHAEL T CLEARY
SIGNAL RESEARCH CTR
50 UOP PLAZA

DES PLAINES IL 60016-6187
PHONE: 312 391 3448

S D CLEMANS
STERLING WINTHROP
COLUMBIA TURNPIKE

RENSSELAER NY 12144
PHONE: 518 445 8139

RONALD L COCHRAN
ASHLAND CHEMICAL CO
PO BOX 2219

COLUMBUS OH 43216
PHONE. 614 889 4642

ALLEN I COHEN
SQUIBB INST MED RES
PO BOX 191

NEW BRUNSWICK NJ 08902
PHONE· 201 545 2686

RICHARD B COLE
MASS SPECTROMETRY GROUP
NIEHS BLDG 6 ROOM 605
PO BOX 605
RES TRI PK NC 27709
PHONE· 919 541 2964

GEORGE J COLLINS
FINNIGAN MAT
355 RIVER OAKS PKWY

SAN JOSE CA 95134-9990
PHONE· 408 433 4800

KEITH R COMPSON
KRATOS ANALYTICAL INST
170 WILLIAMS DRIVE

RAMSEY NJ 07446
PHONE 201 934 9000

DENISE A CONTOS
1802 ASHLAND AVE

COLUMBUS OH 43212
PHONE 614 422 8190

G L COOK
8220 E GARFIELD M-15

SCOTTSDALE AZ 85257
PHONE. 602 994 3326

ANDREW J CLIFFORD
DEPT OF NUTRITION
UNIV OF CALIFORNIA

DAVIS CA 95616
PHONE 916 752 3376

JOHN T CODY
QUALITY CONTROL DIV
AIR FORCE DRUG TESTING LAB

BROOKS AFB TX 78235-5000
PHONE 512 536 2961

M J COHEN
PCP INC
2155 INDIAN ROAD

W PALM BEACH FL 33409
PHONE 305 683 0507

EMILE COLEMAN
US EPA
26 W ST CLAIR STREET

CINCINNATI OH 45268
PHONE. 513 569 7456

JENNIFER A COLLINS
BIO-ANALYTICAL TECHNOLOGIES
CHDN'S MEMORIAL HOSPITAL
2300 CHDN'S PLAZA
CHICAGO IL 60614
PHONE: 312 880 4306

CONRAD CONE
IFF R&D
1515 HIGHWAY 36

UNION BEACH NJ 07735
PHONE 201 264 6500

D C CONWAY
TEXAS A&M UNIVERISTY
CHEMISTRY DEPT

COLLEGE STN TX 77843
PHONE: 209 845 4034

H D COOK
WESTINGHOUSE
BAPL
PO BOX 79
WEST MIFFLIN PA 15122
PHONE: 412 476 5424

MIDGE L COATES
CHEMISTRY DEPT
UNIV OF CALIFORNIA

RIVERSIDE CA 92521
PHONE. 714 787 4740

ROBERT B CODY
NICOLET INST CO
5225-1 VERONA RD

MADISON WI 53711
PHONE. 608 271 3333

K H COLBERG
AMERICAN CAN CO
TECH SER

BARRINGTON IL 60010
PHONE. 312 381 1900

STEVEN G COLGROVE
RAINTREE APTS
3300 ROLLINGBROOK DRIVE

BAYTOWN TX 77521
PHONE· 713 425 5784

RICHARD J COLTON
NRL
CODE 6170

WASHINGTON DC 20375-2671
PHONE 202 767 2671

JOHN D CONNELL
KRATOS SCIENTIFIC
603 ROSE CT

LISLE IL 60532
PHONE.

R J CONZEMIUS
1211 GARFIELD AVE

AMES IA 50010
PHONE 515 294 5822

J CARTER COOK
UNIV OF ILLINOIS
CHEMICAL SCIENCES

URBANA IL 61801
PHONE 217 333 2545

JOY P COCCHIARA
SHELL DEVELOPMENT CO
PO BOX 1380

HOUSTON TX 77001
PHONE: 713 493 7739

MICHAEL J COGGIOLA
SRI INTERNATIONAL
333 RAVENSWOOD AVE

MENLO PARK CA 94025
PHONE 415 859 3045

BRUCE N COLBY
PACIFIC ANALYTICAL
1989-B PALOMAR OAKS WAY

CARLSBAD CA 92008
PHONE: 619 931 1766

HUMBERTO COLLAZO-LOPEZ
306-4 PENELL CIRCLE

TALLAHASSEE FL 32304
PHONE 904 644 6484

C M COMBS
6814 KEMBELL DR

EVANSVILLE IN 47710
PHONE 812 838 8213

GERALD R CONNER
INFICON LEYBOLD
6500 FLY ROAD

E SYRACUSE NY 13057
PHONE. 315 437 0377

CHARLES J COOK
8301 DITZLER

RAYTOWN MO 64138
PHONE·

KELSEY D COOK
CHEMISTRY DEPT
UNIV OF TENNESSEE

KNOXVILLE TN 37996-1600
PHONE 615 974 8019

R GRAHAM COOKS
PURDUE UNIVERSITY
CHEMISTRY DEPT

W LAFAYETTE IN 47907
PHONE 317 494 5263

W J COOPER
FLORIDA INTERNL UNIV
DRINKING WATER
QUALITY RES CTR
MIAMI FL 33199
PHONE: 305 559 3049

J E COTTON
2512-102 AVE NE

BELLEVUE WA 98004
PHONE 237 5399

J WAYNE COWENS
GCOC ROOM 371
RPMI
666 ELM STREET
BUFFALO NY 14263
PHONE 716 845 3563

A G CRASKE
240 ALPHA DRIVE
PO BOX 11512

PITTSBURGH PA 15238
PHONE: 412 782 3884

THOMAS R CRISWELL
EASTMAN KODAK CO
1254 HOLLEY ROAD

WEBSTER NY 14580
PHONE: 716 477 6733

CATHERINE ANN CROWDER
7038 KINZALOW DRIVE

KNOXVILLE TN 37909
PHONE 615 584 7797

JAMES E CURLETT
CITY OF PHOENIX
1207 WEST 10TH PL

TEMPE AZ 85281
PHONE: 602 262 1855

C V COOPER
NIOSH
4676 COLUMBIA PKWY

CINCINNATI OH 45226
PHONE: 513 684 4258

CATHERINE E COSTELLO
MIT
CHEMISTRY 56-029
77 MASS AVE
CAMBRIDGE MA 02139
PHONE. 617 253 7224

M W COUCH
RESEARCH SERVICES
VA MEDICAL CTR

GAINESVILLE FL 32602
PHONE 904 376 1611

JOHN COWPAR
2860 DOVER DRIVE

BOULDER CO 80303
PHONE:

DAVID CRAWFORD
US DOE
NEW BRUNSWICK LABORATORY
9800 S CASS AVENUE
ARGONNE IL 60438
PHONE:

D R CRONN
RT 2 BOX 596

PULLMAN WA 99163
PHONE 509 335 1526

JAN R CROWLEY
WAYNE STATE UNIV
435 CHEMISTRY

DETROIT MI 48202
PHONE 313 577 3073

BO CURRY
HEWLETT-PACKARD CO
PO BOX 10161

PALO ALTO CA 94303-0871
PHONE 415 857 7660

CHARLES B COOPER
UNIV OF DELAWARE
PHYSICS DEPT

NEWARK DE 19711
PHONE: 302 451 2666

DONNA B COSULICH
LEDERLE LABORATORIES
MIDDLETOWN RD

PEARL RIVER NY 10965
PHONE 914 735 5000

JOHN COUTANT
MERRELL DOW PHARM
2110 E GALBRAITH RD

CINCINNATI OH 45215
PHONE: 513 948 7884

J C CRAIG
UNIV OF CALIFORNIA
PHARMACEUTICAL CHEM
926 MED SCIENCES BLD
SAN FRANCISCO CA 94143
PHONE: 415 476 1225

RICHARD W CRAWFORD
LLNL
PO BOX 808
L 310
LIVERMORE CA 94550
PHONE: 415 422 6309

KEVIN P CROSS
CHEMICAL ABSTRACTS SERVICE
DEPT 23
PO BOX 3012
COLUMBUS OH 43210
PHONE 614 421 3600

P R CUNNINGHAM
5 WESTRIDGE DR

BOLTON CT 06040
PHONE

ZORAH F CURRY
2650 BENTLEY ROAD
APT 14L

MARIETTA GA 30067
PHONE. 404 424 2411

DON A COOPER
RT 2 BOX 302

PURCEVILLE VA 22132
PHONE: 703 285 2583

ROBERT J COTTER
JOHNS HOPKINS UNIV
MID ATLANTIC MS LAB
725 N WOLFE ST
BALTIMORE MD 21205
PHONE: 301 955 3431

THOMAS COVEY
EQUINE DRUG TESTING
CORNELL UNIVAVE
925 WARREN DRIVE
ITHACA NY 14850
PHONE 607 256 6555

PAMELA F CRAIN
UNIV OF UTAH
311A SKAGGS HALL

SALT LAKE CTY UT 84112
PHONE. 801 581 7532

WILLIAM R CREASY
CHEMISTRY DIV
CODE 6110
NAVAL RESEARCH LAB
WASHINGTON DC 20375
PHONE. 202 767 2398

F W CROW
THE UPJOHN CO
UNIT 7832-259-12
7000 PORTAGE ROAD
KALAMAZOO MI 49001
PHONE 616 323 4344

ROBERT CUNNINGHAM
UNIV OF PITTSBURGH
3939 OHARA

PITTSBURGH PA 15260
PHONE: 412 624 0298

H M CURTIS
HALLIBURTON SERVICES
CHEMISTRY DEPT

DUNCAN OK 73533
PHONE. 405 251 3922

RAY D'ALONZO
PROCTER & GAMBLE
NORWICH DIVISION
PO BOX 191
NORWICH NY 13815
PHONE: 607 335 2042

D A DAHL
EG&G IDAHO
PO BOX 1625

IDAHO FALLS ID 83415
PHONE: 208 526 9915

MARIA-LOURDES DAHL
MONSANTO
800 N LINDBERGH

ST LOUIS MO 63167
PHONE. 314 694 5754

JIM DAHLGRAN
BORG WARNER CHEMICAL
PO BOX 68

WASHINGTON WV 26181
PHONE: 304 863 7325

FRED DALE
LID/AFGL
HANSCOM AFB

BEDFORD MA 01731
PHONE:

H S DANACEAU
7 BROOKES AVE

GAITHERSBURG MD 20760
PHONE. 301 977 7737

PRADIP R DAS
SCHERING-PLOUGH CORP
60 ORANGE STREET
B-8B
BLOOMFIELD NJ 07003
PHONE. 201 429 3977

CHHABIL DASS
STOUT NEUROSCIENCES
MASS SPEC LAB
956 COURT ST
MEMPHIS TN 38163
PHONE: 901 528 5488

G D DAVES
LEHIGH UNIV
CHEMISTRY DEPT
SEELEY G MUDD BLDG 6
BETHLEHEM PA 18015
PHONE: 215 861 3471

ARTHUR DAVIDSON
DEA WESTERN FIELD LAB
PO BOX 36075

SAN FRANCISCO CA 94102
PHONE. 415 556 0951

TIM DAVIDSON
3051 MARSHALL APT 5

CINCINNATI OH 45220
PHONE: 513 475 4312

WALTER DAVIDSON
42 HARRISON STREET

CROTON/HUDSON NY 10520
PHONE:

JOHN P DAVIES
1610 NORTH 12TH

LAFAYETTE IN 47906
PHONE 317 742 2583

DEAN V DAVIS
UNOCAL SCIENCE & TECH DIV

BREA CA 92621
PHONE 714 528 7201

FREDDY C DAVIS
AIR FORCE DRUG TESTING LAB
AFDTL/DL

BROOKS AFB TX 78235-5000
PHONE 512 536 2387

MARGARET R DAVIS
261 ROCHELLE AVENUE

PHILADELPHIA PA 19128
PHONE: 215 768 3081

W D DAVIS
R D 5
COUNTY FARM ROAD

BALLSTON SPA NY 12020
PHONE

WILLIAM DAVIS
71 MERBROOK BLVD

NERION PA 19066
PHONE

WILLIAM DAVIS
ATOM SCIENCES
114 RIDGEWAY CTR

OAK RIDGE TN 37830
PHONE. 615 483 1113

WILLIAM E DAVIS
NOR-AM CHEMICAL CO
PO BOX 5130
1740 WHITEHALL RD
N MUSKEGON MI 49445
PHONE 616 744 4711

RICHARD A DAY
UNIV OF CINCINNATI
CHEMISTRY DEPT

CINCINNATI OH 45221
PHONE 513 475 3673

ROBERT DAY
5A BROOKSIDE DRIVE

DRYDEN NY 13053
PHONE 607 755 8312

DONN E DEAL
11761 E HERNDON AVE

CLOVIS CA 93612
PHONE 209 297 1552

MARK A DEARTH
GEOLOGY 541
INDIANA UNIV

BLOOMINGTON IN 47405
PHONE 812 335 6246

B A DEBARBIERI
37 WARREN ST
APT 3A

NUTLEY NJ 07110
PHONE 201 235 2852

JAMES J DECORPO
NAVAL SEA SYS COMM
CODE 05R32

WASHINGTON DC 20362
PHONE 202 692 9462

JOHN A DEFEVER
14469 ELLEN DR

LIVONIA MI 48154
PHONE.

MAX L DEINZER
OREGON STATE UNIV
AGRICUL CHEM DEPT

CORVALLIS OR 97331
PHONE 503 754 2906

DAVID A DEIS
2450 DUNSWORTH DR

COLUMBUS OH 43085
PHONE.

DANA E DEJOHN
WARNER LAMBERT
PO BOX 1047
2800 PLYMOUTH RD
ANN ARBOR MI 48106-1047
PHONE. 313 996 7135

DON C DEJONGH
FINNIGAN CORP
355 RIVER OAKS PKWY

SAN JOSE CA 95134
PHONE: 408 433 4800

MICHAEL J DEKREY
CONOCO INC RE 228
PO BOX 1267

PONCA CITY OK 74603
PHONE 405 767 2945

TOM DELANEY
PROCTER & GAMBLE CO
MIAMI VALLEY LABS

CINCINNATI OH 45247
PHONE

SHERRI-SUE DELBERT
CHEMISTRY DEPT
MICHIGAN STATE UNIV

EAST LANSING MI 48824
PHONE: 517 353 5215

JAMES E DELMORE
R #7 BOX 54

IDAHO FALLS ID 83401
PHONE

WILLIAM DEMAIO
7003 BISSONNET STREET
#1210

HOUSTON TX 77074
PHONE: 713 749 2675

BRUCE R DEMARK
PROCTER & GAMBLE
MIAMI VALLEY LABS
PO BOX 39175
CINCINNATI OH 45247
PHONE 513 245 2572

PLAMEN A DEMIREV
JOHNS HOPKINS UNIV
DEPT OF PHARMACOLOGY
725 N WOLFE STREET
BALTIMORE MD 21205
PHONE. 301 955 3022

DRUE DENTON
UNIV OF CINCINNATI
MEDICAL CTR
HEMATOLOGY-ONCOLOGY
CINCINNATI OH 45267
PHONE: 513 872 7694

CHARLES H DEPUY
UNIV OF COLORADO
CHEMISTRY DEPT
CAMPUS BX 215
BOULDER CO 80309
PHONE: 303 492 7652

HENRY L DEQUASIE
215 MEADOWOOD ROAD SW

FAIRVIEW TN 37062
PHONE: 615 322 2094

FRED L DEROOS
BATTELLE LABS
505 KING AVE

COLUMBUS OH 43201
PHONE 614 424 4247

DOMINIC DESIDERIO
UNIV OF TENNESSEE
RM A218 COLEMAN BLDG
956 COURT
MEMPHIS TN 38163
PHONE:

ANTHONY J DESTEFANO
NORWICH EATON PHARM
PO BOX 191

NORWICH NY 13815
PHONE: 607 335 2603

LEESA DETERDING
MCMS
UNIV OF NEBRASKA

LINCOLN NE 68588
PHONE. 402 472 3507

LISA DETTER
DEPT OF CHEMISTRY
BOX 390
PURDUE UNIV
W LAFAYETTE IN 47907
PHONE 317 494 5462

M S DEVRIES
IBM
K32180
ALMADEN RESEARCH CTR
SAN JOSE CA 95120
PHONE

JOS SIMON DEWIT
DEPT OF CHEMISTRY
UNIV OF NORTH CAROLINA

CHAPEL HILL NC 27514
PHONE:

PATRICIA H DHAHIR
ELI LILLY & CO
WISHARD MEMORIAL HOSPITAL
1001 WEST 10TH STREET
INDIANAPOLIS IN 46202
PHONE. 317 261 4807

SEKSAN DHEANDHANOO
NAT'L BUR OF STANDARDS
A144/BLDG 222

GAITHERSBURG MD 20899
PHONE

J R DIAS
UNIV OF MISSOURI
CHEMISTRY DEPT

KANSAS CITY MO 64110
PHONE: 816 276 1555

V H DIBELER
PO BOX 151

BETHANY BEACH DE 19930
PHONE

KENNETH J DICKENS
VACUMETRICS INC
2261 PALMA DRIVE

VENTURA CA 93003
PHONE. 805 644 7461

L L DICKERSON
2005 S HIGBEE

IDAHO FALLS ID 83401
PHONE 208 526 3035

GERALD C DIDONATO
CHEMISTRY DEPT
INDIANA UNIVERSITY

BLOOMINGTON IN 47401
PHONE 812 335 3436

ANDREA M DIETRICH
UNIV OF N CAROLINA
ENVIR SCI & ENGIN
ROSENAU HALL RM 155
CHAPEL HILL NC 27514
PHONE: 919 966 3862

DONNA K DIETRICH
3446 WE AVENUE

ST ANN MO 63074
PHONE. 314 694 3610

L A DIETZ
1124 MOHEGAN RD

SCHENECTADY NY 12309
PHONE

JOHN J DINO
5706 LOYAL AVENUE

DURHAM NC 27713
PHONE: 549 8263

MARY M DIRR
PROCTER & GAMBLE
11810 E MIAMI RIVER ROAD

CINCINNATI OH 45247
PHONE: 513 245 2258

ROBERT L DITTRICH
RALSTON PURINA CO
900 CHECKERBOARD SQUARE

ST LOUIS MO 63164
PHONE 314 982 3416

MARY A DITUSA
1975 NOTTINGHAM LANE

WHEATON IL 60187
PHONE 312 653 2792

MICHAEL F DIXON
GALILEO ELECTRO-OPTICS
GALILEO PK

STURBRIDGE MA 01518
PHONE: 617 347 9191

A S DOAN
GODDARD SPC FLT CTR
CODE 615

GREENBELT MD 20771
PHONE 344 7511

D L DOERFLER
307 CROYDON LANE

MANCHESTER MO 63021
PHONE. 314 537 6756

JOSEPH R DONNELLY
734 STRAWBERRY PL

HENDERSON NV 89015
PHONE· 702 798 2299

STEVEN B DORN
GEN'L ELEC CORP
R&D BLDG K-1 RM2A40
PO BOX 8
SCHENECTADY NY 12301
PHONE· 518 387 6419

ROBERT C DRAKE
2420 MORNINGSIDE DRIVE

LAWRENCE KS 66046
PHONE 913 864 3223

D L DROPKIN
3408 MORNINGSIDE DR

RALEIGH NC 27607
PHONE· 919 541 2323

KEVIN DUFFIN
CHEMISTRY BLDG
INDIANA UNIV

BLOOMINGTON IN 47405
PHONE 812 335 3436

ROBERT C DUNBAR
CASE WESTERN RESERVE
CHEMISTRY DEPT

CLEVELAND OH 44118
PHONE· 216 368 3712

L R DUSOLD
FDA
HFF-454
200 C ST SW
WASHINGTON DC 20204
PHONE· 202 245 1413

STEVE DOHERTY
CHEMISTRY DEPT
INDIANA UNIV

BLOOMINGTON IN 47405
PHONE· 812 335 3436

FRANKLIN G DOOLITTLE
DEPT OF CHEMISTRY
WASHINGTON STATE UNIV

PULLMAN WA 99163
PHONE: 509 335 1707

MARIE G DORVIL
1085 NW 117TH STREET

MIAMI FL 33168
PHONE: 305 769 1895

PETER A DREIFUSS
W R GRACE CO
WASHINGTON RESEARCH CTR
7379 ROUTE 32
COLUMBIA MD 21044
PHONE 301 531 4504

GEORGE R DUBAY
BRISTOL-MYERS RES
5 RESEARCH PKWY
PO BOX 5100
WALLINGFORD CT 06492-7660
PHONE·

D L DUGGER
114 LEOLEIS DR

MARLBORO MA 01752
PHONE· 617 466 2764

MICHAEL A DUNCAN
DEPT OF CHEMISTRY
UNIV OF GEORGIA

ATHENS GA 30602
PHONE 404 542 2626

R C DUTKY
14112 NEW HAMP AVE

COLESVILLE MD 20904
PHONE: 301 384 5305

MALCOLM DOLE
110 WOOD ROAD M-1

LOS GATOS CA 95030
PHONE 408 354 0478

J WALLACE DOONG
7502 CORPORATE #178

HOUSTON TX 77036
PHONE: 713 943 9776

RALPH C DOUGHERTY
FLORIDA STATE UNIV
CHEMISTRY DEPT

TALLAHASSEE FL 32306
PHONE· 904 644 5725

RUSSELL C DREW
103 CARPENTER DRIVE

STERLING VA 22170
PHONE

B F DUDENBOSTEL
NJ DEP
CN411
380 SCOTCH ROAD
TRENTON NJ 08628
PHONE:

BRUCE E DUMDEI
MDS ADVANCED ANALYTICS
TWO DUNDEE PARK

ANDOVER MA 01810
PHONE· 617 470 1390

RICHARD DUNPHY
MONELL CHEMICAL SENSES CTR
3500 MARKET ST

PHILADELPHIA PA 19104
PHONE 215 898 1031

SHIB PRASAD DUTTA
BIOPHYSICS DEPT
ROSWELL PK MEM INST
666 ELM STREET
BUFFALO NY 14263
PHONE. 716 845 3294

GREGORY G DOLNIKOWSKI
DEPT OF CHEMISTRY
MICHIGAN STATE UNIV

EAST LANSING MI 48824
PHONE: 517 353 6767

R CAMERON DOREY
DEPT OF CHEMISTRY
WICHITA STATE UNIV

WICHITA KS 67208
PHONE· 316 689 3120

ROBERT J DOYLE
NAVAL RESEARCH LAB
CODE 6110

WASHINGTON DC 20375
PHONE· 202 767 3551

TOM J DRISCOLL
NICOLET INSTRUMENTS
215 FOURIER AVENUE

FREMONT CA 94539
PHONE 415 490 8870

DENNIS DUEBELBEIS
ENVIRONMENTAL TRACE
SUBSTANCES RES CTR
ROUTE 3
COLUMBIA MO 65201
PHONE 314 882 2151

DAVID DUMOND
SYMBOLICS CORP

PHONE:

R J DUPZYK
LLL
PO BOX 808 L-396

LIVERMORE CA 94550
PHONE: 415 422 6611

DANIEL M DYE
AIZA CORP
950 PAGE MILL ROAD
PO BOX 10950
PALO ALTO CA 94303
PHONE· 415 494 5302

FAUL P DYMERSKI
CAL LAB EAST
PO BOX 11106

RICHMOND VA 23230
PHONE 804 359 1900

BRIAN ECKENRODE
CHEMISTRY DEPT
MICHIGAN STATE UNIV

EAST LANSING MI 48824
PHONE 517 353 5215

JIM EICHELBERGER
US EPA
26 E ST CLAIR

CINCINNATIE OH 45268
PHONE

JAMES F ELDER
R J REYNOLDS TOBACCO
R & D DEPT
BOWMAN GRAY TECHNICAL CTR
WINSTON-SALEM NC 27102
PHONE. 919 773 4941

POLLY ELLERBE
NAT'L BUR OF STANDARDS
ORGANIC ANALYTICAL DIV

GAITHERSBURG MD 20899
PHONE: 301 921 2153

EDGAR M EMERY
6 HIGHVIEW DRIVE

WOODBRIDGE NJ 07095
PHONE.

PAUL S EPSTEIN
3260 CREEK

ANN ARBOR MI 48104
PHONE. 313 971 3523

JAMES S ERSKINE
DOW CHEMICAL
B-1219

FREEPORT TX 77541
PHONE: 409 238 3244

ISMET DZIDIC
1220 BARTLETT
NO 2

HOUSTON TX 77006
PHONE 713 493 8594

JAMES P EDASERY
72-31 LITTLENECK PWY

GLEN OAKS NY 11004
PHONE. 212 650 6159

W NOEL EINOLF
PHILIP MORRIS USA
RESEARCH CENTER
PO BOX 26583
RICHMOND VA 23261
PHONE: 804 274 2530

VINCENT A ELDER
MARY KAY COSMETICS
PO BOX 47310

DALLAS TX 75247
PHONE 214 638 6750

WILLIAM H ELLIOTT
ST LOUIS UNIV
BIOCHEMISTRY DEPT
1402 S GRAND BLVD
ST LOUIS MO 63104
PHONE. 314 577 8150

JOHN F ENG
DEPT OF CHEMISTRY
PRINCETON UNIV

PRINCETON NJ 08540
PHONE. 609 452 3928

JOHN A ERAS
2020 W BEVERLY BLVD

LOS ANGELES CA 90057
PHONE. 213 974 4647

THOMAS J ESKEW
NUCLIDE CORP
642 E COLLEGE AVE

STATE COLLEGE PA 16801
PHONE: 814 238 0541

R E EBY
955 W OUTER DRIVE

OAK RIDGE TN 37830
PHONE. 615 483 1829

KENNETH W EDGELL
BIONETICS CORP
16 TRIANGLE PARK DR

CINCINNATI OH 45246
PHONE: 513 771 0448

BRIAN EITZER
541 GEOLOGY BLDG
INDIANA UNIV

BLOOMINGTON IN 47405
PHONE 812 335 5976

CLAUDIA H ELKINS
STAUFFER CHEMICAL
EASTERN RESEARCH CENTER

DOBBS FERRY NY 10522
PHONE. 914 693 1200

ROBERT H ELLIS
HEWLETT PACKARD
SCIEN INSTR DIV
1601 CALIFORNIA AVE
PALO ALTO CA 94304
PHONE: 415 857 6090

ROGER E ENGLAND
800 BUCHANAN STREET

ALBANY CA 94710
PHONE: 415 486 3519

ERIC ERICKSON
CHEMISTRY DEPT
MICHIGAN STATE UNIV

EAST LANSING MI 48824
PHONE 517 353 5215

RAMON ESPINO
10372 BRYAN STREET

RIVERSIDE CA 92505
PHONE: 714 354 5954

M W ECHO
WINCO
PO BOX 536

IDAHO FALLS ID 83402
PHONE 208 526 2327

CHARLES G EDMONDS
UNIV OF UTAH
COLLEGE OF PHARMACY
MEDICINAL CHEM DEPT
SALT LAKE CTY UT 84112
PHONE: 801 581 5581

F A ELDER
237 JUDSON ST

WEBSTER NY 14580
PHONE: 422 3179

ROBERT E ELLEFSON
MONSANTO RESEARCH CO
MOUND LAB R171

MIAMISBURG OH 45342
PHONE: 513 865 3791

WILLIAM B EMARY
DEPT OF CHEMISTRY
BOX 402
PURDUE UNIVERSITY
W LAFAYETTE IN 47907
PHONE:

CHRISTIE G ENKE
MICHIGAN STATE UNIV
CHEMISTRY DEPT

EAST LANSING MI 48824
PHONE: 517 535 4511

MITCHELL D ERICKSON
MIDWEST RES INST
425 VOLKER BLVD

KANSAS CITY MO 64110
PHONE. 816 753 7600

BARBARA EVANS
38 EATON STREET

WINCHESTER MA 01890
PHONE: 617 642 0188

BEN M EVANS
CONOCO
PO BOX 1267

PONCA CITY OK 74603
PHONE 405 767 4736

C A EVANS
CHARLES EVANS & ASSOC
301 CHESAPEAKE DR

REDWOOD CITY CA 94063
PHONE 415 369 4567

DANIEL EVANS
152 DAVEY LABORATORY
BOX 31
PENN STATE UNIV
UNIV PARK PA 16802
PHONE: 814 863 3583

JAMES E EVANS
E KENNEDY SHRIVER CT
200 TRAPELO RD

WALTHAM MA 02254
PHONE 617 642 0188

JAMES V EVANS
MILES LABORATORIES
ANALYTICAL RESEARCH
PO BOX 932
ELKHART IN 46515
PHONE: 219 262 7762

KERRY EVEN
38550 ORCHARD HILL DR
HEWLETT-PACKARD

NOVI MI 48050
PHONE: 313 349 9200

J W EWING
1701 LEXINGTON DR

LYNCHBURG VA 24503
PHONE:

JOHN R EYLER
UNIV OF FLORIDA
CHEMISTRY DEPT

GAINESVILLE FL 32611
PHONE 904 392 0532

BARBARA L FABRICANT
OWENS CORNING FIBERGLASS
PO BOX 415

GRANVILLE OH 43023
PHONE: 614 587 7360

I S FAGERSON
UNIV MASSACHUSETTS
CHENOWETH LAB

AMHERST MA 01003
PHONE: 413 545 2278

HENRY M FALES
NAT'L INST OF HEALTH
BLDG 10, ROOM 7N 318

BETHESDA MD 20892
PHONE: 301 496 2135

A M FALICK
SCH OF PHARMACY
PARMACEUTICAL CHEM
UNIV OF CALIFORNIA
SAN FRANCISCO CA 94143-0446
PHONE: 415 666 5160

F C FALKNER
PFIZER INC
METAB

GROTON CT 06340
PHONE 203 441 4697

KAREN FARRELL
NORTH SHORE SANITARY DIST
RUSSELL ROAD
PO BOX 750
GURNEE IL 60031
PHONE 312 623 6060

JACK D FASSETT
NBS
BLDG 221 RM A21

GAITHERSBURG MD 20899
PHONE 301 921 2781

DOUGLAS FAST
CENTERS FOR DISEASE CONTROL
BLDG C17 ROOM 1814

ATLANTA GA 30333
PHONE 404 452 4144

KYM F FAULL
STANFORD UNIVERSITY
PSYCHIATRY DEPT
MEDICAL SCHOOL
STANFORD CA 94305
PHONE 415 497 7205

KENNETH D FAUST
ROCKY MTN ANALYTICAL LAB
5530 MARSHALL ST

ARVADA CO 80002
PHONE 303 421 6611

ANTOINETTE L FAVERO
RUSSELL ROAD
PO BOX 750

GURNEE IL 60031
PHONE 312 623 6060

LOUIS FEIGE
1851 TEAK COURT

HENDERSON NV 89015
PHONE 702 798 2226

VERNON J FEIL
USDA-MRRL
STATE UNIV STATION

FARGO ND 58105
PHONE 701 237 5771

GOTTFRIED FEISTNER
DEPT OF PSYCHIATRY
STANFORD UNIV MEDICAL CTR

STANFORD CA 94305
PHONE: 415 723 7205

JACK R FELKEY
TMS ANALYTICAL
6264 LAPAS TRAIL

INDIANAPOLIS IN 46268
PHONE 317 291 5697

JERRY FELSHER
140 RIDGE ROAD

NEW CITY NY 10956
PHONE 914 634 8905

RONG FENG
CHEMISTRY DEPT
BAKER LAB
CORNELL UNIV
ITHACA NY 14853
PHONE 607 256 3731

JOHN B FENN
ENGINEERING DEPT
YALE UNIV
PO BOX 2159 YALE STATION
NEW HAVEN CT 06520-2159
PHONE

PAUL V FENNESSEY
UNIV OF COLORADO
MED CTR C232
4200 E 9TH AVE
DENVER CO 80262
PHONE 303 394 7286

CATHERINE C FENSELAU
JOHNS HOPKINS UNIV
PHARMACOLOGY DEPT
725 N WOLFE ST
BALTIMORE MD 21205
PHONE 301 955 3420

ANNA M FERGUSON
THERMODYNAMICS RES
REED MCDONALD BLDG
TEXAS A&M UNIV
COLLEGE STATI TX 77843-3111
PHONE: 409 845 4940

G J FERGUSSON
124 NASSAU PLACE

CLAREMONT CA 91711
PHONE 714 626 8258

ROBERTO FERNANDEZ
412 DAVIS ROAD
PO BOX 3326

PASADENA TX 77501
PHONE 713 477 6841

DEAN D FETTEROLF
FED BUREAU OF INVESTIGATION
FORENSIC SCIENCE RESEARCH
FBI ACADEMY
QUANTICO VA 22135
PHONE: 703 640 6131

FRANK H FIELD
ROCKEFELLER UNIV
1230 YORK AVE

NEW YORK NY 10021
PHONE: 212 570 8848

WILLIAM FIES
155 CHEROKEE WAY

PORTOLA VLLY CA 94025
PHONE: 408 433 4800

FRED FINDEIS
DIV OF CHEMISTRY
NAT'L SCIENCE FNDN

WASHINGTON DC 20550
PHONE: 202 357 7503

H H FINEGOLD
RD 1, BOX 165

DALLASTOWN PA 17313
PHONE:

ROBERT E FINNIGAN
FINNIGAN MAT
355 RIVER OAKS PKWY

SAN JOSE CA 95134-9990
PHONE: 408 433 4800

DERRY L FISHEL
KENT STATE UNIV
CHEMISTRY DEPT

KENT OH 44242
PHONE: 216 672 2978

DIXIE L FISHER
ALLERGAN PHARMACEUTICALS
ANALYTICAL CHEMISTRY
2525 DUPONT DRIVE
IRVINE CA 92715
PHONE: 714 752 4500

JAMES R FISHER
1000 W AARON DRIVE I-8

STATE COLLEGE PA 06803
PHONE 814 234 2556

WADE L FITE
EXTREL CORP
240 ALPHA DR
PO BOX 11512
PIITSBURGH PA 15238
PHONE: 412 782 3884

JOHN F FITZGERALD
ETC
284 RARITAN CENTER PWY

EDISON NJ 08837
PHONE:

PAT W FLANAGAN
3008 ELLSWORTH DR

GREENVILLE NC 27834
PHONE: 919 522 6498

ELLEN L FLENTYE
7910 IVANHOE AVE
SUITE 430

LA JOLLA CA 92037
PHONE: 619 456 0669

GERALD D FLESCH
IOWA STATE UNIV
AMES LAB
USDOE
AMES IA 50011
PHONE: 515 294 3887

JANA L FLOREA
CONOCO INC
PO DRAWER 1267
325 R&D
PONCA CITY OK 74603
PHONE 405 767 2954

RICK A FLURER
DEPT OF CHEMISTRY
INDIANA UNIV

BLOOMINGTON IN 47405
PHONE: 812 335 3436

DENIS L FOERST
HEWLETT-PACKARD S/D
1601 CALIFORNIA AVE

PALO ALTO CA 94304
PHONE: 415 857 6025

THEODORE L FOLK
227 WASHINGTON AVE

CUYAHOGA FALL OH 44221
PHONE 216 796 4217

RODGER L FOLTZ
UNIV OF UTAH
CTR HUMAN TOXICOLOGY
38 SKAGGS HALL
SALT LAKE CTY UT 84112
PHONE: 801 581 5117

ROBERT A FORBES
28-29 TOWER DRIVE

W LAFAYETTE IN 47906
PHONE: 317 463 6799

CECIL FORD
CNA INSURANCE
OCCUPATIONAL HEALTH LAB
CNA PLAZA 3 WEST
CHICAGO IL 60685
PHONE: 312 822 5884

JOSEPH H FORD
USDA, APHIS, PPQ
NMRAL
PO BOX 3209
GULFPORT MS 39505-3209
PHONE:

JOHN B FOREHAND
A H ROBINS INC
1211 SHERWOOD AVE

RICHMOND VA 23220
PHONE:

FREDERICK FOREMAN
MONSANTO CO
MAIL ZONE U3G
800 NORTH LINDBERGH
ST LOUIS MO 63133
PHONE:

PAUL A FORSHEY
PROCTER & GAMBLE
6100 CENTER HILL ROAD

CINCINNATI OH 45224
PHONE: 513 659 6804

HOLLY A FORTNUM
DEPT OF CHEMISTRY BOX 155
MICHIGAN STATE UNIV

EAST LANSING MI 48824
PHONE. 517 349 2783

G O FOSS
FARRELL ROAD

NEWTOWN CT 06470
PHONE: 203 834 6343

KIRK B FOSTER
11549 HARLAN STREET

BROOMFIELD CO 80020
PHONE: 303 466 7156

NORMAN G FOSTER
2719 ROBINWOOD LANE

DENTON TX 76201
PHONE: 817 387 4840

H G FOUDA
PFIZER INC
DRUG METABOLISM

GROTON CT 06340
PHONE.

ROBERT E FRAAS
28 FOUNTAIN CIRCLE

RICHMOND KY 40475
PHONE.

ANA FRAIMAN
9232 TRIPP

SKOKIE IL 60076
PHONE: 312 677 3368

DAVID F FRALEY
903 SARBROOK DR

CINCINNATI OH 45231
PHONE: 513 627 6412

THOMAS J FRANCL
AGRICULTURAL RES DIV
AMERICAN CYANAMID CO
PO BOX 400
PRINCETON NJ 08690
PHONE: 609 799 0400

PAULA FRANCOM
38 SKAGGS HALL
CTR FOR HUMAN TOXICOLOGY
UNIV OF UTAH
SALT LAKE CTY UT 84112
PHONE

D J FRANK
8790 C ALLISON DRIVE

WESTMINSTER CO 80005
PHONE: 303 966 7855

LESLEY R FRANK
10807 LOMBARDY RD

SILVER SPRING MD 20901
PHONE 301 443 1640

JAMES C FRANKLIN
141 CUMBERLAND VIEW

OAK RIDGE TN 37830
PHONE 615 574 2284

BLAIR A FRASER
FDA
BOB/DBB/8800
ROCKVILLE PIKE
BETHESDA MD 20892
PHONE 301 496 1840

WILLIAM FRASURE
ANALYTICAL SPECIALTIES
326 MARION AVE

ST LOUIS MO 63119
PHONE 314 962 8648

ROYAL B FREAS
NAVAL RESEARCH LAB
CHEMISTRY DIV
CODE 6110
WASHINGTON DC 20375-5000
PHONE 202 767 3551

DONNAJEAN A FREDEEN
DEPT OF CHEMISTRY
UNIV OF BRIDGEPORT

BRIDGEPORT CT 06601
PHONE 203 576 4439

J P FREEMAN
1500 ROCK

PINE BLUFF AR 71602
PHONE 501 541 4369

LOUIS C FREES
INFICON LEYBOLD
6500 FLY ROAD

E SYRACUSE NY 13057
PHONE: 315 437 0377

KELLY D FREGIEN
UNIV OF MINN HOSP
GC-MS LAB
BOX 198 MAYO BLDG
MINNEAPOLIS MN 55455
PHONE 612 373 8772

CARL B FREIDHOFF
JOHNS HOPKINS UNIV
REMSEN HALL
34TH & N CHARLES STREETS
BALTIMORE MD 21218
PHONE 301 338 7454

BEN S FREISER
PURDUE UNIVERSITY
CHEMISTRY DEPT

W LAFAYETTE IN 47907
PHONE.

PATRICIA J K FRENCH
AMERICAN CYANAMID
PO BOX 400

PRINCETON NJ 08540
PHONE

ROBERT S FREUND
AT&T BELL LABS
600 MOUNTAIN AVE
ROOM 1D-256
MURRAY HILL NJ 07974
PHONE

NELSON M FREW
WOODS HOLE OCEAN INS
FYE BUIDLING

WOODS HOLE MA 02543
PHONE. 617 548 1400

CARL FREY
459 GRANITE SPRINGS

YORKTWN HGTS NY 10598
PHONE 914 742 4558

MARGARET A FRISCH
IBM RESEARCH CENTER
PO BOX 218

YORKTWN HGTS NY 10598
PHONE 914 945 1037

STEVEN W FROELICHER
2817 BLAIRMONT DRIVE

MIDLAND MI 48640
PHONE.

EMIL W FU
SANDOZ INC
59 ROUTE 10
BLDG 404 RM 376
E HANOVER NJ 07936
PHONE 201 386 8121

ROGER G FUELSTER
US GOV'T DEA
NORTH CENTRAL LAB
RM 500 610 S CANAL
CHICAGO IL 60607
PHONE 312 353 3640

RALPH W FUHRHOP
618 HOLLYWOOD PLACE

WEBSTER GROVE MO 63119
PHONE 314 275 7272

JOHN D FUHRMAN
MONSANTO UIC
800 N LINDBERGH BLVD

ST LOUIS MO 63167
PHONE 314 694 4238

MIEKO FUJIWARA
MONSANTO CO
AA1F
700 CHESTERFIELD VILL PWY
CHESTERFIELD MO 63198
PHONE 314 537 6271

ELAINE K FUKUDA
HOFFMAN LAROCHE
340 KINGSLAND ST

NUTLEY NJ 07110
PHONE 201 235 2019

LESLIE FUNDAKOWSKI
DEPT OF CHEMISTRY
UNIV OF DELAWARE

NEWARK DE 19711
PHONE. 302 451 2917

CAROL FUNG KEE FUNG
737 NE 9TH STREET

GAINESVILLE FL 32601
PHONE

PHILLIP T FUNKE
E R SQUIBB
PO BOX 4000

PRINCETON NJ 08540
PHONE 609 921 4993

DIANE L FURIO
PROCTER & GAMBLE
MIAMI VALLEY LABS
PO BOX 39175
CINCINNATI OH 45247
PHONE 513 245 2155

ED FURLONG
SPEA LABORATORY
ROOM 541 GEOLOGY
INDIANA UNIV
BLOOMINGTON IN 47401
PHONE 812 335 1217

JORGE FURLONG
DEPT OF CHEMISTRY
BAKER LABORATORY
CORNELL UNIV
ITHACA NY 14853
PHONE. 607 255 3731

RAYMOND L FURNER
NEUROSCIENCES PROG
UNIV OF ALABAMA

BIRMINGHAM AL 35294
PHONE. 205 934 2443

J H FUTRELL
UNIV OF UTAH
CHEMISTRY DEPT

SALT LAKE CTY UT 84112
PHONE 801 581 7307

WILLIAM G GABODA
BETZ LABORATORIES
4636 SOMERTON RD

TREVOSE PA 19047
PHONE 215 355 3300

P JANE GALE
RCA
DAVID SARNOFF RES CTR
PO BOX 432
PRINCETON NJ 08543-0432
PHONE: 609 734 3053

THEODORE J GALEN
5006 SHADY OAKS LANE

FRIENDSWOOD TX 77546
PHONE 713 483 4641

KENNETH L GALLAHER
STANDARD OIL CO
4440 WARRENSVILLE RD

CLEVELAND OH 44128
PHONE. 216 581 5826

EMILIO J GALLEGOS
CHEVRON
PO BOX 1627

RICHMOND CA 94804
PHONE 415 620 4113

W A GARLAND
DEPT DRUG METABOLISM

HOFFMANN-LA ROCHE
NUTLEY NJ 07110
PHONE: 201 235 2137

ERNEST L GARNER
NAT'L BUR STANDARDS
BLDG 221 ROOM B362

GAITHERSBURG MD 20899
PHONE

JOEL GARRELL
MECHANICAL ENGINEERING DEPT
UNIV OF TEXAS

AUSTIN TX 78712
PHONE: 512 471 5730

JOHN H GARRETT
WRIGHT STATE UNIV
BREHM LAB

DAYTON OH 45435
PHONE

DANIEL GARTEIZ
FINNIGAN MAT
355 RIVER OAKS PWY

SAN JOSE CA 95134
PHONE:

M L GAY
328 EAGLE HARBOR SO

LAUREL MD 20707
PHONE. 301 498 0245

RICHARD GEDAMKE
AYERST LABS RESEARCH
CN 8000

PRINCETON NJ 08540
PHONE

RICHARD A GEHLBACH
ATEC ASSOC INC
5150 EAST 65TH

INDIANAPOLIS IN 46220
PHONE: 317 849 4990

MICHAEL J GEHRON
DEPT OF CHEMISTRY
UNIV OF FLORIDA

GAINESVILLE FL 32611
PHONE. 904 392 0515

DAVID L GEIGER
2502 CROSS COUNTRY ROAD

FAIRBORN OH 45324
PHONE 513 255 2631

PAUL R GEISSLER
EXXON CHEMICAL CO
PO BOX 241

BATON ROUGE LA 70821
PHONE 504 359 4644

GREGORY I GELLENE
DEPT OF CHEMISTRY
UNIV OF NOTRE DAME

NOTRE DAME IN 46556
PHONE: 219 239 7837

GARY L GERMANN
1101 CRESCENT DRIVE

SPRINGFIELD IL 62704
PHONE. 217 782 8389

TIM GETEK
DEPT OF CHEMISTRY
UNIV OF HOUSTON

HOUSTON TX 77004
PHONE. 713 749 2675

SAHBA GHADERI
NICOLET INST CORP
ANAL BLDG
5225 VERONA RD
MADISON WI 53771
PHONE. 608 271 3333

BENJAMIN Y GIANG
STAUFFER RESEARCH
1200 SO 47TH ST

RICHMOND CA 94804
PHONE. 415 231 1118

DARYL GIBLIN
DEPT OF CHEMISTRY
UNIV OF NEBRASKA

LINCOLN NE 68588
PHONE: 402 472 3507

BRADFORD W GIBSON
DEPT OF PHARMACEUTICAL CHEM
UNIV OF CALIFORNIA

SAN FRANCISCO CA 94143
PHONE

GRAHAM GIBSON
4 ELENA COURT M

MEDFORD NJ 08055
PHONE 609 654 1862

JAMES H GIBSON
STANDARD OIL CO
4440 WARRENSVILLE CTR ROAD

CLEVELAND OH 44128
PHONE 216 581 5145

JEAN LUC GIGUET
DELSI INSTRUMENTS
10 KINGSBRIDGE ROAD

FAIRFIELD NJ 07006
PHONE. 201 227 7690

PHYLLIS W GILBERT
THE CLOROX CO
7200 JOHNSON DRIVE
PO BOX 493
PLEASANTON CA 94566
PHONE 415 847 6601

JOHN T GILL
MONSANTO RESEARCH CORP
MOUND FACILITY

MIAMISBURG OH 45342
PHONE:

BETH GILLECE-CASTRO
2035 9TH AVE
UNIV OF CALIFORNIA

SAN FRANCISCO CA 94116
PHONE. 415 476 5129

GREG GILLEN
DEPT OF CHEMISTRY
ARIZONA STATE UNIV

TEMPE AZ 85281
PHONE 609 965 4236

KEITH T GILLEN
SRI INTERNATIONAL
333 RAVENSWOOD AVE

MENLO PARK CA 94025
PHONE: 415 859 3250

K A GINGERICH
TEXAS A&M UNIVERSITY
CHEMISTRY DEPT

COLLEGE STN TX 77843
PHONE 409 845 2431

EDWARD GLICK
US EPA
26 WEST ST CLAIR

CINCINNATI OH 45268
PHONE

DOUGLAS E GOERINGER
OAK RIDGE NAT'L LAB
PO BOX Y BLDG 9735

OAK RIDGE TN 37831
PHONE 615 574 2452

PAUL C GOODLEY
HEWLETT PACKARD
SCI INST DIV
1601 CALIFORNIA AVE
PALO ALTO CA 94304
PHONE 415 857 6194

W PERRY GORDON
9550 N ZIONSVILLE ROAD

INDIANAPOLIS IN 46268
PHONE

JOSEPH J GRABOWSKI
DEPT OF CHEMISTRY
HARVARD UNIV
12 OXFORD STREET
CAMBRIDGE MA 02138
PHONE 617 495 4130

SUSAN H GRAHAM
6255 LONDON DRIVE

NEW ORLEANS LA 70122
PHONE. 504 394 2233

P W GILLES
UNIV OF KANSAS
CHEMISTRY DEPT

LAWRENCE KS 66045
PHONE

ANNE B GIORDANI
MT SINAI SCH OF MEDICINE
22/70 ANNENBERG BLDG
1 GUSTAVE LEVY PLACE
NEW YORK NY 10029
PHONE 212 650 5960

R E GLICK
FLORIDA STATE UNIV
CHEMISTRY DEPT

TALLAHASSEE FL 32306
PHONE 904 644 4824

ANN G GOETZ
HOFFMANN-LAROCHE
BLDG 71
340 KINGSLAND ST
NUTLEY NJ 07110
PHONE. 201 235 2058

GEORGE W GOODLOE
1359-A HAMPTON DRIVE

AUBURN AL 36830
PHONE. 205 826 5066

GWEN D GORETSAS
HEWLETT-PACKARD
2025 LARPENTEUR

ST PAUL MN 55113
PHONE 612 644 1100

DONALD G GRACZYK
ARGONNE NAT'L LAB
CHEMICAL TOXICOLOGY DIV
9700 S CASS AVENUE
ARGONNE IL 60439
PHONE 312 972 4460

ANDREW H GRANGE
935 SE 16TH AVE
NO 10

PORTLAND OR 97214
PHONE. 503 690 1084

TODD A GILLESPIE
UNIV OF FLORIDA
LEIGH HALL BOX 122

GAINESVILLE FL 32611
PHONE. 904 392 0515

GARY G GIRDAUKAS
42 S SERENITY WAY

GREENWOOD IN 46142
PHONE.

GARY L GLISH
OAK RIDGE NATL LAB
PO BOX Y
BLDG 9735
OAK RIDGE TN 37831
PHONE 615 574 2456

MILTON W GOHEEN
1211 KNOLLWOOD CT

RICHLAND WA 99352
PHONE: 509 376 3358

DENNIS GOODPASTURE
675 BROOKSEDGE BLVD

WESTERVILLE OH 43081
PHONE 614 891 3344

LEO A GORMAN
VG INSTRUMENTS
134 JUNEDALE DR

CINCINNATI OH 45218
PHONE. 513 825 1790

H H GRADE
GENERAL ELECTRIC CO
R&D CENTER
BLDG K-1 PO BOX 8
SCHENECTADY NY 12301
PHONE 518 387 6419

GERALD W GRANTHAM
FINNIGAN MAT
355 RIVER OAKS PWY

SAN JOSE CA 95134
PHONE.

JEROME P GILMAN
803 CASHEW CT APT K

BEL AIR MD 21014
PHONE: 301 671 3753

O L GLAESMANN
DOW CHEMICAL
PO BOX BB
ENVIRONMENTAL SERV
FREEPORT TX 77541
PHONE. 409 238 2804

DAVID R GODWIN
NDRC LABORATORIES INC
3553 MILLER PARK DRIVE

GARLAND TX 45042
PHONE: 214 233 9801

A A GOLDBERG
115 LIVINGSTON AVE

EDISON NJ 08820
PHONE. 201 906 6814

S M GORDON
IITRI
CHEMISTRY DIVISION
10 W 35 ST
CHICAGO IL 60616
PHONE: 312 567 4374

JOHN D GORSUCH
GENCORP
RESEARCH DIV
2990 GILCHRIST ROAD
AKRON OH 44305
PHONE 216 798 4025

WILLIAM L GRADY
114 SPRINGHOUSE ROAD

SAVANNAH GA 31419
PHONE 912 238 7779

PETER W GRAVES
DETECTOR TECHNOLOGY
PO BOX K-300

BROOKFIELD MA 01506
PHONE 617 867 4030

CHARLES L GRAY
SDS BIOTECH
PO BOX 348

PAINESVILLE OH 44077-0348
PHONE: 216 357 3343

ROGER J GREATHEAD
KRATOS ANALYTICAL
170 WILLIAMS DR

RAMSEY NJ 07466
PHONE

S H GREENHOUSE
51 SCHUYLER AVE
APT 3 G

STAMFORD CT 06902
PHONE 203 348 7331

JOSEPH F GREER
CIBA GEIGY
BLDG 6 J210
556 MORRIS AVENUE
SUMMIT NJ 07901
PHONE: 201 277 7143

DIETER P GRIFFIS
N CAROLINA STATE UNIV
PO BOX 7903

RALEIGH NC 27695-7903
PHONE 919 737 2348

QUIRINUS G GRINDSTAFF
MARTIN MARIETTA
Y-12 PLANT
PO BOX Y BLDG 9995
OAK RIDGE TN 37831
PHONE 615 574 0679

MARVIN F GROSTIC
THE UPJOHN CO
DEPT 7820
7000 PORTAGE ROAD
KALAMAZOO MI 49001
PHONE 616 323 2804

J B GRUTKA
659 LANDAU AVE

JOLIET IL 60432
PHONE:

JOHN W GRAY
GALILEO ELEC-OPTICS
GALILEO PARK

STURBRIDGE MA 01518
PHONE 617 347 9191

JOHN GREAVES
SCH OF MARINE SCIENCE
COLLEGE OF WM & MARY

GLOUCESTER PT VA 23062
PHONE 804 642 7247

R CLIVE GREENOUGH
29 LYNWOOD DRIVE

MILLDALE CT 06467
PHONE: 203 288 3518

HUGH GREGG
LLNL
PO BOX 808 L-310

LIVERMORE CA 94550
PHONE 415 423 7501

RONALD D GRIGSBY
MASSPEC INC
275 TURKEY CREEK RD

BARTLESVILLE OK 74006-8034
PHONE 918 337 4376

GEORGE GRINS
7011 BLACKBERRY DR

ARLINGTON TX 76016
PHONE 817 467 0211

A A GROTE
NIOSH
4676 COLUMBIA PKWY

CINCINNATI OH 45226
PHONE 513 841 4308

ROBERT M GRUVER
PENN STATE UNIV
BORLAND BLDG

UNIVERSITY PA PA 16802
PHONE 814 863 2966

WESLEY A GRAY
MEDICAL SCHOOL
CASE WESTERN RESERVE UNIV

CLEVELAND OH
PHONE:

LARRY A GREEN
708 UNION ROAD

MICKLETON NJ 08056
PHONE 609 423 1040

GIL J GREENWOOD
PHILLIPS PETROLEUM
117 CL

BARTLESVILLE OK 74003
PHONE 918 661 7939

KAY SUE GREGORSKI
USDA, ARS
WESTERN REGIONAL RES CTR
800 BUCHANAN STREET
BERKELEY CA 94710
PHONE:

CASEY C GRIMM
DEPT OF CHEMISTRY
FLORIDA STATE UNIV

TALLAHASSEE FL 32306
PHONE: 904 644 6484

GARY GROENEWOLD
BRISTOL-MYERS CO
PRDD, BLDG 23A-338
PO BOX 4755
SYRACUSE NY 13221-4755
PHONE 315 432 2265

FREDERICK W GROTHKOPP
1766 COTTAGE GROVE DR

ENCINITAS CA 92024
PHONE 619 477 4173

BRIDGET P GUCCIONE
GENCORP
ANALYTICAL RESEARCH
2990 GILCHRIST ROAD
AKRON OH 44305
PHONE: 216 798 4028

MICHAEL GRAYSON
3433 BLUFFVIEW DR

ST CHARLES MO 63303
PHONE 314 233 2541

FRANK T GREENE
MIDWEST RESEARCH INST
425 VOLKER BLVD

KANSAS CITY MO 64110
PHONE 816 753 7600

GARY GREER
901 WATCH HILL ROAD

MIDLOTHIAN VA 23113
PHONE 804 379 0330

STANLEY P GRIFF
5 OAKWOOD TERRACE

ROCKAWAY NJ 07866
PHONE 201 627 7580

ERIC P GRIMSRUD
CHEMISTRY DEPT
MONTANA STATE UNIV

BOZEMAN MT 59717
PHONE: 406 994 5418

MICHAEL L GROSS
UNIV OF NEBRASKA
CHEMISTRY DEPT

LINCOLN NE 68588
PHONE 402 472 2794

IAN GROVE
VG INSTRUMENTS
300 BROAD STREET

STAMFORD CT 06901
PHONE: 203 322 4546

CHRISTIAN GUENAT
NIEHS
PO BOX 12233

RES TRI PK NC 27709
PHONE 919 541 2964

J G GUERRERA
27 MIRIAM DRIVE

MATAWAN NJ 07747
PHONE.

RICHARD J GUIDOBONI
NORTHERN ANAL LAB
7 TOPSFIELD DR

NASHUA NH 03062
PHONE: 603 673 1420

RAY F HAACK
4049 VIA MAYISOL
APT 118

LOS ANGELES CA 90042
PHONE: 818 354 6568

MARK E HAIL
301 LEIGH HALL
UNIV OF FLORIDA

GAINESVILLE FL 32611
PHONE 904 392 0515

MYNARD C HAMMING
CONOCO INC

PONCA CITY OK 74603
PHONE. 405 767 5671

CAROL A HANEY
204 TRAILS END CT

RALEIGH NC 27614
PHONE 919 737 3746

GORDON E HANSEN
BOEHRINGER-INGELHEIM
RES & DEV CTR
175 BRIAR RIDGE RD
RIDGEFIELD CT 06877
PHONE. 203 748 4200

KEVIN L HARBOL
DEPT OF CHEMISTRY
UNIV OF KENTUCKY

LEXINGTON KY 40506
PHONE: 606 257 6957

ROGER GUEVREMONT
DEPT OF CHEMISTRY
UNIV OF FLORIDA

GAINESVILLE FL 32611
PHONE.

WILSON M GULICK
MICH TECH UNIV
CHEM & CHEM ENGIN

HOUGHTON MI 49931
PHONE. 906 487 2296

DAVID L HACHEY
BAYLOR COLL OF MED
PEDIATRICS DEPT
1200 MOUR SAND
HOUSTON TX 77030
PHONE: 713 799 6002

DAVID J HAJDAZZ
DEPT OF CHEMISTRY BOX 468
PURDUE UNIV

W LAFAYETTE IN 47907
PHONE:

CLAY HAMNER
CAL LAB EAST
PO BOX 11106

RICHMOND VA 23230
PHONE. 804 359 1900

ALAN HANNA
2514 PRAIRIE ROAD

MADISON WI 53711
PHONE 608 273 0058

CURT HANSON
4328 NAGLE STREET

BRYON TX 77801
PHONE.

DWAYNE HARDIN
RADIAN CORPORATION
8501 MOPAC BLVD

AUSTIN TX 78766
PHONE: 512 454 4797

H Y GUH
PFIZER INC
EASTERN POINT RD

GROTON CT 06340
PHONE:

JOHN P GUTE
6414 GLENGARRY

WHITTIER CA 90606-1514
PHONE. 613 699 0405

WILLIAM F HADDON
35 WILLOW AVE

LARKSPUR CA 94939-1321
PHONE 415 486 3693

ROBERT J HALE
TENNESSEE EASTMAN CO
B-150 RESEARCH
PO BOX 1972
KINGSPORT TN 37662
PHONE 615 229 3066

CHRISTINE V HAMPTON
22260 INNSBROOK DR

NORTHVILLE MI 48167
PHONE.

ROBERT E HANNAH
2840 NESTLING RD

PHILADELPHIA PA 19154
PHONE. 215 278 7434

SHINJI HARA
JEOL USA
11 DEARBORN ROAD

PEABODY MA 01960
PHONE

D R HARDY
NAVAL RESEARCH LAB
CODE 6180

WASHINGTON DC 20375
PHONE 202 767 3559

DAVID M GUIDO
THE UPJOHN CO
7234-25-11

KALAMAZOO MI 49001
PHONE. 616 385 5461

JAMES W GUTHRIE
1119 UPLAND DRIVE NE

ALBUQUERQUE NM 87112
PHONE: 505 846 4266

LYNN R HAGEMAN
NESTLES FOODS QAL
809 COLLINS ROAD

MARYVILLE OH 43040
PHONE.

CARL G HAMMAR
UNIV HOSPITAL N429
ANESTHESIOLOGY DEPT
410 W 10TH AVE
COLUMBUS OH 43210
PHONE 614 421 8487

OWEN W HAND
DEPT OF CHEMISTRY BOX 473
PURDUE UNIV

W LAFAYETTE IN 47907
PHONE 317 494 5264

R J HANRAHAN
UNIV OF FLORIDA
NUCLEAR SCIENCE
RM 406
GAINESVILLE FL 32611
PHONE: 904 392 1442

KEN-ICHI HARADA
RAL SCH OF CHEMICAL SCIENCE
UNIV OF ILLINOIS
1209 W CALIFORNIA ST
URBANA IL 61801
PHONE 217 333 0655

RITA H HARDY
UNIV OF KENTUCKY
3548 LAREDO DR

LEXINGTON KY 40502
PHONE 606 252 5535

KIM HARICH
VIRGINIA TECH
DEPT OF BIOCHEMISTRY

BLACKSBURG VA 24061
PHONE.

R L HARLESS
701 WHITE OAK DR

CARY NC 27511
PHONE 919 541 2248

ALAN D HARMON
MCCORMICK & CO
RES & DEV LABS
202 WIGHT AVE
HUNT VALLEY MD 21031
PHONE: 301 667 7458

PETER E HAROLDSEN
UNIV COLO SCH MED
4200 E 9TH AVE C236
PHARMACOLOGY DEPT
DENVER CO 80262
PHONE 303 394 8961

D N HARPOLD
GODDARD SPC FLT CTR
CODE 615

GREENBELT MD 20771
PHONE· 301 344 8184

WILLIAM L HARRINGTON
RCA LABORATORIES
DAVID SARNOFF RES CT

PRINCETON NJ 08540
PHONE· 609 734 2415

GAIL HARRIS
NICOLET INSTRUMENTS
5225-1 VERONA ROAD

MADISON WI 53711
PHONE· 608 271 3333

ROBERT E HARRIS
BOX 41022

BRECKSVILLE OH 44141-0422
PHONE· 216 447 5369

C BRETT HARRISON
EXTREL CORP
PO BOX 11512

PITTSBURGH PA 15238
PHONE 412 782 3884

JAMES F HARRISON
DEPT OF CHEMISTRY
MICHIGAN STATE UNIV

EAST LANSING MI 48823
PHONE 517 353 9410

ROBERT H HARRISON
BROWARD SHERIFFS OFFICE
CRIME LABORATORY
201 SE 6TH STREET
FT LAUDERDALE FL 33301
PHONE:

WILLARD W HARRISON
UNIV OF VIRGINIA
CHEMISTRY DEPT

CHARLOTTESVLL VA 22901
PHONE: 804 924 3435

KEVIN J HART
DEPT OF CHEMISTRY
MICHIGAN STATE UNIV

EAST LANSING MI 48824
PHONE. 517 353 5215

NEIL R HARTMAN
MAYO CLINIC
740 GUGGENHEIM BLDG

ROCHESTER MN 55905
PHONE: 507 284 4212

THOMAS G HARTMAN
63 VISTA AVENUE

STATEN ISLAND NY 10304
PHONE: 201 932 9684

D J HARVAN
701 W CORNWALLIS ROAD

DURHAM NC 27707
PHONE: 919 544 5720

PAUL HARVATH
BUICK MOTOR DIV
BLDG 85, DIV 46-83
CHEMISTRY LAB
FLINT MI 48550
PHONE 313 236 0241

GEORGE J HARVEY
PROCTER & GAMBLE
11520 REED HARTMAN HWY

CINCINNATI OH 45241
PHONE

T MICHAEL HARVEY
VG INSTRUMENTS
PO BOX 12554

RES TRI PK NC 27709
PHONE.

HANAA HASHEM
SCH OF PHARMACY
1100 SALK HALL
UNIV OF PITTSBURGH
PITTSBURGH PA 15213
PHONE:

J RONALD HASS
TRIANGLE LABORATORIES
PO BOX 13485

RES TRI PK NC 27709
PHONE

FRANK W HATCH
BOEHRINGER INGELHEIM
90 EAST RIDGE
PO BOX 368
RIDGEFIELD CT 06877
PHONE 203 748 4200

CAROLINE HATTON
DEPT OF PHARMACOLOGY
UCLA SCH OF MEDICINE
23-278 CHS
LOS ANGELES CA 90024
PHONE: 213 206 6656

SUSAN HATTOX
BOEHRINGER INGELHEIM
175 BRIAR RIDGE RD

RIDGEFIELD CT 06877
PHONE: 203 748 4200

R L HAWKS
5429 31ST STREET NW

WASHINGTON DC 20015
PHONE 301 443 5280

RUTH HAWLEY-FEDDER
LLNL
L-310
PO BOX 808
LIVERMORE CA 94550
PHONE: 415 422 6328

DAVID A HAYES
12400 MOSSY BARK TRAIL

AUSTIN TX 78750
PHONE 512 454 4797

JOHN M HAYES
INDIANA UNIV
BIOGEOCHEM LABS
GEOLOGY BLDG
BLOOMINGTON IN 47405-5101
PHONE: 812 335 5610

MARION E HAYES
GALILEO ELCTRO-OPTICS
GALILEO PARK

STURBRIDGE MA 01518
PHONE.

MICHAEL J HAYES
CIBA-GEIGY CORP
444 SAW MILL RIVER ROAD

ARDSLEY NY 10502
PHONE· 914 478 3131

ROGER HAYES
UCHSC
4200 E 9TH AVE C232

DENVER CO 80262
PHONE· 303 394 8961

TIMOTHY L HAYES
BATTELLE MEMORIAL INST
505 KING AVENUE

COLUMBUS· OH 43201
PHONE

MARK J HAYWARD
649 NORTH 7TH STREET
NO 1

LAFAYETTE IN 47905
PHONE· 317 423 4403

EUGENE C HEATH
HARRIS LABS
PO BOX 80837

LINCOLN NE 68501
PHONE. 402 476 2811

CLYDE HEDIN
1020 WOODBRIDGE DR

LAS VEGAS NV 89108
PHONE: 702 798 2231

CURT E HEINE
DEPT OF CHEMISTRY
MICHIGAN STATE UNIV

EAST LANSING MI 48824
PHONE: 517 353 6767

ROBERT HELLMANN
WESTINGHOUSE MATERIALS CO
PO BOX 398704

CINCINNATI OH 45239
PHONE: 513 738 6551

T R HENDERSON
5609 DON FELIPE CT SW

ALBUQUERQUE NM 87105
PHONE· 505 831 1111

GLEN HERMAN
OCCIDENTAL CHEM CO
LONG RD

GRAND ISLAND NY 14072
PHONE.

RICHARD F HERZOG
9221 W BROWARD BLVD
NO 2304

PLANTATION FL 33324
PHONE·

KELLY HEAD
NORTH SHORE SANITARY DIST
PO BOX 750

GURNEE IL 60031
PHONE. 312 623 6060

L C HEATH
MISSISSIPPI CRIME LB
PO BOX 5008

JACKSON MS 39216
PHONE

DAVID L HEIKES
FDA
1009 CHERRY

KANSAS CITY MO 64106
PHONE: 816 374 5524

THOMAS M HEINZE
1701 EAST 10TH STREET

PAWHUSKA OK 74056
PHONE

PHILIP H HEMBERGER
LOS ALAMOS NAT'L LAB
GROUP CHM-1, MS G740
PO BOX 1663
LOS ALAMOS NM 87545
PHONE: 505 667 9903

JACK D HENION
CORNELL UNIVERSITY
EQUINE DRUG TESTING
925 WARREN ROAD
ITHACA NY 14850
PHONE: 607 256 6556

DAVID A HEROLD
UNIV OF VIRGINIA
PATHOLOGY DEPT
MEDICAL CTR
CHARLOTTESVLL VA 22908
PHONE: 804 924 5691

KENNETH R HESS
CHEMISTRY DEPT
UNIV OF VIRGINIA

CHARLOTTSVLL VA 22901
PHONE 804 924 7180

BRYAN HEARN
305 LEIGH HALL
DEPT OF CHEMISTRY
UNIV OF FLORIDA
GAINESVILLE FL 32611
PHONE. 392 0536

H D HECK
CIIT
PO BOX 12137

RES TRI PK NC 27709
PHONE: 919 541 2070

WAYNE HEIMERMANN
RT 2 BOX 193

AUSTIN MN 55912
PHONE: 301 948 3817

DAVID N HELLER
PO BOX 33342

BALTIMORE MD 21218
PHONE: 301 955 6961

MARK E HEMLING
SMITH KLINE & FRENCH F-90
1500 SPRING GARDEN ST
PO BOX 7929
PHILADELPHIA PA 19101
PHONE. 215 751 4783

RICHARD A HEPPNER
APPLIED SCIENCE DIV
2771 N GAREY AVENUE

POMONA CA 91767
PHONE:

G R HERTEL
UNIV CENTRAL FLORIDA
CHEMISTRY DEPT
PO BOX 25000
ORLANDO FL 32816
PHONE: 305 275 2246

ROBERT HETTICH
DEPT OF CHEMISTRY
PURDUE UNIV

W LAFAYETTE IN 47907
PHONE· 317 494 5271

JOHN HEARN
FINNIGAN MAT
355 RIVER OAKS PKWY

SAN JOSE CA 95134-9990
PHONE· 408 433 4800

WILLIAM L HECKLE
2312 FAIRVIEW AVENUE

CINCINNATI OH 45219
PHONE·

RICHARD E HEIN
NICOLET INSTRUMENTS
5225 VERONA RD

MADISON WI 53711
PHONE.

STEPHEN R HELLER
USDA-ARS, ASRI-MDCL
ROOM 56 BLDG 007
BARC-WEST
BELTSVILLE MD 20705
PHONE. 301 344 1709

M J HENCHMAN
BRANDEIS UNIV
CHEMISTRY DEPT

WALTHAM MA 02254
PHONE 617 861 4028

GUOR-RONG HER
HARVARD SCH OF PUBLIC HLTH
DEPT OF NUTRITION
665 HUNTINGTON AVE
BOSTON MA 02115
PHONE: 617 752 0652

HARRY S HERTZ
NBS
A309 CHEMISTRY

GAITHERSBURG MD 20899
PHONE: 301 921 2851

CHARLES A HETZEL
150 SPRING LANE

PHILADELPHIA PA 19128
PHONE.

DENNIS L HEURING
TMS ANAL SERVICES
6264 LAPAS TRAIL

INDIANAPOLIS IN 46268
PHONE: 317 291 5697

TETSUO HIGUCHI
JEOL
11 DEARBORN ROAD

PEABODY MA 01960
PHONE.

DAVID R HILKER
17 VAN BUREN AVE

E GREENBUSH NY 12061
PHONE: 518 474 1675

RANDY G HILLIARD
BROWARD SHERIFFS OFFICE
CRIME LABORATORY
201 SE 6TH STREET
ST LAUDERDALE FL 33301
PHONE.

HARRY B HINES
VILLANOVA UNIV
CHEMISTRY DEPT

VILLANOVA PA 19085
PHONE· 215 645 4840

VEI-SHI HO
MI DEPT OF NAT RESOURCES
ENVIRONMENTAL LAB
31 S CLIPPERT ST
LANSING MI 48912
PHONE: 517 373 2197

HENRY T HOFFMAN
22 VANDER VEER DR

LAWRENCEVILLE NJ 08648
PHONE: 609 737 5540

J F HOLLAND
MICHIGAN STATE UNIV
BIOCHEMISTRY DEPT

EAST LANSING MI 48824
PHONE

BRUCE J HIDY
BATTELLE LABS
505 KING AVE

COLUMBUS OH 43201
PHONE: 614 424 4591

DAVID A HIKADE
OWENS-CORNING FIBERGLASS
ROUTE 16

GRANVILLE OH 43023
PHONE: 614 587 8126

JAMES AMHERST HILL
MIT
CHEMISTRY 56-016
77 MASS AVE
CAMBRIDGE MA 02139
PHONE: 617 253 7236

LAURENCE R HILPERT
NAT'L BUR STAN
BLDG 222 RM A-113

WASHINGTON DC 20234
PHONE. 301 963 7370

DAVID S HIRANO
ARCO PLANT CELL RESEARCH
6560 TRINITY COURT

DUBLIN CA 94568
PHONE. 415 833 3457

J R HOBBS
DOT/TSC
CODE 48
KENDALL SQUARE
CAMBRIDGE MA 02142
PHONE: 617 494 2534

MICHAEL K HOFFMAN
US DEPT OF AGRICULTURE
300 12TH STREET SW

WASHINGTON DC 20250
PHONE: 202 447 3695

JAMES S HOLLER
CENTER DISEASE CNTRL
TOXI BRANCH C17-1814

ATLANTA GA 30333
PHONE: 404 452 4144

PETER M HIERL
UNIV OF KANSAS
CHEMISTRY DEPT

LAWRENCE KS 66044
PHONE· 913 864 3019

D L HILDENBRAND
SRI INTERNATIONAL

MENLO PARK CA 94025
PHONE· 415 859 3436

JOHN C HILL
1501 HARVEY ROAD
PENTHOUSE

COLLEGE STN TX 77840
PHONE:

GEORGE W HIME
15501 SW 106 AVE

MIAMI FL 33157
PHONE. 305 549 7347

RONALD A HITES
INDIANA UNIV
SPEA 410 H

BLOOMINGTON IN 47405
PHONE· 812 335 0193

D L HOBROCK
8736 MALTBIE RD

CENTERVILLE OH 45459
PHONE: 513 865 4064

CARL HOGBERG
6901 BRYN MAWR DR

AUSTIN TX 78723
PHONE: 512 458 7587

ROBERT W HOLMAN
DEPT OF CHEMISTRY
756 HAMILTON HALL
UNIV OF NEBRASKA
LINCOLN NE 68588
PHONE 402 472 3507

CHARLES E HIGNITE
IBM BLDG E35-013
DEPT E35
5600 COTTLE RD
SAN JOSE CA 95120
PHONE·

FRED D HILEMAN
MONSANTO U1F
800 N LINDBERGH BLVD
PO BOX 8
ST LOUIS MO 63167
PHONE. 314 694 1275

JOSEPH F HILLER
DOW CHEMICAL CO
574 BLDG

MIDLAND MI 48667
PHONE. 517 636 2126

DAVID M HINDENLANG
ALLIED CORP
PO BOX 1021R

MORRISTOWN NJ 07960
PHONE· 201 455 2071

ALLAN HLAVAC
STERLING-WINTHROP RESEARCH
COLUMBIA PIKE

RENSSELAER NY 12144
PHONE· 518 445 8140

JIMMIE HODGESON
US EPA
EMSL
26 WEST ST CLAIR STREET
CINCINNATI OH 45268
PHONE.

JOE HOHMANN
NICOLET INSTRUMENT CORP
5225-1 VERONA ROAD

MADISONGE WI 53711
PHONE:

W F HOLMES
WASHINGTON UNIV
BIOCHEMISTRY DEPT
660 S EUCLID
ST LOUIS MO 63110
PHONE:

STEVE HOLSHOUSER
MARTIN-MARIETTA ENERGY SYS
PO BOX 1410

PADUCAH KY 42001
PHONE

JAMES R HOLTSCLAW
486 WILLOW LANE

PALM HARBOR FL 33563
PHONE.

RICHARD E HONIG
RCA LABORATORIES

PRINCETON NJ 08540
PHONE. 609 921 7824

JEFF P HONOVICH
PHARMACOLOGY DEPT
JOHNS HOPKINS UNIV
725 N WOLFE STREET
BALTIMORE MD 21205
PHONE 301 955 3022

ROBIN J HOOD
CHEMISTRY DEPT
75 CHEMISTRY
WAYNE STATE UNIV
DETROIT MI 48202
PHONE· 313 577 2046

JOHN J HOPPE
VACUMETRICS INC
2261-#1 PALMA DR

VENTURA CA 93003-5789
PHONE 805 644 7461

JOSEPH P HOPPESCH
BORG-WARNER RESEARCH
WOLF & ALGONQUIN RDS

DES PLAINES IL 60018
PHONE 312 827 3131

EVAN C HORNING
11610 STARWOOD DR

HOUSTON TX 77024
PHONE: 713 799 4721

MARJORIE G HORNING
BAYLOR COLL MEDICINE
INST LIPID RESEARCH
TEXAS MEDICAL CENTER
HOUSTON TX 77030
PHONE. 713 799 4721

STEVEN R HORNING
DEPT OF CHEMISTRY BOX 477
PURDUE UNIV

W LAFAYETTE IN 47907
PHONE.

K R HOUSTON
413 FOREST OAKS LANE

LAKE JACKSON TX 77556
PHONE 409 297 5814

WILLIAM N HOWALD
DEPT OF MEDICINAL CHEMISTRY
UNIV OF WASHINGTON

SEATTLE WA 98195
PHONE· 206 543 6439

STEPHEN LEE HOWARD
4709 SOUTH 1175 WEST

SALT LAKE CTY UT 84123
PHONE

J R HOYLAND
DURYEA ASSOCIATES
701 ALPHA DRIVE

PITTSBURGH PA 15238
PHONE 412 963 7262

DAVID W HOYT
FINNIGAN MAT
355 RIVER OAKS PKWY

SAN JOSE CA 95134
PHONE. 408 433 4800

MARILYN P HOYT
6 HOWELL DRIVE

ANDOVER MA 01810
PHONE· 617 258 3083

J D HRIBAR
G D SEARLE & CO
4901 SEARLE PKWY

SKOKIE IL 60077
PHONE· 312 982 7505

TACHENG HSIEH
SANDOZ CROP PROTECTION
ANAL RESEARCH
341 E OHIO ST
CHICAGO IL 60611
PHONE. 312 670 4823

THOMAS C HSIEH
DEPT OF FOOD SCIENCE
LOUISIANA ST UNIV

BATON ROUGE LA 70803-1806
PHONE 504 388 5206

ANNJIA T HSU
CHEMISTRY DEPT
OHIO STATE UNIV
140 W 18TH AVENUE
COLUMBUS OH 43210
PHONE 614 422 0480

BIH-HSIUNG HSU
121-12 MARSHALL

W LAFAYETTE IN 47906
PHONE 317 494 5262

C SAM HSU
EXXON RES & ENGIN
CLINTON TOWNSHIP

ANNANDALE NJ 08801
PHONE 201 730 7228

CHIEN-PING HSU
CHAMPION INT'L CORP
TECHNICAL CTR
WEST NYACK ROAD
WEST NYACK NY 10994
PHONE. 914 578 7005

FONG FU HSU
DEPT OF MEDICINAL CHEMISTRY
UNIV OF UTAH

SALT LAKE CTY UT 84112
PHONE

FRANCIS S HSU
PHILIP MORRIS USA
PO BOX 26583

RICHMOND VA 23261
PHONE 804 274 2641

J P HSU
6127 VALLEY BAY

SAN ANTONIO TX 78250
PHONE 512 522 2228

HUA CHING HU
11 BENFORD DR

PRINCETON JCN NJ 08550
PHONE. 609 452 2300

FRANCIS Y HUANG
12821 WEST GOLDEN LANE

SAN ANTONIO TX 78249
PHONE.

SUNKWEI HUANG
MIDWEST CTR MASS SP
CHEMISTRY DEPT
UNIV OF NEBRASKA
LINCOLN NE 68588
PHONE. 402 472 3507

YONGGING HUANG
DEPT OF CHEMISTRY
PURDUE UNIV

W LAFAYETTE IN 47907
PHONE 317 494 5271

YUCHI HUANG
NICOLET INSTRUMENTS
5225-1 VERONA ROAD

MADISON WI 53711
PHONE·

LEE HUBBARD
MEDICAL UNIV OF S CAROLINA
PHARMACOLOGY DEPT

CHARLESTON SC 29425
PHONE:

W C HUBBARD
NIH NCI
BLDG 37 RM 5B22

BETHESDA MD 20205
PHONE 301 496 2970

F G HUDDA
36 PERRY AVE

LATHAM NY 12110
PHONE: 518 387 6665

CHARLES E HUDSON
MARINE BIOMEDICAL INST
200 UNIVERSITY BLVD

GALVESTON TX 77550
PHONE. 409 761 2939

JAMES E HUDSON
ALCON LABORATORIES
PO BOX 1959

FORT WORTH TX 76101
PHONE: 817 551 8113

STEVEN M HUES
DEPT OF CHEMISTRY
ARIZONA STATE UNIV

TEMPE AZ 85287
PHONE 602 965 4236

B MASON HUGHES
1065 CAMARGO

BALLWIN MO 63011
PHONE.

C G HUGHES
UNIV OF KENTUCKY
TOBACCO & HEALTH

LEXINGTON KY 40506
PHONE 606 257 9318

DAVID B HUGHES
34 LANGHORNE CR

NEWPORT NEWS VA 23606
PHONE.

HELEN HUGHES
INST FOR LIPID RES
BAYLOR COLL OF MED
1200 MOURSUND
HOUSTON TX 77030
PHONE: 713 799 4210

JOHN M HUGHES
HEWLETT-PACKARD CO
PO BOX 58019

SANTA CLARA CA 95052-8019
PHONE 408 988 7289

INGEMAR HULTHAGE
CARNEGIE-MELLON UNIV
ROBOTICS

PITTSBURGH PA 15213
PHONE: 412 268 8816

SUSAN V HUMMEL
PO BOX 16602

ARLINGTON VA 22215
PHONE:

HOYING L HUNG
CHEMISTRY DEPT
NORTHWESTERN UNIV
2145 SHERIDAN RD
EVANSTON IL 60201-2974
PHONE 312 491 5514

BONNIE HUNT
3712 WINGATE

CARROLLTON TX 75007
PHONE

DONALD F HUNT
UNIV OF VIRGINIA
CHEMISTRY DEPT
MCCORMICK ROAD
CHARLOTTESVLL VA 22901
PHONE 804 924 3610

JERRY E HUNT
CHEM DIV 200 C173
ARGONNE NAT'L LAB
9700 S CASS AVE
ARGONNE IL 60439
PHONE: 312 972 3517

SHARON HUNT
3M CENTER
BLDG 201-1W-29

ST PAUL MN 55144
PHONE 612 736 3525

R L HUNTER
ION SPEC CORP
ONE LONGSTREET

IRVINE CA 92714
PHONE: 714 857 0793

W T HUNTRESS
JET PROPULSION LAB
L83-301

PASADENA CA 91109
PHONE: 818 354 8275

H E HURST
UNIV OF LOUISVILLE
MED SCHOOL
DEPT PHARM & TOX
LOUISVILLE KY 40292
PHONE. 502 588 5291

JIM HURST
FINNIGAN MAT
355 RIVER OAKS PKWY

SAN JOSE CA 95134
PHONE 408 433 4800

PAUL M HYDE
LSUMC
BIOCHEMISTRY DEPT
1901 PERDIDO ST
NEW ORLEANS LA 70112-1393
PHONE 504 568 6585

CHARLES R IDEN
SUNY-STONY BROOK
PHARMACOLOGY DEPT

STONY BROOK NY 11794
PHONE 516 246 2298

ELAINE C IGO
134 GROVE STREET

MELROSE MA 02176
PHONE:

CARL F IJAMES
DEPT OF CHEMISTRY
UNIV OF CALIFORNIA

RIVERSIDE CA 92521
PHONE 714 787 4740

ANDREAS J ILLIES
CHEMISTRY DEPT
AUBURN UNIV

AUBURN AL 36849
PHONE 205 826 4043

RAFAEL N INFANTE
CATHOLIC UNIV
CHEMISTRY DEPT

PONCE PR 00732
PHONE 809 844 4150

L L INGRAM
PO DRAWER FP

MISSISSIPPI S MS 39762
PHONE: 601 325 3102

RUTH R INNERS
MCNEIL PHARMACEUTIC
CHEMICAL RESEARCH
WELSH & MCKEAN ROADS
SPRING HOUSE PA 19477-0776
PHONE 215 628 5648

SAM E INSALACO
PO BOX 551

FINDLAY OH 45839
PHONE 419 423 3526

JOHN C IRELAND
US EPA 8016
26 WEST ST CLAIR ROOM 687

CINCINNATI OH 45268
PHONE 513 569 7329

A P IRSA
BROOKHAVEN NATL LAB
CHEMISTRY DEPT

UPTON NY 11973
PHONE 516 282 4326

ROBERT K ISENSEE
ONEIDA RES SERVICE
ONE HALSEY ROAD

WHITESBORO NY 13492
PHONE. 315 736 3050

DAVID WANG IVERSON
DELSI INSTRUMENTS
10 KINGSBRIDGE ROAD

FAIRFIELD NJ 07006
PHONE 201 227 7690

DENLEY B JACOBSON
DEPT OF CHEMISTRY 127-72
CALIF INST OF TECHNOLOGY

PASADENA CA 91125
PHONE· 818 356 6543

ALAN T JAMES
EXXON PRODUC. RES
PO BOX 2189

HOUSTON TX 77001
PHONE· 713 965 4158

CHARLES H JARBOE
UNIV OF LOUISVILLE
PHAMACOLOGY & TOX

LOUISVILLE KY 40292
PHONE 502 588 5158

BARBARA JELUS-TYROR
DELSI INSTRUMENTS
10 KINGSBRIDGE ROAD

FAIRFIELD NJ 07006
PHONE 201 227 7690

ALFRED H JENSON
662 ARBOR VALLEY

CAMPBELL HALL NY 10916
PHONE 201 934 9000

G A ST JOHN
SRI INTERNATIONAL
333 RAVENSWOOD AVE

MENLO PARK CA 94025
PHONE 859 3621

ILEANA ISERN-FLECHA
CHEMISTRY DEPT
BOX 504
PURDUE UNIV
W LAFAYETTE IN 47906
PHONE· 317 494 6898

J M JACKSON
MARTIN MARIETTA
ENERGY SYSTEMS INC
PO BOX 1410
PADUCAH KY 42001
PHONE 502 444 6311

PETER JAHNKE
FINNIGAN MAT
355 RIVER OAKS PWY

SAN JOSE CA 95134
PHONE: 408 433 4800

RUBY H JAMES
SOUTHERN RES INST
2000 9TH AVE SOUTH

BIRMINGHAM AL 35255-5305
PHONE 205 323 6592

IAN JARDINE
MAYO CLINIC
PHARMACOLOGY DEPT
200 1ST STREET SW
ROCHESTER MN 55905
PHONE· 507 284 4178

D J JENDEN
CTR FOR HEALTH SCIENCES
PHARMACOLOGY DEPT
UNIV OF CALIFORNIA
LOS ANGELES CA 90024
PHONE 213 825 6694

BRIAN A JEROME
OAK RIDGE NAT'L LAB
BLDG 3550
PO BOX X
OAK RIDGE TN 37831
PHONE 615 574 6167

B M JOHNSON
PFIZER INC
CENTRAL RESEARCH

GROTON CT 06340
PHONE. 203 441 3789

S C ISRAEL
UNIV OF LOWELL
CHEMISTRY DEPT

LOWELL MA 01854
PHONE. 617 452 5000

THOMAS C JACKSON
EASTMAN KODAK
RESEARCH LABS
1669 LAKE AVENUE
ROCHESTER NY 14650
PHONE· 716 477 8515

EDWARD M JAKUBOWSKI
US ARMY MRICD
1285 JAMISON COURT

BELCAMP MD 21017
PHONE·

GENE C JAMIESON
ZOECON CORP
975 CALIFORNIA AVE
PO BOX 10975
PALO ALTO CA 94304
PHONE. 415 857 1130

J A JARRELL
11 HYDE STREET

NEWTON HGHLND MA 02161
PHONE· 617 478 2000

NANCY JEAN JENSEN
MCMS

UNIV OF NEBRASKA
LINCOLN NE 68588-0362
PHONE. 402 472 3507

EMILE C JOEL
2408 17TH PLACE SE

WASHINGTON DC 20020
PHONE 301 921 2781

CARL G JOHNSON
123 FYE LABORATORY
WOODS HOLE OCEAN INST

WOODS HOLE MA 02543
PHONE. 617 548 1400

PHILLIP ISSENBERG
UNIV OF NEBRASKA
EPPLEY INST
MEDICAL CENTER
OMAHA NE 68105
PHONE: 402 559 4473

THOMAS J JACKSON
1614 RICHFOREST

RICHARDSON TX 75081
PHONE. 214 851 8456

GEORGE JAKUBOWSKI
TRAVENOL LABORATORIES
6301 LINCOLN AVE

MORTON GROVE IL 60053
PHONE. 312 965 4700

JOHN JANZER
MATTSON INSTRUMENTS
6333 ODANA ROAD

MADISON WI 53719
PHONE: 608 273 2370

KOKA JAYASIMHULU
UNIV OF CINCINNATI
700 MORGAN HALL

CINCINNATI OH 45219
PHONE 513 872 6349

T E JENSEN
5574 CASTLETON DR

W BLOOMFIELD MI 48033
PHONE. 313 322 4598

CAROLYN JOHLMAN
CHEMISTRY DEPT
UNIV OF CALIFORNIA

RIVERSIDE CA 92521-0403
PHONE 714 787 4740

ERIC K JOHNSON
FINNIGAN MAT
355 RIVER OAKS PARKWAY

SAN JOSE CA 95134
PHONE 408 433 4800

JAN JOHNSON
DEPT OF STATE POLICE
BUR OF FORENSIC SCIENCES
215 W LAWRENCE
SPRINGFIELD IL 62704
PHONE. 217 782 7430

P E JOHNSON
HUMAN NUTRITION LAB
BOX 7166 UNIV STATN

GRAND FORKS ND 58202
PHONE: 701 795 8416

MARK JOHNSTON
NICOLET INSTRUMENTS
5225-1 VERONA ROAD

MADISON WI 53711
PHONE. 608 271 3333

E G JONES
SYSTEMS RESEARCH LAB
RES APPLICATIONS DIV
2800 INDIAN RIPPLE
DAYTON OH 45440
PHONE: 513 426 6000

CHARLES M JUDSON
UNIV OF KANSAS
CHEMISTRY DEPT

LAWRENCE KS 66044
PHONE. 913 864 3223

LONNIE G JUSTICE
HEWLETT PACKARD
675 BROOKSEDGE BLVD

WESTERVILLE OH 43081
PHONE 614 891 3344

HENRY T KALINOSKI
BATTELLE PACIFIC NW LABS
PO BOX 999

RICHLAND WA 99352
PHONE 509 376 1656

ARTHUR KANT
139 WOODRIDGE RD

WAYLAND MA 01778
PHONE

JODIE V JOHNSON
2124 NE 7 ST

GAINESVILLE FL 32609
PHONE: 904 392 0515

RICHARD S JOHNSON
MIT
CHEMISTRY 56-016
77 MASS AVENUE
CAMBRIDGE MA 02139
PHONE: 617 253 7236

MURRAY V JOHNSTON
DEPT OF CHEMISTRY
CAMPUS BOX 215
UNIV OF COLORADO
BOULDER CO 80309-0215
PHONE: 303 492 5033

F E JONES
536 24TH SW

MIAMI OK 74354
PHONE. 918 542 9801

GREGORY A JUNGCLAUS
MIDWEST RES INST
425 VOLKER BLVD

KANSAS CITY MO 64110
PHONE: 816 753 7600

MALCOLM KAHN
301 WICHITA TRAIL

FRANKLIN LAKE NJ 07417
PHONE

GEORGE J KALLOS
DOW CHEMICAL CO
BLDG 574

MIDLAND MI 48640
PHONE: 517 636 5340

IZET M KAPETANOVIC
NIH NINCDS
BLDG 36 ROOM 5D-21

BETHESDA MD 20205
PHONE. 301 496 6777

JUDITH A JOHNSON
STERLING-WINTHROP RESEARCH
81 COLUMBIA TURNPIKE

RENSSELAER NY 12144
PHONE: 518 445 8885

ROBERT L JOHNSON
119 HOLLOWOAK CT

CARY NC 27511
PHONE:

RICHARD M JOHNSTON
FINNIGAN CORP
355 RIVER OAKS PKWY

SAN JOSE CA 95134
PHONE: 408 433 4800

GILBERT G JONES
AMOCO RESEARCH CTR MSB-5
PO BOX 400

NAPERVILLE IL 60566
PHONE. 312 420 5773

GREGOR A JUNK
US DOE
AMES LAB
IOWA STATE UNIV
AMES IA 50011
PHONE

ISHENKUMBA A KAHWA
CHEMISTRY DEPT
LOUISIANA STATE UNIV

BATON ROUGE LA 70803
PHONE: 504 388 5811

M S KAMINSKY
ARGONNE NAT'L LAB-20
MATERIAL SCI & TECH
9700 S CASS AVE
ARGONNE IL 60439
PHONE: 312 972 4074

J J KARLINER
CIBA-GEIGY CORP
ANALYTICAL DEPT

ARDSLEY NY 10502
PHONE: 914 478 3131

KENNETH L JOHNSON
3600 BENTON STREET
No 33

SANTA CLARA CA 95051
PHONE 408 247 1663

W H JOHNSON
UNIV OF MINNESOTA
PHYSICS DEPT

MINNEAPOLIS MN 55455
PHONE: 612 373 5218

A DANIEL JONES
FAC FOR ADVANCED INSTR
9 HUTCHISON HALL
UNIV OF CALIFORNIA
DAVIS CA 95616
PHONE: 916 752 6272

HARLAN JONES
365 ELIZABETH ST
NO 4

SALT LAKE CTY UT 84102
PHONE:

JEANETTE JURUSIK
NYS DEPT OF HEALTH
WCL&R
EMPIRE STATE PLAZA
ALBANY NY 12201
PHONE: 518 473 4871

ROBERT G KALEY
MONSANTO
800 N LINDBERGH

ST LOUIS MO 63167
PHONE: 314 694 8558

JOHN DE KANEL
DIV OF PARI-MUTUEL WAGERING
1350 NW 12TH AVE ROOM 507

MIAMI FL 33136-2169
PHONE: 305 325 2671

TOM KARNS
UNIV OF OKLAHOMA
CHEMISTRY DEPT
620 PARRINGTON OVAL
NORMAN OK 73019
PHONE 405 325 2843

DANIEL B KASSEL
333 CHEMISTRY BLDG
DEPT OF CHEMISTRY
MICHIGAN STATE UNIV
EAST LANSING MI 48824
PHONE·

PATRICK E KASTL
DOW CHEMICAL USA
TOXICOLOGY
1803 BLDG
MIDLAND MI 48640
PHONE. 517 636 2060

VISWANATHAM KATTA
DEPT OF CHEMISTRY
UNIV OF HOUSTON

HOUSTON TX 77004
PHONE:

ROBERT N KATZ
ROCKEFELLER UNIV
BOX 253
1230 YORK AVENUE
NEW YORK NY 10021
PHONE. 212 570 5674

KATHLEEN A KAYGANICH
DEPT OF CHEMISTRY
MICHIGAN STATE UNIV

EAST LANSING MI 48824
PHONE 517 353 0612

G L KEARNS
1504 SAN CARLOS BAY DRIVE

SANIBEL ISLND FL 33957
PHONE

RONALD KEEFE
INTERNATIONAL PAPER CO
PO BOX 797

TUXEDO PARK NY 10987
PHONE

GARY W KEEN
CONOCO INC
1000 S PINE

PONCA CITY OK 74601
PHONE: 405 767 2468

JOSEPH B KEENAGHAN
FINNIGAN MAT
1383 PICCARD DR
SUITE 100
ROCKVILLE MD 20850
PHONE· 301 948 1067

PAUL R KELLER
PROCTER & GAMBLE
11520 REED HARTMAN

CINCINNATI OH 45241
PHONE.

JAMES A KELLEY
NIH
NCI MED CHEM SEC
BLDG 37 RM 6D23
BETHESDA MD 20892
PHONE 301 496 3597

MICHAEL A KELLEY
98 COPPER MINE ROAD

FARMINGTON CT 06032
PHONE: 203 283 8235

PAUL E KELLEY
FINNIGAN MAT
355 RIVER OAKS PKWY

SAN JOSE CA 95134
PHONE 408 433 4800

SHARON L KELLY
RORER GROUP
ANALYTICAL DEPT
1 SCARSDALE ROAD
TUCKAHOE NY 10707
PHONE· 914 779 6300

LEONID KELNER
10401 GROSVENOR DR #1101

ROCKVILLE MD 20852
PHONE 703 530 2374

DAVID L KEMP
1813 RIDGE ROAD

MARTINSVILLE NJ 08836
PHONE: 201 228 5538

TREVOR R KEMP
KRATOS ANALYTICAL
170 WILLIAMS DRIVE

RAMSEY NJ 07446
PHONE

PAUL C KEMPER
DEPT OF CHEMISTRY
UNIV OF CALIFORNIA

SANTA BARBARA CA 93106
PHONE 805 961 2673

MARIANNE KEMPFF
1116 SUFFIELD

BIRMINGHAM MI 48009
PHONE· 313 577 3072

ERIC J KEMPSTER
2178 POMPEY-FABIUS ROAD

FABIUS NY 13063
PHONE. 315 677 3833

J M KENNISH
UNIV OF ALASKA
CHEMISTRY DEPT
3211 PROVIDENCE DR
ANCHORAGE AK 99508
PHONE 907 786 1236

DAVID V KENNY
338 ESSEX STREET

SWAMPSCOTT MA 01907
PHONE· 617 592 1315

LLOYD KENT
KRATOS
46A WALNUT STREET

PEMPTON LAKES NJ 07442
PHONE: 201 934 9000

RICHARD H KENT
REG FORENSIC LAB
27 WOODLAND RD

PAINESVILLE OH 44077
PHONE. 216 325 9517

HILKKA KENTTAMAA
PURDUE UNIV
CHEMISTRY DEPT

W LAFAYETTE IN 47907
PHONE 317 494 5264

CHRISTINE N KENYON
451 HOMER AVENUE

PALO ALTO CA 94301
PHONE 408 725 8111

THOMAS W KEOUGH
9896 BARNSLEY CT

CINCINNATI OH 45242
PHONE. 513 245 2486

EDWARD H KERNS
BRISTOL MYERS CO
2404 PENNSYLVANIA AVE

EVANSVILLE IN 47721
PHONE· 812 838 8225

SUHAS KETKAR
EXTREL CORP
PO BOX 11512

PITTSBURGH PA 15238
PHONE· 412 782 3884

J K KHANDELWAL
MT SINAI MED SCHOOL
PHARMACOLOGY DEPT
100 ST AND 5TH AVE
NEW YORK NY 10029
PHONE: 212 650 5603

MOHAN KHARE
EA ENGINEERING SCI & TECH
15 LOVETON CIRCLE

SPARKS MD 21152
PHONE. 301 771 4950

H GOBIND KHORANA
MIT
CHEMISTRY 18-511

CAMBRIDGE MA 02139
PHONE

DAVID KIDWELL
NAVAL RES LAB
CODE 6170

WASHINGTON DC 20375
PHONE 202 767 3575

W E KILLINGER
W R GRACE & CO
RESEARCH DIV
7379 ROUTE 32
COLUMBIA MD 21044
PHONE 301 531 4479

LEWIS B KILLMER
325 N EDGMONT ST

MEDIA PA 19063
PHONE 215 751 3499

HEE-YONG KIM
261 CONGRESSIONAL LANE
#308

ROCKVILLE MD 20852
PHONE 301 496 4900

BRENDA J KIMBLE
AMPHION ASSOCIATES
PO BOX 1608

LAFAYETTE CA 94549
PHONE: 415 372 8260

CAROL F KING
DYNAMAC CORP
11140 ROCKVILLE PIKE

ROCKVILLE MD 20852
PHONE

FRED L KING
DEPT OF CHEMISTRY
MCCORMICK ROAD
UNIV OF VIRGINIA
CHARLOTTESVLL VA 22901
PHONE: 804 924 7180

JACK KING
4302 MEADOWBANK

SEABROOK TX 77586
PHONE 713 474 2730

ROY W KING
UNIV OF FLORIDA
CHEMISTRY DEPT

GAINESVILLE FL 32611
PHONE 904 392 0592

SHERRILL KING
W R GRACE & CO
CRYOVAC DIV
PO BOX 464
DUNCAN SC 29334
PHONE 803 433 2559

DONNA J KINNEY
4 HARRIET ST

ALBANY NY 12205
PHONE 518 474 1675

GARY R KINSEL
CAMPUS BOX 215
UNIV OF COLORADO

BOULDER CO 80309-0215
PHONE

ROBIN KINSER
PHILIP MORRIS USA
RESEARCH CENTER
PO BOX 26583
RICHMOND VA 23261
PHONE 804 274 5905

JAMES A KINSINGER
NICOLET ANAL INST
5225 VERONA RD
PO BOX 4508
MADISON WI 53711-0508
PHONE 608 271 3333

T H KINSTLE
BOWLING GREEN ST UNIV
CHEMISTRY DEPT

BOWLING GREEN OH 43403
PHONE 419 372 2658

MICHAEL KINTER
BOX 168
UNIV OF VA MEDICAL CTR

CHARLOTTESVLL VA 22901
PHONE:

MIKE KINTER
DEPT OF PATHOLOGY
CLINICAL LABS BOX 168
UNIV OF VA MEDIVAL CTR
CHARLOTTESVLL VA 22908
PHONE 804 924 9204

JEFFREY P KIPLINGER
5414 WAYNE STREET

RALEIGH NC 27606
PHONE 919 683 6076

MARION C KIRK
SOUTHERN RES INST
2000-9TH AVE S
BOX 55305
BIRMINGHAM AL 35255
PHONE 205 323 6592

NADIA D KIRZECKY
AMER CYANAMID CO
PO BOX 400

PRINCETON NJ 08540
PHONE 609 799 0400

ROBERT W KISER
9-CP BLDG
UNIV OF KENTUCKY

LEXINGTON KY 40506
PHONE 606 257 4622

PETER T KISSINGER
BIOANALYTICAL SYS
2701 KENT AVE

W LAFAYETTE IN 47906
PHONE 317 463 4527

F G KITSON
3 HARTFORD PLACE

NEWARK DE 19711
PHONE 302 772 3543

MICHAEL KLANECKY
443 WRIGHT STREET
NO 307

LAKEWOOD CO 80228
PHONE: 303 966 4788

KALVIN E KLATT
LOS ALAMOS NAT'L LABS
PO BOX 1663

LOS ALAMOS NM 67544
PHONE

E R KLEIN
6608 FANNIN AVE
SUITE 601

HOUSTON TX 77030
PHONE 713 799 6183

PETER D KLEIN
6608 FANNIN AVE
RM 519

HOUSTON TX 77030
PHONE 713 799 6001

RON KLUSMAN
DEPT OF CHEM/GEOCHEMISTRY
COLORADO SCH OF MINES

GOLDEN CO 80401
PHONE:

DANIEL R KNAPP
MED UNIV S CAROLINA
PHARMACOLOGY DEPT
171 ASHLEY AVE
CHARLESTON SC 29425
PHONE 803 792 2471

GARY D KNERR
411 N ALMON
NO 523

MOSCOW ID 83843
PHONE 208 885 6756

T C KNIGHT
2370 S BRENTWOOD ST

LAKEWOOD CO 80227
PHONE 303 977 4241

W B KNIGHTON
FRANKLIN & MARSHALL
CHEMISTRY DEPT
BOX 3003
LANCASTER PA 17604
PHONE 717 291 4124

FRITZ J KNORR
SURFACE SCIENCE LABS
465 NATIONAL AVE

MTN VIEW CA 94043
PHONE: 415 962 8780

B E KNOX
PENN STATE UNIV
MATERIALS RES LAB

UNIVERSITY PA PA 16802
PHONE 814 865 1168

CHARLES KOCH
ASSOCIATED LABS
806 NORTH BATAVIA

ORANGE CA 92668
PHONE: 714 771 6900

HANS KOCH

PHONE:

CHRIS KOEGEL
MERRELL-DOW
2110 E GALBRAITH ROAD

CINCINNATI OH 45215
PHONE.

CATHY J KOLANOWSKI
2144 TANSEL ROAD

INDIANAPOLIS IN 46234
PHONE: 317 271 0347

ERIC W KOLODWIEJ
DEPT OF MEDICINAL CHEMISTRY
PHARMACY BLDG
PURDUE UNIV
W LAFAYETTE IN 47907
PHONE 317 494 6917

M G KOLOR
GENERAL FOODS CORP
555 SO BROADWAY

TARRYTOWN NY 10591
PHONE 914 335 6459

RICHARD W KONDRAT
CHEMISTRY DEPT
UNIV OF CALIFORNIA

RIVERSIDE CA 92521
PHONE: 714 787 5287

WALTER A KORFMACHER
NCTR
CHEMISTRY DIV
HFT-154
JEFFERSON AR 72079
PHONE.

RICHARD A KORNFELD
2667-C HYDRAULIC ROAD

CHARLOTTESVLL VA 22901
PHONE.

TIM KOSCHMANN
XEROX AI SYSTEMS
450 ALGONQUIN ROAD

ARLINGTON HTS IL 60005
PHONE: 312 981 7447

MARK E KOSLIN
9803 FREMONT AVE

MONTCLAIR CA 91763
PHONE 714 593 3581

JAMES G KOSTELC
MONSANTO CO
MAIL ZONE BB21
700 CHESTERFIELD VILL PWY
CHESTERFIELD MO 63198
PHONE 314 537 6218

KAREN KOTZ-GEBEL
32 MIDDLESEX ROAD

MATAWAN NJ 07747
PHONE: 201 225 5600

S W KRASNER
METRO WATER DIST
WATER QUALITY BRANCH
700 NORTH MORENO AVE
LA VERNE CA 91750
PHONE: 714 593 7474

JOHN M KRECISZ
SCA CHEMICAL SERVICES
11700 S STONY ISLAND

CHICAGO IL 60617
PHONE. 312 646 5700

MARY J KREEK
ROCKEFELLER UNIV
1230 YORK AVE

NEW YORK NY 10021
PHONE: 212 570 8248

GERHARD M KRESBACH
NORTHEASTERN UNIV
BARNETT INSTITUTE
360 HUNTINGTON AVE
BOSTON MA 02115
PHONE: 617 437 2794

THOMAS KRICK
UNIV OF MINNESOTA
BIOCHEMISTRY DEPT
1479 GORTNER AVE
ST PAUL MN 55108
PHONE. 612 373 1456

THAIYA KRISHNAMURTHY
US ARMY
CHEM RES & DEV CTR
CRDEC
ABG MD 21005
PHONE: 301 671 2255

MICHAEL J KRISTO
CHEMISTRY DEPT
MICHIGAN STATE UNIV

EAST LANSING MI 48824
PHONE: 517 353 5215

KYLE J KROHA
CHEMISTRY DEPT
CHEMISTRY BLDG
INDIANA UNIV
BLOOMINGTON IN 47405
PHONE 812 335 3436

FRANCIE M KUBIAK
MILES LABORATORIES
1127 MYRTLE ST BOX 40

ELKHART IN 46514
PHONE: 219 262 7979

DOUGLAS W KUEHL
EPA
6201 CONGDON BLVD

DULUTH MN 55804
PHONE: 218 720 5558

W F KUHN
PHILIP MORRIS USA
RESEARCH CENTER
PO BOX 26583
RICHMOND VA 23261
PHONE. 804 274 3918

NARAYAN KUMAR
AMERICAN WATER WORKS
1115 S ILLINOIS ST

BELLEVILLE IL 62221
PHONE 618 235 3600

DURGA KUMARI
DEPT OF FOREST PRODUCTS
UNIV OF MINNESOTA

ST PAUL MN 55108
PHONE:

NICHOLAS J KURLICK
ENVIRESPONSE INC
GSA RARITAN DEPOT BLDG 209
WOODBRIDGE AVE
EDISON NJ 08837
PHONE: 201 548 9660

PHILLIP A KUYKENDALL
FINNIGAN MAT
355 RIVER OAKS PKWY

SAN JOSE CA 95134
PHONE. 408 433 4800

GILLES LABELLE
CAMBRIDGE ISOTOPE LABS
20 COMMERCE WAY

WOBURN MA 01801
PHONE: 617 938 0067

JACQUES L LABROSSE
BALZERS
8 SAGAMORE PARK RD

[illegible]SON NH 03051
[illegible]HONE 603 889 6888

MARTIN P LACEY
PROCTER & GAMBLE
MIAMI VALLEY LABS
PO BOX 39175
CINCINNATI OH 45247
PHONE:

C ROBERT LAGERGREN
2110 HOWELL AVE

RICHLAND WA 99352
PHONE: 509 373 3872

JOHN G LAMBERTON
REICHHOLD CHEMICALS
PO BOX 1433

PENSACOLA FL 32596
PHONE:

FRED W LAMPE
PENN STATE UNIV
152 DAVEY LAB

UNIVERSITY PK PA 16802
PHONE: 814 865 6553

RUSSELL F LANG
US DEPT OF COMMERCE
NOAA/AOML
4301 RICKENBACKER CSWY
MIAMI FL 33149
PHONE: 305 361 4387

MARK A LAPACK
ANALYTICAL LABS
DOW CHEMICAL CO

MIDLAND MI 48640
PHONE: 517 636 6329

ROBERT P LATTIMER
B F GOODRICH R & D
9921 BRECKSVILLE RD

BRECKSVILLE OH 44141
PHONE: 216 447 5369

DAVID W LAW
SKCL TOXICOLOGY DEPT
1075 FIRST AVENUE

KG OF PRUSSIA PA 19406
PHONE. 215 962 7673

CAROL LACING
NORTH SHORE SANITARY DIST
PO BOX 750

GURNEE IL 60031
PHONE: 312 623 6060

WILLIAM M LAGNA
11209 SANDYVALE ROAD

BRADSHAW MD 21021
PHONE. 301 592 9610

STEPHEN A LAMMERT
FINNIGAN MAT
355 RIVER OAKS PKWY

SAN JOSE CA 95134-9990
PHONE. 408 433 4800

DONALD P LAND
CHEMISTRY DEPT
UNIV OF CALIFORNIA

IRVINE CA 92717
PHONE:

H G LANGER
DOW CHEMICAL
PO BOX 400

WAYLAND MA 01778
PHONE: 617 651 9634

RICK LAPP
HAMILTON HALL RM 28
UNIV OF NEBRASKA

LINCOLN NE 68588
PHONE: 402 472 3499

R KAZMER LATVEN
HEWLETT PACKARD
3003 SCOTT BLVD

SANTA CLARA CA 95050
PHONE 408 857 2517

JULIE K LAWRENCE
1320 1/2 W EDWARDS

SPRINGFIELD IL 62704
PHONE: 217 782 7430

A L LAFLEUR
16 WALL STREET

ARLINGTON MA 02174
PHONE: 617 253 3499

S T LAI
69 SCANTIC DRIVE

E LONGMEADOW MA 01028
PHONE

CAROLEJEAN H LAMOUREUX
METABOLISM & RADIATION
RESEARCH LABORATORY
STATE UNIV STATION
FARGO ND 58105
PHONE: 701 237 5771

DOROTHY C LANE
4209 COMANCHE DRIVE

LARAMIE WY 82070
PHONE 307 721 2352

PATRICK LANGVARDT
DOW CHEMICAL CO
1803 BLDG

MIDLAND MI 48640
PHONE 517 636 1108

BARBARA LARKA
6818 WOODHILL TRAIL

EDEN PRAIRIE MN 55344
PHONE 612 645 3601

M T LAUG
ARGONNE NATIONAL LAB
PO BOX 2528

IDAHO FALLS ID 83401
PHONE: 208 526 7319

JACKSON O LAY
NAT'L CTR FOR TOX RESEARCH
HFT-1S4R

JEFFERSON AR 72079
PHONE: 501 541 4364

LAWRENCE E LAFLEUR
NCASI
PO BOX 458

CORVALLIS OR 97339
PHONE: 503 754 2015

ROGER A LAINE
BIOCHEMISTRY DEPT
LOUISIANA STATE UNIV
322 CHOPPIN HALL
BATON ROUGE LA 70803
PHONE

LES LAMPARSKI
DOW CHEMICAL
BLDG 57408, L-233

MIDLAND MI 48667
PHONE:

JACK LANG
GOODYEAR ATOMIC CORP
DEPT 513 MS 2229
PO BOX 628
PIKETON OH 45661-0628
PHONE: 614 289 2331

VICKI LANYON
HEWLETT-PACKARD
1200 E DIEHL ROAD

NAPERVILLE IL 60566
PHONE:

EDMUND A LARKA
6818 WOODHILL TRAIL

EDEN PRAIRIE MN 55344
PHONE: 612 373 2366

FRANK H LAUKIEN
4 TROWBRIDGE PLACE
APT 4C

CAMBRIDGE MA 02138
PHONE 617 864 2181

JOHN J LEARY
MICHIGAN STATE UNIV
CHEMISTRY DEPT

EAST LANSING MI 48824
PHONE 517 353 6767

JULIE A LEARY
MASS SPECTROMETRY LAB
COLL OF CHEM, 8 LEWIS HALL
UNIV OF CALIFORNIA
BERKELEY CA 94720
PHONE 415 642 0701

LEO M LECH
DEPT OF CHEMISTRY
PURDUE UNIV

W LAFAYETTE IN 47907
PHONE: 317 494 5271

EDWARD B LEDFORD
201 NORTH 8TH STREET
SUITE 201

LINCOLN NE 68508
PHONE: 402 475 7640

EDGAR D LEE
CORNELL UNIV
EQUINE DRUG TESTING
925 WARREN DRIVE
ITHACA NY 14850
PHONE: 607 255 6555

MIKE S LEE
CHEMISTRY DEPT
LEIGH HALL BOX 356
UNIV OF FLORIDA
GAINESVILLE FL 32611
PHONE 904 392 0515

TERRY D LEE
CITY OF HOPE
IMMUNOLOGY DEPT
1450 E DUARTE RD
DUARTE CA 91010
PHONE 818 357 9711

JANET M LEE-WUEBBELS
1764 SOUTH WISTERIA

ST CHARLES MO 63303
PHONE 314 694 1273

H F LEFEVRE
LEFEVRE ENGINEERING
2945 BURRVILLE RD

FORT RECOVERY OH 45846
PHONE 419 375 4104

MICHAEL G LEGENDRE
US DEPT OF AG
1100 ROBT E LEE BLVD
PO BOX 19687
NEW ORLEANS LA 70179
PHONE.

KASSU LEGESSE
BECKMAN RESEARCH INST
DIV OF IMMUNOLOGY
1450 E DUARTE ROAD
DUARTE CA 91010
PHONE

A M LEGRAND
WESTINGHOUSE NFD
PO DRAWER R

COLUMBIA SC 29250
PHONE 803 776 2610

JIM LEHMAN
DEPT OF CHEMISTRY
ARIZONA STATE UNIV

TEMPE AZ 85287
PHONE 602 965 6193

THOMAS A LEHMAN
PO BOX 435

N NEWTON KS 67117
PHONE 316 283 2500

CHRIS P LEIBMAN
UT STATION
PO BOX 16433

KNOXVILLE TN 37916
PHONE 615 574 2455

DOUGLAS A LEICH
LLNL - L-232
PO BOX 808 MAIL CODE L-231

LIVERMORE CA 94550
PHONE 415 422 6637

THOMAS LEIKER
BUR OF RECLAMATION M/C 1523
DENVER FEDERAL CTR
PO BOX 25007
DENVER CO 80225
PHONE

FREDRIC D LEIPZIGER
NOR ANALYTICAL LAB
3 NORTHERN BLVD

AMHERST NH 03031
PHONE 603 673 1420

ROBERT E LEMIEUX
1211 SHERWOOD AVE

RICHMOND VA 23220
PHONE

FRANK LEMUNYON
4414 NW 79TH TERRACE

KANSAS CITY MO 67151
PHONE

R ESPINOSA LENIZ
1200 N QUEEN ST
NO 402

ARLINGTON VA 22209
PHONE 703 237 1733

S R LEONE
UNIV OF COLORADO
JILA CAMPUS BOX 440

BOULDER CO 80309-0440
PHONE: 303 492 5128

MILTON I LEVENBERG
ABBOTT LABS
DEPT 417, AP9

ABBOTT PARK IL 60064
PHONE 312 937 2080

C ANTHONY LEWIS
SCH OF GEOLOGY & GEOPHYSICS
850 VAN VLEET OVAL

NORMAN OK 73019
PHONE.

DOUGLAS E LEWIS
BIO-ANALYTICAL TECHNOLOGIES
2300 CHILDREN'S PLAZA

CHICAGO IL 60614
PHONE. 312 880 3889

SYDELL LEWIS
ROHM & HAAS
8838 CREFELD STREET

PHILADELPHIA PA 19118
PHONE

L M LIBBEY
OREGON STATE UNIV
DPT FOOD SCI/TECH

CORVALLIS OR 97331
PHONE 503 754 4636

DAN LIBERATO
NIH
BLDG 6 RM 136

BETHESDA MD 20205
PHONE 301 496 5531

MARK LICHTENWALNER
NAT'L MED SERVICES INC
2300 STRATFORD AVENUE

WILLOW GROVE PA 19090
PHONE 215 657 4900

J G LIEHR
UNIV OF TEXAS
MEDICAL BRANCH

GALVESTON TX 77550-2774
PHONE

JERROLD M LIESCH
MERCK INSTITUTE
R80 M223
PO BOX 2000
RAHWAY NJ 07065
PHONE 201 574 5546

KAREN J LIGHT
1992 LAC DU MONT

HASLETT MI 48840
PHONE 517 339 3475

W V LIGON
GENERAL ELECTRIC COD
R&D CENTER
BLDG K1 PO BOX 8
SCHENECTADY NY 12301
PHONE. 518 385 8647

WILLIAM LIJINSKY
NCI FREDERICK CANCER
RESEARCH FACILITY
PO BOX B
FREDERICK MD 21701
PHONE 301 695 1221

H K LIM
CTR FOR HUMAN TOXICOLOGY
38 SKAGGS HALL
UNIV OF UTAH
SALT LAKE CTY UT 84112
PHONE

DENIS C K LIN
ENVIR TEST & CERT CO
284 RARITAN CTR PKWY
PO BOX 7808
EDISON NJ 08837-7808
PHONE: 201 225 6707

DING-PING LIN
3967 IVERNESS LANE

W BLOOMFIELD MI 48033
PHONE 313 855 6196

YONG Y LIN
INST FOR BASIC RESEARCH
1050 FOREST HILL RD

STATEN ISLAND NY 10314
PHONE 718 494 5242

KENNETH A LINCOLN
2016 STOCKBRIDGE AVE

REDWOOD CITY CA 94061
PHONE 415 694 5373

JAMES R LINDSAY
US GEOLOGICAL SURVEY
MAIL STOP 938
345 MIDDLEFIELD RD
MENLO PARK CA 94025
PHONE 415 323 8111

N C LING
THE SALK INSTITUTE
BOX 85800

SAN DIEGO CA 92138
PHONE 619 453 4100

RICHARD W LINTON
CHEMISTRY DEPT
UNIV OF N CAROLINA

CHAPEL HILL NC 27514
PHONE: 919 962 2303

CAROL A LISEK
MAYO CLINIC
PHARMACOLOGY DEPT
200 FIRST STREET SW
ROCHESTER MN 55905
PHONE 504 284 4224

ANITA KAY LISTER
YOUNG GRAD HOUSE
ROOM 0244-0

W LAFAYETTE IN 47906
PHONE: 317 494 6311

DAVID T LITTLE
KRATOS ANALYTICAL
2209 QUARTER MASTER

RESTON VA 22091
PHONE: 703 860 8878

DOROTHY LITTLE
FRICK CHEMICAL LAB
ROOM 25
PRINCETON UNIV
PRINCETON NJ 08540
PHONE 609 452 3928

JAMES L LITTLE
TENN EASTMAN KODAK C
BLDG 231

KINGSPORT TN 37662
PHONE 615 229 5651

DUANE LITTLEJOHN
NICOLET INSTRUMENTS
5225-1 VERONA ROAD

MADISON WI 53711
PHONE:

JAMES F LITTON
LOCKHEED MISSILES & SPACE
0/48-92 B/195B
1111 LOCKHEED WAY
SUNNYVALE CA 94088-3504
PHONE 408 756 3236

NORMAN W LIU
SEARLE RES LAB
4901 SEARLE PKWY

SKOKIE IL 60077
PHONE 312 982 8847

RAY H LIU
CRIMINAL JUSTICE
UNIV OF ALABAMA

BIRMINGHAM AL 35226
PHONE 205 934 2069

YA-MEI LIU
101-14 MARRIED STUD COURTS

W LAFAYETTE IN 47906
PHONE: 317 743 6659

H A LLOYD
NIH
BLDG 10 RM 7N312

BETHESDA MD 20892
PHONE: 301 496 3376

JOHN R LLOYD
ORTHO PHARMACEUTICAL
RT 202

RARITAN NJ 08869
PHONE: 201 524 2185

HSI H LO
PERKIN-ELMER
APPLIED SCIENCE DIV
2771 NORTH GAREY AVE
POMONA CA 91767
PHONE: 714 593 3581

JOHN LOGSDON
9909 HOYT WAY

WESTMINSTER CO 80030
PHONE: 303 421 6611

STANTON LOH
BAKER LAB
CORNELL UNIV

ITHACA NY 14853-1301
PHONE: 607 256 3726

JAMES E LONGBOTTOM
US EPA
26 WEST ST CLAIR STREET

CINCINNATI OH 45268
PHONE

JOSEPH A LOO
CHEMISTRY DEPT
BAKER LAB
CORNELL UNIV
ITHACA NY 14853
PHONE: 607 255 3731

LAZARO LOPEZ
SUBURBAN LAB, INC
4140 LITT DRIVE

HILLSIDE IL 60162
PHONE: 312 544 3260

V V LOPEZ-AVILA
ACUREX CORP
485 CLYDE AVE

MNTN VIEW CA 94039
PHONE: 415 964 3200

HARVEY LOUCKS
HEWLETT-PACKARD
SCIENTIFIC INSTRUMENTS
1601 CALIFORNIA AVE
PALO ALTO CA 94304
PHONE 415 857 6989

EDWARD D LOUGHRAN
LOS ALAMOS NAT'L LAB
PO BOX 1663
MS C920
LOS ALAMOS NM 87545
PHONE 505 667 4894

JOHN N LOURIS
CHEMISTRY DEPT
BOX 589
PURDUE UNIV
W LAFAYETTE IN 47907
PHONE: 317 494 6898

NORMAN LOW
HEWLETT-PACKARD
1601 CALIFORNIA AVE

PALO ALTO CA 94304
PHONE: 415 857 7381

DAVID M LUBMAN
CHEMISTRY DEPT
UNIV OF MICHIGAN

ANN ARBOR MI 48109
PHONE. 313 764 1669

WILLIAM J LUKSEMBURG
RADIAN CORP
10395 OLD PLACERVILLE ROAD

SACRAMENTO CA 95827
PHONE 916 362 5332

HENRY E LUMPKIN
1600 DEEP WOOD DR

ROUND ROCK TX 78681
PHONE: 512 255 8386

WILLIAM R LUSBY
8028 NEW RIGGS RD

ADELPHI MD 20783
PHONE: 301 344 2389

MICHAEL LUTZ
CHEMISTRY DEPT
UNIV OF CALIFORNIA

IRVINE CA 92717
PHONE 714 856 5682

KENNETH V LYKINS
VACUMETRICS INC
2261-#1 PALMA DR

VENTURA CA 93003-5789
PHONE· 805 644 7461

PAUL LYNE
2532 VAN HISE AVENUE

MADISON WI 53705
PHONE: 608 262 1845

PHILIP A LYON
3M COMPANY
CENTRAL RESEARCH
201 BW 09
ST PAUL MN 55144
PHONE: 612 736 3525

LESLIE T LYTLE
4305 MINUTEMAN DR

CINCINNATI OH 45245
PHONE 412 487 4500

ABDUL MABUD
108-7 MARRIED STUDENT CT

W LAFAYETTE IN 47906
PHONE 317 743 8141

JOHN L MACDONALD
RALSTON PURINA CO
3RS CHECKERBOARD SQ

ST LOUIS MO 63164
PHONE· 314 982 3038

RONALD D MACFARLANE
TEXAS A&M UNIVERSITY
CHEMISTRY DEPT

COLLEGE STN TX 77843
PHONE. 409 845 2021

TIM MACMAHON
DEPT OF CHEMISTRY
PURDUE UNIV

W LAFAYETTE IN 47907
PHONE 317 494 5271

ROBERT J MADDEN
793 LIND PLACE

MASON OH 45040
PHONE 513 782 4700

JAMES M MADSON
MCDONNELL DOUGLAS
DEPT 223 BLDG 110
PO BOX 516
ST LOUIS MO 63166
PHONE. 314 233 2544

C W MAGEE
RCA LABORATORIES

PRINCETON NJ 08540
PHONE· 609 734 2519

DONALD F MAGIN
PHILIP MORRIS R&D
BOX 26583

RICHMOND VA 23261
PHONE 804 274 4153

PAUL MAHAFFY
CODE 615-1
GODDARD SPACE FLIGHT CTR

GREENBELT MD 20771
PHONE 301 344 8054

N H MAHLE
DOW CHEMICAL CO
574 BLDG

MIDLAND MI 48640
PHONE 517 636 9691

KENNETH O MAHLER
SCI GLASS ENGIN
2007 KRAMER LANE
SUITE 100
AUSTIN TX 78758
PHONE

JOHN MAHONEY
PHRASOR SCIENTIFIC
1536 HIGHLAND AVE

DUARTE CA 91010
PHONE. 213 357 3201

G J MAINS
301 E REDBUD DR

STILLWATER OK 74074
PHONE. 405 624 5941

J O MALBICA
ICI AMERICAS INC
BIOMEDICAL RES LAB

WILMINGTON DE 19897
PHONE 302 575 2268

SIMIN D MALEKNIA
DEPT OF CHEMISTRY
56-028
M I T
CAMBRIDGE MA 02139
PHONE 617 253 7229

LARRY MALLIS
TEXAS A&M UNIV
CHEMISTRY DEPT

COLLEGE STN TX 77843
PHONE.

DAVID A MALTBY
PEDIATRIC METABOLISM
BOX 3028
DUKE MEDICAL CTR
DURHAM NC 27710
PHONE 919 684 2036

RAYMOND MANDRA
SUN VALLEY HEIGHTS RD
PO BOX 324

CROTON FALLS NY 10519
PHONE 914 335 6208

SURAJ P MANRAO
MERCK & CO
ISOTOPES R33-50
PO BOX 2000
RAHWAY NJ 07065
PHONE· 201 574 4207

J J MANURA
SCIENTIFIC INSTR SERVICES
ROUTE 179
RD 2, BOX 198
RINGOES NJ 08551-9675
PHONE 201 788 5550

JOSEPH M MARASCO
479 BROOKSIDE LANE

SOMERVILLE NJ 08876
PHONE. 201 560 0076

DEAN MARBURY
19 PINNACLE ROAD

DURHAM NC 27705
PHONE: 919 544 5729

ALVIN B MARCUS
6 BAYARD ROAD
APT 859

PITTSBURGH PA 15213-1946
PHONE: 412 624 5160

KEN MARCUS
DEPT OF CHEMISTRY
CLEMSON UNIVERSITY

CLEMSON SC 29631
PHONE.

RICHARD K MARCUS
CHEMISTRY DEPT
UNIV OF VIRGINIA

CHARLOTTESVLL VA 22901
PHONE 804 924 7180

JAY A MARK
HUNTINGTON BCH POLICE
2000 MAIN STREET

HUNTINGTON BC CA 92648
PHONE: 714 536 5682

SANFORD P MARKEY
NIMH NIH
BLDG 10-3D40
9000 ROCKVILLE PIKE
BETHESDA MD 20892
PHONE. 301 496 2151

PHILLIP MARQUIS
UNIV OF WISCONSIC
CLSES
6201 CONGDON BLVD
DULUTH MN 55804
PHONE: 218 720 5558

TERRY D MARRIOTT
RICE UNIV
CHEMISTRY DEPT
PO BOX 1892
HOUSTON TX 77251
PHONE. 713 527 8101

PHILIP G MARSH
OCCIDENTAL CHEMICAL CORP
TECHNOLOGY CTR
2801 LONG ROAD
GRAND ISLAND NY 14072-2390
PHONE:

ALAN G MARSHALL
CHEMISTRY DEPT
140 W 18TH AVE
OHIO STATE UNIV
COLUMBUS OH 43210
PHONE. 614 422 3446

D J MARSHALL
PO BOX 315

ACTON MA 01720
PHONE· 617 263 2936

EDWIN MARTI
122 SUNNY MEADE LN
NO 2

MADISON WI 53713
PHONE 608 262 4523

JERRY D MARTIN
3304 OTIS

MODESTO CA 95350
PHONE: 209 529 2671

LOUIS MARTIN
CIBA GEIGY
556 MORRIS AVENUE

SUMMIT NJ 07901
PHONE 201 277 7143

ROBERTO MARTIN
8066 GREENRIDGE DR, #44

OAKLAND CA 94605
PHONE. 415 633 6184

STEPHEN A MARTIN
MIT
BLDG 56-035
77 MASSACHUSETTS AVE
CAMBRIDGE MA 02139
PHONE: 617 253 7233

PETER MARTINELLI
149-11 ARNOLD DRIVE

W LAFAYETTE IN 47906
PHONE.

RICHARD I MARTINEZ
A147 CHEMISTRY
NAT'L BUR OF STANDARDS

GAITHERSBURG MD 20878
PHONE·

DAVID MARTINSEN
AMERICAN CHEMICAL SOCIETY
1155 16TH STREET NW

WASHINGTON DC 20036
PHONE. 202 452 2110

FLOYD C MASELES
UNIV OF TEXAS
2.204A WELCH HALL
CHEMISTRY DEPT
AUSTIN TX 78712
PHONE 512 471 5484

W RODNEY MATHEWS ·
THE UPJOHN CO
LIPIDS RESEARCH L5-11

KALAMAZOO MI 49001
PHONE 616 385 7507

DWIGHT E MATTHEWS
WASHINGTON UNIV
METABOLISM DIV
SCHOOL OF MEDICINE
ST LOUIS MO 63110
PHONE 314 362 7877

DAVID R MATTSON
MATTSON INSTRUMENTS
6333 ODANA ROAD

MADISON WI 53719
PHONE 608 273 2370

JEAN E MATUSIK
FOOD & DRUG ADMN

2 LOPA COURT
GAITHERSBURG MD 20878
PHONE. 202 245 1371

KENNETH P MATUSZAK
UNIV OF FLORIDA
401 LEIGH HALL

GAINESVILLE FL 32611
PHONE: 904 392 0515

R K MAULDIN
CELANESE FIBERS
PO BOX 32414

CHARLOTTE NC 28232
PHONE 704 554 3134

M M MAUTNER
NBS

GAITHERSBURG MD 20899
PHONE. 301 921 2784

RALPH J MAY
GENERAL ELECTRIC
BLDG K-1 RM 2A40

SCHENECTADY NY 12308
PHONE: 518 387 6419

JANET A MAYERNIK
A724 CRABTREE HALL
UNIV OF PITTSBURGH

PITTSBURGH PA 15261
PHONE·

SUEANN MAZER
RESEARCH INST - RM KL102
UNIV OF DAYTON
300 COLLEGE PARK
DAYTON OH 45469
PHONE· 513 229 2806

DALE MAZOROW
RHO-CHEM CORP
425 ISIS

INGLEWOOD CA 90301
PHONE 818 368 1115

DAVID J MCADOO
62 LE BRUN COURT W

GALVESTON TX 77551
PHONE· 409 761 2939

LINDA MCCARRAHER
CHEMISTRY DEPT
MICHIGAN STATE UNIV

EAST LANSING MI 48824
PHONE:

CRAIG A MCCLELLAND
M&M/MARS, INC
HIGH STREET

HACKETTSTOWN NJ 07840
PHONE 201 852 1000

WILLIAM MCCLENNEN
BIOMATERIALS PROFILING CTR
391 S CHIPETA WAY SUITE F

SALT LAKE CTY UT 84108
PHONE 801 581 8431

TERRENCE MCCORMICK
E R SQUIBB & SONS
PO BOX 4000

PRINCETON NJ 08543-4000
PHONE 609 921 5439

D A MCCRERY
BLDG B1219
DOW CHEMICAL-TX OPERATIONS

FREEPORT TX 77541
PHONE: 409 238 3244

STEPHEN W MCELVANY
11726 S LAUREL DRIVE
APT 2A

LAUREL MD 20708
PHONE 202 767 2398

J H MCGLOTTEN
SCHERING CORP
GALLOPING HILL ROAD

KENILWORTH NJ 07033
PHONE: 201 558 5881

J A MCHUGH
GENERAL ELECTRIC CO
KNOLLS ATOM POW LAB
PO BOX 1072
SCHENECTADY NY 12301
PHONE 518 393 6611

JEFF MCKINLEY
722 N INDIANA AVENUE

BLOOMINGTON IN 47401
PHONE

MATTHEW A MCLEAN
UNIV OF HOUSTON
DEPT OF CHEMISTRY
4800 CALHOUN
HOUSTON TX 77004
PHONE 713 749 2646

JAMES A MCCLOSKEY
UNIV OF UTAH
COLLEGE OF PHARMACY
MEDICINAL CHEM DEPT
SALT LAKE CTY UT 84112
PHONE. 801 581 5581

WILLIAM E MCCORMICK
ARMCO INC
703 CURTIS STREET

MIDDLETOWN OH 45043
PHONE: 513 425 2638

KENNETH E MCCULLOH
10304 ST ALBANS DR

BETHESDA MD 20814
PHONE. 301 530 1617

CHARLES N MCEWEN
DUPONT COMPANY
CENTRAL RES DEPT
EXPER STN 228
WILMINGTON DE 19898
PHONE 302 772 2952

STEVEN R MCGOWN
DEPT OF BIOCHEMISTRY
PS II
OKLAHOMA STATE UNIV
STILLWATER OK 74075
PHONE: 405 624 6202

D J MCINTOSH
UNIV OF ALASKA
INST MARINE SCIENCE

FAIRBANKS AK 99775-1080
PHONE 907 474 6731

H S MCKOWN
393 EAST DRIVE

OAK RIDGE TN 37830
PHONE: 615 574 2454

SCOTT A MCLUCKEY
OAK RIDGE NAT'L LABORATORY
BLDG 9735
PO BOX Y
OAK RIDGE TN 37831
PHONE 615 574 2454

C R MCCLURE
FINNIGAN MAT
355 RIVER OAKS PWY

SAN JOSE CA 95134-9990
PHONE 408 946 4848

MICHAEL MCCOWN
VESTEC CORP
9299 KIRBY DRIVE

HOUSTON TX 77054
PHONE 713 796 9677

R N MCDONALD
KANSAS STATE UNIV
CHEMISTRY DEPT
WILLARD HALL
MANHATTAN KS 66506
PHONE. 913 532 6680

WILLIAM H MCFADDEN
FINNIGAN MAT
355 RIVER OAKS PKWY

SAN JOSE CA 95134
PHONE 408 433 4800

J M MCGUIRE
ATHENS ENVIRONMENTAL
RESEARCH LABORATORY
COLLEGE STATION RD
ATHENS GA 30613
PHONE 404 546 3185

ROBERT T MCIVER
UNIV OF CALIFORNIA
CHEMISTRY DEPT

IRVINE CA 92717
PHONE 714 856 6085

FRED W MCLAFFERTY
CORNELL UNIVERSITY
CHEMISTRY DEPT
BAKER LABORATORY
ITHACA NY 14853
PHONE: 607 256 5100

JOHN MCMAHON
7672 TIMBER CIRCLE
NO 2

HUNTNGTN BCH CA 92648
PHONE. 213 306 4200

GARY A MCCLUSKY
WARNER LAMBERT CO
PO BOX 1047

ANN ARBOR MI 48106-1047
PHONE 313 996 7525

J M MCCREA
PO BOX 172

MONROEVILLE PA 15146-0172
PHONE 412 242 0448

RICHARD A MCDONIE
UNION CARBIDE TECH CTR
BLDG 770 ROOM 118
PO BOX 8361
S CHARLESTON WV 25303
PHONE: 304 747 4591

DONALD D MCFALL
PPG INDUSTRIES
PO BOX 31

BARBERTON OH 44203
PHONE: 216 848 4161

JEFFREY M MCGUIRE
HERCULES INC
RESEARCH CENTER

WILMINGTON DE 19894
PHONE 302 995 3294

KEITH B MCKELLOP
BOEHRINGER INGELHEIM
RES & DEV
175 BRIAR RIDGE RD
RIDGEFIELD CT 06877
PHONE 203 748 4200

R DAVID MCLANE
PROCTER & GAMBLE
11511 REED HARTMAN HWY

CINCINNATI OH 45241
PHONE: 513 530 3081

WALTER J MCMURRAY
YALE UNIV SCH OF MEDICINE
333 CEDAR STREET

NEW HAVEN CT 06510
PHONE. 203 785 4525

RICHARD MCNAUGHT
GENERAL FOODS CORP
TECHNICAL CTR

WHITE PLAINS NY 10625
PHONE 914 335 6806

CATHERINE J MCNEAL
TEXAS A&M UNIVERSITY
CHEMISTRY DEPT

COLLEGE STN TX 77843
PHONE: 409 845 2355

RUSSELL D MCNIECE
AQUALAB INC
9909 BURNET ROAD

AUSTIN TX 78758
PHONE

J H MCREYNOLDS
SUNY MEDICAL SCHOOL
BIOPHYSICAL SCIENCE
118 CARY HALL
BUFFALO NY 14214
PHONE: 716 831 3245

B D MCVEETY
INDIANA UNIV
ROOM 541
GEOLOGY BLDG
BLOOMINGTON IN 47405
PHONE 812 335 5976

GINA M MEAGHER
COMMERCIAL TESTING
490 ORCHARD ST

GOLDEN CO 80401
PHONE 303 278 9521

J C MEANS
UNIV OF MARYLAND
CHESAPEAKE BIOL LAB
PO BOX 38
SOLOMONS MD 20688
PHONE 301 326 4281

WILMA K MECKSTROTH
OHIO STATE UNIV
944 BRICE ROAD

REYNOLDSBURG OH 43068
PHONE. 614 366 3321

PATRICK W MEEHAN
BATTELLE COL LABS
505 KING AVE

COLUMBUS OH 43201
PHONE. 614 424 7936

JON R MEEK
AMERICAN CYANAMID
PO BOX 400

PRINCETON NJ 08540
PHONE

H H MEHNERT
US GEOLOGICAL SURVEY
ISOTOPE GEOLOGY

DENVER CO 80225
PHONE 303 236 7882

T K MEHRHOFF
14120 82ND AVE N

SEMINOLE FL 33542
PHONE: 813 541 8769

STANLEY MEISELMAN
NAT'L BUR OF STANDARDS
BLDG 222 ROOM A113

GAITHERSBURG MD 20899
PHONE. 301 921 2153

GERRY G MEISELS
UNIV OF NEBRASKA
1223 OLDFATHER HALL

LINCOLN NE 68588-0312
PHONE 402/472-6262

S J MELFORD
DEPAUL UNIVERSITY
CHEMISTRY DEPT

CHICAGO IL 60614
PHONE 312 341 8180

G E MELLEN
935 HUGHES DR

ST ALBANS WV 25177
PHONE 304 727 8126

BENNETT MELNICK
3040 W CHASE

CHICAGO IL 60645
PHONE

MARCIA MEREDITH
TETRA TECH INC
11820 NORTHUP WAY
SUITE 100
BELLEVUE WA 98005-1927
PHONE

GUY L MERRILL
24 SOUTHBURY RD

CLIFTON PARK NY 12065
PHONE. 518 393 6611

CLIMACO J METRAL
309 BOXFORD COURT

FREDERICK MD 21701
PHONE: 301 695 1226

H L MEUZELAAR
BIOMATERIALS PROFILING CTR
391 S CHIPETA WAY

SALT LAKE CTY UT 84108
PHONE.

V D MEYER
GTE LIGHTING PRODUCTS
100 ENDICOTT ST

DANVERS MA 01923
PHONE. 617 777 1900

MICHAEL C MEYERS
4334 DEER SPRING ROAD

MIDDLETOWN MD 21769
PHONE: 301 459 2940

SEYMOUR MEYERSON
650 N TIPPECANOE ST

GARY IN 46403
PHONE 219 938 1933

I I MICHAEL
AFGL-PHG
STOP 30

HANSCOM AFB MA 01731
PHONE

JOSEF MICHL
CHEMISTRY DEPT
UNIV OF UTAH

SALT LAKE CTY UT 84112
PHONE. 801 581 8549

JOHN A MICHNOWICZ
HEWLETT PACKARD
1601 CALIFORNIA AVE

PALO ALTO CA 94304
PHONE: 415 857 5481

M A MICKE
DEPT OF BIOCHEMISTRY
MICHIGAN STATE UNIV

EAST LANSING MI 48824
PHONE: 517 353 0612

DUANE L MICKELSON
THE UPJOHN CO
LOC 1140-230-2

KALAMAZOO MI 49001
PHONE: 616 323 4031

DAVID MICKUNAS
MSD ADVANCED ANALYTICS
2 DUNDEE PARK

ANDOVER MA 01810
PHONE. 617 470 1390

RICHARD M MILBERG
UNIV OF ILLINOIS
SCH OF CHEM SCIENCES
505 S MATHEWS
URBANA IL 61801
PHONE. 217 333 2545

JEFFREY ROBERT MILLARD
CHEMISTRY DEPT
INDIANA UNIV

BLOOMINGTON IN 47405
PHONE: 812 335 7723

WILLIAM G MILLEN
AMERICAN CYANAMID
PO BOX 400

PRINCETON NJ 08540
PHONE 609 799 0400

CHARLES M MILLER
MS J-514
LOS ALAMOS NATL LAB

LOS ALAMOS NM 87545
PHONE 505 667 4546

DAVID L MILLER
EG&G IDAHO INC
PO BOX 1625

IDAHO FALLS ID 83415
PHONE:

DEBORAH MILLER
UNION CARBIDE
BLDG 770-318
PO BOX 8361
S CHARLESTON WV 25303
PHONE 304 747 4463

DENNIS A MILLER
MICH TECH UNIV
CHEM & CHEM ENGIN

HOUGHTON MI 49931
PHONE 906 487 2059

LELAND V MILLER
UNIV OF COLORADO
HEALTH SCIENCE CTR C232
4200 E 9TH
DENVER CO 80262
PHONE 303 394 8126

MARK L MILLER
MONSANTO POLYMER PRODUCTS
260 SPRINGSIDE DR

AKRON OH 44313
PHONE 216 668 8244

ROBERT A MILLER
2610 GILLIS FALLS ROAD

WOODBINE MD 21797
PHONE:

DAVID S MILLINGTON
DEPT OF PEDIATRICS
BOX 3028
DUKE UNIV MED CTR
DURHAM NC 27710
PHONE: 919 684 2036

T A MILNE
SERI
1617 COLE BLVD

GOLDEN CO 80401
PHONE 303 231 1440

ROBERT D MINARD
PENN STATE UNIV
152 DAVEY LAB

UNIV PARK PA 16802
PHONE 814 865 2202

JAMES MING
NASA/GODDARD SPACE CENTER
CODE 313
BLDG 22 ROOM 349
GREENBELT MD 20771
PHONE

DONALD M MINTZ
1610 BELLEVILLE WAY

SUNNYVALE CA 94087
PHONE 415 493 4000

STEPHEN R MISSLER
13755 GREYWOOD

SUGAR LAND TX 77478
PHONE 713 432 2572

LAURA A MITACEK
DU PAGE COUNTY CRIME LAB
501 NORTH COUNTY FARM ROAD

WHEATON IL 60187
PHONE 312 682 7817

RONALD K MITCHUM
US EPA
PO BOX 15027

LAS VEGAS NV 89114-5027
PHONE 702/798-2103

KEI MIYANO
F A I HUTCHINSON HALL
ROOM 9
UNIV OF CALIFORNIA
DAVIS CA 95611
PHONE 916 752 6272

JOERG MOENIG
DEPT OF CHEMISTRY
UNIV OF CALIFORNIA

RIVERSIDE CA 92507
PHONE 714 787 3657

MEHDI MOINI
CHEMISTRY DEPT
UNIV OF FLORIDA

GAINESVILLE FL 32611
PHONE

MARK TWINING MOJESKY
DEPT OF CHEMISTRY
CHEM/PHYS BLDG ROOM 4
UNIV OF KENTUCKY
LEXINGTON KY 40506
PHONE 606 257 6957

JAMES MONCUR
LOCKHEED
3251 HANOVER ST

PALO ALTO CA 94304
PHONE: 415 424 2533

KARIN MONSON-KIRLAND
ICI AMERICAS INC
BMRD L-215
CONCORD PK & MURPHY
WILMINGTON DE 19897
PHONE 302 575 2277

RICHARD M MONTGOMERY
243 EAST GLEN AVE

RIDGEWOOD NJ 07450-1709
PHONE 914 357 2000

J ROBERT MOONEY
STANDARD OIL CO
4440 WARRENSVILLE CTR ROAD

CLEVELAND OH 44128
PHONE 216 586 5824

CATHERINE A MOORE
DEPT OF CHEMISTRY
UNIV OF CALIFORNIA

IRVINE CA 91717
PHONE: 714 856 5682

JOHN A MOORE
DOW CORNING CORP
3901 S SAGINAW RD
BOX 1592 NO 21
MIDLAND MI 48640-0995
PHONE: 517 496 5711

LARRY J MOORE
ATOM SCIENCES INC
114 RIDGEWAY CTR

OAK RIDGE TN 37830
PHONE 615 483 1113

LAWRIE MOORE
KRATOS ANALYTICAL
170 WILLIAMS DRIVE

RAMSEY NJ 07446
PHONE:

ERICH MORAINE
R J BRUNFELDT CO
PO BOX 2066

BARTLESVILLE OK 74005
PHONE 918 336 4467

SHARON PALLANTE MORELL
JOHNS HOPKINS UNIV
PHARMACOLOGY DEPT
725 N WOLFE ST
BALTIMORE MD 21205
PHONE 301 955 6961

JOHN J MORELLI
309 S AIKEN AVENUE
APT 4

PITTSBURGH PA 15232
PHONE: 412 624 2799

KENT MORRILL
TENN EASTMAN CO
B150
PO BOX 1972
KINGSPORT TN 37662
PHONE: 615 229 3066

CLARENCE J MORRIS
LLNL
PO BOX 808

LIVERMORE CA 94550
PHONE: 415 422 5779

FRANK MORRIS
HOLLY OAK TERRACE
301 MAPLE AVE

WILMINGTON DE 19809
PHONE 302 575 8410

G H MORRISON
CORNELL UNIVERSITY
CHEMISTRY DEPT
BAKER LABORATORY
ITHACA NY 14853-1301
PHONE 607 256 3614

THOMAS H MORTON
UNIV OF CALIFORNIA
CHEMISTRY DEPT

RIVERSIDE CA 92521
PHONE: 617 495 4022

NEIL MOSESMAN
SUPELCO INC
SUPELCO PARK

BELLEFONTE PA 16823-0048
PHONE: 814 359 3441

SANDRA L MUELLER
ABBOTT LABS
D-417 AP9

ABBOTT PARK IL 60064
PHONE. 312 937 2081

M LUIS MUGA
TOFTEC
PO BOX 12877

GAINESVILLE FL 32604
PHONE: 904 392 1441

ANTHONY M MUJSCE
AT&T BELL LABORATORIES
600 MOUNTAIN AVE

MURRAY HILL NJ 07974
PHONE: 201 582 6249

STEVEN L MULLEN
CHEMISTRY DEPT BOX 253
OHIO STATE UNIV
140 W 18TH AVENUE
COLUMBUS OH 43210
PHONE: 614 422 4214

C E MULLER
4139 BELLAIRE BLVD

HOUSTON TX 77025
PHONE: 713 665 2115

MOHAMMAD M MUMTAZ
PREVENTATIVE MEDICINE
COMMUNITY HEALTH F-17
UNIV OF TX MED BRNCH
GALVESTON TX 77550
PHONE: 409 761 1128

IN K MUN
1 APPLE COURT

NANUET NY 10954
PHONE: 212 305 1230

DAVID J MUNCH
US EPA
26 W ST CLAIR STREET

CINCINNATI OH 45268
PHONE.

JEAN W MUNCH
US EPA
26 W ST CLAIR STREET

CINCINNATI OH 45268
PHONE 513 569 7465

BURNABY MUNSON
UNIV OF DELAWARE
CHEMISTRY DEPT

NEWARK DE 19711
PHONE. 302 451 2340

EDMOND MURAD
AF GEOPHYSICS LAB
PHK

HANSCOM AFB MA 01731
PHONE: 617 861 3176

STANLEY MURAKAMI
SYNTEX CORP
3401 HILLVIEW AVENUE

PALO ALTO CA 94304
PHONE: 415 855 5692

SANDRA MURAWSKI
447 RAL BOX 97-5
1209 W CALIFORNIA

URBANA IL 61801
PHONE. 217 333 0655

CONSTANCE M MURPHY
JOHNS HOPKINS UNIV
725 N WOLFE STREET

BALTIMORE MD 21205
PHONE: 301 955 6961

ROBERT C MURPHY
UNIV OF COLORADO
MEDICAL CENTER
PHARMCOLOGY DEPT
DENVER CO 80262
PHONE: 303 394 8962

JOHN S MURRAY
4227 WOODLAND DR

INDIANAPOLIS IN 46254
PHONE: 317 243 8305

G M MUSCHIK
NCI-FREDERICK CANCER
RESEARCH FACILITY
PO BOX B BLDG 467
FREDERICK MD 21701
PHONE 301 695 1226

E E MUSCHLITZ
UNIV OF FLORIDA
CHEMISTRY DEPT

GAINESVILLE FL 32611
PHONE: 904 392 2006

BRIAN D MUSSELMAN
MICHIGAN STATE UNIV
BIOCHEMISTRY DEPT
MASS SPEC FACILITY
EAST LANSING MI 48824
PHONE: 517 353 0612

STEVE MUSSER
DEPT MCPG
UNIV OF MARYLAND
20 N PINE STREET
BALTIMORE MD 21201
PHONE:

CLIFFORD E MYERS
SUNY @ BINGHAMTON
CHEMISTRY DEPT

BINGHAMTON NY 13901
PHONE: 607 798 2229

LESTER MYERS
MASON & HANGER
PO BOX 30020

AMARILLO TX 79177
PHONE: 806 381 4208

M'CHAEL MYERS
NICOLET INSTRUMENTS
5225-1 VERONA ROAD

MADISON WI 53711
PHONE: 608 271 3333

N N NARASIMHACHARI
MEDICAL COL VIRGINIA
PSYCHIATRY DEPT
BOX 710
RICHMOND VA 23298
PHONE 804 786 5360

BOB NEAL
PROCTER & GAMBLE
MIAMI VALLEY LABORATORIES
PO BOX 39175
CINCINNATI OH 45247
PHONE 513 245 2178

DAVID NEAL
PROCTER & GAMBLE
MIAMI VALLEY LABORATORIES
PO BOX 39175
CINCINNATI OH 45247
PHONE: 513 245 2258

CHAD C NELSON
311A SKAGGS HALL
UNIV OF UTAH

SALT LAKE CTY UT 84114
PHONE: 801 581 5582

PAUL R NELSON
DEPT OF CHEMISTRY
GEORGIA TECH

ATLANTA GA 30332
PHONE· 404 894 4070

ROBERT J NELSON
NORTHEASTERN UNIV
CHEMISTRY DEPT
360 HUNTINGTON AVE
BOSTON MA 02115
PHONE. 617 437 5069

SIDNEY D NELSON
UNIV OF WASHINGTON
DEPT MEDICINAL CHEM
BLDG 20
SEATTLE WA 98195
PHONE 206 543 1419

VINCENT P NERO
TEXACO INC
BOX 509

BEACON NY 12508
PHONE 914 831 3400

ROBERT A NESMAN
SCIEX
263 ROCHESTER HILL RD

ROCHESTER NH 03867
PHONE

THOMAS A NEUBECKER
MIAMI VALLEY LABS
PO BOX 39175

CINCINNATI OH 45247
PHONE·

BRUCE NEWCOME
CHEMISTRY DEPT
MICHIGAN STATE UNIV

EAST LANSING MI 48824
PHONE.

A S NEWTON
1665 THOUSAND OAKS

BERKELEY CA 94707
PHONE. 415 486 5040

JOHN C NEWTON
LAW LIV NAT'L LAB
L-310
PO BOX 808
LIVERMORE CA 94550
PHONE. 415 422 6892

KENNETH T NG
CIBA-GEIGY CORP
444 SAW MILL RIVER ROAD

ARDSLEY NY 10502
PHONE 914 478 3131

KWOKEI J NG
SCHERING CORP
60 ORANGE STREET B-6-139

BLOOMFIELD NJ 07003
PHONE. 201 429 4211

NIMH-THUY L NGUYEN
SUN SO
ARD 2
PO BOX 1135
MARCUS HOOK PA 19061
PHONE.

LAURENCE NIELSEN
UNION CAMP CORP
PO BOX 6941

LAWRENCEVILLE NJ 08648
PHONE. 609 896 1200

HASSO B NIEMANN
NASA GODDARD SPACE
FLIGHT CTR
CODE 615
GREENBELT MD 20771
PHONE. 301 344 8706

A O NIER
UNIV OF MINNESOTA
PHYSICS/ASTRONOMY

MINNEAPOLIS MN 55455
PHONE 612 373 3325

JOHN A NIKORA
B F GOODRICH CENTER
CHEMISTRY DIVISION
PO BOX 122
AVON LAKE OH 44012
PHONE 216 933 0288

TOSHIHIDE NISHIMURA
UNIV OF NEBRASKA
524 HAMILTON HALL

LINCOLN NE 68588
PHONE. 402 472 3517

ALBERT J NITOWSKI
63 GALPIN STREET

NAGATUCK CT 06770
PHONE 203 723 3495

ROY W NOBLE
MONSANTO CO
MAIL CODE U1F
800 N LINDBERGH BLVD
ST LOUIS MO 63167
PHONE 513 694 1272

JAMES S NOONAN
OHIO STATE UNIV
1935 COFFEY ROAD

COLUMBUS OH 43210
PHONE 614 422 4299

ERIC J NORMAN
1044 SUNWOOD CT

CINCINNATI OH 45231
PHONE. 513 872 4233

JAMES D NORMAN
T107 N F D C
TENN VALLEY AUTHORITY

SHEFFIELD AL 35660
PHONE. 205 386 2371

D J NORTHINGTON
WEST COAST ANAL SERVICE
9840 ALBURTIS AVE

SANTA FE CA 90670
PHONE 213 948 2225

DANIEL L NORWOOD
RESEARCH TRIANGLE INST
PO BOX 12194

RES TRI PK NC 27709
PHONE 919 541 5928

BOBETTE D NOURSE
CHEMISTRY DEPT C/O ENKE
MICHIGAN STATE UNIV

EAST LANSING MI 48824
PHONE 517 353 5215

FRANK P NOVAK
UNIV OF PITTSBURGH
CHEMISTRY DEPT

PITTSBURGH PA 15260
PHONE 412 624 2799

LYDIA NUWAYSIR
3637 CANYON CREST DRIVE
APT H 206

RIVERSIDE CA 92507
PHONE: 714 684 9729

ANNE D O'DONNELL
13651 LAMON

CRESTWOOD IL 60445
PHONE 312 388 0486

J T O'DONOVAN
FINNIGAN INSTRUMENTS
1383 PICCARD DR #100

ROCKVILLE MD 20850
PHONE 301 948 1067

ANTHONY O'KEEFE
NAVAL RESEARCH LABORATORY
CODE 6110

WASHINGTON DC 20375
PHONE· 202 767 2398

JOHN R O'LEAR
CHEMISTRY BLDG
BOX 652
PURDUE UNIV
W LAFAYETTE IN 47906
PHONE: 317 494 5262

REBECCA M O'MALLEY
UNIV OF S FLORIDA
CHEMISTRY DEPT

TAMPA FL 33620
PHONE: 813 935 8120

D W OBLAS
GTE LABS
40 SYLVAN RD

WALTHAM MA 02154
PHONE: 617 466 2456

DAVID R OHORI
ORTHO PHARMACEUTICAL
RT 202

RARITAN NJ 08869
PHONE: 201 524 8738

J A OLIVARES
213 S SHELDON NO 3

AMES IA 50010
PHONE: 509 376 6095

BRUCE ONISKO
STAUFFER CHEMICAL CO
1200 S 47TH STREET

RICHMOND CA 94804
PHONE: 415 231 1058

RON ORLANDO
DEPT OF CHEMISTRY
UNIV OF DELAWARE

NEWARK DE 09702
PHONE: 302 368 8687

CHARLES M OSBURN
OSBURN INSTRUMENT SERVICES
THISBE RANCH
RTE 1
SPARKS NV 89431
PHONE 702 343 1116

FEZA OZTURK
CHEMISTRY DEPT
LEIGH HALL
UNIV OF FLORIDA
GAINESVILLE FL 32611
PHONE: 904 392 0536

F G PADRTA
UOP INC
TEN UOP PLAZA

DES PLAINES IL 60016
PHONE: 312 391 3175

JOHN L OCCOLOWITZ
LILLY CORPORATE CTR
DEPT MC525

INDIANAPOLIS IN 46285
PHONE 317 261 4713

EDWARD L OLBERDING
MERRELL-DOW PHARMACEUTICAL
9550 ZIONSVILLE RD
BLDG 219
INDIANAPOLIS IN 46268
PHONE: 317 873 7149

KEITH L OLSON
GM RESEARCH
ANALYTICAL CHEMISTRY
30500 MOUND ROAD
WARREN MI 48090-9055
PHONE: 313 575 7142

JON D ONSTOT
MIDWEST RES CTR
425 VOLKER BLVD

KANSAS CITY MO 64110
PHONE: 816 753 7600

DENNIS J ORR
FINNIGAN MAT
355 RIVER OAKS PKWY

SAN JOSE CA 95134-9990
PHONE: 408 433 4800

REBECCA OSTERMAN
VESTEC CORP
9299 KIRBY DRIVE

HOUSTON TX 77054
PHONE. 713 796 9677

C F PACHUCKI
GENERAL ELECTRIC CO
KNOLLS ATOM POW LAB
PO BOX 1072
SCHENECTADY NY 12301
PHONE: 518 393 6611

RODNEY P PAGE
ARCO
388 ULTIMO AVENUE

LONG BEACH CA 90814
PHONE

R W ODOM
301 CHESAPEAKE DRIVE

REDWOOD CITY CA 94063
PHONE: 415 572 1601

RONALD G OLDHAM
1410 TARTON

SAN ANTONIO TX 78231
PHONE: 512 650 0695

WILLIAM M OLSON
MST-13 MS-E511
LOS ALAMOS NAT'L LAB

LOS ALAMOS NM 87545
PHONE:

J DOUGLAS OPTHOFF
CLAYTON ENVIRONMENTAL
CONSULTANTS
25711 SOUTHFIELD RD
SOUTHFIELD MI 48075
PHONE. 313 424 8860

ROBERT G ORTH
RT 1 BOX 658A

CEDAR HILL MO 63016
PHONE 314 694 1271

CHARLES OTTO
LLNL
L-310
PO BOX 808
LIVERMORE CA 94550
PHONE: 415 422 6899

ROBIN ROUSH PACHUTA
CHEMISTRY BLDG
BOX 712
PURDUE UNIV
W LAFAYETTE IN 47907
PHONE: 317 494 5262

CYNTHIA A PALMER
ONEIDA RESEARCH SERVICES
ONE HALSEY ROAD

WHITESBORO NY 13492
PHONE: 315 736 3050

TERESA ODOM
FINNIGAN MAT
355 RIVER OAKS PKWY

SAN JOSE CA 95134
PHONE. 408 433 4800

IRVING A OLEARY
THE UPJOHN CO
UNIT 7256-126-2
301 HENRIETTA
KALAMAZOO MI 49001
PHONE: 616 385 4579

JAMES OLTHOFF
JOHNS HOPKINS SCH OF MED
PHARMACOLOGY DEPT
725 N WOLFE ST
BALTIMORE MD 21205
PHONE: 301 955 6961

MARIA L ORDINARIO
SHRADER ANALYTICAL
3814 VINEWOOD

DETROIT MI 48208
PHONE: 313 894 4440

DAVID OSBORNE
520 WAKARA WAY

SALT LAKE CTY UT 84108
PHONE: 801 584 3260

EDWARD B OVERTON
5536 RIVERBEND DRIVE

BATON ROUGE LA 70820
PHONE: 504 388 8521

STEVEN J PACHUTA
BOX 677
CHEMISTRY DEPT
PURDUE UNIV
W LAFAYETTE IN 47907
PHONE: 317 494 5262

PETER T PALMER
CHEMISTRY DEPT
MICHIGAN STATE UNIV

EAST LANSING MI 48824
PHONE: 517 353 5215

JOSEPH C PAN
CHEMISTRY DEPT
29 HAMILTON HALL
UNIV OF NEBRASKA
LINCOLN NE 688588
PHONE. 402 472 3507

EDWARD K PANG
GTE PRODUCTS CORP
100 ENDICOTT STREET

DANVERS MA 01923
PHONE. 617 777 1900

VINCENT M PAPA
UNIV OF ILLINOIS
PEDIATRICS 1218 HA
840 S WOOD
CHICAGO IL 60680
PHONE: 312 996 0930

DAN PARKER
TEKNIVENT CORP
10774 TRENTON AVE

ST LOUIS MO 63132
PHONE 314 429 7272

LES G PARTRIDGE
SYNTEX RESEARCH
3401 HILLVIEW AVE

PALO ALTO CA 94304
PHONE 415 855 5067

ADAM PATKIN
PERKIN-ELMER
761 MAIN AVENUE

NORWALK CT 06859-0090
PHONE 203 762 6804

RAPHE PAVLICK
WESTON INC
7720 LORRAINE ST 102

STOCKTON CA 95210
PHONE 209 957 3405

RICHARD C PEFFER
1100 SALK HALL
UNIV OF PITTSBURGH

PITTSBURGH PA 15261
PHONE 412 624 3285

SHU-TEH PAN
7720 LORRAINE AVE #102

STOCKTON CA 95210
PHONE

HO-MING PANG
CHEMISTRY DEPT
UNIV OF MICHIGAN

ANN ARBOR MI 48109
PHONE 313 764 1669

I A PAPAYANNOPOULOS
M I T.
RM 56-012 CHEM DEPT

CAMBRIDGE MA 02139
PHONE. 617 253 7237

GEORGE A PARKER
METRO WATER QUAL LAB
821 SECOND AVENUE
MAIL STOP LAB
SEATTLE WA 98119
PHONE 206 447 5877

ROSE PASSARELLA
152 DAVEY LABORATORY
BOX 83
PENN STATE UNIV
UNIV PARK PA 16802
PHONE. 814 863 3583

DONALD G PATTERSON
CTR FOR DISEASE CONT
TOXICOLOGY BRANCH

ATLANTA GA 30333
PHONE 404 452 4176

ROBERT J PAWLOSKY
UNIV OF MINNESOTA
495 BORLAUG HALL
1991 BUFORD CR
ST PAUL MN 55104
PHONE

PEURA PEKKA
766 ESCONDIDO VILLAGE

STANFORD CA 94305
PHONE.

R J PANCIROV
EXON RES & ENG CO
CLINTON TOWNSHIP

ANNANDALE NJ 08801
PHONE. 201 730 2229

LEWIS K PANNELL
NIH
BLDG 8 ROOM B2A

BETHESDA MD 20892
PHONE 301 496 4055

DAVID M PAREES
AIR PRODUCTS & CHEM
PO BOX 538

ALLENTOWN PA 18105
PHONE. 215 481 5794

STEVEN PARKHURST
DOW CHEMICAL
EVS-620 BLDG

MIDLAND MI
PHONE

MICHAEL J PASTEL
LEDERLE LABORATORIES
BLDG 65 ROOM 126

PEARL RIVER NY 10965
PHONE. 914 735 5000

PAUL J PAULSEN
NBS
BLDG 221 RM A25

WASHINGTON DC 20234
PHONE: 301 921 2781

DAVID A PEAKE
20 HAMILTON HALL
CHEMISTRY DEPT
UNIV OF NEBRASKA
LINCOLN NE 68588
PHONE 402 472 3507

H E PENA
215 RIO VISTA DR

ST CHARLES MO 63303
PHONE 314 982 5404

R C PANDEY
WAKSMAN INST OF MICRO
PO BOX 759

PISCATAWAY NJ 08854
PHONE 201 932 3067

JOAN PAO
HOFFMANN-LAROCHE INC
BLDG 86

NUTLEY NJ 07110
PHONE 201 235 3167

CAROL E PARKER
PO BOX 232
ROUTE 3

APEX NC 27502
PHONE: 919 541 5008

N H PARSONS
GENERAL ELECTRIC CO
PO BOX 2908

LARGO FL 34294
PHONE. 813 541 8417

SUBHA M PATEL
1573 WASHINGTON VALLEY RD

BRIDGEWATER NJ 08807
PHONE 201 264 4500

J F PAULSON
AFGL-LID

HANSCOM AFB MA 01731
PHONE: 617 861 3124

DAN S PEARCE
HEWLETT PACKARD CO
3200 HANOVER STREET

PALO ALTO CA 94303
PHONE 415 857 7448

M B PENNINGTON
6407 LONGVIEW

SHAWNEE KS 66218-9739
PHONE 816 997 4187

ROBERT E PENROD
NICOLET INSTRUMENTS
5225-1 VERONA ROAD

MADISON WI 53711
PHONE: 608 271 3333

DANIEL PENTEK
YALE UNIV
CHEMICAL INSTR CTR
225 PROSPECT ST
NEW HAVEN CT 06511
PHONE. 203 436 3999

ROBERT J PERCHALSKI
PHARMATEC INC
PO BOX 730

ALACHUA FL 32615
PHONE 904 462 1210

JULIUS PEREL
PHRASOR SCIENTIFIC
1536 HIGHLAND AVE

DUARTE CA 91010
PHONE.

DEBORAH D PERKINS
SCH OF CHEMISTRY
GEORGIA TECH

ATLANTA GA 30332
PHONE: 404 894 4051

PATRICK D PERKINS
HEWLETT-PACKARD
SCIENTIFIC INSTRUMENTS DIV
1601 CALIFORNIA AVE
PALO ALTO CA 94304
PHONE·

RICHARD E PERRIN
MOUNTAIN ROUTE 100

JEMEZ SPRINGS NM 87025
PHONE: 505 667 4755

DONALD L PERRY
8155 JEFFERSON HWY
APT 703

BATON ROUGE LA 70804
PHONE 504 928 0232

PAUL H PETERMAN
1 ROLLINGWOOD WEST DRIVE
ROUTE 5

COLUMBIA MO 65202-9542
PHONE: 314 875 5399

DEANNA L PETERSON
3359 FEDERAL BLVD

DENVER CO 80211
PHONE· 303 623 2500

GLENN S PETERSON
DELSI INSTRUMENTS
10 KINGSBRIDGE ROAD

FAIRFIELD NJ 07006
PHONE 201 227 7690

R J PETERSON
FIRMENICH INC
PO BOX 5880

PRINCETON NJ 08540
PHONE 609 452 1000

G A PETZINGER
9 LAMBERT STREET

WOODBRIDGE NJ 07095
PHONE. 718 965 5722

ALBERT PEYTON
134 C/217
LEDERLE LABS .

PEARL RIVER NY 10965
PHONE· 914 735 5000

CARL D PFAFFENBERGER
3301 NE 5TH AVENUE #1107

MIAMI FL 33137
PHONE. 305 375 3326

DANIEL PHELPS
AMOCO PRODUCTION CO
PO BOX 3385

TULSA OK 74102
PHONE: 918 660 3129

LAWRENCE R PHILLIPS
19820 COCHRANE WAY

GAITHERSBURG MD 20879-1637
PHONE: 301 496 4570

W C PHILLIPS
1108 FRANK DR

CHAMPAIGN IL 61820
PHONE·

DOUGLAS W PHILLIPSON
UNIV OF UTAH
DEPT OF MEDICINAL CHEMISTRY
311A SKAGGS HALL
SALT LAKE CTY UT 84112
PHONE 801 581 7532

MARY JANE PHINNEY
VG INSTRUMENTS
300 BROAD STREET

STAMFORD CT 06901
PHONE: 203 322 4546

WILLIAM M PIERCE
DEPT PHARMACOLOGY & TOXI
HEALTH SCIENCES CTR

LOUISVILLE KY 40292
PHONE. 502 588 5141

DAVID PILOSOF
UNIV OF HOUSTON
CHEMISTRY DEPT
4800 CALHOUN
HOUSTON TX 77004
PHONE.

J DAVID PINKSTON
MIAMI VALLEY LABS
PROCTER & GAMBLE
PO BOX 39175
CINCINNATI OH 45247
PHONE 513 245 2269

J L PINKUS
75 CLEVELAND ROAD

WELLESLEY MA 02181
PHONE· 617 720 6400

JAMES W PINSON
UNIV OF ILL MED CTR
COLL OF PHARMACY
833 S WOOD RM 131 CPL
CHICAGO IL 60612
PHONE:

JAMES W PINSON
AMER LABS & RESEARCH
1008 SOUTHEAST CR

HATTIESBURG MS 39402-1008
PHONE: 601 264 9320

E G PIOTROWSKI
ERRC USDA
600 E MERMAID LN

PHILADELPHIA PA 19118
PHONE· 215 233 6487

ALBERT J PIRONE
10 KENLEIGH CT

WILMINGTON DE 19808
PHONE: 302 575 8385

MATTHEW V PISERCHIO
3420 PLAZA DRIVE

STATE COLLEGE PA 06801
PHONE. 814 238 2331

H O PITTS
1370 CLAREMONT DR

BOULDER CO 80303
PHONE: 303 966 4106

VINCE PIZZITOLA
EXTREL CORP
PO BOX 11512AITH RD

PITTSBURGH PA 15238
PHONE

IRENE PLAKUNOV
3184 EAGLESWAY DR
NO 1636

LAFAYETTE IN 47905
PHONE· 317 477 6160

RONALD D PLATTNER
NORTHERN REG LAB
1815 N UNIVERSITY ST

PEORIA IL 61604
PHONE: 309 685 4011

THOMAS R POFAHL
KRAFT INC
801 WAUKEGAN RD

GLENVIEW IL 60025
PHONE. 312 998 3619

STEVEN C POMERANTZ
DEPT MEDICINAL CHEMISTRY
311A SKAGGS HALL
UNIV OF UTAH
SALT LAKE CTY UT 84112
PHONE: 801 581 5582

BARBARA S PORTZ
U OF CO HEALTH SCI CTR
GI DIV BOX B158
4200 E NINTH AVE
DENVER CO 80262
PHONE. 303 394 7287

LURA J POWELL
411 CHRISTOPHER AVE #22

GAITHERSBURG MD 20879
PHONE. 301 921 3132

BIKASH PRAMANIK
HOWARD HUGHES MEDICAL
UT HEALTH SCI CTR
5323 HARRY HINES BLVD
DALLAS TX 75235-9050
PHONE 214 689 5019

WILLIAM N PRICE
HEWLETT-PACKARD
PO BOX 105005

ATLANTA GA 30339
PHONE: 404 244 2500

THOMAS H PRITCHETT
ENVIRESPONSE INC
GSA RARITAN DEPOT
BLDG 209 BAY F
EDISON NJ 08837
PHONE

CHESTER E PLUCINSKI
18354 W 58TH PLACE #D

GOLDEN CO 80403
PHONE: 303 966 7593

S M POLING
263 S CHESTER AVE

PASADENA CA 91106
PHONE 818 796 0239

BING T POON
WALTER REED ARMY
INST OF RESEARCH
EXPTL THERAPEUTICS
WASHINGTON DC 20307-5100
PHONE 301 427 5426

THOMAS POTTER
GC/MS LABORATORY
UNIV OF MASSACHUSETTS

AMHERST MA 01003
PHONE 413 545 3505

MARK L POWELL
SCHERING CORP
B-6-137
60 ORANGE STREET
BLOOMFIELD NJ 07003
PHONE 201 429 4213

GEORGE PRETI
MONELL CTR
3500 MARKET ST

PHILADELPHIA PA 19104
PHONE. 215 898 4713

R B PRIME
IBM (H20/025)
5600 COTTLE ROAD

SAN JOSE CA 95193
PHONE 408 256 6167

BERTHA L PROCTOR
UNIV OF TEXAS
ENV SCIENCE
BOX 688
RICHARDSON TX 75080
PHONE 214 690 2970

LAWRENCE PODOKSIK
10818 E ANDY STREET

CERITOS CA 90701
PHONE: 213 974 4611

LAWRENCE P POLLACK
15321 DELPHINIUM LANE

ROCKVILLE MD 20853
PHONE: 301 929 1295

JIM POPPITI
FINNIGAN MAT
1383 PICCARD DRIVE
SUITE 100
ROCKVILLE MD 21797
PHONE.

THOMAS C POTTER
MOBIL RESEARCH & DEV

PAULSBORO NJ 08066
PHONE:

ROGER E POWERS
DEPT OF CHEMISTRY
UNIV OF PENNSYLVANIA
231 SOUTH 34TH STREET
PHILADELPHIA PA 19104
PHONE 215 898 8164

JOSEPH F PRICE
4043 FAUNSDALE DRIVE

MONTGOMERY AL 36109-2424
PHONE 205 261 2739

JOHN F PRINCE
1692 N LADDIE CT

BEAVERCREEK OH 45432
PHONE. 202 767 4908

JOHN DAVID PRYNE
PROCTER & GAMBLE
6100 CENTER HILL ROAD

CINCINNATI OH 45224
PHONE: 513 659 2543

MANFRED O POEPPEL
110 PARKER ROAD

SARVER PA 16055
PHONE. 412 782 3884

CHARLES W POLLEY
ARCO CHEMICAL CO
3801 W CHESTER PIKE

NEWTOWN SQ PA 19073
PHONE. 215 359 2440

RICHARD F PORTER
CORNELL UNIVERSITY
CHEMISTRY DEPT

ITHACA NY 14853
PHONE 607 256 3483

DAVID H POWELL
ENVIRON SCI & ENGIN
PO BOX ESE

GAINESVILLE FL 32602
PHONE: 904 332 3318

B N PRAMANIK
SCHERING CORP
60 ORANGE ST

BLOOMFIELD NJ 07003
PHONE 201 429 3993

PHILIP C PRICE
UNION CARBIDE
TECH CTR 770-120
PO BOX 8361
S CHARLESTON WV 25303
PHONE 304 747 5594

D G PRITCHARD
UNIV OF ALABAMA
MICROBIOLOGY DEPT

BIRMINGHAM AL 35294
PHONE. 205 934 6023

HARLAN G PULSIPHER
420 EAST 600 NORTH

BRIGHAM CITY UT 84302
PHONE: 801 863 3303

STEVEN M PYLE
4200 PARADISE ROAD
#3061

LAS VEGAS NV 89109
PHONE 702 798 2529

ELLIOT M RACHLIN
MEDICINAL CHEMISTRY
311A SKAGGS HALL
UNIV OF UTAH
SALT LAKE CIT UT 84112
PHONE 801 581 5581

LEO RAFTOGIANIS
FINNIGAN MAT
355 RIVER OAKS PKWY

SAN JOSE CA 95134
PHONE

L S RAMOS
DEPT OF CHEMISTRY
BG 10
UNIV OF WASHINGTON
SEATTLE WA 98195
PHONE. 206 543 8888

SUDHAKAR G REDDY
DEPT OF CHEMISTRY
UTAH STATE UNIV

LOGAN UT 84322
PHONE 801 750 1624

WILLIAM REENTS
AT&T BELL LABS
ROOM 1A-320
600 MOUNTAIN AVE
MURRAY HILL NJ 07974
PHONE 201 582 2097

DON K REMLING
3246 CURTIS CIRCLE

PLEASANTON CA 94566
PHONE 408 946 4800

STEPHEN REYNOLDS
15719 HAVENHURST DR

HOUSTON TX 77059
PHONE. 713 425 5134

JAMES W PYPER
LLNL
PO BOX 808 L-310

LIVERMORE CA 94550
PHONE. 415 422 7311

BARBARA D RADECKI
BASF CORPORATION
1609 BIDDLE

WYANDOTTE MI 4819248824
PHONE 313 246 6324

A A RAHBEE
AIR FORCE GEOPHYSICS LAB
LSI

HANSCOM AFB MA 01731
PHONE

WARREN RAYFORD
2143 N WELLINGTON

PEORIA IL 61604
PHONE. 309 682 5388

ERIC REDMAN
CHEMISTRY DEPT
UNIV OF CALIFORNIA

RIVERSIDE CA 92521-0403
PHONE. 714 787 3657

VERNON N REINHOLD
HARVARD SCH OF PUBLIC
HEALTH
665 HUNTINGTON AVE
BOSTON MA 02115
PHONE 617 732 0631

DON L REMPEL
UNIV OF NEBRASKA
CHEMISTRY DEPT

LINCOLN NE 68588-0304
PHONE 402 472 3507

W W RICE
121 W MAIDEN LANE

OAK RIDGE TN 37830
PHONE

DIANE QUATTLANDER
THE UPJOHN CO
7171 PORTAGE ROAD

KALAMAZOO MI 49001
PHONE: 616 323 7527

GIL RADOLOVICH
MIDWEST RESEARCH INST
425 VOLKER BLVD

KANSAS CITY MO 64110
PHONE. 816 753 7600

GREGORY S RAHN
ONEIDA RES SERVICE
ONE HALSEY ROAD

WHITESBORO NY 13492
PHONE: 315 736 3050

LEO REAP
WESTERN MI ENVIRONMENTAL
245 EAST LAKEWOOD BLVD

HOLLAND MI 49423
PHONE: 616 396 1209

DOUGLAS REED
SEARLE R&D
4901 SEARLE PKWY

SKOKIE IL 60077
PHONE.

ROBERT W REISER
E I DUPONT
EXPERIMENTAL STATION
AG DEPT BLDG 402
WILMINGTON DE 19898
PHONE 302 772 1434

MICHAEL E RENNEKAMP
DELSI INSTRUMENTS
2756 BELLA VIA AVE

COLUMBUS OH 43229
PHONE 614 882 6511

DOUG E RICKERT
CHEM INDUS INST TOXI
PO BOX 12137

RES TRI PK NC 27709
PHONE. 919 541 2070

B A RABY
1547 ARATA COURT

SAN JOSE CA 95125
PHONE 408 946 8961

THOMAS P RADUS
BETTIS LABS 14D
PO BOX 79

W MIFFLIN PA 15122
PHONE: 412 476 5824

HARRI G RAMJIT
MERCK & CO
28-1F SUMMNEY TOWN PIKE

WEST POINT PA 19486
PHONE: 215 661 5305

CARL E RECHSTEINER
CHEVRON RES CORP
POB 1627 RM 41-3240

RICHMOND CA 94802
PHONE: 415 620 5095

DWIGHT REED
FORENSIC SCI SERVICE
PO BOX 449

SANTA ANA CA 92702
PHONE 714 834 3073

R F REITER
13422 BROKEN BR CT

CHANTILLY VA 22021
PHONE. 703 892 6000

JOHNNY D REYNOLDS
3932 PAPERMILL SQUARE
APT H

KNOXVILLE TN 37919
PHONE: 615 974 8679

DOUGLAS P RIDGE
UNIV OF DELAWARE
CHEMISTRY DEPT

NEWARK DE 19711
PHONE: 302 451 1197

DOUGLAS A RIDOLFI
1920 N MARIANNA AVE #212

LOS ANGELES CA 90032
PHONE. 213 255 3073

NICK RINGO
EXTREL CORP
PO BOX 11512

PITTSBURGH PA 15238
PHONE.

DON J RIZZO
GENERAL FOODS CORP
555 SO BROADWAY

TARRYTOWN NY 10591
PHONE: 914 335 6807

DWIGHT F ROBERTS
ENVIR SCI & ENGIN
PO BOX ESE

GAINESVILLE FL 32602
PHONE 904 332 3318

DOUGLAS W ROBINSON
PENNWALT
900 FIRST AVE
BOX C
KG OF PRUSSIA PA 19406
PHONE 215 337 6563

HENRY RODRIGUEZ
460 PT BRUNO BLVD

S SAN FRAN CA 94080
PHONE.

DENNIS K ROHRBAUGH
125 FAIRMONT DR

BEL AIR MD 21014
PHONE. 301 671 2366

PETER ROLLER
NIH
NCI
BLDG 37 RM 3B-27
BETHESDA MD 20892
PHONE. 301 496 1323

TIM L RILEY
326 E KINGSLEY

ANN ARBOR MI 48104
PHONE: 313 996 4046

GREGORY D RISKA
280 RIVER ROAD APT 35B

PISCATAWAY NJ 08854
PHONE: 201 878 7598

JOHN A G ROACH
FDA
HFF-424
200 C STREET SW
WASHINGTON DC 20204
PHONE 202 245 1371

GERALD D ROBERTS
SMITHKLINE & FRENCH LABS
1500 SPRING GARDEN ST
PO BOX 7929
PHILADELPHIA PA 19101
PHONE 215 751 4503

JOHN ROBOZ
MT SINAI SCH OF MED
1 GUSTAVE LEVY PL

NEW YORK NY 10029
PHONE 212 650 7382

PEDRO A RODRIGUEZ
PROCTER & GAMBLE CO
PO BOX 39175

CINCINNATI OH 45249
PHONE.

WILLIAM K ROHWEDDER
USDA
N REGIONAL RESEARCH
3900 N STABLE CT 205
PEORIA IL 61614
PHONE 309 685 4011

JOHN M ROMAN
NCI-FCRF
PROGRAM RESOURCES
PO BOX B
FREDERICK MD 21701
PHONE. 301 695 1226

KENNETH L RINEHART
UNIV OF ILLINOIS
CHEM 454 ROGER ADAMS
1209 W CALIFORNIA ST
URBANA IL 61801
PHONE 217 333 0627

NELSON H RISSER
LANCASTER LABORATORIES
2425 NEW HOLLAND PIKE

LANCASTER PA 17601
PHONE: 717 656 2301

EUGENE F ROBBINS
UNIV OF ILLINOIS
RES RESOURCES CTR M/C 937
PO BOX 6998
CHICAGO IL 60680
PHONE: 312 996 7462

DONALD H ROBERTSON
S.A.T.L.
ANAL CHEM GRP
US ARMY NATICK LABS
NATICK MA 01760-5020
PHONE 617 651 5535

ALAN L ROCKWOOD
DEPT OF CHEMISTRY
UNIV OF HOUSTON

HOUSTON TX 77004
PHONE

STEPHEN P ROGERS
5526 E CHEERY LYNN

PHOENIX AZ 85018
PHONE 602 244 3711

DONALD J ROKOP
LANL
BOX 1663

LOS ALAMOS NM 87545
PHONE. 505 667 7796

LUSHAN RONG
35 NOYES LABORATORY BOX 51
UNIV OF IL CHEMISTRY DEPT
505 S MATHEWS AVENUE
URBANA IL 61801
PHONE

RUSSELL D RING
BASF WYANDOTTE CORP
1419 BIDDLE AVE

WYANDOTTE MI 48192-3736
PHONE. 313 246 6325

ANASTASIA RIZWANIUK
HOECHST-ROUSSEL
ROUTE 202-206 NORTH

SOMERVILLE NJ 08876
PHONE: 201 231 2652

RONNY C ROBBINS
2403 ROTH

EDGEWOOD MD 21040
PHONE 671 4253

RUSSELL ROBINS
THE UPJOHN CO
7832-259-12
7000 PORTAGE RD
PORTAGE MI 49008
PHONE.

ALLAN ROCZKO
CHEMISTRY BLDG BOX 85
UNIV OF PITTSBURGH

PITTSBURGH PA 15260
PHONE

P F ROGERSON
EPA
ENVIRON RES LAB
SO FERRY ROAD
NARRAGANSETT RI 02882
PHONE 401 789 1071

LINDA ROLL
CHEMISTRY DEPT
INDIANA UNIV

BLOOMINGTON IN 47405
PHONE. 812 335 1217

DEBRA J ROSANO
ARTHUR D LITTLE INC
15 ACORN PARK

CAMBRIDGE MA 02140
PHONE. 617 864 5770

LAURA M ROSATO
6SPH/IEHS
UNIV OF PITTSBURGH
130 DESOTO STREET
PITTSBURGH PA 15261
PHONE:

T L ROSE
97 BARTLETT HILL RD

CONCORD MA 01742
PHONE:

ANN ROSECRANCE
JTC ENVIRONMENTAL CONSUL
4 RESEARCH PLACE

ROCKVILLE MD 20850
PHONE:

JOSEPH D ROSEN
DEPT FOOD SCIENCE
COOK COLLEGE
RUTGERS UNIV
NEW BRUNSWICK NJ 08903
PHONE: 201 932 9667

ROBERT T ROSEN
CTR FOR ADVANCED FOOD TECH
COOK COLLEGE
RUTGERS UNIV
NEW BRUNSWICK NJ 08903
PHONE: 201 932 8306

EARL ROSENBERG
SUBURBAN LABORATORIES
4140 LITT DRIVE

HILLSIDE IL 60162
PHONE:

MARK ROSS
CODE 6110
NAVAL RES LAB

WASHINGTON DC 20375-5000
PHONE: 202 767 3148

COLLEEN E ROSTAD
US GEOLOGICAL SURVEY
WRD
5293 WARD ROAD
ARVADA CO 80002
PHONE: 236 3616

SUSAN ROTTSCHAEFER
1195 HART LANE

HARTSVILLE PA 18974
PHONE: 215 270 7948

K L ROWLAND
CHEMISTRY DIV
NAT'L CTR TOXICOLOGY RES

JEFFERSON AR 72212
PHONE: 501 541 4287

RAYMOND L ROY
DETECTOR TECHNOLOGY
PO BOX K-300

BROOKFIELD MA 01506
PHONE 617 867 4030

TIM ROY
MOBIL OIL
TOXICOLOGY DIV
PO BOX 1029
PRINCETON NJ 08540
PHONE: 609 737 5509

MELVIN D ROZEBOOM
STAUFFER CHEMICAL CO
EASTERN RESEARCH CTR

DOBBS FERRY NY 10522
PHONE. 914 639 1200

A L ROZEK
465 W DOMINION DR
UNIT 306

WOOD DALE IL 60191
PHONE: 312 670 4824

MARTIN A RUDAT
DUPONT
TEXTILE FIBERS
EXP STATION E302
WILMINGTON DE 19898
PHONE. 302 772 2634

PATRICK J RUDEWICZ
709 SWEDELAND ROAD

SWEDELAND PA 19479
PHONE: 215 768 3011

M R RUECKER
PERKIN-ELMER CORP
APPLIED SCIENCE DIV
2771 N GAREY AVE
POMONA CA 91767
PHONE: 714 593 3581

D H RUSSELL
TEXAS A&M UNIV
CHEMISTRY DEPT

COLLEGE STN TX 77843
PHONE. 409 845 3345

JOHN W RUSSELL
BRISTOL MYERS
PHARMACEUTICAL R&D
2404 PENN AVENUE
EVANSVILLE IN 47721
PHONE: 812 838 8384

M E RUSSELL
NORTHERN ILLINOIS UNIV
CHEMISTRY DEPT

DEKALB IL 60115
PHONE· 815 753 6881

JOHN M RUTH
PO BOX 450

COLLEGE PARK MD 20740
PHONE. 301 344 3136

PHILIP W RYAN
PACIFIC ANALYTICAL
1989-B PALOMAR OAKS WAY

CARLSBAD CA 92008
PHONE: 619 931 1766

ROBERT J RYBA
STANDARD OIL INDIANA
PO BOX 400

NAPERVILLE IL 60566
PHONE: 312 420 5966

F M SAAD
MICHIGAN PUB HEALTH
3500 N LOGAN ST

LANSING MI 48909
PHONE: 517 373 1422

F E SAALFELD
5510 VENTNOR LANE

SPRINGFIELD VA 22151
PHONE. 202 696 4101

THOMAS M SACK
MIDWEST RESEARCH INST
425 VOLKER BLVD

KANSAS CITY MO 64110
PHONE· 816 753 7600

ELAINE SALADINO
FINNIGAN MAT
1801 BITTERSWEET LANE

MT PROSPECT IL 60056
PHONE: 312 827 4096

LARRY SALLANS
2655 MULL AVENUE

COPLEY OH 44321
PHONE: 216 848 4161

G E SALSER
17 ARTHUR PLACE

YONKERS NY 10701
PHONE. 201 894 6266

VINCENT G SALTAMACH
COLUMBIA UNIV
BOX 555 HAVEMEYER
119TH ST & BROADWAY
NEW YORK NY 10027
PHONE· 212 280 2165

MARY E SALYAN
10423 WILLAMETTE
MERIDIAN ROAD NW

SILVERDALE WA 98383
PHONE: 206 476 8092

MARTY SAMMONS
PROCTER & GAMBLE CO
PO BOX 39175

CINCINNATI OH 45247
PHONE

R H BARRY SAMPLE
INDIANA UNIV SCH OF MED
DEPT OF PATHOLOGY
635 BARNHILL DRIVE/MS 157
INDIANAPOLIS IN 46223
PHONE 317 264 2158

MADELINE P SAMPSON
12110 HUNTINGTON PK

HOUSTON TX 77099
PHONE: 713 527 8101

PAUL C SAMSON
SIGNAL RESEARCH CTR
50 EAST ALGONQUIN ROAD
BOX 5016
DES PLAINES IL 60017-5016
PHONE 312 391 3378

JOHN M SANDERS
SDS BIOTECH CORP
PO BOX 348

PAINESVILLE OH 44077
PHONE 216 357 3349

PHILLIP E SANDERS
UNIV OF ILLINOIS
VET MED BASIC SCI BLDG 1623
2001 S LINCOLN AVE
URBANA IL 61001
PHONE 217 244 1571

ROBERT A SANDERS
PROCTER & GAMBLE CO
6071 CENTER HILL RD

CINCINNATI OH 45224
PHONE 513 659 7865

GARY L SANTEE
EASTMAN KODAK
150 BELMEADE ROAD

ROCHESTER NY 14617
PHONE: 716 722 3194

SITTHIVET SANTIKARN
HARVARD SCH OF PUB HEALTH
DEPT OF NUTRITION
665 HUNTINGTON AVE
BOSTON MA 02115
PHONE 617 732 0632

IVAN SANTOS
CHEMISTRY DEPT
OHIO STATE UNIV
140 W 18TH AVENUE
COLUMBUS OH 43210
PHONE 614 422 0480

JEFFREY SANTROCK
GENERAL MOTORS RESEARCH
BIOMEDICAL SCIENCE DEPT

WARREN MI 48090-9055
PHONE 313 575 3484

G G SANZONE
VIRGINIA POLYTECH
CHEMISTRY DEPT

BLACKSBURG VA 24061
PHONE: 703 961 5294

I M SARASOHN
DUPONT
KINSTON PLANT
PO BOX 800
KINSTON NC 28501
PHONE: 919 522 6468

F G SATKIEWICZ
JOHN HOPKINS UNIV
APL
JOHNS HOPKINS RD
LAUREL MD 20707
PHONE 301 953 6247

JIM SATKOWSKI
RTE 3, BOX 226

BARNWELL SC 29812
PHONE 803 557 4341

DUANE SATZGER
1141 CENTRAL PWY

CINCINNATI OH 45202
PHONE

JANICE R SAUCERMAN
MEAD JOHNSON & CO
2404 PENNSYLVANIA AVE

EVANSVILLE IN 47721
PHONE 812 429 7914

ANDREW D SAUTER
2356 AQUA VISTA

HENDERSON NV 89015
PHONE 702 454 7884

PHIL SAVICKAS
DOW CHEMICAL CO
BLDG 574

MIDLAND MI 48640
PHONE 517 636 8728

M D SCAMUFFA
3019 MONTFORD

SUGARLAND TX 77478
PHONE 713 776 6038

GALE F SCANLAN
MAYO CLINIC
738 GUGGENHEIM
200 1ST STREET SW
ROCHESTER MN 55901
PHONE 507 284 4213

M D SCANLON
57 MARIEMONT AVE

BUFFALO NY 14220
PHONE 716 631 5733

WILLIAM SCHAEFER
DEPT OF PHARMACOLOGY
VANDERBILT UNIVERSITY

NASHVILLE TN 37221
PHONE

RICHARD SCHAEFFER
EXTREL CORP
PO BOX 11512

PITTSBURGH PA 15238
PHONE 412 782 3884

MARLENE E SCHAPS
3700 WATONGA
APT 2406

HOUSTON TX 77092
PHONE 713 686 2818

RICHARD H SCHEEL
MICH PUBLIC HEALTH
CEHS EPIDEMIOLOGY STUD DIV
3500 N LOGAN ST
LANSING MI 48909
PHONE 517 373 7336

THOMAS A SCHEHL
4400 LONGBOW DR

TITUSVILLE FL 32796
PHONE 305 867 3080

STEVEN M SCHEIFERS
31 GOLDEN AVENUE
APT 23B

BATTLE CREEK MI 49015
PHONE 616 961 2096

S E SCHEPPELE
BARTLESVILLE ENERGY
TECHNOLOGY CENTER
PO BOX 1398 DOE
BARTLESVILLE OK 74003
PHONE 918 337 4414

KEVIN L SCHEY
3554 A CHAUNCEY ST E DR

LAFAYETTE IN 47905
PHONE 317 494 5264

S M SCHILDCROUT
YOUNGSTOWN STATE UNIV
CHEMISTRY DEPT

YOUNGSTOWN OH 44555
PHONE 216 742 7114

STEVEN SCHILL
INFICON
6500 FLY ROAD

E SYRACUSE NY 13057
PHONE 315 437 0377

ALLEN W SCHINSKY
11326 LOVELAND

LIVONIA MI 48150
PHONE: 313 424 8860

ANDREW SCHKUTA
CAMBRIDGE ANAL ASSOC
1106 COMMONWEALTH

BOSTON MA 02215
PHONE. 617 232 2207

R J SCHMITT
SRI INTERNATIONAL
333 RAVENWOOD AVE
PS 219
MENLO PARK CA 94025
PHONE 415 859 5579

ROBERT J SCHOCK
2305 WESTBURY ROAD

LANSING MI 48906
PHONE

DONALD L SCHOOLEY
MILES LABORATORIES
PO BOX 932

ELKHART IN 46515
PHONE 219 262 7804

E M SCHREIBER
22 FAIRFIELD CT

PITTSBURGH PA 15201
PHONE 412 362 3598

ADAM J SCHUBERT
ARCO PETROLEUM PRODUCTS
1350 WEST 8TH STREET

LONG BEACH CA 90813
PHONE 213 437 8002

K E SCHWARZ
HP SCIENTIFIC INSTR
1601 CALIFORNIA AVE

PALO ALTO CA 94304
PHONE. 415 857 6056

L JOSEPH SEARS
CHEMISTRY DEPT
MONTANA STATE UNIV

BOZEMAN MT 59717
PHONE. 406 994 4801

JOHN J SCHLAGER
DEPT PHARM & TOX
HEALTH SCIENCE CTR
UNIV OF LOUISVILLE
LOUISVILLE KY 40292
PHONE: 502 588 5199

DEBBIE SCHMITZ
PROCTER & GAMBLE
6100 CENTER HILL ROAD

CINCINNATI OH 45224
PHONE:

DALE A SCHOELLER
UNIV OF CHICAGO
BOX 163
5841 S MARYLAND AVE
CHICAGO IL 60637
PHONE. 312 962 6561

DAVID M SCHRADER
CHEMISTRY DEPT
MARQUETTE UNIV

MILWAUKEE WI 53233
PHONE 414 224 3332

J M SCHROEER
ILLINOIS STATE UNIV
PHYSICS DEPT

NORMAL IL 61761
PHONE 309 438 5193

JAMIE SCHULTZ
UNIV OF PITTSBURGH
3939 OHARA STREET

PITTSBURGH PA 15260
PHONE 412 624 4966

HUBERT A SCOBLE
MIT
CHEMISTRY DEPT
ROOM 56-028
CAMBRIDGE MA 02139
PHONE: 617 253 7229

R D SEDGWICK
ALLIED CORP
CORPORATE TECHNOLOGY
PO BOX 1021R
MORRISTOWN NJ 07960
PHONE. 201 455 2977

CHARLES E SCHMIDT
PETC-DOE
PO BOX 10940

PITTSBURGH PA 15236
PHONE

H K SCHNOES
UNIV OF WISCONSIN
BIOCHEMISTRY DEPT

MADISON WI 53706
PHONE 608 262 0650

ALAN E SCHOEN
655 S FAIR OAKS K215

SUNNYVALE CA 94086
PHONE: 408 946 4848

MAUREEN A SCHRADER
3229 MERRICK LANE # 3B

INDIANAPOLIS IN 46222
PHONE 317 924 2274

JOSEPH N SCHROEPFER
3M
3M CENTER
BLDG 201-1W
ST PAUL MN 55144
PHONE.

WILLIAM G SCHULZE
MILLER BREWING CO
3939 W HIGHLAND BLVD

MILWAUKEE WI 53108
PHONE

R G SCOTT
ARGONNE NATIONAL LAB
D-200
9700 S CASS AVE
ARGONNE IL 60439
PHONE. 312 972 3529

ROSALIND SEGESTA
9837 MINT STREET

BATON ROUGE LA 70809
PHONE 504 292 0755

JOHN G SCHMIDT
BRISTOL-MYERS CO
2404 PENNSYLVANIA

EVANSVILLE IN 47721
PHONE: 812 838 8225

WILLIAM C SCHNUTE
FINNIGAN CORP
355 RIVER OAKS PKWY

SAN JOSE CA 95134
PHONE 408 433 4800

DONALD M SCHOENGOLD
3655 STORRIE CT

LAS VEGAS NV 89103
PHONE: 702 739 3142

KARL H SCHRAM
UNIV OF ARIZONA
COLLEGE OF PHARMACY

TUCSON AZ 85721
PHONE: 602 626 5630

LEONARD SCHRONK
WYETH LABS
ROOM C084
PO BOX 8299
PHILADELPHIA PA 19101
PHONE: 215 341 2565

JAE C SCHWARTZ
3554 A CHAUNCEY CT E DR

LAFAYETTE IN 47905
PHONE: 317 494 5262

RICHARD SCOTT
ACUREX CORP
405 CLYDE AVENUE

MTN VIEW CA 94039
PHONE

WILLIAM E SEIFERT
UNIV OF TX MED SCH
PO BOX 20708

HOUSTON TX 77225-0708
PHONE. 713 792 5612

MUSTAFA I SELIM
DEPT OF CHEMISTRY
MURRAY STATE UNIV

MURRAY KY 42071
PHONE 502 762 2584

SATINDER K SETHI
TRAVENOL LABS
6301 LINCOLN AVE

MORTON GROVE IL 60053
PHONE 312 965 4700

LEWIS A SHADOFF
DOW CHEMICAL CO
574 BLDG

MIDLAND MI 48676
PHONE 517 636 5584

T E SHARP
LOCKHEED RES LAB
3251 HANOVER
D93-50 B204
PALO ALTO CA 94304
PHONE 415 493 1545

PAUL W SHEARER
HERCULES INC
RESEARCH CENTER

WILMINGTON DE 19899
PHONE 302 995 3258

LAWSON E SHERMAN
TEXACO INC
PO BOX 509

BEACON NY 12505
PHONE 914 831 3400

YOSUKE SHIGEMATSU
808-I CHERRY LANE

EAST LANSING MI 48823
PHONE 517 355 8134

RONALD SHOMO
CHEMISTRY DEPT BOX 169
OHIO STATE UNIV
140 W 18TH AVENUE
COLUMBUS OH 43210
PHONE 614 422 0480

DILIP K SENSHARMA
UCLA
CHEMISTRY DEPT
405 HILGARD AVENUE
LOS ANGELES CA 90024
PHONE 213 825 9810

JEFFREY SHABANOWITZ
UNIV OF VIRGINIA
CHEMISTRY DEPT

CHARLOTTESVLL VA 22901
PHONE 804 924 7994

FRANCIS J SHALA
353 DERBY DOWNS RD

NEWARK OH 43055
PHONE 614 587 7233

THOMAS R SHARP
DEPT OF CHEMISTRY
CTR FOR CHEM CHAR & ANAL
TEXAS A&M UNIVERSITY
COLLEGE STN TX 77843-3144
PHONE 409 845 8404

EDWARD W SHEEHAN
1100 SALK HALL
PHARMACOLOGY & TOXICOLOGY
UNIV OF PITTSBURGH
PITTSBURGH PA 15261
PHONE 412 624 3285

PAUL L SHERMAN
MONSANTO - U1F
800 N LINDBERGH BLVD

ST LOUIS MO 63167
PHONE 314 694 3519

MING-CHUEN SHIH
6820 MARBURY ROAD

BETHESDA MD 20817
PHONE

FRED L SHORE
RADIAN CORPORATION
PO BOX 9948

AUSTIN TX 78766
PHONE 512 454 4797

ROBERT SERFASS
DEPT OF FOODS & NUTRITION
105 MACKAY HALL
IOWA STATE UNIV
AMES IA 50011
PHONE

W M SHACKELFORD
US EPA
MD-34

RES TRI PK NC 27711
PHONE 919 541 1190

LAMAAT M SHALABY
DUPONT EXPER STA
AGRICULTURAL DEPT
E402 3112
WILMINGTON DE 19898
PHONE 302 772 3481

KIM M SHAW
STANDARD OIL CO
4440 WARRENSVILLE CTR ROAD

CLEVELAND OH 44128
PHONE 216 581 5174

DENISE A SHEPPERD
ROY F WESTON INC
256 WELSH ROAD

LIONVILLE PA 19353
PHONE 215 524 0180

WILLIAM R SHERMAN
WASHINGTON UNIV
SCHOOL OF MEDICINE
PSYCHIATRY DEPT
ST LOUIS MO 63110
PHONE 314 362 7013

TSUNG-MING A SHIH
USA MED RES INST
CHEM DEF
BLDG E-3100
APG MD 21010-5425
PHONE 301 671 3414

JOHN S SHOWELL
NAT'L SCIENCE FNDN
1800 G STREET NW

WASHINGTON DC 20550
PHONE 202 357 7501

KENNETH SETCHELL
CHLDN'S HOSPITAL MED CTR
CLINICAL MASS SPECTROMETRY
ELLAND & BETHESDA AVENUES
CINCINNATI OH 45229
PHONE 513 559 8442

CEDRIC H SHACKLETON
OAKLAND CHDN'S HOSP
747 52ND STREET

OAKLAND CA 94609
PHONE 415 428 3604

A G SHARKEY
321 OLD ENGINEERING HALL
UNIV OF PITTSBURGH

PITTSBURGH PA 15260
PHONE 412 624 7990

J PAUL SHEA
5041 E SHERWOOD DRIVE

NEWBURGH IN 47630
PHONE 812 429 8349

JAMES SHERFINSKI
NICOLET INSTRUMENTS
5225-1 VERONA ROAD

MADISON WI 53711
PHONE

D CRAIG SHEW
SMITH & SHEW
PO BOX 1373

ADA OK 74821-1373
PHONE

CHARLES J SHIMANSKAS
CIBA-GEIGY CORP
444 SAW MILL RIVER ROAD

ARDSLEY NY 10502
PHONE 914 478 3131

STEPHEN SHRADER
SHRADER ANAL LAB
3814 VINEWOOD

DETROIT MI 48208
PHONE 313 894 4440

ANIL K SHUKLA
DEPT OF CHEMISTRY
UNIV OF UTAH

SALT LAKE CTY UT 84112
PHONE. 801 581 4614

MELVIN W SIEGEL
ROBOTICS INSTITUTE
CARNEGIE-MELLON UNIV

PITTSBURGH PA 15213
PHONE. 412 578 8802

A H SILVER
1 OVERBROOK PLACE

HILLSDALE NJ 07642
PHONE: 201 943 7100

BERND R SIMONEIT
OREGON STATE UNIV
COLL OF OCEANOGRAPHY

CORVALLIS OR 97331
PHONE 503 754 2895

MARK R SINE
2631 E US 22 & 3

MORROW OH 45152
PHONE 513 245 2554

EVERETTE SIZEMORE
DELSI INSTRUMENTS
10 KINGSBRIDGE ROAD

FAIRFIELD NJ 07006
PHONE. 201 227 7690

J J SLOVINSKI
12537 W FIRST PLACE

LAKEWOOD CO 80228
PHONE

CHERYL A SMITH
MULTI TECH LABORATORIES
320 TESCONI CIRCLE UNIT R

SANTA ROSA CA 95401
PHONE 707 544 5570

RANDY SHUL
152 DAVEY LAB, BOX 90
CHEMISTRY DEPT
PENN STATE UNIV
UNIV PARK PA 16801
PHONE. 814 863 3583

MARY LOU SIGSBY
1008 BRAYTON CT

RALEIGH NC 27606
PHONE:

R W SILVERMAN
UNIV OF CALIFORNIA
PHARMACOLOGY DEPT
CTR FOR HEALTH SCI
LOS ANGELES CA 90024
PHONE 213 825 5448

D S SIMONS
NBS
BLDG 222 RM A121

GAITHERSBURG MD 20899
PHONE 301 963 7908

RAJESH SINGHA
32 MINE BROOK ROAD
APT 96

EDISON NJ 08820
PHONE: 201 548 5963

JOHN SLAYBACK
ONEIDA RESEARCH SERVICES
ONE HALSEY ROAD

WHITESBORO NY 13492
PHONE 315 736 3050

REIN SMIT
VESTEC CORP
9299 KIRBY DRIVE

HOUSTON TX 77089
PHONE 713 796 9677

DANNE E SMITH
36 STONE RUN ROAD

BEDMINSTER NJ 07921
PHONE. 201 685 7555

GARY D SIDES
1732 TAHITI LANE

ALABASTER AL 35007
PHONE 323 6592

STERLING W SIGSWORTH
152 DAVEY LABORATORY
BOX 99
PENN STATE UNIV
UNIV PARK PA 16802
PHONE 814 863 3583

JOHN SIMMS
620 CLEVELAND AVENUE

HAMILTON OH 45013
PHONE:

WILLIAM J SIMONSICK
DUPONT MARSHALL RES LAB
3500 GRAYS FERRY AVE

PHILADELPHIA PA 19146
PHONE 215 339 6269

KATHLEEN E SINGLETON
SOUTHERN RESEARCH INST
PO BOX 55305

BIRMINGHAM AL 35255-5305
PHONE: 205 323 6592

L E SLIVON
BATTELLE LABS
505 KING AVE

COLUMBUS OH 43201
PHONE. 614 424 4274

ARTHUR SMITH
TEKNIVENT
10774 TRENTON AVENUE

ST LOUIS MO 63132
PHONE: 314 429 7272

DAVID E SMITH
3665 EL GRANDE

SAN JOSE CA 95132
PHONE 408 433 4800

MARSHALL M SIEGEL
LEDERLE LABS
AMERICAN CYANAMID

PEARL RIVER NY 10965
PHONE:

ARTHUR D SILL
ANALYTICAL CHEMISTRY
MERRELL DOW RESEARCH INST
2110 E GALBRAITH ROAD
CINCINNATI OH 45215
PHONE

NANNETTE SIMON
2260 BASELINE ROAD
APT 6

GRAND ISLAND NY 14072
PHONE 716 773 5427

CHUNG HANG SIN
CHEMISTRY DEPT
UNIV OF MICHIGAN
930 N UNIVERSITY
ANN ARBOR MI 48109
PHONE. 313 764 1669

M P SINHA
JET PROPULSION LAB
MS 11-116
4800 OAK GROVE DR
PASADENA CA 91103
PHONE:

CLOIS J SLOCUM
US EPA
26 W ST CLAIR STREET

CINCINNATI OH 45268
PHONE 513 569 7281

CHARLES A SMITH
17669 SAN VICENTE

FNTN VALLEY CA 92708
PHONE. 714 896 5280

DAVID H SMITH
ORNL UNION CARBIDE
PO BOX Y BLDG 9735

OAK RIDGE TN 37831
PHONE: 615 574 2454

DAVID LEE SMITH
MEDICINAL CHEM DEPT
PURDUE UNIV

W LAFAYETTE IN 47907
PHONE: 317 494 6094

JOHNNY SMITH
TVA
2314 NORWOOD BLVD

FLORENCE AL 35630
PHONE: 205 386 2371

RICHARD D SMITH
BATTELLE-NW
BLDG 329 AREA 300

RICHLAND WA 99352
PHONE: 509 376 0723

CHARLES R SNELLING
EXXON R&D LABS
PO BOX 2226

BATON ROUGE LA 70821
PHONE. 504 359 8361

JOHN D SNYDER
700 HAWLEY ROAD

MASON MI 48854
PHONE

B H SOLKA
7813 W ROSEDALE

CHICAGO IL 60631
PHONE 312 567 5290

B D SOLTMANN
1909 BRIDGEPORT DR

RALEIGH NC 27609
PHONE: 919 847 0744

VIRENDRA K SOOD
THE UPJOHN CO
UNIT 7256-126-2

KALAMAZOO MI 49001
PHONE: 616 385 6430

GARMON BROOKS SMITH
US EPA
PO BOX 1198

ADA OK 74820
PHONE: 405 332 8800

LAURENCE A SMITH
PROCTER & GAMBLE CO
IVORYDALE TECH CTR
5299 SPRING GROVE AVE
CINCINNATI OH 45217
PHONE. 513 627 5082

RICHARD W SMITH
NIEHS
PO BOX 12233

RES TRI PK NC 27709
PHONE: 919 541 2964

L T SNIEGOSKI
NAT'L BUR OF STAN
BLDG 222 RM A361

GAITHERSBURG MD 20899
PHONE: 301 921 2867

INGVAR E SODAL
6595 ODELL PLACE
SUITE M

BOULDER CO 80301
PHONE 303 444 1861

JEROME J SOLOMON
NEW YORK UNIV MED CTR
ENVIRONMENTAL MEDICINE

TUXEDO PARK NY 10987
PHONE 914 351 4398

NANCY SOMERS
101-5 RAL
DEPT OF CHEMISTRY
UNIV OF ILLINOIS
URBANA IL 61820
PHONE:

G W SOVOCOOL
3155 HIGHVIEW DR

HENDERSON NV 89015
PHONE 702 798 2212

HOWARD E SMITH
BAKER LABORATORY BOX 334
CORNELL UNIV

ITHACA NY 14853
PHONE. 607 255 3884

PAUL V SMITH
FDA LAB
10 WEST 35TH STREET

CHICAGO IL 60616
PHONE: 312 886 7074

ROBERT F SMITH
ROUTE 5
BOX 136

MURPHY NC 28906
PHONE: 704/837-7086

JOSEPH T SNODGRASS
DEPT OF CHEMISTRY
JOHNS HOPKINS UNIV

BALTIMORE MD 21218
PHONE: 301 338 7454

STEVE SOKOLOW
FINNIGAN MAT
355 RIVER OAKS PWY

SAN JOSE CA 95134
PHONE 408 433 4800

MALCOLM D SOLOMON
HEWLETT-PACKARD CO
PO BOX 10161

PALO ALTO CA 94303-0871
PHONE: 415 857 7634

PETER F SOMSSICH
36 RAVINE ROAD

AMHERST NH 03031
PHONE. 617 777 1900

GLENN E SPANGLER
BENDIX ESD
1400 TAYLOR AVE
PO BOX 9840
BALTIMORE MD 21284-9840
PHONE: 301 321 5261

JAMES S SMITH
7A GRACE'S DRIVE

COATESVILLE PA 19320
PHONE: 215 692 5770

R A SMITH
RADIAN CORPORATION
PO BOX 9948
8501 MOPAC BLVD
AUSTIN TX 78766
PHONE. 512 454 4797

RONALD G SMITH
MONSANTO AG PRODUCTS
700 CHESTERFLD VILLAGE PKWY

CHESTERFIELD MO 63017
PHONE: 314 537 6275

A PETER SNYDER
422 CAMPUS HILL DRIVE

BEL AIR MD 21014
PHONE 301 671 2416

JOSEPH G SOLCH
8370 HEILMAN DR

NEW CARLISLE OH 45344
PHONE 513 873 2202

RICHARD T SOLSTEN
MONSANTO CO AA1F
LIFE SCIENCES RES CTR
700 CHESTERFIELD VILL PARK
CHESTERFIELD MO 63198
PHONE 314 537 6272

BAN-HUAT SONG
6810 NEWLIGHT COURT

FT WASHINGTON MD 20744-1036
PHONE 301 894 4347

DAVID SPARKMAN
1172 RIDGE DRIVE

MOUNTAINSIDE NJ 07092
PHONE: 201 376 1300

DAVID N SPEIS
ETC CORP
PO BOX 7808

EDISON NJ 08818-7808
PHONE. 201 225 6759

G N SPOKES
US TESTNG
1415 PARK AVE

HOBOKEN NJ 07030
PHONE 201 792 2400

GEORGE STAFFORD
FINNIGAN MAT
355 RIVER OAKS PKWY

SAN JOSE CA 95134
PHONE. 408 433 4800

C G STANDARD
MONSANTO CO
PO BOX 1311

TEXAS CITY TX 77590
PHONE 409 942 3519

W L STEBBINGS
3M COMPANY
PO BOX 33221

ST PAUL MN 55133
PHONE 612 733 4891

DANNY O STENE
4200 EAST 9TH
UNIV OF CO HEAL SCI CTR
SCH OF MED BOX 236
DENVER CO 80226
PHONE 303 394 8961

RICHARD STEPNOWSKI
CHEMISTRY DEPT
MICHIGAN STATE UNIV

EAST LANSING MI 48824
PHONE 517 353 6495

R N STILLWELL
10 DANIELS DRIVE

BEDFORD MA 01730
PHONE. 617 239 0128

ROBERT B SPENCER
5121 FLAMBEAU RD

MADISON WI 53705
PHONE 608 271 3333

RUSSELL C SPREEN
STUART PHARMACEUTICALS
RT 202 & MURPHY ROAD

WILMINGTON DE 19897
PHONE 302 575 3999

VASSILIS STAMOUDIS
GEOCHEM & ENVIRON INSTRU
ER-362
ARGONNE NAT'L LAB
ARGONNE IL 60439
PHONE.

MICHELE S STANLEY
CHEMISTRY DEPT BOX 267
INDIANA UNIV

BLOOMINGTON IN 47405
PHONE: 812 335 3436

JOHN D STEIN
GENERAL ELECTRIC
1334 KATHY CT

LIVERMORE CA 94550
PHONE:

LAURA J STEPHENS
SHRADER ANALYTICAL
3814 VINEWOOD

DETROIT MI 48208
PHONE 313 894 4440

FREDERICK A STEVIE
AT&T BELL LABS
ROOM 2C-070
555 UNION BLVD
ALLENTOWN PA 18103
PHONE 215 439 7169

W SARA STILLWELL
MIT
APPLIED BIOLOGICAL SCIENCE

CAMBRIDGE MA 02139
PHONE 617 253 3118

J A SPHON
FDA
HFF-426
200 C STREET SW
WASHINGTON DC 20204
PHONE 202 472 9144

ROBERT R SQUIRES
CHEMISTRY DEPT
PURDUE UNIV

W LAFAYETTE IN 47907
PHONE: 317 494 7322

JEFFREY A STAMP
153 E LITTLE CANADA ROAD
#219

ST PAUL MN 55117
PHONE 612 624 1295

DOUGLAS B STAUFFER
CORNELL UNIV
BAKER LAB
BOX 68
ITHACA NY 14853
PHONE: 607 255 3726

URS STEINER
FINNIGAN CORP
355 RIVER OAKS PKWY

SAN JOSE CA 95134
PHONE: 408 433 4800

JAMES L STEPHENSON
2402 OMEGA ROAD

RICHMOND VA 23228
PHONE: 804 266 1732

D W STEWART
675 BEACH AVE

ROCHESTER NY 14612
PHONE:

JAMES J STOFFELS
BATTELLE-NW
BLDG 320 AREA 300
PO BOX 999
RICHLAND WA 99352
PHONE. 509 376 2142

DAVID E SPLICHAL
615 HIGHLAND AVENUE
APT 6

SALINA KS 67401
PHONE. 913 823 5242

ALLAN E STAFFORD
1083 HARBOR WAY

RODEO CA 94572
PHONE. 415 486 3657

DION A STAMS
812 SPRUCE STREET

RIVERSIDE CA 92507
PHONE. 714 787 3657

JAMES L STAUFFER
UNIV OF UTAH
311 A SKAGGS HALL

SALT LAKE CTY UT 84112
PHONE: 801 581 7532

ELIZ A STEMMLER
541 GEOLOGY BLDG
INDIANA UNIV

BLOOMINGTON IN 47405
PHONE 812 335 5424

MYRON STEPHENSON
US EPA
COLLEGE STATION ROAD

ATHENS GA 30613
PHONE.

DWIGHT D STIFF
5700 BUNKER HILL STREET
NO 804

PITTSBURGH PA 15206
PHONE. 412 362 2194

MARTIN STOGNIEW
PO BOX 25

BLOOMING GROV NY 10914
PHONE:

HOWARD A STORMS
GENERAL ELECTRIC CO
M/C V08
PO BOX 460
PLEASANTON CA 94566
PHONE: 415 862 4527

DARYL P STRANDBERGH
8924 PERRIN

LIVONIA MI 48150
PHONE: 313 424 8860

J M STRONG
13103 BLUHILL RD

SILVER SPRING MD 20906
PHONE: 301 496 4116

G P STURM
NAT'L INST FOR PETRO
AND ENERGY RES
PO BOX 2128
BARTLESVILLE OK 74005
PHONE 918 337 4314

CLINT SULFRIDGE
158 WADDELL CIRCLE

OAK RIDGE TN 37830
PHONE: 615 574 2438

TERRY L SUMPTER
DEPT OF CHEMISTRY
UNIV OF TENNESSEE

KNOXVILLE TN 37996
PHONE 615 974 6578

SEFIK SUZER
DEPT OF CHEMISTRY
MCCORMICK ROAD
UNIV OF VIRGINIA
CHARLTTSVLL VA 22901
PHONE. 804 924 6844

ROBERT SWAIM
FINNIGAN MAT
PO BOX 5997

KINGWOOD TX 77325
PHONE: 713 360 2740

MICHAEL STORY
FINNIGAN MAT
355 RIVER OAKS PWY

SAN JOSES CA 95134
PHONE 408 433 4800

KENNETH M STRAUB
SMITH KLINE & FRENCH LABS
MAIL CODE J 100
620 ALLENDALE ROAD
KING PRUSSIA PA 19406
PHONE. 215 768 3125

SUSAN E STRONG
HEWLETT PACKARD
1601 CALIFORNIA AVE

PALO ALTO CA 94304
PHONE: 415 857 7890

DAVID L STYRIS
205 CRAIGHILL

RICHLAND WA 99352
PHONE: 509 376 1907

H R SULLIVAN
ELI LILLY CO
RESEARCH LABS
307 E MCCARTY ST
INDIANAPOLIS IN 46285
PHONE.

TUNG SUN
USDA-FSIS
PO BOX 6085

ATHENS GA 30604
PHONE: 404 546 3571

ROBERT K SUZUKI
25 HICKORY PLACE
APT H-4

CHATHAM NJ 07928
PHONE: 201 380 8520

ADRIAN SWANSON
INTERPOLL, INC
4500 BALL ROAD NE

CIRCLE PINES MN 55014
PHONE 612 786 6020

JAYNE STOUT
PO BOX 10

CHART LEY MA 02712
PHONE: 617 226 2348

ROBERT J STRIFE
MIAMI VALLEY LABS
PROCTER & GAMBLE
PO BOX 39175
CINCINNATI OH 45247
PHONE. 513 245 2655

JOHN T STULTS
MICHIGAN STATE UNIV
CHEMISTRY DEPT

EAST LANSING MI 48824
PHONE 517 353 6767

T C K SU
SMU
CHEMISTRY DEPT

N DARTMOUTH MA 02747
PHONE: 617 999 8235

RICHARD E SULLIVAN
APT NO 52
23251 LOS ALISOS

EL TORO CA 92630
PHONE 213 933 5991

YIPING SUN
DEPT MEDICINAL CHEMISTRY
SCH OF PHARMACY
PURDUE UNIV
W LAFAYETTE IN 47907
PHONE:

H J SVEC
IOWA STATE UNIV
CHEMISTRY DEPT

AMES IA 50011
PHONE: 515 294 6486

JEFFREY D SWEATLOCK
435 HAWKINS GRAD HOUSE

W LAFAYETTE IN 47906
PHONE

STEVEN J STOUT
AMERICAN CYANIMID
AGRICULTURAL DIV
PO BOX 400
PRINCETON NJ 08540
PHONE: 609 799 0400

JUSTIN G STROH
UNIV OF ILLINOIS
BOX 101-5
1209 W CALIFORNIA
URBANA IL 61801
PHONE: 217 333 0655

CATHERINE M STUPAK
BALZERS
8 SAGAMORE PARK RD

HUDSON NH 03051
PHONE: 603 889 6888

CHUCK SUEPER
BATTELLE MEM INST
ROOM 7244
505 KING AVENUE
COLUMBUS OH 43201
PHONE. 614 424 4243

R L SUMMERS
700 W MURRILL

BAYTOWN TX 77520
PHONE 713 470 3464

SOMCHAI SUWANRUMPHA
DEPT OF CHEMISTRY
UNIV OF HOUSTON
UNIVERSITY PARK
HOUSTON TX 77004
PHONE 713 743 2675

DEBORAH L SWACKHAMER
GEOLOGY BLDG RM 541
INDIANA UNIV

BLOOMINGTON IN 47405
PHONE. 812 335 1005

CHARLES C SWEELEY
MICHIGAN STATE UNIV
BIOCHEMISTRY DEPT

EAST LANSING MI 48824
PHONE: 517 353 3257

KEVIN M SWEENEY
6500 CREEKWOOD CT

MOBILE AL 36609
PHONE: 205 470 3243

JOHN SYKA
FINNIGAN MAT
355 RIVER OAKS PKWY

SAN JOSE CA 95134
PHONE: 408 433 4800

M W TABOR
18 JUNEFIELD AVE

CINCINNATI OH 45218
PHONE: 513 872 4830

CALVIN K TANAKA
CALIF ANALYTICAL LAB
2544 INDUSTRIAL BLVD

W SACRAMENTO CA 95691
PHONE: 916 372 1393

LESTER TAYLOR
BURROUGHS WELLCOME
3030 CORNWALLIS ROAD

RES TRI PK NC 27709
PHONE:

R G TEECE
UNIV OF ARIZONA
COLLEGE OF PHARMACY
PHARMACEUTICAL SCIENCE
TUCSON AZ 85721
PHONE: 602 626 3434

TERRYANN N TERNES
MARTIN MARIETTA ENERGY SYS
BLDG 9995 MS 01
PO BOX Y
OAK RIDGE TN 37831
PHONE: 615 574 2354

DAVID W THOMAS
SRI INTERNATIONAL
ROOM AB-011
333 RAVENSWOOD AVE
MENLO PARK CA 94025
PHONE: 415 859 3787

BRIAN J SWEETMAN
VANDERBILT UNIV
PHARMACOLOGY DEPT

NASHVILLE TN 37232
PHONE: 615 322 2094

DEBORAH A SZARO
26 WALNUT STREET

FOXBORO MA 02035
PHONE: 617 253 1806

JUANITA R TACKETT
MONSANTO RESEARCH CORP
PO BOX 32

MIAMISBURG OH 45342
PHONE: 513 865 3790

K K TANAKA
YALE UNIVERSITY
HUMAN GENETICS
MEDICAL SCHOOL
NEW HAVEN CT 06510
PHONE: 203 785 2659

M L TAYLOR
BREHM LABORATORY
WRIGHT STATE UNIV

DAYTON OH 45435
PHONE: 513 873 3119

RICHARD M TEETER
CHEVRON RESEARCH
PO BOX 1627

RICHMOND CA 94802-0627
PHONE: 415 620 3078

D T TERWILLIGER
6350 OAK CREEK DR

CINCINNATI OH 45247
PHONE: 513 684 7329

DEBORAH A THOMAS
3500 SUTHERLAND AVE
H202

KNOXVILLE TN 37919
PHONE: 615 584 4835

JANET AREY SWEETMAN
AIR POLLUTION RES CTR
UNIV OF CALIFORNIA

RIVERSIDE CA 92521
PHONE: 714 787 3502

P P SZCZEPANIK-VANLEEUWEN
UNIV OF IL MEDICAL CTR
COLL OF PHARMACY RM 131 CPL
833 S WOOD
CHICAGO IL 60612
PHONE: 312 966 2927

C R PETE TALLEY
E I DUPONT
EXPERIMENTAL STATION
PETRO CHEM BLDG 336
WILMINGTON DE 19898
PHONE: 302 772 2142

SHENG-YUH TANG
N I P E R
PO BOX 2128

BARTLESVILLE OK 74005
PHONE: 918 337 4484

PAUL A TAYLOR
2544 INDUSTRIAL BLVD

W SACRAMENTO CA 95691
PHONE: 916 372 1393

ROGER TEMBREULL
2109 MEDFORD ROAD #29

ANN ARBOR MI 48104
PHONE: 313 764 1669

ED TEWS
DEPT OF CHEMISTRY
PURDUE UNIV

W LAFAYETTE IN 47907
PHONE: 317 494 5271

FAIRWELL THOMAS
NIH
BLDG 10 RM 7N115

BETHESDA MD 20892
PHONE: 301 496 6508

DENNIS F H SWIJTER
AIR PRODUCTS & CHEMICALS
PO BOX 538

ALLENTOWN PA 18105
PHONE: 215 481 4629

VINCENT TABONE
FINNIGAN CORP
355 RIVER OAKS PKWY

SAN JOSE CA 95134
PHONE: 408 433 4800

Y L TAN
DOE
ENVIRON MEAS LAB
376 HUDSON ST
NEW YORK NY 10014
PHONE: 212 620 3481

JAMES W TAYLOR
UNIV OF WISCONSIN
CHEMISTRY DEPT
1101 UNIVERSITY AVE
MADISON WI 53706
PHONE: 608 262 4561

RON TECKLENBURG
TEXAS A&M UNIVERSITY
DEPT OF CHEMISTRY

COLLEGE STN TX 77843
PHONE:

JAMES L TEMPLETON
BETZ LABORATORIES
9669 GROGANS MILL ROAD

THE WOODLANDS TX 77380
PHONE: 713 367 6201

BERTA L THOMAS
BATTELLE PACIFIC NW LABS
PO NOX 999

RICHLAND WA 99352
PHONE: 209 376 4637

MICHAEL J THOMAS
BIOCHEMISTRY DEPT
BOWMAN GRAY SCH MED
300 S HAWTHORNE RD
WINSTON-SALEM NC 27103
PHONE: 919 748 2313

QUENT THOMAS
FINNIGAN INSTITUTE
4450 CARVER WOODS ROAD

CINCINNATI OH 45242
PHONE.

JOHN J THOMPSON
ALLIED CHEMICAL
20 PEABODY ST

BUFFALO NY 14210
PHONE 716 827 6374

NORBERT THONNARD
ATOM SCIENCES
114 RIDGEWAY CTR

OAK RIDGE TN 37830
PHONE 615 483 1113

ALLSUP THURMAN
BURROUGHS WELLCOME
3030 CORNWALLIS ROAD

RES TRI PK NC 27709
PHONE 919 248 4544

G S TINT
EAST ORANGE VA HOSP

EAST ORANGE NJ 07019
PHONE 201 676 1000

EMIRGUL TOLUN
UTCHS
STOUT NEUROSCIENCE LAB
956 COURT AVENUE
MEMPHIS TN 38163
PHONE 901 528 5488

DANIEL D TONG
FINNIGAN MAT INSTITUTE
CARVER WOODS DRIVE

CINCINNATI OH 45242
PHONE 513 891 4560

ANIBAL TORRES
SK&F LABORATORIES
PO BOX 2700

GUAYAMA PR 00654
PHONE 809 864 4545

TIMOTHY THOMAS
CHEMISTRY DEPT
UNIV OF MISSOURI

KANSAS CITY MO 64110
PHONE. 816 276 1555

K R THOMPSON
NUCLEAR DATA INC
GOLF & MEACHAM RD

SCHAUMBURG IL 60196
PHONE 312 884 3741

KELLY R THORNBURG
MIDWEST RESEARCH INST
425 VOLKER BLVD

KANSAS CITY MO 64110
PHONE. 816 753 7600

THOMAS O TIERNAN
WRIGHT STATE UNIV
BREHM LAB

DAYTON OH 45431
PHONE· 513 873 2202

SUSAN S TJOA
UCHSC
4200 E 9TH AVE C232

DENVER CO 80262
PHONE 303 394 8175

ALBERT D TOMASSIAN
PERKIN-ELMER CORP
2771 N GAREY AVENUE

POMONA CA 91767
PHONE·

HUA-YI TONG
DEPT OF OCEANOGRAPHY
TEXAS A & M UNIV

COLLEGE STN TX 77843
PHONE 409 845 2986

JOHN P TOTH
PESTICIDE RESEARCH LAB
UNIV OF FLORIDA

GAINESVILLE FL 32611
PHONE. 904 392 1978

MICHAEL M THOMASON
SOUTHERN RES INST
2000 9TH AVENUE SOUTH

BIRMINGHAM AL 35255
PHONE 205 323 6592

RICHARD M THOMPSON
BATTELLE LABS
505 KING AVE

COLUMBUS OH 43201
PHONE· 614 424 4620

JOHN R THORP
HEWLETT-PACKARD
10535 HARWIN

HOUTON TX
PHONE:

SANDRA J TILLIN
USDA-WRRC
800 BUCHANAN ST

ALBANY CA 94710
PHONE 415 486 3139

PETER J TODD
OAK RIDGE NAT'L LAB
PO BOX Y BLDG 9735

OAK RIDGE TN 37831
PHONE· 615 574 2455

KENNETH B TOMER
MIDWEST CTR FOR MASS
CHEMISTRY DEPT
UNIV OF NEBRASKA
LINCOLN NE 68588-0362
PHONE· 402 472 1684

STEPHEN S TONG
CORNING GLASS WKS
SULLIVAN PK FR-18

CORNING NY 14831
PHONE· 607 974 3363

JAMES C TOU
DOW CHEMICAL CO
ANALYTICAL LAB
B-574
MIDLAND MI 48640
PHONE 517 636 2551

FREDERICK A THOME
R J REYNOLDS TOBACCO
BOWMAN GRAY TECH CTR

WINS-SALEM NC 27102
PHONE: 919 773 4936

MICHAEL L THOMSON
AMERICAN CYANAMID
AGRICULTURAL DIV
PO BOX 400
PRINCETON NJ 08540
PHONE 609 799 0400

AL THRUSTON
US EPA
COLLEGE STATION ROAD

ATHENS GA 30613
PHONE

EDMUND TING
LA COUNTY SHERIFF
CRIMINALISTICS LAB
2020 W BEVERLY BLVD
LOS ANGELES CA 90057
PHONE 213 974 4647

LASZLO TOKES
SYNTEX RESEARCH
3401 HILLVIEW AVE

PALO ALTO CA 94304
PHONE· 415 855 5713

YVES G TONDEUR
6540 ROMANCE CIRCLE

LAS VEGAS NV 89108
PHONE 702 739 3142

PAUL C TOREN
MONSANTO CO
800 N LINDBERGH BLVD

ST LOUIS MO 63167
PHONE

JOE C TRACY
OAK RIDGE NAT'L LABORATORY
BLDG 9204-3 MS 1
PO BOX Y
OAK RIDGE TN 37831
PHONE

WILLIAM F TRAGER
UNIV OF WASHINGTON
MEDICINAL CHEM
BAGLEY HALL BG-20
SEATTLE WA 98195
PHONE. 206 543 7025

JOSEPH A TRAINA
BERLEY LABORATORIES
110 E HANOVER AVE

CEDAR KNOLLS NJ 07927
PHONE 201 540 8700

THOMAS M TRAINOR
NORTHEASTERN UNIV
CHEMISTRY DEPT
360 HUNTINGTON AVE
BOSTON MA 02115
PHONE· 617 437 2794

VINH THI TRAN
ROY F WESTON INC
256 WELSH POOL ROAD

LIONVILLE PA 19853
PHONE. 215 524 0180

CHERYL ANN TREESE
202 ELMHURST DRIVE
NO H36

OAK RIDGE TN 37830
PHONE 615 483 5620

MICHAEL L TREHY
MONSANTO U4G
800 N LINDBERGH BLVD

ST LOUIS MO 63167
PHONE. 314 694 1515

FRANK L TRENSCH
208 MARY DRIVE

OLDSMAR FL 33557
PHONE.

JOANN TRIMBLE
UNIV OF TENNESSEE
COLEMAN BLDG, RM 2A09
956 COURT ST
MEMPHIS TN 38163
PHONE: 901 528 5488

ROBERT L TROTTIER
LOCTITE CORP
705 N MOUNTAIN RD

NEWINGTON CT 06111
PHONE 203 278 1280

JEAN-LUC TRUCHE
HEWLETT-PACKARD
SCIENTIFIC INSTRUMENTS DIV
1601 CALIFORNIA AVE
PALO ALTO CA 94304
PHONE·

B P TSAI
UNIV OF MINNESOTA
CHEMISTRY DEPT

DULUTH MN 55812
PHONE· 218 726 7585

CHENG-WEN TSAI
1603 VIKING CT #205

PEORIA IL 61614
PHONE·

ROBERT TSAI
LOCTITE PUERTO RICO
PO BOX 669

SABANA GRANDE PR 00747
PHONE· 809 873 6500

RUSHUNG TSAO
DEPT OF CHEMISTRY
UNIV OF CALIFORNIA

RIVERSIDE CA 92521
PHONE: 714 787 5287

ANTHONY TSARBOPOULOS
MAYO CLINIC
DEPT OF PHARMACOLOGY
GUGGENHEIM BLVD
ROCHESTER MN 55905
PHONE: 507 284 2565

K Y TSERNG
CLINICAL PHARMACOLOGY
VA MEDICAL CTR
10701 EAST BLVD
CLEVELAND OH 44106
PHONE:

BRIAN J TUCKER
NEW JERSEY DEPT OF HEALTH
CN360 ROOM L435

TRENTON NJ 08625
PHONE: 609 984 7255

ROBERT L TUCKER
CLOROX CO
7200 JOHNSON DR
PO BOX 493
PLEASANTON CA 94566
PHONE. 415 847 6651

WILLIAM O TUCKER
ROUTE 7
BOX 198

CLINTON TN 37716
PHONE: 615 574 2419

ALBERT TUINMAN
CANCER RESEARCH INST
ARIZONA STATE UNIV

TEMPE AZ 85283
PHONE: 602 965 1872

JERRY A TURBETT
TURBETT ASSOC
PO BOX 352

BOULDER CO 80306
PHONE 303 442 4838

MAX J TURNER
CIIT
PO BOX 12137

RES TRI PK NC 27709
PHONE: 919 541 2070

JUDITH TURNLAND
USDA
WESTERN HUMAN NUTRITION CTR

BERKELEY CA 94710
PHONE:

JOHN R TUSCHALL
NORTHRUP SERVICES
PO BOX 12313

RES TRI PK NC 27709
PHONE: 919 549 0611

W J TUTING
409 E MCFARLAN ST

DOVER NJ 07801
PHONE 201 368 1707

LINDSAY TYCER
1975 JERLYN

DENHAM SPRING LA 70726
PHONE 504 359 2199

ANDREW N TYLER
METABOLISM DIV
WASHINGTON UNIV MED SCH

ST LOUIS MO 63110
PHONE. 314 302 6929

GED TYROR
3656 WOODS RD

WILLIAMSON NY 14589-9533
PHONE:

HAROLD R UDSETH
BATTELLE NORTHWEST
PO BOX 999

RICHLAND WA 99352
PHONE: 509 376 1656

STANLEY ULICK
VA HOSPITAL

BRONX NY 10468
PHONE:

STEVE E UNGER
SQUIBB INST FOR MEDICAL
RESEARCH
PO BOX 4000
PRINCETON NJ 08543-4000
PHONE 609 921 4987

BILLY T UPCHURCH
1213 BLUEBIRD DRIVE

VIRGINA BEACH VA 23451
PHONE. 804 431 0415

ROGER UPHAM
TWIN CITY TESTING CO
662 CROMWELL AVE

ST PAUL MN 55114
PHONE 612 641 9486

AUSRINE K VALAITIS
7431 S MAPLEWOOD AVENUE

CHICAGO IL 60629
PHONE 312 793 4766

RICHARD B VANBREEMEN
DEPT OF CHEMISTRY BOX 8204
NORTH CAROLINA STATE UNIV

RALEIGH NC 27695
PHONE.

G G VANDERVELDE
16440 GREENWOOD AVE

S HOLLAND IL 60473
PHONE 312 841 8360

RICK VANVOROUS
690 WESTERN HILLS DR

RIO RANCHO NM 87124
PHONE. 505 892 4166

MADAN VERMA
CIBA GEIGY CORPORATION
AG DIVISION
PO BOX 18300
GREENSBORO NC 27419
PHONE 919 292 7100

M M VESTLING
CHEMISTRY DEPT
SUNY COLL @ BROCKPORT

BROCKPORT NY 14420
PHONE 716 395 5594

RICHARD VICKERS
5 GOLFERS WAY SOUTH

THORNDALE PA 09372
PHONE 215 383 6225

BERNARD L UPSHULTE
DASCOMB RESEARCH PARK
PO BOX 3100

ANDOVER MA 01810
PHONE: 617 475 9030

HERMAN VALENTE
NYS DEPT OF HEALTH
WADSWORTH CTR FOR
LABS & RES ESP
ALBANY NY 12220
PHONE 518 474 7054

W J VANDENHEUVEL
MERCK SHARP & DOHME
RESEARCH LABORATORY
PO BOX 2000
RAHWAY NJ 07065
PHONE 201 574 5443

F M VANE
HOFFMANN-LAROCHE INC

NUTLEY NJ 07110
PHONE 201 235 2919

PHILIP VARGHESE
DEPT OF MECHANICAL ENGIN
UNIV OF TEXAS

AUSTIN TX 78712
PHONE. 512 471 3110

WILLIAM J VERRET
6608 HORNWOOD

HOUSTON TX 77074
PHONE 713 954 6771

STEPHEN W VEYSEY
85A GILMAN HALL
IOWA STATE UNIV

AMES IA 50011
PHONE 515 294 5958

NANCY E VIEIRA
NICHD, LTPB
BLDG 6, RM 136
9000 ROCKVILLE PIKE
BETHESDA MD 20205
PHONE 301 496 5531

MICHAEL J URBAN
RD 1 BOX 167-F

JACKSON NJ 08527
PHONE: 201 321 6689

J L VALENTINE
ORAL ROBERTS UNIV
SCHOOL OF MEDICINE
8181 SOUTH LEWIS
TULSA OK 74170
PHONE 918 493 8833

MARINUS VANDENHUL
1215 N NEVADA
SUITE # 1

COLORADO SPRG CO 80903
PHONE

SCOTT W VANETTEN
160 MILLERICK AVE

LAWRENCEVILLE NJ 08648
PHONE: 609 452 9050

LAWRENCE F VASSAMILLET
VARIAN SPECIALTY METALS
3515 GROVE CITY ROAD

GROVE CITY OH 43123
PHONE:

CHRISTINA H VESTAL
VESTEC CORP
9299 KIRBY DRIVE

HOUSTON TX 77054
PHONE 713 796 9677

DOM VICCHIO
UNIV OF MARYLAND
SCH OF PHARMACY
20 N PINE ST
BALTIMORE MD 21201
PHONE 301 528 2980

DAN VILLALANTI
SHELL DEVELOPMENT
PO BOX 1380

HOUTON TX 77001
PHONE.

O MANUEL UY
JOHNS HOPKINS UNIV APL
JOHNS HOPKINS ROAD

LAUREL MD 20707
PHONE: 301 953 5334

PAUL P VALLON
ESTEE LAUDER INC
125 PINE LAWN RD

MELVILLE NY 11747
PHONE. 516 531 1500

ROY W VANDERHAAR
AMOCO CORPORATION
PO BOX 400 - MS B-5

NAPERVILLE IL 60566
PHONE 312 420 5240

AGNES VANLANGENHOVE
ENSECO INC
205 ALEWIFE BROOK PKWY

CAMBRIDGE MA 02138
PHONE 617 611 3111

CAROL VELSKO
LLNL
PO BOX 808, L-232

LIVERMORE CA 94550
PHONE. 415 423 6256

MARVIN L VESTAL
VESTEC
9299 KIRBY DRIVE

HOUSTON TX 77054
PHONE 713 749 2675

GEORGE H VICKERS
DEPT OF CHEMISTRY
INDIANA UNIV

BLOOMINGTON IN 47405
PHONE: 812 335 7905

S K VISWANADHAM
CHEMISTRY DEPT
BOX 10
UNIV OF PITTSBURGH
PITTSBURGH PA 15260
PHONE: 412 624 3088

T S VISWANATHAN
8409 WEST 90TH ST

OVERLAND PARK KS 66212
PHONE 913 236 3881

ROBERT D VOYKSNER
204 TRAIL'S END CT

RALEIGH NC 27614
PHONE 919 541 6697

RICHARD W WADE
520 WAKARA WAY

SALT LAKE CTY UT 84108
PHONE 801 583 3600

GUENTER WAGNER
FINNIGAN MAT
355 RIVER OAKS PKWY

SAN JOSE CA 95134
PHONE 408 433 4800

KENNETH M WALKER
BROWN & WILLIAMSON TOBACCO
PO BOX 35090

LOUISVILLE KY 40232
PHONE 502 568 7986

BING HUANG WANG
CHEMISTRY DEPT
BAKER LABORATORY
CORNELL UNIV
ITHACA NY 14853
PHONE 607 255 3731

M M WANG
CHEMISTRY DEPT
OHIO STATE UNIV
140 W 18TH AVENUE
COLUMBUS OH 43210
PHONE 614 422 0480

CHARLES D WARNER
DEPT OF CHEMISTRY
HASTINGS COLLEGE

HASTINGS NE 68901
PHONE

DAVID W VONENDT
CAL-MSC
SMITHSONIAN INSTN

WASHINGTON DC 20560
PHONE 202 287 3721

JAMES VRBANAC
MED UNIV OF SC
PHARMACOLOGY DEPT

CHARLESTON SC 29425
PHONE 803 792 2471

P A WADSWORTH
814 CHEVY CHASE CIR

SUGAR LAND TX 77478
PHONE 713 491 4754

L C WAGNER
2030 TOWNGATE DRIVE

GARLAND TX 75041
PHONE 214 995 2294

RAYMOND L WALKER
ORNL MARTIN MARIETTA
PO BOX Y BLDG 9735
Y-12 PLANT
OAK RIDGE TN 37831
PHONE 615 574 2449

J L WANG
BECKMAN INDUSTRIAL
4141 PALM STREET

FULLERTON CA 92635
PHONE 714 447 2337

S-I WANG
ABBOTT LABS
D-417 ABBOTT PARK
RTS 137 & 143
N CHICAGO IL 60064
PHONE 312 937 2082

BETHANNE WARRACK
SQUIBB INST FOR MED RES
PO BOX 4000

PRINCETON NJ 08543-4000
PHONE 609 921 5429

KENT J VOORHEES
COLORADO SCH MINES
CHEMISTRY DEPT

GOLDEN CO 80401
PHONE 273 3616

TIMOTHY WACHS
CORNELL UNIVERSITY
CHEMISTRY DEPT

ITHACA NY 14853
PHONE 607 256 4914

BRUCE F WAGNER
IT CORPORATION
312 DIRECTORS DRIVE

KNOXVILLE TN 37923
PHONE 615 690 3211

AUSTIN L WAHRHAFTIG
UNIV OF UTAH
CHEMISTRY DEPT

SALT LAKE CTY UT 84112
PHONE 801 581 6048

GEORGE R WALLER
OKLAHOMA STATE UNIV
BIOCHEMISTRY DEPT

STILLWATER OK 74078
PHONE 405 624 6199

JEFF WANG
ABBOTT LABORATORIES
ABBOTT PARK

N CHICAGO IL 60064
PHONE

T HELEN WANG
PENNZOIL PRODUCTS CO
TECHNOLOGY DIV
PO BOX 7569
WOODLANDS TX 77387
PHONE 713 363 8049

PHIL WARREN
FINNIGAN MAT
355 RIVER OAKS PKWY

SAN JOSE CA 95134-9990
PHONE 408 433 4800

PAUL VOUROS
NORTHEASTERN UNIV
INST CHEMICAL ANAL

BOSTON MA 02115
PHONE 617 437 2840

ADRIAN P WADE
CHEMISTRY DEPT
MICHIGAN STATE UNIV

EAST LANSING MI 48824
PHONE

DAVID A WAGNER
49 SYMPHONY ROAD
APT 24

BOSTON MA 02115
PHONE 617 722 3000

MICHAEL A WAKEFIELD
1211 BURNHAM DRIVE

SAN JOSE CA 95132
PHONE 408 272 2166

FRED WALLS
PHARM CHEMISTRY
UNIV OF CALIFORNIA

SAN FRANCISCO CA 94143
PHONE 415 476 4894

JIA-SHEN WANG
CLAIROL INC
2 BLACHLEY RD

STAMFORD CT 06922
PHONE 203 357 5089

WAYNE WARGO
ROSS LABORATORIES
625 CLEVELAND ROAD

COLUMBUS OH 43216
PHONE 614 227 3456

ROBERT W WARREN
SUN REFINING & MFG
ARD
PO BOX 1135
MARCUS HOOK PA 19061
PHONE 215 447 1814

VIRGIL L WARREN
PINE BLUFF ARSENAL
QUALITY ASSURANCE
LABORATORY
PINE BLUFF AR 71611
PHONE: 501 541 3157

CLIFFORD H WATSON
LEIGH HALL BOX 554

UNIV OF FLORIDA
GAINESVILLE FL 32611
PHONE: 904 376 5816

GORDON W WEBB
770 STIMSON

IDAHO FALLS ID 83402
PHONE: 208 526 3048

N C A WEERASINGHE
DEPT OF CHEMISTRY
MCMS
UNIV OF NEBRASKA
LINCOLN NE 68588
PHONE 402 472 5554

ROBERT J WEINKAM
ALLERGAN PHARM
2525 DUPONT DR

IRVINE CA 92715
PHONE: 714 955 6713

T J WEISMANN
106 SHORT ST

PITTSBURGH PA 15237
PHONE 412 434 5824

MICHAEL J WELCH
NAT'L BUR OF STAN
RM A-113 BLDG 222

GAITHERSBURG MD 20899
PHONE: 301 921 2153

BERND WENCLAWIAK
DEPT OF CHEMISTRY
UNIV OF TOLEDO
2801 W BANCROFT STREET
TOLEDO OH 43606
PHONE 419 537 2664

JUNE GOMPF WASCHE
ENVIRONMENTAL ENTERPRISES
10147 SPRINGFIELD PK

CINCINNATI OH 45215
PHONE. 513 772 2818

J THROCK WATSON
DEPT BIOCHEMISTRY
MICHIGAN STATE UNIV

EAST LANSING MI 48824
PHONE: 517 353 0855

HUGH M WEBB
3746 SAN REMO DR

SANTA BARBARA CA 93105
PHONE: 805 961 4252

ANNEMARIE WEGMANN-SZENTE
STANFORD UNIV
CHEMISTRY DEPT
GC-MS LABS
STANFORD CA 94305
PHONE 415 497 2859

SUSAN T WEINTRAUB
UT HEALTH SCI CTR
7703 FLOYD CURL DR

SAN ANTONIO TX 78284
PHONE 512 691 6121

MARK WEISS
BRUKER INSTRUMENTS
MANNING PARK BLVD

BILLERICA MA 01821
PHONE

DAVID G WELKIE
PERKIN-ELMER CORP
6509 FLYING CLOUD DR

EDEN PRAIRIE MN 55344
PHONE. 612 828 6215

CHRYS WESDEMIOTIS
BOX 441 BAKER LABORATORY
CORNELL UNIV

ITHACA NY 14853
PHONE: 607 255 3731

BRUCE A WASILCHUK
DEPT OF CHEMISTRY
NORTHEASTERN UNIV
360 HUNTINGTON AVE
BOSTON MA 02115
PHONE: 617 437 2794

JAMES G WATT
FINNIGAN CORP
355 RIVER OAKS PKWY

SAN JOSE CA 95134
PHONE: 408 433 4800

MICHAEL WEBER-GRABAU
FINNIGAN MAT
355 RIVER OAKS PWY

SAN JOSE CA 95134
PHONE: 408 433 4800

LEO A WEIBEL
HAZLETON LABS
PO BOX 7545

MADISON WI 53707
PHONE: 608 241 4471

MIRYAM WEISBERGER
NERMAG
10 KINGSBRIDGE ROAD

FAIRFIELD NJ 07006
PHONE: 201 227 7690

ADRIAN WEISZ
NAT'L INST HEALTH
BLDG 10 ROOM 3N325

BETHESDA MD 20892
PHONE 301 496 2151

ROBERT R WELLER
GRAD SCH OF PUBLIC HEALTH
DEPT OF IEHS
UNIV OF PITTSBURGH
PITTSBURGH PA 15261
PHONE 412 624 5573

DAVID S WESLEY
ASHLAND PETROLEUM CO
PO BOX 391

ASHLAND KY 41101
PHONE. 606 329 3333

MARVIN ALAN WATKINS
4970 DAVIS ROAD

WINSTON-SALEM NC 27105
PHONE: 919 767 7964

CLARA WEBB
DOW CHEMICAL CO
B-1222 BLDG

FREEPORT TX 77541
PHONE. 409 238 2924

G H WEDDLE
FAIRFIELD UNIV
CHEMISTRY DEPT

FAIRFIELD CT 06430
PHONE: 203 254 4000

DAVID A WEIL
GOODYEAR TIRE & RUBBER CO
142 GOODYEAR BLVD ROOM 200

AKRON OH 44305
PHONE 216 796 1998

C R WEISENBERGER
OHIO STATE UNIV
CHEMISTRY DEPT
140 W 13TH AVE
COLUMBUS OH 43210
PHONE.

KENNETH J WELCH
SC JOHNSON & SON INC
ANAL R&D STA MS 056
1525 HOWE ST
RACINE WI 53403-5011
PHONE: 414 631 2993

JOHN WELLS
11929 VENICE BLVD H215

LOS ANGELES CA 90066
PHONE 213 398 5372

JAY Y WESTCOTT
UNIV OF CO HSC
BOX B-133 CVP DEPT
4200 E NINTH AVE
DENVER CO 80262
PHONE. 303 394 8591

PATRICIA A WESTMARK
MERRELL DOW PHARMACEUTICALS
2110 E GALBRAITH ROAD

CINCINNATI OH 45215
PHONE 513 948 3110

H R WETHERELL
MSP LAB
714 SO HARRISON

EAST LANSING MI 48823
PHONE 517 337 6191

EARL L WHITE
R J REYNOLDS TOBACCO CO
BOWMAN GRAY TECH CTR

WINSTON-SALEM NC 27102
PHONE 919 773 4015

ROBERT H WHITE
DEPT OF BIOCHEMISTRY
VPI & SU

BLACKSBURG VA 24061
PHONE

JOSEPH WICHMANN
WALLACE LABS
HALF ACRE ROAD

CRANBURY NJ 08512
PHONE

MARK D WIEDERHOLD
SEC OF MEDICAL ONCOLOGY
RUSH MEDICIAL COLL
1725 WEST HARRISON
CHICAGO IL 60612
PHONE 312 942 2249

BRUCE E WILKES
ENVIRONMENTAL ANALYTICAL
5176 CRYSTAL DRIVE

CROSS LANES WV 25313-1940
PHONE 304 776 2730

DALE A WILLCOX
218 W CHESTNUT ST

MACUNGIE PA 18062
PHONE 215 481 7977

DAVID G WESTMORELAND
ROHM & HAAS CO
727 NORRISTOWN RD

SPRING HOUSE PA 19477
PHONE 215 641 2033

JEFF R WETZLER
WESTINGHOUSE-BETTIS
PO BOX 79

WEST MIFFLIN PA 15122-0079
PHONE 412 476 5839

ED WHITE
NBS
A113 CHEMISTRY

GAITHERSBURG MD 20899
PHONE 301 921 2153

CRAIG M WHITEHOUSE
YALE UNIV
ENGIN DEPT MASON LAB
9 HILLHOUSE AVE
NEW HAVEN CT 06520
PHONE 203 436 1767

JOSEPH K WICHMANN
WALLACE LABORATORIES
HALF ACRE ROAD

CRANBURY NJ 08512
PHONE 609 655 6630

RICHARD A WIELESEK
UNIV OF OREGON
CHEMISTRY DEPT

EUGENE OR 97403
PHONE 503 686 4641

P S WILKES
FDA
60 EIGHTH ST NE

ATLANTA GA 30309
PHONE 404 347 4002

JIM WILLEY
8194 FLOWER COURT

ARVADA CO 80005
PHONE

ALAN F WESTON
OCCIDENTAL CHEMICAL
360 RAINBOW BLVD S BOX 728

NIAGRA FALLS NY 14302
PHONE 716 286 3607

CONRAD WHEELER
3235 VICENTE STREET
No 2

SAN FRANCISCO CA 94116
PHONE 415 561 2635

F A WHITE
RENSSELAER POLY INST
NUCLEAR ENG DEPT

TROY NY 12181
PHONE 518 270 6398

JOANNE O WHITNEY
131 TERESITA BLVD

SAN FRANCISCO CA 94127
PHONE 415 566 7755

MARGARET E WICKHAM
MIDWEST RES INST
425 VOLKER BLVD

KANSAS CITY MO 64110
PHONE 816 753 7600

JAMES T WILDER
SIMSPEC
1474 FIELDCREST CIR

PLEASANT HILL CA 94523
PHONE 415 229 0325

CHARLES L WILKINS
UNIV OF CALIFORNIA
CHEMISTRY DEPARTMENT

RIVERSIDE CA 92521-0403
PHONE 714 787 3518

EVAN WILLIAMS
BAKER LAB
DEPT OF CHEMISTRY
CORNELL UNIV
ITHACA NY 14853
PHONE 607 256 3731

CHARLES WESTON
ETC CORP
284 RARITAN CTR PWY

EDISON NJ 08837
PHONE

J W WHEELER
10019 REDDICK DRIVE

SILVER SPRING MD 20901
PHONE 202 636 6910

KEVIN D WHITE
FDA
HFF-424
200 C STREET SW
WASHINGTON DC 20204
PHONE 202 245 1371

N F WHITTAKER
NIH
BLDG 4 RM B2-37

BETHESDA MD 20205
PHONE 301 496 4055

ROBERT L WIECZOREK
100 DEFOREST AVENUE
TECHNICAL CTR

EAST HANOVER NJ 07936
PHONE 201 884 4000

ZBIGNIEW A WILK
CHEMISTRY DEPT BOX 56
UNIV OF PITTSBURGH

PITTSBURGH PA 15260
PHONE 412 624 2799

JOANN WILKINSON
S-CUBED
PO BOX 1620

LA JOLLA CA 92038
PHONE

FRED P WILLIAMS
RESEARCH TRIANGLE INST
PO BOX 12194

RES TRI PK NC 27709
PHONE 919 541 6699

PETER WILLIAMS
ARIZONA STATE UNIV
CHEMISTRY DEPT

TEMPE AZ 85287
PHONE. 602 965 4107

TODD D WILLIAMS
CHEMISTRY DEPT
AUBERT HALL
UNIV OF MAINE
ORONO ME 04469
PHONE. 207 581 1169

TYLON O WILLINGHAM
ENVIRESPONSE
BLDG 209 BAY F
WOODBRIDGE AVE
EDISON NJ 08837
PHONE 201 548 9660

ROBERT D WILLIS
ATOM SCIENCES
114 RIDGEWAY CTR

OAK RIDGE TN 37830
PHONE: 615 483 1113

ROSS C WILLOUGHBY
EXTREL
240 ALPHA DRIVE

PITTSBURGH PA 15238
PHONE 412 782 3884

GREGORY M WILLS
GALILEO ELECTRO OPTICS CORP
GALILEO PARK

STURBRIDGE MA 01566
PHONE 617 347 9191

DANIEL A WILSON
CHEMISTRY DEPT
INDIANA UNIV

BLOOMINGTON IN 47405
PHONE: 812 335 7905

MARK WILSON
BALZERS
8 SAGAMORE PARK RD

HUDSON NH 03051
PHONE: 603 889 6888

RANDALL L WILSON
COLL OF VETERINARY MEDICINE
OHIO STATE UNIV
1935 COFFEY ROAD
COLUMBUS OH 43210
PHONE: 614 424 5594

WILLEM WINDIG
391 S CHIPETA WAY
SUITE F
RESEARCH PARK
SALT LAKE CTY UT 84108
PHONE· 201 328 3889

BRIAN WINGER
608-2 YOUNG GRADUATE HOUSE

W LAFAYETTE IN 47906
PHONE: 317 743 9057

C R WINKELMAN
1570 SIMMONS DR

CLEARWATER FL 33516
PHONE. 813 447 7157

PAUL WINKLER
SCH OF CHEMISTRY
PO BOX 163
GEORGIA TECH
ATLANTA GA 30332
PHONE·

D L WINMILL
HERCULES INC
RESEARCH CENTER

WILMINGTON DE 19899
PHONE 302 995 3267

DOUGLAS J WINTERS
MORTON THIOKOL INC
CHEMICAL DIV RES CTR

WOODSTOCK IL 60098
PHONE 815 338 1800

MARCUS B WISE
OAK RIDGE NAT'L LAB
4500-S MS-E160
PO BOX X
OAK RIDGE TN 37830
PHONE· 615 576 6691

JOHN S WISHNOK
MIT
APPLIED BIOLOGICAL SCI
ROOM 56-313
CAMBRIDGE MA 02139
PHONE

THOMAS A WITTSTRUCK
NUCLIDE CORP
AGV DIVISION
PO BOX 315
ACTON MA 01720
PHONE 617 263 2936

MARTA H WOLFE
SHRINERS HOSP

610 TEXAS AVE
GALVESTON TX 77550
PHONE· 409 761 6575

ROBERT R WOLFE
SHRINERS HOSPITAL
METABOLISM UNIT
610 TEXAS AVE
GALVESTON TX 77550
PHONE:

BURT WOLFF
DEPT OF CHEMISTRY
FLORIDA STATE UNIV

TALLAHASSEE FL 32306
PHONE

W ALAN WOLSTENHOLME
VG INSTRUMENTS
300 BROAD STREET

STAMFORD CT 06901
PHONE 203 322 4546

CARLA M WONG
LLL
PO BOX 808 L-365

LIVERMORE CA 94550
PHONE 415 422 0435

LAN K WONG
UNIV OF PITTSBURGH
SCHOOL OF PHARMACY
804 SALK HALL
PITTSBURGH PA 15261
PHONE: 412 624 3268

WILLIAM W WONG
MEDICAL TOWERS BLDG
6608 FANNIN AVENUE

HOUSTON TX 77030
PHONE 713 799 6187

G M WOOD
2 LITTLE BLUFF RD

NEWPORT NEWS VA 23606
PHONE. 804 865 2466

KARL V WOOD
PURDUE UNIV
FUELS ANAL LAB
CHEMISTRY BLDG
W LAFAYETTE IN 47907
PHONE 317 494 7357

NEVILLE WOOD
BASF ARC

RES TRI PK NC 27709
PHONE

PAUL L WOOD
CIBA GEIGY
556 MORRIS AVE

SUMMIT NJ 07901
PHONE. 201 277 5741

J W WOODS
8 RICHARDS RD

LYNNFIELD MA 01940
PHONE. 617 246 0040

J R WOOLSTON
RCA LABORATORIES

PRINCETON NJ 08540
PHONE: 609 734 3108

DEREK WORKMAN
CHEMISTRY BOX 826
PURDUE UNIVERSITY

W LAFAYETTE IN 47907
.:ONE

BARRY WRIGHT
EXTREL CORP
PO BOX 11512

PITTSBURGH PA 15238
PHONE 412 782 3884

CHARLES J WRIGHT
1210 MAJESTIC WAY

WEBSTER NY 14580
PHONE: 716 477 6733

LARRY G WRIGHT
CHEMISTRY DEPT
PURDUE UNIV

W LAFAYETTE IN 47907
PHONE 317 743 8531

LYNN H WRIGHT
US EPA
EMSL MD-78

RES TRI PARK NC 27711
PHONE 919 541 2951

NANCY E H WRIGHT
SUN REFINING & MARKETING
PO BOX 1135

MARCUS HOOK PA 19061
PHONE. 215 447 1815

JOHN WRONKA
DEPT OF CHEMISTRY
NORTHEASTERN UNIV
360 HUNTINGTON AVE
BOSTON MA 02115
PHONE:

RICHARD WU
WRIGHT STATE UNIV
BREHM LAB

DAYTON OH 45435
PHONE. 513 873 3194

JANET LEE WUEBBELS
MONSANTO CO
800 N LINDBERGH BLVD

ST LOUIS MO 63167
PHONE: 314 694 1273

DITTMAR WULFF
HEWLETT-PACKARD
1285 ELLWANGER DRIVE

PHOENIXVILLE PA 19460
PHONE

JEFF R WYATT
NRL
CODE 6110

WASHINGTON DC 20375-5000
PHONE. 202 767 3244

VICKI H WYSOCKI
CHEMISTRY DEPT
BOX 482
PURDUE UNIV
W LAFAYETTE IN 47907
PHONE: 317 494 6898

JIANG XIANG-YU
318 PHARMACY BLDG
PURDUE UNIV

W LAFAYETTE IN 47907
PHONE.

GEORGE F YAMNITZKY
NORTH CENTRAL LABORATORY
ROOM 500
610 SOUTH CANAL STREET
CHICAGO IL 60607
PHONE 312 353 3640

MARK YANCEY
DEPT OF CHEMISTRY
INDIANA UNIV

BLOOMINGTON IN 47405
PHONE: 812 335 7008

CATHY YANG
DEPT OF CHEMISTRY
UNIV OF CALIFORNIA

RIVERSIDE CA 92521
PHONE: 714 787 4740

LILLY YANG
VESTEC CORP
9299 KIRBY DRIVE

HOUSTON TX 77054
PHONE. 713 796 9677

MO YANG
CHEMISTRY DEPT
INDIANA UNIVERSITY

BLOOMINGTON IN 47405
PHONE:

SONG-CHENG YANG
NIMH
BLDG 10 3040

BETHESDA MD 20892
PHONE:

JOHN R YATES
DEPT OF CHEMISTRY
MCCORMICK RD
UNIV OF VIRGINIA
CHARLOTTESVLL VA 22901
PHONE: 804 924 7994

RAZIEH YAZDANPARAST
MDCH
PHARMACY SCHOOL
PURDUE UNIV
W LAFAYETTE IN 47907
PHONE: 317 494 1449

GEORGE YEFCHAK
CHEMISTRY DEPT
MICHIGAN STATE UNIV

EAST LANSING MI 48824
PHONE 517 353 5215

LAUREN M YELLE
ARTHUR D LITTLE INC
15 ACORN PARK

CAMBRIDGE MA 02140
PHONE: 617 864 5770

RICHARD O YELTON
FINNIGAN CORP
4450 CARVER WOODS DRIVE

CINCINNATI OH 45242
PHONE 513 865 4403

ANDREW J YENCHA
SUNY-ALBANY
CHEMISTRY DEPT

ALBANY NY 12222
PHONE: 518 442 4416

ALFRED L YERGEY
NIH
BLDG 6 RM 136

BETHESDA MD 20205
PHONE: 301 496 5531

JAMES A YERGEY
NIAAA/LCSNIH
BLDG 10 RM 3C218

BETHESDA MD 20205
PHONE 301 496 4900

W D YONEKAWA
NIH
BLDG 36 RM 5D21

BETHESDA MD 20205
PHONE 301 496 6777

MATTHIAS YOONG
6904 DOVE STREET

VENTURA CA 93003
PHONE. 818 787 7380

GLENN YOSHIMURA
4336 MAIN

SKOKIE IL 60076
PHONE

RICHARD A YOST
UNIV OF FLORIDA
CHEMISTRY DEPT

GAINESVILLE FL 32611
PHONE 904 392 0557

DAVID C YOUNG
41 GRANFIELD AVE
APT 2

ROSLINDALE MA 02131
PHONE: 617 325 8040

SO HUN YOUNG
DEPT OF CHEMISTRY
CASE WESTERN RESERVE UNIV

CLEVELAND OH 44106
PHONE

STEVEN E YOUNG
2455 THADDEUS

MOUNTAIN VIEW CA 94043
PHONE 415 859 4806

TIM L YOUNGLESS
CHEVRON CHEMICAL CO
1862 KINGWOOD DR

KINGWOOD TX 77339
PHONE: 713 359 6541

M J YOUSSEFI
UNION CARBIDE
PO BOX 670

BOUND BROOK NJ 08805
PHONE 201 563 5075

KYUNG YU
AFAMRL-THT
AREA B BLDG 79
WRIGHT PATTERSON
A F BASE OH 45433-6573
PHONE. 513 255 3364

MING L YU
IBM RESEARCH CENTER
PO BOX 218

YORKTOWN HGHT NY 10598
PHONE: 914 945 2564

T Y YU
PETROLITE CORP
TRETOLITE DIVISION
369 MARSHALL AVE
ST LOUIS MO 63119
PHONE

MARC YUDKOFF
CHDN'S HOSP OF PHIL
1 CHILDREN'S CTR

PHILADELPHIA PA 19104
PHONE

M F ZABIELSKI
UNITED TECH RES CTR
SILVER LANE, MS 30

EAST HARTFORD CT 06108
PHONE: 203 727 7431

DANIEL W ZAHAREVITZ
4702 SHARON ROAD

CAMP SPRINGS MD 20748
PHONE 301 496 4116

DONALD ZAKETT
DOW CHEMICAL CO
ANAL LABS 574 BLDG

MIDLAND MI 48867
PHONE

JULIE A ZALIKOWSKI
3413 NE LEMOLO SHORE DR

POULSBO WA 98370
PHONE 206 373 1127

RICHARD G ZAYLSKIE
USDA AG RES SERVICE
STATE UNIV STATION
PO BOX 5674
FARGO ND 58105
PHONE 701 237 5771

JAMES M ZECHMAN
SCHERING CORP
60 ORANGE STREET B1

BLOOMFIELD NJ 07003
PHONE

QINGMEI ZHA
DEPT OF CHEMISTRY
642 HAMILTON HALL
UNIV OF NEBRASKA
LINCOLN NE 68588-0304
PHONE. 402 472 3517

MEI-YI ZHANG
BOX 285
BAKER LABORATORY
CORNELL UNIV
ITHACA NY 14853-1301
PHONE: 607 255 3731

BARBARA ZIELINSKA
STATEWIDE AIR POLLUTION
RESEARCH CTR
UNIV OF CALIFORNIA
RIVERSIDE CA 92521
PHONE

KIMBERLY J ZILIS
ROCKY MTN ANALYTICAL LAB
5530 MARSHALL ST

ARVADA CO 80002
PHONE 303 421 6611

JEFFREY ZIMMERMAN
14401 HELLENIC DRIVE B6

TAMPA FL 33613
PHONE 813 971 0992

MICHAEL L ZIMMERMAN
BATTELLE COLUMBUS LABS
505 KING AVENUE

COLUMBUS OH 43214
PHONE

DEBORAH L ZINK
MERCK SHARP & DOHME
PO BOX 2000 R80M-223

RAHWAY NJ 07065
PHONE: 201 574 7207

MARK ZINKL
HEWLETT-PACKARD
13001 HOLLENBURG DRIVE

BRIDGETON MO 63044
PHONE

JOSEPH A ZIRROLLI
FJSRL-NC

US AIR FORCE
ACADEMY CO 80840
PHONE 303 472 2655

JAMES J ZOLDAK
MDS ADVANCED ANALYTICS
2 DUNDEE PARK

ANDOVER MA 01810
PHONE 617 470 1390

ROSALIE M ZUBYK
230 SUMMIT HOUSE

WEST CHESTER PA 19380
PHONE

FRANK S ABBOTT
FAC OF PHARMACEUTICAL SCI
UNIV OF BRITISH COLUMBIA

VANCOUVER, BC V6T 1W5
PHONE. 604 228 2566

GINETTE BAUME
ANALYTECH INST & SERVICE
100 ALEXIS NIHON BLVD
SUITE 575
ST LAURENT QUEBEC H4M 2P1
PHONE· 514 744 5519

M J BERTRAND
UNIV OF MONTREAL
CHEMISTRY DEPT
C P. 6128 STATION A
MONTREAL QUEBEC H3C 3J7
PHONE.

J A BUCKLEY
SCIEX INC
55 GLENCAMERON RD
SUITE 202
THORNHILL ONT L3T 1P2
PHONE: 416 881 4646

M B COMISAROW
UNIV BRIT COLUMBIA
CHEMISTRY DEPT
2036 MAIN MALL
VANCOUVER BC V6T 1Y6
PHONE:

PAUL A D'AGOSTINO
275 11TH STREET NE
MEDICINE HAT

ALBERTA T1A 6A8
PHONE·

RICHARD W EDOM
COLL OF PHARMACY
UNIV OF SASKATCHEWAN

SASKATOON SASK S7N 0W0
PHONE: 306 966 6343

JIM FEDORA
ESSO PETROLEUM CANADA
RESEARCH DIVISION
PO BOX 3022
SARNIA ONT N7T 7M1
PHONE·

PETER ARROWSMITH
SCIEX
55 GLENCAMERON ROAD

THORNHILL ONTARIO L3T 1P2
PHONE·

SYLVIE BEAUDET
UNIV OF QUEBEC
CHEMISTRY DEPT
PO BOX 8888 STAT 'A'
MONTREAL QUE H3C 3P8
PHONE. 514 282 3048

RON F BONNER
SCIEX
55 GLENCAMERON RD

THORNHILL ONT L3T 1P2
PHONE: 416 881 4646

PETER BURGERS
DEPT CHIMIE
UNIV LAVAL

LAVAL QUEBEC G1K 7P4
PHONE. 418 656 2266

PIERRE L COULOMBE
ANALYTECH
742 MOONEY'S BAY PL

OTTAWA ONTARIO K1V 9R2
PHONE

W R DAVIDSON
SCIEX INC
55 GLENCAMERON RD
SUITE 202
THORNHILL ONT L3T 1P2
PHONE: 416 881 4646

G K EIGENDORF
UNIV BRIT COLUMBIA
CHEMISTRY DEPT
2036 MAIN MALL
VANCOUVER BC V6T 1Y6
PHONE 604 228 3235

H PETER FISCHER
PETRO CANADA
RES & DEV DEPT
2489 N SHERIDAN WAY
MISSISSAUGA ONT L5K 1A8
PHONE·

GUY P ARSENAULT
RR 2
MIDDLE ROAD

KINGSTON ONT K7L 5H6
PHONE 613 545 7484

RONALD C BEAVIS
PHYSICS DEPT
UNIV OF MANITOBA

WINNIPEG MAN R3T 2N2
PHONE· 204 942 9358

CLAUDE BOUDONNAIS
ANALYTECH INST & SERVICE
100 ALEXIS NIHON BLVD
SUITE 575
ST LAURENT QUEBEC H4M 2P1
PHONE: 514 744 5519

JOHN M CARRON
WGNL DOE CC1W
867 LAKESHORE ROAD

BURLINGTON ONTARIO L7R 4A6
PHONE:

IAIN H CROCKER
BOX 496
DEEP RIVER

ONTARIO K0J 1P0
PHONE. 613 584 3311

PETER H DAWSON
NAT'L RESEARCH COUNCIL
MICROSCTRUCTURAL SCIENCES
MONTREAL ROAD
OTTAWA ONTARIO K1A 0R6
PHONE· 613 993 9369

WERNER E ENS
UNIV OF MANITOBA
PHYSICS DEPT

WINNIPEG MANITOBA R3T 2N2
PHONE·

I P FISHER
GULF CANADA LTD
RESEARCH & DEVELOP
2489 N SHERIDAN WAY
SHERIDAN PK ONT L5K 1A8
PHONE: 416 822 6770

TERRENCE ASHE
ESSO PETROLEUM CANADA
PO BOX 3022

SARNIA ONTARIO N7T 7M1
PHONE. 519 339 2870

F M BENOIT
HEALTH-WELFARE DEPT
ENVIRONMENTAL HEALTH
TUNNEYS PASTURE
OTTAWA ONTARIO K1A 0L2
PHONE:

ROBERT K BOYD
UNIV OF GUELPH
CHEMISTRY DEPT

GUELPH ONTARIO N1G 2W1
PHONE· 519 824 4120

SWAPAN K CHOWDHURY
DEPT OF CHEMISTRY
UNIV OF ALBERTA

EDMONTON ALBERTA T6G 2G2
PHONE. 403 432 3205

DOUG CROSBY
SHELL CANADA LTD
OAKVILLE RESEARCH CTR
3415 LAKESHORE ROAD W
OAKVILLE ONTARIO L6J 5C7
PHONE: 416 827 1141

DAVID A DURDEN
PSYCHIATRIC RES DIV
A114 CMR BLDG
UNIV OF SASKATCHEWAN
SASKATOON SASK S7N 0W0
PHONE· 306 664 6912

M J EVANS
CHEMISTRY DEPT
UNIV OF MONTREAL
C P 6210 SUCCA
MONTREAL QUE H3C 3J7
PHONE· 514 343 6884

CLAUDE J FORTIN
LAB DE POLICE SCIENTIFIQUE
1701 PARTHENAIS, 5TH FL

MONTREAL QUE H2K 3S7
PHONE 514 873 2704

M G FOSTER
ZENON ENVIRONMENTAL
845 HARRINGTON CT

BURLINGTON ONT L7N 3P3
PHONE 416 639 6320

BERNARD F FRANCIS
SHELL RESEARCH CTR
3415 LAKESHORE RD W

OAKVILLE ONTARIO L6J 5C7
PHONE 416 827 1141

J B FRENCH
4 THORNBANK RD

THORNHILL ONT L4J 2A2
PHONE: 416 667 7706

JOHN FULFORD
SCIEX
55 GLENCAMERON ROAD

THORNHILL ONTARIO L3T 1P2
PHONE

JUANITA N GEARING
DEPT FISHERIES & OCEANS
901 CAP DIAMANT
B P 15500
QUEBEC QUEBEC G1K 7Y7
PHONE 418 648 7781

HUGH A GILLIS
NAT'L RESEARCH COUNCIL
1411 OXFORD ST

HALIFAX NS B3H 3Z1
PHONE: 902 426 7936

LAWRENCE W GREEN
ATOMIC ENERGY OF CAN
CHALK RIVER NUC LAB

CHALK RIVER ONT K0J 1J0
PHONE: 613 584 3311

ALEX G HARRISON
UNIV OF TORONTO
CHEMISTRY DEPT

TORONTO ONT M5S 1A1
PHONE: 416 978 3577

J M HARTWELL
CIL INC
2101 HADWEN RD
SHERIDAN PK RES COMM
MISSISSAUGA ONT L5K 2L3
PHONE 416 823 7160

JOHN HEADLEY
ALBERTA ENVIRON CTR
CHEMISTRY WING
PO BAG 4000
VEGREVILLE ALBERTA T0B 4L0
PHONE 403 632 6761

J A HERMAN
UNIVERSITE LAVAL
CHEMISTRY DEPT

QUEBEC QUEBEC G1K 7P4
PHONE 418 656 3848

K K HERMAN
UNIVERSITE LAVAL
CHEMISTRY DEPT

QUEBEC QUEBEC G1K 7P4
PHONE 418 616 5691

ALAN M HOGG
UNIV OF ALBERTA
CHEMISTRY DEPT

EDMONTON ALBERTA T6G 2G2
PHONE 403 432 5577

LAWRENCE R HOGGE
NAT'L RES COUNCIL
110 GYMNASIUM RD

SASKATOON SASK S7N 0W9
PHONE 306 975 4193

ANDREW HOLMES
HEALTH & WELFARE
HEALTH PROT BRN
2301 MIDLAND AVE
SCARBOROUGH ONT M1P 4R7
PHONE

JOHN L HOLMES
UNIV OF OTTAWA
CHEMISTRY DEPT

OTTAWA ONTARIO K1N 9B4
PHONE 613 231 2239

MICHAEL G IKONOMOU
CHEMISTRY DEPT
UNIV OF ALBERTA

EDMONTON ALBERTA T6G 2G2
PHONE 403 432 3502

W D JAMIESON
NRC
1411 OXFORD ST

HALIFAX NS B3H 3Z1
PHONE 902 426 8279

MAUREEN KALLOO
MSD ISOTOPES
PO BOX 899

PTE CLAIRE QUEBEC J4Z 2X5
PHONE

JAMES KAPRON
DEPT OF CHEMISTRY
MCMASTER UNIV

HAMILTON ONTARIO L8S 4M1
PHONE 416 525 9140

C W KAZAKOFF
UNIV OF OTTAWA
CHEMISTRY DEPT

OTTAWA ONTARIO K1N 9B4
PHONE 614 231 4039

PAUL KEBARLE
UNIV OF ALBERTA
CHEMISTRY DEPT

EDMONTON ALBERTA T6G 2G2
PHONE. 403 432 3469

H J KOCH
MSD ISOTOPES
TRANSCANADA HWY

KIRKLAND QUEBEC
PHONE.

J R KRAUSE
UNIV OF OTTAWA
CHEMISTRY DEPT

OTTAWA ONTARIO K1N 9B4
PHONE 613 231 4039

D A LANE
31 DE VERE GDNS

TORONTO ONTARIO M5M 3E6
PHONE 416 667 4965

BENJAMIN P LAU
HEALTH & WELFARE CAN
FOOD RESEARCH
TUNNEY'S PASTURE
OTTAWA ONTARIO K1A 0L2
PHONE 416 993 4994

JACQUES LESAGE
IRSST
505 OUEST DE MAISONNEUVE

MONTREAL QUEBEC H3A 3C2
PHONE 514 288 1551

D L LEWIS
DEPT OF AGRICULTURE
TOXICOLOGY LAB
BOX 8070 6909-116TH
EDMONTON ALBERTA T6H 4P2
PHONE. 403 436 8410

FREDERICK P LOSSING
UNIV OF OTTAWA
CHEMISTRY DEPT

OTTAWA ONTARIO K1N 9B4
PHONE 613 231 4039

D B MACLEAN
MCMASTER UNIVERSITY
CHEMISTRY DEPT

HAMILTON ONTARIO L8S 4M1
PHONE. 416 525 9140

DENNIS E MAIN
UNIV OF MANITOBA
PHYSICS DEPT

WINNIPEG MAN R3T 2N2
PHONE:

GREG MALIS
LAB SERVICES BLDG #22
ROOM B5
CENTRAL EXPERIMENTAL FARM
OTTAWA ONTARIO K1A 0C6
PHONE.

ORVAL MAMER
MCGILL UNIV
1130 PINE AVE WEST

MONTREAL QUEBEC H3A 1A3
PHONE

L J MCBURNEY
DCIEM
PO BOX 2000

DOWNSVIEW ONT M3M 3B9
PHONE 416 635 2130

GORDON MCKAY
COLL OF PHARMACY
UNIV OF SASKATCHEWAN

SASKATOON SASK S7N 0W0
PHONE. 306 966 6361

JACK M MILLER
BROCK UNIV
CHEMISTRY DEPT

ST CATHERINES ONT L2S 3A1
PHONE· 416 688 5550

RONALD B NEW
CHEMISTRY DEPT
UNIV OF WINDSOR

WINDSOR ONT N9B 3P4
PHONE 519 253 4232

F I ONUSKA
CCIW-AMRS
PO BOX 5050

BURLINGTON ONT L7R 4A6
PHONE: 416 637 4635

GIOVANNI PERLUZZO
GENIE PHYSIQUE
ECOLE POLYTECHNIQUE
C P 6079 SUCC A
MONTREAL H3C 3A7
PHONE 514 340 4956

LOUIS RAMALEY
DALHOUSIE UNIVERSITY
CHEMISTRY DEPT

HALIFAX NS B3H 4J3
PHONE. 902 424 3305

ANDRE MARTINEAU
INRS - SANTE
7401 HOCHELAGA

MONTREAL QUEBEC H1N 3M5
PHONE· 514 253 2832

DOUG MCCLURE
RCM POLICE FORENSIC LAB
PO BOX 8885

OTTAWA ONTARIO K1G 3M8
PHONE· 613 993 0645

ROGER MERCER
80 ST GEORGE STREET

TORONTO ONTARIO M5S 1A1
PHONE

ALEXANDER A MOMMERS
CHEMISTRY DEPT
UNIV OF OTTAWA
365 NICHOLASS ST
OTTAWA ONTARIO K1N 9B4
PHONE 613 564 4039

TARAS W OBAL
CHEMISTRY DEPT
UNIV OF WINDSOR
401 SUNSET AVENUE
WINDSOR ONTARIO N9B 3P4
PHONE 519 253 4232

E R PAQUIN
MINISTERE AGRICULTURE
2700 RUE EINSTEIN
LOCAL C2-105
SAINTE FOY QUE G1P 3W8
PHONE 418 643 5126

D W PRIDDLE
UNIV OF TORONTO
CHEMISTRY DEPT

TORONTO ONTARIO M5S 1A1
PHONE 416 978 5088

MARK L J REIMER
CHEMISTRY DEPT
UNIV OF MANITOBA

WINNIPEG MANITOBA R3T 2N2
PHONE 204 474 9761

ROBERT MASSE
INRS-SANTE
7401 HOCHELAGA

MONTREAL QUEBEC H1N 3M5
PHONE 514 253 2832

D L MCGILLIVRAY
UNIV OF VICTORIA
CHEMISTRY DEPT

VICTORIA BC V8W 2Y2
PHONE 604 721 7183

F Y MESSIER
ENV QUEBEC
850 BOUL VANIER
ST VINCENT DE PAUL (LAVAL)
QUEBEC H7C 2M7
PHONE: 514 873 3072

JANE MONTGOMERY
BIOMEDICAL MASS SPEC
1130 PINE AVE W

MONTREAL QUE H3A 1A3
PHONE. 514 392 6716

JAMES OLSEN
DEPT OF CHEMISTRY
UNIV OF WINDSOR

WINDSOR ONT N9B 1T3
PHONE 519 253 4232

J R PARE
1245 WALKLEY RD
NO 1103

OTTAWA ONT K1V 9S5
PHONE· 613 995 3700

LIONEL R PROVOST
DEFENSE RES ESTAB
SUFFIELD
RALSTON
ALBERTA T0J 2N0
PHONE

ERIC J REINER
50 CORDOVA AVE
APT 2003

ISLINGTON ONT M9A 4X6
PHONE: 416 978 3571

LUI MATTIAZZI
RAYONICS SCIENTIFIC
585 CANARCTIC DRIVE

DOWNSVIEW ONTARIO M3J 2P9
PHONE: 416 736 1600

DOUGLAS E MCINTYRE
HEWLETT-PACKARD CANADA
6877 GOREWAY DR

MISSISSAUGA ONT L4V 1M8
PHONE:

W F MILES
MASS SPEC LAB
LAB SERVICES DIV
BLDG #22 C.E F
OTTAWA ONTARIO K1A 0C5
PHONE· 613 995 4907

J E MORGAN
MORGAN SCHAFFER CORP
5110 COURTRAI AVE

MONTREAL QUE H3W 1A7
PHONE:

J B OLTHETEN
2545 DE MINIAC

MONTREAL QUEBEC H4S 1E5
PHONE. 514 337 4343

O O PELLETIER
HEALTH PROTECTION BR
ROOM 277 HPB BLDG
TUNNEYS PASTURE
OTTAWA ONTARIO K1A 0L2
PHONE

M A QUILLIAM
MCMASTER UNIVERSITY
CHEMISTRY DEPT

HAMILTON ONTARIO L8S 4M1
PHONE 416 525 9140

R T RYE
CONCORDIA UNIV
CHEMISTRY DEPT
1455 DE MAISONNEUVE
MONTREAL QUEBEC H3G 1M8
PHONE: 514 848 3344

R W SADLIER
12 BAL HARBOUR DR

GRIMSBY ONT L3M 4P9
PHONE.

JEAN-PIERRE SCHMIT
UNIV OF QUEBEC
CHEMISTRY DEPT
CP 8888 SUCCURSALE A
MONTREAL PQ H3C 3P8
PHONE: 514 282 3048

BRUNO SCHUELER
PHYSICS DEPT
UNIV OF MANITOBA

WINNIPEG MAN R3T 2N2
PHONE 204 474 9358

BORI I SHUSHAN
SCIEX
55 GLENCAMERON RD

THORNHILL ONT L3T 1P2
PHONE: 416 881 4646

RICHARD W SMITH
CHEMISTRY DEPT
MCMASTER UNIV
1280 MAIN STREET W
HAMILTON ONTARIO L8S 4M1
PHONE· 416 525 9140

KENNETH STANDING
UNIV OF MANITOBA
PHYSICS DEPT

WINNIPEG MANITOBA R3T 2N2
PHONE 204 474 9358

J A STONE
QUEEN'S UNIVERSITY
CHEMISTRY DEPT

KINGSTON ONTARIO K7L 3N6
PHONE· 613 547 3161

NEIL STOOK
179 COLONNADE ROAD

NEPEAN ONTARIO
PHONE

WING-FUNG SUN
HEALTH PROTECTION BRANCH
FOOD RESEARCH DIVISION
HEALTH & WELFARE CANADA
OTTAWA ONTARIO K1A 0L2
PHONE:

JAN A SUNNER
DEPT OF CHEMISTRY
UNIV OF ALBERTA

EDMONTON ALBERTA T6G 2G2
PHONE: 403 432 3502

JAN E SZULEJKO
DEPT OF CHEMISTRY
UNIV OF WATERLOO

WATERLOO ONT N2L 1K1
PHONE: 519 885 1211

U Y TAGUCHI
ONTARIO MIN ENVIRONMENT
125 RESOURCES ROAD
PO BPX 213
REXDALE ONTARIO M9W 5L1
PHONE 416 248 3755

XUEJUN TANG
DEPT OF PHYSICS
UNIV OF MANITOBA

WINNIPEG MANITOBA R3T 2N2
PHONE

PIERRE THIBAULT
10344 PARTHENAIS

MONTREAL H2B 2L7
PHONE· 514 384 6787

H M TOSINE
DRINKING WATER ORGANICS
RESOURCES RD
PO BOX 213
REXDALE ONTARIO M9W 5L1
PHONE 416 248 7484

DAVE WADDELL
DEPT OF CHEM & BIOCHEM
UNIV OF GUELPH

GUELPH ONTARIO N1H 2T8
PHONE.

J B WESTMORE
UNIV OF MANITOBA
CHEMISTRY DEPT

WINNIPEG MAN R3T 2N2
PHONE 204 474 9761

S K WONG
UNIV WESTERN ONTARIO
CHEMISTRY DEPT

LONDON ONTARIO N6A 5B7
PHONE· 519 679 2796

GORDON W WOOD
UNIV OF WINDSOR
VICE PRESIDENT ACADEMIC

WINDSOR ONTARIO N9B 3P4
PHONE· 519 253 4232

RAGHAV YAMDAGNI
UNIV OF CALGARY
CHEMISTRY DEPT

CALGARY ALB T2N 1N4
PHONE· 403 220 5890

ALEX E YOUNG
DEPT OF CHEMISTRY
UNIV OF TORONTO
80 ST GEORGE STREET
TORONTO M5S 1A1
PHONE· 416 978 3571

J J ZAMECNIK
CAMU
HEALTH & WELFARE CAN
BOX 1035 POST STA B
DOWNSVIEW ONT M3M 5V5
PHONE: 416 630 8503

DIMO ZIDAROV
OFF 8
5265 COTE STE CATHERINE

MONTREAL QUEBEC H3W 1N2
PHONE 514 343 7555

PHONE

H H ADLERCREUTZ
MEILAHTI HOSPITAL
CLINICAL CHEMISTRY

00290 HELSINKI 29 011 358
FINLAND

TEODOR AST
FACULTY OF TECHNOLOGY &
METALLURGY
KARNEGIJEVA
11000 BELGRADE
YUGOSLAVIA

M L BENNETT
BHP MELBOURNE RES LA
PO BOX 264

CLAYTON VIC 3168
AUSTRALIA

JOHN C BILL
207 CREWE ROAD

SANDBACH
CHESHIRE
ENGLAND

RENE N BOTTER
CEN SACLAY DPC

91191 GIF SUR YVETTE
CEDEX
FRANCE

R Y VAN FOSSEN BRAVO
PUC DEPTO QUIMICA
R M SAO VICENTE,225
22.453 - GAVEA
RIO DE JANEIRO-RJ 021 274
BRAZIL

PROF H BUDZIKIEWICZ
INST. ORG CHEM
GREINSTR 4

5000 KOELN 41
WEST GERMANY

J S COTTRELL
KRATOS
BARTON DOCK RD
URMSTON
MANCHESTER M31 2LD
ENGLAND

MARTIN P ALLEMANN
SPECTROSPIN AG
INDUSTRIESTR 26

8117 FALLENDEN
SWITZERLAND

GRAHAM ATKIN
VG GAS ANALYSIS SYSTEMS
ASTON WAY
MIDDLEWICH
CW10 OHT
ENGLAND

ALFRED BENNINGHOVEN
PHYSIKALISCHES INST
UNIV MUNSTER
DOMAGKSTR 75
4400 MUNSTER
WEST GERMANY

WALTER BLACKSTOCK
GLAXO GROUP RESEARCH LTD
PHYSICAL CHEM DEPT
GREENFORD ROAD, GREENFORD
MIDDLESEX UB6 0HE
ENGLAND

D V BOWEN
PFIZER CENTRAL RES
SANDWICH

KENT CT13 9NJ 0304 61
ENGLAND

CHARLES J W BROOKS
UNIV OF GLASGOW
CHEMISTRY DEPT

GLASGOW G12 8QQ 041 339
SCOTLAND

JEAN CESARIO
SEAIN - Bat 91
CEN/SACLAY
91191 GIF/YVETTE
CEDEX
FRANCE

ANTHONY G CRAIG
DEPT OF IMMUNOLOGY
BIOMEDICAL CENTER
UPPSALA UNIV BOX 582
S-75123 UPPSALA
SWEDEN

R T APLIN
DYSON PERRINS LAB
OXFORD UNIVERSITY
SOUTH PARKS ROAD
OXFORD OX1 3QY
ENGLAND

R H BATEMAN
VG ANALYTICAL
FLOATS ROAD
WYTHENSHAWE
MANCHESTER M23 9LE
ENGLAND

A J BERRY
DEPT OF CHEMISTRY
UNIVERSITY COLLEGE
PO BOX 78
CARDIFF CF1 1XL
UNITED KINGDOM

A J BOERBOOM
A DURER STR 25-2

1077 LT AMSTERDAM 31 20 6
NETHERLANDS

WILLI BRAND
FINNIGAN MAT
BARKHAUSENSTR 2

D-2800 BREMEN 14
WEST GERMANY

A P BRUINS
STATE UNIVERSITY
PHARMACY DEPT
A DEUSINGLN 2
9713-AW GRONINGEN 50 1161
NETHERLANDS

ROLANDO CHRISTIAN
9 RUE DE LA PRAIRIE

92160 ANTONY
FRANCE

JEAN CZUCZWA
EAWAG

DUBENDORF CH-8600
SWITZERLAND

EMANUELE ARLANDINI
FARMITALIA-CERBA
VIA GRACCHI, NO 35

MILANO
ITALY

CLAUDE BEAUGRAND
NERMAG
49 QUAI DU HALAGE

RUEIL MALMAISON
F 92500 FRANCE

KIRIT H BHATT
PHARMACOLOGY/TOXICOLOGY
UNIV OF KUWAIT
PO BOX 24923
SAFAT
KUWAIT 13110

PETER BOTT
VG ANALYTICAL
FLOATS ROAD
WYTHENSHAWE
MANCHESTER
ENGLAND M23 9LE

M C TEN NOEVER DE BRAUW
TNO-CIVO
PO BOX 360

3700 AJ ZEIST
NETHERLANDS

CURT BRUNNEE
FINNIGAN MAT
BARKHAUSENSTR 2
POSTFACH 14 4062
D-2800 BREMEN 10
WEST GERMANY

MAGDA M CLAEYS
UNIV INSTELL ANTWERP
PHARMACY DEPT
UNIVERSITEITSPLEIN 1
B-2610 WILRIJK 03 828
BELGIUM

PETER D'ARCY
VG MASSLAB
TUDOR ROAD
ALTRINCHAM
CHESHIRE SK8 3DW
ENGLAND

OLOF DAHLMAN
SWEDISH TOBACCO CO
BOX 17007

STOCKHOLM
SWEDEN S-104 62

T S DAVIS
VG ANALYTICAL
FLOATS ROAD
WYTHENSHAWE
MANCHESTER
ENGLAND M23 9LE

F F DEGREVE
CEGEDUR PECHINEY
CENTRE DE RECHERCHES
BP 27
38340 VOREPPE
FRANCE

DR DELAROFF
ROUSSEL-UCLAF
102-111 ROUTE DE NOISY

93230 ROMAINVILLE
FRANCE

PROF G DEMORTIER
DEPT OF PHYSICS
FNDP
61 RUE DE BRUXELLES
B5000 NAMUR
BELGIUM

J J DEUTSCH
21 HAMASOREET
RACHEL ST

JERUSALEM
ISRAEL

GERD DIELMANN
FINNIGAN MAT
BARKHAUSENSTR 2
POSTFACH 144062
2800 BREMEN
WEST GERMANY

PETER DOBBERSTEIN
FINNIGAN MAT
BARKHAUSENSTR 2
POSTFACH 144062
2800 BREMEN
WEST GERMANY

STEPHEN DOWN
MASS SPECTROMETRY DATA CTR
ROYAL SOC OF CHEMISTRY
UNIV OF NOTTINGHAM
NOTTINGHAM NG7 2RD
UNITED KINGDOM

J D DROWART
VRIJE UNIV BRUSSELS
PLEINLAAN 2

B-1050 BRUSSELS
BELGIUM

A M DUFFIELD
UNIV NEW SOUTH WALES
CLINIC PHARMACOLOGY
PO BOX 1
KENSINGTON NSW 02 697
AUSTRALIA 2033

GERRY ELLIOTT
KRATOS ANALYTICAL
BARTON DOCK ROAD
URMSTON
MANCHESTER
ENGLAND

E E ESMANS
UNIV ANTWERPEN
ORGANISCHE SCHEIKUND
GROENENBORGLN 171
B-2020 ANTWERPEN 218 02
BELGIUM

R F EVANS
QUEENSLAND UNIV
CHEMISTRY DEPT

ST LUCIA QNLAND 40
AUSTRALIA

SID EVANS
KRATOS
BARTON DOCK ROAD
URMSTON
MANCHESTER M31 2LD
ENGLAND

S M FACCHETTI
CCR-EURATOM
RADIOCHEMISTRY DIV

21020 ISPRA-VARESE 0332 78
ITALY

PAUL FARROW
VG MASSLAB
TUDOR ROAD
ALTRINCHAM
CHESHIRE WA14 5RZ
ENGLAND

M A FERREIRA
DEPT OF CHEMISTRY
FAC OF SCIENCES
UNIVERSITY OF LISBON
1294 LISBON CODEX
PORTUGAL

ROBERT W FINNEY
INVESESK RESEARCH INT'L
INVESESK GATE
MUSSELBURGH
EH21 7UB
SCOTLAND

DANIEL J FRAISSE
SPEC DE MASSE
SCA-CNRS
BP 22
69390-VERNAISON
FRANCE

H G FRANK
UNIV TUEBINGEN
INST TOXIKOLOGIE
WILHELMSTR 56
D 7400 TUEBINGEN 7071 29
FED REP GERMANY

JOCHEN FRANZEN
BRUKER FRANZEN ANALYTIK
KALLENTURMER HEERSRT 122

D-2800 BREMEN
WEST GERMANY

RUDIGER FREY
BRUKER FRANZEN ANALYTIK Gmbh
KATTENTURMER HEERSTR 122

D-2800 BREMEN 61
WEST GERMANY

MARLIN FRIESEN
IARC/CIRC
150 COURS A THOMAS

69372 LYON
FRANCE

TOSHIHIRO FUJII
NAT'L INST FOR ENVIRONMENTAL
STUDIES
YATABE-MACHI, TSUKUBA
IBARAKI 305
JAPAN

JEAN F GAL
UNIV DE NICE
CAMPUS VALROSE
LAB CHIMIE PHYS ORG
NICE 06034 CEDEX 93 51 9
FRANCE

DAVID E GAMES
UNIVERSITY COLLEGE
CHEMISTRY DEPT
PO BOX 78
CARDIFF CF1 1XL 0222 44
WALES

MATS GARLE
HUDDINGE UNIV HOSP
CLINICAL PHARMACOLOG
C1-68
S-14186 HUDDINGE
SWEDEN

S J GASKELL
TENOVUS INSTITUTE
WELSH NAT'L SCH MED

CARDIFF CF4 4XX 222 755
WALES

T T GAUMANN
EPFL-ECUBLENS
INST DE CHIMIE PHYS

CH-1015 LAUSANNE
SWITZERLAND

CHRIS F GELIJKENS
PARKLAAN 78

B-2700 ST-NIKLAAS
BELGIUM

E E GELPI
RD GUINARDO 5 7

08024 BARCELONA 34 3 20
SPAIN

MICHAEL GEORGIEFF
INST FUR ANESTHESIOLOGIE
KLINIKUM MANNHEIM
THEODOR-KUTZER-UFER
6800 MANNHEIM
FED REP GERMANY

SIMON GOSS
PHYSICAL CHEMISTRY
LA TROBE UNIV
BUNDOORA
VICTORIA 3083
AUSTRALIA

THOMAS R GOVERS
AIR LIQUIDE
CTR RECHERCHE
CLAUDE DELORME
JOVY EN JOSAS
78350 FRANCE

B N GREEN
VG ANALYTICALD
FLOATS ROAD
WYTHENSHAWE
MANCHESTER M23 9LE
ENGLAND

DAVID T GREEN
PPF INT'L LTD
KENNINGTON ROAD
ASHFORD
KENT TN240LT 0233 44
UK

FIONA GREER
M-SCAN LTD
SILWOOD PARK
SUNNINGHILL
ASCOT
ENGLAND SLS 7P2

I K GREGOR
CHEMISTRY SCHOOL
UNIV OF NSW

KENSINGTON NSW 203 61 2 69
AUSTRALIA

PETER GROSSMANN
SPECTROSPIN AG
INDUSTRIESTRASSE 26

CH-8117 FALLANDEN
SWITZERLAND

JUERGEN GROTEMEYER
INST F PHYSIKALISCHE CHEMIE
TECHNISCHE UNIV MUNCHEN
LICHENTENBERGSTR 4
8046 GARCHING
WEST GERMANY

LUTZ GROTJAHN
GBF
MASCHERODER WEG 1

D-3300 BRAUNSCHWEI
W GERMANY

HANS-FRIEDRICH GRUTZMACHER
FAKULTAT FUR CHEMIE
UNIV BIELEFELD
P B 8640
4800 BIELEFELD
WEST GERMANY

CHRISTINE HAFOK
ERNST-BOEHRINGER-INST FUR
ARZNEIMITTELFORSCHUNG
DR BOEHRINGER-GASSE 5-11
A-1121 VIENNA
AUSTRIA

ROBERT J HAGEMANN
CEN FAR/SEA
BP No 6
92265 FONTENAY AUX
ROSES CEDEX
FRANCE

J H HAHN
MAX PLANCK INST CHEM
SAARSTR 23

D-6500 MAINZ
WEST GERMANY

D J HARVEY
OXFORD UNIVERSITY
PHARMACOLOGY DEPT
SOUTH PARKS RD
OXFORD OX1 3QT 0865 51
ENGLAND

YUTAKA HASHIMOTO
31-12 SHIMO 3-CHOME
KITA-KU

TOKYO 115 03 901
JAPAN

P A HAUG
FELDBERG STR 24

D-6095 GINSHEIM 06144 3
WEST GERMANY

D D HENNEBERG
MPI-KOHLENFORSCHUNG

D-433 MULHEIM/RUHR
WEST GERMANY

ANTTI HESSO
INST OF OCCUPATIONAL
HEALTH
HAARTMANNINKATU 1
SF-00290 HELSINKI
FINLAND

K G HEUMANN
UNIV REGENSBURG
CHEMISCHES INSTITUT
UNIVERSTITAETS STR 31
D-84 REGENSBURG 941 943
WEST GERMANY

TONY HICKSON
VG INSTRUMENTS
3 TUDOR ROAD
ALTRINCHAM
CHESHIRE
U K.

FRANZ HILLENKAMP
INST F BIOPHYSIK
UNIV FRANKFURT
THEODOR STERN KAI 7
D-6000 FRANKFURT 69 6301
WEST GERMANY

KENZO HIRAOKA
YAMANASHI UNIVERSITY
FACULTY ENGINEERING
TAKEDA 4
KOFU 400 0552 52
JAPAN

EDMOND DE HOFFMANN
PL PASTEUR 1 BOX 17

LOUVAIN-LA-NEUVE
B-1348 BELGIUM

P T HOLLAND
RUAKURA AG RES CTR

HAMILTON
NEW ZEALAND

M A HOURIEH
PO BOX 686

ALEPPO 236136
SYRIA

W K HUBER
BALZERS AG

FL 9496 BALZERS
LIECHTENSTEIN

JOHAN INGELS
BELIGIAN INST FOR
SPACE AERONOMY
RINGLAAN 3
B-1180 BRUSSELS
BELGIUM

J A IRLAM
KRATOS LTD
BARTON DOCK ROAD
URMSTON
MANCHESTER M31 2LD
ENGLAND

SABURO ISHII
JEOL LTD
NAKAGAMI CHO 1418
AKISHIMA SHI
TOKYO 196 0425 43
JAPAN

A H JACKSON
UNIVERSITY COLLEGE
CHEMISTRY DEPT

CARDIFF CF1 1XL
WALES

J E JALONEN
UNIV OF TURKU
CHEMISTRY DEPT

20500 TURKU 50
FINLAND

KEITH R JENNINGS
UNIV OF WARWICK
GIBBET HILL ROAD
CHEMISTRY DEPT
COVENTRY CV4 7AL 203 240
ENGLAND

D D JONES
VG ANALYTICAL
FLOATS ROAD
WYTHENSHAWE
MANCHESTER
ENGLAND M23 9LE

DANIEL JOULAIN
P ROBERTET ET CIE
B P 100

06333 GRASSE
FRANCE

T T KAISER
MAX PLANK INSTITUT
SAARSTRASSE 23

D-6500 MAINZ
W GERMANY

H H KAMBARA
HITACHI LTD
ADVANCED RESEARCH LAB
KOKUBUNJI
TOKYO 185
JAPAN

IVAN KAMENSKY
PO BOX 15045

S-75215 UPPSALA
SWEDEN

CONCETTA KASCHERES
RUA DR ANTONIO HOSSRI 388

CAMPINAS
SOA PAULO 13100
BRAZIL

HARTMUT KAUFMANN
FINNIGAN MAT
BARKHAUSENSTR 2

2800 BREMEN
W GERMANY

SUSAN KENNERLEY
KRATOS ANALYTICAL INSTRUMENTS
BARTON DOCK ROAD
URMSTON
MANCHESTER
ENGLAND

M S KIM
SEOUL NATIONAL UNIV
CHEMISTRY DEPT
COLL OF NATURAL SCI
SEOUL 151 877 010
KOREA

IKUMI KIMURA
FACULTY OF PHARMACY
MEIJO UNIVERSITY
TEMPAKU
NAGOYA 468
JAPAN

GRAHAM S KING
ICI PLANT PROTECTION DIV
METAB & RESIDUE SECTION
JEALOTTS HILL
BRACKNELL BERK
ENGLAND

ANTHONY KINSELLA
VG ISOTOPES
ION PATH ROAD THREE
WINSFORD
CHESHIRE
ENGLAND

PIETER KISTEMAKER
FOM INST FOR ATOMIC &
MOLECULAR PHYSICS
KRUISLAAN 407
1098 SJ AMSTERDAM
NETHERLANDS

HANS KNOF
AM FORSTTEICH 15/17

D-2000 NORDERSTEDT
WEST GERMANY

K K KODERA
31-2
SHIMOGAMOKITAZONOCHO
SAKYO
KYOTO 606
JAPAN

WILFRIED A KOENIG
UNIV HAMBURG
INST F ORGAN CHEMIE
M-L-KING-PLATZ6
D-2000 HAMBURG 13
W GERMANY

PETER KOFEL
SPECTROSPIN AG
INDUSTRIESTR 26

CH-8117 FALLANDEN
SWITZERLAND

JURGEN A KOPRIO
BALZERS
DEPT ECA

9496 BALZERS 075 447
LIECHTENSTEIN

S S KROLIK
VG ANALYTICAL
FLOATS ROAD
WYTHENSHAWE
MANCHESTER M23 9LE
ENGLAND

GIJI KUBOTA
1418 NAKAGAMI

AKISHIMA
TOKYO 196
JAPAN

WILLIAM LAUWERS
JANSSEN PHARMACEUTIC
TURNHOUTSE BAAN 30

B-2340 BEERSE
BELGIUM

A M LAWSON
CLINICAL RES CENTRE
HARROW

LONDON HA1 3UJ 01 864
ENGLAND

PIET A LECLERCQ
EINDHOVEN UNIV TECH
PO BOX 513

5600-MB EINDHOVEN
NETHERLANDS

ANDRE P DE LEENHEER
STATE UNIV OF GENT
RIJVISSCHEPARK 18

B-9710 GENT
BELGIUM

J J LETCHER
VG ANALYTICAL
FLOATS ROAD
WYTHENSHAWE
MANCHESTER
ENGLAND M23 9LE

IVOR LEWIS
DEPT OF CHEMISTRY
KING'S COLLEGE LONDON
STRAND
LONDON WC2R 2LS
ENGLAND

CHAVA LIFSHITZ
HEBREW UNIV
PHYSICAL CHEM DEPT
MAIL CODE 91904
JERUSALEM 02 5853
ISRAEL

CLAES LINDBERG
PHARMACOKINETICS LAB
AB DRACO
BOX 34
LUND S-22100
SWEDEN

H BERNHARD LINDEN
PO BOX 61 03 07

D-2800 BREMEN 61
W GERMANY

BUKO LINDNER
FORSCHUNGSINSTITUT BORSTEL
PARKALLES 10

D-2061 BORSTEL
WEST GERMANY

MICHAEL W LINSCHEID
SPEKTROCHEM
BUNSEN-KIRCHHOFF
STR 11
D-4600 DORTMUND 1
W GERMANY

P A LONGEVIALLE
ICSN CNRS

91190 SIF SUR
YVETTE
FRANCE

NORMAN LYNAUGH
VG MASSLAB
ALTRINCHAM

CHESHIRE
ENGLAND

ALLAN MACCOLL
UNIVERSITY COLLEGE
CHEMISTRY DEPT
20 GORDON ST
LONDON WC1H 0AJ
ENGLAND

C G MACDONALD
46 MIRNING CRESCENT

ARANDA 2614
AUSTRALIA

J K MACLEOD
AUSTRALIA NAT UNIV
RES SCHOOL OF CHEM
PO BOX 4
CANBERRA ACT 2600
AUSTRALIA

MARTYN MACPHERSON
BP RESEARCH CTR
CHERTSEY ROAD
SUNBURY ON THAMES
MIDDLESEX TW16 7LN
ENGLAND

A I MALLET
INSTITUTE OF DERMATOLOGY
HOMERTON GROVE

LONDON E9 6BX
ENGLAND

A A MANDELBAUM
TECHNION
CHEMISTRY DEPT

HAIFA 32000
ISRAEL

M F MAQUIN
SOCIETE ROUSSEL UCLAF
SPECTROMETRIE DE MASSE
102 ROUTE DE NOISY
93230 ROMAIVILLE 021 471
FRANCE

K M MARNELA
TAMPERE UNIV
PO BOX 607

33101 TAMPERE 10
FINLAND

KATSUYOSHI MASUDA
FACULTY OF PHARMACY
MEIJO UNIVERSITY
TEMPAKU
NAGOYA 468
JAPAN

ISAMU MATSUMOTO
INST HUMAN GENETICS
KANAZAWA MED UNIV
UCHINADA KAHOKU-GUN
ISHIKAWA 920-02 0762 86
JAPAN

T T MATSUO
INST OF PHYSICS
COLLEGE OF GENERAL EDUCATION
OSAKA UNIVERSITY
TOYONAKA 560
JAPAN

HAJIME MATSUSHIMA
HAMAMATSU UNIV SCH OF MEDICINE
3600 HANDA-CHO
HAMAMATSU 431-31

JAPAN

M A MCDOWELL
VG MASSLAB
3 TUDOR ROAD

ALTRINCHAM
ENGLAND WA14SR2

RUSSELL G MCLOUGHLIN
15 VIVIAN STREET

IVANHOE VIC
3079 AUSTRALIA

G G MELLERIO
UNIVERSITY OF PAVIA
C G S LAB MS
VIA TARAMELLI 10
27100 PAVIA 382 216
ITALY

TOM MERREN
VG ISOTOPES
ION PATH ROAD THREE
WINSFORD
CHESHIRE
ENGLAND

B J MILLARD
VG ANALYTICAL
FLOATS ROAD
WYTHENSHAWE
MANCHESTER
ENGLAND M23 9LE

BRIAN J MILLARD
VG ANALYTICAL LTD
FLOATS ROAD
WYTHENSHAWE
MANCHESTER M23 9LE
ENGLAND

HUBERT J MILON
NESTEC SA
RESEARCH DEPT (LABIOR)

ORBE 1350 24 42 1
SWITZERLAND

TOKUO MIZUNO
JEOL
1418 NAKAGAMI
AKISHIMA
TOKYO 196
JAPAN

R R MOFFETT
VG ANALYTICAL
FLOATS ROAD
WYTHENSHAWE
MANCHESTER
ENGLAND M23 9LE

JOHN J MONAGHAN
ICI MOND DIVISION
PO BOX 8
THE HEATH RUNCORN
CHESHIRE WA7 4OD
UNITED KINGDOM

E E MONTER
ZEISIGWEG 6

D5653 LEICHLINGEN
WEST GERMANY

L E MOORE
KRATOS
BARTON DOCK ROAD
URMSTON
MANCHESTER M31 2LD
ENGLAND

H R MORRIS
IMPERIAL COLLEGE
BIOCHEMISTRY DEPT

LONDON SW7 2AZ
ENGLAND

J D MORRISON
LA TROBE UNIVERSITY
PHYSICAL CHEMISTRY
BUNDOORA
MELBOURNE VIC 3083 03 479
AUSTRALIA

B J MULADY
VG ANALYTICAL
FLOATS ROAD
WYTHENSHAWE
MANCHESTER M23 9GL
ENGLAND

YUZO NAKAGAWA
SHIONOGI RESEARCH LABS
FUKUSHIMA-KU

OSAKA 553
JAPAN

ULRICH NEUERT
WERTHERSTR 163

4800 BIELEFELD 1
WEST GERMANY

N M NIBBERING
JANSHOF 39

1391-XK ABCOUDE 020 522
NETHERLANDS

A J NICHOLSON
6 SCOTT ST

HAWTHORN 3122
AUSTRALIA

R R OWEN
VG ANALYTICAL
FLOATS ROAD
WYTHENSHAWE
MANCHESTER
ENGLAND M23 9LE

T I PLATZNER
NRCN
PO BOX 9001

BEER SHEVA
ISRAEL

JOHN A RACE
VG ANALYTICAL LTD
FLOATS ROAD
WYTHENSHAWE
MANCHESTER M23 9LE 061 945
ENGLAND

GUY RICART
UNIV OF LILLE
UER CHIMIE BAT C4
5G655 VILLENEUVE
D'ASCO CEDEX
FRANCE

FRANZ W ROLLGEN
INST PHYSICAL CHEM
UNIV OF BONN
WEGELERSTR 12
D-5300 BONN
W GERMANY

EGMONT SCHALLER
HOLZWEG 7

D-7803 HEUWEILER 0761 51
W GERMANY

ULRICH J G SEYDEL
FORSCHUNGSINSTITUT
BIOPHYSICS DIV
PASKALLEE 10
D-2061 BORSTEL 04537 1
FED REP GERMANY

EWALD NIEHUIS
PHYS INST UNIV MUNSTER
DOMAGHSTR 75

4400 MUNSTER
F R GERMANY

JANET OXFORD
GLAXO GROUP RESEARCH
BIOCHEM PHARMACOLOGY
PRIORY STREET, WARE
HERTFORDSHIRE
UK

CHRIS J PORTER
VG ANALYTICAL
FLOATS ROAD
WYTHENSHAWE
MANCHESTER
ENGLAND M23 9LE

JAMES C RAMAGE
VG GAS ANALYSIS LTD
HOLMES CHAPEL ROAD
MIDDLEWICH
CHESHIRE
ENGLAND

WILHELM J RICHTER
CIBA GEIGY
K 127.508

CH-4002 BASEL
SWITZERLAND

KEITH ROLLINS
VG MASSLAB LTD
3 TUDOR ROAD
ALTRINCHAM
CHESHIRE
ENGLAND

U P SCHLUNEGGER
UNIVERSITAT BERN
INSTIT ORGAN CHEMIE
FREIESTRASSE 3
CH-3012 BERN 031 65
SWITZERLAND

YUKIO SHIMIZU
KOGAI-SHIGEN
KENKYUSHO
YATABE
IBARAKI 305 0298 54
JAPAN

TAMOTSU NODA
TOYOHASHI UNIV OF
TECHNOLOGY
TEMPAKU-CHO
TOYOHASHI 440 0532 47
JAPAN

V C PARR
VG ANALYTICAL
FLOATS ROAD
WYTHENSHAW
MANCHESTER
ENGLAND

PATRICK POWERS
16 MORETON AVENUE
HARPENDEN

HERTS AL5 2ET 1 637 9
ENGLAND

JACQUES RAPIN
SWISS FEDERAL INST OF TECH
EPFL-ECUBLENS

CH-1015 LAUSANNE
SWITZERLAND

W W RIEPE
BERBAU-FORSCHUNG GMB
FRANZ-FISCHER-WEG 61

D-4300 ESSEN 13
WEST GERMANY

PETER RYAN
KRATOS
BARTON DOCK RD
URMSTON
MANCHESTER M31 2LD
U.K

ERICH R SCHMID
UNIVERSITAT WIEN
INST F ANAL CHEMIE
WAHRINGERSTRASSE 38
A-1090 VIENNA 0222 34
AUSTRIA

CHARLES SMITH
VG ANALYTICAL
TUDOR ROAD
ALTRINCHAM
CHESHIRE
ENGLAND

J J OGDEN
BRIT NUCLEAR FUELS
BLDG 202 MASS SPEC
BNFL CAPENHURST
CHESTER CHIGER 051 339
UK

BEATRICE PELLI
CONS NAX DELLA RICERCHE
AREA DI RECERCA DI PADOVA
CORSO STATI UNITI 4
35020 CAMIN
ITALY

JOHN PRATT
KRATOS ANALYTICAL
BARTON DOCK ROAD
URMSTON
MANCHESTER M31 2LD
ENGLAND

MARTIN RESCH
FRANZ-BRACHT-STR 47

D-4350RECKLINGHAUS
FED REP GERMANY

J D ROBINSON
VG ANALYTICAL
FLOATS ROAD
WYNTHENSHAWE
MANCHESTER
ENGLAND

G G SCHADEN
FACHBER
PHARMAZIE D UNIV

D-3550 MARBURG 06421 2
WEST GERMANY

JAMES SCRIVENS
ICI PETROCHEMICALS
RESEARCH DEPT
PO BOX 90
WILTON CLEVELAND
ENGLAND TS6 8JE

J F SMITH
LA TROBE UNIVERSITY

BUNDOORA VIC 3083
AUSTRALIA

R D SMITH
THE LITTLE HOUSE
BOVINGDON GREEN
BOVINGDON
HERTS HP3 OLD 44 442
ENGLAND

JOHN D SPENCE
ICI PLANT PROTECTION DIV
JEALOTTS HILL

BRACKNELL RG2 6EY
ENGLAND

W W STECKELMACHER
177 RUSPER RD
IFIELD CRAWLEY

SUSSEX RH11 0HT 0293 21
ENGLAND

B P STIMPSON
AERE HARWELL
INSTR & APPLIED
PHYSICS DIV BD148
OXFORDSHIRE OX11 0 0235 24
ENGLAND

MAKOTO SUZUKI
MEIJO UNIVERSITY
PHARMACY FACULTY
TEMPAKU
NAGOYA 468 052 832
JAPAN

RAFFAELE TABACCHI
UNIV DE NEUCHATEL
INST DE CHIMIE
AV DE BELLEVAUX 51
CH-2000 NEUCHATEL
SWITZERLAND

AKIRA TATEMATSU
MEIJO UNIVERSITY
PHARMACY FACULTY
TEMPAKU
NAGOYA 468 052 832
JAPAN

J P THENOT
LERS
SYNTHELABO
58 RUE DE LA GLACIERE
75013 PARIS
FRANCE

JOHN F J TODD
UNIV CHEM LABORATORY
UNIV OF KENT
CANTERBURY
KENT CT2 7NH 0227 66
UK

J C TRAEGER
LA TROBE UNIVERSITY
PHYSICAL CHEMISTRY

BUNDOORA VIC 3083
AUSTRALIA

PIETRO TRALDI
CONS NAX DELLA RECERCHE
AREA DI RECERCA DE PADOVA
CORSO STATI UNITI 4
35020 CAMIN
ITALY

GERHARD TRESSL
HEWLETT PACKARD
HERREN BERGERSTR 110

703 BOEBLINGEN
W GERMANY

C W TSANG
APPLIED SCIENCE
HONG KONG POLYTECH
HUNG HOM
KOWLOON 3 63834
HONG KONG

M M TSUCHIYA
4 37 27 KUGAYAMA
SUGINIMI KU

TOKYO 168 03 812
JAPAN

P J TURNER
VG MICROMASS LTD
ION PATH
ROAD THREE
WINSFORD CHESHIRE
ENGLAND

PIRJO VAINIOTALO
UNIV OF JOENSUU
DEPT OF CHEMISTRY
PO BOX 111
SF-80101 JOENSUU
FINLAND

SOPHIE VAJTA
32 RUE DE GOMETZ

BURES-SUR-YVETTE
91440 FRANCE

DR J VANDERGREEF
CIVO-TNO
PO BOX 360

3700 AJ ZEIST 03404 5
NETHERLANDS

RONALD VANDOORN
ROYAL DUTCH
SHELL LAB
POSTBUS 3003
1003AA AMSTERDAM 020 303
NETHERLANDS

FRANCESCA VENTURA
INST DE QUIMICA BIO-ORGANICA
J GIRONA SALGADO 18-26

08034 BARCELONA
SPAIN

PAUL VIGNY
INSTITUTE CURIE
11 RUE P ET M CURIE

75231 PARIS CEDEX 329 12
FRANCE

ADAM VINCZE
ISRAEL INST BIOL RES
PO BOX 19

NESS ZIONA 70450 972 8 4
ISRAEL

KARL PETER WANCZEK
PARKALLEE 197

D-2800 BREMEN
WEST GERMANY

CHRISTOPHER D WATTS
WATER RESEARCH CTR
PO BOX 16 HENLEY RD
MEDMENHAM
MARLOW BUCKS 0491 57
ENGLAND

PATRICK WEHRUNG
UNIV DE STRASBOURG
DEPT DE CHIMIE
1 RUE BLAISE PASCAL
F-67008 STRASBOURG
FRANCE

GARY D WILLETT
DEPT OF PHY CHEM
UNIV OF N S W
PO BOX 1 KENSINGTON
N S W 2033
AUSTRALIA

H W WILSON
ASHGROVE
THE CRESCENT
BUSBY
GLASGOW G76 8HT
SCOTLAND

HERMANN WOLLNIK
UNIVERSITY GIESSEN
H BUFF RING 16

6300 GIESSEN
WEST GERMANY

CHOON WONG
AUSTRALIAN NAT'L UNIV
RSBS
PO BOX 275
CANBERRA ACT
AUSTRALIA 2601

DAVID WOOD
52 POISEBROOK ROAD
OFFERTON

CHESHIRE SK2 5JF
ENGLAND

ZIRO YAMAIZUMI
NAT'L CANCER CENTER INST
BIOLOGY DIV
5-1-1 TSUKIJI CHUO-K
TOKYO 104
JAPAN

JEHUDA YINON
WEIZMANN INSTITUTE
ISOTOPE RESEARCH

REHOVOT 76100 08 4825
ISRAEL

L F ZERILLI
GRUPPO LEPETIT
VIA DURANDO 38

20158 MILANO
ITALY

MARKUS ZOLLINGER
RAINSTRASSE 20

CH-8610 USTER
SWITZERLAND